F 1103

ACADÉMIE DE LA RÉPUBLIQUE SOCIALISTE DE ROUMANIE

REFERÁLVA

REVUE ROUMAINE DE CHIMIE

TOME 23
N° 1
Janvier 1978

EDITURA ACADEMIEI REPUBLICII SOCIALISTE ROMÂNIA

Rev. Roumaine Chim.

RECHAX, 23, *1*, p. 1–160 (1978), Bucarest

ACADÉMIE DE LA RÉPUBLIQUE SOCIALISTE DE ROUMANIE

COMITÉ DE RÉDACTION

Rédacteur en chef :

I. G. MURGULESCU, membre de l'Académie de la République Socialiste de Roumanie

Rédacteurs en chef adjoints :

A. T. BALABAN et V. EM. SAHINI, membres correspondants de l'Académie de la République Socialiste de Roumanie

Collège de rédaction :

EM. BRATU, ELENA CEAUŞESCU, ECATERINA CIORĂNESCU-NENITZESCU, C. DRĂGULESCU, CR. SIMIONESCU, membres de l'Académie de la République Socialiste de Roumanie; P. SPACU, membre correspondant de l'Académie de la République Socialiste de Roumanie; MARGARETA AVRAM, I. HAIDUC, D. I. MARCHIDAN, I. MOLDOVAN, G. NIAC et D. SĂNDULESCU

La Revue Roumaine de Chimie paraît 10 fois par an. Toute commande de l'étranger (fascicules ou abonnements) sera adressée à ILEXIM – Serviciul Export-Import Carte (Livres)/Serviciul Export-Import Presă (Revues), P.O.B. 136–137, télex 11226, 3, str. 13 Decembrie, Bucarest, Roumanie.

Les manuscrits, les livres et les revues proposés en échange, ainsi que toute correspondance seront envoyés à la rédaction :

REVUE ROUMAINE DE CHIMIE

125, Calea Victoriei, Bucarest, téléphone 50 76 80

EDITURA ACADEMIEI REPUBLICII SOCIALISTE ROMÂNIA

125, Calea Victoriei, 71021, Bucarest, Roumanie, téléphone 50 76 80

REVUE ROUMAINE
DE
CHIMIE

ORSZÁGOS MŰSZAKI KÖNYVTÁR ÉS DOKUMENTÁCIÓS KÖZPONT 1883
1978 FEB 14

Tome 23, N°. 1 Janvier 1978

C. BENDIC, MIHAELA HILLEBRAND and V. E. SAHINI, Computer program for S.C.F.-C.I. calculations. I. Closed shell systems 3–17

D. I. MARCHIDAN and M. CIOPEC, Thermodynamic properties of maleic, trimellitic and pyromellitic anhydrides 19–29

K. SINGH, The limiting apparent molal volumes of ions in N-methylacetamide 31–36

E. J. BARAN, Vibrational spectrum of β-vanadylsulfate (in German) 37–43

L. G. IONESCU, Entropy of some simple gas-water clathrates 45–53

R N. S. BIRADAR, V. B. MAHALE and B. R. HAVINALE, Four and six coordinate complexes of Zn(II) with aroyl hydrazones 55–61

R MARIA VĂGĂONESCU, S. MAGER and LUCIA MUNTEANU, Molecular complexes of nitrophenols with hexamethylenetetramine and their isomers 63–71

M. F. EL-NEWAIHY, E. I. ENAYAT, M. R. SALEM and H. A. ABDEL HAMID, Condensation of 3,4-disubstituted benzophenones with dimethyl homophthalate 73–78

S. H. ETAIW, F. A. ANWER and F. M. ISSA, Electronic spectra and structure of 4-arylhydrazono-3-methyl-5-pyrazolones 79–87

CR. I. SIMIONESCU, S. DUMITRIU, V. I. POPA, V. BULACOVSCHI and B. SIMIONESCU, Chemical model for the synthesis of living matter (in French) 89–102

J. V. KNOP, N. TRINAJSTIĆ, M. MILUN and S. PEJAKOVIĆ, Conformational analysis and electronic structure of thienylpyridines 103–110

R GEORGETA M. GHERASIM and LEONIA STOICESCU-CRIVETZ, Thermal and photoinduced polymerization of N,N′-bismaleimide 111–118

R I. PETRARIU and EUGENIA BĂRBÎNȚĂ, Interaction between chloromethylated styrene–divinylbenzene and dimethylformamide 119–123

C. LITEANU and T. HODIȘAN, Optimization of the separation process in temperature gradient chromatography. II. Determination of the minimum chromatographing time necessary for the separation of some component mixtures by applying a constant temperature gradient 125–131

S. GOCAN, C. KONNERT and H. VOIK, Separation of polyphenols by thin layer chromatography with orthogonal temperature gradient (in German) 133–135

Rev. Roumaine Chim., 23, *1*, p. 1–160 (1978), Bucares

ELENA HOPÎRTEAN and EUGENIA ŞTEFĂNIGĂ, Liquid membrane-electrodes. XII. Liquid membrane-electrodes for perchlorate, thiocyanate, tetrafluoroborate and nitrate based on triphenylmethane dyes 137–142

A. T. BALABAN, ILEANA I. STĂNOIU, F. CHIRALEU and I. MOŢOC, Isotopic exchange of active methyl groups. XI. Kinetics of deuteriation of 2,6-diaryl-4-methylpyrylium salts 143–146

ANDREEA SECARĂ, A. TURCU and E. SEGAL, Kinetic investigation of some molecular complexes between 1,3,7,9-tetranitrophenothiazine-5-oxide and amines 147–155

BOOK REVIEWS 157–160

Revue Roumaine de Chimie, **23**, *1*, 3–17 (1978)

COMPUTER PROGRAM FOR S.C.F.-C.I. CALCULATIONS

I. CLOSED SHELL SYSTEMS

C. BENDIC, MIHAELA HILLEBRAND and V. E. SAHINI
Department of Physical Chemistry, Polytechnic Institute, B-dul Republicii 13, Bucharest, Romania

Received April 26, 1977

A program written in FORTRAN IV for S.C.F.-C.I. calculations is given. The electronic properties and reactivity indices of π-electron systems can be calculated.

The increasing interest in the electronic structure and reactivity of large organic compounds requires fast calculations of the electronic properties in the ground and excited states, using relatively few parameters.

In this paper, a program written in FORTRAN IV is given which allows calculations for π-electron systems, using the semiempirical S.C.F.-P.P.P. method.[1,2] This program was conceived to obtain the electronic properties of both ground and excited states, with and without taking into account the configurational interaction. The convergence of eigenvectors was chosen from the different selfconsistency criteria. The iterative S.C.F. procedure is continued untill the difference between the same components of the eigenvectors obtained in two consecutive iterations does not exceed 0.0005. The program is stopped after 20 iterations even if the selfconsistency is not yet reached. The best method to improve the rate of convergence was found to change the starting Huckel parameters. In order to reduce the running time, only the $M(I, J)$, $J \geqslant I$ elements of the symmetrical matrices are calculated.

The program is schematically presented in Fig. 1.

For an easier manipulation, the program was assembled from 14 subprograms. If some properties are not desired, the respective subroutines can be left out.

The main operations handled by every subprogram are summarised in the following:

— SUBROUTINE COORA	the atomic position coordinates and the interatomic distances are calculated by a method already described[3].

---

[1] J. A. Pople, *Trans. Faraday Soc.*, **49**, 1375 (1953).

[2] R. Pariser and R. G. Parr, *J. Chem. Phys.*, **21**, 767 (1953).

[3] M. Gheorghiu and P. Filip, "Aplicaţiile Calculatoarelor în Chimie", Ed. Ştiinţifică, Bucureşti, 1973, p. 237.

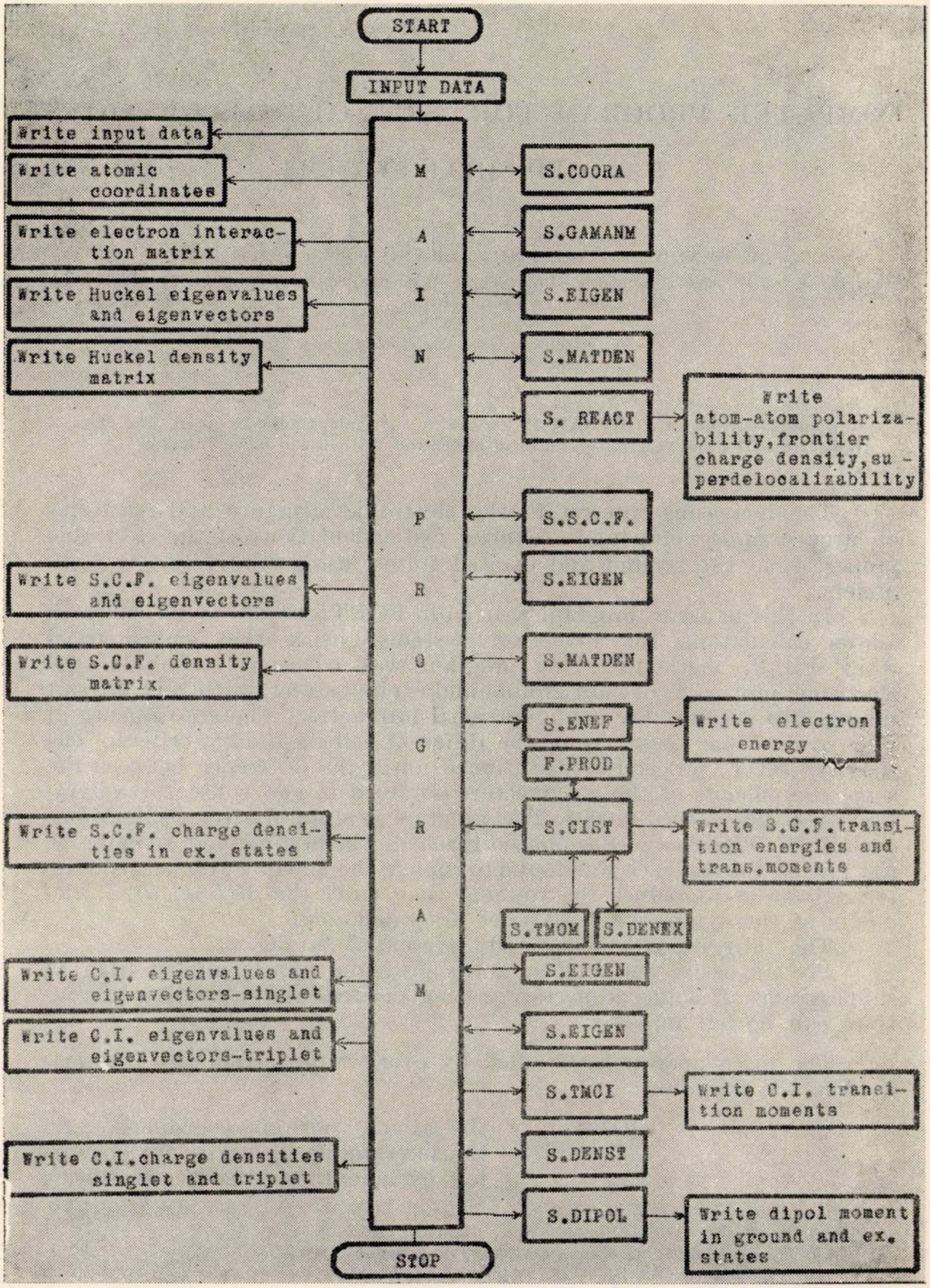
START
INPUT DATA
MAIN PROGRAM
Write input data
Write atomic coordinates
S.COORA
Write electron interaction matrix
S.GAMANM
Write Huckel eigenvalues and eigenvectors
S.EIGEN
Write Huckel density matrix
S.MATDEN
S. REACT
Write atom-atom polarizability, frontier charge density, superdelocalizability
S.S.C.F.
Write S.C.F. eigenvalues and eigenvectors
S.EIGEN
Write S.C.F. density matrix
S.MATDEN
S.ENEF
Write electron energy
F.PROD
Write S.C.F. charge densities in ex. states
S.CIST
Write S.C.F. transition energies and trans. moments
S.TMOM
S.DENEX
Write C.I. eigenvalues and eigenvectors-singlet
S.EIGEN
Write C.I. eigenvalues and eigenvectors-triplet
S.EIGEN
S.TMCI
Write C.I. transition moments
Write C.I. charge densities singlet and triplet
S.DENST
S.DIPOL
Write dipol moment in ground and ex. states
STOP

Fig. 1

— SUBROUTINE GAMANM calculates the two-centre bielectronic repulsions using the Nishimoto-Mataga approximation[4].

$$\gamma_{\mu\nu} = \frac{14.3897}{a_{\mu\nu} + r_{\mu\nu}}; \quad a_{\mu\nu} = \frac{28.7794}{\gamma_{\mu\mu} + \gamma_{\nu\nu}};$$

$$\gamma_{\mu\mu} = I_{\mu} - A_{\mu} \tag{1}$$

— SUBROUTINE MATDEN calculates the charge and bond order matrix

$$P_{\mu\mu} = \sum_{i=1}^{all} n_i \, c_{i\mu}^2 \tag{2}$$

— SUBROUTINE SCF calculates the elements of the S.C.F. energy matrix

$$\begin{aligned} F_{\mu\mu} &= I_{\mu} + 1/2 P_{\mu\mu} \gamma_{\mu\mu} - \sum_{\nu \neq \mu} (Z_{\nu} - P_{\nu\nu}) \gamma_{\mu\nu} \\ F_{\mu\nu} &= \beta_{\mu\nu} - 1/2 P_{\mu\nu} \gamma_{\mu\nu} \end{aligned} \tag{3}$$

— SUBROUTINE ENEF calculates the π-electron energy in the ground state

$$E = \sum_i (I_i + \varepsilon_i) \tag{4}$$

— SUBROUTINE CIST calculates the elements of the configurational interaction matrix and the S.C.F. singlet and triplet electronic transition energy.

$$\begin{aligned} ({}^1V_{i-j} \,|H|\, {}^1V_{i-j}) &= \varepsilon_j - \varepsilon_i - (ii/jj) + \\ &\quad + 2(ij/ij) \\ ({}^1V_{i-j} \,|H|\, {}^1V_{k-l}) &= 2(ij/kl) - (ik/jl) \\ ({}^3V_{i-j} \,|H|\, {}^3V_{i-j}) &= \varepsilon_j - \varepsilon_i - (ii/jj) \\ ({}^3V_{i-j} \,|H|\, {}^3V_{k-l}) &= -\,(ik/jl) \\ {}^{1,3}V_{i-j} &= 1/\sqrt{2}\,(\chi_{i-\bar{j}} \mp \chi_{\bar{i}-j}) \end{aligned} \tag{5}$$

$$(ij/kl) = \sum_{\mu} \sum_{\nu} c_{i\mu} \, c_{j\mu} \, \gamma_{\mu\nu} \, c_{k\nu} \, c_{l\nu}$$

---

[4] K. Nishimoto and N. Mataga, *Z. phys. Chem.* (*Frankfurt*), **13**, 140 (1957).

This subroutine claims for a subprogram function PROD and two subroutines TMOM and DENEX.

— FUNCTION PROD

$$\mathrm{PROD}\,(I,\ J,\ K,\ L) = (ij/kl) \tag{6}$$

— SUBROUTINE TMOM calculates the S.C.F. transition moments and their components.

$$M_x\,(i \to j) = \sqrt{2} \sum_{\mu} c_{i\mu}\,(ex_\mu) c_{j\mu} \tag{7}$$

— SUBROUTINE DENEX calculates the S.C.F. atomic charge densities in the excited states (eq. 2).

The next subroutines are concerned with the properties in the excited states obtained by the interaction of the ${}^{1,3}V_{i-j}$ configurations.

$${}^{1,3}\psi_k = \sum_{i-j} {}^{1,3}(a_{i-j})_k\, {}^{1,3}V_{i-j} \tag{8}$$

where $(a_{i-j})_k$ stands for the coefficient of the S.C.F. excited configuration ${}^{1,3}V_{i-j}$ in function ψ_K.

— SUBROUTINE DENST calculates the atomic charge densities for ψ_K.[5,6]

$${}^{1,3}P_{\mu\mu} = q_\mu + \sum_{i-j,k-l} {}^{1,3}a_{i-j}\,{}^{1,3}a_{k-l}\,(c_{j\mu}c_{l\mu}\delta_{ik} - c_{i\mu}\,c_{k\mu}\delta_{jl}) \tag{9}$$

— SUBROUTINE TMCI calculates the C.I. transition moments and their components.

$$M_x(\mathrm{C.I.}) = \int V_0 \sum_{\mu} ex_\mu\, {}^1\psi_K = \sum_{i-j} {}^1a_{i-j}\, M_x\,(i \to j) \tag{10}$$

— SUBROUTINE REACT calculates the atom-atom polarizability, the frontier charge density and the superdelocalizability for the elec-

---

[5] V. I. Danilov, I. A. Krugliac and V. I. Pecenaia, *Theor. Chim. Acta*, **13**, 288 (1969).

[6] V. I. Danilov, I. A. Krugliac and V. I. Pecenaia, *Theor. exp. Khim*, **5**, 669. (1969).

trophilic, radicalic and nucleophilic substitution.

$$\pi_{\mu\nu} = 4 \sum_{i}^{\text{occ}} \sum_{j}^{\text{unocc}} \frac{c_{i\mu}\, c_{i\nu}\, c_{j\mu}\, c_{j\nu}}{\varepsilon_i - \varepsilon_j}$$

$$f_\mu = (2 - n_e)c^2_{f\mu} + n_e\, c^2_{(f+1)\mu} \qquad (11)$$

$$S_\mu = \sum_j (n_j - n_e)c^2_{j\mu}/\varepsilon_j$$

$n_e = 0$, electrophilic substitution; $n_e = 1$, radicalic substitution, $n_e = 2$, nucleophilic substitution.

— SUBROUTINE DIPOL calculates the π dipol moment both in the ground and first excited states. (S.C.F. and C.I.)

— SUBROUTINE EIGEN the subroutine EIGEN[7] is used to diagonalise the Huckel, S.C.F. and C.I. matrices.

All the symboles used in equations (1)—(11) have the usual meaning. The following symboles are used for the different variables in the program :

N : the numbers of π electron centers

M : the number of the occupied molecular orbitals.

NJ, NS : numbers which define the lowest $(M - NJ)$ and the highest $(M + NS)$ orbital included in the configurational interaction.

NCI : the order of the configurational interaction matrix.

FCD, FSD, FSR1, FSR2, FSR3 : FORMAT instructions for reading and writing the input and output data.

A(I), A1(I), A2(I) : upper diagonal elements of a matrix taken as a row vector $(a_{11}, a_{12}, a_{22}, a_{,13}, a_{23})$: this form is claimed by the subroutine EIGEN. A, A1, A2 stand for the Huckel, S.C.F. and C.I. matrices, respectively. After the matrix diagonalisation, the elements $A(I(I+1)/2)$ represent the corresponding eigenvalues.

R(I), R1(I), R(I) : components of the eigenvectors belonging to Huckel S.C.F. and C.I. matrices, respectively.

HO(I,J) : the element of the monoelectronic hamiltonian matrix.

G(I) : the monocentre repulsion integral.

EN(I) : the number of electrons in a molecular orbital

Z(I) : the charge of the atomic core.

RAB, RBC, RCD : the interatomic distances between different pairs of the A, B, C, D atoms.

NA, NB, NC, ND : atomic labels for the atoms A, B, C, D.

TETA, BCD, ABCD : the ABC, BCD, respectively the dihedral $ABCD$ angles.

X(I), Y(I), ZET(I) : atomic position coordinates.

---

[7] ''Scientific Subroutine Package, IBM System 360''.

RAZA (I, J) : the interatomic distance.
GAMA (I, J) : the two-centre interaction integral.
ICONT : the number of iterations.
C(I, J), CV(I, J) : the elements of the S.C.F. eigenvector matrix ; two different matrices are necessary to compare the values obtained by two successive iterations $(CV(I,J) = -C(I,J))$.
P(I, J) : the atomic charge and bond order.
ENER(I) : S.C.F. molecular orbital energy.
EFUND : the π electron energy.
PI(I, J) : atom-atom polarizability.
F(I) : frontier charge density.
S(I) : superdelocalizability.
TMX, TMY, TMZ, TM2 : the components and the square of the S.C.F. transition moments.
TMCIX, TMCIY, TMCIZ, TMCI2 : the components and the square of the C.I. singlet transition moments.
DEX (I, J) : the S.C.F. charge density of atom J in the excited configuration I.
DENS(I, J), DENT(I, J) : the charge density of atom J in the excited singlet and triplet state I after the configurational interaction.
DX1, DY1, DZ1, DIP1 : the components and the dipol moment in the S.C.F. ground state.
DX2, DY2, DZ2, DIP2 : the components and the dipol moment in the first excited S.C.F. state.
DX3, DY3, DZ3, DIP3 : the components and the dipol moment in the first C.I. excited state.

INPUT DATA

The input data are read in the following sequence :
— N, M, NJ, NS, NCI (5I2)
— FCD (18A4)
— FSD (18A4)
— FSR1 (18A4)
— FSR2 (18A4)
— FSR3 (18A4)
— (A(I), I = 1, K) (FCD)
— ((HO(I, J), J=1, N), I = 1, N) (FCD)
— (G(I), I = 1, N) (FCD)
— (EN(I), I = 1, N) (FCD)
— (Z(I), I = 1, N) (FCD)
— RAB, RBC, TETA (2F5.3, F6.2)

This card is necessary to obtain the coordinates of the first three atoms ; the initial system is chosen as the coordinates of these atoms can be easily computed. The origin is fixed on the atom A and the X axis along the AB bond.* TETA is taken considering the reference system translated in B with the X pointing towards C.

---

* For more details see the reference [3].

The following (N—3) cards contain sequences required to calculate the coordinates of the D atoms; a sequence has the general form :
— NA, NB, NC, ND, RCD, BCD, ABCD (4I3, 3F10.5)

The sequence can be chosen arbitrarily, provided the coordinates of the considered A, B, C, atoms have been computed from the previous sequences; if the molecule is folded about an axis passing through two nonbonded atoms, when atom D is not in the same plane as A, it is indicated to use a sequence in which the nonbonded atoms play the role of the B, C atoms. The *ABC* and *ABCD* angles are taken in a local reference system, resulted by translation of the initial system in C, followed by rotations around *Z*, *Y*, and *X* axis, to obtain *X* axis pointing towards B and a positive *Y* coordinate for the atom A.

OUTPUT DATA

The program prints the input data (FSD) and the following results :
- atomic coordinates (3(4x,F8.4));
- the matrix of the interatomic distances (FSR2);
- the matrix of bielectronic interaction integrals (FSR2);
- Huckel results :
  - eigenvalues and eigenvectors (FSR1);
  - charge and bond order matrix (FSR2);
  - atom-atom polarizability matrix (FSR2);
- frontier charge densities and superdelocalizabilities for electrophilic, radicalic and nucleophilic substitution (I4, 2F9.3,3x, 2F9.3, 3x, 2F9.3);
- S.C.F. results :
  - eigenvalues and eigenvectors (FSR1);
  - charge and bond order matrix (FSR2);
  - π dipol moment and its components in the ground state (4F12.5)
  - π dipol moment and its components in the first excited state (4F12.5);
  - π electron energy in the ground state (F12.5);
  - number of iterations (I3);
  - energies of the singlet and triplet transitions and the transition moments of the singlet states (2I4, 6F12.4);
  - atomic charge densities in excited states (2I3,3x, 16F7.4);
- C.I. results :
  - C.I. singlet and triplet eigenvalues and eigenvectors (FSR3);
  - C.I. transition moments (I4,4(5x, F9.5));
  - atomic charge densities in the C.I. singlet and triplet states* (FSR2);
  - dipol moment and its components in the first C.I. excited state (4F12.5);

In order to check the validity of the program, the results were compared with those given by Solony et al.,[8] for pyrrole, thiophene and furane.

---

* The atomic charge densities are listed starting from the configuration of highest energy.

[8] N. Solony, F. W. Birss and J. B. Greenshields, *Canad. J. Chem.*, **43**, 1569 (1965).

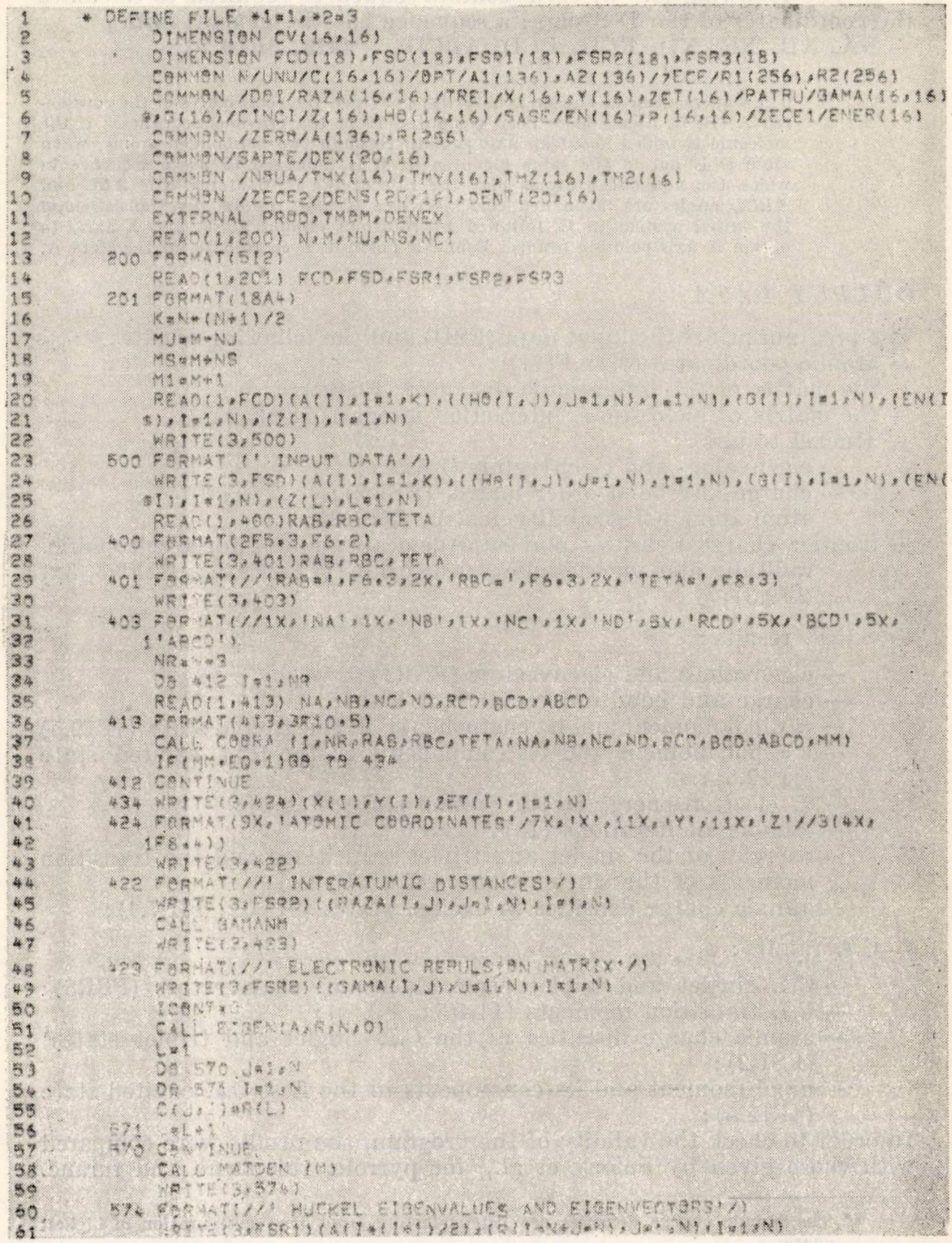

```
      * DEFINE FILE *1=1,*2=3
        DIMENSIØN CV(16,16)
        DIMENSIØN FCD(18),FSD(18),FSR1(18),FSR2(18),FSR3(18)
        CØMMØN N/UNU/C(16,16)/ØPT/A1(136),A2(136)/ZECE/R1(256),R2(256)
        CØMMØN /DØI/RAZA(16,16)/TREI/X(16),Y(16),ZET(16)/PATRU/GAMA(16,16)
       *,G(16)/CINCI/Z(16),HØ(16,16)/SASE/EN(16),P(16,16)/ZECE1/ENER(16)
        CØMMØN /ZERØ/A(136),R(256)
        CØMMØN/SAPTE/DEX(20,16)
        CØMMØN /NØUA/TMX(16),TMY(16),TMZ(16),TM2(16)
        CØMMØN /ZECE2/DENS(20,16),DENT(20,16)
        EXTERNAL PRØD,TMØM,DENEX
        READ(1,200) N,M,MU,NS,NCI
    200 FØRMAT(5I2)
        READ(1,201) FCD,FSD,FSR1,FSR2,FSR3
    201 FØRMAT(18A4)
        K=N*(N+1)/2
        MJ=M-NJ
        MS=M+NS
        M1=M+1
        READ(1,FCD)(A(I),I=1,K),((HØ(I,J),J=1,N),I=1,N),(G(I),I=1,N),(EN(I
       $),I=1,N),(Z(I),I=1,N)
        WRITE(3,500)
    500 FØRMAT (' INPUT DATA'/)
        WRITE(3,FSD)(A(I),I=1,K),((HØ(I,J),J=1,N),I=1,N),(G(I),I=1,N),(EN(
       *I),I=1,N),(Z(L),L=1,N)
        READ(1,400)RAB,RBC,TETA
    400 FØRMAT(2F5.3,F6.2)
        WRITE(3,401)RAB,RBC,TETA
    401 FØRMAT(//'RAB=',F6.3,2X,'RBC=',F6.3,2X,'TETA=',F8.3)
        WRITE(3,403)
    403 FØRMAT(//1X,'NA',1X,'NB',1X,'NC',1X,'ND',6X,'RCD',5X,'BCD',5X,
       1'ABCD')
        NR=N-3
        DØ 412 I=1,NR
        READ(1,413) NA,NB,NC,ND,RCD,BCD,ABCD
    413 FØRMAT(4I3,3F10.5)
        CALL CØØRA (I,NR,RAB,RBC,TETA,NA,NB,NC,ND,RCD,BCD,ABCD,MM)
        IF(MM.EQ.1)GØ TØ 434
    412 CØNTINUE
    434 WRITE(3,424)(X(I),Y(I),ZET(I),I=1,N)
    424 FØRMAT(9X,'ATØMIC CØØRDINATES'/7X,'X',11X,'Y',11X,'Z'//3(4X,
       1F8.4))
        WRITE(3,422)
    422 FØRMAT(//' INTERATUMIC DISTANCES'/)
        WRITE(3,FSR2)((RAZA(I,J),J=1,N),I=1,N)
        CALL GAMANM
        WRITE(3,423)
    423 FØRMAT(//' ELECTRØNIC REPULSIØN MATRIX'/)
        WRITE(3,FSR2)((GAMA(I,J),J=1,N),I=1,N)
        ICØNT=0
        CALL EIGEN(A,R,N,0)
        L=1
        DØ 570 J=1,N
        DØ 571 I=1,N
        C(J,I)=R(L)
    571 L=L+1
    570 CØNTINUE
        CALL MATDEN (M)
        WRITE(3,574)
    574 FØRMAT(//' HUCKEL EIGENVALUES AND EIGENVECTØRS'/)
        WRITE(3,FSR1)(A(I*(I+1)/2),(R(I-N+J*N),J=1,N),I=1,N)
```

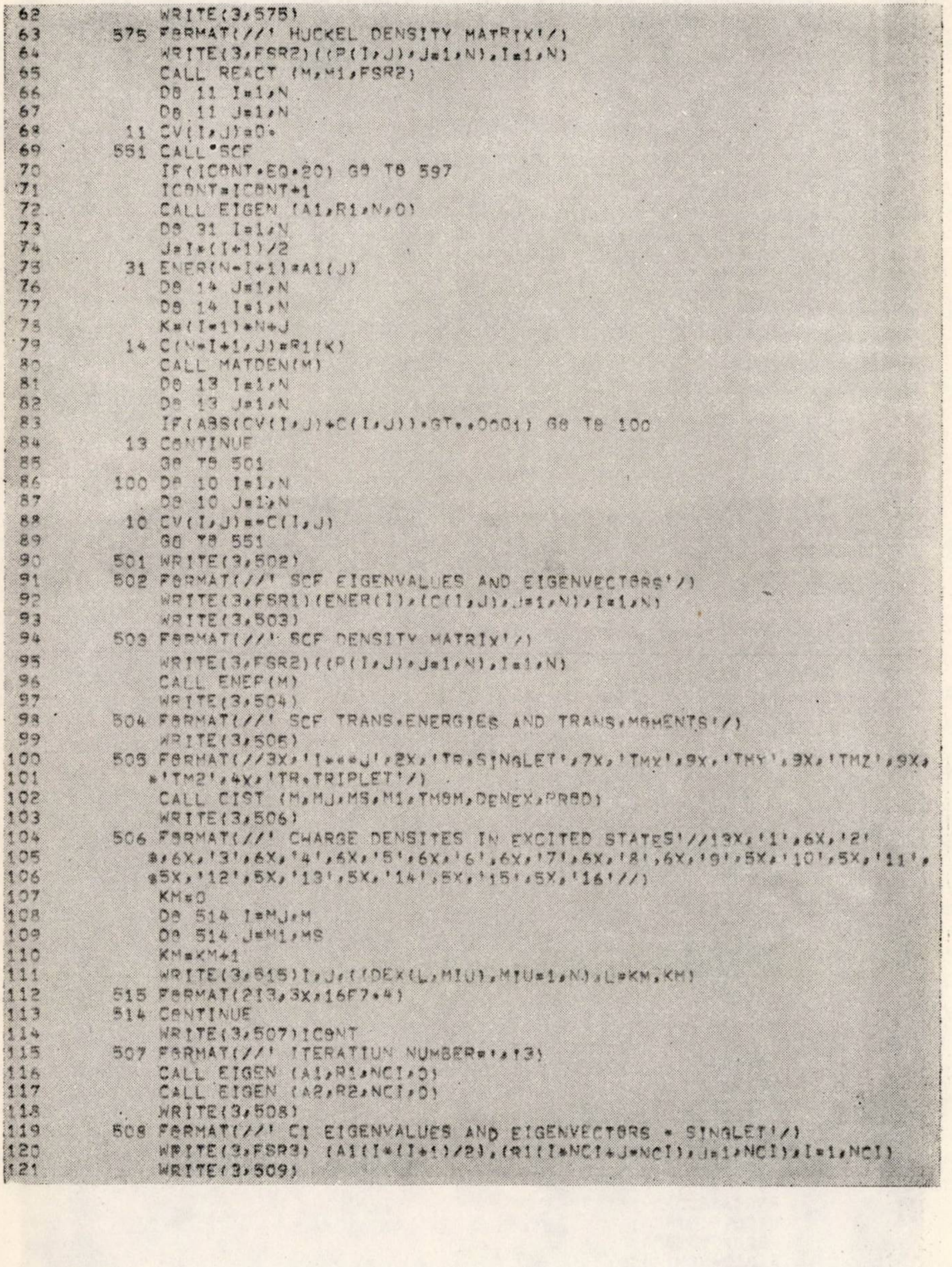

```
      WRITE(3,575)
  575 FØRMAT(//' HUCKEL DENSITY MATRIX'/)
      WRITE(3,FSR2)((P(I,J),J=1,N),I=1,N)
      CALL REACT (M,M1,FSR2)
      DØ 11 I=1,N
      DØ 11 J=1,N
   11 CV(I,J)=0.
  551 CALL SCF
      IF(ICØNT.EQ.20) GØ TØ 597
      ICØNT=ICØNT+1
      CALL EIGEN (A1,R1,N,0)
      DØ 31 I=1,N
      J=I*(I+1)/2
   31 ENER(N-I+1)=A1(J)
      DØ 14 J=1,N
      DØ 14 I=1,N
      K=(I-1)*N+J
   14 C(N-I+1,J)=R1(K)
      CALL MATDEN(M)
      DØ 13 I=1,N
      DØ 13 J=1,N
      IF(ABS(CV(I,J)+C(I,J)).GT..0001) GØ TØ 100
   13 CØNTINUE
      GØ TØ 501
  100 DØ 10 I=1,N
      DØ 10 J=1,N
   10 CV(I,J)=-C(I,J)
      GØ TØ 551
  501 WRITE(3,502)
  502 FØRMAT(//' SCF EIGENVALUES AND EIGENVECTØRS'/)
      WRITE(3,FSR1)(ENER(I),(C(I,J),J=1,N),I=1,N)
      WRITE(3,503)
  503 FØRMAT(//' SCF DENSITY MATRIX'/)
      WRITE(3,FSR2)((P(I,J),J=1,N),I=1,N)
      CALL ENEF(M)
      WRITE(3,504)
  504 FØRMAT(//' SCF TRANS.ENERGIES AND TRANS.MØMENTS'/)
      WRITE(3,505)
  505 FØRMAT(//3X,'I***J',2X,'TR.SINGLET',7X,'TMX',9X,'TMY',9X,'TMZ',9X,
     *'TM2',4X,'TR.TRIPLET'/)
      CALL CIST (M,MJ,MS,M1,TMØM,DENEX,PRØD)
      WRITE(3,506)
  506 FØRMAT(//' CHARGE DENSITES IN EXCITED STATES'//13X,'1',6X,'2'
     *,6X,'3',6X,'4',6X,'5',6X,'6',6X,'7',6X,'8',6X,'9',5X,'10',5X,'11',
     *5X,'12',5X,'13',5X,'14',5X,'15',5X,'16'//)
      KM=0
      DØ 514 I=MJ,M
      DØ 514 J=M1,MS
      KM=KM+1
      WRITE(3,515)I,J,((DEX(L,MIU),MIU=1,N),L=KM,KM)
  515 FØRMAT(2I3,3X,16F7.4)
  514 CØNTINUE
      WRITE(3,507)ICØNT
  507 FØRMAT(//' ITERATIUN NUMBER=',I3)
      CALL EIGEN (A1,R1,NCI,0)
      CALL EIGEN (A2,R2,NCI,0)
      WRITE(3,508)
  508 FØRMAT(//' CI EIGENVALUES AND EIGENVECTØRS - SINGLET'/)
      WRITE(3,FSR3) (A1(I*(I+1)/2),(R1(I*NCI+J-NCI),J=1,NCI),I=1,NCI)
      WRITE(3,509)
  509 FØRMAT(//' CI EIGENVALUES AND EIGENVECTØRS - TRIPLET'/)
      WRITE(3,FSR3) (A2(I*(I+1)/2),(R2(I*NCI+J-NCI),J=1,NCI),I=1,NCI)
      WRITE(3,511)
  511 FØRMAT(//' CI TRANS.MØMENTS'//1X,'CIF',8X,'TMCIX',9X,'TMCIY
     $',9X,'TMCIZ',9X,'TMCI2'/)
      CALL TMCI(NCI)
      CALL DENST(M,MJ,MS,NCI,M1)
      WRITE(3,512)
  512 FØRMAT(//' CI CHARGE DENSITIES - SINGLET'/)
      WRITE(3,FSR2)((DENS(NC,MIU),MIU=1,N),NC=1,NCI)
      WRITE(3,513)
  513 FØRMAT(//' CI CHARGE DENSITIES - TRIPLET'/)
      WRITE(3,FSR2)((DENT(NC,MIU),MIU=1,N),NC=1,NCI)
      CALL DIPØL (NJ,NS,NCI)
      GØ TØ 599
  597 WRITE(3,598)
  598 FØRMAT(//' STØP, ICØNT=20 '/)
  599 STØP
      END

      SUBRØUTINE CØØRA(I,NR,RAB,RBC,TETA,NA,NB,NC,ND,RCD,BCD,ABCD,M)
      CØMMØN N/DØI/RAZA(16,16)/TREI/X(16),Y(16),ZET(16)
      IF(I-1)431,431,432
  431 TETA=TETA*3.1415926/180
      DØ 402 J=1,3
      X(J)=0.
      Y(J)=0.
  402 ZET(J)=0.
      X(2)=RAB
      X(3)=RAB-RBC*CØS(TETA)
      Y(3)=RBC*SIN(TETA)
      DØ 411 J=4,N
  411 X(J)=10000
  432 IF(ABS(X(NA))+ABS(X(NB))+ABS(X(NC))-10000) 415,414,414
  414 WRITE(3,416) I
  416 FØRMAT(//' WRUNG SEQUENCE NR=',I2)
      STØP
  415 WRITE(3,417)NA,NB,NC,ND,RCD,BCD,ABCD
  417 FØRMAT(//1X,4(I2,1X),F8.3,F9.2,F7.2)
      XAT=X(NA)-X(NC)
      YAT=Y(NA)-Y(NC)
      ZAT=ZET(NA)-ZET(NC)
      XBT=X(NB)-X(NC)
      YBT=Y(NB)-Y(NC)
      ZBT=ZET(NB)-ZET(NC)
      XY=SQRT(XBT*XBT+YBT*YBT)
      CØSAL=XBT/XY
      SINAL=YBT/XY
      XRZ=CØSAL*XAT+SINAL*YAT
      YRZ=CØSAL*YAT-SINAL*XAT
      ZRZ=ZAT
      RBC=SQRT(XBT*XBT+YBT*YBT+ZBT*ZBT)
      SINBE=ZBT/RBC
      CØSBE=SQRT(1.-SINBE*SINBE)
      XRY=XRZ*CØSBE+ZRZ*SINBE
      YRY=YRZ
      ZRY=ZRZ*CØSBE-XRZ*SINBE
      YZ=SQRT(YRY*YRY+ZRY*ZRY)
      CØSGA=YRY/YZ
      SINGA=ZRY/YZ
      BCD=BCD*3.1415926/180
      ABCD=ABCD*3.1415926/180
      SBCD=SIN(BCD)
      CBCD=CØS(BCD)
      SABCD=SIN(ABCD)
      CABCD=CØS(ABCD)
      XD=RCD*CBCD
```

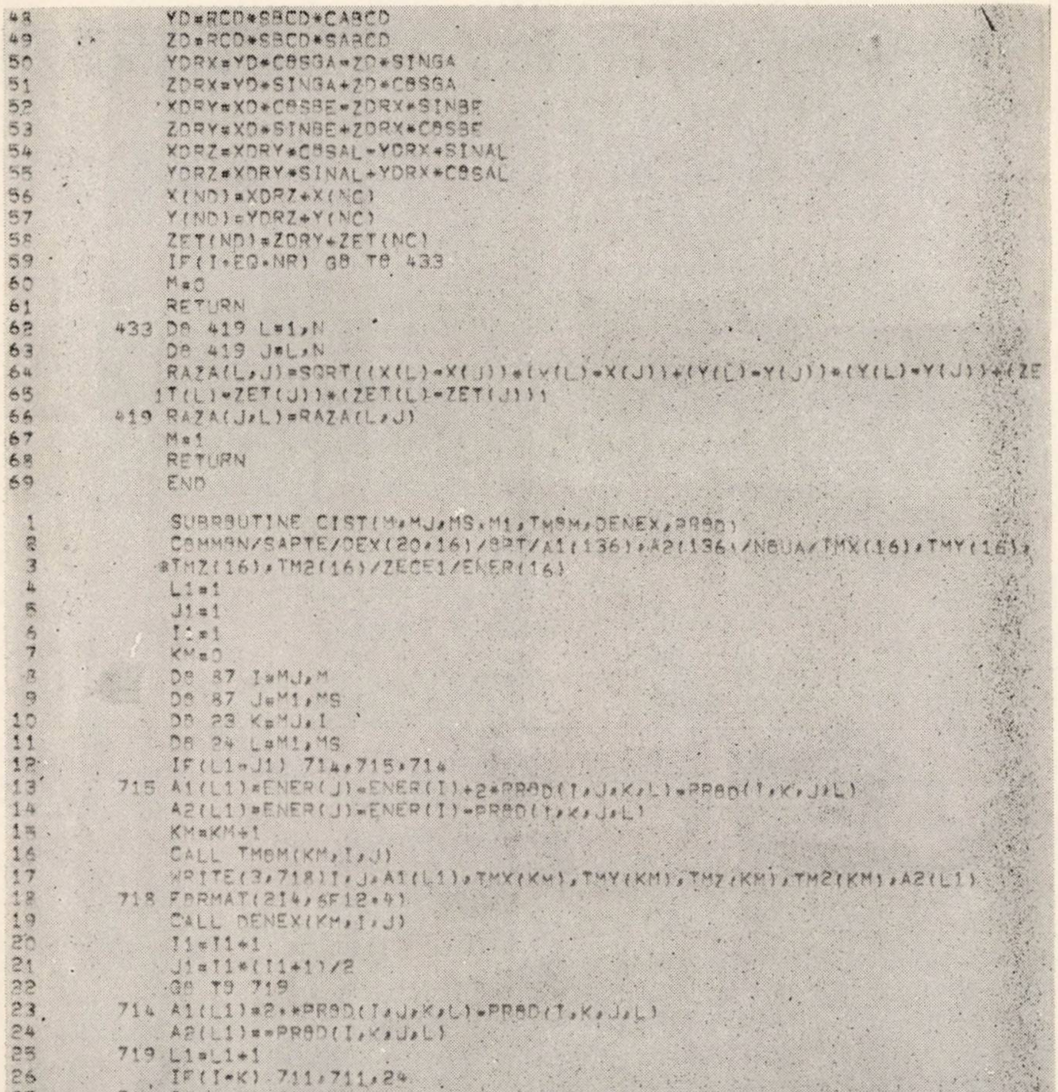

```
      YD=RCD*SBCD*CABCD
      ZD=RCD*SBCD*SABCD
      YDRX=YD*CØSGA-ZD*SINGA
      ZDRX=YD*SINGA+ZD*CØSGA
      XDRY=XD*CØSBE-ZDRX*SINBE
      ZDRY=XD*SINBE+ZDRX*CØSBE
      XDRZ=XDRY*CØSAL-YDRX*SINAL
      YDRZ=XDRY*SINAL+YDRX*CØSAL
      X(ND)=XDRZ+X(NC)
      Y(ND)=YDRZ+Y(NC)
      ZET(ND)=ZDRY+ZET(NC)
      IF(I.EQ.NR) GØ TØ 433
      M=0
      RETURN
  433 DØ 419 L=1,N
      DØ 419 J=L,N
      RAZA(L,J)=SQRT((X(L)-X(J))*(X(L)-X(J))+(Y(L)-Y(J))*(Y(L)-Y(J))+(ZE
     1T(L)-ZET(J))*(ZET(L)-ZET(J)))
  419 RAZA(J,L)=RAZA(L,J)
      M=1
      RETURN
      END

      SUBRØUTINE CIST(M,MJ,MS,M1,TMØM,DENEX,PRØD)
      CØMMØN/SAPTE/DEX(20,16)/ØPT/A1(136),A2(136)/NØUA/TMX(16),TMY(16),
     *TMZ(16),TM2(16)/ZECE1/ENER(16)
      L1=1
      J1=1
      I1=1
      KM=0
      DØ 87 I=MJ,M
      DØ 87 J=M1,MS
      DØ 23 K=MJ,I
      DØ 24 L=M1,MS
      IF(L1-J1) 714,715,714
  715 A1(L1)=ENER(J)-ENER(I)+2*PRØD(I,J,K,L)-PRØD(I,K,J,L)
      A2(L1)=ENER(J)-ENER(I)-PRØD(I,K,J,L)
      KM=KM+1
      CALL TMØM(KM,I,J)
      WRITE(3,718)I,J,A1(L1),TMX(KM),TMY(KM),TMZ(KM),TM2(KM),A2(L1)
  718 FØRMAT(2I4,6F12.4)
      CALL DENEX(KM,I,J)
      I1=I1+1
      J1=I1*(I1+1)/2
      GØ TØ 719
  714 A1(L1)=2.*PRØD(I,J,K,L)-PRØD(I,K,J,L)
      A2(L1)=-PRØD(I,K,J,L)
  719 L1=L1+1
      IF(I-K) 711,711,24
  711 IF(L-J) 24,23,23
   24 CØNTINUE
   23 CØNTINUE
   87 CØNTINUE
      RETURN
      END



      SUBRØUTINE DENEX(KM,I,J)
      CØMMØN N/UNU/C(16,16)/SASE/EN(16),P(16,16)/SAPTE/DEX(20,16)
      DØ 721 MIU=1,N
  721 DEX(KM,MIU)=P(MIU,MIU)-C(I,MIU)*C(I,MIU)+C(J,MIU)*C(J,MIU)
      RETURN
      END
```

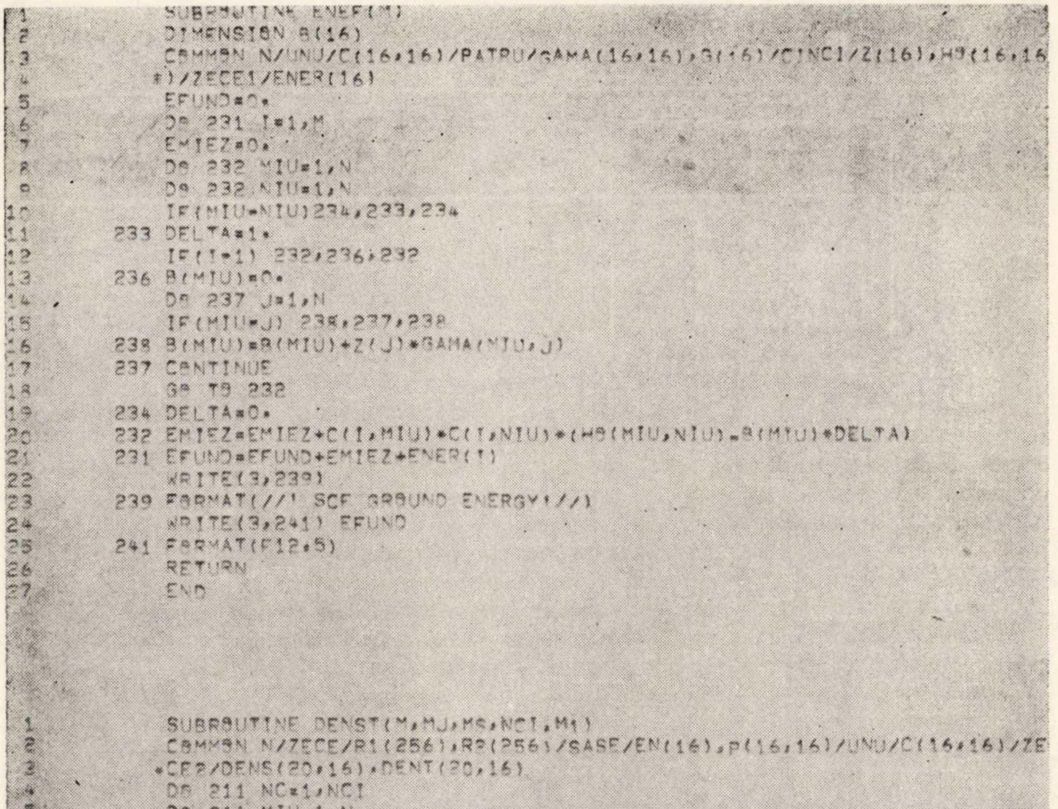

```
      SUBRØUTINE ENER(M)
      DIMENSIØN B(16)
      CØMMØN N/UNU/C(16,16)/PATRU/GAMA(16,16),G(16)/CINCI/Z(16),HØ(16,16
     *)/ZECE1/ENER(16)
      EFUND=0.
      DØ 231 I=1,M
      EMIEZ=0.
      DØ 232 MIU=1,N
      DØ 232 NIU=1,N
      IF(MIU-NIU)234,233,234
  233 DELTA=1.
      IF(I-1) 232,236,232
  236 B(MIU)=0.
      DØ 237 J=1,N
      IF(MIU-J) 238,237,238
  238 B(MIU)=B(MIU)+Z(J)*GAMA(MIU,J)
  237 CØNTINUE
      GØ TØ 232
  234 DELTA=0.
  232 EMIEZ=EMIEZ+C(I,MIU)*C(I,NIU)*(HØ(MIU,NIU)-B(MIU)*DELTA)
  231 EFUND=EFUND+EMIEZ*ENER(I)
      WRITE(3,239)
  239 FØRMAT(//' SCF GRØUND ENERGY'//)
      WRITE(3,241) EFUND
  241 FØRMAT(F12.5)
      RETURN
      END
```

```
      SUBRØUTINE DENST(M,MJ,MS,NCI,M1)
      CØMMØN N/ZECE/R1(256),R2(256)/SASE/EN(16),P(16,16)/UNU/C(16,16)/ZE
     *CE2/DENS(20,16),DENT(20,16)
      DØ 211 NC=1,NCI
      DØ 211 MIU=1,N
      I1=NC*NCI-NCI+1
      DENS(NC,MIU)=P(MIU,MIU)
      DENT(NC,MIU)=P(MIU,MIU)
      DØ 212 I=MJ,M
      DØ 213 J=M1,MS
      I2=NC*NCI-NCI+1
      DØ 214 K=MJ,M
      DØ 215 L=M1,MS
      IF(I-K) 217,216,217
  216 DELTA1=1.
      GØ TØ 218
  217 DELTA1=0.
  218 IF(J-L) 221,219,221
  219 DELTA2=1.
      GØ TØ 222
  221 DELTA2=0.
  222 DENS(NC,MIU)=DENS(NC,MIU)+R1(I1)*R1(I2)*(C(J,MIU)*C(L,MIU)*DELTA1
     *-C(I,MIU)*C(K,MIU)*DELTA2)
      DENT(NC,MIU)=DENT(NC,MIU)+R2(I2)*R2(I1)*(C(J,MIU)*C(L,MIU)*DELTA1-
     *C(I,MIU)*C(K,MIU)*DELTA2)
  215 I2=I2+1
  214 CØNTINUE
  213 I1=I1+1
  212 CØNTINUE
  211 CØNTINUE
      RETURN
      END
```

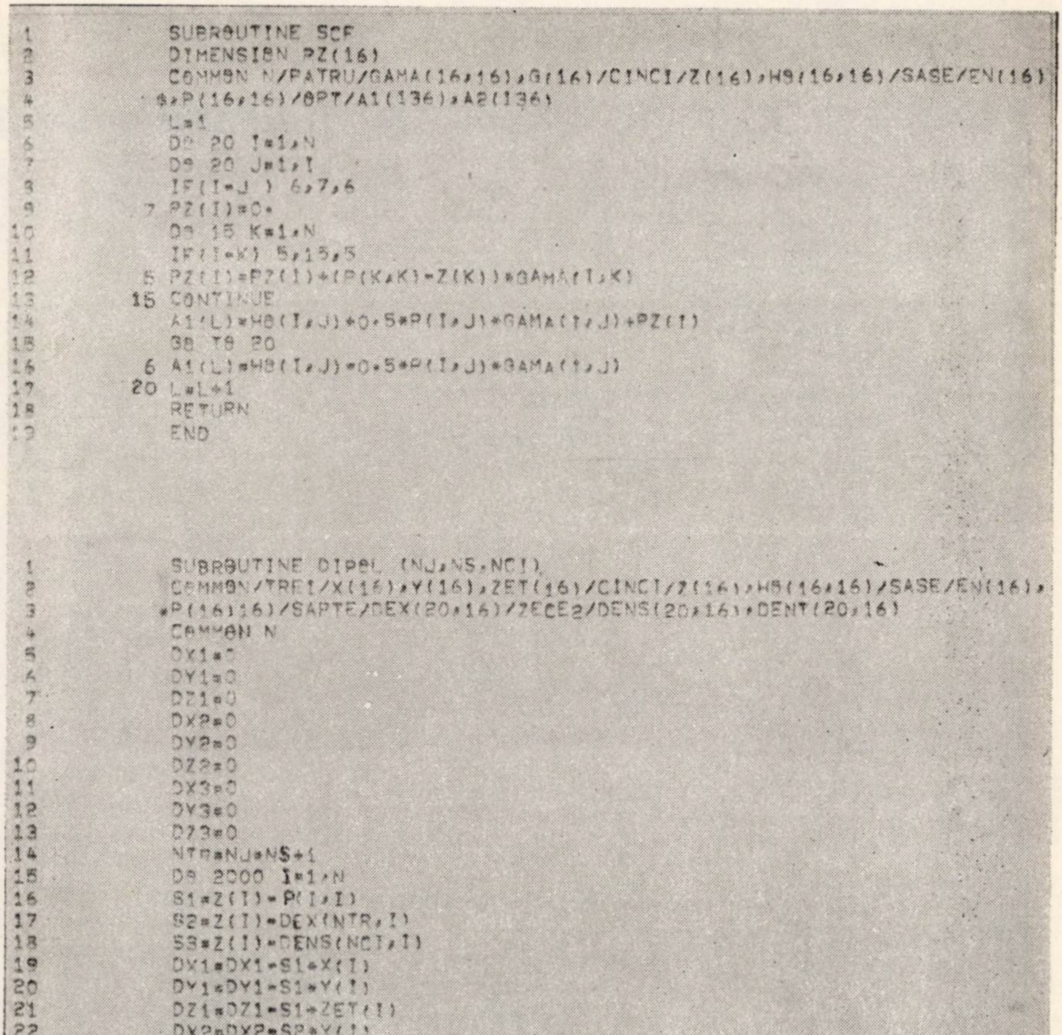

```
      SUBRØUTINE SCF
      DIMENSIØN PZ(16)
      CØMMØN N/PATRU/GAMA(16,16),G(16)/CINCI/Z(16),HØ(16,16)/SASE/EN(16)
     $,P(16,16)/ØPT/A1(136),A2(136)
      L=1
      DØ 20 I=1,N
      DØ 20 J=1,I
      IF(I-J ) 6,7,6
    7 PZ(I)=0.
      DØ 15 K=1,N
      IF(I-K) 5,15,5
    5 PZ(I)=PZ(I)+(P(K,K)-Z(K))*GAMA(I,K)
   15 CONTINUE
      A1(L)=HØ(I,J)+0.5*P(I,J)*GAMA(I,J)+PZ(I)
      GØ TØ 20
    6 A1(L)=HØ(I,J)-0.5*P(I,J)*GAMA(I,J)
   20 L=L+1
      RETURN
      END
```

```
      SUBRØUTINE DIPØL (NJ,NS,NCI)
      CØMMØN/TREI/X(16),Y(16),ZET(16)/CINCI/Z(16),HØ(16,16)/SASE/EN(16),
     *P(16,16)/SAPTE/DEX(20,16)/ZECE2/DENS(20,16),DENT(20,16)
      CØMMØN N
      DX1=0
      DY1=0
      DZ1=0
      DX2=0
      DY2=0
      DZ2=0
      DX3=0
      DY3=0
      DZ3=0
      NTR=NJ*NS+1
      DØ 2000 I=1,N
      S1=Z(I)-P(I,I)
      S2=Z(I)-DEX(NTR,I)
      S3=Z(I)-DENS(NCI,I)
      DX1=DX1-S1*X(I)
      DY1=DY1-S1*Y(I)
      DZ1=DZ1-S1*ZET(I)
      DX2=DX2-S2*Y(I)
      DY2=DY2-S2*Y(I)
      DZ2=DZ2-S2*ZET(I)
      DX3=DX3-S3*X(I)
      DY3=DY3-S3*Y(I)
 2000 DZ3=DZ3-S3*ZET(I)
      DIP1=4.8*SQRT(DX1*DX1+DY1*DY1+DZ1*DZ1)
      DIP2=4.8*SQRT(DX2*DX2+DY2*DY2+DZ2*DZ2)
      DIP3=4.8*SQRT(DX3*DX3+DY3*DY3+DZ3*DZ3)
      WRITE(3,2001)DX1,DY1,DZ1,DIP1,DX2,DY2,DZ2,DIP2,DX3,DY3,DZ3,DIP3
 2001 FØRMAT(//13X,'MX',10X,'MY',10X,'MZ',6X,'DIPØL MØMENT'//'SCF',3X,
     *4F12.5/'EX.SCF',4F12.5/'EX.CI',1X,4F12.5)
      RETURN
      END
```

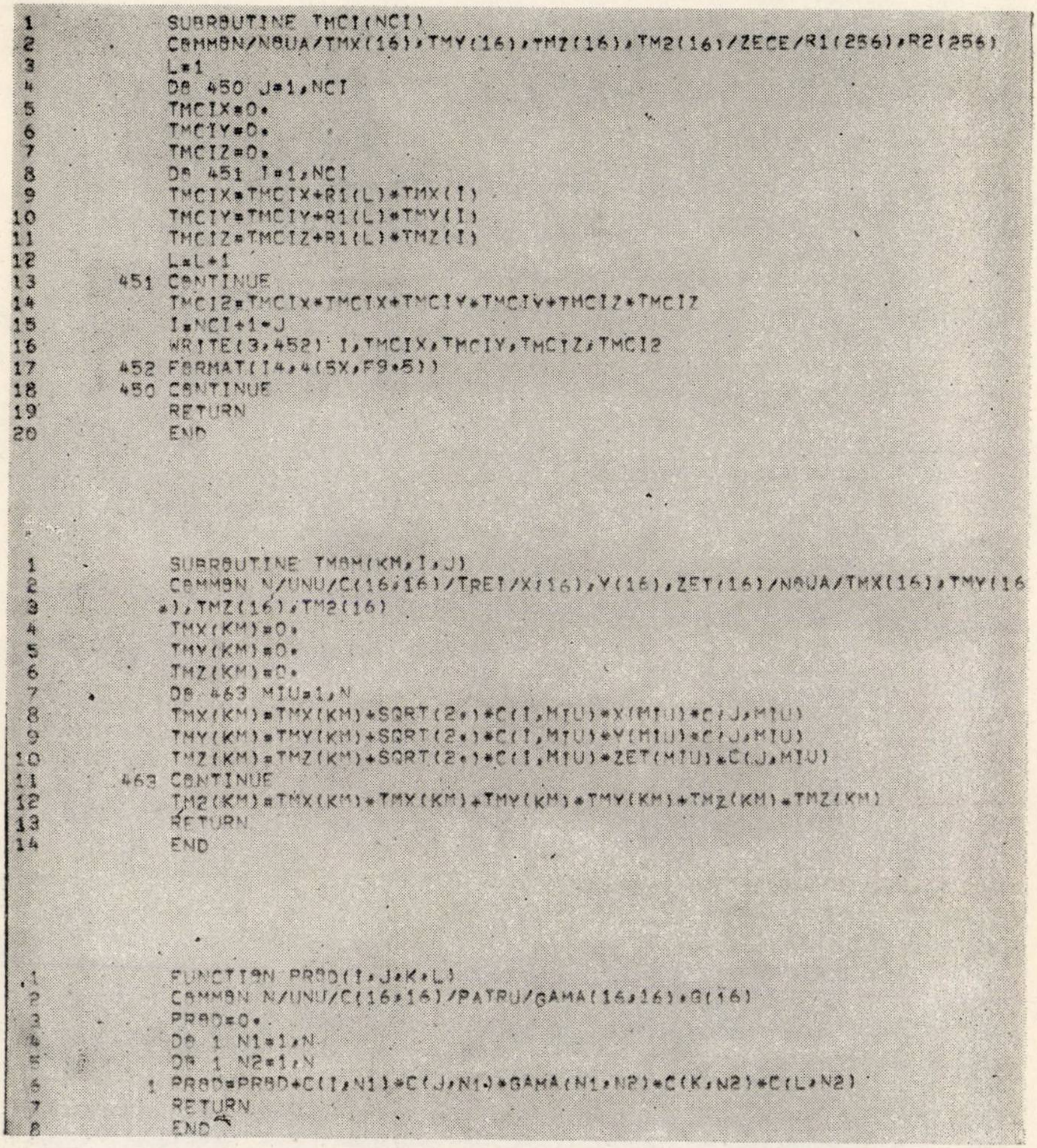

```
      SUBRØUTINE TMCI(NCI)
      CØMMØN/NØUA/TMX(16),TMY(16),TMZ(16),TM2(16)/ZECE/R1(256),R2(256)
      L=1
      DØ 450 J=1,NCI
      TMCIX=0.
      TMCIY=0.
      TMCIZ=0.
      DØ 451 I=1,NCI
      TMCIX=TMCIX+R1(L)*TMX(I)
      TMCIY=TMCIY+R1(L)*TMY(I)
      TMCIZ=TMCIZ+R1(L)*TMZ(I)
      L=L+1
  451 CØNTINUE
      TMCI2=TMCIX*TMCIX+TMCIY*TMCIY+TMCIZ*TMCIZ
      I=NCI+1-J
      WRITE(3,452) I,TMCIX,TMCIY,TMCIZ,TMCI2
  452 FØRMAT(I4,4(5X,F9.5))
  450 CØNTINUE
      RETURN
      END
```

```
      SUBRØUTINE TMØM(KM,I,J)
      CØMMØN N/UNU/C(16,16)/TREI/X(16),Y(16),ZET(16)/NØUA/TMX(16),TMY(16
     *),TMZ(16),TM2(16)
      TMX(KM)=0.
      TMY(KM)=0.
      TMZ(KM)=0.
      DØ 463 MIU=1,N
      TMX(KM)=TMX(KM)+SQRT(2.)*C(I,MIU)*X(MIU)*C(J,MIU)
      TMY(KM)=TMY(KM)+SQRT(2.)*C(I,MIU)*Y(MIU)*C(J,MIU)
      TMZ(KM)=TMZ(KM)+SQRT(2.)*C(I,MIU)*ZET(MIU)*C(J,MIU)
  463 CØNTINUE
      TM2(KM)=TMX(KM)*TMX(KM)+TMY(KM)*TMY(KM)+TMZ(KM)*TMZ(KM)
      RETURN
      END
```

```
      FUNCTIØN PRØD(I,J,K,L)
      CØMMØN N/UNU/C(16,16)/PATRU/GAMA(16,16),G(16)
      PRØD=0.
      DØ 1 N1=1,N
      DØ 1 N2=1,N
    1 PRØD=PRØD+C(I,N1)*C(J,N1)*GAMA(N1,N2)*C(K,N2)*C(L,N2)
      RETURN
      END
```

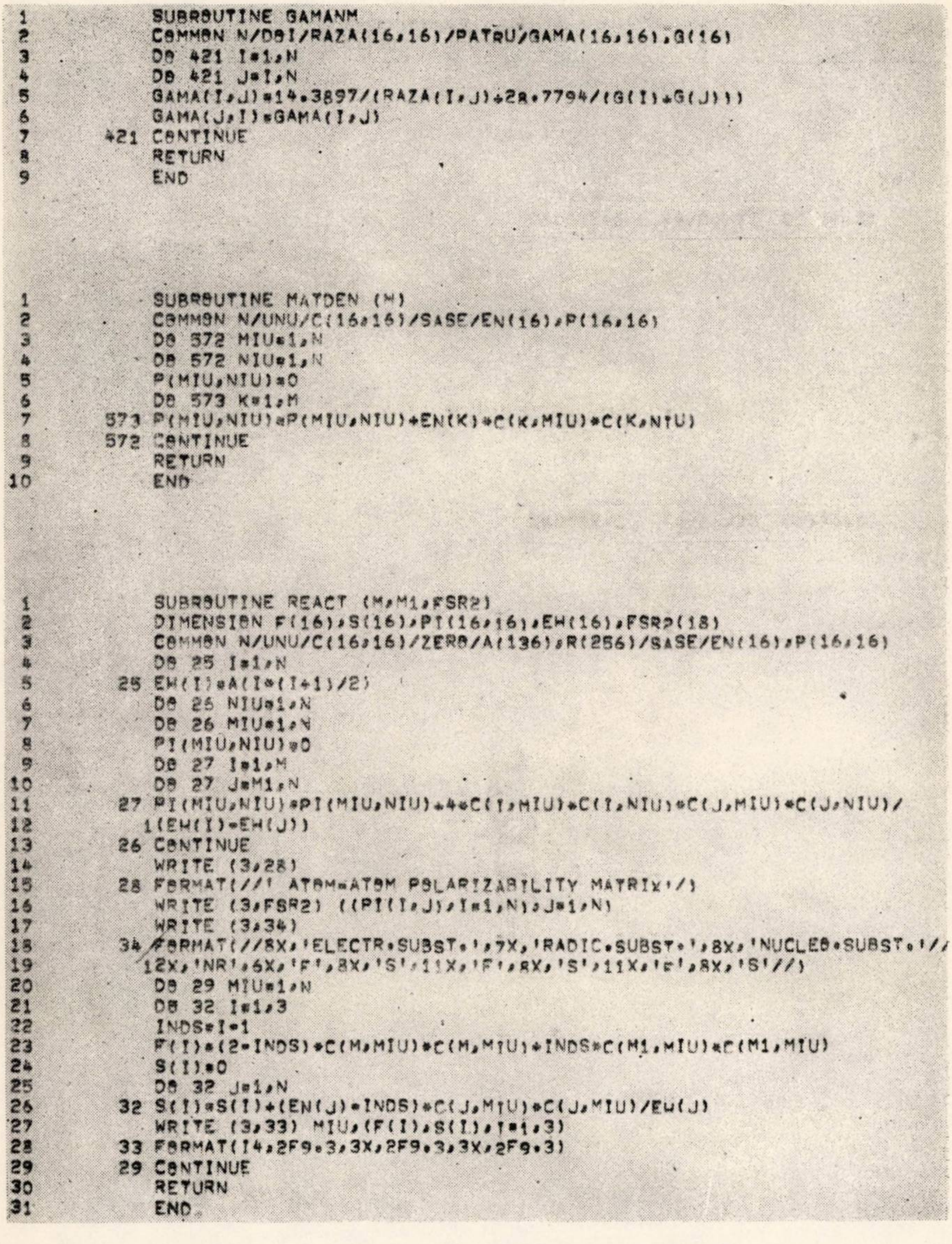

```
      SUBRØUTINE GAMANM
      CØMMØN N/DØI/RAZA(16,16)/PATRU/GAMA(16,16),G(16)
      DØ 421 I=1,N
      DØ 421 J=I,N
      GAMA(I,J)=14.3897/(RAZA(I,J)+28.7794/(G(I)+G(J)))
      GAMA(J,I)=GAMA(I,J)
  421 CØNTINUE
      RETURN
      END
```

```
      SUBRØUTINE MATDEN (M)
      CØMMØN N/UNU/C(16,16)/SASE/EN(16),P(16,16)
      DØ 572 MIU=1,N
      DØ 572 NIU=1,N
      P(MIU,NIU)=0
      DØ 573 K=1,M
  573 P(MIU,NIU)=P(MIU,NIU)+EN(K)*C(K,MIU)*C(K,NIU)
  572 CØNTINUE
      RETURN
      END
```

```
      SUBRØUTINE REACT (M,M1,FSR2)
      DIMENSIØN F(16),S(16),PI(16,16),EH(16),FSR2(18)
      CØMMØN N/UNU/C(16,16)/ZERØ/A(136),R(256)/SASE/EN(16),P(16,16)
      DØ 25 I=1,N
   25 EH(I)=A(I*(I+1)/2)
      DØ 26 NIU=1,N
      DØ 26 MIU=1,N
      PI(MIU,NIU)=0
      DØ 27 I=1,M
      DØ 27 J=M1,N
   27 PI(MIU,NIU)=PI(MIU,NIU)+4*C(I,MIU)*C(I,NIU)*C(J,MIU)*C(J,NIU)/
     1(EH(I)-EH(J))
   26 CØNTINUE
      WRITE (3,28)
   28 FØRMAT(//' ATØM-ATØM PØLARIZABILITY MATRIX'/)
      WRITE (3,FSR2) ((PI(I,J),I=1,N),J=1,N)
      WRITE (3,34)
   34 FØRMAT(//8X,'ELECTR.SUBST.',7X,'RADIC.SUBST.',8X,'NUCLEØ.SUBST.'//
     12X,'NR',6X,'F',8X,'S',11X,'F',8X,'S',11X,'F',8X,'S'//)
      DØ 29 MIU=1,N
      DØ 32 I=1,3
      INDS=I-1
      F(I)=(2-INDS)*C(M,MIU)*C(M,MIU)+INDS*C(M1,MIU)*C(M1,MIU)
      S(I)=0
      DØ 32 J=1,N
   32 S(I)=S(I)+(EN(J)-INDS)*C(J,MIU)*C(J,MIU)/EH(J)
      WRITE (3,33) MIU,(F(I),S(I),I=1,3)
   33 FØRMAT(I4,2F9.3,3X,2F9.3,3X,2F9.3)
   29 CØNTINUE
      RETURN
      END
```

Revue Roumaine de Chimie, 23, 1, 19–29 (1978)

THERMODYNAMIC PROPERTIES OF MALEIC, TRIMELLITIC AND PYROMELLITIC ANHYDRIDES

D. I. MARCHIDAN and M. CIOPEC
Center of Physical Chemistry, Spl. Independenţei 202, Bucharest, Romania.

Received February 19, 1977

The values of thermodynamic functions of maleic and trimellitic anhydrides and pyromellitic dianhydride in nonreacting conditions, within the 298.15 – 550 K temperature range are given. The relative enthalpy is obtained from calorimetric data by drop calorimetry. The heat capacity and relative entropy are functions derived from the previous. The parameters of solid-liquid transition have been determined by means of the discontinuity of temperature variation of relative enthalpy : $T_{\text{fusion}} = 325.65$ K, $\Delta H_{\text{fusion}} = 2929.380$ cal. mol^{-1} for maleic anhydride; $T_{\text{fusion}} = 385$ K, $\Delta H_{\text{fusion}} = 2501.133$ cal. mol^{-1} for trimellitic anhydride and $T_{\text{fusion}} = 557.15$ K, $\Delta H_{\text{fusion}} = 3783$ cal. mol^{-1} for pyromellitic dianhydride. The experimental data have been employed as corrections for the contribution of the container and thus the thermodynamic functions of V2A steel (out of which the container was machined) have been evaluated.

The usual international tables[1] list as thermodynamic properties of a substance the relative enthalpy* $\{H^0(T) - H^0(298.15\text{K})\}$, the heat capacity, C_p^0, the relative entropy $\{S^0(T) - S^0(298.15\text{ K})\}$, the enthalpy of formation $\Delta_f H^0(T)$, the free enthalpy of formation $\Delta_f G^0(T)$ and their temperature variation. The first three quantities refer to the substance in nonreacting state and allow calculation of the last two when the standard enthalpy of formation $\Delta_f H^0(298{,}15\text{ K})$ and standard entropy of formation $\Delta_f S^0(298{,}15\text{ K})$ are known.

PROCEDURE OF EVALUATION OF THERMODYNAMIC FUNCTIONS OF NONREACTING SYSTEMS

To evaluate the thermodynamic properties of substances in nonreacting state, a block-type drop calorimeter with isothermal jacket, designed by the authors (CALOR – 01, prototype which has been approved and represents an improved variant of calorimeters previously described[5-7]) was used.

---

* The terms and units employed in this work are according to recommendations of IUPAC[2] (International Union of Pure and Applied Chemistry), The International System of Units[3] and of International Practical Temperature Scale[4].

[1] D. R. Stull (Editor), "JANAF Thermochemical Tables", Dow Chemical Co., Midland, Mich., 1965, N°PB 168–370.

[2] * * * "A Guide to Procedure for the Publication of Thermodynamic Data", IUPAC, Butterworths, London, 1972.

[3] I. Iscrulescu, Gh. Ispăşoiu and V. Petrescu, "Sistemul Internaţional de Unităţi de Măsură", Editura Tehnică, Bucureşti, 1970, p. 60.

[4] * * * "The International Practical Temperature Scale of 1968", National Physical Laboratory, London Her Majesty's Stationary Office, 1969, p. 7.

Since this calorimeter is equipped with a matching block which allows the obtaining, directly on the recorder, of calorimetric curves (the increase of block temperature as against the quasi-constant temperature of the jacket), Δh determined experimentally has been converted into relative enthalpy by the equation

$$\{H^0(T) - H^0(298.15\ \mathrm{K})\} = \frac{M}{m}\{(\Delta h_1 - \Delta h_2)\, k_s + Q^r + Q^b\} \tag{1}$$

where Δh_1 is the (corrected) deviation for the container with sample;
Δh_2 is the (corrected) deviation for container without sample;
k_s the calibration constant of the calorimeter in cal. mm^{-1} for a certain scale (s) of the recorder;
Q^r the heat lost during drop;
Q^b the heat retained by the sample due to the fact that the final equilibrium temperature of block-sample system is superior to 25°C (298.15 K);
$\frac{M}{m}$ the number of moles of substance in the container.

Q^r and Q^b are corrections whose average weights is 0.1 % of the thermal effect to be determined. Their evaluation is made by usual methods of calculation. [8]

The calibration constant, k_s, was determined with known amounts of heat introduced into the block either by Joule effect (by means of calibration heater) or by a standard substance (synthetic sapphire, NBS Standard Reference Material No. 720) whose variation enthalpy versus temperature is known.[9]

The results obtained with these measurements have allowed establishing of the performance of the prototype:

— operating temperature range: 300 — 1300 K;
— thermal effect (heat content): 170 — 5050 cal.;
— reproducibility of heat content mesurements: 99.55 — 99.70 per cent;
— sensitivity: 0.797 — 12.250 cal. depending on measuring scale;
— precission in measurements of heat content: better than 99.7 per cent.

The relative enthalpy calculated from experimental data by eq. (1) is a function on temperature:

$$\{H^0(T) - H^0(298.15\ \mathrm{K})\} = f(T) \tag{2}$$

This function has been obtained by least square computer processing of data; use has been made of an improved variant of TERMOX program [10] which allows finding directly the equation for which deviation of experimental points from calculated curve is minimal; the final results are tabulated and both calculated and experimental curves are plotted.

From $f(T)$ in eq. (2) the other thermodynamic quantities characteristic of the nonreacting systems may be deduced:

— heat capacity $C_p^0 = \frac{\partial}{\partial T}\{H^0(T) - H^0(298.15\ \mathrm{K})\}$ (3)

and

— relative entropy $\{S^0(T) - S^0(298.15\ \mathrm{K})\} = \int_{298.15}^{T} \frac{C_p^0}{T}\,\mathrm{d}T.$ (4)

---

[5] D. I. Marchidan and M. Ciopec, *Studii şi cercetări Chim. Acad. R.S.R.*, **17**, 737 (1969).
[6] D. I. Marchidan and M. Ciopec, *Rev. Roumaine de Chimie*, **16**, 1145 (1967).
[7] D. I. Marchidan, M. Ciopec and Al. Bîrhală, *Rev. Chim. (Bucureşti)*, **27**, 394 (1976).
[8] A. C. Macleod, *J. Chem. Thermodynamics*, **4**, 391 (1972).
[9] D. E. Fredrickson and M. G. Chasanov, *J. Chem. Thermodynamics*, **2**, 623 (1970).
[10] M. Ciopec, Doctoral Thesis, Centre of physical chemistry, Bucharest, 1975, p. 160.

RESULTS

Since a very important correction Δh_2 (for container without sample) intervenes in eq. (1), a first set of runs with the V2A stainless steel container has preceded calorimetric determinations on anhydrides.

A container of V2A steel of about 30 grams has been used; the conversion of deviations into enthalpy according to eq. (1) has yilded the following temperature dependence over the 298.15 – 586 K range

$$\{H^0(T) - H^0(298.15\ \mathrm{K})\} = -2718.829 + 9.119\ (T/K)\ \mathrm{cal.\ mol^{-1}} \qquad (5)$$

The standard deviation of experimental data from calculated curve is $\pm$ 3.686 cal. mol^{-1} that is $\pm$ 0.242 per cent.

Equations (3) and (4) have been used in the deduction of characteristic equations for heat capacity and relative entropy;

$$C_p^0 = 9.119\ \mathrm{cal.mol^{-1}.K^{-1}} \qquad (6)$$

$$\{S^0(T) - S^0(298.15\ \mathrm{K})\} = -51.965 + 21.001 \log(T/K)\ \mathrm{cal.\ mol^{-1}.K^{-1}} \qquad (7)$$

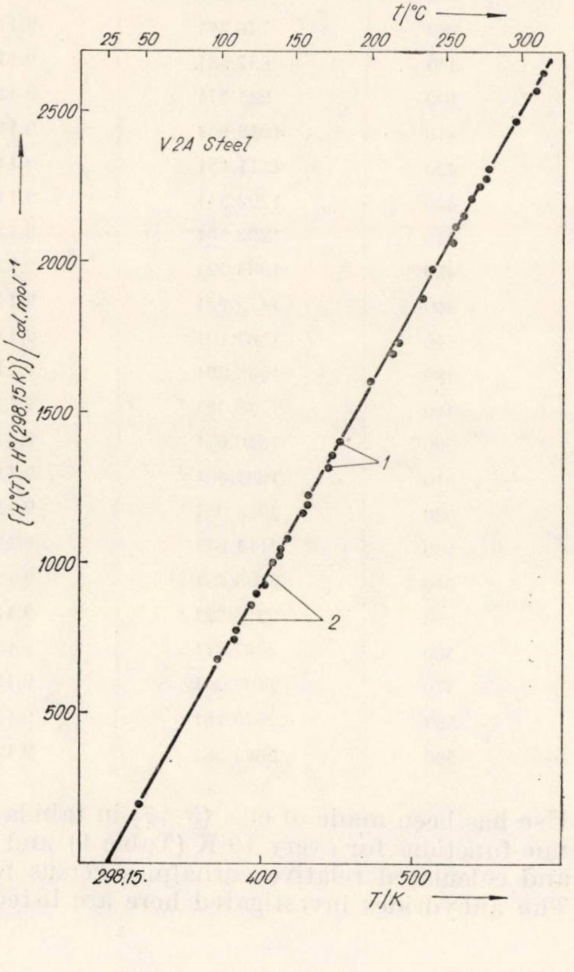

Fig. 1. Relative enthalpy of V2A steel *vs* temperature:

1. experimental; *2.* calculated.

Table 1

Values of thermodynamic functions for V^{2}A steel

T	$\{(H^0(T) - H^0(298.15\ \mathrm{K})\}$	C_p°	$S^0(T) - S^0(298.15\ \mathrm{K})$
K	cal. mol^{-1}	cal. mol$^{-1}\cdot$K^{-1}	cal. mol$^{-1}\cdot$K^{-1}
298.15	0.0	9.119	0.0
300	16.871	9.119	0.057
310	108.061	9.119	0.356
320	199.251	9.119	0.645
330	290.441	9.119	0.926
340	381.631	9.119	1.198
350	472.821	9.119	1.463
360	564.041	9.119	1.719
370	655.201	9.119	1.969
380	746.391	9.119	2.213
390	837.581	9.119	2.450
400	928.771	9.119	2.680
410	1019.961	9.119	2.906
420	1111.151	9.119	3.126
430	1202.341	9.119	3.340
440	1293.531	9.119	3.550
450	1384.721	9.119	3.755
460	1475.911	9.119	3.956
470	1567.101	9.119	4.152
480	1658.291	9.119	4.344
490	1749.481	9.119	4.532
500	1840.671	9.119	4.716
510	1931.861	9.119	4.896
520	2023.051	9.119	5.074
530	2114.241	9.119	5.247
540	2205.431	9.119	5.394
550	2296.621	9.119	5.585
560	2387.811	9.119	5.750
570	2497.001	9.119	5.911
580	2570.191	9.119	6.070
590	2661.381	9.119	6.225

Use has been made of eqs. (5—7) in tabulation of the main thermodynamic functions for every 10 K (Table 1) and in plotting both experimental and calculated relative enthalpies versus temperature (figure 1). The anhydrides investigated here are listed in Table 2.

Table 2

Studied anhydrides by drop calorimetry

Name	Formula	Molecular weight (grams)	Temperature of melting °C	
			literature[11-12]	D.T.A.
malleic anhydride (anhydride of *cis*-butendioic acid) *	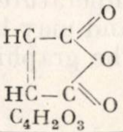 $C_4H_2O_3$	98.06	52.8 52.6	52.6
trimellitic anhydride (1 :2 anhydride of 1,2,4, benzentricarboxylic acid)*	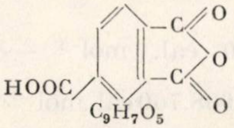 $C_9H_7O_5$	192.14		114
pyromellitic dianhydride (1 :2, 4 :5 dianhydride of 1,2,4,5 benzentetracarboxylic acid)*	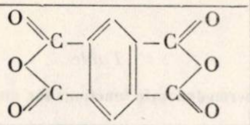 $C_{10}H_2O_6$	218.19	284 296	286

* Names approved by the International Union of Chemists (IUC) [12]

The equations of temperature variation of relative enthalpy and of thermodynamic functions are as follows :

Maleic anhydride

Solid state : 298.15 — 325.15 K

$$\{H^0(T) - H^0(298.15\text{ K})\} = -4781.891 + 16.063\ (T/K)\ \text{cal. mol}^{-1} \quad (8)$$

Standard deviation = ± 8.348 cal. mol^{-1} that is ±2.62 per cent.

$$C_p^0 = 11.063\ \text{cal. mol}^{-1}\ .\text{K}^{-1} \quad (9)$$

$$\{S^0(T) - S^0\,(298.15\text{ K})\} = -152.751 + 61.732 \log\,(T/\text{K})\,\text{cal. mol}^{-1}.\text{K}^{-1} \quad (10)$$

Liquid state : 327.5 — 469.15 K

$$\{H^0(T) - H^0(298.15\text{ K})\} = -5371.277 + 22.805\ (T/\text{K})\ \text{cal.mol}^{-1} \quad (11)$$

---

[11] D'ANS, LAX, "Taschenbuch für Chemiker und Physiker", Band II, Springer Verlag, Berlin, 1964.

[12] * * * "Handbook of Chemistry and Physics", 55th edition, CRC-Press, Cleveland, U.S.A.

Standard deviation $= \pm\, 19.007$ cal. mol^{-1}, that is $\pm\, 0.37$ per cent.

$$C_p^0 = 26.805 \text{ cal. mol}^{-1}\,.\text{K}^{-1} \tag{12}$$

$$\{S^0(T) - S^0(298.15\text{ K})\} = -\,152.751 + 61.732\ \log\,(T/\text{K})\text{ cal. mol}^{-1}.\text{K}^{-1} \tag{13}$$

The discontinuity in temperature variation of relative enthalpy is due to solid-liquid transition and may be employed in evaluation of parameters of this transition [13]. The graphic method as well as eqs. (8) and (11) yield :

$T_{\text{fusion}} = 325.65$ K

$$\Delta H_{\text{fusion}} = \left\langle \begin{array}{l} \nearrow \text{graphic} = 2950 \ \text{ cal. } \ \text{mol}^{-1} \\ \searrow \text{calculated} = 2908.760\,\text{cal. mol}^{-1} \end{array} \right\rangle \Rightarrow (\Delta H_{\text{fusion}})_{\text{medium}} = 2929.380\text{cal.mol}^{-1}$$

Table 3

Value of thermodynamic functions for maleic anhydride

T	$\{H^\circ(T) - H^\circ(298{,}15\text{ K})\}$	C_p°	$\{S^0(T) - S^\circ(298{,}15\text{ K})\}$
K	cal. mol^{-1}	cal. mol^{-1}.K^{-1}	
298.15	0.0	16.063	0.0
300	37.156	16.063	7.530
310	197.791	16.063	8.219
320	358.425	16.063	8.651
330	3474.547	26.805	2.699
340	3742.602	26.805	3.499
350	4010.658	26.805	4.276
360	4278.714	26.805	5.023
370	4546.769	26.805	5.766
380	4814.824	26.805	6.480
390	5082.879	26.805	7.177
400	5350.935	26.805	7.856
410	5618.990	26.805	8.517
420	5887.045	26.805	9.163
430	6155.101	26.805	9.794
440	6423.156	26.805	10.410
450	6691.211	26.805	11.013
460	6959.267	26.805	11.602
470	7227.322	26.805	12.179
480	7495.377	26.805	12.743

---

[13] T. B. Douglas and E. G. King, in "Experimental Thermodynamics", vol. 1, Chapter 8, J. P. McCullough and D. W. Scott editors, Butterworths, London, 1968.

As in the previous case, the values of thermodynamic functions are tabulated and the temperature variation of relative enthalpy both experimental and calculated is plotted.

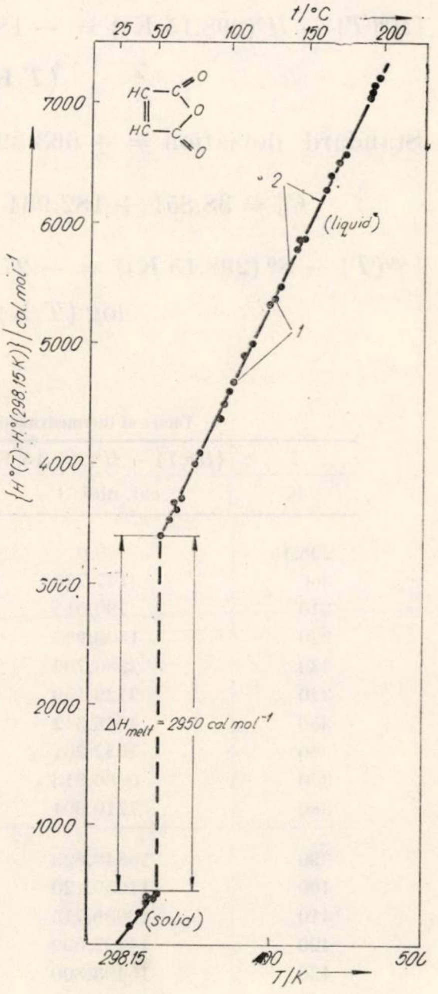

Fig. 2. Relative enthalpy of maleic anhydride *vs* temperature :

1. experimental ; 2. calculated.

Trimellitic anhydride.

Solid state : 298.15 — 385 K

$$\{H^0(T) - H^0(298.15\ \mathrm{K})\} = 12842 - 145.416\ (T/\mathrm{K}) + 343.673 \times 10^{-3}\ (T/\mathrm{K})^2\ \mathrm{cal.\ mol^{-1}} \qquad (14)$$

Standard deviation $= \pm\ 176.119$ cal. $\mathrm{mol^{-1}}$ that is ± 3.32 per cent.

$$C_p^0 = 687.346 \times 10^{-3}\ (T/\mathrm{K}) - 145.416\ \mathrm{cal.\ mol^{-1}.K^{-1}} \qquad (15)$$

$$\{S^0(T) - S^0(298.15\ \mathrm{K})\} = 623.737 + 687.346 \times 10^{-3}\ (T/\mathrm{K}) - 334.893\ \log(T/\mathrm{K})\ \mathrm{cal.mol^{-1}.K^{-1}} \quad (16)$$

Liquid state : 385−536 K

$$\{H^0(T) - H^0(298.15\ \mathrm{K})\} = -18219.890 + 38.851\ (T/\mathrm{K}) + 91.492 \times 10^{-3}\ (T/\mathrm{K})^2\ \mathrm{cal.\ mol^{-1}} \quad (17)$$

Standard deviation = ± 663.391 cal. $\mathrm{mol^{-1}}$ that is ± 3.28 per cent

$$C_p^0 = 38.851 + 182.984 \times 10^{-3}\ (T/\mathrm{K})\ \mathrm{cal.\ mol^{-1}.K^{-1}} \quad (18)$$

$$\{S^0(T) - S^0(298.15\ \mathrm{K})\} = -275.953 + 182.984 \times 10^{-3}\ (T/\mathrm{K}) + 89.474\ \log(T/\mathrm{K})\ \mathrm{cal.\ mol^{-1}.K^{-1}} \quad (19)$$

Table 4

Values of thermodynamic functions for trimellitic anhydride

T	$\{H^0(T) - H^\circ(298{,}15\ \mathrm{K})\}$	C_p°	$\{S^\circ(T) - S^\circ(298{,}15\ \mathrm{K})\}$
K	cal. $\mathrm{mol^{-1}}$	cal. $\mathrm{mol^{-1}.K^{-1}}$	
298.15	0.0	59.516	0.0
300	147.770	60.787	0.370
310	790.015	67.661	2.475
320	1500.995	74.534	4.730
330	2280.709	81.408	7.130
340	3129.159	88.281	9.660
350	4046.342	95.155	12.317
360	5032.261	102.028	15.094
370	6086.913	108.902	17.983
380	7210.301	115.775	20.978
390	10848.823	110.215	27.243
400	11960.120	112.044	30.057
410	13089.715	113.874	32.846
420	14237.609	115.704	35.613
430	15403.800	117.534	38.357
440	16588.291	119.363	41.080
450	17791.080	121.193	43.783
460	19012.167	123.023	46.467
470	20251.553	124.853	49.133
480	21509.237	126.683	51.780
490	22785.219	128.513	54.412
500	24079.500	130.343	57.027
510	25392.079	132.173	59.626
520	26722.957	134.002	62.210
530	28072.133	135.832	64.780
540	29439.607	137.662	67.336

The processing of information supplied by discontinuity in relative enthalpy temperature variation (due to fusion of substance) has yielded the following results :

$T_{\text{fusion}} = 385$ K

$$\Delta H_{\text{fusion}} = \begin{cases} \nearrow \text{graphic} = 2500 \text{ cal. mol}^{-1} \\ \searrow \text{calculated} = 2502.266 \text{ cal. mol}^{-1} \end{cases} \Rightarrow (\Delta H_{\text{fusion}})_{\text{medium}} = 2501.133 \text{ cal. mol}^{-1}$$

Equations (14)-(19) have been employed in tabulation of the main thermodynamic functions; plots have been drown of temperature variation of experimental relative enthalpy in comparison with the calculated curve.

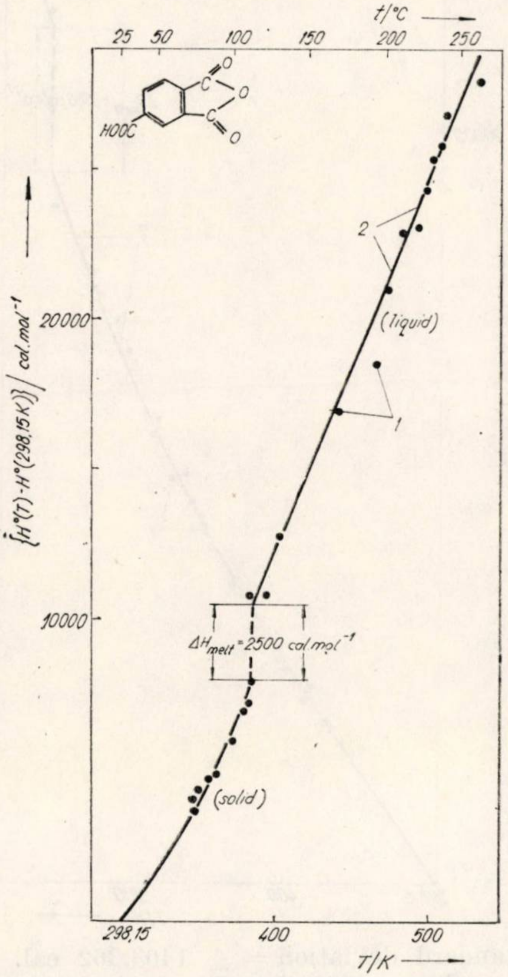

Fig. 3. Relative enthalpy of trimellitic anhydride *vs* temperature :
1. experimental; *2.* calculated.

Pyromellitic anhydride

Solid state : 298.15 – 557.15 K

$$\{H^0(T) - H^0(298.15 \text{ K})\} = -28488.398 + 167.726(T/\text{K}) - 349.220 \times 10^{-3}(T/\text{K})^2 + 359.359 \times 10^{-6}(T/\text{K})^3 \text{cal.mol}^{-1} \quad (20)$$

Standard deviation = ± 165.307 cal. mol^{-1} that is ± 1.5 per cent.

$$C_p^0 = 167.726 - 698.440 \times 10^{-3}(T/\text{K}) + 1078.077 \times 10^{-6} (T/\text{K})^2 \text{ cal. mol}^{-1}.\text{K}^{-1} \quad (21)$$

$$\{S^0(T) - S^0(298.15\text{K})\} = -794.912 + 386.273 \log(T/\text{K}) - 698.440 \times 10^{-3}(T/\text{K}) + 539.038 \times 10^{-6}(T/\text{K})^2 \text{ cal. mol}^{-1}.\text{K}^{-1} \quad (22)$$

Liquid state : 557.15 – 578.15 K

$$\{H^0(T) - H^0(298.15\ \mathrm{K})\} = 5467.338 \times 10^3 - 27.515 \times 10^3(T/\mathrm{K}) + + 45.959\ (T/\mathrm{K})^2 - 253.318 \times 10^{-4}\ (T/\mathrm{K})^3\ \mathrm{cal.\ mol^{-1}} \qquad (23)$$

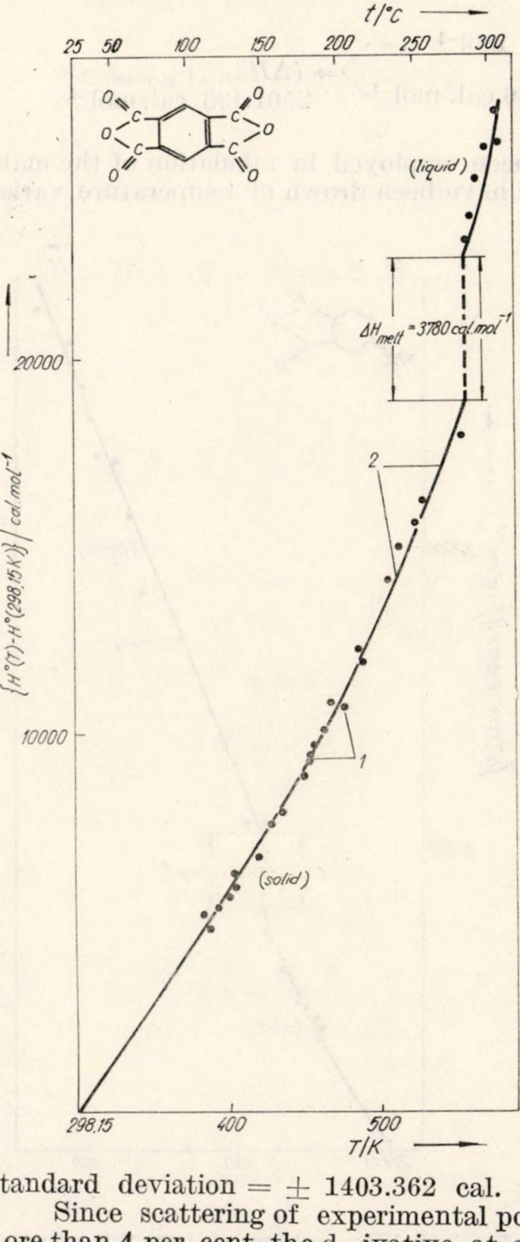

Fig. 4. Relative enthalpy of pyromellitic dianhydride *vs* temperature :

1. experimental; *2.* calculated

Standard deviation = ± 1403.362 cal. mol⁻¹, that is ± 5.76 per cent.

Since scattering of experimental points around calculated curve is more than 4 per cent, the derivative at eq. (23) does not describe accurately the dependence of heat capacity on temperature. However eqs. (20) and (23) estimate the thermal effect associated to melting of substance

$T_{\text{fusion}} = 557.15\ \text{K}$

$$\Delta H_{\text{fusion}} \begin{matrix} \nearrow \text{graphic} = 3780\ \text{cal. mol}^{-1} \\ \searrow \text{calculated} = 3786\ \text{cal. mol}^{-1} \end{matrix} \Rightarrow (\Delta H_{\text{fusion}})_{\text{medium}} = 3783\ \text{cal. mol}^{-1}$$

Equations (20) — (23) have been used in tabulation of the main thermodynamic quantities and in plotting the temperature variation of experimental and calculated relative enthalpies.

Table 5

Values of thermodynamic functions for piromellitic dianhydride

T	$\{H^\circ(T) - H^\circ(298.15\ \text{K})\}$	C_p°	$\{S^\circ(T) - S^\circ(298.15\text{K})\}$
K	cal. mol^{-1}	cal. mol^{-1} .K^{-1}	
298.15	0.0	55.316	0.0
300	102.295	55.221	0.913
310	837.044	54.812	2.718
320	1384.030	54.620	4.456
330	1930.168	54.643	6.136
340	2477.616	54.882	7.773
350	3028.529	55.336	9.371
360	3585.063	56.006	10.938
370	4149.375	56.891	12.486
380	4723.621	57.993	14.017
390	5309.956	59.310	15.540
400	5910.538	60.842	17.063
410	6527.521	62.590	18.586
420	7163.063	64.554	20.120
430	7819.320	66.733	21.665
440	8489.447	69.128	23.225
450	9202.600	71.738	24.808
460	9933.937	74.575	26.418
470	10694.613	77.606	28.054
480	11486.784	80.863	29.722
490	12312.607	84.337	31.427
500	13174.237	88.025	33.167
510	14073.830	91.929	34.948
520	15013.544	96.049	36.772
530	15995.534	100.385	38.646
540	17021.955	104.935	40.562
550	18094.965	109.702	42.532
560	23011.011	126.922	
570	24595.062	187.354	
580	26707.438	232.587	

CONCLUSIONS

The data obtained for the three studied substances allow calculation of thermodynamic functions which characterize the formation of these substances; likewise calculations could be made of thermal effects of some reactions whose reactants are the substances studied in this work.

Revue Roumaine de Chimie, **23**, *1*, 31 – 36 (1978)

THE LIMITING APPARENT MOLAL VOLUMES OF IONS IN N-METHYLACETAMIDE

KHUSHWANT SINGH

Chemistry Department B.S.N.V. Degree College Lucknow, (U.P.) India

Received July 25, 1975

The apparent molal volumes, Φv, of some uniunivalent electrolytes have been determined by using pyknometers of about 50 ml capacity down to 0.1 m and limiting apparent molal volume, Φ^0, have been obtained by extrapolating Φ_V vs. $\sqrt{c}$ curves to zero concentration. The Φ^0 of different salts, studied in this investigation have been shown to be additive in NMA as reported in water, formamide and NMP An attempt has been made to divide Φ^0 of salts into ionic contribution Φ^0_+ and Φ^0_- and $Ø^\circ$ (ion) has been examined assuming it to be difference between the intrinsic volume of the ion, Φ^0 (int) and the electrostriction volume Φ^0 (elect.).

INTRODUCTION

The additive nature of the limiting apparent molal volume, Φ^0, of electrolytes has been found to be true in a variety of solvents like water,[1] formamide [2,3] N-methylpropionamide,[4] within experimental error, however, the division of Φ^0 of electrolytes into their ionic components cannot be normally made by direct experimental technique[5]. Once the Φ^0 of an ion is estimated by some relations and then Φ^0 of other ions can be obtained by application of additivity law.

In the present communication, Φ^0 of different salts in NMA have been divided into their ionic components and Φ^0 (ion) of different ions has been determined by using the method suggested by Mukerjee[6] due to its simple and appealing assumptions. These values have been used to discuss ion-solvent interaction in NMA.

[1] A. M. Couture and K. J. Laidler, *Canad. J. Chem.*, **34,** 1209 (1956).

[2] R. Gopal and R. K. Srivastava, *J. Indian Chem. Soc.*, **40,** 99 (1963).

[3] R. Gopal and R. K. Srivastava, *J. Phys. Chem.*, **66,** 2704 (1962).

[4] F. J. Millero, *J. Phys. Chem.*, **72,** 3209 (1968).

[5] R. Zena and E. Yeager, *J. Phys. Chem.*, **70,** 954 (1966). Reported the first estimates of 0° (ion) based on direct experimental methods using an ultrasonic technique.

[6] P. Mukerjee, *J. Phys. Chem.*, **65,** 744 (1961).

EXPERIMENTAL

The A.R. (B.D.H.) samples of common salts used in this investigation were recrystallised several times from conductivity water, dried in a hot air oven and stored in a vacuum desiccator until used. N-methylacetamide (DPI, USA) was purified in the usual manner[7] and the samples having specific conductance of 10^{-6} mho or less were used. Solutions were prepared on the molal basis and their densities at 35° were measured in a large thermostat, running at 35 ± 0.005° or better, with pyknometers described elsewhere[8]. The accuracy of density measurements is expected to be better than 0.001 %[9].

From the density data in the 0.005 to 0.1 m concentration range, the apparent molal volume, Φ_v was calculated in the usual manner and the Φ_v vs. $\sqrt{c}$ curves were drawn in different cases.

RESULTS AND DISCUSSION

ADDITIVITY OF Φ^0 OF ELECTROLYTES AND LIMITING APPARENT MOLAL VOLUMES OF IONS Φ^0_+ AND Φ^0_-

The limiting apparent molal volumes of NaCl, NaBr, $NaNO_3$, NaI, KBr, KNO_3, KI, NH_4Cl, NH_4Br, NH_4NO_3 and NH_4I in NMA were obtained as 26.0, 32.6, 35.0, 42.0, 40.2, 42.8, 45.8, 35.5, 44.7, 47.3 and 51.7 respectively by extrapolating the corresponding plots of their apparent molal volume Φ_v vs. $\sqrt{c}$ to infinite dilution. The additivity law in NMA is found to be applicable and the average differences in Φ^0 of nitratebromide, iodide-chloride, Potassium-sodium, ammonium-potassium and ammonium-sodium salts are found to be 2.5, 16.1, 6.4, 4.5 and 12.2 respectively.

Table 1
The φ° of some common ions in NMA at 35°

Ion	Crystal radius in Å	$\overset{\circ}{\varphi}_{(\text{ion})}$ (ml/mole)	$\overset{\circ}{\varphi}_{(\text{ion})}$ (ml/mole) (Corrected graphically)
Na^+	0.95	0.0	3.4
K^+	1.33	6.4	9.8
NH_4^+	1.60	12.2	15.6
Cl^-	1.81	25.9	22.5
Br^-	1.95	32.6	28.2
NO_3^-	2.03	35.1	31.7
I^-	2.16	42.0	38.6

For the division of Φ^0 of salts into ionic contribution, the method suggested by Mukerjee [6] may be employed. The procedure is as follows:

Assuming $\Phi^{0+}_{(Na)}$ to be 0.0 ml/mole, $\Phi^{0-}_{(Br)}$ and $\Phi^{0-}_{(I)}$ were calculated from $\Phi^0(NaBr)$ and $\Phi^0(NaI)$ values as 32.6 and 42.0 respectively. The values of Φ° for the other ions were then calculated from the average difference. The values of the limiting ionic volumes of some common and compact ions in NMA at 35°, thus obtained, are given in column 3 of Table 1. These values for different ions have been plotted against the cube of ionic radius given by Pauling[10]. These plots are given in Fig. 1. The cations appear to fall on one line and the anions on the other; these two lines, one for the cations and the other for the anions, can be made to overlap, if $\Phi^0(Na^+)$ is assigned 3.4 ml/mole value. These values of Φ^0 for some common ions, after adjustment are given in column 4 of Table I.

---

[7] R. Gopal, M. A. Siddiqui and K. Singh, *Z. phys. Chem. (Frankfurt)*, **75**, 7–14 (1971).

[8] K. Singh, *Z. phys. Chem. (Frankfurt)*, **95**, 297 (1975).

[9] R. Gopal and K. Singh, *Z. phys. Chem. (Frankfurt)*, **69**, 81 (1970).

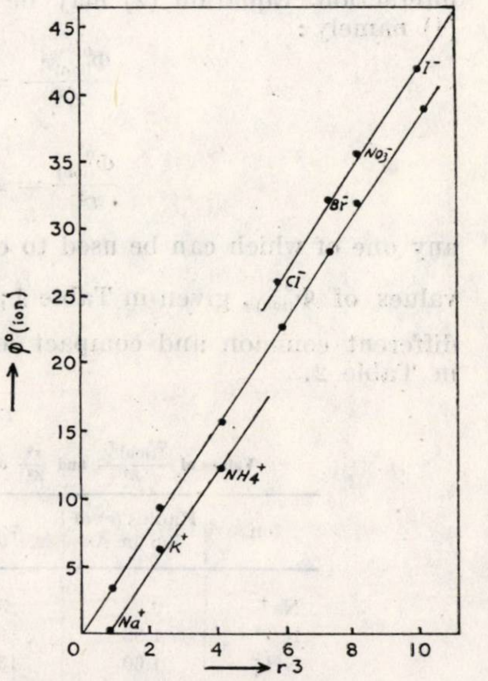

Fig. 1. — The Φ° for ions in NMA as a function of r^3 (the crystal radius in Å units).

The individual Φ^0(ion) value, despite of dependence on one or more assumptions can be used to throw light on the nature of ion-solvent interaction in a more elegant and convincing manner than the Φ^0 value of the salt. In this section, an attempt has been made to study ion-solvent interaction between ions and NMA molecules from the point of view of limiting apparent ionic volumes.

The limiting apparent molal volumes of an ion may be assumed to be the sum of two major components[6,11-13]

$$\Phi^0_{(\text{ion})} = \Phi^0_{(\text{int})} + \Phi^0_{(\text{elect.})} \qquad (1)$$

where $\Phi^0_{(\text{int.})}$ is the intrinsic volume of the ion which takes into account void space effect and $\Phi^0_{(\text{elect.})}$, the electrostriction limiting apparent molal volume is the contribution of electrostriction due to ion-solvent interaction. A number of relations have been proposed, connecting these two effects with the radius of the ion. The most successful semiempirical correlation of $\Phi^0_{(\text{ion})}$ in water has been made with equation of the form[6,11,13]

$$\Phi^0_{(\text{ion})} = Ar^3 - \frac{Bz^2}{r} \qquad (2)$$

where A and B are constant, r the radius of the ion in solution (usually taken to be the crystal radius) and Z is the charge on the ion. The first term on the right-hand side of equation (2) represents the positive contribution to the volume due to the space occupied by the ion i.e., ion cavity and the second term, the decrease in volume due to compression of solvent around the ion (electrostriction effect). Since equation (2) is semi-empirical in nature, therefore, determination of *A* and *B* in other solvent (NMA) may lead to better understanding of ion-solvent interaction. Equation (2) may be rearranged to give equations (3) and (4) namely:

---

[10] L. Pauling, "The Nature of Chemical Bond", 3rd edition, Cornell University Press Ithaca, New York, 1940.

[11] L. G. Hepler, *J. Phys. Chem.*, **61**, 1426 (1957).

[12] B. E. Conway, R. E. Verrall and J. E. Desnoyers, *Z. phys. Chem.* (*Frankfurt*) **157**, 230 (1965).

[13] E. Glueckauf, *Trans. Fruday Soc.*, **61**, 914 (1965).

$$\frac{\Phi^0_{(\text{ion})} r}{Z^2} = \frac{A r^4}{Z^2} - B \tag{3}$$

$$\frac{\Phi^0_{(\text{ion})}}{r^3} = A - \frac{B Z^2}{r^4} \tag{4}$$

any one of which can be used to evaluate constants A and B using the values of $\Phi^0_{(\text{ion})}$, given in Table 1; the values of $\frac{\Phi^0_{(\text{ion})} r}{Z^2}$ and $\frac{r^4}{Z^2}$ for different common and compact ions have been calculated and are given in Table 2.

Table 2

Values of $\frac{\varphi^\circ_{(\text{ion})}\, r}{Z^2}$ and $\frac{r^4}{Z^2}$ of some common ions in NMA at 35°

Ion	Radius (*r*) of ion in Å	$\varphi^\circ_{(\text{ion})}$	$\frac{\varphi^\circ_{(\text{ion})}\, r}{Z^2}$	$\frac{r^4}{z^2}$
Na^+	0.95	3.4	3.23	0.81
K^+	1.33	9.8	13.03	3.13
NH_4^+	1.60	15.6	24.96	6.55
Cl^-	1.81	22.5	40.72	10.73
Br^-	1.95	28.2	54.99	14.47
NO_3^-	2.03	31.7	64.35	16.98
I^-	2.16	38.6	83.38	21.76

The plot of $\frac{\Phi^0_{(\text{ion})} r}{Z^2}$ vs. $\frac{r^4}{Z^2}$ is shown in Fig. 2. From the slope and intercept of the linear curve, the constants *A* and *B* have been evaluated to be 4.0 and 1.5, respectively.

The true intrinsic limiting apparent molal "nonhydrated" volume of an ion in solution, $\Phi^0_{(\text{int.})}$ cannot be measured directly and is usually calculated from the crystal radius (*r*) of the ion. Assuming ions to be hard sphere and the volume of an ion, as given by $\frac{4}{3}\pi r^3$, to represent the volume of an ion cavity, one can write,

$$\Phi^0_{(\text{int.})} = \frac{4}{3}\pi r^3\, \mathrm{N} \times 10^{-24} \tag{5}$$

$$= 2.52\ r^3$$

where r is the crystal radius in Å units and N, the Avogadro's number. Thus the value of A as given by equation (5) is 2.52 which is smaller than 4.0, obtained from graph 2. So it appears that the volume of the ion in solution increases by about 58% in NMA as compared to the crystal volume. It has been suggested that $\Phi^0_{(\text{int.})}$ increases by 32% in Methanol,[14] 77% in water 6. The possible factors which have been suggested to be responsible for the larger $\Phi^0_{(\text{int.})}$ value are (i) the radius of the ion in solution is larger than the radius of the ion in crystal because of the difference in environments and (ii) there is an additional free volume associated with ions in solution due to improper packing of solvent molecules around the ions.

The theoretical prediction of the electrostriction caused by various ions appears to be difficult due to uncertainty of the nature of interaction between ion and solvent molecule. Thus theoretical calculation of B of equation (2) and the electrostriction caused by an ion in NMA, is not possible because calculation of B theoretically[15] from the equation

$$\Phi^0_{(\text{elect.})} = -\frac{NZ^2e^2}{2\varepsilon r}\left(\frac{\partial \ln \varepsilon}{\partial p}\right) = -BZ^2/\gamma \qquad (6)$$

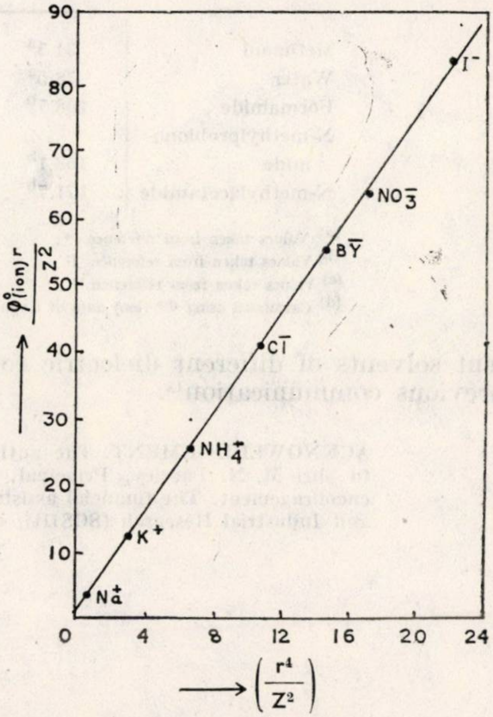

Fig. 2. – Plot of $\frac{\Phi^0_{(\text{ion})}\nu}{Z^2}$ vs. $\frac{r^4}{Z^2}$ for some ions in NMA at 35°.

would require the pressure dependence of the dielectric constant of the solvent which is not available for NMA. However one can compare the values of constant 'B' in some solvents which may give an idea of the relative electrostriction effects in them. Table 3 lists the values of 'B' in different solvents along with the dielectric constant of the solvent. From Table 3 it appears that the value of 'B' is inversely proportional to the dielectric constant, ε, of the solvent which is in approximate agreement with the theoretical prediction of equation (6) provided, $(\partial \ln \varepsilon/\partial P)$ is assumed to be almost the same for different solvents. Qualitatively, it can be stated that ion-dipole interaction gets weaker the larger the dielectric constant of the medium which is easily convincing. This deduction may also be justified by comparing Φ^0 of salts in diffe-

---

[14] F. J. Millero, *J. Phys. Chem.*, **73,** 2417 (1969).

[15] P. Drude and W. Nernst, *Z. phys. Chem.* (*Frankfurt*), **15,** 79 (1894).

Table 3

Constant '*B*' in some solvents

Solvent	Dielectric constant (ε)	Temperature	Constant '*B*' of equation (2)
Methanol	31.5^a	25°	16^c
Water	78.5^a	25°	8^c
Formamide	108.7^b	25°	2^d
N-methylprobionamide	163.1^b	25°	3^c
N-methylacetamide	171.7^b	35°	1.5

(a) Values taken from reference[16];
(b) Values taken from reference[17];
(c) Values taken from reference[14];
(d) Calculated using Φ^0 (ion) data of Gopal and Srivastava[2,3].

rent solvents of different dielectric constant as has been done in the previous communication[18].

ACKNOWLEDGEMENT. The author wishes to express his sincere thanks to Shri M. N. Pandey, Principal, B. S. N. V. Degree College, Lucknow for encouragement. The financial assistance given by the State Council of Scientific and Industrial Research (SCSIR), U.P. is gratefully acknowledged.

---

[16] H. S. Harned and B. B. Owen, "Physical Chemistry of Electrolitic Solutions", Reinhold Publishing Corporation, New York, 1958.

[17] S. J. Bass, W. I. Nathan, R. M. Meighan and R. H. Cole, *J. Phys. Chem.* **68**, 509 (1964).

[18] R. Gopal and K. Singh, *Z. phys. Chem.* (*Frankfurt*), **91**, 106 (1974).

Revue Roumaine de Chimie, 23, 1, 37–43 (1978)

DAS SCHWINGUNGSSPEKTRUM VON β-VANADYLSULFAT

ENRIQUE J. BARAN

Cátedra de Química Inorgánica, Facultad de Ciencias Exactas, Universidad Nacional de La Plata. La Plata, Rep. Argentina.

Eingegangen am 6. August 1975

Die Infrarot- und Raman-Spektren von β-$VOSO_4$ wurden gemessen und an Hand der bekannten kristallographischen Daten diskutiert. Die Deutung wurde durch die theoretische Faktorgruppenanalyse des gesamten Gitters unterstützt. Auch einige Bindungseigenschaften des VO^{2+}-Ions wurden berechnet und besprochen.

Seit einiger Zeit beschäftigen wir uns mit strukturellen und spektroskopischen Untersuchungen an Oxoanionen des Vanadins (vgl. z.B.[1–8]). Um weitere Einsicht in die Schwingungseigenschaften solcher Systeme zu erhalten, erschien es interessant auch einige andere Verbindungen, welche gleichfalls V-O-Bindungen enthalten, näher zu untersuchen und zu charakterisieren.

In vorliegender Arbeit wollen wir die Ergebnisse der spektroskopischen Untersuchung von β-$VOSO_4$ mitteilen.

ZUR KRISTALLSTRUKTUR VON β-$VOSO_4$

Wasserfreies Vanadylsulfat tritt bekannterweise in zwei Modifikationen auf,[9,10] eine ist tetragonal (α-$VOSO_4$) und die andere orthorhombisch (β-$VOSO_4$); dazu sind auch noch mehrere hydratisierte Formen bekannt.[9]

---

[1] E. J. Baran und P. J. Aymonino, *Z. anorg. Chem.*, **383**, 226 (1971).

[2] E. J. Baran, P. J. Aymonino und A. Müller, *J. Mol. Struct.*, **11**, 453 (1972).

[3] E. J Baran und P. J. Aymonino, *Z. anorg. Chem.*, **390**, 77 (1972).

[4] E. J. Baran, *Monatsh.*, **103**, 1684 (1972).

[5] J. C. Pedregosa, E. J. Baran und P. J. Aymonino, *Z. Krist.*, **137**, 221 (1973).

[6] J. C. Pedregosa, E. J. Baran und P. J. Aymonino, *Z. anorg. allg. Chem.* **404**, 308 (1974).

[7] E. J. Baran, *Monatsh.*, **106**, 1 (1975).

[8] E. J. Baran, I. L. Botto, J. C. Pedregosa und P. J. Aymonino, *Z. anorg. Chem.*, im Druck.

[9] G. Ladwig, *Z. anorg. Chem.*, **364**, 225 (1969).

[10] J. M. Longo und R. J. Arnott, *J. Solid State Chem.*, **1**, 394 (1970).

Die Kristallstruktur von β-$VOSO_4$ wurde von Kierkegaard und Longo[11] bestimmt; die Substanz kristallisiert in der orthorhombischen Raumgruppe *Pnma* mit vier Formeleinheiten in einer Elementarzelle der Dimensionen $a = 7{,}371$ Å, $b = 6{,}269$ Å und $c = 7{,}082$ Å. Die Struktur ist ein dreidimensionales Netz das von verzerrten VO_6-Oktaeder-Ketten gebildet wird, welche durch SO_4-Tetraeder verbunden sind.

Die VO_6- „Oktaeder" besitzen einen ganz kurzen V-O-Abstand von 1,59 Å der in *trans*-Stellung zu einer längeren V-O-Bindung (2,28Å) steht; die anderen vier Abstände sind praktisch identisch und betragen ungefähr 2,03 Å. Ähnliche Koordinationsverhältnisse werden auch bei zahlreichen anderen Vanadylverbindungen gefunden (vgl. z.B.[12]).

FAKTORGRUPPENANALYSE DES β-$VOSO_4$-GITTERS

An Hand der eben besprochenen kristallographischen Daten haben wir als erstes eine Faktorgruppenanalyse des gesamten Gitters durchgeführt um so einen kompletten Einblick in seine Schwingungseigenschaften zu erhalten. Dazu haben wir die Tabellen von Adams und Newton[13] (vgl. auch[14,15]) zusammen mit den aus der Strukturuntersuchung bekannten Punktlagen der verschiedenen Atomsorten benutzt.

Das Ergebnis dieser Analyse ist Tab. 1 zu entnehmen. Vom theoretischen Standpunkt her ist eine solche Analyse sehr wichtig und aufschlußreich, denn sie erlaubt die richtige Symmetrie der verschiedenen Schwingungen zu erhalten sowie die im Gitter gültigen Auswahlregeln zu bestimmen.

SCHWINGUNGSSPEKTRUM VON β-$VOSO_4$

Die durchgeführte Faktorgruppenanalyse gibt, wie eben bemerkt, Information über die verschiedenen Bewegungen aller Bausteine des Gitters. Uns interessieren aber vor allem die inneren Schwingungen der Gruppierungen welche im Gitter vorhanden sind. Wie aus Tab. 1 ersichtlich ist, liegen vierzig solcher Schwingungen vor, d.h.:

$$\Gamma_{\text{inn. Schw.}} = 7A_g + 3B_{1g} + 7B_{2g} + 3B_{3g} + 3A_u + 7B_{1u} + 3B_{2u} + 7B_{3u}$$

Von diesen sind alle Spezies gerader Parität nur im Ramaneffekt aktiv und alle mit ungerader Parität (mit Ausnahme von A_u, welche inaktiv ist) nur im IR-Spektrum erlaubt.[16]

Da wir lediglich IR- una Raman-Spektren vom mikrokristallinen Pulver messen konnten und über keine zusätzlichen Daten (wie z.B.

---

[11] P. Kierkegaard und J. M. Longo, *Acta Chem. Scand.*, **19**, 1906 (1965).

[12] J. Selbin, *Chem. Rev.*, **65**, 153 (1965).

[13] D. M. Adams und D. C. Newton, „Tables for Factor Group and Point Group Analysis". Beckman RIIC Ltd. Croydon, England, 1970.

[14] D. M. Adams und D. C. Newton, *J. Chem. Soc.* **A 1970**, 2822.

[15] D. M. Adams, *Coord. Chem. Rev.*, **10**, 183 (1973).

[16] S. D. Ross, „Inorganic Infrared and Raman Spectra", Mc. Graw Hill, London, 1972.

Raman-Einkristallmessungen und IR-Messungen mit polarisiertem Licht an dünnen Kristallplättchen) verfügen, erscheint die Totalzuordnung einer so großen Anzahl von Phononen praktisch unmöglich. Wir haben also im vornherein auf eine solche Totalzuordnung verzichtet und uns mit einer einfacheren Betrachtung begnügt.

Tabelle 1

Faktorgruppenanalyse des β-$VOSO_4$-Gitters

Atom	Anzahl und Lage	A_g	B_{1g}	B_{2g}	B_{3g}	A_u	B_{1u}	B_{2u}	B_{3u}
V	4c	2	1	2	1	1	2	1	2
S	4c	2	1	2	1	1	2	1	2
O_{II}	4c	2	1	2	1	1	2	1	2
O_{III}	4c	2	1	2	1	1	2	1	2
O_{IV}	4c	2	1	2	1	1	2	1	2
O_I	8d	3	3	3	3	3	3	3	3
$N_{Tot.}$ (= 3N = 84)		13	8	13	8	8	13	8	13
$T_{Akust.}$ (= 3)		0	0	0	0	0	1	1	1
$T_{Tot.}$ (= 24)		4	2	4	2	2	4	2	4
R (= 20)		2	3	2	3	3	2	3	2
$N_{Int.}$ (= 40)[a]		7	3	7	3	3	7	3	7

[a] $N_{Int.} = N_{Tot.} - T_{Tot.} - R$.

Auf Abb. 1 ist das IR-Spektrum im Bereich zwischen 1300 und 200 cm^{-1} zu ersehen. Das erhaltene Raman-Spektrum war nicht so gut definiert, so daß auf eine Wiedergabe verzichtet wurde. Das auf Abb. 1 wiedergegebene Spektrum erscheint weitaus deutlicher ausgeprägt und besser definiert als ein früher publiziertes, aber nicht näher diskutiertes Spektrum derselben Substanz [17].

Zur Deutung des gesamten Schwingungsspektrums erschien es nützlich und vorteilhaft dieses in zwei Bereiche zu teilen und diese separat zu diskutieren.

a) *Bereich 1300—600 cm^{-1}*:

In diesem ersten Bereich erwartet man die inneren Schwingungen des SO_4^{2-}-Ions sowie diejenige der kurzen V-O-Bindung.

Tab. 2 wiedergibt die in diesem Bereich getroffene Zuordnung der gemessenen IR-und Raman-Spektren.

Interessant ist zu bemerken, daß die antisymmetrische Valenzschwingung des Sulfat-Ions (ν_3), bloß zweifach aufspaltet, obwohl die Lagesymmetrie dieses Ions im Gitter C_s ist[11] und somit die Entartung total aufgehoben sein müßte (vgl. z.B.[16]); ähnlich verhält sich auch die antisymmetrische Deformation (ν_4). Dies bedeutet, daß die reelle Störung der SO_4-Gruppen geringer als erwartet, und annähernd C_{3v} ist.

---

[17] L. D. FREDERICKSON und D. M. HAUSEN, *Analyt. Chem.*, **35**, 818 (1963).

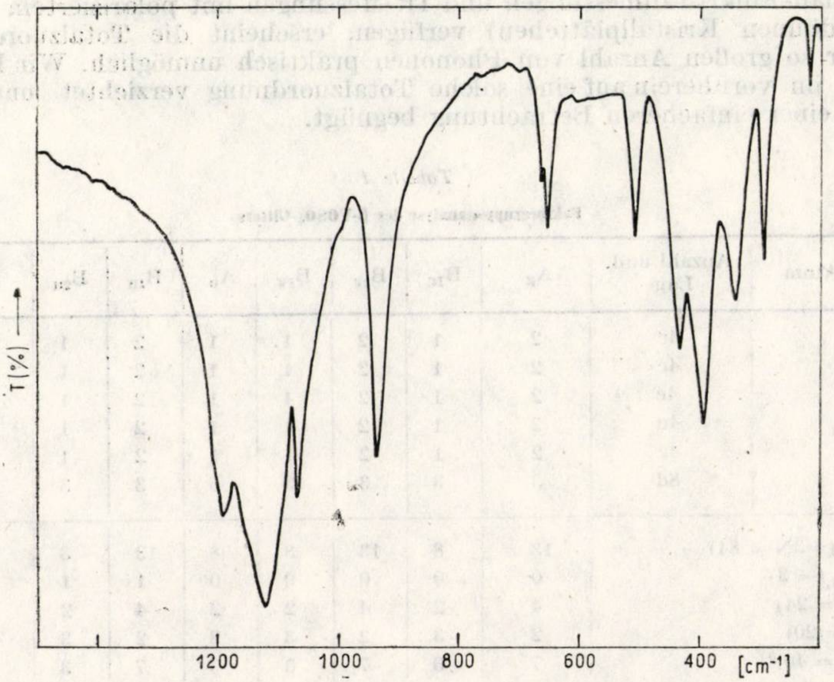

Abb. 1. — Infrarotspektrum von β-$VOSO_4$.

Tabelle 2

Innere Schwingungen vin β-$VOSO_4$ im Bereich zwischen 1300 und 600 cm^{-1}

Infrarot	Raman	Zuordnung
1192	—	
1120	1112 m	$\nu_3(SO_4^{2-})$
—	1095 s	
1070	1075 m	$\nu_1(SO_4^{2-})$
938	923 sSt	$\nu(VO)$
667	655(?) sS	$\nu_4(SO_4^{2-})$
654		

sSt: sehr stark; m: mittelstark; s: schwach; sS: sehr schwach

Die symmetrische Valenzschwingung, ν_1, erscheint imIR-Spektrum als scharfe und gut definierte Bande bei 1070 cm^{-1}; auffallenderweise tritt sie aber im Ramanspektrum nur ziemlich schwach hervor.

Die ziemlich hohe Lage der Valenzschwingungsbanden ist charakteristisch für als Liganden fungierende Sulfatgruppen (vgl. z.B.[18,19]); in wäßriger Lösung liegt ν_1 bei 981 cm^{-1} und ν_3 bei 1104 cm^{1-} (vgl.[16]). Auch im IR-Spektrum von α-$VOSO_4$ zeigt sich eine ähnliche Verschiebung der Lage der SO_4^{2-}-Schwingungen.[9]

Die V-O-Valenzschwingung ist die intensivste Linie im Raman-Spektrum und sie tritt auch sehr stark im IR-Spektrum auf. Die Tatsache, daß der Frequenzunterschied beim Vergleich der entsprechenden

---

[18] K. Nakamoto, „Infrared Spectra of Inorganic and Coordination Compounds", J. Wiley, New York, 1969.

[19] H. Siebert, „Anwendungen der Schwingungsspektroskopie in der anorganischen Chemie", Springer Verlag, Berlin, 1966.

Bande auf beiden Spektren 15 cm^{-1} beträgt, läßt sich ganz einfach erklären bedenkt man, daß die IR-und Raman-Schwingungen verschiedenen Phononen angehören, wie bereits aus der Faktorgruppenanalyse ersichtlich ist. Auch bei entsprechenden Sulfat-Banden zeigen sich solche Frequenzunterschiede deutlich.

Das spektroskopische Verhalten dieser VO-Bindung interessiert uns, wie in der Einleitung gesagt wurde, ganz besonders. An Hand des einfachen „Zweimassenmodells" haben wir die Kraftkonstante dieser Bindung abgeschätzt und einen Wert von 6,33 mdyn/Å erhalten, was wiederum zu einem Bindungsgrad (berechnet nach Siebert[19]) von 1,7 führt. Erwartungsgemäß liegt die erhaltene Kraftkonstante sehr hoch im Vergleich mit den Werten die bei anderen Oxovanadinverbindungen berechnet wurden; sie beträgt z.B. für VO_4^{3-}(Lösung) 4,58 mdyn/Å [20]; für VO_4^{3-} im $Sr_3(VO_4)_2$ 4,60 mdyn/Å[21]; für die endständigen VO_3-Gruppen im $V_2O_7^{4-}$-Ion in Lösung 5,21 mdyn/Å[21] und für die endständigen VO_2-Gruppen bei einigen Metavanadaten ca. 6,1 mdyn/Å.[22]

Weiterhin war es auch interessant näheres über die mittlere Schwingungsamplitude von dieser starken VO-Bindung zu erfahren. An Hand der einfachen Methode von Kimura und Kimura[23] (vgl. auch[24]) haben wir die Amplitudenwerte für dieselbe im Temperaturbereich zwischen 0 und 1000 K berechnet. Die Ergebnisse sind Tab. 3 zu entnehmen. Hieraus ist ersichtlich, daß diese starke Metall-Sauerstoff-Bindung eine nur ganz geringe Temperaturabhängigkeit aufweist. Die erhaltenen mittleren Schwingungsamplituden liegen aber etwas höher als z.B. bei VOF_3 oder $VOCl_3$ (0,0366 Å bzw. 0,0369 Å bei 298 K) [25] aber niedriger als z.B. beim VO_4^{3-}-Ion (0,043 Å bei 298 K).[25,26]

b) *Bereich 600—200 cm^{-1}:*

In diesen Bereich müßte man die restlichen Schwingungen der verzerrten VO_6-Oktaeder und die symmetrische Deformationsschwingung, ν_2, des SO_4^{2-}-Ions erwarten. Letztere Schwingung müßte im IR-Spektrum ganz schwach und im Raman-Spektrum intensiver auftreten.[27,28] In Lösung liegt diese Schwingung bei 451 cm^{-1};[16] in diesem Bereich und auch in der nahen Umgebung zeigt aber das Ramanspektrum keine einzige Bande; dieselbe erreicht also wahrscheinlich im vorliegenden Fall auch im Ramaneffekt nicht genügend Intensität, sie kann aber auch stärker verschoben sein oder stark mit den anderen, bei tieferen Frequenzen beobachteten Schwingungen, gekoppelt sein.

---

[20] A. Müller und B. Krebs, *J. Mol. Spectroscopy*, **24**, 180 (1967).

[21] J. C. Pedregosa, Dissertation. Universidad Nac. de San Luis, 1975.

[22] E. J. Baran, in Vorbereitung.

[23] K. Kimura und M. Kimura, *J. Chem. Phys.*, **25**, 362 (1956).

[24] E. J. Baran, *Z. phys. Chem.*, (*Leipzig*), **255**, 1022 (1974).

[25] A. Müller, E. J. Baran und K. H. Schmidt, Characteristic Mean Amplitudes of Vibration in „Molecular Structures and Vibrations" (S. J. CYVIN, Herausg.), Elsvier, Amsterdam, 1968.

[26] E. J. Baran, *Monatsh.*, **106**, 121 (1975).

[27] N. Weinstock, H. Schulze und A. Müller, *J. Chem. Phys.*, **59**, 5063 (1973).

[28] A. Müller, N. Weinstock und E. J. Baran, in Vorbereitung.

Für ein gestauchtes VO_6-Oktaeder, mit annähernd C_{4v}-Symmetrie werden vier entartete und sieben nicht entartete Schwingungen erwartet; von diesen sind acht $(4A_1+4E)$ IR- und Raman-aktiv und drei $(2B_1+B_2)$ nur Ramanaktiv (vgl. z.B.[29]). Eine der A_1-Schwingungen dieses Oktaeders ist die der bereits im anderen Bereich erwähnte und diskutierte kurze VO-Bindung. Die Zuordnung der anderen Oktaederschwingungen ist weitaus schwieriger, besonders wegen des nicht gut definierten Ramanspektrums und weil auch im tieferen Bereich Gitterschwingungen des T- oder -R Typs auftreten können, dessen Anzahl gemäß Tab. 1 ja auch ziemlich groß ist.

Tabelle 3

Mittlere Schwingungsamplitude der VO-Bindung in β-$VOSO_4$ bei verschiedenen Temperaturen

Temp. (°K)	u_{VO} (Å)
0	0,038
100	0,038
200	0,038
300	0,039
400	0,040
500	0,041
600	0,043
700	0,044
800	0,046
900	0,048
1000	0,050

Tabelle 4

IR- und Raman-Spektrum von β-$VOSO_4$ zwischen 600 und 200 cm^{-1}

Infrarot	Raman
508	—
432	427 (?) sS
393	396 sS
—	359 St
341	340(?) sS
—	328 m
—	307 (?) sS
294	288 s
—	266 m
221	—

St : stark; m : mittelstark;
s : schwach;
sS : sehr schwach

Tab. 4 wiedergibt eine Zusammenstellung aller in diesem Bereich beobachteten Banden ohne nähere Zuordnung.

Zusammenfassend, kann man also sagen, daß die Zuordnung im Bereich der höheren Frequenzen ziemlich eindeutig ist; die Symmetrie der SO_4^{2-}-Gruppen ist im Gitter annähernd C_{3v} und auch die kurze und starke VO-Bindung ist deutlich festzustellen. Bei den niederen Frequenzen dagegen, ist eine eindeutige Zuordnung nicht mehr möglich, die meisten beobachteten Banden sind aber sicherlich an V-O-Schwingungen der verzerrten VO_6-Oktaeder zuzuschreiben.

[29] B. Jezowska-Trzebiatowska, J. Hanuza und M. Baluka, *Acta Phys. Polon.*, **A38**, 563 (1970).

EXPERIMENTELLER TEIL

Das β-$VOSO_4$ wurde durch Reaktion zweischen V_2O_5 und H_2SO_4 hergestellt [30] und durch sein Pulverdiagramm [11] charakterisiert.

Das IR-Spektrum wurde an CsJ-Presslingen des Kristallpulvers mit einem Perkin Elmer 180 Spektralphotometer gemessen. Die Raman-Spektren wurden mit einem Apparat der Fa. Coderg (Typ PHO) unter Anwendung der 5682 Å-Linie eines Kr-Lasers der Fa. Spectra Physics aufgenommen.

Sämtliche Berechnungen wurden an einem IBM-360-Computer (CESPI-Universidad Nacional de La Plata) durchgeführt.

Diese Arbeit wurde mit Unterstützung der „Alexander von Humboldt"-Stiftung (Bonn—Bad Godesberg, BRD) und des „Consejo Nacional des Investigaciones Científicas y Técnicas de la República Argentina" durchgeführt. Wir danken auch Herrn Dr. K. H. Schmidt, Universität Dortmund, für die Messung der Spektren.

---

[30] G. Brauer, „Handbuch der Präparativen Anorganischen Chemie", F. Enke Vlg., Stuttgart, 1962.

Revue Roumaine de Chimie, 23, 1, 45–53 (1978)

ENTROPY OF SOME SIMPLE GAS-WATER CLATHRATES[1]

LAVINEL G. IONESCU
Department of Chemistry, University of Detroit, Michigan 48221

Received August 21, 1975

The present paper discusses some approaches that can be used to determine the entropy change for the formation of simple gaswater clathrates. A simple method considering the entropies of phase transitions of the gas and water is presented in detail. Comparison of values obtained by this approximate method to results determined from experimental measurements shows good agreement.

1. INTRODUCTION

A clathrate is a "compound" consisting of two distinct components, the host and the guest. The guest, usually a gas or a liquid, is held in a cage provided by the crystalline lattice of the host. In fact, the word clathrate was proposed by Powell[2] from the Latin *clathratus*, which means enclosed by gratings or a cage. The clathrates in which water is the host and a gas is the guest are also commonly called gas hydrates. The forces holding a clathrate together are usually of the Van der Waals type, so clathrates are not really chemical compounds in a genuine sense.

Davy and Faraday originally discovered clathrates when they studied the solubility of chlorine in water about 1810, and Villard [3] was the first to prepare a noble gas clathrate when he prepared the argon-water clathrate in 1896. Clathrates were the subject of many investigations by Villard, Rozeboom and De Forcrand toward the end of the 19th and the begining of the 20th century. Later, they were studied with considerable interest by Tamman and by Von Stackelberg and his associates.

Many kinds of clathrates are known. Water, for example, forms clathrates with some of the noble gases, simple hydrocarbons such as methane, ethane, ethylene, acetylene, and other small molecules like hydrogen sulfide, methyl chloride, phosphine, arsine, etc. Hydroquinone, α-cyclodextrin, monoamminenickel (II) cyanide and Dianin's compound form a variety of clathrates. An unusual system that might also involve clathrate formation reported by Booth and Willson[4] is Ar-BF_3, where both of the components are gases, but form various solid stoichiometric compounds at high pressure and low temperature.

---

[1] Presented in part at the Fall Meeting of the New Mexico Academy of Science held at Las Vegas, N. Mexico, October 12, 1974.

[2] H. M. POWELL, *J. Chem. Soc.*, **1950**, 298, 300, 468.

[3] P. VILLARD, *Compt. rend.*, **123**, 377 (1896).

The properties and some of the uses of clathrates have been reviewed extensively in the literature.[5-14] Hydroquinone clathrates have been used for the storage and transportation of noble gases, monoamminenickel(II) cyanide has been employed in the purification of benzene, and clathrates have been proposed for storage of natural gas to conserve space and as regenerable life support for certain gases in space cabins.[16] It is well known that gas hydrate formation takes place in both plant and animal tissues.[17-18] Clathrates have been used as a model for anesthesia and the interaction of respiratory pigments with gases. [19-20] The problem of hydrate formation in natural gas is of significant economic importance in regard to its transportation in pipelines and its liquefaction [21]. Purification or desalination of water with gas hydrates is a very active area of research today, especially since the gas hydrate approach appears to provide more economical routes than other available techniques.[22] In addition to large deposits on earth, the presence of gas hydrates has been suggested in other parts of the solar system and the Universe. Methane hydrates may exist on Uranus, Neptune, Saturn and Jupiter.[23] Carbon dioxide hydrates have been proposed as the main components of the Martian cap[24] and hydrates of carbon dioxide, methane, ethylene and other molecules are believed to exist in the heads of comets.[25]

---

[4] H. S Booth and K. S. Willson, *J. Amer. Chem. Soc.*, **57**, 2273, 2280 (1935).

[5] W. M Deaton and E. M Frost, *U. S Bur. Mines Monograph*, No. 8, 23 (1949).

[6] L. Mandelcorn, *Chem. Rev*, **59**, 827 (1959).

[7] M. Hagan, "Clathrate Inclusion Compounds", Reinhold Publ. Co., New York, 1962.

[8] W. Child, *Quart. Rev.*, **18**, 34 (1964).

[9] L. Mandelcorn, Ed., "Nonstoichiometric Compounds", Academic Press, New York, 1964.

[10] G. A. Jeffrey and R K. McMullan, *Progr. Inorg. Chem.*, **8**, 43 (1967).

[11] G. Gawalek, "Inclusion Compounds : Addition Compounds, Clathrates, Physicochemical Separating and Measuring Methods", Verlag Deut. Wissenschaft., Berlin, 1969.

[12] D. W. Davidson in "Water — A Comprehensive Treatise", F. Franks Ed , Vol 2, p. 115ff, Plenum Press, London, 1973.

[13] H. Fernandez, *Rev. Asoc. Bioquim. Argent.*, **33**, 178, 198 (1968).

[14] E. C. Makin, *Separ. Purif. Methods*, **1**, 371 (1972).

[15] B. Miller and E. R. Strong, *Amer. Gas Assoc. Proc.*, p. 80, 1945.

[16] R. B. Martin, NASA Spec. Publ., SP-234, pp. 379—389, 1969.

[17] G. Van Hulle and O. Fennema, *Cryobiology*, **7**, 228 (1971).

[18] G. Van Hulle and O. Fennema, *Cryobiology*, **8**, 91 (1971).

[19] L. Pauling, *Science*, **134**, 15 (1961).

[20] E. Rothstein and R. M. Featherstone, *J. Mol. Biol.*, **50**, 199 (1970).

[21] A. Lapin and S. J. Cinnamon, *Bull. Inst. Int. Froid, Anéxe*, **1**, 198 (1969).

[22] A. J. Barduhn, H. E. Towlson and Yee Chien Hu, *Amer. Inst. Chem. Eng. J.*, **8**, 176 (1962).

[23] S. L. Miller, *Proc. Nat. Acad. Sci. U.S.*, **47**, 1798 (1961).

[24] S. L. Miller and W. D. Smythe, *Science*, **170**, 531 (1970).

[25] A. H. Delsemme and D. C. Miller, *Planet. Space Sci.*, **18**, 717 (1970).

The stoichiometry of the gas hydrates was studied by Villard,[3,26,27] De Forcrand, [28-33] and by Von Stackelberg and his associates.[34,35] For most of the simple clathrates the ideal stoichiometric ratio is usually six moles of water to one mole of gas. The structure of the gas hydrates was elucidated mainly by Von Stackelberg and his coworkers [34-42] by means of x-ray analysis, and was confirmed by Claussen,[43] Pauling and Marsh[33] and Jeffrey and McMullan.[10,45]

Crystallographic studies of the gas hydrates indicate that there are two crystalline forms, both cubic, one with a lattice constant of 12Å and the other of 17Å.[34,38] The smaller structure, also called type I, is usually present in simple clathrates formed by molecules smaller than 5.5Å in diameter. The larger structure or type II is more common in double or mixed hydrates and is commonly formed when the gas molecules are large. The type I unit cell consists ideally of 48 water molecules and 8 gas molecules with the resulting stoichiometry $\mathrm{Gas}\cdot 6H_2O$. However, the eight cavities present are not all geometrically equivalent. They are all surrounded by 28 water molecules, but two of the "cages" or "holes" are somewhat larger than the rest. The smaller cavities, with the water molecules arranged regularly about the center of the hole have a diameter of about 5.3Å. The remaining six have a diameter of 5.9Å. Actually the water : gas stoichiometric ratio varies from less than six to less than eight, depending upon which cavities are occupied. Gases with small molecular diameters do not form clathrates even at high pressures because they are too small to be trapped in the cage of the crystalline lattice.

For the type II structure, the unit cell consists of 136 water molecules and contains eight large cavities with a diameter of about 6.8Å and sixteen smaller ones with a diameter of 5.0Å. The water : gas stoichiometric ratio depends again on the degree of occupancy of the two kinds of cavities, the ratio of 17 :1 being achieved when all the large cavities are occupied.

---

[26] P. Villard, *Ann. Chim. Phys.*, **11**, 289 (1897).
[27] P. Villard, *Compt. rend.*, **106**, 1602 (1888).
[28] R. De Forcrand, *Compt. rend.*, **134**, 836 (1902).
[29] R. De Forcrand, *Compt. rend.*, **135**, 959 (1902).
[30] R. De Forcrand, *ibid.*, **134**, 991 (1902)
[31] R. De Forcrand, *Ann. Chim. Phys.*, **29**, 36 (1903).
[32] R. De Forcrand, *Compt. rend.*, **176**, 355 (1923).
[33] R. De Forcrand, *ibid.*, **181**, 15 (1935).
[34] M. Von Stackelberg, *Naturwiss.*, **36**, 327, 359 (1949).
[35] M. Von Stackelberg and H. Müller, *ibid.*, **38**, 456 (1951).
[36] M. Von Stackelberg and H. Müller, *ibid.*, **39**, 20 (1952).
[37] M. Von Stackelberg and H. Frühbuss, *Elektrochem.*, **58**, 99 (1954).
[38] M. Von Stackelberg and H. Müller, *ibid.*, **58**, 25 (1954).
[39] M. Von Stackelberg and H. Müller, *J. Chem. Phys.*, **19**, 1319 (1951).
[40] M. Von Stackelberg and W. Jahns, *Elektrochem.*, **58**, 162 (1954).
[41] M. Von Stackelberg and W. Meinhold, *ibid.*, **58**, 40 (1954).
[42] M. Von Stackelberg and W. Meuthen, *ibid.*, **62**, 130 (1958).
[43] W. F. Claussen, *J. Chem. Phys.*, **19**, 259, 662, 1425 (1951).
[44] L. Pauling and R. E. Marsh, *Proc. Nat. Acad. Sci. U.S.*, **38**, 112 (1952).
[45] R. K. McMullan and J. A. Jeffrey, *J. Phys. Chem.*, **42**, 2725 (1965).

2. THERMODYNAMICS OF CLATHRATE FORMATION

A statistical mechanical treatment of gas hydrates based on the Lennard-Jones and Devonshire method has been presented by Plateeuw and Van der Waals[46,47] and others.[48] The model is satisfactory and in general the calculated results agree well with experimental values.

From a classical thermodynamic viewpoint, the formation of a simple gas hydrate with 6 :1 stoichiometry can be represented by equation (1).

$$G(g) + 6\,H_2O(1) \rightarrow G\cdot 6H_2O(s) \tag{1}$$

where G represents any gas that forms clathrates. The equilibrium constant for the reaction above, K_a, based on the activities of the reactants and products is given by equation (2).

$$K_a = \frac{a_G\,.\,6H_2O}{a_G\cdot a_{H_2O^6}} \tag{2}$$

Assuming that the activities of the solid clathrate and liquid water are approximately unity, and that the activity of the gas is about the same as its pressure, $a = P$, then a new equilibrium constant, K_p, is given by the expression

$$K_p = \frac{1}{P_G} \tag{3}$$

The equilibrium constant, K_p, can then be obtained at a given temperature by merely substituting the equilibrium pressure of the gas, P_G, i.e. the dissociation pressure of the clathrate, P_{diss}, in equation (3). This equation, of course, has a standard state for the gas of 1 atm of pressure.

The standard heat of reaction, ΔH^0_r, of a gas with water to form a clathrate according to equation (1) can be determined using the Clausius-Clapeyron equation in the form given by (4) and making a plot of log P_{diss} versus (1/T). Using common thermodynamic relations

$$\frac{d\log P}{d(1/T)} = \frac{-\Delta H^0_{\text{vap}}}{2.303R} \tag{4}$$

where $\Delta H^0_{\text{vap}} = -\Delta H^0_r$ for reaction (1)
one can also obtain the standard free energy, ΔG^0_{rT}, and standard entropy, ΔS^0_r, for reaction (1) at a given temperature T.

$$\Delta G^0_{r_T} = -RT\ln K_p \tag{5}$$

$$\Delta S^0_r = \frac{\Delta H^0_r - \Delta HG^0_{r_T}}{T} \tag{6}$$

---

[46] J. C. Platteeuw and J. H. Van der Waals, *Molec. Phys.*, **1**, 91 (1958).

[47] J. H. Van der Waals and J. C. Platteeuw in "Advances in Chemical Physics", Vol. 2. I. Prigogine, Ed., pp. 1–57, Interscience Publishers, New York, 1959.

[48] R. M. Barrer and W. I. Stuart, *Proc. Roy. Soc.*, **A 243**, 172 (1957).

Standard heats of reaction for clathrate formation, ΔH_r^0's, according to the reaction given by (1). and dissociation pressures, P_{diss}'s, have been reported in the literature and the corresponding ΔG_r^0 and ΔS_r^0 can be calculated from experimental data.

3. CONSIDERATION OF ENTROPY

The consideration of entropy changes for chemical processes can often provide additional insight and information about the nature of these phenomena, beyond the simple concept of increase of order or disorder in the system. For example, entropy gradients can be used to obtain information about conformational changes in proteins [20,49] and many interactions at specific sites. Clathrates provide such an example of weak interactions at specific sites and have been used as models for anesthesia and the binding of respiratory pigments with gases.[19,20] In addition, the economic importance of clathrates, as well as the fact that they provide an "ideal" system for the study of the properties of an universal solvent like water, make a better understanding of gas hydrates desirable.

The entropy changes for the formation of simple gas hydrates can be determined in several ways, besides the statistical mechanical method[46–49] and the thermodynamic relation given by equation (6). Some of these may involve processes described by equations (7—11), which are somewhat different from that described by equation (1).

$$G(1) + 6H_2O(1) \rightarrow G \cdot 6H_2O(s) \tag{7}$$

$$G(soln) + 6\,H_2O(1) \rightarrow G \cdot 6H_2O(s) \tag{8}$$

$$G(1) + 6H_2O(s) \rightarrow G \cdot 6H_2O(s) \tag{9}$$

$$G(soln) + 6\,H_2O(s) \rightarrow G \cdot 6H_2O(s) \tag{10}$$

$$G(s) + 6\,H_2O(s) \rightarrow G \cdot 6H_2O(s) \tag{11}$$

Von Stackelberg[34] has estimated an approximate entropy change of — 36 to — 41 eu for the formation of a typical gas hydrate or clathrate according to equation (7). This value was obtained by taking into account the entropy of freezing of 6 moles of liquid water at 0° C, i.e. — 31 eu, and the entropy required to transfer a gas from the liquid state into the clathrate lattice. He assumed this second term to be about equal to the entropy of solidification of the substance forming the hydrate and of the order of —5 to —10 eu. If one considers that the gas molecule is usually free to rotate in the crystalline cage, the second term is reduced by about 5 eu. This method yields only a rough value for the entropy change of the process described by equation (7) and employs liquid gas and water as the standard states.

---

[49] G. J. Ewing and L. G. Ionescu, *J. Phys. Chem.*, **76**, 591 (1972).

Consideration of the entropy of dilution or mixing of the substance G forming the clathrate[50] leads only to approximate estimates of the entropy changes for the processes described by equations (7) and (8). The mixing process assumes by definition a random distribution in the system, and this is of course, not the case for the highly ordered clathrates. The entropy of mixing, $\Delta S_{\mathrm{mixing}}$, is given by the expression

$$\Delta S_{\mathrm{mixing}} = -R \sum x_i \ln x_i \qquad (12)$$

where $\Delta S_{\mathrm{mixing}}$ = entropy of mixing per mole of mixture

R = gas constant

x_i = mole fraction of substance i

For a system containing only a gas and water, the entropy mixing, $\Delta S_{\mathrm{mixing}}$, is given by equation (13).

$$\Delta S_{\mathrm{mixing}} = -R(x_G \ln x_G + x_{H_2O} \ln x_{H_2O}) \qquad (13)$$

where

x_G = mole fraction of gas G

x_{H_2O} = mole fraction of water

R = gas constant = 1.987 cal deg mole

We will use $Xe \cdot 6H_2O$[50-52] as an example. The mixing of xenon with water is described by equation (14). For the case of xenon

$$Xe(1) + \text{excess } H_2O(1) \rightarrow Xe(\text{soln}) \qquad \Delta S_{\mathrm{mixing}} \qquad (14)$$

at 1 atm and 0°C, the solution contains 1.053×10^{-2} mole of xenon [53] and 55.56 moles of water. This corresponds to $x_{Xe} = 1.895 \times 10^{-4}$ and $x_{H_2O} = 9.998 \times 10^{-1}$, or a $\Delta S_{\mathrm{mixing}}$ of +19.1 eu.

The conditions of 1 atm and 0°C chosen for the solution of liquid xenon in water represent hypothetical extrapolation conditions for state parameters.

The entropy change for the formation of the clathrate according to equation (7) corresponds to the sum of the entropy changes for the three processes described below.

$$\begin{array}{lr}
Xe(g) + 6H_2O(1) \rightarrow Xe \cdot 6H_2O(s) \quad \Delta S_f^0 & (1) \\
Xe(1) + \text{excess } H_2O(1) \rightarrow Xe(\text{soln}) \; \Delta S_{\mathrm{mixing}} & (14) \\
Xe(\text{soln}) \rightarrow Xe(g) + \text{excess } H_2O(-1) - \Delta S_{\mathrm{soln}} & (15) \\
\hline
Xe(1) + 6H_2O(1) \rightarrow Xe \cdot 6H_2O(s) & (7)
\end{array}$$

---

[50] L. G. Ionescu, Doctoral Dissertation, New Mexico State University, Las Cruces, N. M., 1970.

[51] L. G. Ionescu, *Rev. Roumaine Chim.*, **18**, 1731 (1973).

[52] G. J. Ewing and L. G. Ionescu, *J. Chem. and Eng. Data*, **19**, 367 (1974).

[53] D. Wood and R. Caputi, U. S. Naval Radiological Defense Laboratory, Report TR-988, San Francisco, California, 1966.

The heat of solution determined experimentally for xenon is -5.70 kcal/mole.[50] This gives a value of -20.9 eu for ΔS_{soln} at 0°C. The entropy change for the process described by equation (7) is then $-57.6 + 19.1 - (-20.9)$ or -17.6 eu. This is not in very good agreement with the value of Von Stackelberg [34], as one might expect for the aforementioned reasons.

The entropy change for the process involving the formation of the clathrate according to equation (8) is readily obtained by considering equations (1) and (15). It is given by the difference between ΔS^0_r and

$$\mathrm{Xe(g)} + 6\mathrm{H_2O(1)} \rightarrow \mathrm{Xe}\ 6\mathrm{H_2O(s)} \qquad \Delta S^0_r \tag{1}$$

$$\underline{\mathrm{Xe(soln)} \rightarrow \mathrm{Xe(g)} + \text{excess } \mathrm{H_2O(1)}} - \Delta S_{soln} \tag{15}$$

$$\mathrm{Xe(soln)} + 6\mathrm{H_2O(1)} \rightarrow \mathrm{Xe}\cdot 6\mathrm{H_2O(s)} \tag{8}$$

ΔS_{soln}, i.e. $-57.6 - (-20.9)$ and corresponds to -36.7 eu. This is rather different from -24.3 eu obtained for reaction (8) by means of thermodynamic relation (6) from experimental data.

A simple way to estimate the standard entropy change, ΔS^0_r, for clathrate formation according to reaction (1) is by consideration of the entropy changes for the following processes.

$$\mathrm{G(g)} \rightarrow \mathrm{G(1)} \qquad \Delta S^0_{\text{G condensation}} \tag{16}$$

$$\mathrm{G(1)} \rightarrow \mathrm{G(s)} \qquad \Delta S^0_{\text{G solidification}} \tag{17}$$

$$\mathrm{H_2O(1)} \rightarrow \mathrm{H_2O(s)} \qquad \Delta S^0_{\mathrm{H_2O}\text{ solidification}} \tag{18}$$

Assuming that the reaction described by equation (11) proceeds with near zero entropy change, ΔS^0_r for reaction (1) is given by equation (19).

$$\Delta S^0_r = \sum \Delta S^0_{\text{G condens}} + \Delta S^0_{\text{G solidif}} + 6\,\Delta S^0_{\mathrm{H_2O}\text{ solidif}} \tag{19}$$

Values for the entropy of solidification and condensation for many gases forming clathrates are readily available in the literature[54]. We have estimated ΔS^0_r for some simple noble gas hydrates by means of equations (19) and have also calculated values for ΔS^0_r at 0° C by means of thermodynamic relation (6) and experimental ΔH^0_r's and P_{diss}'s reported in the literature. The results obtained are given in Table 1. Similar thermodynamic properties obtained for other simple gas hydrates are given in Table 2. As one might expect, the value of ΔS^0_r does not vary much for small temperature ranges. In fact, on the basis of experimental data for $\mathrm{Xe}\cdot 6\mathrm{H_2O}$,[50,52] ΔS^0_r was found to vary less than 0.1 eu from 0° to 12°.

---

[54] F. D. Rossini, D. W. Wagman, W. H. Evans, S. Levine and I. Jaffe, "Selected Values of Chemical Thermodynamic Properties", Circular 500, Nat. Bur. Stand., U. S. Government Printing Office, Washington, D.C., 1952.

Table 1

Entropy of some noble gas water clathrates

Clathrate	Experimental Dissociation Pressure at 0°C (atm)	Experimental ΔH_r^0 (kcal/mole)	Estimated ΔS_r^0 from liquid H_2O and gas at 1 atm (eu)	ΔS_r^0 from liquid H_2O and gas at 1 atm calculated from experimental data at 0°C (eu)
$Ar \cdot 6H_2O$	95.5[46]	−13.3[32]	−52.8	−57.7
$Kr \cdot 6H_2O$	14.5[46]	−13.9[34]	−52.9	−56.2
$Xe \cdot 6H_2O$	1.52[52]	−15.5[52]	−53.2	−57.6
$Rn \cdot 6H_2O$	0.5*[55]	—	−53.6	

* Estimated value

Table 2

Entropy of other simple gas hydrates

Clathrate	Experimental Dissociation Pressure at 0°C (atm)	Experimental ΔH_r^0 (kcal/mol)	Estimated ΔS_r^0 from liquid H_2O and gas at 1 atm (eu)	ΔS_r^0 from liquid H_2O and gas at 1 atm calculated from experimental data at 0°C (eu)
$CH_4 \cdot 6H_2O$	26.0[56]	−14.5[34]	−51.5	−59.6
$C_2H_6 \cdot 6H_2O$	5.20[56]	−15.0[34]	−58.2	−58.2
$C_2H_4 \cdot 6H_2O$	5.50[34]	−15.2[34]	−57.7	−59.0
$C_2H_2 \cdot 6H_2O$	5.70[57]	−15.0[34]	−58.6	−58.4
$H_2S \cdot 6H_2O$	0.962[38]	−16.3[29]	−55.5	−59.6
$H_2Se \cdot 6H_2O$	0.455[38]	−16.8[29]	−54.4	−59.9
$H_2Te \cdot 6H_2O$	—	—	−56.5	—
$PH_3 \cdot 6H_2O$	1.60[38]	−16.4[38]	−52.3	−61.0
$AsH_3 \cdot 6H_2O$	0.807[38]	—	−55.0	—
$SO_2 \cdot 6H_2O$	0.391[38]	−16.6[38]	−63.1	−58.9
$Cl_2 \cdot 6H_2O$	0.332[38]	−16.0[38]	−60.8	−56.4
$N_2O \cdot 6H_2O$	10.0[38]	−14.7[38]	−61.5	−58.4
$CO_2 \cdot 6H_2O$	12.3[38]	−14.4[38]	−62.5	−57.7

4. DISCUSSION AND CONCLUSIONS

An analysis of the results summarized in Table I indicates that ΔS_r^0 values estimated for simple noble gas hydrates differ from those calculated from experimental data by about −4 to −6 eu. This amounts to about 10% discrepancy between the two set of values. The results obtained for other simple gas hydrates in general show differences of

---

[55] M. VON STACKELBERG, *Elektrochem.*, **58**, 104 (1954).

[56] O. L. ROBERTS, E. R. BROWNSCOMBE and L. S. HOWE, *Oil Gas J.*, **39**, 37 (1940).

[57] P. VILLARD, *Ann. Chim. Phys.*, **11**, 7 (1897).

0 to -10 eu, with the exception of Cl_2, SO_2. N_2O and CO_2 clathrates where the difference is of the order of $+4$ eu.

This would appear to suggest that the assumption that reaction (11) proceeds with near zero entropy is not correct. The simplified treatment according to equation (19) does not take into account the motion of guest molecules in the gas hydrate. This subject has been studied in detail for various systems especially by McDowell [58,59] and by Davidson[12,60] and their associates. In general, the contribution to entropy due to the motion of guest molecules, varies with the type of molecule and the lattice that provides the cage and can range from about 1 to 10 eu.

The tabulated data for the various phase transitions[54] used in the estimates is probably very accurate, but such is not the case for the experimental standard heats of reaction, ΔH_r^0's, and the dissociation pressure for the clathrates, P_{diss}'s, reported in the literature. The ability of certain gases present as impurities to stabilize clathrates is well known The values presented for ΔH_r^0 and P_{diss} for some gas hydrate systems vary considerably and it is difficult to determine which are the correct ones. For example, reported values for ΔH_r^0 for $Ar \cdot 6H_2O$ vary from -13.3[32] to -14.9 kcal/mole [32] and for P_{diss} from 95.5[46] to 105 atm[3].

The treatment using entropies of phase transitions assumes an ideal gas-water stoichiometry of 1 :6. The value of this ratio depends to a great extent on the occupancy of the cages and in most of the systems considered above, this exact ratio is seldom reached.

The method described by equation (19) is rather approximate and is probably similar to the empirical rule of Barclay and Butler[61] modified by Franck and Evans [62] for the determination of the entropy of vaporization of molecules from aqueous solutions for the special case where there is a strong interaction between solute and solvent. Trouton's rule, is of course, a similar equation describing the entropy of vaporization of pure liquids at the boiling point.

Of the methods described above, the statistical mechanical treatment proposed by Platteeuw and Van der Waals [46,47] and modified by Barrer and Stuart [48] gives the more precise estimates but it involves laborious numerical calculations and requires valuable computer time. The approximate method given by equation (19) is very rapid and convenient.

ACKNOWLEDGEMENT. **The author wishes to express his sincere thanks to Professors Gordon J. Ewing of New Mexico State University, Las Cruces and Joseph A. Schufle of New Mexico Highlands University, Las Vegas for their helpful comments.**

---

[58] C. A. McDowell and P. R. Raghunathan, *J. Molec. Struct.*, **5,** 433 (1970).

[59] A. W. K. Khanzada and C. A. McDowell, *ibid.*, **7,** 241 (1971).

[60] D. W. Davidson, *Canad. J. Chem.*, **49,** 1224 (1971).

[61] I. M. Barclay and J. A. V. Butler, *Trans. Faraday Soc.*, **34,** 1445 (1938).

[62] H. S. Franck and M. S. Evans, *J. Chem. Phys.*, **13,** 507 (1945).

Revue Roumaine de Chimie, **23**, *1*, 55 – 61 (1978)

FOUR AND SIX COORDINATE COMPLEXES OF Zn(II) WITH AROYL HYDRAZONES

N. S. BIRADAR*, V. B. MAHALE and B. R. HAVINALE
Department of Chemistry, Karnatak University, Dharwar-580003, India

Received August 1, 1975

A few complexes of Zn(II) have been prepared by reacting zinc acetate with aroyl hydrazones in aqueous ethanolic medium. The elemental analyses indicate 1 : 2 or 1 : 1 stoichiometry depending on the ligands. On the basis of the infrared spectral studies, coordination number four and six have been suggested.

INTRODUCTION

Hydrazones are known for their varied behaviour in the complexes.[1–8] One can predict the following four types of formulation in salicylidene salicylhydrazone depending on the involvement of the coordination sites viz. C=N and C=O and active group –OH on the aldehyde residue.

The structures A, B and C depict different modes of attachment of the ligand to the metal ion in the *keto form* : A, monovalent tridentate, B, monovalent bidentate and C, neutral bidentate. In the *enol form* such type of ligands probably show bivalent tridentate behaviour (D). It is possible to know the mode of bond formation and the form of the ligand in the complexes with the help of spectroscopic data.

Though much work is done on the transition metal complexes[1–8] with hydrazones, considerably less is known about zinc (II) hydrazone

---

* For correspondence.

[1] P. V. Gogorishvilli, M. V. Karkarashvilli and D. Z. Kalandrishvilli, *Zhur. neorg. Khim.*, **14**, 1516 (1969); *Chem Abstr.*, **71**, 66805 (1969).

[2] K. Nagano, H. Kinoshita and A. Hirakawa, *Chem. Pharm. Bull.*, **12**, 1198 (1964).

[3] R. C. Aggarwal and A. Bahadur, *Indian J. Chem.*, **7**, 1038 (1969).

[4] J. F. Alcock, R. J. Baker and A. A. Daimantis, *Austral. J. Chem.*, **25**, 289 (1972).

[5] L. El-Sayed and M. F. Iskander, *J. Inorg. Nuclear Chem.*, **33**, 435 (1971).

[6] M. F. Iskander, S. E. Zayman, M. A. Khalifa and L. El-Sayed, *J. Inorg. Nuclear Chem.*, **36**, 551 (1974).

[7] L. El-Sayed, M. F. Iskander and A. El-Toukhy, *J. Inorg. Nuclear Chem.*, **36**, 1739 (1974).

[8] K. K. Narang and Miss A. Aggarwal, *Inorg. Chim. Acta*, **9**, 137 (1974).

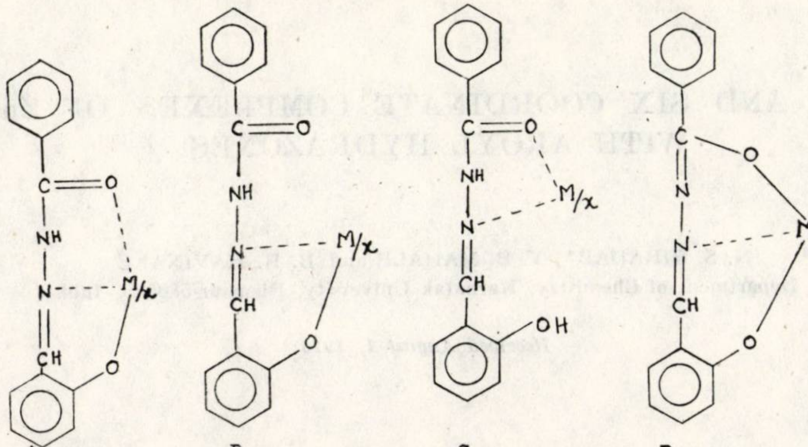

A B C D

complexes.[9–11] In this paper synthesis and spectral results of a few zinc (II) complexes with the following hydrazones are reported.

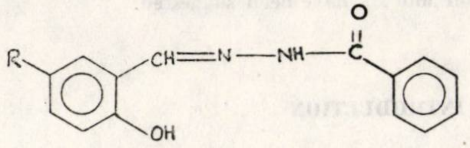

I R = H

II R = CH_3

III R = Cl

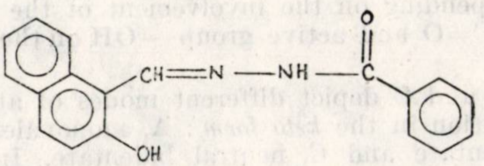

IV

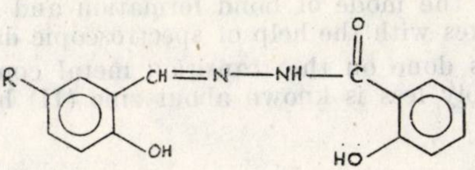

V R = H

VI R = CH_3

VII R = Cl

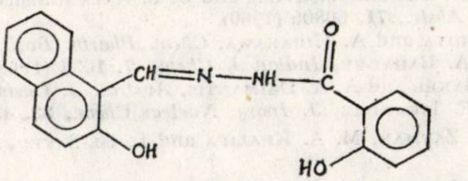

VIII

---

[9] J. F. Geldard and F. Lions, *J. Amer. Chem. Soc.*, **84**, 2262 (1962).

[10] G. S. Vasilikiotis and Th. A. Kouimtzis, *Microchem*, J., **18**, 85 (1973).

[11] I. M. Issa, R. M. Issa, Y. M. Temerk and M. M. Ghoneim, *Monatsh.*, **104**, 963 (1973).

EXPERIMENTAL

MATERIALS AND METHOD

Ethylbenzoate, methylsalicylate and hydrazine hydrate used for preparing the hydrazides were of reagent grade.

Zinc acetate was an analytical reagent. Benzoyl hydrazide and *o*-hydroxy-benzoylhydrazide were prepared according to the standard method.[12] The substituted aldehydes were prepared according to Duff's method.[13]

The hydrazones were prepared by the reaction of benzoylhydrazide or *o*-hydroxy benzoylhydrazide (0.1M) with corresponding aldehydes (0.1M) in ethanol.

PREPARATION OF THE COMPLEXES

To an ethanolic solution containing 0.2M of hydrazide and aldehyde, an aqueous zinc acetate solution (0.1M) was added. The reaction mixture was heated for a while on water bath and the complex precipitated was filtered and washed free from the ligand with ethanol and finally with ether and dried in vacuum over P_2O_5.

In the case of *o*-hydroxy-benzoylhydrazide 0.1M of the hydrazide and 0.1M of the corresponding aldehydes were used for the preparation of complexes.

ELEMENTAL ANALYSIS

Zinc in the complexes is estimated volumetrically using EDTA[14] and nitrogen by Dumas method. Carbon and hydrogen were determined by microanalytical method. The results of the elemental analysis are shown in Table 1.

PHYSICAL MEASUREMENTS

The conductivity measurements are done on an ELICO-CM-82 conductivity bridge with a cell having cell constant 0.829 cm^{-1}. The IR spectra of the ligands and the complexes in nujol mull were recorded on Beckmann IR-20 in the region of 4000–650 cm^{-1}.

RESULTS AND DISCUSSION

The complexes are yellow in colour, insoluble in common organic solvents. However they are soluble to some extent in DMF, DMSO and pyridine. The analytical results shown in Table 1 agree with the formula containing two molecules of ligand per atom of zinc in the complexes IX to XII and one molecule of ligand in the complexes XIII–XVI.

CONDUCTANCE

The molar conductance values of the complexes in DMSO at the concentration $\sim 10^{-3}$M are too low to measure for any dissociation of the complexes in the solvent. Hence the complexes are non-electrolytes.

---

[12] A. I. Vogel, "A Text Book of Practical Organic Chemistry", Longmans Green, London, 1968.

[13] J. C. Duff, *J. Chem. Soc.*, **1941,** 547.

[14] A. I. Vogel, "A Text Book of Quantitative Inorganic Analysis", Longmans Green, London, 1969.

Table 1

Elemental analysis of Zn(II) complexes with aroyl hydrazones

S. N°	Ligand N°	Complex N°	Empirical formula	% Zn		%N		%C		% H	
				Found	*Calcd.*	*Found.*	*Calcd.*	*Found*	*Calcd.*	*Found*	*Calcd.*
1	I	IX	$(C_{14}H_{11}N_2O_2)_2Zn$	11.74	12.03	9.85	10.30	61.38	61.84	3.46	4.05
2	II	X	$(C_{15}H_{13}N_2O_2)_2Zn$	11.57	11.44	9.79	9.80	62.63	63.01	4.33	4.55
3	III	XI	$(C_{14}H_{10}N_2O_2Cl)_2Zn$	10.33	10.68	8.67	9.15	55.04	54.87	3.15	3.27
4	IV	XII	$(C_{18}H_{13}N_2O_2)_2Zn$	9.92	10.16	8.39	8.71	66.71	67.15	4.59	4.04
5	V	XIII	$(C_{14}H_{10}N_2O_3)Zn$	20.36	20.46	8.90	8.77	51.53	52.59	3.65	3.13
6	VI	XIV	$(C_{15}H_{12}N_2O_3)Zn$	19.45	19.61	8.78	8.40	52.62	50.40	3.76	3.60
7	VII	XV	$(C_{14}H_9N_2O_3Cl)Zn$	18.31	18.48	8.01	7.91	47.40	47.47	2.78	2.54
8	VIII	XVI	$(C_{18}H_{12}N_2O_3)Zn$	17.60	17.70	7.10	7.58	59.12	58.48	3.44	3.25

INFRARED SPECTRA

The important infrared bands are listed in Table 2 along with their assignments.

The broad band of medium intensity around 3200 cm^{-1} and broad weak band in the region 2800–2700 cm^{-1} observed for the ligands I–VIII are respectively assigned to the ν(NH)[15] and intramolecularly hydrogen bonded OH vibrations. Similar types of broad weak band due to hydrogen bonded OH is also reported in salicylidene anilines.[16] In the ligands V to VIII one can expect two types of intramolecular hydro-

Table 2

Important infrared frequencies (in cm^{-1}) of Zn(II) complexes with aroyl hydrazones and their assignments

S. N°	Ligand N°.	Complex N°.	ν(NH)	ν(C=O)	ν(C = N)	ν(C = C)	ν(C–O)
1	I	IX	3140	1625	1585	1585 1547 1505	1325
2	II	X	3140	1640	1615	1585 1545 1503	1320
3	III	XI	3140	1620	1580	1580 1555 1498	1322
4	IV	XII	3140	1620	1580	1580 1550 1500	1310
5	V	XIII	—	—	1630 1610	1590 1560 1525	1335 1295
6	VI	XIV	—	—	1640 1615	1598 1562 1515	1330 1295
7	VII	XV	—	—	1642 1616	1590 1555 1530	1330 1282
8	VIII	XVI	—	—	1630 1618	1590 1555 1520	1328 1295

In the ligands, the following assignments may be made: ν(NH)∼ 3200 cm^{-1}, ν(Intramolecular hydrogen bonded –OH) 2800–2700 cm^{-1}, ν (C=O) 1670–1650 cm^{-1}, ν(C=N) 1625–1610 cm^{-1} and ν(C–O) ∼1280 cm^{-1}

---

[15] C.N.R. Rao "Chemical Applications of Infrared Spectroscopy", Academic Press, New York, 1962.

[16] N.S. Biradar and V. H. Kulkarni, *J. Inorg. Nuclear Chem.*, **33**, 2451 (1971).

gen bonded $-OH$, one with azomethine-N- and other with carbonyl oxygen.

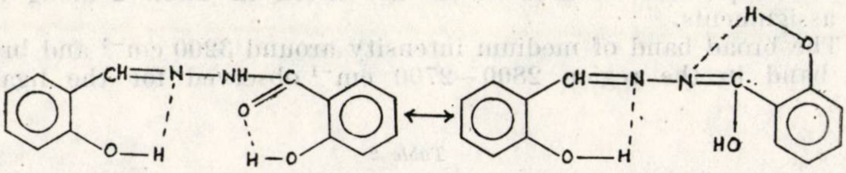

In the ligands, two intense bands are observed in the region 1670—1610 cm^{-1}. Of these, the band in the region 1670—1650 cm^{-1} is assigned to $\nu(C{=}N)$.[16,17]

In the complexes of the ligands I—IV the band due to $\nu(NH)$ is retained, and others due to $\nu(C{=}O)$ and $\nu(C{=}N)$ shift to the lower frequency indicating that both $C{=}O$ and $C{=}N$ are coordinatively bonded to the zinc ion through —O— and —N— respectively. This suggests that the ligands exist in the *keto form.*

In the complexes of the ligands V—VIII the band due to $\nu(NH)$ is absent. The $C{=}N$ band shows low frequency shift, suggesting coordination through —N— of the $C{=}N$ group. An intense band observed in the region 1642—1630 cm^{-1} may be assigned to $\nu(C{=}N)$ generated due to the enolic form of the ligand. The phenolic $C-O$ band around 1280 cm^{-1} appears in the region 1325—1300 cm^{-1} and the band due to intramolecular hydrogen bonded $-OH$ disappears in the complexes, IX—XII. However, it is retained in the complexes XIII—XVI, and may be due to the OH, on the hydrazide residue, intramolecularly hydrogen bonded to the —N— of the free $(C{=}N)$ group. All these evidences show that in these complexes the ligands exist in the *enol form.*

The complexes of the ligands I—IV have 1 : 2 stoichiometry and spectral evidences show that the ligands behave as tridentate coordinating through $C{=}O$, $C{=}N$ and oxygen of OH group.

Hence complexes have coordination number six.

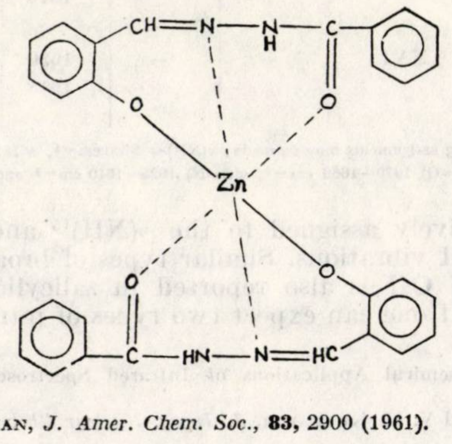

---

[17] H. H. FREEDMAN, *J. Amer. Chem. Soc.*, **83**, 2900 (1961).

The complexes of the ligands V—VIII have 1 :1 stoichiometry. All the coordinating groups and one of the active groups are involved in the bond formation. Thus these ligands show tridentate behaviour and complexes appear to have coordination number three. It seems improbable in view of the known complexes of coordination number four.[18]

In order to keep the minimum coordination number, the complexes must have undergone dimerisation. The examples of dimeric complexes with such type of ligands are numerous in the literature.[19] However, the dimeric nature of the complexes can not be substantiated by the molecular weight determination because of their insolubility.

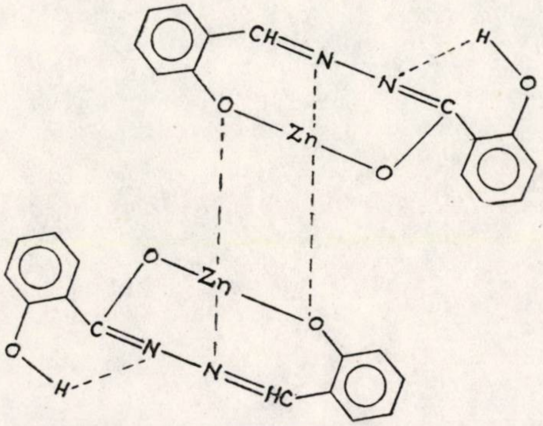

ACKNOWLEDGEMENTS. One of the authors, (B.R.H.) is thankful to Prof. E. S. Jayadevappa, Head of the Department of Chemistry, Karnatak University Dharwar, for laboratory facilities and encouragement. Thanks are also due to Dr. V. H. Kulkarni.

---

[18] F. A. Cotton and G. Wilkinson, "Advanced Inorganic Chemistry", Wiley Eastern, New Delhi, 1972.

[19] R. H. Holm, G. W. Everett, Jr. and A. Chakravorty, *Progr. Inorg. Chem.*, **7**, 83 (1966).

Revue Roumaine de Chimie, **23**, *1*, 63–71 (1978)

MOLECULAR COMPLEXES OF NITROPHENOLS WITH HEXAMETHYLENETETRAMINE AND THEIR ISOMERS

MARIA VĂGĂONESCU, SORIN MAGER and LUCIA MUNTEANU

Department of Organic Chemistry Babeş-Bolyai University, Cluj-Napoca Str. Arany Janos 11, Romania

Received August 8, 1975

The molecular complexes of hexamethylenetetramine with nitrophenols, nitroanisoles and chlorophenols have been studied and the phenomenon of the complexisomerism has been demonstrated by means of IR, UV and NMR studies. The molecular complexes formed in the molecular ratio 1 : 1 and 1 : 2 show in the case of one isomer a hydrogen-bonded structure and in the case of the second one, an EDA (electronodonor-acceptor) type structure. The NMR spectra point out a noteworthy difference between the chemical shifts of the aromatic protons in the hexamethylenetetramine-2,4-dinitrophenol complex and the same protons in the free 2,4-dinitrophenol.

In a previous paper the possibility of molecular complexes formation between mono-, di- and trinitrophenols and hexamethylenetetramine (HMT) has been shown.[1] Since the melting point (143°) of the molecular complex I, obtained by us from *p*-nitrophenol (*p*NP) and HMT[1] differs from that (128–129°) of the complex mentioned in the literature,[2] we attributed this difference to a complexisomerism. The phenomenon of the complexisomerism, also mentioned in other cases,[3–6] is due to different possibilities of binding the components in a complex. The first complexisomers separations have been mentioned in the case of the molecular complexes of picric acid with amines and it has been established that isomerisation can occur under the influence of different factors as temperature, solvent etc.[4,7,8]

The purpose of this paper is to point out the complexisomerism under the temperature influence, in the case of the molecular complexes of mono-, di- and trinitrophenols with HMT.

---

[1] M. Vagaonescu and M. Ionescu, *Rev. Roumaine Chim.*, **16**, 105 (1971).
[2] J. C. Duff and E. Y. Bills, *J. Chem. Soc.*, **1934**, 1305.
[3] P. Hepp, *Liebigs Ann. Chem.*, **215**, 357 (1882).
[4] E. Hertel, *Liebigs Ann. Chem.*, **451**, 179 (1927).
[5] I. Ostromisslensky, *Ber. dtsch. Chem. Ges.*, **268**, 1344 (1911).
[6] O. Dimroth and C. Bamberger, *Liebigs Ann. Chem.*, **438**, 67 (1924).
[7] G. Briegleb, "Elektronen-Donator-Acceptor-Komplexe", Springer Verlag, Berlin, 1961 p. 180, 193.
[8] G. Briegleb, Y. Czekalla and A. Hauser, *Z. phys. Chem. (Frankfurt)*, **21**, 99 (1959).

In attempting to clear up the structure of these complexes we have investigated their IR, NMR and UV spectra, in comparison with those of the initial compounds. Some modifications which appear in the spectra confirm the formation of a hydrogen bond between the phenolic OH and the N atom of HMT in the case of hydrogen bond (H.b) complex type, while in the case of electronodonor-acceptor (EDA) complexes an n-π interaction is to be found between the N atom from HMT (donor) and one of the nitro groups from the respective nitrophenol (acceptor).

The complex I (pNP-HMT) of yellow colour, with m.p. = 143° by slow heating at 140°, turns into its isomer II, of brown-reddish colour, with m.p. 128–129°. The identical elemental microanalysis of the two products confirm the existence of the complexisomerism. From the data of the spectral analysis (IR, UV and NMR) the structure of these complexes could be determined: complex I is formed through hydrogen bond, while its isomer II is an EDA complex of n-π type:

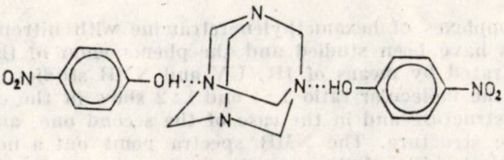

I; m.p.=143°

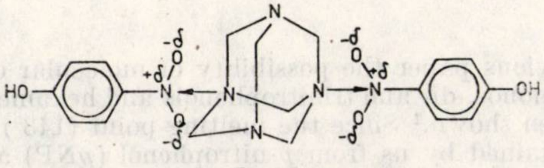

II; m.p.=128° – 129°

In the IR spectrum of complex I, as compared to those of the components, no vibration of the OH from 3300 cm^{-1} is to be seen, this being shifted towards lower frequencies, at 3020–3200 cm^{-1}, owing to the involvement of the OH in a hydrogen bond.

The NMR spectrum of this complex shows, by means of peak intensities, the molar ratio 2:1 (pNP–HMT) of the components; the comparison of this spectrum with the one of the pNP, recorded in the same conditions, demonstrates the disappearance of the characteristic peak of the phenolic OH ($\tau = -0.97$ ppm) as a consequence of the formation of hydrogen bond with the N atom of the HMT.

As distinguished from complex I, in the IR spectrum of its isomer II, the vibration of the free OH at 3300 cm^{-1} is to be found, resulting that this complex is not formed by hydrogen bond; it is an EDA complex. The overall effect of the charge transfer is a shift of the antisymmetric stretching vibration of the nitro group involved in the complex. Thus in its IR spectrum, the nitro antisymmetric stretching vibration appears at 1470–1495 cm^{-1}(instead of 1500–1515 cm^{-1}) showing that the charge transfer is localized at the nitro group.

The UV spectra of these two complexes (I and II) as compared to that of the *p*NP (Fig. 1) confirm also the EDA type complex for the isomer II through the appearance of the broad intense band at $\lambda_{max} = 390$ nm ($\varepsilon = 585$). This bathochromic shift ($\lambda_{max} = 313$ nm for *p*NP) indicates the so-called "charge transfer (CT) band" which usually characterizes the EDA complexes.[9]

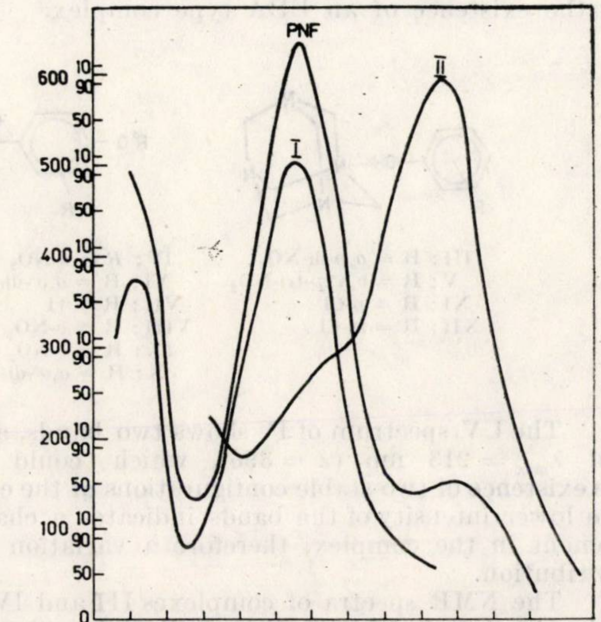

Fig. 1. — UV absorption spectra for *p*NF and complexes I and II.

The molecular complex III (2,4-DNP-HMT) of yellow colour with m.p. 167—168°,[1] by slow heating at 150°, changes into its isomer IV, of brown-reddish colour with m.p. 90—105°, having identical elemental microanalysis with the first one. The IR spectrum of III indicates the possibility for the formation of H.b type complex, the absorption of the OH group being shifted from 3275—3280 cm^{-1} to 3260 cm^{-1}. At the same time the ν_{C-OH} absorption is shifted from 1120 cm^{-1} (in the 2,4-DNP) to 1135—1140 cm^{-1}. The broad band from 2260—2520 cm^{-1} could be attributed to the stretching vibration $\nu_{\overset{+}{N}H}$, due to the formation of an ionic bond $>C-O^{-}\ldots H\overset{+}{N}<$ including the hydrogen bond, too. As a result of a salt formation, this band is called "salt band" (Salzbande).[4,10]

---

[9] R. S. Mulliken, *J. Amer. Chem. Soc.*, **72**, 600 (1950); *J. Amer. Chem. Soc.*, **74**, 811 (1952).

[10] G. Briegleb and H. Delle, *Electrochem.*, **64**, 347 (1960).

In the IR spectrum of complex IV, as distinguished from that of complex III, two nitro antisymmetric stretching vibrations appear at 1530 cm^{-1} and 1575 cm^{-1}. The ν_{C-N} absorption from 1380 cm^{-1} (in HMT) disappears also, as a result of the formation of the new bond $-\overset{\diagdown}{\underset{\diagup}{N}} \overset{-\delta o}{\underset{-\delta o}{\longrightarrow}} \overset{\diagdown}{\underset{\diagup}{N}}-$ in the complex. The disappearance of the "salt band" is also a proof for the existence of an EDA type complex.

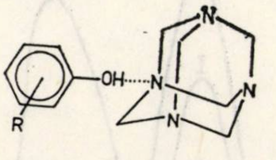

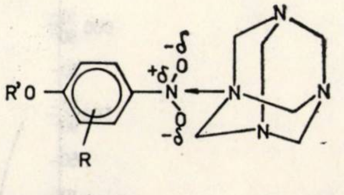

III; $R = o,p\text{-di-}NO_2$
V; $R = o,o',p\text{-tri-}NO_2$
XI; $R = p\text{-}Cl$
XII; $R = m\text{-}Cl$

IV; $R = o\text{-}NO_2$ $R' = H$
VI; $R = o,o'\text{-di-}NO_2$ $R' = H$
VII; $R = H$ $R' = Na$
VIII; $R = o\text{-}NO_2$ $R' = Na$
IX; $R = o\text{-}NO_2$ $R' = CH_3$
X; $R = o,o'\text{-di-}NO_2$ $R' = CH_3$

The UV spectrum of IV shows two bands, at $\lambda_{max} = 356$ nm ($\varepsilon = 435$) and $\lambda_{max} = 213$ nm ($\varepsilon = 396$), which could be explained through the existence of two stable configurations of the complex in the solution.[11] The lower intensity of the bands indicates a change of the transitional moment in the complex, therefore a variation of the electronic charge distribution.

The NMR spectra of complexes III and IV confirm also the molar ratio 1 :1, which had been established by elemental microanalysis, as well as by colorimetric extinction measurements.[1] In connection with the NMR spectra noteworthy are the outstanding differences which had been observed in the chemical shifts of the aromatic protons in the molecular complex III, as compared to those of the 2,4-DNP. The spectrum of 2,4-DNP in hexadeuterated dimethylsulfoxide (d_6 DMS) shows the following chemical shifts of the protons *a*, *b* and *c* (Fig. 2) $\tau_{H_a} = 1.35$ ppm, $\tau_{H_b} = 1.68$ ppm and $\tau_{H_c} = 2.70$ ppm. (The broader peak at $\tau = 3.07$ ppm belongs to the proton of the phenolic OH, superposed with the signal of the protons existent in the water traces of d_6 DMS, used as solvent). The spectrum of the complex shows the same coupling pattern and the same coupling constants : $J_{ab} = 2.9$ Hz and $J_{bc} = 9$ Hz, but different chemical shifts for the protons *b* and *c*: $\tau_{H_b} = 2.13$ ppm and $\tau_{H_c} = 3.52$ ppm, for which the following differences appear : $\Delta_{H_b} = 0.45$ ppm and $\Delta_{H_c} = 0.82$ ppm. These differences are probably due to a steric disposition of the 2,4-DNP molecule in the complex, in such a way that the *b* and *c* protons should be situated in the region in which HMT shows a shielding effect. This effect is not felt by the proton *a*, isolated between the two nitro groups from the positions 2 and 4. This phenomenon had been obvious only in the case of the 2,4-DNP asymmetric complex, while in the case of the other symmetric complexes of *p*NP and 2,4,6-TNP it could not be observed.

---

[11] G. Briegleb and J. Czekalla, *Angew. Chem.*, **72**, 401 (1960).

Complex V (2,4,6-TNP-HMT), of yellow colour and m.p. = 177—178°, of H.b type, by slow heating at 160°, changes into its isomer VI, of brown-reddish colour, with m.p. = 79—95°. The IR spectrum of V proves the hydrogen bond formation, as the OH vibration is shifted from 3110—3120 cm^{-1} in 2,4,6 - TNP, to 2920—70 cm^{-1} in the complex. At the same time the ν_{C-OH} vibration is also modified appearing in the complex at 1170 cm^{-1} (instead of 1150 cm^{-1} in 2,4,6-TNP). The appearance of the broad band from 2470—2610 cm^{-1} could be attributed to the salt formation as in the case of complex III. The IR spectrum of VI, as compared to that of V, shows some modifications which plead for an EDA complex. Thus in its spectrum the OH vibration from 2,4,6-TNP at 3110—3120 cm^{-1} is to be found again; in exchange the salt band disappears and the two NO_2 antisymmetric vibrations appear at 1530 cm^{-1} and 1565 cm^{-1}.

In the UV spectrum of VI only one absorption appears at $\lambda_{max} = 352$ nm (in 2,4,6-TNP $\lambda_{max} = 360$nm, $\varepsilon = 738$) with a lower intensity, $\varepsilon = 441$. Therefore it is about a variation of the electronic charge distribution in the complex.

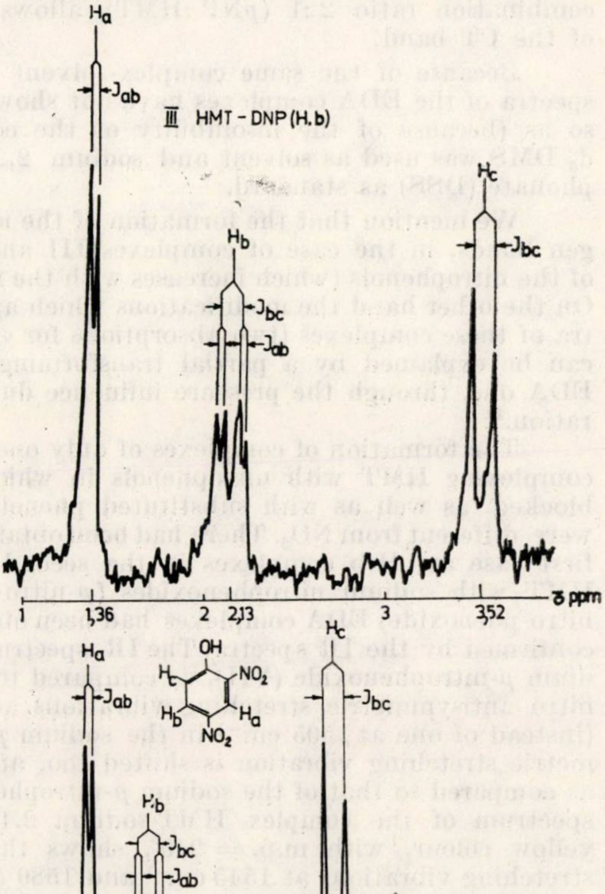

Fig. 2. — NMR spectra for 2,4-NDF and complex III.

The UV spectra do not offer in this case edifying data concerning the complex isomers because in the alcoholic solution in which the spectra were run, the complex isomers of EDA type show the tendency to be decomposed in components, a fact mentioned in the literature, too.[7] In the case of complex II its bigger stability, probably due to the combination ratio 2 :1 (*p*NP :HMT), allows the clear-cut appearance of the CT band.

Because of the same complex-solvent interaction, even the NMR spectra of the EDA complexes have not shown edifying results, the more so as (because of the insolubility of the complexes in other solvents) d_6 DMS was used as solvent and sodium 2,2-dimethyl-2-sylapentanesulphonate (DSS) as standard.

We mention that the formation of the ionic bonds, including hydrogen bonds, in the case of complexes III and IV, is due to the acidity of the nitrophenols (which increases with the number of the nitro groups). On the other hand the modifications which appear only in some IR spectra of these complexes (two absorptions for ν_{NO_2} antisym. instead of one) can be explained by a partial transforming of a H.b complex into an EDA one, through the pressure influence during the KBr pellets preparation.[12]

The formation of complexes of only one type had been achieved by complexing HMT with nitrophenols in which the OH group had been blocked, as well as with substituted phenols in which the substituents were different from NO_2. There had been obtained EDA complexes in the first case and H.b complexes in the second one. Thus by complexing HMT with sodium nitrophenoxides (*p*-nitro-, 2,4-dinitro- and 2,4,6-trinitro-phenoxide) EDA complexes had been obtained, a fact that had been confirmed by the IR spectra. The IR spectrum of the complex HMT-sodium *p*-nitrophenoxide (VII), as compared to its components, shows two nitro antisymmetric stretching vibrations at 1470 cm^{-1} and 1490 cm^{-1} (instead of one at 1505 cm^{-1} in the sodium *p*-nitrophenoxide). The symmetric stretching vibration is shifted too, at 1375 cm^{-1} in the complex, as compared to that of the sodium *p*-nitrophenoxide (1315 cm^{-1}). The IR spectrum of the complex HMT-sodium 2,4-dinitrophenoxid (VIII), of yellow colour, with m.p. = 240°, shows the two nitro antisymmetric stretching vibrations at 1545 cm^{-1} and 1580 cm^{-1}, and the nitro symmetric stretching vibration at 1355 cm^{-1}. In the IR spectrum of VIII some modifications appear, as compared to those of the sodium 2,4-dinitrophenoxide, in the range of ν_{C-O} and ν_{C-N} stretching vibrations. Thus the two ν_{C-O} antisymmetric stretching vibrations from 1290 cm^{-1} and 1020 cm^{-1}, plead for the presence of a *p*-quinoid structure in the complex. On the other hand the appearance of the maximum at 820 cm^{-1}, for the ν_{C-N} stretching vibration, indicates changes at the nitro group.

Nitroanisoles with HMT, form also EDA complexes, confirmed by spectral analysis. Thus the IR spectrum of the complex HMT-2,4-dinitroanisole (IX), of yellow colour, with m.p. = 196 – 198°, shows two nitro antisymmetric stretching vibrations, at 1540 – 1560 cm^{-1} and 1572 cm^{-1} (instead of only one, at 1545 cm^{-1}, in the 2,4-dinitroanisole). The nitro symmetric stretching vibration is also shifted from 1352–1360 cm^{-1} to 1330 cm^{-1} in the complex. In the IR spectrum of the complex HMT-2,4,6-trinitroanisole (X), of yellow colour, with m.p. = 201°, two nitro antisymmetric stretching vibrations appear also at 1520–1530 cm^{-1} and 1565 cm^{-1} (instead of one at 1545–1565 cm^{-1} in the 2,4,6-trinitroanisole). The elemental microanalysis pleads for the molar ratio 1 : 1 of the components, in the case of nitroanisoles complexes.

---

[12] G. Briegleb, "Elektronen-Donator-Acceptor-Komplexe", Springer Verlag, Berlin, 1961, p. 105.

H.b complexes had been prepared from HMT and chlorophenols. The elemental microanalysis shows the molar ratio 1 : 1 between the components, and the IR spectra show the formation of the hydrogen bonds through the shift of the OH vibration to lower frequencies : 3010–3130 cm^{-1} in the case of the complex HMT-*p*-chlorophenol (XI), of light yellow colour, with m.p. = 96–98° (as compared to ν_{OH} = 3608 cm^{-1} in the free *p*-chlorophenol) and 3025–3114 cm^{-1} in the HMT-*m*-chlorophenol complex (XII), of yellow colour and m.p. = 100–103° (as compared to ν_{OH} = 3600 cm^{-1} in the free *m*-chlorophenol).

CONCLUSIONS

— The complexisomerism had been pointed out under the influence of temperature, in the case of molecular complexes HMT-nitrophenols, obtaining H.b complexes, of yellow colour with high melting points and EDA complexes, of brown reddish colour and lower melting points.

— EDA complexes of nitrophenols with blocked OH had been prepared, and H.b complexes of substituted phenols, in which the substituents were different from NO_2.

— The formation of these complexes occurred in molecular ratio 1 :1 and 1 :2, as proved by elemental microanalysis and NMR data.

— The type of complex (EDA or H.b) has been identified from the data of the IR spectral analysis (modifications of the ν_{NO_2} antisym. ν_{OH} and ν_{C-OH} vibrations), the UV spectral analysis (bathochromic and hypsochromic effect, appearance of CT bands) and the NMR spectral analysis (peak intensities, chemical shifts and coupling constants). Noteworthy in the last case are the differences observed between the chemical shifts of the aromatic protons of the 2,4-DNP-HMT complex (H.b) and those of the 2,4-DNP.

EXPERIMENTAL

The isomers of molecular complexes nitrophenols-HMT have been prepared either by heating over 140° the components, or by heating the preformed complexes without solvent. The purification has been made by washing with diethyl ether.

Table 1

Analytical data for molecular complexes I–XII

Complex	Molec. formula complex type	C $\%^{\text{calc.}}_{\text{found}}$	H $\%^{\text{calc.}}_{\text{found}}$	m.p.°C	spectral bands *	
					IR (cm^{-1})	UV (nm)
I (*p*NP-HMT)	$C_{18}H_{22}O_6N_6$ H.b	51.67 51.62	5.26 5.30	143	ν_{OH} 3020–3200 (3300)	
II (*p*NP-HMT)	$C_{18}H_{22}O_6N_6$ EDA	51.67 52.06	5.26 5.25	128–129	ν_{OH} 3300(3300) ν_{NO_2} a.1470–95 (1500–15)	λ_{max}390 ; ε = 585 (λ_{max}= 313)
III (2,4-DNP-HMT)	$C_{12}H_{16}O_5N_6$ H.b	44.41 44.52	4.93 4.68	167–168	ν_{OH} 3260 (3275–80) ν_{C-OH} 1135–40 (1120) ν_{NH} 2260–2520	
IV (2,4-DNP-HMT)	$C_{12}H_{16}O_5N_6$ EDA	44.41 44.79	4.93 5.20	90–105	ν_{NO_2} a 1530, 1575	λ_{max}356 ; ε = 435 (λ_{max}213 ; ε = 396)
V (2,4,6-TNP-HMT)	$C_{12}H_{15}O_7N_7$ H.b	39.11 39.40	4.06 4.32	177–178	ν_{OH} 2920–70 (3110–20) ν_{C-OH} 1170 (1150) $\nu_{\overset{+}{N}H}$ 2470–2610	
VI (2,4,6-TNP-HMT)	$C_{12}H_{15}O_7N_7$ EDA	39.11 38.82	4.06 4.31	79–95	ν_{OH} 3110–20(3110–20) ν_{NO_2} a. 1530, 1565	λ_{max}352 ; ε = 441 (λ_{max}360 ; ε = 738)
VII (Na*p*NP-HMT)	$C_{18}H_{20}O_6N_6Na_2$ EDA	46.75 47.32	4.32 4.76		ν_{NO_2} a. 1470, 1490 (1505) ν_{NO_2} s. 1375 (1315)	
VIII (Na 2,4-DNP-HMT)	$C_{12}H_{15}O_5N_6Na$ EDA	41.61 41.92	4.33 4.80	240	ν_{NO_2} a. 1545, 1580 ν_{NO_2} s. 1355 ν_{C-O} a. 1290, 1020 ν_{C-N} 820	
IX (2,4-DNA-HMT)	$C_{13}H_{10}O_5N_6$ EDA	46.15 46.50	5.32 5.80	196–198	ν_{NO_2} a. 1540–1560, 1572 (1545) ν_{NO_2} s. 1330 (1352–1360)	
X (2,4,6-TNA-HMT)	$C_{13}H_{17}O_7N_7$ EDA	40.80 40.90	4.43 4.51	201	ν_{NO_2} a. 1520–30, 1565 (1545–65)	
XI (*p*CP-HMT)	$C_{12}H_{17}ON_4Cl$ H.b	54.40 54.72	5.54 5.90	96–98	ν_{OH} 3010–3130 (3608)	
XII (*m*CP-HMT)	$C_{12}H_{17}ON_4Cl$ H.b	54.40 54.60	5.54 5.82	100–103	ν_{OH} 3025–3114 (3600)	

* In brackets are given (for comparison) the vibrations of nitrophenols nitrophenolates, nitroanisoles and chlorophenols which participate to the formation of complexes.

The complexes VII—X have been prepared in the following way: VII, VIII by heating 0.5 g HMT in 0.5 ml water, with 0.5 g sodium nitrophenoxide in 0.5 ml water for 60 minutes on the water bath; IX by heating 0.5 g HMT with 0.7 g 2,4-dinitroanisole, for 60 minutes at 90°; X by heating 0.5 g HMT in 0.5 ml water with 0.87 g 2,4,6-trinitroanisole in 10 ml ethyl alcohol, for 30 minutes on the water bath.

The analysis data are shown in Table 1.

The IR spectra were recorded in KBr pellets with an UR 10 C. Zeiss-Jena spectrophotometer.

The UV determinations were performed in alcoholic solution, having as witness proof ethyl alcohol of 96%. The determined extinctions were represented *versus* λ (220 — 400 nm); a V. S.U. 1 spectrophotometer has been used.

The NMR spectra have been performed in d_6-dimethylsulfoxid solution, using a Tesla B.S. 487 C 80 MHz spectrometer.

Sodium 2,2-dimethyl-2-sylapenthane-sulfonate (DSS) has been used as standard.

Revue Roumaine de Chimie, 23, 1, 73–78 (1978)

CONDENSATION OF 3,4-DISUBSTITUTED BENZOPHENONES WITH DIMETHYL HOMOPHTHALATE

M. F. EL-NEWAIHY, E. I. ENAYAT, M. R. SALEM, and H. A. ABDEL HAMID
Department of Chemistry, Faculty of Science, Ain Shams University, Cairo, Egypt

Received June 2, 1975

3,4-Dimethoxy- and 3,4-dichlorobenzophenone condense with dimethyl homophthalate in the presence of sodium hydride to give the expected stereoisomeric half-esters 1 and 2. The (Z)-configuration 2 was favoured in the two cases. The configuration was determined by cyclisation of the derived dibasic acids 3 and 4 to the oxo-indenyl acids 7 and 8, also obtained by the action of aluminium chloride on the anhydrides 5 and 6. Structures are supported by IR spectroscopic evidence. The ratio of isomers is interpreted in terms of the relative ease of ring cleavage of the intermediate δ-lactones 9 and 10.

In a previous investigation,[1] the ratio of stereoisomeric half-esters obtained from the condensation of *p*-methyl, *p*-methoxy- and *p*-chlorobenzophenone with dimethyl homophthalate was interpreted in terms of the polar effect of the substituent in influencing the relative ease of ring cleavage of the δ-lactonic intermediate.

In the present work, 3,4-dimethoxy- and 3,4-dichlorobenzophenone were condensed with dimethyl homophthalate in the presence of sodium hydride, whereby each of the expected half-esters 1 and 2*a*, *b* was obtained in pure form. They exhibited $\nu C{=}O$ at 1715–1725 cm^{-1} for α,β-unsaturated ester[2a] and at 1698 cm^{-1} for aryl-conjugated carboxyl groups.[2b] The ultraviolet spectra of the half-esters (λ_{max} : ~ 235–245, 302–315 nm. ; ϵ *Ca* 19000, 9000) ; exhibited the expected effect of substituents ; but no significant difference was observed in the spectra of each *cis-trans* pair.

The configuration of the half-esters was determined *via* the derived dibasic acids 3 and 4*a*,*b*. These were obtained in pure state from the respective half-esters, indicating that no *cis-trans* isomerisation occurred during saponification. The diacids showed carbonyl bands at *Ca* 1700 and 1685 cm^{-1} for α,β-unsaturated and aryl-conjugated carboxyl groups.[2b]

Upon treatment with concentrated sulphuric acid (0°, 1 hr.), one of the isomeric β-3,4-dimethoxyphenyl acids gave a 30% yield of the 3-phenyl-5,6-dimethoxyindenyl acid 7 whose structure is discussed latter; whereas no indenyl acid could be isolated from the second isomer. The (Z)-configuration 4*a* was thus assigned to the former diacid. The validity of this conclusion can be clarified as follows. It had been observed,[1] that under similar conditions the (Z)- and (E)-β-*p*-anisyl diacids (analogous to 4 and 3) gave the 3-phenyl-6-methoxy indenyl acid (analogous to 7) in 60 and 10% yields respectively. These results were attributed to enhanced *cis-trans* isomerisation being faster than ring closure at the phenyl group; a factor that will also operate in the present case. Furthermore, it is noticeable that the (Z)-dimethoxy acid 4*a* cyclises in a yield almost half that achieved with the β-*p*-anisyl analogue in spite of the fact that it has a more activated aromatic nucleus. This is probably due to sulphonation and subsequent water-solubilisation of the 5,6-dimethoxy indenyl acid 7, an interpretation that is born out by the observed deep red colour of the aqueous layer obtained during working out. These two complicating factors might be responsible for the lack of isolating a cyclisation product from the (E)-dimethoxy acid 3*a*.

---

[1] M. F. El-Newaihy, M. R. Salem, and H. A. Abdel Hamid, *J. prakt. Chem.* (under press).

[2] L. J. Bellamy, "The Infrared Spectra of Complex Molecules", Wiley, New York, 1958 (a) p. 179 (b) p. 162 (c) p. 125 (d) p. 149 (e) p. 65.

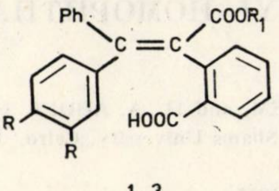

1, 3

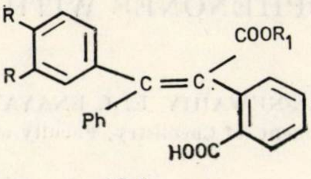

2, 4

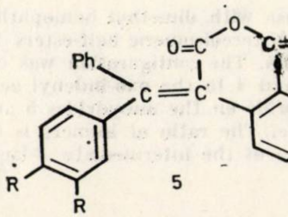

5

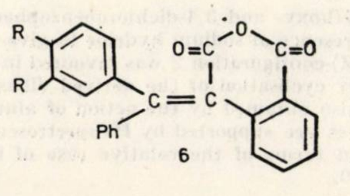

6

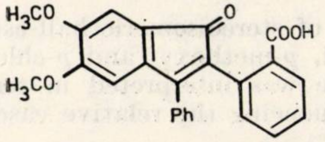

7

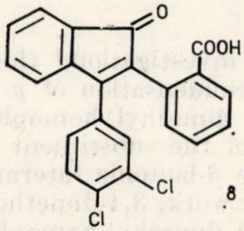

8

	a	b
R	OCH$_3$	Cl

	R$_1$
1, 2	CH$_3$
2, 4	H

The isomeric β-3,4-dichlorophenyl acids 3*b* and 4*b* gave the 3-(3′,4′-dichlorophenyl)indenyl acid 8 as the sole cyclisation product, and the (E)-configuration 3*b* was assigned to the diacid cyclising in higher yield (88% compared to 44%). The failure of the (Z)-β-3,4-dichlorophenyl diacid 4*b* to give its own cyclisation product can be attributed to *cis-trans* isomerisation being faster than ring closure at the deactivated aromatic ring. A similar behaviour was displayed by the isomeric β-*p*-chlorophenyl diacids.[1]

ACTION OF ALUMINIUM CHLORIDE ON THE ANHYDRIDES 5 AND 6

The β-3,4-dichlorophenyl dibasic acids *3b* and *4b* were converted (by heating with acetyl chloride in presence of pyridine) to the corresponding cyclic anhydrides *5b* and *6b* in pure state, thus excluding the occurrence of *cis-trans* isomerisation. The resulting anhydrides exhibited the expected carbonyl coupling bands (at *Ca* 1785 and 1750 cm^{-1}).[2e] As with the preceding diacids, the isomeric anhydrides *5b* and *6b* gave (upon treatment with aluminium chloride) the 3-(3′,4′-dichlorophenyl) indenyl acid 8 as the sole cyclisation product, and the (E)-configuration *5b* was assigned to the one cyclising in higher yield.

In spite of the addition of pyridine to neutralise the acids liberated during anhydride formation, the isomeric β-3,4-dimethoxyphenyl dibasic acids *3a* and *4a* gave (in comparably high yields) the (E)-anhydride *5a* whose configuration was revealed by saponification to the (E)-diacid *3a*. Isomerisation enhanced by the *p*-methoxy group, as well as attractive forces between the 3,4-dimethoxyphenyl group and the carbonyl-bearing phenyl group might account for this behaviour which was also observed with the isomeric β-*p*-anisyl diacids.[1] The cyclisation of the (E) anhydride *5a* to give only the 5,6-dimethoxy indenyl acid reflects the possibility of enhanced *cis-trans* isomerisation being faster than ring closure at phenyl. Again, a similar behaviour has been observed for the (E)-β-*p*-anisyl anhydride.[1]

STRUCTURE OF THE OXO-INDENYL ACIDS

Apart from differentiation between the 3-phenyl and 3-aryl isomers 7 and 8, the structure suggested for these compounds is based upon (i) elemental analysis; (ii) colour (yellow to red); (iii) formation of sodium salts; (iv) infrared bands at 1715 and 1685 cm^{-1} expected for α, β-unsaturated ring ketonic[2d] and aryl conjugated carboxyl group.[2b]

The 5,6-dimethoxy indenyl acid 7 was identified *via* two strong bands at 700 and 875 cm^{-1} due to out-of-plane deformations of the 5-adjacent and single *para*-hydrogens,[2e] respectively. The structure of the 3-(3′,4′-dichlorophenyl) indenyl acid 8 is suggested from the mere fact of its formation as the sole cyclisation products of the isomeric diacids 3 and *4b* as well as the derived anhydrides 5 and *6b*. Furthermore, it exhibited a medium band at 885 cm^{-1} due to γ C—H of a single aromatic hydrogen.[2e]

INTERPRETATION OF ISOMER RATIOS

In a recent investigation,[1] it has been found that the (Z)-configuration (analogous to 2) predominated in the condensation involving *p*-methyl- and *p*-methoxybenzophenone, whereas the (E)-isomer (analogous to 1) was favoured with *p*-chlorobenzophenone. In the present investigation, however, the (Z)-configuration (2) is favoured with both 3,4-dimethoxy- and 3,4-dichlorobenzophenone indicating that polar effects are not a controlling factor. Due to a *m*-substituent, a 3,4-disubstituted aryl group is expected to interfere sterically to a certain extent with an adjacent *cis* group especially if butressing effects of adjacent groups in the aromatic ring are taken into consideration. Although such interference might operate to favour the formation of 9 (Ar *cis* to H)[3–5] yet it will retard its subsequent ring cleavage (Ar now becoming *cis* to $C_6H_4COO^-$). The formation of the (Z)-half-esters 2*a* and *b* (derived from 10) in larger amounts suggests that the ease of ring cleavage is the controlling factor.

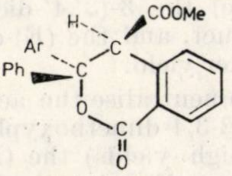

9

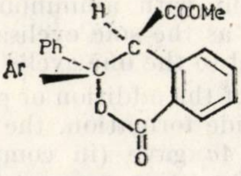

10

EXPERIMENTAL PART

Melting points are not corrected. Infrared (KBr) spectra were measured on Unicam SP. 1200 Infracord, electronic spectra on Perkin-Elmer Spectracord Model 4000A Spectrophotometers.

(A) *Stobbe condensation*. Dimethyl homophthalate (2 mol.), the ketone (1 mol.), and sodium hydride (2 mol.) in excess dry benzene were heated at 70° with stirring for 35 hrs., and the reaction mixture worked up as usual.[1,6] 3,4-Dimethoxybenzophenone (20 g.) gave a crude half-ester mixture (23 g.) from which the less soluble (Z)-half-ester was isolated from the (E)-isomer by fractional crystallisation from ethanol. 3,4-Dichlorobenzophenone (20 g.) gave a half-ester mixture (26 g.) from which the (E)-isomer was isolated by its solubility in boiling cyclohexane.

The percent ratio of (E)- and (Z)-isomers in the half-ester mixture are given in Table 1, in each case the difference from 100% was an inseperable semisolid mixture.

Table 1

Methyl (E)- and (Z)-α-*o*-carboxyphenyl-β-arylcinnamates (1 *a*, *b* and 2 *a*,*b*)

Nr.	m.p. (°C) Solvent of cryst.	% ratio of isomers	Formula	Analysis C Calcd	C Found	H Calcd	H Found	Cl Calcd	Cl Found
1*a*	160–162 Ethanol	30	$C_{25}H_{22}O_6$	71.76	71.30	5.3	4.8		
2*a*	204–206 Ethanol	51	$C_{25}H_{22}O_6$	71.76	71.40	5.3	5.4		
1*b*	161–163 Cyclohexane	30	$C_{23}H_{16}O_4Cl_2$	64.6	64.8	3.7	4.0	16.6	16.5
2*b*	211–213 Ethanol	53	$C_{23}H_{16}O_4Cl_2$	64.6	65.4	3.7	4.0	16.6	16.1

---

[3] F. G. Baddar, M. F. El-Newaihy, and M. S. Ayoub, *J. Chem. Soc., Sect. C*, **1971**, 3333.

[4] W. I. Awad, F. G. Baddar, F. A. Fouli, S.M.A. Omran, and M. I. Selim, *J. Chem. Soc., Sect. C*, **1968**, 507.

[5] M. F. El-Newaihy, and M. A. El-Hashash, *J. Chem. Soc., Sect. C*, **1971**, 785.

[6] H.J.E. Lowenthal, and R. Pappo, *J. Chem. Soc.*, **1952**, 4799.

(B) *Saponification of the half-esters* 1*a*, *b and* 2*a*, *b into the dibasic acids* 3*a*,*b and* 4*a*, *b*. The half-ester was refluxed with 10 % aqueous sodium hydroxide (10 ml. per g. ester) for 3 hrs. (yield, 90—95 %); see Table 2.

Table 2

(E)- and (Z)-α-*o*-Carboxyphenyl-β-arylcinnamic acids (3 and 4 *a*,*b*)

Nr.	m.p. (°C)^{a} Solvent$_{b}$ of cryst.	Formula	Analysis					
			Calcd	*Found*	*Calcd*	*Found*	*Calcd*	*Found*
			C		H		Cl	
3a	135	$C_{24}H_{20}O_6$	71.28	71.76	4.99	5.05		
4a	227	$C_{24}H_{20}O_6$	71.28	71.80	4.99	5.10		
3b	190	$C_{22}H_{14}O_4Cl_2$	63.92	63.90	3.38	3.20	17.18	16.40
4b	210	$C_{22}H_{14}O_4Cl_2$	63.92	63.60	3.38	3.20	17.18	16.80

a: With decomposition *b:* Ethyl acetate

(C) *Conversion of the dibasic acids* 3*a*,*b and* 4*a*, *b to the cyclic anhydrides* 5 *and* 6. To a cold solution of the dibasic acid in benzene, pyridine (15 ml. per g. acid) was added at one time, followed by dropwise addition of acetyl chloride (15 ml. per g. acid). After refluxing for $\frac{1}{2}$ hr., the reaction mixture was poured onto ice-cold water, the organic material taken up in ether, and unchanged acid extracted with sodium carbonate solution. The anhydrides were obtained in 75—95 % yields (Table 3). *Note:* Both isomeric (E)- and (Z)-β-3,4-dimethoxyphenyl diacids *3a* and *4a* gave the (E)-anhydride *5a* in 85 and 95 % yields, respectively.

Table 3

(E)- and (Z)-α-*o*-Carboxyphenyl-β-arylcinnamic acid anhydrides 5 and 6

Nr.	m.p. (°C)^{a} Solvent of cryst.	Formula	Analysis					
			Calcd	*Found*	*Calcd*	*Found*	*Calcd*	*Found*
			C		H		Cl	
5a	155—156 l.p.; yellow	$C_{24}H_{18}O_5$	74.6	74.0	4.7	4.6		
5b	228—229 bz.; yellow	$C_{22}H_{12}O_3Cl_2$	66.84	67.4	3.03	2.9	17.97	17.6
6b	155—156 bz.; yellow	$C_{22}H_{12}O_3Cl_2$	66.84	66.7	3.03	2.5	17.97	17.8

l.p. = light petroleum (b.p. 100—120°); bz = benzene

(D) *Cyclisation of the dibasic acids* 3*a*,*b and* 4*a*,*b to the indenyl acids* 7 *and* 8 *with concentrated sulphuric acid*. The dibasic acid was added portionwise to concentrated sulphuric acid kept at 0°C (10 ml. per g. acid), the reaction mixture left at the same temperature for one hr., then poured onto ice-cold water and the organic material taken up in ether. Upon extraction with sodium carbonate solution (10 %), the sodium salt of the oxo-indenyl acid precipitated and was filtered off, suspended in water, acidified, and the resulting indenyl acid extracted with ether.

The (E)-β-3,4-dimethoxyphenyl dibasic acid *3a* gave no indenyl acid upon treatment with concentrated sulphuric acid.

The (Z)-β-3,4-dimethoxyphenyl dibasic acid *4a* (0.5 g.) gave 2-*o-carboxyphenyl*-3-*phenyl*-5,6-*dimethoxyind*-2-*enone* 7 (30 % yield) as red crystals, m.p. 227—228° (from benzene). *(Found:* C, 75.1; H, 5.0. $C_{24}H_{18}O_5$ requires: C, 74.6; H, 4.7 %).

Either the (E)- or (Z)-α-o-carboxyphenyl-β-3,4-dichlorocinnamic acids 3*b* and 4*b* (1g.) gave *2-o-carboxyphenyl-3-(3′, 4′-dichlorophenyl)-ind-2-enone* 8 (88 and 44% yield, respectively) as yellow crystals, m.p. 182–183° (from benzene). *(Found:* C, 67.4; H, 2.9; Cl. 17.7. $C_{22}H_{12}O_3Cl_2$ requires : C, 66.84; H, 3.03; Cl, 17.97 %).

(E) *Action of aluminium chloride on the anhydrides* 5*a*, *b and* 6*b*. To a stirred cold solution of the anhydride (1 mol.) in dry nitrobenzene (30 ml. per 1 g. anhydride), aluminium chloride (1.2 mol.) was added, and stirring continued for 6 hrs. at room temperature, then left to stand overnight. The resulting oxo-indenyl acid was isolated as usual and crystallised from benzene.

The (E)-β-3,4-dimethoxyanhydride 5*a* (1 g.) gave the above-mentioned dimethoxyindenyl acid 7 in 71 % yield. The (E)- and (Z)-β-3,4-dichlorophenyl anhydrides (1 g.) gave the above-mentioned dichloroindenyl acid 8 in 80 and 50% yields, respectively.

Revue Roumaine de Chimie, **23**, *1*. 79–87 (1978)

ELECTRONIC SPECTRA AND STRUCTURE OF 4-ARYLHYDRAZONO-3-METHYL-5-PYRAZOLONES

S. H. ETAIW, F. A. ANWER and F. M. ISSA
Chemistry Department, Faculty of Science, Tanta University, A. R. Egypt.

Received August 8, 1975

The electronic absorption spectra of some 4-arylhydrazono-3-methyl-5-pyrazolones in the UV and visible regions are studied. The assignment of the observed bands to certain electronic transitions is attempted by comparing the spectra of these compounds with that of heterocyclic carbonyls and some anils. Solvent and substituent effects are also considered. The important bands in the IR-spectra are assigned and discussed in relation to molecular structure.

INTRODUCTION

The absorption spectra of carbonyl and anil compounds have been the subject of many investigations.[1–9] However, the spectra of 4-arylhydrazono-3-methyl-5-pyrazolones were not the subject of any investigation. The present study is devoted to visible and spectrophotometric investigation of these compounds. Band assignment and solvent shifts of absorption bands are reviewed, and correlations with various solvent properties are discussed.

EXPERIMENTAL

Solvents were extensively purified to remove impurities that may interact with the solute molecules and to be spectrally transparent in the region down to 200 nm [10].

---

[1] P. G. Furrell, *Canad. J. Chem.*, **46,** 3684 (1968).

[2] J. M. Hearn, *J. Chem. Soc.*, **1951,** 3318.

[3] R. A. Morton, and V. T. ErIam, *J. Chem. Soc.*, **1941,** 159.

[4] R. H. Peter, and H. H. Summer, *J. Chem. Soc.*, **1953,** 2101.

[5] Z. Yoshida, and F. Takabayaski, *Tetrahedron*, **24,** 933 (1968).

[6] M. A. El-Bayoumi, M. El-Aasser and F. Abdel-Halim, *J. Amer. Chem. Soc.*, **93,** 586 (1971).

[7] G. O. Dudek, and E. P. Dudek ; *J. Amer. Chem. Soc.*, **88,** 2407 (1967).

[8] V. L. Minkin, O. A. Osipov and V. A. Kogan ; *Doklady Akad. Nauk. S.S.S.R.*, **145,** 336 (1952).

[9] R. M. Issa, A. A. El-Samahy and S. H. Etaiw, *Z. phys. Chem.* (*Leipzig*), **255,** 853 (1974).

[10] A. I. Vogel, "Practical Organic Chemistry", Longmans, London,1956.

The compounds were prepared by coupling the diazonium salt of substituted anilines (1 mole) with acetoacetic ester (1 mole in ethanol) in the presence of sodium acetate on cold. The precipitated products were filtered, dried, then refluxed with hydrazine hydrate (1 :1 mole) for about 2 hours on a water bath. The precipitated 4-arylhydrazono-3-methyl-5-pyrazolones were filtered and recrystallised from ethanol.[11] Electronic spectra were recorded on a UNICAM S.P. 800 self-recording quartz spectrophotometer using 1 cm matched silica cells. Infrared absorption spectra were recorded on the UNICAM S.P. 1200 G infrared spectrophotometer.

RESULTS AND DISCUSSIONS

The compounds under investigation have the general structure:

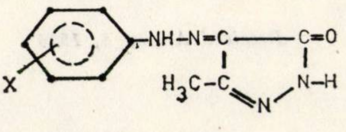

in which X = H(I), p-OCH_3(II), p-OH(III), p-CH_3(IV), p-Cl(V), p-Br(VI), p-COOH(VII), p-NO_2(VIII), m-NO_2(IX), o-OCH_3(X), o-CH_3(XI), o-Cl(XII), o-COOH(XIII), o-NO_2(XIV).

Electronic spectra in ethanol comprise four absorption bands (Table 1) The first three bands located near 253, 260 and 335 nm show very little solvent effect, being thus due to local electronic excitations. They are characterized by high molar absorptivity, so they are of $\pi-\pi^*$ type.

Table 1

The electronic absorption spectra of 4-arylhydrazono-3-methyl-5-pyrazolones in ethanol

λ_{max}=nm $\varepsilon_{max}10^{-4}$=cm² mole^{-1}

Compound	^1L_a		^1L_b		$\pi-\pi$ of C=O and C=N groups		C.T.	
	λ_{max}	$\varepsilon_{max}\cdot10^{-4}$	λ_{max}	$\varepsilon_{max}\cdot10^{-4}$	λ_{max}	$\varepsilon_{max}\cdot10^{-4}$	λ_{max}	$\varepsilon_{max}\cdot^{-}10^4$
H	251	1.35	258	1.30	335	0.89	409	1.44
p-OCH_3	—	—	261	1.10	—	—	432	2.16
p-OH	—	—	265	0.96	—	—	438	1.60
p-CH_3	254	1.20	262	1.17	340	1.09	418	1.80
p-Cl	253	1.50	260	1.40	336	1.30	412	2.10
p-Br	253	1.10	260	1.00	335	0.92	411	1.37
p-COOH	—	—	270	set	—	—	408	—
p-NO_2	253	1.72	—	—	344	1.59	407	2.10
m-NO_2	252	1.46	—	—	345	1.68	400	1.40
o-OCH_3	255	1.18	—	—	—	—	430	1.77
o-CH_3	252	1.32	260	1.30	336	0.99	416	1.61
o-Cl	254	1.40	262	1.30	338	1.03	404	1.47
o-COOH	—	—	—	—	—	—	410	set
o-NO_2	250	1.98	275	1.67	350	1.96	420	1.98

The first two bands can be assigned to ($^1L_a \rightarrow 1$ A) and ($^1L_b \leftarrow 1$ A) transitions respectively. The band near 335 nm is a broad and composite one. It represents different types of transition which may involve the $\pi-\pi^*$ transition of the carbonyl function and the $\pi-\pi^*$ transition of the anil group influenced by charge transfer (C.T.) from the arylhydrazone system. This is substantially supported by the fact that the band is remarkably affected by the nature and position of the substituent X. However, it is slightly sensitive to solvent effects. Also, benzanils and phenylhydrazones absorb near 338 nm. This band was assigned to a $\pi-\pi^*$ transition involving the whole molecule, influenced by C.T. interaction.[9]

---

[11] R. V. Rothenburg, *Ber. dtsch. Chem. Ges.*, **27**, 790 (1894).

The bands due to $n-\pi^*$ transition are expected to appear in the region of the third band. Since these bands usually exhibit low extinction, they are obscured by the more intense bands due to the $\pi-\pi^*$ transitions.

The band on longer wavelength side, located within the range of 400–438 nm, is broad and solvent sensitive. It may correspond to a C.T. transition. The C.T. originates from the substituted phenyl ring to the carbonyl group by resonance and from the hetero ring by induction. The band is highly influenced by the nature and position of the substituent X. Donor groups cause a red shift while acceptor ones cause a blue shift relative to the non-substituted compound (I). *o*-Substituted compounds show a blue shift which can be attributed to steric effects. Generally, the observed λ_{max} and ε_{max} changes run in a more or less regular manner with the electron donor-acceptor character of the X-substituent. This fact finds support in the approximate linear corelation between λ_{max} and σ (the Hammett constant) as shown in Fig. 1. The compounds display the keto-enol tautomerism.

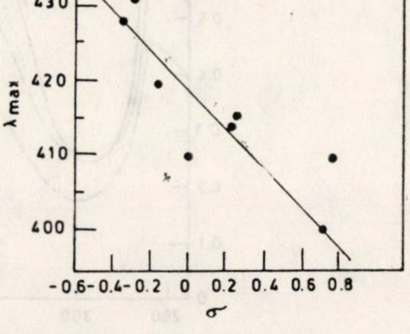

Fig.1. — The relation between λ_{max} of C.T. band and π in CCl_4.

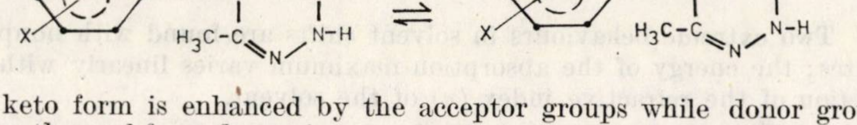

The keto form is enhanced by the acceptor groups while donor groups favour the enol form due to increased polarization of the carbonyl group.

SOLVENT EFFECTS

Bands due to intramolecular charge transfer interaction are usually solvent sensitive, while LE bands are relatively insensitive to change of solvent polarity. The spectra in different solvents of a typical compound

(IV) are represented in Fig. 2; all the results are depicted in Table 2. The C.T. band of the present compounds shows some solvent-dependence.

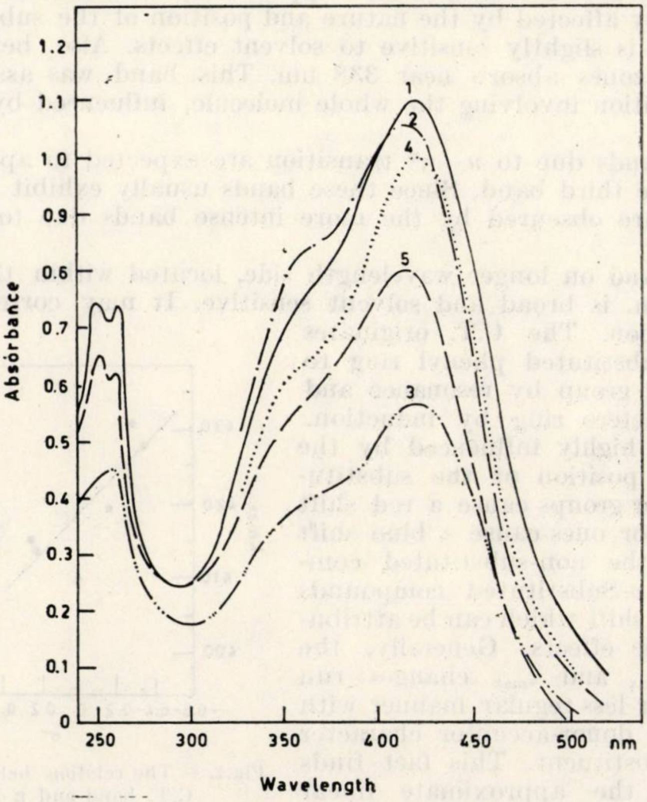

Fig.2. — Spectra of IV in different organic solvents.
1 — Ethanol 0.60×10^{-4} M; 2 — Acetone 0.4649×10^{-4} M;
3 — $CHCl_3$ 0.2619×10^{-4} M; 4 — CCl_4 0.3846×10^{-4} M;
5 — Cyclohexane (Saturated).

Two extreme behaviours in solvent shifts are found with nonpolar solutes; the energy of the absorption maximum varies linearly with the function of the refractive index (n) of the solvent.

$$(n^2) = \frac{2(n^2 - 1)}{2n^2 + 1}$$

This type of shift results from dispersion forces between the solute and the solvent and is of small magnitude. With polar solutes the energy of the absorption maximum would vary in accordance with the func-

Table 2

The electronic absorption spectra of 4-arylhydrazono-3-methyl-5-pyrazolones in different organic solvents

$\lambda_{max} = \text{nm}$ $\varepsilon_{max} \cdot 10^{-4} = \text{cm}^2\ \text{mole}^{-1}$

Compound	^1L_a			^1L_b					$\pi-\pi^*$ of C = O and C=N groups								
	Ethanol		Cyclohexane*	Ethanol		$CHCl_3$		Cyclohexane*	Ethanol		Acetone		$CHCl_3$		CCl_4		Cyclohexane*
X	λ_{max}	ε_{max}	λ_{max}	λ_{max}	ε_{max}	λ_{max}	ε_{max}	λ_{max}	λ_{max}	ε_{max}	λ_{max}	ε_{max}	λ_{max}	ε_{max}	λ_{max}	ε_{max}	λ_{max}
H	251	1.35	250	258	1.30	258	1.60	258	335	0.89	334	0.12	334	1.04	334	1.71	335
p-OCH_3	—	—	250	261	1.10	260	1.73	260	—	—	—	—	—	—	—	—	—
p-OH	—	—	—	265	0.96	265	*	263	—	—	—	—	—	—	—	—	—
p-CH_3	254	1.20	254	262	1.17	260	1.63	262	340	1.09	336	1.58	337	1.43	335	1.91	334
p-Cl	253	1.50	252	260	1.40	260	1.45	260	336	1.30	336	1.21	334	1.35	337	*	334
p-Br	253	1.10	252	260	1.00	263	1.02	260	335	0.92	335	1.68	336	1.82	335	*	235
p-COOH	—	—	—	270	*	268	*	266	—	—	—	—	—	—	—	—	—
p-NO_2	253	1.72	250	—	—	—	—	—	334	1.59	344	1.52	343	*	337	*	322
m-NO_2	252	1.46	249	—	—	—	—	260	345	1.68	344	1.70	350	*	347	*	339
o-OCH_3	255	1.18	255	—	—	265	1.20	—	—	—	—	—	—	—	—	—	—
o-CH_3	252	1.32	252	260	1.30	262	1.30	260	336	0.99	336	1.10	338	1.23	337	1.21	338
o-Cl	254	1.40	255	262	1.30	265	1.57	263	338	1.03	338	1.13	340	1.73	338	1.40	338
o-COOH	—	—	—	—	—	—	—	—	—	—	—	—	—	—	—	—	—
o-NO_2	250	1.98	—	275	1.67	278	1.32	272	350	1.96	348	1.12	352	1.48	350	2.21	337

* Saturated solution.

Table 2 (continued)

Compound	C.T.								
	Ethanol		Acetone		$CHCl_3$		CCl		Cyclohexane*
X	λ_{max}	ε_{max}	λ_{max}	ε_{max}	λ_{max}	ε_{max}	λ_{max}	ε_{max}	λ_{max}
H	409	1.44	404	1.88	412	1.58	410	2.35	407
p-OCH_3	432	2.16	426	2.29	434	2.70	432	*	420
p-OH	438	1.60	430	2.0	430	*	428	*	424
p-CH_3	418	1.80	414	2.28	420	2.10	419	2.60	414
p-Br	411	1.37	406	2.10	417	2.30	416	*	401
p-COOH	408	*	402	*	400	*	398	*	395
p-NO_2	407	2.10	410	2.10	414	*	410	*	403
m-NO_2	400	1.40	400	1.27	402	*	400	*	400
o-OCH_3	430	1.77	424	2.10	432	1.90	430	*	424
o-CH_3	416	1.61	413	1.70	422	1.85	420	1.80	410
o-Cl	404	1.47	396	1.58	414	2.20	410	1.80	408
o-COOH	410	*	410	*	414	*	—	—	402
o-NO_2	420	1.98	418	0.92	425	1.50	419	2.44	406

* Saturated solution.

tion of the dielectric constant (D).

$$(D) = \frac{2\,(D-1)}{2\,D+1}$$

The plots of $\bar{\nu}$ max against $f(D)$ are more or less linear relations (Fig. 3). However, the solute-solvent systems cannot be considered purely as a dipole-dielectric interaction, deviation from the $f(D)$ plot is often evidence that the so-called "specific association" occurs usually much stronger than the dielectric stabilization. Ethanol, acetone and $CHCl_3$ molecules can undergo molecular compound formation, when these solvents are strongly bound through an intermolecular hydrogen bond to the solute. The magnitude of the shift runs in the order :

$CHCl_3 > CCl_4 \geqslant$ ethanol $>$ cyclohexane $\simeq$ acetone. It is surprising that the C.T. band is red shifted in non-polar solvents compared to polar ones. This may be due to the fact that acetone and ethanol favours the enolic form. Acetone molecules can form a strong hydrogen bond with the hydroxyl hydrogen atom. This interaction antagonises the C.T. from the phenyl group to the five membered ring. On the other hand, ethanol molecules form two types of hydrogen bonds, one with the proton of the hydroxyl group and the other with the hydroxyl oxygen atom. The last type decreases the antagonism, thus the C.T. band in ethanol is red shifted as compared to acetone. In case of $CHCl_3$, CCl_4 and cyclohexane the shift is in accordance with the increasing solvent polarity.

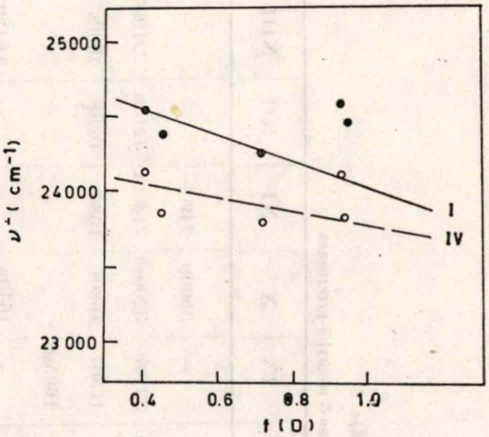

Fig. 3. — Solvent shift of I and IV (C. T. band).

IR-SPECTRA

The important bands in the IR-spectra of the compounds under investigation are reported in Table 3 ; they are interpreted to the possible extent in the relation to molecular structure. A broad band appears within the 3338—3500 cm^{-1} region which corresponds to the stretching vibrations of the OH-group. The appearance as well as the broadened and the low frequency of that band support the occurrence of keto-enol tautomerism with such compounds. The ν_{OH} band is only observed in the IR-spectra of the compounds containing the donor groups. This substantiates the above-mentioned opinion that the donor groups favour the enol form. The ν_{NH} band appears, as a medium broad one within

Table 3

IR-spectra of 4-arylhydrazono-3-methyl-5-pyrazoones

Compound I	II	III	IV	V	VI	VII	VIII	IX	X″	XI	XII	XIII	XIV	Band assignment
3338m	3500m	3290b	3470b	3500b	—	3410b	—	—	3500b	3490b	—	—	—	ν_{OH}
3195b	3185b	3180b	3190m	3210m	3200b	3290s	3220b	3210b	3200sh	3180m	3215b	3210b	3240s	ν_{NH}
1670s	1670s	1660s	1670s	1675s	1672s	1685s	1675s	1680s	1680s	1680s	1670s	1690s	1685s	$\nu_{C=O}$
1660sh	—	1650sh	—	—	—	—	—	1665sh	—	—	—	—	—	$\nu_{C=N}$
1640sh	1640sh	1640sh	—	—	—	1645sh	—	—	1640w	—	—	1645m	—	$\nu_{N=N}$
1600s	1610s	1590s	1608s	1600m	1585s	1510m	1610m	1590w	1605m	1600s	1600sh	1590m	1610m	$\nu_{C=C}$
1560b	1555s	1555s	1560b	1575s	1565s	1560s	1575m	1555s	1570s	1570s	1570s	1530s	1575s	,,
1490s	1500m	1480s	1490s	1490s	—	—	1500s	1485m	1490w	1490s	1502s	1485s	1500s	,,
1390w	1390s	1360w	1380s	1415m	1375w	1380s	1375s	1380s	1390w	1395w	1390m	1380s	1380s	δ_{C-H}
1250s	1250s	1250s	1255s	1257s	1250s	1250s	1240s	1240s	1260s	1255b	1250b	1280s	1270s	ν_{C-O}
1215sh	1230w	1220s	1210w	—	—	1215w	1210m	1210s	1210s	1230s	1212s	1210s	1220w	δ_{OH}

s = strong m = medium sh = shoulder b = broad the 3180—3280 cm^{-1} region, in the spectra of all compounds. The plot of ν_{NH} with σ (Hammett constant) Fig. 4A, is a more or less linear relation with a positive slope indicating that the N—H bond order increases

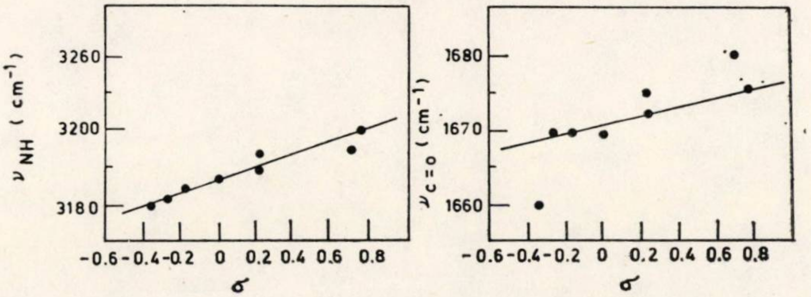

Fig. 4. — ν_{NH} and $\nu_{C=O}$–σ relationship.

with decreasing the donor character of (X). The somewhat low frequency values of the ν_{NH} may arise from possible intramolecular association through hydrogen bonding.

The spectra show a strong band near 1670 cm^{-1} which can be assigned to the stretching frequency of the carbonyl group. Also, the plot of $\nu_{C=O}$ as a function of σ (Fig. 4B) is a linear relation with positive slope. Thus, the frequency of the carbonyl group decreases with increased donor character of the substituent (X), which is in accordance with common behaviour.

The $\nu_{C=N}$ and $\nu_{N=N}$ bands are observed near 1650 and 1640 cm^{-1} respectively in the spectra of I, II and III as shoulders, the bands are strongly interacted with those due to $\nu_{C=O}$. Resonance through the molecule influences the bond order of C=N and N=N groups, consequently the frequency values of the two groups change in the same way. The band due to the ethylenic bond is strongly merged with the ring vibration band near 1600 cm^{-1} accordingly its behaviour cannot be pointed out with certainity.

Revue Roumaine de Chimie, 23, *1*, 89–102 (1978)

MODÈLE CHIMIQUE DE SYNTHÈSE DES PRÉCURSEURS DE LA MATIÈRE VIVANTE

CR. I. SIMIONESCU, S. DUMITRIU, V. I. POPA, V. BULACOVSCHI
et B. SIMIONESCU
Institut Polytechnique, Jassy, Roumanie

Reçu le 3 septembre 1976

On a établi un modèle chimique de synthèse des précurseurs de la matière vivante en tenant compte de la composition de l'atmosphère primaire, des sources d'énergie et des catalyseurs. La décomposition des mélanges CH_4/H_2O, CH_4/NH_3 et $CH_4/NH_3/H_2O$ dans le plasma haute fréquence a conduit à la formation des aldéhydes, alcools, acides, cétones, amines et nitriles, intermédiaires dans la synthèse de biomonomères. L'influence de différents paramètres, des catalyseurs, du pH et des sources d'énergie a été étudiée.

La synthèse des composés d'intérêt biologique a été réalisée dans le processus d'évolution chimique, soit spontanément, conséquence de l'interaction chimique, soit par autocatalyse, soit par l'utilisation de l'énergie extérieure et des catalyseurs exogènes. De ce fait, l'établissement d'un modèle chimique de synthèse des précurseurs de la matière vivante doit tenir compte de la composition de l'atmosphère primaire, des sources d'énergie et des catalyseurs.

Nos recherches ont été réalisées dans des atmosphères réductrices formées de méthane, d'ammoniac et d'eau (justifiées thermodynamiquement[1]), en utilisant comme sources d'énergie le plasma haute fréquence et les radiations en UV et comme catalyseurs de différentes roches et argiles.

L'éclaircissement des conditions de réaction et des substances qui se forment dans l'atmosphère mentionnée a imposé l'étude de la décomposition dans le plasma de chaque composant [2,3] des mélanges binaires[3–5] et enfin ternaires.[5]

La décomposition du méthane dans le plasma froid a été réalisée à une pression de 3 mm Hg dans une installation travaillant en système stationnaire, liée à un chromatographe des gaz pour l'analyse continue des produits de réaction.[2] Les analyses ont montré la formation, dans les conditions de travail adoptées, des composés suivants : H_2, C_2H_2, C_2H_4 et C_2H_6. Les concentrations des produits signalés dans le mélange final sont influencées par la durée de la décharge (figure 1) et la puissance d'alimentation (figure 2).

---

[1] W. R. Eck, M. D. Dayhoff, E. R. Rippincott et Y. T. Pratt, *Science*, **153**, 628 (1966).

[2] Cr. Simionescu, S. Dumitriu, V. Bulacovschi et D. Onac, *Z. Naturforsch.*, **30b**, 516 (1975).

[3] Cr. Simionescu, S. Dumitriu, et V. I. Popa, *Z. Naturforsch.*, **31b**, 466 (1976).

[4] Cr. Simionescu, S. Dumitriu, V. Bulacovschi et V. I. Popa, *Z. Naturforsch.*, en cours de publication.

[5] Cr. Simionescu, S. Dumitriu, V. Bulacovschi, B. Simionescu et V. I. Popa, *Compt. rend.*, c, 283, 515 (1976).

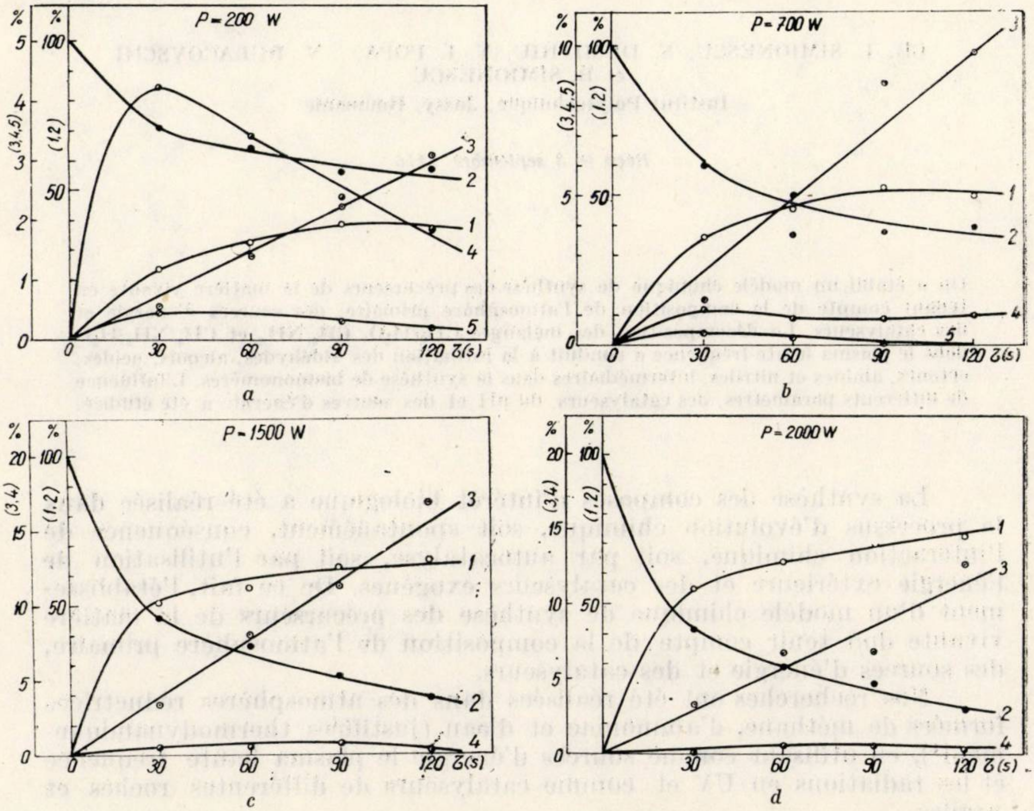

Fig. 1. — Diagrammes cinétiques pour la décomposition du méthane en temps : *a* – 200 W ; *b* – 700 W ; c – 1500 W ; *d* – 2000 W.

Les données résultées ont permis d'établir des mécanismes probables pour les réactions qui se déroulent à différentes puissances d'alimentation. Jusqu'à 700 W on propose le mécanisme de décomposition en chaîne du méthane :

$$CH_4^{*} \rightarrow CH_2: + H_2 \tag{1}$$

$$CH_2: + CH_4 \rightarrow 2CH_3^{\bullet} \rightleftharpoons C_2H_6 \tag{2}$$

$$CH_3^{\bullet} + CH_4 \rightarrow C_2H_6 + H^{\bullet} \tag{3}$$

$$H^{\bullet} + CH_4 \rightarrow H_2 + CH_3^{\bullet} \tag{4}$$

$$H^{\bullet} + CH_3^{\bullet} + M \rightarrow CH_4 + M \tag{5}$$

$$C_2H_6 \xrightarrow{-H_2} C_2H_4 \xrightarrow{-H_2} C_2H_2 \tag{6}$$

Simultanément avec la réalisation de l'équilibre $C_2H_6 \rightleftharpoons 2CH_3^{\bullet}$, la réaction (7) doit être prise en considération :

$$CH_2 : + CH_4 \rightarrow C_2H_4 + H_2 \qquad (7)$$

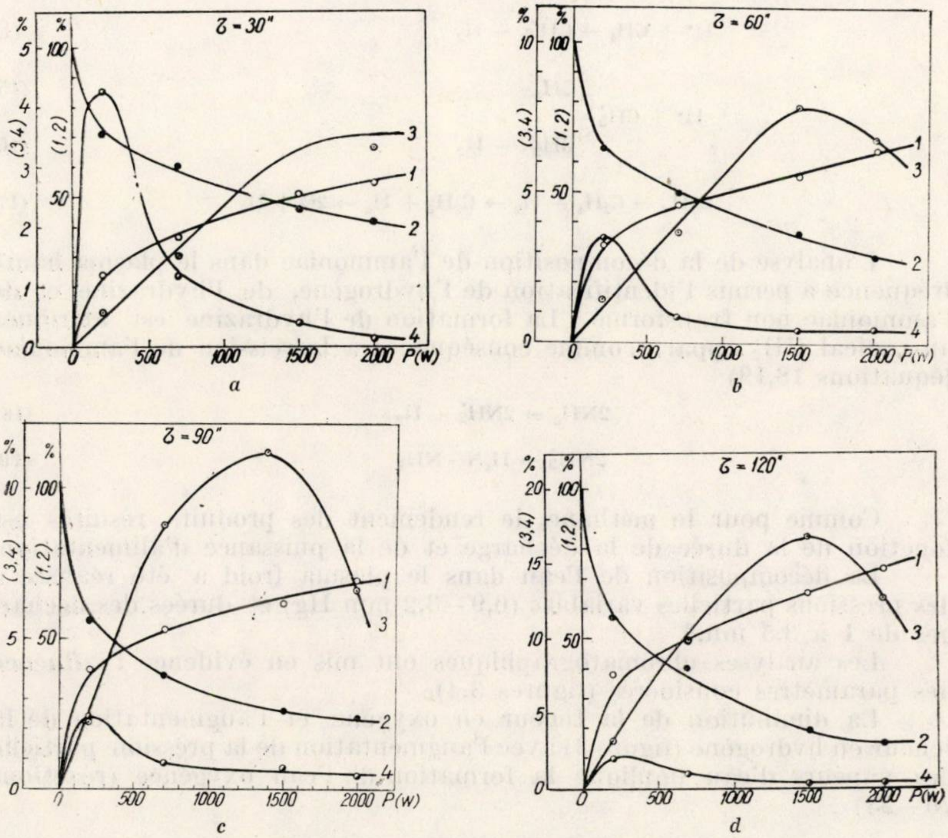

a b

c d

Fig. 2. — Courbes de conversion des produits formés par la décomposition du méthane fonction de la puissance d'alimentation :

1 – H_2 ; 2 – CH_4 ; 3 – C_2H_2 ; 4 – C_2H_4 ;
a – 30 sec ; b — 60 sec ; c – 90 sec ; d – 120 sec.

Un mécanisme de décomposition en chaîne dégénérative correspond pour les puissances d'alimentation plus élevées (jusqu'au 2000 W) :

$$CH_4 \rightarrow CH_2 : + H_2 \qquad (8)$$

$$CH_2 : + CH_4 \begin{array}{l} \nearrow C_2H_4 + H_2 \qquad (9) \\ \rightarrow 2CH_3^{\bullet} \\ \quad \downarrow\uparrow \\ \searrow C_2H_6 \qquad (10) \end{array}$$

$$CH_2: + CH_2: \rightarrow C_2H_2 + H_2 \qquad (11)$$

$$CH_3^\bullet + CH_4 \rightarrow C_2H_6 + H^\bullet \qquad (12))$$

$$CH_3^\bullet + CH_2: \rightarrow C_2H_2 + H_2 + H^\bullet \qquad (13)$$

$$H^\bullet + CH_4 \rightarrow CH_3^\bullet + H_2 \qquad (14$$

$$H^\bullet + CH_3^\bullet \begin{array}{l} \nearrow CH_4 \qquad (15) \\ \searrow CH_2: + H_2 \qquad (16) \end{array}$$

$$C_2H_6 \rightarrow C_2H_4 + H_2 \rightarrow C_2H_2 + H_2 \rightarrow 2C + H_2 \qquad (17)$$

L'analyse de la décomposition de l'ammoniac dans le plasma haute fréquence a permis l'identification de l'hydrogène, de l'hydrazine et de l'ammoniac non transformé.[2] La formation de l'hydrazine est attribuée au radical $NH_2^\bullet$ apparu comme conséquence à la scission de l'ammoniac (équations 18,19)

$$2NH_3 \rightarrow 2NH_2^\bullet + H_2 \qquad (18)$$

$$2NH_2^\bullet \rightarrow H_2N-NH_2 \qquad (19)$$

Comme pour le méthane, le rendement des produits résultés est fonction de la durée de la décharge et de la puissance d'alimentation.

La décomposition de l'eau dans le plasma froid a été réalisée à des pressions partielles variables (0,9—3,2 mm Hg) et durées des décharges de 1 à 3,5 mn.[3]

Les analyses chromatographiques ont mis en évidence l'influence des paramètres considérés (figures 3,4).

La diminution de la teneur en oxygène et l'augmentation de la teneur en hydrogène (figure 3) avec l'augmentation de la pression partielle des vapeurs d'eau implique la formation de l'eau oxygénée (réactions 20—23)

$$H_2O \rightarrow H^\bullet + HO^\bullet \qquad (20)$$

$$HO^\bullet + HO^\bullet \rightarrow H_2O + O \qquad (21)$$

$$H^\bullet + O_2 \rightarrow HO_2^\bullet \qquad (22)$$

$$HO_2^\bullet + H_2 \rightarrow H_2O_2 + H^\bullet \qquad (23)$$

L'augmentation de la durée de la décharge (figure 4) détermine une augmentation de la concentration des radicaux qui se forment, tout en étant favorable à une diversité de réactions :

$$2HO_2^\bullet \xrightarrow{M} H_2O_2 + O_2 \qquad (24)$$

$$H^\bullet + HO_2^\bullet \xrightarrow{M} H_2O_2 \qquad (25)$$

$$H^{\bullet} + HO_2^{\bullet} \longrightarrow 2HO^{\bullet} \qquad (26)$$

$$H^{\bullet} + HO_2^{\bullet} \xrightarrow{M} H_2 + O_2 \qquad (27)$$

$$HO. + HO_2^{\bullet} \xrightarrow{M} H_2O + O_2 \qquad (28)$$

Ainsi s'explique la diminution de la concentration en hydrogène qui est fourni uniquement par la réaction (27), tandis que l'augmentation correspondante de la concentration en oxygène peut être expliquée par les réactions (24), (27) et (28).

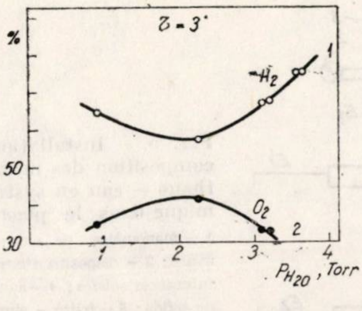

Fig. 3. — Influence de la pression partielle des vapeurs d'eau sur la composition du mélange final : 1 — H_2 ; 2 — O_2 ; τ décharge = 3 minutes.

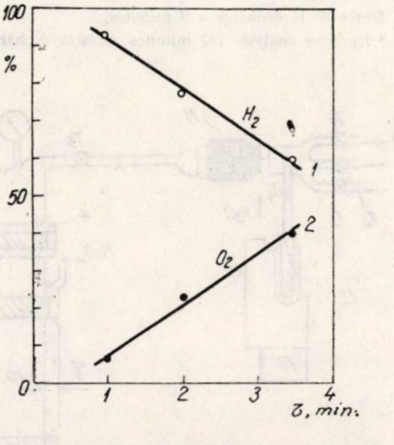

Fig. 4. — Influence de la durée de la décharge sur la concentration des composants du mélange final : 1 — H_2 ; 2 — O_2 ; p_{H_2O} = 3,2 mm Hg

La décomposition des mélanges CH_4-H_2O dans le plasma froid conduit à la formation d'une gamme variée de composés (tableau 1) déterminée particulièrement par les réactions de recombinaison des radicaux formés des scissions des deux molécules.[3] De même, ne sont pas à exclure les réactions possibles entre les espèces actives, réactions qui modifient fortement la composition et la nature des composants du système en temps.

L'analyse de la décomposition des mélanges CH_4-H_2O dans le plasma froid, en système stationnaire, montre que la nature et la composition des produits formés sont dépendantes du rapport des deux composants, de la durée de la décharge et de la durée de conservation dans le réacteur.

L'utilisation d'un réacteur dynamique (figure 5) et le captage des produits de réaction à basse température, tout en simulant mieux certaines réactions de l'ère primaire, conduisent à la synthèse d'un plus grand

Tableau 1

Produits formés par la décomposition des mélanges CH_4-H_2O en plasma froid, en système stationnaire

$r=P_{CH_4}/P_{H_2O}$	H_2	O_2	C_2H_2	C_2H_4	C_2H_2	CH_3CHO	CH_2O	CH_3OH	C_2H_5OH + CO	HCOOH
Torr/Torr	%									
0.40	28,1	22,5	0,6	6,0	0,4	0,5		2,3	2,0	—
0,40*	46,1	9,1	2,3	16,4	—	—	0,7	—	1,0	14,1
1,87	36,1	10,6	3,4	2,2	—	3,5	6,1	—	—	—

Durée de la décharge = 3 minutes.

* Epreuve analysée 137 minutes après la décharge.

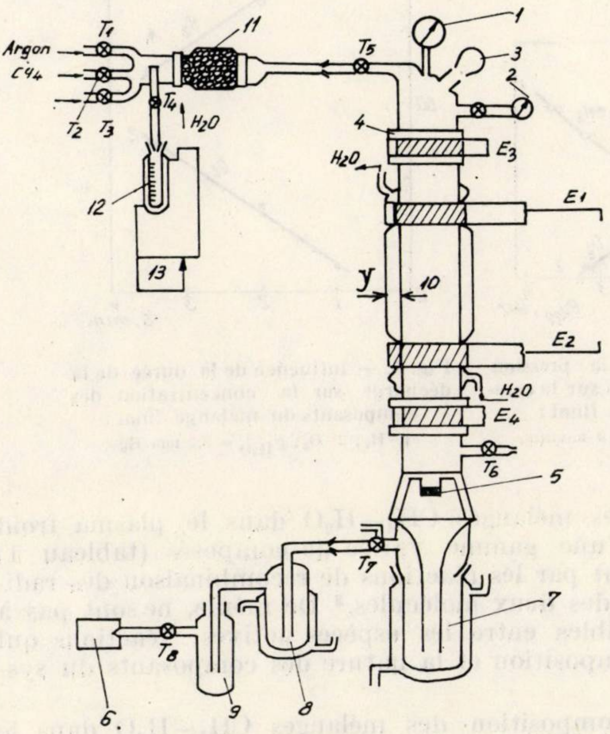

Fig. 5. — Installation de décomposition des mélanges méthane — eau en système dynamique dans le plasma froid : 1 — manomètre de vide ; 2 — vacuomètre ; 3 — dispositif d'introduction des substances solides ; 4 — anneaux isolants de téflon ; 5 — fritte — support pour les catalyseur ; 6 — pompe à vide ; 7,8,9- récipients pour condenser et collecter les produits de réaction (N_2 liquide) ; 10 — espace de réaction ; 11- — mélangeur des gaz ; 12 — ampoule contenant de l'eau thermostatée ; $T-T_8$-robinets ; E_1, E_2— électrodes alimentées au courant haute fréquence ; E_3, E_4 — 7 électrodes qui limitent le plasma.

nombre de composés — aldéhydes, cétones, alcools, acides — précurseurs possibles des biomonomères (tableau 2)[4].

L'analyse de la phase liquide collectée après le dégel a montré que la concentration des produits résultés est fonction du rapport CH_4/ /H_2O, de l'épaisseur de la couche d'eau de refroidissement (Y), de la

Tableau 2

Composition de la phase liquide résultée par la décomposition des mélanges CH_4-H_2O en système dynamique

CH_4/H_2O	Y	Aldéhyde formique	Aldéhyde acétique	Acétone	Méthyl-éthyl cétone	Alcool méthylique	Alcool éthylique	Alcool isopropylique	Alcool butylique sec.	Alcool butylique tert.	Acide formique	Acide acétique
Torr/ml.h^{-1}	mm	g/µl.10^7										
36,76 (2,5/0,068)	8	87,77	18,89	9,23	—	28,52	4,69	—	—	—	0,62	—
96,09 (3,2/0,033)	8	438,87	91,53	65,64	11,18	47,12	25,83	5,89	7,28	33,74	64,15	32,16
96,09*	8	62,69	58,40	35,89	9,09	42,98	14,09	4,75	8,27	17,06	63,37	34,94
68,75 (2,75/0,040)	1	1360,50	20,61	23,58	9,36	34,72	42,85	3,96	9,92	33,16	15,53	19,96
93,45** (3,0/0,032)	1	1304,07	27,48	28,71	10,48	57,87	93,93	7,11	7,72	60,46	31,29	13,31
92,59*** (3,0/0,0324)	1	789,80	18,89	47,18	18,18	76,05	131,51	4,71	8,82	109,23	12,51	23,85

* Epreuve analysée après 200 h ;** – irradiation UV pendant le dégel ; *** – irradiation UV pendant la synthèse.

présence des radiations UV pendant la décharge ou pendant le dégel et de la durée de conservation à la température normale.

L'augmentation du rapport CH_4/H_2O provoque une concentration des produits de réaction (figure 6,7) et diversifie leur gamme (tableau 2).

L'analyse de la phase gazeuse a mis en évidence la formation des hydrocarbures C_2-C_4 (tableau 3,4).

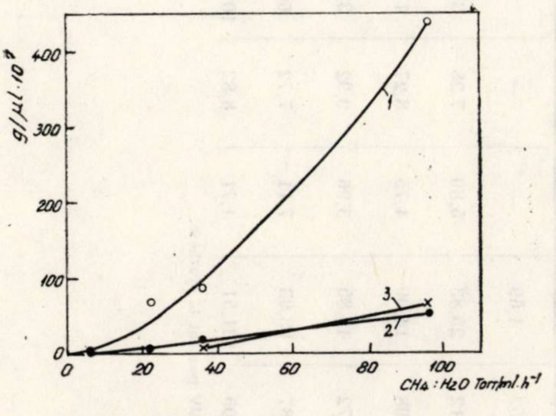

Fig. 6. — Influence du rapport CH_4/H_2O sur la concentration en aldéhydes et cétones :

1 – Aldéhyde formique ; 2 – Aldéhyde acétique ; 3 – Acétone.

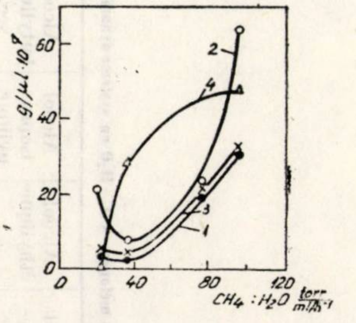

Fig. 7. — Influence du rapport CH_4/H_2O sur la concentration en alcools et acides :

1 – Acide acétique ; 2 – Acide formique ; 3 – Alcool butylique tertiaire ; 4 – Alcool méthylique.

Tableau 3

Composition de la phase gazeuse résultée par la décomposition des mélanges CH_4-H_2O dans le plasma froid

CH_4/H_2O	Durée de conservation	CH_4	CO_2	C_2H_4	C_3H_8	C_4
Torr/ml. h^{-1}	h	%				
68,75	0	0,06	7,77	10,25	58,00	4,51
96,09	0	2,38	2,20	10,34	51,87	10,88
	0	5,05	16,60	17,09	41,47	20,78
93,45*	18	4,22	11,10	17,28	54,00	5,35
	0	0,12	7,48	6,43	49,09	7,77
92,59**	23	0,07	1,34	3,00	35,32	2,27

* Irradiation UV pendant le dégel ; ** irradiation UV pendant la synthèse

Tableau 4

Composition de la fraction C_4 résultée par la décomposition des mélanges CH_4-H_2O dans le plasma froid

CH_4/H_2O	n-Butane	*cis*-Butène	*trans*-Butène	Isobutène + butadiène
Torr/ml. h^{-1}	%			
68,75	3,89	0,69	0,24	0,52
93,45*	6,87	0,21	0,49	1,47
92,59**	9,26	7,71	0,54	1,38

* – irradiation UV pendant le dégel; ** – irradiation UV pendant la synthèse.

On propose les réactions suivantes pour la synthèse des produits mentionnés :

$$CH_3^{\bullet} + O_2 \rightarrow [CH_3O_2^{\bullet} \rightarrow \dot{C}H_2OOH] \rightarrow CH_2O + HO^{\bullet} \qquad (29)$$

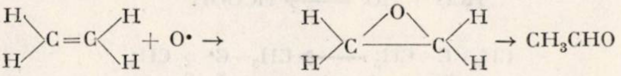

(30)

$$CH_3CHO + CH_3^{\bullet} \rightarrow CH_4 + CH_3\dot{C} = O \qquad (31)$$

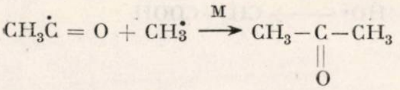

(32)

$$CH_3\dot{C} = O + CH_3^{\bullet} \xrightarrow{M} CH_3-\underset{\underset{O}{\|}}{C}-CH_3$$

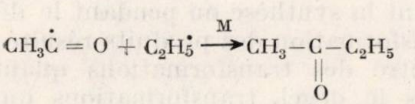

(33)

$$CH_3\dot{C} = O + C_2H_5^{\bullet} \xrightarrow{M} CH_3-\underset{\underset{O}{\|}}{C}-C_2H_5$$

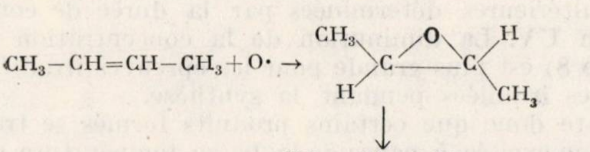

(34)

$$CH_3-CH=CH-CH_3 + O^{\bullet} \rightarrow \ldots \rightarrow CH_3-CO-C_2H_5$$

$$CH_3^{\bullet} + HO^{\bullet} \xrightarrow{M} CH_3OH \qquad (35)$$

$$C_2H_5^{\bullet} + HO^{\bullet} \xrightarrow{M} C_2H_5OH \qquad (36)$$

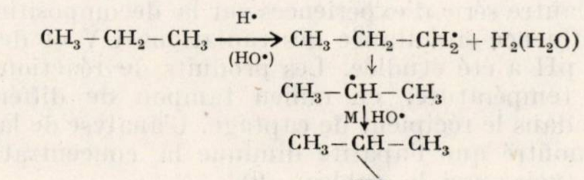

(37)

$$CH_3-CH_2-CH_3 \xrightarrow[(HO^{\bullet})]{H^{\bullet}} CH_3-CH_2-CH_2^{\bullet} + H_2(H_2O) \downarrow CH_3-\dot{C}H-CH_3 \xrightarrow{M,\ HO^{\bullet}} CH_3-\underset{HO}{CH}-CH_3$$

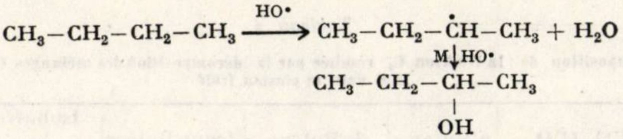

$$CH_3-CH_2-CH_2-CH_3 \xrightarrow{HO^\bullet} CH_3-CH_2-\dot{C}H-CH_3 + H_2O \xrightarrow[M]{HO^\bullet} CH_3-CH_2-CH(OH)-CH_3 \quad (38)$$

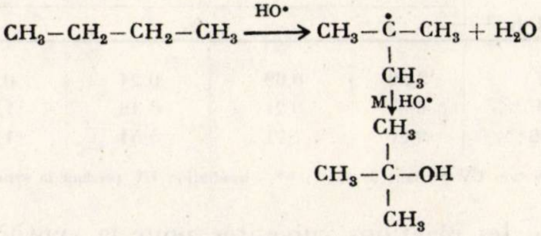

$$CH_3-CH_2-CH_2-CH_3 \xrightarrow{HO^\bullet} CH_3-\dot{C}(CH_3)-CH_3 + H_2O \xrightarrow[M]{HO^\bullet} CH_3-C(CH_3)(OH)-CH_3 \quad (39)$$

$$CH_2O + HO^\bullet \longrightarrow H_2O + H\dot{C}O \quad (40)$$

$$H\dot{C}O + HO^\bullet \xrightarrow{M} HCOOH \quad (41)$$

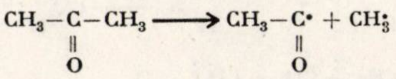

$$CH_3-\underset{\underset{O}{\|}}{C}-CH_3 \longrightarrow CH_3-\underset{\underset{O}{\|}}{C^\bullet} + CH_3^\bullet \quad (42)$$

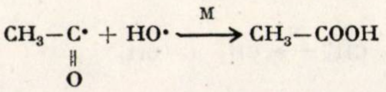

$$CH_3-\underset{\underset{O}{\|}}{C^\bullet} + HO^\bullet \xrightarrow{M} CH_3-COOH \quad (43)$$

L'irradiation UV pendant la synthèse ou pendant le dégel influence tant la formation que la transformation des produits résultés (tableau 2).

Les analyses ont montré des transformations quantitatives des composants longtemps après le dégel, transformations qui impliquent des réactions ultérieures déterminées par la durée de conservation et par l'irradiation UV. La diminution de la concentration en aldéhyde formique (figure 8) est plus grande pour les épreuves irradiées, en particulier pour celles irradiées pendant la synthèse.

On constate donc que certains produits formés se trouvent longtemps sous forme excitée à cause de la basse température de condensation. Ultérieurement, ces molécules excitées participent aux réactions secondaires d'où résultent ou des produits dont l'identification par chromatographie est possible, ou des produits de couleur brune (polymères acétyléniques ramifiés) qui se déposent en temps.

Ainsi on démontre la coopération de différentes formes d'énergie et on justifie les conditions expérimentales choisies.

Dans une autre série d'expériences sur la décomposition du mélange CH_4-H_2O, l'influence simultanée des radiations UV et des catalyseurs, pour différents pH a été étudiée. Les produits de réactions ont été collectés à basse température, en milieu tampon de différents pH, sur apatite déposée dans le récipient de captage. L'analyse de la phase liquide (tableau 5) a montré que l'apatite diminue la concentration de l'aldéhyde formique (voir aussi le tableau 2).

Tableau 5

Composition de la phase liquide résultée par la décomposition des mélanges $CH_4 - H_2O$ en présence de l'apatite dans le plasma froid

CH_4/H_2O	Durée d'irradiation	pH	Aldéhyde formique	Aldéhyde acétique	Acétone	Méthyl-éthyl-cétone	Alcool méthylique	Alcool éthylique	Alcool isopropylique	Alcool butylique sec.	Alcool butylique tert.	Acide formique	Acide acétique
Torr/ /ml.h^{-1}	h		$g/\mu l\ .10^7$										
53,72	3	—	33,22	20,61	17,43	3,63	28,60	2,70	8,16	5,84	6,14	7,82	16,19
70,68	11	—	—	—	13,33	5,59	17,03	—	—	3,31	1,95	12,51	20,30
68,59	—	2	—	—	28,71	12,58	38,02	9,39	10,30	22,43	7,72	35,98	39,93
68,59	23	2	—	—	30,76	15,38	38,02	7,63	7,93	18,75	17,55	19,55	33,27
71,43	3	8	22,88	13,74	29,74	4,19	20,66	5,46	14,51	8,82	22,04	13,30	26,62
64,43	28	10	135,42	—	9,84	6,43	—	23,48	4,20	12,46	24,38	27,38	16,97

L'introduction des solutions tampon à pH alcalin ou acide cause une diminution de concentration de l'aldéhyde formique ou même sa disparition totale de la phase liquide.

L'apatite — qui retient et concentre les produits — et le pH sont des conditions favorables au déroulement des réactions qui engagent particulièrement l'aldéhyde formique. Les données préliminaires, en révélant la présence des sucres et des composés organiques au phosphore, confirment l'existence de telles transformations.

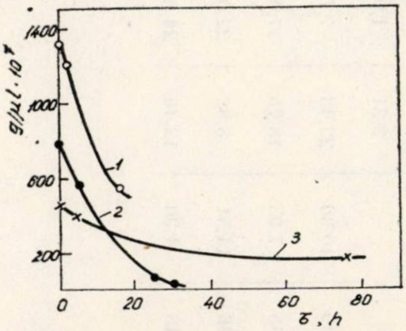

Fig. 8. — Variation de la concentration en aldéhyde formique avec la durée de conservation :

1 — irradiation UV pendant le dégel ($CH_4/H_2O = 93{,}45$ Torr/ml.h^{-1}) ; 2 — irradiation UV pendant la décomposition ($CH_4/H_2O = 92{,}59$ Torr/ml.h^{-1}) 3 — épreuve non irradiée($CH_4/H_2O = 96{,}09$ Totrr/ml.h^{-1}).

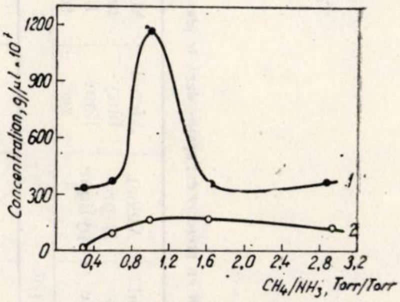

Fig. 9. — Influence du rapport CH_4/NH_3 sur la concentration de l'acide cyanhydrique et de l'acétonitrile dans la phase liquide :

1 — HCN ; 2 — CH_3CN.

Les radiations UV ont aussi produit une diminution de la concentration des aldéhydes, cétones et alcools, tout en augmentant l'acidité organique.

Les produits de réaction obtenus par la décomposition à haute fréquence des mélanges $CH_4—NH_3$ ont des concentrations dépendantes du rapport CH_4/NH_3 (tableau 6)[5].

Tableau

Compositon de la phase gazeuse résultée par la décompositio

CH_4/NH_3 Torr/Torr	CH_4	C_2H_4	n-C_4H_{10}	C_5	C_6
					%
0,35	—	—	—	—	—
0,60	0,15	—	0,23	0,23	0,16
1,00	0,19	—	0,23	0,12	0,01
1,64	0,04	2,44	0,16	0,21	0,03
2,90	—	0,39	0,23	0,12	0,03

Son augmentation jusqu'à 1,00 est favorable à la formation de l'acide cyanhydrique qui a une concentration maximum tant dans la phase gazeuse (tableau 6) que dans la phase liquide (figure 9).

La concentration des radicaux méthyle augmente et ils réagissent avec les radicaux NH : pour conduire à l'acide cyanhydrique

$$\begin{tikzcd} CH_3^\bullet + NH: \arrow[r] & CH_3NH^* \arrow[r, "M"] \arrow[d] & CH_3NH^\bullet \\ & HCN+H_2+H^\bullet & \end{tikzcd} \qquad (44)$$

La diminution de la concentration de l'ammoniac dans le mélange de départ accroît sa stabilité[6] et la quantité d'acide cyanhydrique dans les produits formés diminue. Cette stabilité croissante de l'ammoniac est confirmée par sa variation de concentration en phase liquide (fig. 10).

L'introduction de l'eau dans le système méthane-ammoniac modifie la composition du produit résulté particulièrement sous aspect quantitatif (tab. 7)

Dans ce cas résultent d'importantes quantités d'acide cyanhydrique, intermédiaire majeur dans la synthèse des acides aminés et des hydroxyacides. On constate aussi la présence de l'acétonitrile, important dans la formation des purines et pyrimidines.

L'étude de la décomposition des mélanges $CH_4-NH_3-H_2O$ a mis en évidence la formation d'un grand nombre de combinaisons chimiques réactives (aldéhydes, alcools, acides, cétones, amines, nitriles), intermédiaires capables de se recombiner diversement pour conduire aux biomonomères. Les récentes observations radio-astronomiques qui montrent l'existence de ces composés dans l'espace cosmique[7-9] soulignent le rôle important qu'ils ont eu pour l'apparition de la vie sur la Terre (figure 11).[10]

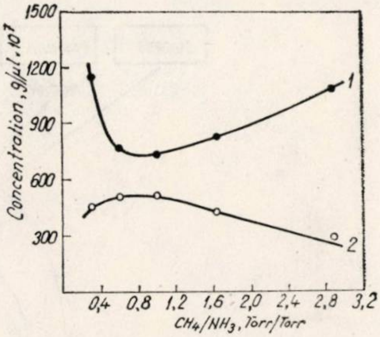

Fig. 10. — Influence du rapport CH_4/NH_3 sur la concentration de l'ammoniac et de la méthylamine dans la phase liquide.
1 – NH_3 ; 2 – CH_3NH_2.

6

des mélanges CH_4-NH_3 – dans le plasma froid

HCN	CH_3CN	$CH_2=CH-CN$	CH_3NH_2	$(CH_3)_2NH$
	0,06	—	traces	traces
49,32	0,19	0,11	0,56	0,17
80,52	0,21	0,08	5,20	0,58
65,50	0,35	0,28	2,76	0,52
60,81	0,26	0,09	2,66	0,41

---

[6] G. Toupance, F. Raulin et R. Buvet, *Origins of Life*, **6**, 83 (1975).

[7] D. Buhl, *Sky and Teleskope*, **45**, 2 (1973).

[8] R. D. Brown, *Chem. Brit.*, **9**, 450 (1973).

[9] M. Calvin, *La Recherche*, **5**, 44 (1974).

Tableau 7

Composition de la phase liquide résultée par la décomposition du mélange $CH_4/NH_3/H_2O$ dans le plasma froid *

$CH_4/NH_3/H_2O$	NH_3	HCN	CH_3NH_2	CH_3CN	$CH_2 = CH-CN$
Torr/Torr/ml.h^{-1}	g/µl.10^7				
2,5/5,0/0,00044	1703,12	335,36	354,32	8739,51	57,94
4,6/2,8/0,00369	3116,40	2280,48	381,82	3,20	139,46
4,2/2,1/0,00074	2862,50	1475,60	253,53	23,24	512,63

* On indique seulement les principaux composés.

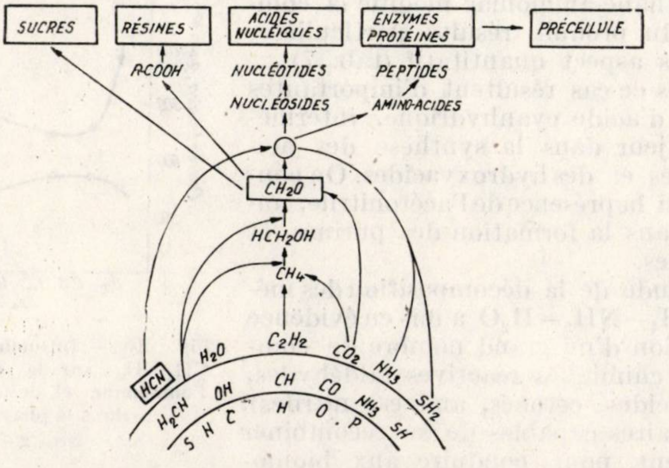
SUCRES
RÉSINES
ACIDES NUCLÉIQUES
ENZYMES PROTÉINES
PRÉCELLULE
R-COOH
NUCLÉOTIDES
NUCLÉOSIDES
PEPTIDES
AMINO-ACIDES
CH2O
HCH2OH
CH4
HCN
H2O
C2H2
CO2
NH3
SH2
H2CH
OH
CH
CO
NH3
S H C
H
O . P
SH

Fig. 11. — Relation probable entre la chémogenèse et la biogenèse.

D'autre part, une série de données expérimentales[11–17] confirme les possibilités de synthèse des sucres, bases, acides nucléiques et amino-acides par la décomposition des mélanges méthane — ammoniac — eau dans le plasma froid.

L'utilisation de systèmes catalytiques et de radiations UV améliore les rendements des biomonomères et confère un support réel pour le modèle de synthèse chimique des précurseurs de la matière vivante.

---

[10] A. A. Titaev, "Evolutsia organiccheskikh soedinenii na zemle", Ed. Nauka, Moskva 1974, p. 110.

[11] Cr. Simionescu, N. Asandei et F. Deneș, *Compt. rend. D*, **273**, 599 (1971).

[12] Cr. Simionescu, F. Denèș et M. Macoveanu, *Doklady Akad. Nauk S.S.S.R.*, **207**, 469 (1972).

[13] Cr. Simionescu, F. Denèș et E. Schneider, *Compt. rend. D.*, **275**, 703 (1972).

[14] Cr. Simionescu, F. Denèș et M. Macoveanu, *Biopolymers*, **12**, 237 (1973).

[15] Cr. Simionescu, F. Denèș, D. Onac et G. Bloos, *Biopolymers*, **13**, 943 (1974).

[16] Cr. Simionescu, F. Denèș et M. Dragnea, *Compt. rend. C*, **278**, 29 (1974).

[17] Cr. Simionescu, T Lixandru, C Gorea et V Gorduza, *Compts rend C*, **280**, 685 (1975).

Revue Roumaine de Chimie, 23, 1, 103–110 (1978)

CONFORMATIONAL ANALYSIS AND ELECTRONIC STRUCTURE OF THIENYLPYRIDINES

J. V. KNOP and N. TRINAJSTIĆ [1]
Rechenzentrum der Universität Düsseldorf, 4000 Düsseldorf, BRD

M. MILUN [2] and S. PEJAKOVIĆ
The Rugjer Bošković Institute, P.O.B. 1016, 41000 Zagreb, Croatia, Yugoslavia

Received August 21, 1975

The conformation of six isomeric thienylpyridines is studied using the extended Hückel theory. The most preferred conformational arrangement is found to be the twisted ($\theta \approx 30°$) *syn* form for the 2,2′-, 4,2′-, 2,3′-, and 3,3′- isomers and the twisted ($\theta \approx 150°$) *anti* form for the 3,2′- and 4,3′- isomers. The CNDO/2 method and the Pople-Segal approach are employed to calculate the net atomic charges and the dipole moments of the thienylpyridines, respectively. The UV spectra of these molecules are predicted from the Pariser-Parr SCF MO method.

INTRODUCTION

Thienylpyridines are heteroconjugated compounds consisting of thiophen and pyridine ring systems linked together through an essentially single bond. There are six isomeric thienylpyridines possible : 2-/2′-thienyl/ /pyridine (1), 3-/2′-thienyl/-pyridine (2),4-/2′-thienyl/-pyridine (3),2-/3′-thienyl/-pyridine (4), 3-/3′-thienyl/-pyridine (5), and 4-/3′-thienyl-pyridine (6). We shall denote these molecules in a shorthand notation as 2,2′-, 3,2′-, 4,2′-, 2,3′- 3,3′-, and 4,3′-isomers. Their atomic skeletal structures are given in Fig. 1.

Thermodynamic stability of the thienylpyridines is expected to be considerable because these molecules consist of two (weakly interacting) aromatic molecules — thiophene and pyridine — which are stable compounds. One can indeed approximately evaluate their index of aromatic stabilisation (A_S) using formula[3]

$$A_S(A-B) = A_S(A) + A_S(B)$$

Since A_S (thiophene) = 6.5 kcal/mole[4] and A_S (pyridine) = 23.1 kcal/mole,[5] the A_S index of the thienylpyridines is approximately 30 kcal/mole.

---

[1] Visiting Professor from the Rugjer Bošković Institute, P.O.B. 1016, 41001 Zagreb, Croatia, Yugoslavia.

[2] Permanent address : The Pharmaceutical and Chemical Works "Pliva", Zagreb, Croaţia, 41000, Yugoslavia.

[3] N. Trinajstić, *Record Chem. Progress* **32,** 85 (1971).

[4] M.J.S. Dewar and N. Trinajstić, *J. Amer. Chem. Soc.,* **92,** 1453 (1970).

[5] M.J.S. Dewar and N. Trinajstić, *Theoret. Chim. Acta,* **17,** 235 (1970).

This result agrees with experimental findings: all six isomeric thyenylpyridines are prepared and behave like aromatic compounds.[6–10] Futhermore, these compounds are able to coordinate some metals/ Ni^{2+}, Cu^{2+}, Zn^{2+} /[7,11] and also possess an interesting photochemical behaviour[7]. Besides, isomeric thienylpyridines are compounds of pharmaceutical interest. For example, the 2,2′-isomer is an active compound in the inhibition of gastric secretion without anticholinergic and ganglionic blocking activity [12].

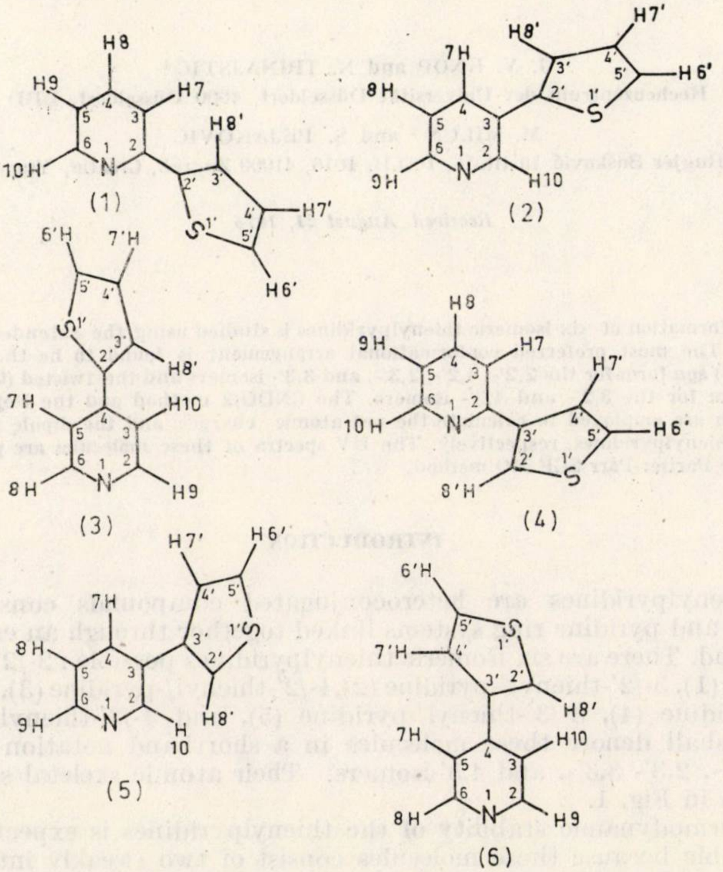

Fig. 1. — Geometries and atom numbering of isomeric thienylpyridines.

---

[6] K. Kahman, H. Sigel, and H. Erlenmeyer, *Helv. Chim. Acta*, **47**, 1754 (1964).

[7] H. Wynberg, T. J. van Bergen, and R. M. Kellogg, *J. Org. Chem.*, **34**, 3175 (1969).

[8] F. Eloy and A. Deryckere, *Chim. Theor.*, **1970**, 416.

[9] T. Kauffmann, E. Wienhöfer, and A. Woltermann, *Angew. Chem.*, **83**, 796 (1971); T. Kauffmann, *ibid.*, **83**, 798 (1971).

[10] H. S. Ryang and H. Sakurai, *J.C.S. Chem. Comm.*, **1972**, 594.

[11] H. Sigel, H. Wynberg, T. J. van Bergen, and K. Kahman, *Helv. Chim. Acta*, **55**, 610 (1972).

[12] D. E. Butler, P. Bass, I. C. Nordin, P. G. Hauck, Jr., and J. Y. L'Italien, *J. Med. Chem.*, **14**, 575 (1971).

This all makes the investigation of the eletronic structure of the thienylpyridines timely and desirable. The only theoretical study so far performed on these molecules was an attempt to correlate the ground state basicities with the π-electron energies obtained from HMO and SCF MO calculations.[13]

CONFORMATIONAL ANALYSIS

For molecules formed by two conjugated rings joined by an essentially single bond, such as thienylpyridines, there are two opposing effects mainly responsible for the equilibrium conformation : the conjugative effect and the steric effect. The conjugative effect between the aromatic rings tends to keep them coplanar, whereas the steric effect is minimal when the terminal units are perpendicular. The equilibrium conformation of the molecule is determined by a delicate balance of these two effects. It is therefore necessary to include both effects in the calculations in order to provide a reliable estimate for the potential energy function of rotation about the inter-ring bond. Our experience[14] is that the simplest method to be used in such a case is the Extended Hückel Theory (EHT) in the framework of the Hoffmann's variant,[15] since its wide application to a number of organic, inorganic and biological compounds provides a good test of this method to cope with conformational problems on a qualitative level.

The standard EHT is used.[15] All valence electrons were explicitly treated and all overlap integrals were included. The Slater orbital exponents are used for *s* and *p* valence orbitals of C, N, and S. The exponent 1.3 instead of the usual value 1.0 is used[17] for the *ls* orbital of the hydrogen atom. No use has been made of the *d*-orbitals on S in view of the minor role played by these orbitals in bonding as shown recently by an *ab initio* treatment of thiophene[18] and by the unrestricted Hartree-Fock spin density calculations on sulphurcontaining aromatic radicals.[19] Galasso, De Alti, and Bigotto[20] have also shown that the inclusion of sulphur *d*-orbitals causes no change in the geometry and has only a small effect on the height of the rotational barrier in systems like phenyl-thiophenes and diphenyl-sulphide. The valence state ionization potentials were taken from Hoffmann and I Imamura[17] for H, C, N, and from Hinze and Jaffé[21] for S.

---

[13] E. Bowhuis and M. J. Janssen, *Tetrahedron Lett.*, **1972,** 233.

[14] V. Galasso and N. Trinajstić, *Tetrahedron*, **28,** 2799, 4419 (1972). Galasso, M. Milun, and N. Trinajstić, *Z. Naturforsch.*, **28b,** 464 (1973).

[15] R. Hoffmann, *J. Chem. Phys.*, **39,** 1397 (1963).

[16] J. R. Hoyland, in "Molecular Orbital Studies in Chemical Pharmacology", Edited by L. B. Kier, Springer-Verlag, New York, 1970, p. 31. L. B. Kier, "Molecular Orbital Theory in Drug Research, " Academic Press, New York 1971, p. 164.

[17] R. Hoffmann and I. Imamura, *Biopolymers*, **7,** 207 (1968).

[18] S. Polezzo, M. P. Stabilini, and M. Simonetta, *Mol. Phys.*, **17,** 609 (1969), D. T. Clark, and D. R. Armstrong, *J.C.S Chem. Comm.*, **1970,** 319. B. Ross and P. Siegbahn. *Theoret. Chim. Acta* **21,** 369 (1971), U. Gelius, B. Ross, and P. Siegbahn, *ibid.* **27,** 171 (1972).

[19] D. N. Nanda and P. T. Narasimhan, *Mol. Phys.* **24,** 1341 (1972).

[20] V. Galasso and G. De Alzi, *Tetrahedron* **27,** 4947 (1971), V. Galasso, G. De Alti and A. Bigotto, *ibid.* **27,** 6151 (1971).

[21] J. Hinze and H. H. Jaffé, *J. Amer. Chem. Soc.*, **84,** 540 (1962).

Since the structural data are lacking, the idealized structures of the thienylpyridines have been formed by connecting the actual geometries of thiophene [22] and pyridine [23] with an inter-ring bond of 1.48 Å. The potential energy function of each molecule has been calculated with respect to the variation of the angle of twist around the inter-ring bond in the range of 0°—180° with scanning of 30°. The plots of the calculated total energy vs. the angle of twist are given in Fig. 2. The following conformational information for the isomeric thienylpyridines is obtained : the most preferred conformational arrangement is the twisted ($0 \approx 30°$) *syn* form for the 2,2′-, 4,2′-, 2,3′-, and 3,3′-isomers, and the twisted ($0 \approx 150°$) *anti* form for the 3,2′- and 4,3′-isomers. These theoretical findings cannot be at present checked with direct experimental information since these are lacking, but they can perhaps stimulate further research in determining the structure of the thienylpyridines especially since these compounds are of potential interest in medicinal chemistry. Perhaps it is of some interest to compare our results with those obtained for the thienylbenzenes. [20] (2-thienyl)-benzene (7) and (3-thienyl)-benzene (8) are predicted [20] to have an equilibrium conformation twisted by about 37° from planar geometry. Since thienylbenzenes and the thienylpyridines differ only in one position (the CH group in the former being replaced by a nitrogen atom in the later) the difference in the value of the angle of twist may be attributed to the difference in the interactions *s*. . .*s*, *s*. . .*p*. and *p*. . .*p* between the heteroatoms and the neighbouring H atom on the phenyl ring.

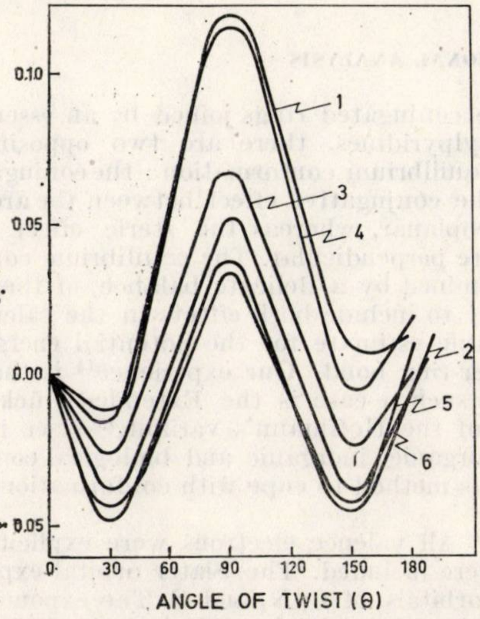

Fig. 2. — Extended Hückel energy vs. the angle of twist for 2-/2′-thienyl/pyridine, (1), 3-/2′-thienyl/pyridine (2), 4-/2′-thienyl/pyridine (3), 2-/3′-thienyl/pyridine (4), 3-/3′-thienyl/pyridine (5) and 4-/3′-thienyl/pyridine (6). The energy zero has been arbitrarily assigned to the planar *syn* conformation.

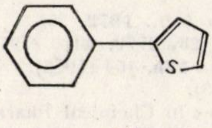

(7)

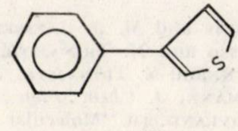

(8)

---

[22] B. Bak, D. Christensen, L. Hansen-Nygaard, and J. Rastrup-Andersen, *J. Mol. Spectroscopy*, **7**, 58 (1961).

[23] B. Bak, L. Hansen-Nygaard, and Rastrup-Andersen, *ibid.*, **2**, 361 (1958).

ELECTRONIC STRUCTURE

Since the CNDO/2 method[24] provides more reliable atomic charges than EHT, especially for systems containing heteroatoms, the charge distribution for the two more favourable conformations of each molecule has been calculated using CNDO/2 method. The parametrization scheme has been taken from Sichel and Whitehead[25] (ionization potentials and one-centre two-electron Coulomb integrals) and from Burns[26] (orbital exponents for all orbitals but 1*s* on hydrogen, where a value of 1.2 has been used). The resonance integrals have been taken from calculations of the standard Wolfsberg-Helmholtz formula[27] with K=1 and the two-centre two-electron Coulomb integrals using the Ohno-Mataga-Nishimoto relation.[28] The net atomic charges thus obtained are given in Table 1.

Table 1

Net atomic charges of thienylpyridines

ISOMER	2,2′		3,2′		4,2′	
TWIST ANGLE / ATOM	30°	150°	30°	150°	30°	150°
N−1	−0.40317	−0.41780	−0.36141	−0.36287	−0.39658	−0.39644
C−2	0.30261	0.30343	0.01768	0.01802	0.16237	0.16225
C−3	0.22564	0.22802	0.18039	0.19031	−0.11816	−0.11470
C−4	−0.10099	− 0.10165	0.19625	0.19603	0.22222	0.22146
C−5	0.06104	0.05972	−0.07278	−0.07109	0.22254	0.22273
C−6	−0.11592	−0.10516	0.02851	0.01887	−0.10898	−0.11165
H−7	0.00107	0.00059	0.00424	0.01200	0.02819	0.02778
H−8	0.02289	0.02299	0.00220	0.00221	−0.00165	−0.00106
H−9	0.01194	0.01221	0.02214	0.02200	−0.00098	−0.00150
H−10	0.02438	0.03307	0.02139	0.0146	0.02663	0.02691
S−1′	−0.06956	−0.09852	−0.09955	0.09920	−0.08745	−0.08772
C−2′	−0.02855	−0.02411	−0.05732	0.05671	−0.01889	−0.01880
C−3′	−0.00261	−0.00540	−0.05334	−0.05208	−0.07288	−0.07283
C−4′	−0.04106	−0.02165	0.00324	0.00239	−0.42852	−0.42823
C−5′	0.03270	0.02743	− 0.02788	−0.02788	0.08238	0.08211
H−6′	0.01817	0.02594	0.04415	0.04421	0.39908	0.39903
H−7′	0.01661	0.01686	0.01750	0.01726	0.04288	0.04285
H−8′	0.04479	0.04403	0.01997	0.01901	0.04780	004781
(D) DIPOLE MOMENT	4.815	1.659	2.186	5.114	6.768	6.765

---

[24] J. A. Pople, D. P. Santry, and G. A. Segal, *J. Chem. Phys.*, **43,** 5129 (1965). J. A. Pople and G. A. Segal, *ibid.*, **44,** 3289 (1966).

[25] J. M. Sichel and M. A. Whitehead, *Theoret. Chim. Acta*, **7,** 32 (1967).

[26] G. Burns, *J. Chem. Phys.*, **41,** 1521 (1964).

[27] M. Wolfsgerg and L. Helmholtz, *J. Chem. Phys.*, **20,** 837 (1952).

[28] N. Mataga and K. Nishimoto *Z. phys. Chem.* (*Frankfurt*) **13,** 764 (1956). K. Ohno, *Theoret. Chim. Acta*, **2,** 219 (1964).

Table 1 continued

ISOMER	2,3′		3,3′		4,3′	
TWIST ANGLE	30°	150°	30°	150°	30°	150°
ATOM						
N−1	−0.41173	−0.41211	−0.36757	−0.36764	−0.38878	−0.38878
C−2	0.27529	0.27600	−0.01219	−0.01219	0.11848	0.11848
C−3	−0.11165	−0.11201	0.02163	0.02175	−0.10964	−0.10959
C−4	0.05824	0.05840	−0.07435	−0.07435	0.22283	0.22296
C−5	−0.09718	−0.09742	0.20141	0.20148	0.22178	0.22162
C−6	0.22364	0.22382	0.18845	0.18822	−0.11561	−0.11564
H−7	0.02221	0.02229	0.01263	0.01298	0.02036	0.02026
H−8	0.01066	0.01058	0.02148	0.02153	−0.00075	−0.00079
H−9	0.02123	0.02122	0.00068	0.00068	−0.00063	−0.00059
H−10	−0.00049	−0.00045	0.00123	0.00085	0.02184	0.02192
S−1′	−0.07835	−0.07877	−0.07657	−0.07747	−0.07211	−0.07206
C−2′	−0.01730	−0.01638	−0.05696	−0.05625	−0.01414	−0.01409
C−3′	−0.01058	−0.02556	0.07100	0.07104	−0.02474	−0.02500
C−4′	0.03987	0.03745	−0.03045	−0.03127	0.05189	0.05181
C−5′	−0.01488	−0.02700	−0.01371	−0.01300	−0.04640	−0.04602
H−6′	0.04674	0.05422	0.04526	0.04552	0.04826	0.04846
H−7′	0.02833	0.02022	0.01991	0.02093	0.02186	0.02157
H−8′	0.04595	0.04548	0.04812	0.04717	0.04551	0.04549
(D) DIPOLE MOMENT	3.557	4.985	4.067	1.643	1.744	1.810

The charge distribution shows that the S and N atoms attain a negative charge and that thus both atoms act as electron acceptors. The overall charge distribution in a molecule is reflected to some extent by the dipole moment which has been in our examples evaluated by the Pople-Segal approach.[24] Calculated dipole moments are also reported in Table 1.

ELECTRONIC SPECTRA

Electronic spectra are calculated using the Pariser-Parr SCF MO method with limited CI[29]. For one-centre repulsion and one-electron core resonance integrals the values of Gleir et al.[30] were used. Two centre repulsion integrals were determined in the Mataga-Nishimoto way.[31] Sulphur was considered without *d*-orbitals for the same reasons as stated before.[32] In Table 2 we predict the UV spectral characteristic of compounds (1)—(6) in their *syn* and *anti* forms. Transition energies are given up to 6eV. Oscillator strenghts (f) are given, too. Unfortunately there is no experimental evidence to check our results.

[29] R. Pariser and R. G. Parr, *J. Chem. Phys.*, **21,** 466, 767 (1953).

[30] G. Glier, F. Dietz, M. Scholz, and G. Fischer, *Tetrahedron,* **28,** 5779 (1972).

[31] N. Mataga and K. Nishimoto, see ref. 28.

[32] see ref. 18.

However, the survey of calculated results shows no difference between the two conformational forms. This is in agreement with findings for the other similar systems.[33,34]

An additional point that we wish to discuss is the shift observed in the calculated first transition energy/which mostly consists of the transition from 6. to 7. MO (95%) of 2,3'-, 3,3'-, and 4,3'- isomers when compared with 2,2'- (0.28 eV), 3,2'- (0.23eV) and 4,2'- isomers (0.35eV). This effect can be anticipated following the simple graph theoretical thinking[35,36] by taking into account only carbon π-electron lattices of the thiophen part of the molecule.

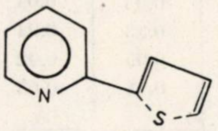

2,2'-

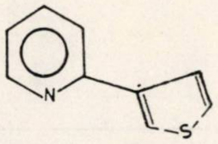

2,3'-

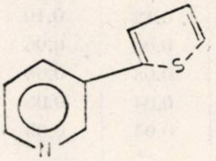

3,2'-

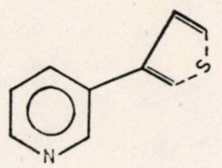

3,3'-

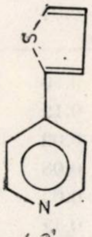

4,2'-

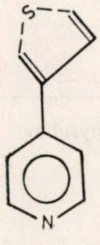

4,3'-

Similar rationalisation was successfully used, for example, in the case of bithienyls and related compounds.[37,38] We have found that the increase of the number of carbon atoms with three C-neighbours causes an increase in the first transition energy.[39]

---

[33] A. J. Wachters and D. W, Davies, *Tetrahedron*, **20**, 2841 (1964).

[34] L. Klasinc, N. Trinajstić, and E. Pop, *Rev. Roumaine Chim.*, **18,** 89 (1973).

[35] I. Gutman and N. Trinajstić, *Chem. Phys. Lett.*, **17**, 535 (1972), Croat. Chem. Acta **46**, 423 (1974). J. V. Knop, N. Trinajstić, I. Gutman and L. Klasinc, *Naturwiss.*, **60,** 475 (1973).

[36] See, for example, also I. Gutman, and N. Trinajstić, *Topics Curr. Chem.*, **42,** 49, (1973).

[37] R. M. Kellogg, A. P. Schaap, and H. Wynberg, *J. Org. Chem.*, **34,** 343 (1969).

[38] M. Milun and N. Trinajstić, *Spectroscopy Lett.*, **6,** 329 (1973).

[39] I. Gutman, B. Ruščić, N. Trinajstić, and C. F. Wilcox, Jr. *J. Chem. Phys.* **62** 2770 (1974).

Table 2

Calculated singlet-singlet transition energies (ΔE) and oscillator strengths (f) of isomeric thienylpyridines

Molecule	ΔE/eV/		f	
	syn	anti	syn	anti
2-/2′-thienyl/pyridine	3.22	3.23	0.78	0.79
	4.32	4.45	0.14	0.05
	4.75	4.81	0.03	0.04
	4.96	4.97	0.23	0.24
	5.72	5.81	0.05	0.02
	5.96	6.01	0.11	0.03
3-/2′-thienyl/pyridine	3.38	3.38	0.31	0.30
	4.37	4.36	0.61	0.69
	4.68	4.67	0.12	0.10
	4.89	4.86	0.05	0.06
	5.10	5.25	0.08	0.06
	5.73	5.75	0.04	0.05
	5.93	5.94	0.04	0.03
4-/2′-thienyl/pyridine	3.67	3.67	0.77	0.79
	4.05	4.07	0.24	0.20
	4.57	4.55	0.17	0.15
	5.58	5.53	0.15	0.10
	5.96	5.97	0.01	0.01
2-/3′-thienyl/pyridine	3.50	3.55	0.52	0.60
	4.26	4.08	0.13	0.12
	5.06	5.01	0.32	0.02
	5.23	5.19	0.16	0.08
	5.57	5.55	0.02	0.03
	5.70	5.78	0.29	0.42
3-/3′-thienyl/pyridine	3.61	3.60	0.23	0.23
	4.39	4.42	0.22	0.20
	4.85	4.92	0.20	0.32
	5.09	5.06	0.01	0.06
	5.24	5.25	0.02	0.09
	5.55	5.55	0.69	0.54
4-/3′-thienyl/pyridine	4.02	4.01	0.24	0.24
	4.12	4.15	0.32	0.30
	4.58	4.50	0.39	0.40
	5.38	5.39	0.42	0.45
	5.75	5.76	0.08	0.05

Revue Roumaine de Chimie, **23**, *1*, 111—118 (1978)

THERMAL AND PHOTOINDUCED POLYMERIZATION OF N,N′-BISMALEIMIDE

GEORGETA M. GHERASIM and LEONIA STOICESCU-CRIVETZ
Institute of Macromolecular Chemistry "P. Poni", 41 A Aleea Gr. Ghica-Vodă, Iassy, Romania

Received May 20, 1975

Thermal and photochemical free-radical homopolymerizations of N,N′-bismaleimide were studied to obtain a new polybismaleimide. Infrared spectra and elemental analysis of the polymer showed that it is composed alternatively of cyclobutane and bisimide rings, except for the polymer obtained by melting. Thermogravimetric and differential thermal analysis curves showed that the polymer is less stable than the reported polybismalimides due to the less stable nitrogen-nitrogen groups. It was assumed that the polymer could be obtained by a repeated $2_\pi + 2_\pi$ photocycloaddition process.

INTRODUCTION

Free-radical polymerization of the bismaleimide type compounds (Ia) has been previously reported.[1–7] Their thermal polymerization,[1,2] photopolymerization in the solid state[3–5] and solution[6,7] using either ultraviolet light[4,6] or γ-ray irradiation[3] have been investigated. However, a study on the thermal and photoinduced polymerization of N,N′-bismaleimide (Ib) has not been carried out yet.

In the present paper, we report the thermal and photochemical free-radical homopolymerization of N,N′-bismaleimide (Ib), as well as the properties and the structure of the resulting polybismaleimide. The monomer, which was prepared a while ago[8] is obtained quite easily and shows rather good solubility and thermal stability properties. N,N′-Bismaleimide contains two electron-withdrawing carbon-carbon double bonds and the imide rings are directly bound through the nitrogen atoms.[8]

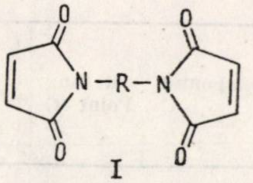

I

(a) R = alkyl or aryl :
(b) R = without radical.

---

[1] M. Russo, *Mater. Plast. ed Elast.*, **36**, 746 (1970).

[2] G. Menges and R. Kleinholz, *Plastverarbeiter*, **5**, 21(1970).

[3] V. S. Ivanov, I. P. Bezhan and L. K. Levando, *Vestnik. Leningrad Univ., Fiz., Khim.*, **20**, 157 (1965).

[4] J. G. Smets and F. C. De Schryver, (Agfa-Gevaert A.-G.), Ger. Offen. Pat. 1.963.731,3 Sept. 1970; *Chem. Abstr.*, **73**, 104343 (1970).

[5] V. S. Ivanov, I. P. Kopteva and L. K. Levando, U.S.S.R. Pat. 164 678, 19 Aug. 1964; *Chem. Abstr.*, **62**, 2886 (1965).

[6] F.C. De Schryver, N. Boens and J. G. Smets, *J. Polymer Sci.*, **A1**, 1687 (1972),

[7] F. C. De Schryver, W. J. Feast and J. G. Smets, *J. Polymer Sci.*, **A1**, 1939 (1970).

[8] E. Hedaya, R. L. Hinman and S Theodoropulos, *J. Org. Chem.*, **31**, 1311 (1966).

MONOMER SYNTHESIS

N,N′-Bismaleimide (Ib) was prepared according to Hedaya et al.[8] Their method was slightly modified to obtain purer products and higher yields. The Diels-Alder reaction of the maleic anhydride with furan gave the adduct (II) which treated with hydrazine led to the bisimide (III). Thermal cracking of the bisimide (III) gave N,N′-bismaleimide (Ib).

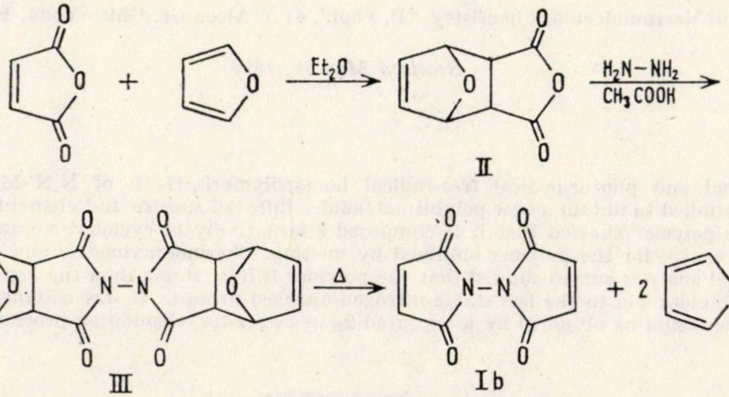

The melting points, yields and elemental analysis are summarized in Table 1.

Table 1

Monomer and intermediates

Compound	Melting Point °C	Yield %	Elemental Analyses % Calculated C	H	N	Found C	H	N
(II)	122-3	72 Lit.[9] 70	57.83	3.63	—	58.06	3.79	—
(III)	171-2 Lit.[8] 171-3	73 Lit.[8] 56	58.53	3.68	8.53	58.62	3.99	8.30
(Ib)	179−181 Lit.[8] 176-8	87	50.00	2.04	14.58	49.98	2.05	14.50

POLYMER SYNTHESIS

N,N′-Bismaleimide (Ib) was subjected to both solid and solution phase thermal and photoinduced polymerization using or not a free-radical initiator (benzoyl peroxide), under a dry nitrogen atmosphere.

---

[9] Rex E. Lidov (to Shell Development Co.), U.S. Pat. 2.733.248, 31 Jan. 1956; *Chem. Abstr.*, **50**, 13094 (1956).

All polymerization reactions — except those carried out in the melting state — led to the same structure (IV).

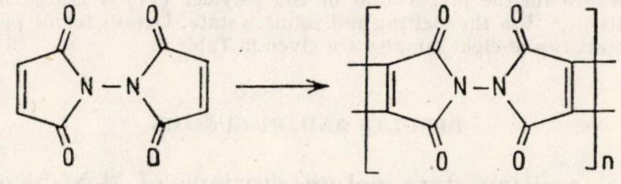

Ib IV

The results showed that the rate of the polymerization and the inherent viscosity were maximal in the photochemical process; when an initiator was used, both the rate of the polymerization and the inherent viscosity were increased. The solution and suspension phase reactions were generally accompanied by the coloration of the polymerization system.

EXPERIMENTAL

All melting points were taken in open capillaries using a GALLENKAMP melting point apparatus. The carbon, hydrogen and nitrogen microanalyses were carried out using an Elemental Analyzer Mod. 1102 CARLO ERBA. Infrared spectra were recorded on UNICAM-SP-200 Spectrophotometer, in potassium bromide pellets. A MOM-BUDAPEST Thermal Analyzer was used for the thermogravimetric and differential thermal analyses. The viscosities were measured using an Ostwaldt viscometer. The samples were irradiated with ultraviolet light using an UV-IR apparatus (220 V, AP-STAS-6048-59), the infrared rays being shielded.

MATERIALS

Commercial maleic anhydride was purified by recrystallization from chloroform. All solvents were purified just before use by the usual methods. N-Methyl-2-pyrrolidone (NMP) was purified by vacuum distillation and stored over molecular sieves.

3,6-Endoxo-1,2,3,6-tetrahydrophthalic anhydride (II). [9]

The following were introduced into a 250 ml single-necked flask fitted with a reflux condenser topped with a calcium chloride drying tube (without stirring) : 68 g (1 mole) furan, 98 g (1 mole) maleic anhydride and 200 ml anhydrous ether. The mixture was held at room temperature overnight and the resulting crystals were collected washed with cold ether and vacuum-dried. Yield 72% (II), m.p. 122—3°.

N,N'-bis (7-Oxabicyclo-2.2.1.5.-heptendicarboximide (III)[8].

The following were introduced into a 1500 ml three-necked flask fitted with a reflux condenser, a stirrer and a thermometer : 166 g (1 mole) anhydride (II) and 750 ml glacial acetic acid. 25 g (0.5 moles) 99% hydrazine hydrate was added over a period of 30 minutes with vigorous stirring, at 26°. The mixture was kept at room temperature for 1 hour and at 50—60° for an additional hour, then left at room temperature overnight. The white precipitate was filtered off, washed thoroughly with methanol and dried in vacuum for 24 hours. Yield 73% (III), m.p. 171—2°.

N,N'-Bismaleimide (Ib)[8].

The bisimide (III) (4 g, 0.0122 moles) was heated over a sand bath at 180—190°. The solid melted slowly with visible furan evolution. After 5 minutes the yellow liquid was cooled.

Recrystallization of the residue from cyclohexanone and after that from benzen gave 2 g (87% yield) of white needls, m.p. 179–181°.

Poly-N,N′-bismaleimide (IV).

The procedure for the preparation of the polymer (IV) is general for all free-radical homopolymerizations,[1-7] in the melting and solution state. Details for all polymerization reactions and characteristics of eight samples are given in Table 2.

RESULTS AND DISCUSSION

Thermal melting state polymerizations of N,N′-bismaleimide (Ib) were carried out at a little higher temperature than its melting point. Light brown, insoluble, infusible, transparent polymers were obtained. These polymers were identified as polyimides by means of infrared spectroscopy (Fig. 1) and elemental analysis (Table 2). Photochemical polymerizations of N,N′-bismaleimide, in acetone suspension, carried out at 100° for 72 hours, gave a brown amorphous product. All the polymers were insoluble in usual organic solvents and acids, partially soluble in hot concentrated sulphuric acid. This insolubility pleads for a mechanism leading to crosslinkages due to the relative easiness of the maleimides to undergo vinyl polymerization.[10,11] The infrared spectra of different polymer samples (Fig. 1, curves 1, 2, 5,6) often show traces of unsaturation absorptions at 1565 and 3050 cm^{-1}.

Our investigations were directed towards the solution phase polymerization reactions which were carried out thermally and photochemically using or not a free-radical initiator.

Thermal and photochemical polymerization of N,N′-bismaleimide (Ib), carried out by the solution technique in NMP, led to a brown powder. All the products were completely soluble in the following solvents : dimethylformamide, dimethylsulfoxide, NMP, dimethylacetamide. On account of their solubility in the above-mentioned solvents, we could assume that the crosslinkages was very low.

On the other hand, since under our experimental conditions all light energy was absorbed by acetophenone sensitizer — in the photoinduced polymerizations — it was assumed that the reaction proceeds by way of the attack of the acetophenone triplet on a maleimide unit in its ground state[4]. The same assumption has been made for the thermal energy, in the thermal polymerization reactions using an initiator.

The infrared spectra[15] provided further support for the assigned structure (IV). A typical spectrum (Fig. 1, curves 3, 4, 7,8) showed characteristic broad peaks of a polymeric material; in addition, the comparison with the monomer spectrum[8] (Fig. 1, curve 0) showed that the double-bond C=C stretching frequencies at 1570 and 3100 cm^{-1} have disappeared and the antisymmetric and symmetric stretching frequencies of the imide system at 1739 and 1870 cm^{-1} (shoulder) respectively, have remained.

---

[10] Y. Nakayama and J. G. Smets, *J. Polymer Sci.*, **A1**, 1619 (1967).

[11] M. Yamada, I. Takasa and N. Koutou, *J. Polymer Sci.*, (B), **6**, 883 (1968).

Table 2

The reaction conditions and the characteristics of poly-N'N'-bismaleimide

Method		Reaction conditions	Yield %	Colour	$[\eta]$ inh	Elemental Analyses[c]		
						Found %		
Phase	Initiator					C	H	N
A. Thermal polymerization								
solid	none	182°, 30 min. 185°, 30 min. 190°, 5 min.	—	light brown, transparent	0.08[b]	50.49	2.22	13.85
solid	benzoyl peroxide[d]	182°, 30 min. 185°, 30 min. 190°, 5 min.	—	dark brown, amorphous	0.12[b]	49.52	2.11	13.78
NMP solution	none	100°, 72 h.	46[f]	bright brown[e]	0.28[g]	50.40	2.09	14.02
NMP solution	benzoyl[a] peroxide	100°, 72 h.	58[f]	bright brown[e]	0.60[g]	50.88	2.27	13.88
B. Photoinduced polymerization								
solid	none	acetone suspension, 0.02 moles acetophenone, 100°, 72 h.	18[a]	brown amorphous	0.18[b]	50.42	2.56	13.47
solid	benzoyl peroxide[d]	acetone suspension, 0.02 moles acetophenone, 100°, 72 h.	30[a]	brown amorphous	0.21[b]	49.68	2.31	13.91
NMP solution	none	0.02 moles acetophenone 100°, 40 h.	60[f]	bright brown[e]	0.25[g]	50.17	2.13	13.98
NMP solution	benzoyl peroxide[d]	0.02 moles acetophenone 100°, 40 h.	69[f]	briwht brown[e]	0.35[g]	49.76	1.94	14.22

a. Samples were several times methanol washed; b. In sulfuric acid at 20°, conc. = 0.5%; c. Calculated for $C_8H_4N_2O_4$°: C = 50%, H = 2.04%, N = 14.58%; d. 0.004 g for 0.01 moles monomer; e. Polymer colour after drying at 150° for 16 h.; f. Samples were precipitated with ether and dried at 150° for 16 h.; g. In NMP at 20°, conc. = 0.5%.

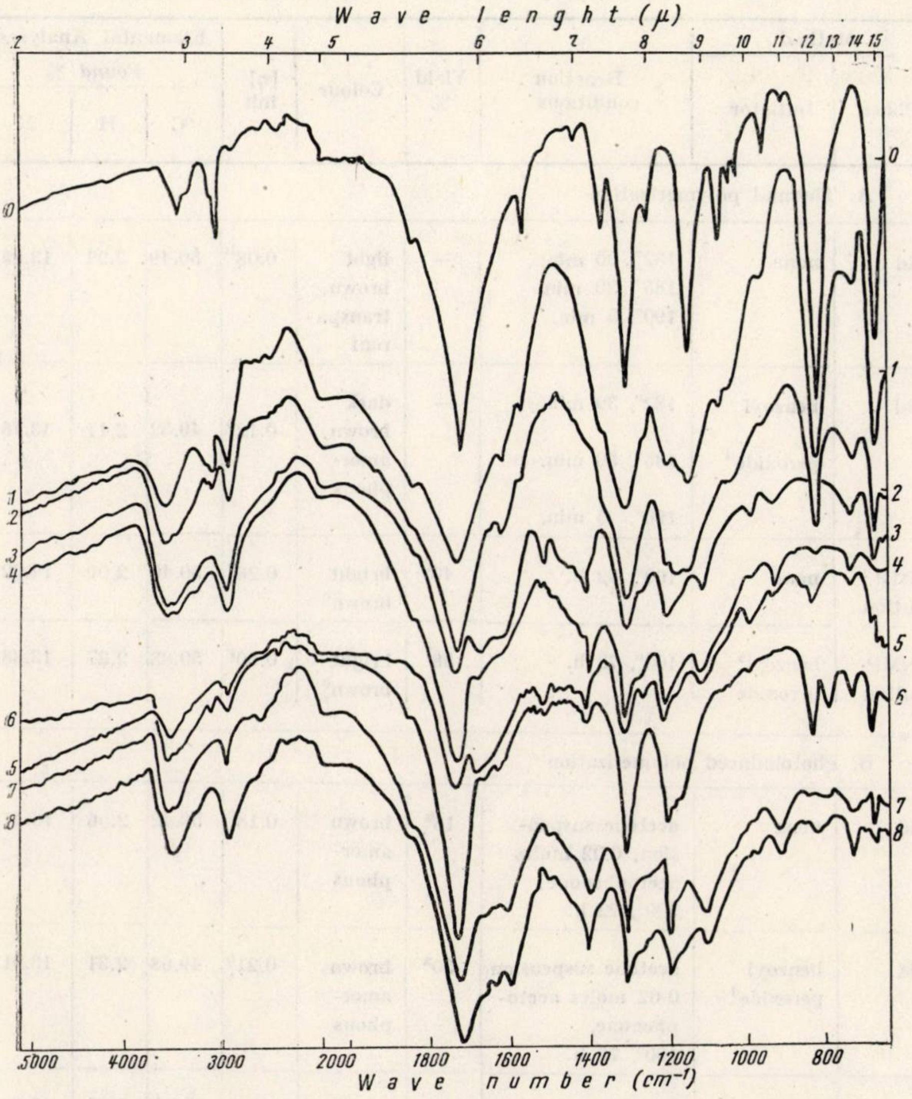

Fig. 1. — Infrared spectra of the monomer and poly-N,N′-bismaleimide : O : N,N′-bismaleimide ; 1 : polymer obtained by thermal polymerization in the melting state without initiator ; 2 : polymer obtained by thermal polymerization in the melting state using an initiator ; 3 : polymer obtained by thermal polymerization in NMP solution without initiator ; 4 : polymer obtained by thermal polymerization in NMP solution using an initiator ; 5 : polymer obtained by photoirradiation in the suspension phase without initiator ; 6 : polymer obtained by photoirradiation in the suspension phase using an initiator ; 7 : polymer obtained by photoirradiation in NMP solution without initiator ; 8 : polymer obtained by photoirradiation in NMP solution using an initiator.

On the other hand, the appearance of other new peaks at about 2910 cm^{-1} (CH), 933, 1000 and 1200 cm^{-1} (cyclobutane ring)[12] indicated that the polymerization reactions have taken place.

Since the four spectra (Fig. 1, cuves 3, 4, 7,8) were nearly identical, it was assumed that benzoyl peroxide acted as initiator.

In general, the absorption peaks of poly-N,N'-bismaleimide were lower compared to the corresponding peaks of the monomer (Fig. 1).

When the reactions were performed using a free-radical initiator, a high molecular polyimide was obtained. Figures 2 and 3 show the rate of the thermal and photochemical homopolymerization of N,N'-bismaleimide (Ib), in terms of the inherent viscosity of the polymer. The absence of the initiator led to low inherent viscosity. The photoirradiation accelerated the polymerization (Fig. 2 and 3).

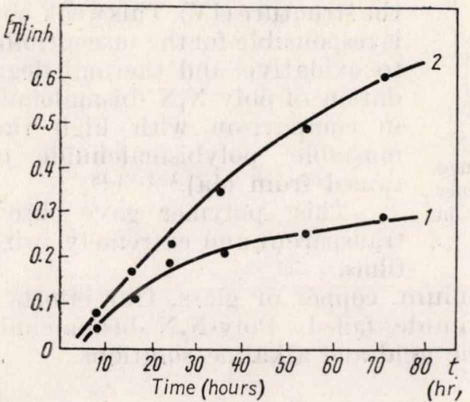

Fig. 2. — Inherent viscosity variations depending on the time of the thermal polymerization in NMP: 1-without initiator; 2-using an initiator.

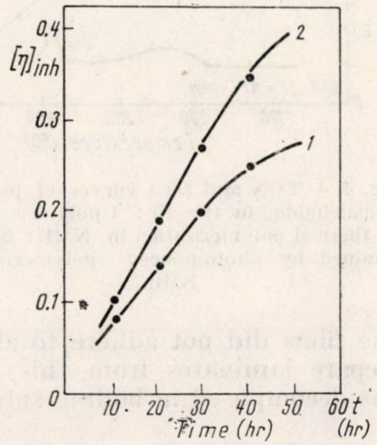

Fig. 3 — Inherent viscosity variations depending on the irradiation-time of the photoinduced polymerization in NMP: 1-without initiator; 2-using an initiator.

The thermal stability of the polymer was evaluated by the differential thermal analysis (DTA) and the thermogravimetric analysis (TGA), in the air. The DTA and TGA curves of the poly-N,N'-bismaleimide are given in Figure 4. DTA curve of the polymer obtained by the thermal polymerization in NMP, showed two characteristic exothermal peaks at about 200° (broad and low) and 395° (sharp); the first one correlated well with the first weight loss temperature in TGA curve, but the second corresponded to the total degradation of the polymer. This is indicative of a rather severe susceptibility to oxidative and thermal degradation a little below 200°. Poly-N,N'-bismaleimide obtained by the photoinduced polymerization in NMP, showed only a very low broad peak at about 200°. Decomposition temperature of both thermal and photochemical polymers, determined by TGA, were around 200°.

---

[12] Y. Lord and N. Nakagawa, *J. Chem. Phys.*, **39**, 2951 (1963).

It may be concluded from the results that the thermal stability of poly-N,N′-bismaleimide reported in this paper is nearly comparable to that of a melamine-cured polyacrylate with five different polyether-based polyurethanes[13] or other low thermal stability polymers (Fig. 4).

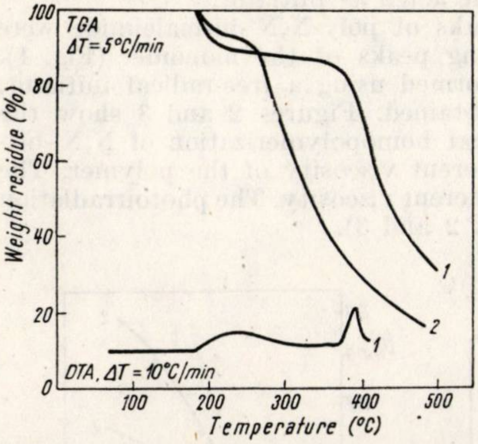

Fig. 4. — TGA and DTA curves of poly-N,N′-bismaleimide, in the air: 1-polymer obtained by thermal polymerization in NMP; 2-polymer obtained by photoinduced polymerization in NMP.

The polymer chain is made up of bissuccinimide units linked by cyclobutane rings. Since the repeating unit is symmetrical, no possibility exists for stereoisomerism.

Poly-N,N′-bismaleimide contains a nitrogen-nitrogen single-bond linking the two imide rings in the backbone as it is shown in the structure (IV). This weak bond is responsible for the susceptibility to oxidative and thermal degradation of poly-N,N′-bismaleimide in comparison with high thermostable polybismaleimide obtained from (Ia).[1-7,14,15]

This polymer gave brown transparent and extremely brittle films. The films did not adhere to aluminium, copper or glass. Our efforts to prepare laminates from this polyimide failed. Poly-N,N′-bismaleimide was decomposed in boiling sulphuric acid and alkaline solutions.

CONCLUSIONS

The thermal and photoinduced polycycloaddition of N,N′-bismaleimide led to a new polyimide. This reaction can be used in the synthesis of polymers containing cyclobutane units which are difficult to obtain by the usual polymerization techniques. N,N′-Bismaleimide showed the highest reactivity when it was polymerized by the solution phase photoirradiation. When a sensitizer was used a higher polymerization rate was observed.

ACKNOWLEDGEMNT. The authors are deeply indebted to Mr. Gh. Stoica, Mrs. M. Tumurug and Mrs. V. Grădinaru for the elemental analyses, to Mrs. C. Bernic for the spectral data and to Mrs. Z. Ciobanu for the thermogravimetric and differential thermal analyses.

---

[13] K. C. Frisch, D. Klempner and S. Migdal, *J. Polymer Sci., Polymer Chem. Ed.*, **12**, 885 (1974).

[14] J. Put and F. C. De Schryver, *J. Amer. Chem. Soc.*, **95**, 137 (1973).

[15] P. Bassignana, C. Cogrossi, G. P. Mattiot and M. Gillio-Tos, *Spectrochim. Acta*, **18**, 809 (1962).

Revue Roumaine de Chimie, 23, 1, 119–123 (1978)

INTERACTION BETWEEN CHLOROMETHYLATED STYRENE–DIVINYLBENZENE AND DIMETHYLFORMAMIDE

I. PETRARIU and EUGENIA BĂRBÎNȚĂ
"Petru Poni" Institute of Macromolecular Chemistry, Iassy, Aleea Gr. Ghica Vodă 41 A

Received May 16, 1974
Completed May 4, 1976

Studies were made on the addition reaction of dimethylamine, resulted from dimethylformamide decomposition, to a chloromethylated styrene—divinylbenzene gel copolymer, leading to the obtainment of a weakly basic anion exchanger. The physico-chemical characteristics of the weakly basic anion exchanger were estimated by exchange capacity and thermal analysis.

Amination of chloromethylated styrene-divinylbenzene copolymers (Co—CM) in view of obtaining anion-exchangers takes usually place either with primary, secondary or tertiary amines or with diamines or polyamines or even with aminoalcohols or tertiary aminothioalcohols.

In view of amination, Co-CM is previously swollen in an adequate solvent (dioxane, 1,2-dichloroethane, dimethylformamide, acetone, benzene, etc.) adding amine thereafter and conducting the reaction between 25–150° for 5–48 hrs.

The literature data indicate the use of dimethylformamide (DMF) either as a catalytic agent in a series of reactions such as substitution,[1–4] elimination,[5–7] cyclization,[8] polymerization,[9] etc., or as a reactant in synthesis of aldehydes,[10] nitriles,[11] heterocyclic compounds[12–13] etc.

[1] G. C. Finger and C. W. Kruse, *J. Amer. Chem. Soc.*, **78,** 6034 (1956).
[2] F. J. Marshall and W. N. Cannon, *J. Org. Chem.*, **1956,** 245.
[3] H. B. Donahoe, R. J. Seiwald, M. M. C. Neuman and K. K Kimura, *J. Org. Chem.*, **1957,** 68.
[4] M. S. Newman and S. Otsuka, *J. Org. Chem.*, **1958,** 797.
[5] E. C. Taylor jr. and A. E. Martin, *J. Amer. Chem. Soc.*, **74,** 6295 (1952).
[6] C. S. Harvel and M. M. Martin, *J. Amer. Chem. Soc.*, **80,** 6600 (1958).
[7] K. D. Gundermann and R. Thomas, *Chem. Ber.*, **92,** 1503 (1959).
[8] N. W. Gabel and S. B. Binkley, *J. Org. Chem.*, **1958,** 643.
[9] C. H. Bamford, A. D. Jenkins and R. Johnston, *Proc. Roy. Soc.*, **239A,** 214 (1957).
[10] Z. Arnold, *Coll. Czech. Chem. Comm.*, **25,** 1313 (1960).
[11] Z. Arnold, *Coll. Czech. Chem. Comm.*, **26,** 1113 (1961).
[12] H. Gold, *Angew. Chem.*, **72,** 956 (1960).
[13] L. Joseph and A. H. Albert, *J. Heterocyclic Chem.*, **3,** 107 (1966).

Mention is also made of DMF interaction with aromatic isocyanates,[14–16] benzene derivatives possessing various functional groups[17–19] alkyl, acid chlorides or anhydrides,[20] etc.

It is known that at 150°, in the presence of HCl or of bases DMF starts decomposing into dimethylamine and carbon oxide.[17,21] This fact must be considered in the amination of chloromethylated copolymers with various amines with a high boiling point which enables the amination reaction to be conducted in DMF at a temperature of over 120°.

In the case in which one aims at obtaining a monofunctional basic polyelectrolyte, the use of DMF as reaction medium should be avoided since dimethylamine resulted from decomposition will also participate in the reaction in addition to the added amine, leading to a polyfunctional basic polyelectrolyte.

Since no references have been made in the literature concerning the interaction between Co-CM and DMF, the present paper undertakes to provide some clarifications on this reaction monitoring the manner in which dimethylamine resulted from DMF decomposition participates in the reaction forming a weakly basic anion exchanger.

MATERIALS AND METHODS

– Styrene copolymerization with 8 % divinylbenzene took place in suspension.[22]

After copolymerization, the resulted beads were washed with water and passed through a sieve in a wet state, the fraction included between 0.4–0.8 mm being retained.

– Monochlorodimethylether (MCDE) was redistilled prior to use (b.p. = 58 – 60°, $n_D^{25} = 1.3949$ and $\rho_{25} = 1.062$).

– Zinc chloride was dehydrated by melting prior to use.

– N,N-dimethylformamide (DMF) was purified by passing through molecular sieves[16] (b.p.$_{760\ mm}$ = 153° and $\rho_{25} = 0.9445$).

– Chloromethylation of styrene-divinylbenzene copolymer was performed with MCDE in presence of $ZnCl_2$.[23].

The chloromethylated copolymer had a 21.0 % Cl content which corresponds to a 90.4% conversion degree.

The Co-CM amination reaction with DMF was conducted in a 3-neck flask fitted with a stirrer, reflux cooler and a thermometer according to optimum stability conditions described in the section of results and discussion.

Co-CM was slowly stirred for 5–168 hrs at 153° in DMF in a gravimetric ratio Co-CM/DMF = 1/20. After the completion of the reaction, anionite beads were placed on a filtration funnel, they were washed with a 4 % HCl solution and allowed to stand in HCl for 24 hrs. Then anionite was converted into OH form by treating with a 4% NaOH solution and was eventually washed with acetone in a filtering plate-containing column, and then with distilled water until total disappearance of OH^- ion. The nitrogen content in the basic exchanger obtained in this way varies depending on the reaction conditions between 3.15–5.26 %, which corresponds to an exchange capacity ranging between 2.08–3.48 mech/g.

---

[14] K. Thinius and L. Hintzenstern, *Plast. und Kautchuk*, **1**, 375 (1959).

[15] M. L. Weiner, *J. Org. Chem.*, **1969**, 2245.

[16] L. I. Kopusov and V. V. Zharkov, *Sintez i Fiz. Khim. Polimerov.* **8**, 58 (1971).

[17] E. Felstead, H. C. Fielding and B. J. Wakefied, *J. Chem. Soc. (C)*, **1966**, 708.

[18] R. S. Asquith, W. M. Lord, A. T. Peters and F. Wallace, *J. Chem. Soc. (C)*, **1966**, 95.

[19] J. M. Birchall, R. N. Huszoldine and J. O. Morley, *J. Chem. Soc. (C)*, **1970**, 456.

[20] G. M. Coppinger, *J. Amer. Chem. Soc.*, **76**, 1372 (1954).

[21] A. B. Thomas and E. G. Rochow, *J. Amer. Chem. Soc.*, **79**, 1843 (1957).

[22] I. Petrariu and J. Stamberg, *Coll. Czech. Chem. Comm.*, **32**, 798 (1957).

[23] A. Carpov, D. Drăgan and I. Petrariu, *Rev. Roumaine Chim.*, **17**, 1923 (1972).

The total exchange capacity was determined according to Stamberg.[24]

IR spectra of the obtained samples of anion exchangers were recorded on a SP Unicam spectrophotometer applying KBr method.

The thermal stability was estimated using the thermogravimetric and the thermodifferential analysis by means of a Paulik and Erdey derivatograph in the presence of air with a 9,8°/min heating rate.

Nitrogen analyses were performed according to Kjeldahl.

RESULTS AND DISCUSSION

Since the chloromethylated styrene-divinylbenzene copolymer is sufficiently reactive, it was used as a support to bind dimethylamine resulted from the DMF splitting reaction.

Schematically, the reactions may be represented as follows :

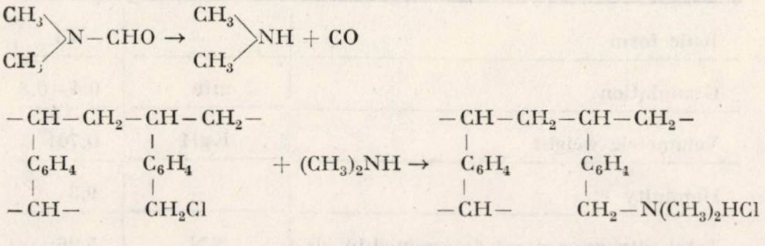

$$(CH_3)_2N-CHO \rightarrow (CH_3)_2NH + CO$$

Since the heating duration of DMF at 153° plays an important role in its decomposition, a series of experiments were made in which Co-CM was heated together with DMF at various reaction intervals.

Table 1 presents data referring to the amination degree of Co-CM with dimethylamine resulted from DMF decomposition. It is observed that as the DMF heating time increases the amount of dimethylamine released from its decomposition increases and consequently the nitrogen content in Co-CM and aminate reaches higher values.

Table 1

Amination of Co-CM with DMF, depending on reaction duration. Conditions of reaction : gravimetric ratio Co-CM/DMF = 1/20 ; the reaction temperature = 153°.

Duration of reaction hrs	N %	Total exchange capacity calculated from the nitrogen content (mech/g)	Exchange capacity determined experimentally (mech/g)
5	3.15	2.25	2.08
12	3.32	2.37	2.19
24	3.77	2.69	2.56
72	4.55	3.25	3.14
168	5.26	3.75	3.48

---

[24] J. Stamberg and F. Yurachika, *Zhur. priklad. Khim.*, **35**, 2295 (1962).

By calculating the theoretical exchange capacities in the nitrogen content determined from the elementary analysis and by comparing these values to the exchange capacities experimentally determined by column dynamic method, one finds a good agreement.

The weakly basic anion exchanger obtained under optimum conditions in this manner was analyzed and the basic physicochemical characteristics are given in table 2.

Table 2 .

Physico-chemical characteristics of the weakly basic anion exchanger obtained by reaction of Co-CM with dimethylamine resulted from the degradation

Characteristics	Unity of measurement	Value
Ionic form	—	Cl
Granulation	mm	0.4—0.8
Volumetric weight	Kg/1	0.701
Humidity %	—	9.3
Total nitrogen content determined by elementaly analysis	%N	5.26
Total exchange capacity (calculated by nitrogen content)	mech/g	3.75
Total exchange capacity experimentally determined	mech/g	3.48

From the analysis of data presented in this table results that it is possible to obtain in this way a weakly basic anion exchanger with a rather high exchange capacity (3.48 mech/g), after a sufficiently long reaction time (168 hrs).

As to thermal stability of this resulted anionite, fig. 1 shows that the weight losses of samples undergoing a thermal treatment fail to present essential differences even though they have a different nitrogen content. All samples are stable up to 50°. The thermogravimetric and thermodifferential analysis carried out in air atmosphere with rate of heating 9°/min. on the anionite whose characteristics were revealed in table 2 and is given in figure 2.

CONCLUSIONS

1. Studies were made on the addition reaction of dimethylamine to Co-CM resulted from dimethylformamide decomposition.

2. Physico-chemical characteristics of the weakly basic anion exchanger obtained in this way were determined.

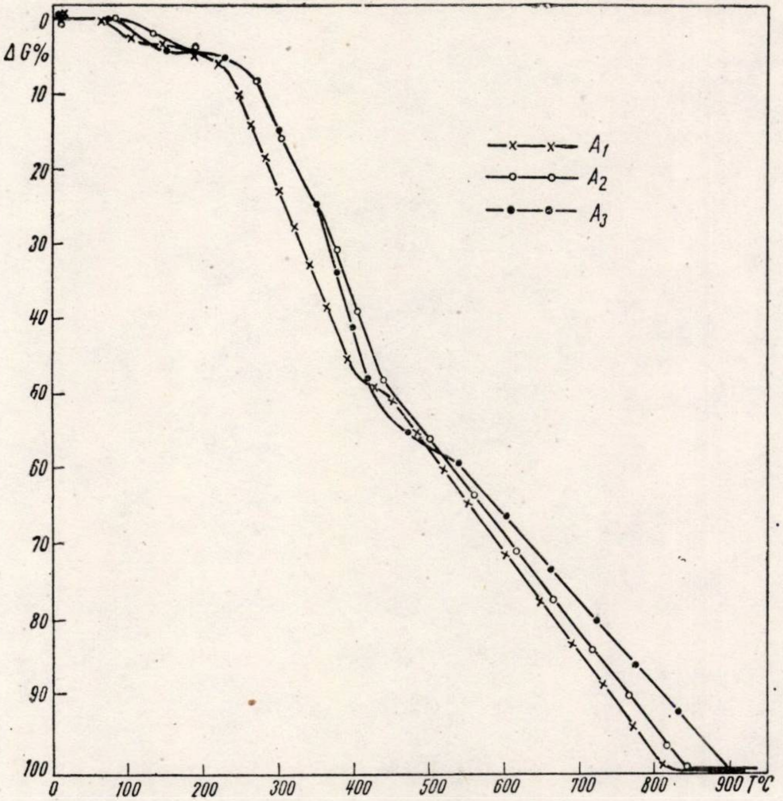

Fig. 1. — The thermogravimetric curves in air atmosphere, heating rate 9°/min. of some weakly basic anion exchangers with variable nitrogen content.

$A_1 = 5.26\%N$; $A_2 = 4.55\%N$; $A_3 = 3.77\%N$.

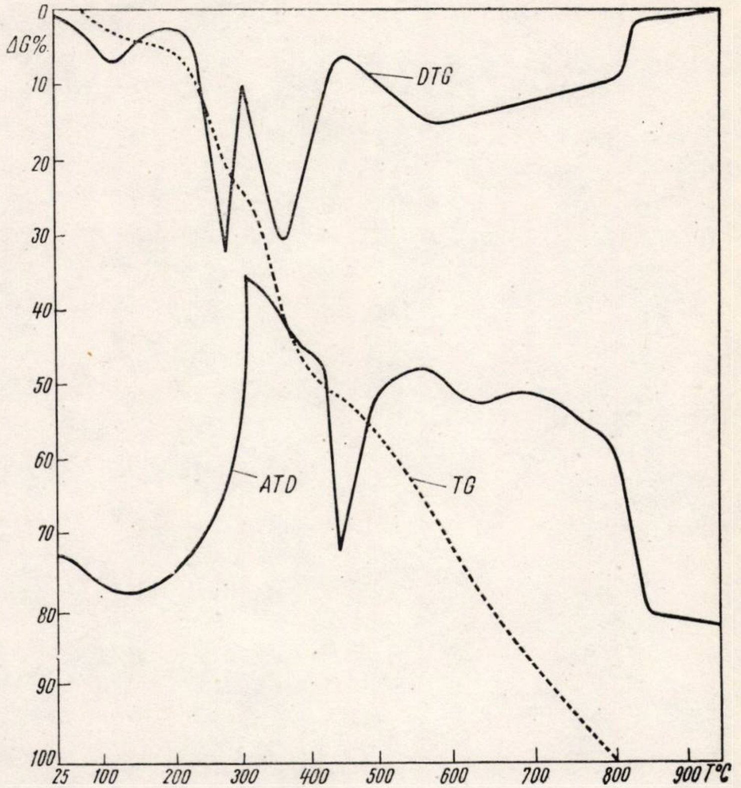

Fig. 2. — Thermal decomposition of a weakly basic anion exchanger obtained by the reaction of Co-CM and dimethylamine resulted from the degradation of dimethylformamide.

Revue Roumaine de Chimie, **23**, *1*, 125 – 131 (1978)

OPTIMIZATION OF THE SEPARATION PROCESS IN TEMPERATURE GRADIENT CHROMATOGRAPHY.II[1]

DETERMINATION OF THE MINIMUM CHROMATOGRAPHING TIME NECESSARY FOR THE SEPARATION OF SOME COMPONENT MIXTURES BY APPLYING A CONSTANT TEMPERATURE GRADIENT

C. LITEANU and T. HODIŞAN
Department of Analytical Chemistry, University of Cluj-Napoca, str. Arany János nr. 11, Cluj-Napoca

Received July 18, 1975

The paper introduces a method for the optimization of thin-layer chromatographic separations with a temperature gradient, in relation to the chromatographing time. A mathematical relation resolution-time enables the calculation of the necessary time for obtaining an optimum resolution between the pairs of adjacent zones so that the separation of the global mixture be quantitatively achieved. The resolution obtained in the case of the temperature gradient is higher than the theoretical one, due to the flattening of zones during the chromatographic process.

A first aspect referring to the optimization of the separation process in thin-layer chromatography temperature gradient is to determine a quantitative relation which should reflect the resolution variation when working with different values of the temperature gradient.[1] Therefore while working with different temperature gradients, the point was to determine the value of the gradient for which one obtains an optimum resolution.

Another aspect that will be approached in this paper, relates to the developing time which is also a basic parameter of optimization. In this sense, an equation was deduced which illustrates the dependence between the R_f values of the components under study and their resolution.

As it is known, $R_s = \Delta z/4\sigma$, Δz being the difference between the position of the peaks in the densitogram of the two components and σ-the standard deviation of zones. Δz is a magnitude measured on the densitogram, yet it may be expressed by an equation in the form :

$$\Delta z \simeq \Delta R_f \cdot h_e \tag{1}$$

in which ΔR_f is the difference between the R_f values of the two components and h_e – the height reached by the eluent front.

---

[1] Part I: T. Hodişan and C. Liteanu, *Rev. Roumaine Chim.*, **22**, 1539 (1977).

Equation (1) is only approximate for the following reasons : R_f values are always measured in the centre of zones, but the maximum concentration inducing the peak of the densitogram may not be assigned to the very centre of the zone, particularly in the case of components whose concentration has an asymmetrical zone distribution. In such a case it is obvious that $\Delta z \neq \Delta R_f \cdot h_e$.

The second reason which is far more important relates to the zone shape. It has been experimentally found[2] that in temperature gradient chromatography, the zone shape changes with the gradient increase passing from circular to elliptical with the small axis oriented towards migration. Nevertheless the same change in the zone shape may also occur in a constant gradient in parallel with the increase of the chromatographing time. Zones become narrower and narrower tending to be distributed under the form of a line, for a sufficiently long chromatographing time. The decrease of the zone standard deviation with the *chromatographing time* for three aminoacids is exhibited in Fig. 1.

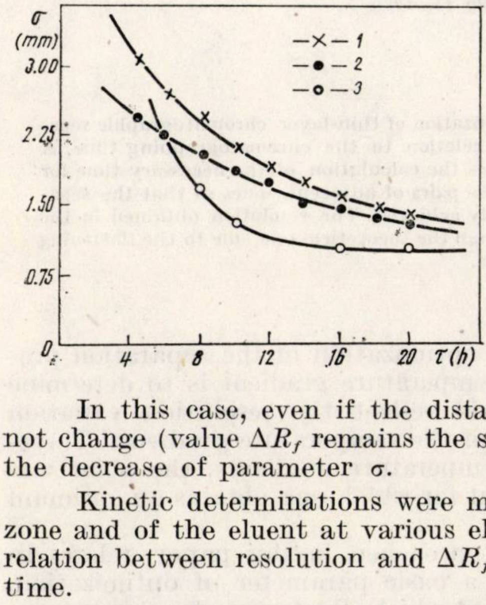

Fig. 1. — Variation of the standard deviation σ of three aminoacids : (1) alanine, (2) glutamic acid and (3) glutamine with the chromatographing time, at grad.t. = const. = 1.07°C/cm. Support, microcrystalline cellulose, eluent, the organic phase of the mixture : n-butanol-acetic acid-water (40 :10 : 50, v/v).

In this case, even if the distance between the zone centres does not change (value ΔR_f remains the same) the resolution increases due to the decrease of parameter σ.

Kinetic determinations were made with regard to the shift of the zone and of the eluent at various elution times, in order to establish a relation between resolution and ΔR_f, respectively the chromatographing time.

It was shown[3] that in temperature gradient chromatography, the zone migration takes place according to an equation in the form :

$$h_z = b\,\tau^m \qquad (2)$$

In log form one obtains :

$$\log h_z = \log b + m \log \tau \qquad (3)$$

---

[2] T. Hodişan, S. Bândeanu and C. Liteanu, *Stud. Univ. Babeş-Bolyai*, Chem., (2) **17,** 119 (1972).

[3] S. Gocan and C. Liteanu, *Bull. Soc. chim. France*, **1969,** 1409.

The ascending speed of the eluent in the temperature gradient chromatography is described[3] by an equation having the form:

$$h_e = \frac{\tau}{A + B\tau} \tag{4}$$

or

$$1/h_e = B + A.1/\tau \tag{5}$$

By replacing magnitudes h_z and h_e given by equations (2) and (4), respectively in the retention expression: $R_f = h_z/h_e$, one obtains[3]:

$$R_f = b(A\,\tau^{m-1} + B\,\tau^{m}) \tag{6}$$

which, for two components, may be written:

$$R_{f_1} = b_1(A\,\tau^{m_1-1} + B\,\tau^{m_1}) \tag{7}$$

and respectively:

$$R_{f_2} = b_2(A\,\tau^{m_2-1} + B\,\tau^{m_2}) \tag{8}$$

Knowing that $R_s = \Delta z/4\,\sigma$ and considering both relation (1) and the fact that, as illustrated in figure 1, the standard deviation varies with the developing time, one may write:

$$R_s = \frac{h_e \times \Delta\, R_f}{4\,\sigma} = \frac{h_e\,[b_1(A\,\tau^{m_1-1} + B\,\tau^{m_1}) - b_2(A\,\tau^{m_2-1} + B\,\tau^{m_2})]}{2(\sigma_1 + \sigma_2)} \tag{9}$$

By replacing the constants in this equation for each mixture and by conditioning that $R_s = 1.0$, one may determine the value of the chromatographing time τ at which the chromatographic process should be discontinued.

The validity of these equations will be verified below for two amino-acid mixtures formed of alanine-glutamic acid and alanine-glutamine.

The results concerning the variation of R_f values and of the resolution, respectively, for the two mixtures are listed in Figs. 2 and 3 which show that the resolution of the components of each mixture rises with the chromatographing time, reaching a maximum value precisely when the component with the higher R_f reaches the eluent front.

Figs. 4 and 5 respectively illustrate the ascending height of the zone given by equation (2) for the components of the two amino acid mixtures.

The linearization of these curves (equation 3) is plotted in Figs. 6 and 7 respectively, for the components of the two mixtures. The resulted

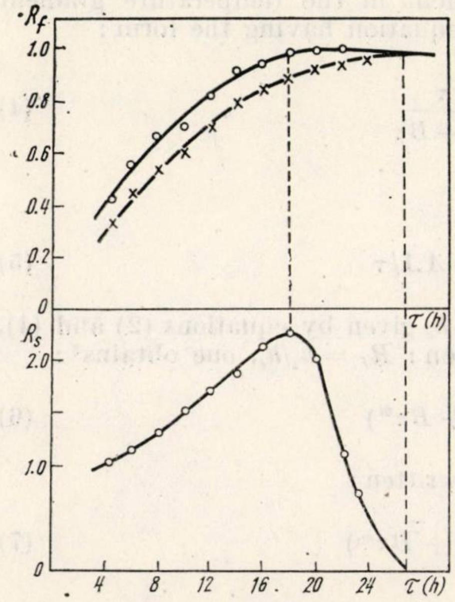

Fig. 2. — Variation of R_f values and of the resolution of the mixture alanine-glutamic acid with the chromatographing time, at a grad. t = const. = 1.07°C/cm. The support and the eluent are identical to those in Fig. 1.

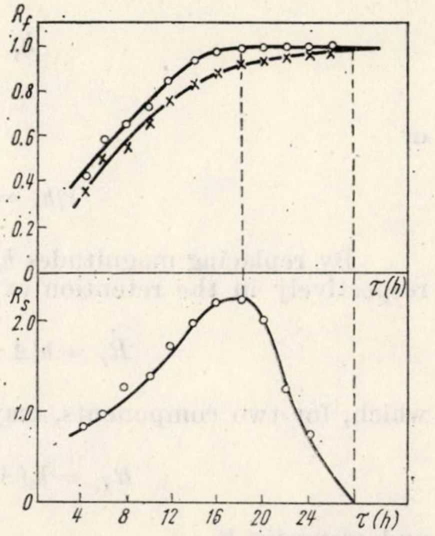

Fig. 3. — Variation of R_f values and of the resolution of the alanine-glutamine mixture with the chromatographing time at a grad. t = 1.07°C/cm. The support and the eluent are identical to those in Fig. 1.

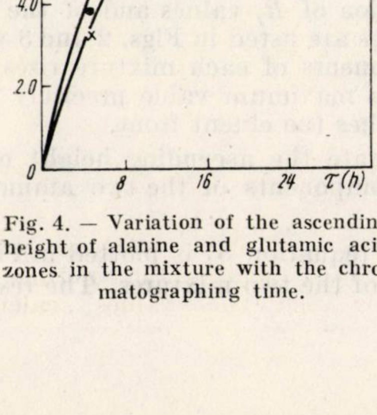

Fig. 4. — Variation of the ascending height of alanine and glutamic acid zones in the mixture with the chromatographing time.

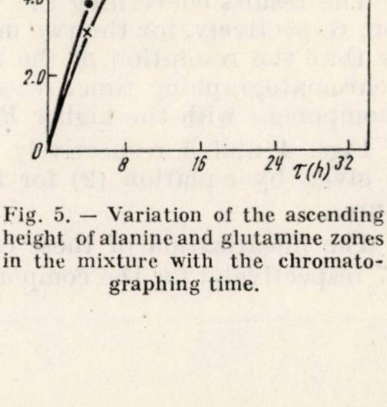

Fig. 5. — Variation of the ascending height of alanine and glutamine zones in the mixture with the chromatographing time.

straight lines were used to determine constants b and m for each mixture. Constants A and B of equation (5) are determined from the kinetics of the eluent's migration by plot $1/h_e = f(1/\tau)$ (Fig. 8).

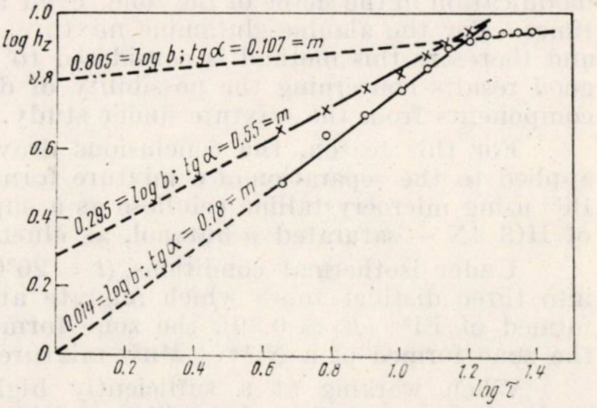

Fig. 6. — Linearized plot of eqn. (2) under the form of eqn (3) for alanine and glutamic acid.

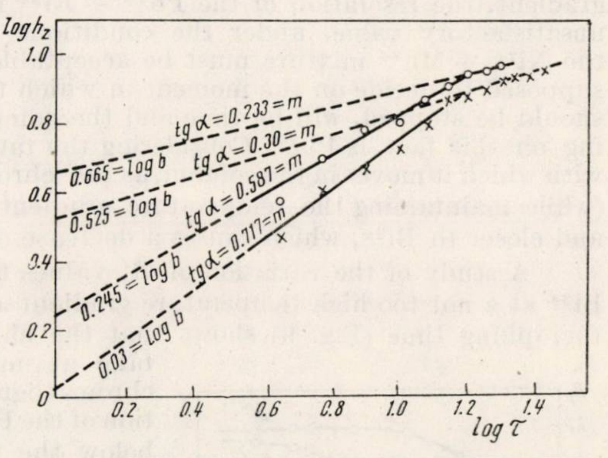

Fig. 7. — The same plot of Fig. 6 for the alanine-glutamine mixture.

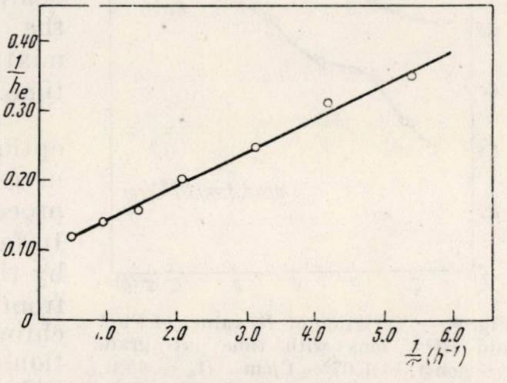

Fig. 8. — Variation of the reciprocal value of the ascending height of the eluent ($1/h_e$) as a function of $1/\tau$.

By replacing constants : b, m, A and B for each system in equation (9) one may determine that value of the chromatographing time τ for which $R_s = 1.0$. The consistence between the values calculated in this manner and those obtained from the zone densitograms in general is satisfactory. Certain differences appearing may be explained by the asymmetrical distribution of the components concentration and by the modification in the shape of the zone, even at reduced chromatographing times.[2] For the alanine-glutamine mixture, the agreement is very good and therefore this method is considered to yield, in general, sufficiently good results concerning the possibility of determining the resolution of components from the mixture under study.

For this reason, the conclusions drawn in this paper have been applied to the separation of a mixture formed of Ni^{2+}, Mn^{2+}, Pb^{2+} and Bi^{3+} using microcrystalline celullose as a support and a mixture formed of HCl 4N — saturated *n*-butanol, as eluent.

Under isothermal conditions ($t = 20°C$) the mixture is separated into three distinct zones which migrate at different speeds: the zone formed of Bi^{3+} ($R_f \simeq 0.80$), the zone formed of Pb^{2+} ($R_f \simeq 0.40$) and the zone formed of a $Ni^{2+} + Mn^{2+}$ mixture ($R_f \simeq 0.25$).

When working at a sufficiently high value of the temperature gradient, the resolution of the $Pb^{2+} + Bi^{3+}$ mixture risks to drop to an unsatisfactory value, under the conditions in which the resolution of the $Ni^{2+} + Mn^{2+}$ mixture must be acceptable. In this case, the variable supposed to decide on the moment in which the chromatographic process should be stopped, will be time and the component of the mixture deciding on this fact, is Pb^{2+}. Considering the rather high value of the speed with which it moves in the column, as the chromatographic time, increases (while maintaining the temperature gradient constant), Pb^{2+} gets closer and closer to Bi^{3+}, which causes a decrease of the resolution.

A study of the variation of R_f values for the individual ions Pb^{2+}, Bi^{3+} at a not too high temperature gradient as a function of the chromatographing time (Fig. 9) shows that the chromatographic process may take at most 10 hours; for longer chromatographing times, the resolution of the $Pb^{2+} + Bi^{3+}$ mixture decreases below the acceptable value whereas the resolution of the $Ni^{2+} + Mn^{2+}$ mixture increases with the developing time.

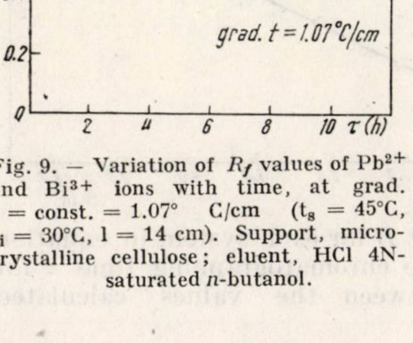

Fig. 9. — Variation of R_f values of Pb^{2+} and Bi^{3+} ions with time, at grad. t = const. = 1.07° C/cm ($t_s = 45°C$, $t_i = 30°C$, l = 14 cm). Support, microcrystalline cellulose; eluent, HCl 4N-saturated *n*-butanol.

Figure 9 shows that in order to optimize the separation process also in relation to time, chromatographic process may be stopped after 9 hours. In fact this value has also been obtained by the previously described method, from R_f values obtained with different chromatographing times. The condition was that the resolution of the $Pb^{2+} + Bi^{3+}$ mixture be equal to unity, while assuming an arbitrary value for the standard deviation of zones.

By conducting the chromatographic process at the same value of the temperature gradient (1.07°C/cm) for 9 hours, both mixtures were quantitatively separated having a very good resolution ($R_s = 1.32$ for $Ni^{2+} + Mn^{2+}$ and $R_s = 1.50$ for $Pb^{2+} + Bi^{3+}$).

The aspect of completely separated zones is exhibited in Fig. 10.

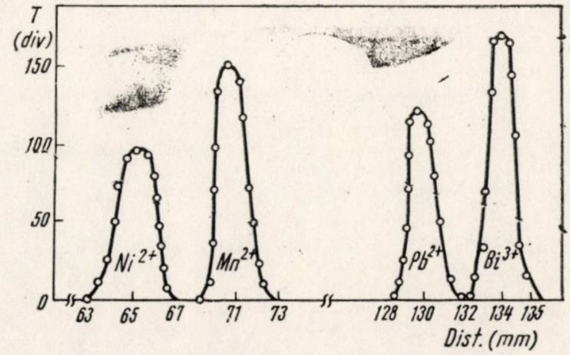

Fig. 10. — Aspect of the zones of the global mixture after a 9 hours'chromatographing time.

The fact of obtaining for the $Pb^{2+} + Bi^{3+}$ mixture a higher resolution than that imposed by eqn. (9) is explained by the modification of the shape of the zone under the conditions of the temperature gradient. At the end of the chromatographic process, the Bi^{3+} zone appears as a very flattened ellipse. In fact, in most cases the experimentally obtained resolution will outweigh that resulted from eqn. (9).

Revue Roumaine de Chimie, 23, 1, 133–135 (1978)

TRENNUNG EINIGER POLYPHENOLE DURCH DÜNNSCHICHTCHROMATOGRAPHIE MIT ORTHOGONALEM TEMPERATURGRADIENT

S. GOCAN, C. KONNERT und H. VOIK
Lehrstuhl für analytische Chemie der Universität ,,Babeş-Bolyai'',
Str. Arany János Nr. 11, Cluj-Napoca, Rumänien

Eingegangen am 1. August 1975

Es werden die Vorteile der Anwendung des orthogonalen Temperaturgradienten an einer S-Kammer bei der Trennung eines Polyphenolgemischs gezeigt. Die Trennung erfolgte auf mit 20% Polyamid imprägnierten Silikagelschichten. Als Laufmittel wurde ein Gemisch von Benzol-Eisessig-Methanol (45 : 4 : 8 v/v) verwendet.

In einer vor kurzem veröffentlichten Arbeit[1] wurde gezeigt, daß mit Polyamid imprägnierte Silikagelschichten mit Erfolg zur Trennung phenolischer Substanzen verwendet werden können. Das verwendete Fließmittel ist verschieden polar abhängig von dem zu trennenden Gemisch. Sind im Gemisch Komponenten gleicher Polarität, so werden diese auf der gleichen Strecke wandern und ihre Trennung in isothermen Bedingungen ist nicht möglich. Deshalb wurde die Trennung solcher Komponenten im orthogonalen Temperaturgradient versucht.

Der positive Einfluß des orthogonalen Temperaturgradienten auf die Trennergebnisse wurde schon bei der Trennung von Farbstoffen[2] und Aminosäuren[3,4] ersichtlich, wo das Erhöhen des angewendeten orthogonalen Temperaturgradienten zum differenzierten Wachsen der R_f-Werte führte. Da ein Teil des Fließmittels, dank der höheren Temperatur, von der Schicht verdampft, wird ein zusätzliches Fließmittelvolumen ΔV die Schicht durchsetzen. Gleichzeitig ändert sich die Zusammensetzung des Fließmittels und zwar wächst die Konzentration der Komponente mit dem höchsten Siedepunkt. Es kommt also zu einer selektiven Verdampfung des Fließmittels. Der orthogonale Temperaturgradient führt zum Verringern der Trennstufenhöhe H, die transversale Diffusion wird größer als die longitudinale, was zu einer Verengung der Zonen und zu einer besseren Trennung führt.

[1] S. GOCAN und C. KONNERT, *Stud. Univ. ,,Babeş-Bolyai'', Chem.*, **22**, 39 (1977).
[2] S. GOCAN, *Stud. Univ. ,,Babeş-Bolyai'', Chem.*, **20**, 33 (1975).
[3] S. GOCAN und C. KYRI, *Rev. Roumaine Chim.*, **19**, 1957 (1974).
[4] S. GOCAN und C. KYRI, wird veröffentlicht.

Experimenteller Teil : Die Dünnschichten wurden aus mit 20% Polyamid imprägniertem Silikagelpulver unter Verwendung eines organischen Bindemittels erhalten.

Zur Trennung des aus Phenol, Pirokatechin, Resorzin, Pyrogallol und Fluoroglucin gebildeten Substanzgemisches wurde als Fließmittel : Benzol-Eisessig-Methanol (45 : 4 : 8 v/v) verwendet. Die Entwicklung erfolgte auf Glasplatten 10 × 14 cm in einer S-Kammer. Auf die beiden Platten der Kammer wurden zwei Heizplatten angebracht, [5] die einen Temperaturunterschied zwischen den beiden gegenüberliegenden Platten der *S*-Kammer gewährleisteten, und zwar derart, daß die DC-Platte bei einer Temperatur t_2 größer ist als die Temperatur t_1 der Gegenplatte. Die Distanz *d* zwischen DC-Platte und Gegenplatte betrug 3 mm. Der orthogonale Temperaturgradient (senkrecht auf die Schicht und Fließrichtung) wurde nach folgender Gleichung berechnet : $0\text{-grad}.t=(t_2 - t_1)/d$ (°/mm). Der Nachweis erfolgte durch Besprühen mit diazotierter Sulfanilsäure gefolgt von 10% Natriumhydroxidlösung.

Ergebnisse : Zur Trennung des Polyphenolgemisches wurden zwei orthogonale Temperaturgradienten angewendet und zwar $0\text{-grad}.t = (40 - 20)/3 = 6{,}66°/\text{mm}$ und $0\text{-grad}.t = (50-20)/3 = 10°/\text{mm}$. Stellt man die R_f-Werte der Polyphenole als Funktion des orthogonalen Temperaturgradienten dar, so erhält man das Schaubild aus Abbildung 1. Die R_f-Werte wachsen mit steigendem orthogonalem Temperaturgradient bei konstanter Entwicklungsdauer (30 Minuten) an.

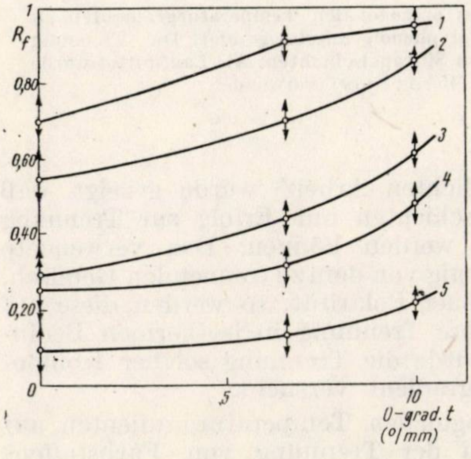

Abb. 1. — Abhängigkeit der R_f-Werte von orthogonalen Temperaturgradienten. Entwicklungsdauer : 30 Minuten. Komponenten : *1*, Phenol, *2*, Pirokatechin, *3*, Resorzin, *4*, Pyrogallol, *5*, Fluoroglucin

Ebenso bemerkt man die Verengung der Zonen im Gradient. Auf der Abbildung geben die mit Pfeilen begrenzten Strecken die Länge der der Fließrichtung parallelen Achsen der Zonen in R_f-Einheiten an. Wenn in isothermen Bedingungen ($0\text{-grad}.t = 0°/\text{mm}$) Resorzin und Pyrogallol dank ihrer annähernd gleichen Polarität noch ungetrennt waren, so ändert sich das bei Anwendung der orthogonalen Temperaturgradienten. Man erhält eine Trennung dieser beiden Komponenten schon bei $0\text{-grad}.t = 6{,}66°/\text{mm}$, während bei $0\text{-grad}.t = 10°/\text{mm}$ sich diese Trennung bedeutend verbessert.

Arbeitet man mit konstantem Temperaturgradient und ändert sich die Entwicklungsdauer, so erhält man die Ergebnisse aus Abbildung 2 ($0\text{-grad}.t = (40 - 20)/3 = 6{,}66°/\text{mm}$) und Abbildung 3 ($0\text{-grad}.t = (50-20)/3 = 10°/\text{mm}$).

Man bemerkt, daß das Verlängern der Entwicklungsdauer einen positiven Einfluß auf die Trennung der Komponenten hat, da es zu höheren R_f-Werten und kompakteren Zonen führt. Aber eine zu lange Entwicklungszeit führt zur Verschlechterung der Auflösung. So z.B. ist für $0\text{-grad}.t = 6{,}66°/\text{mm}$ die beste Entwicklungsdauer 60 Minuten (Abb. 2 und 4) ; nach 90 Minuten sind die Zonen des Phenols und Pirokatechins sehr nahe aneinandergerückt. Für einen $0\text{-grad}.t = 10°/\text{mm}$

---

[5] A. NIEDERWIESER, *Chromatographia*, **2**, 362 (1964).

passiert das schon nach 60 Minuten; nach 90 Minuten sind die Zonen von Phenol, Pirokatechin und Resorzin überlagert (Abb. 3).

Durch Anwendung des orthogonalen Temperaturgradienten und einer passenden Entwicklungsdauer kann man alle fünf Polyphenole trennen. Der orthogonale Temperaturgradient ist vor allem für die Trennung der Polyphenole gleicher Polarität geeignet.

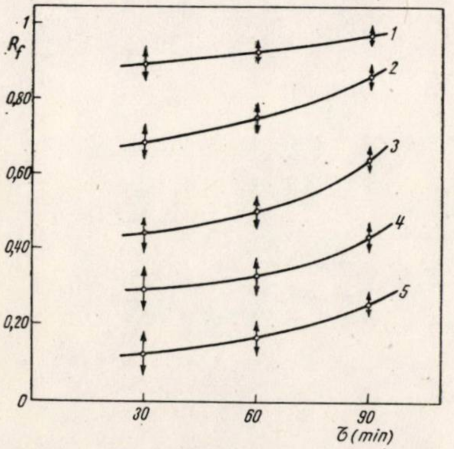

Abb. 2. — Abhängigkeit der R_f-Werte von der Entwicklungsdauer. 0-grad.$t = (40 - 20)/3 = 6{,}66°/\text{mm}$; Komponenten:
1, Phenol; *2*, Pirokatechin; *3*, Resorzin; *4*, Pyrogaloll; *5*, Fluoroglucin.

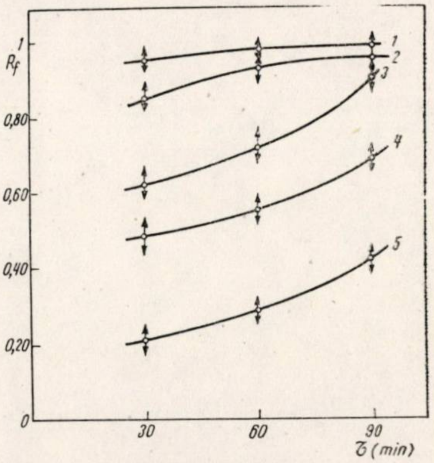

Abb. 3. — Abhängigkeit der R_f-Werte von der Entwicklungsdauer. 0-grad.$t = (50 - 20)/3 = 10°/\text{mm}$; Komponenten:
1, Phenol; *2*, Pirokatechin; *3*, Resorzin; *4*, Pyrogallol; *5*, Fluoroglucin.

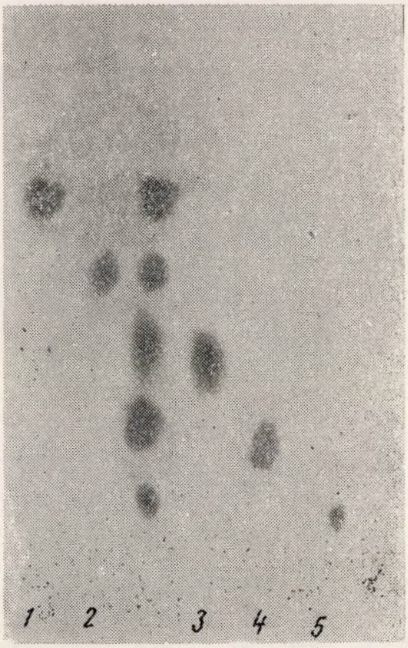

Abb. 4. — Chromatogramm. Komponenten:
1, Phenol; *2*, Pirokatechin; *3*, Resorzin; *4*, Pyrogallol; *5*, Fluoroglucin.
0-grad.$t = (40-20)/3 = 6{,}66°/\text{mm}$; Entwicklungsdauer: 60 Minuten.

Revue Roumaine de Chimie, **23**, *1*, 137–142 (1978)

LIQUID MEMBRANE-ELECTRODES. XII*

LIQUID MEMBRANE-ELECTRODES FOR PERCHLORATE, THIOCYANATE, TETRAFLUOROBORATE AND NITRATE BASED ON TRIPHENYLMETHANE DYES

ELENA HOPÎRTEAN and EUGENIA ŞTEFĂNIGĂ
Department of Analytical Chemistry, University of Cluj-Napoca, str. Arany J. nr. 11,
Cluj-Napoca, Romania

Received August 14, 1975

The results obtained in a study concerning the obtention of liquid membrane-electrodes for perchlorate, thiocyanate, tetrafluoroborate and nitrate anions, using triphenylmethane dyes as active electrode components, are presented. Malachite green, fuchsine, crystal violet, methyl violet, gentiana violet and alkali blue in nitrobenzene or tetrachloroethane, were used. The practical nernstian response in the largest concentration interval was obtained for perchlorate with gentiana violet and fuchsine ($10^{-1}-2\times10^{-5}$M), for thiocyanate with gentiana violet and alkali blue ($10^{-1}-4\times10^{-5}$M), for tetrafluoroborate with malachite green ($10^{-1}-6.3\times10^{-5}$ M) and for nitrate with crystal violet ($10^{-1}-2.5\times10^{-5}$ M) and with gentiana violet ($10^{-1}-6.3\times10^{-5}$M).

INTRODUCTION

Lately triphenylmethane dyes have been used as electrode active components for anions. Thus, crystal violet[1-6] was used for liquid membrane-electrodes sensitive towards organic anions, such as: benzenesulphonate,[1,5] dodecylbenzenesulphonate,[1] toluenesulphonate,[5] naphthalenesulphonate,[5] maleate,[3,6] phthalate,[3,6] *p*-aminosalicylate,[2] salicylate,[2] trifluoroacetate.[4] Liquid electrodes based on malachite green, methyl violet and fuchsine, were tested towards aromatic sulphonic compounds[5] too, but the results obtained were poorer than those obtained with crystal violet. Brilliant green has been used as electrode component for tetrathiocyanatozincate[7] and tetrafluoroborate,[8] respectively.

---

* Part XI: E. Hopîrtean, E. Ştefănigă and C. Liteanu, *Rev. Roumaine Chim.*, **22**, 653 (1977).

[1] N. Ishibashi and H. Kohara, *Bunseki Kagaku*, **21**, 100 (1972); *Chem. Abstr.* **76**, 107667 (1972).

[2] K. Kina, M. Mackava and N. Ishibashi, *Bull. Chem. Soc. Japan*, **46**, 2773 (1973).

[3] N. Ishibashi, A. Jyo and M. Yonemitsu, *Chem. Lett.*, **1973**, 483.

[4] N. Ishibashi and A. Jyo, *Mikrochem. J.*, **18**, 220 (1973).

[5] N. Ishibashi, H. Kohara and K. Horinouchi, *Talanta*, **20**, 867 (1973).

[6] A. Jyo, M. Yonemitsu and N. Ishibashi, *Bull. Chem. Soc. Japan*, **46**, 3734 (1973).

[7] A. S. Fogg, M. Duzinkewycz and A. S. Pathan, *Analyt. Lett.*, **6**, 1101 (1973).

[8] A. S. Fogg, A. S. Pathan and D. Th. Burns, *Analyt. Lett.*, **7**, 545 (1974).

In this paper, the obtention and the behaviour of a series of liquid membrane-electrodes for perchlorate, thiocyanate, tetrafluoroborate and nitrate, are presented. The electrode active components are triphenylmethane dyes: crystal violet (CV), malachite green (MG), methyl violet (MV), fuchsine (F), gentiana violet (GV) and alkali blue (AB). We mention that CV, MG, MV and F have been used by other authors,[5] too, for obtention of liquid electrodes for organic anions, but GV and AB have not been used till now. The solvent used were nitrobenzene and tetrachloroethane.

EXPERIMENTAL

Electrode active components. Triphenylmethane dyes studied were: 4,4′-dimethylaminotriphenylmethane (malachite green), *p*-rosaniline chloride (fuchsine), pentamethyl-*p*-rosaniline chloride (methyl violet), hexamethyl-*p*-rosaniline chloride (crystal violet), pentamethyl-and hexamethyl-*p*-rosaniline chloride mixture (gentiana violet) and the monosulphonic derivative of aniline blue (alkali blue). Solutions (c = 0.1 %) in nitrobenzene and tetrachloroethane were prepared from these compounds. These solutions were used to prepare the organic electrode active solutions for perchlorate, thiocyanate, tetrafluoroborate and nitrate. For this, the chloride ion from the organic phase was changed with the corresponding anion, from a 1M aqueous solution, using extraction method. Equal volumes of the two phases were used.

Liquid membrane-electrodes. Each membrane electrode was obtained by soaking the pores of a glass frit G_4, made hydrophobic, attached to the extremity of a glass tube (Ø = 15 mm), by the electrode active compound in nitrobenzene or tetrachloroethane solution, obtained by extraction. The organic solution was used as internal solution, too. The inner, respectively the outer reference electrodes were of the SCE type, with salt bridge and ceramic junction.

Potential measurements have been performed at room temperature, in nonstirred solutions, using a MV-85 pH-meter (± 1 mV precision). The reproducibility of the slope of electrode functions is in the accuracy range of the device used, and the standard potential of the electrodes was reproducible with a ± 2 mV precision.

Reagents and standard solutions. All reagents were of analytical grade. Standard 10^{-1}—10^{-6} M solutions have been prepared by successive dilutions of the corresponding 1M stock solution. A constant ionic strength has been maintained (J = 0.15 M), adjusting the ionic strength with 5×10^{-2} M Na_2SO_4 solution. Twice distilled water has been used.

RESULTS AND DISCUSSIONS

Fig. 1 shows the electrode functions obtained for perchlorate with gentiana violet in nitrobenzene. Gentiana violet was used as chloride salt (curve 1), respectively as perchlorate salt (after extraction) (curve 2). An abnormal response and poor repeatability have been obtained if GV was used as chloride salt. GV perchlorate gives a practical nernstian response, stable towards perchlorate in a large concentration range. This finding holds also, for the electrode response towards thiocyanate, tetrafluoroborate and nitrate, as well as for the electrode response of the other compounds towards all these anions. Therefore, the method of obtaining the liquid membrane-electrodes, using the triphenylmethane dye as a salt of the anion to-be tested, was adopted. Subsequently, the electrodes elaborated for perchlorate, thiocyanate, tetrafluoroborate and nitrate have been tested.

The electrode functions for perchlorate, obtained for the six electrode components in nitrobenzene are shown in Fig. 2, those obtained

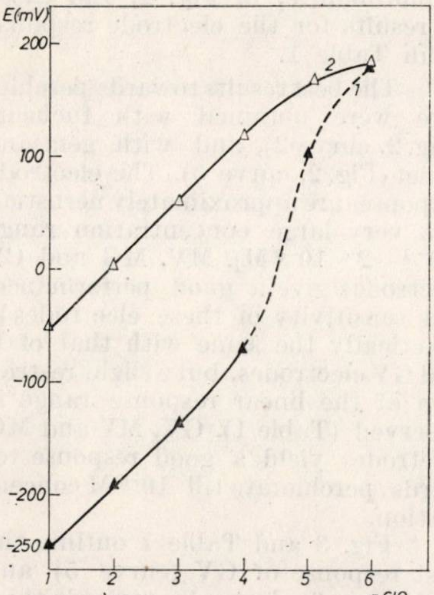

Fig. 1. — Electrode functions for perchlorate.

1 - GV as chloride salt; 2-GV as perchlorate salt.

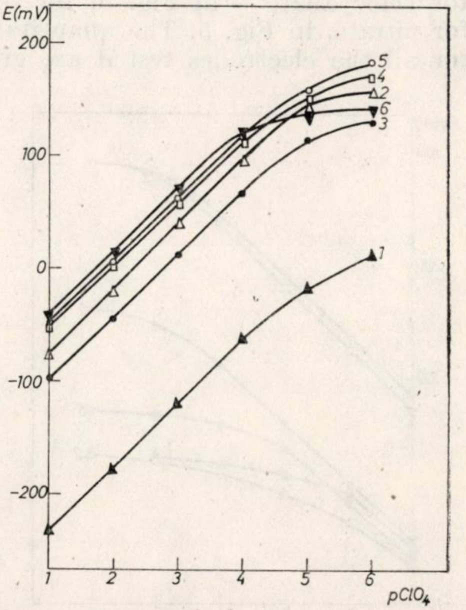

Fig. 2. — Electrode function for perchlorate.

1-MG; 2-F; 3-MV; 4-CV; 5-GV; 6-AB. Nitrobenzene is the solvent.

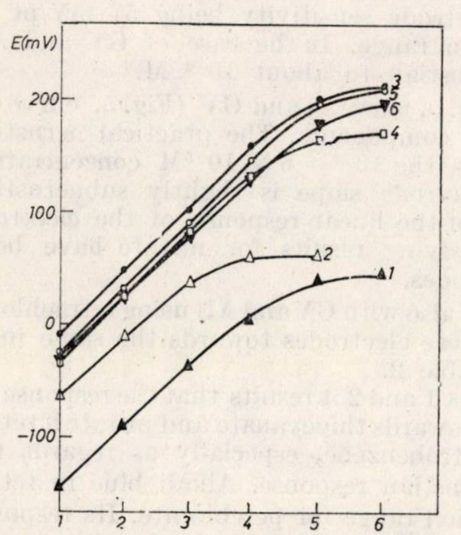

Fig. 3. — Electrode functions for thiocyanate.

1-MG; 2-F; 3-MV; 4-CV; 5-GV; 6-AB. Nitrobenzene is the solvent.

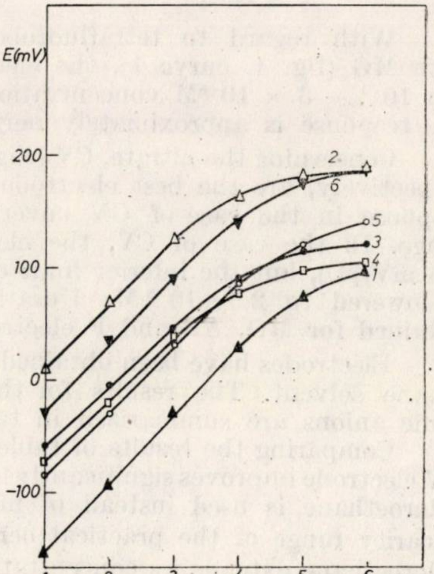

Fig. 4. — Electrode functions for tetrafluoroborate.

1-MG; 2-F; 3-MV; 4-CV; 5-GV; 6-AB. Nitrobenzene is the solvent.

for thiocyanate — in Fig. 3, for tetrafluoroborate, in Fig. 4, and those for nitrate, in Fig. 5. The quantitative results for the electrode response for all the electrodes tested are given in Table 1.

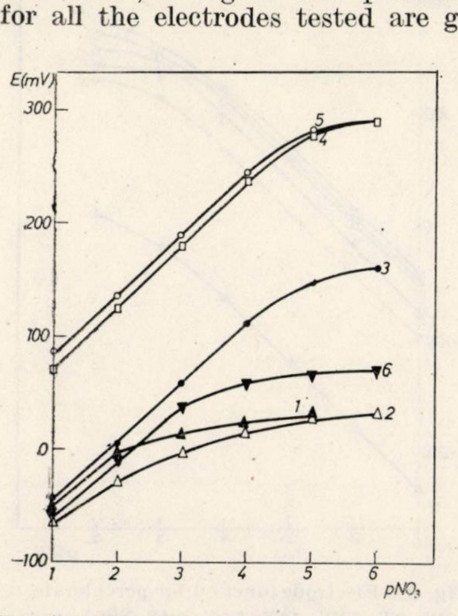

Fig. 5. — Electrode functions for nitrate. 1-MG; 2-F; 3-MV; 4-CV; 5-GV; 6-AB. Nitrobenzene is the solvent.

The best results towards perchlorate were obtained with fuchsine (Fig. 2, curve 2), and with gentiana violet (Fig. 2, curve 5). The electrode responses are approximately nernstian in a very large concentration range (10^{-1}–2×10^{-5} M). MV, MG and CV electrodes give a good performance. The sensitivity of these electrodes is practically the same with that of F and GV electrodes, but a slight restriction of the linear response range is observed (Table 1). GV, MV and MG electrodes yield a good response towards perchlorate till 10^{-6} M concentration.

Fig. 3 and Table 1 outline the best response of GV (curve 5) and AB (curve 6) electrodes towards thiocyanate. Excepting fuchsine (curve 2), all the electrode compounds have a good response for thiocyanate in a large concentration range (Table 1).

With regard to tetrafluoroborate, the best result was obtained with MG (fig. 4, curve 1), the electrode sensitivity being 57 mV/pC in the $10^{-1} - 3 \times 10^{-5}$M concentration range. In the case of GV and AB the response is approximately nernstian to about 10^{-4} M.

Concerning the nitrate, CV (Fig. 5, curve 4) and GV (Fig. 5, curve 5), respectively, are the best electrode components. The practical nernstian response in the case of GV covers the $10^{-1} - 6 \times 10^{-5}$M concentration range. In the case of CV, the electrode slope is slightly subnernstian (55 mV/pC), but the inferior limit of the linear response of the electrode is lowered to 2.5×10^{-5} M. Unsatisfying results for nitrate have been obtained for MG, AB and F electrodes.

Electrodes have been obtained also with GV and AB using tetrachloroethane solvent. The results for these electrodes towards the same inorganic anions are summarized in table 2.

Comparing the results of tables 1 and 2 it results that the response of GV electrode improves significantly towards thiocyanate and nitrate if tetrachloroethane is used instead of nitrobenzene, especially as regards the linearity range of the practical nernstian response. Alkali blue in tetrachloroethane extends its concentration range for perchlorate. Its response towards nitrate is clearly improved in tetrachloroethane both by increasing the sensitivity from 48 mV in nitrobenzene to 53 mV in tetrachloroethane, and by decreasing the lower concentration limit of the linear response.

Table 1

Electrode behaviour of some triphenylmethane dyes in nitrobenzene towards the following anions: ClO_4^-, SCN^-, BF_4^- and NO_3^-

Anion	Malachite Green		Fuchsine		Methyl Violet		Crystal Violet		Gentiana Violet		Alkali Blue	
	Conc. range (M)	Slope (mV)	Conc. range (M)	Slope (mV)	Conc. range (M)	Slope (mV)	Conc. range (M)	Slope (mV)	Conc. range (M)	Slope (mV)	Conc. range (M)	Slope (mV)
ClO_4^-	$10^{-1}-3\times10^{-5}$	57	$10^{-1}-2\times10^{-5}$	58	$10^{-1}-3\times10^{-5}$	56	$10^{-1}-6.3\times10^{-5}$	56	$10^{-1}-2\times10^{-5}$	56	$10^{-1}1.6\times10^{-4}$	56
SCN^-	$10^{-1}-3\times10^{-4}$	53	$10^{-1}-10^{-3}$	54	$10^{-1}-4\times10^{-4}$	55.5	$10^{-1}-2\times10^{-4}$	55	$10^{-1}-5\times10^{-5}$	57	$10^{-1}-4\times10^{-5}$	55
BF_4^-	$10^{-1}-6.3\times10^{-5}$	57	$10^{-1}-3\times10^{-4}$	55	$10^{-1}-5\times10^{-4}$	54	$10^{-1}-5\times10^{-4}$	56	$10^{-1}-1.5\times10^{-4}$	56	$10^{-1}-10^{-4}$	56
NO_3^-	$10^{-1}-10^{-2}$	48	$10^{-1}6.3\times10^{-4}$	30	$5\times10^{-1}-10^{-4}$	53	$10^{-1}2.5\times10^{-5}$	55	$10^{-1}-6.3\times10^{-5}$	57	$10^{-1}-10^{-3}$	48

Table 2

Electrode behaviour of some triphenylmethane dyes towards the following anions : ClO_4^- , SCN^- , BF_4^- and NO_3^- . The solvent was tetrachloroethane

Electrode component Anion	Gentiana Violet		Alkali Blue	
	Concentration range	Slope (mV)	Concentration range	Slope (mV)
ClO_4^-	$10^{-1}-1.2\times10^{-5}$M	56	$10^{-1}-3.2\times10^{-5}$M	56
SCN^-	$10^{-1}-1.6\times10^{-4}$M	56	$10^{-1}-3.2\times10^{-4}$M	56
BF_4^-	$10^{-1}-10^{-5}$M	59	$10^{-1}-5\times10^{-5}$M	56.5
NO_3^-	$10^{-1}-10^{-5}$M	57	$10^{-1}-2\times10^{-4}$M	53

The practical insignificant structure differences between CV, MV and GV (triphenylmethane dyes with three auxochromes), are reflected in their similar electrode responses. The best response given by GV toward all four anions tested has to be emphasized (table 1) Fuchsine, whose N-alkyl derivatives are the above mentioned dyes, gives a good response only in the case of perchlorate. It means that the electrode response towards the anions is improved by alkylating the amino groups of *p*-rosaniline (CV, MV and GV). The increased hydrophobic character of these groups determines a rise of the distribution ratio of the electrode component between the organic and the aqueous phases.

Malachite green, a basic triphenylmethane dye with two auxochromes (the two amino groups are fully methylated), has outpassed the response of the basic triphenylmethane dyes with three auxochromes concerning the response towards tetrafluoroborate (Table 1).

Alkali blue, the monosulphonic derivative of aniline blue (triphenyl-derivative of *p*-rosaniline) is not more hydrophobic than GV, CV and MV so that its electrode behaviour is inferior to that of these three compounds.

Beside the kind of the electrode active component correlated especially with its distribution coefficient between the organic and the aqueous phases, the role of the solvent dielectric constant is decisive for the liquid membrane-electrode response.[5,9] From the obtained results it follows that tetrachloroethane, a newly used solvent for this kind of electrode component, is, like nitrobenzene, a very good solvent in order to achieve membrane-electrodes with liquid ion exchangers.

The response rate of the obtained electrodes is very high, the equilibrium being reached in a few seconds in more concentrated solutions than 10^{-4}M. In $10^{-5}-10^{-6}$M solutions, the equilibrium potential is reached in maximum 3—4 minutes.

In conclusion, in order to obtain liquid membrane-electrodes sensitive to perchlorate, thiocyanate, tetrafluoroborate and nitrate anions, the respective anion salt of the triphenylmethane dye, in nitrobenzene or tetrachloroethane solvent, may be successfully used. The results thus obtained allow the extension of the electrode active compound series for inorganic anions.

[9] E. Hopîrtean, E. Ştefănigă, C. Liteanu and I. Gusan, *Rev. Chim.* (*Bucureşti*), **27**, 346 (1976).

Revue Roumaine de Chimie, **23**, *1*, 143–146 (1978)

ISOTOPIC EXCHANGE OF ACTIVE METHYL GROUPS. XI[1]

KINETICS OF DEUTERIATION OF 2,6-DIARYL-4-METHYLPYRYLIUM SALTS

A. T. BALABAN[a], ILEANA I. STĂNOIU[b], F. CHIRALEU[c] and I. MOŢOC[d]

[a] The Polytechnic, Department of Organic Chemistry, Bucharest
[b] Institute of Atomic Physics, Bucharest
[c] Centre of Organic Chemistry, Bucharest
[d] Department of Physical Chemistry, Timişoara University

Received July 23 1977

The deuteriation of 2,6-diphenyl-4-methylpyrylium chloroaluminate, 2,6-di-*p*-tolyl- and -*p*-anisyl-4-methylpyrylium perchlorates was followed kinetically by ^{1}H-NMR spectroscopy in a mixture of hexadeuterioacetone and buffered D_2O. The Hammett plot gives best correlation with σ_p^+ values, and the ρ value agrees with the intermediate formation of a γ-methylenepyran.

In previous parts of this series, ^{1}H-NMR spectroscopy was used to evidence that the side-chain deuteriation of pyrylium salts with α- or γ-methyl[2–4] or -isopropyl groups[5,6] proceeds about ten times faster in γ than in α, about three times faster for an isopropyl hydrogen than for a methyl hydrogen,[5] and appreciably faster* for 2,6-diaryl-4-methylpyrylium than for 2,6-dialkylpyrylium salts (for the 4-methyl hydrogens).[4] Activation parameters were determined for 2,4,6-trimethylpyrylium,[3] 2,6-diethyl-4-methylpyrylium,[7] 2,6-diisopropyl-4-methylpyrylium, 2,6-dimethyl-4-ethylpyrylium,[7] 2,6-dimethyl-4-isopropylpyrylium,[6] and 2,4-dimethyl-6-isopropylpyrylium perchlorates.[5] These kinetic data, the isotope effects,[6] and HMO calculations,[8] all indicate that the isotopic exchange proceeds *via* methylenepyran (anhydrobase) intermediates.

---

* Quantitative rate measurements for 2,6-diaryl-4-methylpyrylium salts are first reported in the present paper.

[1] Part X, I. I. Stănoiu, A. T. Balaban and F. Chiraleu, *Rev. Roumaine Chim.* **22,** 1499 (1977).

[2] E. Gârd, A. Vasilescu, G. D. Mateescu and A. T. Balaban, *J. Labelled Comp.* **3,** 196 (1967).

[3] E. Gârd, I. Stănoiu, F. Chiraleu and A. T. Balaban, *Rev. Roumaine Chim.* **18,** 257 (1973).

[4] E. Gârd, I. Bally, A. Vasilescu, A. Arsene and A. T. Balaban, *J. Labelled Comp.* **1,** 182 (1965).

[5] I. I. Stănoiu, E. Gârd, C. Uncuţa, F Chiraleu and A. T. Balaban, *Rev. Roumaine Chim.*, **22,** 1359 (1977).

[6] I. I. Stănoiu, F. Chiraleu, E. Gârd and A. T. Balaban, *Rev. Roumaine Chim.* **22,** 117 (1977).

[7] I. I. Stănoiu, E. Gârd, F. Chiraleu and A. T. Balaban (in press).

The present paper reports the results of a kinetic study for the deuteriation of 2,6-diaryl-4-methylpyrylium salts, where both α-aryl groups are phenyl, *p*-tolyl, or *p*-anisyl. Despite the restricted number of *para*-substituents, a Hammett correlation was attempted.

EXPERIMENTAL PART

2,6-Diphenyl-4-methylpyrylium chloroaluminate was prepared by dibenzoylation of isobutene, from benzoyl chloride, t-butyl chloride, and anhydrous aluminium chloride.[9] 2,6-Di-*p*-tolyl-4-methylpyrylium and 2,6-di-*p*-anisyl-4-methylpyrylium perchlorates were obtained similarly, using *p*-toluyl and *p*-anisyl chlorides, respectively, and precipitating the perchlorates from the aqueous solutions of the chloroaluminates with $HClO_4$; all salts were recrystallized from acetic acid. [10]

The preparation of buffered D_2O solutions was described earlier.[6]

^1H-NMR spectra were determined with a Varian A-60A instrument. Solutions of pyrylium salt in hexadeuterioacetone were treated with buffered D_2O (electrochemically determined pH = 1.4), about five moles of D_2O per mole of pyrylium salt, kept in a thermostat bath at 38° and the ^1H-NMR spectra were recorded at specified times, also at 38° in the NMR spectrometer.

The small amount of non-deuteriated acetone in the solvent served as an internal standard for the integrator of the NMR instrument. Three integral curves were recorded rapidly at each specified time for the γ-methyl (noted by *A* in Table 1 and the kinetic expressions beneath this table) and the acetone protons. The calculation of the reaction rate was effected as described earlier, by the least-square method, using the ratio of the acetone

Table 1

Experimental kinetic data for the deuteriation of 2,6-diaryl-4-methylpyrylium salts at 38°

Phenyl			*p*-Tolyl			*p*-Anisyl		
Time hrs	Averaged peak area (mm)		Time hrs	Averaged peak area (mm)		Time hrs	Averaged peak area (mm)	
	γ-Me *A*	Me_2CO		γ-Me *A*	Me_2CO		γ-Me *A*	Me_2CO
0	56.0	23.7	0	71.2	56.5	0	34.0	27.3
0.033	42.0	20.3	0.033	60.2	55.0	0.025	32.8	27.0
0.067	27.1	21.8	0.067	49.5	54.2	0.050	32.0	27.5
0.100	20.6	20.5	0.167	37.5	55.0	0.083	30.2	25.8
0.133	15.0	20.8	0.175	27.8	55.2	0.133	28.0	27.2
0.167	10.2	20.2	0.233	20.3	55.5	0.200	25.8	25.5
0.200	8.2	20.5	0.300	15.8	57.5	0.267	21.2	25.5
—	—	—	0.367	12.8	56.8	0.350	19.0	27.2
—	—	—	—	—	—	0.467	15.5	27.2
—	—	—	—	—	—	0.583	11.4	27.2

Rate equations:

I, R = H: $-\lg A = 0.033 + 4.49\,t$, $k = 4.49\ \mathrm{h}^{-1}$

I, R = Me: $-\lg A = 0.032 + 2.06\,t$, $k = 2.06\ \mathrm{h}^{-1}$

I, R = OMe: $-\lg A = 0.006 + 0.784\,t$, $k = 0.784\ \mathrm{h}^{-1}$

[8] C. C. Renția, A. T. Balaban and Z. Simon, *Rev. Roumaine Chim.* **11,** 1193 (1966).

[9] A. T. Balaban and C. D. Nenitzescu, *Liebigs Ann. Chem.* **625,** 74 (1959).

[10] A. T. Balaban, M. Gavăt, P. T. Frangopol, M. Mocanu and C. D. Nenitzescu, *Rev. Roumaine Chim.* **9,** 79 (1964).

protons as a correction factor for the small fluctuations of the integrator sensitivity; from the three curves, an average was calculated, indicated in Table 1, and this average value was corrected and then expressed as a semilogarithmic expression *versus* time.

Table 1 presents the experimental averaged results, and the rate expressions obtained by a least-square analysis. The time is given in hrs^{-1} in order to have the same rate units as in previous papers in this series,[1-6] though the present reactions are faster than all previously investigated deuteriations.

DISCUSSION OF THE RESULTS

It is evident from Table 1 that the higher the electron-donating ability of the α-aryl group in the pyrylium cation I, the lower is the isotopic exchange rate. This results was expected and can be accounted for by the reaction mechanism involving the intermediate formation of the anhydrobase (methylenepyran) II: qualitatively expressed, electron-donating groups increase the electron density on α- and γ-positions of the pyrylium ring, slowing thereby the deprotonation of the γ-methyl group.

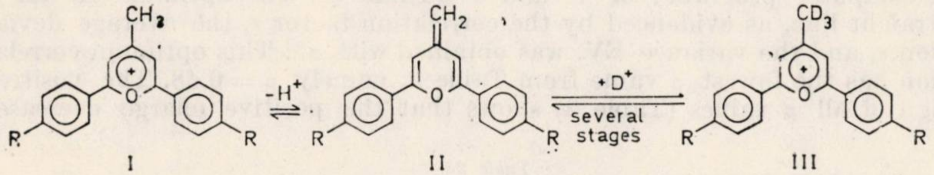

Despite the fact that only three kinds of α-aryl groups are available, one may attempt a Hammett correlation. The literature on this topic is increasing steadily, with books,[11-17] symposia,[18-19] reviews,[20-29] and

---

[11] L. P. Hammett, "Physical Organic Chemistry", 2nd Ed., McGraw-Hill, New York, 1970.

[12] J. E. Leffler and E. Grunwald, "Rates and Equilibria of Organic Reactions", Wiley, New York, 1963.

[13] C. D. Johnson, "The Hammett Equation", At the University Press, Cambridge, 1973.

[14] P. R. Wells, "Linear Free Energy Relationships", Academic Press, London, 1968.

[15] Yu. A. Zhdanov and V. I. Minkin, "Korrelatsionnyi analiz v organicheskoi khimii", Izd. Rostovskogo Universiteta, 1966.

[16] O. Exner, in "Advances in Linear Free Energy Relationships" (N. B. Chapman and J. Shorter, ed.), Plenum Press, London, 1972.

[17] J. Shorter, "Correlation Analysis in Organic Chemistry. An Introduction to Linear Free Energy Relationships", Clarendon Press, Oxford, 1973.

[18] C. D. Ritchie, in "Papers of the Symposium on Linear Free Energy Correlations", Durham, 1964, p. 107.

[19] V. A. Palm, in "Trudy konferentsii po problemam primeneniya korrelatsionnykh uravnenii v organicheskoi khimii", vol. 1, p. 3, Tartuskii Gosud. Univ., Tartu, 1962.

[20] P. R. Wells, *Chem. Rev.* **63**, 171 (1963).

[21] P. R. Wells, S. Ehrenson and R. W. Taft, *Progr. Phys. Org. Chem.* **6**, 147 (1968).

[22] H. H. Jaffé, *Chem. Rev.* **53**, 191 (1953).

[23] C. D. Ritchie and W. F. Sager, *Progr. Phys. Org. Chem.* **2**, 323 (1964).

[24] M. Charton, *Chemtech*, 502 (1974); 245 (1975); *Progr. Phys. Org. Chem.* **8**, 235 (1971); **10**, 81 (1973).

[25] D. Fărcașiu, *Studii Cercetări Chim. Acad. R. S. România*, **14**, 37 (1966).

[26] S. Ehrenson, *Progr. Phys. Org. Chem.* **2**, 195 (1964).

[27] L. M. Stock and H. C. Brown, *Adv. Phys. Org. Chem.* **1**, 35 (1963).

[28] V. Palm, *Usp. Khim.* **31**, 471 (1961).

[29] H. H. Jaffé and H. L. Jones, *Adv. Heterocyclic Chem.* **3**, 209 (1964);

a journal[30] devoted to such extrathermodynamic correlations (linear free energy relationships).

In the present case, involving the deprotonation of a methyl group *meta* relatively to two *para*-substituted aryl groups, there are three questions to be taken into account:

(i) Will the combined effect of the two aryl groups be twice as large as that of one group?

(ii) Should σ_p or σ_m values be employed?

(iii) Should one try the correlation with σ, σ^n, σ^+ or σ^0?

The first question is the easiest and may be answered in the affirmative. The second question is rather tricky. A literature analysis made by Silberg and Silberg[31] revealed that pK_a values of 4′-substituted 3-biphenylcarboxylic acids[32] correlate excellently ($r = 0.996$) with σ_p values, hence for the present case the sigma constants will be taken for the *para* series. The reply to the third question cannot be guessed *a priori*, therefore an empirical approach was followed.

From the various types of sigma constants, three were tested with a computer program: σ, σ^+ and σ^0 (Table 2). The optimum fit for a straight line, as evidenced by the correlation factor r, the average deviation s, and the variance EV, was obtained with σ^+. This optimum correlation has the lowest ρ value from Table 2, namely $\rho = 0.48$. The positive sign of all ρ values (Table 2) shows that the positive charge decreases in the transition state,[33] as expected for the proton transfer to a base if the rate-determining step is the formation of the anhydrobase II:

Table 2

Hammett correlations

Sigma	R in I			Calculated expression	Correlation indices		
	H	Me	OMe		r	s	EV
σ_p	0	−0.170	−0.268	$\lg k = 0.686 + 2 \times 1.87$	0.976	0.082	0.907
σ_p^+	0	−0.311	−0.78	$\lg k = 0.640 + 2 \times 0.48$	0.999	0.017	0.996
σ_p^0	0	−0.15	−0.16	$\lg k = 0.683 + 2 \times 2.16$	0.916	0.153	0.678

$$\mathrm{I} \rightarrow \mathrm{II} + \mathrm{H}^+$$

The present data also evidence that the pyrylium ring has a transmissive capacity for electronic efects comparable to that of a phenyl ring.

ACKNOWLEDGEMENT. Discussions with Drs. I. Silberg and F. Badea are gratefully acknowledged.

---

[30] V. A. Palm (editor), *Organic Reactivity*, **1**, 247 (1964).

[31] S. Silberg and I. Silberg, (to be published).

[32] T. Drapala and J. Moldawski, *Rocz. Chem.* **38**, 1593 (1964).

[33] F. Badea, "Reaction Mechanisms in Organic Chemistry", Abacus Press, Tunbridge Wells, **1977**, p. 122.

Revue Roumaine de Chimie, **23**, *1*, 147 – 155 (1978)

KINETIC INVESTIGATION OF SOME MOLECULAR COMPLEXES BETWEEN 1,3,7,9-TETRANITROPHENOTHIAZINE-5-OXIDE AND AMINES

ANDREEA SECARĂ*, A. TURCU** and E. SEGAL*

* Polytechnical Institute of Bucharest, Institute of Chemistry, Departament of Physical Chemistry and Electrochemical Technology,

** University of Bucharest, Faculty of Biology, Department of Biochemistry

Received November 13, 1976

The results obtained by the kinetic study of the thermal decomposition of the complexes given by 1,3,7,9-tetranitrophenothiazine-5-oxide with ammonia, some aliphatic amines and morpholine, are presented.

Following the studies[1–3] concerning the molecular complexes of the 1,3,7,9-tetranitrophenothiazine-5-oxide with ammonia and some organic bases, we should like to bring up a kinetic approach of the unexplosive thermal decomposition of these compounds.

EXPERIMENTAL

The substances have been ground and sorted through sieves able to retain a medium size of 0.11 mm. Experience proved that, in some cases, the grains passing through the sieve meshes have an apparent size, exhibiting rather a conglomerate structure of particles with smaller size.[4] In order to determine the true particle size, the X-ray difraction method has been applied. A Phillips diffractometer PW 1349/30 has been used.

The heating curves necessary to determine the values of the kinetic parameters have been obtained using a derivatograph NOM-Budapest type Paulik-Paulik-Erdey.

To get the necessary data for the kinetic analysis, the substances have been heated with different values of the heating rate. Two methods given by Freeman-Carroll[5] and Coats-Redfern[6] were applied for the evaluation of the kinetic parameters.

RESULTS AND DISCUSSION

The crystal grain sizes have been evaluated using Scherrer's formula : [7]

$$L = \frac{0.9\ \lambda}{(W_x - \omega)\cos\theta}$$

---

[1] A. Turcu and M. Răileanu, *Rev. Roumaine Chim.*, **14**, 1579 (1969).

[2] M. Răileanu, M. Olteanu, I. Radulian, C. Volanschi, A. Turcu and H. Căldăraru, *Rev. Roumaine Chim.*, **16**, 1269 (1971).

[3] A. Turcu, *Rev. Roumaine Chim.*, **22**, 1363 (1977).

[4] I. G. Murgulescu and E. Segal, *Rev. Roumaine Chim.*, **10**, 4 (1965).

[5] E. S. Freeman and B. Carroll, *J. Phys. Chem.*, **62**, 394 (1958).

[6] A. W. Coats and T. P. Redfern, *Nature*, **201**, 68 (1964).

[7] W. B. Innes, "Experimental Methods in Catalytic Research" edited by B. Anderson, Academic Press, New York-London, 1968, p. 84.

where :

L — is medium size of the crystal grain,

λ — is the wave length of the monochromatic applied radiation (a copper anticathode has been used with $\lambda_{K\alpha} = 1.5418$Å).

W_x — is the half-width of a line chosen for determination in radians

ω — is the half-width of a line exhibited by a well crystallised material expressed in the same units, and

θ — is the Bragg angle.

A polycrystalline silicium pellet has been used as a standard. In this way, the following L-values have been obtained :

— for the complex with diethylamine $L = 51$ Å
— for the complex with triethylamine $L = 204$ Å
— for the complex with methylamine $L = 51$ Å

The complexes with ethylamine, propylamine, ammonia and morpholine exhibit lines whose half widths are smaller than the standard ones. In these cases, it is not possible to apply Scherrer's formula, because the grain sizes are higher, approaching the apparent ones.

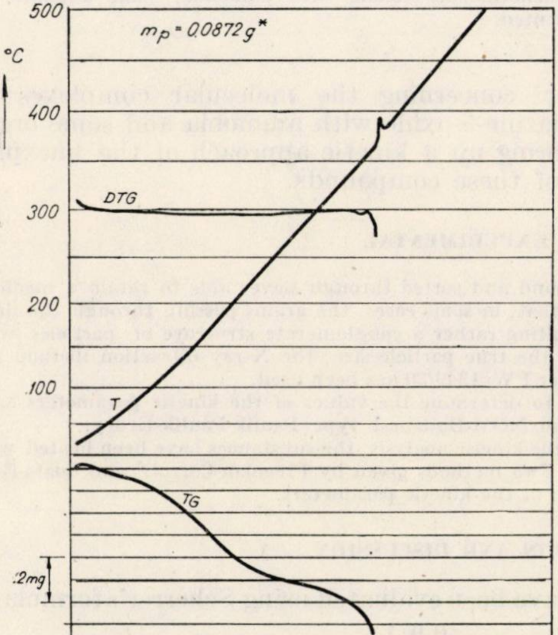

*mp = initial weight of the powder

Fig. 1. — The derivatogram of decomposition of the complex with ammonia.

Passing to the description of the results obtained for the unexplosive thermal decomposition of the analysed complexes, we present below (Fig. 1) the derivatogram of the complex with ammonia, corresponding to its heating up to 500°.

It can be noticed that decomposition takes place in a unique process, developing with maximum rate at 290°, temperature which is conventionally considered to be the reaction temperature. The decomposition process is described by a chemical equation as follows :

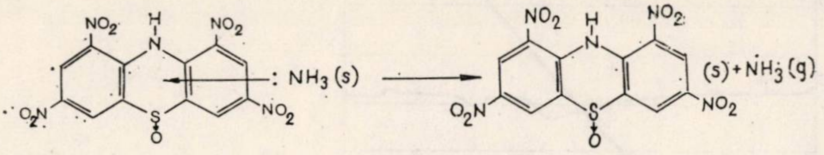

I

The values of the kinetic parameters of the reaction (I) including the reaction order (n), the preexponential factor (A) and the activation energy (E) are shown in Table 1.

Table 1

Kinetic parameters values for reaction I

$\frac{dT}{dt}$ °/min	n	E kcal/mole		A s^{-1}	
		Freeman	Coats	Freeman	Coats
5.83	0.3	8.641	8.641	2.10^2	$2.66.10^2$

The structure of the complexes with the other donors (methylamine, ethylamine, diethylamine, triethylamine, propylamine and morpholine) is in the main the same. Their decomposing process is also analogous.

Figure 2 gives the derivatogram corresponding to the decomposition of the complex with methylamine which takes place at 150°.

The values of the kinetic parameters for the reaction are shown in Table 2.

Table 2

Kinetic parameters values for the reaction

$\frac{dT}{dt}$ °/min	n	E kcal/mole		A s^{-1}	
		Freeman	Coats	Freeman	Coats
5.27	0.4	14.233	14.868	$0.7.10^3$	9.10^4
2.47	0.4	14.267	14.557	1.10^3	$6.5.10^3$

As concerns the complex with ethylamine whose derivatogram is shown in Figure 3, the decomposition develops at 130° and has the following kinetic parameters shown in Table 3 :

Table 3

Kinetic parameters values for the reaction

$\frac{dT}{dt}$ °/min	n	E kcal/mole		A s^{-1}	
		Freeman	Coats	Freeman	Coats
6.36	0.3	17.5	17.9	$3.9.10^5$	$5.3.10^6$
1.89	0.3	19.2	18.1	$3.3.10^6$	$5.1.10^6$

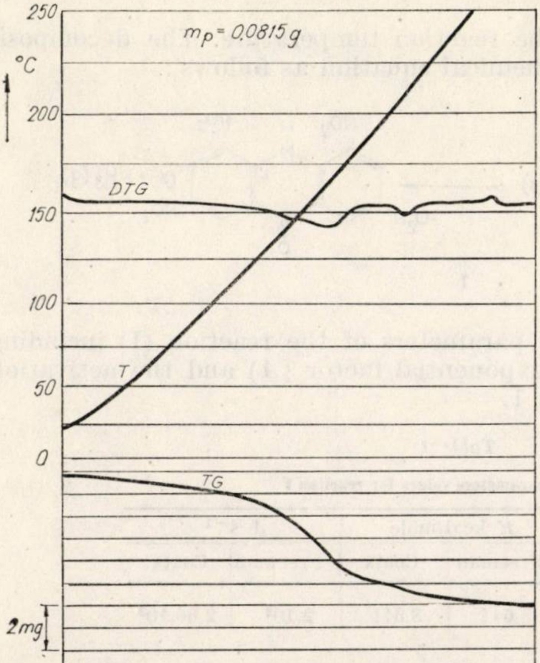

Fig. 2. — The derivatogram of decomposition of the complex with methylamine.

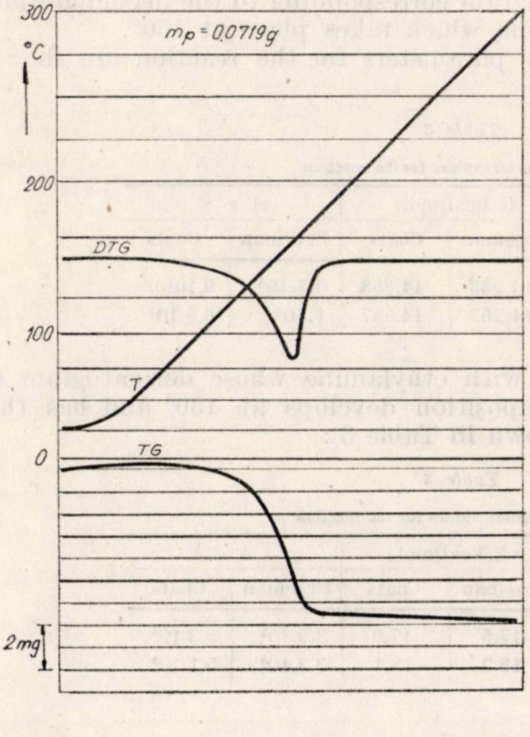

Fig. 3. — The derivatogram of decomposition of the complex with ethylamine.

The derivatogram corresponding to the decomposition of the complex with diethylamine is shown in Fig. 4. The decomposition takes place at 180°, the values of the kinetic parameters being given in Table 4.

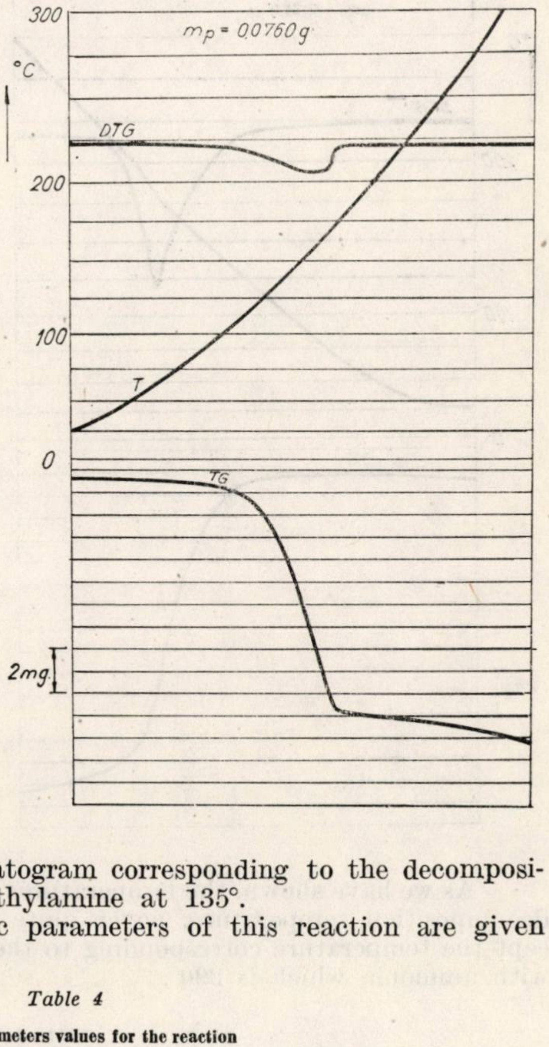

Fig. 4. – The derivatogram of decomposition of the complex with dyethylamine.

Figure 5 shows the derivatogram corresponding to the decomposition of the complex with triethylamine at 135°.

The values of the kinetic parameters of this reaction are given in Table 5.

Table 4

Kinetic parameters values for the reaction

$\frac{dT}{dt}$ °/min	n	E kcal/mole		A s^{-1}	
		Freeman	Coats	Freeman	Coats
1.59	0.25	17	17	$0.5.10^5$	$3.4.10^5$

Figure 6 shows the derivatogram of the decomposition of the complex with propylamine at 150°.

The kinetic data for the reaction are shown in Table 6.

The complex with morpholine decomposes itself at 160°.

The derivatogram is shown in Fig. 7, and the kinetic parameters are given in Table 7.

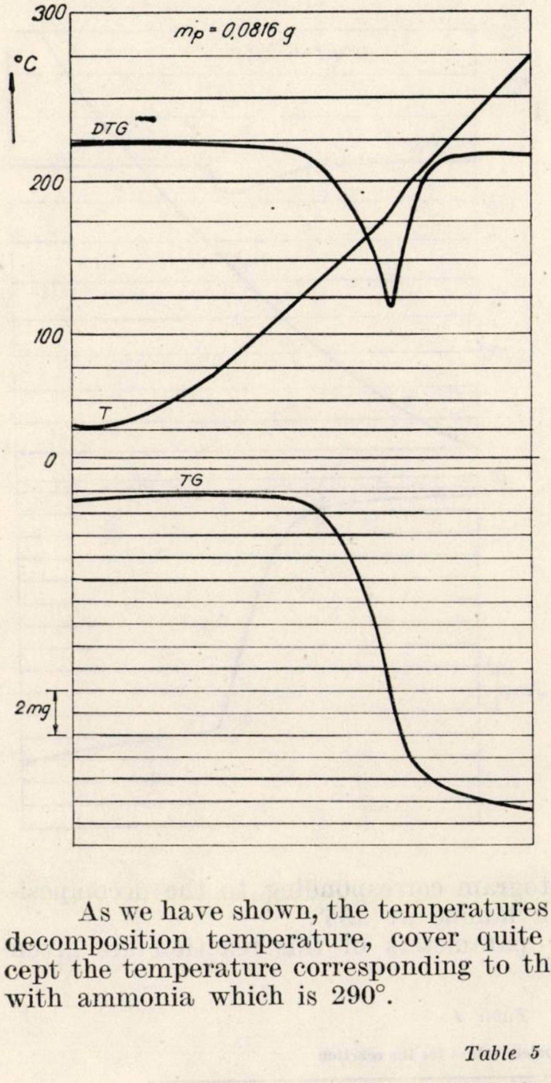

Fig. 5. – The derivatogram of decomposition of the complex with triethylamine.

As we have shown, the temperatures corresponding to the maximum decomposition temperature, cover quite a small range (130–180°), except the temperature corresponding to the decomposition of the complex with ammonia which is 290°.

Table 5

Kinetic parameters values for the reaction

$\frac{dT}{dt}$ °/min	n	E kcal/mole		A s^{-1}	
		Freeman	Coats	Freeman	Coats
12.72	0.35	17	17.64	$1.3.10^5$	$1.4.10^6$
6.36	0.27	16	16	$5.7.10^4$	$1.5.10^5$
2.14	0.3	16.1	16.36	$2.8.10^4$	$2.2.10^5$
1.34	0.3	16.14	16.54	$3.2.10^4$	$2.9.10^5$

After the careful analysis of the experimental results, we can conclude that the values of the kinetic parameters are not sensitive to the change of the heating rate, that is for the maximum values of this parameter we get results which are quite comparable with the extrapolated ones for heating-rate.

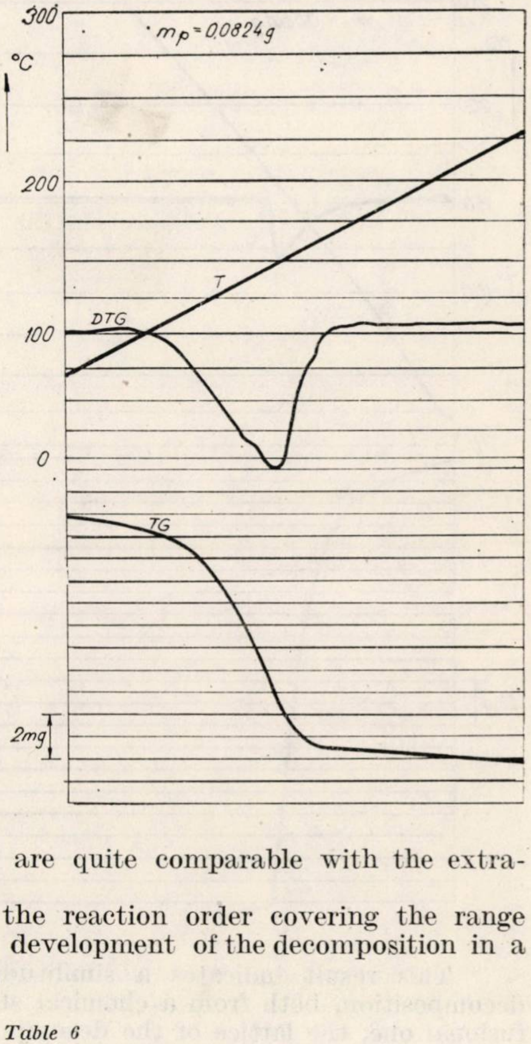

Fig. 6. — The derivatogram of decomposition of the complex with propylamine.

The fractionary values of the reaction order covering the range from 0.25 up to 0.40 show the development of the decomposition in a mixed kinetic-diffusional regime[8].

Table 6

Kinetic parameters values for the reaction

$\frac{dT}{dt}$(°/min)	n	E (kcal/mole)		A (s)$^{-1}$	
		Freeman	Coats	Freeman	Coats
6.46	0.4	17	18.3	$0.7.10^6$	$1.3.10^7$
2.44	0.36	18.9	18.5	2.10^6	$1.7.10^7$
1.31	0.38	18.3	18.3	$1.9.10^7$	$0.99.10^7$

---

[8] I. G. MURGULESCU, D. FĂTU and E. SEGAL, *J. Thermal Anal.*, **1**, 97 (1969).

It can also be noticed that the values of the kinetic parameters for the investigated reactions within the limits of experimental errors, do not differ too much.

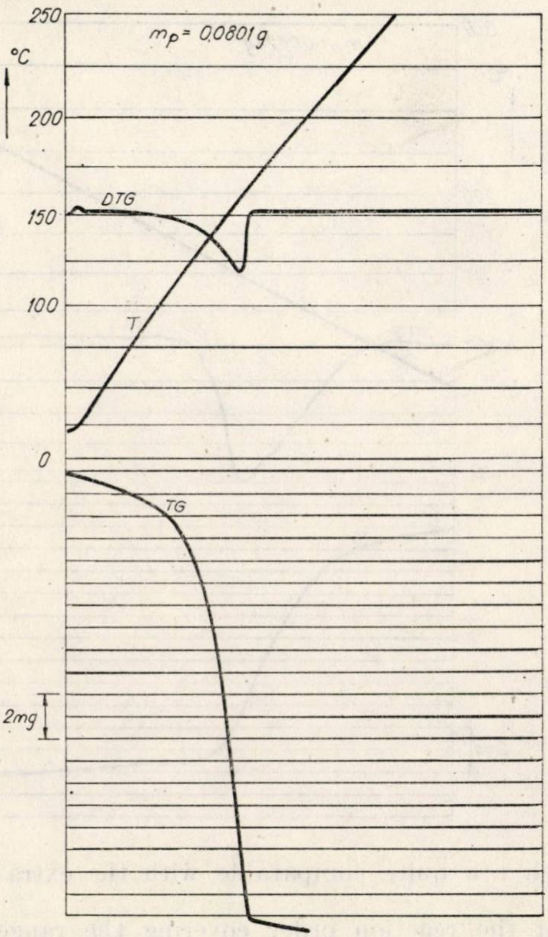

Fig. 7. — The derivatogram of decomposition of the complex with morpholine.

This result indicates a similitude concerning the mechanism of decomposition, both from a chemical standpoint and mainly from a diffusional one, the lattice of the decomposed substance through which the volatile component is eliminated, being the same.

Table 7

Kinetic parameters values for the reaction

$\frac{dT}{dt}$ (°/min)	n	E(kcal/mole)		$A(s^{-1})$	
		Freeman	Coats	Freeman	Coats
2.625	0.4	19.193	18.838	$7.8.10^5$	7.10^6
1.69	0.4	19.248	18.9	$5.6.10^5$	$6.3.10^6$

CONCLUSION

The decomposition of the analysed complexes takes place with the formation of 1,3,7,9-tetranitrophenothiazine-5-oxide in solid phase, and the elimination of the ammonia, amines and morpholine in vapour phase.

The values of the kinetic parameters of decomposition are close to one another, proving the existence of a mainly diffusional mechanism through the same lattice.

Revue Roumaine de Chimie, **23**, *1*, 157–160 (1978)

COMPTES RENDUS

"NMR-Basic Principles and Progress" ed. : P. Diehl, E. Fluck and R. Kosfeld, vol. 12, Björn Lindman and Sture Forsén, "Chlorine, Bromine and Iodine NMR. Physico-Chemical and Biological Applications". Springer Verlag, Berlin, 1976, 368 p.

Although halogens are known as "the most perfect series" from the periodic table, some special physical and chemical properties of fluorine in comparison with chlorine, bromine and iodine are also well known. The same discrepancy occurs also in NMR properties where fluorine nucleus posseses a spherical distribution of nuclear charge whereas all stable isotopes of the other halogens (^{35}Cl, ^{37}Cl, ^{79}Br, ^{81}Br, ^{127}I) have nuclear quadrupole moments. These quadrupole moments determine practically all the NMR characteristics of chlorine, bromine and iodine.

The present book shows how, in spite of the known difficulties in the study of NMR spectra of nuclei with electric quadrupole moments, Chlorine-, Bromine- and Iodine-NMR have brought a considerable amount of useful data for physicists and chemists.

The book is divided in two main parts, the former discussing the NMR of covalent halogen compounds (of Cl, Br, I) and the latter the NMR of halide ions.

Chapter 1, "Introductory Aspects", presents clearly and in an accessible form the characteristic features of halogen NMR, classified according to static parameters (quadrupole splittings, nuclear shieldings and spin-spin couplings) and dynamic ones (quadrupole relaxations and other relaxation mechanisms). Nevertheless in the introduction of the following 7 Chapters the main theoretic principles involved (applicable to all quadrupolar nuclei) are resumed in an abstracted form in order to facilitate the understanding of the reader who performs only a selective reading.

The covalent halogen NMR spectra are presented in Chapters 2, "Relaxation in Molecules or Ions with Covalently Bonded Halogens"; 3, "Shielding Effects in Covalent Halogen Compounds" and 4, "Scalar Spin Couplings". Some relevant characteristics of these spectra are underlined e.g. : the quadrupole relaxation as the most important relaxation mechanism; the importance of studying halogen relaxation in liquids in order to test the applicability of theoretical models of motion in liquids; the experimental difficulties encountered in determinations of chemical shifts (line width of about 10 kHz, corresponding to 2000 ppm at an observing frequency of 5 MHz); the availability of shielding data only for covalent chlorine; the impossibility of direct determination of spin-spin coupling constants due to the very effective relaxations; the limited data for halogen couplings (all indirectly determined, only for one- or two-bond couplings and without a sign attribution).

The NMR spectra of halide ions are presented in the following Chapters : 5, "Relaxation of Chloride, Bromide and Iodide Ions"; 6, "Shielding of Halide Ions" and 7, "Quadrupole Splittings in Liquid Crystals".

The large development of NMR studies of halide ions in solutions is mainly due to the good resolution of spectra, which follow from the decreased operativity of quadrupole relaxation mechanism due to the very small field gradients at the nuclei.

In connection with quadrupole relaxation of halide ions in solution, which is "by far the most studied aspect of Cl-, Br- and I-NMR", the authors present in 100 pages a survey of literature data, including topics as : relaxations in infinitely dilute aqueous solutions, relaxations in aqueous solutions of alkali halides and other inorganic halides (the influence of halide concentration, temperature etc. being stressed), halide ions in surfactant systems and in mixed solvents and chemical exchange of halide ions.

Concerning the chemical shifts of halogens from halide ions the distinction between shift values of "free" and "hydrated" ion is first underlined, then different methods of calculation and estimation of shieldings are presented. The influence of salt concentration on Cl-, Br,- and I-chemical shifts in halide aqueous solutions, often expressed through linear correlations, is also described.

In Chapter 8 the applications of halogen NMR in the study of biological systems are reviewed. The basis of such studies is "chemical amplification", the effect of modification of relaxation times (T_1 and T_2) due to the efficiency of the quadrupole relaxation mechanism involving that part of halogen nuclei liganded on a protein (or other molecule with biological interest) found in an aqueous halide ion solution. The abundant material (76 pages) presents two types of studies namely : the studies of halide ions binding to native metal containing- or metal-free-proteins (e.g. : carbonic anhydrase, alcohol dehydrogenase, alkaline phosphatase etc.) and studies of halide ions binding to proteins where an artificial metal label is attached (e.g. hemoglobin). In this connection different parameters obtained from such experiments are discussed : binding constants of halide ions ; stoichiometry of metal reactive groups on a protein ; quadrupole coupling constants of halide ions in macromolecular binding sites ; rates and activation parameters of halide ion exchange etc.

In Chapter 9, "Studies of the Perchlorate Ion", the NMR characteristics of this ion — which are different from those of both covalent chlorine and chloride ions — are discussed.

The entire book is written in a clear and even didactic style. Thus, when the presentation of halogen NMR parameters is made, frequent comparisons with the more usual parameters of non-quadrupolar nuclei are discussed in order to clarify the differences.

Results obtained in the authors'laboratory from University of Lund (often unpublished ones) are mentioned throughout the book, e.g. : calculations of chlorine chemical shifts in chlorometanes, medium effects on the shielding of chlorine, the study of ClO_4^- in connexion with protein chemistry etc.

The various tables of data and numerous references (530, up to january, 1976) are of great value and could be considered a real collection of NMR data for chlorine, bromine and iodine.

In my opinion this useful and interesting book greatly contributes to deny the slogan "NMR is dead", which appeared in the late 1960's among some scientists.

M. Banciu

"NMR-Basic Principles and Progress", ed. : P. Diehl, E. Fluck and R. Kosfeld, vol. 13, "Introductory Essays", ed. by M.M. Pintar, Springer Verlag, Berlin, Heidelberg, New York, 1976, 154 p. 48 fig.

The book contains 11 essays which were presented as lectures at the 4th Waterloo International Summer School on Nuclear Magnetic Resonance (June 1975, University of Waterloo, Canada). It is mentioned that the contributions are introductory and were not intended to be review papers.

All the papers develop interesting and modern problems of nuclear magnetic resonance, topics which are discussed from a theoretical point of view. It depends only upon the particular interest of the reader in order to assess which lecture suits better his interest. Therefore we would like to limit ourselves only to mention the titles and the authors (all well-known scientists in the field) : A Guide to Relaxation Theory (A.G. Redfield) ; Thermodynamics of Spin Systems in Solids (J. Jeener) ; Coherent Averaging and Double Resonance in Solids (J. S. Waugh) ; Macroscopic Dipole Coherence Phenomena (E. L. Hahn) ; Nuclear Spins and Non Resonant Electromagnetic Phenomena (G. J. Bene) ; Nuclear Spin Relaxation in Molecular Hydrogen (F. R. Mc Court) ; Longitudinal Nuclear Spin Relaxation Time Measurements in Molecular Gases (R. L. Armstrong) ; Spin-Lattice Relaxation in Nematic Liquid Crystals Via the Modulation of the Intramolecular Dipolar Interactions by Order Fluctuation (R. Blinc) ; NMR Studies of Molecular Tunnelling (S. Clough) ; Effect of Molecular Tunnelling on NMR Absorption and Relaxation in Solids (M. M. Pintar) and How to Build a Fourier Transform NMR Spectrometer for Biochemical Applications (A. G. Redfield).

From the different characteristic features of the book we can mention only a few : the direct style ; the elegant and attractive presentation (e.g. the lecture "Nuclear Spins and Non Resonant Electromagnetic Phenomena" by G.J. Bene and "Longitudinal Nuclear Spin Relaxation Time Measurements in Molecular Gases" by R. L. Armstrong), the rigorous mathematical treatment (e.g. in "Spin-Lattice Relaxation in Nematic Liquid Crystals" by R. Blinc), the adequate illustration of the text with figures, schemes or diagrams and the good printing of the book.

The article "How to Build a Fourier Transform NMR Spectrometer for Biochemical Applications" by A.G. Redfield deserves a special mention due to its very practical character ; the described constructions and operation as well as the recomendations greatly contributes to "make Fourier transform spectrometers more convenient and less formidable looking to the novices".

In conclusion, the 13th volume of the series "NMR-Basic Principles and Progress" is a collection of interesting lectures, discussing various aspects of modern NMR spectroscopy and we believe that it would be useful for a large number of physical chemists and molecular physicists.

M. Banciu

"Tetrahedron Reports" (numbers 15, 16, 17 and 19), Pergamon Press, Oxford, 1976

With these Reports the "Tetrahedron" continues the recent series of reviews concerning modern aspects of organic chemistry.

The Report N°. 15 : *Catecholborane. A New Hydroboration Reagent*, is written by Clinton F. Lane and George W. Kabalka. In ten pages (64 references) the authors describe the applicability of a new hydroboration reagent, namely catecholborane (1,3,2-benzodioxaborole), which could be conveniently prepared from catechol with BH_3.THF, and shows remarkable stability in dry air. In description of hydroboration of alkenes the nearly quantitative yields, the stereoselectivity of the reaction as well as some synthetic applications of B-alkylcatecholboranes obtained from such reactions (e.g. the oxidation to alcohols with H_2O_2/NaOH or the conversion to "mixed" trialkylboranes) are presented.

The hydroboration of alkynes with catecholborane, which affords in a regioselective and stereospecific manner *B*-alkenylcatecholboranes is then presented and some synthetic applications of such boranes are mentioned (e.g. : stereospecific synthesis of alkenes or of alkenylmercurials, synthesis of alkenyl iodides with retention of configuration and synthesis of alkenyl bromides with inversion of configuration and synthesis of alkenyl bromides with inversion of configuration). Characteristic experimental procedures are given throughout the report.

The Report No 16 : *Ynamine: A versatile Tool in Organic Synthesis* (38 pages) is written by Jaqueline Ficini. After a short introduction in which the characteristic features of ynamines chemistry are stressed and useful comparisons with related compounds (e.g. enamines) are mentioned the following two main sections describe: "Addition reactions of ynamines leading to the formation of C—C bonds" and "Cycloaddition reactions with ynamines". The very rich chemical literature of the domain is presented not exhaustively but in a way which "show through various examples the unusual capability of ynamines and the new pathways which are made available to synthesis by this versatile tool". From the addition reactions, the regiospecific acylation of cyclenones, the synthesis of heterocyclic compounds and of spiranes as well as the formation of γ-unsaturated amides deserve special mention. From cycloadditions of ynamines some interesting examples should be also cited : synthesis of unsaturated amides (from carbonyl derivatives), synthesis of cyclobutenones and allenes (from ketenes) first synthesis of amino-γ-pyranes (from ethylenic ketones) and the selective cycloadditions with cyclenones. The applicability of ynamines in stereospecific synthesis of some chiral compounds (e.g. juvabione) is stressed.

The complex problems of ynamine chemistry are presented (116 references from which 45 by J. Ficini) in a very clear and easily understandable fashion, confirming, thus again the statement : "ce que l'on conçoit bien s'énonce clairement".

The Report No. 17 : *The Organic Photochemistry of Benzene. I*, by D. Bruce-Smith and A. Gilbert, presents in 18 pages (113 references) the photoisomerization reactions of benzenes. The brief introduction contains a discussion of the UV-spectrum of benzene and an orbital-symmetry approach for photoisomerisations and cycloadditions of benzene. In the following sections the photoisomerisations of unsubstituted benzene and of substituted benzenes (hexafluorobenzene, alkylbenzenes, dialkylbezenes, tri-*t*-butylbenzenes) are described. In all cases mechanistic pictures are presented. Some interesting results from the field are detailed e.g. : isolation of tri-*t*-butyl-Dewar-benzene on irradiation of the very crowded 1,2,4-tri-*t*-butylbenzene ("a striking example of creative reasoning"), the ring transpositions which give rise to apparent shifts of alkyls on irradiation of alkylbenzenes. The review clearly demonstrates that the "photochemistry of benzene is much more varied than the thermal chemistry".

A minor observation could be made concerning the lack of uniformity for some units (namely wavelengths in Å and nm at the same page 6 ; energies in kcal/mol and kJ/mole).

The Report No. 19 : *New Horizons in Carbonyl Chemistry: Reagents for Nucleophilic Acylation* (29 pages, 261 references) is written by O. William Lever, jr. The author presents a very interesting review concerning the nucleophilic acylation, method in which "formally at least, the carbonyl carbon atom abandons its traditional role and functions as a nucleophilic center". Such reactions, including a polarity inversion (also known as "symmetrization of reactivity", "charge affinity inversion", or as "Umpolung") offer a powerful strategy in organic chemistry, conducting to rich series of new reagents which could function as synthetic equivalents ("synthons" of normally inaccessible intermediates. Although the described reactions do not create novel functionalities, the major interest lies "in utilization of starting materials altogether different from those in conventional procedures". The descriptive material presents the available synthons of elusive carbonyl anion. The most useful reagents for nucleophilic acylation are realised starting from halides ($RX \rightarrow R-CO^-$) or from aldehydes ($RCO \rightarrow RCO^-$). From the numerous interesting reactions we mention : the utility of protected cyanohydrin anions for ketone synthesis (procedure developed as a consequence of the clear understanding of mechanism of benzoin condensation) and the large development of 1,3-ditiane-anions, the most versatile and accessible reagents in nucleophilic acylation.

The present review greatly contributes to a better understanding of the polarity inversion and through its very rich material could offer the reader new ideas in this interesting field.

M. Banciu

"Journal of Power Sources". Vol. 1, N° 1 and N° 2, Elsevier Sequoia S.A., Switzerland, Ed. D. H. Collins

In recent years, there has been a steady growth of scientific interest and research into the problems of non-mechanical generation, storage and conversion of electrical power.

Unfortunately until last year there was not a single international journal in this field, the scientific papers being printed in different publications.

Starting from 1976, Elsevier Scientific Publishing Company is publishing the Journal of Power Sources, an international journal edited by D. H. Collins and having an editorial board representative of industry and research institutes throughout the world. The scope of the journal is to bring together work from many scientific disciplines related with the subject of non-mechanical generation of electrical power.

The idea of bringing together internationally in one journal all the work on power sources, which until recently was published in different scientific publications, is a very good one giving the possibility to the scientist to obtain the necessary information in a more direct way.

This new publication met a very important need in the field of power sources in a period when the importance of the problem has been emphasized by the energy crises.

The first two numbers dealt mainly with problem related with lead-acid batteries, zinc-air, nickel-cadmium, fuel cells, solid state batteries, sodium/sulphur and metal/halogen batteries.

From these two numbers of the journal someone can notice the important impact which the electrochemical research has in this field, all the papers being in fact electrochemical work, no papers dealing with thermoionic, thermo-electric and isotope-generator being published so far in this journal.

No doubt that from now on every research worker in this field has to read the Journal of Power Sources, the only international publication on the non-mechanical generation, storage and conversion of electrical power.

N. Totir

NOTE POUR LES AUTEURS

La Revue Roumaine de Chimie publie des articles en anglais, français, russe, allemand ou espagnol. Les auteurs sont priés d'envoyer des articles et des comptes rendus inédits.

Les manuscrits seront dactylographiés à deux intervalles. La bibliographie, les tableaux et la légende des figures seront placés après le texte.

Si l'article fait partie d'une série numérotée, le titre de la partie précédente sera indiqué dans une note au bas de la première page.

Chaque article sera précédé d'un résumé comprenant quinze lignes au maximum.

Les références bibliographiques dans le texte seront faites par des exposants sans parenthèse et paraîtront comme des notes au bas de chaque page.

Les publications périodiques mentionnées dans la bibliographie seront présentées suivant les prescriptions internationales : le nom de l'auteur précédé de l'initiale du prénom, le titre du périodique abbrégé conformément à « Chemical Abstracts » et souligné par une ligne, le numéro du tome, indiqué par des chiffres arabes et souligné par deux lignes, suivi de la première page de l'article ; à la fin, l'année de la parution sera placée entre parenthèses. Le numéro de la revue ne sera pas indiqué si les pages du volume sont numérotées consécutivement. Pour les revues dont les tomes ne sont pas numérotés (par ex. Bull. Soc. Chim. France, etc.), l'année de la parution soulignée par deux lignes précèdera l'indication de la page.

Les textes des livres ou traités incluеront : les noms des auteurs, les initiales du prénom, le titre du livre entre guillemets et sans être souligné, le numéro du tome précédé par l'abbréviation « vol. » (ou « Bd. »), le numéro de l'édition, les éditions (the publisher), la localité de la parution et la page de la référence précédée par l'abbréviation « p. » (ou « S. »).

Les brevets seront indiqués comme suit : l'auteur ou la firme, le pays et le numéro du brevet, la date et la revue (Chem. Abstr.). Par ex. : M. Jones (to Union Carbide Co.), Brit. Pat. 601 238, 2 Sept. 1959, *Chem. Abstr.*, **54**, 12808 (1960).

Si la référence n'a pas été lue en original, on indiquera aussi la revue de références consultée.

Les diagrammes seront tracés à l'encre de Chine sur papier calque. Les tableaux et les figures (en nombre strictement nécessaire) seront numérotés par des chiffres arabes et leur explication sera donnée dans la légende des figures. Prière de ne pas inscrire les mêmes données dans les tableaux et les figures. Chaque tableau aura un titre. On indiquera dans le texte la place approximative des tableaux et des figures. Les formules chimiques seront incluses dans le texte ; en outre, elles seront transcrites sur papier calque, à l'encre de Chine.

Les auteurs sont priés d'indiquer les caractères italiques (en soulignant les lettres au crayon), ainsi que tout autre caractère spécial ; les préfixes *ortho*, *meta*, *para*, *cis*, *trans*, etc. seront soulignés pour indiquer leurs caractères italiques et ne seront jamais écrits avec des majuscules.

Aucune correction à la main ne sera admise sur le manuscrit. Les corrections seront frappées à la machine. Les lettres grecques ou d'autres symboles spéciaux seront insérés à la main à l'encre clairement.

Le manuscrit sera signé par l'auteur

Le colonne-titre aura 50 lettres au maximum.

L'entière responsabilité du contenu des articles appartient aux auteurs.

TRAVAUX PARUS AUX ÉDITIONS DE L'ACADÉMIE DE LA RÉPUBLIQUE SOCIALISTE DE ROUMANIE

C. DRĂGULESCU, E. PETROVICI, **Chimia structurală modernă. Chimia coordinanței** (La Chimie structurale moderne. La Chimie de la coordinence), 1977, 947 p., 70 lei.

I. G. MURGULESCU, **Introducere în Chimia fizică. Vol. I. 1. Atomi, molecule, legătură chimică** (Introduction à la Chimie Physique, Ier vol. 1. Atomes, molécules, liaison chimique), 1976, 560 p., 36 lei.

E. P. BALTĂ, E. BALTĂ, **Introduction to the physical chemistry of the vitreous state**, coédition avec Abacus Press, 1976, 287 p., 31 lei.

H. I. GĂLĂŢEANU, **Radiochimia aplicată. Metode şi probleme** (La radiochimie appliquée. Méthodes et problèmes), 1976, 307 p., 19 lei.

C. V. UGLEA, **Cromatografia pe gel permeabil. Noi domenii de aplicare** (La chromatographie sur gel perméable. Nouveaux domaines d'application), 1976, 120 p., 6,75 lei.

FR. A. GOTHARD, **Echilibre lichid-vapori. I. Baze teoretice şi metode de calcul** (Equilibres liquide-vapeurs. I. Bases théoriques et méthodes de calcul), 1975, 262 p., 28 lei.

CONST. GH. MACAROVICI, DAN MACAROVICI, **Chimia oxizilor dubli şi utilizările lor** (La Chimie des oxydes doubles et leur utilisation), 1975, 194 p., 13 lei.

ELENA CEAUŞESCU, **Research work on synthesis and caracterization of macromolecular compounds. Contributions**, 1974, 251 p., 20 lei.

I. ZUGRĂVESCU et MAGDA PETROVANU, **Chimia N-Ilidelor** (La Chimie des N-Ilures, 1974, 347 p., 19 lei.

MARGARETA AVRAM, **Antidăunători** (Pesticides), 1974, 494 p., 41 lei.

CR. SIMIONESCU, VIORICA RUSAN et N. POPA, **Chimia algelor marine** (La Chimie des algues marines), 1974, 211 p., 18 lei.

TIBERIU NĂŞCUŢIU, **Metode radiochimice de analiză** (Méthodes radiochimiques d'analyse), 1973, 384 p., 23 lei.

MARIA FITI, **Dozimetria chimică a radiaţiilor ionizante** (Le dosimétrie chimique des radiations ionisantes), 1973, 240 p., 13,50 lei.

MIHAI FLORESCU, **Eficienţa economică a cercetării ştiinţifice** (L'efficience économique de la recherche scientifique), 1972, 115 p., 15 lei.

GEORGETA LĂZĂRESCU, **Sistematizarea informaţiilor în Chimia organică** (La systématisation des informations dans la Chimie organique), 1972, 252 p., 10,50 lei.

I. P. INFORMAŢIA c. 7622

43 426

Lei 25.—

F 1103

ACADÉMIE DE LA RÉPUBLIQUE SOCIALISTE DE ROUMANIE

REFERALVA

REVUE ROUMAINE DE CHIMIE

TOME 23
N° 2
Février 1978

EDITURA ACADEMIEI REPUBLICII SOCIALISTE ROMÂNIA
Rev. Roumaine Chim.
RRCHAX, 23, 2, p. 161–312 (1978), Bucarest

ACADÉMIE DE LA RÉPUBLIQUE SOCIALISTE DE ROUMANIE

COMITÉ DE RÉDACTION

Rédacteur en chef:

I. G. MURGULESCU, membre de l'Académie de la République Socialiste de Roumanie

Rédacteurs en chef adjoints:

A. T. BALABAN et V. EM. SAHINI, membres correspondants de l'Académie de la République Socialiste de Roumanie

Collège de rédaction:

EM. BRATU, ELENA CEAUȘESCU, ECATERINA CIORĂNESCU-NENITZESCU, |C. DRĂGULESCU|, CR. SIMIONESCU, membres de l'Académie de la République Socialiste de Roumanie; P. SPACU, membre correspondant de l'Académie de la République Socialiste de Roumanie; MARGARETA AVRAM, I. HAIDUC, D. I. MARCHIDAN, I. MOLDOVAN, G. NIAC et D. SĂNDULESCU

La Revue Roumaine de Chimie parait 10 fois par an. Toute commande de l'étranger (fascicules ou abonnements) sera adressée à : 70116, ILEXIM Departamentul Export-Import Carte (Livres)/Departamentul Export-Import Presă (Revues), P.O.B. 136—137 télex 11226, Bucarest 12, 3, str. 13 Decembrie, Roumanie

Les manuscrits, les livres et les revues proposés en échange ainsi que toute correspondance seront envoyés à la rédaction :

REVUE ROUMAINE DE CHIMIE

23, str. Dumbrava Roșie, Bucarest, 9, Roumanie, téléphone 12 41 60

EDITURA ACADEMIEI REPUBLICII SOCIALISTE ROMÂNIA

71021, 125, Calea Victoriei, Bucarest, Roumanie, téléphone : 50 76 80

REVUE ROUMAINE DE CHIMIE

1978 MAR. 9

Tome 23, N° 2 Février 1978

V. E. SAHINI, V. CONSTANTIN, I. ŞERBAN and C. VLĂDESCU, Electron impact-induced fragmentation of dibenzo/b,e/oxepin-11-one and dibenzo/b,e/thiepin-11-one 163–169

R A. SWINARSKI and W. KLAFKOWSKI, Influence of the origin of iron oxide on the catalytic activity of the catalyst (in French) 171–178

S. SENENT, L. FERRARI and A. ARRANZ, Kinetic study of the reduction of Cr(VI) by hydrazine (in Spanish) 179–186

A. T. BALABAN, ILEANA I. STĂNOIU and F. CHIRALEU, Isotope effects in lanthanide-induced shifts of ^{1}H–NMR spectra of selectively side-chain deuteriated pyridines 187–196

NORA RĂDULESCU and C. SÂRBU, Solvent and medium basicity effects on the reaction of 5-chloro-2-pentanone with sodium methoxide 197–202

S. DESHERCES, J. BARRANS and J. L. ROUBATY, Synthesis of 4-hydroxy-Δ^2-oxadiazolines-1,2,4 (in French) 203–208

R I. DRIMUŞ and L. PAPAHAGI, On the influence of the chain length of n-alkanes on the composition of monocarboxylic acids formed by catalytic autoxidation of n-alkanes in liquid phase with molecular oxygen (in German) . . 209–214

A. C. BANCIU, O. CONSTANTINESCU and P. SPACU, EPR study of chelate complexes with Cu(II)–N(sp^2) bonds 215–223

L. CORMOŞ, A. POP and LUCIA ORBU, Contributions to the study of the catalytic activity of some $n\mathrm{SiO_2}.m\mathrm{Al_2O_3}.x\mathrm{H_2O}$ systems in the decomposition reaction of cumene hydroperoxide. V. Influence of the reaction medium . . 225–231

J. M. CACHAZA, J. CASADO and A. VARELA, Study of Arbuzov reactions. II. Reactions between trialkylphosphites and ethyl bromides (in Spanish) 233–236

R CR. I. SIMIONESCU, D. FELDMAN and VIOLETA NUŢĂ, Copolymerization of acrylonitrile with methacrylic esters in the presence of organo-metallic catalysts 237–250

R D. F. ANGHEL and GEORGETA POPESCU, Anionic surfactant analysis from micellar solutions 251–253

C. CINCU and C. BOGHINĂ, Unperturbed dimensions of copolymers. Poly(N-vinylcaprolactam-diethylfumarate) alternating copolymer 255–260

GH. DRĂGAN, Amorphous-crystalline coupling in polyethylene. V. Lamellar recrystallization in shear history 261–264

R S. GOCAN, T. HODIŞAN, H. NAŞCU and CARMEN GEORGESCU, Separation and determination of phenol and salicylic acid in industrial wastes 265–268

Rev. Roumaine Chim. 23, 2, p. 161–312 (1978), Bucarest

R A. M. QURESHI and S. A. MALIK, A modified non cyanide scheme for the qualitative chemical analysis of the group II A sulphides 269–271
R ELENA HOPÎRTEAN and ELISABETA VERESS, Ion selective membrane-electrodes for organic analysis. I. Liquid membrane-electrode for some organic anions based on cetylpyridinium salt 273–279
L. CAMPANELLA, T. FERRI and D. GOZZI, Pyridinemonocarboxylate ion selective electrodes 281–286
E. CORDOŞ and GEORGETA BĂRCEANU, Evaluation of a methane-oxygen-air flame for atomic emission 287–294
W. SCHMIDT, D. MARANDIUC, A. NEMEŞ and G. OSTROGOVICH, Enhancement of exactitude and reduction of time in planimetry of this layer chromatograms (in German) 295–299
D. IORDACHE, On the vibrational anharmonicities of the furan molecule . . . 301–307

BOOK REVIEWS 309–311

Revue Roumaine de Chimie, **23**, *2*, 163–169 (1978)

ELECTRON IMPACT-INDUCED FRAGMENTATION OF DIBENZO/b,e/OXEPIN-11-ONE AND DIBENZO/b,e/THIEPIN-11-ONE

V. E. SAHINI[a], V. CONSTANTIN[a], I. ŞERBAN[a] and C. VLĂDESCU[b]

[a] The Polytechnic Institute Bucharest, Institute of Chemistry, Department of Physical Chemistry, Bd. Republicii 13, Bucharest, Romania

[b] Institute of Internal Medicine of the Academy of Medical Sciences, Şos.Ştefan cel Mare 19, Bucharest, Romania

Received January 29, 1977

The 50 eV mass spectra of dibenzo/b, e/oxepin-11-one and dibenzo/b, e/thiepin-11-one are reported and discussed. The compounds present a high stability to electron impact. The main fragmentation pathways depend upon the nature of the heteroatom in the central seven-membered ring. The ionization potentials and the appearance potentials for the more relevant fragments are reported.

The dibenzoheterocyclic compounds containing a seven member intermediate cycle have been scarcely studied in mass spectrometry.[1,2] The use of dibenzo/b, e/thiepin-11-one for the synthesis of medicines such as prothiadene [3] justifies the interest in the study of their fragmentation to electron impact. The compounds studied in this work have the following structure :

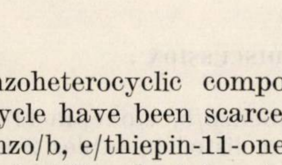

X = O, M = 210
X = S, M = 226

and contain two specific fragmentation centres : the X heteroatom in 5 position and the carbonyl group in 11 position.

---

[1] G. H. Wahr jr., *Org. Mass Spectrom.*, **3**, 1349 (1970).

[2] A. Maquestieu, Y. van Haverbeke and F. Delalieu, *Org. Mass Spectrom.*, **5**, 1015 (1971).

[3] M. Rajner, E. Svatek, I. Metisova and M. Protiva, *Coll. Czech. Chem. Comm.*, **34**, 1963 (1969).

EXPERIMENTAL

Mass spectra were recorded with a MI—1305 mass spectrometer using the direct evaporation sample in the ion source, at 50 eV energy of electron beam. The emission current was kept at 1.5 mA. In order to obtain a low electron energy, the mass spectrometer was modified in the original circuitry of the ionization voltage.[4]

The ionization efficiency (IE) curves were obtained by reducing the electron ionizing voltage (by means of a ten turn helical potentiometer which permitted resetting to ±0.01 volt) in 0.1 volt steps and by recording the ion current of the investigated ion on a digital voltmeter. During recording of IE curves the emission current was kept at 0.1 mA. The mercury, present in the ion source from diffusion pumps of the mass spectrometer, was used to calibrate the energy scale. The threshold voltage was evaluated by the extrapolated voltage differences to zero ion current method.[5]

Table 1

The ionization potentials and the appearance potentials of fragment ions (volts)

	Dibenzo/b,e/oxepin-11-one M=210, IP = 9.63 V.				Dibenzo/b,e/thiepin-11-one M = 226, IP = 9.21 V.				
m/e	209	182	181	152	225	198	197	194	193
AP	10.8	11.5	12.4	13.8	10.4	9.75	11,15	9 45	10,5

The results given in table 1 are average values from 3—4 determinations, the maximum deviation being ± 0.05 volt for parent ions and ±0.15 volt for fragment ions. Since it was not possible to vary the partial pressures of gases in the ion source, the IE curves were frequently unparallel, particularly for fragment ions. For this reason the absolute values of appearance potentials for some fragments may possibly be affected by an error higher than indicated above.

RESULTS AND DISCUSSION

The 50 eV mass spectra of dibenzo/b, e/oxepin-11-one (DBO) and dibenzo/b, e/thiepin-11-one (DBT) are listed in tables 2 and 3. The mass spectra in the range of higher masses (above m/e 180) were also run at low electron voltages (15—20 volt) in order to choose the proper fragmentation routes. Since the appearance potentials have been measured for the main fragments, these low voltage mass spectra have not been included.

Table 2

Mass Spectrum of Dibenzo/b, e/oxepin-11-one

m/e	212	211	210	209	182	181	165	154	153	152	151
Rel. int.	1.5	15.5	100	35	24	85	11	9	30	36	10

m/e	128	127	126	115	105	92	91	90	89	77	76
Rel. int.	6	7	4	5	6	4	9	10	18	10	14

Peaks having an intensity lower than 3% of the base peak are not included. Metastable peaks are found at m/e values of 155 to 157 and 129. Doubly charged ions are found at m/e values of 105.5, 104.5, 91.5 (1% rel. int.), 90.5 (1.5%), 82.5, 81.5, 76.5 (1.8%) and 69.5; except otherwise indicated, the other doubly charged ions have an intensity lower than 0.3%.

---

[4] V. E. Sahini, L. Rădulescu and V. Constatin, (forthcoming).

[5] J. W. Warren, *Nature*, **165**, 810 (1950).

Table 3

Mass Spectrum of Dibenzo/b, e/thiepin-11-one

m/e	228	227	226	225	198	197	196	195	194	193	180
Rel. int.	4	17	100	36	8	45	8	7	12	51	3
m/e	171	166	165	164	163	153	152	151	139	121	115
Rel. int.	4	7	42	6	5	6	12	4	4	7	3
m/e	113	108	98	97	91	90	89	83	82	77	76
Rel. int.	4	3	4	4	3	4	12	4	4	7	6

Peaks having an intensity lower than 3% of the base peak are not included. Metastable peaks are found at m/e values of 170 to 174, 164 to 166 and 136 to 144. Doubly charged ions are found at m/e values of 113,5, 112.5, 98.5 (1.8% rel. int.), 97.5 (1.7%), 96.5, 86.5, 85.5 (1%), 82.5 (2.2%), 81.5, 76.5 and 69.5 ; unless otherwise for indicated, the other doubly charged ions have an intensity lower than 0.3%.

The studied compounds present a high stability to electron bombardment the molecular ions constituting the base peak (and around 15% of total ionization) in both spectra. The fragmentation of molecular ions yields a relatively small number of specific ions whose origin and structure may be generally derived from the mass spectra and from the study of these compounds at low electron energy.

MASS SPECTRUM OF DIBENZO/b,e/OXEPIN-11-ONE (DBO)

Examination of the DBO mass spectrum revealed two metastable transitions (table 2) which, correlated with the mechanical information derived from the spectra, allow to establish the main fragmentation route of the molecular ion (scheme 1).

$$\begin{tikzcd}
m/e\ 210 \arrow[r, "-H"] & m/e209 \arrow[r, "-CO"] & m/e\ 181 \arrow[r, "-CO"] & m/e\ 153 \arrow[r, "-H"] \arrow[d, "-C_2H_2"] & m/e\ 152 \arrow[r] \arrow[d, "-C_2H_2"] & m/e\ 76 \\
 & & & m/e\ 127 & m/e\ 126 &
\end{tikzcd}$$

Scheme 1.

It is observed that this route includes almost all the major peaks from the mass spectrum of DBO.

The study of the low voltage spectra indicated that while the relative intensity of m/e 181 and m/e 153 peaks diminished, the relative intensity of m/e 182 and m/e 154 peaks increased as the energy decreased. This behaviour suggests the existence of a second fragmentation route, initiated by loss of a CO molecule directly from the molecular ion (scheme 2) :

$$\begin{tikzcd}
m/e\ 210 \arrow[r, "-CO"] & m/e\ 182 \arrow[r, "-CO"] \arrow[d, "-H"] & m/e\ 154 \arrow[r] \arrow[d, "-C_2H_2"] & m/e\ 77 \\
 & m/e\ 181 & m/e\ 128 &
\end{tikzcd}$$

Scheme 2

The major fragmentation pathways of DBO under electron impact and the possible structures suggested for the main ions are presented in scheme 3. The main feature of DBO decomposition under electron impact is the succesive loss of two molecules of carbon monoxide from the $M^{+\cdot}$ molecular ion and/or from the $(M-1)^+$ ion, leading to ions m/e 182 and m/e 154 and/or m/e 181 and m/e 153, respectively.

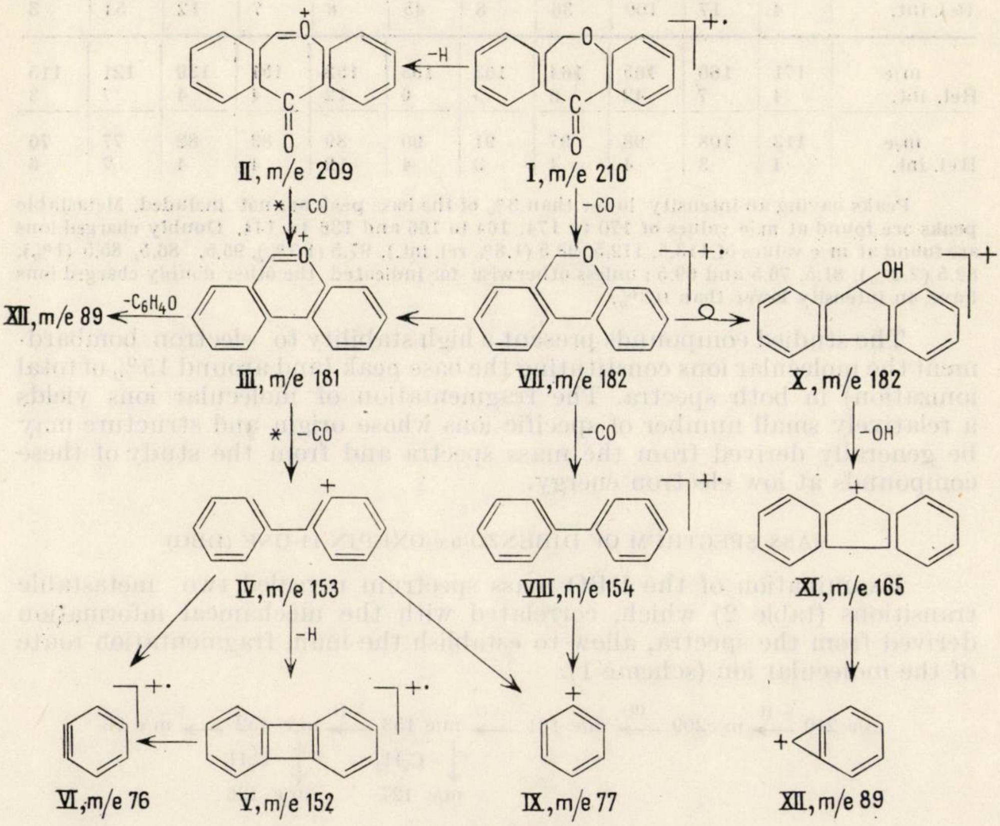

Scheme 3

The first CO molecule eliminated presumably originates in the 11 position of carbonyl group, while the second implies the carbon atom in 6 position of the initial DBO molecule. The high intensity of the m/e 181 and 182 ions suggests a stable, closed ring structure, of the phenanthrene skeleton type.

The elimination of the second CO molecule from III, m/e 181 and VII, m/e 182 ions is accompanied by the migration of the hydrogen atom (or atoms, respectively) towards the ring skeleton leading to the biphenyl-type ions IV, m/e 153 and VIII, m/e 154, respectively. The high relative intensity of the m/e 152 odd-electron ion suggests a particularly stable structure of this ion in the ringed form of the biphenylene ion V, which presents a higher degree of charge delocalization throughout the skeleton than the m/e 154 or m/e 153 biphenyltype ions.

The ions situated at mass numbers lower than m/e 152 have generally small intensities, except those around m/e 127, m/e 89 and m/e 76 mass numbers. The m/e 128-m/e 126 ion group arises from the m/e

154-m/e 152 ion group by the respective loss of a stable acetylene molecule and their structures can be assumed to be a naphthalene ring type. The benzocyclopropenyl cation XII structure is usually proposed[6,7] for the strong peak m/e 89, which in DBO mass spectrum results from a splitting of III,m/e 181 and XI, m/e 165 ions. The m/e 77 and m/e 76 ions assumed to have IX-phenyl and VI-dehydrobenzene structures, respectively are formed by the splitting of the biphenyl-type ions (m/e 154 and m/e 153) or the biphenylene ion m/e 152, respectively. A fraction of a few percents of the relative intensity of the m/e 77 and m/e 76 peaks belong to the 154^{++} and 152^{++} doubly-charged ions, as can be seen from the high relative intensity of doubly charged 153^{++}, m/e 76.5 ion. As the splitting of doubly charged ions is also possible at 50 eV, the formation pathways for m/e 76 and m/e 77 peaks may be represented as follows :

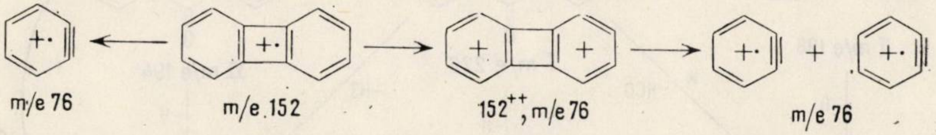

The presence of m/e 165 ion in the mass spectrum of DBO is difficult to explain. An analysis of some possible formation pathways for this ion, suggests that the most probable route is elimination of a OH radical from the m/e 182 ion, after a previous skeletal rearrangement in the X, m/e 182 species (scheme 3).

MASS SPECTRUM OF DIBENZO/b,e/THIEPIN-11-ONE (DBT)

An examination of the mass spectrum of DBT at 50 eV (table 3) reveals five strong peaks at m/e 226, m/e 225, m/e 197, m/e 193 and m/e 165. Among these, the first two peaks are assignable to the $M^{+\cdot}$ molecular ion and the $(M-1)^+$ ion respectively, and the last one represents the $C_{13}H_9^+$ fluorenyl cation, as in the mass spectrum of DBO. The m/e 197 and m/e 193 ions may arise both from the molecular ion and from the m/e 225 ion. The relative intensity of the m/e 198 and m/e 194 peaks presents an important increase in the low energy range, becoming at 15–20 eV comparable with the relative intensity of the m/e 197 and m/e 193 neighbouring strong peaks, respectively. The molecular ion fragmentation process seems therefore to be rather complex, the possible fragmentation pathways being indicated in scheme 4 :

$$\begin{tikzcd}
m/e\ 198 \arrow[d, dashed, "-H"'] & M^{+\cdot} = m/e\ 226 \arrow[l, dashed, "-CO"'] \arrow[r, dashed, "-S"] \arrow[dl, "-HCO"] \arrow[d, "-H"] \arrow[dr, dashed, "-HS"] & m\ e\ 194 \arrow[d, dashed, "-H"] \\
m/e197 & m/e\ 225 \arrow[l, dashed, "-CO"] \arrow[r, "-S"'] & m/e\ 193
\end{tikzcd}$$

Scheme 4

---

[6] L. W. Hall and E. W. Oliver, *Org. Mass Spectrom.*, **2**, 801 (1969).

[7] B. Zeeh and R. Beutler, *Org. Mass Spectrom.*, **1**, 791 (1968).

At 50 eV the m/e 198 and m/e 194 have a lower intensity (only 1% and 4 %, respectively if the isotope contribution of the m/e 197 and m/e 193 ions, respectively is taken into account) and hence, the processes involving the CO and/or S loss directly from the molecular ion are not important at higher energies. On the other hand, the metastable peaks in the mass spectrum (generally diffuse and somewhat uncertainly assignable) seem to indicate two principal fragmentation pathways of the molecular ion (full arrows in scheme 4), which initiate the formation processes of the main peaks in the mass spectrum of DBT at 50 eV (scheme 5).

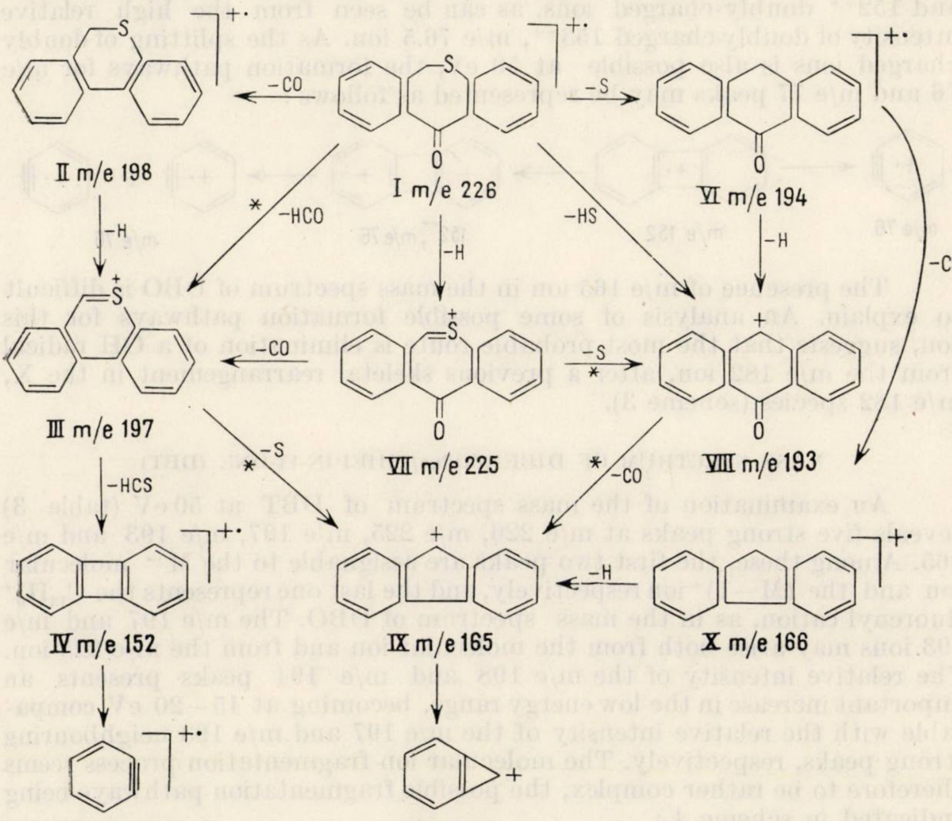

Scheme 5

The m/e 225, m/e 197, m/e 193 and m/e 165 ions of high abundance are even-electron ions and have probably the completely conjugated structures suggested in scheme 5. The III, m/e 197 ion may further decompose by elimination of the HCS (or H + CS) group with the formation of the IV, m/e 152 biphenylene ion, or by loss of the sulphur atom with the formation of the IX, m/e 165 fluorenyl cation, as in the mass spectrum of thioxanthene.[8] However, most of the relative intensity of the IX, m/e 165 peak is likely to arise from the elimination of a CO molecule from the

[8] J. HEISS and K. P. ZELLER, *Org. Mass Spectrom.*, **2**, 819, (1969).

VIII, m/e 193 ion (and in parallel from the m/e 194 → m/e 166 → m/e 165 processes), as in the mass spectrum of anthrone[6] where the m/e 165 ion is the strongest peak of the mass spectrum.

The peaks situated at lower masses than m/e 165 generally have lower intensities than the same number of mass peaks in the mass spectrum of DBO.

A comparison between the mass spectra of DBO and DBT shows that the fragmentation of such compounds to electron impact presents some common features. Thus the elimination process of a hydrogen atom occurs in the same manner in both spectra, the $(M-1)^+$ peak intensity (around 35%) and the activation energy of the processes (around 1.2 eV) being practically identical in both spectra.

The possible elimination routes of the CO group from the 11 position are also the same, leading to the $(M\text{-}29)^+$ ion, exhibiting very intense peaks in both spectra. Nevertheless, a comparison of scheme 3 and 5 shows that the formation process of $(M-29)^+$ ion occurs mainly by the direct loss of HCO in the case of the molecular ion of DBT and by successive loss of two fragments (H and then CO) in the case of the molecular ion of DBO.

The $(M-1)^+$ ion seems to play an important role in the mass spectra. The subsequent decomposition of this ion leads mainly to the m/e 165 cation in the DBT mass spectrum and to m/e 152 radical ion in the DBO mass spectrum. The high stability of the fluorenyl cation compared to that of the biphenylene odd-electron ion could explain why the spectrum at lower masses contains peaks of greater intensity in the case of DBO than in that of DBT.

The presence of m/e 105 peak in DBO mass spectrum and of m/e 121 peak in DBT mass spectrum indicates the existence of a charged fragment of $C_7H_5X^+$ type. These fragments can arise from similar ions, such as the $(M-1)^+$ ion or, more probable from the $(M-29)^+$ ion :

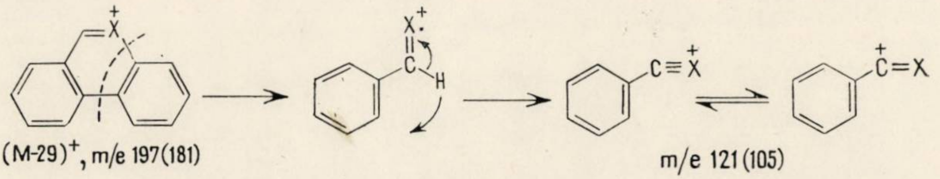

Since in DBO mass spectrum all the neighbouring half-masses peaks of the m/e 105 peak have an relative intensity less than 0.1%, most of the relative intensity of the m/e 105 peak belong presumably to the monocharged $C_7H_5O^+$ ion.

Revue Roumaine de Chimie, **23**, *2*, 171–178 (1978)

L'INFLUENCE DE L'ORIGINE DE L'OXYDE DE FER SUR L'ACTIVITÉ CATALYTIQUE DU CATALYSEUR Fe(III)–O–X (X = Mo, V, W,)

A. SWINARSKI et W. KLAFKOWSKI
Institut de Chimie de l'Université de Toruń
Institut de Chimie de l'Université de Poznań
Pologne

Reçu le 3 septembre 1976

Studies have been carried out on the specific activity, conversion and selectivity of catalyst having the composition Fe(III)–O–X, where X = Mo, V, W, in the reaction of oxidation of methanol to formaldehyde. The catalyst was prepared in two parallel series. In one of them the initial substance was iso-ortho-Fe $(OH)_3$, in the other it was γ-Fe(OOH). Definite differences were found in the effect of each series of the catalyst, in both of which iron was in the form of Fe_2O_3. An attempt has also been presented at elucidating the differences in activity between catalyst containing Mo, V, or W,.

L'aldéhyde formique s'obtient industriellement par l'oxydation ménagée du méthanol. On se sert le plus souvent d'un catalyseur d'oxydation composé d'oxyde de fer (III) et de molybdène (VI).

Trifiro [1] admet que le méthanol absorbé à la surface réagit avec l'oxygène du réseau du catalyseur, et ce dernier se réoxyde ensuite à l'aide de l'oxygène atmosphérique. Wheeler [2] mentionne l'importance de la porosité du catalyseur pour éliminer la concurrence des réactions secondaires d'oxydation de méthanol. Pernicone [3] démontre que la désorption de l'aldéhyde formique de la surface du catalyseur limite la vitesse globale de la réaction, cette constatation étant un appui supplémentaire pour l'importance de la porosité du catalyseur dans ce type de réaction. Suivant Trifiro [4] la sélectivité du catalyseur dans l'oxydation du méthanol à l'aldéhyde formique est liée à la présence de doubles liaisons entre le molybdène et l'oxygène à la surface du catalyseur.

On n'est pas d'accord sur le rôle du Fe^{3+} dans le catalyseur. Les mesures ERP faites pendant la réaction catalytique [5] ont montré que les ions Fe^{3+} se réduisent avant qu'on observe une réduction avancée de Mo (VI).

---

[1] F. Trifiro, V. Vecchi et I. Pasquon, *Kinetika i Kataliz*, **8**, 15 (1969).

[2] A. Wheeler, *J. Catalysis*, **2**, 105 (1955).

[3] N. Pernicone, F. Lazzerin et G. Landzavecchia, *J. Catalysis*, **10**, 83 (1968).

[4] E. Trifiro, P. Centola, J. Pasquon et P. Jim, «Trudy 4-Kongresa po Katalizu» Moscou, 1968, p. 218.

[5] F. Gesmundo, V. Lorenzelli, A. Passerone, P. Rossi et N. Pernicone, *C.R. Acad. Nac. Lincei VIII*, **45**, 368, 1968.

On a effectué ce travail dans le but :

1) de vérifier l'influence de l'origine de l'oxyde ferrique sur l'activité du catalyseur Fe(III)—O—Mo(VI).

2) de constater l'influence de la double liaison entre le Mo(VI) et l'oxygène du catalyseur sur son pouvoir oxydant.

Pour y arriver on a préparé deux séries de catalyseurs une à base d'iso-*ortho*-$Fe(OH)_3$, autre à base de γ-FeOOH, obtenues suivant les méthodes connues.[6] Le second composant du catalyseur a été MoO_3, V_2O_5 ou WO_3.

Pour obtenir le catalyseur homogène d'une certaine composition on a macéré des proportions définies d'iso-*ortho*-$Fe(OH)_3$ ou de γ-FeOOH à l'état humide avec des proportions molaires correspondantes de $(NH_4)_6 Mo_7O_{24}$, NH_4VO_3 ou $(NH_4)_4W_5O_{17}$. Le mélange a été séché pendant 3 h à 120°, ensuite homogénéisé à l'aide d'un mortier, et finalement calciné dans un courant d'air à 450° pendant 4 h. On a séparé le catalyseur à la dimension des grains de 0,07 à 0,15 mm de diamètre.

On a noté par « i » les produits provenant de l'iso-*ortho*-$Fe(OH)_3$, et par « γ » les produits provenant de γ-FeOOH.

RÉSULTATS

Dans la fig. 1 on a représenté la répartition du volume de pores pour les oxydes ferriques Fe_2O_3 provenant de l'iso-*ortho*-$Fe(OH)_3$ et de γ-FeOOH, obtenus dans les mêmes conditions de température que les catalyseurs.

Le maximum du volume de pores pour « i »-Fe_2O_3 est situé vers $r = 2419$ Å. La plupart du volume total des pores (67%) se trouve entre $986 < r < 3571$ Å. Pour γ-Fe_2O_3 le maximum du volume de pores est situé vers $r = 250$ Å, et 45% du volume total se trouve entre $150 < r < 986$ Å.

La répartition du volume de pores pour les catalyseurs à base de « i »-Fe_2O_3 et « γ »-Fe_2O_3 est représentée dans les fig. 2 et 3. Le maximum du volume de pores des catalyseurs est situé dans la même région que celui des oxydes de fer purs qui constituent les catalyseurs.

Les spectres IR de deux séries de catalyseurs à base de MoO_3 sont présentés dans la fig. 4.

Dans une étude détaillée sur les spectres IR du système Fe—O—Mo Barraclough[7] attribue la bande vers 1000 cm^{-1} aux vibrations d'extension de la double liaison $Mo^{6+} = = O^{2-}$, et la bande vers 800 cm^{-1} aux vibrations de la liaison simple Mo—O.

Les spectres IR représentés dans la fig. 5 révèlent l'existence d'une bande vers 1030 cm^{-1} pour le système Fe—O—V et d'une bande vers 825 cm^{-1} pour le système Fe—O—W.

La bande de 1030 cm^{-1} peut être attribuée aux vibrations de la double liaison V = O dans laquelle la force d'attraction entre le métal et l'oxygène est affaiblie, la bande vers 825 cm^{-1} étant attribuée aux vibrations de la liaison simple W—O.

Aux mêmes conditions de température et de vitesse des gaz, on a déterminé l'activité catalytique des catalyseurs dans la réaction d'oxydation du méthanol à l'aldéhyde formique. Les résultats obtenus pour le catalyseur Fe—O—W étant trop faibles pour la température de réaction de 250°, on a été obligé d'augmenter la température de réaction jusqu'à 295°.

---

[6] A. Lewandowski, *Arch. Mineral. Tow. Nauk. Warszawskiego,* **17**, 170 (1947).

[7] G. Barraclough, J. Lewis et R. F. Nyhonn, *J. Chem. Soc.* **35**, 5 (1959).

Les résultats sous forme d'activité spécifique, de taux de conversion et de sélectivité sont réunis dans les figs. 6, 9.

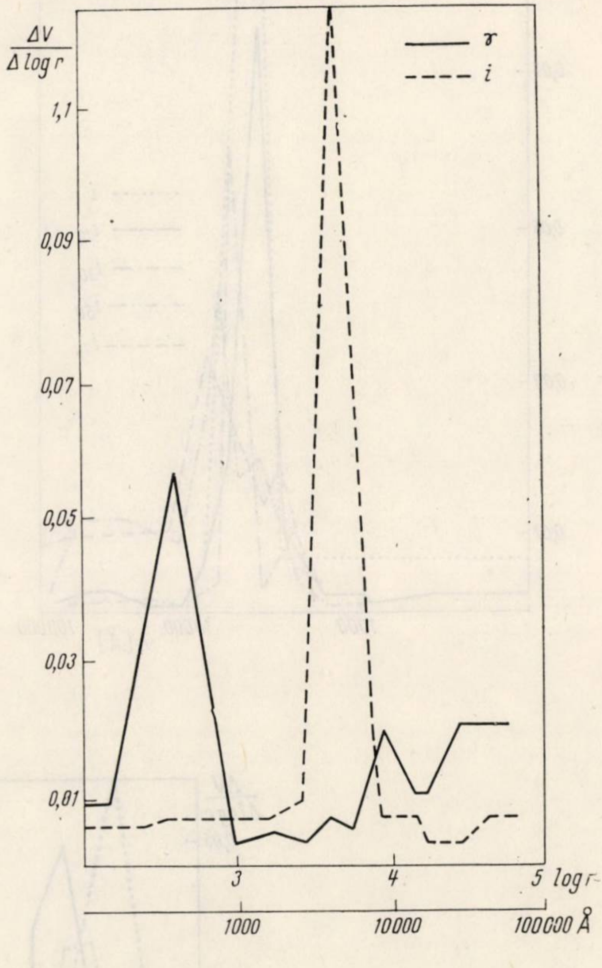

Fig. 1. La répartition du volume de pores de Fe_2O_3 provenant de i-*o*-$Fe_2(OH)_3$ ou de γ-FeOOH.

Les mêmes écarts entre les résultats obtenus pour les échantillons « i » et « γ » se manifestent aussi pour les catalyseurs Fe—O—V. Les catalyseurs Fe—O—W ayant une activité bien plus faible, la différence entre les deux séries « i » et « γ » correspondantes est moins visible (tabl. 1).

DISCUSSIONS

L'analyse comparative des spectres IR (fig. 4 et 5) et de l'activité catalytique des catalyseurs semble confirmer la conception de Trifiro[4] qui attribue la sélectivité du catalyseur à la présence d'une double liaison entre le Mo et l'oxygène. Nous avons constaté une dépendance entre l'exis-

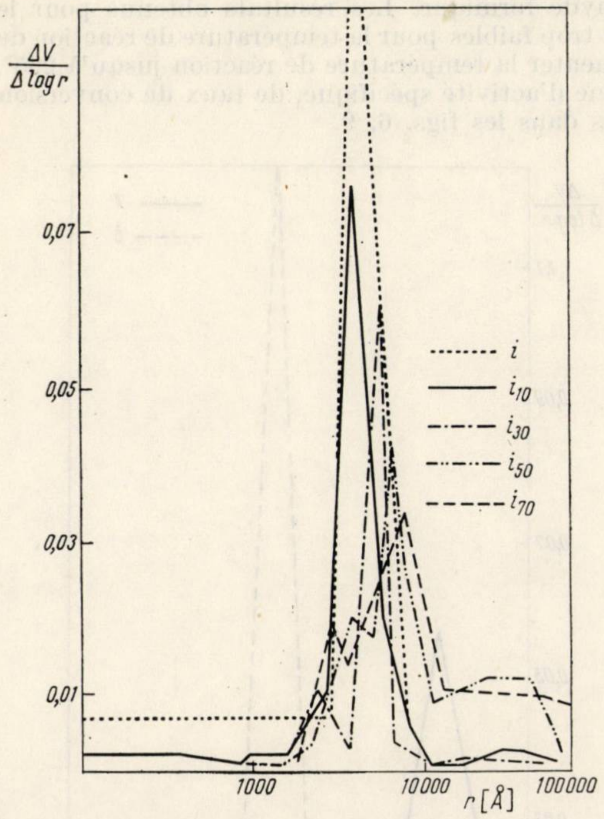

Fig. 2. La répartition du volume de pores de catalyseurs à base de « i »$-Fe_2O_3$ pour les échantillons contenant :

$i_{10}-10\%$ molaires de MoO_3, $i_{30}-30\%$ molaires de MoO_3,
$i_{50}-50\%$ molaires de MoO_3, $i_{70}-70\%$ molaires de MoO_3.

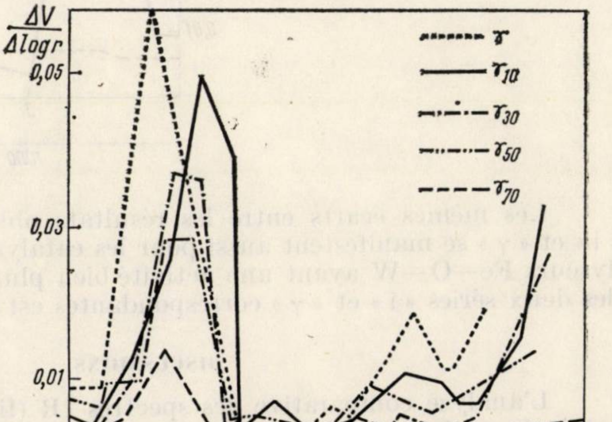

Fig. 3. La répartition du volume de pores de catalyseurs à base de « γ »$-Fe_2O_3$ pour les échantillons contenant :

$\gamma_{10}-10\%$ molaires de MoO_3, $\gamma_{30}-30\%$ molaires de MoO_3
$\gamma_{50}-50\%$ molaires de MoO_3, $\gamma_{70}-70\%$ molaires de MoO_3.

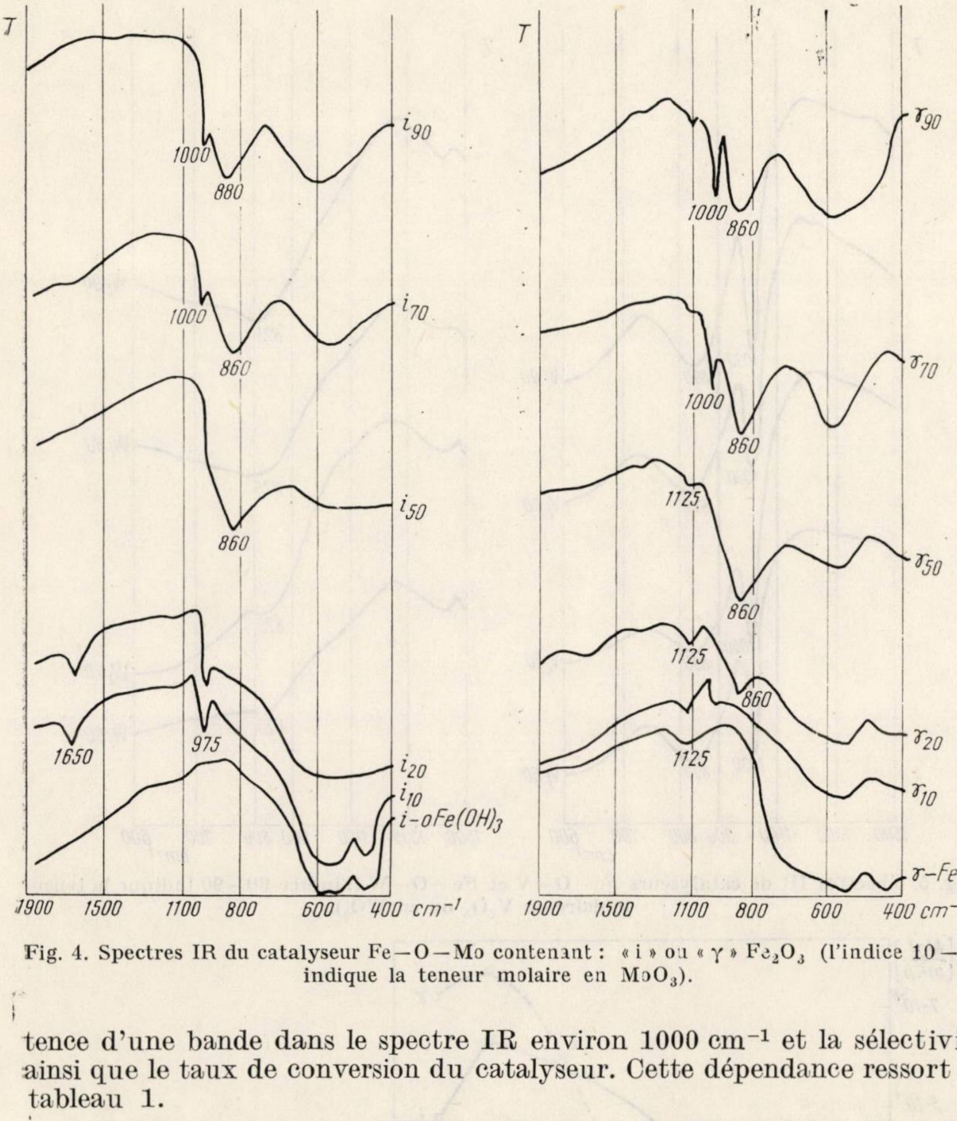

Fig. 4. Spectres IR du catalyseur Fe — O — Mo contenant : « i » ou « γ » Fe_2O_3 (l'indice 10 — 90 indique la teneur molaire en MoO_3).

tence d'une bande dans le spectre IR environ 1000 cm^{-1} et la sélectivité, ainsi que le taux de conversion du catalyseur. Cette dépendance ressort du tableau 1.

Les bandes de spectres IR vers 1000 cm^{-1} et 1030 cm^{-1} dans les catalyseurs Fe — O — Mo, et Fe — O — V, correspondent à un haut degré de sélectivité et de conversion du catalyseur. La bande de 1000 cm^{-1} étant déplacée pour le catalyseur au vanadium jusqu'à 1030 cm^{-1} peut être attribuée à une double liaison plus faible entre le métal et l'oxygène ce qui explique un taux de conversion plus élevé pour le catalyseur à V_2O_5 que celui à MoO_3. Le catalyseur contenant WO_3 manifeste une activité de beaucoup plus faible. Ce fait peut être expliqué par l'absence de la double liaison entre le wolfram et l'oxygène, par conséquent par l'absence de la bande vers 1000 cm^{-1} dans le spectre IR de ce catalyseur.

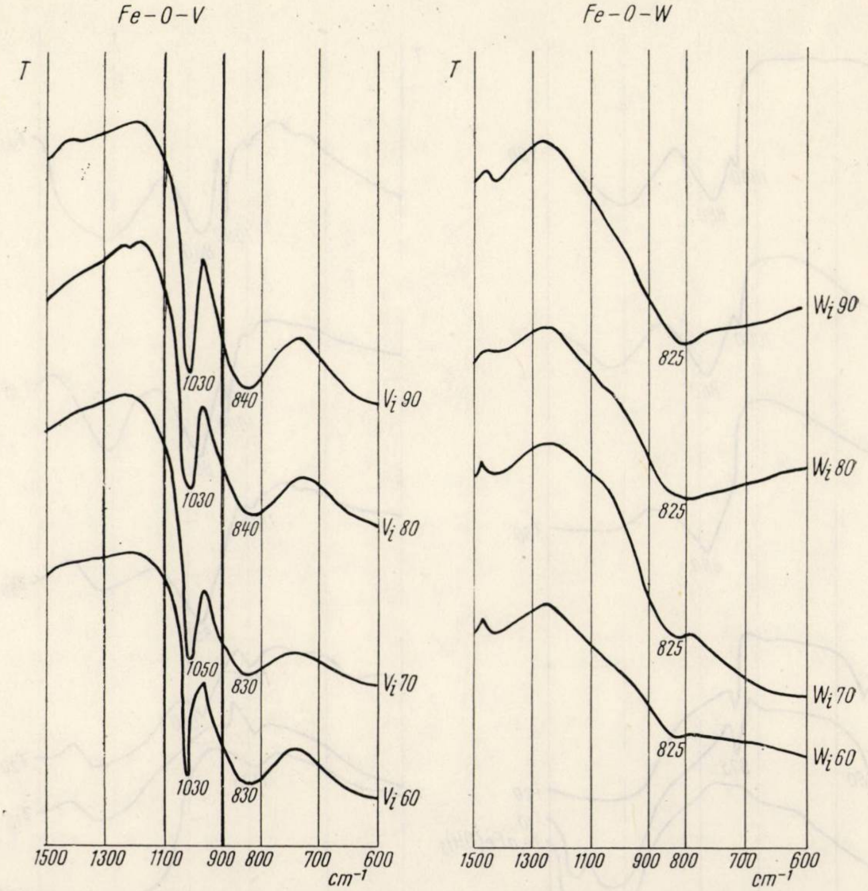

Fig. 5. Spectres IR de catalyseurs Fe – O – V et Fe – O – W (l'indice 60 – 90 indique la teneur molaire en V_2O_5 ou en WO_3).

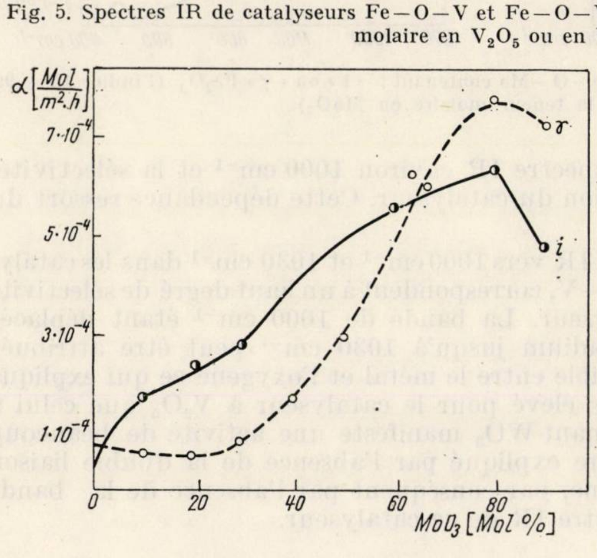

Fig. 6. L'activité spécifique du catalyseur Fe – O – Mo contenant « i » ou « γ » Fe_2O_3.

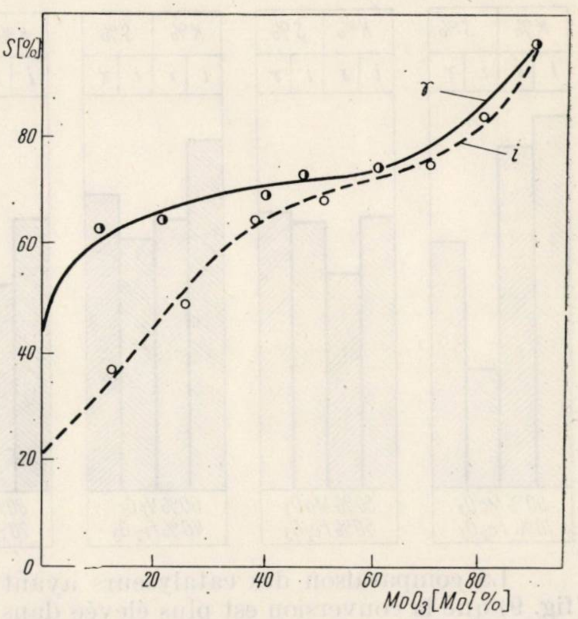

Fig. 7. Sélectivité du catalyseur Fe – O – Mo contenant « i » ou « γ » Fe_2O_3.

L'influence de l'origine de l'oxyde de fer du catalyseur se manifeste nettement dans les fig. 6 – 8. L'origine de l'oxyde de fer laisse une empreinte dans la répartition du volume de pores des catalyseurs (fig. 2 et 3) et dans la position du maximum du volume de pores, même dans le catalyseur qui ne dépasse pas 30% molaires de Fe_2O_3.

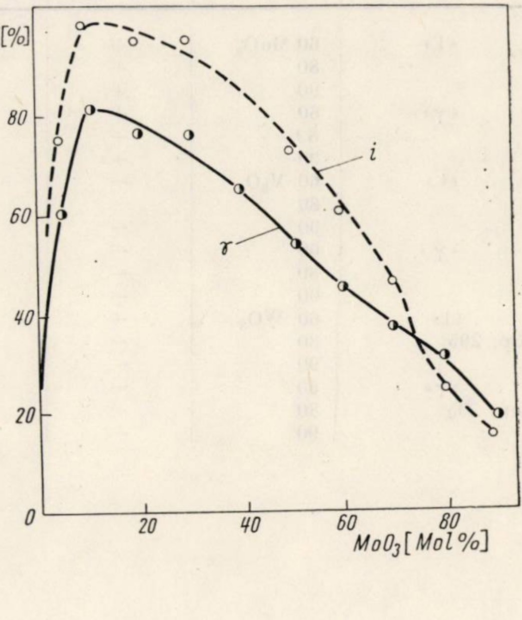

Fig. 8. Taux de conversion du catalyseur Fe – O – Mo contenant « i » ou « γ » Fe_2O_3.

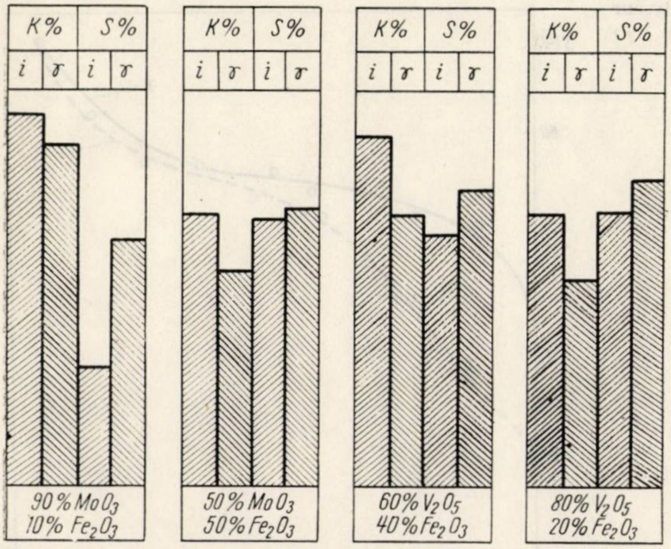

Fig. 9. La comparaison de la conversion (K), et de la sélectivité (S) des catalyseurs Fe – O – Mo et Fe – O – V pour les séries contenant « i » ou « γ » Fe_2O_3.

La comparaison des catalyseurs ayant la même composition révèle (fig. 9) que la conversion est plus élevée dans tous les cas pour les catalyseurs « i ». Par contre, la sélectivité de catalyseurs « γ » est toujours supérieure à celle de catalyseurs « i ».

Tableau 1

Comparaison entre les spectres en IR, la conversion et la sélectivité de catalyseurs

Origine de Fe_2O_3	% molaire du second composant	Bande à 1000 cm^{-1}	Bande à 1030 cm^{-1}	Conversion %	Sélectivité %
« i »	60 MoO_3	+	–	61,4	73,4
	80	+	–	25,2	82,6
	90	+	–	16,6	98,3
« γ »	60	+	–	45,5	75,5
	80	+	–	31,1	90,5
	90	+	–	19,2	96,3
« i »	60 V_2O_5	–	+	91,1	65,3
	80	–	+	70,5	72,1
	90	–	+	50,1	70,5
« γ »	60	–	+	63,4	77,9
	80	–	+	54,2	79,6
	90	–	+	44,7	72,3
« i »	60 WO_3	–	–	75,1	11,7
temp. 295°	80	–	–	62,6	21,6
	90	–	–	48,6	16,5
« γ »	60	–	–	72,4	15,9
temp. 295°	80	–	–	58,2	18,2
	90	–	–	45,4	10,9

Revue Roumaine de Chimie, **23**, 2. 179–186 (1978)

ESTUDIO CINETICO DE LA REDUCCION DEL Cr(VI) POR HIDRACINA

S. SENENT, L. FERRARI y A. ARRANZ

Departamento de Química Física de la Universidad de Valladolid (España)

Recibido 2 de setiembre de 1975

Se ha estudiado la reacción entre el Cr(VI) y la hidracina en medio acuoso entre 25 y 33°. La velocidad específica de reacción se obtuvo espectrofotométricamente, siguiendo el cambio de la absorción del Cr(VI) con el tiempo. La reacción presenta un orden cinético total de dos (siendo uno respecto al Cr(VI) y tambien uno respecto a la hidracina) y una estequiometría de $[Cr(VI)]/[N_2H_4]=1.33$. También se han calculado los valores de la energía, entalpia y entropía de activación. Se propone un mecanismo de reacción consistente con los datos experimentales.

The kinetic of the rection between the Cr(VI) and the hydrazine has been studied in aqueous medium between 25 and 33°. The specific rate of reaction was obtained spectrophotometrically, following changes in the absorbance of Cr(VI) with the time. The reaction exhibits a total second order kinetics, first with respect to the Cr(VI) and also first with respect to N_2H_4) and a stoichiometry of $[Cr(VI)]/[N_2H_4]=1.33$. The values of energy, enthalpy and entropy of activation have also been calculated. A mechanism consistent with the experimental data is suggested

El estudio de procesos redox en los que intervienen aniones de los metales de transición presenta gran interés no sólo desde el punto de vista fisicoquímico, sino también bioquímico y biológico. Por ello no es de extrañar que exista una amplia bibliografía sobre processos de este tipo[1] aunque generalmente los resultados no pasan de ser cualitativos o semicuantitativos, y en muchos casos no tocan su aspecto — cinético y mecanicista. Tal ocurre con la reacción Cr(VI)-hidracina, de la que se conocen pocas contribuciones al estudio de su cinética[2,3] y de ellas sólo la de Beck y Durham[2] aporta un estudio más sistemático, aunque incompleto. El interés de este tema ha constituído el trabajo objeto de estudio en la presente investigación.

---

[1] C. H. Bamford y C. F. H. Tipper (Ed.), "Comprehensive Chemical Kinetics", Vol. 7, Elsevier Publishing Company, London, 1972.

M. T. Beck y D. A. Durham, *J. Inorg. Nuclear Chem.*, **32**, 1971 (1970).

[3] V. M. Ramanujam y N. Venkatasubramanian, *Indian J. Chem.*, **8**, 948 (1970).

PARTE EXPERIMENTAL

Para seguir el curso de la reacción se ha seguido una técnica espectrofotométrica dinámica, eligiendo como especie química de control el Cr(VI), que presenta una intensa banda cuyo máximo aparece a una longitud de onda de 350 nm en las condiciones de trabajo. Es de señalar que tanto la hidracina como los productos de reacción no presentan banda alguna en esta zona del espectro.

Las disoluciones cumplen la ley de Lambert-Beer en los intervalos de concentraciones empleados: $[Cr(VI)] \leqslant 5.10^{-4}M$ y $[HClO_4]$ entre 0,1 M y 5.10^{-3} M. (Los coeficientes de correlación oscilan entre 0,9999 y 1,0073).

Todos los reactivos fueron de pureza "para análisis": dicromato potásico Merck, hidrato de hidracina F.E.R.O.S.A., hidrocloruro de hidracina Schuchardt y ácido perclórico Merck.

Las disoluciones de dicromato se prepararon por pesada directa. Las de hidracina se valoraron con iodato potásico, según el método de Andrews[4] y las de ácido perclórico con óxido de mercurio (II) Merck, con fenolftaleína como indicador.

En todos los experimentos se empleó, para mantener constante la fuerza iónica del medio I, perclorato sódico en concentraciones del orden de 0,3 M.

Se utilizó un espectrofotómetro Perkin-Elmer, mod. 137 U. V. que dispone de portacubetas en el que puede mantenerse constante la temperatura con un error máximo de ± 0,1° mediante le agualanzada por un ultratermostato "Colora". Las disoluciones de los reactivos, una vez que alcanzaban la temperatura de trabajo endicho termostato, se mezclaban e introducían en el espectrofotómetro. Estas manipulaciones podían hacerse en un intervalo máximo de 30 ó. 35 segundos, lo que resultaba imprescindible porque la reacción es bastante rápida y se completa en un periodo que oscila entre 5 y 10 minutos, según las condiciones experimentales de trabajo. El espectrofotómetro permite registrar automáticamente la variación de la absorción en función del tiempo en la longitud de onda elegida para el seguimiento de la reacción.

Las medidas de pH se llevaron a cabo en un pH-metro Radiometer, mod. 26, previamente calibrado con disoluciones reguladoras adecuadas para el intervalo de pH deseado.

RESULTADOS Y DISCUSION

Se ha realizado un estudio sistemático de la influencia de los reactívos, acidez del medio y temperatura sobre la velocidad específica de reacción. Los resultados se recogen en las Tablas I a IV. Las constantes de velocidad se calcularon por el método de integración, aunque en algunos experimentos se aplicaron simultáneamente éste y el de las velocidades iniciales, preferido por otros autores,[2] obteniéndose resultados análogos. Asimismo se comprobó el cuplimiento satisfactorio de la ley de Arrhenius y de la ecuación deducida en la teoría del complejo activado, calculándose la energía, entalpia y entropía de activación.

También se determinó espectrofotométricamente la estequiometría de la reacción en exceso del reactivo hidracina, encontrándose que aquélla es de 4 moles de Cr(VI) por 3 moles de N_2H_4, en concordancia con la determinada para la misma reacción, pero en medio sulfúrico, por otros autores.[3]

A partir de los datos de las tablas siguientes, puede deducirse:

1) La pseudoconstante de velocidad, k_{exp}, es independiente de la concentración de Cr(VI) cualesquiera que sean las concentraciones iniciales de hidracina (tanto en forma de hidrocloruro como de hidrato) y ácido perclóricos

---

[4] A. Vogel, "Química Analítica Cuantitativa", Vol. I, Ed. Kapelusz, Buenos Aires, 1960, pág. 508.

Tabla 1

Influencia de la concentración de Cr(VI)

$T = 25°C$							I = 0,39 N	
$[N_2H_4.HCl]\cdot10^2/M$:	3,52		3,52		3,52		0,352	
$[HClO_4]\cdot10^3/M$:	1,0		5,0		10,0		10,0	
$[Cr(VI)]\cdot10^4/M$	$k_{exp}\cdot10/min^{-1}$	r_{xy}	$k_{exp}\cdot10/min^{-1}$	r_{xy}	$k_{exp}\cdot10/min^{-1}$	r_{xy}	$k_{exp}\cdot10/min^{-1}$	r_{xy}
1,0	0,72	0,9989	—		—		1,08	0,9987
1,5	0,71	9994	2,71	0,9989	4,25	0,9998	1,06	9988
2,0	0,71	9990	2,71	9998	3,82	9987	1,15	9998
2,5	0,71	9987	2,59	9998	3,92	9989	1,06	9998
3,0	0,69	9995	2,45	9995	4,13	9991	1,07	9991
3,5	0,72	9974	2,52	9994	3,87	9997	1,09	9992
4,0	0,73	9979	2,50	9997	3,97	9992	1,04	9997
4,5			2,52	9986	3,95	9988	1,05	9996

Tabla 2

Influencia de la acidez del medio

$T = 25°C$ I = 0,40 M	$[Cr(VI)] = 3.10^{-4}M$	$[N_2H_4\cdot H_2O] = 7.10^{-4}M$
$[HClO_4]\cdot10^2/M$	$k_{exp}\cdot10/min^{-1}$	r_{xy}
1,0	0,231	0,9999
3,0	0,460	9992
6,0	0,784	9973
8,0	0,943	9989
9,0	1,121	9981
10,0	1,203	9991

Tabla 3

Influencia de la concentración de hidracina

$T = 25°C$ I = 0,48M	$[Cr(VI)] = 3.10^{-4}$ M	$[HClO_4] = 0,1$ M
$[N_2H_4\cdot H_2O]\cdot10^4/M$	$k_{exp}\cdot10/min^{-1}$	r_{xy}
0,9	0,153	0,9970
2,0	0,370	9955
3,0	0,419	9987
4,0	0,579	9987
5,0	0,767	9969
6,0	0,904	9983
8,0	1,147	9987
10,0	1,560	9991

Tabla 4

Influencia de la temperatura

	I = 0,34 M	$[Cr(VI)] = 3 \cdot 10^{-4}$M			$[HClO_4]=5 \cdot 10^{-3}$M	
T/°C		$k_{exp} \cdot 10$/min^{-1}				
	$[N_2H_4 \cdot HCl] \cdot 10^3$/M:	5,0	6,0	7,0	8,0	9,0
25		0,450	0,491	0,627	0,723	0,744
27		0,475	0,599	0,679	0,746	0,832
29		0,513	0,639	0,775	0,878	0,957
31		0,613	0,694	0,823	0,928	0,998
33		0,634	0,755	0,869	0,985	1,051
E_a/kJ mol^{-1}		35,5	38,0	31,8	31,8	33,9
$\Delta H^{\neq}/kJ$ mol^{-1}		33,0	35,7	29,4	29,2	30,5
$\Delta S^{\neq}/JK^{-1}$mol^{-1}		−160	−150	−169	−169	−164

$[HClO_4]$/M	$[Cr(VI)] \cdot 10^4$/M	$[N_2H_4 \cdot H_2O] \cdot 10^3$/M	I/M	$k_{exp} \cdot 10$/min^{-1}					E_a/kJmol^{-1}	$\Delta H^{\neq}/kJ$ mol^{-1}	$\Delta S^{\neq}/JK^{-1}$mol^{-1}
				T/°C: 25	27	29	31	33			
0,072	4,0	0,35	0,45	0,488	0,500	0,536	0,644	0,651	31,4	28,8	−173
0,072	4,0	1,0	0,45	1,49	1,53	1,88	1,90	2,11	33,8	31,4	−156
0,13	3,0	0,8	0,47	1,86	1,92	2,21	2,31	2,62	33,0	30,5	−157
0,24	2,0	1,0	0,58	4,01	4,50	4,85	4,90	5,78	30,5	29,4	−135

Los coeficientes de correlación para las constantes de velocidad oscilan entre 0,9976 y 0,9997.

rico, con tal de que puedan considerarse constantes. Por tanto, la dependencia de la velocidad — respecto del Cr(VI) es de la forma:

$$V = -\mathrm{d}[\mathrm{Cr(VI)}]/\mathrm{d}t = k_{\mathrm{exp}}[\mathrm{Cr(VI)}] \tag{1}$$

2) Existe una relación lineal entre éstas pseudoconstantes y la concentración de hidracina,

$$k_{\mathrm{exp}} = c\,[\mathrm{N_2H_4}] \tag{2}$$

3) En el intervalo de acidez estudiado, la dependencia de k_{exp} con la concentración de ácido es:

$$k_{\mathrm{exp}} = a[\mathrm{HClO_4}] + b \tag{3}$$

Todas estas consideraciones parecen conducir a una ecuación de velocidad de la forma:

$$V = \{a'[\mathrm{HClO_4}] + b'\}\,.\,[\mathrm{N_2H_4}]\,.\,[\mathrm{Cr(VI)}] \tag{4}$$

que indica un orden cinético total dos, y órdenes parciales uno respecto de cada reactivo.

De la comparación entre (1) y (4) se deduce que

$$k_{\mathrm{exp}} = \{a'[\mathrm{HClO_4}] + b'\}\,.\,[\mathrm{N_2H_4}] \tag{5}$$

De acuerdo con esta ecuación, existe una correlación lineal entre $k_{\mathrm{exp}}/[\mathrm{N_2H_4}]$ y $[\mathrm{HClO_4}]$, como muestra la fig. 1, construída con los datos de las tablas anteriores. Un ajuste de la recta por el método de los mínimos cuadrados da:

$$a' = 1631\ \mathrm{min^{-1}\,mol^{-2}\,dm^{6}}$$

$$b' = 3.9\ \mathrm{min^{-1}\,mol^{-1}\,dm^{3}}$$

Según se desprende de varios trabajos consultados, [5-7] en los intervalos de acidez y de concentraciones de Cr(VI) y de hidracina estudiados las especies presentes en mayor proporción son $\mathrm{CrO_4H^-}$, $\mathrm{CrO_4H_2}$ y $\mathrm{N_2H_5^+}$. Por otra parte, en la formulación de mecanismos de reacciones de oxidación crómica, se han postulado compuestos intermedios de Cr(IV) y Cr(V) [8]; algunos han sido detectados recientemente [9] mientras que de otros sólo se tienen pruebas indirectas de su existencia.[10,11]

---

[5] J. D. Neuss y W. Rieman, *J. Amer. Chem. Soc.*, **56**, 2238 (1934).

[6] J. Y. Tong y E. L. King, *J. Amer. Chem. Soc.*, **75**, 6180 (1953).

[7] G. P. Haight, D. C. Richardson y N. H. Coburn, *Inorg. Chem.*, **3**, 1777 (1964).

[8] F. H. Westheimer, *Chem. Rev.*, **45**, 491 (1949).

[9] K. B. Wiberg y H. Schafer, *J. Amer. Chem. Soc.*, **89**, 455 (1967).

[10] K. B. Wiberg y S. K. Mukherjee, *J. Amer. Chem. Soc.*, **93**, 2543 (1971).

[11] M. Rahman y J. Rocek, *J. Amer. Chem. Soc.*, **93**, 5462 (1971).

Los resultados obtenidos en este trabajo y los datos recogidos en la literatura sobre reacciones similares parecen estar de acuerdo con el siguiente mecanismo de reacción:

$$\mathrm{CrO_4H^-} + \mathrm{H^+} \overset{K}{\rightleftharpoons} \mathrm{CrO_4H_2} \qquad (6)$$

$$\mathrm{CrO_4H^-} + \mathrm{N_2H_5^+} \underset{k_{-1}}{\overset{k_1}{\rightleftharpoons}} \mathrm{C} \qquad \text{(rápida)} \qquad (7)$$

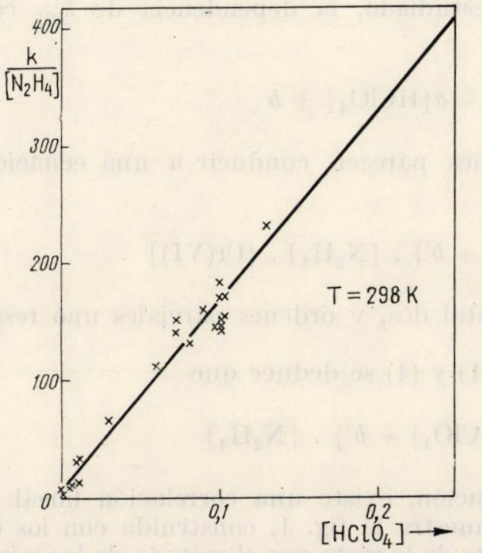

Fig. 1. — Determinación de las constantes *a* y *b′* de la ecuación (5).

$$\mathrm{CrO_4H^-} + \mathrm{C} \xrightarrow{k_2} 2\mathrm{Cr(V)} + \mathrm{N_2H_2} + \mathrm{H_2O} + \mathrm{H^+} \quad \text{(rápida)} \qquad (8)$$

$$2\ \mathrm{Cr(V)} \xrightarrow{k_3} \mathrm{Cr(VI)} + \mathrm{Cr(IV)} \qquad (9)$$

$$\mathrm{Cr(V)} + \mathrm{N_2H_5^+} \xrightarrow{k_4} \mathrm{Cr(III)} + \mathrm{N_2H_2} + \mathrm{H_2O} + \mathrm{H^+} \qquad (10)$$

$$\mathrm{Cr(IV)} + \mathrm{N_2H_5^+} \xrightarrow{k_5} \mathrm{Cr(II)} + \mathrm{N_2H_2} + \mathrm{H_2O} + \mathrm{H^+} \qquad (11)$$

$$\mathrm{CrO_4H^-} + \mathrm{Cr(II)} \xrightarrow{k_6} \mathrm{Cr(V)} + \mathrm{Cr(III)} \qquad (12)$$

$$2\mathrm{N_2H_2} \xrightarrow{k_7} \mathrm{N_4H_4} \qquad (13)$$

$$\mathrm{N_4H_4} + \mathrm{H^+} \xrightarrow{k_8} \mathrm{N_2} + \mathrm{N_2H_5^+} \qquad (14)$$

Independiente y simultáneamente, la especie química $\mathrm{CrO_4H_2}$ puede dar lugar a otra serie de reacciones totalmente análogas.

No existe evidencia experimental directa de la formación del complejo hidracina—Cr(VI), representado por C en las ecuaciones (7) y (8), pero los valores fuertemente negativos encontrados invariablemente para la entropía de activación, los valores relativamente bajos de $\Delta H^{\neq}$[12] y la correlación lineal existente entre $1/k_{\mathrm{exp}}$ y $1/[N_2H_4]$ parecen indicar la formación de un complejo antes de la reacción principal. Se ha observado en varias ocasiones un orden cinético dos en reacciones que transcurren a través de un complejo intermedio si la constante de equilibrio de formación del complejo no es muy grande.[13, 14] Este complejo es probable que, por reacción con otra molécula de CrO_4H^-, se descomponga en Cr(V) y — N_2H_2. La estequiometría de la reacción, la ecuación de velocidad y los productos finales de oxidación de la hidracina —N_2 y H_2O—[15] están en concordancia con la ecuación (8).

En mecanismos de reducción del Cr(VI) ha sido frecuentemente postulada [8, 16] la reacción :

$$\mathrm{Cr(VI)} + \mathrm{Cr(IV)} \longrightarrow 2\,\mathrm{Cr(V)}$$

que parece bastante improbable [17] pues debe ir acompañada de un cambio positivo de entalpía libre de más de 80 kJ mol^{-1}. Por ello, se ha incluído la reacción inversa, es decir, la dismutación del Cr(V), en el mecanismo de reacción.

No se conocen con seguridad las reactividades de las especies Cr(IV) y Cr(V), aunque es de esperar sea alta. Wetton e Higginson (loc. cit.) aseguran que el Cr(IV) es un oxidante enérgico, por lo que es probable reaccionen con la hidracina para transformarse finalmente en Cr(III) estable. Además, de la estimación indirecta de los potenciales redox de los pares $\mathrm{Cr(V)/Cr^{+++}}$, $\mathrm{Cr\ (IV)/Cr^{++}}$ y N_2H_2/N_2H_4 se deduce que las reacciones (10) y (11) son termodinámicamente posibles. Otro tanto puede decirse de (12), de la que existen pruebas experimentales.[18, 19] Los productos intermedios de la oxidación de la hidracina están bien estudiados, tanto si el oxidante toma un sólo electrón por molécula de reductor como si toma dos, que es lo que parece suceder en esta reacción según se deduce de su estequiometría y productos finales.[15, 20, 21]

---

[12] J. P. Hunt, "Metal Ions in Aqueous Solution", W. A. Benjamin, Inc., New York, 1963, pág. 114.

[13] H. L. Hintz y D. C. Johnson, *J. Org. Chem.*, **32**, 556 (1967).

[14] K. Jijee, M. Santappa, *Proc. Indian. Acad. Sc.*, **69**, 117 (1969).

[15] (a) W. C. E. Higginson, D. Sutton y P. Wright, *J. Chem. Soc.*, **1953** ; 1380.
(b) W. C. E. Higginson y D. Sutton, *J. Chem. Soc.*, **1953** ; 1402.
(c) W. C. E. Higginson y P. Wright, *J. Chem. Soc.*, **1955** ; 1551.

[16] R. Stewart, "Oxidation Mechanisms", Benjamin, New York, 1964, Cap. 4.

[17] E. A. M. Wetton y W. C. E. Higginson, *J. Chem. Soc.*, **1965** ; 5890.

[18] L. S. Hegedus y A. Haim, *Inorg. Chem.*, **6**, 664 (1967).

[19] J. C. Kenny y D. W. Carlyde, *Inorg. Chem.*, **12**, 1952 (1973).

[20] R. E. Kirk y A. W. Browne, *J. Amer. Chem. Soc.*, **50**, 337 (1928).

[21] T. Huang y J. T. Spence, *J. Phys. Chem.*, **72**, 4198 (1968).

La aplicación de la aproximación del estado estacionario al esquema propuesto conduce a una expresión análoga a (4) si se cumple la condición de que

$$k_2[\mathrm{CrO_4H^-}] \gg k_{-1}$$

$$k_2'\mathrm{K}[\mathrm{H^+}][\mathrm{CrO_4H^-}] \gg k'_{-1}$$

hipótesis lógica pues, dada la gran velocidad con que transcurre la reacción total, la descomposición del complejo ha de producirse preférentemente a través de la reacción (8).

AGRADECIMIENTO. Uno de los autores (A. A.) desea expresar su agradecimiento a la Dirección General de Universidades e Investigación por la concesión de una Beca del Plan de Formación de Personal Investigador (cursos 1971–72, 72–73 y 73–74) con cuya ayuda se ha realizado este trabajo.

Revue Roumaine de Chimie, 23, 2, 187–196 (1978)

ISOTOPE EFFECTS IN LANTHANIDE-INDUCED SHIFTS OF ^{1}H-NMR SPECTRA OF SELECTIVELY SIDE-CHAIN DEUTERIATED PYRIDINES[1]

ALEXANDRU T. BALABAN, [a,b,c] ILEANA I. STĂNOIU [b] and FILIP CHIRALEU[d]

[a] Department of Organic Chemistry, The Polytechnic Institute, Bucharest, Romania
[b] Institute for Atomic Physics, P.O.B. 5206, Bucharest, Romania
[c] Correspondence should be addressed to [a]
[d] Research Centre for Organic Chemistry, Bucharest, Romania

Received August 2, 1977

Europium tris(dipivaloylmethanate), Eu(dpm)$_3$, shifts the ^{1}H-NMR peaks due to the β-protons of 2,4,6-tri-d$_3$-methylpyridine **8** or of 2,6-di-d$_3$-methyl-4-methylpyridine **10** with 6% more than the β-protons of the non-deuteriated *sym*-collidine **7** or of the 4-d$_3$-methyl-2,6-dimethylpyridine **9**. Analogous effects were observed with selectively deuteriated 2,6-diethyl-4-methylpyridines **11**–**14**. α-Isopropyl **(15–18)** or t-butyl groups **(19, 20)** prevent the formation of complexes with Eu(dpm)$_3$. These results indicate a steric origin of this secondary isotope effect exerted by Eu(dpm)$_3$ on ^{1}H-NMR induced shifts.

INTRODUCTION

2,4,6-Trimethylpyrylium salts **1** which are easily accessible,[2] may be readily deuteriated at the methyl groups by heating at 80–100° in deuterium oxide.[3] Kinetic analysis by means of ^{1}H-NMR spectra revealed that the 4-methyl group is deuteriated about 12 times faster than the α (2- and 6-) methyl groups.[4] This was interpreted [4] as being due to the higher concentration of the 4*H*-methylenepyran intermediate **2** of the γ-methyl hydrogen exchange; being symmetrical, **2** has a lower energy than the 2*H*-methylenepyran intermediate **4** of the α-methyl hydrogen exchange, which is formed in smaller amounts (scheme 1). Hückel MO calculations of **2** and **4** agree with this interpretation,[5] and the small kinetic isotope effect[6] of these deuteriation/de-deuteriation reactions, $k_H/k_D = 1.6$, is in agreement with the formation of methylenepyran intermediates (anhydrobases).

---

[1] Preliminary communication, A. T. Balaban, I. I. Stănoiu and F. Chiraleu, *J. C. S. Chem. Comm.*, **1976**, 984.

[2] A. T. Balaban and C. D. Nenitzescu, *Org. Synth. Coll.* Vol. **5**, 1106; K. Hafner and H. Kaiser, *ibid.* 1108; A. T. Balaban and A. J. Boulton, *ibid.* 1112, 1114 (1973).

[3] A. T. Balaban, E. Gârd, A. Vasilescu and A. Barabas, *J. Labelled Comp.* **1**, 266 (1965).

[4] E. Gârd, A. Vasilescu, G. D. Mateescu and A. T. Balaban, *J. Labelled Comp.*, **3**, 196 (1967); E. Gârd, I. I. Stănoiu, F. Chiraleu and A. T. Balaban, *Rev. Roumaine Chim.*, **18**, 257 (1973).

[5] C. C. Renţia, A. T. Balaban and Z. Simon, *Rev. Roumaine Chim.*, **11**, 1193 (1966); G. V. Boyd, *ibid.*, **12**, 1133 (1967).

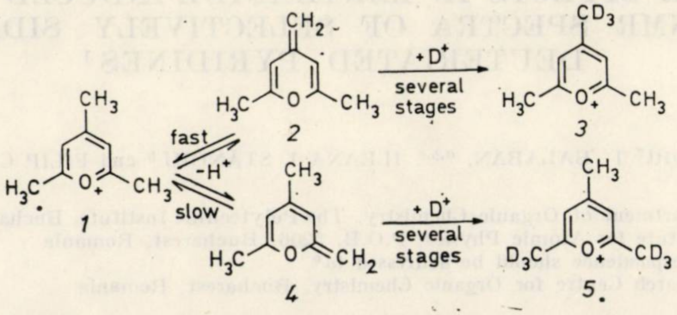

Scheme 1. — Mechanism of α- and γ-deuteriation of alkyl side-chains in pyrylium salts.

This difference in reaction rates allowed the preparation of four selectively side-chain deuteriated pyrylium salts, **1**, **3**, **5**, and **6** as indicated in scheme 2 : on heating **1** (as perchlorate) in D_2O at 80° for 10 minutes, the product is 2,6-dimethyl-4-d_3-methylpyrylium perchlorate **3** (isotopic purity about 85 % ; the ^{1}H-NMR spectrum reveals the presence of partly α-deuteriated isotopic impurities). Longer heating in D_2O (one hour at 100°) converts **1** into 2,4,6-tri-d_3-methylpyrylium perchlorate **6** (isotopic purity 98—99 %). Complete deuteriation of **1**, i.e., including exchange of aromatic protons, requires under these conditions very long reaction times (refluxation for one week) and the mechanism probably involves ring opening to the pseudobase. By de-deuteriating product **6** at 80° in H_2O for 20 min (twice as long as for γ-deuteriation owing to the kinetic isotope effect), again the 4-methyl reacts faster, affording 2,6-di-d_3-methyl-4-methylpyrylium perchlorate **5** (isotopic purity about 85 %).

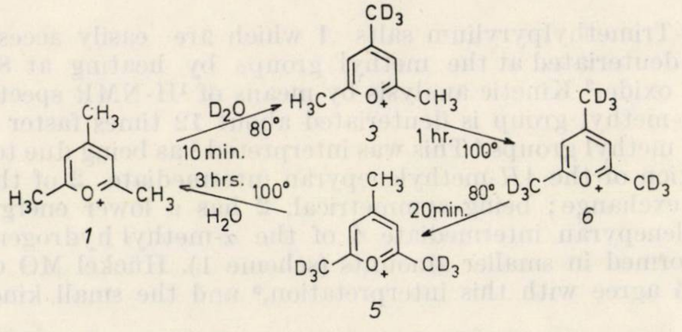

Scheme 2. — Preparation of selectively-deuteriated 2,4,6-trimethyl-pyrylium perchlorates **1**, **3**, **5**, and **6**.

---

[6] I. I. Stănoiu, F. Chiraleu, E. Gârd and A. T. Balaban, *Rev. Roumaine Chim.*, **22**, 117 (1977).

On reacting pyrylium salts **1, 6, 3,** and **5** with aqueous ammonia in the cold, *sym*-collidines **7—10**, respectively were obtained, with isotopic purities similar to those of the corresponding pyrylium salts since the conversion of a pyrylium salt into a pyridine is much faster than the isotopic exchange.

Similar reactions allowed the preparation of 2,6-diethyl-4-methylpyridines **11—14** selectively deuteriated in the benzylic positions, starting from 2,6-diethyl-4-methylpyrylium perchlorate [7] (scheme 3).

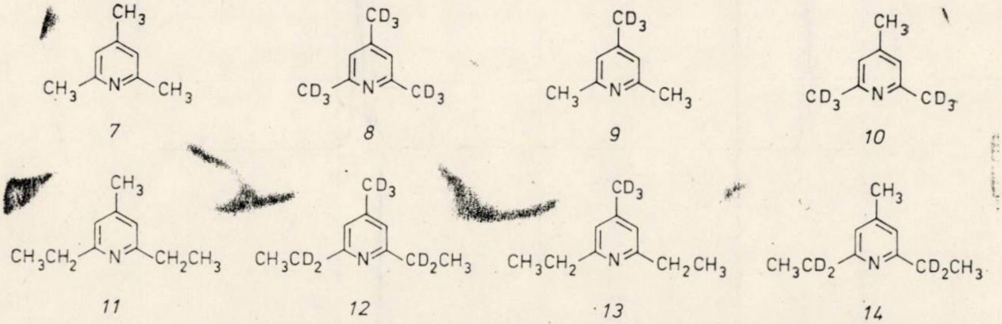

Scheme 3. — Selectively deuteriated 2,4,6-trimethylpyridines **7—10** and 2,6-diethyl-4-methylpyridines **11—14** forming complexes with LSR such as $Eu(dpm)_3$.

^{1}H-NMR Spectra of pyridines **7—14** are in agreement with their structures and isotopic purities (figs. 1 and 2).

In connection with a study of the lanthanide-induced shifts (LIS) in the NMR spectra of substituted pyridines,[8] and with the reported [9–14] isotope effects observed with deuteriated substrates, we investigated the effect of the tris (dipivaloylmethanato) europium chelate, $Eu(dpm)_3$, as lanthanide shift reagent (LSR) on the proton chemical shifts of pyridines **7—14**. Carbon disulphide was selected as solvent because it was reported to afford larger chemical shifts with LSR than other solvents.[15]

EXPERIMENTAL PART

Pyrylium salts. 2,4,6-Trimethylpyrylium perchlorate was prepared from t-butanol, acetic anhydride and perchloric acid.[2] 2,6-Diethyl-4-methylpyrylium perchlorate was obtained[7] from propionyl chloride and aluminium chloride, into whose mixture t-butyl chloride was added; after hydrolysis, addition of perchloric acid caused the crystallization of the pyry-

---

[7] A. T. Balaban and C. D. Nenitzescu, *Liebigs Ann. Chem.*, **625**, 74 (1959).

[8] A. T. Balaban, A. Bota, F. Chiraleu, E. Sliam, A. Haneș and C. Drăghici, *Rev. Roumaine Chim.*, **22**, 1003 (1977).

[9] G. V. Smith, W. A. Boyd and C. C. Hinckley, *J. Amer. Chem. Soc.*, **93**, 6319 (1971).

[10] C. C. Hinckley, W. A. Boyd and G. V. Smith, *Tetrahedron Letters*, **1972**, 879.

[11] C. C. Hinckley, W. A. Boyd, G. V. Smith and F. Behbahany, in "Nuclear Magnetic Resonance Shift Reagents" (editor R. E. Sievers), Academic Press, New York, 1973, p. 1.

[12] D. S. Dyer, J. A. Cunningham, J. J. Brooks and R. E. Rondeau, *ibid.* p. 21.

[13] J. J. Brooks and R. E. Sievers, *J. Chromatogr. Sci.* **11**, 303 (1973); J. K. M. Sanders and D. H. Williams, *Chem. Comm.*, **1972**, 436.

[14] C. H. De Puy, P. C. Fünfschilling and J. M. Olson, *J. Amer. Chem. Soc.*, **98**, 276 (1976); A. F. Cockerill, G. L. O. Davies, R. C. Harden, and D. M. Rackham, *Chem. Rev.*, **73**, 553, 571 (1973).

[15] D. B. Walters, *Analyt. Chim. Acta*, **60**, 421 (1972).

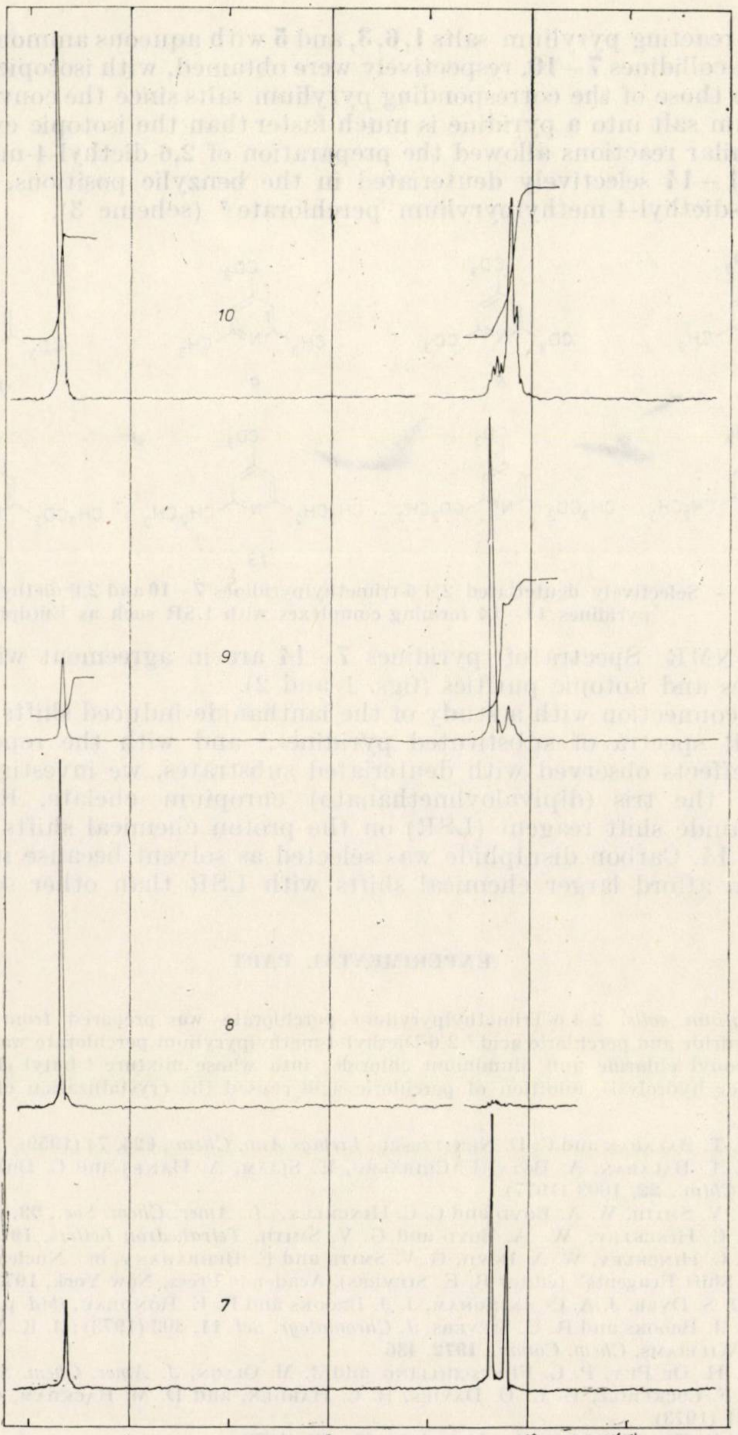

Fig. 1. — ^{1}H-NMR Spectra of selectively deuteriated 2,4,6-trimethylpyridines **7 – 10** in CS_2.

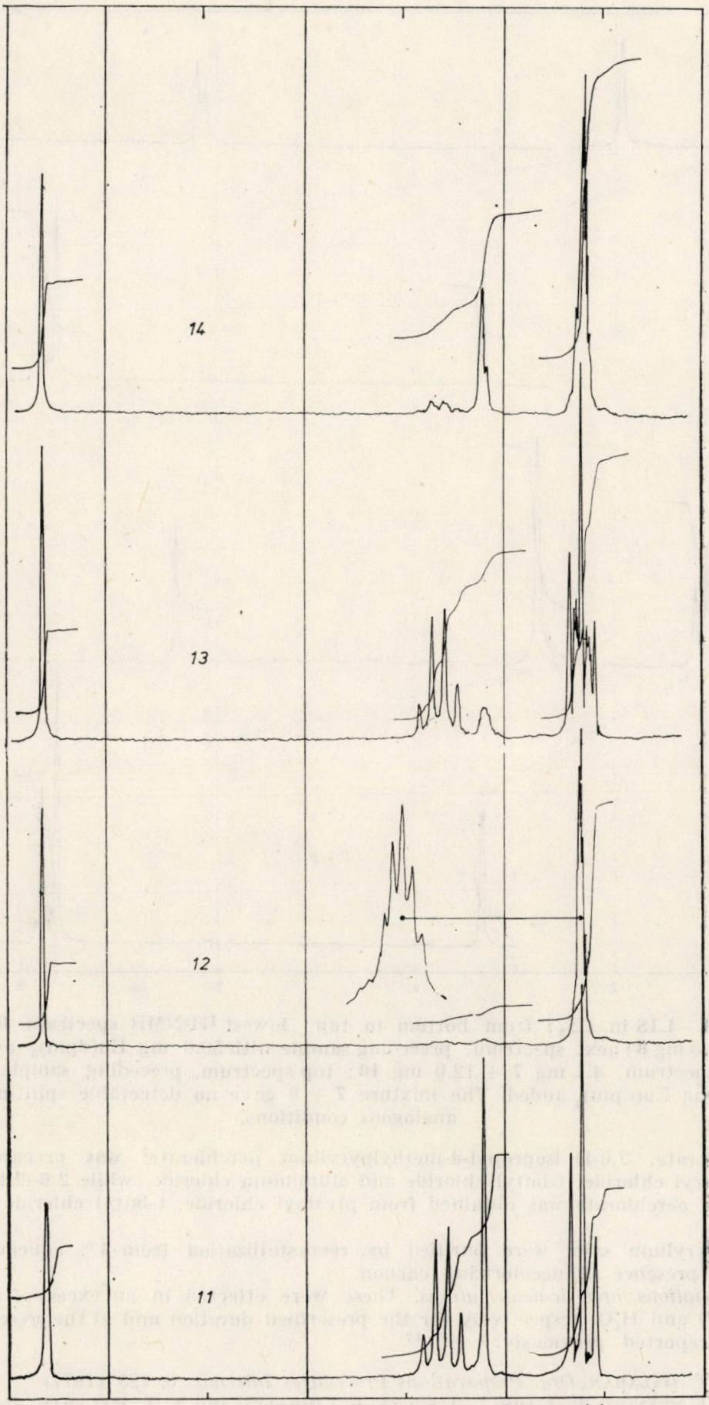

Fig. 2. — ^{1}H-NMR Spectra of selectively deuteriated 2,6-diethyl-4-methyl-pyridines **11**–**14** in CS_2 (sweep width 500 Hz); the insert for **12** was recorded with sweep width 100 Hz.

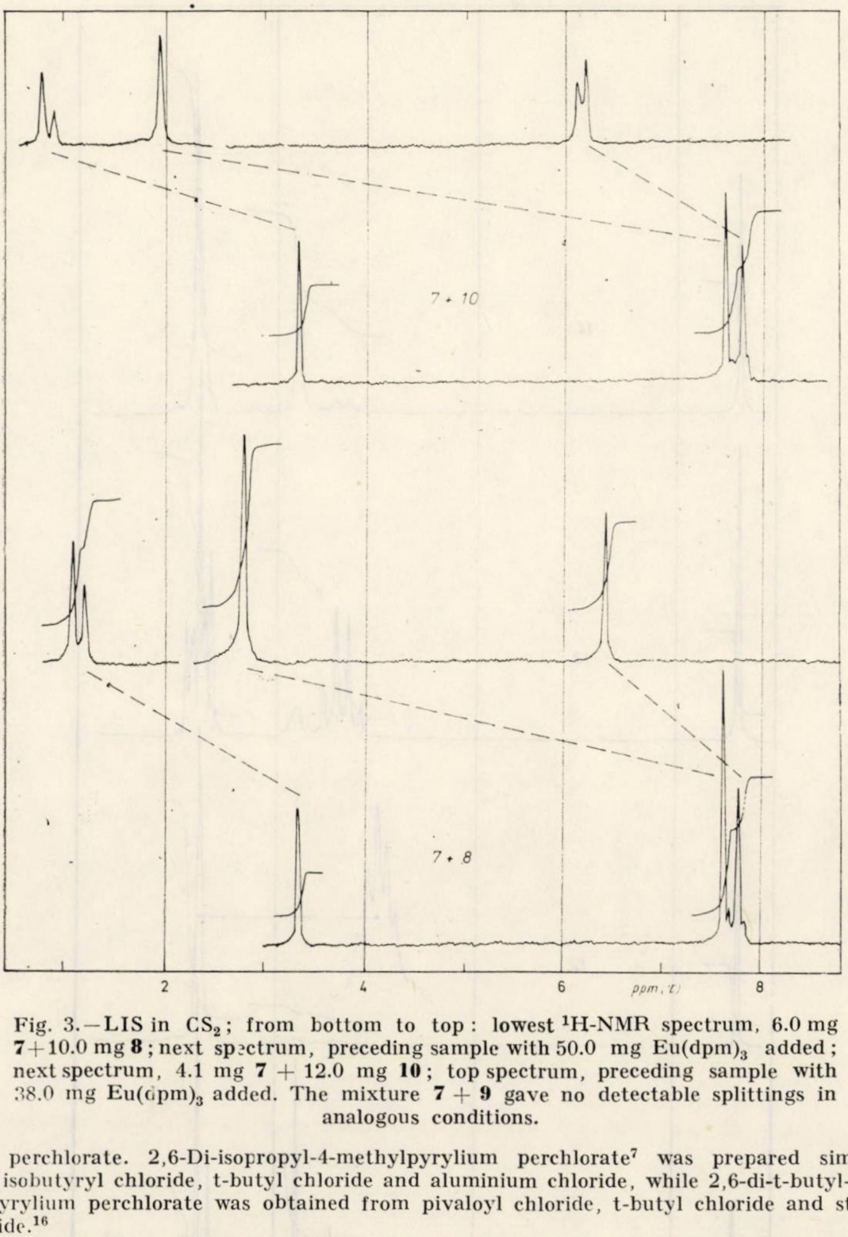

Fig. 3.—LIS in CS_2; from bottom to top: lowest ^{1}H-NMR spectrum, 6.0 mg **7**+10.0 mg **8**; next spectrum, preceding sample with 50.0 mg $Eu(dpm)_3$ added; next spectrum, 4.1 mg **7** + 12.0 mg **10**; top spectrum, preceding sample with 38.0 mg $Eu(dpm)_3$ added. The mixture **7** + **9** gave no detectable splittings in analogous conditions.

lium perchlorate. 2,6-Di-isopropyl-4-methylpyrylium perchlorate[7] was prepared similarly from isobutyryl chloride, t-butyl chloride and aluminium chloride, while 2,6-di-t-butyl-4-methylpyrylium perchlorate was obtained from pivaloyl chloride, t-butyl chloride and stannic chloride.[16]

All pyrylium salts were purified by recrystallization from 1% aqueous perchloric acid in the presence of decolorizing carbon.

Deuteriations and de-deuteriations. These were effected in an excess of non-buffered distilled D_2O and H_2O, respectively for the prescribed duration and at the prescribed temperature, as reported previously.[3, 4, 6, 17]

---

[16] A. T. Balaban, *Org. Preparations Procedures Internat.* **9**, 125 (1977)

[17] I. I. Stănoiu, E. Gârd, C. Uncuța, F. Chiraleu and A. T. Balaban, *Rev. Roumaine Chim.*, **22**, 1359 (1977).

2) γ-Deuteriation does not influence the MIS value, as evidenced by the absence of any detectable splitting in the mixtures **9** + **7** or **13** + **11** (a splitting corresponding to a total isotope effect of 0.2% would have been detectable, i.e., 0.07% per deuterium atom at the γ-methyl), as well as by the practical identity of the effects for **8** and **10**, or for **12** and **14**.

3) The absolute MIS values for the α,α-diethylpyridines **11**–**14** are appreciably smaller than those of **7**–**10** which have methyl groups in α-positions.

With bulkier α-substituents like isopropyl (**15**–**18** in scheme 4) where selective deuteriation was also effected,[6] or like t-butyl (**19** and **20** in scheme 4) no lanthanide-induced shifts were observed at all under the same conditions, either with Eu(dpm)$_3$ or with Eu (fod)$_3$; these pyridines do not form therefore complexes with the LSR.

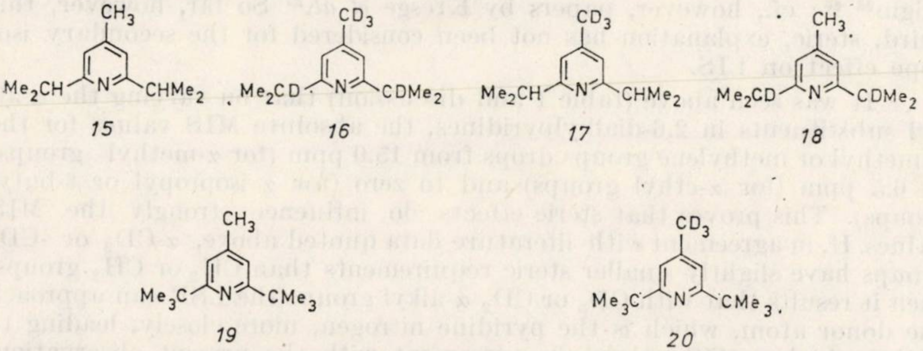

Scheme 4. — Selectively deuteriated 2,6-diisopropyl-4-methylpyridines **15**–**18** and 2,6-di-t-butyl-4-methylpyridines **19**–**20**, which do not form complexes with LSR.

Hinckley, the discoverer of LSR,[18] also discovered [9–11] that geminally deuteriated alcohols have slightly larger (with 1–2%) MIS values than their non-deuteriated counterparts. He advanced [9] two hypotheses to explain this behaviour: the possibility of an influence *via* hydrogen bonds between the geminal proton/deuteron and an oxygen atom of the europium β-diketonate (this hypothesis was soon discarded [11]) or the enhancement of the basicity of the donor atom (hydroxyl oxygen) which interacts with the europium chelate. This latter hypothesis gained support from the observation [19] that CD$_3$ or CD$_2$ groups are electron-releasing relative to CH$_3$ or CH$_2$ groups.

However, if this were the origin of the isotope effect on LIS, it would be expected that the electron-releasing power should be comparable for α- and for γ-methyl or methylene groups. Indeed, control measurements evidenced a monotonous increase in the series **7**, **9**, **10**, and **8**, whose pK$_a$ values are: 7.45, 7.47, 7.49, and 7.53, respectively (the precision of the electrochemical method was about 0.01 pK unit), i.e., an increase of approximately 0.025 pK$_a$ units per CD$_3$ group replacing a CH$_3$ group.[20]

---

[18] C. C. Hinckley, *J. Amer. Chem. Soc.*, **91**, 5160 (1969); cf. R. von Ammon and R. D. Fischer, *Angew. Chem.*, **84**, 737 (1972); *Angew. Chem. Internat. Edit.*, **11**, 675 (1972).

[19] E. A. Halevi, M. Nussim and A. Ron, *J. Chem. Soc.*, **1963**, 866; H. S. Klein and A. Streitwieser Jr., *Chem. and Ind.*, **1961**, 180.

[20] A. T. Balaban, I. I. Stănoiu and E. Gârd, *Rev. Roumaine Chim*,. **22**, 1191 (1977).

Hence, it must be admitted that the enhancement of the basicity is not the main factor which causes the secondary isotope effect on LIS. A different rationale must therefore be proposed, assuming a steric origin of this effect. It is known [21] that the deuterium atom has smaller covalent and Van der Waals radii than protium, and this explains the lower rotation barriers of *o,o'*-dibromobiphenyls when their remaining *ortho*-hydrogens undergo deuteriation,[22] leading to faster racemizations. Similar phenomena were observed by Mislow *et al.*, [23] for the racemization of 4,5-dimethyl (or di-d_3-methyl, respectively)-9,10-dihydrophenanthrene. Indeed, H.C. Brown advocated that most or all secondary isotope effects have a steric origin[24-26]; cf., however, papers by Kresge *et al.*[27] So far, however, this third, steric, explanation has not been considered for the secondary isotope effect on LIS.

It was seen above (table 1 and discussion) that on varying the α-alkyl substituents in 2,6-dialkylpyridines, the absolute MIS values for the α-methyl or methylene groups drops from 15.0 ppm (for α-methyl groups) to 6.5 ppm (for α-ethyl groups) and to zero (for α-isopropyl or t-butyl groups). This proves that steric effects do influence strongly the MIS values. If, in agreement with literature data quoted above, α-CD_3 or -CD_2 groups have slightly smaller steric requirements than CH_3 or CH_2 groups, then it results that with CD_3 or CD_2 α-alkyl groups the LSR can approach the donor atom, which is the pyridine nitrogen, more closely, leading to slightly higher MIS values, in agreement with the present observation. Should the steric origin of these effects be the determing factor, rather than the inductive enhancement of the basicity, the absence of any secondary isotope effect on MIS values with γ-deuteriated methyl groups is easily understandable.

In considering the secondary isotope effects due to deuterium (recent reviews by Halevi, [28] Thornton,[29] Laszlo and Welvart,[30] and in the book edited by Collins and Bowman [31-33]), due attention must be paid to the criticisms [29,31-33] made both to Halevi's inductive model, [19,28] and to Bartell's steric model [34]: actually, the effects are *on* the isotopic atom (i.e., on its vibrational force constants) rather than *of* the isotopic atom.[33]

---

[21] K. Clusius and K. Weigand, *Z. physik. Chem.* **B**, **46**, 1 (1940).

[22] L. Melander and R. E. Carter, *J. Amer. Chem. Soc.*, **86**, 295 (1964); *Acta Chem. Scand.*, **18**, 1138 (1964).

[23] K. Mislow, R. Graewe, A. J. Gordon and G. H. Wahl Jr., *J. Amer. Chem. Soc.*, **85**, 1199 (1963); **86**, 1733 (1964).

[24] H. C. Brown and G. J. McDonald, *J. Amer. Chem. Soc.*, **88**, 2514 (1966).

[25] H. C. Brown, M. E. Azzaro, J. G. Koelling and G. J. McDonald, *J. Amer. Chem. Soc.*, **88**, 2520 (1966).

[26] H. C. Brown, "Boranes in organic Chemistry", Cornell Univ. Press, Ithaca, N. Y., 1972, pp. 66 and 71.

[27] A. J. Kresge and R. J. Preto, *J. Amer. Chem. Soc.*, **89**, 5510 (1967).

[28] E. A. Halevi, *Progr. Phys. Org. Chem.*, **1**, 109 (1963).

[29] E. R. Thornton, *Ann. Rev. Phys. Chem.*, **17**, 349 (1966).

[30] P. Laszlo and T. Welvart, *Bull. Soc. Chim. France*, **1966**, 2412.

[31] M. A. Van Hook, in "Isotope Effects in Chemical Reactions" (editors C. J. Collins and N. S. Bowman), Van Nostrand — Reinhold Co., New York, 1970, p. 60.

[32] J. V. Shiner, Jr., *ibid.*, p. 90.

[33] E. K. Thornton and E. R. Thornton, *ibid.*, p. 213.

[34] L. S. Bartell, *Tetrahedron Letters*, **1960**, 13,; *J. Amer. Chem. Soc.*, **83**, 3567 (1961).

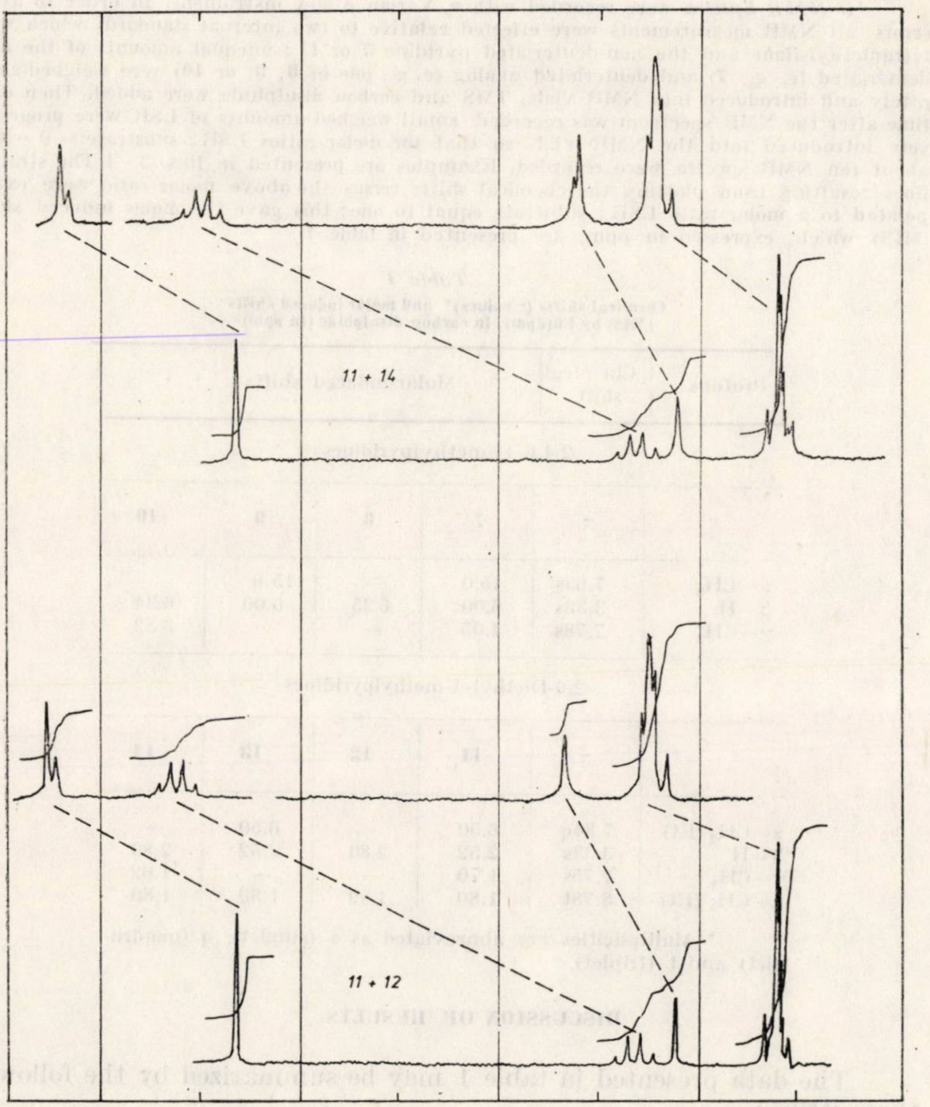

Fig. 4. — LIS in CS_2; from bottom to top: lowest ^{1}H-NMR spectrum 4.0 mg **11** + 9.0 mg **12;** next spectrum, preceding sample with 41.4 mg $Eu(dpm)_3$ added; next spectrum, 2.8 mg **11** + 7.0 mg **14**; top spectrum, preceding sample with 39.1 mg $Eu(dpm)_3$ added. The mixture **11** + **13** gave no detectable splitting in analogous conditions.

Substituted pyridines were prepared by introducing the deuteriated or non-deuteriated pyrylium perchlorates into a cold agitated mixture of excess aqueous ammonia and ether, separating the ethereal layer, and purifying the resulted pyridine by extraction into 10% hydrochloric acid and alkalinization of the acid aqueous layer; the pyridines were extracted with ether, dried over powdered sodium hydroxide and distilled under reduced pressure.

^{1}H-NMR Spectra were recorded with a Varian A-60A instrument. In order to avoid errors, all NMR measurements were effected relative to two internal standards which were tetramethylsilane and the non-deuteriated pyridine **7** or **11** : unequal amounts of the non-deuteriated (e. g., **7**) and deuteriated analog (e. g., one of **8**, **9**, or **10**) were weighed accurately and introduced into NMR vials, TMS and carbon disulphide were added. Then each time after the NMR spectrum was recorded, small weighed amounts of LSR were progressively introduced into the NMR vial, so that for molar ratios LSR : substrate = 0 – 0.7, about ten NMR spectra were recorded. Examples are presented in figs. 3–4. The straight lines resulting from plotting the chemical shifts *versus* the above molar ratio were extrapolated to a molar ratio LSR : substrate equal to one; this gave the molar induced shifts (MIS) which, expressed in ppm, are presented in table 1.

Table 1

Chemical shifts (τ values)* and molar induced shifts (MIS) by Eu(dpm)$_3$ in carbon disulphide (in ppm)

Protons	Chemical shift	Molar-induced shifts			
2,4,6-Trimethylpyridines					
	τ	**7**	**8**	**9**	**10**
$\alpha-CH_3$	7.63s	15.0	—	15.0	—
$\beta-H$	3.33s	6.00	6.35	6.00	6.34
$\gamma-CH_3$	7.78s	4.05	—	—	3.82
2,6-Diethyl-4-methylpyridines					
	τ	**11**	**12**	**13**	**14**
$\alpha-CH_2$ (Et)	7.34q	6.50	—	6.50	—
$\beta-H$	3.33s	2.52	2.80	2.52	2.80
$\gamma-CH_3$	7.75s	1.70	—	—	1.62
$\alpha-CH_3$ (Et)	8.78t	1.80	1.89	1.80	1.89

* Multiplicities are abbreviated as s (singlet), q (quadruplet) and t (triplet).

DISCUSSION OF RESULTS

The data presented in table 1 may be summarized by the following three items :

1) In the presence of LSR, pyridines possessing α-deuteriated substituents exhibit a larger MIS than the non-deuteriated reference compound, for the protons present in both systems : the MIS increment is, for the β-protons, about 6% for **8** and **10** relative to **7**, and about 4% for **12** and **14** relative to **11**. This isotope effect amounts in both cases to about 1% per one deuterium atom at the α-methyl or α-methylene group. The isotope effect is smaller for the methyl protons of the ethyl group in **12** and **14**, but it is readily detectable. We cannot explain at present the inverse isotope effect for the γ-methyl group in **10** relative to **7**, and in **14** relative to **11** (cf. figs 3 and 4).

Revue Roumaine de Chimie, **23**, *2*, 197–202 (1978)

SOLVENT AND MEDIUM BASICITY EFFECTS ON THE REACTION OF 5-CHLORO-2-PENTANONE WITH SODIUM METHOXIDE

NORA RĂDULESCU and C. SÂRBU

Chemical and Pharmaceutical Research Institute, Şos. Vitan, 112, Bucharest, Romania

Received November 23, 1975

The reaction of 5-chloro-2-pentanone with sodium methoxide in three different solvents : benzene, methanol, dimethylsulfoxide was investigated. In each solvent the reaction yielded only methyl cyclopropyl ketone via a γ elimination. The reaction kinetics was investigated in methanol-dimethylsulfoxide and methanol-benzene mixtures. Assumptions are made concerning the assignment of the γ elimination between E_1 cb and E_2 mechanisms, based on the medium basicity and solvent effect.

*

The base catalysed cyclisation of 5-chloro-2-pentanone to methyl-cyclopropyl ketone via a γ elimination is well known. In spite of numerous information regarding the experimental conditions of this reaction,[1–3] few data concerning the medium basicity and solvent effects are found in the literature.[4] No kinetic data are reported and any mechanism was proposed.

It was assumed [5] that the preferential cyclisation to a three-membered ring and the absence of the five-membered one is determined by a solvent effect. Later, Bartsch,[4] studying the cyclisation of 5-chloro-2-pentanone in various base-solvent systems found that the solvation hypothesis for the preferential formation of a three-membered ring is inapplicable to this case.

The present work deals with the reaction of 5-chloro-2-pentanone with sodium methoxide in three different solvents : benzene, methanol and dimethylsulfoxide. The solvent effect on the nature of the reaction products, as well as on kinetics is investigated. Correlations between the rate constants and the medium and solvent properties are established in order to clear up the reaction mechanism.

[1] G. W. Cannon, R. C. Ellis and I. R. Leal, "Organic Synthesis Coll". Vol. IV, Wiley, New York, 1963, p. 597.

[2] L. S. Smith and E. R. Rogier, *J. Amer. Chem. Soc.*, **73**, 4049 (1951).

[3] M. Julia, S. Julia and Y. Noël, *Bull. Soc. chim. France.*, **1960**, 1708.

[4] R. A. Bartsch and D. M. Cook, *J. Org. Chem.*, **1970**, 1714.

[5] E. Schmitz, *Angew. Chem.*, **76**, 197 (1964).

In the reaction of 5-chloro-2-pentanone with sodium methoxide as basic and nucleophilic reagent, the formation of methyl cyclopropyl ketone together with the nucleophilic substitution product and the β and ε elimination products can be assumed.

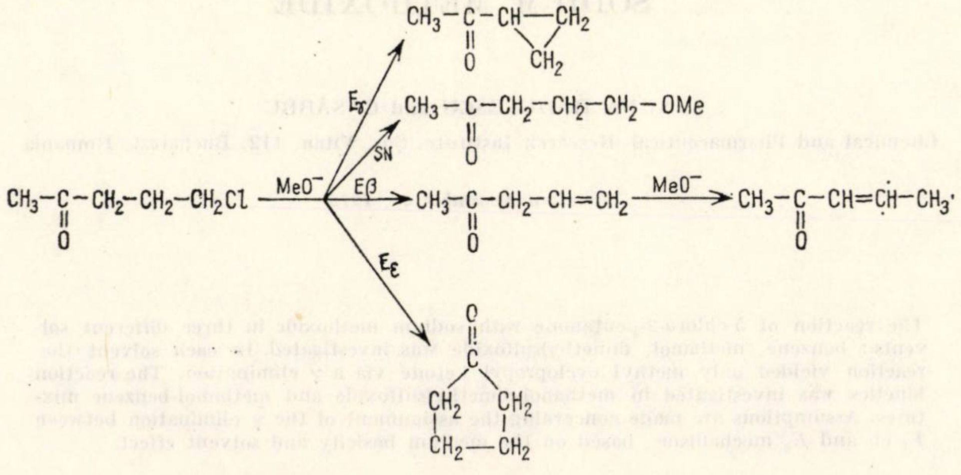
CH3–C–CH–CH2 (O, CH2)
Eγ
CH3–C–CH2–CH2–CH2–OMe
SN
CH3–C–CH2–CH2–CH2Cl
MeO⁻
Eβ
CH3–C–CH2–CH=CH2
MeO⁻
CH3–C–CH=CH–CH3
Eε
O
C
CH2 CH2
CH2–CH2

The standards of all these products were prepared and their presence into the reaction mixture was investigated by v.p.c. analysis. In all solvents (benzene, methanol, dimenthylsulfoxide) at temperatures ranging from 0 to 60°, the formation of methyl cyclopropyl ketone by a γ elimination was the only reaction observed. No solvent effect on the reaction products was noticed.

Two possible mechanisms are generally accepted for the elimination reactions:

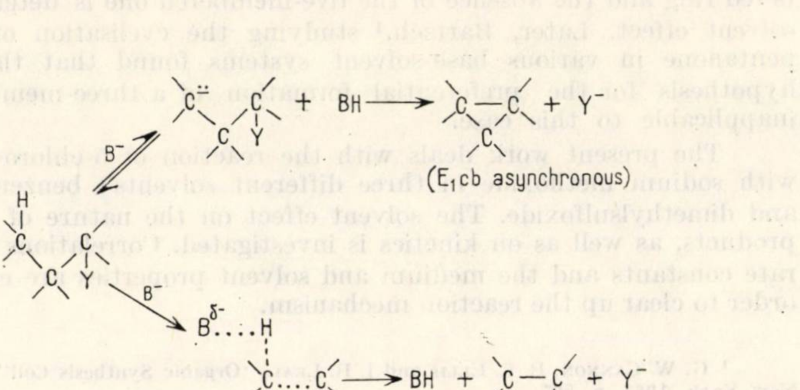
C C Y + BH C–C + Y⁻ C
B⁻
(E1cb asynchronous)
H C C C Y
B⁻
B^δ-....H
C....C C Y^δ-
BH + C–C + Y⁻ C
(E2 synchronous)

The differential criteria of the two mechanisms reviewed previously by Lennan [6] and recently by Saunders [7] offer, in few cases only, the possibility of reliable assignment of the investigated reaction to one of them. Both mechanisms are bordering situations of small probability; there is no net limit between them; a large spectrum of transition states is involved between the E_1 *cb* and E_2 mechanisms.[8,9]

A kinetic distinction between these mechanisms is not possible as both involve usually second-order kinetics. It was considered that some correlations between the rate constants, the medium basicity and solvent properties will supply indications concerning the distinction between the two mechanisms. If the observed correlations are similar to those established in carbanionic reactions, a transition state with a carbanionic character, as in the E_1 *cb* mechanism, can be assumed.

The fact that methyl cyclopropyl ketone was the only observed product in the investigated reaction, simplified the kinetic experiments. They were performed by simple argentimetric titration of the halogen ion, formed in the γ elimination. The results of the kinetic experiments are summarized in table 1.

Table 1

Second-order rate constants, $k_2 10^4$ l/mol.s in methanol-dimethylsulfoxide mixtures at various temperatures, (5-chloro-2-pentanone = 0.02 to 0.2 M/l, MeONa = 0.05 to 0.5 M/l

$k_2 \cdot 10^4$ l/mol.s	t°	0	10	20	30	40	50	60
MeOH—0%	DMSO	0.5	1.7	5.0	15.5	45.5	115.0	270.0
MeOH—25%	DMSO	1.9	5.7	20.0	57.0	145.0	—	—
MeOH—50%	DMSO	14.0	43.0	162.0	460.0	—	—	—
MeOH—76.5%	DMSO	560.0	900.0	—	—	—	—	—
MeOH—90%	DMSO	17400.0	—	—	—	—	—	—

An important increase of about 10^5 in the reaction rate is noticed if the composition of the mixture changes from 100% methanol to 90% dimethylsulfoxide. The increase of the methoxide ion basicity and the preferential stabilisation of the transition state by dimethylsulfoxide are probably responsible, like in other cases, [10, 11] for the reaction rate increase.

Cram and coworkers [10, 12] studied the basic properties of natrium methoxyde in methanol-dimethylsulfoxide mixtures at various ratios. A H_- function was proposed,[12] as a property of the medium that measures the ability of that medium to remove a proton from weak acids under equilibrium conditions. For certain carbanionic reactions (racemisation of 2-methyl-3-phenylpropionitrile) a linear correlation has been established between the H-function and the negative logarithm of the second-order rate constant k_2. Fig. 1 reproduces this correlation (dotted line) at 25° ; the same dependence is plotted for the rate constant determined in the reaction of 5-chloro-2-pentanone with sodium methoxide (full lines) at 0° and 10°.

---

[6] D. J. Mc. Lennan, *Quart. Rev.*, **21**, 490 (1967).

[7] W. H. Saunders, Jr., *Acc. Chem. Res.*, **9**, 19 (1976).

[8] J. F. Bunnett, *Angew. Chem.*, **74**, 731 (1962).

[9] W. H. Saunders, Jr. and A. F. Cockerill "Mechanisms of Elimination Reactions", Wiley-Interscience, New York, 1973, chap. 2.

[10] D. J. Cram "Fundamentals of Carbanion Chemistry", Academic Press, New York, 1965, p. 36.

[11] C. Reichardt "Lösungsmitteleffecte in der organischen Chemie", Verlag Chemie, G.m.b.H., Weinheim, 1969, p. 93.

[12] R. Steward, J. F. O'Donnell, D. J. Cram and B. Rickborn, *Tetrahedron.*, **18**, 317 (1962).

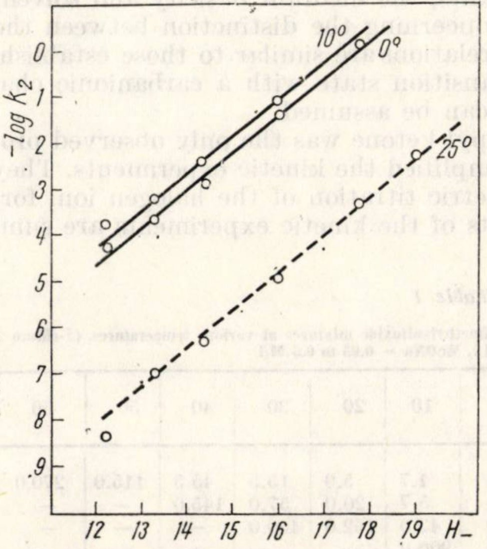

Fig. 1. — Plot of H_- vs — log k_2 for the methoxide catalyzed racemisation of 2-methyl-3-phenylpropionitrile at 25° (dotted line) and for the methoxyde catalyzed γ elimination of 5-chloro-2-pentanone at 0 and 10° (full lines).

The linear correlations for the γ elimination from 5-chloro-2-pentanone at two different temperatures are close to those previously established by Cram[10, 12] for the methoxide catalysed racemisation of 2-methyl-3-phenylpropionitrile. The slopes of these lines measure the reaction sensitivity to changes of the medium basicity.[13] Their values of 0.8 are characteristic of carbanionic reactions.[6] Therefore, it is possible to assume for the investigated γ elimination a transition state having a pronounced carbanionic character as in an E_1cb mechanism.

Both mechanisms assume that in the transition state of the investigated γ elimination the methoxide ion charge is distributed on several atoms. According to Hughes-Ingold's solvent theory[14–16] a decrease of the reaction rate with increase of solvent polarity is expected. For the investigation of the solvent effect on the reaction rate, kinetic experiments were carried out in methanol and benzene-methanol mixtures. The results are given in table 2.

---

[13] J. E. LEFFLER and E. GRUNDWALD, "Rates and Equilibria of Organic Reactions", Wiley, New York, 1963, p. 235.

[14] E. D. HUGHES and C. K. INGOLD, *J. Chem. Soc.*, **1935**, 244.

[15] C. K. INGOLD "Structure and Mechanism in Organic Chemistry", Cornell University Press, Ithaca, 1953, p. 345.

[16] D. V. BANTHORPE, "Elimination Reactions", Elsevier, Amsterdam, 1963, chap. 2.

Table 2

Second-order rate constants $k_2.10^4$ l/mol.s in benzene-methanol-mixture at different temperatures, [5-chloro-2-pentanone] = 0.05 M/l, [MeONa] = 0.1 M/l

t^c / $k_2\ 10^4$ l/mol· s		20	30	40	50
MeOH—0 %	benzene	5.0	15.5	45.0	115.0
MeOH—25 %	benzene	5.5	17.0	50.0	140.0
MeOH—50 %	benzene	7.6	27.0	78.0	260.0
MeOH—75 %	benzene	9.8	35.0	103.0	410.0
MeOH—90 %	benzene	16.0	55.0	158.0	—

In agreement with Hughes-Ingold's theory a slight increase of the reaction rate was observed as the solvent composition changes from 100% methanol to 90% benzene. The solvent effect is reduced; this might be due to the fact that in the transition state the methoxide ion charge is distributed on a small part of the attacked molecule. In fact in a transition state having a carbanionic character as in an $E_1\,cb$ mechanism, the methoxide ion charge is distributed only on the acidic carbon atom, unlike in the transition state of the E_2 mechanism where the charge is distributed on the whole molecule. Based on the observed solvent effect we assume, for the investigated γ elimination, that a transition state with a carbanionic character as in an $E_1\,cb$ mechanism is much more probable.

CONCLUSIONS

The reaction of 5-chloro-2-pentanone with sodium methoxide was investigated in three solvents: benzene, methanol and dimethylsulfoxide at temperatures ranging from 0 to 60°; the only reaction observed was the formation of methyl cyclopropyl ketone via a γ elimination. No solvent effect on the nature of the reaction products was noticed.

Kinetic experiments carried out in methanol-dimethylsulfoxide and methanol-benzene mixtures and the observed medium basicity and solvent effects point out that a transition state having a pronounced carbaninonic character as in an E_1cb mechanism could be involved in the formation of methyl cyclopropyl ketone from 5-chloro-2-pentanone and sodium methoxide.

EXPERIMENTAL PART

5-Chloro-2-pentanone[17]: A mixture of 25 g αacetyl-γ butirolactone, 78 ml hydrochloric acid and 230 ml benzene was heated at 45—50°. The mixture was stirred at this temperature for 5 hrs and then cooled at room temperature. The benzenic layer was removed and the aqueous layer was twice extracted with 50 ml benzene. The combined extracts dried on anhydrous sodium sulfate, concentrated and vacuum distilled, gave 25.5 g 5-chloro-2-pentanone b. p. 80—82°/30 mm.

Methyl cyclopropyl ketone was prepared from 5-chloro-2-pentanone and sodium hydroxide in aqueous solution[1]: b. p. 110—112° n_D^{25} 1.4226.

---

[17] N. Rădulescu, M. Iulian, I. P. Ambrus and V. Tamaş, Romanian Pat. 77626—1974.

5-Methoxy-2-pentanone was obtained from 2-methyl-2-(3-chloro-propyl)-1,3-dioxolan[18–19] and sodium methoxide followed by acid hydrolysis in a similar way to that described for other 5-alcoxy-2-pentanones[19]: b. p. 97°/35 mm, n_D^{20} 1.4148, semicarbazone m. p. 119°.[20]

Methyl propenyl ketone was prepared by Grignard's method[21]: b. p. 122°, n_D^{20} 1.4350. Cyclopentanone (Merck) was used without further purification.

The solvents: anhydrous methanol reagent grade (Reactivul) was distilled over magnesium; commercial benzene was dried on sodium and distilled, dimethylsulfoxide p. a. (U. C. B). was used without further purification.

V. p. c. analyse was performed on a Carlo Erba 2400 v Fractovap with flame ionisation detector, with a 5% silicone SE 30 on Chromosorb W, column (1 m/6 mm diam) at 110° with a hydrogen rate flow of 60 ml/min.

Kinetic experiments: measured quantities of 5-chloro-2-pentanone and sodium methoxide solutions at given concentrations were placed in two concentric isolated spaces of the same glass ampule. The ampules were sealed, thermostated at the desired temperature for 2 minutes and the reagents mixed by upsetting the ampules. At established times the ampule was opened and the reaction quenched by adding a 1:1 mixture of methanol: acetic acid. The halogen ion content was titrated with 0.01 N silver nitrate in the presence of eosine indicator. The error of these determinations is about ± 8%.

ACKNOWLEDGEMENT. The authors are indebted to Professor Valeriu Vântu, Gas and Petroleum Institute, Ploiești, Romania, for his careful guidance and valuable advice.

---

[18] Y. Inoue and Y. Ban, *J. Chem. Soc. C.*, **1970**, 602.

[19] Unilever Ldt., Brit. Pat. 1016516–1966; *Chem. Abstr.*, **64**, 14095 (1966).

[20] O. S. Stepanova, *Zhur. obshchei Khim.*, **32**, 3295 (1962).

[21] M. V. Grignard and M. Fluchaire, *Ann. Chim. (France)*, **9**, 10 (1928).

Revue Roumaine de Chimie, **23**, *3*, 203–208 (1978)

SYNTHÈSE DE 4-HYDROXY-Δ^2-OXADIAZOLINES-1,2,4

S. DESHERCES*, J. BARRANS** et J. L. ROUBATY*
*Laboratoire des hétérocycles du phosphore et de l'azote 118, Route de Narbonne,
31 400, TOULOUSE, FRANCE
**L. A. 199 C.N.R.S. 39, Bd du 11 Novembre 1918, 69 626, VILLEURBANNE, FRANCE
* Adresse actuelle : B. P. 92 CENTRE UNIVERSITAIRE
TLEMCEN (ALGÉRIE)

Reçu le 11 septembre 1975

De nouvelles 4-hydroxy-Δ^2-oxadiazolines-1,2,4 ont été préparées par action d'aldéhydes sur des N-hydroxy-amidoximes. Cette méthode permet d'obtenir ces composés avec des restes alkyles en 3. Certains composés ont été étudiés par spectrographie I. R. et de R. M. N. du proton. Un mécanisme de réaction est proposé.

INTRODUCTION

Les N-hydroxy-amidoximes sont connues depuis 1898 où Ley, par action de la benzalchloroxime sur l'hydroxylamine, a pu préparer la N-hydroxy-benzal-doxime :[1]

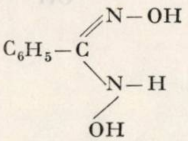

L'obtention de N-hydroxy-amidoximes à reste alkyle est possible par action de l'hydroxylamine sur les amidoximes. Ces dernières, par une réaction de transposition conduisent à la formation de composés du type :[2]

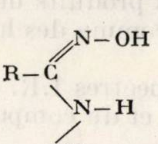

Nous avons utilisé ces N-hydroxy-amidoximes pour la synthèse de 4-hydroxy-Δ^2-oxadiazolines-1, 2, 4. Certains de ces composés peuvent être préparés par action de BF_5 (qui agit comme catalyseur) sur un mélange d'oxyde de benzonitrile et d'oxime.[3] Cette méthode ne permet pas d'obtenir de 4-hydroxy-Δ^2-oxadiazolines-1, 2, 4 avec un reste alkyle en 3.

---

[1] H. Ley, *Ber, dtsch. Chem. Ges.*, **1898**, 2126.

[2] J. Armand, *Compt. rend.*, **262 C**, 592 (1968).

Les résultats sont donnés par le tableau 1.

Tableau 1

Résultats expérimentaux

Réactifs *	Conditions expérimentales	Produit formé**
$R_1 = C_6H_5$ $R_2 = C_2H_5$	Et_2O, 20°C 10 mm	(a) N hydroxy-Δ^2-oxadiazoline 1, 2, 4, pF : 116°
$R_1 = C_6H_5$ $R_2 = pNO_2C_6H_5$	CH_3OH, 40°C 1 heure	(b) -id- pF : 186–8°
$R_1 = CH_3$ $R_2 = C_2H_5$	CH_3OH, 20°C 10 mn	(c) -id- huile
$R_1 = CH_3$ $R_2 = pNO_2C_6H_5$	CH_3OH, 40°C 5 mn	(d) -id- solid jaune pF : pyrolyse
$R_1 = CH_3$ $R_2 = pOCH_3C_6H_5$	CH_3OH, 40°C	(e) -id- solide blanc pF : pyrolyse

* N-hydroxy-amidoxime

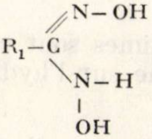

$R_1-C(=N-OH)-NH-OH$

aldéhyde :

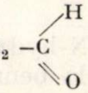

$R_2-C(H)=O$

**

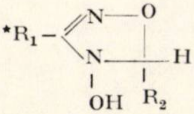

INTERPRÉTATION ET DISCUSSION DES RÉSULTATS

Nous avons considéré nos produits de départ comme étant des amidoximes N substituées et non comme des hydroxylamines.

Ce choix tient compte :

— de la similitude des spectres I.R. en solution dans CCl_4 des amidoximes secondaires d'une part et du composé :

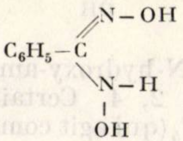

$C_6H_5-C(=N-OH)-NH-OH$

d'autre part.

---

[3] S. Morocchi et A. Ricca, *Chimica e Industria*, **49**, 629 (1967).

Ce dernier montre en effet une bande ν_{OH} libre vers 3610 cm^{-1} bande caractéristique des composés :

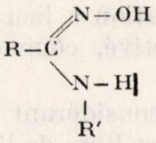

où R est un reste aromatique ;

— du fait qu'ils conduisent à la formation d'hétérocycles analogues à ceux obtenus avec les amidoximes dans des conditions similaires.

C'est pourquoi nous proposons un mécanisme de réaction analogue à celui déjà étudié par Malavaud.[4]

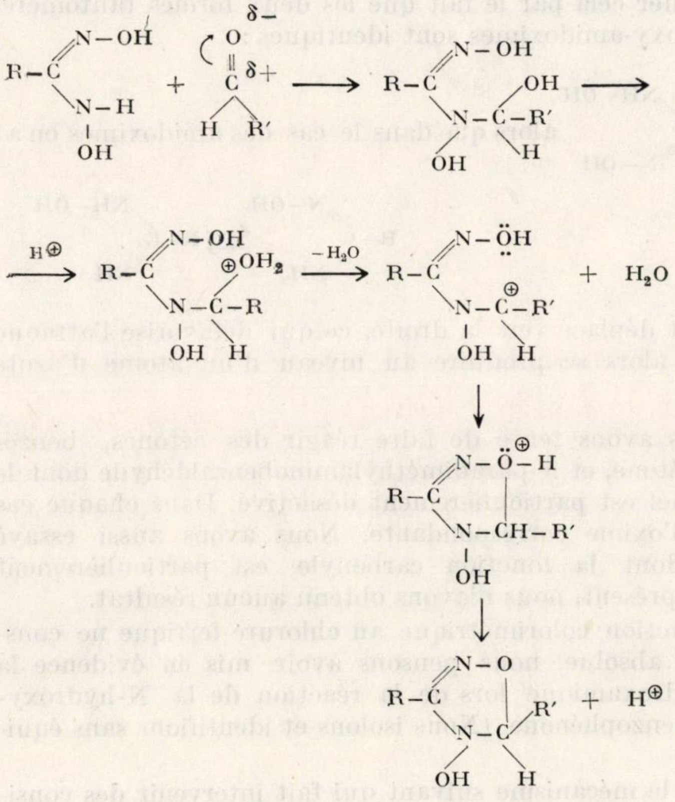

Nous avons remarqué que la réactivité des N-hydroxy-amidoximes est de beaucoup supérieure à celle des amidoximes. En effet :

1) la vitesse des réactions est beaucoup plus grande (quelques minutes suffisent dans la plupart des cas), alors que dans des conditions ana-

---

[4] C. Malavaud « Synthèse et étude structurale de quelques dérivés de l'$H_{4.5}$ oxadiazoline 1, 2, 4 », thèse, Toulouse, 1971.

logues la réaction demande de nombreuses heures en ce qui concerne les amidoximes ;

2) la réaction de cyclisation a lieu même avec des molécules où le carbone est relativement désactivé, comme par exemple le *para*-métoxybenzaldéhyde.

Cela suppose donc, en considérant le mécanisme proposé, une plus grande disponibilité du doublet libre de l'azote dans le cas de N-hydroxyamidoximes

Or, en spectroscopie infra-rouge, nous avons observé une fréquence NH relativement basse par rapport à celle des amidoximes (3335 cm^{-1}) en ce qui concerne le spectre de la N-hydroxybenzaldoxime. Ceci prouve un état d'hybridation de l'azote en question très proche de sp^3.

On peut expliquer cela par le fait que les deux formes tautomères possibles des N-hydroxy-amidoximes sont identiques :

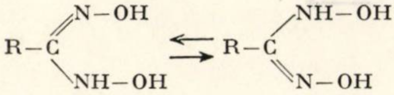

alors que dans le cas des amidoximes on a :

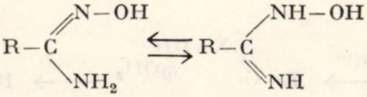

avec l'équilibre plutôt déplacé vers la droite, ce qui défavorise l'attaque électrophile qui doit alors se produire au niveau d'un atome d'azote hybridé sp^2.

Remarque. Nous avons tenté de faire réagir des cétones, benzophénone et phénylacétone, et le paradiméthylaminobenzaldéhyde dont le groupement fonctionnel est particulièrement désactivé. Dans chaque cas nous avons obtenu l'oxime correspondante. Nous avons aussi essayé l'hexafluoroacétone dont la fonction carbonyle est particulièrement activée, mais jusqu'à présent, nous n'avons obtenu aucun résultat.

Bien que la réaction colorimétrique au chlorure ferrique ne constitue pas une preuve absolue, nous pensons avoir mis en évidence la formation d'acide hydroxamique lors de la réaction de la N-hydroxybenzaldoxime sur la benzophénone. (Nous isolons et identifions sans équivoque l'oxime.)

Nous proposons le mécanisme suivant qui fait intervenir des considérations d'ordre stérique :

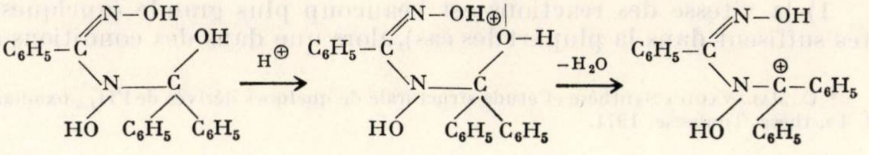

A ce stade la cyclisation est peu probable vu la taille des substituants portés par le carbone et :

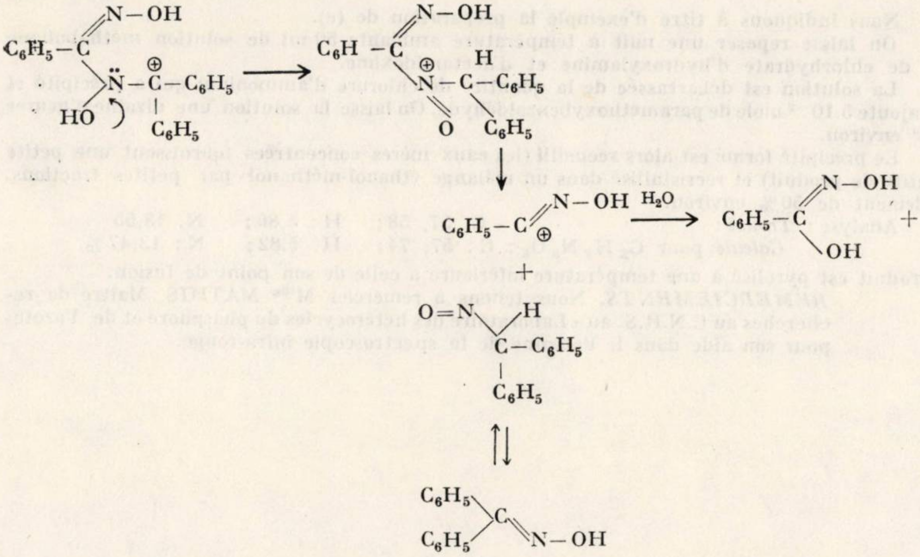

ÉTUDE SPECTROGRAPHIQUE DES COMPOSÉS PRÉPARÉS

Vu la faible solubilité de ce genre de composés en général, et tout particulièrement dans CCl_4, l'étude spectrographique est délicate.

Nous avons pu malgré tout étudier la fréquence ν_{OH} libre dans plusieurs cas en utilisant des cuves à face NaCl jusqu'à 7 cm de longueur.

En solution dans le DMSO D6 nous avons observé en R.M.N. du proton le déplacement chimique du proton lié au carbone asymétrique. L'environnement immédiat de ce carbone est le même pour nos composés que pour les Δ^2-oxadiazolines-1, 2, 4 étudiées par Malavaud.[4] Nous avons constaté que le remplacement du proton de l'azote par un radical hydroxy ne modifie pratiquement pas le déplacement chimique du proton lié au carbone asymétrique.

Dans le cas du composé (a) le signal dû aux protons $-CH_2-$ liés au carbone asymétrique est apparemment très complexe et se présente sous la forme d'un quintuplet aux raies très élargies. On a affaire en réalité au recouvrement de deux quadruplets et ce, par influence du carbone asymétrique.

Par une analyse du premier ordre nous avons pu mesurer les constantes de couplage :

$$J_{CH-CH_ACH_B} = 6\ H_z \text{ et } J_{CH_AH_B-CH_3} = 7{,}5\ H_z$$

Tableau 2

Données spectroscopiques

Composé	Fréquence ν_{OH} libre*	δ^1 H 10^{-6} **
(a)	3579 – 80	5,6
(b)		4,85
(c)	3578 – 79	5,15
(d)	3571 – 73	4,38

* Exprimée en cm^{-1}, en solution dans CCl_4 ;
** en solution dans DMSO D6.

Les données spectroscopiques sont données dans le tableau 2.

PARTIE EXPÉRIMENTALE

Nous indiquons à titre d'exemple la préparation de (e).

On laisse reposer une nuit à température ambiante 50 ml de solution méthabolique 1 M de chlorhydrate d'hydroxylamine et d'acétamidoxime.

La solution est débarrassée de la quantité de chlorure d'ammonium qui a précipité et on y ajoute 5.10^{-2} mole de paraméthoxybenzaldéhyde. On laisse la solution une dizaine d'heures à 40° environ.

Le précipité formé est alors recueilli (les eaux mères concentrées fournissent une petite quantité de produit) et recristallisé dans un mélange éthanol-méthanol par petites fractions. Rendement de 50 % environ.

Analyse : *Trouvé* :	C, 57, 58 ;	H : 5,86 ;	N, 13,55
Calculé pour $C_x H_y N_z O_k$:	C : 57, 74 ;	H 5.82 ;	N : 13,47 %

Le produit est pyrolisé à une température inférieure à celle de son point de fusion.

REMERCIEMENTS. Nous tenons à remercier Mme MATHIS, Maître de recherches au C.N.R.S. au « Laboratoire des hétérocycles du phosphore et de l'azote » pour son aide dans le domaine de la spectroscopie infra-rouge.

Revue Roumanie de Chimie, 23, 2, 209–214(1978)

ÜBER DEN EINFLUSS DER KETTENLÄNGE DER n-ALKANE AUF DIE ZUSAMMENSETZUNG DER MONOKARBOXYLSÄUREN DIE SICH DURCH DIE KATALYTISCHE OXYDATION DER n-ALKANE IN DER FLÜSSIGEN PHASE MIT MOLEKULARSAUERSTOFF ERGEBEN

I. DRIMUŞ und L. PAPAHAGI
Fakultät für angewandte Chemie des Polytechnischen Institutes in Bukarest, Lehrstuhl für organische Chemie und Verfahrenstechnik auf dem Gebiet der organischen Chemie, Calea Victoriei 149, Bukarest.

Eingegangen am 31. August 1975

Zur Festlegung der Lagen in denen der Riß der Kette der n-Alkane während des katalytischen Oxydationsvorganges mit Molekolarsauerstoff stattfindet, wurde der Einfluß der Kettenlänge mancher n-Alkane (n-Dekan, n-Undekan, n-Dodekan, n-Tridekan und n-Tetradekan) auf die Zusammensetzung der sich als Folge der Oxydation ergebenden Monokarbarboxylsäuren untersucht.

EINFÜHRUNG

Im Rahmen der Festlegung des Oxydationsmechanismus der n-Alkane in der flüssigen Phase mit molekularem Sauerstoff stellt die Bestimmung derjenigen Lagen, in denen der Riß der n-Alkanketten stattfindet, eine wichtige Frage dar. Es wurden mehrere Annahmen im Zusammenhang mit dieser Frage geäußert. Darunter sind die folgenden die wichtigsten :

a. G. Damkohler, I. Leibnitz und andere Forscher sind der Meinung, daß der Sauerstoff anfangs das am Rande der Kette vorhandene Kohlenstoffatom angreift.[1,2] Diese Annahme wurde experimentell nicht mit Sicherheit bestätigt und erklärt desgleichen nicht in einem zufriedenstellenden Maße die Bildung der Sauerstoffsäuren als auch die Dynamik des Vorganges.

b. Iwanow [3] erachtet, daß bei niedrigen Temperaturen der Angriff nur in Lage 2 erfolgen würde, was jedoch weniger wahrscheinlich erscheint.

---

[1] G. Damkohler, *Chem. Phys.*, **51**, 123 (1943).
[2] Leibnitz, *J. prakt. Chem.*, 227 (1957).
[3] K. Iwanow, *Doklady Akad. Nauk. S.S.S.R.*, **72**, 903 (1950).

c. Pritzkow [4], Benton [5] und Pardun[6] betrachten, daß der Angriff in gleichem Maße bei sämtlichen sekundären Kohlenstoffatomen stattfinden könnte.

d. Grün [7], Prückner [8] teilen die Meinung derjenigen Forscher die erachten, daß der Angriff des Sauerstoffes bei den Methylengruppen erfolgt und daß derselbe um so leichter stattfindet, je größer das Kohlenwasserstoffmolekül ist und je näher die Methylengruppen zu der Mitte der Kette gelegen sind.

Die ersten drei Annahmen wurden durch die im Laufe der letzten Jahre durch Rasumowski [9] und Drimuş, [10,11] veröffentlichten Arbeiten widerlegt.

Da eine Reihe von experimentellen Schwierigkeiten die Abscheidung und Bestimmung derjenigen Hydroperoxyd-Isomere nicht gestatten, die die ersten sich aus der Oxydation ergebenen Verbindungen darstellen, und auch nicht der Isomere der Alkohole und der Ketone (Nebenprodukte, in deren Rahmen die Lage der Funktionsgruppierung im Hydroperoxyd beibehalten wird) um die Art und Weise festzustellen, in welcher der Molekularsauerstoff auf die Karbokette der n-Alkane wirkt, haben wir die Zusammensetzung der Monokarboxylsäuren in Betracht gezogen, die chromatographisch abgeschieden und bestimmt werden können.

Es wurde bei geringen Konversionen gearbeitet, da im vorliegenden Falle die oxydativen Zersetzungen der Monokarboxylsäuren vernachlässigbar sind und jedes Paar von gebildeten Komplementärsäuren eine Gesamtatomzahl aufweisen wird, die gleich derjenigen der n-Alkanmoleküle ist. Es konnten Schlußfolgerungen im Zusammenhang mit derjenigen Lage festgelegt werden, in der der erste Angriff seitens des Sauerstoffes auf die Karbokette des n-Alkans stattgefunden hat; die Festlegung derselben erfolgte auf Grund der Zusammensetzung des sich als Folge der Oxydation ergebenden Säurengemisches. Das Studium wurde auf einer Anzahl von fünf n-Alkane hoher Reinheit (n-Dekan, n-Undekan, n-Dodekan, n-Tridekan und n-Tetradekan) vorgenommen.

VERSUCHSTEIL

Die Oxydationsvorgänge erfolgten in einem Reaktor aus Rasothermglas, mit einem Inhalt von 80 ml, der elektrisch beheizt wird und dessen Temperatur auf 140° eingestellt wurde, und in den eine Menge von 40 g Alkan eingeführt wurde. Der Sauerstofffluß betrug 5 l/h. Als Katalysator wurde das Kobaltnaphtenat im Verhältnis von 1 Mol Katalysationsmittel auf 100 Mol n-Alkan verwendent.

Analysen. In einem Zeitabstand von je 30 Minuten wurde die Säurezahl und die Peroxydzahl der Reaktionsmasse bestimmt.

Aus der Reaktionsmasse wurden die Säuren gemäß dem in Abb. 1 gezeigten Schema abgeschieden. Die Säuren wurden als solche chromatographisch bestimmt, um die Zusammensetzung des Gemisches feststellen zu können.

---

[4] W. Pritzkow, *Z. anorg. Chem.*, **67**, 399 (1955).

[5] I. Benton und M. M. Wirth, *Nature*, **171**, 4345, 269 (1953).

[6] N. Pardun und M. Kuchinka, *Erdöl und Kohle*, **3**, 109 (1950).

[7] A. Grün und E. Ulbrich, *Z. anorg. Chem.*, **36**, 125 (1923).

[8] H. Prückner, *Chem. Teh.*, **5**, 193 (1952).

[9] S. D. Rasumowski, *Zhur. priklad. Khim.*, **41**, 863 (1968).

[10] I. Drimuş und C. Florescu, *Rev. Chim.*, *(Bucureşti)*, **24**, 249 (1973).

[11] I. Drimuş und L. Papahagi, *Rev. Roumaine Chim.*, **20**, 7 (1975).

ERGEBNISSE

Die Oxydation der fünf n-Alkane wird bis zum Erreichen einer Säurezahl zwischen 35–45 mg KOH/g durchgeführt. Die Änderung der Säurezahlen und der Peroxydzahlen während des Oxydationsvorganges der fünf n-Alkane wird in Tabelle 1 gezeigt

Die Angaben gemäß Tabelle 1 gestatten die Feststellung, daß die Ansammlung der Peroxyde mit geringen Geschwindigkeiten erfolgt (der Höchstwert der Peroxydzahl überschreitet nicht 1mg O/g), wobei die Ansammlungsgeschwindigkeiten der Säuren im Falle der Oxydation der fünf n-Alkane beiläufig gleich sind.

Als Folge der Bearbeitung der Oxydate gemäß dem Schema der Beilage 1 wurden die Monokarboxylsäuren abgeschieden, die 1 bis 14 Kohlenstoffatome im Molekül enthalten.

Die Zusammensetzung der Säuregemische wurde chromatographisch bestimmt. Wir weisen darauf hin, daß die Ameisensäure mit Hilfe der angewandten chromatographischen Methode nicht identifiziert werden konnte.

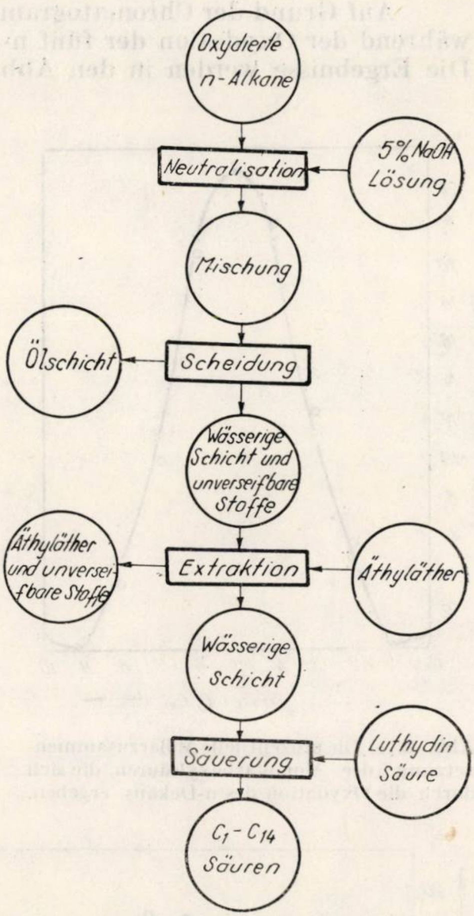
Oxydierte n-Alkane
Neutralisation
5% NaOH Lösung
Mischung
Ölschicht
Scheidung
Wässerige Schicht und unverseifbare Stoffe
Äthyläther und unverseifbare Stoffe
Extraktion
Äthyläther
Wässerige Schicht
Luthydin Säure
Säuerung
C_1-C_{14} Säuren

Abb. 1. — Schema der Bearbeitung des Oxydates hinsichtlich der Abscheidung der Säuren.

Tabelle 1

Die Veränderung der Säurezahl (mg KOH/g)und der Peroxydzahl (mg O/g) während der Oxydation von n-Alkanen, katalytisch bei 140°

n-Alkan	Oxydationszeit (Minuten)							
	S.Z.				P.Z.			
	30	60	90	120	30	60	90	120
n-Dekan	13,40	23,50	36,90	42,20	0,15	0,35	0,60	0,51
n-Undekan	13,41	19,96	29,95	40,80	0,30	0,48	0,68	0,57
n-Dodekan	12,12	19,65	27,30	39,40	0,26	0,43	0,66	0,54
n-Tridekan	10,21	18,35	28,90	36,70	0,17	0,43	0,77	0,62
n-Tetradekan	9,09	18,10	24,30	36,36	0,23	0,40	0,64	0,52

Auf Grund der Chromatogramme wurden die Molarprozente der sich während der Oxydation der fünf n-Alkane ergebenden Säuren berechnet. Die Ergebnisse werden in den Abbildungen 2–6 gezeigt.

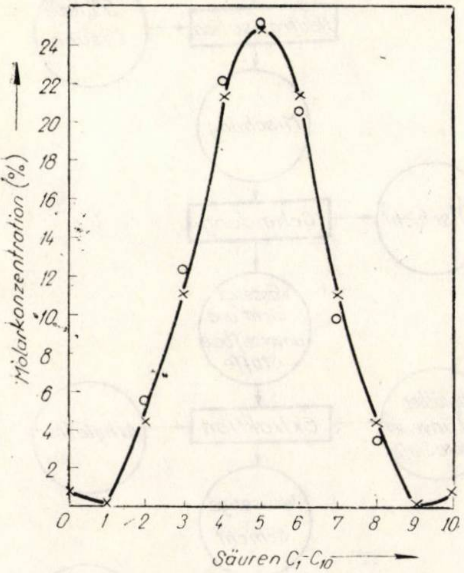

Abb. 2. — Die prozentuelle Molarzusammensetzung der Monokarboxylsäuren, die sich durch die Oxydation des n-Dekans ergeben.

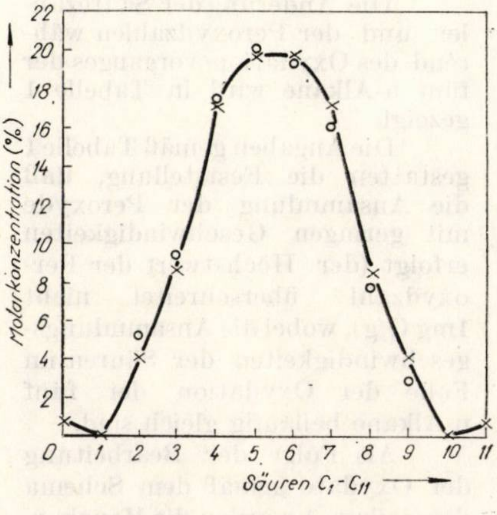

Abb. 3. — Die prozentuelle Molarzusammensetzung der Monokarboxylsäuren, die sich durch die Oxydation des n-Undekans ergeben.

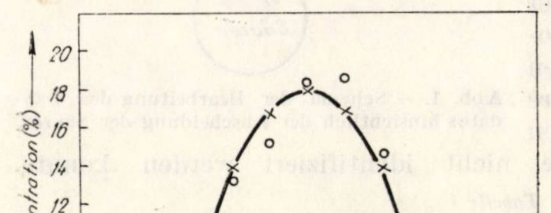

Abb. 4. — Die prozentuelle Molarzusammensetzung der Monokarboxylsäuren, die sich durch die Oxydation des n-Dodekans ergeben.

Es kann festgestellt werden, daß für die n-Alkane mit 10 und 11 Kohlenstoffatomen im Molekül die Höchstkonzentrationen die für Säuren mit 4, 5 und 6 Kohlenstoffatomen im Molekül erhalten werden. Für die n-Alkane mit 12, 13 und 14 Kohlenstoffatomen im Molekül weisen die Säuren mit 5, 6, 7 und 8 Kohlenstoffatomen die Höchstkonzentrationen auf.

Wird angenommen, daß durch den Riß der n-Alkankette zwei komplementäre Säuren entstehen, die zusammen dieselbe Kohlenstoffatomanzahl aufweisen wie das ursprüngliche n-Alkan ist es mölglich anzunehmen, daß die prozentuelle

Molarkonzentration dieselben Werte für die komplementären Säuren aufweisen wird.

Im allgemeinen wird die Säure C_m, wo m die Anzahl der Kohlenstoffatome seines Moleküls darstellt, einer komplementären Säure C_{n-m} entsprechen, worin n die Anzahl der Kohlenstoffatome des Alkanmoleküls ist, woraus sich die zwei Säuren gebildet haben. Die Molarkonzentration wird für die Säuren C_m und C_{n-m} gleich sein.

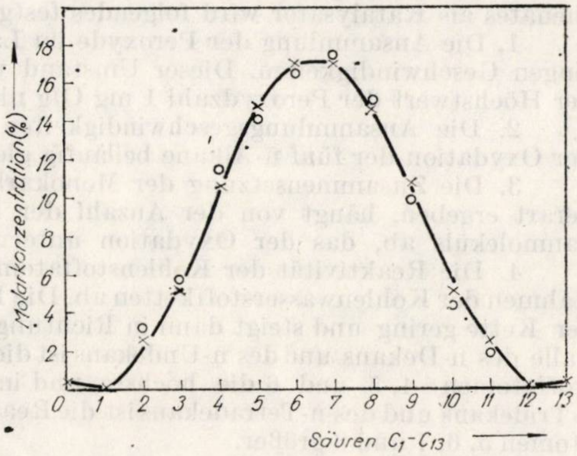

Abb. 5. – Die prozentuelle Molarzusammensetzung der Monokarboxylsäuren, die sich durch die Oxydation des n-Trodekans ergeben.

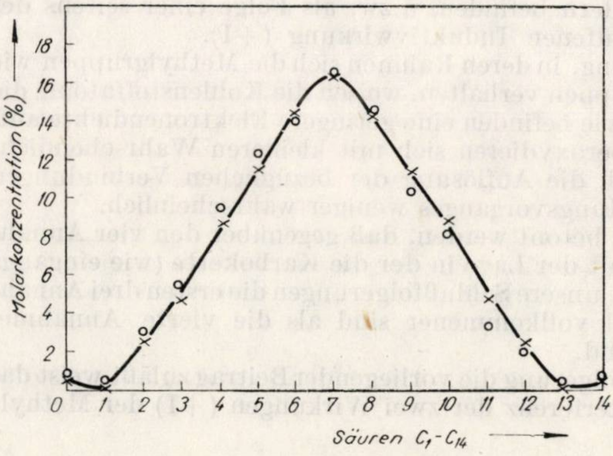

Abb. 6. – Die prozentuelle Molarzusammensetzung der Monokarboxylsäuren, die sich durch die Oxydation des n-Tetradekans ergeben.

Auf Grund dieser Betrachtungen wurden die theoretischen Molarkonzentrationen berechnet, die in die Diagramme der Abbildungen 2–6 neben den exprimentell bestimmten Werten aufgetragen wurden.

Die erhaltenen Werte sind für die Arbeitsbedingungen kennzeichnend. Die Anwesenheit sonstiger Katalysatoren oder die Durchführung der Oxydationen bei großen Konversionen bedingen eine Änderung des Spektrums der Säurezusammensetzung.

SCHLUSSFOLGERUNGEN

Als Folge der Oxydation der n-Alkane mit 10, 11, 12, 13 und 14 Kohlenstoffatomen im Molekül, in der flüssigen Phase, mit Molekularsauerstoff bei einer Temperatur von 140° und in Anwesenheit des Kobaltnaphthenates als Katalysator wird folgendes festgestellt:

1. Die Ansammlung der Peroxyde im Laufe der Zeit erfolgt mit geringen Geschwindigkeiten. Dieser Umstand wird dadurch bestätigt, daß der Höchstwert der Peroxydzahl 1 mg O/g nicht überschreitet.

2. Die Ansammlungsgeschwindigkeiten der Säuren sind im Falle der Oxydation der fünf n-Alkane beiläufig gleich.

3. Die Zusammensetzung der Monokarboxylsäuregemische die sich derart ergeben, hängt von der Anzahl der Kohlenstoffatome des n-Alkanmoleküls ab, das der Oxydation unterworfen wurde.

4. Die Reaktivität der Kohlenstoffatome hängt von deren Lage im Rahmen der Kohlenwasserstoffketten ab. Die Reaktivität ist an den Enden der Kette gering und steigt dann in Richtung der Mitte derselben an. Im Falle des n-Dekans und des n-Undekans ist die Reaktivität bei den Kohlenstoffatomen 4, 5 und 6 die höchste, und im Falle des n-Dodekans, des n-Tridekans und des n-Tetradekans ist die Reaktivität bei den Kohlenstoffatomen 5, 6, 7 und 8 größer.

5. Wir sind der Meinung, daß dieses Verhalten durch eine Verringerung der Reaktivität der Kohlenstoffatome erklärt werden kann, die sich nahe den Kettenrändern befinden, u.zw. als Folge einer seitens der Methylgruppen hervorgerufenen Induktivwirkung (+I).

Wegen dieser Wirkung, in deren Rahmen sich die Methylgruppen wie elektronenabstoßende Gruppen verhalten, weisen die Kohlenstoffatome die sich in der Nähe der Methyle befinden eine geringere Elektronendichte auf. Diese Kohlenstoffatome peroxydieren sich mit kleineren Wahrscheinlichkeiten und daher ist auch die Auflösung der bezüglichen Verbindungen im Rahmen des Säurebildungsvorganges weniger wahrscheinlich.

Es soll der Umstand betont werden, daß gegenüber den vier Annahmen im Zusammenhang mit der Lage in der die Karbokette (wie eingangs erwähnt) angegriffen wird, unsere Schlußfolgerungen die ersten drei Annahmen widerlegen und viel vollkommener sind als die vierte Annahme, mit welcher sie ähnlich sind.

6. Die letzte Schlußfolgerung die vorliegender Beitrag zuläßt weist darauf hin, daß es keine Interferenz der zwei Wirkungen (+I) der Methylrandgruppen gibt.

Revue Roumaine de Chimie, **23**, *2*, 215–223 (1978)

EPR STUDY OF CHELATE COMPLEXES WITH $Cu(II) — N(sp^2)$ BONDS

A. C. BANCIU *, O. CONSTANTINESCU ** and P. SPACU *

* Centre of Physical Chemistry, Str. Dumbrava Roșie, 23, Bucharest, Romania

** Institute for Atomic Physics (I.F.A.), Bucharest-Măgurele, Romania

Received June 25, 1976

The paper studies the EPR spectra of three tetracoordinated Cu(II) chelate complexes, formed with ligands from the class of 1-methyl-2-carbethoxy-glyoxalanil-(1)-phenylhydrazones-(2), substituted at the benzene ring of the hydrazone group. In solid magnetic dilution in the analogous Ni(II) complex, the Cu(II) complex formed with the *p*-NO_2- substituted ligand exhibits a super-hyperfine structure formed of 13 lines with a 16.7 G* separation. This indicates the interaction of the unpaired electron of Cu(II) with the nuclei of six nitrogen atoms from the chelate chains of the molecule : the four donor nitrogen atoms as well as the other two nitrogen atoms which are directly bound to the donor atoms.

INTRODUCTION

In a recent paper,[1] we have described the synthesis and the physico-chemical properties (IR and electronic spectra, molar electric conductivities and magnetic moments) of four new Cu(II) chelate complexes.

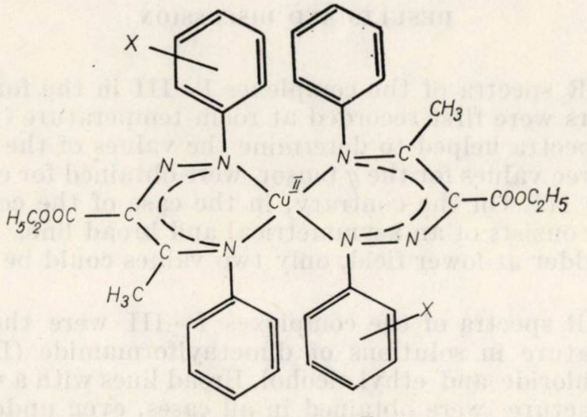

I: X=H ; II: X=p−CH_3 ; III: X=p−NO_2

---

* One Gauss (G) equals 10^{-4} Tesla.

[1] A. C. Banciu and P. Spacu, *Rev. Roumaine Chim.*, **21**, 1331 (1976).

They are formed with organic ligands from the class of 1-methyl-2-carbethoxy-glyoxalanil-(1)-phenylhydrazones-(2) differently substituted at the benzene ring of the hydrazone group. The electronic spectra of the new complexes are rich in bands within the 350—1200 nm range. They indicate for the Cu (II)-N chemical bonds in complexes, as very probable, an intermediate geometrical structure, between the square-planar and the tetrahedral, yet closer to the latter.

This study is concerned with the EPP spectra of three of the new Cu(II) complexes, i.e. complexes I—III.

EXPERIMENTAL

The chemical synthesis of the complexes I—III has been described in a previous paper.[1]

The samples of solid magnetic dilution of complex III were prepared by coprecipitation. A small amount of Cu(II) ions was thus doped into the lattice of the similar Ni(II) complex which is diamagnetic, therefore square-planar. Through precipitation of Ni(II) ions by the organic ligand, a small amount of the Ni(II) salt — 0.7% of the theoretically required $NiCl_2.6H_2O$ — was replaced by the equivalent amount of $CuCl_2.2H_2O$. The Cu(II) ions which were not included in the lattice of the diamagnetic Ni(II) complex (dark violet) by coprecipitation, were separated in the form of the pure Cu(II) complex, III (dark blue-green). In organic solvents the Cu(II) complex is much more readily soluble than the Ni(II) one. Thus, the small amount of Cu(II) pure complex III which separated as a mechanical impurity of the Ni(II) complex was removed by repeated washing with small amounts of ethyl alcohol. From the amount of pure Cu(II) complex which was separated, it was established that in the sample of solid magnetic dilution of complex III, which was studied by EPR, the substitutional Cu(II) ions represent less than 0.3% of the total metal ions.

The EPR spectra of the complexes in the solid state (polycrystalline powders) as well in solutions were recorded at room temperature and at 77 K. A spectrograph operating in the X band and having high frequency modulated magnetic field (100 kHz) was used for this purpose. The values of the *g* tensor were determined by means of DPPH and Mn(II) standards.

The X-ray diffraction spectra were recorded on a Debye-Scherrer camera using the CuKα radiation supplied by a TUR-M 60 generator and filtered with nickel.

RESULTS AND DISCUSSION

The EPR spectra of the complexes I—III in the form of polycrystalline powders were first recorded at room temperature (Fig. 1).

These spectra helped to determine the values of the *g* tensor listed in table 1. Three values for the *g* tensor were obtained for each of the complexes II and III. On the contrary, in the case of the complex I, since its spectrum consists of an asymmetrical and broad line, which presents only one shoulder at lower field, only two values could be determined for the *g* tensor.

The EPR spectra of the complexes I—III were then recorded at room temperature in solutions of dimethylformamide (DMF), benzene, carbon tetrachloride and ethyl alcohol. Broad lines with a weakly resolved hyperfine structure were obtained in all cases, even under conditions of maximum dilution permitted by the recording procedure. This is probably due to a line broadening effect. The hyperfine structure results from the interaction between the unpaired "3d" electron of the Cu(II) ion and the ^{63}Cu and ^{65}Cu nuclear spins.

In its turn, at liquid nitrogen temperature (77 K) the solutions of the studied complexes I–III exhibit EPR spectra with two noticeable sets of hyperfine lines, which correspond to $g_{\parallel}$ and $g_{\perp}$ (fig. 2).

In all cases, the set of four hyperfine structure lines corresponding to $g_{\parallel}$ is well resolved. Conversely, the hyperfine structure components corresponding to $g_{\perp}$ overlap the superhyperfine structure components. The super-hyperfine structure is caused by the interaction between the unpaired electron of the Cu(II) ion and the nuclei of the nitrogen atoms of the ligands. These spectra helped to determine accurately the values of the $g_{\parallel}$ and $A_{\parallel}$ parameters (the error in g values was below ± 0.0010) and also, less accurately, the values of the $g_{\perp}$ and $A_{\perp}$ parameters (the error in g values was ±0.0015). The results obtained by the study of complexes in DMF solutions are summarized in table 2.

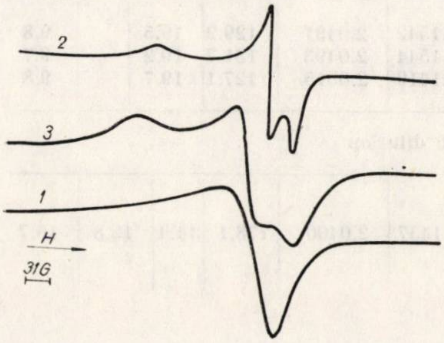

Fig. 1. – EPR spectra of polycrystalline powders of Cu(II) complexes, recorded at room temperature. *1*: complex I; *2*: complex II; *3*: complex III.

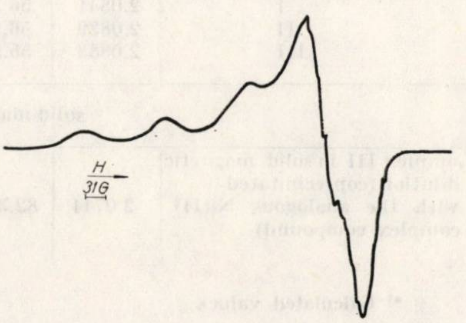

Fig. 2. – EPR spectrum of complex compund II recorded on frozen DMF solution (77 K).

Table 1

Values of the g-tensor for Cu(II) complexes in the form of polycrystalline powder

Complex compound	g_1	g_2	g_3	g_n
I	2.1461		2.0423	2.0769
II	2.1688	2.0597	2.0359	2.0885
III	2.1841	2.0748	2.0274	2.0954

In the case of the spectra recorded at room temperature, which have only a weakly resolved hyperfine structure, table 2 shows for the g and A tensors the *calculated* isotropic values (g_0 and A_0). These were calculated by means of Kivelson's[2]:

$$g_0 = \frac{1}{3}(g_{\parallel} + 2g_{\perp}) \tag{1}$$

---

[2] K. Kivelson, *J. Chem. Phys.*, **33**, 1094 (1960).

Table 2

EPR parameters of Cu(II) complex compounds

Complex compound	g_0 *)	A_0*) [G]	$g_{\|\|}$	$g_\perp$	$A_{\|\|}$ [G]	$A_\perp$ [G]	$A_{\|\|}^{(N)}$ [G]	$A_\perp^{(N)}$ [G]
	DMS solution		frozen DMF solution (77 K)					
I	2.0841	56.3	2.1542	2.0491	129.2	19.5		9.8
II	2.0839	56.9	2.1544	2.0493	131.7	19.2		9.7
III	2.0883	55.5	2.1619	2.0515	127.1	19.7		9.8
	solid magnetic dilution							
Complex III in solid magnetic dilution (coprecipitated with the analogous Ni(II) complex compound)	2.0744	82.3	2.1457	2.0400	178.1	34.4	13.8	16.7

*) Calculated values

and McConnell's[3]

$$A_0 = \frac{1}{3}\,(A_{||} + 2A_\perp) \tag{2}$$

relations.

As can be seen (table 2), in DMF solutions the complexes I and II present very similar values for the EPR parameters. Therefore, the substitution by $-\mathrm{CH_3}$ of the hydrogen atoms from the *para* positions of two of the four benzene rings which are bonded to the donor nitrogen atoms (i.e. the transition from complex I to complex II) does not significantly modify the EPR spectra of the complexes. In contrast, greater differences can be observed between the EPR parameters of the two mentioned complexes, on the one hand, and those of the complex III, on the other. This is particularly true in the case of the g and g_0 values. The substitution of the hydrogen atoms from the *para* positions of two of the four benzene rings bound to the donor nitrogen atoms, by $-\mathrm{NO_2}$ groups, which are endowed with strong electronic (inductive and mesomeric) effects (i.e. the transition from complex I to complex III) influences to a larger extent the EPR spectra of the complexes, than the substitution by $-\mathrm{CH_3}$ groups, which are endowed only with weak inductive effect.

As shown in a previous work,[1] the electronic spectra of the complexes I–III indicate for the involved Cu(II)-N chemical bonds (i.e. for the Cu(II)-$\mathrm{N_4}$ chromophore) a very plausible intermediate geometrical structure between square-planar and tetrahedral, which is closer to the latter mentioned limit structure.

---

[3] H. M. McConnell, *J. Chem. Phys.*, **25**, 709 (1956).

It is of interest to see what results would be obtained from the data supplied by EPR spectra, if an arbitrary and opposed hypothesis were accepted, i.e. that in the complexes I—III the Cu(II)—N_4 chromophore presents at most only a small distortion from the regular square-planar structure. It is known[4] that the detailed theoretical handling of the EPR spectra of the Cu(II) complexes with a square-planar structure has long been solved and is frequently used in current studies. In the case of a square-planar structure the LCAO-MO scheme for the D_{4h} symmetry gives the following relations for the antibonding molecular orbitals of the complexes[5–7]

$$\Psi_{B_{1g}} = \alpha d_{x^2-y^2} - \frac{1}{2}\alpha'(-\sigma_x^{(1)} + \sigma_y^{(2)} + \sigma_x^{(3)} - \sigma_y^{(4)}) \tag{3}$$

$$\Psi_{B_{2g}} = \beta d_{xy} - \frac{1}{2}(1-\beta^2)^{1/2}(p_y^{(1)} + p_x^{(2)} - p_y^{(3)} - p_x^{(4)}) \tag{4}$$

$$\Psi_{E_g}\begin{cases} \delta d_{xz} - \dfrac{1}{\sqrt{2}}(1-\delta^2)^{1/2}(p_z^{(1)} - p_z^{(3)}) & (5) \\ \delta d_{yz} - \dfrac{1}{\sqrt{2}}(1-\delta^2)^{1/2}(p_z^{(2)} - p_z^{(4)}) & (6) \end{cases}$$

where $\sigma^{(i)} = np^{(i)} \mp (1-n^2)^{1/2} s^{(i)}$ represent the sp^2 hybrid orbitals of the donor nitrogen atoms ($n = \sqrt{2/3}$), the α, β and δ coefficients (more specifically, the values α^2, β^2 and δ^2) express the covalent character of the σ, π-in-plane and, respectively, π-out-of-plane bonds, while all the other symbols assume the usual significance from the MO-calculations.

The α, β and δ coefficients in the above formulae could be determined from the known relations of Abragam and Pryce,[8] Maki and McGarvey[5] and Kivelson and Neiman[7], which relate them to the EPR parameters ($g_\parallel$, $g_\perp$, $A_\parallel$ and $A_\perp$) of the spin hamiltonian. In addition to several known magnitudes, the calculus would also involve the ΔE_{xy} and ΔE_{xz} energies of some d-d transitions from the optical spectra, which are[1] of 12 900 cm^{-1} and 17100 cm^{-1} respectively, in the case of the complexes in question. This calculus, based on the arbitrary hypothesis of a square-planar structure of the Cu(II)-N bonds in complexes, would lead in the case of the complexes I—III to the following values of the mentioned coefficients: 1) $\alpha^2 = 0.57 \ldots 0.58$ (inidicating an appreciable covalency of the σ bonds); 2) $\beta^2 = 0.64 \ldots 0.68$ (indicating a marked covalent character of the π-in-plane bonds; and 3) $\delta^2 = 0.96 \ldots 0.99$ (indicating a very low covalency for the π out-of-plane bonds). The markedly subunitary values of the

---

[4] O. Cozar and V. Mercea, *Studii și Cercetări Fiz. Acad. R.S.R.*, **28**, 142 (1976).

[5] A. N. Maki and B. R. McGarvey, *J. Chem. Phys.*, **29**, 31, 35 (1958).

[6] E. M. Roberts and W. S. Koski, *J. Amer. Chem. Soc.*, **82**, 3006 (1960).

[7] D. Kivelson and R. Neiman, *J. Chem. Phys.*, **35**, 149 (1961).

[8] A. Abragam and M. H. L. Pryce, *Proc. Roy. Soc.*, **A 205**, 136 (1951); **A 206**, 164 (1951).

β^2 coefficients are surprising, because, as has been shown,[1] in the new complexes I—III all the donor nitrogen atoms are found in sp^2 hybridization and, therefore, no π-in-plane bonds exists in these complexes ! (The d_{xy} orbital is a nonbonding orbital in the case of the square-planar coordination by means of nitrogen atoms in sp^2 hybridization). Evidently, the found α^2 and δ^2 coefficients are in no way more plausible than the β^2 coefficient, because all the cited coefficients intervene concomitantly in the mentioned formulas [5,7,8] involved in the calculus. Their values are determined with the same degree of plausibility and with the same error. In the case of really square-planar complexes of Cu(II), such as those formed with phthalocyanine,[9] with ethyoporphyrine-II,[6] with tetraphenylporphine,[10] etc., complexes which also present donor nitrogen atoms in sp^2 hybridization, the above-mentioned calculus helps to obtain for β^2 values which practically coincide to unity. These are plausible because they tally with the nonexistence of π-in-plane bonds (see relation (4) above). The erroneous result obtained by this calculus shows that the premise — that of a square-planar structure — is erroneous. The necessary result, therefore, is that the structure of the Cu(II)-N_4 chromophore is much closer to tetrahedral than to square-planar. The electronic spectra of the complexes have indicated the same thing.[1]

In the case of complex III, formed by the Cu(II) ion with the anion of 1-methyl-2-carbethoxy-glyoxalanil-(1)-*p*-nitro-phenyl-hydrazone- (2) as ligand, solid magnetic dilutions of the Cu (II) ions were also prepared. Thus, Cu(II) ions were substituted by coprecipitation, in the diamagnetic lattice of the Ni(II) complex, which is similar to the above complex III. Fig. 3 illustrates the EPR spectrum of a solid magnetic dilution of Cu(II) ions in the diamagnetic lattice of the similar Ni (II) complex (complex III magnetically diluted in the corresponding Ni(II) complex).

Besides the hyperfine structure corresponding to $g_{||}$ and $g_{\perp}$ a super-hyperfine structure was also revealed on the components corresponding to $M_I = -1/2$ and $M_I = -3/2$. This could be properly analysed on the additional absorption line observed in the spectrum at high field. Here, the super-hyperfine structure does not overlap other components. [11,12] The analysis of the structure model recorded on this component has shown the existence of 13 lines of super-hyperfine structure with a separation of 16.7 G (fig. 4).

This super-hyperfine structure model was considered to be conditioned by the interaction of the magnetic moment of the unpaired Cu(II) electron with the magnetic moments of six equivalent or approximately equivalent nitrogen atoms from the organic part of the molecule. (For nitrogen the nuclear spin quantum number $I = 1$; $(2nI + 1) = 13$ and hence $n = 6$). In other words, there exists a probability greater than zero, that the unpaired electron of the central Cu(II) ion will also be found for a while on six nitrogen atoms in the organic part of the molecule (i.e.

---

[9] C. M. Guzi, J. B. Raynor and M. C. R. Symons, *J. Chem. Soc.*, **A. 1969**, 2299.

[10] J. Assour, *J. Chem. Phys.*, **43**, 2477 (1965).

[11] G. M. Iarin, *Zhur. strukt. Khim.*, **6**, 548 (1965).

[12] G. M. Iarin, *Teoret. i Exp. Khimiia*, **4**, 245 (1968).

extended molecular orbital, covalency !). These atoms are as follows: the four donor nitrogen atoms and, also, the other two nitrogen atoms in the chelate chains of the molecule which are directly bound to two of the above-mentioned donor atoms (see formula III).

The parameters of the EPR spectrum of complex III found in solid magnetic dilution in the analogous Ni(II) complex were also summarized in table 2.

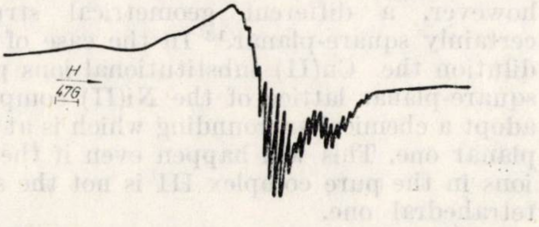

Fig. 3. — EPR spectrum of the sample of solid magnetic dilution of Cu(II) ions in the lattice of the Ni(II) complex compound which is analogous to the Cu(II) complex compound III.

The EPR spectra recorded both in frozen solutions and in the solid magnetic dilution can be properly described by means of an axial-symmetric spin hamiltonian of the form

$$\mathcal{H} = g_{\parallel} \beta H_z S_z + g_{\perp} \beta (H_x S_x + H_y S_y) + A_{\parallel} I_z S_z + A_{\perp} (I_x S_x + I_y S_y) + \sum_{i=1}^{6} A_{\parallel}^{(N)} I_z^{(N)i} S_z + \sum_{i=1}^{6} A_{\perp}^{(N)} (I_x^{(N)i} S_x + I_y^{(N)i} S_y), \qquad (7)$$

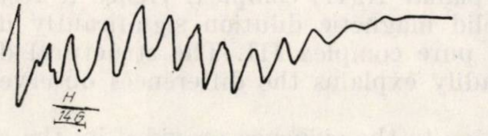

Fig. 4. — The super-hyperfine structure recorded on the hyperfine structure component in the EPR spectrum of the sample of solid magnetic dilution of Cu(II) ions.

where g is the spectroscopic splitting tensor; A is the tensor of the hyperfine structure; the indices $_{\parallel}$ and $\perp$ designate the values of the tensors in the direction of the symmetry axis and, respectively, in a plane perpendicular to the crystal symmetry axis (z axis) β is the Bohr magneton; S is the overall electronic spin; I is the nuclear spin angular momentum; H is the external statical magnetic field; the indices x, y and z designate the values of the respective magnitudes in the direction of the crystal rectangular axes, x, y and z; the exponential indices (N) indicate the values of the respective magnitudes assigned to the nitrogen atoms and the magnitudes without this index belong to the central Cu(II) ion. In the present case $S = 1/2$; $I = 3/2$; $I^{(N)} = 1$ and $g_{\parallel}$, $g_{\perp}$, $A_{\parallel}$, $A_{\perp}$ $A_{\parallel}^{(N)}$ and $A_{\perp}^{(N)}$ have the values summarized in table 2.

Table 2 shows that the sample of the solid magnetic dilution of complex III in the diamagnetic lattice of the analogous Ni(II) complex differs much more significantly from complexes I—III than these latter complexes differ from each other. One can see the differences between the values of the EPR parameters of complex III solid magnetic dilution and the same values of the pure complex III found in frozen DMF solutions. Such differences in EPR spectra can be explained by the modifications occurring with the penetration of Cu(II) substitutional ions into the diamagnetic lattice of the Ni(II) complex. Some data mentioned before have indicated that the structure of complex III is closer to tetrahedral than to square-planar. In turn, the Ni(II) complex used as a magnetic dilutant which from the standpoint of its rough structure is analogous to complex III possesses, however, a different geometrical structure. It is diamagnetic, hence certainly square-planar.[13] In the case of the complex III solid magnetic dilution the Cu(II) substitutional ions penetrated into the diamagnetic, square-planar lattice of the Ni(II) complex are forced by the lattice to adopt a chemical surrounding which is at least close to the regular square-planar one. This will happen even if the chemical surrounding of Cu(II) ions in the pure complex III is not the square-planar, being close to the tetrahedral one.

This modification was confirmed by X-ray diffraction spectra. They were recorded for the following three compounds : 1) the pure complex III ; 2) the similar Ni(II) complex used as a magnetic dilutant and 3) the sample of solid magnetic dilution of Cu(II) ions in the lattice of the Ni(II) diamagnetic complex (complex III magnetically diluted in the similar Ni(II) complex). The diffraction lines summarized in table 3 positively show that the first two cited complexes clearly differ from each other.

The sample of the solid magnetic dilution of Cu(II) ions (complex III diluted in the similar Ni(II) complex) presents an intermediate structure between the first two mentioned complexes, yet much closer to that of the diamagnetic, square-planar Ni(II) complex. Hence it results that complex III found in a solid magnetic dilution significantly differs in point of structure from the pure complex III. The structural difference outlined in this manner readily explains the differences observed in the EPR spectra.

In conclusion, in addition to the evidence provided by the electronic spectra (presented in [1]) and by the EPR spectra of complexes I—III (interpreted above), these structural differences between the pure complex III and the solid magnetic dilution of Cu(II) ions also indicate for the Cu(II)—N chemical bonds in complexes I—III a structure which is relatively close to the tetrahedral one.

---

[13] A. C. Banciu and C. I. Lepădatu, *Z. phys. Chem. (Frankfurt)*, **97**, 197 (1975).

Table 3

The X-ray diffraction lines [Å] of the complexes

Cu (II) complex III	The sample of magnetic dilution of Cu (II) ions in the lattice of the Ni(II) complex	The diamagnetic Ni(II) complex, analogous to the Cu (II) complex III
		13.2
		9.95
		8.24
		7.39
	6.89	
		6.31
	6.05	
		5.99
		5.61
	5.57	
	4.918	
4.754		
4.500	4.502	
		4.199
4.135	4.147	
4.022		
	3.801	3.805
3.767		
3.607		
		3.554
	3.508	
	3.412	
3.322		
	3.235	3.237
3.216		
3.157		
3.057		3.055
3.001		
	2.986	2.971
2.809	2.792	
2.639	2.646	
		2.595
	2.524	
2.479		
2.446		
	2.401	2.417
2.348		
2.305		
	2.279	2.289
2.230		
2.162		
	2.095	2.098
2.041		
	2.035	2.033
1.965		
	1.929	1.920
1.901	1.891	
		1.861
		1.819
	1.763	

Revue Roumaine de Chimie, **23**, *2*, 225–231 (1978)

CONTRIBUTIONS TO THE STUDY OF THE CATALYTIC ACTIVITY OF SOME $nSiO_2.mAl_2O_3.xH_2O$ SYSTEMS IN THE DECOMPOSITION REACTION OF CUMENE HYDROPEROXIDE. V*

INFLUENCE OF THE REACTION MEDIUM**

L. CORMOŞ, A. POP and LUCIA ORBU

Department of Organic and Technological Chemistry of the Faculty of Chemistry, Cluj-Napoca,
str. Arany J. 11, Romania

Received October 11, 1975

While performing the decomposition of cumene hydroperoxide in n-heptane, *m*-diisopropylbenzene, cumene, *o*-xylene, *m*-xylene, toluene, benzene and dioxan whose electron-donor effect increases in the above-mentioned order, the authors have found that the more pronounced the solvent donor effect, the more reduced is the catalytic activity. Practically, the reaction will not occur in benzene and dioxan and the reaction rate is maximum in n-heptane. The ratio of reaction rate values in solvents, following the above order, is ; 1 : 0.875 : 0.323 :0.720 :0.050 : 0.022 : 0.0001 : 0.00009.

In a series of papers [1–4] we have investigated various aspects of cumene hydroperoxide decomposition on synthetic alumino-silicates. It is known that in reactions occurring in the presence of a solvent, the latter may constitute merely a physical medium in which the reaction takes place, yet in most cases it is also involved in the process development. Studies are often made on the influence of the solvent character on the catalytic activity by the solvent interaction with the catalyst.

Such studies regarding the cumene hydroperoxide decomposition are described in the literature in the case of homogeneous catalysis.[5]

In a previous paper [2] we have shown that the reaction rate of the cumene hydroperoxide decomposition increases linearly with the increase of the catalyst nonprotonic acidity, a fact which has prompted us to conclude that this acidity form is the active factor of the catalyst.

---

* Part IV. L. Cormoş and S. Popica, *Stud.Univ. Babeş-Bolyai, Chem.*, **19**, 19 (1974).

** Paper presented at the "4-th Republican Conference of General and Applied Physical Chemistry", Bucharest Sept. 2–5, 1974.

[1] A. Pop, P. Kröbl, L. Cormoş and Gy. Lenhyel, *Stud. Univ. Babeş-Bolyai, Chem.*, **12**, 89 (1967).

[2] A. Pop and L. Cormoş, *Stud. Univ. Babeş-Bolyai, Chem.*, **16**, 61 (1971).

[3] A. Pop and L. Cormoş, *Stud. Univ. Babeş-Bolyai, Chem.*, **16**, 101 (1971).

[4] L. Cormoş and S. Popica, *Stud. Univ. Babeş-Bolyai, Chem.*, **19**, 19 (1974).

[5] A. Pop and L. Cormoş, *Studii şi Cercetări Chim. Acad. R. S. Romania*, **18**, 1009 (1970).

To verify this finding we have undertaken to conduct the reaction in solvents with a Lewis base character (electron-donors), considering that they should have a great influence in the process. Accordingly we have studied under this aspect aromatic hydrocarbons, n-heptane and dioxan as solvents.

EXPERIMENTAL

The macrokinetics of the decomposition reaction of some cumene hydroperoxide solutions was investigated in the following solvents : *m*-diisopropylbenzene, cumene, xylenes, toluene, benzene, n-heptane and dioxan. The hydroperoxide concentration in such solvents was 10%. Our experiments made use of 25 ml solution and 2 g catalyst in each case. A synthetic aluminosilicate catalyst with 33.6% Al_2O_3 content obtained by the method of co-precipitation was used in all the experiments.[1] The catalyst samples were subjected to a thermal treatment at 580° for 3 hr. All the tests employed a catalyst type having a 0.1—0.2 mm granulation. Experiments were conducted in a static working system [1] in a glass reactor fitted with a cooling system and with continuous mixing of the reactants and of the catalyst in suspension.

For each solvent used as a reaction medium, experiments were conducted at three different temperatures, i.e. at 20 ; 30 and 40°. The temperature was kept constant throughout the experiments with a 0.1° variation. Three determinations were performed for each separate temperature and the data obtained as an arithmetic mean of the three determinations were used for the calculation. Practically, the reaction was monitored by withdrawing samples of 0.5 ml each and by dosing the undecomposed cumene hydroperoxide.[6]

RESULTS AND DISCUSSION

Taking into account the fact that in industrial practice, the cumene hydroperoxide is an intermediate in the production of phenol, as it results as a cumene hxydroperoxide solution in cumene, most attempts to decompose this hydroperoxide were made with cumene as reaction medium.

In relation to this solvent taken as a standard, the solvents used by us may be grouped into two classes :

1. Solvents in which the reaction rate of hydroperoxide decomposition is higher than in the case in which the reaction occurs in cumene ;
2. Solvents in which the decomposition reaction takes place at a lower rate than in the case of performing it in cumene.

The first group of solvents includes n-heptane and *m*-diisopropylbenzene. The data obtained in the decomposition of a solution with 0.719 moles/l concentration of cumene hydroperoxide in n-heptane and in *m*-diisopropylbenzene, respectively, for the three working temperatures, are listed in table 1.

Based on the conversions presented in these tables, lg $\frac{100}{100-\alpha}$ was calculated and plotted versus time, as seen in fig. 1.

This figure illustrates that, for conversions included between 10—95%, the points are satisfactorily ranged on the straight lines and the decomposition reactions occur, in such conditions, following a first-order kinetics relative to hydroperoxide. In the case of conversions below 10% probably due to the activated adsorption heat and to the relatively high reactant concentration, the heat released in the process is significant and the experimental data are somehow more dispersed.

---

[6] H. Hook and H. Kropf, *Angew. Chem.*, **69**, 313 (1957).

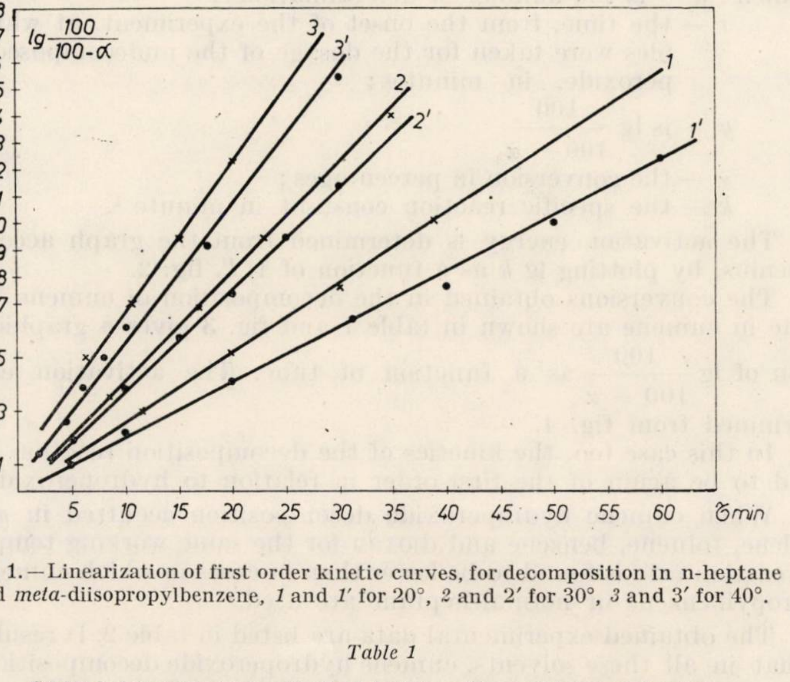

Fig. 1.—Linearization of first order kinetic curves, for decomposition in n-heptane and *meta*-diisopropylbenzene, *1* and *1'* for 20°, *2* and 2' for 30°, *3* and 3' for 40°.

Table 1

Cumene hydroperoxide decomposition in : n-heptane, *m*-diisopropyl-benzene and cumene

Time in min.	Conversion %								
	20°	30°	40°	20°	30°	40°	20°	30°	40°
	n—heptane			*m*-diisopropylbenzene			cumene		
2	—	—	27.53	—	—	27.53	—	—	—
4	—	—	44.92	—	—	44.92	—	—	—
5	20.29	34.78	—	20.29	34.78	—	9.95	16.03	20.29
6	—	—	59.42	—	—	59.42	—	—	—
8	—	—	68.11	—	—	68.11	—	—	—
10	40.57	57.92	75.36	40.57	57.92	75.36	—	—	40.57
15	—	73.18	94.20	—	73.92	94.20	12.97	25.19	—
20	60.86	81.88	97.10	60.96	81.88	97.10	—	—	60.84
25	—	88.40	—	—	88.40	—	—	—	—
30	76.81	92.75	—	76.81	92.75	—	22.13	42.74	76.81
40	82.60	—	—	82.60	—	—	—	—	82.60
50	89.85	—	—	89.85	—	—	—	—	89.85
60	94.20	—	—	94.20	—	—	—	68.70	94.20
90	—	—	—	—	—	—	56.48	84.73	—
140	—	—	—	—	—	—	—	93.89	—
150	—	—	—	—	—	—	75.57	—	—
200	—	—	—	—	—	—	84.73	—	—

The specific reaction rates were calculated by the least squares method[7] using relation:

$$k = \frac{n\sum xy - \sum x \sum y}{n\sum x^2 - (\sum x)^2}$$

in which: n — is the number of determinations;

x — the time, from the onset of the experiment, at which samples were taken for the dosage of the undecomposed hydroperoxide, in minutes;

y — is $\lg \frac{100}{100 - \alpha}$

α — the conversion in percentages;

k — the specific reaction constant in minute^{-1}.

The activation energy is determined from the graph according to Arrhenius, by plotting $\lg k$ as a function of $1/T$, fig. 2.

The conversions obtained in the decomposition of cumene hydroperoxide in cumene are shown in table 1 and fig. 3 gives a graphic presentation of $\lg \frac{100}{100 - \alpha}$ as a function of time. The activation energy is determined from fig. 4.

In this case too, the kinetics of the decomposition reaction has been found to be again of the first-order in relation to hydroperoxide.

When cumene hydroperoxide decomposition occurred in *m*-xylene, *o*-xylene, toluene, benzene and dioxan for the same working temperature, the reaction rate is found to be lower than in cases in which cumene, *m*-diisopropylbenzene or normal-heptane are used.

The obtained experimental data are listed in table 2. It results thereof that in all these solvents, cumene hydroperoxide decomposition occurs according to a first-order kinetics in relation to hydroperoxide.

The experimental data thus obtained were used to calculate the specific reaction rates and the activation energies presented in table 3.

From the data in table 3, it results that the reaction rates for the same temperature decrease following the order: n-heptane $>$ *m*-diisopropylbenzene $>$ cumene $>$ *o*-xylene $>$ *m*-xylene $>$ toluene $>$ benzene $>$ dioxan.

In the case of cumene hydroperoxide decomposition in benzene and dioxan, the specific reaction rates are lower than in n-heptane by three orders of magnitude.

We interpret such experimental results as follows: all solvents used are considered to be electron-donors, a property which becomes more marked following the order: n-heptane $<$ *m*-diisopropylbenzene $<$ cumene $<$ $<$ *o*-xylene $<$ *m*-xylene $<$ toluene $<$ benzene $<$ dioxan. In another paper[2] we have shown that the active centers of the aluminosilica catalyst are the tricoordinated aluminium atoms in the system, electron-acceptors and hence Lewis acids. The presence of such large amounts of solvents

---

[7] I. I. JOFFE and L. M. PISMEN, "Cataliza eterogenă în ingineria chimică" Ed. Tehnică, Bucureşti, 1967, p. 378.

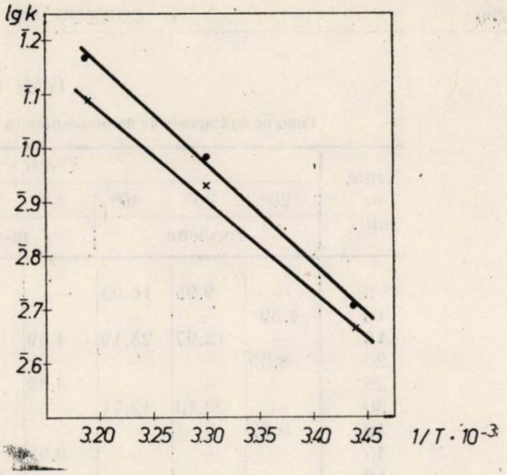

Fig. 2. — Graphical determination of the activation energy, based on Arrhenius equation for decomposition in : ● — n-heptane, + *meta* diisopropylbenzene.

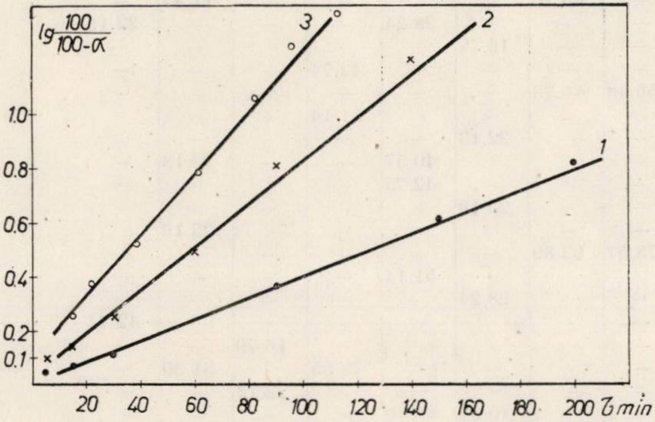

Fig. 3. — Linearization of first order kinetic curves, for decomposition in cumene : *1* for 20°, *2* for 30°, *3* for 40°.

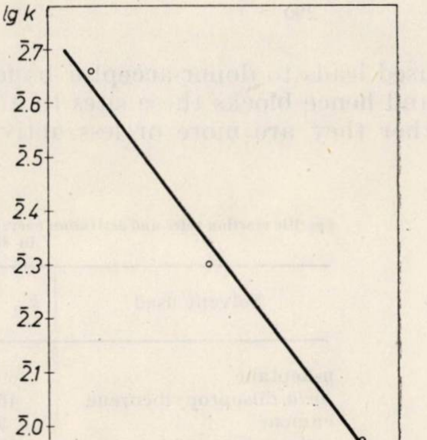

Fig. 4. — Graphical determination of the activation energy, based on Arrhenius equation, for decomposition in cumene.

Table 2

Cumene hydroperoxide decomposition in : *o*-xylene, *m*-xylene and toluene

Time in min.	Conversion %								
	20°	30°	40°	20°	30°	40°	20°	30°	40°
	o-xylene			*m*-xylene			toluene		
5	—	9.95	16.03	—	—	—	—	—	—
10	4.59	—	—	—	—	—	—	—	—
15	—	12.97	25.19	4.59	—	—	—	4.56	—
20	8.39	—	—	—	9.92	12.97	—	—	—
25	—	—	—	8.39	—	—	—	—	—
30	—	22.13	42.74	—	—	—	—	—	11.45
40	9.92	—	—	—	—	25.19	4.59	8.39	—
45	—	—	—	9.92	—	—	—	—	—
50	—	—	—	—	22.13	—	—	—	—
60	—	—	68.70	—	—	—	—	11.45	—
70	16.79	—	—	—	28.24	—	—	—	22.13
75	—	—	—	16.79	—	—	—	—	—
80	—	—	—	—	—	42.74	—	—	—
90	—	56.48	84.73	—	—	—	—	—	—
100	22.13	—	—	—	—	51.14	—	—	—
105	—	—	—	22.13	—	—	—	—	—
110	—	—	—	—	40.57	—	—	22.13	—
125	—	—	—	—	42.75	—	—	—	—
130	—	—	—	25.19	—	—	—	—	—
140	—	—	—	—	—	—	—	25.19	—
150	—	75.57	93.89	—	—	—	—	—	—
160	28.24	—	—	—	51.14	—	—	—	—
170	—	—	—	28.24	—	—	—	—	—
180	—	—	—	—	—	—	—	—	42.74
190	—	—	—	—	—	—	16.79	—	—
200	—	—	—	—	—	75.55	—	31.30	—
240	—	—	—	—	—	—	22.13	—	—
250	—	—	—	40.57	68.70	—	—	—	—
260	—	—	—	—	—	—	—	—	56.48
280	—	—	—	—	—	—	—	42.74	—
290	—	—	—	—	—	—	25.19	—	—

used leads to donor-acceptor bonds with the active centers of the catalyst and hence blocks these sites to a larger or smaller extent, depending whether they are more or less active donors and hence stronger or weaker

Table 3

Specific reaction rates and activation energies of the cumene hydroperoxide decomposition reaction in different solvents

Solvent used	$k_{20} \cdot 10^3$	$k_{30} \cdot 10^3$	$k_{40} \cdot 10^3$	E_a kcal/mole
n-heptane	60.5	106.5	140.2	7.23
meta-diisopropylbenzene	46.0	87.5	122.7	7.90
cumene	9.4	19.9	46.0	12.50
ortho-xylene	3.3	9.35	16.84	13.02
meta-xylene	1.94	4.51	7.05	13.50
toluene	1.013	2.35	3.10	17.20
benzene	—	—	0.022	—
dioxan	—	—	0.013	—

Lewis bases. Actually, the same as other researchers [8-11] we have used such substances to determine the nonprotonic acidity of aluminosilicate systems.

The results obtained positively confirm that both the interpretation of the catalytic action of aluminosilicate systems and our attempt to give a schematic representation of the reaction mechanism in this process are correct.

As a matter of fact, the given interpretations are also confirmed by the reaction kinetics which is certainly a first-order kinetics in all the cases.

---

[8] I. Trambouze, *Comp. rend.*, **233**, 648 (1951).

[9] A. Pop and L. Cormoş, *Stud. Univ. Babeş-Bolyai, Chem.*, **17**, 37(1972).

[10] A. Pop and L. Cormoş, *Rev. Chim. (Bucureşti)*, **23**, 347 (1972).

[11] A. Pop and L. Cormoş, "Lucrările celei de a III-a Conferinţe Naţionale de Chimie Analitică", vol. II. Metode optice, Braşov-Romania 22–26 Sept. 1971, p. 307.

Revue Roumaine de Chimie, 23, 2, 233–236 (1978)

ESTUDIO DE REACCIONES DE ARBUZOV. II[1]

REACCIONES ENTRE TRIALQUIL FOSFITOS Y BROMURO DE ETILO

J. M. CACHAZA, J. CASADO y A. VARELA
Departamento de Química Física. Universidad de Santiago. España
Laboratorio de Investigaciones Químicas, C.S.I.C.

Recibido 29 de Mayo de 1975

The reaction mechanism that has been proposed in a previous paper for some Arbuzov's reactions has been confirmed and generalized.

I. INTRODUCCIÓN

En un trabajo realizado anteriormente,[1] se ha llevado a cabo un estudio cinético de las reacciones entre trietil, tributil y trifenil fosfitos con yoduros de alquilo, en disolución de acetonitrilo, utilizando la conductimetría como técnica de trabajo. Se postuló un mecanismo que interpretó satisfactoriamente los resultados experimentales, que se han demostrado en discrepancia con los obtenidos por Buck y Yoke,[2] mediante una técnica de trabajo análoga, para la reacción entre tributil fosfito y yoduro de etilo. En cambio, se encuentran en la misma línea de los resultados de Aksnes y Aksnes [3] utilizando la espectrografía como técnica de trabajo.

En este trabajo se da cuenta de los resultados obtenidos al estudiar las reacciones de trietil fosfito (TEtP) y tributil fosfito (TBuP) con bromuro de etilo.

II PARTE EXPERIMENTAL

La técnica utilizada y detalles complementarios son los mismos que ya se han descrito en un trabajo previo (loc. cit.)

---

[1] J. M. Cachaza, J. Casado y A. Varela, *Rev. Roumaine Chim.*, **22**, 213 (1977).
[2] F. C. Buck y J. T. Yoke, *J. Org. Chem.*, **27**, 3675 (1962).
[3] G. Aksnes y D. Aksnes, *Acta Chem. Scand.*, **17**, 2121 (1963) ; **18**, 38 (1964) ; **19**, 898 (1965).

III. RESULTADOS

La primera serie de reacciones se encaminó a la determinación del orden global de reacción y estudio que, sobre la constante de velocidad, ejerce la concentración inicial de reactivos.

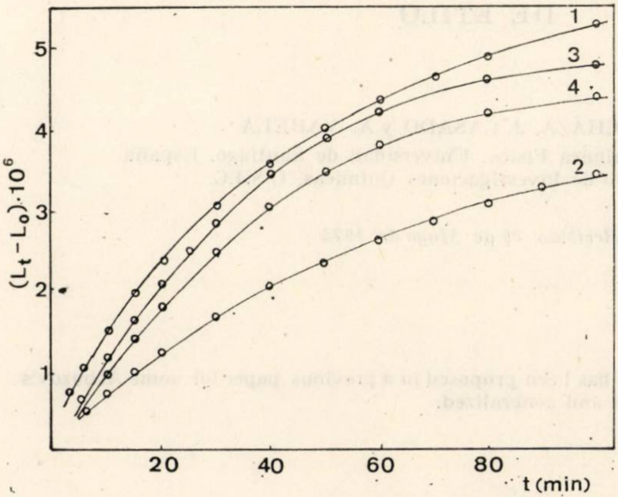

Fig. 1. — Variación de la conductividad (expresada en siemens) con el tiempo para las reacciones: (1), TEtP + BrEt, $c_i = 0{,}1908$ M, 30°C; (2), TEtP + BrEt, $c_i = 0{,}1431$ M, 30°C; (3), TBuP + BrEt, $c_i = 0{,}1865$ M, 30°C; (4), TBuP + BrEt, $c_i = 0{,}1732$ M, 30°C.

Los datos experimentales de conductividades y tiempos (Fig. 1) se han ajustado a una ecuación integrada de orden dos, de la forma:

$$\boxed{\frac{1}{L_t - L_0} = \frac{C}{a} + \frac{C}{a^2 \cdot k} \cdot \frac{1}{t}} \qquad (1)$$

en la que a representa la concentración inicial de reactivos, L_0 la conductividad inicial, L_t la conductividad a tiempo t, y C el coeficiente de proporcionalidad entre concentración y conductividad:

$$x = C(L_t - L_0) \qquad (2)$$

En la Fig. 2 puede observarse el cumplimiento de la linealidad que implica la ecuación (1). Los valores de las constantes de velocidad se recogen en la Tabla 1.

Para tratar de confirmar el orden global dos en las reacciones estudiadas, se determinaron órdenes parciales mediante la técnica de aislamiento, encontrando orden parcial unitario respecto a cada reactivo.

Mediante el método de Guggenheim se calcularon las constantes de velocidad de orden uno de las que, a título de ejemplo, se resumen algunas — Tabla 2 — correspondientes a la reacción entre tributil fosfito y bromuro de etilo.

Fig. 2. — Comprobación de la ecuación (1).

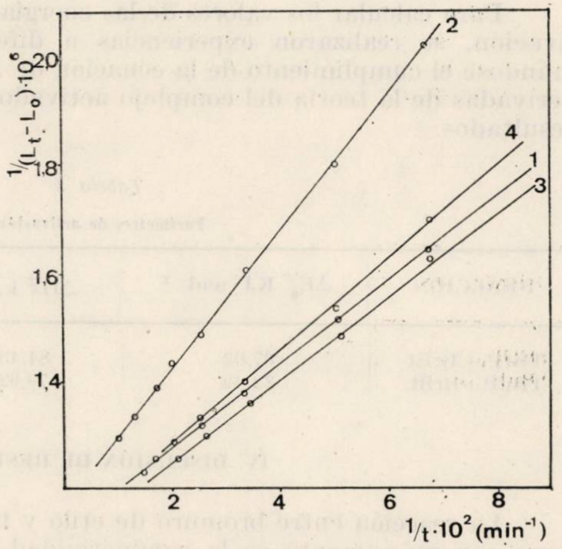

Tabla 1

Cálculo de la constante de velocidad de orden dos

(TEtP) mol · l^{-1}	(BrEt) mol · l^{-1}	$k_{303} \cdot 10^3$ l · mol^{-1} · s^{-1}
0,1812	0,2004	1,13
0,1359	0,1503	1,72
0,0906	0,1002	3,58
0,0543	0,0606	5,05
(TBuP) mol · l^{-1}	(BrEt) mol · l^{-1}	$k_{303} \cdot 10^3$ l · mol^{-1} s^{-1}
0,1872	0,1959	1,32
0,1738	0,1725	1,44
0,1604	0,1593	1,52
0,1337	0,1327	1,29

Tabla 2

Método de aislamiento

(TBuP) mol · l^{-1}	(BrEt) mol · l^{-1}	$k_{303} \cdot 10^4$ s^{-1}
0,3209	0,0797	3,77
0,3276	0.0730	3,40
0,3343	0,0664	3,22
0,3477	0,0531	2,71

Para calcular los valores de las energías, entalpias y entropías de activación, se realizaron experiencias a diferentes temperaturas, confirmándose el cumplimiento de la ecuación de Arrhenius y de las previsiones derivadas de la teoría del complejo activado. La tabla 3 dá cuenta de los resultados.

Tabela 3

Parámetres de activación

REACCION	$\Delta E_a^{\neq}$ KJ · mol^{-1}	$\Delta H^{\neq}$ kJ · mol^{-1}	$\Delta S^{\neq}$ J · mol^{-1}K^{-1}
TEtP + BrEt	87,02	84,43	−18,01
TBuP + BrBt	82,42	79,92	−35,82

IV. DISCUSIÓN DE RESULTADOS

La reacción entre bromuro de etilo y trietil y tributil fosfitos transcurre con un aumento en la conductividad del sistema reaccionante, sin que pueda apreciarse descenso de la misma una vez alcanzado el valor máximo. El comportamiento es análogo al que presentan las reacciones en que el bromuro de etilo es substituido por yoduro de etilo (Cfr. 1). Sin embargo, el intervalo de variación de la conductividad es mucho mayor para las reacciones en que interviene el yoduro de etilo.

El hecho de que no se haya observado un descenso en la conductividad encuentra apoyo en los resultados negativos encontrados al tratar de detectar la presencia del grupo P = 0 en los productos de reacción mediante espectrografía de IR.

Por lo demás, los resultados obtenidos pueden ser inscritos en el marco general del mecanismo propuesto (Cfr. 1.).

Al igual que para el yoduro de etilo, las reacciones con bromuro de etilo transcurren con una entropía de activación de signo negativo, pero su valor absoluto es mucho menor en el caso del bromuro de etilo. Esto parece indicar que el complejo intermedio, de naturaleza polar, debe encontrarse más disociado en el caso del yoduro de etilo, con la consiguiente intervención de fenómenos de solvatación que conduzcan a valores más negativos en la entropías de activación. La mayor variación en la conductividad es una confirmación del carácter más iónico del complejo en las reacciones en que interviene yoduro de etilo, lo que puede atribuirse a una mayor labilidad del enlace carbono-iodo frente al carbono-bromo.

Revue Roumaine de Chimie, **23**, *2*. 237 – 250 (1978)

COPOLYMERIZATION OF ACRYLONITRILE WITH METHACRYLIC ESTERS IN THE PRESENCE OF ORGANO-METALLIC CATALYSTS

CR. I. SIMIONESCU, D. FELDMAN and VIOLETA NUȚĂ
Institute of Macromolecular Chemistry "P. Poni" Jassy,
Aleea Grigore Ghica Vodă 41-A

Received December 15, 1976

Acrylonitrile copolymerization with methacrylic esters (e.g. methyl-, butyl- and lauryl methycrylate) and epichlorohydrin with Al*(iso*-$C_4H_9)_3$ in the presence of different co-catalysts was studied. The influence of the catalysts on the kinetic of the copolymerization and terpolymerization with methyl methacrylate and epichlorohydrin was followed. The nature of obtained products was discussed in all cases.

INTRODUCTION

The polymers synthesized with organo-metallic catalysts are the subject of many papers. [1–19]

---

[1] G. Natta, *Angew. Chem.*, **69**, 686 (1967).
[2] I. Benedek, N. Asandei and Cr. I. Simionescu, *European Polymer Sci*, **7**, 995 (1971).
[3] Cr. I. Simionescu, I. Benedek and N. Asandei, *European Polymer Sci.*, **7**, 1549 (1971).
[4] Cr. I. Simionescu, N. Asandei and I. Benedek, *European Polymer Sci.*, **7**, 1561 (1971).
[5] L. C. Anand, A. B. Deshpande and S. L. Kapur, *Chem. Ind.*, **34**, 1457 (1966).
[6] Y. Amerik, W. I. Reynolds and J. E. Guillet, *J. Polymer Sci.*, *A–1*, **9**, 531 (1971).
[7] A. C. Cheswarth, R. N. Haszeldine and P. J. T. Tait, Abstracts – IUPAC International Symposium on Macromolecules, Aberdeen, 1973, p. 387.
[8] R. N. Haszeldine, T. G. Hyde and P. J. T. Tait, *Polymer*, **14**, 224 (1973).
[9] N. G. Gaylord and B. K. Patnaik, *J. Polymer Sci.*, *B*, **10**, 653 (1972).
[10] U. Giannini and S. Cesca, *Chim. Ind.* (*Milan*), **44**, 371 (1962).
[11] W. P. Baker, Jr., *J. Polymer Sci.*, **42**, 578 (1960).
[12] E. A. H. Hopkins and M. L. Miller, *Polymer*, **4**, 75 (1963).
[13] E. J. Vandenberg, *J. Polymer Sci.*, *A*, **1**, 207 (1963).
[14] G. Natta, H. Dall'Asta, G. Mazzanti, U. Giannini and S. Cesca, *Angew. Chem.*, **71**, 205 (1959).
[15] H. Wexler and J. A. Manson, *J. Polymer Sci.*, *A*, **3**, 2903 (1965).
[16] J. Furukawa, E. Kobayashi and J. Yamauchi, *Polymer J.*, **2**, 407 (1971).
[17] Ikeda Masanori, Hirano Tsuneo and Tsunuta Teiji, *Makromol. Chem.*, **150**, 127 (1971).
[18] Suzuki Yuji and Saito Mitsutoka, *J. Polymer Sci.*, *A–1*, **9**, 3639 (1971).
[19] Yamada Akira and Yanagita Masaya, *J. Polymer Sci.*, *B*, **10**, 91 (1972).

Methyl methacrylate (MMA) polymerization with organo-lithium compounds was much studied,[20-23] but owing to the complexity of the process, the kinetic data are very different from one author to the other.

On the basis of kinetic measurements made at MMA polymerization with lithium-butyl (LiBu), Korotkov and coworkers[24] proposed a mechanism which admits that in the initiation step an isomerizable complex is formed.

The literature data[25-27] show that such catalysts disappear from the reaction medium immediately after the mixing of reactants and that the initiation develops suddenly.

The influence of the reaction medium on the development of MMA polymerization with organo-metallic compounds and on the structure of polymers was studied by Glusker,[28] Goode[29] and Smets.[30]

In the case of polymerization of acrylic esters with organo-metallic compounds the polymer yield as well as its structure depend on the nature of esteric group. The greater is the esteric group (butyl, t-butyl, cyclohexyl, lauryl), the higher the conversion.[31-33]

It was also established that when acrylonitrile (AN) is polymerized with organo-metallic derivatives the initiation is instantaneous and that early in the process two competitive reactions occur : polymerization and olygomerization.[34,35]

Unlike other polar monomers which were polymerized with organo-magnesium derivatives, in the case of methacrylonitrile (MAN) polymerization with Mg and Be organo-metallic compounds,[36,37] the catalytic activity increases with temperature. The nature of the organic rest from the catalyst molecule influences its activity, e.g. aliphatic derivatives are more active than the aromatic ones.

---

[20] T. G. Fox, B. S. Garrett, W. E. Goode, S. Gratch, J. F. Kincaid, A. Spell and J. D. Straupe, *J. Amer. Chem. Soc.*, **80**, 1768 (1958).

[21] F. Wenger, *Chem Ind. (London)*, 1094 (1959).

[22] R. K. Graham, D. L. Dunkelberg and E. S. Cohn, *J. Polymer Sci.*, **42**, 501 (1960).

[23] P. Rempp, V. J. Volkov, J. Parrod and C. Sadron, *Bull. Soc. Chim. France*, 1919 (1960).

[24] A. A. Korotkov, S. P. Mitsengendler and V. N. Krasulina, *J. Polymer Sci.*, **53**, 217 (1961).

[25] B. J. Cottam, D. M. Willes and S. Bywater, *Canad. J. Chem.*, **41**, 1905 (1963).

[26] N. Kawabata and T. Tsuruta, *Makromol. Chem.*, **86**, 231 (1965).

[27] D. L. Glusker, E. Stiles and B. Yoncoskie, *J. Polymer Sci.*, **49**, 297 (1961).

[28] D. L. Glusker, E. Stiles and B. Yoncoskie, *J. Amer. Chem. Soc.*, **86**, 187 (1964).

[29] W. E. Goode, F. H. Owens, R. P. Fellmann, W. H. Snyder and J. E. Moore, *J. Polymer Sci.*, **46**, 317 (1960).

[30] G. L. Aboe and G. Smets, *J. Polymer Sci.*, *A—1*, **5**, 1325 (1967).

[31] M. L. Miller and C. E. Rauhur, *J. Polymer Sci.*, **38**, 63 (1959).

[32] B. S. Garrett, W. E. Goode, S. Gratch, J. F. Kincaid, C. L. Levesque, A. Spell, J. D. Stroupe and W. H. Watanabe, *J. Amer. Chem. Soc.*, **81**, 1007 (1959).

[33] T. Tsuruta, T. Makimcto and Y. Nakayama, *Makromol. Chem.*, **90**, 12 (1966).

[34] I. G. Krasnoselskaya and B. L. Erusalimski, *Vysokomol. Soedineniya*, **12**, 2233 (1970).

[35] B. L. Erusalimski, I. G. Krasnoselskaya, V. N. Krasulina, A. V. Novoselova and E. V. Zashtsherinsky, *European Polymer J.*, **6**, 1391 (1970).

[36] G. Natta and G. Dall'Asta, *Chim. Ind. (Milano)*, **46**, 1429 (1964).

[37] Y. Joh, T. Yashihara, Y. Kotake, F. Ido and K. Nakatsuka, *J. Polymer Sci.*, *B*, **3**, 933 (1965).

Simionescu and coworkers [38] studied AN polymerization in the presence of catalytic systems composed of an aluminium-alkyl derivative and various cocatalysts and obtained interesting data regarding the influence of the catalytic system on the polymerization process and on the properties of the resulted products.

The wider utilization of AN copolymers suggests the study of their synthesis by a similar catalytic process using various systems for initiation.

In this paper the AN copolymerization with methacrylic esters and epichlorohydrin (ECH) is investigated, using various catalytic systems, chosen on the basis of the results obtained earlier.[38]

EXPERIMENTAL

AN copolymerization with various comonomers, was made in the conditions mentioned in the previous paper.[38]

Monomers and benzene were dried on metallic sodium or with molecular sieves and purified by repeated distillation under vacuum in an inert atmosphere. Benzene was used as reaction medium.

Various catalyst-cocatalyst systems, like : Al$(iso\text{-}C_4H_9)_3$, $TiCl_3$, $VoCl_3$, Sn $(C_6H_5)_4$, were used for initiation.

RESULTS AND DISCUSSION

In order to establish an adequate catalytic system which permits to obtain AN copolymers in favourable circumstances, copolymerization of AN with MMA, butyl- (BMA), or lauryl methacrylate (LMA) was studied; the ternary systems with ECH were also investigated, using Al $(iso-C_4H_9)_3$ with or without cocatalysts.

The results are presented for each system as follows.

1. AN–MMA COPOLYMERIZATION

Similarly to AN polymerization,[38] the use of different catalytic systems formed by an aluminium-alkyl compound and a cocatalyst was followed, for AN copolymerization either with MMA or with MMA and ECH.

Experimental data are presented in table 1.

As one can see from this table Al$(iso-C_4H_9)_3$ copolymerizes the AN–MMA system, but the obtained yields are very small.

Taking into account the data regarding the nitrogen amount (6.48%), by calculation, the following composition of the copolymer is established (sample 1, table 1); 46.98% moles AN and 53.02% moles MMA, respectively hence a supraunitary ratio between the MMA/AN units from the copolymer (MMA $>$ AN).

From IR study of the copolymer (sample 1), one can see that: the peak from 2280 cm^{-1} frequency belongs to the vibrations of $\nu(-C \equiv N)$ groups from the units neighbouring with the ester units, and the peak from 2395 cm^{-1} frequency corresponds to units with $-C\equiv N$ groups which are at the ends of the macromolecular chain.[39,40] The acrylic groups ($-COOCH_3$) appear through an intense absorption band at 1720 cm^{-1} frequency which is specific to the esteric group of MMA $\nu(-C=0)$.[40]

---

[38] Cr. I. Simionescu, D. Feldman and V. Nuţă, *Rev. Roumaine Chim.*, **6**, 927 (1976).

Table 1

AN-MMA copolymerization with binary and ternary catalytic systems

N°	I/M mole/mole	I/(M + S) mole/mole	Catalytic system: $Al(i-Bu)_3$ ml	$Al(i-Bu)_3$ mole	Cocatalysts 1 ml	Cocatalysts 1 mole	Cocatalysts 2 ml	Cocatalysts 2 mole	Al/Cocatalyst ratio mole/mole	Conv. % gv.	Obs.
1	0.200	0.036	2.00	0.0080	—	—	—	—	—	0.95	*a*
					$VOCl_3$						
2	0.050	0.009	0.50	0.0019	0.10	0.57×10^{-4}	—	—	33.33	11.14	*b*
					$Sn(C_6H_5)_4$						
3	0.200	0.036	2.00	0.0080	0.01g	0.23×10^{-4}	—	—	347.00	20.93*	*a*
4	0.124	0.032	2.00	0.0080	—	—	—	—	—	12.25*	*c*
					$TiCl_3$		$VOCl_3$				
5	0.051	0.009	0.50	0.0019	0.20	0.64×10^{-4}	0.10	0.57×10^{-4}	15.70	3.60*	*a*
					$VOCl_3$		$Sn(C_6H_5)_4$				
6	0.050	0.009	0.50	0.0019	0.10	0.57×10^{-4}	0.01g	0.23×10^{-4}	23.75	10.13*	*a*
					$Sn(C_6H_5)_4$						
7	0.125	0.033	2.00	0.0080	0.01g	0.23×10^{-4}	—	—	348.00	22.15*	*c*

I — catalyst ; M — monomer ; S — solvent ; 40° ; 25 h ; molar ratio.

M/S = 0.22, except the samples 4 and 7 where M/S = 0.36 ; $Al(i-Bu)_3$ was used as a toluene solution of 60 g/l.

* After substraction of ash

[a] Copolymer AN-MMA ; [b] Copolymer AN-MMA (minerals as traces) ;
[c] Terpolymer AN—MMA—ECH ([ECH] = 0.025 moles).

The band from 3420 cm^{-1} frequency belongs to the superior harmonic vibration which is probably superposed also on $-OH$ groups that are due to the water traces from the KBr tablet.

The presence of a small number of double bands is noticed at 1640 cm^{-1} frequency.[39,40] Such microstructural defects are not numerous on the macromolecular chain.

At 1460 cm^{-1} frequency a broad peak appears which belongs to methylic and methylenic groups of the copolymer.

---

[39] M. Avram and Gh. D. Mateescu, "Spectroscopia în infraroşu. Aplicaţii în chimia organică", Ed. tehnică, Bucharest, 1966.

[40] L. J. Bellamy, "The Infra-Red Spectra of Complex Molecules", Wiley Inc., New York, 1966, pp. 34, 178, 263.

In order to increase the copolymer yield, besides Al $(iso-C_4H_9)_3$ the catalytic system was modified by introduction of $VOCl_3$ and $Sn(C_6H_5)_4$; their presence, as in the case of AN homopolymerization,conducted to higher conversions.[38]

Regarding the influence of protonic reagents, one remarks that in the presence of cyclic ethers (ECH), conversion increased similarly to AN homopolymerization.[38]

In all experiments, conversion did not exceed 20 %.

In the presence of $VOCl_3$ or Sn $(C_6H_5)_4$ (samples 2 and 3), Al$(iso-C_4H_9)_3$ led to a conversion of 10–20%. The yield of the terpolymerization of AN + MMA + ECH was of the same magnitude.

Excepting the system with $VOCl_3$, in all the other cases the copolymer had a high amount of minerals, e.g. 13% for the copolymer with ECH and 22% for the sample with $Sn(C_6H_5)_4$, resulting from catalysts.

The following data : %N = 1.70 and %Cl = 17.70 of the terpolymer (sample 4, table 1), are used to establish its composition : 12.34% moles AN, 49.84% moles ECH and 37.82% moles MMA.

These data show that the amount of ECH prevails in copolymer composition.

IR spectrum of the product proves the presence of all three monomers. Successive extractions of homopolymers, made in order to clear up the nature of this polymer, show that in the applied experimental conditions it is possible to obtain an AN–MMA–ECH terpolymer.

In the case of sample 3 of table 1, the IR spectrum of AN–MMA copolymer is modified in comparison with that of PMMA, which can be explained by a pronounced complexation of organo-tin compound by polar groups.

AN–MMA copolymer synthesized with soluble Ziegler-Natta catalysts at different temperatures presents also absorptions common to radical — obtained copolymer (absorption near 1740 cm^{-1} frequency). On the other hand this polymer has characteristic peaks in the 1660–1640 cm^{-1} range of frequency (due to C = C and C = N bands) and at 1280 cm^{-1} bands which exist in spectra of copolymers synthesized with soluble Ziegler-Natta catalysts.

In the case of the polymerization of stabilized or purified monomers the same yields were obtained at small duration (about one hour); this excludes the possibility of a radical polymerization mechanism, in which case the influence of inhibitors is remarkable.

These observations as well as the IR spectroscopic data plead in favour of a polymerization mechanism different from the radical or ordinary ionic one.

The copolymer synthesized with catalytic system Al $(iso-C_4H_9)_3$ — Sn $(C_6H_5)_4$ (sample 7, table 1) was obtained with higher yield. From the elemental analysis of the product the following results are to be retained : %N — 2.00 %Cl — 20.26.

The copolymer was extracted with hot dimethylformamide (DMF) and hot cylclohexanone (CH), being a good solvent for PECH.[41] A soluble part and an insoluble part were obtained after extraction. The elemental analysis of these fractions are expounded in table 2.

---

[41] M. Dimonie and I. Gavăt, *European Polymer J.*, *4*, 541 (1968).

IR study of the soluble fraction shows the presence of absorptions characteristic of AN at 2280 cm^{-1} and at 2390 cm^{-1} $\nu(-C\equiv N)$, of the same specific to ECH at 1120 cm^{-1} $\nu(-C-O-C-)$ and of absorptions characteristic of MMA at 1720 cm^{-1} and 1730 cm^{-1}, the last one is split (because the copolymer has two types of $C=O$ bands).[40] The intense absorption range from 1620–1660 cm^{-1} (a composite one) pleads for the existence of some double bands at the edges and inside some cyclic units. In the range of 1440–1470 cm^{-1}, where two bands apear for $-CH_3$ and $-CH_2$ (probably from MMA and ECH). The IR data show the existence of the terpolymer.

Table 2

Results of the elemental analysis of the soluble and insoluble in CH fractions of the terpolymer AN – MMA – ECH

	Elemental analysis *			
	C** %	H** %	N %	Cl %
Soluble fraction	48.50	6.31	1.95	19.80
Insoluble fraction	58.65	6.23	8.75	6.55

* These values are calculated again after having subtracted the residue content (mineral substances).

** Calculated on basis of nitrogen and chlorine analysis.

Unlike the fraction insoluble in CH, the soluble fraction is characterized by a high chlorine content and a low nitrogen amount. These data plead in favour of formation of a terpolymer in which ECH (soluble fraction), or vinyl comonomers (insoluble fraction) is predominant.

NMR spectrum (Jeol JNM–C–60 HL), characteristic of AN–MMA–ECH terpolymer is presented in fig. 1.

NMR spectrum of the protons from this copolymer (fig. 1) permits to identify the following signals : the signal from 2.20 ppm and 2.5 ppm coming out from the methylene protons of the AN units,[42,43] the signal from 0.9 ppm and 1.35 ppm given by the methyl and methylene protons from MMA and the signal from 3.50 ppm belonging to the methyl protons also from MMA,[43,44] as well as the signal from 3.55 ppm as being a part of the complex given by the methylene protons from ECH.[45] The other signals are, unfortunately, hidden by the strong signals of some impurities as : dimethylsulphoxide-d_6, water from the solvent or sample and dioxan from the sample. So, the signal of the methyn proton from AN which is normally appearing at 3.25 ppm [42,43] is covered by signals coming from the water of the solvent, and the strong signal from 3.70 ppm coming from dioxan covers the signals of methin and methylen protons from ECH.

---

[42] K. Matsuzaki, T. Dryu and K. Ishiagure, *J. Polymer Sci.*, *B*, **4**, 93 (1966).

[43] Catalog JEOL, vol. 2.

[44] F. A. Bovey, *Pure and Applied Chem.*, **12**, 525 (1966).

[45] Tables of correlation VARIAN.

The shape of the methylene and methyn signals from AN, MMA and ECH are not sufficiently clear to permit conclusions about the concatenation of these units.

In order to establish the best synthesis conditions, the influence of different parameters on terpolymerization of AN—MMA—ECH system

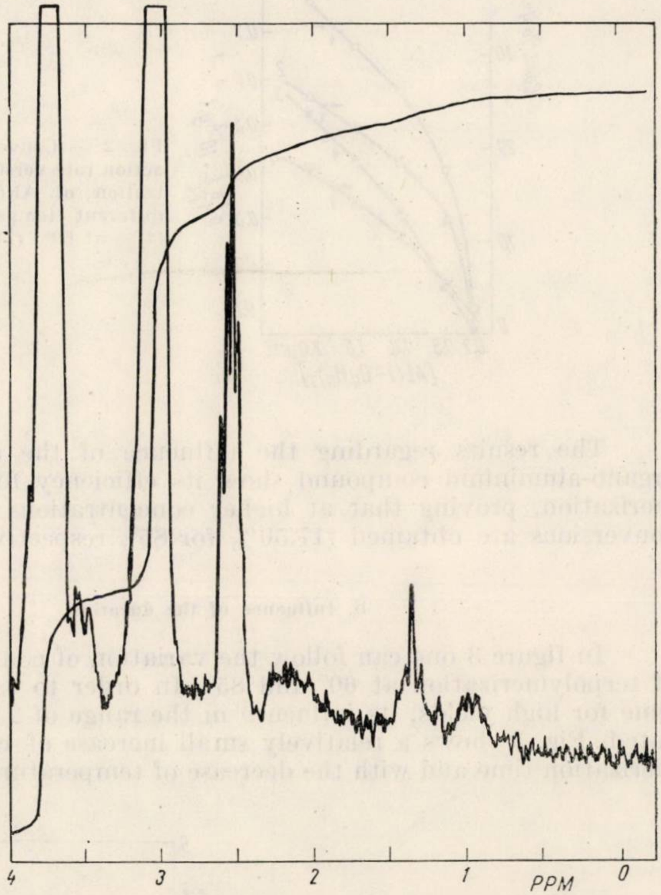

Fig. 1. — RMN spectrum of the soluble fraction of the AN-MMA-ECH terpolymer.

was followed, using as catalysts $Al(iso-C_4H_9)_3$ and $Sn(C_6H_5)_4$ which gave the best results regarding the conversion.

a. Influence of organo-aluminium compound

Working conditions: molar ratio M/S = 0.36; Sn $(C_6H_5)_4$ concentration, 0.23×10^{-4} moles; total concentration of monomers (M), 0.0643 moles; solvent (S) (benzene) concentration, 0.179 moles; duration, 2 hours; $Al(iso-C_4H_9)_3$ between 0.0019—0.0080 moles; temperatures, 60° and 85°. The organo-aluminium compound was used as toluene solution.

From the experimental data presented in fig. 2, a pronounced increase of the rate of reaction with the amount of $Al(iso-C_4H_9)_3$ could be remarked. At the same time, the rate decreases with the increase of temperature. This fact could be explained by the destruction of the catalyst.

Terpolymerizations at 85° conduct to smaller conversions than those carried out at 60°.

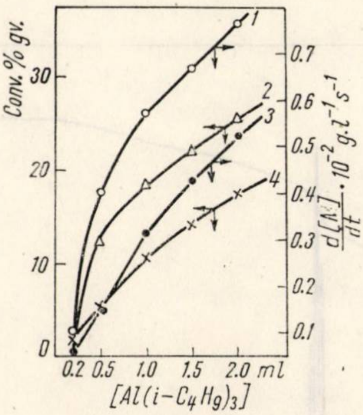

Fig. 2. — Conversion and reaction rate versus the concentration of $Al(iso-C_4H_9)_3$ at different temperatures: (*1*), (*2*) — at 60°; (*3*), (*4*)— at 85°.

The results regarding the influence of the concentration of the organo-aluminium compound show its efficiency for the studied copolymerization, proving that at higher concentrations (0.008 moles) higher conversions are obtained (17.50% for 85°, respectively 25.50% for 60°).

b. Influence of the duration

In figure 3 one can follow the variation of conversion with the time of terpolymerization at 60° and 85°. In order to establish the optimum time for high yields, its influence in the range of 2—12 hrs. was investigated. Fig. 3 shows a relatively small increase of conversion with polymerization time and with the decrease of temperature.

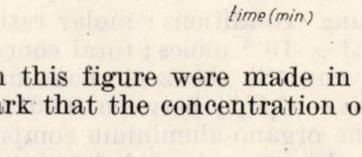

Fig. 3. — Conversion versus time of copolymerization at different temperatures: (*1*) — at 60°; (*2*) — at 85°.

The experiments presented in this figure were made in conditions described at point a, with the remark that the concentration of $Al(iso-C_4H_9)_3$ was 0.0008 moles.

The data in figures 2 and 3 point to an increase of conversion both with organo-aluminium compound concentration and with reaction time;

practically it is advantageous to increase the total concentration of the initiator because this increase conducts to a conversion from 25.50% for a reaction time from 2 hours ((fig. 2, curve 2).

c. Influence other factors (temperature, I/M and I/(M + S) ratio)

The experiments were made at 60° and 85°. According to the data presented in figures 2 and 3 the increase of the temperature determines the decrease of the reaction rate.

Table 3

Influence of the molar ratio I/M and I/M and I/(M + S) on the AN – MMA – ECH terpolymer conversion (time = 120 min.)

N°	I/M mole/mole	I/(M+S) mole/mole	[Al $(iso-C_4H_9)_3$] ml	[Al $(iso-C_4H_9)_3$] mole	Conversion % grav. Temp. 60°	Conversion % grav. Temp. 85°
1	0.013	0.0034	0.20	0.0008	2.33	1.97
2	0.030	0.0080	0.50	0.0019	12.70	5.20
3	0.063	0.0160	1.00	0.0039	18.38	10.50
4	0.090	0.0240	1.50	0.0058	22.20	14.30
5	0.124	0.0330	2.00	0.0080	25.50	17.65

I — catalyst ; M — monomer ; S — solvent.

The follow up of the influence of the molar ratios catalyst/monomer (fig. 4) and catalyst/(monomer + solvent) — (fig. 5) — on the terpolymer yield at 60° and 85° conducts to the conclusion that as they increase the conversion rises also, up to a maximum value at a molar ratio of catalyst/monomer = 0.124 and of catalyst/(monomer + solvent) = 0.033 (table 3).

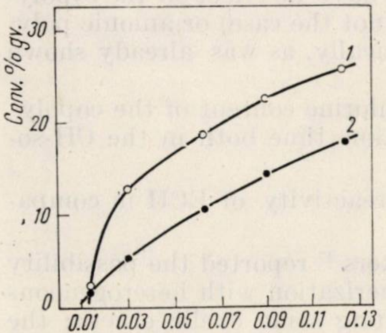

Fig. 4. — Copolymer yield versus the molar ratio I/M, at different temperatures : (*1*) — at 60° ; (*2*) — at 85°.

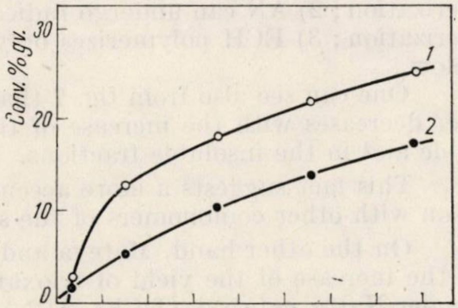

Fig. 5. — Copolymer yield versus the molar ratio I/(M+S), at different temperatures : (*1*) — at 60° ; (*2*) — at 85°.

As a result of the study of AN—MMA copolymerization in the presence of Sn $(C_6H_5)_4$, Al$(iso-C_4H_9)_3$ and ECH, by chemical methods (successive extractions, elemental analysis) and physical methods (IR and NMR spectroscopy), one establishes the formation of AN–MMA–ECH terpolymer; regarding the mechanism of this terpolymerization some difficulties appear because the main two comonomers polymerize by different ionic mechanisms (i.e., AN polymerizes anionically, and ECH polymerizes mostly cationicaly). As we remarked in a previous paper [38] the synthesis of an AN–ECH binary copolymer with Al (iso-$C_4H_9)_3$ + $Sn(C_6H_5)_4$ catalytic system is possible. At the same time we must mention that ECH homopolymerizes with this catalytic complex.

Studying polymerization and copolymerization of ECH with alkyl-aluminium or alkyl-aluminium – water system, Saegusa and coworkers,[46] presume the existence of two competitive mechanisms, i.e. cationic and coordinative respectively.

According to the data of the elemental analysis (low content of chlorine), the copolymer obtained with the catalytic complex Al*(iso*–$C_4H_9)_3$ – $Sn(C_6H_5)_4$ contains homopolymer, fact proved also by the weight decrease of the product after having extracted with dioxan or CH and DMF specific solvents for PECH and respectively PAN. Presuming that the increase of the yield of the product (fig. 2) results also by formation of PECH, it is possible that the chlorine amount of the obtained product increases at the same time with the increase of the Al/Cocatalyst ratio. The data of fig. 6 confirm this hypothesis.

The chlorine content of the obtained terpolymer increases at the same time as aluminium compound concentration reaching a maximum at a concentration of 0.008 moles Al*(iso*–$C_4H_9)_3$.

The results and the possibility of obtaining AN–ECH binary copolymers with the mentioned catalytic system suggest that the copolymerization mechanism is ionic. The following observations support this affirmation : 1) the radical inhibitors (hydroquinone) have no effect on the copolymerization ; 2) AN can undergo radical (it is not the case) or anionic polymerization ; 3) ECH polymerizes only cationically, as was already shown below.

One can see also from fig. 7 that the chlorine content of the copolymer decreases with the increase of the reaction time both in the CH-soluble and in the insoluble fractions.

This fact suggests a more accentuated reactivity of ECH in comparison with other comonomers of the system.

On the other hand, Mateva and coworkers [47] reported the possibility of the increase of the yield of trioxan polymerization with heterogeneous Ziegler-Natta catalyst ($TiCl_4$–AlR_3) by adding some cyclic ethers; the authors explained this phenomenon by the formation of a coordination cyclic complex between $TiCl_4$, AlR_3 and ECH, which decomposes in cationic active species.

At the same time we must mention that these authors [47] copolymerized also AN with ECH in the presence of $TiCl_4$–$Al(C_2H_5)_3$ complex; as already mentioned this reaction may be performed also with the catalytic system Al*(iso*–$C_4H_9)_3$ – $Sn(C_6H_5)_4$.[38]

---

[46] T. Saegusa, T. Ueshima and S. Tomita, *Makromol. Chem.*, **107**, 131 (1967).

[47] R. Mateva, V. Kabaiwanov and M. Natov, *Makromol. Chem.*, **109**, 231 (1967).

According to literature data,[48] the addition of Lewis bases (simple cyclic ethers) to aluminium-alkyls increases their catalytic activity in vinyl polymerization. It was supposed to be a radical mechanism for these reactions.

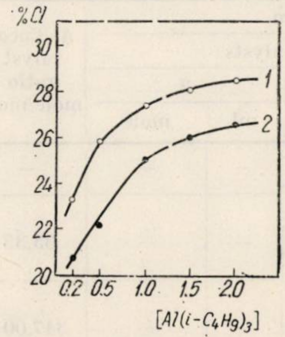

Fig. 6. — Chlorine content of the synthesized products at 60° :

(*1*) and 85° *2*), with Al(*iso*$-C_4H_9)_3$ $-Sn(C_6H_5)_4$ plotted against Al(*iso*$-C_4H_9)_3$ concentration.

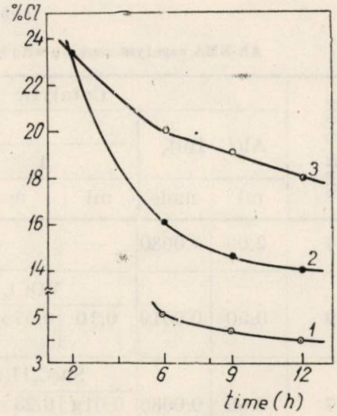

Fig. 7. — Chlorine content of the AN-MMA-ECH terpolymer synthesized at 60°, with Al(*iso*-$C_4H_9)_3-Sn(C_6H_5)_4$ plotted against reaction time :

(*1*) Chlorine content variation of the CH-insoluble fraction; (*2*) Chlorine content variation of the CH-soluble fraction; (*3*) Total chlorine content variation of the terpolymer.

Owing to the complexity of the process, and especially to the great number of compunds, the mechanism on which AN—MMA—ECH terpolymer synthesis is based is not yet elucidated, being one of our main concerns.

2. AN—BMA COPOLYMERIZATION

The copolymerization of AN and BMA and the terpolymerization of AN, BMA and ECH were made in similar conditions and the influence of methacrylic monomer on conversion was investigated. Experimental data are presented in table 4.

Results of table 4 show that similarly to AN—MMA copolymerization the aluminium-alkyl derivative catalyzes copolymerization of AN and BMA with very low yields.

A content of N = 5.23 % was established for the copolymerization product (sample 1, table 4), hence a composition of the copolymer determined by calculation of 38 % moles AN and 62 % moles BMA.

In order to increase the conversion, the use of some cocatalytic additions was experimented also in this case.

---

[48] D. S. Breslow, D. L. Christman, H. H. Espy and C. A. Lukach, *Appl. Polymer Sci.*, **11**, 73 (1967).

$Al(iso-C_4H_9)_3$ and cocatalysts as : $VOCl_4$ or $Sn(C_6H_5)_4$ (samples 2 and 3, table 4) conduct to conversions of 10–20%. AN + BMA + ECH terpolymerization (sample 4, table 4) was performed with conversions of analogous values.

Table 4

AN-BMA copolymerization with binary and ternary catalytic systems

N°.	I/M mole/mole	I/(M+S) mole/mole	Catalytic system						Al/Cocatalyst ratio mole/mole	Conv. % gv.	Obs.
			$Al(i-Bu)_3$		Cocatalysts						
					1		2				
			ml	mole	ml	mole	ml	mole			
1	0.220	0.037	2.00	0.0080	—	—	—	—	—	2.20	*a*
					$VOCl_3$						
2	0.054	0.009	0.50	0.0019	0.10	0.57×10^{-4}	—	—	33.33	8.66	*b*
					$Sn(C_6H_5)_4$						
3	0.220	0.037	2.00	0.0080	0.01g	0.23×10^{-4}	—	—	347.00	22.23*	*a*
4	0.130	0.033	2.00	0.0080	—	—	—	—	—	21.53*	*c*
					$TiCl_3$		$VOCl_3$				
5	0.055	0.0093	0.50	0.0019	0.20	0.64×10^{-4}	0.10	0.57×10^{-4}	15.70	3.29*	*a*
					$VOCl_3$		$Sn(C_6H_5)_4$				
6	0.054	0.0092	0.50	0.0019	0.10	0.57×10^{-4}	0.01g	0.23×10^{-4}	23.75	11.17*	*a*
					$Sn(C_6H_5)_4$						
7	0.131	0.0334	2.00	0.0080	0.01g	0.23×10^{-4}	—	—	348.00	23.78*	*c*

I — catalyst ; M — monomer ; S — solvent ; 40° ; 25 h ; molar ratio M/S = 0.20, except the samples 4 and 7 where M/S = 0.34 ; $Al(i-Bu)_3$ was used as a toluene solution of 60 g/l.

* After subtraction of ash ;

[a] Copolymer AN–BMA ; [b] Copolymer AN–BMA (minerals as traces) ; [c] Terpolymer AN–BMA–ECH ([ECH] = 0.025 moles).

After having removed the homopolymers, the terpolymer (sample 4, table 4) has %N = 1.40, %Cl = 18.20, which leads to a composition of : 10.20% moles AN, 51.24% moles ECH and 38.56% moles BMA.

The data prove that the reaction product has both units of vinyl comonomers and ECH units, the latter prevailing.

IR spectrum confirms the presence of characteristic peaks and the NMR spectrum puts into evidence the existence of all three monomers, so that it can be said that an AN–BMA–ECH terpolymer was formed.

Regarding the possibility of obtaining some suitable conversions it is also necessary to use high amounts of catalyst.

Using the same quantities of catalysts this system was characterized by higher conversions than those having MMA as comonomer (see run 4 in tables 1 and 4).

The data of samples 5,6 and 7 (table 4) prove that the used catalytic systems conducted to higher conversions than in the case of the system with MMA (see table 1).

Elemental analysis of the terpolymer synthesized with the binary catalytic system Al*(iso*$-C_4H_9)_3 - Sn(C_6H_5)_4$ (sample 7) gave higher nitrogen and chlorine percentages (%N = 1.63 and %Cl = 21.10) than those obtained only with Al*(iso*$-C_4H_9)_3$ (sample 4).

Subsequent treatment of the copolymer (sample 7) and the established observations are in good agreement with those of the system with MMA.

3. AN–LMA COPOLYMERIZATION

AN–LMA copolymerization conducted to the results presented in table 5.

Table 5

AN-LMA copolymerization with binary and ternary catalytic systems

N°.	I/M mole/mole	I/(M + S) mole/mole	Catalytic system						Al/Cocatalyst ratio mole/mole	Conv. % gv.	Obs.
			Al(i−Bu)$_3$		Cocatalysts						
					1		2				
			ml	mole	ml	mole	ml	mole			
1	0.240	0.037	2.00	0.0080	—	—	—	—	—	3.25	*a*
					VOCl$_3$						
2	0.058	0.009	0.50	0.0019	0.10	0.57×10^{-4}	—	—	33.33	9.05	*b*
					Sn(C$_6$H$_5$)$_4$						
3	0.240	0.037	2.00	0.0080	001.g	0.23×10^{-4}	—	—	347.00	26.63*	*a*
4	0.137	0.034	2.00	0.0080	—	—	—	—	—	23.25*	*c*
					TiCl$_3$		VOCl$_3$				
5	0.060	0.0093	0.50	0.0019	0.20	0.64×10^{-4}	0.10	0.57×10^{-4}	15.70	3.41*	*a*
					VOCl$_3$		Sn(C$_6$H$_5$)$_4$				
6	0.059	0.0092	0.50	0.0019	0.10	0.57×10^{-4}	0.01g	0.23×10^{-4}	23.75	12.08*	*a*
					Sn(C$_6$H$_5$)$_4$						
7	0.137	0.0337	2.00	0.0080	0.01g	0.23×10^{-4}	—	—	348.00	24.66*	*c*

I – catalyst ; M – monomer ; S – solvent ; 40° ; 25 h : molar ratio

M/S = 0.18, except the samples 4 and 7 where M/S = 0.33 ; Al(i−Bu)$_3$ was used as a toluene solution of 60 g/l.

* After substraction of ash

[a] Copolymer AN-LMA : [b] Copolymer AN-LMA (minerals as traces) ; [c] Terpolymer AN–LMA–ECH ([ECH] = 0.025 moles).

Their examination show that one obtains conversions slightly higher than for the systems with MMA or BMA, but they remain in the same range of magnitude order.

The AN—LMA copolymer synthesized with Al*(iso*—$C_4H_9)_3$ (sample 1, table 5) has a content of %N = 4.20; calculation established a composition of 30.40% moles AN and 69.60% moles LMA respectively.

From those data and from that of nitrogen analysis of AN—MMA and AN—BMA copolymers synthesized in same conditions, one can see, that the molecular weight of methacrylic comonomer increases as the nitrogen percentage of samples decreases.

AN—LMA—ECH copolymerization (samples 4 and 7 in table 5) occurred with higher conversions than when MMA (run 4 and 7 in table 1), or BMA (run 4 and 7 in table 4) were used as comonomers.

The nitrogen and chlorine analysis of the AN—LMA—ECH terpolymer, synthesized with Al*(iso*—$C_4H_9)_3$ (sample 4, table 5) is as follows: %N = 1.28, %Cl = 19.18, hence to a composition of: 9.30% moles AN, 54% moles ECH and 36.70% moles LMA.

These data show that similarly to previous monomers copolymerizations, the reaction product is a terpolymer in which ECH units are predominant.

It should be mentioned that also in the case of AN—LMA—ECH terpolymer IR spectrum confirms the presence of peaks characteristic of all three comonomers.

Elemental analysis of the terpolymer (sample 7) exhibits also in this case somehow high nitrogen and chlorine percentages (%N = 1.32 and %Cl = 22.72) than in the case of the terpolymer obtained with Al*(iso*—$C_4H_9)_3$ as catalyst (run 4).

Extracted copolymer with hot DMF and CH conducts to obtention of two fractions, one soluble in CH and one unsoluble, similarly to terpolymers with MMA and BMA.

CONCLUSIONS

1. AN copolymerization and terpolymerization with MMA, BMA, LMA and respectively ECH, was studied using various catalytic systems containing Al*(iso*—$C_4H_9)_3$.

2. Binary systems with $VOCl_3$ and $Sn(C_6H_5)_4$ conduct to conversions of about 20%. The system Al*(iso* — $C_4H_9)_3$ — $Sn(C_6H_5)_4$ provides higher conversions for copolymers with ECH.

3. The copolymer yield increases with the increase of length of methacrylic esther chain.

4. The catalytic activity of the system Al*(iso*—$C_4H_9)_3$ — Sn $(C_6H_5)_4$ decreases with the increase of temperature.

Revue Roumaine de Chimie, **23**, 2, 251–253 (1978)

ANIONIC SURFACTANT ANALYSIS FROM MICELLAR SOLUTIONS

D. F. ANGHEL and GEORGETA POPESCU

The "P. Poni" Institute for Macromolecular Chemistry, Department of Colloids, Bucharest 7000, Str. Dumbrava Roşie, Nr. 18

Received October 14, 1975

The anionic surfactant content of micellar solutions used in the process of oil recovery was checked up by the twophase titration method using various indicators: methylene blue, bromocresol green and dimidium bromide-disulphine blue VN. The nonionic surfactants and the alcohols do not interfere. The bromocresol green method gives higher values when the hydrocarbon of the micellar solution contains fatty acids. The presence of crude oil entails difficulties in the end-point determination.

Micellar solutions usually called microemulsions, swollen micelles, soluble oils or transparent dispersions are made of hydrocarbon, water (including electrolytes), surfactant and cosurfactant (a polar organic substance like alcohols). Micellar solutions have been highly developed in processes of oil recovery [1–4] and well stimulation.[5,6] Unfortunately, there are no literature data available about the analysis of the surfactant contained in these systems. By this communication we report the results obtained in this field by the methylene blue,[7] bromocresol green [8] and mixed indicator (dimidiun bromide and disulphine blue VN)[9] methods. The interferences from nonionic surfactants, hydrocarbons and alcohols are also considered.

Micellar solutions were prepared with anionic surfactants i.e. sodium alkylaryl sulphonate (equivalent molecular weight, $M_e = 325$) and petroleum sulphonate (Petronate TRS–10, $M_e = 420$, from Witco Chemical Co., Sonnenborn Division), sometimes mixed with nonionic surfactants AF–31 (alkylphenol polyoxyethylene ether) or AG–22 (oxyethy-

---

[1] W. B. Gogarty, Paper SPE 1847–A presented at the 42nd Annual Fall Meeting of Society of Petroleum Engineers of AIME, October 1–4, 1967.

[2] W. B. Gogarty and W. C. Tosch, *J. Pet Tech.*, **1968,** 1407.

[3] W. B. Bleakley, *Oil and Gas Journal*, November **1971,** 49.

[4] W. B. Gogarty and J. A. Davis Jr., *World Oil*, March **1973,** 53.

[5] W. B. Gogarty, W. L. Kinney and W. B. Kirk, *J. Pet. Tech.*, **1970,** 1577.

[6] J. P. Moran and W. N. Maxwell, Paper SPE 2842 presented at SPE Meeting on Practical Aspects of Improved Recovery Techniques, Forth Worth, Texas, March 8–10, 1970.

[7] S. R. Epton, *Nature*, **160,** 795 (1947); *Trans. Faraday Soc.*, **44,** 226 (1948).

[8] B. M. Milwidsky and S. Holtzman, *Soap Chem. Spec.*, **42,** 83 (1966); M. Bares, *Tenside*, **6,** 312 (1969).

[9] V. W. Reid, G. F. Longman and E. Heinerth, *Tenside*, **4,** 292 (1967).

lated fatty alcohol). n-Amyl alcohol, fusel oil and heavy oil (a residue obtained from butanol preparation by oxo-synthesis) were used as cosurfactants. Fresh water, together with hydrocarbons i.e. kerosene, gas oil and crude oil, was used.

Details on analytical methods are given in the above mentioned papers.[7–9] However, we must point out the titrant which was in all cases the 0.004 M benzylalkyldimethyl ammonium chloride (BAC) solution made with BAC p.a., M = 365.5 (Schuchardt) and standardized against the 0.004 M sodium dodecyl sulphate (SDS) solution. This SDS p.a. was also supplied by Schuchardt.

Table 1

Anionic surfactant analysis from micellar solutions

Run n°	Methylene Blue method (% w/v)	Mixed Indicator method (% w/v)	Bromocresol Green method (% w/v)
1	8.00	8.59	8.59
2	5.39	6.95	7.11
3	12.18	11.15	10.96
4	11.25	10.77	10.97
5	8.95	8.62	8.68
6	7.17	6.65	7.27

The content of micellar solutions in anionic surfactant determined by these three methods is shown in Table 1. We found out that the last two methods had a better behaviour, the differences being of about ± 2%. The methylene blue method leads to more erroneous results (up to 11% for the solution no. 3). These differences could be due to the interferences with other components of the micellar solution and to the difficulties in end-point determination by the presence of coloured hydrocarbon like crude oil. A higher value obtained for the solution no. 6 by bromocresol green method is due to the presence of fatty acids in the hydrocarbon. In alkaline conditions they become soaps and are detected by this method.

In order to establish the influences performed by other components on the micellar solution content in anionic surfactant, the cosurfactant and the hydrocarbon have been added in turn, to the surfactant solution, determining every time the surfactant content of the new formed system. The results are given in Table 2. A better behaviour of the bromocresol green and mixed indicator methods are pointed out once more. Interferences of other components are in this case small. Now, it is much more evident that only in the presence of hydrocarbons which contain fatty acids (the acidity number of gas oil used in run no. 6 is 8 mg KOH/100 g) erroneous values are obtained, the nonionic surfactant and the cosurfactant having no influence.

To conclude, in determination of anionic surfactant from micellar solutions, the bromocresol green and the mixed indicator methods provide the best results. The cosurfactant and the nonionic surfactants do not interfere, but the bromocresol green method is seriously affected when the hydrocarbon contains fatty acids. Sometimes, when crude oil is used to prepare micellar solutions, difficulties may occur in the end point determination, by the methylene blue and mixed indicator methods.

Table 2

The influence of the components of the micellar solution on the anionic surfactant content determined by various methods

Run n°	Component added	% on Active added	Methylene Blue method (% w/v)	Mixed Indicator method (% w/v)	Bromocresol Green method (% w/v)
1	—	—	7.85	8.63	8.55
	Fusel Oil	0−200	7.95	8.67	8.63
	AF−31[a]	0−200	8.04	8.65	8.70
	Kerosene	0−200	8.00	8.59	8.59
2	—	—	5.42	6.96	7.10
	$\mathrm{n-C_5}$ alcohol	0−200	5.40	6.96	7.10
	Tzicleni Crude Oil	0−300	5.39	6.95	7.11
3	—	—	11.30	11.15	10.99
	AG−22[b]	0−200	11.70	11.17	10.98
	Carbunesti Crude Oil	0−250	12.18	11.15	10.96
4	—	—	11.12	10.76	11.00
	AG−22[b]	0−200	11.11	10.74	10.85
	Surani Crude Oil	0−250	11.25	10.77	10.97
5	—	—	8.55	8.73	8.55
	Fusel Oil	0−300	8.52	8.56	8.63
	AF−31[a]	0−200	8.56	8.61	8.67
	Kerosene	0−300	8.53	8.62	8.68
6	—	—	7.07	6.61	6.86
	Heavy Oil[c]	0−320	7.07	6.54	6.80
	AF−31[a]	0−320	7.11	6.59	6.82
	Gas Oil	0−300	7.17	6.65	7.27

[a] AF−31 is an alkylphenol polyoxyethylene ether;

[b] AG−22 is an oxyethylated fatty alcohol;

[c] Heavy oil is a residue obtained from butanol preparation by oxo-synthesis.

Revue Roumaine de Chimie, 23, 2, 255–260 (1978)

UNPERTURBED DIMENSIONS OF COPOLYMERS. POLY(N-VINYLCAPROLACTAM-DIETHYLFUMARATE) ALTERNATING COPOLYMER

C. CINCU and C. BOGHINĂ

Laboratory of Macromolecular Chemistry, Polytechnic Institute, Calea Victoriei 149,
Bucharest, Romania

Received September 11, 1975

Kuhn-Mark-Houwink-Sakurada (KMHS) relations were obtained in benzene (B) and chloroform (C) at 25° for poly (N-vinylcaprolactam-diethylfumarate) (NVC-DEF) alternating copolymer. The values of the unperturbed dimensions, K_θ or $A=(\bar{r}_0^2/M)^{1/2}$ and conformational parameter σ have been determined using five known extrapolation techniques. Using Flory-Fox-Schaefgen method, the values of K_θ, A or σ are smaller than those obtained by other methods.

1. INTRODUCTION

The unperturbed dimensions of the polymer chains $K_\theta = \O_0 \dfrac{\bar{r}_0^2}{M}$ or $A = (r_0^2/M)^{1/2}$, where $\O_0$ is the hydrodynamic constant, M is molecular weight and r_0^2 is the mean-square-end-to-end distance of the polymer chain in the unperturbed state, and conformational parameter σ reflect the chain conformation and the flexibility of these polymers. The parameter is defined as follows:

$$\sigma = \bar{r}_0^2/\bar{r}_{01}^2 \tag{1}$$

where $\bar{r}_{01}^2$ is the mean-square-end-to-end distance for a chain in which the internal rotation about the C—C bond of the main chain is completely free.

The evaluation of these dimensions is of great interest because of their connection with the fundamental properties of the polymer chain.

For the (NVC—DEF) alternating copolymer the values of K_θ, A and σ must be governed by the molar volume of substituents and their distribution along the chain. On the other hand, electrostatic forces induced by the neighbouring — $COOC_2H_5$ groups in the main chain are expected to favour the "trans" conformation in this copolymer.

2. EXPERIMENTAL

2.1. MATERIALS AND COPOLYMERIZATION

The monomers N-vinylcaprolactam (NVC)[1–3] and diethylfumarate (DEF)[4] were obtained by distillation under nitrogen at reduced pressure.

The copolymerization[5] was carried out in bulk at 60°, α, α′-azobis-izobituronitrile (AIBN) being used as initiator. The molar ratios VCL/DEF and AIBN/VCL were 9/11 and $10^{-3}/3.77$, respectively.

The copolymer was dissolved in diethylene dioxide, precipitated in petroleum ether and dried in vacuum at 40°.

2.2. CHEMICAL COMPOSITION

The chemical composition was calculated on the basis of the nitrogen content determined by micro-Dumas analysis.

2.3. FRACTIONATION OF COPOLYMER

The copolymer has been fractionated by column elution with benzene-petroleum ether.

2.4. DIFFERENTIAL REFRACTIVE INDEX INCREMENT AND LIGHT SCATTERING

The differential refractive index increment, d*n*/d*c* (*n* is the refractive index and *c* is the weight concentration of the solution) was measured in methyl ethyl cetone (MEK) at 25° with a Zeiss interferometer.

Light scattering measurements were carried out at 25±0.1° in MEK with a "Sofica" photogoniodifusometer. Dust free solutions and solvent were obtained by filtration through a No 5 porosity glass filter under pressure directly into the cells. The instrument was calibrated using a standard scattering glass (standard benzene). For pure benzene in unpolarized light, the Rayleigh ratio $R=16.3\times10^{-6}\,\text{cm}^{-1}$ ($\lambda=5461$ Å, $t=25°$) was used.

The interpretation of the scattering data was based on the Zimm method.[6] For (VCL-DEF) alternating copolymer, the true molecular weight $\overline{M}_w$ is obtained by usual treatment to be applied to homopolymers.[7,8]

2.5. INTRINSIC VISCOSITY

The viscosities of the solutions and solvents were determined in benzene and chloroform at 25±0.1° with a modified suspended level viscometer for which kinetic energy corrections were negligible.

The intrinsic viscosity $[\eta]$ was evaluated using the graph of η_{sp}/c vs concentration according to the relationship[9]

$$\eta_{sp}/c=[\eta]+k_{Hg}\cdot[\eta]^2.c \tag{2}$$

---

[1] W. E. Hanford and D. L. Fuller, *Ind. Eng. Chem.*, **40,** 1179 (1948).

[2] F. M. Shostakovskii, *Izvest. Akad. Nauk S.S.S.R., Otdel. khim. Nauk*, **1953,** 108.

[3] F. M. Shostakovskii, F. P. Sidelkovskaya and M. G. Zelenskaya, *Doklady Akad. Nauk S.S.S.R.*, **1952,** 643.

[4] A. I. Vogel, "Practical Organic Chemistry", III Ed., Akademie Verlag, Berlin 1956, p. 383.

[5] C. Boghină, D. Thesis, Polytechnic Institute, Bucharest, 1975.

[6] B. H. Zimm, *J. Chem. Phys.*, **16,** 1099 (1948).

[7] W. Bushuk and H. Benoit, *Canad. J. Chem.*, **36,** 1616 (1958).

[8] M. Leng and H. Benoit, *J. Chim. phys.*, **58,** 480 (1961).

[9] M. L. Huggins, *J. Amer. Chem. Soc.*, **64,** 2716 (1942).

3. RESULTS AND DISCUSSION

The content of nitrogen and the differential refractive index increment (table 1) show that all fractions of the copolymer have the same composition : VCL/DEF = 1/1 (mole/mole). The copolymerization constants [5] $r_1 = 0.004$ and $r_2 = 0.07$ also prove that this copolymer is nearly an alternating copolymer.

Table 1

The nitrogen content and values of d*n*/d*c* for (VCL–DEF) alternating copolymers fractions

Fraction	Content of nitrogen (Wt. %)	VCL/DEF (mole/mole)	d*n*/d*c* (cm^3/g) in MEK
4	4.66	1 : 1	0,121
5	4.55	1 : 1	0.122
6	4.39	1 : 1	0.120
7	4.83	1 : 1	0.120
8	4.55	1 : 1	0.119
9	4.67	1 : 1	0.122
10	4.53	1 : 1	0.121
11	4.59	1 : 1	0.118
12	—	—	0.118
13	—	—	0.120
Unfractionated	4.50	1 : 1	0.121

The molecular weights ($\bar{M}_w$) and the intrinsic viscosities for the fractions of this copolymer are shown in table 2.

Table 2

Viscosities and molecular weight ($\bar{M}_w$) for (VCL–DEF) alternating copolymer fractions

Fraction	Molecular weight $\bar{M}_w \times 10^{-3}$	Intrinsic viscosity, $[\eta]$ (cm^3/g)	
		Benzene	Chloroform
3	175.6	58.0	63.0
4	260.3	74.0	84.2
5	380.5	96.7	110.0
6	552.5	135.0	123.3
7	631.6	142.0	163.0
8	772.2	162.0	191.0
9	854.7	170.0	198.0
10	997.0	189.0	208.0
11	1039.5	222.6	253.0
12	1127.0	224.0	255.0
13	1263.0	238.0	272.0

3.1. KUHN-MARK-HOUWINK-SAKURADA EQUATIONS

The plots of $\log [\eta]$ vs $\log \bar{M}_w$ for (VCL–DEF) alternating copolymer fractions in benzene and chloroform are shown in fig. 1.

According to the K. M. H. S. equation:

$$[\eta] = KM^a \tag{3}$$

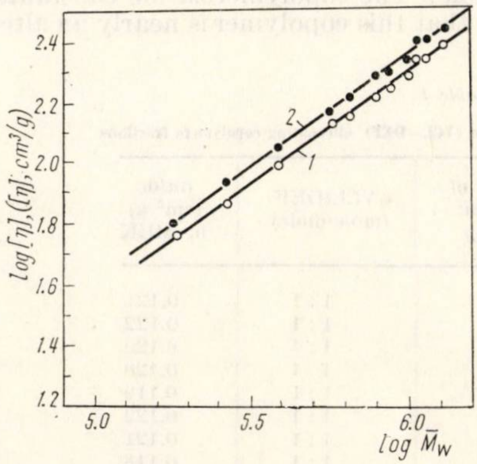

Fig. 1. – The graph of log $[\eta]$ as a function of log $\overline{M}_w$ for (VCL-DEF) alternating copolymer fractions in benzene (*1*) and chloroform (*2*).

the following relations were obtained : ($[\eta]$ in cm³/g at 30°)

$$[\eta] = 9.03 \times 10^{-3} M^{0.724} \quad \text{in benzene}$$

$$[\eta] = 9.33 \times 10^{-3} \; M^{0.730} \quad \text{in chloroform}$$

All linear extrapolations in this study were made by the least-squares method to obtain the best mathematical fit of the data.

3.2. UNPERTURBED DIMENSIONS

The unperturbed dimensions of the copolymer chains were obtained from measurements in nonideal solvents using the following extrapolation : Flory-Fox[10]-Schaefgen[11] (Method FFS), Stockmayer-Fixman[12] (Method SF), Kurata-Stockmayer-Roig[13,14] (Method KSR), Inagaki-Suzaki-Kurata[15] (Method ISK) and Patel[16] (Method P).

The graphs are shown in fig. 2 (Methods FFS and P), fig. 3 (Method SF), fig. 4 (Method KSR) and fig. 5 (Method ISK).

Generally, the graphs are linear and the intercept with the ordinate does not vary with the nature of the solvent in benzene and chloroform.

[10] P. J. Flory and T. G. Fox, *J. Amer. Chem. Soc.*, **73**, 1904 (1951).

[11] I. R. Schaefgen and P. J. Flory, *J. Amer. Chem. Soc.*, **70**, 2709 (1948).

[12] W. H. Stockmayer and M. Fixman, *J. Polymer. Sci. C.*, **1**, 137 (1963).

[13] M. Kurata, W. H. Stockmayer and H. Roig, *J. Chem. Phys.*, **33**, 151 (1960).

[14] M. Kurata and W. H. Stockmayer, *Adv. Polymer Sci.*, **3**, 196 (1963).

[15] H. Inagaki, H. Suzuki and M. Kurata, *J. Polymer Sci. C.*, **15**, 409 (1966).

[16] J. R. Patel, C. K. Patel and R. D. Patel, *Makromol. Chem.*, **115**, 178 (1968).

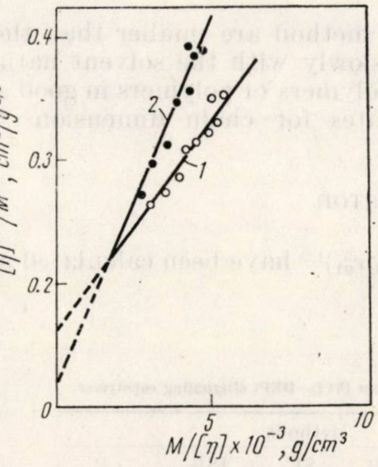

Fig. 2. — The graph of $[\eta]^{2/3}/M^{1/3}$ as a function of $M/[\eta]$ for (VCL — DEF) alternating copolymer fractions (Method FFS and P) in benzene (*1*) and chloroform (*2*).

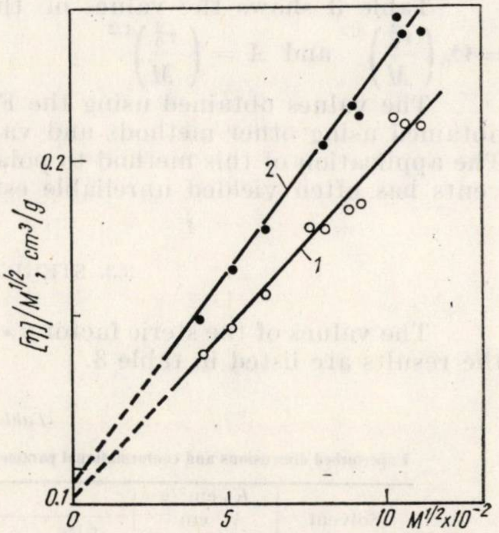

Fig. 3. — The graph of $[\eta]/M^{1/2}$ as a function of $M^{1/2}$ for (VCL-DEF) alternating copolymer fractions (Method SF) in benzene (*1*) and chloroform (*2*).

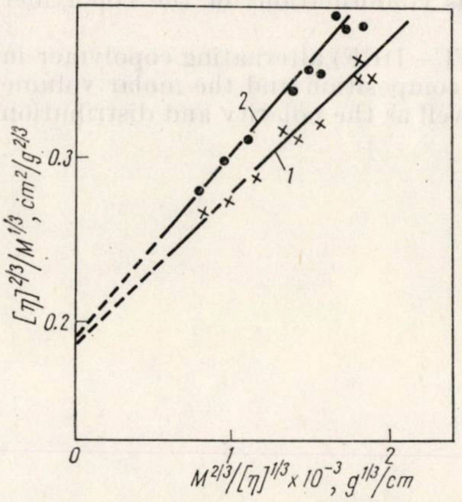

Fig. 4. — The graph of $[\eta]^{2/3}/M^{1/3}$ as a function of $M^{2/3}/[\eta]^{1/3}$ for (VCL-DEF) alternating copolymer fractions (Method KSR) in benzene (*1*) and chloroform (*2*).

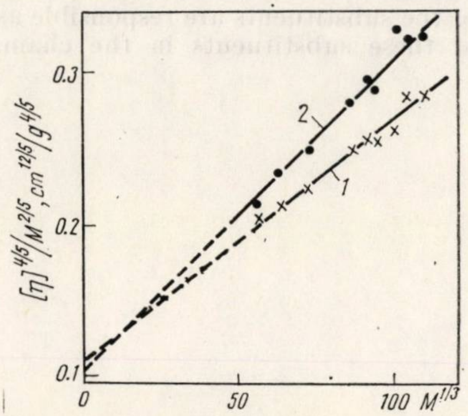

Fig. 5. — The graph of $[\eta]^{4/5}/M^{2/5}$ as a function of $M^{1/3}$ for (VCL—DEF) alternating copolymer (Method ISK) in benzene (*1*) and chloroform (*2*).

Table 3 shows the values of the unperturbed dimensions $K_\theta = \text{Ø}_0 \left(\frac{\bar{r}_0^2}{M} \right)^{3/2}$ and $A = \left(\frac{\bar{r}_0^2}{M} \right)^{1/2}$

The values obtained using the FFS method are smaller than those obtained using other methods and vary slowly with the solvent nature. The application of this method to polar polymers or polymers in good solvents has often yielded unreliable estimates for chain dimensions. [14,16]

3.3. STERIC FACTOR

The values of the steric factor $\sigma = (\bar{r}_0^2/\bar{r}_{01}^2)^{1/2}$ have been calculated and the results are listed in table 3.

Table 3

Unperturbed dimensions and conformational parameter σ for (VCL–DEF) alternating copolymer

Solvent	K_θ, cm^3/g A, cm σ	Methods				
		FFS	KSR	SF	ISK	P
Chloroform	$K_\theta \times 10^2$	4.2	7.75	9.5	9.3	10.3
	$A \times 10^{11}$	525.3	646.1	691.7	687.8	771.0
	σ	2.12	2.61	2.79	2.78	2.87
Benzene	$K_\theta \times 10^2$	6.4	7.74	9.5	9.34	10.3
	$A \times 10^{11}$	606.4	646.1	691.7	687.0	711.0
	σ	2.45	2.61	2.79	2.78	2.87

These values show that the trans conformations of the copolymer segments predominate in the chains.

For this increased rigidity of (NVC–DEF) alternating copolymer in benzene and chloroform the chemical composition and the molar volume of the substituents are responsible as well as the polarity and distribution of these substituents in the chain.

Revue Roumaine de Chimie, **23**, *2*, 261—264 (1978)

AMORPHOUS-CRYSTALLINE COUPLING IN POLYETHYLENE. V[1]

LAMELLAR RECRYSTALLIZATION IN SHEAR HISTORY

GH. DRĂGAN
Institute of Chemical Research, ICECHIM, Spl. Independenţei 202, Bucharest, Romania

Received October 22, 1975

The field of shearings associated with twist disclination at the interface between the lamellar fragment and the local amorphous domain developed by precipitation of chemical decorated defects is pointed out. The binary system of chlorinated high density polyethylene (CPE) and poly(vinyl chloride) (PVC) is studied for a clearer amorphous-crystalline coupling. According to the theoretical results (Chou 1971) and to the previous model for this coupling in CPE samples, it has been considered that twist disclination state relaxes through a viscous mode by reciprocal lamellar rotation and approaches along maximum shear lines. Thus, it is supposed that in compression moulded plates made of rolled sheets, these lines are developed as dark lines, because of the separation of the lamellar-fragment local amorphous interaction domains from the rest of amorphous lattice of PVC.

In the field of polymeric materials processing, the notion of *composite material* has been used in recent time. Morphologically speaking , this notion supposes the existence of many phases. The crystalline polymers represent a typical case whose morphology consists of crystalline and amorphous phases, and whose interaction is studied in the present series,[1–4] for the particular case of polyethylene (PE).

It has been established that after treatments the two phases tend to be more separated, and their interaction *to equilibrium* consists in an interlamellar order. Between the two processes that occur during annealing of this amorphous-crystalline morphology, [4] the most important one, responsible for interlamellar order (detected by order-disorder transition T_m^1),[2] is the migration of the lamellar defects. This process is localized at a lamellar level for the case of a high density PE with chemical decorated defects by photochlorination.[3,4] The interlamellar order is achieved between the resulted lamellar fragments by coherent precipitation of defects in local amorphous domains. The proposed interaction between lamellar fragments and local amorphous domains for the particular case of lamellar defects annealing,[4] is similar with the initial model for interlamellar order detected in the *row crystallized* material by nucleation along the shear lines.[5] In this last case it is observed that the lamellae are equidistantly distributed along a shear line which is parallel to |001| direction, and their interaction with amorphous domains takes place principally on a habit face parallel to this direction. In this way the T_m^1 effect observed for injection moulded samples,[2] is explained by twist disclination relaxation associated to this interaction; this, because in flash calorimetry, a heat pulse is followed by an annealing period. A similar type morphology is observed in a material subjected to shear stresses for temperatures below T_m^0 (plastic deformation).[5] The kinetics of migration of the defects induced by γ-irradiation in PE,[6] point out $\boldsymbol{T} = (|100| + (1/m)\,|010|)(001)$[1,4] ($m \simeq 2.5$) as the main glide direction which establishes the habit face for interaction in disclination state.

---

[1] GH. DRGA N, Part IV, *Rev. Roumaine Chim.*, **21**, 1537 (1976).
[2] GH. DRĂGAN, *Materiale Plastice*, **10**, 87 (1973).
[3] GH. DRĂGAN, *Rev. Roumaine Chim.*, **20**, 687 (1975).
[4] GH. DRĂGAN, *Rev. Roumaine Chim.*, **21**, 1381 (1976).

This work reports additional observations on amorphous-crystalline coupling in high density PE with chemically decorated defects by chlorination. The CPE samples [1,3,4] are compounded with poly (vinyl chloride) (PVC) for a clearer evidence of the local amorphous-crystalline coupling in local order against the order induced in row crystallization. In this way the lamellae are separated by PVC species, since the initial amorphous domains in CPE samples for 40% chlorine content are also PVC species.[3] The observations presented here, lead to the conclusion that the local interlamellar order is maintained above T_m^0 in the absence of shear stresses, and the lamellar fragments become oriented during recrystallization by the twist disclination memory effect, thus developing the maximum shear lines induced in the first row crystallization.

EXPERIMENTAL

CPE and PVC compounds in portion of 20% and 80%, respectively, are studied with emphasis on the sample previously denoted CPE 3.[4] These compounds were processed in three distinct stages:

1. The defects annealing in PE before and/or after chlorination. This treatment was performed in fluidized bed for 3 hours at 125°.

2. The compounding was performed on a mixing mill at a temperature of 10° above T_m^0(T_m^0 is the observed melting point by DTA). The shear ratio, the distance between cylinders and the mixing time were identical data for all the samples. The thickness of the resulted sheets ranges within 0.8—1.2 mm.

3. The compression moulding of superposed rolled sheets. The preheating temperature was 10° above T_m^0.

The observations were performed on the sections of the resulted plates after careful splintering.

Table 1

The thermal treatments applied on PE before and/or after chlorination(125° for 3 hours in 1-st stage)

Sample	Before chlorination	After chlorination
I	unannealed	unannealed
II	unannealed	annealed
III	annealed	unannealed
IV	annealed	annealed

---

[5] GH. DRĂGAN, "Morphology of Polymers. Principles of Characterization and Processing", Lectures, ICECHIM, Bucharest, June 1974.

[6] T. NAGASAWA and K. KOBAYASHI, *J. Appl. Phys.*, **43**, 2067 (1972).

Fig. 1.— The cross-section of the processed samples I—IV.

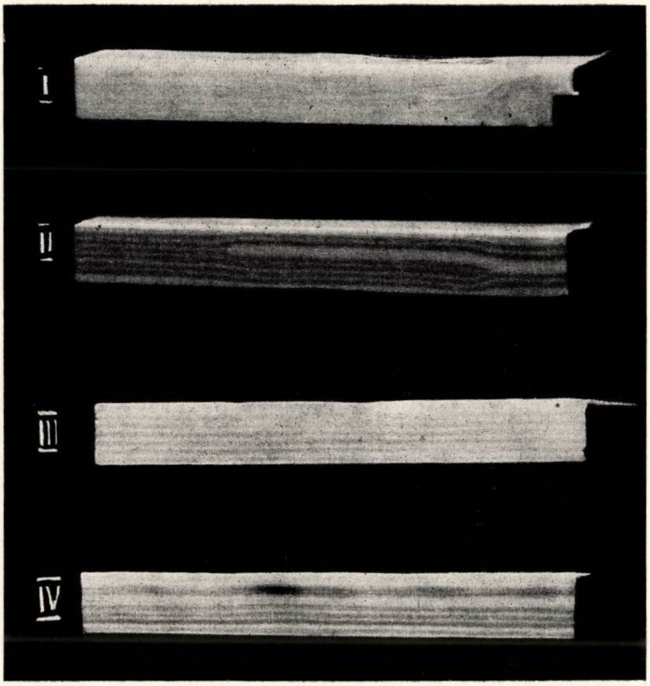

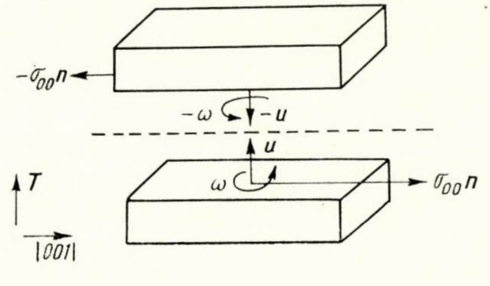
$-\sigma_{00}n$
$-\omega$
$-u$
u
T
ω
$\sigma_{00}n$
|001|

Fig. 2. — Schematic outline of the disclination state in the recrystallization history of lamellar fragments.

DISCUSSIONS

The compounds resulted after mixing (2nd stage) had a homogeneous appearence. It may be considered that when withdrawing the sheet from the mixing mill the material is suddenly cooled, freezing by row crystallization the interlamellar order along the shear lines. Dark-coloured lines appear in the cross sections of the compression moulded plates, parallel to initial shear lines and in equal number with the superposed rolled sheets. This development phenomenon for the shear direction in rolled sheets is observed to be strongly correlated with annealing in CPE (1st stage) namely with the local amorphous domains performed in lamellar morphology.[4] Although these observations have been performed on numerous samples, differing by the PE sort, the applied treatments (1st stage) and the ratio between the CPE and PVC quantities, to draw conclusions four samples were selected which differ only by the conditions of the 1st stage (Table I). For all these compounds CPE samples with equal chlorine content (40 ± 0.5%) were produced.

This phenomenon may be explained on the basis of the model for the amorphous-crystalline coupling previously established,[3,4] by studying the coherent precipitation process of the decorated defects on glide direction T.[6] Towards equilibrium, the local amorphous domains interact with lamellar fragments by shear stresses.[4] This order of lamellar fragments has been called *local interlamellar order*. Amorphous domains of initial PE which have been preferentially attacked by chlorination, become essentially PVC species,[4] and lose their identity by compounding with PVC. In this way immediately after rolling (2nd stage) the lamellae (sample I) or lamellar fragments (samples II—IV) are homogeneously distributed in the material. Because of sudden cooling, the crystallization "freezes" the lamellar order, adequate to row crystallization along shear lines. During recrystallization the amorphous local domains reveal their identity regrouping lamellar fragments, characteristic of the samples II—IV, in interlamellar local order by relaxation of the twist disclination state[4].

Fig. 2 reproduces schematically this regrouping process taken over from the previously proposed model (Ref. 4, fig.10) having in view the attraction process for lamellar fragments towards a preferential shear line induced in the rolled sheet. Recently it has been theoretically established [7] that for two materials with different Poisson constants and whose interaction consists mainly of shear stresses on the separation interface, the elastic energy relaxes by reciprocal approaching and rotating about an axis normal on the interface. This interaction (twist disclination) is just the present case for the local amorphous-crystalline coupling.[4] From these observations and the representation in fig. 2, it results that an attraction takes place between lamellar fragments by the local amorphous layer towards the maximum shear lines frozen during row crystallization. From the theoretical data [7] there results that on approaching these fragments for minimizing the elastic energy (in this case the minimum shear stresses), a reciprocal rotation of lamellar fragments takes place about ***T*** direction with an angle $\omega \sim \sigma_{00}$, the so-called disclination power. This should correspond to the observations on the reciprocal rotation of lamellae about |010| direction with an angle depending on the value of the shear stresses imposed in plastic deformation.[5] The direction ***n*** of the shear stresses, coincides with the chain axis, and the interlamellar order resulted during the first crystallization corresponds to the nematic structure with the *director* ***n***. In addition, for the compounds with greater CPE contents, the occurrence of a cleavage process of the plates along the shear direction has been observed.

---

[7] T. W. Chou, *J. Appl. Phys.*, **42**, 4931 (1971).

CONCLUSIONS

The experimental data presented here complete the model previously defined [4] for the twist disclination existing in the local amorphous-crystalline coupling in PE with chemical decorated defects. This completion is based on the following two main considerations : (i) the memory effect of the local interlamellar order above T_m^0 in isostatic conditions (in the absence of an external shear field), and (ii) the colour effect for the separation lines of the interaction between the local amorphous domains and the lamellar fragments from the rest of the PVC homogeneous lattice.

For the first consideration recent studies [8] show that just for the case of PE, the structure of the interlamellar order (called sometimes internodular order) is observed also above T_m^0. Both for the case of polymers and for micromolecular materials, the paracrystalline structure for the solid state is maintained above T_m^0 in the absence of flow.[9] Hoseman and coworkers have studied in detail this structure in the melts of the metals. Very recently they found a nematic structure for the PE static melt.[10] Because of this second assumption it is considered that the local interlamellar order is maintained whereas the elastic energy associated to this interaction vanishes by a viscous mode.[4]

The development process of the maximum shear lines is supported by the second hypothesis. The arguments on which this assumption is based have been previously pointed out, and are as follows :[4]

— the local amorphous domains have both the chemical and morphological structure which differ from the amorphous phase of PVC ;

— these local amorphous domains remain separated from the initial amorphous phase of PE, as a result of the relaxation process, and

— because of this relaxation of the twist disclination state, and regrouping of the lamellar fragments along the maximum shear lines (after the disclination theory),[6] these lines are mainly made of lamellar fragments and local amorphous domains for which a colour effect may be considered. Subsequent studies will establish directly the composition for these lines developed by the colour effect observed.

[8] K. Neki and P. H. Geil, *J. Macromol. Sci. — Phys.*, **B8**, 295 (1973).

[9] A. F. Scrishevski, "The Structural Analysis of the Liquids", Vishaia Shkola, Moscow, 1971.

[10] R. Hoseman, J. Loboda-Cackovic and H. Cackovic, *Ber. Bunsengesellschaft Phys. Chem.*, **77**, 1044 (1973).

Revue Roumaine de Chimie, 23, 2, 265–268 (1978)

SEPARATION AND DETERMINATION OF PHENOL AND SALICYLIC ACID IN INDUSTRIAL WASTES

S. GOCAN [*], T. HODIŞAN [*], H. NAŞCU [*] and CARMEN GEORGESCU [**]
[*] Department of Analytical Chemistry, "Babeş-Bolyai"
University, Cluj-Napoca, str. Arany Janos 11
[**] "Sinteza" Chemical Enterprise, Oradea

Received August 1, 1975

The separation of the two components occurred on a thin layer of silicagel R using as a mobile phase benzene-ethyl acetate (1 : 1, v/v). The column separation was performed on silicagel RC (pH = 9 and particle size 160–70 μm) by stepwise elution : phenol with benzene-ethyl acetate (8 : 1, v/v) and salicylic acid with benzene-methanol (3 : 1, v/v). The two components were determined photocolorimetrically and volumetrically.

Owing to the extended water consumption, the frequent pollution of this major component of the environment requires a special attention. As a result of the tremendous development of the chemical industry in our country it has been estimated that about 18 tons of phenols and their derivatives are daily discharged into rivers.[1] Their presence in the respective water courses provides significant damage and harmful influences on aquatic flora and fauna.

In this context, the present paper provides the possibility of separating and quantitatively determining phenol and salicylic acid, components appearing either as raw material (phenol)or as reaction intermediates (salicylic acid) in the process of producing acetosalicylic acid (aspirin). By developing this method it becomes possible to control the degree of water-pollution, particularly by phenol.

In order to establish a method for the separation and determination of these two components by column chromatography, we first achieved the separation by thin layer chromatography and this enabled us to effect the transposition on column. The literature reports a number of papers[2-4] which discuss the problem of transposing the results obtained by thin layer chromatography when developing a column chromatographic method.

Separation by thin-layer chromatography. The two components were separated using silicagel R as support and the benzene-ethyl acetate system (1 : 1, v/v) as mobile phase.

---

[1] G. Ghimicescu and I. Hîncu, "Chimia şi controlul poluării apei", Ed. Tehnică, Bucharest, 1974, p. 3.

[2] O. E. Schultz and R. Camberg, *J. Chromatogr.*, **32,** 346(1967).

[3] H. Schlitt and F. Geiss, *J. Chromatogr.*, **67,** 261(1972).

[4] F. Geiss and H. Schlitt, *J. Chromatogr.*, **82,** 5(1973).

Stahl and Dumont[5] have shown that the pH of the chromatographic support largely influences the R_f values in the case of ionisable components. If the silicagel thin layer has a larger pH than the pK_A values of the acid components subjected to separation, R_f values will generally become zero for all the components and the separation will not occur. To obtain differences between R_f values of the components, the pH of the support have to be smaller than their pK_A values.

In the case of a mixture of phenol ($pK_A = 9.99$) and salicylic acid ($pK_{A_1} = 2.98$ and $pK_{A_2} = 13.44$), a study was undertaken on the R_f variation as a function of the pH of the layer. Chromatographic plates of silicagel R having different pH values were prepared for this purpose.

Developing took place in an S chamber on glass plates (10 × 14 cm).

The visualisation reagent used consisted of a mixture of: $FeCl_3$ and 10% solution and $K_3[Fe(CN)_6]$ 2% solution in a ratio 2 :1, v/v. After spraying this reagent onto plate, the phenol spot is identified by its blue colour while the spot of salicylic acid is brown.

The results obtained are illustrated in fig. 1. The arrows indicate the spot size in R_f units. An analysis of results has shown that phenol is washed off by the eluent and carried in the front. In turn, in the case of salicylic acid, the two steps in variation of R_f values versus pH values corresponding to pK_{A_1} and pK_{A_2} values are visible.

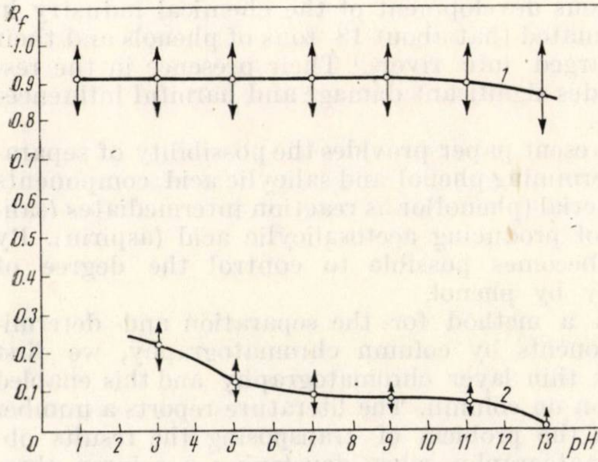

Fig. 1. — Variation of R_f values as a function of the pH of the silicagel thin layer. Eluent: benzene-ethyl acetate (1: 1, v/v).

1. Phenol; *2.* Salicylic acid.

Separation by column chromatography. The results obtained by thin layer chromatography have enabled us to develop a column separation method by stepwise elution.

The column was manufactured from glass tube having a length of 18 cm and an inner diameter of 1 cm. It was filled with silicagel R(pH=9) having a granulation of 160−70 μm. To obtain a total separation of phenol and salicylic acid mixture, it is sufficient to have a 14 cm long column filling which was slightly compressed in advance by tapping the column.

---

[5] E. Stahl and E. Dumont, *J. Chromatogr. Sci.*, **7**, 517(1969).

The stationary phase permits the stepwise elution of components which makes method safe and handier. Phenol was eluted using the benzene-ethyl acetate system (8 : 1, v/v) whereas the elution of the salicylic acid required a much stronger eluent; the benzene-methanol system (3 :1, v/v) was used to this effect.

Approximately 10 ml of the first eluent is passed into column prepared as described above, introducing then 0.5 ml of a synthetic sample (phenol 0.5%; salicylic acid 0.1%). The elution of both components takes place at a 0.5 ml/min flow rate.

The elution curves plotted in fig. 2 shows that phenol has a retention volume $V_R = 15$ ml and the elution is practically complete in a 35 ml volume. Elution is then continued with the second eluent. The salicylic acid is found to be totally eluted in a volume of approximately 35 ml.

Determination of phenol and of salicylic acid. 75 ml water is added to the phenol (respectively salicylic acid) sample withdrawn from the column efluent, leaving it on the water bath until total evaporation of the organic phase. The aqueous solution is then made up to the mark in a 100 ml graduated flask.

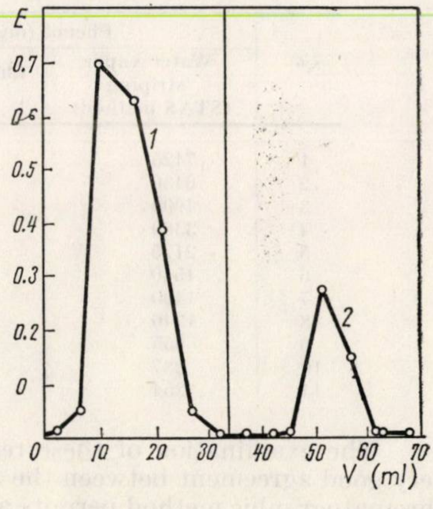

Fig. 2. —Elution curves. Column : length 14 cm and diameter 1 cm; Filling: Silicagel RC (pH = 9 and particle size 160—70 um).

1. Phenol eluted with benzene—ethyl acetate (8: 1, v/v).
2. Salicylic acid eluted with benzene — methanol (3 : 1, v/v). Flow rate 0.5 ml/min.

The determination of phenol and of salicylic acid takes place volumetrically by the method involving bromate-bromide or photocolorimetrically: phenol with the diazonium salt of sulphanilic acid and salicylic acid with $FeCl_3$ at pH = 2.—2.5 or with any other adequate reagent. The results obtained are listed in table 1.

Both the photocolorimetrical and the volumetrical method were further applied to the determination of phenol and of salicylic acid in industrial wastes, after their previous column separation. The chromatographic method was, in this way, compared with the STAS method (water vapor striping) for phenol determination. The results are given in table 2 :

Table 1

Results obtained from the determination of phenol and of salicylic acid

Introduced amount (mg)	Found amount			
	Photometric (mg)	Error (%)	Volumetric (mg)	Error (%)
Phenol 2.50	2.43	−2.8	2.55	+2.0
	2.60	+4.0	2.25	−10.0
	2.35	−6.0	2.40	− 4.0
	2.45	−2.0	2.56	+ 2.4
Salicylic acid 1.00	0.92	−8.0	0.90	−10.0
	0.95	−5.0	0.95	−5.0
	0.98	−2.0	0.97	−3.0
	1.05	+5.0	1.06	+ 6.0

Table 2

Determination of phenol and of salicylic acid by column chromatography and STAS method

N⁰	Phenol (mg/l)		Salicylic acid (mg/l)
	Water vapor striping ; (STAS method)	Chromatographic method	Chromatographic method
1	7425	7426	2580
2	6430	6450	1830
3	4900	4880	1082
4	3380	3340	1172
5	2125	2160	875
6	1540	1590	626
7	1490	1463	314
8	1240	1200	263
9	955	864	115
10	287	298	65
11	254	251	92

The examination of these results leads us to the conclusion that a very good agreement between the two methods exists. In addition the chromatographic method permits also the consecutive determination of salicilic acid.

The determination limit was found to be 40 μg/sample.

Revue Roumaine de Chimie, 23, 2, 269–271 (1978)

A MODIFIED NON CYANIDE SCHEME FOR THE QUALITATIVE CHEMICAL ANALYSIS OF THE GROUP II A SULPHIDES

A. M. QURESHI* and S. A. MALIK**

*Department of Chemistry, University of Nigeria, Nsukka, Nigeria
** Department of Chemistry, Makerere University, Kampala, Uganda

Received September 25, 1975

The paper describes a modified scheme of analysis of group II A sulphides. An effective separation of lead(II) from bismuth(III) with 5 M aqueous sodium hydroxide and non cyanide detection of cadmium(II) in presence of copper(II) using 0.5 M hot ammonium oxalate solution is discussed. The lower limit of cations concentration is 1.50 mg per ml except copper(II) which is easily detected up to 0.40 mg per ml. Cadmium(II) to copper (II) limit ratio is 1 : 1.

INTRODUCTION

The qualitative scheme of chemical analysis is still an important aid in the teaching of chemistry. Attempts have always been made to get the traditional procedures of a more simple and less expensive analysis. Toxic hydrogen sulphide had been replaced by thioacetamide [1] and altogether a new scheme avoiding the precipitation of sulphides has been reported [2]. The non-cyanide detection of cadmium(II) in the presence of copper(II) has received much attention[3-6] to avoid highly poisonous KCN in the laboratories at the elementary level but it seems that most of the reagents have not yet come in use [7,8]. Further HNO_3 has solvent effect on $PbSO_4$ so the precipitation of lead(II) is never complete unless the solution is evaporated to expell all the nitric acid. If much care is not taken, the bismuth(III) ion may be partially converted to insoluble basic bismuth sulphate which precipitates out along with lead sulphate. Tracer technique

---

[1] H. H. Barber and E. Grzeskowiak, *Analyt. Chem.*, **21**, 192 (1949).

[2] P. Lumme and J. Tummavouri, *Acta. Chem. Scand.*, **27**, 851 (1973).

[3] R. Chandra, *J. Chem. Educ.*, **38**, 409 (1961).

[4] T. H. Whitehead and G. K. Hatcher, *J. Chem. Educ.*, **39**, 399 (1962).

[5] R. L. Dutta and S. D. Choudhury, *J. Chem. Educ.*, **40**, 414 (1963).

[6] R. E. D. Clark, "Semimicro Inorganic Qualitative Analysis", Pergamon Press, London, 1965.

[7] C. H. Sorum, "Introduction to Semimicro Qualitative Analysis", 4th Edition, Prentice Hall, New York, 1967.

[8] A. I. Vogel, "Text Book of Macro and Semimicro Qualitative Inorganic Analysis", 4th Edition, Longmans, London, 1964.

Table 1

Separation of group II a sulphides

Boil for one minute the precipitates of HgS, PbS ,Bi_2S_3, CuS and CdS with 3M HNO_3 and centrifuge

<table>
<tr><td rowspan="5">*Residue:* Dissolve in aqua regia, evaporate to dryness and perform confirmatory test for mercury(II)</td><td colspan="5">*Centrifugate:* Treat with 5M NaOH dropwise until the supernatant liquid does not give any precipitate on further addition. Now add 5 drops in excess. Shake and centrifuge.</td></tr>
<tr><td colspan="4">*Residue:* Add 5 M HCl to just dissolve the precipitates. Warm the solution and treat with 6M NH_4OH until the solution is well alkaline then add 10 drops in excess. Shake and centrifuge.</td><td rowspan="4">*Centrifugate:* Acidify with 5M CH_3COOH and perform confirmatory test for lead(II).</td></tr>
<tr><td rowspan="3">*Residue:* Dissolve in 5M HCl and perform confirmatory test for bismuth (III).</td><td colspan="3">*Centrifugate:* (a) If colourless, Cu(II) is absent, perform directly confirmatory test for Cd(II).
(b) If deep blue, Cd(II) may be present but Cu(II) is definitely present. So divide the centrifugate into two parts.</td></tr>
<tr><td rowspan="2">I
Acidify the first part with 5M CH_3COOH and perform confirmatory test for copper(II).</td><td colspan="2">II
In the second part add a few drops of 5M CH_3COOH until the solution is just acidic. Now treat with hot 0.5M $(NH_4)_2C_2O_4$ dropwise until the supernatant liquid gives no precipitate on further addition. Add 10 drops of the reagent in excess. Shake and centrifuge.</td></tr>
<tr><td>*Residue:* Dissolve in 2M HCl and perform confirmatory test for cadmium(II).</td><td>*Centrifugate:* Blue, copper (II) is present. Evaporate with Conc. HNO_3 to decompose oxalato complex and perform additional confirmatory test for copper(II).</td></tr>
</table>

has shown that the separation of lead(II) and bismuth(III) as sulphate is not very effective and sodium hydroxide has been found an excellent reagent for their separation[9].

We have modified the scheme of qualitative analysis of group II A sulphides to give effective separation of lead(II) from bismuth(III) and detect cadmium(II) in presence of copper(II) without using potassium cyanide.

DISCUSSION

2 ml of aqueous solution containing 50 mg of the mixture of the nitrates of Hg(II), Pb(II), Bi(III), Cu(II) and Cd(II) was treated with 1 drop of 2 M HCl. Hydrogen sulphide was then bubbled in hot solution for 2 minutes to precipitate the corresponding sulphides.

The group II A sulphides dissolve in 3M HNO_3 except HgS. The resulting solution when treated with excess of 5M NaOH, precipitated the hydroxides of Bi(III), Cu(II) and Cd(II) and left the lead(II) in solution as, $Pb(OH)_4^{2-}$, the tetrahydroxo-plumbate(II) ion. It is well known that $Cu(OH)_2$ and $Cd(OH)_2$ with excess of NH_4OH forms $Cu(NH_3)_4^{2+}$ and $Cd(NH_3)_4^{2+}$ ions whereas $Bi(OH)_3$ has no effect but the coprecipitation of sodium hydroxide with Bi(III), Cu(II) and Cd(II) hydroxides prevented the direct separation of these hydroxides. They were, therefore, first dissolved in 5 M HCl and then treated with excess of NH_4OH to keep copper (II) and cadmium(II) in solution and precipitate only $Bi(OH)_3$. In the absence of mineral acids cadmium(II) was precipitated as white cadmium oxalate and copper(II) remained in solution in the form of complex $Cu(C_2O_4)_2^{2-}$ ion.

Table 1 describes the detail procedure of separation. Confirmatory tests were performed as given in reference [8]. The procedure is useful for cations up to a minimum concentration of 1.50 mg per ml except copper (II) which can easily be detected even up to 0.40 mg per ml. The lower limit ratio for Cd(II) to Cu(II) has been found to be 1 : 1.

---

[9] A. O'Donnell, *J. Chem. Educ.*, **40**, 415 (1963).

Revue Roumaine de Chimie, **23**, *2*, 273–279 (1978)

ION SELECTIVE MEMBRANE-ELECTRODES FOR ORGANIC ANALYSIS. I

LIQUID MEMBRANE-ELECTRODE FOR SOME ORGANIC ANIONS BASED ON CETYLPYRIDINIUM SALT

ELENA HOPÎRTEAN and ELISABETA VERESS

Department of Analytical Chemistry, University of Cluj-Napoca, str. Arany J. nr. 11, Cluj-Napoca, Romania

Received August 14, 1975

The results obtained by studying the performance of the liquid membrane-electrode from cetylpyridinium bromide in nitrobenzene, are presented. The electrode gives a good response towards : biphthalate, phenylacetate, benzoate, *o*- and *p*-chlorobenzoate, sebacate, salicylate, 3,5-dinitrobenzoate, *o*-nitrobenzoate, 5,5-diethylbarbiturate, cholate, sulphanilate anions. The nernstian response of the electrode towards biphthalate has to be underlined (slope 59.5 mV in the $10^{-1}-10^{-4}$ concentration range) in the case in which the liquid membrane has been obtained with an organic solution resulting from extraction of an aqueous biphthalate solution and a cetylpyridinium bromide solution in nitrobenzene.

INTRODUCTION

Simultaneously with the liquid membrane-electrodes development for inorganic anions, the field of liquid electrodes for organic anions has lately been widely developed. This fact has to be underlined especially as many of these anions are water pollutants. On the other hand, a number of organic anions are of interest from industrial or biological points of view.

In order to obtain liquid membrane-electrodes for organic anions, the following types of substances have been used as active electrode components : quaternary ammonium salts, [1–12] the salts of crystal vio-

---

[1] C. J. Coetzee and H. Freiser, *Analyt. Chem.*, **40**, 2071 (1968).

[2] C. J. Coetzee and H. Freiser, *Analyt. Chem.*, **41**, 1128 (1969).

[3] M. Matsui and H. Freiser, *Analyt. Lett.*, **3**, 161 (1970).

[4] H. J. James, G. P. Carmack and H. Freiser, *Analyt. Chem.*, **44**, 853 (1972).

[5] H. J. James, G. P. Carmack and H. Freiser, *Analyt. Chem.*, **44**, 856 (1972).

[6] B. J. Birch and D. E. Clarke, *Analyt. Chim. Acta*, **61**, 159 (1972).

[7] N. Ishibashi, A. Jyo and K. Matsumoto, *Chem. Lett.*, **1973**, 1297.

[8] T. Fujinaga, S. Okazaki and H. Freiser, *Analyt. Chem.*, **46**, 1842 (1974).

[9] T. Shigematsu, A. Ota and M. Matsui, *Bull. Inst. Chem., Res. Kyoto Univ.*, **51**, 268 (1973) ; *Chem. Abstr.* **81**, 72303 (1974).

[10] Gr. Popa, B. Geafar and C. Luca, *Rev. Chim.* (*Bucureşti*), **25**, 748 (1974).

[11] C. Luca, Gh. Semenescu and C. Nedea, *Rev. Chim.* (*Bucureşti*), **25**, 1015 (1974).

[12] L. P. Sedysheva, B. M. Vrevskii and E. S. Roskin, *Zhur. priklad. Khim.*, **45**, 2331 (1972).

let,[13-18] the salts of the complex cations of iron with phenantroline,[14,16,18,19] or even plasticizers of polyvinylchloride.[20] The response was studied of different electrodes towards a series of surfactants : *p*-toluenesulphonate,[1,2,4,8,11] benzenesulphonate,[13,17] dodecylbenzenesulphonate,[12,13] dodecylsulphate,[6,10] α-naphthalenesulphonate,[7,17] *i*-laurylbenzenesulphonate,[8] *n*-laurylbenzenesulphonate,[8] *n*-octylsulphate,[8] laurylsulphate.[8]

The response was studied of some liquid electrodes towards the anions of the following amino acids : tryptophan,[3,4] phenylalanine,[3-5] leucine,[3-5] methionine,[3,4] glutamic acid[3], glycine[4], serine,[4] alanine,[4] valine[4]. The response of the liquid membrane-electrodes was studied also in the following series of anions : acetate,[1,2,4,5] formate,[1,2,4] propionate,[1,2,4] oxalate,[1,2,5] benzoate,[1,2,4,9] salicylate,[1,2,4,5,9,14] *p*-aminosalicylate,[14] maleate,[15,18] biphthalate,[7,15,18] trifluoroacetate,[16] dehydroacetate,[9] cyclohexylsulphamate,[9] *p*-hydroxybenzoate,[9] crotonate,[4] capronate,[4] *n*-octanoate,[4] and *n*-decanoate.

The present paper deals with the response of the liquid membrane-electrodes — elaborated by using a cetylpyridinium salt in nitrobenzene — towards a series of organic anions : biphthalate, benzoate, *o*-chlorobenzoate, *p*-chlorobenzoate, phenylacetate, sebacate, salicylate, 3,5-dinitrobenzoate, *o*-nitrobenzoate, 5,5-diethylbarbiturate, cholate and sulphanilate.

EXPERIMENTAL

The liquid membrane-electrode **was obtained by soaking the pores of a glass frit G_4, made hydrophobic, attached to the extremity of a glass tube (∅ = 15 mm), with the solution of cetylpyridinium bromide (c = 0.05%) in nitrobenzene. The organic solution was also used as internal solution. The standard calomel electrode was used, both as inner and outer reference electrode.**

Potential measurements **have been performed with a MV−85 pH-meter (±1 mV precision), by measuring the e.m.f. of the electrochemical cell :**

SCE ‖ Internal organic solution | Liquid membrane in glass frit | Test solution ‖ SCE

Potential measurements were performed at room temperature in nonstirred solutions.

Reagents and standard solutions. **Analytical grade reagents were used. Standard solutions of the natrium salts of the organic monovalent anions tested were prepared in the 10^{-1}–10^{-5}M concentration range, by successive dilutions of a 10^{-1} M stock solution, adjusting the ionic strength with Na_2SO_4 10^{-1}M. A constant ionic strength was used (J = 0.1 M).**

RESULTS AND DISCUSSIONS

The electrode functions obtained for a series of anions of organic acids presenting industrial or biological interest were determined. The results are given in table 1.

---

[13] N. Ishibashi and H. Kohara, *Bunseki Kagaku*, **21**, 100 (1972); *Chem. Abstr.*, **76**, 107667 (1972).

[14] K. Kina, M. Maekava and N. Ishibashi, *Bull. Chem. Soc. Japan*, **46**, 2773 (1973).

[15] N. Ishibashi, A. Jyo and M. Yonemitsu, *Chem. Lett.*, **1973**, 483.

[16] N. Ishibashi, and A. Jyo, *Mikrochem. J.*, **18**, 220 (1973).

[17] N. Ishibashi, H. Kohara and K. Horinouchi, *Talanta*, **20**, 867 (1973).

[18] A. Jyo, M. Yonemitsu and N. Ishibashi, *Bull. Chem. Soc. Japan*, **46**, 3734 (1973).

[19] B. J. Birch and D. E. Clarke, *Analyt. Chim. Acta*, **67**, 387 (1973).

[20] T. Higuchi, C. R. Illian and J. L. Tossounian, *Analyt. Chem.*, **42**, 1674 (1970).

These data show that the electrode response is approximately nernstian for the following anions: biphthalate, benzoate, *o*-chlorobenzoate, *p*-chlorobenzoate, phenylacetate and sebacate, the concentration range of the linear response being narrowed for benzoate and phenylacetate. The electrode sensitivity is satisfying for salicylate, 3,5-dinitrobenzoate, *o*-nitrobenzoate, 5,5-diethylbarbiturate, cholate and sulphanilate anions.

Table 1

Electrode behaviour of the liquid membrane from cetylpyridinium bromide 0.05% in nitrobenzene towards different organic anions

Anion	Linear response range (M)	Sensitivity (mV)
Biphthalate	$10^{-1}-3.2\times10^{-4}$	58
Salicylate	$10^{-1}-3.2\times10^{-4}$	52
Phenylacetate	$5.6\times10^{-2}-5\times10^{-4}$	59
Sebacate	$10^{-2}-1.6\times10^{-4}$	56
Cholate	$5.6\times10^{-2}-10^{-4}$	51
5,5-Diethylbarbiturate	$10^{-1}-5.6\times10^{-4}$	50
Sulphanylate	$10^{-1}-4.5\times10^{-4}$	50
Malonate	$10^{-1}-1.8\times10^{-4}$	48
Succinate	$10^{-1}-10^{-2}$	48
Benzoate	$4.5\times10^{-2}-3.2\times10^{-4}$	54
o-Chlorobenzoate	$10^{-1}-3.2\times10^{-4}$	54
p-Chlorobenzoate	$10^{-1}-1.8\times10^{-4}$	54
o-Nitrobenzoate	$10^{-1}-2.8\times10^{-4}$	50.5
m-Nitrobenzoate	$10^{-1}-2\times10^{-4}$	45
p-Nitrobenzoate	$10^{-1}-2.8\times10^{-4}$	48
3,5-Dinitrobenzoate	$10^{-1}-10^{-4}$	51

For the remaining anions tested the electrode has a sensitivity below 50 mV for a concentration decade. Fig. 1 shows the electrode functions for some anions towards which a good electrode response was obtained.

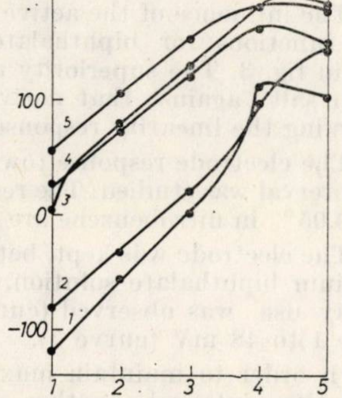

Fig. 1. — Electrode function for different organic anions.

1, biphthalate; *2*, salicylate; *3*, cholate; *4*, malonate; *5*, 5,5-diethylbarbiturate.

The influence of the kind and number of substituents of benzoate anion upon the electrode response is illustrated in fig. 2.

In the case of chlorobenzoates (fig. 2*a*, and table 1), an extension of the linear response range was obtained as compared to benzoate. The electrode sensitivity was not modified. In the case of nitrobenzoates a more complex situation arises (fig. 2*b*). Anions with a single nitrosubstituent have a linearity range from 10^{-1} to approximately 3×10^{-4}M, being slightly more extended in the case of *m*-nitrobenzoate as compared to *o*-, resp. *p*-nitrobenzoates. The electrode sensitivity is lowest in the case of *m*-nitrobenzoate. Both the sensitivity and the linearity range are the highest in the case of 3,5-dinitrobenzoate.

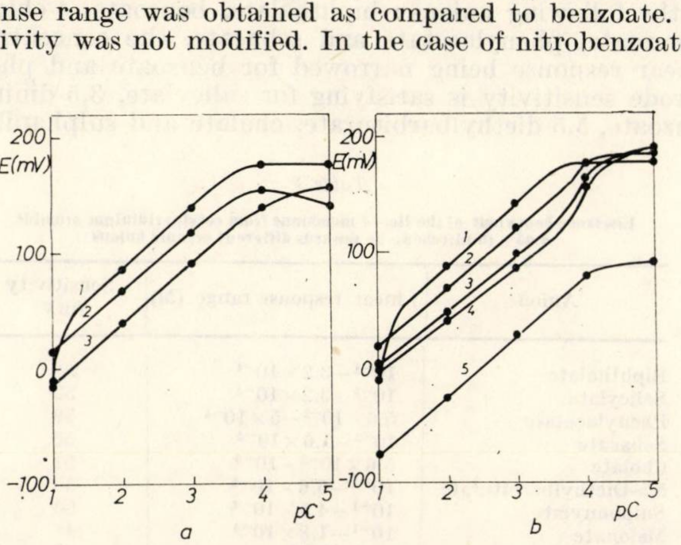

Fig. 2. — Influence of the substituents of benzoate anion on the electrode behaviour.

a) Chlorobenzoates : *1*, benzoate ; *2*, *o*-chlorobenzoate ; *3*, *p*-chlorobenzoate. *b)* Nitrobenzoates : *1*, benzoate ; *2*, *o*-nitrobenzoate ; *3*, *p*-nitrobenzoate ; *4*, *m*-nitrobenzoate ; *5*,3,5-dinitrobenzoate.

The influence of the active electrode component type upon the electrode functions for biphthalate, salicylate and 3,5-dinitrobenzoate is given in fig. 3. The superiority of the electrode obtained from cetylpyridinium salt against that derived from $[\mathrm{Ni}\ (\text{o-phen})_3]^{2+}$ salt, especially concerning the linearity response range, was established.

The electrode response towards biphthalate related to the operating time interval was studied. The results obtained with cetyl-pyridinium bromide 0.05% in nitrobenzene are given in fig. 4.

The electrode was kept, between the measurements series, in a 10^{-1}M potassium biphthalate solution. A desensitisation of the electrode after a 6-day use was observed (curve 3), the slope decreasing from 59 mV (curve 1)to 48 mV (curve 3).

In order to maintain maximum sensitivity of the electrode for a longer time interval, another preparation mode for liquid membrane was used. The cetylpyridinium biphthalate was extracted in nitrobenzene solution, using nitrobenzene saturated with cetylpyridinium bromide and a 10^{-1}M aqueous biphthalate solution. The liquid membrane-electrodes were obtained diluting the organic extract with nitrobenzene in the 1 : 1, 1 : 2, 1 : 3 and 1 : 4 ratios. These electrodes were consequently tested on biphthalate. The results thus obtained are given in table 2. The best behaviour

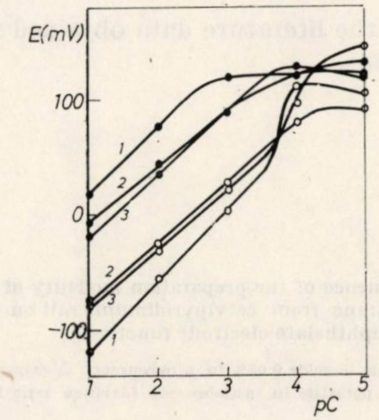

Fig. 3. — Influence of the electrode component type of the liquid membrane on electrode behaviour towards some organic anions.

—o— cetylpyridinium bromide 0.05% in nitrobenzene;

—●— $[Ni(o\text{-}phen)_3](ClO_4)_2$ 0.01% in nitrobenzene.

1, biphthalate; *2*,3,5-dinitrobenzoate; *3*, salicylate.

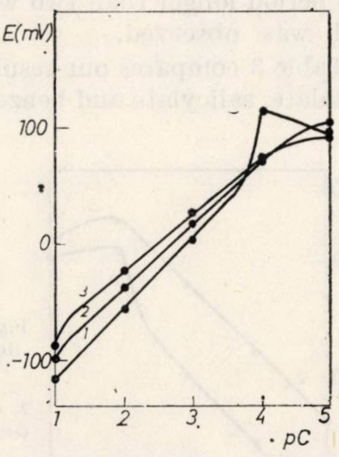

Fig. 4. — Behaviour in time towards biphthalate of the liquid membrane-electrode from cetylpyridinium bromide 0.05% in nitrobenzene

1, after 1 day; *2*, after 2 days; *3*, after 6 days.

Table 2

Comparative data of liquid membrane-electrodes for the anions: biphthalate, salicylate and benzoate

Anion	Sensitivity (mV)	Linear response range (M)	References
Benzoate	53	$10^{-1}-10^{-3}$	4,5
	Nernst	$10^{-1}-10^{-3}$	9
	58.5	$10^{-1}-10^{-3}$	1
	54	$4.5\times10^{-2}-3.2\times10^{-4}$	own results
Salicylate	53	$10^{-1}-10^{-3}$	4,5
	56	$10^{-1}-10^{-3}$	1
	Nernst	$10^{-1}-10^{-3}$	9
	60	$10^{-1}-10^{-5}$	14
	52	$10^{-1}-3.2\times10^{-4}$	own results
Biphthalate	57	$10^{-2}-10^{-4}$	18*
	58	$10^{-2}-10^{-4}$	18*
	58	$10^{-1}-3.5\times10^{-5}$	15
	59.5	$10^{-1}-10^{-4}$	own results

* Results have been obtained with different electrodes.

was obtained in the case of the electrode with a 1 : 2 dilution ratio. Fig.5 underlines the importance, for the electrode response, of the method used to obtain the liquid membrane. We mention that the electrode obtained with cetylpyridinium biphthalate maintains its sensitivity (fig. 5, curve 2) over a period longer than two weeks. A slight change of the standard potential was observed.

Table 3 compares our results with the literature data obtained with biphthalate, salicylate and benzoate anions.

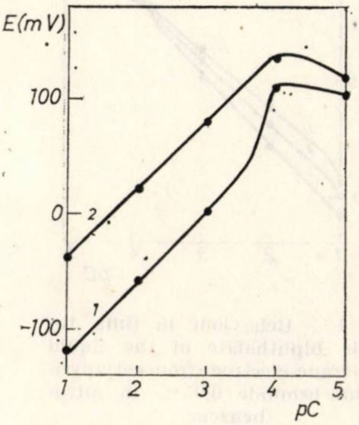

Fig. 5. — Influence of the preparation modality of the liquid membrane from cetylpyridinium salt on the biphthalate electrode function.

1, cetylpyridinium bromide 0.05% in nitrobenzene; *2*, extract of cetylpyridinium phthalate in nitrobenzene (dilution ratio 1 :2).

Table 3

Electrode characteristics of the membrane from cetylpyridinium biphthalate in nitrobenzene as a function of its concentration

Dilution ratio (extract : nitrobenzene)	Linear response range (M)	Sensitivity (mV)
Undiluted extract	$10^{-1}-10^{-3}$	59.5
1 : 1	$10^{-1}-3.7\times10^{-4}$	60.5
1 : 2	$10^{-1}-10^{-4}$	59.5
1 : 3	$10^{-1}-1.5\times10^{-4}$	58.5
1 : 4	Too high electrical resistance of the membrane	

The reproducibility of the electrode functions is high for all the tested anions , e.g. for biphthalate — with the cetylpyridinium biphthalate electrode, and for the other anions even with the cetylpyridinium bromide electrode, used after a few hours of conditioning in the 10^{-1}M solution of the respective anion. All results given in the paper represent the mean of the three determinations. The standard deviation is below ±1 mV, so that the accuracy of measurements is in the precision range of the apparatus used.

Concerning the response time of the electrode, it is 2—5 min in the solutions with concentrations higher than 10^{-3} M, 8—10 min in 10^{-4}M solutions and approx. 15 min in 10^{-5}M solutions. The rate of the electrode response was generally lower towards organic anions as compared with inorganic ones.

CONCLUSIONS

An anion-sensitive liquid membrane-electrode was obtained, using a new electrode component viz., a cetylpyridinium salt. The electrode response towards 16 organic anions of which only benzoate, biphthalate and salicylate are discussed in the literature, was tested. The electrode has a good sensitivity (a slight subnernstian response) towards the following anions: benzoate, *o*-chlorobenzoate, *p*-chlorobenzoate, phenylacetate, sebacate, salicylate, 3,5-dinitrobenzoate, *o*-nitrobenzoate, 5,5-diethylbarbiturate, cholate and sulphanilate. Improving the preparation technique of the liquid membrane, a nernstian response was obtained (59.5 mV sensitivity) towards biphthalate in a large concentration range (10^{-1}—10^{-4}M).

Revue Roumaine de Chimie **23**, *2*, 281–286 (1978)

PYRIDINEMONOCARBOXYLATE ION SELECTIVE ELECTRODES

L. CAMPANELLA, T. FERRI [a] and D. GOZZI [b]
[a] Institute of Analytical Chemistry, Rome University, Italy
[b] Institute of Physical Chemistry, Rome University, Italy

Received October 2, 1975

Two new membrane electrodes are prepared and employed to determine nicotinate ion concentration. Copper nicotinate and nicotinic esther, particularly cetyl nicotinate, are the sensor compounds in the two electrodes. Both electrodes behave satisfactorily; the solid membrane electrode is characterized by better mechanical properties and a more stable signal, the liquid one by a higher selectivity; anyway both electrodes appear to be sensitive to nicotinate isomers.

The determination of nicotinic acid is an analytical problem of great interest because of the biological activity [1,2] of this substance and its derivatives, particularly its amide, connected with the liver functions in the presence of PP vitamin in the human body.

Quantitative analysis of nicotinic acid can be performed by spectrophotometry,[3] acid-base potentiometry and polarography[4]; but in all these cases the analysis conditions must be rigorously chosen, the techniques being quite long and non-specific.

In this paper we describe a study concerning the employment of some new membrane electrodes for the determination of nicotinic acid.

The study was performed according to two different programs: heterogeneous solid membrane electrodes (copper nicotinate as sensor. and liquid membrane electrodes (an esther of nicotinic acid as sensor).

EXPERIMENTAL

a) In the case of heterogeneous solid membrane electrodes, (fig. 1), the sensor was dipped into different media (polythene, silicon rubber, paraffin) which acted as binding material and contained graphithe as conducting material. Copper nicotinate was obtained as described in the

---

[1] M. AIAZZI MANCINI and L. DONATELLI, "Trattato di Farmacologia", Vallardi Ed., Vallardi, Padova, 1964.

[2] H. W. DOUGHERTY and P. I. POLLAK, "Medicinal Chemistry", Burger Ed., Interscience Publishers, Inc., New York, 1970.

[3] E. B. HUGHES, H. H. JELLINEK and B. AMBROSE, *J. Phys. Colloid. Chemistry*, **53**, 1649, (1973).

[4] L. CAMPANELLA and G. DE ANGELIS, *Rev. Roumaine Chim.*, **18**, 1649 (1973).

literature[5]. The membrane was prepared by weighing the needed amounts of the different constituting materials, by mixing them well together and by melting the mixture under pressure in an adequate mold. For such a membrane the thickness was about 1 mm and the electrical resistance ranged from 10 to 30 KΩ.

In the case of liquid membrane electrodes, (fig. 2), the sensor, if solid at room temperature, was present in the molten state or as solution in heavy aliphatic ethers ($c = 1.10^{-2} \div 1.10^{-1}$M). The experimental conditions must be such as ($[H^+] \geqslant 3M$) to ensure the rapid acid hydrolysis of the esther, on which the functioning of the electrode is based, because of the influence of addition of nicotinic acid. The measurement cell was in this case the following

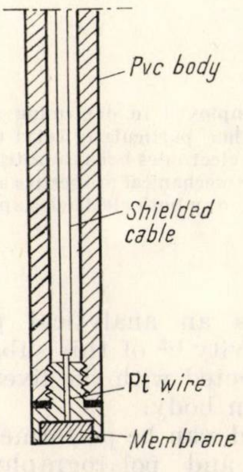

Fig. 1. — Heterogeneous solid membrane electrode.

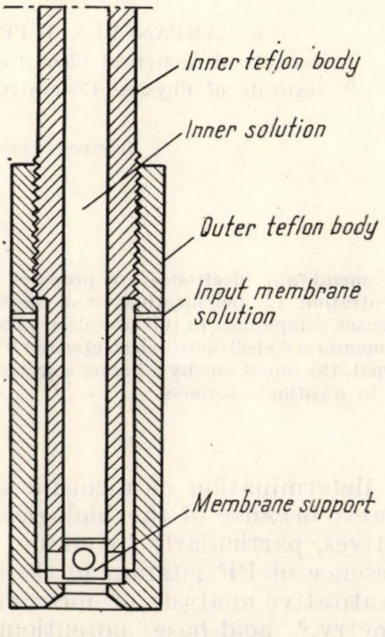

Fig. 2. — Liquid membrane electrode.

Pt, molten esther (50°)
or
esther solution
or
pure liquid esther (25°)

| ($C_5H_4NH)^+COOH$, $HClO_4$ 3M || reference electrode

millipore membrane (10 mμ)
or sintered glass

The tested esthers were cethyl-, cyclohexyl-, 2-hexadecanyl-, 2-octyl-, isoamyl-nicotinate, all these answering satisfactorily to the requirement for very low solubility and great viscosity.

b) For all the electrodes prepared the calibration curve was determined according to the following procedure : conditioning in buffered nicotinic (tris, pH = 8) solutions, immersion in buffer solution without nicotinic acid, waiting for signal stability of e.m.f., addition of known amounts of nicotinic acid, measurement of the new tension value. The values recorded after each addition were plotted against the logarithm of nicotinic acid concentration corrected for dilution, and considering the diagram with the three possible species of the acid.

---

[5] E. G. Cox, W. Wardlaw and V. C. Webster, *J. Chem. Soc.*, **1936**, 775.

c) Selectivity constants are determined by the two ions mixture method.[6]

RESULTS AND DISCUSSION

Heterogeneous solid membrane electrodes are characterized by a slope corresponding to a univalent potential determining anion, (59 ± 1) mV/concentration decade. Their behaviour is not influenced by the concentration of the ionic strength buffer. The response time depends on the

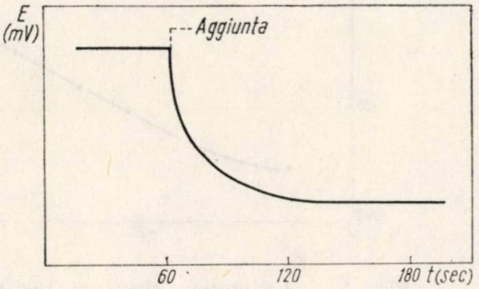

Fig. 3. — Response time of the heterogeneous solid membrane electrode.

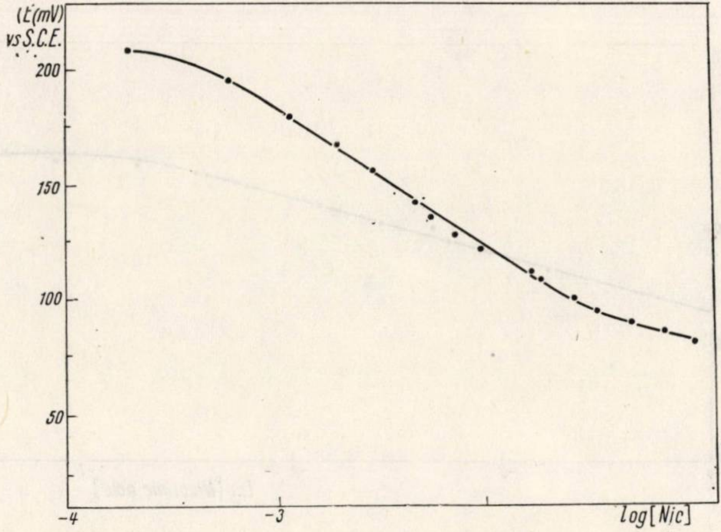

Fig. 4. — Calibration curve of the heterogeneous solid membrane electrode.

---

[6] G. J. Moody, J.D.R. Thomas, "*Selective Ions Sensitive Electrodes,*" Merrow Technical Library, London, 1971.

conditions of sensor, preparation anyway less than two minutes (fig. 3). The response linearity is observed in the range $5.10^{-4} \div 5.10^{-2}$M, (fig. 4), the lower limit being fixed by the solubility of the copper nicotinate and the upper one by the sensible variation of the ionic strength. It was observed that the electrode is sensitive to copper (II) ions, (fig. 5), with a good linear answer in the concentration range $7.10^{-3} \div 5.10^{-1}$M.

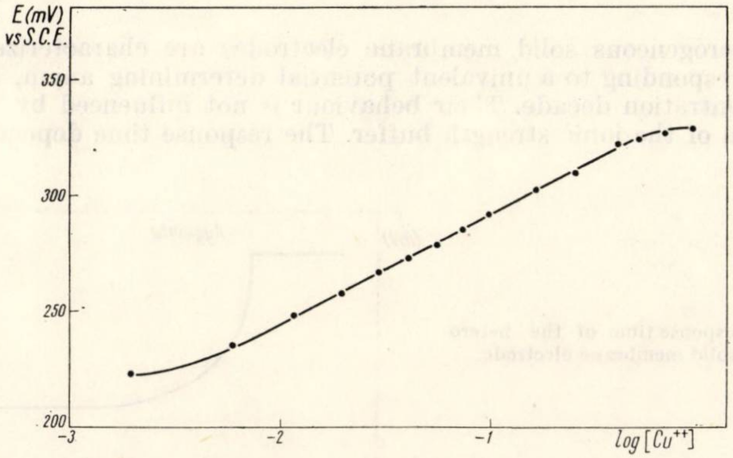

Fig. 5. — Calibration curve of the heterogeneous solid membrane electrode for copper ions.

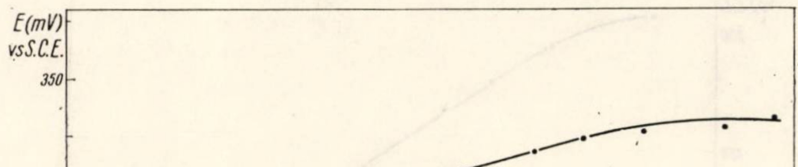

Fig. 6. — Calibration curve of the liquid membrane electrode.

The slope, (48 ± 1)mV/concentration decade, is quite far from the theoretical value. Aliphatic acid anions (formate, acetate, oxalate, citrate) do not interfere, whereas aromatic ones (benzoate, phthalate, p-toluensulfonate) especially those of nicotinic acid isomers, are strongly interfering.

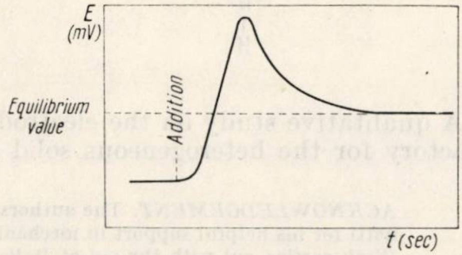

Fig. 7. — Response time of the liquid membrane electrode.

For such as aromatic anions the selectivity constants are respectively 1.1, 0.5, 0.8 for the three considered ions.

This kind of electrodes are mechanically advantageous, compact, requiring no inner reference, and giving a fast enough response.

Liquid membrane electrodes are characterized by a slope of (25 ± 1) mV/concentration decade. The linear response is observed in the range $1.10^{-4} \div 5.10^{-1}$M (fig. 6).

The recorded signal after each addition has the behaviour shown in (fig. 7), the response time being almost the same as in the case of heterogeneous solid membrane electrode; as nicotinic acid concentration increases the response time decreases. Among the tested esthers, the best results are obtained with cethylnicotinate, which the figures refer to . The greatest disadvantage of this kind of electrodes is due to the high experimental temperature (50°), required and at this temperature some esthers are not stable. In order to solve this problem solutions are used in place of molten esther; in this case the electrode always contains an inner reference and supplying system. The results are quite similar but the signal stability is lower.

About the selectivity of experimental results it can be concluded that these electrodes are more selective than solid membrane ones : this is probably due to the fact that esther liquid membranes are sensitive to protonated cationic species, so that all those acids unable to exist as cations do not interfere.

The slope value 25 mV/concentration decade can be explained by the double positive charge of the species which controls the rate of hydrolysis reactions on which electrode functioning is based.

This species results from the water addition to carbonyl with formation of a charged intermediate in the rate determining the step of the reaction, the protonation of nitrogen being justified by the free acidity of the reaction medium.

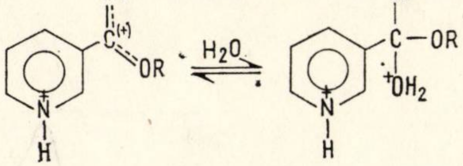

A qualitative study on the electrode reproducibility shows its being satisfactory for the heterogeneous solid membrane electrode only.

ACKNOWLEDGEMENT. The authors wish to thank the technician Sesto Simonetti for his helpful support in mechanical and construction problems.
Work carried out with the aid of Italian CNR.
Part of this paper was presented at "EUROANALYSIS II" — 25—30 August 1975—Budapest, Hungary.

Revue Roumaine de Chimie, **23**, *2*, 287–294 (1978)

EVALUATION OF A METHANE–OXYGEN–AIR FLAME FOR ATOMIC EMISSION

E. CORDOŞ and GEORGETA BĂRCEANU

University "Babeş-Bolyai" Cluj-Napoca, Department of Chemistry, Division of Analytical Chemistry, Arany János 11

Received October 4, 1975

The methane-oxygen-air flame is characterized from the analytical point of view in atomic emission spectroscopy. Two different burners, adapted to this flame were built: one for a turbulent flame and another for laminar flame. The analytical signal generated by the flame was integrated in two ways: at the nominal wavelength and during spectral line scanning. The data obtained for Ca and Li show that determinations accuracy and calibration curves linearity are similar for both types of flames. The detection limits are in the 25–450 ng/ml range. The integration at the nominal wavelength yields a better sensitivity. The integration during scanning gives sufficient accuracy to allow the use of this procedure in multielemental analysis instruments.

In recent years the flame spectrometry has achieved important advances by introducing new techniques and by improving the instrumentation performances. The atom reservoir on which measurements are made, the flame, has been the subject of special attention concerning both new types of nebulizer and burners and the use of new fuels and oxidizers.[1–6]

The methane based flame is known [7–8] but its use in flame spectrometry was empirical, the methane being considered merely a substitute for propane or butane. There is no detailed study on the analytical feasibility of this flame, its optical background, calibration curves shape, detection limits, etc.

The methane is the hydrocarbon with the highest hydrogen percentage and one of the smallest burning velocities.[9] This means a long residence time of the sample in the flame and consequently a good sensitivity for most determinations, even at lower temperatures. Therefore in the present paper a preliminary study is accomplished concerning the obtaining of a

---

[1] H. V. Malmstadt and E. Cordoş, *Amer. Lab.*, **4** (8) 35 (1972).

[2] G. F. Kirkbright and M. Marshall, *Analyt. Chem.*, **44**, 1288 (1972).

[3] R. F. Browner and D. C. Manning, *Analyt. Chem.*, **44**, 843 (1972).

[4] M. B. Denton and H. V. Malmstadt, *Analyt. Chem.*, **44**, 241 (1972).

[5] Y. Mitzutani and A. Nakajima, *Combust. Flame*, **19**, 203 (1972).

[6] T. R. Copeland, K. W. Olson and R. K. Skogerboe, *Analyt. Chem.*, **44**, 1471 (1972).

[7] P. Datta, B. M. Hayward and S. B. Reed, *Combust. Flame*, **17**, 399 (1971).

[8] P. Datta and S. B. Reed, *Combust. Flame*, **19**, 89 (1972).

[9] R. Gunther and G. Janisch, *Combust. Flame*, **19**, 49 (1972).

methane-oxygen turbulent (total consumption) flame and a methane-oxygen-air laminar flame. The flame performance has been characterized by means of calibration curves and detection limits in atomic emission for calcium and lithium, whose resonance lines are sufficiently apart from each other in visible spectrum. The atomic emission signal of these elements was integrated in two modes : at the nominal wavelength and by scanning on a ± 1 nm interval around this wavelength.

EXPERIMENTAL PART

The instrumentation consists of two main units : the spectrophotometric unit and the data handling and control unit. Both units have been built according to the modular principle, either from commercial available modules or from modules built in our laboratory. The block diagram of the instrumentation is given in fig. 1.

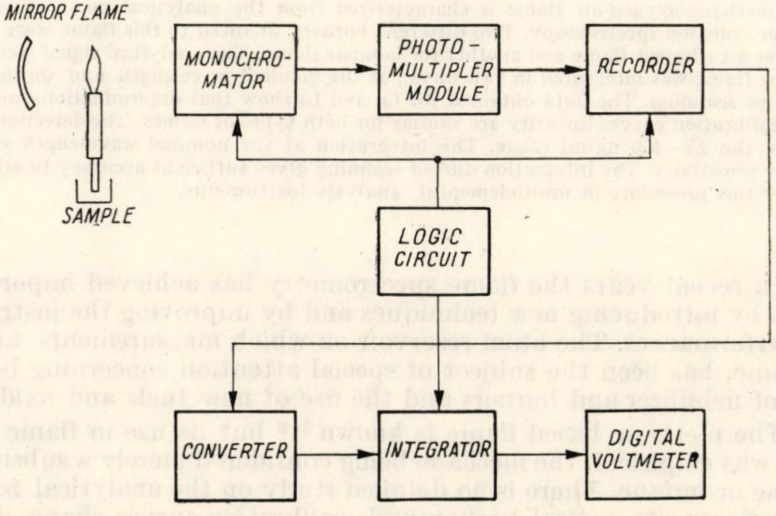

Fig. 1. — Block diagram of the spectrophotometric unit and of the data handling and control unit.

The burner with nebulization system, the sample cup and the mirror are mounted on a Heath EU-700-20 flame module. The emitted wavelength is selected with a Heath Eu-700 monochromator and converted into a current by a 1P28A photomultiplier housed by a Heath Eu-701-30 photomultiplier module. The photocurrent is measured with a Heath Eu-28 B recorder.

The signal from the recorder auxiliary output which is identical with the input signal, is used for further handling. The current from this output is amplified by a current-to-voltage converter and fed to an integrator. The integrated signal is finally measured by a four-digit digitvoltmeter built in our laboratory. A logic circuit controls the integration time and the integrator function. The same logic circuit provides the monochromator scanning over a predetermined wavelength interval and a synchronous advance of the recorder paper. The part of the instrumentation built in our laboratory is described below.

The flame and the burner. The turbulent flame has been provided by a Beckman 4020 burner. This burner is not designed for use with fuels of low burning velocity as the methane. Therefore an external hose with a supplementary port for oxygen has been added (fig. 2). This outer sheat of oxygen maintains the flame "attached" on the burner and provides a mechanical protection.

The gas flows for which the flame yields optimum results are : methane 1.90 l/min, oxygen for sample aspiration and burning 2 l/min and outer sheat oxygen 0.9 l/min.

The burner for laminar flame consists of a stainless steel mixing chamber and a head with two tubes. The nebulizer is a Beckman burner placed in a side inlet of the mixing chamber (fig. 3). A spoiler, made from a steel bead is placed in front of the aerosols stream in order to increase the homogeneity and the proportion of smaller droplets. The excess of solution is drained through the lower part of the burner.

The burner head made of two pieces allows oxygen to be used both inside and outside the flame. Through the right port and a series of channels oxygen is fed between the exit holes for methane-air mixture. In this way the flame temperature could be controlled. The oxygen fed through the left tube forms a sheat around the flame. This improves the burning conditions and gives a better mechanical stability.

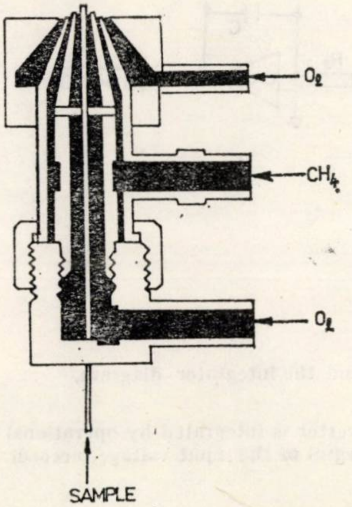

Fig. 2. — The total consumption burner for methane-oxygen flame.

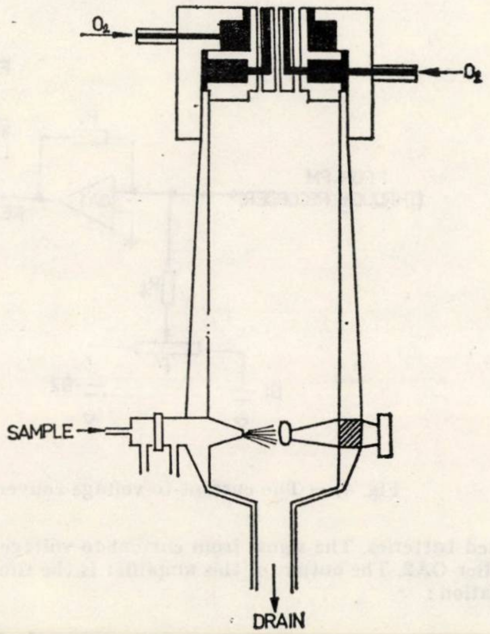

Fig. 3. — The burner for methane-air-oxygen laminar flame.

The integrator and the current-to-voltage convertor. The photocurrent-to-voltage conversion and the integration was accomplished by two operational amplifiers Burr-Brown 3308/12 C. The amplifier OA 1, having a R_1 feedback resistor was the converter (fig. 4). The value of the resistor R_1 can be evaluated using equation (1).

$$R_1 = -\frac{e_0(1+A)}{i_{in}\,A} \text{ ohms,} \tag{1}$$

where : e_0 — output signal (volts) ;
i_{in} — input current (amps) ;
A — amplification.

Since for our amplifiers $A = 100,000$ the equation (1) becomes :

$$R_1 = -\frac{e_0}{i_{in}}. \tag{2}$$

At an output voltage of 1V and input currents of 10^{-6} to 10^{-7} A, the R_1 value ranges between 1 Mohm and 10 Mohms.

To compensate for the flame background current and the current from recorder amplifier a d.c. offset is connected to the summing point. This d.c. offset which can compensate in both positive and negative range is made from resistor R_4, potentiometer P and two 1.5 V

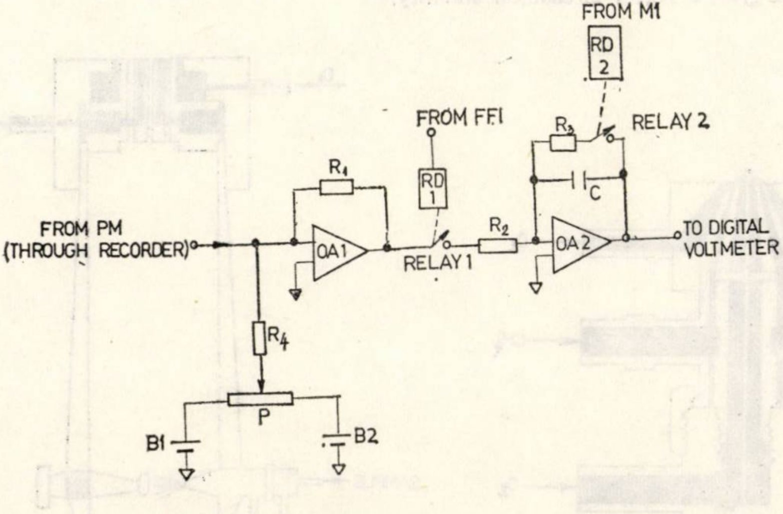

Fig. 4. — The current-to-voltage converter and the integrator diagram.

dried batteries. The signal from current-to-voltage converter is integrated by operational amplifier OA2. The output of this amplifier is the time integral of the input voltage, according to relation :

$$e_0 = -\frac{1}{RC}\int_0^t e_{in}\,dt. \tag{3}$$

The OA1 output is fed to the OA2 input through relay 1 which is closed by the logic circuit on a predetermined time t. Relay 2, parallel with capacitor C, allows the integration to occur only when it is open. R_3 resistor is a buffer resistor which limits the current during the shorting of capacitor C.

The logic circuit (fig. 5) :

(1) provides the integration time with a precision of one hundredth of a second; (2) synchronizes the monochromator with the recorder and the integrator (both the monochromator and the recorder work only during the integration time); (3) opens relay 2 and closes relay 1; (4) erases the old result from the integrator, prior to the start of a new measurement.

The logic circuit is made up of a four decade decimal counter (DCU—1—4) a flip-flop FF—1, three monostables M1—M3 and two NAN D gates G1 to G2.

At the start command the monostable M1 goes to "O" for about 3 s, as is set by the R_{M1} resistor. By this the integration capacitor is shortened. At the end of the 3s the monostable 1 activates the monostable M2 which changes its state for 0.5 s. At the end of this

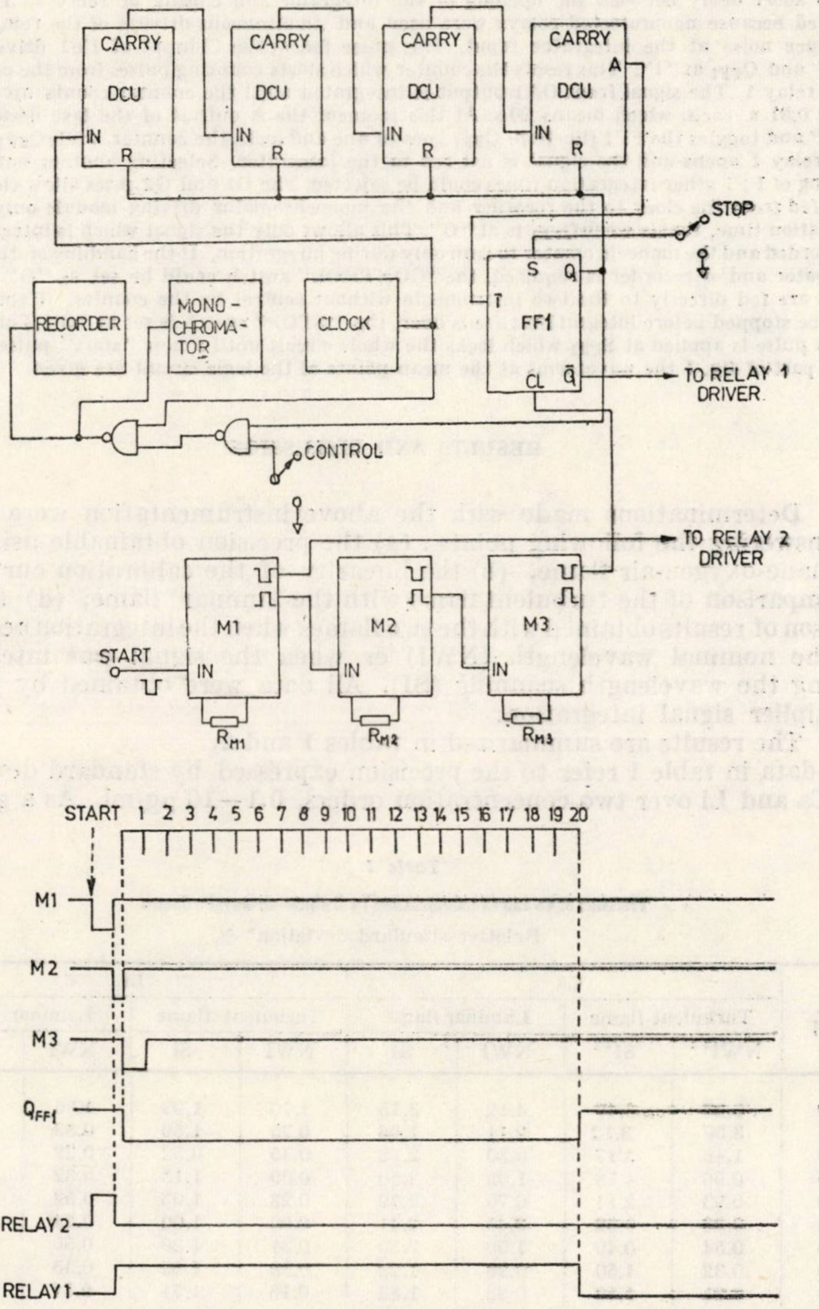
CARRY
DCU
IN
R
CARRY
DCU
IN
R
CARRY
DCU
IN
R
CARRY
A
DCU
IN
R
STOP
S
Q
T
FF1
CL
Q̄
TO RELAY 1 DRIVER
RECORDER
MONO-CHROMATOR
CLOCK
CONTROL
TO RELAY 2 DRIVER
M1
M2
M3
START
IN
IN
IN
R_{M1}
R_{M2}
R_{M3}
START 1 2 3 4 5 6 7 8 9 10 11 12 13 14 15 16 17 18 19 20
M1
M2
M3
Q_{FF1}
RELAY 2
RELAY 1

Fig. 5. — The logic circuit diagram (upper) and the waveform of circuit main points (lower).

period M2 activates M3 which sends a short pulse at the Cl input of FF 1. The M2 role is to provide a short delay between the opening of the integrator and closing of relay 1. This was required because nonprotected relays were used and simultaneous driving of the relays could introduce noise at the integrator input. The pulse fed at the Cl input of FF1 drives Q_{FF1} to "O" and Q_{FF1} at "1". This resets the counter which starts counting pulses from the clock and closes relay 1. The signal from OA1 output is integrated until the counter counts up to 2000 pulses 0.01 s each, which means 20 s. At this moment the A output of the last decade goes to "O" and toggles the FF1 flip-flop. Q_{FF1} goes to one and locks the counter while Q_{FF1} goes to zero, relay 1 opens and the signal is not fed to the integrator. Selecting another output for toggling of FF1 other integration times could be selected. The G1 and G2 gates allow the pulses to be fed from the clock to the recorder and the monochromator driving module only during integration time, that is when Q_{FF1} is at "O". This allows only the signal which is integrated to be recorded and the monochromator to scan only during integration. If the handling of the monochromator and/or recorder is required, the "CONTROL" switch could be set at "O" and the pulses are fed directly to the two instruments without control by the counter. If the circuit must be stopped before integration time is over, the "STOP" switch is set at "O". This means that a pulse is applied at S_{FF1} which locks the whole circuit until a new "start" pulse. In the lower part of fig. 5 the waveforms at the mean points of the logic circuit are given.

RESULTS AND DISCUSSION

Determinations made with the above instrumentation were aimed at answering the following points : (a) the precision obtainable using the methane-oxygen-air flame, (b) the linearity of the calibration curves (c) a comparison of the turbulent flame with the laminar flame, (d) a comparison of results obtained with the two flames when the integration occurred at the nominal wavelength (NWI) or when the signal was integrated during the wavelength scanning (SI). All data were obtained by photomultiplier signal integration.

The results are summarized in tables 1 and 2.

The data in table 1 refer to the precision expressed by standard deviation for Ca and Li over two concentration orders, 0.1—10 μg/ml. As a general

Table 1

Precision of Ca and Li determination in methane-air-oxygen flames

Relative standard deviation* %

Conc. μg/ml	Ca				Li			
	Turbulent flame		Laminar flame		Turbulent flame		Laminar flame	
	NWI**	SI**	NWI	SI	NWI	Si	NWI	SI
0.10	5.27	3.47	4.12	3.15	1.70	1.93	1.96	1.80
0.25	3.50	3.12	2.11	1.96	0.75	1.69	0.83	1.79
0.50	1.46	3.17	0,80	2.18	0.45	0.52	0.29	1.71
0.75	0.56	4.18	1.05	2.50	0.09	1.13	0.32	0.62
1.00	0.93	2.14	0.70	2.79	0.23	1.03	0.52	0.47
2.50	0.38	0.52	0.45	2.41	0.06	1.00	0.24	0.88
5.00	0.54	0.49	1.00	2.32	0.31	1.29	0.55	1.07
7.50	0.32	1.50	0.26	1.28	0.38	1.65	0.45	1.32
10.00	0.21	1.53	0.33	1.82	0.16	1.71	0.54	1.48

* Calculated from 10 determinations;

** NWI — Nominal Wavelength (λ_0) Integration. Ca $\lambda_0 = 422.7$ nm; Li $\lambda_0 = 670.8$ nm, SI — Scanning Integration from $\lambda_0 - 1$ nm to $\lambda_0 + 1$ nm.

Table 2

Linearity and detection limits for Ca and Li determinations in methane-air-oxygen flames

			Turbulent flame		Laminar flame	
			Calibration curve equation*	ts	Calibration curve equation	ts
Ca 422.7 nm	Conc. range : 0.1–1.0 μg/ml	NWI	$y = 15.1 + 2595.2x$	6.0	$y = 0.5 + 370.5x$	2.5
		SI	$y = 10.3 + 1505.1x$	8.1	$y = 0.3 + 169.0x$	3.9
	Conc. range : 1.0–10.0 μg/ml	NWI	$y = 8.7 + 260.4x$	13.6	$y = -0.4 + 36.9x$	1.4
		SI	$y = -0.1 + 146.9x$	4.6	$y = 0.5 + 16.2x$	1.4
	Detection limit ng/ml	NWI	87		140	
		SI	160.		419	
Li 670.8 nm	Conc. range : 0.1–1.0 μg/ml	NWI	$y = -23.2 + 3789.6\,x$	5.2	$y = -1.2 + 609.9x$	2.3
		SI	$y = 28.9 + 2166.6x$	3.0	$y = -0.3 + 348.7x$	2.1
	Conc. range : 1.0–10.0 μg/ml	NWI	$y = -8.5 + 366.6x$	4.4	$y = 0.3 + 64.8x$	3.0
		SI	$y = -9.1 + 197.5x$	5.2	$y = 0.5 + 36.5x$	2.1
	Detection limit ng/ml	NWI	30		25	
		SI	60		45	

* y – arbitrary units on digitvoltmeter ; x – concentration in μg/ml

feature, the precision is better for Li than for Ca, regardless of the determination technique or flame type. The precision with laminar flame is of about the same magnitude as for turbulent flame. As expected, the standard deviation decreases with concentration (signal/noise ratio improvement), but this decrease is more obvious when the nominal wavelength integration is used. This could be explained by the fact that the area resulting from NWI is larger than that obtained by SI. This gives a better signal/noise ratio in the first case and consequently a better precision. However, the errors with scanning integration keep around 1–4%. It means that a multielemental analysis is possible, conditioned by the automatic movement of the monochromator from a wavelength to another. Since the stop of the monochromator with high precision, at a given wavelength is a complicated matter,[10] the determination could be performed in simpler conditions by slowing down the monochromator close to the desired wavelength and integrating the spectral line during scanning.

---

[10] E. CORDOŞ and H. V. MALMSTADT, *Analyt. Chem.*, **45**, 425 (1972).

In the considered spectral and concentration ranges (422.7 to 670.8 nm and 0.1—10 μg/ml) there is no significant difference between the precision with laminar or turbulent flames. In selecting the flame type one must consider other parameters, the most important being the interfering factors. The calibration curves were calculated by the least square method. In all cases the points are on a straight line, within a narrow dispersion band, calculated after Liteanu-Mioşcu.[11] As could be seen the slope is higher for nominal wavelength integration which is also explained by the larger integrated area.

The detection limits (table 2) are in the ng/ml range. The limits obtained by NWI are about half from that obtained by SI. It should be noted that for Ca the turbulent flame gives better detection limits than the laminar flame. This is due to the higher temperature of the turbulent flame and lack of interfering agents in the standards. For lithium the situation is reversed, the laminar flame being better. This is due to the lower spectral background of this flame at 670.8 nm as compared with 422.7 nm. Since even in relatively low temperature flame the lithium compounds yields easily free atoms, at higher temperature their number does not increase as much as the flame background.

It can be considered that the methane-oxygen-air flame is useful for elements determination by atomic emission in the visible range of the spectrum. The burners used permit to control the flame temperature, especially for laminar flame, and to obtain reproducible data. Although the detection limits are in the same range as those mentioned for other flames, the authors consider that because of the differences in instrumentation and measurement system a comparison cannot be made for the time being. A fair comparison could be made only by using the other flames in the same instrumental conditions.

---

[11] C. Liteanu and M. Mioşcu, *Studii şi Cercetări Chim. Acad. Bucureşti*, **17**, 899 (1969).

Revue Roumaine de Chimie, 23, 2, 295–299(1978)

ERHÖHUNG DER GENAUIGKEIT UND VERKÜRZUNG DES ZEITAUFWANDS BEI DER FLECKENPLANIMETRIE IN DER DÜNNSCHICHTCHROMATOGRAPHIE *

W. SCHMIDT, D. MARANDIUC, A. NEMEŞ und G. OSTROGOVICH

Laboratorium für organische Chemie und Farbstoffe, Chemiezentrum Timişoara,
Bd. Mihai Viteazul 24, R. S. România

Eingegangen am 11. Oktober 1975

Durch Projektieren der Flecken eines entwickelten Chromatogramms mit einem Epidiaskop bei etwa achtfacher linearer Vergrößerung, kann der Fehler bei der Planimetrierung einer Fleckenoberfläche von 80 mm² unter 1 % gehalten werden. Der Zeitaufwand bei der Bestimmung der Oberfläche kann um etwa 80 % herabgesetz werden, wenn die Planimetrierung durch elektronische Bestimmung der Kapazität einer metallisierten Oberfläche ersetzt wird. Die Verfahren wurden bei der Analyse von Verbindungen mit mehrfachen stickstoffhaltigen Funktionen angewendet, wo die Bildung des Jodations beim Sichtbarmachen mit Chlor-Kaliumjodid-Stärke zu scharf begrenzten Flecken führt.

Die quantitative Auswertung von Dünnschichtchromatogrammen durch Planimetrie der Flecken weist gegenüber anderen quantitativen Methoden den Nachteil geringerer Genauigkeit auf.

Die Genauigkeit der Oberflächenbestimmung bei kreisförmigen oder annähernd kreisförmigen Flecken mit einem Planimeter oder durch graphische Integration wird wesentlich von der Größe der Oberfläche und der Schärfe der Konturen beeinflußt.

Bei der Bestimmung einer kreisförmigen Oberfläche A tritt ein Fehler $\pm \Delta A$ auf, der als eine ringförmige Fläche an der Peripherie des Fleckens gedeutet werden kann. Der relative Fehler $\Delta A/A$ ist direkt proportional mit der Breite des ringförmigen Streifens δ und umgekehrt proportional mit dem Durchmesser der Fläche. Aus der Beziehung

$$\frac{\Delta A}{A} = \frac{\pi \cdot D . \delta}{\frac{\pi}{4} D^2} = \frac{4\delta}{D}$$

folgt, daß durch optische Vergrößerung der Flecken der relative Fehler kleiner wird, wenn δ konstant bleibt, d.h. daß die Schärfe der Konturen durch die Vergrößerung nicht beeinträchtigt wird.

---

* Mitgeteilt auf der 4. Landeskonferenz für allgemeine und angewandte physikalische Chemie, Bukarest, 1.–5. September 1974.

Daraus ergibt sich die prinzipielle Möglichkeit, durch optische Vergrößerung der Flecken auf einem Chromatogramm die Genauigkeit bei der quantitativen Auswertung durch Messung der Fleckenoberfläche zu erhöhen.

EXPERIMENTELLER TEIL

Es wurden Glasplatten, 100 × 150 mm verwendet, die mit Kieselgel G nach Stahl oder mit nach eigenem Verfahren [1] hergestelltem Kieselgel mit Hilfe eines Streichgeräts nach Nybom, [2] eingestellt auf 0,25 mm, beschichtet wurden. Die Schicht wurde durch Ritzen in 15 mm breite Streifen eingeteilt.

Als Laufmittel diente die obere Schicht eines Gemisches aus 75 ml Methyläthylketon und 20 ml wäßriger Lösung von $NaCHCO_3$ 8 g/l bei Verteilungsgleichgewicht (für Biuret) oder Methyläthylketon (für Rhodamin B). Entwickelt wurde bei Kammersättigung. Als Proben dienten eine wäßrige Lösung von Biuret (im Laboratorium dargestellt) und eine 0,05 %ige Lösung von Rhodamin B in Äthanol. Am Start wurden 3 µl Lösung, die 1—25 µg Biuret enthalten, mit Hilfe einer mit Quecksilber geeichten Serumpipette und einer mechanischen Vorrichtung [3] aufgetragen.

Beim Sichtbarmachen durch Chlorieren nach unserer Variante [4] erhält man im Falle des Biurets einige Minuten nach dem Besprühen scharf begrenzte weiße Flecken im Innern von dunkelblauen Flecken mit weniger scharfen äußeren Konturen. Nach etwa einer Stunde sind die Konturen stabil. Die Reagenzlösung, ein Gemisch von gleichen Volumen einer 1 % igen wäßrigen KJ-Lösung und einer 10 %igen wäßrigen Stärkelösung, muß frisch bereitet werden, sonst ist der Fleckenumeriß nicht stabil. Feines Pulverisieren und eine gleichmäßige feine Textur der Schicht sind wesentlich für das Erzielen brauchbarer Flecken. Flecken von Rhodamin B werden ohne weitere Behandlung ausgewertet.

Zum Vergrößern der Flecken wurden zwei Möglichkeiten untersucht:

— Aufsichtprojektion des Chromatogramms, wobei eine etwa achtfache lineare Vergrößerung erzielt wird. Zwei modifizierte Geräte wurden verwendet: ein Epidiaskop I.O.R. Atlat Aped II (mit Halogenbrenner 50 W) und ein Epidiaskop der Firma N. Malinski Leipzig (mi Fluoreszenzbrenner 400 W Electrofar). Mit beiden Geräten wurde eine scharfe Projektion erhalten. Die erforderliche Kühlwirkung wurde durch einen starken Ventilator erreicht.

— Durchsichtprojektion von 24 × 36 mm — Negativen, erhalten durch Photographieren der Chromatogramme. Dabei wird eine etwa vierfache Vergrößerung erreicht.

Eine stärkere Vergrößerung erwies sich als unzweckmäßig, da wegen wachsender Unschärfe der Konturen kein Gewinn an Genauigkeit erzielt werden kann.

Die Fläche, auf welche projektiert wird, muß eben sein (ein Zeichenbrett wurde verwendet) und senkrecht zur optischen Achse des Objektivs stehen. Die senkrechte Stellung und die Qualität des Objektivs können gleichzeitig durch Projektion einer Standardfläche in verschiedenen Bereichen des Projektionsfeldes kontrolliert werden.

Die Konturen der Fläche werden mit einem gut gespitzten harten Bleistift (6H) nachgezogen und die Oberfläche mit Hilfe eines Polarplanimeters MOM K 800 bzw. durch Ausschneiden und Wägen gemmessen. Die Größe der Fläche kann auch mit Hilfe elektronischer Meßmethoden ermittelt werden. [5] Dazu werden die Flecken auf eine ebene beiderseitig metallisierte Plastikfolie projektiert, die Konturen mit einer Nadel in die etwa 10 µ dicke Metallschicht eingeritzt, so daß ein elektrischer Kondensator mit ebenen Platten entsteht, dessen Kapazität mit der Fleckenoberfläche proportional ist. Zur Bestimmung der Kapazität wurde eine Brücke RLG Tesla TM 393 mit manueller Kompensation verwendet. Die verwendete Plastikfolie muß eine gleichmäßige Dicke haben, was durch kreisförmige Proben nachgeprüft werden kann.

---

[1] Rum. Patent 57.736 vom 13. November 1970.

[2] N. Nybom, *Nature*, **198**, 1229 (1963).

[3] W. Schmidt und A. Nemeş, *Rev. Chim. (Bucureşti)*, unter Druck.

[4] A. Nemeş und G. Ostrogovich, *Z. analyt. Chem.*, **275**, *28* (1974).

[5] A. Popa und D. Marandiuc, *Buletin de fotogrammetrie*, **7**, *60* (1972).

ERGEBNISSE UND DISKUSSION

Die Größe der Biuretflecken nach dem Sichtbarmachen hängt von der Temperatur bei der Chlorbehandlung ab.

Durch Chlorbehandlung bei —20° wird die Empfindlichkeit des Nachweises gegenüber der Chlorbehandlung bei Zimmertemperatur auf etwa das Vierfache erhöht.

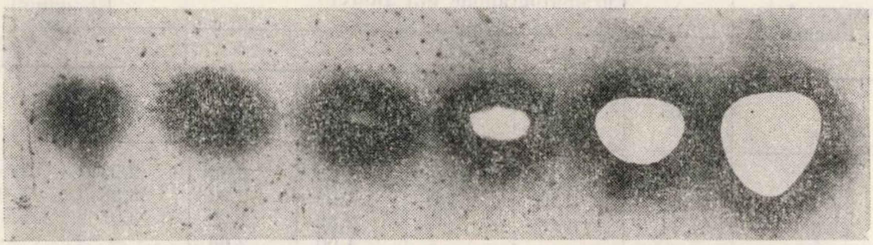

Abb. 1 — Biuretfelcken 1, 2, 3, 4, 8, 12 μg, bei 0° mit Chlor behandelt.

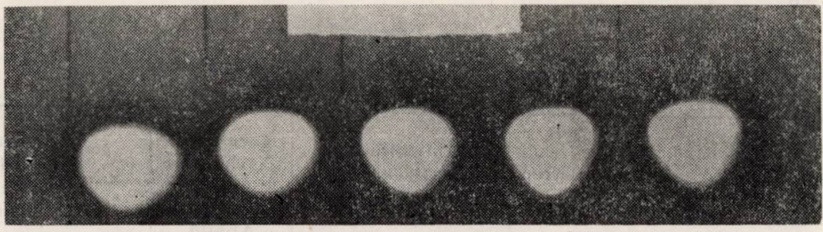

Abb. 2 — Biuretflecken 25 μg, bei 22° mit Chlor behandelt.

Die oben angegebenen Vergrößerungsmaßstäbe entsprechen etwa dem erzielbaren Optimum, so daß stärkeres Vergrößern keine weiteren Vorteile bringt.

Anderseits kann der Zeitaufwand für eine Bestimmung unter Beibehaltung der Genauigkeit auf ein Fünftel gesenkt werden, wenn man die Fleckenoberfläche mit Hilfe elektronischer Methoden mißt.

Die Genauigkeit bei der Messung der Kapazität ist größer als die Genauigkeit beim Nachzeichnen der Konturen. Tabelle 1 und Tabelle 2 geben ein Bild von der mit den beschriebenen Methoden erzielten Genauigkeiten.

Es ist ersichtlich, daß bei Anwendung der beschriebenen Methoden die Standardabweichung bei der Messung der Oberfläche eines Fleckens von Ø etwa 10 mm auf unter 1% gesenkt werden kann. Dadurch dürfte der planimetrischen Auswertung der Flecken eines Chromatogramms neue Möglichkeiten erschlossen werden.

Die Auswertung der Flecken auf den Chromatogrammen 1—3 (Tab. 1) nach einmonatigem Aufbewahren in Laboratoriumsatmosphäre zeigt ein leichtes Ansteigen der s-Werte und der Fleckenoberflächen (Tab. 3).

Gemäß den Daten aus Tabelle 1 ist die Standardabweichung für drei nebeneinanderliegende Flecken kleiner als jene, die für alle Flecken des Chromatogramms berechnet wurde. Die s-Werte beziehen sich in die-

Tabelle 1

Relative Standardabweichungen $s = \sqrt{\frac{\sum_{i=1}^{n}(\bar{x}-x_i)^2}{n-1}}$ **n**

Prozenten berechnet für das Gesamtverfahren für die ganze Platte (5, bzw. 8 Flecken) und für Gruppen von je 3 anliegenden Flecken

Ausgewertete Flecken	Chromatogramme mit Biuret					Chromatogramme mit Rhodamin B	
	1	2	3	4	5	1	2
1—5	5,65	1,99	6,02	—	—	4,76	6,28
1—8	—	—	—	4,90	5,65	—	—
1—3	2,99	1,78	0,63	3,59	3,94	2,93	3,54
2—4	4,32	1,64	0,47	4,29	2,92	3,38	3,40
3—5	4,14	1,59	7,47	2,89	1,72	3,01	4,84
4—6	—	—	—	4,00	2,66	—	—
5—7	—	—	—	3,17	6,94	—	—
6—8	—	—	—	3,75	5,44	—	—

Tabelle 2

Standardabweichungen *s* für die einzelnen Bestimmungen beim Messen der Oberfläche durch Projektion

Lf. Nr.	Vergrößerte Abbildung erhalten durch	Bestimmung der Oberfläche der projektierten Abbildung	Anzahl der Nachzeichnungen am projektierten Abbild	*s* % Durchschnitt	Anzahl der Flecken für die *s* berechnet wurde
1	Manuelles Nachzeichnen der Konturen der Flecken auf Transparent-Zeichenpapier auf weißem reflektierendem Grund mit einem spitzen harten Bleistift (6H)	Mit Polarplanimeter MOM K 800	4	±0,69	5
2	„ „	Ausschneiden und Wägen	4 3	±0,89 ±0,57	95 5
3	Manuelles Nachzeichnen der Konturen der Flecken auf einer beiderseitig metallisierten gleichmäßigen Plastikfolie mit einer harten Nadel.	Messen der Kapazität mit Tesla RLC Bridge TM 393			

Tabelle 3

Vergleich der Genauigkeit der Auswertung unmittelbar nach dem Sichtbarmachen und nach einem Monat

Chromatogramm Nr.	*s* (in Prozenten)			Mittlere Veränderung der Fleckenoberfläche %
	etwa 2 Stunden nach dem Sichtbarmachen		Nach einem Monat	
	Planimetrieren	Ausschneiden und Wägen	Ausschneiden und Wägen	
1	5,65	5,95	6,12	—1,10
2	1,99	1,94	2,17	+2,57
3	6,02	6,29	6,11	+6,67

sem Fall auf das ganze Verfahren vom Auftragen der Probe bis zur Auswertung. Diese Regelmäßigkeit ist eigentlich zu erwarten, doch ihr Nachweis ist an eine entsprechende Genauigkeit des Auswertungsverfahrens gebunden. Derselbe Vorgang wird von Hais [6] im Falle der Papierchromatographie erwähnt, aber mit Variationskoeffizienten von etwa 10%, und von Kirchner [7] bei densitometrischen Untersuchungen (2,5% Unterschied zwischen benachbarten Flecken zum Unterschied von höchstens 5,2% für alle Flecken einer Platte).

---

[6] I. M. Hais, *J. Chromatog.*, **33**, *305* (1968).

[7] J. G. Kirchner, *J. Chromatog.*, **82**, *101* (1973).

Revue Roumaine de Chimie, **23**, *2*, 301 – 307 (1978)

ON THE VIBRATIONAL ANHARMONICITIES OF THE FURAN MOLECULE

DAN IORDACHE
Polytechnic Institute, Department of Physics, Bucharest, Romania

Received October 21, 1975

Accurate estimates for about 80% of the vibrational anharmonicities x_{ss}, corresponding to the furan molecule and to six of its deuterated derivatives have been obtained by means of a special computation program. The detailed analysis of these estimates showed that, the statistical parameters (mean values $\tilde{x}$, quadratic mean deviations σ) of the different groups of similar $x_{ss'}$ constants generally present regular dependences on the order of deuteration and on the types of the implied vibration fundamentals. Based on these correlations both satisfactory estimates for the other $x_{ss'}$ constants could be obtained and even correct assignments of some observed absorption bands of unidentified nature could be made.

1. INTRODUCTION

As it is known, both the complete interpretation of the molecular vibration-rotation spectra [1,2] and the refinement of the molecular effective force-fields and structures to the complete force field and the geometrical structure corresponding to the equilibrium configuration [3-6] require the previously correct estimation of all the vibrational anharmonicity constants $x_{ss'}$ of the studied molecule. Unfortunately, the difficulties implied by this estimation are rapidly increasing with the number of atoms of the molecule, especially if this molecule belongs to a low symmetry point group; for this reason, only the vibrational anharmonicities of the low symmetry molecules with less than 7 atoms [7] and these of the medium- or high-symmetry molecules with less than 20 atoms [2,8] have been systematically studied up to now.

---

[1] H. H. Nielsen, *Phys. Rev.*, **60**, 794 (1941); H. H. Nielsen, *Rev. Mod. Phys.*, **23**, 90 (1951).

[2] Z. Muldakhmetov, *Tr. fiz. Inst. Akad. Nauk SSSR*, **39**, 7 (1967).

[3] Z. Cihla and J. Pliva, *Coll. Czech. Chem. Comm.*, **28**, 1232 (1963).

[4] T. Oka and Y. Morino, *J. Mol. Spectroscopy*, **6**, 472 (1961); Y. Morino, K. Kuchitsu, and T. Oka, *J. Chem. Phys.*, **36**, 1108 (1962); M. Toyama, T. Oka, and Y. Morino, *J. Mol. Spectroscopy*, **13**, 193 (1964).

[5] D. Iordache, *Dissertation*, University of Bucharest, 1971; D. Bârcă-Gălățeanu, D. Iordache, and D. Gavrilă, *Rev. Roumaine Phys.*, **17**, 211 (1972).

[6] A. R. Hoy, I. M. Mills, and G. Strey, *Mol. Phys.*, **24**, 1265 (1972).

[7] W. S. Benedict, N. Gailar, and E. K. Plyler, *J. Chem. Phys.*, **24**, 1139 (1956); C.P. Courtey, *Ann. Soc. sci. Bruxelles*, **73**, 5 (1959); K. Machida, *J. Chem. Phys.*, **44**, 4186 (1966); G. A. Khachkuruzov and I. N. Przhevalski, *Opt. Spektrosk.*, **33**, 237 (1972).

[8] Y. Morino, J. Nakamura, and S. Yamamoto, *Bull. Chem. Soc. Japan*, **38**, 459 (1965); E. W. Jones, R. J. L. Poplewell, and H. W. Thompson, *Spectrochim. Acta*, **22**, 669 (1966); J. McBride and R. W. Nicholls, *J. Phys.*, B, **5**, 408 (1972); R. J. Hayward, B. R. Henry, and W. Siebrand, *J. Mol. Spectroscopy*, **46**, 207 (1973).

The determination of all the $x_{ss'}$ constants corresponding to the more complex molecules probably requires certain improvements of the present estimation procedure and implies, moreover, the use of an adequate computation program. Therefore, the aim of this work is to test — for the furan molecule — the possibilities of our CHCVF computation subprogram,[5] previously elaborated in order to estimate the harmonic components ω_s of the molecular vibration fundamentals (the so-called "zero-order frequencies"), and to obtain some useful conclusions by a detailed analysis of the values corresponding, for the same molecule, to an important number of similar $x_{ss'}$ constants.

2. OBTAINED RESULTS

Starting from the main existing data concerning the vibration spectra of the furan molecule [9,5] and of its deuterated derivatives,[10] taking into account the latest proposed assignments [11,12] for the vibration fundamentals of this molecule and using our CHCVF computation subprogram, we have been able to obtain accurate values for 1293 different $x_{ss'}$ constants and uncertain * values for other 272 such constants from the 1617 $x_{ss'}$ constants corresponding to the furan molecule and to its *2d*-, *3d*-, $2,5d_2$-, $3,4d_2$-, $2,3,5d_3$-and d_4-deuterated derivatives.

As it is proven by the large amplitudes and the considerable superpositions of the confidence-intervals of the $x_{ss'}$ constants corresponding to the different groups of characteristic vibrations and to the different deuterated furans (tables 1 and 2), the dependences of the individual values of the $x_{ss'}$ constants on the order of the considered deuterated derivatives, respectively on the types of the characteristic vibrations, are not too strong, so that these individual values cannot be accurately predicted using exclusively the individual values of other similar $x_{ss'}$ constants. Moreover, as the theoretical expressions of the $x_{ss'}$ constants are generally very complicated[*], it is impossible to estimate the uncertain or unknown values of certain $x_{ss'}$ constants using exclusively these theoretical relations and the accurately determined $x_{ss'}$ values.

---

* If from the observed spectra, for the liquid and the vapour phase of the studied compound have got only considerably different values of a same $x_{ss'}$ constant, or if these values are not in close agreement withthe existing collection data [2,7,8] (being, however, in the range of the theoretically possible values), the resulting value of the $x_{ss'}$ constant is considered as *uncertain*.

[9] H. W. Thompson and R. B. Temple, *Trans. Faraday Soc.*, **41,** 27 (1945); J. Lecompte, *Bull. Soc. chim. France*, **1946,** 415; G. B. Guthrie, D. W. Scott, W. N. Hubbard, C. Katz, J. P. McCullough, M. E. Gross, K. D. Williamson, and G. Waddington, *J. Amer. Chem. Soc.*, **74,** 4662 (1952); B. Bak, S. Brodersen, and L. Hansen, *Acta Chem. Scand.*, **9,** 749 (1955); E. G. Treschova, D. Ekkardt, and Iu. K. Iuriev, *Zhur. fiz. Khim.*, **38,** 295 (1964); J. Loisel, *Compt. rend., sér. B*, **262,** 31 (1966).

[10] M. Rico, M. Barrachina, and J. M. Orza, *Anales real Soc. espan. Fis. Quim., ser. A*, **61,** 141 (1965).

[11] M. Rico, M. Barrachina, and J. M. Orza, *J. Mol. Spectroscopy*, **24,** 133 (1967).

[12] J. Loisel and J. P. Pinan-Lucarré, *Compt. rend., sér. B*, **275,** 141, (1972); J. Loisel, J. P. Pinan-Lucarré, and V. Lorenzelli, *J. Mol. Spectroscopy*, **17,** 341 (1973).

For these reasons, in order to obtain at least certain statistical characterizations of the groups of similar $x_{ss'}$ constants, we carried out a detailed study of these $x_{ss'}$ groups. To this end, denoting by N, Δ, Γ and ν, δ, γ the groups of all the vibration fundamentals of the stretching, in-plane or out-of-plane deformation type of the C—H bonds, respectively of the molecular ring, the $x_{ss'}$ constants were classified as belonging to the 2N, N + N′, N + Δ, ... groups, according to $\omega_s \equiv \omega_{s'} \in N$, $\omega_{s'}\ \omega_{s'} \in N$, $\omega_s \neq \omega_{s'}$, respectively $\omega_s \in N$, $\omega_{s'} \in \Delta$, and so on.

Since for the furan molecule the assignments of all the vibration fundamentals of the N, Γ and γ types are doubless, [11,12] the mean values $\tilde{x} = \frac{1}{N_x} \sum x_i$ and the quadratic mean deviations $\sigma = \sqrt{\frac{1}{N_x} \sum (x_i - \tilde{x})^2}$ of the accurately determined $x_{ss'}$ constants corresponding to the vibration fundamentals of these types were analyzed first. The obtained results (table 1) indicate that, generally, *the algebraic values of the statistical parameters $\tilde{x}$ and σ corresponding to the groups of similar $x_{ss'}$ constants increase both with the order of the deuteration and with the modulus $|\omega_s - \omega_{s'}|$ of the difference of the frequencies of the implied vibration fundamentals.*

A similar analysis of the $x_{ss'}$ values reported by the other existing works [2, 7, 8] shows that the above specified findings of this work remain also valid — sometimes in a somewhat less evident form — for the ensembles involving a relatively reduced number of available $x_{ss'}$ values. The same conclusion is imposed by the examination of the table 2, which indicates the values $\tilde{x}_{2\Delta}$, $\tau_{2\Delta}$, $\tilde{x}_{2\nu}$, $\tau_{2\nu}$, $\tilde{x}_{2\delta}$, $\tau_{2\delta}$ of the statistical parameters of the restricted groups of similar x_{ss} constants corresponding to the undoubtedly assigned vibration fundamentals of the Δ, ν and δ types.

In order to find if the criterion of the minimum values of the reduced deviations associated to the mean values $\tilde{x}$ of the x_{ss} constants can be efficiently used for the assignment of the vibration fundamentals, we computed — for the groups of the mono-and dideuterated furans, for which the number of available x_{ss} values is maximum — the values of the reduced

---

[*] For example, the simplest such expression is :

$$x_{ss} = \frac{1}{4}\left[6k_{ssss} - 15\,\frac{k_{sss}^2}{\omega_s} - \sum_{s'} \frac{k_{sss'}^2}{\omega_{s'}} \cdot \frac{8\omega_s^2 - 3\omega_{s'}^2}{4\omega_s^2 - \omega_{s'}^2} \right], \tag{1}$$

where the normal-coordinate force constants k_{sss}, $k_{sss'}$, k_{ssss} are given in terms of the actual cubic or quartic force-constants k_{ijl}, k_{ijlm}, by relations of the type :

$$k_{sss} = \sum_{i,j,l} k_{ijl} \cdot (D^{-1}L)_{is} \cdot (D^{-1}L)_{js} \cdot (D^{-1}L)_{ls}, \tag{2}$$

by means of the $D^{-1}L$ matrix which expresses the column-vector $\boldsymbol{q}$ of the internal coordinates q_i in terms of the column-vector $\boldsymbol{N}$ of the normal coordinates N_s : $\boldsymbol{q} = D^{-1} \cdot L \cdot \boldsymbol{N}$. (3)

deviations $z_\Delta = \frac{|\tilde{x} - \tilde{x}_{2\Delta}|}{\sigma_{2\Delta}}$, z_ν, z_δ corresponding to the uncertainly assigned vibration fundamentals of furan. The obtained results (table 3) show that the principal components (elementary vibration modes) of the normal vibrations corresponding to the 995 cm^{-1} and 1140 cm^{-1} absorption bands are probably of the ring stretching type, respectively of the C—H bond in-plane deformation type. Moreover, one finds that the weights of the ele-

Table 1

The values (cm^{-1}) of the statistical parameters $\tilde{x}$ and σ of the groups of similar $x_{ss'}$ constants corresponding to the N, Γ and γ types of the implied vibration fundamentals

Type of the $x_{ss'}$ group	Type of the deuterated furans									
	Furan		d—F		d_2—F		d_3—F		d_4—F	
	$\tilde{x}$	σ	$\tilde{x}$	σ	$\tilde{x}$	σ	$\tilde{x}$	σ	$\tilde{x}$	σ
2N	−45.4	6.2	—	—	-35.3	8.4	−16.8	15.5	—	—
N+N′	−43.8	12.2	—	—	−54.5*	25.5	− 2.7	8.2*	—	—
N+Γ	− 1.2	10.4	+ 0.3	10.8	+ 0.6	11.5	+ 1.4	9.9	+ 1.7	11.6
N+γ	—	—	+ 0.9	10.3	+ 1.0	12.5	− 1.0*	8.6	+ 3.7	11.9
2Γ	− 2.8	2.1	− 1.7	3.2	− 1.3	2.2	+ 0.4	1.8	+ 2.8	3.8
Γ+Γ′	− 1.9	2.8	+ 0.2	3.3	− 0.5	5.4	+ 1.2	5.5	+ 0.7	4.0
Γ+γ	− 1.6	4.8	− 2.1	9.0	− 0.7	4.5	+ 0.4	9.1	0.0	10.4
2γ	− 5.8	2.3	− 3.6	5.3	− 1.6	4.0	− 1.8	0.3*	− 0.8	0.3*
γ+γ′	− 5.0	—	+5.5*	6.5	− 2.0	—	− 1.0	—	+ 1.0	—

* Owing to the reduced number of available data concerning the values of the $x_{ss'}$ constants of the corresponding groups, these indicated mean values are less significant.

Table 2

The values (cm^{-1}) of the statistical parameters $\tilde{x}$ and σ of the restricted groups of similar x_{ss} constants corresponding to the undoubtedly assigned vibration fundamentals of the Δ, ν and δ types

The type of the x_{ss} group	The order of the deuteration									
	0		1		2		3		4	
	$\tilde{x}$	σ	$\tilde{x}$	σ	$\tilde{x}$	σ	$\tilde{x}$	σ	$\tilde{x}$	σ
2Δ	− 4.1	3.1	−3.0	3.2	−1.7	4.5	+3.5	6.5	+3.5	6.0
2ν	−11.5	5.0	−5.8	9.7	−4.1	9.6	+6.0*	12.0	+4.8	11.8
2δ	− 3.4	2.4	−1.2	4.5	−3.0*	1.5	+0.8	7.3	+1.5	12.0

* Owing to the reduced number of available data concerning the values of the x_{ss} constants of the corresponding groups, these indicated mean values are less significant.

mentary vibration modes of the Δ, ν and δ types in the normal vibration modes corresponding to the 1180 cm^{-1} and 1040 cm^{-1} bands are comparable, the δ and ν modes being probably preponderant in the first case, and the Δ and ν modes in the second one. All these conclusions are in good agreement with the results of the work,[12] obtained by means of the classical assignment criteria.

Table 3

The values of the statistical parameters $\tilde{x}$, σ (cm^{-1}) $z_\Delta = \frac{|\tilde{x} - \tilde{x}_{2\Delta}|}{\sigma_{2\Delta}}$, z_ν and z_δ of the groups of accurate x_{ss} estimates corresponding — for the mono- and dideuterated furans — to the uncertainly assigned vibration fundamentals of furan

$\tilde{\nu}_s$ (cm^{-1})	The order of the deuteration								Assignments		
	1				2				Ref. 11	Ref. 12	This work
	$\tilde{x}$; σ	z_Δ	z_ν	z_δ	$\tilde{x}$; σ	z_Δ	z_ν	z_δ			
1180	−1.2 ;4.9	0.56	0.47	0	−3.8 ;4.7	0.51	0.03	0.53	Δ	δ	$\delta+\nu$
1140	−3.0 ;1.2	0	0.29	0.40	−2.2 ;1.1	0.11	0.20	0.53	ν	Δ	Δ
1040	−2.3 ;1.4	0.22	0.36	0.24	+1.0 ;5.0	0.60	0.53	2.67	$\nu+\delta$	Δ	$\Delta+\nu$
995	−6.3 ;3.8	1.03	0.05	1.13	−8.0 ;3.7	1.40	0.41	3.33	Δ	ν	ν

Using the accurately determined values of certain $x_{ss'}$ constants and the estimates offered by the determined confidence-intervals for the other $x_{ss'}$ constants, the direct estimates Ω_s of the zero-order frequencies :

$$\Omega_s = \tilde{\nu}_s - x_{ss} - \frac{1}{2} \cdot \sum_{s'} x_{ss'}, \tag{4}$$

as well as their quadratic mean errors :

$$\sum\nolimits_s = \sqrt{\tau^2(\tilde{\nu}_s) + \mathrm{Cov}(\tilde{\nu}_s,\ x_{ss}) + \sigma^2(x_{ss}) + \sum_{s'} [\mathrm{Cov}(\tilde{\nu}_s,\ x_{ss'}) + \frac{1}{4} \cdot \sigma^2(x_{ss'}) + \mathrm{Cov}(x_{ss},\ x_{ss'})]},$$

implied by the quadratic mean errors and the covariances corresponding to the observed wavenumbers $\tilde{\nu}_s$ of the absorption bands identified — in the accepted assignment [12] — with the ν_s vibration fundamentals, respectively to the estimates of the x_{ss} and $x_{ss'}$ constants, were obtained. Finally, the adjusted values ω_s of these Ω_s estimates, satisfying both the complete isotopic rules (CIR) and the condition : $\sum_s \left(\frac{\omega_s}{\Omega_s} - 1\right)^2 = \text{minimum}$, (5) have been determined by means of the same CHCVF computation program. The obtained Ω_s, $\sum_s$ and ω_s values, together with the observed wavenumbers $\tilde{\nu}_s$ corresponding to the out-of-plane vibration fundamentals of the furan molecule are presented in table 4.

Table 4

The observed wavenumbers ($\tilde{\nu}$), the confidence-intervals ($\Omega \pm \Sigma$) of the direct estimates of the zero order frequencies, and the adjusted by CIR harmonic components (ω) corresponding to the out-of-plane fundamental vibrations of furan and its deuterated derivatives (cm^{-1})

Normal mode of vibration		Molecule						
		Furan	2d−F	3d−F	2,5 d_2−F	3,4d_2−F	2,3,5d_3−F	d_4−F
$\nu_9(A_2)$	$\tilde{\nu}$	(863)	860	849	(849)	780	828	(725)
	$\Omega\pm\Sigma$	855±10.6	860± 7.6	833±12.1	843±16.4	792±20.5	844±16.4	740± 9.7
	ω	850.42	847.92	837.89	849.39	792.90	848.86	740.74
$\nu_{10}(A_2)$	$\tilde{\nu}$	728	658	646	644	(666)	582	572
	$\Omega\pm\Sigma$	769±10.0	687±22.5	700±28.0	681±17.1	677±19.7	611±14.6	586±22.7
	ω	764.34	688.44	701.04	679.73	677.08	610.36	589.85
$\nu_{11}(A_2)$	$\tilde{\nu}$	613	601	602	524	527	515	(498)
	$\Omega\pm\Sigma$	648±24.0	635± 9.6	636±21.9	556±19.5	571±22.3	550±27.2	527±21.7
	ω	643.52	638.96	635.78	551.64	570.61	548.50	531.39
$\nu_{19}(B_2)$	$\tilde{\nu}$	745	738	729	679	605	666	597
	$\Omega\pm\Sigma$	791±29.5	755±27.2	742±13.8	701±13.7	633±10.8	692±18.4	625±13.3
	ω	794.96	752.14	744.07	703.92	629.94	693.01	617.35
$\nu_{20}(B_2)$	$\tilde{\nu}$	838	814	800	799	806	709	700
	$\Omega\pm\Sigma$	822±22.0	864±13.9	799±13.9	810±18.6	776±21.5	699±11.7	717±18.6
	ω	824.24	851.50	802.74	826.35	782.16	700.19	701.12
$\nu_{21}(B_2)$	$\tilde{\nu}$	603	516	547	506	587	499	500
	$\Omega\pm\Sigma$	626±20.3	536± 7.1	584±12.0	529±17.8	645±36.2	522±15.3	533±24.9
	ω	635.78	543.05	582.99	520.04	642.51	520.20	530.99

CONCLUSIONS

The obtained results impose the following conclusions :

(i) the use of an automatic program for the analysis of the vibration spectra of the second and third order is possible and — for the molecules with many atoms — it is even necessary,

(ii) the statistical parameters (mean values $\tilde{x}$, qudratic mean deviations σ) corresponding to the ensembles of $x_{ss'}$ constants of a same character, present certain regularities (the general increase of the values of these statistical parameters with the order of the deuteration and with the modulus $|\omega_s - \omega_{s'}|$ of the difference of the frequencies corresponding to the implied vibration fundamentals),

(iii) starting from a detailed analysis of the values of the x_{ss}, constants and using the criterion of the "minimum values of the reduced deviations of the mean values of the x_{ss} constants", there are possible even some correct assignments of the observed absorption bands of unidentified nature,

(iv) though the errors affecting the estimates of the zero-order frequencies are relatively large (sometimes — see table 4 — of about 20 — 30 cm^{-1}), undoubtedly one finds that these zero-order frequencies considerably differ from the observed ones, the parameters of the harmonic part of the complete force field being — in consequence — sensibly different [5] from the corresponding constants of the quadratic force field determined without taking into account the vibrational anharmonicities.

Revue Roumaine de Chimie, **23**, 2, 309–311 (1978)

COMPTES RENDUS

C. DRĂGULESCU and E. PETROVICI, "Chimie structurală modernă. Chimia coordinanţei 8" (*Modern Structural Chemistry. The Chemistry of Octacoordination*), Ed. Academiei, Bucharest, 1977, 947 pages.

Although the chemistry of the coordinance may appear to the nonspecialist as limited in scope and of very narrow interest, it actually covers a surprisingly large variety of substances and manages to explain adequately their structure and chemical behaviour. This branch of chemistry has established itself over the years as an independent and self-contained branch of coordination chemistry and the workers in this field may approach a wide range of interesting subjects. Over the past ten years papers reporting new octacoordinated compounds or working out their molecular or crystalline architecture have appeared at a fast pace. Their number, according to the authors, is now well over 3000. Such a diversity of substances, having in common only the same coordination number of the central atoms and including a wide spectrum of complexes, metals, alloys and salts, may prevent attempts at reporting them coherently in a monograph. The task required to systemize and describe exhaustively the known octacoordinated structures, to find a method and a language suitable to encompass the whole variety of structures, and keep abreast of every new publication while writing for updating the material may seem exceedingly difficult. Such a work has however been undertaken by the authors, Prof. Coriolan Drăgulescu, and Dr. Emil Petrovici, both of the Timișoara Polytechnical Institute, themselves original contributors to the field. The resulting work, a rich, 947-page monograph, the first of its kind in the Romanian chemical literature, gives a coherent outline of the chemical structure of the coordination compounds, based on quantum chemistry treatment and the concept of coordinance, describing almost all existing octacoordinated compounds under their various aspects.

The monograph consists of four parts. The first part presents some theoretical aspects of the chemical bond, introducing the reader to this field and acquainting him with the usual concepts of coordination chemistry. It is more of a textbook and can be useful to coordination chemists in general. The second part deals with octacoordination geometries, giving an extensive description of each type of structure, according to the form of the octacoordination polyhedron. The authors make consistent use in their work of the rather obvious fact that knowledge of the coordination polyhedron of each atom and oft he polyhedra space arrangement leads to a complete structural knowledge of the solid. Sometimes, the reduced symmetry of the polyhedra hinders easy description, in which case the authors consider them as distorted forms of some simpler, more symmetrical geometries, such as the cube for most octacoordinated conformations. Such a methodology allows a more systematic approach to structure description. A supplementary chapter in this part deals with the increasingly intriguing variable-coordinance structures.

The last two parts of the monograph (amounting to two thirds of its volume) constitute a thorough compilation of the literature, the reported octacoordinated compounds being classified first according to the generating element and second to the polyatomic ligand groups which provide the coordination polyhedra. The generating elements are presented following their order in the periodic table. As for ligands, the inorganic ones are reported first, followed by the organic ligands in the order of the nature of the atoms making up the functional group. Such a systematic treatment allowed the authors to offer structural data on almost all complexes and other compounds of the about 100 elements which can possibly have the coordination number 8 — the number of overlooked compounds being thus insignificant. In the fourth part, the number of considered polyatomic ligands liable to ensuring octacoordination under various symmetries, amount to about 80, not including their derivatives. A special, but unfortunately too short chapter is devoted to the octacoordinance of the elements having zero oxidation number. In this way, compounds such as $Rh_6(CO)_{16}$ or $La(dipy)_4$, which have stimulated much research of late, are covered.

This wealth of material is excellently illustrated by hundreds of well-drawn and suggestive figures, displaying various polyhedron packings and coordination geometries, and by plenty of structural formulae helping the correct understanding of compound conformation. Hoard's notation, used throughout, turned out to be particularly productive in describing antiprism and trigonal dodecahedron structures. It simplified the overall layout of the book. A good point is that structure descriptions were not burdened with experimental details, available for the interested reader in the references quoted (in the alphabetical order of the first author's name) at the end of the book. Compound retrieval is greatly facilitated by a very detailed subject index.

It should be sadly reminded here that Professor C. Drăgulescu died at the age of 70, just after this book appeared. Well known for his original scientific activity in the fields of inorganic and coordination chemistry, Prof. Drăgulescu was also highly esteemed for his teaching abilities and for the outstanding quality of his textbooks, of which "Modern Inorganic Chemistry", published in 1975, is widely used today by both students and researchers. The clarity of his style makes his books easily readable and the wealth of their information and insight makes them indispensable for any coordination chemist or specialist in such related fields as chemical technology or biochemistry.

Alex. Butucelea
Center of Physical Chemistry

D. NEGOIU and ANGELA KRIZA, "Poluanţi anorganici în aer" (*Inorganic Pollutants in Air*) Ed. Academiei, Bucharest, 1977, 219 pages.

Environment protection has become a major concern not only for scientists and technologists, bur for citizens as well and, consequently, for the law-promoting and law-enforcing bodies in any country. The Romanian government has initiated a comprehensive and long-range programme of preventing further environment deterioration and reducing the levels of existing pollutants. The corresponding law, adopted several years ago, offers a set of standards for industrial or other virtual pollutants, and stipulates fines for any violation of its provisions. At the same time, a complex educational programme has been undertaken to define and popularize the possible sources of air and water pollution, the harmful effects of various pollutants, and the means to prevent the increase of pollution levels and even lower them below sub-noxious values.

This book may be considered as a welcome and valuable contribution to the antipollution campaign. It is a successful attempt to describe the main inorganic compounds having a harmful effect upon the air quality and to suggest the methods for analyzing and purifying industrial gases. The need for such a work in the Romanian literature has long been felt. The chapters of the book are devoted to each inorganic pollutant—carbon monoxide, nitrogen and sulfur oxides, hydrogen sulfide, hydrochloric acid, fluorine and its compounds, chlorine, phosphorus and its compounds, arsenic, mercury. lead, beryllium, cadmium, and copper. Since light is deeply involved in producing smog in urban agglomerations, a separate chapter deals with air pollutants produced photochemically. Another chapter describes succintly the general methods of purifying industrial gases. Each chapter describing a pollutant delineates first the main pollution sources, then the means for controlling the compound emission, its physiological action and, lastly, the methods of its determination in the air. Though such a unitary pattern is obviously helpful to the reader for quick reference, it surely makes the book somewhat tedious to read from cover to cover. The material is well supported by 400 references.

It is a matter of common knowledge to ecologists and environmental chemists that air pollution is much more than the simple sum of its parts ; it is rather the result of a complex interaction of the present pollutants both among themselves and with solar radiation and other atmospheric and biological factors. The authors describe such interactions in each chapter devoted to a particular pollutant and discuss their overall aspects in chapter 7.

Somewhat unfamiliar to the Romanian reader may seem the names used by the authors for certain inorganic substances, e.g. carbon monoxide, diarsenic trisulfide, etc. instead of carbon oxide, arsenic trisulfide or simply sulfide. The latter names have long been used in our chemical nomenclature, but they are often misleading and should be replaced. Rational names as those used by the authors describe better than the traditional ones the compound stoichiometry and they have been already widely accepted in many languages, upon recomandation from the International Union of Pure and Applied Chemistry (IUPAC). Several chemistry books published lately, including this one, have promoted the IUPAC nomenclature, but a real progress could only be made if the Publishing House of the Academy would speed up publication of the new nomenclature of chemical compounds, already completed by a Romanian team, which would contribute significantly to widening the proper usage of substance names in our literature.

The book may be particularly useful to chemical technologists, who have to know the main pollution sources and the means to fight them efficiently, but also to research chemists, teachers and students. Publication of a similar book on organic air (and water) pollutants would be most welcome.

Alex. Butucelea
Center of Physical Chemistry

P. W. SELWOOD, "Chemisorption and Magnetization", Academic Press, New York, 1975, IX + 172 pages.

At present, magnetochemistry is a valuable method for the study of surface phenomena. This book is devoted to the strategy of application of magnetism in chemisorption and heterogenous catalysis. It is a complete revised and enlarged edition of the previous book "Adsorption and Collective Paramagnetism" published by Academic Press in 1962. Change of title has been dictated by changes of emphasys, and removal of the term "collective paramagnetism" in favour of "superparamagnetism". Much more attention is now paied to the particle size determination, and to the number of adsorbent atoms affected when any molecule is adsorbed on a solid surface. Though not exclusively, as before, the author refers chiefly to nickel as adsorbent.

Chapter I is a brief consideration of the basic phenomena in chemisorption and magnetism.

As this book is addressed mainly to the researchers interested in chemosorption and catalysis, an introduction to magnetism is included in chapter II — Superparamagnetism, and chapter III — Magnetization measurements at high M/M_0.

The following chapter describes the particle size determination by means of magnetic methods.

Chapter V deals with applications of magnetization measurements at high M/M_0 to the H_2/Ni, $H_2/Ni\text{-}Cu$, H_2/Co, and H_2/Fe systems.

In chapter VI, magnetization, measurements at low M/M_0 are recorded.

Low-field results for H_2/Ni, H_2/Co, and H_2/Fe are given in chapter VII.

One of the most important problems in the chemisorption — determination of the bond nature and number — is treated in chapters VIII and IX.

Chapter X depicts results for ethylene, ethane, and acetylene; results for benzene are given in the next chapter.

Chapter XII — the last — deals with other systems.

An Appendix, with the symbols and units used in the work, and two indexes — author and subject — are also provided.

The work contains many interesting and pioneering results obtained in the author's laboratory; and Professor Selwood is a well-known and reputed expert in magnetochemistry.

This book will be of great interest and value to research workers engaged in the field of chemosorption or heterogenous catalysis.

T. Chirulescu

CORRIGENDA

A. T. Balaban, *Rev. Roumaine Chim.* **19**, 1611 (1974): Chemical Graphs. XXIII. General Cubic Graphs with One Loop, and Homovalenes or Their Derivatives.

In Table 2 (p. 1613), the last line, for $p-1 = 11$, should have 125 instead of 126, and 601 instead of 502. On p. 1616, line 7, also replace 502 by 601. The numbers of general cubic graphs with one loop, $p-1 = 11$ vertices, β double bonds, and t three-circuits are presented in the following table.

t β	0	1	2	3	4	5	Total
0	3	10	20	18	9	2	62
1	15	48	59	31	10	1	164
2	38	79	58	24	2	—	201
3	44	49	26	6	—	—	125
4	23	17	4	—	—	—	44
5	4	1	—	—	—	—	5
Total	127	204	167	79	21	3	601

* * *

A. T. Balaban, E. M. Palmer and F. Harary, *Rev. Roumaine Chim.* **22**, 517 (1977): Chemical Graphs. XXIX. Numbers of Isomers with Naphthalene and Adamantane Skeletons.

In Table 1 (p. 519), second line from bottom and column headed $x^{14}yz$, replace 16 by 13. On page 522, second line from bottom, replace $48y_1^2y_2^3y_4$ by $48y_1^2y_2^3y_4^2$.

NOTE POUR LES AUTEURS

La Revue Roumaine de Chimie publie des articles en anglais, français, russe, allemand ou espagnol. Les auteurs sont priés d'envoyer des articles et des comptes rendus inédits.

Les manuscrits seront dactylographiés à deux intervalles. La bibliographie, les tableaux et la légende des figures seront placés après le texte.

Si l'article fait partie d'une série numérotée, le titre de la partie précédente sera indiqué dans une note au bas de la première page.

Chaque article sera précédé d'un résumé comprenant quinze lignes au maximum.

Les références bibliographiques dans le texte seront faites par des exposants sans parenthèses et paraîtront comme des notes au bas de chaque page.

Les publications périodiques mentionnées dans la bibliographie seront présentées suivant les prescriptions internationales : le nom de l'auteur précédé de l'initiale du prénom, le titre du périodique abrégé conformément à « Chemical Abstracts », et souligné par une ligne, le numéro du tome indiqué par des chiffres arabes et souligné par deux lignes, suivi de la première page de l'article; à la fin, l'année de la parution sera placée entre parenthèses. Le numéro de la revue ne sera pas indiqué si les pages du volume sont numérotées consécutivement.

Les textes des livres ou traités incluront : les noms des auteurs, les initiales du prénom, le titre du livre entre guillemets et sans être souligné, le numéro du tome précédé par l'abréviation « vol. » (ou « Bd. »), le numéro de l'édition, les éditions (the publisher), la localité de la parution du livre, l'année de la parution et la page de la référence précédée(s) par l'abréviation « p » (ou « S »).

Les brevets seront indiqués comme suit : l'auteur ou la firme, le pays et le numéro du brevet, la date et la revue (Chem. Abstr.). Par ex. : M. Jones (to Union Carbide C°), Brit. Pat. 601 238, 2 Sept. 1959, *Chem. Abstr.*, **54**, 12808 (1960).

Les diagrammes seront tracés à l'encre de Chine sur papier calque. Les tableaux et les figures (en nombre strictement nécessaire) seront numérotés par des chiffres arabes. Les courbes dans les figures seront numérotées par des chiffres arabes et leur explication sera donnée dans la légende des figures. Prière de ne pas inscrire les mêmes données dans les tableaux et les figures. Chaque tableau aura un titre. On indiquera dans le texte la place approximative des tableaux et des figures. Les formules chimiques seront incluses dans le texte; en outre, elles seront transcrites sur papier calque, à l'encre de Chine.

Les auteurs sont priés d'indiquer les caractères italiques (en soulignant les lettres au crayon), ainsi que tout autre caractère spécial; les préfixes *ortho, meta, para, cis, trans*, etc. seront soulignés pour indiquer leurs caractères italiques et ne seront jamais écrits avec des majuscules.

Aucune correction à la main ne sera admise sur le manuscrit. Les corrections seront frappées à la machine. Les lettres grecques ou autres symboles spéciaux seront insérés à la main à l'encre clairement.

Le manuscrit sera signé par l'auteur.

Le colonne-titre aura 50 lettres au maximum.

L'entière responsabilité du contenu des articles appartient aux auteurs.

PRINTED IN ROMANIA

TRAVAUX PARUS AUX ÉDITIONS DE L'ACADÉMIE DE LA RÉPUBLIQUE SOCIALISTE DE ROUMANIE

6 JUN 1978

C. DRĂGULESCU, E. PETROVICI, **Chimie structurală modernă. Chimia coordinanţei** (La chimie structurale moderne. La chimie de la coordinence), 1977, 947 p., 70 lei.

I. G. MURGULESCU, **Introducere în Chimia fizică. Vol. I. 1. Atomi, molecule, legătură chimică** (Introduction à la Chimie Physique, 1er vol. 1. Atomes, molécules, liaison chimique), 1976, 560 p., 36 lei.

E. P. BALTĂ, E. BALTĂ, **Introduction to the physical chemistry of the vitreous state**, coédition avec Abacus Press, 1976, 287 p., 31 lei.

H. I. GĂLĂŢEANU, **Radiochimia aplicată. Metode şi probleme** (La radiochimie appliquée. Méthodes et problèmes), 1976, 307 p., 19 lei.

CONST. V. UGLEA, **Cromatografia pe gel permeabil. Noi domenii de aplicare** (La chromatographie sur gel perméable. Nouveaux domaines d'application), 1976, 123 p., 6,75 lei.

FRANCISC A. GOTHARD, **Echilibre lichid-vapori. I. Baze teoretice şi metode de calcul** (Equilibres liquide-vapeurs. I. Bases théoriques et méthodes de calcul), 1975, 263 p., 2 pl., 28 lei.

CONST. GH. MACAROVICI, D. MACAROVICI, **Chimia oxizilor dubli şi utilizările lor** (La chimie des oxydes doubles et leur utilisation), 1975, 195 p., 13 lei.

M. AVRAM, **Antidăunători** (Pesticides), 1974, 496 p., 41 lei.

ELENA CEAUŞESCU, **Research work on synthesis and characterization of macromolecular compounds. Contributions**, 1974, 251 p., 20 lei.

DUMITRU COSTACHE, **Analiza chimică prin metoda cinetică** (L'Analyse chimique par la méthode cinétique), 1974, 251 p., 20 lei.

G. A. RĂDULESCU, **Proprietăţile ţiţeiurilor româneşti** (Les propriétés des pétroles roumains), 1974, 267 p., 2 pl., 18 lei.

CR. SIMIONESCU, VIORICA RUSAN, V. POPA, **Chimia algelor marine** (La chimie des algues marines), 1974, 212 p., 1 pl., 18 lei.

I. ZUGRĂVESCU, MAGDA PETROVANU, **Chimia n-ilidelor** (La chimie des n-Ilures), 1974, 348 p., 19 lei.

MARIA FITI, **Dozimetria chimică a radiaţiilor ionizante** (La dosimétrie chimique des radiations ionisantes), 1973, 240 p., 13,50 lei.

TIBERIU NĂŞCUŢIU, **Metode radiochimice de analiză** (Méthodes radiochimiques d'analyse), 1973, 384 p., 23 lei.

CRISTOFOR SIMIONESCU, MARGARETA GRIGORAŞ, AGATA CERNĂTESCU ASANDEI, GHEORGHE ROZMARIN, **Chimia lemnului in România. Plopul şi salcia** (La Chimie du bois en Roumanie. Le peuplier et le saule), 1973, 299 p., 13 pl., 26 lei.

MIHAI FLORESCU, **Eficienţa economică a cercetării ştiinţifice** (L'efficience économique de la recherche scientifique), 1972, 115 p., 15 lei.

GEORGETA LĂZĂRESCU, **Sistematizarea informaţiilor în chimia organică** (Systématisation des informations en Chimie organique), 1972, 243 p., 1 pl., 10,50 lei.

I. P. I. c. 7710

43 426

Lei 25.—
$45 (price per year)

F 1103

ACADÉMIE DE LA RÉPUBLIQUE SOCIALISTE DE ROUMANIE

REVUE ROUMAINE DE CHIMIE

TOME 23
N° 3
Mars 1978

EDITURA ACADEMIEI REPUBLICII SOCIALISTE ROMÂNIA

Rev. Roumaine Chim.

RECHAX, 23, 3, p. 313–468 (1978), Bucarest

ACADÉMIE DE LA RÉPUBLIQUE SOCIALISTE DE ROUMANIE

COMITÉ DE RÉDACTION

Rédacteur en chef :

I. G. MURGULESCU, membre de l'Académie de la République Socialiste de Roumanie

Rédacteurs en chef adjoints :

A. T. BALABAN et V. EM. SAHINI, membres correspondants de l'Académie de la République Socialiste de Roumanie

Collège de rédaction :

EM. BRATU, ELENA CEAUŞESCU, ECATERINA CIORĂNESCU-NENITZESCU, C. DRĂGULESCU, CR. SIMIONESCU, membres de l'Académie de la République Socialiste de Roumanie; P. SPACU, membre correspondant de l'Académie de la République Socialiste de Roumanie; MARGARETA AVRAM, I. HAIDUC, D. I. MARCHIDAN, I. MOLDOVAN, G. NIAC et D. SĂNDULESCU

La Revue Roumaine de Chimie paraît 10 fois par an. Toute commande de l'étranger (fascicules ou abonnements) sera adressée à : 70116, ILEXIM—Departamentul Export-Import Presă (Revues)/Departamentul Export-Import Carte (Livres), P.O.Box 136—137, télex 11226, 3, str. 13 Decembrie, Bucarest, Roumanie

Les manuscrits, les livres et les revues proposés en échange, ainsi que toute correspondance seront envoyés à la rédaction :

REVUE ROUMAINE DE CHIMIE

23, str. Dumbrava Roşie, Bucarest 9, Roumanie, téléphone 12 41 60

EDITURA ACADEMIEI REPUBLICII SOCIALISTE ROMÂNIA

71021, 125, Calea Victoriei, Bucarest, Roumanie, téléphone 50 76 80

REVUE ROUMAINE
DE
CHIMIE

1978 MÁR 29

Tome 23, N° 3 Mars 1978

V. E. SAHINI, V. CONSTANTIN, I. ŞERBAN and C. VLĂDESCU, Electron-impact-induced fragmentation of some dibenzo[b,e]thiepines 315–323

R S. STERNBERG and MARIANA TERZI, Surface tension of simple fused halides 325–337

M. ABRAHAM and M. POIRIER, Stability constant of $FeCl_4^-$ in molten $NaFeCl_4$ (in French) 339–350

R MARIA RĂDULESCU, Study of the influence of fluoride contamination on the corrosion of zircaloy-2 in water and steam at high temperature (in French) 351–360

ALA NICOLESCU, MARIANA UDREA and GABRIELA POPA, Comparative study of the adsorption of some cyclic hydrocarbons on active alumina-support for catalysts. I. Determination of adsorption isotherms and of various characteristic thermodynamic values 361–369

D. NEGOIU, VASILICA MUREŞAN and N. MUREŞAN, Contributions to the chemistry of thiocomplexes. VI. Complex compounds of Pt(II) with thioamides of the dibenzofuran series 371–376

V. K. SRIVASTAVA, C. SINGH and B. B. MISRA, Protection of DNA by metal coordinates — A simple stoichiometric study 377–382

I. GUTMAN, M. RANDIĆ and N. TRINAJSTIĆ, Kekulé structures and topology. III. On inseparability of Kekulé structures 383–395

RODICA CRĂCIUNEANU and EUGENIA FLOREAN, Behaviour of 1-Acyl-4-aryl-thiosemicarbazides towards heavy metal ions. IV. Behaviour of Ni(II) towards 1-benzoyl-4-aryl-thiosemicarbazides (in German) 397–405

I. DRIMUŞ, L. PAPAHAGI and C. CRISTESCU, Degradation of peroxides obtained by thermal oxidation of n-dodecane with molecular oxygen. I. Thermal degradation of samples obtained at various conversions. II. Separation of a peroxidic concentrate from n-dodecane oxidized at a law conversion; thermocatalytic degradation of this concentrate (in German) 407–415

R F. MARX, I. MENESSY and D. BECHERESCU, On the formation of high-melting carbides in plasma (in German) 417–427

M. Y. MIRZA, Practical indications for the preparation of ^{99m}-Tc generator for medical use 429–433

R GH. DRĂGAN, Amorphous-crystalline coupling in polyethylene. VI. The study of the morphological changes in high molecular weight polyethylene by compounding with polypropylene 435–443

Rev. Roumaine Chim., **23**, *3*, p. 313–468 (1978), Bucarest.

I. AGHERGHINEI, Considerations upon rationalization of numerical integration of Mayo-Lewis equation 445–448

E. CORDOŞ, I. ANGYALOSI and CĂTĂLINA DIMITRESCU, An automatic system for cyclic chronopotentiometry 449–452

S. MOLDOVEANU, A new type of parametrization among the approximate SCF-LCAO-MO methods 453–465

BOOK REVIEWS 467–468

Revue Roumaine de Chimie, **23**, *3*, 315–323 (1978)

ELECTRON-IMPACT-INDUCED FRAGMENTATION OF SOME DIBENZO[b, e] THIEPINES

V. E. SAHINI*, V. CONSTANTIN*, I, ŞERBAN** and C. VLĂDESCU**

* Polytechnic Institute Bucharest, Institute of Chemistry, Department of Physical Chemistry, Bd. Republicii 13, Bucharest, Romania

** Institute of Internal Medicine of the Academy for Medical Sciences, Şos. Şt. cel Mare 19, Bucharest, Romania

Received June 29, 1977

The 50 eV mass spectra of dibenzo[b, e]thiepine, dibenzo[b, e]thiepine-5,5-dioxide and dibenzo[b, e]thiepine-11-one-5,5-dioxide are reported and discussed. The stability of the molecular ions and their fragmentation markedly depend on the nature of the bridging atom groups in the central seven-membered ring. The ionization potentials and the appearance potentials for the relevant fragments are reported.

A variety of specific fragmentation reactions and interesting rearrangements of the type ABC→AC + B have been established in the gas phase ion chemistry of organosulphur compounds.[1–6] However, although the mass spectra of several classes of sulphur heterocycles have been extensively studied (cf. a comprehensive review[7]) little attention has been directed towards dibenzothiepines.[8–9]

The aim of the present study is an investigation in the electron-impact behaviour of dibenzo[b, e] thiepine (I), dibenzo [b, e] thiepine 5,5-dioxide (II) and dibenzo [b, e] thiepine-11-one-5,5-dioxide (III):

I. $X{=}S$, $Y{=}CH_2$, $M{=}212$
II. $X{=}SO_2$ $Y{=}CH_2$, $M{=}244$
III. $X{=}SO_2$, $Y{=}CO$, $M{=}258$

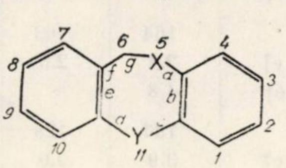

[1] J. Heiss and K. P. Zeller, *Org. Mass Spectrom.*, **2**, 819 (1969).

[2] L. Audier, M. Azzaro, A. Cambon and R. Guedj, *Bull. Soc. chim. France*, **1968**, 1013.

[3] L. Simov and I. G. Taulov, *Org. Mass Spectrom.*, **5**, 1133 (1971).

[4] R. J. Soothill and L. R. Williams, *Org. Mass Spectrom.*, **6**, 141 (1972).

[5] J. H. Bowie, B. K. Simons and S. O. Lawesson, *Rev. Pure Appl. Chem.*, **19**, 61 (1969).

[6] T. H. Kinstle and W. R. Oliver, *Org. Mass Spectrom.*, **6**, 669 (1972).

[7] A. N. Porter and J. Baldes, "Mass Spectrometry of Heterocyclic Compounds", Wiley-Interscience, New York, 1971.

[8] G. H. Wahr, *Org. Mass Spectrum.*, **3**, 1349 (1970).

[9] A. Maquestieu, Y. van Haverbeke and F. Delalieu, *Org. Mass Spectrom.*, **5**, 1015 (1971).

EXPERIMENTAL

Mass spectra were recorded with a MI-1305 mass spectrometer using the direct evaporation of the sample in the ion source, at 50 eV energy of the electron beam. The emission current was kept at 1.5 mA. In order to obtain a low electron energy, the mass spectrometer was modified in the original circuitry of the ionization voltage.[10] The ionization efficiency (*IE*) curves were obtained by reducing the electron ionizing voltage in 0.1 volt steps and by recording the ion current of the investigated ion on a digital voltmeter. During recording of the IE curves the emission current was kept at 0.1 mA. The mercury, present in the ion source from the diffusion pumps of the mass spectrometer, was used to calibrate the electron energy scale. The threshold voltage was evaluated by the method of extrapolated voltage differences to zero ion current.[11–12]

RESULTS AND DISCUSSION

The 50 eV mass spectra of compounds I—III are listed in tables 1—3. Table 1 also gives the mass spectrum of dibenzo[c, e]thiepine, obtained by Maquestieu et al[9]. The ionization and appearance potentials given in table 4 are average values from 3—4 determinations, the maxi-

Table 1

Mass spectra of dibenzo[b, e]thiepine * and dibenzo[c, e]thiepine **

m/e	214	213	212	211	210	209	208	198
Rel. int. [b, e]	5.4	15.8	97.7	15.2	3.2	2.8	3.7	2.1
Rel. int. [c, e]	—	—	100	—	—	—	—	—
m/e	197	196	195	194	185	184	180	179
Rel. int. [b, e]	35.5	1.7	3.0	2.6	1.1	3.3	15.9	100
Rel. int. [c, e]	—	—	—	—	—	—	11.6	64.7
m/e	178	177	176	175	171	167	166	165
Rel. int. [b, e]	75.0	10.0	8.9	1.7	2.3	1.4	3.3	14.3
Rel. int. [c, e]	44.7	—	—	—	—	8.9	33.5	51.6
m/e	164	163	153	152	151	150	139	135
Rel. int. [b, e]	2.4	2.6	2.5	9.8	5.0	2.3	3.3	4.4
Rel. int. [c, e]	4.8	—	2.9	12.5	5.8	—	6.3	—
m/e	134	128	127	126	121	115	92	91
Rel. int. [b, e]	3.9	2.0	1.7	1.2	2.0	3.4	2.3	2.7
Rel. int. [c, e]	—	2.4	2.2	0.5	—	5.5	—	—
m/e	90	89	88	78	77	76	75	69
Rel. int. [b, e]	1.7	14.0	1.6	1.9	4.2	4.9	1.1	2.2

* Peaks having an abundance less than 1% of base peak are not included. Metastable peaks are found at m/e values of 183, 151 and 131 to 127. Doubly-charged ions are found at m/e values of 106.5, 105.5, 104.5, 98.5, 97.5 92.5, 89.5 (4%), 88.5, 82.5(0.6%), 76.5 (0.7%) and 69.5. Unless otherwise stated, the other peaks gave an abundance lessa than 0.5%.

** Taken from reference 9.

---

[10] V. E. Sahini, L. Rădulescu and V. Constantin, to be submitted.

[11] J. W. Warren, *Nature*, **165**, 810 (1950).

[12] J. W. Warren and C. A. Mc Dowell, *Discuss. Faraday Soc.*, **10**, 53 (1951).

Table 2

Mass spectrum of dibenzo[b, e]thiepine-5.5 dioxide

m/e	246	245	244	228	227	226	225	209
Rel. int.	2.3	6.3	38.5	2.8	14.0	3.5	1.9	1.9
m/e	197	196	195	194	193	180	179	178
Rel. int.	5.3	1.2	3.8	3.8	1.7	56.8	100	78.4
m/e	177	176	175	167	166	165	164	163
Rel. int.	15.2	11.1	2.3	1.1	6.2	32.1	18.3	20.8
m/e	154	153	152	151	150	139	128	127
Rel. int.	4.7	3.0	14.0	7.5	2.0	3.3	2.2	1.7
m/e	126	116	115	114	91	90	89	88
Rel. int.	1.5	4.2	3.8	3.6	3.1	3.3	18.0	2.3
m/e	78	77	76					
Rel. int	2.1	4.3	5.6					

Peaks having an abundance less than 1% of base peak are not included. Metastable peaks are found at m/e values of 132, 129 and uncertain at m/e values of 212 to 208 , 153 to 150 and 141 to 138. Doubly-charged ions are found at m/e values of 105.5, 104.5, 98.5, 97.5, 96.5, 90.5, 89.5 (5.4%), 88.5 (1,8%), 87.5, 86.5, 83.5, 82.5 (3.8%) 76.5, 75.5 and 69.5. Unless otherwise stated, the other doubly-charged ions have an abundance less than 0.5%.

Table 3

Mass spectrum of dibenzo[b, e]thiepine-11-one-5,5-dioxide

m/e	260	259	258	195	194	193	167	166
Rel. int.	1.0	2.5	15.3	11.8	75.0	9.0	2.8	27.0
m/e	165	164	163	162	152	140	139	115
Rel. int.	100	13.1	9.5	1.3	2.8	1.4	8.1	4.5
m/e	113	97	96	91	90	89	83	82
Rel. int.	1.4	1.2	1.3	1.4	11.0	16.5	3.5	6.5

Peaks having an abundance less than 1% of base peak are not included. Metastable peaks are found at m/e values of 145 and 140. Doubly-charged ions are found at m/e values of 98.5, 97.5, 96.5, 95.5, 85.5, 84.5, 83.5, 82.5 (5,9%), 81.5, 71.5, and 69.5 (0.9%). Unless otherwise stated, the other peaks have an abundance less than 0.5%.

mum deviation being ± 0.05 volt for the parent ions and ± 0.15 volt for the fragment ions. Since it was not possible to vary the partial pressures of the gases in the ion source, the *IE* curves were frequently unparallel, particulary for fragment ions. For this reason the absolute values of the appearance potentials for some fragments may be affected by an error higher than that indicated above.

The mass spectrum of dibenzo[b, e]thiepine-11-one (IV. X=S, Y=CO, M=226) has been reported in a previous work.[13] The dominating fragmentation routes of this compound are presented in scheme 1, where the m/e values are followed by the relative intensity (%). It appears from this scheme that the fragmentation of the IV molecular ion initiated

---

[13] V. E. Sahini, V. Constantin, I. Serban and C. Vlădescu, *Rev. Roumaine Chim.*, **23**, 163, (1978).

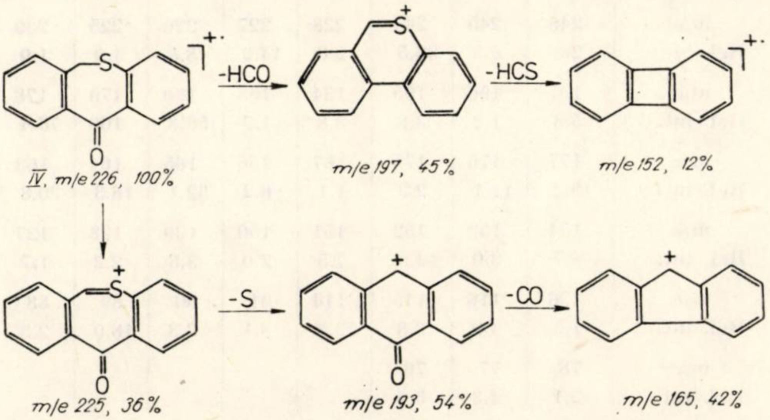

Scheme 1

by the elimination of a hydrogen atom, followed by the elimination of the sulphur atom, produces a higher abundance of ions than the concurrent pathway which begins with the elimination of the HCO group.

Mass spectrum of Dibenzo [b, e] thiepine (I)

Examination of the data in table 1 reveals three primary fragmentation processes $(M-H)^+$, $(M-CH_3)^+$ and $(M-HS)^+$, leading to the formation of *m/e* 211, m/e 197 and *m/e* 179 peaks, the last two processes being supported by appropriate metastable transitions. A fourth primary fragmentation process, consisting in the ejection of a H_2S molecule with the formation of the *m/e* 178 peak is required by energetic considerations; the appearance potential of the *m/e* 178 ion is much closer to that of the molecular ion than those of the other ions in the mass spectrum (table 4), and therefore no other formation routes can be assumed for the *m/e* 178 ion, for example via *m/e* 211 or via *m/e* 179.

Table 4

Ionization potentials and appearance potentials of some fragment ions (eV)

m/e	IP or AP		
	COMPOUND		
	I	II	III
258	—	—	9.70
244	—	9.85	—
227	—	10.30	—
212	8.77	—	—
211	11.40	—	—
197	10.80	—	—
194	—		10.00
180	—	10.20	—
179	11.05	10.35	—
178	9.76	10.00	—
166	—	—	12.20
165	—	10.10	13.25

Apart from the peaks mentioned above, only three peaks *m/e* 165, *m/e* 152 and *m/e* 89 have a relative intensity greater than 5%.

The main routes to obtain the major peaks in the mass spectrum are presented in scheme 2. As expected from the study of the mass spectra of similar compounds[8–9], the most important fragmentation pathways of the molecular ion occur with the elimination of the heteroatom from the central ring either as an HS radical or as an H_2S molecule.

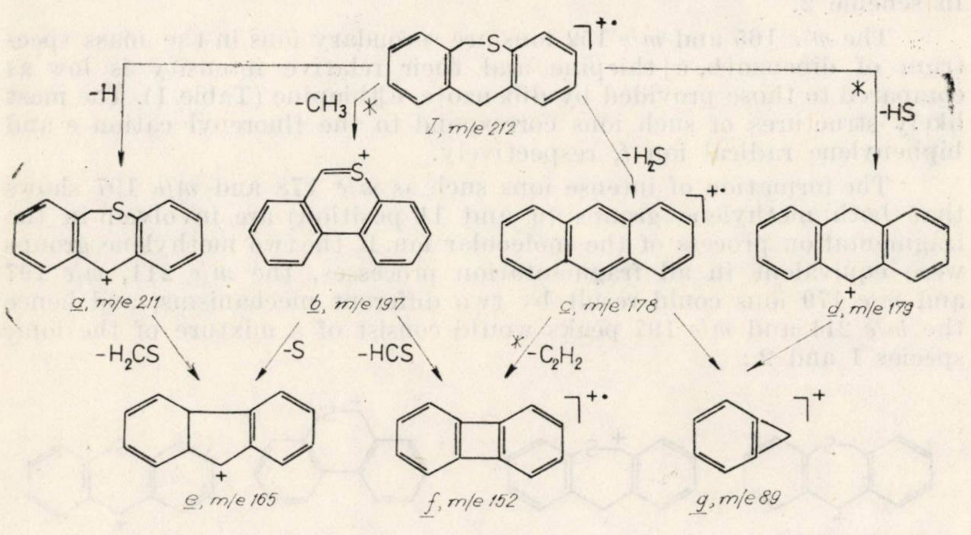

Scheme 2

The *m/e* 179 ion is the base peak of the mass spectrum. Its high abundance suggests a stable structure of *d*-type (scheme 2), in which there is an additional conjugation of π electrons comparatively to the molecular ion. In principle, the *m/e* 179 ion could arise by two different mechanisms, depending on which methylene group (6 or 11 position of the molecule) loses the hydrogen atom to form the ejected HS radical.

The high intensity of the *m/e* 178 odd-electron ion supposes a very stable structure, in this case the most probable being the completely conjugated structure *c* of the anthracene molecular ion.

Both the *d*, *m/e* 179 ion and the *c*, *m/e* 178 ion contribute by splitting to the formation of the *m/e* 89 ion, to which the benzopropenyl cation *g*-structure is usually suggested. A few percents of the relative intensity of the *m/e* 89 peak belong to the 178^{++} doubly-charged ion, as can be observed from the relatively large intensity of the 179^{++}, *m/e* 89.5 doubly-charged ion (Table 1). Since the splitting of doubly-charged ions is also possible at 50 eV, the formation pathways of the *m/e* 89 peak indicated in scheme 2 may be completed as follows:

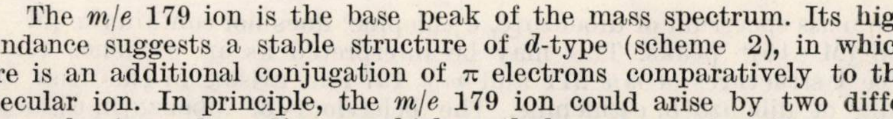

The other two primary fragmentation processes are the elimination of a hydrogen atom with the formation of a *m/e* 211 peak and less expected, the loss of the CH_3 radical leading to the *m/e* 197 peak. The high intensity of the even-electron ions resulted from these processes suggests the stable structures with an additional conjugation presented in scheme 2.

The *m/e* 165 and *m/e* 152 ions are secondary ions in the mass spectrum of dibenzo[b, e] thiepine and their relative intensity is low as compared to those provided by dibenzo[c, e]thiepine (Table 1). The most likely structures of such ions correspond to the fluorenyl cation *e* and biphenylene radical ion *f*, respectively.

The formation of intense ions such as *m/e* 178 and *m/e* 197 shows that both methylene groups (6 and 11 position) are involved in the fragmentation process of the molecular ion. If the two methylene groups were equivalent in all fragmentation processes, the *m/e* 211, *m/e* 197 and *m/e* 179 ions could result by two different mechanisms, and hence the *m/e* 211 and *m/e* 197 peaks would consist of a mixture of the ionic species 1 and 2 :

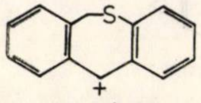
a1, m/e 211

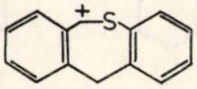
a2, m/e 211

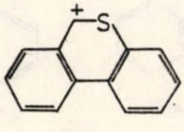
b1, m/e 197

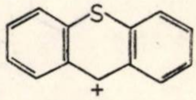
b2, m/e 197

The mass spectrum of dibenzo[c, e]thiepine[8] does not contain the $(M-1)^+$ and $(M-15)^+$ peaks. This may be interpreted as an evidence for the type 1 structures of *m/e* 211 and *m/e* 197 ions arising in the mass spectrum of dibenzo[b, e]thiepine. The behaviour of dibenzo[b, e]thiepine in the substitution reactions points out a much greater reactivity of site 11 in comparison to site 6 (for example on bromination, only the 11 derivative is obtained).

Mass Spectrum of Dibenzo [b, e] thiepine-5,5-dioxide (II)

The molecular ion fragmentation is dominated by the elimination processes of the SO_2 group leading to the prominent ion group *m/e* 180—*m/e* 178 (scheme 3). The appearance potentials of such ions (Table 4) show that the *m/e* 178 ion is directly formed from the molecular ion, by elimination of the H_2SO_2 (or H_2+SO_2) group, in agreement with the metastable transition revealed in the mass spectrum, whereas the *m/e* 179 ion may arise by several routes (directly from molecular ion, via *m/e* 227 or via *m/e* 180).

The main fragmentation process is the expected expulsion of SO_2 providing the stable dihydroanthracene molecular ion *d*, *m/e* 180, which contributes both to the formation of the *e*, *m/e* 179 ion (the base peak of the mass spectrum) and of the fluorenyl cation *g*, *m/e* 165.

The *m/e* 227 peak corresponding to the $(M-OH)^+$ ion is probably formed after a previous rearrangement of the molecular ion in the *a*, *m/e* 244 form, in a similar fashion as in the mass spectra of thioxanthene S, S dioxide and of some phenothiazines S oxide or S,S dioxide.[1-3]

By analogy with compound I, the hydrogen atom participating in the elimination of the neutral group (OH or HSO_2, scheme 3) is supposed to come from position 11. This postulate is substantiated by considering the mass spectrum of compound III, which fails to present the $(M-17)^+$ peak, although the methylene group in position 6 is available for a possible elimination of the OH radical from the molecular ion.

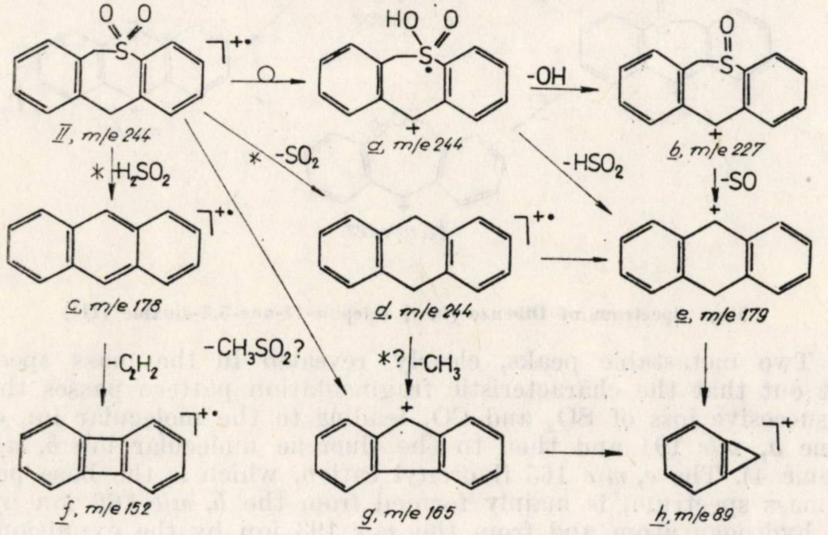

Scheme 3

The *m/e* 165 ion has an unexpected low appearance potential and it is difficult to state whithin the precision limit of our determinations, whether this ion arises via *m/e* 180 (the respective metastable transition is quite weak and cannot be assigned with certainty) or whether it is directly formed by the ejection of CH_3SO_2 radical (or CH_3+SO_2 groups) from the molecular ion, like in the case of dimethyl-benzothiadiazoline-2,2 dioxide.[14]

A significant part of the intensity of the *m/e* 89 peak arises from the 178^{++} doubly-charged ion, as in the mass spectrum of compound I.

The *m/e* 197 peak has a relatively low intensity (5%) in the mass spectrum of compound II. The formation of this peak directly from the molecular ion, as in the mass spectra of compounds I and IV is not probable. It is reasonable to suppose that the *m/e* 197 ion arise from the *b*, *m/e* 227 ion, after a previous skeletal rearrangement in one of the forms *b1* or *b2*, by elimination of the H_2CO (or H_2+CO) group

---

[14] K. C. C. Bancroft, L. H. Morcos Guindi, A. F. Temple and B. J. Millard, *Org. Mass Spectrom.*, **6**, 1313 (1972).

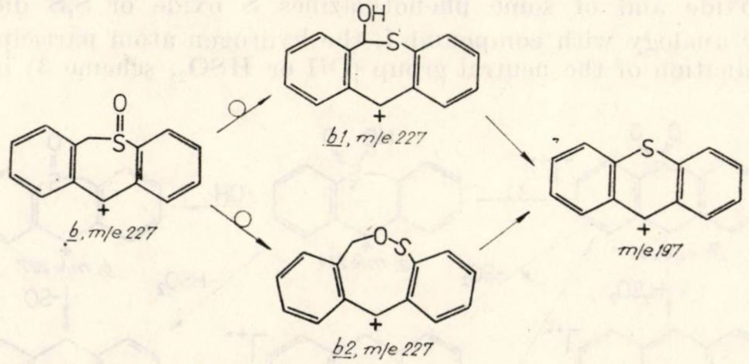

Mass Spectrum of Dibenzo [b, e] thiepine-11-one-5,5-dioxide (III)

Two metastable peaks, clearly revealed in the mass spectrum, point out that the characteristic fragmentation pattern passes through the succesive loss of SO_2 and CO, leading to the molecular ion of anthrone *a*, *m/e* 194 and then to the fluorene molecular ion *b*, *m/e* 166 (scheme 4). The *c*, *m/e* 165 fluorenyl cation, which is the base peak of the mass spectrum, is mainly formed from the *b*, *m/e* 166 ion by loss of a hydrogen atom and from the *m/e* 193 ion by the expulsion of a CO molecule, as in the mass spectrum of compound IV.

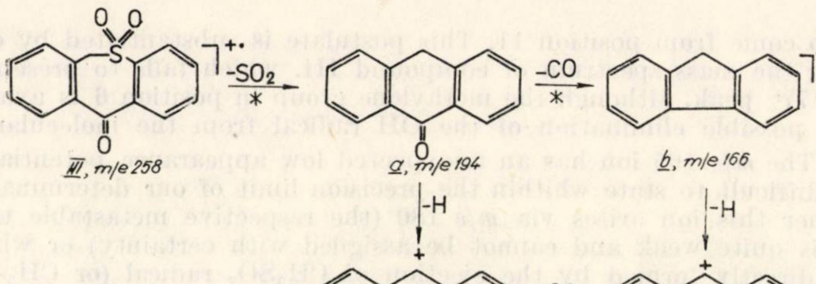

Scheme 4

A detailed inspection of the mass spectra at 50 eV and at 15–20 eV shows that the range *m/e* 258 to *m/e* 195 is practically devoid of peaks. This reveals that no other fragmentation process of the parent ion (i. e M–SO, M–CO or M–OH, as in compound II) is possible. Therefore, excepting the *m/e* 90 and *m/e* 89 peaks which occur with a relative high intensity, the mass spectrum at lower masses than *m/e* 194 is similar to the mass spectrum of anthrone.[15]

The *m/e* 195 peak is not significant in the mas spectrum of compound III, being totally constituted from the isotopic contribution of the *m/e* 194 ion, as can be found out from calculation.

A comparison between the mass spectra of the investigated compounds shows that their fragmentation produces a relatively small number of prominent peaks. Although a great deal of mechanistic information can be derived from the mass spectra and by analogy with the mass spectra of similar compounds, the unambiguous fragmentation patterns may be selected only by use of the energetic information derived from appearance potential measurements.

The stability under electron impact of the dibenzo[b, e]thiepines depend on the nature of the group in site 5 : in X=S compounds the molecular ions have a very great abundence, 98% for I($Y=CH_2$) and 100% for IV($Y=CO$), whereas in $X=SO_2$ compounds the molecular ions appear with a moderate intensity, 39% for II ($Y=CH_2$) and only 15% for III ($Y=CO$). The fragmentation is dominated by the sulphur atom, the main fragmentation pathways being initiated by its elimination in the S, HS or H_2S form for X=S compounds, or in the SO_2, HSO_2 or H_2SO_2 form for $X=SO_2$ compounds.

---

[5] L. V. Hall and R. W. A. Oliver, *Org. Mass Spectrom.*, **2**, 801 (1969).

intensity, the mass spectrum at lower masses than m/e 194 is similar to the mass spectrum of anthrone.[5]

The m/e 195 peak is not significant in the mass spectrum of compound III, being totally constituted from the isotopic contribution of the m/e 194 ion, as can be found out from calculation.

A comparison between the mass spectra of the investigated compounds shows that their fragmentation produces a relatively small number of prominent peaks. Although a great deal of mechanistic information can be derived from the mass spectra and by analogy with the mass spectra of similar compounds, the unambiguous fragmentation patterns may be selected only by use of the energetic information derived from appearance potential measurements.

The stability under electron impact of the dibenzothiepines depends on the nature of the group in site 5: in X = S compounds the molecular ions have a very great abundance, 98% for I (Y = CH_2) and 100% for IV (Y = CO), whereas in X = SO_2 compounds the molecular ions appear with a moderate intensity, 39% for II (Y = CH_2) and only 15% for III (Y = CO). The fragmentation is dominated by the sulphur group, the main fragmentation pathways being initiated by its elimination, in the S, HS or H_2S form for X = S compounds, or in the SO_2, HSO_2 or H_2SO_2 form for X = SO_2 compounds.

---

[5] L. [illegible] and R. W. A. Oliver, Org. Mass Spectrom., 2, 801 (1969).

Revue Roumaine de Chimie, 23, 3, 325—337 (1978)

SURFACE TENSION OF SIMPLE FUSED HALIDES

S. STERNBERG and MARIANA TERZI
Center of Physical Chemistry,
Central Institute of Chemistry
Street Galati 31, Bucharest, Romania

Received November 15, 1975

Some attempts have been made to extend to simple fused salts the equatios which correlate the surface tension with the critical temperature, density, compressibility, viscosity and interaction energy. It was established that Eötvös equation (modified with $k^E=0.5-0.7$ erg/mol$^{2/3}$ K instead of 2.1) applies satisfactorily to molten salts. Cationic and anionic parachors for fused alkali halides have been defined. A new equation relating the surface tension to critical properties of fused alkali halides has been advanced. The product surface tension times compressibility was found to be constant and equal to 3.61 10^{-8} (dyne cm)$^{1/2}$. An exponential equation of the type $\sigma=A\ \exp\,(B/\eta)$ has been established between surface tension and viscosity. A linear dependence of surface enthalpy on the interionic binding energy in fused salts has been found.

Various equations have been proposed[1–5] to correlate the surface tension with other macroscopic properties of molecular liquids (e. g. critical temperature, compressibility, viscosity and interaction energy). Some attempts of extending and perfecting such equations, in order to applay them to fused salts, are presented below.

1. EÖTVÖS EQUATION

Eötvös[6] equation is:

$$\sigma(M/\rho)^{2/3}=k^{E}\,(T_c-T) \qquad (1)$$

where σ is the surface tension, M is the molecular mass, ρ is the density of liquid, T_c is the critical temperature and k^E is Eötvös constant. The value of k^E for "unassociated" liquids (simple fluids and nonpolar organic liquids is known to be about 2.1 erg/mole$^{2/3}$K. The equation

---

[1] J. Pressing, *J. Chem. Phys.*, **54**, 3485 (1971).
[2] J. G. Eberhart, *J. Colloid. Int. Sci.*, **33**, 191 (1970).
[3] F. Kohler, *Monatsh. Chem.*, **103**, 685 (1972).
[4] H. Schonhorn, *J. Chem. and Eng. Data*, **12**, 524 (1967).
[5] N. Dass and Om Singh, *J. Phys. Soc. Japan*, **28**, 806 (1970).
[6] R. Eötvös, *Ann. Physik.*, **27**, 448 (1886).

(1) is valid far from critical region and does not apply to molten metals which have a positive value for $d\sigma/dT$.

Katayama[7] has modified the eq. (1) by including explicitly the gaseous phase density:

$$\sigma[M/(\rho_1-\rho_2)]^{2/3} \quad k^E\,(T_c-T) \tag{2}$$

where ρ_1 and ρ_2 are the densities of liquid and gaseous phases which coexist at equilibrium.

For fused salts the vapour density can be negletcted as it is very small.

Therefore we have calculated the Eötvös constant for many fused alkali halides, according to eq. (1). The values available in literature for critical temperatures and densities[8] have been used.

Two series of critical temperatures have been reported in literature: one given by Kirshenbaum et al[9] and the other theoretically evaluated by Lu et al.[10] Values of the Eötvös constant so calculated are listed in table 1.

The surface tension values for alkali chlorides and bromides are authors' own data[12-16]; the σ values for alkali flourides LiCl and CsBr are those given by Janz[8]. Examination of table 1 suggests several remarks. Firstly, Eötvös constant varies slightly with temperature ($\sim 2\%$). Secondly the k^E for fused alkali halides range between 0.5 and 0.7 erg/mole$^{2/3}$ K values which are much smaller than that for molecular liquids. Thirdly, the k^E values calculated with the two series of the critical temperature values do not agree. The values of T_c given by Kirshenbaum et al[9] were determined from the experimental data unlike the second series of T_c which were theoretically calculated by means of the significant structure theory for liquid state. This could be an explanation of the observed disagreement between the two series of k^E values. The small values of Eötvös constant for molten salts might be explained by the empirical character of Eötvös equation which in fact was established only for liquids at tempertures lower than 373 K. The critical temperatures in molten salt are very high ($\sim 3\,000$ K) compared to their melting temperatures, so that the (T_c-T) difference is much larger than that in the molecular liquids. As $\sigma(M/\rho)^{2/3}$ was of the same order of magnitude both in molten salts and molecular liquids, the lower k^E values in molten salts would result.

Taking into account the reduced reliability of critical temperature values one can say that the Eötvös equation modified by using $k^E=0.5-0.7$ instead of 2.1. erg/mole$^{2/3}$ K, applies satisfactorily to fused salts (alkali halides), contrary to the opinion of the other authors[11].

---

[7] M. Katayama, *Sci. Rept. Tohoku Imp. Univ.*, **4**, 373 (1916).

[8] G. J. Janz, "Molten Salts Handbook", Academic Press, New York, 1967.

[9] A. D. Kirshenbaum, J. A. Cahil, P. J. McGonigal and A. V. Grosse, *J. Inorg. Nuclear Chem.*, **24**, 1287 (1962).

[10] W. C. Lu, T. Ree, V. G. Gerrard and H. Eyring, *J. Chem. Phys.*, **49**, 797 (1968).

[11] H. Bloom, F. G. Davies and D. W. James, *Trans. Faraday Soc.*, **56**, 1179 (1960).

[12] S. Sternberg and M. Terzi, *Rev. Roumaine Chim.*, **15**, 527 (1970).

[13] S. Sternberg and M. Terzi, *J. Chem. Thermodynamics*, **3**, 259 (1971).

[14] S. Sternberg and M. Terzi, *Rev. Roumaine Chim.*, **17**, 1147 (1972).

[15] S. Sternberg and M. Terzi, *Rev. Roumaine Chim.*, **18**, 1319 (1973).

[16] S. Sternberg and M. Terzi, *Rev. Roumaine Chim.*, **20**, 17 (1975).

Table 1

The values of Eötvös constant for fused salts

Salt	T_c, K		T	σ_T	ρ_T	V_m	k^E erg/mole$^{2/3}$K	
	ref. 9	ref. 10	K	erg/cm^2	g/cm^3	cm^3/mole	ref. 9	ref.10
LiF	4 140		1 173	245.4	1.8018	14.39	0.489	—
			1 273	234.5	1.7528	14.80	0.493	—
			1 373	223.6	1.7038	15.22	0.496	—
NaF	4 270	—	1 273	185.2	1.942	21.62	0.479	—
			1 373	177.0	1.886	22.26	0.483	—
LiCl	3 080	—	973	130.8	1.4631	28.97	0.586	—
			1 073	123.9	1.4198	29.85	0.594	—
			1 173	117.0	1.3766	30.79	0.603	—
NaCl	3 400	2 219	1 073	114.9	1.5567	37.54	0.553	1.120
			1 173	105.9	1.5024	38.89	0.546	1.162
			1 273	96.9	1.4481	40.35	0.536	1.205
KCl	3 200	2 144	1 073	96.2	1.5103	49.36	0.608	1.21
			1 173	89.1	1.4520	51.35	0.607	1.26
			1 273	82.0	1.3936	53.50	0.604	1.33
RbCl	3 140	—	1 000	96.4	2.2378	54.03	0.644	—
			1 073	91.0	2.1734	55.63	0.642	—
			1 173	83.5	2.0851	57.93	0.636	—
CsCl	3 040	—	973	86.1	2.7330	61.60	0.649	—
			1 073	79.3	2.6265	64.10	0.646	—
			1 173	72.6	2.5200	66.81	0.640	—
NaBr	3 200	2 804	1 073	100.3	2.2983	44.77	0.594	0.726
			1 173	93.4	2.2166	46.42	0.595	0.735
			1 273	86.6	2.1349	48.19	0.595	0.744
KBr	3 170	2 687	1 073	87.1	2.0728	57.41	0.618	0.803
			1 173	79.5	1.9902	59.79	0.608	0.802
			1 273	72.0	1.9077	62.38	0.597	0.801
RbBr	3 130	—	973	86.0	2.6962	61.34	0.619	—
			1 073	80.6	2.5890	63.87	0.626	—
			1 173	75.1	2.4818	66.64	0.630	—
CsBr	3 045	—	973	79.4	3.0546	89.31	0.765	—
			1 073	73.3	2.9322	93.04	0.763	—
			1 173	67.2	2.8099	97.09	0.758	—
NaI	3 160	—	973	84.4*	2.7039	55.43	0.561	—
			1 073	75.4*	2.6090	57.45	0.538	—
			1 173	66.4*	2.5142	59.62	0.510	—
KI	2 980	2 757	973	77.8*	2.4295	68.33	0.647	0.729
			1 073	69.1*	2.3340	71.13	0.622	0.704
			1 173	60.4*	2.2384	74.16	0.589	0.673

* The surface tension values are obtained by Bloom and collab[11].

2. SUGDEN PARACHOR

Another well-known empirical equation relating the surface tension to the liquid density is the parachor equation found by Sugden[17]:

$$P = \sigma^{1/4} M(\rho_1 - \rho_g). \tag{3}$$

The experimental values of surface tension and density were used to calculate the parachor values for a simple molten salt series. These values are listed in table 2.

Table 2

The parachor values versus temperature for fused salts

Salt	σ_T erg. cm^{-2}	T K	V_m cm^3 mole^{-1}	P erg$^{1/4}$ cm$^{5/2}$ mole		
					exp. average	calc. value
	114.9	1 073	37.54	122.9		
NaCl	105.9	1 173	38.89	124.8	124.8	138.3
	96.9	1 273	40.35	126.6		
	96.2	1 073	49.36	154.6		
KCl	89.1	1 173	51.35	157.7	157.8	164.0
	82.0	1 273	53.50	161.0		
	96.5	1 000	54.03	169.3		
RbCl	91.0	1 073	55.63	171.8	172.1	174.1
	83.5	1 173	57.99	175.3		
	86.1	973	61.60	187.6		
CsCl	79.3	1 073	64.10	181.4	188.0	181.9
	72.6	1 173	66.81	195.0		
	100.3	1 073	44.77	141.7		
NaBr	93.4	1 173	46.42	144.3	144.3	151.3
	86.6	1 273	48.19	147.0		
	87.1	1 073	57.41	175.4		
KBr	79.5	1 173	59.79	178.5	178.5	176.9
	72.0	1 273	62.38	181.7		
	86.1	973	61.34	186.8		
RbBr	80.6	1 073	63.87	191.3	191.4	187.0
	75.2	1 173	66.64	196.2		
	84.4[a]	973	55.43	167.9		
NaI	75.4[a]	1 073	57.45	169.3	169.1	172.0
	66.4[a]	1 173	59.62	170.2		
	77.8[a]	973	68.33	202.9		
KI	69.1[a]	1 073	71.13	205.1	204.9	197.6
	60.4[a]	1 173	74.16	206.8		
RbI	80.3[b]	915	73.14	218.9	218.9	207.7

a values obtained by Bloom and collab.[11]

b value obtained by Jaeger[18]

---

[17] S. Sugden, *J. Chem. Soc.*, **32**, 125 (1924).

[18] F. M. Jaeger, *Z. anorg. Chem.*, **101**, 1 (1917).

One can observe that in salts with a common cation the parachor values increase in the sequence Cl<Br<I, and in those with a common anion, in the sequence Na<K<Rb<Cs; that is, the parachor increases with ionic radii. The parachor variation with temperature is also shown in table 2. On the average, it changes by 3% over a temperature range of 300° for all fused alkali halides. The smallest parachor temperature variation, below 2%, is for KI.

If the additivity of ionic parachors is considered,

$$P_{(+)} + P_{(-)} = P \tag{4}$$

and the ratio of anionic and cationic parachors is proportional to the ratio of ionic radii,

$$\frac{P_{(+)}}{P_{(-)}} = \frac{r_{(+)}}{r_{(-)}} \tag{5}$$

the ionic parachor values can be calculated. The average values of ionic parachors are given in table 3.

Table 3

The average values of ionic parachors in molten salts

P (−) anionic parachors			P(+) cationic parachors			
Cl^-	Br^-	I^-	Na^+	K^+	Rb^+	Cs^+
91.1	104.0	124.7	47.3	72.9	83.0	90.8

The ionic radii employed were taken from reference[19]. It is evident that the ionic parachor values for alkali cations increase in the order Na<K<Rb<Cs and for anions in the order Cl<Br<I. With the average values listed in table 3 we have additively recalculated the molecular parachors, the values of which are given in the seventh column of table 2. There is a good agreement of about ± 5% between the molecular parachors and the experimental ones. The only exception is for NaCl, where a larger difference of 10% is obtained.

3. SURFACE TENSION AND CRITICAL PROPERTIES

Guggenheim[20] applied the principle of corresponding states to the surface tension of liquids and demonstrated that the surface tension of a liquid extrapolated to absloute zero, σ_0, the critical molar volume,

---

[19] L. Pauling "Nature of Chemical Bond", Cornell University Press, New York, 1963 3rd edition.

[20] E. A. Guggenheim, *J. Chem. Phys.*, **13**, 253 (1945).

$V_c = M/\rho_c$, and the critical temperature, T_c are related through the equation:

$$\sigma_0 V_c^{2/3} = K T_c \tag{6}$$

where K is a universal constant. By analysis of the surface tensions and critical properties of simple liquids such as the heavier rare gases, nitrogen and oxygen, Guggenheim[20, 21] showed that $K = 4.3$ erg/mole$^{2/3}$ K.

We tested the applicability of the principle of corresponding states to the surface tension of molten salts by calculating the Guggenheim constant from eq. (6). Table 4 lists the calculated values of K together with σ_0 values and the critical temperatures and volumes given by Lu and coworkes[10].

Table 4

The principle of corresponding states applied to the surface tension of fused salts

Salt	T_c K ref. 10	V_c cm^3/mole ref. 10	σ_0 erg/cm^2 our	 ref. 11	$\sigma_0 V_c^{2/3}/T_c$ erg/mol$^{2/3}$K our	 ref. 11
NaCl	2218.98	152.59	211.5	216.2	2.72	2.78
NaBr	2804.47	360.66	173.5	—	3.13	—
KCl	2144.44	151.13	172.4	175.1	2.28	2.32
KBr	2686.78	458.09	167.9	161.9	3.71	3.58
KI	2757.01	512.35	—	162.4	—	3.77

Clearly $\sigma_0 V_c^{2/3}/T_c$ is not a constant for these liquids and it is less than 4.3 erg/mole$^{2/3}$ K, the value for simple liquids.

As eq. (6) could not be applied to molten salts, a new empirical relation between σ_0, V_c and T_c was proposed:

$$\sigma_0 (V_c - B)^{2/3} = A T_c \tag{7}$$

where A and B are constants. Eq. (7) is equivalent to the following equation:

$$(T_c/\sigma_0)^{3/2} = A^{-3/2}(V_c - B). \tag{8}$$

Its validity is tested in Figure 1 by the linearity of the $(T_c/\sigma_0)^{3/2}$ versus V_c plot for the data in table 4. By least squares analysis of data the constants $A = 5.00$ erg/mole$^{2/3}$ K and $B = -288.61$ cm^3/mole have been obtained. For comparison, Fig. 1 contains also the analogous representation for simple liquids plotted according to eq. (6), namely:

$$(T_c/\sigma_0)^{3/2} = 0.112\ V_c.$$

---

[21] E. A. Guggenheim, *Proc. Phys. Soc.*, **85**, 811 (1965).

A relationship similar to eq. (7) has been found by Eberhart[2] for liquid alkali metals.

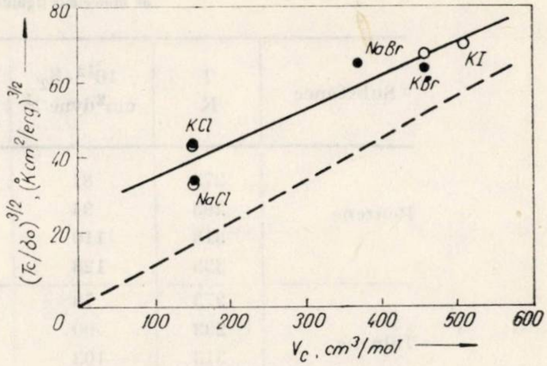

Fig. 1. — The relation between the surface tension and critical properties for fused salts and simple liquids.

● Our data; o data of Bloom and collab.[11]; — fused salts; — — — simple liquids.

Therefore, the relation between surface tension and critical properties predicted by the corresponding states principle is valid for fused salts with some alterations; that is, an additional parameter introduced according to eq. (7).

4. SURFACE TENSION AND COMPRESSIBILITY

A simple relationship between the surface tension and the isothermal compressibility, $\beta_T = -1/V\,(\partial v/\partial P)_T$, has been found by McGowan[22,23] on the basis of some relations previously proposed by Wada[24] and Richards and Mathews[25]:

$$\beta_T \sigma^{3/2} = \text{const.}\ (1.3310^{-8}\ (\text{dyne cm})^{1/2} \tag{9}$$

which holds for unassociated liquids. The product of surface tension and compressibility is independent of temperature and pressure.

We have calculated again this product for some of the molecular liquids, using for isothermal compressibility and surface tension data from reference[26]. These data are listed in table 5. The average value of $\beta_T\,\sigma^{3/2}$ was found to be $1.43\ 10^{-8}$ (dyne cm) $^{1/2}$; it changes a little with temperature (about 2% over a temperature range of 60°).

We tried to extend eq. (9) to molten salts. The results of calculation are given in table 6.

---

[22] J. C. McGowan, *Rec. Trav. chim.*, **76,** 155 (1957).

[23] J. C. McGowan, *Nature,* **210** 1255 (1966).

[24] Y. Wada, *J. Phys. Soc. Japan,* **4,** 280 (1949).

[25] T. W. Richards and J. H. Mathews, *Z. phys. Chem.* (*Frankfurt*), **61,** 449 (1908)

[26] "International Critical Tables", vol. 4, McGraw-Hill, New York, 1928.

Table 5

The relation between the surface tension and isothermal compressibility of molecular liquids

Substance	T K	$10^{12} \cdot \beta_T$ $cm^2 dyne^{-1}$	σ $dyne\ cm^{-1}$	$10^8 \beta_T \sigma^{3/2}$ $dyne^{1/2} cm^{1/2}$
Benzene	273	81	31.58	1.44
	293	94	28.88	1.46
	313	110	26.26	1.48
	333	128	23.72	1.48
Toluene	273	78	30.74	1.33
	293	90	28.43	1.36
	313	103	26.13	1.38
	333	120	23.18	1.39
Chloroform	283	92	28.60	1.41
	293	100	27.24	1.42
	333	141	21.73	1.43
Carbon tetrachloride	283	97	28.00	1.44
	293	105	26.77	1.45
	303	113	25.53	1.46
	333	132	23.14	1.47
Ethylen chloride	283	74	33.6	1.44
	293	80	32.2	1.46
	313	92	29.5	1.47
	333	108	26.7	1.49

The values of isothermal compressibility in fused salts are those obtained by Sternberg and Vasilescu[27] from ultrasonic velocity measurements while the surface tension values are own data[12–16]. For molten alkali halides, the average value of $\beta_T\ \sigma^{3/2}$ is 3.61 10^{-8} (dyne cm)$^{1/2}$, much larger than that of molecular liquids. In silver, magnesium, cadmium and lead halides the product has lower values, on the average 2.46 10^{-8} (dyne cm)$^{1/2}$.

In table 6 the temperature variation of $\beta_T\ \sigma^{3/2}$ in molten salts is also illustrated ; over a temperature range of 100° it increases by ~ 5 %.

In conclusion, we have found that the product of surface tension 3/2 power to isothermal compressibility has a constant value of 3.61 10^{-8} (dyne cm)$^{1/2}$ for all fused alkali halides, value which is much higher than that for molecular liquids.

---

[27] S. Sternberg and V. Vasilescu, *Rev. Roumaine Chim.*, **12**, 1187 (1967) ; *idem*, **13**, 265 (1968) ; *J. Chem. Thermodynamics*, **1**, 595 (1969) ; **3**, 877 (1971).

[28] K. Grjotheim, J. L. Holm, B. Lillebuen and H. A. Oye, *Acta Chem. Scand.* **26** 2050 (1972).

[29] N. K. Boardman, A. R. Palmer and E. Heymann, *Trans. Faraday Soc.*, **51**, 277 (1955).

Table 6

The relation between the surface tension and isothermal compressibility in molten salts

Salt	T K	$10^{12}\beta_T$ $cm^2\ dyne^{-1}$	σ $dyne\ cm^{-1}$	$10^8\beta_T\sigma^{3/2}$ $(dyne\ cm)^{1/2}$
NaCl	1 073	28.2	114.9	3.35
	1 173	33.8	105.9	3.68
KCl	1 073	38.4	96.2	3.62
	1 173	44.0	89.1	3.70
RbCl	1 073	44.5	91.0	3.86
	1 173	52.2	83.5	3.98
CsCl	973	41.6	86.1	3.32
	1 073	49.7	79.3	3.51
NaBr	1 073	35.3	100.3	3.54
	1 173	44.2	93.4	3.98
KBr	1 023	43.2	90.9	3.74
	1 173	54.8	79.5	3.92
RbBr	973	42.5	86.1	3.39
	1 073	53.4	80.6	3.86
NaI	973	35.5	84.4^a	2.75
	1 073	46.4	75.4^a	3.04
AgCl	773	8.9	181.0	2.17
	873	10.3	175.4	2.39
AgBr	773	10.7	158.1	2.13
	873	11.9	154.1	2.27
$MgCl_2$	1 073	52.7	62.1^b	2.57
	1 173	55.3	61.7^b	2.68
	1 273	57.4	61.3^b	2.75
$CdCl_2$	873	29.7	83.9^c	2.28
	973	33.1	81.4^c	2.43
$CdBr_2$	873	41.8	68.4^c	2.36
	973	45.5	64.7^c	2.37
$PbCl_2$	873	17.9	126.1^a	2.53
	973	19.7	115.1^a	2.43

a data of Bloom and collab.[11]; *b*, data of Grjotheim and collab.[28]
b data of Boardman and collab.[29]

5. SURFACE TENSION AND VISCOSITY

Pelofsky[30] has proposed an empirical equation relating the surface tension to the viscosity of a liquid, valid for a large number of organic and inorganic liquid systems:

$$\sigma = Ae^{\frac{B}{\eta}} \tag{10}$$

---

[30] A. H. Pelofsky, *J. Chem. and Eng. Data*, **11**, 394 (1966).

where η is the liquid viscosity, A and B are constants for a given substance.

We tested the applicability of this relation to molten salts, by plotting the logarithmic equation (10).

$$\log \sigma = \frac{B}{2.303\eta} + \log A \tag{11}$$

at different temperatures over a 200° range. In Figures 2 and 3 the viscosity dependence of surface tension at different temperatures for molten NaCl and, respectively KCl was plotted.

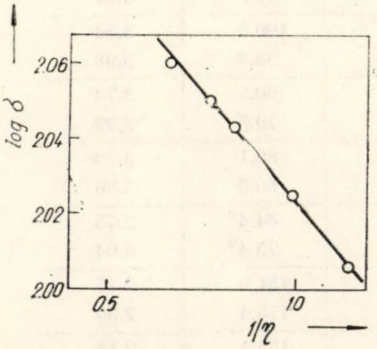

Fig. 2. — Plot of log σ against $1/\eta$ at different temperatures for molten NaCl.

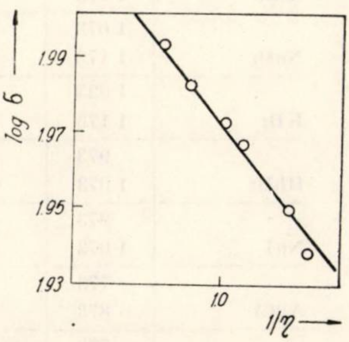

Fig. 3.—Plot of log σ against $1/\eta$ at different temperatures for molten KCl.

Figures 4 and 5 illustrate the viscosity dependence of σ for molten RbCl and CsCl.

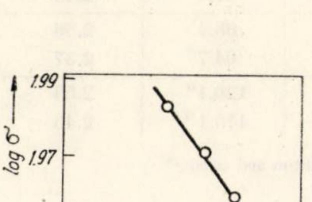

Fig. 4. — Plot of log σ against $1/\eta$ at different temperatures for molten RbCl.

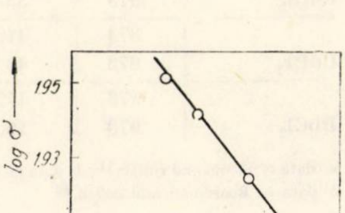

Fig. 5. — Plot of log σ against $1/\eta$ at different temperatures for molten CsCl.

In all the above figures, it is noticeable that the points lie a straight line, which confirms the validity of eq. (10). It was found out that the *A* and *B* constants are characteristic of each salt. Their values were obtained from the least squares analysis and given in table 7.

The viscosity values obtained by Murgulescu and Zuca[31] and our own surface tension values have been used. The *A* constant could be a measure of the surface tension of the solid phase $A = \sigma$ when the viscosity approached ∞.

To sum up, an exponential relation (eq. 10) relating the surface tension to viscosity has been verified for molten alkali chlorides.

Table 7

The A and B constants from equation $\sigma = A\ \exp(B/\eta)$ for alkali chlorides

Salt	A dyne/cm	B CP
NaCl	138.0	−0.2703
KCl	128.3	−0.2376
RbCl	123.3	−0.3212
CsCl	112.3	−0.3001

6. SURFACE TENSION AND INTERIONIC BINDING ENERGY

To see how the surface tension depends on the interionic binding energy, we plotted in Figure 6 the surface tension at a corresponding temperature, T', such as $T'/T_m = 1.05$ (T_m being the melting temperature), versus the lattice energy of the anion-cation bond, for a series of alkali and silver halides.

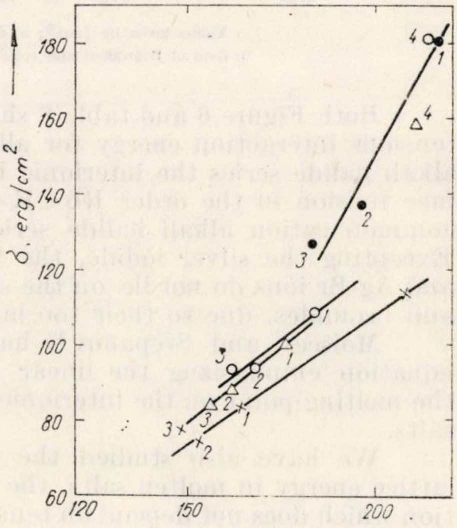

Fig. 6. — The dependence of surface tension on the lattice energy of a single ionic bond for alkali and silver halides.

● Fluorides; o chlorides; Δ broimdes; x iodides; *1*. Na^+; *2*. K^+; *3*. Rb^+; *4*. Ag^+.

The surface tension values for chlorides and bromides are our own data while those for fluorides and iodides are taken from the reference[8]. These values are listed in table 8 together with the corresponding temperatures at which they were evaluated.

---

[31] I. G. Murgulescu and St. Zuca, *Z. phys. Chem.* (*Leipzig*), **218**, 379 (1961) and *ibid* **222**, 300 (1963).

Table 8

The surface tension dependence on the binding energy of anion-cation bond in molten salts

Salt	T' $T'/T_m=1.05$ K	$\sigma_{T'}$ erg/cm^2	H^σ/A^σ erg/cm^2	$-U$ kcal/mole
NaF	1 331	180.5^a	289.6^a	216
KF	1 185	137.2^a	226.1^a	193
RbF	1 100	126.7^a	238.9^a	183
NaCl	1 135	109.3	211.5	184
KCl	1 097	94.5	172.4	168
RbCl	1 040	93.5	171.4	162
AgCl	764	181.5	224.6	214
NaBr	1 071	100.4	173.5	176
KBr	1 057	88.3	167.9	162
RbBr	1 001	84.5	139.1	156
AgBr	738	159.4	188.9	211
NaI	982	83.6^b	171.9^b	164
KI	1 006	74.9^b	162.5^b	153
RbI	959	77.9^a	143.4^a	148
AgI	870	114.5^c	132.8^c	208

a Values given by Janz[8]; b, data of Bloom and collab.[11];
b data of Boardman and collab[28].

Both Figure 6 and table 8 show a linear dependence of the surface tensions interaction energy for all alkali halides. In the common anion alkali halide series the interionic binding energy increases with the surface tension in the order Rb<K<Na. The same finding holds for the common cation alkali halide series the sequence being I<Br<Cl<F. Excepting the silver iodide, the binding energy values between Ag-Cl and Ag-Br ions do not lie on the straight line corresponding to chlorides and bromides, due to their too large values of surface tension.

Moiseev and Stepanov[32] have previously proposed an empirical equation emphasizng the linear dependence of the surface tension at the melting point on the interionic binding energy for a series of molten salts.

We have also studied the surface enthalpy dependence on the lattice energy in molten salts, the surface enthalpy being a surface function which does not depend on temperature. For this purpose we plotted in Figure 7 the surface enthalpy per unit area, H^σ/A^σ versus the lattice energy for all alkali halides.

One can observe a linear dependence, according to the following empirical equation :

$$H^\sigma/A^\sigma = 2.17\,U - 183\ (\text{Kcal}) \qquad (12)$$

---

[32] G. K. Moiseev and G. K. Stepanov, *Trudy Instituta ElectrokhimiiUral. Akad. Nauk S. S. S. R.,* **6**, 47 (1965).

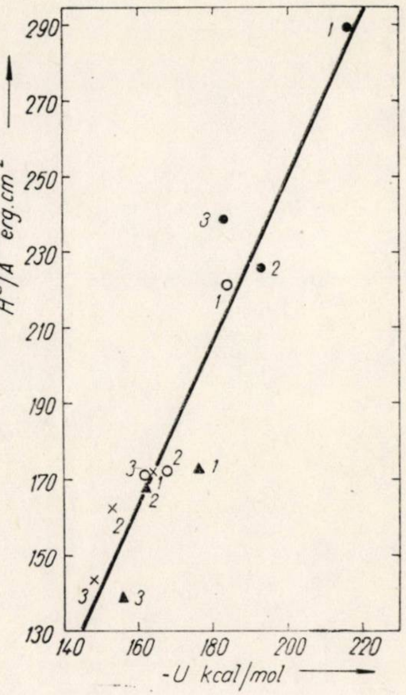

Fig. 7. — The dependence of surface enthalpy per unit area on the binding energy in fused salts.

● Fluorides; o chlorides; ▲ bromides; x iodides; 1. Na^+; 2. K^+; 3. Rb^+.

where A^σ is the surface area of the melt and U is the interionic binding energy.

The data of this plot are given in table 8. The silver halides were not plotted in Figure 7, because the lattice energy values are very closed to each other.

If we convert the units of lattice energy from kcal into erg we obtain the following equation :

$$H^\sigma/A^\sigma = 9.07\ 10^{10} U - 183 \qquad (13)$$

In conclusion, it was shown that according to the empirical eq. (12), both surface tension and surface enthalpy per unit area depend linearly on the binding energy between ions for all molten alkali halides.

Revue Roumaine de Chimie, **23**, *3*, 339–350 (1978)

LA CONSTANTE DE STABILITÉ DE $FeCl_4^-$ DANS LE $NaFeCl_4$ FONDU

M. ABRAHAM et M. POIRIER
Laboratoire d'Electrochimie, Département de chimie
Université de Montréal, Canada

Reçu le 6 novembre 1975

La constante de stabilité de l'ion complexe $FeCl_4^-$ dans le $NaFeCl_4$ fondu est déterminée à partir de mesures de f.é.m. dans l'intervalle de température 180–280°. Cette évaluation est obtenue à l'aide de la notion de fraction ionique mixte et du concept de lacune dans les sels fondus.

The stability constant of the complex ion $FeCl^-$ in molten $NaFeCl_4$ is determined from emf measurements in the temperature range 180–280°. This evaluation is obtained with the notion of mixed ionic fraction and the concept of vacancy in molten salts.

INTRODUCTION

Dans une étude[1] sur le dégagement anodique du chlore à une électrode de carbone vitreux en milieu $FeCl_3$-$NaCl$, on retenait la possibilité que l'ion $FeCl_4^-$ intervienne dans une étape cinétique initiale. Cela dépend de la disponibilité du milieu en cette espèce qui peut vraisemblablement se dissocier plus ou moins pour donner $FeCl_3$ et Cl^-. Nous décrivons ici des résultats concernant ce phénomène de dissociation, obtenus dans l'étude de la f. é. m. d'une pile en fonction de la température. Cette pile est constituée d'une électrode à sodium, d'une électrode à chlore et d'un électrolyte fondu dont la composition correspond à celle du composé $NaFeCl_4$.[2] A cette composition la tension de vapeur de $FeCl_3$ est très faible.[2]

Pour calculer la constante de stabilité de $FeCl_4^-$ et les grandeurs thermodynamiques standards qui s'y rattachent à partir des résultats expérimentaux, nous appliquons une méthode originale d'expression des activités des espèces en milieux fondus. Cette méthode est basée sur les conceptions de structure à lacunes des sels fondus.

---

[1] M. Abraham, M. C. Trudelle et M. Poirier, *J. Appl. Electrochem.*, (sous presse).

[2] M. C. Cook et W. E. Dunn, *J. Phys. Chem.*, **65**, 1505 (1961).

MESURES

Beaucoup d'aspects expérimentaux de ce travail sont bien connus. Certains présentent des difficultés notables mais qu'on peut considérer maintenant comme classiques dans l'électrochimie des sels fondus. Nous décrirons seulement ceux qui nous semblent particuliers.

En 1940, Skobets et Kavetskii[3] proposèrent l'emploi du verre comme électrolyte de jonction séparant le sodium métallique des sels fondus. A haute température cependant, le sodium attaque le verre et l'utilisation d'un amalgame au sodium devient nécessaire. Delimarskii et Khaimovich[4] utilisèrent donc plus tard l'électrode à verre et amalgame. Dans le domaine de température 180—280° où nous opérons, il apparaît qu'il suffit d'employer une électrode à verre avec du sodium au lieu d'amalgame de sodium. Nous utilisons du verre ordinaire au sodium n° 46470 de Kimble C°. D'après Dorémus[5] il n'y a pas de potentiel de diffusion quand le verre et la solution dans laquelle il plonge ne possèdent qu'un seul cation commun. La reproductibilité des électrodes sodium-verre est ± 5 mV.

Lors des premiers essais nous avons utilisé comme conducteur électronique de l'électrode à chlore des tiges de carbone graphitables. La reproductibilité et la stabilité des mesures obtenues avec ces électrodes étaient mauvaises. Il est probable que le chlorure ferrique donne des composés d'insertion dans le graphite.[6] De ce fait, nous utilisons du carbone vitreux. Ces électrodes à chlore ont une reproductibilité de ± 1 mV.

L'électrolyte est préparé par mélange mole pour mole de chlorure ferrique et de chlorure de sodium, directement dans la cellule d'essai, sous azote sec, parce que le chlorure ferrique forme avec l'eau divers composés. La cellule d'essai est chauffée à 200°. On traite l'électrolyte par l'acide chlorhydrique pour décomposer les oxydes de fer et par le chlore pour oxyder le chlorure ferreux. Il faut un traitement par barbotage de chlore pendant six heures pour obtenir des mesures de f. é. m. stables et reproductibles. Les quantités résiduelles d'oxydes de fer et de chlorure ferreux sont difficiles à éviter, en particulier le chlorure ferreux qui se forme par décomposition thermique du chlorure ferrique.[6]

Onze piles sont étudiées entre 180 et 280°. Chaque pile est faite avec de nouvelles électrodes et une préparation récente d'électrolyte.

Une cinquantaine de mesures de f. é. m. en fonction du temps, à températures constantes, donnent des valeurs stables à ± 6 mV, pendant plusieurs heures, qui sont indiquées fig. 1.

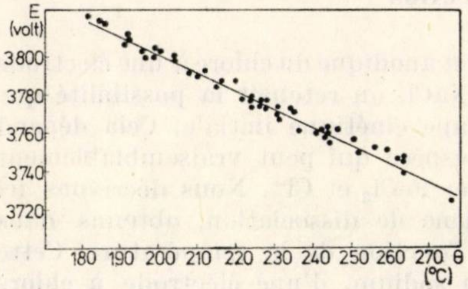

Fig. 1 — F.é.m. en fonction de la température

RÉSULTATS ET DISCUSSION

En appliquant la méthode des moindres carrés aux résultats expérimentaux (fig. 1), on obtient une droite dont l'équation est

$$E = 4.246 - 0.941 \times 10^{-3}\, T$$

---

[3] E. M. Skobets et N. S. Kavetskii, *Zhur, obshchei Khim.*, **10**, 1858 (1940).

[4] Y. K. Delimarskii et R. S. Khaimovich, *Ukrain. khim. Zhur.*, **15**, 77, 340 (1949).

[5] R. H. Doremus, « Glass Electrodes for Hydrogen and Other Cations », G. Eisenman Ed., New York, 1967, p. 113.

[6] L. E. Wilson et N. W. Gregory, *J. Phys. Chem.*, **62**, 433 (1958).

E : f. é. m. de la pile en volt
T : température absolue

Pour exploiter ce résultat deux questions se posent essentiellement au départ : l'évaluation de la f. é. m. standard E^0 et celle des activités des espèces en solution.

Pour simplifier l'écriture de ce qui suit nous utiliserons les indices 0, 1, 2, 3 pour les espèces $FeCl_3$, Cl^-, $FeCl_4^-$, Na^+.

Les mesures étant faites sous une pression de chlore égale à une atmosphère, la f. é. m. de la pile de formation de NaCl doit obéir à l'équation

$$E = E^0 - \frac{RT}{F} \ln (a_1 a_3)$$

a : activité
E^0 représente alors la f. é. m. de la pile de formation de NaCl pur, si on pose que les activités de Na^+ et Cl^- sont égales à un dans NaCl pur.

La solution étant toujours à une température inférieure à celle de fusion de NaCl pur, celui-ci est considéré à l'état surfondu.[7,8] Pour obtenir E^0 on calcule d'abord la variation d'enthalpie libre de la réaction

$$\mathrm{Na}(L) + \frac{1}{2}\,\mathrm{Cl_2}(G) = \mathrm{NaCl}\,(S)$$

On l'obtient par interpolation des résultats de Hamer, Malmberg et Rubin.[9] Ensuite on calcule la variation d'enthalpie libre de la transformation.

$$\mathrm{NaCl}\,(S) = \mathrm{NaCl}\,(L)$$

par l'expression

$$\Delta G = (T_F - T)\,\Delta S_F - \Delta C_P \left[T \ln \frac{T}{T_F} + (T_F - T) \right]$$

On trouve une discussion de cette expression ainsi que les valeurs numériques de T_F, ΔS_F et ΔC_P dans le traité de Lumsden.[7] La somme des deux variations d'enthalpie libre ainsi obtenues donne celle de la réaction

$$\mathrm{Na}\,(L) + \frac{1}{2}\,\mathrm{Cl_2}(G) = \mathrm{NaCl}\,(L)$$

à des températures inférieures à celle de fusion de NaCl. Tous calculs faits, on trouve l'équation

$$E^0 = 3.995 - 0.720 \times 10^{-3}\,T$$

---

[7] J. Lumsden, «Thermodynamics of Molten Salt Mixtures», Academic Press, London, 1966.

[8] K. Grjotheim, K. H. Stern et L. U. Thulin, *Electrochim. Acta*, **15**, 1137 (1970).

[9] W. J. Hamer, M. S. Malmberg et B. Rubin, *J. Electrochem. Soc.*, **103**, 8 (1956).

En milieu fondu, on utilise souvent les fractions ioniques issues du modèle de Temkin[10] pour exprimer les concentrations des espèces en solution. Mais, dans le mélange fondu étudié ici il existe également une espèce neutre : $FeCl_3$. Une analogie existe entre ce cas et celui traité dans un travail précédent[11,12] où un mélange fondu de nitrates contenait des molécules d'eau. On avait alors introduit l'utilisation des fractions ioniques mixtes en posant comme hypothèse de base que l'introduction de molécules d'eau neutres a pour effet de créer des lacunes dans le milieu fondu.

Bien que la composition $NaFeCl_4$ soit obtenue pratiquement en diluant NaCl dans $FeCl_3$ on peut, d'un point de vue thermodynamique, considérer qu'on l'obtient en diluant d'abord NaCl dans un composé hypothétique $NaFeCl_4$ où $FeCl_4^-$ ne subirait pas de dissociation, puis en ajoutant $FeCl_3$.

En désignant par X les fractions ioniques mixtes et par f les coefficients d'activité, la f. é. m. de la pile s'écrit :

$$E = E^0 - \frac{RT}{F} \ln (X_1 X_3) - \frac{RT}{F} \ln (f_1 f_3)$$

Les fractions ioniques mixtes s'évaluent de la façon décrite ci-dessous.

Les cations Na^+ définissent un sous-réseau cationique, les anions Cl^-, $FeCl_4^-$ un sous-réseau anionique. $FeCl_3$ étant neutre peut participer à l'un ou l'autre des deux sous-réseaux. Quand il participe à l'un, cela entraîne l'apparition d'une lacune dans l'autre. Posons :

n_0 : nombre total de molécules $FeCl_3$

N_a et N_c : les nombres de sites anioniques et cationiques libérés de leurs ions par l'apparition de $FeCl_3$ dans une répartition donnée.

Quand il y a n molécules de $FeCl_3$ dans le sous-réseau anionique, il y en a $(n_0 - n)$ dans la sous-réseau cationique. Comme $FeCl_3$ peut se placer indifféremment dans l'un ou l'autre des deux sous-réseaux, il existe $(n_0 + 1)$ possibilités de répartition de $FeCl_3$. Une répartition n est décrite ainsi :

$$\text{sous-réseau anionique} \begin{cases} n_1 \text{ anions } Cl^- \\ n_2 \text{ anions } FeCl_4^- \\ n \text{ molécules } FeCl_3 \\ (N_a - n) \text{ lacunes anioniques} \end{cases}$$

$$\text{sous-réseau cationique} \begin{cases} n_3 \text{ cations } Na^+ \\ (n_0 - n) \text{ molécules } FeCl_3 \\ N_c - (n_0 - n) \text{ lacunes cationiques} \end{cases}$$

---

[10] M. I. Temkin, *Acta Physicochim. U. S. S. R.*, **20**, 411 (1945).

[11] M. Abraham et J. J. Hechler, *Electrochim. Acta*, **17**, 1203 (1972).

[12] M. Abraham et J. J. Hechler, *Electrochim. Acta*. **17**, 1849 (1972).

L'entropie du système correspondant à une configuration où il y a n molécules de $FeCl_3$ dans le sous-réseau anionique et (n_0-n) molécules de $FeCl_3$ dans le sous-réseau cationique s'écrit :

$$S(n) = S_0(n) + \Delta S(n)$$

$\Delta S(n)$: variation d'entropie configurationnelle résultant de l'opération de mélange

$S_0(n)$: ensemble des autres contributions entropiques existant dans les composés NaCl, $FeCl_3$ et $NaFeCl_4^*$ pris séparément, et que l'on suppose se conserver lors du mélange.

* : il s'agit du composé hypothétique $NaFeCl_4$ où $FeCl_4^-$ ne subirait pas de dissociation.

D'après l'hypothèse de Boltzmann :

$$\Delta S(n) = k \ln W(n)$$

avec

$$W(n) = W_+(n) \times W^-(n)$$

$$W_+(n) = \frac{(n_3 + N_c)\,!}{n_3\,!\,(n_0 - n)\,!\,(N_c - n_0 + n)\,!}$$

$$W_-(n) = \frac{(n_1 + n_2 + N_a)\,!}{n_1\,!\,n_2\,!\,n\,!\,(N_a - n)\,!}$$

En appliquant l'approximation de Stirling suivante :

$$\ln x\,! = x \ln x - x$$

on obtient

$$\ln W(n) = n_1 \ln \frac{n_1 + n_2 + N_a}{n_1} + n_2 \ln \frac{n_1 + n_2 + N_a}{n_2} + n_3 \ln \frac{n_3 + N_c}{n_3} +$$

$$+ N_a \ln (n_1 + n_2 + N_a) + N_c \ln (n_3 + N_c) - n \ln n -$$

$$- (n_0 - n) \ln (n_0 - n) - (N_a - n) \ln (N_a - n) -$$

$$- (N_c - n_0 + n) \ln (N_c - n_0 + n)$$

Les molécules de $FeCl_3$ pouvant se distribuer au hasard dans les deux sous-réseaux, les états microscopiques correspondant à $W(0)$, $W(1)$, . . . , $W(n)$, . . . , $W(n_0-1)$, $W(n_0)$ ont même probabilité d'existence. Il en résulte une entropie moyenne de mélange

$$\Delta S = \frac{k}{n_0 + 1} \sum_{n=0}^{n=n_0} \ln W(n)$$

n_0 étant un grand nombre :

$$\Delta S = \frac{k}{n_0}\int_0^{n_0} \ln W(n)\cdot \mathrm{d}n$$

$$\frac{\Delta S}{k} = n_1 \ln \frac{n_1 + n_2 + N_a}{n_1} + n_2 \ln \frac{n_1 + n_2 + N_a}{n_2} + n_3 \ln \frac{n_3 + N_c}{n_3} +$$

$$+ N_a \ln (n_1 + n_2 + N_a) + N_c \ln (n_3 + N_c) - n_0 \ln n_0 -$$

$$- \frac{N_c^2}{2n_0} \ln N_c - \frac{N_a^2}{2n_0} \ln N_a + \frac{(N_c - n_0)^2}{2n_0} \ln (N_c - n_0) +$$

$$+ \frac{(N_a - n_0)^2}{2n_0} \ln (N_a - n_0) + \frac{N_c + N_a}{2}$$

L'idéalité du mélange se traduit par

$$\Delta G = - T \Delta S$$

La variation du potentiel chimique d'une espèce i provenant de l'opération de mélange est alors

$$\Delta \mu_i = - T \frac{\partial \Delta S}{\partial n_i}$$

d'où

$$\Delta \mu_1 = k T \ln \frac{n_1}{n_1 + n_2 + N_a}$$

$$\Delta \mu_2 = k T \ln \frac{n_2}{n_1 + n_2 + N_a}$$

$$\Delta \mu_3 = k T \ln \frac{n_3}{n_3 + N_c}$$

$$\Delta \mu_a = k T \left[- 1 - \ln (n_1 + n_2 + N_a) + \frac{N_a}{n_0} \ln N_a - \right.$$

$$\left. - \frac{(N_a - n_0)}{n_0} \ln (N_a - n_0) \right]$$

$$\Delta\mu_c = kT\left[-1 - \ln(n_3 + N_c) + \frac{N_c}{n_0}\ln N_c - \right.$$

$$\left. - \frac{(N_c - n_0)}{n_0}\ln(N_c - n_0)\right]$$

$$\Delta\mu_0 = kT\left\{1 + \ln n_0 - \frac{N_c^2}{2n_0^2}\ln N_c - \frac{N_a^2}{2n_0^2}\ln N_a + \right.$$

$$+ \frac{N_a - n_0}{2n_0}\left[1 + \frac{N_a + n_0}{n_0}\ln(N - n_0)\right] +$$

$$\left. + \frac{N_c - n_0}{2n_0}\left[1 + \frac{N_c + n_0}{n_0}\ln(N_c - n_0)\right]\right\}$$

Les ions étant monovalents, quand une molécule de $FeCl_3$ est introduite, deux sites sont libérés de leurs ions.

1) un site résulte du départ de l'ion auquel se substitue $FeCl_3$ et qui est occupé par celle-ci ;
2) un suite résulte du départ d'un ion de signe contraire, à proximité par raison d'électroneutralité.

L'introduction de n_0 molécules de $FeCl_3$ provoque le départ de $2n_0$ ions de leurs sites dont un nombre n_0 est occupé par ces n_0 molécules de $FeCl_3$. D'où :

$$2n_0 = N_a + N_c$$

Si les molécules de $FeCl_3$ peuvent se placer indifféremment dans les sous-réseaux anionique ou cationique :

$$N_a = N_c = n_0$$

Alors les variations de potentiels chimiques peuvent s'écrire :

$$\Delta\mu_1 = kT\ln\frac{n_1}{n_1 + n_2 + n_0}$$

$$\Delta\mu_2 = kT\ln\frac{n_2}{n_1 + n_2 + n_0}$$

$$\Delta\mu_3 = kT\ln\frac{n_3}{n_3 + n_0}$$

$$\Delta\mu_a = kT\left(\ln\frac{n_0}{n_1 + n_2 + n_0} - 1\right)$$

$$\Delta\mu_c = kT\left(\ln\frac{n_0}{n_3+n_0} - 1\right) = kT\left(\ln\frac{n_0}{n_1+n_2+n_0} - 1\right)$$

$$\Delta\mu_0 = kT.$$

Comme une molécule de $FeCl_3$ occupe un site libéré $\square^-$ ou $\square^+$ on peut considérer les couples ($\square^-$, $FeCl_3$) et ($\square^+$, $FeCl_3$) comme des entités réactionnelles et écrire :

$$\square^+ + FeCl_3 = (\square^+, FeCl_3)$$

ou

$$\square^- + FeCl_3 = (\square^-, FeCl_3)$$

Les variations de potentiels chimiques de ces couples sont

$$\Delta\mu_{0c} = \Delta\mu_{0a} = \Delta\mu_0 + \Delta\mu_c = \Delta\mu_0 + \Delta\mu_a$$

$$\Delta\mu_{0c} = \Delta\mu_{0a} = kT\ln\frac{n_0}{n_1+n_2+n_0}$$

L'équilibre de formation du complexe s'écrit :

$$(\square^+, FeCl_3) + Cl^- = FeCl_4^- \text{ ou}$$

$$(\square^-, FeCl_3) + Cl^- = FeCl_4$$

Sa constante de stabilité s'exprime par :

$$K = \frac{a_2}{a_1\,a_{0c}} = \frac{a_2}{a_1\,a_{0a}}$$

avec

$$a_1 = \frac{n_1}{n_1+n_2+n_0}$$

$$a_2 = \frac{n_2}{n_1+n_2+n_0}$$

$$a_{0c} = a_{0a} = \frac{n_0}{n_0+n_1+n_2}$$

D'après les expressions de a_1 et a_2 on a :

$$\frac{a_2}{a_1} = \frac{n_2}{n_1}$$

De plus, comme le liquide étudié ici a une composition correspondant à celle du composé défini $NaFeCl_4$:

$$n_0 = n_1$$

d'où, d'une part

$$a_1 = \frac{n_1}{2n_1 + n_2}$$

$$\frac{a_2}{a_1} = \frac{n_2}{n_1} = \frac{1 - 2a_1}{a_1}$$

et d'autre part

$$a_{0c} = a_{0a} = a_1$$

La constante de stabilité du complexe s'exprime finalement par :

$$K = \frac{1 - 2a_1}{a_1^2}$$

c'est-à-dire uniquement en fonction de l'activité de l'ion Cl^-. Les activités «a» se confondent dans ce calcul avec les fractions ioniques mixtes.[11,12] Quand on s'écarte de l'idéalité on utilise les coefficients d'activité «*f*» :

$$K = \frac{1 - 2X_1 f_1}{X_1^2 f_1^2}$$

avec

$$X_1 = \frac{n_1}{n_1 + n_2 + n_0}$$

De la même façon, comme

$$n_3 = n_1 + n_2$$

$$n_0 = n_1$$

$$\frac{n_2}{n_1} = \frac{1 - 2X_1}{X_1}$$

on obtient

$$X_3 = 1 - X_1$$

et la f. é. m. de la pile s'exprime par

$$E = E^0 - \frac{RT}{F} \ln \left[X_1 (1 - X_1)\right] - \frac{RT}{F} \ln (f_1 f_3)$$

D'après Lumsden, Cook et Dunn [7,2] $NaFeCl_4$ forme des solutions proches de l'idéalité avec $FeCl_3$ ou NaCl. S'il en est ainsi, $FeCl_4^-$ doit former des systèmes proches de l'idéalité avec Cl^- et $FeCl_3$ provenant de sa propre dissociation et l'on a

$$E = E^0 - \frac{RT}{F} \ln [X_1 (1 - X_1)]$$

A partir des valeurs mesurées de E et des valeurs calculées de E^0 on obtient les valeurs de X_1 par la relation

$$X_1 = \frac{1 \pm \left\{1 - 4 \exp\left[\frac{F}{RT}(0.221 \times 10^{-3} T - 0.251)\right]\right\}^{\frac{1}{2}}}{2}$$

le signe «moins» doit être retenu car la composition de l'électrolyte est telle que

$$X_1 = \frac{n_1}{n_0 + n_1 + n_2} = \frac{n_1}{2n_1 + n_2} < 0,5$$

Le tableau 1 donne la fraction ionique mixte de Cl^-, la constante de stabilité K du complexe $FeCl_4^-$ et le pourcentage de $FeCl_4^-$ dissocié, à diverses températures comprises entre 185 et 270°.

Tableau 1

Pourcentage de $FeCl_4^-$ dissocié en fonction de la température

θ°C	T°K	$T^{-1} \times 10^3$	X_{Cl^-}	K	% de $FeCl_4^-$ dissocié[4]
185	458	2,18	0,0230	1 800	2,35
210	483	2,07	0,0323	897	3,34
230	503	1,99	0,0414	535	4,32
250	523	1,91	0,0523	327	5,52
270	543	1,84	0,0651	205	6,96

Par application de la relation de Van't Hoff on obtient la variation d'enthalpie standard de la réaction de formation de $FeCl_4^-$. La figure 2 montre que la fonction $\ln K = f(1/T)$ est linéaire. La pente donne

$$\Delta H^0 = -R\,\frac{\mathrm{d}\ln K}{\mathrm{d}(1/T)} = -\,12{,}7 \text{ kilocalorie/mole}$$

De la constante de stabilité on calcule la variation d'enthalpie libre standard de formation de $FeCl_4^-$ par la formule $\Delta G^0 = -RT \ln K$.

Tableau 2

Variation d'enthalpie standard en fonction de la température

T °K	ΔG^0(kilocalorie/mole)
458	−6,8
483	−6,5
503	6,3
523	−6,0
543	5,7

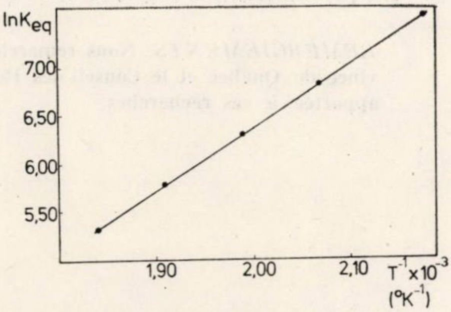

Fig. 2. — Constante de stabilité en fonction de la température.

Le tableau 2 donne les valeurs de ΔG^0 en fonction de la température. On calcule également la variation d'entropie standard de formation du complexe dans ce domaine de température :

$$\Delta S^0 = -\,12{,}8 \text{ calorie/(degré} \times \text{mole)}$$

CONCLUSIONS

Dans des travaux passés, [13–19] l'un de nous et d'autres auteurs avions développé l'idée que le concept de lacune utilisé comme celui de particule devait permettre d'approfondir l'étude des propriétés électrochimiques et thermodynamiques et peut-être, plus encore, celle des propriétés générales liées à l'état liquide. A l'époque, cette démarche pouvait à première vue introduire une complexité supplémentaire dans la description des phénomènes, hors de proportion avec les résultats qu'on en pourrait tirer dans des applications pratiques. Mais, si le concept de lacune ainsi compris correspondait vraiment à une réalité physique

---

[13] M. Abraham et J. Brenet, Colloque «Electrochimie» de l'Association Belge pour favoriser l'étude des verres et composés siliceux, Bruxelles (Octobre 1960).

[14] M. Abraham et J. Brenet, *Compt. rend.*, **251**, 2921 (1960).

[15] M. Abraham, J. Dupuy et J. Brenet, *Compt. rend.*, **252**, 4148 (1961).

[16] M. Abraham, J. Dupuy, J. Guion et J. Brenet, *Compt. rend.*, **254**, 4290 (1962).

[17] M. Abraham, J. Dupuy, J. Guion et J. Brenet, *Electrochim. Acta*, **8**, 125 (1963).

[18] M. Abraham, J. P. Chevillot et J. Brenet, *Compt. rend.*, **256**, 2129 (1963).

[19] M. Abraham, Thèse, Strasbourg (France), 1963.

il devait apparaître un moment où son utilisation permettrait de faire des calculs autrement difficile à envisager. Il en est ainsi d'un travail auquel nous nous sommes déjà référés[12] et de celui décrit ici.

Dans un travail sur la thermodynamique des mélanges de sels fondus Ketelaar et Vos[20] arrivent à la conclusion que seul le modèle de Temkin[10] montre un comportement idéal dans des cas divers. Le modèle que nous avons utilisé constitue une généralisation de celui de Temkin quand on tient compte de la création dans le milieu fondu de lacunes supplémentaires en relation avec l'existence d'espèces neutres.

REMERCIEMENTS. Nous remercions le ministère de l'Education de la Province de Québec et le Conseil des Recherches du Canada pour l'aide financière apportée à ces recherches.

---

[20] J. A. A. Ketelaar et B. Vos, *Monatsh.*, **102**, 1284 (1971).

Revue Roumaine de Chimie, **23**, *3*, 351–360 (1978)

L'ÉTUDE DE L'INFLUENCE D'UNE CONTAMINATION EN FLORURES SUR LA CORROSION DU ZIRCALOY-2 DANS L'EAU ET LA VAPEUR À HAUTE TEMPÉRATURE

MARIA RĂDULESCU
Laboratoire de la corrosion, Institut pour les Technologies Nucléaires, Pitești, Roumanie

Reçu le 13 novembre 1975

La contamination par F^- a été étudiée par deux méthodes : a) l'introduction d'ions F^- dans l'autoclave sous forme de solutions de HF et b) la contamination superficielle du métal par ions F^- provenant du bain de rinçage. Dans le premier cas, on a travaillé parallèlement dans trois autoclaves : l'un à l'eau déminéralisée, l'autre à une solution de HF titrant 1 mg F^{-1} et le troisième à une solution de HF titrant 10 mg F^{-1}. Dans le deuxième cas, on a utilisé deux bains de rinçage : un bain contenant une solution de HF titrant 1 mg F^{-1} et l'autre une solution de HF titrant 10 mg F^{-1}. On a examiné de même, l'influence d'un traitement préalable dans l'eau chaude avant de faire un essai, pendant trois jours, dans la vapeur à 400°– 100 kg/cm². Une partie des résultats obtenus ont été calculés par la méthode gravimétrique et une autre partie est présentée sous forme de micrographies, obtenues au microscope métallographique.

I. INTRODUCTION

Il est connu depuis longtemps, que la contamination grossière des alliages de Zr par différents éléments peut réduire sensiblement leur résistance à la corrosion dans l'eau à haute température et pression. Ainsi, la contamination par N du métal et les dépôts superficiels de florures obtenus comme résultat d'un décapage insatisfaisant ont suscité un intérêt tout particulier.[1-3]

D'habitude, le décapage est effectué avec une solution de 40% (vol) de HNO_3 70% et 3,5%(vol) de HF 50%, qui élimine 1,5–2 mils du métal. Pour cette raison, il est normal qu'un rinçage incorrect ou insuffisant, fait après l'opération de décapage, engendre une corrosion accélérée dans l'eau à haute température, due aux ions F^- à la surface du métal. Cette situation est similaire à celle où des ions F^- sont présents dans la solution qui baigne le métal. Cela peut être une raison de la dégradation prématurée des alliages de Zr existants dans un réacteur nucléaire.[4,5] La source de F^- peut être ou le décapant résiduel resté

---

[1] D. E. Thomas ,,Metallurgy of Zirconium'', par Lustman B. & Kerze F. jun., Mc Graw Hill, New York, 1955, p. 616.
[2] A. Sietnieks et G. Ostberg, *Corrosion J.*, **3**, 7 (1968).
[3] J. T. Demant et J. N. Wanklyn, «AERE» R 4788, (1965).
[4] S. Kass, *Corrosion*, **17**, 566 T (1961).
[5] W. E. Berry, «ASTM» N° 368.

à une surface dû au rinçage inefficace ou les matériaux lesquels, comme résultat de la dégradation, peuvent apporter une contribution en F^- à l'eau. Cette dernière catégorie peut comprendre : 1) la dégradation des matériaux plastiques (fluocarbonates) qui entrent dans la composition des joints ; 2) les décapants résiduels extraits des autres matériaux composants du réacteur nucléaire ; 3) l'introduction accidentelle de l'eau contaminée dans le circuit primaire de refroidissement et 4) la contamination par ions F^- provenant du combustible nucléaire. L'effet des ions F^- peut être jugé par les méthodes gravimétrique et micrographique. L'effet du F^- consiste dans une accélération de la formation d'oxyde blanc de Zr, ZrO_2, sur la surface d'un alliage de Zr.

L'oxyde blanc de ZrO_2 est meilleur isolateur que le ZrO_2 noir formé normalement sur la surface des alliages de Zr de bonne qualité, dans l'eau à haute température. L'oxyde noir passe en oxyde blanc ; cette transition dépend de la température dans les sens que : plus la température est grande, plus la transition est rapide.

II. ÉTUDE EXPÉRIMENTALE

Pour cette étude, la contamination par F^- a été effectuée en utilisant deux méthodes :

1. l'introduction d'ions F^- dans l'autoclave sous forme de solution de HF.
2. La contamination superificielle du métal par ions F^-, provenant du bain de rinçages.

II.1.1. Les essais ont été effectués dans trois autoclaves Prolabo d'un litre, dans les milieux aqueux :

— eau déminéralisée de résistivité $\geqslant 1 \mathrm{M}\Omega$ cm ;
— solution de HF titrant 1 mg l^{-1} de F^- ;
— solution de HF titrant 10 mg l^{-1} de F^-.

La durée des essais a été limitée à trois jours. La concentration des solutions en ions F^- a été vérifiée par dosage de F^- dans la solution, en obtenant les résultats :

Concentration de la solution en F^- (théorique) mg F^-/l	Résultat du dosage de F^- dans une solution initiale mg F^-/l	Résultat du dosage de F^- dans une solution sortie de l'autoclave mg F^-/l
1	1,0±0,1	1,1±0,1
10	8,8±0,8	8,0±0,8

Le dégazage des solutions fluorhydriques a été fait seulement par barbotage d'argon pendant une heure et demie ; on n'a pas fait le dégazage par ébullition à cause du risque de diminution de la teneur en florures dans ces solutions. A l'aide des trois solutions ci-dessus, on a fait trois essais à : 300°, 350° et 400°. Aux essais effectués à 300° et 350°, 5 échantillons ont été placés dans la phase liquide et 5 échantillons dans la phase vapeur ; à l'essai effectué à 400°—100 kg/cm² on a utilisé 10 échantillons. Après chaque essai, on a déterminé les augmentations de poids de chaque échantillon et on a examiné au microscope métallographique l'aspect de la couche d'oxyde et les hydrures formés sur 1—2 échantillons prélevés de chaque groupe. De même on a déterminé la teneur en hydrogène d'un échantillon choisi de chaque groupe.

Après les essais exécutés conformément aux conditions mentionnées on a observé que dans une solution titrant 1 mg F^-/l la position de l'échantillon dans la phase liquide ou à vapeur n'engendre aucun changement. Le tableau 1 révèle que les augmentations de poids des échantillons contaminés dans une solution titrant 1 mg F^-/l et des échantillons témoins — examinés à la même température dans l'eau déminéralisée — sont comparables, à toutes les trois températures. On peut donc conclure que cette faible contamination, par 1 mg F^-/l affecte très peu le comportement à la corrosion du zircaloy-2, au moins dans le cas de ce bref intervalle de trois jours.

D'ailleurs on observe dans la fig. 1 que les échantillons 63 et 66 (tous les deux maintenus pendant trois jours à 350° — le premier dans la phase liquide et le deuxième dans la phase vapeur) présentent un

Tableau 1

Influence de la concentration en ions F^- de la solution mise dans un autoclave sur la corrosion de zircaloy-2 à différentes températures

La contamination mgF^-/l	Phase	$\Delta p'$ mg/dm^2 3 jours à 300°		$\Delta p''$ mg/dm^2 3 jours à 350°		$\Delta p'''$ mg/dm^2 3 jours à 400°	
L'eau déminéralisée	liquide	10,8	(44)	13	(69)	20	(95)
	liquide	9,2	(45)	14,6	(70)	20	(96)
	liquide	10	(46)	15,4	(71)	20	(97)
	vapeur	10	(47)	14,6	(72)	20	(98)
	vapeur	9,2	(48)	15,4	(73)	22,3	(99)
	vapeur	9,2	(49)	13	(74)	20,8	(100)
1	liquide	11,5	(34)	15,4	(60)	23	(75)
	liquide	11,5	(35)	17	(61)	22,3	(76)
	liquide	10	(36)	17,7	(62)	23	(77)
	liquide	9,2	(37)	17	(63)	25,4	(78)
	liquide	11,5	(38)	14	(64)	22,3	(79)
	vapeur	10,8	(39)	15,4	(65)	23,8	(80)
	vapeur	10	(40)	15,4	(66)	21,5	(81)
	vapeur	10,8	(41)	15,4	(67)	23,8	(82)
	vapeur	10	(42)	15,4	(68)	20,8	(83)
	vapeur	11,5	(43)	16,1	(69)	23,8	(84)
10	liquide	28,5	(24)	117,7	(50)	36,9	(85)
	liquide	27,7	(25)	116,9	(51)	30	(86)
	liquide	21,5	(26)	120	(52)	31,5	(87)
	liquide	27	(27)	119,2	(53)	34,6	(88)
	liquide	30	(28)	119,2	(54)	36,9	(89)
	vapeur	14,6	(29)	86,9	(55)	31,5	(90)
	vapeur	13	(30)	87,7	(56)	33,8	(91)
	vapeur	14	(31)	89,2	(57)	34,6	(92)
	vapeur	16	(32)	89,2	(58)	36,1	(93)
	vapeur	14	(33)	90	(59)	33,1	(94)

Les chiffres entre parenthèses indiquent les codes des échantillons.

oxyde noir brillant, comparable à l'oxyde présenté par l'échantillon 74, maintenu dans l'eau déminéralisée dans les mêmes conditions. Une micrographie exécutée sur l'échantillon 62 (fig. 2) révèle l'apparition d'une couche d'oxyde très fine et relativement uniforme. Parallèlement, on a déterminé la teneur en hydrogène de l'échantillon et on a trouvé une valeur de (45±5) ppm. La corrosion réduite de l'échantillon est démontrée de plus, par la faible quantité d'hydrures présentée.

Dans l'essai effectué dans la même solution à 400°, l'augmentation de poids enregistrée est un peu supérieure à celle obtenue à 300° et 350°, les échantillons présentant une surface à taches blanches (voir l'échantillon 81, fig. 1). La micrographie de l'échantillon 75 (fig. 3) révèle une couche d'oxyde à épaisseur irrégulière avec des portions d'oxyde uniformes comme épaisseur, à côté d'autres présentant de petites enflures, ainsi que des ramifications dirigées de l'extérieur vers l'intérieur de l'échantillon. La quantité d'hydrogène (voir tabl. 2) et d'hydrures n'a pas sensiblement varié vis-à-vis des échantillons soumis à l'essai à 300° et 350°. Donc, la corrosion plus forte relevée à 400° est due à la non-uniformité de la couche d'oxyde formée.

Tableau 2

Détermination de la quantité d'hydrogène absorbée par les échantillons soumis à l'essai à la corrosion

Concentration de la solution mgF^-/l	Position dans l'autoclave	$\Delta p'$ mg/dm² 3 jours à 350°	Quantité d'hydrogène correspondant à $\Delta p'$ ppm	$\Delta p''$ mg/dm² 3 jours à 400°	Quantité d'hydrogène correspondant à $\Delta p''$ ppm
Témoin	—	—	6±1 (A1)	—	—
1	liquide	17,7	45±5 (62)	—	—
1	vapeur	15,4	—	23	35±4 (75)
10	liquide	119,2	232±20 (53)	—	—
10	vapeur	36,9	243±25 (55)	36,9	65±7 (89)

Les chiffres entre parenthèses indiquent les codes des échantillons.

L'essai dans une solution contaminée par 10 mg F^-/l (tabl. 1) révèle à partir de 300° des différences entre les augmentations de poids des échantillons contaminés et des échantillons témoins, les premières étant de 2,5—3 fois supérieures aux dernières.

Dans l'essai effectué à 350°, dans la même solution contenant 10 mg F^-/l, cette différence devient très grande, nommément :

$$\Delta p_{\text{témoin}} \simeq \frac{\Delta p_{\text{échantillon contaminé}}}{8}$$

Une caractéristique commune des échantillons soumis à l'essai à 300° et 350° est l'existence d'une différence entre les augmentations de poids présentées par les échantillons en phase liquide et en phase vapeur, les augmentations des premiers étant de 1,1—1,3 fois plus grandes que les autres. Cette attaque plus forte dans la phase liquide que dans la phase vapeur peut être expliquée par une contamination réelle qui est moins grande dans la vapeur. Tandis que dans la phase liquide les échantillons sont continuellement entourés d'une solution contaminée, ceux dans la vapeur sont soumis à une attaque plus faible de HF, puisque dans le volume entier occupé par la phase vapeur il y aura un mélange de gaz : (Ar + vapeurs de la solution contaminée).

L'explication ci-dessus est encore confirmée par l'essai à 400°—100 kg/cm^2, à la fin duquel on a enregistré des augmentations de poids moindres que celles à 350°. En plus s'ajoute le fait qu'à 400° on utilise un volume très petit de solution (48 ml) ce qui explique la concentration de HF en vapeurs si réduite. Les différences enregistrées entre les augmentations de poids mentionnées sont mises en évidence aussi par l'aspect extérieur des échantillons soumis à l'essai à une certaine température, mais en différentes phases (v. fig. 1). Ainsi à l'essai effectué à 350°, l'échantillon 54 maintenu dans le liquide présente une couche d'oxyde moins noire (vers le gris) que l'éch. 57, tenu en vapeur à la même température. Les micrographies de deux échantillons maintenus dans différentes phases (fig. 5), à la même température, révèlent, dans le cas de l'échantillon tenu en vapeur (55) une couche d'oxyde plus mince que celui tenu en liquide (53). En plus, la couche d'oxyde du dernier présente çà et là de petites fissures. De même, la densité des hydrures en 53 est plus grande qu'en 55. La teneur en hydrogène des deux échantillons est grande, mais sans être trop différente d'un échantillon à l'autre. A la surface des échantillons soumis à l'essai à 400°, on observe des taches blanches et des traces blanches (voir l'éch. 92, fig. 1), à l'encontre de l'échantillon 100 soumis à l'essai à la même température dans de l'eau déminéralisée, qui présente une couche d'oxyde noire brillante. L'échantillon 89 soumis à l'essai en solution contaminée à 400° a une couche mince d'oxyde, d'une épaisseur un peu irrégulière ; la quantité d'hydrures est relativement faible, mais la teneur en hydrogène dans l'échantillon est de (65±7) ppm. (fig. 4).

II.1.2. Pour évaleur l'influence d'une préoxydation des échantillons sur leur comportement ultérieur à la corrosion un nombre de 19 échantillons de zircaloy-2 a été préoxydé (1 jour à 300° et 3 jours à 400°) et ensuite soumis à la corrosion dans des solutions contaminées par 1 et 10 mg F$^-$/l pendant 3, 13 et 30 jours, à 350°. Les résultats sont représentés dans le tableau 3, où l'on observe que les échantillons préoxydés, introduits dans une solution contaminée par 1 mg F$^-$/l présentent, après 3 et 13 jours, des augmentations de poids très petites, c'est pourquoi on a considéré qu'il n'est plus nécessaire un essai de 30 jours à 350°. Ces augmentations de poids très petites montrent que la couche d'oxyde formée pendant la préoxydation a été uniforme et compacte, donc une contamination ultérieure due au maintien, pendant 30 jours, dans cette solution titrant 1 mg F$^-$/l, n'influence pas négativement les échantillons. Ce fait est confirmé par l'aspect des échantillons 17 et 23, le premier maintenu en liquide et le dernier dans la vapeur (fig. 6). Dans le cas de la solution titrant 10 mg F$^-$/l, après 3 jours, les augmentations de poids ne sont pas très accusées (excepté les 2 échantillons),

Tableau 3

Essai à la corrosion à 350° C des échantillons préoxydés de Zy-2

Code de l'échantillon	Concentration de la solution mgF⁻/l	Position dans l'autoclave	$\Delta p'$ mg/dm² 3 jours à 350°C	$\Delta p''$ mg/dm² 13 jours à 350°C	$\Delta p'''$ mg/dm² 30 jours à 350°C
1	10	liquide	1,5	9,2	127
2	10	liquide	1,5	14	163
4	10	liquide	27	231	569,2
5	10	liquide	8,5	158	502,3
8	10	liquide	1,5	49,2	Micrographié
9	10	vapeur	0	28,5	,,
10	10	vapeur	0	8,5	91,5
11	10	vapeur	4,6	113	445,4
13	10	vapeur	17	160,8	460,8
14	10	vapeur	0	17,7	158,4
15	1	liquide	1,5	4,6	
16	1	liquide	0,8	2,3	
17	1	liquide	1,5	4,6	
18	1	liquide	0	1,5	
19	1	liquide	0	2,3	
20	1	vapeur	2,3	3,8	
21	1	vapeur	0	2,3	
22	1	vapeur	0,8	3,8	
23	1	vapeur	0	1,5	

en échange, après 13 jours, elles deviennent très grandes et très dispersées comme valeur. Pour cette raison, il n'a pas été possible de tracer une courbe cinétique, Δ_p-temps et par conséquent, les augmentations de poids ont été seulement enregistrées, en exécutant des micrographies sur quelques échantillons sortis de l'autoclave après 13 et 30 jours. Ces valeurs grandes et dispersées sont explicables par une attaque aléatoire de HF sur la couche d'oxyde, fait mis en évidence par l'aspect extérieur des échantillons et de leurs micrographies. Ainsi, la micrographie exécutée sur un échantillon préoxydé – 8 – maintenu dans la phase liquide, révèle l'existence d'une couche d'oxyde très irrégulière comme épaisseur et qui présente çà et là des « poches » d'oxyde (fig. 7). De même, les micrographies exécutées sur les échantillons maintenus pendant 30 jours dans l'autoclave, présentent, en ce qui concerne l'aspect de la couche d'oxyde, deux traits caractéristiques sans tenir compte si les échantillons ont stationné dans la phase liquide ou en vapeur, dans l'autoclave) :

— les échantillons qui ont beaucoup gagné en poids présentent une couche d'oxyde épaisse et régulière (voir la micrographie de l'éch. 4 de la fig. 8).

— les échantillons à petites augmentations de poids présentent une couche d'oxyde irrégulière, mince sur quelques portions et épaisse sur les autres (voir la micrographie de l'éch. 10 de la fig. 9).

La couche épaisse d'oxyde est poreuse, fait mis en évidence par des microfissures apparues et, par conséquent, elle n'a pas un rôle protecteur vis-à-vis du reste du métal. La porosité de cet oxyde est mise en évidence, de plus, par une très grande quantité d'hydrures formée dans l'échantillon 4. Les échantillons de la deuxième catégorie — qui présentent de petites augmentations de poids — ont une faible quantité d'hydrures (fig. 9).

II.2.1. Après décapage fluonitrique et rinçage dans un courant d'eau filtrée pendant une heure, les échantillons de zircaloy-2 ont été contaminés par immersion, pendant 20 heures, dans des solutions titrant 1 et 10 mg F^-/l. On a essayé de faire aussi une contamination dans une solution titrant 100 mg F^-/l, mais on a observé qu'après 4 heures d'immersion dans une telle solution, l'aspect superficiel des échantillons est visiblement modifié, fait montrant le commencement d'une attaque marquante de la solution sur le zircaloy-2. Ensuite, une moitié des échantillons a été laissée sécher en position horizontale et une autre en position verticale. On a effectué après l'essai habituel de réception de ces échantillons. Dans chaque autoclave, en dehors des échantillons contaminés on a introduit comme témoins des échantillons correctement décapés et rincés. On a constaté que dans le cas de la contamination par rinçage dans une solution titrant 1 mg F^-/l, on obtient des augmentations de poids comparables tant pour les échantillons contaminés que pour les témoins (voir tabl. 4). De même, dans la fig. 10 on observe que l'aspect des échantillons de cette catégorie (voir les échantillons F 15, F 8, F 11 et F 3) ne diffère pas beaucoup de celui du temoin A 15. Quoique la contamination de l'échantillon témoin ait été due seulement au maintien dans la même solution qui baignait les échantillons contaminés, pourtant, la micrographie du témoin — A 13 relève le commencement d'une faible attaque, fait mis en évidence par l'apparition de très petits grossissements, situés çà et là sur l'oxyde. Au cas des échantillons contaminés, on observe des grossissements un peu plus grands et plus fréquents que chez les autres (voir la micrographie de l'échantillon F 7, fig. 11). La quantité d'hydrures présentée par des échantillons contaminés et témoins est plus ou moins équivalente.

La contamination par rinçage dans une solution titrant 10 mg F^-/l, révèle même après un stationnement d'un jour à 300° de très grandes différences, concernant l'augmentation en poids entre les échantillons contaminés et témoins (de 7 jusqu'à 20 mg/dm^2, v. tabl. 5). Après l'essai dans la vapeur les augmentations des échantillons témoins sont normales (de 18—20 mg/dm^2), tandis que les autres échantillons contaminés présentent des valeurs près de 37—40 mg/dm^2. La corrosion produite due à un rinçage dans une solution titrant 10 mg F^-/l est mise en évidence aussi par l'aspect extérieur des échantillons G 2 et G 15 (fig. 10) par rapport à l'échantillon témoin A 12. La couche d'oxyde formée sur l'échantillon contaminé a une couleur gris clair, tandis que celle formée sur

Tableau 4

Influence de la contamination superficielle par ions F−, due à un rinçage dans une solution titrant 1 mg/l F−

Code de l'échantillon	Position dans l'autoclave	$\Delta p'$ mg/dm^2 1 jour à 300°C	$\Delta p''$ mg/dm^2 3 jours à 400°C
F 1	liquide	7	19,2
F 2	vapeur	7	19,2
F 3	vapeur	7,7	18,5
F 4	liquide	7	20
F 5	liquide	7	19,2
F 6	vapeur	7	17,7
F 7	vapeur	7,7	18,5
F 8	liquide	7,7	20,8
F 9	vapeur	7	18,5
F 10	liquide	6,1	19,2
F 11	vapeur	7	17,7
F 12	vapeur	7	18,5
F 13	liquide	7	20,8
F 14	vapeur	7,7	19,2
F 15	liquide	5,4	18,5
F 16	liquide	7	20
A 13	vapeur	7,7	18,5
A 15	liquide	7	20

l'échantillon témoin A 11 (fig. 12) est noire, avec quelques petits points gris, dus, probablement, à la contamination par stationnement dans la même solution avec les échantillons contaminés. On a constaté que le séchage en position horizontale ou verticale n'a pas une grande importance, mais seulement la position d'arrangement dans l'autoclave. Ainsi, les échantillons situés dans la phase liquide présentent des augmentations de poids plus grandes que les autres situés dans la vapeur. La couche d'oxyde des échantillons contaminés (voir l'échantillon G 5 de la fig. 12) est un peu irrégulière et plus épaisse qu'au cas de l'échantillon témoin A 11.

II.2.2. Pour cet essai, 16 échantillons de zircaloy-2 ont été décapés et après une heure de maintien dans un courant d'eau filtrée, ils ont été introduits pendant 20 heures dans une solution titrant 10 mg F$^-$/l. Après, une moitié des échantillons ont été séchés en position horizontale et l'autre en position verticale. Sur le support introduit dans l'autoclave, on a arrangé à la même hauteur les échantillons séchés dans différentes positions pour déduire l'influence de la position de séchage sur leur comportement ultérieur à la corrosion. Cet essai a compris l'oxydation pendant un jour à 300° d'une moitié du nombre total des échantillons, plus 2 échantillons témoins (correctement décapés). Après cette opération, ont été introduits dans l'autoclave tant les échantillons préoxydés que les autres non soumis à la préoxydation et soumis pendant 3 jours

Tableau 5

Influence de la contamination superficielle avec des ions F^- due à un rinçage dans une solution titrant 10 mg/l F^-

Code de l'échantillon	Position dans l'autoclave	$\Delta p'$ mg/dm² 1 jour à 300°C	$\Delta p''$ mg/dm² 3 jours à 400°C
G 1	liquide	23	40
G 2	liquide	21,5	39,2
G 3	liquide	20	37,7
G 4	liquide	21,5	40
G 5	liquide	20,8	37,7
G 6	liquide	21,5	39,2
G 7	liquide	20,8	38,5
G 8	liquide	23	39,2
G 9	vapeur	21,5	37
G 10	vapeur	20,8	36,1
G 11	vapeur	20	35,4
G 12	vapeur	21,5	37
G 13	vapeur	20,8	36,1
G 14	vapeur	21,5	37,7
G 15	vapeur	21,5	37
G 16	vapeur	22,3	37
A 11	vapeur	6,1	16,1
A 12	liquide	7	18,4

à 400° — 100 kg/cm². Dans l'autoclave ont été introduits, en plus, 2 échantillons correctement décapés et qui n'ont pas été au préalable préoxydés. Les résultats de cet essai sont représentés dans le tableau 6, où l'on observe que la position de séchage n'affecte pas leur comportement ultérieur à la corrosion. Dans le cas des échantillons témoins — correctement décapés — des valeurs normales ont été obtenues pour les augmentations de poids après l'essai de réception ; un seul échantillon de cette catégorie — immergé dans la phase liquide pendant la préoxydation d'un jour à 300° — a présenté une augmentation de poids plus grande que les autres témoins, fait explicable par une concentration plus grande de HF dans la phase liquide qu'en vapeur où il existe un mélange : (Ar + vapeurs de la solution). La contamination apparue dans la solution résulte du fait que les échantillons contaminés par F^- sont immergés dans cette solution. D'ailleurs la fig. 13 indique que l'aspect des échantillons témoins D 2 et D 8 confirme les observations mentionnées en présentant une couche d'oxyde noire-brillante, parsemée de petits points blancs. La micrographie effectuée sur l'échantillon D 1 (fig. 14) relève une couche d'oxyde mince et approximativement régulière et une petite quantité d'hydrures. Parmi les échantillons contaminés, ceux qui ont été pendant la préoxydation dans la phase liquide présentent des augmentations de poids plus grandes que ceux dans la vapeur ; à leur tour

Tableau 6

Influence d'un traitement thermique préalable des échantillons à 300° C pendant un jour, sur leur comportement ultérieur à la corrosion

Code de l'échantillon	Préparation de l'échantillon	Position pendant le séchage	Position dans l'autoclave	$\Delta p'$ mg/dm^2 1 jour à 300°C	$\Delta p''$ mg/dm^2 3 jours à 400°C
D 1	Dec. ; p. o.	—	liquide	13.8	25,4
D 2	Dec ; p. o.	—	vapeur	7,7	16,1
D 3	C. ; p. o.	vert.	liquide	25,4	41,5
D 4	C. ; p. o.	horiz.	liquide	24,6	40,8
D 5	C. ; p. o.	vert.	liquide	27,7	44,6
D 6	C. ; p. o.	horiz.	liquide	30	47
D 7	C. ; p. o.	vert.	vapeur	23	37
D 8	Dec.	—	liquide	—	19,2
D 9	C. ; p. o.	vert.	vapeur	21,5	35,4
D 10	C. ; p. o.	horiz.	vapeur	21,5	36,1
D 11	C ; p. o.	horiz.	vapeur	23,8	37,7
D 12	C.	horiz.	liquide	—	33,1
D 13	C.	horiz.	liquide	—	35,4
D 14	C.	horiz.	vapeur	—	33,1
D 15	C.	horiz.	vapeur	—	32,3
D 16	C.	vert.	liquide	—	32,3
D 17	C.	vert.	liquide	—	32,3
D 18	C.	vert.	vapeur	—	32,3
D 19	C.	vert.	vapeur	—	33,1
A 16	Dec.	—	vapeur	—	18,5

Dec. – échantillon correctement décapé, C. – échantillon contaminé ; p. o. – échantillon préoxydé.

l'augmentation du poids de ces derniers est plus grande que celle des échantillons non soumis à la préoxydation. Cette affirmation est soutenue par des micrographies. En ce qui concerne l'aspect de la couche d'oxyde des échantillons préoxydés, maintenus dans la phase liquide — D6 — (fig. 14) et dans la vapeur — D11 — (fig. 15), il n'y a aucune différence significative entre eux, les deux catégories présentant une couche d'oxyde pas trop épaisse et partiellement irrégulière. En échange, entre les oxydes formés sur ces échantillons et celui apparu sur un échantillon non soumis à la préoxydation D 15 — (fig. 15) une différence évidente apparaît en ce qui concerne son épaisseur, qui est moins grande dans le dernier cas. De même, la quantité d'hydrures diminue suivant l'ordre : D 6, D 11 et D 15.

Remerciements. **Je remercie M. J. Blanchet, chef du laboratoire de la corrosion du C. E. N. Fontenay aux Roses (France), pour les précieux conseils prodigués au cours de mes travaux expérimentaux.**

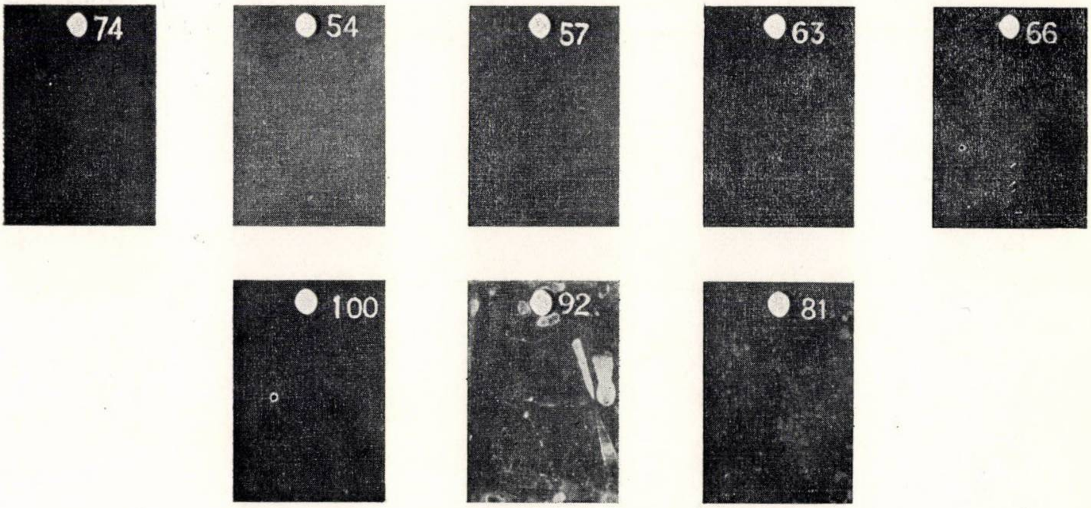

Fig. 1. — L'aspect des échantillons soumis à la corrosion à 300°, 350° et 400°, dans des solutions contenant 1 mgF$^-$/l et 10 mg F$^-$/l.

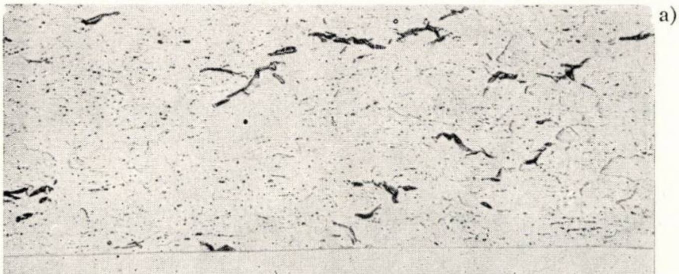

Fig. 2. — Micrographies de l'échantillon n° 62 :

a) hydrures (grossissement × 200). et b) couche d'oxyde (grossissement × 500).

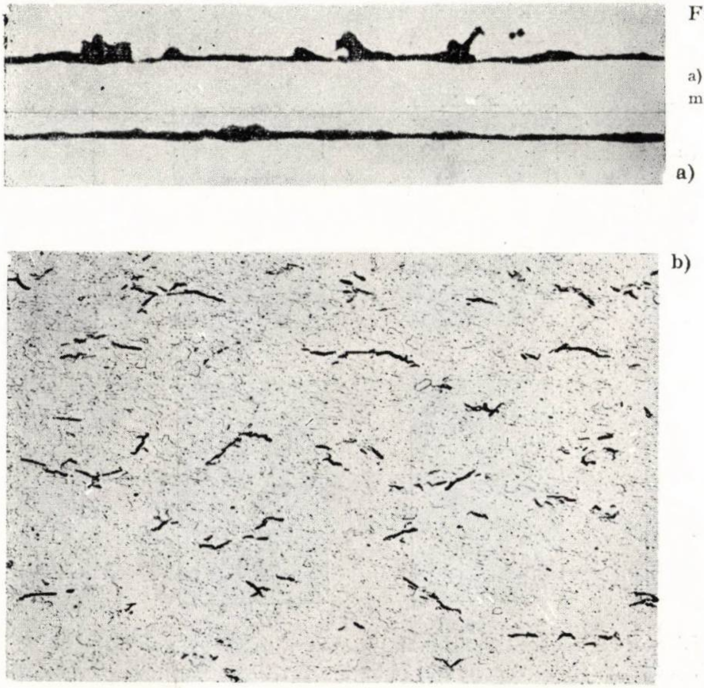

Fig. 3. — Micrographies de l'échantillon n° 75 :

a) couche d'oxyde (le grossissement × 500) et b) hydrures (grossissement × 100).

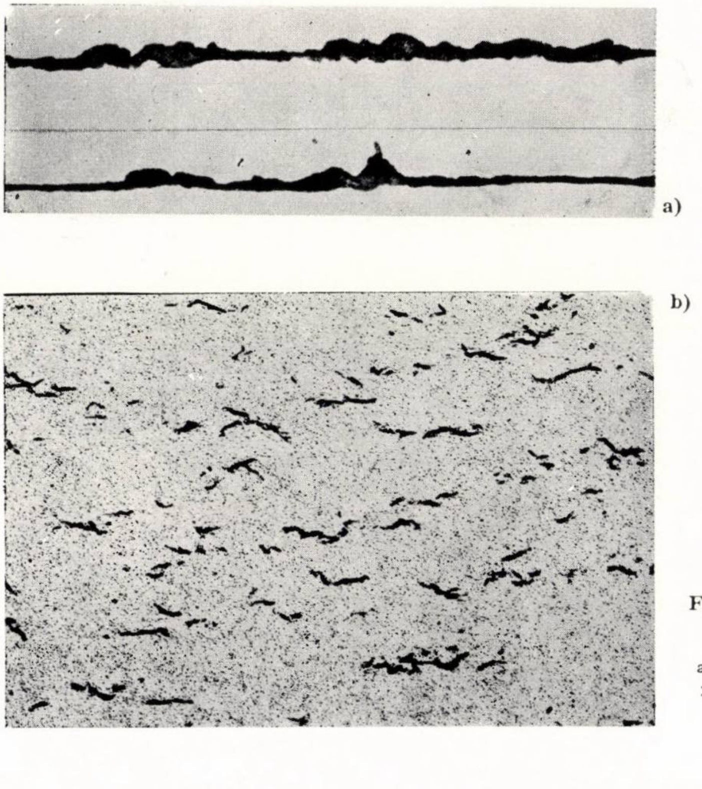

Fig. 4. — Micrographies de l'échantillon n° 89 :

a) couche d'oxyde (grossissement × 500) et b) hydrures (grossissement × 100).

a)

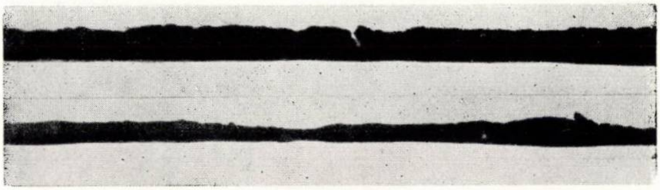

Fig. 5. — Aspect de la couche d'oxyde de :

a) l'échantillon n° 53 et b) l'echantillon n° 55 (grossissement × 500).

b)

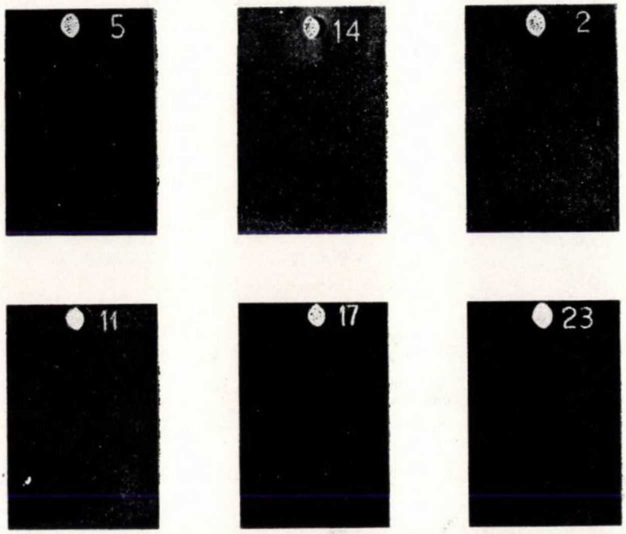

Fig. 6. — Aspect des échantillons préoxydés, soumis après la préoxydation, à la corrosion à 350°, dans des solutions contenant 1 et 10 mgF$^-$/l, à différents intervalles de temps.

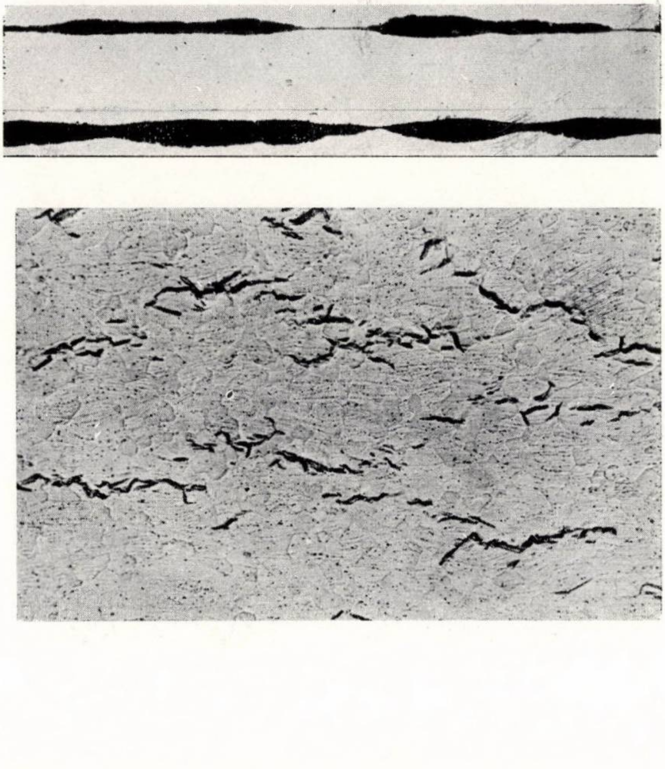

a)

b)

Fig. 7. — Micrographies de l'échantilon n° 8 :

a) couche d'oxyde et b) hydrures (grossissement × 200).

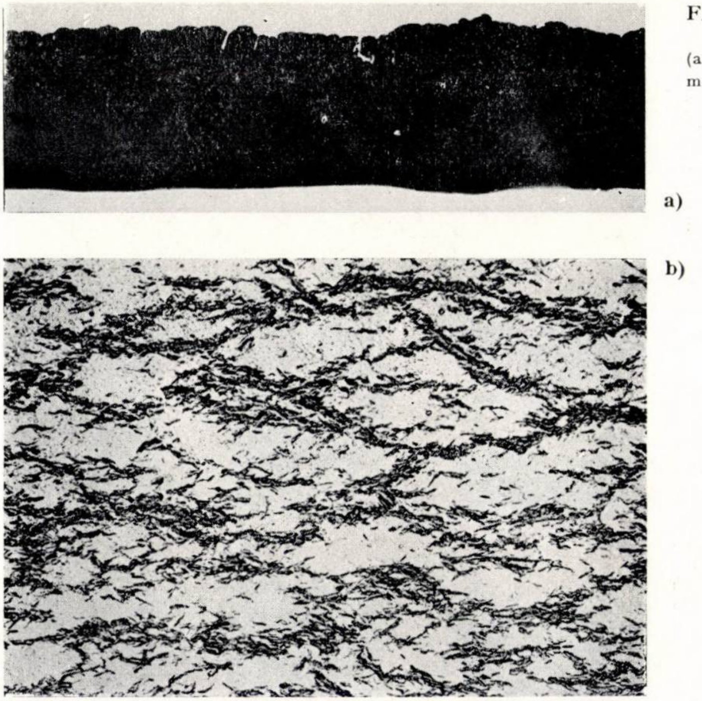

Fig. 8. — Micrographies de l'échantillon n° 4 :
(a couche d'oxyde (grossissement×500) et b) hydrures (grossissement × 100).

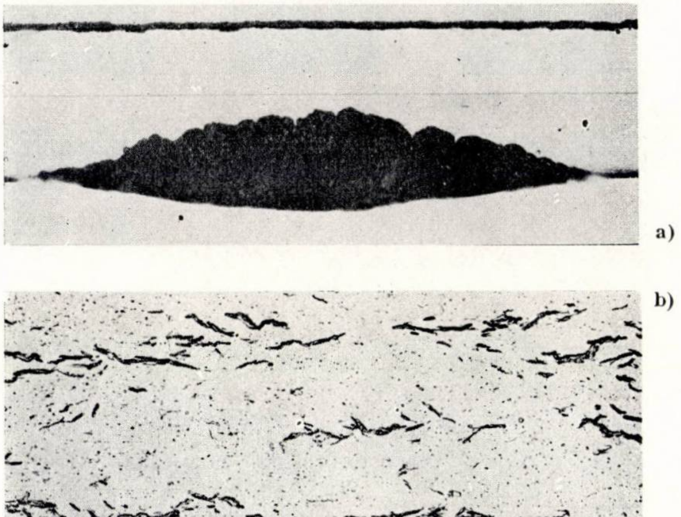

Fig. 9. — Micrographies de l'échantillon n° 10 :
a) couche d'oxyde (grossissement × 500) et b) hydrures (grossissement × 20)

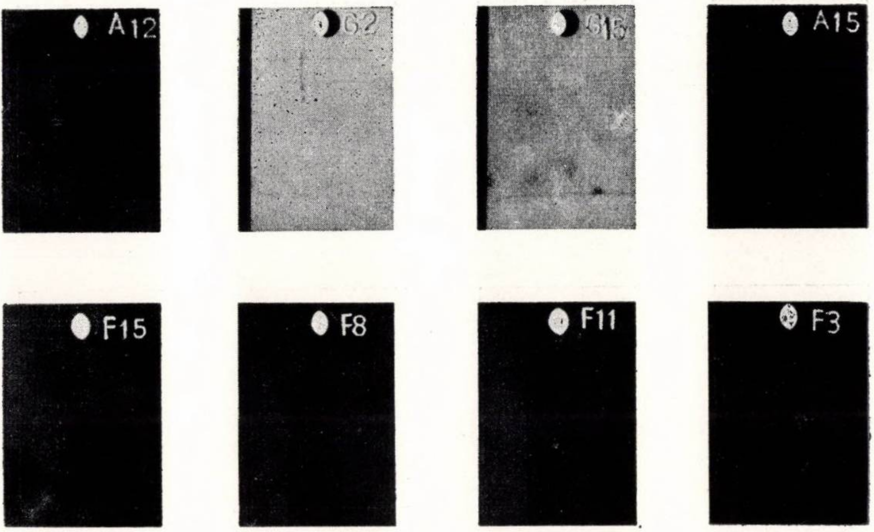

Fig. 10. — Aspect des échantillons contaminés initialement dans une solution contenant 1mgF⁻/l et soumis après à un esssai de réception.

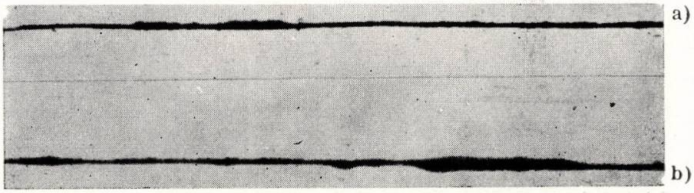

Fig. 11. — Aspect de la couche d'oxyde des échantillons n° A13(a) et F7(b) : grossissement × 500.

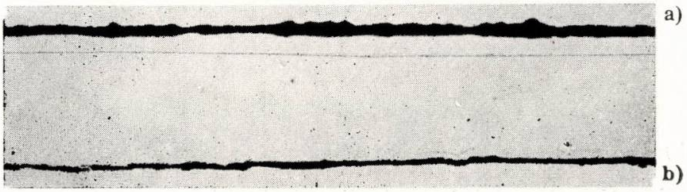

Fig. 12. — Aspect de la couche d'oxyde des échantillons G5(a) et A 11(b) ; grossissement ×500.

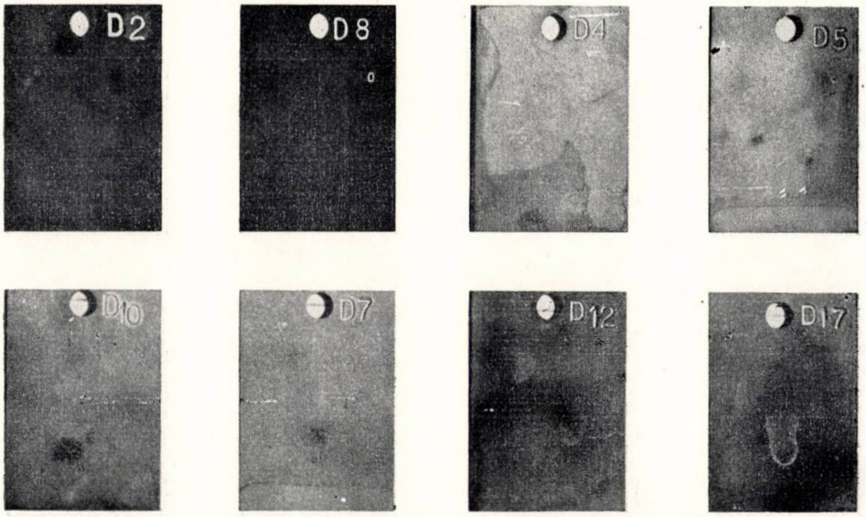

Fig. 13. — Aspect des échantillons contaminés initialement dans une solution contenant 10 mgF$^-$/l et soumis après à un essai de réception.

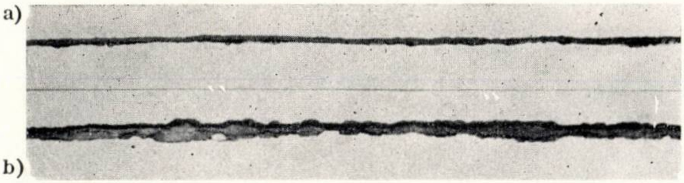

Fig. 14. — Aspect de la couche d'oxyde des échantillons n° D 1(a) et D 6(b); grossissement ×500.

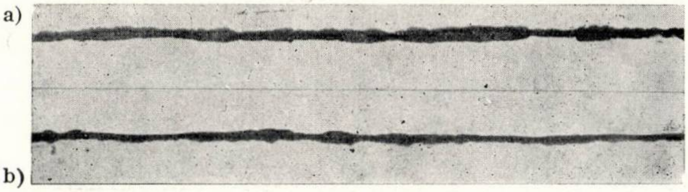

Fig. 15. — Aspect de la couche d'oxyde des échantillons n° D 11 (a) et D 15(b); grossissement ×500.

Revue Roumaine de Chimie, **23**, *3*, 361–369 (1978)

COMPARATIVE STUDY OF THE ADSORPTION OF SOME CYCLIC HYDROCARBONS ON ACTIVE ALUMINA-SUPPORT FOR CATALYSTS. I

DETERMINATION OF ADSORPTION ISOTHERMS AND OF VARIOUS CHARACTERISTIC THERMODYNAMIC VALUES

ALA NICOLESCU, MARIANA UDREA and GABRIELA POPA
Centre of Physical Chemistry, str. Dumbrava Roșie 23, Bucharest 9, Romania

Received July 27, 1976

The gas-chromatographic method was applied to trace the adsorption isotherms of cyclohexane, cyclohexene and benzene (at a small coverage of the surface) on an active catalytic alumina prepared by us by an original method. The specific adsorbate-adsorbent interactions and the influence of π electrons participation in the formation of bonds with the active centers on the alumina surface have been evidenced from the variation of the main adsorption thermodynamic values.

INTRODUCTION

The gas-chromatographic method stands out by the rapidity of adsorption measurements over a large temperature domain and by the simplicity of the standard apparatus used.

It permits a characterization of solid catalysts emphasizing the nature and the role of interactions appearing between reactant molecules and reaction products with surface active centers.[1,2] Likewise, the variation of the main thermodynamic values in the molecules transition from gaseous state into adsorbed state affords a series of conclusions regarding the surface heterogeneity degree and the mechanism of the actual catalytic reaction.[3]

The purpose of the present paper has been to study the behavior of an active catalytic alumina-support for catalysts during the adsorption of cyclohexane, cyclohexene and benzene, under different conditions of catalytic transformations. The criteria used for estimations were

---

[1] S. Ross and J. P. Olivier, "On Physical Adsorption", Interscience Publ., Co., New York, 1964.

[2] A. V. Kiselev and Y. I. Yashin, "Gas Adsorption Chromatography", Nauka Press, Moscow, 1967.

[3] P. Ciambelli, S. Crescitelli, V. De Simone and G. Russo, *Ann. Chim.* (*Ital.*), **63**, 701 (1973).

the variation of the principal thermodynamic values. A subsequent paper will determine the quantitative distribution of the adsorption potential in view of making the fullest possible characterization of the alumina active surface.

EXPERIMENTAL

The study was carried out using a Willy Giede, type GCHF 18.2 chromatograph fitted with a thermal detector (TCD).

A γ aluminium oxide with a specific surface S_{BET} =171 m^2/g prepared by an original method[4] and dennoted Al_2O_3 TC-600 was used as adsorbent.

The column was activated for 24 hr at 150°, in a current of carrier gas-nitrogen.

The working conditions are presented in table 1.

Table 1

Experimental conditions

Stationary phase Al_2O_3TC-600 (21.8 g, granulation $0.16<0<0.315$ mm)

Steel column, 1 m long and with an inlet diameter = 0.6 cm

Adsorbate	T_{column} °C	Flow rate eluent cm^3/min	Pressure drop at
Cyclohexane	120–150	90	0.5–0.51
Cyclohexene	130–170	75	0.37–0.40
Benzene	160–200	100	0.49–0.55

The reactants used were cyclohexane, cyclohexene and benzene of p. a purity.

RESULTS AND DISCUSSION

The adsorption isotherms were determined stepwise[5], assuming the adsorbate distributed between the solid stationary phase Al_2O_3 TC-600 and the mobile phase-nitrogen.

The concentrations in stationary phase C_i^s(g adsorbate/g adsorbent) and in mobile phase C_i^m (g (adsorbate/cm^3 nitrogen) as well as the partial pressure of the component being adsorbed p_i (at) were calculated according to relations :

$$C_i^s = \frac{S_{ads}\cdot g}{S_{peak}G} \tag{1}$$

[4] I. V. Nicolescu, M. Dardan-Udrea, A. Nicolescu, G. Muscă, I. Suciu, V. Părău-şeanu, S. Blejoiu and I. Melichian, Patent RSR, no. 58724, Publ. 28.08.1975.

[5] J. F. K. Huber and R. G. Gerritse, *J. Chromatogr.*, **50**, 137 (1971).

$$C_i^m = \frac{g.w}{F.S_{\text{peak}}} \cdot H \tag{2}$$

$$p_i = \frac{C_i^m}{M_i} \cdot RT \tag{3}$$

where :

S_{ads} = adsorption surface cm^2, S_{peak} = surface of chromatographic peak, cm^2, g = weight of injected sample, g, G = weight of alumina in the column, g, H = height of chromatographic peak, cm, w = paper unrolling speed cm/min, F = carrier gas flow rate, cm^3/min, M_i = molecular mass of the substance adsorbed, g, T = column temperature, K.

The adsorption isotherms were next traced

$$c_i^s = f(p_i) \tag{4}$$

as seen in Figures 1, 2 and 3

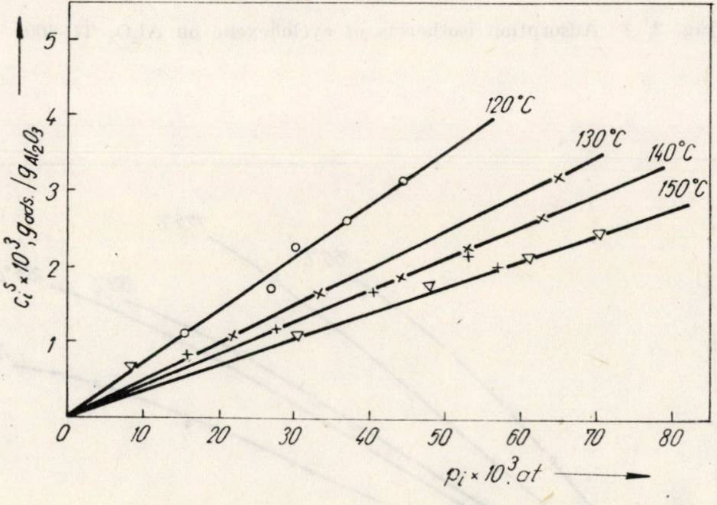

Fig. 1. — Adsorption isotherms of cyclohexane on Al_2O_3 TC-600.

The adsorption isosteric heats were calculated by the Clausius-Clapeyron relation,

$$\Delta H = -R \frac{\mathrm{d} \ln p_i}{\mathrm{d}(1/T)} \tag{5}$$

from the slope of adsorption isosteres presented in Figures 4,5 and 6.

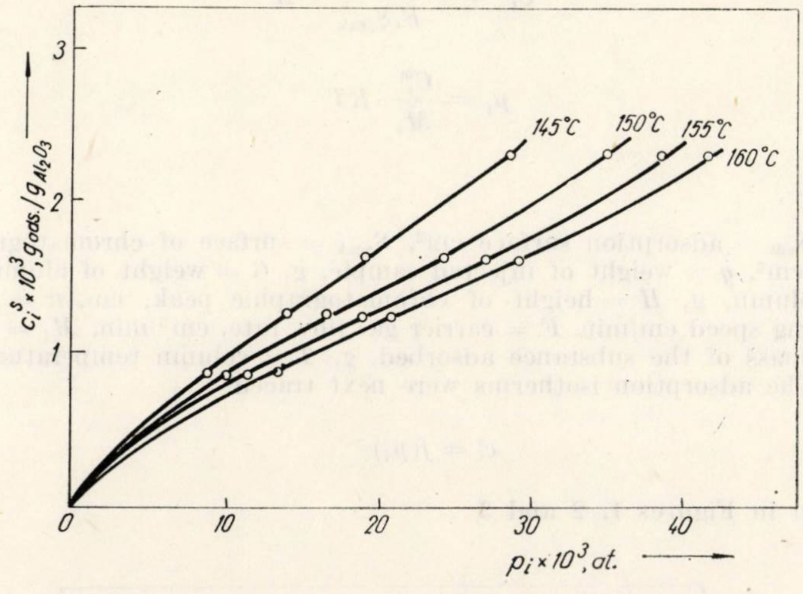

Fig. 2. — Adsorption isotherms of cyclohexene on Al_2O_3 TC-600.

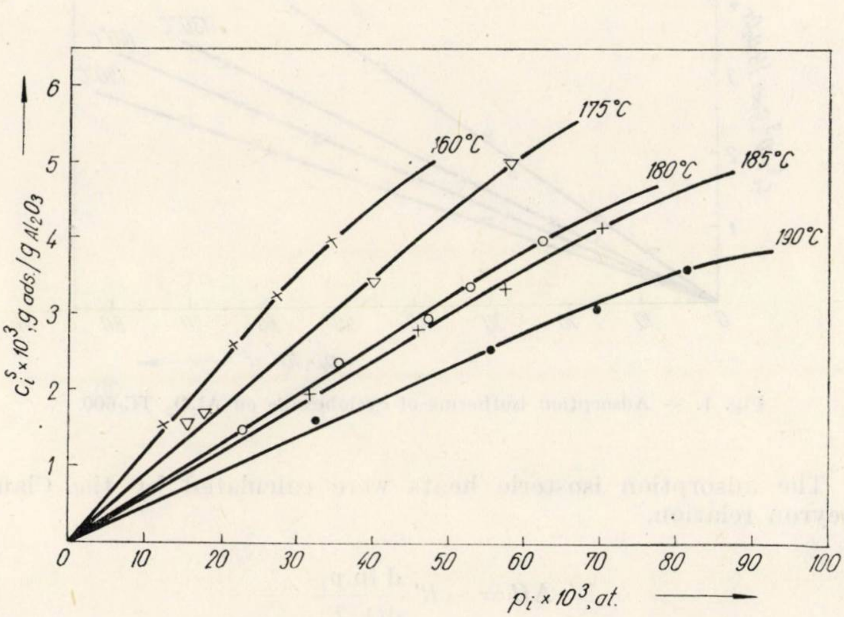

Fig. 3. — Adsorption isotherms of benzene on Al_2O_3 TC-600.

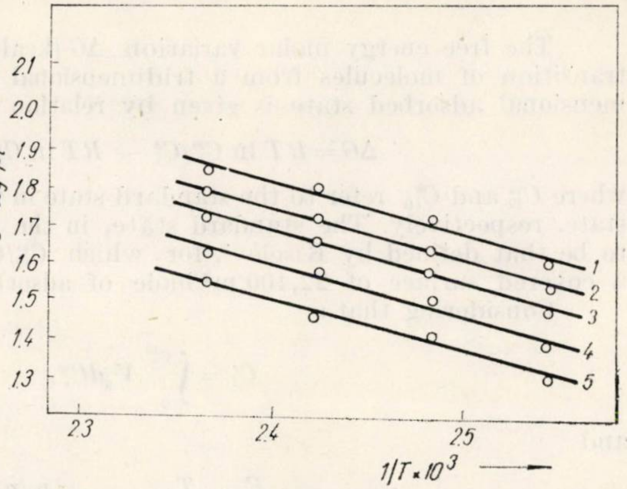

Fig. 4. — Adsorption isosteres of cyclohexane

1. $C_i^s = 2.6.10^{-3}$ g/G, q_{ist} = = 5.94 kcal/mole; 2. $C_i^s = 2.3.10^{-3}$ g/G, q_{ist} = 5.90 kcal/mole; 3. $C_i^s = 2.0.10^{-3}$ g/G, q_{ist} = 5.81 kcal/mole; 4. $C_i^s = 1.6.10^{-3}$ g/G, q_{ist} = 5.81 kcal/mole; 5. $C_{i_4}^s = 1.3.10^{-3}$ g/G, q_{ist} = 5.72 kcal/mole.

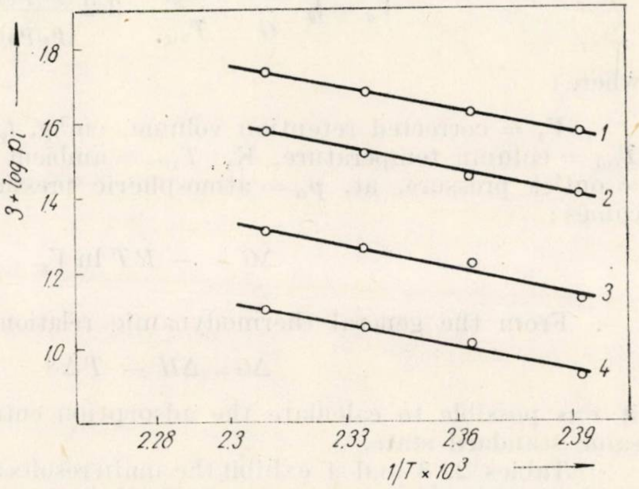

Fig. 5. — Adsorption isosteres of cyclohexene

1. $C_i^s = 2.15 . 10^{-3}$ g/G, q_{ist} = = 8.41 kcal/mole; 2. $C_i^s = 1.59. .10^{-3}$ g/G, q_{ist} = 8.71 kcal/mole; 3. $C_i^s = 1.23.10^{-3}$ g/G, q_{ist} = = 9.43 kcal/mole; 4. $C_i^s = 0{,}75.10^{-3}$ g/G, q_{ist} = 10.28 kcal/mole.

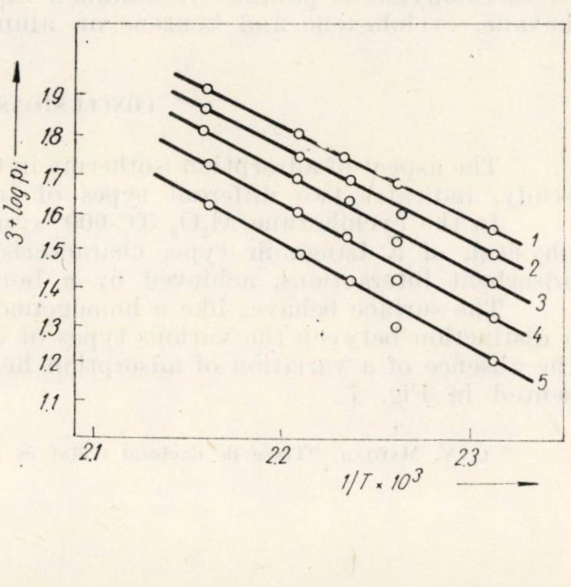

Fig. 6. — Adsorption isosteres of benzene

1. C_i^s =4. 10^{-3} g/G, q_{ist}=11.76 kcal/mole; 2. C_i^s=3.5 ç 10^{-3} g/G, q_{ist}=11.87 kcal/mole; 3. C_i^s=3.0 10^{-3} g/G; q_{ist}=12.06 kcal/mole; 4. C_i^s= 2.5. 10^{-3} g/G; q_{ist} = 12.235 kcal/mole; 5. C_i^s = 2.0. 10^{-3} g/G; q_{ist} = 12 594 kcal/mole.

The free energy molar variation ΔG (kcal/mole) accompanying the transition of molecules from a tridimensional gaseous state to a bidimensional adsorbed state is given by relation :

$$\Delta G = RT \ln C_i^m/C_i^s - RT \ln C_{i0}^m/C_{i0}^s \tag{6}$$

where C_{i0}^m and C_{i0}^s refer to the standard state in unadsorbed and adsorbed state, respectively. The standard state, in the present case, was chosen to be that defined by Kiselev[2], for which $C_{i0}^m/C_{i0}^s = 1$, which supposes a covered surface of 22,400 m^2/mole of adsorbed substance at 273 K.

Considering that :

$$C_i^s = \int_0^{C_2^m} V_g dC_i^m \tag{7}$$

and

$$V_g = t_g \cdot \frac{F}{G} \cdot \frac{T_{\mathrm{col}}}{T_{\mathrm{air}}} \cdot 3/2\, \frac{(p_e/p_0)^2 - 1}{(p_e/p_0)^3 - 1} \tag{8}$$

where :

V_g = corrected retention volume, cm^3/g, t_g = retention time, min, T_{col} = column temperature, K, T_{air} = ambient temperature, K, p_e = = outlet pressure, at, p_0 = atmospheric pressure, at, relation (6) becomes :

$$\Delta G = -RT \ln V_g. \tag{9}$$

From the general thermodynamic relation :

$$\Delta G = \Delta H - T \Delta S \tag{10}$$

it was possible to calculate the adsorption entropy ΔS related to the same standard state.

Tables 2, 3 and 4 exhibit the main results concerning the variation of thermodynamic parameters obtained during the adsorption of cyclohexane, cyclohexene and benzene on alumina TC-600.

CONCLUSIONS

The aspect of adsorption isotherms in the case of the systems under study, indicates two different types of interactions.[6]

In the cyclohexane/Al_2O_3 TC-600 system, the adsorption is purely physical, of a Langmuir type, characteristic of nonspecific adsorbate-adsorbent interactions, achieved by σ bonds.

The surface behaves like a homogeneous entity without permitting a distinction between the various types of centers, a fact resulting from the absence of a variation of adsorption heats with covering degree presented in Fig. 7.

---

[6] C. V. MADJAR, "Thèse de doctorat d'état ès Science Physique", Paris, 1969.

In the case of the systems cyclohexene/Al_2O_3 TC-600 and benzene Al_2O_3 TC-600 a variation of adsorption heats with the covering degree of the surface appears indicating specific adsorbate-adsorbent interactions. The heterogeneity of interactions in such cases may be due to the existence on the alumina surface of two types of active centers with different adsorption potentials, remanent hydroxyl groups and incompletely coordinated Al^{3+} cations, able to form complexes with the π electrons of the reactant.

Table 2

Thermodynamic data obtained for the system Al_2 O_3 TC-600 cyclohexane

Temperature k	Adsorbate	V_R cc^3/g	$-\Delta G$ kcal/mole	$-\Delta S_{exp}$ cal/degree mole
393	2	26.06	2.259	9.10
	4	24.13	2.198	9.25
	6	23.68	2.184	9.29
	8	22.82	2.155	9.36
	10	22.01	2.127	9.44
	15	21.73	2.117	9.46
	20	20.56	2.074	9.57
403	2	21.58	2.165	9.11
	4	20.43	2.121	9.22
	6	19.84	2.098	9.27
	8	19.07	2.066	9.35
	10	18.53	2.043	9.41
	15	17.86	2.014	9.48
	20	16.72	1.961	9.61
413	2	18.53	2.085	9.08
	4	17.58	2.050	9.16
	5	17.25	2.035	9.20
	6	17.04	2.025	9.22
	8	16.36	1.992	9.31
	10	15.82	1.963	9.37
	15	13.60	1.840	9.67
	20	12.97	1.801	9.77
423	2	15.77	2.009	9.05
	4	15.05	1.969	9.14
	6	14.55	1.942	9.21
	8	14.14	1.917	9.26
	10	13.96	1.906	9.28
	15	8.00	1.740	9.67
	20	7.60	1.700	9.77

Table 3

Thermodynamic data obtained for the cyclohexene / Al_2O_3 TC-600

T_{column} °K	Adsorbate	V_R cm³/g	$-\Delta G$ kcal/mole	$-\Delta S_{exp}$ cal/degree mole
418	2	37.20	2.780	17.94
	4	35.03	2.685	16.13
	6	34.35	2.585	14.65
	10	31.58	2.427	14.31
423	2	34.42	2.742	17.82
	4	33.10	2.655	16.01
	6	31.13	2.604	14.43
	10	28.85	2.540	13.87
428	2	31.90	2.677	17.76
	4	29.75	2.591	16.00
	6	28.74	2.561	14.36
	10	26.23	2.489	13.83
433	2	30.05	2.638	17.65
	4	27.82	2.568	16.56
	6	26.23	2.514	14.31
	10	24.28	2.452	13.76

Table 4

Thermodynamic data obtained in the system Al_2O_3 TC-600 benzene

Temperature °k	Adsorbate	$3V_R$ cc/g	$-\Delta G$ kcal/mole	$-\Delta S$ cal/degree mole
433	5	58.52	3.185	20.74
	10	51.81	3.081	20.98
	15	48.32	3.021	21.12
	20	47.17	2.997	21.18
443	5	49.95	3.119	20.42
	10	44.47	3.017	20.65
	15	40.72	2.940	20.83
	20	38.29	2.885	20.95
448	5	43.77	3.037	20.38
	10	39.31	2.941	20.59
	15	35.96	2.862	20.77
	20	33.16	2.790	20.93
453	5	33.98	2.843	20.58
	10	30.00	2.731	20.83
	15	27.16	2.641	25.03
	20	25.38	2.581	21.16
463	5	6.66	2.671	20.51
	10	11.39	2.578	20.71
	15	14.25	2.503	20.87
	20	16.72	2.450	20.99
473	5	7.14	2.650	20.12
	10	13.06	2.529	20.38
	15	16.81	2.462	20.52
	20	19.67	2.404	20.64

In this case, the isotherms may be assumed to be of a Freundlich type, a fact also reported by other authors[3]. The specificity of interactions in terms of the molecular structure appears even more evident from the entropy variation on passing to the adsorbed state, as seen in Fig. 8.

The mobility of the molecule on the surface decreases with the increase of the molecular electronic density, hence in the sense cyclohexane-cyclohexene-benzene.

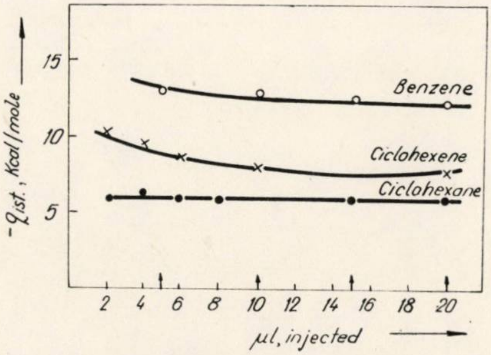

Fig. 7. — The variation of adsorption heats of cyclohexane, cyclohexene and benzene with the covering degree of surface.

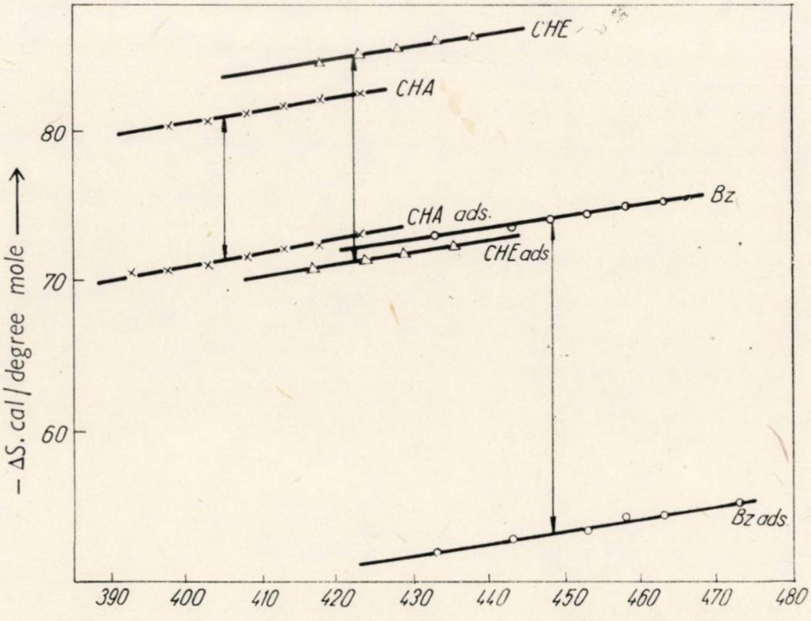

Fig. 8. — The variation of the molar entropy of cyclohexane (CHA), cyclohexene (CHE) and benzene (Bz), by passing from gaseous to the adsorbed state.

Revue Roumaine de Chimie, **23**, *3* 371–376 (1978)

CONTRIBUTIONS TO THE CHEMISTRY OF THIOCOMPLEXES. VI [1]

COMPLEX COMPOUNDS OF Pt(II) WITH THIOAMIDES OF THE DIBENZOFURAN SERIES

DUMITRU NEGOIU*, VASILICA MUREŞAN** and N. MUREŞAN**
* Faculty of Chemistry, Polytechnic Institute Bucharest, Splaiul Independenţei 89
** Faculty of Chemistry, University of Craiova, Al. I. Cuza 13

Received October 27, 1975

Complex compounds of Pt(II) with thioamides of the dibenzofuran series (3-thioacetylamino-dibenzofuran, 3-thiobenzoylamino-dibenzofuran and 3-thiofuroylamino-dibenzofuran) were prepared. These complex compounds were characterized by elemental analysis and by IR, visible and UV spectra as well as by conductivity measurements. The results of these studies lead to the conclusion that the complexes are of type [Pt L Cl_2] in which L is the ligand, i. e. the thioamide of the dibenzofuran series; it acts in the "thioketo" form as a bidentated ligand, leading to a square-planar structure which belongs to the D_4 symmetry group.

In its lower oxidation state (II), platinum shows a more marked class (b) character, respectively that of a soft Lewis acid, as compared to the higher oxidation state (IV).

Literature reports complex compounds of Pt(II) with ligands containing sulphur as donor atom (soft Lewis bases) which exhibit a particular stability, owing to the high affinity of Pt(II) to such ligands. This can be understood on the basis of Pearson's principle of soft and hard acids and bases.[2]

Nevertheless, the number of papers concerned with complex compounds of platinum with thioamides is very reduced[1,3-8] and the number of ligands used is also relatively small (thioacetamide, phenylthioacetamide and its derivatives, thiobenzamide, cynnamthioamide and its derivatives, dithiooxamide and its derivatives). We have investigated further complex compounds of Pt(II) with thioamides[1] in an attempt to extend the existing theoretical and practical information and to provide new data on the complex compounds of Pt(II) with thioamides of the dibenzofuran series : [9] 3-thioacetylamino-dibenzofuran (TAADBF), (I), 3-thiobenzoylamino-dibenzofuran (TBADBF) (II) and 3-thiofuroylamino-dibenzofuran (TFADBF) (III) :

---

[1] Part V: D. Negoiu and V. Mureşan, *Rev. Roumaine Chim.*, **19**, 1031 (1974).

[2] R. G. Pearson, *J. Chem. Educ.*, **45**, 581, 643 (1968).

[3] C. D. Flint and M. Goodgame, *J. Chem. Soc. A.*, **3**, 750 (1968).

[4] Yu. N. Kukushňin, S. A. Simanova and N. N. Knyazeva, *Zhur. neorg. Kkim.*, **16**, 2488 (1971).

[5] Yu. N. Kukushňin, S. A. Simanova and A. P. Alashkevich, *Zhur. priklad. Khim.*, **44**, 1640 (1971).

[6] F. Kaspàrek and J. Mollin, *Coll. Czech. Chem. Comm.*, **25**, 2919 (1960).

[7] I. V. Talmachov and P. V. Rasteghina, *Ukrain. Khim. Zhur.*, **32**, 82 (1966).

[8] W. D. Jakobs, *Analyt. Chem.*, **33**, 1279 (1961).

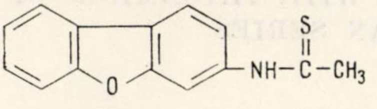

I

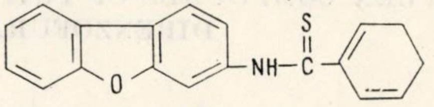

II

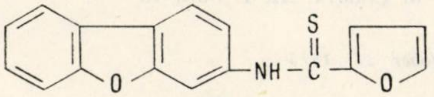

III

RESULTS AND DISCUSSION

Complex compounds of Pt(II) with thioamides of the dibenzofuran series are obtained by adding the thioamide in ethanol solution to a solution containing $[PtCl_4]^{2-}$ under constant stirring. They appear as microcrystalline orange powders, sparingly or partially soluble in inorganic and organic solvents, with melting points higher than the pure thioamides.

The results of the elemental analysis listed in table 1 prove that all these complex compounds are of type : $[PtL\,Cl_2]$ (L=TAADBF, TBADBF, TFADBF).

Table 1

Elemental analysis of Pt(II) complexes

Compound	S%		C%		H%		Colour	m. p. (°C)
	Calcd.	Found	Calcd.	Found	Calcd.	Found		
$[Pt(TAADBF)\,Cl_2]$	6.31	5.98	33.10	34.87	2.09	2.91	orange	152
$[Pt(TBADBF)\,Cl_2]$	5.62	6.12	40.06	41.32	2.28	2.85	orange	147
$[Pt(TFADBF)\,Cl_2]$	5.72	6.20	36.48	37.59	1.96	2.46	orange	—

In order to establish the nature of the bonding in the compounds prepared we have systematized the results of IR spectral analysis in specific domains, both for ligands and for the corresponding complexes[10] (Table 2).

---

[9] V. FĂRCĂȘAN, S. FLOREA and R. BEJU, *Stud. Univ. Babeș-Bolyai, Chemia*, **1970**, 63.
[10] K. A. JENSEN and P. H. NIELSEN, *Acta Chem. Scand.*, **20**, 597 (1966).

Table 2

Characteristic infrared absorption frequencies (cm^{-1}) of ligands and complexes

Compound	3500 — 3000	1 650—1600	1 600—1 350		1 350—900		900—600	
			1 600—1 450	1 450—1 350			900—700	700—600
	νNH_2	δNH_2	νCN coupling C—C	νCN Coupling NH_2	νCS	δNH_2	νNCS	$\nu(C=S)$
TAADBF	3 090 w 2 960 i	1 600 m	1 455 i	1 370 i	1 210 i 1 180 i	958 m	845 i 742 i 722 m	670 m
TBADBF	3 090 w 2 960 m	1 600 m	1 450 i	1 350 i	1 230 i 1 150 i	942 m	748 i	680 i
TFADBF	3 220 i 3 050 sh 2 860 w	1 600 m	1 460 i	1 360 i	1 210 m 1 205 i	952 m	740 i 730 i	660 m
[Pt(TAADBF) Cl_2]	3 030 sh 3 100 sh	1 600 w	1 490 w	1 420 m	1 210 sh 1 180 sh	950 i	845 m 742 m 722 w	670 sh
[Pt(TBADBF) Cl_2]	3 050 w 3 100 sh	1 600 w	1 490 w	1 420 W	1 280 w	940 w	750 m	685 w
[Pt(TFADBF) Cl_2]	3 100 sh 3 150 sh	1 600 w	1 490 sh	1 422 w	1 220 sh	950 m	750 m 725 w	—

i = intense, m = medium, w = weak, sh = shoulder

A comparative interpretation of infrared spectral data suggests that the thioamides act as bidentate ligands in the investigated complex compounds, having both sulphur and nitrogen atoms as donors.

The spectral arguments suggesting the participation of sulphur atom in the "thioketo" form are as follows:

(*a*) the modification of the band at 1 220 cm^{-1} which shows an important contribution of the C=S bond, and which appears in complexes with a much lower intensity or is even levelled off;

(*b*) the disappearance in the complexes of the intense band in the 550–680 cm^{-1} range of the thioamides spectrum, which is generally atributed to the ν C=S vibration.

The evidence with regard to the participation of thioamide group nitrogen in the bonding is supported by the following:

(*a*) in the 3 500–3 000 cm^{-1} range, the bands characteristic of νsym NH_2 and ν asym NH appear in complexes at modified frequencies compared to the respective thioamides, and are much weaker;

(*b*) the band characteristic of the $-NH_2$ group stretching vibration in the 1 650–1 660 cm^{-1} range, occurs at slightly higher frequencies in complexes, and with a variable intensity;

(*c*) the band at ~ 960 cm^{-1} attributed to the $-NH_2$ group stretching vibration, is reduced or totally disappears in complexes.

The spectral analysis in the visible and UV domains was performed in order to establish the coordination geometry of the new complex compounds. Electronic reflectance spectra were recorded in solid powders and are presented in Figures 1 and 2.

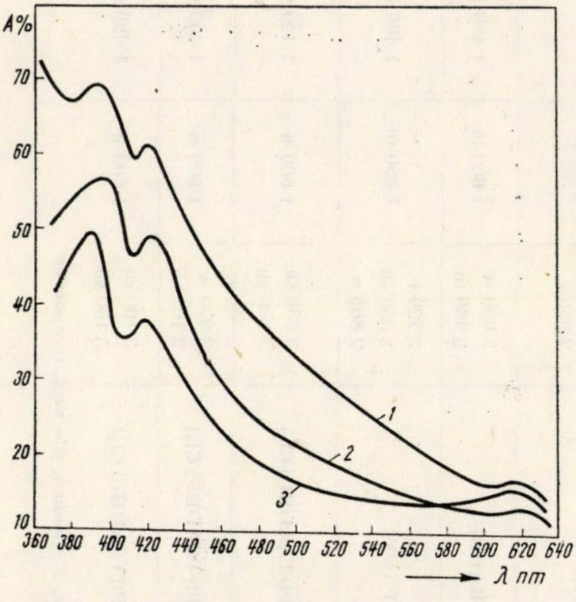

Fig. 1. — Visible electronic reflectance spectra of [Pt(TAADBF) Cl_2] (1), [Pt (TBADBF) Cl_2] (2) and [Pt(TFADBF) Cl_2] (3) complexes.

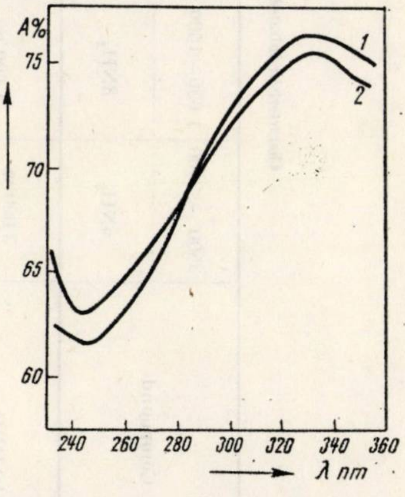

Fig. 2.— UV electronic reflectance spectra of [Pt(TBADBF)Cl_2] (1) and [Pt(TFADBF) Cl_3] (2) complexes.

The bands observed in the electronic absorption spectra of the complexes studied were assigned according to the work of Gray and Ballhausen[11]. They use the molecular orbital approach to explain the spectra of square-planar complexes of the d^8 elements: Ni(II), Pd(II), Pt(II) and Au(III).

The correlation of bands observed in electronic spectra of the platinum (II) complexes with those of $[PtCl_4]^{2-}$ leads us to the following assignments:

(a) the band at 30,303 cm^{-1} (330 nm) is assigned to the $^1A_{1g}\rightarrow{}^1E_g$ transition;

(b) the band at 25,640 cm^{-1} (390 nm) is assigned to the $^1A_{1g}\rightarrow{}^1B_{1g}$ transition;

(c) the band at 23,800 cm^{-1} (420 nm) is assigned to the $^1A_{1g}\rightarrow{}^1A_{2g}$ transition;

(d) the shoulder at 16,129 cm^{-1} (620 nm) is assigned to the $^1A_{1g}\rightarrow\rightarrow{}^3A_{2g}$ transition.

The correspondence of these four bands observed in our complexes with the bands described for $[Pt\,Cl_4]^{2-}$ suggests that they have a similar symmetry, with a square-planar geometry (D_{4h} symmetry).

The study of our complex compounds has been completed with conductivity measurements. The values of molar electric conductivities of the studied complexes in 10^{-4} M acetone solutions are given in table 3. The conductivity data show that the compounds investigated are non-electrolytes.

Table 3

Molar electric conductivity for Pt(II) complexes

Compound	Concentration x.10^{-4}M	Molar conductivity $\lambda(\Omega^{-1}mol^{-1}cm^2)$
$[Pt(TAADBF)Cl_2]$	1.06	1.42
$[Pt(TBADBF)Cl_2]$	0.98	1.07
$[Pt(TFADBF)Cl_2]$	0.97	1.14

EXPERIMENTAL

Reagents: $[PtCl_4]^{2-}$ aqueous solution and thioamide ethanol solutions of analytical (reagent) grade purity were used.

Apparatus: IR spectra were recorded on a Perkin-Elmer 157 instrument in anhydrous KBr pellets; electronic reflectance spectra in the visible and UV range were measured on a VSU-1 Zeiss-Jena spectrophotometer in MgO pellets; the electric conductivitiy was determined by an OK-102/1(made in Hungary) conductivity meter.

Preparation of complexes

Dichloro (3-thioacetylamino-dibenzofuran)-platinum (II)

Ethanolic solution of thioamide was added to a $[Pt\,Cl_4]^{2-}$ aqueous solution under constant stirring, having a 1 : 1 molar ratio. The precipitate formed was allowed to settle during an hour. It was then filtered on a G_4 porosity glass filter, washed with 96$^0/_0$ ethyl alcohol, diethyl-ether, then vacuum-dired. The compounds are orange microcrystalline plastes stable on storage, sparingly soluble in inorganic solvents and with a medium solubility in organic solvents.

Dichloro (3-thiobenzoylamino-dibenzofuran)-platinum (II) and dichloro (3-thiofuroylamino-dibenzofuran)-platinum (II) have been prepared by analogous procedures.

---

[11] H. B. GRAY and C. J. BALLHAUSEN, *J. Amer. Chem. Soc.*, **85**, 260 (1963).

CONCLUSIONS

A correlation of the results obtained from chemical analysis with the results from physico-chemical investigations on complex compounds of [Pt L Cl_2] type (in which L=TAADBF, TBADBF, and TFADBF), suggest the following structural formulation:

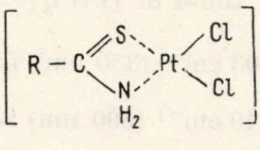

This formulation is supported by the IR spectral analysis, which confirms the involvement of the thioamide sulphur and nitrogen atoms in bonding to the metal. The thioamide group participates in the "thioketo" form.

The given structural formulation also agrees with the conclusions drawn from the spectral analysis in the UV and visible ranges, which indicates a square-planar geometry, belonging to the D_{4h} symmetry group.

An additional argument in support of the given formulation is provided by the results of conductivity determinations, which prove that the thioamide complexes are non-electrolytes, a fact which requires the participation of both chlorine atoms in the achievement of the tetracoordination of platinum (II).

The fact that in our complexes, platinum (II) fails to coordinate two ligand molecules, as in the case of [Pt L_2] Cl_2 type complexes (where L= thioamide of the phenylthioacetamide series)[1] can be explained by the large volume of thioamides of the dibenzofuran series, which produces steric hindrances.

It is worth mentioning the analogy of the properties and structures of Pt(II) and Pd(II) complexes[12] with te thioamides of the dibenzofuran series. This fact is justified by the analogy of the d^8 type electronic configuration, alongside with the analogy of the general properties of platinum metals.

---

[12] D. Negoiu, V. Mureşan and S. Florea, *Rev. Roumaine Chim.*, **18**, 1875 (1973).

Revue Roumaine de Chimie, 23, *3*, 377–382 1978)

PROTECTION OF DNA BY METAL COORDINATES — A SIMPLE STOICHIOMETRIC STUDY

V. K. SRIVASTAVA*, C. SINGH** and B. B. MISRA*

*Department of Chemistry, University of Gorakhpur,
Gorakhpur, (U. P.), INDIA
** Division of Biochemistry, C.D.R.I., Lucknow, U. P., INDIA

Received October 22, 1975

The cationic metal coordinates of Co(III), Cu(II), Cu(I) and Pb(II) showed protection of DNA. The degree of protection was dependent on the geometry of the coordinate and nature of ligands. The protection with $[Co(NH_3)_6]Cl_3$ was 70% whereas it was 35% with $[(CuTu_3)_2]SO_4 2H_2O$. Tm value of metal coordinates-DNA solution was higher than native DNA and the stoichiometry of metal-coordinates-DNA interaction ranged between 0.13 to 0.65.

INTRODUCTION

Metal coordinates radically differ from the parental metal cations in several respects [1,2] including their interaction behaviour with oppositely charged species. This has been verified by the fact that cationic coordinates of Co, Cr and Cu yield cohesive clots with native DNA while the corresponding parental metal cations do not behave alike[3]. Besides, positively charged metal-coordinates behave true chromotropes for inducing metachromasia in acid dyes[4]. A few earlier studies deal with the complex formation behaviour of cationic coordinates with acid polysaccharides, inorganic polyphosphates and acid dyes.[5-7]

In the field of metal cations -DNA interaction it has been established that the divalent cations stabilize[8-11] as well as destabilize DNA

---

[1] M. M. Jones, "Elementary Coordination Chemistry", Prentice Hall. Inc. USA, 1966.

[2] H. I. Emeleus and J. S. Anderson, "Modern Aspects of Inorganic Chemistry", Routledge & W. Paul. Ltd., London, 1949.

[3] C. Singh, *Ind. J. Biochem.*, **7**, 255 (1970).

[4] C. Singh, *Stain Technol.*, **38**, 103 (1963).

[5] M. Stacey and S. A. Barkeley, "Carbohydrates of Living Tissues", Van Nostrand D. Co. Ltd., London, 1962.

[6] J. R. Van Wazer, "Phosphorous and its Compounds", Vol. I, Inter Science Publication Inc., New York, 1958.

[7] C. Singh, *Ind. J. Biochem. Biophys.*, **8**, 45 (1971).

[8] J. Shack and B. S. Bynum, *Nature*, **184**, 635 (1959).

[9] G. Felsenfeld and S. L. Huang, *Biochem. Biophys. Acta*, **51**, 19 (1961).

[10] G. L. Eichhorn and Clark, *Proc. Nat. Acad. Sci. U. S. A.*, **53**, 586 (1965).

[11] W. F. Dove and N. Davidson, *J. Mol. Biol.*, **5**, 467 (1967).

structure against heating.[12–15] It would thus be very interesting to explore whether stable coordinates of such metal cations (with all their valencies satisfied with suitable ligands) would stabilize or destabilize the DNA helix. The present investigation was thus motivated by the expectations that metal cations like Co(III), Pb(II) and Cu(I & II), which normally destabilize the secondary structure of DNA should behave differently once they form cationic metal-coordinates with different ligands. This is because in cationic metal coordinates all the vacant orbitals of metal ions are filled by lone pair of electrons donated by ligands and thus there will be little provision left for their interaction with bases. Besides, the present study also form a simple and reproducible basis for the calculation of stoichiometry of metal coordinate-DNA interactions.

EXPERIMENTAL

All the cationic metal coordinates were prepared by the well-known methods described elsewhere.[16–18] The chemicals of reagent grade were used without further purification. The metal coordinates were recrystalized before use and their purities were checked by TLC and paper chromatography methods. Stock solution of 1 mg/ml of calf thymus DNA was prepared in 10^{-3} M KNO_3 solution and stored in presence of 1 ml chloroform. An aliquot of stock solution was diluted with 1 mM KNO_3 solution to give the required DNA concentration. Varying amounts of cationic metal coordinate solutions (1–40 μg) were added to 2 ml of DNA solution (25 μg/ml) and the total volume of the solutions were adjusted to 3 ml. These were heated to 30, 40, 50, 60, 70, 80, 90 and 100° for 15 minutes, chilled in ice and then optical density were recorded at 260 nm with Backmann DU spectrophotometer model 202. Though the solutions were heated to different temperatures, the increase in optical density upto 70° was not so remarkable as compared to that obtained at higher temperatures. Thus difference in optical density (ΔOD) was determined with different concentrations of metal coordinates. The optical densities so obtained were used for the determination of the Tm values and the percentage protection was calculated by the simple relation mentioned below:

$$\frac{\Delta OD_{DNA} - \Delta OD_{MC}}{\Delta OD_{DNA}} \times 100 \quad (MC = \text{metal coordinates})$$

(OD = Difference of optical densities values taken at room tempeature and after heating to 80° and chilled).

There is minium stress on DNA with no possibility of degradation and thus has the additional advantage over the classical method for the determination of the T_m values.

All experiments were done in the absence of any buffer solution because of possible complications which it can introduce into the system. However, the possibility of effect of pH change obtained by adding metal coordinates to DNA solution on the DNA structure cannot be ruled out. This was ascertained by the following simple measurements.

The pH of DNA solution is 6.2 and its pH rises to 6.7 after heating and cooling. The initial pH of metal coordinates and DNA solution is 5.8 which rises to 6.0 after heating to 90° and cooling. The solution of DNA containing no cationic coordinates was adjusted to pH 5.8. The Tm of this solution was decreased only by 1°, showing thereby that the pH change introduced by the metal coordinates does not affect the DNA structure, analogous to the earlier observation in case of metal cations as reported earlier.[10]

---

[12] T. Yamane and N. Davidson, *Biochem. Biophys. Acta*, **55**, 600 (1962).

[13] S. Hiai, *J. Mol. Biol.*, **11**, 672 (1965).

[14] H. Venner and C. H. Zimmer, *Biopolymers*, **4**, 321 (1966).

[15] J. H. Coates, D. O. Jordan and V. K. Srivastava, *Biochem. Biophys. Res. Commun.*, **20**, 611 (1965).

[16] W. G. Palmer, "Experimental Inorganic Chemistry", Cambridge University Press, 1954.

[17] H. S. Booth, "Inorganic Synthesis", vol. II, Mc. Graw-Hill Book Bo. Inc., New York 1939.

[18] W. C. Fernelius, "Inorganic Synthesis" vol. II, Mc. Graw-Hill Book Co. Inc. New York, 1946.

RESULTS AND DISCUSSION

It was found that (ΔOD) decreased with increasing concentration of all the cationic metal coordinates. The metal coordinates show different constant values beyond which there is no appreciable change in ΔOD and almost forms a plataeu (Figures 1a and 1b).

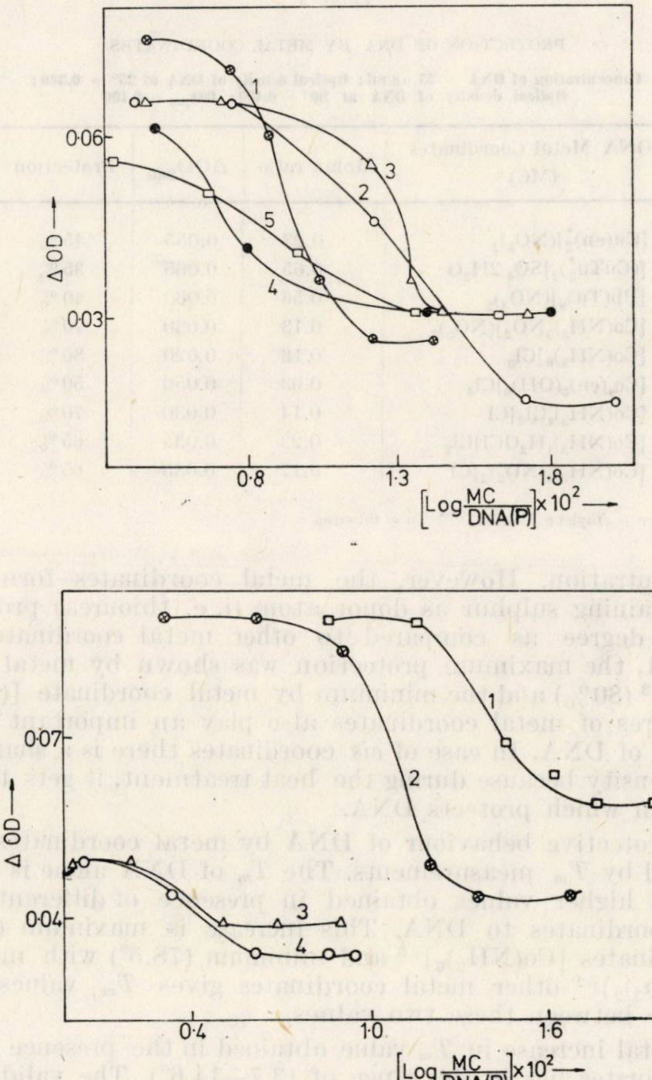

Fig. 1(a). — Dependence of ΔOD on the mole ratio of cationic coordinates to DNA (P) concentration

1. $[Co(NH_3)_4H_2O.Cl]Cl_2$; *2.* $[Co(NH_3)_4]Cl_3$; *3.* $[Co(NH_3)_4(NO_2)_2]Cl$; *4.* $[Co(NH_3)_4Cl_2]Cl$; *5.* $[Co(NH_3)_5NO_2](NO_3)_2$.

(b) — 1. $[Co_4(en)_6(OH)_6]Cl_6$; *2.* $[Cu(en)_2](NO_3)_2$; *3.* $[(CuTu_3)_2](SO_4)_2$; *4.* $[Pb(Tu)_6](NO_3)_2$.

These values were taken into consideration for the calculation of the degree of protection. As summarized in table 1, different metal coordinates produced different degrees of protection. The experiments were followed with different DNA concentration and it was concluded that the protective nature of DNA by metal coordinates was independent of DNA concentration. However, the metal coordinates formed by the ligands containing sulphur as donor atom (i. e. thiourea) protects DNA to a lesser degree as compared to other metal coordinates. As seen from table 1, the maximum protection was shown by metal coordinate $[\mathrm{Co(NH_3)_6}]^{+3}$ (80%) and the minimum by metal coordinate $[\mathrm{(CuTu_3)_2}]^{+2}$. The structures of metal coordinates also play an important role in the stabilization of DNA. In case of *cis* coordinates there is a sharp decrease in optical density because during the heat treatment, it gets transformed to *trans* form which protects DNA.

Table 1

PROTECTION OF DNA BY METAL COORDINATES

Concentration of DNA = 25 μg/ml; Optical density of DNA at 25° = 0.300; Optical density of DNA at 80° = 0.400; OD_{260} = 0.100

DNA Metal Coordinates (MC)	Molar ratio	$\Delta\mathrm{OD}_{260}$	Protection
1. $[\mathrm{Cu(en)}_2^{*}](\mathrm{NO_3})_2$	0.23	0.055	45%
2. $[(\mathrm{CuTu}_3^{*})_2]\mathrm{SO_4\ 2H_2O}$	0.65	0.065	35%
3. $[\mathrm{Pb(Tu)_6}](\mathrm{NO_3})_2$	0.56	0.060	40%
4. $[\mathrm{Co(NH_3)_5NO_2}](\mathrm{NO_3})_2$	0.13	0.030	70%
5. $[\mathrm{Co(NH_3)_6}]\mathrm{Cl_3}$	0.16	0.020	80%
6. $[\mathrm{Co_4(en)_6(OH)_6}]\mathrm{Cl_6}$	0.63	0.050	50%
7. $[\mathrm{Co(NH_3)_4Cl_2}]\mathrm{Cl}$	0.14	0.030	70%
8. $[\mathrm{Co(NH_3)_4H_2OCl}]\mathrm{Cl_2}$	0.23	0.035	65%
9. $[\mathrm{Co(NH_3)_4(NO_2)_2}]\mathrm{Cl}$	0.17	0.035	65%

* en = ethylene diamine, ** Tu = thiourea

The protective behaviour of DNA by metal coordinates is further strengthened by T_m measurements. The T_m of DNA alone is 74.5° which increases to higher values obtained in presence of different mole ratio of metal coordinates to DNA. This increase is maximum (89.0°) with metal coordinates $[\mathrm{Co(NH_3)_6}]^{+3}$ and minimum (78.5°) with metal coordinate $[\mathrm{(CuTu_3)_2}]^{+2}$ other metal coordinates gives T_m values which are intermediate between these two values.

The total increase in T_m value obtained in the presence of different metal coordinates lies in the range of (3.7—14.6°). The validity of such results were confirmed by finding the percentage of protection of DNA by spermine and protamine sulphate which is of the order of 85% and 75% respectively.

As seen from table 2, T_m depends on the nature and geometry of metal coordinates. The details about the role of isomerism may be ascertained by studying the influence of other stable cationic coordinates which involve different metal ion and ligands. Figure 2 shows the plot of T_m against the logarithm of *mole ratio* wherefrom it is observed that T_m increases linearly with increasing *mole ratio.*

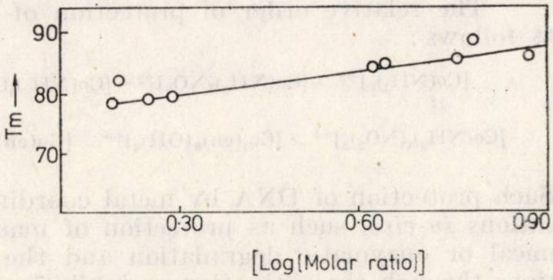

Fig. 2. — Influence of molar ratio (MR) of metal coordinates on helix coil transition (T_m) of DNA.

The mole ratio of metal coordinate-DNA interaction lies between 0.13 to 0.65 (Table 2). This accounts for the apparent stoichiometry of the process. Since the values are less than 1 it is presumed that metal coordinate interact with negatively charged phosphate sites only. This conclusion agrees with earlier results of different metal-DNA interaction, where it was concluded that if the value was less than 1, metal cations were bound to phosphates only and for values of more than 1, they reflect the ability for interacting phosphates as well as bases sites.[10] Thus it can be proposed that amino group of metal coordinates interact with DNA phosphates, charge is clearly not the only consideration although nonspecific effect of a cation shielding phosphates must partly account for the data. This, however, is similar to protection of DNA by spermine and spermidine, where the T_m value of DNA was increased.[19,20]

Table 2

STOICHIOMETRY OF MC-DNA INTERACTIONS

Concentration of DNA = 25 μg/ml; Melting temperature of DNA = 74.5°

Metal Coordinates (MC)	Mol. Wt.	Equivalent charge	Melting temperature	ΔT_m
MC_1	307.54	153.77	84.0°	+9.5°
MC_2	643.88	321.94	78.5°	+4.0°
MC_3	757.80	378.90	79.5°	+5.0°
MC_4	314.14	157.07	86.0°	+11.5°
MC_5	264.48	88.16	89.0°	+14.5°
MC_6	910.44	151.74	82.5°	+8.0°
MC_7	233.41	233.41	81.3°	+7.6°
MC_8	251.32	125.66	84.5°	+10.0°
MC_9	254.53	254.53	85.5°	+11.0°

---

[19] H. R. Mahler and B. D. Mehrotra, *Biochem. Biophys. Acta*, **68**, 211 (1963).

[20] H. R. Mahler and B. D. Mehrotra, *Biochem. Biophys. Res. Commun.*, **4**, 79 (1961).

Tsuboi[21] suggested that both primary and secondary amino groups of spermine interact with four DNA phosphates with the secondary amino group making a bridge across the shallow groove in the double helix while the primary amino groups were bound to adjacent nucleoside phosphate along a single polynucleotide chain.

The relative order of protection of DNA by metal coordinates is as follows :

$$[Co(NH_3)_6]^{+3} > [Co(NH_3)_5NO_2]^{+2} \sim [Co(NH_3)_4Cl_2]^{+1} > [Co(NH_3)_4H_2O.Cl]^{+2} \sim$$

$$[Co(NH_3)_4(NO_2)_2]^{+1} > [Co_4(en)_6(OH)_6]^{+6} > [Cu(en)_2]^{+2} > [Pb(Tu)_6]^{+2} > [(CuTu_3)_2]^{+2}$$

Such protection of DNA by metal coordinates may be important implications *in-vivo*, such as protection of macromolecules against their chemical or enzymatic degradation and the regulation of metabolic reactions through the activation or inhibition of enzyme systems.

ACKNOWLEDGEMENT. The authors are thankful to Prof. R. P. Rastogi, Head, Chemistry Department University of Gorakhpur, Gorakhpur and Dr. C. R. Krishnamurthy, Deputy Director and Head, Biochemistry Division, C.D.R.I., Lucknow for providing necessary facilities and valuable suggestions during the course of this investigation. One of us (BBM) is thankful to SCSIR for financial assistance.

---

[21] M. Tsuboi, *Bull. Chem. Soc. Japan*, **37**, 1514 (1964).

Revue Roumaine de Chimie, **23**, *3*, 383–395 (1978)

KEKULÉ STRUCTURES AND TOPOLOGY. III[1]

ON INSEPARABILITY OF KEKULÉ STRUCTURES

I. GUTMAN*, M. RANDIĆ**, and N. TRINAJSTIĆ*
* The Rugjer Bošković Institute, P. O. B. 1016, 41001 Zagreb,
Croatia, Yugoslavia
** Department of Chemistry, Tufts University, Medford, Mass. 02155, U. S.A.

Received October, 11, 1975

The concept of the parity of Kekulé structures is discussed. Conditions for separability of Kekulé structures into two classes of the opposite parity are given. It is also shown that there are systems for which it is not possible to assign relative parity. The simplest such molecules have three fused odd-membered rings. Few derivatives of this special class of compounds are known. Such compounds show somewhat distinctive properties and it is believed that these are manifestations of their unique structural features.

1. INTRODUCTION

The ability to represent conveniently the results of ambitious theoretical calculations in a way which is analogous to traditional valence bond resonance structures should be of considerable utility in chemistry. Recently some efforts were made to express chemical bonding in terms of resonance between specific types of VB structures in a way which is not only semiquantitative but has also a great appeal to chemical intuition[2,3]. On the other hand, it has been recently reported that empirical and simple VB calculations, based on only Kekulé structures, are in very satisfactory agreement with the thermochemical SCF calculations of resonance energies[4]. Thus, a revived interest in Kekulé valence structural formulae appears not only justified but also rewarding. For instance, a re-examination of conjugated hydrocarbons showed that the Pauling bond orders, which are simply derived from Kekulé structures, are as adequate as the other more elaborate MO counterparts when correlating with experimental carbon-carbon bond lenghts[5].

---

[1] Part II: D. Cvetković, I. Gutman and N. Trinajstić, *Croat. Chem. Acta*, **46**, 15 (1974).

[2] M. H. Whangbo and I. Lee, *J. Amer. Chem. Soc.*, **93**, 2330 (1971).

[3] A. Graovac, I. Gutman, M. Randić, and N. Trinajstić, *J. Amer. Chem. Soc.*, **95**, 6267 (1973).

[4] W. C. Herndon and M. L. Ellzey, Jr., *J. Amer. Chem. Soc.*, **97**, 6631 (1974).

[5] W. C. Herndon, *J. Amer. Chem. Soc.*, **96**, 7605 (1974).

The concept of bond orders may be also extended to larger molecular fragments, such as diene group or individual rings.[6–9]

The important step in improving the initial resonance theory was the recongnition of the fact that some Kekulé structures will make a positive contribution to the stability of the compound, or some other molecular property, while others may make a negative contribution. The simple postulate that the stability of a conjugated molecule is proportional to the number of Kekulé structures[10] (K) requires a revision, because it may lead to false conclusions.[11] This is in particular the case with cyclobutadiene-containing systems.[12] The concept of the parity of Kekulé structures was introduced in order to distinguish the two kinds of structures of *alternant* hydrocarbons.[13]

In this paper we will consider some problems which arise when the concept of partity of Kekulé structures is applied to non-alternant systems. We will see that, while for some systems the extension is straightforward, in other systems the assignment of parity to individual Kekulé structures cannot be achieved in an internally consistent manner. The former class may be called *Kekulé-separable*, i. e., all Kekulé structures may be separated into those belonging to the opposite parity. The latter class represents *Kekulé-inseparable* structures and the conditions which are sufficient for a system to belong to this group are delineated.

2. ON A DEFINITION OF THE PARITY OF KEKULÉ STRUCTURES

Although the notion of the parity of Kekulé structures is relatively old[13], there are difficulties in establishing its theoretical justification. The original formulation of Dewar and Longuet-Higgins[13] that two Kekulé structures are of the *same* parity if one structure is obtained from the other by permutation of an *odd* number of double bonds is not sufficiently general. It, for instance, predicts opposite parity for some structures of pyrene in contradiction to view that all benzenoid systems have structures of the same parity only. Recent interest in application of graph theory to the chemistry of conjugated systems[14] has provided for an alternative definition of the relative parity of Kekulé structures. A superposition of two Kekulé structures leads generally to a structure in which the double bonds form a cyclic arrangement or several cyclic components. The critical quantity which determines the relative parity of two Kekulé structures is the number of cyclic components involving

[6] O. E. Polansky and G. Derflinger, *Internat. J. Quantum Chem.*, **1**, 379 (1967).

[7] H. Sofer, O. E. Polansky, and G. Derflinger, *Monats*, **99**, 1879 (1968).

[8] M. Randić, *Tetrahedron*, **30**, 2067 (1974).

[9] M. Randić, *Tetrahedron*, in press.

[10] G. W. Wheland, "The Theory of Resonance and Its Application to Organic Chemistry", Wiley, New York, 1953.

[11] I. Gutman, N. Trinajstić, and C. F. Wilcox, Jr. *Tetrahedron*, **31**, 143 (1975).

[12] C. F. Wilcox, Jr., *Tetrahedron Lett.*, **(1968)**, 795.

[13] M. J. S. Dewar and H. C. Longuet-Higgins, *Proc. Roy. Soc.*, **A 214**, 482 (1952).

[14] For review see, for example, I. Gutman and N. Trinajstić, *Topics Curr. Chem*, **42**, 49 (1973).

$4m$ carbon atoms.[15–17] Let R_{4m} be the number of ring components of the size $4m$ in the superimposed graph S_{ab}, where a and b refer to individual Kekulé structures. The expression:

$$p_a p_b = (-)^{R_{4m}(S_{ab})} \tag{1}$$

is either positive or negative and the corresponding Kekulé structures are taken as of the *same* or *opposite* parity, respectively. In other words, two Kekulé structures are of the *same* parity if, and only if, R_{4m} is *zero* or *even*. The Kekulé forms of benzenoid systems are of the same parity.[17] For non-benzenoid systems this is no longer the case as illustrated below for benzocyclobutadiene. Benzocyclobutadiene has three Kekulé forms:

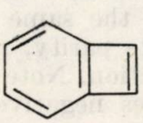
a

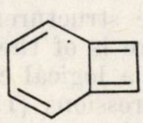
b

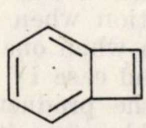
c

They give rise to the following superposition structures:

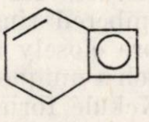
S_{ab}

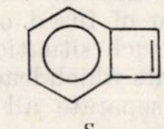
S_{ac}

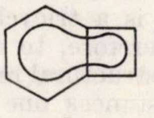
S_{bc}

It follows then that two of three structures are of the same parity (a, c), and one structure (b) is of opposite parity. One can assign to a and c parity value $p=1$ and called them *even* and to structure b parity value -1 and refer to it as *odd*. However, such an assignement does not imply any significance to this, rather than an alternative, assignement. It may be of convenience in situations when an unequal number of structures of opposite parity appear to refer to the more numerous class as even.

The expression (1) can uniquely determine the relative parity of *any two Kekulé forms* of a system including non-benzenoid and non-alternant systems. However, *for systems with three or more Kekulé forms a question of compatibility of such pairwise assignement may be raised.*[18]

---

[15] A. Graovac, I. Gutman, N. Trinajstić, and T. Živković, *Theoret. Chim. Acta*, **26** 67 (1972).

[16] I. Gutman and N. Trinajstić, *Croat. Chem. Acta*, **45**, 539 (1973).

[17] D. Cvetkovic, I. Gutman, and N. Trinajstić, *J. Chem. Phys.*, **61**, 2700 (1974).

[18] I. Gutman and N. Trinajstić, *Croat. Chem. Acta*, **47**, 35 (1975).

If a, b, and c designate three Kekulé structures of an arbitrary system the following situations may arise:

	case I	case II	case III	case IV
Pairs of the same parity	a, b a, c b, c	a, b a, c	a, b	
Pairs of the opposite parity		b, c	a, c b, c	a, b a, c b, c

Only case I and case III are internally consistent and correspond to the situation when all three structures are of the same parity and the situation when one structure is of the opposite parity, respectively. In case II and case IV there is a logical contradiction. Note that in the latter case the product of expressions (1) becomes negative, while for the compatible cases it is positive.

In previous discussions of the parity of Kekulé forms in the literature it was tacitly assumed that a pairwise assignement of the parity does not lead to contradictions. It will be shown here that such an assumption is not always true. The simplest structures for which this is the case is a tricyclic system of fused odd-membered rings. It is of interest, therefore, to examine such situations more closely and to formulate the structural requirements which lead to such a unique condition. In such instances one cannot separate all the Kekulé forms into two classes according to their parity.

If symbols K^+ and K^- stand for the number of Kekulé structures of the opposite parity, the two important structural parameters are given as their sum (K) and their difference (ΔK). The sum gives the total number of Kekulé structures:

$$K = K^+ + K^- \tag{2}$$

The absolute value of the difference

$$\Delta K = |K^+ - K^-| \tag{3}$$

has been called algebraic structure count (ASC)[12,19] or corrected structure count (CSC)[20]. The difference, ΔK, is giving the effective number of structures to be correlated with properties such as molecular stability. Namely, the two kinds of structures of opposite parity make also opposite contribution to molecular stability, thus there is a partial cancellation and formally the system is equivalent to a situation where there are only ΔK structures of the same parity present. Recent analyses of alternant systems have shown that thermodynamic and chemical

---

[19] C. F. Wilcox, Jr., *J. Amer. Chem. Soc.*, **91**, 2732 (1969).

[20] W. C. Herndon, *Tetrahedron*, **29**, 1 (1972).

properties of such molecules are a function of ΔK and not K[11,21]. For example, the total π-electron energy, as derived from Hückel theory, is proportional to ln ΔK[11].

3. MOLECULAR SYSTEMS WITH INCOMPATIBLE PARITY

We have already noticed that incompatibility of an assignment of parity does not allow a logically coherent value to be attributed to a product of three factors $(-)^{R_{4m}(S_{xy})}$. Therefore, a product:

$$(-)^{R_{4m}(S_{ab})+R_{4m}(S_{ac})+R_{4m}(S_{bc})} \tag{4}$$

indicates whether three structures *a*, *b*, and *c* have a logically coherent assignment. When its value is $+1$ we can separate the three structures into the classes of the same or opposite parity, but this is no longer possible when the product is -1. Alternatively the sum

$$R_{4m}(abc) = R_{4m}(S_{ab}) + R_{4m}(S_{ac}) + R_{4m}(S_{bc}) \tag{5}$$

which can be either *even* or *odd*, determines the character of the case. When $R_{4m}(abc)$ is *odd* it is *not* possible to assign the parity type to individual structures without contradicting already made assignments. Generally, for systems with more than three Kekulé structures the same reasoning applies to any triplet of structures, and if there is a single such a triplet with associated $R_{4m}(xyz)$ which is *odd* we confront the case of non separability of Kekulé structures in two classes of opposite parity.

In order to see if conjugated systems can introduce the situations when non-separability of Kekulé forms occur, a systematic examination of topologies of such molecules which can support three or more Kekulé forms need be undertaken. Benzenoid systems, as it has been mentioned, can give rise only to rings of size $4m + 2$, hence all structures are of the same parity and no problem arises. Non-benzenoid alternant systems, as benzocyclobutadiene, do possess structures of opposite parity, but do not introduce incompatibilities. Two fused rings of $4m$ and $4m' + 2$ size, as in benzo-derivatives of cyclobutadiene, produce upon the superposition rings of conjugation of size $4m$, $4m' + 2$, and $4(m + m')$, which is consistent with two structures of the same parity and one of opposite parity. When $4m$ and $4m + 2$ rings are not fused again, as illustrated below, the structures may be separated into two classes of opposite parity:

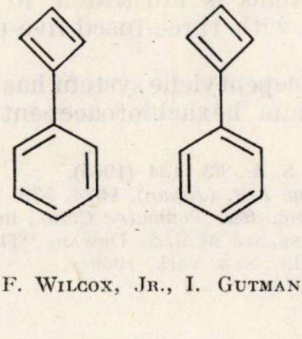

and

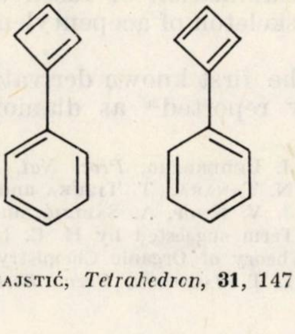

---

[21] C. F. Wilcox, Jr., I. Gutman, and N. Trinajstić, *Tetrahedron*, **31**, 147 (1975).

It may be also easily verified that the same is true in both cases when both rings considered are of $4m$ and $4m'$ size.

Possible source for parity incompatibility are then non-alternant systems. Bicyclic non-laternants, such as pentalene or azulene, have only two Kekulé forms. Tricyclic systems have several topologies[22–24], but for our discussion only three pericondensed rings may introduce a novel situation. Namely, catacondensed rings in a molecule like

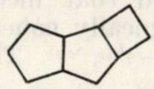

give three Kekulé forms

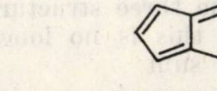

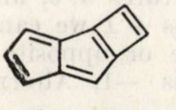

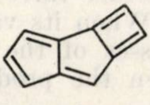

This examination reveals that the central bond in the pentalene part is *single* in all three Kekulé forms, so called *essentially single bond*[25], and as such cannot affect the properties which depend on distribution of double bonds within the skeleton. Hence, for subsequent discussion (i. e. evaluation of $R_{4m}(abc)$), such a bond can be erased, which reduces the system to alternant.

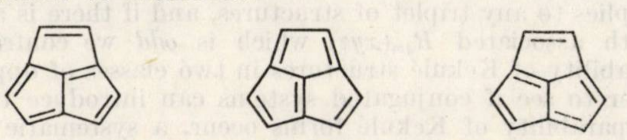

Superposition (graphs) structures

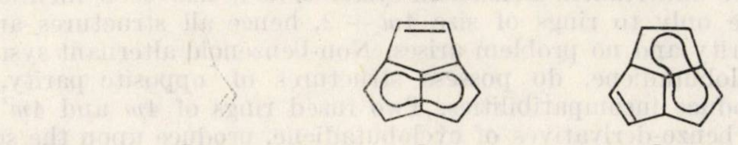

Fig. 1. — Kekulé forms for acepentylene and the resulting superposition structures requiring contradicting opposite parity for each pair of forms.

Examination of fused tricyclic systems is illustrated in Figure 1 on the skeleton of acepentylene (a system with three fused five-membered rings).

The first known derivative of the acepentylene system has been very recently reported[26] as dianion in dilithium hexachloroacepentylendiide,

---

[22] J. Lederberg, *Proc. Nat. Acad. Sci., U. S. A.*, **53**, 134 (1965).

[23] N. Tanaka,. T. Tizuka and T. Kan, *Chem. Lett. (Japan)*, **1974**, 539.

[24] J. V. Knop, A. Sabljić, and N. Trinajstić, *Rev. Roumaine Chim.*, in press.

[25] Term suggested by H. C. Longuet-Higgins, see M. J. S. Dewar, "The Molecular Orbital Theory of Organic Chemistry", McGraw-Hill, New York, 1969.

[26] I. T. Jacobson, *Chem. Scripta*, **4**, 30 (1974).

a stable species at − 70°. Another related nonalternant is acenaphtalene having two six-membered and one five-membered rings fused:

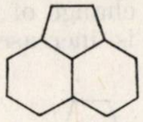

However, in all Kekulé forms the pair of bonds in the five-membered ring of acenaphthalene are always single

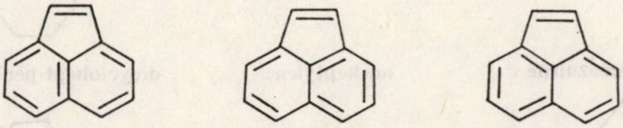

which reduces such structures to alternants upon erasure of essentially single bonds — hence such structures cannot generate parity incompatibility. In acepentylene there are no essentially single bonds and the skeleton cannot be reduced or related to an alternant by the erasure process. The Kekulé forms of acepentylene are shown in Figure 1 together with the superposition formulae. For each pair of structures an eight-membered cycle results as a superposition form indicating that each pair should point to opposite parity of the involved structures—a logical contradiction.

The existence of a system which contradicts the concept of parity is somewhat disturbing and perhaps calls for a revision of the concept or a suitable modification of it. At least, if one has resigned to the fact, one may summarize the finding as indicating that molecules (conjugated systems) can be divided into a class for which parity is meaningful and a class for which (according to the current definition and concept) it cannot be satisfactorily assigned. It is also not an isolated example of a concept with limited application. For instance, there are conjugated molecules for which it is not possible to write a Kekulé structure[27], called non-Kekulé compounds,[28] and which should exhibit special characteristics[29].

4. STRUCTURAL FEATURES OF PARITY INCOMPATIBLE SYSTEMS

Acepentylene is but one example of molecules for which parity concept breaks down. Additional examples are shown in Figure 2. Structurally closely related are aceazulene and aceheptylene in which formally one and two five-membered rings are enlarged to seven-membered rings, respectively. This suggests that an enlargement of a ring by *two* carbon atoms (or more generally by an *even* number of carbon atoms) does not change the character of the system with respect to parity compatibility; such a change can alter the value of $R_{4m}(S_{ab})$, but as each change will appear *twice* (i. e., in two of the three superposition structures), the overall change of $R_{4m}(abc)$ does not occur. What will happen when a ring size is increased by insertion of two carbon atoms is that the type (case) of inconsistency will alter from case IV to case II and vice versa (see Section 2).

---

[27] E. Clar, W. Kemp and D. C. Stewart, *Tetrahedron*, 3, 325 (1958).

[28] Ref., p. 233.

[29] E. Clar, "The Aromatic Sextet", Wiley, London, 1972, Chapter 23.

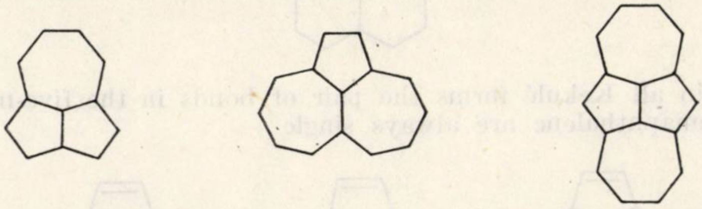

aceazulene

acheptylene

dicyclohept-pentalene

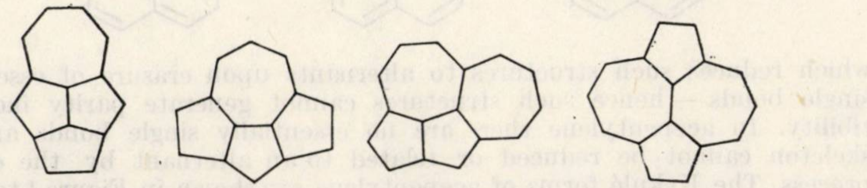

pentaleno — 3, 8, 4, 5, — — bcd) — azulene

pentaleno — (2, 3, 8, 4 — cde) — azulene

pentaleno (6, 6a, 1, 2 — def) — heptalene

azupyrene

Fig. 2. — Several Kekulé inseparable tri- and tetra-cyclic systems having only $4m \pm 1$ rings.

It appears that the presence of three condensed odd-membered rings is an essential element for parity incompatibility. However, a formulation of necessary and sufficient conditions cannot be based on a single type or family of structures. The above discussion on insertion of an even number of carbon atoms only secures that the presence of three fused odd-membered rings is a ***sufficient*** structural requirement. Consider examples shown in Figure 3.

Here *even*-membered rings participate in the fusion, but the respective structures are parity incompatible. It is, therefore, not the parity of fused rings (i. e., even-odd type) which is so important. However, molecules shown in Fig. 3 have ***essentially single bonds*** and when these are erased the molecules are reduced to structures built from three odd-membered rings centrally fused. Thus, it appears that the necessary and sufficient structural conditions for parity incompatibility of Kekulé structures may be a presence of there fused ***essentially*** odd-membered rings, i. e., rings in which bonds which are single throughout the set of Kekulé forms are erased.

The above is true when the system considered ***has only three Kekulé structures*** or when a ***triplet of structures*** of a system having ***many*** structural formulae is considered. For instance, the system shown in Figure 4 has five Kekulé forms and no ***essentially single*** bonds which would allow reduction of the molecular topology.

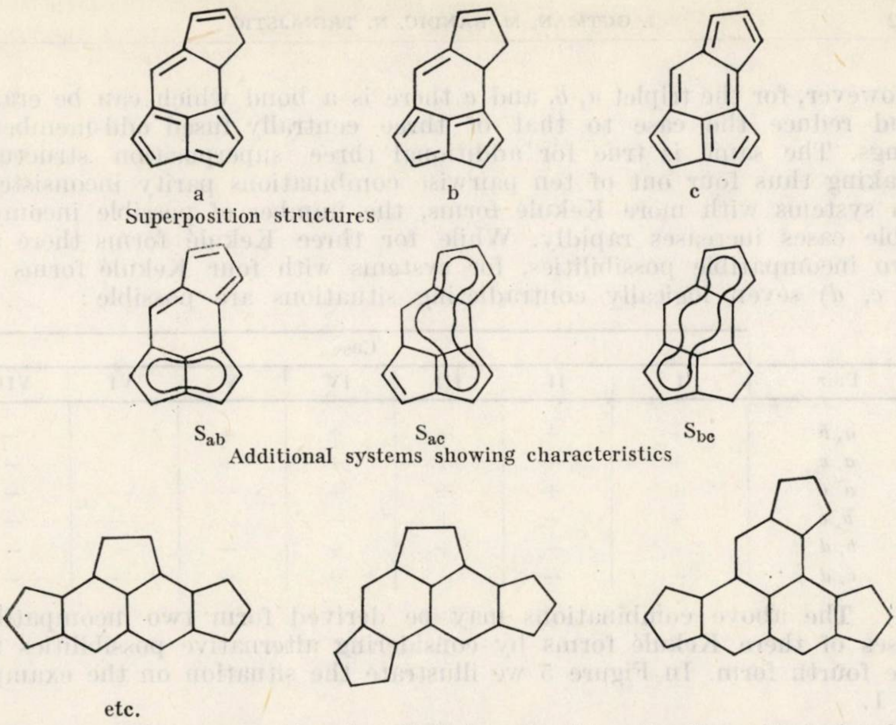
a
b
c
Superposition structures
S_{ab}
S_{ac}
S_{bc}
Additional systems showing characteristics
etc.

Fig. 3. — Kekulé inseparable polycyclic systems involting other than odd-membered rings. All systems, however, may be reduced to *odd*-membered rings when *essentially* single bonds are deleted.

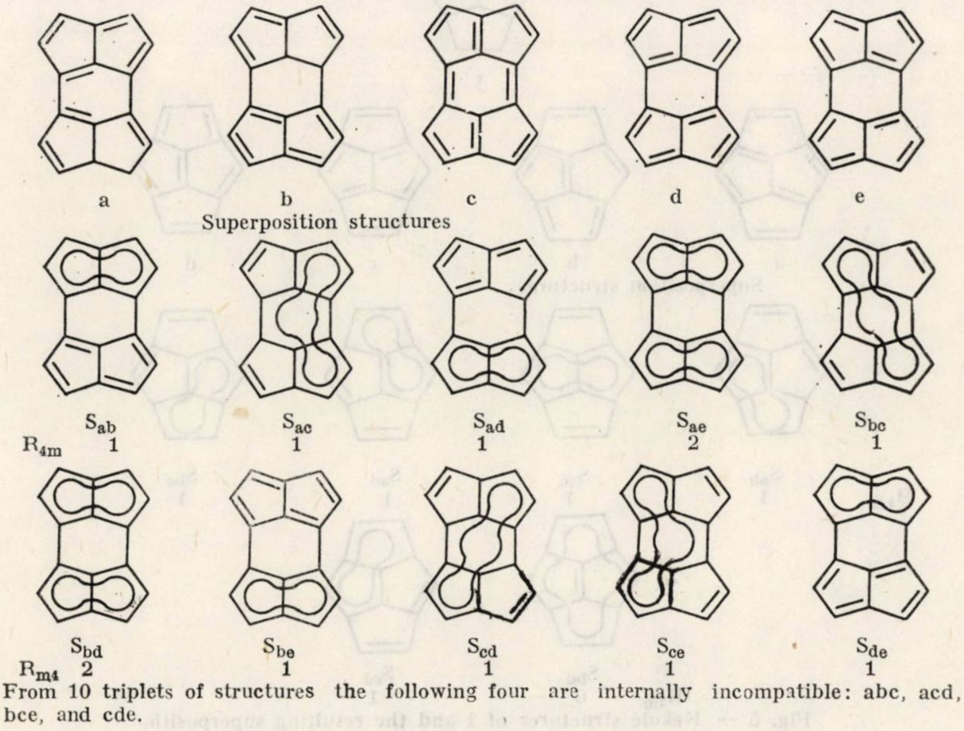
a
b
c
d
e
Superposition structures
S_ab
S_ac
S_ad
S_ae
S_bc
R_4m
1
1
1
2
1
S_bd
S_be
S_cd
S_ce
S_de
R_m4
2
1
1
1
1

From 10 triplets of structures the following four are internally incompatible: abc, acd, bce, and cde.

Fig. 4 — An example of a Kekulé inseparable system, including an *even*-membered ring and having no essential single bonds.

However, for the triplet *a*, *b*, and *c* there is a bond which can be erased and reduce the case to that of three centrally fused odd-membered rings. The same is true for additional three superposition structures making thus four out of ten pairwise combinations parity inconsistent. In systems with more Kekulé forms, the number of possible incompatible cases increases rapidly. While for three Kekulé forms there are two incompatible possibilities, for systems with four Kekulé forms (*a*, *b*, *c*, *d*) seven logically contradicting situations are possible :

	Case						
Pair	I	II	III	IV	V	VI	VII
a, *b*	+	+	−	+	+	+	−
a, *c*	+	+	+	+	+	−	−
a, *d*	+	+	+	+	−	−	−
b, *c*	+	+	+	−	−	−	−
b, *d*	+	−	+	−	−	−	−
c, *d*	−	−	−	−	−	−	−

The above combinations may be derived form two incompatible cases of there Kekulé forms by considering alternative possibilities for the fourth form. In Figure 5 we illustrate the situation on the example of 1.

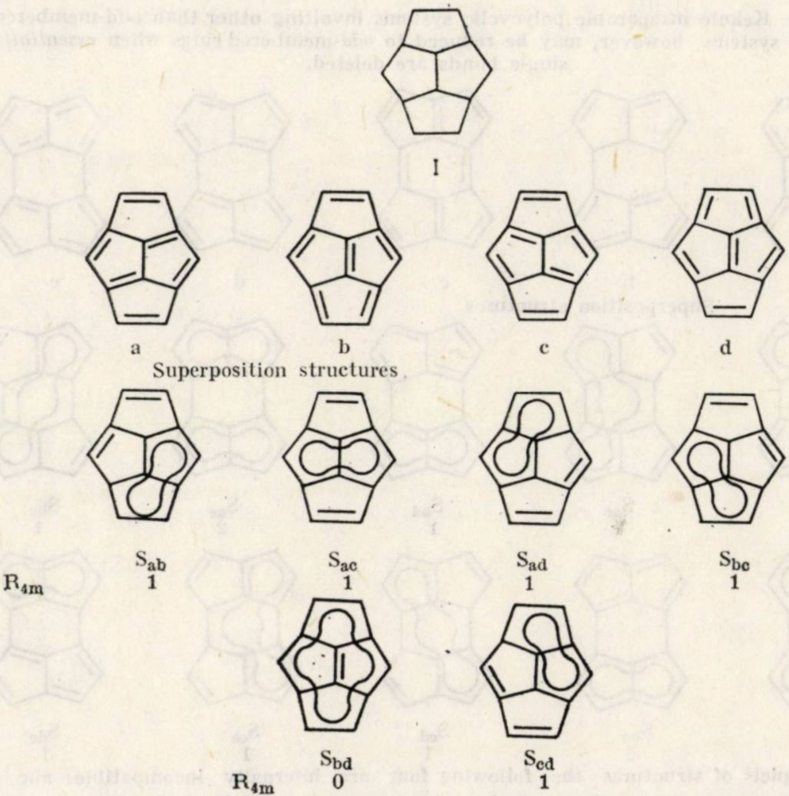

Fig. 5 — Kekulé structures of I and the resulting superposition structures.

Of the resulting six superposition structures only pair (*b*, *d*) is of the same parity. Note also that triplets (*b*, *c*, *d*) and (*a*, *b*, *d*) do not cause incompatibility and the source for inconsistency is, thus, due to the opposite parity of structures *a* and *c*, the essential part of which is given by pentalene skeleton.

5. DISCUSSION

Two questions may be raised in connection with the demonstration of limitation of the concept of parity of Kekulé structures: (1) What are the consequences and how are they reflected on experimental data of conjugated systems and what may be the other theoretical implications; (2) Is it possible to modify the concept and eliminate the inconsistencies? We want to show that even so limited, the concept of parity is indicative of unusual situations in Kekulé inseparable compounds. Most of the molecules shown in Fig. 2 have been synthetized, while in other cases derivatives are known. For instance, tricyclic pentalene derivative II was prepared.[30]

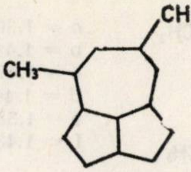

II

Several other tricyclic conjugated hydrocarbons and their derivatives consisting of only five-and seven-membered rings fused in a pericondensed fashion have been also synthetized in recent years mainly by Hafner and co-workers.[31–39] It is interesting to note that hydrocarbon II does not show properties of an azulene system, but it behaves as a polyolefin. However, the related aceheptylene derivative III

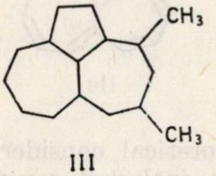

III

[30] K. Hafner and J. Schneider, *Liebigs Ann. Chem.*, **624**, 37 (1959).

[31] K. Hafner, R. Fleischer, and K. Fritz, *Angew. Chem.*. **77**, 42 (1965).

[32] J. Hils, V. Hagen, H. Ludwig, and H. Rühlmann, *Chem. Ber.*, **99**, 776 (1966).

[33] K. Hafner, G. Hafner-Scheneider, and F. Bauer, *Angew. Chem.*, **80**, 801 (1968)

[34] K. Hafner, G. Hafner-Schneider, unpublished work on 3, 5, 8, 10-tetramethylaceheptylene cited in E. Carstensen-Oeser and G. Habermehl, *Angew. Chem.*, **80**, 564 (1968)

[35] A. O. Andersen, Jr., A. A. MacDonald, A. F. Montana, *J. Amer. Chem. Soc.*. **90**, 2993 (1968).

[36] K. Hafner and R. Fleischer, *Angew. Chem.*, **82**, 217 (1970).

[37] C. Jutz and E. Schweiger, *Angew. Chem.*, **83**, 886 (1971).

[38] K. Hafner and F. Bauer, unpublished work on pentaleno (2, 1, 6-def) heptalene cited in Ref. 30.

[39] H. Reel and E. Vogel, *Angew. Chem.*, **84**, 1064 (1972).

appears to exhibit some similarity with azulene.[40]. The situation in such systems, including azulene, is complicated by their susceptibility to charge asymmetry and it is not simple to separate overlapping contributions. It appears, however, that Kekulé inseparable systems do have somewhat different tendencies and resemble polyolefins, or at least deviate from expected behaviour base on fully delocalized picture for π electrons. For example, polarographic reduction potentials of numerous conjugated hydrocarbons have been plotted vs. energies of lowest vacant orbitals.[41] It is found that non-benzenoid non-alternant compounds are reduced more easily than is predicted by MO calculation; the deviations believed to be larger than the experimental error in the measurements of the reduction potentials. Several of nonbenzenoid hydrocarbons have been compounds or derivatives of systems for which parity incompatibility arises, azapyrene showing unusually large departure from the correlation. For few of compounds the *x*-ray crystal structure analysis has been reported. These include a tetramethyl derivative of aceheptylene[34] :

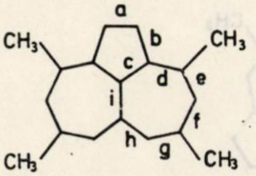

a = 1.39 Å
b = 1.41 Å
c = 1.47 Å
d = 1.44 Å
e = 1.38 Å
f = 1.43 Å
g = 1.36 Å
h = 1.45 Å
i = 1.43 Å

Some alternation of observed carbon-carbon bond lengths is in agreement with predictions of MO theory. These results are also qualitatively consistent with prediction based on Pauling bond orders obtained by superposition of the three Kekulé structures.

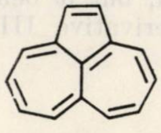
(a)

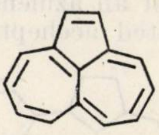
(b)

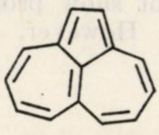
(c)

There are several theoretical considerations of non-benzenoid hydrocarbons, some of which included several of here discussed parity incompatible systems. A representative work includes Hess and Schaad[42] evaluation of π-resonance energies and subsequent semiempirical SCF calculations of Dasgupta and Dasgupta.[43] Similarly, Binsch and Heilbronner[44] considered a tendency in some benzenoid systems, including again few systems of interest here, to localize π electrons in certain bonds.

[40] K. Hafner, *Angew. Chem.*, **75**, 1041 (1963).
[41] A. G. Anderson, Jr., and G. M. Masada, *J. Org. Chem.*, **39**, 572 (1974).
[42] B. A. Hess, Jr., and L. J. Schaad, *J. Org. Chem.*, **36**, 3418 (1971).
[43] A. Dasgupta and N. K. Dasgupta, *Tetrahedron*, **28**, 3587 (1972).
[44] G. Binsch and E. Heilbronner, *Tetrahedron*, **24**, 1215 (1968).

In all this theoretical work, however, there is no indication of *discrimination between parity compatible and parity incompatible systems* and we may say that MO treatments fail to discern something unusual in some non-benzenoid hydrocarbons. Perhaps the only exception may be found in a *failure* of a criterion for aromaticity proposed some time ago by Craig[45] as an indication that perhaps there are differences among non-benzenoid systems. However, ambiguities associated with Craig's aromaticity criterion have lead to a general abandonment of the rule, rather than intriguing a search for its origin (see work of Abramowitch and McEwen[46]). It is intersting to note that systems, like cyclopentaheptalene, for which the prediction of Craig's rule depend on arbitrariness of an assignment of labelling atoms, are those which are parity incompatible. This suggests that perhaps there is a substance in the Craig rules if these can be adapted to concepts and ideas of *topology* and *combinatorics*, rather than *group theory* (symmetry), however, it is outside of the scope of the present work to further elaborate along such speculations.

---

[45] D. P. Craig, *Proc. Roy. Soc.*, **A 200**, 390 (1950); D. P. Craig, *J. Chem., Soc.*, **1951** 3175.

[46] R. A. Abramowitch and K. L. McEwen, *Canad. J. Chem.*, **43**, 2616 (1965).

Revue Roumaine de Chimie, **23**, 3, 397–405 (1978)

DAS VERHALTEN VON 1-ACYL-4-ARYL-THIOSEMICARBAZIDEN GEGENÜBER DEN SCHWERMETALLKATIONEN. IV[1]. DAS VERHALTEN VON Ni(II) GEGENÜBER DEN 1-BENZOYL-4-ARYL-THIOSEMICARBAZIDEN

RODICA CRĂCIUNEANU und EUGENIA FLOREAN
Institut für Medizin und Pharmazie Cluj-Napoca, Pharmazeutische
Fakultät, Lehrstuhl für analytische Chemie, Str. Pasteur 4

Eingegangen am 25. Juni 1975

Die vorliegende Arbeit ist die Fortsetzung einer Reihe von Studien die das Verhalten der 1-Benzoyl-4-R-thiosemicarbaziden zu verschiedenen Metallionen verfolgt mit dem Zweck, sie als analytische Reagenzien zu verwenden. Ni(II) bildet mit den von uns untersuchten 1-Benzoyl-4-R-thiosemicarbaziden ($R = H, C_6H_5-p-C_6H_4-CH_3$, $p-C_6H_4-Br$, $p-C_6H_4-OCH_3$, $p-C_6H_4-OC_2H_5$, α-$C_{10}H_7$, $-CH_2-CH=CH_2$) komplexe Verbindungen deren Entstehung sowohl in Lösungen als auch im festen Zustande nach ihrer Isolierung verfolgt wurde. Die Löslichkeit dieser Verbindungen in verschiedenen organischen Lösungsmitteln, wobei farbige Lösungen entstehen, erlaubte ein photometrisches Studium zwecks Ermittlung des Kombinationsverhältnisses, der Instabilitätskonstanten und quantitativen Bestimmung des Ni(II). Die wahrscheinliche Struktur der im festen Zustande isolierten Verbindungen wurde mit Hilfe der chemischen Analyse und IR Spektren bestimmt.

In den vorangegangenen Mitteilungen dieser Reihe [1–7] wurde ein Studium der Reaktionen zwischen 1-Acyl-4-aryl-thiosemicarbaziden, die bakteriostatische Eigenschaften aufweisen [8–13] und den Kationen der Übergangsmetalle begonnen, wobei die Art und Stellung der Substituenten des Thiosemicarbazidmoleküls sowie die Elektronenkonfiguration der Katione berücksichtigt wurden.

---

[1] R. Crăciuneanu, E. Florean und P. Marcu, *Rev. Roumaine Chim.*, **16**, 951(1971).
[2] R. Crăciuneanu und L. Chiorean, *Die Pharmazie*, **2**, 108(1972).
[3] R. Crăciuneanu und E. Florean, *Rev. Roumaine Chim.*, **14**, 753(1969).
[4] R. Crăciuneanu und E. Florean, *Rev. Roumaine Chim.*, **13**, 105(1968).
[5] R. Crăciuneanu, E. Florean und M. Şerban, „Lucrările celei de-a III-a Conferinţe Naţionale de Chimie Analitică" Braşov, **3**, 215(1971).
[6] R. Crăciuneanu und E. Florean, *Die Pharmazie*, **8**, 462(1969).
[7] R. Crăciuneanu, P. Marcu und I. Pitea, „Lucrările celei de-a III-a Conferinţe Naţionale de Chimie Analitică" Braşov, Bd. **4**, 443, 1971.
[8] N. Buu-Hoi, P. Glay und Ng. Dat Xuong, *Compt. rend.*, **238**, 2582(1959).
[9] V. S. Mishra und R. S. Varma, *J. Indian Chem. Soc.*, **40**, 799(1963).
[10] V. S. Mishra und S. R. Varma, *J. Indian Chem. Soc.*, **39**, 553(1962).
[11] N. P. Buu-Hoi und Ng. Dat Xuong, *Ccmpt. rend.*, **325**, 329(1952).
[12] N. P. Buu-Hoi und Ng. Dat Xuong, *Ccmpt. rend.*, **237**, 498(1953).
[13] Yao-Tsu Chen und Tzi I. Chang, *Chem. Abstr.*, **61**, 3065(1965).

Die vorliegende Arbeit untersucht das Verhalten von Ni(II) Ionen als Komplexgeneratoren gegenüber einer Reihe von Liganden vom Typ der 1-Benzoyl-4-arylthiosemicarbaziden. Es wird der Einfluß der Substituenten am aromatischen Ring auf die Koordinationsfähigkeit, Stabilität und andere Eigenschaften untersucht.

Um einen Zusammenhang zwischen der Interaktion Ni(II)-Ligand und der Natur der elektronenanziehenden bzw. elektronenabweisenden Substituenten an dem 1-Benzoyl-4-arylthiosemicarbazidmolekül zu finden, wurde folgende Serie der in para-Stellung des Phenyls zum N^4 substituierten Verbindungen untersucht :

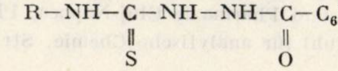

$$R-NH-\underset{\underset{S}{\|}}{C}-NH-NH-\underset{\underset{O}{\|}}{C}-C_6H_5$$

$$R=H,\ C_6H_5-,\ -C_6H_4Br,\ -C_6H_4-CH_3, -C_6H_4-OCH_3,\ -C_6H_1-OC_2H_5,\ -C_{10}H_7,\ -CH_2-CH=CH_2.$$

Ni(II) bildet mit 1-Benzoyl-4-R-thiosemicarbaziden in neutralem oder basischem Milieu, feste Verbindungen oder stark gefärbte Lösungen, die chemisch und physikalisch untersucht wurden um ihre Struktur und Verwendung zu ermitteln.

EXPERIMENTELLER TEIL

1. Das Studium der in festem Zustande isolierten Verbindungen. Synthese, Analyse und Eigenschaften der Verbindungen des Ni(II) mit 1-Benzoyl-4-R thiosemicarbaziden.

Die Verbindungen wurden durch Versetzen einer wäßrigen Lösung von Ni(IJ)(NO_3^-, SO_4^{2-}), bei pH=6−7, mit stochiometrischen Mengen der in Äthanol gelösten entsprechenden Liganden erhalten. Dabei entstehen gelb-orangefarbige Niederschläge die mit einem G_3-Filter filtriert werden. Der Niederschlag wird anschließend mit warmem destilliertem Wasser gewaschen, danach mit Äthanol und schließlich bei 80° im Trockenschrank getrocknet.

Die somit erhaltenen Verbindungen sind mikrokristalline Substanzen von gelber Farbe im Falle von 1-Benzoylthiosemicarbazid (BTSC)und1-Benzoyl-4-allylthiosemicarbazid(BAlTSC) und orangenfarbig im Falle von 1-Benzoyl-4-phenylthiosemicarbazid(BFTSC), 1-Benzoyl-4-tolythiosemicarbazid (BToTSC), 1-Benzoyl-4-bromphenyl-thiosemicarbazid(BBrFTSC), 1-Benzoyl-4-methoxyphenylthiosemicarbazid (BMtxFTSC),1-Benzoyl-4-ethoxyphenylthiosemicarbazid(BEtxFtsc) und 1-Benzoyl-4-α-naphthylthiosemicarbazid(BNTSC).

Diese Komplexverbindungen sind löslich in MeOH, EtOH, Me_2O, DMF, Py und konzentrierten Mineralsäuren aber in Wasser schwer löslich.

Die Zusammensetzung der aus der Lösung isolierten Verbindungen wurde durch quantitative Analyse von Ni(II), Schwefel und Stickstoff bestimmt. Ni(II) wurde gravimetrisch durch Fällung mit Dimethylglyoxim und der Schwefel als $BaSO_4$ bestimmt, wobei die Verbindung zuerst mit $KMnO_4$ im alkalischen Milieu zersetzt wurde. Der Stickstoff wurde mit Hilfe der Mikromethode nach Pregl bestimmt. Aus der Tabelle 1 geht hervor, daß ein Kombinationsverhältnis 1Ni(II) : 2L vorliegt.

Infrarot-spektrophotometrische Untersuchung. Die IR-Spektren der synthetisierten und analysierten Verbindung des Ni(II) mit 1-B-4-RTSC wurden im festen Zustande als KBr-Preßlinge im Bereich von 500−3 500 cm^{-1} aufgenommen. Tabelle 2 gibt die charkteristischen Banden der IR-Spektren, deren Auswertung im Vergleich zu den Spektren der Liganden erfolgte.

Tabelle 1

Die Ergebnisse der chemischen Analyse der Verbindungen des Ni(II) mit 1-Benzoyl-4-R-TSC

Lfd. Nr.	Komplex	Mgw. Komplex	Farbe	Ni%		S%		N%	
				Theor.	Exp.	Theor.	Exp.	Theor.	Exp.
I	$Ni(BTSC)_2$	447,182	gelb-orange	23,22	23,02	12,67	12,48	18,78	18,44
II	$Ni\ (BFTSC)_2$	599,379	gelb-orange	9,79	9,83	10,20	10,40	14,02	13,87
III	$Ni\ (BBrFTSC)_2$	751,182	orange	7,93	7,44	8,66	8,74	—	—
IV	$Ni\ (BToTSC)_2$	627,434	gelb-orange	9,35	9,26	10,22	10,35		—
V	$Ni\ (BMtxFTSC)_2$	659,432	orange	8,90	8,31	9,72	9,80		
VI	$Ni\ (BEtxFTSC)_2$	687,476	orange	8,54	8,39	9,32	9,62		
VII	$Ni\ (BNTSC)_2$	703,512	gelb-orange	8,34	8,11	9,11	9,21	—	—
VIII	$Ni\ (BAlTSC)_2$	527,310	gelb-orange	11,13	10,87	12,16	12,48	—	

Tabelle 2

Die IR-Absorptionsspektren der Verbindungen des Ni(II) mit 1-B-4R-TSC

Komplex / Bereich Abs. cm^{-1}	3 500 – 2 900 (νNH_2, νNH)	1 700 – 1 600 ($\nu C = O$)	1 600 – 1 200 ($\nu C{-}N$, $\nu C{=}S$) (δNH, $\nu C{=}O$)	1 250 – 900 ($\nu C{=}S$, $\nu C{-}N$) (δNH)	900 – 600 ($\nu C{=}S$, $\nu C{-}N$)	500 – 400 ($\nu M{-}N$)
$Ni\ (BTSC)_2$	3 480 3 340 3 180	1 610	1 490 1 340	1 168 1 090 912	798 752 700	455
$Ni\ (BFTSC)_2$	3 320 3 190	1 615	1 570 1 530 1 470 1 414 1 365	1 230 1 105 940	780 751 698	435
$Ni\ (BBrFTSC)_2$	3 320 3 160	1 600	1 550 1 490 1 470 1 385 1 345	1 220 1 100 935	825 750 698	445
$Ni(BMtxFTSC)_2$	3 313 3 188	1 608	1 558 1 518 1 432	1 255 1 100	833 750 690	442
$Ni\ (BAlTSC)_2$	3 342 3 190	1 640 1 610	1 552 1 518 1 485 1 415	1 230 1 130 935	795 750 695	455

Im Bereich von 2 900—3 500 cm^{-1} erscheint die individuelle νNH Valenzschwingung. Im Bereiche 1600—1700 cm^{-1} treten charakteristische und intense Banden auf,[14,15] die der amidischen νCO-Valenzschwingung zugeschrieben werden können. Dies zeigt, daß diese Gruppe durch Koordinierung nicht betroffen wurde [16-18].

Im Bereich der ,,N—C=S" gekoppelten Schwingungen I und II, verschieben sich im Falle von Ni(BTSC)$_2$ die zwischen 1520—1572 cm^{-1} befindlichen Banden der Liganden um 87 cm^{-1} nach niedriegeren Wellenzahlen. Im Falle der übrigen Verbindungen erschienen die Banden mit einer verminderten Intensität, gespalten und verbreitet im Bereich von 1518—1570cm^{-1}[19,20] Ähnlich anderen Verbindungen, werden auch hier ausgeprägte Absorptionsbanden im Bereich 1340—1415 cm^{-1} beobachtet. Diese werden den Molekülen durch Koordination aufgetretener Veränderungen zugeschrieben wobei der ,,C=N"-Doppelbindungscharakter dem der einfachen Bindung vorherrscht, eine Beobachtung die mit anderen für ähnlichen in der Literatur angegebenen Fällen übereinstimmt.[21-24]

Der für ,,Amido III"-Valenzschwingung zugeschriebene Bereich III, der in den Spektren der Liganden zwischen 1238—1243 cm^{-1} auftritt, weist im Falle der Komplexverbindungen Banden mit bedeutend verringter Intensität auf die um 20—50 cm^{-1} gegen kleinere Wellenzahlen verschoben sind. In der für die gekoppelten Schwingungen ,,N—C=S" zugeschriebenen Bereichen III und IV mit den Banden zwischen 900—1200 und 620—850 cm^{-1} sind die spektralen Veränderungen charakteristisch für die Einbeziehung dieser Gruppe in die Komplexbildung, da die Banden eine kleinere Intensität aufweisen, gespalten und verbreitet sind. Im Bereich 400—500 cm^{-1} weisen alle Verbindungen schwache Absorptionsbanden N—Ni,[25-27] deren Stellung auf einen betont kovalenten Charakter dieser Bindung hinweist.

2. Das Studium der Systeme Ni(II)-1-Benzoyl-4R-thiosemicarbazide in Lösung

Da Ni(II) beim alkalischen pH(8—10) mit 1-Benzoyl-4R-TSC Komplexverbindungen bildet, die gelb-braune Färbung aufweisen und in MeOH, EtOH, Me$_2$O, DMF löslich sind, wurden die Systeme in Lösung photometrisch und spektrophotometrisch untersucht.

Die Bestimmung des Kombinationsverhältnisses Ni(II): L. Dafür wurde die Methode der äquimolekulären Serien von Job[28] verwendet. Zu diesem Zweck wurden 3 Serien von Konzentrationen von 10^{-2}M, 2, 5.10^{-3} M und 5,10^{-3} M dargestellt, wobei in allen Fällen das Absorptionsmaximum beim Verhältnis 1Ni(II): 2L vorlag. In Abbildung 1 sind die Absorbtionskurven für c=2,5.10^{-3}M zu sehen.

---

[14] M. Avram und Gh. Mateescu, ,,Spectroscopia în infraroşu. Aplicaţii în chimia organică, Ed. tehnică, Bucureşti, 1966.

[15] L. J. Bellamy, ,,The Infra-Red Spectra of Complex Molecules", Methuen, London, 1959.

[16] S. S. Bogomolov und I. Y. Postivskii, *Doklady Akad. Nauk. S.S.S.R.*, **91**, 1111 (1953).

[17] M. Mashima, *Bull. Chem. Soc. Japan*, **36**, 210 (1963; *ibidem*, **37**, 974(1964).

[18] N. Dutta Ahmed und P. K. Mandal, *J. Inorg. Nuclear Chem*, **28**, 2215(1966).

[19] P. B. Bowman und I. B. Rogers, *J. Inorg. Nuclear Chem.*, **28**, 1963(1966).

[20] I. Smith, B. Holt und R. Cadin, *J. Amer. Chem. Soc.*, **86**, 3017(1964).

[21] R. S. Postavi und C. N. Rao, *J. Inorg. Nuclear Chem.*, **29**, 971(1967).

[22] S. Suzuki, *Null. Chem. Soc. Japan*, **35**, 1456 (1962).

[23] K. Swaminathan und H. M. Irving, *J. Inorg. Nuclear Chem.*, **28**, 171(1966).

[24] N. Israily, P. Gonzerh und P. P. Souchay, *Rev. Chim. Minérale*, **3**, 897(196

[25] S. F. Svatos und C. Curran, *J. Amer. Chem. Soc.*, **77**, 6159(1955).

[26] C. N. Rao und P. Venkataraghavan, *Spectrochim. Acta*, **18**, 451(1962).

[27] L. C. Thomson und R. O. Mayer, *J. Inorg. Nuclear Chem.*, **27**, 1652(1965).

[28] P. Job, *Liebigs Ann. Chem.*, **6**, 97(1936); *ibidem*, **9**, 113 (1928).

Bestimmung der Instabilitätskonstanten. Dazu wurde die Methode der nichtäquimolekulären Serien von Job[28] verwendet, die Berechnung dieser Werte erfolgte nach der Formel:

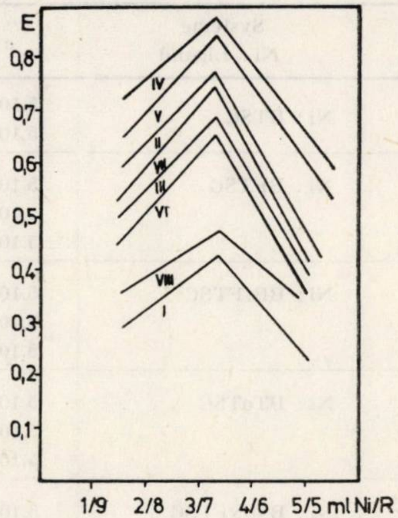

Abb. 1. Bestimmung des Kombinationsverhältnisses Ni : L mit Hilfe der äquimolekularen Serien.

$$K = \frac{c^{m+n-1}\, p^{n-1}\, [(pm + n)\, x - n]^{m+n}}{m^{n-1}\, n^{m-1}\, [n - (m + n)\, x]\, (p - 1)^{m+n-1}}$$

wobei:

c = molare Konzentration der Ni(II)-Lösung.
p = das Verhältnis der molaren Konzentrationen der Ni(II)-Lösung.
m und n = die Koeffizienten der beiden Komponenten des Komplexmoleküls.
x = 1/10 des Ligandlösungsvolumens für welches der Extinktionswert maximal ist.

Tabelle 3 zeigt die Instabilitätskonstanten der Komplexe des Ni(II) mit 1-B-4-RTSC.

Spektrophotometrische Untersuchung in UV. Die Absorbtionsspektren in UV der Ni(II) Komplexe mit 1-Benzoyl-4R-thiosemicarbaziden wurden in Lösungen von c $\approx 10^{-5}$M in MeOH ausgeführt. Die Bestimmungen erfolgten mit einem Spektrophotometer VSU-2P Zeiss-Jena mit 1 cm Küvette an. Methanollösung, im Bereich von 200—400 nm. Die Auswertung erfolgte im Vergleich zu den UV-Spektren der Liganden die unter denselben Bedingungen ausgeführt wurden. Tabelle 4 zeigt die UV-Absorptionsmaxima der Liganden und ihrer entsprechenden Komplexe. Aus den UV-Spektren der Liganden können Absorptionsmaxima zwischen 301—312 nm ($\varepsilon = 4{,}22.10^4$ l/mol. cm) festgestellt werden denen Übergänge vom Typ $\pi - \pi^*$ zugesprochen werden können. [29–32]

3. Analytische Verwendungen

Bestimmung des Anwendungsbereiches des Lambert-Beerschen Gesetzes. Dieses erfolgte durch Bestimmung der optimalen Bedingungen der Bildung von komplexen Kombinationen (Wellenlänge, Zeit pH, Reagenzüberschuß). Die Farbreaktion findet bei pH = 8—10 statt, der durch Zugabe von 1M NaOH erreicht wird. Die maximale Extinktion wird nach 10—15 Minuten nach Vermischen der Reaktanten beobachtet, die erhaltene Lösung ist cca 2 Stunden stabil mit Ausnahme der Kombinationen des Ni(II) mit BTSC und BAlTSC, deren Stabilität cca 30 Minuten andauert. Um den Verwendungsbereich des Lambert-Beerschen Gesetzes zu ermitteln wurde folgendermaßen gearbeitet. Der Lösung von 10^{-2} M Ni(II), vorher mit

---

[29] E. Angelescu und F. Cornea, ,,Probleme teoretice de chimie organică'', Ed. did. și ped., București, 1969.

[30] C. N. Rao, ,,Ultraviolet and Visible Spectroscopy'', Butterworths, London, 1967.

[31] M. J. Jenssen, *Rec. Trav. chim.*, **79**, 454(1960); *ibidem*, **79**, 1066(1960).

[32] L. Helmholtz und R. P. Kruh, *J. Amer. Chem. Soc.*, **74**, 1176(1952).

Tabelle 3

Die Instabilitätskonstanten der Komplexe des Ni(II) mit 1-Benzoyl-4R-TSC

Lfd. Nr.	Systeme Ni : Ligand	c	p	x	K mittel
I	Ni : BTSC	5.10^{-3}	3	0,520	$8{,}54.10^{-6}$
		5.10^{-3}	4	0,460	
II	Ni : BFTSC	5.10^{-3}	2	0,540	$4{,}07.10^{-7}$
		5.10^{-3}	3	0,440	
		5.10^{-3}	4	0,380	
III	Ni : BBrFTSC	5.10^{-3}	2	0,540	$6{,}64.10^{-7}$
		5.10^{-3}	3	0,460	
		5.10^{-3}	4	0,400	
IV	Ni : BToTSC	5.10^{-3}	2	0,525	$6{,}10.10^{-8}$
		5.10^{-3}	3	0,425	
		5.10^{-3}	4	0,350	
V	Ni : BMtxFTSC	5.10^{-3}	2	0,510	$0{,}71.10^{-8}$
		5.10^{-3}	3	0,410	
		5.10^{-3}	4	0,350	
VI	Ni : BEtxFTSC	5.10^{-3}	2	0,520	$0{,}57.10^{-8}$
		5.10^{-3}	3	0,410	
		5.10^{-3}	4	0,345	
VII	Ni : BNTSC	5.10^{-3}	2	0,560	$1{,}42.10^{-6}$
		5.10^{-3}	3	0,460	
		5.10^{-3}	4	0,380	
VIII	Ni : BAlTSC	5.10^{-3}	3	0,500	$3{,}39.10^{-6}$
		5.10^{-3}	4	0,420	

Tabelle 4

Die Absorptionsmaxima in UV.

Lfd. Nr.	Ligand	λ_{max} nm	$\varepsilon.10^4$ l/mol.cm	Ni (II) Komplexe λ_{max} nm	$\varepsilon.10^4$ l/mol.cm
I	BTSC	244	2,07	258	2,23
II	BFTSC	230	2,31	275	2,95
III	BBrFTSC	232	2,29	278	3,59
IV	BToTSC	238	2,18	270	3,60
V	BMtxFTSC	236	2,13	267	3,48
VI	BEtxFTSC	238	2,01	270	2,49
VII	BNTSC	300	0,36	318	2,55
VIII	BAlTSC	316	0,12	322	1,85
	BAlTSC	244	1,97	260	4,35

cca 1 ml Me_2O verdünnt, wurden 10 ml Reagens 1 % gelöst in $Me_2O : H_2O$, 1 : 1, anschließend 1 M Na H zugegeben und dann wurde sie mit Me_2O zu 25 ml verdünnt. Tabelle 5 zeigt die Grenzen, zwischen denen Ni(II) bestimmt werden kann in μg Ni/ml und die nach Sandell berechnete Empfindlichkeit der Reaktion.[33]

Tabelle 5

Der Anwendungsbereich des Lambert-Beerschen Gesetzes.

Lfd. Nr.	Reagens	Minimal-quant. μg/ml	Maximal-quant. μg/ml	Empfindlichkeit μg/cm²
I	BTSC	5,87	70,45	0,52
II	BFTSC	7,54	82,19	0,55
III	BBrFTSC	5,87	58,70	0,47
IV	BToTSC	5,87	93,94	0,51
V	BMtFTSC	5,87	70,45	0,44
VI	BEtxFTSC	8,87	70,45	0,44
VII	BNTSC	5,70	82,19	0,65
VIII	BAlTSC	5,87	35,23	0,42

AUSWERTUNG DER ERGEBNISSE

Aus den Untersuchungen die sowohl auf die im festen Zustande gewonnenen Verbindungen als auch auf die in Lösung befindlichen Systemen zwischen Ni(II) und 1-Benzoyl-4-R-thiosemicarbaziden ausgeführt wurden, konnte ein Zusammenhang zwischen der Basizität der Liganden und den Eigenschaften der Komplexe festgestellt werden. Das Komplexbildungsvermögen bzw. die Basizität der Liganden ist von dem induktiven + I und − I Einfluß der Gruppen $-CH_3$, $-Br$, $-OCH_3$, $-OC_2H_5$, −α-Naphtyl, −Allyl abhängig, welcher die Elektronendichte um das Stickstoff- und Schwefelatom vergrößert oder herabsetzt :

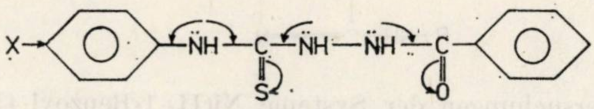

X = Effekt (+ I)

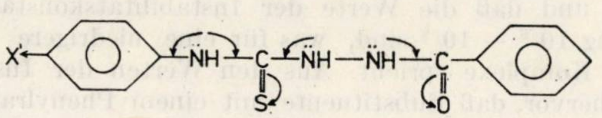

X = Effekt (− I)

Es konnte damit qualitativ eine Verminderung der Löslichkeit und eine Zunahme der Farbintensität der Komplexe beobachtet werden die von den Derivaten der 1-Benzoyl-4R-thiosemikarbazide, die im Molekül Gruppen mit —I Effekten (—Br, $-OCH_3$, $-OC_2H_5$) enthalten, abstammen.

---

[33] E. B. Sandell, „Colorimetric Determination of Traces of Metals'', Interscience Publication, New York, 1959, S. 80.

Aus dem Studium der IR-Absorptionsspektren der Komplexe, verglichen mit denen der Liganden, konnten deutliche Veränderungen in den Bereichen der gemischten gekoppelten „N—C=S" Schwingungen beobachtet werden, die charakteristisch für die Einbeziehung dieser Gruppe in die Koordination des Metalls sind. Anderseits wurde auch noch beobachtet, daß in den Bereichen die den „N—C=O" Valenzschwingungen zugeschrieben werden, die Spektren derKomplexe keine wesentlichen Änderungen aufweisen, was darauf hinweist, daß diese Gruppe von der Metallkoordination nicht betroffen ist. Alle Komplexe weisen im Bereich von 400—500 cm^{-1} Absorptionsbanden auf, die der Bindung N—Ni zugeschrieben werden können, wobei der kovalente Charakter dieser Bindung betont wird.

Aus den Daten der chemischen Analyse, des Koordinationsverhältnisses und der IR-Spektren kann folgende wahrscheinliche Strukturformel abgeleitet werden:

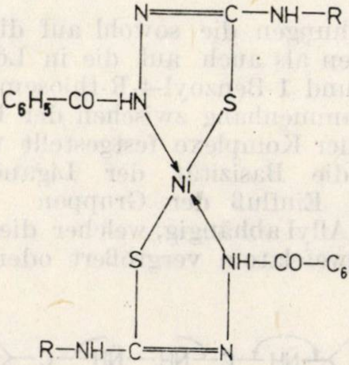

Aus den Untersuchungen der Systeme Ni(II)-1-Benzoyl-4R-thiosemikarbazide wurde festgestellt, daß das Kombinationsverhältnis Ni(II) :L, 1 : 2 beträgt und daß die Werte der Instabilitätskonstanten von der Größenordnung 10^{-6} — 10^{-8} sind, was für eine niedrigere Stabilität der entstandenen Komplexe spricht. Aus den Werten der Instabilitätskonstanten geht hervor, daß Substituente mit einem Phenylradikal in Stellung 4 des 1-Benzoyl-4R-TSC zu einer Zunahme der Stabilität des Komplexes führen. Der Beitrag des α-Naphtyls ist kleiner als der des Phenylradikals, aber er ist größer als der des Allylradikals. Es ist offensichtlich die Stabilitätszunahme der Komplexe bei der Einführung in der *para*-Stellung am Benzolring der CH_3-Gruppe (mit + I-Effekt) sowie der Gruppen $-OCH_3$ und $-OC_2H_5$. Dies im Unterschied zum Bromsubstituenten, welcher einen — I Effekt aufweist. Es kann eine

Parallele zwischen der Stabilität der Komplexverbindungen und der Basizität der Liganden festgestellt werden als Folge des Einflusses der Substituenten, welcher die Elektronendichte um das Stickstoff- und Schwefelatom beeinflußt.

Die UV-Absorptionsspektren der Ni(II)-Komplexe verglichen mit denen der Liganden weisen hypsochrome Verschiebungen auf (32—56 nm), besonders ausgeprägt bei den Verbindungen mit BTSC, BAlTSC, BMtxFTSC und BETxFTSC, und batochrome Verschiebungen bei den Verbindungen mit BNTSC. Die Werte der molaren Extinktionskoeffizienten (1,85—3,60.10^4l/mol.cm) werden durch Koordination nicht wesentlich beeinflußt.

Das Studium des Systems Ni(II)-1-Benzoyl-4R-TSC in Lösung ermöglichte die Ausarbeitung einer photometrischen Methode zur quantitativen Bestimmung des Ni(II) in Grenzen zwischen 5,70—93,94 μg Ni(II)/ml, anwendbar auch zur Analyse von Erzen, Legierungen, usw.

Revue Roumaine de Chimie, 23, 3, 407—415 (1978)

DER ABBAU DER BEI DER THERMISCHEN OXYDATION DES n-DODEKANS MIT MOLEKULARSAUERSTOFF ERHALTENEN PEROXYDE

I. DER THERMISCHE ABBAU DER SICH BEI VERSCHIEDENEN KONVERSIONEN ERGEBENDEN PROBEN

II. DAS ABSCHEIDEN EINES PEROXYDISCHEN KONZENTRATES AUS DEM BEI GERINGER KONVERSION OXYDIERTEN n-DODEKAN: DER THERMOKATALYTISCHE ABBAU DIESES KONZENTRATES

IOSIF DRIMUŞ*, LAMBRACHE PAPAHAGI und CONSTANTIN CRISTESCU

Fakultät für angewandte Chemie des Polytechnischen Instituts in Bukarest, Lehrstuhl für organische Chemie und Verfahrenstechnik auf dem Gebiet der organischen Chemie, Calea Victoriei 149, Bukarest

Eingegangen am 31.August 1975

Es wurde die Frage des thermischen Abbaues der bei verschiedenen Konversionen im Rahmen der thermischen Oxydation des n-Dodekans mit molekularem Sauerstoff sich ergebenden Proben als auch die Frage des thermokatalytischen Abbaues (als Katalysatoren, Naphtenate des Li, Na, K, Rb, Cs, Cu, Ag, Be,Mg, Ca, Sr, Ba, Zn, Cd, Hg, Al, La, Ce, Cr, Mn, Fe, Co, Ni) eines peroxydischen Konzentrates, das aus dem bei geringer Konversion oxydierten n-Dodekan abgeschieden wurde, untersucht.

EINFÜHRUNG

Die bedeutenden Anwendungen der Peroxyde und der Hydroperoxyde bedingen während der letzten Zeit neue Forschungen im Zusammenhang mit den Eigenschaften und Merkmalen dieser Stoffe.

Wie bekannt, stellen die Alkylhydroperoxyde ein Zwischenstadium im Rahmen des Oxydationsvorganges der Paraffine dar, eines komplizierten Vorganges, bestehend aus einer Reihe von Reaktionen die nacheinander bzw. gleichzeitig vor sich gehen und die letzthin zu einem komplexen Gemisch von oxygenierten Produkten führen.

Die Zersetzung der Peroxyde ist von besonderem Interesse.

Als Folge des Vorhandenseins im Molekül der peroxydischen Stoffe einer Peroxy-Gruppe, deren Bindungsenergie cca. 37 kcal/Mol beträgt, geben alle diese Stoffe Sauerstoff ab und zersetzen sich bei hohen Temperaturen, bei Ablauf der Zeit und insbesondere unter dem Einfluß der verschiedenen chemischen Stoffe, Reagenzien oder Katalysatoren.

Die katalytische Zersetzung der Hydroperoxyde, die wichtige Zwischenprodukte darstellen, ist durch die eigentliche chemische Umwandlung bedingt, der dieselben bestimmt sind. So z. B. sollen die Hydroperoxyde der oberen Alkane derart im Rahmen der Industrie der Fettsäuren zersetzt werden, daß mit einer höchsten Ausbeute Fettsäuren erhalten werden können.

---

* Decesed 1978

Die thermische Zersetzung der Isopropylen-Hydroperoxyde stellte den Gegenstand zahlreicher Arbeiten und Patente dar, worunter wir eine Reihe von Systematisierungsbeiträgen anführen. [1-4]

Manche Verfasser[5] stellten fest, daß die Zersetzung des Kumol-Hydroperoxydes autokatalytisch erfolgt und daß im Gemisch mit dem Kumol die Reaktionen bei einem Null-Orden der Reaktion abläuft, wobei andere Verfasser[6] behaupten, daß bei sehr geringen Konzentrationen die Zersetzung des II. Ordens ist. Mit dem Steigen der Hydroperoxydkonzentration findet folglich eine Erhöhung des Reaktionsordens statt.

Forschungen in der Sowjetunion stellten fest,[7] daß die Zersetzung in Lösemittel der Hydroperoxyde von der Bildung der organischen Säuren beeinflußt wird; Die Kinetik der Zersetzung hängt unmittelbar von der Konzentration der Hydroperoxyde in der Lösung ab. Die Zersetzungsreaktion wird von der Art des verwendeten Lösungsmittels in einem hohen Maße beeinflußt.

Was das Gefüge der Zersetzungsprodukte anbelangt scheint es, daß sowohl die thermische Zersetzung als auch die katalytische Zersetzung mit manchen Ausnahmen zu denselben Produkten führen. [8]

Die Peroxyde weisen im allgemeinen ein den Hydroperoxyden gleiches Verhalten auf,[9] wie aus dem Wert der Halbwertzeit und der für die Zersetzung nötigen Aktivierungsenergie gefolgert werden konnte.

Die katalytische Zersetzung der Hydroperoxyde stellte den Gegenstand von Sonderstudien dar, wobei dieselben Zwischenprodukte von einigen wichtigen Vorgängen darstellen.

Zur Zersetzung der Hydroperoxyde werden gegenwärtig einige Schematas besprochen, worunter die folgenden wichtiger sind:

— das Schema von Langenbeck-Pritzkow, das eine Disproportionierung gegenüber der Bildung einer Ketone als Hauptreaktion und eines sec-Alkohols als Nebenreaktion[10-12] vorraussetzt;

— das Schema von Zyshckowski[13-16] setzt die Bildung von zwei Alkoholen und des Formaldehyds voraus;

— ein anderes Schema ist jenes von Rieche, [16] das die Bildung von Äther voraussetzt;

---

[1] S. W. Zagorodnyi, *Uspekhi Khim*, **30**, 345 (1961).

[2] B. D. Kriyalow und P. Gergheew, *Khim. Nauk i Prom.*, **1**, 287 (1956).

[3] M. S. Nemtzow u. a., *Khim. Nauk i Prom.*, **2**, 306 (1957).

[4] H. Hock und H. Kropf, *Z. angew. Chem.*, **69**, 313 (1951).

[5] P. G. Sergeew, „Okislenie uglewodorodow wy schidkoi fase", Isd. A. N., S.S.S.R., Moskau, **1959**, S. 207.

[6] Huan Vao Tun, *Ref. Zhur. Khim.*, **1959**, 56413.

[7] W. A. Redoskin und W. A. Suschanow, „Khimia Perekisnych Soedinenyi", Izd. Akad. Nauk, S.S.S.S.R., Moskau, 1963, S. 207.,

[8] Y. Fushisaki und M. Saito, *Bull. Univ. Osaka Prefect. Ser. AG*, **1958**, 1955.

[9] D. F. Doehnert und O. L. Mageli, „Ann. Techn. Management, Conf. Reinforced. Plastics", Div. Soc. Plastues Ind. Inc. 13 Sekt. 1 B S 1 (1958); *Chem Abstr.*, **53**, 185341 (1959).

[10] W. Langenbeck und W. Pritzkow, *Chem. Technik*, **2**, 116 (1950).

[11] W. Langenbeck und W. Pritzkow, *Chem. Technik*, **4**, 391 (1952).

[12] W. Pritzkow, *Liebigs Ann. Chem.*, **597**, 167 (1955).

[13] W. K. Zyschkowski, *Nowosti Neothianoi Techn.*, **9**, 17 (1956).

[14] W. K. Zyschkowschi, *Zhur. priklad. Khim.*, **31**, 440 (1958).

[15] W. K. Zyschkowschi, *Zhur. priklad. Khim.*, **28**, 772 (1953).

[16] W. Rieche, *Angew. Chem.*, **51**, 707 (1938).

— ein letztes wichtigeres Schema[17] setzt desgleichen die Bildung eines Äthers voraus.

Die derart entstandenen Produkte reagieren zweifelsohne weiter und ergeben eine große Reihe von Produkten, die üblicherweise bei der Zersetzung der Hydroperoxyde erhalten werden.

Was die Aktivität der Zersetzungskatalysatoren anbelangt, bestehen sogar im Zusammenhang mit den meisten angewendeten, wie Mangan und Kobalt, zahlreiche Unstimmigkeiten.

Wie die Hydroperoxyde, stellten die Peroxyde den Gegenstand derjenigen Zersetzungsstudien dar, die mit Hilfe verschiedener Kationen durchgeführt worden sind. Diese Studien begrenzen sich auf die Prüfung insbesondere des Mechanismus durch den die Zersetzung stattfindet.

I. DER THERMISCHE ABBAU DER SICH BEI VERSCHIEDENEN KONVERSIONEN ERGEBENDEN PROBEN

Experimenteller Teil

Die Oxydation zwecks Erhaltung der Hydroperoxyde erfolgte in einem Glasreaktor mit einem Inhalt von 400 cm³, der elektrisch beheizt wird und bei einer auf 155° eingestellten Temperatur, wobei in denselben 250 cm³ n-Dodekan eingeführt wurde. Über eine poröse Glasplatte (G3) wurden 50 Liter Sauerstoff pro Stunde eingeleitet.

In Zeitabständen von je 20 Minuten wurden während der Versuchszeit Proben genommen, die ebenfalls bei 155° dem thermischen Abbau unterworfen wurden, jedoch ohne Durchleiten von Sauerstoff. Die Apparatur besteht aus einer Glaszelle, die mit : Mantel (durch welchen Mineralöl von einem Thermostaten zirkuliert), Thermometer, Durchperlstutzen für das Schutzgas, Stutzen zur Entnahme der Flüssigkeitsproben, Stutzen zur Abfuhr de Gases versehen ist.

ERGEBNISSE

Die im Rahmen dieses ersten Teiles der Arbeit erzielten Ergebnisse werden in Tabelle 1 und in Abb. 1 gezeigt. Die Angaben gemäß Tabelle 1 wurden in das Diagramm der Abb. 2 eingetragen, das den Vergleich

Tabelle 1

Halbwertzeit bei verschiedenen Konversionen

Lfd. No.	Oxydationszeit Minuten	Halbwertzeit Minuten
1	20	600
2	40	180
3	60	45
4	80	28
5	100	15
6	120	13
7	140	8
8	160	7
9	180	6,5

---

[17] H. Pardun und I. Kuchinka, *Erdöl u. Kohle*, 3, 109 (1950).

des Wertes der Halbwertzeit bei gleichen Konzentrationen gestattet. Demzufolge kann festgestellt werden, daß z. B. einer Konzentration von 5 mg aktivem Sauerstoff im steigenden Teil der Kurve eine Halbwertzeit von 43′ entspricht, während denselben Konzentrationen, jedoch im fallenden Teil der Kurve, eine Halbwertzeit von nur 9 Minuten entspricht.

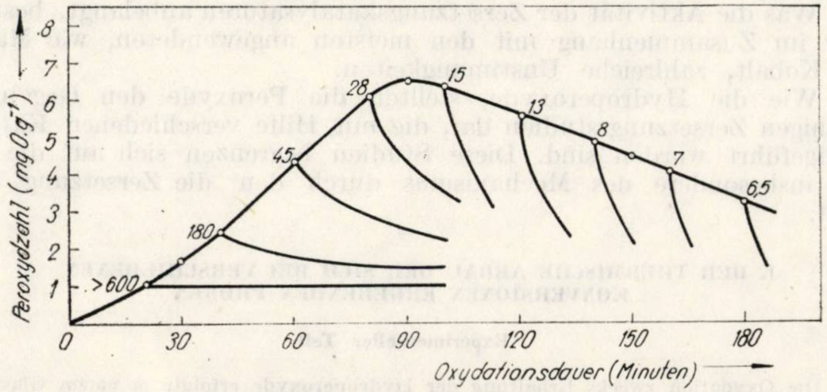

Abb. 1 — Die Änderung der Peroxydzahl in Abhängigkeit von der Zeit bei dem thermischen Abbau bei 155° der durch Oxydation des n-Dodekans erhaltenen Peroxyde.

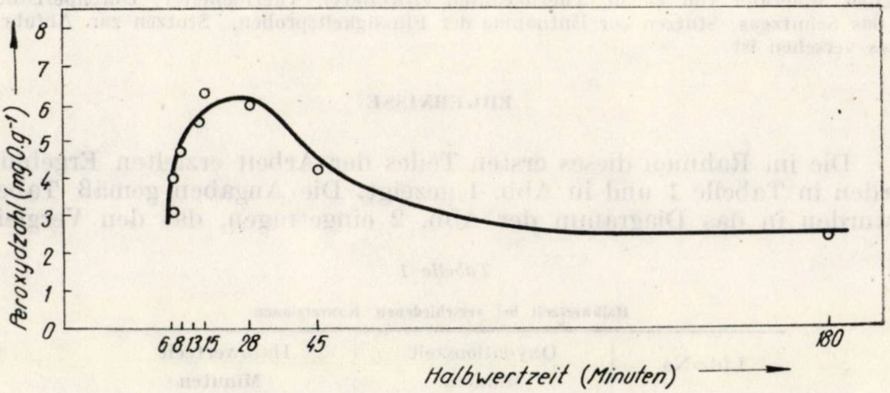

Abb. 2 — Die Änderung der Peroxydzahl in Abhängigkeit von der Halbwertzeit.

Diese Differenzen können in erster Reihe durch den Umstand erklärt werden, daß die im Rahmen des ersten Teiles der Reaktion gebildeten Dodezylhydroperoxyde eine größere Beständigkeit als die in die folgenden Stufen gebildeten Peroxydprodukte aufweisen, die sich bei größeren Konversionen ansammeln.

II. ABSCHEIDEN EINES PEROXYDISCHEN KONZENTRATES AUS DEM OXYDIERTEN n-DODEKAN BEI GERINGER KONVERSION; DER THERMO-KATALYTISCHE ABBAU DIESES KONZENTRATES

Experimenteller Teil

Die Oxydation fand in derselben Apparatur und unter denselben Bedingungen statt, wie für Thema I gezeigt. Um aus dem oxydierten n-Dodekan eine größere Menge Dodezylhydroperoxyde abzuscheiden, haben wir erachtet, daß die günstigste Oxydationskonversion nicht dem Spitzenwert der Ansammlung von aktivem Sauerstoff entspricht, sondern links dieses Maximums gelegen ist. Bei Arbeit mit geringen Konversionen erhielten wir folglich ein peroxydisches Konzentrat mit einem höheren Gehalt an Dodezylperoxyden.

Die Oxydationsdauer betrug 60 Minuten. Während der Oxydation wurden in Zeitabständen von je 10 Minuten Proben zur Bestimmung der Peroxydzahl und der Säurezahl genommen.

Das oxydierte Erzeugnis wurde der folgenden Bearbeitung zwecks Abscheidung eines peroxydischen Konzentrates unterworfen:

a. Auszug der Peroxyde mit Methanol;

b. Destillation des Methanols zwecks Erhaltung eines Konzentrates von Hydroperoxyden und Säuren;

c. Die Neutralisierung der Säuren aus dem Hydroperoxydkonzentrat mit 5%-igen NaOH-Lösung;

d. das Waschen und Trocknen des Konzentrates zur Beseitigung der Spuren der alkalischen Lösung und der Säuren;

e. die Reinigung des Produktes durch molekulare Destillation (10^{-3} mm HgS).

Als Folge dieser Arbeitsgänge wurde ein Hydroperoxydkonzentrat mit einer Peroxydzahl von 63,7 mg O/g erhalten.

Weiter wurden aus dem Peroxydkonzentrat Proben aufbereitet, die eine bestimmte Peroxydzahl aufweisen und die einen thermischen und thermo-katalytischen Abbau bei Temperaturen von 60° und 90° in Anwesenheit von Li, Na, K, Rb, Cs, Be, Mg, Ca, Sr, Ba, La, Ce, Cr, Men, Fe, Co, Ni, Cu, Ag, Cd, Hg, Al unterworfen wurden. Die Apparatur ist gleich derjenigen bei Thema I gezeigten. Jede Probe besteht aus: einem Gramm Hydroperoxydkonzentrat, einem Gramm Katalysator und 20 Gramm n-Dodekan. Die Peroxydzahl der Probe ohne Katalysator beträgt 3,34 mg O/g.

Die Konzentration des Hydroperoxydes wurde durch dessen Dosierung auf jodometrischem Wege verfolgt.

ERGEBNISSE

Durch Vergleich der Peroxydzahl in Abhängigkeit von der Zeit bei Temperaturen von 60° bzw. 90° für die verschiedenen Katalysationsmittel (Abbildungen 3—8) kann festgestellt werden, daß im allgemeinen die Kationen (oder die Katalysationsmittel) zwei Wirkungsarten aufweisen: sie katalysieren die Zersetzung oder sind unempfindlich.

Die Abbildungen 3—9 gestatten den Einfluß von Kationen der Metalle der Gruppen I, II, III, VI, VII und VIII als auch den Einfluß der Temperatur auf die Zersetzung der Hydroperoxyde zu verfolgen.

Aus den Abbildungen 4—7 ist klar ersichtlich, daß die Metalle der Gruppe I (Untergruppe A und B) und II (Untergruppe A und B) den Zersetzungsvorgang der Hydroperoxyde begünstigen.

Die Untergruppe B der I. Gruppe (Abb. 5) weist auf eine Hemmungstendenz der Zersetzung u. zw. in Abhängigkeit vom Steigen des Atomgewichtes des Grundstoffes hin. Dieselbe Tendenz kann auch bei der Gruppe I, Untergruppe A festgestellt werden.

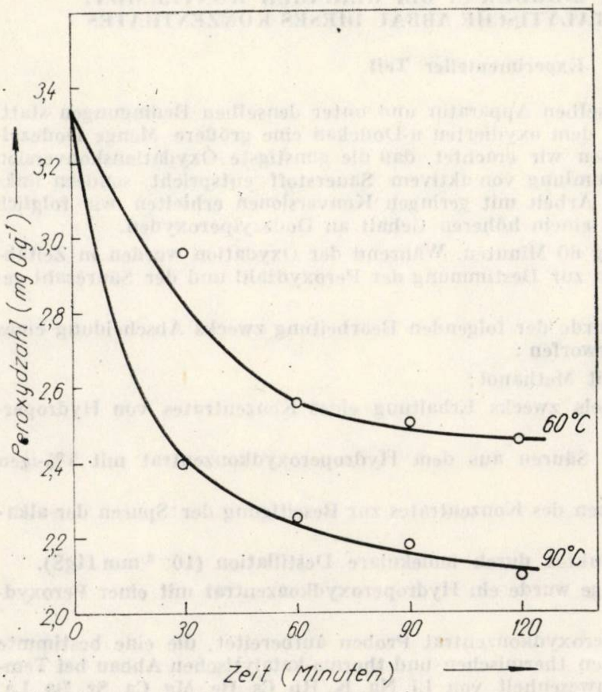

Abb. 3 – Die Änderung der Peroxydzahl in Abhängigkeit von der Zeit im Falle des thermischen Abbaues.

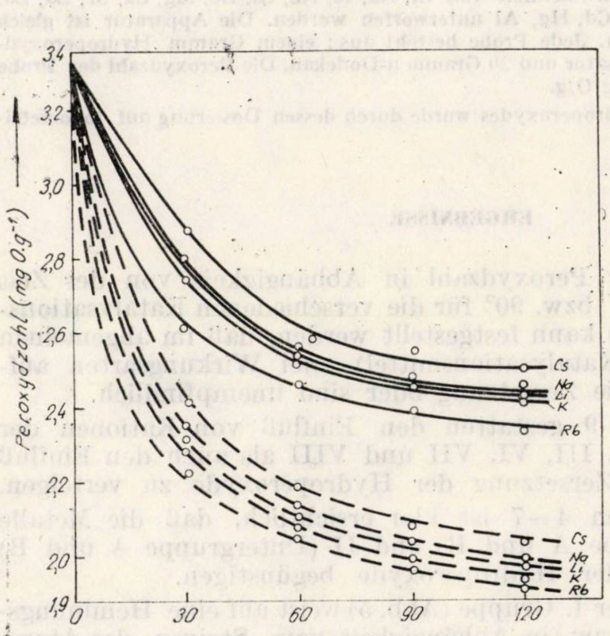

Abb. 4 – Die Änderung der Peroxydzahl in Abhängigkeit von der Zeit für die Katalysatoren auf Grund der Metalle der Gruppe A.

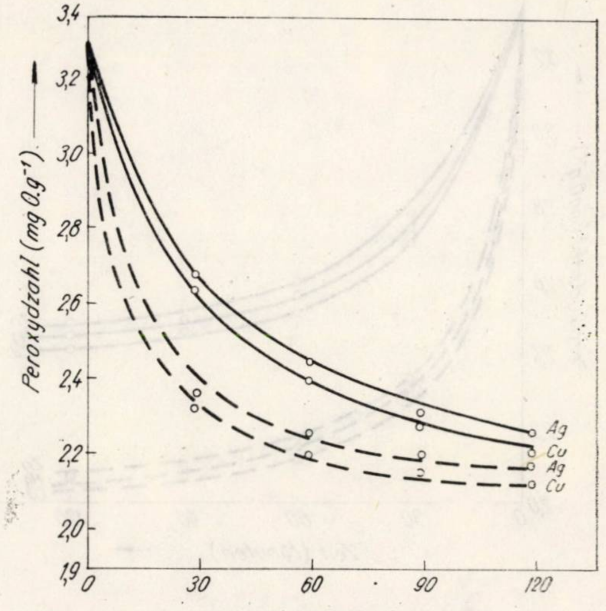

Abb. 5 — Die Änderung der Peroxydzahl in Abhängigkeit von der Zeit für die Katalysatoren auf Grund der Metalle der Gruppe I B.

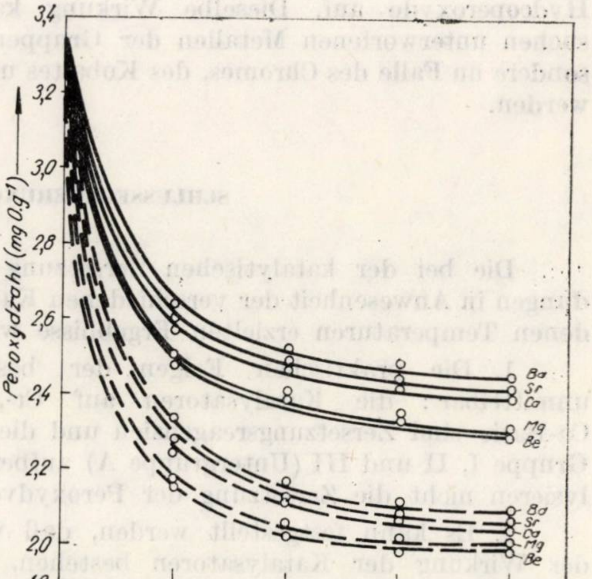

Abb. 6 — Die Änderung der Peroxydzahl in Abhängigkeit von der Zeit für die Katalysatoren auf Grund der Metalle der Gruppe II A.

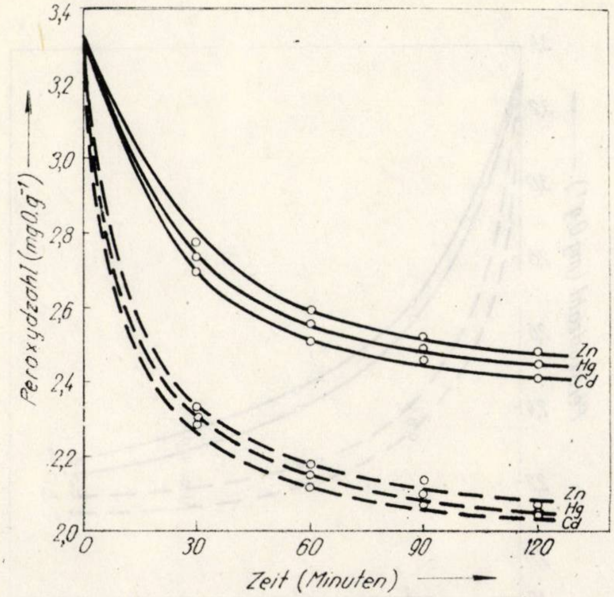

Abb. 7 – Die Änderung der Peroxydzahl in Abhängigkeit von der Zeit für die Katalysatoren auf Grund der Metalle der Gruppe II B.

Im Rahmen der Gruppe III (Abb. 8) weisen die anderen Metalle, mit Ausnahme des Aluminiums, eine starke Zersetzungswirkung der Hydroperoxyde auf. Dieselbe Wirkung kann auch bei den den Versuchen unterworfenen Metallen der Gruppen VI, VII und VIII (insbesondere im Falle des Chromes, des Kobaltes und des Mangans) festgestellt werden.

SCHLUSSFOLGERUNGEN

Die bei der katalytischen Zersetzung der peroxydischen Verbindungen in Anwesenheit der verschiedenen Katalysatoren und bei verschiedenen Temperaturen erzielten Ergebnisse weisen auf folgendes hin:

1. Die praktischen Folgen der beschriebenen Versuche sind unmittelbar: die Katalysatoren auf Cr-, Mn-, Co-, Ni-, La- und Ca-Basis sind Zersetzungsreagenzien und die auf Grund der Metalle der Gruppe I, II und III (Untergruppe A) aufbereiteten Katalysatoren katalysieren nicht die Zersetzung der Peroxydverbindungen.

2. Es kann festgestellt werden, daß verschiedene Schwankungen der Wirkung der Katalysatoren bestehen, Schwankungen die erstens von der Art des Kations und der Temperatur abhängig sind.

3. Es kann festgestellt werden, daß die höchste katalytische Wirkung vom gleichzeitigen Vorhandensein der folgenden Faktoren bedingt ist:

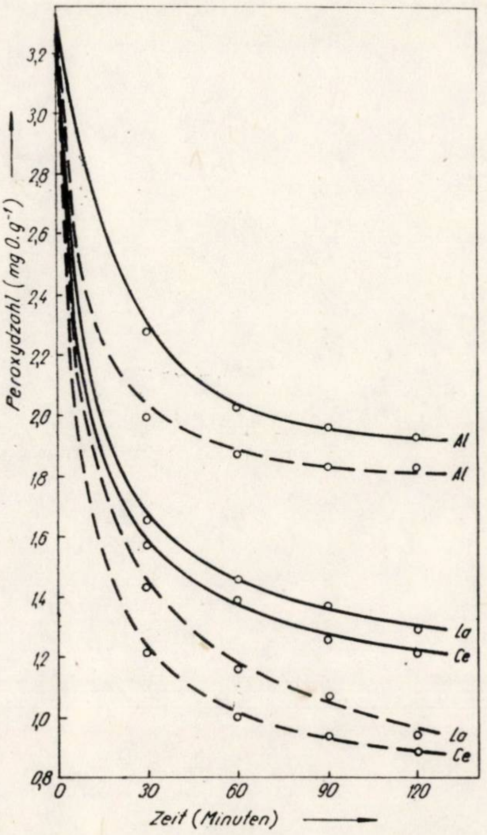

Abb. 8 – Die Änderung der Peroxydzahl in Abhängigkeit von der Zeit für die Katalysatoren auf Grund der Metalle der Gruppe III.

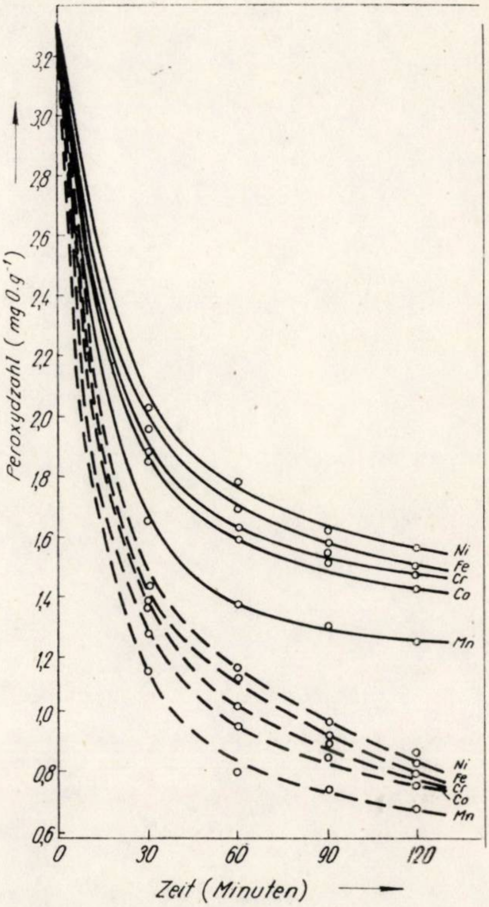

Abb. 9 – Die Änderung der Peroxydzahl in Abhängigkeit von der Zeit für die Katalysatoren auf Grund von Metallen der Gruppen VI, VII und VIII.

– dem Vorhandensein von einer ungeraden Anzahl von Elektronen auf der letzten Schicht des Atomes;

– dem Vorhandensein einer veränderlichen Wertigkeit.

Falls nur eine dieser Bedingungen erfüllt ist, weist das Kation eine schwache katalytische Wirkung auf.

Revue Roumaine de Chimie, 23, 3, 417–427 (1978)

ÜBER DIE ENTSTEHUNG EINIGER HOCHSCHMELZENDER KARBIDE IM PLASMASTRAHL

F. MARX, I. MENESSY und D. BECHERESCU
Laboratorium für Silikattechnik, Technische Hochschule „Traian Vuia",
1900 Timişoara, Bul. 30 Decembrie Nr. 2
Rumänien

Eingegangen am 15. November 1975

Die vorliegende Arbeit untersucht die Entstehung einiger Karbide der Übergansmetalle beim Erhitzen eines Gemisches von Metalloxid und Kohlenstoff mit Hilfe eines Argon-Plasmastrahls. An Hand von röntgenographischen Analysen der Reaktionsprodukte wurde auf den Einfluß von Rohstoffversatz und thermischer Behandlung auf den Verlauf der Hochtemperaturreduktion näher eingegangen. An den erhaltenen Karbiden werden Gitterkonstanten bestimmt und thermische Analysen durchgeführt. Der Verlauf der DTA- und DTG-Kurven zwischen 20 und 1500°, bei Erwärmung der Karbide in Anwesenheit von Luftsauerstoff, wird besprochen. Für die Phasen TiC, TaC und WC wurde an Hand der Gewichtszunahme während der Oxidationsreaktion die genaue Zusammensetzung ermittelt.

EINFÜHRUNG

In einer vorhergegangenen Arbeit,[1] welche die Verwendung von Plasmabrennern bei der Herstellung feuerfester Boride der Übergangsmetalle zum Gegenstand hatte, wurde die Bildung von Karbiden als Zwischenstufe der carbonthermischen Hochtemperaturreduktion einiger Metalloxide nachgewiesen.

In der vorliegenden Arbeit soll die Entstehung der Karbide unter den Bedingungen einer thermischen Behandlung, die mit jener, welche bei der Herstellung der Boride beschrieben wurde, analog ist, untersucht werden, mit der Absicht, die stabilen Phasen festzulegen, sowie die Zusammensetzung von nichtstöchiometrischen Verbindungen, die in reinem Zustand erhalten würden, zu bestimmen.

Bekanntlich sind die Karbide der Übergangsmetalle der 4.,5. und 6. Gruppe des Periodensystems Anlagerungsverbindungen mit breiten Homogenitätsbereichen. Ihre Entstehung beim Erhitzen eines Gemisches von Metalloxid und Kohlenstoff verläuft im Temperaturbereich zwischen 1900 und 2 800° und in schützender Atmosphäre, wobei Konzentration des Kohlenstoffs im Ausgangsgemisch und Parameter der thermischen Behandlung die wichtigsten Faktoren sind, welche den Verlauf des Umwandlungsprozesses bestimmen.

---

[1] F. Marx, I. Menessy und D. Becherescu, *Keram. Z.*, **26**, *382*(1974).

Die in der Literatur[2,3] beschriebenen Methoden zur Herstellung der schwerschmelzenden Karbide bestehen im Wesentlichen aus: direkter Verbindung der Elemente, Reaktion der Metalloxide mit Kohlenstoff, Spaltung von Halogenverbindungen oder Carbonylen der Metalle, Elektrolyse von Gemischen geschmolzener Salze, Karburierung von Metallen in der Gasphase. Unter diesen Verfahren gilt als wirtschaftlich bedeutendstes die Reaktion zwischen Metalloxiden und Kohlenstoff.

ENTSTEHUNG DER KARBIDE IM REAKTIONSGEMISCH

Im Hinblick auf eine Untersuchung der Bildung von Karbiden im Plasmastrahl, wurde von Rohstoffgemischen mit einem Kohlenstoffgehalt ausgegangen, welcher zumindest der stoechiometrischen Menge entsprach, die zur Entstehung der beständigsten Phase nötig ist. Eine Reihe von Voruntersuchungen hatten ergeben, daß bei einigen Systemen eine vollständige Umwandlung des Oxids in das betreffende Karbid in stoechiometrischen Gemischen stattfindet (Me_2O_5-C und MeO_3-C), während bei anderen Systemen ein Überschuß an Kohlenstoff nötig ist (MeO_2-C). In jenen Fällen, in welchen die Karbide als Zwischenstufe bei der Synthese von Boriden beobachtet wurden, erfolgte die thermische Behandlung unter identischen Bedingungen, durch Aufheizung des Reaktionsgemisches mit dem Plasmastrahl, unter Einsatz eines geschlossenen porösen Graphitreaktors.[1] Die durchgeführten Versuche hatten ergeben, daß nach etwa 20 Minuten Erwärmung die oberste Schicht des Reaktorinhalts vollständig oder teilweise in das Karbid umgewandelt wurde. Die röntgenographische Analyse tiefer gelegener Schichten, nach Abschreckung des Reaktors, ermöglichte die Festlegung von Phasenzusammensetzungen, die bestimmten Abschnitten des Reaktionsverlaufs entsprachen. In solchen Fällen, wo das Karbid nicht als Übergangsphase bei der Herstellung der Boride aufgetreten war, erfolgten die Untersuchungen, betreffend die Entstehung von Karbiden, durch eine unmittelbare Einführung des Reaktionsgemisches in die Flamme eines Argon-Plasmabrenners, wobei die in[4] beschriebene Arbeitsweise angewandt wurde.

Die Auswertung der röntgenographischen Daten ergaben, daß im Verlauf des Reaktionsprozesses im System TiO_2-C das Karbid TiC im selben Maß an Konzentration gewinnt, in welchem der Anteil an TiO_2 geringer wird, ohne ein Auftreten anderer Etappen der Hochtemperaturreduktion. In Abb. 1 ist das Beugungsspektrum einer nahezu vollständig umgwandelten Probe wiedergegeben. Man ersieht daraus die Anwesenheit einer kleinen Menge von restlichem TiO_2, neben dem in großer Konzentration entstandenen TiC. Eine Verlängerung der thermischen Behandlung führte zur Bildung eines Karbids von rönthenographischer Reinheit.

---

[2] I. E. Campbell und E. M. Sherwood, „High-Temperature Materials and Technology", J. Wiley, New York, 1967, S. 317.

[3] F. Eisenkolb, „Fortschritte der Pulvermetallurgie", Band 2, Akademie-Verlag, Berlin, 1963, S. 481.

[4] D. Becherescu, F. Winter und F. Marx, *Bul. St. Tehn. I.P.T.*, **10**, *389*(1965).

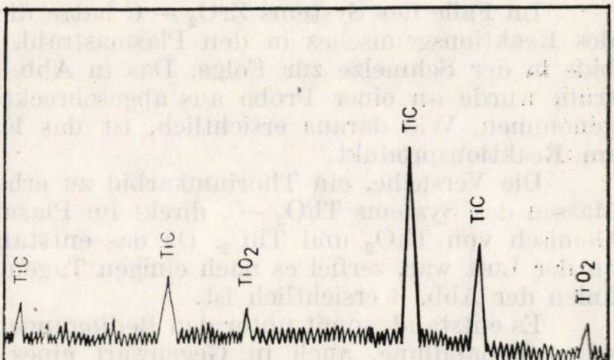

Abb. 1 Beugungsspektrum des entstandenen TiC.

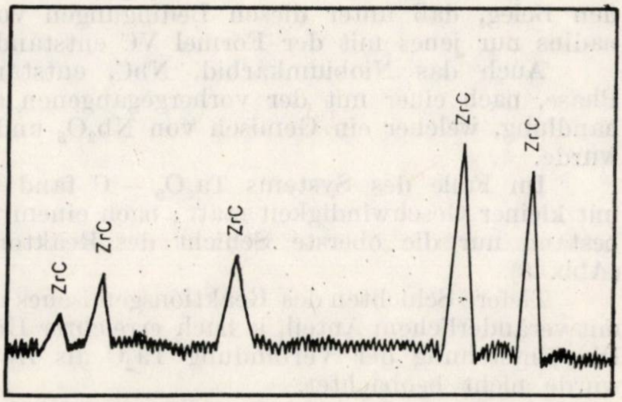

Abb. 2 Beugungsspektrum des entstandenen ZrC.

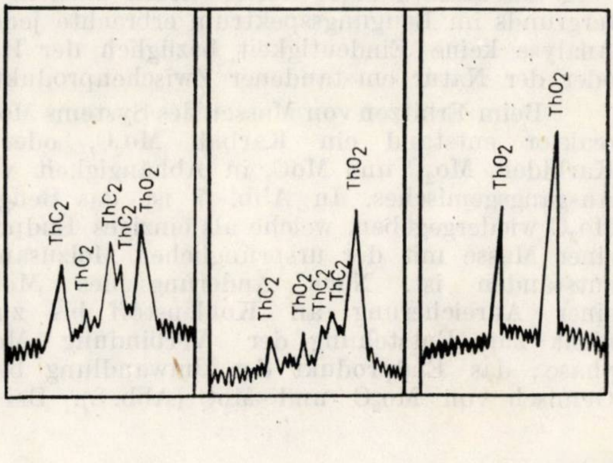

Abb. 3 Beugungslinien des Gemisches $ThC_2 + ThO_2$

a) 30 Minuten nach der thermischen Behandlung. b) Nach 7 Tagen. c) Nach 30 Tagen.

Im Falle des Systems ZrO_2 — C hatte die unmittelbare Einführung des Reaktionsgemisches in den Plasmastrahl, die Entstehung des Karbids in der Schmelze zur Folge. Das in Abb. 2 gezeigte Beugungsspektrum wurde an einer Probe aus abgeschreckten Schmelztröpfchen aufgenommen. Wie daraus ersichtlich, ist das Karbid ZrC alleinige Phase im Reaktionsprodukt.

Die Versuche, ein Thoriumkarbid zu erhalten, durch Erhitzen von Massen des Systems ThO_2—C, direkt im Plasmastrahl, führten zu einem Gemisch von ThO_2 und ThC_2. Da das entstandene Karbid unbeständig an der Luft war, zerfiel es nach einigen Tagen, wie aus den Beugungslinien der Abb. 3 ersichtlich ist.

Es entstand somit unter den Bedingungen der angewandten thermischen Behandlung, auch in Gegenwart eines Überschusses an Kohlenstoff, kein reines Karbid, ohne einen Gehalt an nichtumgewandeltem ThO_2.

Im System V_2O_5 — C entstand, nach einem Erhitzen von 20 Minuten im Graphitreaktor, eine Karbidphase als einziges Endprodukt der Reaktion. Das in Abb. 4 wiedergegebene Beugungsspektrum erbrachte den Beleg, daß unter diesen Bedingungen von den Karbiden des Vanadins nur jenes mit der Formel VC entstanden ist.

Auch das Niobiumkarbid, NbC, entstand gleichfalls als einzige Phase, nach einer mit der vorhergegangenen analogen thermischen Behandlung, welcher ein Gemisch von Nb_2O_5 und Kohlenstoff unterworfen wurde.

Im Falle des Systems Ta_2O_5 — C fand die Bildung des Karbids mit kleiner Geschwindigkeit statt; nach einem Erhitzen von 20 Minuten bestand nur die oberste Schicht des Reaktorinhalts aus reinem TaC. (Abb. 5).

Tiefere Schichten des Reaktionsgemisches enthielten Ta_2O_5 und TaC, mit veränderlichem Anteil, je nach erreichter Höchsttemperatur. (Abb. 6). Die Entstehung der Verbindung Ta_2C als Zwischenstufe der Reaktion wurde nicht beobachtet.

Bei den Massen des Systems Cr_2O_3—C wurde erneut die Methode der unmittelbaren Einführung der Reaktionspartner in die Plasmaflamme verwendet. In der erstarrten Schmelze konnte auf röntgenographischem Weg das Karbid Cr_3C_2 nachgewiesen werden. Wegen eines starken Untergrunds im Beugungsspektrum erbrachte jedoch die diffraktometrische Analyse keine Eindeutigkeit bezüglich der Reinheit des Endproduktes oder der Natur entstandener Zwischenprodukte.

Beim Erhitzen von Massen des Systems MoO_3—C im porösen Graphitreaktor entstand ein Karbid, Mo_2C, oder ein Gemisch von zwei Karbiden, Mo_2C und MoC, in Abhängigkeit vom Kohlenstoffgehalt des Ausgangsgemisches. In Abb. 7 ist das Beugungsspektrum der Phase Mo_2C wiedergegeben, welche als einziges Endprodukt durch das Erhitzen einer Masse mit der ursprünglichen Molzusammensetzung $2MoO_3 + 7C$ entstanden ist. Nach Änderung des Molverhältnisses im Sinne einer Anreicherung an Kohlenstoff bis zu $1MoO_3 + 4C$, kam es nicht zur Entstehung der Verbindung MoC als einzige Karbidphase; das Endprodukt der Umwandlung bestand immer aus einem Gemisch von Mo_2C und MoC (Abb. 8). Bei einer Verlängerung der

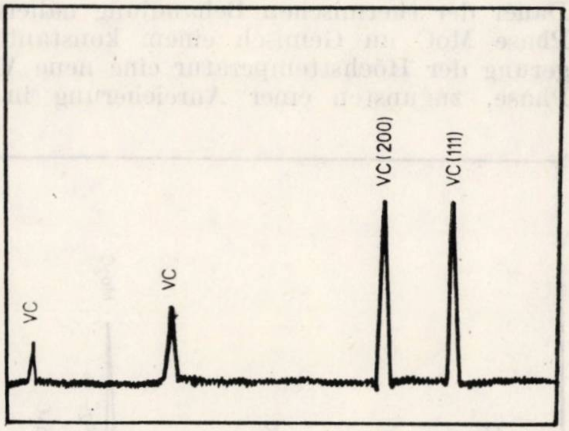

Abb. 4 Beugungsspektrum des entstandenen VC.

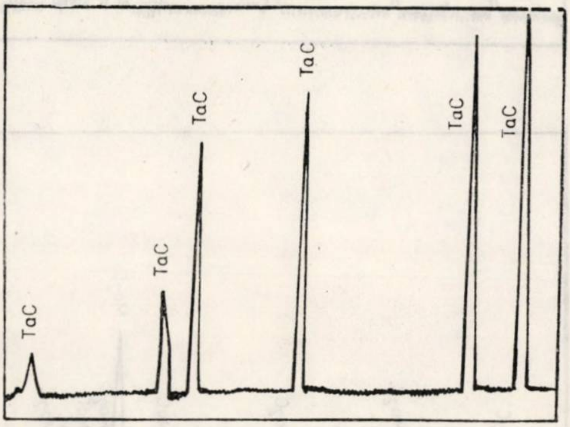

Abb. 5 Beugungsspektrum einer vollständig umgewandelten Masse des Systems Ta_2O_5-C.

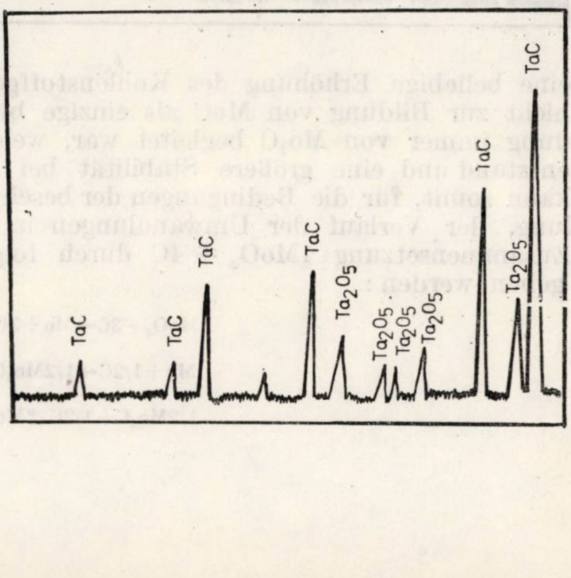

Abb. 6 Beugungsspektrum einer teilweise umgewandelten Masse des Systems Ta_2O_5.

Dauer der thermischen Behandlung näherte sich die Konzentration der Phase MoC im Gemisch einem konstanten Wert, während eine Steigerung der Höchsttemperatur eine neue Verringerung des Anteils dieser Phase, zugunsten einer Anreicherung in Mo_2C, zur Folge hat. Auch eine beliebige Erhöhung des Kohlenstoffgehaltes im Rohgemisch führte nicht zur Bildung von MoC als einzige binäre Phase, da diese Verbindung immer von Mo_2C begleitet war, welches zu Beginn der Reaktion entstand und eine größere Stabilität bei Hochtemperatur aufwies. Es kann somit, für die Bedingungen der beschriebenen thermischen Behandlung, der Verlauf der Umwandlungen in einer Masse mit der molaren Zusammensetzung $1MoO_3 + 4C$ durch folgende Gleichungen wiedergegeben werden:

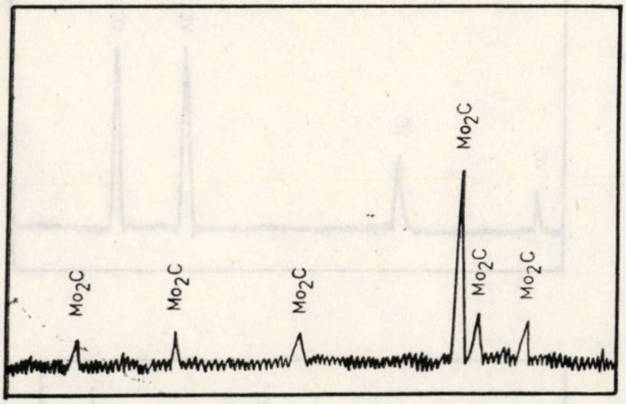

Abb. 7 Beugungsspektrum der Phase Mo_2C.

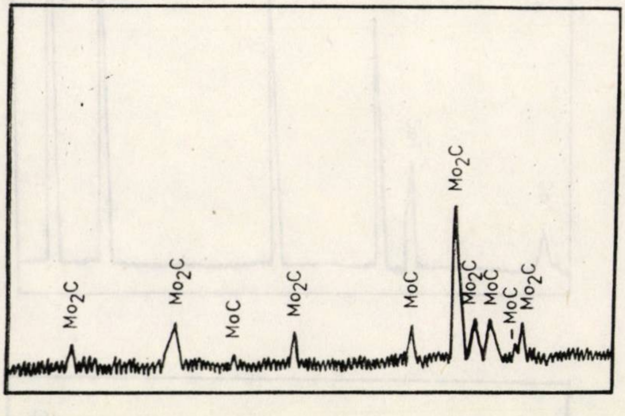

Abb. 8 Beugungsspektrum des Phasengemisches Mo_2C+MoC.

$$MoO_3+3C \rightarrow Mo+3CO$$

$$Mo+1/2C \rightarrow 1/2Mo_2C$$

$$1/2Mo_2C+1/2C \rightleftarrows MoC$$

Da eine Steigerung der Temperatur das Gleichgewicht nach links verschiebt, entstand die Verbindung MoC nicht als alleinige Karbidphase.

Ein umgekehrtes Verhalten wurde bei Massen des Systems WO_3-C beobachtet. Obwolhl auch hier, im Falle eines Rohstoffgemisches der molaren Zusammensetzung $1WO_3 + 4C$, zuerst die Phase $\alpha - W_2C$ entstand, verblieb die Verbindung WC die einzige binäre Phase nach einer Verlängerung der thermischen Behandlung. In Abb. 9 ist das Beugungsspektrum des so entstandenen Karbids wiedergegeben.

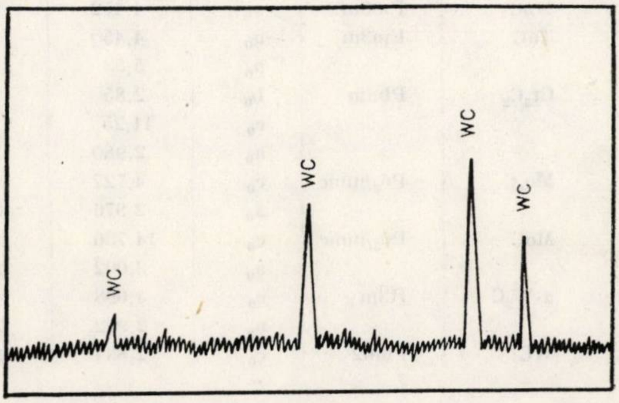

Abb. 9 Beugungsspektrum des entstandenen WC.

Wurde von einem Rohstoffgemisch der Zusammensetzung $2WO_3 + 7C$ ausgegangen, entstand wieder als erste binäre Phase das $\alpha - W_2C$, jedoch vor dem Verschwinden des Oxids WO_3 erschien auch die Phase WC, sowie metallisches Wolfram. Die röntgenographische Analyse des Reaktionsgemisches nach verschiedenen Abschnitten der thermischen Behandlung ergab folgenden Verlauf der Umwandlungen:

$$2WO_3+6C \rightarrow 2W+6CO$$

$$2W+C \rightarrow W_2C$$

$$W_2C \rightleftarrows W+WC$$

Da die beiden letzten Reaktionen im selben Temperaturbereich stattfinden und ein Anwachsen der Höchsttemperatur das Gleichgewicht nach rechts verschob, entstand die Verbindung W_2C nicht als einzige Karbidphase.

DIE GITTERKONSTANTEN DER ENTSTANDENEN KARBIDE

Die infolge der thermischen Behandlung entstandenen Karbide besitzen Beugungslinien, welche nahe bei den Werten liegen, die in der Literatur für die betreffenden Phasen angegeben sind. Die Berechnung der Gitterkonstanten erfolgte an Hand der gegebenen Miller-Indizes sowie der für das jeweilige Kristallsystem gültigen geometrischen Beziehungen. In der Tabelle 1 sind die erhaltenen Ergebnisse, im Vergleich mit Literaturdaten, zusammengestellt.

Tabelle 1

Gitterkonstanten der Karbidphasen

Karbid	Raumgruppe	Gitterkonstante, Å		Literaturwerte, Å	
		Symbol	Wert	ASTM-Karte	Andere Quellen
TiC	Fm3m	a_0	4,328	4,328	4,321[5]
ZrC	Fm3m	a_0	4,692	4,698	4,688[6]
VC	Fm3m	a_0	4,158	4,16	4,182[7]
NbC	Fm3m	a_0	4,472	4,470	4,469[8]
TaC	Fm3m	a_0	4,450	4,456	4,457[9]
Cr_3C_2	Pbnm	a_0	5,53	5,52	5,53[2]
		b_0	2,85	2,82	2,83
		c_0	11,25	11,46	11,48
Mo_2C	$P6_3/mmc$	a_0	2,980	2,994	3,002[2]
		c_0	4,727	4,722	4,724
MoC	$P6_3/mmc$	a_0	2,976	3,01	2,989[10]
		c_0	14,736	14,61	2,809
α-W_2C	$R\bar{3}m$	a_0	3,002	2,99	3,00[11]
		c_0	4,698	4,72	4,73
WC	$P\bar{6}m2$	a_0	2,902	2,91	2,908[12]
		c_0	2,834	2,84	2,837

THERMISCHE ANALYSEN

Der breite Homogenitätsbereich, der für die untersuchten Verbindungen charakteristisch ist, bewirkt, daß die röntgenographische Strukturanalyse mit Genauigkeit nur die Festlegung der anwesenden Phasen ermöglicht, während eine Bestimmung der Zusammensetzung auf Grund von schwachen Verschiebungen der Beugungslinien nur zu annähernden Ergebnissen führt. So ändert sich, gemäß Literaturangaben,[13] beim Titankarbid die Gitterkonstante nur um den Betrag von etwa 0,04 Å, bei einer Änderung der Zusammensetzung innerhalb eines Existenzbereiches, dessen Grenzen den Formeln $TiC_{1,0}$ und $TiC_{0,5}$ entsprechen. Es erwies sich daher als zweckmäßig, eine komplette thermogravimetrische Untersuchung der hergestellten Karbide durchzuführen. Die erhaltenen Ergebnisse — in den Abb. 10 bis 14 wiedergegeben — erlaubten sowohl eine Bestimmung der Zusammensetzung, als auch der Oxidationsbeständigkeit der Karbide bei Erwärmung an der Luft, in pulverförmigem Zustand.

[5] S. Fujishire, *J. Phys. Soc. Japan*, **16**, 1780(1961).

[6] H. Suzuki, S. Kimura und T. Hozaka, *Bull. Tokyo Inst. Technol.*; **1963**, 159.

[7] Er. Rudy, F. Benesovsky und El. Rudy, *Monatsh.*, **93**, *693* (1962).

[8] N. Terao, *Jap. J. Appl. Phys.*, **3**, *104*(1964).

[9] A. L. Bowman, *J. Phys. Chem.*, **65**, *1596*(1961).

[10] G. V. Samsonov, „Tugoplavkie Soedineniya", Metallurgizdat, Moskva, 1963, S. 25.

[11] A. Epstein und I. G. Geib, *J. Electrochem. Soc.*, **106**, *995*(1959).

[12] J. Liciejewicz, *Acta Cryst.*, **14**, *200*(1961).

[13] I. I. Timofeewa und L. A. Klotshkow, „Tugoplavkie karbidy", Naukowa Dubka, Kiew, 1970, S. 143.

Die in den Abb. 10 bis 14 enthaltenen Thermogramme ergaben, daß bei allen untersuchten Verbindungen eine Temperaturerhöhung auf 100–200° einen schwachen Gewichtsverlust zur Folge hat; dieser wird einer Ausscheidung von Kohlenstoff zugeschrieben, der in äußerst fein verteilter Form vorliegt und im Verlauf der Reinigungsprozesse nicht entfernt werden konnte. Der geringe Anteil dieses Verlustes, (0,1–0,5%) bezeugt indessen die Wirksamkeit der verwendeten Trennungsverfahren.

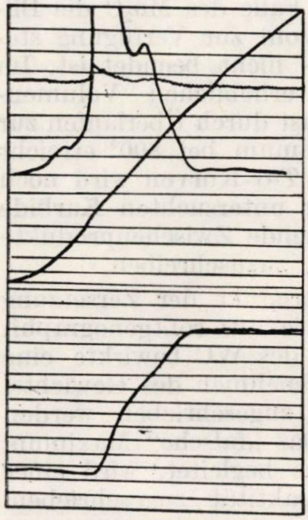

Abb. 10 Thermogramm der Zersetzung des TiC.

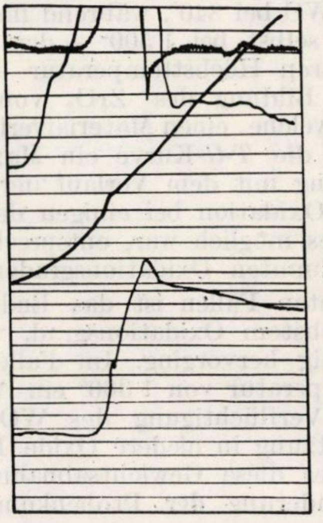

Abb. 11 Thermogramm der Zersetzung des ZrC.

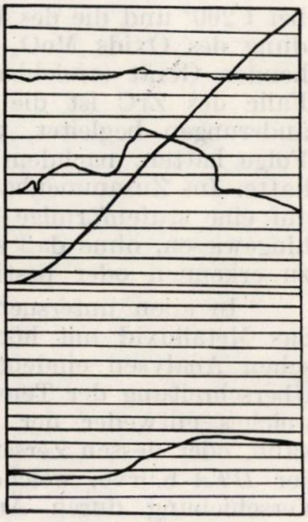

Abb. 12 Thermogramm der Zersetzung des TaC.

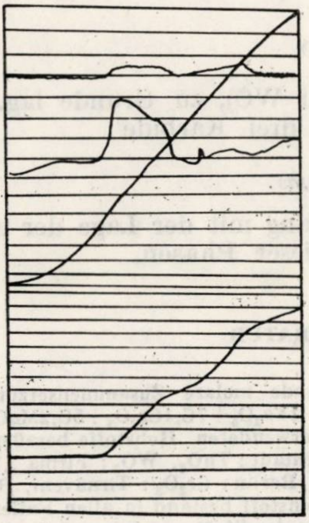

Abb. 13 Thermogramm der Zersetzung des Mo_2C.

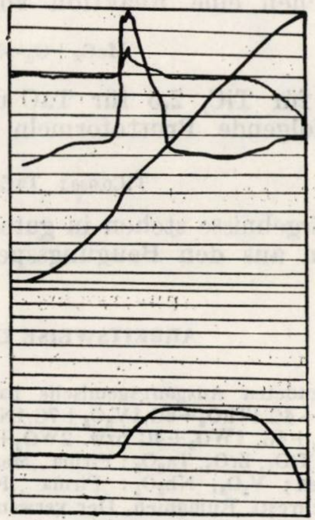

Abb. 14 Thermogramm der Zersetzung des WC.

An der Luft in Pulverform geglüht, weisen die Karbide einen ziemlich engen Bereich thermischer Beständigkeit auf, wonach eine Oxidation einsetzt, die für alle untersuchten Verbindungen stark exotherm ist. Der Beginn des Oxidationsprozesses hängt von der Art des Karbids ab und liegt bei 450° für die Phase TiC, 500° für ZrC, 560° für TaC, 400° für Mo_2C und 550° für WC. Die Temperatur, welche das Ende der Oxidation kennzeichnet, weist bedeutend größere Schwankungen auf. So ist die Oxidation des TiC bei etwa 1 100° beendet, diejenige des TaC bei 1 200° und die des WC bei 840°, während im Falle des Mo_2C die Bildung des Oxids MoO_3 selbst bei 1 500° – der vom zur Verfügung stehenden Gerät erreichbaren Höchsttemperatur — nicht beendet ist. Im Falle des ZrC ist die Bildung des ZrO_2 von erheblichen Volumenänderungen begleitet, welche einen Materialverlust durch Überlaufen zur Folge hatten, nachdem die *T-G*-Kurve ein Maximum bei 800° erreicht hatte. Im Zusammenhang mit dem Verlauf der *T-G*-Kurven wird noch auf eine stufenförmige Oxidation bei einigen der untersuchten Karbide hingewiesen, ohne daß es möglich war, entsprechende Zwischenprodukte zu erkennen oder bestimmten Oxidationsgraden zuzuschreiben.

In allen untersuchten Fällen ist das Endprodukt der Zersetzung das Metalloxid mit höchstem Oxidationsgrad, wie aus röntgenographischen Analysen eindeutig hervorging. Im Falle des WC bewirkte eine Überschreitung der Temperatur von 1 300° ein Abnehmen des Gewichts, welches entweder der Verflüchtigung des WO_3 zugeschrieben werden kann, oder dessen Zersetzung in niedere Oxide. Das „falsche" Maximum der *DTA*-Kurve, welches diese Gewichtsabnahme begleitet, wird einer Verschiebung durch Änderung der Probenkompaktität zugeschrieben.

Aus den weiter oben gezeigten Abbildungen geht somit hervor, daß nur die Thermogramme von 3 Proben (TiC, TaC, WC) zu quantitativen Bestimmungen verwendet werden können. An Hand von Berechnungen, welchen eine Reaktion vom Typ.

$$MeC_x + O_2 \rightarrow MeO_y + xCO,$$

(wobei $y=2$ für TiC, 2,5 für TaC und 3 für WC), zu Grunde lag, ergaben sich folgende Bruttoformeln für die drei Karbide:

$$TiC_{0,966}; \quad TaC_{0,97}; \quad WC_{0,973}.$$

Diese Ergebnisse stehen in gutem Einklang mit der Lage der wichtigsten Linien aus den Beugungsspektren dieser Phasen.

ARBEITSWEISE UND APPARATUR

Die verwendeten Ausgangsgemische hatten folgende molare Zusammensetzungen: $1TiO_2+4C$, $1ZrO_2+4C$, $1ThO_2+6C$, $1V_2O_5+7C$, $1Nb_2O_5+7C$, $1Ta_2O_5+7C$, $1Cr_2O_3+5C$, $2MoO_3 + +7C$ bzw. $1MoO_3+4C$, $1WO_3+4C$ bzw. $2WO_3+7C$. Die verwendeten Rohstoffe besaßen folgende Herkunft: TiO_2, ZrO_2, Ta_2O_5: Firma „Merck", Darmstadt; ThO_2, WO_3: Firma „Schuchardt", München; V_2O_5, Nb_2O_5: Firma „Kahlbaum", Berlin; Cr_2O_3: Tîrnăveni, Rumänien; MoO_3: București, Rumänien. Der verwendete Kohlenstoff bestand in allen Fällen aus Ruß, hergestellt in Copșa Mică, Rumänien. Das Vermischen der Stoffe erfolgte auf trockenem Weg, in einer Labormühle vom Typ „Pulverisette". Der verwendete Plasmabrenner ist in[4] beschrieben. Die diffraktometrischen Analysen erfolgten auf einem Apparat TUR-M 61 Dres-

ANNOUNCEMENTS

27th IUPAC CONGRESS

The 27th IUPAC congress is to be held at Finlandia Hall in Helsinki, Finland, August 27th—31st, 1979.

The scientific programme includes the following main sections and subsections

1. *Trace element analysis*

   Agricultural and food chemistry
   Biological and clinical chemistry
   Environmental chemistry
   Geochemistry
   Instrumental techniques in trace element analysis

2. *Modern methods in clinical chemistry*

   Competitive binding assays
   Enzymatic kinetic methods for non-enzymatic components
   Analysis of tissue specimens by ultramicro methods
   Gas chromatography, mass spectrometry and electron spin resonance in clinical chemistry

3. *Chemistry and biology of cell membrane carbohydrates*

   Symposium on structure and analysis of complex oligosaccharides
   Analytical developments in the determination of structures of complex carbohydrates
   Biological functions of membrane carbohydrates
   Purification of membrane clycoproteins

4. *Chemistry and technology of natural polymers and their degradation products*

   Cellulose
   Starch
   Other polysaccharides
   Lignin
   Other phenolic polymers
   Physical characterization of natural polymers

5. *Biotechnology and Bioengineering*

   Industrial production of enzymes
   Biotechnology in pulp and paper industry
   Design and operation of fermentors
   Mathematical models of fermentation processes

6. *Mineral recources in Northern Europe*

Authors wishing to present papers should provide titles and an English summary (of about 28–32 lines) in dublicate as soon as possible and in any case in sufficient time to enable the programme to be completed by 31 December 1978.

The second circular including details of the programme, technical information and registration forms will be sent in autumn 1978.
The final deadline date for abstracts will also be announced.

All correspondence should be addressed to

27th IUPAC Congress
P.O. Box 13244
SF–00131 HELSINKI 13
Finland
Cable: Finncongress
Phone: 90–174415

den, mit Horizontalgoniometer und linearem Impulsdichteschreiber. Es wurde die CuK_{α}-Strahlung verwendet, bei einer Drehgeschwindigkeit des Zählrohrs von 0,25°/Min.

Die thermischen Analysen wurden auf einem Derivatographen vom Typ Paulik Paulik Erdelyi durchgeführt, unter Verwendung eines Heizofens mit der Höchsttemperatur 1500°. Die Erwärmung der Proben erfolgte in einem Platintiegel, bei einer Aufheizungsgeschwindigkeit von 10°/Min.

ZUSAMMENFASSUNG

1. Die Erhitzung auf Hochtemperaturen im Plasmastrahl der Gemische von Metalloxiden und Kohlenstoff führte zur Entstehung folgender Karbide als einzige binäre Phasen im Reaktionsprodukt: TiC, ZrC, VC, NbC, TaC, Mo_2C und WC. Im Gemisch mit anderen Phasen entstanden die Karbide MoC, Cr_3C_2, ThC_2 und W_2C.

2. Die Karbide welche allein entstehen, sind — abgesehen von überschüssigem Kohlenstoff — von röntgenographischer Reinheit. Durch thermogravimetrische Analyse gelang die Bestimmung der genauen stöchiometrischen Zusammensetzung der Karbide des Titans, Tantals und Wolframs, u. zw. $TiC_{0.966}$ $TaC_{0.97}$ sowie $WC_{0.973}$.

3. In fein verteiltem Zustand besitzen die erhaltenen Karbide eine geringe Oxidationsbeständigkeit. So zerfällt ThC_2 schon bei gewöhnlicher Temperatur, während andere Karbide zwischen 400 und 600° mit dem Luftsauerstoff reagieren und höhere Oxide bilden.

den, mit Horizontalgoniometer und äusserem Impulsdichteschreiber. Es wurde die CoKα-Strahlung verwendet, bei einer Drehgeschwindigkeit des Zählrohrs von 0,25°/Min.

Die thermischen Analysen wurden mit einem Derivatographen vom Typ Paulik-Paulik-Erdey durchgeführt, unter Verwendung eines Heizofens mit der Hochtemperatur 1500°. Die Erwärmung der Proben erfolgte in einem Platintiegel, bei einer Aufheizungsgeschwindigkeit von 10°/Min.

ZUSAMMENFASSUNG

1. Die Erhitzung auf Hochtemperaturen im Plasmastrahl der Gemische von Metalloxiden und Kohlenstoff führte zur Entstehung folgender Karbide als einzige binäre Phasen im Reaktionsprodukt: TiC, ZrC, VC, NbC, TaC, Mo_2C und WC. Im Gemisch mit anderen Phasen entstanden die Karbide MoC, Cr_3C_2, ThC_2 und W_2C.

2. Die Karbide welche allein entstehen, sind — abgesehen von überschüssigem Kohlenstoff — von röntgenographischer Reinheit. Durch thermogravimetrische Analyse gelang die Bestimmung der genauen stöchiometrischen Zusammensetzung der Karbide des Titans, Tantals und Wolframs, u. zw. $TiC_{0,88}$, $TaC_{0,97}$ sowie $WC_{0,973}$.

3. In fein verteiltem Zustand besitzen die erhaltenen Karbide eine geringe Oxidationsbeständigkeit. So zerfällt ThC_2 schon bei gewöhnlicher Temperatur, während andere Karbide zwischen 400 und 600° mit dem Luftsauerstoff reagieren und höhere Oxide bilden.

Revue Roumaine de Chimie, **23**, *3*, 429–433 (1978)

PRACTICAL INDICATIONS FOR THE PREPARATION OF ^{99m}Tc GENERATOR FOR MEDICAL USE

M. Y. MIRZA*
Dept. of Chemistry,
University of Nigeria, Nsukka,
Nigeria

Technetium – 99 m generator of high specific activity and radiochemical purity was prepared from the neutron irradiated molybdenum oxide. The effect of pH of the feed solution, velocity and the volume of eluant, total concentration of molybdenum, nature and length of column and elution yield were studied. Quantitative adsorption of Mo^{99} was achieved by the control of pH of the feed solution, thus making it possible to supply the generators of 100–150 mCi activity which were ready for despatch in 45 minutes after the end of irradiation.

INTRODUCTION

The desirable characteristics i. e. the short half life of ^{99m}Tc (6.0 hr) with the emission of only one gamma ray of 140 keV in the absence of beta particles and rapid clearance from the blood makes this nuclide ideal for scanning for liver, spleen and bone marrow.

Several technetium – 99m generators are reported in the literature [1–18] while a few of them are now commercially available. The difference among the proposed generators concern the separation techniques used as well as the source of ^{99}Mo. Fission of ^{235}U gives rise to high specific activity ^{99}Mo but it contains undersirable contaminants like ^{103}Ru, ^{131}I, ^{132}I which are difficult to remove or require elaborate procedures.

---

* Work was performed in Pakistan.

[1] D. G. Stang Jr., (Coordinator) BNL-864 (T-347) (1964).

[2] W. D. Tucker, M. W. Green, A. Weiss and A.P. Murrenhoff BNL-3746 (1958).

[3] W. D. Tucker, R. F. Doering, M. W. Green and L. G. Stang Jr. *Trans. Am. Nucl. Soc.*, **3**, 2 (1960).

[4] W. D. Tucker, M. W. Green and A. P. Murrenhoff, *Atompraxis*, **5**, 163 (1962).

[5] R. Muenze, *Kernenergie*, **4**, 808 (1961).

[6] N. B. Mikheeve, M. El-Garhy and Z. Moustafa, *Atompraxis*, **10**, 263 (1964).

[7] J. F. Allen, *Int. J. Appl. Rad. Isotopes*, **15**, 333 (1965).

[8] P. Richards, *Int. J. Appl. Rad. Isotopes*, **17**, 427 (1966).

[9] M. El-Garhy, S. Bayomy and S. Al-Eley, *Rad. Chim. Acta*, **7**, 163 (1967).

[10] H. Levy, P. Reinhold and P. Wolf, *Rad. Chim. Acta*, **7**, 168 (1971).

[11] T. Lengyl, *Magyar Kémi Lapjá*, **19**, 428 (1964).

[12] J. J. Pinajian, *Int. J. Appl. Rad. Isotopes*, **17**, 664 (1964).

[13] S. Meloni and A. Nrandone, *Int. J. Appl. Rad. Isot.*, **19**, 164 (1968).

[14] S. Bulbulian and H. Sorantin, *Kerntechnik*, **8**, 118 (1966).

[15] E. P. Belkas and D. C. Perricos, *Rad. Chim. Acta*, **11**, 56 1969).

[16] K. Albin, *Nucleonika*, **14**, 261 (1969).

[17] A. Karpeles and M. C. Palcos CNEA-267 (1970) Argentina.

[18] M. Y. Mirza, PINSTECH-72-1 (1972).

In the ion exchange procedures ^{99}Mo parent is adsorbed on a material with strong sorption properties i. e. alumina,[1-11,17] iron oxide[14] while the ^{99m}Tc daughter is eluted with different eluants. A few good solvent extraction procedures[5,19] for the separation of ^{99m}Tc using methyl-ethyl-ketone from 6M NaOH are also reported.[15] Quality control of ^{99m}Tc generators has also been mentioned.[20]

In the first few preparations quantitative adsorption of ^{99}Mo could not be achieved resulting in making the generator of low specific activity. However, the contamination of ^{99}Mo was observed by washing the column with saline solution for 5—6 hours. The present work was undertaken to streamline the production procedure for ^{99m}Tc generator of high specific activity which was achieved by adsorbing ^{99}Mo activities on alumina column at a controlled pH. The generator was ready for despatch in 45 min after the end of irradiation. Elution of such generators for 10 days gave no detectable molybdenum. The use of zirconium oxide as column material was found unsuitable for the generator.

EXPERIMENTAL

Reagents and Apparatus

All the reagents used were of AnalaR grade and pyrogen free water was used in making the solutions. A $\beta-\gamma$ ionization chamber was used for measuring the final yield and 1024 multichannel ND 4410 computerized analyser system coupled with 3×3 in NaI(Tl) crystal for radiochemical purity.

Column Preparation

The column material (alumina) was water graded and the heaviest 10% and the lightest 10% fractions were discarded followed by preconditioning with 0.9% NaCl solution. Various columns with sintered glass plug N° 2 were packed with the prepared material to a height of 1 to 4 cm and tamped to restrict the flow rate of required velocity. For the supply of generator the alumina was packed to a height of 4 cm in a glass cartridge of 2 cm internal diameter having penicillin vial openings on both sides with sintered glass plug N° 2 on the lower end. After loading, both the openings were closed with rubber stoppers. The inlet and the outlet of the generator were provided by means of syringes.

Target Preparation

1.5 gram of MoO_3 encapsulated in a quartz ampule was sealed in a standard aluminium can and irradiated in the core of PARR-1 for 100 hours with a thermal neutron flux of 2×10^{13} n/sec/cm^2 and fast neutron flux of 1×10^{12} n/sec/cm^2. During the irradiation 264mCi ^{99}Mo, 64 mCi^{101}Mo, 3.2 mCi^{99} Mo, 3.0 mCi^{92}Nb, 134 uCi^{95}Nb, 2.17 uCi^{95}Zr, 1.2 uCi^{97}Zr were calculated to be increased.

Procedure

The irradiated molybdenum oxide was dissolved in 10 ml of 25% ammonia solution at 50—60° to get ammonium molybdate. The ammonical solution of ^{99}Mo was evaporated almost to dryness and the activities taken up in 5 ml of 0.9% NaCl solution (isotonic saline

---

[19] N. K. Baisha, R. B. Heslop and A. C. Ramsay, *Radiochem. Radioanal. Letter*, **4**, 15(1970).

[20] L. Oniciu and G. B. Cook, *J. Radioanal. Chem.*, **13**, 247 (1973).

solution). The pH of the solution was adjusted at 5.0 to 5.5 by the addition of a few drops of diluted hydrochloric acid. The solution was passed through the glass cartridge containing alumina preconditioned with saline solution. The flow of the solution was regulated at 6–7 drops/min to allow the quantitative adsorption of molybdenum activities. The column was washed with 10 ml of saline solution to remove the negligible amount of unadsorbed molybdenum. The ^{99m}Tc activities increased after some time could be quantitatively eluted with 10 ml of saline solution with no detectable molybdenum contamination.

Quality Control

No effort was made to determine the lower oxidation states of technetium present in the eluted solution of sodium technetate. Since we used Al_2O_3 column there was a possibility of aluminium contamination in the eluate. The absence of ^{99}Mo coming along with ^{99m}Tc was established by gamma ray spectroscopy.

Determination of aluminium traces[21]

The eluate containing sodium technetate was adjusted at pH 3.0 ± 0.1 by the addition of sodium acetate buffer solution. 0.001 M methyl thymol blue solution was added and heated at 65–70° for about 15 minutes. The solution was cooled to room temperature and the absorption was measured at 555 mμ after half an hour against a reagent blank similarly prepared.

RESULTS AND DISCUSSION

Optimum growth of ^{99m}Tc occurs at 22–24 hrs when it reaches the maximum value and can be eluted daily as long as ^{99}Mo furnishes a useful amount of ^{99m}Tc. Maximum adsorption of ^{99}Mo (ammonium molybdate) on alumina bed was found to be dependent on various factors, most important among them being the pH of the parent solution. The effect of pH on the adsorption on molybdenum is given in table 1.

Table 1

Effect of pH on the adsorption of molybdenum on alumina

pH	% total activity adsorbed*
10.0	20–25
9.0	25–30
8.0	35–40
7.0	70–75
6.0	80–85
5.0–5.5	95–100
4.0	60–65

* Mean of four experiments

At pH above 7 the adsorption is less than 40% while it is quantitative at pH 5.0–5.5. The complete adsorption of molybdenum at acidic pH is due to the fact that like tungsten and unlike zirconium and uranium, it gets hydrolyzed at low pH and polymerizes with the increase in the concentration giving rise to polybasic and heteropoly basic anionic

---

[21] T. V. Malkov, N. D. Medvedeva and K. B. Yatsimirski, *Zhur. neorg. Khim.*, **9**, 2347 (1964).

species which are strongly adsorbed on alumina while monobasic pertechnetate ions are only moderately held and can be easily eluted. At high pH, polymerization of molybdenum occurs with no possibility for the formation of highly charged anionic species. At low pH, dibasic anionic species are formed with less possibility of adsorption. Thus in the present work the ideal pH was found to be 5.0—5.5. The velocity of inflow of feed solution (ammonium molybdate) was adjusted at 8—10 drops per min. Increase in the velocity of the solution decreased the adsorption. Length of alumina bed is also important in making an efficient generator system. Among the various columns those of 4.0 and 4.5 cm length respectively were found out to be more appropriate where no leakage of ^{99}Mo could be observed.

Elution of ^{99m}Tc was carried out with sterile isotonic saline solution at pH 5.8—6.5. Complete recovery was achieved with 10 ml of saline solution in about 5—6 min. Under these conditions, the eluted ^{99m}Tc activity does not contain any detectable ^{99}Mo as shown in Figure 1

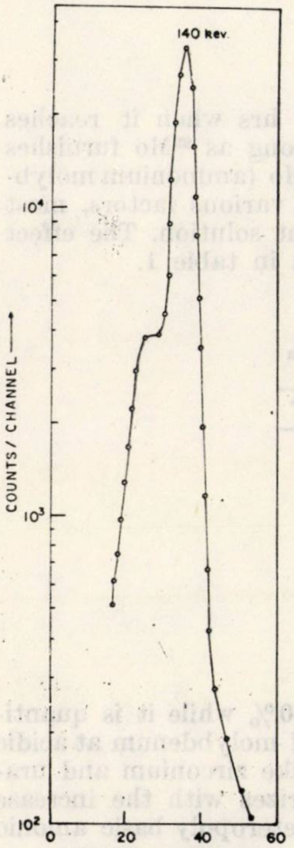

Fig. 1. — Gamma spectra of ^{99m}Tc eluted from ^{99}Mo.

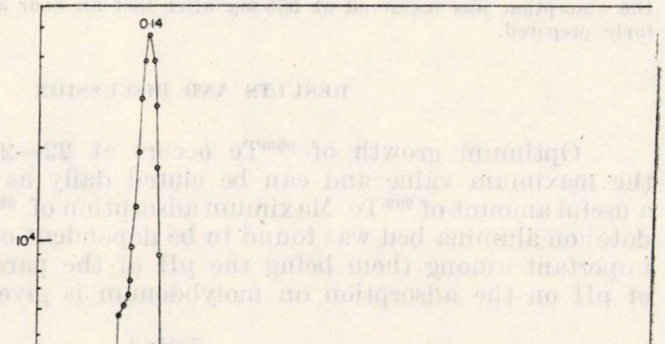

Fig. 2. — Gamma spectra of ^{99}Mo—^{99m}Tc system.

and can be compared with the gamma spectrum of ^{99}Mo — ^{99m}Tc mixture as shown in Figure 2. If ^{99m}Tc is in equilibrium with ^{99}Mo, the yield of the eluted ^{99m}Tc will be about 80%. It is impossible to reach a yield of 100% as part of ^{99}Mo decays to longer lived ^{99}Tc.

The concentration of molybdenum required for adsorption on alumina depends upon the available surface area. Under the optimum conditions used, 300 mg of molybdenum could be easily adsorbed on the column of 20 grams of alumina without any leakage of molybdenum. A comparison was made between alumina and zirconium oxide (100—200 mesh) as column materials. Zirconium oxide was prepared locally by fusing zirconium nitrate at 600°. A fraction of 100—200 mesh was selected and packed in the column having the same dimensions as that of alumina. Elution study with such column showed an appreciable leakage of ^{99}Mo along with ^{99m}Tc activity and moreover, a manyfold volume of the saline solution was required to elute technetium.

Revue Roumaine de Chimie, 23, 3, 435–443 (1978)

AMORPHOUS-CRYSTALLINE COUPLING IN POLYETHYLENE. VI[1]

THE STUDY OF THE MORPHOLOGICAL CHANGES IN HIGH MOLECULAR WEIGHT POLYETHYLENE BY COMPOUNDING WITH POLYPROPYLENE

GHEORGHE DRĂGAN
Institute of Chemical Research, ICECHIM, Spl. Independenței 202, Bucharest Romania

Received October 22, 1975

The amorphous-crystalline coupling in the high molecular weight polyethylene ($M_w \sim 10^6$) is studied by differential thermal analysis (DTA). It is considered that the melting endotherm changes its shape together with the change in the morphology of the composite material. The original polyethylene (as resulted from synthesis) analyzed with and without transfer medium, is studied comparatively to the compound with polypropylene. For this last case the amorphous-crystalline coupling performed by row or quiescent crystallization is damaged by polypropylene coupling. The observed changes on thermograms are explained by the energy transfer topology during DTA round of the melting. These results are considered consistent with the idea of the energy dissipation modes coupling recently approached in the first order transitions.

INTRODUCTION

The lamellar habit is the most frequent crystalline morphology in polyethylene (PE) for a large range of crystallization conditions; but in turn, as was pointed out in previous works,[1–5] both these conditions and the treatments applied to the polymers in solid state (below T_m^0), considerably change the amorphous-crystalline coupling. In all these works the manner for revealing these changes is mainly based on the dynamic calorimetric analysis for the transitions of the order-disorder type specific of the interlamellar order.[2] For the PE samples previously considered, two distinct interlamellar orders were established,[1] namely: an order performed by the crystallization conditions,[2] and a local order between the lamellar fragments resulting from the coherent precipitation of the lamellar defects in amorphous local domains.[1,3–5] The two are connected with the shear stresses from the interface between the amorphous domain and lamella (or lamellar fragment) imposed during crystallization, [1,2] respectively during defects precipitation.[4] This amorphous-crystalline coupling expressed by the elastic interaction between the two phases is described by the twist disclination state for the particular case when the stress tensor contains only the shear components in the interface.[1] In this way the two interlamellar orders are equivalent, such an order is also achieved by plastic deformation where the shear components prevail in the interface,[6] and for which T_m^1 transition is also characteristic.[7] In all these cases it is considered that the amorphous-crystalline coupling is performed on the habit face parallel to $|001|$ direction (the chain axis), because the (001) faces are not affected.[4] For the local interlamellar order, for example, the glide direction ($\vec{T} = (|100| + (1/2.5)|010|)$) is considered to define the habit face which separates the lamellar fragment from the local amorphous domain.[4] The crystallization conditions influence also the crystalline habit,[8] but this is not yet known in detail for PE.

---

[1] Part V: Gh. Drăgan, *Rev. Roumaine Chim.*, **22**, 261 (1977).
[2] Gh. Drăgan, *Materiale Plastice*, **10**, 87 (1973).
[3] Gh. Drăgan, *Rev. Roumaine Chim.*, **20**, 687 (1975).
[4] Gh. Drăgan, *Rev. Roumaine Chim.*, **21**, 1381 (1976).
[5] Gh. Drăgan, *Rev. Roumaine Chim.*, **21**, 1537 (1976).

The present work resumes the study of the high molecular weight PE ($M_w \sim 10^6$) previously denoted as PEAS, and for which a net T_m^1 effect mainly originating from row crystallization was observed by flash adiabatic calorimetry.[2] In the meantime their morphology was studied[9] in a similar manner as for the three LPE types previously considered.[1,3–5] The kinetics of the defects precipitation is observed to be extended on a larger range because of a high melting point T_m^0 (140–142°).[9] This precipitation process has also a gravitational effect, but comparatively to the CPE samples,[5] this polymer has some peculiarities.[9] The amorphous-crystalline coupling for row crystallization conditions is studied also[2] on compound samples with polypropylene (PP) because this polymer does not flow in the melt state for sufficiently high stresses (the melt index is zero). Although the DTA results are not qualitatively comparable to those obtained from the flash adiabatic calorimetry,[2] these are suitable for qualitative observations on the disclination states of the composite materials. In addition, this study points out the topological aspect of the heat transfer during the DTA round, whose importance was revealed also in the case of the CPE morphology.[5] The DTA thermograms for the LPE samples, especially for the CPE samples,[4] have revealed a direct correspondence between the height and the area of the melting peak, for the two effects T_m^0 and T_m^1, and for the three sets of composite materials. In the case of PEAS samples, it was observed that this correspondence was not maintained,[9] which indicates changes in the energy transfer topology during melting in the DTA round. These changes may be explained by the specific mode-mode coupling in the energy dissipation.

---

[6] GH. DRĂGAN, "Morphology of Polymers. Principles of Characterization and Processing", Lectures, ICECHIM, Bucharest, June 1974.

[7] G. C. ADAMS, *J. Polymer Sci.*, **A2**, **9**, 1235 (1971).

[8] P. HARTMAN, *Rendiconti della Societa Italiana di Mineralogia e Petrologia*, **29**, 153 (1973).

[9] GH. DRĂGAN, unpublished data.

EXPERIMENTAL

The PE powder sample as resulted from synthesis is analyzed in the same way as the LPE and CPE samples,[4] by its behaviour during annealing in the range of 115—136°. The annealing and the DTA study have been carried out on the samples similarly prepared and grouped in the three sets after composition, namely: dry annealed and DTA samples (I); dry annealed and medium DTA (II), and medium annealed and DTA (III).

The morphology of the row crystallized PE is studied on the compound with 50% PP, by using Charpy little specimens after STAS 5801-73 obtained by injection moulded at one end in the cold mould. The sample for the DTA round is cut along the longitudinal axis, with the DTA cell length.[4] Thus it has been observed,[9] that, for these specimens, the fragment placed at the opposite gate presents the maximum T^1_m effect, while the middle fragment has not this effect. This would correspond to the fact that the shear lines are suddenly frozen in the first portion, while in the second the quiescent conditions perform a spherulitic texture.[6] The good reproducibility of this effect was established by considering the effect h_{2PE} (see below) on 2—5 samples for the same injection moulding conditions and subsequent treatments. The annealing of the PE and compound samples was performed in the metallic block together with LPE and CPE samples.[4] For good thermal contact with metallic walls both during annealing and in the DTA round, each sample is wrapped in an aluminium foil and compressed in the respective orifice.

The used DTA apparatus was previously described.[4] For better reliability of the described observations the three round speeds denoted as $K1$, $K2$ and $K3$, were used.

RESULTS AND DISCUSSIONS

The melting point for crystalline phase in polymers was expressed by the characteristic parameters of the lamellar habit in the well known Hoffman's theory.[10] In this way the unusually high melting interval for the high molecular weight PE[9] is explained by the existence of large-sized lamellae on direction |001|, of fibrilar type. A similar habit was provided by this theory also in the case of high pressure crystallization for the linear species with relatively low molecular weight ($2-5\times10^4$).[11]

Attention was drawn previously[3] that the melting process, as any other critical phenomenon has an extension on the temperature and time scale. On the other hand their kinetics evolves as a function of the testing method, or more precisely, of the response function of the considered thermodynamic system.[6] For example, the interlamellar order is detected by the T^1_m effect which is differently observed by the flash adiabatic calorimetry[2] and by the DTA. Although in the two cases the same response function is considered as the temperature variation during the heat flow absorption, the extension of the process on the temperature scale is more strict in the first system. This fact may be explained by the different contribution in the response function of the dissipation mode coupling.[12] For the endothermal process in DTA associated to the amorphous-crystalline coupling in PE, the choice of the peak top as the transition temperature is an approximation which may supply orientative information within the limits of Hoffman's theory. For this reason the study of the shape of the endotherm is more important, namely the time evolution of the difference temperature $\theta(t)$ between the two DTA cells. The changes that occur in the shape may be interpreted as contributions of the energy dissipation modes in the composite material.

---

[10] J. Hoffman and J. Weeks, *J. Res. Nat. Bur. Standards*, **66**, 13 (1965).

[11] D. C. Bassett and B. Turner, *Phil. Mag.*, **28**, 285 (1973).

[12] L. P. Kadanoff and J. Swift, *Phys. Rev.*, **166**, 89 (1968).

The results considered below refer to the changes in the melting endotherm of the high molecular weight PE samples, and are classified in three distinct groups:

(*a*) results obtained on the initial polymer analyzed in the three specified sets (Figures 1, 2);

(*b*) results obtained on the compounds with PP which exhibit the orientation effect defined by the peak height h_{2PE}(Figure 3);

(*c*) results obtained on the compound with PP, in which the effect h_{2PE} is negligible (spherulitic texture morphology) (Figures 4, 5).

(*a*) The first group immediately shows the deviation from the correspondence between the melting enthalpy (ΔH_m^{PE}) and the height of the respective endotherm T_m^0, denoted by h_{1PE} in the time dependence during annealing in set III (Figure 1). In the considered annealing conditions no assymetry is observed in the shape of the peak which would indicate a T_m^1 effect. Otherwise the IR spectra are characteristic of the essentially linear PE species and show no considerable changes for the conformational defects during annealing. [9] The abrupt fall in ΔH_m^{PE} for the compositions in the sets II and III (Figure 2*b* and respectively Figures 1 and 2*c*) shows the fragmentation of the lamellae on | 001 | direction, similarly with those observed in the LPE 2 and CPE 2 samples because of the silicon oil diffusion. The heat of diffusion is superposed over the ΔH_m^{PE} effect occurring on the whole as a saturation process after the amplitude dependence on a logarithm of the annealing time (t_a) (Figure 1, set III), but as an activation process after the dependence on the annealing temperature (T_a) (Figure 2*a*, set II). For the set III from Figure 2*c*, because the annealing time is sufficiently large, ΔH_m^{PE} remains practically constant, and the lamellar segmentation occurs during annealing and not in the DTA round. The value in this case is very close to the saturation value from Figure 1*a*. It is worth noting the difference of 20 calories per gram of polymer between the two compositions: dry (set I) and with medium (set III, corresponding to Figure 1 at 10^2 min, or Figure 2*a* and 2*c* at T_a 130°). The set I shows that both ΔH_m^{PE} estimated as $\int_{t_1}^{t_2} \theta(t)dt$ (t_1 and t_2 are the input, respectively the finish moment of the transformation process) is function of the transfer medium between the material component which transforms the cell wall too.

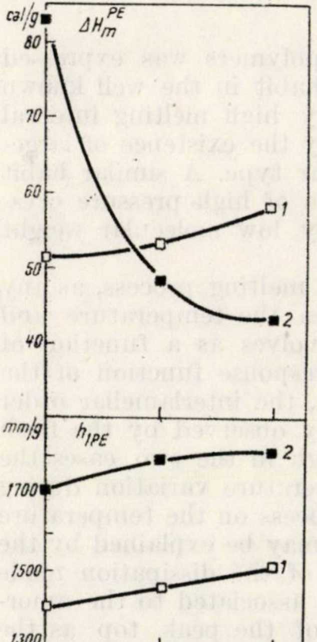

Fig. 1. — Dependence of the melting enthalpy and of the melting peak height on annealing time for dry annealed PE samples at T_a=124°, and DTA round speed Kl. (*1*, dry DTA, *2*, medium DTA).

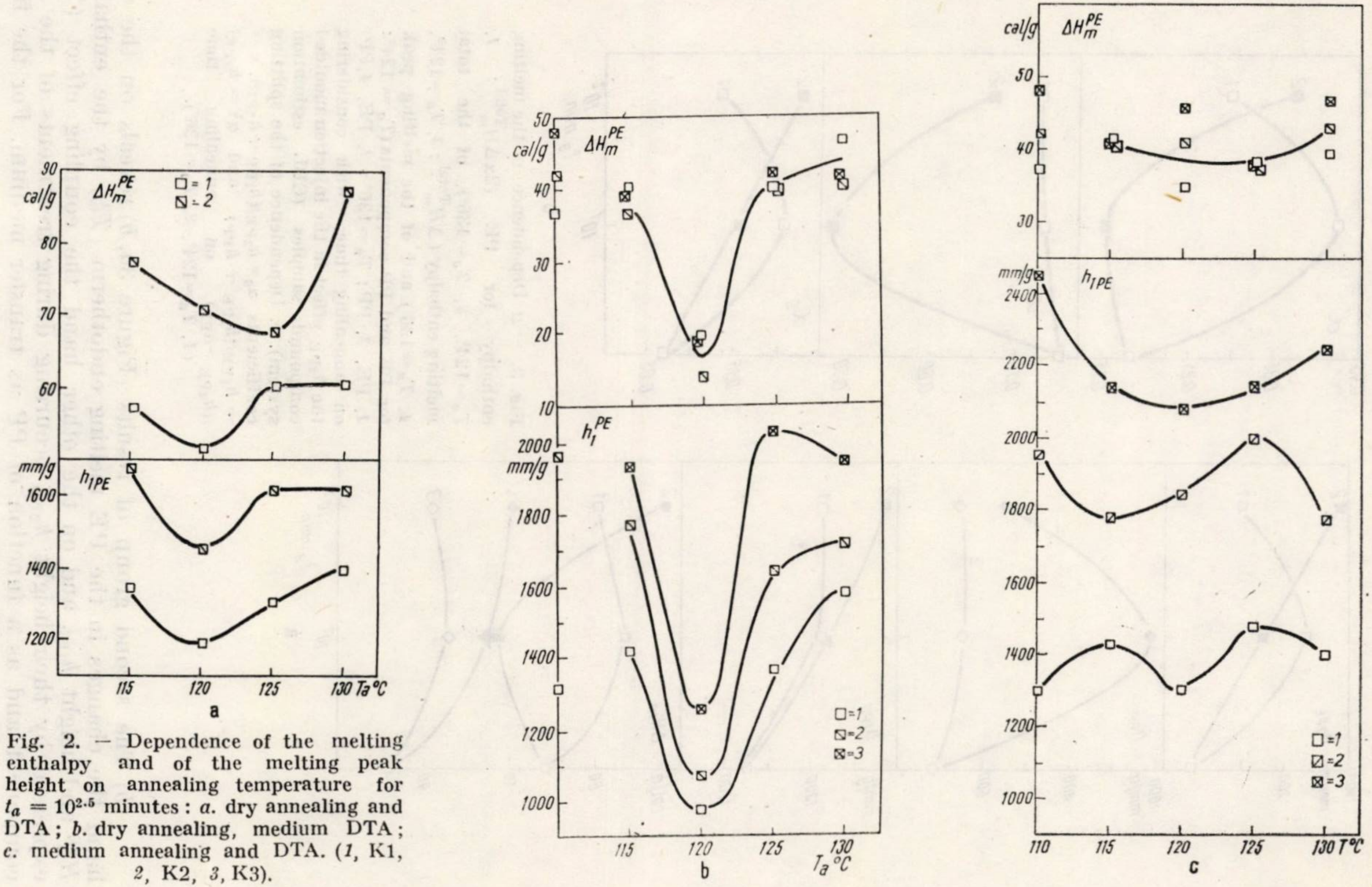

Fig. 2. — Dependence of the melting enthalpy and of the melting peak height on annealing temperature for $t_a = 10^{2.5}$ minutes : *a*. dry annealing and DTA ; *b*. dry annealing, medium DTA ; *c*. medium annealing and DTA. (*1*, K1, *2*, K2, *3*, K3).

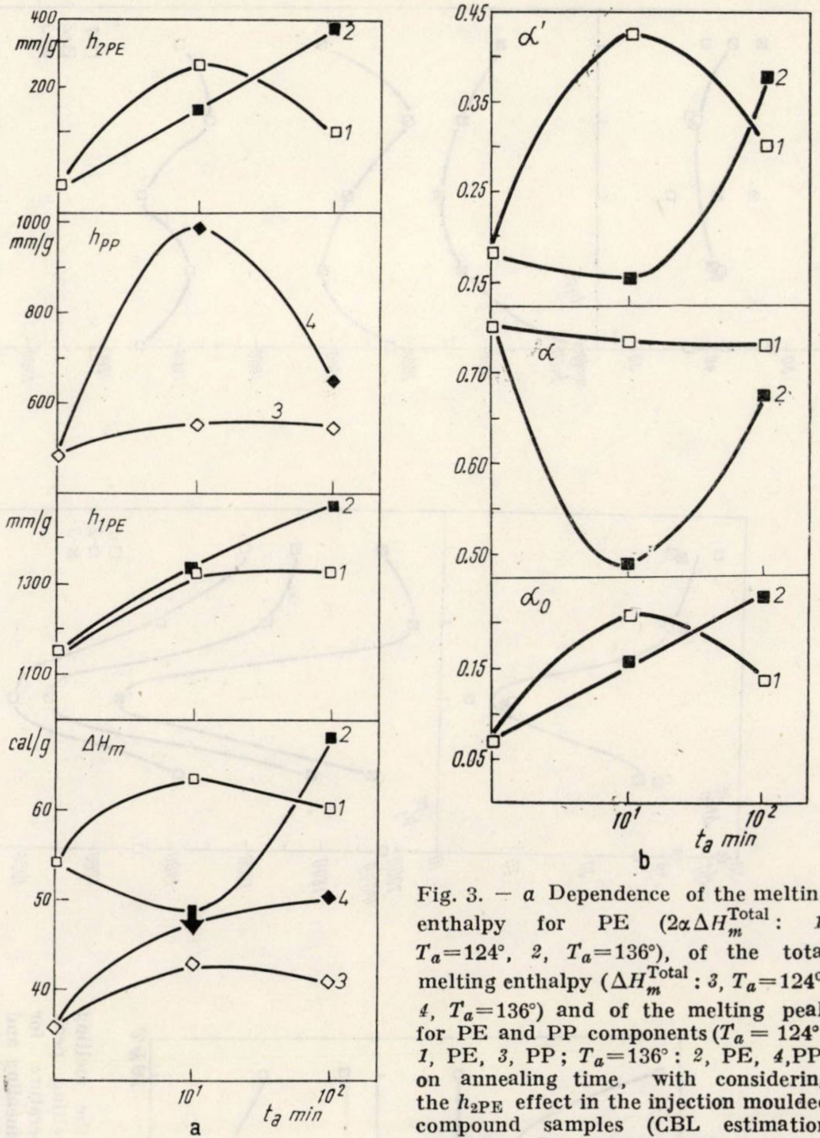

Fig. 3. — *a* Dependence of the melting enthalpy for PE ($2\alpha\Delta H_m^{\text{Total}}$: *1*, $T_a=124°$, *2*, $T_a=136°$), of the total melting enthalpy ($\Delta H_m^{\text{Total}}$: *3*, $T_a=124°$, *4*, $T_a=136°$) and of the melting peak for PE and PP components ($T_a = 124°$: *1*, PE, *3*, PP; $T_a=136°$: *2*, PE, *4*, PP) on annealing time, with considering the h_{2PE} effect in the injection moulded compound samples (CBL estimation system). *b*. Dependence of the splitting coefficients $\alpha_0=h_{2PE}/(h_{1PE}+h_{2PE})$, $\alpha = h_{1PE}/(h_{1PE}+h_{PP})$ and $\alpha^1 = h_{2PE}/(h_{2PE}+h_{PP})$ on annealing time (*1*, $T_a=124°$, *2*, $T_a=136°$).

(*b*) The second group of results (Figure 3*a*, *b*) reveals on the one hand the changes in the PE melting endotherm (T_m^0) by the enthalpy H_m^{PE} and height h_{1PE}, and on the other hand the coupling effect (T_m^1) expressed by their height h_{2PE}, occurring during treatments of the PE component and as a function of PP as transfer medium. For the first

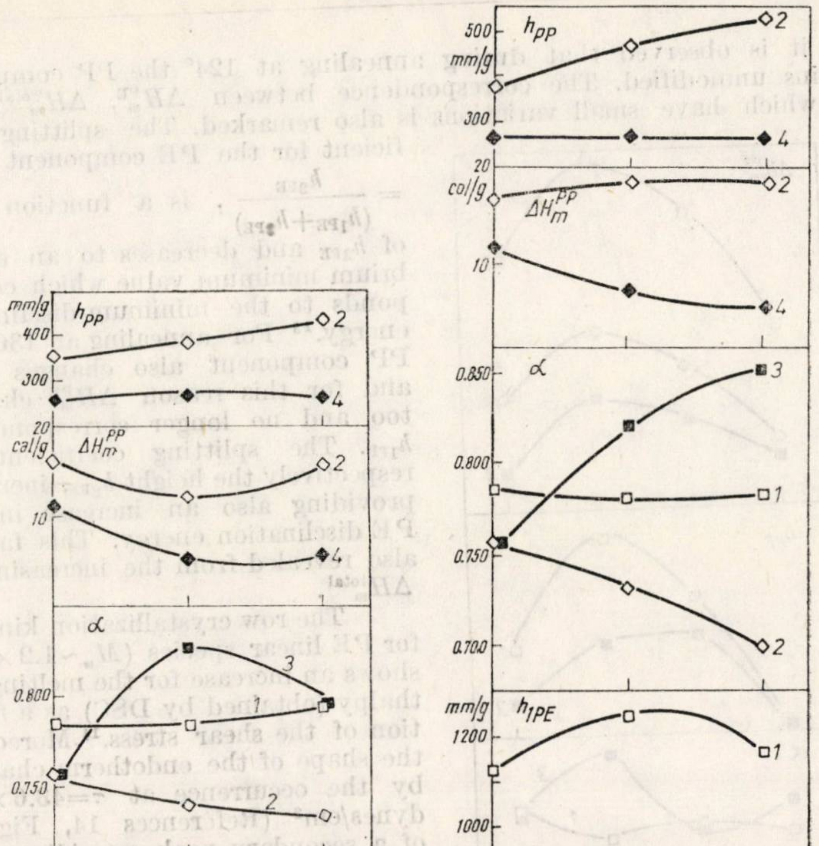

Fig. 4. — *a*. Dependence of the melting enthalpy, of the height of the peaks and of the splitting coefficient α between components on the annealing time with elimination of the h_{2PE} effect, by using the CBL system (*1*, PE, *2*, PP) and IBL system (*3*, PE, *4*, PP) for the injection moulded compound samples. *b*. The splitting coefficient was estimated by the heights ratio (*1*, IBL, *2*, CBL) and by the areas ratio in IBL system (*3*).

case it is observed that during annealing at 124° the PP component remains unmodified. The correspondence between ΔH_m^{PE}, $\Delta H_m^{\mathrm{Total}}$, and $h_{1\mathrm{PE}}$ which have small variations is also remarked. The splitting coefficient for the PE component $\alpha_0 = \dfrac{h_{2\mathrm{PE}}}{(h_{1\mathrm{PE}}+h_{2\mathrm{PE}})}$, is a function only of $h_{2\mathrm{PE}}$ and decreases to an equilibrium minimum value which corresponds to the minimum disclination energy.[13] For annealing at 136° the PP component also changes (h_{PP}), and for this reason ΔH_m^{PE} changes too and no longer corresponds to $h_{1\mathrm{PE}}$. The splitting coefficient α_0, respectively the height $h_{2\mathrm{PE}}$, increases providing also an increase in the PE disclination energy. This fact is also revealed from the increasing of $\Delta H_m^{\mathrm{total}}$.

The row crystallization kinetics for PE linear species ($M_w \sim 1.2\times10^5$) shows an increase for the melting enthalpy (obtained by DSC) as a function of the shear stress.[14] Moreover, the shape of the endotherm changes by the occurrence at $\tau = 43.6\times10^5$ dynes/cm² (References 14, Fig. 1) of a secondary peak providing precisely the interlamellar order.

(*c*) For the last group of results (Figures 4 and 5) the interlamellar order effect in PE is eliminated ($h_{2\mathrm{PE}}=0$). For the two annealing conditions for which the PP component as transfer medium is unperturbed ($T_a=124°$) and respectively changed ($T_a=136°$), the two endotherms which interfere have been estimated in their common baseline system (CBL) and

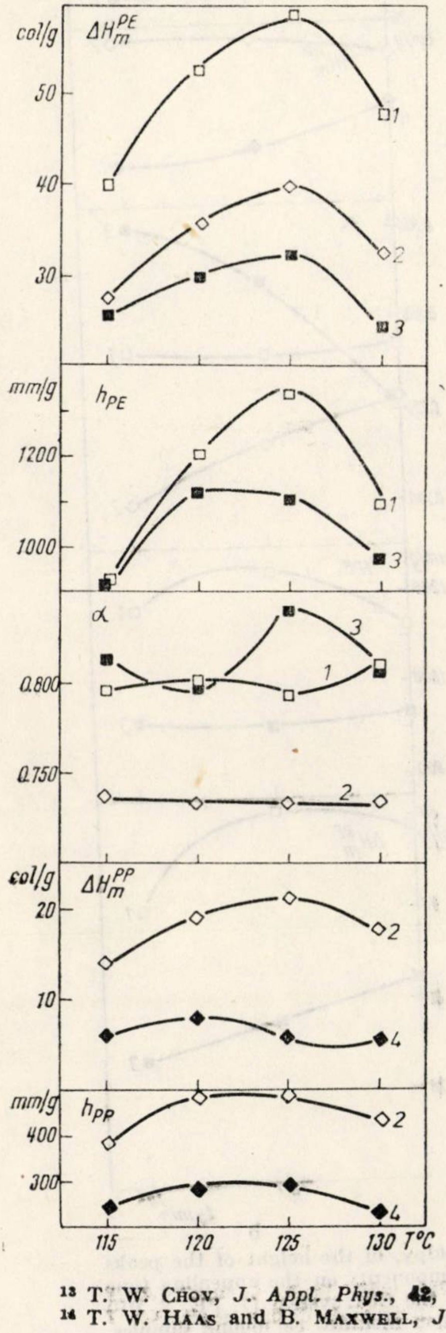

Fig. 5. — Dependence of the melting enthalpies, of the height of the melting peaks and of the splitting coefficient α, for the PE and PP components on annealing temperature for the injection moulded samples, with the elimination of the $h_{2\mathrm{PE}}$ effect. The same observations hold for the splitting coefficient α as in Fig. 4. (CBL system: *1*, PE, *2*, PP; IBL system: *3*, PE, *4*, PP).

---

[13] T. W. CHOW, *J. Appl. Phys.*, **42**, 4931 (1971).

[14] T. W. HAAS and B. MAXWELL, *J. Appl. Polymer Sci.*, **14**, 2407 (1970).

individual baseline system (IBL). A suitable speed of the paper has been chosen in recording the thermogram for better separation of the two effects in the IBL system. The interference point is not on the CBL, a difference is observed in the values of the two estimations. In both estimation systems and for the two treatments conditions sensible changes are observed neither for PE nor for PP component (Figure 4 *a*, *b*). Also the good correspondence between ΔH_m and h_1 is maintained for both components. The same good correspondence is also observed for the behaviour during isochronous annealing (Figure 5), where the splitting coefficient α between the components remains also unperturbed. This coefficient estimated in IBL system by the ratio of the areas shows a change in correspondence between ΔH_m and h_1 which occurs in this estimation system. In the last two groups of results the values of ΔH_m^{PE} are close, but differ from those in the set III of the first group.

Revue Roumaine de Chimie, 23, 3, 445–448 (1978

CONSIDERATIONS UPON RATIONALIZATION OF NUMERICAL INTEGRATION OF MAYO-LEWIS EQUATION

I. AGHERGHINEI
"P. Poni" Institute of Macromolecular Chemistry,
Aleea Gr. Ghica Vodă 41/A, Jassy

Received November 15, 1975

A method is proposed for the rationalization of numerical integration of Mayo-Lewis differential equation for radical copolymerization, starting from the observation that this equation is of homogeneous type : $y' = f(y/x)$.

The kinetics of polymer radical copolymerization leads to the Mayo-Lewis equation :[1]

$$\frac{\mathrm{d}M_1}{\mathrm{d}M_2} = \frac{M_1}{M_2}\,\frac{r_1M_1 + M_2}{r_2M_2 + M_1} \tag{1}$$

where M_1 and M_2 are molar concentrations of the two monomers in reactant mixture, and r_1 and r_2 are the reactively ratios of monomers.

The equation (1) is a homogeneous differential equation. Indeed, noting the ratio M_1/M_2 equal with u, equation (1) can be written :

$$\frac{\mathrm{d}M_1}{\mathrm{d}M_2} = u\,\frac{r_1u + 1}{r_2 + u} = f(u) \tag{2}$$

In the hypothesis $M_2 \neq 0$, the differential equation which corresponds to the new variable u is an equation with separable variables and its solution can be easily determined.[2] For the first time, the solution of this equation was obtained by Mayo and Lewis[1] as follows :

$$\log\frac{M_2}{M_{20}} = \frac{r_2}{1-r_2}\log\frac{M_{20}M_1}{M_{10}M_2} - \frac{1-r_1r_2}{(1-r_1)(1-r_2)}\log\frac{(r_1-1)(M_1/M_2)-r_2+1}{(r_1-1)(M_{10}/M_{20})-r_2+1} \tag{3}$$

where M_{10} and M_{20} are initial values of M_1 and M_2.

---

[1] Cr. I. Simionescu and C. Oprea, "Tratat de chimia compuşilor macromoleculari," vol. 1, Editura didactică şi pedagogică, Bucureşti, 1973, pp. 514 and 516.

[2] D. V. Ionescu, ,,Ecuaţii diferenţiale şi integrale", Editura didactică şi pedagogică, Bucureşti, 1964, pp. 22 and 165.

In most cases expression (3) is not used due to its complicated form and instead of this expression it is preferable to use the numerical integration of equation (1), in accord with one of methods given in the literature.[2] On the other hand, owing to a necessity of practical order, the numerical integration of this equation is effectuated for a certain number of initial conditions. In this situation the rationalization of the numerical integration of equation (1) starts from the following observation: the integral curves of equation (1) can be inferred from one another by a homothetic transformation versus the origin.[2] We recall here that a homothetic transformation of a figure into another one is that transformation in which the corresponding points are placed in a straight line towards a fixed point named the centre of homothety, and the ratio of distances from this point to corresponding points is constant and is named the ratio of homothety (the power of homothety).

Taking into account the above observation we conclude that it enables us to rationalize the integration of equation (1) either with the help of a numerical calculator or in the absence of such an apparatus. Indeed, let us consider that we have already made a first numerical integration of equation (1) for the initial conditions M_{10} and M_{20}, and that we want to make a new integration of this equation for the initial conditions M'_{10} and M'_{20}. In accordance with the above observation, in order to obtain a new integral curve it is enough to effectuate a homothetic transformation of the first curve versus the origin, where the ratio of homothety is established considering the straight line which crosses the origin, and the point of co-ordinates (M'_{10}, M'_{20}). We shall try now to study in detail when such a procedure is possible. It is necessary for this to determine the position of integral curves versus the axis of co-ordinates and the azeotropic straight line, $M_1=((1-r_2)/(1-r_1))M_2$ and the sign of the second derivative.

Calculating the second derivative the following expression is obtained:

$$\frac{d^2M_1}{dM_2^2}=\frac{M_1}{M_2}\frac{r_1M_1+M_2}{(r_2M_2+M_1)^2}\left[\frac{r_2M_2}{r_2M_2+M_1}+\right.$$

$$\left.+\frac{r_1M_1}{r_1M_1+M_2}\right][M_2(1-r_1)-M_1(1-r_1)].$$

One can observe that the sign of the second derivative depends only on the sign of expression:

$$E=M_2(1-r_2)-M_1(1-r_1) \tag{4}$$

Hence, supposing $E>0$, the curve will be convex, and for $E<0$, the curve will be concave.

To determine the position of integral curves versus the axis of co-ordinates and the azeotropic straight line, we resort to the theory of homogeneous equations.[2] In accordance with this theory it is necessary to establish the value of the following integral:

$$I = \int_{u_0}^{u} \frac{dv}{f(v)-v}$$

when $u \to 0$, $(1-r_2)/(1-r_1), \infty$. Effectuating the integral we shall get the following expression:

$$\frac{r_2}{1-r_2} \ln |u| - \frac{1-r_1 r_2}{(1-r_1)(1-r_2)} \ln \left| u - \frac{1-r_2}{1-r_1} \right|$$

The values of the required limits will be as follows:

$$\lim_{u \to 0} I = \begin{cases} -\infty, & \text{if } r_2<1 \\ \infty, & \text{if } r_2>1 \end{cases}$$

$$\lim_{u \to \infty} I = \begin{cases} -\infty, & \text{if } r_1<1 \\ \infty, & \text{if } r_1>1 \end{cases}$$

$$\lim_{u \to \frac{1-r_2}{1-r_1}} I = \begin{cases} -\infty, & \text{if } r_1>1 \text{ and } r_2>1 \\ \infty, & \text{if } r_1<1 \text{ and } r_2<1 \end{cases}$$

The following conclusions can be drawn on the basis of the above results:

(*a*) If $r_1>1$, $r_2>1$, the axes OM_1 and OM_2 are asymptotical directions of the integral curves. When M_1 and M_2 tend toward 0, the ratio M_1/M_2 tends toward $(1-r_2)/(1-r_1)$ (Figure 1*a*).

(*b*) If $r_1<1$, $r_2<1$, the azeotropic straight line is an asymptotical direction of the integral curves. For the above curves, if M_1 and M_2 tend toward 0, the ratio M_1/M_2 will tend toward ∞, while for the lower curves as against this straight line, this ratio will tend toward zero (Figure 1*b*).

(*c*) If $r_1>1$, $r_2<1$, OM_1 axis is an asymptotical direction. When M_1 and M_2 tend toward 0, the ratio M_1/M_2 will tend toward 0 (Figure 1*c*).

(*d*) If $r_1<1$, $r_2>1$, OM_2 axis become an asymptotical direction. When M_1 and M_2 tend toward 0, the ratio M_1/M_2 tends toward ∞ (Figure 1*d*).

Before going on, it is necessary to make the observation that all the curvatures of the integral curves plotted in Figure 1, are in a good agreement with the relation (4).

Returning to the initial problem, we can see that Figure 1 gives the possibility to establish the initial compositions for which the integration with the aid of a homothetic transformation is possible. For example, if $r_1 > 1$, $r_2 < 1$ all the initial compositions (M'_{10}, M'_{20}) which satisfy the inequality :

$$\frac{M'_{10}}{M'_{20}} \leqslant \frac{M_{10}}{M_{20}}$$

can be integrated in this mode.

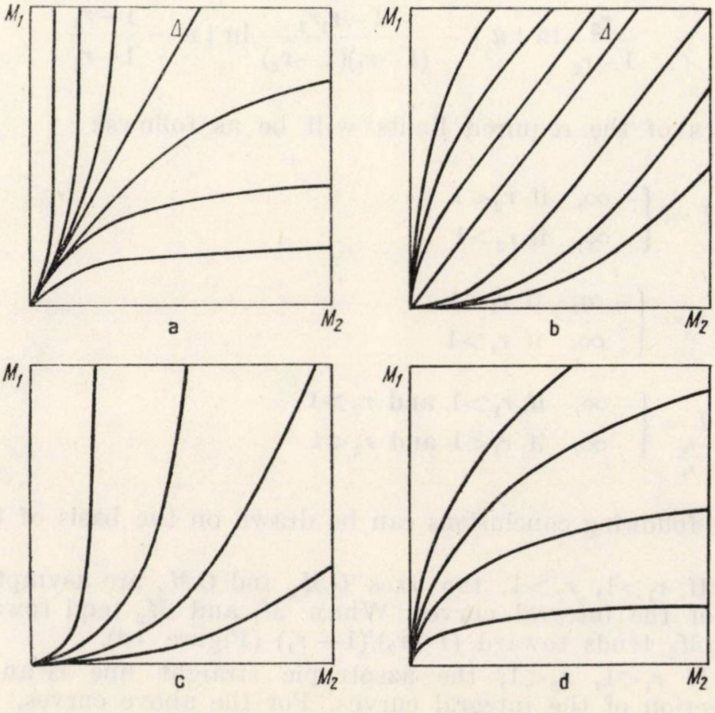

Fig. 1. — Integral curves of equation (1) : (*a*) $r_1 > 1$, $r_2 > 1$, Δ azeotropic straight line ; (*b*) $r_1 < 1$, $r_2 < 1$, Δ azeotropic straight line ; (*c*) $r_1 > 1$, $r_2 < 1$; (*d*) $r_1 < 1$, $r_2 > 1$.

In conclusion, let us make some observations :

1. In order to determine the ratio of homothety with a good precision degree, it is necessary that M_{10}/M_{20} and M'_{10}/M'_{20} ratios should not differ too much from one another.

2. It is possible that the distance between a pair of successive points obtained by homothetic tansformation be longer than that of their corresponding points. This distance evidently depends in a direct relationship on the ratio of homothety. But it is clear that if the first integral puts at our disposal a sufficient number of points, the negative effect of this "rarefaction" will be adequately attenuated.

Revue Roumaine de Chimie, **23**, *3*, 449–452 (1978)

AN AUTOMATIC SYSTEM FOR CYCLIC CHRONOPOTENTIOMETRY

E. CORDOŞ, I. ANGYALOSI and CĂTĂLINA DIMITRESCU
University "Babeş-Bolyai" Cluj-Napoca, Department of Chemistry, Division of Analytical Chemistry, Arany Jànos 11

Received October 14, 1975

The polarity change in cyclic chronopotentiometry implies the use of proper electronic instrumentation. An electronic device, able to reverse the polarity of the electrolytic cell when the voltage difference between the indicating electrode and the reference electrode reaches a predetermined level is presented in the paper. The instrument is based on a dual differential comparator, available as integrated circuit.

The cyclic chronopotentiometry was introduced by Herman and Bard[1] and consists in reversing the current polarity each time when it reaches a predetermined level.

The same authors[2] and later Vuković and Pravdić[3] developed the theory of electrochemical processes which occur in this method. Since the manual accomplishing of operations connected with cyclic chronopotentiometry is a difficult task, a series of instruments based on tubes[4] or transistors[5], were built. In the present paper it is for the first time that an integrated circuit CLB 2711-C, dual differential comparator is used. It allows a great simplification of instrumentation and a fast operation of mechanical or electronic switching system.

BLOCK DIAGRAM

The working principle of the automatic system for cyclic chronopotentiometry is illustrated in Figure 1.

The electrolytic cell is power supplied through a polarity control so that a working electrode could become anode or cathode as a result of an external command. The voltage difference between the indicating and reference electrodes is fed to a differential comparator whose output voltage can suddenly change between two logic levels "0" and "1".

---

[1] H. B. Herman and A. J. Bard, *Analyt. Chem.*, **35**, 1121 (1963).
[2] H. B. Herman and A. J. Bard, *J. Electrochem. Soc.*, **115**, 1028 (1968).
[3] M. Vuković and V. Pravdić, *Croat. Chem. Acta*, **42**, 21 (1970).
[4] H. B. Herman and A. J. Bard, *Analyt. Chem.*, **37**, 590 (1965).
[5] T. Rabuzin, G. Smiljanić and F. Iović, *J. Electroanalyt. Chem.*, **27**, 397 (1970).

This change will activate a start-stop circuit which in its turn stops an electronic timer, changes the cell current polarity and locks one of the dual comparator amplifiers. The chronopotentiometric curve could be recorded and the transition time τ could be measured either on recording or readings from the display of the electronic timer.

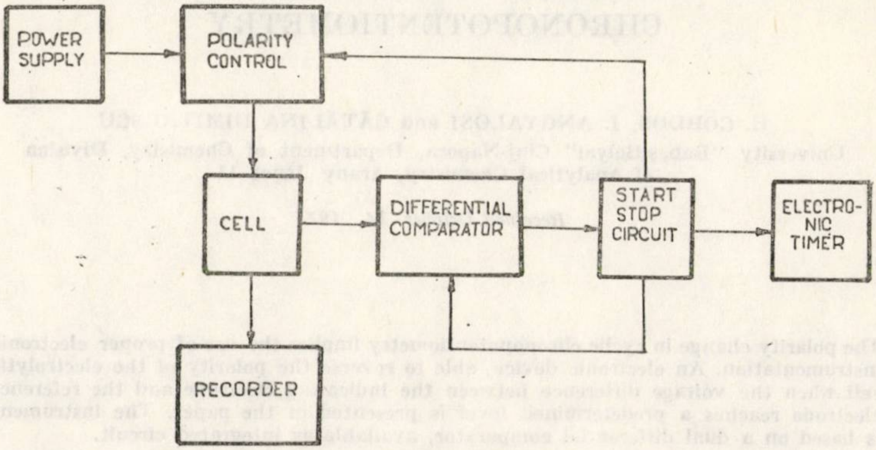

Fig. 1. — Blockdiagram of the automatic system for cyclic chronopotentiometry.

ELECTRONIC CIRCUIT

A shematic of the electronic circuit is given in Figure 2.

The main part is the dual differential comparator, CLB 2711-C (IPRS Băneasa) which contains two differential amplifiers in a single case, DA 1 and DA 2. The input resistance of the amplifiers is 200 ohms and the output positive level ("1") is 4.5 V. The two amplifiers have a common output. By means of two strobe inputs (2 and 5) one or both amplifiers could be locked, so that at the common output the state of the desired amplifier is found. The response time of the amplifiers is about 12 ns which means that practically no error is introduced in determining the transition time. The CLB 2711-C requires two supply voltages: + 12 and − 6 V. The differential input voltage could range at ± 5 V and strobe voltage between 0 and + 5 V. The strobe and output voltage correspond to most frequently logic levels encountered in integrated digital circuits.

The electrolytic cell has tree electrodes, two working electrodes and a reference. One of the working electrodes is the indicating electrode and it is connected with the inverting (−) inputs of the two amplifiers (DA 1 and DA 2). At noninverting (+) inputs a reference voltage is supplied by means of P1 and P2 potentiometer and a 3 V from a stabilized source. The two reference voltages represent the higher and lower limits between which the indicating electrode potential may vary during the chronopotentiometric measurements. When the indicating electrode potential equals the reference voltage, the corresponding amplifier changes its output state from "1" to "0".

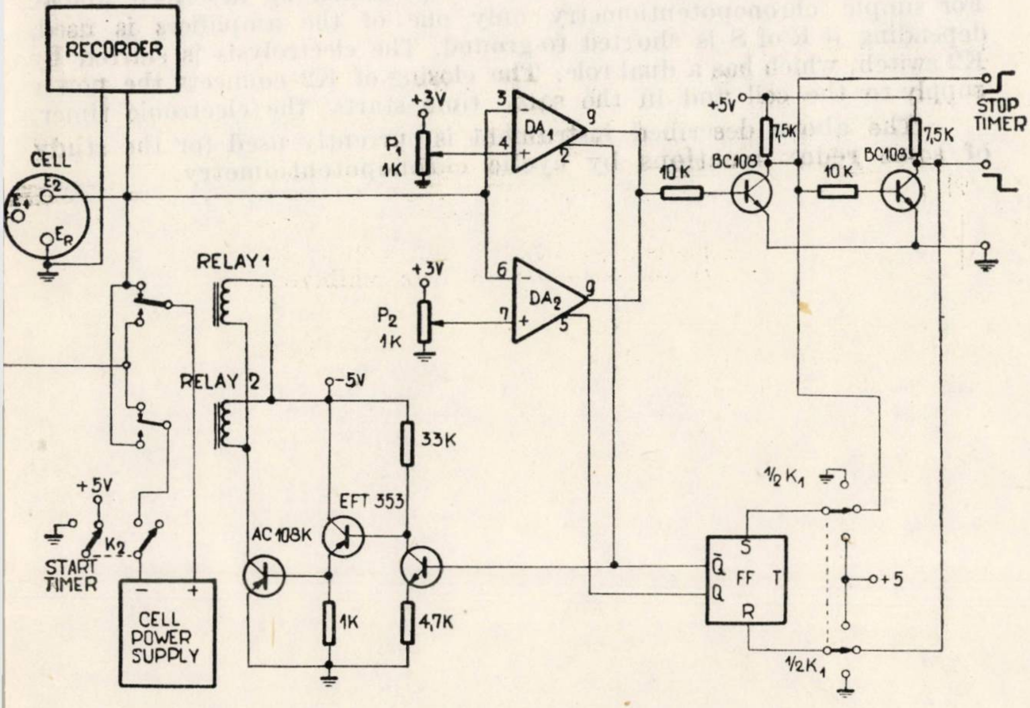
RECORDER
CELL
E2
E1
ER
+3V
P1
1K
3
4
DA1
9
2
+5V
7,5K
7,5K
BC108
BC108
10K
10 K
STOP
TIMER
RELAY 1
+3V
6
7
DA2
9
5
P2
1K
RELAY 2
-5V
33K
EFT 353
AC 108K
1K
4,7K
+5V
K2
START
TIMER
CELL
POWER
SUPPLY
½ K1
S
Q̄
Q
FF
T
R
+5
½ K1

Fig. 2. — Diagram of cyclic chronopotentiometry circuit.

This makes the bistable switch made of transistors T1 and T2 change its state and stop the electronic timer. This type of bistable switch was wired in order to have two complimentary outputs and use that one which is compatible with the available electronic timer. In the present work a "Numeport", IFA Bucharest has been used, with the time base rewired so that the last digit on display should represent hundredths of second.

The two complementary outputs of T1 and T2 drive a flip-flop, FF. The complimentary outputs of this circuit (Q and $\overline{Q}$) controls the strobe so that when an amplifier changes its state it is automatically locked, through the strobe and the other amplifier is unlocked. The unlocking of second amplifier coincides with the cell current polarity reversal, accomplished by relays R1 and R2. These relays are driven by the circuit composed of transistors T3, T4 and T5, driven also by FF. The polarity reversal makes the indicating electrode potential change its sign and turn toward the reference voltage applied to the second amplifier. When this voltage is reached the second amplifier goes to "0" the polarity is reversed again and the first amplifier is unlocked. The reversing operation may take place as many times as required. The K 1 switch selects two working modes of the instrument. If the R and S inputs of FF are directly connected to the T1 and T2 collectors, the two amplifiers are alternatively locked as described above. For simple chronopotentiometry only one of the amplifiers is used, depending if R of S is shorted to ground. The electrolysis is started by K2 switch, which has a dual role. The closing of K2 connects the power supply to the cell and in the same time starts the electronic timer.

The above described instrument is currently used for the study of some redox reactions by cyclic chronopotentiometry.

Revue Roumaine de Chimie, **23**, *3*, 453–465 (1978)

A NEW TYPE OF PARAMETRIZATION AMONG THE APPROXIMATE SCF-LCAO-MO METHODS

S. MOLDOVEANU
I. P. B., National Institute of Chemistry, Faculty of Chemical Technology Bucharest

Received September 3, 1976

A new type of approximate method (named NTP), for SCF-LCAO-MO computation is proposed. The method requires about the same volume of computation as CNDO/2, using unmodified values for fitting constants (valence state ionisation potentials and Slater exponents). The agreement with the experiment regarding the obtained orbital energies and dipole moments for studied organic and inorganic molecules is very good.

The main purpose of this paper is to give a new type of approximate SCF-LCAO-MO method in which the integrals usually computed in NDO[1,2] methods would be more efficiently used, so as to obtain a better agreement with the experiment using a smaller number of adjustable parametres.

In order to reach these purposes, the basic assumption in CNDO, (M)INDO or PNDO methods, namely the orthogonality of the basic set of atomic orbitals is repelled. Thus, the algebraic eigenvalue problem which must be solved in order to obtain orbital energies and molecular orbitals for a molecule, is Roothaan's equation : [3]

$$\mathbf{FC}=\mathbf{SCE} \qquad (1)$$

in which **S** is not the identity matrix. The elements of **S** matrix, using the set $\{\chi_\mu\}$ of atomic orbitals are thus found by integration.

These values are also computed in NDO type methods but only for the purpose of obtaining two-center one electron "resonance" terms $h_{\mu\nu}$.

To compute elements of matrix **F**, according to the new method which will be further referred to as NTP method, some approximations are used as will be seen in the following. In spite of the non orthogonality of the basic set, the volume of computation is about the same as in the CNDO/2 method.

---

[1] J. A. Pople, D. L. Beveridge, and N. S. Ostlund, *Int. J. Quant. Chem.*, **1** S, 293 (1967).

[2] K. R. Roby, *Chem. Physics Letters*, **11**, 6 (1971).

[3] C. C. J. Roothaan, *Rev. Mod. Phys.*, **23**, 69 (1951).

DESCRIPTION OF THE METHOD

In the use of this method for solving Roothaan's equation the first step is the computation of the overlap matrix S. This can be made by standard procedures using Slater orbitals[4] or atomic orbitals as given by Clementi and Roetti [5] and taking into account the angular overlaping.[6]

To evaluate elements $F_{\mu\upsilon}$ of Fock's matrix we shall study first the case $\mu=\nu$. For $F_{\mu\mu}$ elements we may write (using generally accepted notations):

$$F_{\mu\mu} = U^{A}_{\mu\mu} - \sum_{B\neq A} Z_{B}(\mu B \mu) + \left(\sum_{\xi\notin A} + \sum_{\xi\in A}\right) P_{\xi\xi}\left[(\mu\mu \mid \xi\xi) - \frac{1}{2}(\mu\xi \mid \mu\xi)\right] + $$

$$+ \sum_{\xi}\sum_{\neq\zeta} P_{\xi\zeta}\left[(\mu\mu)\,\xi\zeta) - \frac{1}{2}(\mu\xi \mid \mu\zeta)\right] \tag{2}$$

where $\xi \in A$ designates that χ_{ξ} orbital belongs to the A core and where $(\mu B\mu) = \int \chi_{\mu} \frac{1}{r_{B\mu}} \chi_{\mu} dV$.

The following two approximations which do not involve zero overlap justifications will be now introduced:

(*a*) $$U^{A}_{\mu\mu} = -I^{A}_{\mu} - (P_{AA}-1)(\mu\mu \mid \mu\mu) \tag{3}$$

which is a modified formula of $U^{A}_{\mu\mu}$ in comparison with that given by Pople et al.[7] This modification was made in order to account more satisfactorily for the tendency of an atomic orbital to loose electrons.

(*b*) $$\sum_{\xi\notin A} P_{\xi\xi}\left[(\mu\mu \mid \xi\xi) - \frac{1}{2}(\mu\xi \mid \mu\xi)\right] = \sum_{B\neq A}\left(\sum_{\xi\in B} P_{\xi\xi}\right)(\mu B\mu) \tag{4}$$

For the above relation we assume that charge density created by an electron occupying the χ_{ξ} orbital belonging to the B atom is the unity and this is centred in the position of B atom.

Thus we have:

$$\begin{aligned} F_{\mu\mu} = -I^{A}_{\mu} - \sum_{B\neq A} Q_{B}(\mu B\mu) - (P_{AA}-1)(\mu\mu \mid \mu\mu) + \\ + \sum_{\xi\in A} P_{\xi\xi}\left[(\mu\mu \mid \xi\xi) - \frac{1}{2}(\mu\xi \mid \mu\xi)\right] + \\ + \sum_{\xi}\sum_{\zeta} P_{\xi\zeta}\left[(\mu\mu \mid \xi\zeta) - \frac{1}{2}(\mu\xi \mid \mu\zeta)\right] \end{aligned} \tag{5}$$

---

[4] J. A. Pople and D. L. Beveridge, "Approximate Molecular Orbital Theory", McGraw-Hill Book Co., New York, 1970, p. 204.

[5] E. Clementi and C. Roetti, "Atomic Data and Nuclear Data Tables", vol. 14, Nr. 3–4, Academic Press, New York, 1974.

[6] C. E. Schäffer, *Structure and Bonding*, **5**, 68 (1968).

[7] J. A. Pople and G. A. Segall, *J. Chem. Phys.*, **44**, 3289 (1966).

In this expression for $F_{\mu\mu}$, only the first three terms can be easy evaluated namely:

— the ionization potentials for which we have:

$$I_{\mu}^{A}=A(\mu)Q_{A}^{2}+B(\mu)Q_{A}+C(\mu) \tag{6}$$

where $A(\mu)$, $B(\mu)$ and $C(\mu)$ are constants computed from data given in the literature[8,5]. ($A(\mu)$ not necessarily different of zero).

— $(\mu B\mu)$ integrals which can be effectively calculated using Roothaan's formulae,[3] and taking into account the rotation of the coordinate system of each atom as in the case of the overlap,[9] such that the invariance of the method to rotations of each atom is achieved.

— $(\mu\mu \mid \mu\mu)$ integrals which can be also effectively calculated.[2]

The rest of the terms are very difficult to compute. In order to avoid this difficulty, a solution consists in the empirical evaluation of all uncomputed terms such that the results be in agreement with experimental data.

In order to obtain finally this evaluation by means of a single undimensional value for each orbital, we shall write:

$$F_{\mu\mu}=-I_{\mu}^{A}-\sum_{B\neq A}Q_{B}(\mu B\mu)+P\mu\mu(\mu\mu\,|\mu\mu)K_{\mu}^{A} \tag{7}$$

where:

$$K_{\mu}^{A}=-\frac{P_{AA}-1}{P_{\mu\mu}}+\frac{\sum\limits_{\xi\in A}P_{\xi\xi}\left[(\mu\mu\mid\xi\xi)-\frac{1}{2}(\mu\xi\mid\mu\xi)\right]}{P_{\mu\mu}(\mu\mu\mid\mu\mu)}+$$
$$+\frac{\sum\sum\limits_{\xi\neq\zeta}P_{\xi\zeta}\left[(\mu\mu\mid\xi\,\zeta)-\frac{1}{2}(\mu\xi\mid\mu\,\zeta)\right]}{P_{\mu\mu}(\mu\mu\mid\mu\mu)} \tag{8}$$

The value of K_{μ}^{A} depends obviously on a great number of data. However supposing that all orbitals which belong to an atom are orthogonal and of different symmetry,[10] we obtain:

$$K_{A}^{\mu}=\frac{1}{P_{\mu\mu}}+\frac{\sum\sum\limits_{\xi\neq\zeta}P_{\xi\zeta}\left[(\mu\mu\mid\xi\,\zeta)-\frac{1}{2}(\mu\xi|\mu\,\zeta)\right]}{P_{\mu\mu}((\mu\mu\mid\mu\mu)}, \tag{8'}$$

---

[8] O. Sinanoglu, K. Wiberg, "Sigma Molecular Orbital Theory", Yale Univ. Press, New Haven, 1970.

[9] C. I. Lepădatu, private communication.

[10] S. Moldoveanu, "Aplicaţiile teoriei grupurilor în chimie" Editura Ştiinţifică şi Enciclopedică, Bucureşti, 1975.

Supposing that from the integrals which appear in the rel. (8′) only those are not very small, in which the orbitals of bonded atoms of A are involved, we conclude that K^{A}_{μ} can depend only on the χ_μ orbital, A atom and the orbitals of the bonded atoms of A. Thus we expect the K^{A}_{μ} parameter as transferable at least for the same class of molecules in which the neighbours of an atom are the same. Moreover the substitution of a bonded atom from the same row of the periodic table cannot determine too great a variation of K^{A}_{μ}.

As the case $\mu \neq \nu$ is concerned for $F_{\mu\nu}$ elements we may consider :

$$F_{\mu\nu}=S_{\mu\nu}(2-|S_{\mu\nu}|)\,\frac{-I^{A}_{\mu}-I^{B}_{\nu}}{2}-\frac{1}{2}\,P_{\mu\nu}\,\frac{(\mu B\mu)+(\nu A\nu)}{2}$$

$$(\mu B\mu)=0,\ (\nu A\nu)=0 \text{ if } \mu\in B,\ \nu\in A \tag{9}$$

which is in fact a modification of Cusach's approximation[11]. The modification consists in the introduction of a supplementary term in order to better account for the electronic interactions.

Using rel. (7) and (9) for the elements of Fock's matrix, the number of computed integrals is small even in comparison with the most simple methods which use zero overlap approximation because in these methods, overlap integrals are also computed but only in order to obtain one - electron two - center integrals. Thus, the computing problem (1) can be solved using the well-known iterative procedure. From the mathematical point of view this one is well posed in NTP approximation and is invariant when a unitary transformation between the various orbitals of an individual atom is made.

CHOICE OF PARAMETERS IN THE METHOD

Two kinds of data have been used in the applications of the NTP, namely the data regarding atomic and molecular structure and parameters K^{A}_{μ}.

All data regarding atomic and molecular structure are those given in the literature,[4, 5, 8] this being a major advantage of the method proposed in the present paper.

As far as the K^{A}_{μ} parameter is concerned, this was considered as an adjustable parameter which has to make possible not only the estimation of uncomputed integrals in $F_{\mu\nu}$ elements but also a correction of different other errors introduced by used approximations both in the method and in the choice of the form and the number of atomic functions. Thus, K^{A}_{μ} was adjusted for a number of simple molecules including elements in the first three rows of the periodic system, until the agreement of computed orbital energies with experimental ionization potentials[12] was achieved. The obtained values for different molecules are the same even if the bonded atoms with the A atom are changed. Only a few less close values are observed such as the values for K^{H}_{1s} in H_2, K^{N} in N_2, K^{F} in HF and K^{Cl} in HCl in comparison with the same values K^{A} in other compounds. The less close values can be however considered as special cases because of the particularity of molecules in which they were observed.

---

[11] C. L. Cusach, *J. Chem. Phys.*, **43**, 1575 (1965).

[12] T. A. Koopmans, *Physica*, **1**, 104 (1933).

Thus there are two possibilities of application of NTP. The first is to give a standard parametrization for K^{A}_{μ} such that these values be used in all compounds even if the agreement with experiment will be in some cases less good. The second is to make for each molecule a systematic study for K^{A}_{μ} parameters on little and well known molecules in which the same molecular fragments appear as in the given molecule.

Very good results were obtained as will be seen in the followings, even using the first alternative stated above. The proposed standard values for K^{A}_{μ} of different valence orbitals[13] are given in table 1 (3 d orbitals were neglected in all computations).

Table 1

The values of K^{A}_{μ} parameter for valence type Slater orbitals of H, C, N, O, F and single zeta valence orbitals of Si, P, S and Cl

Element and orbital	K^{A}_{μ} value	Element and orbital	K^{A}_{μ} value
H 1s	0.380	F 2p	0.095
C 2s	0.367	Si 3s	0.367
C 2p	0.450	Si 3p	0.300
N 2s	0.350	P 3s	0.350
N 2p	0.150	P 3p	0.075
O 2s	0.340	S 3s	0.330
O 2p	0.110	S 3p	0.045
F 2s	0.320	Cl 3s	0.310
		Cl 3p	0.030

RESULTS CONCERNING THE USABILITY OF THE METHOD

On the basis of the above described method a FORTRAN program was written such that it could be run even on a low performance computer (An IBM 360/30 and a FELIX C-256 were used).

Thus the maximum memory required by the program (splitted in phases) is 50 K for a molecule with 50 orbitals.

The convergence of the results is extremely good such that usually after 4—5 iterations a difference not exceeding 0.005 eV in orbital energies remains.

---

[13] M. Kleiner and R. McWeeny, *Chem. Phys. Letters*, **19**, 476 (1973).

Table 2

Computed orbital energies for some molecules

Molecule and symmetry	MO type	Computed energy (eV)*	Ionisation potential (eV)*	Orbital energies computed by ab initio methods (eV)*
H_2	σ_g	−16.21	15.45	
group $\mathbf{D}\infty h$				
CH_4		−13.00		
	t_1	−13.00	12.99	
group $\mathbf{T}_d$		−13.00		
	$2a_1$	−21.89	∼24	
C_2H_6	e_g	−11.36	11.49	
		−11.36		
staggered	a_{1g}	−11.91	11.49	
(group $\mathbf{D}_{3d}$)	e_u	−14.11		
		−14.18	14.47	
	a_{2u}	−18.81	∼20	
	a_{1g}	−23.95		
C_2H_6	e''	−11.22		
eclipsed		−11.32	—	
(group $\mathbf{D}_{3h}$)	a_1'	−11.78	—	
	e'	−14.13	—	
		−14.23		
	a_2''	−18.79	—	
	a_1'	−23.92	—	
C_3H_8	b_1	−11.01	11.07	
(group $\mathbf{C}_{2v}$)	b_2	−11.01	11.07	
	a_1	−11.01	11.07	
	a_2	−13.02	13.17	
	b_2	−13.01	13.17	
	a_1	−15.10	15.17	
	b_1	−13.13	15.17	
	a_1	−18.21	∼20	
	b_2	−19.31	—	
	a_1	−24.21	—	
C_2H_4	b_{3u}	−10.57	10.48	
(group $\mathbf{D}_{2h}$)	b_{3g}	−11.96	12.50	
	a_g	−14.02	14.93	
	b_{2u}	−14.73	15.63	
	b_{1u}	−18.18	19	
	a_g	−24.20	—	

*1 eV = 0.160219 aJ

Table 2 (continued)

Molecule and symmetry	MO type	Computed energy (eV)*	Ionisation potential (eV)*	Orbitral energies computed by ab initio-methods (eV)*
C_2H_2 (group $\mathbf{D}_{\infty h}$)	π_u	−11.35	11.10	
		−11.35		
	σ_g	−15.91	16.44	
	σ_u	−18.24	18.42	
	σ_g	−26.31	—	
C_5H_6 (group $\mathbf{C}_{2v}$)	a_2	−8.60	8.9	
	b_1	−10.57	—	
	a_1	−10.76	—	
	b_2	−11.32	—	
	b_2	−11.36	—	
	b_1	−11.92	—	
	a_1	−14.61	—	
	a_1	−15.61	—	
	b_2	−16.18	—	
	a_1	−16.73	—	
	b_2	−21.90	—	
	a_1	−22.07	—	
	a_1	−27.30	—	
C_6H_6 (group $\mathbf{D}_{6h}$)	e_{1g}	−9.69	9.25	
		−9.75		
	e_{2g}	−9.92	11.49	
		−10.23		
	b_{2u}	−12.19	12.19	
	a_{2u}	−12.44	—	
	e_{1u}	−12.93	13.67	
		−13.16		
	a_{1g}	−13.84	14.44	
	b_{1u}	−15.81	16.73	
	e_{2g}	−17.61	18.75	
		−17.74		
	e_{1u}	−23.12		
		−223.29	—	
	a_{1g}	−27.62	—	
NH_3 (group $\mathbf{C}_{3v}$)	a_1	−10.33	10.35	−10.03[a]
	e	−15.03	14.95	−15.85
		−15.13		−15.85
	a_1	−23.41	—	−29.92

[a] V. KALDOR and I. SHAVITT, *J. Chem. Phys.*, **45**, 888 (1966).

Table 2 (*continued*)

Molecule and symmetry	MO type	Computed energy (eV)*	Ionisation potential (eV)*	Orbital energies computed by ab initio methods (eV)*
N_2H_4	a_g	− 9.62	9.72	
(group $\mathbf{D_{2h}}$)	b_{3u}	−10.21	—	
	b_{3g}	−12.41	—	
	a_g	−15.46	—	
	b_{2u}	−15.88	—	
	b_{1u}	−19.61	—	
	a_g	−24.21	—	
HCN	π	−14.02	13.91	
(group $\mathbf{C_{\infty v}}$)		−14.02		
	σ	−14.20	—	
	σ	−20.21	—	
	σ	−28.34	—	
C_4NH_5	a_2	−9.234	8.97	−10.55[b]
(group $\mathbf{C_{2v}}$)	b_1	−10.39	—	−11.57
	a_1	−13.24	—	−15.68
	b_2	−14.01	—	−16.32
	b_2	−14.68	—	−16.98
	b_1	−15.21	—	−17.17
	a_1	−15.73	—	−17.62
	a_1	−19.01	—	−21.17
	b_2	−19.81	—	−21.68
	a_1	−20.01	—	−22.44
	b_2	−25.31	—	−28.14
	a_1	−25.89	—	−29.80
	a_1	−31.27	—	−36.01
C_5NH_5	a_2	− 9.40	9.56	−11.05[c]
(group $\mathbf{C_{2v}}$)	b_1	−10.86	—	−11.59
	a_1	−11.50	—	−12.04
	b_2	−12.00	—	−15.13
	b_1	−12.96	—	−15.82
	a_1	−13.17	—	−16.85
	b_2	−13.80	—	−17.63
	a_1	−14.26	—	−18.80
	b_2	−15.19	—	−18.89
	a_1	−16.64	—	−20.68
	b_2	−18.38	—	−24.06
	a_1	−18.45	—	−24.24

[b] E. CLEMENTI, H. CLEMENTI and D. R. DAVIS, *J. Chem. Phys.*, **46**, 4725 (1967).

[c] J. D. PETKE, J. L. WHITTEN and J. A. RYAN, *J. Chem. Phys.*, **48**, 953 (1966).

Table 2 (continued)

Molecule and symmetry	MO type	Computed energy (eV)*	Ionisation potential (eV)*	Orbital energies computed by ab initio methods (eV)*
	b_2	−23.71	—	−29.24
	a_1	−24.41	—	−30.69
	a_1	−29.04	—	−35.23
H_2O	b_1	−12.79	12.61	
(group C_{2v})	a_1	−14.25	14.23	
	b_2	−17.73	18.02	
	a_1	−26.80	—	
CO_2	π_g	−14.69	13.79	
(group $D_{\infty h}$)		−14.69		
	π_u	−17.28	17.59	
		−17.28		
	σ_u	−16.89	18.07	
	σ_g	−19.44	19.36	
	σ_u	−26.88	—	
	σ_g	−31.25	—	
CH_3OH	a	−10.13	10.88	
(group C_1)	a	−11.27	—	
	a	−14.94	—	
	a	−16.49	—	
	a	−16.61	—	
	a	−21.12	—	
	a	−27.30	—	
C_4OH_4	a_2	−8.89	9.03	
(group C_{2v})	b_1	−10.12	—	
	a_1	−10.76	—	
	b_2	−11.45	—	
	b_2	−12.31	—	
	b_1	−14.90	—	
	a_1	−15.12	—	
	a_1	−15.45	—	
	b_2	−17.57	—	
	a_1	−17.90	—	
	b_2	−22.94	—	
	a_1	−23.55	—	
	a_1	−30.42	—	

Table 2 (continued)

Molecule and symmetry	MO type	Computed energy (ev)*	Ionisation potential (eV)*	Orbital energies computed by ab initio methods (eV)*
F_2	π_g	-15.62	15.63	
(group $\mathbf{D}_{\infty h}$)		-15.63		
	σ_g	-17.73	17.35	
	π_u	-18.91	18.46	
		-18.92		
	σ_u	-23.19	—	
	σ_u	-26.37	—	
HF	π	-16.90	16.06	
(group $\mathbf{C}_{\infty v}$)		-16.90		
	σ	-17.32	16.48	
	σ	-33.00	—	
CH_3F	e	-12.65	12.85	
(group $\mathbf{C}_{3v}$)		-12.67		
	a_1	-13.91	14.10	
	e	-16.81	16.89	
		-16.81		
	a_1	-19.21	—	
	a_1	-25.34	—	
CH_2F_2	a_1	-12.81	12.72	
(group $\mathbf{C}_{2v}$)	b_2	-13.08	—	
	b_1	-13.11	—	
	a_1	-13.16	—	
	a_1	-15.37	—	
	b_1	-16.01	—	
	a_1	-16.02	—	
	b_2	-18.18	—	
	a_1	-27.63	—	
	a_2	-31.19	—	
SiH_4	t_1	-11.92		
(group $\mathbf{T}_d$)		-11.92	11.90	
		-11.92		
	a_1	-16.39	—	
CH_3SiH_3	e	-10.28	10.50	
(group $\mathbf{C}_{3v}$)		-10.28	—	
	a_1	-11.00	—	
	e	-12.96		
		-12.97	—	
	a_1	-17.24	—	
	a_1	-21.41	—	

Table 2 (continued)

Molecule and symmetry	MO type	Computed energy (ev)*	Ionisation potential (eV)*	Orbital energies computed by ab initio methods (eV)*
PH_3	a_1	−9.89	9.90	
(group C_{3v})	e	−13.68	–	
		−13.69	–	
	a_1	−19.41		
H_2S	b_1	−10.40	10.48	−10.47[d]
(group C_{2v})	a_1	−14.16	–	−14.73
	b_2	−17.26	–	−18.37
	a_2	−31.45	–	−38.31
CH_3SH	a	−9.45	9.44	−9.44[d]
(group C_1)	a	−11.31	–	
	a	−13.27	–	−13.73
	a	−14.31	–	
	a	−14.41	–	
	a	−17.21	–	−18.94
	a	−32.41	–	−35.48
HCl		−11.73	12.80	
(group $C_{\infty v}$)		−11.73		
		−12.13	–	
		−22.21	–	
CH_3Cl	e	−11.28	11.26	
(group C_{3v})		−11.28		
	a_1	−12.85	–	
	e	−14.16	–	
		−14.18		
	a_1	−18.29	–	
	a_1	−21.43	–	
CH_2Cl	a_1	−11.30	11.33	
(group C_{2v})	b_1	−12.75		
	a_1	−12.78	–	
	b_2	−12.79	–	
	a_1	−15.21	–	
	b_1	−15.98	–	
	a_1	−16.00	–	
	b_2	−18.01	–	
	a_1	−26.31	–	
	a_2	−31.11	–	

[d] S. D. THOMSON, D. G. CARROLL, F. WATSON, M. O. DONNELL, and S. P. MCGLYNN, *J. Chem. Phys.*, **45**, 1367 (1966).

This fast convergence of the procedure and the reduced memory required by a FORTRAN program for NTP, make it suitable for computations on molecules with a relatively great number of atoms. However, in order to verify the method, only results for well-known molecules with relatively small number of atoms will be presented. Orbital energies computed using the method, in comparison with experimental ionization potentials or "ab initio" results are given in table 2.

As one may see from table 2 the agreement with the experiment regarding orbital energies [12] is very good. The symmetry of the computed wave functions is also in agreement with expectations.

Besides the orbital energies, very good results were obtained in the computations by NTP of the charge distributions and of other properties that can be obtained from charge distributions such as dipole moments.

Table 3

Charge densities Q_A and dipole moments for some of the studied molecules

Molecule	Atom	Charge density Q_A	Computed dipole moment (D)*	Experimental dipole moment (D)*
CH_4	C	−0.20	—	—
	H	0.05		
C_2H_6	C	−0.12	—	—
	H	0.04		
NH_3	N	−0.78	1.421	1.468
	H	0.26		
HCN	N	−0.44		
	C	0.36	2.801	2.985
	N	0.08		
H_2O	O	−0.62	1.752	1.870
	H	0.31		
HF	F	−0.40	1.763	1.8195
	H	0.40		
CO_2	O	−0.325	—	
	C	0.65		

** 1 D $3.335640.10^{-30}$ C-m

Another area where the NTP proved satisfactory is the calculation of bond angles. Thus using for the total energy of a molecule the formula :

$$E = \sum_{i=1}^{n} \varepsilon_i + \frac{1}{2} \sum_{\mu} \sum_{\nu} P_{\mu\nu} h_{\mu\nu} - \sum_{A} \sum_{\substack{B \\ A>B}} \frac{Z_A Z_B}{r_{AB}} \qquad (10)$$

a minimum was obtained for values very close to experimental bond angles for studied molecules (in CH_4 109.5° comp., 109.5° exp.; in NH_3 106.4° comp. 106.6° exp.; in H_2O 105.1° comp., 104.45° exp.; in CO_2 180° comp., 180° exp.; în PH_3 95.1° comp., 93.8° exp.; in H_2S 94.2° comp., 93.3° exp.).

As concerns the heats of formation, the use of NTP with the above presented parametrization (table 1) does not lead to good results, but taking the internuclear potential energy as net electrostatic repulsion (see rel. (10)), the result is not surprising. An extensive study of this problem will be made in another paper.

CONCLUSIONS

A new approximate method for SCF-LCAO-MO computations, which made a correct orthogonalization of the atomic basis set is proposed. The method requires a small number of computed integrals and have a very fast convergence of the results.

The approximations include the use of a transferable parameter, which allow to use atomic data of only generally known values[4, 5] and no other experimental or empirical constants.

The calculations can be performed even on low performance computers.

The agreement with experiment of the computed orbital energies (ionization potentials), charge densities (dipole moments) and bonds angles for different molecules including elements in the first three rows of the periodic system is very good in comparison with many other semiempirical methods[14, 15]

ACKNOWLEDGEMENTS. The author expresses his grateful thanks to Dr. C. I. Lepădatu and A. Savin for fruitful discussions. A part of the computations were made at the Computing Centre of the University of Bucharest.* Thanks are also due to M. Pepelea for technical assistance.

---

[14] J. M. MURREL and A. J. HARGET, "Semiempirical SCF-MO-theory of Molecules" Wiley, Interscience, London, 1972.

[15] T. A. HALGREN and W. N. LIPSCOMB, *J. Chem. Phys.*, **58**, 1569 (1973).

* Detailed computer program may be obtained by writing to the author.

Revue Roumaine de Chimie, **23**, *3*, 467 – 468 (1978)

COMPTES RENDUS

"HOCHDRUCK-FLÜSSIGKEITS-CHROMATOGRAPHIE" (HIGH PRESSURE LIQUID CHROMATOGRAPHY). Second edition, Springer-Verlag, Berlin, Heidelberg, New York 1977, 257p., 62 figures, 18 tables.

The second edition of Prof. Engelhard's book (*Angewande Physikalische Chemie*, Universität des Saarlandes) presents in a clear and systematic form, in 12 chapters, the theoretical and major practical fundamentals the experimentalist must know when dealing with high pressure liquid chromatography.

The first five chapters deal with general theoretical principles of liquid chromatography, with description of equipment, stationary and mobile phases employed in high pressure experiments.

The following seven chapters are devoted to detailing the notions mentioned in earlier chapters in order to provide the reader with practical solutions.

Each chapter includes a rich, updated bibliography.

In chapter I, the author presents a general classification of chromatographic methods, then, in chapter II,he expounds the main, theoretical notions which underlie chromatographic separation in liquid phase.

In chapter III, the equipment employed in high pressure liquid chromatography is described. The description is systematic and gradual; it begins with the principle diagram, operation and procedure of assembling a fully equipped apparatus. Then the operation of components is thoroughly described.

Chapter IV deals in detail with detection systems and detectors. The author ascribes careful attention to each aspect without overlooking any detection system employed at present in high pressure liquid chromatography.

Chapter V presents the stationary phases for adsorption, partition and ion exchange chromatography, the recently introduced chemically bonded phases are also included. At the end of this chapter a list of all producers of stationary phases used by high pressure liquid chromatography is supplied.

The major theoretical and practical aspects regarding adsorption (solid-liquid partition) chromatography make up the topic of chapter VI. The presentation is made according to the nature of the stationary phase : polar (silicagel, aluminium oxide, polyamide) and nonpolar (chemically bonded), the latter meant for separations based on "reversed phases". Special attention is paid to the stationary phase-compound-mobile phase correlation ; therefore the influence of compound structure is also discussed. This chapter is concluded by several examples of separation of compounds by adsorption chromatography.

Chapter VII is devoted to liquid-liquid partition. The approach is similar to that in the previous chapter. This chapter also offers, in the end, several examples of separation.

Chapter VIII, specialized in ion exchange, starts up with the theory of ion-exchange separation. Various ion exchangers are further considered and the main parameters that may optimize separation are discussed. Examples of ion-exchange separation are also supplied.

Chapter IX focuses on separation through differentiated gel permeation with its applications in polymers.

In chapter X, the author systematizes the main criteria which would allow using this or that method (from among adsorption, liquid-liquid partition, ion exchange and gel permeation).

Chapter XI, entitled "Special techniques", deals with the problems of preparative, quantitative and trace analysis chromatography.

In the last chapter the author discusses the problems related to the purity of the solvent employed as a mobile phase.

The book ends by a presentation of producers of equipment and materials relevant to high pressure liquid chromatography.

The content and structure of Prof. Engelhardt's book recommend it as a precious practical guide for those who wish to initiate or specialize in high pressure liquid chromatography.

Dr. Titus Constantinescu

G. E. BAIULESCU and V. V. COŞOFREŢ: "Applications of ion-selective membrane electrodes in organic analysis" (in Ellis Horwood Ltd. series in Analytical Chemistry, Ed. Dr. R. A. Chalmers) John Wiley & Sons, New York, London, Sydney, Toronto, 1977, 235 p.

During the last decade various types of ion-selective membrane electrodes have been produced, and numerous papers have developed their theoretical and experimental aspects At the same time the performances of such electrodes have been successfully extended to include organic analysis. Employed as electrochemical sensors, the ion-selective membrane electrodes are able to measure selectively and continuously the activity of a particular ion in a sample solution. In addition, numerous analysis methods for organic substances by using these electrodes have been recently described, the procedures being remarkable for their rapidity and accuracy. This explains why the ion-selective membrane electrodes have already been used not only in direct potentiometric determinations, bipotentiometric or potentiometric titrations, but also in kinetic and mechanism studies, biochemical and biomedical research, soil analysis, etc.

It is the purpose of this book to present available systems for the ion-selective membrane electrodes technique and their numerous uses in organic analysis.

After a short introduction which aims to present the field and to classify the ion-selective membrane electrodes the content of the book is divided into two parts.

The first part entitled "Theoretical considerations" contains the general principles of the selective membranes (chap. 1), considerations concerning the selectivity and the response time of the electrodes and the current analytical techniques (chap. 2, 3, 4). Another chapter (chap. 5) refers to the behaviour of such electrodes in non-aqueous media, familiar to organic chemistry. All the aspects are presented in a clear and concise manner which assures a good understanding of the second part.

The second, and the main part of this book, is entitled "Applications in organic analysis". Several chapters (6 to 17) of this part, deal with the ion-selective membrane electrodes applications in various classes of organic compounds analysis such as: halogenated compounds, hydroxy compounds, sulphur compounds, boron and arsenic compounds, compounds containing nitrogen and other functional groups, carboxylic acids and derivatives, derivatives of carbonic acid, hydroxy carboxylic acids, sugar and derivatives, heterocyclic aromatic compounds, enzymes. A particular treatment of the ion-selective membrane electrodes applications in analysis of sulphur compounds, where prof. G. E. Baiulescu (Polytechnic Institute of Bucharest) and Dr. V. V. Coşofreţ (Institute of Chemical and Pharmaceutical Research Bucharest) have remarkable contributions, is to be noticed. A rich bibliography is attached o every chapter, amounting to 664 references.

The book is the first to discuss the applications of ion-selective membrane electrodes in organic analysis and its concise and clear style, the exhaustive treatment of the subject are to be mentioned.

This book is highly recommended, being useful to analysts working in various fields: organic chemistry, electrochemistry, biology, biochemistry, clinical chemistry, physiology and pharmacy.

Nora Rădulescu

NOTE POUR LES AUTEURS

La Revue Roumaine de Chimie publie des articles en anglais, français, russe, allemand ou espagnol. Les auteurs sont priés d'envoyer des articles et des comptes rendus inédits.

Les manuscrits seront dactylographiés à deux intervalles. La bibliographie, les tableaux et la légende des figures seront placés après le texte.

Si l'article fait partie d'une série numérotée, le titre de la partie précédente sera indiqué dans une note au bas de la première page.

Chaque article sera précédé d'un résumé comprenant quinze lignes au maximum. Les références bibliographiques dans le texte seront faites par des exposants sans parenthèses et paraîtront comme des notes au bas de chaque page.

Les publications périodiques mentionnées dans la bibliographie seront présentées suivant les prescriptions internationales : le nom de l'auteur précédé de l'initiale du prénom, le titre du périodique abrégé conformément à «Chemical Abstracts», et souligné par une ligne, le numéro du tome indiqué par des chiffres arabes et souligné par deux lignes, suivi de la première page de l'article ; à la fin, l'année de la parution sera placée entre parenthèses. Le numéro de la revue ne sera pas indiqué si les pages du volume sont numérotées consécutivement.

Les textes des livres ou traités incluront : les noms des auteurs, les initiales du prénom le titre du livre entre guillemets et sans être souligné, le numéro du tome précédé par l'abréviation «vol.» (ou «Bd»), le numéro de l'édition, les éditions (the publisher), la localité de la parution du livre, l'année de la parution et la page de la référence précédée(s) par l'abréviation «p» (ou «S»).

Les brevets seront indiqués comme suit : l'auteur ou la firme, le pays et le numéro du brevet, la date et la revue (Chem. Abstr.). Par ex. : M. Jones (to Union Carbide C^{o}), Brit. Pat. 601 238,2 Sept. 1959, Chem. Abstr., 54, 12808 (1960).

Les diagrammes seront tracés à l'encre de Chine sur papier calque. Les tableaux et les figures (en nombre strictement nécessaire) seront numérotés par des chiffres arabes. Les courbes dans les figures seront numérotées par des chiffres arabes et leur explication sera donnée dans la légende des figures. Prière de ne pas inscrire les mêmes données dans les tableaux et les figures. Chaque tableau aura un titre. On indiquera dans le texte la place approximative des tableaux et des figures. Les formules chimiques seront incluses dans le texte ; en outre, elles seront transcrites sur papier calque, à l'encre de Chine.

Les auteurs sont priés d'indiquer les caractères italiques (en soulignant les lettres au crayon), ainsi que tout autre caractère spécial ; les préfixes *ortho*, *meta*, *para*, *cis*, *trans*, etc. seront soulignés pour indiquer leurs caractères italiques et ne seront jamais écrits avec des majuscules.

Aucune correction à la main ne sera admise sur le manuscrit. Les corrections seront frappées à la machine. Les lettres grecques ou autres symboles spéciaux seront insérés à la main à l'encre clairement.

Le manuscrit sera signé par l'auteur.

Le colonne-titre aura 50 lettres au maximum.

L'entière responsabilité du contenu des articles appartient aux auteurs.

TRAVAUX PARUS AUX ÉDITIONS DE L'ACADÉMIE DE LA RÉPUBLIQUE SOCIALISTE DE ROUMANIE

C. DRĂGULESCU, E. PETROVICI **Chimie structurală modernă. Chimia coordinaţiei 8** (Chimie structurale moderne. La Chimie de la coordinence 8), 1977, 947 p., 70 lei.

P. BALTĂ, E. BALTĂ, **Introduction to the physical chemistry of the vitreous state**, coédition avec Abacus Press, Kent, 1976, 287 p., 31 lei.

I. G. MURGULESCU, **Introducere în chimia fizică. Vol. I. 1. Atomi. Molecule. Legătură chimică** (Introduction à la Chimie physique. 1er vol. 1re Partie. Atomes. Molécules. Liaison chimique), 1976, 560 p., 2 pl., 36 lei.

GR. POPA, ŞERBAN MOLDOVEANU, **Reactivii organici în chimia analitică** (Les réactifs organiques dans la chimie analytique), 1976, 255 p., 18 lei.

I. ZUGRĂVESCU, MAGDA PETROVEANU, **N-ylid Chemistry**, 1976, coédition avec McGraw-Hill International Book Company, SUA, 396 p., 33 lei.

C. V. UGLEA, **Cromatografia pe gel permeabil. Noi domenii de aplicare** (La Chromatographie sur gel perméable. Nouveaux domaines d'application), 1976, 123 p., 6, 75 lei.

I. GĂLĂŢEANU, **Radiochimia aplicată. Metode şi probleme** (La radiochimie appliquée. Methodes et problèmes), 1976, 307 p., 19 lei.

FRANCISC A. GOTHARD, **Echilibre lichid-vapori. I. Baze teoretice şi metode de calcul** (Equilibres liquide-vapeurs. I. Bases théoriques et méthodes de calcul), 1975, 263p., 2 pl., 28 lei.

CONST. GH. MACAROVICI, D. MACAROVICI, **Chimia oxizilor dubli şi utilizările lor** (La chimie des oxydes doubles et leur utilisation), 1975, 195 p., 13 lei.

ELENA CEAUŞESCU, **Research work on synthesis and characterization of macromolecular compounds. Contributions**, 1974, 251 p., 20 lei.

M. AVRAM, **Antidăunători** (Pesticides), 1974, 496 p., 41 lei.

DUMITRU COSTACHE, **Analiza chimică prin metoda cinetică** (L'Analyse chimique par la méthode cinétique), 1974, 276 p., 15,50 lei.

G. A RĂDULESCU, **Proprietăţile ţiţeiurilor româneşti** (Les propriétés des pétroles roumains), 1974, 267 p., 2 pl., 18 lei.

CR. SIMIONESCU, VIORICA RUSAN, V. POPA, **Chimia algelor marine** (La chimie des algues marines), 1974, 212 p., 1 pl., 18 lei.

MARIA FITI, **Dozimetria chimică a radiaţiilor ionizante** (La dosimétrie chimique des radiations ionisantes), 1973, 240 p., 13,50 lei.

TIBERIU NĂŞCUŢIU, **Metode radiochimice de analiză** (Méthodes radiochimiques d'analyse), 1973, 384 p., 23 lei.

CRISTOFOR SIMIONESCU, MARGARETA GRIGORAŞ, AGATA CERNĂTESCU-ASANDEI, GHEORGHE ROZMARIN, **Chimia lemnului în România. Plopul şi salcia** (La Chimie du bois en Roumanie. Le peuplier et le saule), 1973, 299 p., 13 pl., 26 lei.

MIHAI FLORESCU, **Eficienţa economică a cercetării ştiinţifice** (L'Efficience économique de la recherches scientifique), 1972, 115 p., 15 lei.

GEORGETA LĂZĂRESCU, **Sistematizarea informaţiilor în chimia organică** (La systématisation des informations en Chimie organique), 1972, 243 p., 1 pl., 10,50 lei.

I. P. INFORMAŢIA c. 7739

43 426

Lei 25.—
$45 (pour un abonnement annuel)

=1103

ACADÉMIE DE LA RÉPUBLIQUE SOCIALISTE DE ROUMANIE

R
REZERVA

REVUE ROUMAINE DE CHIMIE

TOME 23
N° 4
Avril 1978

EDITURA ACADEMIEI REPUBLICII SOCIALISTE ROMÂNIA

Rev. Roumaine Chim.

RECHAX, 23, 4, p. 469–640 (1978), Bucarest

ACADÉMIE DE LA RÉPUBLIQUE SOCIALISTE DE ROUMANIE

COMITÉ DE RÉDACTION

Rédacteur en chef:

I. G. MURGULESCU, membre de l'Académie de la République Socialiste de Roumanie

Rédacteurs en chef adjoints:

A. T. BALABAN et V. EM. SAHINI, membres correspondants de l'Académie de la République Socialiste de Roumanie

Collège de rédaction:

EM. BRATU, ELENA CEAUŞESCU, ECATERINA CIORĂNESCU-NENITZESCU, C. DRĂGULESCU, CR. SIMIONESCU, membres de l'Académie de la République Socialiste de Roumanie; P. SPACU, membre correspondant de l'Académie de la République Socialiste de Roumanie; MARGARETA AVRAM, I. HAIDUC, D. I. MARCHIDAN, I. MOLDOVAN, G. NIAC et D. SĂNDULESCU

La Revue Roumaine de Chimie paraît 10 fois par an. Toute commande de l'étranger (fascicules ou abonnements) sera adressée à ILEXIM — Departamentul Export-Import Carte (Livres)/Departamentul Export-Import Presă (Revues), P.O.B. 136—137, télex 11226, 70116 Bucarest, 3, str. 13 Decembrie, Roumanie

Les manuscrits, les livres et les revues proposés en échange, ainsi que toute correspondance seront envoyés à la rédaction :

REVUE ROUMAINE DE CHIMIE

23, str. Dumbrava Roşie, Bucarest, Roumanie, téléphone 12 41 60

EDITURA ACADEMIEI REPUBLICII SOCIALISTE ROMÂNIA
125, Calea Victoriei, 71021 Bucarest, Roumanie, téléphone 50 76 80

REVUE ROUMAINE DE CHIMIE

KÖNYVTÁRES KÖZPONT
183

Tome 23, Nº 4 Avril 1978

R I. G. MURGULESCU and GABRIELA MINCU, Kinetics and mechanism of oxidoreduction. Reaction of the bisoxalatodiaquo Co(III) complex with iodide ion in acid medium 471–477
V. E. SAHINI, V. CONSTANTIN and I. ŞERBAN, Determination of ionization potentials using a MI-1305 mass spectrometer 479–482
V. E. SAHINI and LILIANA TELEA, Molecular interactions in anisidine. III. IR spectra and heats of dilution 483–487
P. ROTARU, G. NIAC and S. I. BLEJOIU, Method for calculating heats of decomposition from thermogravimetric data (in French) 489–493
D. W. CLACK and M. MONSHI, Molecular orbital calculations on transition metal complexes. XII. Unpaired electron distributions. 495–504
S. STERNBERG and T. VIŞAN, Cyclic voltammetry of strontium deposition and dissolution in molten potassium nitrate 505–513
C.-E. MOROŞANU and E. SEGAL, *In situ* evaluation of the chemical vapor deposition rates of some thin films on silicon by infrared interference 515–522
M. VLAD, Perturbation approaches for kinetics of isotope exchange reactions 523–526
R ELENA CONSTANTINESCU and V. BRÎNZOI, Anodic oxidation of primary alcohols 527–534
R SIMONA BĂDILESCU, VOICA TĂLPUŞ and RODICA RACOTĂ, Infrared spectral study of hydrogen bonding in ethyl alcohol absorbed in polyethylene sheets 535–540
M. VLAD, Fluctuation phenomena in diffusion 541–547
K. SINGH, D. N. BAJPAI and B. K. DWIVEDI, Apparent molal volumes of some common salts in methanol-water mixtures 549–553
R. K. JAIN and H. C. GAUR, Generalized potential-time equations for A. C. chronopotenţiometry: application to quasi-reversible processes 555–558
IOANA JITARU and MARIA BREZEANU, Cobalt complex compounds with 3-amino-1-propanol 559–568
I. A. KHAN, ABDU-SSALAM M. CACA and Z. H. FAROOQI, Studies on coordination compounds, 2-thiosalicylic acid complexes of copper(II) 569–572
DOINA OŞIANU, ELENA NICOARĂ and C. BODEA, Inchain-epoxides of carotenoids. VI. Isomerizations and rearrangements of canthaxanthin-inchain-epoxides 573–576
S. H. DOSS, Sultam synthesis (in German) 577–580

Revue Roumaine Chim. 23, 4, 469–640 (1978) Bucarest

A. I. BLAGA, R. F. PAPE and T. CHIRILĂ, Acid-catalysed acetalisation. I. The influence of kind and concentration of acid catalysts on synthesis of bis-1,1-(2′,2′-ethylhexyloxy)-2-methylpropane 581–586

R A. S. HAMMAM and H. S. EL-KASHEF, Heterocyclic quinones. X. Synthesis and antibacterial screening of new thiazolocarbazoloquinones 587–593

ALICE MARIE GLATZ, V. DRĂGUȚAN, Z. ARVAY, C. DRĂGHICI and A. C. RĂZUȘ, Different behaviour of isomeric arylbenzylketones towards phosphorus pentachloride 595–601

O. HOROWITZ, On triazines. LVI. HMO calculations for derivatives of 1,3,5-triazine (in German) 603–611

S. S. SRIMALI, N. D. SHARMA, S. KUMAR and B. C. JOSHI, Proton-catalysed rearrangement of sulphonamide to sulphone. I. Conversion of substituted arylquinolylamine sulphonamide to the isomeric substituted diarylsulphone 613–616

I. M. ISSA, A. A. EL SAMAHY, R. M. ISSA and H. S. EL KASHEF, Preparation and spectrophotometric studies of some quinoneanils 617–624

V. D. LAMBRINO and R. S. NISTOR, Determination of the repartition of elements in a bentonite by means of X-ray analyzer with electronic microprobe. (in French) 625–627

R GH. DRĂGAN, Amorphous-crystalline coupling in polyethylene. VII. Study of the crystallization kinetics in the approximation of the purely thermal dissipative coupling 629–635

BOOK REVIEWS 637–639

Revue Roumaine de Chimie, **23**, *4*, 471–477 (1978)

KINETICS AND MECHANISM OF OXIDOREDUCTION

REACTION OF THE BISOXALATODIAQUO Co (III) COMPLEX WITH IODIDE ION IN ACID MEDIUM

I. G. MURGULESCU and GABRIELA MINCU
Institute of Chemistry, Department of Physical Chemistry, Bd. Republicii 13, Bucharest

Received June 18, 1977

This paper deals with the kinetics and mechanism of the reaction between the complex ion $[Co(C_2O_4)_2(H_2O)_2]^-$ and I^- taking into account the catalytic effect of hydrogen ion. The activation parameters are calculated from the rate constant values obtained at various temperatures. A reaction mechanism is proposed according to these data.

The oxidoreduction reactions of the transition metal complexes in aqueous solution catalysed by hydrogen ion have been frequently studied.[1-4]

In acid media, the oxalato-complexes undergo intramolecular redox decomposition leading to Co(II) as final product.[5,6]

In the present paper, the intermolecular oxidoreduction reaction of bisoxalatodiaquo Co(III) complex with iodide ion, in hydrochloric acid medium was studied. The reaction is moderately fast and there are no data in literature on this subject.

EXPERIMENTAL

The reaction half time lies between 60 and 100 sec. It was not possible to follow the kinetics of this reaction spectrophotometrically because of the too high molar absorptivity of the final product, iodine, needing a very thin cell where there is not possible a fast mixing of the reactants. On the other hand, the absorption band of the complex (~600 nm) overlaps the band tail of iodine whose intensity increases gradually during the reaction. For these reasons we considered as an adequate technique for our measurements the clock method used

[1] R. Davies and A. D. Sykes, *J. Chem. Soc. A*, **1968**, 2237.
[2] H. A. Liebbarfsky and A. Mohamed, *J. Amer. Chem. Soc.*, **55**, 3977 (1933).
[3] I. Bîldea and G. Niac, *Inorg. Chem.*, **7**, 1232 (1968).
[4] L. J. Kirschenbaun and J. R. Sutter, *J. Phys. Chem.*, **70**, 3863 (1966).
[5] I. G. Murgulescu and T. Oncescu, *Z. phys. Chem.* (*Leipzig*), **214**, 238 (1960).
[6] I. G. Murgulescu and G. Mincu, *Rev. Roumaine Chim.*, **16**, 1033 (1971).

also by Shurwell[7,8] for the other redox reactions of the iodide. It consists in measuring the necessary time for the consumption of a given amount of the complex. The resulting iodine is removed by adding necessary sodium-thiosulphate amounts corresponding to a certain complex conversion.

. The Durrant's salt, necessary to prepare the bisoxalatodiaquo complex in acid medium, was obtained as indicated in literature.[9] Kalium iodide and hydrochloric acid were of analytical reagent grade "Analar" BDH and "Merck", respectively. The sodium thiosulphate (Reactivul) was recrystallized.

The reaction was performed in a thermostated vessel under continuous magnetic stirring. The concentrated sodium thiosulphate solution was added with a micropipette to avoid an excessive dilution of the solution. The concentration of the unreacted complex was calculated taking into account the successive dilution of the medium.

RESULTS

All the experiments were performed in excess iodide at the ionic strength up to 0.5 M. The kinetic data verified a first order low in respect to complex for conversions up to 70—80 % as can be seen in Figure 1.

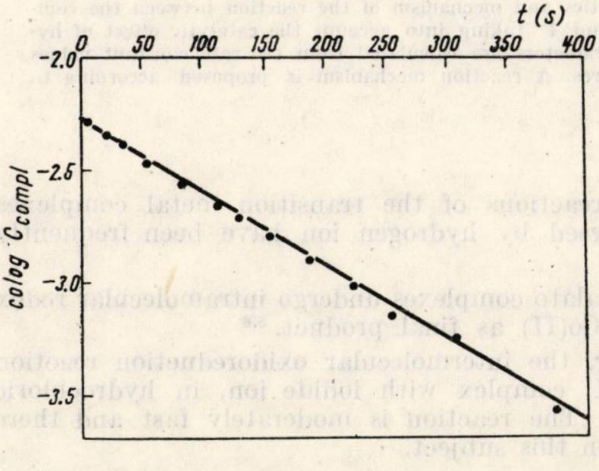

Fig. 1. — The plot of the complex concentration versus time at 25°; $C_{\text{compl}} = 5.22.10^{-3}$ M; $C_{I^-} = 0.209$ M; $C_{H_3O^+} =$ $= 0.104$ M

The slope of the line, calculated by the least squares method gives a rate constant $k_I = 0.00720\ \text{sec}^{-1}$. We carried out our experiments at different initial complex concentrations and at various excess iodide concentrations at a constant hydrogen ion concentration $C_{H_3O^+}$ (the total concentration of the acid). The ratio between the first order rate constant k_I and the excess iodide concentration, gives the second order constant $k_{II_{\text{exp}}} = k_I/C_{I^-}$ (Table 1).

Experiments at various hydrochloric acid concentration were also performed keeping the initial reactant concentrations constant. One obtained a linear dependence of the rate constant.

---

[7] H. Shurwell, *J. Chem. Educ.*, **44**, 677 (1967).

[8] G. Mincu, *Studii și Cercetări Chim., Acad. București*, **20**, 533 (1972).

[9] R. G. Durrant, *J. Chem. Soc.*, **1905**, 176.

Table 1

The first and second order rate constants for the reaction between $[Co(C_2O_4)_2(H_2O)_2]^-$ and I^- in acid medium for different initial concentrations of the reactants
($T = 25°$ $C_{H_3O^+} = 0.104M$)

$C_{compl}.10^3M$	$C_{I^-}.10M$	$k_I.10^3s^{-1}$	$k_{II_{exp}}.10^2 = \frac{k_I}{C_{I^-}}.10^2M^{-1}s^{-1}$
2.61	2.09	7.27	3.50
5.22	2.09	7.15	3.42
7.81	2.09	7.17	3.43
5.22	0.523	1.68	3.21
5.22	1.05	3.56	3.39
5.22	1.57	5.59	3.56
5.21	3.13	10.51	3.36

$k_{II} = (3.41 \pm 0.13).10^{-2}$

The relationship between k_I and $C_{H_3O^+}$ is given by:

$$k_I = (k_0 + k' C_{H_3O^+})\, C_{I^-} \tag{1}$$

and therefore the second order rate constant can be calculated by the equation:

$$k_{II_{calc}} = k_0 + k'\, C_{H_3O^+} \tag{2}$$

In Figure 2, the intercept k_0 and the slope k' are the rate constants of the uncatalysed and hydrogen ion catalysed reactions, respectively (Table 2)

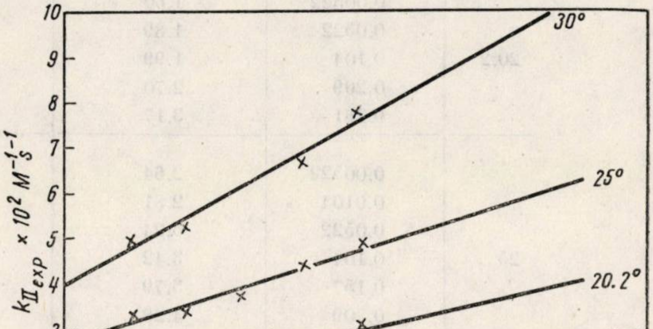

Fig. 2. — The plot of the rate constants $k_{II_{exp}}$ versus hydrochloric acid concentrations $C_{H_3O^+}$ at various temperatures.

Table 2

The rate constants k_0 and k' at different temperatures
$C_{I^-} = 0.209 M$ $C_{compl} = 5.22.10^{-3}$ M

$T°$	$k_0.10^2 M^{-1}s^{-1}$	$k'.10^2 M^{-1}s^{-1}$
15.2	0.933	3.33
20.2	1.52	5.88
25	2.69	7.64
30	4.05	15.06

The relationship (2) holds for all working temperatures as can be seen in Figure 2.

Using the k_0 and k' values from the table 2 and the relationship (2), the values of constants $k_{II_{calc}}$ for different temperatures and hydrogen ion concentration were calculated and given in table 3.

Table 3

The rate constants k_{II} for the reaction between $[Co(C_2O_4)_2(H_2O)_2]^-$ and I^- at different temperatures and hydrogen ion concentrations
($C_{I^-} = 0.209$ M $C_{compl} = 5.22r10^{-3}$ M)

$T°$	$C_{H_3O^+}$ M	$k_{II_{calc}}.10^2 M^{-1}s^{-1}$	$k_{II_{exp}}.10^2 M^{-1}s^{-1}$
15.2	0.0522	1.10	1.11
	0.104	1.28	1.28
	0.209	1.65	1.63
	0.261	1.78	1.80
20.2	0.00522	1.60	1.55
	0.0522	1.89	1.83
	0.104	1.99	2.13
	0.209	2.70	2.75
	0.261	3.17	3.05
25	0.00522	2.64	2.73
	0.0104	2.81	2.77
	0.0522	3.24	3.09
	0.104	3.42	3.43
	0.157	3.79	3.89
	0.209	4.28	4.29
	0.261	4.74	4.68
30	0.0522	4.93	4.84
	0.104	5.53	5.62
	0 209	7.08	7.20
	0.261	8.09	7.98

In the last column of the table 3 are given the values of the rate constant $k_{\text{II}_{\text{exp}}}$ obtained directly from experiments. These ones agreed very well with the calculated values $k_{\text{II}_{\text{calc}}}$.

The data from tables 2 and 3 were used to plot log k_0, log k' and log k_{II} against $1/T$ (Figure 3), the activation energies being the same within the limits of the experimental errors (17.1±0.3 kcal/mol).

The preexponential factors are practically constant (11.27 M^{-1} s^{-1}) as well as the activation entropies (−9 u.e.).

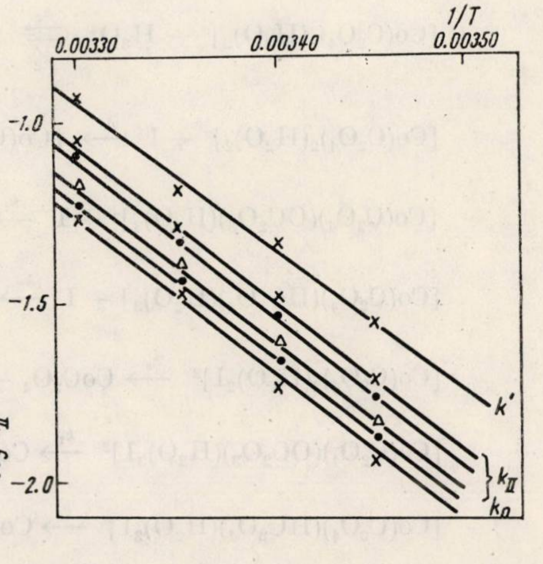

Fig. 3. — The plot of log k versus $1/T$; k_0=uncatalysed reaction rate constant; k_{II} =total rate constant; k' =catalysed reaction rate constant.

DISCUSSION

Our experimental data showed that the reaction is first order in respect with both rectants $[Co(C_2O_4)_2(H_2O)_2^-]$ and I^-, the reaction rate being given by the equation (3):

$$-\frac{dC_{\text{compl Co(III)}}}{dt} = [k_0 + k'\,C_{H_3O^+}]\,C_D\,C_{I^-} \qquad (3)$$

were C_D stands for the bisoxalatodiaquo complex concentration. This complex can be obtained only in solution by mixing stoechiometrically equivalent amounts of hydroxoaquo Co(III) complex and hydrochloric acid, when the following equilibrium establishes.[10,11]

$$[Co(C_2O_4)_2H_2O\,OH]^{2-} + H_3O^+ \overset{K}{\rightleftharpoons} [Co(C_2O_4)_2(H_2O)_2]^- + H_2O \qquad (A)$$

---

[10] G. Spacu, I. G. Murgulescu and M. Vancea, *Z. anorg. Chem.*, **220**, 1 (1934).

[11] A. W. Adamson and H. Ogata *J. Inorg. Nucl. Chem.*, **6**, 319 (1958).

The existence of this equilibrium is supported by the pH increase during the mixing.

In the presence of I^- an electron transfer from I^- to Co(III) occurs. According to our experimental data we suggest the following reaction mechanism :

$$[Co(C_2O_4)_2\,(H_2O)_2]^- + H_2O \underset{k_1'}{\overset{k_1}{\rightleftharpoons}} [Co(C_2O_4)(OC_2O_3)(H_2O)_3]^- \qquad (a)$$

$$[Co(C_2O_4)_2(H_2O)_2]^- + H_3O^+ \underset{k_2'}{\overset{k_2}{\rightleftharpoons}} [Co(C_2O_4)(HC_2O_4)(H_2O)_3] \qquad (b)$$

$$[Co(C_2O_4)_2(H_2O)_2]^- + I^- \xrightarrow{k_3} [Co(C_2O_4)_2(H_2O)_2\,I]^{2-} \qquad (c)$$

$$[Co(C_2O_4)(OC_2O_3)(H_2O)_3]^- + I^- \xrightarrow{k_4} [Co[C_2O_4)(OC_2O_3)(H_2O)_3I]^{2-} \qquad (d)$$

$$[Co(C_2O_4)(HC_2O_4)(H_2O)_3] + I^- \xrightarrow{k_5} [Co(C_2O_4)(HC_2O_4)(H_2O)_3\,I]^- \qquad (e)$$

$$[Co(C_2O_4)_2(H_2O)_2I]^{2-} \xrightarrow{k_6} CoC_2O_4 + C_2O_4^{2-} + 1/2I_2 + 2H_2O \qquad (f)$$

$$[Co(C_2O_4)(OC_2O_3)(H_2O)_3I]^{2-} \xrightarrow{k_7} CoC_2O_4 + C_2O_4^{2-} + 1/2I_2 + 3H_2O \qquad (g)$$

$$[Co(C_2O_4)(HC_2O_4)(H_2O)_3I]^- \xrightarrow{k_8} CoC_2O_4 + HC_2O_4^- + 1/2I_2 + 3H_2O \qquad (h)$$

The initial bisoxalatodiaquo complex of Co(III) (D) is involved in the aquation (a) and protonation (b) fast preequilibria giving the aquated (DA) and protonated (DH) complexes. This behaviour is common for all oxalic complexes of the transition metals.[12-15] The three complexes of Co(III) are simultaneously reduced by I^- in the slow parallel steps (c) (d) and (e).

It is difficult to specify the structure of such activated complexes. In any cases a structure with the decrease of freedom is expected, the involved processes occurring between species with the same charges (c), (d) or, even without charge (e), what explains the negative value of the activation entropy. Because the last process (e) is faster and therefore determining step, the activation entropy obtained for the high acid concentration, is less negative (−8.8 u. e.) than in the case of a zero excess acid (−9.3 u. e). The intermediates thus obtained lead to the final products in the fast steps (f), (g) and (h).

---

[12] G. M. Haris and F. D. Graziano, *J. Phys. Chem.*, **63**, 330 (1959).

[13] T. Oncescu and E. Pantazi, to be published.

[14] G. M. Haris and K. V. Kriohnamurty, *J. Phys. Chem.*, **64**, 346 (1960).

[15] G. M. Haris and D. Barton, *Inorg. Chem.*, **1**, 251 (1962).

Only $[Co(C_2O_4)_2(H_2O)_2]^-$ ion (and both aquated (DA) and protonated (DH)forms) reacts with I^-, because in acid excess the equilibrium (A) is shifted towards this complex ion. On the other hand, the reaction between $[Co(C_2O_4)_2H_2O\,OH]^{2-}$ and I^- has a half time of several orders of magnitude larger than the reaction in acid medium[16] (30 min as compared to 2–3 sec) in agreement with our supposition.

We did not take into account in this system, the thermal decomposition[5,6] of $[Co(C_2O_4)_2(H_2O)_2]^-$ because its half time is long enough (30 min) and therefore the $C_2O_4^{\cdot-}$ radical do not appear in the solution to compete with the redox reaction. We proved its absence by the fact that we did not obtain the polymerisation of acrylonitrile added in this system.[17]

The experiments using kalium chloride instead hydrogen chloride, showed that the rate constants are independent on the KCl concentration. This result agrees with the mechanism of H_3O^+ catalysis and with the supposition that the step (e) is the limiting one.

The rate equations for the three complex species of Co(III) are:

$$-\frac{dC_D}{dt} = k_1 C_D C_{H_2O} - k_1' C_{DA} + k_2 C_D C_{H_3O^+} - k_2' C_{DH} + k_3 C_D C_{I^-} \qquad (4)$$

$$-\frac{dC_{DA}}{dt} = -k_1 C_D C_{H_2O} + k_1' C_{DA} + k_4 C_{DA} C_{I^-} \qquad (5)$$

$$-\frac{dC_{DH}}{dt} = -k_2 C_D C_{H_3O^+} + k_2' C_{DA} + k_5 C_{DH} C_{I^-} \qquad (6)$$

By summing equations (4), (5) and (6) we get:

$$-\frac{d(C_D + C_{DA} + C_{DH})}{dt} = (k_3 C_D + k_4 C_{DA} + k_5 C_{DH})\, C_{I^-} \qquad (7)$$

Taking into account the relationship between the concentrations C_{DA}, C_{DH} and equilibrium constants K_1 and K_2 of the preequilibria (a) and (b) one gets:

$$-\frac{d(C_D + C_{DA} + C_{DH})}{dt} = (k_3 + k_4 K_1 C_{H_2O} + k_5 K_2 C_{H_3O^+})\, C_D C_{I^-} \qquad (8)$$

In this equation the sum of the first tow terms is the constant k_0 and the product $k_5 K_2$ is the constant k', so that it can be rewritten:

$$-\frac{d(C_D + C_{DA} + C_{DH})}{dt} = (k_0 + k' C_{H_3O^+}) C_D C_{I^-} \qquad (9)$$

As we can see it is similar to the experimental relationship (3) verified by our data.

---

[16] I. G. Murgulescu and G. Mincu, to be published.

[17] T. Oncescu, *Rev. Roumaine Chim.*, **15**, 209 (1970).

Revue Roumaine de Chimie, **23**, *4*, 479–482 (1978)

DETERMINATION OF IONIZATION POTENTIALS USING A MI-1305 MASS SPECTROMETER

V. E. SAHINI, V. CONSTANTIN and I. ŞERBAN

Department of Physical Chemistry, Institute of Chemistry, Polytechnic Institute Bucharest, Bd. Republicii 13, Bucharest

Received June 29, 1977

The ionizing voltage circuit of MI-1305 mass spectrometer was modified in order to extend the ionizing voltage range under 20 volts. To avoid the difficulties connected with the measurement of small voltage changes operated at high potential, the ionizing voltage has been simulated so that the ionization efficiency curves could be plotted directly on the chart paper of an X–Y recorder.

The MI-1305 mass spectrometer (60° sectored field type, 300 resolution, 1–400 range for mass numbers) is designed for routine isotope abundance measurement. It is equipped with a fairly simple electron bombardment ion source with drawing-out potential instead of pusher plate. This instrument cannot be directly used to obtain the ionization potentials because the emission current is stabilised only for 25–100 volt range of ionizing voltage, while the values of ionization potentials commonly are found around 7–15 volt range.

Kowalsky and Henrych[1] pointed out that a few modifications in the 12 unit of MI-1305 mass spectrometer are necessary in order to obtain a low ionizing voltage; they constructed a device which allow the plotting of the ionization efficiency (*IE*) curve of a given ion on the chart tape of the ion current (amplified) recorder. However, this procedure seems to be not suitable to establish the electron energy scale (i. e. recording the *IE* curve of an internal standard together with that of the sample) and therefore, the ionization potential of the ion under investigation is difficult to obtain.

In this paper is presented a modification of the MI-1305 mass spectrometer which permits a rapid determination of the *IE* curves, from which ionization potentials reproducibile whithin ± 0.03 volt can be obtained. Based on the idea of Bhattacharya et al,[2] this modification consist in the measurement of a low voltage (supplied from batteries) instead of the actual ionizing voltage operated at high potential (4 kV for MI-1305 mass spectrometer), as shown in Figure 1.

---

[1] Z. Kowalsky and R. Henrych, *Nukleonica*, **14**, 299 (1969).

[2] A. K. Bhattacharya, L. D. Smithson and D. W. Hurley, *Rev. Sci. Instr.*, **41**, 1111 (1970).

The ionizing voltage variable potentiometer (R_9 in the original circuit diagram of 12 unit) was replaced by a dual variable resistor P_1-P_2 (2×10 k) connected with a 10 turn 1k helical potentiometer (HP_1). The voltage across the HP_1 potentiometer was adjusted at 10.00 volts. The variable tap on this helipot provides the variable ionizing voltage which is applied to the anode of the electron gun. A second 10 turn helical potentiometer (HP_2) is connected in the divider string of the low voltage supply unit. The shafts of both helipots were fitted to an insulated gear drive which allows a simultaneous mechanical movement of the front potentiometers within the whole 10 turn range. The variable tap on the HP_2 helipot will therefore provide a low voltage proportional to the change in ionizing voltage operated at high potential. Since the time constant for the ion current amplifier of the MI-1305 mass spectrometer is up to five seconds, the recording of *IE* curves must be done smoothly. For this purpose, a sinchronous motor was attached through a suitable reduction gearing to the insulated gear drive of the helipot shafts. The time taken for a complete 10.00 volts (10 turn) range is three minutes.

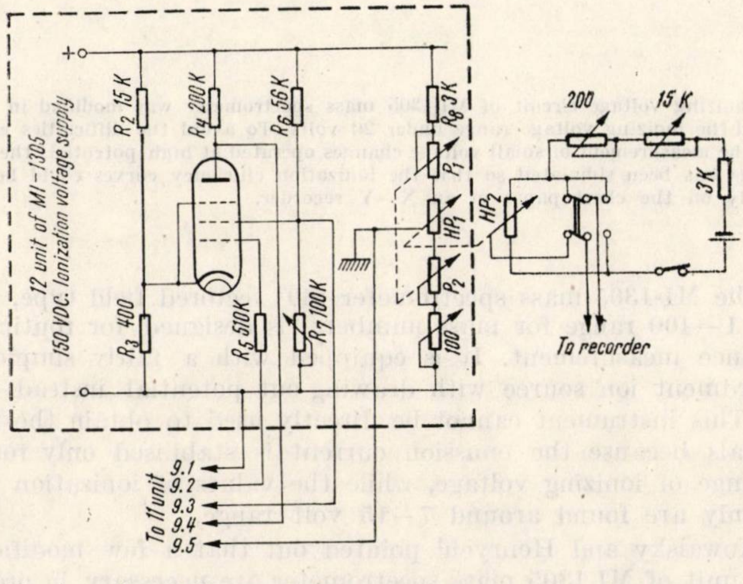

Fig. 1. — Circuit diagram of units employed to generate ionizing voltage and simulated low voltage.

The *IE* curves can be automatically plotted by means of an X–Y recorder: the low voltage provided by HP_2 helipot is applied to one axis, while the ion current taken from the output of the dc amplifier constitutes the input signal for the other axis.

Due to contact potentials in the electron gun and to other complex effects in the ionization chamber, a calibration of the energy scale becomes necessary. The simplest way to do this is to use as reference a calibrating gas admitted into the ion source simultaneously with the sample. To avoid the drifts in the experimental conditions it is desirable that the measurements of *IE* curves to be carried out, one after another, in a time as short as possible.

A number of experimental factors which influence the shape of *IE* curves through excessive tailing have been observed.[3] Among these, the magnetic field for aligning the electron beam through the slits of ionization chamber plays an important role. A careful adjustement of the permanent magnet was practically necessary after 5—6 pairs of curves. Another effect is due to the electron collector potential, which in original circuitry is negative with respect to ionization chamber. In our determination, the collector potential is operated at the same potential as the ionization chamber.

The various methods available for the determination of ionization potentials are discussed at length in some books and reviews.[4–7] The method employed in this work is based on the usual mass spectrometric methods.[8–9] The partial pressures of the standard and sample in the gaseous mixture are arbitrarily adjusted to obtain the parallelism between the initial linear portions of *IE* curves. Better results are obtained when the *IE* curves are parallel up to onset of ionization. In our experiments this parallelism occurs when the ion currents are equalised at an ionizing voltage of 30 volts. The difference between the parallel parts of *IE* curves is taken as the difference between the ionization potentials.

For a complete determination of a pair of *IE* curves (for sample and calibrating ion) about 5 to 10 minutes are required (as compared to the manual determination, where the whole process takes 1/2 to 1 hour).

To check the reproducibility of the ionization potentials with the MI-1305 mass spectrometer modified as described above, several gaseous compounds with known ionization potential were used. The results given in table 1 are average values from 5 scannings, the maximum deviation being $\pm$ 0.03 volt. It can be observed that our values are within the range of ionization potentials reported by different authors.

---

[3] V. E. Sahini, V. Constantin and L. Rădulescu, to be submitted.

[4] F. H. Field and J. L. Franklin, "Electron Impact Phenomena", Academic Press, New York, 1957, p. 12—36 and 281.

[5] A. C. McDowell, "Mass Spectrometry", Mc Graw-Hill, New York, 1963, p. 506—588.

[6] R. W. Kiser, "Introduction to Mass Spectrometry", Prentice Hall, Englewood Cliffs, 1965, p. 162—207.

[7] J. E. Collin, in "Mass Spectrometry", ed. by R. I. Reed, Academic Press, 1965, p. 183—222.

[8] J. W. Warren, *Nature*, **165**, 810 (1950).

[9] F. P. Lossing, A. W. Tickner and W. A. Bryce, *J. Chem. Phys.*, **19**, 1254 (1951).

Table 1

Ionization potentials of N_2, N_2O, CO_2 and CH_3OH

Compound	Cal. gas	IP (volts)	Literature
N_2	Ar	15.58 ± 0.02	S : 15.576 ;[6,12] PI : 15.576 ;[12] EI: 15.57,[11] 15.60,[10] 15.66,[11] 15.57(1d), 15.63(RPD)[12]
N_2O	Ar	12.91 ± 0.03	S : 12.889 ;[13] PI : 12.882,[13] 12.886,[13] 12.83,[7] 12.89 ;[6] EI : 13.01 – 13.10[7]
CO_2	Ar	13.89 ± 0.03	S : 13.78 ;[7,12] PI : 13.775 ;[13] EI : 13.78, 13.88,[11] 13.85,[10] 13.95,[8] 13.78(1d), 13.85(RPD)[12]
CH_3OH	Hg	10.90 ± 0.03	S : 10.8 ;[6] PI : 10.52, 10.85 ;[6] EI : 10.80 – 10.86 – 10.97,[4,6] 10.85(RPD)[14]

IPs for the calibrating gases were taken as 15.76 (Ar) and 10.44 (Hg).[15]
S-spectroscopic value, PI-photon impact method, EI-electron impact methods, RPD-retarding potential difference, 1d-first derivative of IE curve.

---

[10] R. E. Honig, *J. Chem. Phys.*, **16**, 105 (1947).

[11] J. D. Morrison, *J. Chem. Phys.*, **19**, 1305 (1951).

[12] J. Momigny and E. Derouane, *Adv. Mass Spectrom.*, **4**, 607 (1968).

[13] V. H. Diebler and J. A. Walker, *Adv. Mass Spectrom.*, **4**, 767 (1968).

[14] S. Tsuda and W. Hamill, *Adv. Mass Spectrom.*, **3**, 249 (1963).

[15] D. C. Frost, C. A. McDowell, J. S. Sandhu and D. A. Wroom, *Adv. Mass Spectrom.*, **4**, 781 (1968).

Revue Roumaine de Chimie, **23**, *4*, 483–487 (1978)

MOLECULAR INTERACTIONS IN ANISIDINE. III[1]

IR SPECTRA AND HEATS OF DILUTION

V. E. SAHINI and LILIANA TELEA
Center of Physical Chemistry
Bucharest, Splaiul Independenţei, 202 A

Received June 29, 1977

The solvent effect upon the NH_2 band parameters of the infrared spectra of the anisidine isomers has been investigated; in the case of the *ortho* isomer the intramolecular interaction has been considered. Formation of a 1 :1 molecular complex of all isomers with dioxane has been evidenced. Spectral data have been compared to some calorimetric measurements.

INTRODUCTION

Anisidine isomers have, like all primary amines, two IR absorption bands that may be associated with the symmetrical and asymmetrical NH_2 stretching vibrations. If the two NH bonds are different as a result of inter- and intramolecular interactions, subsequent modifications will occur in the vibrational spectra of molecules. The paper deals with the influence of the solvent and of the intramolecular interaction upon the NH_2 stretching band parameters in the IR spectra of anisidines. The existence of a 1 :1 anisidine-dioxane complex has been evidenced. The thermodynamic parameters K and ΔH, characteristic of the intermolecular association, have been determined from calorimetric measurements and have been compared with the previously obtained values from UV data.[1]

EXPERIMENTAL

IR spectra have been obtained in the region 3300–3600 cm^{-1} with a UR 10 spectrophotometer in *n*-hexane, carbon tetrachloride and dioxane, as well as in *n*-hexane-dioxane mixtures. The amine concentration has been $\sim 5.10^{-2}$ M and the amount of dioxane in solvent mixtures has been varied between 0.1–0.6 M.

Heats of dilution have been measured by means of an adiabatic calorimeter[2] which consists of a Dewar flask ($\sim 50\ cm^3$) with a stirrer, a thermistor, a submerged pipette ($\sim 1\ cm^3$) with a bent up delivery tube. The Dewar flask has been immersed in a thermostat. 1 ml of dioxane solution of various concentrations has been succesively added to the 5.10^{-2} M solution of anisidine in *n*-hexane extant in the Dewar flask. Increases in temperature have been measured with a thermistor ($R_{25°} = 10,000\ \Omega$) set in a Wheatstone bridge.

---

[1] Part II, V. E. Sahini and L. Telea, *Rev. Roumaine Chim.*, **21**, 645 (1976).
[2] S. N. Vinogradov and T. H. Linell, *J. Chem. Phys.*, **23**, 93 (1955).

RESULTS AND DISCUSSIONS

The HNH apparent bond angle (θ) and the stretching force constant (k_{NH}) have been calculated using the Linett equations.[3] The results are presented in table 1, in comparison with aniline.

Table

Solvent effect upon the fundamental

Compound	pK	n-hexane				carbon
		ν_{as} (cm^{-1})	ν_s (cm^{-1})	$k.10^{-5}$ ($dyne.cm^{-1}$)	θ (°C)	ν_{as} (cm^{-1})
aniline	4.69	3485	3399	6.52	112°	3481
o-anisidine	4.53	3492	3398	6.53	114°9′	3488
m-anisidine	4.23	3486	3401	6.52	111°43′	3483
p-anisidine	5.34	3468	3388	6.47	110°29′	3463

As it can be observed, the frequencies of the vibrational NH_2 bands, especially the symmetrical ones, are significantly shifted to shorter wavenumbers in dioxane. The greatest shift occurs for the *meta*-anisidine, the most basic of the amines studied. Both the *ortho* and *para* isomers are comparable in point of frequency shift despite their differences in pK values, because of the intramolecular interaction.

The k and θ values in *n*-hexane and carbon tetrachloride are quite constant; only in dioxane we observe a noticeable increase in θ and a coresponding diminution of k, proving the amine-dioxane interaction. In *ortho*-anisidine, the "k" and "θ" increase is due to the enhancement of the conjugation of the lone pair aminic electrons with the aromatic π system, as a result of the intramolecular hydrogen bonding. In table 2 a correlation of k_{NH} with the charge density on the amino nitrogen is evidenced: the force constant increases with the decrease of the nitrogen charge density.

In order to better point the differences in the amine-dioxane interaction, their spectra have been studied in inert solvent-proton acceptor mixtures. The donor concentration has been kept constant and the variable acceptor (dioxane) concentration was as low as to make the intermolecular hydrogen bonding evident.[4]

---

[3] J. W. LINETT, *Trans. Faraday Soc.*, **41**, 223 (1945).

[4] A. ALLERHAND and P. R. SCHLEYER, *J. Amer. Chem. Soc.*, **85**, 371 (1962).

The symmetrical NH_2 stretching vibration is shifted more than the antisymmetrical one and splits as the dioxane concentration increases. While the absorption attributed to the formation of the complex develops into a separate peak at 0.3 M dioxane for the *meta*- and *para*-anisidine, in the *ortho* isomer the splitting is distinct only at 0.6 M dioxane. We note also that the resulting frequency shifts $\Delta\nu$ corelate with the basicity of amine except for the same *ortho* derivative (see Table 3).

1

NH_2 stretching band parameters

Solvent						
tetrachloride			dioxane			
ν_s (cm^{-1})	$k.10^{-5}$ ($dyne.cm^{-1}$)	θ (°C)	ν_{as} (cm^{-1})	ν_s (cm^{-1})	$k.10^{-5}$ ($dyne.cm^{-1}$)	θ (°C)
3394	6.51	112°19′	3456	3366	6.40	113°18′
3396	6.52	113°38′	3465	3370	6.42	114°38′
3398	6.51	111°45′	3457	3367	6.40	113°18′
3383	6.44	110°31′	3443	3360	6.37	111°32′

Table 2

Correlation of the NH stretching force constant with the nitrogen charge density

Compound	$k_{NH}.10^{-5}$	q_N(HMO)[1]
aniline	6.52	1.917
o-anisidine	6.53	1.904
m-anisidine	6.52	1.917
p-anisidine	6.47	1.922

Therefore, the greater shift of the symmetrical NH_2 vibrational band and its splitting in solvent mixtures point to the formation of a 1 :1 complex of anisidine isomers with dioxane, formation which is a little hindered in the *ortho*-isomer, due to intramolecular interaction.

The intermolecular association with dioxane has been also investigated by direct calorimetric measurements at 25°.

If the complex formation is represented by the equation:

$$A(s) + B(s) \rightleftarrows AB(s) \qquad (1)$$

Table 3

Fundamental NH stretching frequencies in n-hexane-dioxane mixtures

Compound	ν_s free	ν_s bonded*	ν_{as}	$\Delta\nu$**	pK
aniline	3 399	3381	3 482	18	4.69
o-anisidine	3 398	(3384)	3 490	14	4.53
m-anisidine	3 401	3381	3 484	20	4.23
p-anisidine	3 388	3373	3 465	15	5.34

* – dioxane 0.3 m – n-hexane

** – ν_{sym} (free) – ν_{sym} (bonded)

in which *s* indicates that the species are in diluted solution in solvent *s*, the equilibrium constant is :

$$K = \frac{c}{(c_A - c)(c_B - c)} \tag{2}$$

where c_A and c_B represent the initial concentrations of anisidine and dioxane respectively and c the equilibrium complex concentration.

The effect of the formation of n mole of complex AB is related to the ΔH interaction enthalpy as follows :

$$Q = n \cdot \Delta H = c . V . \Delta H \tag{3}$$

where V is the volume of solution in the calorimeter. The heat effect of reaction (1) represents the difference between the enthalpy change Q_1 (measured after a solution of dioxane has been added to a diluted solution of anisidine in n-hexane), and the extraneous effect Q_2 – heat of dilution of dioxane in n-hexane (determined in a separate experiment) :

$$Q = Q_1 - Q_2$$

Using a K value determined independently (i. e. from spectroscopic measurements) one can calculate a set of c values for a series of c_A and c_B/according to (2)/ and from

$$\Delta H = \frac{Q}{c \cdot V} \tag{3'}$$

a value of ΔH is obtained ; it is very sensitive to variations in K when the latter is small.[5] In order to obtain simultaneously both K and ΔH we have used a method similar to that of Zeegers-Huyskens.[6] For each set of experimental data (c_A, c_B, V, Q) we have calculated ΔH from equations (2) and (3′) for a range of K values, selecting for the best K, the values giving a constant ΔH. In table 4 are presented K and ΔH obtained for the anisidine-dioxane complex.

---

[5] L. Lamberts, *Ind. chim. belge*, **36**, 347 (1971).

[6] L. Lamberts and Th. Zeegers-Huyskens, *J. Chim. phys.*, **60**, 435 (1963).

Table 4

Thermodynamic parameters of the anisidine-dioxane complex obtained from calorimetric measurements at 25°C

Compound	K (l.mole^{-1})	ΔH (kcal/mole)
o-anisidine	0.35	7.46
m-anisidine	0.50	8.0
p-anisidine	0.40	7.54

The values are a little greater (especially ΔH) as compared with those previously obtained from the UV spectra,[1] but the tendency of complex formation remains in the same sequence : *meta-*, *para-*, *ortho.*

The advantage of the calorimetric method is that it permits the direct evaluation of ΔH of complex formation without recourse to the van't Hoff equation and the uncertainities derived from differentiation of experimental results. But it is rather difficult to choose the appropriate $K:\Delta H$ values and if the presence of the complex is certain, to determine its composition, equilibrium constant and heat of formation, further detailed calorimetric measurements are required.

CONCLUSIONS

Investigations based on methods discussed in this paper have shown that a hydrogen bonded intermolecular complex is formed between anisidine isomers and proton acceptor dioxane, as proved by our previous dipole-moment and UV measurements.

Revue Roumaine de Chimie, **23**, *4*, 489–493 (1978)

MÉTHODE POUR LE CALCUL DE LA CHALEUR DE DÉCOMPOSITION À L'AIDE DES DONNÉES THERMOGRAVIMÉTRIQUES

P. ROTARU*, G. NIAC et S. I. BLEJOIU**

* Centre de Recherches pour les Engrais et les Produits Spéciaux Craiova

** Centrale Industrielle d'Engrais Chimiques Craiova

Reçu le 12 janvier 1977

Une équation mentionnée dans la littérature est employée pour le calcul de la chaleur de décomposition au cas des processus simples du type :

$$A_s \rightarrow \nu_b B_s + \nu_g G,$$

à l'aide de données facilement accessibles par des mesurages de longueur sur le diagramme de décomposition. La méthode ne requiert pas d'analyses thermogravimétriques et thermodifférentielles supplémentaires des substances étalon. Les valeurs obtenues pour la chaleur de décomposition du carbonate de calcium sont proches de la valeur rapportée par la littérature, ce qui témoigne de la validité de l'équation, aussi bien que de la véridicité des suppositions faites pour sa déduction.

1. INTRODUCTION

Les méthodes employées dans l'analyse thermique différentielle pour la détermination de la chaleur de décomposition ont pour point de départ la proportionnalité prouvée entre l'aire de la courbe thermodifférentielle et la chaleur de réaction.[1] Ces méthodes supposent la mesure, par un moyen quelconque, de l'aire fermée par la courbe thermodifférentielle et l'abscisse (T ou t) et sa comparaison avec l'aire de la courbe ATD au cas d'une substance à la chaleur de transformation connue. La substance de comparaison est choisie afin qu'elle subisse la transformation dans un intervalle de température le plus proche possible de celui de la décomposition de l'échantillon étudié.

Traoré[2] a trouvé pour la dépendance du temps par rapport au degré de transformation α des relations théoriques dans quelques cas simples de processus physiques et chimiques étudiés de façon thermodifférentielle par l'élévation constante de la température.[2–4] Ces travaux sont purement théoriques.

Dans ce qui suit, en utilisant une relation, déduite par Traoré on détermine la chaleur de décomposition, à l'aide des données thermogravimétriques et thermodifférentielles.

---

[1] D. Fătu, *J. Thermal Anal.*, **1**, 285 (1969).

[2] K. Traoré, *J. Thermal Anal.*, **4**, 12 (1972).

[3] K. Traoré, *J. Thermal Anal.*, **4**, 123 (1972).

[4] K. Traoré, *J. Thermal Anal.*, **4**, 135 (1972).

II. LA PRÉSENTATION DE L'ÉQUATION

Au cas d'une décomposition simple dont l'équation chimique est :

$$A_s \rightarrow \nu_b B_s + \nu_g G \tag{R1}$$

(A_s, B_s étant des substances solides, et G une substance gazeuse), Traoré[1,2] a déduit la relation :

$$\frac{\partial \ln \alpha_m}{\partial t} = \frac{\lambda_r}{\sigma} \frac{(Ø - 1)\,\theta . c_a}{q} \tag{1}$$

valable dans le maximum de la courbe ATD (quand $\frac{\mathrm{d}}{\mathrm{d}t}\Delta T = 0$), qui coïncide généralement avec le maximum de la courbe DTG. Au maximum de la courbe DTG ou ATD, le degré de conversion est :

$$\alpha_m = \frac{x_m}{x_\infty} \tag{2}$$

et le reste des grandeurs a les significations :

λ_r — le coefficient de transmission de la chaleur vers le système de référence (creuset de référence + substance de référence), fonction de la géométrie du système dans le four, de l'atmosphère dans le four et des autres facteurs.

θ — vitesse de chauffage ; $\theta = \mathrm{d}T/\mathrm{d}t$, exprimée en K/s

$$Ø = \frac{R_b c_b + R_g c_g}{R_a c_a} \text{ où } R_a = \frac{[A_s]}{\nu_g [G]},\ R_b = \frac{\nu_b [B_s]}{\nu_g [G]},\ R_g = \frac{\nu_g [G]}{\nu_g [G]},$$

où $[A_s]$, $[B_s]$, $[G]$, 1, ν_g, ν_f sont les masses moléculaires, c'est-à-dire les coefficients stœchiométriques des substances A_s, B_s, G et c_a, c_b, c_g leurs chaleurs spécifiques (en cal/g).

$q = \frac{\partial Q}{\partial x}$ — la chaleur consommée dans le processus de décomposition pour un gramme de gaz. On peut considérer que sa valeur est constante, pour le domaine assez restreint de température dans lequel a lieu la décomposition.

$\sigma = \frac{M_r c_r + M_{rc}\, c_{rc}}{\rho}$ où ρ est un coefficient fonction des caractéristiques électriques et géométriques du four, et M_r, M_{rc}, c_r, c_{rc} sont les masses et les chaleurs spécifiques de la substance de référence et du creuset où se trouve la substance de référence.

En remplaçant dans l'équation (1), donnée par Traoré, α_m de (2) on peut expliquer la chaleur du processus q (rapportée à un gramme de gaz résulté) :

$$q = \frac{\lambda_r}{\sigma} \frac{x_m}{\partial x_m/\partial t} (Ø - 1) c_a\, \theta \tag{3}$$

La majorité des grandeurs dans la relation (3) sont connues ou mesurables, les seules qui présentent des difficultés de détermination sont λ_r et σ, paramètres dépendants de la construction de l'appareil.

Le rapport λ_r/σ est égal à l'unité, comme on peut voir plus clairement si l'on quitte pour le moment l'équation (3) et on se réfère à une autre équation déduite par Traoré [3] laquelle se rapporte au processus de fusion :

$$\Delta T = \frac{\lambda_r \theta_t}{\sigma} t \qquad (4)$$

où $\Delta T = T_{rf} - T_i$ est la différence entre la température de l'échantillon témoin à la fin de la fusion et la température isotherme à laquelle la fusion a lieu.

t — l'intervalle de temps dans lequel se produit la fusion.

θ_t — la vitesse de chauffage du four où la fusion a lieu, les autres grandeurs étant connues.

On étudie la signification de la grandeur ΔT, qui est la différence entre deux températures : l'une identique à tout moment à celle du four (la température du système de référence) et l'autre constante (la température de fusion pour la substance en question). Donc, le rapport $\Delta T/t$ représente la vitesse même de croissement de la température (de chauffage) notée dans ce cas θ_t, c'est-à-dire

$$\theta_t = \frac{\mathrm{d}T}{\mathrm{d}t} = \frac{\Delta T}{t}$$

Il résulte de ce qui précède et de la relation (4) que la valeur du rapport λ_r/σ ne peut être que l'unité, lorsque la température du système de référence est à tout moment identique à celle du four. Le rapport est addimensionnel.

En supposant que la fusion a lieu en conditions de travail identiques à celles de la décomposition, à savoir : la même substance de référence dans la même quantité, le même programme de croissement de la température dans le même intervalle de température ou presque le même intervalle de température, tous les deux processus étant endothermes, on suppose que le rapport λ_r/σ a la valeur 1 pour le processus de décomposition aussi, car ce rapport ne dépend pas du processus mais de la construction du four et du système de référence.

Tel que montré, la relation (3) peut revêtir la forme :

$$q = \frac{\partial Q}{\partial x} = \frac{x_m}{\partial x_m/\partial t} (\text{Ø} - 1) c_a \cdot \theta \qquad (5)$$

ou

$$q = \frac{\partial Q}{\partial x} = \frac{x_m}{\partial x_m/\partial t} \cdot \frac{\nu_b [B_s] c_b + \nu_g [G] c_g - [A_s] c_a}{A_s} \cdot \theta \qquad (5')$$

ou

$$q=\frac{\partial Q}{\partial x}=\frac{x_m}{\partial x_m/\partial t}\,\frac{\nu_b C_{pBs}+\nu_g C_{pG}-C_{pAS}}{[A_s]}\cdot\theta \qquad (5'')$$

où C_p représente la capacité calorique molaire pour chaque composant.

III. VÉRIFICATION EXPÉRIMENTALE

La validité de l'équation (5″) a été vérifiée au cas de la décomposition du carbonate de calcium, pour lequel on a comparé la chaleur trouvée avec l'équation (5″), de la courbe thermogravimétrique, avec la valeur rapportée par la littérature.

On a décomposé un carbonate de calcium *p.a.* livré par la firme Merck et comme substance inerte (de référence) on a employé de l'alumine calciné à 1373 K. La décomposition a été effectuée en présence de l'aire à une thermobalance de type SETARAM, munie d'un enregistreur qui trace les courbes : T, ATD, DTG, TG. L'intervalle de temps entre deux impressions consecutives de points sur la courbe de température, obtenu par la médiation sur un intervalle de temps suffisamment long est de 53,8 s. De même, la mesure des courbes TG et DTG permet le calcul de la perte en poids de l'échantillon à un certain moment, respectivement de la dérivée de la perte en poids, c'est-à-dire de la vitesse de perte en poids de l'échantillon à ce moment-là.

Tableau 1

Données expérimentales

$x_m.10^2$ (g)	$\partial x_m/\partial t.10^7$ (g/s)	$q=\partial Q/\partial x$ (cal/g)	0,44 q (cal/g)
5,7647	4.345	901,72	396,8
3,7853	2,951	871,72	383,6
4,5362	3,196	964,65	409,4
5,342	4,061	894,02	393,4

La température peut être connue avec une précision de 0,1°.

L'équation de la décomposition du carbonate de calcium est :

$$CaCO_3 \rightarrow CaO + CO_2 \qquad (R2)$$

Le maximum pour les courbes ATD, DTG et l'inflexion pour la courbe TG sont obtenus à 1224 K. Les capacités caloriques molaires à cette température pour chaque substance ont été calculées d'après Karapetiantz,[5] en obtenant pour le carbonate de calcium 30,98 cal/mol.K, pour l'oxyde de calcium 12,988 cal/mol.K et pour le bioxyde de carbone 13,0577 cal/mol.K.

---

[5] M. H. KARAPETIANTZ, "Termodinamica chimică", Ed. tehnică, Bucarest, 1956, annexe I.

Toutes les quatre décompositions du carbonate de calcium ont été effectuées, en vertu du même programme de chauffage, la vitesse de l'élévation de la température étant $\theta = 0{,}135$ K/s. Avec les étalonnages correspondants on a obtenu les valeurs pour x_m, $\partial x_m/\partial t$ par des mesures directes sur les diagrammes de décomposition.

A l'aide de la relation (5″) on a calculé q. Un calcul simple fait le passage de la chaleur nécessaire pour obtenir un gramme de CO_2 par la décomposition du carbonate de calcium, vers la chaleur nécessaire pour la décomposition d'un gramme de carbonate de calcium.

Les valeurs obtenues par la méthode décrite concordant, dans la limite des erreurs expérimentales, avec la valeur 404 cal/g trouvée dans la littérature,[6] la moyenne étant 396 cal/g, et l'écart carré moyen de 8,5 cal/g en distribution Student pour un seuil de signification de 0,05 dans ce cas le facteur Student étant 3,18.

IV. CONCLUSIONS

Par le processus de fusion, on a montré que le rapport λ_r/σ des équations théoriques de Traoré est égal à l'unité.

Sur cette base on a proposé une équation pour le calcul de la chaleur de décomposition à l'aide de la courbe thermogravimétrique.

On a vérifié la relation dans le cas de la décomposition du carbonate de calcium, à l'aide des courbes TG et DTG, et on a trouvé une bonne concordance avec la valeur donnée dans la littérature.

---

[6] P. GARN, "Thermal Methods of Chemical Investigation", Academic Press, New York, 1965.

Revue Roumaine de Chimie, **23**, *4*, 495–504 (1978)

MOLECULAR ORBITAL CALCULATIONS ON TRANSITION METAL COMPLEXES. XII*

UNPAIRED ELECTRON DISTRIBUTIONS

DENIS W. CLACK and MAHMOUD MONSHI
Dept. of Inorganic Chemistry, University College,
P.O. Box 78, Cardiff CFI IXL, United Kingdom

Received February 16, 1976

Molecular orbital calculations have been made with and without inclusion of exchange interactions, to examine the mechanisms of spin delocalisation in a range of transition metal complexes. Spin transfer coefficients to orbitals on atoms adjacent to and further removed from the paramagnetic transition metal ion are compared with experimentally derived values and in general good agreement is found for both the signs, when these are known, and the magnitude of the transferred spin. The importance of direct delocalisation, spin polarisation and the nodal properties of the molecular orbitals and their contributions to the spin transfer values is discussed.

INTRODUCTION

Molecular orbital calculations for transition metal systems have been used in the main to describe the bonding modes and related quantities such as covalency, and electronic properties have been correlated with experimental data obtained from u. v.-visible or u. v. photoelectron spectroscopic studies. In some cases electron spin resonance g parameters have been calculated[1] but there have been few attempts to obtain unpaired electron densities from such calculations.[2–4] Data of this latter type may be used to assign hyperfine coupling to magnetic nuclei in the e. s. r. spectra of such complexes and therefore provides a sensitive test for any molecular orbital theory.

Calculations of the Huckel type and various modifications of this method have proved to be extremely useful for analysing and assigning electron spin resonance spectra of aromatic type radicals[5] but no single method has as yet been applied in depth to transitional complexes. In view of the importance of coulomb and exchange terms in determining the spin properties within these systems it is clear that an adequate description of the distribution of unpaired electrons will only be obtained if electron-electron terms of both these types are included in the calculations, which may either employ restricted or unrestricted Hartree-Fock procedures.

---

* Part XI, D. W. Clack and M. Monshi, *Mol. Phys*, accepted for publication.

[1] K. E. Falk, E. Ivanova, B. Roos and T. Vanngard, *Inorg. Chem.*, **9**, 556 (1970).

[2] S. Larsson, *Theor. Chim. Acta.*, **39**, 173 (1975).

[3] R. D. Brown and P. G. Burton, *Theor. Chim. Acta.*, **18**, 309 (1970).

[4] D. W. Clack, N. S. Hush and J. R. Yandle, *J. Chem. Phys.*, **57**, 3503 (1972).

[5] A. Streiweiser, "Molecular Orbital Theory for Organic Chemists", Wiley, New York, (1961).

On a one-electron model delocalisation of the magnetic electrons arises from a mixing of some fraction (b^2) of the ligand wavefunction (Φ_{Lig}) with that of the central metal ion d-wavefunction (Φ_{3d}) as given by equation (1) where ψ_{mol} is a normalised molecular orbital. This picture is frequently used to estimate mixing coefficients from hyperfine

$$\psi_{\mathrm{mol}} = a\Phi_{3d} \pm b\Phi_{\mathrm{Lig}} \tag{1}$$

coupling constants.[6,7] For example, the observed isotropic fluorine coupling in $KNi(Mg)F_3$ arises through direct σ-delocalisation of the 'nickel' e_g electrons into the fluorine $2s$ orbitals. On the other hand this mechanism does not account for the observed fluorine $2s$ spin density in the complex $[CrF_6]^{3-}$, which formally contains only t_{2g} π-type unpaired electrons. In this case spin density in the ligand σ-orbitals must occur by polarisation *via* exchange interactions. In other cases the nodal properties of the molecular orbitals containing the unpaired electrons may play a decisive role in determining the magnitude of the spin density transferred to the ligands.

We have therefore examined the spin distribution of a range of transition metal complexes using an intermediate neglect of differential overlap method which satisfies the above requirement at the lowest level of approximation. Results are reported for delocalisation to atoms bonded directly to the transition metal ion and also to centres further removed from the metal ion, and are compared with spin parameters derived from electron spin and nuclear magnetic resonance spectral measurements.

METHOD

The INDO method for transitional elements together with the relevant parameterisation have been described elsewhere.[8] The calculations were made within the unrestricted Hartree-Fock formalism with the orbital spin densities obtained as differences between the α and β electron occupancies. Although the unrestricted wavefunctions are not true eigen-functions of the S^2 operator the expectation values $<S^2>$ for the species studied were close to those anticipated for the pure spin components. On this basis contamination from states of higher spin multiplicity is not serious, as was previously found with organic radicals[9], and results are given without annihilation of these components of higher spin multiplicity.

Comparison of the calculated "S" spin densities with those derived from isotropic couplings is not strictly valid since the computations use Slater-type atomic orbitals which are nodal at the nucleus. One way to overcome this difficulty is to derive an empirical value for the quantity $\frac{8\pi}{3} g\beta\gamma h |\psi_0^2|$ y plotting calculated spin densities against observed coupling

---

[6] H. R. GERSMANN and J. D. SWALEN, *J. Chem. Phys.*, **36**, 3221 (1962).

[7] J. OWEN and J. H. M. THORNLEY, *Rept. Progr. Phys.*, **29**, 675 (1966).

[8] D. W. CLACK, *Mol. Phys.*, **27**, 1513 (1974).

[9] D. L. BEVERIDGE and P. A. DOBOSH, *J. Chem. Phys.*, **48**, 5532 (1968).

constants[10]. It has been shown that the empirical values of 539.86 gauss for ^1H is not very different from the theoretical value of 506.82 gauss, however for other elements significant differences between experimental and theoretical values were found. Alternatively one may simply compare relative values of these spin densities and ignore the absolute magnitudes. In view of the fact that the computed spin densities in this work are always of similar magnitude to the experimentally derived values we have chosen to give the actual values obtained.

Parallel calculations were also made neglecting the one-centre exchange integrals (CNDO approximation) in order to investigate the relative importance of both direct delocalisation and polarisation in the spin transfer process. Molecular structures were taken from the available literature.

RESULTS

METAL IONS IN FLUORIDE LATTICES

Nuclear magnetic and electron spin resonance data for these systems have yielded both the isotropic and anisotropic coupling to the ^{19}F nucleus, which may be used to obtain '*s*' and '*p*' type spin densities on the fluoride ligand.[7] Calculations to evaluate the fluorine hyperfine coupling have been in the main for $[Ni^{II}F_6]$ although Brown has examined a series of hexafluoride complexes and CNDO computed transferred spin densities have also been reported.[3,4]

Table 1 gives the computed $2s$, $2p_\sigma$ and $2p_\pi$ fluorine spin densities together with the experimentally derived f_s and $(f_\sigma - f_\pi)$.[7] One striking feature of the results is the large resultant negative spin densities in the $2s$ and $2p_\sigma$ orbitals in the INDO calculation but not present using the CNDO method for the complexes $[V^{II}F_6]$, $[Cr^{III}F_6]$ and $[Mn^{IV}F_6]$. Thus it is evident that the simplistic one-electron picture is inappropriate for a description of spin delocalisation. For these d^3 systems which have a t_{2g}^3 configuration in octahedral symmetry, a one-electron picture can only produce unpaired spin in p_π type orbitals, while for $Ni^{II}(d^8)$ with the configuration $t_{2g}^6\,e_g^2$ the picture leads only to σ-type $(2s, 2p_\sigma)$ ligand spin density. This model has been used to interpret the observed magnitude and signs of the ^{19}F coupling constants where the derived $(f_\sigma - f_\pi)$ of negative sign was assumed to be due wholly to f_π for the d^3 complexes, while the positive value of $(f_\sigma - f_\pi)$ for $[Ni^{II}\,F_6]$ was considered to originate from f_σ only.[7]

The calculations indicate that for the complexes with electronic configurations d^5, d^6, d^7, and d^8 the σ-transfer dominates the $(f_\sigma - f_\pi)$ values with π-transfer relatively small except for $[Fe^{III}\,F_6]$. However, the results show that for the d^3 species the overall $(f_\sigma - f_\pi)$ is composed of a large negative contribution from σ-delocalisation which clearly arises through exchange polarisation since no such values arose in the CNDO calculations. The mechanism for this type of polarisation was first proposed by Orgel[11] and involves a movement of 1 from the ligands to the metal, brought about by $d-d$ exchange terms, thereby leaving a negative spin density on the ligands. The relative contributions of

---

[10] J. A. Pople and D. L. Beveridge, "Approximate Molecular Orbital Theory", Mc Graw-Hill, New York, 1970.

[11] L. E. Orgel, *J. Chem. Phys.*, **30**, 1617 (1959).

Table 1

Spin Transfer Coefficients (%) for Metal Ions in Fluoride Lattices

	CNDO			Expt.	INDO			f_s		
	f_σ	f_π	$f_\sigma - f_\pi$	f_ρ	$f_\sigma - f_\pi$	f_σ	f_π	INDO	CNDO	Expt.
V^{II}	0.0	0.3	−0.3	−2.8	−0.93	−0.67	0.26	−0.15	0.0	−0.072
Cr^{III}	−0.01	0.73	−0.74	−4.9	−2.16	−1.52	0.64	−0.18	−0.01	−0.021
Mr^{IV}	−0.02	2.34	−2.36	−9.2	−4.12	−2.33	1.79	−0.17	−0.03	0.1
Cr^{I}	1.24	0.11	1.13	−1.5	0.69	0.74	0.05	0.05	0.28	0.64
Mn^{II}	2.45	0.20	2.25	0.2−1.2	1.53	1.63	0.10	0.10	0.34	0.5
Fe^{III}	7.44	0.72	6.72	3.4	5.33	5.85	0.52	0.35	0.62	0.8
Fe^{II}	2.04	0.14	1.90	2.45	1.37	1.40	0.03	0.07	0.27	0.45
Fe^{I}	0.78	−0.01	0.79	2.2	0.54	0.52	−0.02	0.02	0.15	0.48
Co^{II}	1.76	0.01	1.75	2.4	1.23	1.22	−0.01	0.06	0.21	0.52
Ni^{III}	8.25	−0.05	8.30	8.6	6.04	6.08	0.04	0.13	0.31	0.68
Ni^{II}	1.4	0.01	1.39	3.1	1.07	1.04	−0.03	0.06	0.15	0.53

$f_\rho = f_\sigma - f_\pi$ for d^8, d^5 and d^3 ions. f_ρ is defined in ref. 7 for d^6 and d^7 ions.

f_σ and f_π are essentially the same as those obtained by Brown[3] using calculations at similar level of aproximation, and the overall agreement of the INDO spin densities with the experimental $(f_\sigma - f_\pi)$ values is very satisfactory. Recent studies using the $X\alpha$ multiple scattering method have also shown the importance of a negative f_σ in the d^3 systems.[2]

The computed INDO 2s spin densities are all smaller than the corresponding CNDO values. In absolute terms the agreement with experiment is less satisfactory however, it is significant that Pople's correlation of isotropic ^{19}F couplings showed that the computed fluorine 2s spin densities were also all smaller than indicated by experiment by a factor of about 2.5.[10]

It is worth examining how the exchange process above leads to smaller values for f_s and f_σ with negative values for the d^3 complex ions. In these latter complexes where the metal e_g orbitals are empty the results show that the bonding e_g $(\uparrow)$ orbitals have a larger contribution from the metal when exchange terms are included but that the reverse is true for the bonding e_g $(\downarrow)$ orbitals. This produces a net 7% *excess* of $\uparrow$ in the metal $d_{x^2-y^2}$ and d_z2 orbitals which may be attributed to the inclusion of $d-d$ exchange terms. It is not possible to have a movement of $\uparrow$ towards the metal in this way for high-spin ions with more than five d-electrons since all e_g $(\uparrow)$ orbitals are filled and any change in the form of the molecular orbitals has no effect on the final electron $(\uparrow)$ count. The e_g $(\downarrow)$ bonding orbitals are however occupied and any change in their form will affect the overall difference between spin $\uparrow$ and spin $\downarrow$ occupancies (i. e. f_s and f_σ). For $[\mathrm{Fe^{III}F_6}]$ the calculations show that this e_g $(\downarrow)$ bonding orbital is localised more on the ligands when exchange terms are included. Thus for both $[\mathrm{Cr^{III}F_6}]$ and $[\mathrm{Fe^{III}F_6}]$ the exchange process results in a larger amount of spin $\downarrow$ residing on the ligands and on this basis the spin differences f_s and f_σ are more negative. Although it is clearly not possible to attribute the spin transfer to any specific molecular orbitals in the d^3 complexes, the spin distribution seems to be fairly well represented by the open shell spin $\downarrow$ orbitals for the other complexes.

HEXA AQUO COMPLEXES

We have previously reported CNDO type calculations for these complex ions[12] and shown that the observed proton spin densities[13,14] may be rationalised in terms of a pseudo tetrahedrally bound oxygen atom in all complexes. Calculations using a planar 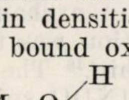 $\mathrm{M{-}O}\langle^{\mathrm{H}}_{\mathrm{H}}$ fragment resulted in far too much spin being transferred through the e_s orbitals. INDO calculated hydrogen 1s spin densities using the same geometry as previously are given in column 2 of table 2. With the exception of $[Cr^{III}(H_2O)_6]^{3+}$ all the values are smaller than those obtained using the CNDO method (column 1, Table 2) and the good agreement with the experimentally derived values is lost. Working on the assumption that the coordination geometry about oxygen in all these complexes is identical we found that a small change in the angle between the M—O bond and the H_2O plane from 125° to 132° led to calculated spin transfer coefficients which were again in good agreement with experiment (column 3, Table 2). It was found that neither the spin ↑ nor the spin ↓ open-shell orbitals alone could be used to describe the spin distribution in these complexes.

---

[12] D. W. Clack and M. S. Farrimond, *L. Chem. Soc.*, (*A*), **1971**, 299.

[13] Z. Luz and R. G. Shullman, *J. Chem. Phys.*, **43**, 3750 (1965).

[14] B. B. Wayland and W. L. Rice, *Inorg. Chem.*, **5**, 54 (1966).

Table 2

% Proton Spin Densities for hexa aquo metal ions

	INDO		CNDO	
	125° (Tetrahedral)	132°	125° (Tetrahedral)	Experimental
$[Cu(H_2O)_6]^{2+}$	0.02	0.03	0.05	0.01
$[Ni(H_2O)_6]^{2+}$	0.05	0.09	0.08	0.03
$[Co(H_2O)_6]^{2+}$	0.07	0.13	0.10	0.11
$[Fe(H_2O)_6]^{2+}$	0.09	0.17	0.14	0.14
$[Mn(H_2O)_6]^{2+}$	0.13	0.22	0.19	0.22
$[Fe(H_2O_6]^{3+}$	0.2	0.39	0.41	0.42
$[Cr(H_2O)_6]^{3+}$	0.42	0.42	0.40	0.42

METALLOCENES

Both ^1H and ^{13}C nuclear magnetic resonance shifts [15,16] have been reported for some of these complexes from which it is possible to derive hydrogen 1*s* and carbon 2*s* spin densities. The sign of the resonance shift changes along the series vanadocene to nickelocene, with vanadocene showing a net positive (↑) spin density at the protons and a negative (↓) spin density in the carbon 2*s* orbital while the reverse applied for nickelocene. One-electron extended Huckel type calculations have been used[17] to account for the spin transfer process to the protons and an exchange type mechanism for the carbon $2p_\pi$-hydrogen 1*s* interaction was taken into account empirically using the McConnell relationship.[18] The results agreed very well with experiment. The CNDO and INDO spin densities are given in table 3. The results for vanadocene $(e_{2g}^2 a_{1g}^1)$ and chromocene $(e_{2g}^3\, a_{1g}^1)$ are in very good agreement with the experimentally derived values for both the magnitude and the sign of the transferred spin. The net positive (↑) spin density on the

---

[15] M. F. Rettig and R. S. Drago, *J. Amer. Chem. Soc.*, **91**, 1361 (1969).

[16] P. K. Burket, H. P. Fritz, F. H. Kohler and H. Rupp, *J. Organomet. Chem.*, **24**, 59 (1970).

[17] M. F. Rettig and R. S. Drago, *J. Amer. Chem. Soc.*, **91**, 3432 (1969).

[18] H. M. McConnell, *J. Chem. Phys.*, **24**, 764 (1956).

protons is dominated by direct delocalisation *via* the a_{1g} molecular orbital as was also found with the extended Huckel calculations and in view of this there is little difference between the INDO and CNDO computed spin densities. The net negative (↓) spin density in the carbon $2s$ orbitals arises by a similar mechanism to that which produces negative spin density in the fluorine $2s$ orbitals of $[Cr^{III}F_6]$ described above, i. e. by spin polarisation through the e_{1g} orbitals. The observed change in sign of the carbon $2s$ spin density is reproduced by the calculations for cobaltocene and nickelocene although the calculated values are smaller than those observed by a factor of about three. In view of the fact that this positive spin density in the carbon $2s$ orbitals arises by direct delocalisation *via* the e_{1g} orbitals it appears that the covalency within this orbital is underestimated by the calculations. This probably explains why the calculations fail to produce a negative (↓) spin density at the protons for cobaltocene and nickelocene in view of the importance of the carbon $2p_\pi$-hydrogen $1s$ exchange polarisation. The INDO calculations do however yield considerably more negative spin density than the CNDO results for these two complexes, although it is insufficient to reverse the sign of the net spin difference density [(↑)−(↓)].

Table 3

Carbon 2 *s* and Hydrogen 1 *s* Transferred Spin Densities (%) for Cyclopentadienyl metal complexes

	Carbon $2s$			Hydrogen $1s$		
	CNDO	INDO	Expt	CNDO	INDO	Expt.
Vanadocene	−0.05	−0.11	−0.12	0.40	0.39	0.49
Chromocene	−0.06	−0.10	−0.07	0.44	0.40	0.49
Manganocene	0.05	0.08	—	0.50	0.36	—
Ferricenium	−0.02	−0.05	—	0.13	−0.01	0.04
Cobaltocene	0.04	0.05	0.18	0.14	0.06	−0.20
Nickelocene	0.05	0.09	0.28	0.12	0.03	−0.49

Table 4

Calculated and Experimental Spin Transfer Coefficients (%) to hydrogen for some Transition Metal Complexes

	CNDO	INDO	Experimental
$[VBz_2]$	0.52	0.63	+0.80
$[CrBz_2]^+$	0.41	0.41	+0.63
$[Cu(sal)_2]$ N−H	0.19	0.26	—
$(Cu-\hat{N}-H=108°)$ C−H	0.47	0.55	1.09
$[Cr(O)(C_2H_4O_2)_2]^-$	+0.01	−0.05	0.12
oxygen $2s$	+0.14	−0.04	0.08

BIS-BENZENE VANADIUM AND CHROMIUM CATION

These axially symmetric d^5 complexes posses a ${}^2A_{1g}$ ($e_{2g}^4\, a_{1g}^1$) ground state and in the light of the spin transfer results for the structurally similar metallocenes, significant proton spin densities are to be expected. The calculated transferred spin densities (Table 4) accord well with the e. s.r. derived values[19-22] for both molecules and it is evident that direct delocalisation *via* the a_{1g} molecular orbital is almost entirely responsible for the observed values. Other workers have also found this to be the case.[23,24] It is of interest to note that the calculations suggest very little spin transfer ($-0.02\,\%$) to the $2s$ orbitals of the benzene ring carbon atoms. This reflects the composition of the open shell a_{1g} orbital which contains less than 1% carbon $2s$ with about $3\,{}^1/_2\%$ contribution from hydrogen $1s$.

HEXACYANO COMPLEXES

Carbon and nitrogen spin densities for $[\mathrm{Fe^{III}(CN)_6}]^{3-}$ and $[\mathrm{Cr^{III}(CN)_6}]^{3-}$, which have the respective electronic configurations t_{2g}^5 and t_{2g}^3, have been indicated by ^{13}C and ^{14}N magnetic resonance studies.[25-28] Although cyano complexes are generally considered to be fairly covalent the results surprisingly showed little spin density transferred to the carbon $2p_\pi$ orbitals. Apart from the nitrogen $2s$ value, the signs and magnitudes of the INDO calculated transferred $2s$ spin densities are in excellent agreement with the experimental values. (Table 5). The mechanism by which the negative spin density arises at the carbon atoms is by exchange polarisation, similar to that in the $[\mathrm{Cr^{III}F_6}]$ species. Although the nitrogen shift appears to be considerably smaller in $[\mathrm{Cr(CN)_6}]^{3-}$ than in $[\mathrm{Fe(CN)_6}]^{3-}$ it is hard to rationalise this in terms of their electronic configurations. The longer metal to carbon bond[29] in the hexacyanochromate ion might be expected to have some effect on reducing the transferred spin density, but even using this distance the calculated value is ~ 4 times the experimental value.

Although the nitrogen atom is further from the metal than the carbon atom in both complexes the computed nitrogen $2p_\pi$ spin density is larger than the carbon $2p_\pi$ density. The calculations suggest that this occurs because the open shell t_{2g} molecular orbital is almost non-bonding in these complexes with the carbon atoms lying near to a nodal

---

[19] R. Prins and F. J. Reinders, *Chem. Phys. Letts*, **3**, 45 (1969).

[20] Y. S. Karimov, V. M. Chibrikin and I. F. Shchegolev, *J. Phys. Chem. Solids*, **24**, 1683 (1963).

[21] S. E. Anderson and R. S. Drago, *J. Amer. Chem. Soc.*, **92**, 4244 (1970).

[22] K. H. Hausser, *Z. Naturforsch*, **16a**, 1190 (1961).

[23] S. E. Anderson and R. S. Drago, *Inorg. Chem.*, **11**, 1564 (1972).

[24] R. Prins, *J. Chem. Phys.*, **50**, 4804 (1969).

[25] A. Loewenstein, M. Shporer and G. Navon, *J. Amer. Chem. Soc.*, **85**, 2855 (1963).

[26] M. Shporer, G. Ron, A. Loewenstein and G. Navon, *Inorg. Chem.*, **4**, 358 (1965).

[27] H. Kuska and M. T. Rogers, *J. Chem. Phys.*, **41**, 3802 (1964).

[28] D. G. Davis and R. J. Kurland, *J. Chem. Phys.*, **46**, 388 (1967).

[29] N. G. Vannerberg and S. Jagner, *Acta. Chem. Scand.*. A28, 623 (1974).

Table 5

Spin Transfer Coefficient s(%) to carbon and nitrogen in hexa-cyano complexes

			CNDO	INDO	Experimental
$[Cr(CN)_6]^{3-}$	C	2s	-0.06	-3.03	-2.6
		$2p_\sigma$	-0.05	-2.87	$P_\sigma - P_\pi = -2.7$
		$2p_\pi$	-1.18	-2.04	
	N	2s	0.0	$+0.21$	$+0.05$
		$2p_\sigma$	0.0	-0.71	—
		$2p_\pi$	$+1.92$	$+2.88$	—
$[Fe(CN)_6]^{3-}$	C	2s	-0.03	-1.08	-1.06
		$2p_\sigma$	-0.03	-1.06	$+1.0, -1.0, +3.0$
		$2p_\pi$	-1.01	-0.74	
	N	2s	0.0	$+0.10$	$+0.14$
		$2p_\sigma$	0.0	-0.23	—
		$2p_\pi$	$+1.80$	$+1.05$	—

surface. On this basis positive (1) spin density is transferred only to the nitrogen $2p_\pi$ orbitals with the negative density arising in the carbon $2p_\pi$ orbitals by polarisation. This model provides an explanation for the failure to observe any significant carbon p-type spin density.

BIS SALICYLIDENEIMINATO COPPER

We have previously[30] given CNDO results for this complex which failed to produce the correct relative magnitudes of the spin density transferred to the hydrogen atoms of the imino carbon and nitrogen.[31] The positions of these hydrogen atoms are not known and we previously assumed a N$-$H bond distance of 1.03 Å with $Cu-\hat{N}-H=122°$. We have now found that the computed spin transfer to this hydrogen is very dependent on its position; thus bending the $Cu-\hat{N}-H$ angle from 108° to 122°, which increases the distance of this hydrogen from the nodal plane from 0.82 Å to 1.15 Å, changed the spin density from 0.19% to 0.74%. Thus it appears that the lack of hyperfine coupling to this proton is due to the closeness of this hydrogen to the nodal plane, as was previously suggested.[31] The calculations give essentially the same spin transfer using CNDO and INDO methods and on this basis the spin delocalisation is largely *via* σ-delocalisation.

CHROMYL ETHYLENE GLYCOLATE ANION

Despite the fact that the hydrogen atoms lie ~3.5 Å from the paramagnetic centre, coupling to these protons is observed in the e. s. r. spectrum.[32] CNDO calculations yielded small positive spin densities at these atoms while calculations which included exchange terms produced significant negative spin densities. Substantial positive oxygen 2s spin density occurs by σ-delocalisation which is reduced to a negative value by exchange polarisation (Table 4). These quantities should be compared with the small value (0.08%) of unknown sign indicated by ^{17}O studies. The INDO values are in reasonably good agreement with the experimental values.

---

[30] D. W. Clack and M. S. Farrimond, *J. Chem. Soc.*, (*Dalton*), 1972, **29**.

[31] A. H. Maki and B. R. McGarvey, *J. Chem. Phys.*, **29**, 35 (1958).

[32] C. J. Winscom, *Mol. Phys.*, **28**, 1579 (1974).

CONCLUSIONS

These results have accounted for the positive spin density that may be transferred to orbitals on ligand atoms bonded directly to the metal ion as in the σ-orbitals of $[Ni^{II}F_6]$ or p_π orbitals of $[Cr^{III}F_6]$, or further removed from the metal as is the case for the hydrogen atoms in the aquometal complexes, bisbenzene species and bissalicylideneiminato copper, by direct delocalisation *via* molecular orbital formation. Small positive spin densities may be reduced or even made to change sign by exchange interactions with neighbouring atoms as in the case of the metallocene complexes and the chromylethyleneglycolate anion. Exchange terms clearly are responsible for the negative spin densities in σ-type orbitals of $[Cr^{III}F_6]$ and cyano complexes, and the nodal properties of the molecular orbitals involved in spin delocalisation in bissalicylideneiminato copper and cyano complexes play an important role in determining the low spin transfer observed to the hydrogen and carbon atoms respectively in these molecules.

M.M. thanks the University of Ryadh, Saudi Arabia, for financial support.

Revue Roumaine de Chimie, **23**, *4*, 505–513 (1978)

CYCLIC VOLTAMMETRY OF STRONTIUM DEPOSITION AND DISSOLUTION IN MOLTEN POTASSIUM NITRATE

S. STERNBERG and T. VIȘAN
Dept. of Physical Chemistry and Electrochemical Technology, Polytechnical Institute
Bucharest

Received September 6, 1976

Cyclic voltammograms were obtained in molten systems $KNO_3-Sr(NO_3)_2$ and KNO_3-SrCl_2 at various potential sweep rates and Sr(II) concentrations. The temperature was maintained constant at 400°. A mechanism for cathodic discharge of the alkaline-earth ions in molten KNO_3 is proposed. The standard potential differences for the cathodic reduction of K(I), Ca(II), Sr(II) and Ba(II) have been calculated from thermodynamic data.

1. INTRODUCTION

Voltammetry with triangular varying potential (cyclic voltammetry) has found wide application in analysis and in investigation of electrode processes mechanism. The first study of a given electrochemical process is often carried out using polarographic technique. At elevated temperatures, the polarography has the disadvantage to use the large polarization times so that it is difficult to eliminate the convective transport of ions to the electrode surface.

The difficulty can be eliminated using chronopotentiometry or voltammetric techniques (linear sweep voltammetry and cyclic voltammetry) where polarization times of only a few seconds are employed.

The chronopotentiometry in molten nitrates has been widely used by us[1,2] whereas the voltammetric techniques have only recently attracted attention.

Francini *et al.*[3,4] used the dropping mercury electrode to study the voltammetric behaviour of several cations and anions in molten nitrates. The cathodic deposition of metals by linear sweep voltammetry was investigated in $NaNO_3-KNO_3$ eutectic [5] at platinum wire electrodes. The reduction of Ag(I) and Pb(II) in molten $NaNO_3-Ba(NO_3)_2$ eutectic

---

[1] S. Sternberg and C. Herdlicka, *Rev. Roumaine Chim.*, **14**, 991 (1969); **15**, 343 (1970).

[2] S. Sternberg and T. Vișan, *Rev. Roumaine Chim.*, **18**, 221 (1973).

[3] M. Francini, S. Martini and C. Monfrini, *Electrochim. Metall.*, **2**, 325 (1967).

[4] M. Francini and S. Martini, *Electrochim. Acta*, **13**, 851 (1968).

[5] G. Mamantov, J. M. Strong and F. R. Clayton, Jr., *Analyt. Chem.*, **40**, 488 (1968).

at platinum wire electrodes was also studied by Behl and Gaur.[6] The cathodic process of Pb(II) is complicated by the reaction of deposited liquid metal with the nitrate solvent to form the oxide.

The technique of cyclic voltammetry was employed by us to study the reduction of Ag(I) in molten KNO_3 at platinum foil electrodes. It was shown that the electrochemical process : $Ag(I)+e=Ag$ in molten nitrates is reversibly and diffusion controlled over the concentration range and sweep rates studied.

In the previous paper the cathodic deposition of Sr(II) ion in molten KNO_3 was studied by means of the chronopotentiometric method. It was the purpose of this work to report the results of cyclic voltammetry of the same system Sr(II)/molten KNO_3 at 400°.

2. EXPERIMENTAL

Voltammetric experiments were made with the conventional technique. The working assembly for the potentiodynamic measurements and the electrolysis cell were identically with those described in the previous paper[7]. Smooth platinum foil electrodes (working electrode and counterelectrode) of 1 cm^2 and 4 cm^2 respectively, were used. The platinum foils were spotwelded to platinum wires sealed in the glass tubes. An Ag wire/0.01 M $AgNO_3$ in 1 kg KNO_3, was the reference electrode. A standard pretreatment was given to the Pt electrodes before each experiments, consisting of heating in a flame for 1 min. The potential was swept in cathodic direction and back by means of a triangular wave generator in conjuction with a d. c. power supply. The electrode potential was also controlled by electronic Philips voltmeter type PM-2440. The cyclograms (cyclic voltammograms) were recorded (the first 3—6 cycles) on a XY recorder Philips. Experiments were carried out at 400° in $KNO_3-Sr(NO_3)_2$ and KNO_3-SrCl_2 solutions, with Sr(II) concentrations of $0.8-12.0\times10^{-2}$ mol/l. The strontium salts were dried by heating at about 200°C for 24 hours, whereas the KNO_3 solvent was recryistallised from bidistilled water and twice melted.

3. RESULTS AND DISSCUSION

Cyclic voltammograms were recorded at different sweep rates between 0.005 and 1.2 V/s, starting of stationary potential in cathodic direction. Figures 1—3 show the cyclic repetitive voltammograms obtained in $KNO_3-Sr(NO_3)_2$ and KNO_3-SrCl_2 solutions at various potential sweep rates and concentrations. The curves plotted in Figures 2—3 are representative and correspond to the "steady state" situation in which further potential cycling resulted in superimposable traces.

During the first sweep the cathodic current peak is observed at about $-0.9\div-1.1$ V and during the returning half-cycle an anodic current peak appears at *ca* $-0.3\div-0.4$ V. The peak potential separation was found to be about 0.5 V.

On the cyclograms of KNO_3 solvent no electrode process was detected in the same potential range, in agreement with previous workers in molten nitrates.[8]

---

[6] W. K. BEHL and H. C. GAUR, A II-a Conferinţă Republicană de Chimie Fizică Generală şi Aplicată, Vol. II, Bucureşti 1970, p. 187.

[7] T. VIŞAN, D. P. GEANĂ and S. STERNBERG, *Rev. Roumaine Chim.*, **21**, 1153 (1976).

[8] S. SHIBATA and M. P. SUMINO, *Electrochim. Acta*, **20**, 871 (1975).

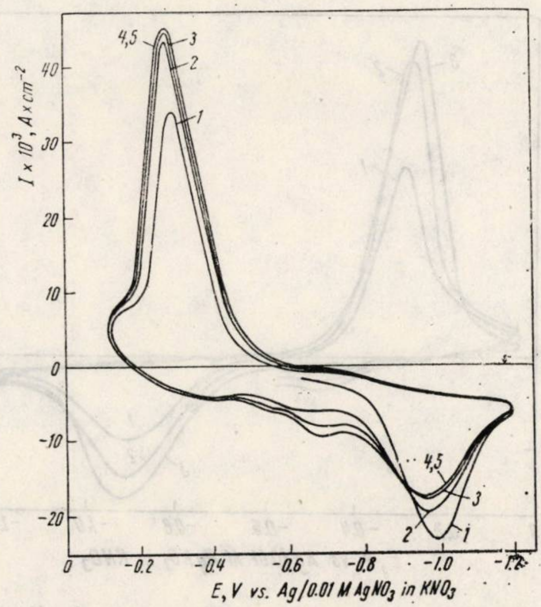

Fig. 1. — Repetitive voltammograms covering the cathodic potential region (−0.1 to −1.2 V) Pt/$KNO_3-Sr(NO_3)_2$; $c=4.25\times10^{-2}$ mol/l; sweep rate 0.33 V/s; temp. 400°.

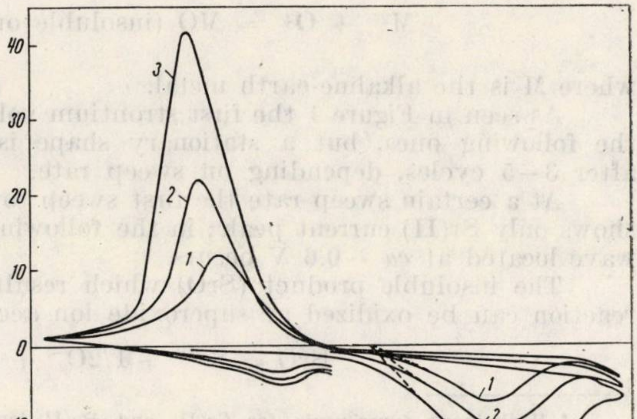

Fig. 2. — Voltammograms (first cycle) in $KNO_3-Sr(NO_3)_2$ system at 400°. Pt electrode; Sr^{2+} conc. 2.46×10^{-2} mol/l; sweep rates: 1—0.032 V/s; 2—0.096 V/s; 3—0.256 V/s.

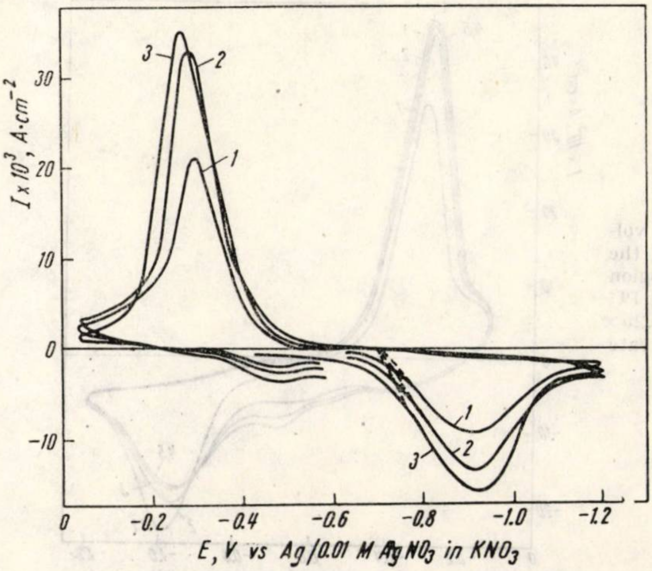

Fig. 3. — Voltammograms (first cycle) in KNO_3-SrCl_2 system at 400°. Pt electrode; Sr^{2+} conc. 4.3×10^{-2} mol/l; sweep rates: 1—0.072 V/s; 2—0.24 V/s; 3—0.36 V/s.

In all the cases the cyclograms of alkaline-earth metal ion/KNO_3 systems * present a great difference $\Delta E_p = E_p$ anodic $- E_p$ cathodic because the charge transfer is complicated by the presence of NO_3^- solvent ion.

No gaseous products were detected on the cathode in any potentials examined. The following cathodic mechanism involving charge transfer followed by an irreversible chemical reaction was proposed:

$$NO_3^- + 2e = NO_2^- + O^{2-} \text{ (soluble)} \tag{1}$$

$$M^{2+} + O^{2-} = MO \text{ (insoluble or soluble)} \tag{2}$$

where M is the alkaline-earth metal.

As seen in Figure 1 the first strontium voltammogram differs from the following ones, but a stationary shape is reached approximately after 3—5 cycles, depending on sweep rate.

At a certain sweep rate the first sweep towards cathodic potential shows only Sr(II) current peak; in the following cycles a new cathodic wave located at *ca* —0.6 V occurs.

The insoluble product (SrO) which results in the main cathodic reaction can be oxidized at superoxide ion according to reaction:

$$SrO = Sr^{2+} + 1/2O_2^- + 3/2e. \tag{3}$$

---

* Preliminary experiments for Ca(II) and Ba(II) ions in molten KNO_3 solvent in the same conditions (sweep rate, ion concentration and temperature) show similarly cathodic peaks at about — 0.7 and — 1.2 V and anodic peaks at ~ — 0.05 and ~ —0.65 V respectively. In Ba(II)/KNO_3 system an additional anodic peak is observed in the region $-1 \div -0.8$ V. This peak can be attributed to the dissolution of the cathodic product deposited by the electrochemical reduction of the K(I) solvent ion.

The sharp anodic peak of voltammogram corresponds to this anodic reaction of dissolution. The ratio of anodic to cathodic peak current (I_{pa}/I_{pc}) is 1.3—1.8. This is a criterion to demonstrate the presence of coupled chemical reaction in the cathodic process.

The presence of a new cathodic current peak in the repetitive voltammograms was assigned to the electrochemical reduction of superoxide ion at peroxide :

$$O_2^- + e = O_2^{2-} \tag{4}$$

The peak currents of strontium reduction were found to increase with sweep rate. As seen in Figures 2—3 the main cathodic peak shifts to more negative potential when the sweep rate was increased, while the position of the second cathodic peak lies practically unchanged. This suggests that the O_2^- electrochemical reduction appears as a reversible process, whereas the observed shift in strontium peak potential with sweep rate may be attributed to the irreversible formation of strontium oxide film at platinum/melt interface. We assume that over a complete cycle the oxide film formed on cathodic sweep was dissolved in the anodic sweep. The ratio between anodic and cathodic peak areas was found approximately 1.1—1.4.

At any Sr(II) concentration a linear relationship between the peak current density (I_{pc}) and the square root of sweep rate ($v^{1/2}$) is obtained (Figures 4—5). This demonstrates that the electrochemical reduction of Sr(II) ion is diffusion controlled.

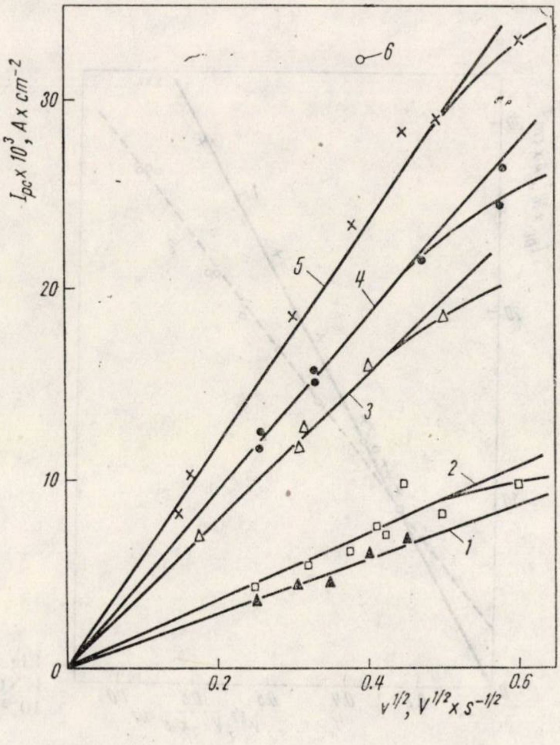

Fig. 4. — Variation of I_p cathodic (first cycle) with $v^{1/2}$ at 400°. Sr^{2+} concentrations : 1—0.86 × 10^{-2} mol/l $Sr(NO_3)_2$; 2—1.7 × 10^{-2} mol/l $SrCl_2$; 3—2.46 × 10^{-2} mol/l $Sr(NO_3)_2$; 4—3 × 10^{-2} mol/l $Sr(NO_3)_2$; 5—4.3 × 10^{-2} mol/l $SrCl_2$; 6—6 × 10^{-2} mol/l $Sr(NO_3)_2$.

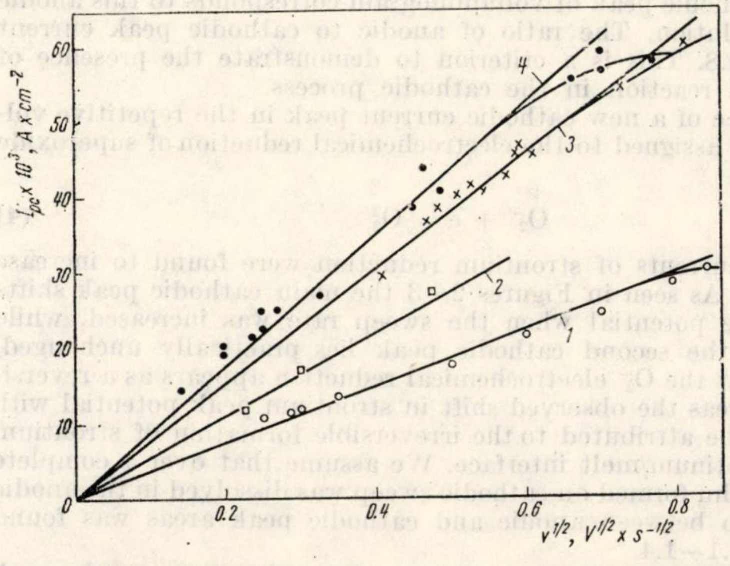

Fig. 5. — Variation of $I_{p\ \text{cathodic}}$ (first cycle) with $v^{1/2}$ at 400°. Sr^{2+} concentrations : 1—4.25×10^{-2} mol/l $Sr(NO_3)_2$; 2—6.77×10^{-2} mol/l $Sr(NO_3)_2$; 3—7.25×10^{-2} mol/l $Sr(NO_3)_2$; 4—10.7×10^{-2} mol/l $Sr(NO_3)_2$.

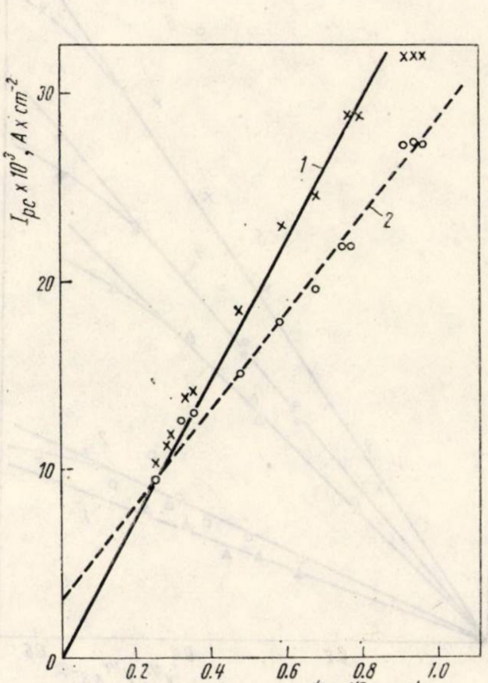

Fig. 6. — Variation of $I_{p\ \text{cathodic}}$ with $v^{1/2}$ $KNO_3 - Sr(NO_3)_2$; temp. 400° ; $c = 4.25 \times 10^{-2}$ mol/l ; 1—for the first cycle ; 2—after reaching of the stationary shape.

The solid line plotted in Figure 6 represents the peak heights for the first sweep. The broken line refers to the repetitive voltammograms, when a stationary situation is reached. This straightline does not intercept the origin of coordinates confirming the occurrence of a complex electrode process.

In a first approximation the diffusion coefficient of Sr(II) ion(D, cm^2/s) can be evaluated from the relation :[9]

$$I_p = \frac{1.082\,(nF)^{3/2}\,cD^{1/2}\,v^{1/2}}{(\pi RT)^{1/2}} \tag{5}$$

where c is Sr(II) concentration and the other symbols have their common signification.

The slopes of linear plots of Figures 4–5 vs. Sr(II) concentration are plotted in Figure 7. The slope of this last straightline was found equal to 11.1×10^2 $V.cm^3/(s^{1/2}.mol)$ at 400°.

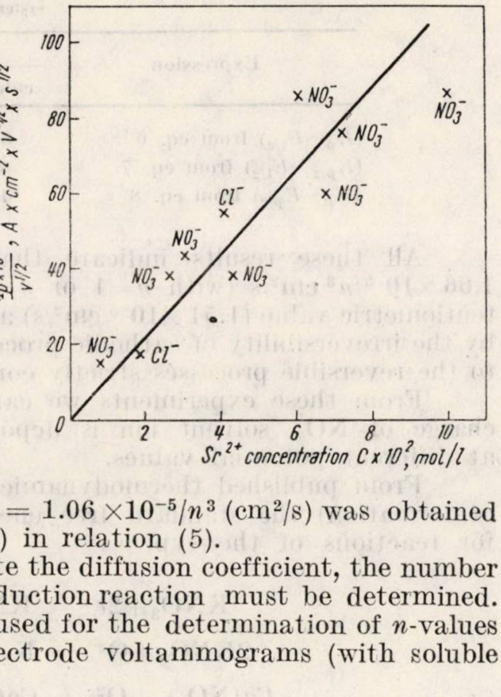

Fig. 7. — Variation of $I_p \times v^{-1/2}$ with conc. of Sr^{2+} at 400°.

The diffusion coefficient $D_{Sr^{2+}} = 1.06 \times 10^{-5}/n^3$ (cm^2/s) was obtained inserting the slope value $I_p/(v^{1/2}.c)$ in relation (5).

Therefore, to correctly estimate the diffusion coefficient, the number of electrons involved in electroreduction reaction must be determined.

The equations that are often used for the determination of n-values in the case of stationary plane electrode voltammograms (with soluble product) are :

$$E_p = E_{1/2} - 1.109\frac{RT}{nF} \tag{6}$$

$$E_{p/2} = E_{1/2} + 1.09\frac{RT}{nF} \tag{7}$$

---

[9] T. Berzins and P. Delahay, *J. Amer. Chem. Soc.*, **75**, 555 (1953).

For the reversible cathodic process involving an insoluble product the $(E_p - E_{p/2})$ difference may be expressed as

$$E_p - E_{p/2} = -0.7725 \frac{RT}{nF} \tag{8}$$

where E_p is the peak potential and $E_{p/2}$ the half-peak potential.

$E_{1/2}$ is the half-wave potential from classical polarography and it can be estimated on cyclic voltammogram at the point where the current density is 85.17 % I_p.

Because the cathodic peak is broad extending over a range of 10—50 mV, it is convenient to use the half-peak potential, namely the relation (7).

The calculated n-values from the equations (6—8) are given in table 1.

Table 1

The n-values as yielded by cyclic voltammetric data equations. Pt/KNO_3 – $Sr(NO_3)_2$ system

Expression	Value, mV		n-value
	calculated	found	
$(E_p - E_{1/2})$ from eq. 6	$64.5/n$	60	1.07
$(E_{p/2} - E_{1/2})$ from eq. 7	$63/n$	60	1.05
$(E_p - E_{p/2})$ from eq. 8	$44.8/n$	120	0.373

All these results indicate that the voltammetric $D_{Sr^{2+}}$ value $1.06 \times 10^{-5}/n^3$ cm²/s (with $n=1$ or $n=2$) is smaller than the chronopotentiometric value (1.54×10^{-5} cm²/s) at 400° . This disagreement is caused by the irreversibility of cathodic process[10], but the relation (5) is applied to the reversible processes strictly controlled by diffusion.

From these experiments we can suppose that the cathodic discharge of NO_3^- solvent ion is depolarized by the alkaline-earth ions at different potential values.

From published thermodynamic data[11] (the standard free energies of formation) the standard free energy changes have been calculated for reactions of the type:

$$KNO_3 + 2e = KNO_2 + O^{2-} \tag{9}$$

$$2KNO_3 + O^{2-} = K_2O + 2NO_3^- \tag{10}$$

$$Ca(NO_3)_2 + O^{2-} = CaO + 2NO_3^- \tag{11}$$

$$Sr(NO_3)_2 + O^{2-} = SrO + 2NO_3^- \tag{12}$$

$$Ba(NO_3)_2 + O^{2-} = BaO + 2NO_3^- \tag{13}$$

---

[10] R. S. Nicholson and I. Shain, *Analyt. Chem.*, **36**, 706 (1964).

[11] * * * Selected Values of Chemical Thermodynamic Properties, part I, N. B. S., Circular 500, 1961.

From these values and the relationship

$$\Delta E = E_{M_2} - E_{M_1} = \frac{-(\Delta G_{M_1(NO_3)_2} + \Delta G_{M_2O} - \Delta G_{M_2(NO_3)_2} - \Delta G_{M_1O})}{0.239\ nF} \qquad (14)$$

the standard potential differences were calculated and listed in table 2.

It was also observed that linear cathodic sections of all voltammograms at different sweep rates intersect in one point on the axis of potential, *i. e.* for Sr(II) ion/molten KNO_3 at −0.8 V (Figures 2–3).

Table 2

Comparison of the standard potential differences ($E_{M_2} - E_{M_1}$) with the voltammetric potential differences. Pt/alkaline-earth ion in molten KNO_3

Ion pairs	$/E_{M_2} - E_{M_1}/$differences, volts	
	experimental[a] (673K)	calculated ($n = 2$; 298K)
Ca – Sr	0.35	0.46
Sr – Ba	0.13	0.12
Ca – Ba	0 48	0.58
Ba – K	0.75	0.85
Sr – K	0.88	0.97
Ca – K	1.23	1.43

[a] The potential difference (Sr-K) has been determined in this work; the other potential difference values were reported in another paper.[12]

The use of these values for differences $E_{M_2} - E_{M_1}$ has given the results presented in table 2. The values calculated with $n = 2$ in equation (14) coincide reasonably well with those derived from experimental voltammetric curves using either the peak potentials, or the half-peak potentials or the intersections on the axis of potential, as described above.

---

[12] S. Sternberg and T. Vişan, *Electrochem. Acta*, to be published.

Revue Roumaine de Chimie, **23**, *4*, 515–522 (1978)

IN SITU EVALUATION OF THE CHEMICAL VAPOR DEPOSITION RATES OF SOME THIN FILMS ON SILICON BY INFRARED INTERFERENCE

CONSTANTIN-EUGEN MOROŞANU * and EUGEN SEGAL **

* Chemical vapor deposition group, Research Institute for Electronic Components ICCE, Str. Erou Iancu Nicolae 32 B, Bucharest R 72996

** Chair of Physical Chemistry and Electrochemical Technology, Polytechnic Institute of Bucharest, Bulevardul Republicii 13

Received February 19, 1976

The results obtained by evaluating the deposition rates of some thin films of materials used in silicon semiconductor technology using a technique based on infrared radiation interference, are presented.

INTRODUCTION

The technique of evaluation of the thin film thickness using interference data allows *in situ* studies of these films and is recommended for kinetic studies.[1-7]

We present the results obtained by applying the technique based on infrared radiation interference to determine the deposition rates of some thin films used in silicon technology.

The method is based on the interference of the infrared radiations emitted from a slice through a thin film whose thickness is varying with time. The intensity of the emitted radiation shows maxima and minima at distances determined by the wavelength of the radiation and the refractive index of the deposited film. Due to absorption of the emitted radiation in the deposited film, the amplitude of the emitted radiation waves decreases with increasing thickness. The distance between two adjacent maxima or minima does not depend on temperature, support and thickness of the deposited film. Measuring this distance and the number of complete cycles we can evaluate the thickness of the deposited films and by recording the time, we can also evaluate the deposition rate of the thin film.

---

[1] D. J. Dumin, *Rev. Sci. Instr.*, **38**, 1107 (1967).

[2] J. F. Roberts, C. A. Clark and A. C. Dumbri, *Rev. Sci. Instr.*, **41**, 247 (1970).

[3] T. I. Kamins and C. J. Dell'Oca, *J. Electrochem. Soc.*, **119**, 112 (1972).

[4] K. Sugawara, T. Yoshimi, H. Okuyama and T. Shirasu, *J. Electrochem. Soc.*, **121**, 1233 (1974).

[5] K. Sugawara, T. Yoshimi, H. Okuyama and Y. Homma, *J. Electrochem. Soc.*, **121**, 1235 (1974).

[6] K. Sugawara, Y. Nakazawa and T. Yoshimi, *J. Electrochem. Soc.*, **123**, 586 (1976).

[7] K. Sugawara, T. Yoshimi, Y. Nakazawa and K. Itoh, *J. Electrochem. Soc.*, **123**, 759 (1976).

EXPERIMENTAL

The gases used (supplied by the Matheson Co.) were: 5% monosilane in U.H.P. nitrogen; carbon dioxide 99.99%; ammonia 99.99%. Line oxygen and nitrogen of 99.99% purity were also used.

The depositions have been performed by passing gaseous reactants at constant flow rates on silicon wafers (250 μ thickness, 32 or 38 mm diameter) in a RF-heated, horizontal, air-cooled reactor.

An outline of the equipment for chemical vapor depositions is given in Figure 1.

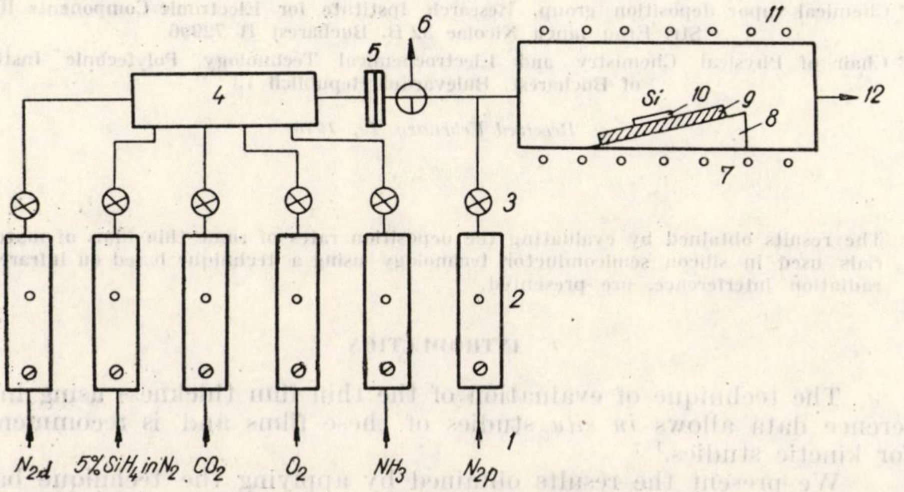

Fig. 1. — An outline of the CVD apparatus. *1* — gases, *2* — flowmeters, *3* — shut-off valves, *4* — mixing chamber, *5* — Millipore filter, *6* — 3-way valve, *7* — quartz reactor, *8* — quartz craddle, *9* — graphite susceptor, *10* — silicon wafer, *11* — R. F. coil, *12* — exhaust.

The equipment contains the following parts: a RF generator, hoods with gas cylinders, a gas distribution panel, a horizontal reactor cabinet, an infrared pyrometer for temperature measurement and for *in situ* monitoring of these depositions, a burner for residual gases.

The gas distribution panel contains Sho Rate 150 Brooks flow-meters including needle valves and Whitey shut-off valves. Pipes are made from AISI-316 stainless, fittings are Swagelok-type.

The horizontal quartz reactor (72 × 34 mm cross-section) was air-cooled. In the reactor, the wafers were placed on a high purity graphite susceptor, located on a quartz craddle.

Nitrogen was used as an inert gas as well as a dilution gas. The nitrogen for dilution N_{2d} was introduced in the mixing chamber together with the reactive gases. The inert nitrogen, N_{2p} was purged directly into the reactor thus protecting the silicon wafers. In some experiments, both kinds of nitrogen sources have been used, because a higher flow rate minimalizes homogeneous reaction and improves the uniformity of the deposited layer.

The temperature was kept constant, with an accuracy of ± 10°, its value being checked on the graphite susceptor before and after the deposition, with the help of the infrared pyrometer.

The following depositions have been carried out in nitrogen atmosphere on uncoated Si, or on single or double submicronic films of coated silicon: polycrystalline silicon obtained by monosilane pyrolytic decomposition, silicon dioxide obtained by oxidation of monosilane in oxygen, or in carbon dioxide, silicon nitride obtained by nitridation of silane with ammonia.

Thickness and deposition rate measurements of the deposited films, have been performed by an infrared pyrometer (IRCON-model 300 LC). The system contains an optical part including PbS detector sensitive in the 2—2.6 μ range (max. sensitivity at 2.4 μ), an amplifier unit and a strip-chart recorder. The temperature range of the pyrometer is 60—1700°. The pyrometer is focused on silicon wafer through the quartz wall of the reactor.

The system for deposition monitoring with an infrared pyrometer is given in Figure 2 and Figure 3 outlines the interference phenomenon of the emitted infrared radiations for uncoated silicon (1) and for single (2) or double (3) coated silicon.

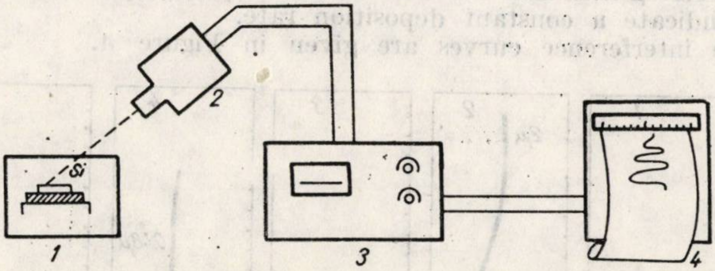

Fig. 2. — In process thickness and deposition rate measurement device. *1* — quartz reactor, *2* — optical head, *3* — amplifier unit, *4* — recorder.

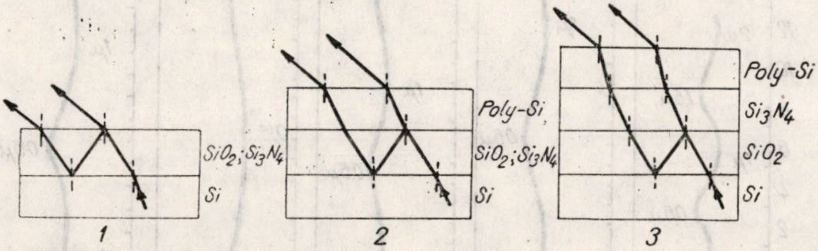

Fig. 3. — Interference occuring in a growing thin film on uncoated, single or two-layer coated silicon.

In the following, the curves output signal of the infrared pyrometer versus time for different deposition processes, temperature and gas flow rates being kept constant, are given. To calibrate the interference curves, thickness determinations have been carried out with a Talysurf IV instrument.

RESULTS AND DISSCUSIONS

A. DEPOSITIONS ON UNCOATED SILICON

1. Deposition of silicon dioxide films by the reaction between monosilane and carbon dioxide

Deposition conditions :

(a) — temperature $t=840°$ (corrected for silicon emissivity),

— pure monosilane flow rate $F_{SiH_4}=5.6$, 8.2 and 11.2 cm³/min,

— carbon dioxide flow rate $F_{CO_2}=3.87$ l/min,

— dilution nitrogen flow rate $F_{N_{2d}}=6.00$ l/min.

— deposition rate $d=800$, 1 050 and 1660 Å/min respectively.

(b) — $t = 775°$ and $715°$; $F_{\mathrm{SiH}_4} = 11.2$ cm³/min ; $F_{\mathrm{CO}_2} = 3.87$ l/min ; $F_{\mathrm{N}_{2d}} = 6$ l/min ; $d = 1\,000$ and 230 Å/min respectively.

First maximum of the interference curve is recorded at 0.5 μ thickness, a cycle corresponding to 1μ thickness. When monosilane flow rate is increased, the distance between extremes decreases, which clearly shows an increase of the deposition rate. At a relatively low temperature (715°) the interference curve is similar, but a new minimum corresponding to a 0.16 μ thickness becomes evident. The analyses of the obtained curves, indicate a constant deposition rate.

The interference curves are given in Figure 4.

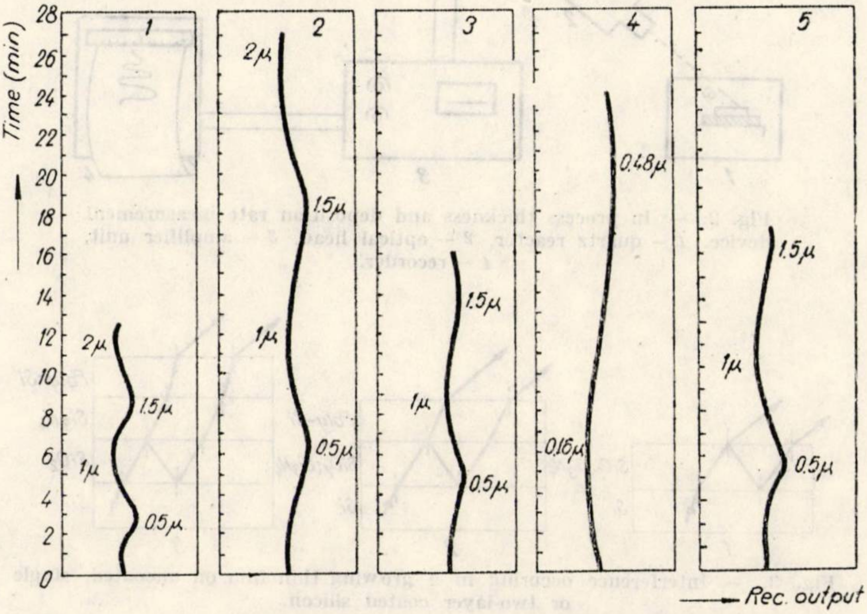

Fig. 4. — Silicon dioxide deposition by monosilane-carbon dioxide system on uncoated silicon. *1* — d = 1660 Å/min, *2* — *d* = 800 Å/min, *3* — *d* = 1050 Å/min, *4* — *d* = 230 Å/min, *5* — *d* = 1 000 Å/min.

2. Deposition of silicon dioxide films obtained by the reaction of silane with oxygen

Deposition conditions : $t = 700°$; $F_{\mathrm{SiH}_4} = 5.6$ cm³/min ; $F_{\mathrm{O}_2} = 1.2$ l/min ; $F_{\mathrm{N}_{2d}} = 9$ l/min ; $d = 400$ Å/min.

Similar curves were obtained for SiO_2 deposition by reaction of monosilane with oxygen, on silicon precoated with a thin film of polycrystalline silicon.

The curves are given in Figure 5.

3. Silicon nitride deposition in the monosilane-ammonia system

Deposition parameters : $t = 840°$; $F_{\mathrm{SiH}_4} = 11.25$ and

15.00 cm³/min ; $F_{\mathrm{NH}_3} = 11.25$ l/min ; $F_{\mathrm{N}_{2d}} = 11.6$ l/min

$F_{\mathrm{N}_{2p}} = 7.87$ l/min ; $d = 750$ and 1 000 Å/min respectively.

The deposition rate is determined with the help of the following extremes: 0.12 μ; 0.28 μ; 0.46 μ; 0.80 μ; etc., a cycle corresponding to 0.34/μ thickness. (Figure 6)

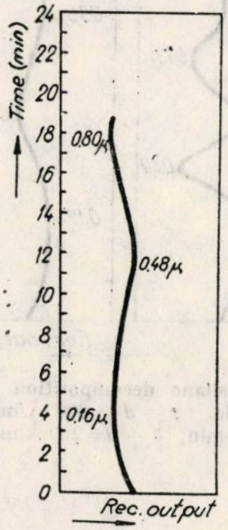

Fig. 5. — Silicon dioxide deposition by monosilane - oxygen system on uncoated and polysilicon coated silicon wafers, $d = 400$ Å/min.

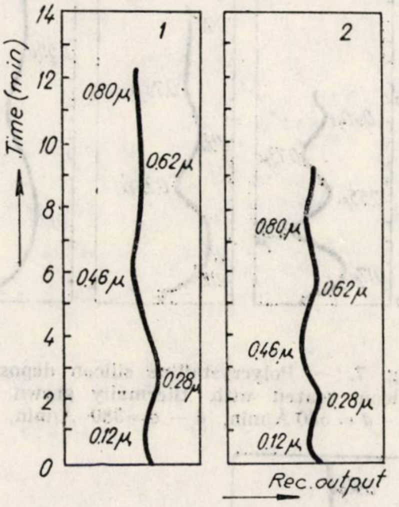

Fig. 6. — Silicon nitride deposition by monosilane-ammonia system on uncoated silicon. *1* — $d = 750$ Å/min, *2* — $d = 1\,000$ Å/min.

B. DEPOSITIONS ON SILICON PRECOATED WITH A SINGLE FILM

1. Deposition of polycrystalline silicon on silicon precoated with thermally grown silicon dioxide

Deposition conditions: $t = 840°$; $F_{\mathrm{SiH_4}} = 5.6$, 8.4 and 11.2 cm³/min; $F_{\mathrm{N}_{2d}} = 9.00$ l/min; $F_{\mathrm{N}_{2d}} = 6.30$ l/min; $d = 380$, 580 and 800 Å/min respectively.

The curves are similar to that obtained by Kamins,[3] but with a higher number of extremes (0.17 μ; 0.39 μ; 0.55 μ; 0.73 μ; 0.9 μ; 10.7 μ; 1.24 μ; and 1.41 μ).

Maintaining the monosilane flow rate at 5.6 cm³/min and varying the temperature at 940° and 800° deposition rates of 640 Å/min and 290 Å/min, respectively were obtained (Figure 7).

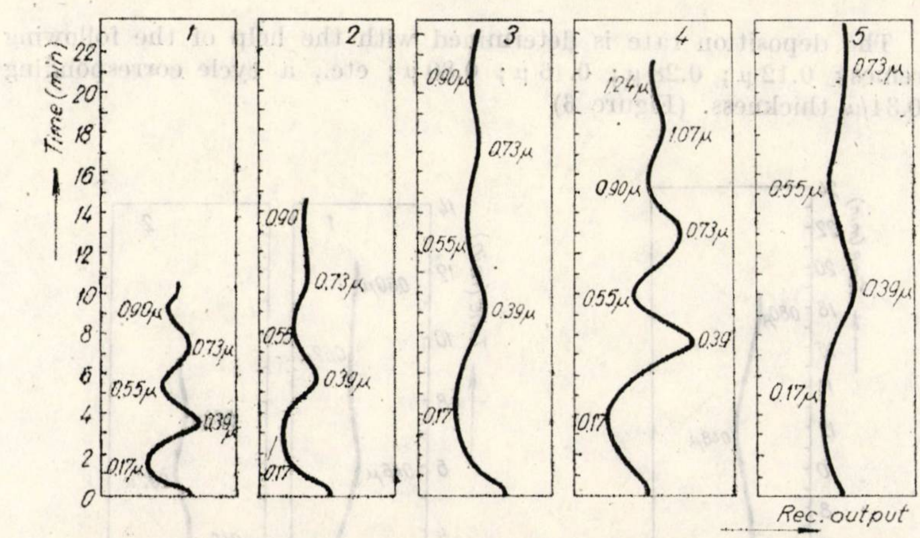

Fig. 7. — Polycrystalline silicon deposition by monosilane decomposition on silicon coated with thermally grown silicon dioxide. *1* — *d* = 800 Å/min, *2* — *d* = 580 Å/min, *3* — *d* = 380 Å/min, *4* — *d* = 640 Å/min, *5* — *d* = 290 Å/min.

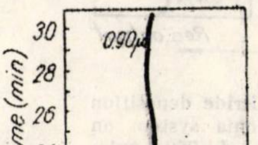

Fig. 8. — Polycrystalline silicon deposition on silicon coated with silicon nitride. *1* — *d* = 210 Å/min, *2* — *d* = 290 Å/min.

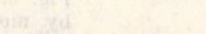

Fig. 9. — Silicon dioxide deposition by monosilane - carbon dioxide system on silicon precoated with polysilicon. *d* = 830 Å/m.

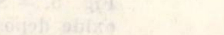

Fig. 10. — Silicon dioxide deposition by monosilane - carbon dioxide. SYSTEM on Silicon precoated with silicon nitride. *d* = 1 000 Å/min.

2. Deposition of polycrystalline silicon, on silicon precoated with silicon nitride

Deposition conditions: $t = 800°$; $F_{SiH_4} = 4.2$ and 5.6 cm³/min; $F_{N_{2d}} = 9$ l/min; $F_{N_{2p}} = 6.3$ l/min; $d = 210$ and 290 Å/min respectively (Figure 8).

3. Deposition of silicon dioxide by monosilane-carbon dioxide system on silicon precoated with polycrystalline silicon

Deposition conditions: $t = 840°$; $F_{SiH_4} = 8.4$ cm³/min; $F_{CO_2} = 3.87$ l/min; $F_{N_{2d}} = 6.00$ l/min; $d = 830$ Å/min (Figure 9).

4. Deposition of silicon dioxide by reaction of monosilane with carbon dioxide on silicon precoated with silicon nitride

Deposition conditions: $t = 840°$; $F_{SiH_4} = 8.4$ cm³/min; $F_{CO_2} = 3.87$ l/min; $F_{N_{2d}} = 6$ l/min; $d = 1\,000$ Å/min (Figure 10).

5. Deposition of silicon nitride by monosilane-ammonia system on silicon precoated with silicon dioxide

Deposition conditions: *a.* $t = 840°$; $F_{SiH_4} = 1.4$; 2.8; and 8.4 cm³/min; $F_{NH_3} = 1.275$ l/min; $F_{N_{2d}} = 6$ l/min; $d = 100$; 230 and 650 Å/min; respectively, *b.* $t = 785°$ and $710°$; $F_{SiH_4} = 8.4$ cm³/min; $F_{NH_3} = 1.275$ l/min; $F_{N_{2d}} = 6$ l/min; $d = 300$ and 180 Å/min respectively.

The determination of the deposition rate is similar to that of silicon nitride deposition on uncoated silicon (Figure 11).

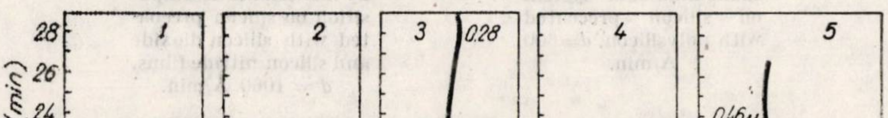

Fig. 11. — Silicon nitride deposition by monosilane-ammonia system on silicon precoated with thermally grown silicon dioxide. *1* — $d = 650$ Å/min, *2* — $d = 230$ Å/min, *3* — $d = 100$ Å/min, *4* — $d = 300$ Å/min, *5* — $d = 180$ Å/min.

6. Deposition of silicon nitride by monosilane-ammonia reaction on silicon precoated with polycrystalline silicon

Deposition conditions: $t = 840°$; $F_{SiH_4} = 8.4$ cm³/min; $F_{NH_3} = 1.275$ l/min; $F_{N_{2d}} = 6$ l/min; $d = 600$ Å/min (Figure 12).

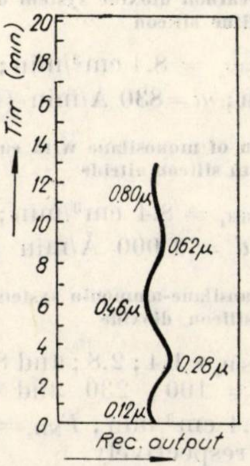

Fig. 12. — Silicon nitride deposition by monosilane-ammonia system on silicon precoated with polysilicon, $d = 600$ Å/min.

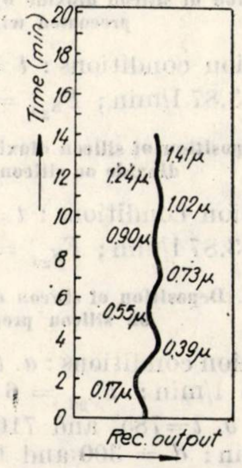

Fig. 13. — Polycrystalline silicon deposition by monosilane decomposition on silicon precoated with silicon dioxide and silicon nitride films. $d = 1060$ Å/min.

C. DEPOSITIONS ON TWO-LAYER COVERED SILICON

1. Depositions of polycrystalline silicon by thermal decomposition of monosilane on silicon precoated with thermal silicon dioxide and pyrolytic silicon nitride

Deposition conditions: $t = 800°$; $F_{SiH_4} = 11.2$ cm³/min; $F_{N_{2d}} = 9$ l/min; $F_{N_{2p}} = 6.3$ l/min; $d = 1\,060$ Å/min (Figure 13).

CONCLUSIONS

Infrared radiation interference method allows an *in situ* control of the thickness and the deposition rate of some thin films used in silicon technology.

Revue Roumaine de Chimie, **23**, *4*, 523 – 526 (1978)

PERTURBATION APPROACHES FOR KINETICS OF ISOTOPE EXCHANGE REACTIONS

M. VLAD

Polytechnical Institute of Bucharest, Institute of Chemistry, Department of Physical Chemistry and Electrochemical Technology, Bd. Republicii 13

Received January 21, 1976

This work presents two approximate methods for integration of the rate equations $-\mathrm{d}a_i/\mathrm{d}t = \mathrm{d}a_i^*/\mathrm{d}t = \sum_{j\neq i}(k_{ji}a_j^*a_i - k_{ij}a_i^*a_j)$ $i = 1,\ldots,n$ $(k_{ij} \gg k_{ij} - k_{ji} \neq 0)$ corresponding to the isotope exchange reactions $A_i^* + A_j \underset{k_{ji}}{\overset{k_{ij}}{\rightleftarrows}} A_j^* + A_i$ $n \geqslant i > j \geqslant 1$.

Let us consider the reactions of isotope exchange [1-4]

$$A_i^* + A_j \underset{k_{ji}}{\overset{k_{ij}}{\rightleftarrows}} A_j^* + A_i \qquad n \geqslant i > j \geqslant 1. \tag{1}$$

The corresponding rate equations are :

$$-\mathrm{d}a_i/\mathrm{d}t = \mathrm{d}a_i^*/\mathrm{d}t = \sum_{j\neq i}(k_{ji}a_j^*a_i - k_{ij}a_i^*a_j) \quad i = 1,\ldots, n \tag{2}$$

or

$$a_i + a_i^* = b_i \quad i = 1,\ldots, n \tag{3}$$

and

$$\mathrm{d}a_i^*/\mathrm{d}t = \sum_{j\neq i}(k_{ji}b_ia_j^* - k_{ij}b_ja_i^*) + \sum_{j\neq i}(k_{ij} - k_{ji})a_i^*a_j^* \quad i = 1,\ldots, n \tag{3'}$$

where $a_i = [A_i]$, $a_i^* = [A_i^*]$ $i = 1,\ldots, n$ and b_i is the total amount of the compound A_i (labeled and unlabeled) $i = 1,\ldots, n$.

If $\beta_{ij} = k_{ij} - k_{ji} = 0$ the rate equations (3′) can be easily integrated. Indeed, for $\beta_{ij} = 0$ Eqs. (3′) become :

$$\mathrm{d}\mathbf{a}^*/\mathrm{d}t = \boldsymbol{\lambda}\mathbf{a}^* \tag{4}$$

---

[1] H. A. McKay, *Nature*, **142**, 957 (1938).

[2] L. R. Darbee, F. E. Jenkins and G. M. Harris, *J. Chem. Phys.*, **25**, 605 (1956).

[3] S. Z. Roginski, "Teoreticheskie osnovy izotopnyh metodov izucheniya khimicheskih reaktsii", Izd. A.N. S.S.S.R., Moskva, 1956.

[4] L. Melander, "Isotope Effects on Reaction Rates", The Ronald Press Company, New York, 1960.

where

$$\mathbf{a}^* = (a_i^*)\ \ i = 1, \ldots, n\,;\ \ \boldsymbol{\lambda} = ||\,\lambda_{ij}\,||,\ \ \lambda_{ij} = k_{ji} b_i\ \ j \neq i,\ \ \lambda_{ii} = -\sum_{j \neq i} \lambda_{ji}\ \ i, j = 1, \ldots, n.$$

The solution of matrix differential equation (4) which fulfils the initial condition $\mathbf{a}^*(t = 0) = \mathbf{a}_0^*$ is[5]

$$\mathbf{a}^*(t) = \mathbf{Z}(t)\mathbf{a}_0^* \tag{5}$$

with

$$\mathbf{Z}(t) \triangleq \exp(\boldsymbol{\lambda} t) = ||\,\eta_{ij}(t)\,||.$$

In fact $k_{ij} \gg \beta_{ij} \neq 0$ and then (5) represents only an approximate solution of Eqs. (3′). Further on, we aim to obtain more accurate expressions for $\mathbf{a}^*(t)$. To achieve this, we shall generalize two techniques used in the theory of quasi steady state approximation.[6, 7]

THE METHOD OF CORRECTION PARAMETERS

The solution of Eqs. (3′) may be written in the form

$$\mathbf{a}^* = \mathbf{Z}(t)[\mathbf{I} + \boldsymbol{\Phi}(t)]\mathbf{a}_0^*\ \ (\boldsymbol{\Phi} = ||\,\varphi_{ij}\,||\ \ i, j = 1, \ldots, n). \tag{6}$$

As $k_{ij} \gg \beta_{ij} \neq 0$ the correction parameters φ_{ij} are small. $(\forall\ |\varphi_{ij}| \ll 1)$. It follows that:

$$a_i^* a_j^* = \sum_{\sigma,\omega} \sum_{\sigma',\omega'} \eta_{i\sigma}\eta_{j\sigma'}(\delta_{\sigma\omega} + \varphi_{\sigma\omega})(\delta_{\sigma'\omega'} + \varphi_{\sigma'\omega'}) \cong$$

$$\cong \sum_{\sigma,\omega} \sum_{\sigma',\omega'} \eta_{i\sigma}\eta_{j\sigma'}(\delta_{\sigma\omega}\delta_{\sigma'\omega'} + \varphi_{\sigma\omega}\delta_{\sigma'\omega'} + \varphi_{\sigma'\omega'}\delta_{\sigma\omega}) \tag{7}$$

By introducing the notations

$$\mathbf{x} = (x_i) = \mathbf{Z}\boldsymbol{\Phi}\mathbf{a}_0^*\ \ i = 1, \ldots, n \text{ and } \mathbf{a}^{*(0)} = \mathbf{Z}\mathbf{a}_0^*$$

Eqs. (6) and (7) become

$$\mathbf{a}^* = \mathbf{a}^{*(0)} + \mathbf{x} \tag{6′}$$

and

$$a_i^* a_j^* = a_i^{*(0)} a_j^{*(0)} + x_i a_j^{*(0)} + x_j a_i^{*(0)}.$$

Inserting Eqs. (6′) and (7′) into (3′) we get

$$\mathrm{d}x_i/\mathrm{d}t + \mathrm{d}a_i^{*(0)}/\mathrm{d}t = \sum_j \lambda_{ij} a_j^{*(0)} + \sum_j \lambda_{ij} x_j + a_i^{*(0)} \sum_{j \neq i} \beta_{ij} a_j^{*(0)} +$$

$$+ x_i \sum_{j \neq i} \beta_{ij} a_j^{*(0)} + a_i^{*(0)} \sum_{j \neq i} \beta_{ij} x_j.$$

---

[5] L. M. Pismen and I. I. Ioffe, *Kinetika i Kataliz*, **2**, 606 (1961).

[6] J. G. Giddings and H. K. Shin, *Trans Faraday Soc*, **57**, 468 (1961).

[7] J. R. Bowen, A. Acrivos and A. K. Oppenheim, *Chem. Eng. Sci.*, **18**, 177 (1963).

But

$$\mathrm{d}a_i^{*(0)}/\mathrm{d}t = \sum_j \lambda_{ij} a_j^{*(0)} \tag{4'}$$

and then

$$\mathrm{d}\mathbf{x}/\mathrm{d}t = \boldsymbol{\lambda}\mathbf{x} + \boldsymbol{\mu}(t)\mathbf{x} + \mathbf{U}_0(t) \tag{8}$$

where

$$\boldsymbol{\mu} = ||\mu_{ij}||, \ \ \mu_{ij} = \beta_{ij} a_i^{*(0)} \ \ i \neq j, \ \ \mu_{ii} = \sum_{j \neq i} \beta_{ij} a_j^{*(0)} \ \ i, j = 1, \ldots, n$$

$$\mathbf{U}_0 = (U_{0i}), \ \ U_{0i} = a_i^{*(0)} \sum_{j \neq i} \beta_{ij} a_j^{*(0)} \quad i = 1, \ldots, n.$$

Integration of Eq. (8) gives:

$$\mathbf{x}(t) = \int_0^t \mathbf{Z}(t-\tau)\,\boldsymbol{\mu}(\tau)\,\mathbf{x}(\tau)\,\mathrm{d}\tau + \int_0^t \mathbf{Z}(t-\tau)\mathbf{U}_0(\tau)\,\mathrm{d}\tau \tag{9}$$

(9) is a Volterra matrix integral equation of the second kind. Its solution is

$$\mathbf{x}(t) = \sum_{n=0}^{\infty} \boldsymbol{\psi}_n(t) \tag{10}$$

with

$$\boldsymbol{\psi}_0(t) = \int_0^t \mathbf{Z}(t-\tau)\mathbf{U}_0(\tau)\,\mathrm{d}\tau\,; \ \ \boldsymbol{\psi}_{n+1}(t) = \int_0^t \mathbf{Z}(t-\tau)\boldsymbol{\mu}(\tau)\boldsymbol{\psi}_n(\tau)\mathrm{d}\tau \quad n = 0,1,\ldots$$

Hence

$$\mathbf{a}^*(t) \cong \mathbf{a}^{*(0)}(t) + \int_0^t \mathbf{Z}(t-\tau)\,\mathbf{U}_0(\tau)\mathrm{d}\tau +$$

$$+ \int_0^t \int_0^\tau \mathbf{Z}(t-\tau)\,\boldsymbol{\mu}(\tau)\,\mathbf{Z}(\tau-\tau')\,\boldsymbol{\mu}(\tau')\,\mathbf{U}_0(\tau)\,\mathrm{d}\tau\,\mathrm{d}\tau' + \ldots$$

Holding the first two terms, we obtain:

$$a_i^*(t) \cong \sum_j \eta_{ij}(t) a_{0j}^* + \sum_k \sum_{l \neq k} \sum_\sigma \sum_\omega \beta_{kl} \int_0^t \eta_{ik}(t-\tau)\,\eta_{k\sigma}(\tau)\,\eta_{l\omega}(\tau)\,a_{0\sigma}^*\,a_{0\omega}^*\,\mathrm{d}\tau \tag{12}$$

A GENERAL PERTURBATION APPROACH

Writing the functions a_i in the form

$$a_i^*(t) = \sum_{\forall\, m_{\alpha\xi}=0}^{\infty} \prod_{\alpha,\xi=1}^{n} \beta_{\alpha\xi}^{m_{\alpha\xi}}\ g_j(\mathbf{M}, t)$$

$\beta_{ii}=0$ $i=1,\ldots,n$; $\mathbf{M}=||m_{\alpha\xi}||$ $\alpha,\ \xi=1,\ldots,n$; $g_j(\mathbf{0},0)=a_{0j}^*$; $g_j(\mathbf{M}\neq\mathbf{0},0)=0$

Eqs. (7) become :

$$\sum_{\forall\, m_{\alpha\xi}=0}^{\infty} \prod_{\alpha,\xi=1}^{n} \beta_{\alpha\xi}^{m_{\alpha\xi}} \left(\frac{\mathrm{d}g_i}{\mathrm{d}t}(\mathbf{M}, t) - \sum_{j} \lambda_{ij}\, g_j(\mathbf{M}, t) \right) -$$

$$- \sum_{j} \sum_{\forall\, m_{\alpha\xi}=1}^{\infty} \prod_{\alpha,\xi=1}^{n} \beta_{\alpha\xi}^{m_{\alpha\xi}}\, \beta_{ij} \sum_{\mathbf{M}'=\mathbf{0}}^{\mathbf{M}} g_i(\mathbf{M} - \mathbf{M}', t)\, g_j(\mathbf{M}, t) \equiv 0. \tag{14}$$

In order that the identity (14) may hold, it is necessary that

$$\frac{\mathrm{d}g_i}{\mathrm{d}t}(\mathbf{0}, t) = \sum_{j} \lambda_{ij}\, g_j(\mathbf{0}, t), \;\; g_i(\mathbf{0}, 0) = a_{0i}^{*} \;\; i = 1, \ldots, n \tag{15}$$

and

$$\frac{\mathrm{d}g_i}{\mathrm{d}t}(\mathbf{M}, t) = \sum_{j} \lambda_{ij} g_j(\mathbf{M}, t) - \sum_{j=j_1, j_2, \ldots} \sum_{\mathbf{M}'=\mathbf{0}}^{\mathbf{M}''_{ij}} g_i(\mathbf{M}''_{ij} - \mathbf{M}', t)\, g_j(\mathbf{M}', t),$$

$$\mathbf{M}''_{ij} = \mathbf{M} - \| \delta_{\alpha i} \delta_{\xi j} \|, \;\; m_{ij\alpha} \geqslant 1, \;\; \alpha \geqslant 1, \;\; g_i(\mathbf{M}, 0) = 0 \tag{16}$$

Eqs. (15) and (16) allow us to find the functions $g_i(\mathbf{M}, t)$. We get :

$$\frac{\mathrm{d}\mathbf{g}}{\mathrm{d}t}(\mathbf{0}, t) = \boldsymbol{\lambda}\mathbf{g}(\mathbf{0}, t)\,; \quad \mathbf{g}(\mathbf{0}, t) = \mathbf{Z}(t)\mathbf{a}_0^{*} \tag{17}$$

$$\frac{\mathrm{d}\mathbf{g}^{(\sigma\omega)}(t)}{\mathrm{d}t} = \boldsymbol{\lambda}\mathbf{g}^{(\sigma\omega)}(t) + \mathbf{H}^{(\sigma\omega)}(t)\,; \;\; \mathbf{g}^{(\sigma\omega)}(t) = \int_0^t \mathbf{Z}(t-\tau)\, \mathbf{H}^{(\sigma\omega)}(\tau)\, \mathrm{d}\tau \tag{17'}$$

. . . .

where

$$g_i(\mathbf{M} = \| \delta_{\alpha\sigma}\, \delta_{\xi\omega} \|, t) = g_i^{(\sigma\omega)}, \;\; H_i^{(\sigma\omega)}(t) = \delta_{i\sigma}\, g_i(\mathbf{0}, t)\, g_\omega(\mathbf{0}, t).$$

Then

$$a_i^{*}(t) = \sum_{j} \eta_{ij}(t) a_{0j}^{*} + \sum_{\sigma} \sum_{\omega} \sum_{k} \beta_{\sigma\omega} \int_0^t \eta_{ik}(t-\tau)\, H_k^{(\sigma\omega)}(\tau)\, \mathrm{d}\tau + \ldots \tag{18}$$

$$a_i^{*}(t) \cong \sum_{j} \eta_{ij}(t) a_{0j}^{*} + \sum_{\sigma} \sum_{\omega} \sum_{r} \sum_{v} \beta_{\sigma\omega} \int_0^t \eta_{i\sigma}(t-\tau)\, \eta_{\sigma r}(\tau)\, \eta_{\omega v}(\tau)\, a_{0r}^{*} a_{0v}^{*}\, \mathrm{d}\tau \tag{18'}$$

We found again Eq. (12)

ACKNOWLEDGEMENT. The author wishes to thank E. Segal, V. Mincu and C. Bendic for their help and encouragement.

Revue Roumaine de Chimie, **23**, *4*, 527–534 (1978)

ANODIC OXIDATION OF PRIMARY ALCOHOLS

ELENA CONSTANTINESCU and VIOREL BRÎNZOI
Institute of Chemistry, Faculty of Chemistry, Department of Physical Chemistry,
Bd. Republicii 13, Bucharest

Received November 19, 1975

Using the potentiostatic method and smooth platinum electrodes, the anodic oxidation of the following primary alcohols: methanol, ethanol, *n*-propanol, *n*-butanol, isobutanol and *n*-pentanol in 1N H_2SO_4 have been investigated. The anodic oxidation curves exibit the same shape. The current peaks occur typically in the same range of potential regardless of the nature and concentration of oxidized substance. The similarity in electrochemical behaviour of the alcohols leads to a common anodic oxidation mechanism.

INTRODUCTION

The study of electrochemical oxidation of organic compounds has received considerable attention during the last decade particularly because of the increased interest for fuel cells technology.

The study requires the analysis of:

— electrode-kinetics problems involving the determination of reaction rates depending on the electric parameter — the electrode potential;

— usual thermal kinetics problems concernning reactants' and intermediates' concentrations;

— catalysis problems concerning electrode nature influence on reaction rates.

From all these groups of problems we have chosen the first one, applied to the following primary alcohols: methanol, ethanol, *n*-propanol, *n*-butanol, isobutanol and *n*-pentanol.

EXPERIMENTAL

The experiments were carried out in an electrolytic glass cell with separate anodic and cathodic compartiments (Figure 1).

As working electrode, a smooth platinum plate with a geometrical area of 1 cm^2, as counter and reference electrode, a platinum wire of about 0.8 mm Ø and the saturated calomel electrode respectively were used. The working and the reference electrodes were connected by a Haber Luggin capillary.

The smooth platinum electrode was controlled, varied and measured by means of a Tacussel potentiostatic equipment made up of a PRT 20–2 potentiostat, a 9/A Servovit automatic pilot and a S6/G4R millivoltmeter. The current-potential curves were obtained by means of a Graphispot recording galvanometer.

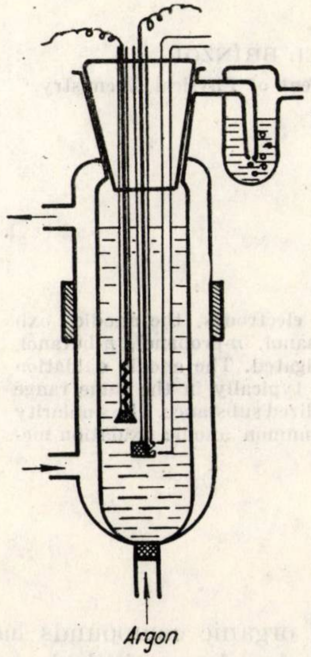

Fig. 1. — Electrolytic cell.

Before each electrochemical measurements the electrodes were treated by repeated anodic and cathodic polarisation as was recommended by Bagotzky.[1]

The solutions have been prepared from p. a. reagents and doubly distilled water. The supporting electrolyte was 1 N H_2SO_4.

All the measurements were performed in the presence of pure argon bubbled through the electrolytic cell. The temperature was kept constant by recirculating a water current from a thermostat bath. A linear potential increase in a range of potential: (–200 mV) – (+1400 mV) either single sweep or in cycles has been imposed.

RESULTS

The controlled potential anodic polarization curves of the studied primary alcohols has pointed out several regularities, noticed by the other authors too. Even in the case of other substances which are oxidized in the same potential region, they exhibit similar curves with current maxima and minima located within the same range of potential regardless of the nature and the concentration of organic compounds [1-4].

In the case of anodic potential sweep two current-peaks (i_{p_1} and i_{p_2}) are noticed on the polarization curve within the range of potential 500–600 mV and 950–1050 mV (E. S. C.) respectively. At the reverse potential sweep the curves exhibit only one maximum within the range of potential of 200–400 mV (E. S. C.). (Figure 2). A growth of the height of peak current-densities with temperature is noticed and also a tendency of approach between the two peaks.

METHANOL

In the case of methanol, the experiments have been carried out with 1 M alcohol concentration at 25° and a voltage sweep rate v = 1100 mV/mn.

---

[1] V. S. Bagotzky and Yu. B. Vasilyev, *Electrochim. Acta*, **9**, 869 (1964).
[2] M. W. Breiter and S. Gilman, *J. Electrochem. Soc.*, **109**, 622, 1099 (1962).
[3] M. W. Breiter and S. Gilman, *Electrochim. Acta.*, **8**, 447, 457 (1963).
[4] R. P. Buck and L. R. Griffith, *J. Electrochem. Soc.*, **109**, 1005 (1962).

The methanol oxidation rate dependence on temperature has been also studied. All the characteristic magnitudes of the recorded anodic polarization curves are given in the table 1.

Table 1

Methanol oxidation rate dependence on temperature at $v = 1000$ mV/mn

	$t°$	E_{p_1} (mV)	E_{p_2} (mV)	i_{p_1} (mA/cm²)	i_{p_2} (mA/cm²)
1M Methanol in 1N H_2SO_4	25°	587	1060	1.71	1.41
	30°	551	1054	2.87	2.01
	40°	552	1054	5.7	2.76
	50°	550	1018	11.2	3.8

ETHANOL

In the case of ethanol, the experiments have been carried out with 0.2 M alcohol concentration at 25° and at the following voltage sweep rates (v) : 400 mV/mn, 600 mV/mn, 800 mV/mn (Figure 2) and 1100 mV/mn.

The height of the peak current-densities increases with the voltage sweep rate for both i_{p_1} and i_{p_2}, without any influence on the potential range within the peaks are located.

All the characteristic magnitudes of the recorded curves are given in the table 2.

The plot of the i_{p_1} or i_{p_2} vs. v (Figure 3) gives a linear dependence according to Nicholson's equation :[5]

$$i_p = (1 - \theta)\frac{KF}{RT}v. \quad \text{or} \quad i_p = \text{const.}\, v.$$

The ethanol oxidation rate dependence on temperature has been also studied. There has been used 0.2 M ethanol at the following temperatures : 25°, 45° and 65° and a voltage sweep rate $v=1100$ mV/mn (Figure 4).

A remarkable growth of the height of peak-current densities with temperature is noticed and $i_{p_1} > i_{p_2}$.

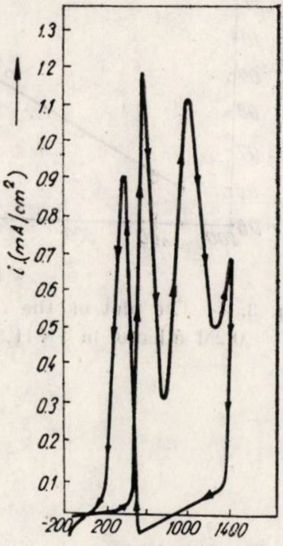

Fig. 2.— Current-potential curve for 0.2M ethanol in 1N H_2SO_4 at 25°±0.1° and a voltage sweep rate of 800 mV/mn.

The plot of log i_{p_1} or i_{p_2} vs. 1/T leads to a straight line according to Arrhenius type equation :

$$i_p = A \exp(-E/RT) \text{ or } \ln i_p = \ln A - \frac{E}{RT}$$

---

[5] R. S. Nicholson and I. Shain, *Analyt. Chem.*, **36**, 706 (1964).

Table 2

The oxidation peaks height dependence on the voltage sweep rate at 25°

	v (mV/mn)	E_{p_1} (mV)	E_{p_2} (mV)	i_{p_1}(mA/cm²)	i_{p_2}(mA/cm²)
0.2 M Ethanol in 1N H_2SO_4	400	572	998	1.23	0.62
	600	580	1 000	1.29	0.73
	800	546	973	1.32	0.88
	1 100	570	1 009	1.41	0.96

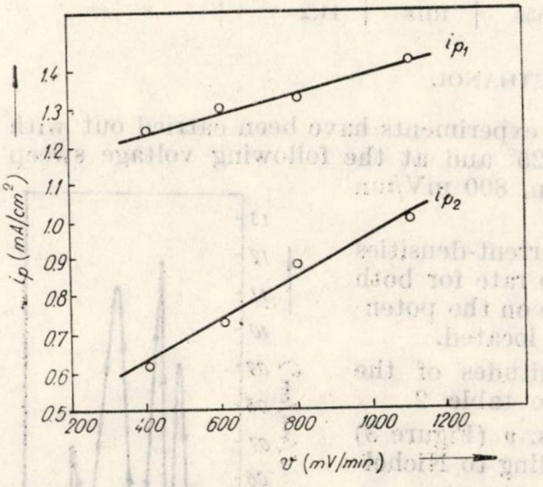

Fig. 3. — The plot of the i_{p_1} and i_{p_2} vs. v for 0.2M ethanol in 1N H_2SO_4 at 25±0.1°.

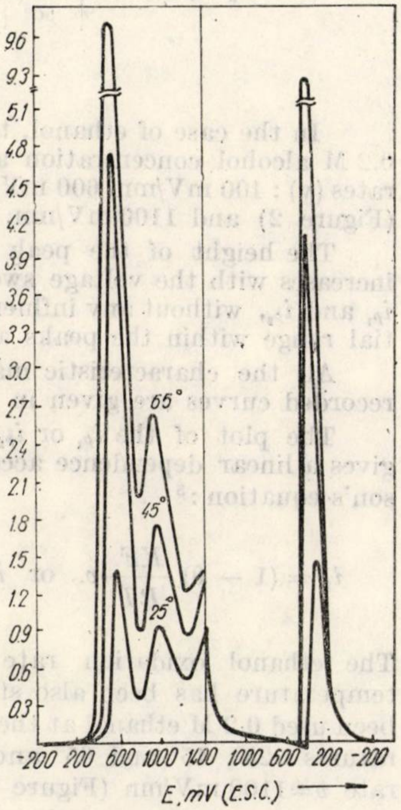

Fig. 4. — Current-potential curves for 0.2M ethanol in 1N H_2SO_4 at 25°, 45°, 65° and a voltage sweep rate of 1100 mV/mn.

The values of apparent energy of activation are ≃ 9 Kcal/mol and ≃ 5 Kcal/mol respectively.

n-PROPANOL

In the case of *n*-propanol anodic oxidation, the curves exhibit the same shape as with the other alcohols. Curves with two current peaks located in the same range of potentials are obtained (Figure 5).

The oxidation rate grows by *n*-propanol concentration increase. The concentrations are the following ones : 0.05 M, 0.2 M and 0.8 M. Current peaks occur invariably in the same potential ranges and are not influenced by alcohol concentration. The results are illustrated by table 3.

A linear dependence of current density i_{p_1} or i_{p_2} with alcohol concentration is noticed.

For the 0.2 M alcohol concentration has been studied the dependence of n-propanol oxidation rate with temperature. It may be noticed that $i_{p_1} > i_{p_2}$ and that both current maxima increase with temperature (see Table 4).

From the plotting of log i_{p_1} and log i_{p_2} vs. $^1/T$ the following values of apparent energy of activation may be found : 7Kcal/mol and 6 Kcal/mol.

There have been recorded current-potential curves for the voltage sweep rates v : 400 ; 600 ; 800 ; 1100 mV/mn at 25° and for 0.2 M alcohol concentration.

The magnitudes of these curves are shown in table 5.

We may notice an increase of the alcohol oxidation rate with the sweep rate.

The values of i_{p_1}, i_{p_2} are very close to each other.

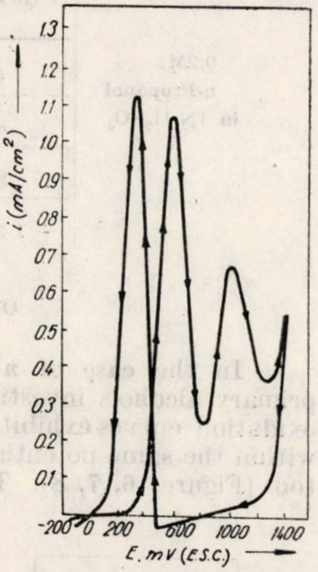

Fig. 5. — Current-potential curve for 0.2M *n*-propanol in 1N H_2SO_4 at 25°±0.1° and a voltage sweep rate of 1100 mV/mn.

Table 3

***n*-Propanol oxidation rate dependence on concentration at 25° and v = 1 000 mV/mn**

Alcohol + 1N H_2SO_4	E_{p_1}(mV)	E_{p_2}(mV)	i_{p_1}(mA/cm²)	i_{p_2}(mA/cm²)
n-Propanol 0.05M	606	1046	0.32	0.34
n-Propanol 0.2M	569	1009	1.09	1.02
n-Propanol 0.8M	606	1009	2.61	2.52

Table 4

***n*-Propanol oxidation rate dependence on temperature at 25° and c = 0.2M**

	t°	E_{p_1}(mV)	E_{p_2}(mV)	i_{p_1}(mA/cm²)	i_{p_2}(mA/cm²)
0.2M *n*-Propanol in 1N HS_2O_4	25°	569	1009	1.20	1.11
	45°	569	991	2.67	2.19
	65°	643	991	5.37	3.24

Table 5

The oxidation peaks height dependence on the voltage sweep rate at 25°

	v (mV/mn)	E_{p_1}(mV)	E_{p_2}(mV)	i_{p_1}(mA/cm²)	i_{p_2}(mA/cm²)
0.2M *n*-Propanol in 1N H_2SO_4	400	572	1025	0.96	0.72
	600	580	1020	1.12	0.83
	800	573	1026	1.20	0.94
	1 100	569	1009	1.23	1.02

OTHER PRIMARY ALCOHOLS

In the case of *n*-butanol, isobutanol and *n*-pentanol, the other primary alcohols investigated by us, it may be noticed that the anodic oxidation curves exhibit the same shape. The current peaks are located within the same potential ranges as with the first three primary alcohols too (Figures 6, 7, 8). Taking into account the results presented one can conclude that the growth of the hydrocarbon chain does not influence the potential range within which the oxidation peaks are located. The only influence which can be noticed consists in the decrease of the oxidation peaks height with the hydrocarbon chain length (see Table 6).

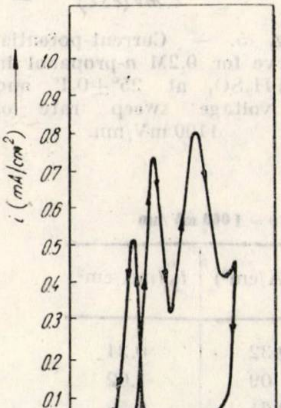

Fig. 6. — The plot of the log *i* vs. log *c* for 0.05M, 0.2M and 0.8M *n*-propanol at 25±0.1° and a voltage sweep rate of 1 100 mV/mn.

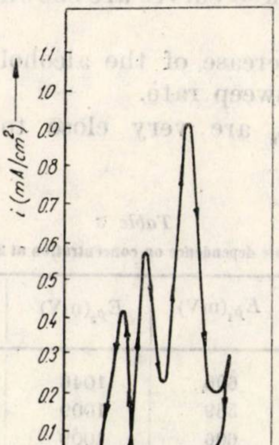

Fig. 7. — Current-potential curve for 0.2M *n*-butanol in 1N H_2SO_4 at 25°±0.1° and a voltage sweep rate of 1 100 mV/mn.

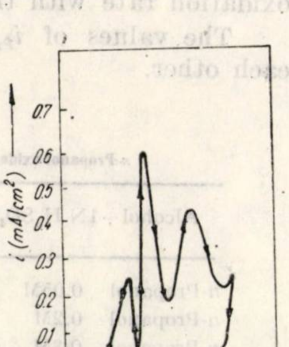

Fig. 8. — Current-potential curve for 0.2M isobutanol in 1N H_2SO_4 at 25°±0.1° and a voltage sweep rate of 1 100 mV/mn.

Table 6

The oxidation peaks height dependence on the hydrocarbon chain length at 25° and voltage sweep rate $v = 1100$ mV/mn

Alcohol + 1N H_2SO_4		E_{p_1} (mV)	E_{p_2}(mV)	i_{p_1}(mA/cm^2)	i_{p_2}(mA/cm^2)
n-ethanol	0.2M	569	1009	1.41	0.96
n-propanol	0.2M	569	1009	0.93	1.15
n-butanol	0.2M	606	1046	0.73	0.79

DISCUSSION

The analysis of the oxidation curves of the studied primary alcohols indicates two current peaks and a corresponding number of minima dividing the oxidation range into a number of separate regions regardless of the nature and concentration of alcohols.

The phenomena observed depend on the conditions of the experiments. The same regularities are observed by other researchers as well, working even with other organic compounds under the same conditions.[1–4]

The minima zones mark a slowing down of the reaction and indicate the presence of several different oxygen types adsorbed on the platinum electrode. The beginning of the oxygen adsorption zones coincides with the current decrease beginning on the anodic polarization curves and the end of these zones with the current minimum density.

The dependence of the logarithm of oxidation rate upon potential on the ascending sections of polarisation curves is linear, and has a slope of 0.11—0.12 (for instance, methanol). The kinetic equation can be written :

$$i = k \exp (\beta F \varphi / RT)$$

where $\beta = 0.5$

On the descending sections where the reaction is slowed down by adsorbed oxygen, a linear dependence of oxidation rate upon potential is also observed with the same value of the slope, but of opposite sign.

Since in these potential zones the amount of adsorbed oxygen rises lineary with potential increase, the kinetic equation for this part of curves can be written :

$$i = k \exp (- K'[\mathrm{O}_{\mathrm{ads}}]) \cdot \exp (\beta F \varphi / RT)$$

i. e. inhibition of the reaction grows exponentially with the amount of adsorbed oxygen.

In the potential zone of the second current-increase the current in general comprises the oxidation current in the presence of adsorbed oxygen and the residual oxidation current in those zones of the surface that are not yet subject to the action of the adsorbed oxygen.

Consequently, we may say that the anodic oxidation processes of organic compounds may be accelerated by a potential shift towards the more positive magnitudes and in the presence of adsorbed oxygen.

The kinetic equation of dependence of the reaction rate of alcohol on its concentration is the following one:

$$i = kc^{\alpha}.$$

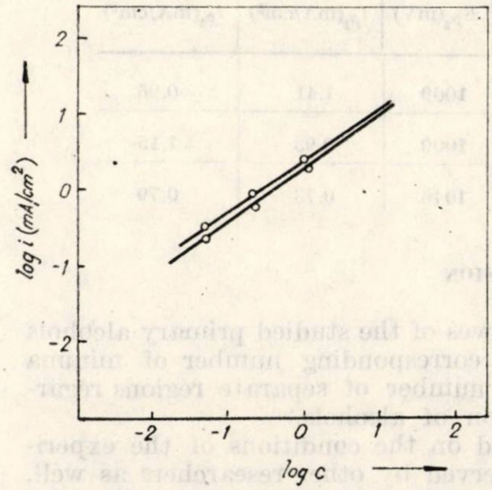

Fig. 9. — Current-potential curve for 0.05M *n*-pentanol in 1N H_2SO_4 at 25°±0.1° and a voltage sweep rate of 1100 mV/mn.

The plot of the log i vs. log c leads for all studied alcohols potentials to a sub-unitary value for the reaction order $0 < \alpha < 1$. As an example has been chosen the case of propanol (Figure 9).

This indicates that reactant particles are adsorbed on the unhomogeneous surface of platinum.

In the potential range of the first peak it may be assumed, according to Rightmire's[6] arguments in the case of ethanol, that there is a radical of the form $CH_3-\underset{\cdot}{C}H-OH$ and in the range of the second peak a radical of the form $CH_3-CH_2-O^{\cdot}$.

Through analogy we may assume the formation of some radicals of the same type in the case of the other studied alcohols $R-CH-OH$ and $R-\underset{\cdot}{C}H_2-O^{\cdot}$ respectively.

The oxidation process would take place in two steps, according to the scheme:

$$R-CH_2-OH \rightarrow R-\underset{\cdot}{C}H-OH + H^+ + e^-$$
$$R-\underset{\bullet}{C}H-OH \rightarrow R-CHO + H^+ + e^-$$

the first one rapidly, and the second one slowly, R being-CH_3, $-C_2H_5$, $-C_3H_7$, $-C_4H_9$.

Thus, if we compare the obtained curves between them under the same experimental conditions one can conclude that the anodic oxidation of primary alcohols occurs according to the same mechanism.

On basis of the results obtained by us and by others and particularly on basis of Bagotzky's[1,7] studies we may suppose that alcohols are subject to dissociative chemisorption on the surface of the platinum electrode, accompanied by the direct oxidation of the resulting radicals.

---

[6] R. A. Rightmire, R. L. Rowland, D. L. Boos and D. L. Beals, *J. Electrochem. Soc.*, **111**, 242 (1964).

[7] V. S. Bagotzky and Yu. B. Vasilyev, *Electrochim. Acta*, **11**, 1439 (1966).

Revue Roumaine de Chimie, **23**, *4*, 535–540 (1978)

INFRARED SPECTRAL STUDY OF HYDROGEN BONDING IN ETHYL ALCOHOL ABSORBED IN POLYETHYLENE SHEETS

SIMONA BĂDILESCU, VOICA TĂLPUŞ and RODICA RACOTĂ
Spectroscopy Laboratory, Petrochemical Works Piteşti

Received January 6, 1976

A spectral study of hydrogen bonding in ethyl alcohol absorbed in polyethylene sheet was performed and the different associated species present in the amorphous region of the polymer, were evidenced. The influence of the temperature and of the microstructure of the polymer amorphous phase on the liquid absorption have been studied.

INTRODUCTION

Transparent polyethylene (PE) sheets were used for a long time in spectroscopy, either to protect the potassium bromide windows against to aggresive solution [1-7] or as matrix material for solid samples.[8,9] A sealed liquid cell with PE windows for far infrared region was also described by Tsasas.[7] Polyethylene is an optical material affording a good transmittance in the infrared excepting the following spectral ranges: 700–800, 1200–1400 and 2700–3000 cm^{-1} which are covered by the strong methyl- and methylene- absorption. [10-13]

In a recent paper [14] it was reported that PE sheets have been used as matrix for liquids by swelling the PE sheet into the studied liquid.

The dependence of liquid absorption on polymer structure (crystallinity degree, branching, molecular weight distribution) has been evidenced in an earlier study. [15]

---

[1] T. Robinson, *Nature*, **184**, 448 (1959).

[2] G. J. Lawson and J. W. Purdie, *Chem. and Ind.*, 1961 508

[3] F. F. Ferrand, *Appl. Spectroscopy*, **16**, 23 (1962).

[4] I. Cohen, *J. Chem. Educ.*, **39**, 262 (1958).

[5] A. D. E. Pullen and J. Mc. C. Pollock, *Trans. Faraday Soc.*, **54**, 11 (1958).

[6] P. A. Giguere and R. Savoie, *Canad. J. Chem.*, **38**, 2467 (1960).

[7] A. T. Tsatsas and W. M. Risen Jr., *Appl. Spectroscopy*, **24**, 383 (1970).

[8] L. May and K. Schwing, *Appl. Spectroscopy*, **17**, 166 (1963).

[9] J. W. Brasch and R. J. Jakobsen, *Spectrochim. Acta*, **20**, 1644 (1964).

[10] J. J. Fox and A. E. Martin, *Proc. Roy. Soc.*, **A175**, 208 (1940).

[11] L. H. Cross, R. D. Richards and H. A. Willis, *Discuss. Faraday Soc.*, **9**, 235 (1950).

[12] F. M. Rugg, J. J. Smith and L. H. Waterman, *J. Polymer Sci.*, **11**, 1 (1953).

[13] S. Badilescu, M. Toader, H. Oprea and I. I. Badilescu, *Materiale Plastice*, **7**, 468 (1970).

[14] N. A. Minaeva and N. A. Chiumaevski, *Zhur priklad Spektr.*, **22**, 729 (1975).

[15] S. Badilescu, V. Talpus, R. Schiau and I. Gonciulea, *Materiale Plastice*, in press

In this paper, we wish to report some results concerning the hydrogen bonding in ethyl alcohol in a PE matrix.

EXPERIMENTAL

The pressing ensemble in two plane brass plates sandwiched between other two steel ones. The polymeric material was placed between the brass plates and pressed on an electrical press at 150° for 5 minutes at 50 Kgf/cm^2 with a preheating time of 5 minutes and a cooling time of 5 minutes at 40°. Rectangular pieces with a thickness of 0.25 ± 0.02 mm were cut from the sheet. The sample, supported in a special holder, was immersed into the studied liquid. Spectra were run on a grating spectrophotometer Grubb Parson. In the reference beam, PE sheet of the same grade was placed.

The desorption of the sheets were performed by heating at about 60° and checked up spectrophotometrically.

RESULTS AND DISCUSSIONS

The properties of the PE grades used as matrix material are given in table 1. Figure 1 gives the change of O—H stretching frequencie belonging to the different polymer species over a period of ten hours The absorption at different temperatures (43—a, 50° — b and 60°—c) for oligomer (1) and higher polymer species of ethyl alcohol (2) are presented in Figure 2. The liquid absorption in the sheet was followed by means of absorbance value. The relative concentration of different species expressed by means of the absorbance ratio (E_1/E_2) is represented in Figure 3.

Figure 4 shows comparatively the liquid absorption in the two polymer grades. The results obtained for an annealed sheet (by absorption and subsequent desorption) are recorded in Figure 5.

Table 1

Structural peculiarities of the used PE grades

Grade	Density (g/cm^3)	Branching degree (CH$_3$/1000C)	Melt Flow Index (g/10′)	Nonnewtonian Flow Index
A	0.970	1	5.5	26
B	0.953	3—5	0.9	24

The spectrum of ethyl alcohol in PE matrix shows in the 3000 cm^{-1} range two well defined bands: a band near 3585 cm^{-1}, which may be due to H — bonded O—H in the dimer or trimer species, and a much broader band near 3330 cm^{-1} which was assigned to the polymer species. There has been considerable discussion about the various associated species which are present in alcohol solution. Recent calculations by Murthy et al.,[16] as well as the experimental work of Bellamy and Pace[17]

---

[16] A. S. N. Murthy, R. E. Davis and C. N. R. Rao, *Theor. Chim. Acta*, **13**, 81 (1968).
[17] L. J. Bellamy and R. J. Pace, *Spectrochim. Acta*, **22**, 525 (1966).

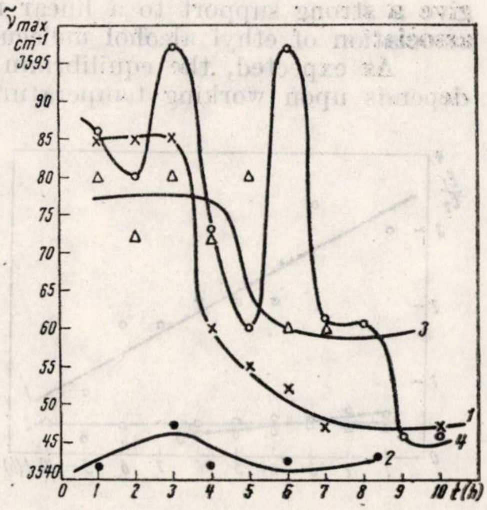

Fig. 1. — The change of O—H stretching frequencies belonging to the different alcohol polymer species absorbed in PE sheet.

1 —PE(A) at 50°; 2—PE(A) at 60°; 3—PE(B) at 60°; 4—PE (A) at 50° (in mixed alcohol — acetone oligomer species)

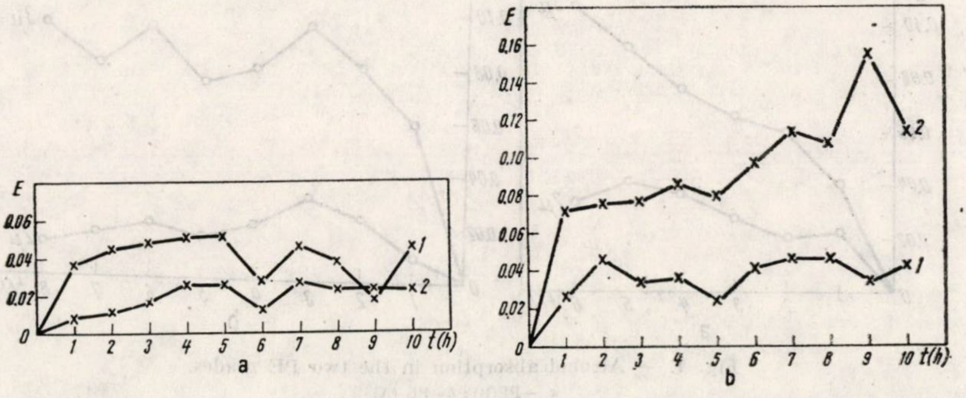

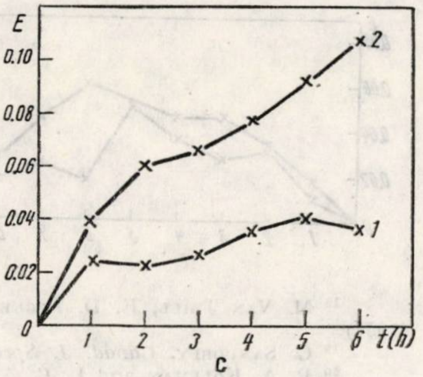

Fig. 2. — The absorption at different temperatures (40°—*a*, 50°—*b* and 60°—*c*) for oligomer (1) and higher polymer species of ethyl alcohol (2).

give a strong support to a linear rather than cyclic dimer and trimer association of ethyl alcohol molecules.[18]

As expected, the equilibrium between different associated species depends upon working temperature and polymer structure. [19,20]

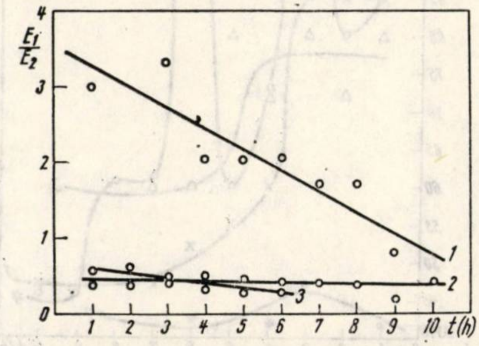

Fig. 3. — The relative concentration of different species absorbed in PE (E_1 — absorbance corresponding to oligomers; E_2 — absorbance corresponding to polymer species).
1 – 40° ; 2—50° ; 3 – 60°

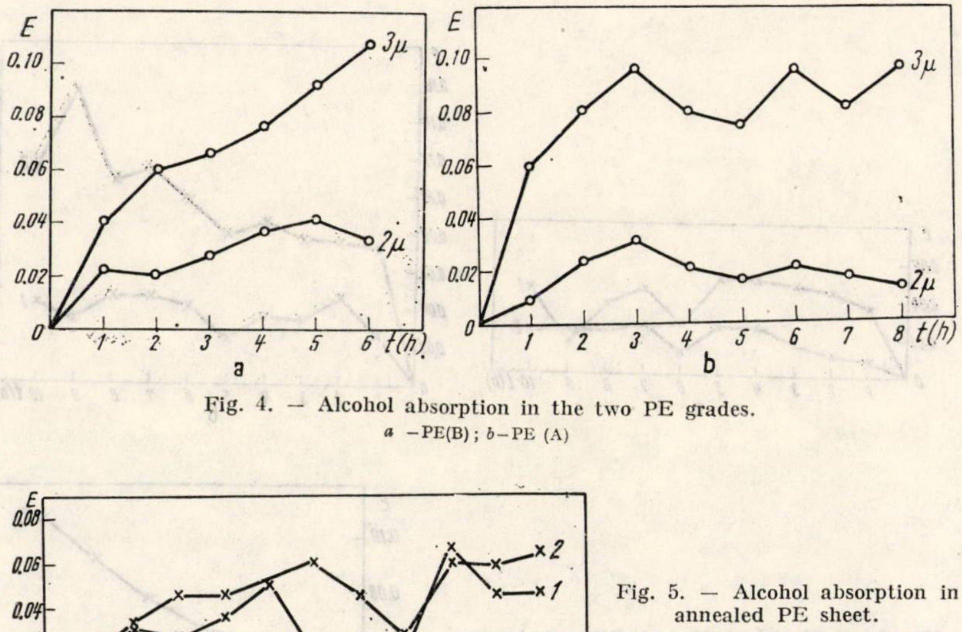

Fig. 4. — Alcohol absorption in the two PE grades.
a – PE(B) ; *b* – PE (A)

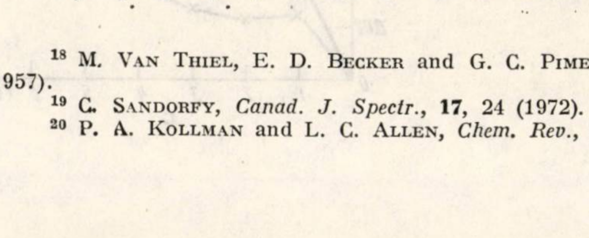

Fig. 5. — Alcohol absorption in annealed PE sheet.
1—new sheet, *2* – annealed sheet.

---

[18] M. Van Thiel, E. D. Becker and G. C. Pimentel, *J. Chem. Phys.*, **27**, 95, 486 (1957).

[19] C. Sandorfy, *Canad. J. Spectr.*, **17**, 24 (1972).

[20] P. A. Kollman and L. C. Allen, *Chem. Rev.*, **72**, 285 (1972).

It is well known [21,22] that the liquid absorption is determined mainly by the amorphous phase content in PE.

Klute[23] introduced the idea that the absorption would be position-dependent on a micro-scale in the amorphous phase. The molecular or associated species diffusing near crystallite surfaces are more impeded than those which are further away, because the segments of polymer chain are less free to undergo rotatory movements. Thus, even some of amorphous phase may be equivalent of blind pores which play no part in the absorption. The oligomers (dimers and trimers) may be absorbed in the small channels between lamellae in the polymer spherulites. The absorption of linear trimers and tetramers of alcohol in the enlarged channels of PE increases rapidly with the temperature (Figures 1—2). Figure 2 shows increases and descreases of absorption over a period of time, but a gradual increase tendency of absorbed liquid amount at 50 and 60°, is obviously.

The slight absorption observed at 40° (2a) remains roughly constant over a long period. The ratio between oligomers and higher polymer species decreases over a period of ten hours (Figure 3). This behaviour becomes more pronounced at 40° (3—1) when there are a greater amount of oligomers than higher species owing to the macromolecular chain rigidity. The great absorption at 50 and 60° could be due to the system expanse; the microbrownian movements of chains became more intensive and so the permeability towards higher polymer species is favoured.

The greater absorption of ethyl alcohol in grade B polyethylene agrees with an increased contents of amorphous phase and a greater branching degree of this type of polymer as it was evidenced by DTA and X-ray measurements. Dimers of alcohol (3580 cm^{-1}) were evidenced over a period of 8—10 hours in the spectrum (Figure 1—1) when probably they are disposed in the very narrow channels. The results are in agreement with the low value of melt flow index which indicates the chain rigidity.

The polymer matrix was expanded by means of subsequent absorption and desorption. Figure 5 shows the increased absorption in such type of system. The results correspond to Michaels[24] and Baddour[25] conclusion concerning the increased permeability after swelling the sheet in penetrants such as p-xylene.

The absorption of alcohol dimer (3585 cm^{-1}) is less difficult than that of the mixed dimer (alcohol—acetone) 3597 cm^{-1}. The latter has been evidenced in the spectrum only after a period of three hours immersion (Figures 1—4). This mixed dimer appears only after a period of six hours when also the absorbed amount (Figure 2) increases. The

---

[21] A. Renfrew and P. Morgan, "Polyethene. The Technology and Uses of Ethylene Polymers", London, Iliffe Ltd., 1960.

[22] J. Crank and G. S. Park, "Diffusion in Polymers", Academic Press, London, 1968.

[23] C. H. Klute, *J. Appl. Polymer Sci.*, **1**, 340 (1959).

[24] A. S. Michaels, R. F. Baddour, H. J. Bixler and C. Y. Choo, *Ind. Engng. Chem. Process design and Develop.*, **1**, 14 (1962).

[25] R. F. Baddour, A. S. Michaels, H. J. Bixler, R. P. De Filippi and J. A. Barrie, *J. Appl. Polymer Sci.*, **8**, 897 (1964).

broad band near 3380 cm^{-1} corresponds to higher mixed polymer species. PE (grade B) absorbs exclusively the oligomers species (3585 cm^{-1} of alcohol, whose dimension increases over a period of time (ν_{max} shifts to 3547 cm^{-1}). Similarly the mixed higher polymer species afforded smaller dimension (3420 cm^{-1}) comparatively with the corresponding polymer alcohol species. The results are in accordance with the greater chain rigidity.

The amorphous phase of PE could be a good matrix for liquids too, and many problems concerning the structure of liquids and solutions would be studied by means of this new method.

Revue Roumaine de Chimie, **23**, *4*, 541 – 547 (1978)

FLUCTUATION PHENOMENA IN DIFFUSION

M. VLAD

Polytechnical Institute of Bucharest, Institute of Chemistry, Department of Physical Chemistry and Electrochemical Technology, Bd. Republicii 13

Received January 21, 1976

A simple stochastic model for diffusion phenomenon is developed. By using the technique of master equation, it is possible to derive the correlation functions of concentration and of Langevin noise source.

The purpose of this paper is to present a general algorithm for calculating the concentration fluctuations which occur during the diffusion of a simple fluid. The suggested algorithm is inspired mainly from the works of Landau's school. [1–3]

Let us consider the non-stationary diffusion of a simple fluid in a closed system. We divide the system volume into n cells and denote by N_i the number of fluid molecules contained in the cell i. Supposing that the probability of transition i → j is equal to

$$p_{ij} = k_{ij}\, N_i\, \Delta t + 0(\Delta t^2) \tag{1}$$

we can prove that the probability distribution $\mathrm{P}(N_1, \ldots, N_n, \mathrm{t}) = P(\mathbf{N}, \mathrm{t})$ verifies the equation

$$\frac{\mathrm{d}P}{\mathrm{d}t} = \sum_{i} \sum_{j \neq i} k_{ij}[(N_i + 1)P(N_i + 1,\ N_j - 1) - N_i\, P] \tag{2}$$

with

$$P(\mathbf{N}, 0) \begin{cases} 1 \text{ if } \mathbf{N} = \mathbf{N}_0 \\ 0 \text{ if } \mathbf{N} \neq \mathbf{N}_0 \end{cases}$$

---

[1] L. Landau and E. Lifchitz, "Physique statistique", Ed. Mir, Moscou, 1967, p. 414.

[2] L. Landau and E. Lifchitz, "Mécanique des fluides", Ed. Mir, Moscou, 1971, p. 653.

[3] L. Landau and E. Lifchitz, "Electrodinamique des milieux continus", Ed. Mir. Moscou, 1969, p. 466.

(2) is the well-known master equation used in the theory of relaxation phenomena[4] and in stochastic theory of reaction rates.[5–8] Its integration gives

$$G(\mathbf{s}, t) = \sum_{\forall N_i} \prod_i s_i^{N_i} P(\mathbf{N}, t) = \prod_i \Big(\sum_j \eta_{ji}(t) s_j \Big)^{N_{0i}} \tag{3}$$

and then:

$$G(s_k, t) = \prod_i (1 + (s_k - 1)\, \eta_{ki}(t))^{N_{0i}} \tag{3'}$$

Using Eq. (3) we obtain[4–8]

$$\mathrm{d}\overline{\mathbf{N}}/\mathrm{d}t = \mathbf{K}^+ \overline{\mathbf{N}} \tag{4}$$

$$\overline{\mathbf{N}} = \mathbf{E}(t)\, \mathbf{N}_0 \tag{5}$$

$$\mathbf{M}(t) = \overline{\Delta\mathbf{N}(t)\, \Delta\mathbf{N}^+(t)} = \Big\| \sum_\alpha (\delta_{ij} - \eta_{j\alpha}(t))\, \eta_{i\alpha}(t) N_{0\alpha} \Big\| \tag{6}$$

$$\begin{aligned} \overline{\Delta\mathbf{N}(t_1)\, \Delta\mathbf{N}^+(t_2)} &= h(-\tau)\, \mathbf{E}(|\tau|)\, \mathbf{M}(t) + h(\tau)\, \mathbf{M}(t)\, \mathbf{E}^+(|\tau|) = \\ &= \Big\| \sum_\alpha N_{0\alpha}[(\eta_{ij}(|\tau|) - \eta_{i\alpha}(t + |\tau|))\eta_{j\alpha}(t) h(-\tau) + (\eta_{ji}(|\tau|) - \\ &\quad - \eta_{j\alpha}(t + |\tau|))\, \eta_{i\alpha}(t)\, h(\tau)] \Big\| \end{aligned} \tag{7}$$

$$\begin{aligned} \mathbf{C}(t_1, t_2) = \overline{\mathbf{F}(t_1)\, \mathbf{F}^+(t_2)} &= \delta(\tau)[4\mathbf{D}(t) + \mathbf{M}(t)\, \mathbf{K} + \mathbf{K}^+\, \mathbf{M}(t)] = \\ &= \delta(\tau)[2\mathbf{D}(t) - \mathrm{d}\mathbf{M}(t)/\mathrm{d}t] \end{aligned} \tag{8}$$

$$\overline{\Delta\mathbf{N}(t_1)\, \mathbf{F}^+(t_2)} = 2h(-\tau)\, \mathbf{E}(|\tau|)\, \mathbf{D}(t) \tag{9}$$

$$\overline{\mathbf{F}(t_1)\, \Delta\mathbf{N}^+(t_2)} = 2h(\tau)\, \mathbf{D}(t)\, \mathbf{E}^+(|\tau|) \tag{10}$$

where

$$\mathbf{K} = \| k_{ij} \|, \; k_{ii} = -\sum_{j \neq i} k_{ij}.$$

$$\mathbf{E}(t) = \exp(\mathbf{K}^+ t) = \| \eta_{ij}(t) \|$$

$$\tau = t_2 - t_1, \; t = \min(t_1, t_2), \; h(t < 0) = 0, \; h(t > 0) = 1$$

---

[4] L. M. Krieger, and P. J. Gans, *J. Chem. Phys.*, **32**, 247 (1960).
[5] I. G. Darvey and P. J. Staff, *J. Chem. Phys.*, **44**, 990 (1966).
[6] M. Vlad and E. Segal, *Rev. Roumaine Chim.*, **21**, 667 (1976).
[7] M. Vlad and E. Segal, *Rev. Roumaine Chim.*, **21**, 1311 (1976).
[8] M. Vlad and E. Segal, *Rev. Roumaine Chim.*, **21**, 1319 (1976).

$$2\mathbf{D} = \mathrm{d}\mathbf{M}/\mathrm{d}t - \mathbf{K}^{+}\,\mathbf{M} - \mathbf{MK} = \| \, \delta_{ij} \sum_{\lambda \neq i} (k_{\lambda i}\, \bar{N}_{\lambda} + k_{i\lambda}\, \bar{N}_{i}) +$$

$$+ (1 - \delta_{ij})\,(k_{ij}\, \bar{N}_{i} + k_{ji}\, N_{j}) \, \|$$

and $\mathbf{F}(t)$ is the vector of noise sources, defined by the equation

$$\mathrm{d}\mathbf{N}/\mathrm{d}t = \mathbf{K}^{+}\,\mathbf{N} + \mathbf{F}(t).$$

Passing to continuous variables ($n \rightarrow \infty$) we have

$$i \rightarrow (x_1, x_2, x_3) = (x, y, z) = \vec{r}$$

$$N_{0i} \rightarrow C_0(\vec{r})\ \mathrm{dxdydz} = C_0(\vec{r})\mathrm{d}\vec{r}$$

$$N_i(t) \rightarrow C(\vec{r}, t)\, \mathrm{d}\vec{r}$$

$$\eta_{ij}(t) \rightarrow G(\vec{r}, \vec{r}', t)\, \mathrm{d}\vec{r}$$

$$F_i\,(t) \rightarrow \sigma\,(\vec{r},\ t)\mathrm{d}\vec{r}$$

$$k_{ij} = \left[\frac{\partial}{\partial t}\ \mathbf{E}(0)\right]_{ij} \rightarrow \beta(\vec{r},\vec{r}')\ \mathrm{d}\vec{r}' = \frac{\partial G\ (\vec{r}', \vec{r}, 0)}{\partial t}\ \mathrm{d}\vec{r}'$$

As[6,7]

$$\sum_i \eta_{ij}(t) = 1$$

$$\eta_{ij}(0) = \delta_{ij}$$

$$\eta_{ij}\,(\infty) = p_i = \bar{N}_i(\infty) / \sum_i \bar{N}_i(\infty)$$

$$\sum_j k_{ij} = 0$$

it folows that

$$\int_V G(\vec{r}, \vec{r}', t)\mathrm{d}\vec{r} = 1 \tag{11}$$

$$G(\vec{r}, \vec{r}',0) = \delta\,(\vec{r} - \vec{r}') \tag{12}$$

$$G(\vec{r}, \vec{r}', \infty) = \bar{C}(\vec{r}, \infty) \Big\backslash \int_V \bar{C}(\vec{r}, \infty)\, d\vec{r} = 1/V \tag{13}$$

$$\int_V \frac{\partial G(\vec{r}', \vec{r}, 0)}{\partial t}\, d\vec{r}' = 0 \tag{14}$$

The principle of microscopic reversibility requires[7]

$$\eta_{ij}\, p_j = \eta_{ji}\, p_i. \tag{15}$$

Then

$$G(\vec{r}, \vec{r}', t) = G(\vec{r}', \vec{r}, t). \tag{16}$$

For n → ∞ Eq. (4) becomes

$$\frac{\partial \bar{C}\ \ \vec{r}, t)}{\partial t} = \lim_{\forall \Delta x_j \to 0} \sum_{i=1}^{3} \sum_{k=1}^{2} [\beta(\vec{r}^{ik}, \vec{r})\, \bar{C}(\vec{r}^{ik}, t) - \beta(\vec{r}, \vec{r}^{ik})\, \bar{C}(\vec{r}; t)] \prod_j \Delta x_j \tag{17}$$

where $x_j^{ik} - x_j = (-1)^k\, \delta_{ij}\, \Delta x_j$.

But

$$\bar{C}(\vec{r}^{ik}, t) \cong \bar{C}(\vec{r}, t) + \sum_{j=1}^{3} (x_j^{ik} - x_j) \frac{\partial \bar{C}}{\partial x_j} + \frac{1}{2} \sum_{j,l=1}^{3} (x_j^{ik} - x_j)(x_l^{ik} - x_l) \frac{\partial^2 \bar{C}}{\partial x_l \partial x_k}$$

Supposing that

$$\lim_{\forall \Delta x_j \to 0} \sum_k (-1)^k \Delta x_i \prod_\alpha \Delta x_\alpha\, \beta(\vec{r}^{ik}, \vec{r}) = 0$$

and

$$\lim_{\forall \Delta x_j \to 0} \sum_k (\Delta x_i)^2 \prod_\alpha \Delta x_\alpha\ \beta(\vec{r}^{ik}, \vec{r}) = 2D_i \neq f(\vec{r}$$

we obtain

$$\frac{\partial \bar{C}}{\partial t} = D_1 \frac{\partial^2 \bar{C}}{\partial x_1^2} + D_2 \frac{\partial^2 \bar{C}}{\partial x_2^2} + D_3 \frac{\partial^2 \bar{C}}{\partial x_3^2} \tag{18}$$

We found so the well-known differential equation of diffusion Eq. (5) leads to

$$\bar{C}(\vec{r}, t) = \int_V G(\vec{r}, \vec{r}', t)\ C_0(\vec{r}')\, d\vec{r}' \tag{19}$$

From Eq. (19) folows that $G(\vec{r}, \vec{r}\,', t)$ is the Green function attached to the diffusion equation (18).
Similarly

$$\lim_{\Delta V \to 0} \frac{\overline{\Delta N^2(\vec{r}, t)}}{\Delta V} = \bar{C}(\vec{r}, t) \tag{20}$$

$$\overline{\Delta C(\vec{r}_1, t)\, \Delta C(\vec{r}_2, t)} = \delta(\vec{r}_1 - \vec{r}_2)\, \bar{C}(\vec{r}_1, t) - \int_V G(\vec{r}_1, \vec{r}, t)\, G(\vec{r}_2, \vec{r}, t)\, C_0(\vec{r})\, \mathrm{d}\vec{r} \tag{20'}$$

$$\overline{\Delta C(\vec{r}_1, t_1)\, \Delta C(\vec{r}_2, t_2)} = \int_V [(G(\vec{r}_1, \vec{r}_2, |\tau|) - G(\vec{r}_1, \vec{r}, t + |\tau|))\, G(\vec{r}_2, \vec{r}, t)$$

$$h(-\tau) + (G(\vec{r}_2, \vec{r}_1, |\tau|) - G(\vec{r}_2, \vec{r}, t + |\tau|))\, G(\vec{r}_1, \vec{r}, t) h(\tau)]\, C_0(\vec{r})\, \mathrm{d}\vec{r} \tag{21}$$

$$\overline{\sigma(\vec{r}_1, t_1)\ \sigma(\vec{r}_2, t_2)} = \delta(\tau) \Big[\delta(\vec{r}_1 - \vec{r}_2) \int_V \beta(\vec{r}, \vec{r}_1)\, \bar{C}(\vec{r}, t)\, \mathrm{d}\vec{r} -$$

$$- \beta(\vec{r}_1, \vec{r}_2)\, \bar{C}(\vec{r}_1, t) - \beta(\vec{r}_2, \vec{r}_1)\, \bar{C}(\vec{r}_2, t) - \frac{\partial}{\partial t} \overline{\Delta C(\vec{r}_1, t)\, \Delta C(\vec{r}_2, t)} \Big] \tag{22}$$

$$\overline{\Delta C(\vec{r}_1, t_1)\, \sigma(\vec{r}_2, t_2)} = h(-\tau) \int_V [(G(\vec{r}_1, \vec{r}_2, |\tau|) - G(\vec{r}_1, \vec{r}, |\tau|))\ \beta(\vec{r}, \vec{r}_2)\, \bar{C}(\vec{r}, t) -$$

$$- G(\vec{r}_1, \vec{r}, |\tau|)\, \beta(\vec{r}_2, \vec{r})\, \bar{C}(\vec{r}_2, t)]\, \mathrm{d}\vec{r} \tag{23}$$

and

$$G(s(\vec{r}), t) = \exp \Big[\int_V \ln (1 + (s(\vec{r}) - 1) G(\vec{r}, r_1, t)\, \Delta V(\vec{r}))\ C_0(\vec{r}_1,)\, \mathrm{d}\vec{r}_1] \cong$$

$$\cong \exp [(s - 1)\, \Delta V(r)\, \bar{C}(\vec{r}, t)] \tag{24}$$

Thus

$$P(N(\vec{r}), t) \cong \frac{(\bar{C} \Delta V)^N}{N\,!}\, C^{-\bar{C}\Delta V} \tag{24'}$$

At equilibrium ($t \to \infty$, $\bar{C}(\vec{r}) = \text{const}$) the equations derived above become

$$\overline{\Delta C(\vec{r}_1)\ \Delta C(\vec{r}_2)} = \delta(\vec{r}_2 - \vec{r}_1)\ \bar{C} - \bar{C}/V \tag{20''}$$

$$\overline{\Delta C(\vec{r}_1, t_1) \Delta C(\vec{r}_2, t_2)} = G(\vec{r}_1, \vec{r}_2, |\tau|)\ \bar{C} - \bar{C}/V \tag{21'}$$

$$\begin{aligned}\overline{\sigma(\vec{r}_1,\ t_1)\ \sigma(\vec{r}_2,\ t_2)} &= -2\delta(-\tau)\beta(\vec{r}, \vec{r}_2)\ \bar{C} = \\ &= -2\delta(\tau)\ \beta(\vec{r}_2, \vec{r}_1)\ \bar{C}\end{aligned} \tag{22'}$$

$$\begin{aligned}\overline{\Delta C(\vec{r}_1, t_1)\ \sigma(\vec{r}_2,\ t_2)} &= -2h(-\tau)\ \bar{C} \int_V G(\vec{r}_1, \vec{r}, |\tau|)\ \beta(\vec{r}, \vec{r}_2)\ \mathrm{d}\vec{r} = \\ &= -2h(-\tau)\ \bar{C} \int_V G(\vec{r}_1, \vec{r},\ \tau)\ \beta(\vec{r}_2, \vec{r})\ \mathrm{d}\vec{r}.\end{aligned} \tag{23'}$$

Taking the Fourier transforms of Eqs. (21′)–(23′), we get

$$\begin{aligned}\overline{\Delta C(\vec{r}_1, \omega_1)\ \Delta C(\vec{r}_2, \omega_2)} &= \frac{1}{(2\pi)^2} \iint_{-\infty}^{+\infty} \overline{\Delta C(\vec{r}_1, t_1)\ \Delta C(\vec{r}_2, t_2)}\ \mathrm{e}^{-i\omega_1 t_1 - i\omega_2 t_2}\,\mathrm{d}t_1\,\mathrm{d}t_2 = \\ &= \delta(\omega_1 + \omega_2)[(g^+(\vec{r}_1, \vec{r}_2, \omega_1) + g^+(\vec{r}_1, \vec{r}_2, -\omega_1))\ \bar{C} - \delta(\omega_1)\ \bar{C}/V]\end{aligned} \tag{25}$$

$$\overline{\sigma(\vec{r}_1,\ \omega_1)\ \sigma(\vec{r}_2,\ \omega_2)} = -\frac{1}{\pi}\,\delta(\omega_1 + \omega_2)\ \beta(\vec{r}_1, \vec{r})\ \bar{C} \tag{26}$$

$$\overline{\Delta C(\vec{r}_1,\ \omega_1)\ \sigma(\vec{r}_2,\ \omega_2)} = -2\delta(\omega_1 + \omega_2)\ \bar{C} \int_V g^+(\vec{r}_1, \vec{r},\ \omega_1)\ \beta(\vec{r}, \vec{r}_2)\mathrm{d}\vec{r} \tag{27}$$

where

$$g^+(\vec{r}_1, \vec{r}_2, \omega) = \frac{1}{2\pi} \int_0^\infty G(\vec{r}_1, \vec{r}_2,\ \tau)\ \mathrm{e}^{-i\omega\tau}\ \mathrm{d}\tau.$$

In the case of an infinite ($V=\infty$) and izotropic ($D_1=D_2=D_3=D$) medium we have:

$$G(\vec{r}, \vec{r}', |\tau|)=\frac{1}{(4\pi D|\tau|)^{3/2}}\exp\left[-\frac{(\vec{r}-\vec{r}')^2}{4D|\tau|}\right]$$

and then

$$\overline{\Delta C(\vec{r}_1, t_1)\,\Delta C(\vec{r}_2, t_2)}=\frac{\bar{C}}{(4\pi D|\tau|)^{3/2}}\exp\left[-\frac{(\vec{r}_1-\vec{r}_2)^2}{4D|\tau|}\right] \tag{28}$$

$$\overline{\Delta C(\vec{r}_1, \omega_1)\,\Delta C(\vec{r}_2, \omega_2)}=\frac{\delta(\omega_1+\omega_2)\bar{C}}{8\pi^2 D\sqrt{(\vec{r}_1-\vec{r}_2)^2}}\,e^{-\sqrt{\frac{\omega_1}{2D}(\vec{r}_1-\vec{r}_2)^2}}\cos\left[\sqrt{\frac{\omega_1}{2D}(\vec{r}_1-\vec{r}_2)^2}\right] \tag{29}$$

ACKNOWLEDGEMENT The author is grateful to professor Eugen Segal for his suggestions.

Revue Roumaine de Chimie, **23**, *4*, 549–553 (1978)

APPARENT MOLAL VOLUMES OF SOME COMMON SALTS IN METHANOL—WATER MIXTURES

K. SINGH*, D. N. BAJPAI and B. K. DWIVEDI

Chemistry Department,
B.S.N.V. Degree College,
Lucknow, India

Received December 11, 1975

Apparent molal volumes of four uni-univalent salts namely NH_4Cl, NH_4Br, NH_4I and NH_4NO_3 have been determined in 9.47%, 19.84%, 34.84% and 42.10% methanol-water mixtures at 25°. The limiting apparent molal volumes ($\varphi°$) have been obtained in the usual manner and is found to be dependent on the solvent composition i. e., decreases with increase in the methanol content in the mixture. The results indicate that the plots of φ_v vs. $\sqrt{c}$ are almost straight line and have a positive slope for all the salts in all the mixtures. The experimental results are expressed in terms of ion-solvent and ion-ion interaction together with structure of binary solvent and role of dielectric constant of the medium.

INTRODUCTION

In continuation of our previous studies[1–4] on the apparent molal volume of tetraalkylammonium and common salts in different solvents, we now have determined the apparent molal volume of some common uni-univalent electrolytes in a series of methanol-water mixtures at 25°. Although a significant amount of work on apparent molal volume in aqueous and non-aqueous solvents is available, little work has been reported on the same heading in mixed solvents. [5–9]

Padova[10] reported the apparent molal volume of some salts in ethanol-water and acetone-water mixtures at 25° and interpreted the results in terms of ion-solvent interaction and solvated molar volumes as a function of bulk dielectric constant of the solvent. Baron[11] has investigated the effect of composition of components on molar volumes of sodium bromide in methanol-water mixtures. It seems, therefore, desirable to extend the same study to some methanol-water mixtures of known dielectric constant.[12] It is the aim of present work to use methanol-water mixture for examining the effect of dielectric constant and solvent composition on the limiting apparent molal volume and slope, *Sv*, of the φ_v vs. $\sqrt{c}$ curves.

---

* To whom all correspondence should be addressed.

[1] R. Gopal and K. Singh, *Z. phys. Chem. (Frankfurt)*, **75**, 219 (1971).

[2] R. Gopal, M. A. Siddiqi and K. Singh, *Z. phys. Chem. (Frankfurt)*, **75**, 7 (1971).

[3] R. Gopal and K. Singh, *Z. phys. Chem. (Frankfurt)*, **19**, 98 (1974).

[4] K. Singh, *Indian J. Chem.*, **13**, 51 (1975).

[5] D. Fennel Evans and P. Gardan, *J. phys. Chem.*, **72**, 9 (1968).

[6] D. Fennel Evans and P. Gardan, *J. phys. Chem.*, **73**, 158 (1969).

[7] R. L. Ray and D. Fennel Evans, *J. phys. Chem.*, **69**, 4216 (1965).

[8] B. R. Cho, *J. Korean Chem. Soc.*, **15**, 95 (1971).

[9] B. R. Cho, Y. J. Lee and I. Lee, *J. Korean Chem. Soc.*, **15**, 159 (1971).

[10] J. Padova, *J. Chem. Phys.*, **39**, 2599 (1963).

[11] M. Baron, *Tr. Leningr. Teknol. Inst. im. Lensoveta*, **37**, 10 (1957); *C. A., Bull Cancer Progr.*, **53**, 2751 (1959).

EXPERIMENTAL

The B. D. H. (A. R.) samples of common electrolytes were purified by repeated crystallisation from conductivity water. The purified samples were dried in a hot air oven and stored in a vacuum desiccator.

Conductivity water was prepared by redistillation of distilled water containing a little potassium permanganate through a block of condenser and saving only middle fraction. The specific conductance of the sample used was 1.0×10^{-6} ohm^{-1} cm^{-1} at 25°.

B. D. H. methyl alcohol (A. R.) was kept overnight over freshly ignited quicklime and then distilled. The middle fraction of the distilled is being redistilled and its purity was checked by density and refractive index measurements.

Stock solutions of mixed solvents were prepared by calculating the required volumes using density data in a water thermostat running at $25 \pm .005°$. All salts solutions were prepared on molal basis and converted to molarities from the known density.[13]

The density of solutions was determined with a dilatometer of about 40 ml. capacity, the stem of which was graduated in 0.01 ml (accuracy "A" from VEB Glasswerke, Stutzerbach, Thüringen, Germany). The volume change on the stem could be read to $\pm .002$ ml within an error not exceeding $\pm .001$ ml with the help of a magnifying glass. The dilatometer for density measurement was calibrated with conductivity water and the accuracy of measurements was checked against some test solutions of known accurate density. The density data obtained agreed with the literature values within $\pm .001$ to $\pm .003\%$. Duplicate measurements were made each solution and the average value being taken.

From the density, apparent molal volume, φ_v, was calculated using the equation namely,

$$\varphi_v = \frac{1000(d_0 - d)}{mdd_0} + \frac{M}{d}$$

The terms used have their usual significance. Density measurements for each salt were carried out in each methanol-water mixture over a concentration range of 0.1 to 0.5 M.

RESULTS AND DISCUSSION

From the values of apparent molal volumes, φv, for different common salts in different mixtures at 25° φ_v vs. $\sqrt{c}$ curves have been drawn. An illustrative examples of the plots are demonstrated for NH_4Cl in Figure 1. In all the cases, φ_v was found to vary linearly with $\sqrt{c}$ over the concentration range studied here and so they fit in the Masson's equation namely,

$$\varphi_v = \varphi^0 + Sv\sqrt{c} \qquad (1)$$

---

[12] K. P. ANDERSON, E. A. BUTLER and E. M. WOOLLEY, *J. Phys. Chem.*, **77**, 2565 (1973).

[13] J. E. DESNOYERS, G. E. PELLETER and C. JOLICOEUR, *Canad. J. Chem.*, **43**, 3232 (1965).

Sv used in equation (1) is the theoretical slope and is given by

$$Sv = KW^{3/2} \tag{2}$$

Where W is valence factor given by number ϑ_i of ions of species i formed by one molecule of electrolyte and valence Z_i according

$$W = \sum \vartheta_i z_i^2 \tag{3}$$

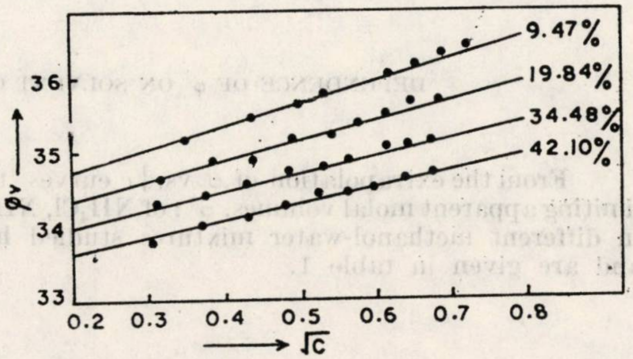

Fig. 1. — Apparent molal volumes of NH_4Cl in various methanol-water mixtures at 25°.

The slope K in equation (2) is given by the expression namely,

$$K = N^2 e^3 \left(\frac{8\pi}{1\,000\,\varepsilon^3 RT} \right)^{1/2} \left(\frac{\partial \ln \varepsilon}{\partial P} - \frac{\beta}{3} \right) \tag{4}$$

Here N is Avogadro's number, ε and β are dielectric constant and compressibility of the solvent respectively and the other terms have their usual meaning.

The slope, Sv, of the φ_v vs. $\sqrt{c}$ curves for all the salts in all the four mixtures under investigation is positive as reported in aqueous solution.[14]

As the present data correspond to higher concentrations, it is not possible to use the data for testing the applicability of Debye-Hückel limiting law. Also, theoretical calculation of limiting slope from equation (IV) is not possible in methanol-water mixture due to lack of required data on the dielectric constant (ε) and its pressure relationship and the compressibility of the solvent. It appears, therefore, advisable not to attach too much quantitative significance to the Sv values and make deductions therefrom about the ion-solvent interaction. Only the dependence of apparent molal volume on concentration and composition should be used to throw light on the mode of ion-solvent interaction in methanol-water mixtures.

---

[14] H. S. HARNED and B. B. OWENS, "Physical Chemistry of Electrolytic Solutions" Reinhold Publishing Corporation, New York, 1958.

DEPENDENCE OF φ_v ON CONCENTRATION

The positive concentration dependence of φ_v may be due to electrostatic ion-ion interaction and less compactness of the ion-solvent complex i. e., partial reduction of solvent dipoles by the presence of ions in solution is greater (the greater this reduction, the smaller extent of solvation and larger the apparent molal volume). The largest value in most concentrated solution indicates that the number of solvent molecules available for each ion is least due to increase in number of ions.

DEPENDENCE OF φ° ON SOLVENT COMPOSITION

From the extrapolation of φ_v vs. $\sqrt{c}$ curves to infinite dilution, the limiting apparent molal volumes, φ° : of NH_4Cl, NH_4Br, NH_4I and NH_4NO_3 in different methanol-water mixtures studied here have been obtained and are given in table 1.

Table 1

Limiting apparent molal volume, θ° of some salts in methanol-water mixtures at 25°

Percent (by Weight) of methanol in the mixture	θ° in ml $mole^{-1}$ for			
	NH_4Cl	NH_4Br	NH_4I	NH_4NO_3
9.47 ($\varepsilon_{25^\circ} = 74.36$)	34.75	42.95	96.95	38.50
19.84 ($\varepsilon_{25^\circ} = 69.28$)	34.35	42.75	96.75	48.20
34.48 ($\varepsilon_{25^\circ} = 62,19$)	34.00	42.35	96.60	47.95
42.10 ($\varepsilon_{25^\circ} = 58.61$)	33.65	42.00	96.50	47.65

The variation of limiting apparent molal volume, φ°, of common salts studied may be used as a tool to throw some light on the varying structure of solvent system. From table 1, it appears that limiting apparent molal volume decreases with increase of methanol content in the mixture. This change in limiting apparent molal volume, φ°, may be due to structuredness of water because it may be suggested[15] that structure of water is promoted by initial addition of methanol probably as a result of hydrophobic interactions between the methanol and the water. In addition, fitness of solute molecule in preformed hole before dissolution may also contribute to this change of φ° with solvent composition.

---

[15] I. Lee and J. B. Hyne, *Canad. J. Chem.*, **46**, 2333 (1968).

DEPENDENCE OF φ° ON DIELECTRIC CONSTANT OF THE SOLVENT

From the table 1, it is clear that dielectric constant of the mixed solvent decreases with increase in methanol content of the mixture and decreasing trend in limiting apparent molal volume, φ°, with decrease indielectric constant of the medium is very much noticeable. This decreasing trend shows that electrostriction effect would be smaller and the smaller φ°(salt), the lower the dielectric constant of the medium. Thus the general conclusion from the present study is that the smaller dielectric constant favours a smaller value of limiting apparent molal volume, θ°, as a result of weaker electrostatic ion-solvent interaction. With respect to dependence of θ° on composition of the solvent and dielectric constant of the medium, further investigations are in progress.

ACKNOWLEDGEMENTS. The authors express their deep sense of gratitude to Shri M. N. Pandey, Principal, B. S. N. V. Degree College, Lucknow for his encouragement.

Financial assistance given by State Council of Scientific and Industrial Research, (SCSIR), U. P. is gratefully acknowledged.

Revue Roumaine de Chimie, 23, 4, 555–558 (1978)

GENERALIZED POTENTIAL-TIME EQUATIONS FOR A. C. CHRONOPOTENTIOMETRY

APPLICATION TO QUASI-REVERSIBLE PROCESSES

RAKESH K. JAIN and HARISH C. GAUR*
Department of Chemistry, University of Delhi, Delhi, —110007 (India)

Received November 19, 1975

Generalized potential-time equations for quasi-reversible process for A. C. Chronopotentiometry are given. Equations for reversible and totally irreversible processes are shown to be limiting cases.

INTRODUCTION

A method of electrolysis at controlled current in which an alternating current is superimposed upon a constant electrolysis current (A. C. Chronopotentiometry) was first introduced by Takemori *et al.*[1] and a theoretical treatment for reversible waves was given. It was shown that alternating component of the potential of the polarized electrode became very large at the transition time (τ), enabling a precise determination of the latter. A treatment of totally irreversible processes was given by Gaur and Jindal.[2] In both the above, the reduced species was soluble. In this communication generalized potential-time equations for quasi-reversible processes are given where the reduced species may or may not be soluble. Reversible and totally irreversible processes are shown to be limiting cases.

THEORETICAL ANALYSIS

For a first order electrode reaction

$$O + ne = R \text{ (Soluble)} \qquad \text{I}$$

the rate of the reaction is

$$\frac{dN_O}{dt} = -\frac{dN_R}{dt} k_f C_O(0, t) - k_b C_R(0, t) \qquad (1)$$

---

* To whom correspondence should be addressed.

[1] Y. Takemori, T. Kambara, M. Senda and I. Tachi, *J. Phys. Chem.*, **61**, 968 (1957).

[2] H. C. Gaur and H. L. Jindal, *J. Electroanalyt. Chem.*, **14**, 297 (1967).

where C_O and C_R are the concentrations of oxidized and reduced species, k_f and k_b are the rate constants for the forward and backward processes. Expressing k's in terms of the electrode potential from the theory of absolute reaction rates[3] the above equations can be expressed as

$$\frac{dN_O}{dt} = -\frac{dN_R}{dt} = k_{s,h}\theta^{\alpha}[C_O(0, t) - C_R(0, t)/\theta] \tag{2}$$

where $k_{s,h}$ is the heterogeneous rate constant at the electrode potential (E) equal to formal potential (E°), α is the transfer coefficient and

$$\theta = \exp\left[\frac{nF}{RT}(E^{\circ\prime} - E)\right].$$

Equating the products of the rate of transformation, the area of the electrode surface and charge nF involved in the reduction of one mole of 0 with the electrolysis constant, we have

$$\frac{i + B\sin\omega t}{nFA} = k_{s,h}\theta^{\alpha}[C_O(0, t) - C_R(0, t)/\theta] \tag{3}$$

Solving Fick's equation for linear diffusion[4], $\dfrac{\partial C}{\partial t} = D\dfrac{\partial^2 C}{\partial x^2}$ for the above boundary conditions, and assuming C_R^0 as the initial concentration of R, one has following Takemori *et al*.[1] equations:

$$C_O(0, t) = C_O^0 - \frac{1}{nFAD_O^{1/2}}\left\{\frac{2it^{1/2}}{\pi^{1/2}} + \frac{B\sin(\omega t - \pi/4)}{\omega^{1/2}}\right\} \tag{4}$$

and

$$C_R(0, t) = C_R^0 + \frac{1}{nFAD_R^{1/2}}\left\{\frac{2it^{1/2}}{\pi^{1/2}} + \frac{B\sin(\omega t - \pi/4)}{\omega^{1/2}}\right\} \tag{5}$$

Substituting the values of $C_O(0, t)$ and $C_R(0, t)$ from equations (4) and (5) into equation (3) one obtains

$$\begin{aligned}\frac{i + B\sin\omega t}{nFA} = k_{s,h}\theta^{\alpha}\Bigg[\, & C_O^0 - \frac{1}{nFAD_O^{1/2}}\left\{\frac{2it^{1/2}}{\pi^{1/2}} + \frac{B\sin(\omega t - \pi/4)}{\omega^{1/2}}\right\} - \\ & - C_R^0 + \frac{1}{nFAD_R^{1/2}\theta}\left\{\frac{2it^{1/2}}{\pi^{1/2}} + \frac{B\sin(\omega t - \pi/4)}{\omega^{1/2}}\right\}\Bigg]\end{aligned}$$

---

[3] S. GLASSTONE, J. K. LAIDLER and H. EYRING, "The Theory of Rate Processes", McGraw-Hill Inc., New York, 1941.

[4] A. FICK, *Pogg. Ann.*, **94**, 59 (1855).

which can be rearranged in the form

$$\frac{t^{1/2}}{\tau^{1/2}} = \left[1 - \frac{1}{\theta}\frac{C_{\mathrm{R}}^0}{C_{\mathrm{O}}^0} - \frac{D_0^{1/2}\pi^{1/2}}{2k_{s,h}\,\theta^{\alpha}\,\tau^{1/2}}\left(1 + \frac{B\sin\omega t}{i}\right)\right]\left(\frac{\theta\Phi}{1+\theta\Phi}\right) - \frac{\pi^{1/2}\,B\sin(\omega t - \pi/4)}{2i\,\tau^{1/2}\,\omega^{1/2}} \tag{6}$$

where τ is the transition time defined by the Sand equation [5]

$$\tau^{1/2} = \frac{nFAD_0^{1/2}\,\pi^{1/2}\,C_{\mathrm{O}}^0}{2i}$$

When R is an insoluble equation (3) would be modified to

$$\frac{i + B\sin\omega t}{nFA} = R_{s,h}\,\theta^{\alpha}[C_{\mathrm{O}}(0,\,t) - {}^1/\theta] \tag{7}$$

analogue of equation (6) being

$$\frac{t^{1/2}}{\tau^{1/2}} = 1 - \frac{\pi^{1/2}B\sin(\omega t - \pi/4)}{2i\omega^{1/2}\,\pi^{1/2}} - \frac{D^{1/2}\,\pi^{1/2}}{2ik_{s,h}\,\theta^{\alpha}}(i + B\sin\omega t) - \frac{nFAD_{\mathrm{O}}^{1/2}\pi^{1/2}}{2i\,\theta\,\tau^{1/2}} \tag{8}$$

Equations (6) and (8) correspond to the reversible case and obey Nernst equation when the factor $\dfrac{D_{\mathrm{O}}\,\pi^{1/2}}{2ik_{s,h}\,\theta^{\alpha}\,\tau^{1/2}}(i + B\sin\omega t)$ becomes negligible. Under this condition the corresponding potential-time equations, when R is soluble and insoluble at the electrode are

$$E = E^{\circ} + \frac{RT}{nF}\ln\Phi + \frac{RT}{nF}\ln\left(\frac{\tau^{1/2} - t^{1/2}}{\dfrac{C_{\mathrm{R}}^0}{C_{\mathrm{O}}^0}\,\Phi t^{1/2} + t^{1/2}}\right) + \frac{RT}{nF}\ln\left(\frac{1 - \dfrac{x}{\tau^{1/2} - t^{1/2}}\sin(\omega t - \pi/4)}{1 + \dfrac{x}{\dfrac{C_{\mathrm{R}}^0}{C_{\mathrm{O}}^0}\,\Phi\,\tau^{1/2} + t^{1/2}}\sin(\omega t - \pi/4)}\right) \tag{9}$$

and

$$E = E^{\circ} + \frac{RT}{nF}\ln\left\{\frac{2i(\tau^{1/2} - t^{1/2})}{\pi^{1/2}\,nFAD_{\mathrm{O}}^{1/2}}\right\} + \frac{RT}{nF}\ln\left\{1 - \frac{x}{\tau^{1/2} - t^{1/2}}\sin(\omega t - \pi/4)\right\} \tag{10}$$

---

[5] H. F. S. Sand, *Phil. Mag.*, **1**, 45 (1901).

respectively λ where $x = \dfrac{\pi^{1/2} B}{2i\omega^{1/2}}$

Equations (9) and (10) are similar to those derived by Takemori *et al.*,[1] and Bansal and Jindal.[6]

Equations (7) and (8) reduce to that for a totally irreversible charge-transfer processes[2], under the following conditions:

$$\theta\Phi \gg 1$$

or

$$1 - \frac{C_{\mathrm{R}}^{0}}{C_{\mathrm{O}}^{0}} \ll \frac{i + B\sin\omega t}{nFAC_{\mathrm{O}}^{0} k_{s,h}\,\theta^{\alpha}}$$

the potential-time equations being

$$E = E^{\circ} + \frac{RT}{\alpha nF}\ln\left\{\frac{2k_{s,h}\,(\tau^{1/2} - t^{1/2})}{D_{\mathrm{O}}^{1/2}\pi^{1/2}}\right\} + \frac{RT}{\alpha nF}\ln\left\{\frac{i - \dfrac{B\pi^{1/2}\sin(\omega t - \pi/4)}{2\omega^{1/2}(\tau^{1/2} - t^{1/2})}}{i + B\sin\omega t}\right\}$$

which is independent of the solubility of R. If the mass-transfer and charge-transfer proceeses have comparable rates (quasi-reversible) equations (6) and (8) must be used.

ACKNOWLEDGEMENT. The authors express their sincere gratitude to Professor Dr. R. Tamamushi, Institute of Physical and Chemical Research, Wako, Saitama (Japan) for reading through the manuscript and helpful comments, to the University Grants Commission, New Delhi for financial assistance of the project and to the Centre of Advanced Study in Chemistry (University of Delhi) for a Junior Research Fellowship to one of them (RKJ).

---

[6] N. P. Bansal and H. L. Jindal, *J. Indian Chem. Soc.*, **49**, 957 (1972).

Revue Roumaine de Chimie, **23**, *4*, 559–568 (1978)

COBALT COMPLEX COMPOUNDS WITH 3-AMINO-1-PROPANOL

IOANA JITARU and MARIA BREZEANU

Polytechnic Institute Bucharest, Department of Chemistry, Laboratory of Inorganic Chemistry, Splaiul Independenţei, 87, Bucharest, Romania

Received March 27, 1976

A series of cobalt complex compounds with 3-amino-1-propanol have been obtained; they are of the following general types: $[Co(AOH)_3]X_2$ ($X=1/2\ SO_4$); $[Co(AOH)_3]X_3.nH_2O$ ($X=Cl$, NO_3, CH_3COO, $n=1$; $X=1/2SO_4$, $n=4$); $[Co(AOH)_2(AO)]X_2.nH_2O$ ($X=Cl$, $n=3$; $X=Br$, CNS, $n=1$; $X=NO_3$, CH_3COO, $1/2SO_4$, $n=2$) and $[Co(AOH)(AO)_2]X.nH_2O$ ($X=Cl$, NO_3, CH_3COO, $n=2$). The complexes obtained have been characterized by elemental analysis, molecular weight determinations, electric conductivity measurements, electronic and vibrational spectra. Attempts have been made to assign the most probable stereochemistry on the base of data thus obtained.

In a number of earlier papers we have reported the results obtained in the study of some copper (II),[1] and chromium (III)[2] complex compounds with 3-amino-1-propanol (monopropanolamine). The ability of propanolamine to act both as neutral ligand and as anionic ligand has been demonstrated in these papers.

The present paper reports the results obtained in the synthesis and characterization of some cobalt (II) and cobalt (III) complex compounds with 3-amino-1-propanol.

The compounds obtained belong to the following general types: $[Co(AOH)_3]X_2$ ($X=1/2\ SO_4$); $[Co(AOH)_3]X_3.nH_2O$($X=Cl$, NO_3, CH_3COO, $n=1$; $X=1/2SO_4$, $n=4$); $[Co(AOH)_2(AO)]X_2.nH_2O$ ($X=Cl$, $n=3$; $X=Br$, CNS, $n=1$; $X=NO_3$, $CH_3COO.1/2SO_4$, $n=2$); $[Co(AOH)(AO)_2]X.nH_2O$ ($X=Cl$, NO_3, CH_3COO, $n=2$) where $AOH=H_2N-(CH_2)_3-OH$ and $AO=H_2N-(CH_2)_3-O^-$.

These compounds have been characterized by elemental analysis, molecular weight determinations, electric conductivitity measurements, electronic and vibrational spectra.

RESULTS AND DISCUSSION

With the purpose of obtaining cobalt complex compounds with variously coordinating manners of monopropanolamine, the synthesis was conducted under different conditions with regard to the component ratio, the pH of the reaction medium, the nature of the cobalt salt anion.

---

[1] M. Brezeanu and I. Jitaru, *Rev. Roumaine Chim.*, **18**, 2039 (1973).

[2] M. Brezeanu and I. Jitaru, *Rev. Roumaine Chim.*, (in press).

In addition to such factors, the oxidation state of the metal ion should be considered carefully, since the reducing character of monopropanolamine affords a stabilization of some Co(II) complex compounds.

The conditions under which such compounds were obtained and the possibilities of mutual interconversions are shown in the scheme below:

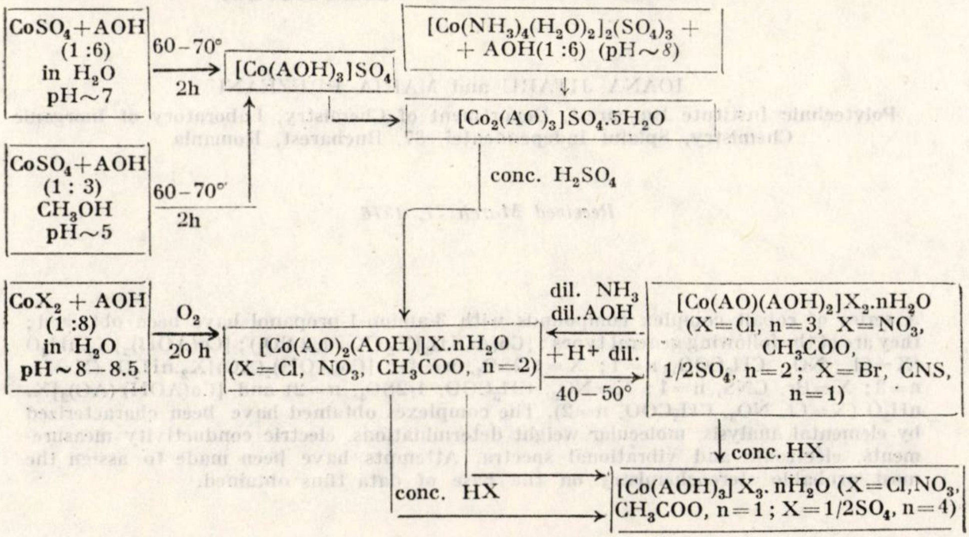
$CoSO_4$+AOH (1:6) in H_2O pH~7
60–70° 2h
$[Co(AOH)_3]SO_4$
$[Co(NH_3)_4(H_2O)_2]_2(SO_4)_3$ + + AOH(1:6) (pH~8)
$[Co_2(AO)_3]SO_4.5H_2O$
$CoSO_4$+AOH (1:3) CH_3OH pH~5
60–70° 2h
conc. H_2SO_4
CoX_2 + AOH (1:8) in H_2O pH~8–8.5
O_2 20 h
$[Co(AO)_2(AOH)]X.nH_2O$ (X=Cl, NO_3, CH_3COO, n=2)
dil. NH_3 dil.AOH
+H+ dil. 40–50°
$[Co(AO)(AOH)_2]X_2.nH_2O$ (X=Cl, n=3, X=NO_3, CH_3COO, 1/2SO_4, n=2; X=Br, CNS, n=1)
conc. HX
conc. HX
$[Co(AOH)_3]X_3.nH_2O$ (X=Cl,NO_3, CH_3COO, n=1; X=1/2SO_4, n=4)

In the direct reaction between cobalt (II) sulphate and monopropanolamine, at a cobalt (II) : AOH molar ratio varying from 1:3 to 1:6, in methanol or in aqueous solution, the compound obtained is $[Co(AOH)_3]SO_4$. It is relatively stable in the air; however, after about two weeks, it undergoes an oxidation process, resulting in a binuclear complex compound with the following formula, found by chemical analysis: $[Co_2(AO)_3]SO_4.5H_2O$.

The data regarding the synthesis of this compound and its behaviour in acid medium have established the simultaneous presence of cobalt (II) and coblat (III).

Under similar conditions, cobalt (II) chloride and nitrate fail to lead to well defined compounds.

In order to obtain pure cobalt (II) complex compounds with monopropanolamine, metallic cobalt in powder form was also used as a starting material. But neither in such conditions was it possible to separate a well-defined compound.

While only one complex compound for cobalt (II) was obtained, we succeeded in obtaining a relatively large number of cobalt (III) complex compounds, by conducting the synthesis under conditions supposed to favour the stabilization of such compounds.

It is also worth mentioning that the synthesis of cobalt (III) compounds was conducted under certain conditions so as to enable the monopropanolamine ligand to act in the form of various species.

Cobalt (II) was oxidized to cobalt (III) by means of the atmospheric oxygen.

Compounds of $[Co(AOH)(AO)_2]X$ type were generally obtained in a basic medium (which favours the presence of monopropanolamine as an anionic species), at a pH ranging between 8.5 and 10 and with a molar ratio of the components, varying from 1 : 8 to 1 : 10.

All the attempts made to obtain compounds of the type $[Co(AO)_3]$ ($pH \sim 10$, Co(II) : AOH molar ratio from 1 : 10 to 1 : 20) resulted in the isolation of compounds $[Co(AOH)(AO)_2]X.nH_2O$ in which only two monopropanolamine ligands act as anionic species, as can be easily seen.

Likewise, we failed to obtain by direct synthesis complex compounds of cobalt containig only neutral monopropanolamine as ligand. Compounds of the type $[Co(AOH)_2(AO)]X_2$ and $[Co(AOH)_3]X_3$, respectively, were obtained by the action of the appropriate acids on compounds $[Co(AO)_3(AOH)]X$. The formation of one or the other of the two types of compounds depends on the initial acid concentration and also on the subsequent work-up of the solutions obtained (see the Experimental Data).

Some of these compounds are interconvertible. The acid-base type equilibria in which they can participate (see the scheme above) explain why the formation of such a large number of complex species is possible. Thus, for instance, compounds of type $[Co(AOH)(AO)_2]X$ treated with dilute acids (molar ratio complex compound : acid=1 : 1) lead to red-purple solutions from which compounds $[Co(AOH)_2(AO)]X_2$ can be separated by a subsequent work-up.

By treating compounds $[Co(AOH)_2(AO)]X_2$ with weakly basic solutions (2% ammonia solution or 3% monopropanolamine solution) the former are changed to the parent compounds, $[Co(AOH)(AO)_2]X$, according to the reaction :

$$[Co(AOH)_2(AO)]X_2 + NH_4OH \rightarrow [Co(AOH)(AO)_2]X + NH_4X + H_2O.$$

The action of concentrated acids on compounds $[Co(AOH)(AO)_2]X$ or $[Co(AOH)_2(AO)]X_2$, followed by the evaporation of the solutions thus obtained in open air caused the separation of red-brown compounds of type $[Co(AOH)_3]X_2$.

Molecular weight determinations. Table 1 gives the molecular weights obtained for some compounds investigated.

Table 1

Molecular weights and melting points of some studied compounds

Compound	Melting point (°C)	Molecular weight	
		calcd.	*found*
$[Co(AOH)_3]SO_4$	180	380.01	382.05
$[Co(AO)_2(AOH)_2]Cl.2H_2O$	150 (dec.)	353.48	348.10
$[Co(AO)(AOH)_2]Cl_2.3H_2O$	135 (dec.)	407.94	400.40
$[Co(AOH)_3]Cl_3.H_2O$	160 (dec.)	408.36	410.35
$[Co_2(AO)_3]SO_4.H_2O$	175	525.96	530.10

$AOH = HO-(CH_2)_3-NH_2$ and $AO = H_2N-(CH_2)_3-O^-$.

Molar electric conductivity measurements. The formulation assigned to the complex compounds investigated was confirmed by the determination of their molar electric conductivities. (Table 2).

Electronic spectra. The probable structure of the compounds investigated was assigned on the basis of their electronic spectra.

Table 2

Molar electric conductivities of the studied compounds

Compound	Molar electric conductivity ($\Omega^{-1}cm^2mol^{-1}$)	Electrolyte type
$[Co(AOH)_3]SO_4$	90.30	1 : 1
$[Co(AO)_2(AOH)]Cl.2H_2O$	80.20	1 : 1
$[Co(AO)_2(AOH)]NO_3.2H_2O$	80.10	1 : 1
$[Co(AO)_2(AOH)]CH_3COO.2H_2O$	85.20	1 : 1
$[Co(AO)(AOH)_2]Cl_2.3H_2O$	150.30	1 : 2
$[Co(AO)(AOH)_2]Br_2.H_2O$	148.10	1 : 2
$[Co(AO)(AOH)_2]\ (CNS)_2.2H_2O$	150.20	1 : 2
$[Co(AO)\ (AOH)_2]\ (NO_3)_2.2H_2O$	145.40	1 : 2
$[Co(AO)\ (AOH)_2]\ (CH_3COO)_2.2H_2O$	160.30	1 : 2
$[Co(AO)\ (AOH)_2]SO_4.2H_2O$	85.50	1 : 1
$[Co(AOH)_3]Cl_3.H_2O$	230.15	1 : 3
$[Co(AOH)_3]\ (NO_3)_3.H_2O$	220.90	1 : 3
$[Co(AOH)_3]\ (CH_3COO)_3.H_2O$	230.50	1 : 3
$[Co(AOH)_3]_2(SO_4)_3.4H_2O$	410.20	2 : 3
$[Co_2(AO)_3]SO_4.H_2O$	80.20	1 : 1

10^{-3} M solutions, t = 25°C, DMF solvent.

The spectrum of compound $[Co(AOH)_3]SO_4$ (Figure 1) may be interpreted as indicating an octahedral configuration around the cobalt (II) ion (d^7).[3,4] Thus, the band appearing at 1170 nm (8550 cm^{-1}) may be assigned to a ${}^4T_{2g} \leftarrow {}^4T_{1g}$ transition, the band at 475 nm (21.250 cm^{-1})

---

[3] J. Fergusson, *J. Chem. Phys.*, **39**, 116 (1963).

[4] A. B. P. Lever, "Inorganic Electronic Spectroscopy", Academic Press, New York, 1968, p. 309.

to a ${}^4T_{1g}(P) \leftarrow {}^4T_{1g}$ transition and the weak band appearing at about 600 nm (16.600 cm^{-1}) to a ${}^4A_{2g} \leftarrow {}^4T_{1g}$ transition.

An analysis of electronic reflectance spectra, recorded for compounds $[Co(AOH)_3]X_3.nH_2O$ (X=Cl, NO_3, CH_3COO, n=1; X=1/2SO_4, n=4) (Figure 2) shows many similarities with regard to the position of absorption bands and their relative intensities. This suggests that their most likely structure is low-spin octahedral type.[5] The bands occurring in the spectra of these compounds can be assigned as follows:

— the band at 370 nm (27.000 cm^{-1}) to a ${}^1T_{2g} \leftarrow {}^1A_{1g}$ transition;

— the band at 525 nm (19.050 cm^{-1}) to a ${}^1T_{1g} \leftarrow {}^1A_{1g}$ transition and

— the low intensity band at 1 000 nm (10.000 cm^{-1}) to a ${}^3T_{1g} \leftarrow {}^1A_{1g}$ spin-forbidden transition.

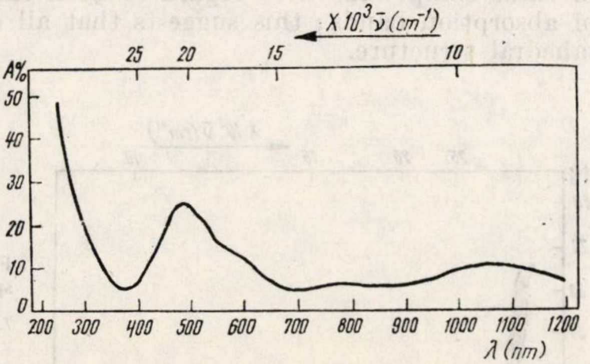

Fig. 1. — Electronic reflectance spectrum of compound $[Co(AOH)_3]SO_4$.

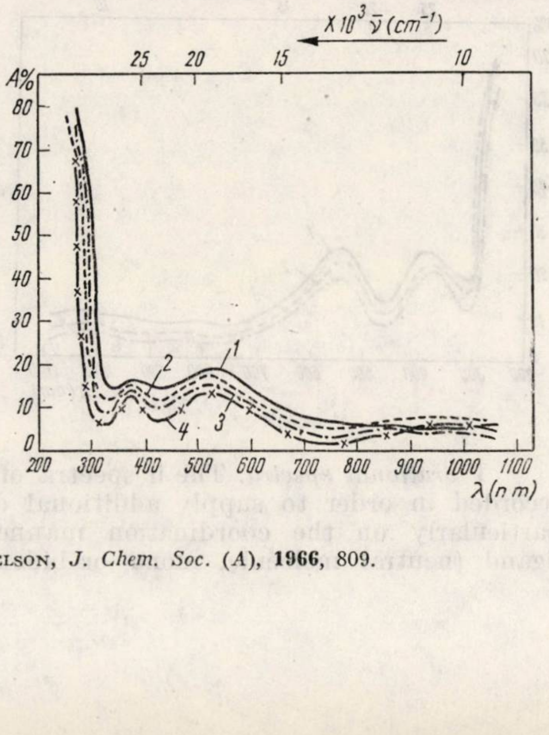

Fig. 2.—Electronic reflectance spectra of compounds:
1. $[Co(AOH)_3]Cl_3.H_2O$ (———); *2.* $[Co(AOH)_3](NO_3)_3.H_2O$ (------); *3.* $[Co(AOH)_3](CH_3COO)_3 \cdot H_2O$ (-.-.-.-); *4.* $[Co(AOH)_3]_2(SO_4)_3.4H_2O$ (-×-×-×-).

---

[5] A. B. P. Lever and S. M. Nelson, *J. Chem. Soc.* (*A*), **1966**, 809.

Figures 3 and 4 exhibit the electronic reflectance spectra of compounds $[Co(AOH)_2(AO)]X_2.nH_2O$ (X=Cl, n=3, X=Br, CNS, n=1; X=NO_3, CH_3COO, 1/2 SO_4, n=2) and $[Co(AOH)(AO)_2]X.nH_2O$ (X=Cl, NO_3, CH_3COO, n=2) respectively.

A comparative study reveals a close similarity between the spectra of these compounds with regard to both the number and the position of absorption bands; this suggests that all of them have the same octahedral structure.

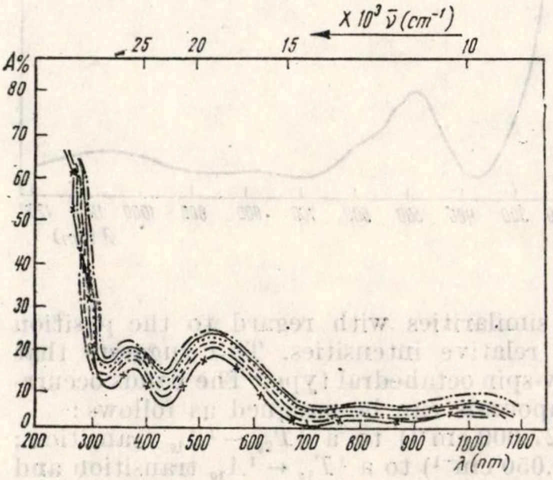

Fig. 3. — Electronic reflectance spectra of compounds:

1. $[Co(AOH)_2(AO]\ Cl_2.3H_2O$ (–...–...–...–);
2. $[Co(AOH)_2(AO)]\ Br_2.H_2O$ (———);
3. $[Co(AOH)_2(AO)\ ]\ CNS)_2.H_2O$ (...........);
4. $[Co(AOH)_2(AO)]\ (NO_3)_2.2H_2O$ (-----);
5. $[Co(AOH)_2(AO)]\ (CH_3COO)_2.2H_2O$ (–.–.–);
6. $[Co(AOH)_2(AO)]SO_4.2H_2O$ (–×–×–×–).

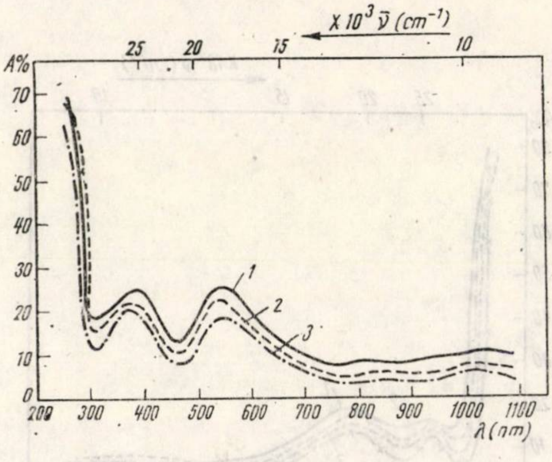

Fig. 4. — Electronic reflectance spectra of compounds: 1. $[Co(AOH)(AO)_2]\ Cl.2H_2O$ (———); 2. $[Co(AOH)(AO)_2]NO_3.2H_2O$ (-----) and 3 $[Co(AOH)(AO)_2]CH_3COO.2H_2O$ (–.–.–.–).

Vibrational spectra. The ir spectra of compounds investigated were recorded in order to supply additional data on their stereochemistry, particularly on the coordination manner of the monopropanolamine ligand (neutral molecule, mono- or bidentate anion) and also on the behaviour of anions (coordinated or in the ionization outer sphere). From this point of view, of interest are the range of O—H (ν_{OH}), C—O (ν_{CO}) and N—H (ν_{asNH}, ν_{sNH}) stretching vibrations of the monopropanolamine ligand, and on the other hand, the range where absorption can be assigned to the stretching modes of anions.

The complex compounds investigated generally contain water of crystallization, which obscure the O—H (ν_{OH}) stretching vibration range of aminoalcohol. In this case, the coordination manner of aminoalcohol was established only on the basis of its N—H (ν_{sNH} and ν_{asNH}) stretching vibration and on its bending vibrations (δ_{NH_2}).

Table 3 shows the ir frequencies characteristic of some studied compounds and the probable assignments. The ir frequencies characteristic of the free ligand are also indicated for comparison.

An analysis of the data leads to the following conclusions relative to the coordination manner of the monopropanolamine ligands:

— the frequency of the N—H (ν_{asNH}, respectively ν_{sNH}) stretching vibration (δ_{NH_2}) shifted towards lower values in all the complex compounds under study, relative to the free ligand, indicate its coordination through the nitrogen of the amino group;

— the frequency of the O—H (ν_{OH}) stretching vibration appearing in the spectrum of the cobalt (II) compound, $[Co(AOH)_3]SO_4$ at 3300 cm^{-1}, markedly shifted relative to the free aminoalcohol (3450 cm^{-1}), indicates the presence of monopropanolamine as a neutral, bidentate ligand;

— in the spectra of compounds $[Co(AOH)_3]X_3.nH_2O$ (X=Cl, NO_3, CH_3COO, n=1; X=1/2SO_4, n=4); $[Co(AOH)_2(AO)]X_2.nH_2O$ (X=Cl, NO_3, CH_3COO, n=2) (table 3 gives one compound of each type) the absorption band assigned to the stretching vibration O—H of aminoalcohol is very likely to be overlapped by the bands asigned to the vibration modes of the water of crystallization;

— in the spectra of compounds having the formula $[Co(AOH)_2(AO)]X_2.nH_2O$ and $[Co(AOH)(AO)_2]X.nH_2O$ the absorption band assigned to the C—O (ν_{CO}) stretching vibration appears split into two components, indicating that in all these compounds, monopropanolamine acts both as a neutral ligand and as anionic ligand;

— the bands occurring in the ranges which can be assigned to the vibration modes of SO_4^{2-}, CH_3COO^-, CNS^- and NO_3^- anions indicate their presence as uncoordinated ionic species.[6-11]

---

[6] K. Nakamoto, "Infrared Spectra of Inorganic Coordination Compounds", Academic Press, New York, 1963, p. 165.

[7] B. E. Gatehouse, S. E. Livingstone and R. S. Nyholm, *J. Chem. Soc.*, **1957**, 4222.

[8] K. Nakamoto, *J. Amer. Chem. Soc.*, **78**, 1347 (1956).

[9] E. Uhling and K. Staiger, *Z. anorg. Chem*, **360**, 39 (1968).

[10] N. F. Curtis, *J. Chem. Soc.*, **1968**, 1579.

[11] K. Nakamoto, *Inorg. Chem.*, **4**, 804 (1966).

Table

IR frequencies of some cobalt-propanolamine

Compound	ν_{OH}	ν_{asNH}	ν_{sNH}	δ_{NH_2}
AOH	3450 (s, b)	3290 (s, b)	3170 (sh)	1615 (m, b)
$[Co(AOH)_3]SO_4$	3300 (s, b)	3220 (m, b)	3100 (w, b)	1590 (m)
$[Co(AOH)(AO)_2]CH_3.COO.\ 2H_2O$	3320 (m, b)	3280 (m, b)	3080 (w, b)	H_2O bands
$[Co(AOH)_2(AO)](CNS)_2.\ 2H_2O$	3310 (m, b)	3270 (m, b)	3080 (w, b)	H_2O bands
$[Co(AOH)_3](NO_3)_3.H_2O$	3310 (m, b)	3280 (m, b)	3070 (w, b)	H_2O bands

EXPERIMENTAL

1-SYNTHESIS OF COMPLEXES

1. $[Co(AOH)_3]SO_4$. To a solution obtained by dissolving 0.25 g $CoSO_4.7H_2O$ in a minimal amount of water, was added approx. 2.20 cc aqueous solution of 3-amino-1-propanol (1 :5) corresponding to a cobalt (III) : AOH molar ratio = 1 :6. The solution obtained was heated for about 2 hrs on a water bath, at 60—70°, adding small amounts of water in the meantime. When the separation of pink crystals began, the solution was cooled and left in a vacuum dessiccator over P_4O_{10}.

The solid deposited was filtered, washed with ethyl alcohol and ether and dried in a dessiccator. The same compound was also obtained by adding approx 2.20 cc methanolic solution of 3-amino-1-propanol (1 :5) corresponding to a Co(II) : AOH molar ratio = 1 :3, to a finaly ground-suspension of 0.25 g $CoSO_4.7H_2O$ in methanol. After the maceration of cobalt sulphate, the solution was filtered and concentrated over P_4O_{10} in a dessiccator. The crystals separated after a few days were filtered, washed with methanol and ether and dried in a dessiccator.
Calcd. for $CoC_9H_{27}N_3O_3SO_4$:Co %, 15.50 ; N %, 11.05 ; SO_4 %, 25.26 ;
Found : Co %, 15.40 ; N %, 11.10 ; SO_4 %, 25.10.

In the compound $[Co(AOH)_3]SO_4$ is allowed to stand for 1—2 weeks in open atmosphere its colour changes from pink to dark red, this being accompanied by a gain in weight of about 37.80 %.

2. $[Co_2(AO)_3(H_2O)_3]SO_4.2H_2O$. The dark red crystals obtained by keeping the above compound in the air were worked up again with a mixture of water and ethanol (1 :5), filtered, washed with this mixture until the filtrate turned almost colourless, and then washed with ethanol and ether.

The same compound can also be obtained by heating for a long time (3—4 hr.) on a water bath at 70—80° a concentrated aqueous solution of $[Co(NH_3)_4 (H_2O)_2]_2(SO_4)_3.3H_2O$ added with an amount of 3-amino-1-propanol corresponding to a cobalt (III) : AOH molar ratio = 1 :6.

Fresh water amounts are added during evaporation. After filtration the solution is evaporated on a water bath until a dark red crystalline substance separates. It is filtered and washed with water, ethanol and ether in small amounts.
Calcd. for $Co_2C_9H_{30}N_3O_6SO_4.2H_2O$: Co %, 22.41 ; N %, 7.99 ; SO_4 %, 18.26 ; H_2O %, 6.84 ;
Found : Co %, 22.50 ; N %, 8.10 ; SO_4 %, 18.43 ; H_2O %, 6.57.

3. $[Co(AOH)(AO)_2]X.nH_2O$ (X = Cl, NO_3, CH_3COO, n = 2). To a concentrated aqueous solution of cobalt salt (0.5 g $CoX_2.nH_2O$) was added an amount of aqueous solution (1 :1)

3

complex compounds and their probable assignments

ν_{CO}	$\nu_{SO(SO_4)}$	$\nu_{OCO(CH_3COO)}$	$\nu_{CN(CNS)}$ $\nu_{CS(CNS)}$	$\nu_{NO(NO_3)}$
1055 (s)				
1045 (a)	1140 (s) (ν_3) 625 (s) (ν_4)			
1040 – 1020 (sh)		1405(s) (ν_{sOCO}) 1570 (s) (ν_{asOCO})		
1040 – 1020 (sh)			1960 (s) (ν_{CN}) 960 (s) (ν_{CS})	
1040 (m, b)				1385 (s) (ν_1) 830 (m) (ν_2)

of 3-amino-1-propanol corresponding to a cobalt(II) : AOH molar ratio = 1 :8 (i. e. approx. 2.5 cc solution of 3-amino-1-propanol in water (1 :1) for X=Cl, CH_3COO and respectively approx. 2 cc for $X=NO_3$). An air flow was passed through the solution thus obtained, for approx. 20 hrs. The resulted red-purple solution was filtered to remove the traces of cobalt hydroxide and concentrated in a dessiccator over P_4O_{10}. After 5 – 6 days, a pink-purple crystalline substance is separated. It is filtered, washed with a mixture of water and ethanol (1 :5) and then with ether.

Calcd. for $CoC_9H_{25}N_3O_3Cl.2H_2O$: Co %, 16.67 ; N %, 11.88 ; Cl %, 10.03 ; H_2O %, 10.19 ;
Found : Co %, 16.90 ; N %, 11.95 ; Cl %, 10.14 ; H_2O %, 9.75.
Calcd. for $CoC_9H_{25}N_4O_6.2H_2O$: Co %, 15.50 ; N %, 14.74 ; C %, 28.44 ; H_2O %, 9.47 ;
Found : Co %, 15.35 ; N %, 14.93 ; C %, 28.70 ; H_2O %, 8.85.
Calcd. for $CoC_{11}H_{28}N_3O_5.2H_2O$: Co %, 15.63 ; N %, 11.14 ; C %, 31.85 ; H_2O %, 9.55.
Found : Co %, 15.50 ; N %, 11.30 ; C %, 32.30 ; H_2O %, 8.90.

4. $[Co(AOH)_2(AO)]X_2.nH_2O$ (X=Cl, n=3 ; $X=NO_3$, CH_3COO, $1/2SO_4$, n=2 ;
X=Br, CNS, n=1).

The chloride, bromide and sulphate were obtained by treating the solution obtained from 0.90 g $[Co(AOH)(AO)_2]Cl.2H_2O$ in approx. 20 cc water, at 40 – 50° with approx. 5 cc HCl 0.5 M (X=Cl), approx. 5 ml HBr 1M, (X=Br) and respectively approx. 5 cc H_2SO_4 0.5 M ($X=1/2SO_4$). From the solution thus obtained, pink-purple compounds separate on storage. They are filtered and washed with a mixture of water, ethanol and ether (1 :5 :2). The thiocyanate precipitates immediately if a concentrated aqueous solution of KSCN is added to the solution obtained from 0.90 g $[Co(AOH)(AO)_2]Cl.2H_2O$ in approx. 20 cc water and approx. 5 cc HCl 1M.

The nitrate and the acetate are obtained in a similar manner, starting however from $[Co(AOH)(AO)_2](NO_3).2H_2O$ and $[Co(AOH)(AO)_2]CH_3COO.2H_2O$ respectively.

Calcd. for $CoC_9H_{26}N_3O_3Cl_2.3H_2O$: Co %, 14.44 ; N % ; 10.30 ; Cl %, 17.38 ; H_2O %, 13,14 ;
Found : Co %, 14.55 ; N %, 10.35 ; Cl %, 17.50 ; H_2O %, 12.50.
Calcd. for $CoC_9H_{26}N_3O_3Br_2.H_2O$: Co %, 12.79 ; N %, 9.11 ; Br %, 34.77 ; H_2O %, 3.93.
Found : Co %, 13.05 ; N %, 9.32 ; Br %, 34.75 ; H_2O %, 3.50.
Calcd. for $CoC_6H_{29}N_3O_3CNS.H_2O$: Co %, 14.12 ; N %, 16.78 ; CNS %, 27.84 ; H_2O %, 4.31 ;
Found : Co %, 14,35 ; N %, 16.90 ; CNS %, 28.10 ; H_2O %, 3.80.
Calcd. for $CoC_9H_{26}N_5O_9.2H_2O$: Co %, 13.30 ; N %, 15.80 ; C %, 24.39 ; H_2O %, 8.13 ;
Found : Co %, 13.53 ; N %, 15.95 ; C %, 24.70 ; H_2O %, 7.80 ;
Calcd. for $CoC_{13}H_{32}N_3O_7.2H_2O$: Co %, 13.48 ; N %, 9.61 ; C %, 35.72 ; H_2O %, 8.25 ;
Found : Co %, 13.60 ; N %, 9.85 ; C %, 35.90 ; H_2O %, 7.85.
Calcd. for $CoC_9H_{26}N_3O_3SO_4.2H_2O$: Co %, 14.19 ; N %, 10.12 ; SO_4 %, 23.14 ; H_2O %, 8.67 ;

Found: Co%, 14.30; N%, 10.15; SO_4%, 23.35; H_2O%, 8.99.

5. $[Co(AOH)_3]X_3.nH_2O$ (X=Cl, NO_3, CH_3COO, n=1; X=1/2SO_4, n=4). Approx. 0.25 g $[Co(AOH)(AO)_2]Cl.2H_2O$, $[Co(AOH)(AO)_2](NO_3)_2.H_2O$ or $[Co(AOH)(AO)_2]CH_3COO.2H_2O$ respectively are dissolved in approx. 10 cc concentrated HCl, concentrated HNO_3, or glacial CH_3COOH respectively. After a few days, the solution is filtered and evaporated in the air. A treatment with acetone leads to the separation of red-brown substances which are filtered and washed with a mixture of water and acetone (1:5).

The compound $[Co(AOH)_3]_2(SO_4)_3.4H_2O$ is obtained by dissolving approx. 0.25 g $[Co_2(AO)_3]SO_4.H_2O$ in 10 cc water and by adding approx. 5 cc conc. H_2SO_4. The resulted solution is concentrated in a dessiccator over P_4O_{10}, until brown-reddish crystals appear, which are filtered and washed with ethanol and ether.

Calcd. for $CoC_9H_{27}N_3Cl_3.H_2O$: Co%, 14.43; N%, 10.29; Cl%, 26.04; H_2O%, 4.41;
Found: Co%, 14.53; N%, 10.50; Cl%, 26.10; H_2O%, 3.70.
Calcd. for $CoC_9H_{27}N_6O_{12}.H_2O$: Co%, 12.07; N%, 17.22; C%, 22.15; H_2O%, 3.69;
Found: Co%, 12.17; N%, 17.35; C%, 22.50; H_2O%, 3.10.
Calcd. for $CoC_{15}H_{36}N_3O_9.H_2O$: Co%, 12.30; N%, 8.77; C%, 37.60; H_2O%, 3.75;
Found: Co%, 12.65; N%, 8.90; C%, 37.90; H_2O%, 3.20.
Calcd. for $Co_2C_{18}H_{54}N_6O_6(SO_4)_3.4H_2O$: Co%, 12.70; N%, 9.05; SO_4%, 31.04; H_2O%, 7.76.
Found: Co%, 12.80; N%, 9.29; SO_4%, 31.20; H_2O%, 7.20.

Molecular weight measurements. The molecular weights of the studied compounds were determined by means of the Rast method. The solvent used for this purpose was camphor.

Molar electric conductivity measurements. Molar electric conductivity determinations were performed on a K. Zeiss Jena type II conductometer with the cell constant k=0.52. Dimethylformamide solutions 10^{-3} M were used at a temperature of 25°.

The assignment of the electrolyte type was made by applying the procedure reported in the literature for dimethylformamide.

Electronic spectra. Electronic reflectance spectra were recorded at room temperature using a K. Zeiss Jena VSU-1 Spectrophotometer. The reference material used was magnesium oxide. The electronic spectra in solution were recorded at room temperature using a VSU 2-G Spectrophotometer K. Zeiss Jena.

Vibrational spectra. IR spectra were recorded by means of a Perkin-Elmer Spectrophotometer in Nujol suspension or in KBr pellets.

Revue Roumaine de Chimie, 23, 4, 569 – 572 (1978)

STUDIES ON COORDINATION COMPOUNDS, 2-THIOSALICYLIC ACID COMPLEXES OF COPPER (II)

IRSHAD A. KHAN*, ABDU-SSALAM M. CACA* and Z. H. FAROOQI**
* Department of Chemistry, University of Tripoli, Tripoli, Libya
** P. C. S. I. R. Laboratories Karachi-39, Pakistan

Received December 2, 1975

Present work consists of synthesis, chemical and spectral studies of some new copper complexes containing ligands i. e. 2-thiosalicylic acid and water molecules within coordination sphere, bearing the general formula $[CuL_2(OH_2)_2]X_2$ (where L=2-thiosalicylic acid; X=Cl, Br, NO_3 or $\frac{1}{2}SO_4$). The I. R. spectra suggest the bonding through thio group.

In recent years a great deal of interest has been directed towards coordination compounds of ligands containing more than one potential donar group. In the whole survey, none of the workers tried to prepare complexes of 2-thiosalicylic acid with copper (II) containing water molecules in coordination sphere. During recent years much work has been carried out on thiosalicylic acid but investigation has largely been oriented towards the mixed ligands.[1,2] Clifford and Sargent[3,4] prepared such complexes in liquid hydrogen fluoride but without water in the coordination sphere. Kumar et al.[5] have reported thiosalicylic acid urenyl $(UO_2)^{2+}$ complexes containing water in the coordination sphere.

Now we have prepared the complexes of 2-thiosalicylic acid with copper (II) having two moles of water coordinated with metal atom. The general formula for the complexes is proposed to $[ML_2(OH_2)_2]X_2$. The metal to be tried is copper, anions under consideration are chloride, bromide, nitrate and sulphate. The ligand introduced is 2-thiosalicylic acid.

RESULTS AND DISCUSSION

All the compounds described here are new and have a stoichiometry corresponding to $[Cu(2\text{-thiosalicylic acid})_2(OH_2)]X_2$, where X is Cl, Br, NO_3 or $1/2SO_4$. The water molecules are not easily expelled and

---

[1] W. Hieber and K. Kaiser, *Z. anorg. Chem.*, **358**, 271 (1968).

[2] S. Dubey, A. M. Bhandari, S. N., Misra and R. N. Kapoor, *Indian J. Chem.*, **8**, 97 (1970).

[3] A. F. Clifford and J. Sargent, *J. Amer. Chem. Soc.*, **79**, 4041 (1957).

[4] M. V. Reddy and P. K. Bhattacharya, *J. Inorg. Nuclear Chem.*, **32**, 2321 (1970).

[5] A. N. Kumar, H. L. Nigam and M. Katyal, *Bull. Chem. Soc. Japan*, **40**, 788 (1967).

hence must be in the coordination sphere. Being insoluble in most of the organic solvents and to a certain extent in water also, they can be regarded polymeric in nature. The spectra of these compounds have the C—S frequency occuring at lower wave lengths indicating the participation of the thio groups in compound formation. The colour of the complexes changes during the filtration process or when they are brought in open air; it might happen due to the change of oxidation state of the metal atom. Most probably the molecular are distroted tetrahedrally in shape as the ligands are large in size. Analysis and other characteristics of these compounds have been tabulated in table 1.

Table 1

Analysis, melting points and state of the complexes

Compond	Metal %		C %	H %	S %	M.P.	Colour
$[Cu(thiosal)_2(OH_2)_2]Cl_2$	*Found*	13.73	35.36	3.19	13.12	275d	green
	Calcd	13.27	35.10	3.34	13.37		
$[Cu(thiosal)_2(OH_2)_2]Br_2$	*Found*	11.69	29.23	2.27	11.72	269d	green
	Calcd	11.19	29.60	2.81	11.27		
$[Cu(thiosal)_2(OH_2)_2](NO_3)_2$	*Found*	12.10	31.82	2.98	12.32	285d	dark green
	Calcd	11.95	31.60	3.01	12.04		
$[Cu(thiosal)_2(OH_2)_2]SO_4$	*Found*	12.16	33.61	3.66	—	274d	dark brown
	Calcd	12.60	33.35	3.17	—		

Infrared spectra of the compounds and of 2-thiosalicylic acid are recorded in table 2. Spectrum observed for free 2-thiosalicylic acid in the region of 700—2 000 cm^{-1} agrees well with those reported by other workers.[6,7] The literature reveals some attempts by Pettit and Eilbeck[8,9] to investigate complex forming tendencies of oxygen and sulphur containing ligands.[10] Sulphur is known to form weak M—L II-bonds whereas M—O bond is only σ in character.

The reported band of aromatic ring at 3030 cm^{-1} disappeared both in 2-thiosalicylic acid and in the complexes, attributed to —CH=CH— stretching, due to the electron attracting substituent in the ring causing hinderence in the delocalization of electrons. I. R. spectra are almost the same of chloro, bromo compounds but some shifting occurs in nitro and sulphato compounds which is most probably due to the steric differences of the groups.

The absorptions observed at 3420 and 3422 cm^{-1} in the spectra of the compounds proved that water is coordinated to the metal atom.

[6] A. Wagner, H. J. Becher and K. G. Kottenhahen, *Chem. Ber.*, **89**, 1708 (1956).

[7] A. K. Kumar and H. L. Nigam, *Indian J. Chem.*, **4**, 472 (1966).

[8] L. D. Pettit, A. Royston and R. J. Whewell, *J. Chem. Soc.*, **1968**, 2009.

[9] W. J. Eilbeck, F. Holmes, T. W. Thomas and G. William, *J. Chem. Soc.*, **1968**, 2348.

[10] S. Ahrland, J. Chatt and N. R. Davis, *Quart. Rev.*, **265**, 12 (1958).

Table 2

I-R. absorption frequencies for 2-thiosalicylic acid and its complexes

HSC_6H_4COOH	$[Cu(thiosal)_2(OH_2)_2]Cl_2$	$[Cu(thiosal)_2(OH_2)_2]Br_2$	$[Cu (thiosal)_2(OH_2)_2](NO_3)_2$	$[Cu(thiosal)_2(OH_2)_2]SO_4$
—	3 420 s	3 420 s	3 420 s	3 422 s
2 520 s	—	—	—	—
1 680 vs	1 613 vs	1 613 vs	1 655 m	1 682 m
1 398 ss	1 398 s	1 398 s	1 390 vs	1 421 m
1 312 s	1 300 w	1 300 w	1 321 w	1 330 s
1 288 s	1 280 w	1 280 w	1 270 w	1 280 w
1 268 s	1 264 m	1 264 m	1 250 m	1 247 s
1 165 s	1 165 m	1 165 m	1 150 m	1 195 vs
1 152 s	1 111 w	1 111 w	1 112 w	1 135 w
1 058 m	1 089 m	1 089 m	1 050 w	1 089 m
1 039 vs	1 039 w	1 039 w	1 035 s	1 031 s
893 s	843 m	841 w	850 m	810 w
800 w	758 m	760 s	749 vs	770 s
740 vs	740 s	740 s	720 s	752 m
705 m	702 m	702 m	702 w	719 s

This band is absent in the spectrum of 2-thiosalicylic acid and a weak band observed at 2520 cm^{-1} has been assigned to S—H stretching vibration by Wagner et al.[6] This type of absorption, however has not been observed in this work, since coordination through sulphur must bring some changes in S—H bond character. The absorption observed at 1613, 1655 and 1682 cm^{-1} may conveniently be assigned to C=O stretching vibrations corresponding to 1680 cm^{-1} in free thiosalicylic acid. The absorptions in the region 1421—1247 cm^{-1} are assigned to C=O stretching in plane deformation mode. The region 1200—950 cm^{-1} reveals the aromatic C—H stretching in plane deformation characteristics of 1 : 2 disubstituted aromatic rings while the second region 900—730 cm^{-1} of interest is the one due to the out of plane hydrogen deformation vibrations. The bands observed at 700—719 cm^{-1} corresponding to 705 cm^{-1} band of 2-thiosalicylic acid may be attributed to C—S stretching. The slight shift is atributed to coordination of sulphur to metal atom. This reason is also confirmed by the fact that the band at 2520 cm^{-1} disappeared in the complexes attributing to S—H stretching.

EXPERIMENTAL

[Cu(2-thiosalicylic acid)$_2$ $(OH_2)_2$]Cl_2. A mixture of 2-thiosalicylic acid and partly dehydrated cupric chloride (molar proportion 4 :1) in anhydrous methanol was refluxed and stirred for 30 minutes. The resulting yellow precipitate changed to green during filtration process. The amorphous green product was washed thoroughly with anhydrous methanol and dried in vacuum. Yield 61 %. Stable in air.

[Cu(2-thiosalicyclic acid)$_2$ $(OH_2)_2$]X_2. The above mentioned procedure was adopted to prepare the bromo and nitro compounds (X=Br or NO_3). Green amorphous compounds were obtained from the resulting solutions. Yield 61 % and 59 % respectively. Stable in air.

[Cu(2-thiosalicylic acid)$_2$ $(OH_2)_2$]SO_4. Procedure adopted was the same as described above, maintaining the refluxing and stirring time one hour. The resulting yellow precipitate turned to brownish black during filtration process. The amorphous product was washed with anhydrous methanol and dried in vacuum. Yield 60 %. Stable in air.

I. R. spectra were run on a Beckman I. R.-4 spectrophotometer using KBr pellets and Nujol mull.

Revue Roumaine de Chimie, 23, 4, 573–576 (1978

INCHAIN-EPOXIDES OF CAROTENOIDS. VI[1]

ISOMERIZATIONS AND REARRANGEMENTS OF CANTHAXANTHIN-INCHAIN-EPOXIDES

DOINA OŞIANU, ELENA NICOARĂ and C. BODEA
Institute of Agronomy "Dr. Petru Groza", Department of Chemistry and Biochemistry,
Str. Mănăştur 3, Cluj-Napoca, Romania

Received December 16, 1975

Canthaxanthin-inchain-epoxides are isomerized into inchain ketones by ring opening under the action of perchloric acid. On treatment with diluted alkali or acid, 11,12-epoxy-canthaxanthin rearranges to 9,12-furanoid oxide. In acid medium this rearrangement is followed by another one resulting in migration of epoxidic oxygen from the nonmethylated 11,12 to the methylated 9,10 position.

To enlarge our general knowledges on the chemical behaviour of inchain-epoxides of carotenoids, we have now investigated the action of some hydrolytic epoxy-ring opening reagents on canthaxanthin inchain-epoxides described in previous papers.[1–3]

Sondheimer[4] has performed the hydrolytic opening of the epoxidic ring of epoxy-steroids under the action of perchloric acid in watery acetone, leading to diols. Acting with this reagent on 9,10- and 13,14-epoxy-canthaxanthin (I, II) both having the epoxidic group attached to a methylated bond, and on 11,12-epoxy-canthaxanthin (III), in which the 11,12-bond is nonmethylated, we observed no difference in the behaviour of the two types of inchain-epoxides. But the epoxidic group undergoes isomerization into keto-group instead of hydrolytic opening, the three inchain-epoxides being converted into 10-keto-, 14-keto- and 12-keto-canthaxanthin respectively (IV, V, VI). Reduction of these triketones with $NaBH_4$ yields the corresponding triols, namely 10-hydroxy-9,10-dihydro-, 13-hydroxy-13,14-dihydro- and 12-hydroxy-11,12-dihydro-isozeaxanthin (VII, VIII, IX) (Scheme 1).

It should be pointed out that the presence of the inchaincarbonyl group in the triketo-compounds IV, V, VI, could not be detected by IR-spectroscopy being allylic, like the two carbonyl groups at C_4 and $C_{4'}$. To identify the inchain-carbonyl group we have first reduced III with $NaBH_4$ and the resulted 11,12-epoxy-isozeaxanthin (X) was con-

---

[1] Part V : D. Oşianu, E. Nicoară and C. Bodea, *Rev. Roumaine Chim.*, **22**, 1085 (1977).
[2] E. Nicoară, D. Oşianu and C. Bodea, *Rev. Roumaine Chim.*, **15**, 1965 (1970).
[3] D. Oşianu, E. Nicoară and C. Bodea, *Rev. Roumaine Chim.*, **16**, 765 (1971).
[4] F. Sondheimer, *J. Amer. Chem. Soc.*, **76**, 5020 (1954).

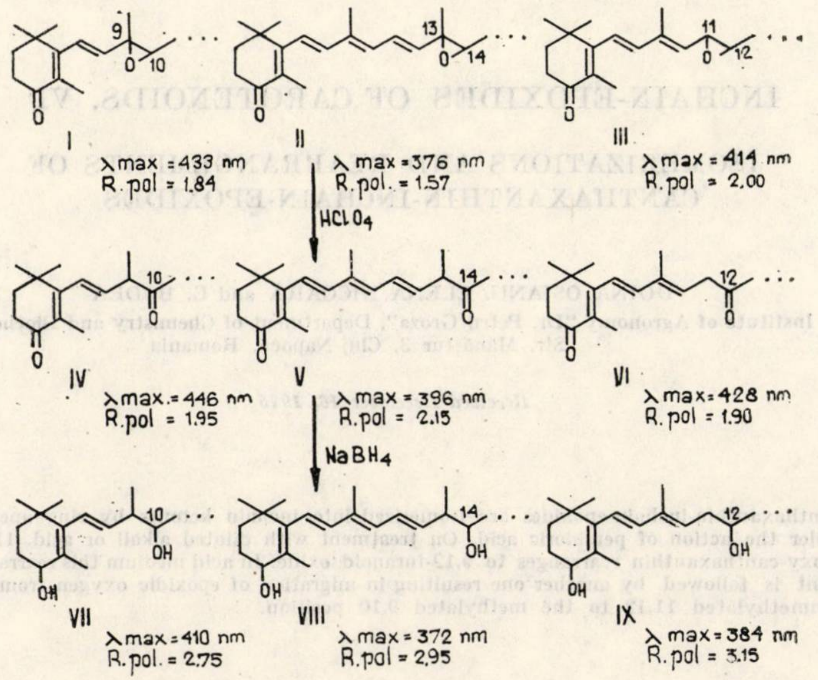
9
10
13
14
11
12
I
λmax = 433 nm
R. pol = 1.84
II
λmax = 376 nm
R. pol. = 1.57
III
λmax = 414 nm
R. pol = 2.00
HClO4
IV
λmax. = 446 nm
R. pol = 1.95
V
λmax = 396 nm
R. pol = 2.15
VI
λmax = 428 nm
R. pol = 1.90
NaBH4
VII
λmax = 410 nm
R. pol. = 2.75
VIII
λmax = 372 nm
R. pol = 2.95
IX
λmax = 384 nm
R. pol = 3.15

Scheme 1

verted thereafter by ring opening with perchloric acid into 12-keto-isozeaxanthin (XI) (Scheme 2). The IR-spectrum of XI showed a sharp band characteristic of a carbonyl group, located at 1610 cm^{-1}, with a hypsochromic shift as compared to the position of the carbonyl band of the triketone VI, due probably to the formation of intermolecular or even intramolecular hydrogen bonds.

Another reagent frequently used to achieve hydrolytic opening of the epoxidic ring is alcoholic alkali. Such a ring opening has been performed in the case of 5,6-epoxy-carotenoids.[5]

On treatment of the 9,10- and 13,14-epoxides (I, II) with alcoholic NaOH or KOH we could observe only deepoxidation, the epoxides reverting to canthaxanthin. Conversely, only part of the 11,12-epoxide (III) belonging to the "nonmethylated" type, underwent deepoxidation, the main transformation being a rearrangement ot 9,12-furanoid oxide (XII)[1] and to a keto-compound identical with 12-keto-canthaxanthin (VI) obtained by ring opening of III by the action of perchloric acid. Further treatment of the furanoid oxide (XII) with alcoholic alkali gave the same 12-keto-canthaxanthin (VI) by ring opening (Scheme 3).

---

[5] W. V. Bush and L. Zechmeister, *J. Amer. Chem. Soc.*, **80**, 2991 (1958).

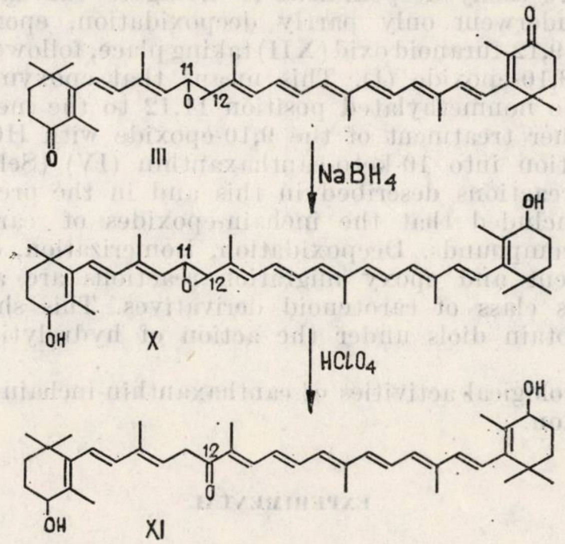
O
11
12
O
O
III
NaBH4
OH
11
12
O
OH
X
HClO4
OH
12
O
OH
XI

Scheme 2

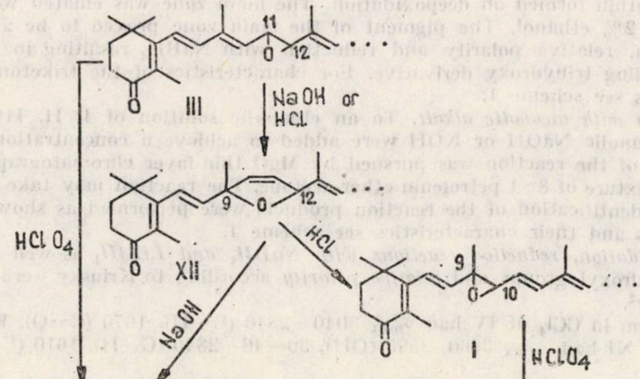
11
O
12
O
III
NaOH or
HCl
9
O
12
O
XII
HClO4
HCl
NaOH
9
O
10
O
I
HClO4
12
O
O
VI
10
O
O
IV

Scheme 3

Interesting is the behaviour of the 11,12-epoxide (III) towards methanol acidified with HCl. While in this condition the 9,10- and 13,14-epoxides are easily deepoxidized reverting to canthaxanthin, the 11-12-epoxide underwent only partly deepoxidation, epoxide-furanoid rearrangement to 9,12-furanoid oxid (XII) taking place, followed by another one leading to 9,10-epoxide (I). This means that epoxymigration has occurred from the nonmethylated position 11,12 to the methylated position 9,10. Further treatment of the 9,10-epoxide with $HClO_4$ resulted in the isomerization into 10-keto-canthaxanthin (IV) (Scheme 3).

From the reactions described in this and in the previous papers it should be concluded that the inchain-epoxides of carotenoids are highly reactive compounds. Deepoxidation, isomerization, epoxide-furanoid rearrangement and epoxy migration reactions are attesting the reactivity of this class of carotenoid derivatives. This should explain the failure to obtain diols under the action of hydrolytic epoxy-ring opening reagents.

Eventual biological activities of canthaxanthin-inchain-epoxides are under investigation.

EXPERIMENTAL

1. *Reaction with perchloric acid.* An acetonic solution of the inchain-epoxides I, II or III, was treated with 15% aqueous $HClO_4$, in the molar ratio 1 : 1. The solution turned green. After keeping the mixture for three hours at room temperature, in the dark, the acid was neutralized with a saturated $NaHCO_3$ solution up to pH 7. Petroleum ether was added and after washing off with water, the pigments were separated on a MgO column. Developing was performed with petroleum ether containing up to 10% acetone. The column showed that the main reaction product is accompanied by small quantities of the starting epoxide and of canthaxanthin formed on deepoxidation. The main zone was eluted with petroleum ether containing 2% ethanol. The pigment of the main zone proved to be a triketone by electronic spectra, relative polarity and reduction with $NaBH_4$ resulting in the formation of the corresponding trihydroxy derivative. For characteristics of the triketones and trihydroxy derivatives see scheme 1.

2. *Reaction with alcoholic alkali.* To an ethanolic solution of I, II, III or IV small quantities of ethanolic NaOH or KOH were added to achieve a concentration of 0.1% alkali. The course of the reaction was pursued by MgO thin-layer chromatography, using for development a mixture of 8 : 1 petroleum ether-acetone. The reaction may take several hours. Separation and identification of the reaction products were performed as shown above. For reaction products and their characteristics see scheme 1.

3. *Deepoxidation, reduction reactions with $NaBH_4$ and $LiAlH_4$* as well as *elimination* of the allylic hydroxyl groups and *relative polarity* according to Krinsky were performed as shown previously[2].

IR spectrum in CCl_4 of IV had ν_{max} 3040—2840 (C—H), 1670 (C=O), 963 (all trans), cm^{-1} and that of XI had ν_{max} 3660, 3595 (OH), 30—40—2840 (C—H), 1610 (C=O), 965 (all trans), cm^{-1}.

This work is part of a joint research program between our Department and the Department of Food and Resource Chemistry, University of Rhode Island, Kingston, Rhode Island, U. S. A.

Revue Roumaine de Chimie, 23, 4, 577–580 (1978)

SYNTHESE VON SULTAMEN*

S. H. DOSS**
National Research Center Sh. El Tahrir, Dokki, Kairo, VAR-Ägypten

Eingegangen am 30. Dezember 1975

Die Synthese eines N-Undecylsultams, eines *o*-Hydroxyphenyl-sultams und eines 1,4-Bisultamyl-n-butans sowie deren spektroskopische Identifizierung werden beschrieben.

N-Undecylamin und *o*-Aminophenol reagieren, wie andere primäre Amine auch, mit 4-Chlor-*n*-butan-1-sulfonylchlorid in normaler Weise zu den entsprechenden N-(4-Chlor-n-butansulfonyl)-Verbindungen I und II.

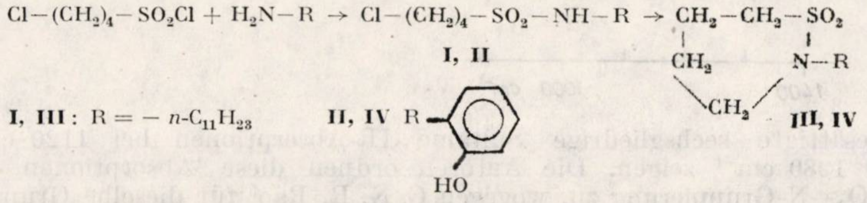

$$Cl-(CH_2)_4-SO_2Cl + H_2N-R \rightarrow \underset{\text{I, II}}{Cl-(CH_2)_4-SO_2-NH-R} \rightarrow \text{III, IV}$$

I, III : $R = -n\text{-}C_{11}H_{23}$

Aus dem n-Undecylderivat I konnte zum ersten Mal ein Sultam (III) mit einer längeren aliphatischen Seitenkette am Sultam-Stickstoff hergestellt werden. Das *o*-Hydroxyphenylderivat II führt zu einem auf Grund der phenolischen Hydroxylgruppe in Alkali löslichen Sultam (IV).

Die Kondensation von 4-Chlor-*n*-butan-1-sulfonylchlorid mit 1,4-Diamino-*n*-butan liefert, analog den obigen Reaktionen, eine N,N-Bis-(4-chlor-*n*-butan-sulfonyl)-Verbindung (V), aus der das Bis-Sultam VI hergestellt werden konnte.[1]

$$2Cl-(CH_2)_4-SO_2Cl + H_2N-(CH_2)_4-NH_2 \rightarrow Cl(CH_2)_4-SO_2-NH-(CH_2)_4-NH-SO_2-(CH_2)_4Cl$$

V

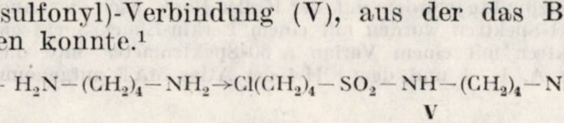

VI

---

* Meinem verehrten Lehrer, Herrn Professor Dr. B. Helferich, dem ich für die stete Förderung dieser Arbeit danke, zum 88. Geburtstag gewidmet.

** z. Zt. Fachbereich 14 — Organische Chemie, Universität des Saarlandes, D 6600 Saarbrücken, BRD.

[1] B. Helferich und S. H. Doss, *Liebigs Ann. Chem.*, **741**, 139 (1970); **747**, 107 (1971)

Die Strukturen der neuen Verbindungen wurden durch Analyse und spektroskopische Methoden bewiesen.

Die $>$NH-Gruppe in den Verbindungen I, II, V konnte IR-spektroskopisch (Banden bei 3280 cm^{-1} und 3260 cm^{-1}) und ^1H-NMR-spektroskopisch (Singulett bei $\tau = 5.5$ ppm [2])) nachgewiesen werden.

Bei den Sultamen III, IV und VI fehlen diese Signale. Dafür treten im IR-Spektrum die charakteristischen Sultam-Banden[3] bei 1291—1270 cm^{-1} auf (s. Abb. 1). Kürzlich berichteten Zeid und Ismail,[4] daß manche ungesättigte sechsgliedrige Sultame IR-Absorptionen bei 1120 cm^{-1} und 1280 cm^{-1} zeigen. Die Autoren ordnen diese Absorptionen der $-SO_2-N$-Gruppierung zu, wogegen C. N. R. Rao[5] für dieselbe Gruppierung Banden bei 1180—1140 cm^{-1} (s) und 1370 cm^{-1} (s) angibt. Nach unseren früheren Ergebnissen[3] vermuten wir, daß die Bande bei 1280 cm^{-1} für den Sultamring charakteristisch ist.

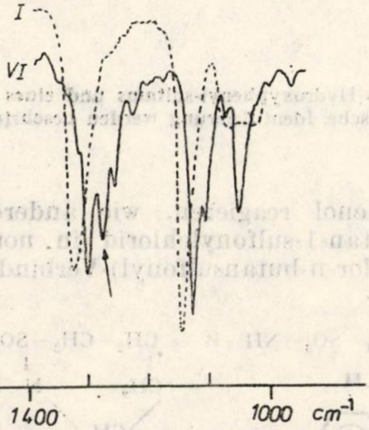

Abb. 1 — Infrarotspektren der Verbindungen I und VI

BESCHREIBUNG DER VERSUCHE

Die Schmelzpunkte wurden auf der Kofler-Bank nach der Anordnung von Weygand bestimmt. Die IR-Spektren wurden mit einem Perkin-Elmer Spektrometer, Modell 221, die Kernresonanzspektren mit einem Varian A 60-Spektrometer und die Massenspektren mit einem Gerät der A. E. I und dem CH-4 der Atlas MAT. aufgenommen.

N-(4-CHLOR-*n*-BUTAN-1-SULPHONYL)-*n*-UNDECYLAMIN (I)

8,5 g (0,05 Mol) *n*-Undecylamin werden in Natronlauge (2 g NaOH in 30 ml Wasser) gelöst und unter Rühren und Eiskühlung mit 0,06 Mol 4-Chlor-*n*-butan-1-sulphochlorid tropfenweise versetzt (ca. 30 Min.). Nach weiteren 12 Stunden bei Raumtemperatur wird der

[2] S. H. Doss, *Rev. Roumaine Chim.*, **17**, 905 (1972).

[3] S. H. Doss, *Chem. & Ind.*, **1971**, 961 ; *Acta Chem. Acad. Sci. Hung.*, **72**, 341 (1972) ; *Rev. Roumaine Chim.*, **17**, 1611 (1972) ; *Chem. Rev.* im Druck ; B. Helferich und S. H. Doss, *Liebigs Ann. Chem.*, **756**, 170 (1972).

[4] I. Zeid und I. Ismail, *J. prakt. Chem.*, **314**, 367 (1972).

[5] C. N. R. Rao in „Chemical Applications of Infrared Spectroscopy", Academic Press, New York, 1963, S. 296.

Niederschlag abgesaugt, mit Wasser gewaschen, getrocknet (Ausbeute: 12 g) und dreimal aus je 100 ml Methanol umkristallisiert.

Ausbeute: 10,5 g (65 %). Die feinen weißen Blättchen schmelzen bei 85°.

$C_{15}H_{32}ClNO_2S$ Ber. : C 55, 38 H 9,84 S 9,81
Gef. : C 55,15 H 9,72 S 9,94

Die Substanz ist leicht löslich in Aceton, Chloroform und Acetonitril, schwer löslich in Äther und unlöslich in Alkohol, Benzol, Petroläther und Wasser.

N-(*n*-UNDECYL)-BUTANSULTAM-(1,4) (III)

6,5 g (0,02 Mol) der Substanz I werden in Natronlauge (1,5 g NaOH in 50 ml Wasser) gelöst und 8 Stdn. unter Rückfluß gekocht. Der dabei entstehende Niederschlag (5,2 g) wird dreimal aus ca. 80 ml Petroläther umkristallisiert.

Ausbeute: 5,0 g (82 %). Schmp.: 78–79°.

Die Substanz hält sehr hartnäckig Wasser zurück. Selbst die bei 50° i. Vak. getrocknete Verbindung enthält noch 1 Mol Wasser pro Formeleinheit. MS :[6] $m/e = 279(M^+)$; ber. : 289,42.

$C_{15}H_{31}NO_2S \times H_2O$ Ber. : C 58,63 H 10,10 S 10,43
Gef. : C 59,15 H 10,77 S 10,06

Die Substanz ist leicht löslich in Aceton, mäßig löslich in Benzol und Chloroform, schwer löslich in Alkohol, Äther und Petroläther und unlöslich in Wasser.

N-(4-CHLOR-*n*-BUTAN-1-SULPHONYL)-*o*-AMINOPHENOL (II)

5,45 g (0,05 Mol) *o*-Aminophenol werden in Natronlauge (2 g NaOH in 40 ml Wasser) gelöst und unter Rühren bei Raumtempeartur mit 0,06 Mol 4-Chlor-*n*-butan-1-sulphochlorid versetzt (ca. 30 Min.). Nach weiterem Rühren (14 Stdn.) wird das ausgeschiedene Öl mit Äther aufgenommen. Die Ätherlösung wird mit Wasser gewaschen, mit Na_2SO_4 getrocknet und i. Vak. eingedampft. Der Rückstand wird in 100 ml Methanol aufgenommen, die Lösung mit Aktivkohle weitgehend entfärbt und die Substanz durch Zugabe von 100 ml Wasser ausgefällt. Sie wird zweimal in 100 ml Methanol aufgenommen und mit 100 ml Wasser wieder ausgefällt.

Ausbeute: 8,0 g (69 %). Die fast farblosen Kristalle schmelzen bei 50–51°.

$C_{10}H_{14}ClNO_3S$: Ber. : S 12,16 N 5,35
Gef. : S 12,55 N 5,85.

Die Substanz ist leicht löslich in Äther, Chloroform, Benzol, Aceton und Alkohol und unlöslich in Petroläther und Wasser.

o-HYDROXYBENZOL-N-BUTANSULTAM-(1.4) (IV)

Eine Lösung von 10 g (0,038 Mol) der Substanz II in Natronlauge (2 g NaOH in 50 ml Wasser) wird eine Stunde unter Rückfluß gekocht, mit Äther zur Entfernung einer kleinen Menge Öl ausgeschüttelt und mit 2n HCl bis zur sauren Reaktion versetzt. Der dabei ausfallende kristalline Niederschlag (6,5 g) wird 2 mal aus Wasser/Methanol (je 30 ml) umkristallisiert.

Ausbeute: 6,2 g (72 %). Die fast farblosen Kristalle schmelzen bei 156–157°.

$C_{10}H_{13}NO_3S$ Ber. : C 52,86 H 5,72 N 6,16 S 14,10
Gef. : C 53,46 H 5,68 N 6,58 S 14,23.

Die Substanz ist leicht löslich in Aceton, mäßig löslich in Äther und Methanol und unlöslich in Benzol, Petroläther und Wasser.

---

[6] H. D. BECKY, H. R. SCHULTEN, G. ECKHARDT und S. H. DOSS, *Tetrahedron*, **29**, 386 (1973).

BIS-1,4-(4-CHLOR-*n*-BUTAN-1-SULPHONAMIDO)-*n*-BUTAN (V)

1,7 g (0,02 Mol) 1,4-Diamino-*n*-butan werden in Natronlauge (1,6 g NaOH in 20 ml Wasser) gelöst und unter Rühren und Eiskühlung tropfenweise mit 0,05 Mol 4-Chlor-*n*-butan-1-sulphochlorid versetzt (ca. 13 Min.). Nach weiteren 2 Stdn. bei Raumtemperatur wird der entstandene kristalline Niederschlag abgesaugt und aus 80 ml Aceton umkristallisiert. Ausbeute : 3,6 g (45 %). Schmp. 137 – 139°.

$C_{12}H_{26}Cl_2N_2O_4S_2$	Ber. :	N 7,07	S 16,16
	Gef. :	N 6,92	S 16,29

Die Substanz ist leicht löslich in Benzol, Aceton und Dimethylsulphoxid, mäßig löslich in Chloroform und schwer- bis unlöslich in Alkohol, Tetrahydrofuran und Wasser.

BIS-1,4-(N-BUTANSULTAMYL-1′.4′)-*n*-BUTAN (VI)

1 g (0,0025 Mol) der Verbindung V wird in Natronlauge (0,5 g NaOH in 30 ml Wasser) gelöst und eine Stunde unter Rückfluß gekocht. Der zunächst ölige, beim Abkühlen kristallisierende Niederschlag wird abgesaugt und aus 20 ml Methanol umkristallisiert. Ausbeute : 0,7 g (86 %). Schmp. 141 – 142°.

$C_{12}H_{24}N_2O_4S_2$:	Ber. :	C 44,44	H 7,40
	Gef. :	C 44,25	H 7,37

Die Substanz ist leicht löslich in Benzol und Chloroform, mäßig löslich in Aceton und schwer- bis unlöslich in Alkohol, Äther, Tetrahydrofuran und Wassser.

Herrn Dr. H. Kober danke ich für die Durchsicht des Manuskripts.

Revue Roumaine de Chimie, 23, 4, 581–586 (1978

ACID-CATALYSED ACETALISATION. I

THE INFLUENCE OF KIND AND CONCENTRATION OF ACID CATALYSTS ON SYNTHESIS OF BIS-1,1-(2′,2′-ETHYLHEXYLOXY)-2-METHYLPROPANE

AUREL I. BLAGA*, RICHARD F. PAPE and TRAIAN CHIRILĂ
ICECHIM Chemical Research Staff of Petrochemical Works "Solventul"
spl. N. Titulescu nr. 31, Timişoara 1900

Received January 26, 1976

The most commonly used method for the nucleophilic addition of alcohols to carbonyl compounds (direct acetalisation or ketalisation) consists in a direct protolytic catalysis, which was very much employed, but not much studied. In this paper, results of a comparative study on three acid catalysts used in reaction between isobutyraldehyde and 2-ethylhexanol are communicated.

The main method for synthesis of acetals and ketals is the nucleophilic addition or exchange of alcohols (or other compounds) to (as such or modified) carbonyl groups; this method includes many synthetic variants, from those the most important being the acid-catalysed reaction between aldehydes (ketones) and alcohols (namley direct acetalisation or ketalisation). In this respect, the direct protolytic catalysis (by proton-donating compounds) is very much used.

We can classify the agents of direct acetalisation so:

— *mineral and organic acids* (direct protolytic catalysis);

— *Lewis acids* (probably an indirect protolytic catalysis rather than a specific catalysis);

— *salts and oxides* (as dehydrating agents); the employment of alkaline bisulphates implies a direct protolytic catalysis. The employment of so-called "catalytic dehydrators" (the mixture of an acid catalyst with a mineral salt-drying agent) led to satisfactory results;[1]

— *ion-exchange resins of strong acid cationic type*;

— *activated natural aluminium silicates.*

In a previous paper,[2] we already have made an attempt to classify the cyclic acetalisation agents.

*** Present address: Industrial Central of Drugs, Cosmetics, Dyestuffs and Varnishes, bd. I. Şulea nr. 309, sector IV, Bucureşti.**

[1] V. I. Stenberg, G. F. Vesley and D. Kubik, *J. Org. Chem.*, 36, 2550 (1971).

[2] A. Blaga, R. Vlădea and T. Chirilă, *Bul. şt. tehn. Inst. Politeh. Timişoara, Ser. Chimie*, 19 (33), 139 (1974).

The first syntheses of acetals were performed without catalysts, both in acyclic[3] and in cyclic[4,5] series. In fact, an acid-catalysed (by traces of acid from carbonylic compound) reaction has taken place. The protolytic catalysis was firstly introduced few years later. [6–14]

Direct acetalisation is a nucleophilic addition of alkoxyl groups from alcohol to carbonylic carbon from aldehyde RCHO. The first step in this reaction is the formation of a hemiacetal (I), which may take place either in acid or in basic catalysis.[15] The second step (formation of acetal) requires *only* acid catalysts. This step through the route of the resonance-stabilised (and solvated) ion (II) evolves. The ionic species (II) is the essential intermediate of this reaction, which is formed only in presence of hydrogen ions (direct or indirect protolytic catalysis). Between carbenium ion (IIb) and oxonium ion (IIa) a mesomerism exists.[16]

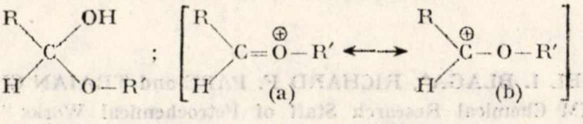

(I) (II)

In this paper, the authors are dealing with the synthesis of bis-1,1-(2′,2′-ethylhexyloxy)-2-methyl-propane (III) by direct acetalisation of isobutyraldehyde with 2-ethylhexanol in presence of some different acid catalysts (direct protolytic catalysis). The attention was mainly focused on the effect of change of catalyst kind and of increase of catalyst amount upon the rate of reaction, the yield, the purity and the colour of main product — the acetal (III).

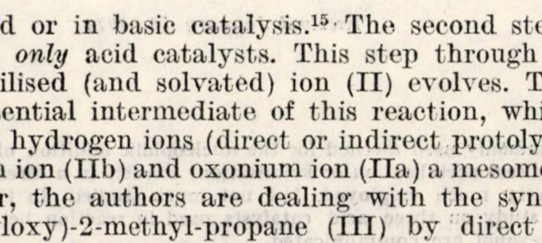

(III)

---

[3] A. Geuther, *Liebigs Ann. Chem.*, **126**, 62 (1872).

[4] A. Wurtz, *Liebigs Ann. Chem.*, **120**, 328 (1861).

[5] Th. Harnitzky and N. Menschutkine, *Liebigs Ann. Chem.*, **136**, 126 (1865).

[6] E. Fischer, *Ber. dtsch. chem. Ges.*, **28**, 1145 (1895).

[7] E. Fischer and G. Giebe, *Ber. dtsch. chem. Ges.*, **30**, 3053 (1897).

[8] E. Fischer and G. Giebe, *Ber. dtsch. chem. Ges.*, **31**, 545 (1898).

[9] J. Meunier, *Compt. rend.*, **106**, 1425, 1732 (1888).

[10] J. Meunier, *Ann. Chim. phys.*, *VI*, **22**, 424 (1891).

[11] E. Fischer, *Ber. dtsch. chem. Ges.*, **26**, 637 (1893).

[12] E. Fischer, *Ber. dtsch. chem. Ges.*, **27**, 1524 (1894).

[13] A. Verley, *Compt. rend.*, **128**, 314 (1899); *Chem. Zentr.*, **1899 (I)**, 564.

[14] A. Verley, *Bull. Soc. chim France*, *III*, **21**, 275 (1899); *Chem. Zentr.*, **1899 (I)**, 919.

[15] J. D. Roberts and M. Caserio, "Basic Principles of Organic Chemistry", Benjamin Inc., New York, 1965, p. 443–446.

[16] C. A. Buehler and D. E. Pearson, "Survey of Organic Syntheses", Wiley-Interscience, New York, 1970, p. 514–516.

Acetal formation is an equilibrium reaction, and to obtain high yelds, one of the products must be continuously removed from system. In the preparation of high-boiling acetals, e. g. acetal (III), the water arised from reaction has to be removed, in these circumstances as azeotrope with one of the raw materials.

The compound (III) was very little studied. One synthesis is only quoted,[17] which was carried out in presence of sulphuric acid as catalyst, with gradually added excess of isobutyraldehyde and two hours refluxing. The practical importance of this compound is also little studied.[18,19]

EXPERIMENTAL

Benzene sulphonic acid $C_6H_5SO_3H \cdot H_2O$ (Carlo Erba), sulphuric acid G. R. of 1.84 density (UCB) and anhydrous potassium bisulphate $KHSO_4$ ("Reactivul") were employed as catalysts.

Isobutyraldehyde of 94—96% purity and 2-ethylhexanol of 99—99.5% purity were products of technical grade (CIPA Rîmnicu Vîlcea).

Both Panradl's[17] and our experiments have proved that the use of an isobutyraldehyde excess is more advantageous than use of a 2-ethylhexanol excess. The resulted water is continuously removed by azeotropic distillation, in the beginning as binary azeotrope with isobutyraldehyde (b. p. 64.3°)[20] or, probably, as ternary azeotrope (we have not found data concerning it); in the end, if isobutyraldehyde remains in excess of that was theoretically needed and 2-ethylhexanol is exhausted, in system will establish a more reduced refluxing temperature than if 2-ethylhexanol would remain in excess (his azeotrope with water :[20] b. p. 99.1°). We have observed two advantages of this choice :

— a shorter reaction time;

— a decreasing with 50—70 degrees of maximum temperature at the end of reaction, that entails few possibilities to occur side reactions and leads to a less coloured product.

In all syntheses, the molar ratio isobutyraldehyde/2-ethylhexanol was 0.75/1.00 (theoretically 0.5/1.0).

All reactions were carried out in a three-necked reaction vessel provided with Dean-Stark trap, Liebig condenser, stirrer and thermometer. Electric heating was employed.

Firstly, 130.2 g (1 mol) 2-ethylhexanol was mixed with catalyst, and then 54.1 g (0.75 mol) isobutyraldehyde was added under vigorous stirring. A rapid rise of temperature (19—23 degrees) was observed in mixture (exothermal process). After about ten minutes, the temperature was stabilized and heating was started. After 30 minutes, the value of temperature has reached 78—81°, when in trap the first condensate drops have appeared. The reaction was continued with refluxing until no water drops were separated in condensate. The cooled crude mixture was weighed, analyzed, neutralized with aqueous sodium hydroxide (2—5%) and purified by vacuum distillation (7 mm Hg). The analysis of crude and pure products was carried out by gas-chromatography, using a Fractovap 2400 T gas-chromatograph under the following conditions: 4 mm × 1.5 m column packed with 15% Carbowax 20 M on Chromosorb P (AW), 60—80 mesh, at 180°, using H.W.D. and hydrogene as carrier gas (40 ml/min).

Table 1 shows the data of main syntheses.

During the syntheses, the removed water was continuously measured, water percentage being plotted as function of time (time is zero in the moment of appearance of first drop of water in trap). We have thus expressed the rate of reaction as the rate of removing of water that is formed in reaction.

Figure 1 shows the influence of molar ratio choice on the rate of reaction. Figures 2, 3 and 4 plot the curves for separated water percentage as function of refluxing time.

---

[17] R. Panradl, *Riechstoffe u. Aromen*, **6**, 33, 65 (1956); *Chem. Abstr.*, **50**, 13796 (1956).

[18] BASF, Fr. Pat. 1 533 896, 19 Jul. 1968; *Chem. Abstr.*, **71**, 31443 (1969).

[19] J. W. Hartmann, G. Schnell, E. Schmidt and F. Gress (to BASF), Ger. Pat. 1 278 514, 26 Sept. 1968; *Chem. Abstr.*, **70**, 48183 (1969).

[20] S. K. Ogorodnikov, T. M. Lesteva and V. B. Kogan, "Azeotropnye smesy", Izd. Khimiya, Leningrad, 1971, p. 66, 92.

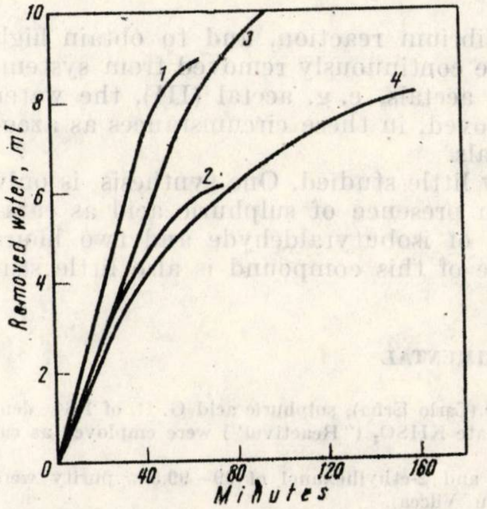

Fig. 1. — The dependence of amount of resulted water upon the molar ratio isobutyraldehyde/2-ethylhexanol for two different catalysts in same concentration presented as a function of time: *1*—0.1044% mol benzene sulphoic acid and molar ratio 0.75/1.00; *2*—0.1044% mol benzene sulphonic acid and molar ratio 0.44/1.00; *3*—0.2251% mol potassium bisulphate and molar ratio 0.75/1.00; *4*—0.2251% mol potassium bisulphate and molar ratio 0.38/1.00.

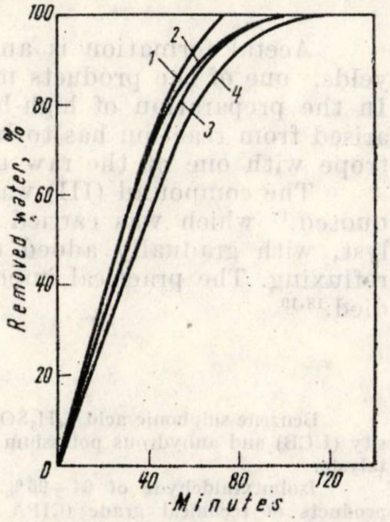

Fig. 2. — The influence of catalyst concentration on the rate of acetalisation.

Catalyst: benzene sulphonic acid; molar ratio isobutyraldehyde/2—ethylhexanol = 0.75/1.00; *1*—0.3133% mol; *2*—0.2049% mol; *3*—0.1566% mol; *4*—0.0522% mol.

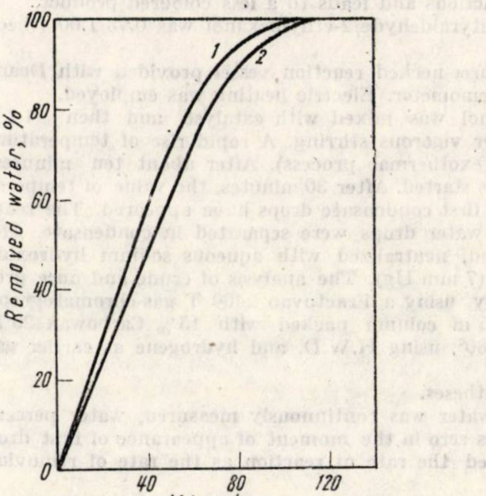

Fig. 3. — The influence of catalyst concentration on the rate of acetalisation.

Catalyst: sulphuric acid; molar ratio sobutyraldehyde/2 — ethylhexanol = 0.75/1.00; *1* — 0.3752% mol; *2* — 0.1876% mol.

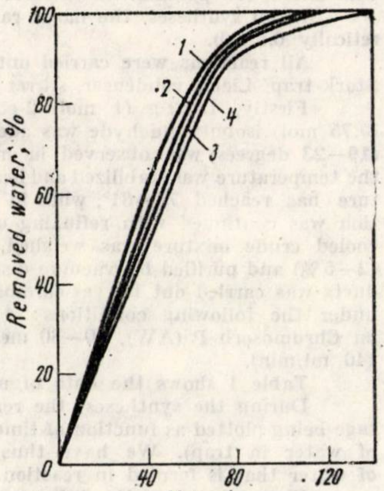

Fig. 4. — The influence of catalyst concentration on the rate of acetalisation.

Catalyst: potassium bisulphate; molar ratio sobutyraldehyde/2—ethylhexanol = 0.75/1.00; *1*—0.5405% mol; *2*—0.4053% mol *3*—0.2702% mol; *4* — 0.1351% mol.

Table 1

The data of synthetic experiments

Catalyst			Total time, minutes	Max. temp., °C	Total removed water, ml	Purity of crude products, %	Yield, %
Kind	Amount, g	Molar concn., %					
BSA*	0.092	0.0522	111	128	10.1	84.3	93.3
,,	0.276	0.1566	97	126	9.5	86.1	93.5
,,	0.361	0.2049	95	128	10.3	82.5	92.6
,,	0.552	0.3133	75	129	9.8	82.3	91.5
H_2SO_4	0.184	0.1876	116	132	9.4	81.6	91.8
,,	0.368	0.3752	107	134	9.3	80.1	90.0
$KHSO_4$	0.184	0.1351	130	121	9.6	84.1	93.2
,,	0.368	0.2702	116	113	9.6	83.3	93.4
,,	0.552	0.4053	110	118	9.6	82.9	93.1
,,	0.736	0.5405	104	119	9.7	83.0	93.0

* Benzene sulphonic acid.

The colouring of crude products was studied with a Lovibond 1 000 comparator.

Table 2 presents the physical characteristics of pure acetal (III), by comparison with the compound obtained by Panradl.[17]

Table 2

The main physical properties of bis-1, 1-(2',2'-ethylhexyloxy)-2-methyl-propane

Property	Purity, %	B. p. at 7 mm Hg, °C	Density at 20°, g/cc	n_D^{20}	Viscosity, cP
Our product	98,5	152-4	0.849*	1.4367	7.42**
Panradl's product[17]	—	154-5	0.848	1.3468	—

* 50 cc pycnometer.
** Höppler viscosimeter.

The acetal (III) was studied by infrared spectroscopy (film), using a Specord 71 IR apparatus. Four absorption bands were identified in the region 1 000—1 200 cm^{-1}, that is characteristic for C—O—C—O—C (acetal).[21,22] The four bands are situated at : 1050 cm^{-1}, 1110 cm^{-1}, 1125 cm^{-1} and 1190 cm^{-1}. Infrared spectrum showed the absence of hydroxyl and carbonyl groups.

---

[21] H. Tchamler and R. Leutner, *Monatsh.*, **83**, 1502 (1952).
[22] J. Radell and R. Rondeau, *J. Chem. and Eng. Data*, **16**, 104 (1971).

CONCLUSIONS

1. The rate of acetalisation increases with increasing concentrations of catalysts (Figures 2—4). Small amounts of catalysts generally lead to great reaction times and to increased temperatures at the end of reactions. Greater concentrations of sulphuric acid cause an increase of rate of acetalisation, but a greater final temperature in reaction mixture (more than other catalysts, sulphuric acid probably implies side reactions, hence high-boiling co-products).

2. The purities of crude products and the reaction yields do not perform conclusive variations so that we could advance some statement. The employment of sulphuric acid leads to the smallest purities and yields (side reactions) (Table 1).

3. The employment of sulphuric acid as catalyst led to the most strengthened colouring of crude products. For all catalysts, the increase of concentration causes the intensification of colouring.

4. In this work, the best results from almost all points of view were obtained with potassium bisulphate, although it is hard to make a differentiation between potassium bisulphate and benzene sulphonic acid as catalysts.

5. Generally, there is an optimum concentration for each catalyst. This concentration assures the most favourable results concerning rate of reaction, purity, yield a. s. o. This optimum range seems to be 0.1 — 0.2% mol for benzene sulphonic acid and 0.3 — 0.5% mol for potassium bisulphate (percentage is given to amount of 2-ethylhexanol).

Revue Roumaine de Chimie, 23, 4, 587–593 (1978)

HETEROCYCLIC QUINONES. X[*)]

SYNTHESIS AND ANTIBACTERIAL SCREENING OF NEW THIAZOLOCARBAZOLOQUINONES

A. S. HAMMAM and H. S. EL-KASHEF
Department of Chemistry, Faculty of Science, Assiut University,
Assiut, Egypt

Received December 11, 1975

A series of 2-aminothiazoles bearing substituents in the 4-and/or 5-positions (IIa-h) were condensed with 4,4'-dimethoxydiquinone (I) to give new thiazolocarbazoloquinones (IIIa-h). The carbethoxy derivative (IIi), however, was unable to react with (I) except after hydrolysis of the corresponding carboxylic acid derivative (IIj), followed by neutralization to salt. None of the aminothiazoles (II) could substitute the quinonoid methoxyl group of the resulting compounds (III). The latter products exhibited antibacterial activity against a wide range of microbes.

We have recently reported[1] that sulphonamides interact with dimethoxydiquinone (I) under specified conditions to give coloured sulphonamides in which the aromatic amino group[a)] became replaced by a carbazoloquinone nucleus.

These products showed *in vitro* antibacterial activity comparable with sulphamethoxazole and interesting results were specifically obtained with the sulphathiazole product. Such observations together with the increasing interest in the biological application of thiazole derivatives,[2] have prompted us to synthesize a new series of substituted thiazolocarbazoloquinones in an endeavour to testing their antibacterial activity, hoping that a combination of the favourable properties of both the carbazoloquinone and the substituted thiazole may be achieved.

[*)] Part IX. Novel dibenzocarbazoloquinones from di-α-naphthoquinone and primary amines. (In press in *Canadian Journal of Chemistry*).

[a)] Sulphaguanidine differed from other sulphonamides in affecting the initial carbazolation reaction through the guanidino and not the aromatic amino group[1].

[1] A. S. Hammam and M. A. El-Dawy, "4th Congress of Arab Pharmacists Union" (1974) 29 Oct. — 1 Nov., Cairo (Abstracts, p. 52).

[2] H. J. Chlorke, *J. Amer. Chem. Soc.*, **37**, 229 (1939).

2-Aminothiazoles carrying substituents in the 4- and/or 5-positions (IIa-i) were prepared by the method of King *et al.*,[3,4] through the interaction of ketones with thiourea in presence of iodine.

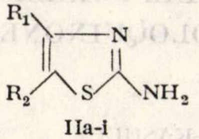

IIa-i

II	R_1	R_2
a	C_6H_5	H
b	C_6H_5	CH_3
c	$p\text{-}CH_3.C_6H_4$	H
d	$p\text{-}CH_3.C_6H_4$	CH_3
e	$p\text{-}CH_3O.C_6H_4$	H
f	$p\text{-}Br-C_6H_4$	H
g	CH_3	H
h	CH_3	CH_3
i	CH_3	COOEt

These thiazoles were then interacted with I in dioxan or acetylene tetrachloride as a reaction medium to give the corresponding thiazolocarbazoloquinones (IIIa-h) in almost quantitative yields.

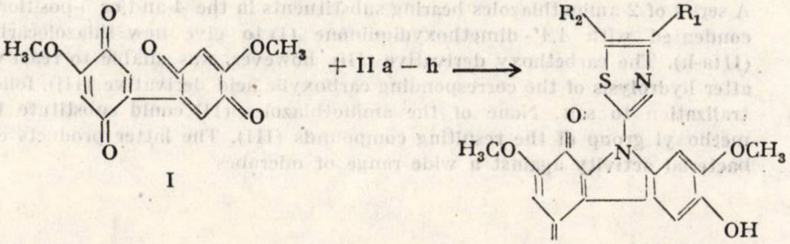

I

IIIa-h

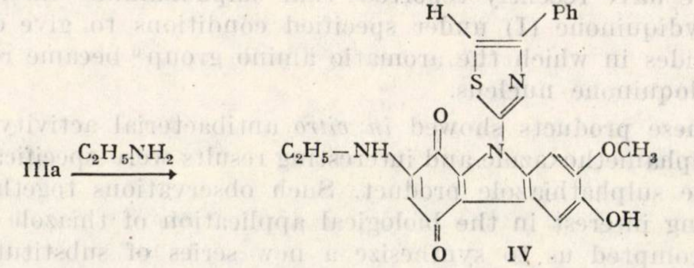

IV

On performing the reaction in ethanol, however, more time was required to accomplish the reaction and relatively low yields resulted with the concomitant production of varying amounts of the blue violet material (V), the latter being formed as a partial reduction product of I.[5] Thus dioxan and acetylene tetrachloride, in view of their high boiling points, good dissolving power and low reducing properties were preferable over alcohol as a reaction medium for this reaction.

---

[3] L. C. King and R. J. Hlavacek, *J. Amer. Chem. Soc.*, **72**, 3722 (1950).

[4] R. M. Dodson and L. C. King, *J. Amer. Chem. Soc.*, **67**, 2242 (1945).

[5] G. Erdtmann, *Proc. Roy. Soc.*, **143a**, 211 (1934).

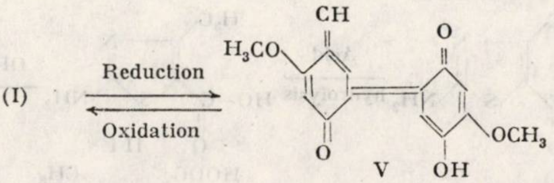

The production of the blue violet material (V) was previously observed during the carbazolation of I with aromatic amines, whereby, it resulted in varying amounts depending on the basic strength of such amines. [6-8] On the other hand, this material was never produced during the reaction of the relatively more basic aliphatic amines.[6,7] The reactivity of aminothiazoles (IIa-h) is therefore analogous to that of aromatic and not aliphatic amines. This conclusion was verified by the failure to affect the substitution of the quinonoid methoxyl group in compounds III by a thiazole-amino group through prolonged reflux with excess amino thiazoles. Such a substitution reaction is established to be readily affected by aliphatic and not aromatic amines. [6-8]

A difference in the rate of formation of compounds III from I and II, was also remarkable in the present study. Thus, aminothiazoles with electron releasing substituents such as IIh (where $R_1=R_2=CH_3$) accomplished the reaction more readily than those with electron withdrawing groups, e. g. IIf (where $R_1=p$-bromophenyl and $R_2=CH_3$).

It is also noteworthy to find out that the aminothiazole IIi, having a carbethoxy substituent in position 5, was unable to react with I although it carries an electron releasing CH_3 group in position 4. The deactivating effect of the carbonyl of the carbethoxy group seems to be so prominent that it prevents completely the aminothiazole to behave as a nucleophile, a condition that should be fulfilled in order that the carbazolation reaction proceeds. This result is analogous to our previous observation on p-amino acetophenone which failed to react with I[6].

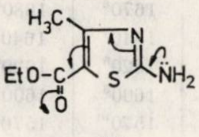

IIi

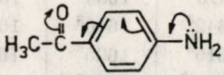

On cancelling the electron withdrawing effect of the carbonyl group in IIi by hydrolysis of the carbethoxy substituent to give the corresponding 5-carboxylic acid derivative (IIj), followed by incorporating the carboxylic group into a process of self resonance through transformation to salt, a reaction could be readily accomplished with I to give the corresponding thiazolocarbazoloquinone (IIIj).

---

[6] A. M. OSMAN and A. S. HAMMAM, *Egypt. J. Chem.*, **15**, 213 (1972).

[7] A. M. OSMAN, A. S. HAMMAM and H. S. EL-KASHEF, *Egypt. J. Chem.*, **15**, 277 (1972).

[8] A. S. HAMMAM, *Egypt. J. Chem.*, **15**, 291 (1972).

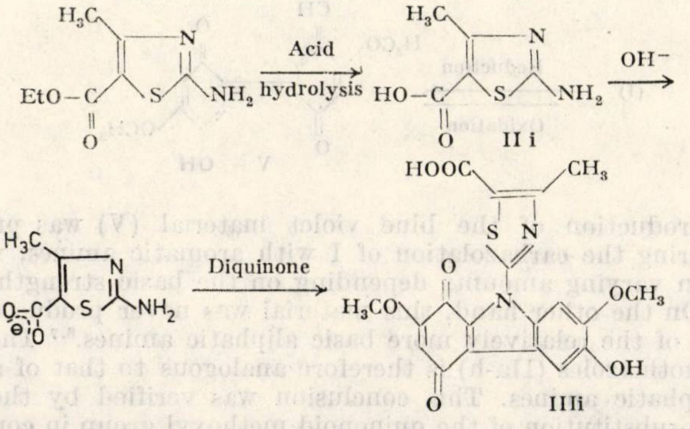

The spectra of the compounds III were measured in their region and the results obtained were in consistance with the structures proposed. These spectra showed vibrational frequencies corresponding to O−H, C=O and C=C of quinones, C−O−C, and C=N of the thiazole ring (Table 1).

Table 1

Infrared spectral data of thiazolocarbazoloquinones III

IIIa	IIIb	IIIc	IIId	IIIe	IIIg	IIIh	Band assignment
3400^{b}	3460^{b}	3460^{b}	3370^{b}	3390^{b}	3340^{b}	3360^{b}	ν O—H bonded
3070^{w}	3050^{w}	3090^{w}	3050^{w}	3100^{w}	3000^{w}	3060^{w}	ν C—H aromatic
3010^{w}	3020^{w}	3040^{w}	3010^{w}	3070^{w}		3020^{w}	
2940^{w}	2960^{w}	2945^{w}	2960^{w}	2985^{w}	2940^{w}	2960^{w}	ν as C−H aliphatic
2830^{w}	2870^{w}	2875^{w}	2870^{w}	2880^{w}	2860^{w}	2880^{w}	νs C−H aliphatic
1660^{s}	1680^{s}	1676^{s}	1680^{s}	1670^{s}	1670^{s}	1680^{s}	νC=O of quinone
1650^{s}	1650^{s}	1642^{s}	1640^{s}	1640^{s}	1640^{s}	1640^{s}	ν C=N of thiazole
1620^{s}	1620^{s}	1615^{s}	1625^{s}	1620^{s}	1620^{s}	1620^{s}	
1610^{s}	1600^{sh}	1600^{sh}	1600^{s}	1600^{s}	1600^{s}	1600^{s}	ν C=C skeletal vibrations
1585^{m}	1580^{sh}	1580^{m}	1570^{sh}	1590^{s}	1570^{m}	1570^{m}	
1510^{m}	— —	— —	1510^{m}	— —	1480^{m}	1510^{m}	
1430^{w}	1540^{m}	— —	1450^{s}	— —	— —	1450^{s}	
1530^{m}	1540^{m}	1530^{m}	1530^{m}	1530^{m}	1520^{m}	1530^{m}	Thiazole I band [9]
1250^{s}	1235^{s}	1250^{s}	1230^{m}	1260^{s}	1230^{s}	1200^{s}	ν as C−O−C
1040^{s}	1045^{s}	1040^{m}	1040^{m}	1030^{m}	1040^{m}	1040^{m}	ν s C−O−C
850^{m}	860^{m}	800^{s}	850^{m}	850^{m}	820^{s}	850^{m}	ν C−H ν aromatic
730^{s}	780^{m}	750^{s}	830^{m}	— —	— —	— —	
710^{m}	710^{m}	— —	— —	— —	— —	— —	

---

[9] Randall, Fowler, Fuson and Dangl : "Infrared Determination of Organic Structures" D. Van Nostrand Co., Inc., New York, 1949.

In vitro antibacterial screening of selected members of compounds III was also performed on 14 strains of different pathogenic bacteria and the minimum inhibitory concentrations (MIC) in micrograms per ml. were determined (Table 2). With the exception of *Shigella sonnei*, the growth of the other 13 microbes was inhibited by the compounds under test. It is also interesting to point out that the MIC figures obtained were lower than the corresponding figures given by analogous carbazoloquinones containing a sulphonamide[1] or even a penicillanic acid moiety.[10]

Table 2

Antibacterial activity of selected thiazolocarbazoloquinones III *in vitro*

Strains		Minimum inhibitory concentrations (MIC) in μg/ml.			
		IIIc	IIId	IIIb	IIIh
Staphylococcus aureus	195	100	50	50	12.5
Staphylococcus aureus	200	100	100	100	50
Staphyloccocus aureus	205	100	100	6.25	3.12
Escherichia coli	30	25	12.5	12.5	1.56
Escherichia coli	10	100	100	50	12.5
Klebsiella pneumoniae	81	50	50	25	3.12
Proteus spp. indole (−)	125	100	100	100	50
Proteus spp. indole (−)	127	100	50	25	25
Proteus spp. indole (+)	130	100	50	12.5	12.5
Pseudomonas aeruginosa	21	100	100	100	50
Pseudomonas aeruginosa	22	100	100	100	100
Pseudomonas aeruginosa	13	100	100	100	50
Shigella sonnei		>100	>100	>100	100
Salmonella para typhi B		50	25	100	50

MIC in Brain Heart Infunsion Broth. Used concentrations: 0.39, 0.78, 1.56, 3.12, 6.25, 12.5, 25, 50 and 100 μg/ml.

EXPERIMENTAL

All melting points are uncorrected. The ir spectra were measured on a Perkin Elmer Infracord Model 137 using KBr Wafer technique.

4-and/or 5-substituted aminothiazoles IIa-i: These were prepared by the procedure of King *et al.*[3,4]

4,4′-Dimethoxydiquinone I: This was prepared by a modified[8] procedure of Erdtmanen.[5]

THIAZOLOCARBAZOLOQUINONES IIIA-H

General method of preparation: A mixture of the diquinone I (1.37 g., 5 m mole) and the aminothiazole IIa-h (5 m mole) was covered with 30—40 ml acetylene tetrachloride and refluxed for 0.5—1.5 hrs. where it gave a deep coloured solution (reddish-orange to brownish-violet). The reaction mixture was then cooled to room temperature, filtered, concentrated to one half of its volume and then diluted with two volumes of petroleum ether (b. p. 40—60°). The precipitated dark solid was collected, dried and recrystallised from the proper solvent (Table 3).

---

[10] G. Cocuxxa, Univ. of Catania, Italy (Personal communication).

Table 3

Thiazolocarbazoloquinones III

Compound	Reaction % yield		time min.		Solvent	Colour of the product	m. p.°	Formula	Analysis %					
									Required			Found		
	A	B	A	B					C	H	N	C	H	N
IIIa	60	90	80	71	Dioxan	Brownish violet	210 (sint.)	$C_{23}H_{16}O_5N_2S$	63.89	3.70	6.48	63.77	3.52	6.40
IIIb	50	60	Quant.	82.5	Dioxan	Dark red	173	$C_{24}H_{18}O_5N_2S$	64.57	4.03	6.28	64.21	3.97	6.35
IIIc	45	60	Quant.	81.7	Ethanol	Dark violet	>350	$C_{24}H_{18}O_5N_2S$	64.57	4.03	6.28	64.19	4.15	6.48
IIId	40	60	Quant.	83	Ethanol	Orange red	262	$C_{25}H_{20}O_5N_2S$	65.22	4.35	6.09	65.21	4.33	6.22
IIIe	60	90	Quant.	80	Excess ethanol	Violet	>350 (sint.)	$C_{24}H_{18}O_6N_2S$	62.34	3.90	6.06	62.55	3.71	6.00
IIIf	90	150	70	55	Excess ethanol	Dark brown	221 (sint.)	$C_{23}H_{15}O_5N_2SBr$	54.01	2.94	5.48	54.37	2.88	5.52
IIIg	40	60	Quant.	92	Excess ethanol	Brownish red	242	$C_{18}H_{14}N_2O_5S$	58.38	3.78	7.57	58.18	4.01	7.67
IIIh	30	40	Quant.	Quant.	Ethanol-methanol	Orange red	235	$C_{19}H_{16}N_2O_5S$	59.37	4.17	7.29	59.29	3.99	7.15

(A) In Dioxan or acetylene tetrachloride

(B) In Ethanlo.

When the reaction was performed in dioxan instead of acetylene tetrachloride, the dilution of the concentrated filtrate was done with water instead of petroleum ether.

When ethanol was used as a reaction medium, the time of reflux ranged from 40—150 minutes and the yields were relatively low (Table 3). Variable amounts of the blue violet material V usually precipitated during reflux and were removed by filtration from the hot reaction mixture.

Attempted reaction of thiazolocarbazoloquinone IIIh with an excess of 4,5-dimethyl-2-aminothiazole IIh.

A mixture of IIIh (0.768 g, 2 m mole) and IIh (0.374 g, 3 m mole) was refluxed for 3 hrs. in ethanol (40 ml.). The resulting brownish red solution was concentrated to one half of its volume, acidified with concentrated hydrochloric acid and cooled. A red solid separated out which gave on recrystallisation from an ethanol-methanol mixture orange red needles of the starting material IIIh, m .p. and mixed m. p. with an authentic sample was 235°. (Found : N; 7.51 $C_{19}H_{16}N_2O_5S$; required : N; 7.29).

Reaction of ethylamine with the thiazolocarbazoloquinone IIIa : 0.864 g (2 m mole) of IIIa was treated with an excess amount of ethylamine solution (2 ml, 30 %). The mixture was refluxed in alcohol for 30 minutes during which the resulting greenish brown reaction liquor changed to brown and a dark brown solid precipitated. The latter was collected (0.7 g) and recrystallised from dioxan into brown platelets of 2-ethylamino-6-hydroxy-7-methoxy-9-(4-phenylthiazol-2-yl)-carbazole-1,4-quinone IV, m. p. > 320° (sint.) (Found : N; 9.52 $C_{24}H_{19}O_4N_3S$ required : N; 9.44).

Attempted reaction of 4-methyl-5-carbethoxy-2-aminothiazole IIi with I :

A mixture of IIi (0.93 g, 5 m mole) and I (1.37 g, 5 m mole) was covered with dioxane (30 ml) and refluxed for 2 hrs. The resulting dark yellow solution was cooled when yellow needles of I precipitated unchanged. Concentration of the reaction liquor and cooling precipitated the remainder of I. After removing I, the concentrate was diluted with water when it precipitated colourless crystals of IIi.

On repeating the above reaction in alcohol instead of dioxan most of the diquinone was reduced to the blue violet product V.

2-Amino-3-methyl-4-thiazole carboxylic acid IIj :

4 g of IIi was dissolved in 50 ml ethanol-water mixture (1 :1). The solution was treated with concentrated hydrochloric acid (25 ml) and gently refluxed for 5 hrs. The mixture was then cooled and neutralized with an aqueous solution of sodium acetate when a flocculant white solid precipitated which was filtered, washed with excess water and recrystallised from aqueous ethanol into long fluffy white needles of IIi, yield quantitative, m. p. 182°. (Found : C, 37.69; H, 3.75; N, 17.71. $C_5H_6O_2N_2S$ required : C, 37.97; H, 3.80; N, 17.72).

Reaction of 2-amino-3-methyl-4-thiazolecarboxylic acid IIi with I :

A mixture of IIi (1.58 g, 10 m mole) and I (2.74 g, 10 m mole) was dissolved in 100 ml of dioxan and treated with 0.84 g $NaHCO_3$ dissolved in 5 ml of water. The mixture was then refluxed for 30 minutes when a deep magenta red colour developed and a red solid precipitated on the wall of the container. The reaction mixture was then acidified with hydrochloric acid and diluted with an equal volume of water. The precipitated red solid was collected (yield, 3.6 g) and recrystallised from ethanol into crimson red platelets of 6-hydroxy-2,7-dimethoxy-9-[3-methyl-4-carboxythiazol-2-yl)-carbazole-1,4-quinone, IIIj, m. p. > 320° (sint.). (Found : C, 52.51; H, 3.38; N, 7.17; $C_{17}H_{14}O_7N_2S$. required : C, 52.31; H, 3.27; N, 7.18

ACKNOWLEDGEMENT. We would like to acknowledge Prof. Dr. G. Cocuxxa, Head of Institute of Microbiology, Catania University, Italy, for the antibacterial screening.

Revue Roumaine de Chimie, **23**, *4*, 595–601 (1978)

DIFFERENT BEHAVIOUR OF ISOMERIC ARYLBENZYLKETONES TOWARDS PHOSPHORUS PENTACHLORIDE

ALICE MARIE GLATZ, VALERIAN DRĂGUŢAN, ZSOLT ARVAY,
CONSTANTIN DRĂGHICI and ALEXANDRU C. RĂZUŞ
Center of Organic Chemistry, Spl. Independenţei 202B, 77201 Bucharest, Romania

Received January 30, 1976

The reaction of *p*-n-butylphenyl-*p'*-ethoxybenzylketone or *p*-n-butylbenzyl-*p'*-ethoxyphenylketone with phosphorus pentachloride in similar conditions yields different major products (monochlorostilbene and dichlorostilbene derivative respectively) depending on the position of the substituents in the aromatic rings. The pathways of the two reactions are discussed.

The isomeric *p*-n-butyl-*p'*-ethoxy-*trans*-1-chlorostilbene (**1**) and *p*-n-butyl-*p'*-ethoxy-*trans*-2-chlorostilbene (**2**) were needed for a study in our laboratory. In order to obatin these two compounds *p*-n-butylphenyl-*p'*-ethoxybenzylketone (**3**) and *p*-n-butylbenzyl-*p'*-ethoxyphenylketone (**4**) were prepared as starting materials. The ketones **3** and **4** were treated with phosphorus pentachloride according to the general procedure of Young, Aviram and Cox.[1] Whereas the ketone **3** gave the expected monochlorostilbene (**1**) (84.0%) the ketone **4**, in the same conditions afforded as main product *p*-n-butyl-*p'*-ethoxy-*trans*-1,2-dichlorostilbene (**5**) (81.0%).

The composition of the reaction mixture was determined by NMR spectrum (see experimental section). As table shows, besides the main products **1** and **5** from the both ketones, two types of products, in significantly different ratios, are formed : a chlorinated ketone (**6** respectively **8**) and a *gem*-dichloride (**7** respectively **9**). From the ketone **3** no dichlorostilbene **5** was detected, whereas from the ketone **4** the corresponding monochlorostilbene **2** was present in the reaction mixture only in traces. The last one, undetectable from the NMR spectrum, was isolated by column chromatography from many experiments and identified by elemental analyses and NMR spectrum.

Attempts to obtain **2** from ketone **4** and PCl_5 by changing the reaction conditions were unfruitful. At lower temperatures (25°) the chloroketone **8** and the *gem*-dichloro compound **9** were formed in larger amounts on the expense of dichlorostilbene **5**. No chlorostilbene was detected in these milder conditions.

---

[1] W. R. Young, A. Aviram and R. J. Cox, *J. Amer. Chem. Soc.*, **94**, 3976 (1972).

Scheme 1

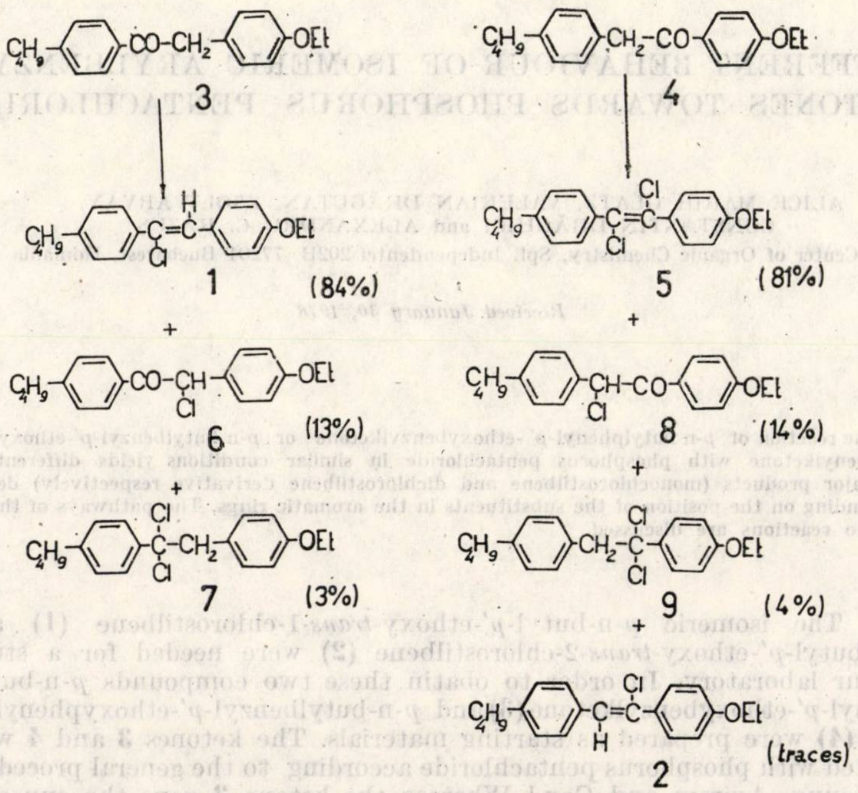

Table 1

Reaction of ketones 3 and 4 with phosphorus pentachloride in methylene chloride under reflux

Exp. N°	Reactants	Reaction time hrs	Reaction products, % mol.[a]				
			1	3	5	6	7
1.	3	5	84.0	0	0	13.0	3.0
			2	4	5	8	9
2.	4	1	0	12.0	67.0	10.0	11.0
3.		5	traces[d]	0	72.0	23.0	4.0
4.		6	traces[d]	0	81.0	14.0	4.0
5.[b]		5	0	51.0	0	38.0	10.0
6.[c]		1/2	0	25.0	23.0	34.0	18.0

a) Calculated from NMR spectra of the crude reaction mixture.

b) Reaction temperature 25°

c Reaction temperature 25° without solvent.

d) Isolated from the reaction products by means of column chromatography

Beteiligung dieses Atomes tritt deutlich hervor, zumal in der hydroxylaminischen Form des Moleküls, so wie es auch die Elektronendichten und Bindungsordnungen bezeugen.

Keiner der oben angegebenen Werte kann als Stabilitätskriterium der Tautomeren betrachtet werden, angesichts ihrer Unsicherheit (Parameterabhängigkeit) und der Vernachlässigung der σ-Elektronen. Um dennoch die Stabilität der Tautomeren besprechen zu können, wurde eine grobe Abschätzung ihrer Gesamtelektronenenergieunterschiede unternommen. Die Gesamtelektronenenergie wurde als die Summe der lokalisierten Einfach- und Doppelbindungsenergien betrachtet, zu der noch die π-Delokalisierungsenergie zukommt. Wir benützten die von Dewar[5] angegebenen Bindungsenergien:

C—N	C=N	C—O	C=O
—3,346 eV	—5,177 eV	—3,999 eV	—7,101 eV

ohne die Folgen der Bindungsabstandsänderungen, im Molekül in Vergleich zu den isolierten Bindungen, in Betracht zu ziehen, da sie in allen Tautomeren ähnlich sein dürften. Andererseits muß der Anteil der in verschiedener Anzahl vorliegenden Bindungen N—H und O—H in die Rechnung miteingezogen werden. Dewars Werte[6] für diese Energien sind:

=N—H (Imino)	$>$N—H (Amino)	O—H
—4,375 eV	—4,202 eV	—4,439 eV

Da wir nur die Energiedifferenzen der einzelnen Tautomeren suchen, wurden nur jene Bindungen mitgerechnet, durch die sich die Tautomere einer Verbindung unterscheiden. Zu diesen Energien wurden die in eV umgerechneten E_R-Werte hinzugefügt, wobei für β der von Streitwieser[3] vorgeschlagene Wert: $\beta = -0{,}69$ eV benützt wurde. Die Ergebnisse sind als E' in Tab. 2 eingetragen.

Die Formen (II) und (IV) erweisen sich, sowohl im Dioxim wie auch im Monoxim, als weniger stabil; der Energieunterschied zu den andern Formen ist recht beträchtlich: etwa 0,9 eV (20 kcal/Mol). Dies Ergebnis ist mit denen zahlreicher anderer MO-Berechnungen für Heterozyklen übereinstimmend, welche die Formen mit Oxogruppen (=O) stabiler als die mit Hydroxygruppen (—OH) finden. Unsere Berechnungen geben ferner an, daß die aromatische Form (IV) energetisch günstiger als (II) ist, allerdings ist der Unterschied gering. Die hier verwendete Annäherung zeigt keinen deutlichen Energieunterschied zwischen (I) und (III); beim Dioxim scheint hier (III) etwas stabiler, aber die Energie einer σ-Bindung N—O in =N—OH dürfte tiefer liegen als in —NH—OH, was zu einer Stabilisierung der Form (I) führen müßte. Fürs Monoxim, bezeichnen die Ergebnisse nach Satz (2) die Form (I) als die stabilste.

Obwohl die HMO-Methode für Spektralberechnungen wenig geeignet zu sein scheint, wurden die Energieunterschiede Δm, die den drei energieärmsten Elektronenübergängen entsprechen sollten, berechnet. Für (Ia) und (IIa) ist die erste Anregungsenergie viel kleiner als für die anderen Formen; dementsprechend zeugt die gelbe Farbe des Dioxims für sein Vorhandensein in Form (I). Aus dem Absorptionsspektrum des Dioxims ergeben sich Maxima bei etwa 320 und 230 nm[7]. Nach Streitwieser[3] gilt, für die Frequenzen der Absorptionsbanden bei aromatischen Kohlenwasserstoffen, die Gleichung: $\gamma(\mathrm{cm}^{-1}) = (19020 \pm 330)\Delta m + (10520 \pm 340)$. Für die Form (I) des Dioxims, können die experimentellen Werte mit folgenden ähnlichen Gleichungen genau wiedergegeben werden:

---

[5] M. J. S. DEWAR, „The MO Theory of Organic Chemistry", McGraw-Hill, New York, 769, S. 381.

[6] N. BODOR, M. J. S. DEWAR und A. J. HARGET, *I. Amer. Chem. Soc.*, **92** 2929 (1970).

$$\gamma(\mathrm{cm}^{-1}) = 23600\Delta m + 11700 \qquad \text{(Satz 1)}$$

$$\gamma(\mathrm{cm}^{-1}) = 24600\Delta m + 7200 \qquad \text{(Satz 2).}$$

Beim Monoxim ist der Energieunterschied zwischen dem höchsten besetzten und dem tiefsten unbesetzten Zustand wesentlich größer als für das Dioxim, in jeder tautomeren Form, und in der Tat ist das Monoxim fast farblos. Für Tautomer (Ib) ist die aus dem ersten Elektronenübergang resultierende Wellenlänge, nach den obigen Formeln berechnet, etwa 290 nm (Parametersatz 1) oder 270 nm (Satz 2).

π-ELEKTRONENVERTEILUNG

Die nach den zwei Parametersätzen berechneten *effektive π-Ladungen* ($n_i - q_i$, wo die Zahl der Elektronen mit denen das Atom i zum π-Elektronensystem beiträgt durch n_i und die Elektronendichte durch q_i bezeichnet sind) der einzelnen Atome im Dioxim und Monoxim sind in Tabelle 3 angeführt. Die Ergebnisse der zwei Parametersätze sind, was die Elektronenverteilung betrifft, in großen Zügen ähnlich, doch die Ladungen sind gewöhnlich für Satz (2) stärker. Die Unterschiede, die nur selten 0,1 übertreffen, können auf Grund der Parameterwerte leicht erklärt werden.

Im Dioxim besitzt der carbonylische O_{10} (Ia, IIIa) die stärkste negative Ladung; der ketoximische N_{11} (Ia, IIa) ist das am stärksten negativ geladene von allen N-Atomen des Moleküls. Der an ihn gebundene O_{12} hat eine sehr schwache positive Ladung, die auf eine sehr schwache Delokalisierung des einsamen Elektronenpaares schließen läßt. Im Monoxim sieht die Elektronenverteilung jener im Dioxim sehr ähnlich, nur beim N_{11}-Atom wird die Ladung viel stärker negativ in der Iminogruppe (Ib, IIb). In Form (I) ist die Gesamtladung des Ringes stark positiv (etwa $+1$); diese Ladung ist in den Formen (II) und (III) zu nur $+0{,}3 \ldots +0{,}4$ reduziert. Die Form (IV) enthält einen negativ geladenen aromatischen Ring; in Folge der Elektronendelokalisierung kommt es zu einem besseren Elektronenausgleich.

Die berechneten *Bindungsordnungen*, p_{ij} hängen auch von den verwendeten Parametern ab, sind aber fast dieselben fürs Dioxim (Tabelle 4) und Monoxim. Mit Ausnahme des Ringes in Form (IV), deuten sie auf eine ziemlich schwache Delokalisierung; besonders mit Satz (1)

---

[7] I. Cădariu, E. Gavrilă und G. Niac, *Z. phys. Chem. (Leipzig)*, **242**, 391 (1969).

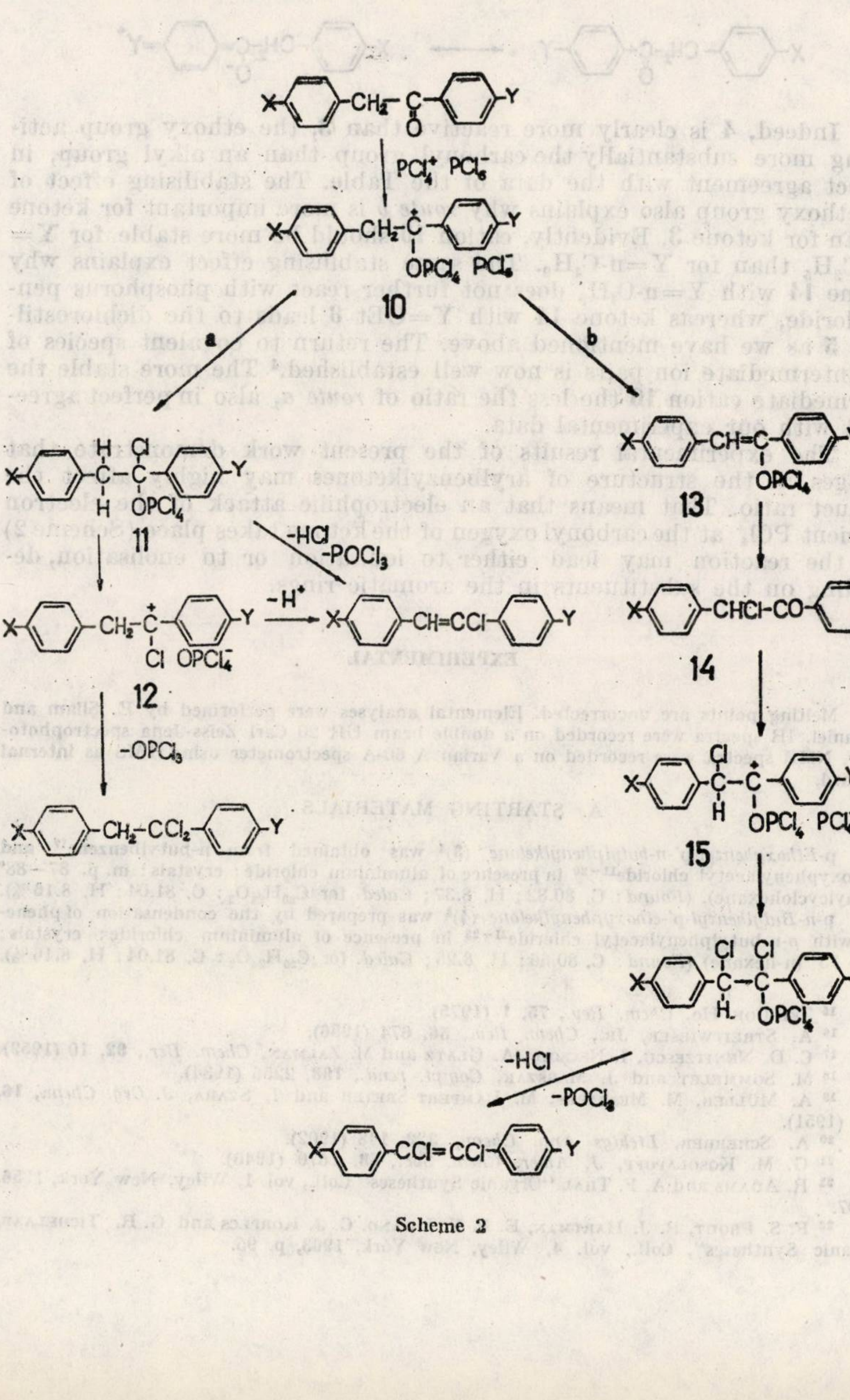
X
Y
PCl$_4^+$ PCl$_6^-$
OPCl$_4$ PCl$_6^-$
10
a
b
11
-HCl
-POCl$_3$
-H$^+$
12
-OPCl$_3$
13
14
15
-HCl
-POCl$_3$

Scheme 2

group. The effect of the ethoxy group[15] is transmitted through benzene ring[16] conjugated with CO group favouring the electron shift toward oxygen.

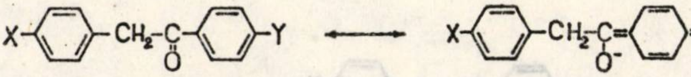

Indeed, **4** is clearly more reactive than **3**, the ethoxy group activating more substantially the carbonyl group than an alkyl group, in perfect agreement with the data of the Table. The stabilising effect of the ethoxy group also explains why *route b* is more important for ketone **4** than for ketone **3**. Evidently, cation **10** should be more stable for $Y = OC_2H_5$ than for $Y = n\text{-}C_4H_9$. The same stabilising effect explains why ketone **14** with $Y = n\text{-}C_4H_9$ does not further react with phosphorus pentachloride, whereas ketone **14** with Y=OEt **8** leads to the dichlorostilbene **5** as we have mentioned above. The return to covalent species of the intermediate ion pairs is now well established.[4] The more stable the intermediate cation **10** the less the ratio of *route a*, also in perfect agreement with our experimental data.

The experimental results of the present work demonstrate that changes in the structure of arylbenzylketones may highly affect the product ratio. That means that an electrophilic attack of the electron deficient PCl_4^+ at the carbonyl oxygen of the ketone takes place (Scheme 2) and the reaction may lead either to ionisation or to enolisation, depending on the substituents in the aromatic rings.

EXPERIMENTAL

Melting points are uncorrected. Elemental analyses were performed by E. Şliam and V. Daniel. IR spectra were recorded on a double beam UR 20 Carl Zeiss-Jena spectrophotometer. NMR spectra were recorded on a Varian A 60-A spectrometer using TMS as internal standard.

A. STARTING MATERIALS

p-*Ethoxybenzyl*-p'-*n-butylphenylketone* (**3**)[4] was obtained from n-butylbenzene[17] and *p*-ethoxyphenylacetyl chloride[11–20] in presence of aluminium chloride; crystals; m. p. 87—88° (methylcyclohexane). (*Found*: C, 80.82; H, 8.37; *Calcd.* for $C_{20}H_{24}O_2$: C, 81.04; H, 8.16%).

p-*n-Butylbenzyl*-p'-*ethoxyphenylketone* (**4**)[4] was prepared by the condensation of phenetole with *p*-n-butylphenylacetyl chloride[21–23] in presence of aluminium chloride; crystals; m. p. 75° (n-hexane) (*Found*: C, 80.66; H, 8.25; *Calcd.* for $C_{20}H_{24}O_2$: C, 81.04; H, 8.16%).

[15] Tse-Lok Ho, *Chem. Rev.*, **75**, 1 (1975).

[16] A. Streitwieser, Jr., *Chem. Rev.*, **56**, 674 (1956).

[17] C. D. Nenitzescu, I. Necşoiu, A. Glatz and M. Zalman, *Chem. Ber.*, **92**, 10 (1959).

[18] M. Sommelet and J. Marszak, *Compt. rend.*, **198**, 2256 (1934).

[19] A. Müller, M. Meszares, M. Lampert-Sreter and I. Szara, *J. Org. Chem.*, **16**, 1013 (1951).

[20] A. Scherrer, *Liebigs Ann. Chem.*, **322**, 148 (1902).

[21] G. M. Kosolapoff, *J. Amer. Chem. Soc.*, **68**, 1670 (1946).

[22] R. Adams and A. F. Thal "Organic Syntheses" Coll., vol. 1, Wiley, New York, 1956, p. 107.

[23] F. S. Prout, R. J. Hartman, E. P. Y. Huang, C. J. Korpecs and G. R. Tichelaar, "Organic Syntheses", Coll., vol. 4, Wiley, New York, 1963, p. 95.

B. CHLORINATION REACTIONS OF THE KETONES 3 AND 4

REACTION WITH PHOSPHOURS PENTACHLORIDE (TABLE 1)

p-*n-Butyl*-p′-*ethoxy-1-chloro-trans-stilbene* **(1)**. The chlorination of ketone **1** was performed according to Young, Aviram and Cox.[1] 3 g (0.01 mol) of ketone **3** dissolved in 50 ml of dried methylene chloride was added dropwise to a reaction vessel contaning 3.15 g (0.015 mol) of PCl_5 dissolved in 50 ml of methylene chloride. The solution was stirred and refluxed for 5 hrs. After cooling the red solution was washed with saturated NaCl and $NaHCO_3$ solutions, filtered and the solvent was evaporated. The crude product (3.1 g) analyzed by NMR and IR spectroscopy was eluted with benzene through a column of silica gel. The fractions obtained were recrystallized repeatedly from petroleum ether at — 60° affording chlorostilbene **1** m. p. 29°. *(Found* : C, 76.10; H, 7.58; Cl, 11.13; *Calcd.* for $C_{20}H_{23}OCl$:C, 76.28; H, 7.36; Cl, 11.36%).

NMR spectrum (CCl_4, δ, ppm): 0.75—1.72 (m, 10H); 2.64 (t, 2H, J=7 Hz); 4.04 (q, 2H, J=7.5 Hz); 6.7—7.86 (m, 9H).

IR spectrum (CCl_4, cm^{-1}) : 925 s; 1057 vs; 1122 s, 1180 vs; 1310 s; 2937 vs; 2965 vs; 2990 s; 3035 m; 3090 w.

p-*n-Butyl*-p′-*ethoxy-2-chloro-trans-stilbene* **(2)** was obtained in traces by chlorination of ketone **4** according to the method above and was isolated by means of a chromatographic column packed with silicagel less than 0.08 mm. eluted with benzene; m. p. 39°. *(Found*: C, 75.49; H, 7.41; Cl, 12.04; *Calcd.* for $C_{20}H_{23}OCl$: C, 76.28; H, 7.36; Cl, 11.36%).

NMR spectrum (CCl_4, δ, ppm): 0.85—1.80 (m, 10H); 2.6 (t, 2H, J=6.5 Hz); 4.1 (q, 2H, J=7 Hz); 6.7—7.8 (m, 9H).

IR spectrum (CCl_4, cm^{-1}) : 929 m; 1125 m; 1185 s; 1520 m; 1620 m; 2868 m; 2879 m; 2968 s; 3035 w; 3050 w.

p-*n-Butyl*-p′-*ethoxy-1,2-dichloro-trans-stilbene* **(5)** was obtained in the reaction above and isolated by chromatographic elution, m. p. 71°. *(Found*: C, 68.79; H, 6.61; Cl, 20.06; *Calcd.* for $C_{20}H_{22}OCl_2$: C, 68.77; H, 6.35; Cl, 20.30%).

NMR spectrum (CCl_4, δ, ppm): 0.7—1.8 (m, 10H); 2.6 (t, 2H, J=6.5 Hz); 3.95 (q, 2H, J=7 Hz); 6.5—7.25 (m, 8H).

IR spectrum (CCl_4, cm^{-1}) : 1060 s; 1125 s; 1186 vs; 1267 vs; 1520 m; 1613 s; 2880 w; 2942 s; 2970 s; 3056 vw.

Chloroketone **8** was noticed in all attempts of chlorination of ketone **4** with phosphorus pentachloride by means of NMR spectra.

NMR spectrum (CCl_4, δ, ppm): 0.7—1.7 (m, 10H); 2.57 (t, 2H, J= 7 Hz); 3.96 (q, 2H, J=7 Hz); 3.96 (q, 2H, J=7Hz); 6.14 (s, 1H); 6.7—8.0 (m, 8H).

IR spectrum (CCl_4, cm^{-1}) : 1055 m; 1128 m; 1178 vs; 1270 s; 1610 s; 1701 s; 2880 m; 2940 s; 2970s; 2990 m; 3035 w.

Chloroketone **8** gave with PCl_5 in the same conditions as for ketones **3** and **4** a mixture of 28% **5** and 72% **8**.

gem-Dichloro compound **9** was similarly, observed in small amounts in usual chlorination reactions of ketone **4**.

NMR spectrum (CCl_4, δ, ppm): 0.67—1.75 (m, 10H); 2.54 (t, 2H, J=7 Hz); 3.90 (q, 2H, J=7 Hz); 5.40 (s, 2H); 6.65—7.55 (m, 8H).

IR spectrum (CCl_4, cm^{-1}) : 1055 s; 1180 vs; 1255 s; 1482 m; 1500 m; 1519 m; 2880 m; 2936 s; 3055 w.

An attempt to prepare the compound **9** working without solvent,[3] at 25°, for 1/2 hour yielded (NMR spectrum) 18.0% of **9** beside chloroketone **8** and dichlorostilbene **5**.

C. OTHER ATTEMPTS OF CHLORINATION

Ketone **4** and $POCl_3$ in chloroform under reflux yielded 25% chloroketone **8** beside unchanged ketone **4**.

Ketone **4** with PCl_3 in chloroform under reflux for 5 hrs, gave no chlorination products.

Ketone **4** and $SOCl_2$ under reflux, 5 hrs, gave no chlorination products.

ACKNOWLEDGEMENT. We are grateful to Dr. F. Badea for helpful discussions.

Revue Roumaine de Chimie, 23, 4, 603–611 (1978)

ÜBER TRIAZINE. LVI.

HMO-BERECHNUNGEN AN DERIVATEN DES 1,3,5-TRIAZINS

OSSI HOROWITZ
Lehrstuhl für physikalische Chemie der Babeş-Bolyai Universität, Cluj-Napoca,
Str. Arany János 11

Eingegangen am 3. Februar 1976

Hückels MO-LCAO Methode, mit zwei verschiedenen Parametersätzen, wurde für Berechnungen an je vier tautomeren Formen des 4-Oxo-6-oximintetrahydrotriazinyl-2-formaldoxims und des 4-Oxo-6-iminotetrahydrotriazinyl-2-formaldoxims verwendet. Es wurden Elektronenenergien, Elektronendichten und Bindungsordnungen berechnet und die Stabilität der Tautomeren, ihr Spektrum und die Bindungsabstände abgeschätzt.

HMO-BERECHNUNGEN

Im Anschluß an die Arbeiten einiger Chemiker aus Cluj-Napoca, die Triazine betreffend,[1] wurden Berechnungen mit Hilfe der einfachen Hückelschen MO-LCAO (HMO) Näherung am π-Elektronensystem des 4-Oxo-6-oximintetrahydrotriazinyl-2-formaldoxims (im weiteren kurz Dioxim genannt) und des 4-Oxo-6-iminotetrahydrotriazinyl-2-formaldoxims (kurz Monoxim) durchgeführt. Diesen Verbindungen, zuerst von A. Ostrogovich und I. Cădariu hergestellt,[2] werden die Formeln (Ia), bzw. (Ib) zugeschrieben. Es können aber auch andere tautomere Formen (II–IV), die sich durch die Verteilung der Doppelbindungen und die Art der Substituenten unterscheiden, in Betracht gezogen werden.

Das Modell, auf Grund dessen die Berechnungen durchgeführt wurden (V), besteht aus 12 Atomen und 16 π-Elektronen fürs Dioxim (a), bzw. 11 Atomen und 14 π-Elektronen fürs Monoxim (b). Die tautomeren Formen wurden in den Berechnungen unterschieden durch Benützung verschiedener Parameter für pyridinartige ($=\!N-$) und pyrrolartige ($>\!\ddot{N}-$) Stickstoffatome, so wie für carbonylische ($=\!O$) und hydroxylische ($-\ddot{O}-$) Sauerstoffatome; dasselbe gilt für deren Bindungen mit Kohlen-

---

[1] LV. Mitteilung: E. Gavrilă und I. Cădariu, *Stud. Univ. Babeş-Bolyai, Chem.*, in Vorbereitung

[2] A. Ostrogovich und I. Cădariu, *Gazz. chim. Ital.*, **71**, 505, 524 (1941).

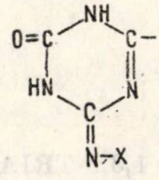

I

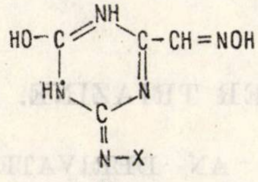

II

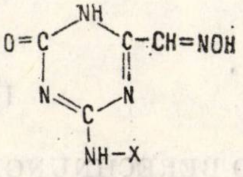

III

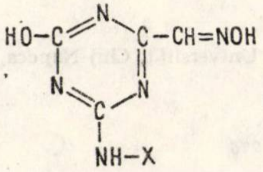

IV

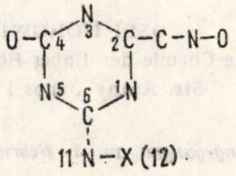

V

$X = \begin{cases} OH & (a) \\ H & (b). \end{cases}$

stoffatome. Das Aminogruppen-N-Atom wurde wie ein pyrrolartiges behandelt. Es wurden zwei verschiedene Parametersätze gewählt :

— die von Streitwieser[3] vorgeschlagenen und in HMO Berechnungen üblichen Parameter :

$$h_C=0\,;\; h_{=N-}=0{,}5\,;\; h_{>\ddot{N}-}=1{,}5\,;\; h_{=O}=1\,;\; h_{-\ddot{O}-}=2\,; \quad (1)$$

$$k_{CC}=1\,;\; k_{CN}=1\,;\; k_{C-\ddot{N}}=0{,}8\,;\; k_{C=O}=1\,;\; k_{C-\ddot{O}}=0{,}8\,;\; k_{NO}=0{,}7.$$

— die von Häfelinger[4] für die Berechnung der Bindungslängen auf Grund der Bindungsordnungen verwendeten Parameter :

$$h_C=0\,;\; h_{=N-}=0{,}8\,;\; h_{>\ddot{N}-}=1{,}5\,;\; h_{=O}=1{,}2\,;\; h_{-\ddot{O}-}=2{,}1\,;$$

$$k_{CC}=1\,;\; k_{CN}=1{,}1\,;\; k_{C-\ddot{N}}=1\,;\; k_{C=O}=1{,}6\,;\; k_{C-\ddot{O}}=1\,;\; k_{NO}=0{,}8. \quad (2)$$

Hier stehen h_X für den Coulombparameter und k_{XY} für den Resonanzparameter. Dieses Verfahren ermöglicht es, den Einfluß der Parameter auf die verschiedenen berechneten Werte abzuschätzen und so die Unsicherheit, die mit der Parameterwahl verbunden ist, zu vermindern. Nach der üblichen HMO-Methode wurden die Eigenwerte und Eigenvektoren erhalten.

ENERGIEWERTE UND ABGELEITETE EIGENSCHAFTEN

Die in Tabelle 1a, b eingetragenen Eigenwerte (es sind die *m*-Werte aus dem Ausdruck : $\varepsilon_\mu=\alpha+m_\mu\beta$ der Energien der Molekülorbitale angegeben) sind vom Parametersatz ziemlich stark abhängig. Für Satz (2),

---

[3] A. Streitwieser, ,,MO Theory for Organic Chemists'', Wiley Inc., New York, 1966, S. 135, 217, 241.

[4] G. Häfelinger, *Chem. Ber.*, **103**, 2902, 2922, 2953, 3289, 3370 (1970).

Tabelle 1a

Eigenwerte *m* der Tautomeren des Dioxims

Form	Ergebnisse nach Satz (1)				Ergebnisse nach Satz (2)			
μ	I	II	III	IV	I	II	III	IV
1	2,6734	2,6853	2,7151	2,7183	3,1796	3,0704	3,1524	3,0592
2	2,3767	2,3729	2,4878	2,5066	2,6357	2,6240	2,7961	2,7557
3	2,3167	2,3648	2,3381	2,3686	2,6157	2,6190	2,6132	2,6157
4	1,9219	2,0776	1,7739	2,0646	2,1868	2,2736	2,1827	2,2766
5	1,7691	1,7985	1,7178	1,5898	2,0479	1,9574	1,9096	1,7892
6	1,1472	1,2771	1,1480	1,2122	1,2769	1,4570	1,2474	1,3848
7	1,0395	0,9639	0,9241	0,8850	1,1701	1,1362	1,0140	1,0868
8	0,5211	0,4432	0,7835	0,8258	0,6772	0,6242	0,9305	0,8996
9	−0,3078	−0,3343	−0,2890	−0,4165	−0,3021	−0,3276	−0,3025	−0,3688
10	−0,9485	−0,9958	−0,8897	−0,9420	−1,2500	−1,0854	−1,1562	−1,0321
11	−1,2287	−1,2338	−1,3662	−1,3280	−1,4493	−1,3197	−1,5176	−1,3843
12	−1,7807	−1,9193	−1,8433	−1,9845	−1,9883	−2,0290	−2,0696	−2,0823

Tabelle 1b

Eigenwerte *m* der Tautomeren des Monoxims

Form	Ergebnisse nach Satz (1)				Ergebnisse nach Satz (2)			
μ	I	II	III	IV	I	II	III	IV
1	2,6488	2,6640	2,6135	2,6265	3,1663	2,0469	3,1216	2,9973
2	2,3589	2,3719	2,3502	2,3687	2,6178	2,6192	2,6134	2,6157
3	1,9704	2,1599	2,0346	2,1905	2,3027	2,4029	2,3810	2,4427
4	1,8271	1,8191	1,7641	1,8273	2,1425	2,0133	2,0906	2,0175
5	1,1472	1,3592	1,2580	1,2893	1,2815	1,5346	1,3184	1,4346
6	1,0843	0,9647	1,0705	1,0022	1,2047	1,1370	1,2043	1,1640
7	0,6816	0,6046	0,7857	0,8572	0,9312	0,8696	0,9973	1,0779
8	−0,2891	−0,3240	−0,2855	−0,4157	−0,2895	−0,3211	−0,2984	−0,3674
9	−0,9420	0,9923	0,8841	−0,9362	−1,2238	−1,0757	−1,1431	−1,0215
10	−1,2109	−1,2103	−1,3650	−1,3260	−1,4492	−1,3010	−1,5175	−1,3804
11	−1,7763	−1,9169	−1,8419	−1,9836	−1,9842	−2,0256	−2,0675	−2,0805

der größere Parameterwerte enthält, sind die negativen Zustände nach unten und die positiven nach oben verschoben. Die in den Formen (I, II) des Dioxims quasidegenerierten Zustände 2 und 3, deren Elektronenverteilungen meistens bei den zwei Oximgruppen konzentriert sind, werden im Monoxim durch einen einzigen Zustand, größtenteils an der Aldoximgruppe lokalisiert, ersetzt. Im Vergleich mit denen der entsprechenden tautomeren Formen des Dioxims, sind die positiven Eigenwerte im Monoxim so gut wie unverändert.

Gesamt-π-Elektronenenergien, *E*, sind in Tabelle 2 angeführt; selbstverständlich sind sie tiefer bei Verwendung des Satzes (2). Die Reihen-

folge der Tautomeren, der wachsenden π-Elektronenenergie gemäß ist : nach Parametersatz (1) : $IV < II < III < I$;
nach Parametersatz (2) : $IV \leqslant III < I \leqslant II$

Tabelle 2

Energiewerte der Tautomeren des Dioxims (a) und Monoxims (b)

Satz	Form	$E(\beta)$	$\Delta E(\beta)$	$E_R\ (\beta)$	$\Delta\Delta E(\beta)$	E_R (eV)	E'(eV)
(1)	Ia	27,5314	11,0314	2,6105	—	−1,801	−16,450
	IIa	27,9663	10,9663	2,7199	—	−1,877	−15,492
	IIIa	27,7765	11,2765	2,8556	—	−1,970	−16,619
	IVa	28,3420	11,3420	3,0956	—	−2,136	−15,751
(2)	Ia	31,5795	13,5795	3,1393	—	−2,166	−16,815
	IIa	31,5236	12,7236	3,3596	—	−2,318	−15,933
	IIIa	31,6918	13,6918	3,2516	—	−2,244	−16,893
	IVa	31,7351	12,9351	3,5711	—	−2,464	−16,079
(1)	Ib	23,4366	10,9366	2,5157	0,0948	−1,736	−20,760
	IIb	23,8869	10,8869	2,6405	0,0794	−1,822	−19,812
	IIIb	23,7530	11,2530	2,8321	0,0235	−1,954	−20,805
	IVb	24,3232	11,3232	3,0768	0,0188	−2,123	−19,940
(2)	Ib	27,2932	13,4932	3,0530	0,0863	−2,107	−21,131
	IIb	27,2467	12,6467	3,2827	0,0769	−2,265	−20,255
	IIIb	27,4530	13,6530	3,2128	0,0388	−2,217	−21,068
	IVb	27,4995	12,8995	3,5355	0,0356	−2,439	−20,256

sowohl für das Dioxim, als auch für das Monoxim. Die benzolartige Form (IV) liegt energetisch am günstigsten, was für HMO-Berechnungen, welche die elektronische Delokalisierung und die von ihr hervorgebrachte Stabilisierung zu übertreiben pflegen, zu erwarten war. Die Energieunterschiede der einzelnen Tautomere sind recht gering, was zu Änderungen in ihrer Reihenfolge beim Parameterwechsel führt.

Zwei weitere Energiewerte wurden in Tabelle 2 eingetragen : ΔE (Energieunterschied des π-Elektronensystems gegenüber den bei den einzelnen Atomen isolierten π-Elektronen) und E_R (Delokalisierungsenergie). Diese wurden berechnet, indem aus den E-Werten die Energien der in Doppelbindungen ($C{=}O, C{=}N$) oder als einsame Elektronenpaare ($\ddot{N}$, $\ddot{O}$) streng lokalisierten π-Elektronen (entsprechend den Formeln I—IV) abgezogen wurden, wobei die Energien der lokalisierten Bindungen mit denselben Parametersätzen berechnet wurden. Auch diesmal sind die Ergebnisse mit Satz (2) tiefer, die Reihenfolge der Tautomeren ist dieselbe beim Dioxim und Monoxim, aber vom Parametersatz abhängig. Die ΔE (oder E_R) Energieunterschiede zwischen den zwei Verbindungen wurden (für entsprechende Tautomere) als $\Delta\Delta E$ in Tab. 2 angegeben und können als Maß der Konjugierung des Atomes O_{12} im Dioxim mit dem übrigen Teil des Moleküls betrachtet werden. Die geringe

The chlorination of **4** with $POCl_3$ in refluxing chloroform (5 hrs) yielded 35% chloroketone **8**, the remainder being unchanged ketone **4**. No reaction could be detected between **4** and PCl_3 or $SOCl_2$ respectively. An effort to prepare chlorostilbene **2** by dehydrochlorination of the *gem*-dichloride **9** also failed. It was not possible to obtain only **9** from **4** by the known procedures[2] (ketone with PCl_5 without any solvent at room temperature). As table shows, a mixture of compounds **5**, **8** and **9** was generated.

The poor tendency of ketone **4** to yield chlorostilbene **2**, in contrast with the behaviour of the isomeric ketone **3** requires an explanation.

It is well known from earlier works[2,3] that ketones with phosphorus pentachloride yield *gem*-dichlorides and chloroalkenes in variable amounts. Later Newman and Wood[4] in order to explain this reaction proposed a mechanism involving two possible pathways starting from a common intermediate, the two above products being obtained. They showed that the product ratios are largely dependent on the reaction conditions. Thus, aromatic ketones (alcoxy group substituted aromatic ring of a benzylic moiety) yield chlorostilbenes.[1,5] α-Chloroacetophenones are chlorinated with phosphorus pentachloride to 1,2-dichloroalkenes.[6] In some instances, at higher temperatures, certain ketones give α-chlorinated ketones.[7]

Depending on the reaction conditions, phosphorus pentachloride may react in two different ways. In one of them it acts as an electrophile. Indeed, by means of X-ray analysis it has been established[8] that even in solid state, phosphorus pentachloride consists of a mixture of covalent molecules in equilibrium with ion pairs :

$$2PCl_5 \rightleftharpoons PCl_4^+ PCl_6^- \qquad (1)$$

Equilibrium (1) is sensitive to medium and temperature changes (Newman and Wood[4]). Carbonyl compounds may solvate specifically the electron deficient cation PCl_4^+, yielding thus in several steps the *gem*-dichloride and/or the monochlorovinylic compound.

At higher temperatures, phosphorus pentachloride reacts as a commonly chlorinating agent [4,7,9,10], dissociating in phosphorus trichloride and molecular chloride :

$$PCl_5 \rightleftharpoons PCl_3 + Cl_2 \qquad (2)$$

---

[2] A. L. Henne and M. W. Renoll, *J. Amer. Chem. Soc.*, **59**, 2435 (1937); P. D. Bartlett and L. J. Rosen, *J. Amer. Chem. Soc.*, **64**, 544 (1942).

[3] A. Favorsky, *J. prakt. Chem.*, (2), **88**, 641 (1913); L. Pfaundler, *Liebigs Ann. Chem.*, **115**, 29 (1860); J. Bredt, *ibid.*, 435, 192 (1924); F. Strauss and A. Berkow, *ibid.*, **401**, 132 (1913).

[4] M. S. Newman and L. L. Wood, jr., *J. Amer. Chem. Soc.*, **81**, 4300 (1959).

[5] T. Nagano, *J. Amer. Chem. Soc.*, **77**, 1691 (1955).

[6] F. Kunckell and K. Eras, *Ber. dtsch. chem. Ges.*, **33**, 3264 (1900); F. Kunckell and R. Koritzky, *ibid.*, **33**, 326 (1900); F. Kunckell and K. Eras, *ibid.*, **36**, 915 (1903).

[7] A. Favorsky, *J. Russ, Phys. chem. Soc.*, **44**, 1339 (1912); C. 1913, I, 1004.

[8] D. Clark, H. M. Powell and A. F. Wells, *J. Chem. Soc.*, **1942**, 642.

[9] A. Asinger, "Chemie und Technologie der Paraffinkohlenwasserstoffe", Akademie Verlag, Berlin, 1956, p. 207.

[10] P. H. Groggins, "Unit Process in Organic Syntheses", McGraw-Hill, New York, 1947, p. 223.

The results obtained in this work rule out equilibrium (2) in explaining the different behaviour of the two isomeric ketones. Indeed, the same mixture is obtained from **4** either in refluxing solvent or at room temperature, with or without solvent (Table 1). The nature of the reaction mixture is thus not temperature dependent, as would be expected if equilibrium (2) would be involved. No reaction was observed between **4** and phosphorus trichloride. Other chlorinating agents, such as $POCl_3$ and $SOCl_2$ fail to lead both to *gem*-dichloride and to chlorostilbene. On the other hand, equilibrium (1) seems to be satisfactory in explaining the experimental data of this work.

In Scheme 2 are represented the transformations of an arylbenzylketone, assuming the initial attack of the electron defficient PCl_4^+. Ion pair **10** is thus formed. This ion pair is a key intermediate in the further transformations of the product. Two routes are possible:

In *route a* (when $Y=C_4H_9$) the chlorostilbene and the *gem*-dichloride are formed in agreement with the reaction mechanism of Newman and Wood.[4] The ion pair **10** collapses to the covalent species **11**. The further ionisation of this one will lead to ion **12**, $POCl_4^-$ ($POCl_3+Cl^-$) being a more efficient leaving group than Cl^-. In the same time the high tendency in the formation of $POCl_3$ may explain the easy formation of monochlorostilbene. The *gem*-dichloride is also formed from **12** by $POCl_3$ elimination. A concerted elimination from **11** is not excluded.

In *route b*, (when Y=OEt) 1,2-dichlorostilbene is the main product. This implies as first step a proton elimination from **10**. Both *a* and *b routes* are competitive.

The products analysis reveals a greater tendency for proton elimination from **10** to the reaction products following the *route b*. Thus the proton elimination from **10** leads to the enol derivative **13**.

A rearrangement of this enol derivative may form the chloroketone **14**, in agreement with the well-known fact[11–14] that enol derivatives are intermediates in the α-halogenation of ketones in acid catalysis. Dichlorostilbenes are formed from these chloroketones in a similar way with the *route a* suffered by the original arylbenzylketone. Cation **15** is formed by the electrophilic attack of PCl_4^+ with further collapse to the dichloro derivative. As an evidence, the ketone **14** leads to the dichlorostilbene **5** as we observed by the independent treatment of ketone **8** with PCl_5. Both routes in the transformation of the intermediates **10** should be available for the arylbenzylketones. However product ratio must depend upon the substituents in the aromatic rings, as well as upon the substituents in the aliphatic chain. The Table shows that the same type of products are formed from both ketones **3** and **4**.

Scheme 2 predicts that the more reactive ketone will be the arylbenzylketone with a Y substituent able to conjugate with the carbonyl

---

[11] A. Lapworth, *J. Chem. Soc.*, **1904**, 80.

[12] M. J. Ronteix and A. Marquet, *Tetrahedron Letters*, **1966**, 5801.

[13] M. Gaudry and A. Marquet, *Tetrahedron*, **26**, 5617 (1970).

[14] Y. Jasor, M. Gaudry, A. Marquet and M. Battahan, *Bull. Soc. chim. France*, **1973**, 2732.

Tabelle 3

Effektive Ladungen, $n_i - q_i$, im Dioxim (a) und Monoxim (b)

Satz	Form	N_1	C_2	N_3	C_4	N_5	C_6	C_7	N_8	O_9	O_{10}	N_{11}	O_{12}
(1)	Ia	−0,2880	+0,2214	+0,2506	+0,3746	+0,2280	+0,1605	+0,0738	−0,0772	+0,0716	−0,6472	−0,4045	+0,0364
	IIa	−0,3117	+0,1844	−0,3336	+0,3386	+0,2526	+0,1597	+0,0835	−0,0926	+0,0686	+0,1006	−0,4784	+0,0284
	IIIa	−0,2774	+0,2565	+0,2817	+0,2840	−0,3510	+0,2580	+0,0722	−0,0490	+0,0751	−0,7065	+0,1473	+0,0091
	IVa	−0,2786	+0,1613	−0,2779	+0,2247	−0,2955	+0,2113	+0,0880	−0,1095	+0,0652	+0,0795	+0,1249	+0,0065
(2)	Ia	−0,3954	+0,2924	+0,3159	+0,2959	+0,2710	+0,2242	+0,1544	−0,1750	+0,0783	−0,5471	−0,5451	+0,0305
	IIa	−0,3934	+0,2503	−0,4067	+0,3662	+0,3399	+0,2190	+0,1619	−0,1916	+0,0715	+0,1366	−0,5810	+0,0274
	IIIa	−0,3873	+0,3017	+0,3368	+0,2626	−0,4941	+0,2759	+0,1551	−0,1690	+0,0790	−0,5794	+0,2052	+0,0133
	IVa	−0,3734	+0,2352	−0,3741	+0,2935	−0,4050	+0,2611	+0,1649	−0,1977	+0,0732	+0,1173	+0,1933	+0,0117
(1)	Ib	−0,2978	+0,2475	+0,2589	+0,3748	+0,2375	+0,2182	+0,0724	−0,0558	+0,0744	−0,6471	−0,4829	—
	IIb	−0,3176	+0,1980	−0,3229	+0,3411	+0,2656	+0,2078	+0,0828	−0,0815	+0,0697	+0,1010	−0,5440	—
	IIIb	−0,2765	+0,2590	+0,2845	+0,2857	−0,3448	+0,2685	+0,0719	−0,0472	+0,0753	−0,7050	+0,1285	—
	IVb	−0,2752	+0,1616	−0,2738	+0,2251	−0,2910	+0,2186	+0,0879	−0,1092	+0,0652	+0,0795	+0,1112	—
(2)	Ib	−0,3995	+0,3083	+0,3246	+0,2962	+0,2830	+0,2738	+0,1540	−0,1651	+0,0799	−0,5469	−0,6081	—
	IIb	−0,3940	+0,2586	−0,3958	+0,3657	+0,3517	+0,2625	+0,1622	−0,1850	+0,0759	+0,1342	−0,6359	—
	IIIb	−0,3864	+0,3050	+0,3404	+0,2636	−0,4843	+0,2942	+0,1548	−0,1670	+0,0793	−0,5784	+0,1789	—
	IVb	−0,3696	+0,2362	−0,3682	+0,2945	−0,3980	+0,2772	+0,1649	−0,1979	+0,0733	+0,1176	+0,1700	—

Tabelle 4

Bindungsordnungen und berechnete Bindungsabstände im Dioxim (a) und Monoxim (b)

Satz	Form	N_1-C_2	C_2-N_3	N_3-C_4	C_4-N_5	N_5-C_6	C_6-N_1	C_2-C_7	C_7-N_8	N_8-O_9	C_4-O_{10}	C_6-N_{11}	$N_{11}-O_{12}$
Bindungsordnungen, p_{ij}													
	Ia	0,7044	0,3697	0,4199	0,4288	0,3245	0,4824	0,4418	0,8616	0,2538	0,6936	0,7693	0,1450
	IIa	0,6488	0,5214	0,6794	0,4470	0,3418	0,5086	0,4134	0,8750	0,2459	0,3638	0,7405	0,1213
(1)	IIIa	0,6692	0,4277	0,4091	0,5754	0,6096	0,5454	0,4337	0,8678	0,2637	0,6062	0,4189	0,0360
	IVa	0,6053	0,5971	0,6187	0,6235	0,6006	0,6039	0,4032	0,8815	0,2387	0,3097	0,3839	0,0284
	Ia	0,6648	0,4780	0,3914	0,4043	0,4076	0,4778	0,3721	0,8776	0,2510	0,7613	0,7112	0,1161
	IIa	0,6325	0,5580	0,6000	0,5095	0,4112	0,5002	0,3612	0,8825	0,2459	0,4234	0,6916	0,1019
(2)	IIIa	0,6494	0,5041	0,3922	0,4772	0,5888	0,5103	0,3672	0,8809	0,2532	0,7226	0,5007	0,0519
	IVa	0,6105	0,5957	0,5787	0,6006	0,5622	0,5551	0,3577	0,8832	0,2395	0,3867	0,4864	0,0474
Bindungsabstände, R_{ij} (in Å)													
	Ia	1,322	1,366	1,386	1,383	1,383	1,366	1,466	1,273	1,381	1,236	1,312	1,431
	IIa	1,330	1,347	1,338	1,359	1,382	1,361	1,469	1,272	1,383	1,322	1,316	1,436
(2)	IIIa	1,326	1,360	1,386	1,366	1,340	1,359	1,467	1,272	1,380	1,246	1,361	1,455
	IVa	1,335	1,339	1,343	1,337	1,346	1,348	1,470	1,271	1,385	1,331	1,364	1,456
	Ib	1,325	1,363	1,386	1,384	1,377	1,363	1,467	1,272	1,379	1,236	1,318	–
	IIb	1,332	1,345	1,338	1,359	1,377	1,357	1,470	1,271	1,383	1,322	1,323	–
(2)	IIIb	1,327	1,359	1,386	1,367	1,337	1,357	1,467	1,272	1,380	1,245	1,367	–
	IVb	1,336	1,338	1,342	1,338	1,344	1,346	1,470	1,271	1,385	1,331	1,370	–

kann man leicht „fast einfache“ und „fast doppelte“ Bindungen erkennen. So ist die aldoximische C_7-N_8 Bindung so gut wie doppelt, eher als die ketoximische C_6-N_{11} (im Dioxim). Dagegen sind die $N-O$ echte einfache Bindungen, zumal in der ketoximischen Gruppe. In der aromatischen Form (IV) findet ein Bindungsausgleich innerhalb des Ringes statt, dafür sind die drei Gruppen mit schwächeren Bindungsordnungen als in den andern Formen an den Ring gekoppelt.

Auf Grund der nach Satz (2) bestimmten Bindungsordnungen wurden auch die Bindungsabstände berechnet, durch die von Häfelinger[4] vorgeschlagenen Gleichungen, der Form :

$$R_{ij} = a - bp_{ij}$$

wo den Parametern a, b folgende Werte zugeschrieben wurden :

	CC	CN	CO	NO
a	1,572	1,478	1,430	1,474
b	0,285	0,234	0,255	0,371

Diese Bindungsabstände (Tab. 4) stimmen mit den experimentell bestimmten Werten für ähnliche Verbindungen überein und können für Berechnungen durch genauere π-Elektronentheorien verwendet werden.

Revue Roumaine de Chimie, **23**, *4*, 613–616 (1978)

PROTON-CATALYSED REARRANGEMENT OF SULPHONAMIDES TO SULPHONES. I

CONVERSION OF SUBSTITUTED ARYLQUINOLYLAMINE SULPHONAMIDE INTO THE ISOMERIC SUBSTITUTED DIARYLSULPHONE

S. S. SRIMALI, NARESH D. SHARMA, SANTOSH KUMAR* and BHUWAN C. JOSHI*
Chemical Laboratories, University of Rajasthan, Jaipur-302004, India

Received November 23, 1975

2-(4-Methoxyanilino)-4-methylquinoline *(1)* was condensed with 2-hydroxy-5-chlorosulphonylbenzoic acid *(2)* to obtain the sulphonamide, 2-[N-(3′-carboxy-4′-hydroxybenzenesulphonyl)-4-methoxyanilino]-4-methylquinoline *(3)*. The sulphonamide 3 was rearranged with sulphuric acid to a sulphone, 2-[2-(3′-carboxy-4′-hydroxybenzenesulphonyl)-4-methoxyanilino]-4-methylquinoline *(4)*. The structures of 3 and 4 were established through elemental analyses and Nmr spectral studies.

DISCUSSION

It has been reported that arenesulphonamides undergo rearrangement besides hydrolysis when treated with concentrated sulphuric acid[1]. Witt and Uermanyi have reported that arenesulphonamides yield mainly ortho-aminosulphones on treating with high concentrations of sulphuric acid.[2] Witt and Halberkamm established that the rearrangement generally takes place at the *ortho* position, when groups like nitro,

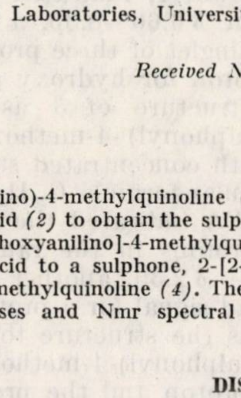

1

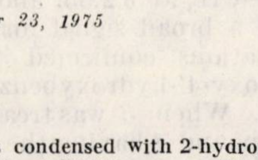

2

---

* For further correspondence

[1] L. A. Warren and S. Smiles, *J. Chem. Soc.*, **1932**, 2775.
[2] O. N. Witt and D. Uermanyi, *Ber. dtsch. Chem. Ges.*, **46**, 296 (1913).

amino, sulphonic acid etc. occupy the para-position.[3,4] Gennaro and Zanger synthesised a number of sulphones by rearranging 1,2,3,4-tetrahydroquinoline sulphonamides with concentrated sulphuric acid.[5] Analogous reactions have recently been investigated in this laboratory with a view to extending their utility as synthetic tools in the preparation of medicinally important sulphones.

On the basis of the observations made by earlier workers, it was thought worthwhile to carry out the rearrangement of the sulphonamide *3*. The elemental analysis of *3* gave molecular formula $C_{24}H_{20}O_6N_2S$. The broad pattern of absorption in the range of 3700–2800 cm^{-1} and a characteristic absorption band at 1710 cm^{-1} in *3* and *4* indicated the presence of carboxyl group in the compounds. The Nmr spectrum of *3* in TFA gave no signal for NH proton. It, however, indicated the presence of twelve aromatic protons in the region δ 6.60–8.30, a singlet of three protons of $C-CH_3$ at δ 2.35, another singlet of three protons of $O-CH_3$ at δ 3.60 and a broad signal for a proton for hydroxy group at δ 5.35. These observations confirmed the structure of *3* as sulphonamide, 2-[N-(3-'carboxy-4'-hydroxybenzene-sulphonyl)-4-methoxyanilino]-4-methylquinoline. When *3* was treated with concentrated sulphuric acid an isomeric compound *4* having the molecular formula $C_{24}H_{20}O_6N_2S$ was obtained. The Nmr spectrum of *4* in TFA indicated the presence of NH proton at δ 10.20, eleven aromatic protons in the range δ 6.50–8.30, a singlet of three protons of $C-CH_3$ at δ 2.30, another singlet of three protons of $O-CH_3$ at δ 3.55 and a broad signal for a proton for hydroxyl at δ 5.35. Based on these observations the structure to *4* was assigned as 2-[2-(3'-carboxy-4'hydroxybenzenesulphonyl)-4-methoxyanilino]-4-methylquinoline. The absence of –NH proton and the presence of twelve aromatic protons in *3*, the presence of –NH proton and only eleven aromatic protons in *4* and the identical molecular formulae of 3 and 4 confirmed that the rearrangement has occurred. The migration could either be to position *3* of the quinoline ring or to the meta-position with respect to methoxyl group in phenyl ring. The Nmr spectra of *3* as well as *4* indicated clearly the presence of a proton at position 3 of the quinoline ring in the vicinity of δ 6.6. This indicates that the sulphone moiety has possibly migrated to the phenyl ring and not to the quinoline ring.

PROPOSED MECHANISM

The transformation of *3* to *4* is a proton-catalysed intra-molecular rearrangement, which possibly takes place through the mechanism as shown in the chart.

The sulphonyl moiety migrates preferentially to the phenyl ring rather than to quinoline ring. This could be due to the fact that the phenyl ring has been activated by the presence of methoxyl group making it more prone to electrophilic attack by the sulphonyl moiety. On

---

[3] J. Halberkamm, *Ber. dtsch. Chem. Ges.*, **54**, 1665 (1921).

[4] O. N. Witt and H. Truttwin, *Ber. dtsch. Chem. Ges.*, **47**, 2786 (1914).

[5] A. R. Gennaro and M. Zanger, *J. Org. Chem.*, **36**, 1321 (1971).

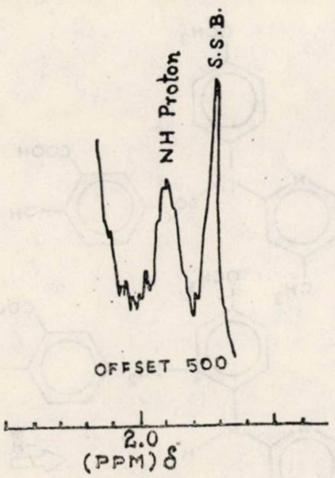

Fig. 1. — Position of NH proton signal in Nmr spectrum of 4 in TFA.

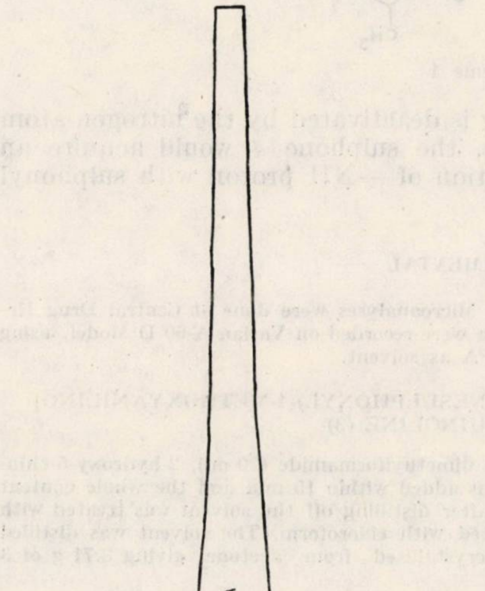

Fig. 2. — Portion of Nmr spectrum of 3 in TFA.

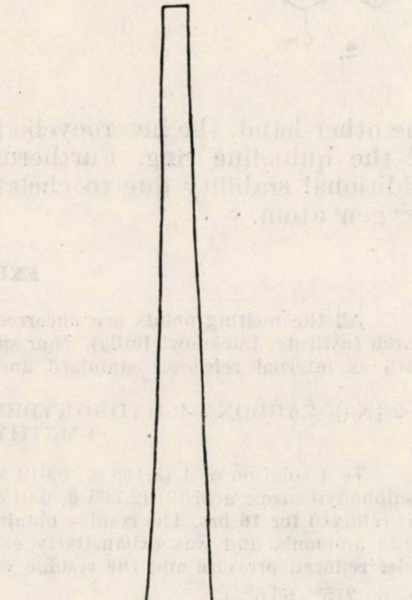

Fig. 3. — Portion of Nmr spectrum of 4 in TFA.

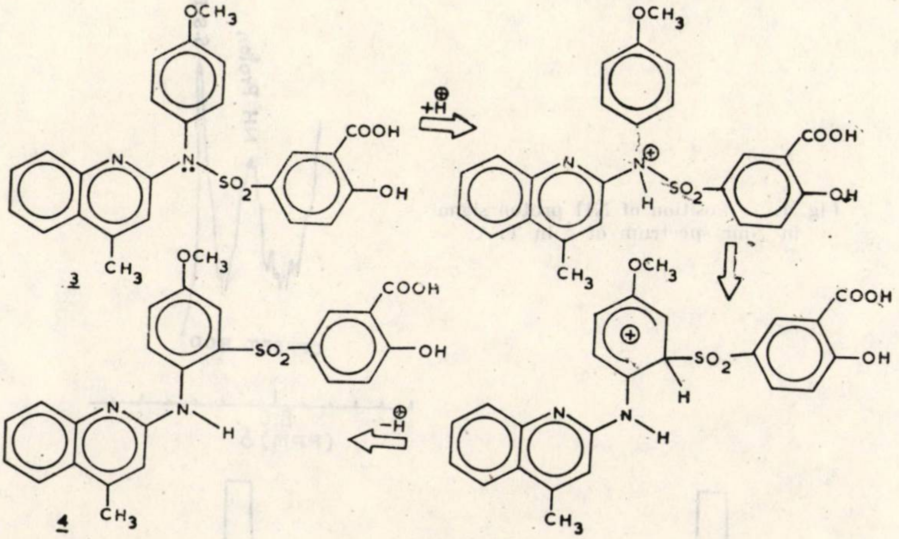

Scheme 1

the other hand, the heterocyclic ring is deactivated by the nitrogen atom of the quinoline ring. Furthermore, the sulphone *4* would acquire an additional stability due to chelatization of —NH proton with sulphonyl oxygen atom.

EXPERIMENTAL

All the melting points are uncorrected. Microanalyses were done at Central Drug Research Institute, Lucknow (India). Nmr spectra were recorded on Varian A-60 D Model, using TMS as internal reference standard and TFA as solvent.

2-[N-(3′-CARBOXY-4′-HYDROXYBENZENESULPHONYL)-4-METHOXYANILINO] -4-METHYLQUINOLINE (3)

To a solution of 1 (3.168 g., 0.012 M) in dimethylformamide (20 ml), 2-hydroxy-5-chlorosulphonylbenzoic acid (2) (2.365 g, 0.01M) was added within 15 min and the whole content was refluxed for 16 hrs. The residue obtained after distilling off the solvent was treated with dilute ammonia and was exhaustively extracted with chloroform. The solvent was distilled under reduced pressure and the residue was crystallised from acetone giving 3.71 g of 3 (m. p. 215°, 66.6%).

2-[2-(3′-CARBOXY-4′-HYDROXYBENZENESULPHONYL)-4-METOXYANILINO] -4-METHYLQUINOLINE (4)

3 (2.320 g., 0.05 M) was added to sulphuric acid (5. ml., sp. gr. 1.84) in one lot. The whole content was kept on boiling water bath for 3 min and poured in crushed ice to give 0.928 g of *4*, which was crystallised from DMF to white solid (m. p. 260° dec. 40%).

Analysis

Calcd. for $C_{24}H_{20}O_6N_2S$: C, 62.06 ; H, 4.31 ; N, 6.03%
Found : *3* C, 62.26 ; H, 4.11 ; N. 6.23% ; *4*
C, 62.15 ; H, 4.33 ; N, 6.15%.

Note (TMS — Tetramethylsilane, TFA — Trifluroacetic acid SSB — Spinning side Band).

ACKNOWLEDGEMENT. The authors thank the Head of the Chemistry Department, University of Rajasthan, Jaipur for providing necessary facilities and one of the authors (NDS) thanks the U. G. C. for financial assistance.

Reuve Roumaine de Chimie, **23**, *4*, 617–624 (1978)

PREPARATION AND SPECTROPHOTOMETRIC STUDIES OF SOME QUINONEANILS

I. M. ISSA, A. A. EL SAMAHY, R. M. ISSA, and H. S. EL KASHEF
Chemistry Department, Faculty of Science, Assiut University A. E. Egypt

Received January 6, 1976

Some quinoneanils were prepared and their spectral behaviour in ethanol was studied. In general the uv spectra of these compounds showed mainly four bands. The shortest wavelength band is due to $\pi \rightarrow \pi^*$ transition within the phenyl ring, whereas the longest one is assigned as a C. T. band. The two intermediate bands are due to the $\pi \rightarrow \pi^*$ transition within the quinone system. The effect of substitution on band position was also investigated.

INTRODUCTION

It is well known that quinoneanils, especially indoaniline dyes, have many applications such as in colour photography [1] and in the preparation of various dyestuffs.[2,3] Quinoneanils were prepared by the oxidation of amines,[4] by the condensation of amines with phenols [5–8] or from nitroso compounds.[9–11] Vittum and Brown[8] showed that N,N-dimethyllindoaniline in cyclohexane has two maxima in the uv range besides the absorption maximum in the visible range (λ_{max} 552 nm). They also pointed out that indoaniline dyes have markedly different absorptions depending on the nature of the substituent group in the oxygen containing ring. Some workers [12] reported that the introduction of electronegative groups in naphthol blue caused deepening of the colour with a bathochrome shift proportional to the electronegativity of the substituent.

[1] R. Fischer; U. S. Patent 1, 102, 028 1914; cf. ref. 8.

[2] E. D. Robinson and D. F. Mason (to Southern Dyestuff Corp.), U. S. 2, 657, 112, Oct. 27 1953; *Chem. Abstr.* **18**. 3679 (1953).

[3] H. Hiyama and K. T. Kogye, *Science and Ind.*, **14**, 694 (1939).

[4] E. Schunck and L. Marchewski, *Ber. dtsch. chem. Ges.*, **25**, 3574 (1892).

[5] G. Heller, *Liebigs Ann. Chem.*, **418**, 259 (1919).

[6] L. Fieser and H. Thompson, *J. Amer. Chem. Soc.*, **61**, 376 (1939).

[7] Gnehm and Bots *J. prakt. Chem.*, **69**, 162 (1904); cf. ref. 6.

[8] P. W. Vittum and G. H. Brown, J. *Amer. Chem. Soc.*, **68**, 2235 (1946).

[9] H. Euler, *Ber. dtsch. Chem. Ges.*, **39**, 1035 (1906).

[10] H. J. Tender and G. Jellinek, *Ber. dtsch. Chem. Ges.*, **87**, 1841-8 (1954).

[11] C. Brömme, *Ber. dtsch. Chem. Ges.* **21**, 391 (1888).

[12] B. S. Portnaya, N. S. Speakukotakil, N. F. Turitsyns, T. P. Bobkova, G. I. Arbuzov and I. I. Levkoev (All-Union Cinophpto Inst., Leningrad), *Zhur. obshchei Khim.*, **26**, 2537 (1969).

In the present work some quinoneanils were prepared and their spectral behaviour in the uv-visible region was studied in an endeavour to point out the important spectra-structure correlations.

EXPERIMENTAL

All the melting points are uncorrected and are determined in open capillary tubes by the use of sulphuric acid m. p. apparatus.

PREPARATION OF QUINONEANILS "GROUP 1"

The procedure of Fieser and Thompson[6] for the preparation of 2′,3′-benzo-1,4-quinoneanil was applied to prepare this group of quinoneanils. The crude product was recrystallized from ethanol (Table 1).

PREPARATION OF QUINONEANILS "GROUP 2"

This group was prepared following the procedure described by Vittum and Brown[8]. The product was recrystallized from the proper solvent (Table 1).

Table 1

Quinoneanils

Compound	Solvent of cryst.	M. P. C°	Found			Formula	Required		
			C	H	N		C	H	N
Ia	E	138	82.81	4.60	6.32	$C_{16}H_{11}NO$	82.40	4.72	6.01
Ib	E	105–107	82.79	4.55	6.23	$C_{16}H_{11}NO$	82.40	4.72	6.01
Ic	E	70	79.50	5.29	7.10	$C_{16}H_{11}NO$	79.19	5.58	7.11
Id	E	89	73.71	5.33	6.59	$C_{13}H_{11}NO_2$	73.24	5.16	6.57
IIa	C	161	74.20	6.25	12.59	$C_{14}H_{14}N_2O$	74.34	6.19	12.39
IIb	*p*(80–100°)	120	74.80	6.92	11.91	$C_{15}H_{16}N_2O$	75.00	6.67	11.67
IIc	*p*(60–80°)	114–115	75.33	6.59	11.55	$C_{15}H_{16}N_2O$	75.00	6.67	11.67
IId	*p*(60–80°)	107–108	75.80	7.13	11.20	$C_{16}H_{18}N_2O$	75.59	7.08	11.02
IIe	*p*(60–100°)	88–89	76.50	7.49	10.66	$C_{17}H_{20}N_2O$	76.12	7.46	10.45
IIIa	*p*(80–100°)	148–149	78.59	5.95	10.19	$C_{18}H_{16}N_2O$	78.26	5.79	10.14
IIIb	*p*(80–100°)	113–115	81.79	3.22	9.45	$C_{20}H_{20}N_2O$	81.63	3.40	9.52
IVa	*p*(60–80°)	170	81.72	4.62	8.71	$C_{22}H_{16}N_2O$	81.17	4.93	8.96
IVb	*p*(80–100°)	236	54.93	3.75	5.93	$C_{22}H_{14}N_2OBr_2$	54.72	3.90	5.80
IVc	E	168	82.13	5.82	7.88	$C_{24}H_{20}N_2O$	81.81	5.68	7.95
IVd	E	220	75.40	5.41	7.28	$C_{24}H_{20}N_2O$	75.00	5.20	7.29
IVe	E	248	74.55	4.61	7.99	$C_{22}H_{16}N_2O$	74.15	4.49	7.86
IVf	E	200	76.39	4.25	13.79	$C_{22}H_{26}N_4O$	76.09	6.39	13.65
IVg	E	169	77.61	7.35	12.10	$C_{30}H_{34}N_4O$	77.25	7.29	12.02

p = Pet. ether.
E = Ethanol
c = Ethyl acetate

PREPARATION OF QUINONEANILS "GROUP 3"

Following the procedure described by Brömme[11] for the preparation of 2-anilino-1,4-naphthoquinoneanil, a new series of quinoneanils were prepared. The crude product was crystallized from the proper solvent (Table 1).

ULTRAVIOLET AND VISIBLE SPECTRAL STUDIES

The recrystallized quinoneanils were dissolved in specially purified solvents and their spectra were read on a Unicam SP 8000 Ultraviolet Recording Spectrophotometer using 1 cm matched silica cells. The values of λ_{max} and ε_{max} for the spectra of the quinoneanils in ethanol are depicted in Table 2.

Table 2

Spectra of quinoneanils in ethanol

Cpd.	$\pi \rightarrow \pi^*$ aromatic				$\pi \rightarrow \pi^*$ quinonoid				C. T.	
					C = O		C = C			
	λ_{max}	$\varepsilon_{max} \times 10^{-4}$	λ_{max}	$\varepsilon_{max} \times 10^{-4}$	λ_{max}	$\varepsilon_{max} \times 10^{-4}$	λ_{max}	$\varepsilon_{max} \times 10^{-4}$	λ_{max}	$\varepsilon_{max} \times 10^{-4}$
Ia	—	—	275	1.23	310	0.73	335	0.31	510	0.25
Ib			270	2.45	290	1.60	315	0.95	490	0.43
Ic			262	1.49	300	1.17	—	—	465	0.51
Id			265	1.76	315	1.07	—	—	493	0.96
Ie			255	1.84	265	1.25	—	—	595	0.96
IIa			275	1.47	300	1.10	350	0.65	610	2.50
IIb			275	2.12	307	0.99	335	0.78	600	2.01
IIc			275	1.67	245	1.25	350	0.65	608	1.89
IId			275	1.43	315	0.93	350	0.71	620	3.25
IIe			275	1.65	303	1.10	365	0.68	620	2.51
IIIa			255	1.99	265	1.88	308	1.15	595	1.38
IIIb			270	1.71	—	—	315	1.07	607	1.51
IVa	250	2.09	280	2.40	295	1.62	340	0.60	470	0.67
IVb	250	2.50	285	2.86	306	1.59	335	0.75	465	0.80
IVc	250	2.42	275	2.72	305	1.60	335	0.86	480	0.79
IVd	245	2.27	275	2.33	—	—	335	0.72	500	0.68
IVe	250	2.27	275	2.24	295	1.85	320	0.97	510	0.72
IVf			260	2.07	285	1.61	332	0.72	565	0.53
IVg			270	2.70	290	2.33	335	1.13	590	0.78

λ_{max} in nm, ε_{max} in mole^{-1} cm^2

RESULTS AND DISCUSSION

The quinoneanils under investigation are divided into three groups. The general formulae of these compounds are given below.

Quinoneanils "Group 1"

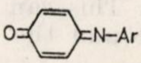

(I)

a : Ar$=\alpha-C_{10}H_7$
b : Ar$=\beta-C_{10}H_7$
c : Ar$=CH_3.C_6H_4$
d : Ar$=CH_3O.C_6H_4$
e : Ar$=HO.C_6H_4$

Quinoneanils "Group 2"

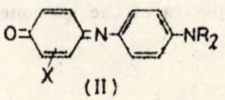

(II)

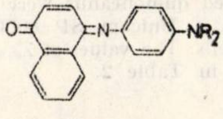

(III)

a : $X=H$, $R=CH_3$
b : $X=2-CH_3$, $R=CH_3$
c : $X=3-CH_3$, $R=CH_3$
d : $X=H$, $R=C_2H_5$
e : $X=2-CH_3$, $R=C_2H_5$

a : $R=CH_3$
b : $R=C_2H_5$

Quinoneanils "Group 3"

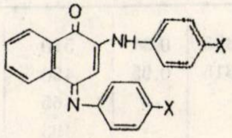

(IV)

a : $X=H$
b : $X=Br$
c : $C=CH_3$
d : $X=OCH_3$
e : $X=OH$
f : $X=N(CH_3)_2$
g : $X=N(C_2H_5)_2$

It is apparent from the data given in table 2 and shown in Figures 1—3 that the spectrum of each compound exhibits mainly four absorption bands. The shorter wavelength band is due to $\pi \rightarrow \pi^*$ transition within the phenyl ring, whereas the longest one can be assigned to an intramolecular charge transfer interaction. The charge transfer probably occurs from the aromatic nucleus as a source to the $C=O$ group as a sink. The two intermediate bands are due to the $\pi \rightarrow \pi^*$ transition within the quinone structure,[13] of which the short wavelength band, in analogy to hydroxyanthraquinone[14] would be assigned to the $\pi \rightarrow \pi^*$ transition of the $C=O$ group while the long one is assigned to the $\pi \rightarrow \pi^*$ of the $C=C$ system (Table 2).

The position of the C. T. band is largely influenced by the nature of the substituent depending on whether it is attached to the aromatic or the quinone ring. It is obvious that the C. T. band exhibited by compound I_c appears at the shortest wavelength. The position of this band is progressively red shifted in the compounds studied in the order $I_c < < I_b < I_d < I_a < I_e < II_a < II_d$. The plot of $1/\lambda_{max}$ of the quinoneanils in ethanol versus the Hammett constant (σ) of the p-substituent yields a linear relationship (Figure 4). However the hydroxy compound I_e is found to deviate slightly from this linear relation. This can be due to the hydrogen bond formation between the solvent and the OH group of the compound rendering this group more polarited, and hence it acts as a higher electron donor than it actually should be.

---

[13] Z. Yoshida and F. Takabayaski, *Tetrahedron,* **24,** 933 (1969).

[14] M. S. El Ezaby, T. M. Salem, A. H. Zowail and R. M. Issa, *J. Chem. Soc.,* **1970,** 1293.

Concerning the quinoneanils 2 and 3, an apparent red shift is observed on changing the R group from the methyl to the ethyl group in both cases. This runs parallel to the stronger mesomeric effect (+M) of the $(C_2H_5)_2N-$ than that of the $(CH_3)_2N-$ group. However, for the quinoneanils II_a or II_d the substitution in the quinone ring by methyl or 2,3-benz substituent results in a small blue shift. The methyl group displays a stronger effect when introduced into the 2- than into the 3-position. As a matter of fact, the electropositive nature of the methyl group antagonizes the charge transfer to the quinone oxygen. The antagonism brought about the $2-CH_3$ group is direct and consequently it causes the stronger effect; whereas that of the $3-CH_3$ group is due to the decreased participation of the dipolar structure to the ground state where the oxygen containing ring becomes less capable of accommodating the negative charge. The antagonizing effect is illustrated in the following two schemes.

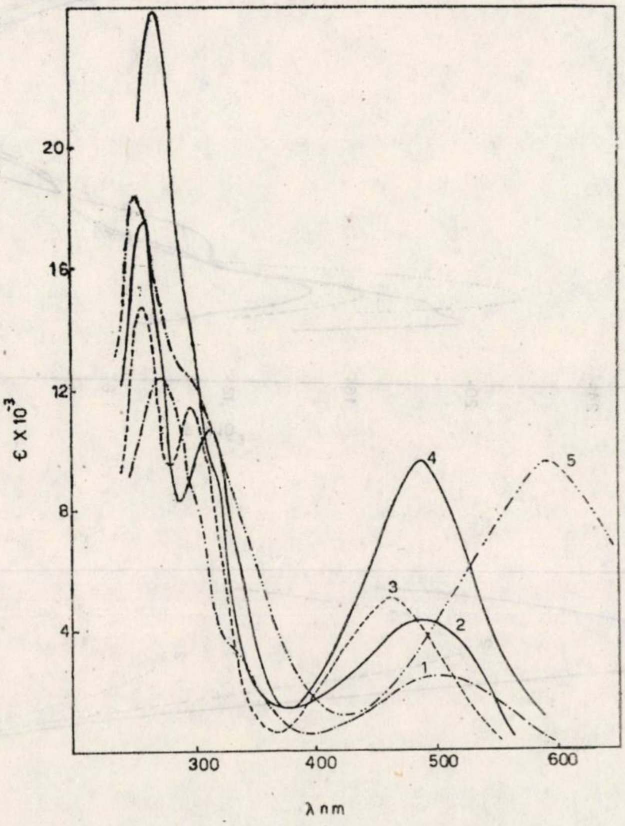

Fig. 1. — Electronic absorption spectra of quinoneanils "Group 1".

1 — Ia; *2* — Ib; *3* — Ic; *4* — Id; *5* — Ie.

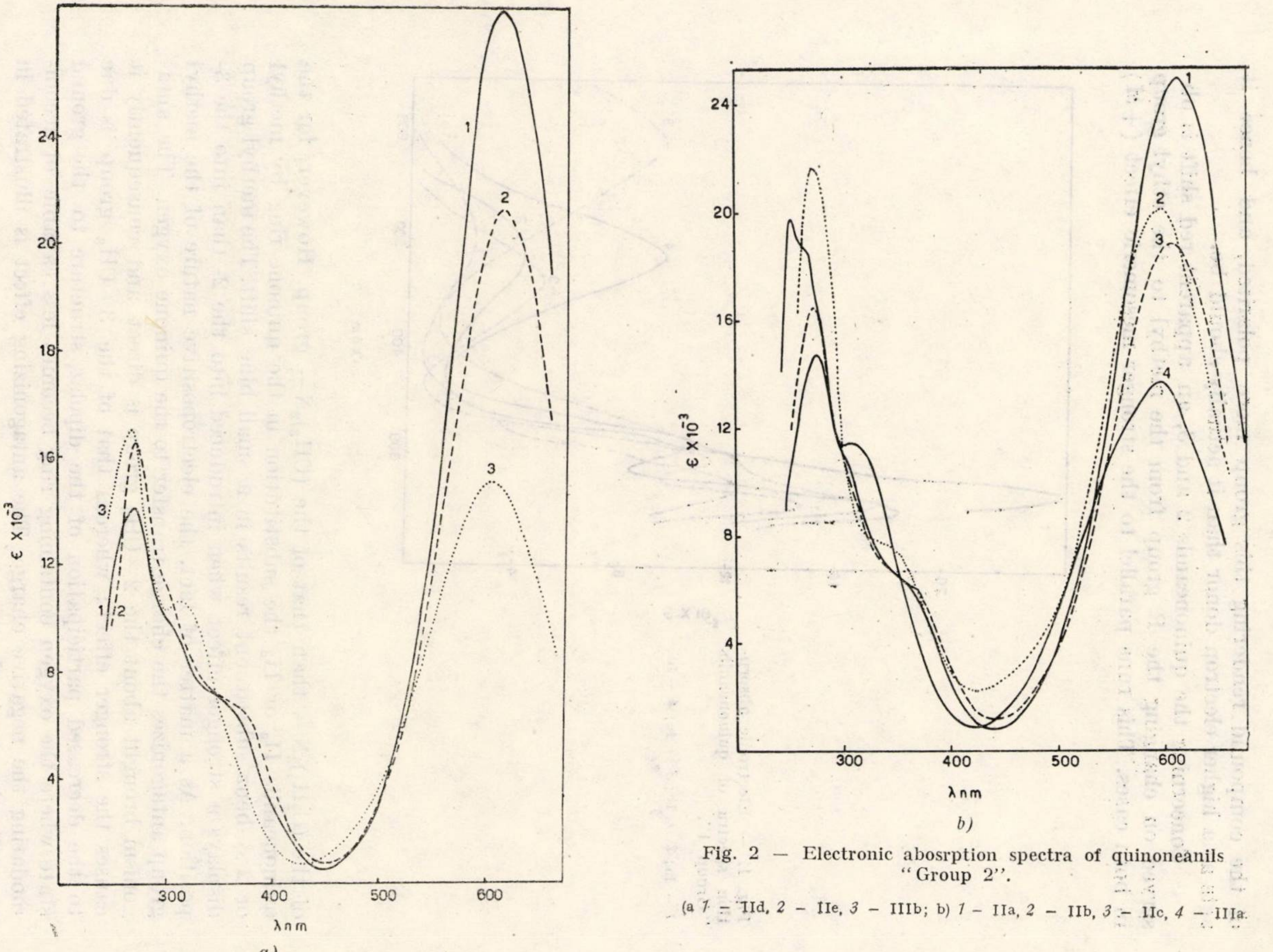

Fig. 2 — Electronic abosrption spectra of quinoneanils "Group 2".

(a *1* — IId, *2* — IIe, *3* — IIIb; b) *1* — IIa, *2* — IIb, *3* — IIc, *4* — IIIa.

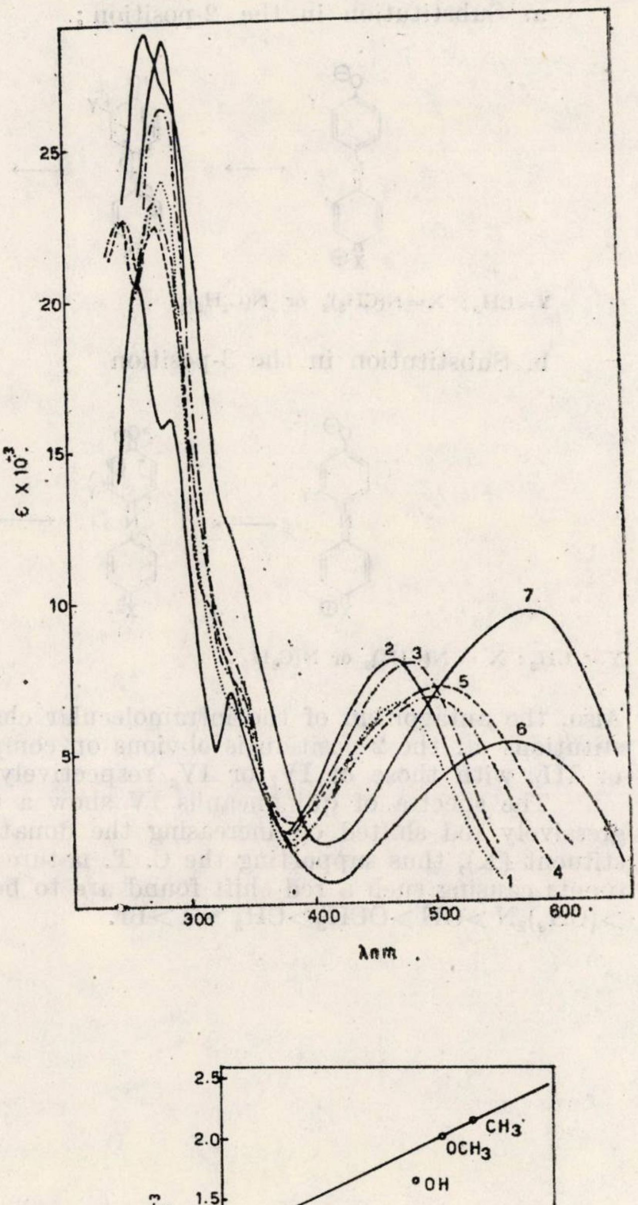

Fig. 3 — Electronic absorption spectra of quinoneanils "Group 3".

1 — IVa; *2*—IVb; *3*—IVc; *4*—IVd; *5* — IVe; *6* — IVf; 7—IVg

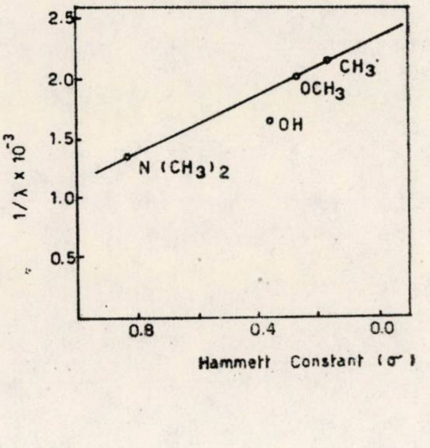

Fig. 4 — 1/ — Relationship.

a. Substitution in the 2-position:

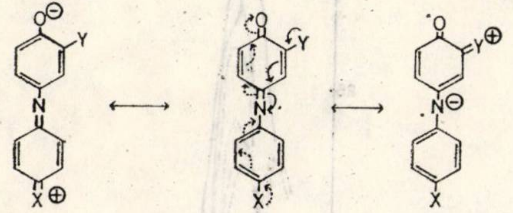

$Y{=}CH_3$; $X{=}N(CH_3)_2$ or $N(C_2H_5)_2$

b. Substitution in the 3-position

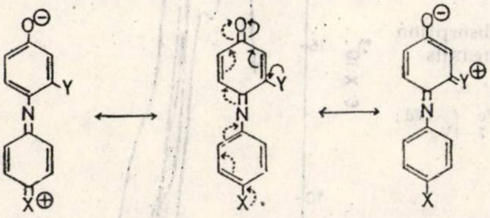

$Y = CH_3$; $X = N(CH_3)_2$ or $N(C_2H_5)_2$

Also, the antagonism of the intramolecular charge transfer by the substitutions at the 2-position is obvious on comparing the spectra of III_a or III_b with those of IV_f or IV_g respectively.

The spectra of quinoneanils IV show a C. T. band which is progressively red shifted on increasing the donating character of the substituent (X), thus supporting the C. T. nature of the band. The substituents causing such a red shift found are to be in the order $(C_2H_5)N >$ $>(CH_3)_2N > OH > OCH_3 > CH_3 > H > Br$.

Revue Roumaine de Chimie, **23**, *4*, 625–627 (1978)

DÉTERMINATION DE LA RÉPARTITION DES ÉLÉMENTS DANS UNE BENTONITE À L'AIDE DU MICROANALYSEUR DES RAYONS À SONDE ÉLECTRONIQUE

V. D. LAMBRINO et R. S. NISTOR
Institut de médecine et pharmacie ,6, str. Traian Vuia Bucarest,

Reçu le 9 janvier 1976

On fait une microanalyse « in situ » par une méthode électronooptique sur une bentonite roumaine qui met en évidence la répartition des éléments sur la surface de l'ordre de 80 × 80 μm.

INTRODUCTION

Il faut remarquer le fait qu'à l'aide de la répartition des éléments on peut étudier les zones d'agglomération de ceux-ci et leur rôle dans la capacité d'échange du matériel. Nous considérons qu'on pourrait étudier suivant cette méthode les nombres des centres d'échange actifs sur l'unité de surface.

Ces études pourraient conduire à l'amélioration de la qualité des catalyseurs ou des échangeurs d'ions.

PRINCIPE DE L'ANALYSE À L'AIDE DE LA MICROSONDE ÉLECTRONIQUE

Un faisceau d'électrons émis par un filament de tungstène réchauffé à 2700 K est collimaté dans le vide à l'aide des lentilles électromagnétiques étant accéléré à des tensions comprises entre 5–50 Kw de manière que dans le plan du foyer du système il tombe sur la preuve à analyser sous forme d'un faisceau très fin Ø=0,3–1 μm nommé sonde électronique.[1,2]

Au point d'impact du faisceau avec la preuve se produisent les radiations X de tous les éléments qui se trouvent dans la preuve.

La captation des différents signaux obtenus comme conséquence de l'interaction du faisceau d'électron avec l'échantillon analysé et leur

---

[1] V. LEROY et L. HABRAKEN, *Rev. Universelle des Mines*, 9 serie, **19**, 3 (1962).

[2] A. H. COMPTON et S. K. ALLISON, « X Rays in Theory and Experiment » Macmillan, New York, 1935, p. 76.

introduction dans l'oscilloscope d'un certain type donne des images. Les images sont :

— électrons absorbés ;

— électrons rétrodiffusés ;

— rayons X (répartition des éléments).

Les informations offertes par les deux premiers types d'images permettent la mise en œuvre de certainnes analyses d'homogénéité et de topographie de la surface. La densité des impulsions est proportionnelle à la concentration de l'élément analysé.

DONNÉES EXPÉRIMENTALES

CARACTÉRISTIQUES DE L'APPAREIL J. X. A.-3A

L'appareil utilisé présente les caractéristiques suivantes :

— résolution 1 μm — 3 μm ;

— les éléments à analyser vont de 5B jusqu'à $_{92}U$;

— limite de détection 10^{-14} g ; (jusqu'à $Z=40$ sensibilité est de l'ordre 10^{-12} g ; pour les éléments avec $Z=41-65$ elle est de l'ordre 10^{-10} g et pour le reste des éléments elle est de l'ordre 10^{-8}g en arrivant jusqu'à ^{238}U à 10^{-6}g) ;

— $\frac{\Delta\lambda}{\lambda} = 10^{-3}$.

Préparation de la preuve pour la microanalyse à l'aide de la microsonde électronique. Pour pouvoir être analysés, les matériaux auraient dû être parfaitement lisses et ensuite couverts d'une couche métallique.

Les preuves doivent être transformées en pastilles à surface parfaitement plane et ensuite couvertes d'une couche métallique, par évaporation dans le vide.

Les preuves soumises à la microanalyse à l'aide de la sonde électronique, ont été la bentonite de Valea Chioarului (VC).

Etant donné que les matériaux présentaient une faible résistance, ils ont été transformés en pastilles, ce qui à conduit à une grande rugosité.

La conductibilité électrique du matériel a été assurée en le couvrant dans le vide d'une pellicule métallique de palladium de quelques centaines de Å. On a utilisé le palladium, pour métallisation grâce à son absence dans la composition des matériaux choisis pour l'analyse.[3]

L'analyse des preuves a été effectuée dans des conditions identiques d'excitation, de tension d'accélération de courant d'épreuve, les surfaces analysées (environ 80/80 μm) étant sélectionnées optiquement, seulement en vue d'éviter une dénivélation (rugosité) marquée de la surface.

RÉSULTATS DE LA MICROANALYSE ET LEUR INTERPRÉTATION

Les recherches effectuées ont envisagé d'obtenir des observations concernant les éléments présents, leur mode de répartition, ainsi que la morphologie de la surface de la preuve.

Les résultats obtenus sur les preuves sont indiqués dans les fig. 1—8.

Les fig. 1 et 2 représentent des images réalisées par des électrons rétrodiffusés, respectivement absorbés sur la même zone du matériel. On peut remarquer la disposition agglomérée de matériel formé par des particules rondes, de 2—5 μm. La rugosité prononcée du matériel

---

[3] V. D. Lambrino, T. Stan, E, Ursu, *Rev. Chim.* (*București*), **21**, 9, 572 (1970).

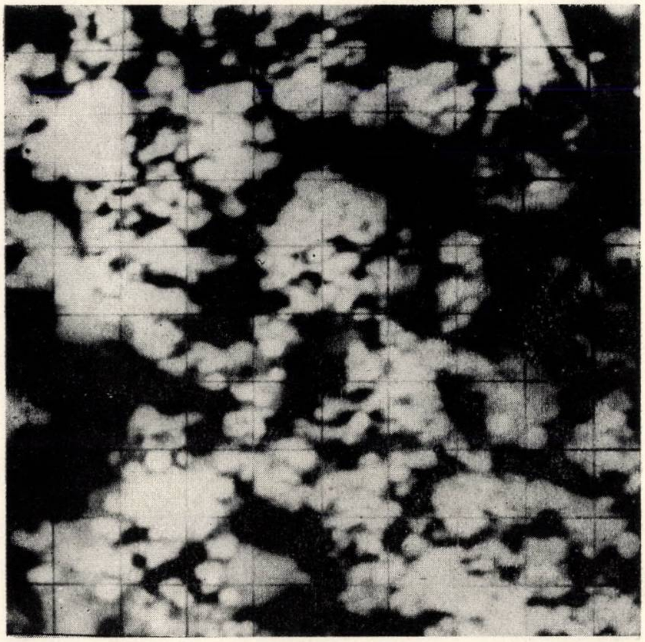

Fig.1. — L'image de la composition de la bentonite de VC (1275×).

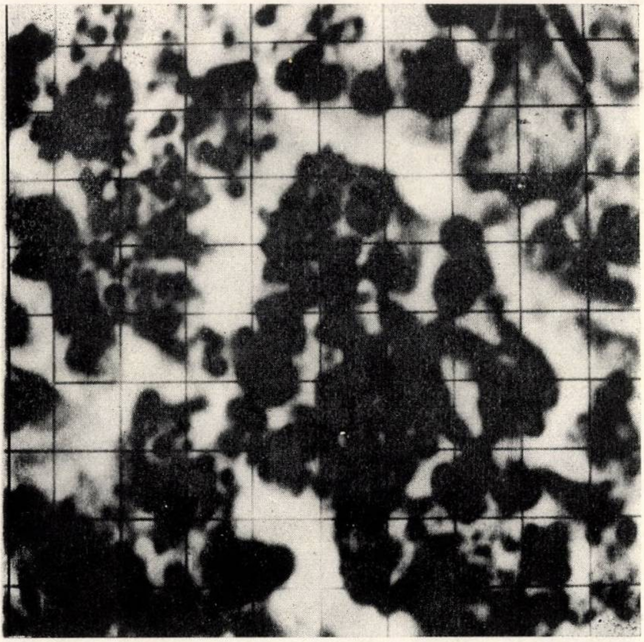

Fig. 2. — L'image d'absorption de la bentonite de VC (1275 ×).

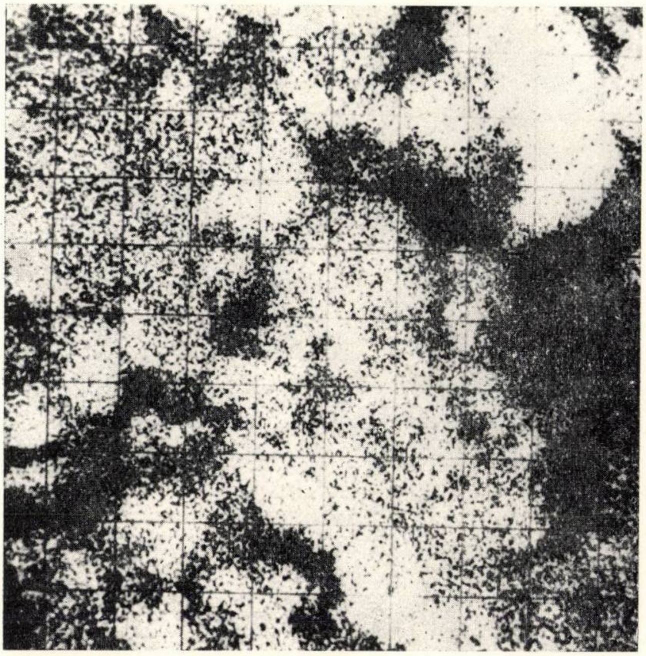

Fig. 3. — Répartition du silicium dans la bentonite de VC (1275 X).

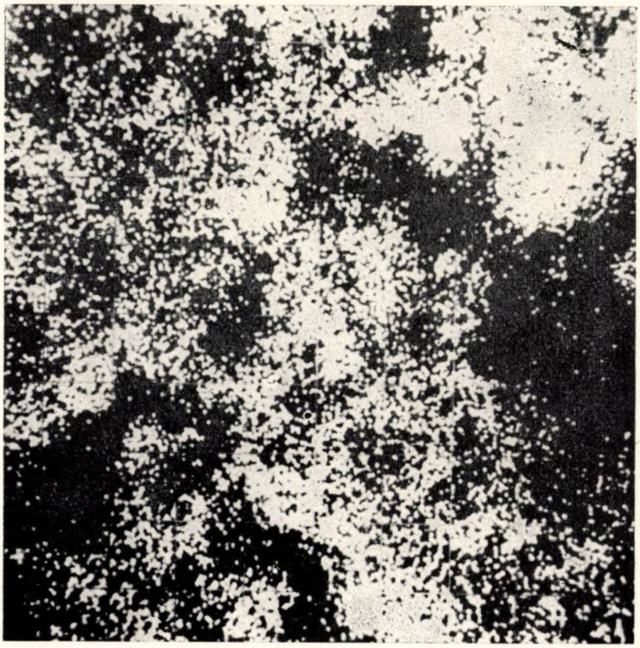

Fig. 4 — Répartition d'aluminium dans la bentonite de VC (1275 X).

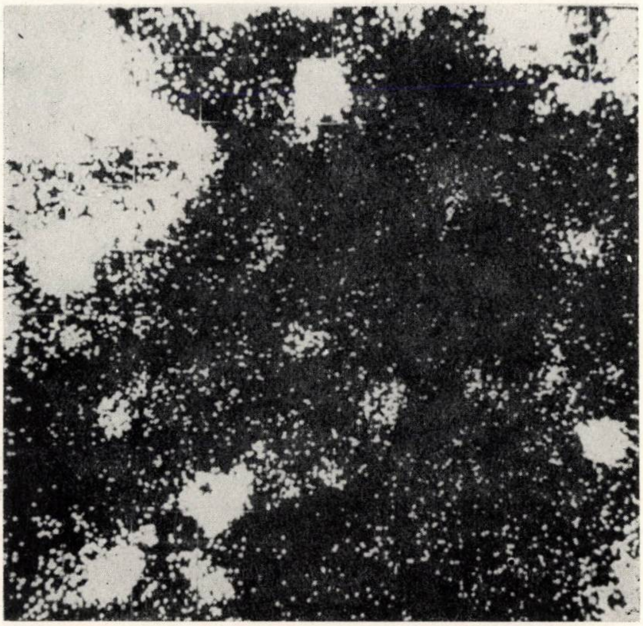

Fig. 5. — Répartition du calcium dans la bentonite de VC (1275 X)

Fig. 6. — Répartition du magnésium dans la bentonite de VC (1275 X).

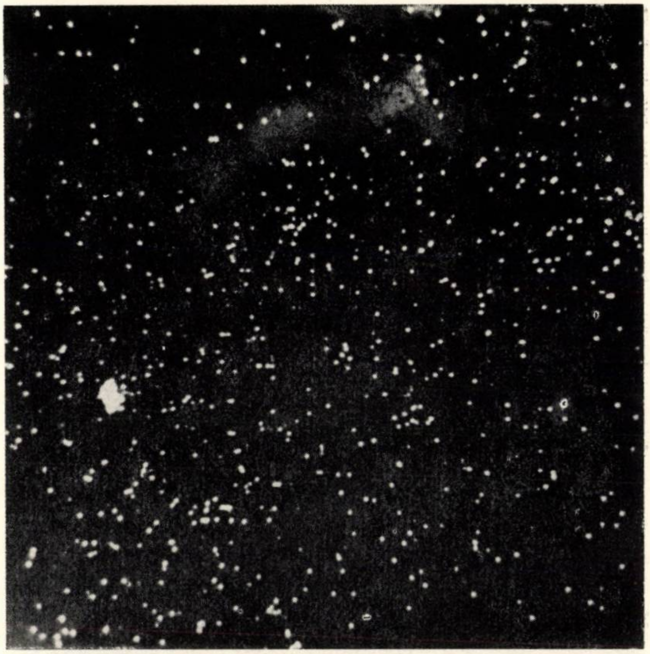

Fig. 7. — Répartition du titane dans la bentonite de VC (1275 X).

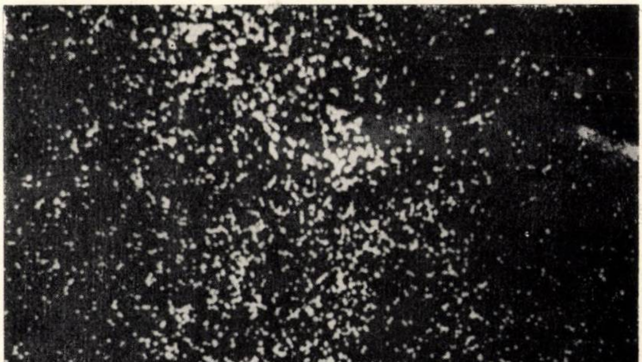

Fig. 8. — Répartition du fer dans la bentonite de VC (1275 X).

observée dans la fig. 1, nous a empêché d'obtenir des analyses quantitatives.

L'analyse qualitative a mis en évidence la présence de l'aluminium, du silice, du calcium, du magnésium, du titane et du fer dans les épreuves.

Les informations concernant la répartition des éléments identifiés sont données dans les fig. 3—8.

En examinant les photos, on constate que *l'aluminium* et *le silice* sont répartis presque uniformément (fig. 3, 4) dans les mêmes zones dans les preuves, ayant des dimensions d'environ 50 µm,

— *le calcium* présente de fortes agrégations se présentant comme un composant distinct sous forme de granules avec le diamètre de 5 à 25 µm (fig. 5) — le *magnésium* se présente comme un élément presque homogène avec de rares concentrations qui accompagne le silicium et l'aluminium (fig. 6).

— *le fer* se présente sous forme de ségrégations (fig. 8), et

— *le titane* se présente uniformément, avec de très rares précipités (fig. 7). Il n'a pas été mis en évidence par la méthode d'analyse chimique classique. [3]

Le sodium et le potassium n'ont pas pu être mis en évidence dans les preuves étudiées, le signal étant situé au niveau du fond.

CONCLUSIONS

L'étude apporte une contribution importante consistant dans le fait que c'est pour la première fois qu'on utilise le microanalyseur, nommé sonde électronique, pour l'étude des bentonites, ce qui a permis de constater leur non-homogénéité et de mieux connaître leur concentration et la répartition des éléments dans la masse du matériel.

C'est aussi à l'aide de la sonde électronique qu'on peut mettre en évidence des éléments qui n'ont pas pu être identifiés par les méthodes chimiques classiques en concentration au-dessous de 10^{-6} g comme dans le cas du titane dans notre étude.

En fait cette analyse est en concordance aussi avec l'analyse des bentonites en infra-rouge par laquelle ont été mises en évidence les liaisons Si—O, Al—O, Ca—O, Mg—O et moins accentuées les liaisons Na—O et K—O. [4]

On constate en même temps la présence du calcium en quantité assez grande, — d'où on peut conclure qu'il s'agit du Ca-montmorillonite, fait confirmé d'autant plus par l'analyse thermodifférentielle. [5]

Le grand avantage de cette méthode consiste dans le fait qu'elle vient compléter l'analyse à l'aide des rayons X,-utilisée pour établir la structure et la composition des bentonites. [6]

L'étude met aussi en évidence la possibilité d'utiliser les bentonites comme échangeurs d'ions pour la séparation des éléments. A l'aide de la méthode décrite on pourrait établir la répartition des éléments séparés complètement ou seulement partiellement, ainsi que la capacité d'échange ionique du matériel.

[4] V. D. Lambrino, *Compt. rend. Acad. bulg., Sci.*, **26**, 483 (1973).

[5] V. D. Lambrino, *Compt. rend. Acad. bulg. Sci.*, **26**, 223 (1973).

[6] V. D. Lambrino, *Compt. rend. Acad. bulg. Sci.*, **26**, 335 (1973).

Revue Roumaine de Chimie, **23**, *4*, 629–635 (1978)

AMORPHOUS-CRYSTALLINE COUPLING IN POLYETHYLENE. VII[1]

STUDY OF THE CRYSTALLIZATION KINETICS IN THE APPROXIMATION OF THE PURELY THERMAL DISSIPATIVE COUPLING

GH. DRĂGAN
Institute of Chemical Research, ICECHIM, Spl. Independenţei 202, Bucharest

Received November 6, 1975

The study of the amorphous-crystalline coupling in polyethylene by means of the dynamic calorimetric methods has revealed the thermal transfer topology specific of the composite nature of this material. The simple model of polyethylene morphology based on the purely thermal dissipative coupling between the two components is analyzed considering the previous results. This situation is considered to be revealed during crystallization as a thermal activated process. The proposed model is developed by means of the mathematical and diagrammatical formalism recently used for the external thermal circuits in the differential thermal analyses. The theoretical results are in good agreement with the experimental results obtained on a conduction calorimetric system for the high density polyethylene samples which are studied in the present series.

The amorphous-crystalline coupling in polyethylene (PE) has been previously[1–6] studied by means of the values which characterize the amplitude of the melting processes denoted as T_m^0 and T_m^1. These two processes characterize the lamellar, respectively interlamellar order and are revealed during dynamic calorimetric rounds, as first order transitions.[2] For the particular case of T_m^1 process, defined as interlamellar coupling effect as a result of an applied treatment, it was established that the viscous mode of the reciprocal rotating and approaching of the lamellae (or lamellar fragments) appears as a secondary dissipation mode during the relaxation of the disclination state.[1,4,6]

The study of first order transitions was started and thoroughly carried on with the liquid-gas transitions. The kinetic coefficients are observed[7] to reveal specific discontinuities of the testing methods in the critical region for this phase transition. But in the beginning of the viscosity measurements in this region, Fixman[8] has found that the critical fluctuations are coming from contributions of the other kinetic coefficients. This model of the dissipation modes coupling in critical domain has been theoretically explained,[9] and was rapidly extended to most first order transitions.[10]

---

[1] Part VI: Gh. Drăgan, *Rev. Roumaine Chim.* **23**, 435 (1978).
[2] Gh. Drăgan, *Materiale Plastice*, **10**, 87 (1973).
[3] Gh. Drăgan, *Rev. Roumaine Chim.*, **20**, 687 (1975).
[4] Gh. Drăgan, *Rev. Roumaine Chim.*, **21**, 1381 (1976).
[5] Gh. Drăgan, *Rev. Roumaine Chim.*, **21**, 1537 (1976).
[6] Gh. Drăgan, *Rev. Roumaine Chim.*, **23**, 361 (1978).
[7] J. V. Sengers, *Ber. Bunsengesellshaft Phys. Chem.*, **76**, 234 (1972).

The dynamic calorimetric methods approached in this series for the study of the PE morphology, have drawn attention on the strong linkage between topology of the thermal transfer and the amorphous-crystalline coupling. In the general context of the first order transitions, it was previously revealed[3] that the transition which characterizes the order at a certain level in the composite material, is remarked in the response function depending on the level-"latice" coupling. The critical behaviour of the magnetic systems, as the closest example to PE, is recently studied by the renormalization group.[11] This analysis is applied on the system Hamiltonian and it is useful to note that it is also based on the composite nature of the magnetic systems. This aspect is the starting point in describing the topology of the thermal transfer for the external circuits in the differential thermal analyses.[12]

A simplified model for the amorphous-crystalline coupling in PE is considered in this work by using the previous formalism, namely, for the case of crystallization this coupling is supposed to be reduced to the purely thermal mode of dissipation. The extraflux of crystallization is shifted from the start of the total transfer by a time period depending on the crystallization temperature. The proposed model ultimately expresses this dependence and is found to be in good agreement with experimental results obtained on a conduction calorimetric system for PE samples previously denoted as LPE. The observed deviations from the theoretical plot are explained by mode-mode coupling.

PURELY THERMAL DISSIPATIVE COUPLING MODEL

The proposed coupling is studied in isothermal conditions, knowing that the morphological changes are thermally activated processes.[2–4] This fact can be expressed by supposing that the C_1 component, which effectivelly changes, has the transfer parameter through the dissipative medium R_0, as depending on the transformation temperature T, after an Arrhenius law

$$\tau_1 \equiv C_1\tilde{R}_0 = \tau_{10}\,e^{-E/\mathfrak{R}T} \tag{1}$$

where $\tilde{R}_0$ is the transfer function of the leakage medium between C_1 and the inert component C_2, τ_{10} is the value of τ_1 for T (in Kelvin degrees)→→0, $\mathfrak{R}$ the gas constant and E the activation energy for the transformation process.

---

[8] M. Fixman, *J. Chem. Phys.*, **36**, 310 (1962).

[9] L. P. Kadanoff and J. Swift, *Phys. Rev.*, **166**, 89 (1968).

[10] K. Kawasaki, *Ann. Phys.*, **61**, 1 (1970).

[11] M. E. Fisher, *Rev. Mod. Phys.*, **46**, 597 (1974).

[12] Gh. Drăgan, *J. Thermal Anal.*, **9**, 405 (1976)

The internal circuit during transformation can be represented as in the diagram a (Figure 1*a*). $T_0(t)$ is the temperature at which for $t=0$ the material has the equilibrium morphology which differs from that at T. C_2 component is directly coupled to the equipotential surface T_0, and its transfer parameter through the medium R is not T dependent.

The change effect w_1 is separated from w_2 as a parasite effect, by superposing the reference circuit C_R in an isothermal and differential calorimetric system (IDCC), where $w_R = w_2$. In this way the response function $\theta(t) = \theta_2(t) - \theta_1(t)$ expresses the contribution of the w_1 effect only, following the relations :[12]

$$\tilde{\theta} = \tilde{R}\,\tilde{w}_1 \tag{2}$$

because

$$\tilde{\theta}_1 \equiv \tilde{T} - \tilde{T}_0 = \tilde{R}(\tilde{w}_1 + \tilde{w}_2) \tag{3}$$

$$\tilde{\theta}_2 \equiv \tilde{T} - \tilde{T}_R = \tilde{R}\,\tilde{w}_2$$

The upper sign defines the Laplace transformation.[12]

The bond diagram in Figure 1b represents the overall circuit in the used IDCC system.

By elimination of w_2 in (3), taking into account the previous constitutive relations[12] for the capacitive storage

$$C_1 p\,\tilde{T}_1 = \tilde{w}_1$$

$$C_2\,p\tilde{T}_0 = \tilde{w}_2 \tag{4}$$

$$C_R\,p\tilde{T}_R = \tilde{w}_2$$

we get

$$\tilde{\theta}(p) = A\,\frac{1}{(1+\tau_1 p)(1+\tau_R\,p)} \tag{5}$$

where $A = \tilde{R} C_R\, C_1/C_2$. In (4) T_1 is the local temperature of the C_1 component during dissipation process, and p is the complex variable for the Laplace transformation of a time dependent function.

By reverse transformation of (5) we obtain : [13]

$$\theta(t) = \frac{A}{\tau_1 - \tau_R}\,(e^{-t/\tau_1} - e^{-t/\tau_R}). \tag{6}$$

---

[13] G. DOETSCH, "Anleitung zum Praktischen Gebrauch der Laplace-Transformation und der Z-Transformation", Munchen, 1967.

The change effect w_1 is revealed experimentally as a peak in $\theta(t)$ dependence, and therefore it is important to correlate the peak time period t_m with the transformation temperature T in this model. By differentiation, from (6) it may obtain:

$$t_m = \frac{\tau_1 \tau_R}{\tau_1 - \tau_R} \ln \frac{\tau_1}{\tau_R} \tag{7}$$

In this result we replace τ_1 by the initial hypothesis (1) and also observing that for $T \to 0$, $\tau_1 \to \tau_R$. For the case $E > 0$, we may write

$$\ln (Tt_m) = -\frac{E}{\mathfrak{R}T} - \ln \left(1 - e^{-E/\mathfrak{R}T}\right) + K \tag{8}$$

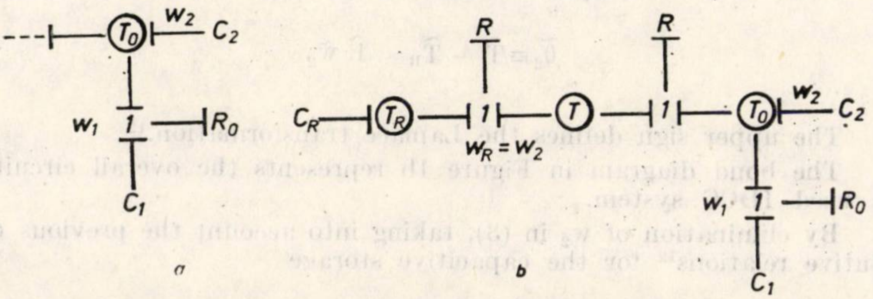

Fig. 1. *a*. Bond diagram of the internal circuit in the crystallizing polyethylene.
b. Bond diagram for the used calorimetric system.

For T belonging in the range

$$T \ll E/\mathfrak{R} \tag{9}$$

equation (8) simply becomes

$$\ln (Tt_m) = -\frac{E}{\mathfrak{R}T} + K \tag{10}$$

For the case in which $E < 0$, equation (8) must be rewritten as

$$\ln (Tt_m) = -\frac{E}{\mathfrak{R}T} - \ln \left(e^{\frac{E}{\mathfrak{R}T}} - 1\right) + K \tag{8'}$$

In this case the linearity between $\ln (t_m T)$ and $1/T$ is maintained only for the restricted range

$$T \sim \frac{E}{\mathfrak{R} \ln 2} \tag{11}$$

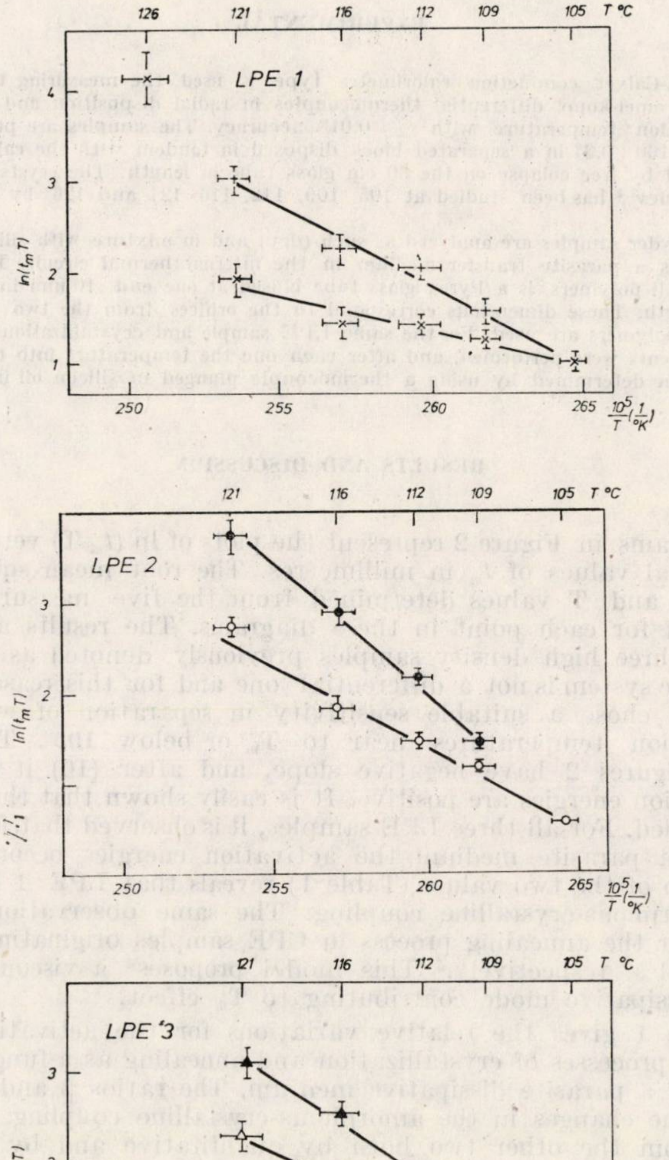

Fig. 2. – Arrhenius plots for the crystallization process in the considered LPE samples : X, ◯, △ dry samples ; +, ●, ▲ medium samples.

EXPERIMENTAL

A Tian-Calvet conduction calorimeter type is used, the measuring block of which contains 16 cromel-kopel differential thermocouples in radial disposition and is maintained at crystallization temperature with ± 0.01° accuracy. The samples are prethermostated 4 minutes at $160 \pm 0.3°$ in a separated block disposed in tandem with the calorimeter and are transferred by free colapse on the 30 cm glass tube in length. The crystallization effect for LPE samples[3,4] has been studied at 105, 109, 112, 116, 121 and 126° by recording $\theta_1(t)$ signal.

The powder samples are analyzed as such (dry) and in mixture with silicon oil (Schuchardt 702) as a parasite transfer medium in the internal thermal circuit. The test piece, the same for all polymers, is a Pyrex glass tube closed at one end, 10 mm in diameter and 45 mm in length. These dimensions correspond to the orifices from the two blocks. Equal quantities of polymers are used. For the same LPE sample and crystallization temperature, five measurements were performed, and after each one the temperature into the calorimeter block has been determined by using a thermocouple plunged in silicon oil in a glass tube.

RESULTS AND DISCUSSION

Diagrams in Figure 2 represent the plots of ln (t_m T) versus 1/T for experimental values of t_m in millimetres. The root mean squares associated to t_m and T values determined from the five measurements are represented for each point in these diagrams. The results are grouped after the three high density samples previously denoted as LPE.[3] The calorimetric system is not a differential one and for this reason it is not possible to chose a suitable sensitivity in separation of w_2 effect for crystallization temperatures near to T_m^0 or below 105°. The straight lines in Figures 2 have negative slope, and after (10) it means that the activation energies are positive. It is easily shown that the condition (9) is satisfied. For all three LPE samples, it is observed that for crystallization with parasite medium the activation energies become greater. The α ratio of the two values (Table 1) reveals that LPE 1 has a more labile amorphous-crystalline coupling. The same observation was also revealed for the annealing process in CPE samples originating from the LPE samples, respectively.[4] This model proposes[4] a viscous mode as a main dissipative mode contributing to T_m^1 effect.

Table 1 gives the relative variations for the activation energies in the two processes of crystallization and annealing as a function of the presence of a parasite dissipative medium. The ratios β and γ allow to compare the changes in the amorphous-crystalline coupling. LPE 1 separates from the other two both by quantitative and by qualitative aspects of the change amplitudes. The qualitative aspect is reduced to the fact that for this sample the ratios β and γ are greater than unity and this explains that by decoration of the lamellar defects in LPE 1 sample the amorphous-crystalline coupling become more labile.

The limitation of the proposed model of this coupling in PE is expected to result both from the condition (9), and from the mode-mode coupling in the dissipative process for all LPE samples. Deviations from the linearity for a temperature near T_m^0 can be observed. The experimental restricted domain for linearity has been verified by the plot of $h/(m\Delta T)$ versus T (h the height of the peak effect w_2, m the sample

Table 1

The activation energies for the crystallization process in LPE samples according to the purely thermal dissipative model of amorphous-crystalline coupling, relative to the activation energies for the annealing process in CPE respective samples [4]

LPE	E_{cryst}^{dry} kcal/mole	E_{cryst}^{medium} kcal/mole	α 1)	β 2)	γ 3)	β/γ
LPE 1	12	42	3.50	3.67	1.26	2.91
LPE 2	44	82	1.86	0.55	0.29	1.90
LPE 3	36	58	1.61	0.67	0.41	1.63

1) $\alpha = (E_{cryst}^{medium} / E_{cryst}^{dry})$.

2) $\beta = (E_{ann} / E_{cryst})$ dry.

3) $\gamma = (E_{ann} / E_{cryst})$ medium; the values for E_{ann} are taken from Table 4, Reference 4 considering B and C parameters.

weight and $\Delta T = 160° - T$). This value remains effectively constant on the linearity range.

For the next studies it is interesting to consider the crystallization process in CPE samples where the annealing process is superposed and which is not purely thermal dissipative. These experiments are possible on a IDCC system only because these processes have a small amplitude effect in CPE samples.

Revue Roumaine de Chimie, 23, 4, 637–639 (1978)

COMPTES RENDUS

LANDOLT-BÖRNSTEIN, "Numerical Data and Functional Relationship in Science and Technology", New Series, II/9, "Magnetic Properties of Free Radicals", Part a, Springer-Verlag, Berlin, Heidelberg, New York, 1977, 341 p.

The present volume of the Landolt-Börnstein new series is a supplement and extension to volume II/1 about magnetic properties of free radicals. It deals with atoms, inorganic radicals and radicals in metal complexes. The free radicals presented in the tables are paramagnetic atoms, molecules and ions which derive their paramagnetism from a single unpaired s- or p-electron.

The volume is organized in two chapters. After a short introduction by Fischer, Morton and Preston present in the first chapter the tabulated magnetic properties of inorganic radicals and von Zelewsky and Daul in the second one the magnetic properties of radicals in metal complexes.

The tables include atoms and atomic ions in ^2S and ^2P states, molecules or molecular ions which arise from the break of a single bond in a diamagnetic organic or inorganic molecule or molecular ion, negative or positive ions of neutral organic or inorganic compounds and several molecules which are paramagnetic in their normal binding states and have one unpaired electron. The tables give the spin-Hamiltonian parameters g and a_χ of free radicals based mainly on spectroscopic measurements on liquid or solid samples. In the tables on inorganic radicals gaseous phase di- and tri-atomic radicals are also included.

The arrangement of the tables facilitates the easy finding of the needed data.

The literature was covered for a period from 1964 to the end of 1975. Some references from 1976 were included as well.

This volume is an excellent supplement to Fischer's first volume on magnetic properties of free radicals published in 1965; the volume upholds the high standards of the well-known Landolt-Börnstein series.

The book is a very useful and precious guide for all theoretical chemists and experimental spectroscopists working in the field.

Valerian Drăguţan

S. R. NIKETIĆ and K. RASMUSSEN, "The Consistent Force Field: A Documentation," X + 212 pp., Springer Verlag, Berlin—Heidelberg—New York, 1977.

Finding the atomic force field accounting for various properties of substances constitutes a relatively old problem of those chemists who attempt to establish a rational correlation between these properties and the forces acting at atomic and molecular level. The most notable effort on these lines is undoubtedly the normal coordinate treatment of molecules, which has been able to correlate satisfactorily the vibrational spectra with suitably chosen valence or other force fields. Methods have also been given for deriving various thermodynamic quantities from an assumed force field model. Interatomic and intermolecular interactions have long been treated on the basis of various force functions. Molecular conformational analyses have been previously carried out based on specific intramolecular force fields and crystal structures elucidated based on plausible intermolecular forces. Such methods proved to be often individually successful in solving the particular problem undertaken, but no adequate force field has yet been found which could explain all these various properties simultaneously. Such a force field which gives reasonable values for vibrational frequencies, enthalpies, molecular conformations, crystal unit cell parameters, etc., has been found in a few cases of very simple systems but its extension to different, even related, molecules turned out eventually to be impracticable.

The heart of the *consistent force field* (CFF) method lies in finding a semiempirical force field on the basis of a set of physical properties coming from very different branches, such as the molecular or crystalline equilibrium conformation, the molecular and lattice vibrational frequencies, the vibrational enthalpy and sublimation energy, or the strain energy in some cases. The energy parameters of such a force field are refined by a least-squares procedure, until the best possible fit is reached between the calculated and observed values of these quantities. The method was initiated, and later improved, by Professor Shneior Lifson and his associates of the Weizmann Institute of Science, Rehovot, Israel. All interatomic interactions are assumed to be additive and mutually independent, so that the potential energy of any system may be formulated as a sum of terms, each of which represents various kinds of interactions, such as bond stretchings, angle bendings, torsions, non-bonded interactions (e.g. of the Lennard-Jones type), and Coulomb interactions. If suitably processed, such a complex potential function may provide numerical values for various quantities of interest which are then compared to the experimental ones; least-squares iteration are then carried out to improve the fit. Both static and dynamic data may be and have in fact been used as observables. The method was applied successfully by its originators to cyclo-and normal-alkanes (both strained and unstrained) and by many workers to various other classes of compounds such as the amides, lactams, pyrrolidones, olefins, transition metal complexes, and even proteins. The idea beyond the method is that finding the right energy parameters for a class of related compounds may help with the prediction of some properties of interest for new compounds in the same class.

The book reviewed herein deals with various aspects of the practical implementation of the CFF method. As the authors point out, there is nothing revolutionary about the method itself and the only purpose of the book is to give a detailed account of the package of programs devised at the Technical University of Denmark for carrying out CFF calculations. The programs were written in FORTRAN IV for the IBM Operating System/370. They consist of independent segments, monitored by a master program, making thus an easy task for any researcher to operate extensions and modifications, to make use of a particular segment according to the problem in hand, and to optimize the overall program package application. Chapters are devoted to molecular topology and geometry, conformational energy and its derivatives, energy minimisation, vibrational calculation, optimisation of energy parameters, and developing a force filed. The program operation is fully described and there are given examples of specific cases. All variables involved are clearly defined from the onset. Several options are offered concerning the choice of the non-bonded type of potential. Minimisation and other calculation algorithms are provided. Unfortunately, no input/output specific examples are given; they would greatly facilitate the program efficient utilization.

An earlier, simpler version of similar programs, written by Warshel and Levitt, is being currently offered by QCPE (under N°. 247). The version described by Niketić and Rasmussen is by far the most complete available today. Understandably, no listing of the program is given in their book, which is intended rather as a complement to the listing itself, as a working tool, and at the same time as a guide to the CFF principles. This documentation, provided with many references and a subject index, can be very useful to physical chemists or physicists concerned with conformational analysis, vibrational spectroscopy and/or thermodynamics, either at the molecular or crystalline level.

Alex. Butucelea

Ion-Selective Electrodes", Second Symposium held at Mátrafüred, Hungary, 18–21 October 1976, Edited by E. Pungor and I. Buzás, Akadémiai Kiadó, Budapest, 1977, 263 p.

This book contains the papers of the 2nd Conference on Ion-Selective Electrodes, held at Mátrafüred, Hungary 1976, and gives a survey of the most recent results obtained by means of ion-selective electrodes.

Specialists of international reputation have dealt with almost all current theoretical and practical problems of the application of the different systems of ion-selective electrodes.

The volume includes five plenary lectures whose titles are given below in brackets after the authors' names. The length of these lectures varies from 12 to 26 pages.

Three plenary lectures examine the properties of recently developed neutral carrier electrodes, as follows:

– W. Simon, W. E. Morf and A. P. Thoma's lecture (Neutral Carrier Ion-Selective Membrane Electrodes) emphasized the design of electrically neutral organic complexing agents, with highly selective liquid membrane electrodes for the measurement of alkaline, alkaline-earth and other metalic ions. Using radio traces technique, ion and ligand profiles within membranes containing such complexing agents have been determined.

— W. E. Morf and W. Simon's lecture (Transport Properties of Neutral Carrier Membranes) describes the permselectivity of carrier membranes for cations from the theoretical stand-point as is observable in both potentiometric measurements and electrodialyses experiments. The response characteristics of ion-selective electrodes based on neutral carrier liquid membranes have been correlated with the ion transport properties of the same macroscopic membranes.

— G. J. Moody and J. D. R. Thomas's lecture (Properties of Ion-Sensing Membranes Based on PVC Matrices) emphasized membranes of liquid ion exchangers and neutral or carged carrier complexes in PVC material. General response and interference characteristics make the electrodes competitive with those of conventional types of liquid membrane electrodes. These aspects of their behaviour are related to solvent extraction phenomena.

The last two lectures described methods of automatic analysis as well as enzymatic analysis by means of ion-selctive electrode.

— E. Pungor, I. Tóth, G. Nagy and Zs. Fehér's lecture (Methods for Automatic Analysis with Ion-Selective Electrodes) presented two techniques based on the flow through analytical channel principle, employing ion-selective electrodes. One of the techniques allows the fast rate of analysis of individual samples in a continously streaming sample. The principle of the other technique is a potentiometric titration carried out in a streaming solution. Both techniques will gain application in the field of automatic analysis.

— G. Johansson and L. Ögren's lecture (Application of Ion-Selective Electrodes to Enzymatic Analysis) presented an enzyme reactor electrode for urease with its kinetics behavior. The combination of an enzyme reaction with an ion-selective electrode opens up a new field of analytical applications, because the enzymes give a high selectivity to the compounded system. Some preliminary results for 1-alanine-dehydrogenase are reported.

At the end of these lectures there are questions and comments on the problems involved.

The fifteen discussion lectures report mainly on the analytical uses, the question of selectivity and sensitivity of the new types of electrodes, new analytical techniques, new design etc.

All discussion lectures as well as questions and comments on the problems involved emphasized an up-to-date report of the most prominent problems dealing with ion-selective electrodes.

The panel "Discussion on Selected Topics of Interest in the Field of Ion-Selective Electrodes", will be of interest in the future research activities of the participants and to all engaged in the field of analytical chemistry.

The printing is accurate, with well drown formulas.

The publication of the material of the Mátrafüred Symposium, will be at great benefit, particulary for those who could not attend the Symposium which formed a wider circle of chemists dealing with physical chemistry, biochemistry or process technology.

Iuliana Vartires

NOTE POUR LES AUTEURS

La Revue Roumaine de Chimie publie des articles en anglais, français, russe, allemand ou espagnol. Les auteurs sont priés d'envoyer des articles et des comptes rendus inédits.

Les manuscrits seront dactylographiés à deux intervalles. La bibliographie, les tableaux et la légende des figures seront placés après le texte.

Si l'article fait partie d'une série numérotée, le titre de la partie précédente sera indiqué dans une note au bas de la première page.

Chaque article sera précédé d'un résumé comprenant quinze lignes au maximum.

Les références bibliographiques dans le texte seront faites par des exposants sans parenthèse et paraîtront comme des notes au bas de chaque page.

Les publications périodiques mentionnées dans la bibliographie seront présentées suivant les prescriptions internationales : le nom de l'auteur précédé de l'initiale du prénom, le titre du périodique abrégé conformément à « Chemical Abstracts » et souligné par une ligne, le numéro du tome, indiqué par des chiffres arabes et souligné par deux lignes, suivi de la première page de l'article ; à la fin, l'année de la parution sera placée entre parenthèses. Le numéro de la revue ne sera pas indiqué si les pages du volume sont numérotées consécutivement. Pour les revues dont les tomes ne sont pas numérotés (par ex. Bull. Soc. Chim. France, etc.), l'année de la parution soulignée par deux lignes précèdera l'indication de la page.

Les textes des livres ou traités inclueront : les noms des auteurs, les initiales du prénom, le titre du livre entre guillemets et sans être souligné, le numéro du tome précédé par l'abbréviation «vol.» (ou «Bd.»), le numéro de l'édition, les éditions (the publisher), la localité de la parution du livre, l'année de la parution et la page de la référence précédée par l'abréviation «p.» (ou «S.»).

Les brevets seront indiqués comme suit : L'auteur ou la firme, le pays et le numéro du brevet, la date et la revue (Chem. Abstr.). Par ex. : M. Jones (to Union Carbide Co.), Brit. Pat. 601 238, 2 septembre 1959, *Chem. Abstr.*, 54, 12808 (1960).

Si la référence n'a pas été lue en original, on indiquera aussi la revue de références consultée.

Les diagrammes seront tracés à l'encre de Chine sur papier calque. Les tableaux et les figures (en nombre strictement nécessaire) seront numérotés par des chiffres arabes et leur explication sera donnée dans la légende des figures. Prière de ne pas inscrire les mêmes données dans les tableaux et les figures. Chaque tableau aura un titre. On indiquera dans le texte la place approximative des tableaux et des figures. Les formules chimiques seront incluses dans le texte ; en outre, elles seront transcrites sur papier calque, à l'encre de Chine.

Les auteurs sont priés d'indiquer les caractères italiques (en soulignant les lettres au crayon), ainsi que tout autre caractère spécial ; les préfixes *ortho*, *meta*, *para*, *cis*, *trans*, etc. seront soulignés pour indiquer leurs caractères italiques et ne seront jamais écrits avec des majuscules.

Aucune correction à main ne sera admise sur le manuscrit. Les corrections seront frappées à la machine. Les lettres grecques ou autres symboles spéciaux seront insérés à la main à l'encre clairement.

Le manuscrit sera signé par l'auteur.

Le colonne-titre aura 50 lettres au maximum.

L'entière responsabilité du contenu des articles appartient aux auteurs.

PRINTED IN ROMANIA

1978 SEP 26

TRAVAUX PARUS AUX ÉDITIONS DE L'ACADÉMIE DE LA RÉPUBLIQUE SOCIALISTE DE ROUMANIE

C. DRĂGULESCU, E. PETROVICI, **Chimia structurală modernă. Chimia coordinanţei 8** (La Chimie structurale moderne. La Chimie de la coordinence 8), 1977, 947 p., 70 lei.

I. G. MURGULESCU, **Introducere in Chimia fizică**, vol. I. **1. Atomi, molecule, legătură chimică** (Introduction à la Chimie physique, Ier vol., 1. Atomes, molécules, liaison chimique), 1976, 560 p., 36 lei.

E. P. BALTĂ, E. BALTĂ, **Introduction to the physical chemistry of the vitreous state**, coédition avec Abacus Press, 1976, 287 p., 31 lei.

H. I. GĂLĂŢEANU, **Radiochimia aplicată. Metode şi probleme** (La radiochimie appliquée. Méthodes et problèmes), 1976, 307 p., 19 lei.

CONST. V. UGLEA, **Cromatografia pe gel permeabil. Noi domenii de aplicare** (La chromatographie sur gel perméable. Nouveaux domaines d'application), 1976, 122 p., 6,75 lei.

GR. POPA, ŞERBAN MOLDOVEANU, **Reactivii organici in chimia analitică** (Les réactifs organiques dans la chimie analytique), 1976, 255 p., 18 lei.

FRANCISC A. GOTHARD, **Echilibre lichid-vapori. I. Baze teoretice şi metode de calcul** (Equilibres liquide-vapeurs. I. Bases théoriques et méthodes de calcul), 1975, 263 p., 2 pl., 28 lei.

CONST. GH. MACAROVICI, D. MACAROVICI, **Chimia oxizilor dubli şi utilizările lor** (La chimie des oxydes doubles et leur utilisation), 1975, 195 p., 13 lei.

M. AVRAM, **Antidăunători** (Pesticides), 1974, 496 p., 41 lei.

ELENA CEAUŞESCU, **Research work on synthesis and characterization of macromolecular compounds. Contributions**, 1974, 251 p., 20 lei.

DUMITRU COSTACHE, **Analiza chimică prin metoda cinetică** (L'Analyse chimique par la méthode cinétique), 1974, 276, p., 15,50 lei.

G. A. RĂDULESCU, **Proprietăţile ţiţeiurilor româneşti** (Les propriétés des pétroles roumains), 1974, 267 p., 2 pl., 18 lei.

CR. SIMIONESCU, VIORICA RUSAN, V. POPA, **Chimia algelor marine** (La chimie des algues marines), 1974, 212 p., 1 pl., 18 lei.

I. ZUGRĂVESCU, MAGDA PETROVANU, **Chimia n-ilidelor** (La chimie des n-Ilures), 1974, 348 p., 19 lei.

MARIA FITI, **Dozimetria chimică a radiaţiilor ionizante** (La dosimétrie chimique des radiations ionisantes), 1973, 240 p., 13,50 lei.

TIBERIU NĂŞCUŢIU, **Metode radiochimice de analiză** (Méthodes radiochimiques d'analyse), 1973, 384 p., 23 lei.

CRISTOFOR SIMIONESCU, MARGARETA GRIGORAŞ, AGATA CERNĂTESCU-ASANDEI, GHEORGHE ROZMARIN, **Chimia lemnului în România. Plopul şi salcia** (La Chimie du bois en Roumanie. Le peuplier et le saule), 1973, 299 p., 13 pl., 26 lei.

MIHAI FLORESCU, **Eficienţa economică a cercetării ştiinţifice** (L'efficience économique de la recherche scientifique), 1972, 115 p., 15 lei.

GEORGETA LĂZĂRESCU, **Sistematizarea informaţiilor în chimia organică** (Systématisation des informations en Chimie organique), 1972, 243 p., 1 pl., 10,50 lei.

I. P. INFORMAŢIA c. 67

43426

Lei 25.—

=1103 04

ACADÉMIE DE LA RÉPUBLIQUE SOCIALISTE DE ROUMANIE

REVUE ROUMAINE DE CHIMIE

R
REFERÁLVA

TOME 23
N° 5
Mai 1978

EDITURA ACADEMIEI REPUBLICII SOCIALISTE ROMÂNIA

Rev. Roumaine Chim.

RRCHAX, 23, 5, p. 641–826 (1978), Bucarest

ACADÉMIE DE LA RÉPUBLIQUE SOCIALISTE DE ROUMANIE

COMITÉ DE RÉDACTION

Rédacteur en chef:

I. G. MURGULESCU, membre de l'Académie de la République Socialiste de Roumanie

Rédacteurs en chef adjoints:

A. T. BALABAN et V. EM. SAHINI, membres correspondants de l'Académie de la République Socialiste de Roumanie

Collège de rédaction:

EM. BRATU, ELENA CEAUŞESCU, ECATERINA CIORĂNESCU-NENITZESCU, C. DRĂGULESCU, CR. SIMIONESCU, membres de l'Académie de la République Socialiste de Roumanie; P. SPACU, membre correspondant de l'Académie de la République Socialiste de Roumanie; MARGARETA AVRAM, I. HAIDUC, D. I. MARCHIDAN, I. MOLDOVAN, G. NIAC et D. SĂNDULESCU

La Revue Roumaine de Chimie paraît 10 fois par an. Toute commande de l'étranger (fascicules ou abonnements) sera adressée à ILEXIM — Departamentul Export-Import Carte (Livres)/Departamentul Export-Import Presă (Revues), P.O.B. 136—137 télex 11226, 3, str. 13 Decembrie, R-70116 Bucarest 12, Roumanie

Les manuscrits, les livres et les revues proposés en échange ainsi que toute correspondance seront envoyés à la rédaction :

REVUE ROUMAINE DE CHIMIE

23, str. Dumbrava Roşie, R-Bucarest, Roumanie, téléphone 12 41 60

EDITURA ACADEMIEI REPUBLICII SOCIALISTE ROMÂNIA

125, Calea Victoriei, R-71021 Bucarest, Roumanie, téléphone 50 76 80

REVUE ROUMAINE DE CHIMIE

ORSZÁGOS MŰSZAKI KÖNYVTÁR ÉS DOKUMENTÁCIÓS KÖZPONT 1983

Tome 23, Nº 5 Mai 1978

V. E. SAHINI, RODICA GRIGOROVICI and A. BUTUCELEA, A modified Urey-Bradley force field for hexahalodisilanes 643–649

A. BUTUCELEA and RODICA GRIGOROVICI, Vibrational symmetry coordinates for some arsenic chalcogenides 651–654

FLORENTINA AVRAMESCU and D. A. ISĂCESCU, Heat of combustion of mono- and difurfurylidene acetone 655–659

A D. A. ISĂCESCU and FLORENTINA AVRAMESCU, Reaction mechanism for the condensation of furfural with acetone catalysed by sodium hydroxide 661–665

R. SINGH, S. PRAKASH and O. PRAKASH, Thermodynamic properties of binary liquid mixtures 667–671

A ELENA CONSTANTINESCU and V. BRÎNZOI, Anodic oxidation of cyclohexanol 673–679

R. MIHAIL, C. V. RADU and I. M. BELCEA, Methods for complex reaction systems equilibrium computation 681–698

MARIA BREZEANU and MAGDALENA, DINCULESCU, Polynuclear complex compounds of iron, cobalt and nickel. III. Mercury-containing complex compounds 699–706

A. C. BANCIU, Electronic spectra and magnetic susceptibilities of some new tetrahedral chelate complexes with $\mathrm{Co}(d^7)-\mathrm{N}(sp^2)$ bonds 707–718

M. S. SUBHANI, Study of the influence of the dielectric constant on the reaction between simple inorganic anions in solution 719–723

A. M. BALINT and F. KEREK. Unidentate copper-amine complexes, a statistical method to evaluate the dissociation constant of labile complexes 725–731

A. T. BALABAN, Chemical graphs. XXXIII. Graphs for intramolecular rearrangements of tetragonal-pyramidal complexes 733–746

M. HASSAN, A.R.O. ABDEL NOUR and A. M. SATTI, The kinetics and reactions of some aryl-substituted epoxides with *t*-butoxide in *t*-butanol. . . . 747–751

A A. C. RĂZUȘ, ZS. ARVAY and ALICE MARIE GLATZ, Aluminium chloride catalyzed reactions of unsaturated acids with benzene. XI. Isomerizations during the reaction of benzene with 4-methyl-2-pentenoic acid 753–758

ABD EL-KADER FATEEN, A. M. KADDAH and Y. M. NAGUIB, Spiro-3-arylidene-1, 2, 3, 4-tetrahydronaphthalene-4-ones. I. Reactions with amines and Friedel-Crafts reactions 759–767

M. MRACEC and Z. SIMON, Hybridization of dicoordinated trivalent and tetracoordinated pentavalent phosphorus in conjugated six-membered rings. . . 769–779

Rev. Roumaine Chim., **23**, *5*, p. 641–826 (1978), Bucarest

MAGDA PETROVANU, I. DRUŢĂ and MAI VAN TRI, Pyridazinium-ylids. IX. Addition of aryl-pyridazinium-ylids on activated olefins (in French) 781–789

ABD EL-KADER FATEEN and A. M. KADDAH, Spiro-3-arylidene-1,2,3,4-tetrahydronaphthalene-4-ones. II. Synthesis of spiropyrazolines 791–796

A I. PETRARIU, MARIA CUJBĂ, IG. POINESCU and CORNELIA LUCA, Degradation of anion exchangers in aggressive medium. IV. Chemical stability of type I macroporous anion exchangers with binary and ternary structure in basic medium 797–803

B. TOKES, Polarographic investigations of the chemical constitution and reaction mechanisms of organic peroxides. I. Conditions of the polarographic analysis of organic peroxides (in Russian) 805–817

A K. K. GIRDHAR, Spectrophotometrical studies of the kinetics of the conversion of ferrocyanide to ferricyanide in the presence of hydrogen peroxide . . 819–824

BOOK REVIEWS 825

Revue Roumaine de Chimie, **23**, *5*, 643–649 (1978)

A MODIFIED UREY-BRADLEY FORCE FIELD FOR HEXAHALODISILANES

V. E. SAHINI, RODICA GRIGOROVICI and A. BUTUCELEA
Center of Physical Chemistry, Spl. Independenței 202,
77208-Bucharest, Romania

Received 20 July, 1977

The UB force field was so modified as to reproduce the observed spectra of the hexahalodisilanes. The estimated force constants are discussed in terms of the strength and nature of the Si—Si and Si—halogen bonds. The assignment of all vibrational bands is also given.

Certain vibrational and bonding effects occurring on the halogenation of ethane were evidenced previously [1] by carrying out a normal coordinate analysis in a Urey-Bradley force field (UBFF). This study suggested to search for similar effects in the series of halogenated ethane analogs, Si_2X_6 (X = F, Cl, Br, I), where problems concerning the strength of the Si—Si bond have been encountered. [2] As the normal coordinate analysis carried out for this series of compounds by Höfler *et al.* [3,4] used a different (GV) force field and a different set of symmetry coordinates, a direct comparison of the results obtained for these two classes of compounds could not be made. Consequently, we carried out the vibrational analysis using a same type of force field as that already used for ethanes.

For reaching a satisfactory agreement between the observed and calculated frequencies of the hexahalodisilanes, several interaction force constants had nevertheless to be included in the UBFF. We found finally an appropriate modified UBFF having a unique structure for all compounds in the series, a feature which is essential for comparing force constant values of compounds belonging to a same series.

METHOD OF CALCULATION

The hexahalodisilanes have a staggered conformation (D_{3d} point symmetry), the representation of the nuclear motions being reducible to $3A_{1g}(\text{R}) + A_{1u}(\text{in}) + 2A_{2u}(\text{ir}) + 3E_g(\text{R}) + 3E_u(\text{ir})$. The geometrical parameters and observed vibrational frequencies of the Si_2X_6 compounds were taken from Refs. 3, 4. The inactive A_{1u} mode (ν_4) was neglected. We used as symmetry coordinates the set already used[1] for hexahaloethanes. Unlike the symmetry coordinates used by Höfler *et al.* [5] our coordinates do not mix the $X-\mathrm{Si}-X$ and $\mathrm{Si}-\mathrm{Si}-X$ bending internal coordinates and include all the redundancies.

---

[1] R. Grigorovici, A. Butucelea, V. E. Sahini and M. K. DeArmond, *Rev. Roumaine Chim.*, **21**, 965 (1976).

[2] Th. G. Spiro, in "Progress in Inorganic Chemistry", Vol. 11, ed. by S. J. Lippard, Wiley, New York, 1970.

[3] F. Höfler, W. Sawodny and E. Hengge, *Spectrochim. Acta*, **26A**, 819 (1970).

[4] F. Höfler, S. Waldhör and E. Hengge, *Spectrochim. Acta*, **28A**, 29 (1972).

The G and F matrices were calculated, and the force constants refined (in 6 iteration cycles) using the programs BGLZ and LSMB written by Shimanouchi *et al.*[6] We used first a simple UBFF, consisting of 8 force constants : $K_{\mathrm{SiSi}}(=K_R)$, $K_{\mathrm{Si}X}(=K_r)$, $H_{\mathrm{SiSi}X}(=H_\alpha)$, $H_{X\mathrm{Si}X}$ $(=H_\beta)$, $F_{\mathrm{Si}X}$, $F'_{\mathrm{Si}X}$, F_{XX} and F'_{XX}. The constants F' were supposed to be equal to $-0.1\,F$. A poor agreement between calculated and observed frequencies was obtained for $\mathrm{Si_2F_6}$, whereas for $\mathrm{Si_2Cl_6}$, $\mathrm{Si_2Br_6}$ and $\mathrm{Si_2I_6}$ this field led to very low values of some diagonal elements of the $\widetilde{J}WJ$ matrix.

The force field was therefore completed with the following interaction force constants (Figure 1) :

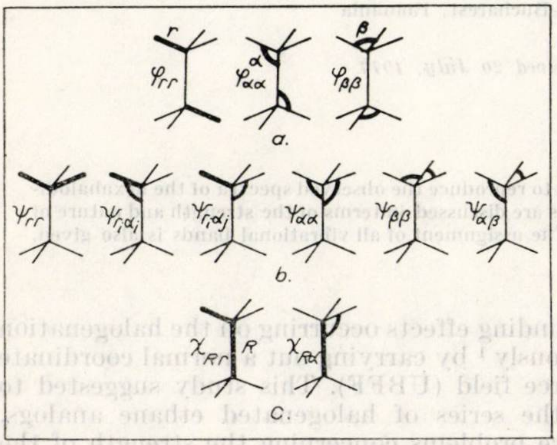

Fig. 1. Interaction force constants in hexahalodisilanes.

(*a*) φ_{rr}, $\varphi_{\alpha\alpha}$, $\varphi_{\beta\beta}$, representing interactions between internal coordinates of the the two $-\mathrm{Si}X_3$ groups ;

(*b*) ψ_{rr}, $\psi_{r_i\alpha_i}$, $\psi_{r_i\alpha_j}$, $\psi_{\alpha\alpha}$, $\psi_{\beta\beta}$, $\psi_{\alpha\beta}$, representing interactions between internal coordinates within a single $-\mathrm{Si}X_3$ group ; and

(*c*) χ_{Rr}, $\chi_{R\alpha}$, representing interactions in which the $\mathrm{Si}-\mathrm{Si}$ bond stretch is involved.

Table

Force constants of the hexahalodisilanes

Compound	UB force constants					
	K_R (1)	K_r (2)	H_α (3)	H_β (4)	$F_{\mathrm{Si}X}$ (5)	F_{XX} (6)
$\mathrm{Si_2F_6}$	2.55	5.71	0.15	0.46	−0.02	−0.05
$\mathrm{Si_2Cl_6}$	2.15	2.61	0.05	0.19	0.11	0.12
$\mathrm{Si_2Br_6}$	1.92	2.05	0.04	0.13	0.15	0.12
$\mathrm{Si_2I_6}$	1.66	1.55	0.02	0.13	0.13	0.02

Since only 11 experimental frequencies are available at most for $\mathrm{Si_2}X_6$ compounds,[3,4] no more than 4 to 5 interaction force constants could be considered at a time in the iteration procedure, in addition to the 6 diagonal UB force constants. The best fit between calculated and observed frequencies was obtained by trial-and-error, with the same set of interaction

[5] M. Pfeiffer and H. J. Spangenberg, *Z. Phys. Chem. (Leipzig)*, **232,** 47 (1966).

[6] T. Shimanouchi, "Normal Coordinate Treatment of Polyatomic Molecules", Tokyo Univ., Tokyo, 1968.

orce constants for each compound in the series, and only with this set (φ_{rr}, $\varphi_{\beta\beta}$, $\psi_{\beta\beta}$ and $\psi_{r_i\alpha_j}$). Other sets of interaction force constants used in various combinations led either to a poorer frequency fit or to the divergence of the iteration process.

RESULTS AND DISCUSSION

The optimum sets of force constants in the MUBFF used, resulting from the simultaneous refinement of the 10 to 11 mentioned force constants, and leading to an exact fit for all frequencies, are given in table 1.

From these, K_r resulted to be equal to the corresponding UB force constants estimated earlier [7] for tetrahalosilanes, while H_β and F_{XX} are larger and smaller, respectively. Moreover, the repulsive force constants F_{SiX} and F_{XX} of Si_2F_6 are negative when considering the φ_{rr} and $\psi_{r_i\alpha_i}$ interactions. For this compound alone, inclusion of the $\psi_{r_i\alpha_i}$ interaction in the MUBFF turned out to be essential in reaching the best frequency fit, and its estimated value to be quite large. All other refined interaction force constants have small values, but their consideration was required in order to reproduce the observed spectra.

Valence force constants for the Si—Si and Si—X bonds (k_R and k_r, respectively) were calculated from these UB force constants according to the relation (1) of Ref. 1. These are also listed in table 1, together with the values obtained by Höfler *et al.* using a valence force field. Both our and Höfler's k_R and k_r values show the same trend upon complete substitution of hydrogen with various halogens in disilane.

Since vibrational frequencies uncorrected for anharmonicity were used throughout our calculation, the "exact frequency fit" referred to above should be given a cautious weight in determining right values for the force constants involved. This is one of the reasons why in discussing the force constant values the emphasis will be on their relative values along the series of hexahalodisilanes.

1

(mdyne/Å) (all dispersions are under ±0.005)

Interaction force constants					Valence force constants			
					This work		Ref. 3, 4	
φ_{rr} (7)	$\varphi_{\beta\beta}$ (8)	$\psi_{\beta\beta}$ (9)	$\psi_{r_i\alpha_i}$ (10)	$\psi_{r_i\alpha_i}$ (11)	k_R	k_r	k_R	k_r
0.06	0.03	0.10	−0.10	0.23	2.47	5.64	2.4±0.2	5.96
−0.07	0.03	0.03	−0.09	—	2.60	2.83	2.4±0.2	2.90
−0.03	0.02	0.01	−0.14	—	2.52	2.29	2.1±0.15	2.30
0.15	0.00	0.01	−0.15	—	2.14	1.66	1.9±0.1	1.70

Frequency assignment. The assignment of all observed frequencies is based on the potential energy distribution obtained using the mentioned sets of force constants, and is listed for each compound in table 2. As may be seen, in passing from light (F, Cl) to heavy (Br, I) substituents in disilane, most of the non-totally symmetrical frequencies can be assigned unambiguously to certain pure normal modes of vibration, while ν_5 and ν_6, as

---

[7] A. Müller, B. Krebs and A. Fadini, *J. Mol. Spectry.*, **24**, 180 (1967).

Table 2

Assignment of the vibration frequencies of Si_2X_6 compounds and potential energy distribution

Species	Mode	X	Obsd. freqs. (cm^{-1})	Potential energy distribution among symmetry coords.[a]	Potential energy distribution for force constants (main contributions, in percents)[b] 1	2	3	4	5	6	7	8	9	10	11	Assignment[c]
A_{1g}	ν_1	F	541	$S_2 + 0.90S_1 + 0.57S'_3$	30	30		11							7	$\nu_s r + \nu R + \delta_s$
		Cl	624	$S_1 + 0.35S_2$	57	20										νR
		Br	562	$S_1 + 0.20S_2$	64	13										
		I	510	S_1	68	11										
	ν_2	F	910	$S_2 + 0.35S_1$	21	56									6	$\nu_s r + \nu R$
		Cl	351	$S_2 + 0.20S_1$	11	62				13						$\nu_s r$
		Br	223	S_2		67				16						
		I	154			72					7					
	ν_3	F	220	$S'_3 + 0.32S_3 + 0.98S_1$	38		13	24	10				10			$\delta_s + \nu R$
		Cl	134	$S'_3 + 0.34S_3$	10		13	34	13	8			10			δ_s
		Br	80	$S'_3 + 0.51S_3$			15	32	22	10						
		I	(51)[d]	$S'_3 + 0.36S_3$			6	48	26							
A_{2u}	ν_5	F	819	S_5		82									6	$\nu_s r$
		Cl	460			73		5								
		Br	329	$S_5 + 0.20S'_6$		55		10	11					12		
		I	255	$S_5 + 0.50S'_6$		42		16	15					17		$\nu_s r + \delta_s$
	ν_6	F	403	$S'_6 + 0.35S_6 + 0.20S_5$		10	20	37					16		7	δ_s
		Cl	241	$S'_6 + 0.41S_6$			16	39		16			11			
		Br	168	$S'_6 + 0.62S_6 + 0.21S_5$		8	14	31		24				10		
		I	116	$S'_6 + 0.48S_6 + 0.81S_5$		28		29						19		$\delta_s + \nu_s r$

Table 2 (continued)

E_g	ν_7	F	971	S_7		84									6	$\nu_a r$
		Cl	593			80										
		Br	473			71								8		
		I	398			63								13		
	ν_8	F	340	S_8				71					15			δ_a
		Cl	212					52		18		8				
		Br	139	$S_8 + 0,41\,S_9$		10	10	35	17	17						$\delta_a + \rho$
		I	94	$S_8 + 0.41\,S_9$		6	5	48	23							
	ν_9	F	203	S_9			75		10						6	ρ
		Cl	127				54	11	26							
		Br	89	$S_9 + 0.52 S_8$			32	21	30	10						$\rho + \delta_a$
		I	$(53)^d$	$S_9 + 0.40 S_8$			14	20	43			9				
E	ν_{10}	F	985	S_{10}		93										$\nu_a r$
		Cl	604			87										
		Br	479			84										
		I	388			75		10			8					
	ν_{11}	F	306	S_{11}				74					16			δ_a
		Cl	179					61		19		10	9			
		Br	114					57		29		8				
		I	81			12		76								
	ν_{12}	F	135	S_{12}			75		10						10	ρ
		Cl	74				67		31							
		Br	50				51		42							
		I	$(31)^d$			10	18		49			10		12		

---

[a] The symmetry coordinates $S_1, \ldots, S_{12}$ were defined in Ref. 1.

[b] For the numbering of the UB and interaction force constants, see table 1.

[c] Abbreviations: νR = Si−Si stretching; $\nu_{s(a)} r$ = symmetric (asymmetric) SiX_3 stretching; $\delta_{s(a)}$ = sym. (asym.) SiX_3 deformation involving the angles α and/or β; ρ = Si−SiX_3 rocking.

[d] Values calculated in Ref. 3.

well as ν_8 and ν_9 modes, mix to a certain small extent with each other, the corresponding frequencies keeping nevertheless their assignment as defined for disilane or ethane. For the totally-symmetrical modes no significant mixing for heavy substituents was observed. However, for the lightest compound of the series, Si_2F_6, a severe mixing of all three A_{1g} modes appears, in agreement with Höfler's results.[4] The motions involved in two of these modes are visualized in Figure 2, together with the corresponding modes in the C_2X_6 (X = F, Cl, Br) series.[1] For all Si_2X_6 compounds except Si_2F_6 the form of these normal modes is similar to that of the corresponding modes of the C_2X_6 compounds. For Si_2F_6 no proper Si–Si stretching vibration exists (see also table 2), a situation met also for the C–C stretching vibration of C_2D_6.[1] In both these compounds the ν_1 and ν_3 modes are strongly coupled. Moreover, these are the lightest compounds in their corresponding series for which the ν_1 frequency becomes higher than ν_3.

In the ethane series, these effects occur when the $m_C/3m_X$ mass ratio reaches a certain critical value, which was found [8] to occur for $m_X = 1.8$ a.m.u. In the disilane series, owing to the increased mass of silicon as compared to that of carbon, the mentioned effects must occur for a heavier substituent than deuterium. As a matter of fact, they are already present in Si_2F_6, having probably occurred somewhere between Si_2D_6 and Si_2F_6 in the series. A more accurate estimate of this critical mass of the substituent could be made by investigating compounds having substituent masses in this range, such as Si_2T_6 or $Si_2(CH_3)_6$.

Force constants. The force constants (Table 1) will be discussed by emphasizing their relative values along the series of hexahalodisilanes. On the other hand, a comparison of these force constant values with the corresponding force constants in the hexahaloethane series will be made, since it is relevant for the nature of the chemical bond in these compounds.

As may be seen from table 1, the k_R values range between 2.1–2.6 mdyne/Å for hexahalodisilanes (with a slight maximum for Si_2Cl_6, following as a matter of fact the variation of the Si–Si stretching frequencies ν_1). A calculation with a similar field for Si_2H_6 yielded a value of 1.74 mdyne/Å. This strengthening of the Si–Si bond upon disilane halogenation, as reflected by the value of k_R, was also observed and discussed by Höfler *et al.*[3,4] It should be observed that the strengthening is not appreciably greater in Si_2F_6 than in the other hexahalodisilanes. As for k_r, it decreases continuously with the electronegativity of the substituent.

When comparing the ethane and disilane series, the different effect of hydrogen substitution with halogens upon the C–C and Si–Si bonds may be noticed. In the ethane series the k_R values were found [1] to be 4.56 mdyne/Å in C_2H_6, and 9.27, 4.23 and 4.15 mdyne/Å in C_2F_6, C_2Cl_6 and C_2Br_6, respectively, showing no strengthening of the C–C bond upon halogenation, except for C_2F_6. In hexahalodisilanes, the slight strengthening of the Si–Si bond upon halogenation was attributed by Höfler *et al.*[3,4] to an increase of the *s* character of the Si–Si bond, and to an additional $(d-d)\ \pi$ contribution to it. Obviously, such an effect can not occur in the hexahaloethanes. A parallel study of the two classes of compounds through a CNDO-type method would be required to confirm the proposed explanation.

---

[8] R. Beldie, A. Butucelea and V. E. Sahini, *Rev. Roumaine Chim.*, **21**, 327 (1976).

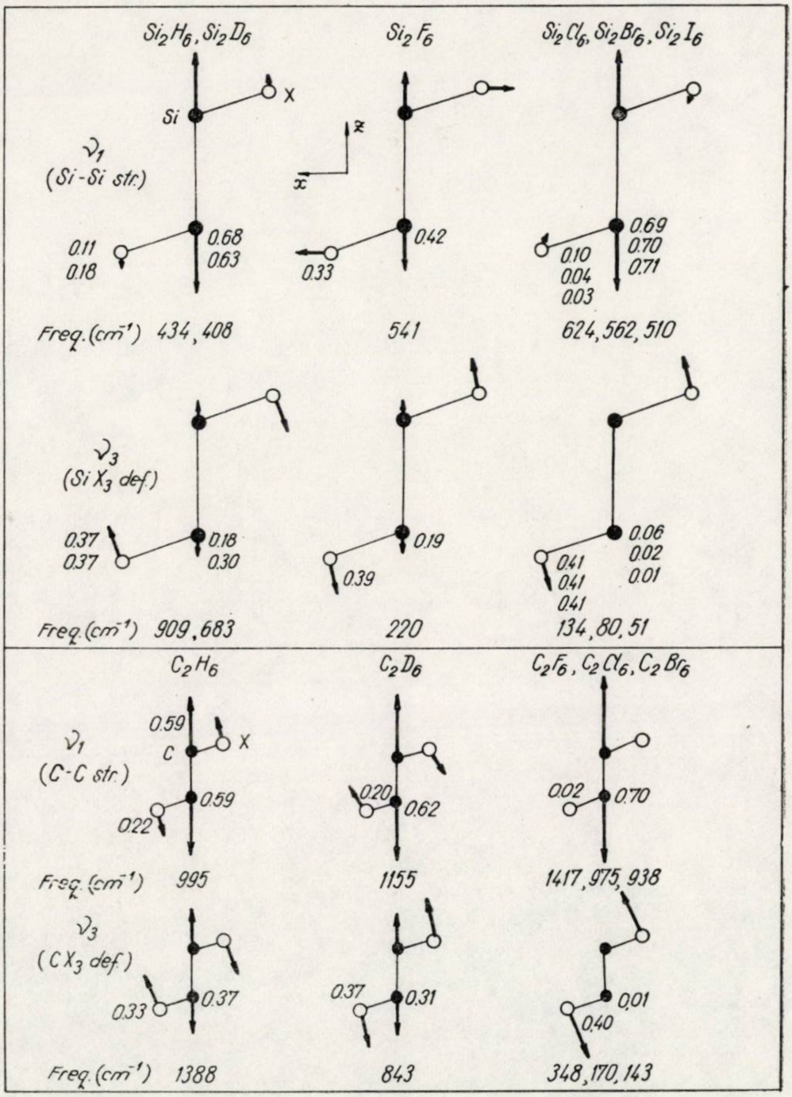
Si_2H_6, Si_2D_6
Si_2F_6
$Si_2Cl_6, Si_2Br_6, Si_2I_6$
X
Si
z
x
ν_1
(Si-Si str.)
0.11
0.18
0.68
0.63
0.42
0.33
0.69
0.70
0.71
0.10
0.04
0.03
Freq.(cm^{-1}) 434, 408
541
624, 562, 510
ν_3
(SiX_3 def.)
0.37
0.37
0.18
0.30
0.19
0.39
0.06
0.02
0.01
0.41
0.41
0.41
Freq.(cm^{-1}) 909, 683
220
134, 80, 51
C_2H_6
C_2D_6
C_2F_6, C_2Cl_6, C_2Br_6
ν_1
(C-C str.)
0.59
C
X
0.59
0.22
0.20
0.62
0.02
0.70
Freq.(cm^{-1}) 995
1155
1417, 975, 938
ν_3
(CX_3 def.)
0.33
0.37
0.37
0.31
0.01
0.40
Freq.(cm^{-1}) 1388
843
348, 170, 143

Fig. 2. — Form of the ν_1 and ν_3 A_{1g} modes in hexahalodisilanes. The arrows represent the relative nuclear displacements, proportional to the values of the L_M matrix elements, written alongside for each compound. The interatomic distances and atomic sizes are not drawn to scale. For simplicity only the xz molecular plane is represented. The corresponding modes in hexahaloethanes are also given for comparison (see text).

In particular, it should be remarked that the outstandingly high value of k_R met in C_2F_6 was not found in the corresponding compound of the disilane series, Si_2F_6. From a practical point of view, this would mean that the highly stabilizing role played by a $-CF_3$ group upon an adjacent bond should not be expected in compounds containing $-SiF_3$ groups.

Revue Roumaine de Chimie, **23**, *5*, 651–654 (1978)

VIBRATIONAL SYMMETRY COORDINATES FOR SOME ARSENIC CHALCOGENIDES

A. BUTUCELEA and RODICA GRIGOROVICI
Center of Physical Chemistry, Spl. Independenţei 202,
Bucharest, Romania

Received June 10, 1977

Internal symmetry coordinates are given for the As_4X_4 (D_{2d}) and As_4X_3 (C_{3v}) ($X = S$, Se, Te) molecular configurations. They may be used in the vibrational analysis of these compounds, or of other compounds with similar configuration.

Arsenic chalcogenide glasses have come to attention because of their semiconducting properties and their subsequent applications in optical information storage or xerography. Elucidation of these properties requires, among others, a good understanding of the vibrational spectra of the compounds involved, As_4X_6, As_4X_4 and As_4X_3 ($X = S$, Se, Te). While carrying out work on these lines, we were faced with the necessity of building up internal symmetry coordinates for various As_4X_n ($n = 3, 4, 6$) molecular configurations likely to be present in the glassy state. In view of their potential usefulness for the normal coordinate analysis of other compounds with similar configuration, we make them available separately of the results of our force constant calculation on arsenic chalcogenides.

For As_4X_6 the symmetry coordinates found by Cyvin [1] during analysis of P_4O_6 or $(CH_2)_6N_4$ can be used, since these molecules and the cage-like As_4X_6 molecular units with T_d symmetry which may be found in the gaseous phase of As_4X_6 have similar configurations. We only give here our original results for the two remaining arsenic chalcogenides.

As_4X_4. The quasi-independent molecular units present [2] in crystalline phase have a cage configuration with the symmetry of the point group D_{2d} (Figure 1). From table 1 it results that the vibration spectra of As_4X_4

---

[1] S. J. Cyvin and B. N. Cyvin, *Z. Naturforsch.*, **26a**, 901 (1971); S. J. Cyvin, Ed., "Molecular Structures and Vibrations," Elsevier, Amsterdam, 1972, p. 283.

[2] T. Ito, *Acta Cryst.*, **5**, 775 (1952); E. J. Smail and G. M. Sheldrick, *Acta Cryst.*, **B29**, 2014 (1973); P. Goldstein and A. Paton, *Acta Cryst.*, **B30**, 915 (1974).

consist of bands of $3A_1(\mathrm{R}) + 2A_2(\mathrm{in}) + 2B_1(\mathrm{R}) + 3B_2(\mathrm{R, ir}) + 4E(\mathrm{R, ir})$ species. The symmetry coordinates of these species were built up by using 18 valence coordinates (the r, s and γ sets). Two symmetrically equivalent sets of 4 valence coordinates each (the angles α and β) were used to build up the redundant symmetry coordinates of $2A_1 + B_1 + B_2 + 2E$ species (Table 1).

The construction of the symmetry coordinates was carried out according to the classical procedure established by Wilson,[3] paying proper attention to the orientation of the generating internal coordinate used for deriving degenerate symmetry coordinates. Moreover, since two symmetry coordinates of species E had to be constructed from a single set of equivalent valence coordinates (e.g. r, see table 1), this set was divided into subsets and the correlation diagram between the group of the initial set and that of the subset was used.[3] The final orthonormal symmetry coordinates, including the redundant ones, are given in table 2.

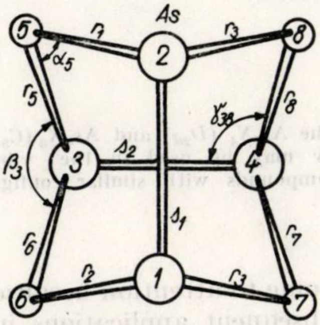

Fig. 1. — Structure and the internal valence coordinates of an As_4X_4 molecular unit.

Table 1

Classification of the normal modes of an As_4X_4 molecular unit and of the redundant coordinates

D_{2d}	$n(r)$	$n(s)$	$n(\alpha)$	$n(\beta)$	$n(\gamma)$	$n(Q)$*	Redundant coordinates
A_1	1	1	1	1	1	3	2
A_2	1	0	0	0	1	2	0
B_1	1	0	1	0	1	2	1
B_2	1	1	0	1	1	3	1
E	2	0	1	1	2	4	2

* Excluding translations and rotations

---

[3] E. B. Wilson, Jr., J. C. Decius and P. C. Cross, "Molecular Vibrations," McGraw-Hill, New York, 1955, pp. 117, 135.

As_4X_3. In crystalline state, this compound consists[4] of As_4X_3 molecular units of C_{3v} symmetry. The reduction of various representations of this molecular group for As_4X_3 units is given in table 3. It results that the normal vibration modes of the As_4X_3 molecule are $4A_1$ (R, ir) + A_2(in) + + $5E$ (R, ir). For building up the corresponding symmetry coordinates

Table 2

Symmetry coordinates of As_4X_4 (D_{2d})
(A single member of the set is given for degenerate coordinates)

$$A_1:\quad S_1 = 1/\sqrt{8}\,(r_1 + r_2 + \ldots + r_8);\; S_2 = 1/\sqrt{2}\,(s_1 + s_2);$$

$$S_3 = 1/\sqrt{8}\,(\gamma_{15} + \gamma_{26} + \gamma_{27} + \gamma_{18} + \gamma_{45} + \gamma_{46} + \gamma_{37} + \gamma_{38});$$

$$S_{\text{red}} = 1/2\,(\alpha_5 + \alpha_6 + \alpha_7 + \alpha_8);\; S_{\text{red}} = 1/2\,(\beta_1 + \beta_2 + \beta_3 + \beta_4)$$

$$A_2:\quad S_4 = 1/\sqrt{8}\,(-r_1 + r_2 - r_3 + r_4 + r_5 - r_6 + r_7 - r_8);$$

$$S_5 = 1/\sqrt{8}\,(-\gamma_{15} + \gamma_{26} - \gamma_{27} + \gamma_{18} + \gamma_{45} - \gamma_{46} + \gamma_{37} - \gamma_{38})$$

$$B_1:\quad S_6 = 1/\sqrt{8}\,(-r_1 + r_2 - r_3 + r_4 - r_5 + r_6 - r_7 + r_8);$$

$$S_7 = 1/\sqrt{8}\,(-\gamma_{15} + \gamma_{26} - \gamma_{27} + \gamma_{18} - \gamma_{45} + \gamma_{46} - \gamma_{37} + \gamma_{38});$$

$$S_{\text{red}} = 1/2\,(-\alpha_5 + \alpha_6 - \alpha_7 + \alpha_8)$$

$$B_2:\quad S_8 = 1/\sqrt{8}\,(r_1 + r_2 + r_3 + r_4 - r_5 - r_6 - r_7 - r_8);\; S_9 = 1/\sqrt{2}\,(s_1 - s_2):$$

$$S_{10} = 1/\sqrt{8}\,(\gamma_{15} + \gamma_{26} + \gamma_{27} + \gamma_{18} - \gamma_{45} - \gamma_{46} - \gamma_{37} - \gamma_{38});$$

$$S_{\text{red}} = 1/2(\beta_1 + \beta_2 - \beta_3 - \beta_4)$$

$$E:\quad S_{11a} = 1/2\,(r_2 - r_4 + r_6 - r_8);\; S_{12a} = 1/2(-r_1 + r_3 + r_5 - r_7);$$

$$S_{13a} = 1/2(\gamma_{26} - \gamma_{18} + \gamma_{46} - \gamma_{38});\; S_{14a} = 1/2\,(-\gamma_{15} + \gamma_{27} + \gamma_{45} - \gamma_{37});$$

$$S_{\text{red},a} = 1/\sqrt{2}\,(\alpha_5 - \alpha_7);\; S_{\text{red},a} = 1/2(\beta_1 - \beta_2 - \beta_3 + \beta_4)$$

Table 3

Classification of the normal modes of an As_4X_3 molecular unit and of the redundant coordinates

C_{3v}	$n(r)$	$n(t)$	$n(s)$	$n(\alpha)$	$n(\beta)$	$n(\gamma)$	$n(\delta)$	$n(Q)$*	Redundant coordinates
A_1	1	1	1	1	1	1	1	4	3
A_2	0	0	0	0	0	1	0	1	0
E	1	1	1	1	1	2	1	5	3

* Excluding translations and rotations

---

[4] H. J. WHITFIELD, *J. Chem. Soc. A*, **1970**, 1800.

15 valence coordinates (r, t, s and γ, defined on Figure 2) were used. The redundant ($3A_1 + 3E$) symmetry coordinates were built up from 9 redundant valence coordinates (the α, β and δ angles).

A procedure identical to that used for As_4X_4 was followed. The results are given in table 4.

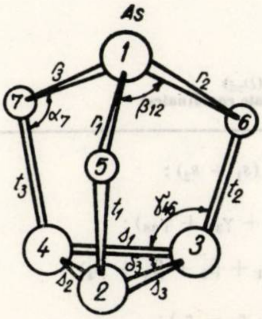

Fig. 2. — Structure and the internal valence coordinates of an As_4X_3 molecular unit.

Table 4

Symmetry coordinates of $As_4\,X_3(C_{3v})$
(A single member of the set is given for degenerate coordinates)

$$A_1:\quad S_1 = 1/\sqrt{3}\,(r_1 + r_2 + r_3)\,;\; S_2 = 1/\sqrt{3}\,(t_1 + t_2 + t_3)\,;\; S_3 = 1/\sqrt{3}\,(s_1 + s_2 + s_3)\,;$$

$$S_4 = 1/\sqrt{6}\,(\gamma_{35} + \gamma_{45} + \gamma_{26} + \gamma_{46} + \gamma_{37} + \gamma_{27})\,;$$

$$S_{\mathrm{red}} = 1/\sqrt{3}\,(\alpha_5 + \alpha_6 + \alpha_7)\,;\; S_{\mathrm{red}} = 1/\sqrt{3}\,(\beta_{12} + \beta_{23} + \beta_{13})\,;$$

$$S_{\mathrm{red}} = 1/\sqrt{3}\,(\delta_2 + \delta_3 + \delta_4)$$

$$A_2:\quad S_5 = 1/\sqrt{6}\,(\gamma_{35} - \gamma_{45} - \gamma_{26} + \gamma_{46} - \gamma_{37} + \gamma_{27})$$

$$E:\quad S_{6a} = 1/2\,(2r_1 - r_2 - r_3)\,;\; S_{7a} = 1/2(2t_1 - t_2 - t_3)\,;\; S_{8a} = 1/2(2s_1 - s_2 - s_3)\,;$$

$$S_{9a} = 1/\sqrt{12}\,(2\gamma_{35} + 2\gamma_{45} - \gamma_{26} - \gamma_{46} - \gamma_{37} - \gamma_{27})\,;$$

$$S_{10a} = 1/2(-\gamma_{26} + \gamma_{46} + \gamma_{37} - \gamma_{27})\,;\; S_{\mathrm{red},a} = 1/2(2\alpha_5 - \alpha_6 - \alpha_7)\,;$$

$$S_{\mathrm{red},a} = 1/2(-\beta_{12} + 2\beta_{23} - \beta_{13})\,;\; S_{\mathrm{red},a} = 1/2(2\delta_2 - \delta_3 - \delta_4)$$

These symmetry coordinates describe appropriately the main nuclear motions expected for the As_4X_4 and As_4X_3 molecular units.

Revue Roumaine de Chimie, 23, 5, 655–659 (1978)

HEAT OF COMBUSTION OF MONO- AND DIFURFURYLIDENE ACETONE

FLORENTINA AVRAMESCU and D. A. ISĂCESCU *
Institute of Chemistry, Faculty of Chemistry, Splaiul Independenţei 89,
Bucharest, Romania

Received February 21, 1976

Heat of combustion of mono- and difurfurylidene acetone has been determined by means of an automatic adiabatic calorimeter bomb Gallenkamp CB–110, at 25°. The standard heats of formation of those two compounds have been determined from the heat of combustion. From the obtained data, the energy of conjugation of F, FAc and F_2Ac has been computed both from heats of combustion and heats of formation.

A previous work [1] has studied the thermic effect of the polymerization reaction in benzene-sulphonic acid catalysis, of furfural (F), monofurfurylidene acetone (FAc) and difurfurylidene acetone (F_2Ac).

Although the results were reproducible and directly applicable in practice, it was necessary to know also the other thermochemical constants : heat of combustion, heat of formation of FAc and F_2Ac for the calculation of their energies of conjugation which make a contribution to the study of polymerization capacity of furfural-acetone monomers.

EXPERIMENTAL PART

PRODUCTS

High purity F, FAc and F_2Ac.

Furfural was purified by coupling with diazotized sulphanilic acid, then refined and recondensed on calcium hydride and closed in vacuum.

Mono- and difurfurylidene acetone of high purity were obtained by fractionated distillation at reduced pressure and repeated recrystallisation as shown in a previous work. [2] For combustion, dry FAc and F_2Ac was used in the form of tablets.

APPARATUS AND PROCEDURE

The heat of combustion was measured with an automatic adiabatic calorimeter bomb Gallenkamp CB–110, at 25° and at an oxygen pressure of 30 atm.

The calorimeter was calibrated with benzoic acid and naphthaline, as standard samples for calorimetry. The heat capacity of the calorimeter was 2458.0± 1 cal/degree.

---

* Deceased, 1977.

[1] I. G. Murgulescu, D. A. Isăcescu, E. Tomuş and F. Tomuş, *Rev. Roumaine Chim.*, **10**, 269 (1965).

[2] D. A. Isăcescu, V. Ursu, I. Rebedea and F. Tomuş, *Anal. Univ. Bucureşti, Chimie*, **14**, 87 (1965).

The combustions were effected in standard conditions, with 1 ml distilled water in the bomb. The correction for nitric acid was maintained under 0.04 of the total heat.

In the course of combustion experiments, the temperature inside the calorimeter was constant at 25°, varying no more than by 0.001°/min. with time.

The corrected temperature values, multiplied by the heat capacity of the calorimetric system and divided by the amount of reagents, gave the heat of combustion, $-\Delta E_c$, cal/g from which $-\Delta H_c$, kcal/mol was then calculated.

RESULTS AND DISCUSSION

1. STANDARD HEATS OF COMBUSTION

The experimental results for combustion at 25° of FAc and F_2Ac with formation of CO_2 and H_2O, are presented in table 1. For verification, the heat of combustion for F was also measured. One can see from table 1 that $-\Delta H_c^0$ for pure furfural is 559.04 ± 0.02 kcal/mol.

Table 1

Heats of combustion

$C = 2458.0 \pm 1$, cal/degree $P_{O_2} = 30$ at $t = 25°$

Substance	m, g	Δt, °C	ΔE_Σ [a] cal	$-\Delta E_c$, cal/g	$-\Delta H_c^0$, kcal/mol
F	1.07120	3.115	1424.14	5818.27	
$M = 96.082$	1.19898	3.418	1425.07	5818.59	559.04 ± 0.02
				Average : 5818.43 ± 0.16	
FAc	1.03210	2.991	16.900	7106.90	
$M = 136.144$	1.03280	2.994	17.630	7108.50	
	1.04490	3.030	20.100	7108.47	968.25 ± 0.37
	1.03250	2.992	15.420	7110.66	
	1.03230	2.990	17.100	7105.10	
	1.03290	2.993	15.100	7107.30	
				Average : 7107.61 ± 2.8	
F_2Ac	1.03835	2.995	16.536	7073.90	
$M = 214.210$	0.99130	2.860	18.500	7072.90	
	1.03900	2.998	18.400	7074.75	1516.17 ± 0.60
	1.03630	2.990	16.250	7076.25	
	1.03924	2.999	15.200	7078.55	
				7074.62	
				Average : 7075.20 ± 2.7	

[a] ΔE_Σ, represents corrections for the heat evolved by burning of wire and cotton. In the case of F a correction is added for the heat evolved by burning of a quantity of paraffin necessary for the fastening of the ampoule in the crucible of the bomb : 11140 cal/g.

We consider that the difference in addition of ~ 1 kcal/mol reported in the literature (560.1) is due to impurities of furfural which are not removed by distillation.

2. STANDARD HEATS OF FORMATION

The standard heat of formation, ΔH_f^0, of F, FAc and F_2Ac, which are presented in table 2 has been determined from the standard heats of combustion of those three products and from those of the component elements, carbon and hydrogen ($\Delta H^0_{c(C)} = -94.0518$ kcal/mol ; $\Delta H^0_{c(H_2)} = -68.3174$ kcal/mol).

Table 2

Heats of formation

Substance	$-\Delta H_f^0$, kcal/mol	ΔH_r^0, kcal/mol
F^a	47.85	
FAc	57.43	22.75
F_2Ac	48.09	34.93

[a] In literature for F : $-\Delta H_f^0 = 46.79$ kcal/mol

The standard heats of reaction, ΔH_r^0, of FAc and F_2Ac were also computed from the heats of combustion of furfural and acetone. The values are also presented in table 3.

Table 3

Energies of conjugation from heats of combustion

Substance	$\Delta H_c(g)$, kcal/mol		E_{conj}, kcal/mol
	calculated	experimental	
F	596.0*	569.37	26.63
	595.8**		
FAc	1022.2	985.73	36.47
	1021.8		36.07
F_2Ac	1607.8	1535.22	72.58
	1601.4		66.18

* by bond constants
** By Konovalov's relation

3. ENERGIES OF CONJUGATION

The data obtained were used to compute the energy of conjugation of F, FAc and F_2Ac both from heats of combustion and heats of formation by the difference between computed and experimental values.

(*a*) The energy of conjugation from heats of combustion was obtained by relation :

$$E_{\text{conj}} = \Delta H_c(\text{g})_{\text{calc}} - \Delta H_c(\text{g})_{\text{exp}} \tag{1}$$

The heats of combustion for the gaseous state, $\Delta H_c(\text{g})_{\text{calc}}$, have been computed by means of the constants of covalent bonds for unconjugated molecules and by means of Konovalov's relation :

$$\Delta H_c = -(48.8\, m + 10.50\, n + x) \tag{2}$$

where m is the number of oxygen atoms required for complete burning of the substance, n is the number of water moles formed and x is a constant correction for a homologous series and which is zero for saturated compounds.

The values thus obtained for $\Delta H_c(\text{g})_{\text{calc}}$ are presented in table 3, which shows a good agreement between the values found by the two calculation methods.

The experimental heats of combustion for gaseous state, $\Delta H_c(\text{g})_{\text{exp}}$, have been obtained having the heats of fusion and vaporization for FAc and F_2Ac. Thus, the heat of fusion for FAc and F_2Ac determined in a previous work [3] are 5.34 and 5.60 kcal/mol respectively. The latent molar heat of vaporization, $\Delta_v H$, of FAc and F_2Ac has been determined by studying the variation of the steam tension with temperature, on the basis of Clapeyron—Clausius equation :

$$\frac{\text{d}\ln p}{\text{d}T} = \frac{\Delta_v H}{RT^2} \tag{3}$$

from the slope of the plot of natural logarithm of the steam pressure, against the inverse of absolute temperature (Figure 1).

The values of $\Delta_v H$, thus computed for FAc and F_2Ac are 13.48 and 17.88 kcal/mol, respectively. For verification, the heat of vaporization of furfural has been obtained in the same manner (Figure 2), 10.40 kcal/mol, being a comparable value with that found in the literature (10.33 kcal/mol).

Therefore, with known heats of sublimation of FAc and F_2Ac (17.48 and 19.05 kcal/mol, respectively) the value of $\Delta H_c(\text{g})_{\text{exp}}$ was determined (Table 3).

By the difference of heats of combustion, there result the corresponding energies of conjugation of F, FAc, F_2Ac presented in table 3.

(*b*) The energy of conjugation from heats of formation was obtained by means of relation :

$$E_{\text{conj}} = \Delta aH_{\text{exp}} - \Delta aH_{\text{calc}} \tag{4}$$

where ΔaH is the atomic heat of formation.

The ΔaH_{exp} values were obtained from heats of formation in gaseous state, heats of dissociation of component elements and from heats of sublimation by means of Hess law.

---

[3] F. Avramescu, *Rev. Roumaine Chim.*, **13** 175 (1968).

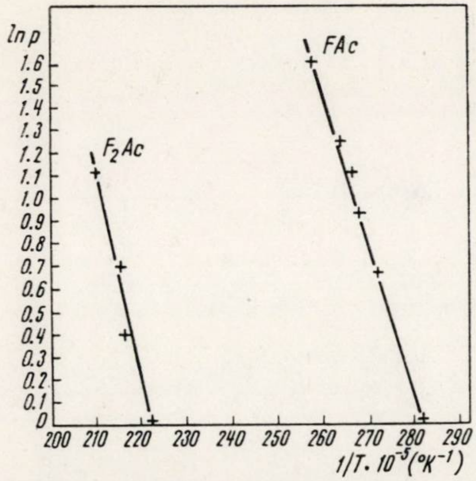

Fig. 1. — The natural logarithms of steam pressure against the inverse of absolute temperature for FAc and F_2Ac.

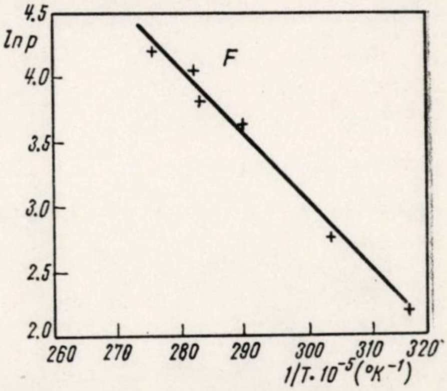

Fig. 2. — The natural logarithms of steam pressure against the inverse of absolute temperature for F.

The values of $\Delta aH_{\mathrm{calc}}$ were obtained from bond energies.

Both the values of heats formation thus obtained and those of the resulted energies of conjugation, are presented in table 4.

Table 4

Energies of conjugation from heats of formation

Substance	$-\Delta\, aH_{\mathrm{exp}}$, kcal/mol	$-\Delta aH_{\mathrm{calc}}$, kcal/mol	E_{conj} kcal/mol.
F	983.32	955.40	28.12
FAc	1564.01	1524.80	39.21
F_2Ac	2333.51	2256.60	76.91

The energy of conjugation (the values average resulting from heats of combustion and formation) increases from F at FAc and F_2Ac in the order : $27.2 < 37.7 < 73.1$ kcal/mol, in accord with their conjugated structure and also with the molecule stabilization.

The presence of furanic cycle by its structure of dienic cyclic ether and the influence of lateral chains of F, FAc, F_2Ac, explain the structural characteristics, the aromatic character, respectively, the reactivity and stability of the corresponding molecule.

CONCLUSIONS

The standard heat of combustion of FAc and F_2Ac was determined. By means of the heats of combustion, the standard heats of formation and the standard heats of reaction for the two compounds were computed.

The energy of conjugation of F, FAc and F_2Ac was also computed from heats of combustion and formation, emphasizing the influence of the nature of the lateral chains on the general structure of the studied compounds, on their reactivity and stability.

Revue Roumaine de Chimie, **23**, *5*, 661–665 (1978)

REACTION MECHANISM FOR THE CONDENSATION OF FURFURAL WITH ACETONE CATALYSED BY SODIUM HYDROXIDE

I. SYSTEMATIZATION AND INTERPRETATION OF EXPERIMENTAL RESULTS

D. A. ISĂCESCU* and FLORENTINA AVRAMESCU

Institute of Chemistry, Faculty of Chemistry, Splaiul
Independenţei 89, Bucharest, Romania

Received February 21, 1976

The paper presents the known condensation mechanisms of furfural with acetone in the NaOH catalysis, as well as a systematization of own experimental data and of those reported in the literature with regard to this reaction.

Furfural-acetone monomers and polymers have acquired a world-wide importance due to their possible use as an organic binder instead of the mineral cement, to obtain organo-mineral concretes with better properties than ordinary concretes, and having a large applicability in the construction field.

Furfural-acetone monomers, monofurfurylidene acetone (FAc) and difurfurylidene acetone (F_2Ac) were obtained by furfural (F) condensation reaction with acetone (Ac) in the NaOH catalysis since 1881 by Schmidt[1] and then by Claisen and Ponder in 1884.[2] Since a rather large number of contributions have subsequently appeared, a rigorous systematization and interpretation of both own experimental results and of those found in the literature were necessary.

The investigations reported in the literature in relation to the reactions which may constitute the formation mechanism of furfural-acetone monomers will be presented in the first place. Our own studies in view of establishing the reaction mechanism will by presented next.

---

* Deceased, 1977

[1] J. G. Schmidt, *Ber. dtsch. chem. Ges.*, **14,** 1459 (1881).
[2] L. Claisen and H. C. Ponder, *Liebigs Ann. Chem.*, **223,** 144 (1884).

1. MECHANISMS REPORTED IN THE LITERATURE

The literature published so far mentions the following formation mechanisms of mono- and difurfurylidene acetone in the alkaline catalysis.

The first mechanism may be considered to be that indicated by Mangini and Andrisano,[3] to obtain mono- and difurfurylidene acetone polymers in the NaOH catalysis, the first stage of which is the monomer formation. The authors consider that for a 1/1 and 1/1.6 F/Ac molar ratio, one obtains FAc which then passes to poly-FAc with different polymerization degrees :

$$1\ \mathrm{F} + 1\ \mathrm{Ac} + 0.25\ \mathrm{NaOH}\ (50\%) \rightarrow \mathrm{FAc} \rightarrow (\mathrm{FAc})_m$$

where

$$m = 12-14 \text{ and } \bar{M} = 1600-1890\,;$$

$$1\ \mathrm{F} + 1.6\ \mathrm{Ac} + 0.25\ \mathrm{NaOH}\ (50\%) \rightarrow \mathrm{FAc} \rightarrow (\mathrm{FAc})_n$$

where

$$n = 9.7 \text{ and } \bar{M} = 1325.$$

For a F/Ac = 2/1 molar ratio, one obtains $\mathrm{F_2Ac}$ which then passes to poly-$\mathrm{F_2Ac}$:

$$2\ \mathrm{F} + 1\ \mathrm{Ac} + 1.74 - 2.5\ \mathrm{NaOH}\ (35-50\%) \rightarrow \mathrm{F_2Ac} \rightarrow (\mathrm{F_2Ac})_x$$

when $\bar{M} = 425-531$.

However, in the same paper, the authors show that the distillation of polymers prepared in such a manner leads to mono- and difurfurylidene acetone in the case of poly-$\mathrm{F_2Ac}$. Hence, the suggested mechanism cannot be the real one.

The second reaction mechanism has been postulated by Isăcescu, Gavăt et al[4] and it relies on the chemical constituents isolated from the final product of the condensation reaction.

As mentioned by the authors[4,5] the total condensation product termed "FA monomer" is not a unitary product. It is a complex mixture formed of the two main products, FAc and $\mathrm{F_2Ac}$, which are the furfural-acetone monomers, of at least three secondary products, diacetone alcohol (DAcAl), mesityl oxide (OM) and lower polymers, and also of F and Ac which do not react.

It has been deduced thereof that the global condensation reaction is actually composed of at least seven consecutive and concurrent reactions :

---

[3] A. Mangini and R. Andrisano, *Ann. Chim. (Ital.)*, **34**, 47 (1944).

[4] D. A. Isăcescu, I. Gavăt, I. V. Ionescu and C. Stoicescu, *Studii și Cercetări Chim. Acad. RPR*, **14**, 211 (1965).

[5] D. A. Isăcescu, I. Gavăt, C. Stoicescu, C. Vass and I. Petruș, *Studii și Cercetări Chim. Acad. RPR*, **14**, 197 (1965).

Reactions between partners of the same kind,

$$\mathrm{Ac + Ac \rightleftharpoons DAcAl \rightarrow OM + H_2O} \qquad \mathrm{I}$$

$$\mathrm{F \rightarrow F{-}CH_2OH + F{-}COOH} \qquad \mathrm{II}$$

Reactions between different partners, F and Ac or F and secondary products,

$$\mathrm{F + Ac \rightarrow FAc + F_2Ac} \qquad \mathrm{III}$$

$$\mathrm{F + DAcAl \rightarrow FAc} \qquad \mathrm{IV}$$

$$\mathrm{F + OM \rightarrow FOM\ (?) + FAc} \qquad \mathrm{V}$$

$$\mathrm{F + FAc \rightarrow F_2Ac} \qquad \mathrm{VI}$$

Reactions with polymer formation,

$$\left.\begin{array}{l} \mathrm{F} \rightarrow \\ \mathrm{FAc} \rightarrow \\ \mathrm{F_2Ac} \rightarrow \\ \mathrm{FOM\ (?)} \rightarrow \end{array}\right\} \text{lower polymers} \qquad \mathrm{VII}$$

The proportion between these reactions, respectively between the compounds obtained, depends on : the F/Ac/NaOH molar ratio, the temperature and reaction time, the solvent absence or presence, the solvent nature and quantity, the order in which reagents have been introduced.

In the condensation reaction, F_2Ac is found to occur even in the conditions of FAc preferential formation, i.e. at a 1F/1Ac molar ratio. This means that the reaction rate of the F_2Ac formation is higher than for FAc or that an intermediate product appears in the reaction, favouring the formation of FAc or of F_2Ac.

The authors feel that the second hypothesis is more likely and that the intermediate product is the FAc anion, formed by means of the acetone anion :

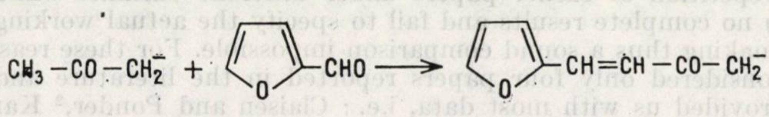
CH3—CO—CH3 + B → CH3—CO—CH2⁻ + BH⁺
CH3—CO—CH2⁻ + O CHO → O CH=CH—CO—CH2⁻

The FAc anion is less stable in water than in alcohol and therefore F_2Ac will almost exclusively form in alcohol :

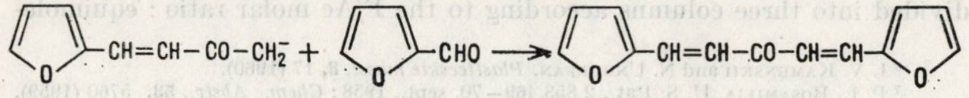

The authors show that for a F/Ac stoichiometric ratio at temperatures of 75—85°, with small NaOH amounts and a short reaction time, the reaction can be conducted towards FAc formation (60—70%) in the presence of water and towards F_2Ac (80%) in the presence of alcohol.

2. OWN INVESTIGATIONS IN VIEW OF ESTABLISHING THE REACTION MECHANISM

In view of establishing the mechanism of F condensation reaction with Ac in the NaOH catalysis, we had to start from a correlation of furfural and acetone reactivities, and also of the compounds resulted from the FAc and F_2Ac reaction, with the reaction medium, the temperature and the catalyst, taking also into account the experimental results reported in published papers.

It was necessary to correlate as many experimental data as possible with our results and observations made during the synthesis, the processing of the total condensation product, the vacuum distillation and also on the behaviour of the distilled products immediately and over time.

Accordingly, we had to develop a critical study of the data published in the literature on this reaction, and to correlate them with the structure and reactivity of reagents, of the reaction compounds and with the factors involved in the reaction.

This approach was necessary as the known mechanisms were general and could not explain the multitude of experimental data which were different and apparently unrelated to each other. Likewise, it is impossible to explain the difficulties encountered in monomers separation and purification, which have direct consequences on their stability and physico-chemical properties.

For these reasons, the study will begin with a systematization and interpretation of our own experimental results and of the most representative ones reported in the literature, in view of emphasizing the influence of the factors on which the multitude of experimental data depends.

3. SYSTEMATIZATION AND INTERPRETATION OF EXPERIMENTAL RESULTS

A critical study of the available papers has shown that some of them are a repetition of earlier papers under different variants while others contain no complete results and fail to specify the actual working conditions, making thus a sound comparison impossible. For these reasons, we have considered only four papers reported in the literature and which have provided us with most data, i.e. : Claisen and Ponder,[2] Kamenskii and Ungurean,[6] Isăcescu and Gavăt [4] and Rosamilia.[7] Our own experimental results were added to these papers.

The results found in these papers are given in a general table (Table 1) divided into three columns according to the F/Ac molar ratio : equimolecular, excess acetone and excess furfural. This presentation is made as a function of two temperature ranges : 10—20° and 70—80°. Each temperature range is presented in relation to two NaOH molar proportions : small amounts of thousandths and hundredths of a mole and larger amounts of tenths of a mole. For each hydroxide proportion, the results are presented in relation to the influence of small water amounts in the NaOH solution, of large added water amounts, of excess acetone and of ethyl alcohol as a solvent. The reaction in phenol medium is presented for one single experiment.[4]

---

[6] I. V. Kamenskii and N. Ungurean, *Plasticeskie massi*, **8,** 17 (1960).

[7] P. L. Rosamilia, U. S. Pat., 2.853.469—70, sept., 1958 ; *Chem. Abstr.*, **53,** 5760 (1959).

In view of better emphasizing the experimental results reported in papers, they have not been presented under an ordinary percent form or in grams, but rather expressed in furfural moles corresponding to the FAc and F_2Ac formation, as free furfural or as polymers, relative to 1 mole of furfural involved in the reaction.

A cursory inspection of the table reveals a large number of blank blocks, which show the lack of a systematic study. Even the available data are complete only for a part of the experiments.

In an attempt to draw the necessary conclusions for establishing the reaction mechanism, we have completed the table with data obtained by our own experiments, on the influence of water and of temperature on the NaOH catalytic action and also on the influence of NaOH taken in similar amounts as those mentioned in the papers written by Kamenskii,[6] Rosamilia [7] and Isăcescu.[4] These data were missing from the table in the case of the F/Ac equimolecular reaction in aqueous medium.

The following findings result from the data given in table 1 :

(*a*) — regardless of the F/Ac/NaOH molar ratio, the monomer formation reaction occurs for F/Ac equimolecular ratio in which only a part furfural (0.5—0.75 moles) is converted into FAc and F_2Ac and the remaining furfural is either free or under the form of polymers ;

(*b*) — in general, F_2Ac forms alongside with FAc and vice-versa, in various proportions, even for a F/Ac equimolecular ratio, which is exclusively for FAc formation (experiment 1a, 3a table 1) ;

(*c*) — exceptions are : the exclusive FAc formation with high excess water (experiment 14 a), with excess water and acetone (experiment 14 b), and with excess acetone (experiment 4 b, 13) ; the exclusive F_2Ac formation in a medium of ethyl alcohol (experiment 15) or a marked F_2Ac preponderance (experiment 27 a, b, c) in an alcohol medium.

CONCLUSIONS

A systematization of our own experimental data and of data found in the literature on the F condensation reaction with Ac in the NaOH catalysis has shown that a large number of experimental results are obtained in this reaction and that they cannot be explained by the known reaction mechanisms already reported in the literature.

All these findings have evidenced the need to establish a reaction mechanism which may explain the catalytic action of sodium hydroxide and the solvent role in conducting the reaction so as to obtain a large and varied number of results, as a function of the working conditions.

Revue Roumaine de Chimie, **23**, *5*, 667–671 (1978)

THERMODYNAMIC PROPERTIES OF BINARY LIQUID MIXTURES

RANANJAY SINGH, SHEO PRAKASH and OM PRAKASH
Chemistry Department, University of Allahabad, Allahabad — India

Received February 28, 1976

Ultrasound velocities, densities, adiabatic compressibilities, intermolecular free lengths, available volumes and free volumes have been computed in four binary liquid-liquid solutions of toluene and cyclohexane in benzene at 20° and of toluene and benzene in chlorobenzene at 30°. The deviations of these properties from the rectilinear nature have been explained on the basis of molecular interaction between the components of the mixtures.

INTRODUCTION

A number of papers [1–7] appeared on the measurements of ultrasound velocity and adiabatic compressibility of binary liquid-liquid mixtures. Kaulgud [4,8] and Reddy et al.[9] have calculated the excess free lengths using the Jacobson's[10] expression. Deshpande and Bhatgadde, [11] Srivastava et al.[12] have published their results on free volume and have demonstrated the existence of molecular interactions in the systems. Recently Prakash et al.[13] have explained the causes of deviations from ideal behaviour with the help of their data on intermolecular free length in binary mixtures.

In the present investigation we are presenting our results of ultrasound velocity (v_L), density (ρ), adiabatic compressibility (β), intermolecular free length (L_f), available volume (V_a) and free volume (V_f) for liquid-

---

[1] I. G. Mikhailov, *Doklady Akad. Nauk. S.S.S.R.*, **81**, 779 (1951).

[2] I. Gabriel and G. Poianni, *Ricerca Sci.*, **24**, 1039 (1954).

[3] K. C. Reddy, S. V. Subrahmanyam and J. Bhimsenachar, *Trans. Faraday Soc.*, **58**, 2352 (1962).

[4] M. V. Kaulgud, *Z. phys. Chem. (Frankfurt)*, **36**, 384 (1963).

[5] R. J. Fort and W. R. Moore, *Trans. Faraday Soc.* **61**, 2102 (1965).

[6] S. Prakash and S. B. Srivastava, *J. Chem. Thermodynamics*, **7**, 997 (1975).

[7] H. Suckmann and A. Bockzek, *Z. phys. Chem. (Frankfurt)*, **29**, 329 (1961).

[8] M. V. Kaulgud, *Acustica*, **10**, 316 (1960).

[9] K. C. Reddy, S. V. Subrahmanyam and J. Bhimsenachar, *J. Phys. Soc. Japan*, **91**, 559 (1964).

[10] B. Jacobson, *Acta Chem. Scand.*, **6**, 1485 (1952).

[11] D. D. Deshpande and L. G. Bhatgadde, *J. Phys. Chem.*, **72**, 261 (1968).

[12] S. B. Srivastava, S. Prakash and O. Prakash, *J. Chim. phys.*, **72**, 115 (1975).

[13] S. Prakash, S. B. Srivastava and O. Prakash, *Ind. J. Pure & Appl. Phys.* **13**, 191 (1975).

liquid binary mixtures of I benzene (A)-toluene (B), II benzene (A)-cyclohexane (B) at 20°, III benzene (A)-chlorobenzene (B) and IV toluene (A)-chlorobenzene (B) at 30°.

EQUATIONS USED FOR CALCULATIONS

The various parameters have been calculated with the help of the following established relations

$$\beta = \frac{1}{v_L^2 \cdot \rho} \tag{1}$$

$$L_f = K \cdot \beta^{1/2} \tag{2}$$

$$V_a = V\left(1 - \frac{v_L}{v_\infty}\right) \tag{3}$$

$$V_f = V\left(\frac{V_g}{v_L}\right)^3 \tag{4}$$

where K is the temperature dependent constant given by Jacobson,[10] $v_\infty = 1600$ m/s, V is the experimental molar volume and v_g is the sound velocity in the vapour phase of the liquid and has been calculated theoretically using the expression

$$v_g = \left[\frac{C_p}{C_v} \cdot \frac{RT}{M}\left\{1 + \frac{9}{128} \cdot \frac{P}{P_c} \cdot \frac{T_c}{T}\left(1 - 6\,\frac{T_c^2}{T^2}\right)\right\}\right]^{1/2} \tag{5}$$

C_p and C_v of the vapours can be calculated by expressions used by Dobratz.[14]

$$C_p = C_v + R\left[1 + \frac{81}{32}\frac{P}{P_c}\left(\frac{T_c}{T}\right)^3\right] \tag{6}$$

and

$$C_v = 3R + \frac{aR}{2} + \sum q_i C_{\nu i} + \frac{3n - 6 - a - \sum q_i}{\sum q_i} \sum q_i C_{\delta i} \tag{7}$$

where a = number of bonds in the molecule permitting free rotations of groups, n = number of atoms in the molecule and q_i = number of bonds of ith type. $C_{\nu i}$ and $C_{\delta i}$ are the Einstein functions at frequencies ν_i and δ_i respectively for the ith type of bonds and are calculated by the quadratic equation of the form

$$C = A + BT + CT^2 \tag{8}$$

---

[14] C. J. Dobratz, *Ind. Eng. Chem.* **33**, 759 (1941).

suggested by Fugassi and Rudy[15] where A, B and C are the constants for different bonding frequencies and are given in a table.[14] v_g in mixture of liquid vapours has been assumed to be additive after some approximations.

EXPERIMENTAL

Debye and Sears[16] light diffraction method has been used for the measurement of ultrasound velocity in the liquid systems. Sound waves were generated at frequency of 5MHz from a generator comprising a gold plated quartz crystal, 2.54 cm in diameter. The test solution was kept in a specially designed cell. The diffraction patterns were photographed and the fringe widths were measured by a travelling microscope made by M/s. Adam Hilga Ltd., London, with a least count of 1×10^{-4} cm.

The liquids used were of AR(BDH) grade and were distilled and purified by standard methods. Densities were measured with the help of a double walled pyknometer and agreed closely with the literature values. Binary solutions of different compositions were prepared by mixing the required volumes of the components in cleaned and dried flasks. The solutions were kept for some time for stabilisation. The cell was thermostated to keep the temperature constant within ±0.1°. The probable error in the measurement of velocity was ±0.15 per cent.

RESULTS AND DISCUSSIONS

The data on sound velocity, density, compressibility, free length, available volume and free volume have been presented in the form of graph. The velocity and compressibility changes with the change in mole fraction of component A of the mixture have been shown in Figure 1. The velocity decreases linearly in I, a little nonlinear increase in III and IV and nonlinear increase in II has been found. The compressibility increases nonlinearly in III and IV and this peculiar behaviour is due to the density of the mixtures which decreases continuously.

Figure 2 is a plot of intermolecular free length and available volume against the composition of the solution. For system I the curve for L_f is linear while for others it is nonlinear. The available volume curves are nonlinear for all of them.

The density and free volume have been plotted in Figure 3. The density decreases in III and IV but increases in I and II. The free volume changes from the ideal behaviour are not important.

The above curves give us the idea about the deviation in above properties from the law of additivity. These deviations actually give the values of the excess properties. The excess values for the system I are extremely low, showing there is not much deviation from ideality. The excess compressibility and excess free length are negative in III and IV but + ve in II. The available volume values change their sign from + ve to − ve in III whereas it is +ve in II and IV. The excess free volume is −ve in III and IV and +ve in II. The results for benzene-cyclohexane agree with those of Piotrowska.[17]

---

[15] P. Fugassi and C. E. Rudy, *Ibid*, **30**, 1029 (1938).

[16] P. Debye, and F. Sears, *Proc. Nat.Acad. Sci. U.S.A.*, **18**, 410 (1932).

[17] A. Piotrowska, *Roczniki Chem.*, **39**, 53 (1965).

Fort and Moore,[5] Deshpande and Bhatgadde[11] and Prakash et al[13] have interpreted that the sign and magnitude of the excess values of above properties determine the strength of interaction between the components of the mixtures. The interaction increases with the increasing negative value. It appears there is no interaction between the components of system I but in the other three, the values support the existence of an interaction which may be of more than one type. The existence of weak dipolar interaction between components of mixtures benzene-chlorobenzene and toluene-chlorobenzene has been demonstrated by Nigam and Singh[18] on the basis of their viscosity values.

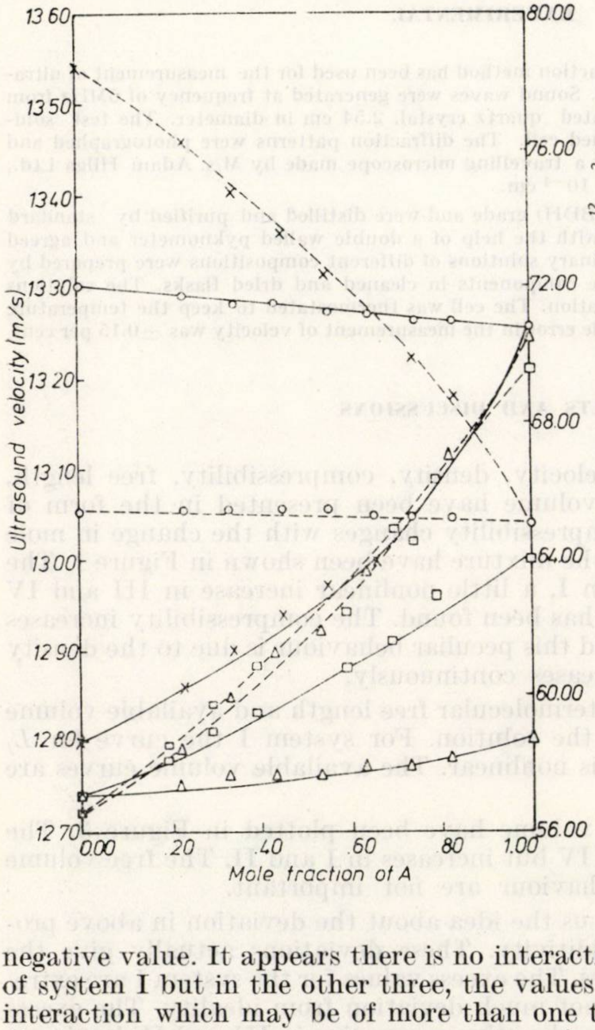

Fig. 1. — Mole fraction vs. ultrasonic velocity and adiabatic compressibility:

—O—O— Benzene + Toluene;

—×—×— Benzene + Cyclohexane;

△ △ Benzene + Chlorobenzene;

—□—□— Toluene + Chlorobenzene;

———— Velocity of ultrasound;

············ adiabatic compressibility.

ACKNOWLEDGEMENT. The financial assistance provided by the State Counci of Scientific and Industrial Research, U.P. is gratefully acknowledged.

---

[18] R. K. Nigam and P. P. Singh, *Indian J. Chem.*, **9**, 691 (1971).

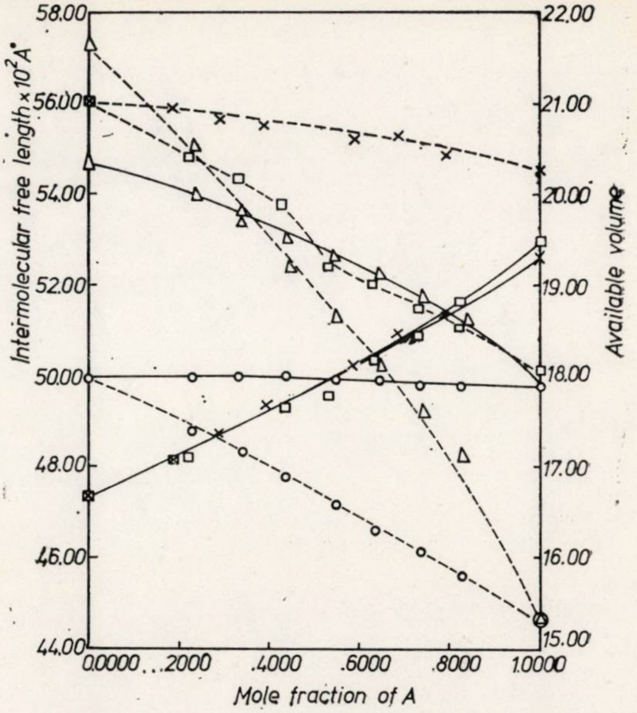

Fig. 2. — Mole fraction vs. intermolecular free length and available volume :

—○—○— Benzene + Toluene ;
—△—△— Benzene + Cyclohexane ;
—□—□— Benzene + Chlorobenzene ;
—×—×— Toluene + Chlorobenzene
———— Intermolecular free length ;
------------ Available volume.

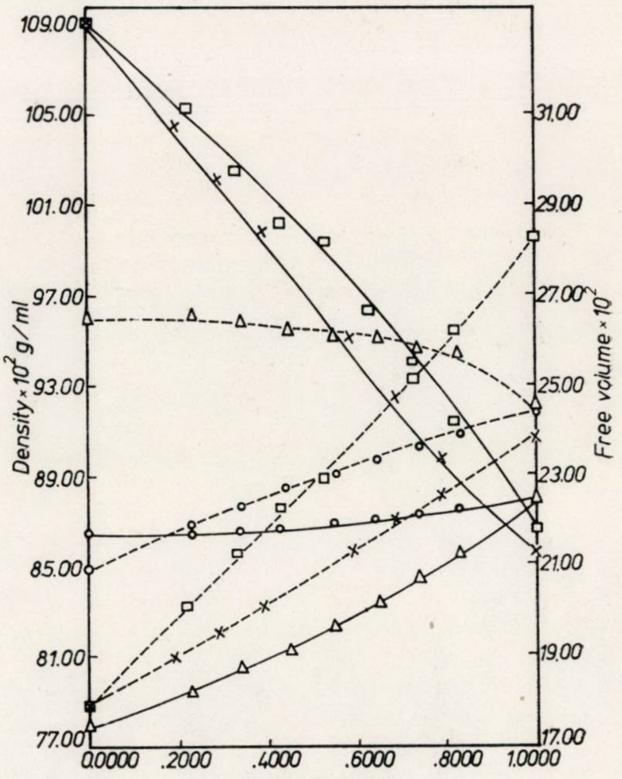

Fig. 3. — Mole fraction vs. density and free volume :

—○—○— Benzene + Toluene ;
—△—△— Benzene + Cyclohexane ;
—□—□— Benzene + Chlorobenzene ;
—×—×— Toluene + Chlorobenzene ;
———— Density ;
------------ Free Volume.

Revue Roumaine de Chimie, 23, 5, 673–679 (1978)

ANODIC OXIDATION OF CYCLOHEXANOL

ELENA CONSTANTINESCU and VIOREL BRÎNZOI
Institute of Chemistry, Faculty of Chemistry,
Department of Physical Chemistry, Bd. Republicii 13, Bucharest, Romania

Received November 19, 1975

Using the potentiostatic method and smooth platinum electrodes the anodic oxidation of cyclohexanol in 1N H_2SO_4 was studied. The analysis of the current-potential curves led to some discussions concerning the mechanism of electrochemical oxidation of the alcohol.

INTRODUCTION

Following our studies[1] on the anodic oxidation of the alcohols we present the results obtained with cyclohexanol. This alcohol has been chosen, taking into account the few studies dedicated to the anodic behaviour of secondary alcohols.[2,3]

There is only one literature reference about cyclohexanol i.e. the paper of Horany and co-workers[3] who applied the galvanostatic method.

Owing to the fact that the potentiostatic method is more suitable for the investigations of anodic oxidation, we used it imposing a linear potential increase in a range of potential : (-200 mV) – ($+1400$ mV) either single sweep or in cycles.

EXPERIMENTAL

Cell and electrodes. The experiments were carried out in an electrolytic glass cell with separate anodic and cathodic compartments on a smooth platinum electrode with a geometrical area of 1 cm^2. As counter and reference electrodes, a platinum wire of about 0.8 mm Ø and the saturated calomel electrode were respectively used. The working and the reference electrodes were connected by a Haber Luggin capillary (Figure 1).

Instrumentation. The smooth platinum electrode was controlled, varied and measured by means of a Tacussel potentiostatic equipment made up of a PRT 20–2 potentiostat, a 9/A Servovit automatic pilot and a S 6/G4R millivoltmeter. The current-potential curves were obtained by means of a Graphispot recording galvanometer.

---

[1] E. Constantinescu and V. Brînzoi, *Rev. Roumaine Chim.*, **673**, 000 (1976).

[2] E. I. Sokolova, S. V. Kalcheva and S. N. Raicheva, *Doklady Bolg. Akad. Nauk.* **26**, 383 (1973).

[3] G. Horany, P. Konig and J. Telcs, *Acta Chim. Acad. Sci. Hung.*, **72**, 165 (1972).

Reagens. The solutions have been prepared from p.a. reagens and twice distilled water. The supporting electrolyte was 1N H_2SO_4.

In order to keep the solutions away from air contamination, pure argon was bubbled through the electrolytic cell.

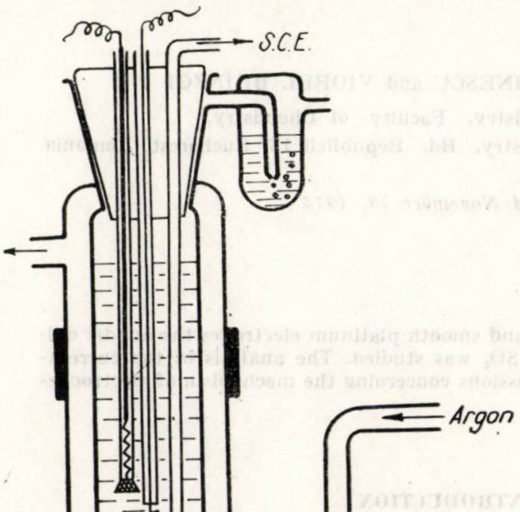

Fig. 1. — Electrolytic cell.

RESULTS

The cyclic voltammograms show that in the case of anodic oxidation of cyclohexanol (Figure 2, curve *2*), in our experimental conditions, two peaks appear in the same range as the oxidation of the adsorbed hydrogen and the formation of oxide layer on the electrode's surface, the former being approximately identical and the latter higher than in the case of the basic solution 1N H_2SO_4 (Figure 2, curve *1*).

CYCLOHEXANOL OXIDATION RATE DEPENDENCE ON CONCENTRATION

There has been analysed the dependence of the oxidation rate on cyclohexanol concentration.

The concentrations in cyclohexanol were the following: 0.01M, 0.05M, 0.08M and 0.1M.

For simplicity there have been indicated only the final curves portions i/E recorded in experimental conditions (25°, voltage sweep rate v of 800 mV/mn in the presence of pure argon) identical to those of the basic electrolytic solution.

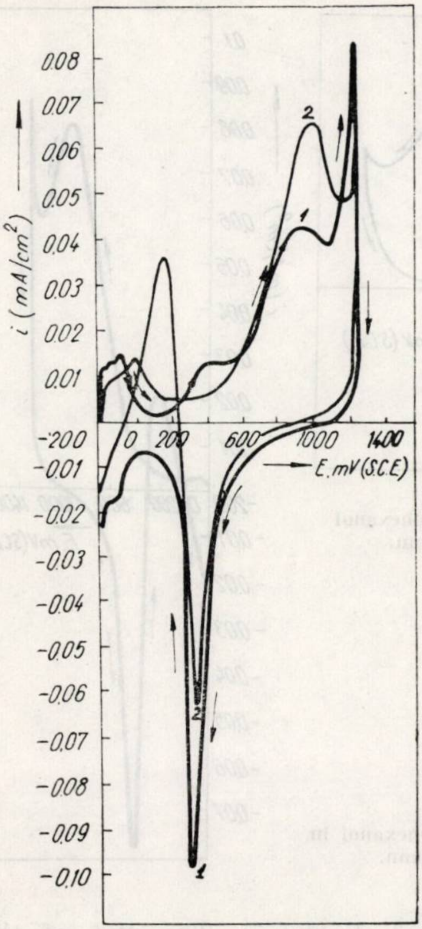

Fig. 2. — Cyclic voltammograms for 0.01M cyclohexanol in 1N H_2SO_4 (curve *2*) and for 1N H_2SO_4 (curve *1*) at 25 ± 0.1° and a voltage sweep rate of 800 mV/mn.

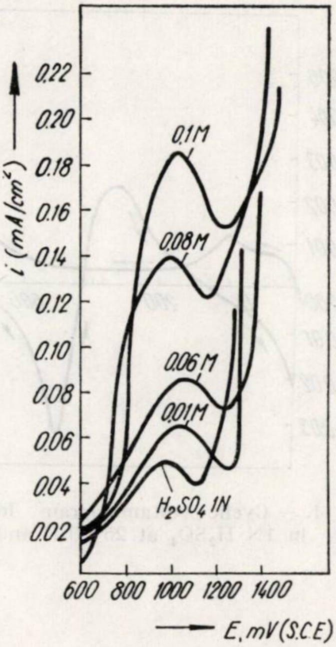

Fig. 3. — Curent-potential curves for cyclohexanol at 25 ± 0.1° and a voltage sweep rate of 800 mV/mn.

The height of the peak current-density i_p increases with the alcohol concentration thus proving the oxidation of the organic compound.

The potential corresponding to the peak current-density E_p lies within the same range of potential : (+950 mV) — (+1050 mV) (S.C.E.) irrespective of cyclohexanol concentration (Figure 3).

CYCLOHEXANOL OXIDATION RATE DEPENDENCE ON VOLTAGE SWEEP RATE

The experiments have been carried out with 0.01 M and 0.2 M cyclohexanol at the following voltage sweep rates : 400 mV/mn ; 600 mV/mn ; 800 mV/mn ; 1000 mV/mn and 1100 mV/mn. Figure 4 represents a cyclic voltammogram for a cyclohexanol concentration of 0.01 M and a voltage sweep rate of 400 mV/mn. For $v = 800$ mV/mn see Figure 2. The height of the peak current density increases with the voltage sweep rate, thus

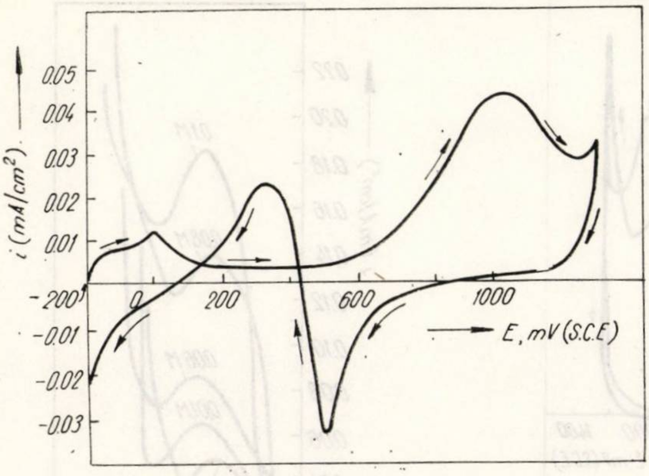

Fig. 4. – Cyclic voltammogram for 0.01M cyclohexanol in 1N H_2SO_4 at 25±0.1° and $v = 400$ mV/mn.

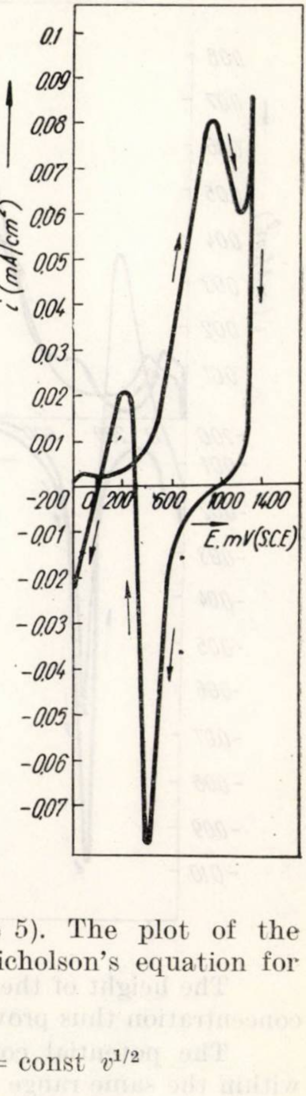

Fig. 5. – Cyclic voltammogram for 0.01M cyclohexanol in 1N H_2SO_4 at 25 ± 0.1° and $v = 1\,100$ mV/mn.

for $v = 1100$ mV/mn, $i_p = 0.080$ mA/cm² (Figure 5). The plot of the i_p vs $v^{1/2}$ gives a linear dependence according to Nicholson's equation for irreversible processes.[4]

$$i_p = 3.10^5 n(RT/b'F)^{1/2} D^{1/2} v^{1/2}\, c \text{ or : } i_p = \text{const } v^{1/2}$$

The experimental data also agree with the following of Nicholson's equations :[5]

$$i_p = (1 - \theta)\,\frac{\beta KF}{RT}\,v\,;\ \text{or}\ i_p = \text{const}.\,v.$$

The rate of oxidation is proportional to voltage sweep rate (Figure 6).

---

[4] R. S. Nicholson, *Analyt. Chem.*, **37**, 1351 (1965).

[5] R. S. Nicholson and I. Shain, *Analyt. Chem.*, **36**, 706 (1964).

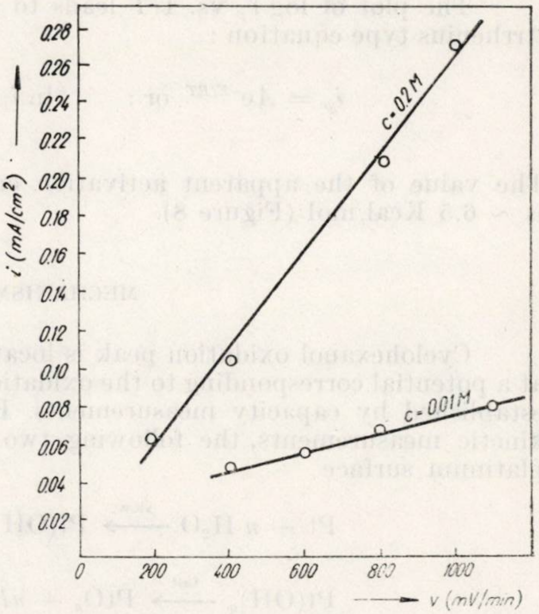

Fig. 6. — The dependence of current-peak density on the voltage sweep rate for 0.2M and 0.01M cyclohexanol in 1N H_2SO_4.

CYCLOHEXANOL OXIDATION RATE DEPENDENCE ON TEMPERATURE

There has been used 0.2 M cyclohexanol at the following temperatures : 25°, 30°, 40°, 50°, 60°, 70°. A growth of the height of peak current density with temperature is noticed ; thus at 25° $i_p = 0.20$ mA/cm² and at 70° it reaches the value $i_p = 0.90$ mA/cm² (Figure 7). The peak lies within the same potential range for all temperatures.

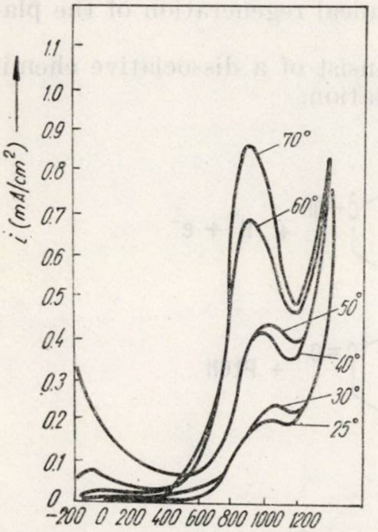

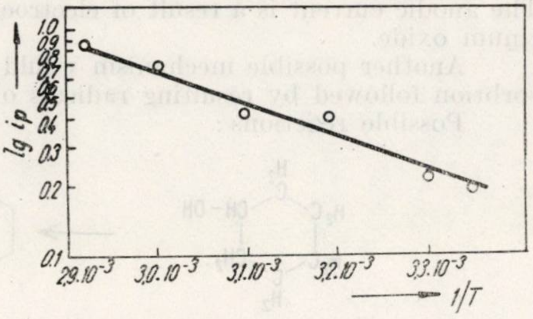

Fig. 8. — The plot log i_p versus $\frac{1}{T}$ for 0.2M cyclohexanol in 1N H_2SO_4.

Fig. 7. — Current-pontential curves for 0.2M cyclohexanol in 1N H_2SO_4 at 25° ; 30° ; 40° ; 50° ; 60° ; 70° and $v = 800$ mV/mn.

The plot of log i_p vs. $1/T$ leads to a straight line, according to an Arrhenius type equation :

$$i_p = A\mathrm{e}^{-E/RT} \quad \text{or :} \qquad \ln i_p = \ln A - \frac{E}{RT}$$

The value of the apparent activation energy calculated from its slope is ~ 6.5 Kcal/mol (Figure 8).

MECHANISM

Cyclohexanol oxidation peak is located on the i/E curves each time at a potential corresponding to the oxidation range of the platinum surface established by capacity measurements. Feldberg[6] suggests, on basis of kinetic measurements, the following two steps oxidation mechanism of platinum surface

$$\mathrm{Pt} + n\,\mathrm{H_2O} \xrightarrow{\text{slow}} \mathrm{Pt(OH)}_n + n\mathrm{H}^+ + ne^-$$

$$\mathrm{Pt(OH)}_n \xrightarrow{\text{fast}} \mathrm{PtO}_n + nH^+ + ne^-$$

Consequently cyclohexanol oxidation could take place by means of platinum oxide, in agreement with the opinion of Bulgarian researchers[2] who consider that alcohol oxidation takes places through a chemical reaction between alcohol and platinum oxide :

$$\mathrm{PtO} + \mathrm{C_6H_{12}O} \rightarrow \mathrm{Pt} + \mathrm{C_6H_{10}O} + \mathrm{H_2O}$$

The anodic current is a result of electrochemical regeneration of the platinum oxide.

Another possible mechanism would consist of a dissociative chemisorbtion followed by resulting radicals oxidation.

Possible reactions :

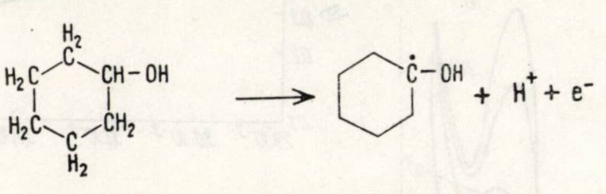

$$\mathrm{PtOH} \longrightarrow \mathrm{PtO} + \mathrm{H}^+ + e^-$$

$$\mathrm{C_6H_{12}O} \longrightarrow \mathrm{C_6H_{10}O} + 2\mathrm{H}^+ + 2\ e^-$$

---

[6] S. W. Feldberg, C. G. Enke and G. E. Breiter, *J. Electrochem. Soc.*, **110**, 826 (1963).

The overall resultant reaction implies two electrons transfer, the final product compound being the corresponding ketone. Ketone presence is illustrated also by Horany [3] in his studies on anodic oxidation of secondary alcohols.

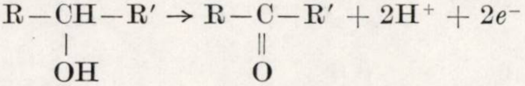

$$\underset{\displaystyle OH}{R-\underset{|}{CH}-R'} \rightarrow \underset{\displaystyle O}{R-\underset{\|}{C}-R'} + 2H^+ + 2e^-$$

If we compare the data for cyclohexanol with those for isopropanol [7] it may be noticed that the last oxidation peaks of the two alcohols situated within the same range of potential (+950 mV) — (+1050 mV) exhibit a quite small difference between the values of peak current densities. Thus, for a 0.2 M concentration, $t = 25°$ and $v = 800$ mV/mn, i_p cyclohexanol $=$ $= 0.22$ mA/cm^2 and i_p isopropanol $= 0.28$ mA/cm^2.

The similarity in electrochemical behaviour of the alcohols shows a common anodic oxidation mechanism which is in good agreement with Bagotzky's [8] dissociative mechanism as a general scheme for organic oxidation.

[7] E. Constantinescu and V. Brînzoi, to be published.

[8] V. S. Bagotzky and Yu. B. Vasilyev, *Electrochim. Acta.*, **9**, 869 (1964); **11**, 1439 (1966).

Revue Roumaine de Chimie, **23**, *5*, 681 – 698 (1978)

METHODS FOR COMPLEX REACTION SYSTEMS EQUILIBRIUM COMPUTATION

RAUL MIHAIL *, CORNELIU V. RADU* and ION M. BELCEA**
* Polytechnic Institute, str. Polizu 1, Bucharest, Romania
** Computing Centre of the Chemical Industry, Spl. Independenţei, 202A, Bucharest, Romania

Received March 6, 1976

Two new procedures are presented for the determination of the chemical equilibrium composition of the complex mixtures by the minimization of the free energy function : a method which differs in principle from those previously described in literature, having a high degree of generality based on Newton's method, and another one which is an improvement of the steepest descent technique application, increasing the precision of calculus and reducing by 10 times the calculation time. Both procedures eliminate the material balance restriction in input data. Results were checked with data from literature, obtained by the minimization method, in the case of hydrazine combustion or by equilibrium constants method, in the case of isopenthane dehydrogenation to isoprene. The agreement is good.

1. INTRODUCTION

The calculation of the chemical reaction equilibrium compositions by the free energy function minimization has been significantly expanded, ever since 1958, when the method was introduced by White, Johnson and Dantzig.[1] The merits of the method are obvious in the case of complex reaction systems, whose many components are simultaneously participating in several reactions. Compared to the other calculus alternative, the method of equilibrium constants, the free energy function minimization requires neither the formulation of the chemical reactions occurring, nor the singling out of certain (or several) molecular species in view of their mathematical processing (algebraic elimination, successive permutation, etc.), the effort imposed on the digital computer being thus smaller. All the same, the literature is pretty poor in presenting the application of the method to some definitely concrete cases of higher complexity, when the method peculiarities and the eventual improvements likely to occur are made more conspicuous.

On the basis of such considerations the aim of this work is many-sided : 1) to show that the initially formulated question of the free energy function minimization falls into the more general class of obtaining one function minimum, by suggesting a new algorithm of the equilibrium composition calculation by the given functional Newton iteration ; 2) to discuss the original solution convergence quality ; 3) to suggest convergence acceleration improved procedures concomitantly with some restriction removal ; 4) to compare the characteristics of the alternatives displayed by the equilibrium composition calculation of the isopenthane dehydrogenation reaction to isoprene, an example selected because it enables reference to the results obtained by the equilibrium constants method, reported in the literature.

---

[1] W. B. White, S. M. Johnson and G. B. Dantzig, *J. Chem. Phys.*, **28**, 751 (1958).

2. FREE ENERGY FUNCTION

The standard molar free energy function F°/RT, is preferred as minimization object instead of the free energy, on account of its fairly slight variation with temperature, allowing for interpolations.[2] The function is scheduled,[3] as such, or it can be calculated from relation $\Delta F = \Delta H - T\Delta S$, also scheduled.[3]

The free energy of a system made up of n chemical species containing x_i moles of species i is expressed as below :

$$F(\mathbf{X}) = \sum_{i=1}^{n} x_i f_i \tag{1}$$

where :

$\mathbf{X} = (x_1, x_2, \ldots, x_n)$ is the composition row vector ;

$$f_i = x_i(c_i + \ln x_i/\bar{x}) \tag{2}$$

$$c_i = (F^0/RT)_i + \ln P ;$$

P = total pressure of the system, atm ;

$$\bar{x} = \sum_{i=1}^{n} x_i \tag{3}$$

The determination of the system equilibrium composition consists in finding a vector $\mathbf{X}$, with non-negative components x_i minimizing (1) and satisfying the following condition of mass conservation :

$$\sum_{i=1}^{n} a_{ij}\, x_i = b_j \qquad j = 1, 2, 3, \ldots, m \tag{4}$$

In the last relation, m is the number of the atomic species available in the system, a_{ij} is a code representing the atom number of element j in species i molecule, whereas b_j is the total number of element j atomic mass, initially present in the system. The a_{ij} terms can form a matrix of a rank equal or smaller than m; only the first alternative, to which the second one can also be reduced with certain logistics will be further considered.

---

[2] K. Suryanarayana, P. H. Reddy and P. S. Murti, *J. Canad. Chem. Eng.*, **49**, 369 (1971).

[3] A. A. Vvedenskii, "Termodinamiceskie rasceti neftehimiceskih proțessov", Gostoptehizdat, Moskva, 1960.

The partial derivatives of the function (1) appear in any of the minimization methods displayed herein, as:

$$\frac{\partial F(\mathbf{X})}{\partial x_i} = c_i + \ln \frac{x_i}{\bar{x}}$$

$$\frac{\partial^2 F(\mathbf{X})}{\partial x_i \partial x_k} = \frac{\bar{x}\,\delta_{ik} - x_i}{x_i\,\bar{x}}$$

where

$$\delta_{ik} = \frac{\partial x_i}{\partial x_k} = \begin{cases} 0 & \text{for } i \neq k \\ 1 & \text{for } i = k \end{cases}$$

is Kronecker's symbol.

3. A GENERAL PROCEDURE FOR THE FREE ENERGY FUNCTION MINIMIZATION

Let us minimize the function

$$F = \sum_{i=1}^{n} (c_j + \ln x_j - \ln \bar{x})\, x_i \tag{5}$$

so that the following restrictions be checked:

$$f_j = \sum_{i=1}^{n} a_{ij}\, x_i - b_j \qquad j = 1, 2, \ldots, m \tag{6}$$

This assumes to find the minimum of the function:

$$\Phi = F + \sum_{j=1}^{m} \lambda_j f_j \tag{7}$$

At the minimum, the conditions given below are to be met:

$$\frac{\partial \Phi}{\partial x_i} = 0, \qquad (i = 1, 2, \ldots, n) \begin{cases} \dfrac{\partial F}{\partial x_i} = 0 \Rightarrow \text{minimum} \\[2ex] \dfrac{\partial f_j}{\partial x_i} = 0 \Rightarrow \text{shifting on surface} \end{cases} \tag{8}$$

$$\frac{\partial \Phi}{\partial \lambda_j} = 0, \; (j = 1, 2, \ldots, m) \Rightarrow \text{surface checking } (f_j = 0) \tag{9}$$

Partial derivatives are

$$\frac{\partial F}{\partial x_k} = c_k + \ln \frac{x_k}{x} \tag{10}$$

$$\frac{\partial f_j}{\partial x_k} = a_{jk} \tag{11}$$

By substituting in (8), (9) one gets :

$$\frac{\partial \Phi}{\partial x_k} = c_k + \ln \frac{x_k}{\bar{x}} \sum_{j=1}^{m} \lambda_j \, a_{jk} = 0 \tag{12}$$

$$\frac{\partial \Phi}{\partial \lambda_k} = \sum_{i=1}^{n} a_{ki} \, x_i - b_k = 0 \tag{13}$$

The following notation was adopted :

$$\mathbf{Y} = (x_1, \, x_2, \, \ldots, \, x_n, \; \lambda_1, \; \lambda_2, \, \ldots, \, \lambda_m) = (y_1, \; y_2, \, \ldots, \, y_p) \tag{14}$$

$$p = n + m$$

whereas relations (12), (13) become

$$\Psi_k = c_k + \ln y_k - \ln \bar{Y} + \sum_{i=n+1}^{p} y_i \, a_{i-n,k} = 0, \tag{15}$$

$$k = 1, \, 2, \, \ldots, \, n$$

$$\Psi_k = \sum_{i=1}^{n} a_{k-n,i} \, y_i - b_{k-n} = 0, \quad k = n + 1, \ldots, p \tag{16}$$

In relation (15) it was assumed : $\bar{Y} = \sum_{i=1}^{n} y_i$.

In order to find the minimum value, the equation set (15), (16) should be solved.

Newton's generalized method can be used :

$$\sum_{i=1}^{p} \frac{\partial \Psi_k}{\partial x_i} \, dx_i = -\Psi_k(\mathbf{X}_0), \qquad k = 1, \, 2, \, \ldots, \, p \tag{17}$$

In this case, the general equation (17) should be written as :
— for (15) :

$$\sum_{i=1}^{p}\left(\frac{\delta_{ik}}{y_k}-\frac{\sum_{j=1}^{n}\delta_{ij}}{\overline{Y}}+\sum_{j=n+1}^{p}\delta_{ij}\,a_{j-n,k}\right)\mathrm{d}y_i=$$

$$=-\left(c_k+\ln y_k-\ln\overline{Y}+\sum_{j=n+1}^{p}y_j\,a_{j-n,k}\right),\qquad k=1,\,2,\,\ldots,\,n \tag{18}$$

— for (16) :

$$\sum_{i=1}^{p}\left(\sum_{j=1}^{n}a_{kj}\,\delta_{ij}\right)\mathrm{d}y_i=-\left(\sum_{j=1}^{n}a_{kj}\,y_j-b_k\right) \tag{19}$$

The system made up of the last two equations can be written in a matrix form. The matrix where the unknown quantitities $\mathrm{d}y_i$, referred to in the convergence condition, are not written, can be partitioned :

$$\begin{array}{l|l|l}
\left(\frac{1}{y_1}-\frac{1}{\overline{Y}}\right),\ -\frac{1}{\overline{Y}},\ldots,-\frac{1}{\overline{Y}}, & a_{11},\,a_{21},\,\ldots,\,a_{m1}, & \begin{array}{l}c_1+y_1-\ln\overline{Y}+\\ \quad+a_{11}\,y_{n+1}+\ldots\\ \quad+a_{m1}\,y_{n+m}\end{array}\\
-\frac{1}{\overline{Y}},\ \left(\frac{1}{y_2}-\frac{1}{\overline{Y}}\right),\ldots,-\frac{1}{\overline{Y}}, & \quad\ldots\ldots & \quad\ldots\ldots\\
\cdot & & \\
\cdot & & \\
\cdot & & \\
-\frac{1}{\overline{Y}},-\frac{1}{\overline{Y}},\ldots,\left(\frac{1}{y_n}-\frac{1}{\overline{Y}}\right), & a_{1n},\,a_{2n},\,\ldots,\,a_{mn}, & \begin{array}{l}c_n+y_n-\ln\overline{Y}+\\ \quad+a_{1n}\,y_{n+1}+\ldots\\ \quad+a_{mn}\,y_{n+m}\end{array}\\
\hline
a_{11},\,a_{12},\,\ldots\qquad,\,a_{1n}, & 0,\,0,\,\ldots,\,0, & \begin{array}{l}a_{11}y_1+a_{12}y_2+\\ \quad+\ldots+a_{1n}y_n\end{array}\\
a_{21},\,a_{22},\,\ldots\qquad,\,a_{2n}, & 0,\,0,\,\ldots,\,0, & \begin{array}{l}a_{21}y_1+a_{22}y_2+\\ \quad+\ldots+a_{2n}y_n\end{array}\\
\cdot & & \\
\cdot & & \\
\cdot & & \\
a_{m1},\,a_{m2},\,\ldots\quad,\,a_{mn}, & 0,\,0,\,\ldots,\,0, & \begin{array}{l}a_{m1}y_1+a_{m2}y_2+\\ \quad+\ldots+a_{mn}y_n\end{array}
\end{array}$$

or :

$$\begin{array}{c|c|c}\mathbf{A} & \mathbf{B} & \mathbf{C}\\ \hline \mathbf{D} & \mathbf{E} & \mathbf{F}\end{array} \tag{21}$$

WORKING PROCEDURE

1. At first any positive solution $\mathbf{Y} = (y_1, y_2, \ldots, y_n)$ is assumed.
2. The input data values are assigned to the elements of the matrix in **B**, **D**, **E**.
3. Then the elements of matrix in **A**, **C**, **F** are calculated by (18), (19).
4. The set obtained thus is solved.
5. It is checked whether the minimum value, $dy_i \leqslant \varepsilon$, is attained; if so, it is continued with 7, if not with 6.
6. The following approximation $y_i^1 = y_i^0 + dy_i$ is computed and it continues with 3.
7. The final results are calculated with values $(y_1, y_2, \ldots, y_n)$.

4. WHITE'S METHOD AND SOME OF ITS CHARACTERISTICS

Starting with any set of positive values:

$$\mathbf{Y} = (y_1,\ y_2,\ \ldots,\ y_n) \tag{22}$$

which fulfil the mass balance equation (4) and considering relation (1) the free energy of the mixture can be expressed as follows:

$$F(\mathbf{X}) = \sum_{i=1}^{n} y_i\, c_i + \sum_{i=1}^{n} y_i \ln y_i - \sum_{i=1}^{n} y_i \ln \bar{y} \tag{23}$$

where:

$$\bar{y} = \sum_{i=1}^{n} y_i \tag{24}$$

Let be: $\Delta_i = x_i - y_i$ and $\bar{\Delta} = \bar{x} - \bar{y}$ (25)

Function $F(\mathbf{Y})$ can be approximated around the point $\mathbf{Y}$ by Taylor's series expansion of which only the first three terms are retained:

$$Q(\mathbf{X}) = F(\mathbf{Y}) + \sum_{i=1}^{n} \frac{\partial F}{\partial x_i}\bigg|_{\mathbf{X}=\mathbf{Y}} \Delta_i + \frac{1}{2\,!} \sum_{i=1}^{n} \sum_{k=1}^{n} \frac{\partial^2 F}{\partial x_i \partial x_k}\bigg|_{\mathbf{X}=\mathbf{Y}} \Delta_i\, \Delta_k \tag{26}$$

By substituting the partial derivatives in relation (26) one obtains:

$$Q(\mathbf{X}) = F(\mathbf{Y}) + \sum_{i=1}^{n} (c_i + \ln y_i - \ln \bar{y})\, \Delta_i + \frac{1}{2} \sum_{i=1}^{n} y_i \left(\frac{\Delta_i}{y_i} - \frac{\bar{\Delta}}{\bar{y}} \right)^2 \tag{27}$$

Since the partial derivatives are non-negative, it results that both $F(\mathbf{X})$ and $Q(\mathbf{X})$ are convex, therefore there is a minimum.

To find the next approximation of the searched solution, min $Q(\mathbf{X})$ is searched with the restrictions:

— material balances (4);

— substance existence $x_i > 0, i = 1, 2, \ldots, n$.

For thus purpose one resorts to the Lagrange multiplier technique generally used to find the extreme value of a function of several variables, when there are still certain additional relations (of type (4)) among the variables.

i.e.

$$G(\mathbf{X}) = Q(\mathbf{X}) + \sum_{j=1}^{m} \pi_j \left(- \sum_{i=1}^{n} a_{ij}\, x_i + b_j \right) \tag{28}$$

where π_j are Lagrange multipliers.

$G(\mathbf{X})$ function minimum is to be found in the point, in which

$$\frac{\partial G(\mathbf{X})}{\partial x_i} = 0 \qquad i = 1, 2, \ldots, n \tag{29}$$

or

$$\frac{\partial G(\mathbf{X})}{\partial x_i} = c_i + \ln \frac{y_i}{\bar{y}} + \frac{x_i}{y_i} - \frac{\bar{x}}{\bar{y}} - \sum_{j=1}^{m} \pi_j\, a_{ij} \tag{30}$$

Equations (3), (4) and (30) form a set of $1 + m + n$ equations with $n + m + 1$ unknown values : $x_1, x_2, \ldots, x_n, \pi_1, \pi_2, \ldots, \pi_m, \bar{x}$.

The multipliers'determination is performed thus :

— as $y_i > 0$, equation (30) can be solved with respect to x_i

$$x_i = - f_i(\mathbf{Y}) + \frac{y_i}{\bar{y}}\, \bar{x} + \left(\sum_{j=1}^{m} \pi_j\, a_{ij} \right) y_i \tag{31}$$

By adding up above i :

$$\sum_{j=1}^{m} \pi_j\, b_j = \sum_{i=1}^{n} f_i(\mathbf{Y}) \tag{32}$$

— by substituting relation (31) in relation (4) it results :

$$\sum_{i=1}^{n} a_{ij} \left[- f_i(\mathbf{Y}) + y_i \frac{\bar{x}}{\bar{y}} + \left(\sum_{j=1}^{m} \pi_j\, a_{ij} \right) y_i \right] = b_j \tag{33}$$

By removing the paranthesis and regrouping the terms one obtains :

$$\sum_{i=1}^{n} a_{ij} \left(\sum_{j=1}^{m} \pi_j\, a_{ij} \right) y_i + b_j \left(\frac{\bar{x}}{\bar{y}} - 1 \right) = \sum_{i=1}^{n} a_{ij}\, f_i(\mathbf{Y})$$

Assuming $\qquad u = \dfrac{\bar{x}}{\bar{y}} - 1$

$$r_{jk} = r_{kj} = \sum_{i=1}^{n} (a_{ij}\, a_{ik})\, y_i \tag{34}$$

a set of $m+1$ linear equations is obtained, with $m+1$ unknown values $\pi_1, \pi_2, \ldots, \pi_m, u$:

$$r_{11}\pi_1 + r_{12}\pi_2 + \ldots + r_{1m}\pi_m + b_1 u = \sum_{i=1}^{n} a_{i1} f_i(\mathbf{Y})$$

$$\vdots$$

$$r_{m1}\pi_1 + r_{m2}\pi_2 + \ldots + r_{mm}\pi_m + b_m u = \sum_{i=1}^{n} a_{im} f_i(\mathbf{Y}) \tag{35}$$

$$b_1\pi_1 + b_2\pi_2 + \ldots + b_m\pi_m + 0u = \sum_{i=1}^{n} f_i(\mathbf{Y})$$

$\bar{x}$ and $\bar{y}$ being correlated by (34).

WORKING PROCEDURE

1. A positive solution $\mathbf{Y} = (y_1, y_2, \ldots, y_n)$ is selected so as to satisfy the material balance.
2. $f_i(\mathbf{Y})$ are calculated with (2).
3. r_{jk} are calculated with (34).
4. The set of equations (35) is solved.
5. Improved values x_i are calculated by (34) and (31).
6. The eventual negative values x_i are eliminated — Remark 1.
7. It is checked if a value as close to minimum as needed was reached — Remark 2.
8. If not, the calculation is resumed at point 2 adopting for y_i the values x_i obtained at point 6.
9. If yes, the final results are calculated.

REMARK 1

The elimination of negative values x_i is done as below : Δ_i is assumed to be the preferred descent direction, but only a fraction $\lambda\Delta_i$ will be covered, λ estimated by taking the following into account :

— $x_i > 0$, i.e. $\dfrac{\partial F(\mathbf{X})}{\partial \lambda}$ is definite ;

— the minimum is not exceeded $\dfrac{\partial F(\mathbf{X})}{\partial \lambda} \leqslant 0$.

By replacing $x_i = y_i + \lambda\,\Delta_i$ in relation (23) one obtains :

$$F(\lambda) = \sum_{i=1}^{n} (y_i + \lambda\Delta_i)\left(c_i + \ln \frac{y_i + \lambda\Delta_i}{\bar{y} + \lambda\,\bar{\Delta}}\right) \tag{36}$$

whose partial derivative is :

$$\frac{\partial F(\lambda)}{\partial \lambda} = \sum_{i=1}^{n} \Delta_i \left(c_i + \ln \frac{y_i + \lambda\Delta_i}{\bar{y} + \lambda\bar{\Delta}}\right) \tag{37}$$

A procedure was indicated in [2] to find the value λ :

1. A small original value, say, $\lambda = 0.0005$ is assumed.
2. The terms $\dfrac{y_i + \lambda\Delta_i}{\bar{y} + \lambda\bar{\Delta}}$ are calculated. If all are positive, it is continued with point 3, if not, with point 5.
3. The value $\dfrac{\partial F(\lambda)}{\partial \lambda}$ is calculated by (37). If all values are negative, it is continued with point 4, if not, with 5.
4. λ is increased by 0.0005 and the calculus from point 2 is resumed.
5. λ is decreased by 0.0005.
6. The new values $x_i = y_i + \lambda\Delta_i$ are calculated

REMARK 2

The minimal vicinity is set up at a value and it is attained when :

$$\lambda\Delta_i \leqslant \varepsilon \qquad i = 1,2,\ldots,n \tag{38}$$

The example from [1] is resumed below.

5. ELIMINATION OF SOME RESTRICTIONS AND CONVERGENCE ACCELERATION IN WHITE'S METHOD

White's method requires that the initial estimations should always verify the mass conservation restriction, equation (4). Though, this can always be met in principle, difficulties appear in practice, on account of the requirement to repeat (as often as possible) calculi with many decimal fractions which are extremely laborious. Errors in the initial estimation, even in the last figure, add up in the course of the calculation, as White's method has no control in this respect ; that is why, results are eventually obtained with no physical meaning.

In comparison with data mentioned in section 4 the following modifications are suggested :

1) — Starting from a vector $(y_1, y_2, \ldots, y_n)$ which does not satisfy equation (4), new values are defined :

$$b'_j = \sum_{i=1}^{n} a_{ij}\, y_i \qquad j = 1, 2, \ldots\, m \tag{39}$$

differing from those of the input data :

$$|\, b'_j - b_j \,| < \varepsilon \tag{40}$$

where ε is the admissible error and the vector $(x_1, x_2, \ldots, x_n)$ is searched to verify it.

Relation (31) introduced into (39) for $\mathbf{X} = \mathbf{Y}$ leads to :

$$\sum_{i=1}^{n} a_{ij} \sum_{j=1}^{m} \pi_j\, a_{ij}\, y_i + b'_j \frac{\bar{x}}{\bar{y}} = \sum_{i=1}^{n} a_{ij} f_i(\mathbf{Y}) + b_j \tag{41}$$

By using the notations :

$$u = \frac{\bar{x}}{\bar{y}} \tag{42}$$

$$r_{jk} = r_{kj} = \sum_{i=1}^{n} (a_{ij}\, a_{kj})\, y_i \tag{43}$$

a set of $m+1$ equations is obtained with $m+1$ unknown values differing from (35), namely :

$$\begin{gathered} r_{11}\,\pi_1 + \ldots + r_{1m}\,\pi_m + b_1'\,u = \sum_{i=1}^{n} a_{i1}\,f_i(\mathbf{Y}) + b_1 \\ \cdot \\ \cdot \\ \cdot \\ r_{m1}\,\pi_1 + \ldots + r_{mm}\,\pi_m + b_m'\,u = \sum_{i=1}^{n} a_{im}f_i(\mathbf{Y}) + b_m \\ b_1'\,\pi_1 + \ldots + b_m'\,\pi + 0u = \sum_{i=1}^{n} f_i(\mathbf{Y}) \end{gathered} \tag{44}$$

$\bar{x}$ and $\bar{y}$ correlated by (42).

Consequently, point 1 in the working procedure is modified, as the positive solution suggested **Y** is no longer required to comply with the material balance.

2) — As procedure [2] presented under remark 1 is rather slow, another one was proposed instead, based on the division of the interval under consideration into halves, which diminishes by 10 times the time of a run on the computer :

1. Let us assume $\lambda_1 = 0.5$, $\lambda_2 = 1.0$
2. The terms $\dfrac{y_i + \lambda\Delta_i}{\bar{y} + \lambda\bar{\Delta}}$ are computed in point λ_1 ; if all are positive, it is continued with point, 3, if not, with point 5.
3. The same terms are computed in point λ_2 ; if they are all positive, then λ takes the value of λ_2 and it is continued with point 7, if not, with point 4.
4. λ_2 takes the value $\lambda_1 + (\lambda_2 - \lambda_1)/2$ and it is continued with point 3.
5. λ_2 takes the value of λ_1 and λ_1 the value of $\lambda_1/2$.
6. The same terms are computed in point λ_1 ; if they are all positive, it is continued with point 4, if not with point 5.
7. The value $\dfrac{\partial F(\lambda)}{\partial \lambda}$ is calculated by (37) ; if it is positive, it is continued with point 9.
8. λ_1 takes the value $\lambda_1 + (\lambda_2 - \lambda_1)/2$, likewise λ_2 and it is continued with point 7.
9. The new values are computed for $x_i = y_i + \lambda\,\Delta_i$.

Further on, two examples of calculations performed by this method are given :

1 — example from [1] ;

2 — example from [4] ;

For example 1, several tests have been made, the concentration vector $\mathbf{Y} = (y_1, y_2, \ldots, y_n)$ taking different values by the program. A computing time variation has been noted, due to the differing number of iterations required to find out the correct solution (see table 1).

For example 2 it was considered $\mathbf{Y} = (0.1)$.

Table 1

Variation of computing time with the values of Y

Y = ( )	.01	.1	.2	.3	.4	.5	.6	.7	.8	.9	.99	.999	1	1.1	1.2	1.3	1.4	1.5
Iterations number	8	6	6	7	8	8	8	8	8	9	9	9	9	9	10	10	11	9
Computing time in seconds	36	30	30	33	37	37	37	38	38	41	41	41	40	41	44	44	47	41

6. ISOPRENE DEHYDROGENATION EQUILIBRIUM

Isoprene can be obtained by isopenthane catalytic dehydrogenation, which occurs is two successive stages :

— isopenthane dehydrogenation to isoamylenes ;

— isoamylenes dehydrogenation to isoprene.

The three isomers of isoamylenes, 2-methyl-1-butene, 2-methyl-2-butene, and 3-methyl-1-butene are obtained. The following equations present the reactions taking place :

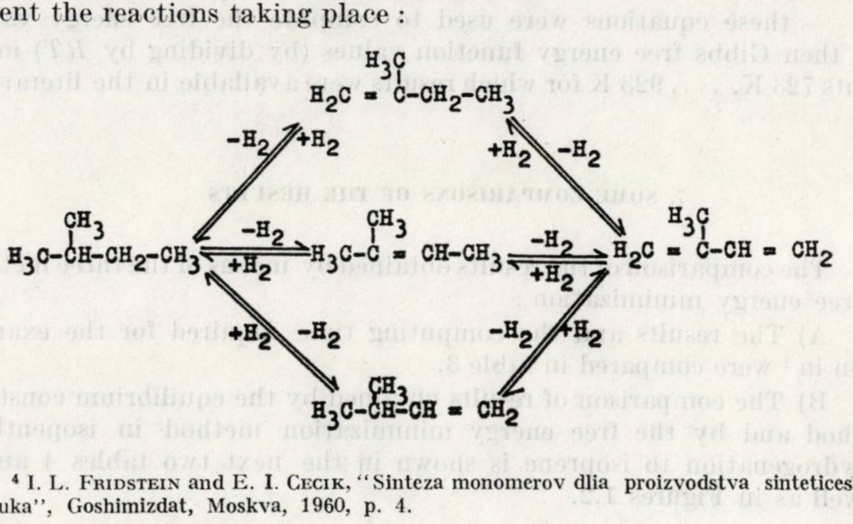

---

[4] I. L. Fridstein and E. I. Cecik, "Sinteza monomerov dlia proizvodstva sinteticeskovo kauciuka", Goshimizdat, Moskva, 1960, p. 4.

Six chemical species are present in the reaction medium any time : isopenthane, three isoamylenes, isoprene and hydrogen. The calculations were made using these six chemical species, but for the sake of clarity the concentrations of the three isoamylenes were given together in plots and tables, whereas hydrogen concentration was no plotted.

The isoprene hydrogenation equilibrium was analysed at the system total pressure of 0.2, 0.3, 1.0 atm, and for isopenthane : isoamylenes feed ratios of 100 : 0, 80 : 20, 70 : 30, 60 : 40 (by weight).

Input data concerning the free energy were obtained as follows:

— the values given in table 2 were taken from the literature [3];

— using the four values for each species, the coefficients of a_i+b_iT equations, which describe the free energy variation of each species in the range 700—1000 K were obtained by regression analysis;

Table 2

Free energy values for the input data preparation

Substance	Formula	Free energy in kcal/mol, at temp.			
		700	800	900	1000 (K)
Isopenthane	C_5H_{12}	45.19	57.88	70.68	83.51
2-methyl-1-butene	C_5H_{10}	51.06	60.37	69.76	79.20
3-methyl-1-butene	C_5H_{10}	53.94	63.64	72.82	82.35
2-methyl-2-butene	C_5H_{10}	50.49	60.05	69.69	79.40
Isoprene	C_5H_8	59.46	65.89	72.40	78.89
Hydrogen	H_2	0	0	0	0

— these equations were used to compute the free energy values, and then Gibbs free energy function values (by dividing by RT) in the points 723 K, . . ., 923 K for which results were available in the literature.[4]

7. SOME COMPARISONS OF THE RESULTS

The comparison of the results obtained by means of the three methods of free energy minimization :

A) The results and the computing time required for the example given in [1] were compared in table 3.

B) The comparison of results obtained by the equilibrium constants method and by the free energy minimization method in isopenthane dehydrogenation to isoprene is shown in the next two tables 4 and 5, as well as in Figures 1,2.

Table 3

Comparisons between results for example 1

Species	Results			
	from [1]	from [1] with [2]	with the general procedure	with the improved procedure
H	0.041	0.041	0.041	0.041
H_2	0.148	0.148	0.148	0.148
H_2O	0.783	0.783	0.783	0.783
N	0.001	0.001	0.001	0.001
N_2	0.485	0.486	0.486	0.485
NH	0.001	0.001	0.001	0.001
NO	0.027	0.027	0.027	0.027
O	0.018	0.018	0.018	0.018
O_2	0.037	0.037	0.037	0.037
OH	0.097	0.097	0.097	0.097
Computing time in seconds	—	192	—	17

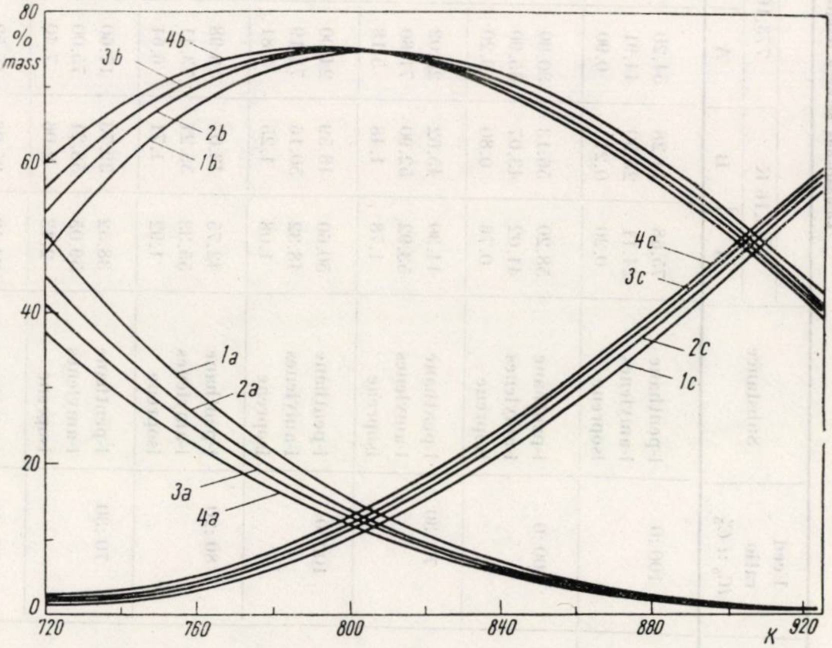

Fig. 1. — Equilibrium composition variation computed with the improved method (total pressure 0.2 atm.):

— concentrations (by weight) for isopenthane (*a*), isoamylenes (*b*), and isoprene (*c*);

— feed ratio isopenthane : isoamylenes (by weight) of 100 : 0(1), 80 : 20(2), 70 : 30(3), 60 : 40(4).

Table 4

Comparisons between results for example 2

Press. atm.	Feed ratio $iC_5 : i\,C_5'$	Substance	Temperature									
			723.16 K		773.16 K		823.16 K		873.16 K		923.16 K	
			A	B	A	B	A	B	A	B	A	B
1	100 :0	i-penthane	75.68	74.28	54.20	54.71	33.07	32.99	16.72	16.40	7.41	7.16
		i-amylenes	24.11	25.50	44.91	44.36	63.90	63.68	74.54	74.19	72.81	71.98
		isoprene	0.20	0.21	0.90	0.93	3.03	3.32	8.74	9.41	19.78	20.86
0.3	100 :0	i-penthane	58.20	56.13	30.90	31.62	14.00	13.89	5.36	5.19	1.99	1.74
		i-amylenes	41.02	43.07	65.90	64.94	75.80	75.13	70.43	69.05	54.30	52.50
		isoprene	0.76	0.80	3.20	3.44	10.20	10.98	24.21	25.76	43.71	45.76
	70 :30	i-penthane	44.30	45.62	23.02	26.19	9.50	11.72	3.62	4.47	1.33	1.52
		i-amylenes	53.92	52.90	71.80	69.11	76.50	75.23	66.75	69.19	49.00	50.32
		isoprene	1.78	1.48	5.18	4.70	14.00	13.05	29.63	28.34	49.67	48.16
0.2	100 :0	i-penthane	50.60	48.59	24.00	24.40	9.70	9.62	3.01	3.26	0.85	0.99
		i-amylenes	48.32	50.16	71.19	70.37	75.45	74.70	64.94	62.82	45.10	45.38
		isoprene	1.08	1.25	4.81	5.23	14.85	15.68	32.05	33.92	54.05	55.43
	80 :20	i-penthane	42.75	43.07	19.98	21.82	7.95	8.68	2.70	2.98	0.84	0.91
		i-amylenes	55.33	55.21	73.41	72.05	75.04	74.20	61.50	61.47	42.05	42.32
		isoprene	1.92	1.71	6.61	6.13	17.01	17.08	35.80	35.55	57.10	56.77
	70 :30	i-penthane	38.52	39.73	17.60	20.33	7.05	8.18	2.46	2.82	0.77	0.87
		i-amylenes	59.05	58.21	75.00	72.93	73.90	73.81	60.00	60.70	40.23	41.59
		isoprene	2.43	2.06	7.40	6.74	19.05	18.01	37.54	36.47	59.00	57.54
	60 :40	i-penthane	34.12	35.98	15.52	18.69	6.27	7.62	2.30	2.66	0.66	0.82
		i-amylenes	62.90	61.48	76.00	73.80	72.92	73.31	58.00	59.74	38.74	40.79
		isoprene	2.98	2.54	8.48	7.51	20.81	19.07	39.07	37.60	60.60	58.38

Table 5

A statistical analysis of results for example 2

Pressure atm.	Feed ratio $iC_5 : iC_5'$	Substance	Average deviation*	Standard deviation** σ	Remarks
1	100 :0	isopenthane	0.512	0.692	
		isoamylenes	0.668	0.787	
		isoprene	0.416	0.583	
0.3	100 :0	isopenthane	0.664	0.991	
		isoamylenes	1.372	1.464	
		isoprene	0.932	1.206	
	70 :30	isopenthane	1.550	1.870	max. deviation
		isoamylenes	1.350	1.539	
		isoprene	0.906	1.017	
0.2	100 :0	isopenthane	0.576	0.926	
		isoamylenes	1.410	1.512	
		isoprene	0.934	1.122	
	80 :20	isopenthane	0.648	0.906	
		isoamylenes	0.516	0.718	
		isoprene	0.268	0.300	min. deviation
	70 :30	isopenthane	1.106	1.438	
		isoamylenes	1.012	1.211	
		isoprene	0.920	0.993	
	60 :40	isopenthane	1.380	1.760	
		isoamylenes	1.560	1.680	
		isoprene	1.368	1.500	

* average deviation $= \dfrac{\sum_{i=1}^{5} |A_i - B_i|}{5}$; ** $\sigma = \sqrt{\dfrac{\sum_{i=1}^{5} (A_i - B_i)^2}{5}}$.

Figure 1 presents the equilibrium concentrations for various feed ratios at a system total pressure of 0.2 atm. Figure 2 gives a comparison between the results from the literature [4] and those obtained in this work, under different working conditions.

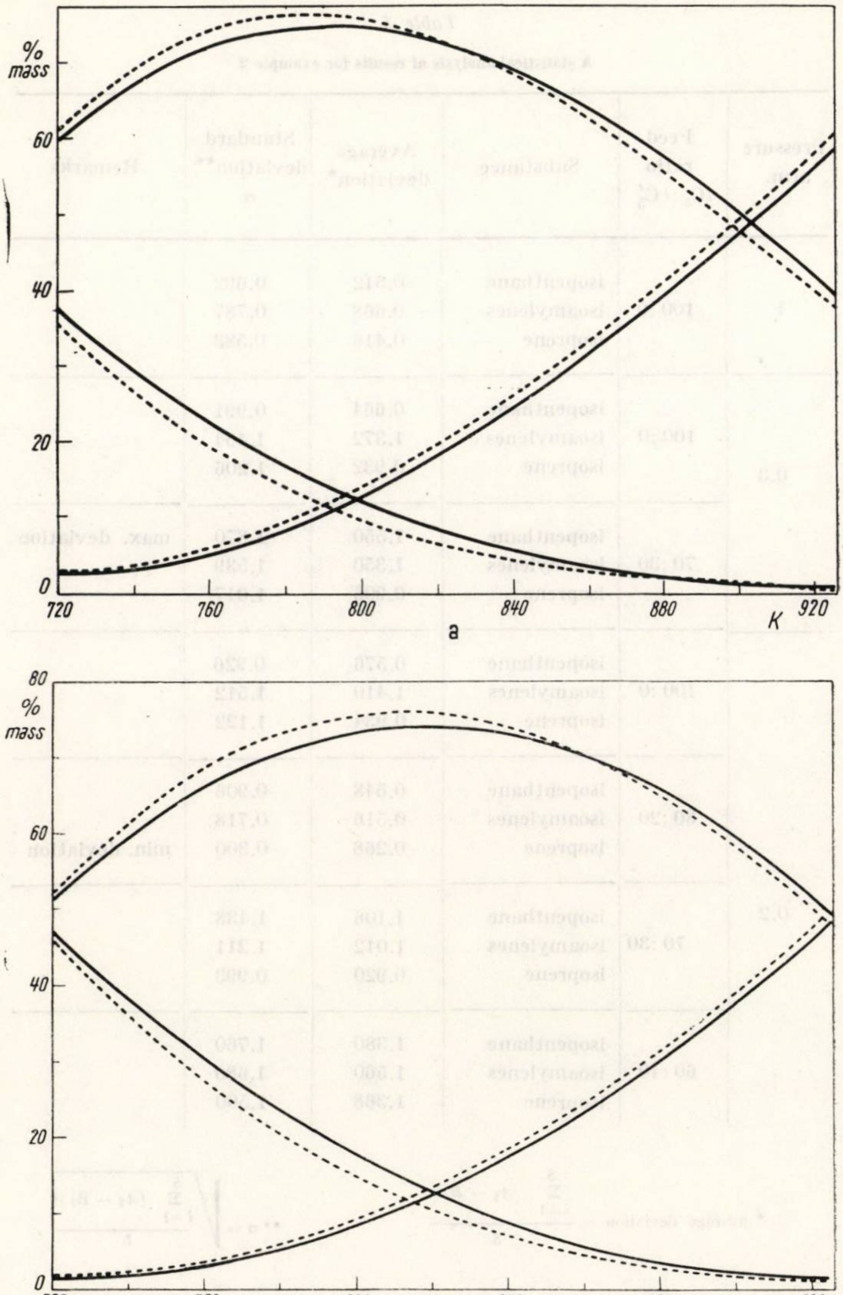

Fig. 2. — Comparisons between the results from [4](------) and those obtained in this work (———):

(a) 0.2 atm., feed ratio isopenthane : isoamylenes of 60 :40
(b) 0.3 ,, ,, ,, ,, ,, ,, 70 :30
(c) 1.0 ,, ,, ,, ,, ,, ,, 100 :00

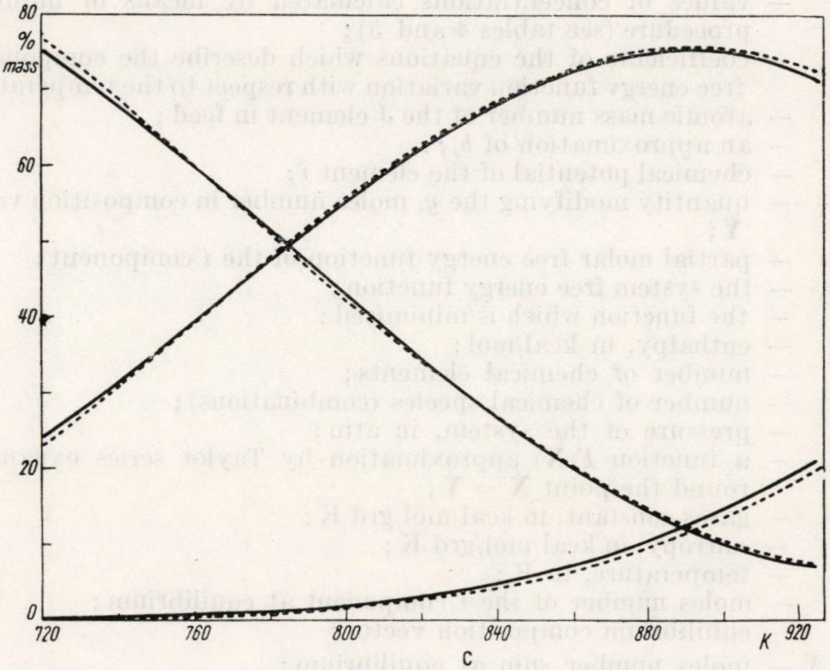

Fig. 2 c.

CONCLUSIONS

Two new procedures are given for finding the chemical equilibrium composition of complex mixtures by the free energy minimization :

— the former is a method which differs in principle from those cited in the literature, being of a high degree of generality ; the restriction of material balance in the input data is eliminated ;

— the latter is achieved by improving the method given in the literature [1,2] ; the improvement consists in the reduction of the computing time, by 10 times, with an increase in the accuracy from $5 \cdot 10^{-3}$ to 10^{-5} and the elimination of the material balance restriction from the input data.

The results were verified both by means of the methods cited in the literature [1,2] and by the equilibrium constants method [4]. The agreement was good.

The calculations were performed with programs written in ALGOL.

NOTATION

a_{ij} — system composition matrix element ;

A — values of concentrations calculated by means of equilibrium constants method (see tables 4 and 5) ;

B — values of concentrations calculated by means of improved procedure (see tables 4 and 5);
a_i, b_i — coefficients of the equations which describe the component i free energy function variation with respect to the temperature;
b_j — atomic mass number of the J element in feed;
b'_j — an approximation of b_j;
c_i — chemical potential of the element i;
$\mathrm{d}y_i$ — quantity modifying the y_i moles number in composition vector $\mathbf{Y}$;
f_i — partial molar free energy function of the i component;
$F(\mathbf{X})$ — the system free energy function;
$G(\mathbf{X})$ — the function which is minimized;
H — enthalpy, in kcal/mol;
m — number of chemical elements;
n — number of chemical species (combinations);
P — pressure of the system, in atm;
$Q(\mathbf{X})$ — a function $F(\mathbf{X})$ approximation by Taylor series expansion, round the point $\mathbf{X} = \mathbf{Y}$;
R — gases constant, in kcal/mol/grd K;
S — entropy, in kcal/mol/grd K;
T — temperature, in K;
x_i — moles number of the i component at equilibrium;
$\mathbf{X}$ — equilibrium composition vector;
$\bar{x}$ or $\bar{X}$ — moles number sum at equilibrium;
y_i — moles number of the i component in suggested (original) composition;
$\mathbf{Y}$ — suggested composition vector;
$\bar{y}$ or $\bar{Y}$ — moles number sum of the suggested composition;
δ_{ik} — Kronecker's symbol;
$\Delta_i = x_i - y_i$;
$\bar{\Delta}$ — differentions Δ_i sum;
ε — admissible error, max Δ_i or max $| b_j - b'_j |$;
λ — fraction of Δ_i covered at a descent;
π_j — Lagrange multipliers;
σ — standard deviation (see table 5);
Φ — more general expression of the minimized function;
Ψ_k — partial derivative on the k direction of the Φ function;

Revue Roumaine de Chimie, **23**, *5*, 699–706 (1978)

POLYNUCLEAR COMPLEX COMPOUNDS OF IRON, COBALT AND NICKEL. III[1]

MERCURY-CONTAINING COMPLEX COMPOUNDS

MARIA BREZEANU and MAGDALENA DINCULESCU
Institute of Chemistry, Laboratory of Inorganic Chemistry,
Splaiul Independenţei 89, Bucharest, Romania

Received November 9, 1976

In the MCl_n-HgCl_2 systems — Base in which M = Fe, Co, Ni, Base = NH_3, en, it was possible to synthesize some polynuclear complex compounds corresponding to the following general formulas : $HgFeCl_{n+1}(NH_3)_{2n}(OH)_{2n+1}(n=1,2,4)$, $HgFe_nCl_{n+1}(en)_n(OH)_{2n+1}$ (n = 1, 2, 4) ; Co_2HgCl_4 $(Base)_2$ $(OH)_2$, Co_4HgCl_4 $(Base)_2$ $(OH)_6$ (Base = NH_3, en) and $NiHgCl_4en_4$. These complex compounds were characterized by elemental chemical analysis, electronic spectra, IR spectra and molecular electric conductivity determinations.

Two previous papers [1,2] have reported the results obtained in the synthesis and characterization of compounds formed in the systems MCl_n-HgCl_2 — Base in which M=Fe, Co, Ni, Base=NH_3, en. The synthesis of these compounds was conducted in conditions in which the amount of iron, cobalt and nickel chloride, respectively, was kept constant while progressively varying the amount of mercury chloride from a 1 : 1 ratio to 1 : 8.

This study was extended to investigate the synthesis and the characterization of compounds obtained in the mentioned systems if the amount of mercury chloride is kept constant while progressively varying the amount of iron, cobalt and nickel chloride, respectively within the same limits of the MCl_n : $HgCl_2$ ratio (from 1 : 1 to 1 : 8).

A series of polynuclear complex compounds containing the mentioned elements were obtained on this occasion and they can be represented by the following general formula : $HgFe_n\ Cl_{n+1}\ (NH_3)_{2n}\ (OH)_{2n+1}$ (n = 1, 2, 4), $HgFe_n\ Cl_{n+1}\ (en)_n(OH)_{2n+1}$ (n = 1, 2, 4) ; $Co_2HgCl_4\ (Base)_2\ (OH)_2$, $Co_4HgCl_4(Base)_2(OH)_6$ (Base = NH_3, en) ; $NiHgCl_4en_4$.

The compounds obtained were characterized by the elemental chemical analysis, electronic and IR spectra, and molecular electric conductivity determinations.

---

[1] Part. II : M. Brezeanu and M. Dinculescu, *Rev. Roumaine Chim.* **22**, 1175 (1977).

[2] Part. I. : M. Brezeanu and M. Dinculescu, *Rev. Roumaine Chim.*, **22**, 539 (1977).

RESULTS AND DISCUSSION

The synthesis of compounds that may be formed in the systems MCl_n-HgCl_2-Base, M=Fe(III), Co(II), Ni(II) was conducted under various conditions with regard to the $MCl_n - HgCl_2$ ratio, i. e. from 1 : 1 to 8 : 1, while keeping constant the amount of mercury chloride.

The influence of the utilized base on the nature of compounds formed in these systems was established using both ammonia and ethylenediamine as a base in otherwise equivalent conditions. The optimal pH for the separation of such compounds is 8.

By conducting the synthesis under different experimental conditions with regard to the above-mentioned parameters it was possible to characterize a series of complex compounds which correspond to the following general formulas : $HgFe_n Cl_{n+1}(NH_3)_{2n} (OH)_{2n+1}$, $HgFe_n Cl_{n+1}(en)_n (OH)_{2n+1}$, n = 1, 2, 4 ; $Co_2HgCl_4(Base)_2(OH)_2$, $Co_4HgCl_4(Base)_2(OH)_6$, Base = NH_3, en ; $NiHgCl_4\ en_4$.

The complex compounds of Fe(III) and Ni(II) exist under the form of one single modification of brown and violet colour, respectively. The complex compounds of cobalt behave differently from this point of view as a function of the utilized base, i. e. the compounds containing ethylendiamine appear under the form of one single (brown) modification whereas two differently coloured modifications (pink and blue) were separated for ammonia-containing compounds.

Thus, compound $Co_2HgCl_4(NH_3)_2(OH)_2$ was obtained in both modifications. The other compounds of Co(II) separated in one single modification, namely, $CoHgCl_2(NH_3)_2(OH)_2$ under the form of the blue modification and $Co_4HgCl_4(NH_3)_2(OH)_6$ under the form of the pink modification. The blue modification represents the stable species in solution. The change to the pink modification in solution is the more difficult as the cobalt amount is smaller. In solid state, the change from one modification to another takes place in time, i. e. the blue modification changes to the pink one. The change is irreversible.

In contrast to the complex compounds of Fe(III), Co(III) and Ni(II) which contain ammonia as a neuter ligand, those with ethylenediamine are characterized by a relatively high thermal stability. Heated to 110°they will not change their colour and their weight remains practically constant. Based on the chemical analyses performed, it was found that on heating to 110° the first compound will decompose losing the whole amount of mercury and ammonia present in the compound. This difference in the behaviour of the two series of compounds can be attributed to the ethylenediamine chelating effect.

The formulation of these complex compunds is a difficult problem due to the fact that it is possible to have direct metal-metal bond as well as bridges of either chlorine or hydroxyl groups, each being able to act as a bridging ligand.

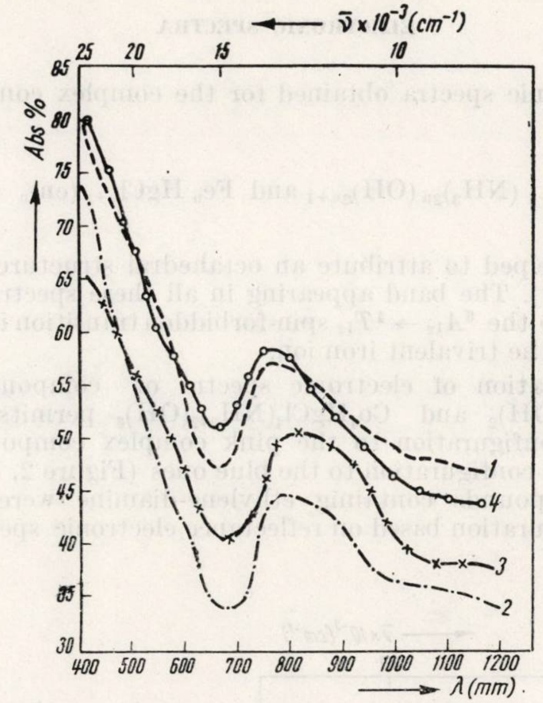

Fig. 1. — Electronic spectra of compounds :
1. $HgFe_4Cl_5en_4(OH)_9$; *2*. $HgFe_2Cl_3en_2(OH)_5$;
3. $HgFe_4Cl_5(NH_3)_8(OH)_9$; *4*. $HgFe_2Cl_3(NH_3)_4(OH)_5$.

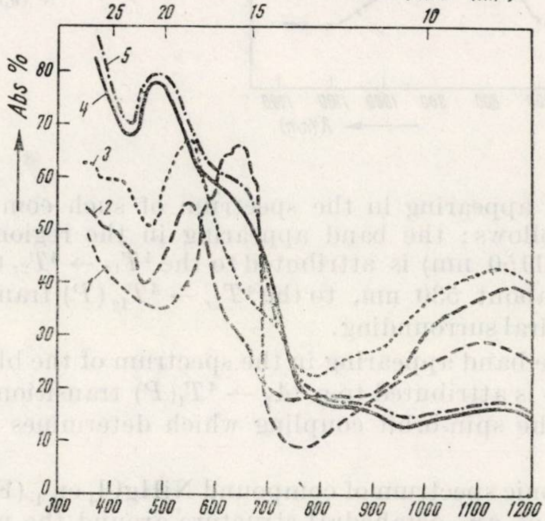

Fig. 2. — Electronic spectra of compounds :
1. $CO_2HgCl_4(NH_3)_2(OH)_2$ (blue) ; *2*. $Co_2HgCl_4(NH_3)_2(OH)_2$(pink) ;
3. $CO_4HgCl_4(NH_3)_2(OH)_6$(pink) ; *4*. $Co_2HgCl_4en_2(OH)_2$; *5*. $CO_4HgCl_4en_2(OH)_6$.

ELECTRONIC SPECTRA

The electronic spectra obtained for the complex compounds of the type :

$$Fe_n\,HgCl_{n+1}\,(NH_3)_{2n}\,(OH)_{2n+1} \text{ and } Fe_n\,HgCl_{n+1}\,(en)_n\,(OH)_{2n+1}$$

where n = 2,4 helped to attribute an octahedral structure to these compounds (Figure 1). The band appearing in all these spectra near 800 nm was attributed to the $^6A_{1g} \rightarrow {}^4T_{1g}$ spin-forbidden transition in an octahedral configuration of the trivalent iron ion.

An examination of electronic spectra of compounds $Co_2HgCl_4(NH_3)_2(OH)_2$ and $Co_4HgCl_4(NH_3)_2(OH)_6$ permits to attribute an octahedral configuration to the pink complex compounds of Co(II) and a tetrahedral configuration to the blue ones (Figure 2, curves 1, 2, 3). The cobalt compounds containig ethylene-diamine were attributed an octahedral configuration based on reflectance electronic spectra (Figure 2, curves 4 and 5).

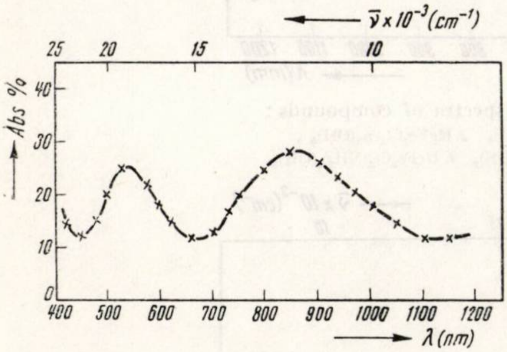

Fig. 3. — Electronic spectrum of compound :
N en$_4$HgC .

The bands appearing in the spectrum of such compounds may be attributed as follows ; the band appearing in the region of long wavelengths (about 1150 nm) is attributed to the $^4T_{1g} \rightarrow {}^4T_{2g}$ transition, while that found at about 530 nm, to the $^4T_{1g} \rightarrow {}^4T_{1g}(P)$ transition, for a d^7 ion in an octahedral surrounding.

The intense band appearing in the spectrum of the blue modification at about 600 nm is attributed to a $^4A_2 \rightarrow {}^4T_1(P)$ transition. Its fine structure is due to the spin-orbit coupling which determines the splitting of term $^4T_1$ (P).

The electronic spectrum of compound $NiHgCl_4\,en_4$ (Figure 3) enables the recognition of an octahedral structure around the nickel atom, the two present bands being attributed to the spinallowed transition : $^3A_{2g}(F) \rightarrow {}^3T_{2g}(F)$, respectively $^3A_{2g}(F) \rightarrow {}^3T_{1g}(\mathrm{F})$.

IR SPECTRA

The vibration spectra of some of the complex compounds obtained were recorded, to obtain additional data on their stereochemistry in order to establish the function of some ligands such as ethylenediamine and the hydroxyl anion.[3-5]

The most important from this point of view are those spectral domains, in which absorption is attributed to the vibration modes of the indicated ligands.

In view of making the most exact possible assignment of absorption bands of the mentioned ligands, table 1 presents comparatively the vibration frequencies characteristic of the free and the coordinated ligands.

Table 1

IR frequencies characteristic of some complex compounds in which Base=NH_3

Compounds	νNH_3	$\delta d(NH_3)$	$\delta s(NH_3)$	pr (NH_3)	$\nu M-N$	νOH (str.)	ν OH (def)
OH free group in primary alcohols	—	—	—	—	—	3590—3650	1260—1350
NH_3	3414—3336	1628	950	—	—	—	—
$[Co(NH_3)_6]Cl_3$	3070	1603	1334	803	=500	—	—
$[Hg(NH_3)_2]Cl_2$	—	—	—	—	$513(A_2)$ $493(A_1)$	—	—
$Co_2HgCl_4(NH_3)_2(OH)_2$ (blue)	2940—2965	1517	1315	770	435 470	3570	1305
$Co_4HgCl_4(NH_3)_2OH)_6$ (pink)	2935—2963	1610	1413	853	430 480	3570	1320

As can be seen in table 1, the spectra of the compounds obtained exhibit the vibration frequencies characteristic of coordinated ammonia. Likewise, the presence in the spectra of the last two compounds of the absorption bands at 3570, 1305 cm^{-1}, respectively 3570, 1320 cm^{-1} attributed to the vibration modes of the hydroxyl group (valency and stretching vibration) indicates its coordination. The shift towards lower frequencies of the bands in question agrees with the literature data.

---

[3] G. Gordon and R. K. Birdwhistell, *J. Amer. Chem. Soc.*, **81**, 3567 (1959).

[4] L. J. Bellamy, "The Infrared Spectra of Complex Molecules", John Wiley Sons, Inc., New York, 1958, p. 102.

[5] K. Nakamoto, "The Infrared Spectra of Inorganic Compounds" Wiley Sons, Inc., New York, 1963, p. 143.

Another spectral domain of interest is that in which absorption is attributed to the ν_{M-N} valency vibration.

The literature shows that the bands appearing in aminocomplexes between 650 and 850 cm^{-1} are attributed to the ν_{M-N} vibration frequencies [5]. Other authors consider however that such bands are due to the "NH_3 rocking" vibration modes and that the ν_{Co-N} vibration frequency appears near 500 cm^{-1} while the band observed is very weak. The frequency of the valency vibration ν_{Hg-N} [6] was found around the value of 500 cm^{-1} for the ion $[Hg(NH_3)_2]^{2+}$. Since, according to literature data both frequencies, ν_{Co-N} and ν_{Hg-N} appear near 500 cm^{-1}, it is hard to attribute the absorption bands existing in the spectra of the studied compounds around this value (Table 1).

For complex compounds in which Base = en, the important domain is that in which absorption is attributed to the vibration modes of ethylenediamine.

An examination of IR spectra of three of the synthesized complex compounds shows again the bands attributed to the vibration modes characteristic of coordinated ethylenediamine (Table 2).

The absorption bands present around a value of 500 cm^{-1} (Table 2) in the IR spectra of such complex compounds were attributed on the basis of literature data, [7] to the metal-ligand metal-nitrogen valency vibration.

Table 2

IR frequencies characteristic of some compounds in which Base = en

Compounds	νNH_2(str.)	νNH_2(def.) asym.	$\nu M-N$	νOH(str.)	νOH(def.)
OH free group in primary alchols	—	—	—	3590—3650	1350—1260
$[Coen_3]Cl_3$	3172 ; 3086	1575	500	—	—
$Co_4HgCl_4en_2(OH)_6$	3220 ; 3154	1590	495 ; 512	3440	1277
$Fe_4HgCl_5en_4(OH)_9$	3190	1585	465	3410	1308
$[Nien_3]Cl_3$	2940 ; 2875	1587 ; 1569	—	—	—
$Nien_4HgCl_4$	2940 ; 2881	1589 ; 1565	477 ; 510	—	—

MOLAR CONDUCTIVITY DETERMINATIONS

The formulations attributed to the studied complexes were also confirmed by determining their molecular electric conductivity. The data obtained (Table 3) show that most complexes obtained are nonelectrolytes.

---

[6] E. P. Bertin and I. Nakagawa, *J. Amer. Chem. Soc.*, **80**, 525 (1958).

[7] D. B. Powel and N. Shephard, *J. Chem. Soc.*, **1112**, 1961.

Table 3

Molecular electric conductivities of complexes obtained in a D.M.F. solution

Compound	Molar conductivity	Type of electrolyte
$HgFeCl_2(NH_3)_2(OH)_3$	26.4	nonelectrolyte
$HgFe_2Cl_3(NH_3)_4(OH)_5$	63.8	1 :1
$HgFe_4Cl_5(NH_3)_8(OH)_9$	77.6	1 :1
$HgFeCl_2en(OH)_3$	18.5	nonelectrolyte
$HgFe_2Cl_3en_2(OH)_5$	60.9	1 :1
$Hg\ Fe_4Cl_5en_4(OH)_9$	78.4	1 :1
$CoHgCl_2(NH_3)_2(OH)_2$ (blue)	13.7	nonelectrolyte
$Co_2HgCl_4(NH_3)_2(OH)_2$ (blue)	17.5	nonelectrolyte
$Co_2HgCl_4(NH_3)_2(OH)_2$ (pink)	13.6	nonelectrolyte
$Co_4HgCl_4(NH_3)_2(OH)_6$ (pink)	45.3	nonelectrolyte
$CoHgCl_4en_2$	10.4	nonelectrolyte
$Co_2HgCl_4en_2\ (OH)_2$	135.4	1 :2
$Co_4HgCl_4en_2(OH)_6$	170.8	1 :2
$NiHgCl_4en_4$	20.3	nonelectrolyte

EXPERIMENTAL SECTION

I. SYNTHESIS AND ANALYSIS OF COMPOUNDS

1. *$HgFe_nCl_{n+1}(NH_3)_{2n}(OH)_{2n+1}$ and $HgFe_nCl_{n+1}(en)_n(OH)_{2n+1}$* (n=1*, 2, 4). 0,25g $HgCl_2$ dissolved in 3 ml water and 2 ml ethyl alcohol. To the solution obtained is added a variable amount of $FeCl_3 \cdot 6H_2O$ i.e. : 0,25 g, 0.5 g, 1 g, corresponding to the $HgCl_2$:$FeCl_3$ ratio of 1 :1, 1 : 2 and 1 :4. Separation of compounds occurs by adding ammonia, respectively ethylenediamine, dropwise up to a pH = 8. After about 24 hr, the separated substances are filtered and washed with alcohol.

The complex compounds for which n = 4 are also obtained at $HgCl_2$: $FeCl_3$ 1 :4 ratios, i.e. 1 : 6, and 1 : 8.

Calculated for $HgFe_2Cl_3(NH_3)_4(OH)_5$: Hg, 35.14 ; Fe, 19.58 ; Cl, 21.61 ; N, 9.79 ; Found : Hg, 35.23 ; Fe, 19.43 ; Cl. 21.54 ; N, 9.83 %.

Calculated for $HgFe_4Cl_5(NH_3)_8(OH)_9$: Hg, 22.55 ; Fe, 25.13 ; Cl, 19.86 ; N, 12.57 ; Found : Hg, 22.63 ; Fe, 25.18 ; Cl, 20.00 ; N, 12.43 %.

Calculated for $HgFe_2Cl_3en_2(OH)_5$: Hg, 32.21 ; Fe, 17.94 ; Cl, 17.06 ; N, 8.97 ; Found : Hg, 32.42 ; Fe, 17.85 ; Cl, 17.16 ; N, 9.15 %.

Calculated for $HgFe_4Cl_5en_4(OH)_9$: Hg, 20.20 ; Fe, 22.52 ; Cl, 17.79 ; N, 11.25 ; Found : Hg, 20.34 ; Fe, 22.63 ; Cl, 17.95 ; N, 11.42 %.

Analysis of compounds in which n = 1 can be found in references 1 and 2.

2. *$Co_2HgCl_4(NH_3)_2(OH)_2$ and $Co_4HgCl_4(NH_3)_2(OH)_6$*. To a solution obtained by dissolving 0.25 g $HgCl_2$ in a minimal amount of water (3 ml) and alcohol (2 ml) is added a variable amount of $CoCl_2 \cdot 6H_2O$, corresponding to a $HgCl_2$: $CoCl_2$ ratio of 1 : 2 and 1 : 4, namely 0.4 g respectively 0.8 g. The solution is vigorously stirred to complete the dissolution of salts. Compounds will be obtained by dropwise addition of ammonia up to a pH = 8. The substances thus obtained are filtered and thoroughly washed with alcohol. The last compound is also obtained for a ratio $HgCl_2$: $CoCl_2$ 1 :4, namely 1 : 6 and 1 : 8.

The first to separate from the solution is the blue modification ; in time, it changes to the pink modifications. The conversion time is the shorter as the cobalt ammount existing in solution is larger. The change from the blue modification to the pink one may also be obtained in solid state, yet the conversion time is much longer.

Calculated for $Co_2HgCl_4(NH_3)_2(OH)_2$ — blue — : Hg, 37.97 ; Co, 22.30 ; Cl, 26.84 ; N, 5.48 ; Found : Hg, 37.52 ; Co, 21.85 ; Cl, 26.53 ; N, 5.10 %.

Calculated for $Co_2HgCl_4(NH_3)_2(OH)_2$—pink— : Hg, 37.59 ; Co, 22.15 ; Cl, 26.74 ; N, 5.37 ; Found : Hg, 37.64 ; Co, 21.93 ; Cl, 26.35 ; N, 5,20 %.

Calculated for $Co_4HgCl_4(NH_3)_2(OH)_6$—pink— : Hg, 28.23 ; Co, 33.12 ; Cl, 19.90 ; N, 3.92 ; Found : Hg, 28,56 ; Co, 33,69 ; Cl, 20.05 ; N, 3.79 % .

3. $Co_2HgCl_4en_2(OH)_2$ *and* $Co_4HgCl_4en_2(OH)_6$. 0.25 g $HgCl_2$ are dissolved in a minimal amount of water (3 ml) and ethyl alcohol (2 ml). To the solution obtained is added a variable amount of $CoCl_2 \cdot 6H_2O$ corresponding to a $HgCl_2 : CoCl_2$ ration of 1 : 1, 1 : 2, 1 : 4, 1 : 6 and 1 : 8, namely : 0.2 g, 0.4 g, 0.8 g, 1.2 g and 1.6 g $CoCl_2$. $6H_2O$. The solution thus obtained is then treated dropwise with ethylendiamine until the separation of a solid compound occurs (pH = 8) The separated brown substance is filtered after 24 hr and thoroughly washed with alcohol.

For a 1 $HgCl_2$: $CoCl_2$ ratio one obtains the compound $Co_2HgCl_4 \cdot en_2(OH)_2$ only if filtering takes place after about two weeks. Under usual conditions, a different compound is separated for this ratio ($CoHgCl_4$ en_2). By working up larger amounts of $CoCl_2$ corresponding to a 1 $HgCl_2$: 4 $CoCl_2$ ratio, the separation of the mentioned compound occurs under normal conditions. For values of the $HgCl_2 : CoCl_2 >$ 1 :4 ratio, i.e. 1 : 6 and 1 : 8, only compound $Co_4HgCl_4en_2(OH)_6$ will be obtained.

Calculated for $Co_2HgCl_4en_2(OH)_2$: Hg, 32.68 ; Co, 19.18 ; Cl, 23.09 ; N, 9.10 ; Found : Hg, 32,46 ; Co, 19.32 ; Cl, 22.91 ; N, 9.23 %.

Calculated for $Co_4HgCl_4en_2(OH)_6$: Hg, 25.09 ; Co, 29.46 ; Cl, 17.60 ; N, 7.01 ; Found : Hg, 24.83 ; Co, 29.23 ; Cl, 17,89 ; N, 6.89 % .

4. $NiHgCl_4en_4$ · 0,25 g $HgCl_2$ are dissolved in 3 ml water and 2 ml alcohol. To the solution obtained is added a variable amount of $NiCl_2$ corresponding to a $HgCl_2 : NiCl_2$ ratio of 1 :1,1 : 2,1 : 4 and 1 :8. The $NiHgCl_4en_4$ compound is obtained only for an excess of nickel chloride (1 $HgCl_2$: 8 $NiCl_2$) when treating the solution obtained with ethylenediamine added dropwise up to pH = 8. The product obtained is filtered after 24 hr.

Calculated : Hg, 31.20 ; Ni, 9.20 ; Cl, 22.15 ; N, 17.47 ; Found : Hg, 31.75 ; Ni, 9.63 ; Cl, 22,95 ; N. 17.93 % .

II. ELECTRONIC SPECTRA

Electronic spectra were recorded at room temperature using VSU_1 spectrophotometer and magnesium oxide as reference.

III. VIBRATION SPECTRA

IR spectra were obtained by means of an UR 20 spectrophotometer using the pelleting technique with potassium bromide.

IV. MOLAR ELECTRIC CONDUCTIVITIES

Molecular electric conductivity measurements were effected on a II conductometer (Czechoslovakia) with constant $K = 0.52$ in D.M.F. solution at 25 degrees. The assignment of the electrolyte type was made according to the indications given in the literature with regard to the methods for establishing the electrolyte type in D.M.F. solutions. [8]

---

[8] D. J. Phillips and S. Y. Tyree, *J. Amer. Chem. Soc.*, **83**, 1806 (1961).

Revue Roumaine de Chimie, **23**, 5, 707–718 (1978)

ELECTRONIC SPECTRA AND MAGNETIC SUSCEPTIBILITIES OF SOME NEW TETRAHEDRAL CHELATE COMPLEXES WITH Co (d^7)—N(sp^2) BONDS

A. C. BANCIU
Center of Physical Chemistry, Bucharest, Str. Dumbrava Roșie,
23 — Romania

Received September 29, 1976

The electronic spectra of some new organic ligands and the electronic spectra and the magnetic susceptibilities of the new tetrahedral Co(II) chelate complexes synthesized with these ligands have been studied. The complexes have identical donor atoms, of nitrogen in sp^2 hybridization. The covalency degree of the Co(II)–N(sp^2) chemical bonds in the complexes has been examined as well as the weight of interactions influencing the values of magnetic susceptibilities (spin-orbit coupling, temperature-independent paramagnetism, and electron delocalization).

Our previous papers [1–5] have described the Co(II) complexes synthesized with the new type I organic ligands, of the class of 1-methyl-2-carbethoxy-glyoxalanil-(1)-phenylhydrazones-(2) differently substituted (Y = H, CH_3, OCH_3, NO_2) at the benzene ring of the hydrazone group.

The present work reports the synthesis of three new type I organic compounds, which are chloro-substituted at the benzene ring of the hydrazone group (Ia–Ic).

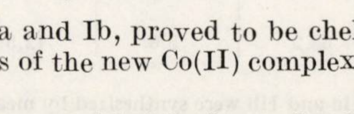

I

a: Y = p-Cl; b: Y = m-Cl; c: Y = o-Cl

Two of them, Ia and Ib, proved to be chelating ligands, since they afforded the synthesis of the new Co(II) complexes, IIa and IIb. The elec-

---

[1] P. Spacu, A. C. Banciu and C. I. Lepădatu, *Rev. Roumaine Chim.*, **18**, 1143 (1973).
[2] A. C. Banciu and P. Spacu, *Rev. Roumaine Chim.*, **19**, 1019 (1974).
[3] A. C. Banciu and P. Spacu, *Rev. Roumaine Chim.*, **19**, 1169 (1974).
[4] A. C. Banciu, *Rev. Roumaine Chim.*, **21**, 1487 (1976).
[5] A. C. Banciu, *Rev. Roumaine Chim.*, under press.

tronic spectra of the organic compounds Ia—Ic and the electronic spectra and the magnetic susceptibilities of the complexes IIa and IIb have been investigated and the results are reported here.

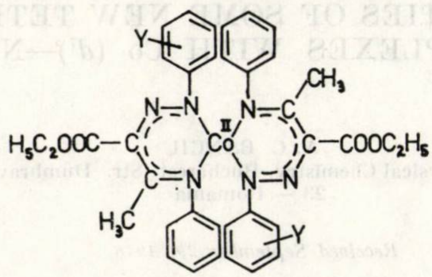

II

a: Y=p-Cl ; b: Y=m-Cl

EXPERIMENTAL

The new organic compounds Ia—Ic were synthesized according to the method described in our previous papers. [1–4] Their analytical data, which are in good agreement with the type I formulas, are listed in table 1.

Table 1

1-Methyl-2-carbethoxy-glyoxalanil-(1)-chlor-phenylhydrazones-(2). Analytical data

Compound	Y	C % calc. found	H % calc. found	N % calc. found	m.p. °C
Ia	$p-$Cl	62.88	5.28	12.22	102—107.5
		62.9	5.8	12.5	
Ib	$m-$Cl	62.88	5.28	12.22	88—91.5
		62.6	5.8	12.5	
Ic	$o-$Cl	62.88	5.28	12.22	126—128.5
		63.2	5.6	12.5	

The new Co(II) complexes IIa and IIb were synthesized by means of the new compounds Ia and Ib, respectively, as described in our previous papers. [1–5] The analytical data of the new complexes, which are in good agreement with their type II formulas, are listed in table 2.

The elemental analysis of Co, C, H and N was performed by usual micromethods.

The absorption spectra were determined on a VSU—2 Carl Zeiss (Jena) spectrophotometer on solutions in absolute ethyl alcohol (organic compounds Ia—Ic) and in acetone (complexes IIa and IIb).

Table 2

Co(II) chelates. Analytical data

Chelate	Y	Co % calc.	Co % found	C % calc.	C % found	H % calc.	H % found	N % calc.	N % found	m.p. °C
IIa	$p-Cl$	7.91	7.7	58.07	57.8	4.60	5.1	11.29	11.8	146−147
IIb	$m-Cl$	7.91	7.6	58.07	57.8	4.60	5.1	11.29	11.7	139−140

The diffuse reflectance spectra of the complexes were determined on a VSU−1 Carl Zeiss (Jena) spectrophotometer, using MgO as standard.

The magnetic susceptibilities were determined at room temperature, in the solid complexes, according to the Faraday method, using Hg [Co(NCS)$_4$] as standard. The magnetic moments were calculated by formula (1),

$$\mu_{eff} = 2{,}828\ [\chi'_M \cdot T]^{1/2}\ \text{B.M.} \qquad (1)$$

where $\chi'_M = \chi_M - \chi_M^{dia}$ is the molar susceptibility corrected for diamagnetism. For both complexes the diamagnetic correction was $\chi_M^{dia} = -376 \times 10^{-6}$ c.g.s.u./mole. On calculating χ_M and χ_M^{dia} the complexes were formulated as monomers, according to the formulas IIa and IIb.

RESULTS AND DISCUSSIONS

Similar to all the other type I compounds which are *ortho*-substituted at the benzene ring of the hydrazone group, the compound Ic has also failed to form complex compounds with the Co(II) ions. In all type I organic compounds, the substituents situated in the *ortho* position at the benzene ring of the hydrazone group hinder sterically the complexation of the metal ions. This fact is not surprising. The *ortho* position at the benzene ring of the hydrazone group is in the vicinity of a nitrogen atom which would form a chemical bond with the central metal ion, if complexation would occur. The magnitude of such steric hindrances is particularly observed in the case of the compound Ic. The latter fails to form complex compounds with the Co(II) ions although it contains, in the *ortho* position, the smallest of the substituents introduced so far (CH_3, OCH_3, NO_2, Cl) in the type I compounds. Thus, the chlorine substituent has a van der Waals radius of only 1.8 Å, smaller than the less bulky substituent CH_3 (~ 2 Å)[6].

However, if the above-mentioned substituents are situated in the *meta* or *para* positions in the benzene ring of the hydrazone group, the complexation of the transition metal ions will be no more sterically hindered. Thus, the compounds Ia and Ib are true chelating ligands. They were used to synthesize the complexes IIa and IIb, respectively.

---

[6] C. D. Nenițescu, "Chimie organică", București, 1966, vol. 1, p. 80.

ELECTRONIC SPECTRA OF THE ORGANIC COMPOUNDS Ia – Ic

The electronic spectra of the free ligands (compounds Ia–Ic) recorded within the 220–450 nm range, on solutions in absolute ethyl alcohol are shown in Figure 1.

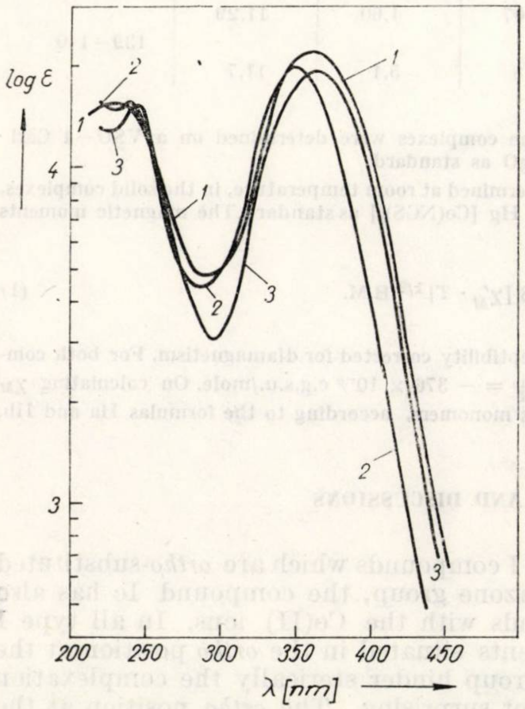

Fig. 1. — Electronic spectra of the organic compounds Ia – Ic.
1. compound Ia ; *2.* compound Ib ; *3.* compound Ic

The most intense bands ($\varepsilon_{\max} \sim 2 \times 10^4$), with maxima situated at 350–365 nm, undoubtedly represent allowed $\pi \rightarrow \pi^*$ transitions. Likewise, the bands with maxima situated at 230–245 nm may be assigned most likely, to some allowed $\pi \rightarrow \pi^*$ transitions. The following considerations support this assignment : 1. The wavelenght at which these bands occur (the $\pi \rightarrow \pi^*$ bands appear within the 200–700 nm range) ; 2. These bands are almost as intense ($\varepsilon_{\max} \sim 1.5 \times 10^4$) as the allowed $\pi \rightarrow \pi^*$ bands of the 350–365 nm range ; 3. When introducing methyl substituents in the chromophore system of some analogous compounds to Ia–Ic, the bands within the 230–245 nm range are also hypsochromically shifted, similar to the allowed $\pi \rightarrow \pi^*$ bands within the 350–365 nm range. (In the organic compounds analogous to Ia–Ic which are, however, not methyl substituted at the carbon atom no. 1 of molecule, the band at ca. 230 nm and ca. 360 nm are both bathochromically shifted, compared to those in the above

Ia—Ic compounds [7]); 4. By varying the used solvent, in the sense of increasing polarity (from n-hexane, of dielectric constant 1.89, to absolute ethyl alcohol, of dielectric constant 24.3) the bands at ca. 230 nm exhibit a negative solvatochromy, being also hypochromically shifted, like the allowed $\pi \to \pi^*$ bands at ca. 360 nm. [7]

Shoulders are observed in the spectra of all compounds Ia—Ic, at ca. 265 nm, representing less intense bands than those first discussed. Their relatively high extinction coefficients ($\varepsilon_{max} \sim 6 \times 10^3$) are very likely caused by some degree of overlap with the more intense bands, at ca. 230 nm. The assignement of the bands at ca. 265 nm is difficult and uncertain. Considering both the spectral range in which they occur, and the values of their extinction, the bands at ca. 265 nm could represent shifted and intensified α-benzene bands, $n \to \sigma^*$ transitions, or $n \to \pi^*$ transitions, or forbidden $\pi \to \pi^*$ transitions.

It is observed (Figure 1) that the electronic spectra of the compounds Ia—Ic are practically extended only to 450 nm wavelenght. This is an important fact in the study of the electronic spectra of the complexes formed by the ligands Ia—Ib with transition metal ions. The bands belonging to the complexes can be clearly observed in such spectra at wavelengths longer than 450 nm. They are not overlapped by more intense bands of the organic ligands.

ELECTRONIC SPECTRA OF THE COMPLEXES IIa AND IIb

As suggested by their composition, both complexes are four-coordinated chelate complexes. Each complex has a set of four identical donor atoms. These are nitrogen atoms in sp^2 hybridization state.

The electronic absorption spectra of the complexes, measured within the 350—450 nm range, on acetone solutions, are shown in Figure 2.

The three bands occurring in the spectrum of each complex are of sensibly different intensities. The very intense bands ($\varepsilon_{max} \sim 2.8 \times 10^4$) with maxima situated at ca 370 nm represent allowed $\pi \to \pi^*$ transitions, belonging to the appropriate organic ligands (Ia and Ib). Even though the two other bands with maxima situated at ca 550 nm ($\varepsilon_{max} \sim 1.3 \times 10^3$) and ca 1040 nm ($\varepsilon_{max} \sim 1 \times 10^2$) differ in their intensity, these are both due to some spin-allowed $d-d$ transitions, proper to the d^7 electronic configuration of the central Co(II) ion in a tetrahedral environment.

The energy expressions for the spin-allowed transitions in a—$d^7(T_d)$ electronic configuration, in the case of a weak coupling, are [8-10]:

$$ {}^4A_2(e^4\,t_2^3) \to {}^4T_2(e^3\,t_2^4) \qquad \Delta \qquad (2) $$

$$ {}^4A_2(e^4\,t_2^3) \to {}^4T_1^a(e^3\,t_2^4) \qquad 1.5\,\Delta + 7.5\,B - Q \qquad (3) $$

$$ {}^4A_2(e^4\,t_2^3) \to {}^4T_1^b\,(e^3\,t_2^4) \qquad 1.5\,\Delta + 7.5\,B + Q \qquad (4) $$

---

[7] A. C. Banciu, Ph. D. Thesis, Polytechnic Institute Bucharest, 1974.

[8] A. B. P. Lever, "Inorganic Electronic Spectroscopy", Elsevier, Amsterdam, 1968, Chapt. 8—9.

[9] Y. Tanabe and S. Sugano, *J. Phys. Soc. Japan*, **9**, 753 (1964).

[10] E. König, *Struct. and Bonding*, **9**, 175 (1971).

where :

$$Q = \frac{1}{2}\,[(0.6\,\Delta - 15\,B)^2 + 0.64\,\Delta^2]^{1/2} \qquad (5)$$

Δ is the orbital splitting parameter (the energy difference between the t_2 and e sublevels), while B is the Racah parameter for the interelectronic repulsion radial integrals ($B_{\mathrm{Co(II)}} = 980$ cm^{-1}).

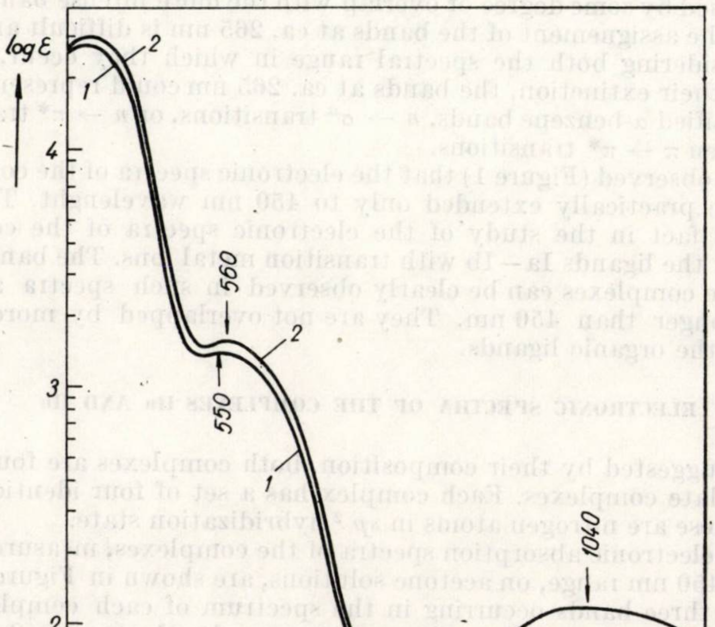

Fig. 2. — Electronic absorption spectra of the complexes IIa and IIb.

1. complex IIa; *2.* complex IIb.

The first of the indicated transitions occurs outside the measured spectral range, in the more-far infrared, at ca 4500–6500 cm^{-1}. This is so since $\Delta_{T_d} = 4/9\ \Delta_{o_h}$ and $\Delta_{o_h} = 10\,000\ \ldots\ 15\,000$ cm^{-1} (relation also valid in the frame of the LCAO-MO[11]).

---

[11] H. H. Schmdtke, *Z. Naturforsch.*, **19a**, 1502 (1964).

The bands occurring in the spectra of the complexes at ca 550 nm and ca 1040 nm are due to the last two of the above indicated transitions :

$$\nu_3({}^4A_2 \rightarrow {}^4T_1^b) = 17\,850 \text{ cm}^{-1} \text{ (560 nm) for the chelate IIa}$$

$$= 18\,200 \text{ cm}^{-1} \text{ (550 nm) for the chelate IIb}$$

$$\nu_2({}^4A_2 \rightarrow {}^4T_1^a) = 9\,600 \text{ cm}^{-1} \text{ (1040 nm) for both chelates IIa and IIb.}$$

Solving the energy expressions of these transitions one obtains the value :

$$\Delta_{1,2} = \frac{0.9\,(\nu_2 + \nu_3) \mp \sqrt{0.81(\nu_2 + \nu_3)^2 - 3.4\,\nu_2\,\nu_3}}{3.6} \text{ cm}^{-1} \qquad (6)$$

and thereby the values

$$B = \frac{(\nu_2 + \nu_3)/2 - 1.5\,\Delta}{7.5} \text{ cm}^{-1} \qquad (7)$$

and

$$\beta = \frac{B}{B_0} = \frac{B}{980} \qquad (8)$$

The determination error of the parameters Δ, B and β depends on the error with which the values ν_3 and ν_2, of the maxima of the bands at ca 550 nm and ca 1 040 nm, are experimentally measured. In our previous works [2-4] we have analysed such determination errors. It was shown [2-4] that the largest possible experimental error, which may have the greatest influence upon the calculated value of the nephelauxetic ratio β, is the determination error of the band ν_3 maximum, at ca 550 nm. It was also shown [2-4] that, if the maximum of the band ν_3 can be located with an error of only ± 5 nm (like in the case of the above mentioned complexes IIa and IIb), then all the cumulated errors of experimental determination of the ν_2 and ν_3 values modify eventually the calculated values of the nephelauxetic ratio β by at most 2 units at the second decimal.

The Δ, B and β values of the complexes IIa and IIb are systematized in table 3.

The values of the nephelauxetic ratio, β, for the type II complexes, substituted at the benzene ring of the hydrazone group are systematized in table 4.

It is observed that of the two new complexes the complex IIa (*p*-Cl-substituted) has practically the same β value as the unsubstituent type II complex. The *p*-Cl substituent will therefore not modify the covalency degree of the metal-ligand bonds in the type II complexes. In the case of this substituent the electronic (inductive and conjugation) effects, which are antagonistic ($-I > +M$), are largely anihilated. For this reason, the chlorine substituent fixed in the *para* position at the benzene ring of the hydrazone group practically fails to modify the electronic density at the

Table 3

The ν_2, ν_3, Δ, B and β values of the new Co(II) complexes

Complex	ν_3	ν_2	Δ [cm^{-1}]	B [cm^{-1}]	β
IIa	560 nm (17850 cm^{-1})	1040 nm (9600 cm^{-1})	5400	750	0.77 ± 0.02
IIb	550 nm (18200 cm^{-1})	1040 nm (9600 cm^{-1})	5390	775	0.79 ± 0.02

donor nitrogen atom which is directly bonded to the substituted benzene ring and, hence, it does not practically modify the covalency degree of the Co (II)—N bonds in type II complexes.

Table 4

The values of the σ^+-Brown constants of the substituents, Y, introduced into the type II complexes, at the benzene ring of the hydrazone group, and the values of the nephelauxetic ratio β, of the corresponding complexes

Type II complex Substituent Y	σ^+ — Brown	β	References
H —	—	$0,76 \pm 0,02$	1
$p-CH_3$ —	−0.306	0.75 ± 0.02	2
$m-CH_3$ —	−0.065	0.75 ± 0.02	2
$p-CH_3O$ —	−0.764	0.71 ± 0.02	3
$m-CH_3O$ —	+0.046	0.76 ± 0.02	3
$p-NO_2$ —	+0.777	0.81 ± 0.04	4
$m-NO_2$ —	+0.662	0.82 ± 0.04	4
$p-Cl$ —	+0,112	9.77 ± 0.02	this paper
$m-Cl$ —	+0.391	0.79 ± 0.02	this paper

The strength of electronic effects of the substituents can be measured by using the values of σ^+ — Brown substituent constants.[12] For the substituents introduced so far in the type II complexes, the σ^+ — Brown constants are also summarized in table 4. It is observed that among all these substituents, only the p-OCH_3 substituent and the NO_2 substituent (regardless of the *para* or *meta* position) exhibit such strong electronic effects, that their σ^+—Brown substituent constants are higher than 0.650, in absolute value. In such substituents, the strong electronic (inductive and conjugation) effects are summed up, being of the same sense. Therefore, when introduced in the type II complexes, at the benzene ring of the hydrazone group, these substituents modify the covalency degree of the metal-ligand chemical bonds to a perceptible extent (which really modifies the value of the nephelauxetic ratio β). The p-OCH_3 substituent increases the covalency degree ($\beta = 0.71 + 0.02$) and the NO_2 substituent decrease it ($\beta \approx 0.82 \pm 0.04$), regardless of the *para* or *meta* position.

---

[12] F. BADEA, "Mecanisme de reacţie în chimia organică", Bucharest, 1971, p 101.

Table 4 also shows that the new complexes IIb (m-Cl-substituted at the benzene ring of the hydrazone group) represents a limit situation in the series of type II complexes, from the point of view of the covalency of the Co(II)—N chemical bonds. The β value of this complex, of $0.79 \pm \pm 0.02$, represents a limit between the high β values just discussed, of 0.82 ± 0.04 (of the complexes 6 and 7 in table 4) on one hand, and the β values of 0.76 ± 0.02 (of the complexes 1, 2, 3, 5 and 8 in table 4) on the other hand. The last mentioned β values indicate, for the Co(II)—N chemical bonds in the complexes, a covalency practically unmodified by the respective substituents (Y = H, p-CH_3, $m-CH_3$, $m-OCH_3$, p-Cl), which have σ^+ — Brown constants smaller than 0.400, in absolute value. The electronic inductive effect ($-I$) of the $m-$Cl substituent (of σ^+ — Brown constant practically equal to 0.400) — which in the *meta* position is not compensated by the opposite $+M$ effect — reaches such a great strength that in the complex IIb the covalency degree of the Co(II)—N chemical bonds is influenced to a limit extent, between a practically negligible one (the complexes 1, 2, 3, 5 and 8 in table 4) and a real one i. e. experimentally perceptible one (the complexes 4, 6 and 7 in table 4).

MAGNETIC SUSCEPTIBILITIES AND MOMENTS

The electronic reflectance spectra recorded on the solid complexes IIa and IIb agree well with their above discussed absorption spectra. This shows that both complexes have, in solutions as well as in solid state, a tetrahedral structure for the Co(II)—N bonds.

Knowing from the electronic spectra the tetrahedral structure of the complexes, and the value of their orbital splitting parameter Δ, the data of the magnetic susceptibility measurements, made on the solid complexes, can be well explained in the following manner.

It is known [13,14] that the magnetic susceptibilities and the magnetic moments of the Co(II) tetrahedral complexes always differ from the spin-only values. For the Co(II) ion, with three unpaired electrons, they are $\chi_M^{s.o.} = 6250 \times 10^{-6}$ c.g.s.u./mole and, respectively, $\mu_{eff}^{s.o.} = 3.87$ B. M. The last value corresponds to formula (9),

$$\mu_{eff}^{s.o.} = [S(S+1)]^{1/2} \quad \text{B.M.} \qquad (9)$$

where $S = 3/2$.

For the complexes with an A ground term, such as the tetrahedral Co (II) ones, fairly exact χ_M and μ_{eff} values (i.e. close to the experimental ones) will be calculated, if the spin-orbit coupling is considered. The latter "mixes in", to a certain extent, the energetical higher states ($^4T_2$ and $^4T_1$

---

[13] B. N. Figgis and J. Lewis, "Progress in Inorganic Chemistry", Vol. 6, Interscience, New York, 1964.

[14] B. N. Figgis, "Introduction to Ligand Fields", Interscience, New York, 1966.

in the T_d Co(II) complexes) with the A ground state. Therefore, although in the complexes with A ground term the orbital contribution to the value of the magnetic susceptibility and moment is, in a first approximation, totaly quenched, a part of it is brought back, as a result of the spin-orbit coupling. Formulas (10) and (11), which take into account the influence of the spin-orbit coupling in the complexes with A ground term, are often considered as statisfactory :

$$\chi_M = (1 - 8\ \lambda/\Delta)\ \chi_M^{\mathrm{s.o.}} \tag{10}$$

$$\mu_{\mathrm{eff}} = (1-4\ \lambda/\Delta)\ \mu_{\mathrm{eff}}^{\mathrm{s.o.}} \tag{11}$$

In these formulas λ is the spin-orbit coupling constant of the free ion, Δ is the orbital splitting parameter and the value $(1-4\ \lambda/\Delta)$ represents the orbital contribution (due to the spin-orbit coupling) to the magnetic moment value.

A temperature independent paramagnetism (TIP), resulted from the higher energy ligand field levels, also contributes, to a smaller extent, to the χ_M value of the Co(II)T_d complexes. For the complexes with A_2 ground term this TIP contribution is given by formula (12).

$$\chi_M\mathrm{TIP} = 8\ N\ \beta^2/\Delta \tag{12}$$

where N = Avogadro's number, β = the Bohr magneton and the product $N\ \beta^2 = 0.261\ \mathrm{cm}^{-1}$. Formula (13) permits to calculate the magnetic susceptibility of the complexes with A_2 ground term, taking into account the spin-orbit coupling and the TIP contribution

$$\chi_M = \chi_M^{\mathrm{s.o.}}\ (1 - 8\ \lambda/\Delta) + 8\ N\ \beta^2/\Delta) \tag{13}$$

Sometimes, the magnetic susceptibility of the T_d Co(II) complexes is also influenced by the electron delocalization, from the t_2 orbitals of the metal ion, into the ligand atoms. The electron delocalization is expressed by the subunitary k factor, which represents the non-delocalization unit. (The value $2(1 - k)$ may be, approximately, regarded as the extent to which the p_π ligand orbitals enter to the molecular orbitals for the *"d"* electrons of the central ion). Formula (14) expresses the magnetic susceptibility of the complexes with A_2 ground term, taking into account the spin-orbit coupling, the TIP and the electron delocalization

$$\chi_M = \chi_M^{\mathrm{s.o.}}\ (1 - 8\ k^2\ \lambda\ /\Delta) + 8\ k^2\ N\ \beta^2/\Delta \tag{14}$$

Knowing $\lambda_{\mathrm{Co(II)}} = -178\ \mathrm{cm}^{-1}$ and the value Δ (determined from the electronic spectra), of $5400\ \mathrm{cm}^{-2}$, for both complexes IIa and IIb, it is possible to establish the weight of the most important effects (spin-orbit coupling, TIP and electron delocalization) which influence the values of the magnetic susceptibilities (and moments) of the Co(II) complexes in question.

Table 5

The χ_M and μ_{eff} values of the new Co(II) complexes

Formulas used for the calculation of χ_M or μ_{eff}	Considered interactions besides the spin-only values	The new complexes IIa and IIb		The complex $Cs_2\,CoCl_4$	
		$\chi_M \times 10^6$ [c.g.s.u./mole]	μ_{eff} [B.M.]	$\chi \times 10^6$ [c.g.s.u/mole]	μ_{eff} [B.M.]
(9)	—	6250	3.87	6250	3.87
(10) and (11)	spin-orbit coupling	7900	4.38	9000	4.65
(13)	spin-orbit coupling and T.I.P.	8290	4.46[a]	9650	4.81
Experimental values (at 298 K) which may be expressed by formula (14)	spin-orbit coupling, T.I.P. and electron delocalization	8440 ± 170[b]	4.49 ± 0.05[a, b]	9250	4.71

[a] Values calculated by means of χ_M, with the formula $\mu_{eff} = 2.828\ [\chi_M . T]\ 1/2$

[b] Experimental values for the complex IIa; the experimental susceptibility is corrected for diamagnetism: $\chi'_M = \chi_M - \chi_M^{dia}$; $\chi_M^{dia} = -\ 376 \times 10{-}^6$ c.g.s.u.

Table 5 summarizes the χ_M and μ_{eff} values calculated for the complexes IIa and IIb with the above formulas. For comparison purposes, the same table lists the corresponding values for a well-known T_d Co(II) complex, $Cs_2[CoCl_4]$, which was also throughly studied from a magnetic point of view.[13,14] It is observed that for the complexes under study, IIa and IIb, the spin-only susceptibility, of 6250×10^{-6} c.g.s.u./mole, represents ca 75 % of the total value of the experimental susceptibility. Another significant contribution is made by the orbital contribution, of ca 1650×10 c.g.s.u./mole, which represents about 20 % of the total value of the experimental susceptibility. Finally, the TIP of ca 390×10^{-6} c.g.s.u./mole (calculated by formula (13)), contributes with up to about 5 % to the total susceptibility value. The TIP contribution is practically equal to the diamagnetic correction (of 376×10^{-6} c.g.s.u./mole) and exceeds the limit of experimental errors (of ± 170 X 10^{-6} c.g.s.u./mole for the complex IIa).

The most interesting result of the magnetic measurements is the fact that in both complexes IIa and IIb, the electron delocalization is practically absent. Indeed, by applying equation (14), for instance in the case of the complex IIa, we have :

$$8400 = 6250 \left(1 + \frac{8k^2(178)}{5400}\right) + 8\,k^2\ \frac{0.261}{5400} \text{ or}$$

$$8400 = 6250 + 1650\ k^2 + 390\ k^2$$

whence the values $k^2 = 1.07$ and $k = 1.03$ are obtained. Evidently, the k value cannot be higher than unity. The small deviation of the k constant from the unitary value is explained, in particular, by the experimental determination error of the susceptibility. For the complex IIa the experimental errors are listed in table 5, while for the complex IIb the experimental errors are somewhat higher, of $\pm 220 \times 10^{-6}$ c.g.s.u./mole for χ_M and of ± 0.08 B.M. for μ_{eff}. Therefore, in the case of the complexes IIa and IIb the magnetic susceptibility is practically influenced only by the spin-only value, by the spin-orbit coupling and by the TIP. The practical absence of electron delocalization ($k \approx 1$) in the complexes IIa and IIb is not surprising. The electron delocalization depends on the extent to which π chemical bonds are formed between the central ion and the ligands atoms. As was shown in an earlier paper, [1] in the case of type II complexes with donor nitrogen atoms in sp^2 hybridization, the coordinative π bonds are very weak, if they ever form. Thus, in such complexes, due to the sp^2 hybridization of the nitrogen atoms, coordinative π bonds situated in the plane of the σ bonds cannot possibly occur. Finally, the out-of-plane π bonds, theoretically possible in the tetrahedral complexes with donor N(sp^2) atoms, appear as practically non-existent in the complexes IIa and IIb. This case differs from that represented, e. g. by the $CoCl_4^{2-}$ complex (see Table 5). In the latter case, the chlorine ligands are able to form π bonds with the central metal ion. The influence of the electron delocalization of the magnetic susceptibility is still perceptible in this complex. It presents $k \approx 0.95$, which indicates a small degree of electron delocalization.

It is of interest to mention that even though they do not exhibit coordinative π bonds, both complexes IIa and IIb show, however, an appreciable covalency degree for the Co(II)—N(sp^2) chemical bonds. This is due to the strong σ chemical bonds between Co(II) and N(sp^2). Thus, in the complexes IIa and IIb the nephelauxetic ratio β has rather small values, of 0.77 and 0.79 respectively. These values are still relatively close to the 0.73 value, in the case of the $CoCl_4^{2-}$ complex, which belongs to the T_d Co(II) complexes with an appreciable covalency for the metal-ligand bonds.

In addition, the appreciable covalency of the type II complexes is also clearly illustrated by the value of their orbital splitting parameter Δ, unusually high for the T_d complexes (of 5400 cm^{-1}, compared to only 3200 cm^{-1}, in the case of the $CoCl_4^{2-}$ complex!). The high Δ value is explained by a strong energy separation between the t_2 (σ antibonding) and e (π antiboding) levels, as a result of a strong σ interaction.

ACKNOWLEDGMENT. **I wish to thank lecturer V. Mincu, from the Polytechnic Institute of Bucharest, for the magnetic susceptibility measurements.**

Revue Roumaine de Chimie, **23**, *5*, 719–723 (1978)

STUDY OF THE INFLUENCE OF THE DIELECTRIC CONSTANT ON THE REACTION BETWEEN SIMPLE INORGANIC ANIONS IN SOLUTION

M. S. SUBHANI
Department of Chemistry, University of Nigeria
Nsukka, Nigeria

Received March 3, 1976

Rate constant of reaction (k'') between the Br^- and BrO_3^- ions was studied at various concentrations of the reaction ions and at various dielectric constants (D) of aqueous ethanol mixtures of 25°. From the plot of log K_0 against $1/D$ the value of r^* and r_{AB}' the radius of the transient species for single and double sphere models were calculated. Comparison of the experimental and theoretical values of r^* and r_{AB} showed that the description of the transient species could best be explained by the single sphere model.

INTRODUCTION

The variation of the specific rate of reaction between any two ionic species as a function of the dielectric constant of medium was studied by Amis, Laidler, and Laidler and Erying. [1-3] Two models were suggested for the shape of activated complex in an ionic reaction, the ‘single sphere’ and the ‘double sphere’ models.[4] The two models give the following equations respectively relating the radius of the activated complex with the specific rate constant.

$$\ln k_0 = \ln k_0' - \frac{e^2}{2\,DKT}\left[\frac{(Z_A + Z_B)^2}{r^*} - \frac{(Z_A)^2}{r_A} - \frac{(Z_B)^2}{r_B}\right] \tag{1}$$

$$\ln k_0 = \ln k' - \frac{(e^2)Z_A Z_B}{DKT\, r_{AB}} \tag{2}$$

where k_0 = specific rate constant at zero ionic strength, k_0' = specific rate constant at infinite dielectric constant, e = charge of an electron, Z_A = valence of the ion A, Z_B = valence of the ion B, D = dielectric constant

---

[1] E. S. Amis, *J. Chem. Educ.*, **29**, 337 (1952).

[2] K. J. Laidler, "Chemical Kinetics", Mc Graw Hill, New York, 1965, p. 212.

[3] K. J. Laidler and H. Erying, *Ann. New York Acad. Sci.*, **39**, 303 (1940).

[4] K. J. Laidler, "Reaction Kinetics", Pergamon, Oxford, 1963, p. 10, 17 and 19.

of the medium, K = Boltzmann constant, T = temperature, r_A = radius of the ion A, r_B = radius of the ion B, r^* = radius of the activated complex for single sphere model, and r_{AB} = radius of the activated complex for the double sphere model.

The reaction between bromide and bromate ions in acidic medium in aqueous ethanol mixture of different dielectric constant was studied in order to find out the dependence of the rate constant on the dielectric of the medium, the reaction between Br^- and BrO_3^- is a fourth order reaction in relatively lower acid concentration.[5-8] However in presence of large excess of hydrogen ions it behaves as pseudo second order reaction.

EXPERIMENTAL

All the chemicals used (Potassium bromide, potassium bromate and sulphuric acid) were of A. R. quality.

All solutions were prepared in triply distilled water.

The dielectric constant for the ethanol water mixture was measured by the method used by Subhani and Lacewala.[9] The velocity of the chemical reaction was measured by mixing 10 ml each of the acidified stock solutions of potassium bromide and potassium bromate in a reaction vessel. Then some volume of the reaction mixture was immediately transfered to the spectrophotometric cell for the estimation of bromine evolved at various intervals of time. Unicam SP 500 nm. the extinction coefficient of bromine solution wavelength was found to be 390 /$cm^2 mole^{-1}$ from the experimentally determined absorption curve for standard solution of bromine. Specific rate constant were determined from the second order plots.

RESULT AND DISCUSSION

The values obtained for the constant of the reaction show that at a constant ionic strength this value rises when the dielectric constant of the medium is lowered. This is presumably due to the increase in the activity of the reactants at lower dielectric constant. It was also noted that in some cases for the same value of the dielectric constant of the medium and for the different concentration of BrO_3^- and Br^- ions a decrease in the ionic strength increases the value for the specific rate constant. This is due to the effect of ionic strength on the specific rate constant as is obvious from the following equation :

$$\ln k'' = \ln k_0 + \frac{e^3}{(DKT)^{3/2}}\left[\frac{8\pi N}{1\,000}\right]^{1/2} Z_A Z_B \sqrt{\mu} \tag{3}$$

where k_0 = specific rate constant at zero ionic strength, N = Avogadro number, μ=ionic strength and k'' the observed specific rate constant at any ionic strength.

k_0 values for each ionic strength were extrapolated from the representations based on eq. 3.

---

[5] W. Judson and T. W. Walter, *J. Chem. Soc.*, **1898**, 410.

[6] C. W. Hinshelewood, *J. Chem. Soc.*, **1947**, 694.

[7] W. C. Bray and P. R. Davis, *J. Amer. Chem. Soc.*, **52**, 1427 (1930).

[8] H. A. Young and W. C. Bray, *J. Amer. Chem. Soc.*, **54**, 4284 (1932).

[9] M. S. Subhani, and Na. H. Lacewala, *J. Math. and Sci.*, **1**, 41 (1974).

Table 1

Values of the specific rate constant (k'') and the dielectric constant of the medium (D) and the concentration of the reactants at 25°C (H^+) = 9×10^{-2} M

Dielectric constant (D)	Concentration of KBr $\times 10^3$ (M)	Concentration of $KBrO_3$ $\times 10^4$(M)	Experimental specific rate constant (k'') $\times 10\,M^{-1}min^{-1}$
79.10	2.5	6.0	6.27
70.30	2.5	6.0	7.23
65.50	2.5	6.0	7.35
56.30	2.5	6.0	8.79
49.10	2.5	6.0	10.06
45.03	2.5	6.0	10.25
41.5	2.5	6.0	10.61
79.10	1.5	3.5	6.19
70.30	1.5	3.5	7.95
65.50	1.5	3.5	7.36
56.30	1.5	3.5	8.87
49.10	1.5	3.5	10.12
45.030	1.5	3.5	10.38
41.50	1.5	3.5	10.84
79.10	1.0	5.0	5.96
70.30	1.0	5.0	7.40
65.50	1.0	5.0	7.24
56.30	1.0	5.0	8.79
49.10	1.0	5.0	10.15
45.030	1.0	5.0	10.39
41.50	1.0	5.0	10.86
79.10	0.75	1.5	6.20
70.30	0.75	1.5	7.14
56.50	0.75	1.5	7.25
49.10	0.75	1.5	10.14
45.04	0.75	1.5	10.43
41.50	0.75	1.5	10.52
79.10	0.5	2.75	5.89
70.30	0.5	2.75	7.03
65.50	0.5	2.75	7.13
56.30	0.5	2.75	8.69
49.10	0.5	2.75	10.03
45.03	0.5	2.75	10.39
41.50	0.5	2.75	10.72
79.10	0.4	0.2	5.84
70.30	0.4	0.2	6.97
65.50	0.4	0.2	7.23
56.30	0.4	0.2	8.88
49.10	0.4	0.2	10.12
45.030	0.4	0.2	10.38
41.50	0.4	0.2	10.84

Table 1 (continued)

Dielectric constant *(D)*	Concentration of $KBr \times 10^3$ (M)	Concentration of $KBrO_3$ $\times 10^4$ (M)	Experimental specific rate constant $(k'') \times 10^{-1}$ min^{-1}
79.10	0.25	0.5	5.89
70.30	0.25	0.5	6.70
65.50	0.25	0.5	7.10
56.30	0.25	0.5	8.73
49.10	0.25	0.5	10.35
45.030	0.25	0.5	10.35
41.50	0.25	0.5	10.94

The plot of logarithm of specific rate constant at zero ionic strength against the reciprocal of the dielectric constant (79 − 41) was a straight line as shown in Figure 1. However, deviation from Figure 1 linearity was observed for values of the dielectric constant below 50. This may be due to the preferential association of water molecules with the reacting ions. Similar behaviour was observed by Scatchard, and Amis and Potts.[10,11]

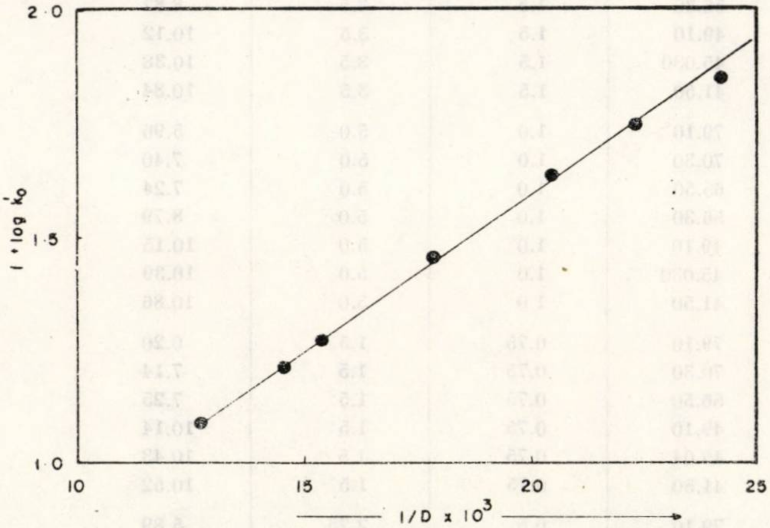

Fig. 1. — Plot of log k'_0 against $\frac{1}{D}$.

The experimental values of r^* and r_{AB} calculated from the slopes of straight lines using equations 1 and 2 respectively, are summarized in table 2.

The rate-determining step

$$H_2BrO_3^+ + Br^- \rightarrow H_2BrO_3Br \text{ (activated complex)} \qquad (4)$$

---

[10] G. S. Scatchard, *J. Chem. Phys.*, **7**, 657 (1939).

[11] E. S. Amis and J. E. Potts, *J. Amer. Chem. Soc.*, **63**, 2883 (1941).

is analogous to

$$H_2BrO_3^+ + I^- \rightarrow H_2BrO_3I \qquad (5)$$

suggested by Subhani and Lacewala [9] in the reaction of iodide and bromate ions in acidic aqueous solution.

The complete mechanism can be written as follows,

$$2H^+ + BrO_3^- \rightleftharpoons H_2BrO_3{}^+ \qquad (6)$$

$$H_2BrO^+ + Br^- \rightleftharpoons H_2BrO_3Br \text{ (activated complex).}$$

$$H_2BrO_3Br \longrightarrow Br - BrO_2 + H_2O \qquad (7)$$

$$Br - BrO_2 + Br^- \longrightarrow Br_2 + BrO_2^- \qquad (8)$$

The activated complex H_2BrO_3Br decomposes to form reactive intermediate $Br - BrO_2$ as given by King and Lister [12] and proposed by Taube and Dodgen. [13]

The experimental value of r^* and r_{AB} are 2.70 Å and 3.95 Å respectively. Theoretical values for the radius of $H_2BrO_3^+$ were calculated assuming that the volume of single sphere equal to the sum of volumes of spheres from which the single sphere has been built up the value for $r_{H_2BrO_3^+}$, was found on calculation to be 2.5 Å theoretical values for r^* and r_{AB} were calculated from the radii of $H_2BrO_3^+$ and Br^-ions (see table 2) are 2.84 Å and 4.45 Å respectively.

Table 2

Experimental and theoretical values of r^1 and r_{AB}

	Experimental values	Theoretical values
r^*	2·70Å	2.84Å
r_{AB}	3.95Å	4.45Å

Comparison of the experimental values with the theoretical values (see table 2) reflects that the shape of the activated complex is more similar to single sphere activated complex.

---

[12] D. E. C. King and M. W. Lister, *Canad. J. Chem.*, **46**, 269 (1968).

[13] H. Taube and H. Dodgen, *J. Amer. Chem. Soc.*, **71**, 3330 (1949).

Revue Roumaine de Chimie, **23**, *5*, 725–731 (1978)

UNIDENTATE COPPER-AMINE COMPLEXES, A STATISTICAL METHOD TO EVALUATE THE DISSOCIATION CONSTANT OF LABILE COMPLEXES

A. M. BALINT and F. KEREK
Centrul de Chimie Timişoara, Bd. M. Viteazul 24,
1900 Timişoara, România

Received February 25, 1976

Several (j = 99) stepwise increasing values between zero and ε_2 are given to the directly not measurable extinction coefficient (ε'_1) of the monoamine species, resulted by the dissociation of the labile $Cu \cdot (succinimidate)_2\ (amine)_2$ complexes (with ε_2 extinction coefficient). The optimal values for ε_1 are selected on hand of statistical criteria, i.e. by the minimal scattering coefficient (χ_j) of the dissociation constants K_{ij}, computed with the assumed ε'_{ij} values. Thus, $K = 2.64 \times 10^{-2}$ mol · l^{-1} have been obtained for *amine* = sec-butylamine and $K = 6.04 \times 10^{-2}$ mol · l^{-1} for *amine* = pyridine in CH_2Cl_2 solutions.

INTRODUCTION

Recently the structural[1] and chiroptical[2] investigations of several $Cu \cdot im_2 \cdot am_2$ (I) (where *im* = imidate anion, such as *su* = *succinimidate*; *am* = sterically not hindered amine) complexes have been performed. The usually pink coloured complexes, firstly obtained by Tschugaeff[3], are readily soluble in chloroform, methylene chloride or benzene, yielding dark blue solutions.

Earlier, authors[4,5] reported some constant extinction values for the absorption band in the visible region at ~ 600 nm. Thus, for instance, an $\varepsilon = 42.7$ l·mol^{-1} cm^{-1} was reported[4] for $Cu \cdot su_2 \cdot py_2$ (*py* = pyridine) at $\lambda = 595$ nm, and an $\varepsilon = 121$ l.mol^{-1} cm^{-1} for[5] $Cu.su_2.pr_2$ (*pr* = isopropylamine) at $\lambda = 630$ nm. These authors claimed the presence of stable complexes in solution assuming thus, that Beer's law is obeyed.

We observed on the contrary, that the extinction values are depending on concentration, which pleads for the lability of the complexes. Thus, for example, if the concentration of $Cu \cdot su_2 \cdot py_2$ varies between c = 0.004 mol · l^{-1} and 0.014 mol · l^{-1} the ε values are changed from $\varepsilon = 30.0$ to $\varepsilon = 37.2$ l·mol^{-1} cm^{-1}.

A similar concentration dependence was observed for the Δε values measured in CD spectroscopy with *am** = optically active amines. Thus, $\Delta\varepsilon = +0.25$ results at 565 nm by c = 0.001 mol · l^{-1} and $\Delta\varepsilon = +0.38$ if c = 0.01 mol · l^{-1} (c = concentrations of the $Cu \cdot su_2(+)bu_2$ complexes with $(+)bu$ = (+) sec-butylamine).

---

[1] F. Kerek and G. Snatzke, *Inorg. Chim. Acta*, **24**, 179 (1977).
[2] F. Kerek and G. Snatzke, *Angew. Chem.*, **87**, 133 (1975).
[3] L. Tschugaeff, *Ber. dtsch. chem. Ges.*, **38**, 2899 (1905).
[4] S. Miki and S. Yamada, *Bull. Chem. Soc. Japan*, **37**, 1044 (1964).
[5] G. Narain and P. Shukla, *Z. anorg. Chem.*, **342**, 221 (1966).

These facts can be explained by the dissociation of (I), according to equation (1):

$$Cu\ su_2\ am_2 \rightleftarrows Cu\ su_2\ am + am \tag{1}$$

The relations suggests investigation of the spectral behaviour at large amine excesses. This was done firstly by chiroptical investigations [1] obtaining already constant $\Delta\varepsilon$ values at [amine]/[$Cu\ su_2\ am_2$] ratios higher than 8. Thus, the $\Delta\varepsilon$ values measured at high amine concentrations correspond to the non-dissociated complexes. For the absorption spectrum of (I), assuming that no further coordination occurs (proved indirectly by chiroptical investigations [1]), the values measured at high amine concentrations can be taken as the extinction coefficients (ε_2) of the bis-amine complexes (I). The very broad absorption band of the bis-amine complexes covered the band of the monoamine species. By dilution only a bathochromic shift of about 50 nm is clearly observable but, isosbestic points cannot be recorded. For this reason, and due to the very small absorption values measured at high dilutions, the molar extinctions (ε_1) of the monoamine species cannot be determined properly. [6]

The dissociation constant (K) of the complexes (I) is given by equation (2):

$$\mathrm{K} = [Cu \cdot su_2 \cdot am]\cdot[am]/[Cu \cdot su_2 \cdot am_2] = c_1 \cdot a/c_2 \tag{2}$$

where: a = concentration of the free amine;
c_2 = concentration of $Cu \cdot su_2 \cdot am_2$ in equilibrium;
c_1 = concentration of $Cu \cdot su_2 \cdot am$ in equilibrium.

Actually, from the absorbance A/d (d = cell thickness) (3) measured at the wavelength λ_2 (see Figure 1)

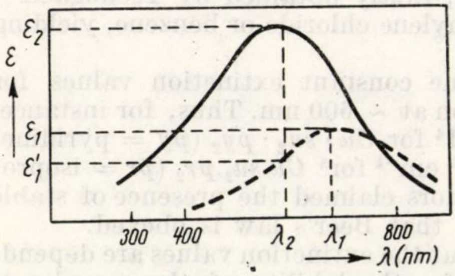

Fig. 1. — Experimental absorption curve (———) of the non-dissociated complex (I) and the hypothetical curve (----------) of the monoamine species,

$$A/d = c_2 \cdot \varepsilon_2 + c_1 \cdot \varepsilon_1' \tag{3}$$

and from the equation (4)

$$c_0 = c_1 + c_2 \tag{4}$$

(where c_0 = initial concentration of $Cu \cdot su_2 \cdot am_2$) the dissociation constant (K) could be computed if the molar extinction (ε_1') of the monoamine species were known. The ε_1' value from relation (3) corresponds to the extinction of the monoamine species at the absorption maximum (λ_2) of the bis-amine species. Figure 1 illustrates the real, experimentally obtained absorption band of a non-dissociated (I), together with the hypothetically assumed shape of the band, corresponding to the monoamine species.

---

[6] W. A. E. McBryde, *Talanta*, **21**, 975 (1974).

In order to determine ε'_1, a computerized statistical method was developed here. For complexes with two identical ligands, like our bis-amine species, the relation (5) is obvious:

$$\varepsilon'_1 = f \cdot \varepsilon_2 ; \qquad 0 < f < 1. \tag{5}$$

Different values are given for f within the $(0, \ldots, 1)$ range, computing for each of them corresponding dissociation constant (K_j). The optimal (K_{opt}) constant is chosen at the minimal value of the "scattering coefficient" $(\chi(j))$, which characterizes quantitatively a statistical behaviour.

RESULTS AND DISCUSSIONS

The absorbancies A_i/d_i have been measured for different initial concentrations of $Cu \cdot su_2 \cdot am_2$ (c_{0i}) with or without amine in excess (a_{ei}). (Tables 1 and 2).

Table 1

The absorbancies measured at 595 nm for different $Cu \cdot su_2 \cdot bu_2$ (c_{0i}) and sec-butylamine (a_{ei}) concentrations

i	c_{0i} mol · l^{-1}	a_{ei} mol · l^{-1}	A_i/d_i cm^{-1}	i	c_{0i} mol · l^{-1}	a_{ei} mol · l^{-1}	A_i/d_i cm^{-1}
1	0.00103	0.00	0.06	30	0.0027	0.195	0.40
2	0.00103	0.00355	0.06	31	0.0027	0.319	0.41
3	0.00103	0.0071	0.06	32	0.0027	0.479	0.42
4	0.00103	0.0106	0.06	33	0.0027	0.710	0.43
5	0.00103	0.0142	0.07	34	0.0036	0.00	0.36
6	0.00103	0.0177	0.08	35	0.0036	0.0142	0.45
7	0.00103	0.0213	0.09	36	0.0036	0.0284	0.49
8	0.00103	0.0391	0.11	37	0.0036	0.0426	0.50
9	0.00103	0.0745	0.13	38	0.0036	0.0568	0.51
10	0.00103	0.163	0.14	39	0.0036	0.071	0.52
11	0.00103	0.323	0.15	40	0.0056	0.00	0.68
12	0.00219	0.00	0.18	41	0.0056	0.0177	0.86
13	0.00219	0.0071	0.19	42	0.0056	0.0355	0.90
14	0.00219	0.0142	0.22	43	0.0056	0.0532	0.92
15	0.00219	0.0213	0.23	44	0.0056	0.071	0.93
16	0.00219	0.0284	0.24	45	0.0056	0.0877	0.94
17	0.00219	0.0355	0.24	46	0.0084	0.00	1.04
18	0.00219	0.0710	0.26	47	0.0084	0.0266	1.29
19	0.00219	0.1420	0.28	48	0.0084	0.0532	1.34
20	0.00219	0.248	0.30	49	0.0084	0.0798	1.37
21	0.00219	0.426	0,32	50	0.0084	0.106	1.37
22	0.00219	0.674	0.32	51	0.0084	0.133	1.40
23	0.0027	0.00	0.24	52	0.0102	0.00	1.36
24	0.0027	0.0106	0.28	53	0.0102	0.0355	1.68
25	0.0027	0.0231	0.30	54	0.0102	0.071	1.70
26	0.0027	0.0319	0.31	55	0.0102	0.106	1.72
27	0.0027	0.0426	0.32	56	0.0102	0.142	1.72
28	0.0027	0.0532	0.33	57	0.0102	0.177	1.72
29	0.0027	0.106	0.38				

$\varepsilon_2 = 167.6$ l · mol^{-1} · cm^{-1}

Table 2

The absorbancies measured at 595 nm for different $Cu \cdot su_2 \cdot py_2$ (c_{0i}) and pyridine (a_{ei}) concentrations

i	c_{0i} mol·l^{-1}	a_{ei} mol·l^{-1}	A_i/d_i cm^{-1}	i	c_{0i} mol·l^{-1}	a_{ei} mol·l^{-1}	A_i/d_i cm^{-1}
1	0.004	0.00	0.12	20	0.0097	0.0485	0.42
2	0.004	0.0496	0.15	21	0.0097	0.121	0.54
3	0.004	0.124	0.20	22	0.0097	0.242	0.66
4	0.004	0.248	0.26	23	0.0097	0.364	0.72
5	0.004	0.372	0.28	24	0.0097	0.606	0.78
6	0.004	0.496	0.30	25	0,0121	0.00	0.44
7	0.0058	0.00	0.18	26	0.0121	0.0496	0.53
8	0.0058	0.0495	0.21	27	0.0121	0.123	0.68
9	0.0058	0.1235	0.28	28	0.0121	0.371	0.88
10	0.0058	0.248	0.36	29	0.0121	0.619	0.95
11	0.0058	0.370	0.40	30	0.0121	1.116	0.98
12	0.0058	0.495	0.43	31	0.0121	1.62	0.98
13	0.0072	0.00	0.22	32	0.0145	0.00	0.54
14	0.0072	0.0489	0.27	33	0.0145	0.0493	0.65
15	0.0072	0.122	0.36	34	0.0145	0.123	0.86
16	0.0072	0.245	0.45	35	0.0145	0.369	1.10
17	0.0072	0.367	0.50	36	0.0145	0.616	1.18
18	0.0072	0.489	0.56	37	0.0145	1.109	1.22
19	0.0097	0.00	0.34	38	0.0145	1.595	1.19

$\varepsilon_2 = 82.0 \text{ l} \cdot \text{mol}^{-1} \text{ cm}^{-1}$

The concentration of the amine (a_i) in equilibrium is the sum of the concentration of the free amine, resulted by dissociation of the complexes (α_i = the dissociation degree), and that of the amine added in excess (a_{ei}) (equation (6)):

$$a_i = \alpha_i c_{0i} + a_{ei} \tag{6}$$

For each ($i = 1, \ldots, N$) measurement j dissociation constants (K_{ij}) are computed, where j is equal to the number of consecutively given f values (equation (5)). For practical purposes, a $j = 99$ corresponding to stepwise (0.01) increase of f, from 0.01 to 0.99, is quite sufficient. The logical diagram of the computational procedure is given by Figure 2.

The scattering coefficient was computed for each step according to equation (7):

$$\chi(j) = \left[\sum_{i=1}^{N} |\,\text{MED}(j) - K_{ij}\,|^2 \right]^{1/2} \cdot (\text{MED}(j))^{-1} \tag{7}$$

where

$$\text{MED}(j) = \frac{1}{N} \sum_{i=1}^{N} K_{ij}. \tag{8}$$

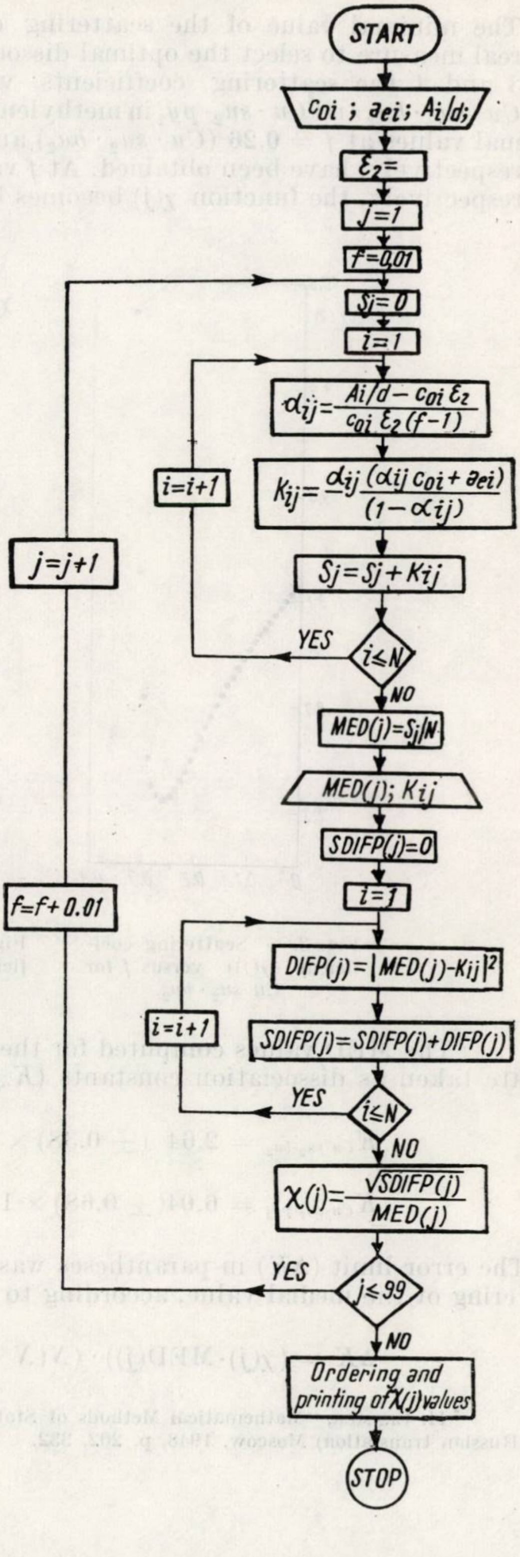
START
c_{oi} ; a_{ei} ; A_i/d;
ε_2 =
j=1
f=0.01
Sj=0
i=1
$\alpha_{ij}=\frac{A_i/d-c_{oi}\varepsilon_2}{c_{oi}\varepsilon_2(f-1)}$
i=i+1
$K_{ij}=\frac{\alpha_{ij}(\alpha_{ij}c_{oi}+a_{ei})}{(1-\alpha_{ij})}$
j=j+1
$S_j=S_j+K_{ij}$
YES
$i\leq N$
NO
$MED(j)=S_j/N$
$MED(j)$; K_{ij}
SDIFP(j)=0
i=1
f=f+0.01
$DIFP(j)=|MED(j)-K_{ij}|^2$
i=i+1
SDIFP(j)=SDIFP(j)+DIFP(j)
YES
$i\leq N$
NO
$\chi(j)=\frac{\sqrt{SDIFP(j)}}{MED(j)}$
YES
$j\leq 99$
NO
Ordering and printing of $\chi(j)$ values
STOP

Fig. 2. — Logical diagram.

The minimal value of the scattering coefficient[7] ($\chi(j)$) seems to be a real measure to select the optimal dissociation constant (K_{opt}). In Figures 3 and 4 the scattering coefficients versus factor f are plotted for $Cu \cdot su_2 \cdot bu_2$ and $Cu \cdot su_2 \cdot py_2$ in methylene chloride solutions. Obvious minimal values at $f = 0.26$ ($Cu \cdot su_2 \cdot bu_2$) and at $f = 0.20$ ($Cu\ su_2py_2$) respectively, have been obtained. At f values higher than 0.32, and 0.35 respectively, the function $\chi(j)$ becomes highly oscillating.

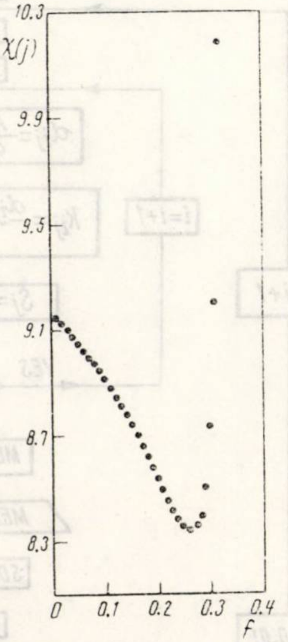

Fig. 3. — Scattering coefficient ($\chi(j)$) versus f for $Cu \cdot su_2 \cdot bu_2$.

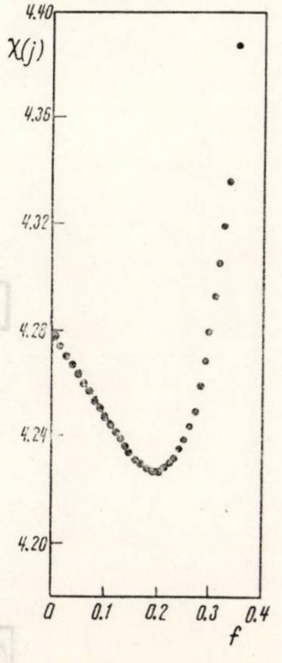

Fig. 4. — Scattering coefficient ($\chi(j)$) versus f for $Cu \cdot su_2 \cdot py_2$.

The MED values computed for the $j = 26$, and $j = 20$ respectively, are taken as dissociation constants (K_{opt}) of each complex :

$$K_{Cu\ su_2 \cdot bu_2} = 2.64 \ (\pm 0.38) \times 10^{-2} \ l \cdot \text{mol}^{-1};$$

$$K_{Cu \cdot su_2 \cdot py_2} = 6.04 (\pm 0.68) \times 10^{-2} \ l \cdot \text{mol}^{-1}.$$

The error limit (ΔK) in parantheses was calculated as the standard scattering of the medial value, according to equation (9) :

$$\Delta K = (\chi(j) \cdot \text{MED}(j)) \cdot (N(N-1))^{-1/2} \qquad (9)$$

---

[7] H. Cramer, "Mathematical Methods of Statistics" 1st Ed., Gosud. Izd. Inostr. Lit., (Russian translation) Moscow, 1948, p. 202, 332.

The above outlined statistical method is able to determine the extinction coefficient of the dissociated, non isolable, species. Thus, it becomes possible to evaluate the dissociation constant of labile complexes, only on hand of measurement of the absorption at a single wave length.

EXPERIMENTAL

The complexes (I) have been prepared from metallic copper, amine and succinimide in ethanolic media.[3] Their composition and structure was checked[8] by combustion analysis, ESR and mass spectra. The initial concentration (c_{0i})of (I) in solutions was calculated directly from the weighed complex and solvent amounts. The amine amounts added in excess have been carefully weighed. Spectra are recorded (at $t = 25°C$) within the 450 – 800 nm range with an UNICAM SP–800 spectrophotometer, using cell thickness $d = 0.5$ or 1.0 cm. The computer program, written in FORTRAN–IV, is available on request. An IRIS–50 computer of the Regional Computer Center of Timişoara was used.

---

[8] J. Hollaender and F. Kerek, submitted to *Inorg. Chim. Acta.*

Revue Roumaine de Chimie 23, 5, 733–746 (1978)

CHEMICAL GRAPHS. XXXIII[1]

GRAPHS FOR INTRAMOLECULAR REARRANGEMENTS OF TETRAGONAL-PYRAMIDAL COMPLEXES

ALEXANDRU T. BALABAN
Department of Organic Chemistry, The Polytechnic, Bucharest,
Romania

Received December 6, 1977

Notations are proposed for pentacoordinated tetragonal-pyramidal complexes with five different ligands, when enantiomerism is, or is not, taken into account. For the seven possible modes of intramolecular rearrangements, reaction graphs are devised showing how the 30 isomers (considering enantiomerism) or 15 isomers (disregarding enantiomerism) are interconnected in these interconversions.

INTRODUCTION

Reaction graphs for intramolecular rearrangements were analyzed in Part XVI of this series for hexacoordinated octahedral complexes,[2] and in Part XIX for pentacoordinated trigonal-bipyramidal complexes.[3] These are the most symmetrical and important 6- and 5-coordinated complexes, respectively, and have therefore received the most detailed consideration. These graphs were reviewed in books by Gielen (for both these types of complexes)[4] and by Luckenbach (only for pentacoordinated phosphorus compounds),[5] as well as in monograph chapters by Gielen[6], by Ugi and coworkers,[7] or by Rouvray and Balaban.[8]

The present paper describes reaction graphs for intramolecular rearrangements of pentacoordinated tetragonal-pyramidal complexes. Though such complexes are less frequently encountered than trigonal-bipyramidal complexes, their importance in organometallic chemistry is rapidly growing. When a metal atom such as molybdenum or tungsten is coordinated to an η^5 -cyclopentadienyl ring and to four other unidentate ligands, the complex possesses a tetragonal-pyramidal geometry with the ring at the apex, as shown by an X-ray analysis of $(C_5H_5)Mo(CO)_3Et$. [9,10]

---

[1] Preceding part, A. T. Balaban, *Croatica Chim. Acta* (in press).

[2] A. T. Balaban, *Rev. Roumaine Chim.*, **18**, 841 (1973).

[3] A. T. Balaban, *Rev. Roumaine Chim.*, **18**, 855 (1973).

[4] M. Gielen, "Stéréochimie Dynamique", Freund Publication House, Tel Aviv, 1974.

[5] R. Luckenbach, "Dynamic Stereochemistry of Phosphorus and Related Elements", Thieme, Stuttgart, 1973, p. 214.

[6] M. Gielen, in "Chemical Applications of Graph Theory" (ed. A. T. Balaban), Academic Press, London, 1976, p. 261.

[7] I. Dugundji, P. Gillespie, D. Marquarding, I. Ugi and F. Ramirez, in "Chemical Applications of Graph Theory" (ed. A. T. Balaban), Academic Press, London, 1976, p. 107.

[8] D. H. Rouvray and A. T. Balaban, in "Applications of Graph Theory" (ed. R. J. Wilson and L. W. Beineke), Academic Press, London, 1979.

Such complexes are stereochemically stable at room temperature : *cis-trans* isomers of $(C_5H_5)Mo(CO)_2(PPh_3)I$ could be separated, and dynamic NMR spectroscopy [11] showed that at elevated temperatures these isomers become converted into an equilibrium mixture. The transition state is probably a trigonal bipyramid (the cyclopentadienyl ring remains at an apical position throughout the process). Similar observations were made polarimetrically for the epimerization of optically active tetragonal-pyramidal complexes.[12]

It should be borne in mind that *vice-versa*, pseudorotations of trigonal-bipyramidal complexes are assumed to proceed through tetragonal-pyramidal transition states.[3]

With five different ligands, tetragonal-pyramidal complexes give rise to 30 isomers existing as 15 pairs of enantiomers. Indeed, the apex may be each of the five ligands, and the remaining four ligands can be arranged in six different circular permutations.

NOTATIONS FOR TETRAGONAL-PYRAMIDAL COMPLEXES WITH FIVE DIFFERENT LIGANDS

We need a short notation for tetragonal-pyramidal complexes with five different ligands, in order to use this notation in the reaction graphs which will be described in the following sections. If the five ligands are denoted by digits 1 through 5, an obvious notation is to list first the ligand at the apex, then to add a comma, and then to list the four ligands at the square base starting with the ligand with the lowest digit and proceeding in anticlockwise order when looking at the base from the apex. This "full notation" can, however, be abbreviated to a "stereochemical notation" without loss of information by omitting the first two digits after the comma : of these, the first digit is always 1, unless 1 appears before the comma as the ligand at the apex, when the first digit after the comma is 2 ; the second digit after the comma can be found by difference, because three digits appear in the stereochemical notation and the fourth is 1 or 2 as shown above.

Figure 1 presents the enantiomeric pair of complexes 1,45 and 1,43 (in stereochemical notation, which will be used henceforth). It is easy to pass from the full notation to the stereochemical notation (omit the first two digits after the comma), and *vice-versa* (insert after the comma 1, unless 1 appears before the comma when 2 should be inserted, follow by the missing fifth digit from the set 1 through 5, and then add the

---

[9] M. J. Bennett and R. Mason, *Proc. Chem. Soc.*, **1963**, 273.

[10] K. W. Barnett and D. W. Slocum, *J. Organomet. Chem.*, **44**, 1 (1972).

[11] L. M. Jackman and F. A. Cotton, "Dynamic Nuclear Magnetic Resonance Spectroscopy", Academic Press, New York, 1975, p. 494.

[12] H. Brunner, *Ann. N. Y. Acad. Sci.*, **239**, 213 (1974) ; *Topics Curr. Chem.*, **56**, 67 (1975) ; *Chemie in Unserer Zeit*, **11**, 157 (1977) and further references therein.

last two digits which in the stereochemical notation were following the comma).

The stereochemical notation includes information about the stereochemistry of the complex. If the stereochemistry is to be disregarded, i.e. if two enantiomeric complexes of a pair are to be treated as the same constitutional isomer, the notation is further abbreviated to a constitutional notation by omitting the last digit as shown by the lowest line of notation in Figure 1.

The rationale behind these notations is the following. It can be observed that the proposed stereochemical notation consists of three digits. The two enantiomers of a pair have the same apex and the same ligand opposing the ligand with the lowest digit at the square base (hence the first two digits, preceding and following the comma, are the same for both enantiomers), but the other two ligands at the base are permuted. Therefore the first two digits of the three composing the stereochemical notation characterize the constitution, and are the only digits retained in the constitutional notation, which disregards enantiomerism. The stereochemical information which discriminates among the two enantiomers of a pair resides in the last, third, digit of the stereochemical notation. To ignore stereoisomerism, therefore, one has to cancel this last digit of the stereochemical notation.

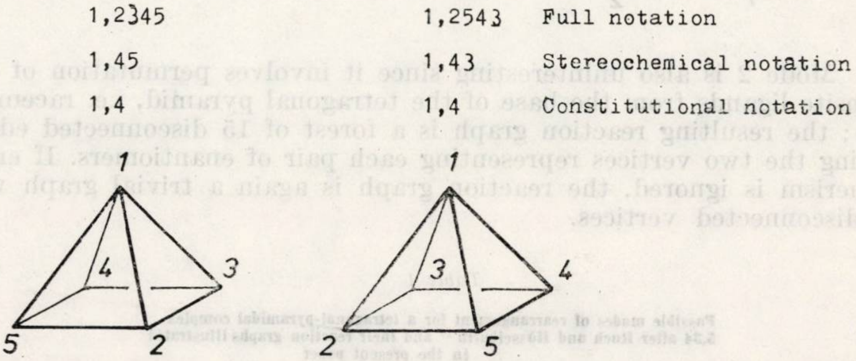

Fig. 1. — Two enantiomeric tetragonal-pyramidal complexes with five different ligands and their notations.

REARRANGEMENT MODES

The permutationally and mechanistically different intramolecular rearrangements of 5- and 6-coordinated complexes were termed "modes of rearrangement" by Musher.[13] Using double cosets, Ruch and Hässelbarth [14] showed how many different modes of rearrangement are possible for various complexes. For the case of a tetragonal-pyramidal complex with stereochemical notation 5,34 presented in Figure 2 ("standard complex"), there are seven possible rearrangement modes listed in table 1.

---

[13] J. I. Musher, *J. Chem. Educ.*, **51**, 94 (1974).

[14] E. Ruch and W. Hässelbarth, *Theor. Chim. Acta*, **29**, 259 (1973).

Mode 1 is trivial (no rearrangement) : it gives rise to a trivial graph with 30 (or 15 when ignoring enantiomerism) disconected vertices.

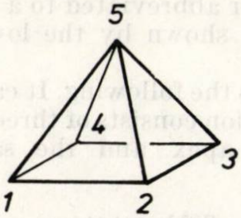

Fig. 2. — Tetragonal-pyramidal complex 5,34 for the definition of rearrangement modes.

Mode 2 is also uninteresting since it involves permutation of two opposite ligands from the base of the tetragonal pyramid, i.e. racemization ; the resulting reaction graph is a forest of 15 disconnected edges, linking the two vertices representing each pair of enantiomers. If enantiomerism is ignored, the reaction graph is again a trivial graph with 15 disconnected vertices.

Table 1

Possible modes of rearrangement for a tetragonal-pyramidal complex 5,34 after Ruch and Hässelbarth [14] and their reaction graphs illustrated in the present paper

Mode	Permutation of ligands	Degree of resulting regular graph	Figures in the present paper	
			Including enantiomerism	Excluding enantiomerism
1	(1)	1	—	—
2	(13)	1	—	—
3	(12)	4	3	
4	(15)	4	4, 5	6, 7
5	(135)	4	8, 9, 10	6,
6	(125)	8	11, 12	13, 14
7	(12) (35)	8	15, 16	13, 14

Mode 3 which involves a trigonal-bipyramidal transition state and thus is probably operating in the complexes described above, permutes two ligands which are adjacent at the base of the pyramid. The apex is not changed. By effecting the permutations, it emerges that the complex 5,34 from Figure 2 may isomerize into (or the vertex of the reaction graph bearing the notation 5,34 is adjacent to) the following four complexes (or vertices, respectively) : 5,42 ; 5,43 ; 5,23 ; 5,24. Therefore the resulting reaction graph consists of five disconnected regular subgraphs of degree four with five vertices each. One of these five disconnected subgraphs is presented in Figure 3.

If enantiomerism is disregarded, vertex 5,4 is adjacent to two vertices : 5,2 and 5,3. The reaction graph in this case consists in five disconnected triangles.

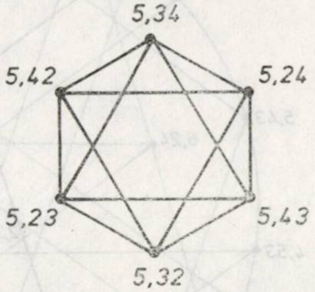

Fig. 3. — Subgraph of the disconnected reaction graph for rearrangement 3, involving permutations of type (12).

REACTION GRAPHS FOR REARRANGEMENT MODE 4

The rearrangement mode 4 involving permutations of type (15) of ligands (for the standard complex presented in Figure 2) gives rise to more interesting reaction graphs. If the apex of the complex 5,34 is permuted with any of the four ligands of the base, the vertex of the reaction graph symbolizing the complex 5,34 is adjacent to the following four vertices : 1,45 ; 2,34 ; 3,54 ; 4,35. By constructing the adjacency matrix of the reaction graph, one can display it for brevity under the form presented in table 2. In order to reduce by half the number of rows

Table 2

Adjacency matrix of the reaction graph for rearrangement mode 4, in abridged form (see text for conventions)

	1,35	1,43	1,53	2,34	2,43	2,53	3,25	3,42	3,52	4,25	4,32	4,52	5,23	5,34	5,43
1,35				*b*	0	0	*b*	0	0	0	0	*a*	0	0	*a*
1,43				0	*a*	0	0	0	*b*	*a*	0	0	0	*b*	0
1,53				0	0	*a*	0	*b*	0	0	*a*	0	*b*	0	0
2,34	*b*	0	0				*b*	0	0	0	*a*	0	0	*a*	0
2,43	0	*a*	0				0	*a*	0	*b*	0	0	0	0	*a*
2,53	0	0	*a*				0	0	*a*	0	0	*b*	*a*	0	0
3,25	*b*	0	0	*b*	0	0				*a*	0	0	*a*	0	0
3,42	0	0	*b*	0	*a*	0				0	*a*	0	0	0	*b*
3,52	0	*b*	0	0	0	*a*				0	0	*a*	0	*b*	0
4,25	0	*a*	0	0	*b*	0	*a*	0	0				*b*	0	0
4,32	0	0	*a*	*a*	0	0	0	*a*	0				0	*b*	0
4,52	*a*	0	0	0	0	*b*	0	0	*a*				0	0	*b*
5,23	0	0	*b*	0	0	*a*	*a*	0	0	*b*	0	0			
5,34	0	*b*	0	*a*	0	0	0	0	*b*	0	*b*	0			
5,43	*a*	0	0	0	*a*	0	0	*b*	0	0	0	*b*			

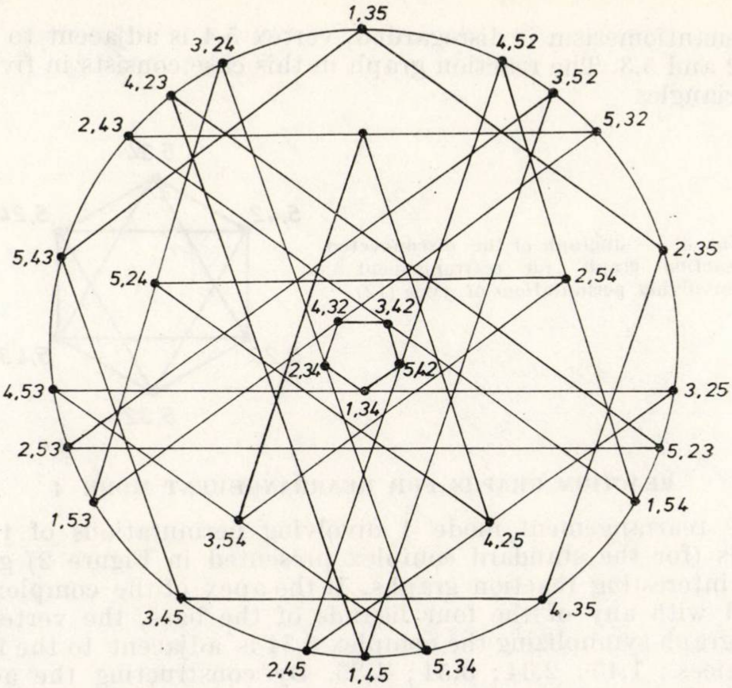
1,35
3,24
4,52
4,23
3,52
2,43
5,32
5,43
2,35
5,24
2,54
4,32
3,42
2,34
5,42
4,53
1,34
3,25
2,53
5,23
1,53
1,54
3,54
4,25
3,45
4,35
2,45
1,45
5,34

Fig. 4. — Representation with fivefold symmetry of the reaction graph for rearrangement mode 4, involving permutations of type (15).

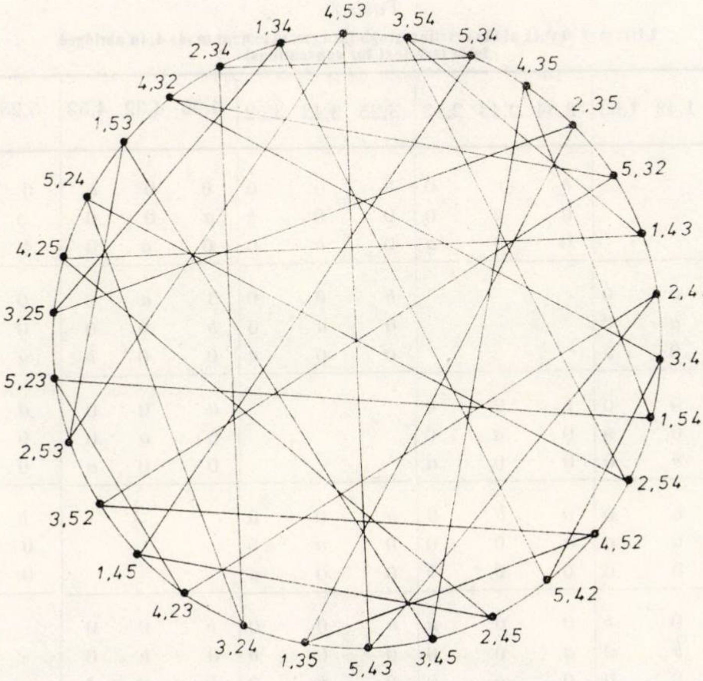
4,53
1,34
3,54
5,34
2,34
4,35
4,32
2,35
1,53
5,32
5,24
1,43
4,25
2,43
3,25
3,42
5,23
1,54
2,53
2,54
3,52
4,52
1,45
5,42
4,23
2,45
3,24
1,35
5,43
3,45

Fig. 5. — Representation emphasizing a Hamiltonian circuit of the same reaction graph as in Fig. 4.

and colums of the adjacency matrix, only one enantiomer of each pair of antipodes is included. Adjacency is symbolized by letter *a* in the place of the conventional digit 1 : if a vertex listed on the left is adjacent to a vertex listed on top of table 2, then at the intersection of that row and column an *a* is to be found. Letter *a* also symbolizes adjacency between the two antipodes of the vertices listed on top and on the left. On the other hand, letter *b* in table 2 indicates that the vertex listed on the left is adjacent to the antipode of the vertex listed on top, or *vice-versa*, that the antipode of the vertex listed on the left is adjacent to the vertex listed on top. A zero or a blank space indicates non-adjacency between vertices.

Two isomorphic representations of the reaction graph for this rearrangement mode are shown in Figures 4 and 5 : the former representation has fivefold symmetry, the latter has threefold symmetry and evidences a Hamiltonian circuit. From the latter representation, other similar representations may be found. Space limitations preclude the display of these other representations, or of representations with two congruent 15-circuits or with three congruent 10-circuits. These can be provided on request. The reaction graph from Figures 4 and 5 is regular of degree four and girth* five.

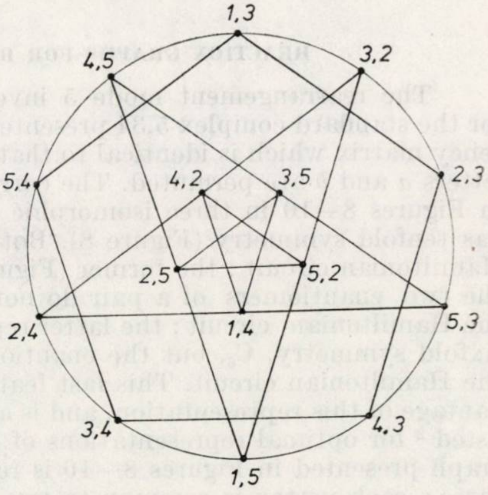

Fig. 6. — Representation with fivefold symmetry of the reaction graph for rearrangement modes 4 and 5, involving permutations of type (15) and (135), respectively, disregarding enantiomerism.

If enantiomerism is disregarded, the 30-vertex graph shown in Figures 4 and 5 reduces to a 15-vertex graph presented in Figures 6 and 7 in two different isomorphic representations : the former has fivefold symmetry, the latter has threefold symmetry and emphasizes a Hamiltonian circuit. This graph is regular of degree four and has girth three. Its adjacency matrix results from table 2 by replacing both letters *a* and *b* by the same adjacency symbol, e.g. the conventional digit 1, and by suppressing the last digit of the vertex notations.

---

* The girth of a graph is the length of its shortest circuit.

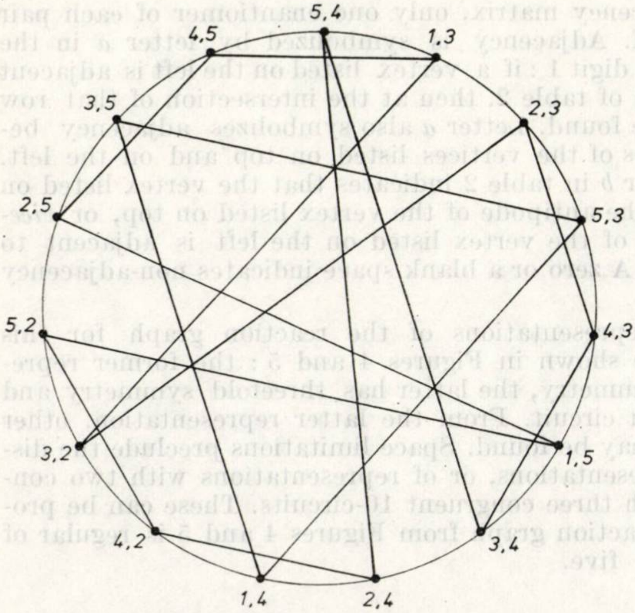

Fig. 7. — Representation emphasizing a Hamiltonian circuit of the same reaction graph as in Fig. 6.

REACTION GRAPHS FOR REARRANGEMENT MODE 5

The rearrangement mode 5 involving permutations of type (135) for the standard complex 5,34 presented in Figure 2 gives rise to an adjacency matrix which is identical to that of table 2 with the exception that letters *a* and *b* are permuted. The corresponding reaction graph is shown in Figures 8—10 in three isomorphic representations, the first of which has tenfold symmetry (Figure 8). Both other representations evidence a Hamiltonian circuit : the former (Figure 9) has sixfold symmetry D_6 but the two enantiomers of a pair do not appear at antipodal positions on the Hamiltonian circuit ; the latter representation (Figure 10) has a lower sixfold symmetry, C_6, but the enantiomers are in antipodal positions on the Hamiltonian circuit. This last feature is a particularly attractive advantage of this representation, and is among the requirements which were listed [2] for optimal representations of such reaction graphs. The reaction graph presented in Figures 8—10 is regular of degree four and has girth three ; each vertex is common to two 3-circuits.

If enantiomerism is disregarded, the 30-vertex graph reduces to the same graph with 15 vertices which was discussed in the preceding section and was represented in Figures 6 and 7. The fact that both reaction graphs for modes 5 and 4 reduce to the same reaction graph when disregarding enantiomerism was to be expected from the relationship between the adjacency rules for modes 5 and 6 (permutation of letters *a* and *b* in Table 2, and replacement of both these letters by the same adjacency symbol on ignoring stereoisomerism).[15]

---

[15] Cf. also D. A. Waller, *Bull. Austral. Math. Soc.*, **14**, 233 (1976) ; ***MatCh*** (in press) ; M. Farzan and D. R. Waller, *Canad. J. Math.*, **29**, 255 (1977).

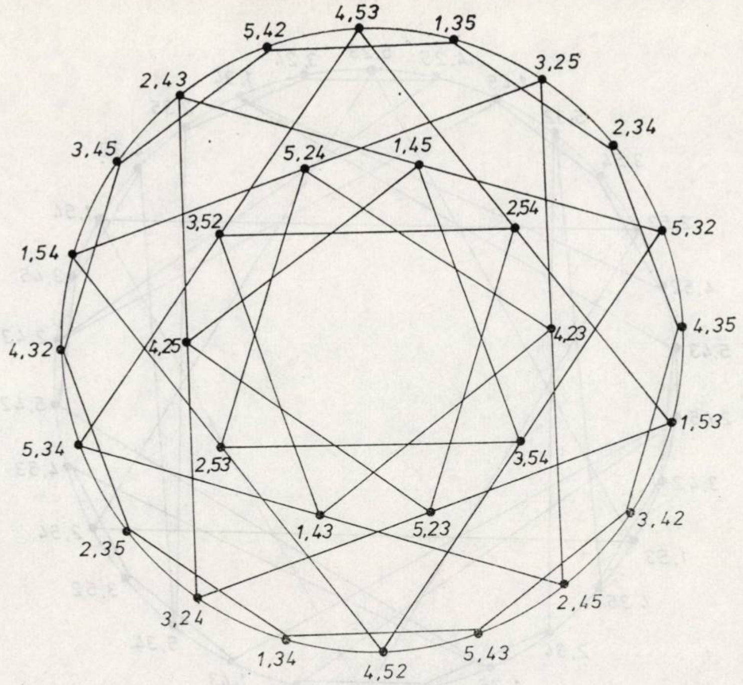
4,53
5,42
1,35
3,25
2,43
2,34
3,45
5,24
1,45
2,54
3,52
5,32
1,54
4,35
4,32
4,25
4,23
1,53
5,34
2,53
3,54
3,42
1,43
5,23
2,35
2,45
3,24
1,34
4,52
5,43

Fig. 8. — Representation with tenfold symmetry of the reaction graph for rearrangement mode 5, involving permutations of type (135).

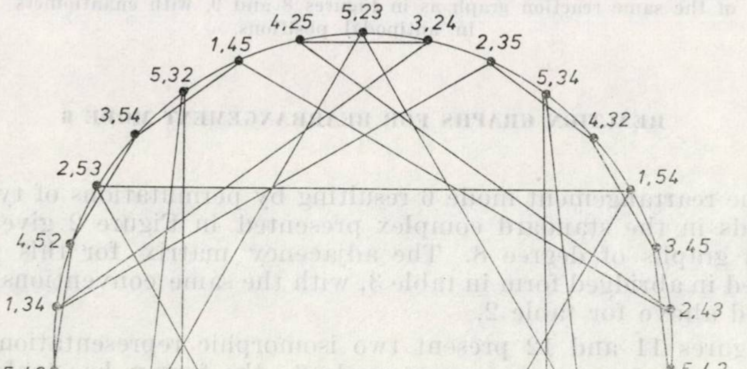
4,25
5,23
3,24
1,45
2,35
5,32
5,34
3,54
4,32
2,53
1,54
4,52
3,45
1,34
2,43
5,42
5,43
4,53
3,42
2,54
1,53
3,52
4,35
1,43
2,34
2,45
1,35
3,25
5,24
4,23

Fig. 9. — Representation with Hamiltonian circuit and D_6 symmetry of the same reaction graph as in Fig. 8.

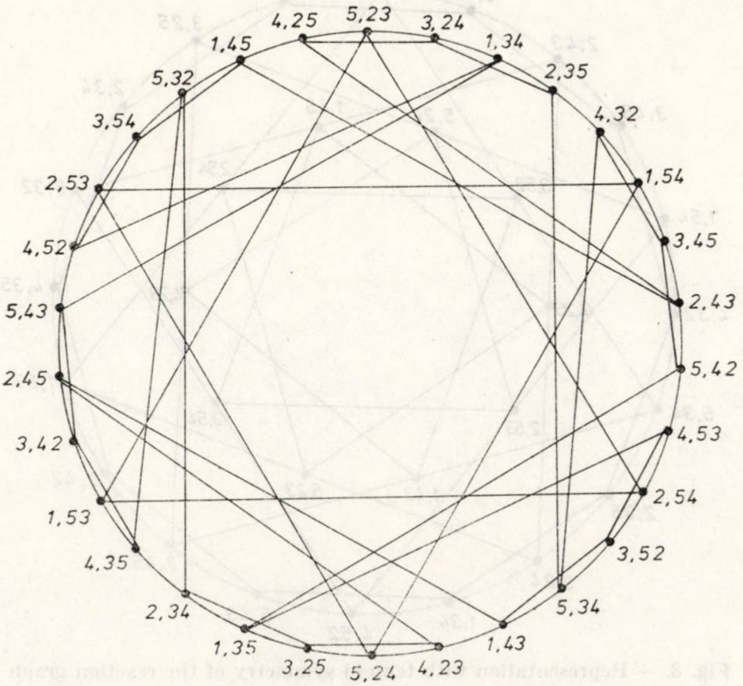

Fig. 10. — Representation with Hamiltonian circuit and C_6 symmetry of the same reaction graph as in Figures 8 and 9, with enantiomers in antipodal positions.

REACTION GRAPHS FOR REARRANGEMENT MODE 6

The rearrangement mode 6 resulting by permutations of type (125) of ligands in the standard complex presented in Figure 2 gives rise to reaction graphs of degree 8. The adjacency matrix for this mode is presented in abridged form in table 3, with the same conventions as those discussed above for table 2.

Figures 11 and 12 present two isomorphic representations of the reaction graph for rearrangement mode 6 : the former has tenfold symmetry, the latter has sixfold symmetry C_6 and a Hamiltonian circuit containing enantiomeric complexes at antipodal positions.

If enantiomerism is disregarded, the adjacency matrix is obtained from table 3 by removing the last digit in the notations of vertices (therefore only 15 vertices are left) and by replacing both letters *a* and *b* by the same adjacency symbol, e.g. the conventional 1. The resulting graph is regular of degree 8 and is presented in two isomorphic representations : in Figure 13 with fivefold symmetry, and in Figure 14 with a Hamiltonian circuit and threefold symmetry.

Table 3

Adjacency matrix, in abridged form, for rearrangement mode 6 (see text for conventions)

	1,35	1,43	1,53	2,34	2,43	2,53	3,25	3,42	3,52	4,25	4,32	4,52	5,23	5,34	5,43
1,35				0	a	b	0	b	a	b	b	0	b	b	0
1,43				b	0	b	a	a	0	0	a	b	b	0	a
1,53				a	b	0	b	0	a	a	0	b	0	b	a
2,34	0	b	a				0	a	b	b	0	b	b	0	b
2,43	a	0	b				b	0	b	0	a	b	a	b	0
2,53	b	b	0				a	b	0	b	a	0	0	b	a
3,25	0	a	b	0	b	a				0	b	b	0	b	b
3,42	b	a	0	a	0	b				b	0	a	a	b	0
3,52	a	0	a	b	b	0				b	a	0	a	0	b
4,25	b	0	a	b	0	b	0	b	b				0	b	b
4,32	b	a	0	0	a	a	b	0	a				b	0	b
4,52	0	b	b	b	b	0	b	a	0				b	b	0
5,23	b	b	0	b	a	0	0	a	a	0	b	b			
5,34	b	0	b	0	b	b	b	b	0	b	0	b			
5,43	0	a	a	b	0	a	b	0	b	b	b	0			

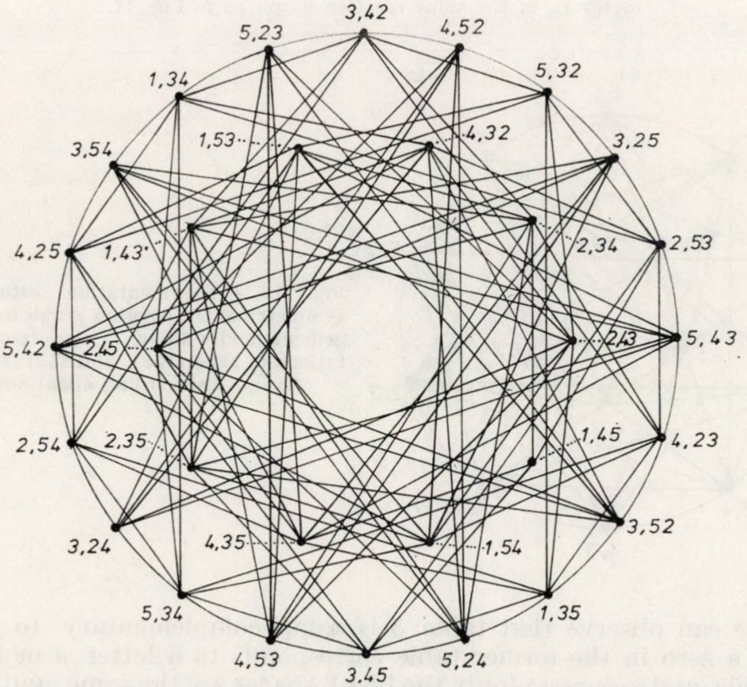
3,42
5,23
4,52
1,34
5,32
1,53
4,32
3,54
3,25
4,25
1,43
2,34
2,53
5,42
2,45
2,43
5,43
2,54
2,35
1,45
4,23
3,52
3,24
4,35
1,54
5,34
1,35
4,53
5,24
3,45

Fig. 11. — Representation with tenfold symmetry of the reaction graph for rearrangement mode 6, involving permutations of type (125).

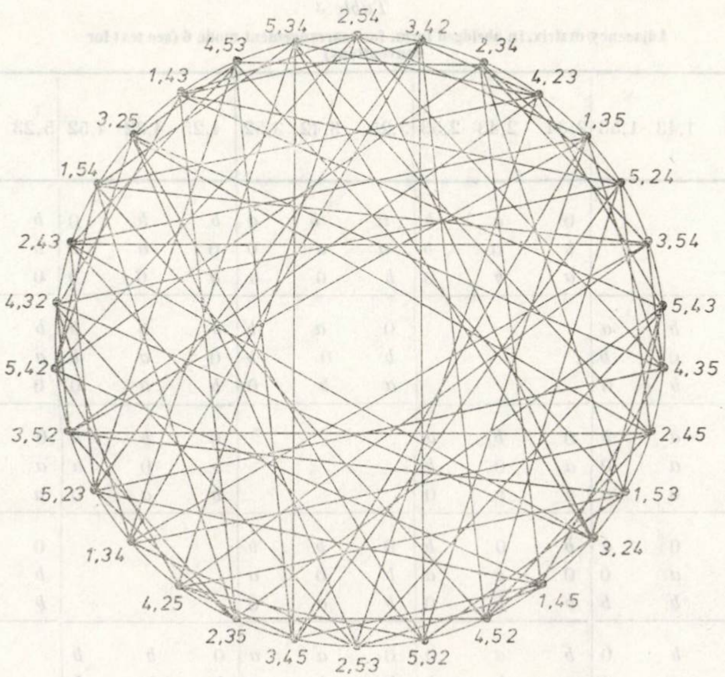
5,34
2,54
3,42
4,53
2,34
1,43
4,23
3,25
1,35
1,54
5,24
2,43
3,54
4,32
5,43
5,42
4,35
3,52
2,45
5,23
1,53
3,24
1,34
4,25
1,45
2,35
4,52
3,45
5,32
2,53

Fig. 12. — Representation with Hamiltonian circuit and sixfold symmetry C_6 of the same reaction graph as in Fig. 11.

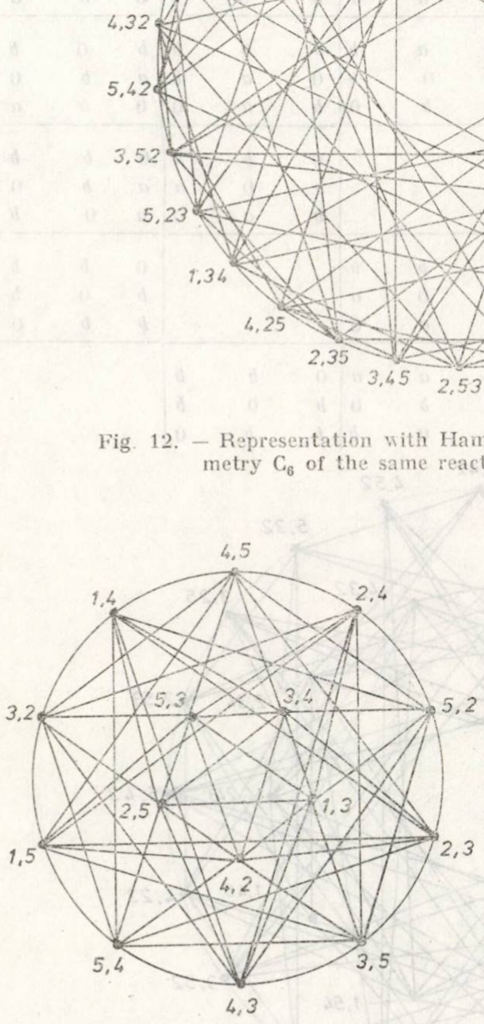
4,5
1,4
2,4
3,2
5,3
3,4
5,2
2,5
1,3
1,5
2,3
4,2
5,4
3,5
4,3

Fig. 13. — Representation with fivefold symmetry of the reaction graph for rearrangement modes 6 and 7, involving permutations of type (125), and (12) (35), respectively, disregarding enantiomerism.

One can observe that table 3 is quasi-complementary to table 2, i.e. that a zero in the former table corresponds to a letter *a* or *b* in the latter table, and *vice-versa* (only the blank spaces are the same, and because

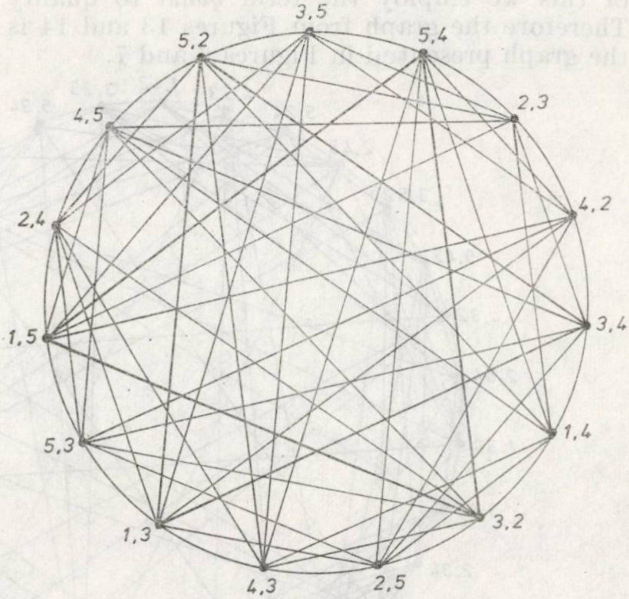
3,5
5,2
5,4
2,3
4,5
4,2
2,4
3,4
1,5
1,4
5,3
3,2
1,3
4,3
2,5

Fig. 14. — Representation with Hamiltonian circuit and threefold symmetry of the same reaction graph as in Fig. 13.

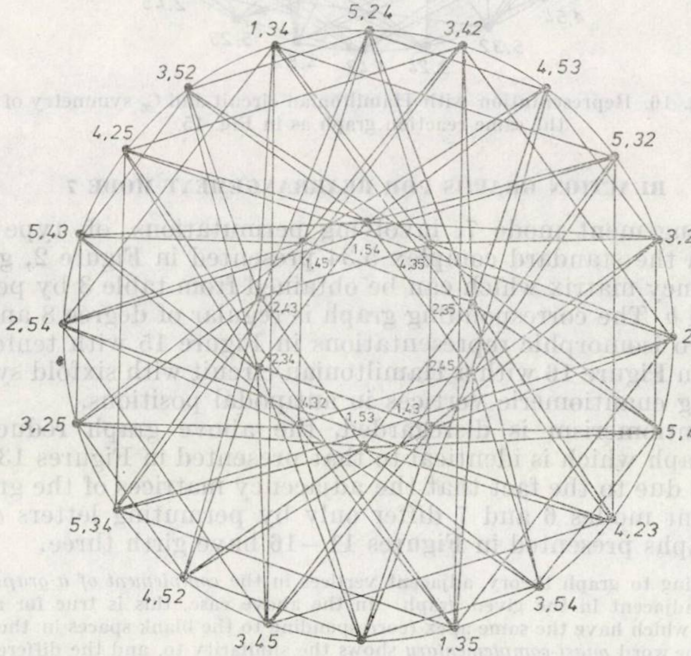
5,24
1,34
3,42
3,52
4,53
4,25
5,32
5,43
3,24
1,45
1,54
4,35
2,43
2,35
2,54
2,53
2,34
2,45
4,32
1,53
1,43
3,25
5,42
5,34
4,23
4,52
3,54
3,45
1,35
5,23

Fig. 15. — Representation with tenfold symmetry of the reaction graph for rearrangement mode 7, involving permutations of type (12)(35).

of this we employ the term *quasi* to qualify the complementarity *). Therefore the graph from Figures 13 and 14 is the quasi-complement of the graph presented in Figures 6 and 7.

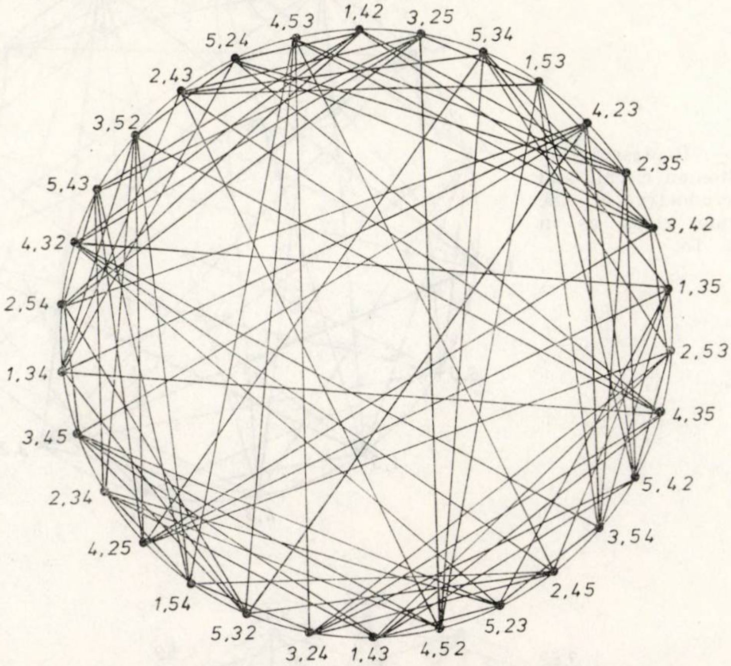

Fig. 16. Representation with Hamiltonian circuit and C_6 symmetry of the same reaction graph as in Fig. 15.

REACTION GRAPHS FOR REARRANGEMENT MODE 7

Rearrangement mode 7, involving permutations of type (12)(35) of ligands in the standard complex 5,34 presented in Figure 2, gives rise to an adjacency matrix which can be obtained from table 3 by permuting letters *a* and *b*. The corresponding graph is regular of degree 8 and is presented in two isomorphic representations in Figure 15 with tenfold symmetry, and in Figure 16 with a Hamiltonian circuit with sixfold symmetry C_6 containing enantiomeric vertices in antipodal positions.

If enantiomerism is disregarded, the above graph reduces to a 15-vertex graph which is identical to that presented in Figures 13 and 14. Again this is due to the fact that the adjacency matrices of the graphs for rearrangement modes 6 and 7 differ only by permuting letters *a* and *b*. All three graphs presented in Figures 11—16 have girth three.

---

* According to graph theory, adjacent vertices in the *complement of a graph* are those which are not adjacent in the given graph. In the above case, this is true for all vertices excepting those which have the same apex (corresponding to the blank spaces in the adjacency matrix). Thus the word *quasi-complementary* shows the similarity to, and the differences from, truly complementary graphs. An analogy may be found in the term *dualist graph* used by Balaban [16] to indicate similarity to, but not identity with, dual graphs when defining and enumerating planar condensed polycyclic systems and tridimensional diamondoid hydrocarbons.

[16] A. T. Balaban, *MatCh*, **2**, 51 (1976) and further references therein.

Revue Roumaine de Chimie, **23**, *5*, 747–751 (1978)

THE KINETICS AND REACTIONS OF SOME ARYL-SUBSTITUTED EPOXIDES WITH *t*-BUTOXIDE IN *t*-BUTANOL

M. HASSAN, A.R.O. ABDEL NOUR and A. M. SATTI
Chemistry Department, University of Khartoum, P.O.B. 321, Khartoum,
Sudan

Received February 17, 1976

The reactions of 1,2-epoxy-3-phenyl propane, its *m*- and *p*-Me, *m*-and *p*-chloro, *p*-*t*-butyl, *p*-F and *p*-MeO derivatives with potassium *t*-butoxide in *t*-butanol have been investigated at 60°. The reactions in all cases resulted in the formation of the corresponding substituted cinnamyl alcohol the production of which has been followed spectrophotometrically. The reaction of 3-phenyl-3-3-dimethyl-1,2-epoxy gave the product expected from the cleavage of the epoxide ring without the production of an allylic product. The plot of the relative rates of reactions against Taft's σ^* constants indicated an approximately linear plot from which a value of $\rho(+0.81)$ was deduced. The reactions proceed via proton abstraction, giving a carbanion which in a concerted reaction affords the unsaturated alcohol. The reaction which was found to be retarded by electron-donating groups reveals the following order :

$$m\text{-Cl} > p\text{-Cl} > \text{H} > p\text{-F} > m\text{-Me} \geqslant p\text{-Me} > p\text{-t-Bu} > p\text{-MeO}$$

The reaction products were isolated in over 80% yield.

Ring cleavage of epoxides in solution involve attach of a nucleophile on one of the ring carbon atoms with displacement of the epoxide ring oxygen. Most of the evidence which accumulated indicated the bimolecular nature of the mechanisms.[1,2] Under conditions of acid catalysis the initial step is protonation of the epoxide oxygen followed by the nucleophilic attack on one of the ring carbon atoms to give, in contrast to reactions in non-acidic media, the abnormal product. It was also concluded that the reaction proceeds by a molecular mechanism in which bond breaking was the major driving force and that the rate was aided by electron releasing substituents, a value of approximately -4.05 being found for ρ.

The reaction of epoxides to give isomerisation products derives from the work of Cope and co-workers.[3] It was found that treatment of compounds like *cis*- and *trans*-4-octene oxides with lithium diethylamide gave

---

[1] R. E. Parker and N. Isaacs, *Chem. Rev.*, 59 (1959).

[2] J. Biggs, N. B. Champion, A. R. Finch and W. Wray, *J. Chem. Soc.*, (B), **1971**, 55.

[3] (a) A. C. Cope and J. K. Heern, *J. Amer. Chem. Soc.*, **87**, 3125 (1965).
(b) A. C. Cope, M. M. Martin and M. A. McKervey, *Quart. Rev.*, **20**, 119 (1966).
(c) A. C. Cope, P. A. Trumbull and E. R. Trumbull, *J. Amer. Chem. Soc.*, **80**, 2844 (1958).

trans-5-octen-4-ol as the major product. It was also shown that the formation of the product proceeds largely by removal of the proton from the α-carbon atom to the oxirane ring rather than by removal of a proton from the ring followed by generation of a carbanion intermediate. To determine which mechanism was followed by the aliphatic epoxides, the reactions were studied with *cis*- and *trans*-4-octene oxide -D_2. The allylic alcohol produced was found by mass spectroscopy to contain 70% in the case of the *cis*- and 84% of D_2 species in the case of the *trans*-isomer. Thus it was concluded that the carbanion mechanism operated in both cases. Further reactions in which strong nucleophiles react with epoxides to yield allylic products include the reactions of unsymmetrical aliphatic epoxides[4] and the reactions of α-pinene and β-isobutylene oxides with lithium diethylamide as well as the reaction of *cis* and *trans*-epoxycyclododecene with *n*-butyl lithium.[5] The reactions of some substituted ethylene oxides with diethylamide were found to give carbonyl compounds, the initial step being again a removal of a proton, this time from the oxirane ring.[3c]

However, the isomerisation of 1,2-epoxy-3-phenylpropane to cinnamyl alcohol has been reported by Haynes, Hilborn, Jones and Sondheimer.[6] They demonstrated that such isomerisations were effected by sodamide in liquid ammonia. The epoxides remain unaffected on treatment with 10% potassium hydroxide.

In the present investigation 1,2-epoxy-3-phenylpropane and some of its aryl substituted derivatives have been reacted with potassium tertiary butoxide in tertiary butanol at 60°. The rates of production of the cinnamyl alcohols were followed spectrophotometrically and the effects of substituents on the rates have been explained.

EXPERIMENTAL

Preparation and purification of materials: The epoxides were prepared by epoxidation of the corresponding allylbenzenes by means of perbenzoic acid in chloroform solution. The allylbenzenes were prepared by coupling of the aryl Grignard reagent and allyl bromide in ether. 1,2-epoxy-3-phenyl propane had b.p. 107–108/26 mm Hg, $n_D^{21.5}$, 1.5222 (lit[7] b. p. 98–100/17 mm Hg). Found C, 80.53; H, 7.53; $C_9H_{10}O$ requires C, 80.59; H, 7.46.% 1,2-epoxy-3 (*p*-chloro-) phenyl propane had b.p. 90°/1.2 mm Hg n_D^{23}, 1.5379. Infrared maxima (wavenumbers in cm^{-1}) 805(s), 935(m) and 1265(m). Found C, 63.77; H, 5.33; Cl, 20.88, C_9H_9ClO requires C, 64.09; H, 5.34, Cl, 21.04.% 1,2-Epoxy-3- (*p*-fluoro)-phenyl propane had b.p. 62–64°/2.0 mm Hg, n_D^{20}, 1.4995. Infrared maxima 820(s), 860(s), 935(m), 1230(m). Found C, 70.20; H, 6.00; C_9H_9FO requires C, 71.05; H, 5.9% 1-2-epoxy-3-(*p*-methyl)-phenyl propane had b.p. 88–89°/0.5 mm Hg, $n_D^{22.5}$, 1.518. Infrared maxima 805 (s), 830 (s), 850(s), 915(w), 935(s), 965(m), and 1265(m). Found C, 80.96; H, 8.34; $C_{10}H_{12}O$ requires C, 81.08; H, 8.11%. The *p*-methoxy derivative had b.p. 119–122°/0.5 mm Hg, n_D^{22} 1.5305, infrared maxima 810(s), 915(s), 1250(s). Found C, 72.67; H, 7.21; $C_{10}H_{12}O_2$ requires C, 73.17; H, 7.32%. The *p*-*t*-butyl epoxide had b.p. 102–103°/1.8 mm Hg, n_D^{26}, 1.5102, infrared maxima, 810(w), 830(s), 935(m) and 1275(m). Found C 81.03; H, 9.29, $C_{13}H_{18}O$ requires C; 82.10, H, 9.47% 1.2-Epoxy-3-(*m*-

---

[4] B. Rickborn and R. P. Thummel, *J. Org. Chem.*, **34**, 3583 (1969).

[5] J. K. Crandall, and. L. H. Chang, *J. Org. Chem.*, **32**, 435 (1967).

[6] L. J. Haynes, I. Heilborn, E. R. Jones and F. Sondheimer, *J. Chem. Soc.*, **1947**, 1583.

[7] J. Lévy and J. Spiras, *Bull. Soc. Chim., France*, **49**, 1823 (1931); *Chem. Abstr.*, **26**, 2429 (1932).

Me-)Phenyl propane had b.p. 73°/0.30 mm Hg, n_D^{25}, 1.5188. Infrared maxima, 780(s), 840(s), 900(w), 945(w), 1265(m). Found C, 80.57 ; H, 8.12. $C_{10}H_{12}O$ requires C, 81.08 ; H, 8.11 % 1,2-epoxy-3(*m*-Cl-)-phenyl-propane had b.p. 87.5/0.17 mm Hg, $n_D^{24.5}$, 1.5367. Infrared maxima 785(s), 840(s), 870(s), 945(m) and 1265(m). Found C, 64.10 ; H, 5.49. $C_9H_9C_{10}$ requires C, 64.09 ; H, 5.34 %.

3-Methyl-3-phenyl-1-butene-oxide was prepared by epoxidation of 3-methyl-3-phenyl-1-butene which was in turn prepared by dehydrochlorination of the corresponding butyl chloride.[8] The epoxide had b.p. 64.66°/0.4 mm Hg n_D^{25}, 1.5127. Infrared maxima 845(s), 920(m) and 1280(s). Found C, 81.39 ; H, 8.76 ; $C_{11}H_{11}O$ requires C, 81.40 ; H, 8.64 %.The chloride was prepared by the action of thionyl chloride on 3-methyl-3-phenylbutan-1-01.[9]

Tertiary butanol was purified by drying over anhydrous potassium carbonate and then distilled from sodium metal,[10] the fraction boiling at 81.5° being collected. The *t*-butoxide was prepared by dissolving a weighed quantity of potassium metal in the alcohol and was standardized by hydrochloric acid using phenolphthalein as indicator. Stock solutions of the epoxide were made by dissolving a known weight of the material in the alcohol made up to a known volume.

Kinetic Measurements : The solutions of epoxide and the base were brought to the temperature of the thermostat (60°) and the reaction which was conducted in a two-necked reaction flask, fitted with a condenser and a silica gel guard tube, was started by adding the reagents so that upon admixture a solution of approximately 8×10^{-3} M in epoxide and $9.0 \times \times 10^{-2}$ M in butoxide was obtained. At convenient intervals 1 ml of the reaction mixture was pipetted and quenched in ethanol in a volumetric flask to give a final concentration of 10^{-6}M. The solutions were then run in a Unicam SP.800 spectrophotometer using silica cells (1 cm wide) and using ethanol in the reference cell. Absorbance of these solutions at a wavelength in the region of 250 nm gave values of A_t (absorbance at time t). By using the relationship :

$$k.t = 2.303 \log_{10} \frac{A_\infty}{A_\infty - A_t}$$

a plot of $\log_{10} \dfrac{A_\infty}{A_\infty - A_t}$ against time gave a straight line the slope of which was used to calculate the first order rate coefficients where

$$k = \text{slope} \times 2.303$$

The following table (1) shows the absorption maxima obtained :

Table 2 gives a summary of the results.

Table 1

Ultra-violet Absorption Maxima of Substituted Allylic products obtained; Measured in Ethanol using 1 cm. wide Silica Cells

Substituent	λ_{max} in nm
H	246.5
p−Cl	256
p−F	250
p−Me	265
p−t−Bu	256.5
p−OMe	277.5
m−Cl	253
m−Me	251

Table 2

Rates of Isomerisation of 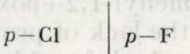

$\mathbf{X-C_6H_4 \cdot CH_2CH - CH_2}$

Substituent X :	H	*p*−Cl	*p*−F	*p*−Me
$k_1 \times 10^5$:	8.8	22.3	5.8	3.10
Substituent X :	*p*−t−Bu	*p*-Me0	*m*−Cl	*m*−Me
$k_1 \times 10^5$:	1.6	0.71	43.5	3.16

---

[8] J. W. Cornforth and R. Robinson, *J. Chem. Soc.*, **1942**, 864.

[9] M. T. Rogert, and D. Davidson, *J. Amer. Chem. Soc.*, **56**, 185 (1934).

[10] N. B. Champion, N. S. Isaacs and R. E. Parker, *J. Chem. Soc.*, **1949**, 1925.

3-Methyl-3-phenyl-1,2-epoxybutane failed to give any allylic product with *t*-butoxide, instead the product showed strong infrared absorption at 3400 cm^{-1} indicating the presence of alcoholic hydroxyl due to normal hydrolytic cleavage to give the hydroxy ether.

DISCUSSION

Kinetics and Mechanisms : The reactions have been found to follow first order kinetics as deduced from the plot of $\log \dfrac{A_\infty}{A_\infty - A_t}$ against time, and from which the rate constants have been calculated. The reactions are of the form

$$-\mathrm{d}/\mathrm{d}t = k\ [\text{epoxide}]$$

Alkaline ring cleavage of epoxides proceeds in either of two ways. First, the classical ring opening giving rise to the normal and/or abnormal products. This type is a nucleophilic attack on an epoxide ring carbon atom where the normal product will be preferred for steric reasons while polar and conjugative effects might act in either direction. As an example the work of Parker *et. al.* [10–14] might be cited.

The second type of ring opening in strongly alkaline media is one which is accompanied by isomerisation giving rise to allylic products. Our results are reasonably interpreted as belonging to the second category in which the production of the allylic alcohol is preceded by proton abstraction from the α-carbon atom to the oxirane ring giving rise to a carbanion which rearranges to the products through a concerted mechanism.

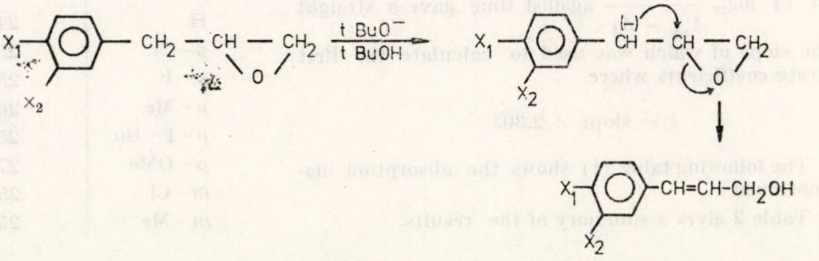

A mechanism for these reactions based on the attack of the nucleophile on the ring carbon atom if considered would be unlikely because such a reaction would give rise to a hydrolytic product which if it underwent elimination would not give cinnamyl alcohol in 87% yield. Further, the failure of 3-methyl-3-phenyl-1,2-epoxybutane to give any allylic product could be explained by the lack of protons at α-carbon atom to the oxirane ring. According to Cope *et. al.* [3] and by using duterium labelling techniques such epoxides react with lithium diethylamide exclusively by a similar

---

[11] N. Isaacs and R. E. Parker, *J. Chem. Soc.*, **1960**, 3497.

[12] J. K. Addy, R. M. Laird and R. E. Parker, *J. Chem. Soc.*, **1961**, 1708.

[13] R. M. Laird and R. E. Parker, *J. Chem. Soc.*, **1963**, 6065.

[14] R. E. Parker and B. W. Rockett, *J. Chem. Soc.*, **1965**, 2569.

carbanion mechanism. Both diethylamide and tertiary butoxide are sufficiently strong nucleophiles to effect this reaction.

Substituent Effects : The reaction rates as determined experimentally follow the order :

$$m\text{—Cl} > p\text{—Cl} > \text{H} > p\text{—F} > m\text{—CH}_3 \geqslant p\text{—CH}_3 > p\text{—}t\text{—Bu} > p\text{—OMe}$$

The sequency of reactivity is consistent with the inductive order of substituents. Those with a $-I$ effect have an accelerating effect on the rate because they facilitate the loss of a proton at the reaction centre. Electron repelling groups such as alkyl have the opposite effect. The *para*-fluoro compound has a slower rate than hydrogen, whereas the inductive order requires $p\text{—F} > p\text{—Cl} > \text{H}$. The order of reactivity shown by our results i.e. $p\text{—Cl} > \text{H} > p\text{—F}$ can only be explained by a greater electron repulsion from the *p*-fluoro-substituent. In the isomerisation reactions of aryl propanes with ethoxide at 81°,[15] which proceeds by a similar mechanism, the same inductive order was observed. Such reactions are known to be aided by groups with $-I$ and not necessarily retarded by groups with a $+I$ effect. However, our present results point very clearly to the retarding effect of the fluorine substituent in these reactions, a fact which cannot be correlated by its inductive effect alone, but rather by the whole of inductive and electronic effects.

Though our present study is not sufficiently extensive to allow a very firm conclusion to be drawn in a quantitative manner, a Hammett plot of the log of rates against σ values indicate an approximately linear plot from which a value of $\rho + 0.8$, for could be deduced. The positive value indicates that the reaction which is aided by electron withdrawal also shows reduced sensitivity to the electronic effects of substituents. In the reactions of aryl propenes with ethoxide, a similar small value for ρ ($+0.5$) was also deduced.[15]

---

[15] M. Hassan and A. R. O. Abdel Nour, *J. Chem. Soc.*, (*B*), **1970**, 1628.

Revue Roumaine de Chimie, 23 5, 753–758 (1978)

ALUMINIUM CHLORIDE CATALYZED REACTIONS OF UNSATURATED ACIDS WITH BENZENE. XI*

ISOMERIZATIONS DURING THE REACTION OF BENZENE WITH 4-METHYL-2-PENTENOIC ACID

A. C. RĂZUŞ, ZS. ARVAY and ALICE MARIE GLATZ
Center of Organic Chemistry, Spl. Independenţei 202-B, R–77 306
Bucharest 15, Romania

Received July 27, 1976

The reaction of 4-methyl-2-pentenoic acid with benzene in the presence of aluminium chloride leads to 4-methyl-3-phenylvaleric, 3-methyl-4-phenyl-2-pentenoic, 3-methyl-4-phenylvaleric, 4-methyl-4-phenylvaleric and 4-methyl-4-phenyl-2-pentenoic acids. The influence of the reaction time was studied. A reaction mechanism scheme was proposed.

Earlier works[1] concerning the aluminium chloride catalyzed reaction of α, β-unsaturated acids with benzene at 45–50° have shown that the reaction products can be explained through a mechanism involving a carbocation resulting from the protonation of the double bond. This first intermediate can react as such with the benzene or can undergo a series of transformations (hydride ions migrations, transpositions or ring openings) to other carbocations which can also react as electrophilic agents.

The transformations which take place during the reaction of 4-methyl-2-pentenoic acid (**1**) with benzene are the object of the present study.

The Friedel-Crafts reaction of this acid was already studied,[2] but in different reaction conditions; consequently these results cannot be compared with the earlier data involving α,β-unsaturated acids.

According to the classical scheme, it was expected that in the reaction of acid **1** with benzene, 4-methyl-4-phenylvaleric (**2**), 4-methyl-3-phenylvaleric (**3**) and 3-methyl-4-phenylvaleric (**4**) acids should be obtained.

---

* Preceding part, V. Drăguţan, L. Stănescu, A. M. Glatz, *Rev. Roumaine Chim.*, **22**, 1045 (1977).

[1] A. M. Glatz, *Rev. Roumaine Chim.*, **19**, 455 (1974).

[2] A. Drusiani, A. G. Giumanini and L. Plessi, *Chim. Ind.* (*Milano*), **55**, 882 (1973).

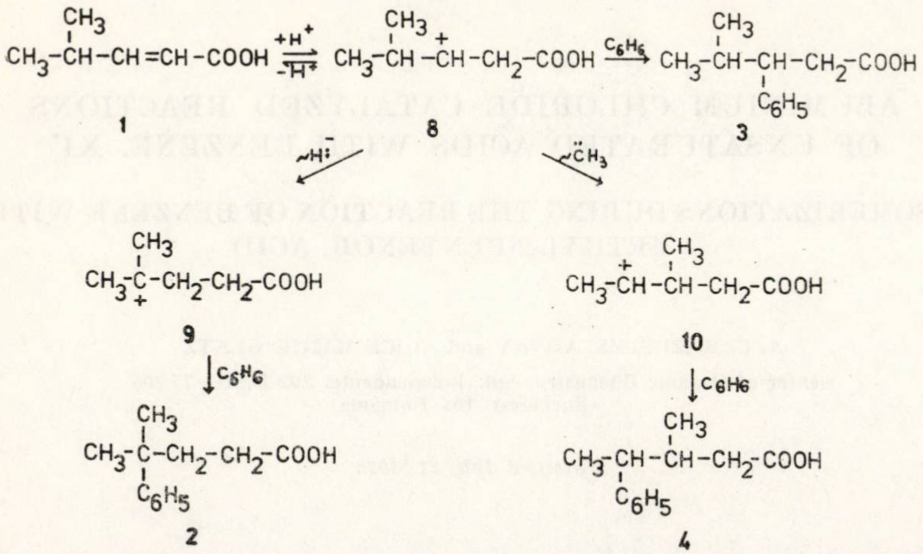

According to this scheme if we consider that the intramolecular hydride migration is as fast as that of the methyl group, acids **2** and **3** should result in amounts comparable to that of acid **4** with rearranged methyl group. Earlier results showed that in the case of α,β-unsaturated acids, the unsaturated phenylated acids are formed only exceptionally (i.e. the formation of 3-phenylindenylacetic acid from indenylideneacetic acid [3]).

In the present paper, the reaction conditions were : unsaturated acid : $AlCl_3$: C_6H_6 was 1 : 1,5 : 20 respectively, temperature 45−50° and different reaction times. After short times, the resulting reaction mixture was directly esterified with diazomethane. After longer times the reaction mixture was neutralized and extracted with ether. The amounts of neutral products from the ethereal solution were negligible even after 570 min. The acid products were esterified with diazomethane. The total yield of the reaction, at short time exceeds 90 %, while at periods longer than one hour it is about 80 %. The analysis of the reaction products was carried out by gas chromatography using authentical samples in order to compare the retention times. In this way the following acids were found in the reaction mixture : 3-methyl-4-phenylvaleric (**3**), 4-methyl-3-phenyl-2-pentenoic (**6**), 4-methyl-3-phenylvaleric (**4**), 4-methyl-4-phenylvaleric (**2**) and 4-methyl-4-phenyl-2-pentenoic (**11**).

3-Methyl-4-phenyl-2-pentenoic (**5**) acid was not found among the products, the retention time of an authentical sample does not coincide with any of the reaction products.

Table 1 presents the reaction products as a function of the reaction time.

The experimental data cannot be explained by the classical scheme discussed above. The unexplained facts are the following : (i) the obtention of a very small proportion of acid **3**, which should result directly by the

---

[3] A. C. Răzuş, F. Chiraleu and A. M. Glatz, *Rev. Roumaine Chim.*, **20**, 781 (1975).

Table 1

V.p.c. analyses of the reaction products*,**

Time min.	Ratio: Phenylated acid / Starting materia	Phenylated acids				
		2	**3**	**4**	**6**	**11**
3	—	50.95	4.58	13.12	14.49	16.05
5	0.16	51.86	3.40	12.40	15.32	11.20
10	0.31	55.64	4.21	14.90	16.65	7.51
60	1.56	56.48	5.53	17.87	18.17	1.95
120	3.22	47.70	11.14	20.33	20.51	0.32
180	16.00	48.95	10.29	19.96	20.80	traces
570	—	48.11	10.50	19.17	22.21	traces

* The results of gas-chromatographic analyses are given in moles per cent.

** 4-Methyl-3-pentenoic acid does not appear among the reaction products. In all samples the presence of small quantities (less than 1%) of 4-methylvaleric acid was observed.

attack of ion **8** formed in the first step and also an unexpectedly great proportion of acids with rearranged methyl group (**4** and **6**); (ii) the formation, even at the very beginning of the reaction, of the unsaturated acid **6** (corresponding to the saturated acid **4**) and the absence of the unsaturated acid **5** (corresponding to the saturated acid **3**), and (iii) the formation of the unsaturated acid **11** as well as the persistence of the starting material (the acid **1**) whose proportions although they decrease in time, are of the same magnitude order as the ratio of the products undergoes significant transformations.

Although the results included under item (i) and partially those of (ii) might be justified also by the contribution of steric factors which should intervene according the scheme 1, this scheme cannot explain the whole set of results.

Considering all the above data a new scheme has to be devised. Scheme 2 takes into account the behaviour of the 4-methyl-2-pentenoic acid (**1**) in this reaction and can explain all the obtained results.

According to this scheme, the protonation of acid **1** forming ion **8** is a rapid reaction but the subsequent phenylation is sterically hindered by the isopropyl group from the α-position.

An intermolecular hydride shift, also a rapid process, leads to the tertiary allylic ion **12**a. This has a suplementary possibility of stabilisation by lactonisation to ion **12**b which can give rise of the starting material as long as it exists in the reaction medium. The reaction of the ion **12** with benzene give the acid **11**. The formation of this acid can be explained by no other precursor. An argument in favour of this is the reaction of the 4-hydroxy-4-methylvaleric acid lactone (**16**) in the same conditions as those described in this paper which give mainly acid **2** (97 %) with small amounts of acid **3** (3 %).

The presence of a small quantity of acid **3** corroborated with the absence of the unsaturated corresponding acid **5** does not exclude the classical way (scheme 1) *via* ion **8**, but the preferred way seems to involve the ion **12**.

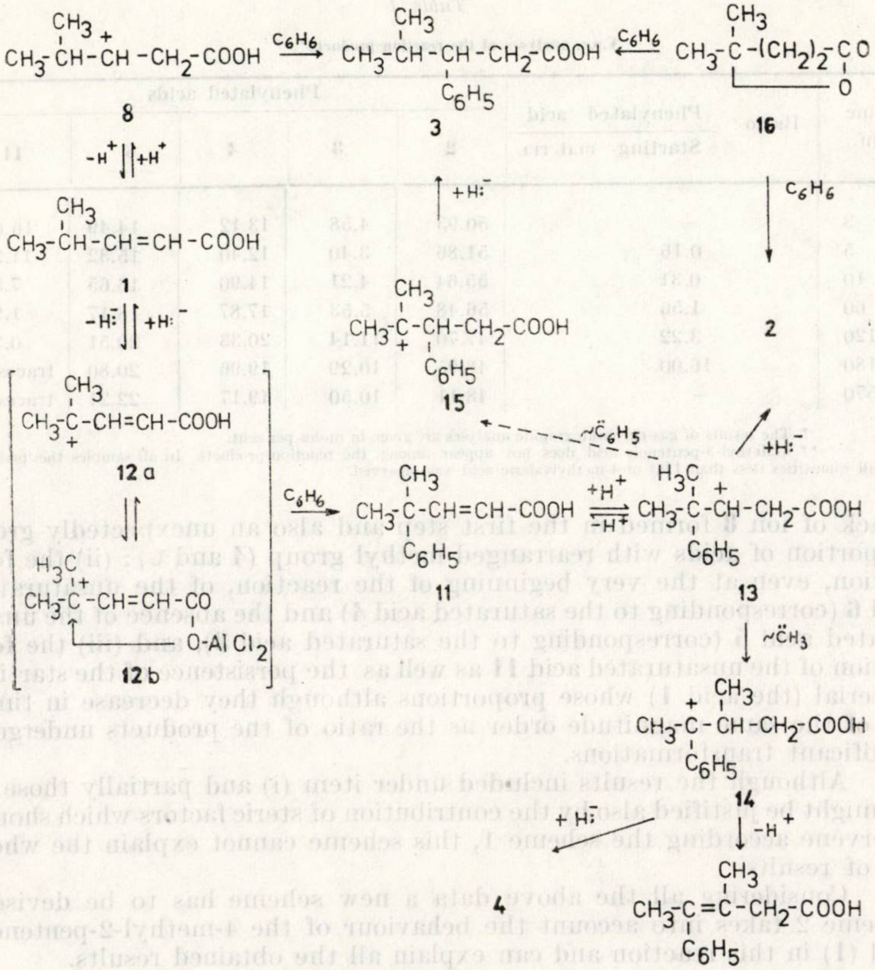

EXPERIMENTAL

All melting points are uncorrected, NMR spectra ($CDCl_3$ or CCl_4, δ in ppm) were recorded on a Varian A 60-A spectrometer, using TMS as internal standard. The v.p.c. analyses were carried out on a Willy Giede gas chromatograph model 18.3, using a 15 % ethyleneglycol succinate + 5 % QF 1/Chromosorb W column, 60 – 80 mesh, temperature 172°.

REACTION OF BENZENE WITH 4-METHYL-2-PENTENOIC ACID (1) OR 4-HYDROXY-4-METHYLVALEROLACTONE (16)

On a suspension of $AlCl_3$ (0.15 moles) in benzene (1.0 mole), a solution of unsaturated acid or lactone (0.1 mole) in benzene (10.0 moles) was dropwise added. The reaction mixture was treated with water and ice, the dried organic layer was esterified with diazomethane. The yields were over 90 %. The reaction mixture at longer times than 60 min. was allowed to cool, treated with ice-water, the organic layer was basified with 10 % aqueous potassium hydroxide and extracted with ether. The aqueous alkaline layer was acidified, extracted with ether, dried over magnesium sulfate and esterified with diazomethane. All ester mixture were distilled under vacuum (0.5 mm). This distillation removes the heavy fraction which disturb the v.p.c. analyses. The yields of these experiences are about 80%. In order to identify the starting material in the reaction mixture by v.p.c. analysis, a temperature program was used at first at 100° for the starting material and then the temperature reached at 172° with a rate of 6°/min.

METHYLPENTENOIC ACIDS

4-Methyl-2-pentenoic acid (**1**) was obtained by Knoevenagel reaction of isobutyraldehyde and malonic acid [4].

NMR spectrum (CCl_4) : 1.1 (doublet, 6H $2CH_3$, $J = 7$ Hz) ; 2.45 (octet, 1H CH−) ; 5.73 (double doublet, 1H, $\alpha{=}CH-$, $J_{trans}{=}15$ Hz, $J_{allylic}{=}1.5$ Hz) ; 7.03 (double doublet, 1H, $\beta-CH{=}$, $J = 6.5$ Hz) ; 12.45 (singlet, 1H, COOH).

V.p.c. analyses (at 100°, column temperature) of the methyl ester indicated a pure product.

The methyl ester of 4-methyl-3-pentenoic acid was prepared by isomerization in alkaline medium of 4-methyl-2-pentenoic acid followed by the esterification with methanol in the presence of sulfuric acid in dichloroethylene.[5] V.p.c. analysis shows a purity of 95% (at 100°). The two esters have different retention times.

4-Hydroxy-4-methylvalerolactone was obtained by a Grignard reaction between levulic acid and methylmagnesium iodide, [6] b.p. 78−80°/2 mm (lit. [6] b.p. 201−206/760 mm).

4-Methyl-4-phenylvaleric acid (**2**) was prepared starting from 2-methyl-2-phenyl-4-pentanone,[6] converted into suitable thiomorpholide, and subsequently hydrolysed to acid **2**, [7] b.p. 130°/2−3 mm (lit. [7] 185−190°/17 mm).

NMR spectrum (CCl_4) ; 1.29 (singlet, 6H, $(CH_3)_2C$) ; 2.0 (singlet, 4H, $-CH_2-CH_2-$) ; 7−7.4 (multiplet, 5H, C_6H_5) ; 11.74 (singlet, 1H, COOH). The methyl ester was obtained by treating with ethereal diazomethane. The v.p.c. analysis gave a single component.

3-METHYL-4-PHENYLVALERIC (4) AND 3-METHYL-4-PHENYL-2-PENTENOIC (6) ACIDS

By Reformatski reaction between acetophenone and ethyl α-bromopropionate the ethyl ester of 3-hydroxy-3-phenyl-2-methylbutyric acid (53%), b.p. 118°/2 mm, was prepared.

By phosphorus pentoxide dehydration [9] of a mixture of the two above esters the unsaturated esters in nearly equal amounts (v.p.c. analysis) was obtained, yield 98%.

NMR spectrum (CCl_4) of the mixture confirms the appearance of the ethyl esters of 2-methyl-3-phenyl-3-butenoic and 2-methyl-3-phenyl-2-butenoic acids ; 1.12 (triplet, 3H, $COOCH_3$) ; 1.33 (doublet, 3H, CH_3-CH first ester) ; 1.75, 2.05 (multiplets, 6H, $2CH_3$ second ester) ; 3.65 (quartet, 1H, $-CH <$, $J = 6.5$ Hz first ester) ; 4.03 (quartet, 2H, CH_2 both esters) ; 5.16, 5.29 (singlets, 2H, $CH_2 <$ first ester) ; 7.0−7.4 (multiplet, 5H, $2C_6H_5$ both esters).

The esters mixture was then hydrolyzed (86%) and the resulted acids hydrogenated at 40 atm in ethanol with 5% Pd/C as catalyst. After working out a red oil was obtained which gave colorless needles of 2-methyl-3-phenylbutyric acid after filtration ; m.p. 130° (from petroeum ether, lit. [8] m.p. 131−132°).

NMR spectrum ($CDCl_3$) : 0.99 (doublet, 3H, αCH_3) ; 1.32 (doublet, 3H, βCH_3) ; 2.4−3.1 (multiplet, 2H, $>CH-CH<$) ; 7.0−7.4 (singlet, 5H, C_6H_5) ; 12.00 (singlet, 1H, COOH).

Arndt−Eistert chain lengthening gave the methyl ester of 3-methyl-4-phenylvaleric acid (**4**). V.p.c. analysis showed the formation of the ester of acid **4** in 90% proportion beside the starting material and small impurities.

NMR spectrum (CCl_4) : 0.80 (multiplet, 3H, CH_3) ; 1.25 (doublet, 3H, CH_3) ; 1.85−2.80 (multiplet, 4H) ; 3.58 (singlet, 3H, $COOCH_3$) ; 7.15 (singlet, 5H, C_6H_5).

---

[4] "Organikum (Organisch chemisches Grundpraktikum)", VEB deutscher Verlag Wissenschaften, Berlin, 1964, p. 446.

[5] J. D. Rogan, *J. Org. Chem.*, **27**, 3910 (1962).

[6] R. T. Arnold, J. S. Buckley jr. and J. Richter, *J. Amer. Chem. Soc.*, **69**, 2323 (1947).

[7] I. P. Labunskii, *Zhurn. org. Khim.*, **28**, 1626 (1958).

[8] R. D. Campbell and N. H. Cromwell, *J. Amer. Chem. Soc.*, **77**, 5169 (1958).

[9] M. C. Kloetzel, *J. Amer. Chem. Soc.*, **62**, 1708 (1940).

[10] C. A. R. Kan and K. S. Norgund, *J. Chem. Soc.*, **1932**, 2461.

The above filtered liquid contains a mixture of 2-methyl-3-phenyl-2-butenoic acid as major product and 20 % 2-methyl-3-phenylbutyric acid (v.p.c. analysis of the methylesters). This mixture gave by Arndt-Eistert chain lengthening 15 % of the methyl ester of 3-methyl-4-phenylvaleric acid (**4**) beside 80 % of the corresponding methyl ester of 3-methyl-4-phenyl-2-pentenoic acid (**6**) (5 % were unidentified compounds).

4-METHYL-3-PHENYLVALERIC (3) AND 4-METHYL-3-PHENYL-2-PENTENOIC (5) ACIDS

A Reformatski reaction between isobutyrophenone and ethyl bromoacetate gave in 62.5 % yield the ester of 3-hydroxy-4-methyl-3-phenylvaleric acid. By subsequent dehydration with phorphorus pentoxide, the ethyl ester of 4-methyl-3-phenyl-2-pentenoic acid (**5**) in 85 % yield was obtained.

NMR spectrum (CCl_4) beside the ethyl group shows the presence of two isomers of the ester of the acid **5** : 1.61 (singlet, 3H, CH_3 *cis* with respect to C_6H_5) ; 1.80 (singlet, 3H, CH_3 *trans* with respect to C_6H_5) ; 3.30 (singlet, 2H, $-CH_2-COOH$) ; 6.7–7.5 (multiplet, 5H, C_6H_5).

The hydrogenation with 5 % Pd/C of the esters in ethanol at atmospheric pressure, for 20 hrs, gave a mixture of saturated esters and starting material. This mixture was saponified. After esterification with ethereal diazomethane, the v.p.c. analysis shows two components in nearly equal proportions.

The *NMR spectrum* (CCl_4) of the mixture, besides the characteristic signals of the 4-methyl-3-phenyl-2-pentenoic acid (**5**), presents also signals of 4-methyl-3-phenylvaleric acid (**3**) : 1.9 (multiplet, 1H, $>CH-CH_3$) ; 2.68 (multiplet, 2H, $-CH_2-COOH$) ; 2.9 (multiplet, 1H, $>CH-C_6H_5$) ; 11.0 (broadened singlet, 1H, COOH both acids).

4-Methyl-4-phenyl-2-pentenoic acid (**11**) was obtained starting from the methyl ester separated by preparative gas-chromatography from the reaction mixture.

NMR spectrum (CCl_4) : 1.47 (singlet, 6H, $2CH_3$) ; 5.76 (doublet, 1H, $-CH=$, $J=16$ Hz) ; 7.20 (doublet, 1H, $=CH-COOH$) ; 7.0–7.4 (multiplet, 5H, C_6H_5) ; 11.35 (broadened signal, 1H, COOH).

Revue Roumaine de Chimie, **23**, *5*, 759–767 (1978)

SPIRO-3-ARYLIDENE-1,2,3,4-TETRAHYDRONAPHTHALENE-4-ONES. I
REACTIONS WITH AMINES AND FRIEDEL-CRAFTS REACTIONS

ABD EL-KADER FATEEN, AHMED MOHAMED KADDAH
and JOUSREY MOUSTAFA NAGUIB
Chemistry Department, Faculty of Science, Ain Shams University,
Cairo, Arab Republic of Egypt

Received March 8, 1976

Spiro-1,2,3,4-tetrahydro-naphthalene-4-one-(1:3′)-2′, 6′-piperidinediones **(1)** condense with different aromatic aldehydes to give spiro-3-arylidene-1, 2, 3,4-tetrahydro-(1:3′)-2′, 6′-piperidinediones**(2a–i)**. Treatment of the freshly prepared dibromo derivatives **3a** and **3b** with excess of different secondary amines gave spiro-3-(α—alkyl—aryl)-1,4-dihydronaphthalene-4-one—(1:3′)—2′ ,6′—piperidinediones **(4a–f)**. The piperidinedione ring of **2b** and **2e** was opened on boiling with sodium hydroxide to give the dicarboxylic acid **5a** and **5b**, which treated with acetylchloride gave the anhydrides **6a** and **6b**. The reaction of the anhydride **6b** with toluene under Friedel—Crafts conditions gave **8**, while **6a** reacts with chlorobenzene under the same conditions to give **9**. Reaction of *p*-anisidine with the anhydride **10** gave **11**. The acid chloride of **12** treated with different amines gives the corresponding amide derivatives **13a–e**. Oxidation of the dicarboxylic acid **14** afforded **15**. The structure of the above products have been established by IR, UV, and elemental analysis.

The interaction of spiro-1,2,3,4-tetrahydro-naphthalene-4-one-(1 :3′)-2′,6′-piperidinediones [1] **(1a–e)** and spiro-1,2,3,4-tetrahydro-(6-chloronaphthalene-4-one)-(1 : 3′)-2′,6′-piperidinediones [2] **(1f–i)** with different aromatic aldehydes in sodium hydroxide solution gave spiro-3-arylidene-1,2,3,4-tetrahydronaphthalene-4-one-(1 : 3′)-2′,6′-piperidinediones **(2a–i)** :

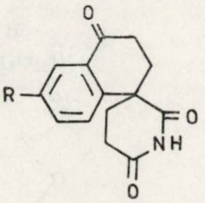

1

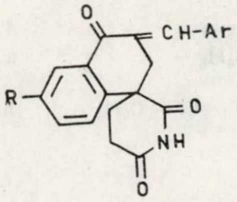

2

1–2	R =	Ar =
a	H	C_6H_5-
b	H	$p-Cl-C_6H_4-$
c	H	$o-Cl-C_6H_4-$
d	H	$p-CH_3-C_6H_4-$
e	H	$p-CH_3O-C_6H_4-$
f	Cl	C_6H_5-
g	Cl	$p-Cl-C_6H_4-$
h	Cl	$o-Cl-C_6H_4-$
i	Cl	$p-CH_3-C_6H_4-$

---

[1] C. F. Koelisch, *J. Org. Chem.*, **25**, 165 (1960).

[2] A. K. Fateen and A. M. Kaddah, *Indian J. Chem.*, **11**, 332 (1973).

The structure of the condensation products **2** was established by elemental analysis, IR and UV spectra. The infrared spectra show a band at 1680 cm^{-1} characteristic of α, β-unsaturated carbonyl stretching frequency.[3] The comparatively low frequency shift is due to the conjugation of the carbonyl group with the olefinic double bond. The IR spectra also show a band at 1720 cm^{-1} characteristic of the stretching of the coupled carbonyl group of the six membered cyclic imides,[3] and a broad band between 2900—3520 cm^{-1} due to stretching vibration of the NH and OH groups.[3] The electronic spectra are very similar to those of chalcones[4] which possesses two absorption maxima at 226 nm (ε_{max} 12000) and 299 nm (ε_{max} 23900). Wiley *et al.*[4] suggested that the lower absorption may be attributed to the carbonyl function shifted under the influence of the auxochromic groups, while the other absorption is due to the ring conjugation with the carbonyl function.

When **2a** and **2c** were allowed to react with bromine in glacial acetic acid, they gave the corresponding dibromoderivatives **3a** and **3b**. These products were isolated in a colourless crystalline form but they acquired a brown colour on standing and did not give correct analysis. Treatment of the freshly prepared spiro-3-bromo-3-(α-arylbromomethyl)-1,2,3,4-tetrahydronaphthalene-4-one-(1 : 3′)-2′,6′-piperidinedione (**3a** and **3b**) with excess of different secondary amines gave spiro-3-(α-arylalkylmethyl)-1,4-dihydronaphthalene-4-one-(1 : 3′)-2′,6′-piperidonedione (**4a—f**).

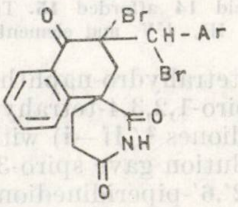

3

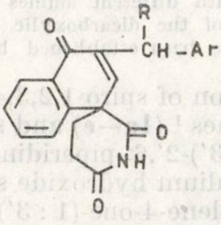

4

3 Ar =	4 Ar =	R =
a C_6H_5 —	**a** C_6H_5 —	$(C_2H_5)_2N$ —
b o — Cl — C_6H_4 —	**b** C_6H_5 —	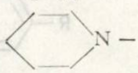
	c C_6H_5 —	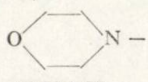
	d o — Cl — C_6H_4 —	$(C_2H_5)_2N$ —
	e o — Cl — C_6H_4 —	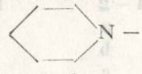
	f o — Cl — C_6H_4 —	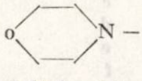

The structure of these products, **4a—f**, was established by elemental analysis, IR and UV spectra. The IR spectra [3] show two bands at 1680 cm^{-1},

---

[3] L. G. Bellamy, "The Infrared Spectra of Complex Molecules" Methuen Co., London 1956, p. 110, 176 and 191.

[4] R. H. Wiley, C. H. Jarboe and H. G. Elbert, *J. Amer. Chem. Soc.*, **77**, 5102 (1965).

1720 cm^{-1} and a broad band at 3270—3660 cm^{-1}. These bands are characteristic of the stretching frequency of the conjugated carbonyl group coupled group of the six-membered cyclic imides and >NH group respectively.

It was found that the piperidinedione ring from **2b** and **2e** was opened on boiling with sodium hydroxide (20%) to give the dicarboxylic acids **5a** and **5b**. When the ketodicarboxylic acids **5a** and **5b** were treated with acetyl chloride, they gave the corresponding anhydrides **6a** and **6b**.

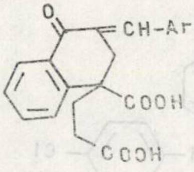

5

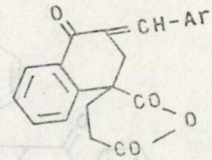

6

5—6 Ar =
a p-Cl — C_6H_4 —
b p-CH_3O — C_6H_4—

The structure of **5a** and **5b** was established by elemental analysis and spectroscopic data. The IR spectra [3] shows the bands characteristic for the stretching frequency of the α, β-unsaturated carbonyl at 1690 cm^{-1}, a band at 1710 cm^{-1} due to the frequency of the carbonyl group of saturated acid and a broad band at 2760—3300 cm^{-1} due to the stretching frequency of the bonded OH group.

The conversion of acids into anhydrides **6** is demonstrated by the disappearance of the ν OH band and the appearance of bands characteristic of anhydrides at 1720 and 1760 cm^{-1}.

The reaction of the anhydride **6b** with toluene under Friedel-Crafts conditions is expected to give two products, depending on the mode of opening the anhydride ring.[2] However the positively charged oxygen in the anhydride-aluminium chloride complex would attract the shared electron pair with the carbon of the carbonyl which is less positive and according to the previous discussion, cleavage of the anhydride should take place as shown in **7** to give finally as product 1-β-(p-methylbenzoylethyl)-3-(p-methoxybenzylidene)-4-oxo-1,2,3,4-tetrahydro-1-naphthoic acid acid(**8**).

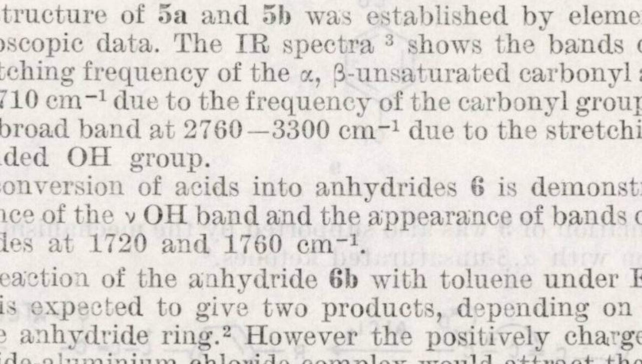

This is supported by the fact that the α, α-gem-dialkylglutaric anhydride reacts with different hydrocarbons in the presence of anhydrous aluminium chloride to give γ-aroyl-α,α-dialkylglutaric acids,[5] which arise from a nucleophilic attack at the carbonyl group far from the α-substituted carbon.

On the other hand, anhydride **6a** reacts with 2 moles of chlorobenzene under Friedel-Crafts conditions, giving 1-β-(*p*-chlorobenzoylethyl)-3-(di-*p*-chlorophenyl)-methyl-4-oxo-1,2,3,4-tetrahydro-1-naphthoic acid (**9**). It was found that the first molecule of chlorobenzene reacts with the anhydride and the other one with the α,β-unsaturated ketonic system.

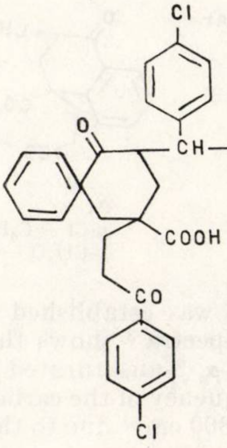

9

The formation of **9** was also supported by the mechanism of Friedel-Crafts reaction with α,β-unsaturated ketones.[6]

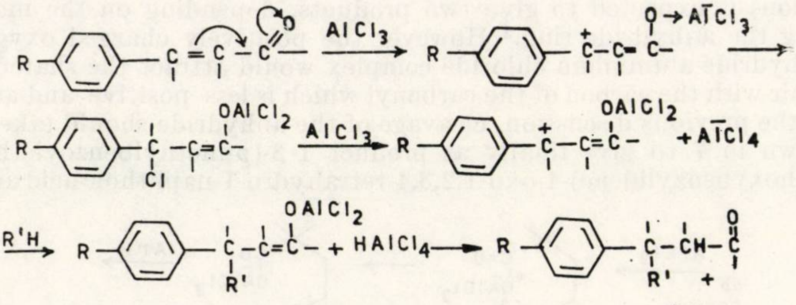

It seems that the attack may preferably take place if R = –Cl. When R = –OCH$_3$, the positive charge on the benzylic carbon atom is partially spoiled by further conjugation and so the compound becomes less reactive towards nucleophilic addition reaction.

---

[5] E. Rothsleim and W. C. Schofield, *J. Chem. Soc.*, **1965**, 4566.

[6] J. Cologne and L. Pichat, *Bull. Soc. chim., France* **1949**, 177.

The IR spectra[3] of the products **8** and **9** show a characteristic stretching frequency of the CO group in conjugation with aromatic rings at 1680 cm^{-1}, a sharp band due to νCO of saturated acids at 1720 cm^{-1} and the band of bonded νOH at 3300–3500 cm^{-1}. The UV spectra shows a very intense band at 245 nm (ε 20656) and a medium intense band at 305 nm (ε_{max} 4750). The former band appears to be due to the red-shifted band-II of benzene, whereas the latter to the red shifted and intensified band-III. The absorption of these compounds is similar to that of **5** which double the intensity because the former compounds contain two isolated chromophores (Ar–CO).

The action of *p*-anisidine on the anhydride [1] **10** should give rise theoretically to either of two possible products depending upon which carbonyl group is preferentially attacked by *p*-anisidine :

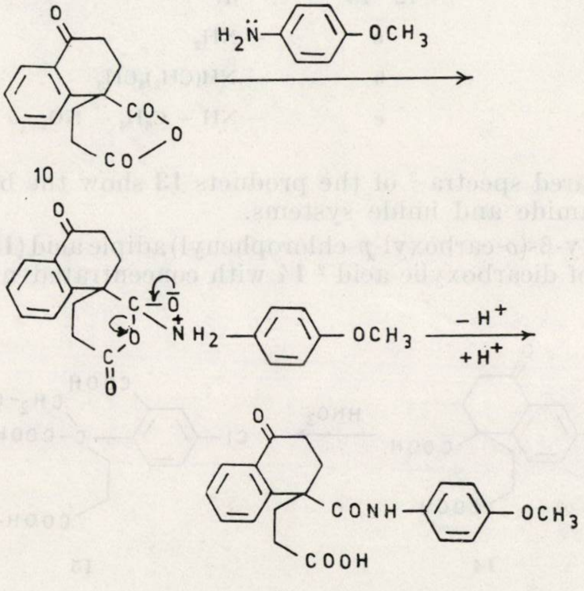

In this case two factors are operating : [2] (*i*) the relative magnitude of the partial positive charge on the carbons of the two carbonyl groups and (*ii*) the steric interference of the spirotetralone ring to nucleophilic attack on the adjacent carbonyl group. However, it is more probable, according to the previous discussion, that the attack takes place at the carbon atom of the adjacent carbonyl group to give finally the product **11**. Moreover, construction of molecular models for **10** illustrates that the spirotetralone ring does not exert any steric interference to an attack at the adjacent carbonyl group.

The structure of the product **11** was established by IR spectra which show bands at 1690 cm^{-1}, 1700 cm^{-1}, 1740 cm^{-1} and a broad band at 3040–3300 cm^{-1} due to the frequency of carbonyl of cyclic ketone, amide, carboxyl and NH & OH respectively. The UV spectrum shows an intense band at 244 nm which is band-II of benzene or red-shifted by conjugation with carbonyl group, and a medium intense band at 290 nm.

The monocarboxylic acid [7] **12** was converted to the acid chloride and then treated with different amines to give the amide derivatives **13a–c**.

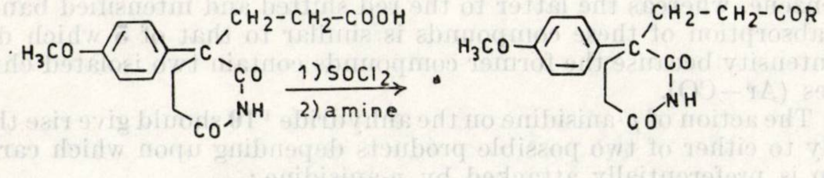

12 **13**

12–13	R
a	$-NH_2$
b	$-NH(CH_2)_3CH_3$
c	$-NH-C_6H_4-NO_2-o$

The infrared spectra [3] of the products **13** show the bands characteristic of the amide and imide systems.

β-Carboxy-β-(*o*-carboxyl-*p*-chlorophenyl) adipic acid (**15**) was obtained by oxidation of dicarboxylic acid [2] **14** with concentrated nitric acid.[1]

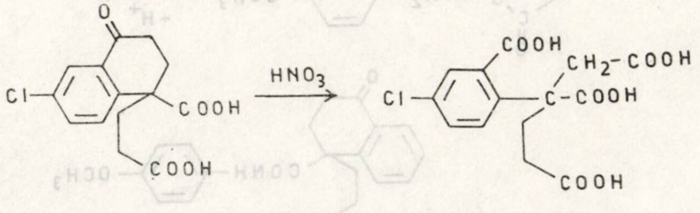

14 **15**

The structure of the product **15** was established by elemental analysis, infrared and electronic spectra. The IR spectrum of **15** shows a broad band at 1720 cm^{-1} due to ν_{CO} of the carboxylic group [3] and also a broad band at 3310–3620 cm^{-1} due to ν_{OH} (bonded) of the acid.[3]

EXPERIMENTAL

All the melting points are uncorrected. The infrared spectra (i.r.) were measured on a SP 1000 PYE UNICAM Spectrophotometer ; the KBr waver technique was used. The electronic spectra were carried out by using a PERKIN-ELMER, Model 402 Ultraviolet Spectrophotometer.

[7] A. K. Fateen and A. M. Kaddah, *Indian J. Chem.*, 11, 225 (1973).

Synthesis of spiro-3-arylidene-1, 2, 3, 4-tetrahydro-naphthalen-4-one (1 :3')-2'-6'-piperidinedione **(2b — i)** :

A solution of (0.01 mole) of 1b—i in 25 ml of NaOH (2%) and ethanol (10 ml) was treated with aromatic aldehyde (0.01 mole), boiled under reflux for 10 minutes, then cooled and acidified with dilute hydrochloric acid. The precipitate of 2b—i was filtered off, dried and recrystallised from a suitable solvent as indicated in table 1.

Table 1

Spiro-3-arylidene-1,2,3,4-tetrahydro-napthalen-4-one-(1 :3')-2',6'- piperidinediones (2b-i) and spiro-3-(α-arylalkylmethyl-) -1,4-dihydro-naphthalen-4-one-(1 :3')-2', 6'-piperidinedione (4a-f).

Product	Recryst. solvent	M. P. °C	Yield %	Molecular formula	Found (%)			Required (%)		
					C	H	N	C	H	N
2b	Ethanol	195	62	$C_{21}H_{16}O_3NCl$	69.1	4.40	3.48	68.9	4.37	3.80
c	Ethanol	206	67	$C_{21}H_{16}O_3NCl^*$	68.4	4.70	3.59	68.9	4.37	3.80
d	Acetic acid	208	58	$C_{22}H_{19}O_3N$	76.9	5.30		76.5	5.40	
e	Acetic acid	221	72	$C_{22}H_{19}O_4N$	72.7	5.30		73.1	5.26	
f	Acetic acid	192	70	$C_{21}H_{16}O_3NCl$	63.3	4.60	3.70	63.9	4.37	3.80
g	Acetic acid	248	68	$C_{21}H_{15}O_3NCl_2$	62.5	4.00		63.0	3.75	
h	Ethanol	189	53	$C_{21}H_{15}O_3NCl_2$	63.2	3.70		63.0	3.75	
i	Acetic acid	187	57	$C_{22}H_{18}O_3NCl$	69.2	4.80		69.5	4.70	
4a	Acetic acid	247	65	$C_{25}H_{26}O_3N_2$	74.38	6.62	6.83	74.62	6.46	6.96
b	Acetic acid	204	59	$C_{26}H_{26}O_3N_2$	74.8	6.4		75.3	6.2	
c	Ethanol	207	59	$C_{25}H_{24}O_4N_2$			6.5			6.7
d	Ethanol	227	60	$C_{25}H_{25}O_3N_2Cl$			6.6			6.4
e	Ethanol	215	55	$C_{26}H_{25}O_3N_2Cl$	69.32	5.64	6.62	69.63	5.57	6.23
f	Ethanol	224	54	$C_{25}H_{23}O_4N_2Cl$	66.83	4.92		66.59	5.1	

* Cl% Found : 9.60% Required : 9.65 %

Action of bromine on spiro-3-arylidene-1, 2, 3, 4-tetrahydronaphthalen-4-one- (1 :3')-2,6'-piperidinedione (**2a** *and* **2e**) :

Bromine (0.01 mole) in glacial acetic acid (10 ml) was added within one hour to a (0.01 mole) stirred solution of **2a** or **2e** in glacial acetic acid (25 ml) at room temperature,then the mixture was poured in ice-water. The solid separated was washed with light petroleum (80°) and dried. The colourless product **3** so obtained decomposed on standing and did not give correct analysis.

Reactions of the dibromo derivatives **3a** *and* **3b** *with secondary amines*:

A mixture of the dibromo compound **3** (1 mole) in benzene (10 ml), and the appropriate secondary amine (10 moles) was allowed to stand at room temperature for 24 hours. The mixture was cooled and treated with dilute hydrochloric acid to react with excess amine, extracted with ether and then evaporated till dryness. The thick oil obtained was triturated with light petroleum (40—60°) to give a solid **(4a—f)** which was recrystallised from a suitable solvent as indicated in table 1.

Hydrolysis of spiro-3-arylidene-1,2,3,4-tetrahydro-naphthalen-4-one-(1 : 3')-2', 6'-piperidinedione **(2b** *and* **2e)** :

A solution of the compound **2b** or **2e** (5 g) in 20% sodium hydroxide (25 ml) was heated under reflux for 4 hours. The mixture was cooled and acidified with conc. hydrochloric acid. A brown oil was obtained which solidified on rubbing with light petroleum (60—80°). The solid **5a** or **5b** was filtered off, dried and crystallised from suitable solvent as indicated in table 2.

Table 2

4-Oxo-3-arylidene-1,2,3,4-tetrahydro-1-naphthoic acid-1-propionic acid (5a and 5b) ; spiro-3-arylidene-1,2,3,4-tetrahydronaphtalene-4-one-(1 :3')-2', 6'- dioxopyran (6a and 6b) ; the products of Friedel-Crafts reaction, 8 and 9, and 3-p-methoxyphenyl-2',6'-piperidinedione-3-propionamide (13a-c).

Compd.	Recryst. solvent	M.P. °C	Yield %	Molecular formula	Found (%)			Required (%)		
					C	H	N	C	H	N
5a	Benzene	221	41	$C_{21}H_{17}O_5Cl^*$						
b	Benzene	178	47	$C_{22}H_{20}O_6$	69.2	5.4		69.5	5.2	
6a	Dry benzene	208	96							
b	Dry toluene	153	97							
8	Benzene/light petroleum (60—80°)	154	39	$C_{29}H_{26}O_5$	76.2	5.6		76.6	5.7	
9	Benzene	165	18	$C_{33}H_{26}O_4Cl_3$	66.2	4.5		66.5	4.6	
13a	Ethanol	206	80	$C_{15}H_{18}O_4N_2$	62.16	6.26		62.07	6.2	
b	Benzene	156	63	$C_{19}H_{26}O_4N_2$	66.8	7.4	8.38	66.9	7.5	8.9
c	Acetic acid	216	61	$C_{21}H_{21}O_6N_3$	61.04	5.01		61.3	5.1	

* Cl % Found : 9.4% Required : 9.2 %

Spiro-3-arylidene-1,2,3,4-tetrahydro-naphthalen-4-one (1 :3')-2, 6'-dioxopyran **(6a** *and* **6b)** :

A solution of **5a** or **5b** (2.5 g) in acetyl chloride (10 ml) was boiled on a water bath for 4 hours. Excess acetyl chloride was removed under vacuum to give a solid which was filtered off, thoroughly washed with light petroleum (60—80°), dried and recrystallised from a suitable solvent as indicated in table 2. The anhydrides obtained **6a** and **6b** were unstable and used immediately in Friedel-Crafts reaction.

Reactions between the anhydrides **6a** *and* **6b** *and chlorobenzene or toluene under Friedel-Crafts conditions* :

Anhydrous aluminium chloride (3 moles) was added portionwise to a cold stirred solution of the anhydride **6a** or **6b** (1 mole) and the appropriated aromatic compound (chlorobenzene or toluene). The mixture was heated under reflux for ten hours and left overnight. It was then decomposed with ice and hydrochloric acid and the organic layer separated and extracted several times with sodium carbonate solution. On acidification of the aqueous layer, a colourless solid separated which recrystallised from a suitable solvent gives **8** and **9** as colourless crystals (Table 2).

*Action of p-anisidine on spiro-1, 2, 3, 4-tetrahydro-naphthalen-4-one-(1 :3′)-2′, 6′-dioxopyran***(10)** :

A mixture of the anhydride **10** (1.5 g) and *p*-anisidine (1 g) was warmed at 100° for two hours. The mixture was cooled and then treated with diluted hydrochloric acid to react with excess *p*-anisidine. The obtained oil was triturated with light petroleum (60—80°) to give a solid which was crystallised from ethanol to give a solid which was crystallised from ethanol to give 4-oxo-1, 2, 3, 4 -tetrahydro-1-naphthyl-1-*p*-methoxyanilide-1-propionic acid **(11)** as colourless crystals, m.p. 199°, Yield : 45% ;
Found : C, 68.64 ; H, 5.42. Required : for $C_{21}H_{21}O_5N$ C, 68.40 ; H, 5.70%.

Synthesis of 3-p-methoxyphenyl-2,6-piperidinedione-3-propionamide derivatives **(13a—e)** :

3-*p*-Methoxyphenyl-2,6-piperidinedione-3-propionic acid **(12a—e)**, (5 g) was treated with thionyl chloride (5 ml) at 40° until complete dissolution. Excess thionyl chloride was removed *in vacuo* and the residue dissolved in dry benzene (30 ml). The acid chloride in benzene (10 ml) was treated with the amine (10 ml) and the mixture was kept for 2—4 hours at room temperature. The solid precipitated was filtered, washed with dilute hydrochloric acid, aqueous sodium carbonate, water, dried and crystallised from a suitable solvent as indicated in table 2.

Synthesis of β-carboxy-β-(o-carboxy-p-chlorophenyl) adipic acid **(15)** :

A solution of 4-oxo-1, 2, 3, 4- tetrahydro-6-chloronaphthoic acid-1-proionic acid **(14)**, (5 g) in hot water (25 ml) was boiled while conc. nitric acid (15 ml) was added dropwise within 30 minutes. The mixture was boiled for half an hour and then poured into cold water. The ether-extract was washed several times with water and dried. An oil was obtained which solidified after trituration with light petroleum (60—80°). It was crystallised from water to give **15** as colourless crystals, m.p. 183°, Yield 51% ; Found : C, 49.00 ; H, 4.0. Required for $C_{14}H_{13}O_8Cl$: C, 48.76 ; H, 3.77%.

Revue Roumaine de Chimie, **23**, *5*, 769–779 (1978)

HYBRIDIZATION OF DICOORDINATED TRIVALENT AND TETRACOORDINATED PENTAVALENT PHOSPHORUS IN CONJUGATED SIX-MEMBERED RINGS

M. MRACEC* and Z. SIMON
Department of Chemistry, University of Timişoara, bd. V. Pârvan 4, Timişoara,
1900, Romania

Received March 17, 1976

The possible hybridizations of dicoordinated trivalent $(\lambda^3 -)$ and tetracoordinated pentavalent $(\lambda^5 -)$ phosphorus are analyzed on hand of $3d$-orbital splitting in C_{2v} potential. The analysis of possible hybridizations demonstrates the necessity to consider $3d$-orbitals, especially for the tetracoordinated pentavalent phosphorus. The real state within a molecule for a third or higher period atom is a mixture of hybridization types allowed by symmetry. One should expect an increasing participation of nd orbitals $(n \geqslant 3)$ to both σ and π-bonds as n increases beyond 3.

The rapid development in synthesis of organophosphorus compounds, especially of conjugated six-membered rings with trivalent dicoordinated phosphorus[1] (λ^3-) and pentavalent tetracoordinated phosphorus[2] (λ^5-), arose an increasing interest in quantum chemical models to explain the nature of phosphorus-bonds in such compounds.

For trivalent dicoordinated phosphorus a model similar to pyridinic nitrogen was assumed from the beginning, based upon work of Brown,[3] and adopted by Vîlceanu et al.[4] Although Brown[3] did not take into account $3d$-orbitals, CNDO/2-calculations of Oehling and Schweig[5] indicate their participation in both σ and π-bonds for six-membered rings. Ab initio calculations of Heilbronner et al.,[6] for the photoelectronic spectrum, concerning the pyridine of λ^3-phosphorin (phosphabenzene) and of arsabenzene and stibabenzene suggest that $3d$-phosphorus orbitals participation is low for bonding, but increased for antibonding levels.

---

* Permanent address : Chemical Research Laboratory "C. P. Solventul" Timişoara, 1900, Timişoara, spl. N. Titulescu, nr. 31, ROMANIA.

[1] G. Märkl, *Angew. Chem.*, **78**, 907 (1966) ; G. Märkl, F. Lieb and A. Merz, *Angew. Chem.*, **79**, 475, 974 (1967) ; P. de Koe and F. Bickelhaupt, *Angew. Chem.*, **79**, 533 (1967) ; K. Dimroth and W. Mach, *Angew. Chem.*, **80**, 489 (1968) ; A. J. Ashe, *J. Amer. Chem. Soc.*, **93**, 3293 (1971).

[2] D. H. Stoker, *J. Amer. Chem. Soc.*, **17**, 275 (1895) ; G. Märkl, *Angew. Chem.*, **75**, 168, 669, 1121 (1963) ; **77**, 1109 (1965) ; G. Märkl and K. H. Heier, *Angew. Chem.*, **84**, 1066 (1972) ; A. Schmidpeter and J. Ebeling, *Chem. Ber.*, **101**, 2602, 3883 (1968) ; M. Davies and A. N. Hughes, *J. Heterocyclic Chem.*, **9**, 1 (1971) ; O. Schaffer and K. Dimroth, *Chem. Ber.*, **108**, 3271, 3281 (1975) ; P. Kieselack, C. Helland and K. Dimroth, *Chem. Ber.*, **108**, 3656 (1975) ; K. Dimroth and P. Kieselack, *Chem. Ber.*, **108**, 3671 (1975).

[3] D. A. Brown, *J. Chem. Soc.*, **1962**, 929.

[4] R. Vîlceanu, A. Balint and Z. Simon, *Anal. Univ. Timişoara, ser. Mat.-Fiz.*, **6**, 337 (1968).

[5] H. Oehling and A. Schweig, *Tetrahedron*, **1970**, 4941 ; H. Oehling, W. Schweig and A. Schweig, *Angew. Chem.*, **83**, 723 (1971) ; A. Schweig, W. Schweig and K. Dimroth, *Angew. Chem.*, **84**, 636 (1972) ; W. Schweig, A. Schweig, F. Bickelhaupt and H. Vermeer, *Angew. Chem.*, **84**, 993 (1972).

In contrast, there were several controverses concerning the model for pentavalent tetracoordinated phosphorus in conjugated six-membered rings. Three models were proposed for λ^5-phosphorus :

i) The antiaromatic (anti Hückel) model of Craig and Paddock [7,8] was put forward to explain electronic structure of phosphonitriles. It was used also by other workers in this field [9] and by Mason [10] — to explain the nature of pentavalent tetracoordinated phosphorus bonds in λ^5-phosphorin cycles. This model implies a d_{xz}-orbitals with two resonance energy integrals, equal but of oposite sign : $\beta_{PC_1} = -\beta_{PC_6}$, eventually also a reduced extent of d_{yz}-orbital.

ii) The Dewar model [11] implies an equal participation of the d_{xz} and d_{yz} orbitals with a conjugation break of at the phosphorus atom.

iii) The Fukui model (aromatic model) put forward by Fukui et al.[12] for organic phosphates, was adopted by Vîlceanu et al.,[13] was used, together with the previous two, in electronic structure of λ^5-phosphorin cycles. The Fukui model implies only one $3d$ orbital, but the $3d_{yz}$-orbital.

---

[6] C. Batich, E. Heilbronner, V. Hornung, A. J. Ashe, D. T. Clark, U. T. Cobley and I. Schanlan, *J. Amer. Chem. Soc.*, **95**, 929 (1973).

[7] D. P. Craig, *Chem. Ind.*, **1958**, 3 ; *J. Chem. Soc.*, **1959**, 997 ; D. P. Craig and N. L. Paddock, *Nature*, **181**, 1052 (1958) ; *J. Chem. Soc.*, **1962**, 4118 ; N. L. Paddock, *Research* (*London*), **13**, 94 (1960) ; *Quart. Rev.* (*London*), **18**, 168 (1964) ; G. R. Branton, C. E. Brion, D. C. Frost, K. A. R. Mitchell and N. L. Paddock, *J. Chem. Soc. A*, **1970**, 151 ; H. P. Calhoun, N. L. Paddock and J. Trotter, *J. Chem. Soc. Dalton*, **1973**, 2708 ; T. N. Ranganathan, S. M. Todd and N. L. Paddock, *Inorg. Chem.*, **12**, 316 (1973) ; R. T. Oakley and N. L. Paddock, *Canad. J. Chem.*, **51**, 520 (1973) ; N. L. Paddock and J. Serreqi, *Canad. J. Chem.*, **52**, 2546 (1974) ; M. W. Douling and N. L. Paddock, *J. Chem. Soc. Dalton*, **1974**, 1022 ; H. T. Searle, Y. Dyson, T. N. Ranganathan and N. L. Paddock, *J. Chem. Soc. Dalton*, **1975**, 202 ; H. P. Calhoun, N. L. Paddock and J. N. Wingfield, *Canad. J. Chem.*, **53**, 1765 (1975).

[8] L. Salem, "The Molecular Orbital Theory of Conjugated Systems", Benjamin Inc., New York, 1966, p. 158 ; H. H. Greenwood, "Computing Methods in Quantum Organic Chemistry", Wiley & Sons Inc., New York, 1972, p. 90.

[9] K. A. R. Mitchell, *J. Chem. Soc. A*, **1968**, 2683 ; *Chem. Rev.*, **69**, 157 (1969) ; M. Pelavin, D. N. Hendrickson, J. M. Hollander and W. L. Jolly, *J. Phys. Chem.*, **74**, 1116 (1970) ; C. Doggett, *J. Chem. Soc. Faraday II*, **1972**, 2075.

[10] S. F. Mason, *Nature*, 205, 495 (1965).

[11] M. J. S. Dewar, E. A. C. Lucken and M. A. Whitehead, *J. Chem. Soc.*, **1960**, 2423.

[12] K. Fukui, K. Morocuma and Ch. Nagata, *Bull. Chem. Soc. Japan*, **33**, 1214 (1960) ; K. Fukui, A. Imamura and Ch. Nagata, *Bull. Chem. Soc. Japan*, **36**, 1450 (1963).

[13] R. Vîlceanu, A. Balint and Z. Simon, *Nature*, **217**, 61 (1968) ; *Rev. Roumaine Chim.*, **13**, 533 (1968) ; R. Vîlceanu, A. Balint, Z. Simon, C. Renţia and G. Unterweger, *Rev. Roumaine Chim.*, **13**, 1923 (1968) ; R. Vîlceanu, A. Balint, M. Mracec and Z. Simon, "Conferinţa Republicană de Chimie Fizică Generală şi Aplicată", Bucharest, 1968, p. 10 ; R. Vîlceanu, A. Balint, Z. Simon and M. Mracec, "Colloques Internationaux du CNRS, nr. 182, Chimie Organique du Phosphore", Paris, 1969, p. 39.

Our HMO calculations[14,15] with all three models applied to conjugated six-membered rings with pentavalent tetracoordinated phosphorus plead for the Fukui model as the most suitable.[15] Only the Fukui model allowed a unitary HMO treatment of the first band in the electronic spectrum of a large variety of compounds of this class.

As a special mention — all these studies used Oy as the C_2 axis.

We shall bring here new arguments concerning participation of $3d$-orbitals in π-bonds of conjugated six-membered rings, for both trivalent dicoordinated and pentavalent tetracoordinated phosphorus. These arguments are based upon a group-theoretical analysis of possible hybrids in Sharma's[16] ideea of partial hybridization.

1. HYBRIDIZATION OF TRIVALENT DICOORDINATED PHOSPHORUS IN CONJUGATED SIX-MEMBERED RINGS

The fundamental state of free phosphorus atom is $3\,{}^4S_{3/2}\,(\mathrm{P}(s^2p^3,\,V_3))$. The L_1-P-L_2 valence angle in conjugated six-membered rings with trivalent dicoordinated phosphorus is of about 103°[17-19] and the cycles are planar.[17,18] The P-atom is thus situated in the field of two identical ligands ($L_1 = L_2 = L$) able to give both σ and π-bonds.

In order that a comparison with the results of Oehling and Schweigh is possible, we shall consider the P-atom in the origin of coordinates, L_1 and L_2 in the xOy plan with the Ox axis bisecting the L_1-P-L_2 angle (Figure 1). Four orientational vectors will be considered for hybrid orbitals : $\mathbf{r}_1$, $\mathbf{r}_2$, $\mathbf{r}_3$ and $\mathbf{r}_4$. Vectors $\mathbf{r}_1$ and $\mathbf{r}_2$ are considered equal and directed towards L_1 and respectively L_2, forming a 103°-angle. They indicate the direction of hybrid orbitals of the σ (P—L) bonds. $\mathbf{r}_3$ is directed on the negative side of the Ox axis at 128.5° angles with $\mathbf{r}_1$ and $\mathbf{r}_2$, and gives the direction for the hybrid orbital which, by similarity with pyridinic nitrogen, contain the electronic lone pair. As the L_1-P-L_2 angle differs from 120°, the value for pyridinic-N, $\mathbf{r}_3$ could be considered equivalent to $\mathbf{r}_1$ and $\mathbf{r}_2$ from a group theoretical point of view. We will consider $\mathbf{r}_3$ nevertheless different in order to have some distinction with respect to $\mathbf{r}_1$ and $\mathbf{r}_2$. The vector $\mathbf{r}_4$ is taken perpendicular to the ($\mathbf{r}_1$, $\mathbf{r}_2$, $\mathbf{r}_3$) plan, directed along the Oz axis and indicates the direction of hybrid orbitals for π-bonds between P and L_1 and L_2 orbitals (see Figure 1).

The point group, to which this ensemble belongs, is, obviously, C_{2v} in contradistinction to pyridinic-N or phenylic-C for which the point group D_{3h} is usually used. As the molecular plan was considered the xOy plan, C_2 must be selected as Ox axis. Thus the σ_v' plan of C_{2v} point group is no longer yOz but xOy and some changes must be considered, in compari-

---

[14] M. Mracec and Z. Simon, "A 2-a Conferință Republicană de Chimie Fizică Generală și Aplicată", Bucharest, 1970, p. 118 ; Z. Szabadai, M. Mracec and M. Mracec, *Anal. Univ. Timișoara, ser. Fiz.-Chim.*, **8**, 145 (1970) ; M. Mracec and M. Mracec, *Anal. Univ. Timișoara. ser. Fiz.-Chim.*, **10**, 61 (1972).

[15] M. Mracec, "A 3-a Conferință Republicană de Chimie Fizică Generală și Aplicată", București, 1972, p. 23 ; M. Mracec and M. Mracec, "A 4-a Conferință Republicană de Chimie Fizică Generală și Aplicată", Bucharest, 1974, p. 11.

[16] C. S. Sharma, *Indian J. Pure Appl. Phys.*, **8**, 15 (1970).

[17] C. J. Bart and J. J. Daly, *Angew. Chem.*, **80**, 843 (1968) ; R. L. Kuczkowski and A. J. Ashe, *J. Mol. Spectroscopy*, **42**, 457 (1972).

[18] U. Thewalt, *Angew. Chem.*, **81**, 783 (1968).

[19] D. Purdela and R. Vîlceanu, "Chimia compușilor organici ai fosforului și ai acizilor lui", Ed. Acad., Bucharest, 1965, p. 25, 111.

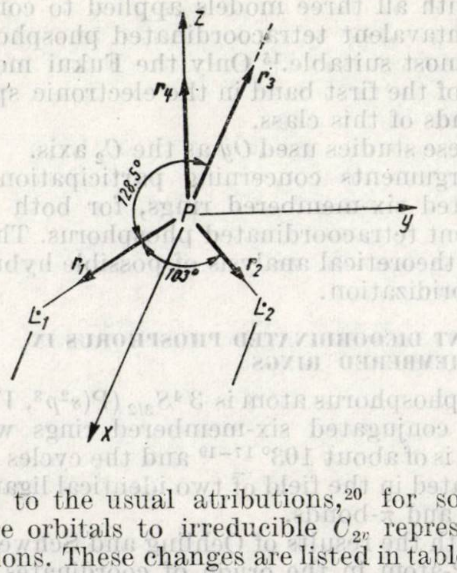

Fig. 1. — Ligand positions and orientations of the directing vectors of the trivalent dicoordinated phosphorus hybrids in conjugated six-membered rings.

son to the usual atributions,[20] for some pure orbitals to irreducible C_{2v} representations. These changes are listed in table 1.

Table 1

Modified C_{2v} group, with Ox as C_2 axis

C_{2v}		
A_1	x	$x^2, y^2, z^2,$
A_2		yz
B_1	z	xz
B_2	y	xy

The irreducible representations according to which the reducible representation of vectors $\mathbf{r}_1$, $\mathbf{r}_2$, $\mathbf{r}_3$, and $\mathbf{r}_4$ is splitted, are $2A_1 + B_1 + B_2$. With data from table 1, these irreducible representations give 24 distinct groups of atomic orbitals which yield hybrids of the required orientations :

$$\begin{array}{ll}
s,\ p_x,\ p_y,\ p_z, & p_x,\ p_y,\ p_z,\ d_{x^2-y^2}, \\
s,\ p_x,\ p_z,\ d_{xy}, & p_x,\ p_z,\ d_{x^2-y^2},\ d_{xy}, \\
s,\ p_x,\ p_y,\ d_{xz}, & p_x,\ p_y,\ d_{x^2-y^2},\ d_{xz}, \\
s,\ p_x,\ d_{xz},\ d_{xy}, & p_x,\ d_{x^2-y^2},\ d_{xz},\ d_{xy}, \\
s,\ p_y,\ p_z,\ d_{x^2-y^2}, & p_x,\ p_y,\ p_z,\ d_{z^2}, \\
s,\ p_z,\ d_{xy},\ d_{x^2-y^2}, & p_x,\ p_z,\ d_{z^2},\ d_{xy}, \\
s,\ p_y,\ d_{xz},\ d_{x^2-y^2}, & p_x,\ p_y,\ d_{z^2},\ d_{xz}, \\
s,\ d_{xz},\ d_{xy},\ d_{x^2-y^2}, & p_x,\ d_{z^2},\ d_{xz},\ d_{xy}, \\
s,\ p_y,\ p_z,\ d_{z^2}, & p_y,\ p_z,\ d_{z^2},\ d_{x^2-y^2}, \\
s,\ p_z,\ d_{z^2},\ d_{xy}, & p_z,\ d_{xy},\ d_{z^2},\ d_{x^2-y^2}, \\
s,\ p_y,\ d_{z^2},\ d_{xz}, & p_y,\ d_{xz},\ d_{z^2},\ d_{x^2-y^2}, \\
s,\ d_{z^2},\ d_{xz},\ d_{xy}, & d_{z^2},\ d_{xz},\ d_{xy},\ d_{x^2-y^2},
\end{array} \tag{1}$$

---

[20] L. H. Hall, "Group Theory and Symmetry in Chemistry", McGrow Hill, New York, 1969, p. 346.

In order to make out the orbitals implied in σ and respectively π bonds we shall consider separately vector $\mathbf{r}_4$ which belongs to B_1. An inspection on table 1 shows that only p_z and d_{xz} belong to this representation. Thus for the π-bonds of trivalent dicoordinated phosphorus, only $3p_z$ and $3d_{xz}$ are available from point of view of symmetries, in agreement with the result of Oehling and Schweig. One may object that if $3p_z$ has one electron and can form π-bonds, implication of the $3d_{xz}$ orbitals is not justified. Now, the difference between *np* and *nd* orbitals, beginning with the third period ($n \geqslant 3$), is not excessively and, by ligand field splitting it may be further reduced. Thus, *np*-level electrons may populate also *nd*-levels, implying also *nd*-orbitals in bonding.

If p_z and d_{xz} orbitals are taken out from the 24 distinct groups (1), following 12 groups rest available for σ-bonds :

$$\begin{array}{ll}
s,\ p_x,\ p_y, & p_x,\ p_y,\ d_{x^2-y^2}, \\
s,\ p_x,\ d_{xy}, & p_x,\ d_{xy},\ d_{x^2-y^2}, \\
s,\ p_y,\ d_{x^2-y^2}, & p_x,\ p_y,\ d_{z^2}, \\
s,\ d_{xy},\ d_{x^2-y^2}, & p_x,\ d_{xy},\ d_{z^2}, \\
s,\ p_y,\ d_{z^2}, & p_y,\ d_{z^2},\ d_{x^2-y^2}, \\
s,\ d_{xy},\ d_{z^2}, & d_{xy},\ d_{z^2},\ d_{x^2-y^2}
\end{array} \tag{2}$$

According to the groups (2), $3d$—P orbitals should be able to participate to σ-bonds also. To make further distinctions between these participating to σ-bonds and lone pairs one observes that $\mathbf{r}_3$ belongs to A_1, while $\mathbf{r}_1$ and $\mathbf{r}_2$ transform according to $A_1 + B_2$. From the irreducible representations of table 1, one observes that only p_x and d_{xy} cannot be implied in the lone pair, while $s, p_x, d_{x^2-y^2}$, and d_{z^2} may be implied both in σ bonds and lone pairs. Oehling and Schweig remark also participation of $3d$ P-orbitals to σ-bonds.

A sequence for splitting of $3d$ orbitals in our ligand field of C_{2v} symmetry, where they transform according to $2A_1 + A_2 + B_1 + B_2$, can be obtained by correlating these irreducible representations with those corresponding to a T_d-ligand field and with some literature figures.[21] Such a sequence, concording with participation of $3d_{xz}$ to π-bond and $3d_{z^2}$, $3d_{x^2-y^2}$, and $3d_{xy}$ to σ-bonds and lone pair is depicted in Figure 2.

One may conclude that a unique hybridization cannot be atributed for heteroatoms of the third and higher periods in conjugated cycles. Any of the 24 possible groups can be considered as hybridization for trivalent dicoordinated phosphorus in our cycles. Thus, only a superposition of these "pure" hybridizations give the real situation and all valence electron calculations for such heteroatoms must take into account also *nd*-orbitals, even if they are unoccupied. The weights of "pure" hybridizations will differ — these in which *d* orbitals predominate, will have a lower weight. For simple Hückel calculations, discussions concerning the "pure" hybridization to be adopted — are senseless. A single superposition hybrid, with orientation required by molecular symmetry, is to be used and characterised by corresponding parameters.

---

[21] A. P. Borisova, Iu. Igonina, D. F. Stepanov and D. I. Ismailov, *Zhur. neorg. Khim.*, **20**, 1876 (1975).

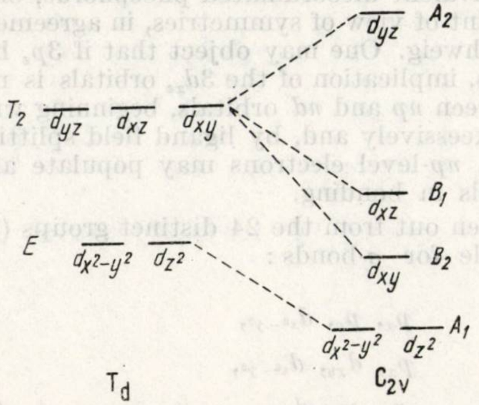

Fig. 2. — Splitting of $3d$ levels in T_d ligand field and their possibilities in C_{2v} ligand field.

2. HYBRIDIZATION OF PENTAVALENT TETRACOORDINATED PHOSPHORUS IN CONJUGATED SIX-MEMBERED RINGS

For pentavalent tetracoordinated phosphorus hybridization in conjugated six-membered rings, two models with one $3d$-orbital in the π-system were used, the antiaromatic [7–10] and the aromatic [12–15], and a single one with two $3d$-orbitals — the Dewar model [8,11–15]. We shall take into account also the possible existence of a π'-system, within the molecular plane, as for the phosphonitrilic systems.[7,8,22,23]

The phosphorus atom is now considered in the field of four ligands : L_1, L_2, L_3, and L_4. L_1 and L_2 will be considered identical ($L_1 = L_2$) and able to give π-bonds with the P-atom (perpendicular to the molecular plane). These ligands may give also π'-bonds with the P-atom in certain situations, as for phosphonitrilic cycles, by donation of the lone pair of the N-atom. The ligands L_3 and L_4 will also be considered as identical but they can give only σ bonds with the P-atom. The L_1-P-L_2 and L_3-P-L_4 angles are different for phosphonitrilic [19,24,25] and λ^5-phosphorin compounds [18,25,26] and different from those corresponding to tetrahedral orientation (see Figures 3 and 4).

We shall consider 6 orientational vectors, $\mathbf{r}_i$ ($i = 1, \ldots, 6$) for the hybrid orbitals. Vectors $\mathbf{r}_1$, $\mathbf{r}_2$, $\mathbf{r}_3$ and $\mathbf{r}_4$ will be oriented towards the L_1, L_2, L_3 and L_4 ligands, indicating the directions of hybrid orbitals which

---

[22] D. W. J. Kruickshank, *J. Chem. Soc.*, **1961**, 5486.

[23] L. Salem, "The Molecular Orbital, Theory of Conjugated Systems", Benjamin Inc., New York, 1966, p. 174.

[24] A. Wilson and D. F. Carroll, *Chem. Ind.*, **1958**, 1558 ; *J. Chem. Soc.*, **1960**, 2548 A. W. Dougill, *J. Chem. Soc.*, **1963**, 3211 ; L. A. Siegel and J. H. van den Hende, *J. Chem. Soc. A*, **1967**, 871 C. J. Bullen, *J. Chem. Soc. A*, **1971**, 1450 ; W. C. Marsh and J. Trotter, *J. Chem. Soc. A*, **1971**, 169.

[25] L. S. Haikin and L. V. Vilkov *Uspekhi Khim.*, **41**, 224 (1972).

[26] J. J. Daly, *J. Chem. Soc. A*, **1970**, 1832.

give the σ-bonds P—L_i ($i = 1, 2, 3, 4$). We shall consider $\mathbf{r}_1 = \mathbf{r}_2$ and $\mathbf{r}_3 = \mathbf{r}_4$. Vector $\mathbf{r}_5$ is perpendicular to the xOy plan, oriented along the Oz axis and indicates the orientation of the hybrid orbital implied in normal π-bonds. Vector $\mathbf{r}_6$ is in the xOy plan and oriented along the negative sense of the Ox axis and corresponds to the hybrid orbital implied in π′-bonds (if their formation is possible). From reasons similar to those presented in the previous paragraph, Ox is considered as the C_2-axis.

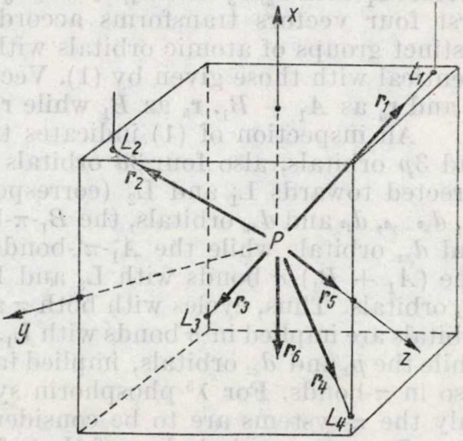

Fig. 3. — Ligand positions and orientations of the directing vectors of the pentavalent tetracoordinated phosphorus hybrids in conjugated six-membered rings, when one hybrid orbital participates at the π system and another one at the π′ system.

These ensemble belong to the C_{2v} point group, not to T_d as one may be tempted to believe. The 6 vectors transform according to irreducible representations $3A_1 + 2B_1 + B_2$. With the data of table 1, one obtains the following 8 distinct groups of atomic orbitals which may form hybrid orbitals with the required orientations :

$$\begin{array}{ll}
s,\ p_x,\ p_y,\ p_z,\ d_{x^2-y^2},\ d_{xz}, & s,\ p_x,\ p_z,\ d_{x^2-y^2},\ d_{xy},\ d_{xz}, \\
s,\ p_x,\ p_y,\ p_z,\ d_{z^2},\ d_{xz}, & s,\ p_x,\ p_z,\ d_{z^2},\ d_{xy},\ d_{xz}, \\
s,\ p_y,\ p_z,\ d_{x^2-y^2},\ d_{z^2},\ d_{xz}, & s,\ p_z,\ d_{x^2-y^2},\ d_{z^2},\ d_{xy},\ d_{xz}, \\
p_x,\ p_y,\ p_z,\ d_{x^2-y^2},\ d_{z^2},\ d_{xz}, & p_x,\ p_z,\ d_{x^2-y^2},\ d_{z^2},\ d_{xy},\ d_{xz},
\end{array} \tag{3}$$

In order to discern the hybridization possibilities of P-atom in λ^5-phosphorin cycles, only the first 5 vectors will be considered, $\mathbf{r}_i$ ($i = 1, \ldots, 5$) which transform according to $2A_1 + 2B_1 + B_2$. With the data of table 1, the following 12 distinct orbital groups are obtained :

$$\begin{array}{ll}
s,\ p_x,\ p_y,\ p_z,\ d_{xz}, & s,\ p_x,\ p_z,\ d_{xy},\ d_{xz}, \\
s,\ p_y,\ p_z,\ d_{x^2-y^2},\ d_{xz}, & s,\ p_z,\ d_{x^2-y^2},\ d_{xy},\ d_{xz}, \\
s,\ p_y,\ p_z,\ d_{z^2},\ d_{xz}, & s,\ p_z,\ d_{z^2},\ d_{xy},\ d_{xz}, \\
p_x,\ p_y,\ p_z,\ d_{x^2-y^2},\ d_{xz}, & p_x,\ p_z,\ d_{x^2-y^2},\ d_{xy},\ d_{xz}, \\
p_x,\ p_y,\ p_z,\ d_{z^2},\ d_{xz}, & p_x,\ p_z,\ d_{z^2},\ d_{xy},\ d_{xz}, \\
p_y,\ p_z,\ d_{z^2},\ d_{x^2-y^2},\ d_{xz}, & p_z,\ d_{z^2},\ d_{x^2-y^2},\ d_{xy},\ d_{xz},
\end{array} \tag{4}$$

In order to discern the orbitals which participate to σ, π and respectively π' bonds, among the possibilities listed in (3) and (4), we shall consider separately the first 4 vectors $\mathbf{r}_i$ ($i=1, 2, 3, 4$) and the groups of vectors $\mathbf{r}_1$ with $\mathbf{r}_2$, $\mathbf{r}_3$ with $\mathbf{r}_4$, $\mathbf{r}_5$ and $\mathbf{r}_6$. The reducible representation of the first four vectors transforms according to $2A_1 + B_1 + B_2$. Hereof, 24 distinct groups of atomic orbitals with required orientations are obtained, identical with those given by (1). Vectors $\mathbf{r}_1$ and $\mathbf{r}_2$ transform as $A_1 + B_2$, $\mathbf{r}_3$ and $\mathbf{r}_4$ as $A_1 + B_1$, $\mathbf{r}_5$ as B_1 while $\mathbf{r}_6$ as A_1.

An inspection of (1) indicates that σ bonds may imply, besides $3s$ and $3p$ orbitals, also four $3d$ orbitals (d_{z^2}, $d_{x^2-y^2}$, d_{xz} and d_{xy}). The σ-bonds directed towards L_1 and L_2 (corresponding to $A_1 + B_2$) imply the s, p_x, p_y, $d_{x^2-y^2}$, d_{z^2} and d_{xy} orbitals, the B_1-π-bonds with these ligands imply the p_z and d_{xz} orbitals while the A_1-π'-bonds — the s, p_x, $d_{x^2-y^2}$ and d_{z^2} orbitals. The $(A_1 + B_1)$-σ bonds with L_3 and L_4 imply the s, p_x, p_z, $d_{x^2-y^2}$, d_{z^2} and d_{xz} orbitals. Thus, cycles with both π and π' bonds, the s, p_x, $d_{x^2-y^2}$ and d_{z^2} orbitals are implied in σ bonds with L_1, L_2, L_3 and L_4 as well as in π'-bonds, while the p_z and d_{xz} orbitals, implied in σ-bonds with L_3 and L_4, are implied also in π-bonds. For λ^5-phosphorin systems, there are no π' systems and only the π-systems are to be considered.

One can conclude hereof that, for the pentavalent tetracoordinated phosphorus in conjugated six-membered rings, $3d$ orbitals are implied both in σ, as in π and π' bonds. There is no reason to assume that the "pure" $3d_{xz}$ orbital is implied only in π-bonds, while the $3d_{xy}$ orbital only in π'-bonds, because the ligand field may type of splitting as depicted in Figure 2. This result agrees with the one of Oehling and Schweig.[5]

Thus for cycles with pentavalent tetracoordinated atoms of the third and higher periods, as for those with trivalent dicoordinated ones of the previous paragraph, mixtures of different weights of several pure hybrids must be considered to be implied in all types of bonds. For naïve method, as the Hückel method for example, one should use hybrid orbitals with certain orientation and symmetry properties, but without specifying their composition.

This model in which we consider one directional vector for hybrid orbitals implied in the π-system and one for these implied in the π' system (where this system exists), will be termed — by similarity with the model used in,[12,14,15] as aromatic or Fukui model, because it transforms according to the same symmetry properties as the original Fukui model.

The analysis of possible hybrids by the group-method, excludes the $3d_{yz}$-orbital from the π-bond. In our coordinate system, this orbital would correspond to the antiaromatic model.[7–10]

In order to analyse a Dewar-type model [8,11] with the pentavalent tetracoordinated phosphorus implied with two $3d$ orbitals to π-bonds in conjugated six-membered rings, we shall keep the previous assumptions concerning the positioning of ligands and of bond angles (see Figure 3 and 4). Now 8 orientational vectors $\mathbf{r}_i$ ($i = 1, \ldots, 8$) will be considered for hybrid orbitals. Vectors $\mathbf{r}_1$—$\mathbf{r}_4$ will be directed towards L_1—L_4, and equal (as length) in pairs, $\mathbf{r}_1 = \mathbf{r}_2$, $\mathbf{r}_3 = \mathbf{r}_4$, corresponding to the P—L_i ($i = 1, \ldots, 4$) σ-bonds. Vectors $\mathbf{r}_5$ and $\mathbf{r}_6$ will be also considered of equal length ($\mathbf{r}_5 = \mathbf{r}_6$) perpendicular on the xOy plan, oriented in the direction of the Oz axis and indicate the direction of hybrid orbitals which shall form π-bonds, with interruption of conjugation at the P-atom. Vectors $\mathbf{r}_7$ and $\mathbf{r}_8$ are also considered of equal length ($\mathbf{r}_7 = \mathbf{r}_8$), in the xOy plan, perpendicular on $\mathbf{r}_5$ and respectively $\mathbf{r}_6$. They indicate the direction of hybrid orbitals implied in π' bonds (if possible) with L_1 and L_2, also with interruption of conjugation at the P-atom. For the π'-system a single directional vector, in the negative sense of the Ox axis, could also have been considered, but this brings no supplementary information, as compared to the previous case.

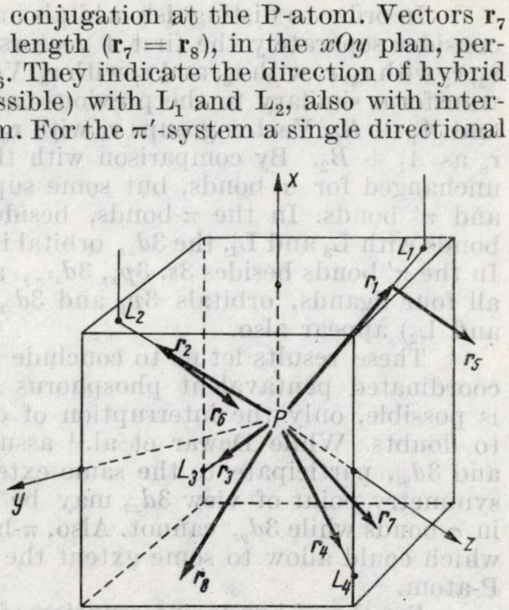

Fig. 4. — Ligand positions and orientations of the directing vectors of the pentavalent tetracoordinated phosphorus hybrids in conjugated six-membered rings, when two hybrid orbitals participate at the π system and other two at the π' system.

The ensemble belongs to the C_{2v} point group and the irreducible representations of the eight vectors transform as $3A_1 + A_2 + 2B_1 + 2B_2$. With the data of table 1, four distinct groups of atomic orbitals are obtained, able to give hybrid orbitals with required orientation :

$$\begin{gathered}
s,\ p_x,\ p_y,\ p_z,\ d_{x^2-y^2},\ d_{xy},\ d_{xz},\ d_{yz},\\
s,\ p_x,\ p_y,\ p_z,\ d_{z^2},\ d_{xy},\ d_{xz},\ d_{yz},\\
s,\ p_y,\ p_z,\ d_{z^2},\ d_{x^2-y^2},\ d_{xy},\ d_{xz},\ d_{yz},\\
p_x,\ p_y,\ p_z,\ d_{z^2},\ d_{x^2-y^2},\ d_{xy},\ d_{xz},\ d_{yz},
\end{gathered} \tag{5}$$

If no π' system is taken into account, the first six vectors are sufficient. They transform as $2A_1 + A_2 + 2B_1 + B_2$ and, with data of table 1, 12 distinct groups of atomic orbitals which can give hybrid orbitals of required orientation are obtained :

$$\begin{array}{llllll}
s,\ p_x,\ p_y, & p_z, & d_{yz},\ d_{xz}, & p_x,\ p_y,\ p_z, & d_{x^2-y^2}, & d_{yz},\ d_{xz},\\
s,\ p_x,\ p_z, & d_{xy}, & d_{yz},\ d_{xz}, & p_x,\ p_z,\ d_{x^2-y^2}, & d_{xy}, & d_{yz},\ d_{xz},\\
s,\ p_y,\ p_z, & d_{x^2-y^2}, & d_{yz},\ d_{xz}, & p_x,\ p_y,\ p_z, & d_{z^2}, & d_{yz},\ d_{xz},\\
s,\ p_z,\ d_{x^2-y^2}, & d_{xy}, & d_{yz},\ d_{xz}, & p_x,\ p_z,\ d_{z^2}, & d_{xy}, & d_{yz},\ d_{xz},\\
s,\ p_y,\ p_z,\ d_{z^2}, & d_{yz}, & d_{xz}, & p_y,\ p_z,\ d_{x^2-y^2}, & d_{z^2}, & d_{yz},\ d_{xz},\\
s,\ p_z,\ d_{z^2},\ d_{xy}, & d_{yz}, & d_{xz}, & p_z,\ d_{z^2},\ d_{x^2-y^2}, & d_{xy}, & d_{yz},\ d_{xz},
\end{array} \tag{6}$$

In order to distinguish orbitals implied in σ, π and π' bonds, we shall consider separately the first 4 vectors and the groups of vectors $\mathbf{r}_1$ with $\mathbf{r}_2$, $\mathbf{r}_3$ with $\mathbf{r}_4$, $\mathbf{r}_5$ with $\mathbf{r}_6$, and $\mathbf{r}_7$ with $\mathbf{r}_8$. Vectors $\mathbf{r}_1 - \mathbf{r}_4$, $\mathbf{r}_1$ with $\mathbf{r}_2$ and $\mathbf{r}_3$ with $\mathbf{r}_4$ transform similary to the previous case, i.e. as $2A_1 + B_1 + B_2$, $A_1 + B_2$ and $A_1 + B_1$. Vector groups $\mathbf{r}_5$ with $\mathbf{r}_6$ transform as $A_2 + B_1$, and $\mathbf{r}_7$ with $\mathbf{r}_8$ as $A_1 + B_2$. By comparison with the previous case, the problem rests unchanged for σ bonds, but some supplimentary problems appear for π and π' bonds. In the π-bonds, besides $3p_z$ and $3d_{xz}$, implied also in σ bonds with L_3 and L_4, the $3d_{yz}$ orbital is also implied (and only in π bonds). In the π' bonds besides $3s$, $3p_x$, $3d_{x^2-y^2}$ and d_{z^2} implied also in σ bonds with all four ligands, orbitals $3p_y$ and $3d_{xy}$ (implied only in σ bonds with L_1 and L_2) appear also.

These results let us to conclude that a Dewar-type model for tetracoordinated pentavalent phosphorus in conjugated six-membered rings is possible, only the interruption of conjugation at the P-atom is open to doubts. While Dewar et al.[11] assume that the two $3d$ orbitals, $3d_{xz}$ and $3d_{yz}$, participate to the same extent in the π-bond system, from the symmetry point of view $3d_{xz}$ may be also implied with a certain weight, in σ-bonds while $3d_{yz}$ cannot. Also, π-bonds may imply also the $3p_z$ orbital which could allow to some extent the continuation of conjugation at the P-atom.

For the π'-bonds, interruption of conjugation at the P-atom is even more difficult to admit, as the $3s$, $3p_x$, $3d_{x^2-y^2}$, and $3d_{z^2}$-bond participate to all four σ-bonds, while $3p_y$ and $3d_{xy}$ participate to the $P-L_1$ and $P-L_2$ σ-bonds. Nevertheless, there may exist two hybrid orbitals able to accept two electrons from the lone pair of the adjacent N-atoms.

This model with two directional vectors for hybrid orbitals implied in the π-system and other two – in the π'- system will be termed by us also Dewar model, by similarity with models known in literature [8,11,12,14,15] and because it transforms according to the same symmetry rules as the original Dewar model.

From the results obtained with the two models one observes that the antiaromatic model of Craig and Paddock [7] does not seem to be allowed by symmetry. The $4n\pi$ electrons rule for aromaticity of phosphonitrilic cycles [7] does not seem necessary, as both the aromatic and the Dewar model may explain stability and planarity of octaatomic phosphonitrilic cycles, as interpenetrations may appear between π, π' and σ-levels due to the participation of $3d$-orbitals in all types of bonds. Even if the antiaro-

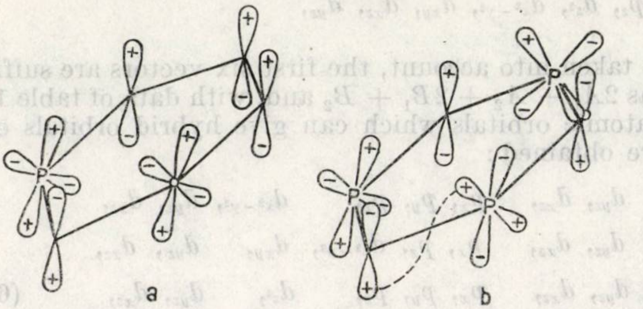

Fig. 5. — Atomic orbital signs with respect to molecular plan of antiaromatic model, in the case of an even number of phosphorus atoms (*a*), and in the case of an odd number of phosphorus atoms (*b*). The dotted line indicates a Möbius-torsion.

matic model would be considered as valid, this could explain only cycles with even numbers of P-atoms. For cycles with an uneven number of P-atoms, a Möbius-torsion of a π-bond should be admitted, destabilising cycles considered as stable. These remarks are evident from an inspection of Figure 5.

CONCLUSIONS

The results obtained for λ^3-phosphorin, λ^5-phosphorin and phosphonitrilic cycles allow us to conclude that $3d$ orbitals have an important role in formation of σ and especially of π-bonds. The low participation of $3d$-orbitals in bonding orbitals of λ^3-phosphorin compounds, as obtained in ab initio calculations by Heilbronner et al.[6] may by due to the reduced ligand field splitting of $3d$ orbital-levels in these compounds, as compared to λ^5-phosphorin compounds. Also this method, although of high sophistication level, gives rather pure agreement with experiment. For compounds of higher period elements in trivalent dicoordinated state (As, Sb) a more significant participation of nd levels is expected, as compared to λ^3-phosphorin compounds, even for ab initio calculations.

The naïve Hückel method is not too efficient in predicting experimental data for these systems and one is obliged to renounce hereby to some classical concepts concerning hybridization concepts usefull to conjugated systems with second period atoms.

Cyclic conjugated compounds with third as higher period atoms should be studied by methods more similar to those used for complex compounds, v.e. a symbiosis of MO methods as used for "usual" organic compounds and respectively for complex compounds is required. The neglect of participation to bonding of free atomic orbitals (above these occupied) may produce errors in interpretation of experimental results.

For arsenium and stibium compounds similar to the phosphorus compounds here discussed similar models may be adopted. Participation of nd orbitals should be even more pronounced in this case and for compounds with atoms of last periods it could be necessary to take into account also f-orbitals participation.

Revue Roumaine de Chimie, **23**, *5*, 781–789 (1978)

PYRIDAZINIUM-YLURES. IX[1]

ADDITION DES ARYL-PYRIDAZINIUM-YLURES SUR LES OLÉFINES ACTIVÉES

MAGDA PETROVANU, ION DRUŢĂ et MAI VAN TRI
Institut Polytechnique « Gh. Asachi », Laboratoire de Chimie organique,
Jassy, 11, str, 23 August, Roumanie

Reçu le 8 mars 1976

L'addition du 3-(phényl)-pyridazinium-phénacylure (III) et du 3,5-diphényl-pyridazinium-phénacylure (X) sur les maléates et fumarates de méthyle et de phényle conduit aux cycloadducts (IV), (V), (VI), (VII), (XI) et (XII). Tenant compte des données résultées de l'analyse chimique et spectrale (spectres I.R. et R.M.N.) il résulte que l'addition des aryl-pyridazinium-ylures sur les oléfines isomères *cis-trans* est bien une *cis* addition.

Les réactions des dipôles 1,3 avec les oléfines activées présentent un grand intérêt tenant compte du fait que l'un des plus importants arguments en faveur d'un mécanisme concerté [1] est constitué par la *cis*-stéréospécificité de la réaction. Les données de la littérature montrent que la majorité des dipôles 1,3 réagissent d'une manière *cis* stéréospécifique avec les dipolarophiles isomères *cis-trans*. Néanmoins, une étude concernant la stéréochimie des réactions des cycloimmonium-ylures en général et des pyridazinium-ylures en particulier avec les oléfines, n'a pas encore été effectuée. [3]

On présente dans ce travail les résultats obtenus concernant la stéréochimie de la cycloaddition des pyridazinium-ylures sur les oléfines activées.

Nous avons choisi comme dipôle 1,3, en premier lieu, le 3-phényl-pyridazinium-phénacylure, obtenu par l'intermédiaire du bromure de N-phénacyle-3-phényl-pyridazinium.

Le sel de cycloimmonium (II) a été obtenu dans la réaction entre la 3-phényl-pyridazine (I) et le bromure de phénacyle.

Du fait que le 3-phényl-pyridazinium-phénacylure (III) obtenu par la déhydrobromuration du sel (II) est instable, dans les réactions concernant cet ylure nous l'avons utilisé « in situ ».

---

[1] Part VIII : Mai Van Tri, M. Petrovanu et I. Druţă, *Buletinul Inst. Politehnic Iaşi*, *3–4*, 45 (1977).

[2] R. Huisgen, *Angew. Chem.*, **75**, 741 (1963).

Pour l'étude de la stéréochimie de la réaction des aryl-pyridazinium-ylures et des dipolarophiles nous avons choisi comme partenaires oléfiniques les esters de l'acide fumarique et maléique

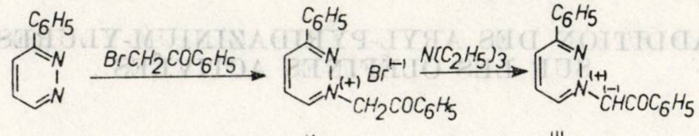
C_6H_5
N
N
$BrCH_2COC_6H_5$
C_6H_5
N
(+)
$Br^{(-)}$
N
$CH_2COC_6H_5$
$N(C_2H_5)_3$
C_6H_5
N
(+)
(−)
N
$\bar{C}HCOC_6H_5$

I II III

En effectuant la réaction entre le maléate de méthyle et le 3-phénylpyridazinium «in situ» en utilisant comme solvant le chlorure de méthylène, à la température ambiante, on a obtenu un produit jaune cristallisé à P.f.158° ; on a attribué à ce produit une structure de tétrahydropyrrolo [1,2—b] pyridazine (IV) tenant compte des analyses chimiques et spectrales.

Dans des conditions identiques l'addition de l'ylure (III) au fumarate de méthyle conduit à un cycloadduct 1 : 1, différent de (IV) à tous les points de vue (point de fusion, aspect, spectres IR et RMN) auquel on a attribué une structure de tétrahydropyrrolo [1,2—b] pyridazine (V).

D'une manière analogue l'addition du 3-phényl-pyridazinium-phénacylure sur le maléate de phényle et le fumarate de phényle conduit à deux cycloadducts différents (VI) et (VII)

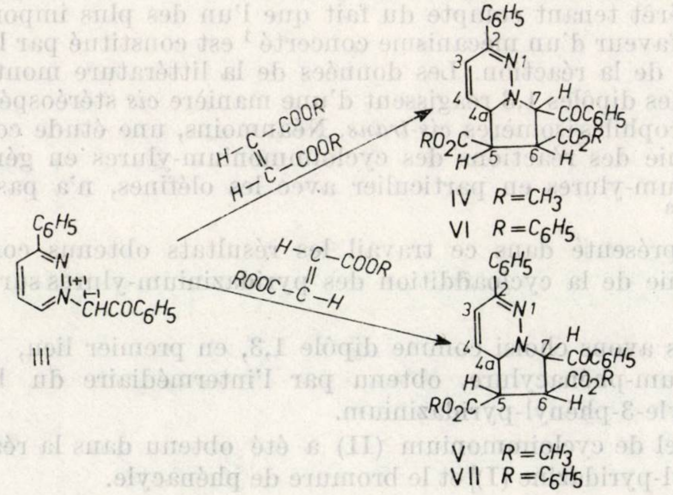
C_6H_5
2
3
N1
4
4a
N
7
H
COC_6H_5
CO_2R
RO_2C
H
5
6
H
H—C—COOR
H—C—COOR
IV R=CH_3
VI R=C_6H_5
C_6H_5
N
(+)
(−)
N
$\bar{C}HCOC_6H_5$
III
H—C—COOR
ROOC—C—H
C_6H_5
2
3
N1
N
7
H
COC_6H_5
CO_2R
4
4a
H
RO_2C
5
6
H
V R=CH_3
VII R=C_6H_5

En comparant les paires (IV)—(V) et (VI)—(VII) on trouve des différences tant en ce qui concerne l'aspect, le point de fusion, qu'en ce qui concerne les spectres I. R. et R.M.N.

Les différences essentielles et importantes visant la détermination des structures sont celles qui apparaissent dans les spectres de R.M.N.

Ainsi, dans le spectre du produit (IV) à l'exception des 10 protons aromatiques qui apparaissent entre δ 7,2—8,5 ppm, le proton H_3 fournit deux doublets à δ = 6,34 ppm.

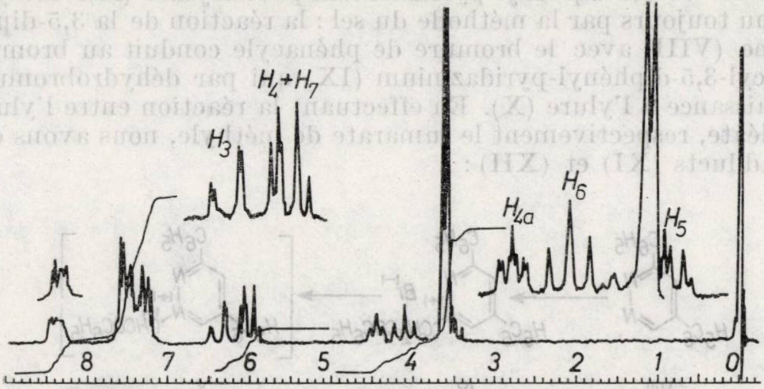

Fig. 1. — Spectre R.M.N. du produit (IV).

A δ = 6 ppm les signaux du proton H_4 (2 doublets) sont superposés à ceux du proton H_7 (un doublet), ces derniers pouvant, toutefois, être identifiés grâce à leur grandeur par rapport aux premiers.

A cause du couplage tant avec les protons H_4, H_5 qu'avec le proton H_3 (long range), le proton H_{4a} donne un multiplet centré à δ = 4,45 ppm. En analysant plus profondément les signaux restants (à l'exception de deux singulets à δ = 3,65 et δ = 3,60 ppm. correspondant sans doute aux groupements carbométhoxyliques) on peut conclure que le triplet à δ = 4,10 ppm correspond au proton H_6 et les quatre signaux à δ = 3,50 ppm sont dus au proton H_5. Le proton H_6 apparaît sous forme de triplet à cause de ses couplages égaux avec les deux protons voisins (H_5 et H_7). Dans le spectre RMN du produit (V) on peut également identifier les signaux des protons H_3, H_4, H_{4a} et H_7 à δ = 6,47, δ = 6,17, δ = 4,40 et δ = 6,01 ppm.

Mais les protons H_5 et H_6 (qui proviennent du fumarate de méthyle) donnent un spectre AB très complexe. Notre tentative d'enregistrer le spectre dans la pyridine ou l'acide trifluoracétique n'a pas conduit aux résultats attendus, les spectres étant indéchiffrables à première vue. Afin de résoudre ce spectre nous avons fait appel à la méthode de la simulation des spectres.

L'étude des valeurs obtenues (Tabl. 1) montre que dans le produit (V) la différence entre les déplacements chimiques des protons H_5 et H_6 est très petite (Δ δ = 0,06 ppm) en comparaison de celle du produit (IV) (Δ δ = 0,6 ppm), ce qui explique le caractère de second ordre du spectre du produit (V).

L'analyse du spectre RMN du produit (VI) a été faite par analogie à celle du spectre du produit (IV). Malgré le fait que la forme des signaux reste presque la même, on observe un déplacement de tous les signaux vers des champs plus faibles, dû à l'influence des noyaux phényliques.

L'analyse du spectre du produit (VII) soulève des difficultés dues au proton H_{4a} qui apparaît, cette fois, très proche de H_5 et H_6, formant un système ABC très complexe.

Pour confirmer les résultats de la réaction entre le 3-phénylpyridazinium-phénacylure et les oléfines isomères *cis-trans* par l'obtention de produits ayant des spectres RMN plus simples, nous avons aussi étudié la réactivité du 3,5-diphényl-pyridazinium-phénacylure (X). Cet ylure a été obtenu toujours par la méthode du sel : la réaction de la 3,5-diphénylpyridazine (VIII) avec le bromure de phénacyle conduit au bromure de N-phénacyl-3,5-diphényl-pyridazinium (IX) qui par déhydrobromuration donne naissance à l'ylure (X). En effectuant la réaction entre l'ylure (X) et le maléate, respectivement le fumarate de méthyle, nous avons obtenu les cyloadducts (XI) et (XII) :

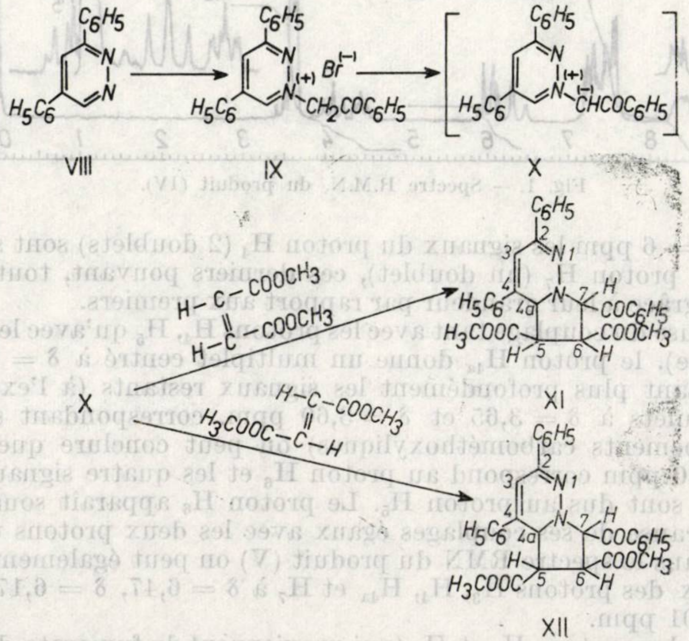

Comme dans les cas précédents, ces deux produits sont différenciés tant par les spectres IR que par les spectres RMN.

Dans le spectre RMN du produit (XI) le singulet à $\delta = 6,71$ ppm est dû à l'absorption du proton H_3. Le déplacement de ce signal en comparaison de celui provenant du produit (IV) est un résultat de l'anisotropie produite par le noyau benzénique en position 4 du bicycle. Le couplage à distance des protons H_3 et H_{4a} disparaît toujours à cause du noyau phénylique, le signal du proton H_{4a} apparaissant, dans ce cas, sous forme de doublet à $\delta = 4,75$ ppm. Le proton H_7 absorbe à $\delta = 6,21$ ppm sous forme de doublet comme suite du couplage avec le proton H_6. Comme dans le cas du produit (IV), le proton H_6 apparaît sous forme de triplet à cause du couplage d'égale intensité avec les deux protons voisins (H_5, H_7).

Malgré le fait que la paire de doublets correspondant au proton H_5 ($\delta = 3,67$) est partiellement masquée par le signal d'un groupement méthylique estérique on peut observer les deux couplages H_{4a} et H_6.

Le spectre RMN du produit (XII) est plus compliqué et il a été très difficile de déterminer les paramètres des protons H_{4a}, H_5, H_6 et H_7. Comme dans le cas du produit (V) on a eu recours à la technique de la simulation.

Dans le spectre du produit (XII) les protons H_7 et H_{4a} apparaissent sous forme de multiplets contenant six signaux et non pas sous forme de doublets comme on s'attendait. Les signaux de faible intensité qui accompagnent les doublets correspondant aux protons H_7 et H_{4a} proviennent d'un nouveau couplage virtuel. [4]

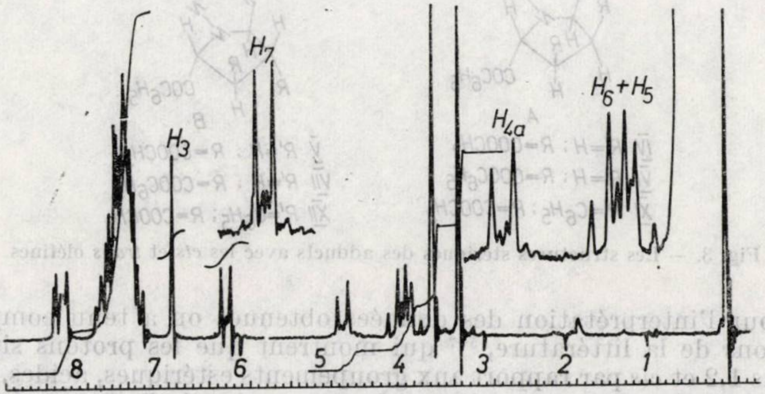

Fig. 2. — Spectre R.M.N. du produit (XII).

Il résulte de l'analyse de tous les cas présentés concernant l'addition des pyridazinium-phénacylures sur les oléfines *cis-trans* que l'on obtient des cycloadducts différents c'est-à-dire que les cycloadducts obtenus à partir des oléfines *cis* diffèrent de ceux obtenus à partir des oléfines *trans*.

Tableau 1

Caractéristiques spectroscopiques des tétrahydropyrrolo-pyridazines

Composé N°	Déplacements chimiques, ppm								Constantes de couplage, Hz					
	H_3	H_4	H_{4a}	H_5	H_6	H_7	OOC | CH_3	OOC | CH_3	$J_{3,4}$	$J_{4,4a}$	$J_{4a,5}$	$J_{5,6}$	$J_{6,7}$	$J_{3,4a}$
IV *cis*	6,34	6,0	4,45	3,50	4,10	6,01	3,65	3,59	10,5	3,9	4,5	7,5	7,5	1,3
V *trans*	6,45	6,12	4,40	3,76	3,70	6,01	3,67	3,62	10,4	4,0	8,2	7,1	7,5	0,5
VI *cis*	6,50	6,15	4,65	3,82	4,45	6,15	—	—	10,5	4,1	4,5	7,5	7,5	0,8
VII *trans*	6,50	6,30	4,50	4,25	4,20	6,12	—	—	9,8	4,1	(a)	(a)	6,0	
XI *cis*	6,71		4,75	3,67	4,24	6,21	3,42	3,62	—	—	5,0	7,5	7,5	—
XII *trans*	6,80		4,70	4,08	3,97	6,18	3,31	3,62	—	—	8,2	7,1	6,75	—

Dans le but d'élucider certains aspects du mécanisme réactionnel des réactions de cycloadditions 1,3-dipolaires des pyridazinium-ylures

---

[3] I. ZUGRĂVESCU et M. PETROVANU, «Chimia N-ilidelor», Ed. Academiei, Bucarest, 1974.

sur les oléfines activées on a essayé d'établir la structure stérique, respectivement les positions relatives des substituants dans le cycle pyrrolidinique.

De l'étude des spectres RMN il résulte que parmi de multiples possibilités, les structures A respectivement B sont les plus probables pour les cycloadducts provenant des oléfines *cis*, respectivement *trans*

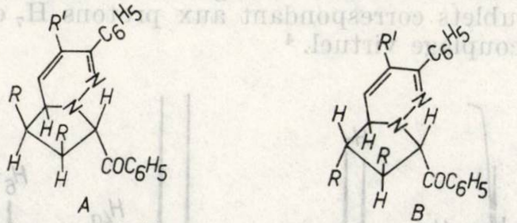

IV $R'=H$; $R=COOCH_3$
VI $R'=H$; $R=COOC_6H_5$
XI $R'=C_6H_5$; $R=COOCH_3$

V $R'=H$; $R=COOCH_3$
VII $R'=H$; $R=COOC_6H_5$
XII $R'=C_6H_5$; $R=COOCH_3$

Fig. 3. — Les structures stériques des adducts avec les *cis* et *trans* oléfines.

Pour l'interprétation des données obtenues on a tenu compte des indications de la littérature, [5-7] qui montrent que les protons situés en positions 1,2 et *cis* par rapport aux groupements estériques, acides, cétoniques et dans des produits cycliques de 5 ou moins de 5 atomes sont plus désécranés qui ceux en position *trans* par rapport aux mêmes groupements. On peut ainsi expliquer le déplacement chimique δ nettement supérieur du proton H_5 dans les produits (V), (VII) et (XII) dans lesquels celui-ci est en position *cis* par rapport au groupement estérique lié au carbone 6 en comparaison du déplacement chimique de ce même proton dans les produits (IV), (VI) et (XI) dans lesquels le proton se trouve en *trans* par rapport au groupement estérique lié au carbone 6.

En même temps la position du proton H_7 en *cis* par rapport au groupement estérique en position 6 est justifiée tant dans les composés provenant des réactions des ylures étudiés avec les oléfines *cis*, que pour ceux provenus à partir des oléfines *trans*, tenant compte du fait que le déplacement chimique de ce dernier est le même ou varie très peu par rapport à la structure stérique des oléfines mises en œuvre.

Ainsi $\delta_{H7}(IV) - \delta_{H7}(V) = 0$ ppm ; $\delta_{H7}(VI) - \delta_{H7}(VII) = 0,03$ ppm et $\delta_{H7}(XI) - \delta_{H7}(XII) = 0,03$ ppm. Les petites différences qui apparaissent dans le cas des deux dernières paires de stéréoisomères sont dues, très probablement, à la torsion des groupements estériques, ce qui mène à une variation de l'angle dièdre formé par ces derniers. Ceci est dû à la présence des noyaux benzéniques qui entrent dans la composition des groupements estériques dans les produits (VI) et (VII) et à la présence du noyau phénylique en position 4 pour les produits (XI) et (XII).

---

[4] L. M. Jackman et S. Sternhell, " Aplication of Nuclear Magnetic Resonance in Organic Chemistry", ed. II, Pergamon Press, Oxford, 1969, p. 147.

[5] T. Texier et R. Carrié, *Compt. rend.*, **269 c**, 709 (1969).

[6] R. Carrié et T. Texier, *Bull. Soc. chim. France*, **1972**, 258.

L'interprétation, de ce point de vue, des données fournies par les spectres RMN conduirait à des résultats contraires en ce qui concerne la configuration des atomes de carbone 6 et 4 *a* par rapport aux autres groupements de la molécule. En effet, l'analyse des spectres obtenus montre que, les déplacements chimiques des protons H_{4a} et H_6 dans les produits (IV), (VI) et (XI) dans lesquels les groupements estériques liés aux carbones 5 sont en *trans* par rapport à ceux-ci sont plus grands que dans les produits (V), (VII) et (XII) dans lesquels ces groupements sont en *cis*.

Mais, tenant compte des données obtenues par Carrié et coll. [5-7] qui ont effectué une étude détaillée concernant la structure pyrrolidinique simple sur des modèles spécialement choisis, on peut affirmer que les structures proposées concordent avec la réalité.

D'après les résultats obtenus par les auteurs mentionnés, il résulte que la présence de deux groupements, parmi lesquels l'un estérique et l'autre cétonique ou nitrilique ou les deux estériques en *cis*, substituant les carbones 3 et 5 (dans notre cas 5 et 7) d'un cycle pyrrolidinique substitué sur tous les carbones par des substituants du second ordre, produit un blindage des protons en 2 et 4 (dans notre cas 4*a* et 6) situés en *cis* par rapport à ces groupements. Pratiquement ces différences sont $\delta_{H6}(IV) - \delta_{H6}(V) = 0{,}4$ ppm ; $\delta_{H6}(VI) - \delta_{H6}(VII) = 0{,}25$ ppm ; $\delta_{H6}(XI) - \delta_{H6}(XII) = 0{,}21$ ppm ; $\delta_{H4a}(IV) - \delta_{H4a}(V) = 0{,}05$ ppm ; $\delta_{H4a}(VI) - \delta_{H4a}(VII) = 0{,}15$ ppm ; $\delta_{H4a}(XI) - \delta_{H4a}(XII) = 0{,}05$ ppm.

Le blindage plus accentué, donc les différences plus marquées entre δ_{H6} [H_6 *trans* par rapport au groupement estérique lié à C_5 (IV), (VI) et (XI)] et δ_{H6}[H_6 *cis* par rapport au groupement esterique lié à C_5 et au groupement cétonique dans (V), (VII) et (XII)] que celles provoquées par les mêmes groupements, dans les mêmes positions et dans les mêmes produits du proton H_{4a}, observées dans le cas de nos produits, sont très probablement dues à l'intercalation plus proche du proton H_6 par rapport au proton H_{4a} entre les deux groupements mentionnés.

Nos essais concernant l'étude de la configuration des produits obtenus, par l'intermédiaire des valeurs des constantes de couplage n'ont pas donné de résultats à cause des torsions des groupements estériques situés en *cis* torsions causées par les empêchements stériques qui conduisent à des variations des angles dièdres entre les protons et par conséquent à des constantes de couplage imprévisibles. D'ailleurs l'existence des empêchements stériques a été mise en évidence par la construction des modèles.

Tenant compte des données présentées il résulte que l'addition des aryl-pyridazinium-phénacylures sur les oléfines est bien une *cis* addition, ce qui confirme la théorie de Huisgen concernant le mécanisme des cycloadditions 3—2 dipolaires.

PARTIE EXPÉRIMENTALE

Les points de fusion ne sont pas corrigés. Les spectres RMN ont été enregistrés sur un spectromètre de type JEOL AH 60. Les expériences de simulation ont été effectuées à l'aide d'accessoires du même appareil.

BROMURE DE N-PHÉNACYL-3-PHÉNYLPYRIDAZINIUM (II)

On dissout 1,56 g (10 mmol) de 3-phényl-pyridazine et 1,99 g (10 mmol) de bromure de phénacyle dans 20 ml d'acétone. On mélange les deux solutions et on laisse le mélange réactionnel à la température ambiante. On filtre le précipité blanchâtre formé et on le recristallise dans un mélange alcool-éther. P. f. 89—90° (déc.) Rd. 3,2 g (90 %). Analyse pour $C_{18}H_{15}N_2OBr$ (355,2) *calculé* : C 60,86 ; H 4,26 ; N 7,88 ; *trouvé* : C 60, 65 ; H 4,40 ; N 8,05. Spectre I.R. (KBr, cm^{-1}) : 1680 (C=O) ; 2950 (CH_2) ; 3000, 3080 (CH) ; 1600, 1460, 1320, 1340 (C—C) ; 1240, 760, 780, 700 (CH).

BROMURE DE N-PHÉNACYL-3,5-DIPHÉNYL-PYRIDAZINIUM (VIII)

On dissout 2,32 g (10 mmole) de 3,5-diphényl-pyridazine et 1,99 g (10 mmole) de bromure de phénacyle dans 25 ml d'acétone. On mélange les deux solutions et on abandonne le mélange réactionnel à la température ambiante pendant 24 heures. On filtre ensuite le précipité formé et on le recristallise dans de l'alcool. On obtient 3 g de sel (70 %). P. f. 232° (déc). Analyse pour $C_{24}H_{19}N_2OBr$ (431) *calculé* : C 66,86 ; H 4,48 ; N 6,49 ; *trouvé* : C 66,57 ; H 4,50 ; N 6,65. Spectre I. R. (KBr, cm^{-1}) : 1680.

MÉTHODE GÉNÉRALE D'OBTENTION DES PRODUITS D'ADDITION DES ARYL-PYRIDAZINIUM-YLURES SUR LES OLÉFINES ACTIVÉES

On suspend 10 mmole bromure de N-phénacyl-aryl-pyridazinium dans 30 ml de chlorure de méthylène et on ajoute 10 mmol composante oléfinique. On refroidit le mélange sur de la glace et on laisse tomber goutte à goutte, en agitant continuellement 1,5 ml de triéthylamine dissoute dans 10 ml de chlorure de méthylène (on a soin de ne pas ajouter une nouvelle goutte de solution de triéthylamine avant la disparition de la couleur rouge provoquée par la goutte précédente). On lave la solution organique 3 fois avec de l'eau (30 ml chaque fois), on sèche la solution organique, on chasse le solvant et on recristallise le résidu dans un solvant approprié.

2-PHÉNYL-*cis*-5,6-DICARBOMÉTHOXY-7-BENZOYL-4a, 5, 6, 7-TÉTRAHYDROPYRROLO [1,2—b] PYRIDAZINE (IV)

On l'obtient suivant la méthode générale à partir de 3,55 g sel (II) et 1,3 ml maléate de méthyle. [8] Le produit obtenu est recristallisé dans un mélange d'alcool + acétonitryle. On l'obtient sous forme de cristaux jaunes à P. f. 156—157° Rd. 3 g (71 %). Analyse pour $C_{24}H_{22}N_2O_5$ (418,5) *calculé* : C 68,88 : H 5,30 ; N 6,69 ; *trouvé* : C 69,10 ; H 5,36 ; N 6,70. Spectre IR (KBr, cm^{-1}) : 1730, 1720 (CO estérique) ; 1680 (CO cétonique) ; 3050 (CH noyau) ; 2950 (CH allyciclique et CH_3) ; 1600, 1580, 1440 et 1390 (C—C, C—N arom) ; 1210 (C—O—C) ; 860, 770, 750 et 695 (δ_{CH}) Spectre RMN ($DCCl_3$, TMS, δ) : multiplet (2H, H ortho dans COC_6H_5) 8,40 ppm ; multiplet (8H aromatiques) 7,20—7,60 ppm ; deux doublets (1H, H_3) 6,34 ppm ; $J_{3.4} = 10,5$ Hz ; $J_{3.4a} = 1,3$ Hz ; doublet (1H, H_7) 6,01 ppm ; $J_{7.6} = 7,5$ Hz ; deux doublets (1H, H_4) 6,00 ppm ; $J_{4.3} = 10,5$ Hz ; $J_{4.4a} = 3,9$ Hz ; multiplet (1H, H_{4a}) 4,45 ppm ; $J_{4a.5} = 4,5$ Hz ; triplet (1H, H_6) 4,10 ppm ; $J_{6,7} = 7,5$ Hz ; $J_{6.5} = 7,5$ Hz ; deux doublets (1H, H_5) 3,50 ppm ; $J_{5,6} = 7,5$ Hz ; $J_{5.4a} = 4,5$ Hz ; singulet (3H, $COOCH_3$) 3,65 ppm ; singulet (3H, $COOCH_3$) 3,59 ppm.

2-PHÉNYL-*cis*-5,6-DICARBOPHÉNOXY-7-BENZOYL-4 a, 5, 6, 7-TÉTRAHYDROPYRROLO [1,2-b] PYRIDAZINE (VI)

On le prépare par la méthode générale à partir de 3,55 g sel (II) et de 2,68 g maléate de phényle [9]. Cristaux jaunes dans de l'acétonitrile. P. f. 167—168°. Rd. 4,2 g (76 %). Analyse pour $C_{34}H_{26}N_2O_5$ (524,6) : *calculé* : C 77,85 ; H 4,99 ; N 5,34 ; *trouvé* : C 77,73 ; H 4,96 ; N 5,16. Spectre IR (KBr, cm^{-1}) : 1730 (CO estérique) ; 1659 (CO cétonique) ; 1180 (C—O—C) ; 3050 (CH noyau) ; 2850 (CH allyciclique) 1580, 1485 et 965 (C—C, C—N arom.) ; 810, 800, 760,740 et 695 (δ_{CH} dans le plan). Spectre RMN ($CDCl_3$, TMS, δ) : multiplet (2 H, H *ortho* dans COC_6H_5) 8,40 ppm ; multiplet (18 H aromatiques) 7,20—7,60 ppm ; deux doublets (1H, H_3) 6,50 ppm, $J_{3,4} = 10,5$ Hz ; $J_{3,4a} = 0,8$ Hz ; deux doublets (1H, H_4) 6,15 ppm ; $J_{4.3} = 10,5$ Hz ; $J_{4.4a} = 4,1$ Hz ; doublet (1H, H_7) 6,15 ppm ; $J_{7.6} = 7,5$ Hz ; multiplet (1H, H_{4a}) 4,65 ppm ; triplet (1H, H_6) 4,45 ppm ; $J_{6.5} = 7,5$ Hz ; $J_{6.7} = 7,5$ Hz ; deux doublets (1H, H_5) 3,82 ppm ; $J_{5.6} = 7,5$ Hz ; $J_{5.4a} = 4,5$ Hz.

---

[7] F. Texier, Thèse, Rennes, 1970.

[8] D. Wolf et van den Straete, *Bull. Soc. chim. belges*, **44**, 293 (1935).

2-PHÉNYL-*trans*-5,6-DICARBOMÉTHOXY-7-BENZOYL-4 a, 5, 6, 7-TÉTRAHYDROPYRROLO [1,2—b] PYRIDAZINE (V)

On l'obtient par la méthode générale à partir de 3,55 g sel (II) et de 1,44 g fumarate de méthyle.[10] P. f. 145° (dans l'acétone). Rd. 2,5 g (60 %). Analyse pour $C_{24}H_{22}N_2O_5$(418,5) *calculé* : C 68,88 ; H 5,30 ; N 6,69 ; *trouvé* : C 68,68 ; H 5,31 ; N 6,77. Spectre I. R. (KBr, cm^{-1}) : 1730 (CO estérique) ; 1682 (CO cétonique) ; 1220 (C—O—C) ; 3050 (CH noyau) ; 2990 (CH allycyclique) et (CH_3) ; 1600, 1585, 1440, 1345, 1280, 935, 925 (C—C, C—N arom.) ; 760, 700 (δ_{CH}). Spectre RMN ($CDCl_3$, TMS, δ) ; multiplet (2H, H *ortho* dans COC_6H_5) 8,20 ppm ; multiplet (8H aromatiques) 720—760 ppm ; deux doublets (1H, H_3) 6,45 ppm ; $J_{3.4} = 10{,}4$ Hz ; deux doublets (1H, H_4) 6,12 ppm ; $J_{4.3} = 10{,}4$ Hz ; $J_{4.4a} = 4{,}9$ Hz ; doublet (1H, H_7) ; $J_{7,6} = 7{,}5$ Hz ; multiplet (1H, H_{4a}) 4,40 ppm.

Calculé :

(H_5) 3,76 ppm, $J_{5.6} = 7{,}1$ Hz ; (H_6) 3,70 ppm ; $J_{6\,5} = 7{,}1$ Hz ; $J_{6,7} = 7{,}5$ Hz singlet (3H, $COOCH_3$) 3,67 ppm ; singlet (3H, $COOCH_3$) 3,62 ppm.

2-PHÉNYL-*trans*-5,6-DICARBOPHÉNOXY-7-BENZOYL-4a 5, 6, 7-TÉTRAHYDROPYRROLO [1,2—b] PYRIDAZINE (VII)

On l'obtient suivant la méthode générale à partir de 3,55 g de sel (II) et de 2,68 g de fumarate de phényle.[9] Après évaporation du solvant, le résidu est dissous dans l'acétone et abandonné pendant 24 heures. On lave les cristaux obtenus avec un mélange d'alcool/acétone 1/10 et recristallise dans de l'acétone. P. f. 140°. Rd. 3,3 g (66 %). Analyse pour $C_{34}H_{26}N_2O_5$(524,6) *calculé* : C 77,85 ; H 4,99 : N 5,34 ; *trouvé* : C 77,91 ; H 4,79 ; N 5,25. Spectre I. R. (KBr, cm^{-1}) : 1740 (CO esterique) ; 1670 (CO cétonique) ; 1200 (C—O—C) ; 3010 (CH noyau) ; 2900 (CH sat.) ; 1585, 1495, 1450, 1320 (C—C, C—N arom.) Spectre R.M.N. ($CDCl_3$, TMS, δ) ; multiplet (2H, H *ortho* dans COC_6H_5) 8,20 ppm ; multiplet (18 H aromatiques) 7,20—7,60 ppm ; deux doublets (1H, H_3) 6,50 ppm, $J_{3.4} = 9{,}8$ Hz ; $J_{3,4a} = 0{,}5$ Hz ; deux doublets (1H, H_4) 6,15 ppm, $J_{4.3} = 9{,}8$, $J_{4.4a} = 4{,}1$ Hz ; doublet (1H, H_7) 6,12 ppm, $J_{7,6} = 7{,}5$ Hz ; multiplet (1H, H_{4a}) 4,60 ppm ; $J_{4a,4} = 4{,}1$ Hz, $J_{4a.5} = 8{,}2$ Hz ; multiplet (2H, $H_5 + H_6$) 4,05—4,5.

2,4-DIPHÉNYL-*cis*-5,6-DICARBOMÉTHOXY-7-BENZOYL-4a, 5, 6, 7-TÉTRAHYDROPYRROLO [1,2—b] PYRIDAZINE (XI)

On traite 4,31 g (10 mmol) de sel (IX) par 1,3 ml (10 mmol) de maléate de méthyle d'après la méthode générale ci-dessus. Après recristallisation dans un mélange d'alcool-acétonitrile on obtient des cristaux jaunes. P. f. 174°. Rd. 3,3 g (63 %). Analyse pour $C_{30}H_{25}N_2O_5$(493,6) : *calculé* : C 73,00 ; H 5,11 ; N 5,67 ; *trouvé* : C 73,14 ; H 5,04 ; N 5,72. Spectre I. R. (KBr, cm^{-1}) : 1730 (CO estérique) ; 1670 (CO cétonique) ; 3050 (CH noyau) ; 2950, 2900 (CH aliphatique) ; 1590, 1500, 1420, 1300 (C—C, C—N arom.) ; 1200, 1180, 1150 (C—O—C) ; 850, 770, 700 (δ_{CH}). Spectre RMN ($CDCl_3$, TMS, δ) : multiplet (2H, H ortho dans COC_6H_5) 8,40 ppm ; multiplet (13 H aromatiques) 6,9—7,6 ppm ; singulet (1H, H_3) 6,71 ppm ; doublet (1H, H_7) 6,21 ppm ; $J_{7.6} = 7{,}5$ Hz ; doublet (1H, H_{4a}) 4,75 ppm, $J_{4a.5} = 5$ Hz ; triplet (1 H, H_6) 4,24 ppm ; $J_{6.5} = 7{,}5$ Hz ; $J_{6.7} = 7{,}5$ Hz ; deux doublets (1H, H_5) 3,67 ppm ; $J_{5.4a} = 5$ Hz ; $J_{5.6} = 7{,}5$ Hz ; singulet (3H, $COOCH_3$) 3,62 ppm ; singlet (3H, $COOCH_3$) 3,42 ppm.

2,4—DIPHÉNYL-*trans*-5,6-DICARBOMÉTHOXY-7-BENZOYL-4a, 5, 6, 7—TÉTRAHYDROPYRROLO [1,2—b] PYRIDAZINE (XII)

On l'obtient par la méthode générale à partir de 4,31 g de sel (IX) et 1,44 g fumarate de méthyle. Par recristallisation dans un mélange acétonitrile-alcool on obtient des cristaux jaunes claires. P.f. 156—157°. Rd 3,8 g (75 %). Analyse pour $C_{30}H_{25}N_2O_5$(493,6) *calculé* : C 73,00 ; H 5,11 ; N 5,67 ; *trouvé* : C 73,22 ; H 5,01 ; N 5,80. Spectre IR (KBr, cm^{-1}) : 1730 (CO estérique) ; 1680 (CO cétonique) ; 3050 (CH noyau) ; 2950 (CH aliphatique) ; 1590, 1580, 1460, 1440, 1340, 1270 (C—C, C—N arom.) ; 1210, 1170 (C—O—C) ; 780, 760, 720, 700 (δ_{CH}) plan. Spectre RMN ($CDCl_3$, TMS, δ) : multiplet (2H, H *ortho* dans COC_6H_5) 8,20 ppm ; multiplet (13 H aromatiques) ; 6,90—7,60 ppm ; singulet (1H, H_3) 6,80 ppm ; ABMX calculé : $\delta_{H7} = 6{,}18$ ppm (6 signaux), $J_{7,6} = 7{,}5$ Hz ; $\delta_{H4a} = 4{,}70$ ppm (6 signaux), $J_{4a.5} = 8{,}2$ Hz ; $\delta_{H5} = 4{,}08$ ppm (multiplet), $J_{5.6} = 7{,}1$ Hz, $J_{5.4a} = 8{,}2$ Hz ; $\delta_{H6} = 3{,}97$ ppm (multiplet) ; $J_{6.5} = 7{,}1$ Hz ; $J_{6.7} = 7{,}5$ Hz ; singlet (3H, $COOCH_3$) 3,62 ppm ; singulet (3H, $COOCH_3$) 3,31 ppm.

---

[9] V. H. Bischoff, *Ber. dtsch. chem. Ges.*, **35**, 4087 (1902).

[10] A. Skrabal et E. Raith, *Monats.*, **42**, 246 (1921).

Revue Roumaine de Chimie, 23, 5, 791–796 (1978)

SPIRO-3-ARYLIDENE-1,2,3,4-TETRAHYDRO-NAPHTHALENE-4-ONES. II[1]

SYNTHESIS OF SPIROPYRAZOLINES

ABD EL-KADER FATEEN and AHMED MOHAMED KADDAH

Chemistry Department, Faculty of Science, Ain Shams University,
Cairo, Arab Republic of Egypt

Received March 9, 1976

Spiro-3-arylidene-1,2,3,4-tetrahydronaphthalene-4-one-(1;3′)-2′,6′-piperidinediones(**1a–e**) react with diazomethane, hydrazinehydrate, phenylhydrazine and benzoylhydrazine to give spiropyrazolines **2**, **7**, **10** and **11** whose structures have been established by elemental analysis, IR, electronic spectra and by characterising the pyrolytic products.

Treatment of spiro-3-arylidene-1,2,3,4-tetrahydronaphthalene-4-one-(1:3′)-2′,6′-piperidinediones[1] (**^{1}a–e**) with diazomethane gave Δ^1-spiropyrazolines **2** or **3**. The mode of addition is similar to that obtained in case of diazomethane addition to arylidene tetralone.[2]

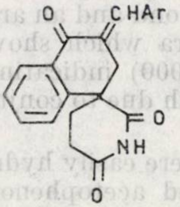

1

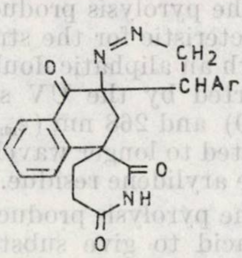

2

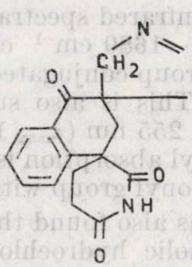

3

1–3	Ar
a;	$- C_6H_5$
b;	$- C_6H_4 - OCH_3-p$
c;	$- C_6H_4Cl-p$
d;	$- C_6H_4 - Cl - o$
e;	$- C_6H_4- CH_3-p$

---

[1] Part I, A. K. Fateen, A. M. Kaddah and Y. M. Naguib *Rev. Roumaine Chim.*, in press.

[2] A. K. Fateen and M. M. Ali, *Indian J. Chem.*, **10**, 968 (1972).

The structure of the products was established by elemental analysis, IR and UV spectra and by thermal decomposition. The IR spectra shows a band characteristic for the stretching frequency of the carbonyl group in the range 1680–1690 cm^{-1}. The increase in frequency of this band in the addition products **2** or **3**, as compared with **1** is due to the non-conjugation of the carbonyl group. [3] The infrared spectra also shows a band at 1730 cm^{-1} characteristic for the stretching frequency of the coupled carbonyl group of the six membered cyclic imides, [3] and a broad band between 3100 – 3640 cm^{-1} due to the stretching vibration of the NH group. [3]

Thermal decomposition of the products by heating for 15 minutes above their melting points gave compounds which can either be derivable from **2** and possessing structure **5** or derivable from **3** and possessing structure **4**.

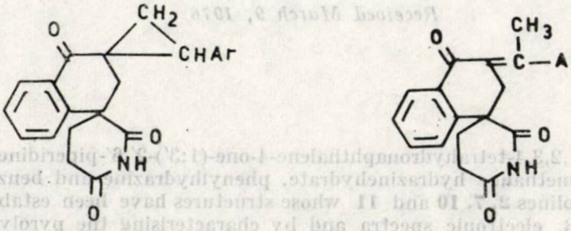

4 **5**

alc. HCl ↓

5–6 Ar =

a; $-C_6H_5$
b; $-C_6H_4-OCH_3-p$
c; $-C_6H_4-Cl-p$
d; $-C_6H_4-Cl-o$
e; $-C_6H_4-CH_3-p$

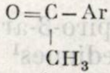

$O{=}\underset{\displaystyle CH_3}{\underset{|}{C}}-Ar$

6

The infrared spectra of the pyrolysis products showed a band in the range 1670–1680 cm^{-1} characteristic for the stretching frequency of the carbonyl group conjugated with an aliphatic double bond and an aromatic nucleus. [3] This is also supported by the UV spectra which shows two maxima at 255 nm (ε_{max} 13000) and 268 nm (ε_{max} 17000) indicating that the carbonyl absorption is shifted to longer wavelength due to conjugation of the carbonyl group with the arylidene residue.

It was also found that the pyrolysis products were easily hydrolysed with alcoholic hydrochloric acid to give substituted acetophenones, **6**, identified as 2,4-dinitrophenylhydrazones. From the above facts it is evident that the pyrolysis products have structure **5** which could only be obtained by the thermal decomposition of **2**, and hence structure **2** could be assigned to the products of interaction of diazomethane with **1**. This is in agreement with Auwers[4] statement that the addition proceeds in such a way that the methylene group is attached to the β-carbon atom.

---

[3] L. G. Bellamy, "The Infrared Spectra of Complex Molecules", Methuen Co., London 1956, p. 116, 119, 184, 191 and 261.

[4] K. V. Auwers and D. Ungemach, *Ber. dtsch. Chem. Ges.*, **66B**. 1205 (1933).

When hydrazine hydrate was allowed to react with **1a**—**e** in ethanol, colourless solid products were obtained which soon darkened and changed to oils. However, when the reaction was carried out in glacial acetic acid, crystalline products were isolated. From analytical data the products were shown to be either acetylpyrazoline derivatives (**7** or **8**) or acetylhydrazone derivatives, **9.**

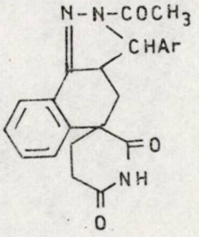

7

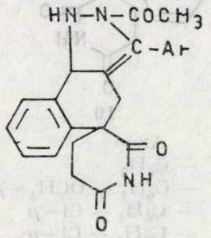

8

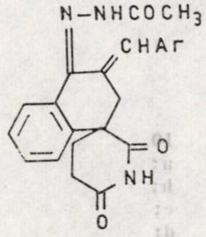

9

7—9	Ar =
a;	$-C_6H_5$
b;	$-C_6H_4-OCH_3-p$
c;	$-C_6H_4-Cl-p$
d;	$-C_6H_4-Cl-o$
e;	$-C_6H_4-CH_3-p$

Structure **9** was excluded, since the UV spectra of the products show only two absorption maxima at 225 nm (ε_{max} 11536) and 297. 5 nm (ε_{max} 18250) characteristic of pyrazolines. [5]

The IR spectra shows a band characteristic for the stretching frequency of C=N group of conjugated cyclic compounds in the range of 1605—1650 cm^{-1}. The conjugation is not apparent in the skeleton **8**. Thus structure **7** was assigned to the products of the reaction.

The IR spectra also shows a band characteristic for the carbonyl stretching frequency of acid amides [3] in the range of 1670—1680 cm^{-1} and shows a band at 1720 cm^{-1} characteristic of the stretching frequency of the coupled carbonyl group of the six membered cyclic imides and a broad band between 2900—3520 cm^{-1} due to the stretching vibration of the NH group. [3]

On the other hand, phenylhydrazine reacted with **1a**—**e** in ethanol to give stable crystalline products whose structures were similarly established as **10a**—**e.** Such structures were confirmed by elemental analysis, IR and UV spectra. The UV spectra of these products showed two absorption maxima at 250 nm (ε_{max} 61843) and 338 nm (ε_{max} 14420) characteristic of pyrazolines [5] except in **10b** which has an additional inflection, attributed to the presence of anisyl group[6] and also by the green fluorescence which was exhibited in solution.[7]

---

[5] G. F. Duffin and J. D. Kendall, *J. Chem. Soc.*, **1954**, 408.

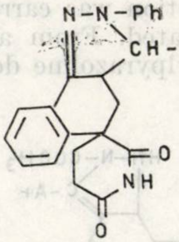

10

10	Ar =
a;	$-C_6H_5$
b;	$-C_6H_4-OCH_3-p$
c;	$-C_6H_4-Cl-p$
d;	$-C_6H_4-Cl-o$
e;	$-C_6H_4-CH_3-p$

Similarly, when benzoylhydrazine was allowed to react with **1a-e** in glacial acetic acid or in ethanol, Δ^2-benzoylpyrazoline derivatives, **11a-e**, were obtained. Their structures were also established by elemental analysis, IR and electronic spectra.

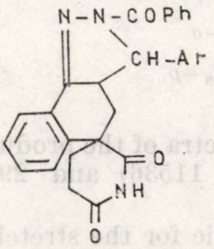

11

11	Ar =
a;	$-C_6H_5$
b;	$-C_6H_4-OCH_3-p$
c;	$-C_6H_4-Cl-p$
d;	$-C_6H_4-Cl-o$
e;	$-C_6H_4-CH_3-p$

EXPERIMENTAL

All the melting points are uncorrected. The infrared spectra (i.r.) were measured on a SP 1000 PYE–UNICAM SPECTROPHOTOMETER; the KBr waver technique was used. The electronic spectra were carried out by using PERKIN–ELMER, Model 402 Ultraviolet Spectrophotometer.

ACTION OF THE DIAZOMETHANE ON SPIRO-3-ARYLIDENE-1,2,3,4-TETRAHYDRONAPHTHALEN-4-ONE-(1 :3′)-2′,6′-PIPERIDINEDIONES(1a–e)

A solution of diazomethane (from 5 g of nitrosomethylurea) in ether (100 ml) was added to a cold solution of **1**(1 g) in tetrahydrofuran (10 ml) and the reaction mixture was left in an ice-box overnight. The viscous oil obtained after distillation of the solvents was triturated with light petroleum (40–60°) to give a solid which crystallised from a suitable solvent to give Δ^1-spiropyrazoline derivatives, **2a–e**, table 1.

---

[6] J. C. J. Schwarz, "Physical Methods in Organic Chemistry", Oliver and Boyed Co., London, 1964, p. 147.

[7] R. C. Elderfield, "Heterocyclic Compounds", Vol. 5, Wiley, New York, 1957, p. 57.

Table 1

Δ^1-spiropyrazolines 2a−e and their pyrolysis products 5a−e

Product	Recryst. solvent	M.P. °C	Yield %	Molecular formula	Analysis					
					Found (%)			Required (%)		
					C	H	N	C	H	N
2a	Benzene/light petroleum (60−80°)	84	62	$C_{22}H_{19}O_3N_3$	70.73	4.96		70.8	5.09	
b	,, ,, ,,	68	44	$C_{23}H_{21}O_4N_3$	67.6	5.0		68.4	5.2	
c	,, ,, ,,	76	67	$C_{22}H_{18}O_3N_3Cl$	63.6	4.48		63.3	4.40	
d	,, ,, ,,	65	52	$C_{22}H_{18}O_3N_3Cl$	63.45	4.37		63.3	4.40	
e	,, ,, ,,	72	47	$C_{23}H_{21}O_3N_3$			10.66			10.85
5a	,, ,, ,,	170	68	$C_{22}H_{19}O_3N$	76.9	5.6		76.5	5.5	
b	Benzene/light petroleum (40−60°)	192	71	$C_{23}H_{21}O_4N$	73.3	5.4		73.6	5.6	
c	Methanol	221	69	$C_{22}H_{18}O_3N\,Cl^*$						
d	,,	203	64	$C_{22}H_{18}O_3N\,Cl$	69.24	4.92		69.56	4.74	
e	,,	215	53	$C_{23}H_{21}O_3N$	76.43	7.94	3.76	76.88	7.85	3.9

* %Cl Found: 9.70; Required: 9.45.

THERMAL DECOMPOSITION OF Δ^1-SPIROPYRAZOLINES 2a−e

The spiropyrazolines **2**(0.5 g) were heated at the melting point till all the gases cease to evolve (about 3 hours). The viscous oil obtained was triturated with light petroleum (40−60°) to yield a solid which crystallised from a suitable solvent affords colourless crystals of the products **5a−e**, table 1.

ACTION OF ALCOHOLIC HYDROCHLORIC ACID ON SPIRO-3-(α-METHYLARYLIDENE)-1,2,3,4-TETRAHYDRO NAPHTHALENE-4-ONE-(1 : 3′)-2′, 6′-PIPERIDINEDIONE (5a−e)

The olefinic derivative **5** (0.25 g) was boiled under reflux with a mixture of conc. hydrochloric acid (5 ml) and ethanol (10 ml) for three hours. On dilution with water, an oily product separated which was extracted with ether. The solvent was driven off to give acetophenone, *p*-methoxyacetophenone, *p*-chloroacetophenone, *o*-chloroacetophenone and *p*-methylacetophenone identified as their 2,4DNPH-derivatives (m. p. and m. m. p. 237°, 220°, 231°, 206° and 258°, respectively).

ACTION OF HYDRAZINE HYDRATE ON SPIRO-3-ARYLIDENE-1,2,3,4-TETRAHYDRONAPHTHALENE-4-ONE-(1 : 3′)-2′, 6′-PIPERIDINEDIONE (1a−e).

Hydrazine hydrate (0.5 ml) was added to the solution of **1**(1 g) dissolved in glacial acetic acid (10 ml). The mixture was heated under reflux for 10−12 hours, then poured on ice-water. The colourless solid products **7** were filtered off, washed with water, dried and crystallised from a suitable solvent as indicated in table 2.

ACTION OF PHENYLHYDRAZINE AND BENZOYLHYDRAZINE ON 1a−e.

Phenylhydrazine (0.5 ml) or benzoylhydrazine (0.5 g) was added to **1** (1 g) in ethanol (10 ml). The mixture was heated under reflux for ten hours on a steam bath, the solution was then concentrated and cooled. The colourless solids separated, **10a−e** or **11a−e**, were filtered

Table 2

Δ^2-**Acetylpyrazoline derivatives, 7a – c, Δ^2-phenylpyrazoline derivatives, 10a – e and Δ^2-benzoylpyrazoline derivatives, 11a–**

Product	Recryst. solvent	M.P. °C	Yield %	Molecular Formula	Analysis					
					Found (%)			Required (%)		
					C	H	N	C	H	N
7a	Ethanol	261	43	$C_{23}H_{21}O_3N_3$	71.1	5.5		71.3	5.4	
b	Ethanol	252	35	$C_{24}H_{23}O_4N_3$	68.92	5.74	10.2	69.06	5.51	10.07
c	Acetic acid	234	64	$C_{23}H_{20}O_3N_3Cl$	65.92	4.56	9.73	65.48	4.70	9.96
d	Acetic acid	208	57	$C_{23}H_{20}O_3N_3Cl$	66.03	4.76		65.48	4.70	
e	Ethanol	257	43	$C_{24}H_{23}O_3N_3$	71.26	5.69	9.89	71.80	5.78	10.47
10a	Ethanol	148	39	$C_{27}H_{23}O_2N_3$	76.50	5.3	9.6	76.95	5.5	9.9
b	,,	144	56	$C_{28}H_{25}O_3N_3$			9.5			9.3
c	,,	137	62	$C_{27}H_{22}O_2N_3Cl$	73.52	4.97	9.35	73.76	4.83	9.22
d	,,	125	59	$C_{27}H_{22}O_2N_3Cl$	73.94	4.58	9.42	73.76	4.83	9.22
e	,,	141	56	$C_{28}H_{25}O_2N_3$	77.40	5.80	9.3	77.22	5.79	9.6
11a	Acetic acid	281	52	$C_{28}H_{23}O_3N_3$	75.07	5.3	9.3	74.81	5.16	9.5
b	,, ,,	198	45	$C_{29}H_{25}O_4N_3$	72.40	5.46		72.63	5.26	
c	,, ,,	204	53	$C_{28}H_{22}O_3N_3Cl$	69.10	4.80		69.49	4.55	
d	,, ,,	195	49	$C_{28}H_{22}O_3N_3Cl$	69.72	4.23	8.85	69.49	4.55	8.68
e	,, ,,	218	37	$C_{29}H_{25}O_3N_3$	75.36	5.28		75.16	5.40	

off, dried and crystallised from a suitable solvent as indicated in table 2. When the reaction was carried out in glacial acetic acid the Δ^2-phenylpyrazoline and Δ^2-benzoylpyrazoline derivatives obtained was found to be identical with that obtained from the above experiment. The identity was confirmed by m. p. and m. m. p.

Revue Roumaine de Chimie, **23**, *5*, 797–803 (1978).

DEGRADATION OF ANION EXCHANGERS IN AGGRESSIVE MEDIUM. IV*

CHEMICAL STABILITY OF TYPE I MACROPOROUS ANION EXCHANGERS WITH BINARY AND TERNARY STRUCTURE IN BASIC MEDIUM

I. PETRARIU, MARIA CUJBĂ, IG. POINESCU and CORNELIA LUCA

Institute of Macromolecular Chemistry "Petru Poni"
Aleea Gr. Ghica Vodă nr. 41 A, Iassy, Romania

Received February 18, 1976

Degradation of type I macroporous strong base anion exchangers with binary and ternary structure in the presence of hydroxyl ions was studied in view of finding the influence of the nature and content of the third comonomer on the chemical stability.
The kinetics of the degradation is illustrated by diagrams and the supposed mechanism of the processes involved is stated.

A series of macroporous strong base anion exchangers has been developed containing quaternary ammonium groups of type $(R^{I}R^{II}R^{III}R^{IV}N)^{+}X^{-}$: R^{I} is derived from a binary copolymer styrene-divinylbenzene (DVB) or ternary copolymer styrene – acrylonitrile – divinylbenzene or styrene – alkylmethacrylate – divinylbenzene and $R^{II} = R^{III} = R^{IV} = CH_3$ and X may be a halogen or hydroxy group.

The anion exchanger in chloride form has been chosen as the resins are usually delivered in this form, and the chloride analyses are relatively simple and very accurate.

It is known that owing to the existence of macropores in the structure of the copolymer pearls macroporous ion exchangers are qualitatively superior to those of the gel-type, [1-4] both chemically and physically. Several samples have a higher porosity and consequently show excellent resistance to organic fouling.

---

* Part. III : I. Petrariu, P. Petrariu, Fl. Popescu and Ig. Poinescu *Materiale Plastice*, **12**, 11 (1975).

[1] W. Busse and E. Schmidt (to Permutit A.-G), Ger. Pat. 1569285, 6 May, 1970 *Chem. Abstr.*, **73** 26244 (1970).

[2] S. N. Ilichev, M. P. Kovaleva, Z. F. Konstantinova and A. M. Soldatenko, URSS. Pat., 267.890, 2 Apr. 1970 ; *Chem. Abstr.* **73**, 67.254 (1970).

[3] M. P. Kovaleva and G. K. Petrova, "Sintez i Svoistva Ionnoobnenit elnyleb Materialov", Nauka, Moscow, 1968, p. 38.

[4] J. Seidl and J. Malinský, *Fortschr. Hochpolym. Forsch.*, **5**, 113 (1967).

It is recommendable to use them as an organic scavenger to remove the more harmful organic substances from the raw water.

Chemical degradation of the macroporous anion exchangers in the presence of hydroxyl ions is much less studied than that of the gel type anion exchangers. [5-8]

The interest in the chemical stability of anion exchangers has appeared with the industrial use of these substances.

The degradation may be caused by breakdown of the polymeric network of the anion exchanger and by changes in the number and nature or the functional groups.

Many papers have reported the quaternary ammonium functional groups change to weakly basic groups and eventually to non-anion exchange groups, occurring during their employment. [5,9-11]

Losses of the operational capacity during their employment, may be caused by fouling of the resins with certain organic materials or by chemical degradation in different aggressive media.

The present paper has given special attention to the influence of the nature and content in the copolymer of the third comonomer as acrylonitrile or the alkyl methacrylate.

EXPERIMENTAL

All the degradation reactions involved macroporous tertiary copolymer pearls, 0.4—0.8 mm in diameter, based on styrene (St)-divinylbenzene (DVB) or styrene-alkyl methacrylatedivinylbenzene [methyl methacrylate (MCMe) and n-butyl methacrylate (MCBu)] prepared by the suspension copolymerization technique. [12-13]

The monomers copolymerization was carried out in the presence of polystyrene (M = = 75.000), gasoline (b.p.125—140°) or toluene as inert media.

The chloromethylation agent was monochlorodimethylether (b.p. 56—60°) and $ZnCl_2$ as a Friedel — Crafts catalyst.

The amination of the chloromethylated copolymers was carried out by trimethylamine (aqueous solution 21 %) for 24 hours at room temperature.

The nitrogen analyses were carried out through the Kjeldahl method. [14] Chlorine was determined by the modified Schöninger method [15].

The experimental equipment used for degradation is shown in Figure 1. It presents some modifications from that given in a previous paper. [5]

The measurement were started on introducing 100 ml 10N NaOH into the reaction flask and heating it to the desired temperature. The absorption vessel was filled with 100 ml distilled water and the flow of nitrogen adjusted to 3.31 ml/s. The intial quantity of 0.1 N H_2SO_4 was added to the absorption vessel and the degradation was started on introducing the weighed sample

---

[5] I. Petrariu and J. Stamberg, *Coll. Czech. Chem. Comm.*, **32**, 798 (1967).

[6] I. Petrariu, P. Petrariu and C. Luca, *Materiale Plastice*, **7**, 71 (1970).

[7] I. Petrariu, S. Drăgan and P. Petrariu, *Rev. Chim. (Bucharest)*, **21**, 207 (1970).

[8] I. Petrariu, O. Petreuş, A. Carpov, C. Luca and M. Dima, *Rev. Chim. (Bucharest)*, **22**, 177 (1971).

[9] I. Petrariu, Thesis, Czechoslovak Academy of Sciences, Prague, 1965.

[10] L. Wirth, *Combustion*, **25**, 49 (1954).

[11] A. L. Wilson, *J. App. Chim.*, **11**, 151 (1961).

[12] Ig. Poinescu, S. Drăgan, S. Maxim and M. Dima, *Rev. Roumaine Chim.*, **20**, 1211 (1975).

[13] S. Maxim, Ig. Poinescu, S. Drăgan and M. Dima, *Rev. Roumaine Chim.* **17**, 1437 (1972).

[14] T. S. Ma and G. Zuazga, *Ind. Eng. Chem. Analyst*, **14**, 280 (1942).

[15] J. Haslam, J. B. Hamilton and D. C. Squirell, *Analyst*, **85**, 556 (1960).

(2mmol) into the reaction flask. The gaseous amine escaping from the reaction mixture was trapped by the acid in the absorption vessel and on reaching the equivalence point determined from the colour change of phenolphtaleine, the time τ was recorded and another portion of 0.1N H_2SO_4 was added. In this way, the course of the degradation was measured over a period of 5 hours at 100°.

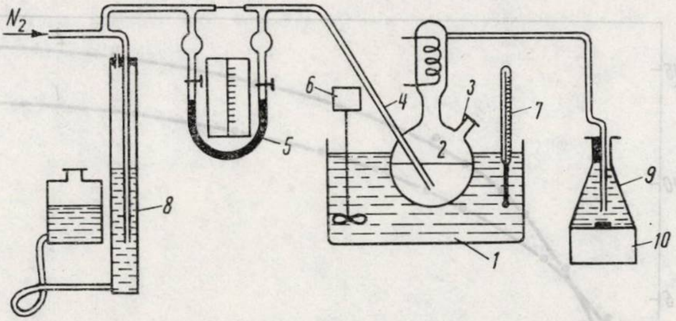

Fig. 1. — Apparatus for measuring the degradation of anion exchangers: *1* — oil bath, *2* — reaction flask (250 ml), *3* — tube for introducing the sample, *4* — tube for introducing nitrogen, *5* — flowmeter, *6* — stirrer, *7* — thermometer, *8* — manostat, *9* — absorption vessel, *10* — electromagnetic stirrer.

RESULTS AND DISCUSSION

Hofmann degradation of the structure $(RN(CH_3)_3^+\ X^-$ with various polymeric substituents R has been studied. In our previous papers [5-6] it was shown that the quaternary ammonium functional groups change during degradation to weakly basic groups (the degradation products were mainly methanol and a polymeric derivative of N,N-dimethylbenzylamine), as well as to a polymeric derivative of benzyl alcohol (the degradation product is trimethyl amine). The latter process is very significant as it destroys the total anion exchange capacity of the exchanger.

The nature and quantity of the third comonomer has an important influence on the chemical stability of the anion exchanger. At the same time, the character of the inert medium used in the polymerization process affects the physical structure of the respective copolymer and also its chemical stability.

As it is shown in Figure 2 an increased percentage of acrylonitrile entails a diminution of the chemical stability.

It is reasonable to assume that the nitrile group existing in the structure of the ternary macroporous copolymer owing to its electron-attracting effect, has a negative influence on the chemical stability, through the decrease of the electron density in the ortho- and para-positions of the benzene nucleus precisely where quaternary ammonium groups are placed. Certainly, a part of — CN groups are transformed into — COOH groups in the presence of sodium hydroxide solution. [16] The same thing holds when the inert medium used is polystyrene (Figure 3).

---

[16] H. Morawetz in "Chemical Reactions of Polymers" Editor E. M. Fettes, Interscience, New York, 1964, p. 10.

The results (Figure 3) show that the binary copolymer (curve 1) is much more resistant from the chemical standpoint than the ternary copolymer containing different percentage of acrylonitrile. To conclude, for a series of copolymers with the same reticulation degree and inert medium, the degradation reaction will be the more favoured as the content of acrylonitryle in the respective copolymer increases (curves 2 and 3). It is to be noted that the same results were obtained degrading anion exchangers synthesized in the presence of toluene as inert medium (Figure 4).

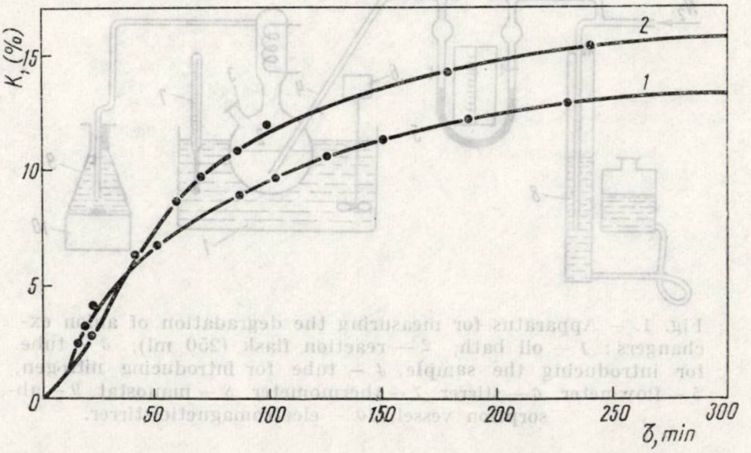

Fig. 2. — The molar conversion of the degradation K, corresponding to time τ. Crosslinking degree with DVB = 18 %, inert medium = gasoline, *1*, 2.26 % acrylonitrile ; *2*, 5.22 % acrylonitrile.

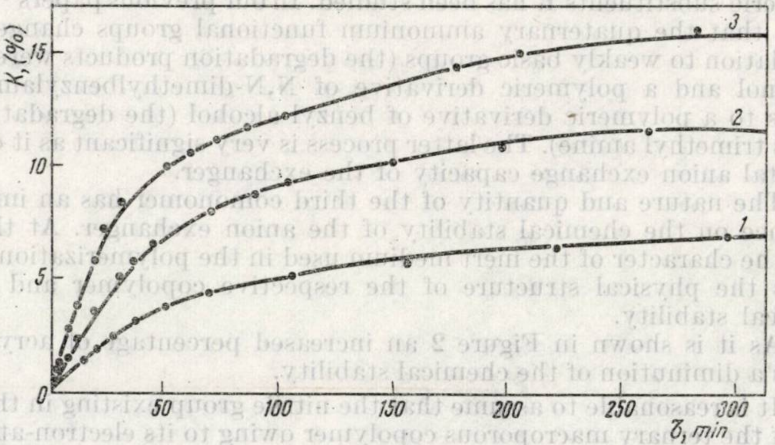

Fig. 3. — Dependence of the transformation degree K on the procentual acrylonitrile content of the macroporous copolymer : Crosslinking degree 8 %, inert medium = polystyrene. *1*, binary copolymer (St — DVB) ; *2*, AN 2 % ; *3*, AN 6.2 %.

Much attention has been paid to the relationship between the crosslinking degree and the degradation process. It is therefore to be expected that the conversion degree should decrease with the increase of the copolymers divinylbenzene. In Figure 5 (curves 1,2) the conversion degree dependent on crosslinking respectively on divinylbenzene percentage in the copolymer is shown.

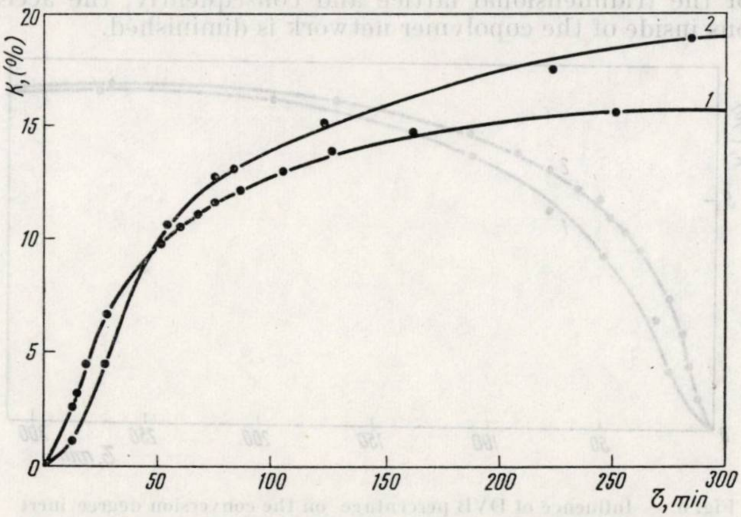

Fig. 4. — Influence of acrylonitrile content on the degradation reaction. DVB — 27 %; inert medium = toluene; *1*, binary copolymer; *2*, ternary copolymer AN 8,4 %.

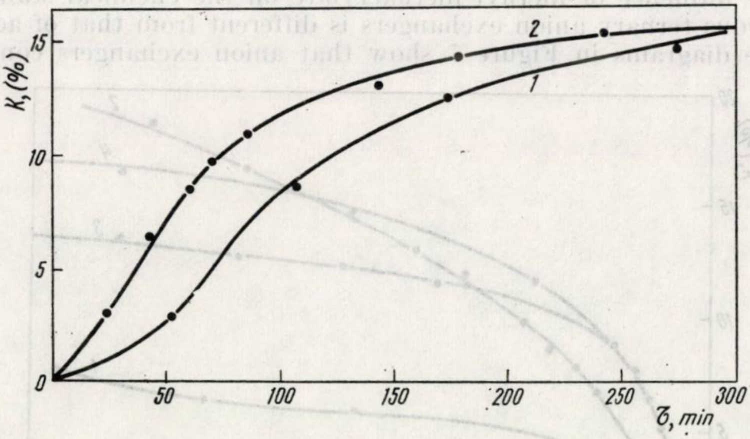

Fig. 5. — Influence of divinylbenzene percentage on the conversion degree : inert medium = polystyrene ; *1*, copolymer containing 10.5 % acrylonitrile and 18 % DVB ; *2*, copolymer containing 10.22 % acrylonitrile and 12 % DVB.

In order to ascertain the validity of this finding also for other comonomers, a few experiments have been made using a ternary copolymer where the third comonomer is methyl methacrylate.

The results in Figure 6 show about the same behaviour during the degradation reaction.

For copolymers with high crosslinking degree there exists a high rigidity of the tridimensional lattice and consequently, the accessibility of OH^- ions inside of the copolymer network is diminished.

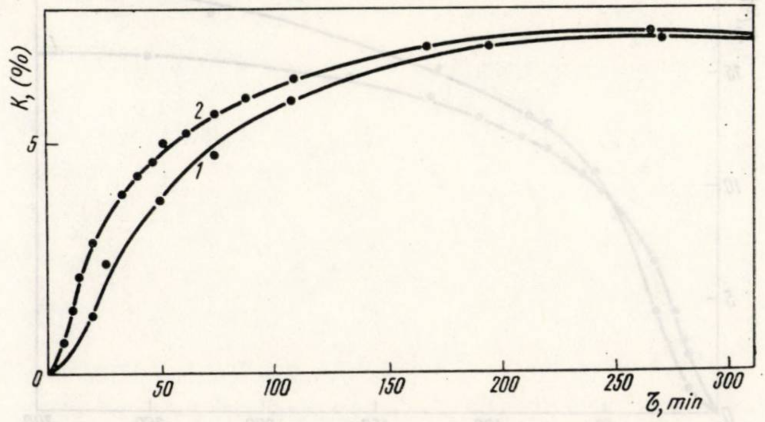

Fig. 6. — Influence of DVB percentage on the conversion degree inert medium = polystyrene *1*, copolymer containing 10 % methyl methacrylate and 12 % DVB ; *2*, copolymer containing 10 % methyl methacrylate and 18 % DVB.

The influence of methyl methacrylate on the chemical stability of macroporous ternary anion exchangers is different from that of acrylonitrile. The diagrams in Figure 7 show that anion exchangers containing

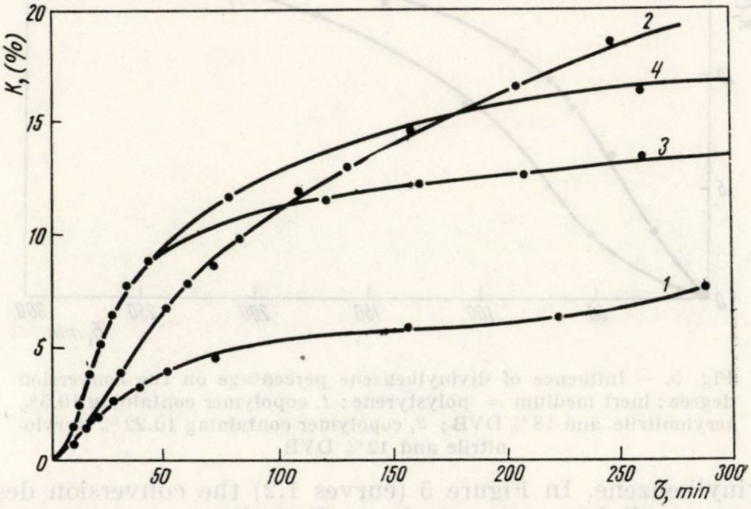

Fig. 7. — Influence of the nature of the third comonomer on the conversion degree : DVB = 8 %, inert medium = polystyrene ; *1*, binary copolymer ; *2*, ternary copolymer containing 19,66 % acrylonitrile ; *3*, ternary copolymer containing 20 % methyl methacrylate ; *4*, ternary copolymer containing 20 % butyl methacrylate.

methyl methacrylate are degraded faster at the beginning of the degradation reaction than are those with acrylonitrile.

This remark stands good only up to two hours degradation time. At longer durations of time, the samples containing acrylonitrile are faster degraded. If we take into account the fact that an anion exchanger containing methyl methacrylate (curve 3) is much more stable than that with butyl methacrylate (curve 4) it is self-evident that the alkyl radical of the ester group has a significant influence on the degradation process.

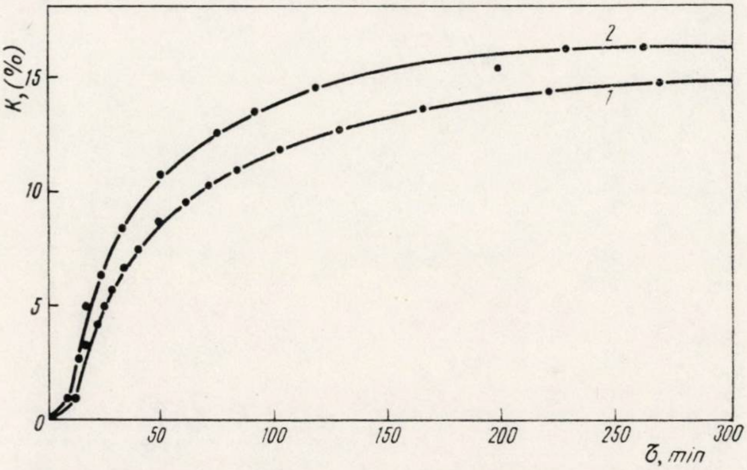

Fig. 8. — Influence of the quantity of the third comonomer on the conversion degree : DVB = 27 %, inert medium = toluene *1*, ternary copolymer containing 5 % methyl methacrylate ; *2*, ternary copolymer containing 2 % methyl methacrylate.

One of the conclusions to be drawn from the experimental data is that the degradation reaction will be favoured by the increase of the volume of the esteric radical of the alkyl methacrylate copolymer. On the other hand, anion exchangers with binary structure are much more stable than those with ternary structure (compare curve 1 with the others).

The insertion of the third comonomer will only improve the physical properties, especially the mechanical qualities of the macroporous copolymer.

The quantity of the third comonomer has also an important influence on the chemical stability. As resulted from the data illustrated in Figure 8 an increased content of the methyl methacrylate (curve 1) causes an improvement in the chemical stability.

CONCLUSIONS

1. The influence of the nature and quantity of the third comonomer on the degradation reaction has been studied as well as the type of the inert medium used in the copolymerization process.

2. It has been found that comonomers as acrylonitrile or alkyl methacrylate included in the copolymer, diminish the chemical stability of anion exchangers.

Revue Roumaine de Chimie, **23**, *5*, 805–817 (1978)

ПОЛЯРОГРАФИЧЕСКИЕ ИССЛЕДОВАНИЯ ХИМИЧЕСКОГО СТРОЕНИЯ И МЕХАНИЗМА РЕАКЦИЙ ОРГАНИЧЕСКИХ ПЕРЕКИСЕЙ. I

УСЛОВИЯ ПОЛЯРОГРАФИЧЕСКОГО АНАЛИЗА ОРГАНИЧЕСКИХ ПЕРЕКИСЕЙ

БЭЛА ТОКЕШ

Лаборатория физической химии,
Медико-фармацевтический Институт
Тыргу-Муреш, улица Г. Маринеску, 38

Получена 28 февраля 1976 г.

Автор предпринял систематическое исследование полярографического поведения трет.-бутилпероксиэфиров, замещённых бензойных кислот. Изучалось влияние различных факторов (растворителя, параметров капилляра, высоты ртутного столба, температуры, концентрации деполяризатора) на параметры полярографической волны, делая выводы о природе тока и обратимости электродного процесса в разных условиях работы. На основе полученных данных, выбрались оптимальные условия полярографического анализа изученных перекисей.

Возрастающая важность органических перекисей, в лабораторных условиях и в химической промышленности, делает необходимым точное определение перекисного кислорода. С этой целью были предложены разные методы, применяемые в различных рабочих условиях, с большим или меньшим успехом. [1–7] Полярография представляет собою один из методов, обеспечивающих самые широкие возможности для изучения представителей этого класса электроактивных соединений, не только с аналитической точки зрения, но и в решении многочисленных других проблем химии перекисей.

Из специальной литературы известно, что при полярографическом восстановлении перекисей, связь O—O необратимо расщепляется, как правило с присоединением двух электронов, а возникающие оксианионы, в протондонорной среде, сбразуют соответствующие гидроксисоедине-

---

[1] Е. Г. Е. Хавкинс, «Органические перекиси их получение и реакции», Изд. «Химия», Москва 1964 стр. 426.

[2] A. G. Davies, ''Organic Peroxides'', Butterworth, London, 1961, стр. 195.

[3] W. R. Lewis, F. W. Quackenbush T. de Vries, *Analyt. Chem.*, **21**, 762 (1949)

[4] L. S. Silbert, *J. Amer. Oil Chemists'Soc.*, **39**, 480 (1962).

[5] М. Ф. Романцев, и Е.С. Левин, *Жур. аналит. хим.*, **18**, 1109 (1963).

[6] A. H. M. Cosijn, *Chem. Weekblad*, **60**, 585 (1964).

[7] R. M. Johnson и J. W. Siddiqui, *J. Polarog. Soc.*, **11**, 72 (1965).

ния. [5,8,9] Учитывая значения потенциалов полуволн органических перекисей, Кута и Какенбуш[10] разделяли эти соединения на 6 групп, позволяя первичное общее ориентирование в их полярографическом анализе.

Знание связи между строением и полярографической восстанавливаемостью перекисей углубилось только после произведения первых систематических исследований Шулцом и Шварцом,[11–13] а дальше Антоновским и сотр.[14–17] Однако эта проблема — как вообще вопрос о количественной связи между полярографическими параметрами и строением, или реакциями органических соединений — в настоящее время далека от полного решения. Литературные данные малочисленные и часто противоречивые. Очевидно, данные полученные из исследования этих вопросов важные и с аналитической точки зрения, способствуя выбору оптимальных условий для анализа перекисных соединений. В самом деле отношение взаимное : для изучения влияния строения на электрохимические свойства деполяризаторов, необходимо зарегистрировать полярографические кривые применимые для количественных измерений.

В наших исследованиях, мы решили ближе рассмотреть несколько классов органических перекисей, в первую очередь замещенные пербензоаты 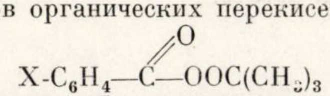 $X\text{-}C_6H_4\text{—}C(=O)\text{—}OOC(CH_3)_3$ и некоторые серии гидроперекисей. В настоящей работе представлены наши результаты о влиянии различных факторов на полярографические параметры изученных перекисей и выбор оптимальных условий их анализа при помощи этого метода.

ЭКСПЕРИМЕНТАЛЬНАЯ ЧАСТЬ

Реактивы. Перэфиры, применяемые для измерений, были синтезированы по известным из литературы методам [2,5,18–26]. Чистота про-

---

[8] В.Д. БЕЗУГЛИЙ и В.Н. ДМИТРИЕВА, *Жур. приклад. хим.*, **31**, 298 (1958).

[9] K. H. SCHWARZ, Dissertation, Humbold-Universität zu Berlin, 1964.

[10] E. J. KUTA и F. W. QUACKENBUSH, *Analyt. Chem.*, **32**, 1069 (1960).

[11] M. SCHULZ и K. H. SCHWARZ, *Uber. dlsch. Akad. Wiss. Berlin*, **6**, 515 (1964).

[12] M. SCHULZ и K. H. SCHWARZ, *Abh. dlsch. Akad. Wiss. Berlin, Kl. Chem., Geol. Biol*, **1964**, 119.

[13] M. SCHULTZ и K. H. SCHWARZ, *Z. Chem.*, **7**, 176 (1967).

[14] В. Л. АНТОНОВСКИЙ, З.С. ФЛОРОВА, Т.Т. СЛЕИНА и М.М. БУЗЛАНОВА, *Жур. общей хим.*, **39**, 268 (1969).

[15] З.С. ФРОЛОВА, М.М. БУЗЛАНОВА, О.Н. РОМАНЦОВА и В.Л. АНТОНОВСКИЙ, *Жур. общей хим.*, **38** 1944 (1968).

[16] В.Л. АНТОНОВСКИЙ, З.С. ФРОЛОВА, Е.В. СКОРОБОГАТОВА, О.Н. РОМАНЦОВА и М.М. БУЗЛАНОВА, *Жур. общей хим.*, **38**, 1948 (1968).

[17] В.Л. АНТОНОВСКИЙ, З.С. ФРОЛОВА, Е.В. СКОРОБОГАТОВА и М.М. БУЗЛАНОВА, *Жур. общей хим.*, **39**, 518 (1969).

[18] «Химия перекисных соединений», Изд. Акад. Наук СССР , Москва, 1963, стр. 279.

[19] С.В. ЗАВГОРОДНИЙ, *Успехи химии*, **30**, 345 (1961).

[20] P. D. BARTLETT и R. R. HIATT, *J. Amer. Chem. Soc.*, **80**, 1398 (1958).

[21] G. A. RUSSEL, *J. Amer. Chem. Soc.*, **78**, 1047 (1956).

[22] N. MILAS и D. SURGENOR, *J. Amer. Chem Soc.*, **68**, 205 (1946).

[23] L. S. SILBERT и D. SWERN, *J. Amer. Chem. Soc.*, **81**, 2364 (1959).

[24] L. S. SILBERT и D. SWERN, *Analyt. Chem.*, **30**, 385 (1958).

[25] Л.С. БОГУСЛАВСКАЯ, *Успехи химии*, **34**, 1199 (1965).

[26] L. S. SILBERT, L. P. WITNAUER, D. SWERN и C. RICCIUTI, *J. Amer. Chem. Soc.*, **81**, 3244 (1959).

дуктов была проверена по содержанию активного кислорода в них, повторяя операцию очищения до достижения уровня $[O] \geqslant 98\%$ по сравнению с вычисленными значениями. Концентрацию перекисного кислорода мы определили с помощью различных вариантов йодометрического метода.[1,6,23,24,27-30]

Чистота всех веществ, применяемых для синтеза и анализа, была порядка р.а.

Приборы. Определения были проведены полярографом ЛП—55А, системы Гейровского, снабжённым регистратором ЕЗ—2. Измерения производились в сосудиках для электролиза формы «Н», окружая рабочий электрод водяной маншеткой для термостатирования ячейки. Постоянство температуры обеспечивалось ультратермостатом Гёпплер, с точностью ±0,05°.

Так как большинство органических перекисей, в водно-спиртовых растворах, восстанавливаются вблизи потенциала каломельного электрода или ртутного анода — общепринятые электроды сравнения —, мы использовали для этого нормальный ртутно-сульфатный электрод (НСЭ): Hg/Hg_2SO_4, раствор I и K_2SO_4, потенциал которого на 0,42 в положительнее потенциала насыщенного каломельного электрода.

В качестве рабочего (индикаторного) электрода применялся ртутно-капельный электрод, имея следующие параметры (в дистиллированной воде, при 0,00 в и $T=293$ К) : $m=1{,}99$ мг сек$^{-1}$, $t_1=3{,}35$ сек, $K = m^{2/3}t_1^{1/6} = 1{,}94$ мг$^{2/3}$ сек$^{-1/2}$.

Для изучения влияния параметров капиляра на электрохимический процесс, мы изготовили, по литературным данным, [31,32] ряд капилярных электродов с принудительным отрывом ртутной капли. Так полученные периоды капания охватили широкий интервал, между 0,32 и 8,19 сек, при постоянной скорости вытекания ртути ($m=1{,}20$ мг сек$^{-1}$).

Ход работы. Для получения удовлетворительной воспроизводимости потенциалов полуволн, порядка 3—4 мв, полярограммы были сняты на растянутой шкале напряжения (25—50 мв/единица по оси абсцисс). Скорость изменения потенциала поддерживалась на постоянном уровне, 1,66 мвсек$^{-1}$.

Удаление растворенного кислорода во всех случаях производилось пропусканием очищенного метана, полученного из светильного газа, через раствор в течение 10 минут, до начала определения. [33,34]

Фоновый раствор содержил в минимальном необходимом количестве желатин (0,005%) для подавления максимумов.

---

[27] V. Karnojitzki, ,,Les peroxides organiques'', Hermann, Paris, 1958, стр. 113.

[28] И.М. Кольтгофф, Р. Белчер, В.А. Стенгер и Г. Мацуяма, «Объемный анализ», т.3, «Практическая часть. Методы окисления-восстановления», Гос. научно-техн. изд. хим. лит., Москва, 1961, стр. 479.

[29] B. Tőkés и B. Barabas, *Revista Medicală* (*Tg.-Mureș*), **8**, 376 (1962).

[30] B. Tőkés, *Revista Medicală* (*Tg.-Mureș*), **10**, 166 (1964).

[31] Е. Н. Скобец и Н. С. Кавецкий, *Заводная лаб.*, **15**, 1299 (1949).

[32] С. Г. Майрановский и Е. Ф. Майрановская, *Извест. Акад. Наук СССР.*, *Отдел хим. наук*, **1961**, 922.

[33] B. Barabas и L. Balogh, *Studii și Cercetări Chim.*, Acad. R.P.R., **5**, 443 (1957).

[34] B. Tőkés, Rev. *Roumaine Chim.*, **13**, 1169 (1968).

РЕЗУЛЬТАТЫ И ИХ ОБСУЖДЕНИЕ

Состав фона. Одна из первичных проблем для анализа по этому методу органических перекисей, является выбор оптимальной среды. В качестве индифферентного электролита, специальная литерарура часто рекомендует раствор LiCl в смеси метиловый спирт — бензол. Полярографические волны записанные в этой среде много раз плохо поддаются анализу из-за несовершенной их формы или появления максимумов неподавленных обыкновенными примесями.[5,7] Лучшие результаты получались используя в качестве индифферентного электролита нитрат аммония, а как растворитель для органических перекисей нерастворимых в воде, рекомендуется ряд органических жидкостей смешивающихся с водой, например: диоксан, метиловый спирт, этиловый спирт, ацетонитрил. При использовании водных смесей этих соединений, содержание воды должно быть как можно большим. [9,11–13]

При проверке ряда растворителей для выбора оптимальных условий полярографического анализа изученных перекисей, мы получали наилучшие полярографические волны используя смеси этилового спирта с водой, а в качестве фона 0,1— 1,0 м растворы серной кислоты. Кривые зарегистрированные в этих средах, близки к идеальной форме, их наклон зависит от концентрации спирта. С ростом концентрации органического растворителя в составе раствора, волны перемещаются в направлении более отрицательных потенциалов, характерно для необратимых

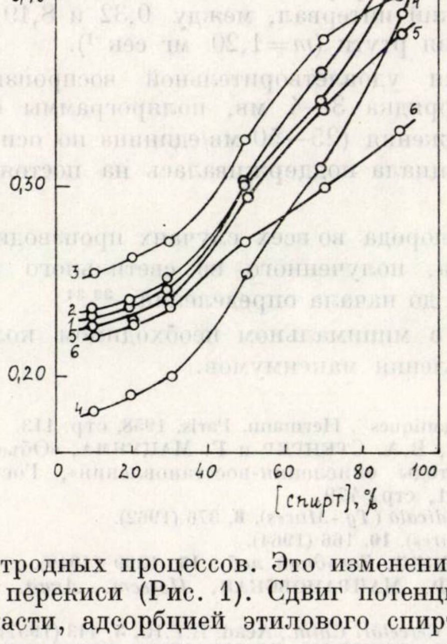

Рис. 1. — Изменение потенциала полуволны в зависимости от концентрации этилового спирта

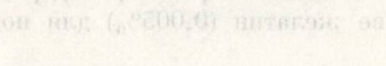

$$n\text{-X-}C_6H_4-\overset{\overset{\displaystyle O}{\|}}{C}-OOC(CH_3)_3.$$

X: (1) CH_5, (2) OCH_3, (3) H, (4) Br, (5) Cl, (6) HO_2. Индифферентный электролит: 0,1м H_2SO_4. $T = 293$ K.

электродных процессов. Это изменение зависит от природы анализируемой перекиси (Рис. 1). Сдвиг потенциалов полуволн можно объяснить, от части, адсорбцией этилового спирта на поверхности электрода, что — вследствие вытеснения молекул деполяризатора — затрудняет перенос электрона и, следовательно, скорость электрохимической реакции уменьшается. [35–39] Направление экспериментального сдвига потенциала полуволн соответствует теоретическому уравнению,[40] которое описывает необратимые полярографические токи, в присутствии адсорбции:

$$\Delta E_{1/2} = \frac{RT}{\alpha n_a F} \ln\left(0{,}155\sqrt{\frac{\nu}{t_1}}\right), \qquad (1)$$

где $\left(\frac{t_1}{\nu}\right)^{1/2}$ — степень заполнения электрода поверхностноактивным веществом. Очевидно, что действие органического растворителя тем сильнее, чем больше адсорбируется деполяризатор на поверхности электрода.

Сдвигу потенциала полуволны к более отрицательным значениям с увеличением концентрации спирта, в то же время может способствовать и первичный эффект среды на неадсорбировнный деполяризатор. На основании теории абсолютных скоростей реакций[41,42] и считая что концентрация активированного комплекса пропорциональна при электродной концентрации деполяризатора, для константы скорости переноса электрона можно написать уравнение:

$$k = k_0 \frac{f}{f^{\neq}}, \qquad (2)$$

где f и $f^{\neq}$ — коэффициенты активности деполяризатора и активированного комплекса, k_0 — константа скорости переноса электрона в чисто водном растворе (f=1). В то время так $f^{\neq}$ мало изменяется при увеличении доли органического растворителя, коэффициент f быстро падает при уменьшении диэлектрической постоянной среды ε, т.е., при возрастании концентрации органического компонента. Это ведёт одновременно к уменьшению значения константы скорости k. Ввиду того, что потенциал полуволны необратимых электродных процессов пропорционален логарифму константы скорости этих реакций: [43,44]

$$E_{1/2} = \frac{RT}{\alpha n_a F} \ln \frac{0{,}886\ k}{D^{1/2}} + \frac{RT}{2\alpha n_a F} \ln t_1, \qquad (3)$$

---

[35] A. Čisak, *Roczniki Chem.*, **36**, 1895 (1962).

[36] K. Schwabe, *Z. phys. Chem. (Leipzig), Sonderheft*, 293 (1958).

[37] K. Schwabe, "Advances in Polarography", Vol. 3, ed. I. Longmuir, Pergamon, London, 1960, стр. 911.

[38] С.Г. Майрановский, «Каталитические и кинетические волны в полярографии», Изд. «Наука», Москва, 1966, стр. 248.

[39] С.Г. Майрановский, «Успехи электрохимии органических соединений», Изд. «Наука», Москва, 1966, стр. 115.

[40] J. Kuta, J. Weber и J. Koutecký, *Coll. Czech. Chem. Comm.*, **25**, 2376 (1960).

[41] S. Glasstone, K. J. Laidler и H. Eyring, "The Theory of Rate Processes", McGraw-Hill "Book Co., New York-London, 1941, стр. 199.

[42] А. П. Томилов, С. Г. Майрановский, М. Я. Фиошин и В. А. Смирнов, «Электрохимия органических соединений», Изд. «Химия», Ленинград, 1968, стр. 68.

[43] А. Н. Фрумкин, В. С. Багоцкий, З. А. Йофа и Б. Н. Кобанов, «Кинетика электродных процессов». МГУ,, Москва, 1952, стр. 172.

[44] J. Koutecký, *Coll. Czech. Chem. Comm.*, **18**, 597 (1953).

изменения значения $\ln k$ отражается через $\Delta E_{1/2}$, т.е. потенциал полуволны сдвигается к более отрицательным значениям, как это выявилось и из наших экспериментальных данных. В случае чистого эффекта: $\ln k \sim \sim \frac{1}{\varepsilon}$ т.е. потенциал полуволны должен изменяться линейно с обратным значением диэлектрической постоянной. Однако, такая линейность в

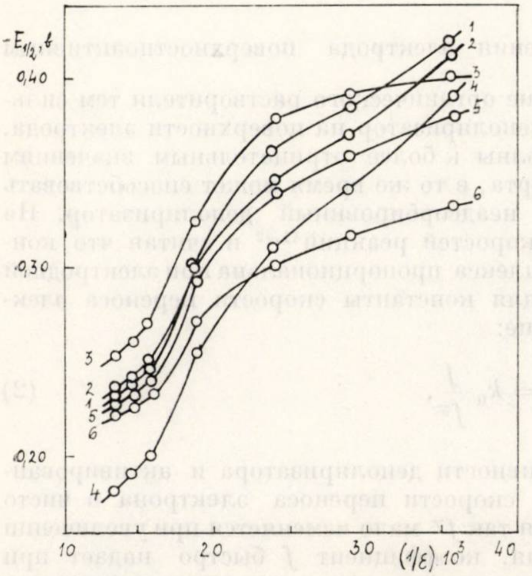

Рис. 2. — Изменение потенциала полуволны в зависимости от обратного значения диэлектрической константы растворителя в серии

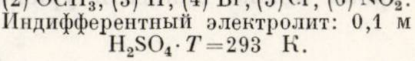

$n\text{-X-}C_6H_4-\overset{\displaystyle O}{\overset{\|}{C}}-COO(CH_3)_3$. X: (1) CH_3, (2) OCH_3, (3) H, (4) Br, (5) Cl, (6) NO_2. Индифферентный электролит: 0,1 м $H_2SO_4 \cdot T = 293$ К.

наших экспериментах не наблюдалась (Рис. 2). Имея в виду общую форму представленных кривых, следует, что в настоящем случае оба эффекта накладываются друг на друга.

С ростом концентрации спирта существенно изменяется и высота полярографической волны. Считая, что механизм электровосстановления остаётся тот же, это изменение можно объяснить прежде всего с изменением коэффициента диффузии деполяризаторов, вследствие изменения вязкости среды и — в меньшей мере — изменений эффективных радиусов сольватированных молекул. Так как вязкость раствора переходит через максимум при 52 объемн. % спирта, силы токов переходят через минимум (Рис. 3). Несовпадение крайный значений вязкости и сил предельных токов отражает неоднородность сольватирования членов реакционной серии и, следовательно, разность их эффективных раудисов. Конечно, в этих последних случаях, величина $\bar{i}_{\text{пр}}\ \eta^{1/2}$ не остается постоянной во всем интервале концентрации спирта.

Параметры капельного электрода. Учитывая что потенциал полуволны необратимых волн зависит от периода капания ртутного электрода, эта зависимость — выраженная уравнением (3) — является экспериментальным пособием распознавания необратимости изученного электродного процесса. Из наклона прямой $(E_{1/2}, \lg t_1)$ можно вычислить произведение αn_a, которое выражает количественно этот характер.

В случае серии перэфиров 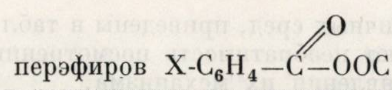 $X\text{-}C_6H_4\text{—}\overset{\displaystyle O}{\overset{/\!/}{C}}\text{—}OOC\,(CH_3)_3$, изменение потенциала полуволны в зависимости от периода капания было изучено методом принудительного отрыва ртутной капли, от четырёх различных капиляров. Точки ($E_{1/2}$, lg t_1) расположены вдоль прямой, в отличном согласии с теорией необратимых электродных процессов, независимо от концентрации спирта в фоне. Уравнение регрессионной линии в случае незамещенного пербензоата, при различных концентрациях этилового спирта, можно выразить в виде:

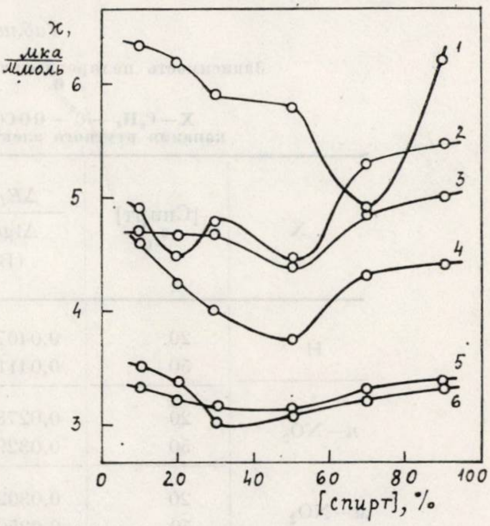

Рис 3. — Изменение константы Илковича $\varkappa = \dfrac{i_{пр}}{C} = 607\ n D^{1/2}\ K$, в зависимости от состава растворителя в серии замещенных пербензоатов. X: (1) H, (2) *п*-Br, (3) *п*-Cl. (4) *п*-OCH_3, (5) *п*-CH_3, (6) *п*-NO_2. Индифферентный электролит: 0,1 м H_2SO_4. $T = 293$ K.

а) В 0 %-ном этиловом спирте:

$$E_{1/2} = (0{,}0388 \pm 0{,}0022)\ \lg\ t_1 - (0{,}2878 \pm 0{,}0011)\ \text{в}$$

$$r = 0{,}997\,; \qquad s_0 = \pm\ 0{,}0022\ \text{в}$$

б) В 20 %-ном этиловом спирте:

$$E_{1/2} = (0{,}0407 \pm 0{,}0022)\ \lg\ t_1 - (0{,}2955 \pm 0{,}0013)\ \text{в}$$

$$r = 0{,}997\,; \qquad s_0 = \pm\ 0{,}0023\ \text{в}$$

в) В 50 %-ном этиловом спирте:

$$E_{1/2} = (0{,}0411 \pm 0{,}0015)\ \lg\ t_1 - (0{,}3585 \pm 0{,}0008)\ \text{в}$$

$$r = 0{,}9987\,; \qquad s_0 = \pm\ 0{,}0016\ \text{в}$$

Для других членов серии получились корреляции то же отличные ($r \geqslant 0{,}99$). Характерные данные, вычисленные методом наименьших квадратов, для двух различных сред, приведены в табл. 1. Эти данные, кроме того что подтверждают необратимость посмотренных процессов, важные и с точки зрения выявления их механизма.

Из эффекта периода капания на силу полярографического предельного тока можно делать выводы о природе последнего. Вообще, $\bar{i}_{\text{пр}} = At_1^a$,

Таблица 1

Зависимость полярографических параметров в серии

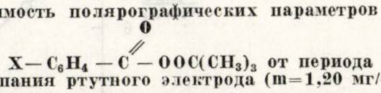

$X-C_6H_4-\overset{\overset{O}{/\!/}}{C}-OOC(CH_3)_3$ **от периода капания ртутного электрода (m=1,20 мг/сек)**

X	[Спирт] %	$\frac{\Delta E_{1/2}}{\Delta \lg t_1}$ (В)	αn_a	$\frac{\Delta \lg \bar{i}_{np}}{\Delta \lg t_1}$
H	20 50	0,0407 0,0411	0,716 0,706	0,192 0,162
$n-NO_2$	20 50	0,0278 0,0329	1,044 0,882	0,208 0,189
$м-NO_2$	20 50	0,0302 0,0250	0,960 1,160	0,178 0,173
$o-NO_2$	20 50	0,0354 0,0436	0,819 0,664	0,195 0,181
$n-Cl$	20 50	0,0426 0,0405	0,681 0,717	0,133 0,158
$м-Cl$	20 50	0,0344 0,0385	0,844 0,754	0,171 0,181
$o-Cl$	20 50	0,0349 0,0374	0,830 0,775	0,184 0,186
$n-Br$	20 50	0,0383 0,0390	0,752 0,744	0,162 0,179
$м-Br$	20 50	0,0324 0,0380	0,896 0,764	0,176 0,185
$n-CH_3$	20 50	0,0407 0,0373	0,713 0,779	0,174 0,199
$o-CH_3$	20 50	0,0426 0,0455	0,682 0,638	0,196 0,162
$n-OCH_3$	20 50	0,0426 0,0338	0,681 0,857	0,208 0,222

где a равняется 1/6 для диффузионных, -1/3 для адсорбционных, и 1/2 для чисто кинетических токов. На основе логарифмического анализа полярографических волн, мы вычислили показатель $a = \dfrac{\Delta \lg \bar{i}}{\Delta \lg t_1}$ пр для данной серии перэфиров. Корреляция ($\lg \bar{i}_{\text{пр}}$, $\lg t_1$) оказалась отличной и в этом случае. Например, для незамещенного перэфира, изученного в тех же средах и с теми же капиллярами, получились следующие уравнения регрессионных линий:

а) В 0%-ном этиловом спирте:

$$\lg \bar{i}_{\text{пр}} = (0{,}198 \pm 0{,}010) \lg t_1 + (1{,}6600 \pm 0{,}0051)$$

$$r = 0{,}998\,; \qquad s_0 = \pm\, 0{,}010$$

б) В 20 %-ном этиловом спирте:

$$\lg \bar{i}_{\text{пр}} = (0{,}192 \pm 0{,}012) \lg t_1 = (1{,}\,6555 \pm 0{,}0063)$$

$$r = 0{,}996\,; \qquad s_0 = \pm\, 0{,}012$$

в) В 50%-ном этиловом спирте:

$$\lg \bar{i}_{\text{пр}} = (0{,}160 \pm 0{,}008) \quad \lg t_1 + (1{,}6245 \pm 0{,}0045)$$

$$r = 0{,}997\,; \qquad s_0 = \pm\, 0{,}009$$

Показатели, полученные для членов серии, приведены в табл. 1. Из экспериментальных данных видно, что сила тока определяется почти исключительно диффузией, параметр a изменяясь в узком диапазоне, между 0,16 и 0,22.

Таблица 2

Значение показателя b в серии 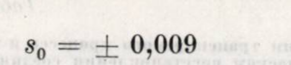
$X-C_6H_4-\overset{\overset{\large O}{\|}}{C}-OOC(CH_3)_3$

X	b	X	b	X	b	X	b
$п-NO_2$	0,56	$п-Cl$	0,58	$п-Br$	0,55	$п-CH_3$	0,58
$м-NO_2$	0,57	$м-Cl$	0,56	$м-Br$	0,58	$о-CH_3$	0,53
$о-NO_2$	0,57	$о-Cl$	0,54	H	0,55	$п-OCH_3$	0,53

Можно прийти к подобному выводу изучая изменение силы предельного тока в зависимости от высоты ртутного столба, на основе выражения: $\bar{i}_{\text{пр}} = Bh^{b}_{\text{Hg}}$ (Табл. 2). Показатель b, определённый из наклона регрессионной линии ($\lg \bar{i}_{\text{пр}}$, $\lg h_{\text{Hg}}$), мало отклонится от величины 0,50, характерной для чисто диффузионных токов.

Температура. Из зависимости высоты полярографических волн от температуры можно так же получить данные о природе транспортного процесса, с помощью которого деполяризатор доставляется к поверхности электрода. Выше приведенные результаты позволяют делать вывод, что при электровосстановлении перэфиров, процессом определяющим силу тока является диффузия. В этом случае можно ожидать, что значение температурного коэффициента тока должен быть около +1,6%/К. Для выражения изученной зависимости, в место температурного коэффициента, мы вычислили — по предложению Влчека[45] — энергию активации транспортного процесса ($Q_{\text{Тр}}$). Для этого, диффузионный коэффициент следует написать в виде:[46]

$$D = D_0 \exp\left(-\frac{Q_{\text{Тр}}}{RT}\right) \tag{4}$$

Подставляя это выражение в уравнение Илковича, получим:

$$\lg \frac{\bar{i}_{\text{пр}}}{m^{2/3}\, t_1^{1/6}} = \lg 607\ n\, C D_0^{1/2} - \frac{Q_{\text{Тр}}}{2 \cdot 2{,}3\ RT} \tag{5}$$

Значение $Q_{\text{тр}}$ вычисляется из наклона прямой, из графика зависимости левой части выражения (5) от $\frac{1}{\text{T}}$. Учитывая, что мы работали в сравнительно узком диапазоне температуры, изменение параметров m и t_1 незначительны, значение энергии активации было вычислено прямо из наклона регрессионной линии $\left(\lg \bar{i}_{\text{пр}},\ \frac{1}{T}\right)$. Значения, полученные таким путём, приведены в табл. 3. Энергии активации транспортного процесса исследуемой реакционной серии находятся в пределах 4,0—7,7 ккал/моль,

Таблица 3

Энергия активации транспортного процесса и температурный коэффициент предельного тока при полярографическом восстановлении соединений X—C_6H_4—COO$(CH_3)_3$. Фон: 0,1 м H_2SO_4 в 20—70%-ном этиловом спирте. Температурный диапазон: 293—313 К.

X	$Q_{\text{Тр}}$	$\frac{1}{\bar{i}_{\text{пр}}} \cdot \frac{\bar{i}_{\text{пр}}}{T} 100$	X	$Q_{\text{Тр}}$	$\frac{1}{\bar{i}_{\text{пр}}} \cdot \frac{\Delta \bar{i}_{\text{пр}}}{\Delta T} 100$
	$\left(\frac{\text{ккал}}{\text{моль}}\right)$	(%/К)		$\left(\frac{\text{ккал}}{\text{моль}}\right)$	(%/К)
п—NO_2	7,0	1.84	*п*—Br	6,9	1,83
м—NO_2	7,2	1,89	*п*—Br	7,7	2,05
о—NO_2	7,0	1,83	H	4,4	1,20
п—Cl	5,6	1,52	*о*—CH_3	4,0	1,17
м—Cl	6,1	1,60	*п*—CH_3	5,2	1,39
о—Cl	7,2	1,88	*п*—OCH_3	6,8	1,78

[45] А. А. Vlcek' *Coll. Czech' Chem. Comm.*, **24**, 2538 (1959).

[46] М. ТЕМКИН, *Жур. физ. хим.*, **22**, 1081 (1948).

соответствуя главным образом диффузионному транспорту. С целью сравнения наших данных с литературными, мы ввели в таблицу и температурные коэффициенты токов. Однако, мы считаем, что использование значения $Q_{\text{Тр}}$ для выражения рассмотренного влияния, является более обосновным, имея в виду, что оно не зависит от экспериментальной температуры и имеет более глубокий физический смысл, чем температурный коэффициент.

В изученном случае, при различных концентрациях этилового спирта в растворителе, мы не наблюдали сколько нибудь осязаемое изменение энергии активации $Q_{\text{Тр}}$.

Концентрация деполяризатора. Зависимость силы предельного тока от концентрации деполяризатора представляет интерес так с аналитической, как и с «диагностической» точки зрения, для выяснения природы тока и механизма электродного процесса. В случае перэфиров, линейнность корреляции значений ($i_{\text{пр}}$, C) оказалась отличной, в данном интервале концентрациий. В 20%-ном этиловом спирте, который чаще всего использовался в качестве растворителя в наших исследованиях, уравнения регрессионных линий членов реакционной серии, представляются следующим образом ($n = 8$, $T = 293$ K, $\langle C \rangle =$ ммоль/литр):

$$X = H \quad : \bar{i}_{np} = (6{,}175 \pm 0{,}012)\, C = (0{,}192 \pm 0{,}022) \text{ мка}$$
$$r = 0{,}9998\,; \quad s_0 = \pm\, 0{,}025 \text{ мка}$$

$$X = o\text{--}NO_2 : \bar{i}_{np} = (3{,}210 \pm 0{,}082)\, C + (0{,}11 \pm 0{,}15) \text{ мка}$$
$$r = 0{,}9980\,; \; s_0 = \pm\, 0{,}17 \text{ мка}$$

$$X = m\text{--}NO_2 : \bar{i}_{np} = (3{,}523 \pm 0{,}022)\, C - (0{,}197 \pm 0{,}028) \text{ мка}$$
$$r = 0{,}9998\,; \; s_0 = \pm\, 0{,}033 \text{ мка}$$

$$X = n\text{--}NO_2 : \bar{i}_{np} = (3{,}\,408 \pm 0{,}059)\, C + (0{,}012 \pm 0{,}025) \text{ мка}$$
$$r = 0{,}9997\,; \quad s_0 = \pm\, 0{,}024 \text{ мка}$$

$$X = o\text{--}Cl : \bar{i}_{np} = (4{,}244 \pm 0{,}046)\, C + (0{,}095 \pm 0{,}043) \text{ мка}$$
$$r = 0{,}99990\,; \; s_0 = \pm\, 0{,}035 \text{ мка}$$

$$X = m\text{--}Cl : \bar{i}_{np} = (4{,}359 \pm 0{,}046)\, C - (0{,}011 \pm 0{,}023) \text{ мка}$$
$$r = 0{,}09995\,; \; s_0 = \pm\, 0{,}034 \text{ мка}$$

$$X = n\text{--}Cl : \bar{i}_{np} = (4{,}880 \pm 0{,}075)\, C - (0{,}068 \pm 0{,}038) \text{ мка}$$
$$r = 0{,}9990\,; \quad s_0 = \pm\, 0{,}026 \text{ мка}$$

$$X = m\text{--}Br : \bar{i}_{np} = (3{,}441 \pm 0{,}074)\, C + (0{,}027 \pm 0{,}031) \text{ мка}$$
$$r = 0{,}9998\,; \; s_0 = \pm\, 0{,}020 \text{ мка}$$

$$X = n\text{--}Br : \bar{i}_{np} = (4{,}58 \pm 0{,}14)\, C - (0{,}044 \pm 0{,}076) \text{ мка}$$
$$r = 0{,}9985\,; \; s_0 = \pm\, 0{,}073 \text{ мка}$$

$$X = o\text{—}CH_3 : \bar{i}_{пр} = (4{,}31 \pm 0{,}16)\,C - (0{,}04 \pm 0{,}10) \text{ мка}$$
$$r = 0{,}9985\,; \; s_0 = \pm\, 0{,}11 \text{ мка}$$

$$X = n\text{—}CH_3 : \bar{i}_{пр} = (0{,}469 \pm 0{,}052)C - (0{,}045 \pm 0{,}022) \text{ мка}$$
$$r = 0{,}9995\,; \quad s_0 = \pm\, 0{,}024 \text{ мка}$$

$$X = n\text{—}OCH_3 : \bar{i}_{пр} = (4{,}244 \pm 0{,}086)\,C + (0{,}029 \pm 0{,}080) \text{ мка}$$
$$r = 0{,}9990\,; \; s_0 = \pm\, 0{,}095 \text{ мка}$$

Из вышепредставленных уравнений следует приложимость уравнения Илковича, в выбранных экспериментальных условиях, позволяя количественно определить перэфиры, так вычислительным, как графическим методом. Средняя относительная ошибка определений характерна полярографическому методу и не превышает предел в ±2—3%. Интервал приложимости уравнения Илковича зависит от конкретного члена серии, мало изменяясь при вариации концентраций спирта в фоне. В табл. 4 показаны значения константы Илковича (*ϰ*) в зависимости от состава растворителя и интервал действительности упомянутого уравнения.

Линейность корреляции предельный ток — концентрация подтверждает доминирующий диффузионный характер полярографического тока, по сравнению с адсорбционным характером, в данных экспериментальных условиях. При бо́льших концентрациях, эта корреляция теряет свою линейность и — соответственно ожиданию — форма кривых напоминает аллюр адсорбционной изотермы (напр. рис. 4).

Таблица 4

Значение константы Илковича ϰ (ма/моль) в зависимости от концентрации этилового спирта в фоне, при полярографировании серии $X—C_6H_4—COOOC(CH_3)_3$

X	Концентрация этилового спирта (%)						Диапазон действительности (M)
	10	20	30	50	70	90	
H	6,37	6,17	5,90	5,76	4,92	6,18	$10^{-4}-10^{-2}$
$n-NO_2$		3,41	3,02	3,12	3,22	3,34	$10^{-4}-7\cdot10^{-4}$
$м-NO_2$	3,55	3,52	3,34	3,02	3,40	3,53	$10^{-4}-2.10^{-3}$
$o-NO_2$	3,29	3,21	3,00	2,96	3,17	3,24	$10^{-4}-3.10^{-3}$
$n-Cl$		4,88	4,79	4,46	4,93	5,00	$10^{-4}-8.10^{-4}$
$м-Cl$	4,36	4,36	4,36	3,99	4,57	4,60	$10^{-4}-10^{-3}$
$o-Cl$	3,93	4,24	4,78	4,55	5,13	5,30	$10^{-4}-10^{-3}$
$n-Br$	4,92	4,58	4,80	4,44	5,27	5,37	$10^{-4}-10^{-3}$
$м-Br$		3,44	3,68	3,42	3,77	3,85	$10^{-4}-7\cdot10^{-4}$
$n-CH_3$	3,30	3,47	3,16	3,16	3,30	3,37	$10^{-4}-10^{-3}$
$o-CH_3$	4,02	4,31	4,17	4,02	4,38	4,43	$10^{-4}-10^{-3}$
$n-OCH_3$	4,61	4,24	4,06	3,76	4,32	4,40	$10^{-4}-2.10^{-3}$

Потенциал полуволны почти независим от концентрации перекисей. Эта независимость позволяет делать некоторые выводы о кинетике и механизме электродного процесса.[47] Эта проблема будет представлять предмет наших следующих сообщений.

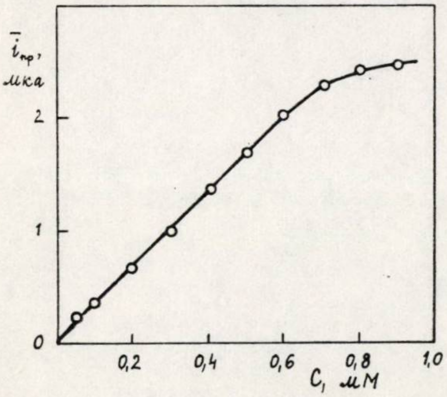

Рис. 4. — Изменение силы тока в зависимости от концентрации перэфира

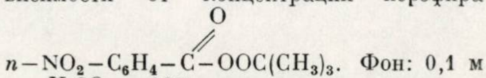
$n\text{-}NO_2-C_6H_4-\overset{O}{\overset{/\!\!/}{C}}-OOC(CH_3)_3$. Фон: 0,1 м H_2SO_4 в 20%-ном этиловом спирте.

ВЫВОДЫ

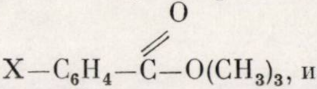

1. На основании изучения влияния различных факторов (растворитель, характеристики капилляра, высота ртутного столба, температура, концентрация деполяризатора) на полярографическое поведение перэфиров типа $X-C_6H_4-\overset{O}{\overset{/\!\!/}{C}}-O(CH_3)_3$, из значения и изменения параметров полярографической волны, делялись некоторые заключения о природе тока и обратимости электродного процесса, в данных экспериментальных условиях. Было показано, что в транспортном процессе доминирует диффузия, а электродная реакция необратима.

2. Были выбраны оптимальные условия полярографического качественного и количественного анализа изученных перекисей, при котором проверялась линейность корреляции предельный ток — концентрация, согласно уравнению Илковича. В качестве фона рекомендуется 0,1 м H_2SO_4 в 20%-ном этиловом спирте, в котором получились наилучшие волны.

---

[47] B. TOKES, Teză de doctorat, Univ. Babeș-Bolyai, Cluj, 1970.

Revue Roumaine de Chimie, **23**, *5*, 819–824 (1978)

SPECTROPHOTOMETRICAL STUDIES OF THE KINETICS OF THE CONVERSION OF FERROCYANIDE TO FERRICYANIDE IN THE PRESENCE OF HYDROGEN PEROXIDE

K. K. GIRDHAR
Department of Chemistry and Biochemistry, Haryana
Agricultural University, Hissar — 125004 (India)

Received September 17, 1975
Completed December 22, 1977

The kinetics of the conversion of ferrocyanide to ferricyanide in the presence of hydrogen peroxide has been studied spectrophotometrically at 4200 A° in the pH range 6.0—8.0 and at different concentrations of hydrogen peroxide and ferrocyanide. A compensating oxidation-reduction type of mechanism involving free radicals has been suggested. Overall the reaction is of second order. It is first order in each hydrogen peroxide and ferrocyanide.

INTRODUCTION

The kinetics of the oxidation reduction reactions involving hydrogen peroxide has been the subject of a large number of studies.[1-2] These systems have been exploited to provide some insight into the mechanism of a rather large body of redox reactions. Interest in radiation chemistry of aqueous solutions where hydrogen peroxide is one of the products and the use of acidic ferrous sulphate solutions as dosimeter in these studies have particularly stimulated[1-4] the investigation of the kinetics of the decomposition of hydrogen peroxide in the presence of Fe^{+2}, Fe^{+3} and their complexes. Recent studies[5-7,13] have shown the possibility of using the aqueous solutions of ferro-and ferricyanides over a range of pH as dosimeter. However, the kinetic studies of the reactions of hydrogen pero-

---

[1] J. H. Baxendale, *Adv. in Catalysis*, **4,** 31 (1952).

[2] J. Weiss, *Adv. in Catalysis*, **4,** 343 (1952).

[3] W. C. Schumb, C. N. Satterfield and R. L. Wantworth, "Hydrogen Peroxide", Reinhold Publishing Corporation, New Delhi, 1955.

[4] J. W. Spinks and R. J. Woods, "An Introduction to Radiation Chemistry", Wiley Inc., New York, 1964.

[5] X. Tarrago, E. Masri and M. Lefort, *Compt. rend*, **244,** 343 (1957).

[6] G. Czapski, J. Rabani and G. Stein, *Trans. Faraday Soc.*, **58,** 2160 (1962).

[7] J. Rabani and G. Stein, *Trans. Faraday Soc.*, **58**. 2150 (1962).

[8] G. Hughes and C. Willis, *J. Chem. Soc. Part IV*, **1962,** 4848.

[9] E. Masri and M. Haisainsky, *J. Chim· Phys.*, **60,** 397 (1963).

[10] G. Hughes and C. Willis, *Discuss. Faraday Soc.*, **36,** 223 (1963).

[11] G. E. Adams, J. W. Boag and B. D. Michael, *Trans. Faraday Soc.*, **61,** 492 (1965).

[12] E. Hayon, *Trans. Faraday Soc.*, **61,** 734 (1965).

[13] J. Rabani and M. S. Matheson, *J. Phys. Chem.*, **70,** 761 (1966).

xide are quite fragmentary.[14–19] The present work was undertaken to study the kinetics of the conversion of ferrocyanide to ferricyanide in the presence of hydrogen peroxide spectrophotometrically.

EXPERIMENTAL

Chemicals. Hydrogen peroxide used was of S. Merck quality. The stabilizers were destroyed by irradiating the sample with unfiltered ultra-violet light for about 10 minutes. All other chemicals used were of BDH, AnalaR quality and were recrystallised before use.

Procedure. Buffer solutions between pH 6 and 8 were prepared from stock solution of disodium hydrogen phosphate and sodium dihydrogen phosphate and their pH was checked with the standard pH meter (Phillip battery Model No. RR−9401).

The system ferro-ferricyanide and hydrogen peroxide is ideal for spectrophotometric studies, as ferrocyanide almost does not absorb at 4200 A° whereas ferricyanide has a large extinction co-efficient ($\varepsilon \approx 1020$). Therefore, to determine how these are interconverted in the presence of hydrogen peroxide, spectrophotometric method was used. The instrument used is Carl Zeiss Spekol 262705.

For low concentration of the reactants, the rates of reactions were not so fast and mixing of the reactants could be done by transferring directly one of the reactants into the other by means of wide mouth-vessels with efficient stirring. However, at higher concentrations the rates being quite fast, these spectrophotometric studies were restricted to lower concentrations. By doing so, mixing could be done in less than two seconds. As the light affected the rate of the reaction, the spectrophotometric cell was exposed only for measurements and then removed immediately to area protected from light. Moreover, fresh reaction mixture was taken after 2 or 3 exposures. Optical densities were recorded at 4 200 A° against time in the pH range 6.0−8.0. The rate constant was calculated and the values of the rate constant at different concentrations of the reactants, pH and temperature, thus determined are given in table 1.

Table 1

Second order Rate Constant under different experimental conditions

Temperature	Conc. of $H_2O_2 \times 10^3$ mole litre^{-1}	Conc. of $Fe(CN_6)^{-4} \times 10^3$ mole litre^{-1}	$R \times 10^6$ mole litre^{-1} sec^{-1}	$R/(H_2O_2)(Fe(CN)^{-4}_6)$ litre mole^{-1} sec^{-1}
		pH = 6.0		
30°	4.0	0.2	0.37	0.46
	1.0	0.2	1.20	0.60
	0.8	1.0	0.41	0,51
	0.5	8.0	1.76	0.44
	0.4	1.0	0.22	0.55
	0.1	8.0	0.47	0.59
	0.1	4.0	0.23	0.58
			Mean	0.53±0.06

[14] W. Kistiakowsky, *Z. phys. Chem.*, **35,** 431 (1900).

[15] B. B. Lal and C. P. Singhal, *Current Science (India)*, **13,** 78 (1944).

[16] K. K. Girdhar and D. V. S. Jain, *J. Inorg. Nuclear Chem.*, **27,** 2653 (1965).

[17] D. V. S. Jain, K. K. Girdhar and I. P. S. Kong, *Indian J. Chem.*, **4,** 305 (1966).

[18] K. K. Girdhar, *Chem. Era*, **11,** 33 (1975).

[19] K. K. Girdhar, *J. Chinese Chem. Soc.* **23,** 233 (1976).

Table 1 *(continued)*

Temperature	Conc. of $H_2O_2 \times 10^3$ mole litre^{-1}	Conc. of $Fe(CN)_6^{-4} \times 10^3$ mole litre^{-1}	$R \times 10^6$ mole litre^{-1} sec^{-1}	$R/(H_2O_2)(Fe(CN)_6^{-4})$ litre mole^{-1} sec^{-1}
25°	2.0	1.0	0.61	0.31
	1.0	1.0	0.37	0.37
	0.8	1.0	0.33	0.41
	0.5	8.0	1.57	0.39
	0.5	4.0	0.97	0.49
	0.5	2.0	0.43	0.43
	0.5	1.0	0.20	0.40
	0.4	1.0	0.17	0.43
	0.4	0.2	0.04	0.50
	0.2	1.0	0.09	0.45
	0.2	0.2	0.014	0.35
	0.1	2.0	0.09	0.45
	0.05	1.6	0.028	0.35
	0.05	8.0	0.15	0.38
			Mean	0.38±0.05
20°	2.73	1.62	1.13	0.26
	2.73	1.00	0.78	0.29
	2.73	0.40	0.38	0.35
	1.37	1.00	0.51	0.37
	0.55	1.00	1.30	0.24
			Mean	0.30±0.05
		pH=7.0		
30°	5.0	4.0	9.57	0.48
	5.0	2.0	3.80	0.38
	4.0	1.0	1.62	0.45
	1.0	1.0	0.44	0.44
	0.8	1.0	0.31	0.39
	0.5	4.0	0.67	0.34
	0.5	2.0	0.42	0.42
	0.1	8.0	0.41	0.51
	0.1	4.0	0.17	0.43
	0.2	1.0	0.09	0.45
			Mean	0.42±0.05
20°	4.0	1.0	0.88	0.22
	2.0	1.0	0.36	0.18
	0.8	1.0	0.16	0.20
	0.5	4.0	0.47	0.24
	0.5	2.0	0.27	0.27
	0.5	1.0	0.14	0.28
	0.4	1.0	0.07	0.18
	0.2	1.0	0.05	0.25
	0.05	4.0	0.04	0.20
	0.05	2.0	0.02	0.20
			Mean	0.22±0.03

Table 1 (continued)

Temperature	Conc. of $H_2O_2 \times 10^3$ mole litre^{-1}	Conc. of $Fe(CN)_6^{-4} \times 10^3$ mole litre^{-1}	$R \times 10^6$ mole litre^{-1} sec^{-1}	$R/(H_2O_2)(Fe(CN)_6^{-4})$ litre mole^{-1} sec^{-1}
	pH=8.0			
25°	1.65	0.33	0.26	0.48
	1.59	0.87	0.45	0.33
	0.44	0.98	0.18	0.42
	0.44	0.76	0.14	0.42
	0.44	0.36	0.08	0.51
			Mean	0.42±0.04
20°	4.0	1.0	0.88	0.22
	0.50	1.0	0.12	0.24
	0.50	4.0	0.47	0.24
	0.50	2.0	0.27	0.27
	0.50	1.0	0.14	0.28
	0.25	1.0	0.06	0.24
	0.13	1.0	0.04	0.31
			Mean	0.26±0.05

RESULTS AND DISCUSSION

In our earlier studies, it has been observed that aquapentacyanoferrate is not the active intermediate in the reaction of hydrogen peroxide with hexacyanoferrates.[18–19] Identical values of first order rate constants in hydrogen peroxide for same initial concentrations of either ferrocyanide or ferricyanide indicate that the catalysis is by compensating oxidation reduction type of mechanism.[18] The steady state ratio of the concentrations of ferrocyanide and ferricyanide seems to be established during very early stages of the reaction. Therefore, it was thought worthwhile to study the inter-conversion of ferrocyanide and ferricyanide in the presence of hydrogen peroxide.

Optical densities of two solutions (i) (ferrocyanide + hydrogen peroxide and (ii) ferricyanide + hydrogen peroxide) were recorded at 4200 Å against time and at pH 8.0, having initially the same concentrations of hydrogen peroxide and ferrocyanide or ferricyanide (Figure 1). Optical density of the solution containing ferrocyanide initially starts with zero, then it rises rapidly and after a while levels off almost to a constant value of optical density. In the ferricyanide[20] solution the optical density starts from a maximum value and decreases rapidly in the beginning but levels off to the same value as in the case of ferrocyanide solution. This clearly shows that whether starting with the solution of ferrocyanide or ferricyanide, after reacting with hydrogen peroxide a stationary state is reached soon with definite ratio of the concentration of ferrocyanide and ferricyanide. At pH 6.0 or below solution under steady state contains mostly ferricyanide and above pH 8.0, it contains mostly ferrocyanide. Therefore, these studies are carried out in the pH range, 6.0–8.0 only.

---

[20] K. K. Girdhar, *Chem. Era*, **11**, 21, (1975).

The levelling off the curves for optical density (Figure 1) with time, gives strong indication that the reaction is taking place by the compensating oxidation reduction type of mechanism. The initial portions of the curves are of interest to obtain the rate constants. Therefore, these portions of the curves are studied in details. In a typical run the optical density was noted at different times and curve drawn was extraploted to zero time. The rate was determined at zero time and rate constant was calculated and found to be a second order. The values of these rate constants at different concentrations of the reactants, pH and temperature, thus determined are given in table 1. The last column in the table gives the value of the second order (first order in each hydrogen peroxide [18] and ferrocyanide) rate constant.

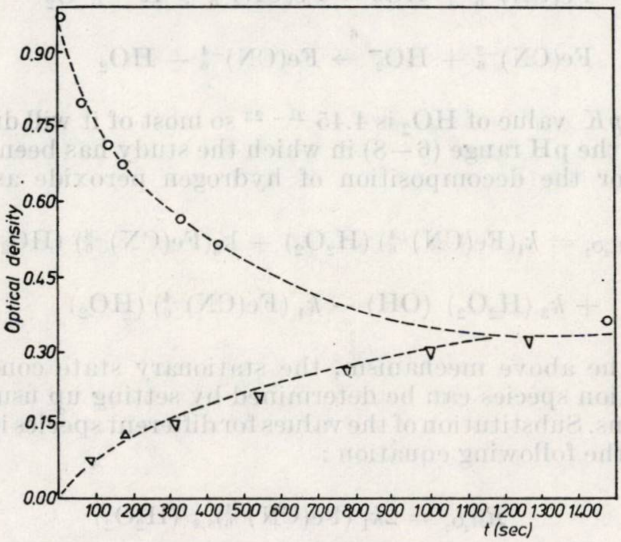

Fig. 1. – Plot between optical density and time

Temperature 20°C; pH 8.0; Conc. of $Fe(CN)_6^{-4}$ 1.0×10^{-3} mole litre^{-1}; Conc. of $Fe(CN)_6^{-3}$ 1.0×10^{-3} mole litre^{-1}; Conc. of H_2O_2 0.5×10^{-3} mole litre^{-1}.

At higher concentrations of hydrogen peroxide (at 10^{-2} mole/litre and above) decrease in the values of second order rate constants was observed for the reaction. This is due to secondary reactions which become important even on small conversions of the hexacyanoferrates at higher concentrations of hydrogen peroxide.

On these basis, it can be concluded that the reaction of hydrogen peroxide with ferro- and ferricyanide takes place through compensating oxidation reduction type of mechanism as given below: [18]

$$Fe(CN)_6^{-4} + H_2O_2 \xrightarrow{1} Fe(CN)_6^{-3} + OH + OH^-$$

$$Fe(CN)_6^{-4} + OH \xrightarrow{2} Fe(CN)_6^{-3} + OH^-$$

$$H_2O_2 + OH \xrightarrow{3} H_2O + HO_2$$

$$Fe(CN)_6^{-4} + HO_2 \xrightarrow{4} Fe(CN)_6^{-3} + HO_2^-$$

$$Fe(CN)_6^{-3} + HO_2 \xrightarrow{5} Fe(CN)_6^{-4} + H^+ + O_2$$

$$Fe(CN)_6^{-3} + HO_2^- \xrightarrow{6} Fe(CN)_6^{-4} + HO_2$$

As the pK value of HO_2 is 4.45 [21-23] so most of it will dissociate into $H^+ + O_2^-$ in the pH range (6—8) in which the study has been carried out. The $R_{H_2O_2}$, for the decomposition of hydrogen peroxide as given by :

$$R_{H_2O_2} = k_1(Fe(CN)_6^{-4})\,(H_2O_2) + k_6(Fe(CN)_6^{-3})\,(HO_2^-)$$
$$+ k_3\,(H_2O_2)\,(OH) - k_4\,(Fe(CN)_6^{-4})\,(HO_2) \qquad (1)$$

From the above mechanism, the stationary state concentration of various reaction species can be determined by setting up usual stationary state equations. Substitution of the values for different species in equation (1) gives rise to the following equation :

$$R_{H_2O_2} = 2k_1\,(Fe(CN)_6^{-4})_{s,s}\;(H_2O_2) \qquad (2)$$

At higher concentration of hydrogen peroxide the equation (2) shows that the $(Fe(CN)_6^{-4})_{s.s}$ concentration is independent of the hydrogen peroxide concentration. If this fact is taken into account then equation for the rate of decomposition of hydrogen peroxide becomes first order in hydrogen peroxide which is in agreement with the data reported earlier. [18] This also clearly shows, at the initial stages, the reaction is of second order, first order in each hydrogen peroxide and ferrocyanide.

ACKNOWLEDGEMENTS. **The author expresses his sincere thanks and heart-felt gratitude to Dr. D.V.S. Jain, Reader in Physical Chemistry, Punjab University, Chandigarh, for his valuable suggestions and helpful criticism. Thanks are also due to Dr. A. D. Taneja, HAU, Hissar, for his help and cooperation.**

---

[21] G. CZAPSKI and B. H. J. BIELSKI, *J. Phys. Chem.*, **67,** 2180 (1963).

[22] G. CZAPSKI and L. M. DORFMAN, *J. Phys. Chem.*, **68,** 1169 (1964).

[23] J. RABANI, W. A. MULAC and M. S. MATHESON, *J. Phys. Chem.*, **69,** 53 (1965).

Revue Roumaine de Chimie, 23, 5, 825 (1978)

COMPTES RENDUS

* * * "Nomenclatura chimiei anorganice" (The Nomenclature of the inorganic chemistry), Academia Republicii Socialiste România, Secţia de Ştiinţe chimice, Colectivul de Nomenclatură chimică, 153 p.

This volume, the first of a large series, deals with the rules for "Nomenclature of Inorganic Chemistry" in a Romanian adaptation.

The work is based on the "1970 Rules" elaborated by the International Union of Pure and Applied Chemistry (IUPAC) and adapted to the Romanian language, by prof. dr. doc. eng. A. Balaban and dr. eng. D. Purdela.

The rules set put here are concerned with the nomenclature of the following inorganic fields : elements (section 1), compounds in general (section 2), ions and radicals (section 3), iso- and hetero-polyanions (section 4), acids (section 5), salts and salt-like compounds (section 6), coordination compounds (section 7), addition compounds (section 8), crystalline phases of variable composition (section 9), polymorphs (section 10) and boron compounds (section 11). Section (7) on coordination compounds is much extended, reflecting the importance of this field in modern inorganic chemistry.

The principale of an alphabetical order of ligands in coordination entities, the rules concerning the designation of ligand positions and the nomenclature of absolute configurations for six-coordonated complexes, based on the octahedron, were adopted.

The alphabetical principle mentioned in connection with section 7 is widely adopted in sections 2 and 6. The section on boron hydrides and their derivatives is also included, but in a reduced manner, while the section which deals with crystalline phases of variable composition is extended.

A preamble is introduced to make clear the precise meaning of some terms within the context of the formal rules.

The most important tables were placed together at the end of the rules and numbered ; an index is also added.

The special merit consists in the fact that this work is not a simple translation of the English or French versions. Certain names and rules appear as inacceptable to Romanian language ; in these cases, adaptation was necessary, but this was done, keeping the changes as small as possible and preserving the spirit of the IUPAC rules.

The purpose of this book is to introduce a uniform chemical nomenclature, in Romanian language, maintaining the spirit of the international model. It is recommended to the chemists from the industry, to the chemical workers and to the teachers and students, who are being trained in the chemical field.

Cristineta Mărculescu

R. J. COX (editor), "Photographic Gelatine, II", New York, Academic Press 1976, XIII + 390 p.

The book contains the proceedings of the third Symposium on photographic gelatine held at Gonville and Caius College and Little Hall, Cambridge, England, in September 1974, sponsored by the Scientific Committee of the Royal Photographic Society.

Gelatine still remains one of the basic raw components for the photographic materials ;. for this reason and for many others applications of this classical natural polymer, its study by physico-chemical methods and the attempt to improvement by different chemical and physical processes is highly opportune.

Twenty-four full papers and three abstracts of fifty-six authors from eight countries are presented in this volume.

Three papers cover the conditions of gelatine molecule itself, ten deal with the structure and properties of the gelatine gel, six outline the chemical properties of the gelatine and five the surface phenomena and crystal growth of silver halide. Only two papers are dealing with the total or partial substitution of gelatine with synthetic water -soluble polymers.

In all cases the papers are original contributions. The work is prefaced by D. L. Nellist and is concluded with a useful subject index.

Anica Ţolea

NOTE POUR LES AUTEURS

La Revue Roumaine de Chimie publie des articles en anglais, français, russe, allemand ou espagnol. Les auteurs sont priés d'envoyer des articles et des comptes rendus inédits.

Les manuscrits seront dactylographiés à deux intervalles. La bibliographie, les tableaux et la légende des figures seront placés après le texte.

Si l'article fait partie d'une série numérotée, le titre de la partie précédente sera indiqué dans une note au bas de la première page.

Chaque article sera précédé d'un résumé comprenant quinze lignes au maximum.

Les références bibliographiques dans le texte seront faites par des exposants sans parenthèse et paraîtront comme des notes au bas de chaque page.

Les publications périodiques mentionnées dans la bibliographie seront présentées suivant les prescriptions internationales : le nom de l'auteur précédé de l'initiale du prénom, le titre de périodique abbrégé conformément à « Chemical Abstracts » et souligné par une ligne, le numéro du tome, indiqué par des chiffres arabes et souligné par deux lignes, suivi de la première page de l'article ; à la fin, l'année de la parution sera placée entre parenthèses. Le numéro de la revue ne sera pas indiqué si les pages du volume sont numérotées consécutivement. Pour les revues dont les tomes ne sont pas numérotés (par ex. Bull. Soc. Chim. France, etc.), l'année de la parution soulignée par deux lignes précédera l'indication de la page.

Les textes des livres ou traités incluéront : les noms des auteurs, les initiales du prénom, le titre du livre entre guillemets et sans être souligné, le numéro du tome précédé par l'abbréviation « vol. » (ou « Bd. »), le numéro de l'édition, les éditions (the publisher), la localité de la parution et la page de la référence précédée par l'abbréviation « p. » (ou « S. »).

Les brevets seront indiqués comme suit : l'auteur ou la firme, le pays et le numéro du brevet, la date et la revue (Chem. Abstr.). Par ex. : M. Jones (to Union Carbide Co.), Brit. Pat. 601 238, 2 Sept. 1959, *Chem. Abstr.*, **54**, 12808 (1960).

Si la référence n'a pas été lue en original, on indiquera aussi la revue de références consultée.

Les diagrammes seront tracés à l'encre de Chine sur papier calque. Les tableaux et les figures (en nombre strictement nécessaire) seront numérotés par des chiffres arabes et leur explication sera donnée dans la légende des figures. Prière de ne pas inscrire les mêmes données dans les tableaux et les figures. Chaque tableau aura un titre. On indiquera dans le texte la place approximative des tableaux et des figures. Les formules chimiques seront incluses dans le texte ; en outre, elles seront transcrites sur papier calque, à l'encre de Chine.

Les auteurs sont priés d'indiquer les caractères italiques (en soulignant les lettres au crayon), ainsi que tout autre caractère spécial ; les préfixes *ortho, meta, para, cis, trans*, etc. seront soulignés pour indiquer leurs caractères italiques et ne seront jamais écrits avec des majuscules.

Aucune correction à la main ne sera admise sur le manuscrit. Les corrections seront frappées à la machine. Les lettres grecques ou d'autres symboles spéciaux seront insérés à la main à l'encre clairement.

Le manuscrit sera signé par l'auteur.

Le colonne-titre aura 50 lettres au maximum.

L'entière responsabilité du contenu des articles appartient aux auteurs.

1978 NOV 9

TRAVAUX PARUS AUX ÉDITIONS DE L'ACADÉMIE DE LA RÉPUBLIQUE SOCIALISTE DE ROUMANIE

I. ZUGRĂVESCU, MAGDA PETROVANU, **N-Ylid Chemistry**, 1977, 396 p., 19 lei.

C. DRĂGULESCU, E. PETROVICI, **Chimie structurală modernă. Chimia coordinanţei 8** (La chimie structurale moderne. La chimie de la coordinence 8), 1977, 947 p., 70 lei.

I. G. MURGULESCU, **Introducere în Chimia fizică. Vol. I. 1. Atomi, molecule, legătură chimică** (Introduction à la Chimie Physique, Ier vol. 1. Atomes, molécules, liaison chimique), 1976, 560 p., 36 lei.

E. P. BALTĂ, E. BALTĂ, **Introduction to the physical chemistry of the vitreous state**, coédition avec Abacus Press, 1976, 287 p., 31 lei.

H. I. GĂLĂŢEANU, **Radiochimia aplicată. Metode şi probleme** (La radiochimie appliquée. Méthodes et problèmes), 1976, 307 p., 19 lei.

CONST. V. UGLEA, **Cromatografia pe gel permeabil. Noi domenii de aplicare** (La chromatographie sur gel perméable. Nouveaux domaines d'application), 1976, 123 p., 6,75 lei.

FRANCISC A. GOTHARD, **Echilibre lichid-vapori. I. Baze teoretice şi metode de calcul** (Equilibres liquide-vapeurs. I. Bases théoriques et méthodes de calcul), 1975, 263 p., 2 pl., 28 lei.

CONST. GH. MACAROVICI, D. MACAROVICI, **Chimia oxizilor dubli şi utilizările lor** (La chimie des oxydes doubles et leur utilisation), 1975, 195 p., 13 lei.

M. AVRAM, **Antidăunători** (Pesticides), 1974, 496 p., 41 lei.

ELENA CEAUŞESCU, **Research work on synthesis and characterization of macromolecular compounds. Contributions**, 1974, 251 p., 20 lei.

DUMITRU COSTACHE, **Analiza chimică prin metoda cinetică** (L'Analyse chimique par la méthode cinétique), 1974, 251 p., 20 lei.

G. A. RĂDULESCU, **Proprietăţile ţiţeiurilor româneşti** (Les propriétés des pétroles roumains), 1974, 267 p., 2 pl., 18 lei.

CR. SIMIONESCU, VIORICA RUSAN, V. POPA, **Chimia algelor marine** (La chimie des algues marines), 1974, 212 p., 1 pl., 18 lei.

MARIA FITI, **Dozimetria chimică a radiaţiilor ionizante** (La dosimétrie chimique des radiations ionisantes), 1973, 240 p., 13,50 lei.

TIBERIU NĂŞCUŢIU, **Metode radiochimice de analiză** (Méthodes radiochimiques d'analyse), 1973, 384 p., 23 lei.

CRISTOFOR SIMIONESCU, MARGARETA GRIGORAŞ, AGATA CERNĂTESCU ASANDEI, GHEORGHE ROZMARIN, **Chimia lemnului în România. Plopul şi salcia** (La Chimie du bois en Roumanie. Le peuplier et le saule), 1973, 299 p., 13 pl., 26 lei.

MIHAI FLORESCU, **Eficienţa economică a cercetării ştiinţifice** (L'efficience économique de la recherche scientifique), 1972, 115 p., 15 lei.

GEORGETA LĂZĂRESCU, **Sistematizarea informaţiilor în chimia organică** (Systématisation des informations en Chimie organique), 1972, 243 p., 1 pl., 10,50 lei.

I. P. Informaţia c. 122

43 426

Lei 25.—
$45 (price per year)

F 1103

ACADÉMIE DE LA RÉPUBLIQUE SOCIALISTE DE ROU[illegible]

REFERÁLVA

REVUE ROUMAINE DE CHIMIE

66

TOME 23
N° 6
Juin 1978

EDITURA A[illegible]EMIEI REPUBLICII SOCIALISTE ROMÂNIA

Rev. Roumaine Chim. RECHAX, 23, *6*, p. 827–986 (1978), Bucarest

ACADÉMIE DE LA RÉPUBLIQUE SOCIALISTE DE ROUMANIE

COMITÉ DE RÉDACTION

Rédacteur en chef :

I. G. MURGULESCU, membre de l'Académie de la République Socialiste de Roumanie

Rédacteurs en chef adjoints :

A. T. BALABAN et V. EM. SAHINI, membres correspondants de l'Académie de la République Socialiste de Roumanie

Collège de rédaction :

EM. BRATU, ELENA CEAUŞESCU, ECATERINA CIORĂNESCU-NENITZESCU, C. DRĂGULESCU, CR. SIMIONESCU, membres de l'Académie de la République Socialiste de Roumanie ; P. SPACU, membre correspondant de l'Académie de la République Socialiste de Roumanie ; MARGARETA AVRAM, I. HAIDUC, D. I. MARCHIDAN, I. MOLDOVAN, G. NIAC et D. SĂNDULESCU

La Revue Roumaine de Chimie paraît 10 fois par an. Toute commande de l'étranger pour les travaux parus aux Editions de l'Académie de la République Socialiste de Roumanie sera adressée à ILEXIM, Departamentul Export-Import Carte (Livres)/Departamentul Export-Import Presă (Revues), P. O. B. 136—137, télex 11226, 3, str, 13 Decembrie, 70116 Bucarest, Roumanie

Les manuscrits, les livres et les revues proposés en échange, ainsi que toute correspondance seront envoyés à la rédaction :

REVUE ROUMAINE DE CHIMIE

125, Calea Victoriei, 71021 Bucarest, Roumanie, téléphone 50 76 80

EDITURA ACADEMIEI REPUBLICII SOCIALISTE ROMÂNIA

125, Calea Victoriei, 71021, Bucarest, Roumanie, téléphone 50 76 80

ORSZÁGOS MŰSZAKI KÖNYVTÁR ÉS DOKUMENTÁCIÓS KÖZPONT

REVUE ROUMAINE DE CHIMIE

Tome, 23, N° 6 Juin 1978

ȘTEFANIA ZUCA, Electrical conductivity and the structure of binary molten alkali halide mixtures 829–833

LUCIA ODOCHIAN and I. A. SCHNEIDER, Some remarks on the heterogeneous character of the low temperature cracking of methane in silica vessels 835–840

S. SENENT, F. MATA and M. A. de la PEÑA, Kinetic study of the oxidation of tertiary amines by permanganate 841–852

LUCIA CIOHODARU, C. C. RENŢIA and I. ZAMFIRESCU, Electronic structure of some stilbene derivatives. VII. MO-LCI-PPP calculations for some polynitro-*trans*-stilbene derivatives 853–859

VALENTINA LĂZĂRESCU and M. F. LĂZĂRESCU, Highly pure gallium obtained by a simple technique 861–864

D. A. ISĂCESCU and FLORENTINA AVRAMESCU, Reaction mechanism for the condensation of furfural with acetone in the catalysis of sodium hydroxide. II. The activated complex and its catalytic action 865–871

D. A. ISĂCESCU and FLORENTINA AVRAMESCU, Reaction mechanism for the condensation of furfural with acetone in the catalysis of sodium hydroxide. III. Solvent influence on the nature of the activated complex and on its catalytic action 873–881

E. BEŁTOWSKA-LEHMAN and A. RIESENKAMPF, Conditions of electrodeposition as a factor influencing the properties of Ni—Fe thin films 883–885

F. THÉOBALD, Oxides and oxide hydrates of vanadium in IV, V and intermediate oxidation state 887–908

MARIA BREZEANU and IOANA JITARU, Nickel (II) coordination compounds with 3-amino-1-propanol 909–915

F. MÁNOK and CS. VÁRHELYI, On the α-dioximine complexes of transition metals. LVI. Some aspects of the polarographic behaviour of the azido-bis-dimethylglyoximine complexes of cobalt (III) 917–920

O. MANTSCH and MARGARETA BUCHWALD, 16α-Methyl Reichstein S 21-acetate from 16-dehydropregnenolone acetate 921–928

L. ROMAN, EUGENIA FLOREAN, MARIA ECHIM-GROSU and EMILIA DORDEA, Study of the reaction between Pb(II) and 5-mercapto-2- amino-1,3,4-thiadiazole. Analytical applications 929–933

A. M. KHALIL, A. A. FADDA and M. M. YOUSIF, The action of aryl-amines on 3-aryl-5-arylmethylenerhodanines 935–941

Rev. Roumaine Chim. **23**, *6*, p. 827–986 (1978) Bucarest

AGLAIA CIOBANU, N. LUCHIAN and VIORICA HAMCIUC, Cyclic organosilicon compounds. Reaction of 1,4-dilithium-1,1,4,4-tetraphenylbutane with organodichlorosilanes 943–950

R I. PETRARIU, LILIANA MONA NEAGU, CORNELIA LUCA, IG. POINESCU and PAMFILIA PETRARIU, Degradation of anion exchangers in agressive medium. V. Effect of hydroxyl ions in the presence of ferric chloride on chemical stability of type I macroporous anion exchangers 951–957

CORNELIA IDIŢOIU and D. AIKENS, Cyclic voltammetry determination of α,α'-dimethylphenyl hydroperoxide 959–965

T. CONSTANTINESCU, ŞTEFANIA ENACHE and R. VASILIEV, Microreactions combined with thin-layer chromatography for the identification of phenothiazine drugs 967–975

C. TĂRĂBĂŞANU-MIHĂILĂ, F. URSEANU, L. FLORU and B. MĂRCULESCU, Heterocyclic compact condensed systems. III. Isomer 9-aminothiazolo[4,5-f]indazole 977–983

COMPTES RENDUS 983–986

Revue Roumaine de Chimie, **23**, *6*, 829–833 (1978)

ELECTRICAL CONDUCTIVITY AND THE STRUCTURE OF BINARY MOLTEN ALKALI HALIDE MIXTURES

ŞTEFANIA ZUCA

Institute of Physical Chemistry, 31, str. Galaţi, Bucharest, Romania

Received December 19, 1976

The electrical conductivity-composition curves in binary molten alkali halide systems with a common ion were discussed in terms of ionic interactions occurring on mixing. It was concluded that the main hindrance in electrical transport in the mixtures depends directly on the nature of the two substituting uncommon ions. It is due to the coulombic interactions in the mixtures with a common cation and to the polarizing effect in those with a common anion. For each of the two studied classes, proper quantitative relationships, $\Delta\lambda$ – distance parameter, were established.

The electrical conductivity of fused alkali halide mixtures was systematically investigated in our laboratory[1–4], both from the theoretical viewpoint of wishing to gain a clearer insight into the behaviour of these liquid mixtures, and from the practical standpoint of wanting to be able to predict the electrical conductivity of fused salt mixtures from the properties of the pure components.

The experimental results obtained in the twelve alkali halide mixtures with a common cation[1,2] and thirty alkali halide mixtures with a common anion[3,4] indicated for equivalent conductivity isotherms systematic negative deviations from additivity. If the obtained $\Delta\lambda$ values were plotted against compositions, the following general trend was noted[1–4]:

— for both kind of mixtures, the $\Delta\lambda$ values increase as the difference between the two uncommon ion radii is larger. Relied on this, we tried to establish in the above named mixtures, some quantitative relationships, $\Delta\lambda$ — distance parameter.

Present paper is concerned with a more comprehensive discussion on this line.

---

[1] S. Zuca and L. Ionescu-Vasu, *Rev. Roumaine Chim.*, **12**, 1285 (1967).

[2] S. Zuca and M. Olteanu, *Rev. Roumaine Chim.*, **13**, 1567 (1968).

[3] S. Zuca and M. Olteanu, *Rev. Roumaine Chimie.*, **15**, 357 (1970).

[4] S. Zuca and M. Olteanu, to be published.

DISCUSSIONS

Many attempts were made by different authors in order to correlate the excess conductivity with the distance parameter. A linear dependence was observed in binary molten nitrate mixtures[5] when $\Delta\lambda$ was plotted against $\frac{d_1 - d_2}{d_1 + d_2}$ so called Tobolsky parameter; for alkali — alkaline earth mixtures, Emons et al.[6,7] used a distance parameter defined as $\frac{d_1 - d_2}{d_1 d_2}$ and more recently we tried[8] to extend the Davis plot for the excess conductivity data in the same class of mixtures, (d_1 and d_2 stand for the interionic separation in single salts).

In order to establish a quantitative correlation in terms of distance parameter in the binary alkali halide mixtures, we have considered the two predominant ionic interactions on mixing: the coulombic interactions between the next nearest neighbours and the polarization of the common anion due to the changes in the cation environment. The change in the cation — cation repulsion on mixing, for a linear group BAC was calculated by Førland as[9,10]:

$$E_c = -e^2 \frac{(d_{AB} - d_{AC})^2}{d_{AB} d_{AC}(d_{AB} + d_{AC})} \qquad (1)$$

According to Lumsden[11,12], the polarization of a linear group BAC is given by:

$$E_p = -\frac{e^2\alpha}{2}\left[\frac{1}{d_{AB}^2} - \frac{1}{d_{AC}^2}\right]^2 \qquad (2)$$

where α is the polarizability of common anion. The polarization occurs because the common anion is subjected to an unsymmetrical electric field, due to the different sizes of the two cations on the opposite sides of the anion.

When $\Delta\lambda$ values were plotted against these two parameters, it could be seen that:

— in binary alkali halide systems with a common cation there is a good proportionality to the coulombic factor but practically no correlation was found with the polarization factor. Figure 1 exemplifies the data for equimolecular mixtures. It is obvious from Figure 1, that within

---

[5] B. de Nooiyer and I.A.A, Ketelaan, *Rec. Trav. Chim.*, **83**, 263 (1964).

[6] H. H. Emons, G. Brautigam and H. Vogt, *Z. anorg. Chem.*, **394**, 263 (1972).

[7] H. Vogt, Thesis, Merseburg, 1971.

[8] S. Zuca and M. Olteanu, *Rev. Roumaine Chim.*, **4**, 449 (1975).

[9] T. Førland, *J. Phys. Chem.*, **59**, 152 (1955).

[10] T. Førland, *Norg. Tekn. Viten Skapakad*, **2**, 4 (1961).

[11] J. Lumsden, *Discuss. Faraday Soc.*, **32**, 138 (1961).

[12] J. Lumsden, "Thermodynamics of Molten Salt Mixtures", Academic Press, London, 1966, p. 70.

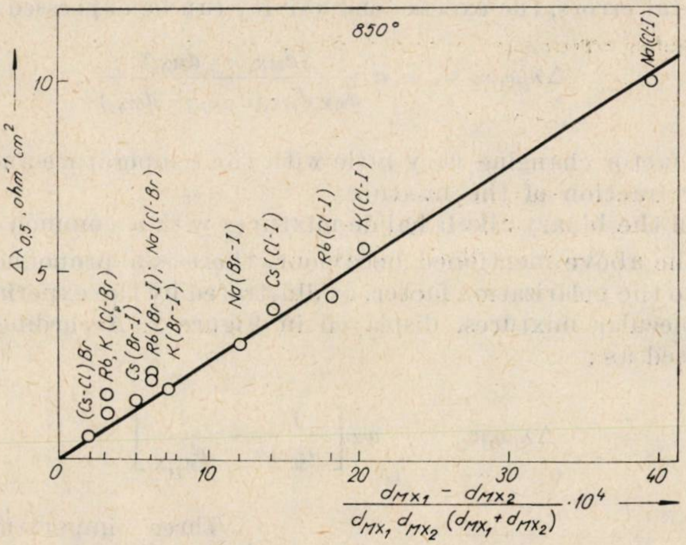

Fig. 1. — $\Delta\lambda_{0.5}$ vs. coulombic factor plot in binary alkali halide mixtures with common cation.

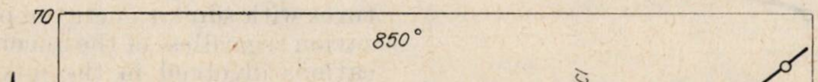

Fig. 2. — $\Delta\lambda_{0.5}$vs. polarization factor plot in binary alkali halide mixtures with common anion.

experimental errors, the excess conductivity can be expressed as :

$$\Delta\lambda/x_1x_2 = -a\frac{(d_{\mathrm{MX}_1} - d_{\mathrm{MX}_2})}{d_{\mathrm{MX}_1}d_{\mathrm{MX}_2}(d_{\mathrm{MX}_1} + d_{\mathrm{MX}_2})} \tag{3}$$

a being a factor changing very little with the temperature and x_1 and x_2, the molar fraction of the mixture.

— in the binary alkali halide mixtures with a common anion, contrary to the above mentioned behaviour, there is a pronounced proportionality to the polarization factor, as illustrated by the experimental data in equimolecular mixtures, displayed in Figure 2. Accordingly, $\Delta\lambda$ can be expressed as :

$$\Delta\lambda/x_1x_2 = -a\alpha\left[\frac{1}{d^2_{\mathrm{M_I X}}} - \frac{1}{d^2_{\mathrm{M_{II} X}}}\right]^2 \tag{4}$$

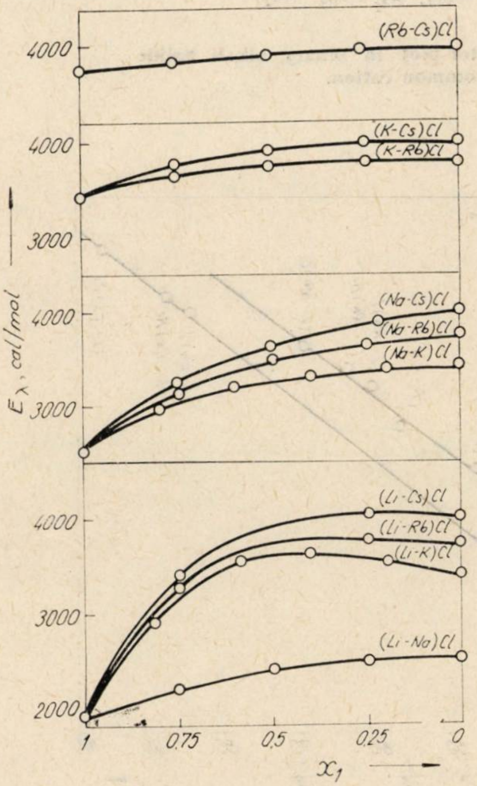

Fig. 3.—E_λ plotted against mole fraction in binary alkali chloride systems.

Three important features with this plot should be noted : 1) $\Delta\lambda$ is increasing as the difference in the polarizing strength of ions ($1/d^2$) is larger ; 2) $\Delta\lambda$'s are equal with each other within the experimental errors, for the mixtures with similar energy of polarization regardless of the uncommon cations involved in the mixture; 3) $\Delta\lambda$ is zero when the substituting cations have a similar polarizing strength, and the system is expected to behave ideally. All these facts can be satisfactorily explained by Lumsden model[11,12].

A special remark concerning (Li—Cs)X and (Na—Cs)X systems is worth to be made here. As seen in the figure, these mixtures must be looked upon as the most noticeable exception as they take a special position in the series. A possible explanation for this behaviour may lie in the fact that the differences between the two uncommon cations are now extremely large (the differences in the Pauling radii are of 0.97Å and of 0.68Å respectively). Thus it is possible that the ionic interactions intensify to such an extent that the simple competitive interionic attractions and the simple associated cation — anion groups are replaced by closer packing formations.

If changes in relative mobility of the ions are to be attributed to the change in the cation — anion bonding energy[11,12] it is reasonable to expect a corresponding change in the activation energy for the electrical conductivity. A plot of E_λ vs. mole fraction, Figure 3, shows indeed the activation energy of the mixtures to be always higher than the one calculated additively. Moreover, the increase of the excess energy follow the development observed for $\Delta\lambda$.

Nevertheless, all the above mentioned results, allow us to conclude that the main hindrance to the electrical transport in binary molten alkali halide systems depends directly on the nature of the uncommon ions in the mixtures. It is due to the coulombic interactions in the mixtures with a common cation and to the polarizing effect in the mixtures with a common anion.

sity to such an extent that the simple competitive interionic transitions and the simple associated cation–anion groups are replaced by closer packing formations.

If changes in relative mobility of the ions are to be ascribed to the change in the extent of [illegible] energy,[illegible] it is reasonable to expect a corresponding change in the activation energy for the electrical conductivity. A plot of E_κ [illegible] from Figure 3, shows indeed the activation energy of the mixtures to be always higher than the one calculated additively. Moreover, the increase of the excess energy follow the development observed for Δ[illegible].

Nevertheless, all the above mentioned results allow us to conclude that the main tendency to the electrical transport in binary molten alkali halide systems depends strongly on the nature of the interaction forces in the mixtures. It is due to the coulombic interactions in the mixtures with a common cation and to the polarization effect in the mixtures with a common anion.

Revue Roumaine de Chimie, **23**, *6*, 835–840 (1978)

SOME REMARKS ON THE HETEROGENEOUS CHARACTER OF THE LOW TEMPERATURE CRACKING OF METHANE IN SILICA VESSELS

LUCIA ODOCHIAN and I. A. SCHNEIDER
Department of Physical Chemistry, Politehnic Institute, Splai Bahlui nr. 71, 6600-Iassy, Romania

Received March 29, 1976

The low temperature thermal degradation of methane (640–670°) in silica vessels shows an important dependence of the overall reaction rate on the reaction pressure and the formed coal deposit, suggesting a pronounced heterogenous character.

In an earlier work[1] about the thermal destruction of methane in a flow system at atmospheric pressure and 1280°K, we were able to show that in the initial stages of the reaction there exists a serious accelerating influence of the silica reactor surface/volum ratio on the rate of hydrogen formation, the main product of the cracking process. However at higher conversion degrees, a retarding effect seems to act too, being also the more important as the surface/volum ratio of the reactor vessel is higher.

Consequently we undertake to examine more detailed these fenomena, studying the thermal destruction of methane in a closed system at lower temperatures, using the apparature described minutely elsewhere.[2]

Taking into account that the overall reaction of ethane formation :

$$2CH_4 \rightarrow C_2H_6 + H_2$$

proceeds without a modification of the mol number, while the ethylene and acethylene formation are accompanied by a rise of the mol number, we wanted to test that in these conditions, ethane is the primary intermediate of the chain dehydrogenation of methane. Thus besides the pressure rise, we also measured the change of the overall thermal conductivity of the system, taking into account the much higher thermal conductivity of the main product, hydrogen.

The only disadvantage of this latter method is the impossibility to evaluate absolute reaction rates, because of the difficulties in calibration.

---

[1] I. Iosif and I. A. Schneider, *Z. phys. Chem.* (*Leipzig*), **237**, 81 (1968).
[2] L. Odochian and I. A. Schneider *Rev. Roumaine Chim.*, **15**, 1647 (1970).

The modifications of both pressure and thermal conductivity during the cracking process were recorded. The obtained curves (Figure 1) show an appreciable difference between the induction periods measured by the manometric and by the thermal conductivity method, the latter being much shorter, and therefore confirming our above supposition.

To obtain an additional evidence that ethane is surely the only primary intermediate, we examined the thermal degradation of methane also in an open system, applying the reaction conditions in which the induction period could be observed only by the thermal conductivity method.

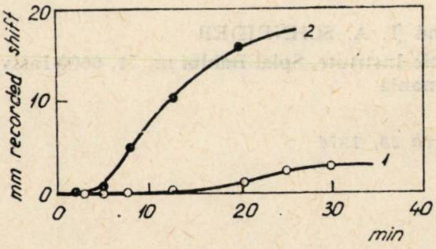

Fig. 1. — Typical conversion curves for the methane degradation at 670° and initial pressure of 65 mmHg recorded by measuring the modification of the overall thermal conductivity (2) and pressure (1).

The corresponding chromatograms obtained on a Carlo Erba Gas-chromatograph G.B. with thermal conductivity detector, using argon as carrier and colums with silicagel, indicate that in these conditions ethane and hydrogen are the only detectable products, formed roughly in echimolecular amounts (see table 1) and this supports the hypothesis that ethane is the primary intermediate.

We mention to have used natural methane of $99.8^{0}/_{0}$ purity, as estabilished also by gas chromatography.

In the closed system, the experimental data concerning the methane cracking in new silica vessels (of 225 cm^3 and a S/V ratio of 1.22 cm^{-1}) as shown in Figure 2 were reproducible only after the reactor was coated by at least nine repeated experiments in constant conditions, burning the deposited carbon black after each experiment, by heating the reactor for 2—3 hours to more than 1000° in the presence of air.

Table 1

The composition of the reaction products of methane cracking in initial stages

CH$_4$ %	H$_2$ %	C$_2$H$_6$ %
99.71	0.046	0.036
99.71	0.037	0.053
99.71	0.042	0.048
99.70	0.050	0.050
99.70	0.049	0.051
99.68	0.065	0.069
99.66	0.069	0.067

The reproducibility of the results in the silica vessels coated in this manner could be preserved, regardless of the subsequent reaction conditions, if the deposited carbon black were always burned.

The thermal destruction of methane in the coated silica vessels at 640, 670 and 700° and at pressures ranging from 30 to 760 mmHg shows a serious dependence of the overall initial reaction rates on the used pressures as seen in Figure 3.

The modification in the slope of the curves obtained suggests also a change of the overall reaction order. The drop of the overall order at lower pressures may be explained by a possible increasing initiation on the reactor wall indicating a partially heterogeneous character of the cracking process.

In addition we observed a decrease of the reaction rate during the degradation process, beginning with higher transformation degrees.

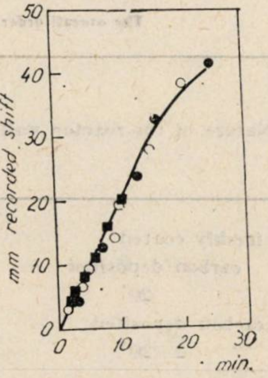

Fig. 2.— Reproducibility of the experimental data in the same working conditions (temperature 670° ; initial pressure 210 mmHg)

(The initial rate was measured by the thermal conductivity method)

○ — exp. no 7 ; ■ — exp. no. 9 ; ● — exp. no.41

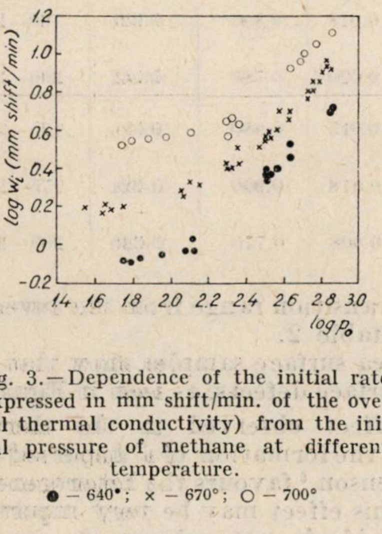

Fig. 3.—Dependence of the initial rate (expressed in mm shift/min. of the overall thermal conductivity) from the initial pressure of methane at different temperature.

● — 640° ; × — 670° ; ○ — 700°

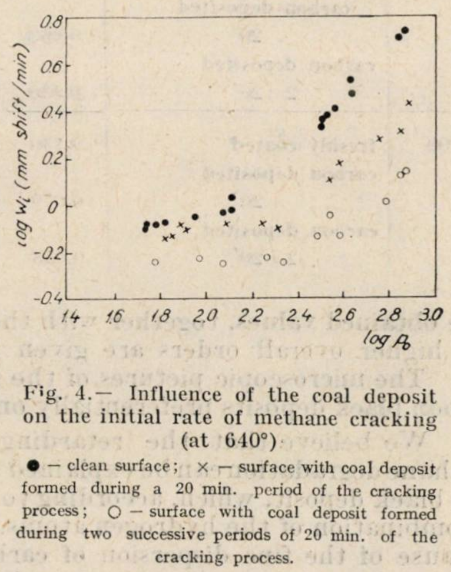

Fig. 4.— Influence of the coal deposit on the initial rate of methane cracking (at 640°)

● — clean surface ; × — surface with coal deposit formed during a 20 min. period of the cracking process ; ○ — surface with coal deposit formed during two successive periods of 20 min. of the cracking process.

We found that in a reactor in which carbon black was deposited on the reactor wall by methane decomposition in the same conditions during two periods of 20 min., the reaction rate was slower than in a reactor in which the deposit was obtained during one single decomposition period of 20 min. and much slower than in a freshly coated reactor, in which the carbon black was burned in the mentioned conditions (see Figure 4).

Besides a decrease of the reaction rate with the increase of the carbon black deposit we observed also a decrease of the overall reaction order and a corresponding shift of the low order region to higher pressures. However, these effects seems to attenuate at higher temperatures.[3]

Using the least squares method we calculated the overall reaction order of the methane cracking in silica vessels at lower and higher pressures.

Table 2

The overall order of the methane cracking in silica vessels

Temp. °C	Nature of the reactor wall	Lower pressure range		Higher pressure range		Transition range
		overall order	standart error	overall order	standart error	mmHg
640	freshly coated	0.119	±0.044	1.070	±0.029	125–175
	carbon deposited 20′	0.080	0.020	0.760	0.040	150–200
	carbon deposited 2×20′	0.030	0.030	0.061	0.041	200–270
670	freshly coated	0.170	0.020	0.960	0.032	120–180
	carbon deposited 20′	0.063	0.018	0.890	0.025	160–250
	carbon deposited 2×20′	0.030	0.020	0.780	0.042	200–300
700	freshly coated	0.130	0.015	0.980	0.015	125–175
	carbon deposited 20′	0.079	0.018	0.900	0.021	175–250
	carbon deposited 2×20′	0.058	0.008	0.770	0.020	200–300

The obtained values, together with the transition range from the lower to the higher overall orders are given in table 2.

The microscopic pictures of the silica surface samples show that the carbon black deposits preferentially on surface defects, as seen in Figure 5.

We believe that the retarding effect observed in the thermal methane degradation can be explained by the formation of a dispersed carbon black deposit, which, according to Benson,[4] favours the heterogeneous recombination of the hydrogen atoms. This effect may be very important because of the fine dispersion of carbon black, not only on the reactor surface, but also in the reactor volume.

This conclusion is somewhat opposed to Palmer's[5] treatment concerning the accelerating effect of the soot nucleation.

[3] L. Odochian and I. A. Schneider, *Rev. Roumaine Chim.*, **17**, 441 (1972).

[4] S. W. Benson, *J. Chem. Phys.*, **38**, 2285 (1963).

[5] H. B. Palmer, J. Lahaye and K.C. Hou, *J. Phys. Chem.*, **72**, 348 (1968).

However, Palmer worked at much higher temperatures and, moreover, he followed the methane decomposition kinetics by carbon film formation. Therefore the initial stages of methane decomposition could possibly have been neglected because the carbon formation is yet not well understood and it may happen also at higher transformation degrees as suggested by Palmer.

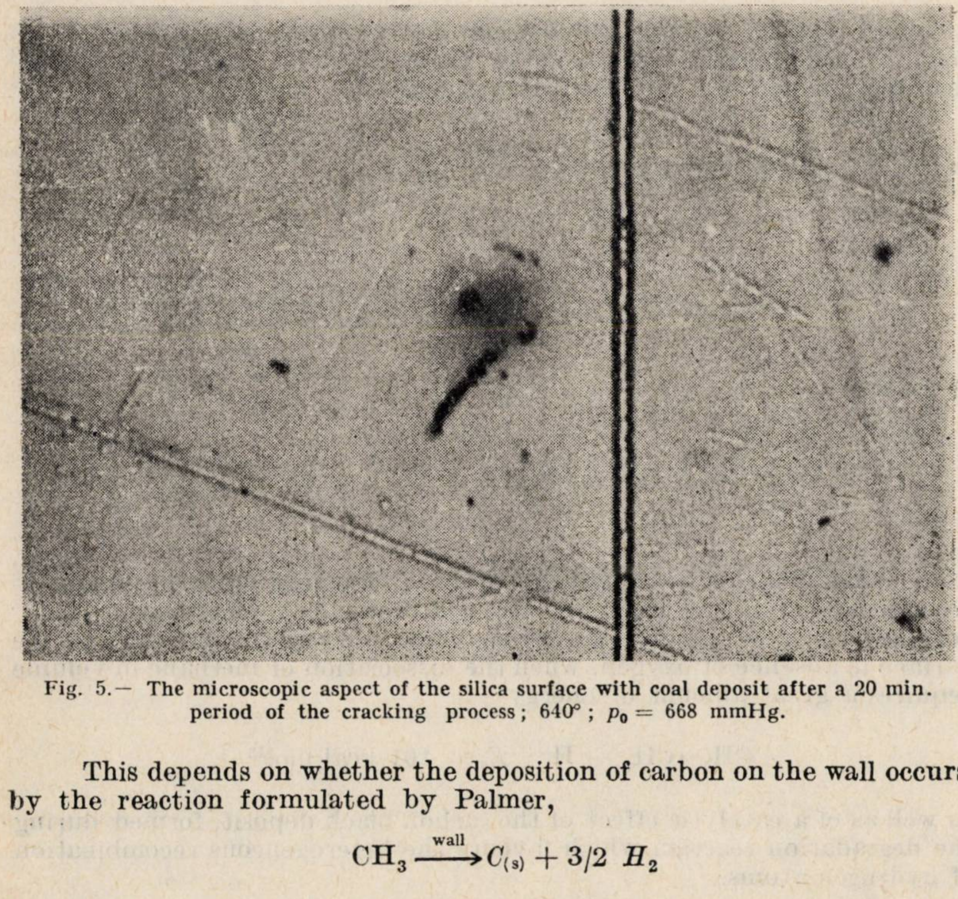

Fig. 5.— The microscopic aspect of the silica surface with coal deposit after a 20 min. period of the cracking process; 640°; $p_0 = 668$ mmHg.

This depends on whether the deposition of carbon on the wall occurs by the reaction formulated by Palmer,

$$CH_3 \xrightarrow{\text{wall}} C_{(s)} + 3/2\ H_2$$

in competition with the reactions of higher hydrocarbon formation, or the carbon formation succeeds the higher hydrocarbon formation, as stated by other authors.[6,7]

An additional study of the wellknown initiation effect of oxygen[8-11] using reaction mixtures with 2% oxygen, showed not only the expected

---

[6] E. N. Eremin, *Zhur. fiz. Khim.*, **49**, 1889 (1975).

[7] I. A. Schneider, *Z. phys. Chem.* (*Leipzig*), **220**, 199 (1962).

[8] M. Letort, *Chem. Rev.*, **197**, 1042 (1933); **200**, 312 (1935).

[9] F. O. Rice and M. Polly, *Trans. Faraday Soc.*, **1939**, 853.

[10] J. Engel, M. Combe, M. Letort and M. Niclause, *Rev. Inst. franc. Petrole*, **12**, 620 (1957).

[11] J. E. Germain and C. Vaniscotte, *Bull. Soc. chim. France*, **1957**, 962.

substantial rise of the overall reaction rate, but also a surprising constancy of the overall reaction order even at lower pressures (Figure 6).

This suggests that the heterogeneous initiation on the surface seems far less favourable than the initiation in volume by disproportionation

$$CH_4 + O_2 \rightarrow CH_3 + HO_2 \quad E_a = 55 \text{ kcal/mol}^{12}$$

although activation energy calculations, using the measured reaction rates for the coal-covered surfaces gave values ranging between 35.4—42.3 kcal/mol, depending on the initial pressure.

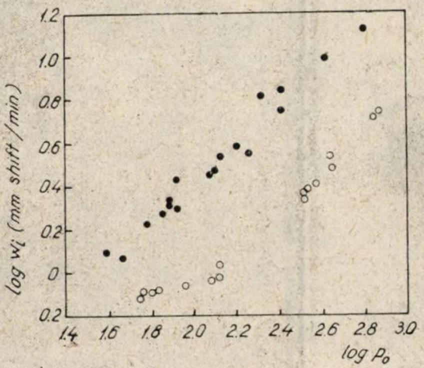

Fig. 6.— Influence of oxygen on the thermal degradation of methane in the pressure range of 40—760 mmHg at 640°;

⊙ — pure methane; ● — methane + 2% O_2 (in volume)

Finally we can therefore suppose that at low temperature and pressures the thermal degradation of methane is a complex homogeneous — heterogeneous process, because of a strong probability of the initiation on the surface in absence of oxygen, when the dissociation of methane in volume requires a great amount of energy

$$CH_4 \rightarrow CH_3 + H \quad E_a = 101 \text{ kcal/mol}^{13}$$

as well as of a catalytic effect of the carbon black deposit, formed during the degradation reaction which favours the heterogeneous recombination of hydrogen atoms.

---

[12] M. Szwarc, *Chem. Rev.*, **47**, 75 (1950).

[13] V. L. Karmilova, N. S. Enikolopian, A. B. Nalbandian and N. N. Semenov, *Zhur. fiz. Khim.*, **6**, 1176 (1960).

Revue Roumaine de Chimie, 23, 6, 841–852(1978)

ESTUDIO CINETICO DE LA OXIDACIÓN PERMANGANICA DE AMINAS TERCIARIAS

S. SENENT, F. MATA, y M.A. de la PEÑA
Departamento de Investigaciones Químicas, C.S.I.C. Sección de Química-Física,
Universidad de Valladolid, España

Received September 17, 1975
Revised November 20, 1976

The kinetics of the reaction between potassium permanganate and trimethyl- a nd triethyl amine has been studied in the range of the neutrality. The rate measurements were made spectrophotometrically at $\lambda = 524$ nm. We investigated the influence of reagent concentrations, ionic strength, acidity of the medium and temperature on the observed rate constant. A reaction mechanism that is in agreement with the results is proposed.

Se ha estudiado la cinética de la reacción entre permanganato potásico y trimetil- y trietil amina en el entorno de la neutralidad. Se midió la velocidad espectrofotometricamente a $\lambda = 524$ nm. Se investigó la influencia de la concentración de reactivos, fuerza iónica, acidez del medio y temperatura sobre la constante experimental de velocidad. Se propone un mecanismo de reacción que está de acuerdo con los resultados.

INTRODUCCIÓN

El presente trabajo recoge los resultados del estudio cinético de la oxidación de la trimetil- y trietil amina con permanganato potásico en medio neutro, problema del que no se conocen antecedentes bibliográficos directos, aunque son numerosos los estudios realizados empleando el permanganato como agente oxidante en medio fuertemente ácido y básico[1–4] así como la degradación de aminas por un gran número de agentes oxidantes[5–7] no llegandose en ellos a resultados concluyentes en puntos tan importantes como el orden de reactividad de las aminas y si el mecanismo transcurre por una cesión de electrones o de átomos de hidrógeno.

Los productos finales de la reacción serán bióxido de manganeso, compuesto insoluble de color marrón, y aldehido; aunque como productos intermedios se obtendrán manganatos y enaminas y/o bases de Schiff, respectivamente. Estas últimas pueden reaccionar con las aminas originales

---

[1] J. Holluta, *Z. phys. Chem.*, **102**, 276 (1922).
[2] J. Holluta, *ibid*, **150A**, 381 (1930).
[3] J. Stamm, *Angew. Chem.*, **47**, 791 (1934).
[4] F. R. Duke, *J. Amer. Chem. Soc.*, **70**, 3975 (1948).
[5] H. William, *J. Org. Chem.*, **32**, 3783 (1967).
[6] S. Eawalay y H. Shechter, *ibid*, **32**, 3129 (1967).
[7] E. Muller en "Houben-Weyl Methoden Der Organischen Chemie", Stuttgard, 1952, p. 976–984.

para dar lugar a productos complejos que sufrirán más tarde oxidación, hidrólisis y degradación. La presencia de los productos finales citados anteriormente, así como de algunas especies intermedias ha sido detectada en nuestros experimentos.

Un interesante trabajo en el que se inicia el tema de nuestra investigación fue el realizado por Rosenblatt y Hull[8] quienes estudiaron la oxidación de la trietil amina por permanganato potásico, aportando un mecanismo para la reacción, teniendo en cuenta la similitud existente entre el dióxido de cloro y el permanganato, en cuanto que ambos son agentes oxidantes muy enérgicos. La reacción fue explicada por el efecto conjunto de la cesión de un electrón y de un átomo de hidrógeno, dependiendo la mayor proporción de una u otra de la estructura de la amina y de la acidez del medio.[9,10] Estudios posteriores de la oxidación de aminas por dióxido de cloro,[11,12] muestran que es la amina libre la especie que controla la velocidad de la reacción y al analizar la influencia que sobre ella ejerce el ión clorito se observa que en las oxidaciones de la trimetil- y trietil amina es predominante la cesión electrónica.

A su vez, existen referencias[13] de que la reacción está facilitada por los substituyentes inductivos de cesión electrónica, de tal forma que el orden de reactividad de las aminas será el siguiente :

$$\text{Terciaria} > \text{Secundaria} > \text{Primaria}$$

y dentro de series alifáticas de aminas terciarias el orden de reactividad estará fijado por el grupo alquílico. Así, Horner y Kirnse,[13] que estudiaron cualitativamente el efecto de los substituyentes muestran que para grupos alquílicos el orden de eliminación es el siguiente :

$$RCH_2 > CH_3 > R_2CH$$

Similarmente, Fouinat y Magat,[14] estudian la reacción entre el permanganato potásico y el peróxido de hidrógeno en medio debilmente alcalino, observando que las curvas velocidad de reacción — tiempo constan de un primer tramo lineal a partir del cual adoptan un perfil de onda lo cual hizo pensar a estos autores que la velocidad de oxidación correspondía a ese primer tramo lineal, debiendose el segundo tramo a una reacción hetereogenea en la superficie del coloide, MnO_2, originado en el curso de la reacción.

EXPERIMENTAL

Se ha utilizado un espectrofotometro Perkin-Elmer, modelo 402, de registro gráfico continuo, que permite realizar exploraciones espectrográficas de una muestra líquida en la región del visible y del ultravioleta.

---

[8] L. A. Hull y D.H. Rosenblatt, *J. Amer. Chem. Soc.*, **89**, 1163 (1967).
[9] R. Stewart y R. Van der Linder, *Discuss. Faraday Soc.*, 1960, 211.
[10] R. Stewart, *J. Amer. Chem. Soc.*, **79**, 3057 (1957).
[11] D. H. Rosenblatt y A. Kenneth, *J. Org. Chem.*, **28**, 2790 (1963).
[12] C. Audeh y S. Lindsay, *J. Chem. Soc.(B)*, 1970, 1280.
[13] L. Horner y W. Kirnse, *Liebigs Ann. Chem.*, **48**, 597 (1956).
[14] F. Fouinat y M. Magat, *J. chim. Phys.*, **47**, 514 (1950).

Como instrumento de medida se empleó un fotocolorímetro Bausch Lomb Spectronic 20 con el que se aplicó la técnica de punto a punto. La constancia de la temperatura se mantuvo con un termostato convencional que garantiza la medida con un error de ±0,05 °C y las medidas del pH se llevaron a cabo con un potenciometro pH-Meter Radiometer, modelo 26, que permite realizar las medidas con un error de ±0,005 u. pH, una vez calibrado para el intervalo de pH de trabajo, mediante soluciones reguladoras adecuadas.

La trietil amina fue Merck ($d^{20} = 0{,}729$ grs cm^{-3} y 99% de riqueza) valorada con ácido clorhídrico, utilizando rojo de metilo como indicador. La trimetil amina fue Schuchard y se utilizó en forma de clorhidrato, preparada por pesada directa y posterior valoración potenciométrica.

Se trabajó en medio tamponado empleando para ello PO_4H_2K y NaOH, ambos Merck.

Técnica utilizada. La especie química de control elegida fue el permanganato potásico. El procedimiento experimental adoptado consistio en un método estático, mediante el cual se determinó a intervalos regulares de tiempo la absorbancia presentada por la especie de control en la longitud de onda característica de la región visible del espectro.

Para llevar a cabo este procedimiento experimental se realizaron previamente exploraciones espectrográficas para tratar de conocer las bandas características de las substancias que intervienen en la reacción, tanto de reactivos y productos como de todas las especies que pudieran interferir en la medida de la absorbancia de la especie de control elegida. El espectro de la especie oxidante en medio neutro presenta la banda más intensa en la región del visible a 524 nm ; comprobándose a esa longitud de onda el cumplimiento de la ley de Beer-Lambert en el rango total de las condiciones de pH de trabajo elegidas. La especie reductora presenta absorbancia unicamente en la zona correspondiente al ultravioleta, y la especie intermedia, manganato, muestra dos bandas intensas a 430 y 600 nm, respectivamente, en la región del visible.

La etapa siguiente fue registrar espectros estáticos y dinámicos del sistema reaccionante, observándose la aparición de un punto isobéstico a 480 nm, que, sin embargo, desaparece a medida que avanza la reacción; modificando sistematicamente las concentraciones de oxidante y reductor, así como el pH del medio, se estudió la posición de dicho punto isobéstico, observándose que en ningún caso se altera su posición por lo que su desaparición es atribuible a las interferencias que crean los productos de la reacción.

En lo que se refiere a las condiciones experimentales, la propria técnica espectrofotométrica utilizada sirvió para determinar el intervalo de concentraciones a manejar ; El rango de pH seleccionado fue desde pH=6 a pH=8, y se trabajó a temperaturas comprendidas entre 21 y 33°C.

La técnica operativa que se siguió en todos los experimentos realizados fue la siguiente: Se colocaban dentro del termostato las disoluciones tamponadas de los dos reactivos, dejándolas un tiempo prudencial para que se alcanzase el equilibrio térmico ; una vez logrado esto, se mezclan ambas disoluciones siendo el volumen total de reacción de 150 mls. y, en este momento, los reactivos tienen la concentración que para cada esperimento se indica en las Tablas que se dan a continuación. A intervalos regulares de tiempo se extraían muestras de la mezcla reaccionante y se medía la absorbancia óptica de la especie química de control.

RESULTADOS

En todos los experimentos cinéticos se ha determinado un orden cinético respecto a la concentración (n_c) o verdadero orden cinético según Letort. La razón principal de esta medida fue la curvatura que adoptaban las gráficas velocidad de reacción — tiempo, transcurrido un 50% de la reacción. A partir de este momento no era posible determinar con garantía la absorbancia de la especie química de control, debido a la aparición de un coloide de color amarillo que dificulta la medida. La aparición de este coloide hizo pensar que el producto de reducción del permanganato es MnO_2[15-18] y que al igual que Fouinat y Magat[14] podemos suponer que el

---

[15] B. Jerowska-Trzebitowska, *Bull. Acad. Polon. Sci. Ser. Sci. Chim.* **2**, 447 (1954).

[16] B. Jerowska-Trzebitowska, *ibid.*, **7**, 405 (1959).

[17] B. Jerowska-Trzebitoeska, *Bull. Acad. Polon. Sci. Ser. Sci. Chim. geol. geograph.*, **7**, 417 (1959).

[18] M. C. R. Symons, *J. Chem. Soc.*, **1953**, 3956.

Tabla 1

Variación de k_{exp} con la concentración de los reactivos

	$k_{exp}/10^3$ min^{-1}	pH = 7,67		T = 25°C	
a)	$[Me_3N.HCl]/10^3M$	$[MnO_4K]/10^5M$			
		5,6	8,0	10,0	12,0	16,0
b)	3,3	4,69(0,9998)	4,39(0,9999)	4,15(0,9996)	3,85(0,9997)	3,59(0,9998)
	4,5	5,82(0,9999)	5,49(0,9999)	5,32(0,9999)	4,97(0,9997)	4,66(0,9997)
	6,0	7,23(0,9993)	6,97(0,9996)	6,59(0,9998)	6,35(0,9999)	5,99(0,9992)
	7,5	8,89(0,9999)	8,45(0,9999)	8,10(0,9996)	7,86(0,9999)	7,22(0,9995)
	10,0	11,32(0,9999)	10,82(0,9999)	10,52(0,9999)	10,12(0,9999)	9,64(0,9997)

n=1 n=0,5	$k_{exp}/10^3$min^{-1} $k_{exp}/10^3$dm$^{3/2}$mol$^{-1/2}$ min$^{-1/2}$	pH=7,67	T=25°C	
$[Et_3N]/10^4$ M	$[MnO_4$ K$]/10^5$ M			
	8,0	10,0	12,0	16,0
n=0,5				
5,0	0,50(0,9998)	0,49(0,9996)	0,50(0,9997)	0,19(0,9995)
8,0	0,97(0,9998)	0,92(0,9998)	0,90(0,9998)	0,96(0,9995)
10,0	1,42(0,9998)	1,42(0,9996)	1,42(0,9994)	1,42(0,9999)
12,0	2,02(0,9995)	2,12(0,9997)	2,07(0,9996)	2,09(0,9997)
n = 1				
15,0	19,77(0,9999)	18,37(0,9999)	17,55(0,9999)	16,46(0,9999)

Los números entre paréntesis se refieren al coeficiente de correlación lineal.

primer tramo lineal de dichas representaciones corresponde a la reacción de oxidación homogénea.

A) Influencia de la concentración de los reactivos

Se determinó el orden cinétio respecto de la especie MnO_4K, utilizando el método de velocidades iniciales. Dicho orden es $n_c = 1$, para la oxidación de la trimetil amina ; mientras que para la oxidación de la trietil amina se encontró un valor de $n_c = 1$, cuando la amina estaba en exceso respecto del oxidante y $n_c = 0{,}5$, en caso contrario. Sin embargo, al aumentar el pH del medio, en estos ultimos casos, el orden era tambien $n_c = 1$. Se trabajó con concentraciones de MnO_4K del orden de 10^{-5} a 10^{-4}, frente a unas concentraciones de amina del orden de 10^{-3} a 10^{-2} M para la trimetil amina y de 10^{-4} a 10^{-3} M en el caso de la trietil amina.

En una primera serie de experimentos se varió sistematicamente la concentración de reductor manteniendo constante la concentración de MnO_4K, acidez del medio y temperatura. La Tabla 1 recoge los resultados obtenidos. Puede verse que la constante experimental de velocidad aumenta conforme lo hace la concentración de amina. En el caso de la trimetil amina los valores de k_{exp} se ajustan a una función lineal de la forma :

$$k_{exp} = m[Me_3N.HCl] + n \tag{1}$$

mientras que en el caso de la trietil amina, tanto cuando el orden cinético respecto del oxidante es 1 como cuando es 0,5, se obtiene una linea recta al representar el cociente $[Et_3N]/k_{exp}$ frente a la concentración de amina, $[Et_3N]$, lo cual permite expresar la constante experimental de velocidad como :

$$k_{exp} = \frac{[Et_3N]}{a - b[Et_3N]} \tag{2}$$

Las ecuaciones (1) y (2) son un hecho muy importante a tener en cuenta al discutir el mecanismo de la reacción.

Cuando se hizo variar unicamente la concentración de MnO_4K las constantes de velocidad de primer orden decrecen frente a la concentración creciente de los iones MnO_4^-. Este efecto ha sido ya encontrado por otros autores[19] en la oxidación permangánica del ácido malónico pero no obstante es de dificil explicación cinética.

B) Influencia de la fuerza iónica

La Tabla 2 da cuenta de los resultados obtenidos en este sentido. En ambas oxidaciones la pendiente de la recta obtenida al representar $\log k_{exp}$ frente a $(I)^{0,5}$(I =fuerza iónica es negativa, lo cual hace pensar que las etapas cinéticas lentas de las oxidaciones transcurren por un mecanismo iónico y a través de iones de carga opuesta.

---

[19] S. SENENT y S. CUADRADO, *Anales real Soc. españ. Fis. Quim.*, **57(B)**, 11 (1961).

Tabla 2

Variación de k_{exp} con la fuerza iónica del medio

$T=25$°C pH=7,0 $[Me_3N.HCl]=8{,}0\ 10^{-2}M$

a) $[ClO_4Na]/10^2M$	$[MnO_4K]=3{,}2\ 10^{-4}M$ $(I)^{1/2}$	$k_{exp}/10^3\ min^{-1}$
6,0	0,41	9,31(0,9996)
4,5	0,39	9,45(0,9998)
3,0	0,37	9,95(0,9996)
1,5	0,35	10,12(0,9998)
0,0	0,33	10,44(0,9999)

b) $[ClO_4Na]/10^2M$	$[MnO_4K]=0{,}8\ 10^{-4}M$ $(I)^{1/2}$	$k_{exp}/10^3\ min^{-1}$
6,0	0,41	9,64(0,9998)
4,5	0,39	9,93(0,9998)
3,0	0,37	10,27(0,9998)
1,5	0,35	10,52(0,9997)
0,0	0,33	10,94(0,9997)

T=25°C pH=6,37 $[Et_3N]=8{,}0\ 10^{-3}M$

c) $[ClO_4Na]/10^2M$	$[MnO_4K]=8{,}0\ 10^{-5}M$ $(I)^{1/2}$	$k_{exp}/10^3\ min^{-1}$
6,0	0,28	14,63(0,9999)
4,5	0,25	15,56(0,9999)
3,0	0,21	16,70(0,9998)
1,5	0,18	17,78(0,9998)
0,0	0,13	19,38(0,9999)

Los números entre parentesis se refieren al coeficiente de correlación lineal.

C) Influencia de la acidez del medio

Se ha comprobado que en ambas oxidaciones la constante experimental de velocidad está muy influenciada por la acidez del medio, tal como afirman algunos otros investigadores.[20] Como puede observarse en la Tabla 3, la constante experimental de velocidad aumenta a medida que lo hace el pH del medio, y se encontro que los valores de la misma se ajustan a una función lineal frente a la concentración de los iones hidroxilo, $[OH^-]$, de pendiente y ordenada en el origen positivas para ambas reacciones. Sin embargo, para los valores más altos de $[OH^-]$, en el intervalo manejado en cada caso, se observó que k_{exp} disminuía ligeramente con $[OH^-]$ para la trimetil amina y, al contrario, k_{exp} aumentaba bruscamente con $[OH^-]$ para la trietil amina. Este último resultado está en la linea de

---

[20] B. Tronov y L. Nikonova, *J. Russ. Phys-Chem. Soc.*, **61**, 541 (1929).

Tabla 3

Variación de k_{exp} con la acidez del medio

a) $k_{exp}/10^3\ \text{min}^{-1}$	$[KMnO_4]=8{,}0\ 10^{-5}$ M		$T=25$°C
pH	$[Me_3N.HCl]/10^2M$		
	2,0	8,8	10,0
6,2			2,43(0,9998)
6,4			3,69(0,9998)
6,6		5,22(0,9996)	5,89(0,9999)
6,8			9,12(0,9998)
7,0	4,68(0,9999)	12,28(0,9998)	13,88(0,9995)
7,2		18,76(0,9994)	20,47(0,9998)
7,4		28,61(0,9993)	31,62(0,9998)
7,6	15,91(0,9995)		45,23(0,9990)
7,8	21,94(0,9993)		
8,0	30,86(0,9993)		

b) $k_{exp}/10^3\ \text{min}^{-1}$	$[KMnO_4]=3{,}2\ 10^{-4}$M		$T=25$°C
pH	$[Et_3N]/10^3M$		
	3,0	4,0	5,0
6,0		0,91(0,9999)	1,35(0,9999)
6,4	1,08(0;9994)	1,38(0,9997)	2,03(0,9997)
6,6	1,35(0,9999)	2,04(0,9999)	2,95(0,9999)
6,8	1,64(0,9999)	3,29(0,9999)	4,83(0,9997)
7,0	2,87(0,9996)	5,08(0,9998)	9,36(0,9996)
7,2	5,57(0,9997)	12,14(0,9995)	44,10(0,9999)

Los números entre parentesis se refieren al coeficiente de correlación lineal.

Tabla 4

Variación de los parámetros de activación con las condiciones de trabajo

a) $T=(21 \text{ a } 29)^{\circ}C$ pH=7,8 $[MnO_4K]=8,0\ 10^{-5}$ M

$[Me_3N.HCl]/10^3$ M	E_a/kJmol^{-1}	$\Delta H^{\neq}$/kJmol^{-1}	$\Delta S^{\neq}$/Jmol^{-1} K^{-1}
15,0	90,91(0,9995)	88,57(0,9994)	+19,45
12,5	87,99(0,9995)	85,56(0,9994)	+ 8,19
10,0	86,86(0,9999)	84,44(1,0000)	+ 2,72
7,5	90,75(0,9989)	88,28(0,9989)	+13,38
5,0	90,75(0,9993)	88,24(0,9993)	+10,20

b) $T=(21 \text{ a } 29)^{\circ}C$ pH=7,2 $[Me_3N.HCl]=10,4\ 10^{-2}$ M

$[KMnO_4]/10^5$ M	E_a/kJmol^{-1}	$\Delta H^{\neq}$/kJmol^{-1}	$\Delta S^{\neq}$/Jmol^{-1} K^{-1}
5,6	70,89(0,9993)	69,68(0,9999)	−52,04
8,0	78,42(0,9999)	75,91(0,9999)	−31,35
10,0	79,38(0,9998)	76,83(0,9999)	−28,42
12,0	79,92(0,9976)	77,45(0,9976)	−26,63
16,0	83,26(0,9992)	79,38(0,9992)	−15,67

c) $T=(21 \text{ a } 29)^{\circ}C$ pH=6,52 $[KMnO_4]=8,0\ 10^{-5}$ M

$[Et_3N]/10^3$ M	E_a/kJmol^{-1}	$\Delta H^{\neq}$/kJmol^{-1}	$\Delta S^{\neq}$/Jmol^{-1} K^{-1}
7,0	93,25(0,9998)	90,79(0,9998)	+18,14
7,5	90,62(0,9997)	88,49(0,9996)	+11,66
8,0	87,11(0,9999)	84,60(0,9997)	− 0,54
8,5	81,93(0,9998)	81,97(0,9998)	− 9,86
9,0	78,00(0,9995)	75,53(0,9995)	−26,17

d) $T=(21 \text{ a } 29)^{\circ}C$ $[Et_3N]=4,0\ 10^{-3}$M $[KMnO_4]=8,0\ 10^{-5}$ M

pH	E_a/kJmol^{-1}	$\Delta H^{\neq}$/kJmol^{-1}	$\Delta S^{\neq}$/Jmol^{-1} K^{-1}
6,8	81,51(0,9983)	79,98(0,9994)	− 23,62
7,0	121,55(0,9992)	118,50(0,9990)	+109,97
7,15	89,95(1,0004)	87,53(0,9995)	+ 12,87

e) $T=(21 \text{ a } 29)^{\circ}$ C $[Et_3N]=8,0\ 10^{-4}$ M $[KMnO_4]=16,0\ 10^{-5}$ M

pH	E_a/kJmol^{-1}	$\Delta H^{\neq}$/kJmol^{-1}	$\Delta S^{\neq}$/Jmol^{-1} K^{-1}
7,15	62,53(0,9997)	60,02(0,9996)	− 99,61
7,3	61,82(0,9991)	59,31(0,9992)	−101,53
7,6	129,24(0,9996)	126,61(0,9992)	+133,93

lo encontrado por Wiberg y Stewart[21,22] en el estudio de la oxidación de aldehidos por permanganato potásico, habiendo observado tambien fuertes cambios en la constante de velocidad con la acidez del medio y apuntando la idea de dos mecanismos diferentes según el pH del medio.

D) Influencia de la temperatura

En la Tabla 4 se da cuenta de los valores obtenidos para los parámetros de activación. Puede verse que las magnitudes de la energía de activación, E_a, y entalpia de activación, $\Delta H^{\neq}$, no cambian sensiblemente con la concentración de los reactivos. Estos mismos parámetros están muy influenciados por la acidez del medio en la reacción de oxidación de la trietil amina pero no así en la oxidación de la trimetil amina. En cuanto a las entropías de activación los resultados obtenidos (valores positivos y negativos) no son concordantes con las ideas de Wiberg y Fox[23] quienes sugieren ordenamientos en el complejo activado para reacciones de este tipo.

DISCUSIÓN

A la vista de los resultados obtenidos, se considera que existen pruebas suficientes para plantear dos mecanismos de reacción distintos, uno para cada amina. Sin embargo, dado que ambas aminas son los primer y segundo término de la misma serie homóloga ambos esquemas deberán tener algunos puntos en común, como se demostrará más adelante.

Comenzaremos discutiendo los resultados referentes a la oxidación de la trimetil amina. Esta amina se empleó en forma de clorhidrato lo cual permite pensar tanto en la especie protonada, $(CH_3)_3NH^+$, como en la especie amina libre, $(CH_3)_3N$, como especies reductoras. La ecuación (3) expresa el equilibrio entre ambas (la constante vale $K = 5{,}4.10^{-5}$, a 25°C) :

$$(CH_3)_3\overset{+}{N}H + OH^- \rightleftharpoons (CH_3)_3N + H_2O \tag{3}$$

y dado el pH de trabajo se puede concluir que la concentración de amina libre es muy inferior a la concentración de amina protonada.

El mecanismo que se propone para la oxidación de esta amina, se esquematiza a continuación :

$$(CH_3)_3\overset{+}{N}H + MnO_4^- \rightarrow X + H^+ \tag{4}$$

$$X + OH^- \rightarrow CH_2 = \overset{+}{N}(CH_3)_2 + H_2O + MnO_4^{=} \tag{5}$$

$$X + (CH_3)_3N \rightarrow 2\ CH_3-\overset{+}{\underset{\cdot}{N}}(CH_3)_2 + MnO_4^{=} \tag{6}$$

$$X \rightarrow CH_2 = \overset{+}{N}(CH_3)_2 + MnO_4H^{=} \tag{7}$$

---

[21] K. Wiberg y R. Stewart, *J. Amer. Chem. Soc.*, **78**, 1214 (1956).
[22] K. Wiberg y R. Stwart, *ibid.*, **77**, 1786 (1955).
[23] K. Wiberg y S. Fox, *ibid.*, **85**, 3487 (1963).

$$CH_3-\underset{\cdot}{\overset{+}{N}}(CH_3)_2 + OH^- \rightarrow CH_2\overset{\cdots}{-}N(CH_3)_2 + H_2O \tag{8}$$

$$CH_2\overset{\cdots}{-}N(CH_3)_2 + MnO_4^{=} + 2H_2O \rightarrow CH_2 = \overset{+}{N}(CH_3)_2 + MnO_2 + 4OH^- \tag{9}$$

$$CH_2 = \overset{+}{N}(CH_3)_2 + H_2O \rightarrow HCOH + HN(CH_3)_2 + H^+ \tag{10}$$

Se admite la formación de un complejo X, de Mn (VI), por reacción de una molécula de amina protonada con el ión permanganato, MnO_4^-, según expresa la ecuación (4). Este complejo X reaccionaría a continuación con los iones OH^- del medio, ecuación (5), con una molécula de amina libre, ecuación (6), o bien sufriría una descomposición monomolecular, ecuación (7), para dar origen, en todos los casos, a Mn(V) y a distintos productos de oxidación de la trimetil amina. Estos últimos darían los productos finales de la reacción a través de los procesos (8),(9), y (10). Se supone que los procesos (5) y (7) son las etapas determinantes de la velocidad de la reacción, de tal forma que:

$$v = k_5[X][OH^-] + k_7[X] \tag{11}$$

Suponiendo que el complejo X alcanza régimen estacionario, es posiblo obtener una expresión para la concentración del mismo, [X], igualands la velocidad del proceso (4) con la suma de las velocidades de los procesoe (5), (6), y (7):

$$[X] = \frac{k_4[(CH_3)_3\overset{+}{N}H][MnO_4^-]}{k_5[OH^-] + k_6[(CH_3)_3N] + k_7} \tag{12}$$

Al substituir [X], dado por la ecuación (12), en la ecuación (11) se obtiene, finalmente, la expresión teórica de la velocidad de la reacción:

$$v = \frac{k_4\{k_5[OH^-] + k_7\}}{k_5[OH^-] + k_6[(CH_3)_3N] + k_7}[(CH_3)_3\overset{+}{N}H][MnO_4^-] \tag{13}$$

La ecuación (13) permite justificar no solamente el orden cinético $n_c = 1$ encontrado respecto de la concentración de la especie oxidante, MnO_4^-, sino también la influencia de la concentración del reductor y de la acidez del medio sobre la constante experimental de velocidad. En efecto, al comparar la referida ecuación (13) con la expresión fenomenológica de la velocidad de la reacción, $v = k_{exp}[MnO_4^-]$, se deduce lo siguiente:

$$k_{exp} = \frac{k_4\{k_5[OH^-] + k_7\}}{k_5[OH^-] + k_6[(CH_3)_3N] + k_7}([CH_3)_3\overset{+}{N}H] \tag{14}$$

y operando,

$$k_{exp} = \frac{k_4\{Kk_5[(CH_3)_3N] + k_7[(CH_3)_3\overset{+}{N}H]\}}{k_5[OH^-] + k_6[(CH_3)_3N] + k_7} \tag{15}$$

donde K es la constante del equilibrio de desprotonación de la trimetil amina, ecuación (3). De acuerdo con los comentarios que se hicieron acerca de la relación $[(CH_3)_3N]/[(CH)_3NH^+]$ (vide supra) es inmediato que la ecuación (15) interpreta teoricamente la ecuación (1), dado que tanto el término $k_4Kk_5[(CH_3)_3N]$ como el denominador, $\{k_5[OH^-]+k_6[(CH_3)_3N]+k_7\}$ no cambian sensiblemente al aumentar la concentración de amina en forma de clorhidrato. Por otra parte, la ecuación (14) interpreta la influencia de la acidez del medio sobre k_{exp}. En efecto, razonando de forma semejante a como se ha hecho en lineas precedentes, es previsible una dependencia lineal de k_{exp} con la concentración de los iones hidroxilo, $[OH^-]$, tal como se ha observado. Sin embargo, a medida que aumenta el pH del medio el término $k_5[OH^-]$, del denominador, es cada vez más alto hasta el punto que su aumento puede hacer descender la magnitud de k_{exp} en relación a los valores previsibles para la misma. Si se analizan los valores de k_{exp} de la Tabla 3 para esta amina se puede comprobar que esto es lo que ocurre en la práctica.

En cuanto a la oxidación de la trietil amina se propone el siguiente mecanismo :

$$(C_2H_5)_3 + MnO_4^- \rightarrow C \tag{16}$$

$$(C_2H_5)_3N + MnO_4^- \rightarrow Y + H^+ \tag{17}$$

$$C + Y + H_2O \rightarrow 2X + OH^- \tag{18}$$

$$C + OH^- \rightarrow Y + H_2O \tag{19}$$

$$C + (C_2H_5)_3N \rightarrow Y + CH_3-CH_2\overset{\cdots}{-}N(C_2H_5)_2 + H^+ \tag{20}$$

$$C \rightarrow Y + H^+ \tag{21}$$

$$X + OH^- \rightarrow CH_3-CH=\overset{+}{N}(C_2H_5)_2 + H_2O + MnO_4^{\equiv} \tag{22}$$

$$X + (C_2H_5)_3N \rightarrow 2\ CH_3-CH_2-\underset{\cdot}{\overset{+}{N}}(C_2H_5)_2 + MnO_4^{\equiv} \tag{23}$$

$$X \rightarrow CH_3-CH=\overset{+}{N}(C_2H_5)_2 + MnO_4^{\equiv} \tag{24}$$

$$\begin{aligned} CH_3-CH_2\overset{\cdots}{-}N(C_2H_5)_2 + MnO_4^{\equiv} \rightarrow CH_3-CH= \overset{+}{N}(C_2H_5)_2 + \\ + MnO_2 + 4OH^- \end{aligned} \tag{25}$$

$$CH_3-CH=\overset{+}{N}(C_2H_5)_2 + H_2O \rightarrow CH_3CHO + HN(C_2H_5)_2 + H^+ \tag{26}$$

Se admite la formación de un complejo de adición C, entre la especie amina libre y el ión permanganato, donde el manganeso actúa como Mn(VII). Simultaneamente se formarían complejos Y, de Mn(V). La reacción entre ambos complejos, ecuación (18), conduce a complejos X, de Mn(VI). En apoyo de esta última hipótesis podemos citar los resultados de Carrington y Symons, [24] por ejemplo. Los complejos C se convertirían en complejos Y por reaccón con los iones OH^- del medio, ecuación (19), con una molécula de amina libre, ecuación (20), o según un proceso monomolecular, ecuación (21). En cuanto a los complejos X, se admite que sufren transformaciones totalmente semejantes a las consideradas para la oxidación de la trietil amina y se recogen en las ecuaciones (22), (23) y (24). Los productos finales de la reacción se originan mediante los procesos (25) y (26), semejantes a los vistos para la otra amina. Se supone que son los procesos (19) y(21) las etapas lentas determinantes de la velocidad de reacción, tal que :

---

[24] A. Carrington y M. Symons, *J. Chem. Soc.*, **1956**, 3373.

$$v = k_{19}[\mathrm{C}][\mathrm{OH}^-] + k_{21}[\mathrm{C}] \qquad (27)$$

Suponiendo que los complejos Y alcanzan régimen estacionario y aplicando las ideas relativas al mismo es posible obtener una expresión para la concentración de los complejos C, de la forma :

$$[\mathrm{C}] = \frac{k_{17}[(\mathrm{C_2H_5})_3\mathrm{N}]\,[\mathrm{MnO_4^-}]}{k_{18}[\mathrm{Y}][\mathrm{H_2O}] - k_{19}[\mathrm{OH}^-] - k_{20}[(\mathrm{C_2H_5})_3\mathrm{N}] - k_{21}} \qquad (28)$$

y si se substituye [C], dado por la ecuación (28), en la ecuación (27) se obtiene la siguiente expresión teórica para la velocidad de la reacción :

$$v = \{k_{19}[\mathrm{OH}^-] + k_{21}\}\,\frac{k_{17}[(\mathrm{C_2H_5})_3\mathrm{N}]\,[\mathrm{MnO_4^-}]}{\{k_{18}[\mathrm{Y}][\mathrm{H_2O}]\} - k_{19}[\mathrm{OH}^-] - k_{20}[(\mathrm{C_2H_5})_3\mathrm{N}]} \qquad (29)$$

La ecuación (29) justifica el orden cinético $n_c = 1$ encontrado respecto de la concentración del oxidante y, tambien, la dependencia de k_{exp} con la concentración de amina y con la acidez del medio. Efectivamente, cuando se estudió la influencia de la concentración de reductor,amina,se mantuvieron fijas el resto de las condiciones experimentales de trabajo, en particular la acidez del medio y por tanto [OH$^-$]. Si esta última condición se lleva a la ecuación (29) es inmediato comprobar que el resultado así obtenido es consistente con la ecuación (2). Por otra parte, cuando se estudió la influencia de la acidez del medio sobre k_{exp} se varió exclusivamente [OH$^-$] manteniendo constantes el resto de las condiciones. En este caso, la ecuación (29) prevé una dependencia lineal de k_{exp} con [OH$^-$] tal como realmente se ha observado.

Conviene añadir que, a pesar de las analogías entre ambos mecanismos, existen importantes diferencias, a destacar ; mientras en la oxidación de la trimetil amina se supone que las etapas determinates corresponden al paso de Mn(VI) a Mn(V), en la oxidación de la trietil amina se supone que es el paso de Mn(VII) a Mn(V) el que condiciona la velocidad del proceso. Sin embargo, en ambas oxidaciones se trata de procesos con "α-hidrogen abstraction" y "electron abstraction", simultáneas.

Solo destacaremos, como último comentario, que los productos finales de ambas oxidaciones : MnO$_2$, formaldehido y acetaldehido, y las aminas secundarias correspondientes, han sido detectados experimentalmente. El MnO$_2$ se observó en todos los experimentos realizados, los aldehidos fueron detectados con dimedona, y las aminas por espectroscopía de RMN.

Revue Roumaine de Chimie **23**, *6*, 853–859 (1978)

ELECTRONIC STRUCTURE OF SOME STILBENE DERIVATIVES. VII[1]

MO-LCI-PPP CALCULATIONS FOR SOME POLYNITRO-*TRANS*-STILBENE DERIVATIVES

LUCIA CIOHODARU*, C.C. RENTIA ** and I. ZAMFIRESCU**

*Department of Physical Chemistry, National Institute of Chemistry, str. Polizu 1, Bucharest, Romania

**Institute of Atomic Physics, Bucharest Romania

Received March 25, 1976

Calculations were performed, using the method of molecular orbitals, within the framework of Pariser-Parr-Pople approximation, of six *trans*-stilbene derivatives containing from two to four nitro groups. A number of 16 monoexcited configurations were taken into account. The results gave satisfactory agreement with the electronic absorption spectra of the same stilbene derivatives. Absorption band assignments were proposed.

INTRODUCTION

There are available literature data in connection with the LCAO-MO-SCF calculations of the unsubstituded *trans*-stilbene ; the calculations are performed using various theoretical approximations : taking into account all monoexcited configurations ;[2–4] "β-variable" approximation ;[5] semiempirical PPP method ;[6] Bloor approximation ;[7] improved Adams-Miller approximation ;[8] Fischer-Hjalmars method, using spectral data in order to calculate the electron repulsion integrals ;[9] FE-MO-CI method ;[10] CNDO/2 method.[11]

As regards the substituted stilbene derivatives, there are literature data referring to the calculations of phenil- and diphenil-stilbene, using the FE-MO-CI method,[10] as well as to the calculations of the electronic transitions using the model of the unidimensional potential gap.[12,13]

---

[1] Part VI : L. Ciohodaru, *Rev. Roumaine Chim.*, **22**, 1315 (1977).

[2] R. Basu, *Theor. Chim. Acta*, **2**, 215 (1964).

[3] D. L. Beveridge and H. H. Jaffé, *J. Amer. Chem. Soc.*, **87**, 5340 (1965).

[4] H. A. Perkampus and J. V. Knop, *Theor. Chim. Acta*, **6**, 45 (1966).

[5] K. Nishimoto and L. S. Forster, *Theor. Chim. Acta*, **3**, 407 (1965).

[6] P. Lindner and O. Martenson, *Theor. Chim. Acta*, **7**, 150 (1967).

[7] J. E. Bloor, B. R. Gibson and. N. Brearley, *Theor. Chim. Acta*, **8**, 35 (1967).

[8] O. W. Adams and R. L. Miller, *Theor. Chim. Acta*, **12**, 151 (1968).

[9] I. Fischer-Hjalmars and M. Sundborn, *Acta Chem. Scand.*, **22**, 607 (1968).

[10] R. Gase, *Z. phys. Chem. (Leipzig)*, **239**, 307 (1968).

[11] S. Ljunggren and G. Wettermark, *Theor. Chim. Acta*, **19**, 326 (1970).

In order to obtain new information in connection with the correlations between the calculated modifications of the electronic energies in the stilbene derivatives and their experimental electronic spectra, calculations were performed in the present paper according to the MO method, within a PPP type approximation, taking into account 16 monoexcited configurations for six *trans*-stilbene derivatives containing from two to four nitro groups.

MO CALCULATIONS

The calculations were performed using a LCAO—MO—LCI—PPP type method,[14,15] which took into account the electron repulsions and antisymmetrized wave function and depended on the Roothan's iterative formalism.[16]

The various type of integrals appearing in calculations were simplified using the ZDO approximation ; those remaining were identified by empirical values (atomic valence state ionization potentials, corresponding to certain hybridization state = *I*) or were calculated within the approximations based on the Coulombian repulsion of some punctiform charges.

The resonance integral values correspond to the literature data.[17]

The one-center repulsion integrals were estimated initially from both the valence state ionization potential values (*I*) and the valence state electron affinities (*A*) of the σ- and π-electronic systems.[18] The corresponding values were approximated, during calculations, after every iteration, according to the Harada's formula,[19] depending on the modification of the σ- and π-charge distribution.

The two-center repulsion integrals were calculated in the Nishimoto-Mataga manner,[17] improved by Ohno.[20]

Although our treatment is based on the $\sigma-\pi$ separation, we take into account the σ-system by means of an iterative procedure, using the same approximation as Del Re method.[21,22] The overlap integrals were estimated in every iteration.

The procedure deals with "closed-shell" and is of use for the calculation of lower spectral states by means of the limited configuration interaction (LCI).[23]

Therefore, our calculation process employs a series of calculating approximations from the literature. On the basis of this process, C. Renţia and I. Zamfirescu have written a computing program which has been carried out on an IBM 370/135 computer.

The Hückel matrices of the π-electron systems have been written, using the parameters of heteroatoms given in a previous paper.[24]

The Z effective charge of atoms have been calculated according to the Slater's rules.[25]

---

[12] H. Kuhn, *Helv. Chim. Acta*, **31**, 1780 (1948).

[13] W. Kuhn, *J. Chem. Phys.*, **17**, 1198 (1949).

[14] R. Pariser and R. G. Parr, *J. Chem. Phys.*, **21**, 466, 767 (1953).

[15] J. A. Pople, *Trans. Faraday Soc.*, **49**, 1735 (1953).

[16] C. J. Roothan, *Rev. Mod. Phys.*, **23**, 69 (1951).

[17] K. Nishimoto and N. Mataga, *Z. phys. Chem (Frankfurt)*, **12**, 335 (1957); ibid. **13**, 140 (1957).

[18] J. Hincze and H. H. Jaffé, *J. Amer. Chem. Soc.*, **84**, 540 (1962).

[19] Y. Harada, *Mol. Phys.*, **8**, 272 (1964).

[20] K. Ohno, *Theor. Chim. Acta*, **2**, 219 (1964).

[21] G. Del Re, *J. Chem. Soc.*, **1958**, 4031.

[22] G. Del Re and B. Pullman, *J. Chem. Phys.*, **62**, 942 (1965).

[23] J. A. Pople, *Proc. Phys. Soc.*, **A 68**, 81 (1955).

[24] L. Ciohodaru, *Rev. Roumaine Chim.*, **22**, 983 (1977).

[25] J. C. Slater, *Phys. Rev.*, **36**, 57 (1930).

The coordinates of atoms in the molecule of the unsubstituted *trans*-stilbene have been calculated using the X-ray diffraction data,[26] but for our studied polynitro-*trans*-stilbene derivatives literature data are missing ; therefore, approximate values for bond lengths and angles were employed.[27]

RESULTS AND DISCUSSION

The stilbene derivatives which we refer to in the present paper agree with the following general formula :

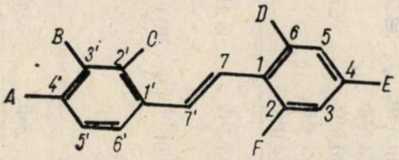

The substituents (A—F) are listed in table 1.

The syntheses of these derivatives, according to the literature data, have been previously reported.[28]

To make it short, we shall not reproduce all our calculated energies, but quote only the relevant results for our *trans*-stilbene derivatives.

Table 1

The substituents of the studied stilbene derivatives

Deriv. N°	A	B	C	D	E	F	Comments
1	H	H	H	H	NO_2	NO_2	
2	H	H	NO_2	H	NO_2	NO_2	positional isomers
3	H	NO_2	H	H	NO_2	NO_2	
4	NO_2	H	H	H	NO_2	NO_2	
5	H	H	H	NO_2	NO_2	NO_2	
6	NO_2	H	H	NO_2	NO_2	NO_2	

Table 2 contains the assignments of the *A* and *B* absorption bands proposed for our stilbenes, by way of comparison between the SCF-LCI calculation results and the experimental data obtained from the electronic spectra of the same stilbene derivatives. [28]

In order to realize the accuracy of our calculation process, table 2 contains also the data for the unsubstituted *trans*-stilbene recalculated using the above explained process.

Examining the data obtained by means of the LCI-PPP calculation and by comparison of these data with the experimental spectral data (UV-visible) the following conclusions may be drawn :

1. The presence of nitro groups in molecules of *trans*-stilbene derivatives leads to the decrease of the energy difference between the ground

---

[26] J. M. ROBERTSON and I. WOODWARD, *Proc. Roy. Soc.*, **A 162**, 568 (1937).

[27] "Tables of Interatomic Distances and Configurations in Molecules and Ions", The Chemical Society, London, 1958.

[28] L. CIOHODARU and A. MEGHEA, *Rev. Roumaine Chim.*, **21**, 1127 (1976).

Table 2

The assignments of the *A* and *B* absorption bands proposed for the studied *trans*-nitro-stilbenes (All molecules are assumed to have a planar conformation ; ΔE in *eV* ; Singlet configurations $^1\Phi_{i\leftarrow k'}$ correspond to transfer of a π electron from an occupied MO Φ_i of the ground state configuration to an unoccupied MO $\Phi_{k'}$)

Der. No	Band	ΔE_{exp}^{a}	f_{exp}	ΔE_{calc}^{b} ($^1\Phi_{i\rightarrow k'}$)	ΔE_{calc}^{c}			ΔE_{calc}^{d}		
					ΔE_{calc}	f_{calc}	Wt. % of most important spin configurations	ΔE_{calc}	f_{calc}	Wt. % of most important spin configuration
trans-stilbene	*A*	4.21^{e}	0.886	5.0193($^1\Phi_{7-8'}$)	4.9946	1.4663	98$^1\Phi_{7-8'}$	4.6344	0.0472	40.5$^1\Phi_{7-9'}$; 32.2$^1\Phi_{6-8'}$; 13.8$^1\Phi_{4-10'}$; 13.5$^1\Phi_{5-11'}$
								4.6401	0.0005	40.6$^1\Phi_{7-10'}$; 31.6$^1\Phi_{5-8'}$; 14.0$^1\Phi_{4-9'}$; 13.4$^1\Phi_{6-11'}$
								4.8583	1.6364	92.0$^1\Phi_{7-8'}$
	B	5.42		5.6579($^1\Phi_{7-10'}$)	5.4424	0.1571	63.6$^1\Phi_{7-9'}$; 36.5$^1\Phi_{6-8'}$	5.7356	0.0005	43.7$^1\Phi_{5-8'}$; 39.1$^1\Phi_{7-10'}$; 9.5$^1\Phi_{6-11'}$;
				5.6951($^1\Phi_{7-9'}$)	6.1555	1.3363	63.0$^1\Phi_{6-8'}$; 35.8$^1\Phi_{7-9'}$	5.9029	1.6985	44.0$^1\Phi_{6-8'}$; 40.6$^1\Phi_{7-9'}$
				5.8501($^1\Phi_{5-8'}$)						
				5.8901($^1\Phi_{6-8'}$)						
1	*A*	3.50	0.695	4.5606($^1\Phi_{11-12'}$)				4.2132	1.2338	75.2$^1\Phi_{11-12'}$; 8.3$^1\Phi_{11-13'}$; 5.5$^1\Phi_{9-12'}$
	B	3.39	0.979	4.9916($^1\Phi_{11-13'}$)				4.5340	0.0616	35.6$^1\Phi_{11-15'}$; 27.9$^1\Phi_{10-14'}$; 22.4$^1\Phi_{10-12'}$; 7.7$^1\Phi_{9-15'}$
				5.5107($^1\Phi_{11-15'}$)				4.6609	0.7044	70.8$^1\Phi_{11-13'}$; 12.8$^1\Phi_{11-12'}$; 11.4$^1\Phi_{9-13'}$
				5.7544($^1\Phi_{8-12'}$)				5.4810	0.3591	42.6$^1\Phi_{8-12'}$; 41.6$^1\Phi_{9-12'}$; 5.4$^1\Phi_{8-13'}$
				5.7988($^1\Phi_{9-12'}$)				5.5642	0.8501	28.0$^1\Phi_{11-14'}$; 22.0$^1\Phi_{11-15'}$; 19.2$^1\Phi_{10-12'}$; 10.8$^1\Phi_{9-12'}$; 10.5$^1\Phi_{10-14'}$
				5.8841($^1\Phi_{11-14'}$)				5.6914	0.6247	21.8$^1\Phi_{11-14'}$; 21.4$\Phi_{11-15'}$; 20.5$^1\Phi_{8-12'}$; 11.8$^1\Phi_{10-12'}$; 6.2$^1\Phi_{8-13'}$; 5.7$^1\Phi_{9-13'}$
				5.8909($^1\Phi_{10-12'}$)						

2	*A*	3.64	0.654	$4.4169(^1\Phi_{13-14'})$				4.1301	1.1039	$64.8^1\Phi_{13-14'}$; $14.9^1\Phi_{13-15'}$; $8.4^1\Phi_{13-16'}$
	B	5.16[e]		$4.7133(^1\Phi_{13-15'})$				4.4355	0.1463	$39.4^1\Phi_{13-16'}$; $29.8^1\Phi_{13-15'}$; $9.7^1\Phi_{12-14'}$; $9.0^1\Phi_{12-17'}$
				$4.9499(^1\Phi_{13-16})$				4.6560	0.7913	$43.2^1\Phi_{13-15'}$; $29.5^1\Phi_{13-14'}$; $10.6^1\Phi_{13-16'}$; $5.3^1\Phi_{12-14'}$
				$5.4696(^1\Phi_{13-17'})$				5.3129	0.2313	$77.5^1\Phi_{13-17'}$; $10.0^1\Phi_{11-14'}$; $5.5^1\Phi_{10-14'}$
				$5.7950(^1\Phi_{10-14'})$				5.4772	0.9330	$35.6^1\Phi_{13-16'}$; $33.7^1\Phi_{12-14'}$; $27.4^1\Phi_{12-17'}$
								5.6881	0.7525	$75.0^1\Phi_{10-14'}$; $9.7^1\Phi_{13-17'}$
3	*A*	3.64	0.664	$4.5446(^1\Phi_{13-14'})$	4.5079	1.1428	$90.1^1\Phi_{13-14'}$; $9.8^1\Phi_{13-15'}$	4.2923	1.1434	$67.0^1\Phi_{13-14'}$; $19.2^1\Phi_{13-15'}$
	B	5.06	1.331	$4.8427(^1\Phi_{13-15'})$	4.8784	0.6064	$90.1^1\Phi_{13-15'}$; $9.8^1\Phi_{13-14}$	4.4704	0.2225	$24.9^1\Phi_{13-16'}$; $17.6^1\Phi_{13-17'}$; $16.4^1\Phi_{12-14'}$; $13.7^1\Phi_{12-16'}$; $9.7^1\Phi_{12-17'}$; $5.7^1\Phi_{13-15'}$; $5.4^1\Phi_{10-16'}$
				$5.4426(^1\Phi_{13-16'})$						
				$5.4426(^1\Phi_{13-17'})$				4.6349	0.7810	$61.1^1\Phi_{13-15'}$; $25.0^1\Phi_{13-14'}$; $7.5^1\Phi_{10-15'}$
				$5.8102(^1\Phi_{12-16'})$				5.4926	0.5545	$59.0^1\Phi_{13-17'}$; $14.1^1\Phi_{10-14'}$; $9.5^1\Phi_{12-14'}$; $8.4^1\Phi_{12-17'}$; $6.1^1\Phi_{13-16'}$
								5.5495	0.9633	$48.5^1\Phi_{13-16'}$; $22.0^1\Phi_{12-14'}$; $11.4^1\Phi_{12-16'}$; $6.9^1\Phi_{10-14'}$; $6.0^1\Phi_{12-17}$
								5.8940	0.8270	$56.1^1\Phi_{12-16}$; $31.0^1\Phi_{12-17'}$
4	*A*	3.52	0.825	$4.5583(^1\Phi_{13-14'})$	4.5204	1.1693	$91.0^1\Phi_{13-14'}$; $9.0^1\Phi_{13-15'}$	4.4362	1.1679	$67.8^1\Phi_{13-14'}$; $18.3^1\Phi_{13-15'}$
5	*A*	3.54	0.504	$4.1299(^1\Phi_{13-14'})$	4.1157	0.9733	$92.0^1\Phi_{13-14'}$; $7.9^1\Phi_{13-15'}$	3.7996	0.8461	$54.0^1\Phi_{13-15'}$; $29.0^1\Phi_{13-14'}$; $12.1^1\Phi_{11-15'}$
								3.8711	0.8051	$58.8^1\Phi_{13-14'}$; $25.8^1\Phi_{13-15'}$; $7.6^1\Phi_{11-15'}$; $5.7^1\Phi_{11-14'}$
6	*A*	3.99	1.018	$4.1298(^1\Phi_{15-16'})$	4.1121	1.0472	$89.4^1\Phi_{15-16'}$; $10.7^1\Phi_{15-17'}$	3.8751	1.0438	$47.1^1\Phi_{15-17'}$; $41.5^1\Phi_{15-16'}$; $6.0^1\Phi_{13-17'}$
				$4.2426(^1\Phi_{15-17'})$	4.2570	0.3935	$89.4^1\Phi_{15-17'}$; $10.7^1\Phi_{15-16'}$	3.9492	0.7368	$49.5^1\Phi_{15-16'}$; $38.9^1\Phi_{15-17'}$; $7.2^1\Phi_{13-17}$

a $-\Delta E_{exp}$ taken from a previous paper;[28]

b $-\Delta E_{calc}$ akng into account only the ground state configuration;

c $-\Delta E_{calc}$ taking into account 4 monoexcited configurations;

d $-\Delta E_{calc}$ taking into account 16 monoexcited configurations;

e $-$ *B* the band did not appear completely in our experimental conditions.[28]

Table 3

The modification of the S – S transition energies for 2,4-dinitro-*trans*-stilbene, assuming that *ortho* nitro group is rotated out of the benzene ring plane at different degrees (ΔE in *eV*; ΔE_{exp} is 3.50(A) and 5.39 (B); ΔE_{calc} taking into account 16 spin configurations; $^1\Phi_{i\to k'}$, has the same significance shown in Table 2)

Band	ΔE_{calc}	f_{calc}	0° Wt% of most important spin configurations	ΔE_{calc}	f_{calc}	5° Wt% of most important spin configurations
A	4.2132	1.2338	75.2$^1\Phi_{11-12'}$; 8.3$^1\Phi_{11-13'}$; 5.5$^1\Phi_{9-12'}$	4.5186	1.3285	76.5$^1\Phi_{11-12'}$; 13.5$^1\Phi_{9-12'}$
B	4.5340	0.0616	35.6$^1\Phi_{11-15'}$; 27.9$^1\Phi_{10-14}$; 22.4$^1\Phi_{10-12'}$; 7.7$^1\Phi_{9-15'}$	5.0445	0.1363	42.0$^1\Phi_{11-15'}$; 22.9$^1\Phi_{10-14'}$; 21.4$^1\Phi_{10-12'}$ 8.8$^1\Phi_{9-15'}$
	4.6609	0.7044	70.8$^1\Phi_{11-13'}$; 12.8$^1\Phi_{11-12'}$; 11.4$^1\Phi_{9-13'}$	5.2210	0.6338	69.0$^1\Phi_{11-13'}$; 16.3$^1\Phi_{9-13'}$
	5.4810	0.3591	42.6$^1\Phi_{8-12'}$; 41.6$^1\Phi_{9-12'}$; 5.4$^1\Phi_{8-13'}$	5.9843	0.5385	39.8$^1\Phi_{9-12'}$; 22.4$^1\Phi_{11-14'}$; 13.8$^1\Phi_{10-15'}$ 9.5$^1\Phi_{8-12'}$
	5.5642	0.8501	28.0$^1\Phi_{11-14'}$; 22.0$^1\Phi_{11-15'}$; 19.2$^1\Phi_{10-12'}$; 10.8$^{11}\Phi_{9-12'}$; 10.5$^1\Phi_{10-14'}$	6.2330	0.9993	43.6$^1\Phi_{10-12'}$; 38.4$^1\Phi_{11-15'}$; 8.6$^1\Phi_{10-14'}$
	5.6914	0.6247	21.8$^1\Phi_{11-14'}$; 21.4$^1\Phi_{11-15'}$; 20.5$^1\Phi_{8-12'}$; 11.8$^1\Phi_{10-12'}$; 6.2$^1\Phi_{8-13'}$; 5.7$^1\Phi_{9-13'}$	6.3420	0.2896	38.2$^1\Phi_{8-12'}$; 22.9$^1\Phi_{10-15'}$; 8.9$^1\Phi_{8-13'}$; 7.3$^1\Phi_{11-14'}$
			15°			30°
A	4.5391	1.3350	76.0$^1\Phi_{11-12'}$; 13.4$^1\Phi_{9-12'}$	4.5273	1.3085	76.0$^1\Phi_{11-12'}$; 14.1$^1\Phi_{9-12'}$
B	5.0417	0.1502	42.0$^1\Phi_{11-15'}$; 23.5$^1\Phi_{10-14'}$; 22.5$^1\Phi_{10-12'}$; 8.3$^1\Phi_{9-15'}$	5.0405	0.1472	41.1$^1\Phi_{11-15'}$; 24.9$^1\Phi_{10-12'}$; 23.44$^1\Phi_{10-14'}$ 7.4$^1\Phi_{9-15'}$
	5.2517	0.6080	67.0$^1\Phi_{11-13'}$; 17.0$^1\Phi_{9-13'}$	5.2630	0.5942	64.0$^1\Phi_{11-13'}$; 17.2$^1\Phi_{9-13'}$
	5.9905	0.5392	40.0$^1\Phi_{9-12'}$; 23.1$^1\Phi_{11-14'}$; 14.5$^1\Phi_{10-15'}$; 7.7$^1\Phi_{8-12'}$	5.9739	0.5689	40.6$^1\Phi_{9-12'}$; 20.6$^1\Phi_{11-14'}$; 12.8$^1\Phi_{10-15'}$; 7.8$^1\Phi_{8-12'}$
	6.2306	1.0118	43.5$^1\Phi_{10-12'}$; 39.6$^1\Phi_{11-15'}$; 8.4$^1\Phi_{10-14'}$	6.1997	0.9986	43.2$^1\Phi_{10-12'}$; 41.3$^1\Phi_{11-15'}$; 7.1 $\Phi_{10-14'}$
	6.3747	0.3482	37.5$^1\Phi_{8-12'}$; 35.7$^1\Phi_{10-15'}$; 6.0$^1\Phi_{9-12'}$	6.3713	0.4508	42.0$^1\Phi_{10-15'}$; 34.0$^1\Phi_{8-12'}$
			45°			90°
A	4.5109	1.2767	76.0$^1\Phi_{11-12'}$; 14.7$^1\Phi_{9-12'}$	4.5261	1.2666	75.1$^1\Phi_{11-12'}$; 15.2$^1\Phi_{9-12'}$
B	5.0360	0.1399	39.4$^1\Phi_{11-15'}$; 27.8 $\Phi_{10-12'}$; 23.3$^1\Phi_{10-14'}$	5.0174	0.1314	37.0$^1\Phi_{11-15'}$; 31.2$^1\Phi_{10-12'}$; 23.7$^1\Phi_{10-14'}$ 5.6$^1\Phi_{9-15'}$
	5.2607	0.5750	61.0$^1\Phi_{11-13'}$; 16.5$^1\Phi_{9-13'}$	5.2670	0.5279	55.0$^1\Phi_{11-13'}$; 15.8$^1\Phi_{9-13'}$; 7.4$^1\Phi_{9-12'}$; 7.3$^1\Phi_{8-12'}$; 6.5$^1\Phi_{-11-12'}$
	5.9445	0.6047	40.5$^1\Phi_{9-12'}$; 17.4$^1\Phi_{11-14'}$; 10.0$^1\Phi_{10-15'}$; 8.8$^1\Phi_{9-13'}$; 8.8$^1\Phi_{11-13'}$; 7.3$^1\Phi_{8-12'}$	5.9210	0.6224	38.7$^1\Phi_{9-12'}$; 15.4$^1\Phi_{11-14'}$; 12.4$^1\Phi_{11-13'}$; 11.6$^1\Phi_{9-13'}$; 8.0$^1\Phi_{10-15'}$; 6.3$^1\Phi_{8-12'}$
	6.1627	0.9851	43.1$^1\Phi_{11-15'}$; 42.3$^1\Phi_{10-12'}$	6.1373	0.9962	46.5$^1\Phi_{11-15'}$; 40.5$^1\Phi_{10-12'}$
	6.3499	0.4700	40.6$^1\Phi_{10-15'}$; 32.8$^1\Phi_{8-12'}$	6.3379	0.5775	47.4$^1\Phi_{10-15'}$; 30.9$^1\Phi_{10-14'}$; 6.7$^1\Phi_{11-13'}$; 6.5$^1\Phi_{11-14'}$

state and the first excited state, regardless of their number and position; this decrease correlates well with $\lambda_{A_{\max}}$[28] of the S—S corresponding transition appearing in the electronic absorption spectrum. A similar conclusion has been reached from the HMO calculations. [22] This fact represents a support of the statement that for such large molecules, for which SCF calculations are laborious, the results of the HMO calculations may be employed especially when we need relative values for certain parameters or characteristics in a series of close related molecules.

2. The diagrams of the π-energy levels are changed due to the influence of the substituents, reaching similar findings with those previously reported.[24]

3. In comparison with the neglect of the configuration interaction, the calculated transition energy from the ground state to a singlet state represents a better approximation, depending on the number of monoexcited configurations taken into account, for the *A* band but no for the *B* band. The calculated energy values are nearer to the experimental values if we take into account a number of 16 monoexcited configurations instead of a smaller number (4).

4. It may be considered that the calculated values of the transition energies for the polynitro-*trans*-stibene derivatives dealt with in this paper are in good agreement with the experimental values. We can mention that the best agreement may be observed in the *A* band of the compounds N° **5** and **6**.

5. The calculated bands are generally composed from many transitions ; the values of the oscillator strength point out the allowed and forbidden transitions ; the assignments based on the symmetry considerations could not be made for our stilbene derivatives.

6. The satisfactory agreement of the results of the MO-LCI-PPP calculation with the experimental results obtained from the electronic absorption spectra together with our previously reported conclusions drawn from UV and IR spectra,[28,29] confirm the *trans* geometry of the studied stilbene derivatives.

7. This agreement also confirms the assumption that these stilbene derivatives show a great tendency to adopt a planar conformation, the existing out-of-plane deviation, due to the *ortho* nitro group, being small. Again it emphasises the conclusion resulted from our previous papers.[28,29] In order to confirm this affirmation we present as example (Table 3) the modifications of the S-S transition energy values corresponding to the *A* and *B* bands of 2,4-dinitro-*trans*-stilbene assuming that *ortho* nitro group is rotated out of the benzene ring plane at different degrees. We can see that the difference between the calculated transition energy values and the experimental ones is reasonable for the planar conformation.

---

[29] L. Ciohodaru, *Rev. Roumaine Chim.*, **22**, 163 (1977).

Revue Roumaine de Chimie, **23**, *6*, 861 – 864 (1978)

HIGHLY PURE GALLIUM OBTAINED BY A SIMPLE TECHNIQUE

VALENTINA LĂZĂRESCU* and M.F. LĂZĂRESCU

R & D Laboratories Radio Components and Semiconductor Devices Co., Str. Erou Iancu Nicolae nr. 32, Bucharest, Romania

Received March 27, 1976

A new technique for obtaining highly pure gallium is presented. The procedure consists of acid treatment, followed by heating under vacuum and repeated crystallizations, alternating with acid washings. High yields of purified product are obtained.

Since 1952 when Welker[1] published his classical paper on new semiconducting compounds and applied it for patents on III—V compound semiconductor devices, the purification of III Group and V Group elements has attracted much research effort. It is evident that a startling innovation in purification methods could hardly be introduced, progress can rather be made by use of combinations of methods and by refinements in existing techniques and procedures.

There are two types of methods for gallium purification :

(1) Those acting directly on gallium in the metallic state : acid treatment,[2,3] treatments with oxygen or other gases,[4,5] heating under vacuum,[6-9]

---

* Present address : Center of Physical Chemistry, Str. Dumbrava Roșie 23, Bucharest, Romania

[1] H. Welker, *Z. Naturforsch.*, **7a**, 744 (1952).

[2] E. Papp and K. Solymar, *Femipari Kutato Intezet Kölemenyei (Hung)*, **4**, 117 (1960) ; *Chem. Abstr.*, **55**, 22023 (1961).

[3] S. M. Kulifay (to Monsanto Co), U.S. Pat. 3, 166, 405, Jan. 19, 1965 ; *Chem. Abstr.*, **62**, 8794 (1965).

[4] R. J. Sime and J. L. Margrave, *J. Phys. Chem.*, **60**, 810 (1956).

[5] H. Merkel (to Siemens), U.S. Pat. 2, 927, 853, March 8, 1960 ; *Chem. Abstr.*, **54**, 10799 (1960).

[6] W. M. Craig and G. W. Drake, *J. Amer. Chem. Soc.*, **56**, 584 (1934).

[7] R. Reinmann, *Schweiz. Arch.*, **1**, 39 (1960).

[8] F. D. Rosi, D. Meyerhofer and R. V. Jensen, *J. Appl. Phys.*, **31**, 1105 (1960).

[9] L. Sakavarelidze, A. A. Mirtskhulava and Z. V. Lobzhanidze, *Soobshch. Akad. Nauk. Gruz. S.S.R.*, **67**, 61 (1972).

vacuum distillation,[10] fractional crystallization and zone refining, [10-12] action of other liquid metals (Hg). [13]

(2) Those operating on a gallium compound : electrolysis, [14,15] solvent extraction of $GaCl_3$[16], distillation or disproportion of gallium halides, [17,18] zone refining of $GaCl_3$, [19] formation of organometallic compounds. [20]

The method proposed here consists of the following sequence of operations : H_2SO_4 treatments, heating under vacuum and repeated crystallizations, alternating with nitric acid and deionized water washings.

The starting gallium (a by-product from the aluminum industry) was of 96.5% purity and the main impurities were Zn 3.5%, Hg 0.01%, Fe 0.01%, Cu, Si, Mg, Pb, Al, Ti, Ca 0.01%. Some of them are eliminated by the preliminary H_2SO_4 treatment (Zn, Fe) or by heating under vacuum (Hg, Pb). The remaining ones are removed in the third stage, using the property of gallium oxide film to retain traces impurities.

ACID TREATMENT

Nitric acid and hydrochloric acid washings were used separately or alternately by a great number of authors[2,3] for gallium purification. These two acids dissolve the oxidized gallium, remove some of the impurities and reduce the other. Because nitric acid has the tendency to disperse gallium and hydrochloric acid on the contrary, to aglomerate it, these two washings must be associated.

However, this treatment causes an important loss of gallium because both nitric and hydrochloric acids attack this metal, even at room temperature. This is why we propose to perform this preliminary purification in a different way. We have found that conc. H_2SO_4 washings are very efficient and have the advantage of a better yield. With 3—4 washings of 15—20 minutes each, we have succeeded in completely eliminating some impurities and decreasing the content of others. After this stage, traces of Hg, and Cu were still present. The process efficiency will be increased if the washings are carried out under magnetic stirring. Acid consumption is about 3 ml per gram of gallium to be purified and the quality must be of electronic grade. The yield after this first stage is of 91.66%.

---

[10] O. Klug, *Neue Hütte*, **12**, 722 (1968).

[11] R. Degeilh and C. Blaizat (to Produits Semiconducteurs), Fr. Pat. 1, 382, 904 Dec. 24, 1964 ; *Chem. Abstr.*, **62**, 11292 (1965).

[12] R. V. Ivanova and A. A. Belskii, *Nauch. Tr. Nauch. — Issled. Proekt. Inst. Redkometal. Prom.*, **38**, 109 (1972) ; *Chem. Abstr.*, **80**, 98667 (1974).

[13] H. G. Plust (to Siemens), Ger. Pat. 1, 022, 012, Jan. 2, 1958 ; *Chem. Abstr.*, **54**, 9707 (1960).

[14] R. Raffaeloff and E. Yellin, *J. Less. Common. Metals*, **19**, 63 (1969).

[15] I. Somosi, B. Toth and Z. Pais, Hung. Tejes 4935, Aug. 28, 1972 ; *Chem. Abstr.*, **78**, 60884 (1973).

[16] A. R. Powel, *J. Appl. Chem.*, **1**, 541 (1951).

[17] L. A. Niselson, N. N. Alekseeva and R. V. Ivanova, *Izvest. Akad. Nauk. S.S.S.R. Metal*, **1965**, 40.

[18] S. A. Vysotskii, L. A. Firsanova and L. Osipova, *Izvest. Akad. Nauk. S.S.S.R. Metal*, **1971**, 52.

[19] N. Goldsmith, A. Mayer and L. Vieland, *J. Less. Common, Metals*, **4**, 464 (1962).

[20] Siemens-Schuckertwerke AG, Brit. Pat. 1, 001, 482, Aug. 18, 1965 ; *Chem. Abstr.* **63**, 12730 (1965).

HEATING UNDER VACUUM

The low vapour pressure of gallium at a fairly high temperature (0.001 torr at 1000°) makes possible the removal of various volatile impurities like Hg, Mg and Ca, as well as halides and dissolved gases.[6-8]

The extraction of impurities depends on temperature and vacuum conditions, and on the time of heating. Generally, a good efficiency of the process is conditioned by a low temperature treatment in high vacuum for a long time, rather than by a higher temperature and slighty lower vacuum. Moreover at higher temperatures, the problem of gallium contamination by crucibles may be more critical than in other methods of purification.

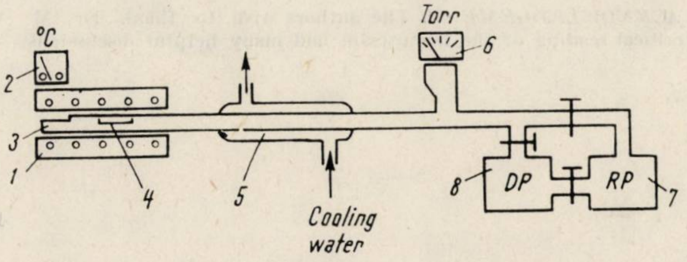

Fig. 1.— Arrangement for gallium heating under vacuum
1) furnace; *2*)furnace control thermocouple; *3*) quartz container; *4*) quartz crucible; *5*) condenser; *6*) Penning vacuum gauge; *7*) rotary vacuum pump; *8*) diffusion vacuum pump.

For this operation we have used a quartz container, heated at a temperature of 750—800°, in a vacuum of 10^{-5} torr. For a sample of about 100 g, the treatment was conducted for 18—20 hours. The arrangement employed is shown schematically in Figure 1.

After this stage, spectral analysis of the gallium sample has indicated only small traces of copper.

CRYSTALLIZATIONS ALTERNATING WITH ACID WASHINGS

The next stage of gallium purification had to solve the problem of copper removal. For this purpose we have used a simple but efficient method, repeated solidifications of the metal alternating with nitric acid and deionized water washings. Solid gallium does not react with nitric acid while copper traces do. The thin film of oxide covering the crystallized-gallium has a tendency to retain part of the foreign elements, so that after 30—40 such operations, copper content is reducing to 2 ppm. Since the impurities to be measured are present only at the ppm level the deionized washing water should have a resistivity of at least 10^6 ohm cm and nitric acid must be of electronic purity.

Traces of remaining impurities in high purity gallium were determined spectrographically, after the separation of the matrix by extraction of $[GaCl]^{3-}$ into Et_2O from 6M HCl. The impurities were preconcentrated on a powder graphite collector (20—50 mg) and excited in a spark discharge by using graphite electrode.[21]

The end product analysis has indicated 2 ppm Cu, Hg + Ni + Pb + +Fe< 5 ppm.

CONCLUSIONS

By using the simple technique described, which does not require an intricate apparatus, it is possible to obtain a higher purity gallium (99.999%). Another advantage of this method should also be mentioned, namely, its good yield (>80%).

ACKNOWLEDGEMENT. The authors wish to thank Dr. M. Vass for the critical reading of the manuscript and many helpful discussions.

---

[21] W. Sokolowska, *Pr. Nauk. Inst. Chem. Nieorg. Met. Pierwiatskow RzadkichPolitech. Wraclaw*, **17**, 405 (1973); *Chem. Abstr.*, **80**, 152435 (1974).

Revue Roumaine de Chimie, 23, 6, 865–871 (1978)

REACTION MECHANISM FOR THE CONDENSATION OF FURFURAL WITH ACETONE IN THE CATALYSIS OF SODIUM HYDROXIDE. II[1]

THE ACTIVATED COMPLEX AND ITS CATALYTIC ACTION

D.A. ISĂCESCU* and FLORENTINA AVRAMESCU

Institute of Chemistry, Faculty of Chemistry, Splaiul Independenţei N° 89,
Bucharest, Romania

Received February 21, 1976

The paper presents the general mechanism of the furfural condensation reaction with acetone, explaining the form in which sodium hydroxide — activated complex acts catalytically. The general mechanism explains the formation of the main reaction compounds, FAc and F_2Ac.

The multitude of experimental data systematized in a previous paper[1] can be integrated in a reaction mechanism capable of emphasizing the factors and the phenomena involved in the furfural (F) condensation reaction with acetone (Ac) in the catalysis of sodium hydroxide and at the same time capable of explaining the large and varied number of results, by dividing the factors specified in table 1[1] into two groups, according to the nature of their involvement.

The first group consists of the factors involved in all the reactions regardless of the working conditions.

We refer to the reaction course under the influence of such factors as being the general mechanism.

The second group is formed of factors constituting the working conditions and influencing the general mechanism. We refer to the reaction course under the influence of such conditions as being the particularities of the general mechanism.

---

* Deceased 1977

[1] Part I: D. A. Isăcescu and F. Avramescu, *Rev. Roumaine Chim.*, 23, 661 (1978).

The two parts are closely correlated forming a unitary whole which constitutes the mechanism established by us.

The reaction mechanism was established keeping into account the systematization and interpretation of our own experimental data and of those reported in the literature presented in a previous paper[1] as well as the formation of intermediate compounds theoretically deduced from the effects of the dynamic delocalization of electrons in the reagents molecules (F, Ac) under the catalyst influence and also the nature of the reaction conditions.

GENERAL MECHANISM

The general mechanism is influenced by reagents, by the catalyst and by the solvent nature as NaOH dissolution medium.

In the first place, it is necessary to establish what is the catalytic action of sodium hydroxide, respectively, of the form in which it acts catalytically. The fact mentioned in the literature, that NaOH acts by the hydroxyl ion, is a general statement which fails to explain the manner in which it acts.

a) The form in which sodium hydroxide, activated complex, acts catalytically

We considered the first step of the mechanism as being the reaction between furfural and sodium hydroxide.

Under the influence of the electrostatic field produced by Na$^+$ and HO$^-$ ions, the static shift of electrons in the furfural molecule passes to a dynamical delocalization with the formation of two centers, anionoid and cationoid.

The two centers form a polar bond and constitute the field in which the reaction with the catalyst occurs.

A sodium hydroxy-furfuraldehydate complex (1) is formed :

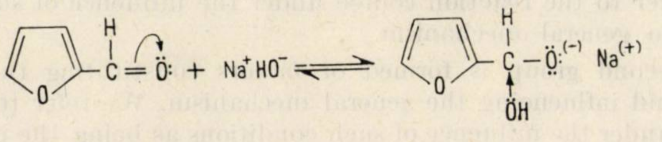

1

which represents the form in which NaOH acts catalytically and at the same time, the furfural activation form. This is the activated complex of the reaction.

The structure of the actived complex is influenced by the solvent nature as dissolution medium of sodium hydroxide.

When the solvent is water, the activated complex is sodium hydroxy-furfuraldehydate.

When the NaOH solution is prepared in ethyl alcohol, sodium ethoxide will form and the activated complex will be sodium ethoxy-furfuraldehydate

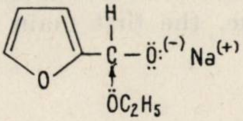

Sodium phenoxide forms in the presence of furfural as a solvent and the activated complex is sodium phenoxy-furfuraldehydate:

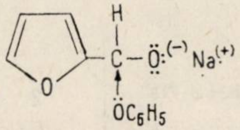

Identifying by R the hydrogen atom in the OH group, ethyl in the OC_2H_5 group and phenyl in the $-OC_6H_5$ group, which are linked at the cationoid center, the general form of the activated complex sodium R-oxy-furfuraldehydate results:

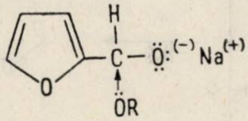

The formation of the activated complex was proven by:

— the initial endothermic effect in the reaction, measured as will be shown when discussing the influence of water as a solvent and by,

— the isolation of sodium phenoxy-furfuraldehydate, as will be shown when discussing the influence of phenol as a solvent.

The formation of sodium R-oxy-furfuraldehydate activated complex is the first step of the reaction mechanism.

b) Catalytic action of the activated complex on acetone

The second step of the reaction mechanism consists of the catalytic action of the activated complex on acetone by its activation with the removal of a proton and the formation of acetone monocarbanion.

The acetone monocarbanion substitutes the OR group in the complex with the formation of a reactive and unstable intermediate, sodium acetonyl-furfuraldehydate (2) which passes to the respective carbinol (3) with catalyst recovery. By elimination of intramolecular water it results in monofurfurylidene acetone, the first main reaction product :

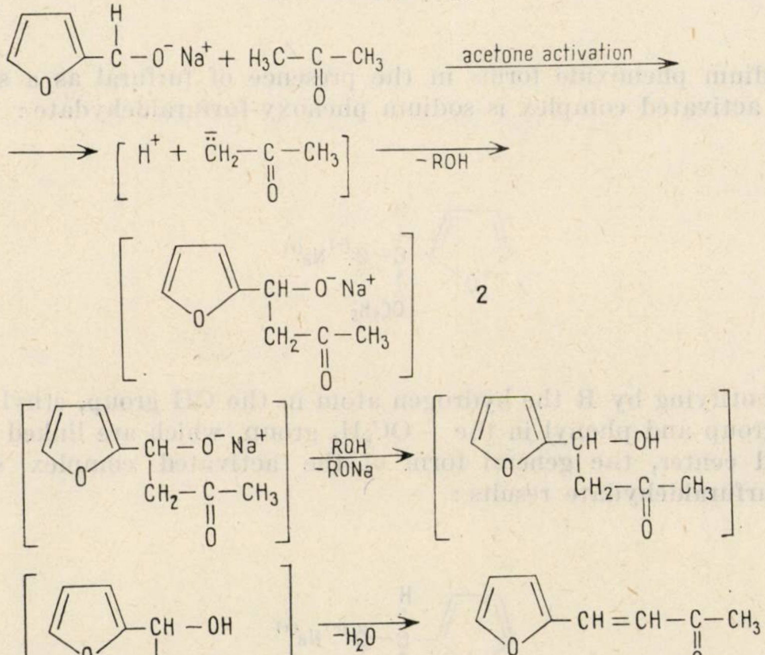

c) Catalytic action of the activated complex on monofurfurylidene acetone

The third step of the mechanism consists of the activation of FAc formed in the second step under the influence of a new molecule of sodium R-oxi-furfuraldehydate, respectively of a new furfural molecule with the removal of a proton and the formation of FAc monocarbanion.

The same mechanism shown in the condensation of the activated complex with acetone leads to the formation of sodium furfurylidene acetonyl furfuraldehydate (4) which passes to the respective carbinol (5) and the latter passes to F_2Ac which is the second main reaction product:

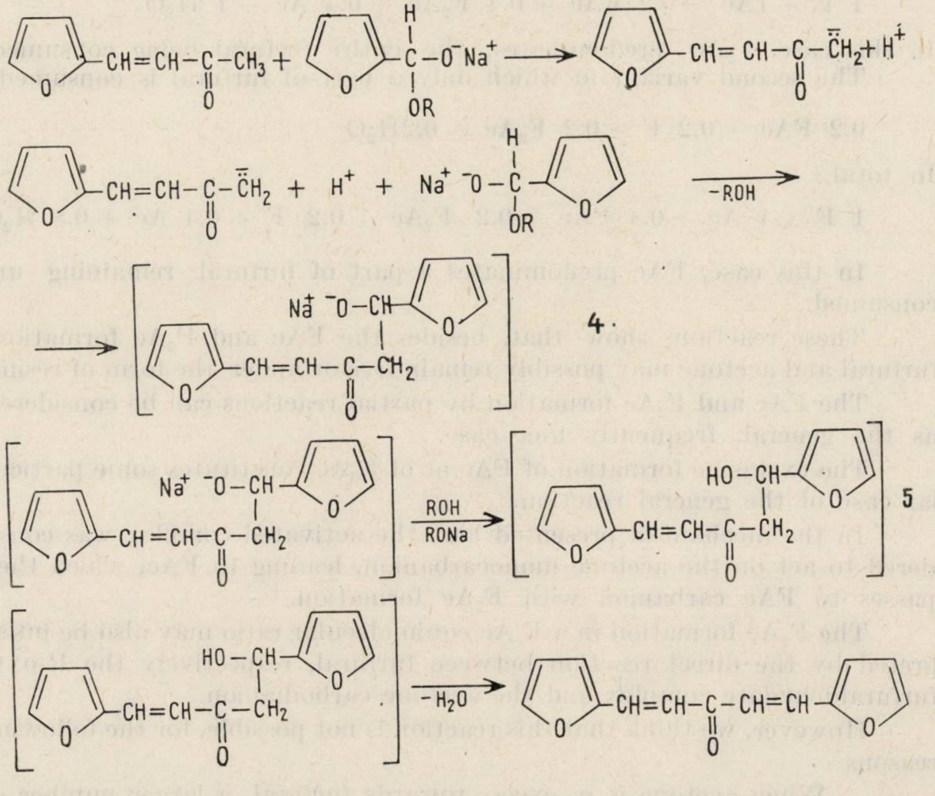

F_2Ac

It results from this mechanism that F_2Ac has formed passing through FAc.

The second step of the mechanism occurs for an 1F/1Ac molar ratio and the third step, for a 2F/1Ac ratio.

At a first sight the two steps seem to be the only possible ones.

In reality it has been experimentally found that FAc and F_2Ac are obtained even for an 1F/1Ac molar ratio (which was an exclusive condition for FAc formation).

In this case it is obvious that their formation occurs by a partial transformation of FAc to F_2Ac.

Briefly, this can be formulated by the following example:

$$1\ \mathrm{F} + 1\ \mathrm{Ac} \rightarrow 0.6\ \mathrm{FAc} + 0.4\ \mathrm{F} + 0.4\ \mathrm{Ac} + 0.6\ \mathrm{H_2O}$$

Two variants result thence, one in which the remaining furfural is consumed :

$$0.4\ \mathrm{FAc} + 0.4\ \mathrm{F} \rightarrow 0.4\ \mathrm{F_2Ac} + 0.4\ \mathrm{H_2O}$$

In total :

$$1\ \mathrm{F} + 1\mathrm{Ac} \rightarrow 0.2\ \mathrm{FAc} + 0.4\ \mathrm{F_2Ac} + 0.4\ \mathrm{Ac} + 1\ \mathrm{H_2O}$$

In this case, F_2Ac predominates, the entire furfural being consumed.

The second variant in which only a part of furfural is consumed :

$$0.2\ \mathrm{FAc} + 0.2\ \mathrm{F} \rightarrow 0.2\ \mathrm{F_2Ac} + 0.2\mathrm{H_2O}$$

In total :

$$1\ \mathrm{F} + 1\ \mathrm{Ac} \rightarrow 0.4\ \mathrm{FAc} + 0.2\ \mathrm{F_2Ac} + 0.2\ \mathrm{F} + 0.4\ \mathrm{Ac} + 0.8\ \mathrm{H_2O}$$

In this case, FAc predominates a part of furfural remaining unconsumed.

These reactions show that, besides the FAc and F_2Ac formation, furfural and acetone may possibly remain free or under the form of resins.

The FAc and F_2Ac formation by partial reactions can be considered as the general, frequently met case.

The exclusive formation of FAc or of F_2Ac constitutes some particular case of the general reaction.

In the mechanism presented here the activated complex was considered to act on the acetone monocarbanion, leading to FAc, which then passes to FAc carbanion with F_2Ac formation.

The F_2Ac formation in a F/Ac equimolecular ratio may also be interpreted by the direct reaction between furfural, respectively the R-oxyfurfuraldehydate complex and the acetone carbodianion.

However, we think that this reaction is not possible, for the following reasons :

— When acetone is in excess towards furfural, a larger number of acetone carbodianions should exist and hence more F_2Ac should form. However, it has been experimentally found, that at 20°, the F_2Ac amount decreases and the FAc amount increases with the increase of the excess acetone.

— The FAc carbanion is much more reactive than acetone carbodianion. For these reasons it reacts readily with the activated complex forming F_2Ac. F_2Ac appears two minutes after FAc formation even in excess furfural. If F_2Ac were formed by acetone carbodianion, its presence would have to be revealed at the very beginning of the reaction rather than two minutes later, as experimentally found.

— The likelihood of acetone carbodianion participation in the condensation reaction could be considered for a 2F/1Ac molar ratio.

In this case, since there are two furfural molecules for one acetone molecule, the probability of a simultaneous collision of the activated complex with acetone carbodianion can be accepted. Nevertheless, it has been experimentally found that FAc will always form alongside with large F_2Ac amounts.

The FAc formation is possible only with acetone monocarbanion. This means that also for a 2F/1Ac molar ratio, FAc forms first. As its carbanion is very reactive, it reacts with a new activated complex molecule, forming F_2Ac.

For the above mentioned reasons, it results that furfural changes to form F_2Ac passing through FAc.

This change explains why FAc will always be found alongside with F_2Ac, except for certain cases.

The data presented so far on the F condensation reaction with Ac in NaOH catalysis, in which the working conditions were disregarded, constitutes the general mechanism which explains the formation of the main reaction compounds, FAc, F_2Ac as well as furfural and acetone which do not react.

Revue Roumaine de Chimie, 23, 6, 873–881 (1978)

REACTION MECHANISM FOR THE CONDENSATION OF FURFURAL WITH ACETONE IN THE CATALYSIS OF SODIUM HYDROXIDE. III[1]

SOLVENT INFLUENCE ON THE NATURE OF THE ACTIVATED COMPLEX AND ON ITS CATALYTIC ACTION

D. A. ISĂCESCU* and FLORENTINA AVRAMESCU
Institute of Chemistry, Faculty of Chemistry, Splaiul Independenţei N° 89, Bucharest, Romania

Received February 21, 1976

The paper presents the influence of phenol as a solvent on the nature of the activated complex and on its catalytic action in the condensation reaction of furfural with acetone, explaining the formation of the main reaction compounds, of secondary products and of polymers.

As shown in the previous paper[1], the particularities of the reaction mechanism are determined by factors which constitute the working conditions, i.e. the solvent nature and amount used, the catalyst, the temperature and the ratio between reagents. These factors lead to various forms of activated complexes, to the appearance of a cocatalyst and to various reaction systems.

The activated complexes, the cocatalyst and the reaction systems activate in a different manner the mobility of electrons in the molecules of furfural (F) and acetone (Ac) which are involved in the general mechanism and the mobility of electrons in the molecule of the formed monofurfurylidene acetone (FAc), providing an explanation to the large and varied number of results.[1,2]

The general mechanism presented by us accounts for the formation of FAc and of F_2Ac (difurfurylidene acetone). However it fails to elucidate the conditions for the exclusive formation of FAc or of F_2Ac, the formation of F_2Ac alongside with FAc with or without predominance, for a F/Ac equimolecular ratio, the formation of secondary products and of polymers.

This part of the mechanism will be elucidated if we consider :

— the solvent nature (water, alcohol or phenol) as a medium for dissolving NaOH with formation of sodium hydroxy-, ethoxy- or phenoxy-furfuraldehydate acting with different intensities ;

---

* Deceased 1977

[1] Part II : D. A. Isăcescu and F. Avramescu, *Rev. Roumaine Chim.*, 23, 865 (1978).

[2] D. A. Isăcescu and F. Avramescu, *Rev. Roumaine Chim.*, **23**, 661 (1978).

— the solvent nature and amount as a reaction medium, with the formation of a homogeneous or a heterogeneous system;

— the NaOH amount in the total reaction mixture, respectively the F/NaOH/solvent molar ratio in 100 g mixture of the reaction components and

— the temperature at which the condensation reaction occurs, i.e. 10—20° and 75°.

The solvents used in the F condensation reaction with Ac are: water, acetone, ethyl alcohol and phenol, and the NaOH solution was prepared in water, ethyl alcohol or phenol.

We shall present in turn the influence of each separate solvent in relation to the other factors under consideration.

1. PHENOL AS A SOLVENT

Furfural, acetone and phenol are totally dissolved in each other forming a homogeneous system. Sodium hydroxide dissolves in phenol with the formation of sodium phenoxide.

According to the general reaction mechanism previously shown[1] sodium phenoxide reacts with furfural forming a larger phenoxy-furfuraldehydate anion which is the activated complex. Because of the remaining phenoxyl, the anionoid center of the aldehydate acquires a more pronounced electronegative character. The electrostatic field of the complex becomes more marked acting with intensity on acetone with FAc formation, and after its formation, another complex molecule acts on FAc, forming F_2Ac. However in these consecutive reactions, FAc cannot be totally transformed to F_2Ac due to the fact that, in parallel with the two reactions, the activated complex acts directly on furfural.

Under the influence of sodium phenoxy-furfuraldehydate, the carbonyl group of another furfural molecule will be activated leading to the formation of a larger sodium furfurylate phenoxy-furfuraldehydate anion:

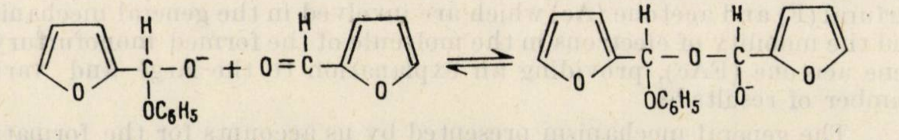

This anion has a high reactivity. The following phenomena take place therein: the migration of the negative charge from oxygen towards the carbon atom, respectively towards the hydrogen atom which passes to a hybride ion and its transfer to the carbon to which the phenolate radical is bound. At the same time, the phenoxyl ion which has previously been coordinatively bound, is detached. The structure of the resulted product is that of furfuryl furoate:

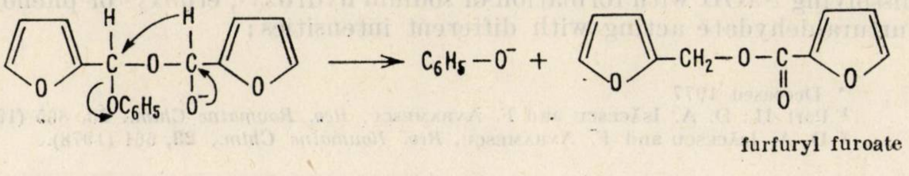

As the medium is anhydrous, the ester is stable and it may be isolated quantitatively. The detached phenoxyl ion forms a new activated complex which leads to the formation of another ester molecule.

If the reaction takes place with hydrated phenoxide, the activated complex formed undergoes partial hydrolysis, with the formation of a phenol molecule and of a hydroxy-furfuraldehydate anion :

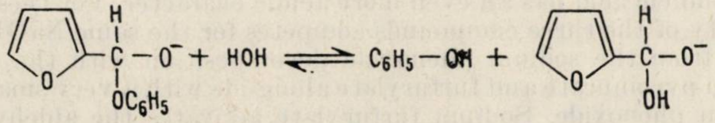

The formed anion activates a new furfural molecule with the formation of a larger anion :

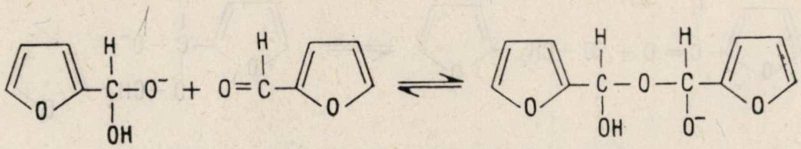

which eliminates a hydroxyl ion by the same previous mechanism, with the formation of the same ester, furfuryl furoate :

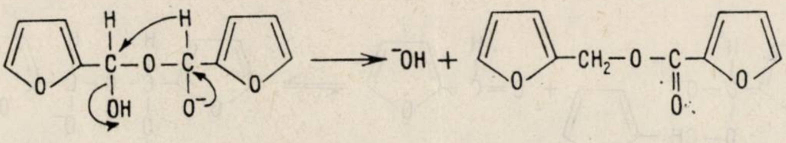

The medium containing the water of hydration of sodium phenoxide causes the released ⁻OH to hydrolize ester in furfurylic alcohol and sodium pyromucate :

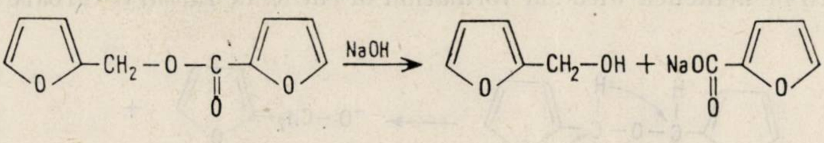

which are the two components of the Cannizzaro reaction of furfural.

In the presented mechanism we have experimentally proved each step : aldehydate, ester, alcohol and acid. We must now show what happens to the two components, furfuryl alcohol and pyromucic acid.

To this end, we have considered the protolytic constant of phenol, of furfural alcohol and of the pyromucic acid :

Substance	K_p
Phenol	$1.77.10^{-10}$
Furfuryl alcohol	$2.81.10^{-10}$
Pyromucic acid	$71.0.10^{-5}$

As can be seen, furfuryl alcohol has a more acidic character than phenol, and pyromucic acid has an even more acidic character. For these reasons, the acidity of the three compounds competes for the same NaOH amount resulted from the sodium phenoxide decomposition with the formation of sodium pyromucate and furfurylate alongside with a very small amount of sodium phenoxide. Sodium furfurylate activates the aldehyde group of furfural by the same mechanism as sodium phenoxide, leading to the formation of an intermediate furfuryl-oxy-furfuraldehydate anion which is a new type of activated complex :

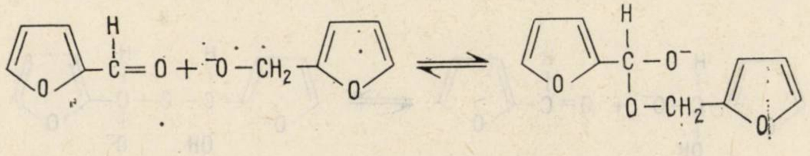

Due to the furfuryl alcohol rest, the reactivity of this complex is much higher than that of the phenoxy-furfuraldehydate and the intensity of its electrostatic field is much higher. It activates a new furfural molecule which is added to the anionoid center of the activated complex forming a larger anion intermediate :

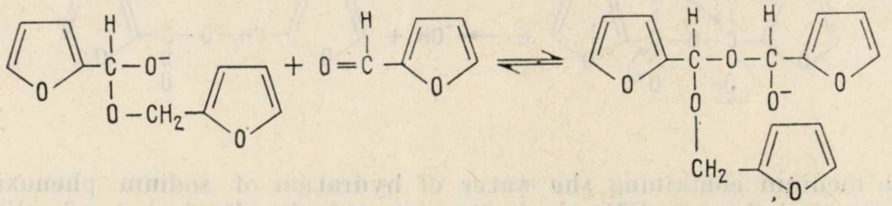

The same migration mechanism of the hydride ion causes a furfurylate ion to be detached with the formation of the same furfuryl furoate ester :

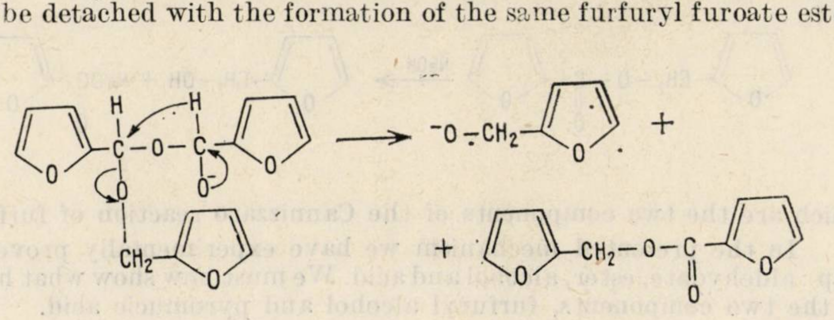

Further, under the influence of the hydroxyl ion, the furfuryl furoate hydrolizes according to the following mechanism. The ^{-}OH ion is added to the C=O double bond of the ester with the formation of a new intermediate anion :

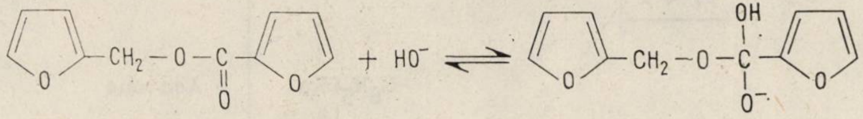

This anion splits into a furfurylate ion and pyromucic acid. The latter eliminates the proton passing to the 2-furan-carboxylate anion :

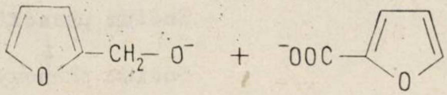

The furfurylate anion is again involved in the reaction with another furfural molecule closing a ring. As a result of these reactions, more and more furfuryl alcohol and pyromucic acid are being formed. The furfurylate anion, being a reaction product with a strong catalytic action, plays the role of a coaccelerator of the Cannizzaro reaction. This action becomes more marked as the amount of furfuryl alcohol increases, producing an autocatalytic shock. This shock determines the reaction acceleration and its exotherm, rapidly reaching temperatures of 75—90°. A rapid conversion of furfural to furfuryl alcohol takes place. The rate of this conversion is higher than that of the reaction between furfural and FAc, and this explains why approx. 0.5 moles of the furfural involved in the reaction is no more free to transform the entire FAc into F_2Ac. However the mechanism has not been completed here since an interaction between furfuryl alcohol and phenoxylate ion occurs simultaneously with the mentioned reactions, with the formation of a black resin.

The separations of phenoxy-furfuraldehydate, of furfuryl furoate and of furfuryl alcohol and piromucic acid, respectively, are evidences in favour of the mechanism established. This mechanism becomes clearer if we develop a general chart integrating the intermediate reaction products and the resulted final products, as a function of temperature and of the furfural amount involved in the reaction (experiment 27 d table 1 of the previous paper[2]).

This chart reveals three temperature ranges. In the upper part, the temperatures ranging between 10—20°, in the middle, an interval ranging between 20—40° and at the bottom the interval ranging between 40—75° (particularly 75°).

The activated complex of sodium phenoxy-furfuraldehydate, mono- and difurfurylidene acetone, form between 10—20° ; 0.44 moles of furfural are consumed here.

General chart

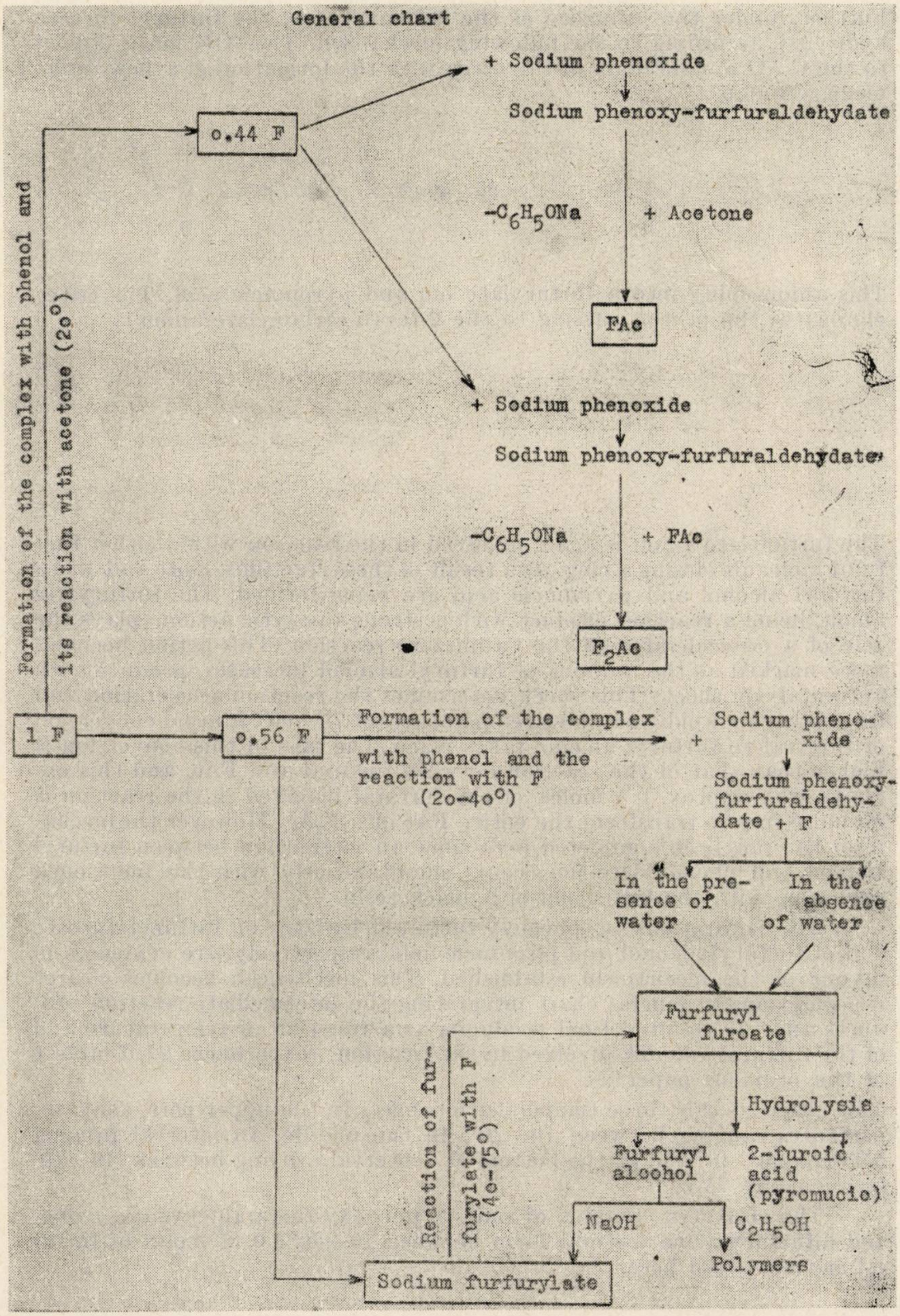
+ Sodium phenoxide
Sodium phenoxy-furfuraldehydate
o.44 F
Formation of the complex with phenol and its reaction with acetone (2o°)
−C6H5ONa
+ Acetone
FAc
+ Sodium phenoxide
Sodium phenoxy-furfuraldehydate
−C6H5ONa
+ FAc
F2Ac
1 F
o.56 F
Formation of the complex with phenol and the reaction with F (2o–4o°)
+ Sodium phenoxide
Sodium phenoxy-furfuraldehydate + F
In the presence of water
In the absence of water
Furfuryl furoate
Hydrolysis
Furfuryl alcohol
2-furoic acid (pyromucic)
NaOH
C2H5OH
Polymers
Reaction of furfurylate with F (4o–75°)
Sodium furfurylate

Between 20—40° we observe the formation of furfuryl furoate under the influence of a new phenoxy-furfuraldehydate molecule formed at 20°.

Between 40—55°, the formation of ester is accentuated. Likewise, its hydrolysis also begins in the presence of water traces resulted from condensation, with the formation of furfuryl alcohol and pyromucic acid. The hydrolysis reaction rate increases within the 65—80° interval. At the sametime, the formed furfuryl alcohol is transformed to sodium furfurylate which becomes a stronger catalyst than sodium phenoxy-furfuraldehydate. Under its influence, the entire remaining furfural is transformed to furfuryl alcohol and pyromucic acid by means of furfuryl furoate. The increased amount of furfuryl alcohol, and of sodium furfurylate, respectively, determines an accelerated catalysis of the reaction. Eventually, the formed furfuryl alcohol reacts with phenol. 0.56 moles of furfural are consumed in the furfural reaction with sodium phenoxy-furfuraldehydate and furfurylate.

The main conclusion drawn thereof is that the furfural condensation reaction with acetone in excess furfural is produced under the action of two catalysts, sodium phenoxy-furfuraldehydate and sodium furfurylate.

Sodium phenoxy-furfuraldehydate participates in the formation of FAc, F_2Ac and of a certain amount of furfuryl furoate whose hydrolysis may lead to a minimum amount of furfuryl alcohol which acts catalytically as sodium furfurylate.

Sodium furfurylate participates in the transformation of the remaining furfural to ester and into furfuryl alcohol and pyromucic acid respectively, which then condense with phenol leading to the formation of resins.

Therefore, two reactions are competing at temperature intervals ranging within 20—40—55° and 65—80°. One is produced by the catalytic action of phenoxy-furfuraldehydate and another is produced by the autocatalytic shock of furfurylate which transforms most part of furfural.

Both compete for the formation of furfuryl furoate which is found in the center of the transformation reactions of furfural which has not reacted with acetone.

It results that all the transformation reactions of the free furfural lead to furfuryl furoate and start from it. In these transformations, the motive force of the reaction is the tendency of the oxygen with negative charge found in the four large intermediate anions, to form a C=O double bond, a fact which leads to the formation of the hydride ion and to its transfer to the cationoid center which determines phenoxylate or furfurylate radicals to be detached. The furfurylate ion determines the autocatalytic shock which leads to the furfural final transformation.

FAc and F_2Ac, even in excess furfural, will always occur in the furfural condensation reaction with acetone, in exclusive conditions for F_2Ac formation. This is due to the fact that FAc has not sufficient furfural to change to F_2Ac, since furfural is transformed to ester and then to furfuryl alcohol and pyromucic acid. The larger F_2Ac proportion is explained by the higher reactivity of the phenoxy-furfuraldehydate complex which rapidly activates FAc leading to the formation of F_2Ac. Considering that only 0.44 moles of furfural change to FAc and F_2Ac, it means that the condensation reaction has occurred for an equimolecular ratio (0.5 F/0.5 Ac). The remaining 0.56 F moles do not participate in the formation of FAc and F_2Ac but in the formation reaction of furfuryl furoate and furfuryl alcohol, respectively, which will condense with phenol forming large resin amounts both during the reaction and during the F_2Ac distillation.

With a small phenol amount, polymerization will continue until the entire existing phenol has been consumed. Then the Cannizzaro reaction continues by itself under the catalytic action of sodium furfurylate.

With a larger phenol amount, reaching mole to mole proportions relative to F (like in the case of the experiment under discussion) and if the reaction is not moderated by cooling, the furfural conversion by the Cannizzaro reaction will superpose the polymerization reaction in which furfuryl alcohol competes with furfural, for a similar phenol amount, with the formation of a black polymer.

Since the colour of F, FAc and F_2Ac polymers obtained in an alkaline medium is from yellow to brown, it results that the black polymers have not occurred in an alkaline medium, but rather in an acidic medium.[3,4] The yellow polymers obtained in the basic catalysis have an intact furan ring, since it is not sensitive to the NaOH action. Black polymers occur in the catalysis of pyromucic acid when the furan ring breaks off. The breaking action of the ring, particularly in F, becomes more intense during distillation when an oxidation phenomenon also occurs. Indeed, the large amount of free pyromucic acid catalyzes at high temperatures (75°, and in vacuum distillation 180°/0.5 mm Hg) the polymerization of furfuryl alcohol and of furfural with phenol.

When phenol is in excess towards F, a fusible and soluble polymer is obtained and when F is in excess,[4] an infusible and insoluble polymer having a tridimensional structure, is obtained.

The formation of pyromucic acid and of furfuryl alcohol explains also other experimental findings published in a previous paper[5].

When the initial NaOH amount is small, the pH is below 7 on completion of the reaction. This is explained by the large amount of pyromucic acid and of furfuryl alcohol being formed which lead to sodium pyromucate and furfurylate, respectively. The more F remains unconverted to FAc and F_2Ac, the more pyromucic acid and furfuryl alcohol will form. A small part of the pyromucic acid neutralizes small NaOH amounts while most part remains free, lending an acid pH to the medium.

It has also been found[5] that "in the neutralization of the reaction mixture at pH = 7, the acid amount required is smaller than that corresponding to the NaOH involved in the reaction".

The use of a smaller acid amount for neutralization is due to the fact that most NaOH was consumed to form sodium pyromucate and furfurylate. During the total reaction, pyromucic acid and furfuryl alcohol can

---

[3] D. A. Isăcescu, V. Ursu and N. Goldenberg, *Studii şi Cercetări Chim. Acad RPR*, **2**, 235 (1954).

[4] D. A. Isăcescu and V. Ursu, *Studii şi Cercetări Chim. Acad. RPR*, **3**, 275 (1955).

[5] D. A. Isăcescu, I. Gavăţ, I. V. Ionescu and C. Stoicescu, *Studii şi Cercetări Chim. Acad. RPR*, **14**, 211 (1965).

be neither isolated nor identified since they belong to the constitution of the polymers being formed, or are included therein.

When the neutralization of the reaction product takes place before washing it, the polymers amount is bigger because of the polymerization of furfuryl alcohol and possibly of the free phenol. By washing the reaction product with water before neutralization, they are eliminated and the polymer amount is smaller.

EXPERIMENTAL SECTION

When the F condensation reaction with acetone occurs in a phenol medium with sodium phenoxide solution, a large amount of polymers is obtained at 75°, as shown in a previous paper,[2] starting from 1 F mole, 0.5 Ac moles, 0.4 C_6H_5OH moles, and 0.003 NaOH moles. 0.018 FAc moles and 0.21 F_2Ac moles were thus obtained and the remaining F, 0.56 moles, were converted to polymers (21 g).

Since this experiment cannot elucidate the reasons for the formation of the above components in various proportions, experiments were performed with each separate component, furfural or acetone.

Acetone with phenol forms diacetone alcohol in the presence of phenoxide. Furfural as such, with sodium phenoxide forms furfuryl alcohol, pyromucic acid and polymers.

We have obtained important data from experiments carried on with furfural purified under certain conditions, dissolved in a large amount of dry benzene, leading to an almost colourless solution. A phenol sodium phenoxide benzene solution was added to the solution cooled below 0 , while vigorously stirring. Shortly thereafter, the solution became turbid due to a fine yellow suspension. After stirring was discontinued, the suspension deposited. By stirring again, the suspension disappeared and the solution was allowed to warm up, reaching 40—50°.

The experiment was resumed, and as soon as the suspension appeared, it was rapidly filtered through a funnel cooled with ice. Since the filtered product had an oily aspect, it was washed with dry benzene. An almost yellow powder was obtained.

A part of this powder heated at a flame on a platinum blade, burned leaving a residue which being further heated, caused the flame to turn dark yellow, which is characteristic for sodium.

Another part of the powder was introduced into water and dissolved, the reaction being weakly alkaline. By CO_2 bubbling, a strong phenol odour appeared. A part of this solution with hydrochloride of anthranilic acid produces an intense violet colouration, characteristic of furfural. Another part of the solution treated with bromine water, yields tribromophenol.

The experimental studies have suggested that the yellow powder is sodium phenoxyfurfuraldehydate. This idea was also supported by the fact that the powder left in the reaction medium from which it was extracted, triggers a reaction which may become violent.

The third experiment made in the cold and then on heating and reaching almost the benzene boiling point, has revealed nothing. If the heated solution is distilled to remove benzene and vacuum-distillation is then continued, one obtains a product which distils at 122°/2mm Hg that corresponds to furfuryl furoate.

The fourth experiment was made under the same conditions as the preceding one, except for the fact that some water was introduced while heating. The reaction was accelerated and the content was pushed into the refrigerator. At the same time, the solution turned black, with the formation of a polymer.

These findings have indicated the formation of the activated complex and the mechanism by which it acts.

Revue Roumaine de Chimie, **23**, *6*, 883–885 (1978)

CONDITIONS OF ELECTRODEPOSITION AS A FACTOR INFLUENCING THE PROPERTIES OF Ni-Fe THIN FILMS

E. BEŁTOWSKA-LEHMAN and A. RIESENKAMPF
Polish Academy of Sciences, Institute of Metallurgy Cracow, Poland

Received April 7, 1976

The results obtained in the course of investigation on electrodeposition of thin Ni80Fe20 films on flat copper substrate are given. The influence of some electrochemical factors on the properties of magnetic thin films are discussed. A method for pretreatment of the substrate surface ensuring obtaining films with satisfactory rectangularity of the hysteresis loop has been developed.

INTRODUCTION

Electrodeposition belongs to well-known methods for obtaining magnetic thin films.[1] The principal advantage of this method consists in the fact that the necessary apparatus is not expensive and very simple as the processes are carried out under atmospheric pressure in aqueous solutions at temperatures not exceeding some dozens of degrees centigrade. Introducing appropriate addition agents into the electrolyte and changing the parameters of electrolysis one can relatively easily control the composition and properties of deposited films. Films obtained by this method can be used in producing elements for microelectronics, for computer memory elements and used in sound-recording.

This paper deals with thin magnetic soft permalloy films of approximate composition Ni80Fe20.

EXPERIMENTAL

Thin permalloy films electrodeposited on flat copper substrates 0.2 mm thick were investigated. After preliminary treatment the surface of the substrate was covered with the alloy in an electrolytic cell placed in Helmholtz coils. By means of these coils the films could be electrodeposited in magnetic fields of different intensities and orientations. As feeding sources an electronic galvanostat or a potentiostat type ZE-21 "Chemipan" were used. The mean chemical composition of obtained films was determined by the AAS method. The microstructure of the substrate as well as that of electrodeposited thin films were investigated by methods of optical microscopy. The state of the surface of specimens was investigated by means of a scanning microanalyzer Jeol JXA-50, profilograms were registered using a Taylor-Hobson Talysurf profilograph. The thickness of films was determined from parameters of electrolysis and in some cases also using the interferometrical method of Tolansky, by means of an interference microscope type IPCW-1. The coercive force and the rectangularity of the hysteresis loop were measured by means of a hysteresograph.

---

[1] L. F. Iljušenko, "*Elektrolitičeski osaždiennyje magnitnyje plenki*", Izd. Nauki i Technika, Minsk, 1972.

INFLUENCE OF ELECTROCHEMICAL PARAMETERS ON THE COMPOSITION OF ELECTRODEPOSITED THIN FILMS

Basing on the relation between the Fe-content in the alloy and the Fe-content in the solution (Figure 1) for six baths differing in the $FeSO_4 \cdot 7H_2O$ content only, the electrolyte of the composition: 15 g/l $FeSO_4 \cdot 7H_2O$; 212 g/l $NiSO_4 \cdot 7H_2O$; 25 g/l H_3BO_3 was chosen. The observed relation agrees well with that described in the paper.[2] The temperature of the electrolyte amounted to 50°. From this bath, films of different thicknesses were deposited galvanostatically at the following cathodic current densities: 1, 3, 4 and 6 A/dm². Figure 2 shows the relation between the Fecontent in the film and its thickness for investigated current densities. As easily seen from the figure the differences in the film composition increase with increasing cathodic current density; the Fe-content decreases with increasing film thickness.

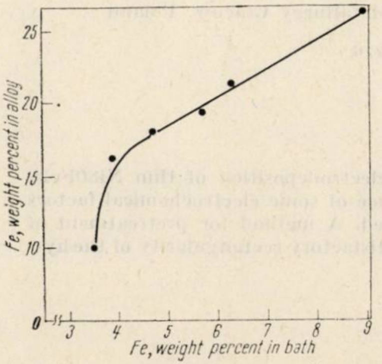

Fig. 1. — The dependence of the Fe-content in deposit on the Fe-content in bath.

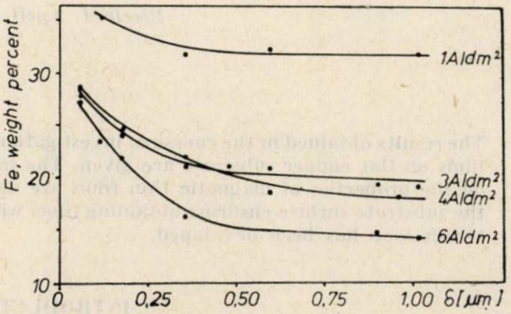

Fig. 2.— Relation between Fe-content and film thickness for different current densities.

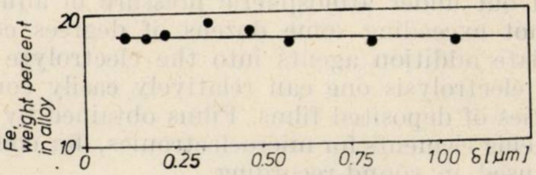

Fig. 3. — The dependence of the Fe-content in film obtained in potentiostatic conditions on its thickness.

Basing on these results the following parameters have been assumed as the most favourable: $D_k = 4$ A/dm², film thickness greater than 0.4 μm. A positive influence of an external magnetic field applied during the electrodeposition could be also observed. Films were obtained in magnetic fields of the intensity of 100 Oe. To improve the homogeneity of the chemical composition the electrolysis was also carried out at a constant cathodic potential controlled using a potentiostat.[3] Figure 3 shows the thickness-dependence of the Fe-content in films which were electrodeposited in described conditions. As evident, in potentiostatic conditions the homogeneity of chemical composition of electrodeposited films and therefore also of their magnetic properties in function of the film thickness were much better.

---

[2] A. Brenner, "Electrodeposition of Alloys", vol. II, Academic Press, New York 1963, p. 268.

[3] F. H. Edelman, *J. Electrochem. Soc.*, **109**, 440 (1962).

PREPARATION OF SUBSTRATE SURFACES

Literature data and own experimental results indicated that at given conditions of electrolysis the properties of obtained films are determined by the substrate smoothness which depends on the method of pretreatment of its surface[4]. This is due to the fact that very thin films inherit the structure of the substrate. Copper substrates were heated at 600° and then covered with permalloy films of the following thicknesses: 0.06 m (Figure 4), 0.96 μm and 2.28 μm (Figure 5). Comparative examination of microstructures of these surfaces leads immediately to the conclusion that only relatively thick films exhibit structures differing from those of substrates. Investigations by means of a scanning microanalyzer show that the surface of a copper substrate, as obtained after rolling, is rough with scratches resulting from this operation. To obtain samples of possibly smooth surfaces the following method has been developed and experimentally checked. The samples were annealed during 2 hours at 600°, and after them chemically polished with a solution of concentrated nitric, orthofosforic and acetic acids. The best smoothness of the surface could be obtained in the case of samples which were subjected to all operations mentioned above and covered additionally with a film of bright copper. Better smoothness of the surface is also corroborated by results of profilographic measurements (Figure 6). Comparing the relation between H_c and film thickness (Figure 7) for films deposited on previously heated substrates /curve 1/ and on substrates with intermediate bright copper films/curve 2/ it could be stated that in the second case the course of this relation is more favourable.

Thin films electrodeposited on surfaces prepared previously in the described manner exhibited a good rectangularity of the hysteresis loop (Figure 8) and a very good reproducibility of magnetic properties. The homogeneity of the Fe-distribution along the film was also investigated using a X-ray microanalyzer. The obtained results (Figure 9) were satisfactory.

CONCLUSION

In the result of the investigations a method has been developed to obtain substrate surfaces of sufficient smoothness for electrodeposition of Ni80Fe20 films. Thin magnetic films electrodeposited on these surfaces exhibited satisfactory magnetic properties and a good rectangularity of the hysteresis loop. Using galvanostatic feeding it could be stated that films of constant chemical composition can be obtained only when their thickness surpasses 0.4 μm; in potentiostatic conditions satisfactory films can be obtained at smaller thicknesses.

---

[4] Y. Uehara *Jap. J. Appl. Phys.*, **2**, 451 (1963).

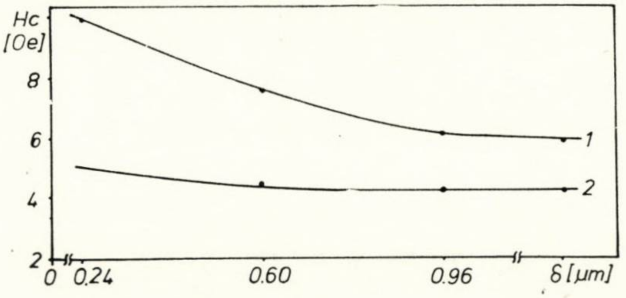

Fig. 7. — Relation between the coercive force H_c and the thickness of the films:

1 — films deposited on annealed and polished substrates; 2 — films deposited on bright copper substrate.

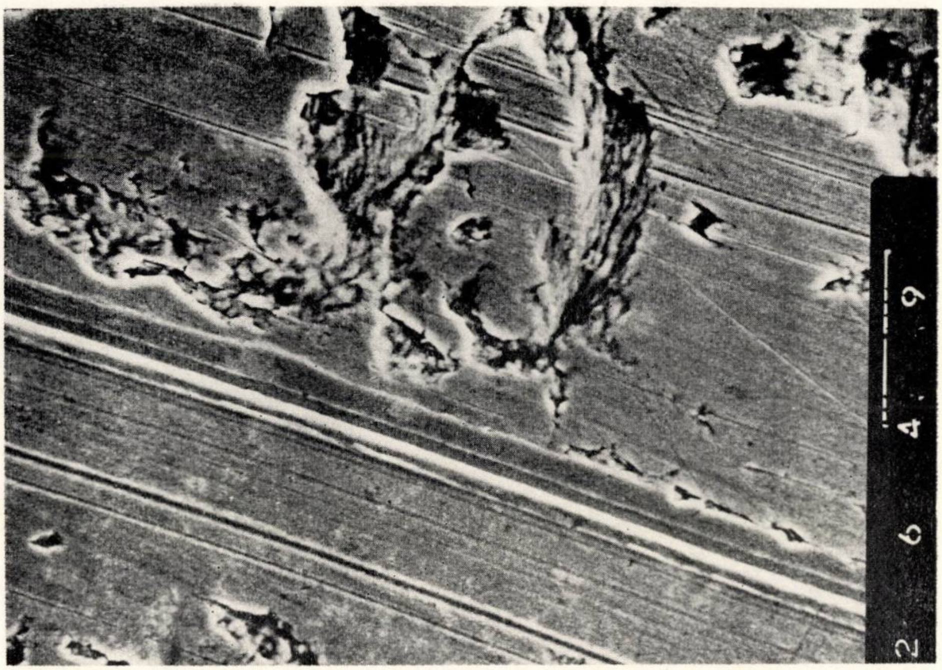

Fig. 8. — Hysteresis loop in the easy direction for a film 0.96 μm thick.

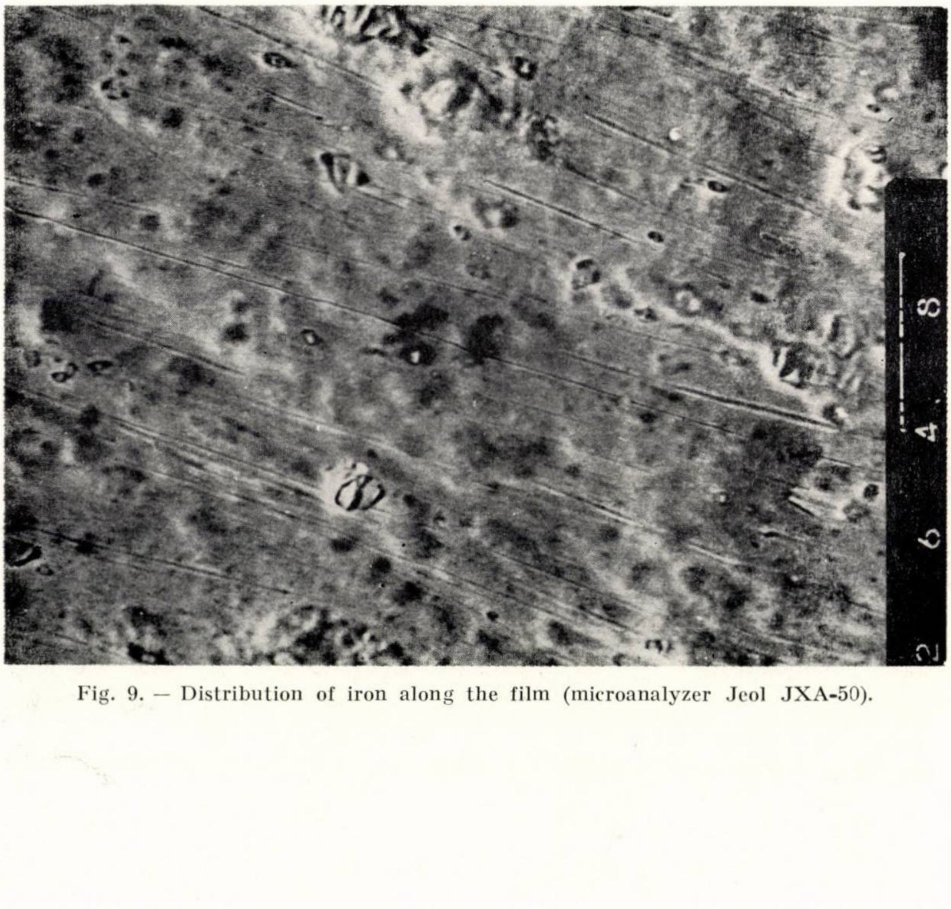

Fig. 9. — Distribution of iron along the film (microanalyzer Jeol JXA-50).

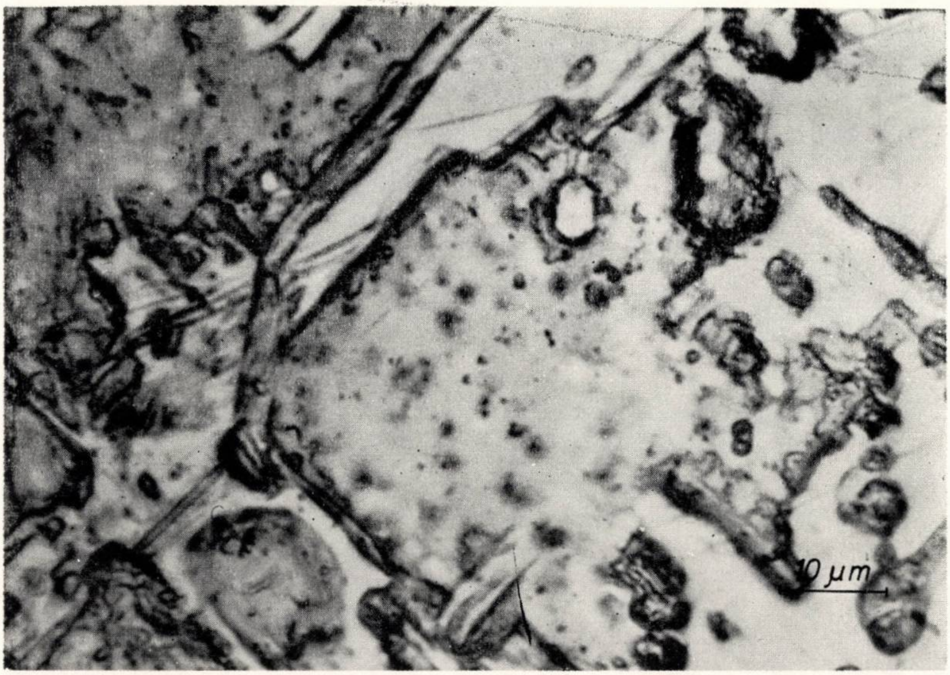

Fig. 4. — Microstructure of NiFe film 0.06 µm thick.

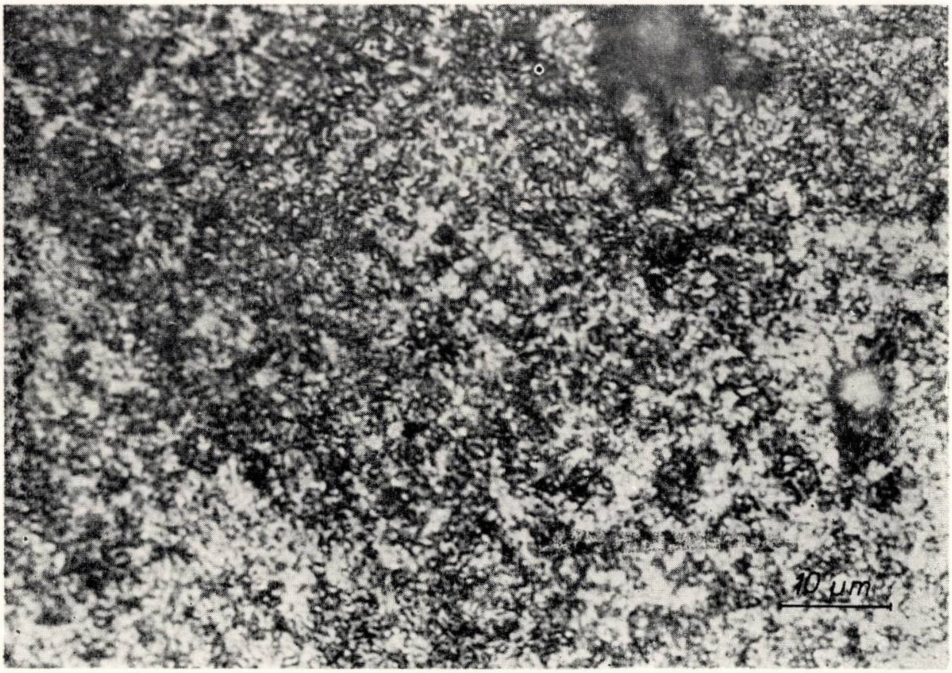

Fig. 5. — Microstructure of NiFe film 2.28 µm thick.

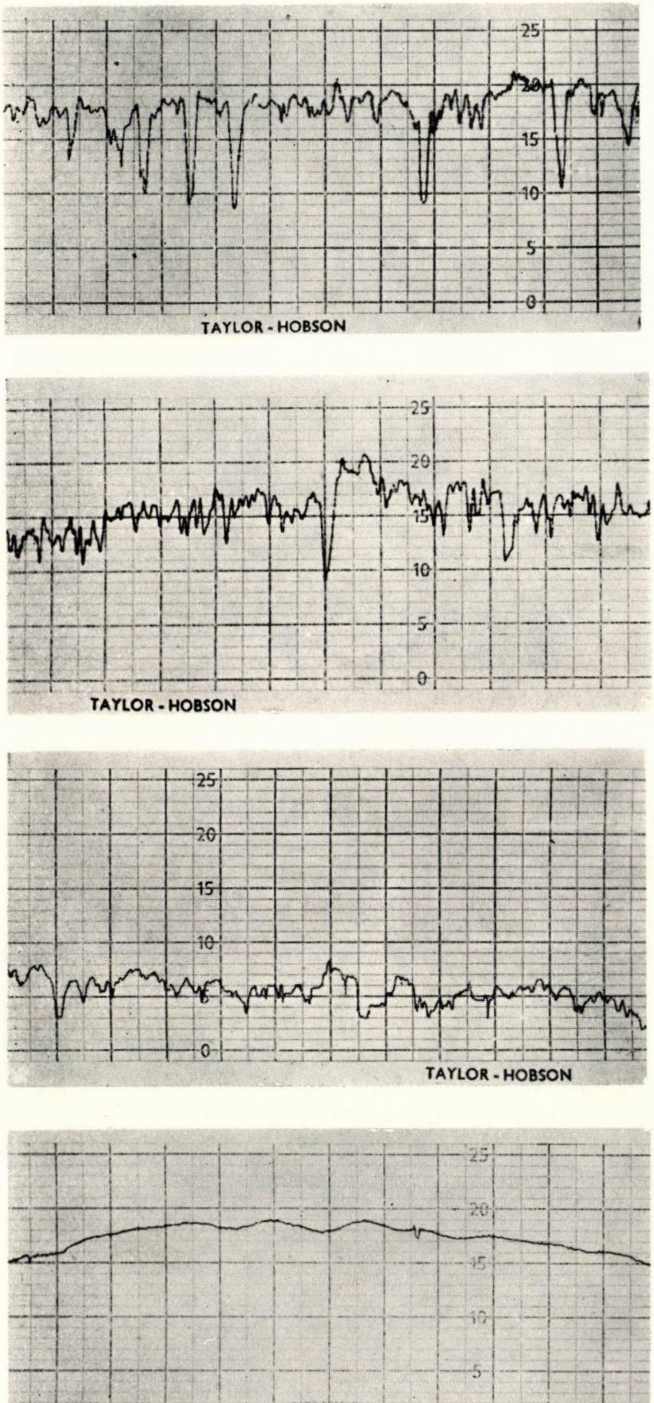

Fig. 6. — Profilograms of copper substrates :

a) initial state ; b) after chemical polishing ; c) after annealing and polishing ; d) after annealing and plating with an intermediate ; bright copper layer.

Revue Roumaine de Chimie, **23**, *6*, 887–908 (1978)

OXYDES ET HYDRATES D'OXYDES DU VANADIUM
AUX DEGRÉS D'OXYDATION IV, V ET INTERMÉDIAIRES

FRANÇOIS THÉOBALD
Laboratoire de Chimie Physique, Faculté des Sciences et des Techniques,
32, rue Mégevand, 25030 Besançon, France

Reçu le 25 mars 1976

De nombreux corps solides existent dans le domaine $V_2O_4-V_2O_5-H_2O$ entre 0°C et 500°C. Nous avons préparé 2 oxydes et 3 hydrates nouveaux et comparé leurs propriétés avec celles des oxydes et hydrates (ou hydroxydes) déjà connus. A part une ou deux exceptions, cet ensemble est relativement homogène du point de vue des propriétés physiques car les oxydes et hydrates possèdent certains éléments de structure identiques. Pour la même raison les propriétés chimiques des oxydes sont aussi voisines. Par contre les hydrates sont plus variés car l'élément hydrogène est lié de plusieurs façons différentes.

INTRODUCTION

Nous nous sommes proposé de rechercher et d'étudier les oxydes et hydroxydes on hydrates d'oxydes de vanadium existant à une *température t inférieure à 500°* et dans lesquels le degré d'oxydation du vanadium est compris entre 4 et 5.

Jusqu'à présent, seul le domaine des températures supérieurs à 500° (ou n'existent que des oxydes) avait été étudié complètement [1à7]. Le domaine inférieur à 500° avait fait l'objet aussi de nombreux travaux mais les résultats étaient souvent fragmentaires voire contradictoires. C'est pourquoi nous avons développé systématiquement certains procédés susceptibles de nous conduire aux oxydes et hydrates cherchés :

a) l'étude du système : oxyde de vanadium (IV) — oxyde de vanadium (V) dans les conditions hydrothermales[8]

b) l'oxydation des hydrates de vanadium (IV) par l'air

c) la réduction de V_2O_5 par les gaz et vapeurs[9]

---

[1] H. G. Bachmann, F. R. Ahmed & W. H. Barnes, *Z. Krist.*, **115**, 110 (1961).
[2] H. G. Bachmann & W. H. Barnes, *ibid.*, 215.
[3] G. Andersson, *Acta Chem. Scand.*, **10**, 623 (1956).
[4] F. Aebi, *Helv. Chimica Acta*, **31**, 8 (1948).
[5] D. Thomas, J. Tudo & G. Tridot, *Compt rend.*, série C, **265**, 183 (1967).
[6] S. Andersson, J. Galy & K. A. Wilhelmi, *Acta Chem. Scand.*, **24**, 1473 (1970).
[7] K. Kosuge, *J. Phys. Chem. Solids*, **28**, 1613 (1967).
[8] F. Théobald, *Canad. J. Chem.*, 1976 (sous presse).
[9] F. Théobald, R. Cabala & J. Bernard, *Compte rend.*, série C, **269**, 1209 (1969).

d) la calcination des vanadates d'ammonium (V)
e) la calcination ou dessiccation des hydrates

Le présent travail consiste en :
- une présentation d'ensemble des phases solides obtenues
- la délimitation de leurs domaines d'existence
- l'examen de leurs relations structurales.

PRÉSENTATION D'ENSEMBLE

Diverses méthodes en particulier la radiocristallographie, la diffraction électronique et la spectroscopie infra-rouge ont permis de confirmer l'existence de quelques phases déjà observées par d'autres auteurs et de mettre en évidence plusieurs phases nouvelles. La figure 1 montre par exemple les solides obtenus par la méthode hydrothermale. Nous pouvons donc dresser la liste de oxydes et hydrates de vanadium dont l'existence est certaine ou probable (tableau 1).

A l'opposé, nous avons montré que de nombreux produits étaient faussement considérés comme des hydrates, en particulier que le composé que Glemser[10] a formulé $V_3O_5(OH)_4$ est en réalité $(NH_4)_2V_3O_8-\varphi$[11] et qu'il n'existe aucun hydrate au degré d'oxydation + 5[12]).

Enfin rappelons que nous n'avons pas retrouvé l'oxyde ,,$V_6O_{13}(C)$ de SATA''[13]) mais nous ne pouvons ni confirmer, ni infirmer son existence.

La formule V_4O_9 attribuée par Wilhelmi & coll.[14] à l'une de leurs préparations est douteuse car ce composé ressemble à V_3O_7,H_2O.

DOMAINES D'EXISTENCE ET STABILITÉ DES PHASES

1. Stabilité thermique

a) Calcination sous vide: Les résultats essentiels peuvent être schématisés comme suit :

$$\begin{array}{llll}
\mathrm{VO_2(B)} & \xrightarrow{400-450} \mathrm{V_2O_4} & \text{Ref.} & ^{15} \\
\mathrm{VO_2}(A) & \xrightarrow{450-500} \mathrm{V_2O_4} & ,, & ^{16} \\
\mathrm{V_6O_{13}} & \xrightarrow{710} \mathrm{VO_2 + V_2O_5} & ,, & ^{4} \\
\mathrm{V_4O_9} & \xrightarrow{450} \mathrm{V_3O_7 + V_6O_{13}} & ,, & ^{9} \\
\mathrm{V_3O_7} & \xrightarrow{670} \mathrm{V_6O_{13} + V_2O_5} & ,, & ^{5,7}
\end{array}$$

---

[10] O. GLEMSER & E. SCHWARZMANN, *Z. anorg. Chem.*, **278**, 249 (1955).

[11] J. BERNARD, F. THÉOBALD & A. VIDONNE, *Bull. Soc. chim. France*, **1970**, 2108.

[12] F. THÉOBALD, *Bull. Soc. chim. France*, **1975**, 1607.

[13] T. SATA, E. KOMADA, Y. ITO, *Kogyo Kagaku Zasshi (J. Chem. Soc. Japan, Ind. Chem. Sect.)*, **71**, 643, 647 (+p. A43) (1968).

[14] K. A. WILHELMI & K. WALTERSSON, *Acta Chem. Scand.*, **24**, 3409 (1970).

[15] F. THÉOBALD, *J. Solid. State Chem.*, **17**, 431 (1976).

[16] F. THÉOBALD & J. BERNARD, *Compt. rend.*, **268** C, 60 (1969).

Tableau 1

Tableau des oxydes et hydrates de vanadium rencontrés au-dessous de 500°C

	Corps déjà identifiés par d'autres auteurs	Corps nouveaux et Corps retrouvés (oui)	Méthodes employées ici	
			préparation	obtention
Au voisinage du degré d'oxydation 4 du vanadium				
oxydes :	VO_2 rutile	oui	c	a, e
	VO_2 monoclinique	oui		
	VO_2 (Z), (T), (M) etc ... (=rutile déformé)	oui		a
	VO_2 paramontroséite	non retrouvé mais possible		
	VO_2 (B)	oui ; caractérisé avec précision	c	d
		$VO_2(A)$	a	
hydrates :	VO_2, H_2O (GAIN)	oui (VO_2, 1,05H_2O)	[10]	a
	$VO(OH)_2$ (duttonite)	oui	a	
	$VO(OH)_2$ (SCHWARZMANN)	oui (VO_2, 0,84H_2O) (~lenoblite)	a	
	$3V_2O_4$, $4H_2O$ (doloresite)	oui		a
Au degré 4,33				
oxydes :	V_6O_{13}(> 170°K)	oui	c, a	d
	V_6O_{13}(< 170°K)	non étudié ici		
Au degré 4,50				
oxyde :		V_4O_9	c	
Au degré 4,66				
oxyde :	V_3O_7	oui		a, d, e
hydrates :		V_3O_7, H_2O	a	
		hydrate intermédiaire possible		
Au degré 4,80				
hydrates :		$V_2O_{4\ 80}$.3,5H_2O ~ navajoïte	a	b
		$V_2O_{4\ 80}$.0,5H_2O ≠ bariandite	e	b
Au degré 4,85	corvusite	non retrouvé mais possible		
hydrate :				
Au degré 5				
oxyde :	V_2O_5 =shcherbinaïte	oui		a

Note ; les lettres a, b, c, d, e des 2 dernières colonnes renvoient aux méthodes citées dans l'introduction

$$VO_2, H_2O(\text{GAIN}) \xrightarrow{150-220} VO_2 \text{ amorphe} \xrightarrow{300-340} V_2O_4 \text{ rutile}$$ [17]

$$VO(OH)_2 \text{ (duttonite)} \xrightarrow{200-250} VO_2 \text{ amorphe} \xrightarrow{300-340} V_2O_4 \text{ rutile}$$ [18]

$$VO_2,O,84H_2O \text{ (Schwarzmann)} \xrightarrow{160-220} VO_2 \text{ amorphe} \xrightarrow{300-340} V_2O_4 \text{ rutile}$$ [19]

$$V_3O_7, H_2O \xrightarrow{300-380} V_3O_7$$ [20]

$$V_2O_{4.80}\ 3{,}5H_2O \xleftrightarrow{20^\circ} V_2O_{4.80},O,5H_2O \xrightarrow{\sim 250^\circ} V_3O_7 + V_2O_5$$ [21.22]

La plupart des réactions indiquées sont irréversibles ou difficilement «renversables».

Dans certains cas on remarque qu'il y a des analogies de structure entre les corps de départ et d'arrivée : décomposition de V_6O_{13}, V_3O_7, H_2O et $V_2O_{4.80}$, nH_2O. Nous y reviendrons par la suite (§ D).

Dans le cas de $V_2O_{4.80}$, nH_2O on note que la réaction de déshydratation est réversible au moins si la teneur en eau ne descend pas au-dessous de $n = 0{,}5$: l'hydrate $V_2O_{4.80}$, $3{,}5H_2O$ séché sous vide à la température ambiante perd de la vapeur d'eau pour donner $V_2O_{4.80}$, $O{,}5H_2O$. Celui-ci, mouillé, redonne $V_2O_{4.80}$, $3{,}5\ H_2O$.

De plus l'équilibre de la vapeur d'eau avec $V_2O_{4.80}$, $O{,}0{,}5H_2O$ est divariant. Ce corps peut fixer presque 3 molécules d'eau (pour 2 atomes de V) sans que sa structure change.

b) Conditions hydrothermales: Nous avons établi un diagramme (figure 1) qui permet de prévoir les réactions qui se produisent dans les conditions hydrothermales. Cependant dans quelques cas, le traitement hydrothermal ne donne pas le résultat escompté tout simplement parce que des facteurs cinétiques s'y opposent, soit que les composés soient trop bien cristallisés, soit qu'il se forme une couche protectrice : ce dernier cas est sans doute celui du traitement hydrothermal de V_3O_7 : il se forme seulement une couche superficielle de V_3O_7, H_2O qui stoppe toute hydratation en profondeur.

L'oxyde V_4O_9 obtenu en réduisant V_2O_5 par les vapeurs organiques vers 300° se singularise parmi les oxydes de vanadium. En effet le traitement hydrothermal montre une réactivité exceptionnelle de ce composé pour l'eau puisqu'il réagit dès 70° (figure 2). Tous les autres oxydes de vanadium voisins résistent à des températures bien plus élevées ($> 200°$). Par ailleurs la densité de V_4O_9 ($d = 3{,}31\ g/cm^3$) est anormalement basse comparée à celles des autres oxydes. Ces faits s'expli-

---

[17] G. Gain, *Compte rend.*, **143**, 823 (1906) ; *Ann. Chim. (France)*, **14**, 224 (1908).

[18] R. T. Evans Jr.& M.E. Mrose, *Acta Cryst.*, **11**, 56 (1958).
H. T. Evans, *Geol. Survey Research Bulletin*, **1960**, (N° 203), B 443–6.

[19] E. Schwarzmann, R. Bak & R. Birkenberg, *Z. Naturforsch.*, **27B**, 1003 (1972).

[20] F. Théobald &R. Cabala, *Compt. rend.*, **270C**, 2138 (1970).

[21] F. Théobald &F. Cesbron, *ibid.*, **271C**, 364 (1970).

[22] F. Théobald, Thèse, Besançon, 1er février 1975, CNRS : AO 3998.

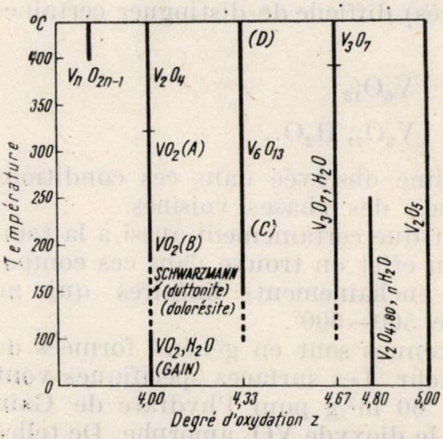

Fig. 1. — Système $VO_2-V_2O_5-H_2O$ dans les conditions hydrothermales.
(sous une pression voisine de la pression saturante P_0 de la vapeur d'eau)

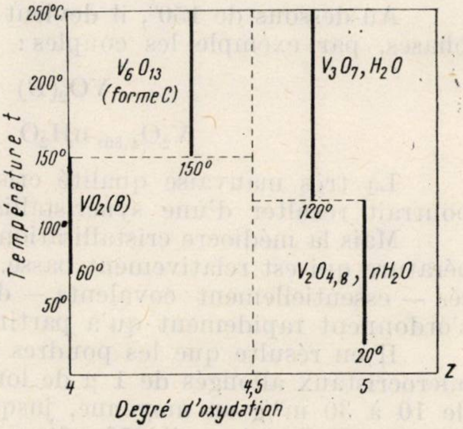

Fig. 2. — Traitement hydrothermal de V_4O_9 ($z = 4{,}5$).
Panorama des phases obtenues.
Pour chaque température *t*, les phases *observées* correspondent aux traits pleins verticaux que rencontre la droite horizontale d'ordonnée *t*.

queraient assez bien si l'on admettait que la structure de V_4O_9 fût déficitaire en oxygène par rapport aux structures des oxydes tels que V_2O_5, V_6O_{13} ou V_3O_7.

2. Limites de composition

L'examen radiocristallographique suggère que les oxydes préparés à basse température ont un domaine de composition assez vaste. En particulier pour les oxydes *nouveaux*, on obtient les limites approximatives suivantes du degré d'oxydation z :

$VO_2(B)$ paraît pour de $z = 3{,}89$ à $z = 4{,}09$

$VO_2(A)$ $z = 3{,}9$ / $4{,}04$

V_4O_9 $z = 4{,}46$ / $4{,}53$

Au contraire, dans le cas des hydrates, le degré d'oxydation est en général mieux défini :

$VO_2, 1{,}05H_2O$ (GAIN) $z \sim 4{,}00 \pm 0{,}01$

$VO_2, 0{,}84H_2O$ (SCHWARZMANN) $z \sim 4{,}00$ / $4{,}05$

$VO(OH)_2$ (duttonite) $z \sim 4{,}00 \pm 0{,}03$

dolorésite $z \sim 3{,}95$ / $4{,}00$

V_3O_7, H_2O $z \sim 4{,}67 \pm 0{,}02$

$V_2O_{4,80}, nH_2O$ $z \sim 4{,}77$ / $4{,}82$

Au-dessous de 150°, il devient (très) difficile de distinguer certaines phases, par exemple les couples :

$$VO_2(B) \quad \text{et} \quad V_6O_{13}$$

$$V_2O_{4.80}, nH_2O \quad \text{et} \quad V_3O_7, H_2O.$$

La très mauvaise qualité cristalline observée dans ces conditions pourrait résulter d'une syncristallisation des phases voisines.

Mais la médiocre cristallisation est due certainement aussi à la température qui est relativement basse. En effet on trouve dans ces composés — essentiellement covalents — des enchaînements linéaires qui ne s'ordonnent rapidement qu'à partir de 500—600°.

Il en résulte que les poudres obtenues sont en général formées de microcristaux allongés de 1 μ de longueur. Les surfaces spécifiques vont de 10 à 30 m^2/g en moyenne, jusqu'à 60 m^2/g pour l'hydrate de Gain VO_2, $1{,}05H_2O$ et jusqu'à 250 m^2/g pour le dioxyde VO_2 amorphe. De telles surfaces sont suffisamment importantes pour expliquer, au moins en partie, les écarts à la stœchiométrie (non-stœchiométrie de surface).

3. Modalités de l'oxydation par l'air à la température ambiante

Les composés ne s'oxydent pas très rapidement à l'air. Mais si la surface spécifique est grande, l'oxydation par l'air devient gênante. Ce cas a été rencontré en particulier avec l'hydrate de Gain ($S = 50$ m^2/g) et avec le dioxyde amorphe ($S = 200$ m^2/g).

Oxydation de l'hydrate de Gain VO_2,$1{,}05H_2O$. Parmi tous les hydrates de synthèse aux degrés 4,00, 4,66 et 4,80 l'hydrate de Gain est l'hydrate le plus intéressant à étudier du point de vue de l'oxydation, parce que ce composé appartient au degré d'oxydation inférieur du domaine étudié, parce que sa préparation conduit à des échantillons dont la composition est très reproductible et surtout parce que sa surface spécifique est grande.

L'oxydation initiale est très rapide. En quelques minutes le degré d'oxydation moyen passe de la valeur 4 à la valeur 4,04. Nous avons suivi cette oxydation par une méthode volumétrique en utilisant l'oxygène sous diverses pressions (figure 3). Cette première étape est une chimisorption. Elle est importante parce que la surface spécifique est importante.

Ensuite l'oxydation ralentit considérablement ; cependant elle se poursuit inexorablement pendant des années. L'évolution des spectres de réflectance diffusés dans le visible a permis d'analyser les étapes de l'oxydation.

Avec l'air sec il se forme d'abord $V_2O_{4.80}$,$0{,}5H_2O$ violet foncé qui se recouvre d'une couche très mince de V_2O_5 jaune — si fine qu'elle laisse transparaître l'hydrate sous-jacent.

En présence d'eau, dans l'air humide il se forme à la fois l'hydrate inférieur $V_2O_{4.80}$,$0{,}5H_2O$ et l'hydrate supérieur $V_2O_{4.80}$, $3{,}5H_2O$, qui se recouvre également de V_2O_5 protecteur. Même après des années la transformation en V_2O_5 à 20° n'est pas totale. Le schéma d'oxydation est donc le suivant :

$$VO_2, 1{,}05H_2O\ (\text{Gain}) \rightarrow V_2O_{4.80}, 0{,}5 \ \text{ou}\ 3{,}5H_2O \rightarrow V_2O_5$$

Par contre on n'observe aucun composé cristallisé aux degrés d'oxydation 4,33,4,50 ou 4,66.

L'oxydation de l'hydrate de Schwarzmann VO_2, $0{,}84H_2O$ est semblable mais plus lente. La duttonite et l'hydrate V_3O_7, H_2O sont beaucoup moins oxydables, notamment parce que leurs surfaces spécifiques sont plus faibles.

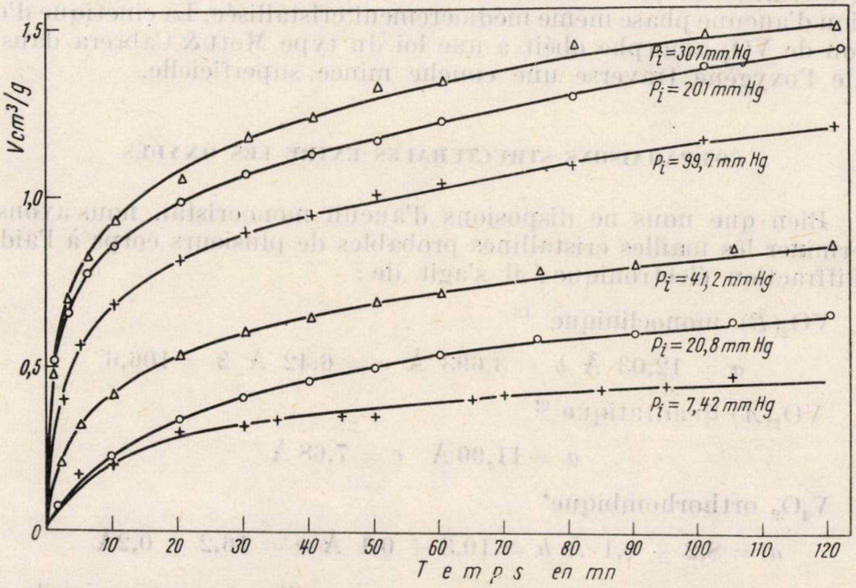

Fig. 3. — Oxydation de l'hydrate de Gain par l'oxygène à 20° (surface spécifique : environ 40 m²/g ; V = volume d'oxygène fixé en cm³/g)

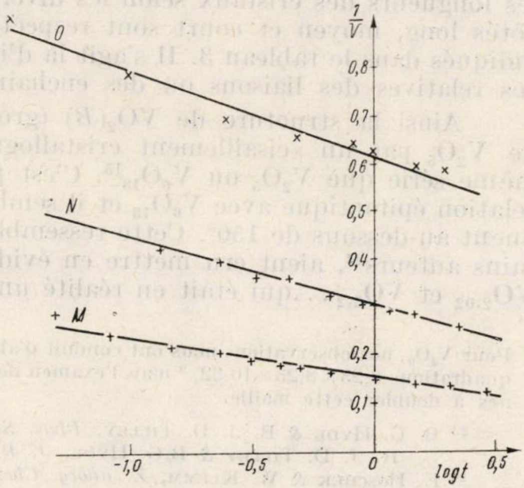

Fig. 4. — Oxydation de l'oxyde VO_2 amorphe par l'oxygène à 22,4°.

Pression : 260 torrs.

V : volume fixé en cm³/g, t : temps en heures.

M : 160 m²/g ; N : 112 m²/g ; O : 54 m²/g.

C'est pour la même raison que l'oxydation à 20° des divers oxydes est négligeable sauf celle du *dioxyde de vanadium* VO_2 *amorphe* très différent de ce point de vue du dioxyde rutile correspondant.

Oxydation du dioxyde VO_2 *amorphe:* Le dioxyde est obtenu en calcinant l'hydrate de Gain à 250° sous vide. L'oxydation initiale à 20° est assez rapide (figure 4) et passe probablement par les mêmes étapes que pour l'hydrate de Gain mais la diffraction X ne permet d'observer la formation d'aucune phase même médiocrement cristallisée. La cinétique d'oxydation de VO_2 amorphe obéit à une loi du type Mott & Cabrera dans laquelle l'oxygène traverse une couche mince superficielle.

COMPARAISONS STRUCTURALES ENTRE LES OXYDES

Bien que nous ne disposions d'aucun monocristal, nous avons pu déterminer les mailles cristallines probables de plusieurs corps à l'aide de la diffraction électronique ; il s'agit de :

$VO_2(B)$ monoclinique [15]

$$a = 12{,}03 \text{ Å} \quad b = 3{,}693 \text{ Å} \quad c = 6{,}42 \text{ Å} \quad \beta = 106{,}6°$$

$VO_2(A)$ quadratique [25]

$$a = 11{,}90 \text{ Å} \quad c = 7{,}68 \text{ Å}$$

V_4O_9 orthorhombique*

$$a = 8{,}2 \pm 0{,}1 \text{ Å} \quad b = 10{,}3 \pm 0{,}1 \text{ Å} \quad c = 16{,}2 \pm 0{,}2 \text{Å}$$

Si l'on compare ces résultats avec les mailles des autres oxydes déjà connus V_2O_5, V_6O_{13} et V_3O_7 (tableau 2) il apparaît que $VO_2(B)$ présente en commun avec ces derniers le paramètre $b \sim 3{,}69$ Å.

Par ailleurs, la microscopie électronique nous a permis de comparer les longueurs des cristaux selon les diverses dimensions : par exemple les côtés long, moyen et court sont respectivement parallèles aux vecteurs indiqués dans le tableau 3. Il s'agit là d'indications précieuses sur les forces relatives des liaisons ou des enchaînements présents.

Ainsi la structure de $VO_2(B)$ (groupe spatial $C2/m = C^3_{2h}$) dérive de V_2O_5 par un «cisaillement cristallographique». Elle appartient à la même série que V_2O_5 ou V_6O_{13}[15]. C'est pourquoi $VO_2(B)$ peut entrer en relation épitactique avec V_6O_{13} et il semble que ce soit le cas le plus fréquent au-dessous de 150°. Cette ressemblance explique d'ailleurs que certains auteurs[24], aient cru mettre en évidence une phase homogène entre $VO_{2,02}$ et $VO_{2,2}$...qui était en réalité un mélange de $VO_2(B)$ et V_6O_{13}.

---

* Pour V_4O_9, nos observations nous ont conduit d'abord à une maille orthorhombique pseudo-quadratique 8,23×8,23×10,32, [9] mais l'examen des travaux de Hyde et Tilley[23] nous a amenés à doubler cette maille.

[23] B. G. Hyde & R. J. D. Tilley, *Phys. Stat. Sol.* (a) **2**, 749 (1970).
R. J. D. Tilley & B.G. Hyde, *J. Phys. Chem. Solids*, **31**, 1613 (1970).

[24] E. Hoschek & W. Klemm, *Z. anorg. Chem.*, **242**, 63 (1939).
Ibid., **226**, 359 (1936).

Tableau 2

Cristaux dont un des paramètres de maille avoisine 3,6 Å

	Paramètre voisin de 3,6 Å	Autre paramètre
V_2O_5	3,56 Å	11,51 Å (a)
V_3O_7	3,68	
V_6O_{13}	3,67	11,90 (a)
$VO_2(B)$	3,69	12,03 (a)
V_3O_7, H_2O	3,63	
bariandite $V_2O_4.4V_2O_5.12H_2O$	3,63	11,60 (a)
navajoïte $V_2O_5.3H_2O$	3,65	12,25 (c)
pseudo-navajoïte	3,64	11,86
corvusite $V_2O_4.6V_2O_5.xH_2O$	3,65	11,6 (a)
pseudo-corvusite $V_2O_4.5V_2O_5.xH_2O$	3,66	11,69
hewettite $CaV_6O_{16}.nH_2O$	3,60	12,23
barnesite $Na_2V_6O_{12}.3H_2O$	3,60	12,17
fernandinite $CaO..V_2O_4.5V_2O_5.14H_2O$	3,67	11,69
grantsite $Na_4(CaSr)_xV^{IV}_{2x}VO^{V}_{12-2x}O_{32}.8H_2O$	3,60	12,41
LiV_2O_5	3,61	
NaV_2O_5	3,61	11,33
$\delta-Ag_{1-x}V_2O_5$	3,66	11,73
$Al_{0,33}V_2O_5-\theta$	3,67	12,19
$Fe_{0,33}V_2O_5-\theta$	3,68	12,19
A cette liste, on peut peut-être ajouter : $VO_2(A)$	$c=2\times3,84=7,68$	11,90

Au contraire, l'oxyde VO_2 rutile, qui est le terme supérieur de la série V_nO_{2n-1} est nettement plus dense et moins réactif que $VO_2(B)$. Les oxydes VO_2 (monoclinique ordinaire) et $VO_2(Z)$ (T) (O) ou(M) s'apparentent aussi à la structure rutile puisqu'ils en dérivent par des distorsions.

Finalement il n'y a que deux oxydes qui apparaissent isolés dans leur comportement $VO_2(A)$ et V_4O_9 :

$VO_2(A)$ apparaît dans les réactions hydrothermales comme un intermédiaire entre $VO_2(B)$ et VO_2 (rutile). La structure de $VO_2(A)$ n'est pas encore connue mais nous supposons que la filiation de ce corps...

$$VO_2(B) \xrightarrow{220°} VO_2(A) \xrightarrow{320°} VO_2 \text{ (rutile)}$$

recouvre une relation structurale et nous espérons qu'il sera possible d'en déduire la structure cherchée.

V_4O_9 occupe une place à part car c'est le moins dense des oxydes : il semble dériver de V_2O_5 par le départ de certains atomes d'oxygène et une réorganisation du réseau mais sans modification notable du volume global.

V_4O_9 est présent dans les catalyseurs d'oxydation en fonctionnement puisque nous avons décelé ses raies caractéristiques dans les spectres des catalyseurs V_2O_5—MoO_3 publiés par Tarama et ses collaborateurs.[25] On peut s'attendre à ce qu'il joue un rôle non négligeable dans la catalyse à cause de son caractère lacunaire.

Spectres infrarouges des oxydes $VO_2(B)$, $VO_2(A)$ et V_4O_9

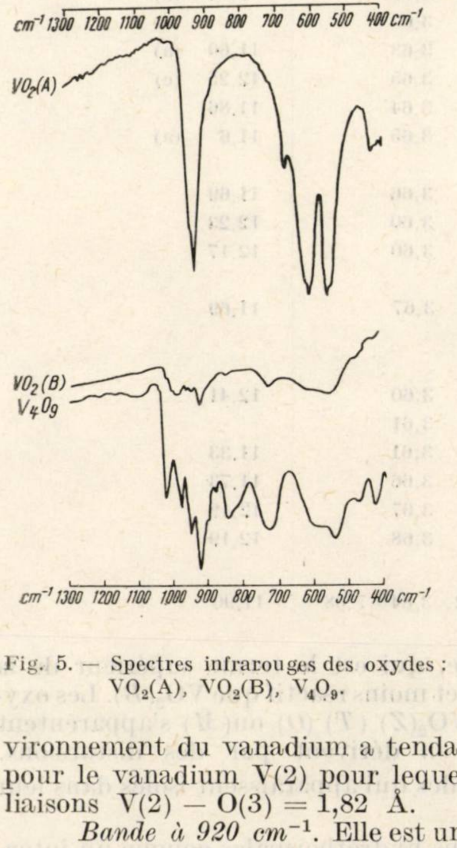

Fig. 5. — Spectres infrarouges des oxydes : $VO_2(A)$, $VO_2(B)$, V_4O_9.

Nous avons tracé les spectres infra-rouges de 3 oxydes originaux $VO_2(B)$, $VO_2(A)$ et V_4O_9 (figure 5). Ils ont montré dans tous les cas l'absence des bandes $\nu(O-H)$ et $\delta(H-O-H)$.

Oxyde $VO_2(B)$

980 cm^{-1}, 950, 920, 720, 615 et 540 cm^{-1}

Le spectre infra-rouge est très médiocre (comme celui de V_6O_{13}). Dans la région 900—1000 cm^{-1}, il y a plusieurs bandes alors que la région correspondante du spectre de V_2O_5 n'en comporte qu'une :

Bande à 980 cm^{-1}. L'abaissement de la fréquence $\nu\,(V = O)$ par rapport à V_2O_5 montre que la liaison est plus longue. Effectivement dans V_2O_5 $V-O_1 = 1{,}54$ Å, alors que dans $VO_2(B)$: $V(1) - O(1) = 1{,}65$ Å*.

Bande à 950 cm^{-1} (très faible). Elle peut être attribuée à une autre liaison $V{=}O$. D'après Sathyanarayana, la fréquence est abaissée si l'environnement du vanadium a tendance à devenir octaèdrique. C'est le cas pour le vanadium V(2) pour lequel la liaison la plus courte est une des liaisons $V(2) - O(3) = 1{,}82$ Å.

Bande à 920 cm^{-1}. Elle est une des plus fortes bandes. Nous l'attribuons à des vibrations d'élongation des liaisons V—O les plus longues.

Oxyde $VO_2(A)$

940 cm^{-1} TF ; 675 m ; 610 F ; 558 F ; 430m

La bande à 940 cm^{-1} montre qu'il n'y a pas de liaison V—O très courte comme dans V_2O_5.

---

[25] K Tarama, S. Teranishi & S. Yoshida, *Bull. Inst. Chem. Res., Kyoto Univ.*, 46, 185 (1968).

* Pour la nomenclature des atomes se reporter aux références [1 et 15].

Oxyde V_4O_9

Le spectre obtenu ne dépend pas du réducteur employé : 1025 cm^{-1} mF ; 977 mF ; 950 mF ; 925 F ; 900 f ; 880 f ; 848 mF ; 820 épaule ; 730 F ; 590 F épaul' ; 542 F ; 500 épaule ; 475 m ; 428 m.

Ce qui frappe d'emblée dans ce spectre, c'est la présence de bandes relativement fines et nombreuses en comparaison des autres oxydes. Il ne serait pas étonnant que cela soit dû au caractère lacunaire de la structure, où des groupements bien individualisés peuvent se manifester.

En résumé, les spectres infra-rouges montrent que :

— dans $VO_2(B)$, les longueurs des liaisons V—O déduites de l'étude radiocristallographique sont compatibles avec les fréquences $\nu(V-O)$.

— dans $VO_2(A)$, l'environnement du vanadium est beaucoup plus symétrique que dans $VO_2(B)$ ou V_2O_5.

— V_4O_9 est probablement l'oxyde ayant la structure la plus compliquée.

COMPARAISONS STRUCTURALES ENTRE LES OXYDES ET LES HYDRATES

Nous avons pu déterminer aussi les mailles probables de quelques hydrates, ainsi que le nombre de motifs par maille, les directions d'élongation des cristaux, etc.

V_3O_7, H_2O orthorhombique[20]

$a = 9{,}34 \pm 0{,}04 Å \quad b = 17{,}0 \pm 0{,}1 Å \quad c = 3{,}626 \pm 0{,}005$ Å

$V_2O_{4.80}$,$0{,}5H_2O$ monoclinique[21]

$a = 11{,}6 \quad b = 3{,}63 \quad c = 14{,}33 \quad \beta = 101{,}4°$

$V_2O_{4.80}$,$3{,}5H_2O$ monoclinique[21]

$a = 12{,}25 \quad b = 3{,}65 \quad c = 17{,}43 \quad \beta = 97°$

Les directions de croissance des cristaux sont données dans le tableau 3.

Les analogies relevées entre les structures des oxydes V_2O_5, V_6O_{13}, $VO_2(B)$ et V_3O_7 s'étendent à ces hydrates, ainsi d'ailleurs qu'à un certain nombre de sels ou bronzes. Le tableau 2 montre en effet que le paramètre 3,6 Å est commun à toutes ces mailles. C'est le signe de *l'existence dans ces composés de chaînes doubles* (figure 6). *Ces corps forment des cristaux allongés dans la direction définie par ces chaînes et fréquemment aplatis selon une direction perpendiculaire.* Il en résulte des orientations particulières (groupements en fibres) que l'on rencontre dans la nature (cristaux minéralogiques) ou sur le porteéchantillon du microscope électronique. D'ailleurs de ce point de vue les hydrates ne diffèrent pas fondamentalement des oxydes puisque *tous les oxydes et hydrates dans lesquels le degré d'oxydation du vanadium est supérieur à 4 ($z > 4$) ont des structures de ce type, sauf peut-être* V_4O_9.

Bien que les composés, dans lesquels le degré d'oxydation du vanadium est inférieur à 4, ne fassent pas partie du domaine étudié, il est utile

Tableau 3

Directions d'elongation des cristaux

dans l'ordre : côtés long, moyen court

$VO_2(B)$	:	$\vec{b}, \vec{a}, \vec{c}$
$VO_2(A)$	:	$\vec{c}, \vec{a}$ (ou $\vec{b}$)
V_6O_{13}		$\vec{b}, \vec{a}, \vec{c}$
V_4O_9	:	$(\vec{a}, \vec{b}), \vec{c}$
V_3O_7, H_2O	:	$\vec{c}, \vec{a}, \vec{b}$
$V_2O_{4,80}, 0{,}5H_2O$	:	$\vec{b}, \vec{a}, \vec{c}$
$V_2O_{4,80}, 3{,}5H_2O$	:	$\vec{b}, \vec{a}, \vec{c}$
duttonite	:	l'élongation correspond à un paramètre de 6 Å

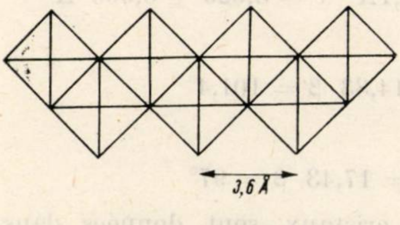

Fig. 6. — Enchainement double existant dans V_2O_5 ; V_6O_{13} ; $VO_2(B)$; V_3O_7 V_3O_7, H_2O ; $V_2O_{4,8}$, nH_2O, etc

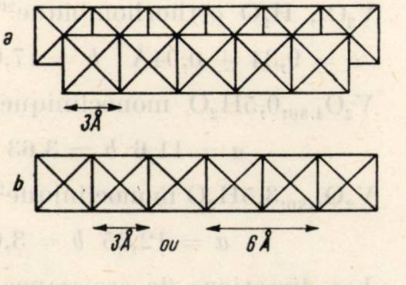

Fig. 7 *a*) — Enchainement double existant dans la (proto)dolorésite, la (para) montroséite et la häggite ; *b* —Enchainement simple existant dans la (para)-montroséite, la duttonite, la (proto)-dolorésite, VO_2 (rutile).

de remarquer qu'un grand nombre de ceux dont on connait la structure sont formés de chaines d'un autre type (figure 7), qui conduisent à un paramètre de 3 ou 6 Å.

Au degré d'oxydation 4, les deux types coexistent et sont représentés par des oxydes ou des hydrates :

paramètre 3,6 Å : $VO_2(B)$

paramètre 3 ou 6 Å : duttonite, VO_2 (rutile), etc...

Cependant nous ne pouvons pas affirmer que toutes les structures se rangent dans ces 2 catégories car certaines ne sont pas encore connues du tout ($VO_2(A)$, hydrates de Gain et de Schwarzmann).

Relations topochimiques entre hydrates et oxydes

Nous avons vu que $VO_2(B)$ et V_6O_{13} pouvaient coexister en relations topotactiques. Des phénomènes du même genre se rencontrent lors de la décomposition de certains hydrates.

1) Déshydratation de V_3O_7, H_2O

V_3O_7,H_2O se décompose entre 330 et 380° en V_3O_7et H_2O ; V_3O_7 cristallise tout de suite

$$V_3O_7,H_2O \rightarrow V_3O_7 + H_2O\nearrow$$

La diffraction X ne montre pas de phase intermédiaire mais une altération de V_3O_7,H_2O dans laquelle un certain nombre de raies s'affaiblissent (figure 8). On note particulièrement la diminution d'intensité des raies suivantes :

8,2 Å (1 1 0) ; 2,08 (3 6 0) ; 2,06 (1 8 0) ; 1,915 (3 7 0)

mais aussi de

8,5 Å (0 2 0) ; 4,82 (1 3 0) ; 4,67 (2 0 0) ; 3,14 (2 4 0).

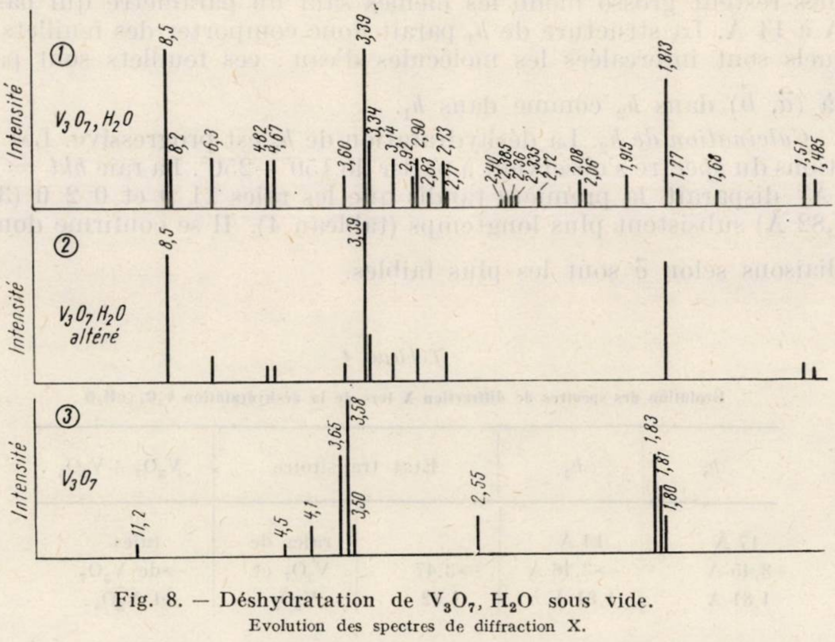

Fig. 8. — Déshydratation de V_3O_7, H_2O sous vide.
Evolution des spectres de diffraction X.

Toutes ces raies sont du type *hko*. Au contraire, les raies qui font intervenir $\vec{c}$ restent fortes jusqu'au moment où V_3O_7 apparaît. Ces observations conduisent à admettre que :

— V_3O_7,H_2O *comme* V_3O_7 *comporte des enchaînements d'octaèdres* VO_6 *(peut-être seulement des bipyramides* VO_5*) liés par des arêtes qui se développent suivant la direction* $\vec{c}$.

— *Ces chaînes sont liées les unes aux autres par divers types de liaisons, sans doute des liaisons V—O—V mais certainement aussi des liaisons hydrogène comme dans la duttonite. Les molécules d'eau participent à la stabilité de l'édifice.*

— *Lorsque les molécules d'eau sont éliminées par chauffage, le cristal se disloque mais les chaînes d'octaèdres se conservent puis se réorganisent au moment de la cristallisation de* V_3O_7.

2) Déshydratation de $V_2O_{4,80}, nH_2O$

Nous avons déjà indiqué que l'hydrate $V_2O_{4,80},3,5H_2O$ (h_1) donne par simple séchage un hydrate $V_2O_{4,80},0,5H_2O$ (h_2) qui lui-même donne après chauffage un mélange de V_3O_7 et V_2O_5

$$h_1 \rightarrow h_2 \rightarrow V_3O_7 + V_2O_5$$

Examinons l'évolution des paramètres au cours de ces deux étapes.

Séchage de h_1 en h_2. Lors du passage de h_1 à h_2 les paramètres de mailles restent grosso modo les mêmes sauf un paramètre qui passe de 17 Å à 14 Å. La structure de h_1 paraît donc comporter des feuillets entre lesquels sont intercalées les molécules d'eau : ces feuillets sont parallèles à $(\vec{a}, \vec{b})$ dans h_2 comme dans h_1.

Calcination de h_2. La déshydratation de h_2 est progressive. Les modifications du spectre s'observent à partir de 150°—250°. La raie $hkl = 0\ 0\ 1$ (14 Å) disparaît la première tandis que les raies 11 0 et 0 2 0 (3,47 Å et 1,82 Å) subsistent plus longtemps (tableau 4). Il se confirme donc que les liaisons selon $\vec{c}$ sont les plus faibles.

Tableau 4

Évolution des spectres de diffraction X lors de la déshydratation $V_2O_{4,8}nH_2O$

h_1	h_2	Etat transitoire		$V_3O_7 + V_2O_5$
17 Å	14 Å		raies de	raies
3,45 Å	→3,46 Å	→3,47	V_3O_7 et	→de V_3O_7
1,81 Å	1,81 Å	1,82	V_2O_5	et V_2O_5

On peut remarquer aussi que la densité augmente, ce qui est normal (h_1 :2,56 g/cm³ ; h_2 : 2,7 ; V_3O_7 : 3,5 et V_2O_5 : 3,4).

La succession des deux déshydratations peut donc s'interpréter comme une contraction de la structure par élimination de «l'eau» entre des plans d'atomes, plans qui ne disparaissent que lorsque la déshydratation est complète. Mais les chaînes d'octaèdres (paramètre 3,6 Å) *se conservent de h_1 à V_2O_5 et V_3O_7 tout au long de la transformation.*

3) Déshydratation des hydrates de vanadium (IV)

Les hydrates de Gain, de Schwarzmann et la duttonite se déshydratent en V_2O_4 en donnant intermédiairement un produit qui paraît amorphe entre 250° et 300° environ c'est-à-dire sur un intervalle de température assez grand.

Ceci nous incite à penser que ces 3 hydrates ont des structures qui n'ont pas beaucoup de points communs avec le dioxyde rutile.

En résumé, la comparaison des hydrates et des oxydes de vanadium, dans lesquels le degré d'oxydation est strictement supérieur à 4 ($z > 4$) montre que l'on trouve dans ces composés des enchaînements d'octaèdres VO_6 ou de bipyramides VO_5 du même genre que celui de la figure 6. Ces enchaînements se conservent lorsqu'on décompose les hydrates en les oxydes correspondants. Au degré d'oxydation 4 ce type d'enchaînement est encore présent dans $VO_2(B)$ mais le dioxyde VO_2 rutile et les hydrates possèdent des enchaînements différents.

COMPARAISON ENTRE LES HYDRATES

Si l'on considère maintenant l'ensemble des hydrates en tant que tels, on s'aperçoit qu'ils ne possèdent pas une véritable unité puisqu'ils présentent à peu près tous les types d'hydratation possibles.

Ces différences on les pressent déjà dans la précision plus ou moins grande avec laquelle la composition est définie. Par exemple, pour V_3O_7, H_2O et pour la duttonite $VO(OH)_2$ la teneur en hydrogène est parfaitement reproductible et elle prend des valeurs qui sont des fractions simples. Au contraire dans l'hydrate de Gain et l'hydrate de Schwarzmann le teneur en eau peut être qualifiée de non stœchiométrique. Enfin dans $V_2O_{4.80}$, nH_2O la teneur en eau est très variable.

L'oxydabilité par l'air (§ B, 3) est une propriété qui rapproche les hydrates de Gain et de Schwarzmann et les différencie de la duttonite.

La température de déshydratation variant de 20° à 380° (cf. §B.1) montre que la force de la liaison qui retient les molécules d'eau dans le réseau est très variable. Mais on ne peut pas déduire de la température de déshydratation — sans autre renseignement — si l'eau qui s'en va, préexistait dans la molécule où s'est formée par recombinaison des $-OH$. En effet, les molécules d'eau liées par liaisons hydrogène ou coordinées au cation central se comportent très différemment.

Spectres infrarouges des hydrates

Les spectres I.R. de l'hydrate de Gain[26] de la duttonite[27] et de l'hydrate de Schwarzmann[19] ont déjà été publiés. Mais un nouvel examen nous a donné des renseignements complémentaires sur la nature de l'eau ou des hydroxyles présents. Nous avons tracé aussi les spectres infrarouges de V_3O_7,H_2O et de $V_2O_{4,80}$, nH_2O.

---

[26] C. Cabannes-Ott, *Compt. rend.*, **242**, 2825 (1956). *Ann. Chim. (France)*, **5**, 905, (1960).

[27] E. Schwarzmann, *Z. Naturforsch.*, **25B**, 1485 (1970).

Duttonite.	2 900 cm^{-1}	F	ν(O—H), liaisons hydrogène
	1 130	F	δ(—OH) ou 2 × 570 cm^{-1}(?)
	1 015	m	ν(V—O)(V—O = 1,65 Å)
	980	m	ν(V—O)
	940	mF	ν(V—O)
	etc...		

La position de la bande ν(O—H) vers 2 900 cm^{-1} donne la longueur des liaisons hydrogène : 2,7 Å. Ceci correspond exactement à la structure décrite par Evans et coll. :[18]

— il n'y a pas de groupement —OH libre qui donnerait une bande plus étroite vers 3 500 cm^{1-}.

— il n'y a pas de molécules d'eau qui donnerait la bande de déformation δ(H—O—H) vers 1 600 cm^{-1}.

La bande à 1 015 cm^{-1} est ν(V—O) pour la liaison V—O la plus courte. Il existe en effet dans l'entourage de chaque atome de vanadium un atome d'oxygène situé à 1,65 Å seulement.

Ces renseignements, quoiqu'en nombre limité, justifient parfaitement l'écriture de la formule : $VO(OH)_2$.

L'ensemble des données relatives à ν(V—O) permet de tracer la figure 9.

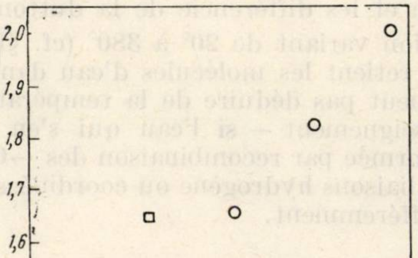

Fig. 9. — Variation de la fréquence de vibration ν(V—O) en fonction de la longueur de la liaison.
+ V_2O_5 ○ VO_2(B) □ duttonite.

Hydrate de Gain. Le spectre infrarouge a déjà été étudié en partie par C. Cabannes-Ott.[26] L'action prolongée et répétée de l'eau lourde sur l'hydrate rose en tube scellé nous a permis de deutérier partiellement ce corps et de poursuivre l'interprétation (figure 10).

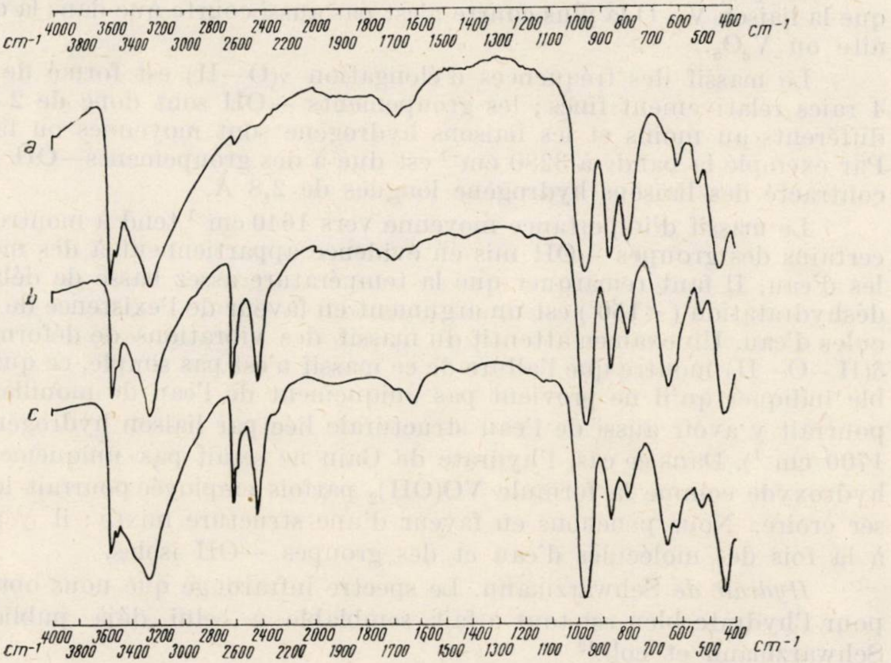

Fig. 10. — Spectres infrarouges de l'hydrate de Gain plus ou moins deutérié (a, b, c).

Spectre intra-rouge de l'hydrate de GAIN et action de l'eau lourde

(Correspondance des raies :
⇒sûre ; →presque sûre ou probable ; ⇢possible ou douteuse)

eau légère			eau lourde	
3 560 cm^{-1}	F	⇒	2 633 cm^{-1} (r=1,35)	massif ν(O−H) ou ν(O−D)
3 520	m	⇒	2 610	
3 380	f (épaul^{t}, douteux)			
3 280	mF	→	2 455	
		⇢	2 320 (épaul^{t})	
1 640	F	→	1 410 m	δ(H−O−H)
1 125	tf			δ(OH) ?
965	TF	⇒	965	ν(V=O)
870	F	⇒	651	δ(V−OH), γ(V−OH) ou librations (V−OH$_2$)
805	F	→	580 (épaul^{t})	
650	tf (douteux)			
618	m	⇒	618	
565	tf (douteux)			
530	m	⇒	530	
455	F	⇒	455	

La position de la bande ν(V=O) vers 965 cm^{-1} permet d'affirmer que la liaison V—O la plus courte n'est pas aussi courte que dans la duttonite ou V_2O_5.

Le massif des fréquences d'élongation ν(O—H) est formé de 3 ou 4 raies relativement fines ; les groupements —OH sont donc de 2 types différents au moins et les liaisons hydrogène sont moyennes ou faibles. Par exemple la bande à 3280 cm^{-1} est due à des groupements—OH ayant contracté des liaisons hydrogène longues de 2,8 Å.

Le massif d'importance moyenne vers 1640 cm^{-1} tend à montrer que certains des groupes —OH mis en évidence appartiennent à des molécules d'eau. Il faut remarquer que la température assez basse de début de déshydratation ($<150°$) est un argument en faveur de l'existence de molécules d'eau. Un examen attentif du massif des vibrations de déformation δ(H—O—H) montre que l'allure de ce massif n'est pas simple, ce qui semble indiquer qu'il ne provient pas uniquement de l'eau de mouillage : il pourrait y avoir aussi de l'eau structurale liée par liaison hydrogène (~ 1700 cm^{-1}). Dans ce cas, l'hydrate de Gain ne serait pas uniquement un hydroxyde comme la formule $VO(OH)_2$ parfois employée pourrait le laisser croire. Nous penchons en faveur d'une structure mixte : il y aurait à la fois des molécules d'eau et des groupes —OH isolés.

Hydrate de Schwarzmann. Le spectre infrarouge que nous obtenons pour l'hydrate bleu est tout à fait semblable à celui déjà publié par Schwarzmann et coll.[19]

3 360 cm^{-1}	TF	et assez étroit	ν(OH)	960 cm^{-1}	F	fine	ν(V—O)
3 060	F	large	ν(O—H) liaisons...H	890	F	fine	
1 970	f	épaul^t	combinaisons ou	795	F		
1 935	m		harmoniques	558	mF		
1 630	mf		δ(H—O—H)	532	mF		
1 033	F	fine	ν(V=O) très courte	445	F		
987	F	fine	ν(V—O)				

La bande à 3360 cm^{-1} est due à l'élongation de groupements O—H presque libres. La bande à 3060 cm^{-1} correspond à des groupements O—H ayant contracté des liaisons H de force moyenne. La présence de molécules d'eau est encore plus douteuse que pour l'hydrate de Gain, bien que nous observions la bande δ(H—O—H) vers 1630 cm^{-1} : cette bande peut être due uniquement à l'eau de mouillage.

La bande à 1033 cm^{-1} provient de l'élongation *d'une liaison* $V = O$ *très courte*. Les bandes à 987 et 962 cm^{-1} appartiennent probablement aussi à des liaisons V—O ce qui indique que la structure est relativement complexe (à titre de comparaison il y a dans le domaine 940—1035 cm^{-1} une bande pour V_2O_5, une bande pour l'hydrate de Gain et trois bandes pour la duttonite.

L'hydrate V_3O_7,H_2O. Le traitement par l'eau lourde à 350° a permis une substitution isotopique presque complète de H par D comme le montre la figure 11.

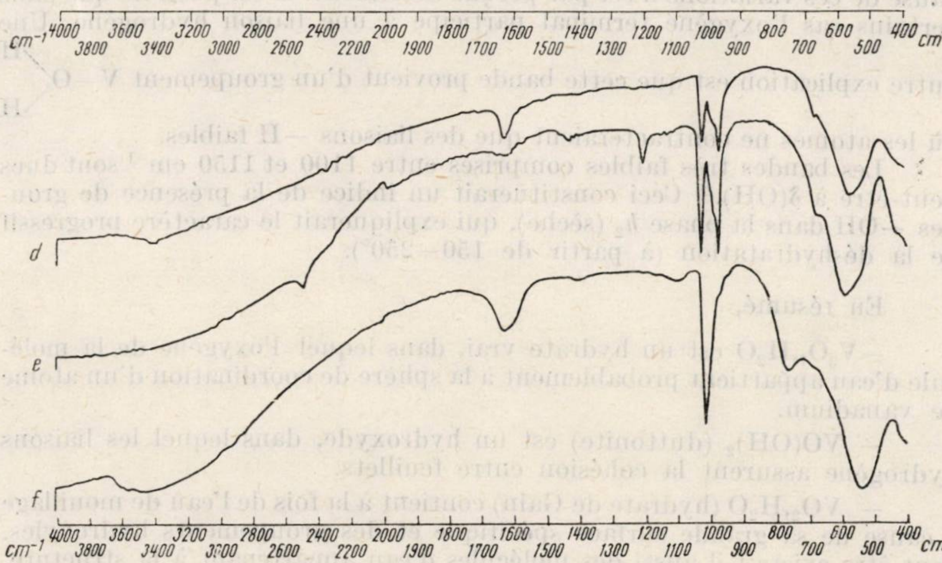

Fig. 11. — Spectres infrarouges de l'hydrate V_3O_7,H_2O plus ou moins deutérié (d, e) et de $V_2O_{4.8}$, nH_2O (f).

eau légère				eau lourde		
3 420 cm^{-1}	m	large	⇒	2 520 cm^{-1}	m	ν(O—H) ou ν(O—D)
1 630	mF	nette	⇒	1 208	mF nette	δ(H—O—H) ou δ(D—O—D)
1 020	F		⇒	1 020		ν(V=O) V—O courte
990	f	épaul^t	⇒	990		
970	F		⇒	970		
667	tf	douteux	→	667		
565	TF	large	→	580		

La bande à 1630cm^{-1} prouve la présence de molécules d'eau. La bande à 3420 cm^{-1} indique que les liaisons hydrogène sont faibles. Par ailleurs, la déshydratation de V_3O_7,H_2O montre que les molécules d'eau sont liées assez fortement, sans doute sont-elles coordinées directement aux atomes de vanadium $V-OH_2$.

Le composé V_3O ,H_2O *apparaît donc nettement comme un hydrate.*

L'hydrate $V_2O_{4,80},nH_2O$ *(phases* h_1 *et* h_2*).*

La figure 11 montre le spectre d'un échantillon de cette phase. L'allure médiocre du spectre s'explique par la mauvaise cristallisation. Il s'agit d'un échantillon de phase «mouillée» h_1. Il n'y a d'ailleurs pratiquement pas de différence par rapport à h_2. Seul le massif ν(O—H) vers 3450 cm^{-1} est plus large parce que les liaisons hydrogène sont plus nombreuses dans la phase mouillée que dans la phase sèche.

La bande à 1630 cm^{-1} confirme qu'il existe des molécules d'eau.

La bande à 1030 cm^{-1} est sans doute due à ν(V=O). Elle est plus ou moins forte et plus ou moins intense selon les échantillons, mais la cause de ces variations n'est par perçue nettement. Il est possible que dans certains cas l'oxygène terminal participe à une liaison hydrogène. Une autre explication est que cette bande provient d'un groupement $\mathrm{V{-}O}{<}^{\mathrm{H}}_{\mathrm{H}}$ où les atomes ne contracteraient que des liaisons —H faibles.

Les bandes très faibles comprises entre 1100 et 1150 cm^{-1} sont dues peut-être à $\delta(OH)$.[28] Ceci constituerait un indice de la présence de groupes —OH dans la phase h_2 (sèche), qui expliquerait le caractère progressif de la déshydratation (à partir de 150—250°).

En résumé,

—V_3O_7,H_2O est un hydrate vrai, dans lequel l'oxygène de la molécule d'eau appartient probablement à la sphère de coordination d'un atome de vanadium.

— $VO(OH)_2$ (duttonite) est un hydroxyde, dans lequel les liaisons hydrogène assurent la cohésion entre feuillets.

— VO_2,H_2O (hydrate de Gain) contient à la fois de l'eau de mouillage à cause de sa grande surface spécifique et des groupements hydroxyles. Peut-être existe-t-il aussi des molécules d'eau appartenant à la structure.

Un des caractères les plus troublants de l'hydrate de Gain est sa médiocre cristallisation. Peut-être faudra-t-il pour expliquer sa structure, s'orienter vers un modèle à structure lamellaire du type $Ni(OH_2)$ dans lequel les feuillets normaux emprisonnent des couches d'ions provenant de la solution.

— $VO_2,0{,}85H_2O$ (hydrate de Schwarzmann) présente beaucoup d'analogies avec le précédent, mais il est mieux cristallisé.

— $V_2O_{4,80},0{,}5H_2O$ est susceptible de fixer de l'eau réversiblement. Cette eau est sans doute liée par des liaisons hydrogène aux atomes d'oxygène du réseau. Elle est mobile et le solide devient le siège d'un équilibre divariant. Il est probable que l'eau s'insère dans des micropores ou entre des feuillets de la structure.

D'autre part la «déshydratation» de $V_2O_{4,80},0{,}5H_2O$ s'accompagne d'une dismutation (il n'y a pas d'oxyde correspondant au degré d'oxydation 4,80), ce qui nous incite à penser qu'une partie de l'hydrogène de la formule appartient en réalité à un groupement —OH. La formule la plus correcte serait intermédiaire entre $V_2O_{4,8},0{,}5H_2O$ et $V_2O_{4,3}(OH)$.

Remarquons que plus le degré d'oxydation est élevé, moins la «teneur en eau» des hydrates ou des hydroxydes est grande.

z	4	4,66	4.80	5
nombre d'atomes H par atome V	~ 2	0,66	0,5*	0

Ceci est conforme à ce qu'on observe fréquemment pour les autres éléments.

---

* Nous ne considérons pas ici l'hydrate supérieur où l'eau est très peu liée.

COMPARAISON DES HYDRATES AVEC LES MINÉRAUX

Dans 5 cas, il a été possible d'identifier un composé naturel et un hydrate synthétique ou tout au moins de montrer leur étroite parenté.

$VO(OH)_2$ =duttonite

$VO_2,0{,}85H_2O$ (Schwarzmann) $\simeq$ lenoblite[29,30]

$3V_2O_4,4H_2O$ = dolorésite[31]

$V_2O_{4,80},0{,}5H_2O$ $\neq$ bariandite[32]

$V_2O_{4,80},3{,}5H_2O$ $\simeq$ navajoïte[33]

De plus la corvusite[34] paraît très voisine de la bariandite mais ses caractères sont beaucoup moins bien définis.

Ces comparaisons nous ont été extrêmement utiles pour préciser les caractères de chaque phase : la composition chimique, le spectre infrarouge et parfois la maille cristalline et la structure, etc...

Par contre nous n'avons pas trouvé jusqu'à présent de correspondant naturel pour l'hydrate de Gain ; il peut y avoir à cela deux raisons :
— ou bien le corps s'oxyde trop vite
— ou bien les conditions géologiques sont telles que l'hydrate de Gain ne puisse pas se former. Ce cas peut se rencontrer si la température est supérieure à 120°.

Oxydation. Il est assez curieux de constater que l'oxydation naturelle des hydrates minéralogiques est comparable à celle de l'hydrate de Gain. Nous avons vu en effet que, à 20° :

$$VO_2,1{,}05H_2O\ (\text{Gain}) \rightarrow V_2O_{4,80},\ nH_2O\ (h_1 \text{ ou } h_2)$$

Or,d'après la disposition naturelle des couches de minéraux, Evans[35] a proposé le schéma suivant pour l'oxydation de la dolorésite :

dolorésite → corvusite → navajoite

Donc dans la nature comme au laboratoire on n'observe aucun composé intermédiaire entre $z = 4$ et $z = 4{,}8$ et les produits finaux sont les mêmes.

Conditions hydrothermales. On ne trouve dans la nature pratiquement que des hydrates. Les seuls oxydes naturels connus sont V_2O_5 et la paramontroséite. Mais si l'on remarque qu'il n'existe aucun hydrate synthétique au degré +5 et que, au degré +4, la paramontroséite est en fait

---

[28] R. Franck, *Rev. Chim. Min.*, **10**, 795 (1973).
[29] F. Cesbron &H. Vachey, *Bull. Soc. Fr. Min. Crist.*, **93**, 235 (1970).
[30] I. G. Smyslova & V. A. Shitov, *Zap. Vses. Mineral. Obshchest*, **105**, 488 (1971).
[31] H. T. Evans & M. F. Mrose, *Amer. Mineralogist*, **45**, 1144 (1960).
[32] F. Cesbron & H. Vachey, *Bull. Soc. Fr. Min. Crist.*, **94**, 49 (1971).
[33] A. D. Weeks, M. E. Thompson & A. M. Sherwood, *Amer. Min.*, **40**, 207 (1955).
[34] M. Ross, *Amer. Min.*, **44**, 322 (1959).
[35] H. T. Evans & R. M. Garrels, *Geochimica & Cosmochimica Acta*, **15**, 131 (1958).

un hydrate déshydrogéné, il se confirme que les conditions hydrothermales jouent un rôle très important dans la minéralogie de l'élément vanadium.

Inversement nos résultats nous permettent de déduire certaines propriétés des minéraux. Par exemple, la bariandite ne doit pas exister au-dessus de 250°C et la navajoïte probablement pas non plus, etc...Ces résultats peuvent être utiles aux géochimistes.

Dimensions des cristaux. Les cristaux naturels sont toujours très petits, allongés et aplatis exactement comme ceux que nous avons observés au microscope électronique. L'espoir d'obtenir au laboratoire des cristaux de taille suffisante pour une étude radiocristallographique est donc très faible.

CONCLUSION

L'étude du système $V_2O_4-V_2O_5-H_2O$ permet de préparer des phases nouvelles dans le domaine 0–500°C : $VO_2(A)$; $VO_2(B)$; V_4O_9 ; V_3O_7,H_2O ; $V_2O_{4.8},0,5H_2O$; $V_2O_{4.8},3,5H_2O$.

La détermination de la structure de $VO_2(B)$ montre qu'il dérive de V_2O_5 ou de V_6O_{13} par un cisaillement cristallographique et comporte des doubles chaînes d'octaèdres. Ce type de chaînes est retrouvé aussi dans un certain nombre d'hydrates que l'eau soit faiblement liée comme dans $V_2O_{4.80},3,5H_2O$, moyennement liée comme dans $V_2O_{4.80},0,5H_2O$ ou fortement liée comme dans V_3O_7,H_2O. Des relations topochimiques sont observées lorsque les hydrates se décomposent en oxydes.

L'étude infra-rouge montre que les hydrates et hydroxydes présentent à peu près tous les types d'«hydratation» possibles : molécule d'eau $-OH_2$ faisant partie de la sphère de coordination d'un atome de vanadium (V_3O_7,H_2O), groupement $-OH$ (duttonite, hydrates de Schwarzmann et de Gain), eau de mouillage (hydrates de V(IV), eau fixée par liaisons hydrogène ($V_2O_{4.80},nH_2O$).

Revue Roumaine de Chimie, 23, 6, 909–915(1978)

NICKEL (II) COORDINATION COMPOUNDS WITH 3-AMINO-1-PROPANOL

MARIA BREZEANU and IOANA JITARU

Institute of Chemistry, Faculty of Chemistry, Laboratory of Inorganic Chemistry,
Splaiul Independenţei, 89, IV, Bucharest, Romania

Received November 24, 1976

A series of Ni(II) complex compounds with 3-amino-1-propanol have been obtained and they correspond to the following geneal types $[Ni(AOH)_3]X_2(X=Cl, Br, NO_3, 1/2SO_4)$; $[Ni(AOH)_4]Cl_2$ and $[Ni(AOH)Cl_2]$ where $AOH=H_2N-(CH_2)_3-OH$ and $AO=(H_2N-(CH_2)_3-O)^-$. These compounds were characterized by elemental chemical analysis, molecular electrical conductivity measurements, electronic and vibrational spectra. On the base of the data obtained, attempts are made to attribute the most probable stereochemistry of the compounds under study.

By carrying on the study of the coordination capacity of some higher aminoalcohols, we have succeeded in characterizing some new complex compounds of chromium (III), cobalt (II) and (III) and copper (II) with 3-amino-1-propanol.[1-3]

In this paper we report the result obtained in the study of the coordination capacity of 3-amino-1-propanol relative to nickel (II) salts.

On this occasion we have been able to characterize a series of complex compounds of nickel (II) belonging to the following general types: $[Ni(AOH)_3]X_2(X = Cl, Br, NO_3, 1/2SO_4)$; $[Ni(AOH)_4]X_2$ $(X = Cl)$; $[Ni(AOH)X_2]$ $(X = Cl)$.

The compounds obtained were characterized by elemental chemical analysis, molecular electrical conductivity determinations, electronic and vibrational spectra.

RESULTS AND DISCUSSION

In view of obtaining a series of nickel (II) complex compounds with monopropanolamine with various coordination possibilities of this ligand, we have studied, like in previous works, the variation of the following experimental conditions: the pH of the reaction medium, the nickel (II) : AOH molar ratio, the nature of anion X, the solvent nature and the temperature.

---

[1] M. Brezeanu, and I. Jitaru, *Rev. Roumaine Chim.*, **18**, 2039 (1973).

[2] M. Brezeanu and I. Jitaru, *Rev. Roumaine Chim.*, **22**, 371 (1977).

[3] M. Brezeanu and I. Jitaru, *Rev. Roumaine Chim.*, in press.

It should be mentioned that unlike all the other investigated cations[1-3], in the case of nickel (II), we have failed to isolate complex compounds in which monopropanolamine would act as a mono- or bidentate anionic ligand.

As also indicated by the types of compounds presented above, monopropanolamine is found to exhibit a pronounced tendency to behave like a neutral, mono- and especially bidentate ligand, relative to the nickel (II) salts.

The $[Ni(AOH)_4]Cl_2$ compound which is in fact the only of this type obtained in the study carried out, in which monopropanolamine behaves like a monodentate neutral ligand coordinated by nitrogen, is far less stable than compounds in which it acts as a bidentate ligand.

Compounds of the form $[Ni(AOH)_3]X_2$ ($X = Cl$, Br, $NO_3 . 1/2SO_4$) were obtained in the reaction between nickel (II) anhydrous halides respectively nickel (II) anhydrous nitrate and sulphate and monopropanolamine in methyl alcohol at a 1 : 3 molar ratio.

In the absence of the solvent at a molar ratio nickel (II) anhydrous chloride : monopropanolamine which varies from 1 : 4 to 1 : 6 we obtained a compound of the form $[Ni(AOH)_4]Cl_2$ which was assigned an octahedral structure based on electronic spectra.

This thing leads to the conclusion that two monopropanolamine molecules act very likely as bidentate ligands while the other two act like monodentate ligands coordinated by means of nitrogen.

In order to assure a sufficiently alkaline medium that may cause monopropanolamine to behave as an anionic ligand, the synthesis was conducted in an aqueous solution. However these conditions have not permitted the isolation of well-defined compounds.

The instability of such compounds in aqueous solution, attributed to their marked hydrolysis tendency accounts for the failure to obtain nickel (II) compounds containing monopropanolamine as an anionic ligand.

Conducting the synthesis in a weak acidic medium ($pH \sim 3.5-4$) obtained by a molar ratio nickel (II) : $AOH = 1 : 1$ in an acetone medium, we succeeded in isolating a complex chloride of the type $[Ni(AOH)Cl_2]$ with a square-planar configuration assigned on the base of the electronic spectrum.

The attempts to obtain compounds of a similar type from the nickel (II) nitrate and sulphate, respectively, under analogous experimental conditions to those mentioned above, have failed to yield results.

This different behaviour was attributed to the different coordination capacity of the anions in question.

Molecular electrical conductivity determinations. The formulation attributed to the complex compounds under study in the sense of establishing the electrolyte type, was confirmed by the determination of their molecular electrical conductivities.

The data obtained (Table 1) confirm the electrolyte nature of the great majority of nickel (II) compounds.

Electronic spectra. To confirm the formulation attributed to the complex compounds of nickel (II) based on chemical data and on molecular electrical conductivity determinations, their electronic reflexion spectra were also recorded.

Table 1

Molecular electrical conductivities of complex compounds studied

Compund	Molecular electrical conductivity* ($\Omega^{-1}cm^2mol^{-1}$)	Electrolyte type
$[Ni(AOH)_3^{**}]Cl_2$	135.20	1 : 2
$[Ni(AOH)_3]Br_2$	130.80	1 : 2
$[Ni(AOH)_3](NO_3)_2$	140.20	1 : 2
$[Ni(AOH)_3]SO_4$	80.45	1 : 1
$[Ni(AOH)_4]Cl_2$	165.30	1 : 2
$[Ni(AOH)Cl_2]$	20.30	non-electrolyte

*10^{-3}M solutions in DMF, $t = 25°$;
**$AOH = H_2N-(CH_2)_3-OH$.

Figure 1 exhibits the electronic spectra of compounds $[Ni(AOH)_3]X_2$ ($X = Cl, Br, NO_3, 1/2SO_4$) as well as those of compound $[Ni(AOH)_4]Cl_2$.

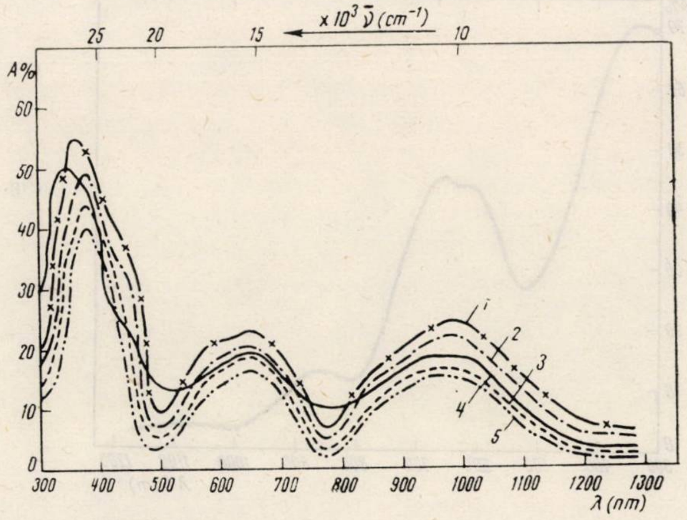

Fig. 1. — Electronic reflexion spectra of compounds :
1. $[Ni(AOH)_3]Cl_2$;
2. $[Ni(AOH)_3]Br_2$;
3. $[Ni(AOH)_3](NO_3)_2$;
4. $[Ni(AOH)_3]SO_4$ and
5. $[Ni(AOH)_4]Cl_2$

As can be readily seen, these spectra are very similar with regard to the number of bands and also their position and they can be satisfactorily interpreted in the terms of an octahedral structure.[4]

---

[4] A. B. P. Lever, "Inorganic Electronic Spectroscopy", Academic Press, New York 1968, p. 320.

Based on the Tanabe Sigano diagram for a d^8 ion in an octahedral symmetry field, the bands appearing in the spectra of such compounds may be attributed as follows :

— the first band appearing at 370 nm (27 030 cm^{-1}) with a shoulder towards 420 nm may be attributed to the $^3T_{1g}(P) \leftarrow {}^3A_{2g}$ transition and the shoulder to the $^1T_{1g} \leftarrow {}^3A_{2g}$ transition ;

— the structured band appearing within the 580—660 nm range (16 260 cm^{-1}) may be attributed to the $^3T_{1g}(F) \leftarrow {}^3A_{2g}$ transition ;

— the band appearing in the near infrared range at 970—980 nm (10 250 cm^{-1}) may be attributed to the $^3T_{2g}(F) \leftarrow {}^3A_{2g}$ transition.

The splitting of the band attributed to the $^3T_{1g}(F) \leftarrow {}^3A_{2g}$ transition is usually interpreted either on the base of a spin-orbit coupling which determines the overlapping of states $^3T_{1g}(F)$ and ^1E_g or on the base of a supplementary forbidden transition at the ^1E_g level.

An octahedral configuration for the central metallic ion of compound $[Ni(AOH)_4]\ Cl_2$ is possible only by admitting that two of the four monopropanolamine molecules act as bidentate ligands and the other two, as monodentate ligands. This behaviour is also confirmed by the data from the vibrational spectra, as shown below.

A study of the absorption spectrum recorded for compound $[Ni(AOH)Cl_2]$ (Figure 2), spectrum which does not present absorption bands below 10.000 cm^{-1} leads to the conclusion of a square-planar configuration ; the band appearing at approx. 600 nm (16 600 cm^{-1}) may be attributed to a $^1A_{2g} \leftarrow {}^1A_{1g}(b_{1g} \leftarrow b_{2g})$ transition and the intense band appearing at approx. 330 nm (30 300 cm^{-1}) to the $^1B_{1g} \leftarrow {}^1A_{1g}\ (b_{1g} \leftarrow a_{1g})$ transition.[5]

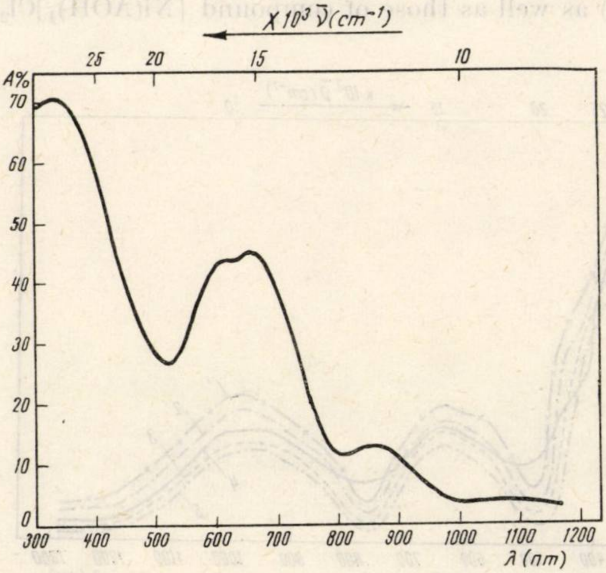

Fig. 2. — Electronic reflexion spectrum of compound : $[Ni(AOH)Cl_2]$.

---

[5] S. Buffagni, L. E. Vallerio and J. V. Quagliano, *Inorg. Chem.*, **3**, 480 (1964).

Vibrational spectra. To provide additional data on the stereochemistry of the studied compounds, in particular on the coordination manner of the monopropanolamine ligand (neutral molecule, mono- or bidentate anion) and also on the behaviour of anions (coordinated or in the ionization sphere), the IR spectra of these compounds were recorded.

The spectrum of the free ligand was also recorded in view of a most correct assignment of IR spectra of the complex compounds under study.

Table 2 presents the characteristic IR frequencies and their probable assignments in the complex compounds under study.

Table 2

Characteristic IR frequencies of compounds studied and probable assignments

Compound	ν_{OH}	ν_{asNH}	ν_{sNH}	δ_{NH_2}	ν_{CO}	ν_{NO} (NO_3)	ν_{SO} (SO_4)
AOH	3450 (s, b)	3290 (s, b)	3170 (sh)	1615 (m, b)	1055 (s)	—	—
$[Ni(AOH)_3(NO_3)_2$	3280 (s, b)	3220 (m, b)	3090 (w, b)	1580 (m)	1055 (s)	1380 (s) 830 (s)	
$[Ni(AOH)_3]SO_4$	3290 (s, b)	3220 (m, b)	3080 (w, b)	1580 (m)	1045 (s)	—	1140(s) 625(s)
$[Ni(AOH)Cl_2$	3290 (s, b)	3230 (m, b)	3090 (w, b)	1590 (m)	1045 (s)	—	—
$[Bi(AOH)_4]Cl_2$	3430 (s, b) 3280(sh)	3200 (m, b)	3050 (w, b)	1580 (m)	1045 (s)	—	—

s-strong, m-medium, w-weak, b-broad
AOH= $H_2N-(CH_2)_3-OH$.

A comparative examination of the data presented in this table suggests several conclusions on the coordination manner of aminoalcohol and on the function of the respective anions, i.e. :

— the shift towards lower of the characteristic frequencies of the vibrational modes of the amino group ($\nu_{as}NH$, ν_sNH, respectively δ_{NH_2}) for all the studied compounds, indicated the coordination of the monopropanolamine ligand by means of the nitrogen from the amino group ;

— the shift of the O—H valency vibration frequency towards lower frequencies (3280 cm^{-1} respectively 3290 cm^{-1} for compounds $[Ni(AOH)_3]X_2$ (X = Cl, Br, NO_3, $1/2SO_4$) respectively $[Ni(AOH)Cl_2]$ relative to the free ligand indicates monopropanolamine coordinations a bidentate neutral molecule (by means of oxygen of the hydroxyl group) ;

— in the spectrum of compound $[Ni(AOH)_4]Cl_2$ the absorption band attributed to the O—H stretching vibration appears split (3450 cm^{-1} respectively 3290 cm^{-1}) which may suggest the interpretation that a part of the aminoalcohol molecules are coordinated as bidentate ligands and the other part, as monodentate ligands ;

— the absorption bands attributed to the vibration modes of nitrate respectively sulphate anions indicate their presence as ionic uncoordinated species, as also resulted from the data included in table 2. [6,7]

EXPERIMENTAL DATA

I. Synthesis of complexes

1. $[Ni(AOH)_3]X_2$ (X=Cl, Br, NO_3, $1/2SO_4$). The chloride and bromide of the series is separated from the solution obtained by adding over nickel (II) anhydrous halides an amount of 1 : 5 solution of 3-amino-1-propanol in methanol corresponding to a 1 : 3 nickel(II) : AOH molar ratio. The blue substances obtained are filtered and washed with anhydrous methanol.

The nitrate and the sulphate of the series are obtained by adding a methanolic solution of 3-amino-1-propanol (1 : 5) to a concentrated methanol solution of nickel nitrate or sulphate. The blue-green solution thus obtained is filtered and concentrated in dessiccator on P_4O_{10}. A blue-green substance is formed after a few days and it is filtered and washed with small amounts or anhydrous methanol.

Calcd. :	Ni%, 16.53 ;	N%, 11.84 ;	Cl%, 19.50 ;	$[NiC_9H_{27}O_3N_3]Cl_2$
Found :	16.35 ;	11.94 ;	19.65.	
Calcd. :	Ni%, 13.22 ;	N%, 9.46 ;	Br%, 36.00 ;	$[NiC_9H_{27}O_3N_3]Br_2$
Found :	13.25 ;	9.60 ;	35.92.	
Calcd. :	Ni%, 14.38 ;	N%, 17.16 ;	C%, 26.49 ;	$[NiC_9H_{27}O_3N_3]NO_3$
Found :	14.50 ;	17.05 ;	26.10.	
Calcd. :	Ni%, 15.44 ;	N%, 11.05 ;	SO_4% 25.27 ;	$[NiC_9H_{27}O_3N_3]_2SO_4$
Found :	15.60 ;	11.20 ;	25.05.	

2. $[Ni(AOH)_4]Cl_2$. To 0.10 g anhydrous $NiCl_2$ is added approx. 1.50 cc solution of 3-amino-1-propanol in methanol (1 : 5) (molar ratio nickel(II) : AOH$\geqslant$1 : 4).

The dark blue solution is concentrated on a water bath almost to dryness. The blue substance which is formed is worked up with a small amount of methanol, it is filtered off and washed with methanol.

Calcd. :	Ni%, 13.65 ;	N%, 13.02 ;	Cl%, 16.48 ;	$NiC_{12}H_{27}O_4N_4Cl_2$
Found :	13.60 ;	13.15 ;	16.60.	

3. $[Ni(AOH)Cl_2]$.0.25 g anhydrous $NiCl_2$ are dissolved in approx. 0.20 cc 3-amino-1-propanol (molar ratio nickel(II) : AOH$\leqslant$1 : 1). The mixture is worked up with 5–6 cc acetone obtaining a crystalline yellow-green substance which is filtered and washed with small amounts of acetone.

Calcd. :	Ni%, 28.67 ;	N%, 6.84 ;	Cl%, 34.68 ;	$[NiC_3H_9ONCl_2]$
Found :	28.50 ;	7.10 ;	34.30.	

---

[6] K. Nakamoto, *Inorg. Chem.*, **4**, 804 (1966).

[7] B. E. Gatehouse, S. E. Livingstone and R. S. Nyholm, *J. Chem. Soc.*, **1957**, 4222.

II. Molecular electrical conductivity measurements

Molecular electrical conductivity measurements were performed on a Karl Zeiss Jena type II (Czechoslovakia) conductometer with k=0.52 cell constant. The electrolyte type was assigned on the base of indications found in the literature with regard to the determination methods of the electrolyte type in dimethylformamide solution.

III. Electronic spectra

The electronic reflexion spectra were recorded at room temperature using a K. Zeiss Jena VSU 1 spectrophotometer and the reference material was magnesium oxide. The electronic spectra in solution were recorded at room tempearture using VSU 2G spectrophotometer.

VI. Vibrational spectra

IR spectra were recorded on a Perkin Elmers spectrophotometer in KBr pellets.

Revue Roumaine de Chimie, 23, 6, 917–920 (1978)

ON THE α-DIOXIMINE COMPLEXES OF TRANSITION METALS. LVI*

SOME ASPECTS OF THE POLAROGRAPHIC BEHAVIOUR OF THE AZIDO-BIS-DIMETHYLGLYOXIMINE COMPLEXES OF COBALT (III)

F. MÁNOK and CS. VÁRHELYI

Faculty of Chemistry, Babeş-Bolyai University, Str. Arany János 11,
Cluj-Napoca, Romania

Received March 20, 1976

The anodic oxidation of some azido-complexes of the type $[Co(DH)_2(N_3)X]^-$(DH_2=dimethylglyoxime, X=Cl, Br, I, N_3) was studied at the mercury dropping electrode. It was found that the coordinated azide is oxidized more easily than the ionic one. The coordinated halogens give no anodic wave. The halogen ions eliberated during the aquation process can be measured on the basis of their distinct anodic waves. Concentration data obtained on this way can be used for kinetic studies.

The polarographic behaviour of the azido-complexes of transition metals was very little investigated. Only a single paper[1] deals with the polarographic determination of the coordinated azide in the presence of free azide ions. The method is based on the anodic oxidation both of the coordinated and ionic azide on the mercury dropping electrode in 0.1 M KNO_3 supporting electrolyte. The polarograms of the various azido-derivatives with two distinct anodic waves enable us the simultaneous determination of the coordinated and free azides. The following complexes: $[Co(NH_3)(N_3)](ClO_4)_2$, $[Co(NH_3)_4(N_3)_2]N_3$, *cis*- and *trans*,-$[Co(en)_2(N_3)_2]NO_3$, $[Co(dien)(N_3)_3]$ ("en" = ethylenediamine, "dien" = diethylenetriamine) were investigated. The coordinated azido-group was observed to be oxidized easier ($E_{1/2} = +0.11 - 0.17$ V vs. SCE) in the case of various azido-ammino-cobalt (III)-complexes as compared to the free, non bonded N_3^- ($E_{1/2} = +0.200 - 0.270$ V vs SCE).

The present paper has studied the anodic oxidation on the mercury dropping electrode of the following mixed azido-dimethyl-glyoximino-cobalt (III)-complexes: [2] $H[Co(DH)_2(N_3)_2]$, $H[Co(DH)_2(N_3)Cl]$, $H[Co(DH)_2(N_3)Br]$ and $H[Co(DH)_2(N_3)I]$.

The polarographic measurements were carried out in 0.1 M $NaClO_4$ supporting electrolyte, without maximum suppressor.

---

* Part LV. Cs. Várhelyi, A. Benkö, M. Somay and A. Koch, *Acta Chim. Acad. Sci. Hung*, vol. ovo (1978)

[1] L. F. Druding, D. M. Lukaszewski and F. D. Sancilio, *Analyt. Chem.*, **47**, 176 (1975).

[2] Z. Finta and Cs. Várhelyi, *J. Inorg. Nuclear Chem.*, **36**, 2199 (1974).

The anodic oxidation of $[Co(DH)_2(N_3)_2]^-$ begins in the negative range of polarization, at -0.100 V vs. SCE. The anodic wave, with a half-wave potential value of $+0.055$ V vs. SCE is well formed.

It is worth mentioning that the anodic oxidation of mercury in these conditions, in the absence of complexing anions for this metal begins at $+0.400$ V vs. SCE.

The height of the anodic wave increases linearly with the concentration of the diazido-complex in the conc. range of $10^{-4} - 10^{-3}$ M/lit. The polarogram of a $5 . 10^{-4}$ M solution of $[Co(DH)_2(N_3)_2]^-$ is represented in Figure 1 *a*. Curve *b* in the same figure represents the polarogram of the above complex in the presence of equal quantity of free NaN_3 ($5 . 10^{-4}$ M). In the latter case a second, well defined, wave appears, with a half-wave potential of $+0.270$ V. The height of this second wave is approximately half of the first one. This means, the first wave corresponds to the oxidation of the coordinated azide and the second to the ionic one.

The presence of two dioximine ligands bonded in the equatorial plane of the $[Co(DH)_2(N_3)X]^-$ octahedral complexes makes easier the oxidation of the *trans* situated azido-groups, as compared with the azido-amino-cobalt (III)-complexes (e.g. $[Co(NH_3)(N_3)]^{2+}$, $[Co(en)_2(N_3)_2]^+$, etc. with $E_{1/2} = +0.110 - 0.170$ V vs. SCE). The oxidation of the $[Co(DH)_2(N_3)X]^-$ complexes takes place at more negative potential values. Both the shape and the height of the polarograms of $[Co(DH)_2(N_3)_2]^-$ remain unchanged on standing 1 h, showing that ligand exchange reactions (aquation) do not take place in the mentioned conditions.

The coordinated azido-group remains unaltered also in the case of $[Co(DH)_2(N_3)X]^-$ complexes ($X = Cl, Br, I$), but the coordinated halogens undergo an aquation process with a measurable reaction rate.

The polarograms of a $5 . 10^{-4}$ M soln $[Co(DH)_2(N_3)Cl]^-$ were run immediately after dissolution of the sample and on standing after 1/2, 1 and 2 hrs, respectively. In this latter cases appear two distinct waves with $E_{1/2} = +0.065$ V and $+ 0.280$ V vs. SCE, respectively. The height of the first wave is the half value as compared with that of the $[Co(DH)_2(N_3)_2]^-$ and remains unchanged during the above mentioned time period. This wave appears due to the oxidation of the coordinated azido-group. The height of the second wave increases with time and equals the height of the first one after 2 hours. This second wave appears during the aquation of the $[Co(DH)_2(N_3)Cl]^-$ leading to the liberation of chloride ions. The anodic oxidation of free Cl^- is responsible for the appearance of this wave. The coordinated bonded halogens cannot be oxidized in this way.

The literature data[3,4] show that the anodic oxidation of the halogen and pseudohalogen ions cannot be a simple oxidation process. The anodic wave, which appears in this case, is due to the anodic oxidation of mercury followed by the complexation of Hg(I) and Hg(II) with the above mentioned anions in a complicated process. Because of their pseudohalogenoid character, similar electrode reactions should be expected for the azides. This expected similarity has been found to exist.

---

[3] J. Revenda, *Coll. Czech. Chem. Comm.*, **6**, 453 (1934).

[4] I. M. Kolthoff and C. S. Miller, *J. Amer. Chem. Soc.*, **63**, 1405 (1941).

The polarograms of the $[Co(DH)_2(N_3)I]^-$ (conc. $= 5.10^{-4}$M) were taken in analogous conditions after dissolution and 2 hours standing. In the case of the freshly prepared solutions only a single wave appears with $E_{1/2} = +0.105$ V vs. SCE, with a height equal with that of a 5.10^{-4}M solution of NaN_3, indicating the anodic oxidation of the coordinated azido-group. After 2 hours of standing there appears a second smaller wave too, at more positive potential values, indicating the anodic oxidation of the eliberated I^- ions. These measurements show the exchange of iodine with water molecules to occur much slower as compared with that of the chloride in $[Co(DH)_2(N_3)Cl]^-$.

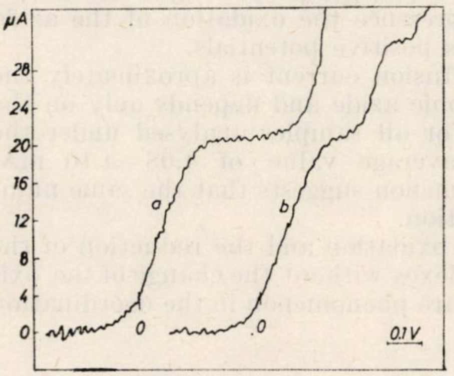

Fig. 1. *a* — The polarogram of a 5.10^{-4} M solution of $[Co(DH)_2(N_3)_2]^-$; *b* — the polarogram of $[Co(DH)_2(N_3)_2]$ in the presence of free $NaN_3(5.10^{-4}M)$.

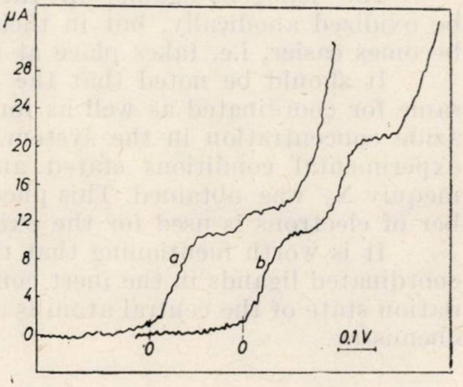

Fig. 2. *a* — The polarograms of $[Co(DH)_2(N_3)_2]^-$ Conc. 5.10^{-4}M) ; *a* — after dissolution ; *b* — after 2 hrs standing.

Fig. 3. *a* — The polarogram of $[Co(DH)_2(N_3)Br]^-$; *b* — the polarogram of $[Co(DH)_2(N_3)I]$.

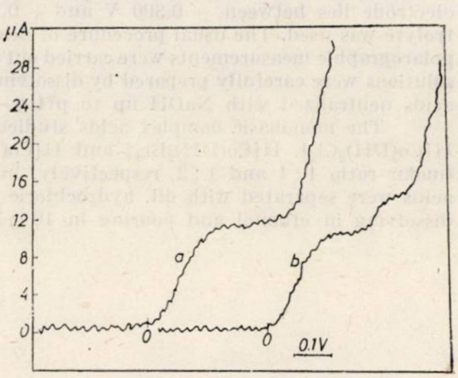

Analogous measurements were carried out on the bromo-azido-derivative : $[Co(DH)_2(N_3)Br]^-$.(5.10^{-4}M soln).

It was observed that the halogen exchange rate is smaller than in the case of the chloro-derivative, but is faster as compared with the $[Co(DH)_2(N_3)I]^-$.

The halogen exchange orders found polarographically agree with those obtained by means of potentiometric titrations. [2]

For the $[Co(DH)_2(N_3)(NCS)]^-$ and $[Co(DH)_2(N_3)(NCSe)]^-$ a lower NCS^- and $NCSe^-$ substitution rate is expected that for the iodine derivative. The azido-groups in the $[Co(DH)_2(N_3)_2]^-$ and $[Co(DH_2(H)_2O)(N_3)]$ complexes formed by the aquation of the halogeno-azido-derivatives do not undergo a substitution reaction with water molecules under the above experimental conditions. The different shifts of the half-wave potentials of the coordinated azido-groups in the studied azido-complexes, as compared with that of the ionic N_3^- ion, can be explained by means of the coordination effect of the *trans* situated X-ligands.

The halogeno-ligands in the $[Co(DH)_2(N_3)X]^-$-complexes cannot be oxidized anodically, but in their presence the oxidation of the azide becomes easier, i.e. takes place at less positive potentials.

It should be noted that the diffusion current is aproximately the same for coordinated as well as for ionic azide and depends only on the azide concentration in the system. For all samples analysed under the experimental conditions stated an average value of 4.08—4.10 mA/mequiv N_3^- was obtained. This phenomenon suggests that the same number of electrons is used for the oxidation.

It is worth mentioning that the oxidation and the reduction of the coordinated ligands in the inert complexes without the change of the oxidation state of the central atom is a rare phenomenon in the coordination chemistry.

EXPERIMENTAL PART

The polarograms were taken with a Radelkis — OH-102 type polarograph using a conventional polarographic cell with a saturated calomel counter electrode, connected to the cell by means of an agar-agar bridge (1 M KNO_3). The polarization range of the mercury dropping electrode lies between — 0.300 V and + 0.500 V vs. SCE. 0.1 Mol $NaClO_4$ supporting electrolyte was used. The usual procedure of deaeration with purified methane was followed. The polarographic measurements were carried out at 20° under thermostated conditions. 10^{-4}—10^{-3}M solutions were carefully prepared by dissolving the $H[Co(DH)_2(N_3)X]$ (X=Cl,Br, I,N_3) complex acids neutralized with NaOH up to pH 6—7 in 0.1 M $NaClO_4$.

The monobasic complex acids studied were prepared by a substitution reaction from $H[Co(DH)_2Cl_2]$, $H[Co(DH)_2Br_2]$ and $H[Co(DH)_2I_2]$ with a stoechiometric amount of NaN_3 (molar ratio 1 : 1 and 1 : 2, respectively, in diluted ethanol (70%). The corresponding azido-acids were separated with dil. hydrochloric acid (1 : 2). The crude products were purified by dissolving in ethanol and pouring in 10% HCl solution.

Revue Roumaine de Chimie, **23**, *6*, 921 – 928(1978)

16α-METHYL REICHSTEIN S 21-ACETAT AUS 16-DEHYDRO-PREGNENOLON ACETAT

O. MANTSCH und MARGARETA BUCHWALD
Chemisch-Pharmazeutisches Forschungsinstitut Cluj-Napoca,
Str. Fabricii Nr. 126

Eingegangen am 29. März 1976

Ausgehend von 16-Dehydro-pregnenolon Acetat wird ein Syntheseweg zur Herstellung von 16α-Methyl Reichstein S 21-Acetat, einer wichtigen Schlüsselverbindung in der Dexamethason-Synthese, beschrieben. Die hierbei erzielte Gesamtausbeute beträgt 26%.

Eine bemerkenswerte Anzahl von Arbeiten die auf dem Gebiet der Steroidchemie durchgeführt wurden bezweckten Wirkungsveränderungen und -steigerungen von biologisch aktiven Steroidverbindungen zu erzielen. Nennenswerte Änderungen wurden vor allem bei denjenigen Abkömmlingen des Hydrocortisons beobachtet, die in unmittelbarer Nähe der funktionellen Gruppen Strukturveränderungen aufweisen. So konnte z. B. durch Einführung eines 16α-Methyl-Substituenten in das Hydrocortison oder Prednisolon-Molekül [1,2] ein Ansteigen der antiinflamatorischen Eigenschaften und ein gleichzeitiges Absinken der Natriumretention beobachtet werden. Die gleichen Erscheinungen wurden auch bei den 16α-Methyl-Derivaten der 9-Fluor[3,4], 6-Fluor [5,6], als auch bei den 6,9-Difluor[7,8]-Corticosteroiden festgestellt. Zu diesen antiinflamatorisch aktiven Verbindungen gehört auch das Dexamethason (16α-Methyl-9α-fluor-prednisolon), das schon in sehr kleinen Mengen wirksam ist. Bei seiner Herstellung spielt die Verbindung 16α-Methyl Reichstein S eine

---

[1] G. E. Arth, D. B. R. Johnston, J. Fried, W. W. Spooncer, D. R. Hoff und L. H. Sarett, *J. Amer. Chem. Soc.*, **80**, 3160 (1958).

[2] E. P. Oliveto, R. Rausser, A. L. Nussbaum, W. Gebert, E. B. Hershberg, S. Tolksdorf, M. Eisler und P. L. Perlman, *J. Amer. Chem. Soc.*, **80**, 4428 (1958).

[3] G. E. Arth, J. Fried, D. B. R. Johnston, D. R. Hoff, L. H. Sarett, R. H. Silber, H. C. Stoerk und C. A. Winter, *J. Amer. Chem. Soc.*, **80**, 3161 (1958).

[4] E. P. Oliveto, R. Rausser, L. Weber, Al. L. Nussbaum, W. Gebert, C. T. Coniglio, E. B. Hershberg, S. Tolksdorf, M. Eisler, P. L. Perlman und M. M. Pechet, *J. Amer. Chem. Soc.*, **80**, 4431 (1958).

[5] J. A. Edwards, A. Zaffaroni, H. J. Ringold und C. Djerassi, *Proc. Chem. Soc.*, **1959**, 87.

[6] J. A. Edwards, H. J. Ringold und C. Djerassi, *J. Amer. Chem. Soc.*, **82**, 2318 (1960).

[7] J. A. Edwards, H. J. Ringold und C. Djerassi, *J. Amer. Chem. Soc.*, **81**, 3156 (1959).

[8] W. P. Schneider, J. H. Lincoln, G. B. Spero, H. C. Murray und J. L. Thompson, *J. Amer. Chem. Soc.*, **81**, 3167 (1959).

wichtige Rolle, da man von dieser, durch mikrobiologische Hydroxylierung, zu Derivaten der Corticosteroidreihe und folglich auch zum Dexamethason gelangen kann.

In der vorliegenden Arbeit beschreiben wir deswegen einen Weg, der die Herstellung dieser Schlüsselverbindung aus 16-Dehydro-pregnenolon Acetat, mit guten Ausbeuten, nach folgendem Reaktionschema, ermöglicht :

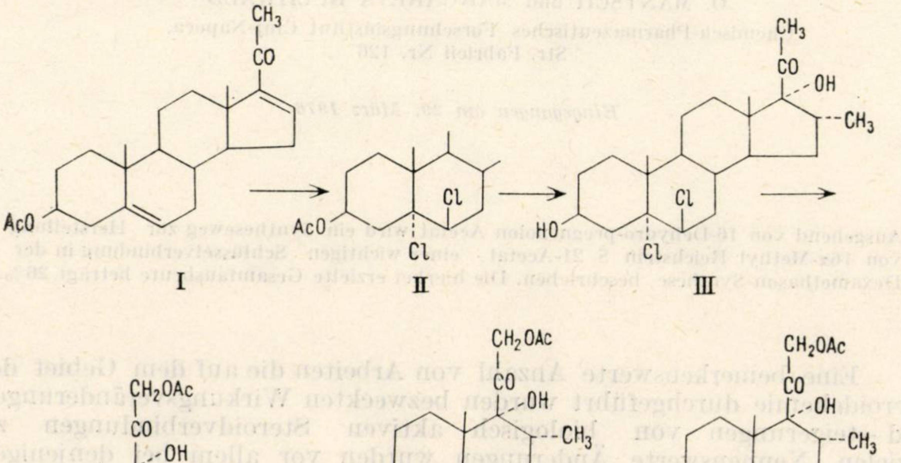

Bezüglich der vorhandenen Literaturangaben muß erwähnt werden, daß fast alle Beschreibungen in Patentschriften vorliegen. Meistens handelt es sich um sehr summarische Mitteilungen in denen oft keine Angaben über die erhaltenen Ausbeuten gemacht werden. Betreffs der angewandten Methoden als auch der Reaktionsfolgen, vermittels welcher man zur Verbindung 16α-Methyl Reichstein S gelangen kann, sei erwähnt, daß diese sich ebenfalls voneinander unterscheiden. Aus den vorhandenen Daten kann man trotzdem eine Gesamtausbeute von 7–18% abschätzen.

Der erste Schritt in der oben angegebenen Reaktionsfolge besteht in einer Anlagerung von Chlor an die 5,6-Doppelbindung, die in Gegenwart von Pyridin[9–11] durchgeführt werden kann. Die hierfür bekannten Beschreibungen beziehen sich jedoch auf Stoffe, die in ihrem Molekül nur eine, und nicht zwei, Doppelbindungen enthalten. Nur in einer ein-

[9] F. A. Cutler, Jr., L. Mandell, D. Shew, J. F. Fisher, und J. M. Chemerda, *J. Org. Chem.*, **24**, 1621 (1959).

[10] E. Batres, T. Cardenas, J. A. Edwards, G. Monroy, O. Mancera, C. Djerassi und H. J. Ringold, *J. Org. Chem.*, **26**, 871 (1961)

[11] Schering Corp , U.S. Pat. 3.290.338, 6/Dec. 1966 ; *Chem. Abstr.*, **67**, 3198 (1967).

zigen Patentschrift[12] wird diese Reaktion auch im Falle des 16-Dehydropregnenolon Acetates (I) angewendet, ohne jedoch eine Aussage über die erzielten Ausbeuten zu machen.

Die Herstellung von 17α-hydroxylierten 16α-Methyl-Derivaten erfordert wegen der stereospezifischen Lage der Substituenten jedoch eine gewisse Reihenfolge in ihrer Einführung. Aus diesem Grunde wird zuerst der 16α-Methyl-Substituent vermittels einer 1,4-Anlagerung von Grignard-Reagenz an das Δ^{16}-20-Keto-System [1,2,4,6,10,11,13-15] einer schon von Marker[16] beschriebenen Reaktion, eingeführt und dann die 17α-Hydroxylgruppe nach der Methode von Gallagher[17] (Enolisierung des C-20-Ketons, Epoxydierung des erhaltenen Enolacetates und Öffnung des Epoxydringes). Wegen der, vom 16α-Methyl-Substituenten ausgeübten, sterischen Hinderung verläuft die Enolisierung langsamer als im Falle von in 16-Stellung unsubstituierten Verbindungen,[18] so daß mit Hilfe dieser Reaktionsfolge keine großen Ausbeuten erzielt werden können. Die Tatsache, daß die Anlagerung von Grignard-Reaktiv in Anwesenheit von Kupferchlorür große Ausbeuten ergibt, führte Heusler und Mitarb.[18] zur Annahme, daß in der Reaktionslösung die 20-Ketogruppe praktisch vollständig in einer nicht-ketonischen Form vorliegt und daß diese Form ein Enolat-Metallsalz darstellt, in dem die 17,20-Enol-Doppelbindung bereits entstanden war, bevor der erwähnte sterische Effekt wirksam werden konnte. Durch Zersetzung dieses Enolates mit Essigsäurechlorid gelang es direkt das entsprechende Enolacetat zu erhalten. Nach Epoxydierung der 17,20-Enol-Doppelbindung und Öffnung des Epoxydringes erhielten sie 17α-hydroxylierte 16α-Methyl-Derivate in Ausbeuten von über 70%.

Diese Methode ist auch im Falle des 16α-Dehydro-pregnenolon Acetates[12](I) angewendet worden, ohne jedoch die erhaltenen Ausbeuten mitzuteilen.

Die 21-Acetoxy-Gruppe wird in zwei Stufen eingeführt und zwar durch Bromierung der Verbindung III. und anschließender Substitution des Broms durch die Acetoxy-Gruppe. [1,2,4,6,12,19-22]

Das Δ^4-3-Keto-System erhält man vermittels einer Dehalogenierungsreaktion in Gegenwart von Zink[12,22] oder Chromchlorür. [20]

Wir führten die Anlagerung von Chlor an die 5,6-Doppelbindung in einer Chloroformlösung und in Gegenwart von Pyridin durch, wobei eine Chlorlösung in Tetrachlorkohlenstoff verwendet wurde. In diesen Bedingungen bildet sich neben der 5α,6β-Dichlor-Verbindung II stets auch eine andere Substanz, wahrscheinlich eine Tetrachlor-Verbindung. Diese Nebenreaktion findet nicht mehr statt, wenn man in einer Tetrachlorkohlenstoff-Lösung arbeitet, da in diesem Falle die Reaktion viel langsamer verläuft. Die Ausbeuten betragen jedoch nur ungefähr 50%. Die besten Ergebnisse wurden in einer Benzol-Lösung mit einem Überschuß von 30% Chlor und 0,5 Mol Pyridin für 1 Mol 16-Dehydro-pregnenolon Acetat (I) erzielt, wobei die 5α, 6β-Dichlor-Verbindung II in einer Ausbeute von 75% erhalten wurde.

---

[12] P. L., Julian, E. Huang und A. Magnani, U.S. Pat. 3.030.389, 17, Apr. 1962; *Chem. Abstr.*, **57**, 11278 (1962).

[13] Syntex S.A., U.S.Pat. 2983737, 9. Mai 1959; *Chem. Abstr.*, **55**, 21171 (1961).

[14] Schering Akt.-Ges., Pat. Ger. 1082595, 2. Juni 1960; *Chem. Abstr.*, **55**, 16604(1961).

[15] Upjohn Co., U.S. Pat. 3174965, 23. März 1965; *Chem. Abstr.*, **62**, 16344 (1965).

[16] R. E. Marker und H. M. Crooks, *J. Amer. Chem. Soc.*, **64**, 1280 (1942).

[17] B. A. Koechlin, D. L. Garmaise, Th. H. Kritchevsky und T. F. Gallagher, *J. Amer. Chem. Soc.*, **71**, 3262 (1949).

[18] K. Heusler, J. Keberle, C. Meystre, H. Ueberwasser, P. Wieland, G. Anner und A. Wettstein, *Helv. Chim. Acta*, **42**, 2043 (1959).

[19] L. Ehmann, K. Heusler, Ch. Meystre, P. Wieland, G. Anner und A. Wettstein, *Helv. Chim. Acta*, **42**, 2548 (1959).

[20] Merck & Co., Inc., U.S.Pat. 3068228, 11. Dez. 1962; *Chem. Abstr.*, **58**, 10278 (1963).

[21] Ciba Soc. An., F. Pat. 1272486, 2. Feb. 1959; *Chem. Zentr.*, **1966**, 12–1775.

[22] F. A. Cutler, Jr., L. Mandell, J. F. Fisher, D. Shew und J. M. Chemerda, *J. Org. Chem.*, **24**, 1629 (1959).

Zur Einführung des 16α-Methyl-Substituenten, als auch der 17α-Hydroxy-Gruppe bedienten wir uns des von Heusler und Mitarb.[18] beschriebenen Verfahrens. Nach Hinzugabe von Acetylchlorid zu dem durch Anlagerung von Grignard-Reagenz an das Δ^{16}-20-Keto-System erhalten Enolatsalz konnten wir, vermittels Dünnschichtchromatographie, die Bildung des entsprechenden 20-Enolacetates nachweisen. Nach durchgeführter Epoxydierung, sowohl mit Monoperphthalsäure als auch mit Peressigsäure, und Verseifung erhielten wir jedoch nicht das erwartete 5α,6β-Dichlor-16α-methyl-pregnan-3β, 17α-diol-20-on (III), sondern die in 17-Stellung unsubstituierte 16α-Methyl-Verbindung.

Es wird darauf hingewiesen,[18] daß sich der Tetrahydrofuranring in den Bedingungen dieser Grignard-Reaktion teilweise öffnet und daß nach Hinzugabe von Acetylchlorid eine Verbindung entsteht, die sowohl die Krystallisierung des Enolacetates, als auch die Epoxydierungsreaktion stört. Tatsächlich tritt fast gleich nach Hinzugabe von Peressigsäure zur Enolacetatlösung eine rosa Färbung auf, die sich in kurzer Zeit verstärkt und rot bis schwarz wird. Diese Verfärbung ist dem Jod zuzuschreiben, das aus einem Nebenprodukt durch die Persäure in Freiheit gesetzt wird.

Aus diesem Grunde versuchten wir an Stelle von Tetrahydrofuran ein anderes Lösungsmittel zu verwenden. Die in Äther und Benzol durchgeführten Versuche ergaben jedoch negative Ergebnisse. In diesen Lösungsmitteln verläuft die Reaktion nur teilweise in der gewünschten Richtung, denn es bilden sich auch andere Verbindungen, die wahrscheinlich einer Grignard-Reaktion des C-20-Ketons zuzuschreiben sind.

Die Einführung des 16α-Methyl-Substituenten wurde auch mit Methylmagnesiumbromid versucht, unter Annahme, daß dieses Reagenz weniger aktiv ist als das entsprechende Jodid und demnach auch die Nebenreaktionen weniger begünstigt. In diesem Falle kann das Aufreten von Jod während der Epoxydierung tatsächlich nicht mehr beobachtet werden. Nach Öffnung des Epoxydringes erhält man jedoch zwei Verbindungen, von denen die eine als das 5α, 6β-Dichlor-16α-methyl-pregnan-3β-ol-20-on identifiziert werden konnte, die andere hingegen ist das erwartete Reaktionsprodukt und zwar das 5α,6β-Dichlor-16α-methyl-pregnan-3β,17α-diol-20-on (III).

Die Bildung von 5α,6β-Dichlor-16α-methyl-pregnan-3β-01-20-on kann mehreren Gründen zugeschrieben werden. Einer dieser Gründe könnte eine unvollständige Enolacetylierung sein. Durch Änderung der Reaktionsbedingungen konnten wir jedoch keinen Einfluß auf den Reaktionsgang beobachten.

Eine andere Möglichkeit wäre eine eventuelle Spaltung des Enolacetates während der Aufarbeitung des Reaktionsgemisches, denn Enolacetate sind empfindlich sowohl Säuren, als auch Basen gegenüber. Es erweckt jedoch den Anschein, daß während der Aufarbeitung keine wesentlichen Änderungen des Enolacetates auftreten, denn auch in dem Falle einer Aufarbeitung in neutralen Bedingungen erhielten wir am Ende der Reaktionsfolge immer ein Gemisch von zwei Verbindungen.

Eine letzte Möglichkeit wäre die einer unvollständigen Epoxydierung. Einige Autoren[19,23] empfehlen hierzu eine Reaktionsdauer von 2—4 Tagen, andere[12,24] hingegen unterbrechen die Reaktion schon nach 24 Stunden.

Trotz einer Reaktionsdauer von 1—4 Tagen in Gegenwart von Kaliumacetat, um eine Spaltung des gebildeten Epoxydringes zu verhindern, erhielten wir immer ein Gemisch von zwei Verbindungen. Auch bei einem Anstieg von 2 auf 4 Mol Persäure für 1 Mol Enolacetat wurden dieselben Resultate erhalten. Hingegen konnten wir feststellen, daß eine Verminderung von Kaliumacetat ein einheitlicheres Reaktionsprodukt ergibt. Aus diesem Grunde wurde die Reaktion auch in Abwesenheit von Kaliumacetat durchgeführt, wobei wir ein fast einheitliches Reaktionsprodukt erhielten. Die Epoxydierungsreaktion kann nach zwei Tagen als beendet betrachtet werden.

Aus dem oben erwähnten geht hervor, daß bei Anwendung von Methylmagnesiumjodid als Methylierungsmittel eine Nebenreaktion stattfinden muß, wobei eine Verbindung entsteht, die dann die Epoxydierung des Enolacetates hindert. Diese Nebenreaktion kann jedoch durch Senkung der Temperatur wesentlich zurückgedrängt werden. Wird z. B. Acetylchlorid bei 0° ins Reaktionsgemisch eingetragen, dann erhält man nach durchgeführter Epoxydierung und Verseifung das erwartete Reaktionsprodukt und zwar das 5α,6β-Dichlor-16α-methyl-pregnan-3β,17α-diol-20-on (III). Auch in diesen Bedingungen wird während der Epoxydierungsreaktion noch etwas Jod in Freiheit gesetzt. Diese Tatsache weist darauf hin, daß, wenn auch in begrenztem Maße, doch noch eine Nebenreaktion stattfindet. Die Lösung färbt sich aber bedeutend weniger intensiv als im Falle einer, bei Zimmertemperatur durchgeführten Enolacetylierung. Um diese unerwünschte Nebenreaktion weitgehend zu unterdrücken, versuchten wir die Herstellung des gewünschten Enolacetates auch durch Hinzugabe von Essigsäureanhydrid zu dem, nach durchgeführter Grignardierung, gebildetem Enolat. Das auf diese Weise erhaltene Enolacetat konnte nun tatsächlich, ohne daß dabei Jod in Freiheit gesetzt wird, epoxydiert werden, wobei man die gewünschte Verbindung III in einer Ausbeute von 80% erhält.

Die 21-Acetoxy-Gruppe führten wir in zwei Stufen ein und zwar mit Hilfe einer Bromierungsreaktion und anschließender Substitution des Broms durch die Acetoxy-Gruppe.

Als Katalysator für die Bromierungsreaktion verwendeten wir zunächst Bromwasserstoffsäure in Essigsäure und als Lösungsmittel Chlo-

---

[23] A. Wettstein, G. Anner, Ch. Meystre, P. Wieland, L. Ehmann, K. Heusler, A. Hunger und J. Kebrle, U.S.Pat. 3026340, 20. März 1962; *Chem. Abstr.*, **57**, 13839 (1962).

[24] P. L. Julian und J. M. Hill, U.S.Pat. 3231568, 25. Jan. 1966; *Chem. Abstr.*, **64**, 9802 (1966).

roform. Die 21-Brom-Verbindung wurde nicht isoliert, sondern, nach Aufarbeitung des Reaktionsgemisches, in die 21-Acetoxy-Verbindung IV überführt. In diesen Bedingungen gelang es jedoch nicht die 21-Acetoxy-Verbindung IV in kristalliner Form zu erhalten.

Wird hingegen gasförmige Salzsäure als Initiator für die Bromierungsreaktion verwendet, dann verläuft die Reaktion anfangs mit einer bemerkenswerten Geschwindigkeit, die jedoch wesentlich abnimmt, wenn ungefähr die Hälfte der Brommenge eingetragen worden ist. In einigen Fällen konnte die 21-Acetoxy-Verbindung IV isoliert werden, jedoch liegen die Ausbeuten unter 50%.

Durch Hinzugabe von Ethanol oder Methanol zum Reaktionsgemisch stellt man ein Anwachsen der Ausbeuten fest, ohne jedoch konstante und reproduzierbare Ergebnisse zu erhalten. Wird hingegen während der ganzen Reaktionsdauer ein schwacher Strom gasförmiger Salzsäure durch das Reaktionsgemisch geleitet, dann verläuft die Bromierung normal und man erhält, nach ausgeführter Substitutionsereaktion, die 21-Acetoxy-Verbindung IV in einer Ausbeute von 70%.

Die Oxydation der 3β-Hydroxyl-Gruppe zum entsprechenden C-3-Keton führten wir in Aceton mit einer wässerigen, mit Schwefelsäure angesäuerten, Chromtrioxyd-Lösung durch. Die Ausbeuten betrugen ungefähr 90%.

Das Δ^4-3-Keto-System erhält man, ausgehend von der Verbindung V, durch Eliminierung des Chlors und Isomerisierung der 5,6-Doppelbindung in 4,5-Stellung.

Wir konnten festellen, daß die Eliminierung von Chlor am besten mit Zink in wässerigem Methanol (90-Volum %) verläuft. In diesen Bedingungen wird das Chlor praktisch vollkommen eliminiert, wenn man das Reaktionsgemisch eine Stunde unter Rückfluß kocht.

Die entstandene 5,6-Doppelbindung isomerisiert hingegen ziemlich schwer, obwohl erwähnt wird, daß die Isomerisierung gleichzeitig mit der Chloreliminierung, im Verlauf von 2 Stunden, stattfindet, wenn die Reaktion in Gegenwart von Essigsäure durchgeführt wird.[12]

Aus unseren Versuchen geht jedoch hervor, daß diese Isomerisierung sogar unter Rückfluß, im Verlauf von 2—3 Stunden, noch nicht beendet ist. Aus diesem Grunde versuchten wir die Reaktion in Methanol und in Gegenwart von p-Toluol-sulfonsäure und Essigsäure durchzuführen. In diesen Bedingungen konnten wir nach Verlauf von 2 Stunden keine Ausgangsverbindung mehr nachweisen. Zur Durchführung dieser beiden Stufen, und zwar, die der Eliminierung und Isomerisierung der Doppelbindung, ist es nicht nötig, daß die entstandene Δ^5-Verbindung isoliert wird, sondern, nach Beendigung der Eliminierungsreaktion fügt man Essigsäure und p-Toluol-sulfonsäure hinzu und erhält direkt, in einem Schritt, die Δ^4-3-Keto-Verbindung und zwar das gewünschte 16α-Methyl Reichstein S 21-Acetat (VI).

Die Eliminierung von Chlor und Isomerisierung der Doppelbindung kann auch mit Zink in Dichlormethan und in Gegenwart von Essigsäure durchgeführt werden. Das Reaktionsgemisch muß aber hierbei 10 Stunden unter Rückfluß gerührt werden. Die Gesamtausbeute für beide Stufen beträgt 70%.

BESCHREIBUNG DER VERSUCHE

Die Schmelzpunkte sind nicht korrigiert. Alle spezifischen Drehungen wurden in Chloroform als 1 proz. Lösung aufgenommen.

5α,6β-Dichlor-Δ^{16}-pregnen-3β-ol-20-on-3-Acetat (II)

100 g 16-Dehydro-pregnenolon Acetat (I) werden in 4 l Benzol gelöst und unter Rühren 1 l Benzol abdestilliert. Zu der auf 10—13° abgekühlten Lösung fügt man unter Rühren 11,3 ml Pyridin und dann innerhalb von 30 Minuten 26 g Chlor in 372 ml Tetrachlorkohlenstoff hinzu (7 g Cl_2/100 ml). Während der Reaktionsdauer muß die Temperatur auf 10—13° gehalten werden. Anschließend wird noch 5 Minuten gerührt, dann 1 Liter 1 proz. Salzsäurelösung hinzugegeben und nach weiteren 5 Minuten die organische Phase abgetrennt, mit 500 ml gesättigter Natriumbicarbonat und dann mit 500 ml gesättigter Natriumchloridlösung gewaschen, im Vakuum eingeengt und der Rückstand in 2 l heißem, 2 ml Pyridin enthaltendem, Methanol gelöst. Hiernach werden 1,2 1 Methanol abdestilliert, abgekühlt und filtriert. Man erhält 90 g 5α, 6β-Dichlor-Δ^{16}-pregnen-3β-01-20-on 3-Acetat (II) vom Schmelzpunkt 151-3°. Ausbeute : 75%.

Umgelöst aus Methanol erhält man II vom F. 153-4° und $(\alpha)_D = -31{,}5°$.

Gefunden : C, 64,60 ; H, 7,74 ; Cl, 16,30. Berechnet für
$C_{23}H_{32}Cl_2O_3$ C, 64,58 ; H, 7,55 ; Cl, 16,60%.

5α,6β-Dichlor-16α-methyl-pregnan-3β,17α-diol-20-on (III)

Aus 25,4 g Magnesium, suspendiert in 880 ml Äther, und 81 ml Methyljodid in 290 ml Äther wird Grignard-Reagenz hergestellt. Ein Teil des Äthers wird abdestilliert bis man eine Temperatur von 40° erreicht. Unter Rühren fügt man 1,43 l gereinigtes Tetrahydrofuran hinzu und destilliert fortlaufend bis die Dämpfe eine Temperatur von 55° erreichen. In das auf 5° abgekühlte Grignard-Reagenz trägt man dann 0,9 g Kupferchlorür und hiernach 90 g der Verbindung II, gelöst in 450 ml Tetrahydrofuran, ein. Hierbei soll die Temperatur 15° nicht überschreiten. Es werden noch 30 Minuten bei Zimmertemperatur gerührt, dann auf 0° abgekühlt und 143 ml Essigsäureanhydrid in 143 ml Tetrahydrofuran hinzugeben, wobei die Temperatur 5° nicht überschreiten soll. Man rührt anschließend 30 Minuten bei 0° und fügt dann unter guter Kühlung 800 ml 10 proz. Ammoniumchloridlösung und hierauf 650 ml Benzol hinzu. Es werden noch 2 Stunden bei Zimmertemperatur gerührt, dann die Benzolschicht abgetrennt und mit 230 ml 10 proz. Thiosulfatlösung, 350 ml Wasser, 2×350 ml gesättigter Natriumbicarbonatlösung und schließlich mit 350 ml gesättigter Natriumchloridlösung gewaschen.

Die organische Lösung wird im Vakuum eingeengt und der erhaltene Rückstand in 900 ml Chloroform gelöst. Zu dieser Lösung fügt man 310 ml Peressigsäure (13 g Persäure/100 ml) hinzu und rührt 48 Stunden bei Zimmertemperatur. Nach Hinzugabe von 300 ml Wasser wird abgetrennt und mit 2×300 ml Wasser, 350 ml gesättigter Natriumbicarbonatlösung, 300 ml 10 proz. Natriumsulfitlösung und schließlich mit 350 ml Wasser gewaschen.

Die Chloroformlösung wird im Vakuum eingeengt und zum Rückstand, unter Rühren, 900 ml Methanol hinzugefügt. Zu der erhaltenen kristallinen Suspension gibt man 860 ml 3,5 proz. methanolische Natriumhydroxydlösung und rührt 2 Stunden bei Zimmertemperatur, wobei man anfangs eine Lösung erhält aus der dann die Verbindung III ausfällt. Das Reaktionsgemisch wird mit 37 ml Essigsäure neutralisiert und nach Hinzugabe von 550 ml Wasser 24 Stunden stehen gelassen. Man erhält 70,5 g 5α,6β-Dichlor-16α-methyl-pregnan-3β, 17α-diol-20-on (III) vom F. 212-4° Ausbeute : 80%.

Umgelöst aus Methanol erhält man III vom F. 213-5° und $(\alpha)_D = -68{,}4°$.

Gefunden : C, 63,13 ; H, 8,61 ; Cl, 17,22. Berechnet für
$C_{22}H_{34}Cl_2O_3$ C, 63,29 ; H, 8,21 ; Cl, 17,00%.

5α,6β-Dichlor-16α-methyl-pregnan-3β,17α,21-triol-20-on 21-Acetat (IV)

70,5 g III werden in einem Gemisch von 1 400 ml Chloroform und 350 ml Methanol gelöst und durch die Lösung gasförmige Salzsäure hindurchgeleitet. Unter Rühren fügt man bei Zimmertemperatur, im Verlaufe einer Stunde, 9 ml Brom in 550 ml Chloroform hinzu.

Während der ganzen Reaktionsdauer wird gasförmige Salzsäure eingeleitet. Die Chloroformlösung wird dann zweimal mit je 650 ml Wasser gewaschen und anschließend im Vakuum eingeengt (die Temperatur des Wasserbades soll hierbei 50° nicht überschreiten).

Der erhaltene Rückstand wird in 1 400 ml Aceton gelöst und nach Hinzugabe von 85 g geschmolzenem Kaliumacetat, 6,5 ml Essigsäure und 6,5 g Kaliumjodid 4 Stunden unter Rückfluß gerührt. Anschließend werden ungefähr 1 000 ml Aceton abdestilliert und dann auf 0—5° abgekühlt. Unter Rühren fügt man langsam 1 000 ml Wasser hinzu und nach einer Stunde wird die ausgeschiedene Verbindung IV abgesaugt und mit Wasser gewaschen. Die an der Luf getrocknete Rohverbindung (80 g) wird 30 Minuten lang mit 800 ml Äther unter Rückfluß mazeriert, dann 400 ml Äther abdestilliert und nach dem Erkalten filtriert. Man erhält 56 g IV vom F. 184-6°. Ausbeute : 70%.

Zur Analyse wurde aus Äther umgelöst. F. 186-9° und $(\alpha)_D = -25,3°$.

Gefunden : C, 60,55 ; H, 7,84 ; Cl, 14,84. Berechnet für
$C_{24}H_{36}Cl_2O_5$ C, 60,62 ; H, 7,62 ; Cl, 14,92%.

5α,6β-Dichlor-16α-methyl-pregnan-17α,21-diol-3,20-dion 21-Acetat (V)

Zu einer auf 0° abgekühlten Lösung der Verbindung IV (56 g) in 560 ml Aceton fügt man unter Rühren 66 ml Chromtrioxydlösung hinzu (hergestellt aus 17,2 g CrO_3, 15 ml konz. H_2SO_4 und Wasser ad 66 ml). Man rührt 20 Minuten bei 0—5° und zersetzt dann das überschüssige Oxydationsmittel mit 280 ml 10 proz. Kaliummetabisulfitlösung, fügt 1 000 ml Wasser hinzu, filtriert nach 30 Minuten die ausgeschiedene Verbindung und wäscht 3 mal mit je 60 ml Methanol. Man erhält 50 g V vom F. 169-70°. Ausbeute : 90%.

Umgelöst aus Dichlormethan/Methanol erhält man V vom F.171-172.°

Gefunden : C, 61,15 ; H, 7,35 ; Cl, 15,00 Berechnet für
$C_{24}H_{34}Cl_2O_5$ C, 60,86 ; H, 7,24 ; Cl, 14,98%.

16α-Methyl Reichstein S 21-Acetat (VI)

A) Zu einer Lösung von 20 g V in 200 ml Dichlormethan und 180 ml Methanol werden 20 ml Wasser und 20 g Zinkstaub gegeben und das Gemisch 2 Stunden unter Rückfluß gehalten. Anschließend wird vom Zink abfiltriert und nach Hinzugabe von 20 ml Eisessig und 0,6 g p-Toluol-sulfonsäure 2 Stunden gekocht und dann vom Lösungsmittel so viel abdestilliert bis die Dämpfe 60° erreichen. Nach Abkühlen erhält man 11,9 g VI vom F. 161—3°. Ausbeute : 70%.

B) 30 g V werden in 550 ml Dichloromethan gelöst und 60 ml Eissessig und 11 g Zinkstaub hinzugegeben. Man rührt 10 Stunden unter Rückfluß, filtriert vom Zink und wäscht die organische Lösung 2 mal mit je 200 ml Wasser, 200 ml Natriumbicarbonatlösung und weiter mit 200 ml Wasser. Nach Trocknen über Magnesiumsulfat werden 165 ml Dichlormethan abdestilliert, zu der Lösung 390 ml Methanol hinzugegeben und fortlaufend eingeengt bis die Dämpfe 60° erreichen, über Kohle filtriert und abgekühlt. Man erhält 17,9 g VI vom F. 162-4° ; $\alpha_{max} = 241$ nm ; log $\varepsilon = 4,20$.

Gefunden : C, 71,54 ; H, 8,70 ; Berechnet für $C_{24}H_{34}O_5$
C, 71,59 ; H, 8,51%.

Revue Roumaine de Chimie, **23**, *6*, 929–933(1978)

L'ÉTUDE DE LA RÉACTION ENTRE LE Pb(II) ET LE 5-MERCAPTO-2-AMINO-1,3,4-THIADIAZOLE. APPLICATIONS ANALYTIQUES

LIVIU ROMAN, EUGENIA FLOREAN, MARIA ECHIM-GROSU
et EMILIA DORDEA
Faculté de Pharmacie, I. M. F. de Cluj-Napoca, Discipline de Chimie analytique
str. Pasteur, 4

Reçu le 19 mars 1976

On a étudié la réaction entre le Pb(II) et le 5-mercapto-2-amino-1,3,4-thiadiazole à des fins d'applications dans l'analyse qualitative et quantitative. En mettant à profit la méthode conductimétrique on a déterminé la conductivité équivalente à une dilution infinie Λ_0 et la constante de dissociation ($K = 3{,}34.10^{-6}$) du ligand, à 25°C ± 0,2. Au moyen de la méthode conductimétrique et de l'analyse chimique de la combinaison on a déterminé le rapport de combinaison Pb : L(1 :2). En vue de l'application de la réaction entre le Pb(II) et le 5-mercapto-2-amino-1,3,4-thiadiazole en chimie analytique qualitative et quantitative, on a déterminé la sensibilité de la réaction ($L_r = 0{,}26$ µg, $L_d = 1 :19.323$, $pD = 4{,}28$), ainsi que le produit de solubilité du complexe dans l'eau, $P_s = 1{,}87.10^{-12}$, et dans l'éthanol 50%, $P_s = 8{,}44.10^{-14}$, ce qui a permis d'élaborer une méthode gravimétrique rapide de dosage du Pb(II), avec une précision de ± 0,27% et une méthode conductimétrique avec une erreur de ± 0,32%.

La littérature cite de nombreuses méthodes de détermination quantitative du Pb(II), en particulier avec des réactifs organiques contenant du soufre, avec lesquels le plomb forme des chélates, souvent à coloration caractéristique et très stables. Parmi les réactifs organiques (au soufre), utilisés au dosage du Pb(II), on peut citer la thio-urée,[1-3] la thionalide,[4-7] le mercaptobenzthiazole, [8-9] la dithizone, [10] le diéthyldithiocarbamate,[11-12] et d'autres.

---

[1] C. Mahr et H. Ohle, *Z. anorg. Chem.*, **234**, 224 (1937).

[2] C. Mahr, *Mikrochim. Acta*, **26**, 27 (1939).

[3] Ch. C. Miller et L. R. Currie, *Analyst*, **75**, 467 (1950).

[4] R. Berg et E. S. Fahrenkamp, *Z. analyt. Chem.*, **112**, 161 (1938) ; **115**, 205 (1938).

[5] Ch. Cimerman et M. Ariel, *Analyt. Chim. Acta*, **12**, 13 (1955) ; **14**, 48 (1956).

[6] Ch. Cimerman et M. Ariel, *Z. analyt. Chem.*, **148**, 381 (1955/1956) ; **154**, 280 (1957)

[7] H. Lilie, *Z. analyt. Chem.*, **159** ,196 (1958).

[8] Gh. Spacu et M. Kuras, *Z. analyt. Chem.*, **104**, 88 (1936).

[9] Ch. Cimerman et D. Bogia, *Analyt. Chim. Acta*, **12**, 218 (1955).

[10] I. M. Kolthoff, P. J. Elving et E. B. Sandell, "Treatise on Analytical Chemistry", Part. II, vol. 6, Interscience, New York, 1966.

[11] I. V. Tertooleu, *Z. analyt. Chem.*, **167**, 401 (1959).

[12] K. C. Srivastava et K. Samir, *Chem. Age* (*India*), **18**, 209 (1967).

En poursuivant des recherches antérieures portant sur la valorisation des réactifs organiques avec du soufre, tels que la bisthio-urée,[13] l'alylbithio-urée,[14] la phénylbisthio-urée, la nphtylbisthio-urée[15] et certains dérivés disubstitués de la bisthio-urée,[16] ainsi que quelques produits de cyclisation avec un noyau mercaptothiadiazolique,[17] dans le présent travail on étudie la réaction entre le Pb(II) et le 5-mercapto-2-amino-1,3,4-thiadiazole (MATD), en vue de l'utilisation pratique de ce réactif dans le dosage conductimétrique et gravimétrique du plomb. A cette fin, utilisant des méthodes chimiques et physico-chimiques, on a effectué une étude portant à la fois sur le ligand et sur la combinaison formée, ainsi que sur les conditions de formation, leurs propriétés et composition.

PARTIE EXPÉRIMENTALE

La détermination de la constante de dissociation du 5-mercapto-2-amino-1,3,4-thiadiazole a été effectuée au moyen de la méthode conductimétrique. A cette fin on a déterminé la conductivité moléculaire à dilution infinie Λ_0 à 25°C ± 0,2 et à diverses concentrations (M/80, M/160, M/320, M/640, M/1 280). Au calcul de la constante de dissociation on a utilisé la relation :

$$K = \frac{\Lambda_m^2}{\Lambda_0(\Lambda_0 - \Lambda_m)v}$$

où Λ_m = la conductivité moléculaire à une certaine concentration

Λ_0 = la conductivité moléculaire à dilution infinie

v = volume de la solution.

La constante moyenne de dissociation du 5-mercapto-2-amino-1,3,4-thiadiazole a la valeur $K = 3{,}34.10^{-6}$.

Synthèse, composition et propriétés du complexe $Pb(MATD)_2$. L'ion Pb(II) forme avec le MATD, en milieu hydro-alcoolique, à pH 6,5—10, en présence d'ammoniac, à chaud, un précipité jaune cristallin, difficilement soluble dans l'eau, le méthanol, l'éthanol, le dioxanne, l'acétone, soluble dans la pyridine et des acides dilués.

La composition chimique de ce complexe a été établie au moyen de l'analyse chimique élémentaire et de la détermination du rapport de combinaison Pb : L par la méthode conductimétrique (fig. 1), qui est de 1 : 2.

La sensibilité de la réaction entre le Pb(II) et MATD a été déterminée aussi sur papier de filtre que sur plaque de porcelaine. Les limites de détection et de dilution comportent les valeurs : $L_r = 0{,}26$ µg $L_d = 1:19.323$, $pD = 4{,}28$, respectivement, $L_r = 5{,}17$ µg, $L_d = 1:144.927$, $pD = 5.15$.

Il a été déterminé conductimétriquement le produit de solubilité du complexe $Pb(MATD)_2$, en utilisant la relation $P_s = m^m.n^n.\ C^{m+n}$. À cette fin on a déterminé la concentration à l'équilibre, respectivement la solubilité de la combinaison, au moyen de mesures conductimétriques dans l'eau, l'éthanol 50% et l'éthanol 100%. en utilisant l'équation suivante :

$$C = \frac{1\,000.\lambda}{\Lambda_s}$$

où Λ_s = conductivité moléculaire de la combinaison dans $\Omega.cm^2.mole^{-1}$

λ = conductivité de la solution

C = concentration, respectivement la solubilité en moles/l

---

[13] L. Roman, "Thèse de doctorat", Univ. Babeş-Bolyai, Cluj, 1968.

[14] E. Popper, L. Roman, P. Marcu, M. Bojiţă et M. Şerban, *Rev. Roumaine Chim.*, **16**, 569 (1971).

[15] E. Popper, L. Popa, V. Junie, et L. Roman, *Studii şi Cercetări Chim. Acad. Bucureşti*, **8**, 269 (1957).

[16] E. Popper, N. Ariton et R. Popa-Crăciuneanu, *Studii şi Cercetări Chim. Acad. Bucureşti*, **7**, 85 (1956).

[17] E. Popper, V. Junie et L. Popa, *Studii şi Cercetări Chim. Acad. Cluj*, **7**, 89 (1956).

Le produit de solubilité de la combinaison, à la température de 25°C ± 0,2 est de $1{,}87.10^{-12}$ dans l'eau, tandis que dans l'éthanol 50% il est de $8{,}44.10^{-14}$, ce qui justifie l'utilisation du 5-mercapto-2-amino-1,3,4-thiadiazole comme réactif pour la détermination gravimétrique du plomb.

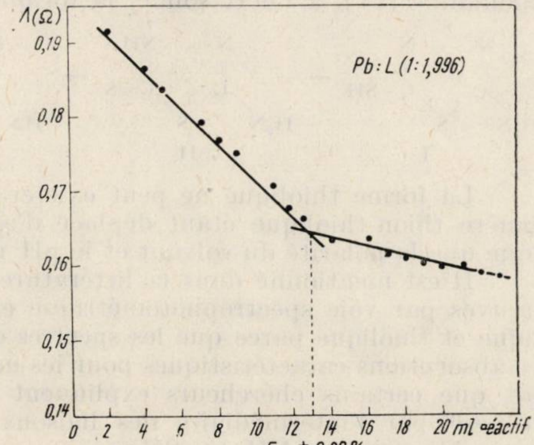

Fig. 1. — Le titrage conductimétrique du Pb(II) avec 5-mercapto-2-amino-1,3,4-thiadiazole.

Dosage gravimétrique rapide du plomb. Les échantillons d'azotate de plomb 10^{-1} M, contenant 20 à 70 mg de Pb(II), sont additionnés de solution de 5-mercapto-2-amino-1,3,4-thiadiazole 1% et d'un ml de solution diluée d'ammoniac. On dilue à l'éthanol 50% et on abandonne au bain-marie. Le précipité cristallin obtenu est filtré sur creuset filtrant G_4, lavé à l'éthanol 50%, puis à éthanol absolu et à l'éther, puis desséché sous vide et pesé. Les données expérimentales sont consignées au tableau 1.

Tableau 1

Le dosage gravimétrique rapide du plomb

N°	Pb(II) à déterminer g	Pb(II) trouvé g	Pb(II) %	L'erreur % par rapport à la moyenne des déterminations	Résultats du calcul statistique
1	0,06228	0,06236	100,38	+0,10	$\overline{X}=100{,}28$
2	0,02076	0,02091	100,78	+0,50	$S_{\overline{X}}=0{,}1101$
3	0,06228	0,06227	99,87	−0,27	$n=7$
4	0,04975	0,04990	100,90	+0,62	$\alpha=0{,}95$
5	0,06228	0,06140	98,89	−0,39	$t\alpha=2{,}45$
6	0,04152	0,04130	99,55	−0,75	$P=100{,}28\pm$
7	0,06228	0,06318	100,48	+0,20	$\pm 0{,}27\%$

Dosage conductimétrique du plomb. On a procédé au titrage conductimétrique d'une solution de nitrate de plomb 10^{-2} M, par une solution de réactif 10^{-2} M dans de l'éthanol 50%, avec utilisation d'un conductimètre du type OK 102 Radelkiss à électrode de platine. La courbe de titrage est représentée à la fig. 1. Les déterminations peuvent être effectuées avec une erreur relative de ± 0,32%.

RÉSULTATS ET DISCUSSIONS

La structure de 5-mercapto-2-amino-1,3,4-thiadiazole peut être formulée[18] comme : thiolamine (I), thionamine (II), thiolimine(III) ou thionimine (IV), à l'état solide, la formule plus probable étant (II) :

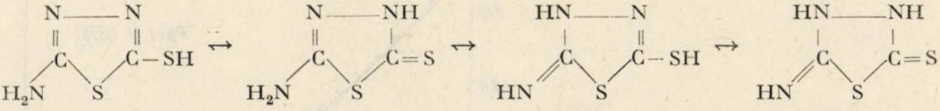

I II III IV

La forme thiolique ne peut exister qu'en solution, l'équilibre tautomère thion-thiolique étant déplacé d'autant plus vers la forme thiolique que la polarité du solvant et le pH de la solution sont plus élevés.

Il est mentionné dans la littérature qu'on ne peut pas fournir des preuves par voie spectrophotométrique en I. R. pour la structure thionique et thiolique parce que les spectres en I. R. ne font pas apparaître les absorptions caractéristiques pour les modes de vibration νNH et νSH, fait que certains chercheurs expliquent par la dimérisation des deux formes[19] par l'intermédiaire des liaisons d'hydrogène qui s'établissent entre les groupes NH et SH :

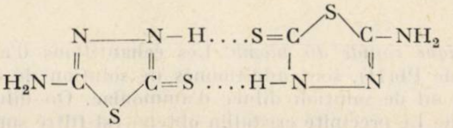

Le titrage enthalpimétrique du phénylaminomercaptothiadiazole, [20] réactif à structure similaire à celle du mercaptoaminothiadiazole, a démontré que sous la forme thiolique il se comporte comme un acide faible. Afin de confirmer ce fait, on a déterminé par voie conductimétrique la constante de dissociation du 5-mercapto-2-amino-1,3,4-thiadiazole ($K = 3{,}34.10^{-6}$).

La sensibilité de la réaction du Pb(II) avec MATD est plus grande que la sensibilité de la réaction de cet ion avec la benzidine, la thiourée, environ du même ordre de grandeur que la sensibilité de la réaction avec rhodizonate de natrium ($L_r = 0{,}1$ μg), mais six fois environ moins sensible que la réaction avec dithizone ($L_r = 0{,}04$ μg). Par ailleurs, le produit de solubilité de la combinaison $Pb(MATD)_2$ est plus petit de quatre ordres de grandeur environ (dix mille fois) que le produit de solubilité du sulfate de plomb ($P_s = 2{,}2.10^{-8}$) dans l'eau et de six ordres de grandeur dans l'éthanol 50%.

Ces résultats justifient l'utilisation du 5-mercapto-2-amino-1,3,4-thiadiazole comme réactif pour l'identification du Pb(II) et pour la détermination gravimétrique rapide de cet ion (tableau 1). D'ailleurs, l'estimation statistique des résultats expérimentaux confirme l'exactitude et la grande précision de cette méthode, qui est de ± 0,27 %.

---

[18] N. Petri, *Z. Naturforsch.*, **17 b**, 278 (1962).

[19] D. Bernard, J. Fabian et H. P. Koch, *J. Chem. Soc.*, **1949**, 2442.

[20] E. Popper, L. Roman et P. Marcu, *Talanta*, **11**, 515 (1964).

La réaction du Pb(II) avec le MATD est interférée par les ions Ag(I), Cu(II), Zn(II), Cd(II), Bi(III), Fe(III), Co(II) et Ni(II). Les complexes de Zn(II), Bi(III), Co(II) et Ni(II) sont solubles dans l'alcool, ceux de Ag(I), Cu(II) et Cd(II) sont solubles dans l'ammoniac et celui de Hg(II) dans le cjanure de potassium. En conséquence, les ions gênants peuvent être masqués par dissolution ou complexation.

En conclusion, il résulte de l'étude sur la réaction du Pb(II) avec le 5-mercapto-2-amino-1,3,4-thiadiazole que la réaction est extrêmement sensible, que le complexe est beaucoup plus difficilement soluble que le sulfate de plomb, qu'il dépose facilement et que la durée d'une détermination est courte. On peut procéder à des déterminations de plomb aussi en présence d'autres ions qui interfèrent, mais que l'on peut masquer. Le réactif est accessible et peut être préparé en grandes quantités puisqu'il constitue une matière première pour l'industrie des médicaments.

Revue Roumaine de Chimie, **23**, *6*, 935–941 (1978)

THE ACTION OF ARYLAMINES ON 3-ARYL-5-ARYLMETHYLENERHODANINES

A. M. KHALIL*, A. A. FADDA and M. M. YOUSIF
Chemistry Department, Al-Mansoura Faculty of Science, Al-Mansoura,
A. R. E. (Egypt)

Received March 16, 1976

2-Arylimino-3-aryl-5-arylmethylene-4-thiazolidinones were prepared by the interaction of primary aromatic amines with 3-aryl-5-arylmethylenerhodanines in the presence of freshly fused sodium acetate. The same thiazolidinones were also obtained by condensation of 2-arylimino-3-aryl-4-thiazolidinones with aldehydes.

Although many reactions of rhodanine derivatives with a variety of reagents have been reported in the literature, [1] the reaction of such compounds with amines and similar compounds has not been thoroughly investigated.

It has been reported that, if 3-phenylrhodanine is heated with aniline for one hour at 160–170°, the attack of the thione group is followed by cleavage of the ring and thiocarbanilide is formed. [2] The presence of substituents in the 5-position, as in 5-benzylidenerhodanine, stabilizes the thiazolidine ring, and aniline converts the sulphur of the thione group to the phenyliminoderivative. [2-3] 3-Benzylideneaminorhodanine, if heated with aniline at 100°, rearranges into 3-amino-4-benzylidenerhodanine. [4]

On the other hand, it has been reported that amines, both primary and secondary, react with 5-(1-ethoxyalkylidene) rhodanines and their 3-substituted derivatives to give 5-(1-aminoalkylidene) rhodanines. [2,5-7]

---

* Present address : Department of Chemistry, Faculty of Science, King Abdulaziz University, P. O. Box 1540 Jeddah, Saudi Arabia

[1] F. C. Brown, *Chem. Rev.*, **61**, 463 (1963).

[2] C. Granacher, *Helv. Chim. Acta*, **3**, 152 (1920).

[3] F. B. Dains, and S. I. Davis, *Univ. Kansas Sci. Bull.*, **15**, 265 (1924); *Chem. Abstr.*, **20**, 600 (1926).

[4] H. Ueda, and M. Ohta, *Nippon Kagaku Zasshi*, **77**, 1520 (1956); *Chem. Abstr.*, **53**, 5248 (1959).

[5] Farbwerke Hoechst A.G. Vorm Meister Lucius U. Bruning; German Patent, 834104 (1952); *Chem. Abstr.*, **50**, 402 (1956).

[6] C. P. Lo, *J. Amer. Chem. Soc.*, **80**, 3466 (1958).

[7] Z. P. Sytnik, L. D. Zhilina, and E. B. Lifshits, *Doklady Akad. Nauk S.S.S.R.*, **114**, 343 (1957); *Chem. Abstr.*, **52**, 369 (1958).

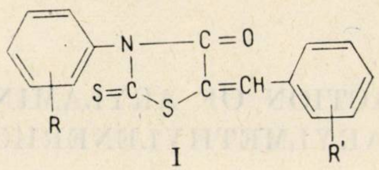

I

	R	R′		R	R′
(I 1)	H	H	(I 2)	H	*o*-NO$_2$
(I 3)	H	*m*-NO$_2$	(I 4)	*p*-Cl	H
(I 5)	*p*-Cl	*o*-NO$_2$	(I 6)	*p*-Me	H
(I 7)	*p*-Me	*o*-NO$_2$	(I 8)	*p*-Me	*m*-NO$_2$
(I 9)	*m*-NO$_2$	H			

In this communication the reaction of 3-aryl-5-arylmethylenerhodanines with various primary aromatic amines under different reaction conditions is reported. Thus, the fusion of 3-aryl-5-arylmethylenerhodanines (I 1–9) with the amines: aniline, *p*-anisidine, *p*-bromoaniline, *o*-chloroaniline, *m*-chloroaniline, *p*-chloroaniline, *o*-nitroaniline, *p*-nitroaniline, *o*-toluidine, *m*-toluidine and *p*-toluidine in the presence of freshly fused sodium acetate gave the corresponding 2-arylimino-3-aryl-5-arylmethylene-4-thiazolidinones (II 1–46).

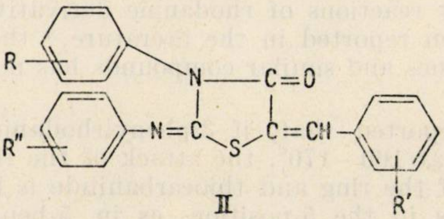

II

	R	R′	R″		R	R′	R″
(II 1)	H	H	H	(II 2)	H	H	*p*-Me
(II 3)	H	H	*o*-Cl	(II 4)	H	H	*m*-Cl
(II 5)	H	H	*p*-Cl	(II 6)	H	H	*o*-NO$_2$
(II 7)	H	*o*-NO$_2$	H	(II 8)	H	*o*-NO$_2$	*m*-Me
(II 9)	H	*o*-NO$_2$	*p*-Me	(II 10)	H	*o*-NO$_2$	*o*-Cl
(II 11)	H	*o*-NO$_2$	*m*-Cl	(II 12)	H	*o*-NO$_2$	*o*-NO$_2$
(II 13)	H	*m*-NO$_2$	H	(II 14)	H	*m*-NO$_2$	*o*-Me
(II 15)	H	*m*-NO$_2$	*o*-Cl	(II 16)	H	*m*-NO$_2$	*m*-Cl
(II 17)	H	*m*-NO$_2$	*p*-Cl	(II 18)	*p*-Cl	H	H
(II 19)	*p*-Cl	H	*p*-Me	(II 20)	*p*-Cl	H	*p*-Cl
(II 21)	*p*-Cl	*o*-NO$_2$	H	(II 22)	*p*-Cl	*o*-NO$_2$	*o*-Me
(II 23)	*p*-Cl	*o*-NO$_2$	*m*-Me	(II 24)	*p*-Cl	*o*-NO$_2$	*p*-Me
(II 25)	*p*-Cl	*o*-NO$_2$	*m*-Cl	(II 26)	*p*-Cl	*o*-NO$_2$	*p*-Cl
(II 27)	*p*-Me	H	H	(II 28)	*p*-Me	H	*m*-Cl
(II 29)	*p*-Me	H	*p*-Cl	(II 30)	*p*-Me	H	*p*-Br
(II 31)	*p*-Me	H	*p*-OMe	(II 32)	*p*-Me	*o*-NO$_2$	*m*-Me
(II 33)	*p*-Me	*o*-NO$_2$	*p*-Me	(II 34)	*p*-Me	*o*-NO$_2$	*p*-Cl
(II 35)	*p*-Me	*o*-NO$_2$	*p*-Br	(II 36)	*p*-Me	*o*-NO$_2$	*p*-NO$_2$
(II 37)	*p*-Me	*m*-NO$_2$	H	(II 38)	*p*-Me	*m*-NO$_2$	*m*-Me
(II 39)	*p*-Me	*m*-NO$_2$	*p*-Me	(II 40)	*p*-Me	*m*-NO$_2$	*p*-OMe
(II 41)	*p*-Me	*m*-NO$_2$	*p*-NO$_2$	(II 42)	*m*-NO$_2$	H	*m*-Me
(II 43)	*m*-NO$_2$	H	*p*-Me	(II 44)	*m*-NO$_2$	H	*p*-Cl
(II 45)	*m*-NO$_2$	H	*p*-Br	(II 46)	*m*-NO$_2$	H	*p*-OMe

The above products were characterized by analysis and by infrared measurements which showed stretching frequencies at about 1 720 cm^{-1} and at 1 640 cm^{-1} characteristic for the carbonyl group of 4-thiazolidinone ring and for $-C=N-$ group respectively.[8]

Also the structure of the above 2-arylimino-3-aryl-5-arylmethylene-4-thiazolidinones (II) was established by comparison of the infrared spectra and mixed melting point determination with authentic sample prepared by condensation of 2-arylimino-3-aryl-4-thiazolidinones (III 1—10) with aromatic aldehydes to give the corresponding 2-arylimino-3-aryl-5-arylmethylene-4-thiazolidinones (II 1—6, 27, 32—34).

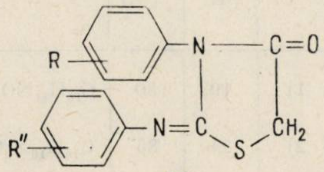

III

	R	R''		R	R''
(III 1)	H	H	(III 2)	H	*p*-Me
(III 3)	H	*o*-Cl	(III 4)	H	*m*-Cl
(III 5)	H	*p*-Cl	(III 6)	H	*o*-NO$_2$
(III 7)	*p*-Me	H	(III 8)	*p*-Me	*m*-Me
(III 9)	*p*-Me	*p*-Me	(III 10)	*p*-Me	*p*-Cl

When the above reaction between amines and 3-aryl-5-arylmethylenerhodanines (I 1—9) was carried out in acetic acid and in the presence of freshly fused sodium acetate, a remarkable evolution of hydrogen sulphide was observed and the corresponding 2-arylimino-3-aryl-5 arylmethylene-4-thiazolidinones (II 1—46) were obtained after a reflux period of approximately 120 hrs.

The identity of the 2-arylimino-3-aryl-5-arylmethylene-4-thiazolidinones obtained by direct fusion of (I) with amines with those obtained by the interaction of (I) with amines in acetic acid containing catalytic amount of sodium acetate was established by: i) analytical figures, ii) mixed melting point determination and iii) infrared measurements.

EXPERIMENTAL

Analytical data were determined in the microanalytical unit Cairo University. Infrared spectra were recorded on a SP 1 000 Pye-Unicam spectrophotometer. Melting points are uncorrected.

Synthesis of 3-aryl-5-arylmethylenerhodanines (I 1—9): 3-Aryl-5-arylmethylenerhodanines (I 1—9) were prepared according to the method of Sahoo *et al*[9] as follows:

---

[8] L. J. Bellmey, "The Infrared Spectra of Complex Molecules", Wiley, New York, 1966.

[9] B. Sahoo, P. B. Tripathy, and M. K. Rout, *J. Indian Chem. Soc.*, **36**, 421(1959).

A mixture of 3-arylrhodanine (0.1 mole), the appropriate aldehyde (0.11 mole), glacial acetic acid (30 ml) and freshly fused sodium acetate (0.5 g) was refluxed on a hot plate for 2 hrs. The reaction mixture was cooled and the product collected by filtration. Recrystallization from acetic acid gave the 3-aryl-5-arylmethylene-rhodanines (I 1—9) (cf. Table 1) as yellow crystals.

Table 1

3-Aryl-5-arylmethylenerhodanines (I)

Substituent in 3-phenyl- R	Substituent in 5-benzylidene R	Product	M. P. °C	Yield (%)	Formula	Analysis (%) Found Calcd. C	H	N
H	H	(I 1)	195	80	$C_{16}H_{11}NOS_2$	64.5	3.5	4.6
						64.7	3.7	4.7
H	o-NO_2	(I 2)	240	85	$C_{16}H_{10}N_2O_3S_2$	56.0	2.8	8.0
						56.1	2.9	8.2
H	m-NO_2	(I 3)	248	78	$C_{16}H_{10}N_2O_3S_2$	55.9	2.9	8.1
						56.1	2.9	8.2
p-Cl	H	(I 4)	182	81	$C_{16}H_{10}ClNOS_2$	57.8	3.3	4.1
						57.9	3.0	4.2
p-Cl	o-NO_2	(I 5)	199	85	$C_{16}H_9ClN_2O_3S_2$	50.8	2.4	7.3
						51.0	2.4	7.4
p-Me	H	(I 6)	183	87	$C_{17}H_{13}NOS_2$	65.6	4.2	4.5
						65.6	4.1	4.5
p-Me	o-NO_2	(I 7)	180	89	$C_{17}H_{12}N_2O_3S_2$	57.3	3.4	7.8
						57.3	3.4	7.9
p-Me	m-NO_2	(I 8)	238	79	$C_{17}H_{12}N_2O_3S_2$	57.3	3.3	7.8
						57.4	3.4	7.9
m-NO_2	H	(I 9)	240	83	$C_{16}H_{10}N_2O_3S_2$	56.2	3.0	8.2
						56.1	2.9	8.1

The above products were characterized by analysis and infrared measurements which showed stretching frequencies at 1 730 cm^{-1} and at 1 480 cm^{-1}characteristic for the carbonyl group of rhodanine ring and for $N-C=S$ group respectively.

Reactions of 3-arylmethylenerhodanines with amines :

A mixture of 3-aryl-5-arylmethylenerhodanine (I 1—9) (0.1 mole), the appropriate amine (0.11 mole), and freshly fused sodium acetate (0.5 g) was heated on oil-bath at 160—170° until the evolution of hydrogen sulphide ceased (2—4 hrs). The product was cooled and washed with concentrated hydrochloric acid (10 ml) to remove the unreacted amine, then with water (10 ml). The product obtained was recrystallized from acetic acid to give 2-arylimino-3-aryl-5-arylmethylene-4-thiazolidinones (II 1—46) (cf. Table 2).

Reaction of 2-arylimino-3-arylrhodanines with aldehydes :

A mixture of 2-arylimino-3-arylrhodanine (III 1—10) (0.1 mole), the appropriate aldehyde (0.11 mole), glacial acetic acid (30 ml), and freshly fused sodium acetate (0.5 g) was refluxed on hot plate for 2 hrs. The reaction mixture was cooled and the product collected by filtration. Recrystallization from acetic acid gave the 2-arylimino-3-aryl-5-arylmethylene-rhodanines (II 1—6, 27, 32—34). Melting points were not depressed when admixed with specimens prepared as described before.

Table 2

2-Arylimino-3-aryl-5-arylmethylene-4-thiazolidinones (II). R Substituent in 3-phenyl-; R′ Substituent in 5-benzylidene-; R″ Substituent in 2-phenylimino

Thiazolidinone	R	R′	R″	M. P. °C	Yield (%)	Formula	Analysis (%) Found Calcd. C	H	N
(II 1)[a]	H	H	H	206	60	$C_{22}H_{16}N_2OS$	74.1	4.4	7.8
							74.2	4.5	7.9
(II 2)[b]	H	H	*p*-Me	168	55	$C_{23}H_{18}N_2OS$	74.5	5.0	7.4
							74.6	4.9	7.6
(II 3)[c]	H	H	*o*-Cl	190	62	$C_{22}H_{15}ClN_2OS$	67.4	3.6	7.1
							67.6	3.8	7.2
(II 4)[c]	H	H	*m*-Cl	193	59	$C_{22}H_{15}ClN_2OS$	67.5	3.7	7.0
							67.6	3.8	7.2
(II 5)[c]	H	H	*p*-Cl	192	65	$C_{22}H_{15}ClN_2OS$	67.6	3.7	7.3
							67.6	3.8	7.2
(II 6)[d]	H	H	*o*-NO$_2$	193	56	$C_{22}H_{15}N_3O_3S$	65.6	3.7	10.3
							65.8	3.7	10.5
(II 7)[c]	H	*o*-NO$_2$	H	170	58	$C_{22}H_{15}N_3O_3S$	65.6	3.8	10.6
							65.8	3.7	10.5
(II 8)[c]	H	*o*-NO$_2$	*m*-Me	245	63	$C_{23}H_{17}N_3O_3S$	66.4	4.0	10.0
							66.5	4.1	10.1
(II 9)[a]	H	*o*-NO$_2$	*p*-Me	200	66	$C_{23}H_{17}N_3O_3S$	66.3	4.1	10.2
							66.5	4.1	10.1
(II 10)[c]	H	*o*-NO$_2$	*o*-Cl	220	61	$C_{22}H_{14}ClN_3O_3S$	60.4	3.0	9.5
							60.6	3.2	9.6
(II 11)[c]	H	*o*-NO$_2$	*m*-Cl	210	62	$C_{22}H_{14}ClN_3O_3S$	60.5	3.1	9.5
							60.6	3.2	9.6
(II 12)[c]	H	*o*-NO$_2$	*o*-NO$_2$	190	57	$C_{22}H_{14}N_4O_5S$	59.2	3.3	12.5
							59.2	3.1	12.6
(II 13)[a]	H	*m*-NO$_2$	H	170	60	$C_{22}H_{15}N_3O_3S$	65.5	3.5	10.4
							65.8	3.7	10.5
(II 14)[c]	H	*m*-NO$_2$	*o*-Me	220	61	$C_{23}H_{17}N_3O_3S$	66.5	4.2	10.0
							66.5	4.1	10.1
(II 15)[c]	H	*m*-NO$_2$	*o*-Cl	180	69	$C_{22}H_{14}ClN_3O_3S$	61.0	3.2	9.5
							60.6	3.2	9.6
(II 16)[b]	H	*m*-NO$_2$	*m*-Cl	240	56	$C_{22}H_{14}ClN_3O_3S$	60.7	3.4	9.7
							60.6	3.2	9.6
(II 17)[c]	H	*m*-NO$_2$	*p*-Cl	198	64	$C_{22}H_{14}ClN_3O_3S$	60.8	3.3	9.6
							60.6	3.2	9.6
(II 18)[c]	*p*-Cl	H	H	184	69	$C_{22}H_{15}ClN_2OS$	67.3	3.8	7.2
							67.6	3.8	7.2
(II 19)[d]	*p*-Cl	H	*p*-Me	232	76	$C_{23}H_{17}ClN_2OS$	68.4	4.3	6.9
							68.2	4.2	6.9

a-Light brown; b-Green; c-Brown; d-Yellow; e-Red; f-Orange

Table 2 (continued)

Thiazolidinone	R	R′	R″	M. P. °C	Yield (%)	Formula	Analysis (%) Found Calcd.		
							C	H	N
(II 20)[d]	*p*-Cl	H	*p*-Cl	210	74	$C_{22}H_{14}Cl_2N_2OS$	62.1 62.1	3.2 3.3	6.6 6.6
(II 21)[c]	*p*-Cl	*o*-NO$_2$	H	270	79	$C_{22}H_{14}ClN_3O_3S$	60.5 60.6	3.2 3.2	9.5 9.6
(II 22)[c]	*p*-Cl	*o*-NO$_2$	*o*-Me	210	76	$C_{23}H_{16}ClN_3O_3S$	61.6 61.4	3.4 3.6	9.1 9.3
(II 23)[c]	*p*-Cl	*o*-NO$_2$	*m*-Me	230	70	$C_{23}H_{16}ClN_3O_3S$	61.3 61.4	3.5 3.6	9.2 9.3
(II 24)[a]	*p*-Cl	*o*-NO$_2$	*p*-Me	241	78	$C_{23}H_{16}ClN_3O_3S$	61.2 61.4	3.6 3.6	9.0 9.3
(II 25)[a]	*p*-Cl	*o*-NO$_2$	*m*-Cl	180	70	$C_{22}H_{13}Cl_2N_3O_3S$	56.0 56.2	2.6 2.8	8.7 8.9
(II 26)[c]	*p*-Cl	*o*-NO$_2$	*p*-Cl	262	75	$C_{22}H_{13}Cl_2N_3O_3S$	56.1 56.2	2.9 2.8	8.6 8.9
(II 27)[a]	*p*-Me	H	H	242	74	$C_{23}H_{18}N_2OS$	74.5 74.6	5.1 4.9	7.8 7.6
(II 28)[c]	*p*-Me	H	*m*-Cl	162	67	$C_{23}H_{17}ClN_2OS$	68.0 68.2	4.3 4.2	7.0 6.9
(II 29)[c]	*p*-Me	H	*p*-Cl	153	77	$C_{23}H_{17}ClN_2OS$	68.1 68.2	4.2 4.2	6.8 6.9
(II 30)[e]	*p*-Me	H	*p*-Br	156	73	$C_{23}H_{17}BrN_2OS$	61.3 61.5	4.0 3.8	6.3 6.2
(II 31)[b]	*p*-Me	H	*p*-OMe	168	67	$C_{24}H_{20}N_2O_2S$	72.1 72.0	5.1 5.0	7.0 7.0
(II 32)[f]	*p*-Me	*o*-NO$_2$	*m*-Me	189	78	$C_{24}H_{19}N_3O_3S$	67.2 67.1	4.4 4.4	9.9 9.8
(II 33)[d]	*p*-Me	*o*-NO$_2$	*p*-Me	262	80	$C_{24}H_{19}N_3O_3S$	67.0 67.1	4.5 4.4	9.8 9.8
(II 34)[d]	*p*-Me	*o*-NO$_2$	*p*-Cl	198	83	$C_{23}H_{16}ClN_3O_3S$	61.3 61.4	3.6 3.6	9.2 9.3
(II 35)[d]	*p*-Me	*o*-NO$_2$	*p*-Br	190	82	$C_{23}H_{16}BrN_3O_3S$	55.8 55.9	3.3 3.2	8.6 8.5
(II 36)[b]	*p*-Me	*o*-NO$_2$	*p*-NO$_2$	167	74	$C_{23}H_{16}N_4O_5S$	59.9 60.0	3.6 3.5	12.1 12.2
(II 37)[d]	*p*-Me	*m*-NO$_2$	H	158	69	$C_{23}H_{17}N_3O_3S$	66.6 66.5	4.2 4.1	10.0 10.1
(II 38)[b]	*p*-Me	*m*-NO$_2$	*m*-Me	154	73	$C_{24}H_{19}N_3O_3S$	67.0 67.1	4.3 4.4	9.7 9.8
(II 39)[c]	*p*-Me	*m*-NO$_2$	*p*-Me	195	82	$C_{24}H_{19}N_3O_3S$	67.1 67.1	4.2 4.4	9.7 9.8
(II 40)[b]	*p*-Me	*m*-NO$_2$	*p*-OMe	178	74	$C_{24}H_{19}N_3O_4S$	64.6 64.7	4.3 4.3	9.3 9.4

Table 2 (continued)

Thiazolidinone	R	R′	R″	M. P. °C	Yield (%)	Formula	Analysis (%) Found Calcd. C	H	N
(II 41)[c]	*p*-Me	*m*-NO$_2$	*p*-NO$_2$	165	76	$C_{23}H_{16}N_4O_5S$	60.0 60.0	3.5 3.5	12.4 12.2
(II 42)[f]	*m*-NO$_2$	H	*m*-Me	163	73	$C_{23}H_{17}N_3O_3S$	66.4 66.5	4.2 4.1	10.0 10.1
(II 43)[f]	*m*-NO$_2$	H	*p*-Me	173	68	$C_{23}H_{17}N_3O_3S$	66.5 66.5	4.2 4.1	10.3 10.1
(II 44)[c]	*m*-NO$_2$	H	*p*-Cl	198	81	$C_{22}H_{14}ClN_3O_3S$	60.5 60.6	3.3 3.2	9.5 9.6
(II 45)[c]	*m*-NO$_2$	H	*p*-Br	203	77	$C_{22}H_{14}BrN_3O_3S$	54.9 55.0	3.0 2.9	8.6 8.8
(II 46)[b]	*m*-NO$_2$	H	*p*-OMe	207	86	$C_{23}H_{17}N_3O_4S$	64.1 64.0	3.9 3.9	9.7 9.8

Reaction of 3-aryl-5-arylmethylenerhodanines with amines in acetic acid:

A mixture of 3-aryl-5-arylmethylenerhodanine (I 1—9) (0.005 mole), and primary aromatic amines (0.006 mole), in acetic acid (20 ml) containing freshly fused sodium acetate (0.2 g) was heated under reflux until the evolution of hydrogen sulphide ceased (about 120 hrs). The reaction mixture was cooled and the precipitated solid was collected by filtration. Recrystallization of the product from acetic acid gave 2-arylimino-3-aryl-5-arylmethylene-4-thiazolidinones (II 1—46) with correct melting points, elemental analyis and infrared spectra.

Revue Roumaine de Chimie, **23**, *6*, 943–950 (1978)

CYCLIC ORGANOSILICON COMPOUNDS. REACTION OF 1,4-DILITHIUM-1,1,4,4-TETRAPHENYLBUTANE WITH ORGANODICHLOROSILANES

AGLAIA CIOBANU, N. LUCHIAN and VIORICA HAMCIUC
Institute of Macromolecular Chemistry "Petru Poni"
Aleea Gr. Ghica Vodă 41 A, Iassy, Romania

Received March 16, 1976

New cyclic organosilicon compounds were obtained by coupling between 1,4-dilithium-1,1,4,4-tetraphenylbutane and dichlorodiphenylsilane, dichlorodimethylsilane and dichloromethylsilane. The chemical analysis, molecular mass determination, IR and NMR spectra have shown that the new compounds have been formed by ring closure through a siloxane bond (compounds I and II) or through $Si(H)CH_3$ bridges between two molecules of 1,1,4,4-tetraphenylbutane in positions 1 and 4 (compound III). The thermogravimetric analysis indicates a thermal stability of compounds up to 280–380°.

The formation of addition compounds of alkali metals with hydrocarbons containing double bonds has been known for a long time. Thus Schlenk et al.[1–4] have described various classes of organic compounds containing double bonds, able to add alkali metals, in anhydrous ethyl ether, with the formation of some intensely coloured complexes. Among these, 1,4-diphenylethylene has a special behaviour. Its reaction product with sodium or lithium is 1,4-disodium- or 1,4-dilithium-1,1,4,4-tetraphenylbutane, resulted from the coupling of two ion radicals :

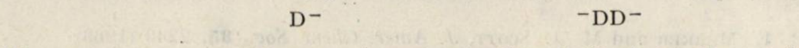

The reaction equilibrium is practically shifted to the right[5,6] as it follows from the value of the equilibrium constant for the dissociation process :

$$2D^- \rightleftharpoons {}^-DD^- \qquad K \geqslant 10^7 \text{ mol/l.}$$

---

[1] W. Schlenk, J. Appenrodt, A. Michael and A. Thal, *Ber. dtsch. chem. Ges.*, **47**, 473 (1914).

[2] W. Schlenk and E. Bergman, *Liebigs Ann. Chem.*, **463**, 1 (1928).

[3] W. Schlenk and E. Bergman, *Liebigs Ann. Chem.*, **463**, 98 (1928).

[4] W. Schlenk, E. Bergman and E. Haak, *Ber. dtsch. chem. Ges.*, **62**, 1771 (1929).

[5] J. Jagur, M. Levy, M. Feld and M. Szwarc, *Trans. Faraday Soc.*, **58**, 2168 (1962).

[6] J. Jagur, H. Monteiro and M. Szwarc, *Trans. Faraday Soc.*, **59**, 1353 (1963).

Because of the presence of two metal atoms 1,4-disodium-1,1,4,4-tetraphenylbutane may undergo coupling with organohalogensilanes to give some new organosilicon compounds.

Such reactions e. g. the condensation of organomagnesium compounds with alkylchlorosilanes, [7-13] the reaction of finely divided sodium with organohalogensilanes and organic halides, [14] the reaction of organosodium or -lithium derivatives with trialkyl (aryl) chlorosilanes[15,16] and finally, the reaction of organolithium derivatives with organohalogensilanes, [17-21] have been investigated extensively.

The present paper deals with the preparation and with some physico-chemical characteristics of compounds resulted from the 1,4-dilithium-1,1,4,4,-tetraphenylbutane reaction with dichlorodiphenylsilane,dichlorodimethylsilane and dichloromethylsilane.

EXPERIMENTAL

1,1-Diphenylethylene was prepared according to the method reported in the literature[22]. It was stirred in an ether solution with small lithium grains, to give 1,4-dilithium-1-1,4,4-tetraphenylbutane.

Dichlorodiphenylsilane, dichlorodimethylsilane and dichloromethylsilane used for syntheses were of 98—99% purity.

Diethyl ether was dried and distilled from sodium while the other solvents were purified by distillation.

The IR spectra were recorded by means of a Perkin-Elmer model 577 spectrophotometer, within the 4 000—200 cm^{-1} region. Samples were pelletted with KBr. For comparison, the IR spectrum of 1,1,4,4-tetraphenylbutane was recorded under similar conditions.

---

[7] L. H. Sommer, L. J. Tyler and F. C. Whitmore, *J. Amer. Chem Soc.*, **70**, 2872 (1948).

[8] A. D. Petrov and V. P. Mironov, *Izvest. Akad. Nauk. S.S.S.R., Otdel. khim. Nauk.*, **1952**, 635.

[9] A. D. Petrov and L. L. Shchukovskaja, *Izvest. Akad. Nauk. S.S.S.R., Otdel, khim. Nauk*, **1952**, 564.

[10] A. D. Petrov and G. I. Nikishin, *Izvest. Akad. Nauk. S.S.S.R., Otdel. khim. Nauk.*, **1952**, 1128.

[11] K. A. Andrianov and N. V. Delazari, *Doklady Akad. Nauk. S.S.S.R.* **122**, 393 (1958).

[12] R. E. Merker and M. J. Scott, *J. Amer. Chem. Soc.*, **85**, 2243 (1963).

[13] *idem*, *J. Amer. Chem. Soc.*, **86**, 953 (1964).

[14] M. Kanazashi, *Bull. Chem. Soc. Japan*, **26**, 493 (1953) ; *Chem. Abstr.*, **49**, 11578 (1955).

[15] A. G. Brook, H. Gilman and L. S. Miller, *J. Amer. Chem. Soc.*, **75**, 4759 (1953).

[16] Brit. Patent 988320, 28 oct. 1963, *Chem. Abstr.*, **63**, 632 (1965).

[17] A. D. Petrov and V. P. Lavrishchev, *Izvest. Akad. Nauk. Otdel. khim. Nauk. S.S.SR.* **1952**, 1125.

[18] A. D. Petrov and G. I. Nikishin, *Doklady Akad. Nauk. S.S.S.R.*, **93**, 1049 (1953)

[19] A. D. Petrov and G. I. Nikishin, *Zhur, obshchei Khim.*, **26**, 1233 (1956).

[20] K. Oita and H. Gilman, *J. Amer. Chem. Soc.*, **79**, 339 (1957).

[21] K. A. Andrianov, A. I. Nogaideli, N. I. Ciobanianu, N. N. Makarova and P.S. Tketelashvili, *Vysokomol. Soedinenya*, **6**, 1195 (1975).

[22] M. Tissier and V. Guignard, *Compt. rend.*, **132**, 1182 (1901).

DTA and DTG curves were recorded using a MOM Paulik-Paulik-Erdey derivatograph with 9°/min. heating rate, within a temperature range of 20—800°.

NMR spectra were recorded on a JEOL 60 MHz device in carbon tetrachloride solution using tetramethylsilane as internal standard.

1,1,3,3,4,4,7,7-octaphenyl-2-oxa-1,3-disilacycloheptane (I)

Freshly prepared 1,1-diphenylethylene (14 g), 300 ml anhydrous ethyl ether and 1.5 g lithium metal in small pieces were stirred together in a 500 ml three-neck flask provided with dropping funnel and reflux condenser protected against moisture with a tube of anhydrous calcium chloride. Dark red prismatic crystals deposited from the red solution after approx. 20 hrs of stirring. Dichlorodiphenylsilane (22 g) was added dropwise to this suspension, with stirring, the content of the funnel being protected by a weak strom of dry nitrogen. The colour of the solution changed from red to yellow, with the disappearance of red crystals and the appearance of a white lithium chloride precipitate. The reaction was exothermal and it took 80 hours. The clear ethereal solution was siphoned into a three-neck dry flask under a nitrogen strom, after the lithium chloride precipitate has deposited. The yellow substance left after the distillation of diethyl ether was solved in acetone and precipitated with ethyl alcohol. The product was purified by solving in acetone and precipitating with ethyl alcohol. A white slighty yellowish, flocculent crystalline product was separated. It was filtered, washed with ethyl alcohol and dried. M. p. 185°, yield 2.5 g (10%). The product was soluble in benzene and carbon tetrachloride.

Anal. Calcd. for $C_{52}H_{44}OSi_2$: C, 84.32; H, 5.94; Si, 7.56; mol. wt. 740. Found: C, 84.15; H, 5.99; Si, 7.57; mol. wt. 722 (determined cryoscopically in benzene).

1,1,3,3-Tetramethyl-4,4,7,7-tetraphenyl-2-oxa-1,3-disilacycloheptane (II)

The manner of preparation was similar, the dichlorodimethylsilane amount used being 11.25 g. The reaction time was 50 hours. The compound obtained was a white-yellowish crystalline product, m. p. 171°, yield 2g (10%).

Anal. Calcd. for $C_{32}H_{36}OSi_2$: C, 78.04; H, 7.31; Si, 11.38; mol. wt. 492. Found: C, 80.30; H, 7.12; Si, 11.52; mol. wt. 507 (determined cryoscopically in benzene).

1,6-Dimethyl-2,2,5,5,7,7,10,10-octaphenyl-1,6-disilacyclodecane (III)

The same procedure was used for the synthesis. The dichloromethylsilane amount was 7.3 g. The reaction time was 45 hours.

After removal of diethyl ether, the product obtained was dissolved in n-hexane and precipitated with acetone. The compound was purified by solving in n-hexane and precipitating with acetone. A shiny white crystalline substance was separated, m. p. 164° yield 2.3 g (16%).

Anal. Calcd. for $C_{58}H_{56}Si_2$: C, 86.01; H, 6.93; Si, 6.93; mol. wt. 808. Found: C, 86.20; H, 7.12; Si, 6.75; mol. wt. 809 (determined cryoscopically in benzene).

RESULTS AND DISCUSSIONS

The reaction between 1,4-dilithium-1,1,4,4-tetraphenylbutane and dichlorodiphenylsilane or dichlorodimethylsilane leads, in the first step, to the substitution of lithium atoms by two chlorodiphenylsilyl and chlorodimethylsilyl groups respectively, with the formation of lithium chloride, probably according to the following reaction scheme :

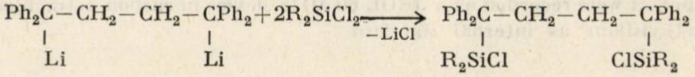

$$\underset{\substack{|\\ \mathrm{Li}}}{\mathrm{Ph_2C}}-\mathrm{CH_2}-\mathrm{CH_2}-\underset{\substack{|\\ \mathrm{Li}}}{\mathrm{CPh_2}}+2\mathrm{R_2SiCl_2}\xrightarrow[-\mathrm{LiCl}]{}\underset{\substack{|\\ \mathrm{R_2SiCl}}}{\mathrm{Ph_2C}}-\mathrm{CH_2}-\mathrm{CH_2}-\underset{\substack{|\\ \mathrm{ClSiR_2}}}{\mathrm{CPh_2}}$$

R = Me, Ph.

Hydrolysis of the chlorodiphenylsilyl groups leads to the formation of a siloxane bond and ring closure :

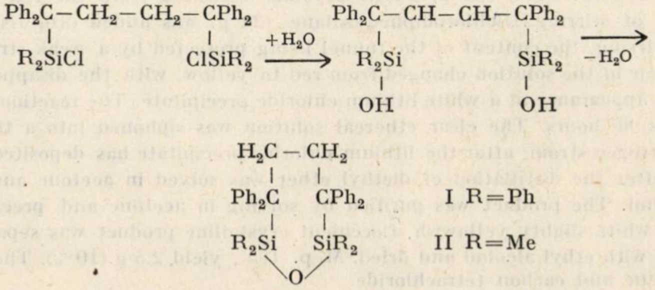

$$\underset{\substack{|\\ \mathrm{R_2SiCl}}}{\mathrm{Ph_2C}}-\mathrm{CH_2}-\mathrm{CH_2}-\underset{\substack{|\\ \mathrm{ClSiR_2}}}{\mathrm{CPh_2}}\xrightarrow{+\mathrm{H_2O}}\underset{\substack{|\\ \mathrm{R_2Si}\\ |\\ \mathrm{OH}}}{\mathrm{Ph_2C}}-\mathrm{CH}-\mathrm{CH}-\underset{\substack{|\\ \mathrm{SiR_2}\\ |\\ \mathrm{OH}}}{\mathrm{CPh_2}}\xrightarrow{-\mathrm{H_2O}}$$

I R=Ph

II R=Me

I, II

The source of water is the wet solvent.

A similar hydrolysis during the coupling of organochlorosilanes with organolithium reagents has been previously reported. Thus Andrianov and coworkers[21] have studied the reaction of 1,4-dilithium-1,4-dihydronaphthalene with trichlorophenylsilane and the product obtained, regardless of the working conditions, was bis-[1,4-bis-(phenyldichlorosilyl) dihydronaphthalene] cyclodioxide according to the scheme :

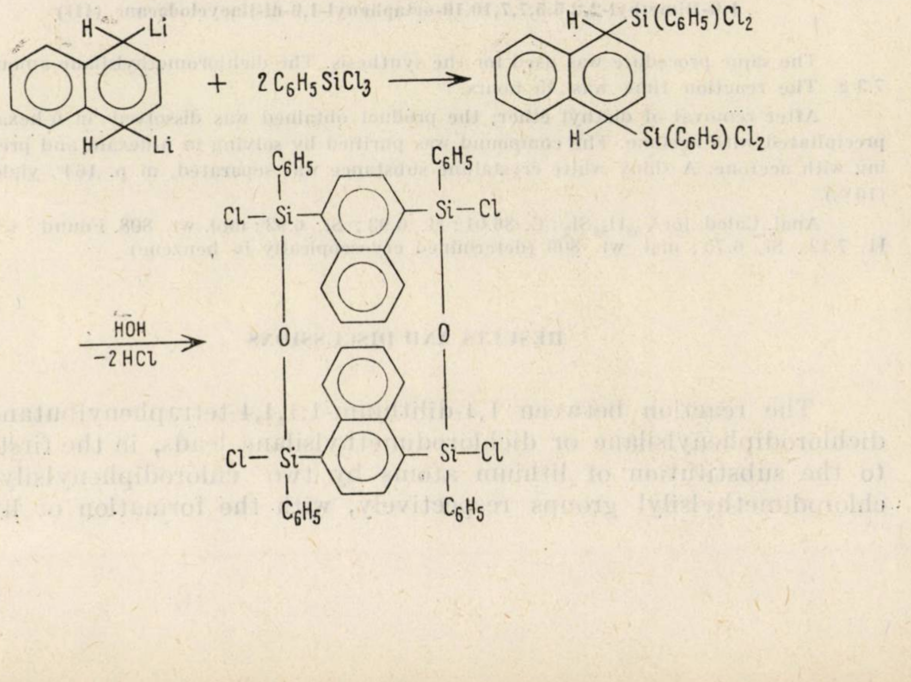

as well as the dimer of this product. Further hydrolitic polycondensation reactions have resulted in polycyclic compounds, and eventually in reticulated polymer products of the type :

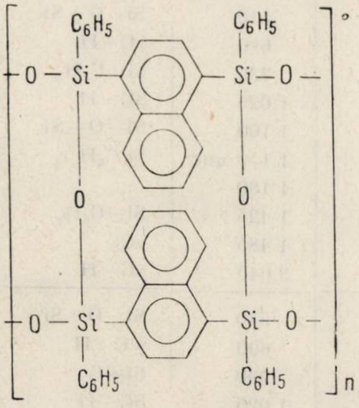

In our work it has been observed that chloromethylsilanes reacts faster with 1,4-dilithium-1,1,4,4-tetraphenylbutane than dichlorodiphenylsilane, i. e. 50 and 45 hours compared to 80 hours of reaction required for obtaining product I. Similar observations have been made by Carraher and Dammeier[23] in the synthesis of some silicon polyesters.

Generally, the IR absorption bands of the compounds prepared occur at shorter wavelengths, compared to those of the starting hydrocarbon (Table 1). Thus, the C—H bond out-of-plane stretching vibrations of the benzene molecule appear 15 cm^{-1} lower, the C—H valency vibrations in benzene, 20 cm^{-1} lower, a fact explained by some authors[24] by the decrease in the silicon electronegativity.

DTA and DTG curves of compounds I and II show them to be stable up to a temperature of 360° (I) and 380° (II), respectively. Heating beyond these temperatures will cause weight losses. Within the temperature, ranges of 360—370° (I), 380—400° (II) and 500—540° and 540—580° respectively, the decomposition products formed are stable.

DTA and DTG curves of the two products were also recorded maintaining approximately constant the temperature, within the limits 360—370° and 380—400° during two hours. From the DTG curves the weight loss is 21% and 20%, (I) and 32% and 7% respectively, (II). After heating, samples were taken from the residue to record their IR absorption spectra. The values of absorption bands frequencies observed are presented in table 2, compared to those of compounds prior heating.

---

[23] Ch. E. Carraher, jr, and R. L. Dammeier, *Makromol. Chem.*, **141**, 251 (1971).
[24] T. Srivastava and M. Onyszchuk, *Canad. J. Chem.*, **41**, 1244 (1963).

Table 1

IR absorption spectra of the compound obtained

Compound	Frequency cm^{-1}	Assignments	Values reported in the literature
I	510	Si–O–Si	520[25]
	690	γC–H	690–710[26]
	730	$Si-C_6H_5$	700–740[27]
	1 025	βC–H	1037[28]
	1 100	Si–O–Si	1020–1110[29]
	1 150 and 1 180	$Si(C_6H_5)_2$	1130[29]
	1 425	$Si-C_6H_5$	1430[30]
	1 485	νCC	1475–1525[31]
	3 040	νC–H .	3027–3039[32]
II	540	Si–O–Si	520[25]
	690	γ C–H	690–710[26]
	790	Si–C	770–850[29-30]
	1 025	βC–H	1037[28]
	1 100	Si–O–Si	1020–1110[29]
	1 250	$Si-CH_3$	1250–1280[33]
	1 485	νCC	1475–1525[31]
	3020	νC–H	3027–3039[32]
III	690	γC–H	690–710[26]
	790	Si–C	770–850[29-30]
	940	Si–H	910–1000[29]
	1 250	$Si-CH_3$	1250–1280[33]
	1 480	νCC	1475–1525[31]
	2 125	Si–H	2080–2270[34]
	3 010	νC–H	3027–3039[32]
1,1,4,4-tretraphenylbutan	710	γC–H	690–710[26]
	1 040	βC–H	1037
1,1,4,4-tetraphenylbutane	1 490	νCC	1475–1525[31]
	1 600	νCC	1580–1600[35]
	3 020	νC–H	3027–3039[32]

[25] H. KRIEGSMANN, *Z. Elektrochem.*, **61**, 1088 (1957).

[26] N. SHEPPARD and D. M. SIMPSON, *Quart. Rev.*, **7**, 19 (1953).

[27] L. SPIALTER, D. C. PRIEST and C. W. HARRIS, *J. Amer. Chem. Soc.*, **77**, 6227 (1955).

[28] M. AVRAM and GH. MATEESCU, "Spectroscopia în infraroşu. Aplicaţii în chimia organică", Ed. Tehnică, Bucureşti, 1966, p. 266.

[29] A. L SMITH, *Spectrochim. Acta*, **16**, 87 (1960).

[30] C. W. YOUNG, P. C. SERVAIS, C. C. CURRIE and M. J. HUNTER, *J. Amer. Chem. Soc.*, **70**, 3758 (1948).

[31] L. J. BELLAMY "The Infrared Spectra of Complex Molecules", Methuen Co., London, 1959, p. 69.

[32] S. E. WIBERLEY, S. C. BUNCE and W. H. BAUER, *Analyt. Chem.*, **32**, 217 (1960).

[33] N. WRIGHT and M. J. HUNTER, *J. Amer. Chem. Soc.*, **69**, 803 (1947).

[34] S. E. WESTERMARK, *Acta Chem. Scand.*, **9**, 947 (1955).

[35] L. J. BELLAMY, loc. cit. (ref. 31), p. 72.

For product I the 21% and 20% weight losses indicate the splitting of two phenyl groups from the silicon atoms when heated in air, with the formation of new siloxane bonds. Also, two other phenyl groups were split from the tetraphenylbutane chain and a C—C double bond appeared. The calculated weight change caused by the loss of two benzene molecules, is 20%. The modifications of the IR spectrum (the disappearance of bands at 1 150 and 1 180 cm^{-1}, characteristic of the $Si(C_6H_5)_2$ bond and also the appearance of bands at 610 and 1 650 cm^{-1} specific of alkenes) support this suggestion.

Table 2

IR absorption spectra of compounds I and II before and after heating

Compound	Unheated sample	Heated sample	Assignment
	Frequency cm^{-1}	Frequency cm^{-1}	
I	510	510	Si—O—Si
	—	610	C—H (alkene)
	690	690	γC—H
	730	735 v. w.	$Si-C_6H_5$
	1 025—1 100	1 000—1 130	βC—H; Si—O—Si
	1 150—1 180	—	$Si(C_6H_5)_2$
	1 425	1 425	$Si-C_6H_5$
	1 485	1 480	ν CC
	—	1 650	νC=C
	3 040	3 040	νC—H
II	540	—	Si—O—Si
	690	690	γC—H
	790	750—900	Si—C
	1 025—1 100	1 000—1 100	βC—H; Si—O—Si
	1 250	1 255	$Si-CH_3$
	1 485	1 485 v.w.	νCC
	—	1 650	νC=C
	3 020	3 020	νC—H

For compound II, the 32% and 7% weight losses may be attributed to the splitting of two phenyl groups from the tetraphenylbutane fragment (theoretically 31.7%) and of two methyl groups at the two silicon atoms (theoretically 6.09%) with the rearrangement of the molecule.

The analytical data, the determined molecular weights, together with the IR data on compounds I and II are in agreement with the pro posed structures.

Dichloromethylsilane reacts with 1,4-dilithium-1,1,4,4-tetraphenylbutane to form a silicon-containing heterocyclic compound :

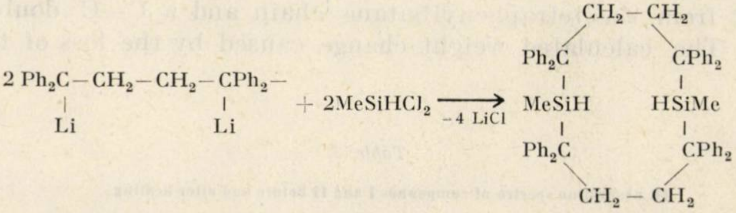

III

The IR spectrum of this compound fails to exhibit absorption bands around 520 and 1 100 cm^{-1}, characteristic of the siloxane bond. Absorption bands specific of the Si−H bond are present at 940 and 2 125 cm^{-1} (Table 1). DTA and DTG curves show that this compound is stable up to a temperature of 280°. Beyond this temperature, the product undergoes fast decomposition, leaving a residue of silicon dioxide.

The NMR spectra of the three products exhibit signal due to the protons of phenyl, methyl, methylene and Si−H groups (Table 3). The integrated signal area ratio between the protons of methylene, methyl, phenyl and Si−H groups suggest the proposed structures.

Table 3

Chemical shifts[a] (ppm) of protons in the compounds prepared

Compound	δ(Si−H)	δ(CH$_2$)	δ(Ph)
I	—	2.22	6.90
II	—	2.65	7.10
III	5.60	3.02	7.50
1,1,4,4-tetraphenylbutane	—	2.00	7.05

[a] measured relative to tetramethylsilane

Revue Roumaine de Chimie, **23**, *6*, 951–957 (1978)

DEGRADATION OF ANION EXCHANGERS IN AGRESSIVE MEDIUM. V.*

EFFECT OF HYDROXYL IONS IN THE PRESENCE OF FERRIC CHLORIDE ON CHEMICAL STABILITY OF TYPE I MACROPOROUS ANION EXCHANGERS

I. PETRARIU, LILIANA MONA NEAGU, CORNELIA LUCA,
IG. POINESCU and PAMFILIA PETRARIU
Institute of Macromolecular Chemistry "Petru Poni" Aleea Gr. Ghica Vodă
nr. 41 A, Iassy, Romania

Received February 18, 1976

We have studied the structural changes in the anion exchangers during the degradative process in the presence of hydroxyl ions and $FeCl_3$. Particular emphasis has been placed on the effect of variations of cross-linkage, inert medium and the nature of the third comonomer.

The previous papers[1–4] have studied the chemical stability of styrene-divinylbenzene type anion exchangers in presence of hydroxyl ions and oxidizing agents.

It is known that the chemical degradation can be accelerated by elevated temperatures[5] as well as by the catalytic activity of metals[6–7].

Anion exchangers are subject to oxidative attack when used in the aggressive waters containig dissolved oxygen or residual levels of chlorine.

The oxidation can also be accelerated by traces of iron or copper that may also be present in the water. The oxidation results in de-crosslinking of the resin and a consequent increase in the moisture content. This, in turn, results in high pressure drop across the bed and eventual bead breakdown.

An appreciable attention has been devoted to studies on the chemical stability of the macroporous strong base ion exchangers as they exhibit a greater range of affinity values for the more common anions that do gel type anion exchangers.

---

* Part IV : See reference 10

[1] I. Petrariu and J. Stamberg, *Coll. Czech. Chem. Comm.*, **32**, 798 (1967).

[2] I. Petrariu, S. Drăgan and P. Petrariu, *Rev. Chim. (București)*, **21**, 207 (1970).

[3] I. Petrariu, P. Petrariu, Fl. Popescu and C. Luca, *Rev. Roumaine Chim.*, **20**, 839 (1975).

[4] I. Petrariu, P. Petrariu, Fl. Popescu and S. Drăgan, *Rev. Roumaine Chim.*, **20** 1167 (1975).

[5] Z. Vasicek, J. Stamberg and O. Dufka, *Coll. Czech. Chem. Comm.*, **36,** 1817 (1971).

[6] R. Kunin and N. W. Frisch, *Ind. Eng. Chem.*, **49**, 1365 (1957).

[7] T. Mizuno, *Nippon Kagaku Zasshi*, **69**, 1254 (1966); *Chem. Abstr.*, **65**, 17125 (1966).

This paper will describe the chemical degradation of macroporous anion exchangers by hydroxyl ions at an elevated temperature in presence of $FeCl_3$, factors which cause complex changes in the structure of ionogenic groups.

EXPERIMENTAL

Chloromethylated macroporous ternary copolymers[8-9] have been used, the third comonomer of which is acrylonitrile or methyl methacrylate.

The amination of chloromethylated-copolymers was carried out with trimethylamine 21% in aqueous solution, at 24° for 6 hours.

Strong base macroporous anion exchangers based on styrene. (St)-acrylonitrile(AN)-divinylbenzene(DVB) or styrene-methyl-methacrylate(MCMe)-divinylbenzene copolymers obtained by copolymerization of monomers in the presence of inert medium as polystyrene, gasoline (b. p. 125–140°) or toluene were degraded.

Degradation was carried out on 2 meq. anion exchanger and 12 meq. of $FeCl_3$ in 20 ml, 10 N.NaOH at 50–100° for 5 hours.

The apparatus used for degradation was described in a previous paper.[10]

The apparent and specific density of the macroporous ternary copolymers was calculated by indications of Kunin et al.[11]

The macroporous anion exchangers were characterized by the exchange capacity and nitrogen analyses. [12]

Changes in the number and nature of the functional groups were investigated by determining the strongly and weakly basic capacities of the sample.

The acrylonitrile amount of the macroporous ternary copolymer was computed from nitrogen analysis, while the methylmethacrylate percentage has taken into account the MCMe monomer amount introduced in the copolymerization reaction.

This hypothesis was checked by calculating the structure of macroporous anionites obtained from these copolymers.[13-14]

The main characteristics of the ternary copolymers subjected to degradation are given in table 1.

Table 1

Chief characteristics of the ternary copolymers

Sample	Inert medium	Chemical structure			Exchange capacity meq/g			Coefficient of		Density	
		DVB %	AN %	MCMe %	C_{wb}	C_{sb}	C_t	methanol g/g	toluene g/g	apparent	skeletal
301	Benzine	18	2.26	—	0.18	2.59	2.77	0.46	1.46	0.7285	1.1448
303	Benzine	18	28.2	—	0.29	2.26	2.55	1.55	2.09	0.3875	1.0723
307	Polystyrene	8	—	—	0.19	3.58	3.77	0.14	1.12	1.0145	1.0745
311	Polystyrene	8	19.66	—	0.26	1.89	2.15	0.53	1.13	0.976	1.0975
314	Toluene	27	—	—	0.18	2.47	2.65	0.49	0.97	0.7391	1.0223
317	Toluene	27	8.4	—	0.27	2.07	2.34	0.94	1.39	0.9683	1.091
325	Polystyrene	8	—	20	0.45	2.96	3.41	0.40	1.04	0.7898	1.0265
331	Benzine	18	—	10	0.43	2.34	2.77	0.25	1.09	0.9496	1.0711

---

[8] Ig. Poinescu, S. Drăgan, S. Maxim and M. Dima, *Rev. Roumaine Chim.*, **20**, 1311 (1975)·

[9] Ig. Poinescu, S. Drăgan and M. Dima, *Rev. Roumaine Chim.*, (in press).

[10] I. Petrariu, M. Cujbă, Ig. Poinescu and C. Luca, *Rev. Roumaine Chim.*, (in press).

[11] R. Kunin, F. E. Meitzner, A. J. Oline, S. Fischer and N. Frisch, *Ind. Eng. Chem. Res. Develop.*, **1**, 140 (1967).

[12] T. S. Ma and G. Zuazaga, *Ind. Eng. Chem. Analyst*, **14**, 280 (1942).

[13] H. S. Pinner and T. Alfrey Jr., *J. Polymer Sci.*, **23**, 533 (1957).

[14] I. Scondac and M. Dima, *Studii şi Cercetări St. Chim. Fil. Iaşi*, **13**, 217 (1962).

RESULTS AND DISCUSSION

It is known that the strongly basic capacity decreases, the weakly basic capacity increases.[15] It appears therefore that part of strongly basic groups change to weakly basic groups.

The increase in the weakly basic capacity of the anion exchanger depending on temperature is shown in table 2.

Table 2

Influence of temperature and aggressive medium ($NaOH + FeCl_3$) on weakly basic capacity of anion exchangers (in Cl^- form)

Degradation temperature °C	Weakly basic capacity (meq/g)							
	301	303	307	311	314	317	325	331
—	0.18	0.29	0.19	0.26	0.18	0.27	0.45	0.43
50	0.31	0.29	0.63	0.32	0.21	0.31	0.64	0.52
80	0.44	0.34	0.71	0.52	0.37	0.36	0.96	0.72
100	0.57	0.44	0.94	0.54	0.60	0.45	1.28	0.98

If one compares the increases in capacity for the samples synthetized in presence of gasoline (i. e. samples 301, 303 and 331 which possess the same cross-linking degree) it can be noticed that this increase varies in the order: 301 > 331 > 303.

When the inert medium is toluene (samples 314 and 317) at the same degree of reticulation at 50° one notices a maximum shifting of increasing in anion exchangers with ternary structure (sample 317). At 80° and 100° binary copolymer (sample 314) exhibits a maximum increasing in weakly basic capacity against the ternary copolymer.

Approximately the same remarks have been also made for anion exchangers synthetized in the presence of polystyrene as inert medium (samples 307, 311 and 325).

This fact may be explained if one admits that during degradation the quaternary nitrogen is progressively transformed to tertiary, secondary and primary nitrogen and finally (at very high temperature, over 100°) degraded to a nonbasic product.[16–18]

Strongly basic capacity values are given in table 3.

A study of curves *1* and *2* (Figure 1) representing the experimental results for two anion exchangers having the same cross-linking degree, copolymerized in gasoline medium but with different amount of the third comonomer (AN) shows that the third comonomer quantity does not cause a significant change in the strongly basic capacity, but its nature (curve *3*) has an important significance.

---

[15] A. L. Wilson, *J. Appl. Chem.*, **11**, 151 (1961).

[16] N. W. Frisch and R. Kunin, *Ind. Eng. Chem.*, **49**, 1365 (1957).

[17] N. W. Frisch and R. Kunin, *J. Am. Water Works Assoc.*, **52**, 875 (1960).

[18] L. F. Wirth Jr., C. A. Feldt and K. Odland, *Ind. Eng. Chem*, **53**, 638 (1961).

Table 3

Influence of temperature and aggressive medium ($NaOH + FeCl_3$) on strongly basic capacity anion exchangers (in Cl^- form)

Degradation temperature °C	Strongly basic capacity (meq/g)							
	301	303	307	311	314	317	325	331
—	2.59	2.26	3.58	1.89	2.47	2.07	2.96	2.34
50	2.20	1.55	2.86	1.41	2.41	1.99	2.69	2.13
80	2.01	1.25	2.71	1.29	2.04	1.84	2.52	1.60
100	1.81	1.05	1.71	1.25	1.39	1.35	1.72	1.36

The influence of the third comonomer on the chemical stability is shown in Figure 2. From the data presented in Figure 2 it is noticed that the binary copolymer (curve *1*) exhibits a good chemical stability compared with the ternary copolymer (curve *2*).

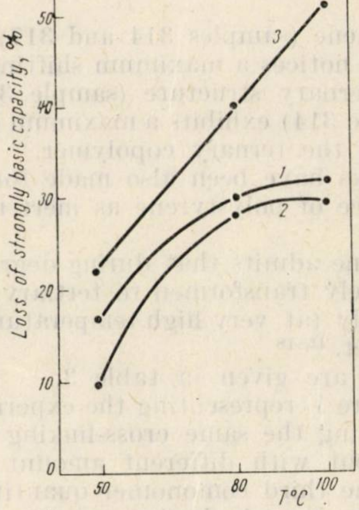

Fig. 1. — Effect of temperature on strongly basic capacities.

1 — sample 301 (DVB 18% and AN 2.26%);
2 — sample 303 (DVB 18% and AN 28.2%);
3 — sample 331 (DVB 18% and MCMe10%);
Gasoline as inert medium.

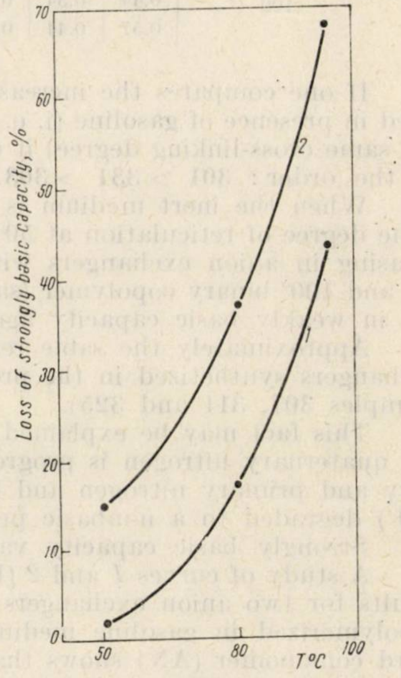

Fig. 2. — Effect of temperature on strongly basic capacities.

1 — sample 314 (DVB 27%, binary copolymer);
2 — sample 317 DVB 27%, ternary copolymer); Toluene as inert medium.

In connection with these observations it was found advisable to study the loss of total capacity as a function of temperature (Table 4). Attention has been focussed on the third comonomer influence. (Figure 3).

Table 4

Influence of temperature and aggressive medium ($NaOH + FeCl_3$) on total basic capacity of anion exchangers (in Cl – form)

Degradation temperature °C	Total basic capacity (meq/g)							
	301	303	307	311	314	317	325	331
—	2.77	2.55	3.77	2.15	2.65	2.34	3.41	2.77
50	2.51	1.84	3.63	1.85	2.62	2.30	3.33	2.65
80	2.45	1.59	3.53	1.81	2.40	2.20	3.20	2.32
100	2.39	1.49	2.65	1.79	1.99	1.80	3.00	2.11

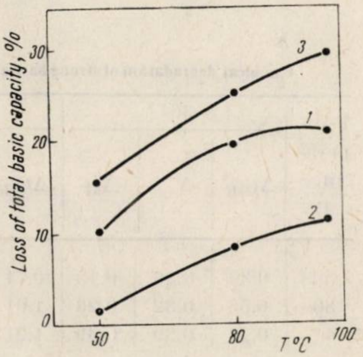

Fig. 3. – Effect of temperature on total basic capacities.

Curves *1*–*3* the same notations and characteristics as in Fig. 1.

To some extent, the same conclusions can be drawn from the experimental data on the total basic capacity as was noticed with the strongly basic capacity. Its decrease may also be attributed to the following effects: firstly, part of strongly basic groups may change directly to non-exchanging groups and, secondary, weakly basic groups themselves may change to non-exchanging groups. [15]

By comparing the results given in Figure 1 and Figure 3 it can be ettled that the rate of the strongly basic capacity loss is much higher than that of the total basic capacity.

With respect to the basic coefficient it is to be noted that a temperature increase determines a decrease of the basic coefficient (Table 5).

These differences in basicity as a function of temperature may be connected with the nature of basic groups initially available in the structure of the anion exchanger.

Table 5

Influence of temperature and aggressive medium ($NaOH + FeCl_3$) on basic coefficient of anion exchangers (in Cl−form)

Degradation temperature °C	Basic coefficient							
	301	303	307	311	314	317	325	331
—	0.93	0.88	0.95	0.87	0.93	0.88	0.86	0.84
50	0.88	0.84	0.78	0.76	0.92	0.86	0.80	0.80
80	0.82	0.78	0.77	0.71	0.85	0.84	0.78	0.69
100	0.76	0.70	0.64	0.69	0.69	0.75	0.57	0.64

Considering that the loss of the strongly basic capacity (ΔC_{sb} follows two paths : [3] a dealkylation reaction (Δ_{al}) and a deamination reaction (Δ_{am}) it can be concluded that both the dealkylation and deamination reactions cooperate in the chemical degradation (Table 6).

Table

Chemical degradation of strong base anion exchangers in aggressive medium ($NaOH + FeCl_3$) at different

Temperature °C	301			303			307			311		
	ΔC_{sb}	Δ_{am}	Δ_{al}	ΔC_{sb}	Δ_{am}	Δ_{al}	ΔC_{sb}	Δ_{am}	Δ_{al}	ΔC_{sb}	Δ_{am}	Δ_{al}
50	0.39	0.26	0.13	0.71	0.71	0.00	0.72	0.28	0.44	0.48	0.42	0.06
80	0.58	0.32	0.26	1.01	0.96	0.05	0.87	0.35	0.52	0.60	0.34	0.26
100	0.78	0.39	0.39	1.21	1.06	0.15	1.87	1.12	0.75	0.64	0.36	0.28

In some respects, it has to be pointed out that the physical structure of the copolymer plays a secondary part in the degradation process. Thus, the porosity of the copolymers, the plasticizing effect which increases with the increase of the hydrocarbonated radical of the methacrylic esthers, [19–20] the nature of the inert medium used in the copolymerization process of the monomers as well as the nature of the third comonomer are factors which are involved in the chemical degradation.

CONCLUSIONS

1. The influence of the copolymer cross-linking degree on the chemical stability of macroporous Type-1 strong base anion exchangers as well as the nature and quantity of the third comonomer was outlined.

---

[19] I. SAKURADA, YU. SAKAGUCHI, T. ONO and T. UEDA, *Kobunski Kagaku*, **22**, 696 (1965) ; *Chem. Abstr.*, **64**, 12828 (1966).

[20] S. YOSHIKAWA and O. KIM, *Bull. Chem. Soc. Japan*, **39**, 1515 (1966).

2. During the degradation reaction the strongly basic capacity and to a small extent, also the total capacity, decreased while the weakly basic capacity, increased.

3. The loss of total basic capacities was much higher initially but then it decreased gradually until it became approximately constant.

6

temperature through dealkylation (Δ_{al}) and deamination (Δ_{am}) reactions

314			317			325			331		
ΔC_{sb}	Δ_{am}	Δ_{al}	ΔC_{sb}	Δ_{am}	Δ_{al}	ΔC_{sb}	Δ_{am}	Δ_{al}	ΔC_{bs}	Δ_{am}	Δ_{al}
0.06	0.03	0.03	0.075	0.033	0.042	0.27	0.08	0.19	0.22	0.12	0.10
0.43	0.25	0.18	0.23	0.13	0.10	0.44	2.21	0.23	0.74	0.45	0.29
1.08	0.66	0.42	0.72	0.53	0.19	1.24	0.42	0.82	0.99	0.66	0.33

Revue Roumaine de Chimie, **23**, *6*, 959–965(1978)

CYCLIC VOLTAMMETRY DETERMINATION OF α,α'-DIMETHYLPHENYL HYDROPEROXIDE

CORNELIA IDIȚOIU[a] and DAVID AIKENS[b]
[a]University of Timişoara, 1900 Timişoara, Romania.
[b]Rensselaer Polytechnic Institute, School of Science Department of Chemistry,
Troy, N. Y., 12180, U. S. A.

Received March 23, 1976

A new method for α,α'-dimethylphenyl hydroperoxide (cumyl hydroperoxide) determination by cyclic voltammetry was developed. Relative errors E_r, statistical parameters $\bar{s}_{I_i}$; $\bar{s}_{\bar{I}_j}$; $\bar{s}_{C_i}$; $\bar{s}_{\bar{C}_i}$ were calculated and some statistical checks were performed. The method has an average error below 2%, is sensitive for 10^{-4} M–10^{-3} M range of concentration, is suited with organic media, the addition of acetone, phenol, α-methylstyrene, acetophenone, 2-phenyl-2-propanol and 2-phenylpropane, had no influence and it needs some minutes only. The method is appropiate in a set of measurements, particularly for the phenol-acetone industry as well as for kinetic studies.

In the last time organic peroxides become of greater interest because of their manifold use as intermediates in industrial synthesis, polymerization initiators, oxidizing agents, [1–4] as well as of their incidence in food, [5] polymer and petrochemical products. [3]

α,α'-Dimethylphenyl hydroperoxide (cumyl hydroperoxide) besides being an intermediate in phenol-acetone manufacture, has a large use as a polymerization initiator in the rubber industry and an oxidizing agent in organic media. [6] For its determination, the methods proposed are of as various principles as: iodometric, [7–8] colorimetric, [9] polarographic, [11] chromatographic, [12,13] etc. However, out of these, the methods

---

[1] A. V. Tobolsky, and R. B. Mesrobian, "Organic Peroxides", Interscience, New York, 1954.

[2] A. C. Davies, "Organic Peroxides", Butterworth, London, 1961.

[3] D. Swern, editor "Organic Peroxides", vol. I, Wiley-Interscience, New York, 1970, vol. II, 1971; vol. III, 1972.

[4] R. M. Johnson and I. W. Siddiqi, "The Determination of Organic Peroxides", In the Series "Organic Functional Group Analysis", Pergamon Press, London, 1970.

[5] K. A. Williams, "Oils, Fats and Fatty Foods", Churchill, London, 1966.

[6] V. J. Karnojitzky, *Chimie et Industrie*, **93**, 529 (1965).

[7] G. P. Armstrong, R. H. Hall and D. C. Quin, *J. Chem. Soc.*, **1950**, 666.

[8] L. Tsuk and G. M. Zollner, *Magyar Kém. Lapja*, **14**, 417 (1959).

[9] M. Ionescu and C. Popescu, *Bull Soc. Stiinţe, Romania*, **3**, 387 (1938). *Chem. Abstr.*, **33**, 9193 (1939).

[10] I. M. Kolthoff, E. J. Meehan, S. Bruckenstein and H. Minato, *Microchem. J.*, **4**, 33 (1960).

[11] C. O. Willit, C. Riccuiti, H. B. Knight and D. Swern, *Analyt. Chem.*, **24**, 785 (1952).

[12] S. W. Bukata, L. L. Zabrocki and M. E. McLaughlin, *Analyt. Chem.*, **35**, 885 (1963).

[13] P. P. Ruban and A. N. Korol, *Zavodskaya Lab.*, **37**, 772 (1971).

with an error below 2% are rather laborious, [7,8,10] while the rapid ones are less accurate or lack reproducibility. [12,13]

Cyclic voltammetry, a most modern and quick electro-chemical means of analysis,[14] offered a chance for a determination method, both rapid and accurate, which is suitable in a set of measurements, particularly for kinetic studies, or for acetone-phenol industry.

EXPERIMENTAL

The chemical : methanol, benzene, acetone, acetophenone, 2-phenylpropane (cumene) α-methylstyrene, 2-phenyl-2-propanol, were of AR (analytical reagent) purity, manufactured by Krackeler & Campbell Incorporation. Acetone was distilled, but the rest of reagents were used without further purification. In order to avoid air humidity absorption, all chemical were kept into a dry box. Technical α,α'-dimethylphenyl hydroperoxide (cumyl hydroperoxide) was purified as Na salt in the following conditions : the product was precipitated with 30% aqueous NaOH below 0°C, washed with an acetone benzene (1 : 1) mixture, and dried for about 2 hrs in a vacuum oven (40° and ~ 10 mm Hg). The such obtained sodium salt was mixed with deionized water to form a paste which was bubbled with CO_2 until the lower aqueous layer became clear. The superior oleic layer of hydroperoxide was extracted with petroleum ether (l. b. p.), washed with deionized water until neutral reaction and concentrated in a circular evaporator (40° and 10 mm Hg). This product was distilled in N_2 atmosphere (2.5×10^{-2} mm Hg, 45°) keeping the middle fraction only. The colorless oleic product obtained was α,α'-dimethylphenyl hydroperoxide of 99.98%purity (by iodometric determination[7]). A 0.1 M solution in 1 : 1 methanol : benzene mixture was prepared and samples of 20—50 μ 1 were taken to calibrate the curves.

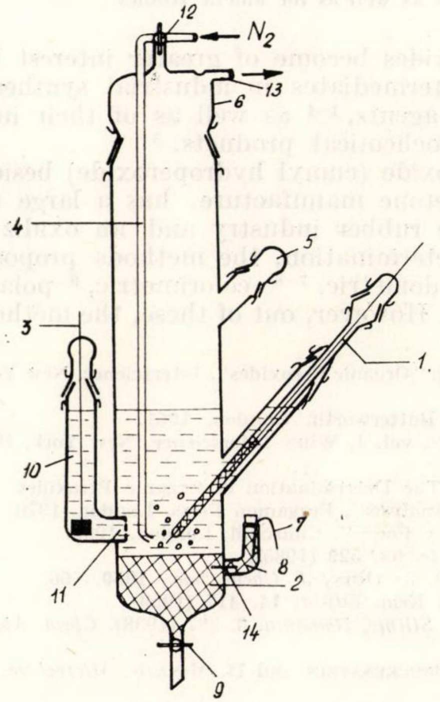

Fig. 1.— The cell : *1*—working electrode ; *2*—reference electrode ; *3*—auxiliary electrode ; *4*—tube for nitrogen ; *5*—samples opening ; *6*—cell's lid ; *7*—Ag mobile connection; *8* — mercury-filled lateral tube ; *9*—discharge stopcock ; *10*—lateral tube for auxiliary electrode ; *11*—frit ; *12*—three-way pressure stopcock ; *13*—gas outlet ; *14*—platinum connection.

---

[14] H. H. Willard, L. L. Merrit and J. A. Dean, "Instrumental Methods of Analysis", Fifth Edition, D. Van Nostrand Comp., New York, 1974.

An electrochemical pyrex cell (Ø = 26 mm, height = 150 mm Figure 1) was designed and materialized. The lid 6 of the cell has a three-way pressure stopcock 12, connected to a 4 mm Ø tube (for N_2), and a gas outlet 13.

Working electrode 1, a platinum wire of 0.21 mm Ø and 4 mm exterior length, was welded into a 4 mm Ø glass tube, filled with mercury in order to make the contact with the instrument. Both for facilitating mercury introduction and electrode-cell connection, joints of 14/20 fastened with steel springs were used.

Reference electrode 2, in fact a 5 ml mercury pool, was attached to the instrument, both with a platinum connection 14 welded into the cell wall and a mobile connection 7. The last one was introduced into the mercury-filled lateral tube 8. The discharge of mercury from the cell was facilitated by the stopcock 9.

Auxiliary compensation electrode 3, made from 0.2 × 0.2 × 0.6 mm platinum foil and 0.25 mm Ø platinum wire, was welded to the lid of lateral tube 10, in order to connect it to the instrument. The connection between auxiliary electrode 3 and the bulk of the cell was facilitated by frit 11. For samples, opening 5 was equiped.

The cell conceived in this way, proved to be an operative, easy to handle and to clean one. It also offers the possibility of an efficient medium deoxygenation and electrode depolarization. By stopcock 12, the components can be mixed quickly and the medium maintained under nitrogen.

The instrument to which the cell shown in Figure 1, was connected, a P.A.R. (Princeton Applied Research) Model 170 (Electrochemistry System) and a x−y recorder, a built-in three electrode system with I.R. compensation and three independent operating sections, which allowed the performance of almost any known electrochemical experiment.

Working procedure was as follows : 20 ml of 0.3 M LiCl in methanol-benzene 1 : 1 mixture were introduced into the cell and deoxygenated by bubbling with solvent saturated nitrogen for about 30 minutes. The cell was connected to the instrument with the following parameters : initial potential − 0.3 V ; final potential − 1.0 V ; current : 50 μA ; scane rate 100 mV/sec ; single scane. The bubbling of nitrogen was interrupted and a background recording was taken curve *1,* Figure 2). If a slight maximum due to oxygen, at 0.45 V was noticed, the deoxygenation had to be continued until it vanished. Then with a suitable syringe, a sample of 20−50 μl was introduced into the cell, mixed by bubbling more nitrogen and interrupted during the recording of the sample. After each recording, the working electrode had to be depolarised by bubbling nitrogen for 2−3 minutes and then checking of reproducibility was made. After ten hours or more of utilisation it happened sometimes, that working electrode got too polarised and had to be cleaned electrochemically as follows : the electrode was introduced into the cell

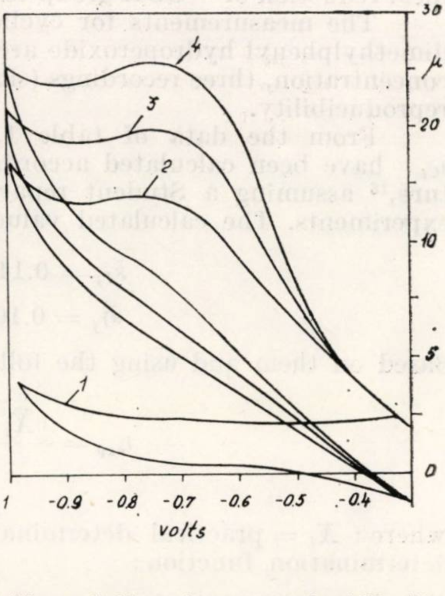

Fig. 2.— Cathodical reduction curves for αα'—dimethylphenyl hydroperoxide determination by cyclic voltammetry. *1* — the deoxygenated background ; *2* — 4.55 × 10^{-4} M.1^{-1} cumyl hydroperoxide ; *3*— 9.55 × 10^{-4} M.1^{-1} cumyl hydroperoxide ; *4* — 12.75 × 10^{-4} M.1^{-1} cumyl hydroperoxide .

containing the deoxygenated background only and cyclic potentials of relatively high frequency (20 V/sec) in the working range (0.3—1.0 V) were applied for a couple of minutes, followed by bubbling nitrogen.

In the above conditions α, α'-dimethylphenyl hydroperoxide had the cythodical reduction maxima for the —OOH group, at —0.74 V, which were found to be reproducible and their heights directly proportional with the concentrations. Figure 2 contains the curves recorded for some concentrations of hydroperoxide : curve *2* :4.55×10^{-4}M.1^{-1} ; curve *3* : 9.55×10^{-4} M.1^{-1} ; curve *4* : 12.75×10^{-4} M.1^{-1}. Although cathodical maxima were not very sharp, they were however reproducible and easy to use for concentrations measurements.

RESULTS AND DISCUSSIONS

Although by similitude with tert-butyl hydroperoxide[15] it can be assumed that cathodical reduction of α,α'-dimethylphenyl hydroperoxide would take place by the following steps:

$$C_6H_5{-}C(CH_3)_2{-}OOH + e^- \rightarrow C_6H_5{-}C(CH_3)_2{-}O\cdot + OH^- \tag{1}$$

$$C_6H_5{-}C(CH_3){-}O\cdot + e^- \rightarrow C_6H_5{-}C(CH_3)_2{-}O^- \tag{2}$$

$$C_6H_5{-}C(CH_3){-}O^- + H^+ \rightarrow C_6H_5{-}C(CH_3)_2{-}OH \tag{3}$$

we did not obtain a maximum for each transferred electron, but one maximum for the overall process only. This fact is possibly due to the rate of the electron transfer reaction which is higher than the scan rate. On the other side, there was no anodical wave (Figure 2), as the cathodical reduction of —OOH group to —OH group is an irreversible process.[14]

The measurements for cyclic voltammetric determination of α,α'-dimethylphenyl hydroperoxide are presented in table 1. For each known concentration, three recordings (single scan) were taken, in order to check reproducibility.

From the data of table 1, statistical parameters $\bar{s}_{I_j}$; $\bar{s}_{\bar{I}_j}$; $\bar{s}_{C_i}$; $\bar{s}_{\bar{C}_i}$ have been calculated according to the method described in literature,[16] assuming a Student repartition of errors, because of less than experiments. The calculated values of these parameters are:

$$\begin{aligned} \bar{s}_{I_j} &= 0.144 \;\; \bar{s}_{C_i} = 0.027 \\ \bar{s}_{\bar{I}_j} &= 0.102 \;\; \bar{s}_{\bar{C}_i} = 0.008 \end{aligned} \tag{4}$$

Based on them and using the following relation :[16]

$$t_{\text{exp}} = \frac{|\bar{X}_i - X_i|}{\bar{s}} \leqslant t_{QK} \tag{5}$$

where : X_i = practical determination function ; X_i = the most probable determination function ;

---

[15] T. I. JURJENKO, A. A. ZANIKO, O. K. SERBIUKOVA and I. I. LUKHANOVA, "Uspekhi Khimii Organiceskih Perekisnîh Soedinenii i Autookisleniia", Izdatelistvo Khimia, Moskova 1969, p. 450.

[16] I. SILBERG, T. A. CRIȘAN, C. BAIULESCU and I. C. CIUREA, "Metode Fizice de Analiză în Chimia Analitică", vol. 6, C.D.I.C.P., București, 1970.

Table 1

Measurements for cyclic voltammetry determination of, α,α' – dimethyl-phenyl-hydroperoxide

Nº	$\overset{*}{C}_{HP}.10^4$ introduced	Current $I(\mu A)$ 1	2	3	Average current $(\mu A)\bar{I}$	$\overset{**}{\bar{C}}_{HP}.10^4(M.1^{-1})$	$C_i - \bar{C}$	$E_r\%$
1.	0	2.50	2.50	2.50	2.50	0	0	0
2.	0.91	4.25	4.00	4.00	4.08	0.89	+0.02	+2.1
3.	1.36	5.00	4.75	5.00	4.92	1.34	+0.02	+1.4
4.	1.82	6.00	5.75	5.75	5.83	1.83	−0.01	−0.55
5.	2.71	7.50	7.25	7.50	7.42	2.69	+0.02	+0.74
6.	3.19	8.50	8.50	8.25	8.42	3.23	−0.04	−1.25
7.	3.62	9.00	9.25	9.00	9.08	3.59	+0.03	+0.83
8.	4.55	11.00	10.75	10.75	10.83	4.53	+0.02	+0.44
9.	5.36	12.50	12.25	12.50	12.33	5.34	+0.02	+0.37
10.	6.42	14.50	14.25	14.25	14.33	6.42	0.00	+0.00
11.	7.28	16.00	16.00	16.00	16.00	7.23	+0.05	+0.69
12.	8.60	18.25	18.50	18.25	18.33	8.58	+0.02	+0.23
13.	10.01	21.00	20.75	21.00	20.92	9.98	+0.03	+0.03
14.	11.00	23.00	22.75	22.75	22.83	11.02	−0.02	−0.18

$\overset{*}{C}_{HP}$= concentration of introduced hydroperoxide

$\overset{**}{C}_{HP}$= average determination of hydroperoxide concentration

the following statistical checks were made :

a) If the relation (5) is respected even for the largest deviation of the current $\bar{I}_i - I_i$ from the most probable line.

b) If the relation (5) is true even for the largest deviation of concentrations $\bar{c}_i - c_i$ from the most probable line, taking $t_{QK} = 2.23$ as $K = 12$ (for the concentrations) when $0 < Q \leqslant 0.05$; and $t_{QK} = 4.30$ (for the currents) when Q is the same as above. From this :

$$t_{exp_{I_i}} = \frac{0.170}{0.144} = 1.18 < 4.3. \qquad (6)$$

$$t_{exp_{C_i}} = \frac{0.050}{0.027} = 1.85 < 2.23 \qquad (7)$$

which leads to a positive answer both for point a and b.

From the data set of table 1, the most probable line equation was determined, as follows :

$$\bar{C}_i = -1.316 + 0.540\, I_i \quad (\bar{C}_i = \text{moles. liter}^{-1}.10^{-4}) \qquad (8)$$

and using the equation : [16,17]

$$L_I = \bar{X} \pm \frac{t_{QK} \cdot \bar{s}}{\sqrt{n}} = \bar{X} \pm t_{QK} \cdot \bar{s}_X \qquad (9)$$

the confidence limit L_I was calculated, taking $n = 12$, $t_{QK} = 2.23$ $(0 < Q \leqslant 0.05)$:

$$L_I = \bar{X} \pm 0.227. \qquad (10)$$

Using (8) and (10) equations of both superior and inferior lines, which determine the dispersion band of the experimental data around the most probable line, are :

$$\bar{C}_{i\ \mathrm{sup.}} = -\,1.088 + 0.540\ \bar{I}_i \quad (C_i = \text{moles.liter}^{-1}.10^{-4}) \qquad (11)$$

$$\bar{C}_{i\ \mathrm{inf.}} = -\,1.544 + 0.540\ I_i \quad (C_i = \text{moles.liter}^{-1}.10^{-4}) \qquad (12)$$

Figure 3 presents the most probable calibration line for cyclic voltammetric determination of α,α'-dimethylphenyl hydroperoxide.

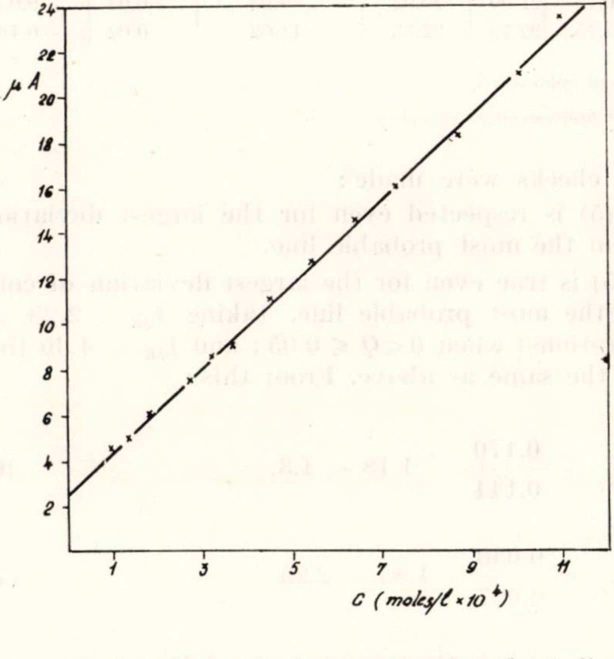

Fig. 3. – The calibration curve for cyclic voltammetry determination of α,α'–dimethylphenyl hydroperoxide.

In another set of experiments, the influence of some acid decomposition products of hydroperoxide as : acetone, phenol, 2-phenylpro-

---

[17] W. E. HARRIS and B. KRATOCHVIL, "Chemical Separations and Measurements Background and Procedures for Modern Analysis", W.B. Saunders Comp., Philadelphia, 1974, p. 40.

pane, α-methylstyrene, acetophenone and 2-phenyl-2-propanol, upon determination was investigated. The results of these measurements are presented in table 2. Each determination is an average of three measurements. The above additions, were prepared as 0.1 M solutions in 1/1 methanol : benzene mixture and samples of 50–90 μ 1 were introduced into the cell. The data of table 2 show that the above reagents had influence neither upon the reduction potential nor upon the current.

Table 2

Selectivity testing for the cyclic voltammetry determination of $\alpha\alpha'$-dimethylphenyl hydroperoxide

N°	Reagents added into the cell	$C.10^4$ $(M.1^{-1})$	Potential (V)	Current (μA)	Note
1.	Background : 0.3M LiCl in benzene-acetone 1/1 mixture	—	—	2.50	Background current according to curve 1, Fig. 2
2.	α,α'-dimethylphenyl hydroperoxide	3.20	−0.74	8.50	mixture 1 plus hydroperoxide
3.	acetone	4.36	−0.74	8.50	mixture 2 plus acetone
4.	phenol	3.11	−0.74	8.40	mixture 3 plus phenol
5.	2-phenylpropane (cumene)	3.57	−0.74	8.50	mixture 4 plus cumene
6.	2-phenyl-2-propanol	2.76	0.74	8.50	mixture 5 plus 2-phenyl-2-propanol
7.	acetophenone	4.16	−0.74	8.40	mixture 6 plus acetophenone
8.	α-methylstyrene	2.54	0.74	8.50	mixture 7 plus α-methylstyrene

As a conclusion, this method has a sensitivity of 10^{-4} M.1^{-1}, an accuracy more than 98% and it needs for determination less than five minutes. It is appropiate for sets of measurements in organic media, as in the phenol-acetone industry, because decomposition reaction products had no influence upon determination, or in kinetic studies, when rapidity and sensitivity are required.

AKNOWLEDGMENT. Cornelia Idiţoiu was a Fulbright grant recipient at Rensselaer Polytechnic Institute, which is greatfully acknowledged. She thanks also to Dr. K. W. Fung for helpful discussion.

Revue Roumaine de Chimie, **23**, *6*, 967–975(1978)

MICROREACTIONS COMBINED WITH THIN-LAYER CHROMATOGRAPHY FOR THE IDENTIFICATION OF PHENOTHIAZINE DRUGS

TITUS CONSTANTINESCU*, ŞTEFANIA ENACHE**[a] and ROSTISLAV VASILIEV**

* Centre of Physical Chemistry, Splaiul Independenţei 202–A, Bucharest, Romania
** State Institute for Drug Control and Pharmaceutical Research, Aviator Sănătescu, 48, Bucharest, Romania

Received May 12, 1976

A procedure which combines *in situ* hydrolysis with thin-layer chromatography techniques has been given for the separation and identification of a series of phenothiazine drugs. The sensitivity of the method is in the range of 50–100 micrograms. The technique can also be applied for the study of the corresponding sulphoxides and sulphones. The same method can be extended to dibenzoazepine drugs.

Drugs derived from phenothiazine are generally characterized by two specific substitutions: an alkylamine chain at the heterocyclic nitrogen and some simple radicals at C-2 (Formula I, R=S, Figure 1). The number of different compounds is rather large, in view of the possible combinations of the two series of substituents, and it is difficult to give a general porcedure for their TLC analysis[1-9].

Instead, a two-step procedure is proposed, which considerably increases the number of compounds that can be identified without interferences: the R″ substituent is identified first by *in situ* hydrolysis of compounds I and II (Figure 1), followed by the TLC of the last ones; the R′ substituent is then determined by a second TLC procedure, using standards with the R″ substituent established in the first step. This method can be applied regardless of the position of R″, as well as for sulphoxides and sulphones. The same method can be extended to dibenzazepine drugs.

---

[a] Deceased Ianuary 1978

[1] E. Sthal, "Thin-Layer Chromatography", Springer Verlag, Heidelberg, 1967, p. 483.

[2] T. Y. Mellinger and C. E. Keeler, *J. Pharm. Sci.*, **51**, 1169 (1962).

[3] Y. L. Kiger and Y. G. Kiger, *Ann. Pharm. Franc.*, **23**, 489 (1965).

[4] Y. Kofoed, C. Fabierkiewicz and G.N.W. Lucas, *J. Chromatogr.*, **23**, 410 (1966).

[5] C. Fabierkiewicz and G. Cimbura, *J. Chromatogr.*, **53**, 413 (1970).

[6] A. De Leenheer, *J. Chromatogr.*, **75**, 79 (1973).

[7] J. E. Forrest and R. A. Hancock, *J. Chromatogr.*, **75**, 156 (1973).

[8] W. N. French, F. F. Matsui and D. L. Robertson, *J. Chromatogr.*, **97**, 223 (1974).

[9] E. Pawelczyk and B. Marciniec, *Die Pharmazie*, **29**, 585 (1974).

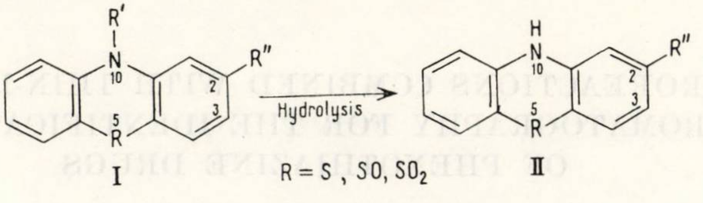

Fig. 1.— The *in situ* hydrolysis reaction of 2,10-disubstituted phenothiazine derivatives.

EXPERIMENTAL

Compounds and Reagents

The investigated phenothiazines were commercially available and are presented in table 1. The corresponding sulphoxides were prepared as previously reported[10], excepting XIIa—c, which were obtained from Sandoz.

For *in situ* hydrolysis 67% hydriodic acid (Merck)—H_2O (1 :3 V/V) was used.

TLC working conditions

Stationary phase : Silicagel G or GF_{254} (Merck), with the following layer thickness : a) 500 microns for preparative purposes (20 × 20 cm plates, non-activated, dried for 24 hours at room temperature) ; b) 250 microns for analytical purposes (20 × 20 cm plates, non-activated, as above, or activated for one hour at 110°).

Mobile phase (Developers) : $S_1 =$ petroleum ether (30—60°) — toluene (5 :5 V/V) ; $S_2 =$ *n*-heptane benzene acetone methanol (2 :4 :3 :1 V/V)[10] ; $S_3 =$ benzene-acetone-ethyl alcohol (95%) — ammonia (25%) (5 :4 :0.5 :0.5 V/V) ; [10]$S_4 =$ petroleum ether (30—60°)—toluene-acetone-methanol (5 :3.5 :1 :0.5 V/V). The separations have been carried out according to the ascendent uni-dimensional technique (over a distance of 10—15 cm) in non-saturated atmosphere for S_1, S_2, S_4 and in saturated atmosphere for S_3.[10]

DETECTION $D_1 =$ localization in UV light (254 nm) when fluorescent support is used ; $D_2 =$ spraying with a H_2SO_4 solution (10 ml H_2SO_4 (conc.) + 10 ml H_2O + 20 ml of ethyl alcohol).[11]

The samples were applied on the chromatographic plates as aqueous solutions in the case of the hydrochloric derivatives and as alcoholic solutions for the salts of organic acids.

Hydrolysis in preparative conditions of compounds I, R = S (Table 1). Isolation and characterization of the hydrolysis products

Compound which have been hydrolysed in preparative conditions are listed in table 2. Samples of 50 milligrams were applied as strips on each of ten GF_{254} silicagel preparative chromatoplates. The chromatoplates were dried for 10 minutes at room temperature, then HI solution was applied over the samples (50 microliters plate), and the chromatoplates were further heated for approximately 30 minutes at 180—200°. Then development with S_1 at room temperature was performed and the plates were dried again 10 minutes at room temperature (in the dark), after which the detection was carried out in UV light and by spraying with D_2 (in the "control area" only).

The hydrolysis products were eluted with a hot mixture of *n*-hexane-toluene (7 :3 V/V) and the resulting solution was concentrated in vacuum (up to approximately 0.5 ml). The crystallized products were obtained by cooling and their purity was checked by TLC using activated silicagel, the S_1 developer and detection with D_2. Further sublimation under vacuum did not enhance the melting points. The identity of type II products was established by the tests indicated in table 2 — where we have also mentioned the R_f values, as well as the detection behaviour.

---

[10] S. Enache, T. Constantinescu and R. Vasiliev, *Farmacia, (Bucharest)*, **25**, 95 (1977).

[11] T. Constantinescu and S. Enache, *Farmacia (Bucharest)*, **24**, 227 (1976).

Table 1

The investigated phenothiazines

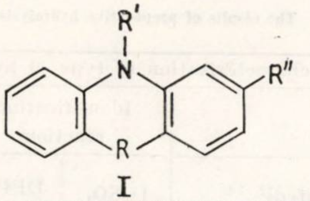

I

	R'	R''	R
III	$CH_2-CHMe-NMe_2$	H	S
IIIa	——,,——	H	SO
IV	$(CH_2)_3-NMe_2$	Cl	S
IVa	——,,——	Cl	SO
V	$CO-(CH_2)_2-NEt_2$	Cl	S
Va	——,,——	Cl	SO
VI	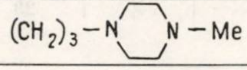	Cl	S
VIa	——,,——	Cl	SO
VII	$(CH_2)_3-NMe_2$	CF_3	S
VIIa	——,,——	CF_3	SO
VIII	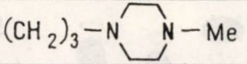	CF_3	S
VIIIa	——,,——	CF_3	SO
IX	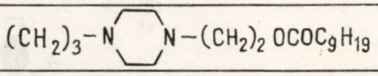 (CH2)3—N N—(CH2)2 OCOC9H19	CF_3	S
IXa	——,,——	CF_3	SO
X	$CH_2-CH(CH_3)-NMe_2$	OMe	S
Xa	——,,——	OMe	SO
XI	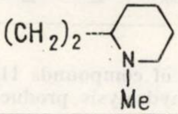	SMe	S
XIa	——,,——	SMe	SO
XII	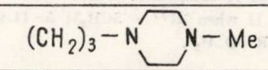	SEt	S
XIIa	——,,——	SEt	SO
XIIb	——,,——	SEt	S
XIIc	——,,——	SEt	SO

Table 2

The results of preparative hydrolysis

Parent compounds N° from Table 1	The characterization of type II hydrolysis products					
	m. p. °C		Identification reaction		TLC data	
	found	cited[12–14]	H_2SO_4	DPPH	$R_f \times 100$	D_2
VII	187	188–189 188–190	+	+	75	Orange-red
IV	198	196–199	+	+	64	Red
V	198	196–199	+	+	64	Red
III	181	180–185	+	+	53	Orange-red
XI	139	138–139 138–140	+	+	44	Blue-green
X	184	—	+	+	23	Violet

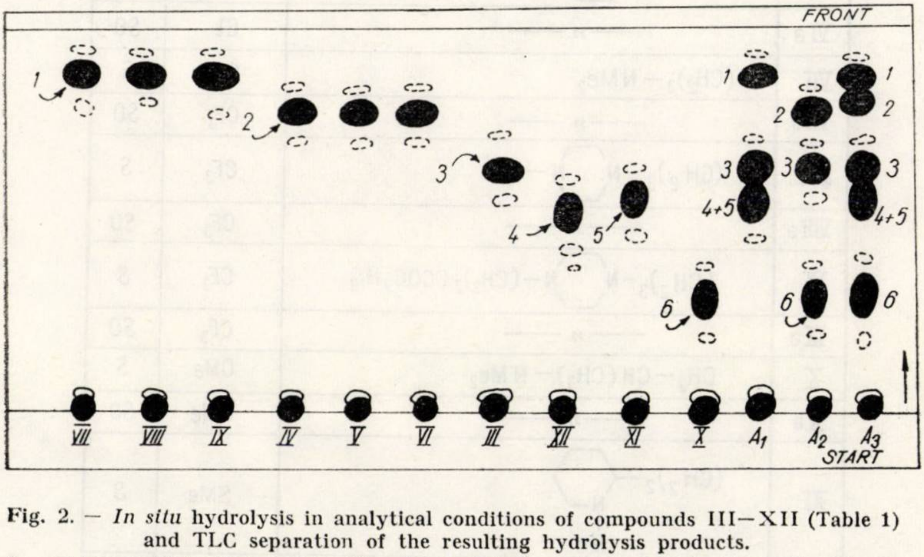

Fig. 2. — *In situ* hydrolysis in analytical conditions of compounds III—XII (Table 1) and TLC separation of the resulting hydrolysis products.

A_1 = mixture of VII (or VIII, or IX) + III + XII (or XI): A_2 = mixture of IV (for V, or VI) + III + X; $A_3 = A_1 + A_2$: Spots 1–6 corespond to the following type II compounds (Figure 1): 1 = II when ($R'' = CF_3$); 2 = II when ($R'' = Cl$); 3 = II when ($R'' = H$); 4 = II when ($R'' = SCH_3$); 5 = II when ($R'' = SC_2H_5$): 6 = II when ($R = OCH_3$).

---

[12] The Aldrich Europe Catalogue — Handbook of Organic and Biochemicals, 1975, 1976, p. 178, 581, 699.

[13] N. L. SMITH, *J. Org. Chem.*, **15**, 1125 (1950).

[14] E. A. NODIFF, S. LIPCHUTZ, P. N. CRAIG and M. GORDON, *J. Org. Chem.*, **25**, 60 (1960).

Analytical procedure for the identification of type I compounds (R = S)

The procedure involves two stages : a) the *in situ* hydrolysis of type I compounds (Figure 1), followed by TLC identification of the hydrolysis products and thus of the nature and the position of the substituent on the aromatic nucleus (R″) ; b) TLC identification of the nitrogen substituent (R′).

a) *Identification of the substituent on the aromatic nucleus* (R″). Samples of 50 to 100 micrograms were applied on the start line of an analytic, non activated chromatoplate. Standards of different type I compounds, with various R″ were applied next to the sample individually, or in mixtures ; 10 microliters of HI solution were applied over the sample and the "standard mixtures". The hydrolysis operations were carried out, followed by development and detection in the conditions mentioned for the preparative study. A typical chromatogram, obtained by this technique is presented in Figure 2. By comparison with the hydrolysis products of the standards, one can infer which is the R′ substituent of an unknown sample.

b) *Identification of the nitrogen substituent* (R′). Samples of 50 to 100 micrograms were applied on an activated analytical chromatoplate. Type I standards were applied in similar amounts, next to the sample, all of them having the R″ substituent identified in the first step. The chromatoplate was then developed with S_2 or S_3, dried at room temperature and the detection was carried out with D_2. Comparison with the standards led to the identification of the nitrogen substituent (R′). Thus the complete identity of the initial sample could be established. The R_f values and the detection behaviour of the investigated 2,10-disubstituted phenothiazines are presented in table 3.

Table 3

Chromatographic behaviour of type I compounds (phenothiazine bases)

N° of compound in Table 1	pK_b[19]	$R_f \times 100$		Detection with D_2
		S_2	S_3	
III	4.90	4.3	67	Orange-red
III a	—	7.5	30	Red
IV	4.78	50	77	Red
IV a	—	7	34	Red
V	—	80	81	Red
Vak	—	7.5	72	Red
VI	6.46 ; 10.40	34	59	Red
VI a	—	—	—	—
VII	4.59	50	66	Orange-yellow
VII a	—	10	42	Orange-red
VIII	5.60 ; 10.10	38	55	Orange-yellow
VIII a	—	0	27	Orange-red
IX	—	86	94	Orange-yellow
IX a	—	7.5	25	Orange-red
X	4.85	52	87	Violet
X a	—	10	43	Blue
XI	4.84	40	70	Blue-green
XI a	—	6	22	Yellow-brown
XII	—	34	62	Blue-green
XII a	—	—	30	Yellow-brown
XII b	—	—	32	Violet
XII c	—	—	12	Red

TLC conditions for the oxidation products of compounds II

Stationary phase : Activated silicagel G (Merck). For the separation of the dimers derived from compounds II the S_1 developer was used ; the order of the spots was as follows : R^f (3,10′ — or 7,10′ — diphenothiazine) $< R_f$ (II) $< R_f$(1,10′ — or 9,10′ — diphenothiazine). For the separation of phenothiazones, sulphoxides and sulphones, which had $R_f = 0$ in the previous conditions, S_4 was used as developer. The results are : R_f (sulphoxides) $< R_f$ (phenothiazones) $< R_f$(II). The detection was effected with D_1 and D_2.

RESULTS AND DISCUSSION

In situ hydrolysis and the identification of the products

The possibility of *in situ* hydrolysis of the N—C bond on silicagel has already been described for some aromatic amines. [15] We have also noted this possibility, in our previous studies for simple phenothiazines[11] (Figure 3). The present work is in fact an extension of this study[11] to the group of phenothiazine drugs.

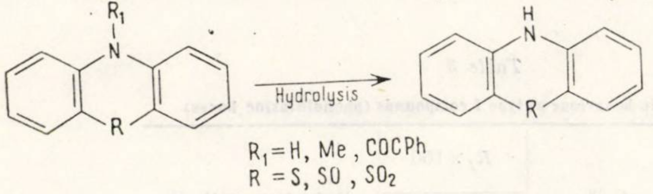

Fig. 3. — *Insitu* hydrolysis of some N-substituted phenothiazine derivatives.[11]

The hydrolysis of type I compounds has been found to depend on a series of factors such as the stationary phase used, reaction time and temperature, as well as the structure of the compounds involved. [11]

Both Al_2O_3 (Merck) and the silicagel or Al_2O_3 ready-for-use plates (D. C. Fertigplatten or Alufolien, Merck) did not provide satisfactory results. These experimental facts, correlated with our previous results[11] suggest that the hydrolysis process at the C—N—10 bond is catalyzed by a surface with Brönsted acid centers (silicagel). This is why addition of HI was advantageous and enhanced the reaction.

The hydrolysis of compounds I is influenced by the nature of the R radical only, the reaction rate decreasing in the series $H > Cl > SR > > CF_3 \geqslant OAlK$. The working conditions described in the Experimental Section were selected to provide for the conversion of all compounds. On the other hand, rising the temperature or the reaction time leads to unwanted oxidation processes. [11] Heat will result in decreased hydrolysis yields. Thus oxidation of compounds I takes place at R (leading to sulphoxides) or/and in the alkyl-amine chain (R′), when N-oxides and N-dealkylated compounds result. Compounds II are also subject to oxidation, leading to phenothiazones, sulphoxides and dimers. [11] The TLC working conditions were selected so that all oxidation products (excepting the dimers) and initial compound I should have $R_f = 0$; in these conditions the dimers could be well separated from compounds II.

---

[15] C. Prandi, *J. Chromatogr.*, **48**, 214 (1970).

The type II hydrolysis of the C—N—10 bond was probed by two reactions (Figure 4) : (i) with concentrated H_2SO_4, when the corresponding cation-radicals (IIa) were identified by ESR, and (ii) with DPPH, when the reduced form ($DPPH_2$) was identified by TLC, and a neutral radical (IIb) or (IIc), [16–18] was observed by ESR. The melting points finally certified the actual structure of the products (the nature of R″).

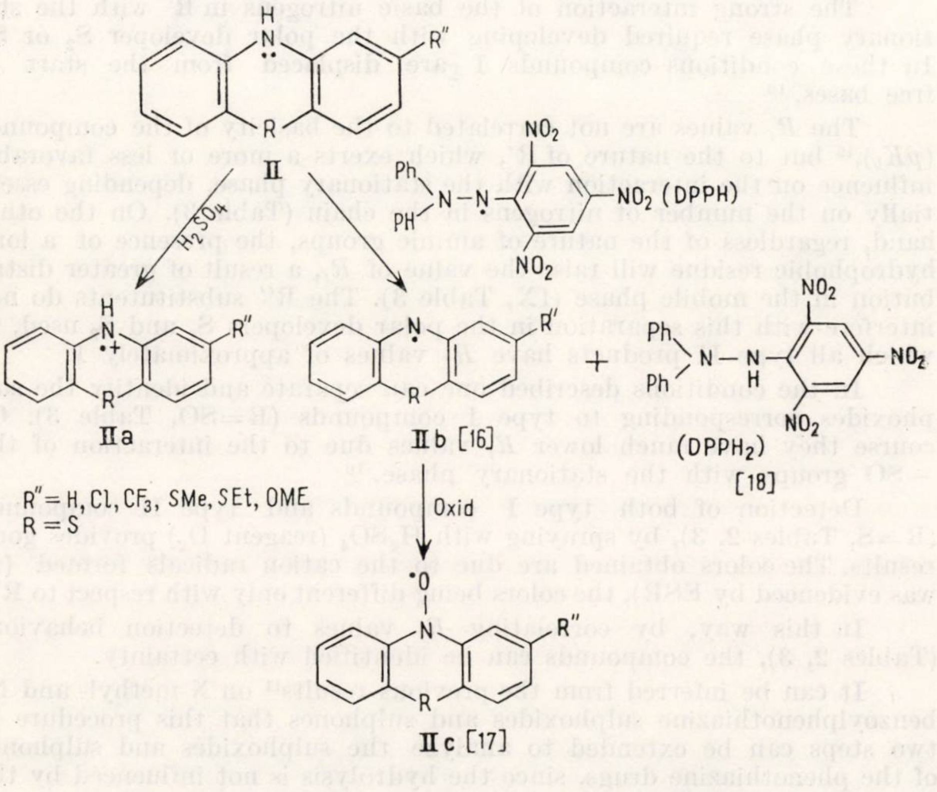
H
N
R″
R
II
Ph
Ph
N—N
NO2
NO2 (DPPH)
NO2
SO4H2
H
N
•+
R″
R
IIa
N
R″
R
IIb [16]
+
Ph
Ph
N—N
H
NO2
NO2
NO2
(DPPH2)
[18]
R″ = H, Cl, CF3, SMe, SEt, OME
R = S
Oxid
O
N
R″
R
IIc [17]

Fig. 4. — Identification reactions for hydrolysis products II.

Analytical conditions

The choice of silicagel as stationary phase for hydrolysis and of the slightly polar developer S_1 was discussed with the preparative working conditions.

The separation of compounds II in these conditions was achieved especially as a result of the inductive effect (—I) introduced by the R″ substituent (Figure 2, Table 2). The more pronounced is this effect (the case of halogens), the lower becomes the basicity of the nitrogen and the lower the interaction with the stationary phase. When heteroatoms are present in R″ (X, XI, Table 2) the −I effect is low and interactions through lone pair electrons may take place, both effects leading to low R_f values.

---

[16] C. Jackson, N.K.D. Patel, *Tetrahedron Letters*, **24**, 2255 (1967).

[17] M. F. Clim, B. C. Gilbert and P. Hanson, *J. Chem. Soc.*, (*B*), **1970**, 1700.

[18] T. Constantinescu and S. Enache, *Farmacia* (*Bucharest*), **20**, 591 (1972).

In the Experimental part we also report TLC conditions for the analysis of the oxidation products from II.

Concerning the conditions for the TLC of compounds I, some points are worth to be discussed.

The strong interaction of the basic nitrogens in R′ with the stationary phase required developing with the polar developer S_2 or S_3. In these conditions compounds I are displaced from the start as free bases.[10]

The R_f values are not correlated to the basicity of the compounds (pK_b),[19] but to the nature of R′, which exerts a more or less favorable influence on the interaction with the stationary phase, depending essentially on the number of nitrogens in the chain (Table 3). On the other hand, regardless of the nature of aminic groups, the presence of a long hydrophobic residue will raise the value of R_f, a result of greater distribution in the mobile phase (IX, Table 3). The R″ substitutents do not interfere with this separation in the polar developers S_2 and S_3 used, in which all type II products have R_f values of approximately 1.

In the conditions described one can separate and identify the sulphoxides corresponding to type I compounds (R=SO, Table 3). Of course they have much lower R_f values due to the interaction of the −SO groups with the stationary phase.[10]

Detection of both type I compounds and type II compounds (R=S, Tables 2, 3), by spraying with H_2SO_4 (reagent D_2) provides good results. The colors obtained are due to the cation radicals formed (as was evidenced by ESR), the colors being different only with respect to R″.

In this way, by correlating R_f values to detection behaviour (Tables 2, 3), the compounds can be identified with certainty.

It can be inferred from the previous results[11] on N-methyl- and N-benzoylphenothiazine sulphoxides and sulphones that this procedure in two steps can be extended to analyze the sulphoxides and sulphones of the phenothiazine drugs, since the hydrolysis is not influenced by the nature of R′ and R.

The sensitivity of the procedure described ranges between 50−100 micrograms of compound and is conditioned by the following points: the hydrolysis reaction is not quantitative; secondary oxidation processes take place; the sensitivity to detection with H_2SO_4 is of approximately 10 micrograms of compound.[10] These values are satisfactory for the currently performed analyses in pharmaceutical laboratories. These limits can be further lowered when fluorescent supports are used.

The method described can be extended, as shown by our preliminary work, to the study of some therapeutical analogs of phenothiazines of the dibenzoazepines series. Thus dibenzoazepines (Figure 5) could be analyzed by TLC following hydrolysis in the conditions described for phenothiazines.

---

[19] L. G. Chatten and L. E. Harris, *Analyt. Chem.*, **34**, 1495 (1962).

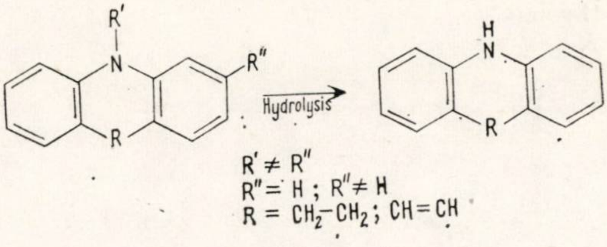

Fig. 5. — The *in situ* hydrolysis reaction of the dibenzoazepine derivatives.

For detection the D_1 method and spraying with aqueous 5% solution of $K_2Cr_2O_7$ diluted (1 : 1 V/V) with ethanol[6] are indicated.

For other therapeutical analogs as benzdiazepines or thioxanthenes the method was found unsuitable. This fact represents a possibility to distinguish them from the other heterocyclic drugs.

ACKNOWLEDGEMENTS. We thank Agneta Caragheorgheopol and Horia Căldăraru from the Centre of Physical Chemistry of Bucharest for the ESR measurements.

Revue Roumaine de Chimie, 23, 6, 977–982 (1978)

HETEROCYCLIC COMPACT CONDENSED SYSTEMS III[1]

ISOMER 9-AMINOTHIAZOLO [4,5-f] INDAZOLE

C. TĂRĂBĂŞANU-MIHĂILĂ, F. URSEANU, L. FLORU and B. MĂRCULESCU*

Laboratory for the Technology of Aromatic Intermediates and Organic Dyes, Polytechnic Institute, Bucharest, Calea Victoriei 149 and

* Laboratory of Macromolecular Chemistry, Polytechnic Institute, Calea Victoriei 149, Bucharest, Romania

Received April 29, 1976

A new possibility for synthesis of isomer 9-aminothiazolo [4,5-f] indazole and its derivatives-dispersion and catonic dyes was studied.

1. INTRODUCTION

9-Aminothiazolo [4,5—f] indazoles have been synthetised by Bellavita[2] in 1968, for pharmaceutical purposes.

In our earlier papers[1, 3] we described various new possibilities for the synthesis of the compound I, as well as the ways of obtaining some dispersion and cationic dyes, derivatives with remarkable tinctorial properties.

The introduction of the compact condensed thiazolo-indazole system into the structure of days proved a possibility of extending the field of the colour shade and of increasing the colour yields, by comparison with similar compounds with indazole or benzthiazole structures.

In the present paper we report on the results of our experimental investigations regarding the synthesis of the compound II and its monoazoic derivatives, which are valuable cationic and dispersion dyes.

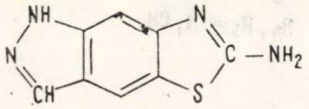

I

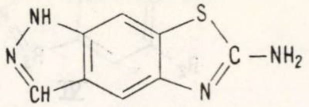

II

---

[1] C. Tărăbăşanu-Mihăilă, L. Floru and M. Olteanu, *Rev. Roumaine Chim.*, **18**, 2113 (1973).

[2] C. Bellavita, N. Martani and F. A. Amaldo, *Ann. Chim. (Ital.)*, **58**, 823 (1968).

[3] C. Tărăbăşanu-Mihăilă, L. Floru, E. Baltă and A. Predescu, *Rev. Roumaine Chim.*, **18**, 889 (1973).

2. RESULTS AND DISCUSSIONS

2. 1. Synthesis of compound II

9-Aminothiazolo [4,5—f] indazole (II) was obtained according to the following reaction sequence :

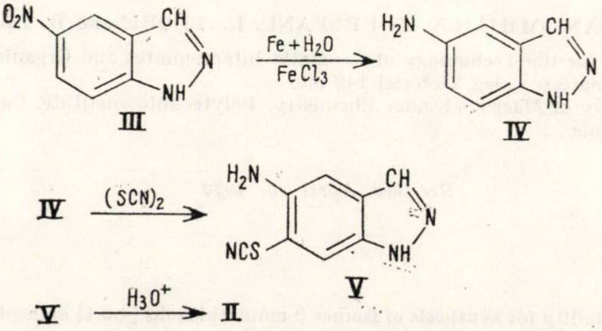

5-Nitroindazole (III) was prepared by the method described by Meunier[4] (m.p. 208—209°). Its reduction to 5-aminoindazole (IV) was carried out with iron in aqueous medium, in the presence of ferrous chloride as electrolyte.

For the reasons already mentioned in our preceding papers[1, 3] we used the thermal decomposition reaction of cupric thiocyanide as dithiocyanate source, and not the action of bromine on the alkaline thiocyanides as it was proposed by Bellavita[2].

$$2Cu(SCN)_2 \rightarrow Cu\ SCN + (SCN)_2$$

2. 2. IR Spectral behaviour of the compound II

Considering Sullivan's observations that in the heterocyclic derivatives of type VI[5, 6]

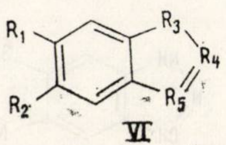

VI

$R_3 = CH_2, O, NH, CO, SO_2$

$R_4, R_5 = N, CH$

the overall shape of the spectrum is affected by the nature of the R_1 and R_2 substituents only by the introduction of their characteristic bands, it would be expected that the derivatives of type II to obey this rule, their spectra showing an additive character. We extended Sullivan's finding to the compounds of type I where two compact condensed heterocyclic systems retain their spectral individuality.

---

[4] J. Meunier, *Bull. Soc. chim. France*, **1904**, 641.

[5] D. G. O'Sullivan and J. Sedler, *J. Org. Chem.*, **22**, 283 (1957).

[6] D. G. O'Sullivan, *J. Chem. Soc.*, **1960**, 3.278

From the spectral data presented in table 1 it may be seen that this is a real fact. The main fundamental bands of the compounds with indazole rests (III and IV) as well as of those of benzothiazole (VII) reappear in the spectrum of 9-aminothiazolo [4,5-f] indazole (II).

Table 1

IR – bands of the compounds II and IV

II	3425 s			2 225 s	2 950 s	2 900 s
IV		3 360 m	3385–3050 s			
II	2 740 m	1 760 s	1 650 m	1 600 s	1 580 m	
IV				1 620 s		1 530 s
II	1 480 s	1 430 w	1 400 w		1 355 m	
IV	1 460 m			1 380 s		
II	1 325 m	1 265 s	1 195 s	1 140 m	1 110 m	
IV	1 340 s	1 245 s	1 185 s			
II	1 090 s	1 040 m	1 000 w	980 m	930 m	850 m
IV	1 085 s			960 s		
II	830 w	815 s		750 m	655 m	
IV	840 w	820 m	795 w	740 m		
II	625 m	600 w	555 m	455 m	425 m	
IV	625 m					

The following bands have been assigned:

1. Bands situated at 655 and 625 cm^{-1}, corresponding to the C–S bond, as it was established by Suresh et al.[7]

2. Bands situated at 980–850 cm^{-1}, characteristic for the thiazole system.[3]

3. Bands situated at 1620 and 1580 cm^{-1}, characteristic for the benzothiazole rest.[8–9]

4. All bands typical of the indazole system, situated at 1480, 1325, 1265, 1140, 1110, 1040, 850 and 750 cm^{-1}.

Vibration frequency of the C=N bond which is situated in the range 1660–1620 cm^{-1} for the indazoles, appears in the IR spectrum of the compound II at 1620 cm^{-1}.

---

[7] K. S. Suresh, J. Ramachandran and G. N. R. Rac, *J. Sci. Ind. Rec. India*, **208**, 2031 (1961).

[8] J. M. Bonnier, M. Gelus and B. Papoz, *Bull. Soc. chim. France*, **1965**, 2485.

[9] A. Taurins, J. G. E. Fenyes and R. N. Janes, *Canad. J. Chem.*, **35**, 423 (1957).

9-Aminothiazolo [4,5-f] indazole has very weak harmonic bands, between 2000–1650 cm^{-1} (indicated in table 1). That is also a common feature of all indazole compounds.[6]

The maximum at 1480 cm^{-1} may be assigned to the ∂_{NH} deformation or to a cycle vibration.

The broad band situated between 3385–3050 cm^{-1} probably includes ν_{HH} involved in strong intermolecular hydrogen bonds ; one of the characteristic ν_{CH} bands (situated at 3065 cm^{-1} for the compound I), as well as ν_{NH_2} sim (at 3385 cm^{-1} in the case of the compound VII).

5. In addition, for 9-aminothiazolo [4,5-f] indazole the following bands have been assigned :

$$\nu_{CH} = 2950 \text{ cm}^{-1} \text{ and } \nu_{NH_2} \text{ asim.} = 3425 \text{ cm}^{-1}.$$

It has been found a great similarity between the IR spectral behaviour of the products I and II, in both cases the IR spectra having a pronounced additive character.

2.3. Dispersion dyes, derivatives of the compound II

The synthesis of monoazoic compounds was carried out according to the following reaction sequence :

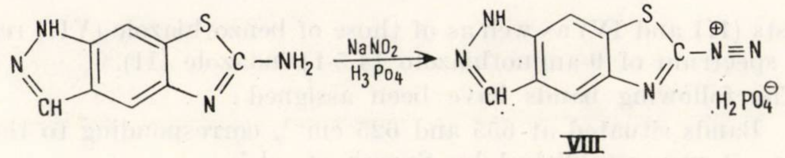

VIII

(5)

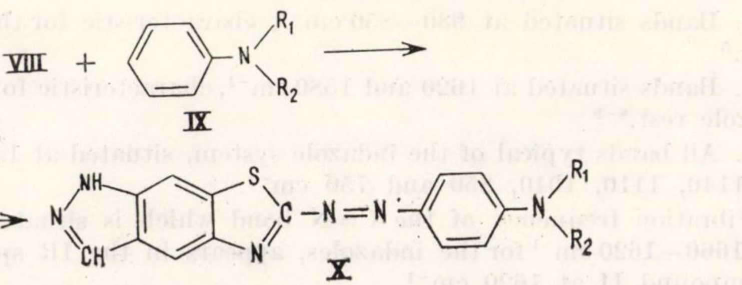

(6)

Table 2 gives the data regarding the synthesis and the tinctorial properties of the compounds of type X, which have been found to be remarkable dyes for cellulose acetate and polyester fibres.

Table 2

Data regarding the synthesis and tinctorial properties of the compounds X

R_1	R_2	Obtaining of the compound VIII					Coupling reaction				Tinctorial results	
		Comp. II g	Solvent (ml)	$NaNO_2$ g	Temp. °C	Time hrs.	Comp. IX g	Solvent (ml)	Temp. °C	%	Colour on cellulose acetate	Colour on polyester fibres
H	CH_3	10	H_2SO_4 (35)	2.6	0	4	4.2	CH_3COOH 70% (60)	0	65	orange	red-orange
CH_3	CH_3	10	H_3PO_4 (25)	2.6	−15	2.5	4.5	CH_3COOH 70% (60)	0	70	red-violet	cherry-coloured
C_2H_5	C_2H_5	10	HCl 15% (25)	2.6	−5	4	5	H_2O (200)	0	60	cherry-coloured	cherry-coloured
C_2H_5	C_2H_4OH	10	H_3PO_4 (25)	2.4	−15	2.5	8.2	H_2O (200)	0	55	cherry-coloured	cherry-coloured

2.4 Cationic dyes

As it was shown in our earlier paper[3], by methylation of the compact condensed thiazolo-indazole system, the methyl group is grafted at the nitrogen atom of the thiazole rest.

Using as methylation agent-dimethyl sulfate in aqueous medium (7.5% compound X, 50% water, 42.5% dimethyl sulfate, at 65–70°) one obtains the products XI which are dyes with remarkable properties for dyeing polyacrylic fibres in dark blue-violet colour shades.

Table 3

Tinctorial properties of compounds XI

R_1	R_2	Colour on polyacrylic fibres
H	CH_3	blue-red
CH_3	CH_3	blue
C_2H_5	C_2H_5	blue
C_2H_5	C_2H_4OH	blue-violet

In table 3 the data regarding tinctorial properties of the compounds XI are presented :

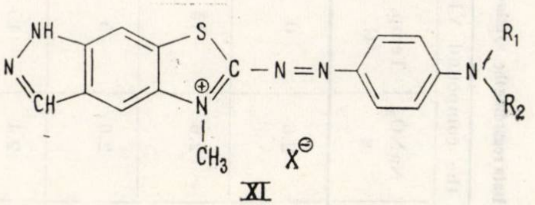

XI

EXPERIMENTAL

Synthesis of 9-aminothiazolo [4,5-f] izomer indazole

Introduce 620 ml glacial acetic acid into a 2.5 liter 3-neck flask, equipped with stirrer, reflux refrigerator and thermometer. When the temperature reaches 10° (external cooling) add 121.6 g ammonium thiocyanide under vigourous stirring, then 200.4 g crystallised copper sulfate. The colour of the reaction mixture turns black owing to the $Cu(SCH)_2$ formation.

Add 20 g 5-amino-indazole, keeping the temperature constant at 10°. Continue stirring for 90 minutes at 10° and then increase slowly the temperature up to 40° during a time interval of 90 minutes. Keep the reaction mixture at this temperature under stirring for 6 hours.

The reaction mass turns yellowish-brown owing to the formation of cuprous thiocyanide.

Pour the mixture from the neck-flask into 1500 ml at 80° and keep the formed suspension under stirring. Add to the filtrate 6 g animal charcoal and filter it again at 80°.

After cooling up to 20°, alkalinize the filtrate with $NaHCO_3$ up to pH = 8.5.

The resulting precipitate, 9-amino-thiazolo [4,5-f] izomer indazole is filtered and dried at 40—50°.

One obtains 15 g of the product II (yield : 65 %). Its purification was carried out by successive precipitation from an alcohol-water mixture.

The elementary analysis for $C_6H_6H_4S$ gave : N% calc. 29.47%, found 29.70% ; S% calc. 16.84% ; found 17.00%.

The infrared spectra were taken in KBr disk using a UR-10 spectrophotometer.

4. CONCLUSIONS

1. A new method for the synthesis of izomer 9-amino-thiazolo [4,5-f] indazole was established, using cupric thiocyanide as dithiocyanate source.

2. The introduction of this heterocycle into the structure of azoic dispersion and cationic dyes leads to products with remarkable tinctorial properties, applicable in the dyeing of the hydrophobic synthetic fibres. These products are not reported in the literature.

Revue Roumaine de Chimie, **23,** *6*, 985–988 (1978)

COMPTES RENDUS

A. GRAOVAC, I. GUTMAN, and N. N. TRINAJSTIĆ, "Topological Approach to the Chemistry of Conjugated Molecules", Springer, Berlin — Heidelberg — New York, 1977, 123 p.

As part 4 of the series entitled "Lecture Notes in Chemistry", Springer Verlag has published by direct reproduction of the authors' manuscript an interesting exposition on applications of graph theory and topology to theoretical organic chemistry.

After a brief introduction, the second chapter (44 pages) presents basic definitions of graph theory, making thus the review understandable for a wider audience, even without a background in this field. A glossary is given for correspondences between graph-theoretical and quantum-chemical terms. The graph-theoretical definitions are given in detailed form, introducing also directed graphs, though these are little used in the review. The mathematical treatment is judiciously balanced so that it is within grasp of most theoretical, and many organic chemists ; even though it does make use of matrix algebra, the present book exemplifies many results also by simpler, more intuitive methods.

A central part of this second chapter is occupied by the Sachs theorem which was used extensively by the Yugoslav school of chemically-oriented graph-theorists in order to obtain important results. It is gratifying to read a clear exposition of their main achievements written in a systematic exposition.

The third chapter (31 pages) discusses the total pi-electron energy of conjugated systems. The importance of the topological approach is that it often gives quite accurate results without having recourse to elaborate calculations or to computer programs. The fact that the eigenvalues of the adjacency matrix **A** are identical to the energies of the molecular orbitals (MO's) (in β units, relatively to the Coulomb integral α taken as zero) obtained by the Hückel MO method demonstrates that the topology of the molecule, as expressed by its adjacency matrix **A**, determines its energy.

The approximate McClelland formula relating the pi-electron energy E_{pi} to the number of vertices (N) and edges (M) in the molecular graph of a completely conjugated compound

$$E_{pi} = 0.92\sqrt{MN}$$

illustrates the fact that about 95% of the pi-electron energy is determined by the magnitude of the molecule. However, for discriminating among energies of isomeric systems, further refinements are necessary. The authors indicate such refinements which result in adding further topological terms to the McClelland formula. Among acyclic conjugated systems, the highest E_{pi} corresponds to the linear polyene, followed by the 3-vinylpolyene. The authors show how branching affects E_{pi}, leading to violations of the basic postulate of resonance theory : a highly branched "comb graph" with $N \geqslant 18$ atoms has a lower E_{pi} than an isomeric 2-methylenepolyene system, though the latter has fewer Kekulé structures than the former.

The Hückel rule and its generalized forms are easily obtained by means of the graph-theoretical approach. No mention is made, however, of cata-condensed systems which obey the Hückel rule, yet do not have a closed pi-electron shell, as first observed by Bochvar. An important development of the last two decades is the recognition starting with Dewar, Longuet-Higgins and Coulson in 1952 that the stability of conjugated systems correlates with the algebraic structure count (ASC) rather than with the number K of Kekulé structures. This was further developed by C.F. Wilcox Jr., W.C. Herndon, J. Kruszewski and T.M. Krygowski, and by the Yugoslav authors. The early successes of resonance theory, which are still exposed in most textbooks of organic chemistry, are due to the fortuitous coincidence that, for benzenoid systems, K = ASC. The general expression for an arbitrary conjugated system is, however,

$$\det \mathbf{A} = (-1)^{N/2}(\mathrm{ASC})^2.$$

Thus, for instance, on treating the adjacency matrices of [4]-, [6]-, and [8]-annulene as determinants, one obtains det **A** = 0, 4, and 0, respectively. This indicates that for [6]annulene (benzene) there are 2 Kekulé structures of the same parity, while for cyclobutadiene and cycloöctatetraene there are two structures each of opposite parity. This explains why the former is aromatic while the latter are not.

Chapter 4 (16 pages) discusses the resonance (delocalization) energy, showing the improvement brought by Dewar when defining what is now known as Dewar resonance energy. The authors show that a simpler but as, or more, powerful tool is the topological resonance energy defined and calculated by using the Sachs theorem. Examples of applications are given for conjugated hydrocarbons, heterocyclics, and ions, i.e. cases where the Dewar resonance energy is not easily calculated.

In the fifth and last chapter (19 pages), by making use of Dewar's PMO approach and by fragmenting the molecules into systems possessing non-bonding MO's (NBMO's), the localization energies and reactivities (regioselectivities) may be predicted. The eigenvectors of NBMO's can be obtained graphically very easily, without laborious computations. Thus the reactivity order *peri* $> \alpha > \beta$ for anthracene, and the tricky order $\beta > \alpha$ in biphenylene result without difficulty.

The book is easy to read, and gives a unified treatment of important findings which should be incorporated into the present-day teaching of organic and theoretical chemistry at all levels. Each chapter has a brief summary. The bibliography of 166 quotations up to, and including 1977, serves well the reader. A subject index is a useful help. Typing errors are few. In two cases, definitions are given after the first mention of the topic, where the index does not prove to be of assistance : algebraic structure count, ASC, pages 54 and 71 ; and the trace of a matrix, pages 16 and 52. For the Western reader, the extensive quotation of the Yugoslav literature will be very useful ; less useful in this case appear books such as A.A. Zykov's on graphs (when R.J. Wilson's book is not quoted) or A.G. Kurosh's book on higher algebra, because they are in Russian. One reference which would have been appropriate (because it was a similar review) was written by D.H. Rouvray as a book chapter. On page 22 it would have been relevant to mention that at long last the four colour problem (or conjecture) has now become the Four Colour Theorem.

In conclusion, the Lecture Notes analyzed here are highly recommended to all those interested in modern developments concerning theoretical organic chemistry, chemical applications of graph theory and topology, as well as teaching modern organic chemistry to chemistry students.

Alexandru T. Balaban

LANDOLT-BØRNSTEIN, "Numerical Data and Functional Relationships in Science and Technology," New Series, II/9, Magnetic Properties of Free Radicals, Part b, Springer-Verlag, Berlin-Heidelberg-New York, 1977, 782 p.

Published only a few months after the first part of the volume II/9, the second part, II/9b, is a new supplement to volume II/1 "Magnetic Properties of Free Radicals", published in 1965 in the Landolt-Børnstein new series. This part compiles the magnetic properties (the spin-Hamiltonian parameters g and a_r) for organic C-centered radicals reported in the literature since 1964.

The first chapter, written by Fischer and Paul, deals with the magnetic properties of nonconjugated carbon radicals. In the class of nonconjugated carbon radicals alkyl radicals and σ-electronic carbon radicals are included. The group of alkyl radicals is further divided into the subgroups of primary, secondary and tertiary alkyl radicals for which the radical carbon is a part of an acyclic structure and the subgroups of mono- and polycyclic alkyl radicals. Within the group of σ-electronic carbon radicals the subgroups of vinyl, aryl and acyl type radicals are distinguished.

The second chapter, written by Berndt, tabulates the magnetic properties of carbon radicals with conjugated π-systems. It contains the conjugated systems with 3 π-electrons (allyl, substituted allyl, cyclopropenyl, propargyl, et. al.), 5 π-electrons (pentadienyl, pentadiinyl, cyclopentadienyl, cyclohexadienyl, et. al.), 7 π-electrons (heptatrienyl, cycloheptatrienyl, cyclooctatrienyl, benzyl, et. al.), 9 π-electrons (cyclooctatetraenylmethyl, indenyl, et. al.), 11 π-electrons (anion radicals from methylnaphtyl ketone, α-naphtonic acid, et al.), 13 π-electrons (perinaphtenyl, diphenylmethyl, fluorenyl, et. al.) and 19 π-electrons (triphenylmethyl, 9-phenylfluorenyl, 9-phenylxanthyl, et. al.).

The volume is a comprehensive compilation of information published in this field since 1964. The first chapter covers the literature from 1964 to the end of 1975 and the second one from 1964 to the end of 1976. Some important references of early 1976 and 1977, respectively, were included as well.

The book is an excellent source of bibliography and represents a precious guide for theoretical chemists and experimental spectroscopists working in organic radical chemistry.

V. Drăguţan

A. OZAKI, "Isotopic studies in heterogeneous catalysis", Academic Press, New York, 1977, 239 pp.

A milestone in the investigation of the mechanisms of chemical reactions was the discovery of deuterium in 1931. Soon after this, isotopic methods have become of great utility in understanding the chemical reactions, especially heterogeneous catalytic ones such as hydrogenation, isomerization and oxidation of olefins, and ammonia synthesis.

A correct use of the isotopic data may reveal the unknown steps of the reactions, and thus it may lead to the true mechanism. Also, isotopic information are sometimes used as a tool for confirmation of a proposed mechanism. In other way, utility of the applications of isotopic techniques to heterogeneous catalysis research is illustrated by the great number of recent publications in this field.

The present volume reviews the fundamental principles of isotopic studies, as well as the applications of isotopes to the heterogeneous catalysis. Chapter 1 has an introductory character. Chapters 2 and 3 present various exchange reactions and their applications. Reaction path studies, as determined by the use of tracers, are the subject of Chapter 4. Chapter 5 deals with relative rates of the elementary steps involved in the reaction path. The last chapter discusses the isotope effects, which are quite important as ones of the few sources of information on the reacting molecules.

The topics covered are of current interest, and at present no other updated reviews are available. This monograph is clearly and concisely written, and provide a convenient-to-use and comprehensive source of current knowledge in the field. The book is recommended without any reservation to all who are involved in the catalytic reaction research.

T. Chirulescu

STRUCTURE AND BONDING vol. 29 Springer Verlag, Berlin, 1976, 219 p.

Under the title "Biochemistry", the 29th volume of the series contains four large sections. The object of the first "The molecular basis of dinitrogen fixation" by W.G. Zumft is a study about new insights into the biological reduction of dinitrogen and the biocatalyst nitrogenase. Dinitrogen fixation is a mode of transmition a reduced form of nitrogen to bacteria and plants, protein synthesis being affected in this way. Nitrogenase, a complex of two different proteins, containing molybdenum and iron-sulphur groups, catalyzes a reductive breakdown of the nitrogen molecule, to ammonia molecule. During this reaction, ATP is hydrolysed to ADP, through a complex formation with divalent metal ions, before interacting with the enzyme. The presented studies about molecular weight, oxygen sensitivity and cold inactivation, as well as the spectroscopic properties (optically, EPR and Mösbauer spectra) allow a first probing of the enzyme at the molecular level. Many general schemes of the nitrogenase reaction mechanism are described, but some discrepancies appear which probably will be improved in the near future by anaerobic techniques. The role of metals in dinitrogen fixation is recognized, especially with respects to molybdenum and iron ; both can be coordination centers for substrates and/or redox components. The dinitrogen-metal complexes and their reduction in organic solvents lead to a chemical model for studing the nitrogenase. At present one considers that the active site of nitrogenase involves a nitrogen molecule bridged between a dimetal site, but the structure of the prosthetic groups of the nitrogenase components, the role of molybdenum in enzyme catalysis and the mechanism of ATP action, remaining to be elucidated. Genetic research will certainly have also a great impact on the new N_2-fixing biosystems.

In the second paper "The uptake of Elements by biological Systems" J.J.R. Frausto da Silva and R.J.P. Williams present an overall involvement of inorganic elements in biology as well as the general features of the uptake of these elements. The inorganic elements which are considered include the closed shell metals, especially of group IA and II A and a large group of non-metals. The uptake of an element is affected by the pH, ionic strength, redox potential, solvent and chemical composition of biological media. Anions can be selectively sorbed by biological systems as readily as cations and also elements are taken up as neutral molecules. The authors put into evidence that incorporation of metal ions into specific sites is governed by thermodynamic and kinetic factors and only in this manner it is possible to distinguish the method by which biology absorbs, separates and concentrates the 20—30 important elements which it uses. Of a great interest is the parallel, presented in a suggestive Table, between the function and the chemical characteristics of the anions and the cations in a biological system.

The purpose of the 3rd paper "The δ-aminolevulinate Dehydratases : Molecular and Environmental Properties" by A.M. Cheh and J.B. Neilands is to describe recent findings pertaining to the biochemical and environmental properties of the enzyme ALA-D (δ-aminolevulinic acid dehydratase). First, the authors give a review of the enzyme catalysed reactions, the assay and the purification methods. The molecular and especially the catalytic properties of liver ALA-D are discussed, taking into account the influence of metal ions. A large part is devoted to the role of zinc and it is concluded that evidence from *in vivo* experiments, suggests that Zn^{++} is required for the synthesis of ALA-D. On the other hand this enzyme is considered to be the most sensitive to environmental exposure to lead and the ALA-D level of erythrocites is presented as a specific indicator of body burden of lead.

Chapter four "The Biological Chemistry of Gold" by P.J. Sadler is concerned with the molecular basis of the biological effects of gold compounds. Here, the two major areas of interest are gold as a metallodrug and as a heavy atom label. The discussion proceeds by examining the involvement of gold in its various oxidation states and the reactivity of gold complexes towards ligand displacement reactions and redox processes. A great part is devoted to Au(I) compounds which have an antiinflamatory activity, but in solution they are too toxic, for clinical use. It is suggested that the few detailed studies of Au(I) binding sites on large molecules such as proteins must be supplied by labelling studies on crystalline proteins for the specific investigation of the coordination geometry for the bound gold ion. Many Au(III) compounds are strong oxidising agents and when used as drugs, they can be reduced to Au(I) *in vivo*. Au (II) compounds are very instable in aqueous solution, but they might be of importance as intermediates in redox reactions of Au(I) and Au(III) when one electron redox reagents are used. In the field of chemotherapy, gold drugs should be viewed not only as a potential cure for a disease, but also as a probe for discovering the cause.

The material included in the volume is presented in a clear and concise manner; it might be extremely useful to all those concerned with research or development in the biochemistry field. Each paper ends with very large up-to-date references.

C. Mărculescu

NOTE POUR LES AUTEURS

La Revue Roumaine de Chimie publie des articles en anglais, français, russe, allemand ou espagnol. Les auteurs sont priés d'envoyer des articles et des comptes rendus inédits.

Les manuscrits seront dactylographiés à deux intervalles. La bibliographie, les tableaux et la légende des figures seront placés après le texte.

Si l'article fait partie d'une série numérotée, le titre de la partie précédente sera indiqué dans une note au bas de la première page.

Chaque article sera précédé d'un résumé comprenant quinze lignes au maximum. Les références bibliographiques dans le texte seront faites par des exposants sans parenthèses et paraîtront comme des notes au bas de chaque page.

Les publications périodiques mentionnées dans la bibliographie seront présentées suivant les prescriptions internationales : le nom de l'auteur précédé de l'initiale du prénom, le titre du périodique abrégé conformément à « Chemical Abstracts », et souligné par une ligne, le numéro du tome indiqué par des chiffres arabes et souligné par deux lignes, suivi de la première page de l'article ; à la fin, l'année de la parution sera placée entre parenthèses. Le numéro de la revue ne sera pas indiqué si les pages du volume sont numérotées consécutivement.

Les textes des livres ou traités incluront : les noms des auteurs, les initiales du prénom, le titre du livre entre guillemets et sans être souligné, le numéro du tome précédé par l'abréviation « vol. » ou (« Bd »), le numéro de l'édition, les éditions (the publisher), la localité de la parution du livre, l'année de la parution et la page de la référence précédée(s) par l'abréviation « p » (ou « S »).

Les brevets seront indiqués comme suit : l'auteur ou la firme, le pays et le numéro du brevet, la date et la revue (Chem. Abstr.). Par ex. : M. Jones (to Union Carbide C^{o}), Brit. Pat. 601 238,2 Sept. 1959, Chem. Abstr., **54**, 12808 (1960).

Les diagrammes seront tracés à l'encre de Chine sur papier calque. Les tableaux et les figures (en nombre strictement nécessaire) seront numérotés par des chiffres arabes. Les courbes dans les figures seront numérotées par des chiffres arabes et leur explication sera donnée dans la légende des figures. Prière de ne pas inscrire les mêmes données dans les tableaux et les figures. Chaque tableau aura un titre. On indiquera dans le texte la place approximative des tableaux et des figures. Les formules chimiques seront incluses dans le texte ; en outre, elles seront transcrites sur papier calque, à l'encre de Chine.

Les auteurs sont priés d'indiquer les caractères italiques (en soulignant les lettres au crayon), ainsi que tout autre caractère spécial ; les préfixes *ortho*, *meta*, *para*, *cis*, *trans*, etc. seront soulignés pour indiquer leurs caractères italiques et ne seront jamais écrits avec des majuscules.

Aucune correction à la main ne sera admise sur le manuscrit. Les corrections seront frappées à la machine. Les lettres grecques ou autres symboles spéciaux seront insérés à la main à l'encre clairement.

Le manuscrit sera signé par l'auteur.

Le colonne-titre aura 50 lettres au maximum.

L'entière responsabilité du contenu des articles appartient aux auteurs.

NOTE POUR LES AUTEURS

La Revue Roumaine de Chimie publie des articles en anglais, français, russe, allemand et espagnol. Les auteurs sont priés d'envoyer des articles et des comptes rendus inédits.

Les manuscrits seront dactylographiés à double interligne. La bibliographie, les tableaux et la légende des figures seront placés après le texte.

Si l'article fait partie d'une série numérotée, le titre de la partie précédente sera indiqué dans une note au bas de la première page.

Chaque article sera précédé d'un résumé comprenant quinze lignes au maximum. Les références bibliographiques dans le texte seront notées par des exposants sans parenthèses et paraîtront comme des notes au bas de chaque page.

Les publications périodiques mentionnées dans la bibliographie seront présentées suivant les prescriptions internationales : le nom de l'auteur précédé de l'initiale du prénom, le titre du périodique abrégé conformément à « Chemical Abstracts », et souligné par une ligne, le numéro du tome indiqué par des chiffres arabes et souligné par deux lignes, suivi de la première page de l'article ; à la fin, l'année de la parution sera placée entre parenthèses. Le numéro de la revue ne sera pas indiqué si les pages du volume sont numérotées consécutivement.

Les textes des livres ou traités incluront : les noms des auteurs, les initiales du prénom, le titre du livre entre guillemets et sans être souligné, le numéro du tome précédé par l'abréviation « vol. » ou (« Bd »), le numéro de l'édition, les éditions (the publisher), la localité de la parution du livre, l'année de la parution et la page de la référence précédée(s) par l'abréviation « p. » (ou « S. »).

Les brevets seront indiqués comme suit : l'auteur ou la firme, le pays et le numéro du brevet, la date et la revue (Chem. Abstr.). Par ex. : 5. Union Carbide Co., Belg. Pat. 601 238.2 Sept. 1959. Chem. Abstr., 54, 12986 (1960).

Les diagrammes seront tracés à l'encre de Chine sur papier calque. Les tableaux et les figures (en nombre strictement nécessaire) seront numérotés par des chiffres arabes. Les courbes dans les figures seront numérotées par des chiffres arabes et leur explication sera donnée dans la légende des figures. L'auteur ne répétera pas les mêmes données dans les tableaux et les figures. Chaque tableau aura un titre. On indiquera dans le texte la place approximative des tableaux et des figures. Les formules chimiques seront incluses dans le texte ; en outre, elles seront transcrites sur papier calque, à l'encre de Chine.

Les auteurs sont priés d'indiquer les caractères italiques en soulignant les lettres ou mots, ainsi que tout autre caractère spécial. Les préfixes trans, cis, para, etc. seront soulignés pour indiquer leurs caractères italiques et ne seront jamais écrits avec des majuscules.

Aucune correction à la main ne sera admise sur le manuscrit. Les corrections seront frappées à la machine. Les lettres grecques ou autres symboles spéciaux seront insérés à la main à l'encre de Chine.

Le manuscrit sera signé par l'auteur.

Le colonne-titre aura 50 lettres au maximum.

L'entière responsabilité du contenu des articles appartient aux auteurs.

1978 NOV 9 1

TRAVAUX PARUS AUX ÉDITIONS DE L'ACADÉMIE DE LA RÉPUBLIQUE SOCIALISTE DE ROUMANIE

H. D. PURDELA (sous la direction), **Nomenclatura Chimiei anorganice** (La nomenclature de la Chimie Inorganique), 1977, 153 p., 11,50 lei.

C. DRĂGULESCU, E. PETROVICI, **Chimia structurală modernă. Chimia coordinanţei 8** (La Chimie structurale moderne. La Chimie de la coordinence 8), 1977, 947 p., 70 lei.

I. G. MURGULESCU, **Introducere în Chimia fizică, vol. I. 1. Atomi, molecule, legătură chimică** (Introduction à la Chimie physique, Ier vol., 1re Partie. Atomes. Molécules. Liaison chimique), 1976, 560 p., 2 pl., 36 lei.

P. BALTĂ, E. BALTĂ, **Introduction to the physical chemistry of the vitreous state**, coédition avec Abacus Press, 1976, 287 p., 31 lei.

I. GĂLĂŢEANU, **Radiochimia aplicată. Metode şi probleme** (La radiochimie appliquée. Méthodes et problèmes), 1976, 307 p., 19 lei.

CONST. V. UGLEA, **Cromatografia pe gel permeabil. Noi domenii de aplicare** (La chromatographie sur gel perméable. Nouveaux domaines d'application), 1976, 122 p., 6,75 lei.

GR. POPA, ŞERBAN MOLDOVEANU, **Reactivii organici în chimia analitică** (Les réactifs organiques dans la chimie analytique), 1976, 255 p., 18 lei.

I. ZUGRĂVESCU, MAGDA PETROVANU, **N-ylid Chemistry**, coédition avec McGraw Hill International Book Company, SUA, 396, p., 33 lei.

FRANCISC A. GOTHARD, **Echilibre lichid-vapori. I. Baze teoretice şi metode de calcul** (Equilibres liquide-vapeurs. I. Bases théoriques et méthodes de calcul), 1975, 263 p., 2 pl., 28 lei.

CONST. GH. MACAROVICI, D. MACAROVICI, **Chimia oxizilor dubli şi utilizările lor** (La chimie des oxydes doubles et leur utilisation), 1975, 195 p., 13 lei.

M. AVRAM, **Antidăunători** (Pesticides), 1974, 496 p., 41 lei.

ELENA CEAUŞESCU, **Research work on synthesis and characterization of macromolecular sompounds. Contributions**, 1974, 251 p., 20 lei.

DUMITRU COSTACHE, **Analiza chimică prin metoda cinetică** (L'Analyse chimique par la méthode cinétique), 1974, 276 p., 15,50 lei.

G. A. RĂDULESCU, **Proprietăţile ţiţeiurilor româneşti** (Les propriétés des pétroles roumains), 1974, 267 p., 2 pl., 18 lei.

CR. SIMIONESCU, VIORICA RUSAN, V. POPA, **Chimia algelor marine** (La chimie des algues marines), 1974, 212 p., 1 pl., 18 lei.

MARIA FITI, **Dozimetria chimică a radiaţiilor ionizante** (La dosimétrie chimique des radiations ionisantes), 1973, 240 p., 13,50 lei.

TIBERIU NĂŞCUŢIU, **Metode radiochimice de analiză** (Méthodes radiochimiques d'analyse), 1973, 384 p., 23 lei.

CRISTOFOR SIMIONESCU, MARGARETA GRIGORAŞ, AGATA CERNĂTESCU-ASANDEI, GHEORGHE ROZMARIN, **Chimia lemnului în România. Plopul şi salcia** (La Chimie du bois en Roumanie. Le peuplier et le saule), 1973, 299 p., 13 pl., 26 lei.

MIHAI FLORESCU, **Eficienţa economică a cercetării ştiinţifice** (L'efficience économique de la recherche scientifique), 1972, 115 p., 15 lei.

I. P. INFORMAŢIA c. 238

43426

Lei 25.—

$ 45 (price per year)

04 F 1103

ACADÉMIE DE LA RÉPUBLIQUE SOCIALISTE DE ROUMANIE

REFERÁLVA

R

REVUE ROUMAINE DE CHIMIE

66

TOME 23
N° 7
Juillet 1978

EDITURA ACADEMIEI REPUBLICII SOCIALISTE ROMÂNIA

Rev. Roumaine Chim.

RERCHAX, 23, 7, p. 989—1160, (1978), Bucarest

ACADÉMIE DE LA RÉPUBLIQUE SOCIALISTE DE ROUMANIE

COMITÉ DE RÉDACTION

Rédacteur en chef:

I. G. MURGULESCU, membre de l'Académie de la République Socialiste de Roumanie

Rédacteurs en chef adjoints:

A. T. BALABAN et V. EM. SAHINI, membres correspondants de l'Académie de la République Socialiste de Roumanie

Collège de rédaction:

EM. BRATU, ELENA CEAUŞESCU, ECATERINA CIORĂNESCU-NENITZESCU, CR. SIMIONESCU, membres de l'Académie de la République Socialiste de Roumanie ; P. SPACU, membre correspondant de l'Académie de la République Socialiste de Roumanie ; MARGARETA AVRAM, I. HAIDUC, D. I. MARCHIDAN, I. MOLDOVAN, G. NIAC et D. SĂNDULESCU

La Revue Roumaine de Chimie paraît 10 fois par an. Toute commande de l'étranger pour les travaux parus aux Editions de l'Académie de la République Socialiste de Roumanie sera adressée à ILEXIM, Departamentul Export—Import Carte (Livres)/Departamentul Export—Import Presă (Revues), P.O.B. 136—137, télex 11226, 3, str. 13 Decembrie, 70116 Bucarest, Roumanie

Les manuscrits, les livres et les revues proposés en échange, ainsi que toute correspondance seront envoyés à la rédaction :

REVUE ROUMAINE DE CHIMIE

125, Calea Victoriei, Bucarest, Roumanie, téléphone 50 76 80

EDITURA ACADEMIEI REPUBLICII SOCIALISTE ROMÂNIA

125, Calea Victoriei, 71021, Bucarest, Roumanie, téléphone 50 76 80

ORSZÁGOS MŰSZAKI KÖNYVTÁR ÉS DOKUMENTÁCIÓS KÖZPONT
1983

REVUE ROUMANIE
DE
CHIMIE

Tome 23, N° 7 Juillet 1978

R I. G. MURGULESCU and MELANIA BOZEŞANU, Some peculiarities of the slow oxidation reaction of methane 991–994

ŞTEFANIA ZUCA and MARIELA CONSTANTINESCU, Cationic tracer-diffusion coefficients in molten $(Tl-Alk)NO_3$ systems 995–998

M. VLAD and E. SEGAL, Langmuir's rate equation for catalytic heterogeneous reactions and the principle of detailed balance 999–1001

O. PESHEV, A remark on oxygen adsorption at semiconducting CdS . . . 1003–1004

R AURELIA MEGHEA, The kinetics of the oxidation of aniline with sodium chlorite 1005–1011

MARILENA ŞERBAN, Lindemann law of melting 1013–1021

N. I. IONESCU and P. BANYAI, Influence of oxygen on the dark conductivity of metal-free phthalocyanine 1023–1027

D. FĂTU, Decomposition of solids by volumetric measurements : kinetic study (in French) 1029–1033

CONSTANTIN GH. MACAROVICI and SILVIA BARBU, Metallocomplexes of salicylaldehyde-thiocarbohydrazone (in German) 1035–1042

D. NEGOIU and MARIA NEGOIU, Complex compounds with tri-*p*-xylylphosphine 1043–1048

V. K. SRIVASTAVA, P. K. BANERJI and G. P. SRIVASTAVA, Dielectric behaviour of DNA-metal complexes 1049–1053

ALICE VASILESCU and TATIANA ONCESCU, Dynamics of the ligand exchange in uranyl bis-(chelated) complexes. II. Configurational rearrangement of bis-(benzoylacetonate) uranyl chelate 1055–1059

R S. MAGER, I. HOPÂRTEAN, FLORICA PAIU and RUXANDRA ŢĂRANU, Determination of benzaldehyde in the catalytical oxidation products of toluene, by gas chromatography 1061–1064

ALEXANDRU T. BALABAN and MIRCEA D. GHEORGHIU, Solvent- and lanthanide-induced shifts in the ^1H-NMR spectra of 4-acetonylidene-2,6-dimethyl-[4H] pyran and its tautomeric protonated pyrylium cations 1065–1077

C. TĂRĂBĂŞANU-MIHĂILĂ, C. ZAHARIA, L. FLORU, F. URSEANU and B. MĂRCULESCU, Heterocyclic compact condensed systems. IV. Linear bis pyrazolo [2,3-d], [8,9-d] *trans*-quinacridone 1079–1084

M. ANWAR, F. I. ABDEL-HAY and M. FAHMY, Reactions on 2-phenyl-3-amino-4(3H) quinazolone 1085–1091

Rev. Roumaine Chim., **23**, *7*, p. 989–1160 (1978), Bucarest

F. GÖNCZY, A. BALOG, E. VARGHA, D. BREAZU and ILONA HALLER, Peptides. XVI. The use of β-dicarbonyl N-protected methionine and tryptophan in peptide synthesis 1093–1107

R I. PETRARIU, MONA LILIANA NEAGU, IG. POINESCU, CORNELIA LUCA and PAMFILIA PETRARIU, Degradation of anion exchangers in aggressive medium. VI. Effect of hydroxyl ions in the presence of $CuCl_2$ on the chemical stability of macroporous strongly basic quaternary ammonium anion exchangers 1109–1115

R M. S. SUBHANI and M. KHALID, Pulse radiolysis and flash photolysis studies of SeO_4^{2-} anion in aqueous solution 1117–1127

M. S. SUBHANI and Z. KAUSER, Flash photolysis decomposition of sulphate and sulphite anions in aqueous solution 1129–1137

R K. K. KAKKAR and D. C. RUPAINWAR, Extraction of thallium (III) from its chloride and bromide solutions with isoamyl alcohol (IAA) and amyl acetate (AA) 1139–1142

H. D. SCHELL, M. ŞERBAN, M. A. MATEESCU and TR. BENŢIA, Acid and alkali amylose ionic exchanger (in German) 1143–1147

G. N. RAO, V. KUMAR and H. KHAS, Polarography of methioninate complexes of cadmium (II), lead (II) and zinc (II) 1149–1152

A. K. SINGH, M. KATYAL and R. P. SINGH, Spectrophotometric determination of iridium (III) with substituted pyrimidinethiols 1153–1156

BOOKS REVIEWS 1157–1159

Revue Roumaine de Chimie, 23, 7, 991–994 (1978)

SOME PECULIARITIES OF THE SLOW OXIDATION REACTION OF METHANE

I. G. MURGULESCU and MELANIA BOZEŞANU
Center of Physical Chemistry, Street Spl. Independenţei 202, Bucharest, Romania

Received May 31, 1977

The kinetic study of the slow oxidation reaction of methane at temperatures up to 750° proves that the methane cracking occurs parallelly to the oxidation reaction, C_2H_6, C_2H_4 and C_2H_2 being its main products.

The reaction of methane slow oxidation like the oxidation of other saturated hydrocarbons exhibits special characteristics due to the chain mechanism with degenerated branching.

Among these, the most representative and frequently investigated have been the negative temperature coefficient, cool flame and two stage ignition. It should also be mentioned that the total activation energy depends on the composition of initial reaction mixture and on the temperature range which also influences the orders of reaction with respect to every reactant.

Although good deal of the slow oxidation reaction of methane has been issued, the nature of its peculiarities is far from elucidated.

In the first part of this work, the authors have conducted experiments under dynamic conditions, in silica vessels, over a 550–750° temperature range with mixtures of $2CH_4 + O_2$ and $CH_4 + O_2$, and have determined the activation energy and the rection order.[1]

RESULTS

I. The study of the relation between the concentration of CO and the reaction time has shown that for the $2CH_4 + O_2$ initial mixture, up to 650°, the curves of CO accumulation have the characteristic shape of chain reaction with degenerated branching (the first part corresponding to the induction period is followed by a section corresponding to a maximum rate of CO accumulation; finally a stationary concentration is reached), as one can notice in Figure 1 (a, b).

---

[1] I. G. Murgulescu and M. Bozeşanu, *Rev. Roumaine Chim.*, **17**, 1637 (1972).

As the temperature increases above 650° and the reaction time exceeds a certain limit, the CO concentration suddenly decreases (Figure 1, c, d) while the CO_2 concentration becomes greater as seen in Figure 2, c.

This is probably accounted for by a delayed explosion of CO, which occurs only when the concentration of CO reaches a limit value.

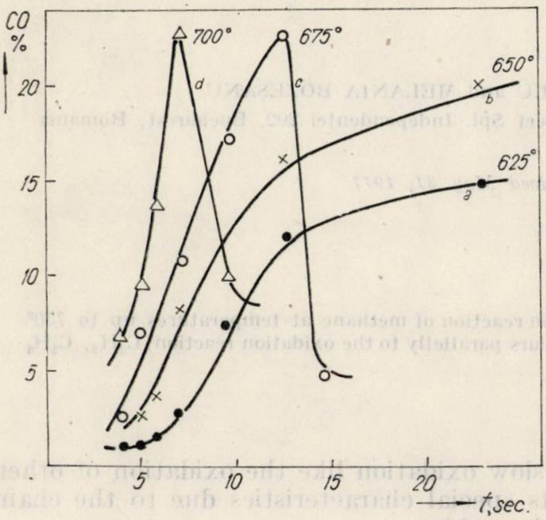

Fig. 1. — Variation of CO concentration with reaction time, for the $2CH_4 + O_2$ mixture in the temperature range of 625—700°.

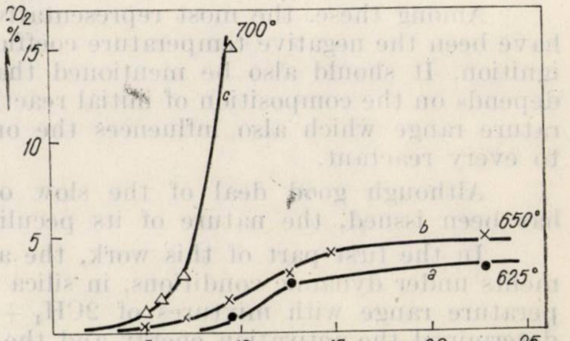

Fig. 2. — Variation of CO_2 concentration with reaction time, for the $2CH_4 + O_2$ mixture in the temperature range of 625—700°.

The same phenomenon was noticed by Hoare and Walsh [2] and by Luquin and James [3] during methane oxidation under static conditions. Luquin and James claim that whenever methane concentration in the initial reaction mixture is higher than 45% the explosion of CO does not occur. Working in dynamic conditions and at atmospheric pressure the authors noticed that the explosion of CO (its further oxidation) occurs in the initial reaction mixture of composition $2CH_4 + O_2$ (66%CH_4) but not in the mixture $3CH_4 + O_2$ (75%CH_4).

---

[2] D. E. Hoare and A. D. Walsh, "Fifth Symposium on Combustion", Academic Press, New York, 1955, p. 467, 474.

[3] H. James and M. Luquin, *J. Chim. phys.*, **70**, 422 (1973).

For the $CH_4 + O_2$ initial reaction mixture the explosion of CO occurs at considerably lower temperatures and reaction time.

II. The gaseous reaction products have been chromatographically analysed, using a 25% dimethylsulpholan column impregnated on chromosorb of suitable granulation (30—60 mesh).

The analysis has evidenced the existence besides oxidation of a cracking process, which has been confirmed by the presence in the reaction products of small amounts of ethane and ethylene.

The following reactions may account for the formation of ethane and ethylene.[4,5,6]

$$2CH_3 \rightarrow C_2H_6$$

$$C_2H_6 \rightarrow C_2H_4 + H_2$$

The accumulation of hydrogen and ethylene is presented in Figures 3 and 4.

It was established that oxidation of CO to CO_2 is accompanied by disappearance of ethane and ethylene (Figure 5) and the appearance of acetylene.

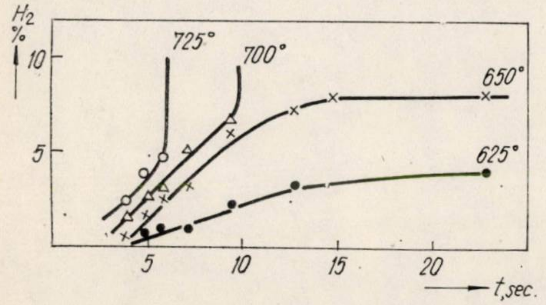

Fig. 3. — Variation of H_2 concentration with reaction time, for the $2CH_4 + O_2$ mixture in the temperature range of 625—725°.

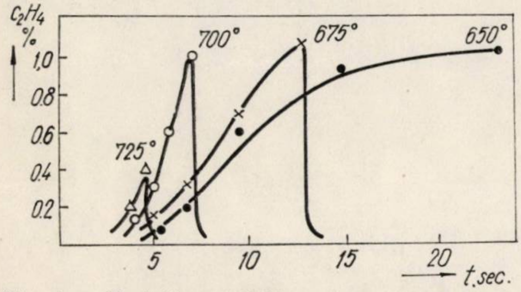

Fig. 4. — Variation of C_2H_4 concentration with reaction time, for the $2CH_4 + O_2$ mixture in the temperature range of 650—725°.

83/1.

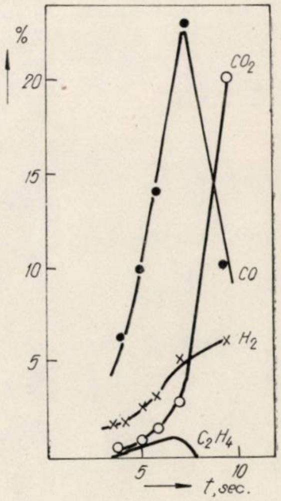

Fig. 5. — Cumulation as a function of time of the gaseous reaction products, CO, CO_2, H_2, C_2H_4, for the $2CH_4+O_2$ mixture at 675°.

---

[4] I. G. Murgulescu and I. A. Schneider, *Z. phys. Chem. (Leipzig)*, **218**, 338 (1961).

[5] R. N. Pease, *J. Amer. Chem. Soc.*, **50**, 1179 (1928).

[6] K. I. Leidler and B. W. Wojiechowski, *Proc. Roy. Soc. A*, **260**, 91 (1961).

The evolution in time of acetylene concentration at different temperatures is shown in table 1, for the $2CH_4 + O_2$ reaction mixture.

Acetylene has not been reported so far to be one of the products of methane slow oxidation reaction at a rather low temperature.

Acetylene could be a secondary product of the ethylene oxidation reaction, formed in its turn during the slow oxidation of methane.

In conclusion it could be stated that the explosion of CO occurring at certain temperatures and reaction times in methane oxidation is closely related to the oxidative cracking of C_2H_4, resulting mainly in acetylene formation.

Table 1

Variation of C_2H_2 concentration with temperature for the $2CH_4 + O_2$ initial mixture

T°	675	700	725	750
%C_2H_2	traces	0.37	1.0	1.2

Revue Roumaine de Chimie, **23**, 7, 995–998 (1978)

CATIONIC TRACER-DIFFUSION COEFFICIENTS IN MOLTEN (Tl–Alk)NO_3 SYSTEMS

ŞTEFANIA ZUCA and MARIELA CONSTANTINESCU
Center of Physical Chemistry, Splaiul Independenţei 202, Bucharest, Romania

Received December 19, 1976

The cationic tracer-diffusion coefficients in the fused (Tl–K)NO_3 and (Tl–Cs)NO_3 systems have been investigated as a function of both temperature and composition. The obtained diffusion isotherms in (Tl–Alk)NO_3 series are discussed in terms of noncoulombic contributions due to the polarizing interactions in such mixtures.

A previous paper by the authors[1] has reported the cationic tracer diffusion coefficients in molten (Tl–Na)NO_3 and (Tl–Rb)NO_3 systems as a function of temperature and composition. The ionic size and polarizability of the two uncommon ions of the mixture proved to be the relevant parameters in explaining the diffusion isotherm development. In order to extend the established regularities, the other two systems of the series were investigated: (Tl–K)NO_3 and (Tl–Cs)NO_3, for which no data are available in literature.

RESULTS AND DISCUSSIONS

The "diffusion-into-the capillary" method was used for the tracer-diffusion coefficient measurements. Details and operation were reported elsewhere[2] and it is sufficient to note that the pure KNO_3 and $CsNO_3$ were p.a. grade quality reagents and that $^{204}Tl^+$, $^{42}K^+$ and $^{134}Cs^+$ isotopes were used as tracers.

The experimental tracer-diffusion coefficients for both cations are summarized in tables 1 and 2 for (Tl–K)NO_3 and (Tl–Cs)NO_3 respectively.

The diffusion isotherms at 320° are illustrated in Figure 1 for D_{Tl^+} and in Figure 2 for D_{Alk^+}. For completness the previous data for (Tl–Na)NO_3 and (Tl–Rb)NO_3 mixtures[1] are also given. The values of cationic self-diffusion coefficients in single nitrates were taken from our previous papers.[2,3]

---

[1] S. Zuca and M. Constantinescu, *Z. Naturforsch.*, **32 a**, 1435 (1977).
[2] S. Zuca and M. Constantinescu, *Rev. Roumaine Chim.*, **17**, 385 (1972).
[3] S. Zuca and M. Constantinescu, *Z. Naturforsch.*, **32 a**, 1433 (1977).

Table 1

Cationic tracer-diffusion coefficients in molten (Tl – K)NO$_3$ mixtures

x_{TlNO_3}	t	D_{Tl^+} .10^5 cm^2 · sec.$^{-1}$	x_{KNO_3}	t	D_{K^+} .10^5 cm^2 · sec.$^{-1}$
0.75	264	1.04	0.75	317	1.31
	269	1.14		328	1.41
	286	1.43		349	1.72
	302	1.61		360	1.74
	307	1.65		374	1.99
	309	1.72			
	325	1.91	0.50	277	1.13
	260	1.02		297	1.32
				317	1.51
0.50	275	1.14		332	1.72
	283	1.17		361	2.08
	298	1.36			
	305	1.48	0.25	262	1.04
	318	1.59		294	1.36
	352	2.07		311	1.65
				342	2.07
0.25	313	1.30		353	2.26
	326	1.52			
	347	1.72			
	359	1.90			
	379	2.18			
0.10	340	1.45			
	347	1.52			
	372	1.80			
	384	1.90			
	386	1.94			
	416	2.39			

Inspection of Figures 1 and 2 points out the different behaviour of the studied mixtures. Thus, there is a linear dependence of D_{M^+} on concentration in (Tl—K)NO$_3$ and (Tl—Rb)NO$_3$ systems, while the other two systems show systematic negative deviations from linearity. As already mentioned, [1,4] these trends could be well accounted for, by Lumsden's model [5] of the competitive attractions of anion environement. The polarization energy of the common anion by the two uncommon cations in the mixtures is given as : [5]

$$E_p = -\frac{\alpha e^2}{2}\left[\frac{1}{r_{AB}^2} - \frac{1}{r_{AC}^2}\right]^2$$

---

[4] S. Zuca and M. Constantinescu, *Z. Naturforsch.*, **29 a,** 497 (1974).

[5] J. Lumsden, *Discuss. Faraday Soc.*, **32,** 138 (1961).

Table 2

Cationic tracer-diffusion coefficients in molten (Tl – Cs)NO_3 mixtures

x_{TlNO_3}	t	$D^{+}_{Tl}\cdot 10^5$ $cm^2\cdot sec^{-1}$
0.75	264	0.93
	297	1.12
	317	1.55
	327	1.71
	364	2.20
0.50	321	1.10
	330	1.17
	337	1.23
	350	1.34
	360	1.58
0.25	357	1.39
	367	1.45
	376	1.60
	405	1.87
	414	2.10
	424	2.16
0.10	411	2.00
	425	2.22
	451	2.46
	457	2.54
	472	2.72
	508	3.35

x_{CsNO_3}	t	$D^{+}_{Cs}\cdot 10^5$ $cm^2\cdot sec^{-1}$
0.75	360	1.20
	380	1.55
	384	1.59
	396	1.69
	405	1.78
	418	2.08
0.50	327	1.12
	335	1.16
	359	1.50
	362	1.50
	371	1.71
	386	1.96
0.25	272	1.05
	316	1.54
	321	1.64
	347	2.18
0.10	244	0.87
	261	1.04
	275	1.12
	280	1.19
	306	1.44
	313	1.73
	321	1.75

Accordingly, if the two cations have similar radii, $E_p = 0$, and the system is expected to behave ideally. This is the case of (Tl–K)NO_3 and (Tl–Rb)NO_3 mixtures, where the two substituting cations are almost similarly sized, (the Pauling radii are $r_{Tl^+} = 1.40$Å, $r_{K^+} = 1.33$ Å and $r_{Rb^+} = 1.46$ Å).

If the two cations in the mixture are of different sizes, the polarization interactions occur, which causes an increased (or reduced) hindrance of the relative anion-cation motion,[4-7] determining the deviation of diffusion coefficients from linearity. As follows from (1), the effect must be more marked as the difference in sizes of the two cations increases, what is confirmed by the experimental data in Figures 1 and 2 ;indeed the deviation from linearity of diffusion isotherms is larger for (Tl–Na)NO_3 than for (Tl–Cs)NO_3 and so is the difference of Pauling cationic radii (0.42 Å and 0.26 Å respectively).

[6] C. T. Moynihan and R. W. Laity, *J. Phys. Chem.*, **68**, 631 (1964).
[7] S. Forcheri and V. Wagner, *Z. Naturforsch.*, **22 a**, 1171 (1967).

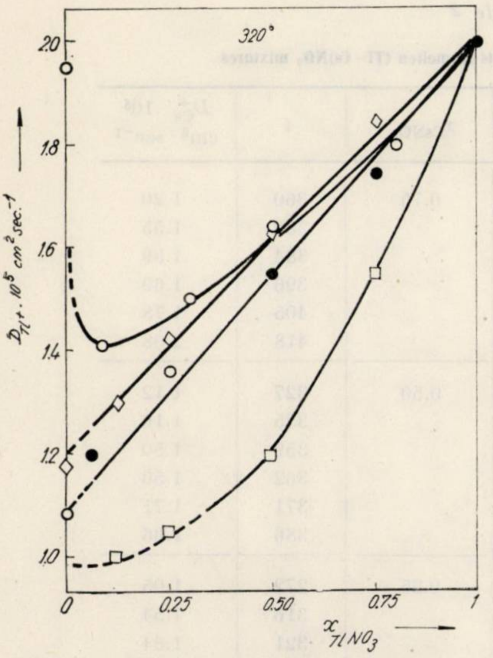

Fig. 1. — D_{Tl^+} vs. composition in molten $(Tl-Alk)NO_3$ mixtures.
○ $NaNO_3$; ◇ KNO_3 ; ● $RbNO_3$; □ $CsNO_3$

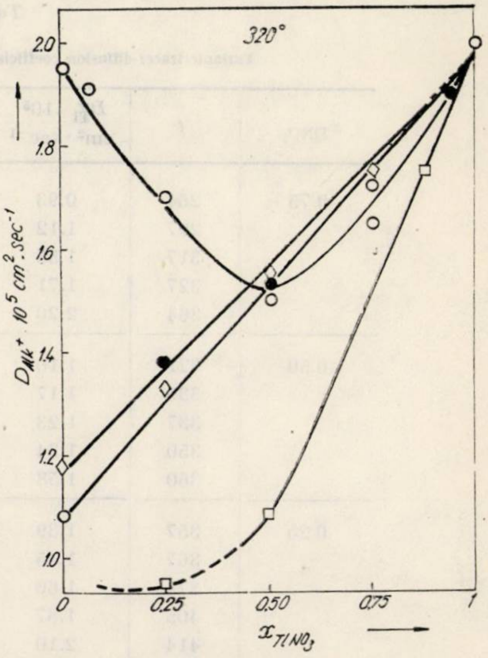

Fig. 2. — D_{Alk^+} vs. composition in molten $(Tl-Alk)NO_3$ mixtures.
○ D_{Na^+} ; ◇ D_{K^+} ; ● D_{Rb^+} ; □ D_{Cs^+}.

Moreover, in $(Tl-Na)NO_3$ system, the formation of some ionic agglomerates with Na^+ laying in the second sphere of coordination may be assumed,[1] due of the high polarizing strength of Na^+ ion and of more easily polarized NO_3^- ion in $TlNO_3$ melt.[8–10]

In conclusion, we consider that the present study establishes the important part played by the noncoulombic contributions not only in determining the equilibrium properties,[11] but the transport properties as well.

---

[8] G. J. Janz, R. P. T. Tomkins, H. Siegenthaler, K. Balasubrahmanyan, and S. W. Lurie, *J. Phys. Chem.*, **75**, 4025 (1971).

[9] D. W. James, R. D. Carlisle and W. H. Leong, *Austral. J. Chem.*, **23**, 1779 (1970).

[10] D. W. James and W. H. Leong, *Trans. Faraday Soc.*, **66**, 1948 (1970).

[11] O. J. Kleppa and L. S. Hersh, *J. Chem. Phys.*, **36**, 544 (1962).

Revue Roumaine de Chimie, **23**, 7, 999–1001 (1978)

LANGMUIR'S RATE EQUATION FOR CATALYTIC HETEROGENEOUS REACTIONS AND THE PRINCIPLE OF DETAILED BALANCE

M. VLAD and E. SEGAL
Polytechnical Institute of Bucharest, National Institute of Chemistry,
Department of Physical Chemistry and Electrochemical Technology,
Bd. Republicii nr. 13, Bucharest, Romania

Received February 28, 1976

Starting from the principle of detailed balance, this note presents a new demonstration of Langmuir's rate equation for catalytic heterogeneous reactions, accompanied by an increase of the number of molecules.

Taking into account Langmuir's work and using the second principle of thermodynamics, Temkine[1] proved that, if for a heterogeneous catalytic reaction

$$\sum_{i=1}^{s} \nu_i A_i \rightleftarrows \sum_{i=1}^{s} \nu'_i A_i, \tag{1}$$

we have $\Delta\nu = \sum_{i=1}^{s} (\nu_i - \nu'_i) > 0$, and if the rate of the forward reaction obeys the mass action law

$$r^+ = k^+ \Pi\, \theta_i^{\nu_i} \tag{2}$$

then the rate of the backward reaction is given by

$$r^- = k^- \Pi\, \theta_i^{\nu'_i} \theta_0^{\Delta\nu} \tag{3}$$

where $\theta_0 = 1 - \Sigma\, \theta_i$ is the fraction of free (uncovered) surface of catalyst.

In this note we shall prove that Eq. (3) is a consequence of a very general principle of statistical mechanics, namely the principle of detailed balance.[2,3]

---

[1] I. Langmuir, *J. Amer. Chem. Soc.*, **38**, 2217 (1916).
M. I. Temkine, *Zhur. fiz. Khim.*, **11**, 169 (1938).
S. L. Kiperman, "Vvedenye v kinetiku gheteroghennykh kataliticheskykh reactsii", Nauka, Moscow, 1964, p. 134.

[2] G. N. Lewis, *Proc. Nat. Acad. Sci. U.S.A.*, **11**, 179 (1925).

[3] R. C. Tolman, "The Principles of Statistical Mechanics", Oxford University Press., London, 1938, p. 160.

Supposing, for the sake of simplicity, that every reactant molecule interacts only with one active centre and that the reaction (1) occurs both in bulk and on surface, it turns out that in the system the following processes take place :

$$(0) \qquad \sum_{i=1}^{s} \nu_i A_i \rightleftarrows \sum_{i=1}^{s} \nu_i' A_i$$

$$(i) \qquad A_i + * \rightleftarrows A_i^* \qquad i = 1, \ldots, s \tag{4}$$

$$(s+1) \qquad \sum_{i=1}^{s} \nu_i A_i^* \rightleftarrows \sum_{i=1}^{s} \nu_i' A_i^* + \Delta\nu *$$

to which the following rate equations corresponds

$$(0) \qquad r_0^+ = k_0^+ \, \Pi \, A_i^{\nu_i}, \quad r_0^- = k_0^- \, \Pi \, A_i^{\nu_i'},$$

$$(i) \qquad r_i^+ = k_i^+ \, \theta_0 A_i, \quad r_i^- = k_i^- \, \theta_i \qquad i = 1, \ldots, s, \tag{5}$$

$$(s+1) \qquad r_{s+1}^+ = k_{s+1}^+ \, \Pi \, \theta_i^{\nu_i}, \; r_{s+1}^- = ?.$$

The principle of detailed balance states that, at equilibrium [2,3]

$$\bar{r}_i^+ = \bar{r}_i^- \qquad i = 0, \ldots, s+1 \tag{6}$$

whence we get

$$k_0^+ \, \Pi \, \bar{A}_i^{\nu_i} = k_0^- \, \Pi \, \bar{A}_i^{\nu_i'}, \tag{7}$$

$$k_i^+ \bar{\theta}_0 \bar{A}_i = k_i^- \bar{\theta}_i \qquad i = 1, \ldots, s \tag{8}$$

and

$$k_{s+1}^+ \, \Pi \, \bar{\theta}_i^{\nu_i} = \bar{r}_{s+1}^- \tag{9}$$

Supposing now that the rate r_{s+1}^- may be expressed in the classical form

$$r_{s+1}^- = g(T) \, f(\theta_0, \ldots, \theta_s) \tag{10}$$

where $g(T)$ and $f(\theta_0, \ldots, \theta_s)$ depends only on temperature and respectively on composition, from Eqs. (7), (8) and (9) we obtain :

$$\frac{\Pi \bar{\theta}_i^{\nu_i'} \bar{\theta}_0^{\Delta\nu}}{\Pi \bar{\theta}_i^{\nu_i}} = \frac{k_0^+}{k_0^-} \prod_{i=1}^{s} \left(\frac{k_i^+}{k_i^-} \right)^{\nu_i' - \nu_i} = \text{const} \tag{11}$$

and

$$\frac{f(\bar{\theta}_0, \ldots, \bar{\theta}_s)}{\Pi \bar{\theta}_i^{\nu_i}} = \frac{k_{s+1}^+}{g(T)} = \text{const} \tag{12}$$

In order that Eqs. (11) and (12) may hold simultaneously it is necessary that

$$f(\bar{\theta}_0, \ldots, \bar{\theta}_s) = \varepsilon \Pi \bar{\theta}_i^{\nu_i'} \bar{\theta}_0^{\Delta\nu} \tag{13}$$

and

$$g(T) = \frac{1}{\varepsilon} k_{s+1}^{+} \frac{k_0^-}{k_0^+} \prod_{i=1}^{s} \left(\frac{k_i^-}{k_i^+} \right)^{\nu_i' - \nu_i} \tag{14}$$

with

$$\varepsilon \neq \varphi(T, \bar{\theta}_0, \ldots, \bar{\theta}_s)$$

Insertion of Eqs. (13) and (14) into Eq. (10) leads to Langmuir's rate equation

$$r_{s+1}^- = k_{s+1}^- \Pi \theta_i^{\nu_i'} \theta_0^{\Delta\nu} \tag{15}$$

where

$$k_{s+1}^- = k_{s+1}^+ \frac{k_0^-}{k_0^+} \prod_{i=1}^{s} \left(\frac{k_i^-}{k_i^+} \right)^{\nu_i' - \nu_i} \tag{16}$$

Revue Roumaine de Chimie, 23, 7, 1003–1004 (1978)

A REMARK ON OXYGEN ADSORPTION AT SEMICONDUCTING CdS

O. PESHEV
Institute of General and Inorganic Chemistry, Bulgarian Academy of Sciences,
1000 Sofia, Bulgaria

Received May 5, 1976

Experimental data on oxygen adsorption at semiconducting CdS are reinterpreted so as to avoid the necessity of dealing with extremely low values (10^{-23} cm^2) of the cross section for electron capture by neutrally adsorbed oxygen as well as with a Henry isotherm up to monolayer coverage (10^{15} cm^{-2}).

Semiconducting CdS/oxygen is a system almost unique as an opportunity to check on adsorption theories. This is due mainly to the work of Many et al.[1–4] whose results, being both exhaustive and quantitative, are of principal importance. Consistent in itself, the intepretation given to them by the authors has two intriguing features : 1) physical adsorption must follow a linear dependence of surface coverage (θ) on pressure (P)— Henry isotherm, in the range of θ-values from zero up to the monolayer (10^{15} cm^{-2}) ; 2) the cross section for electron capture by neutral molecules of adsorbed oxygen (A_n) turns out 10^{-23} cm^2.

In [5,6] we have suggested an alternative interpretation based on the coexistence of physically and chemically adsorbed molecules at the surface. Only chemisorbed molecules are supposed to capture electrons since physisorbed species are not likely to create surface states 0.9 eV below the conduction band where the surface level of oxygen on CdS has been found to lie. Thus we identify the density M_P of the adsorbed molecules available for electron capture with the density N° of the neutral ("weak") form of chemisorption. If the quantity N° is small, its linear dependence on P will not seem surprising.

Assuming $N^\circ = 10^8$ cm^{-2} (instead of $M_P = 10^{15}$ cm^{-2} as accepted in [1,2]) we have kept unchanged the measured value of the product $A_n M_P = 10^{-8}$, all quantities referring to $P = 1$ atm. In this way we have obtained for the density of occupied surface states (charged, or

---

[1] A. Many, J. Shappir and U. Shaked, *Surface Sci.*, **14**, 156 (1969).

[2] J. Shappir and A. Many, *ibid.*, **14**, 169 (1969).

[3] A. Many and A. Katzir, *ibid.*, **6**, 279 (1967).

[4] A. Many, *CRC Critical Revs. Solid State Sci.*, **4**, 515 (1974).

[5] O. Peshev, *Lett. Nuovo Cimento*, **4**, 91 (1972).

[6] O. Peshev, *Comms. Dept. Chem. Bulg. Acad. Sci.*, **5**, 199 (1972).

"strong" form of chemisorption) $N^- = 10^{12}$ cm^{-2}, which coincides with the density of charged species (n_t) determined experimentally, and a reasonable value 10^{-16} cm^2 for A_n. But now chemisorbed molecules ($N^\circ + N^-$) are only a small fraction of the total amount of oxygen present on the surface since $\theta = 10^{15}$ cm^{-2} at $P = 1$ atm. [7]

As stated in,[4] the above mechanism is not ruled out by the experimental data. At the same time two difficulties connected with it have been pointed out : a) reducing the number of molecules active in electron capturing by a factor of 10^7 would mean an erratic and noisy relaxation in surface conductance at low pressures, which is not the case,b) it remains to explain the low values of the cross section for hole capture by charged oxygen molecules, $A_p = 10^{-20} \div 10^{-24}$ cm^2. It is our purpose to show that both of them could be alleviated to some extent.

First, the observed macroscopic kinetics of surface charging and, hence, of conductance relaxation are determined by the product $A_n M_P$. Replacing M_P by N° has not altered the value of this product : there are, indeed, 10^7 times less molecules capable of capturing an electron but each of them proves to be just as many times more active in doing it. Now why is it that with low values of $A_n M_P$ the relaxation in surface conductance is neither erratic nor noisy? For example, at $P = 10^{-5}$ torr where, according to,[1,2] $A_n M_P = 10^{-23} \cdot 10^7 = 10^{-16}$ while, according to,[5,6] $A_n M_P = 10^{-16} \cdot 1 = 10^{-16}$? Both interpretations are equally liable to this question.

In both of them smoothing is due to a statistically large number: in the former — that of less quick captures ($M_P = 10^7$ cm^{-2}), in the latter — that of capturing acts (separated by intervals $\sim 10^{-6}$ sec., i.e. 10^7 times shorter and more numerous).

Second, small values of A_p (as compared to those of A_n) might well be due to poor communication of chemisorbed oxygen with the valence band in contrast to that with the conduction band. A surface contamination by $CdSO_4$ was suggested in Weber's work [8] and accepted in.[4] It is equivalent to sulphide ions being replaced, at least partly, by sulphate ions at the surface. If so, neutrally chemisorbed oxygen will extract electrons pertaining to the valence band of CdS, i.e. from sulphide anions, at a very low rate. Then the reverse process consisting in capturing of holes by charged oxygen molecules will also be very slow on the ground of detailed balance considerations.

An experimentum crucis for the mechanisms under discussion would be the independent measurement of two quantities : oxygen adsorbed and density of surface states created by it.

---

[7] K. J. Haas, D. C. Fox and M. J. Katz, *J. Phys. Chem. Solids*, **26**, 1779 (1965).
[8] E.-H. Weber, *Phys. Status Solidi*, **36**, 175 (1969).

Revue Roumaine de Chimie, **23**, 7, 1005–1011 (1978)

THE KINETICS OF THE OXIDATION OF ANILINE WITH SODIUM CHLORITE

AURELIA MEGHEA
Department of Physical Chemistry, Polytechnic Institute,
St. Polizu 1, Bucharest, Romania

Received April 7, 1976

The kinetics of the oxidation of aniline with sodium chlorite in acidic medium was followed by means of spectrophotometrical analysis. It was found that there are two reaction stages, linearly independent, involving coloured products. The apparent rate constants of the two slow stages of the complex reaction system, as well as the influence of HCl concentration on these rate constants were determined.

The oxidation of aromatic amines is a very complex reaction, leading to a great variety of compounds. The structure and nature of these compounds depend on the nature of amine, the oxidizing agent as well as the oxidation conditions.

There is a small number of recent works dealing with the kinetics of these complex systems. The rigorous kinetic investigations of the oxidation of aniline with agents providing oxygen to the aniline molecule were performed.[1–5] But, when the oxidizing agent abstracts hydrogen from the amino group, the known kinetic studies [6–8] have only a qualitative character; in this case, a series of intermediates or final products are hardly identified.

In a series of previous works, we used sodium chlorite as oxidizing agent which abstracts hydrogen from some aromatic amines.[9–12] One

---

[1] K. M. Ibne-Rasa and J. O. Edwards, *J. Amer. Chem. Soc.*, **84**, 763 (1962).

[2] S. Kashino, Y. Migino and S. Hasegawa, *Bull. Chem. Soc. Japan*, **40**, 2004 (1967).

[3] N. M. Beileryan, M. G. Gevorkyan and O. A. Cealtikyan, *Doklady Akad. Nauk Armyan. S.S.R.*, **48**, 49 (1969).

[4] N. Venkatasubramanian and A. Sabesan, *Canad. J. Chem.*, **47**, 3710 (1969).

[5] G. R. Howe and R. R. Hiatt, *J. Org. Chem.*, **35**, 4007 (1970).

[6] M. G. Gevorkyan, N. M. Beileryan and O. A. Cealtikyan, *Arm. Khim. Zhur.*, **22**, 88 (1969).

[7] K. B. Iaţimirski and G. S. Nicolov, *Zhur. fiz. Khim.*, **44**, 1400 (1970).

[8] P. S. Radhakrishnamurti and R. K. Panda, *Indian J. Chem.*, **8**, 946 (1970).

[9] F. M. Albert and A. Meghea, *Rev. Roumaine Chim.*, **15**, 395 (1970).

[10] F. M. Albert, A. Meghea and C. Panait, *Anal. Univ. Buc. (seria St. Nat.-Chimie)*, **19**, 87 (1970).

[11] F. M. Albert, A. Meghea and C. Panait, *Anal. Univ. Buc. (seria St. Nat.-Chimie)*, **20**, 153 (1971).

[12] A. Meghea and C. Panait, *Rev. Chim. (Bucureşti)*, **27**, 286 (1976).

of these works[11] contains kinetic data for the oxidation of aniline with sodium chlorite in various solvents; the results and discussion have had only a preliminary qualitative character.

The present paper aims at a more complete kinetic characterization of this reaction; the experimental conditions are more rigorous. Simultaneously, we begin a systematic study of the results.

EXPERIMENTAL

Aniline was distilled on zinc powder before every kinetic measurement (b.p. 38.5° at 0.2 mm Hg).

Bidistilled water was used for the preparation of the reactant solutions. On dissolving, aniline gives aniline hydrochloride.

pH(1.5—2.5) was established using 0.1 M HCl. Generally, we used an excess of oxidizing agent (1M $NaClO_2$).

The ionic strength was fixed at a constant value (0.25 M) using a NaCl solution. The volume of the reaction mixture had a constant value (5 ml).

The kinetic measurements were carried out by means of a VSU-1 spectrophotometer. The vats containing the witness sample (bidistilled water) and the reaction mixture were placed in a thermostated cavity (25 ± 0.1°), adapted to apparatus. The solutions were previously and separately thermostated, during 20 minutes.

The aqueous solutions of the reactants don't absorb over 400 nm; therefore, the kinetics was followed at a wavelength of $\lambda = 530$ nm, corresponding to the absorption maximum of the first coloured compound (violet) which appears in these conditions.

In order to define more accurately the positions of the visible absorption bands of the reaction products, as well as to obtain a preliminary picture of the optical evolution of the reaction, we recorded the spectra of the reaction mixture at equal time intervals, after the beginning of the reaction, using an Optica Milano spectrophotometer.

RESULTS AND DISCUSSION

1. Reaction stages

As results from Figure 1, in the oxidation reaction of aniline with sodium chlorite, a violet compound having the absorption maximum at $\lambda = 530$ nm (curves no. 1—2) appears very quickly. This maximum decreases slowly (curves no. 3—6), as a new absorption band due to a yellow product appears and develops at $\lambda = 350-380$ nm. The inverse evolution in time of the two absorption bands determines the appearance of an isobestic point at 420 nm.

Using Mauser's results[13,14] concerning the kinetic development of the reaction spectra, it was found that the components of this reaction, absorbing in visible region, participate in two reaction stages, linearly independent.

Mauser gives a general scheme for the determination of minimum number (s) of the reaction stages, linearly independent, using Lambert-Beer's law and determining the total variation in time of the extinction at different wavelengths ($\Delta E_\lambda(t)$):

$$\Delta E_\lambda(t) = \sum_{k=1}^{s} Q_{\lambda k} \cdot L_k(t) \tag{1}$$

---

[13] H. Mauser, *Z. Naturforsch.*, **23 b**, 1021, 1025 (1968).

[14] H. Lachman, Dissertation, Tübingen, 1973.

where $Q_{\lambda k}$ contains factors independently on time (thickness of absorption layer, molar extinction coefficients, stoichiometric coefficients) and $L_k(t)$ represents the extent of reaction.

When the reaction develops in a single stage ($s = 1$), we may write the equation (1) at two wavelengths; an expression of a line passing through origin is obtained:

$$\Delta E_{\lambda_1}(t) = \frac{Q_{\lambda_1}}{Q_{\lambda_2}} \Delta E_{\lambda_2}(t) \qquad (2)$$

This is "the diagram of the extinction differences".

In a similar manner, when the reaction develops in two linearly independent stages ($s = 2$), we may write:

$$\Delta E_{\lambda_1}(t) = a \Delta E_{\lambda_2}(t) + b \Delta E_{\lambda_3}(t) \qquad (3)$$

or

$$\frac{\Delta E_{\lambda_1}(t)}{\Delta E_{\lambda_3}(t)} = b + a \frac{\Delta E_{\lambda_2}(t)}{\Delta E_{\lambda_3}(t)} \qquad (4)$$

This is "the diagram of the quotients of the extinction differences". The straight line cannot be obtained if $s > 2$.

Using these relations for our reaction spectra recorded in Figure 1, ΔE_{375}, ΔE_{460} and ΔE_{530} are obtained.

If we plot these values according to the equations (2) and (4), a straight line is obtained only for the diagram of the quotients of the extinction differences (Figure 2). This fact points out two linearly independent reaction stages. It must be emphasized that only the components absorbing in visible give the two reaction stages; therefore, it is possible to exist more reaction stages.

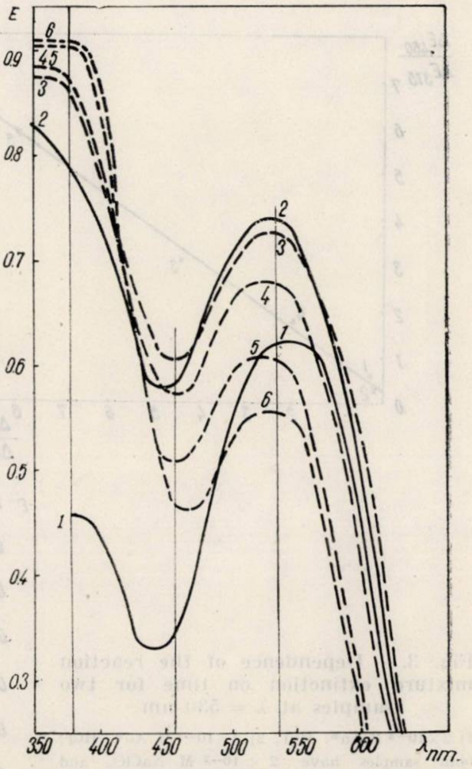

Fig. 1. — Absorption spectra of the oxidation products of aniline, recorded at 6 minutes time interval after the beginning of the reaction, in order 1—6, successively. The reaction mixture contains: 0.1 M An*. HCl (0.2 ml), 0.1 M HCl (1 ml), 1 M NaCl (0.78 ml), H_2O (2.02 ml) and 0.1 M $NaClO_2$ (1 ml).

* An-aniline

The isobestic point at 420 nm also confirms the obtained results ($s = 2$ reaction stages, not $s = 1$); in this point intersect only the reaction spectra obtained after a certain reaction time. Simultaneously, this means that the rate of the second stage is slower than the rate of the first stage.

2. The reaction orders and the rate constants

The curves in Figure 3 show an aspect specific to an intermediate, pointing out that there is a series of successive reactions.

In order to determine the reaction order and the apparent rate constants of the two consecutive reaction stages, we examined separately both the linear initial and the linear final part of the curves.

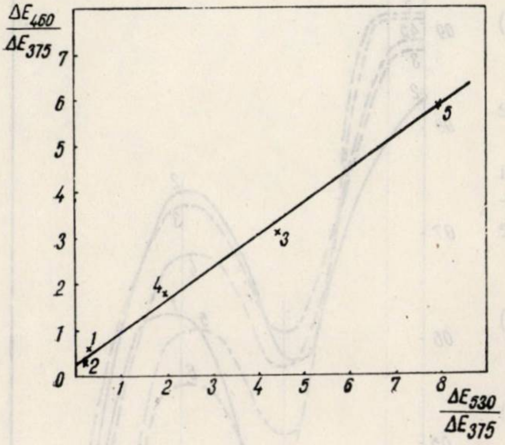

Fig. 2. — Diagram of the quotients of extinction differences.

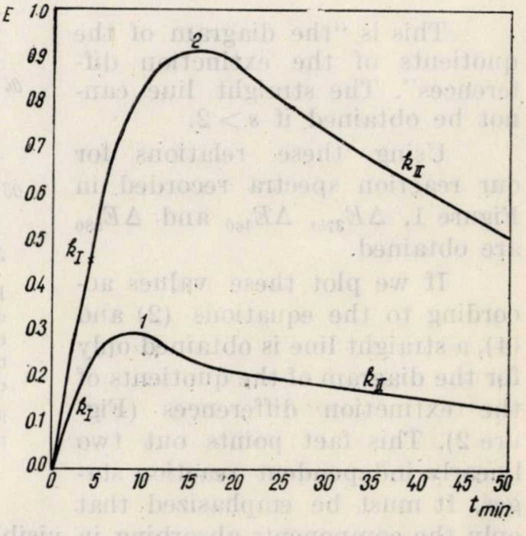

Fig. 3. — Dependence of the reaction mixture extinction on time for two samples at $\lambda = 530$ nm

1) 2×10^{-3} M An*. HCl; 2) 4×10^{-3} M An*. HCl; both samples have 2×10^{-2} M $NaClO_2$ and 2×10^{-2} M HCl, at $\mu^{**}_{NaCl} = 0.25$ M

* An-aniline

** μ-ionic strength

The partial reaction orders of the first stage (the order I with respect to amine and the order I with respect to oxidizing agent) were determined using the tangents method. Therefore, the violet compound, spectrophotometrically proved, results from a stage of order II, which is rate-determining.

The data for calculations are listed in table 1; the least square analysis was employed.

Table 1

Data used in calculation of the partial reaction orders

$C^{*)}_{An} \times 10^3$ (mol/l)	2	3	4	6	8	$n_{An} = 0.92$
$v = \frac{dE}{dt}$	0.057	0.065	0.097	0.140	0.192	
$C^{**)}_{NaClO_2} \times 10^2$ (mol/l)	2	3	4	6		$n_{NaClO_2} = 1.11$
$v = \frac{dE}{dt}$	0.066	0.133	0.177	0.245		

*) – when $C_{NaClO_2} = 2 \times 10^{-2}$M
**) – when $C_{An.HCl} = 3 \times 10^{-3}$M

The kinetic data obtained for some samples having different initial concentrations of aniline hydrochloride were studied graphically in semi-logarithmic coordinates ($t/\log E$). Thus, the apparent rate constants (pseudomonomolecular) for the two independent reaction stages, whose existence was spectrophotometrically proved, were calculated: $k_{I} = 0.331$ min^{-1} and $k_{II} = 0.0186$ min^{-1}.

3. The influence of pH

pH is one of the main factors which determine the mechanism, the nature of the products and the reaction rate of the oxidation of the aromatic amines; pH also influences the nature of the oxidizing species which intervene when sodium chlorite is used as oxidizing agent.[10]

In the oxidation of aniline with sodium chlorite, the violet coloured product is obtained in acidic medium (pH $= 1.5-2.5$). In this small pH-interval, the reaction rate generally increases depending on the added amount of HCl (Figures 4 and 5).

For the first analysed stage (k_{I}) it can be noticed a complex variation, the linearity being sharply interrupted at $[HCl] = 2 \times 10^{-2}$M. This behaviour is probably due to some modifications in the equilibrium determining the nature of the oxidizing species in acidic medium: $ClO_2^- \rightleftharpoons ClO_2^{\cdot} + e^-$.

For the last stage of reaction, spectrophotometrically followed (k_{II}), it was found a linear dependence, in logarithmic coordinates, whose slope closed to 1 suggests a catalytic effect through hydrogens ions.

On the whole, it can be noticed a differentiated influence of the amount of added HCl in the reaction mixture on the two reaction stages, spectrophotometrically studied. This fact is better evidenced through the analysis of the maximum of the kinetic curve $E = f(t)$, using samples with different HCl concentrations (Figure 4). It is clear that the greater k_{I} than k_{II} is the more marked the maximum of the kinetic curve.

The curve $E_{max} = f([HCl])$ (Figure 6) has a decreasing aspect, which points out that in the reaction system $[H^+]$ accelerates to a greater extent k_{II} stage with respect to k_I, leading to the smaller and smaller maxima. The curve is formed from two linear parts m_1 and m_2; the initial slope is sharply modified at HCl concentrations greater than 2×10^{-2} M. At the same value of [HCl] a sharply variation of the rate of the first reaction stage (Fig. 4) has been noticed.

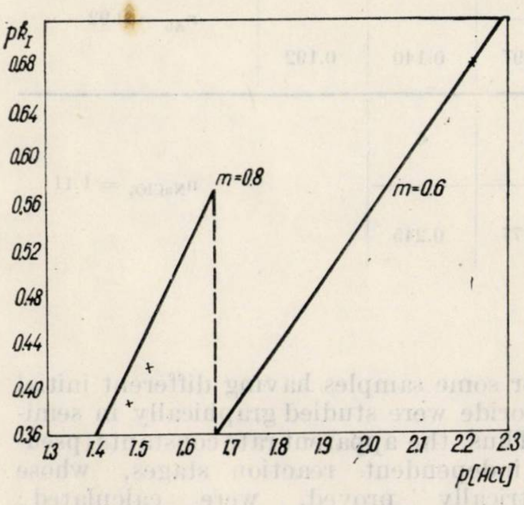

Fig. 4. — Influence of [HCl] on the initial rate of aniline oxidation.

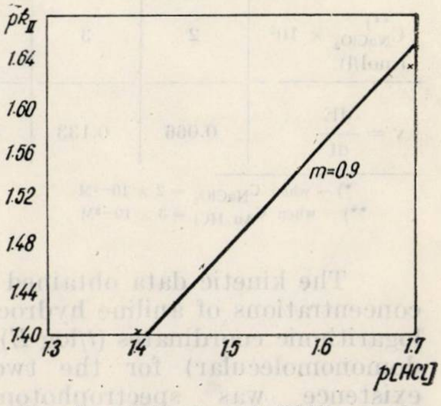

Fig. 5. — Influence of [HCl] on the rate of last stage of aniline oxidation.

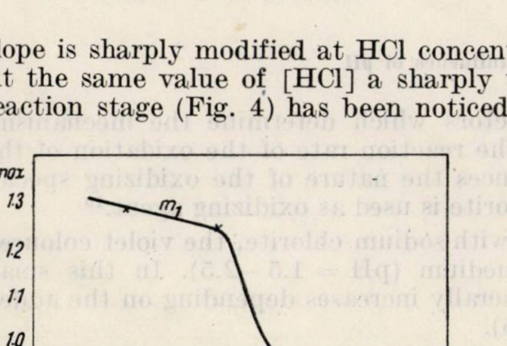

Fig. 6. — Influence of [HCl] on the intensity of maximum of the kinetic curve.

A comparison of the two slopes ($m_2 > m_1$) leads to the conclusion that at the increasing [HCl], the last stage of reaction, leading to the yellow compound, is favoured.

It is possible that the same general mechanism, involving $k_I < k_{II}$ (therefore the violet intermediate couldn't be evidenced, having a too small concentration, practically stationary) leads, in a direct manner, to the yellow compound, observed experimentally, in more acidic medium ($[HCl] > 4 \times 10^{-2}$ M).

On the basis of these kinetic results as well as of the available literature data, the first stage, rate-determining, could be attributed to an oxidizing attack on the nitrogen atom of the amino group; the final slow stage could be attributed to the acidic hydrolysis of one of the intermediates.

TO CONCLUDE, the following may be stated:

1. The analysis of the visible spectra of reaction allows to establish the existence of two linearly independent reaction stages, during the oxidation of aniline with sodium chlorite in acidic medium.

2. The apparent rate constants of two successive and relatively slow stages have been calculated on the basis of kinetic data at $\lambda = 530$ nm. The first stage is of total order II, i.e. of order I with respect to aniline and also of order I with respect to the oxidizing agent.

3. The complex and differentiated influence of the HCl-concentration on the two apparent rate constants was evidenced. A catalytic effect through hydrogen ions was noticed in the last stage.

In a subsequent paper a possible mechanism for the oxidation of aniline with sodium chlorite will be discussed and verified by means of a computer.

Revue Roumaine de Chimie, **23**, 1013–1021 1978

LINDEMANN LAW OF MELTING

MARILENA ŞERBAN
Chemistry Institute, Department of Physical Chemistry,
Bd. Republicii 13, Bucharest, Romania

Received June 3, 1976

It has been found that the ratio between the mean vibration amplitude and the interatomic distance, at the melting point, is not the same for all monoatomic solids, as assumed by Lindemann. This ratio depends upon the atomic arrangement and the interatomic forces. Starting from Mott relation and assuming that at the melting point the vibration frequency of liquid particles obeys a relation similar to the Lindemann relation, it has been proved that the mean vibration amplitude in liquid state is a higher fraction of the interatomic distance. The rise of the mean vibration amplitude is largely due to the occurrence of holes.

I. VIBRATION FREQUENCY OF SOLID PARTICLES AT MELTING POINT – LINDEMANN RELATION

In a previous paper,[1] we have used the relation:

$$\nu = 2.8 \times 10^{12} \sqrt{\frac{T_m}{M V_m^{2/3}}} \qquad (1)$$

for evaluating the vibration frequency of metal atoms in solid state, at the melting point. The coefficient, empirically deduced by Lindemann, may be shown to represent a mean value, generally valid for all metals.

In order to deduce this relation,[2] Lindemann assumed that melting takes place when the mean amplitude of the atomic vibration reaches a particular fraction of the interatomic distance. His deduction is based on Einstein approximation.

According to it, the kinetic energy of a vibratory atom with two degrees of freedom, at the melting point, is given by the relation:

$$\frac{E}{3} = \frac{R}{N} \frac{\beta\nu}{\exp(\beta\nu/T_m) - 1} \qquad (2)$$

---

[1] I. G. Murgulescu and M. Şerban, *Rev. Roumaine Chim.*, **19**, 1417 (1974).

[2] K. Jellinek, "Lehrbuch der Physikalischen Chemie", II Band, Stuttgart, 1928, p. 521–523.

which, if $\beta\nu/T_m \ll 1$, becomes :

$$\frac{E}{3} = \frac{R}{N}\, T_m \tag{3}$$

On the other hand, this harmonic oscillator possesses in its equilibrium position a kinetic energy :

$$\frac{E}{3} = \int_0^{\bar{r}\rho/2} Dx\,\mathrm{d}x = \frac{D\bar{r}^2\rho^2}{8}, \tag{4}$$

for a coordinate axis. D is the force constant, $\bar{r}$ is the mean separation between two neighbouring atomic centers in solid state and $\bar{r}\rho/2$ – the distance covered by the atom which, by leaving its equilibrium position, performs an oscillation. ρ represents the ratio between the mean amplitude and the interatomic distance ; it rises with the temperature, reaching a maximum at the melting point.

From relations (3) and (4) it follows :

$$D = \frac{8\,R\,T_m}{\bar{r}^2\rho^2 N} \tag{5}$$

Since

$$\nu = \frac{1}{2\pi}\sqrt{\frac{D}{m}}, \tag{6}$$

by introducing relation (5) into relation (6) it results :

$$\nu = \frac{1}{2\pi}\sqrt{\frac{8\,R\,T_m}{\bar{r}^2\rho^2 M}}. \tag{7}$$

Starting from this equation, Lindemann comes to the general relation :

$$\nu = \mathrm{const}\sqrt{\frac{T_m}{M\,V^{2/3}}}, \tag{8}$$

when $\bar{r}$ is proportional to $V^{1/3}$ and assuming that this proportion, as well as ρ, are the same for all monoatomic solids.

If we introduce the exact relation between $\bar{r}$ and V :

$$\bar{r} = \gamma^{1/3}\left(\frac{V}{N}\right)^{1/3} \tag{9}$$

we shall obtain :

$$\nu = \frac{(2R)^{1/2}\,N^{1/3}}{\pi\,\gamma^{1/3}}\;\frac{1}{\rho}\sqrt{\frac{T_m}{M V_m^{2/3}}}, \tag{10}$$

where γ is $\sqrt{2}$ for f.c.c. and c.h. structure, $3\sqrt{3}/4$ for the b.c.c. structure, 1 for the hexagonal structure and $3\sqrt{3}/8$ for the tetragonal structure.

If we consider ρ to have the mean value given by Lindemann, 0.12, and γ the mean value of the above figures, 1.121, the coefficient of eq. (10) is found to be the very value empirically deduced by Lindemann, 2.8×10^{12}.

It goes without saying that substituting γ by the values corresponding to each type of structure, ρ assumes values dependent on the respective structure.

In order to show this, the vibration frequency in eq. (10) was substituted by the values obtained from the θ characteristic temperatures; taking V_m the volume of a gram atom of the solid substance at the melting point, we calculated ρ for a number of normal metals.

The obtained values, as well as the data used, are shown in table 1. The T_m and V_m values have been taken from our previous papers; new data have been used for iron.[8] As for θ, the values taken from references [3] and [4] have been obtained from elastic data and those from reference [5] have been roentgenographically obtained.

The ρ values obtained by means of relation (10) exhibit a wide dispersion depending on the characteristic temperature. However, a certain tendency to group is noticeable : alkali metals, with the exception of lithium, have the value 0.13 while compact crystalline structure metals have a value ranging between 0.10 and 0.11. Cadmium and mercury are exceptions. The values found for the two types of iron structure are smaller.

In the case of tin, the calculations were made with extrapolated volume at the melting point, using the data of α allotropic form existing at low temperatures with a tetragonal structure. In the literature [9] 0.13 is given for ρ, at 293 K, corresponding to $\theta = 260$ K.

Table 2 reports the ρ values obtained by other authors, maintaining their notations. Starting from the different models of lattice dynamics, they deduced Lindemann relation whose coefficient is expressed as a function of the elastic and lattice constants.

The data in 2, 3, 4 and 6 columns were calculated with constants evaluated at room temperature; for those in column 5, extrapolated constants at the melting point were used.

According to table 2, a great diversity of the results is noticeable; the values corresponding to roentgenographic θ are the highest ($\theta_r < \theta_e < \theta_D$ are mentioned, where θ_D is obtained from specific heats and θ_e, from elastic data).

---

[3] K. C. Sharma and S. K. Joshi, *Phil. Mag.*, **13**, 881 (1966).

[4] B. N. Oshcherin, *Izv. Vyssh. Ucheb. Zaved., Fiz.*, **15**, 73 (1972).

[5] V. P. Mikhalchenko and V. B. Lototskii, *Fiz. Tverd. Tela*, **13**, 2048 (1971).

[6] C. J. Smithells, "Metals Reference Book", vol. I, 2nd ed., Butterworths Scientific Publications, London, 1955, p. 161.

[7] "American Institute of Physics Handbook", Mc. Graw-Hill Book Company, Inc., New York, 1957, Section, 4, p. 48.

[8] P. Pascal, "Nouveau traité de chimie minerale", vol. XVII, Fasc. 1, 1967, p. 135.

[9] "Gmelins Handbuch der Anorganischen Chemie", 8. Auflage, System-Nummer 46, Teil B, 1971, p. 149–150.

Table 1

ρ values obtained by eq. (10) by means of characteristic temperature

Element	γ	T_m, K	V_m, cc/gatom	θ, K					ρ				
Li	$3\sqrt{3}/4$	453.7	13.368	365.5[3]	317.2[4]	353[5]	363[6]	430[7]	0.142[3]	0.164[4]	0.147[5]	—[6]	—[7]
Na		371	24.12	164	144.3	152	202	160	0.129	0.147	0.139	0.105	—
K		336.6	45.97	99.4	—	—	163	100	0.126	—	—	0.077	—
Rb		312	56.50	—	—	—	58	59	—	—	—	0.131	—
Cs		301.8	71.15	—	—	—	42	43	—	—	—	0.132	—
Cu	$\sqrt{2}$	1356.2	7.527	349.3	345	318	315	343	0.100	0.101	0.110	—	—
Ag		1234	10.90	227.6	226.4	211	215	229	0.099	0.100	0.107	—	—
Au		1336.2	10.694	165.0	161.6	160	170	164	0.107	—	0.110	—	—
Mg		924.2	14.716	—	386	—	290	342	—	0.097	—	0.129	0.109
Zn		692.7	9.538	—	324	—	213	235	—	0.070	—	0.107	0.097
Cd		594.2	13.367	—	214	—	172	165	—	0.067	—	0.084	0.087
Hg		234.3	14.134	—	—	—	97	75	—	—	—	0.068	0.088
Al		933.3	10.502	417	430.5	383	394	375	0.095	0.092	0.104	—	0.106
Pb		600.6	18.758	106.3	105.3	81	88	96.3	0.089	0.090	0.117	0.108	0.099
Co		1765	7.071	—	453	—	385	385	—	0.093	—	0.110	—
Ni		1726	7.048	478.6	475.9	418	375	413	0.088	0.088	0.100	0.112	—
γ	$\sqrt{2}$		7.632		473					0.093			
Fe		1809		496.2			420	355	—			—	0.124
δ	$3\sqrt{3}/4$		7.663			423					0.104		
Sn	$3\sqrt{3}/8$	505.1	20.680	—	—	—	260	195	—	—	—	0.055	0.074

Our results agree with Gilvarry's results,[12] who obtained $\rho = 0.13$ for alkali metals and $\rho = 0.11$ for compact metals, using extrapolated data at the melting point.

Table 2

ρ values reported from references

Element	$\gamma_m^{1/2}$ (3)	$\gamma_m^{1/2}$ (4)	$\gamma_p^{1/2}$ (5)	δ (10)	$X_m^{1/2}$ (11)
Li	0.160	0.210	0.174	0.116	0.154
Na	0.144	0.188	0.160	0.111	0.143
K	0.142	—	—	0.112	0.129
Rb	—	—	—	0.115	0.138
Cs	—	—	—	0.111	0.142
Cu	0.115	0.128	0.133	0.068	0.105
Ag	0.114	0.127	0.130	0.071	0.105
Au	0.122	0.129	0.132	0.073	0.105
Mg	—	0.122	—	—	—
Zn	—	0.089	—	—	—
Cd	—	0.084	—	—	—
Hg	—	—	—	—	—
Al	0.107	0.115	0.125	—	0.104
Pb	0.102	0.113	0.140	0.065	0.102
Co	—	0.118	—	—	—
Ni	0.101	0.112	0.122	0.077	0.096
Fe	0.100	0.115	0.123	—	0.098
		(fcc)	(bcc)		(bcc)
Sn	—	—	—	—	—

The differences between the values obtained by various authors are not exclusively due to the θ values chosen by them; the deduced relations are different through their coefficient.

Our conclusions are the same: the ratio between the mean vibration amplitude and the interatomic distance at the melting point depends upon the structure of the solids and the nature of the binding forces between particles. Thus, the ratio is higher with b.c.c. metals as compared to compact metals; it is also higher with van der Waals solids of noble gases as compared to metals with the same structure.[13] It is different with b.c.c. metals belonging to different groups of periodic table.

The higher ρ in the case of alkali metals can be explained, on the one hand by their rarefied crystalline structure and, on the other hand, by their weaker binding energies.

[10] J. N. Shapiro, *Phys. Rev. B*, **1**, 3982 (1970).

[11] A. K. Shingh and P. K. Sharma, *Canad. J. Phys.*, **46**, 1677 (1968).

[12] J. J. Gilvarry, *Phys. Rev.*, **102**, 308 (1956); **103**, 1700 (1956); **104**, 908 (1956).

[13] N. P. Gupta, *Solid State Comm.*, **13**, 69 (1973).

As seen in Figure 1, the W total binding energy of alkali metals has smaller values, the curves occurring in the range of higher volumes.[14] With these metals, the amplitude is much higher being less limited both by the arrangement of the particles and by the repulsive energy; the interatomic distance is greater too.

As for iron, its binding energy being comparable to that of nickel and consequently higher than the energy of alkali metals, the ρ ratio of b.c.c. form is smaller. Owing to the smaller interatomic distance its vibration amplitude is much smaller. For the compact form, ρ is, as expected, smaller and in spite of the relation $\bar{r}(\delta) < \bar{r}(\gamma)$ its amplitude is smaller.

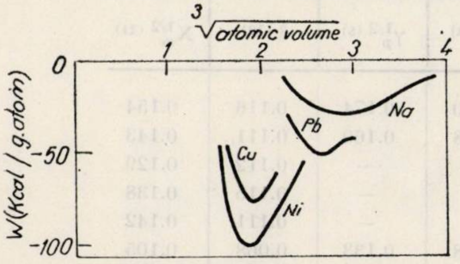

Fig. 1. — Binding energy of the metal as a function of atomic volume.

In the case of noble gas crystals the ratio obtained by Gupta is higher than the ratio of the metals with similar structure, van der Waals bonds existing between particles. Their vibration amplitude is much higher.

It follows that Lindemann assumption on the constancy of ρ is not correct. The coefficient of eq. (8) will be 2.8×10^{12} for compact metals if $\rho = 0.11$ and 2.44×10^{12} for alkali metals if $\rho = 0.13$. In the case of tin, the value deduced here seems to be too small. The value found in the literature leads to the coefficient 3.08×10^{12}.

The accuracy of these data is conditioned by the characteristic temperature; the corresponding values for the melting temperature should be used.

A relation similar to that between θ and T_m in eq. (8) was empirically obtained by Mukherjee[15] between θ and E_f — the necessary energy to form holes in compact solid metals. Starting from this similitude, Mukherjee co-related T_m to this energy. March[16] deduced Mukherjee relation by means of the screening electronic theory. Lindemann relation was deduced[17] by combining the screening electronic theory with the Bragg-Williams theory for an order-disorder transition. In keeping with this deduction, a general Lindemann coefficient is foreseen, but not a very exact one. It is suggested[18] that electronic screening in compact metals is much different from that in b.c.c. metals, which is in accordance with the above mentioned conclusions.

---

[14] N. F. Mott and E. H. Jones, "The Theory of the Properties of Metals and Alloys", Dover Publications Inc., New York, 1958, chap. I, 4 and 5.

[15] K. Mukherjee, *Phil. Mag.*, **12**, 915 (1965).

[16] N. H. March, *Phys. Letters*, **20**, 231 (1966).

[17] J. E. Enderby and N. H. March, *Proc. Phys. Soc.*, **88**, 717 (1966).

[18] N. H. March, "Liquid Metals", Pergamon Press, Oxford, 1968, chap. 6.

II. VIBRATION FREQUENCY OF LIQUID PARTICLES AT MELTING POINT – MOTT RELATION

It has been noticed that for many metals the sound velocity in the melt at the melting point is about that in the crystal. Rao [19] explains this by the rise of the vibration amplitude on melting.

Melting is accompanied by the occurrence of holes and with some elements by a more compact re-arrangement of particles and even by a change in the nature of interactions. Assuming that all monoatomic liquids exhibit a compact packing, we expect the occurrence of the holes to lead to a rise of the mean vibration amplitude.

With a view to quantitatively appreciate the rise of ρ, we started from the following observations:

1. In Note II[1] we proposed Mott relation for evaluating the vibration frequency of liquid monoatomic particles:

$$\frac{\nu_S}{\nu_L} = e^{L/3RT_m} \tag{11}$$

which is valid provided that the melting should be accompanied by a positive change volume.

2. We expected the expression of the vibration frequency of liquid particles at the melting point to be similar to eq. (10).If, as experimentally proved with most of the metals, the interatomic distance is not changed on melting, eq. (9) will be maintained. Introduced into eq. (7) it leads to the expression:

$$\nu_L = \frac{(2R)^{1/2}N^{1/3}}{\pi\gamma^{1/3}}\,\frac{1}{\rho_L}\sqrt{\frac{T_m}{MV_m^{2/3}}} \tag{12}$$

which differs from eq. (10) by ρ_L – the ratio between the mean vibration amplitude of liquid particles and the interatomic distance.

Thus, we obtain the simple relation:

$$\frac{\nu_S}{\nu_L} = \frac{\rho_L}{\rho_S} \tag{13}$$

which allows the evaluation of ρ_L. Since the interatomic distance remains constant on melting, the ratio of the frequencies is inversely proportional with the ratio of the very amplitudes.

Table 3 lists the obtained ρ_L values. The compact metals Zn, Cd, Hg were neglected as we suggested that some of their particles are found in the vicinity of the melting temperature as dimers.[20] An equation similar to eq. (10) is not valid for such elements. In the case of tin a similar situation has been found.

As expected, the mean vibration amplitude represents in melts, at the melting point, a higher fraction of the interatomic distance. The rise is higher with compact metals. The difference between the corresponding values of the two groups of metals becomes smaller as compared to solid state, ρ_L remaining smaller with compact metal melts.

---

[19] M. R. Rao, *Current Sci.*, **13**, 225 (1944).

[20] I. G. Murgulescu and M. Şerban, *Rev. Roumaine Chim.*, **17**, 431 (1972).

Liquid lithium, as well as in its solid state, exhibits a higher value. As for iron, the ratio ν_S/ν_L was separately calculated using for L the values 4400 and 3300 cal/g. atom for the form γ, respectively form δ.[21]

Table 3

ρ_L values obtained by equation (13)

Element	ν_S/ν_L	$(\nu_S/\nu_L)_{av}$	ρ_S	ρ_L
Li	1.305[1]	1.305	0.14	0.18
Na	1.347			
K	1.336	1.335	0.13	0.17
Rb	1.335			
Cs	1.324			
Cu	1.478			
Ag	1.449			
Au	1.477			
Mg	1.483			
Al	1.553	1.465	0.11	0.16
Pb	1.376			
Co	1.426			
Ni	1.480			
Fe(γ)	1.505	1.505	0.093	0.14
Fe(δ)	1.359	1.359	0.10	0.14

The results normally lead to only one value corresponding to its molten state. The ρ_S values in the literature lead to $\rho_L = 0.17$.

Taking into account the data presented in a previous note,[22] it can be seen in table 1 that all compact metal melts present the mean coordination number 11.4, while alkali melts present a theoretical number 10.8. Starting from these data we assumed that by rearrangement the particles of alkali melts are also compactely packed, but exhibiting a larger number of holes.

This higher degree of compactness might explain the lower rise of ρ with alkali metals. Trying to calculate the vibration frequency of a compact solid derived from a b.c.c. solid,[22] one finds that ρ_S is not much affected by compactness.

The small difference between the coordination numbers of the two groups of melts may explain closeness between the ρ_L values.

---

[21] A. R. Ubbelohde, "Melting and Crystal Structure", Clarendon Press, Oxford, 1965, p. 173.

[22] M. Şerban, *Rev. Roumaine Chim.*, **16**, 13 (1971).

The results must be also discussed from the interaction energy viewpoint. We expect the energies to be smaller in liquid state, a fact which could have a greater influence on the change of the compact metal amplitudes; a tendency toward uniformity may also be expected here.

If the rise of the mean vibration amplitude is exclusively due to the occurrence of holes, the apparent rise of the interatomic distance equivalent to the rise of ρ should be identical with the apparent rise equivalent to the decrease of the coordination number.

From the ratio ρ_L/ρ_S, when the atomic diameter is constant, it follows that $\bar{r}_L/\bar{r}_S = 1.060$ with compact metals and $\bar{r}_L/\bar{r}_S = 1.048$ with alkali metals. When taking into account compactness with the latter metals, the ratio becomes: $\bar{r}_L/0.92^{1/3}\ \bar{r}_S = 1.077$.[22]

By means of relation (3) in reference [22], the change of the coordination number from 12 to 11.4 is found to be equivalent to the apparent rise of the interatomic distance $\bar{r}_L/\bar{r}_S = 1.017$, while the change from 12 to 10.8 is equivalent to the apparent rise $\bar{r}_L/\bar{r}_S = 1.036$.

It can be observed that, mostly with alkali metals the occurrence of holes explains to a great extent the rise of the mean vibration amplitude on melting. But this rise is not conditioned only by this occurrence of holes.

The restoring force opperating in vibrations is correlated to the energy involved in a certain disorder and through it with the change of the corresponding melting entropy. With metals, this change is given by the sum of the changes of three components: positional disorder entropy, vibrational entropy and electronic entropy.

As mentioned in reference [21], chap. 8, the difference between ν_S and ν_L obtained with Mott relation is due to the total change of the melting entropy. As we have demonstrated, this difference is primarily explained by the change of volume, which is exclusively due to the occurrence of holes in accordance with the results seen in reference.[22] The occurrence of this positional disorder can determine an increasing scattering of conduction electrons, which can explain a rise in the mean vibration amplitude. Moreover, an influence of the partly anharmonic character of the liquid particle vibrations may occur.[23]

The data presented in this paper lead to the conclusion that the contribution of the changes of vibrational and electronic entropies cannot be overlooked. The estimation of the sum of the changes of the positional disorder entropy and electronic entropy by communal entropy leads with compact metals to a very small change of the vibration frequency, due to a vibrational entropy change. Unfortunately the three contributions of entropy cannot be separately evaluated, since they cannot be dealt with independently.

The obtained results show that the melting properties change in such a way that a uniformity of the general behaviour of metallic melts corresponding to solids with clearly different behaviours is reached.

---

[23] J. S. Dugdale and D. K. C. McDonald. *Phys. Rev.*, **96**, 57 (1954).

Revue Roumaine de Chimie, **23**, 7, 1023–1027 (1978)

INFLUENCE OF OXYGEN ON THE DARK CONDUCTIVITY OF METAL-FREE PHTHALOCYANINE

N. I. IONESCU and P. BANYAI
Institute of Physical Chemistry, Bucharest,
Str. Galaţi 31, Romania

Received June 9, 1976

The presence of oxygen at pressures between 30 and 430 torr increases the dark conductivity of thin metal-free phthalocyanine films. The kinetic law of this process was determined.

The phthalocyanines, typical representatives of dyes with semiconductor properties, present a great interest. These substances have a planar structure and a high chemical stability, being much used together with anthracene in studies concerning the conduction mechanism in organic semiconductors.[1] The phthalocyanines can also be used as model substances in the simulation of some biological processes, because their chemical structure is closely related to the porphyrines, the basic structure of hemoglobin and chlorophyll.

The results obtained till now concerning the oxygen influence on the dark conductivity of metal-free phthalocyanine (H_2-Phc) do not permit a clear interpretation of the conduction mechanism.[2-4]

That is why, in the present paper, we aim to study the influence of oxygen on the dark conductivity of thin metal-free phthalocyanine films.

EXPERIMENTAL

The vacuum apparatus

A usual high vacuum installation, whose scheme is given in Figure 1, was used. The pressure of the introduced oxygen was measured with a Hg-manometer.

The experimental cell

The cell (Figure 2) was made of rasotherm glass, after a model used in studies of some electrical properties of thin metallic films in the process of gas chemisorption.

The thin phthalocyanine film was obtained by vacuum evaporation. The evaporation source was a small molibden basket made of wire having 0.3 mm diameter welded to two tungsten wires with 1 mm diameter, which are the metallic passages through the glass. The phthalocyanine powder was in a quartz cone inside the basket.

---

[1] J. H. Sharp and M. Smith, *Phys. Chem.*, **10**, 435 (1970).

[2] A. T. Vartanian and J. A. Karpovici, *Zhur. fiz. Khim. U.S.S.R.*, **32**, 178 (1953).

[3] J. Kaufhold and K. Hauffe, *Z. Elektrochem.*, **69**, 168 (1965).

[4] K. J. Beales, D. D. Eley, D. J. Hazeldine and T. F. Palmer in "Katalyse an Phthalocyaninen" ed H. Kropf and F. Steinbach, G. Thieme, Stuttgart, 1973, p. 1.

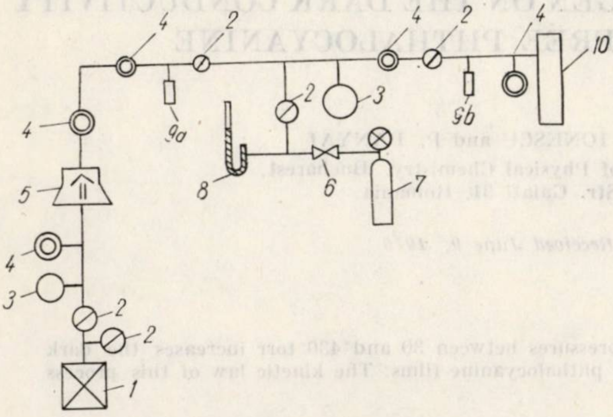

Fig. 1. — The installation used for the study of the surface interaction between metal-free phthalocyanine film and oxygen.
1 = preliminary vacuum pump; *2* = vacuum stopcock; *3* = preliminary vacuum vessel; *4* = trap for liquid nitrogen; *5* = diffusion pump; *6* = needle valve; *7* = oxygen bomb; *8* = Hg manometer; *9a* = Pirani gauge; *9b* = ionization gauge; *10* = experimental cell.

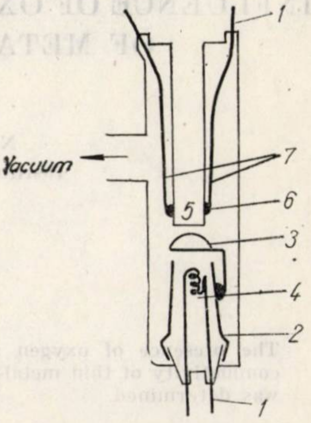

Fig. 2. — Experimental cell.
1 = tungsten electrodes; *2* = canalizing tube; *3* = mobile screen; *4* = evaporation source; *5* = support test-tube; *6* = platinum electrodes; *7* = nickel electrodes.

To protect the support during the outgassing of the filament and until the evaporation temperature of the source was obtained, as well as for the limiting of the evaporated fascicle, a glass canalizing tube was used. This one was fixed to the inner side of the tube through a greasless grinding, being also equipped with a mobile screen which can be operated from the outside by means of a magnet.

The condensation of the film takes place on the plane bottom of the quartz support test tube which is optically polished. A band of one mm width was delimited on the surface of the support. On the rest, a thin platinum film, in contact with two platinum wires, was chemically deposited. These two platinum wires are also welded to tungsten wires.

The cell, including the inner of the support test tube was introduced as much as the geometry of the system allows, in a thermostat with silicon oil.

The substance

Metal-free phthalocyanine (TH. Schuchardt and BASF) purified by vacuum sublimation [5] was used.

The measurements of the dark current

The dark current was measured with a 610 CR Keithley electrometer using a Tesla power supply. The applied field was 500 V/cm. Between 0—2000 V/cm, within the 30—250° temperature interval, the clean or with oxygen covered films have presented an ohmic behaviour. This behaviour was observed by other researchers too.[3] The current of the clean support was less than 10^{-13} A, the detection limit of the electrometer.

---

[5] N. I. Ionescu, R. Schuster, D. Trestianu and A. Mihăilescu, *Z. Chem.*, **15**, 495 (1975).

The description of an experiment

An experiment concerning the superficial interaction between metal-free phthalocyanine and oxygen looks as follows :

After a vacuum of minimum 1.10^{-5} torr was obtained the outgassing of the evaporation source began. After outgassing, the screen of the canalizing tube was removed and the deposition of the film took place. During the deposition the pressure was between $5.10^{-5}-1.10^{-4}$ torr. The temperature of the support test tube was 120°.

After the deposition, the film was heated for two hours at 250°. Then the cell was brought at the working temperature and the initial dark current was measured.

Oxygen at definite pressures was then introduced and the change of the current in time at a constant temperature was followed.

A metal-free phthalocyanine film was used in several experiments because the oxygen can be removed from the film by a special treatment. The current reaching its initial value was also observed in this case.[3]

In order to obtain reproducible results, it was necessary to introduce and pump oxygen for several times.

All the described experiences were performed on such films.

RESULTS AND DISCUSSIONS

The introduction of oxygen in the installation at pressures of 30, 50, 130, 275 and 430 torr produces the increase of the dark current of the film which can be observed in Figure 3. The metal-free phthalocyanine film was maintained at 235°. The variations of the dark current, which are proportional with the variations of the dark conductivity, are oxygen pressures depending.

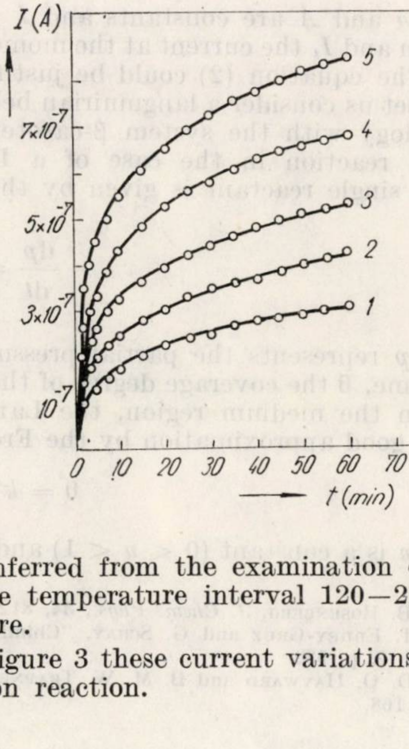

Fig. 3. — The oxygen influence on the dark conductivity of a metal-free phthalocyanine film at 235°.

1 = The pressure of oxygen 30 torr; 2 = the pressure of oxygen 50 torr; 3 = the pressure of oxygen 130 torr; 4 = the pressure of oxygen 275 torr; 5 = the pressure of oxygen 430 torr.

Similar conclusions can be inferred from the examination of the other current variations within the temperature interval 120–215° at the same oxygen pressures as before.

As it can be observed from Figure 3 these current variations have the general aspect of an adsorption reaction.

The surface interaction between metal-free phthalocyanine and oxygen has a kinetic evolution. After proving different kinetic laws, it results that the current variation versus time has the form of a straight line (Figure 4) in a double logarithmic representation. This law was found for all investigated temperatures. Figure 4 represents only the values obtained for temperature 235°.

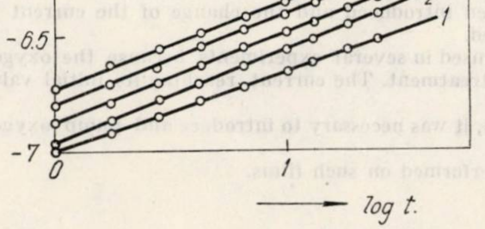

Fig. 4. — The determination of the constants *a* and *A* at 235°.

1 = the pressure of oxygen 30 torr; *2* = the pressure of oxygen 50 torr; *3* = the pressure of oxygen 130 torr; *4* = the pressure of oxygen 275 torr; *5* = the pressure of oxygen 430 torr.

From figure 4 it results:

$$\log I = a \log t + \log A \tag{1}$$

or

$$I = At^a \tag{2}$$

where a and A are constants and $I = I_t - I_0$, I_0 being the current in vacuum and I_t the current at the moment t, after gas introduction.

The equation (2) could be justified as follows:

Let us consider a langmuirian behaviour for the system H_2-Phc/O_2, in analogy with the system β-carotene[6] for instance. The rate of the surface reaction in the case of a Langmuir-Hinshelwood mechanism with a single reactant is given by the relationship:

$$-\frac{dp}{dt} = k\theta \tag{3}$$

where p represents the partial pressure of the reacting introduced gas, t the time, θ the coverage degree of the surface and k a constant.

In the medium region, the Langmuir isotherm can be described with a good approximation by the Freundlich isotherm:[7,8]

$$\theta = k'p^n \tag{4}$$

where n is a constant ($0 < n < 1$) and k' a constant.

---

[6] B. Rosenberg, *J. Chem. Phys.*, **34**, 812 (1961).

[7] T. Erdey-Gruz and G. Schay, "Chimie fizică teoretică", Ed. Tehnică, Bucureşti, 1958, vol. 2, p. 582.

[8] D. O. Hayward and B. M. W. Trapnell, "Chemisorption", Butterworths, London, 1964, p. 168.

By means of relation (4) equation (3) becomes:

$$-\frac{\mathrm{d}p}{\mathrm{d}t} = Kp^{n} \tag{5}$$

where $K = kk'$, which by integration leads to:

$$p = Bt^{\frac{1}{1-n}} \tag{6}$$

B being a global constant.

If we admit that the current variations are proportional to the coverage degree, then:

$$I = \alpha\theta \tag{7}$$

where α is a constant.

By means of (4) and (6) relation (7) becomes:

$$I = At^{a} \tag{8}$$

where $A = \alpha k'[1 - n) K]^{a}$ and $a = n/1 - n$, which is just equation (2).

Table 1

The values of the constant *a* at different pressures

T(°C)	235	215	190	165	140	120
a	0.30 ± 0.04	0.33 ± 0.03	0.36 ± 0.02	0.45 ± 0.02	0.48 ± 0.03	0.49 ± 0.04

Because the experimental data show that $a < 1$ (Table 1) it results that $n < 0.5$, according to the existence conditions for the relationship (4). One can also observe from the signification of the a constant that this must be pressure independent, a fact which was experimentally proved.

We can conclude as a result of our experiments that oxygen increases the dark conductivity of a metal-free phthalocyanine film according to a determined kinetic law.

ACKNOWLEDGEMENTS. The authors wish to thank to the Alexander von Humboldt-Foundation for the award of an electrometer. The metal-free and copper-phthalocyanine were kindly donated by the firms "Badische Anilin und Soda Fabrik" and "Th. Schuchardt".

Revue Roumaine de Chimie, 23, 7, 1029–1033 (1978

ÉTUDE CINÉTIQUE DE LA DÉCOMPOSITION DES SOLIDES, PAR MESURAGES VOLUMÉTRIQUES

D. FĂTU

Chaire de Chimie Physique et Technologie Electrochimique,
Institut Polytechnique Bd. Republicii Nr. 13, Bucarest, Roumanie

Reçu le 5 juillet 1976

On présente le schéma d'un dispositif permettant l'enregistrement du volume de gaz dégagé par la décomposition des solides en conditions isothermes. Les courbes ainsi obtenues permettent de caractériser du point de vue cinétique le système étudié. Les valeurs des paramètres cinétiques des processus de décomposition thermique de l'hexammine du chlorure de nickel et du permanganate de potassium calculées à l'aide des courbes volumétriques sont en concordance avec celles obtenues par d'autres méthodes.

L'évolution cinétique des processus du type :

$$A(s) \to B(s) + C(g)$$

dans lesquels un solide $A(s)$, soumis à une décomposition thermique, se transforme dans un autre solide $B(s)$, en éliminant la composante volatile $C(g)$, est fréquemment caractérisée à l'aide de la méthode de l'analyse thermogravimétrique (ATG) et thermogravimétrique dérivée (ATGD).[1–3].

Si l'on ne dispose pas d'une thermobalance on peut suivre l'évolution de la décomposition thermique en mesurant le volume de la composante volatile $C(g)$ à l'aide d'une burette à gaz. Bien que fort accessible, cette méthode n'est pas applicable dans des conditions expérimentales où la réaction se déroule à grande vitesse. Pour cette raison on a construit un dispositif qui permet l'enregistrement du volume de gaz dégagé. Un tel dispositif peut être utilisé également dans l'analyse thermovolumétrique.[4]

LE DISPOSITIF EXPÉRIMENTAL

Le dispositif expérimental dont le schéma est présenté dans la figure 1 comporte trois parties :

---

[1] J. H. Flynn et L. A. Wall, *J. Res. Nat. Bur. Stand.*, **70 A**, 487 (1966).

[2] D. Fătu, *Studii şi Cercetări Chim., Bucureşti*, **19**, 849 (1971).

[3] J. Sestak, *Thermochim. Acta*, **7**, 333 (1973).

[4] L. G. Berg, "Vedenie v termografiyu" Izd. Acad. Nauk S.S.S.R., Moscou, p. 251.

1 — La partie centrale de l'installation est constituée par le réacteur *R* qui comprend un tube en verre, résistant aux chocs thermiques, placé dans le four électrique *C*. L'échantillon est introduit dans la nacelle *N*, laquelle est liée au noyau en fer *P*, encastré en verre. En agissant de l'extérieur, à l'aide d'un aimant, sur le noyau en fer, l'échantillon est introduit — ou ôté — de la zone de réaction, à température élevée, sans ouvrir le rodage du réacteur.

2— Le dispositif d'enregistrement du volume de gaz dégagé. Celui-ci consiste d'un tube en verre à section constante dans lequel est placé au long de l'axe le fil en platine *F*. Les extrémités du tube en verre sont raccordées, par des tuyaux en caoutchouc, au réacteur et au réservoir à mercure. Le fil en platine est inséré dans un pont de Wheatstone alimenté par une source de courant continu du type Multistab I.F.A., ou par un accumulateur.

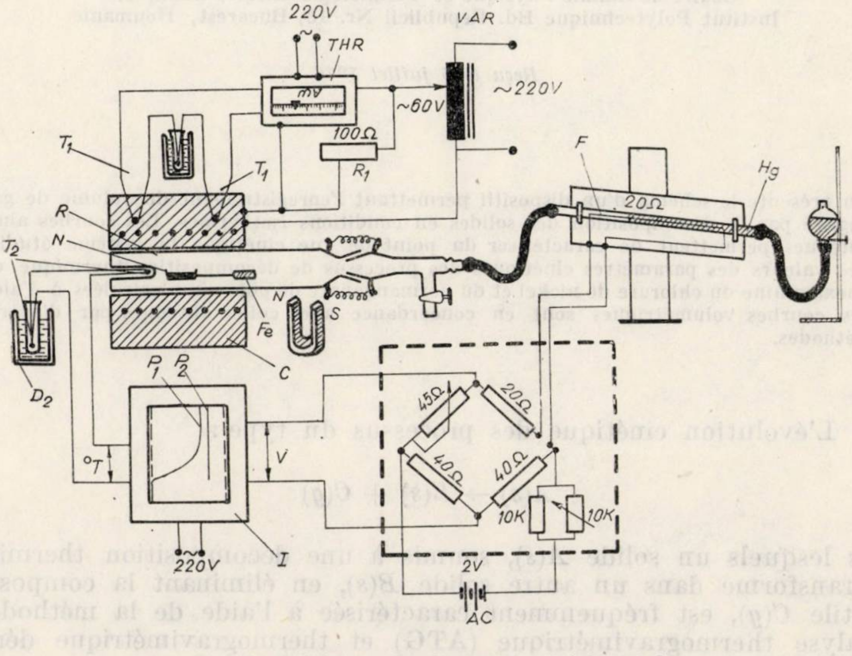

Fig. 1. — Schéma du dispositif expérimental :

R — réacteur ; *C* — four électrique ; *N* — nacelle de l'échantillon ; *P* — noyau en fer ; *M* — aimant ; *F* — fil en platine ; *Ac* — accumulateur ; P_1, P_2 — plumes de l'enregistreur ; T_1, T_2 — thermocouple fer-constantane ; VAR — autotransformateur ; R_1 — résistance électrique ; *THR* — thermorégulateur ; *R* — résistance du four ; *D* — récipient Dewar ; *I* — enregistreur.

Le fonctionnement du dispositif est basé sur le fait que le gaz dégagé par la décomposition thermique chasse le mercure du tube, en libérant par étapes le fil en platine. Par conséquent, le pont Wheatstone est déséquilibré et la tension générée est inscrite sur le diagramme par la plume P_1. On obtient ainsi la courbe $V = V(t)$ du volume de gaz, en fonction du temps, le déplacement de la plume étant 1 cm pour 2.10^{-2}cm^3 gaz dégagé. Il faut mentionner que la déviation de la plume est proportionnelle à la quantité du gaz dégagé à condition que le processus se déroule dans des conditions isotherm-isobares. Si l'inclinaison du tube à mercure est insignifiante on peut négliger la variation de la pression en raison du dénivellement du mercure. D'ailleurs connaissant l'angle d'inclinaison du tube on peut calculer la valeur réelle du volume de gaz.

La plume P_2 de l'enregistreur inscrit les valeurs de la température du réacteur à l'aide du thermocouple fer-constantane T_2.

3 — Le dispositif pour régler la température. Le four électrique est alimenté à l'aide d'un autotransformateur VAR par la résistance R_1 (100 Ω). Le thermorégulateur THR (du type Automatica) est muni d'un relais à mercure qui permet de court-circuiter ou d'introduire en circuit la résistance R_1 en modifiant la force électrique et maintenir la température constante entre 50 et 300° à une précision de $\pm 0,5°$.

RÉSULTATS ET DISCUSSIONS

a) Décomposition de l'hexamine du chlorure de nickel

Pour une première vérification du dispositif expérimental, on a étudié la décomposition de l'hexamine de chlorure de nickel.

Ce processus conduit à dégagement d'ammoniaque, en se déroulant conformément à l'équation stœchiométrique :

$$[Ni(NH_3)_6]\,Cl_2 \rightarrow [Ni(NH_3)_2]\,Cl_2 + 4NH_3 \qquad \text{(I)}$$

Dans des conditions plus énergiques la décomposition est totale, jusqu'au chlorure de nickel. Les courbes expérimentales sont présentées dans la figure 2. Au lieu du volume de gaz dégagé on a indiqué la fraction du réactant non décomposé $(1-\alpha)$ en fonction du temps, où α représente le degré de décomposition.

On peut observer que dans le domaine $0{,}05 \leqslant \alpha \leqslant 0{,}90$ les courbes présentent une portion linéaire caractérisée par la valeur constante de la vitesse de réaction :

$$\mathrm{d}\alpha/\mathrm{d}t = k \qquad (1)$$

où t — temps ; k — constante de vitesse.

Par conséquent, on peut facilement calculer les valeurs de la constante de vitesse, à différentes températures, en déterminant les coefficients directeurs des droites présentés dans la figure 2.

Du diagramme d'Arrhenius (fig. 3) on obtient pour l'énergie d'activation une valeur de 15,1 kcal/mole. Les méthodes thermogravimétriques [5] indiquent une valeur de 14,4 kcal/mole. Donc l'accord entre les deux méthodes est satisfaisant. La valeur nulle de l'ordre de réaction montre que dans les conditions données l'étape limitante de vitesse n'est

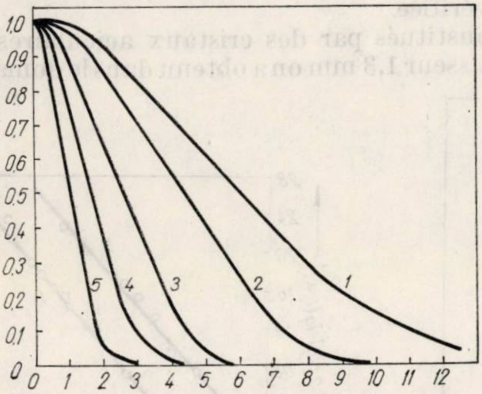

Fig. 2. — Courbes de la décomposition de $[Ni(NH_3)_6]\,Cl_2$:
1, 160° ; *2*, 170° ; *3*, 181° ; *4*, 192° · *5*, 202°.

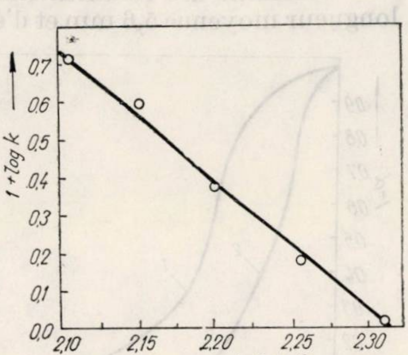

Fig. 3. — Diagramme d'Arrhenius pour la décomposition de $[Ni(NH_3)_6]\,Cl_2$.

---

[5] I. G. Murgulescu, E. Segal et D. Fătu, *Rev. Roumaine Chim.*, **11**, 291 (1966).

pas l'acte chimique, mais le processus de diffusion de la composante volatile à l'interface solide-gaz. Le gradient de concentration de la composante volatile à travers la phase solide varie de façon appréciable seulement au début et à la fin de la réaction.

Pour des valeurs moyennes du degré de décomposition, la valeur du gradient peut être assimilée à une constante, de sorte que la vitesse d'élimination de la composante volatile reste aussi constante ce qui se traduit par l'existence de la portion linéaire sur les courbes $(1 - \alpha) = f(t)$.

b) Décomposition du $KMnO_4$

Le processus de décomposition du permanganate de potassium qui se déroule conformément à l'équation stœchiométrique :

$$2KMnO_4(s) \rightarrow MnO_2(s) + K_2MnO_4(s) + O_2(g)$$

peut également être étudié du point de vue cinétique par l'enregistrement du volume d'oxygène dégagé dans des conditions isothermes. Les courbes correspondantes pour ce processus sont présentées dans la figure 4.

La forme de sigmoïde de ces courbes peut être expliquée du point de vue théorique si l'on considère le processus d'interaction des germes de matériel décomposé qui surgissent sur la surface des cristaux pendant la réaction. Envisageant un tel modèle on aboutit à l'équation de Avrami-Erofeev :

$$\alpha = 1 - \exp(-kt^n) \tag{2}$$

laquelle peut être linéarisée en prenant des logarithmes :

$$\lg[-\lg(1 - \alpha)] = \lg(k/2{,}303) + n \lg t \tag{3}$$

où k et n sont des constantes.

Les diagrammes linéaires présentés dans la figure 5 montrent que l'équation Avrami-Erofeev est vérifiée.

Prenant des échantillons constitués par des cristaux aciculaires de longueur moyenne 5,6 mm et d'épaisseur 1,3 mm on a obtenu dans le domaine

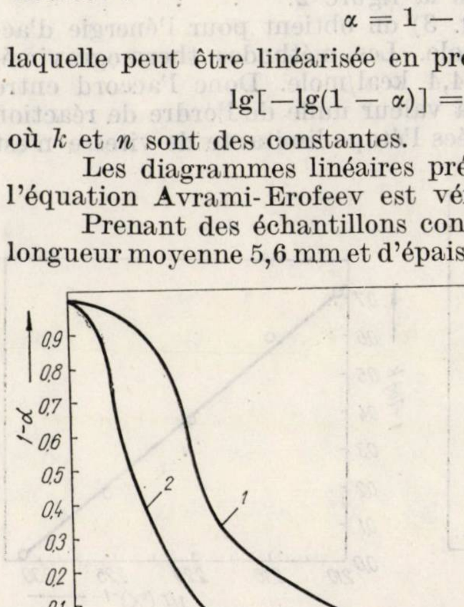

Fig. 4. — Courbes de la décomposition du permanganate de potassium :
1, 274° ; 2, 300°.

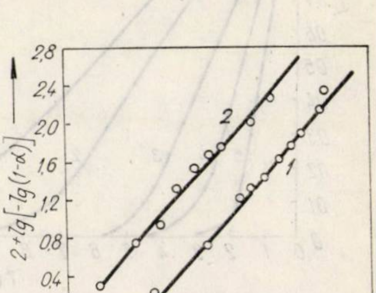

Fig. 5. — Diagramme Avrami-Erofeev pour la décomposition de $KMnO_4$:
1, 274° ; 2, 300°.

de température 262—300° les valeurs : $E = 41,3$ kcal/mole et $n = 2,3$. Dans le cas des échantillons en poudre ($0,09 < \Phi < 0,10$ mm) on a trouvé :

$$E = 39,2 \text{ kcal/mole} \quad \text{et} \quad n = 2,8$$

Ces dernières valeurs sont très proches de celles trouvées par Satava [6] dans des conditions non isothermes.

La variation des paramètres cinétiques dans le cas des réactions de décomposition des solides avec la granulométrie de l'échantillon peut être expliquée par la modification du nombre et de la distribution des centres actifs sur la surface.

Il est à signaler que les données expérimentales concernant la décomposition du permanganate de potassium peuvent également être décrites à l'aide de l'équation de Prout et Tomkins, fondée sur le modèle de la nucléation en chaîne ramifiée :

$$\ln(\alpha/1 - \alpha) = kt + C \tag{4}$$

où k et C sont des constantes.

Le diagramme obtenu est présentée dans la figure 6.

On peut observer que la droite correspondant à l'équation (4) change de pente pour la valeur $\alpha = 0,5$, c'est-à-dire pour le point d'inflexion de la courbe α, t. Par conséquent pour la description d'une courbe expérimentale il faut considérer deux valeurs du paramètre k (2, 31, respectif, 1,41 min^{-1}) ce qui constitue un désavantage par rapport à l'équation de Avrami-Erofeev.

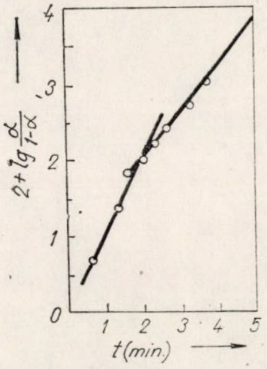

Fig. 6. — Diagramme Prout-Tomkins pour la décomposition de $KMnO_4$.

CONCLUSIONS

— Le dispositif expérimental décrit permet de tracer les courbes de la variation du volume de gaz dégagé pendant les réactions du type :

$$A(s) \rightarrow B(s) + C(g)$$

— Les renseignements fournis par les courbes de variation du volume de gaz en fonction du temps, permettent le calcul des paramètres cinétiques.

— Les valeurs des paramètres cinétiques — obtenues par la méthode volumétrique — pour la décomposition du $[Ni(NH_3)_6]Cl_2$ et $KMnO_4$ concordent d'une manière satisfaisante aux résultats trouvés par la méthode thermogravimétrique.

---

[6] V. Satava, "Thermal Analysis", vol. 2 (Proceedings of Third International Conference of Thermal Analysis 1971), Birkhäuser Verlag, Basel, 1972, p. 373.

Revue Roumaine de Chimie, **23**, 7, 1035–1042 (1978)

METALLKOMPLEXE DES SALICYLALDEHYD–THIOCARBOHYDRAZONS

CONST. GH. MACAROVICI * und SILVIA BARBU **
* ,,Babes-Bolyai“-Universität Cluj-Napoca, Chemie Fakultät, Str. Arany János Nr. 11
** Medizinisch-Pharmazeutisches Institut Cluj-Napoca,
Pharmazeutische Fakultät, Str. I. Creangă Nr. 12 Rumänien

Eingegangen am 24. Mai 1976

Es wurden Metallkomplexe des Salicylaldehyd-thiocarbohydrazons vom Typ $MLCl_2$, $ML_2(SCN)_2$ und $MLSO_4$ mit einigen Übergangsmetallionen synthetisiert. Das thermische Verhalten der synthetisierten Komplexe wurde derivatographisch untersucht. Für die Strukturaufklärung und Feststellung der an der Koordinativbindung beteiligten elektronenabgebenden Gruppen wurden die Elektronen- und IR-Spektren untersucht.

Burns,[1] bzw. Dutt und Chakder,[2-4] beschäftigten sich in ihren Arbeiten mit der Problematik der koordinativen Fähigkeit des Thiocarbohydrazids und seiner Derivate, synthetisierten und studierten auf Grund der Analogie zum Thiosemicarbazid, einige seiner Komplexverbindungen mit Übergangsmetallionen.

Die Thiocarbohydrazone, Azomethinderivate des Thiocarbohydrazids, entsprechend der allgemeinen Formel $H_2N-NH-CS-NH-N=$ $=CH-R$, sind eine Ligandenklasse mit interessanten Koordinierungseigenschaften, durch die im Molekül vorhandenen, elektronenabgebenden Gruppen.

In der vorliegenden Arbeit werden die Ergebnisse des physikalisch-chemischen Studiums bezüglich der Koordinierungsfähigkeiten des Salicylaldehyd-thiocarbohydratons (S–TCH) vorgelegt. In diesem Sinne synthetisierten und charakterisierten wir die Metallkomplexe des S–TCH(L) vom Typ $MLCl_2$, $ML_2(SCN)_2$ und $MLSO_4$, wo M=Fe, Co, Ni, Zn, Cd, Hg, Pd.

EXPERIMENTELLER TEIL

Herstellung der Komplexe

a) *Komplexe vom Typ* $MLCl_2$. Zu einer alkoholischen Lösung des Liganden wird im Molverhältnis 1 : 1 die hydroalkoholische Lösung des Metallchlorids hinzugefügt und auf dem Wasserbade 30 Minuten lang erwärmt. Man fügt Natriumcetatlösung hinzu, um ein pH = 6 zu erreichen.

---

[1] G. R. Burns, *Inorg. Chem.*, **7**, 227 (1968).
[2] N. K. Dutt und N. C. Chakder, *J. Inorg. Nuclear Chem.*, **32**, 2303 (1970).
[3] N. K. Dutt und N. C. Chakder, *J. Inorg. Nuclear Chem.*, **33**, 393 (1971).
[4] N. K. Dutt und N. C. Chakder, *Inorg. Chim. Acta*, **5**, 188 (1971).

Die durch Abkühlung gefällten komplexen Chloride werden durch Umkristallisierung aus Alkohol gereinigt.

b) *Komplexe vom Typ $ML_2(SCN)_2$.* Die alkoholische Lösung des Metallthiocyanids wird aus Kaliumthiocyanid und dem Metallnitrat hergestellt. Das Filtrat wird der alkoholischen Lösung des Liganden im Molverhältnis 1 : 2 hinzugefügt. Das Gemisch wird 30 Minuten auf dem Wasserbad erwärmt. Nach dem Abkühlen gibt man soviel Wasser hinzu bis die Metallkomplexe ausfallen. Die Reinigung wird durch Umkristallisierung aus Alkohol vorgenommen.

c) *Komplexe vom Typ $MLSO_4$.* Einer Metallsulfatlösung, hergestellt durch Auflösen von 0,01 Mol in der kleinstmöglichsten Menge Alkohol-Wasser (1 : 1), wird die Ligandenlösung, hergestellt durch Auflösen von 0,02 Mol in der kleinsten Menge Alkohol, hinzugefügt. Die Mischung wird ungefähr 30 Minuten auf dem Wasserbad erwärmt, dann abgekühlt und nachher mit Wasser verdünnt bis der Niederschlag ausfällt, abfiltriert und mit einem Gemisch Alkohol-Wasser (1 : 1) gewaschen.

Die synthetisierten Metallkomplexe werden bei Raumtemperatur getrocknet.

Tabelle 1 enthält die Ergebnisse der Elementaranalyse und des magnetischen Studiums. Die Komplexverbindungen des S—TCH sind leicht löslich in Lösungsmittel mit basischem Charakter (Dimethylformamid, Pyridin, Natriumhydroxid), wenig löslich in Methyl- und Äthylalkohol, unlöslich in Wasser.

Physikalische Messungen: Das thermische Verhalten wurde mit Hilfe des Derivatographen vom Typ Erdely-Paulik-Paulik untersucht. Die elektronischen Spektren wurden mit Hilfe eines VSU-2P Carl Zeiss-Jena Spektrophotometers aufgenommen. Die magnetische Suszeptibilität wurde bei Raumtemperatur mit Hilfe der mit $Hg[Co(SCN)_4]$ geeichten Faraday-Waage ermittelt. Das magnetische Moment wurde mit Hilfe der Gleichung $\mu_{eff} = 2{,}84\sqrt{\chi_H \cdot T^0}$ berechnet. Die IR-Spektren wurden mit Hilfe eines UR-10 Carl Zeiss Jena Spektrophotometers zwischen 3600—400 cm^{-1} aufgezeichnet, unter Anwendung von KBr-Pastillen.

ERGEBNISSE UND DISKUSSIONEN

Der Komplex $Ni(S-TCH)_2(SCN)_2$ wurde im Vergleich zum freien Liganden[5] derivatographisch untersucht. Die dem Derivatogramm entnommenen Daten wurden mit den Resultaten der stöchiometrischen Berechnung verglichen. Im Derivatogramm des Komplexes als auch in jenem des freien Liganden kann man zwei Zersetzungsstufen des Ligandenmoleküls beobachten, und zwar : bis zu 300° findet die Pyrolyse der desulfurierten Seitenkette statt, während am Ende der aromatische Rest abgetrennt wird. Der Pyrolyserückstand der Verbindung $Ni(S-TCH)_2(SCN)_2$ ist NiO, die erhaltenen Mengen sind in guter Übereinstimmung mit dem Kombinationsverhältnis M : L : SCN von 1 : 2 : 2 und wurden auf Grund der Elementaranalyse bestimmt.

Die elektronischen Spektren der Komplexe mit Ionen mit unvollständigen *d*-Orbitalen wurden in diffuser Reflexion aufgezeichnet.

Die Lage der charakteristischen Banden (siehe Tabelle 3) befürwortet hexakoordinierte Ionen für die Komplexe des Fe(III), Co(II) und Ni(II), mit Ausnahme des Pd(II)-Ions, das tetrakoordiniert ist und eine planar-quadratische Symmetrie aufweist.

Die Lage der ν_1-Bande im Falle des Komplexes $Ni(S-TCH)_2(SCN)_2$ befürwortet eine oktaedrische Symmetrie, die durch den Wert des magnetischen Momentes[6-8] bewiesen ist.

[5] S. Barbu und C. Gh. Macarovici, *Rev. Roumaine Chim.*, **22**, 000 (1977).

[6] D. Sutton, „Electronic Spectra of Transition Metal Complexes", Mc. Graw-Hill, London, 1969.

[7] F. A. Cotton und D. M. L. Goodgame, *J. Amer. Chem. Soc.*, **82**, 5771 (1960).

[8] D. M. Goodgame und F. A. Cotton, *J. Amer. Chem. Soc.*, **82**, 5774 (1960).

Tabelle 1

Ergebnisse der Elementaranalyse und des magnetischen Studiums

Verbindung	Farbe	N%		S%		M%		Cl%		$\chi_{M_{cor}} \cdot 10^6$	μ_{eff} MB
		Ber.	Gef.	Ber.	Gef.	Ber.	Gef.	Ber.	Gef.		
$Fe(S-TCH)Cl_2$	braun	16,62	16,17	9,51	10,02	16,57	17,05	21,04	21,50		
$Co(S-TCH)Cl_2$	braun	16,47	16,68	9,42	8,99	17,33	16,97	20,85	21,21	10682	5,05
$Ni(S-TCH)Cl_2$	braun	16,48	15,96	9,43	8,97	17,27	16,92	20,86	21,38		
$Zn(S-TCH)Cl_2$	gelb-grün	16,16	16,60	9,25	8,78	18,86	18,38	20,48	20,02		
$Cd(S-TCH)Cl_2 \cdot 2H_2O$	gelb-grün	13,04	12,68	7,46	6,98	26,16	25,82	16,52	16,11		
$Hg(S-TCH)Cl_2$	gelb-grün	11,62	11,23	6,65	6,10	41,62	40,71	14,73	13,92		
$Pd(S-TCH)Cl_2$	gelb	14,45	14,90	8,27	8,71	27,44	27,02	18,31	18,02		
$Co(S-TCH)_2(SCN)_2$	braun	23,51	23,53	21,53	21,20	9,89	10,02	—	—	10429	4,99
$Ni(S-TCH)_2(SCN)_2$	gelb	23,52	23,28	21,54	21,27	9,86	10,28	—	—	3583	2,91
$Ni(S-TCH)SO_4$	braun	15,35	14,98	17,54	16,98	16,08	15,53	—	—		

Tabelle 2

Pyrolysediagramm des $Ni(S-TCH)_2(SCN)_2$

Temperatur (°C)	Thermische Effekte (°C)		Gewichtsverlust %		Phänomen
	Endo	Exo	Ber.	Gef.	
200	120	–	9,23	8,02	CN-Abtrennung
300	–	220	28,57	30,20	Pyrolyse der desulfurierten Seitenkette
400	–	385	10,27	10,72	2S-Abtrennung
500	–	440 490	31,28 10,27	29,03 9,23	Pyrolyse des Molekülrestes und S-Abtrennung
800	800	–	12,52	13,58	NiO

Die größere Anzahl der Banden für diese Verbindungen weisen auf eine niedrigere Symmetrie hin, der Oktaeder ist distorsioniert. Das Vorhandensein einer Schulter bei ungefähr 8200 cm^{-1} könnte der Zweiteilung der Bande ν_1 zugeschrieben werden, die durch eine Spin-Orbital-Kopplung hervorgerufen wird.[9,10]

Wegen den Distorsionserscheinungen, die die Zweiteilung der Banden hervorrufen, entspricht die dem Ni(II)-Ion umgebende Geometrie der D_{4h} Symmetrie.

Aus den elektronischen Spektren der Komplexe der Salicylaldehydthiocarbohydrazons ist eine Interferenz der ν_3-Banden mit den charakteristischen $\pi-\pi^*$-Übergängen des Liganden ersichtlich, die bei 30300 cm^{-1} auftreten [5] und eine hohe Intensität aufweisen.

Im Spektrum des Komplexes des Eisen (III) sind zusätzliche Banden ersichtlich, die Ladungsübergängen vom Typ L → M zugeschrieben werden, hervorgerufen durch den Oxydationszustand 3^+ des Eisens, die die Kristallfeldübergänge teilweise oder ganz verdecken können.[11]

Für die Komplexverbindungen des S—TCH mit Metallionen der d^{10}-Struktur wurden elektronische Spektren im Bereich 400—200 nm in methanolischer Lösung aufgezeichnet (Tabelle 4). Die gelb-grüne Farbe der Verbindungen mit d^{10}-Ionen als Komplexbildner kann mit Hilfe von Zwischenligandübergängen erklärt werden, da der von uns benutzte Ligand cromophore Gruppen enthält.[5]

Im Spektrum des S—TCH-Komplexes mit d^{10}-Ionen erscheinen bathocrome Verschiebungen der $\pi-\pi^*$-Bande der Verbindungen $Zn(S-TCH)Cl_2$ und $Cd(S-TCH)Cl_2 \cdot 2H_2O$ als auch Intensitätsänderungen, als Resultat der Beteiligung des Chromophors $\gt C=S$ an der Metall-Ligand-Bindung.

---

[9] O. G. Holmes und D. S. McClure, *J. Chem. Phys.*, **26**, 1686 (1957).

[10] A. D. Liehr und C. J. Ballhausen, *Ann. Phys.*, **6**, 134 (1959).

[11] P. Day und K. C. Jørgensen, *J. Chem. Soc.*, **1964**, 6226.

Tabelle 3

Elektronische Spektren in diffuser Reflexion

Verbindung	ν cm^{-1}/Zuschreibung						
Fe(S–TCH)Cl$_2$	27000	26900 $^4E_g \leftarrow {}^6A_{1g}$	18500 S	16600 $^4T_{1g} \leftarrow {}^6A_{1g}$			
Co(S–TCH)Cl$_2$		23200 $^4T_{1g}(P) \leftarrow {}^4T_{1g}(F)$		16600 $^4A_{2g}(F) \leftarrow T_{1g}(F)$			
Ni(S–TCH)Cl$_2$	27000	25000–23300 $^3T_{1g}(F) \leftarrow {}^3A_{2g}(F)$		16600 $^3T_{1g}(F) \leftarrow {}^3A_{2g}(F)$			
Pd(S–TCH)Cl$_2$	27000 $^1E_g \leftarrow {}^1A_g$			16400 $^3E_g \leftarrow A_{1g}$			
Co(S–TCH)$_2$(SCN)$_2$	27000	25000 $^4T_{1g}(P) \leftarrow {}^4T_{1g}(F)$		16400 $^4A_{2f}(F) \leftarrow {}^4T_{1g}(F)$	15230	14000	
Ni(S–TCH)$_2$(SCN)$_2$		24300 $^3T_{1g}(P) \leftarrow {}^3A_{2g}(F)$		16900 $^3T_{1g}(F) \leftarrow {}^3A_{2g}(F)$	13100	10300 S $^3T_{2g}(F) \leftarrow {}^3A_{2g}(F)$	9600 8200 S
Ni(S–TCH)SO$_4$		23200 $^3T_{1g}(P) \leftarrow {}^3A_{2g}(F)$		15300 $^3T_{1g}(F) \leftarrow {}^3A_{2g}(F)$			

S = Schulter

Tabelle 4

Elektronenspektren im UV-Bereich der Komplexe mit d^{10}-Ionen

Verbindung	$\pi-\pi^*$		Andere Banden	
	λ_{max} nm	$\varepsilon(mol^{-1}cm^{-1})$	λ_{max} nm	$\varepsilon(mol^{-1}cm^{-1})$
$Zn(S-TCH)Cl_2$	340	34411	—	—
$Cd(S-TCH)Cl_2 \cdot 2H_2O$	380	6777	300	7717
$Hg(S-TCH)Cl_2$	330	11468	290	10362

Das Spektrum im IR-Bereich wurde mit dem IR-Spektrum des freien Liganden [5] verglichen, um die an der koordinativen Bindung beteiligten elektronenabgebenden Gruppen der Ligandenmoleküls festzustellen. Die Charakteristika der IR-Spektren der untersuchten Verbindungen, in den Tabellen 5 und 6 wiedergegeben, zeigen essentielle Veränderungen für die $\nu NH_2-(3400-2900\ cm^{-1})$, $\nu C-N$ und $\nu C=S$-Schwingungen. So erscheint der Frequenzbereich für Valenzschwingungen der NH_2 und NH-Gruppen im Spektrum der Komplexverbindungen als eine sehr breite Bande.

Diese Form des Spektrums unterstreicht die Beteiligung der Hydrazingruppe an der Metall-Ligand-Bindung durch den Terminalstickstoff.[12]

Der Bereich des Schwingungspaares νCN und $\nu C=S$ von ungefähr 1280 cm^{-1} ist im Spektrum der Komplexverbindungen nach einer höheren Wellenzahl verschoben, mit Ausnahme des $Fe(S-TCH)Cl_2$-Spektrums. Diese Veränderung kann als Folge einer Symmetrieänderung durch eine Koordinationsbeteiligung des $C=S$-Gruppe erklärt werden; in diesem Falle ist die Beteiligung der potenziellen Energie der $C-N$-Gruppe größer.[13]

Die Beteiligung der $C=S$-Gruppe an der Metall-Ligand-Bindung verändert die Schwingungsbeteiligung $\nu C-N$ im Bereich 800—700 cm^{-1}. Das Spektrum der Komplexe zeigt keine essentiellen Veränderungen in diesem Bereich.

Die Form des Spektrums der Komplexe im Frequenzbereich der Schwingungen $\nu C=N$ und δNH_2 ermöglicht eine Beteiligung der Azomethingruppe an der Koordinativbindung auszuschließen, da die NH_2 Deformationsschwingung („scissoring") unabhängig von der Metall-Ligand-Bindung ist.

Der gemeinsame Effekt mehrerer Faktoren ist auch im Bereiche der NH_2-Deformationsschwingung („rocking") anzutreffen. Der Beitrag der NH_2-Gruppe an der Metall-Ligand-Bindung veranlaßt das Wachsen der ρ-Schwingungskraftkonstanten, also eine Erhöhung der Schwingungsfrequenz. Aber da die Deformationsschwingung („rocking") sehr empfindlich für eine Änderung der Bindungsstärke ist, könnte man annehmen, daß der gemeinsame Effekt dieser Faktoren keine Veränderungen veranlaßt.[14–16]

---

[12] M. Mashima, *Bull. Chem. Soc. Japan*, **37**, 974 (1964).

[13] A. Yamaguki, R. B. Penland, S. Mizushima, T. J. Lane, C. Curran und J. V. Quagliano, *J. Amer. Chem. Soc.*, **80**, 527 (1958).

[14] J. Fujita, K. Naramoto und M. Kobayashi, *J. Amer. Chem. Soc.*, **78**, 3295 (1956).

[15] S. Mizushima, I. Nakagawa und J. V. Quagliano, *J. Chem. Phys.*, **23** 1367 (1955).

[16] M. Kobayashi und J. Fujita, *J. Chem. Phys.*, **23**, 1354 (1955).

Tabelle 5

IR-Spektren der S-TCH Komplexe mit Metallionen mit unvollständig besetzten *d*-Orbitalen

$\mathrm{Fe(S-TCH)Cl}$	$\mathrm{Co(S-TCH)Cl_2}$	$\mathrm{Ni(S-TCH)Cl_2}$	$\mathrm{Pd(S-TCH)Cl_2}$	$\mathrm{Co(S-TCH)_2(SCN)_2}$	$\mathrm{Ni(S-TCH)_2(SCN)_2}$	$\mathrm{Ni(S-TCH)SO_4}$	Zuschreibung
3075 schw breite Bande	3080 schw breite Bande	breite Bande	breite Bande	breite Bande	breite Bande	breite Bande	νNH_2 νNH
-	-			2090 m	2112 i		$\nu C \equiv N$
1630 1608	1615 i	1620 i	1630 i	1610 i	1615 i	1605	$\nu C = N$ δNH_2
1590 S 1560 m 1495 m 1377 m 1305 m	1550 m 1505 S 1450 m 1380 S 1350 S	1560 i 1380 i	1562 i 1500 m 1405 m 1370 m	1545 m 1500 m 1478 m 1450 m 1390 m	1555 i 1480 S 1385 m	1545 i 1475 m 1450 m 1380 m	$WNH + \nu C-N$ $\nu C-N + WCH$
1280 m	1300 m	1300 i	1290 i	1305 m	1280 mi	1300 S	$\nu C-N$ $\nu C = S$
1210 1160	1210 m 1160	1220 i 1160 i	1205 m 1160 m	1210 i 1160 i	1220 mi 1160 mi	1210 m 1160 m	ρNH_2
1120 schw 1040 schw 960 schw	1135 m 1030 1050 965 schw 920 schw	1120 m 1040 m 970 m 920 m	1050 m 960 m 920 schw 910 schw	1038 schw 960 schw 920 schw 868 schw	1120 m 962 schw	1115 m 1045 S 960 schw 920 schw 870 schw	δNCS WNH_2 $\nu C-NN$ $\nu C-N$
760 i	805 schw 760 i	860 m 765 i	840 schw 800 m 750 i	820 schw 800 schw 760 mi	762 i	825 schw 765 i	$\nu C = S$ $\nu C-N$

---

i = intensiv ; m = mittel ; schw = schwach ; S = Schulter.

Tabelle 6

IR-Spektren der Komplexe von d^{10}-Ionen

$Zn(S-TCH)Cl_2$	$Cd(S-TCH)Cl_2 \cdot 2H_2O$	$Hg(S-TCH)Cl_2$	Zuschreibung
3140–3160 m	3190–3290 m	3260 schw	νNH_2 νNH
3000 m	3025 schw	3075 schw	
		breite Bande	
1625 i	1615 i	1690 S	$\nu C = N$ δNH_2
		1630	
1570 i	1555 i	1590 S	$W\ NH + \nu C-N$
1495 i	1500 S	1540 i	$\nu C-N + W\ NH$
1460 m	1450 schw	1495 m	
1400 m	1382 m	1400 m	
1360 m		1350 m	
1320 m	1290 i	1305 S	$\nu C-N$ $\nu C = S$
1290 i		1278 i	
1245 m	1245 S	1245 m	
1205 m	1200 m	1205 m	ρNH_2
1180 m	1160 m	1160 i	
1160 m	1120 schw		
1040 schw	1045 schw	1050 m	δNCS
965 m	965	958 m	$W\ NH_2$
900 schw	918	910 m	$\nu C\ NH$
	845 schw	868 schw	$\nu C-N$
	810 schw	845 schw	
800		800 m	$\nu C = N$ $\nu C-N$
765 S	760 m	760 i	
755 i			

i = intensiv ; m = mittel ; schw = schwach ; S = Schulter

Die Lage des charakteristischen Piks für die $\nu C \equiv N$ Schwingungsart in Thiocyanatkomplexen mit S—TCH, empfiehlt eine Brückenbindung des SCN^--Ions für den Fall, daß der Komplexbildner das Co(II)-Ion ist und eine Bindung über Schwefel im Falle des Ni(II)-Komplexes. [17,18]

Zusammenfassend kann gesagt werden, daß das Salicylaldehydthiocarbohydrazon sich im Falle der von uns synthetisierten Verbindungen als zweiwertiger Ligand verhält ; die an der koordinativen Bindung beteiligten Gruppen sind die Thiol- und Hydrazingruppe. Die Azomethingruppe ist nicht beteiligt. Die Schlußfolgerung steht im Einklang mit den Voraussetzungen, die auch auf Grund der theoretischen Erkenntnisse gemacht werden können, daß jene Gruppen, die ein freies Elektronenpaar in einem sp^3-Hybrid besitzen, basischer sind als jene, die das Elektronenpaar in einem sp^2-Hybrid besitzen. Dieses verhält sich so, dank dem geringeren Beitrag des Schwefels im Falle der sp^3-Hybride.

---

[17] S. Arhland, J. Chatt und N. R. Davies, *Quart. Rev.*, **12**, 265 (1958).
[18] R. G. Pearson, *J. Amer. Chem. Soc.*, **85**, 3533 (1963).

Revue Roumaine de Chimie, **23**, 7, 1043–1048 (1978)

COMPLEX COMPOUNDS WITH TRI-*p*-XYLYLPHOSPHINE

D. NEGOIU and MARIA NEGOIU
Institute of Chemistry, Department of Chemistry and Anorganic Technology, Splaiul Independenței 89, Bucharest, Romania

Received May 7, 1976

The preparation and chemical analysis of the complex compounds of the type HgX_2R, where X = Cl, Br, I and R = $(p\text{-xylyl})_3P$, are presented. The substances obtained have been studied from the point of view of their chemical stability by means of thermogravimetric methods. The structure of the compounds obtained has been established using IR and NMR spectral data.

In the last years, the noticeable ability of the phosphines to form complex compounds with transition metal ions has been investigated by many authors. It has been thus obtained a lot of coordination compounds containing as ligands phosphines or their derivatives having organic radicals instead of halide ions.

Since 1940, mercury complexes with tertiary phosphines[1] have been reported in the literature. Other new compounds of mercury halides with phosphine oxides, sulphides and selenides have been also reported.[2–5]

The aim of the present note is to investigate the obtainment of complex compounds of the type HgX_2R, where X=Cl, Br, I and R=$(p\text{-xylyl})_3P$, as well as the study of their main properties.

RESULTS AND DISCUSSION

To study the thermal behaviour of the newly synthesized compounds the thermogravimetric method has been used. The four thermogravimetric curves corresponding to differential thermal analysis (DTA), thermogravimetry (TG), derivative-thermogravimetry (DTG) and to the temperature variation (T), have been recorded for each complex compound. Figure 1 shows the thermal behaviour of the compound obtained in the reaction between HgI_2 and $(p\text{-xylyl})_3P$. The common feature of all diagrams consists in the fact that the thermolysis process takes place in two stages, which could be both ascribed to the successive decomposition of the original compounds followed by the formation of intermediate unstable products.

---

[1] R. C. Evans and F. Mann, *J. Chem. Soc.*, **1940**, 1209.
[2] J. A. Dalziel, C. Holding and B. E. Wattes, *J. Chem. Soc.* (*A*), **1967**, 358.
[3] M. G. King and G. P. McQuillan, *J. Chem. Soc.* (*A*), **1967**, 898.
[4] M. Negoiu and P. Spacu, *Anal. Univ. Buc.*, **19**, 93 (1970).
[5] M. Negoiu and P. Spacu, *Anal. Univ. Buc.*, **20**, 71 (1971).

It should be emphasized that the two stages are accompanied by an exothermal effect which may be observed on the DTA curves.

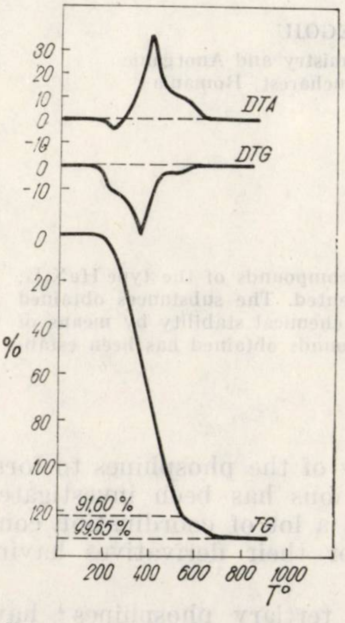

Fig. 1. — The derivatogram of $HgI_2P(p\text{-xylyl})_3$ (3).

One may state from the TG curve that the decomposition process of $HgI_2P(p\text{-xylyl})_3$ begins at 210° and ends at 680° (Table 1). The 235°, 220° and 210° temperatures correspond to those points where the substances **1**, **2**, **3** began to melt with decomposition. Endothermal effects correspond to these points on the DTA curves.

It may be remarked a lowering in the melting point values going from the compound containing mercury (II) chloride to that containing mercury (II) iodide.

The weight losses observed in the TG curves do not however suggest the formation of intermediate compounds having well established structure. This conclusion is also supported by the data summarized in table 2.

Another conclusion is the fact that the whole quantity of substance volatilizes from the crucible at temperatures higher than 680°.

To elucidate the structure of the compounds of the type HgX_2PR_3, the IR and NMR spectra have also been recorded.

Table 1

Thermal properties of $HgX_2P(p\text{-xylyl})_3$

Compound	Maximum stability temperature (°C)	Temperature of the second stage (°C)	Final temperature (°C)
(1) $HgCl_2P(p\text{-xylyl})_3$	235	380	660
(2) $HgBr_2P(p\text{-xylyl})_3$	220	400	620
(3) $HgI_2P(p\text{-xylyl})_3$	210	550	680

Table 2

Weight loss of $HgX_2P(p\text{-xylyl})_3$

Compound	Theoretical %			Experimental %		
	1 molec. phosphine	1 molec. HgX_2	Total	I stage	II stage	Total
(1) $HgCl_2P(p\text{-xylyl})_3$	55.97	44.03	100	84	15.80	99.80
(2) $HgBr_2P(p\text{-xylyl})_3$	48.60	51.40	100	82.30	16.65	98.95
(3) $HgI_2P(p\text{-xylyl})_3$	43.17	56.83	100	91.60	8.05	99.65

The experimental data obtained for the 400—3600 cm^{-1} range are presented in table 3.

Unfortunately it was not possible to assign all the absorption bands occurring in the IR spectrum, due to the great number of atoms contained in the ligand molecula, as well as of its asymmetry. No absorption bands due to vibrations of Hg—X bond have been observed within the frequency domain studied herein. The vibration bands presented in table 3 have been assigned as follows.

Table 3

IR spectra of $HgCl_2PR_3$ (1) ; $HgBr_2PR_3$ (2) and HgI_2PR_3 (3) (KBr; cm^{-1})

(1)	3500 m	3030 m		2920 s	2870 m	1570 w	1495 s	1450 s
(2)	3515 m	3020 m		2915 s	2860 m	1570 w	1495 s	1445 s
(3)	3500 m	3020 m	2950 m	2915 s	2850 m	1570 w	1495 s	1450 m
(1)	1390 s	1290 s	1210 m	1155 m	1075 w	1040 w	820 s	740 w
(2)	1390 s	1290 s	1210 m	1155 m	1070 w	1040 w	820 s	740 w
(3)	1352 m	1290 m	1210 m	1150 m	1075 w	1035 w	820 s	740 w
(1)	710 w	565 w	555 w	545 w	510 m	492 s	455 m	410 w
(2)	710 w	565 w	555 w	545 w	515 m	492 s	460 m	410 w
(3)	710 m		560 w	545 w	505 m	480 m	460 m	410 w

s = strong; m = medium; w = weak

Frequency bands at 1495 cm^{-1}, 1450 cm^{-1} and 1570 cm^{-1} have been ascribed as being due to the ν_{C-C} vibration of aromatic ring.[6] The absorption bands between 2915—2950 cm^{-1} are proper to the antisymmetric ν_{CH_3} vibration and those between 2850—2870 cm^{-1} would correspond to the symmetric ν_{CH_3} vibration.

The bands placed in the 750—650 cm^{-1} and 1400—1100 cm^{-1} domains have been ascribed to the vibration frequency of C—P bond.[7]

The single bands from these domains put in evidence in the IR spectra of the compounds prepared, are those occurring at 710 and 740 cm^{-1}. The absorption bands from the other domain are of no use for our compounds, because they overlap with those due to ν_{C-C} vibration of the aromatic ring, occurring in the same domain. The bands between 3020—3030 cm^{-1} are characteristic to the stretching C—H(ν_{C-H}) vibrations, shifted towards higher wavenumbers (3013 cm^{-1}) in the case of *p*-xylene.[8]

---

[6] M. Avram and G. Mateescu, "Spectroscopia în infraroşu. Aplicaţii în chimia organică", Editura Tehnică, Bucureşti, 1966, p. 16.

[7] C. N. Rao, "Chemical Applications of Infrared Spectroscopy", Academic Press, London, 1963.

[8] S. C. Wiberley, *Analyt. Chem.*, **32**, 217 (1960).

The bands placed at 820 cm^{-1} are characteristic to the out-of-plane C—H bending vibration (γ_{C-H}). The band situated at 740 cm^{-1}, specific to the benzene having three substituted hydrogens,[6] may also be assigned to the γ_{C-H} vibration.

The mono- and the di-valent mercury ions show a very weak band placed at 720 cm^{-1} in the IR spectrum,[9] which cannot be put in evidence for the compounds studied, due to the interference with the intense ν_{C-P} frequency vibration.

It may be concluded from these considerations that the main absorption bands proper to the ligand are found in the spectra of the complex compounds. Some of these bands are shifted if they are compared with the original bands from the free ligand spectrum. The changes are mainly due to the mercury ion-ligand interactions. The phosphorus atom is directly bound to the aromatic ring, in other words it is not a $-CH_2-$ bridge, its characteristic vibrations being inexistent in the spectrum.

As far as the ligand structure is concerned, one may say that the molecule cannot exist in the planar form due to considerable steric hindrances, which make the molecule get a helical shape, the plane of each aromatic ring being rotated with a "φ" angle. The P—C chemical bonds are of "σ" type, all the "p" orbitals involved in the three aromatic sextets cannot, for these reasons, become parallel to them. This observation agrees with the data existent in the related literature for the substituted triarylmethanes.[10]

This structure is also supported by the nuclear magnetic resonance spectra.

The NMR spectrum of the $HgI_2P(p\text{-xylyl})_3$ compound is shown in Figure 2.

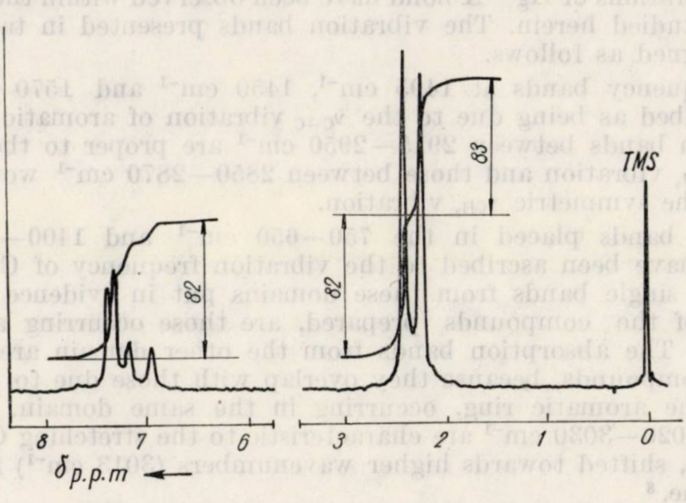

Fig. 2. — NMR spectrum of $HgI_2P(p\text{-xylyl})_3$ **(3)**.

---

[9] R. A. Nyguist, "Infrared Spectra Inorg. Compounds", Academic Press, London, 1971, p. 7.

[10] G. C. Gannon, *Spectrochim. Acta*, **4**, 373 (1951).

One may observe the appearance of two groups of signals. The first one occurs at $\delta = 2.24$ ppm and 2.41 ppm. These two signals are to be ascribed to the methyl groups in the ***ortho*** and in the ***meta*** position.

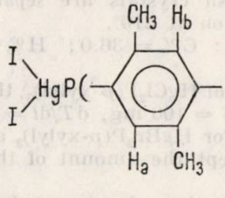

The second group of signals occurs at $\delta = 7.0-7.3$ ppm. These signals are due to the benzene protons (Table 4).

Table 4

NMR-signals of (3) in $CDCl_3$

δppm	Number of protons	Multiplicity	J, Hz	Assignment
2.24	9	singlet		CH_3 (ortho)
2.41	9	singlet		CH_3 (metha)
7.0	3	doublet	14.5	$3H_a$ (vicinal coupling with P)
7.3	6	multiplet		$3H_b + 3H_c$

The ratio between the relative values of the integrals agrees with the number of protons to which the respective signals were assigned. The conclusion drawn from the IR spectra, namely that the phosphorus atom is directly bound to the aromatic ring, without a $-CH_2-$ bridge, is also supported by the NMR spectral data.

EXPERIMENTAL

To obtain the new compounds, mercury (II) halides p.a. Merck and trixylylphosphine synthesized starting[11] from PCl_3 and bromo-*p*-xylene were used.

Dichloro (tri-p-xylylphosphine) mercury (II) $HgCl_2P(p\text{-xylyl})_3$ 0.5 g $HgCl_2$ (2 mmoles) are mixed with 0.7 g $(p\text{-xylyl})_3P$ (2 mmoles), both substances being solved in 25 ml warmed 50° absolute ethanol. The solution is then cooled, a white compound being thus separated. The precipitate is purified through repeated recrystallizations from absolute ethanol. The substance melts with decomposition at 235°.

Analysis $HgCl_2P(p\text{-xylyl})_3$: Calc. : C% = 46.60 ; H% = 4.37 ; Cl% = 11.13 ; Found : C% = 45.92 ; H% = 4.09 ; Cl% = 10.80.

Dibromo (tri-p-xylylphosphine) mercury (II) $HgBr_2P(p\text{-xylyl})_3$ 0.7 g $HgBr_2$ (2 mmoles) are solved in 25 ml absolute ethanol and then added to a warmed 50° solution containing

---

[11] A. Michaelis, *Liebigs Ann. Chem.*, **315**, 98 (1901).

0.7 g $(p\text{-xylyl})_3P$ (2 mmoles) in 25 ml absolute ethanol. The white crystalline precipitate separated from the cooled solution melts with decomposition at 220°.

Analysis $HgBr_2P(p\text{-xylyl})_3$: Calc. : C% = 40.80 ; H% = 3.82 ; Br% = 22.64 ; Found : C% = 40.68 ; H% = 3.80 ; Br% = 22.16.

Diiodo (tri-p-xylylphosphine) mercury (II) $HgI_2P(p\text{-xylyl})_3$ 0.7 g HgI_2 (2 mmoles) in 25 ml absolute ethanol are mixed on the water bath with 0.9 g $(p\text{-xylyl})_3P$ (2 mmoles) in 25 ml absolute ethanol. Fine yellowish crystals are separated from the cooled solution. The substance melts with decomposition at 210°.

Analysis $HgI_2P(p\text{-xylyl})_3$: Calc. : C% = 36.0 ; H% = 3.37 ; I% = 31.71 ; Found : C% = 35.8 ; H% = 3.30 ; I% = 31.50.

For the thermogravimetric study of $HgCl_2P(p\text{-xylyl})_3$, the following experimental conditions have been used : $m = 112.5$ mg, $S = 100$ mg, $dT/dt = 4.9°/\text{min}$, DTA = 1/10, DTG = = 1/20, temperature range 0–1200°. For $HgBr_2P(p\text{-xylyl})_3$ and $HgI_2P(p\text{-xylyl})_3$ the experimental conditions were the same, except the amount of the sample, $m = 101.7$ mg and 132.5 mg respectively.

The IR spectra of the compounds have been recorded on KBr pellets using a Carl Zeiss-Jena UR-10 double-beam spectrophotometer.

The NMR spectrum of $HgI_2P(p\text{-xylyl})_3$ has been obtained with a VARIAN A 60-A spectrometer, the compound being solved in $CDCl_3$ with TMS internal standard.

Revue Roumaine de Chimie, **23**, 7, 1049–1053 (1978)

DIELECTRIC BEHAVIOUR OF DNA-METAL COMPLEXES

V. K. SRIVASTAVA, P. K. BANERJI and G. P. SRIVASTAVA
Department of Chemistry, University of Gorakhpur,
Gorakhpur – 273001, (U.P.), India

Received April 28, 1976

Dielectric dispersion of DNA and DNA-metal complexes were investigated in the frequency range of 50 Hz–5 MHz. The metal cations were found to have a considerable effect on the static dielectric constant and dipole moment of DNA. Dipole moments were estimated from Kirkwood theory. The change in dipole moments of DNA was explained by the structural alterations of DNA obtained by the presence of different metal cations.

INTRODUCTION

The interaction of metal cations with DNA has been very widely studied. The interactions have been found to be dependent not only on the nature of metal cations but on the conformational status of DNA as well.[1–9] Though recently many sensitive and sophisticated techniques have been employed to study the chemical and physical aspects of such interactions, the dielectric method has not been used despite of several reports on the dielectric properties of DNA.[10–17] The present paper deals with the results of dielectric studies of native and denatured DNA's in the presence of metal cations Mg^{+2}, Cu^{+2}, Zn^{+2}, Hg^{+2} and Ag^{+1}.

---

[1] G. L. Eichhorn, *Nature*, **194**, 474 (1962).

[2] H. Venner and Ch. Zimmer, *Biopolymers*, **4**, 321 (1966).

[3] D. W. Gruenwedel and Y. A. Shin, *J. Amer. Chem. Soc.*, **90**, 7223 (1968).

[4] J. H. Coates, D. O. Jordan and V. K. Srivastava, *Biochim. Biophys. Res. Comm.*, **20**, 611 (1965).

[5] S. Hiai, *J. Mol. Biol.*, **11**, 672 (1965).

[6] V. I. Ivanov and L. E. Minchenkovo, *Biokhimia*, **30**, 1213 (1965).

[7] V. K. Srivastava and P. K. Banerji, *Analyst*, **51**, 100 (1975).

[8] V. K. Srivastava and P. K. Banerji, *Chem. Biol. Inter.*, **11**, 307 (1975).

[9] V. K. Srivastava, P. K. Banerji and B. B. Misra, *Biopolymers*, **15**, 227 (1976).

[10] L. G. Allgen, *Acta. Physiol. Scand.*, **22**, 76 (1950).

[11] G. Jungner, I. Jungner and L. G. Allgen, *Nature*, **63**, 849 (1949).

[12] S. Takashima, *Adv. Chem. Ser.*, **63**, 232 (1967).

[13] S. Takashima, *Biopolymers*, **5**, 899 (1967).

[14] S. Takashima, *Biopolymers*, **12**, 145 (1973).

[15] F. Oosawa, *Biopolymers*, **9**, 677 (1970).

[16] D. N. Goswami and N. N. Das Gupta, *Biopolymers*, **12**, 1047 (1973).

[17] D. N. Goswami and N. N. Das Gupta, *Biopolymers*, **13**, 1549 (1974).

MATERIALS AND METHODS

Stock solution of Calf Thymus DNA (obtained as gift from Institute of Biophysics Brno Czechoslavakia) of 1 mg/ml was prepared in 1 mM KNO_3 solution and diluted with the same solution as and when required. Other chemicals used were of reagent grade. Doubly distilled conductivity water was used for making solution. The metal cations solutions were added to native and denatured DNA's (denatured DNA was obtained by heating native DNA solution to 90° for 15 minutes and then shock cooled by using ice cold water) in the mole ratio of 2 : 1. Though the pH of the solution ranged between 5.7—6.1, no buffer solution was used. As suggested earlier, such pH variations did not produce any conformational changes of DNA.[18]

The dielectric measurements were done at 25.8 ± 0.01°. These measurements were made on a special impedance bridge which was a modified form of 1606-A General Radio. The capacity and the resistance of both the cell and solution of DNA with and without metal cation solutions were estimated within the frequency range of 50 Hz—5 M Hz. Both electrode polarization and stray field components were effectively controlled by using guard electrodes and maintaining small distance between them as suggested by Schwann.[19] All observations were made within the least possible time since the dielectric constant of DNA solution changes with time.

The complex dielectric constant of any substance is given by

$$\varepsilon^* = \varepsilon' - i\varepsilon''$$

where ε' and ε'' are the real and imaginary parts of the complex dielectric constant. Dielectric loss (ε'') was calculated using the relationship $\varepsilon'' = (K - K_0)/2\,\Lambda f\,\varepsilon_r$ where K_0 is the low frequency conductance and K the conductance at frequency f, and ε_r is the dielectric constant of the free space. The low and high frequency dielectric constants (ε_0 and ε_∞) were evaluated from Cole — Cole plots.[20] The dielectric data gave an effective molecular moment for DNA and also relaxation time which showed an appreciable distribution factor $(1 - \alpha)$ of Cole — Cole = 0.62. The results were reproducible with fresh solutions of DN .

The dipole moment (μ) was calculated using Kirkwood's relation [21]

$$\mu = 3.3\sqrt{\Delta\varepsilon/c}$$

where $\Delta\varepsilon$ was the dielectric treatment and c is the concentration in mole/ml.

RESULTS

The dielectric dispersion of native DNA, denatured DNA and of their complexes with metal cations are given in Figures 1 and 2. The dielectric dispersion curves reached the static dielectric constant values of 465.0 for native DNA, 187.0 for denatured DNA and 550.0, 526.0, 500.0, 474.0, 462.0 for native DNA complexes with Mn^{+2}, Cu^{+2}, Zn^{+2}, Ag^{+1} and Hg^{+2} and 228.0, 222.5, 298.0, 208.6 and 190.4 for denatured DNA-metal complexes respectively. As compared with native DNA, denatured DNA and the metal complexes with DNA have comparatively lower values of static dielectric constants. The dispersion of DNA — metal complexes were found to occur in a comparatively narrow frequency region.

---

[18] G. L. Eichhorn and P. Clark, *Proc. Nat. Acad. Sci., U.S.A.*, **53**, 586 (1965).

[19] H. P. Schwann, "Physical Techniques in Biological Research", Vol. 6, Academic Press, New York, 1963.

[20] K. S. Cole and R. H. Cole, *J. Chem. Phys.*, **9**, 341 (1941).

[21] J. G. Kirkwood, "Proteins, Amino acids and Peptides", E. J. Cohn & Edsall., Reinhold, New York, 1943.

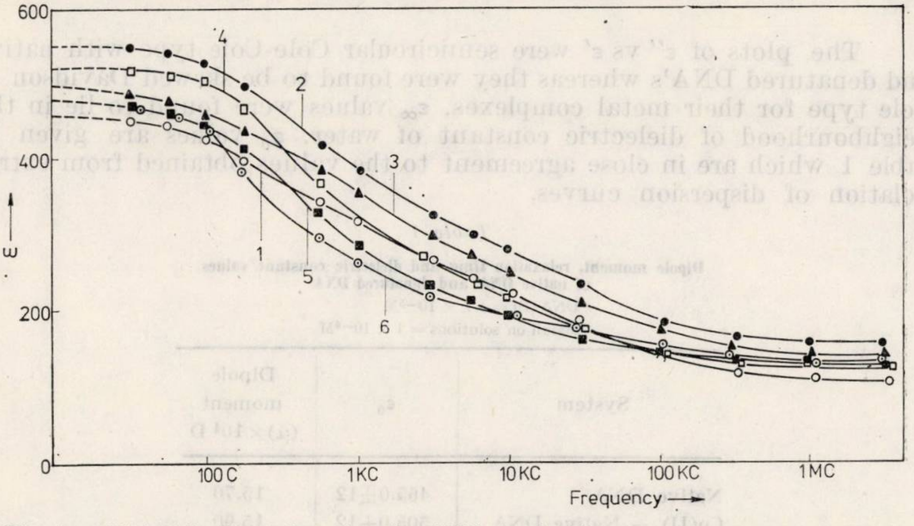

Fig. 1. — Dielectric dispersion of native DNA in the absence and presence of metal ions.

1. native DNA
2. native DNA + Mg (II)
3. native DNA + Cu (II)
4. native DNA + Zn (II)
5. native DNA + Ag (I)
6. native DNA + Hg (II)

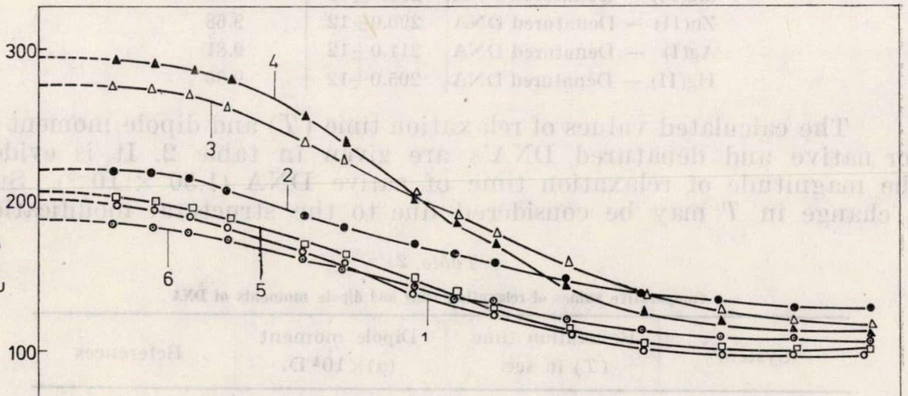

Fig. 2. — Dielectric dispersion of denatured DNA in the absence and presence of metal ions.

1. denatured DNA
2. denatured DNA + Cu (II)
3. denatured DNA + Mg (II)
4. denatured DNA + Zn (II)
5. denatured DNA + Ag (I)
6. denatured DNA + Hg (II)

The plots of ε'' vs ε' were semicircular Cole-Cole type with native and denatured DNA's whereas they were found to be skewed Davidson — Cole type for their metal complexes. ε_∞ values were found to lie in the neighbourhood of dielectric constant of water. ε_0 values are given in table 1 which are in close agreement to the values obtained from extrapolation of dispersion curves.

Table 1

Dipole moment, relaxation time and dielectric constant values of native DNA and denatured DNA

DNA (P) = 4.7×10^{-5}M

Metali on solutions = 1×10^{-4}M

System	ε_0	Dipole moment $(\mu) \times 10^4$ D
Native DNA	465.0±12	15.70
Cu(II) — Native DNA	505.0±12	15.90
Mg(II) — Native DNA	552.5±12	15.61
Zn(II) — Native DNA	525.0±12	15.90
Ag(I) — Native DNA	475.0±12	15.45
Hg(II) — Native DNA	472.5±12	15.55
Denatured DNA	187.0±12	5.69
Cu(II) — Denatured DNA	220.0±12	9.72
Mg(II) — Denatured DNA	280.0±12	10.05
Zn(II) — Denatured DNA	290.0±12	9.68
Ag(I) — Denatured DNA	211.0±12	9.81
Hg(II) — Denatured DNA	205.0±12	9.80

The calculated values of relaxation time (T) and dipole moment (μ) for native and denatured DNA's are given in table 2. It is evident the magnitude of relaxation time of native DNA (1.50×10^{-5}). Such a change in T may be considered due to the structural modifications of DNA. The values of T (1.59×10^{-4}) and μ (15.7×10^4 D) for native DNA in the present investigation compares favourably well with the values as reported by other workers.

Table 2

Comparative values of relaxation time and dipole moments of DNA

System	Relaxation time (T) in sec.	Dipole moment $(\mu) \times 10^4$ D.	References
Native DNA	10^{-3}	3.2	7
Native DNA	1.59×10^{-4}	9.8	17
Native DNA	1.59×10^{-4}	15.7	Present work
Denatured DNA	1.50×10^{-5}	5.69	Present work

$$T = 1.70 \times 10^{-4},\ \mu = 9.8 \times 10^4\ \mathrm{D}^{17} \text{ and } T = 10^{-3},$$

$$\mu = 3.2 \times 10^4\ \mathrm{D}^{22}.$$

---

[22] S. Takashima, *J. Mol. Biol.*, **7**, 455 (1963).

DISCUSSION

The lowering down of relaxation time and dipole moment of DNA from native to denatured states conforms to the fact that the molecule had undergone a change in conformation (Table 1). This is possibly due to orientation polarizability as has been suggested recently.[23] The μ values of DNA are considerably affected by the presence of different metal cations, which is dependent on nature of metal cations and binding sites involved therewith. The counter ion binding by metal cations plays an important role in the electric polarization of DNA. It may thus be suggested that a combination of both orientation as well as induced polarizabilities contribute the observed changes in μ values.

With neutralization of the negative charges by Mg^{+2}, the surface charges are reduced and the μ value is also decreased (15.6×10^4D) was compared to native DNA (15.70×10^4D). Cu^{+2} not only binds to the phosphates stabilizing the ordered structure by counter ion effect but also binds to the bases and competes with the hydrogen bonding of the double helix and thus help to destroy it. Chelate binding of Zn^{+2} to DNA changes the internal conformation and increase the flexibility within DNA to a greater extent than Mg^{+2}. The μ values in these cases have been found to be greater than the μ values of DNA. Hg^{+2} and Ag^{+1} interact with the nucleotide bases so strongly that instead of unwinding they stoichiometrically interpolate between the strands. Consequently very rigid complex is formed which is however removed only by competing complexing agents. The μ values with these metal cations were found to be lower than DNA.

Such variations in μ values occurs due to the structural alterations of DNA in different manner produced by these metal ions. The metal ion induced conformational changes of DNA are better explained by alteration of the winding angle between base pairs. With denatured DNA, the situation is phosphates or bases, the μ values were found to be increased in all cases which were due to the possible involvement of the free exposed nucleotide bases obtained on denaturation of DNA.

ACKNOWLEDGEMENT. The authors are thankful to Prof. R. P. Rastogi,, Head of Chemistry Department, University of Gorakhpur, Gorakhpur, for providing all kinds of necessary facilities. The authors are also thankful to Prof. G. P. Srivastava, Deptt. of Physics, Delhi University, Delhi for allowing us to make dielectric measurements in his laboratory.

---

[23] M. Hauss and J. C. Bernengs, *Biopolymers*, **12**, 215 (1973).

Revue Roumaine de Chimie, **23**, 7, 1055–1059 (1978)

DYNAMICS OF THE LIGAND EXCHANGE IN URANYL BIS-(CHELATED) COMPLEXES. II[1]

CONFIGURATIONAL REARRANGEMENT OF BIS-(BENZOYLACETONATO) URANYL CHELATE

ALICE VASILESCU * and TATIANA ONCESCU **

*Institute for Atomic Physics, P.O. Box 5206, Bucharest, Romania
**Institute of Chemistry, Dept. of Physical Chemistry, Bd. Republicii 13, Bucharest, Romania

Received May 12, 1976

Bis-(benzoylacetonato) uranyl undergoes in deuterochloroform an intramolecular ligand exchange, which is evidenced by DNMR method. The activation parameters are: $E_a = 5.5 \pm 0.3$ kcal/mol, $\log A = 5.43 \pm 0.26$, $\Delta H^{\neq}_{298°K} = 4.9 \pm 0.3$ kcal/mol, $\Delta S^{\neq}_{298°K} = -35.2 \pm 1.2$ eu, $\Delta G^{\neq}_{298°K} = 15.34 \pm 1.08$ kcal/mol. The mechanism supposed to operate is one-end dissociation of the ligand with a TBP transition state.

INTRODUCTION

The intra- and intermolecular ligand exchange in β-ketoenolate complexes focussed attention of numerous investigators in the last years.[1–8] In spite of rich data concerning isomerization and racemization in six-coordinate chelate complexes,[9] as far as we are aware, no studies were published on systems undergoing the following type of rearrangement (Figure 1):

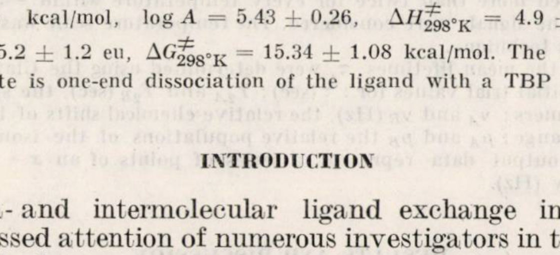

I_a I_b

trans, cis, cis (C_{2v}) *trans, trans, trans* (C_{2h})

Fig. 1. — Type of isomerization of $M(U\text{-chel})_2X_2$ complexes.

---

[1] A. Vasilescu, *Rev. Roumaine Chim.*, **20**, 951 (1975).
[2] A. C. Adams and E. M. Larsen, *Inorg. Chem.*, **5**, 814 (1966).
[3] T. Y. Pinnavaia and R. C. Fay, *Inorg. Chem.*, **5**, 233 (1966); ibid., **7**, 502 (1968).
[4] G. E. Glass and R. S. Tobias, *J. Organometal. Chem.*, **15**, 481 (1968).
[5] A. Barabas, *Inorg. Nuclear Chem. Lett.*, **6**, 744 (1970).
[6] K. Saito and K. Masuda, *Bull. Chem. Soc. Japan*, **41**, 384 (1968); ibid., **43**, 119 (1970).
[7] N. Serpone and R. Ishayek, *Inorg. Chem.*, **13**, 52 (1974).
[8] N. Serpone and K. A. Hersh, *Inorg. Chem.*, **13**, 2901 (1974).
[9] N. Serpone and D. G. Bickely, *Prog. Inorg. Chem.*, **17**, 391 (1972) and references therein.

where the prefixes *trans* and *cis* denote the relative orientations of the X groups, R_1 groups and R_2 groups, respectively.

The uranyl chelates (M=U, X=O) with unsymmetrical ligands ($R_1 \neq R_2$) would illustrate this case, assuming that the uranyl group is linear. In the present work we studied the configurational rearrangement above mentioned in the bis- (benzoylacetonato) uranyl ($R_1=CH_3$, $R_2=C_6H_5$) in deuterochloroform solution by dynamic PMR method.

According to Figure 1, for the bis-(β-diketonate) uranyl complexes the expected PMR signals are : $1R_1$, 1 ring H, 1 R_2 for I_a isomer and 1 R_1, the same 1 ring H, 1 R_2, for the I_b isomer. In the particular case of the bis-(benzylacetonato) uranyl we studied at different temperatures the splitting of the methyl signal.

EXPERIMENTAL

Bis-(benzoylacetonato) uranyl complex was prepared according to ref.[10]. The complex purity was checked by its IR, PMR spectra and the melting point (≃ 140° with dec.). PMR spectra of samples containing 0.0514 g (8.6×10^{-5} mols) in 0.6 ml of $CDCl_3$ were recorded at different temperatures with a variable temperature probe of a NMR Tesla spectrometer operating at 80 MHz. The reproducibility of the spectra was controlled by usual methods. Spectra were recorded more than twice for every temperature within −30° and +25° and averaged shapes of the signals were considered. The temperature scale was calibrated according to the producer's technique.

The values of the mean lifetimes, τ, were determined using the Clatux computer program [11] requiring initial trial values for : τ (sec) ; T_{2A} and T_{2B} (sec), the spin-spin relaxation times for the two isomers ; ν_A and ν_B (Hz), the relative chemical shifts of the isomers in the absence of the exchange ; p_A and p_B the relative populations of the isomers and finally a scaling factor. The output data represent a series of points of an $x-y$ plot, i.e. intensity versus frequency (Hz).

RESULTS AND DISCUSSION

The PMR spectrum of bis-(benzoylacetonato) uranyl in $CDCl_3$ at 25° shows (Figure 2a) : two broad multiplets centered at $\delta=8.27$ and 7.47 ppm belonging to the phenyl group, which is coplanar with the chelate ring, one sharp signal at $\delta=6.49$ ppm corresponding to the methinic protons and finally a relatively broad resonance for methyl protons at $\delta=2.49$ ppm. The narrowing of the methyl signal as the temperature is decreasing can be observed. At +10° the methyl signal splits into a doublet while the methinic resonance remains unchanged and the phenyl region exhibits a rather refined pattern (Figure 2b). With further decrease of the temperature the splitting of the methyl peak into a doublet becomes more pronounced and the phenyl region displays a more complex structure (Figure 2c). The phenomenon is reversible and at +16° the methyl doublet coalesces (Figure 2d).

It is difficult to assign the two methyl signals appearing below +16° as long as the possible isomers, I_a and I_b, can not be isolated. The reported values of the dipole moment of the bis-(benzoylacetonato) uranyl in benzene and carbon tetrachloride solutions are 3.12 and 3.09 D, respectively.[12] These data do not clear up the assignement because the same authors found for bis-(acetylacetonato) uranyl in benzene a dipole moment of 5.12 D. We assume that the more intense high-field methyl peak belongs to the *trans* isomer I_b and the weaker low-field one to the *cis* I_a, relying only on the ring effect of the phenyl group. [13].

---

[10] M. Gilman, R. G. Jones, E. Bindechadler, D. Blume, G. Karmas, G. A. Martin jr., I. F. Nobis, J. R. Thirtle, H. L. Yale and F. A. Joewan, *J. Amer. Chem. Soc.*, **78**, 2790 (1956).

[11] G. Binsch, *J. Amer. Chem. Soc.*, **91**, 1304 (1969).

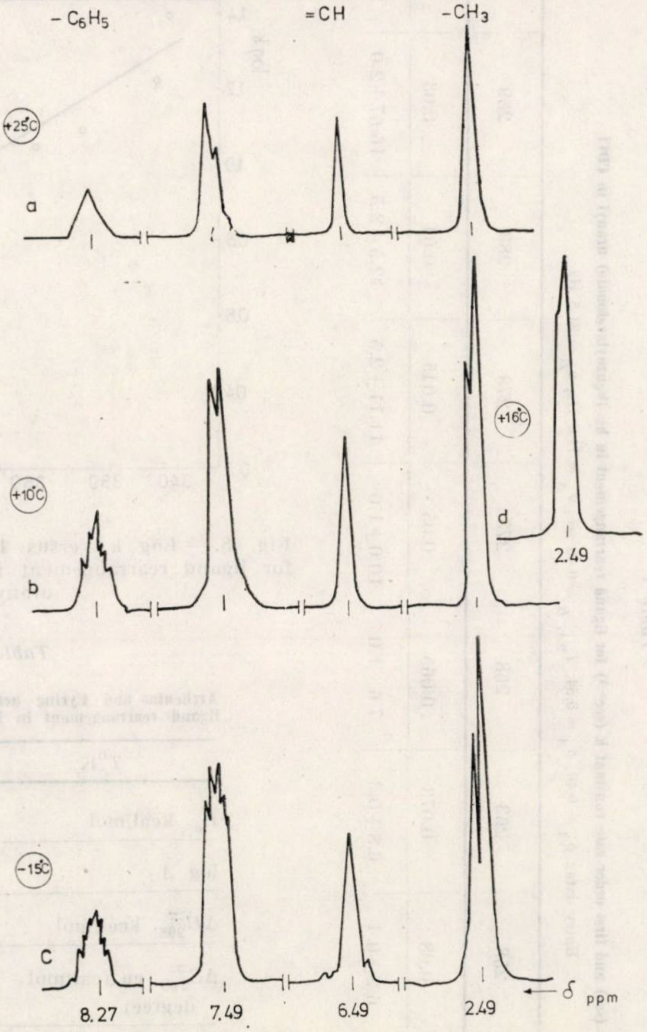

Fig. 2. — PMR spectrum of $UO_2(C_{10}H_9O_2)_2$ in $CDCl_3$ at different temperatures.

In table 1 there are listed the mean lifetime τ values determined by best fitting of the experimental spectra with the calculated ones and the first order rate constant $k=(1/2\tau)$ within $-20°$ and $+20°$. The Arrhenius kinetic parameters obtained from log k versus $1/T$°K least squares plot are : $E_a = 5.5 \pm 0.3$ kcal/mol and log $A = 5.43 \pm 0.26$ (Figure 3). The Eyring activation parameters at 25° are derived from the relationships : $\Delta H^{\neq}_{T^\circ K} = E_a - RT$ and $\Delta S^{\neq}_{T^\circ K} = R[\ln A - \ln RT/Nh] - R$ (Table 2).

---

[12] A. A. Grinberg and A. D. Troitskaia, *Tr. Radiovovo Inst. im. V. G. Khlopina*, **7**, 5 (1956); *Chem. Abstr.* **52**: 24771 (1958).

[13] A. R. Hendrickson and R. L. Martin, *Inorg. Chem.*, **12**, 2582 (1973).

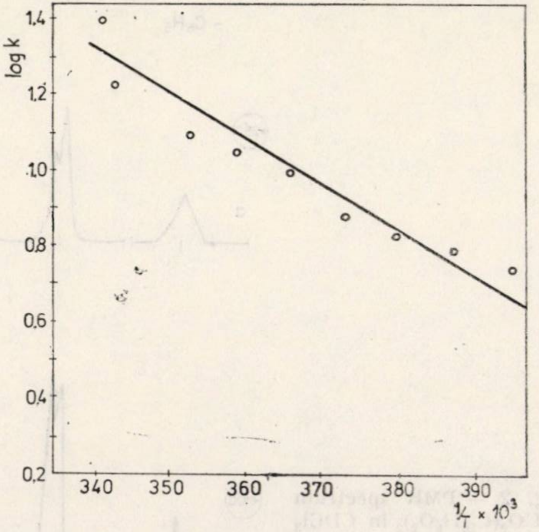

Fig. 3. — Log k versus $1/T^\circ K$ least squares plot for ligand rearrangement in bis-(benzoylacetonato) uranyl.

Table 2

Arrhenius and Eyring activation parameters for ligand rearrangement in $UO_2(C_{10}H_9O_2)_2$ in $CDCl_3$

T^0_cK	289
E_a, kcal/mol	5.5±0.3
log A	5.43±0.26
$\Delta H^{\neq}_{298}$, kcal/mol	4.9±0.3
$\Delta S^{\neq}_{298}$, eu (cal/mol degree)	35.2±1.1
$\Delta G^{\neq}_{298}$, kcal/mol	15.34±1.08
k_{Tc}, sec^{-1}	16.7±2.0
k^*_{298}, sec^{-1}	24.5

* extrapolated value

Table 1

τ values (sec) and first order rate constant k (sec^{-1}) for ligand rearrangement in bis-(benzoylacetonato) uranyl in $CDCl_3$

Entry data : $p_A = 0.46$, $p_A = 0.54$, $T_{2A,\,B} = 0.45$ sec, $\nu_A = 11.6$ Hz, $\nu_B = 31.5$ Hz

T°(K)	253	258	263	268	273	278	283	289	293
τ	0.09	0.08	0.073	0.065	0.05	0.045	0.04	0.03	0.02
k	5.5±0.3	6.2±0.4	6.8±0.3	7.6±1.0	10.0±1.0	11.11±2.5	12.5±3.5	16.67±2.0	25.0±6.3

The mechanisms proposed for the isomerization of the complexes with unsymmetrical ligands of the type M (U-chel)$_2$X$_2$ are[9] : a) the bond rupture of one of the metal-chelate links with the formation of either a trigonal bipyramidal (TBP) or a square pyramidal (SP) intermediate; b) the twist mechanism with the formation of a trigonal prismatic (TP) intermediate, and c) the complete dissociation of one chelate ring within an intermolecular path for ligand exchange. The c) alternative is excluded by our experimental data [14] on the lability of the bis-(benzoylacetonato) uranyl as we observed that the addition of the free ligand to the solution of the complex does not alter the NMR spectrum up to 160°. The twist mechanism b) is not likely to occur without the loss of the uranyl ion linearity, process that would require a much higher activation energy than that found. For the same reason we excluded the square pyramidal intermediate as the result of the bond-rupture alternative a). The linearity of the uranyl group [15,16] is further suppported by our NMR spectra, as found also other authors. [17,18] The remaining path is then the bond-rupture via TBP intermediate (Figure 4):

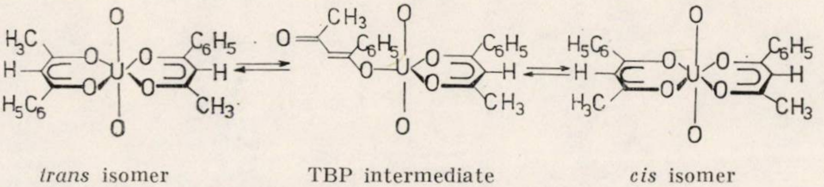
trans isomer TBP intermediate *cis* isomer

Fig. 4. — Bond rupture mechanism via TBP intermediate for ligand isomerization in bis-(benzoylacetonato) uranyl.

This mechanism implies the one-end dissociation of the ligand in the equatorial position, followed by the formation of the TBP intermediate. The structure of the last one allows the rotation of the dangling uni-dentate ligand, its reattachement to the uranium atom and, consequently, the formation of the other isomer. The low negative value of the activation entropy of $- 35.2 \pm 1.2$ eu would suggest some geometric constraints in the transition state to form the proposed TBP intermediate. The conclusion of the available data here presented is that the configurational rearrangement of bis-(benzoylacetonate) uranyl proceeds as an intramolecular ligand exchange.

---

[14] A. Vasilescu, unpublished results.

[15] E. Frasson, G. Bombieri and C. Panattoni, *Nature*, **202**, 1325 (1964).

[16] S. P. McGlynn and J. K. Smith, *J. Mol. Spectroscopy*, **6**, 164 (1961).

[17] Th. H. Sidall III and W. E. Stewart, *J. Inorg. Nuclear Chem.*, **31**, 3557 (1969).

[18] M. M. Dhinga and M. S. Subramanian, *Chem. Phys. Letters*, **30**, 83 (1975).

Revue Roumaine de Chimie, **23**, *7*, 1061–1064 (1978)

DETERMINATION OF BENZALDEHYDE IN THE CATALYTICAL OXIDATION PRODUCTS OF TOLUENE, BY GAS CHROMATOGRAPHY

SORIN MAGER, IONEL HOPÂRTEAN, FLORICA PAIU and RUXANDRA ŢĂRANU
Department of Organic Chemistry, University "Babeş-Bolyai"
11 Arany Janos St., Cluj-Napoca, Romania

Received July 14, 1976

A new gas chromatographic method for determination of small amounts of benzaldehyde in the catalytical oxidation products of toluene (in the manufacture of benzoic acid), using Carbowax 20 M as liquid phase and cyclohexanone as internal standard, has been developed. The accuracy of the method is ± 0.3%.

INTRODUCTION

Among other oxidation products of toluene (benzyl alcohol, biphenyl, *o*- and *m*-methylbiphenyl, benzyl benzoate) in the catalytical presence of cobalt naphenates, benzaldehyde is one of the most valuable by-products. Its presence in the oxidation products of toluene was already reported by Homola and Málek,[1] Manjarrez[2] who also described a gas-chromatographic determination method, by Znamenskaya[3] and by Kazinik.[4–6]

EXPERIMENTAL

The determination of benzaldehyde was carried out in the toluenic solution after the crude product of oxidation was extracted with a 5% aqueous sodium hydroxyde solution for elimination of the benzoic acid which represents the main product of the oxidation reaction.

The chromatogram of the toluenic solution shows the presence of seven products (Figure 1) which were identified as : toluene (0.3), benzaldehyde (0.75), benzyl alcohol (2.05), *m*-methylbiphenyl (3.4), biphenyl (5.6), *o*-methylbiphenyl (7.5) and benzyl benzoate (10.5); retention times are given in brackets.

---

[1] V. Homola and J. Málek, *Chem. prumysl*, **13**, 449 (1963).

[2] A. Manjarrez, *J. Gaz. Chromatog.*, **3**, 140 (1965).

[3] A. P. Znamenskaya, J. G. Solov'eva and N. V. Strokova, *Inform. Sorbshch. Gaz. Nauch-Issled. Proekt. Inst. Azotn. Prom. Prod. Org. Sin.*, **24**, 49 (1969).

[4] E. M. Kazinik, R. S. Iudina, V. V. Platonov and V. K. Leont'eva, *Nauch. Tr. Tul. Gas. Pedagog. Inst.*, **1**, 49 (1968).

[5] E. M. Kazinik, V. N. Kulakov, N. V. Novorusskaya and D. S. Bark, *Tr. Vses., Nauch.-Issled. Proekt. Inst. Monomerov*, **1**, 113 (1969).

[6] E. M. Kazinik, N. V. Novorusskaya, F. P. Sanerich, V. V. Suchkov, E. A. Pasternak and D. S. Bark, *Tr. Vses. Nauch.-Issled. Proekt. Inst. Monomerov*, **2**, 136 (1970).

Determination of benzaldehyde was carried out by means of the internal standard method. Cyclohexanone was proved to be a very suitable internal standard for this purpose.

Calibration curve. For plotting the calibration curve solutions of different known concentrations (between 0.5–3%) of benzaldehyde in toluol, containing all the same concentration of cyclohexanone (2%) were prepared. Solutions were injected in the chromatograph obtaining chromatograms from which the ratios of the areas compound/standard were determined.

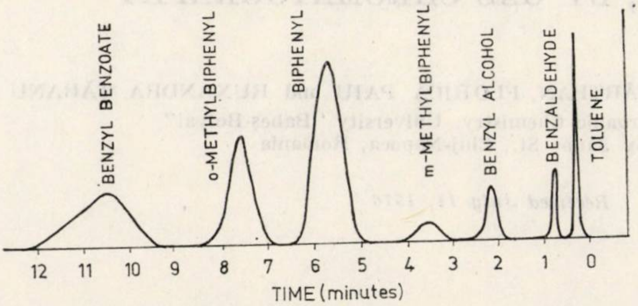

Fig. 1. — The chromatogram of the crude product of the oxidation.

The plot area ratio compound/standard versus concentration ratio compound/standard represents the calibration curve (Figure 2).

For each concentration five determinations were carried out.

The equation of the calibration curve was calculated:

$$y = -0.055 + 1.062\,x$$

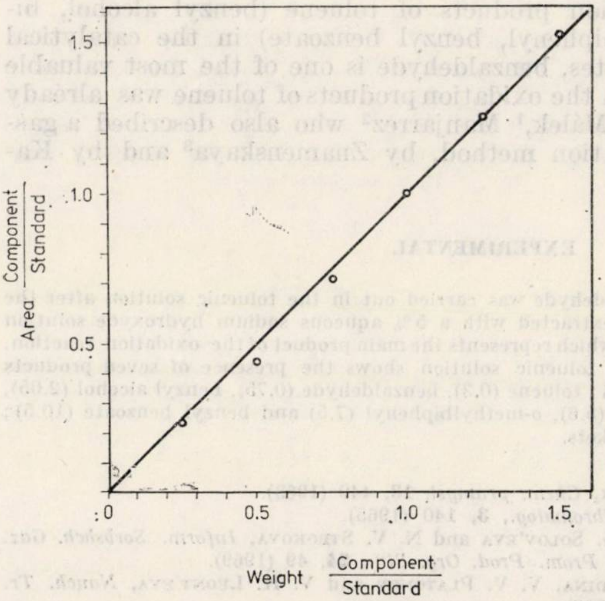

Fig. 2. — Calibration curve.

By means of the "t" test, calculating for $t_{\text{calc.}}$ the value 0.80 which is smaller than $t_{\text{tab.}} = 2.57$, for a 0.95 probability and $k = 5$ freedom degrees, one has verified that the two values, zero and -0.055 do not differ statistically hence the ordinate at origin equals statistically zero.

Using the calibration curve, benzaldehyde was determined in solutions of known concentrations (1, 2 and 3%) by means of the gas chromatographic method (A) comparatively with the volumetric method (B) by titration with hydrochloric hydroxylamine.[7]

For each concentration five determinations were carried out. Results are given in table 1 along with the standard deviations, s and with the percentage errors.

Table 1

The comparative results for the chromatographic (A) and volumetric (B) determinations

Method	Benzaldehyde (g)		s_A	Error
	Weighted	Found		(%)
A	1.0	0.997	0.0208	−0.3
	2.0	1.994	0.0163	−0.3
	3.0	3.004	0.0138	+0.1
B	1.0	1.031	0.0242	+3.1
	2.0	2.018	0.0105	+0.9
	3.0	3.017	0.0102	+0.56

Comparison of the results presented in table 1 shows on the one hand a good agreement between the weighted and experimentally found values and on the other hand the higher accuracy (and rapidity) of the new developed chromatographic method as compared to the volumetrical one.

Sampling procedure. The toluenic solution obtained during the oxidation process of the toluol was washed with a 5% aqueous natrium hydroxyde solution and dried. Five ml toluenic solution (free of benzoic acid) were mixed with 5 ml standard solution (2% cyclohexanone in toluol). One µl from the mixture was injected in the chromatograph. From the obtained chromatograms the area ratios compound/standard were found and from the calibration curve the concentration ratios were determined. Knowing the x and y values, the concentration of benzaldehyde in the analysed sample was calculated.

Apparatus. Determinations were carried out using a CHROMATRON GCHF 18.3–4 chromatograph with flame ionization detector equipped with an electronic integrator G.I.D.2.2. A 2 m inoxidable steel column with a 4 mm diameter packed with 20% Carbowax 20 M on Chromosorb W (60–80 mesh) was used. The speed of the carrier gas (nitrogen) was 33.3 ml/min., the speed of the hydrogen 22 ml/min. and of the air 300 ml/min. Temperature of the column was 130°, of the evaporator 230° and of the detector 230°.

RESULTS

Two sets of determinations were carried out: one concerning the amount of benzaldehyde in the crude product of oxidation, the second one concerning the content in benzaldehyde of the toluenic solution which is recirculated during the oxidation process. In both cases the time dependent variation of the concentration of the benzaldehyde was followed.

Table 2 shows the results of the determinations (I—III) carried out after 6, 10 and 12 hours of oxidation for the crude product, and of the determinations (IV—VII) carried out after 4, 8, 12 hours and at the end of the oxidation, for the toluene which is recirculated during the oxidation reaction; standard deviations are also given.

---

[7] B. S. Hünig, *Liebigs. Ann. Chem.*, **569**, 224 (1950).

While the concentration of benzaldehyde in the crude product becomes smaller as the oxidation time increases, (because of the further oxidation of the aldehyde to acid), the concentration of benzaldehyde in the toluenic solution which is recirculated during the oxidation process is practically constant.

Table 2

Results of the determination of benzaldehyde

Run		Ratio of		Conc. %	s_A
		Areas	Concentrations		
Crude product	I (6 h)	1.14	1.19	2.19	0.030
	II (10 h)	1.16	1.20	1.47	0.050
	III (12 h)	1.00	1.04	1.45	0.056
Recirculated toluene	IV (4 h)	0.22	0.23	0.46	0.020
	V (8 h)	0.245	0.255	0.51	0.014
	VI (12 h)	0.205	0.215	0.43	0.013
	VII*	0.245	0.255	0.51	0.014

* Determination after the oxidation was finished

The developed method, whose accuracy is ± 0.3%, represents a convenient and rapid modality for the determination of small amounts of benzaldehyde in the oxidation products of toluene; it can be used in the case of other similar mixtures, too.

Revue Roumaine de Chimie, **23**, 7, 1065–1077 (1978)

SOLVENT- AND LANTHANIDE-INDUCED SHIFTS IN THE ^1H–NMR SPECTRA OF 4-ACETONYLIDENE-2,6-DIMETHYL-[4H]PYRAN AND ITS TAUTOMERIC PROTONATED PYRYLIUM CATIONS

ALEXANDRU T. BALABAN and MIRCEA D. GHEORGHIU
Organic Chemistry Department, The Polytechnic, Bucharest, Romania

Received December 30, 1977

On the basis of coupling constants and of shifts induced in the ^1H–NMR spectra of the title compound III by dipolar solvents (acetone-d_6, DMSO-d_6) and by aromatic solvents (benzene-d_6), earlier assignments of NMR peaks are revised and interpreted as indicating an *s-cis* conformation. The calculation of molar induced shifts in the presence of $Eu(dpm)_3$, after the McConnell – Robertson equation using Hamilton's agreement factor and the hypothesis significance test, favours the *s-cis* conformation of III also in the complex with the europium chelate. Protonation of compound III affords two tautomeric pyrylium cations, I and II, which coexist in trifluoroacetic acid; addition of acetone-d_6 shifts the equilibrium towards the enolic form II. Aromatic solvent-induced shifts are interpreted in terms of intermolecular charge-transfer complexes by comparison with unpublished X-ray data for N-phenylpyridinium chloride monohydrate. The positive solvatochromy in the UV spectrum of III is in agreement with its structure.

1. INTRODUCTION

While electrophilic diacylation of propene and higher alkenes affords pyrylium salts,[1] triacylation of isobutene and higher branched alkenes yields vinylogous [4H]-pyrones, i. e. 4-(2′-oxoalkylidene)-[4H] pyrans; thus, isobutene, acetyl chloride and aluminium chloride afford 4-acetonylidene-2,6-dimethyl-[4H]pyran (III), [2] which is protonated reversibly to the 4-acetonyl-2,6-dimethylpyrylium cation (I), tautomeric with the enolic 2,6-dimethyl-4-(2′-hydroxy-1′-propenyl)-pyrylium cation (II). On the other hand, 2,3-dimethyl-2-butene, isobutyryl chloride and aluminium chloride yield 2,6-diisopropyl-4-(1′, 1′,3′-trimethylbutan-2′-one-1′-yl)-pyrylium (IV) which cannot be converted into a 4-(2′-oxoalkylidene)-[4H]pyran because it has no benzylic hydrogen at the substituent in position 4.[3] It was reported that 4-(2′-oxoalkylidene)-[4H]pyrans are converted by hydroxylamine into pyridine-N-oxides and/or isoxazolines.[4]

---

[1] Review: A. T. Balaban, W. Schroth and G. Fischer, *Adv. Heterocyclic Chem.*, **10**, 241 (1969).

[2] A. T. Balaban, P. T. Frangopol, A. R. Katritzky and C. D. Nenitzescu, *J. Chem. Soc.*, **1962**, 3889.

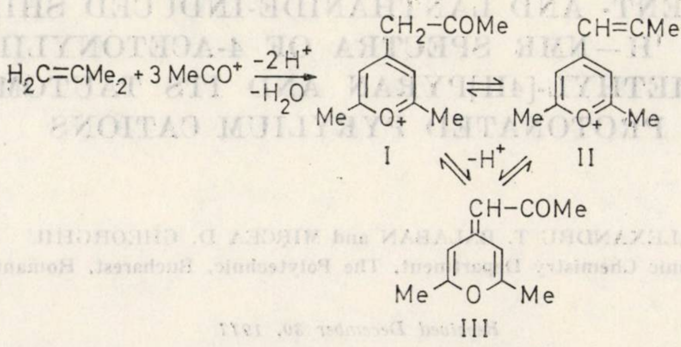

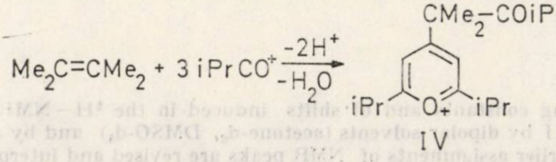

In the present paper we reinvestigate the ^{1}H-NMR assignments of III made earlier,[2] using decoupling experiments and induced NMR shifts. Various solvents have now been used in order to determine the dipolar solvent induced shifts, and aromatic solvent induced shifts (ASIS); also, as lanthanide shift reagent (LSR), tris(dipivaloylmethanato)-europium(III), Eu(dpm)$_3$, was employed in order to determine lanthanide-induced shifts (LIS), expressed quantitatively as molar induced shifts (MIS). These latter data are compared with calculated values in order to determine the geometry of the complex with LSR.

2. DECOUPLING EXPERIMENTS

The ^{1}H-NMR spectrum of 4-acetonylidene-2,6-dimethyl-[4H]pyran (III) in carbon tetrachloride presents three separate methyl peaks (Figure 1); two methyl peaks at lower field, CH_3^A and CH_3^B, are doublets with $J_{AB} = 1$ Hz and are assigned to the two α-standing methyl groups on the pyran ring (further details of this assignment will be discussed later), while the peak at higher field, CH_3^F, is a singlet and is therefore assigned to the acetyl group. In other solvents, the lower-field α-methyl peaks are completely (in C_6D_6) or almost completely overlapped (in D_3C-CO-CD_3, D_3C-SO-CD_3, CS_2), as indicated in table 1; in deuteriochloroform, all three methyl peaks are accidentally degenerate. In addition to the methyl peaks, three one-proton peaks appear at lower field; the two peaks, H^C and H^D, at the lowest field are broad, while the

---

[3] A. T. Balaban, A. Bota and I. I. Stănoiu, *Rev. Roumaine Chim.*, **21**, 1883 (1976).
[4] P. Crabbé, J. Haro and E. Santos, *J. Chem. Soc. Perkin I*, **1975**, 1342.

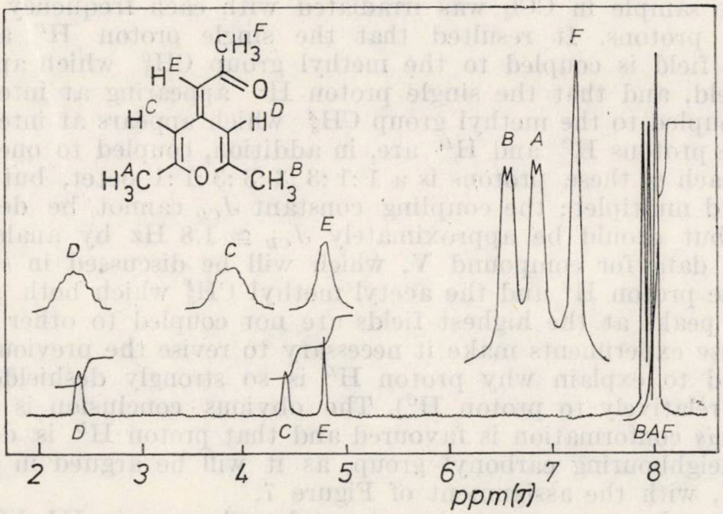

Fig. 1. — ^{1}H—NMR Spectrum of III in CCl$_4$.

Table 1

^{1}H—NMR Spectra of III in various solvents (τ values in ppm), ASIS and MIS values (in ppm

No.	Group	Solvent	CH$_3^F$	CH$_3^A$	CH$_3^B$	H^E	H^C	H^D
1	—	(Ref.[2])	8.00	7.90	7.90	2.40	4.35	4.77
2	i	CCl$_4$	8.01	7.94	7.87	4.77	4.40	2.38
3	i	CS$_2$	8.07	7.93	7.92	4.80	4.41	2.43
4	i	CDCl$_3$	7.90	7.90	7.90	4.63	4.29	2.31
5	ii	(D$_3$C)$_2$CO	8.00	7.90	7.89	4.62	4.19	2.53
6	ii	(D$_3$C)$_2$SO	8.02	7.91	7.90	4.65	4.11	2.49
7	iii	C$_6$D$_6$	7.93	8.34	8.34	4.68	4.59	2.00
ASIS (Δ)			−0.08	0.40	0.47	−0.09	0.19	−0.38
MIS in CCl$_4$			11.5	0.0	1.8	7.5	4.8	16.6
MIS in CS$_2$			13.0	0.0	2.1	8.1	5.0	19.0

third peak, H^E, is a sharp peak. In the previous paper,[2] these peaks were assigned as indicated in the first line of table 1 on the basis of analogies with NMR spectra of [4H]-pyrones and their derivatives: the broad peak H^D at the lowest field was assigned to the exocyclic methine group, while the other close-standing peaks, H^C and H^E, were assigned to the pyranic β-protons.

As shown by the insets in Figure 1, the two lower-field methyl peaks are doublets indicating that the protons of each methyl group are coupled to the neighbouring β-standing pyranic proton. For decoupling, the sample in CCl_4 was irradiated with each frequency of these β-pyranic protons. It resulted that the single proton H^D appearing at lowest field is coupled to the methyl group CH_3^B which appears at lowest field, and that the single proton H^C appearing at intermediate field is coupled to the methyl group CH_3^A which appears at intermediate field. The protons H^C and H^D are, in addition, coupled to one another so that each of these protons is a 1 :1 :3 :3 :3 :1 :1 octet, but appears as a broad multiplet; the coupling constant J_{CD} cannot be determined directly but should be approximately $J_{CD} \cong 1.8$ Hz by analogy with literature data for compound V, which will be discussed in section 7. The single proton H^E and the acetyl methyl CH_3^F which both give rise to sharp peaks at the highest fields are not coupled to other protons.

These experiments make it necessary to revise the previous assignment, and to explain why proton H^D is so strongly deshielded (with 2.0 ppm relatively to proton H^C). The obvious conclusion is that the planar *s-cis* conformation is favoured and that proton H^D is deshielded by the neighbouring carbonyl group, as it will be argued in detail in Section 7, with the assignment of Figure 7.

Although we are aware that the carbonyl group in III differs substantially from a saturated carbonyl group for which the theoretical models were developed, we tried to estimate the relative deshielding of protons H^D and H^C. Calculations were performed assuming an *s-cis* planar conformation for III and including both the anisotropic and the electric effects,[5] for the carbonyl group. The centre of the dipole was assumed to be in the middle of the $C{=}O$ bond. The result accounted only for 30% of the observed deshielding, i. e. a calculated relative deshielding of H^D of 0.7 ppm. Therefore the saturated ketone model is poorly applicable to III, though the deshielding of H^D is confirmed qualitatively.

3. DIPOLAR SOLVENT INDUCED SHIFTS

Table 1 evidences three groups of solvents. Group (i), numbered 2—4, of non-polar solvents, includes halomethanes and carbon disulphide where little interaction between solvent and solute is present. Group (ii) of dipolar solvents, numbered 5 and 6, includes $(D_3C)_2CO$ and $(D_3C)_2SO$ with the anisotropic carbonyl and sulphoxide groupings. Finally, group (iii), number 7, is the aromatic hexadeuteriobenzene with its ring current which gives rise to ASIS and is discussed in the next Section.

The most marked changes in the NMR spectra of III on passing from solvents of group (i) to group (ii) are the following: solvents (ii) deshield proton H^C from the range τ 4.3—4.4. to 4.1—4.2 and shield slightly proton H^D from τ 2.3—2.4 to 2.5. Since compound III is probably appreciably polarized (cf. limiting structures IIIA and IIIB), it is natural that dipolar solvent molecules should exert their most pronounced effects on protons situated close to the axis of the molecular dipole: these are indeed protons H^C and H^D. The experimental results may be accounted for by the effects of the anisotropic solvent molecules

---

[5] J. W. ApSimon, J. Elguero, A. Fruchier, D. Mathieu and R. Phan-Tan-Luu, *Canad. J. Chem.*, **52**, 2296 (1974) and references therein.

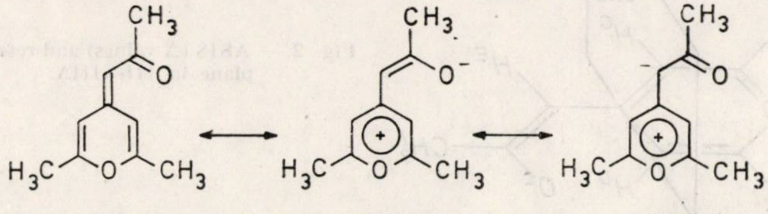

III IIIA IIIB

alone, or by the fact that in dipolar solvents the contribution of limiting structures IIIA and/or IIIB increases, or by a combination of both these effects.

4. AROMATIC SOLVENT INDUCED SHIFTS (ASIS)

The data from table 1 evidence that on passing from the non-polar solvents (i) to aromatic solvents (iii), pronounced changes in chemical shifts occur. The changes are expressed as ASIS, the difference in chemical shifts between the NMR spectra recorded in C_6D_6 and CCl_4:

$$\Delta = \tau(C_6D_6) - \tau(CCl_4)$$

as indicated in the literature.[6-8]

It is seen that the Δ values of protons H^D, H^E and CH_3^F in the vicinity of the carbonyl group are negative, while the remaining protons far from the carbonyl groups are shielded in aromatic solvents (these latter protons have positive Δ values). The model proposed by Connolly and McCrindle,[9] which was also used for α,β-unsaturated ketones,[10] accounts for the ASIS observed with III; however, III is more strongly dipolar than ketones or α,β-unsaturated ketones, so that the reference plane which separates the region of positive and negative Δ values, proposed in the above model,[9] is displaced in III passing no longer through the carbonyl carbon, but through the 4-ring carbon. The benzene molecules clustering around the positive end of the dipole (the pyrylium ring in IIIA) will shield the protons in this moiety of the molecule, cf. Figure 2.

---

[6] P. Laszlo, *Progress in NMR Spectroscopy*, **3**, 231 (1967).

[7] M. Jauquet and P. Laszlo, in "Influence of Solvents on Spectroscopy" (ed. M. R. J. Dack), Wiley, New York, 1975, p. 243.

[8] N. S. Bhacca and D. H. Williams, *Tetrahedron Letters*, **1964**, 3127; "Applications of NMR Spectroscopy in Organic Chemistry. Illustrations from the Steroid Field", Holden-Day, San Francisco, 1964, chap. 7.

[9] J. D. Connolly and R. McCrindle, *Chem. and Ind.*, **1965**, 379.

[10] J. E. Baldwin, *J. Org. Chem.*, **30**, 2423 (1965).

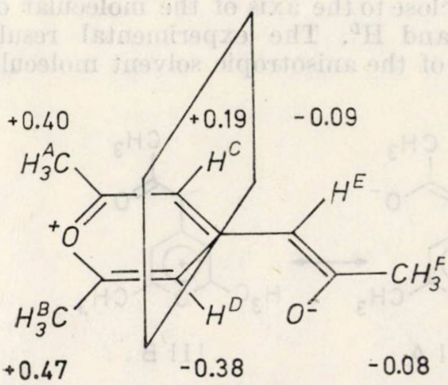

Fig. 2. — ASIS (Δ values) and reference plane in III↔IIIA.

5. INTERMOLECULAR CHARGE-TRANSFER COMPLEXES BETWEEN AROMATIC CATIONS AND BENZENOID AROMATIC RINGS

The association of aromatic solvents with pyrylium salts was observed to give rise to liquid complexes: 2,4,6-trimethylpyrylium tetrachloroferrate with benzene,[11,12] or 2,6-di-t-butyl-4-methylpyrylium chlorostannate(IV) with benzene.[12] Charge-transfer bands were noted to appear on mixing solutions of pyrylium salts as electron acceptors, and of polycyclic benzenoid hydrocarbons (anthracene, pyrene) as electron donors.[13,14] X-Ray diffraction analysis of single crystals of N-phenylpyridinium chloride monohydrate revealed[15] a pairwise antiparallel arrangement of cations, with phenyl over pyridinium rings, which again shows that aromatic benzenic rings interact with aromatic cations, cf. Figures 3–5. These data can be extrapolated to the ASIS reported in the previous Section, and indicate that aromatic benzenoid rings tend to adopt a parallel orientation to the pyrylium rings, above and below these rings. If the deuteriobenzene solvent molecules interact with III as in the above crystal with parallel rings stacked over one another, the observed shielding/deshielding effects in ASIS become easily understandable qualitatively.

6. LANTHANIDE INDUCED SHIFTS (LIS)

It is obvious from formula IIIA that the most negatively charged atom in molecule III is the carbonyl oxygen, which should therefore coordinate with lanthanide shift reagents (LSR). We selected as LSR tris(dipivaloylmethanato)europium(III), Eu(dpm)$_3$, and as solvent carbon

---

[11] A. T. Balaban, E. Romaș and C. C. Renția, *Tetrahedron*, **22**, 1 (1966).
[12] A. T. Balaban, *Org. Preparations Procedures Internat.*, **9**, 125 (1977).
[13] G. Briegleb, G. Betz and W. Heere, *Z. phys. Chem. (Frankfurt)*, **64**, 85 (1969).
[14] C. Parkanyi and C. J. Lev, *Z. Naturforsch.*, **30 b**, 184 (1975).
[15] L. H. Jensen and A. T. Balaban (to be published).

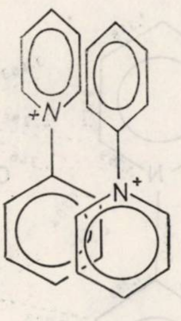

Fig. 3. — Pairwise packing of cations in single crystals of N-phenylpyridinium chloride monohydrate;[15] the average inter-ring torsion angle is 47°.

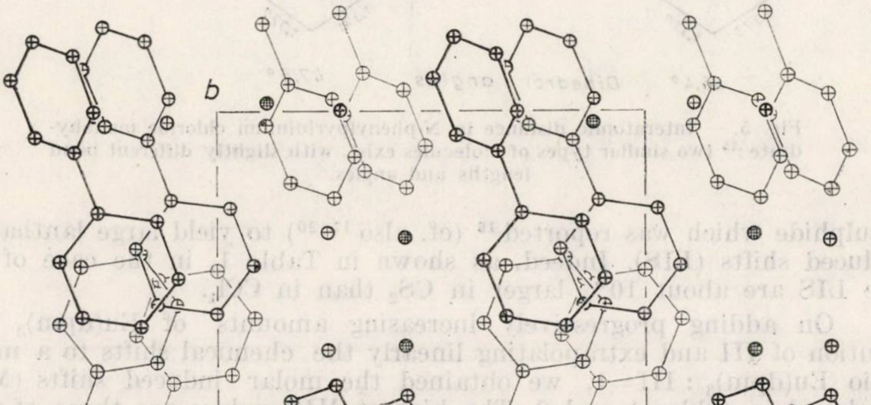

Fig. 4. — Unit cell (viewed along the c axis) of N-phenylpyridinium chloride monohydrate;[15] the isolated atoms are chloride anions and oxygens of water, associated through hydrogen bonds.

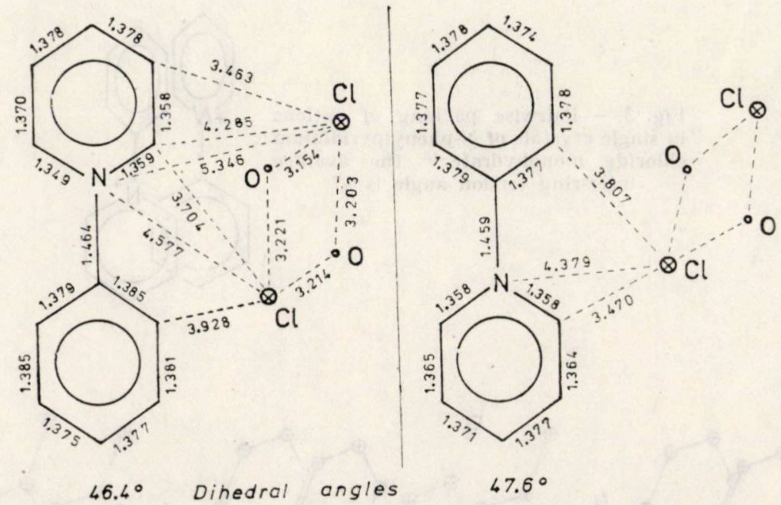
1,378
1,378
3.463
Cl
1.370
1.358
4.285
1,349
N
1,359
5.346
O
3,154
3,704
3.203
1.464
4,577
3,221
O
1,379
1,385
3,214
Cl
3.928
1.385
1.381
1,375
1,377
1,378
1,374
1.377
1.378
Cl
1,379
1,377
O
3,807
1.459
O
4.379
Cl
1,358
N
1,358
3.470
1.365
1.364
1,371
1,377
46.4°
Dihedral angles
47.6°

Fig. 5. — Interatomic distance in N-phenylpyridinium chloride monohydrate;[15] two similar types of molecules exist, with slightly different bond lengths and angles.

disulphide which was reported[16] (cf. also [17–20]) to yield large lanthanide induced shifts (LIS). Indeed, as shown in Table 1, in the case of III the LIS are about 10% larger in CS_2 than in CCl_4.

On adding progressively increasing amounts of $Eu(dpm)_3$ to a solution of III and extrapolating linearly the chemical shifts to a molar ratio $Eu(dpm)_3 : III = 1$, we obtained the molar induced shifts (MIS) displayed in tables 1 and 2. The highest MIS values are those of protons H^D and CH_3^F lying closest to the carbonyl oxygen.

Compound III might exist in several conformations: planar *s-cis* ($\theta = 0°$), planar *s-trans* ($\theta = 180°$), and non-planar conformations differing from both planar extremes in the rotational angle θ around the C—CO bond. A rotational angle θ much different from 0° or 180° (cf. Figure 6) is improbable since it would sacrifice the π-conjugation by decreasing the contribution of structures IIIA and IIIB, so that the planar conformations are energetically the most favoured.

The calculations of lanthanide induced chemical shifts were performed in the assumption that the pseudocontact model of McConnell and Robertson [21] is valid, using a procedure similar to that developed by Willcott, Lenkinski and Davis,[22] and described in more detail in the

---

[16] D. B. Walters, *Analyt. Chim. Acta*, **60**, 421 (1972).

[17] L. Tomić, Z. Majerski, M. Tomić and D. E. Sunko, *Chem. Commun.*, **1971**, 719.

[18] V. Sakaguchi, M. Kunugi, T. Fukumi, S. Tadakoro, A. Yamasahi and S. Fujiwara, *Chem. Letters (Japan)*, **1972**, 177.

[19] C. Freppel, J. C. Florence and J. C. Richter, *Chem and Ind.*, **1972**, 553.

[20] A. T. Balaban, A. Bota, F. Chiraleu, E. Şliam, A. Haneş and C. Drăghici, *Rev. Roumaine Chim.*, **22**, 1003 (1977).

[21] H. M. McConnell and R. E. Robertson, *J. Chem. Phys.*, **29**, 1361 (1958).

[22] M. R. Willcott III, R. E. Lenkinski and R. E. Davis, *J. Amer. Chem. Soc.*, **94**, 1742 (1972).

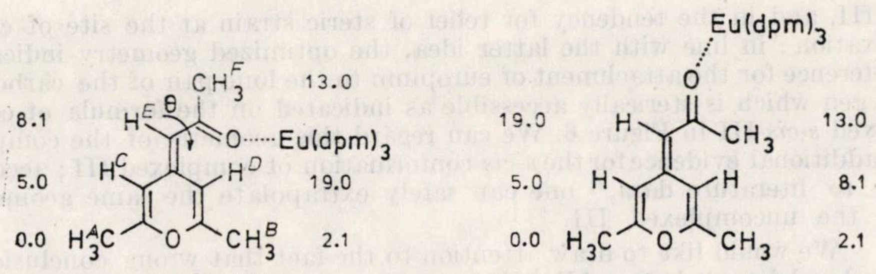

s-cis-III *s-trans*-III

Fig. 6. — Shifts induced by Eu(dpm)$_3$ in the ^{1}H—NMR spectrum of III in CS$_2$ (MIS values in ppm) for the two planar conformers of III; the assignment in the *s-trans* conformer is fictitious and differs from the real one (illustrated for the *s-cis* conformer) by reverting the MIS values of H^D and H^E, as in ref. 2.

experimental part. Methyl groups were treated as free rotors and the calculated induced shifts were taken as the arithmetic mean of at least ten points.

Tables 1 and 2 present the MIS values obtained experimentally and the assignment of these values to protons *A—F* which is based on the previously discussed firm evidence. Table 2 contains the results of calculations. With the given assignment, the result for the *s-cis* conformation gives an agreement factor (AF)[23] of 0.091 which is within the acceptable limits,[24] but is situated close to the upper limit. This may be due to errors resulted from the assumed standard geometrical parameters which were calibrated for unconjugated systems rather than for compounds like III. With the same assignment, an *s-trans* conformation gave an unacceptable AF of over 0.40, which rejects such a conformation with a confidence level of virtually 100%. For the *s-cis* conformation, the oxygen — europium distance of 3.55Å which results for the optimized AF is not excessively higher than the most generally accepted value of 3.0 Å.[25] The difference may originate again in the conjugation

Table 2

Observed (in CS$_2$, ppm) and calculated MIS values for the two conformations of compound III

Conformer	AF	d_{Eu-O} (Å)	Molar induced shifts					
			CH$_3^F$	CH$_3^A$	CH$_3^B$	H^E	H^C	H^D
Observed	—	—	13.0	0.0	2.1	8.1	5.0	19.0
Calc. *s-cis*	0.091	3.55	12.99	1.31	2.71	7.36	3.44	19.36
Calc. *s-trans*	0.037	2.80	12.97	0.45	1.44	7.88[a]	5.43	19.03[a]

[a] Fictitious assignment, with reversed MIS values for these two protons, as in ref. 2.

---

[23] R. E. Davis and M. R. Willcott III, *J. Amer. Chem. Soc.*, **94**, 1744 (1972).
[24] R. E. Lenkinski and J. Reuben, *J. Amer. Chem. Soc.*, **98**, 4065 (1976).
[25] S. Caccamese, P. Finocchiaro, P. Maravigna, G. Montaudo and A. Recca, *Gazz. chim. Ital.*, **107**, 163 (1977).

of III, and in the tendency for relief of steric strain at the site of complexation : in line with the latter idea, the optimized geometry indicates preference for the attachment of europium to the lone pair of the carbonyl oxygen which is sterically accessible as indicated on the formula of complexed *s-cis*-III in Figure 6. We can regard this geometry of the complex as additional evidence for the *s-cis* conformation of complexed III ; according to literature data,[26] one can safely extrapolate the same geometry for the uncomplexed III.

We would like to draw attention to the fact that wrong conclusions, based solely on lower AF values, can sometimes be reached starting from erroneous assignments : if the assignment of MIS values to the protons of III had not been known from independent data such as decoupling, assuming the fictitious assignment presented in Fig. 6 for the *s-trans* conformer, similar calculations led (cf. the last line of Table 2) to an AF value of 0.037, which is beyond the 0.05 experimentally significant perfection limit ; funnily enough, the oxygen — europium distance obtained for this case, 2.80 Å, is close to the value 2.34 Å determined by X-ray diffraction of solid saturated carbonyl complexes.[27] Judging by AF values, assuming the one-dimensional hypothesis, and making use of Lagrange interpolation[28] from Hamilton's tables,[29] one would have obtained a higher confidence level for the *s-trans* conformation which we know, is a false conclusion. Therefore we believe that such calculations for non-rigid carbonyl compounds should be treated with caution, and that additional evidence should be presented, not relying exclusively on best AF values.

Although compound III has two oxygen atoms, we considered that only the carbonyl group is involved in complexation. This assumption is based on the observation that one of the methyl groups flanking the pyranic oxygen heteroatom has a MIS value equal to zero. Since the electronic configuration of III has appreciable contribution of structure IIIA (and somewhat less of IIIB), the positive charge of the pyrylium ring will confer the oxygen heteroatom a negligible Lewis basicity, making it unable to compete with the carbonyl oxygen for the complexation of $Eu(dpm)_3$.

7. CONCLUSIONS ON THE CONFORMATION OF COMPOUND III

The conclusion that the free as well as the complexed compound III in the presence of LSR exists in the *s-cis* conformation agrees with the assignments presented for 2,6-dicarbomethoxy-4-acetonylidene-[4H]-pyran (V) by Ostensen and Undheim.[30] These authors found the NMR chemical shifts indicated in Figure 7, and a coupling constant $J_{3,5}=2.0$ Hz

---

[26] G. Montaudo, V. Librando, S. Caccamese and P. Maravigna, *J. Amer. Chem. Soc.*, **95**, 6365 (1973).

[27] R. E. Cramer and E. Seff, *Chem. Commun.*, **1972**, 400.

[28] Hewlett-Packard, Calculator 9830 Math Pac, Part No. 09830—70000, 9721 M, p. 13.

[29] W. C. Hamilton, *Acta Cryst.*, **18**, 502 (1965).

[30] K. T. Ostensen and K. Undheim, *Acta Chem. Scand.*, **27**, 2814 (1973).

(of course, no other coupling was possible in this compound V). The lower chemical shifts of V relative to III are probably due both to the through-bond electron-attracting effect of the carbomethoxy groups, and to the through-space deshielding effect of the carbomethoxy groups which may assume two different orientations (conformations in plane): this latter effect may account for the difference of 0.3 ppm between differences in τ values of corresponding protons: $(H^C - H^3)-(H^D - H^5)$ for III and V.

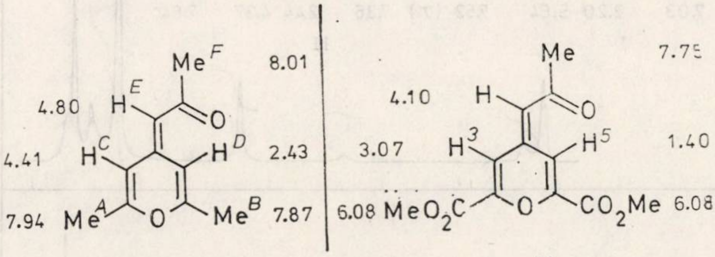

III V

Fig. 7. – Chemical shifts (τ values) of compounds III (in CCl_4) and V (in $CDCl_3$ [30]) in the *s-cis* conformation.

The above authors [30] also found that on protonation, compound V gives a mixture of tautometric pyrylium salts, similarly to the protonation of III which gives I⇌II as will be discussed in the next Section.

The reason for III and V to prefer the *s-cis* conformation is mainly the smaller steric repulsion between the β-pyranic proton and the carbonyl oxygen in this conformation than the repulsion which exists in the *s-trans* conformation between the same proton and the methyl of the acetyl group. An additional factor is the lower electrostatic energy of the *s-cis* conformation (since III has an appreciable dipolar character, cf. IIIA) with the smaller distance between the pyrylium ring and the carbonyl oxygen.

8. ^{1}H-NMR SPECTRA OF TAUTOMERIC PYRYLIUM CATIONS I AND II

If the solvent is trifluoroacetic acid (TFA), the ^{1}H-NMR spectrum of III is completely different from the spectra discussed above and presented in table 1. The new spectrum evidences the cationic species I (protonated at the exocyclic C=C double bond, i. e. the conjugate acid of IIIB) and II (protonated at the carbonyl oxygen, i. e. the conjugate acid of IIIA). In pure TFA, both the ketonic (I) and the enolic species (II) coexist as indicated by Figure 8a, in a ratio of about 75% I and 25% II. In a solvent mixture (20% $D_3C-CO-CD_3$ and 80% TFA), the conjugate acid of III exists exclusively as tautomer II, as seen from Figure 8b, presumably because the enol II forms hydrogen bonds with hexadeuterioacetone. Chemical shifts for I and II are presented on

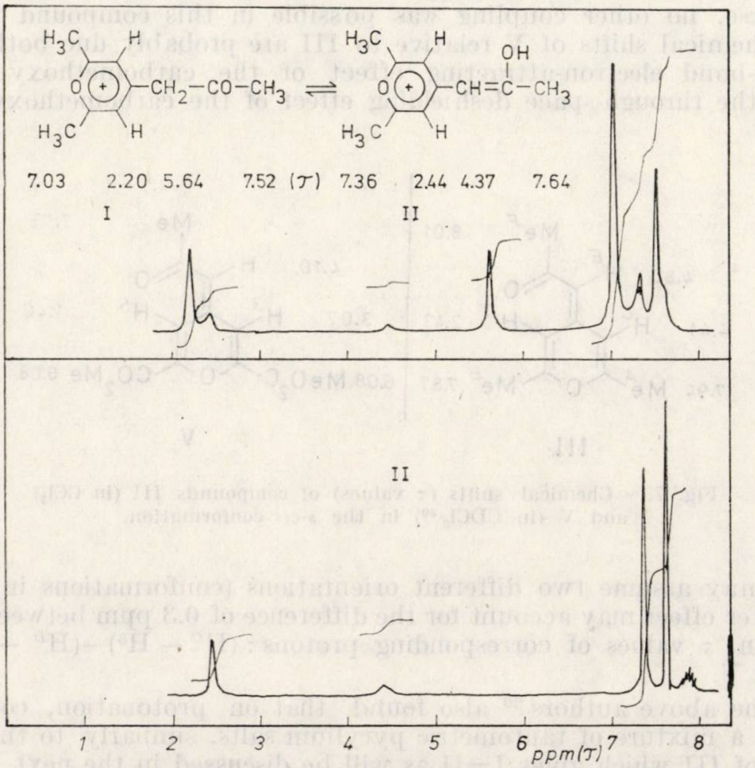

Fig. 8. — a) Upper part : ^{1}H—NMR spectrum of III in trifluoroacetic acid, evidencing a 3 : 1 mixture of cations I and II, respectively ; b) Lower part : ^{1}H—NMR spectrum of III in a 1 : 4 mixture of acetone-d_6 and trifluoroacetic acid, evidencing only cation II (whose enolic proton does not appear in the spectrum, owing to rapid exchange with TFA).

Figure 8a. It will be interesting to determine the constitution of the cation in crystalline salts (picrate, perchlorate) of III, in order to see which tautomer they contain ; the α-pyranylidene isomer (VI), obtained by self-condensation of acetylacetone (as thallium(I) salt in the presence of dichlorodimethylsilane) was found by X-ray diffraction to exist exclusively as enol in the crystal.[31]

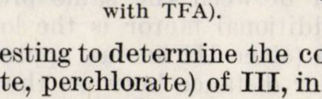

VI

The slightly higher chemical shifts of corresponding protons in the enol II relatively to I (α-methyl, acetyl, and pyrylium ring protons) are explained by the donor effect of the enolic group.

---

[31] N. Serpone and P. H. Bird, *Chem. Commun.*, **1975**, 284.

9. EXPERIMENTAL PART

Compound III was prepared as described earlier,[2] from t-butyl chloride, acetyl chloride and anhydrous aluminium chloride. After hydrolysis, treatment with perchloric acid, and filtration of 2,4,6-trimethylpyrylium perchlorate which results as a side-product, an excess of perchloric acid and diethyl ether were introduced into the filtrate, and the ethereal layer was treated with aqueous ammonia ; the resulted brownish ethereal solution of III was concentrated under reduced pressure until most ether was removed, and petroleum ether was added. Compound III crystallized. It was filtered off and recrystallized from cyclohexane (in which it is fairly soluble) and petroleum ether (in which it is little soluble) in admixture. The infrared absorption spectrum of III was described earlier,[2] but not the *ultraviolet absorption spectrum* ; the UV absorption maxima were determined with a Pye-Unicam SP 1800 instrument : in cyclohexane, $\lambda_{max} = 234$ and 349 nm ; in ethanol, $\lambda_{max}(\varepsilon_{max})$ are 244 nm (12600) and 357 nm (35300) ; the positive solvatochromy of III is in full agreement with its structure and indicates that the excited state possesses a larger contribution of polar structures IIIA and IIIB than the ground state.[32]

^1H—NMR Spectra were recorded with a Varian A-60A spectrometer at 39°. Chemical shifts are expressed as τ values *versus* internal tetramethylsilane.

The lanthanide induced shifts were simulated with the aid of a program written in BASIC and run on a Hewlett-Packard Calculator Model 9830 A, in split precision. The induced shifts were assumed to have a pseudocontact origin and were calculated according to the McConnell—Robertson equation :[21]

$$\delta_i = k(3 \cos^2 \varphi_i - 1)/r_i^3$$

in which δ_i represents the induced chemical shift, φ_i is the angle Eu — O — H^i, r_i represents the distance between the europium and the ith hydrogen, and k is a constant. The rotation of methyl groups was simulated by a subroutine which calculates the coordinates of hydrogens at various angle increments. The europium atom is allowed to move randomly around the coordination site, retaining its coordinates which gave the smallest agreement factor (AF).[22] The significance test of agreement factors, $\mathfrak{R} = AF_1/AF_2$ was calculated using a Lagrange interpolation [28] of Hamilton's values,[29] considering in our case two degrees of freedom.

The coordinates of hydrogen atoms were calculated using a COORD version (QCPE 136) translated in BASIC. The following distances and angles were assumed : (a) for the pyranic ring. C=C 1.34 Å, C—C 1.48 Å, C—O 1.40 Å, C—H 1.09 Å, $C-CH_3$ 1.48 Å ; angles of exocyclic atoms were considered as 120° with respect to the double bonds ; (b) exocyclic bond distances, C=C 1.34 Å, C—C 1.44 Å, $C-CH_3$ 1.50 Å ; C=O 1.20 Å, C—H 1.09 Å, all with 120° angles.

ACKNOWLEDGEMENTS. Thanks are expressed to Mr. N. Bălan for assistance in recording NMR spectra, to Mrs. A. Vasilescu for decoupling experiments with a Tesla NMR instrument operating at 80 MHz, to Mrs. M. Paraschiv for the UV spectra, and to Professor Raymond E. Davis (University of Texas at Austin) for making available a copy of the PRGM program.

---

[32] C. Reichardt, "Lösungsmittel-Effekte in der organischen Chemie", Verlag Chemie, Weinheim/Bergstr., 1969, p. 108.

Revue Roumaine de Chimie, **23**, 7, 1079–1084 (1978)

HETEROCYCLIC COMPACT CONDENSED SYSTEMS. IV[1]

LINEAR BIS PYRAZOLO[2,3-d], [8, 9-d]*trans*-QUINACRIDONE

C. TĂRĂBĂȘANU-MIHĂILĂ, C. ZAHARIA,* L. FLORU, F. URSEANU
and B. MĂRCULESCU **

Laboratory of Technology of Aromatic Intermediates and Organic Dyes, Polytechnic Institute—Bucharest, Calea Victoriei 149, Romania

* Central Laboratory of Spectrofluorimetry, Institute of Virusology "St. Nicolau" 285, Sos. M. Bravu, Bucharest, Romania

** Laboratory of Makromolecular Chemistry, Polytechnic Institute, Bucharest, Calea Victoriei 149, Romania

Received April 28, 1976

The possibility of the synthesis of linear bis pyrazolo [2,3-d], [8,9-d] *trans*-quinacridone by condensation of succinyl succinic ester with 6 amino-indazole, followed by cyclization is studied. The behaviour of the synthetised compound from the spectral point of view in infra-red, emission and excitation is discussed. The tautomeric form which shows affinity towards polyester fibres is specified.

1. INTRODUCTION

Quinacridonic pigments, characterized by a great thermal stability and by insolubility in the most common solvents find in our days a more and more large applicability in the colouring of the plastic masses in the lacquer industry.

Owing to their strong hydrophobic character, quinacridone and its derivatives can not be used in the colouring of the polyester fibres by the means of the technology of application for dispersion dyes.

In the view of decreasing the hydrophobic character we proposed the synthesis of a heterocyclic compact condensed *trans*-quinacridone-pyrazole dye, with applicability in the colouring of polyester fibres. The obtaining of this product was effected according to the following reaction succession :

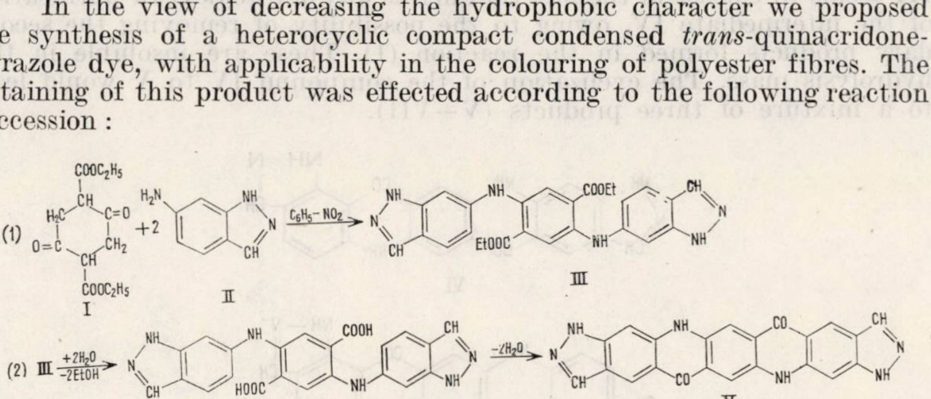

---

[1] C. Tărăbășanu-Mihăilă, L. Floru, B. Mărculescu and F. Urseanu, *Rev. Roumaine Chim.*, **23**, 977 (1978).

2. RESULTS AND DISCUSSION

2.1. Synthesis of linear bis-pyrazolo [2,3-d], [8,9-d] *trans*-quinacridone

The condensation reaction of diethyl ester of the succinyl-succinic acid (I) with 6-amino indazole (II) was carried out in acetic acid-nitrobenzene medium at temperatures situated between 115–125°, during 6–7 hours. The role of nitrobenzene in the reaction is, beside that of the solvent, to oxidize the Schiff base, formed as primary product, to the compound III. The separation of the latter was carried out by the adding of methyl alcohol to the reaction mass.

The yield is situated at about 80%.

The hydrolysis of the diester intermediate III to the compound IV takes place under good conditions by using a water-alcohol-sodium hydroxide mixture at 60–70° as hydrolysis agent. The ratio of the reactants in the hydrolysis mass must be chosen in such a way so that the formed compound IV to be perfectly soluble. Its separation is carried out by acidulation with hydrochloric acid. The yields are 90–95%.

The cyclization of the compound IV to V by dehydration was accomplished either by the action of polyphosphoric acid at 150–180°, or using the ethyl ester of the polyphosphoric acid at 140–160°. In both cases one obtains practically quantitative yields. The purity of the obtained linear [2,3-d], [8,9-d] *trans*-quinacrydone (V) is remarkable. The attempts to use the chlorsulfonic or monohydrated sulfuric acid as cyclization agent did not lead to corresponding results, because the sulfonation reaction appears as a competitive process with the dehydration. For this reason the yields of the compound (V) do not exceed 40–60%.

Moreover, attempts were carried out for the direct cyclization of the intermediate III to V by the removing of alcohol.

Thermal cyclizations at 160° in nitrobenzene or in silicon oil were performed. In this case the yields are great (about 85%), but the purity of the obtained compound V is not satisfactory.

The advantage of the intermediate hydrolysis of the compound III seems to consist in the fact that in this way one achieves a purification of the intermediate IV, owing to the possibility of removing the secondary products formed in the reaction (1). These are insoluble in the hydrolysis mass. The cyclization of the compound IV to V would lead to a mixture of three products (V–VII).

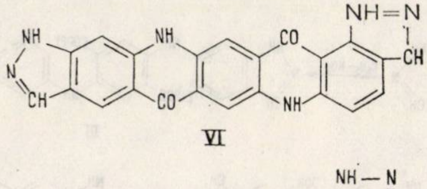

VI

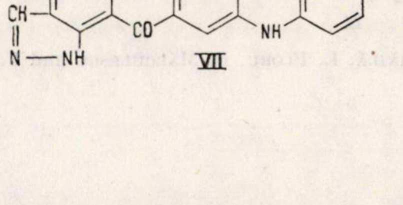

VII

Experimentally one obtains only one compound. After 3 recrystallizations from dimethylformamide of the substance resulted by cyclization, one obtains a pure compound. The purity was checked up by the independence of the emission spectrum on the wave length of the excitation light. This is known as a very sensitive method[2].

Taking into account the cyclization reaction mechanism for the compounds of type III proposed by Altiparmakian,[3] the structure V appears to be the most probable for the synthetized intermediate. The attack of the formed intermediate carbocation is moreprobable in the position 5 of the indazole than in the position 7, with a lower electronic density.

This assumption is in concordance with other data existing in literature, which show that the nucleophilic attack in the case of 6-aminoindazole takes place in the position 7[4].

The attempts to make evident the compounds VI and VII by the bidimensional thin layer chromatography on silica gel support did not lead to conclusive results.

2.2. Infra-red spectral behaviour of the compound V

In table 1 the spectral data regarding linear trans-quinacridone, compound V and 6-aminoindazole are presented. From the great number of the existing bands we proposed to examine only ν_{CO} and ν_{NH}, as a measure of the association of the compound V in solid state and the characteristic bands of the indazole system which are found again in the compound V.

Table 1

Infra-red bands for linear *trans*-quinacridone, compund V, and 6-aminoindazole *

Linear *trans*-quinacridone :	3585 s, 3410 s, 3280 s, 3070 s, 2930 s, 2860 s, 1625 s, 1545 s, 1495 s, 1355 s, 1320 s, 1275 m, 1155 m, 1080, 1030, 1000, 980, 900, 850, 810.
Compound V :	3410 m, 3220 s, 1650 s, 1615 s, 1570 s, 1495 s, 1415 m, 1298, 1170 s, 1040 s, 960, 910 m, 850 m, 795, 680 m, 640 s, 930.
6-aminoindazole :	3440 m, 3360 m, 3130–2980 m, 1620 s, 1490 m, 1455 s, 1390 s, 1330 m, 1310, 1248 m, 1212 m, 1132, 1110, 1070 s, 958 s, 890, 850 s, 785 m, 745.

* Infra-red spectra were taken in a KBr disk using a UR-10 spectrophotometer

The ν_{CO} frequencies are situated at 1625 cm^{-1} in the case of quinacridone and at 1615 cm^{-1} for the compound V.

---

[2] C. N. Zaharia, *Rev. Chim.* (*Bucureşti*), **26**, 255 (1975).
[3] R. H. Altiparmakian, *Helv. Chim. Acta*, **55**, 85 (1972).
[4] R. F. Surean and R. Pernat, *Ind. chim. belge*, *Suppl.*, **2**, 469 (1959).

These values are much lower than those found in the case of substituted diphenylcetones,[5] for which ν_{CO} are situated between 1635—1670 cm^{-1}.

This fact confirms the decreasing of the C=O bond order. This result can be attributed to the formation of the hydrogen intermolecular N—H . . .O=C bonds.

The formation of these bonds also justifies the ν_{NH} frequencies in the quinacridonic rest in the case of the two compounds = 3280 cm^{-1} for quinacridone, 3220 cm^{-1} for the compound V. These frequencies are very low. The bands situated at 1415, 1040, 960, 850 and 795 cm^{-1} in the case of the dye V seem to be characteristic bands of the indazole rest.[6]

The δ_{NH} band is found again in the case of the derivative V at 1495 cm^{-1}. This value is identical in the case of quinacridone and very close to that found for 6-aminoindazole (1490 cm^{-1}).

The C=N stretching vibration which usually is situated in the range from 1660 to 1620 cm^{-1} is found again at 1620 cm^{-1} for 6 amino-indazole and at a greater frequency namely at 1650 cm^{-1} for the compound V.

From the infra red spectral behaviour of the dye V, it may be concluded that in solid state this exists in a strong associated form, the intermolecular hydrogen bridges having an important contribution to the actual state of molecules.

2.3. Excitation and emission spectra of the compound V in solution

The spectral behaviour of the quinacridonic systems has been discussed in an earlier paper. [7] The positions of the O—O bands for the compound V are presented in table 2.

Table 2

The position of the O—O bands (cm^{-1}) for the compound II

Solvent	Dimethyl-formamide	Sulphuric Acid	Polyester
Excitation	19048	18939	20200
Emission	18182	18692	19900
(0—0)	876	247	300

From the examination of these data it follows that in dimenthylformamide the molecular structures corresponding to the emission energy level are considerably different from those corresponding to the ground state. But in sulphuric acid, these differences are much lower, Δ_{O-O} decreasing from 876 up to 247 cm^{-1}, in the case of dimethyl formamide.

---

[5] N. Fusan, M. L. Josian, E. M. Shelton, *J. Amer. Chem. Soc.*, **76**, 2526 (1954).

[6] D. G. O'Sullivan, *J. Chem. Soc.*, **1966**, 3278.

[7] C. N. Zaharia and C. Tărăbăşanu-Mihăilă, *Rev. Roumaine Phys.*, **21**, 359 (1976).

The depencence of excitation and emission maxima on the nature of the solvent is probably due to the change in the ratio between cetonic tautomere V and enolic tautomere VIII in solution.

The cetonic form V predominates in solvents like alkyl formamides. The enolic forms appear in proton donor solvents.

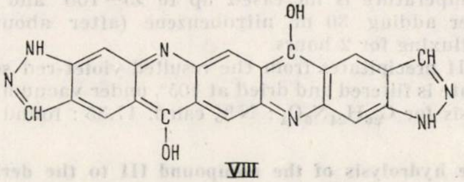

VIII

2.4. Excitation and emission spectra for compound V fixed on polyester fibres

The affinity of the dispersion dye V towards polyester fibres is moderate.

Colourings from dispersions in water and in a dimethyl formamide : water mixture (1 :9 in volume) were performed at 140°. The excitation and emission spectra recorded by reflexion are independent of the nature of the solvent used in the colouring process.

From the Δ_{0-0} value presented in table 2 for the coloured polyester it has been found that this is relatively close to the value obtained for solutions of the compound V in sulfuric acid. This fact involves the existence of small differences between the molecular structure corresponding to the emission energy level and that corresponding to the ground state. Hence, it follows that the enolic form prevails in the coloured polyester fibres.

Studies regarding the infra-red spectral behaviour of the polyester powders coloured with dispersion dyes of type V are in progress in order to clarify the fastening mode of the compound V on polyester fibres. The results of the tinctorial tests that indicate the good resistance of the colouring with the compound V are tabulated in table 3.

Table 3

Results of the tinctorial test for the compound V (colourings on polyester fibres)

% Compound V Vs. the fiber	Colour	Resistance to light	Resistance to wet treatments
1	red-brown	5–6	5
2	brown	6	4–5
3	brown	6	4–5

3. EXPERIMENTAL

3.1. Obtaining of the compound III

8 ml acetic acid and 20 g of compound I are introduced into a four-neck flask equipped with a stirrer, an ascending refrigerent, a thermometer and a dropping funnel. The mixture is heated under stirring at 75—80° till the succinic ester is completely dissolved. Then 24 g 6-amino-indazole are added to the resulted solution. When the reaction mass is homogeneous the temperature is increased up to 95—100° and one starts to add dropwise nitrobenzene. After adding 30 ml nitrobenzene (after about 3 hours) the reaction mass is heated with refluxing for 2 hours.

The compound III precipitates from the resulted violet-red solution by adding 45 ml methanol. The precipitate is filtered and dried at 105°, under vacuum. The yield is about 80%.

Elemental analysis for $C_{26}H_{24}N_6O_4$: N% calcd. 17.35 ; found 17.18.

3.2. The hydrolysis of the compound III to the derivative IV

10 g of compound III are added to a mixture of 50 ml methanol and 50 ml 40% natrium hydroxide solution. The mixture is kept under vigorous stirring at 90—100° for 45—60 minutes. By filtering and acidulation of the filtrate with hydrochloric acid one obtains the derivative IV. The yield is 90—95%.

Elemental analysis for $C_{22}H_{16}N_6O_4$: N% calcd. 19.63 ; found 19.79.

3.3. The cyclization of the intermediate IV

3.3.1. *By using polyphosphoric acid*

10 g of compound IV are dissolved in 60 ml polyphosphoric acid under stirring. The mixture is kept at 120—140° for 3 hours. The compound V precipitates by pouring it into water. The yield is practically quantitative.

3.3.2. *By using the ethyl ester of polyphosphoric acid*

10 g of compound IV are added to 100 ml polyphosphoric acid ethyl ester. The mixture is kept at 140° for 6 hours under stirring. By pouring it into water one obtains the compound V with quantitative yield.

Elemental analysis for $C_{22}H_{12}N_6O_2$: N% calcd. 21.43 ; found 21.60.

3.4. Chromatographic analyses

POLYGRAM-SILG plaques were used. The following eluting agents were employed: formamide water mixtures at different ratios situated between 10%—90%, dimethylformamide in water, dimethyl sulfoxyde, glacial acetic acid, formic acid, pyridine — water mixtures at different ratios, between 10—90%.

CONCLUSIONS

A new heterocyclic compact condensed compound used with good tinctorial results as dispersion dye in the colouring of the polyester fibres was synthetised.

Liner bis-pirazolo[2,3-d], [8,9-d]-*trans*-quinacridone was studied from the spectral point of view in infra-red, emission, and excitation and the tautomere structure which shows probable affinity towards polyester fibres was established.

The obtained results confirm the participation of the enolic form in the tinctorial process and the great contribution of the hydrogen bonds to the actual structure of the compound V in the solid state.

Revue Roumaine de Chimie, 23, 7, 1085–1091 (1978)

REACTIONS ON 2-PHENYL-3-AMINO-4(3H) QUINAZOLONE

M. ANWAR, F. I. ABDEL-HAY and M. FAHMY
Chemistry Department, Faculty of Science, Tanta University, Tanta, A. R. Egypt

Received April 2, 1976

2-Phenyl-3-amino-4 (3H) quinazolone (I) reacts with anhydrides, imides and aryl maleimides to give compounds II. These react with hydrazines, aromatic amines to give III. The reactions of I with ketones, aryl and alkyl halides, diethyl malonate and *p*-toluenesulphonyl chloride were discussed.

2-Aryl-3,1-4H-benzoxazones[1] react with hydrazine hydrate in boiling alcohol to give 2-aryl-3-amino-4(3H) quinazolones (I).[2]

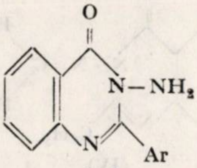

(I)*

I a, Ar = C_6H_5
b, Ar = C_6H_4Cl-p

2-Ethyl-4 (3H) quinazolinone was reported to condense with anhydrides and imides giving the corresponding condensation products.[3] In the present investigation the condesation of compound Ia with phthalic and succinic anhydrides, phthalic and succinic imides and aryl maleimides was studied. The reaction proceeds similarly yielding the condensation products (IIa–f).

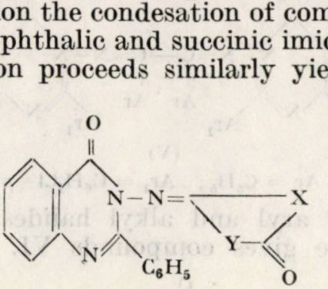

(II)

	Y	X
II a,	O	C_6H_4
b,	NH	C_6H_4
c,	O	CH_2-CH_2
d,	NH	CH_2-CH_2
e,	$N-C_6H_5$	CH=CH
f,	$N-C_6H_4OCH_3-p$	CH=CH

---

* See ref.[2].

[1] D. T. Bain and R. K. Smalley, *J. Chem. Soc.*, **1968**, 1593.

[2] A. Sammour, M. I. B. Selim and M. Anwar, *U.A.R.J. Chem.*, **14**, 197 (1971).

[3] A. Sammour, M. I. B. Selim, M. Elkasaby and M. Abdella, *Acta Chim. Acad. Sci.*, **78**, 293 (1973).

Condesation of IIa, b, e with hydrazines and aromatic amines give compounds (IIIa—d).

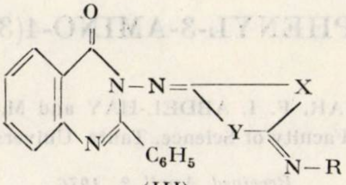

(III)

	Y	X	R
III a,	O	C_6H_4	$NH-C_6H_4NO_2-p$
b,	NH	C_6H_4	$NH-C_6H_5$
c,	$N-C_6H_5$	CH=CH	C_6H_5
d,	NH	C_6H_4	$C_6H_4CH_3-p$

2-Methyl-3,1-4H-benzoxazone was found to condense with ketones yielding the corresponding condensation products.[4] Similarly compound Ia was condensed with acetone and acetophenone to give the condensation products (IVa, b).

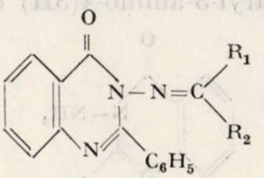

(IV)

IV a, $R_1 = R_2 = CH_3$
b, $R_1 = C_6H_5$; $R_2 = CH_3$

Similarly, two moles of Ib condense with benzil to give compound V.

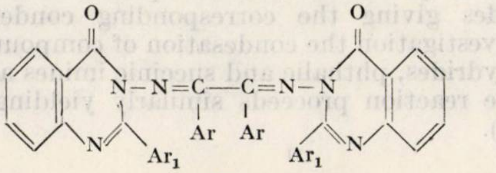

(V)

$Ar = C_6H_5$; $Ar_1 = C_6H_4Cl-p$

Reacting Ia with aryl and alkyl halides, monochloroacetic acid and chloroacetophenone gives compounds VI.

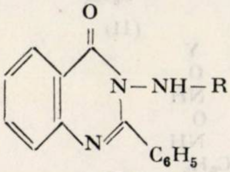

(VI)

VI a, $R = CH_3$; d, $R = C_6H_3(NO_2)_2-(2,4)$
b, $R = C_6H_5$; e, $R = CH_2COOH$
c, $R = C_6H_4NO_2-p$; f, $R = CH_2COC_6H_5$

---

[4] A. Sammour, T. Zimaity and M. Anwar, *Egypt. J. Chem.*, **16**, 215 (1973).

The structures of compounds VI b, c, d were confirmed by the preparation of authentic samples by the reaction of 2-phenyl-3,1-4H-benzoxazone with phenylhydrazine, 4-nitrophenylhydrazine and 2,4-dinitrophenylhydrazine respectively.

The reaction of Ia with ethyl malonate gives compound (VII), which on alkaline hydrolysis gives compound (VIII).

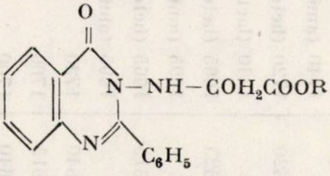

VII, $R = C_2H_5$
VIII, $R = H$

Moreover, Ia reacts with *p*-toluenesulphonylchloride to give compound IX. Alkaline methylation with dimethyl sulphate gives compound X.

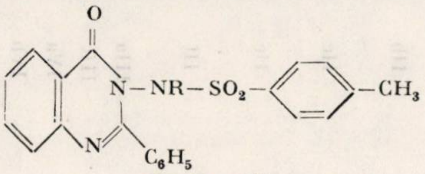

IX, $R = H$
X, $R = CH_3$

Hydrolysis of X with dilute hydrochloric acid gives a compound which is easily confirmed as VIa by m.p. and mixed m.p. determination.

The structure of compounds II−X is confirmed by uv- and ir-measurements.[5,6]

The absorption bands of uv- spectra are listed in table 1. The spectra of these compounds comprise four absorption bands. The first band within the 214−228 nm region corresponds to ^{1}La transition of the phenyl ring. The second band which lies within 232−236 nm region is assigned to the $\pi-\pi^*$ transition of the quinazolone nucleus.

The third band which lies within 270−287 nm region is assigned to ^{1}Lb transition perturbed by the $\pi-\pi^*$ transition of the carbonyl group.

The last band, located over 303 nm region can be assigned to the different types of intramolecular charge transfer within the whole molecule.

Table 2 represents the characteristic ir- spectral bands for compounds II−X. All compounds under investigation show absorption bands for the functional groups besides the three quinazolone skeletal bands. This indeed gives a strong evidence for the structures of compounds prepared.

---

[5] A. M. El-Abbady, M. Anwar, F. I. Abdel-Hay and M. F. Abdel-Megeed, *Egypt. J. Chem.*, **20** (1976) in press.

[6] M. Anwar, M. M. Abou-Sekkina and A. A. Saafan, "XIV Egyptian Conference of Pharmaceutical Science", Abstracts, 1975, p. 86.

Table 1

uv-Spectra of compounds II – VII in methanol (λ max./ε max. $\times 10^{-4}$)

Compound	Band Assignments			
	^1La	$\pi-\pi^*$ Quinazolone	$^1Lb +$ $C=0$	C.T.
IIa	226 4.46	— —	275 1.47	315 0.66
IIb	228 4.49	236 3.64	287 1.15	318 0.59
IIc	227 3.14	— —	272 1.54	316 0.51
IIe	216 5.20	235 5.59	287 2.83	— —
IIf	214 5.76	235 6.19	287 3.18	316 1.86
IIIa	226 6.06	232 5.76	275 2.02	311 0.91
IIIc	— —	234 6.09	284 1.43	303 0.84
IVa	227 2.81	— —	272 1.69	303 1.28
IVb	— —	236 4.76	287 2.46	330 0.61
VIe	228 3.96	— —	282 1.57	319 0.71
VIf	— —	235 5.70	287 2.74	314 1.57
VII	— —	233 2.75	270 3.06	319 1.69

Table 2

ir-Spectra of compounds II – X (KBr; cm^{-1})

Compound	N(tert.)	$\nu(C = N)$	$\nu(C = 0)$	$\nu(NH)$
IIa	1375	1630	1700 (hetero) 1740 (lactone)	
IIb	1380	1620	1690 (hetero) 1740 (amide)	3020—3110
IIc	1360	1620	1720 (hetero) 1740 (lactone)	
IIe	1360	1625	1665 (hetero) 1695 (amide)	
IIf	1370	1615	1665 (hetero) 1695 (amide)	
IIIa	1350	1640	1720	3020—3110
IIIc	1350	1615	1700	
IVa	1350	1640	1700	
IVb	1360	1640	1710	
V	1360	1640	1700	
VIe	1370	1620	1660	3090—3140
VIf	1370	1625	1670	3040—3100
VII	1350	1620	1680	3040—3130
VIII	1360	1620	1675	3040—3150
IX	1360	1625	1680	3040—3200
X	1365	1620	1690	

EXPERIMENTAL

The uv-absorption spectra in methanol were recorded at room temperature by a UNICAM S.P. 8000 spectrophotometer. The ir- spectra were recorded using a UNICAM S.P. 200 G. spectrophotometer. The KBr pellet technique was used. All melting points are not corrected.

Condensation of Ia with anhydrides and imides

A mixture of Ia (0.01 mole), phthalic or succinic anhydrides; phthalic or succinic imides; N-phenyl or N-*p*-anisyl-maleimide (0.01 mole) and anhydrous zinc chloride (0.5 g) was heated (oil-bath) at 200—220° for 5 hrs. The reaction product was washed with water and crystallized from ethyl alcohol to obtain II (yield 75—85%). The data of these products are summarized in table 3.

Table 3

Compounds II and III

Compound	m.p. °C	Formula (Mol. wt)	Analysis Calcd./Found % C	% M	% N
IIa	210	$C_{22}H_{13}N_3O_3$	71.93	3.54	11.47
		(367)	71.80	4.00	11.32
IIb	225	$C_{22}H_{14}N_4O_2$	72.13	3.82	15.30
		(366)	71.89	4.16	15.01
IIc	240	$C_{18}H_{13}N_3O_3$	67.71	4.07	13.16
		(319)	67.56	4.21	13.30
IId	232	$C_{18}H_{14}N_4O_2$	67.92	4.40	17.61
		(318)	67.88	4.24	17.31
IIe	234	$C_{24}H_{18}N_4O_2$	73.46	4.08	14.28
		(392)	73.68	4.26	14.00
IIf	236	$C_{25}H_{18}N_4O_3$	71.09	4.26	13.27
		(422)	71.01	4.36	13.08
IIIa	238	$C_{28}H_{18}N_6O_4$	66.93	3.58	16.73
		(502)	67.12	4.01	16.42
IIIb	231	$C_{28}H_{20}N_6O$	73.68	4.39	18.42
		(456)	73.44	4.52	18.11
IIIc	246	$C_{30}H_{21}N_5O$	77.08	4.49	14.98
		(467)	76.82	4.51	14.66
IIId	219	$C_{29}H_{21}N_5O$	76.48	4.62	15.38
		(455)	76.21	4.84	15.25

Reaction of IIa, b, c with hydrazines and aromatic amines

A solution of II a, b, c (0.01 mole) and *p*-nitrophenylhydrazine, phenylhydrazine, aniline or *p*-toluidine (0.01 mole) in 30 ml ethylic alcohol was refluxed for 5 hrs. The solid separated on cooling was crystallized from benzene to give IIIa—d. (Yield 65—75%). The data of these products are listed in table 3.

Condensation of Ia with ketones

A mixture of Ia (0.01 mole), acetone or acetophenone (0.015 mole) and zinc chloride (0.5 g) was heated in an oil bath at 200—220° for 4 hrs. After cooling the products were washed with water and crystallized from ethylic alcohol to give IVa, b. (Yield 75%). (Table 4).

Condensation of Ib with benzil

A mixture of Ib (0.02 mole), benzil (0.015 mole) and zinc chloride (0.5 g), the reaction mixture was worked as above to give a solid product (V), crystallized from benzene (Yield 70 %). (Table 4).

Table 4

Condensation products of I with acetone, acetophenone and benzil

Compound	m.p. °C	Formula (Mol. wt)	Analysis Calcd./Found %C	%H	%N
IVa	182	$C_{17}H_{15}N_3O$	73.64	5.41	15.16
		(277)	73.26	5.11	15.32
IVb	125	$C_{22}H_{17}N_3O$	77.88	5.01	12.39
		(339)	77.60	4.70	12.43
V	280	$C_{42}H_{26}Cl_2N_6O_2$	70.30	3.63	11.72
		(716.9)	70.01	4.02	11.66

Condensation of Ia with halocompounds

A mixture of Ia (0.01 mole), methyl iodide, bromobenzene, 4-nitrochlorobenzene, 2,4-dinitrochlorobenzene, monochloroacetic acid or chloroacetophenone, (0.02 mole), and 30 ml ethylic alcohol, was heated under reflux for 3 hrs. After cooling, the crystalline solids obtained were crystallized from benzene to give VIa—f. (Yield 65—70 %). The results are listed in Table 5.

Table 5

Condensation products of Ia with ethyl malonate and *p*-toluene sulphonyl chloride

Compound	m.p. °C	Formula (Mol. wt)	Analysis Calcd./Found % C	% H	% N
VIa	254	$C_{15}H_{13}N_3O$	71.79	5.17	16.73
		(251)	71.90	4.70	16.88
VIb	255	$C_{20}H_{15}N_3O$	76.67	4.79	13.41
		(313)	76.44	4.66	13.52
VIc	176	$C_{20}H_{13}N_5O_5$	59.55	3.23	17.37
		(403)	59.43	3.52	17.22
VIe	181	$C_{16}H_{13}N_3O_3$	65.08	4.40	16.27
		(295)	65.40	4.72	16.36
VIf	235	$C_{22}H_{17}N_3O_2$	74.37	4.79	11.83
		(355)	74.51	5.12	11.67
VII	89	$C_{19}H_{17}N_3O_4$	64.95	4.84	11.97
		(351)	64.62	5.11	11.86
VIII	175	$C_{17}H_{13}N_3O_4$	63.16	4.02	13.00
		(323)	62.94	4.36	12.77
IX	215	$C_{21}H_{17}N_3O_3$	70.19	4.74	11.70
		(359)	69.92	4.64	11.51
X	192	$C_{22}H_{19}N_3O_3$	70.78	5.09	11.26
		(373)	70.66	5.24	11.44

Condensation of Ia with phenylhydrazines

A mixture of Ia (0.01 mole), phenylhydrazine, 4-nitrophenylhydrazine or 2,4-dinitrophenylhydrazine (0.01 mole), and 30 ml ethylic alcohol was heated under reflux for 3 hrs. The crystalline solids obtained after cooling were recrystallized from benzene. Yield 85%. The compounds obtained were easily identified as VI b, c, d by m.p. and mixed m.p. (Table 5).

Reaction of Ia with ethyl malonate

A mixture of Ia (0.01 mole), diethylmalonate (0.02 mole), and 30 ml absolute ethylic alcohol, was heated under reflux for 4 hrs. After cooling a colourless crystalline solid was obtained, then recrystallized from methylic alcohol to give VII. Yield 70%. (Table 5).

Hydrolysis of VII

VII (1g) was dissolved in 30 ml ethylic alcohol containing 1 g sodium hydroxide and the reaction mixture was refluxed for 2 hrs. After cooling the product obtained was acidified with ice cold dilute hydrochloric acid and the separated solid was crystallized from benzene to give VIII. Yield 60%. (Table 5).

Condensation of Ia with *p*-toluenesulphonylchloride

A mixture of Ia (0.01 mole), *p*-toluenesulphonylchloride (0.01 mole), and 20 ml pyridine was heated under reflux for 3 hrs. The pyridine was distilled off under reduced pressure and the oil obtained was triturated with light petrol (b.p. 40—60°C) to give after crystallization from benzene the compound IX. Yield 60%. (Table 5).

Methylation of IX with dimethylsulphate

A mixture of IX (1g), (0.03 moles), in 10 ml 1 N sodium hydroxide solution and 8 ml (0.06 moles), dimethylsulphate, was heated at 70—80° for 2 hrs. The product obtained was triturated with light petrol and crystallized from benzene to give X. Yield 65%. (Table 5).

Hydrolysis of X

A suspension of X (1 g), (0.025 mole), in 30 ml diluted hydrochloric acid (1 : 1) was heated under reflux for 2 hrs. After cooling the product was treated with ice-cold sodium bicarbonate solution. The solid obtained was washed with water, then crystallized from benzene. The product was easily identified as VIa by m.p. and mixed m.p.

Revue Roumaine de Chimie, **23**, 7, 1093–1107 (1978)

PEPTIDES. XVI[1]

THE USE OF β-DICARBONYL N-PROTECTED METHIONINE AND TRYPTOPHAN IN PEPTIDE SYNTHESIS

F. GÖNCZY *, A. BALOG *, E. VARGHA **, D. BREAZU * and ILONA HALLER **
* Institute for Chemical and Pharmaceutical Research, Cluj-Napoca, Romania
** Depart. of Organic Chemistry, "Babeş-Bolyai" University, Str. Arany J. No. 11,
3400 Cluj-Napoca, Romania

Received July 16, 1976

Methionine and tryptophan dicyclohexylammonium salts α-amino-protected with CP, AE, AC and BA *** groups (1.1–1.14) were prepared and converted on the one hand, via the mixed anhydride method, into the protected di-**(3.1–3.7, 3.15–3.22)** and tripeptide esters **(5.4–5.6)**, and on the other hand into the appropriate phenacyl esters **(2.1–2.15)**. After removal of the amino protecting groups in acidic medium the corresponding phenacyl ester hydrochlorides **(2.16–2.18)** were obtained and used for the synthesis of the N-protected di-**(3.5, 3.6, 3.8–3.14, 3.17–3.20)** and tripeptide phenacyl esters **(5.1, 5.2, 5.6)** which in acidic medium resulted the adequate di-**(4.1–4.15)** and tripeptide ester hydrochlorides **(5.7–5.9)**.

In the composition of many naturally occurring polypeptides with important biological properties, among other amino acids, there are also methionine and triptophan.[2] For this reason it is important to find methods for the protection and activation of amino acids which make possible the realization of peptide bond between methionine or tryptophan and other amino acids.

Remarkable results have been obtained in our laboratory for the N=α-protection of the amino acids with β-ketoesters and β-diketones as well as for the synthesis of di- and higher peptides with these N-protected compounds applying the mixed anhydride technique.[3] Therefore we have investigated the synthesis of several dipeptides and tripeptides containing methionine and tryptophan. First of all the α-amino group of the methionine and tryptophan was protected with ethyl acetoacetate, 2-ethoxycarbonyl cyclopentanone, acetylacetone and benzoylacetone, and the N-protected compound isolated preferentially as dicyclohexylammonium salt according to the usual method.[3] No difficulties were observed during their preparation and purification both in the L and DL-series except the N-(1-ethoxycarbonyl-propen-2-yl)-L-tryptophan and N-(2-ethoxycarbonyl-cyclopenten-1-yl)-L-tryptophan dicyclohexylammonium salts (**1.11** and **1.9**) which requires special conditions. Surprisingly the crude products were also pure enough for coupling, and reacted with the appropriate amino acid ester resulting in good yields the corresponding N-protected dipeptide ester, which crystallized easily. The good solubility of the N-protected salts in dichlormethane or ethyl acetate is very advantageous for the mixed anhydride formation. The specific rotations of the N-protected salts in methanol at 1% concentration showed an increase function of the protecting group in the following order : CP $<$ AE $<$ $<$ AC $<$ BA. This holds true for the absolute values in the tryptophan series too. These salts are stable compounds, if pure, and no change of the specific rotation and melting point were observed even after a longer period of storage in well closed bottles, but it should be noted their high sensitivity towards acids. The results, constants and analyses are collected together in table 1.

---

* A. Balog deceased in 1976.

** Author to whom correspondence should be addressed.

*** Abbreviations according to IUPAC-IUB Commission on Biochemical Nomenclature, *J. Biol. Chem.*, **247**, 977 (1972); other abbreviations: CP, 2-ethoxycarbonyl-cyclopenten-1-yl, AE, 1-ethoxycarbonyl-propen-2-yl, AC, 1-acetyl-propen-2-yl, BA, 1-benzoyl-propen-2-yl, DCHA, dicyclohexylamine, Bz, benzene, Et_2O ether, EtOAc, ethylacetate, EtOH, ethanol, IpOH, propan-2-ol, MeOH, methanol, P, light petroleum (b.p. 60–80°), DMF, N,N-dimethylformamide.

[1] Previous paper: A. Balog, E. Vargha, D. Breazu, F. Gönczy and L. Beu, *Rev. Roumaine Chim.*, **19**, 689 (1974).

[2] a) E. Schröder and K. Lübke, "The Peptides", Vol. 2, Academic Press, New York, 1965; b) M. Bodánszky and M. Ondetti, "Peptide Synthesis", Interscience Publishers, New York, 1966.

A stepwise buildup of peptides, via the mixed anhydride technique, requires the carboxyl protection of the C-terminal amino acid. For this purpose it is of interest the phenacyl group.[4] While the β-dicarbonyl N-protected phenacyl esters of methionine are readily obtainable by treating the N-protected dicyclohexylammonium salts in acetone or in a mixture of acetone-dimethylformamide with phenacyl bromide, the preparation of the corresponding tryptophan derivatives presents some difficulties. On the whole, N-protected phenacyl esters crystallized well and are relatively stable compounds. Their specific rotation in methanol at 1% concentration shows similar increases, function of the protecting group, as the dicyclohexylammonium salts. The deblocking of the amino group at room temperature by acidification to pH 2.0—1.5 with hydrochloric acid in ethanol or ethyl acetate, occurs without difficulties. The hydrochlorides crystallized well in good yields. The AE and CP residues are removable generally easier than the AC and BA ones. Surprisingly in the methionine series, all the four mentioned protecting groups can be removed without special conditions at room temperature. Data on the phenacyl esters are listed in table 2. We have obtained methionine phenacyl ester hydrochloride (**2.16**) in a more simplified way too, by avoiding the isolation of the intermediate N-protected phenacyl ester (**2.2**) which proved to be enough pure for the further step. We will report the results in the near future.

---

[3] a) A. Balog, D. Breazu, E. Vargha, F. Gönczy and L. Beu, *Rev. Roumaine Chim.*, **15**, 1381 (1970) ; b) A. Balog, E. Vargha, D. Breazu, L. Beu and F. Gönczy, *ibid.*, **15**, 1391 (1970) ; c) C. Daicoviciu, A. Balog, D. Breazu, L. Beu and F. Gönczy, *ibid.*, **16**, 751 (1971) ; d) A. Balog, D. Breazu, C. Daicoviciu, E. Vargha, L. Beu and F. Gönczy, *ibid.*, **16**, 1601 (1971) ; e) E. Vargha, A. Balog, F. Gönczy, D. Breazu and L. Beu, *ibid.*, **18**, 1627 (1973).

[4] G. C. Stelakatos, A. Paganou and L. Zervas, *J. Chem. Soc.*, *(C)*, **1966**, 1199.

The dipeptide and tripeptide esters were prepared by the mixed anhydride coupling procedure, using ethyl chloroformate, isobutyl chloroformate or pivaloyl chloride for the formation of the acylating component, with catalytical amounts of N-methylmorpholine.[5] It is important to eliminate by filtration the dicyclohexylammonium chloride formed in the course of the reaction, since its very low solubility in water renders more difficult the isolation and purification of the water insoluble N-protected dipeptide and tripeptide phenacyl esters. The C-terminal component, i.e. the amino acid phenacyl ester or dipeptide phenacyl ester, was set free from the hydrochloride or hydrobromide with triethylamine in ethyl acetate-methanol in which solvent mixture, with a few exceptions, dissolves these salts and therefore the liberation of the free amino acid phenacyl ester takes place faster and is more complete. In no case the mixed anhydride, the amino acid phenacyl ester or dipeptide phenacyl ester was isolated and it is not necessary to eliminate the formed triethyl ammonium salt owing to its very good solubility in water, in which the protected di- or tripeptide esters are insoluble.

No significant differences were observed in the yields of the N-protected dipeptide or tripeptide phenacyl esters using isobutyl chloroformate or pivaloyl chloride instead of ethyl chloroformate, except for the N-(1-ethoxycarbonyl-propen-2-yl)-L-methionyl-L-asparagine phenacyl ester (**3.1**) in which case the yield increases from 50% to 80%, if the mixed anhydride was prepared with isobutyl chloroformate. These N-protected di- and tripeptide esters crystallized easily from the appropriate solvent.

The removal of the blocking groups was possible under the same conditions as for the N-protected phenacyl esters, i.e. a solution of hydrochloric acid in anhydrous ethanol or ethyl acetate was added at room temperature to adjust the solution or suspension of the protected ester to pH 2.0 to 1.5. This method failed in the case of the N-protected tryptophyl dipeptide esters, because we came upon some difficulties, namely the precipitated substance turned into pink or violet, which indicates some kind of modification in the molecule. The same observations were reported by Boissonnas and coworkers,[6] who intended to remove the benzyloxycarbonyl protecting group from an arginyl-tryptophane methyl ester.

---

[5] G. R. Fosker, N. H. Ch. Nayler and J. A. Wilcox, Brit. Pat., 991, 586, Beecham Research Laboratories Ltd., Brentford, 1962; *Chem. Zentr.*, **1967**, 33 – 1856.

[6] R. A. Boissonnas, St. Guttmann, R. L. Huguenin, P. A. Jaquenoud and E. Sandrin, *Helv. Chim. Acta*, **41**, 1867 (1958).

It was possible to overcome these difficulties carrying out in these cases the removal of the N-protecting group in the presence of diethylphosphonate. The results were satisfactory. Data on the N-protected di- and tripeptide esters and deprotected salts are listed in tables 3–5.

In the experimental part, in addition to the general procedure, there are given typical examples for each group of compounds.

EXPERIMENTAL

All melting points were determined in a capillary and are uncorrected. Rotations were measured with a Metra 400/a Praha type polarimeter in a 2 dm tube at room temperature at 1% concentration. The microanalysis samples were dried for 5–6 hours **in vacuo** at 65° over phosphorus pentoxide. Ascending thin-layer chromatograms were run on Kieselgel-G using the following solvent systems: A, chloroform-methanol (9 : 1), B, benzene-acetone (85 : 15), C, n-propanol-ammonia 25% – water (85 : 7.5 : 7.5) and D, n-propanol-water (7 : 3). Spots were revealed with ninhydrin,[9] chlorine-tolidine-iodine,[10] and in the case of tryptophan containing compounds, with Ehrlich's reagent.[11] In the case of β-dicarbonyl N-protected amino acid derivatives colour spots arose after ninhydrin sprayed plats were heated to 150–170°.

1. β-Dicarbonyl protected amino acid dicyclohexylammonium salts

General procedure. A mixture of the amino acid (20 mmole), of the β-ketoester or β-diketone (20–22 mmole) and of dicyclohexylamine (20 mmole), was boiled under stirring in methanol (30–100 ml) till an almost clear solution resulted. After elimination of the unreacted amino acid, the filtrate was evaporated exhaustively **in vacuo** in a rotary evaporator, usually at a bath temperature of 30–40°, adding benzene to accomplish the azeotropic removal of water. Trituration of the residue with light petroleum (b.p. 60–80°) gave the protected amino acid dicyclohexylammonium salt, which was substantially pure judging by thin-layer chromatography.

1.3. *N-(1-Ethoxycarbonyl-propen-2-yl)*-L*-methionine dicyclohexylammonium salt* (AE–Met–$O^-DCHA\cdot H^+$). L-Methionine (15 g, 0.1 mole), ethyl aceto-acetate (14 ml, 0.11 mole) and dicyclohexylamine (20 ml, 0.1 mole) in methanol (150 ml) were refluxed for 30 min. After the solvent was evaporated off, the residue crystallized from acetone (400 ml) yielding the protected salt (36.8 g, 83%). For constants and analyses see table 1.

1.11. *N-(1-Ethoxycarbonyl-propen-2-yl)*-L*-tryptophan dicyclohexylammonium salt* (AE–Trp–$O^-DCHA\cdot H^+$). A suspension of L-tryptophan (12.25 g, 60 mmole), ethyl acetoacetate (8.4 ml, 66 mmole) and dicyclohexylamine (11.8 ml, 50 mmole) in methanol (100 ml) was refluxed for 10 minutes. After work-up the sticky, amorphous residue was triturated with anhydrous ether (60 ml) and kept at room temperature overnight. The crystalline salt was filtered, washed four times with 10 ml portions of anhydrous ether and air-dried (23.2 g, 78%), mp 118–120°. The crude product was relieved of unreacted tryptophan by refluxing for 5 minutes with ethyl acetate (120 ml). The insoluble solid (2.25 g), mp 253° (decomp.), $[\alpha]_D^{25}$ – 30.9° (c = 1, water) was identified by TLC. The filtered solution was evaporated in a rotary evaporator, the residue was triturated again with anhydrous ether (80 ml) and kept in a refrigerator for one hour. The crystallized product was filtered off and washed thrice with 10 ml portions of anhydrous ether to yield the required protected dicyclohexylammonium salt (18.8 g, 77% calculated on reacted tryptophan). For constants and analyses see Table 1.

2. Phenacyl esters

General procedure. The β-dicarbonyl N-protected amino acid dicyclohexylammonium salt (10 mmole) was suspended in acetone (50 ml) or in a mixture of acetone-dimethylformamide (7 : 2) followed immediately by the addition of phenacyl bromide (10 mmole) and heated

---

[7] G. L. Southard, G. S. Brooke and J. M. Pettee, *Tetrahedron*, **27**, 1359 (1971).

[8] J. M. Davey, A. H. Laird and J. S. Morley, *J. Chem. Soc.* (C), **1966**, 555.

[9] E. D. Moffat and R. L. Lyttle, *Analyt. Chem.*, **31**, 926 (1959).

[10] G. Pataki, *J. Chromatogr.*, **12**, 541 (1963).

[11] R. H. Heacook and M. E. Mahon, *J. Chromatogr.*, **17**, 338 (1965).

Table 1

N-Protected dicyclohexylammonium salts

N°	DCHA Salts	Reaction time min	Yield % [a]	Mp. °C [b]	$[\alpha]_D$ [c]	Formula (M)	Analysis % : Calc./Found				
							C	H	N	S	R_f
1.1	CP-Met	90	85	142–143	– 15.0°	$C_{25}H_{44}N_2O_4S$	64.06	9.46	5.97	6.84	C 0.56
				IpOH		(468.6)	63.88	9.74	5.97	7.75	D 0.63
1.2	CP-DL-Met	90	85	124–125			64.40	9.90	6.14	7.08	
				EtOAc or acetone							
1.3	AE-Met	30	83	140–141	– 5.2°	$C_{23}H_{42}N_2O_4S$	62.40	9.56	6.33	7.24	C 0.31
				acetone		(442.6)	62.31	9.61	6.35	7.65	
1.4	AE-DL-Met	30	94	119–121			62.30	9.73	6.77	7.42	
				EtOAc-Et_2O							
1.5	AC-Met	100	91	136–137	+ 10.0°	$C_{22}H_{40}N_2O_3S$	64.03	9.77	6.36	7.77	C 0.46
				acetone		(412.6)	63.90	9.95	6.36	8.25	D 0.55
1.6	AC-DL-Met	100	73	130–131 [d]			63.43	10.00	7.00	7.75	
1.7	BA-Met [e]	120	69	169–170	+ 21.1° [f]	$C_{27}H_{42}N_2O_3S$	68.31	8.91	5.90	6.75	C 0.54
						(474.7)	—	—	—	—	

---

[a] Yields calculated on purified salts. [b] Solvents used for crystallization are shown under melting point. [c] Rotations were measured at room temperature at 1% concentrations in methanol if not otherwise stated. [d] Purified by refluxing the crude solid for 10 minutes with ether. [e] Reported [7] m.p. 168–170°. [f] (c = 2, EtOAc).

Table 1 (continued)

Nº	DCHA Salts	Reaction time min	Yield %[a)]	Mp. °C [b)]	$[\alpha]_D$ [c)]	Formula (M)	Analysis % : Calc./Found C	H	N	S	R_f
1.8	BA-DL-Met	40	70	145–146							
				Bz-P			68.46	9.30	6.09	6.86	
1.9	CP-Trp	20	88	100–102	−149.8°	$C_{31}H_{45}N_3O_4$	71.09	8.66	8.02		C 0.53
						(523.7)	70.40	8.96	8.25		D 0.67
1.10	CP-DL-Trp	20	86	176–177							
				EtOH			70.28	8.80	8.28		
1.11	AE-Trp [g)]	10	77	117–119 [h)]	−163.1°	$C_{29}H_{43}N_3O_4$	69.98	8.70	8.44		C 0.14
						(497.6)	69.74	8.94	8.70		
1.12	AC-Trp	60	84	185–186	−251.7°	$C_{28}H_{41}N_3O_3$	71.91	8.83	8.98		C 0.57
				BZ		(467.6)	71.77	9.04	9.15		
1.13	AC-DL-Trp	100	55	190–191							
				MeOH			71.80	9.20	8.95		
1.14	BA-DL-Trp [i)]	180	68	137–139		$C_{33}H_{43}N_3O_3$	74.82	8.18	7.93		C 0.54
				EtOH-P		(527.9)	74.52	8.50	7.69		D 0.68
1.15	AE-Asn	50	81	163–164 [j)]	+ 14.5°	$C_{22}H_{39}N_3O_5$	62.10	9.23	9.87		D 0.37
						(425.5)	62.23	9.16	9.58		

---

g) DL-isomer was reported in ref.[3a] mp. 163–164°. h) After trituration with light petroleum. i) L-Isomer reported in lit.[7] j) Purified by refluxing with ethyl acetate and collecting the crystals after standing overnight.

Table 2

Phenacyl esters

Q−X−OPAc

N°	Q	X	Salt	Yield % [a]	Mp. °C [b]	$[\alpha]_D$ [c]	Formula (M)	C	H	N	S	Cl	R_f
								Analysis % : Calc./Found					
2.1	CP	Met		68	66−67 IpOH	+ 45.1°	$C_{21}H_{27}NO_5S$ (405.5)	62.20 62.14	6.71 6.76	3.45 3.56	7.90 8.00		C 0.57
2.2	AE	Met		85	79−80 IpOH	+ 81.2°	$C_{19}H_{25}NO_5S$ (379.4)	60.12 60.50	6.64 6.85	4.69 4.05	8.44 8.56		C 0.56
2.3	AE	DL-Met		90	86−87 EtOH			59.54	6.95	3.51	8.50		
2.4	AC	Met		91	89−91	+ 96.9°	$C_{18}H_{23}NO_4S$ (349.4)	61.87 62.20	6.63 6.90	4.00 4.12	9.17 8.52		C 0.33
2.5	AC	DL-Met		73	72−73 AcOEt-P			61.97	6.85	4.15	9.03		
2.6	BA	Met		85	97−98 IpOH	+100.5°	$C_{23}H_{25}NO_4S$ (411.5)	67.12 67.30	6.12 6.29	3.40 3.58	7.79 7.90		A 0.74
2.7	BA	DL-Met		74	95−96 AcOEt-P			67.30	6.27	3.45	7.63		
2.8	CP	Trp		56	142−145 EtOH	− 72.3° [d]	$C_{27}H_{28}N_2O_5$ (460.5)	70.41 70.69	6.12 6.50	6.20 6.36			B 0.82
2.9	CP	DL-Trp		65	153−154 EtOH			70.30	6.43	6.27			
2.10	AE	Trp		80	130−132 EtOH	− 74.0° [e]	$C_{25}H_{26}N_2O_5$ (434.5)	69.10 69.50	6.03 6.40	6.50 6.70			B 0.76

[a,b,c] See footnote Table 1. [d] At 30°; $[\alpha]_D$ − 58.2° (c = 1, acetone). [e] c = 0.5; $[\alpha]_D$ − 35.7° (c=1, acetone)

Table 2 (continued)

N°	Q	X	Salt	Yield %[a]	Mp· °C[b]	$[\alpha]_D$ [c]	Formula (M)	Analysis %: Calc./Found C	H	N	S	Cl	R_f
2.11	AE	DL-Trp		87	151–152								
					EtOH			69.40	6.39	6.62			
2.12	AC	Trp		84	108–111	−101.0°	$C_{24}H_{24}N_2O_4$	71.28	5.96	6.62			B 0.56
					EtOH		(404.3)	71.12	6.43	7.13			
2.13	AC	DL-Trp		60	137–138								
					EtOH			71.00	6.40	7.05			
2.14	BA	Trp		59	75–95	−165.5[f]	$C_{29}H_{26}N_2O_4$	74.65	5.61	6.00			A 0.74
							(466.5)	75.10	6.20	6.30			
2.15	BA	DL-Trp		68	167–168								
					AcOEt			75.00	6.30	6.20			
2.16	H	Met	HCl[g]	72	162	+ 34.2[h]	$C_{13}H_{18}ClNO_3S$	51.39	5.97	4.60	10.55	11.67	C 0.25
							(303.8)	51.99	6.26	4.95	10.40	11.87	
2.17	H	DL-Met	HCl	85	157								
					MeOH-Et_2O			51.65	6.16	4.50	10.85	11.90	
2.18	H	Trp	HCl	83	158–160	− 4.9°	$C_{19}H_{19}ClN_2O_3$	63.60	5.33	7.81		9.88	A 0.21
							(358.8)	63.14	5.87	7.32		10.15	
2.19	H	Gln	HCl[i]	93	168–169	+ 34.8°	$C_{13}H_{17}ClN_2O_4$	51.99	5.69	9.31		11.79	A 0.62
						(c = 1, H_2O)	(300.7)	51.60	6.20	9.38		12.34	
2.20	H	Ile	HCl	77	168–169	+ 27.7°	$C_{14}H_{20}ClNO_3$	58.84	7.05	9.40		13.41	
							(285.7)	58.66	7.21	9.01		12.60	

---

[f] $[\alpha]_D$ − 96.6° (c = 1, acetone). [g] Easily prepared without the isolation of the intermediate N-protected phenacyl ester. [h] $[\alpha]_D$ + 31.2° (c = 2, water). [i] Prepared from AE−Gln−OPAc (c.f. reference[1]).

Table 3

N-Protected dipeptide esters

N°		Yield % a)	Mp. °C b)	$[\alpha]_D$ c)	Formula (M)	Analysis % : Calc./Found C	H	N	S	R_f
3.1	AE–Met–Asn–OPAc	50	176–177 EtOH	+14.7°	$C_{23}H_{31}N_3O_7S$ (493.5)	55.96 55.50	6.33 6.67	8.51 8.93	6.49 6.75	A 0.14
3.2	AE–Met–Gln–OPAc	53	155–157 EtOH	+23.1° DMF	$C_{24}H_{33}N_3O_7S$ (507.5)	56.78 56.46	6.35 6.90	8.47 8.53	6.31 6.40	A 0.18
3.3	AE–Met–Gly–OMe	72	87–88 EtOH	+64°	$C_{14}H_{24}N_2O_5S$ (332.4)	50.58 50.86	7.27 7.57	8.42 8.58	9.64 9.30	
3.4	AE–Met–Gly–OPAc	68	117–118 EtOH	+65.8°	$C_{21}H_{28}N_2O_6S$ (436.5)	57.78 57.83	6.46 6.50	6.42 6.47	7.34 7.36	A 0.46
3.5	AE–Met–Met–OPAc	59	128–129 EtOH	+32.2°	$C_{24}H_{34}N_2O_6S_2$ (510.6)	56.44 56.40	6.71 7.04	5.48 5.48	12.55 12.40	A 0.87
3.6	AE–DL–Met–DL–Met–OPAc	59	120–121 EtOH			 56.50	 7.16	 6.00	 12.00	
3.7	AE–Met–Ser–OPAc d)	65	144–145 EtOH	+17.2°	$C_{22}H_{30}N_2O_7S$ (466.5)	56.63 56.40	6.48 6.50	6.00 6.67	6.87 6.85	A 0.77
3.8	CP–Gln–Met–OPAc e)	66	187–188 EtOH	+41.3° Dioxan	$C_{26}H_{35}N_3O_7S$ (533.6)	58.51 58.78	6.61 6.80	7.87 8.32	6.30 6.12	
3.9	AE–Gln–Met–OPAc e)	46	178–179 EtOH	+31.6° DMF	$C_{24}H_{33}N_3O_7S$ (507.5)	56.78 56.98	6.55 7.30	8.27 8.90	6.31 6.21	
3.10	AE–Gly–DL–Met–OPAc f)	45	126–128 EtOH		$C_{21}H_{28}N_2O_6S$ (436.5)	57.78 57.58	6.40 6.72	6.42 6.34	7.34 7.50	A 0.26
3.11	AE–Leu–Met–OPAc g)	22	98–99 IpOH	+98.8°	$C_{25}H_{36}N_2O_6S$ (492.5)	60.96 61.01	7.36 7.65	5.68 6.15	6.51 6.15	A 0.85 B 0.50

---

a,b,c) See footnote Table 1. d) Prepared from **1.3** and L-serine phenacyl ester hydrochloride[3d] with ethyl chloroformate. e) By the mixed anhydride coupling procedure from CP–, respectively AE–Gln–O–DCHA·H^+[1]. f) From AE–Gly–O–DCHA·H^+[3a]. With pivaloyl chloride. g) With ethyl chloroformate from AE–Leu–O–DCHA·H^+[3a].

Table 3 (continued)

N°		Yield %[a)]	Mp. °C[b)]	$[\alpha]_D$[c)]	Formula (M)	Analysis %: Calc./Found C	H	N	S	R_f
3.12	AE–Phe–Met–OPAc[h)]	57	151–152	+57.0°	$C_{28}H_{34}N_2O_6S$	63.85	6.50	5.32	6.08	B 0.47
			EtOH	Dioxan	(526.6)	63.80	6.83	5.52	5.90	
3.13	AC–Phe–DL–Met–OPAc[h)]	85	139–140	+93.8°	$C_{27}H_{32}N_2O_5S$	65.28	6.49	5.64	6.45	
			EtOH		(496.60)	65.58	7.00	5.86	6.22	
3.14	CP–Ser–Met–OPAc[i)]	76	150–151	+113.1°	$C_{24}H_{32}N_2O_7S$	58.52	6.54	5.68	6.51	
			EtOH		(492.5)	58.44	6.72	5.89	6.30	
3.15	AE–Trp–Gly–OEt	68	101–103	+85.4°	$C_{21}H_{27}N_3O_5$	62.85	6.78	10.46		
			AcOEt–P		(401.5)	63.10	6.81	10.24		
3.16	AE–DL–Trp–Gly–OEt	81	135–136							
			AcOEt–P			63.33	7.29	10.00		
3.17	AE–Trp–Met–OMe	43	122–123	+81.8°	$C_{23}H_{31}N_3O_5S$	59.85	6.77	9.10	6.94	A. 078
			IpOH		(461.5)	59.80	7.10	9.26	6.63	
3.18	CP–Trp–Met–OPAc	58	138–139	+42.8°	$C_{32}H_{37}N_3O_6S$	64.96	6.30	7.10	5.42	A 0.81
			EtOH		(591.7)	64.83	6.60	7.79	5.31	
3.19	AE–Trp–Met–OPAc	67	103–106	+85.4°	$C_{30}H_{35}N_3O_6S$	63.68	6.23	7.42	5.66	A 0.58
			EtOH		(565.6)	63.80	6.60	7.45	5.46	
3.20	BA–Trp–Met–OPAc	80	144–146	+42.6°	$C_{34}H_{35}N_3O_5S$	68.32	5.90	7.03	5.36	A 0.81
			EtOH		(597.7)	68.23	6.09	7.02	5.31	
3.21	AE–Trp–Phe–OMe	73	108–110	+45.3°	$C_{27}H_{31}N_3O_5$	67.90	6.54	8.80		A 0.57
					(477.5)	67.80	6.67	8.62		
3.22	AE–Trp–Phe–OPAc[j)]	64	153–155	+28.2°	$C_{34}H_{35}N_3O_6$	70.20	6.06	7.22		A 0.60
			Acetone+H_2O		(581.6)	70.40	6.60	7.37		
3.23	AE–Ser–Ile–OMe[k)]	80	136–137	+224°	$C_{16}H_{28}N_2O_6$	55.80	8.12	8.12		
			Et_2O		(344.4)	55.83	8.40	8.30		
3.24	AE–Ser–Ile–OPAc	89	107–108	+162.7°	$C_{23}H_{32}N_2O_7$	61.59	7.19	6.24		B 0.08
			EtOH 50%		(448.5)	61.56	7.45	5.82		

[h)] From AE–, respectively AC–Phe–O– DCHA·H$^+$.[3a] [i)] From CP–Ser–O– DCHA·H$^+$.[3d] [j)] By the mixed anhydride procedure with L phenylalanine phenacyl ester hydrochloride.[3b] [k)] From AE–Ser–O– DCHA·H$^+$.[3d]

Table 4

Dipeptide ester hydrochlorides

$H_2^+-X-Y-OR\cdot Cl^-$

N⁰	X	Y	R	Yield % [a)]	Mp. °C [b)]	$[\alpha]_D$ [c)]	Formula (M)	C	H	N	S	Cl	R_f
4.1	Met D	Asn	PAc	79	181	+ 9.6°	$C_{17}H_{24}ClN_3O_5S$	48.86	5.79	10.05	7.68	8.48	A 0.14
						DMF	(417.8)	48.63	5.90	10.23	7.50	8.30	C 0.31
4.2	Met	Gln	PAc	98	165	+ 4.6°	$C_{18}H_{26}ClN_3O_5S$	50.05	6.06	9.72	7.42	8.20	A 0.19
							(431.9)	49.90	6.50	9.17	6.88	8.50	C 0.33
4.3	Met	Met	PAc	84	138−140	−15.8°	$C_{18}H_{27}ClN_2O_4S_2$	49.70	6.25	6.44	14.74	8.15	A 0.50
							(435.0)	49.48	6.53	6.53	14.64	8.26	C 0.62
4.4	DL-Met	DL-Met	PAc	97	160−162			49.94	6.60	6.54	14.43	8.27	
4.5	Gln	Met	PAc	45	167−168	−13.4°	$C_{18}H_{26}ClN_3O_5S$	50.05	6.06	9.72	7.42	8.20	C 0.52
					MeOH−Et_2O		(431.9)	50.06	6.43	9.54	7.30	8.40	
4.6	Leu	Met	PAc	40	122−125	−13.8°	$C_{19}H_{29}ClN_2O_4S$	54.72	7.01	6.62	7.69	8.50	A 0.59
					IpOH		(416.9)	54.70	7.76	6.43	7.79	8.50	C 0.71
4.7	Phe	Met	PAc	92	152−155	−10.9°	$C_{22}H_{27}ClN_2O_4S$	58.59	6.03	6.21	7.11	7.86	B 0.45
					EtOH		(451.0)	59.10	6.47	6.20	6.96	8.10	

[a,b,c)] See footnote Table 1.

Table 4 (continued)

N⁰	X	Y	R	Yield %[a)]	Mp. °C[b)]	$[\alpha]_D$[c)]	Formula (M)	C	H	N	S	Cl	R_f
4.8	Phe	DL-Met	PAc	50	149–151	+40.5°		58.30	6.43	6.96	6.84	8.70	
4.9	Trp	Gly	Et	86	109–125	−12.1°	$C_{15}H_{20}ClN_3O_3$	55.30	6.18	12.90		10.88	
							(325.7)	55.16	6.64	13.41		11.22	
4.10	DL-Trp	Gly	Et	87	172–174			55.20	6.78	13.22		11.02	
4.11	Trp	Met	Me[d)]	83	92–97	−52.0°	$C_{17}H_{24}ClN_3O_3S$	52.92	6.27	10.89	8.31	9.19	
							(385.8)	52.53	6.65	10.37	8.85	9.80	
4.12	Trp	Met	PAc	70	132–142	−58.8°	$C_{24}H_{28}ClN_3O_4S$	58.82	5.76	8.57	6.54	7.23	
							(490.0)	58.50	6.00	8.33	6.75	7.75	
4.13	Trp	Phe	PAc	99	138–142	−41.8°	$C_{28}H_{28}ClN_3O_4$	66.45	5.57	8.30		7.00	
							(505.9)	66.75	5.80	8.62		7.60	
4.14	Ser	Ile	Me	90	132–133	+23.3°	$C_{10}H_{21}ClN_2O_4$	44.69	7.87	10.42		13.19	
							(268.7)	45.00	8.19	9.58		14.40	
4.15	Ser	Ile	PAc	84	175–178	−20.6°	$C_{17}H_{25}ClN_2O_5$	54.76	6.76	7.51		9.50	
					MeOH–Et_2O		(372.8)	54.80	6.90	7.30		9.90	

[d)] Prepared by Davey and coworkers,[8] from Boc–Trp–Met–OMe, mp. 95–105° (decomp.), no indication for specific rotation.

for 1—2 minutes at a bath temperature of 50°. The dicyclohexylammoniumbromide formed a precipitate. After being kept overnight at room temperature it was collected by filtration, washed with acetone (four times) and the filtrate was then diluted with ice water (350—400 ml). The precipitated thick syrup began to crystallize within a short time. The mixture was allowed to stand at room temperature for 2—3 hours and then it was filtered off, dried and recrystallized from the appropriate solvent.

Removal of the blocking group. A suspension of the β-dicarbonyl protected amino acid phenacyl ester (10 mmole) in anhydrous ethanol or ethyl acetate (10 ml), was treated with 4N hydrogen, chloride in ethyl acetate (10 mmole) to pH 2.0—1.5, and kept 1—2 hours at room temperature. The deposited solid was collected by filtration, washed with cold ethyl acetate and anhydrous acetone. These salts crystallize from ethanol-anhydrous ether.

2.8. *N-(2-Ethoxycarbonyl-cyclopenten-1-yl)-*L*-tryptophan phenacyl ester* (CP—Trp—OPAc). Prepared from **1.9** (5.3 g, 10 mmole) and phenacylbromide (2 g, 10 mmole) in a mixture of acetone-dimethyl-formamide (3 : 1, 40 ml) at room temperature. From the clear solution begins immediately the separation of the dicyclohexylammonium bromide which after being kept overnight, was eliminated by suction, and the filtrate was diluted with ice water (400 ml). The flocky and sticky precipitate stood for two hours in a refrigerator, the liquid was decanted and the remaining crude ester covered with water. After one hour in a refrigerator the slightly sticky mass was filtered and dried in a desiccator. The crude, powdered phenacyl ester (4 g, 86.5 %), mp 124—128°, crystallized from ethanol (50 ml), yielded the pure N-protected ester. For constants and analyses of pure product see table 2.

2.16. L*-Methionine phenacyl ester hydrochloride* (H_2^+—Met—OPAc·Cl^-). A suspension of **2.2** (18 g, 47.5 mmole) in anhydrous ethanol (45 ml), was treated with 4 N hydrogen chloride in ethyl acetate (12 ml, 50 mmole) and kept for 10 minutes at about 40°. The reaction mixture was allowed to stand at room temperature overnight and in the refrigerator for 2 hours more. The deposited solid was collected by filtration, washed with cold ethyl acetate (10 ml) and anhydrous acetone (10 ml). The ester hydrochloride (10.5 g, 72.5 %) proved to be pure without recrystallization (from ethanol-dry ether). For constants and analyses see Table 2.

3. β-Dicarbonyl N-protected dipeptide esters

General procedure. Ethyl chloroformate, isobutyl chloroformate or pivaloyl chloride (20 mmole) was added at —10 to —5° to a stirred solution or suspension of the N-protected amino acid salt in dry tetrahydrofuran or ethyl acetate or dichlormethane (50—100 ml) followed by one drop of methylmorpholine. The mixture was stirred at —10 to —5° for 20—25 minutes and the precipitated dicyclohexylammonium chloride was filtered, washed with dry solvent. A solution in tetrahydrofuran, or ethyl acetate, or ethyl acetate — methanol (100—240 ml) of the amino acid phenacyl ester, set free from the hydrochloride or hydrobromide (20 mmole) with triethylamine (20 mmole) at 0°, was added at —5 to 0° to the stirred mixed anhydride solution. Stirring was continued for two hours. The reaction mixture was then allowed to warm to room temperature and to stand overnight without stirring. A solution (40 ml) of 5 % aqueous sodium hydrogen carbonate and water (100 ml) were added. Upon removal of the organic solvents *in vacuo* at 30—40°, the N-protected peptide ester was left as a crystalline suspension in water, then it was collected by filtration, washed with water, dried and recrystallized from an appropriate solvent.

3.5. *N-(1-Ethoxycarbonyl-propen-2-yl)-*L*-methionyl-*L*-methionine phenacyl ester* (AE—Met—Met—OPAc). The mixed anhydride, prepared from **1.3** (4.5 g, 10 mmole), ethyl chloroformate (1 ml, 10 mmole) and N-methylmorpholine (1—2 drops) in dichlormethane at — 10 to —5°, was treated with the amino component, prepared from **2.16** (3 g, 10 mmole) and triethylamine (1.4 ml, 10 mmole) in ethyl acetate-methanol (5 : 1, 120 ml) at —5 to 0°. After 2 hours of stirring at this temperature, the reaction mixture was kept overnight at room temperature and worked up with a solution (20 ml) of 5 % aqueous sodium hydrogen carbonate and water (50 ml), yielding the crude N-protected dipeptide ester (4.8 g, 94 %), mp 115—122°, which crystallized from ethanol (15 ml) giving the pure product (3 g, 59 %) ; for its constants and analysis see table 3.

3.18. *N-(2-Ethoxycarbonyl-cyclopenten-1-yl)-*L*-tryptophyl-*L*-methionine phenacyl ester* (CP—Trp—Met—OPAc). The mixed anhydride, prepared from **1.9** (3.2 g, 6 mmole), ethyl chloroformate (0.6 ml, 6 mmole) and N-methylmorpholine (1—2 drops) in dichlormethane (30 ml) was treated at —5 to 0° for 2 hours with the phenacylester, prepared from **2.16** (1.85 g, 6 mmole) and triethylamine (0.85 ml, 6 mmole) in ethyl acetate-methanol (10 : 6, 40 ml). After standing overnight at room temperature and work-up, the crude sticky product (3.4 g, 95 %) was recrystallized from ethanol (10 ml) yielding the pure N-protected dipeptide ester (1.8 g, 57 %). For constants and analyses see table 3.

Table 5

Tripeptide phenacyl esters

N°	Tripeptide ester	Yield % [a]	Mp. °C [b]	$[\alpha]_D$ [c]	Formula (M)	Analysis % : Calc./Found					
						C	H	N	S	Cl	R_f
5.1	CP—Asn—Gln—Met—OPAc [d]	35	185—188	+29.0°	$C_{30}H_{41}N_5O_9S$	55.62	6.38	10.81	4.95		A 0.20
			DMF—EtOAc	DMF	(647.7)	55.30	6.90	10.60	4.74		
5.2	AE—Asn—Gln—Met—OPAc	51	173—175	+29.7°	$C_{28}H_{39}N_5O_9S$	54.09	6.32	11.26	5.15		
			DMF—EtOAc	DMF	(621.7)	54.36	6.50	11.60	5.30		
5.3	AE—Leu—Met—Asn—OPAc	84	172—173	+89.6°	$C_{29}H_{42}N_4O_8S$	57.40	6.57	9.23	5.28		A 0.63
				DMF	(606.7)	57.70	7.40	9.22	5.20		
5.4	AE—Met—Ser—Ile—OPAc	67	145—146	+30.2°	$C_{28}H_{41}N_3O_8S$	58.01	7.13	7.24	5.53		
			EtOH		(579.7)	58.00	7.46	7.03	5.36		
5.5	AE—Ser—Met—GlnOPAc	42	184—185	+59.4°	$C_{27}H_{38}N_4O_9S$	54.53	6.44	9.42	5.39		A 0.29
			DMF-acetone	DMF	(594.6)	54.62	6.67	10.10	5.10		
5.6	AC—Trp—Leu—Met—OPAc	43	178—180	—75.6°	$C_{35}H_{44}N_4O_6S$	64.78	6.83	8.63	4.94		A 0.77
			IpOH	DMF	(648.8)	64.21	7.40	8.96	4.70		
5.7	H_2^+—Leu—Met—Asn—OPAc·Cl^-	88	196—197	—16.7°	$C_{23}H_{35}ClN_4O_6S$	52.01	6.44	10.55	6.03	6.67	A 0.42
				H_2O	(531.0)	52.03	7.06	10.69	6.08	7.42	
5.8	H_2^+—Met—Ser—Ile—OPAc·Cl^-	80	171—173	—30.2°	$C_{22}H_{34}ClN_3O_6S$	52.41	8.78	8.33	6.36	7.03	A 0.72
				H_2O	(504.1)	52.45	7.25	8.51	6.14	7.45	
5.9	H_2^+—Trp—Leu—Met—OPAc·Cl^-	96	122	—59.7°	$C_{30}H_{39}ClN_4O_5S$	59.73	6.51	9.29	5.31	5.87	A 0.42
					(603.2)	59.47	6.91	9.77	5.00	6.21	

[a,b] See footnote Table 1. [c] At room temperature at 1% concentration. [d] Prepared from CP—Asn—O^- DCHA·H^+ [1] by the mixed anhydride method with pivaloyl chloride.

4. Dipeptide ester hydrochlorides

Removal of the blocking group occurs in the same conditions as described in general procedure for the N-protected phenacyl esters, but in the case of tryptophyl containing esters the presence of diethylphosphonium is necessary.

4.3. L-*Methionyl*-L-*methionine phenacyl ester hydrochloride* (H_2^+ — Met — Met — OPAc · Cl^-). The N-protected dipeptide ester **3.5** (1.54 g, 3 mmole) in ethyl acetate (8 ml), was acidified with 5 N hydrogen chloride in ethyl acetate (0.7 ml, 3.5 mmole) and was allowed to stand at room temperature overnight. The separated pure hydrochloride (1.1 g, 84 %) was collected by filtration and washed with ethyl acetate. For constants and analyses see Table 4.

4.12. L-*Tryptophyl*-L-*methionine phenacyl ester hydrochloride* (H_2^+ — Trp — Met — OPAc · · Cl^-). The N-protected dipeptide ester **3.18** (0.28 g, 0.5 mmole) suspended in anhydrous ethanol (5 ml) and diethylphosphonate (1 ml) was acidified with 10 N hydrogen chloride in ethyl acetate (0.1 ml, 1 mmole) to pH 1.5. Within 2—3 minutes a clear solution was obtained and kept overnight at room temperature. After diluting with anhydrous ether (80 ml), the precipitated dipeptide ester hydrochloride (0.17 g, 70 %) was collected by filtration and washed with anhydrous ether. For constants and analyses see table 4.

5. Tripeptide esters

General procedure. The mixed anhydride, prepared from the N-protected amino acid dicyclohexylammonium salt, ethyl or isobutyl chloroformate or pivaloyl chloride (one equivalent) in an adequate solvent (tetrahydrofuran, ethyl acetate, dichlormethane) with a catalytic amount of N-methylmorpholine, was treated with the appropriate peptide ester (one equivalent) liberated *in situ* from its hydrochloride with triethylamine (one equivalent) and worked up in the way described in general procedure for the N-protected dipeptide esters.

The conditions were similar with those described in general procedure for the N-protected dipeptide esters.

5.3. *N-(1-Ethoxycarbonyl-propen-2-yl)*-L-*leucyl*-L-*methionyl*-L-*asparagine phenacyl ester* (AE — Leu — Met — Asn — OPAc). The mixed anhydride, prepared from N-(1-ethoxycarbonyl-propen-2-yl)-L-leucine dicyclohexylammonium salt [3a] (0.81 g, 1.91 mmole), isobutyl chloroformate (0.27 ml, 1.91 mmole) and N-methylmorpholine (1 drop) in ethyl acetate (15 ml) at —10 to —5°, was treated with the dipeptide ester, prepared from the hydrochloride **4.1** (0.84 g, 2 mmole) with triethylamine (0.28 ml, 2 mmole) in dichlormethane (15 ml). The N-protected tripeptide ester crystallized from propan-2-ol and gave the pure product. The same yield resulted if ethyl chloroformate in dichlormethane was used instead of isobutyl chloroformate for the anhydride formation. For constants and analyses see table 5.

5.7. L-*Leucyl*-L-*methionyl*-L-*asparagine phenacyl ester hydrochloride* (H_2^+ — Leu — Met — Asn — OPAc · Cl^-). To a suspension of the above N-protected tripeptide ester **5.3** (3.6 g, 6 mmole) in anhydrous ethanol (15 ml), 4 N hydrogen chloride in ethyl acetate (5 ml, 20 mmole) was added. The obtained clear solution turned to a jelly-like mass after one hour at room temperature and solidified next day when triturated with anhydrous ether (150 ml). After standing for three hours in the refrigerator, the crystals were collected by filtration and washed with dry ether. For constants and analyses see table 5.

Revue Roumaine de Chimie, 23, 7, 1109–1115 (1978)

DEGRADATION OF ANION EXCHANGERS IN AGGRESSIVE MEDIUM. VI *

EFFECT OF HYDROXYL IONS IN THE PRESENCE OF $CuCl_2$ ON THE CHEMICAL STABILITY OF MACROPOROUS STRONGLY BASIC QUATERNARY AMMONIUM ANION EXCHANGERS

I. PETRARIU, MONA LILIANA NEAGU, IG. POINESCU, CORNELIA LUCA
and PAMFILIA PETRARIU

Institute of Macromolecular Chemistry "Petru Poni" 41 A,
Gr. Ghica Vodă Alley, 6600 Iassy, Romania

Received April 28, 1976

Degradation results concerning strongly basic macroporous anion exchangers, possessing a binary (ternary) macromolecular network structure, by hydroxyl ions in the presence of $CuCl_2$ are shown in this paper. The influence of a few factors such as the nature and quantity of the third comonomer (acrylonitrile or methyl methacrylate), crosslinking degree, and the nature of the diluent medium, on the chemical stability was pointed out.

It is well known that a series of alternations of the physical and chemical properties of the ion exchangers take place during their industrial application, resulting in the partial loss of their exchange capacity.

This wear process, simultaneous with the macromolecular network mechanical degradation, is recorded by the reference literature under the name of ,,ion exchanger ageing".[1]

The ageing process of anion exchangers is due to some factors as : utilization of the alkaline or oxidizing concentrated solutions, large variation of pH, their industrial utilization at unsuitable temperature, irreversible adsorption of organic materials, etc.

Degradation studies of the ion exchangers had in viev both the ratio exchange between the strongly and weakly basic groups and the skeletal modifications.[2-8] Certain oxidizing agents catalyzed by metals or their salts as $FeCl_3$, $CuSO_4$, etc, reduce to a great extent the strongly basic exchange capacity of anion exchangers.[9-12]

---

* Part V. : I. Petrariu, L. M. Neagu, Ig. Poinescu and P. Petrariu, *Rev. Roumaine Chim.*, (in press).

[1] A. L. Davidov and G. M. Lisovina, *Kolloid Zhur.*, **23**, 145 (1961).

[2] L. Wirth, *Combustion*, **25**, 49 (1954).

[3] M. E. Gilwood, C. Calmon and A. H. Greer, "12th Annual Water Conference Engineering Society, Western Pacific", 1951, p. 119.

[4] R. M. Wheaton and W. C. Bauman, *Ind. Eng. Chem.*, **43**, 1088 (1951).

[5] A. L. Wilson, *J. Appl. Chem.*, **11**, 151 (1961).

[6] I. Petrariu, P. Petrariu and C. Luca, *Materiale Plastice*, **7**, 71 (1970).

[7] I. Petrariu, E. Bărbînță, A. Carpov and Ig. Poinescu, *Materiale Plastice*, **10**, 175 (1973).

[8] I. Petrariu, G. Mocanu, A. Carpov and D. Drăgan, *Materiale Plastice*, **10**, 355 (1973).

The coming out of the macroporous anion exchangers on the industrial scale was determined by the grown interest in the investigation of macromolecular structures, more physically and chemically stable, as compared to the anion exchangers of gel type.

Most of macromolecular networks, used as matrices for the ionogene groups, have a binary (ternary) structure. Introduction of the third comonomer is made generally to improve the ion exchanger mechanical properties.[13-15]

This paper deals with the influence of the third monomer, and the nature of the inert medium used during copolymerization process study, upon the chemical stability of the strongly basic anion exchangers in alkaline media, in the presence of $CuCl_2$.

EXPERIMENTAL

Ternary macroporous copolymers styrene (St) — acrylonitrile (AN) — *p*-divinylbenzene (DVB), and styrene (St) — methyl methacrylate (MCMe) — *p*-divinylbenzene (DVB) were carried out as beads by the suspension copolymerization of the monomers. Polystyrene ($M_w = 7.7 \times 10^5$), gasoline (b.p. 125—140°), and toluene were used as inert media.

The copolymerization technique for these macroporous copolymers was described in a previous paper.[14]

The acrylonitrile amount was calculated according to the nitrogen percentage, and the methyl methacrylate content was taken equal to the monomer quantity introduced into the copolymerization process.[15-16]

Physical and chemical characteristics of the ion exchangers subjected to the degradation reactions are shown in table 1.

Degradation reactions were carried out in a flask of 50 ml. capacity, equipped with an ascending condenser. Macroporous anion exchanger (2 meq.), and then the aggressive mixture (it consists of 15 ml. NaOH 10N, and 12 meq. of $CuCl_2$), were introduced in the flask of 50 ml.

Degradation process was carried out at different temperatures (50°, 80°, and 100°), for five hours.

Finally, after degradation, beads were poured into a column (with fritted disc), where they were washed with distilled water, and then HCl 4% solution, in order to get Cl-form anion exchanger. After that, it was washed with MeOH until all Cl^- ions were removed. Weakly (C_{wb}), strongly (C_{sb}), and remanent total (C_t) capacities were measured for each sample.

Basicity coefficient K_b was defined as the ratio between strongly and total basic capacities.

The exchange capacity losses due to the dealkylation reaction were computed from the weakly exchange basic capacity increase values.

The exchange capacity losses owing to the deamination reaction were calculated from the difference between the strongly basic capacity losses and the increase capacity produced by the weakly basic groups.

---

[9] N. Frisch and R. Kunin, *Ind. Eng. Chem.*, **49**, 1365 (1957).

[10] N. Frisch and R. Kunin, *J. Amer. Water Works Association*, **52**, 875 (1960).

[11] I. Petrariu, P. Petrariu, Fl. Popescu and C. Luca, *Rev. Roumaine Chim.*, **20**, 839 (1975).

[12] I. Petrariu, P. Petrariu, Fl. Popescu and S. Drăgan, *Rev. Roumaine Chim.*, **20**, 1167 (1975).

[13] S. Maxim, Ig. Poinescu, S. Drăgan and M. Dima, *Rev. Roumaine Chim.*, **17**, 1447 (1972).

[14] Ig. Poinescu, S. Drăgan, S. Maxim and M. Dima, *Rev. Roumaine Chim.*, **20**, 1311 (1975).

[15] G. A. Tarasov, *Vysokomol. Soedineniya*, **11**, 1601 (1960).

[16] R. J. Solocombe, *J. Polymer Sci.*, **26**, 9 (1957).

Table 1

Physical and chemical characteristics of the macroporous strong anion exchangers subjected to the chemical degradation study

Sample number	Inert medium	DVB %	AN %	MCMe %	Exchange capacity, meq./g.			Uptake coefficient, g./g.		Density, g./ml.	
					C_{wb}	C_{sb}	C_t	MeOH	Toluene	Specific	Apparent
301	Gasoline	18.0	2.26	—	0.18	2.58	2.76	0.46	1.46	1.1448	0.7285
303	Gasoline	18.0	28.20	—	0.29	2.26	2.55	1.55	2.09	1.0723	0.3875
307	Polystyrene	8.0	—	—	0.19	3.58	3.77	0.14	1.12	1.0745	1.0145
311	Polystyrene	8.0	19.66	—	0.26	1.89	2.15	0.53	1.13	1.0975	0.9760
314	Toluene	27.0	—	—	0.18	2.47	2.65	0.49	0.97	1.0223	0.7391
317	Toluene	27.0	8.40	—	0.27	2.07	2.34	0.94	1.39	1.0910	0.9683
325	Polystyrene	8.0	—	20.00	0.45	2.96	3.41	0.40	0.91	1.0265	0.7898
331	Gasoline	18.0	—	10.00	0.43	2.35	2.78	0.25	1.09	1.0711	0.9496

RESULTS AND DISCUSSION

Chemical degradation of strongly basic anion exchangers, type I, of which macromolecular network consists of St—AN—DVB, or St—McMe—DVB by an aggressive agent, can be described by three important processes:

1. A deamination reaction (Δ_{am}), yields to the trimethylamine scission, and the benzyl alcohol group appearance in the network structure, at the same time. The strongly basic exchange capacity decreases suddenly as a result of this reaction.

2. A dealkylation reaction having as a consequence the scission of a halogenated compound, or methanol (depending on the ionic anion exchanger form subjected to the chemical degradation), while the weakly basic groups remain in matrix. By this reaction, the strongly basic anion exchanger turns partially into a weak base one. As a result of these chemical transformations, the strongly basic capacity decreases, while the weakly basic one (which is initially in the anion exchanger structure) increases.

3. A reaction that alters the macromolecular chain yielding to a decrease of the crosslinking degree. For more severe degradation conditions, the macromolecular network can be entirely rendered soluble, resulting a soluble polyelectrolyte.

Following the weakly basic capacity changeability, under the aggressive media influence, depending upon the chemical structure for an anion exchanger subjected to degradation (Table 2), one notes an increase of the weakly basic exchange capacity simultaneously with the temperature increase. Significant increases of the weakly basic capacity appear for the samples 301, 314, and 325.

Table 2

The effect of the temperature and aggressive medium upon weakly basic exchange capacity

Degradation temperature °C	Remanent weakly basic exchange capacity, meq./g.							
	Sample number							
	301	303	307	311	314	317	325	331
—	0.18	0.29	0.19	0.26	0.18	0.27	0.45	0.43
50°	0.32	0.35	0.31	0.37	0.39	0.34	0.95	0.54
80°	0.42	0.48	0.40	0.50	0.50	0.44	1.09	0.68
100°	0.43	0.49	0.47	0.62	0.52	0.59	1.42	0.81

Taking into account structural characteristics of these samples, (for instance, sample no. 314 is a binary copolymer, while no. 301 and 325 are ternary macromolecular networks), one can note that the existence of the third comonomer in the structure of an anion exchanger does not influence dealkylation reaction, but to a certain extent. This observation is valid for a temperature of degradation below 50°. But, significant differences between samples appear for the temperature range of 80—100°.

The inert medium nature does not affect appreciably the weakly basic exchange capacity increase.

Degradation data for the anion exchangers 301 (ternary copolymer with 2.26 % AN), and 303 (ternary copolymer with 28.20 % AN), show that an increased amount of acrylonitrile gives a small advantage of weakly basic capacity.

An opposite phenomenon can be seen for methyl methacrylate used as the third comonomer (samples 325 and 331), when an increased amount of it determines an adequate increase of the weakly basic capacity.

In another series of experiments, it was followed the strongly basic capacity loss, depending upon degradation temperature (Table 3). From the data analyses showed in table 3, it results that the thermal effect, and the aggressive medium play an important influence in defining the chemical stability of an anion exchanger.

Table 3

The temperature effect and aggressive medium upon the strongly basic exchange capacity

Degradation temperature °C	Strongly basic exchange capacity, meq./g.							
	Sample number							
	301	303	307	311	314	317	325	331
—	2.58	2.26	3.58	1.89	2.47	2.07	2.96	2.35
50°	2.16	2.05	3.33	1.67	2.05	1.65	2.00	1.81
80°	1.81	1.71	3.02	1.50	1.73	1.34	1.24	1.41
100°	1.70	1.58	2.63	1.31	1.31	1.11	0.46	1.14

If one compares sample 307 (binary copolymer) with 311 (ternary copolymer with 19.66 % AN), one notes that the acrylonitrile introduction in large proportion improves to a small extent chemical stability. If the third comonomer is methyl methacrylate (samples 325, 331), the chemical stability decreases sensibly, the values of the strongly basic capacity losses are large. All these observations are valid for the anion exchangers of which macromolecular networks have synthetized in the polystyrene presence as inert medium, with 8.0 % DVB (sample 325), or gasoline with 18.0 % DVB (sample 331).

When toluene is used as inert medium, and for high crosslinking degree (27.0—30.0 % DVB), (Figure 1), one can note that a rise of 8.40 % acrylonitrile (curve 2) diminishes the chemical stability, particularly for the temperature range of 50—80°.

At higher temperature of degradation, the strongly basic capacity losses, for a binary anion exchanger structure (curve 1) get near to those of the ternary anion exchanger capacity (curve 2).

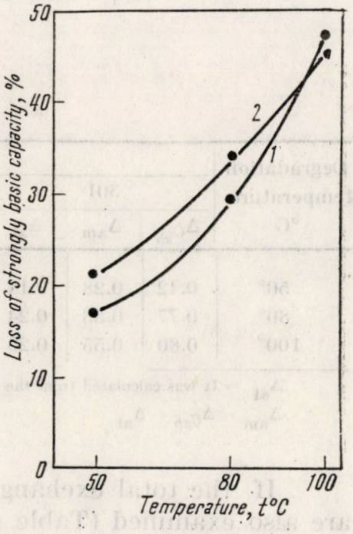

Fig. 1. — Loss variation of the strongly basic exchange capacity, depending upon temperature. Inert medium ; toluene. Curve 1. Sample 314 — binary copolymer structure with 27.0 % DVB ; Curve 2. Sample 317 — ternary copolymer structure with 27.0 % DVB and 8.4 % AN.

Table 4

The temperature influence and aggressive medium upon the total exchange capacity

Degradation temperature °C	Total exchange capacity, meq./g. Sample number							
	301	303	307	311	314	317	325	331
—	2.76	2.55	3.77	2.15	2.65	2.34	3.41	2.78
50°	2.48	2.40	3.64	2.04	2.44	1.99	2.95	2.35
80°	2.23	2.19	3.42	2.00	2.23	1.78	2.33	2.09
100°	2.20	2.07	3.10	1.93	1.83	1.70	1.88	1.95

Table 5

The influence of the thermal effect and aggressive medium upon the basicity coefficient

Degradation temperature °C	Coefficient of basicity, K_b Sample number							
	301	303	307	311	314	317	325	331
—	0.93	0.88	0.95	0.87	0.93	0.88	0.86	0.84
50°	0.87	0.85	0.91	0.81	0.84	0.83	0.67	0.77
80°	0.81	0.78	0.88	0.75	0.77	0.75	0.53	0.67
100°	0.78	0.76	0.84	0.68	0.71	0.65	0.24	0.59

Table

Capacity losses as a result of deamination (Δ_{am}),

Degradation temperature °C	Sample											
	301			303			307			311		
	ΔC_{sb}	Δ_{am}	Δ_{al}	ΔC_{sb}	Δ_{am}	Δ_{al}	ΔC_{sb}	Δ_{am}	Δ_{al}	ΔC_{sb}	Δ_{am}	Δ_{al}
50°	0.42	0.28	0.14	0.21	0.15	0.06	0.25	0.13	0.12	0.22	0.11	0.11
80°	0.77	0.53	0.24	0.55	0.36	0.19	0.56	0.35	0.21	0.39	0.15	0.24
100°	0.80	0.55	0.25	0.68	0.48	0.20	0.95	0.67	0.28	0.58	0.22	0.36

Δ_{al} = It was calculated from the weakly basic exchange capacity increase.

$\Delta_{am} = \Delta_{C_{sb}} - \Delta_{al}$

If the total exchange capacity losses depending upon temperature are also examined (Table 4), one can note that these are much smaller by comparison with the strongly basic capacity losses.

It is also observed that the binary copolymer structure (sample 307), for the temperature range of 50—80° is more chemically stable from the total exchange capacity standpoint, than the ternary one, holding acrylonitrile (samples 301 and 303). Similar results were got for the anion exchanger prepared from a binary copolymer structure (27.0% DVB), carried out in the toluene presence (sample 314). These copolymers are superior to the ternary ones (8.40 % AN, sample 317), for the temperature range of 50—80°.

It also must be pointed out that the introduction of methylmethacrylate decreases to a large extent the chemical stability of the anion exchangers (samples 325 and 331).

Basicity coefficient K_b decreases in proportion as the degradation temperature increases (Table 5) which indicates that the modifications take place at the level of the functional groups.

The basicity coefficient deacrease is better marked for ternary copolymers on the basis of acrylonitrile and methylmethacrylate by comparison with the binary one.

The strongly basic capacity losses, as a result of the two reactions deamination and dealkylation, are shown in table 6.

From the close examination of data showed in table 6, one can note that the degradation of the basic anion exchangers, type I, at 50°, (that possess a binary structure, samples 307 and 314) takes place roughly in equal proportion by both reactions.

In proportion as the degradation temperature increases, the deamination reaction becomes better marked.

The same remarks are also valid for the ternary copolymer on the basis of acrylonitrile and methyl methacrylate carried out in the presence of gasoline (samples 301, 303 and 331), and polystyrene (sample 325).

Sample 311 shows some particular behaviours between 80—100°, i.e. in this temperature range prevails the dealkylation reaction.

6

and dealkylation (Δ_{al})reactions, meq./g.

number

314			317			325			331		
ΔC_{sb}	Δ_{am}	Δ_{al}	ΔC_{sb}	Δ_{am}	Δ_{al}	ΔC_{sb}	Δ_{am}	Δ_{al}	ΔC_{sb}	Δ_{am}	Δ_{al}
0.42	0.21	0.21	0.42	0.35	0.07	0.96	0.46	0.50	0.54	0.43	0.11
0.74	0.42	0.32	0.73	0.56	0.17	1.72	1.08	0.64	0.94	0.69	0.25
1.16	0.82	0.34	0.96	0.64	0.32	2.50	1.53	0.97	1.21	0.83	0.38

CONCLUSIONS

1. It was investigated the aggressive medium influence upon the anion exchanger chemical stability at the functional group level.

2. Nature and quantity of the third comonomer, crosslinking, the inert medium nature influence significantly the degradation reaction by the two mechanisms: deamination and dealkylation.

3. The insertion of the third comonomer (acrylonitrile or methylmethacrylate) in the strongly basic anion exchanger network, diminishes its chemical stability in the order MCMe $>$ AN $>$ binary copolymer.

Revue Roumaine de Chimie, **23**, 7, 1117–1127 (1978)

PULSE RADIOLYSIS AND FLASH PHOTOLYSIS STUDIES OF SeO_4^{2-} ANION IN AQUEOUS SOLUTION

M. S. SUBHANI * and M. KHALID

Department of Chemistry, University of Islamabad, Islamabad, Pakistan

Received April 8, 1976

Pulse radiolysis and flash photolysis studies of Ar, N_2O and O_2 saturated aqueous solution of SeO_4^{2-} anions were carried out. Transient species with $\lambda_{max} = 240$ nm, $\lambda_{max} = 525$ nm were reported in both the cases. The species with $\lambda_{max} = 240$ nm was identified as O_2^- species whereas the species with $\lambda_{max} = 525$ nm was assigned to be SeO_4^- radical anion. In the case of pulse radiolysis the species SeO_4^- radical anion was produced by the reaction

$$OH + SeO_4^{2-} \longrightarrow OH + SeO_4^-$$

whereas in the flash photolysis it was produced by the primary process

$$SeO_4^{2-} H_2O \xrightarrow{h\nu} SeO_4^{2-} H_2^*O \longrightarrow SeO_4^- + e_{aq}^-$$

The species O_2^- and SeO_4^- were found to decay by the second order process. Transient species with $\lambda_{max} = 430$ nm was observed in the case of flash photolysis and was identified as O_3^- radical anion. The species was found to decay by pseudo first order kinetics.

Rate constants for the 2nd order decay of SeO_4^-, O_2^- were determined. The rate constants for the reactions

$$OH + SeO_4^{2-} \longrightarrow OH^- + SeO_4^-$$

$$O^- + SeO_4^{2-} \xrightarrow{H_2O} + SeO_4^- + OH + OH^-$$

$$CO_3^- + SeO_4^{2-} \longrightarrow CO_3^{2-} + SeO_4^-$$

were also determined.

INTRODUCTION

It has been shown with the help of pulse radiolysis technique that hydroxyl radical produced during water radiolysis reacts rapidly with many inorganic reducing anions[1-9] and transient absorbing spectra were observed in some cases.[2,3,4,6,7,8,10] Several new transient spectra have been reported which are due to unstable radical anions produced by electron transfer reactions of the hydroxyl radical.[3,4,6-8,10]

---

* *Present Address;* Department of Chemistry, University of Nigeria, Nsukka, Nigeria

The observations and reaction kinetics of transient species produced in photochemical reaction have been studied for many years. However, relatively few investigations have been made in the vacuum ultra violet region. With the availability of very pure silica transparent down to about 165 nm, it is possible to use the flash photolysis technique for the study of the species absorbing in this region.

The selenate anion in aqueous solution absorbs in the vacuum ultra violet region similar to that of sulphate anion.[1,2,11,12]

No work has apparently been done on the steady state photolysis or flash photolysis of selenate anion in solution.

The present work is concerned with the study of the spectrum and absorbing decay kinetics of the transient species produced on pulse radiolysis and flash photolysis of aqueous solution of selenite anion.

EXPERIMENTAL

All the chemicals used were of A.R. quality. N_2O gas was of anaesthetic grade. Sodium selenite was freshly prepared by the method described by Bagnall.[13]

All solutions were prepared in triply distilled water just before irradiations.

The solutions were saturated with N_2O or Ar gas using normal bubbling procedure.

The pulse radiolysis and flash photolysis set up and detection system used were similar to those described elsewhere.[7,14,15]

(a) PULSE RADIOLYSIS STUDIES

RESULTS AND DISCUSSIONS

10^{-2}M SeO_4^{2-} anion solution Ar saturated or N_2O saturated or O_2 saturated were irradiated with electron pulse.

---

[1] G. E. Adams and J. W. Boag, *Proc. Chem. Soc.*, **1964,** 112.

[2] J. W. Boag and G. E. Adams, "18th Annual Symposium Cellular Radiation Biology" (Houston, March 1964).

[3] G. E. Adams, J. W. Boag and B. D. Michael, *Trans. Faraday Soc.*, **61,** 1674 (1965).

[4] G. E. Adams, J. W. Boag and B. A. Michael, *Proc. Chem. Soc.*, **1964,** 411.

[5] J. P. Keene, *Nature*, **184,** 834 (1960).

[6] G. E. Adams, J. W. Boag, J. Current and B. D. Michael, "Pulse Radiolysis" Ed. by M. Fleet, J. P. Keene, A. J. Swallow and J. H. Baxendale, Academic Press, London, 1965, p. 136.

[7] G. V. Buxton and M. S. Subhani, *J. Chem. Soc. Trans.*, **68,** 947 (1972).

[8] O. Amichai and A. Treinin, *J. Phys. Chem.*, **74,** 830 (1970).

[9] M. Anbar and P. Neta, *Inter. J. Appl. Radiat Isotopes*, **18,** 493 (1967).

[10] (a) G. V. Buntan and F. S. Dainton, *Proc. Roy. Soc.*, **A 304,** 441 (1968).
(b) G. V. Buxton and F. S. Dainton, *Proc. Roy. Soc.*, **A 304,** 427 (1968).

[11] W. Albu and P. Goldfinger, *Z. phys., Chem.*, **16B,** 338 (1932).

[12] E. Rabinowitch, *Rev. Mod. Phys.*, **14,** 112 (1942).

[13] K. W. Bagnall, "Chemistry of Selenium, Tellurium and Polonium," Elsevier Publishing Co., Amsterdam, 1966, p. 72.

[14] K. W. Chambers, E. Collinson, F. S. Dainton, W. A. Seddon and F. Wilkinson, *Trans. Faraday Soc.*, **63,** 1699 (1967).

[15] G. V. Buxton and M. S. Subhani, *J. Chem. Soc., Trans.*, **68,** 958 (1972).

The absorption spectra for the transient species observed were recorded and are shown in Figure 1 and Figure 2.

The spectra have $\lambda_{max} = 240$ nm and $\lambda_{max} = 525$ nm when oxygenated solution was radiolysed. Whereas in the case of N_2O or Ar saturated system only spectrum with $\lambda_{max} = 525$ nm was observed (Figure 2). The two species were found to decay by second order process. The transient absorbing in the far ultra violet region was identified as O_2^- radical anion from its absorption spectrum, life time and decay kinetics reported in the literature.[16,17] The species O_2^- is formed by the process

$$O_2 + e^-_{aq} \rightarrow O_2^- \qquad (1)$$

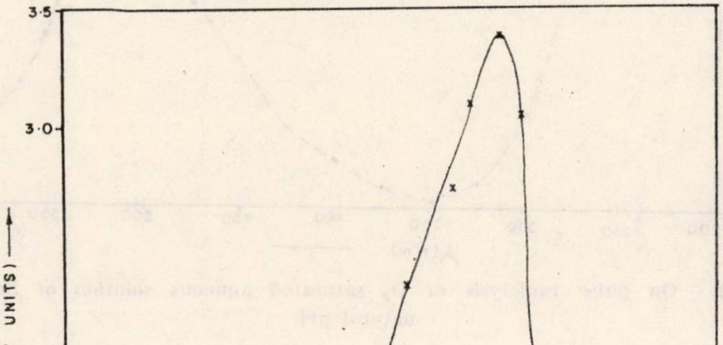

Fig. 1. — On pulse radiolysis of aqueous solution of SeO$_4^{2-}$ at natural pH.

● — (a) Ar saturated; × — (b) N_2O saturated

---

[16] G. Czapski and L. M. Dorfman, *J. Phys. Chem.*, **68**, 1169 (1964).

[17] G. E. Adams, J. W. Boag and B. D. Michael, *Proc. Roy. Soc.*, **A287**, 321 (1965).

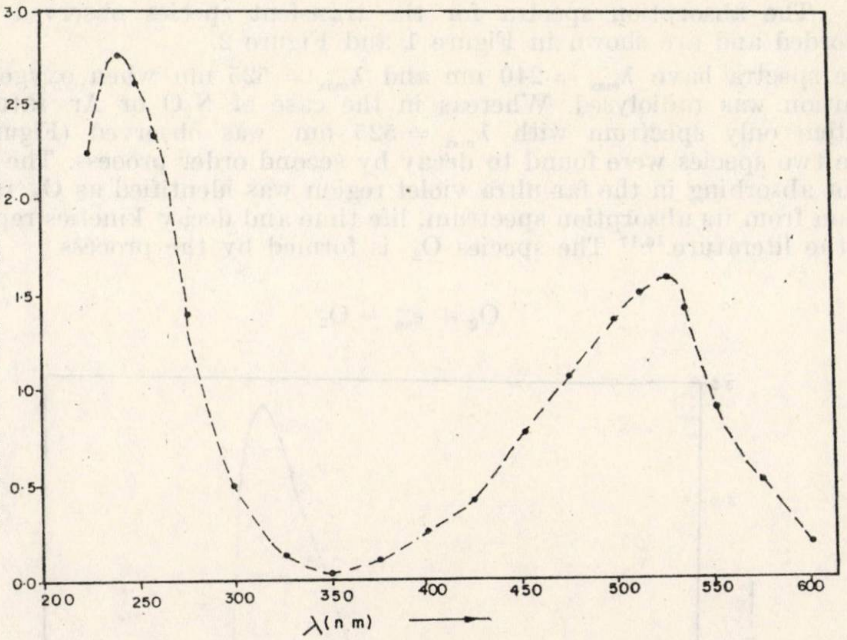

Fig. 2. — On pulse radiolysis of O_2 saturated aqueous solution of SeO_4^{2-} at natural pH.

The other absorption spectrum with $\lambda_{max} = 525$ nm was assigned to SeO_4^- radical anion formed by the reaction of hydroxy radical (produced on radiolysis of water) with SeO_4^{2-} anion,

$$SeO_4^{2-} + OH \rightarrow SeO_4^- + OH^-$$

As shown in Figure 2 no transient species with $\lambda_{max} = 240$ nm was observed in Ar or N_2O saturated system whereas the transient species with λ_{max} 525 nm remained unaffected in case of Ar saturated while in case of N_2O saturated the absorption was almost doubled at $\lambda_{max} = 525$ nm.

The above mentioned experimental observations are the conclusive evidence to support the correct assignment of the spectra shown in Figure 1 and Figure 2.

When O_2 is present the hydrated electron produced on radiolysis reacts with O_2 forming O_2^- radical anion by process (1) and the species O_2^- was found to decay by second order kinetics by the reaction (3)

$$O_2^- + O_2^- \xrightarrow[k_3]{H_2O} H_2O_2 + O_2 + 2OH^- \qquad (3)$$

The values for the rate constant k_3 obtained are shown in table 1.

As in case where N_2O or Ar was present instead of O_2 the process (1) is absent and thus no absorption with $\lambda_{max} = 240$ nm was expected in such cases.

The twice yield of the SeO_4^- radical anion in case of N_2O saturated solution as compared to that of Ar saturated system can be explained on the basis that the hydrated electrons gets converted to OH radical by the reaction.

$$N_2O + e_{aq}^- \xrightarrow{H_2O} OH + OH^- + N_2 \qquad (4)$$

Table 1

(a) Rate constant for the 2nd order decay of O_2^- radical anion at natural pH

λ(nm)	$\frac{2k}{\varepsilon}$ (cm s^{-1})	ε(M^{-1} cm^{-1})	k(M^{-1} s^{-1})
250	1.1×10^5	1030	5.8×10^7

(b) Rate constant (k_5) for the second order decay of SeO_4^- radical anion at natural pH

λ max (nm)	$\frac{2k}{\varepsilon}$ (cm s^{-1})	ε(M^{-1} cm^{-1})	k(M^{-1} s^{-1})
525	1.9×10^6	610	5.5×10^8

(c)

$G(e_{aq}) = 3.2$ [18], $G(Fe(CN)_6^{-3}) = 3.2$ [19]

$G(OH) = 2.9$ [18], $\varepsilon_{420}(Fe(CN)_6^{-3}) = 10^3\ M^{-1}\ cm^{-1}$ [19]

and in case of Ar saturated system they remain unaffected. Thus the yield of OH radical is doubled in case of N_2O saturated system as compared to that of Ar saturated system. The entity with $\lambda_{max} = 525$ nm is most likely to be produced by the reaction of OH radical with SeO_4^{2-} anion by the reaction (2)

$$SeO_4^{2-} + OH \rightarrow SeO_4^- + OH^- \qquad (2)$$

thus resulting in increase of yield in N_2O saturated case.

The transient SeO_4^- radical anion was found to decay by second order kinetics and can be represented as

$$SeO_4^- + SeO_4^- \rightarrow \text{Products} \qquad (5)$$

The rate constant k_5 obtained is given in table 1. The value for the extinction coefficient for the SeO_4^- radical anion used was obtained on the basis of the hypothesis that the transient spectrum reported in this work is due entirely to the reaction between OH radical and SeO_4^{2-} anion. Thus the extinction coefficient can be determined by comparing the optical density produced in ferrocyanide solution with that one produced in the Selenate anion system under identical conditions. The G values for OH and e^-_{aq} are known under such conditions, also the extinction coefficient and G value for $Fe(CN)_6^{3-}$ anion are known and the values are given in table 1.[18,19]

---

[18] G. V. Buxton, *Radiation Res. Rev.*, **1**, 209 (1968).

[19] G. E. Adams, J. W. Boag and B. D. Michael, *Trans. Faraday Soc.*, **61**, 492 (1965).

Reaction of OH and O^-

The rate constants for the reaction of O^- radical anion and OH radical with SeO_4^{2-} anion were measured by the competition method, carbonate anion being used as the reference solute.[4] Since O^- does not react with carbonate anion [20] the competing reactions in alkaline solution can be written as :

$$OH + OH^- \rightleftharpoons O^- + H_2O \tag{6}$$

$$OH + CO_3^{2-} \longrightarrow OH^- + CO_3^- \tag{7}$$

$$OH + SeO_4^{2-} \longrightarrow OH^- + SeO_4^- \tag{2}$$

$$O^- + SeO_4^{2-} \xrightarrow{H_2O} 2OH^- + SeO_4^- \tag{8}$$

The equilibrium (6) is rapidly established [21] and maintained and K_{OH} can be written as

$$K_{OH} = \frac{[O^-][H^+]}{[OH]} \tag{9}$$

but

$$[OH]_{Total} = [OH] + [O^-] \tag{10}$$

in our system, so equation (10) can be written as

$$[OH]_{Total} = [OH] + \frac{K_{OH}}{[H^+]}[OH] \tag{11}$$

In the absence of SeO_4^{2-} anion the total number of hydroxyl radical reacts with CO_3^{2-} anions when the concentration of the latter is sufficiently high so that O^- does not disappears except to form OH radical.

Addition of SeO_4^{2-} anion results in a decrease in the number of OH radicals reacting with carbonate anions and also in the number of O^- radical anions which are converted to OH radicals. Thus the fraction f_{OH} of the total yield of OH radicals which reacts with carbonate anion is given by

$$f_{OH} = \left(1 + (k_2 + k_8)\frac{K_{OH}}{[H^+]}\frac{[SeO_4^{2-}]}{k_7(CO_3^{2-})}\right)^{-1} \tag{12}$$

---

[20] J. L. Weeks and J. Rabani, *J. Phys. Chem.*, **70**, 2100 (1966).

[21] G. V. Buxton, *Trans. Faraday Soc.*, **65**, 2150 (1969).

Experimentally $f = \frac{D}{D_0}$, where D and D_0 are the optical densities due to CO_3^- radical anion at 600 nm in the presence and absence of SeO_4^{2-} anion respectively. Thus,

$$\left(\frac{D_0}{D} - 1\right) = \left(k_2 + k_8 \frac{K_{OH}}{[H^+]}\right) \frac{[SeO_4^{2-}]}{k_7 (CO_3^{2-})}$$

A plot of $\left(\frac{D_0}{D} - 1\right)$ against $\frac{[SeO_4^{2-}]}{[CO_3^{2-}]}$ will have a slope equal to

$$\left(k_2 + k_8 \frac{K_{OH}}{[H^+]}\right) \Big/ k_7$$

From the measurements of the optical densities both in presence and absence of SeO_4^{2-} in N_2O saturated solution at pH 11.2 and 13.1 the values for the rate constants k_2 and k_8 were obtained by solving the simultaneous equations obtained on equating the slopes of the plots. The value for K_{OH} was taken as $10^{-11.9}$ and that of k_7 as 4.2×10^8 M^{-1} S^{-1} reported in the literature.[20, 22]

The values for k_2 and k_8 thus obtained are summarized in table 2.

Table 2

Rate constant for the reaction of OH, O^- and CO_3^- with SeO_4^{2-}

$k(OH + SeO_4^{2-}) = (4.1 \pm 0.5) \times 10^9\ M^{-1}\,s^{-1}$

$k(O^- + SeO_4^{2-}) = (6.8 \pm 0.5) \times 10^8\ M^{-1}\,s^{-1}$

$k(SeO_4^{2-} + CO_3^-) = (4.3 \pm 0.6) \times 10^7\ M^{-1}\,s^{-1}$

It was also observed that the absorption due to CO_3^- decayed more rapidly in the presence of SeO_4^{2-} anion and the rate of decay was found to be proportional to $[SeO_4^{2-}]$. Thus indicating CO_3^- radical anion can oxidize SeO_4^{2-} anion according to the reaction

$$SeO_4^{2-} + CO_3^- \rightarrow SeO_4^- + CO_3^{2-} \qquad (13)$$

At pH 13.1 the rate constant for the reaction was determined and its value is given in table 2.

(b) FLASH PHOTOLYSIS STUDIES
RESULTS AND DISCUSSIONS

The flash photolysis of Ar saturated or oxygen saturated 10^{-2}M aqueous solution of SeO_4^{2-} anion at natural pH gave rise to two transient species, in the case of O_2 saturated and one transient in the case of Ar

---

[22] J. RABANI and M. S. MATHESONS, *J. Phys. Chem.*, **70**, 761 (1966).

saturated systems; absorbing in the region of wavelength 230 nm to 600 nm. One species has a $\lambda_{max} = 520$ nm whereas the other species has $\lambda_{max} = 240$ nm. (Figure 3).
The two transients with $\lambda_{max} = 240$ nm and $\lambda_{max} = 520$ nm were identified as O_2^- and SeO_4^- respectively as their absorption spectra and kinetics were similar to those observed in the above pulse radiolysis work.

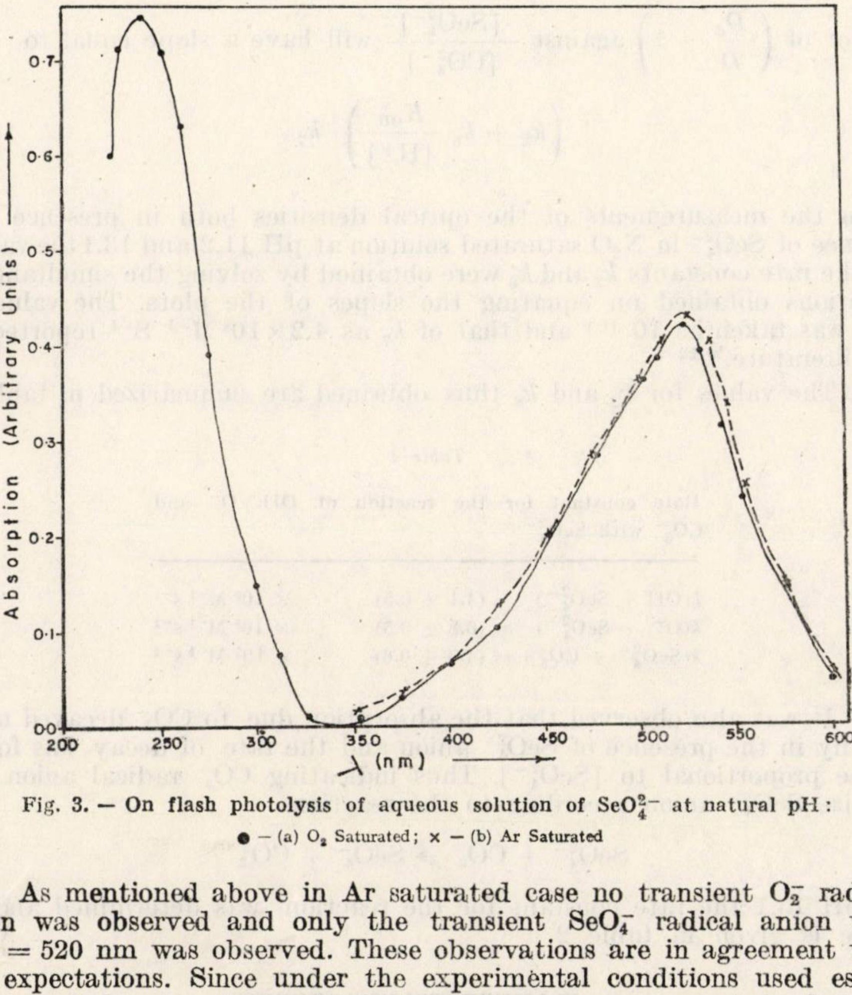

Fig. 3. — On flash photolysis of aqueous solution of SeO_4^{2-} at natural pH :

● — (a) O_2 Saturated; × — (b) Ar Saturated

As mentioned above in Ar saturated case no transient O_2^- radical anion was observed and only the transient SeO_4^- radical anion with $\lambda_{max} = 520$ nm was observed. These observations are in agreement with the expectations. Since under the experimental conditions used essentially no light was absorbed by water, thus one can conclude that the absorbing species O_2^- and SeO_4^- radical anions are produced as a result of the following primary photolytic process

$$SeO_4^{2-} + H_2O \xrightarrow{h\nu} SeO_4^{2-} + H_2O \qquad (14)$$

$$SeO_4^{2-} + H_2O^* \longrightarrow SeO_4^- + e_{aq}^- \qquad (15)$$

followed by

$$O_2 + e^-_{aq} \longrightarrow O_2^- \qquad (1)$$

From the second order plots for the decay of O_2^- and SeO_4^- by processes (3) and (5)

$$O_2^- + O_2^- \xrightarrow{H_2O} H_2O_2 + O_2 + 2OH^- \qquad (3)$$

$$SeO_4^- + SeO_4^- \longrightarrow \text{products} \qquad (5)$$

The value for $\frac{2k}{\varepsilon}$ and k for the reactions were evaluated using

$$\varepsilon_{525}^{SeO_4^-} = 610 \text{ and } \varepsilon_{250}^{O_2^-} = 1030 \text{ M}^{-1}\text{Cm}^{-1}\,{}^{16}$$

The values so obtained are in good agreement with those obtained in (a) and also with the values reported in literature.[17] (Table 3).

Table 3

a) Rate constant for the second order decay of O_2^- radical anion at natural pH

λ(nm)	$\frac{2k}{\varepsilon}$ (cm s^{-1})	ε(M^{-1} cm^{-1})	k(M^{-1} s^{-1})
250	1.20×10^5	1030	6.15×10^7

b) Rate constant for the second order decay of SeO_4^- radical anion at natural pH

λ(nm)	$\frac{2k}{\varepsilon}$ (cm s^{-1})	ε(M^{-1} cm^{-1})	k(M^{-1} s^{-1})
525	1.74×10^6	610	5.3×10^8

The value of the extinction coefficient obtained for SeO_4^- on the basis of equal yield for O_2^- and SeO_4^- radical anion just after the flash was 600 M^{-1}Cm^2 at 520 nm which is in good agreement with the above reported value in (a). Flash photolysis of oxygenated alkaline solution of 2×10^{-2}M SeO_4^{2-} anion at pH 11.8 gave rise to two transient species, one with $\lambda_{max} = 240$ nm and the other transient decaying much slowly with $\lambda_{max} = 430$ nm (Figure 4).

The transient with $\lambda_{max} = 520$ nm disappeared. The species at 430 nm was found to decay by a first order process. In other sets of experiments on flash photolysis of Ar saturated solution of SeO_4^{2-} anions at pH 9.2, SeO_4^- radical anion was observed but was found decaying rapidly by a pseudo first order kinetics. The kinetics was found to depend on OH^- anions concentration. At pH 11.2 all the absorption due to SeO_4^- radical anion disappears when an argen saturated solution of SeO_4^- anion was photolysed. The above mentioned observations can be explained on the basis that SeO_4^- radical anion gets converted to OH radical in alkali solution similar to that proposed for SO_4^- radical anion [23] by the reaction

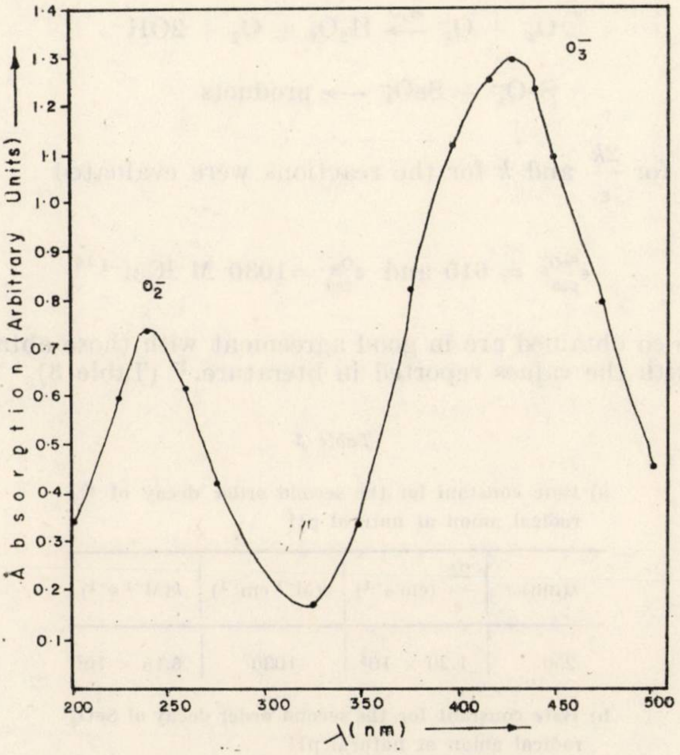

Fig. 4. — On flash photolysis of O_2 saturated aqueous solution of SeO_4^{2-} at pH 11.8.

$$SeO_4^- + H_2O \rightleftharpoons SeO_4^{2-} + OH + H^+ \tag{16}$$

followed by

$$OH + OH^- \rightleftharpoons O^- + H_2O \tag{8}$$

and in presence of O_2

$$O_2 + O^- \rightarrow O_3^- \tag{17}$$

---

[23] M. S. Subhani, (Submitted for publication) *Rev. Roumaine Chim.*

The equilibrium (8) is reported rapidly established[21] and $k_{17} = 2.6 \times 10^9$ $M^{-1} S^{-1}$.[24]

The absorption spectrum with $\lambda_{max} = 430$ nm was similar to that assigned to O_3^- radical anion in pulse radiolysis of oxygenated alkaline aqueous solution.[16,17,24] The mechanism for the first order decay of O_3^- radical anion was not understood.

Addition of OH secavenengus such as methanol reduces the yield of O_3^- considerably which clearly supports the above mentioned reactions 16, 8 and 17. The yield of SeO_4^- radical anion was also found to be doubled in the case of N_2O saturated system as compared to that of Ar saturated system. These results are similar to those observed in (a) and can be explained by reactions (2) and (4).

---

[24] G. E. Adams, J. W. Boag and B. D. Michael, *Nature*, **205**, 898 (1965).

Revue Roumaine de Chimie, **23**, 7, 1129–1137 (1978)

FLASH PHOTOLYSIS DECOMPOSITION OF SULPHATE AND SULPHITE ANIONS IN AQUEOUS SOLUTION

M. SADIQ SUBHANI * and Z. KAUSER
Chemistry Department, University of Islamabad, Islamabad, Pakistan

Received April 8, 1976

The flash photolysis studies of the oxygenated, Ar saturated and N_2O saturated solutions of SO_4^{2-} and SO_3^{2-} anions at natural pH and at alkaline pH were carried out. Two primary photochemical processes

$$SO_4^{2-} + H_2O \xrightarrow{h\nu} SO_4^- + e_{aq}^-$$

and

$$SO_4^{2-} + H_2O \xrightarrow{h\nu} SO_3^- + O^-$$

were suggested. In the case of SO_3^{2-} a primary process

$$SO_3^{2-} + H_2O \xrightarrow{h\nu} SO_3^- + e_{aq}^-$$

was suggested.

The absorption spectra for the transient species SO_4^-, SO_3^-, HSO_3^{2-}, O_3^- and O_2^-, $\lambda_{max} = 445$, $\lambda_{max} = 290$, $\lambda_{max} = 740$ nm $\lambda_{max} = 435$ nm., and $\lambda_{max} = 240$ nm respectively were also reported. The rate constants for the decay O_2^-, SO_4^-, SO_3^- and O_3^- were also evaluated and the values in case of the decay of O_2^- and O_3^- were in good agreement with the literature values.

INTRODUCTION

The absorption spectra of the sulphur polyvalent anions are known in the literature.[1(a)] Albu and Goldfinger [1(b)] have carried out the studies regarding the spectrum of SO_3^{2-} anion and showed that SO_3^{2-} anion absorption spectrum has a long wavelength limit of 260 nm and correspond to the process :

$$SO_3^{2-} + H_2O \xrightarrow{h\nu} SO_3^- + H + OH^- \tag{1}$$

---

* Present Address : Department of Chemistry, University of Nigeria, Nsukka, Nigeria

[1] a) R. Sperling and A. Treinin, *J. Phys. Chem.*, **68**, 893 (1964); *J. Phys. Chem.*, **68**, 897 (1964).
b) W. Albu and P. Goldfinger, *Z. Phys. Chem.*, **16 B**, 338 (1932).
c) M. Smith and M. C. R. Symons, *J. Chem. Phys.*, **25**, 1074 (1956).
d) W. S. Fyfe, *J. Chem. Phys.* **37**, 1894 (1962).
e) A. D. Autrey and R. E. Connick J, *J. Amer. Chem. Soc.*, **73**, 1842 (1951).

Haber and Wans Brough-Jones [2] studied the photochemistry of SO_3^{2-} anion in absence of oxygen. The hydrogen observed in their studies was suggested to be produced by the process

$$H + H \longrightarrow H_2 \tag{2}$$

and another process

$$SO_3^- + SO_3^- \longrightarrow S_2O_6^{2-} \tag{3}$$

was also suggested under the experimental conditions used. The quantum yield reported for the dithionate anion to be of the order of 0.07 at natural pH,-and the possibility of the occurring of the back reaction

$$SO_3^- + H \longrightarrow HSO_3^- \tag{4}$$

was suggested. Backstrome [3,4] studied the inhibiting effect of alcohol on the oxidation of SO_3^{2-} anion in solution. The SO_4^{2-} anion absorbs below 200 nm and its spectrum is characterized as electron transfer spectrum.[5] The charge transfer to the solvent (c.t.t.s.) mechanism in the photolysis of SO_4^{2-} anion can be represented as

$$A_{aq}^{n-} \longrightarrow A_{aq}^{-(n-1)} + e_{aq}^- \tag{5}$$

Using known electron scavenger such as N_2O indirect chemical kinetics evidence was obtained in the photolysis of SO_4^{2-} anion.[6,7] The pulse radiolysis studies of SO_3^{2-} anion and SO_4^{2-} anion in aqueous solution have been carried out and the transient species SO_3^- and SO_4^- radical anions were reported along with their absorption spectra.[8,9,10]

No obvious mechanism was suggested in the past for the photochemical decomposition of SO_3^{2-} and SO_4^{2-} anions in aqueous solution because not much development was made in the flash photolysis technique in the vacuum ultraviolet region. But now it is possible to study and devise experimental set-ups down to 165 nm, because of the availability of very pure silica, with the flash photolysis technique. The work on fash photolysis below 200 nm on water and aqueous system was reported in the literature.[11,12]

In the present paper experiments are described, on the flash photolysis of simple inorganic anions such as SO_4^{2-} and SO_3^{2-} anions in aqueous solution using flash photolysis set-up similar to that described elsewhere.[13,14] The purpose of the present work was to establish various primary photochemical processes occurring in the two photochemical system and to identify the transient produced and to follow their kinetic studies.

---

[2] F. Haber and O. H. Wans Brough-Jones, *Z. Phys. Chem.*, **18B**, 103 (1932).

[3] H. Backstrome, *J. Amer. Chem. Soc.*, **49**, 1460 (1927).

[4] H. Backstrome, *Z. Phys. Chem.*, **25B**, 122 (1934).

[5] E. Rabinowatch, *Rev. Mod. Phys.*, **14**, 112 (1942).

[6] J. Barrett, M. F. Fox and A. L. Mansell, *J. Phys. Chem.*, **69**, 2996 (1965).

[7] F. S. Dainton and P. Fowles, *Proc. Roy. Soc.*, **A 287**, 312 (1965).

[8] E. Huckel, A. Henglein and G. Beck, *Ber. Bunsengesellschaft Phys. Chem.*, **70**, 149 (1966).

[9] G. E. Adams, J. W. Boag and B. D. Michael, *Proc. Chem. Soc.*, **1964**, 411.

[10] G. E. Adams, J. W. Boag and B. D. Michael, *Trans. Faraday Soc.*, **61**, 1674 (1965).

[11] J. H. Baxen Dale, *Radiation Res.*, **17**, 312 (1962).

[12] M. S. Matheson, W. A. Mulac and J. Rabani, *J. Phys. Chem.*, **67**, 2613 (1963).

EXPERIMENTAL

All the chemicals used were of analar grade supplied by Hopkin and Williams and B. D. H.

All solutions were prepared in triply distilled water previously irradiated by gamma ray source.

Solutions were prepared just before irradiation and were saturated with the required gas by the usual bubbling procedure as described elsewhere.[15,16] Fresh sample was used for each measurement. The pHs of the solutions were measured with Pye pH meter previously calibrated just before measurement.

The detail of the flash photolysis set up, flash photolysis lamps, detection system, flow system, flash photolysis cell and shape and duration of the flash used have been described elsewhere.[13,16]

RESULTS AND DISCUSSION

Photolysis of sulphate anion SO_4^{2-}

Oxygen saturated 2×10^{-2}M, aqueous solution of SO_4^{2-} anion at pH 5.5 was photolysed using flash photolysis technique. Two transient species were observed to be produced. One species was found to have an absorption maxima at about 240 nm and the other at 445 nm as shown in (Fig. 1). Their spectra were recorded over a spectrum region 225 to 530 nm. Both the species were found to decay by second order kinetics. The species with maxima at 240 nm was identified as O_2^- radical anion as its absorption spectrum, life time and decay are in agreement with the reported values for O_2^- radical anion in the literature.[17,18] On flash photolysis of 2×10^{-2}M Ar saturated aqueous solution of SO_4^{2-} anions no transient at 230 nm was observed which further supports the transient species O_2^-. The other transient was identified as SO_4^- radical anion as reported in the literature.[19] As no flash energy is absorbed by water under the experimental set-up thus these species most probably are produced as a result of the following primary processes.

$$SO_4^{2-} + H_2O \overset{h\nu}{\rightleftharpoons} SO_4^{2-} + H_2O^* \qquad (6)$$

$$SO_4^{2-} + H_2O^* \longrightarrow SO_4^- + e_{aq}^- \qquad (7)$$

$$O_2 + e_{aq}^- \longrightarrow O_2^- \qquad (8)$$

---

[13] G. V. Buxton and M. S. Subhani, *J. Chem. Soc. Trans. Faraday*, **68**, 958 (1972).

[14] M. S. Subhani, *J. Science and Mathematics*, **2**, 000 (1976).

[15] F. S. Dainton, W. A. Seldon and F. Wilkinson, *Trans. Faraday Soc.*, **63**, 1699 (1967).

[16] M. S. Subhani and T. Kauser, Submitted for publication to *Rev. Roumaine Chim.*

[17] G. Czapski and L. M. Dorfman, *J. Phys. Chem.*, **68**, 1169 (1964).

[18] G. E. Adams, J. W. Boag and B. D. Michael, *Proc. Roy. Soc.*, **A 287**, 321 (1965).

[19] L. Dogliotti and E. Hayon, *J. Phys. Chem.*, **71**, 2511 (1967).

The second order plots were obtained for the decay of both the transient species O_2^- and SO_4^- and can be presented as

$$O_2^- + O_2^- \xrightarrow{2H_2O} H_2O_2 + O_2 + 2OH^- \quad (9)$$

$$SO_4^- + SO_4^- \longrightarrow \text{products} \quad (10)$$

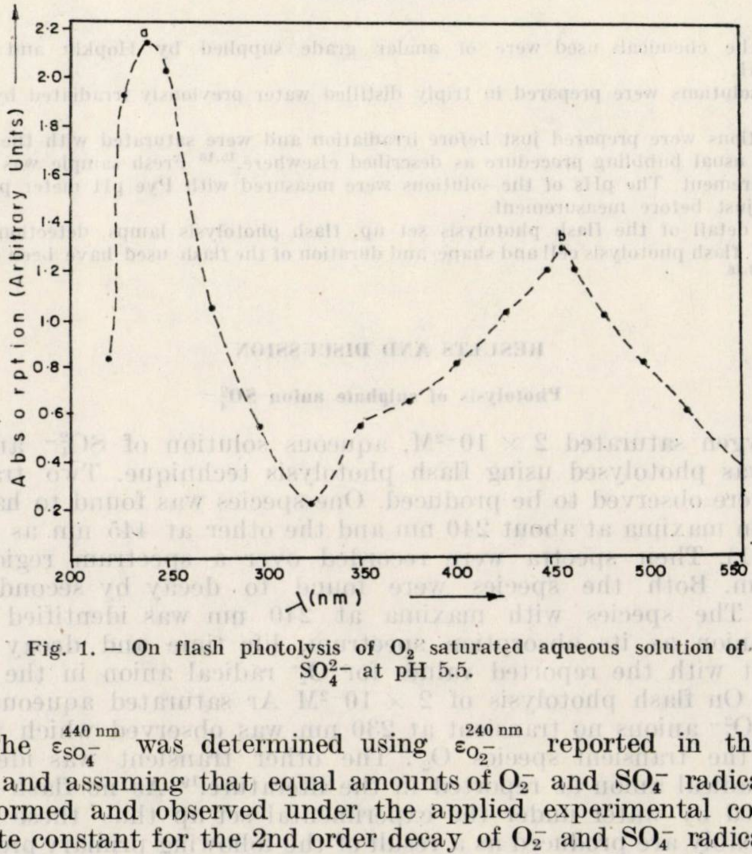

Fig. 1. — On flash photolysis of O_2 saturated aqueous solution of SO_4^{2-} at pH 5.5.

The $\varepsilon_{SO_4^-}^{440\ nm}$ was determined using $\varepsilon_{O_2^-}^{240\ nm}$ reported in the literature[17] and assuming that equal amounts of O_2^- and SO_4^- radical anions were formed and observed under the applied experimental conditions. The rate constant for the 2nd order decay of O_2^- and SO_4^- radical anions was obtained from the plots and values as shown in tables 1 and 2. The value obtained for the rate constant for the second order decay of O_2^- radical anion by the process $O_2^- + O_2^- \rightarrow$ (Table 1) is quite in agreement with the reported value in the literature.[17,18]

Photolysis of alkaline SO_4^{2-} anion

On flash photolysis of oxygen saturated 5×10^{-2}M SO_4^{2-} solution pH 11.5 two transient species were observed, one at $\lambda_{max} = 240$ nm and the other at $\lambda_{max} = 435$ nm. The decay of the species at 435 nm was much slower than that due to SO_4^- radical anion decay.

No absorption spectrum due to SO_4^- radical anion was observed. (Figure 2).

The observations can be explained on the basis of the following reaction mechanism for the formation of O_3^-,

$$SO_4^- + H_2O \longrightarrow SO_4^{2-} + OH + H^+ \tag{11}$$

$$OH + OH^- \longrightarrow O^- + H_2O \tag{12}$$

$$O^- + O_2^- \longrightarrow O_3^- \tag{13}$$

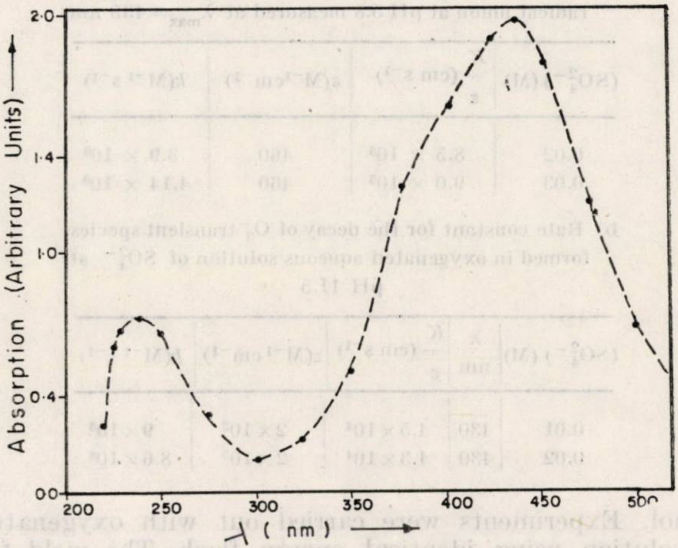

Fig. 2. — On flash photolysis of O_2 saturated SO_4^{2-} aqueous solution at pH 11.5.

Table 1

Rate constant for the decay of O_2^- radical anion at pH 5.8 at $\lambda_{max} = 260$ nm

(SO_4^{2-}) (M)	$\frac{K}{\varepsilon}$ (cm s^{-1})	$\varepsilon(M^{-1}\ cm^{-1})$	$k(M^{-1}\ s^{-1})$
0.02	3.8×10^4	900	3.4×10^7
0.3	4.6×10^4	900	4.14×10^7

Value of K_{12} is $6.2 \times 10^8 M^{-1}$ sec^{-1} and that of K_{13} is $2.6 \times 10^9 M^{-1}$ as reported in the literature.[20,21]

The absorption spectrum at $\lambda_{max} = 435$ nm was similar to that assigned to O_3^- in the pulse radiolysis of alkaline oxygenated water[17,18] and that of flash photolysis of alkaline oxygenated hydrogen peroxide solution.[22] The decay of O_3^- was found to follow first order kinetics.

[20] E. Hayon, *Trans. Faraday Soc.*, **61**, 734 (1965).

[21] G. E. Adams, J. W. Boag and B. D. Michael, *Nature*, **205**, 898 (1965).

[22] J. Heidt and V. R. Landi, *J. Chem. Phys.* **41**, 176 (1964).

When the oxygenated alkaline solution of SO_4^{2-} anion (10^{-2}M) was protolysed in presence of OH radical scavenger such as methanol (10^{-2}M) no transient absorbing species was observed up to 575 nm. These studies indicate that SO_4^- radical anion must probably react with the methanol. Experiments were carried out with oxygenated and Ar saturated solution using identical energy flash. The yield for O_3^- and SO_4^- transients were measured immediately after the flash was over (20 μsec). They are summarized in table 3.

Table 2

a) Bimolecular rate constant for the decay of SO_4^- radical anion at pH 5.8 measured at $\lambda_{max} = 435$ nm

(SO_4^{2-}) (M)	$\frac{K}{\varepsilon}$ (cm s^{-1})	ε($M^{-1}cm^{-1}$)	k($M^{-1}s^{-1}$)
0.02	8.5×10^5	460	3.9×10^8
0.03	9.0×10^5	460	4.14×10^8

b) Rate constant for the decay of O_3^- transient species formed in oxygenated aqueous solution of SO_4^{2-} at pH 11.5

(SO_4^{2-}) (M)	λ nm	$\frac{K}{\varepsilon}$ (cm s^{-1})	ε($M^{-1}cm^{-1}$)	k($M^{-1}s^{-1}$)
0.01	430	4.5×10^4	2×10^3	9×10^8
0.02	430	4.3×10^4	2×10^3	8.6×10^8

Table 3

The yield of O_3^- and SO_4^- radical anions on flash photolysis of 10^{-2} M SO_4^{2-} aqueous solution

	(O_2) μM	(SO_4) μM
Ar saturated	0	2.05
O_2 saturated	3.0	0

These yields indicate that in addition to the primary process

$$SO_4^{2-} + H_2O^* \longrightarrow SO_4^- + e_{aq}^- \quad (7)$$

another primary process

$$OH + OH^- \rightleftharpoons O^- + H_2O$$

$$SO_4^{2-} + H_2O^* \longrightarrow SO_4^{2-} + OH + OH^- \quad (14)$$

may also occur and this process at pH. 11.5 is followed by

$$OH + OH^- \rightleftharpoons O^- + H_2O \quad (15)$$

and in oxygenated alkaline solution the process

$$O^- + O_2 \rightarrow O_3^- \tag{13}$$

and thus resulting in increase of yield of O_3^- as compared to that of SO_4^- transient species immediately after the flash is over. The rate constant for the decay of O_3^- radical anion was measured (Table 2) and was found in agreement with reported value in literature.[18]

Photolysis of sulphite ion

On flash photolysis of aqueous solution of 5×10^{-2}M SO_3^{2-} anion at natural pH both Ar saturated and O_2 saturated a transient species was observed with its absorption spectrum in the wavelength region of 350 nm to 900 nm with $\lambda_{max} = 740$ nm, as shown in Figure 3.

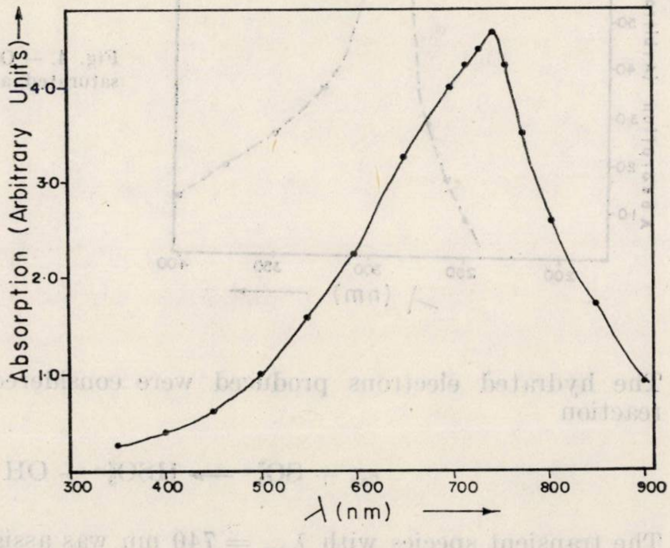

Fig. 3. — On flash photolysis of Ar saturated aqueous solution of SO_3^{2-} at natural pH.

The kinetics of the transient species produced was also studied and was found to obey first order kinetics at various wavelengths in the region of the spectrum of the same absorbing species. The rate constant for the decay of the transient species both in Ar saturated and O_2 saturated, at natural pH, and at alkaline pH, was found to be of the order of

$$K = (2.8 \pm 0.4)\, 10^4 \text{ sec}^{-1}$$

In N_2O saturated solution at natural pH no transient with $\lambda_{max} = 740$ nm was observed whereas a transient species with $\lambda_{max} = 290$ nm and absorbing in the wavelength region of 250 to 400 nm was observed as shown in Figure 4.

The species was found to be a longer lived one and was also produced when Ar and O_2 saturated solution was flash photolysed. The above mentioned experimental observations can be explained on the basis of the following primary photochemical and secondary processes :

$$SO_3^{2-} + H_2O \overset{h\nu}{\rightleftharpoons} SO_3^{2-} + H_2O^* \tag{14}$$

$$SO_3^{2-} + H_2O^* \longrightarrow SO_3^{-} + e_{aq}^{-} \tag{15}$$

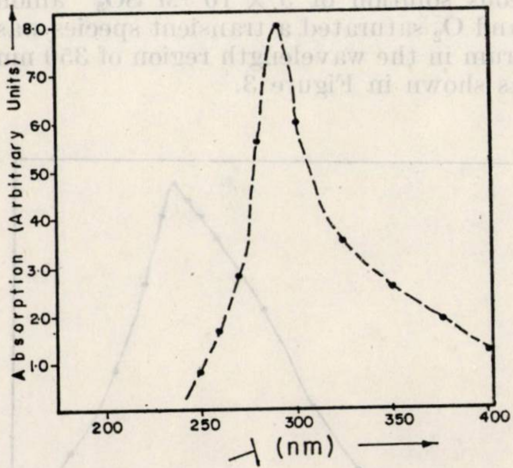

Fig. 4. — On flash photolysis of N_2O saturated aqueous solution of SO_3^{2-} at natural pH.

The hydrated electrons produced were considered to undergo another reaction

$$e_{aq}^{-} + SO_3^{2-} \longrightarrow HSO_3^{2-} + OH^{-} \tag{16}$$

The transient species with $\lambda_{max} = 740$ nm was assigned as HSO_3^{2-} radical and the species with $\lambda_{max} = 290$ nm was identified as SO_3^{-} radical anion as reported in the pulse radiolysis work.[9,10] In order to get further evidence for the type of species mentioned above N_2O saturated solution of SO_3^{2-} anion was photolysed. The absorbing species with $\lambda_{max} = 740$ nm was not observed whereas the species with $\lambda_{max} = 290$ nm was still observed with its yield almost double in magnitude as indicated by its optical density measurements. This can be explained on the basis that all the hydrated electrons produced in the primary photochemical process (15) react with N_2O $k(e_{aq}^{-} + N_2O) = 5.6 \times 10^9 M^{-1}s^{-1}$)[23] under the experimental conditions. Thus no HSO_3^{2-} radical anion was formed by the process (16).

---

[23] M. Anbar and P. Neta, *J. Appl. Radiat. Isotopes*, **18**, 493 (1967).

As mentioned earlier the optical absorption due to the species with $\lambda_{max} = 290$ nm was still observed indicating that electron is not involved into its formation. The increase in its yield may be due to the reaction of SO_3^{2-} with OH radical.

The species SO_3^- radical anion was found to decay by a second order process

$$SO_3^- + SO_3^- \longrightarrow S_2O_6^{2-}$$

forming most probably the stable $S_2O_6^{2-}$ anion. The value for $\frac{2K}{\varepsilon}$ obtained from the kinetics plot was 2.5×10^6 at 290 nm at natural pH.

Thus on the basis of the above mentioned observation and discussions the species with $\lambda_{max} = 290$ nm was assigned to be SO_3^- radical anion whereas that with $\lambda_{max} = 740$ nm was HSO_3^{2-} radical anion.

Revue Roumaine de Chimie, **23**, 7, 1139–1142 (1978)

EXTRACTION OF THALLIUM (III) FROM ITS CHLORIDE AND BROMIDE SOLUTIONS WITH ISOAMYL ALCOHOL (IAA) AND AMYL ACETATE (AA)

K. K. KAKKAR * and D. C. RUPAINWAR **

* Chemistry Department, Lucknow University, Lucknow
** Applied Chemistry Section, Institute of Technology Banaras Hindu University, Varanasi – 221005 (INDIA)

Received April 2, 1977

Thallium (III) has been extracted from its sulphuric acid solution, in the presence of chloride or bromide ions into isoamyl alcohol and amyl acetate. The relation of the distribution coefficient to various factors such as the initial concentration of the hydrogen ion or the halide ion has been evaluated and the best conditions for the extraction of the metal are thereby ascertained. The distribution coefficient increases with increased H^+ ion and metal concentrations and the formula of the extracted species is invariably $HTlX_4$ ($X = Cl^-$, Br^-). The percentage extraction, under the optimum conditions, is comparable to other common oxygenated solvents but is less than that obtained when phosphatic esters e.g. T.B.P. are employed.

INTRODUCTION

During recent years the extraction of thallium (III) from its acidic solutions in halide media has been studied using a number of oxygenated and other solvents.[1-3] The potentialties of two solvents ethyl acetate and fusel oil phosphate (FOP), an ester prepared from the waste product of Indian Alcohol Industries, for the extraction of thallium (III) from chloride solution had been reported from these laboratories.[4-6] This communication describes the extraction of thallium (III) from its chloride and bromide solutions using isoamyl alcohol (IAA)*** and amyl acetate (AA) as solvents.

** To whom all correspondence should be sent.

*** Abbreviations used for the text.

[1] J. A. Dean, *Analyt. Lett,*, **4**, 737 (1971).

[2] V. I. Golavanov, Yu. A. Zolotov and V. A. Zarinskii, *Zhur. neog. Khim.*, **17**, 1114 (1972).

[3] M. B. Chavan and V. M. Shinde, *Chem. Analyt.*, **19**, 1183 (1974).

[4] T. N. Srivastava and D. C. Rupainwar, *Bull. Chem. Soc. Japan*, **38**, 1792 (1965).

[5] T. N. Srivastava and D. C. Rupainwar, *Lab. J. Sci. Tech.*, **9A**, 178 (1971).

[6] K. K. Kakkar and D. C. Rupainwar, *Acta. Chim.* (In Press).

EXPERIMENTAL

1. *Stock solutions of thallium (III)* : The solutions were prepared by dissolving freshly precipitated hydrated thallic oxide in dilute sulphuric acid of known strength and their thallium (III) content was ascertained volumetrically with potassium iodate using methyl orange as an indicator.

2. *Solvents and other solutions* : The solvents isoamyl alcohol (b.r. 130—132°) and amyl acetate (b.p. 140°) were of B.D.H. (AnalaR) grade and used as such after fractional distillation. All the other solutions were prepared from AnalaR compounds and standardised by the usual procedures.

3. *Extraction Procedure* : The solvent used for the extraction experiments was always preequilibriated. Thus 20 ml of an aqueous solution containing the desired amount of H^+ and X^- ions (but no Tl(III); $X = Cl^-$ or Br^-) were taken in a glass-stoppered measuring cylinder and mixed with an equal volume of the solvent. The mixture was shaken for 5 min and allowed to settle. 15 ml of this equilibriated solvent layer was then mixed with 15 ml of thallium (III) solution having corresponding amounts of H^+ and X^- ions and shaken for 5 min. (Preliminary experiments had shown that this time is sufficient to attain the equilibrium). On standing the two layers separated out with negligible change in volumes. The layers were separated, 5 ml aliquots from both the layers were taken and their thallium content was determined. To evaluate the formula of the extracted species 5 ml aliquots from the solvent layer, after each equilibrium, were also taken; their halide content was back washed with distilled water and estimated by Volhard's method.

RESULTS AND DISCUSSIONS

It was originally intended to extract thallium (III), in presence of halide ions, from its perchloric acid solutions since ClO_4^- is more or less a non complexing simple anion. However, on preliminary investigations it was found that when $HClO_4$ is used and its concentration is greater than 3.0 M one of the solvent i.e. amyl acetate becomes completely miscible with the aqueous phase and this has also been observed for the extraction of bismuth (III) with the same solvent.[7] Though this is not the case with isoamyl alcohol yet for the sake of uniformity and comparison of the results of extraction of thallium (III) by these two and other solvents an aqueous phase of $Tl(III)-H_2SO_4-NaX(X = = Cl^-, Br^-)$ was invariably employed for all the subsequent experiments. However, the preliminary extraction experiments on thallium (III)—H_2SO_4 solution (No. X^- ions) have shown that the metal is only negligibly extracted with these solvents.

The results of the effect of the initial concentration of $[H^+]$ ion on the extraction of thallium (IIII) with the two solvents from chloride media are collected in Table 1. It is observed that the distribution coefficient is quite high even at 1.0 M $[H^+]$ and shows a gradual but steady increase. The percentage extraction is as high as 95% at 1.0 M $[H^+]$ and is optimum at 6.0 M $[H^+]$ for isoamyl alcohol and at 8.0 M $[H^+]$ for amyl acetate. On further increasing the initial $[H^+]$ beyond the optimum values the distribution coefficient registers a slight decrease. The empirical formulae of the extracted species given in Table 1 has been worked out by thallium (III), chloride and $[H^+]$ content of the organic layer; the latter was calculated by a method described earlier.[5] The formula of the extracted species up to 2—3 M $[H^+]$ is in between $TlCl_3$

---

[7] H. A. MOTTOLA and SANDELL, *Analyt. Chim. Acta*, **24**, 301 (1961).

Table 1

Extraction of Tl(III) with IAA and AA at different initial $[H^+]$ ions concentrations

Aqueous layer = Organic layer = 15.0 ml;
Initial Tl(III) = 5.98 g/l.

Sl No.	Solvent IAA			Solvent AA		
	Initial $[H^+]$ in Molarity	*D*	Empirical formula	Initial $[H^+]$ in Molarity	*D*	Empirical formula
1	1.06	22.06	$TlCl_3 \cdot 0.71$ HCl	1.21	18.25	$TlCl_3 \cdot 0.61$ HCl
2	1.95	22.59	$TlCl_3 \cdot 0.92$ HCl	2.11	21.00	$TlCl_3 \cdot 0.82$ HCl
3	2.82	24.61	$TlCl_3 \cdot 1.00$ HCl	3.12	27.63	$TlCl_3 \cdot 0.91$ HCl
4	3.61	27.81	$TlCl_3 \cdot 1.10$ HCl	4.01	32.45	$TlCl_3 \cdot 1.00$ HCl
5	4.59	31.83	$TlCl_3 \cdot 1.12$ HCl	5.02	35.22	$TlCl_3 \cdot 1.05$ HCl
6	5.46	33.84	$TlCl_3 \cdot 1.10$ HCl	6.14	35.22	$TlCl_3 \cdot 1.08$ HCl
7	5.90	41.21	$TlCl_3 \cdot 1.15$ HCl	7.04	37.67	$TlCl_3 \cdot 1.10$ HCl
8	6.80	41.21	$TlCl_3 \cdot 1.40$ HCl	8.05	50.32	$TlCl_3 \cdot 1.12$ HCl
9	8.03	31.93	$TlCl_3 \cdot 1.79$ HCl	9.01	42.99	$TlCl_3 \cdot 1.12$ HCl

and $HTlCl_4$ and nearly $HTlCl_4$ afterwards. The higher amount of $[H^+]$ in the organic layer than required for the species $HTlCl_4$ is attributed to the increased co-extraction of the acid due to the formation of mixed ionic clusters as reported earlier.[5] The general behaviour and optimum conditions for the extraction of metal for Tl(III)—H_2SO_4—NaBr system using the same solvents are very similar to that described for the chloride system adt the extracted species are also $HTlBr_4$. Only for the sake of brevity the superfluous details have been omitted. However, the effect of the halide ion ($X^- =$ Cl, Br) concentration on the extraction of Tl(III) at optimum concentration of $[H^+]$ given in Table 2 shows that the halide concentration of 2.0 M produces maximum effect on the distribution coefficient.

Table 2

Effect of the initial halide ion concentration on the distribution coefficient of Tl(III) with solvents IAA and AA

Initial Tl(III) = 5.98 g/l

Sl. No.	NaX in Molarity	Distribution coefficient	X =	0.5	1.0	1.5	2.0	2.5	3.0
1	Solvent IAA		Cl^-	10.57	22.06	33.05	41.21	41.21	41.21
	$[H^+] = 5.99$ M		Br^-	9.83	17.95	27.54	47.88	47.88	47.88
	Solvent AA		Cl^-	11.12	26.06	46.24	50.32	50.32	50.32
	$[H^+] = 8.0$ M.		Br^-	12.52	23.89	40.87	76.75	76.75	76.75

After ascertaining the optimum conditions for the extraction of thallium (III) for the metal-H_2SO_4—NaX system, the effect of the initial metal concentration (up to 20 g/1 — not shown) was also worked out and it has been observed for both solvents that the distribution coefficient rises with the increase in the metal concentration.

Table 3

Comparison of extraction values for Tl(III) from chloride medium with different solvents at varying initial [H+]

Sl. No.	Solvent	Percentage of Extraction at			
		1.0 M	3.0 M	6.0 M	8.0 M
1	Ethylacetate/ Diethylether (8)*	27.26	85.62	97.83	61.73
2	FOP/TBP* (9)	80.30	88.67	98.70	95.35
3	Isoamyl alcohol	95.70	96.51	97.61	96.94
4	Amyl acetate	94.82	96.45	97.23	98.06

* The data are more or less the same for the two solvents and have not been detailed by the authors.[8—9]

When the results of thallium (III) extraction are compared (Table 3) with the results obtained for the chloride media using other oxygenated solvents as extractants, it is observed that though isoamyl alcohol and amyl acetate are less effective at the optimum conditions yet the solvents show better extraction at lower as well as higher $[H^+]$ i.e. up to $\simeq$ 3.0 M and 8.0 M acid concentration. Thus this fact could be utilized for the separation of thallium (III) from aluminium (III), gallium (III) and indium (III) by a batchwise extraction at 1.0 M $[H^+]$ concentration. It is also concluded that the two solvents employed are better than ethyl acetate since they are more resistant to hydrolysis by the acid. The volume changes in the organic layer are negligible which is supported by the higher percentage of extraction at 6.0 N and 8.0 N of $[H^+]$.

ACKNOWLEDGEMENT: The authors are thankful to the Head of the Chemistry Department, Lucknow University for providing laboratory facilities and to State Council of Science and Technology, U.P. for a research grant.

---

[8] E.H. Swift, *J. Amer. Chem. Soc.*, **46**, 2375 (1924).

[9] K. S. Venkateswarlu and P. C. Das, *J. Inorg. Nuclear Chem.*, **25**, 730 (1963).

Revue Roumaine de Chimie, 23, 7, 1143–1147 (1978)

SAURE UND BASISCHE AMYLOSE-IONENAUSTAUSCHER

H. D. SCHELL, M. ŞERBAN *, M. A. MATEESCU und TR. BENŢIA
Institut für Biologische Wissenschaften, Abteilung für Enzymologie, 7000 Bukarest 17, Spl. Independenţei 296
*Institut für Agronomie ,,N. Bălcescu", Lehrstuhl für Chemie, Bukarest, R.S. Rumänien

Eingegangen am 12. Mai 1976

Es werden die Darstellungsmethoden sowie die physikalisch-chemischen und mechanischen Eigenschaften neuer saurer und basischer Ionenaustauscher beschrieben, die durch Einführen von Carboxymethyl- bzw. Diäthylaminoäthyl-Gruppen in das Molekül der mittels Glyceryläther-Brücken vernetzten Amylose erhalten wurden. Die erzielten Verbindungen bilden wasserunlösliche Gele, die, in Chromatographie-Säulen eingeführt, gute Durchflußgeschwindigkeiten gewähren. Die Austauschfähigkeit der dargestellten Stoffe wird von der Menge der in der Reaktion verwendeten Monochloressigsäure bzw. des 1-Chlor-2-diäthylaminoäthan-chlorhydrates bedingt.

Die Ionenaustauschchromatographie stellt zur Zeit eine der wirksamsten und meistverbreiteten analytischen und präparativen Methoden dar, die ganz besonders in den chemischen und biochemischen Labors zur Darstellung und Reinigung verschiedenartigster chemischer und biologisch aktiver Verbindungen angewendet wird. Zu diesem Zweck wurden im Laufe der Zeit eine Reihe von Ionenaustauschern ausgehend von Cellulose, Agarose, Dextran und anderen makromolekularen Verbindungen dargestellt.[1-7] Die weiter unten beschriebenen Verbindungen sollen die Auswahl dieser Stoffe mit neuen sauren und basischen Ionenaustauschern bereichern, die von der Amylose, einem zugänglicheren und relativ billigen Ausgangsprodukt abgehend erzielt wurden. * Die erhaltenen Produkte sind schwach saure (CM-Amylose) oder schwach basische (DEAE-Amylose) Ionenaustauscher und eignen sich zur Trennung und Reinigung biologisch aktiver Makromoleküle, wie Proteine, Enzyme, Nukleinsäuren sowie verschiedener anderer chemischer Stoffe.

---

* Die in der vorliegenden Arbeit beschriebenen Ionenaustauscher sind in Rumänien unter Nr. 62322/1976 patentiert worden.

[1] E. A. PETERSON und H. A. SOBER, *J. Amer. Chem. Soc.*, **78**, 751 (1956).

[2] H. D. SCHELL, V. GHEŢIE und S. MIHĂESCU, *Rev. Roumaine Biochim.*, **5**, 259 (1968).

[3] V. GHEŢIE, H. D. SCHELL und L. BUZILĂ, *Hoppe-Seyler's Z. Physiol. Chem.*, **350**, 1675 (1969).

[4] * * * ,,Ionenaustauscher auf Zellulosebasis", Reanal, Budapest, Ungarn.

[5] * * * ,,Sephadex Ion Exchangers", Pharmacia Fine Chemicals, Uppsala, Sweden, 1973.

[6] M. RYBAN, Z. BRADA und I. M. HAIS, ,,Säulenchromatographie an Cellulose Ionenaustauscher", VEB Gustav Fischer Verlag, Jena, 1966, p. 100.

[7] * * * ,,Serva Cellulose Ionenaustauscher" Serva Entwicklungslabor, Heidelberg, 1962.

Das Darstellungsverfahren der beschriebenen Verbindungen besteht darin, daß die mittels Glyceryläther-Brücken vernetzte Amylose in stark basischem Milieu mit Monochloressigsäure (Reaktionsschema I, II) oder mit 1-Chlor-2-diäthylaminoäthan-Chlorhydrat versetzt wird, wobei den von Peterson und Sober[1] bei der Synthese entsprechender Cellulosederivate und denen von Schell und Gheţie[2,3] im Falle der Herstellung entsprechender Agarosederivate gemachten Hinweisen Rechnung getragen wurde.

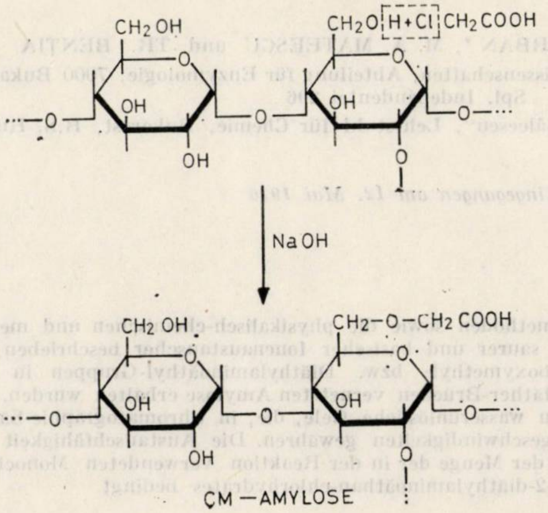
CH₂OH
CH₂O H+Cl CH₂COOH
OH
O
NaOH
CH₂OH
CH₂–O–CH₂COOH
CM —AMYLOSE

Reaktionsschema I. Synthese der CM-Amylose

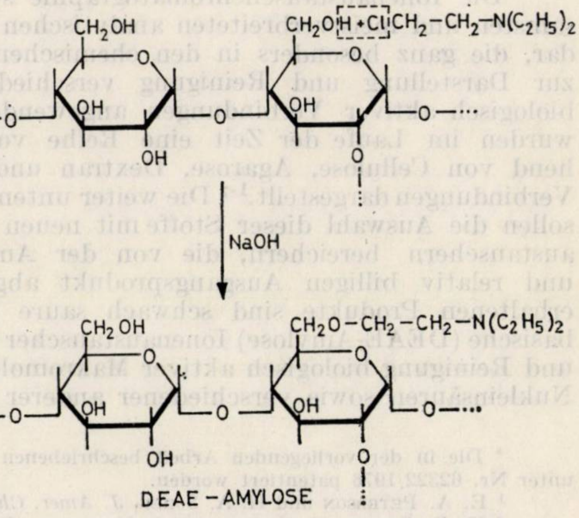
CH₂OH
CH₂O H+Cl CH₂–CH₂–N(C₂H₅)₂
OH
O
NaOH
CH₂OH
CH₂O–CH₂–CH₂–N(C₂H₅)₂
DEAE – AMYLOSE

Reaktionsschema II. Synthese der DEAE-Amylose

MATERIAL UND METHODIK

Darstellung der Carboxymethyl-Amylose (CM-Amylose). Je 20 ml abgesetztes, granuliertes, in Wasser gequollenes Gel der Amylose. X—40*[8] wurden mit 10 ml einer 10 N NaOH-Lösung versetzt, darauf 30 min im Eisbad gerührt und dann ebenfalls im Eisbad und unter Rühren mit je 1 g in 1,2 ml Wasser bzw. 2 g in 2,4 ml Wasser gelöster Monochloressigsäure versetzt. Nach 20—25 min wurde das Reaktionsgemisch im Wasserbad 60 min auf 75—80° erhitzt. Die entstandene CM-Amylose wurde sodann mit destilliertem Wasser bis zur vollkommenen Entfernung des NaOH durch Dekantieren gewaschen, auf dem Büchnertrichter an der Wasserstrahlpumpe kurz mit Eisessigsäure behandelt, sodann erneut mit destilliertem Wasser an der Wasserstrahlpumpe gewaschen, diesmal bis zur völligen Entfernung der Essigsäure und abschließend nach Entwässerung mit Aceton an der Luft getrocknet.

Darstellung der Diäthylaminoäthyl-Amylose (DEAE-Amylose). Je 20 ml wie weiter oben beschriebenes Gel der Amylose X-40 wurden mit 7,5 ml eisgekühlter 7,5 N NaOH-Lösung versetzt und 30 min im Eisbad gerührt. Darauf wurden, ebenfalls im Eisbad und unter Rühren, je 2,5 bzw. 5 g in 5 bzw. in 7 ml Wasser gelöstes 1-Chlor-2-diäthylaminoäthan-Chlorhydrat hinzugesetzt und das Reaktionsgemisch unter zeitweiligem Rühren 60 min im Wasserbad auf 80—85° erhitzt. Die erzielte DEAE-Amylose wurde sodann mehrere Male mit destilliertem Wasser durch Dekantieren gewaschen, an der Wasserstrahlpumpe, abgenutscht, dann gleich anschließend auf dem Büchnertrichter mit je 40 ml 1 N NaOH-Lösung, 1N Salzsäure und wiederum 1N NaOH-Lösung behandelt und über Nacht in verdünnter NaOH-Lösung (0,2 N) stehen gelassen. Tags darauf wurde das granulierte Gel mit destilliertem Wasser bis zur völligen Entfernung des Hydroxyds gewaschen und nach Entwässerung mit Aceton an der Luft getrocknet.

Die *Austauschfähigkeit* der erzielten Produkte wurde durch potentiometrische Titration ermittelt und in mequiv/g Trockengewicht ausgedrückt. Im Falle des sauren Austauschers wurde mit 0,1 N NaOH-Lösung und im Falle des basischen mit 0,1 N Salzsäure titriert.[6]

Die *Quellfähigkeit*, ausgedrückt in ml Gel, die 1 g granuliertes Trockenprodukt durch Quellen in Wasser ergibt, wurde bestimmt, indem eine bekannte Menge des granulierten und getrockneten Ionenaustauschers in einen mit Wasser versehenen Meßzylinder eingetragen und nach einer Stunde Quellung das Gelvolumen abgelesen wurde.[6]

Die *Wasseraufnahmefähigkeit* wurde nach Flodin [9] bestimmt und in Gramm Wasser ausgedrückt, die von einem Gramm Trockensubstanz zurückgehalten werden (water regain).

Der *Feuchtigkeitsgehalt* der dargestellten Ionenaustauscher wurde bestimmt, indem eine an der Luft bei Zimmertemperatur getrocknete Probe vor und nach Trocknung bei 105° auf Gewichtskonstanz genau abgewogen wurde und in g Wasser/100 g Trockensubstanz ausgedrückt.[10]

Die *Trocknung* der granulierten Gele fand nach vorausgehender milden Entwässerung mittels Aceton bei Zimmertemperatur statt.[11,12]

ERGEBNISSE UND DISKUSSIONEN

Wird die durch Glyceryläther-Brücken vernetzte Amylose X-40 in alkalischem Milieu mit Monochloressigsäure oder dem Chlorhydrat des 1-Chlor-2-diäthylaminoäthans versetzt, so erhält man saure bzw. basische Ionenaustauscher, deren Austauschkapazität von der Menge der in der Reaktion zur Anwendung gelangten Reaktanten abhängt, so wie es auch aus den in Abb. 1 und 2 dargestellten Titrationskurven ersichtlich ist.

---

* Der Buchstabe X weist darauf hin, daß es sich um mit Glyceryläther-Brücken vernetzte Amylose handelt, während die darauffolgende Zahl die Epichlorhydrinmenge angibt, die zur Vernetzung von 100 g Amylose verwendet wurde; die Darstellungsmethode dieser Vernetzung ist in einer früheren Arbeit beschrieben worden.[8]

[8] M. Şerban, H. D. Schell und M. A. Mateescu, *Rev. Roumaine Biochim.*, **12**, 187 (1975).

[9] P. Flodin, „Dextran Gels and their Applications in Gel Filtration", Meijels Bokindustri, Uppsala, Sweden, 1962.

[10] M. E. Carsten, „Ion Exchange Celluloses Bibliography", California Corporation for Biochemical Research, Los Angeles, 1962.

[11] H. D. Schell und V. Gheţie, Rumänische Patentschrift Nr. 56403/1971.

[12] V. Gheţie und H. D. Schell, *Experientia*, **27**, 1384 (1971).

So weist z.B. die CM-Amylose, die ausgehend von 20 ml Amylose-Gel und 1 g Monochloressigsäure erhalten wurde, eine Austauschkapazität von 0,8 mequiv/g Trockensubstanz auf (Abb. 1), während bei Anwendung von 2 g Monochloressigsäure eine Austauschkapazität von 1,3 mequiv/g erzielt wird (Abb. 1). Die DEAE-Amylose, die durch Behandlung der erwähnten 20 ml Amylose-Gels mit 2,5 g 1-Chlor-2-diäthylaminoäthan-Chlorhydrat erhalten wurde, weist eine Austauschkapazität von 1 mequiv/g Trockenprodukt auf (Abb. 2), während die durch Hinzufügen von 5 g 1-Chlor-2-diäthylaminoäthan-Chlorhydrat erhaltene DEAE-Amylose eine Austauschkapazität von 1,7 mequiv/g aufweist (Abb.2). Diese Austauschkapazitäten reihen sich gut in die Werte ein, die in der Fachliteratur für CM- und DEAE-Cellulose-Ionenaustauscher (0,7 ± 0,1 mequiv/g)[4] und CM- und DEAE-Sephadex-Ionenaustauscher (4,0 ± 0,5 mequiv/g)[5] angegeben sind und können je nach den Erfordernissen durch Verändern des Verhältnisses der miteinander reagierenden Komponenten auch vergrößert oder verringert werden.

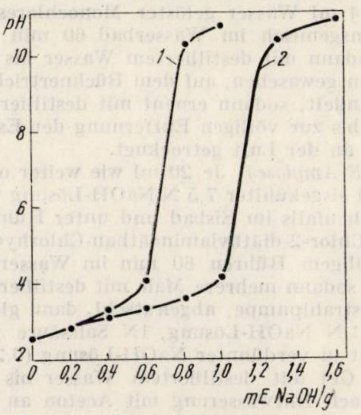

Abb. 1. — Titrationskurven der CM-Amylose

1) Produkt mit der Austauschkapazität 0,8 mequiv/g ; 2) Produkt mit der Austauschkapazität 1,3 mequiv/g.

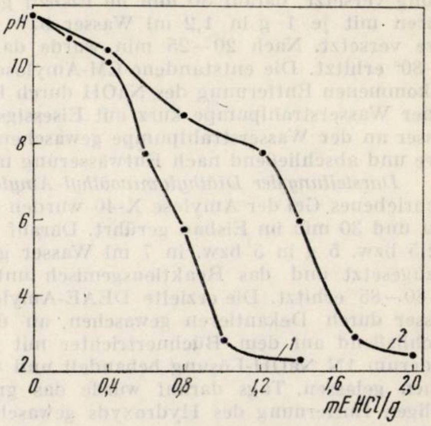

Abb. 2. — Titrationskurven der DEAE-Amylose

1) Produkt mit der Austauschkapazität 1,0 mequiv/g ;
2) Produkt mit der Austauschkapazität 1,7 mequiv/g.

Es wurde die Amylose X-40 als Trägerskelett für die Ionenaustauschergruppen gewählt, weil sie ein entsprechend dichtes Netz von Glyceryläther-Brücken besitzt, die ihr ausgezeichnete mechanische Eigenschaften verleihen und Durchflußgeschwindigkeiten gewährleisten, die denen der handelsüblichen Ionenaustauschern gleichkommen.

Indem wir auch die übrigen physikalisch-chemischen und mechanischen Eigenschaften der CM- und DEAE-Amylose untersuchten, stellten wir — wie es ja anders auch nicht zu erwarten war — Eigenschaften fest, die von denen der vernetzten Amylose zum Teil erheblich abwichen.

Wie aus Tabelle I hervorgeht, wird das Quellvermögen und die Wasseraufnahmefähigkeit der vernetzten Amylose durch Einführen von sauren (CM) und basischen (DEAE) Ionenaustauschergruppen beträchtlich erhöht. Die etwas größeren Werte im Falle des basischen Austauschers werden bedingt durch den etwas ausgeprägteren hydrophilen Charakter der DEAE-Gruppen verglichen mit dem der CM-Gruppen des sauren

Tabelle 1

Die wichtigsten Eigenschaften der von Amylose X-40 erzielten Ionenaustauscher-Gele

Gelart	Austauschfähigkeit (mequiv/g Trockensubstanz)	Quellfähigkeit (ml Gel/g Trockensubstanz)	Wasseraufnahmefähigkeit (water regain) (gH_2O/g Trockensubstanz)	Feuchtigkeitsgehalt (g H_2O/100 g Trockensubstanz)
Vernetzte Amylose X-40	0	4,3	10,9	5,8
Vernetzte CM-Amylose	0,8	7,2	14,4	7,1
	1,3	7,8	17,0	7,3
Vernetzte DEAE-Amylose	1,0	10,5	17,1	7,6
	1.7	12,0	18,6	8,0

Austauschers oder dem der Hydroxyl-Gruppen der als Träger verwendeten vernetzten Amylose.

Aus den von uns erzielten und weiter oben dargelegten Ergebnissen geht hervor, daß die neuen, in dieser Arbeit beschriebenen und von leichter zugänglichem und preiswerterem Ausgangsmaterial abgehend erhaltenen Ionenaustauscher ähnliche physikalisch-chemische und mechanische Eigenschaften aufweisen, wie die zur Zeit verwendeten besitzen.

Das Verhalten in der Ionenaustauschchromatographie sowie das Auflösungsvermögen der dargestellten Verbindungen, verglichen mit anderen zur Zeit angewandten Ionenaustauschern, wird den Gegenstand einer künftigen Mitteilung geben.

SCHLUSSFOLGERUNGEN

1. Behandelt man die mittels Glyceryläther-Brücken vernetzte Amylose in stark basischem Milieu mit Monochloressigsäure oder 1-Chlor-2-diäthylaminoäthan-Chlorhydrat erhält man saure bzw. basische Ionenaustauscher.

2. Die Austauschfähigkeit der neuen Ionenaustauscher kann variiert werden und hängt von der in der Reaktion angewandten Menge der Reaktanten ab.

3. Die Einführung der Ionenaustauscher-Gruppen in das Molekül der vernetzten Amylose verleiht dieser einen ausgeprägteren hydrophilen Charakter.

4. Die erzielte CM- und DEAE-Amylose besitzt vorzügliche physikalisch-chemische und mechanische Eigenschaften, die denen der zur Zeit verwendeten Ionenaustauscher ähnlich sind, was ihre Anwendung in der Ionenaustauschchromatographie gestattet.

Revue Roumaine de Chimie, 23, 7, 1149–1152 (1978)

POLAROGRAPHY OF METHIONINATE COMPLEXES OF CADMIUM (II), LEAD (II) AND ZINC (II)

G. N. RAO * VIJAY KUMAR * and HAUZ KHAS **
* Chemistry Department, Indian Institute of Technology
** N. Delhi 110029, India

Received April 10, 1976

Methioninate complexes of cadmium (II) and lead (II) are reduced reversibly while those of zinc (II) are irreversibly reduced at the dropping mercury electrode. Stability constants (expressed as log values of equilibrium constants for the complex formation) of $Cd(Mt)_3^-$, $Pb(Mt)_1^+$ and $Pb(Mt)_2$ (Mt = methioninate) species are 8.10, 4.30 and 6.10 respectively at 30° and unit ionic strength. Comparison of stability constants of metal complexes of glycinate and methioninate indicates that sulphur is not involved in coordination in the methioninate complexes investigated.

INTRODUCTION

Cadmium (II) complexes of glycine, α-alanine, β-alanine, valine, asparagine, aspartic acid and glutamic acid have been investigated using polarography by Nageswara Rao and Subrahmanya.[1,2] Polarography of lead (II)[3] and zinc (II)[4] complexes with the same amino acids has been reported by the same authors. In the present communication results of the polarographic study of cadmium (II), lead (II) and zinc (II) complexes with a sulphur containing amino acid, DL-methionine $CH_3SCH_2CH(NH_2)COOH$ are described. Such a study is considered useful in view of the current interest in the field of bioinorganic chemistry and metal-peptide interactions.

EXPERIMENTAL

Polarograms were obtained employing Toshniwal manual polarograph and the pH measurements were performed on Elico pH meter. Acid dissociation constant of methionine was determined as described earlier.[1] All experiments were carried out in a thermostat maintained at 30 ± 0.1°. Ionic strength was maintained at unity by adding the requisite amount of potassium nitrate. Gelatin (0.005 %) was included in all solutions to suppress the maxima. Drop time was adjusted to 5 seconds in a normal potassium chloride. All chemicals employed were of reagent quality; stock solution of the amino acid anion was prepared by dissolving a known weight of DL methionine in the requisite amount of sodium hydroxide. The halfwave potentials were reproducible to ± 0.002 volts. Concentration of metal nitrate was maintained at 1 millimolar in all solutions.

---

[1] G. N. Rao and R. S. Subrahmanya, *Proc. Indian Acad. Sci.*, **60A**, 165 (1964).
[2] G. N. Rao and R. S. Subrahmanya, *Current Sci.*, **31**, 55 (1962).
[3] G. N. Rao and R. S. Subrahmanya, *Proc. Indian Acad. Sci.*, **60A**, 185 (1964).
[4] G. N. Rao and R. S. Subrahmanya, *J. Electroanalyt. Chem.*, **9**, 364 (1965).

RESULTS

The acid dissociation constant of methionine (pK = 9.20 at 30°, $\mu = 1.00$) obtained in the present study agrees well with the literature values.[5] Variation of the halfwave potential with the ligand concentration has been studied in all the systems and some of the results are presented in table 1. Reduction process was found to be reversible in systems containing cadmium (II) and lead (II), whereas it is irreversible in solutions containing zinc (II). The values of $E_{\frac{3}{4}} - E_{\frac{1}{4}}$ ranged from 0.030 to 0.034 v in cadmium (II) — methionine system and from 0.027 to 0.030 v in lead (II) — methionine system. In table 1 values of $E_{\frac{3}{4}} - E_{\frac{1}{4}}$ for zinc (II) — methionine system are also listed. Similar results have been obtained previously in systems containing other amino acids.[1 to 4] Application of Lingane's equation to the data in Table 1 shows that three moles of the ligand are attached to each mole of the cadmium (II).

Table 1

Variation of half wave potential with concentration of methioninate
(300°C, $\mu = 1.10$)

Concentration of methioninate (M)	$-E_{\frac{1}{2}}$ vs. S.C.E.(V) Cd(II)	$-E_{\frac{1}{2}}$ vs. S.C.E.(V) Pb(II)	$-E_{\frac{1}{2}}$ vs. S.C.E.(V) Zn(II)	$-E_{\frac{3}{4}} - E_{\frac{1}{4}}$ (V) Zn(II)
0.10	0.750	0.544	1.308	0.044
0.20	0.772	0.556	1.346	0.044
0.30	0.793	0.564	1.356	0.050
0.50	0.812	0.576	1.382	0.048
0.70	0.823	0.582	—	—
1.00	0.833	0.592	1.413	0.046

Stability constant (expressed as log β values in this paper) of the 1 : 3 complex of cadmium (II) with methioninate is calculated to be 8.10. Experiments were also performed at two pH values (9.20 and 11) keeping the methioninate concentration constant. Since the halfwave potentials were independent of pH values at constant methioninate concentration, it was concluded that no mixed hydroxy complexes are formed under the experimental conditions employed. Treatment of the data obtained in lead (II) methioninate systems according to the method described previously,[3] which is based on modified McKenzie-Mellor[6] equation gave the values 4.30 and 6.10 for the stability constants of 1 : 1 and 1 : 2 complexes of lead (II) with methioninate. Employing the equations for irreversible waves as described in earlier papers,[4,6] it was found that 1 : 2 complex of zinc (II) with methioninate is present under the experimental conditions in solution. Experiments carried out at pH 11 in the copper (II) methioninate system showed split waves at all the ligand concentrations employed. The relative heights of the two waves varied with ligand concentration. No conclusion could be reached regarding the stability or stoichiometry of the complex formed. Li and Doody[7] obtained single waves in this system at a lower pH value 8 working with phosphate buffers.

---

[5] L. G. Sillen and A. E. Martell, "Stability Constants of Metal Ion Complexes", The Chemical Soc., London, 1964.

[6] R. S. Subrahmanya, *Proc. Indian Acad. Sci.*, **46**, 443 (1957).

DISCUSSION

Stability constants of methioninate complexes of cadmium (II), lead (II) and zinc (II) have been determined by pH titration method by Li and Manning.[8] For the 1 : 1 complex of lead (II) they obtained a value of 4.40 (25°, $\mu = 0.15$), but precipitation prevented the determination of stability constant of 1 : 2 complex. Lenz and Martell[9] reported a value of 4.38 (25°, $\mu = 0.10$) for the same complex. The value obtained in the present work agrees with these values considering the variation in experimental conditions. Stability constants of some metal complexes of glycinate and methioninate are listed in table 2. It is seen that in all cases the methioninate complexes are less stable than the corresponding glycinate complexes. The lower basicity of methionine (pK = 9.20) compared to glycine[1] (pK = 9.64) is probably responsible for this variation. Sulphur atom is not involved in bond formation in these complexes, as it would have led to the formation of more stable complexes with methionine than glycine, if it were the case. However, it is interesting

Table 2

Stability constants of some metal complexes of glycine and methionine

	Glycinate	Methioninate
Cd (II) 1 : 2	8.08[1]	6.99[8]
Cd (II) 1 : 3	9.78[1]	8.10*
Pb (II) 1 : 1	5.11[3]	4.30*
Pb (II) 1 : 2	7.08[3]	6.10*
Zn (II) 1 : 2	9.19[7]	8.47[8]
Cu (II) 1 : 2	15.10[7]	14.72[8]

Reference numbers are given in brackets
* This work.

---

[7] N. C. Li and R. A. Manning, *J. Amer. Chem. Soc.*, **76**, 221 (1954).

[8] N. C. Li and R. A. Manning, *J. Amer. Chem. Soc.*, **77**, 5225 (1955).

[9] G. R. Lenz and A. E. Martell, *Biochemistry*, **3**, 745 (1964).

to note that Cu (I) forms strong complexes with methionine in which the bonding is supposed to be through sulphur according to the work of Hemmerich [10] who determined the stability constants of several cuprous complexes of biochemical interest utilising the pH titration method in acetonitrile-water solvent system. Since Cu (II) forms a 1 : 2 complex with a stability constant 14.75 in which the bonding is supposed to be through the amino and carboxyl groups, methionine represents a novel situation where the ligand is bound by the same metal through different bonding sites in different oxidation states.

Polarographic technique employing larger ligand concentrations has been effective in determining the stability constants of complexes with highest metal (II) : methioninate stoichiometry with both lead (II) and cadmium (II) while the pH titration method gave evidence for the formation of lower complexes only. Stability constants of the 1 : 2 complexes of amino acids with lead (II) are slightly larger than those of the corresponding cadmium (II) complexes, while the reverse is true in case of EDTA complexes. Surprisingly no more than two bidentate amino acid anion ligands are coordinated to lead (II) even at the highest ligand concentration employed (i.e. 1M) while the relatively smaller cadmium (II) ion is coordinated to three ligands under similar conditions.

---

[10] P. Hemmerich in "The Biochemistry of Copper", Edited by J. Peisach, P. Aisen and W. E. Blumberg, Academic Press, New York, 1966, p. 15.

Revue Roumaine de Chimie, 23, 7, 1153–1156 (1978)

SPECTROPHOTOMETRIC DETERMINATION OF IRIDIUM(III) WITH SUBSTITUTED PYRIMIDINETHIOLS

AJAI K. SINGH, MOHAN KATYAL and R. P. SINGH

Department of Chemistry, University of Delhi, Delhi—110007, India

Received April 20, 1976

1-Anilino- and (2′,4′-dinitroanilino)-4,4,6-trimethyl-1H, 4H-2-pyrimidinethiols react with iridium (III) forming coloured complexes which have been used for their spectrophotometric determination. Optimum conditions for complexation have been established. Beer's law is obeyed. Effects of diverse ions have been investigated and several-fold excess of most of the ions can co-exist in the determination.

Methods for the spectrophotometric determination of iridium are numerous,[1–3] but most of them lack in selectivity or sensitivity or both, and there are objectionable interferences from many of the base and noble metals. In the course of studies on the analytical applications of 2-pyrimidinethioles,[4,5] it has been found that 1-anilino-4,4,6-trimethyl-1H, 4H-2-pyrimidinethiol (ATP, I) and 1-(2′, 4′-dinitroanilino)-4,4,6-trimethyl-1H, 4H-2-pyrimidinethiol (DATP, II) react with iridium (III) forming coloured complexes. In the present paper, the use of the reagents has been described for the spectrophotometric determination of the metal in pure samples and in co-existence with diverse ions.

(ATP, I) R = C_6H_5
(DATP, II) R = $C_6H_3(NO_2)_2$

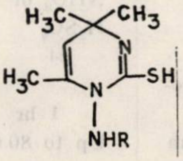

EXPERIMENTAL

Synthesis of ligands : ATP was prepared by the method of Mathes.[6] To synthesize DATP, 2 : 4-dinitrophenylhydrazine (0.02 M ; 3.96 g) and 2-methyl-2-isothiocyano-4-pentanone (0.02 M ; 3.14 g) were taken in 50 ml of ethanol, 3—4 drops of conc. H_2SO_4 added and the mixture refluxed for 5 hr. on a steam bath. The solvent was removed under reduced pressure and the residue washed with water. After 2—3 crystallizations from acetic acid, the m.p. was 223—24°. Calculated : C, 46.29 % ; H, 4.45 % ; N, 20.77 % ; found C, 45.93 % ; H, 5.00 % ; N, 20.46 %.

---

[1] F. E. Beamish, "Analytical Chemistry of Noble Metals," Pergamon, London, 1966, p. 418.

[2] V. K. Rangnekar and S. M. Khopkar, *Chemist-Analyst*, **56**, 84 (1967).

[3] F. G. Nasouri and A. S. Witwit, *Analyt. Chim. Acta*, **50**, 163 (1970).

[4] A. K. Singh, M. Katyal adn R. P. Singh, *Indian J. Chem.*, **53**, p. I (1976).

[5] A. K. Singh, M. Katyal, R. P. Singh and N. K. Ralhan, *Talanta*, **23**, p. I (1976).

[6] R. A. Mathes, *J. Amer. Chem. Soc.*, **75**, 1747 (1953).

Reagents and Chemicals : The standard solution of Ir(III) was prepared by dissolving the appropriate amount of $IrCl_3 . 3H_2O$ (Johnson Mathey) in 1.0 N HCl. The solution was standardized gravimetrically. Standard solutions of the ligands were prepared by dissolving their appropriate amounts in ethanol or methanol.

The pH of the solutions were adjusted with acetate buffers and dilute solutions of NaOH and HCl. All the other reagents used were of analytical grade. Double distilled water was used throughout the work.

Absorbance readings were taken with a Unicam SP 600 spectrophotometer. For pH measurements, a Metrohm pH meter, type E-350 was used.

Working procedure : To a suitable aliquot of iridium solution (Table 1) add 5.0 ml of 0.01 M ATP or DATP solution and 3.0 ml of sodium acetate-hydrochloric acid buffer to adjust the pH around 5.0. Make up the volume to 10.0 ml keeping 50% alcoholic medium. Heat the solution for 75 min. on a steam bath and cool to room temperature. Add 10.0 ml of carbon tetrachloride and shake for 10 min. Allow to settle and remove the organic layer. Measure its absorbance at λ_{max} of the complex against a reagent blank and calculate the amount of iridium from a standard curve.

Table 1

Characteristics of Ir-complexes with ATP and DATP

Characteristic	Ir-complex with ATP		Ir-complex with DATP	
	Yellow	Red	Yellow	Red
λ_{max}(nm)	375	500	385	480
ε_{max} (l. mole^{-1} cm^{-1})	2.0×10^3	1.0×10^4	1.8×10^3	9.0×10^3
Molar excess of the reagent needed for colour development	30-times	20-times	50-times	35-times
Acidity or pH range for max. absorbance	0.1—1.0 N HCl, $HClO_4$, NHO_3 or H_2SO_4	pH 4.0—6.5	0.1—1.0 N HCl, $HClO_4$, HNO_3 or H_2SO_4	pH 3.8—6.8
Stability (hr)	24	24	24	24
Heating needed for colour development	1 hr	1 hr	1 hr	1 hr
Beer's law range, ppm	Up to 80.0	Up to 19.0	Up to 85.0	Up to 20.2
Accurate range of determination, ppm	10.0—65.0	5.0—16.5	10.0—67.5	5.2—17.0
Sandell's sensitivity	0.0961	0.0192	0.106	0.0213
Standard deviation *	0.0068	0.0085	0.0072	0.0048

* Of the absorbance for 9.61 ppm of iridium

RESULTS AND DISCUSSION

Solutions of ATP are colourless while those of DATP are light yellow. When a few drops of alcoholic ATP or DATP solution are heated with dilute iridium (III) solution, two distinct coloured complexes are formed depending upon the acidity or pH of the solution. One of them is formed in highly acidic medium and is not extractable in common organic solvents while the other formed at pH > 3.0 is extractable. The studies in acidic medium have been carried out in 50% methanol or ethanol. The other complex (at pH $>$ 3.0) has been extracted into carbon tetrachloride and investigated. The other solvents like benzene, chloroform, n-butanol and amyl alcohol have been found equally useful. The stoichiometry of the complexes has been ascertained by the methods of continuous variations and logarithmic. Yellow coloured complexes formed in highly acidic medium contain metal and the ligand in 1 : 2 ratio while the complexes at pH $>$ 3.0 contain metal and the ligand in 1 : 3 ratio. The other characteristics of the complexes are summarized in Table 1. The sensitivity of the colour reaction in highly acidic medium is not of high order. Therefore, the red complexes (at pH $>$ 3.0) are used for spectrophotometric determination of the metal and in subsequent investigations.

Effect of diverse ions : The effect of diverse ions in determination of 9.61 ppm of iridium has been investigated. F^-, Cl^-, Br^-, ClO_4^-, CH_3COO^-, SO_4^{2-}, Ca (II), Se (II), Ba (II), Zn (II), Cd (II), Al (III), Ga (III), In (III), Ti (IV), Zr (IV) and Mo (VI) do not interfere even at 10 mg/ml level. However, CN^-, Ru(III), Pd (II), Os (VIII), Pt (IV), Rh (III) and Au (III) affect the determination seriously even at 1—2 ppm level. The tolerance limits of other ions are given in Table 2.

Table 2

Effect of diverse ions

Diverse ion	Tolerance (ppm) in determination of 9.6 ppm Ir with	
	ATP	DATP
I^-	100	50
NO_2^-	80	40
NO_3^-	5,000	5,000
CNS^-	20	10
$S_2O_3^{2-}$	50	20
$C_2O_4^{2-}$	500	500
Tartrate	1,200	1,200
Thiourea	20	20
EDTA	50	50
BO_3^{3-}	1,000	1,000
PO_3^{3-}	1,000	1,000
Citrate	500	500
Ag (I)	50	50
Cu (II)	50	50
Hg (II)	10	10
Sn (IV)	20	10
Pb (II)	100	100
V (IV)	20	20
Mn (II)	50	50
Fe (III)*	50	50
Co (II)	20	20
Ni(II)	20	20

* Masked with F^-

Determination of Ir in presence of Pd and Os : The reaction between iridium and ATP or DATP takes place at elevated temperature while palladium and osmium react completely at room temperature. Based on this behaviour palladium and osmium were extracted into chloroform before heating. The remaining aqueous solution was heated for 75 min. with the ligand solution as described in the procedure and the iridium complex extracted. The absorbance of the extract, even in the presence of 10-fold excess of palladium and osmium, was identical with that found in absence of palladium and osmium.

CONCLUSION

The use of ATP or DATP as a reagent for iridium (III) compares favourably in selectivity and sensitivity with other reagents [1-3] known for this purpose. The present method is simple and affords fairly wide pH range for extraction. ATP is comparatively more sensitive than DATP.

ACKNOWLEDGEMENT. The authors gratefully acknowledge the award of C.S.I.R. fellowship to one of them (A.K.S.).

Revue Roumaine de Chimie, 23, 7, 1157 1159 (1978)

COMPTES RENDUS

"Flavonoids and Bioflavonoids. Current Research Trends" Proceedings of the Fifth Hungarian Bioflavonoid Symposium, Matrafüred, Hungary. Edited by L. Farkas, M. Gábor and F. Kállay, Akadémiai Kiadó, Budapest, 1977, 467 p.

The book represents a collection of the communications which were presented at the 5th Hungarian Bioflavonoid Symposium, held from 25 to 27th May 1977. The book was produced utilising the camera-ready technique, in order to ensure the publication in the same year (1977).

As compared with the book dedicated to the previous symposium (Akadémiai Kiadó, Budapest, 1975, reviewed in *Rev. Roumaine Chim.*, **22**, 313 (1977)), an important increase could be seen in the number of pages (from 286 to 467), contributors (from 46 to 90) and contributions (from 27 to 43). Among the contributors are well-known investigators of this field, from Hungary (L. Farkas, M. Gabor, F. Kállay, R. Bognar) as well as from 10 European countries (J. Chopin, F. Delle Monache, G. B. Marini-Bettòlo, L. A. Griffits, M. N. Zaprometov, H. Wagner).

The subjects of communications cover a large area, starting from the most recent topics of flavonoid chemistry, passing to modern physical methods used for structure determination, reaching then the important aspects of flavonoid biochemistry.

From the numerous interesting problems developed, we could mention here only a few ones, concerning: (a) *structure:* isolation of flavones with triphenylmethane structure, structure of natural procyanidins, synthesis of rare methyl ethers of naturally occurring polyhydroxyflavonols; (b) *reactions:* applications of oxidative rearrangements of chalcones by thallium (III) nitrate, reactions of flavones with hydroxylamine, nucleophylic substitution reaction of flavonoids; (c) *physical methods:* chiroptical techniques (circular dichroism), $^{13}C-NMR$, $^{1}H-NMR$; (d) *biochemistry;* influence of bioflavonoids on the metabolism of vitamin C, synthesis of aromatic compounds in higher plants, absorption and metabolism of flavonoids in man.

Worthy of mention is the communication "New biologically active flavonoid derivatives", by R. Bognar and M. Rákosy. This very interesting survey (with 115 references) begins with the "story" of Szent-Györgyi's vitamin P and continues with an enumeration of the very numerous and important applications of flavonoid in therapy e.g.: drugs for increasing capillary resistance, coronary vasodilators, spasmolytics, muscular relaxants, CNS-stimulants, diuretics, drugs against ulcer and thrombosis as well as antiviral, antitumor and antibiotic action of some flavonoids.

Another interesting subject developed in the book is the study of some *phytoalexins* ("compounds produced in plant cells in response to fungal infection and inhibiting further development of that infection"). In this respect the communications by D. M. X. Donnely, "The synthesis and antifungal activity of 6-a-hydroxy-11-a-methylpterocarpans" and by G. B. Marini-Bettòlo and F. Delle Monache, "Flavonoids with uncommon structures"' are particularly interesting.

This book could be appreciated as a very interesting one for chemists and biochemists with interest in flavonoids; the rapid publication after the Symposium makes the book more valuable and useful.

M. Banciu

E. FLUCK and V. I. GOLDANSKII, eds., "Modern Physics in Chemistry", Academic Press, New York, 1977, vol. 1, 420 pp.

The hyperfine interaction between nuclei and electrons, and interactions between inner and outer electrons, are of great interest to many experimental methods of modern chemistry. The papers, contained in this volume, describe the basic principles of various physical methods such as electron paramagnetic resonance, nuclear quadrupole resonance, X-ray and Mössbauer spectroscopy. More emphasis is placed on the solution of chemical, physico-chemical and biological problems rather than the details of methodology.

In fact, the book edited by Professors Fluck and Goldanskii, is a collection of the following papers :

In the first two chapters V. I. Nefedov and, respectively O. I. Sumbaev discuss "Chemical Effects in X-Ray Spectroscopy", parts I and II.

Chapter III entitled "Electron Spin Resonance" is written by N. N. Bubnov and S.P. Solodonikov.

E. I. Fedin discusses "Nuclear Quadrupole Resonance" in chapter IV.

A review on "Chemically Induced Dynamic Nuclear Polarization" is given by A. L. Buchachenko in chapter V.

The following chapter, written by W. Meisel, deals with "Mössbauer Double Resonance".

In chapter VII V. I. Goldanskii and V. P. Shantorovich write a paper entitled "Positronium in Chemistry".

In the last chapter of the book, V. G. Firsov and L. I. Ponomarov deal with "Mesic Chemistry".

The book ends with an author and a subject index.

The first chapters generally refer to the methods which already found many applications, and they also tend to lay some emphasis on future developments. The last two chapters cover methods which are not yet unanimously adopted in chemistry, but these papers will give a new ground.

The work gives an excellent picture of the way in which modern physics is applied to chemistry. The authors of the chapters have effectively conveyed their sense of excitement about the field and in most instances, have identified those areas where important breakthrough can be predicted. Well written, by reputed experts, this book will be of real value to the scientists and advanced students in all branches of chemistry. Biologists also may have an important profit reading it.

T. Chirulescu

LOUIS P. HAMMETT, „Physikalische organische Chemie", Akademie-Verlag, Berlin, 1976, 413 Seiten.

Das Buch des Professors Louis P. Hammett stellt eine Überarbeitung der ersten Auflage dar, und wuchs aus Vorlesungen und Seminarien heraus, die der Verfasser als Gast mehrerer Institute der Vereinigten Staaten halten konnte.

Die Physikalische organische Chemie beschäftigt sich mit der Untersuchung der Erscheinungen der organischen Chemie mit quantitativen und mathematischen Methoden. Eine der Hauptrichtungen, in denen sich das Fach entwickelte, war die Untersuchung — mit quantitativen Methoden — der Reaktionsmechanismen und der verwandten Probleme des Effektes von Struktur und Umgebung auf die Reaktivität. In keiner anderen Richtung wurden Resultate von so unmittelbar praktischer Bedeutung für das Grundproblem der Chemie, die Kontrolle von chemischen Reaktionen, erzielt. Dieser Teil der physikalischen Chemie ist Gegenstand der vorliegenden Veröffentlichung. Man muß herausstreichen, daß das Buch eine einheitliche und zusammenhängende Behandlung auf der Grundlage von wenigen einfachen Verallgemeinerungen und Theorien bietet. Es werden die Reaktionsgeschwindigkeiten, Gleichgewichte und Mechanismen in der organischen Chemie besprochen.

Das Buch umfaßt zwölf Kapitel, ein Autoren- und ein Sachverzeichnis.

Das erste Kapitel stellt eine Einleitung dar.

Im zweiten Kapitel werden die Grundprinzipien der Thermodynamik von Reaktionen in Lösung dargestellt. Hier werden die Begriffe des chemischen Pontentials und der Aktivität sowie die Gibbs-Duhem-Gleichung erläutert. Es werden die Änderung der Gibbs-Energie bei einer Reaktion, die Konzentrationsabhängigkeit der molaren Enthalpie und der molaren Entropie, sowie der Einfluß der Temperatur auf die Werte der Gleichgewichtskonstante dargestellt. Weiter wird die experimentelle Bestimmung der Enthalpi und der Standard-Entropie einer Reaktion behandelt.

Das dritte Kapitel ist dem Beitrag der statistischen Mechanik zur Bildung erfolgreicher Modelle für chemische Reaktionen gewidmet. Es werden die statistische Mechanik eines idealen Gases und einer gelösten Substanz in verdünnter Lösung, sowie das Problem des Zusammenhangs von Struktur und Reaktivität diskutiert.

Das vierte Kapitel ist der Behandlung von kinetischen Daten gewidmet. Es werden die Beziehung zwischen Geschwindigkeit und Gleichgewicht, die Bestimmung der Reaktionsordnung und das Problem der Präzision behandelt.

Die Theorie des Übergangszustandes und die Katalyse werden ausführlich im fünften Kapitel dargestellt.

Die Besonderheiten einiger Substitutionsreaktionen werden im sechsten Kapitel diskutiert.

Das siebente Kapitel ist auf die Salzeffekte auf Reaktionen in wäßrigen oder nichtwäßrigen Lösungen ausgerichtet, während das achte Kapitel dem Einfluß des Lösungsmittels auf die Reaktivität gewidmet ist.

In den nächsten zwei Kapiteln werden die Besonderheiten der Reaktionen, an denen Säuren und Basen beteiligt sind, behandelt. Die Bestimmung der Azidität, die Aziditätsfunktionen und der Begriff der Basenstärke werden diskutiert. Eine besondere Aufmerksamkeit wird der Geschwindigkeit von Reaktionen, an denen Säuren und Basen beteiligt sind, geschenkt.

Im elften Kapitel werden die quantitativen Beziehungen zwischen Struktur und Reaktivität dargestellt. Dementsprechend werden lineare Freie-Energie-Beziehungen zwischen verschiedenen Reaktionen, sowie der Einfluß von sterischen und induktiven und von Resonanz- und Lösungsmitteleffekten behandelt.

Das letzte Kapitel befaßt sich mit dem Problem des Einflusses der Struktur auf Enthalpie- und Entropieänderungen. Die isokinetische Beziehung zwischen Enthalpie- und Entropieänderungen, sowie die statistisch-mechanischen Betrachtungen werden vorgeführt.

Das Gebiet der Radikal-Reaktionen und die Molekülorbital-Theorie werden in diesem Buch nicht behandelt ; da diese Probleme schon Gegenstände einiger ausführlicheren Bücher waren, zieht der Verfasser vor, sie hier gar nicht zu diskutieren.

Um eine enzyklopädische Prägung zu vermeiden, also die Diskussion aller Reaktionen mit bekannten Mechanismen, zog der Autor es vor Beispiele auszuwählen, die das Vorgehen bei reaktionsmechanistischen Untersuchungen illustrieren. Er hofft indessen, daß die Behandlung der Prinzipien, von denen man bei der Untersuchung von heterolytischen Reaktionen in Lösung Gebrauch macht, gründlich genug ist, so daß das Buch sowohl für den Studenten der physikalischen und der organischen Chemie als auch für den praktisch tätigen Forscher von Nutzen sein wird.

Mihai Dărângă

NOTE POUR LES AUTEURS

La Revue Roumaine de Chimie publie des articles en anglais, français, russe, allemand ou espagnol. Les auteurs sont priés d'envoyer des articles et des comptes rendus inédits.

Les manuscrits seront dactylographiés à deux intervalles. La bibliographie, les tableaux et la légende des figures seront placés après le texte.

Si l'article fait partie d'une série numérotée, le titre de la partie précédente sera indiqué dans une note au bas de la première page.

Chaque article sera précédé d'un résumé comprenant quinze lignes au maximum. Les références bibliographiques dans le texte seront faites par des exposants sans parenthèses et paraîtront comme des notes au bas de chaque page.

Les publications périodiques mentionnées dans la bibliographie seront présentées suivant les prescriptions internationales : le nom de l'auteur précédé de l'initiale du prénom, le titre du périodique abrégé conformément à « Chemical Abstracts », et souligné par une ligne, le numéro du tome indiqué par des chiffres arabes et souligné par deux lignes, suivi de la première page de l'article ; à la fin, l'année de la parution sera placée entre parenthèses. Le numéro de la revue ne sera pas indiqué si les pages du volume sont numérotées consécutivement.

Les textes des livres ou traités inclueront : les noms des auteurs, les initiales du prénom, le titre du livre entre guillemets et sans être souligné, le numéro du tome précédé par l'abréviation « vol. » (ou « Bd. »), le numéro de l'édition, les éditions (the publisher), la localité de la parution du livre, l'année de la parution et la page de la référence précédée(s) par l'abréviation « p » (ou « S »).

Les brevets seront indiqués comme suit : L'auteur ou la firme, le pays et le numéro du brevet, la date et la revue (Chem. Abstr.). Par ex. : M. Jones (to Union Carbide Co.), Brit. Pat. 601 238, 2 sept. 1959, Chem. Abstr., **54**, 12808 (1960).

Les diagrammes seront tracés à l'encre de Chine sur papier calque. Les tableaux et les figures (en nombre strictement nécessaire) seront numérotés par des chiffres arabes. Les courbes dans les figures seront numérotées par des chiffres arabes et leur explication sera donnée dans la légende des figures. Prière de ne pas inscrire les mêmes données dans les tableaux et les figures. Chaque tableau aura un titre. On indiquera dans le texte la place approximative des tableaux et des figures. Les formules chimiques seront incluses dans le texte ; en outre, elles seront transcrites sur papier calque, à l'encre de Chine.

Les auteurs sont priés d'indiquer les caractères italiques (en soulignant les lettres au crayon), ainsi que tout autre caractère spécial : les préfixes *ortho*, *meta*, *para*, *cis*, *trans*, etc. seront soulignés pour indiquer leurs caractères italiques et ne seront jamais écrits avec des majuscules.

Aucune correction à la main ne sera admise sur le manuscrit. Les corrections seront frappées à la machine. Les lettres grecques ou autres symboles spéciaux seront insérés à la main à l'encre clairement.

Le manuscrit sera signé par l'auteur.

Le colonne-titre aura 50 lettres au maximum.

L'entière responsabilité du contenu des articles appartient aux auteurs.

PRINTED IN ROMANIA

TRAVAUX PARUS AUX ÉDITIONS DE L'ACADÉMIE DE LA RÉPUBLIQUE SOCIALISTE DE ROUMANIE

C. DRĂGULESCU, E. PETROVICI, **Chimie structurală modernă. Chimia coordinanţei 8** (Chimie structurale moderne. La Chimie de la coordinence 8), 1977, 947 p., 70 lei.

P. BALTĂ, E. BALTĂ, **Introduction to the physical chemistry of the vitrous state**, coédition avec Abacus Press, Kent, 1976, 287 p., 31 lei.

I. G. MURGULESCU, **Introducere în chimia fizică. Vol. I. 1. Atomi. Molecule. Legătură chimică** (Introduction à la Chimie physique. Ier vol. 1re Partie. Atomes. Molécules. Liaison chimique), 1976, 560 p., 2 pl., 36 lei.

GR. POPA, ŞERBAN MOLDOVEANU, **Reactivii organici în chimia analitică** (Les réactifs organiques dans la Chimie analytique), 1976, 255 p., 18 lei.

I. ZUGRĂVESCU, MAGDA PETROVEANU, **N-ylid Chemistry**, 1976, coédition avec McGraw-Hill International Book Company, SUA, 396 p., 33 lei.

C. V. UGLEA, **Cromatografia pe gel permeabil. Noi domenii de aplicare** (La chromatographie sur gel perméable. Nouveaux domaines d'application), 1976, 123 p., 6,75 lei.

I. GĂLĂŢEANU, **Radiochimia aplicată. Metode şi probleme** (La radiochimie appliquée. Méthodes et problèmes), 1976, 307 p., 19 lei.

FRANCISC A. GOTHARD, **Echilibre lichid-vapori. I. Baze teoretice şi metode de calcul** (Equilibres liquide-vapeurs. I. Bases théoriques et méthodes de calcul), 1975, 263 p., 2 pl., 28 lei.

CONST. GH. MACAROVICI, D. MACAROVICI, **Chimia oxizilor dubli şi utilizările lor** (La chimie des oxydes doubles et leur utilisation), 1975, 195 p., 13 lei.

ELENA CEAUŞESCU, **Research work on synthesis and characterization of macromolecular compounds. Contributions**, 1974, 251 p., 20 lei.

M. AVRAM, **Antidăunători** (Pesticides), 1974, 496 p., 41 lei.

DUMITRU COSTACHE, **Analiza chimică prin metoda cinetică** (L'Analyse chimique par la méthode cinétique), 1974, 276 p., 15,50 lei.

G. A. RĂDULESCU, **Proprietăţile ţiţeiurilor româneşti** (Les propriétés des pétroles roumains), 1974, 267 p., 2 pl., 18 lei.

CR. SIMIONESCU, VIORICA RUSAN, V. POPA, **Chimia algelor marine** (La chimie des algues marines), 1974, 212 p., 1 pl., 18 lei.

MARIA FITI, **Dozimetria chimică a radiaţiilor ionizante** (La dosimétrie chimique des radiations ionisantes), 1973, 240 p., 13,50 lei.

TIBERIU NĂŞCUŢIU, **Metode radiochimice de analiză** (Méthodes radiochimiques d'analyse), 1973, 384 p., 23 lei.

CR. SIMIONESCU, MARGARETA GRIGORAŞ, AGATA CERNĂTESCU-ASANDEI, GH. ROZMARIN, **Chimia lemnului în România. Plopul şi salcia** (La Chimie du bois en Roumanie. Le peuplier et le saule), 1973, 299 p., 13 pl., 26 lei.

MIHAI FLORESCU, **Eficienţa economică a cercetării ştiinţifice** (L'Efficience économique de la recherche scientifique), 1972, 115 p., 15 lei.

1978 NOV 27

I. P. Informaţia. – c. 300

43426

Lei 25.–
$ 45 (price per year)

F 1103

ACADÉMIE DE LA RÉPUBLIQUE SOCIALISTE DE ROUMANIE

REFERÁLVA

REVUE ROUMAINE DE CHIMIE

TOME 23
N° 8
Août 1978

EDITURA ACADEMIEI REPUBLICII SOCIALISTE ROMÂNIA

Rev. Roumaine Chim.

RECHAX, 23, *8*, p. 1161—1350 (1978), Bucarest

ACADÉMIE DE LA RÉPUBLIQUE SOCIALISTE DE ROUMANIE

COMITÉ DE RÉDACTION

Rédacteur en chef:

I. G. MURGULESCU, membre de l'Académie de la République Socialiste de Roumanie

Rédacteurs en chef adjoints:

A. T. BALABAN et V. EM. SAHINI, membres correspondants de l'Académie de la République Socialiste de Roumanie

Collège de rédaction:

EM. BRATU, ELENA CEAUŞESCU, ECATERINA CIORĂNESCU-NENITZESCU, CR. SIMIONESCU, membres de l'Académie de la République Socialiste de Roumanie; P. SPACU, membre correspondant de l'Académie de la République Socialiste de Roumanie; MARGARETA AVRAM, I. HAIDUC, D. I. MARCHIDAN, I. MOLDOVAN, G. NIAC, D. SĂNDULESCU et Z. SIMON

La Revue Roumaine de Chimie paraît 10 fois par an. Toute commande de l'étranger (fascicules ou abonnements) sera adressée à ILEXIM Departamentul Export-Import Carte (Livres)/Departamentul Export-Import Presă (Revues), P.O.B. 136–137, télex 11226, 3 str. 13 Decembrie, 70116 Bucarest 12, Roumanie

Les manuscrits, les livres et les revues proposés en échange, ainsi que toute correspondance seront envoyés à la rédaction:

REVUE ROUMAINE DE CHIMIE

Calea Victoriei, 125, 71021 Bucarest, Roumanie, téléphone 50 76 80

EDITURA ACADEMIEI REPUBLICII SOCIALISTE ROMÂNIA
125, Calea Victoriei, 71021 Bucarest, Roumanie, téléphone 50 76 80

1978 SEP 27
1883

REVUE ROUMAINE DE CHIMIE

Tome 23, N° 8 Août 1978

E. CHIFU, MARIA TOMOAIA, ELENA NICOARĂ and AURORA OLTEANU, Isozeaxanthin films at the oil/water and air/water interfaces 1163–1169

RODICA VÎLCU, MINODORA LECA and MIHAELA OLTEANU, Contraction of polyacrylamides in electrolyte solutions 1171–1178

D. R. ARMSTRONG, R. FORTUNE and P. G. PERKINS, A molecular- orbital study of the ground and excited-state properties of metallocenes of the first-row transition-metal ions. II. 1179–1202

R. H. SCHUSTER und I. A. SCHNEIDER, The environment influence on solvolysis of alkyl halides. III. Observations concerning the solvent dependence of correlation factor log*k* *versus* log$[H_2O]$ (in German) . . . 1203–1212

P. I. PREMOVIČ, *g*-Values of trigonally distorted octahedral d^1 systems: the $Ti(H_2O)_6^{3+}$ complex ion in frozen aqueous solutions 1213–1232

M. VLAD and M. DRAGOŞ, Concentration fluctuations in chemical systems with nondegenerate reactions. A thermodynamic approach 1233–1242

SILVIA BARBU and CONST. GH. MACAROVICI, Physico-chemical study of some thiocarbohydrazone of aromatic and heteroaromatic aldehydes (in German) 1243–1249

A. C. BANCIU, Electronic and IR spectra of some new square-planar complexes with $Ni(d^8)-N(sp^2)$ bonds 1251–1259

N. S. BIRADAR, V. B. MAHALE and B. R. HAVINALE, Divalent manganese complexes with ligands containing O–N–N–O sequence . . . 1261–1266

ANGELA KRIZA and MARTHA NASTA, On titanium (IV) compounds with Schiff bi- and three-dentate bases (in French) 1267–1273

V. KUMARI, R. C. SHARMA and G. K. CHATURVEDI, Potentiometric studies on ternary complexes of Zn(II) 1275–1278

R. S. SINDHU, K. B. PANDEYA and R. P. SINGH, Polarographic behaviour of complexes of cadmium(II) and lead(II) with 3-hydroxypyridine-2-thiol 1279–1282

V. DRĂGUŢAN, ZS. ARVAY and ALICE MARIE GLATZ, Aluminium chloride catalyzed reactions of unsaturated acids with benzene. XII. Methyl esters of cyclohexylideneacetic and 1-cyclohexenylacetic acids 1283–1289

LEELA PARDESHI, A. RASHEED and R. A. BHOBE, Studies in spectral and magnetic properties and non-isothermal decomposition of pyridine adducts of some salts of fatty acids 1291–1301

Rev. Roumaine Chim. **23**, *8*, p. 1161–1350 (1978) Bucarest

SVETLANA DUMITRESCU, V. PERCEC and CR. I. SIMIONESCU, On the polymerization of acetylenic derivatives. XXXI. Electron spin resonance of polyarylacetylene isomers 1303–1311

GH. DRĂGAN, Amorphous-crystalline coupling in polyethylene. VIII. Relativistic effects in disclination state forming processes 1313–1323

J. CLAUS and E. MARÉCHAL, Physico-chemical study of poly(2, 4-dimethylstyrene) obtained by cationic polymerisation (in French) 1325–1335

CECILIA SAVII, T. P. TĂVALĂ, N. GR. BRÎNZAN and G. G. SAVII, Computation program concerning the resulting colour of pigment mixtures . . 1337–1340

M. S. SUBHANI and T. KAUSAR, Flash photolysis study of TeO_3^{2+} anion in aqueous solution 1341–1344

MARIA MIOŞCU and MARIA GREBLĂ, Liquid-liquid interfaces as potentiometric ion-sensors. III. The n-octanol-aqueous solution interface in the acid-base potentiometric titration 1345–1347

BOOK REVIEWS 1349

Revue Roumaine de Chimie, **23**, *8*, 1163–1169 (1978)

ISOZEAXANTHIN FILMS AT THE OIL/WATER AND AIR/WATER INTERFACES

E. CHIFU, MARIA TOMOAIA, ELENA NICOARĂ and AURORA OLTEANU
"Babeş-Bolyai" University, str. Arany János nr. 11,
Department of Physical Chemistry,
Cluj-Napoca, Romania

Received August 10, 1977

Films of all-*trans*-isozeaxanthin at the benzene/water interface and at the air/water interface have been studied by means of interfacial tension and surface pressure measurements. The limiting molecular areas at the two interfaces indicate that the interfacial film (benzene/water) is more expanded than the monomolecular film (air/water). The standard free energy of adsorption at the benzene/water interface and the surface compressional modulus at the air/water interface have been calculated. The results are compared with those previously reported for all-*trans*-canthaxanthin films.

Monomolecular layers and bilayers are artificial systems used to simulate the properties of natural membranes. [1,2]

One of the widely used model systems for biological membranes is the film state [3], which may be looked upon as a half-membrane.

Research on carotenoidic pigments in film is of great interest because these substances are components of biological membranes. [4] The study of carotenoids in film state was started only a few years ago. [5–12]

[1] D. A. CADENHEAD, J. F. DANIELLI and M. D. ROSENBERG, "Progress in Surface and Membrane Science", vol. 9, Acad. Press, New York, 1975, p. 223.

[2] D. A. CADENHEAD, J. F. DANIELLI and M. D. ROSENBERG, "Progress in Surface and Membrane Science", vol. 8, Academic Press, New York, 1974, p. 119.

[3] G. L. GAINES, JR. "Insoluble Monolayers at Liquid – Gas Interfaces", Interscience, New York, 1966.

[4] O. ISLER, "Carotenoids", Birkhäuser Verlag, Basel, 1971.

[5] V. LEJEUNE and C. TRIC, *J. Chim. phys.*, **68**, 105 (1971).

[6] R. E. BROCKMAN and S. S. BRODY, *Z. Naturforsch.*, **26 b**, 119 (1971).

[7] S. S. BRODY, *Z. Naturforsch.*, **28 c**, 97 (1973).

[8] N. YCKOWSKI and S. S. BRODY, *Z. Naturforsch.*, **29 c**, 327 (1974).

[9] R. M. LEBLANC and B. H. ORGER, *Biochim. Biophys. Acta*, **275**, 102 (1972).

[10] S. HOTCHANDANI, R. M. LEBLANC and F. BOUCHER, *Vision Res.*, **15**, 605 (1975).

[11] E. CHIFU, M. TOMOAIA, and A. IOANETTE, *Gazz. chim. Ital.*, **105**, 1225 (1975).

[12] M. TOMOAIA, A. IOANETTE and E. CHIFU, "Proceedings International Conference Colloid and Surface Science", vol. 1, Akad. Kiado, Budapest, 559 (1975).

The aim of the present work is to study the behaviour of all-*trans*-isozeaxanthin at the benzene/water and air/water interfaces. The structure of this compound is shown in Figure 1. Isozeaxanthin is a carotenoidic product of considerable importance to biochemists, because of its role of intermediary in the biosynthesis of ketocarotenoids.

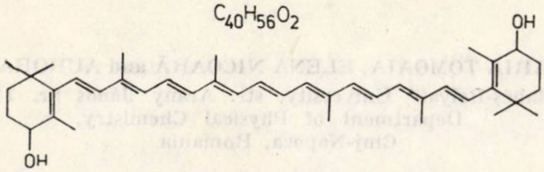

Fig. 1 — Structure of all-*trans*-isozeaxanthin (4,4′ — dihydroxy — β — carotene).

EXPERIMENTAL

The isozeaxanthin used in our experiments was a synthetic product, obtained by the selective reduction of all-*trans*-canthaxanthin. The purity of this substance was checked by thin layer chromatography. As oil phase, reagent grade benzene "Reactivul" București was used and the aqueous phase was doubly-distilled water. Measurements were made on freshly prepared benzene solutions of isozeaxanthin, stored in the dark in order to avoid the possible degradation of the carotenoidic pigment. Two kinds of measurements were performed :

— interfacial tension measurements, at the benzene solution of isozeaxanthin/water interface,

— surface pressure measurements of the monomolecular film of isozeaxanthin at the air/water interface.

The interfacial tensions, σ(dyn/cm), were measured at 25 ± 0.1°C by the du Noüy method, within ± 0.05 dyn/cm, using a double-wired tensiometer, [13] equipped with a platinum ring.

The surface pressures, π (dyn/cm), of the monolayers were measured by means of the Wilhelmy method, [3] using doubly-distilled water as subphase and benzene as spreading liquid. The experimental procedure has been described in our previous report. [11] The accuracy of the surface pressure measurements was of ± 0.5 dyn/cm; the isotherms surface pressure π vs. area A were reproducible to within ± 2 Å^2/molecule.

RESULTS AND DISCUSSION

THE INTERFACIAL FILM OF ISOZEAXANTHIN AT THE BENZENE/WATER INTERFACE

The interfacial tension, σ (dyn/cm), at the interface between benzene solution of isozeaxanthin and water, strongly varies with time, t(min), as can be seen in Figure 2, for some systems of differing concentrations (c, mole/l) of isozeaxanthin. As the static value of the interfacial tension, that one corresponding to the time value of 200 min was taken into account.

By using the static values of the interfacial tension, the isotherm of σ versus the concentration logarithm was constructed, as shown in Figure 3. The linear region slope of the curve was considered since it

[13] G. Piccardi, Ital. Pat. 462316 (1950—1951).

corresponded to low interfacial tension values, i. e. to the closest packing of molecules in the film. [14]

By means of the well-known Gibbs' equation,

$$\frac{\partial \sigma}{\partial \ln c} = - RT\Gamma \qquad (1)$$

Γ, mole/cm^2, being the adsorption, the maximum adsorption was calculated from the slope of the linear portion by means of the least squares method. Hence, the limiting area of the isozeaxanthin at the benzene/water interface was found to be : $A_0 = 74 \pm 2$ Å^2/molecule.

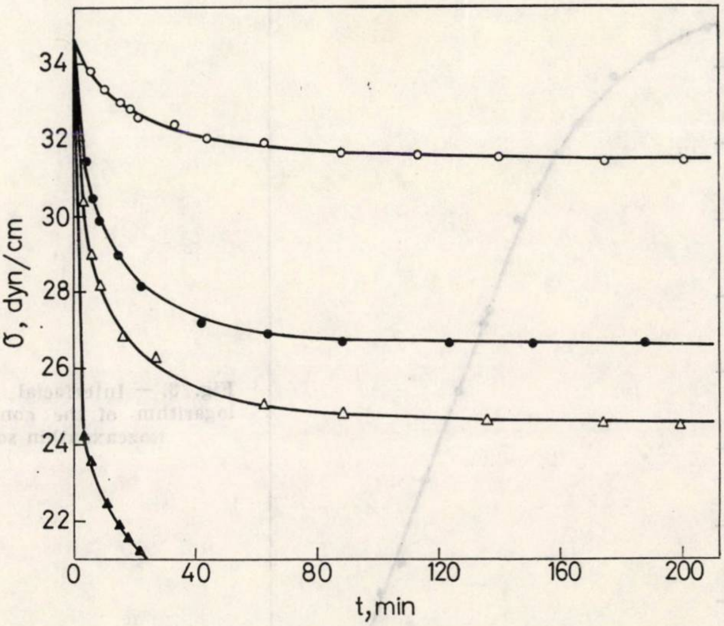

Fig. 2. — Interfacial tension, σ, versus time, t, isotherms for benzene solutions of isozeaxanthin — water. The concentrations of isozeaxanthin (M) are : 4.7×10^{-5} (○); 1.42×10^{-4} (●); 2.0×10^{-4} (△); 5.29×10^{-4} (▲).

The experimental data concerning the static interfacial tension variation as a function of the concentration, respectively the mole fraction of isozeaxanthin, were processed by a computer. It was found that the static interfacial tension dependence on the mole fraction is given by the cubic equation :

$$\sigma = - 5.2438 . 10^{13}\, x^3 + 1.0204 . 10^{10}\, x^2 - 6.9847 . 10^5\, x + 34.28 \qquad (2)$$

---

[14] R. Defay, I. Prigogine, A. Bellemans and D. H. Everett, "Surface Tension and Adsorption", Longmans Green, London, 1966, p. 94.

Furthermore, the standard free energy of adsorption,[15–17] ΔG^0 (kJ/mol), was estimated by the relationship :

$$\Delta G^\circ = -RT\ln\left(\frac{\pi}{x}\right)_0 \frac{x_s}{\pi_s} \tag{3}$$

where π_s is the standard interfacial pressure, independent of the temperature and x_s is the standard mole fraction for the bulk phase. The standard states are $\pi_s = 1$ dyn/cm (or 1mN/m) for the interfacial layer and $x_s = 1$ for the bulk phase, in which the solute would behave as in an ideal dilute solution. The interfacial pressure π equals, as well known, the difference $\sigma_0 - \sigma$, in which σ and σ_0 are the interfacial tensions corresponding to the x and, respectively, the zero value of the mole fraction. The $\left(\frac{\pi}{x}\right)_0$ quantity

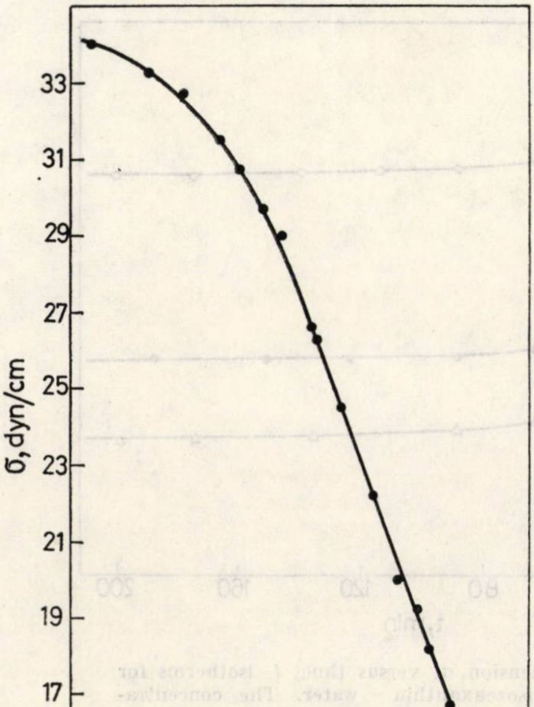

Fig. 3. — Interfacial tension vs. logarithm of the concentration of isozeaxanthin solution.

---

[15] J. J. Betts and B. A. Pethica, *Trans. Faraday Soc.*, **56**, 1515 (1960).

[16] R. Aveyard and B. J. Briscoe, *Trans. Faraday Soc.*, **66**, 2911 (1970).

[17] R. Aveyard and J. Chapman, *Canad. J. Chem.*, **53**, 916 (1975).

in Eq. (3) represents the initial slope of the curve π vs. x, for $x \to 0$. It was evaluated by deriving the equation (2), because :

$$\left(\frac{\pi}{x}\right)_0 = -\left(\frac{\mathrm{d}\sigma}{\mathrm{d}x}\right)_0 \tag{4}$$

By introducing the derivative from (4) into Eq. (3), the standard free energy of adsorption was calculated : $\Delta G^\circ = -33.3 \pm 0.1$ kJ/mol.

For comparison, we have revised our previously published experimental data, [11] concerning the static interfacial tension variation with the mole fraction for the interfacial film of all-*trans*canthaxanthin at the benzene//water interface.

Canthaxanthin (4,4′ — diketo—β—carotene) is a compound having a structure that is similar to isozeaxanthin, but differing from the latter only by the nature of the polar groups (keto-instead of hydroxyl-groups).

By mathematical processing of the experimental data it was found that the dependence of the static interfacial tension on the mole fraction for canthaxanthin was of the same type as in the case of isozeaxanthin :

$$\sigma = -\,6.6439\ 10^{13}\ x^3 + 1.0640\ 10^{10}\,x^2 - 6.2110\ 10^5\,x + 33.54 \tag{5}$$

In the way presented above, by using now Eqs. (5) and (3) the standard free energy value was estimated for the adsorption of canthaxanthin at the benzene/water interface : $\Delta G^\circ = -\,33.0 \pm 0.2$ kJ/mol. One finds that the standard free energies for the adsorption of isozeaxanthin and for that of canthaxanthin at the benzene/water interface are approximately the same. This fact would agree with the small difference between the polarities of the two substances.

THE MONOMOLECULAR FILM OF ISOZEAXANTHIN AT THE AIR/WATER INTERFACE

This film was studied by means of the compression isotherms : surface pressure π vs. area A. In Figure 4, an example is shown, from ten experiments. By extrapolating to $\pi = 0$, the high pressure linear portion of the π vs. A isotherm, the limiting value $A_0 = 60 \pm 2$ Å^2/molecule was obtained, independently of the quantity of spreaded substance.

By the aid of the compression isotherm, the surface compressional modulus,

$$C_s^{-1} = -A\left(\frac{\partial\pi}{\partial A}\right)_T$$

was also evaluated by using the linear-region slope of the isotherm for high pressures, with $A = A_0$. The value $C_s^{-1} = 110$ dyn/cm is found, that is a compressional modulus situated to the inferior limit of the admitted values for the bidimensional state of condensed liquid.[18]

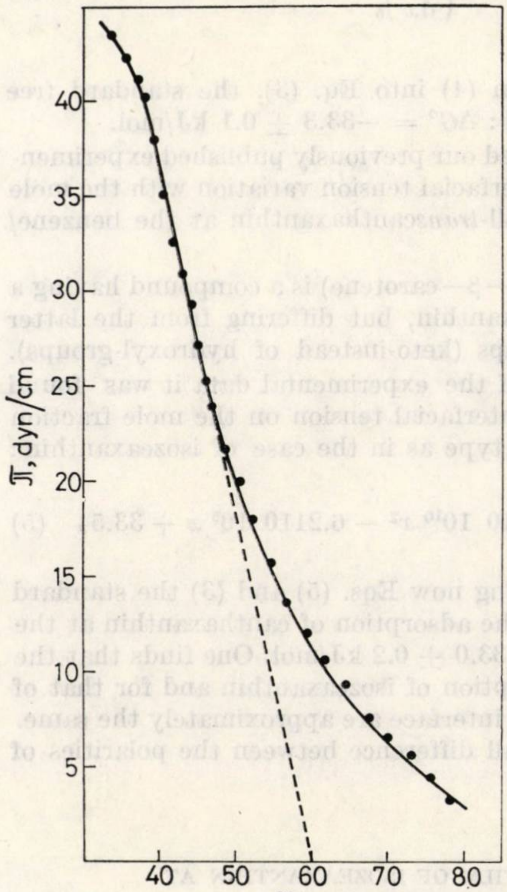

Fig. 4. — Surface pressure, π, vs. area, A, compression isotherm for isozeaxanthin film at the air — water interface.

CONCLUSIONS

We have listed in the table the values of the limiting molecular areas A_0, at the benzene/water and air/water interfaces, as well as those of the standard free energies of adsorption ΔG° (at benzene/water interface), and of the compressional moduli C_s^{-1} (at air/water interface) for the isozeaxanthin films. For comparison, we also present the corresponding values obtained on canthaxanthin.[11]

---

[18] J. T. Davies and E. K. Rideal, "Interfacial Phenomena", Academic Press, New York, 1963, p. 265.

Table 1

Limiting molecular areas, A_0, standard free energies of adsorption ΔG^0, and surface compressional moduli C_s^{-1}, for isozeaxanthin and canthaxanthin films

Film	Interface	A_0 (Å^2/molecule)	$-\Delta G^0$ (kJ/mol)	C_s^{-1} (dyn/cm)
Isozeaxanthin	benzene/water	74±2	33.3±0.1	—
	air/water	60±2	—	110
Canthaxanthin	benzene/water	74±2	33.0±0.2	—
	air/water	60±2	—	145

One finds that the limiting molecular areas are identical at one and the same interface. This suggests an identical orientation of the two sorts of molecules with respect to the interface.

The values of the standard free energies of adsorption are practically the same for the two substances.

The values of the compressional moduli are situated between the admitted limits for the bidimensional state of condensed liquid (100—— 250 dyn/cm).[18]

Relatively large values of the limiting molecular areas, as those obtained by us for isozeaxanthin, were also found in the case of other carotenoids or substances with conjugated polyene chain.[5-12]

These large areas can be explained by the existence of β-ionone rings and side methyl groups, as well as by unsaturation of the chain. Generally,[10,19] the presence of branched or unsaturated chains interferes with the closed packing of the molecules in bidimensional state and results in the expansion of the film.

Comparison of the limiting area values obtained at the benzene/water interface with those obtained at the air/water interface leads us to the conclusion that the film at the benzene/water interface is more expanded than that at the air/water interface. The area increment is due to those benzene molecules which penetrate between the hydrocarbon chains of the interfacial film, tending to reduce attraction among chains.

---

[19] A. W. Adamson, "Physica Chemistry of Surfaces", Interscience, New York, 1967, p. 156.

Revue Roumaine de Chimie, 23, 8, 1171–1178 (1978)

CONTRACTION OF POLYACRYLAMIDES IN ELECTROLYTE SOLUTIONS

RODICA VÎLCU, MINODORA LECA and MIHAELA OLTEANU
Polytechnic Institute of Bucharest, Chemistry Department,
Bld Republicii 13, Romania

Received August 25, 1976

Conformational changes of some polyacrylamides having different degrees of hydrolysis were determined by viscosity measurements. The degrees of hydrolysis were measured by conductometric and pH-metric methods. The behaviour of the unhydrolyzed polyacrylamide in solution having different ionic strength, μ, is similar to that of poly (vinyl alcohol). As the degree of hydrolysis increases, they behave like a weak polyelectrolyte. The contraction of macromolecular chain has been evaluated by the ratios of the intrinsic viscosities : $[\eta]\,\mu/[\eta]_0$ and $[\eta]\,\mu/[\eta]_\infty$. The contraction is enhanced by the degree of hydrolysis and cationic charge at a constant ionic strength.

The adsorption of hydrolyzed and unhydrolyzed polyacrylamides on solid surfaces from aqueous solution is the basic phenomenon of the following applications : soil conditioning,[1–3] secondary recovery of oil and flocculation of mineral suspensions.[4] The adsorption takes place on the solid porous surfaces in the first two cases, while in the last one it occurs on the suspension particles bridging them by polymer molecules.

The adsorption of micromolecular compounds can be characterized either by adsorbed amount or by surface coverage, these two quantities being proportional. The conformation of polyelectrolyte molecules in solution depends on solvent strength, degree of hydrolysis of polyacrylamide and temperature. Depending on these parameters, the macromolecules can be adsorbed either as coils or as roades. The more extended the macromolecule, the higher the surface coverage for the same amount of adsorbed polymer on the surface unit. The number of bounded suspension particles also depends on the extension of macromolecule. Thus, the adsorption of macromolecules having an extended conformation is more suitable from economic point of view.

The water in which polyacrylamides are dissolved can be of various ionic strengths and, besides that, the ionic strength itself can be modified by mineral salts of the environment. In order to predict the efficiency of

---

[1] D. J. Greenland, *Soil Fert.*, **28**, 412, 521 (1965).

[2] M. M. Mortland, *Adv. Agron.*, **22**, 75 (1970).

[3] N. Schamp and J. Huyebroeck, *J. Polymer Sci.: Symposium*, **42**, 553 (1973).

[4] R. W. Slaeter and J. A. Kitchener, *Discuss. Faraday Soc.*, **42**, 267 (1966).

hydrolyzed and unhydrolyzed polyacrylamides, it is very important to know the dependence of the molecular dimension on the ionic strength and degree of hydrolysis.

Using viscosimetric measurements, we have studied the dependence of the molecular dimension on the ionic strength of solution for polyacrylamides having $\overline{M}_v = 3 \times 10^6$ and degrees of hydrolysis of 0 (PAA 0), 22 (PAA22) and 50 per cent (PAA50).

EXPERIMENTAL

Three Romanian-made polyacrylamides having $\overline{M}_v = 3 \times 10^6$ have been studied: PAA 50 as a gel of 8.1 % concentration (produced at Rîşnov), PAA 22 (Medasol 6) and PAA O (RS300) as powders (produced at Mediaş).

Viscosity-average molecular weights, $\overline{M}_v$, were determined, according to STAS 7614–66, with an Ubbelohde viscometer, dissolving the polymer in aqueous 1 kmol/m ^{3} sodium nitrate at 300 K. The molecular weights were calculated by means of the relation :[5]

$$[\eta] = 3.73 \times 10^{-4} M_v^{0.66} \qquad (1)$$

where $[\eta]$ is the intrinsic viscosity determined graphically.

Degrees of hydrolysis were determined both by conductometric and pH-metric methods. In conductometry,[6] 50 cm^3 PAA aqueous solution having 1 kg/m^3 concentration, 5 cm ^{3} 0.1 kmol/m^3 HCl and 100 cm^3 distilled water were titrated with 0.1 kmol/m^3 aqueous sodium hydroxide solution, using a Radelkis conductometer (Hungary). The instrument had a measuring range of 0.1×10^{-6} to 0.5S. The conductivity of solution was plotted against the volume of titrant. The straight line segment lying between the hydrochloric acid neutralization line and the excess sodium hydroxide line is a measure of the total carboxyl content of the sample (Figure 1).

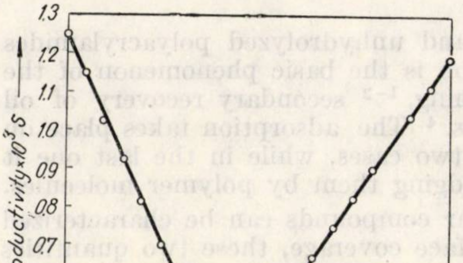

Fig. 1. — Conductometric determination of the degree of hydrolysis (PAA22).

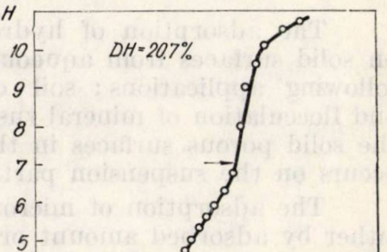

Fig. 2. — pH-metric determination of the degree of hydrolysis (PAA22).

The pH-metric method[7] consists in titrating a similar sample with 0.1 kmol/m ^{3} aqueous sodium hydroxide solution, using a MV84-type pH-meter (G. D. R.), having a GA 50 glass electrode and a calomel one as reference. The pH was plotted in terms of volume of titrant. The volume of base required to bring the polymer solution from pH 3.3 to pH 7.0 gives the total carboxyl content of the sample (Figure 2). The aqueous polymer solution was acidified with a strong mineral acid (HCl) to start from a pH of 3.0 or less. The per cent degree of hydrolysis is given, for both methods, by the relation :

---

[5] "Polyacrylamide" in New Product Bulletin, American Cyanamid Co., New York, 1955.

[6] H. F. Mark, N. G. Gaylor and N. M. Bikales, eds., "Encyclopedia of Polymer Science and Technology", vol. 1, Interscience Publishers, 1964, p. 194.

[7] D. J. Pye and J. A. Patterson, Can. Pat. 522851 (1956), cf. ref. 5.

$$\mathrm{DH}\,\% = \frac{V \times 44}{100 \times a} \tag{2}$$

where V is the base volume, in cm ^{3}, which neutralizes the carboxyl groups, 44 — the equivalent of carboxyl group, in g, and a the weight of polymer, in g. The precision was ± 1 per cent.

If the polymers contain some impurities, better results can be obtained by converting PAA into acid form before analysis by passing the water solution of the sample through a cation exchange resin column of Dowex 50W — X 8 (50 cm^3 1 kg/m^3 PAA solution is passed at a rate of about 1 cm^3/60 s through a column of 1.5 cm inside diameter containing 10 g of Dowex 50 W—X 8 ; the column is then washed with distilled water, obtaining finally a volume of 150 cm ^{3}).

Kinematic viscosities were determined at 298 K by using two Ubbelohde-type suspended level viscometers (Schott — F.R. of Germany) having the K constants 0.004887 (Oa-type) and 0.00976 (I-type) ; the temperature was kept constant within ± 0.05°. The viscometer covered the following viscosity ranges : Oa-type — 0.8×10^{-6} to 5×10^{-6} m^3/s and I-type — 1.2×10^{-6} to 10^{-5} m^3/s. The viscosity ν was then calculated according to the relation :

$$\nu = K(t - t_c) \tag{3}$$

where t_c is the Hagenbach/Couette correction, [8] which takes the kinetic energy into account.

RESULTS AND DISCUSSION

It is well known that intrinsic viscosity is a measure of the size of a macromolecule in solution.[9] The viscometry is the simplest method to study the dependence of macromolecule conformation on the pertinent variables.

The dependence of intrinsic viscosity on flexible macromolecule size was studied theoretically by Flory and Fox. [10] Assimilating the macromolecule to an equivalent sphere having the radius R_e which is ξ times the giration radius R_G, they obtained the following relationship :

$$[\eta] = \Phi(\overline{h^2})^{3/2}/M \tag{4}$$

where $\overline{h^2}$ was average square distance between the two ends, M — molecular weight and $\Phi = 4.291 \times 10^{20} \text{ x } \xi^3$, if $[\eta]$ was expressed in m^3/kg. In terms of the equivalent sphere radius, relation (4) becomes :[11]

$$[\eta] = \frac{1}{3} N R_e^3 / M \tag{5}$$

where N is the Avogadro number. For a given polymer, the ratio of intrinsic viscosities is a measure of the equivalent sphere radius ratio.

The intrinsic viscosity of unhydrolyzed polyacrylamide is relatively small in distilled water. By increasing the ionic strength of solution, the intrinsic viscosity decreases steadily, reaching a constant value (Table 1).

---

[8] W. Weber and W. Fritz, *Rheol. Acta*, **3**, 34 (1963).

[9] R. M. Fuoss, *Discuss. Faraday Soc.*, **11**, 125 (1951).

[10] P. J. Flory and T. G. Fox, Jr., *J. Amer. Chem. Soc.*, **73**, 1904 (1951).

[11] Ch. Tanford, "Physical Chemistry of Macromolecules", Wiley, New York, 1961.

Table 1

Viscometric data for polyacrylamides in aqueous kalium chloride solutions having different ionic strength

Degree of hydrolysis of polyacrylamide, %	μ, kmol/m^3	$1/\mu$	$[\eta]$, m^3/kg	$\frac{[\eta]\mu}{[\eta]_0}$	$\frac{[\eta]\mu}{[\eta]_\infty}$
0	0	∞	0.820	1.000	1.26
	0.125	8	0.670	0.817	1.03
	0.250	4	0.665	0.811	1.02
	0.500	2	0.660	0.805	1.01
	1.000	1	0.660	0.805	1.00
	∞	0	0.650	0.793	1.00
22	0	∞	6.800	1.000	8.70
	0.025	40	2.100	0.309	2.69
	0.075	13.3	1.500	0.220	1.92
	0.125	8	1.25	0.184	1.60
	0.250	4	1.12	0.165	1.43
	1.340	0.75	0.85	0.125	1.09
	∞	0	0.78	0.115	1.00
50	0	∞	10.700	1.000	12.59
	0.025	40	3.150	0.294	3.70
	0.050	20	2.720	0.254	3.20
	0.125	8	2.000	0.187	2.35
	0.250	4	1.500	0.140	1.76
	0.500	2	1.200	0.112	1.41
	1.000	1	1.1700	0.110	1.20
	∞	0	0.850	0.079	1.00

This behaviour is similar to that of poly (vinyl alcohol) [12]. The contraction of equivalent sphere in the ionic electric field can be explained as follows: in the absence of the electric field there is a tendency of mutual compensation of dipoles, so that the rotation of segments is somehow hindered. The macromolecule becomes less flexible and cannot accommodate itself in a minimum volume. In an ionic environment the dipole-moment of macromolecule tends to become higher, this process leading to an augmentation of freedom for rotation which results in a corresponding contraction of the macromolecule.

In electrolyte solutions, the hydrolyzed polyacrylamides behave like weak polyelectrolytes:[13,14] the intrinsic viscosity decreases with increasing ionic strength, μ (Table 1) and so does the slope of the straight line giving the reduced viscosity in terms of concentration. The straight lines $\eta_{SP}/c = f(c)$ for PAA50 at various ionic strength of aqueous kalium hydrochloride solution are plotted in Figure 3.

---

[12] J. Néel and H. Buc, *J. Chim. phys.*, **56**, 768 (1959).

[13] A. Oth and P. Doty, *J. Phys. Chem.*, **26**, 43 (1952).

[14] D. T. F. Pals and J. J. Hermans, *Rec. Trav. chim.*, **71**, 443 (1952).

The weak polyelectrolyte-like behaviour is due to the carboxyl groups resulted by hydrolysis. Therefore, the hydrolyzed polyacrylamides must behave as acrylamide-acrylic acid copolymers having different acrylic acid contents. The carboxyl groups dissociate partially in distilled water, leading to a molecule of weakly charged polymer. The macromolecule occupies a larger volume than the corresponding neutral molecule due to the electrostatic repulsion between the ions belonging to the same chain. If the degree of hydrolysis increases the molecular charge is higher and the volume in which it accommodates must be larger. The experimental results in table 1 confirm this statement.

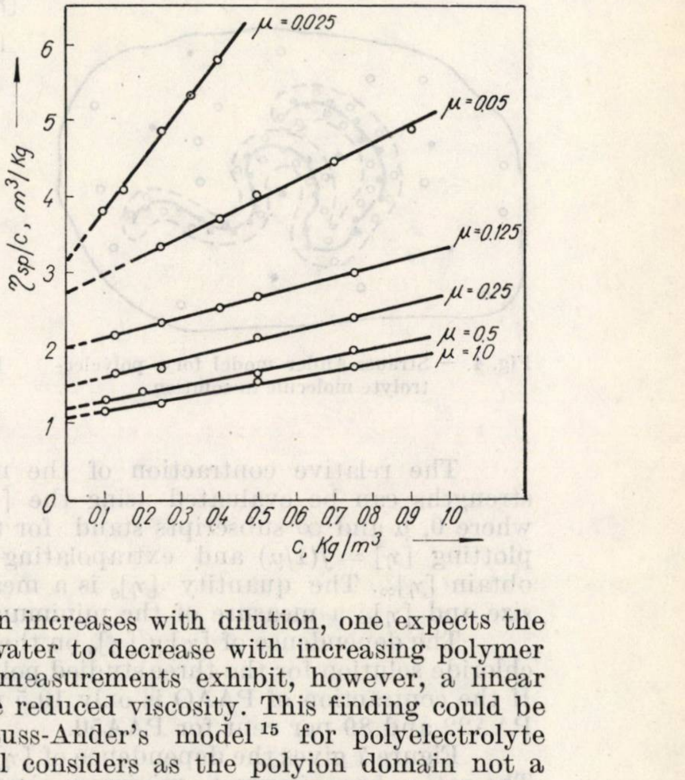

Fig. 3. — Reduced viscosity in terms of concentration at different ionic strengths of aqueous kalium chloride solutions.

As the degree of dissociation increases with dilution, one expects the macromolecule size in distilled water to decrease with increasing polymer concentration. The viscometric measurements exhibit, however, a linear concentration dependence of the reduced viscosity. This finding could be explained in terms of the Strauss-Ander's model[15] for polyelectrolyte solutions (Figure 4). This model considers as the polyion domain not a spherical volume surrounding the coiled polyion as a whole, but rather a sausage-shaped region separated by a membrane from the rest of the solution. For a salt-free polyelectrolyte system, a second layer of ionic atmosphere has to be added to the above model[16] (Figure 4). In the two-layer model the outside membrane separates the polyelectrolyte from the rest of the solution and the inner one separates the "free" counterions from the backbone plus "bound" counterions. As the polyelectrolyte solution is being diluted, both ionic atmospheres will tend to extend. However,

[15] U. P. Strauss and P. Ander, *J. Amer. Chem. Soc.*, **80**, 6494 (1958).
[16] L. Yuan, *J. Polymer Sci.: Symposium*, **45**, 175 (1974).

the expansion of the inner ionic atmosphere is so small compared to that of the outer that it is reasonable to assume it is unchanged.

The number of carboxyl groups being maximum 50 per cent and weak dissociated, the macromolecules are not completely extended in salt-free water and can be assimilated to equivalent spheres.

Adding a strong uni-univalent electrolyte, like kalium chloride, the degree of dissociation is regressed as drastic as the electrolyte concentration is higher. As a result, the repulsive forces decrease, the macromolecule becomes more flexible and the volume in which it accommodates — and consequently the intrinsic viscosity — diminishes sharply.

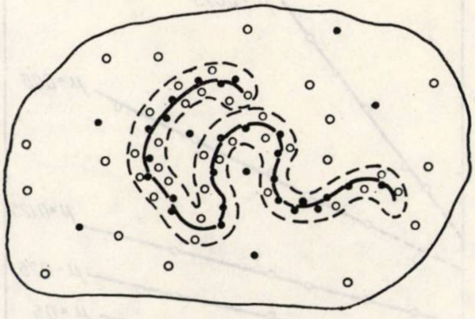

Fig. 4. — Strauss-Ander model for a polyelectrolyte molecule in solution.

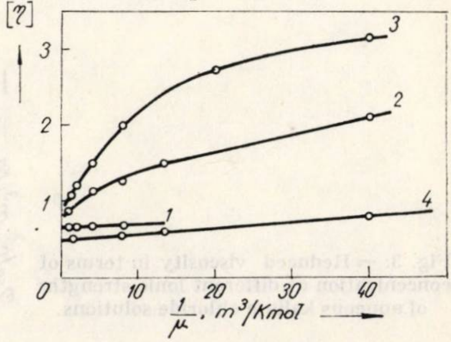

Fig. 5. — Determination of $[\eta]_\infty$: 1 — PAAO in KCl; 2 — PAA22 in KCl; 3 — PAA50 in KCl; 4 — PAA22 in $MgCl_2$.

The relative contraction of the macromolecule at different ionic strengths can be evaluated using the $[\eta]\,\mu/[\eta]_0$ or $[\eta]\mu\,/\,[\eta]_\infty$ ratios, where 0, μ and ∞ subscripts stand for the ionic strength of solution. By plotting $[\eta] = f(1/\mu)$ and extrapolating to $1/\mu = 0$ (Figure 5) one can obtain $[\eta]_\infty$. The quantity $[\eta]_0$ is a measure of the maximum molecular size and $[\eta]_\infty$ a measure of the minimum one.

The dependence of $[\eta]\,\mu/[\eta]_0$ on the ionic strength of aqueous kalium chloride solution for the three studied polyacrylamides is given in Figure 6. If the contraction of PAAO is only 19.5 per cent, it is of 87.5 per cent for PAA22 and 89 per cent for PAA50.

Figure 7 gives the dependence of $[\eta]\,\mu\,/\,[\eta]_\infty$ on the same parameter. The ratio of maximum to minimum sizes is only 1.26 for PAAO, whereas for PAA22 and PAA50 it grows up to 8.70 and respectively 12.60.

The first representation has the advantage to point out the small contractions (characteristic to the unhydrolyzed polymer); the second one shows that, beyond a certain value of the ionic strength which is 0.5 kmol/m³ in this particular case, the ratio of molecular size to the minimum one becomes identical for the hydrolyzed polyacrylamides, while for an ionic strength value of 1.6 kmol/m³ it has the same value for all polyacrylamides.

The solubility of hydrolyzed polyacrylamides is highly dependent on ionic strength if electrolytes have polyvalent counterions. In a

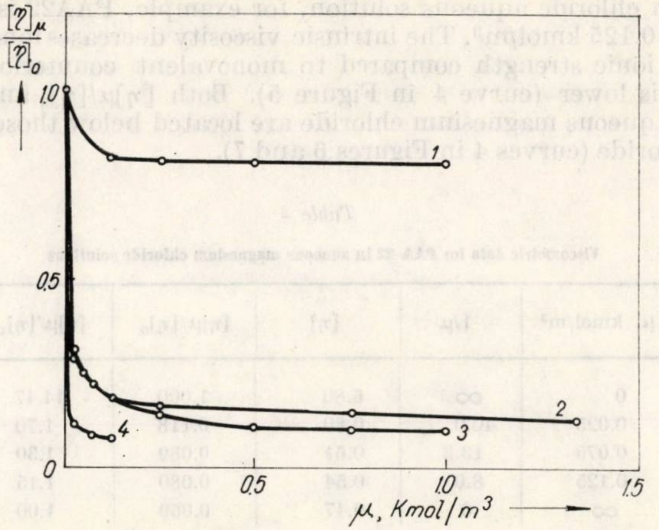

Fig. 6. — $[\eta]_\mu/[\eta]_0$ in terms of ionic strength : 1 — PAAO in KCl ; 2 — PAA22 in KCl ; 3 — PAA50 in KCl ; 4 — PAA22 in $MgCl_2$

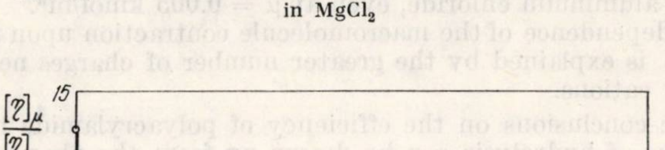

Fig. 7. — $[\eta]_\mu/[\eta]_\infty$ in terms of ionic strength : 1 — PAAO in KCl; 2 — PAA22 in KCl; 3 — PAA50 in KCl; 4 — PAA22 in $MgCl_2$

magnesium chloride aqueous solution, for example, PAA22 is soluble only up to $M=0.125$ kmol/m^3. The intrinsic viscosity decreases much more with increasing ionic strength compared to monovalent counterions (Table 2) and $[\eta]_\infty$ is lower (curve 4 in Figure 5). Both $[\eta]\mu/[\eta]_0$ and $[\eta]\mu/[\eta]_\infty$ curves in aqueous magnesium chloride are located below those for aqueous kalium chloride (curves 4 in Figures 6 and 7).

Table 2

Viscometric data for PAA 22 in aqueous magnesium chloride solutions

μ, kmol/m^3	$1/\mu$	$[\eta]$	$[\eta]\mu/[\eta]_0$	$[\eta]\mu/[\eta]_\infty$
0	∞	6.80	1.000	14.47
0.025	40.0	0.80	0.118	1.70
0.075	13.3	0.61	0.089	1.30
0.125	8.0	0.54	0.080	1.15
∞	0	0.47	0.069	1.00

The hydrolyzed polyacrylamides could not be dissolved in aqueous solution of aluminium chloride, even at $\mu = 0.005$ kmol/m^3.

The dependence of the macromolecule contraction upon the counterion charge is explained by the greater number of charges neutralized by polyvalent cations.

Some conclusions on the efficiency of polyacrylamide having different degrees of hydrolysis can be drawn up from the above findings, regarding both the surface coverage and flocculation capacity.

The unhydrolyzed polyacrylamide is less efficient as much as surface coverage and flocculation capacity, due to its coil conformation in salt-free water. The conformation and subsequently the efficiency are therefore little affected by salt concentration in water.

The size of polyacrylamide molecules becomes 10 times higher as the degree of hydrolysis rises from 0 to 50 per cent.

Increasing the ionic strength, the hydrolyzed polyacrylamides chains shrink appreciably. The higher the degree of hydrolysis the more drastic the shrinkage is and their efficiency decreases ; the efficiency in aqueous kalium chloride solution becomes independent of the degree of hydrolysis at an ionic strength of 1.6 kmol/m^3.

Electrolytes containing bivalent counterions reduce greater both the efficiency and solubility of hydrolyzed polyacrylamides.

The aluminium chloride, even in traces, causes the insolubility of hydrolyzed polyacrylamides.

In order to obtain for the hydrolyzed polyacrylamides an efficiency twice the unhydrolyzed ones efficiency, the following recommendations can be made : for PAA22 the ionic strength has not to exceed 0.50 kmol/m^3 if the counterion is monovalent (K^+) and 0.01 kmol/m^3 if it is bivalent (Mg^{2+}) ; for PAA50 the ionic strength must be below 0.02 kmol/m^3 if the counterion is monovalent (K^+).

Revue Roumaine de Chimie, **23**, *8*, 1179–1202 (1978)

A MOLECULAR-ORBITAL STUDY OF THE GROUND AND EXCITED-STATE PROPERTIES OF METALLOCENES OF THE FIRST-ROW TRANSITION-METAL IONS. II*

D. R. ARMSTRONG, R. FORTUNE and P. G. PERKINS
Department of Pure and Applied Chemistry, University of Strathclyde,
Glasgow Gl 1XL, Scotland

Received September 6, 1976

Molecular-orbital calculations at the CNDO and INDO levels of approximation have been used to study the bonding patterns in mono-substituted ferrocene derivatives of the type Fe(Cp)$_2$ X. The substituent X included H, F, Cl, NH_2, C_2H_4, and CH_3. The effect of substitution on the optical absorption spectra is examined and qualitative agreement with experiment obtained. In addition, unrestricted eigenfunctions are derived for selected open-shell metallocenes and their molecular ions. The bonding schemes resulting from the two computational procedures are found to compare favourably with other data.

Previous molecular-orbital investigations [1–9] of metallocenes of the first-row transition metal ions have resulted in the partial elucidation of the bonding schemes characteristic of these species. However, some uncertainty remains with regard to absolute energy level sequences; e_g for ferrocene, conflicting results are obtained from the various molecular-orbital studies. In addition, contradictory conclusions may be inferred from experimental data. Photoelectron spectroscopic studies of ferrocene [10,11] indicate the outer molecular-orbital sequence $e^*_{1g} > e_{2g} > a_{1g}$:

---

[*] Part I: D. R. Armstrong, R. Fortune and P. G. Perkins, *J. Organometal. Chem.*, **111**, 197 (1976).

[1] A. D. Liehr and C. J. Ballhausen, *Acta. Chem. Scand.*, **11**, 207 (1957).

[2] J. P. Dahl and C. J. Ballhausen, *Kgl. Danske Videnskab., Selskab Mat-Fys. Medd.*, 33 (1961).

[3] R. D. Fischer, *Theoret. Chim. Acta*, **1**, 418 (1963).

[4] A. T. Armstrong, D. B. Carroll and S. P. Mc Glynn, *J. Chem. Phys.*, **47**, 1104 (1967).

[5] J. H. Schachtschneider, R. Prins and P. Ros, *Inorg. Chim. Acta*, **1**, 462 (1967).

[6] I. H. Hillier and R. M. Canadine, *Discuss. Faraday Soc.*, **47**, 27 (1969).

[7] M. Coutiere, J. Demuynck and A. Veillard, *Theoret. Chim. Acta*, **27**, 281 (1972).

[8] T. Ziegler, *Acta Chem. Scand.*, **A28**, 29 (1974).

[9] D. R. Armstrong, R. Fortune and P. G. Perkins, J. Organcmetal. Chem., **111**, 197(1976).

[10] S. Evans, M. L. H. Green, B. Jewitt, A. F. Orchard and C. F. Pygall, *J. Chem. Soc., Faraday Trans. II*, **68**, 1847 (1972).

[11] J. W. Rabalais, L. O. Werne, T. Bergmark, L. Karlsson, M. Hussain and K. Siegbahn, *J. Chem. Phys.*, **57**, 1185 (1972).

conversely, optical absorption spectral data[12,13] evince the sequence $e_{1g}^{*} > a_{1g} > e_{2g}$. *Ab initio* calculation[7] places the e_{2g} level above the a_{1g} level and demonstrates the fallibility of Koopmans'theorem.[14] SFC X_α calculation,[15,16] incorporating the transition-state method,[17,18] provides support for the sequence $e_{1g}^{*} > a_{1g} > e_{2g}$ by accounting accurately for the observed electronic spectrum. Semi-empirical calculations are, in general, not sufficiently sophisticated to distinguish the order and, consequently, both outer orbital sequences have been derived from these calculations.

One possible consideration, which has been largely neglected in this controversy, is the effect on the parent electronic spectrum incurred by ring substitution.[4,19]

METHOD, RESULTS AND DISCUSSION

Both a modified CNDO/2 computational framework,[20] previously employed in the studies of metallocenes,[9] and an INDO approach have been used. The major change from the original CNDO/2 formalism, apart from the use of the Wolfsberg-Helmholtz approximation[21] in place of the traditional bonding parameters,[20] is that valence-shell ionisation potentials are used to estimate the diagonal elements of the initial H matrix. The INDO level of approximation was incorporated into the calculational scheme in order to provide a more satisfactory description of intra-atomic electron interactions. A comparison of the results obtained from the two methods can then be undertaken. Consequently, this work has a twofold purpose. Firstly, to compare the ground and excited states evaluated by both methods as applied to various ferrocene derivatives. Secondly, to examine the compatibility of the two computational frameworks in the determination of open-shell wavefunctions of selected metallocene species.

Incorporation of the INDO parameters[22] gives rise to modified expressions for the core-matrix elements. The equations derived for a metal of outer electronic configuration s^2d^n are listed in Appendix I, those of chromium s^1d^5 are presented in Appendix II. The required metal INDO parameters were extracted from reference.[23] The molecular geometry of the parent ferrocene was assumed to be D_{5d} and the interatomic distances were

---

[12] Y. S. Sohn, D. N. Hendrickson, J. H. Smith and H. B. Gray, *Chem. Phys. Letts.*, **6**, 499 (1970).

[13] Y. S. Sohn, D. N. Hendrickson and. H. B. Gray, *J. Amer. Chem. Soc.*, **93**, 3603 (1971).

[14] T. Koopmans, *Physica*, **1**, 104 (1933).

[15] E. J. Baerends and P. Ros, *Chem. Phys. Letts.*, **23**, 391 (1973).

[16] N. Rösch and K. H. Johnson, *Chem. Phys. Letts.*, **24**, 179 (1974).

[17] J. C. Slaten and K. H. Johnson, *Phys. Rev.*, *B5*, 844 (1972).

[18] K. H. Johnson, *Advances in Quantum Chemistry*, **7**, 143 (1973).

[19] A. T. Armstrong, F. Smith. E. Elder and S. P. McGlynn, *J. Chem. Phys.*, **46**, 4321 (1967).

[20] J. A. Pople and G. A. Segal, *J. Chem. Phys.*, **44**, 3289 (1966).

[21] M. Wolfsberg and L. Helmholtz, *J. Chem. Phys.*, **20**, 837, (1952).

[22] J. A. Pople, D. L. Beveridge and P. A. Dobosh, *J. Chem. Phys.*, **47**, 2026 (1967).

[23] E. Tondello, G. de Michelis, L. Oleari and L. di Sipio, *Coord. Chem. Revs.*, **2**, 65 (1967).

taken from reference.[24] The substituents were assumed to be coplanar with a cyclopentadienyl ring system and their bonding distances were estimated. The atom-numbering system employed in the following discussion is shown in Figure 1. The substituent X is directly bonded to C_1 of the cyclopentadienyl ring system A.

Limited configuration-interaction calculations were employed in the determination of the excited-state properties of ferrocene and its derivatives. All singly excited states (singlet plus triplet) generated by one-electron excitations from the seven highest filled molecular orbitals to the six lowest virtual molecular orbitals were calculated.

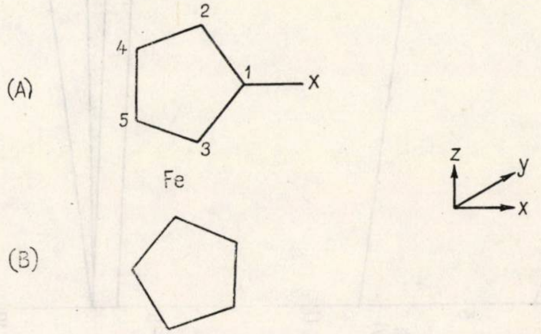

Fig. 1. — The atom-numbering system of substituted ferrocene, $Fe(Cp)_2X$.

a) GROUND AND EXCITED STATES

Initial calculations were carried out on ferrocene in order to determine a suitable value for the Wolfsberg-Helmholtz proportionality constant k. This parameter was systematically increased from 1.0 to 2.0 in both calculational procedures and the results are summarised in Figures 2—5. Figures 2 and 3 show the eigenvalue variations induced by changing the k value as derived by the CNDO and INDO calculations, respectively. Only those levels included in the subsequent configuration-interaction calculations are delineated in these diagrams. Both series of calculations uniformly predict the energy level sequence $e_{2u} > e_{2g} > e_{1g}$ for the virtual molecular orbitals; this result is compatible with previous calculations.[7,15,16] However, the sequences of energy levels found for the filled molecular orbitals differ. The CNDO calculations, except for low values of k, give rise to the energy level ordering $a_{1g} > e_{2g} > e_{1g} > e_{1u}$ whilst the INDO calculations predict the alternative sequence $e_{2g} > a_{1g} > e_{1g} > e_{1u}$. These differences are reflected in the excited-state energies depicted in Figures 4 and 5.

Experimentally, three low-energy transitions, corresponding to the electronic excitations $a_{1g} \rightarrow e_{1g}(^1E_{1g})$ and $e_{2g} \rightarrow e_{1g}(^1E_{1g}, {}^1E_{2g})$, are found at approximately 2.70, 2.98 and 3.82 eV. Clearly, the agreement with

---

[24] R. K. Böhn and A. Haaland, *J. Organometal. Chem.*, **5**, 470 (1966).

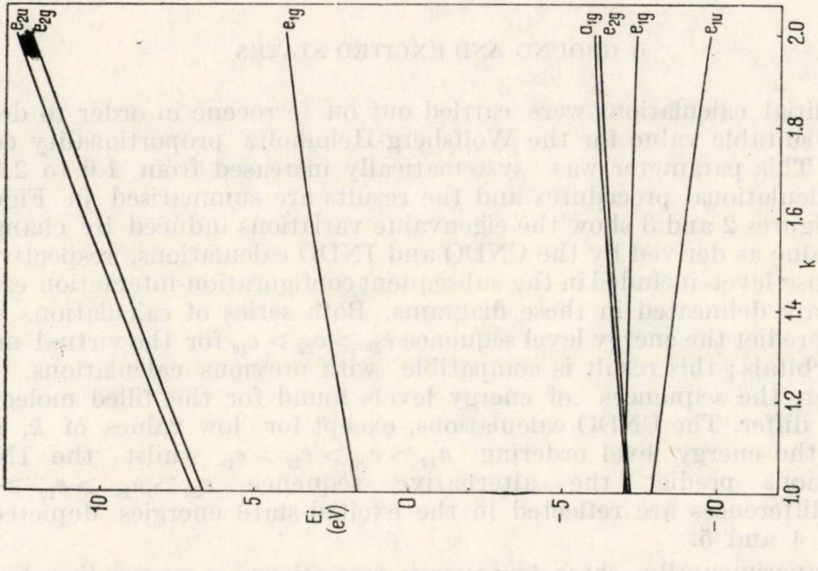

Fig 2 — Variation of eigenvalues of $Fe(Cp)_2$ with k, obtained from CNDO calculations.

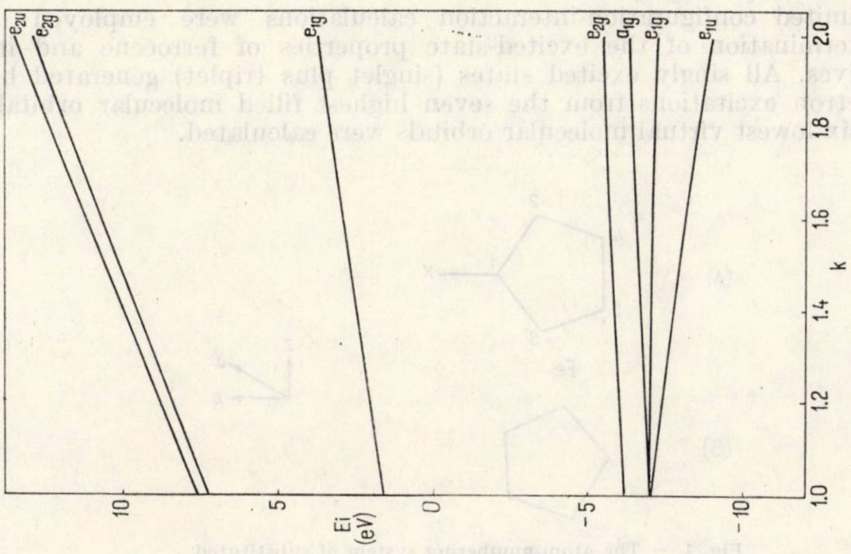

Fig. 3. — Variation of eigenvalues of $Fe(Cp)_2$ with k, obtained from INDO calculations.

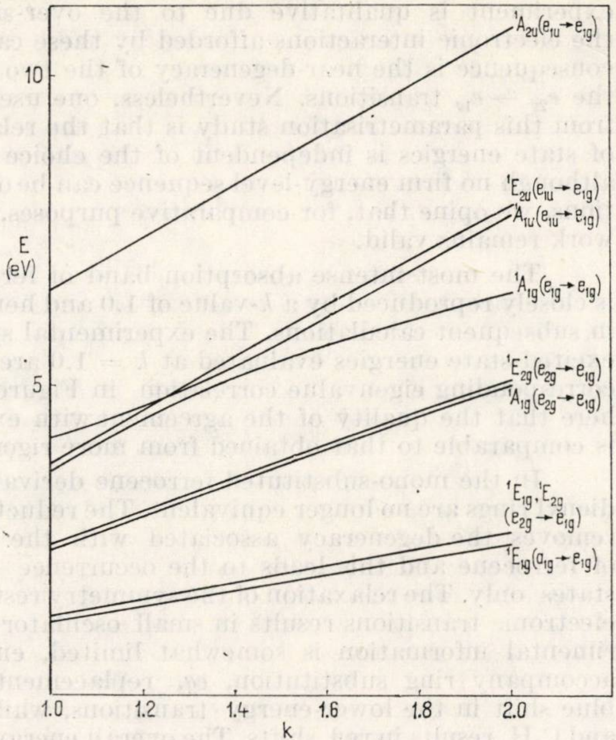

Fig. 4. — Variation of excited states of $Fe(Cp)_2$ with *k*, obtained from CNDO calculations.

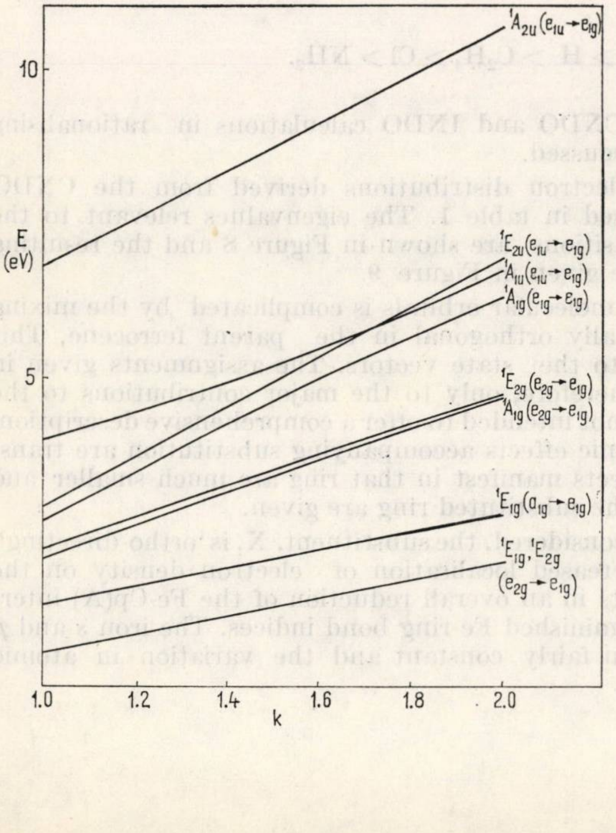

Fig. 5. — Variation of excited states of $Fe(Cp)_2$ with *k*, obtained from INDO calculations.

experiment is qualitative due to the over-simplified representation of the electronic interactions afforded by these calculations. One important consequence is the near-degeneracy of the two excited states arising from the $e_{2g} \rightarrow e_{1g}$ transitions. Nevertheless, one useful feature which emerges from this parametrisation study is that the relative order of the majority of state energies is independent of the choice of the k-value. Therefore, although no firm energy-level sequence can be obtained from these calculations, we opine that, for comparative purposes, the computational framework remains valid.

The most intense absorption band of ferrocene, centred at 6.4 eV, is closely reproduced by a k-value of 1.0 and hence, this value was retained in subsequent calculations. The experimental spectrum and the calculated excited-state energies evaluated at $k = 1.0$ are shown in Figure 6 and the corresponding eigenvalue correlation in Figure 7. It is pertinent to note here that the quality of the agreement with experiment in the latter case is comparable to that obtained from more rigorous calculations. [7]

In the mono-substituted ferrocene derivatives the two cyclopentadienyl rings are no longer equivalent. The reduction in molecular symmetry removes the degeneracy associated with the e-type molecular orbitals of ferrocene and this leads to the occurrence of non-degenerate excited states only. The relaxation of the symmetry restrictions on the low-energy electronic transitions results in small oscillator strengths. Although experimental information is somewhat limited, energy shifts are known to accompany ring substitution, *eg*, replacement of H by CH_3 induces a blue shift in the lower-energy transitions, while substitution by Cl, NH_2 and C_2H_4 results in red shifts. The overall energy order of the first absorption band is

$$CH_3 > H > C_2H_4 > Cl > NH_2.$$

The utility of the CNDO and INDO calculations in rationalising these data will now be discussed.

The ground-state electron distributions derived from the CNDO calculations are summarised in table 1. The eigenvalues relevant to the low-energy electronic transitions are shown in Figure 8 and the resulting excited-state energies are given in Figure 9.

Classification of the molecular orbitals is complicated by the mixing of symmetry types normally orthogonal in the parent ferrocene. This effect is carried through to the state vectors. The assignments given in Figures 8 and 9 relate, therefore, only to the major contributions to the particular vectors and are not intended to offer a comprehensive description. Also, although the electronic effects accompanying substitution are transmitted to ring B, the effects manifest in that ring are much smaller and only data pertaining to the substituted ring are given.

In all the complexes considered, the substituent, X, is 'ortho-directing', towards electrophiles. Increased localisation of electron density on the central metal atom results in an overall reduction of the Fe-Cp(A) interaction, as witnessed by diminished Fe-ring bond indices. The iron s and p orbital occupancies remain fairly constant and the variation in atomic

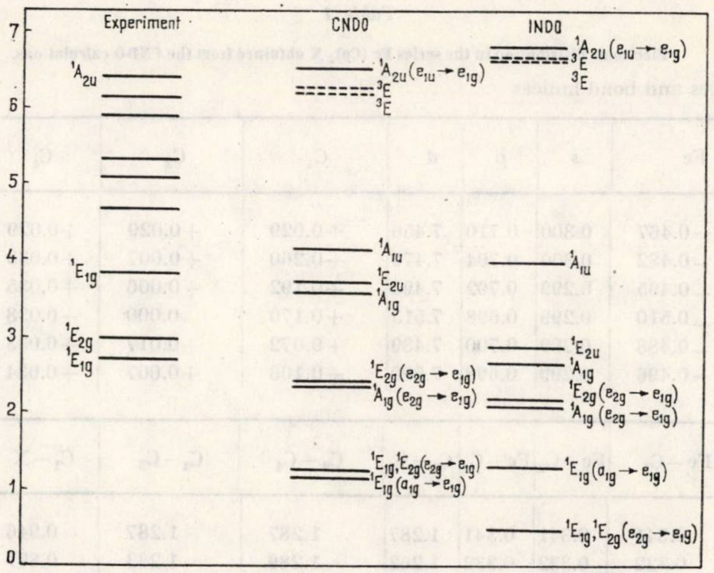

Fig. 6. — Calculated and experimental excited states of $Fe(Cp)_2$.

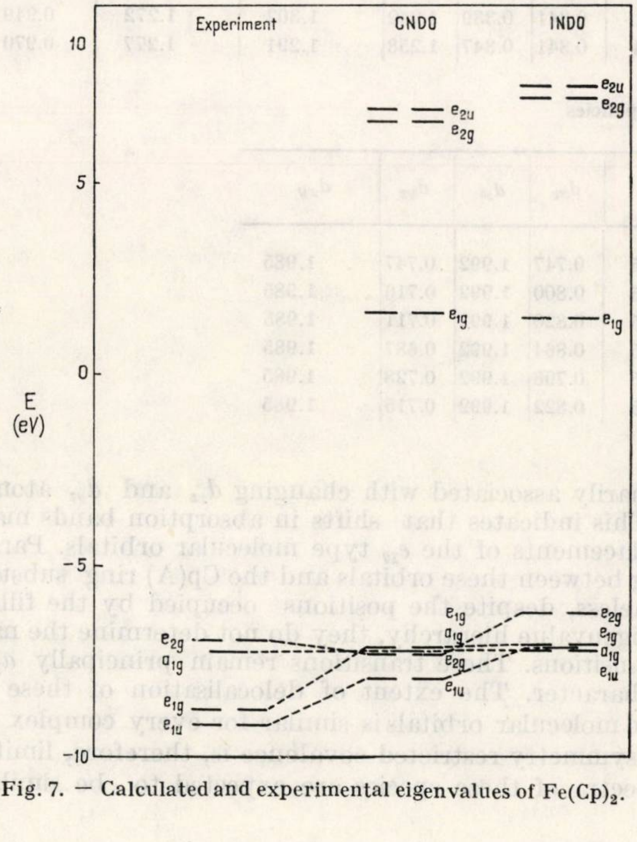

Fig. 7. — Calculated and experimental eigenvalues of $Fe(Cp)_2$.

Table 1

Electronic distribution in the series Fe $(Cp)_2$ X obtained from the CNDO calculations.

Atom charges and bond indices

X	Fe	s	p	d	C_1	C_2	C_4	X
H	−0.467	0.300	0.710	7.456	+0.029	+0.029	+0.029	+0.015
F	−0.482	0.300	0.704	7.479	+0.260	+0.007	+0.033	−0.260
Cl	−0.495	0.299	0.702	7.493	+0.192	+0.006	+0.035	−0.143
NH_2	−0.510	0.299	0.698	7.513	+0.170	0.000	+0.038	−0.231
C_2H_4	−0.488	0.299	0.700	7.489	+0.072	+0.017	+0.033	+0.010
CH_3	−0.496	0.299	0.698	7.500	+0.106	+0.007	+0.034	−0.121

	$Fe-C_1$	$Fe-C_2$	$Fe-C_4$	C_1-C_2	C_2-C_4	C_4-C_5	C_1-X
H	0.341	0.341	0.341	1.287	1.287	1.287	0.946
F	0.322	0.332	0.332	1.262	1.289	1.283	0.897
Cl	0.327	0.330	0.337	1.260	1.294	1.279	0.958
NH_2	0.328	0.338	0.347	1.245	1.295	1.271	1.026
C_2H_4	0.331	0.341	0.339	1.242	1.302	1.272	0.949
CH_3	0.334	0.341	0.347	1.258	1.291	1.277	0.970

Iron d-orbital occupancies

	$d_{x^2-y^2}$	d_{xz}	d_{z^2}	d_{yz}	d_{xy}
H	1.985	0.747	1.992	0.747	1.985
F	1.985	0.800	1.992	0.716	1.985
Cl	1.985	0.820	1.992	0.711	1.985
NH_2	1.985	0.864	1.992	0.687	1.985
C_2H_4	1.985	0.798	1.992	0.728	1.985
CH_3	1.985	0.822	1.992	0.715	1.985

charge is primarily associated with changing d_{xz} and d_{yz} atomic orbital occupancies. This indicates that shifts in absorption bands may relate to the relative placements of the e_{1g} type molecular orbitals. Parallel trends in the bonding between these orbitals and the Cp(A) ring substantiate this view. Nevertheless, despite the positions occupied by the filled e_{1g} type levels in the eigenvalue hierarchy, they do not determine the nature of the low-energy transitions. These transitions remain principally $a_{1g} \rightarrow e_{1g}$ and $e_{2g} \rightarrow e_{1g}$ in character. The extent of delocalisation of these essentially metal localised molecular orbitals is similar for every complex considered. The effect of symmetry-restricted covalence is, therefore, limited and the low-energy spectra of these species are expected to be similar. In each

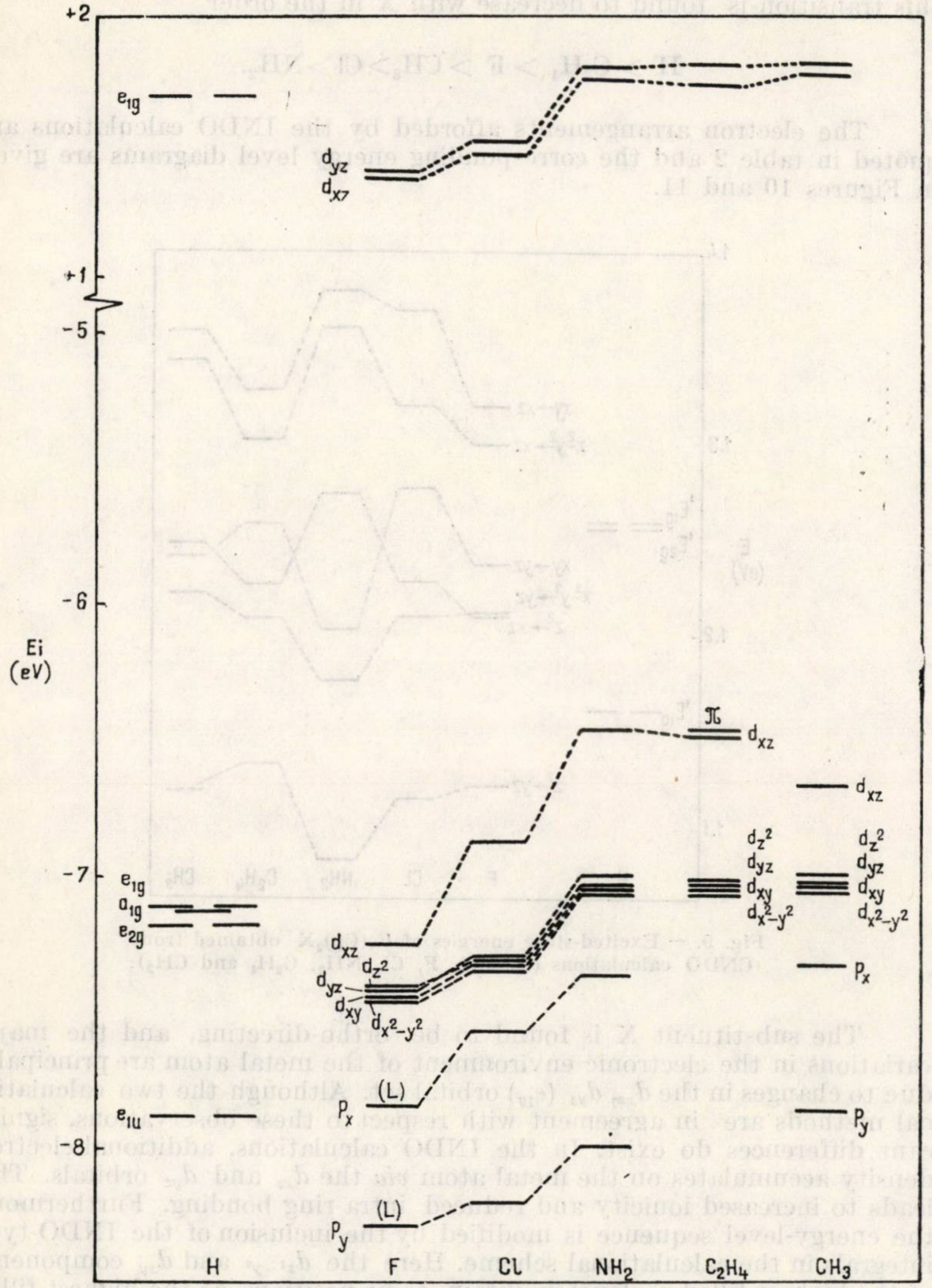

Fig. 8. — Eigenvalues of Fe(Cp)$_2$X obtained from CNDO calculations (X = H, F, Cl, NH$_2$, C$_2$H$_4$ and CH$_3$).

case, the lowest energy transition is the $d_{z^2}(a_{1g}) \rightarrow d_{yz}(e_{1g})$. The energy of this transition is found to decrease with X in the order

$$H > C_2H_4 > F > CH_3 > Cl > NH_2.$$

The electron arrangements afforded by the INDO calculations are quoted in table 2 and the corresponding energy level diagrams are given in Figures 10 and 11.

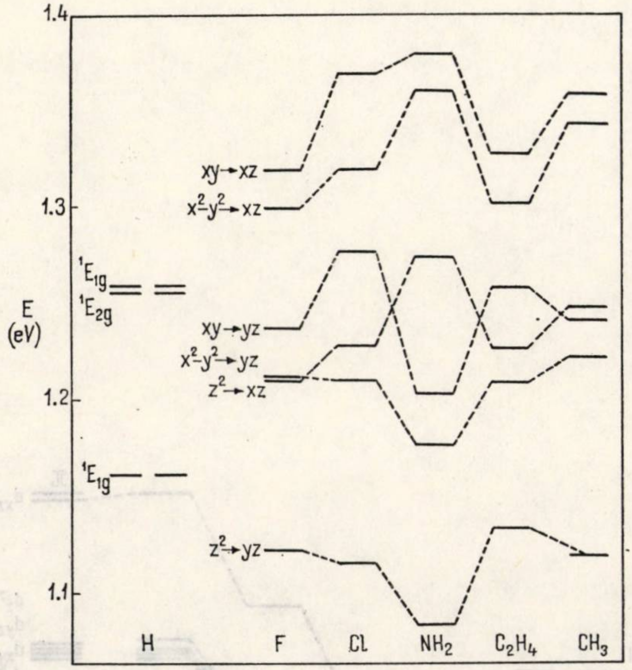

Fig. 9. — Excited-state energies of $Fe(Cp)_2X$ obtained from CNDO calculations ($X = H$, F, Cl, NH_2, C_2H_4 and CH_3).

The substituent X is found to be ortho-directing, and the major variations in the electronic environment of the metal atom are principally due to changes in the d_{xz}, d_{yz} (e_{1g}) orbital set. Although the two calculational methods are in agreement with respect to these observations, significant differences do exist. In the INDO calculations, additional electron density accumulates on the metal atom *via* the d_{xz} and d_{yz} orbitals. This leads to increased ionicity and reduced intra-ring bonding. Furthermore, the energy-level sequence is modified by the inclusion of the INDO-type integrals in the calculational scheme. Here the $d_{x^2-y^2}$ and d_{xy} components of the highest filled e_{2g} level maintain their positions as the highest filled levels when the ligand X is varied and the absorption spectra of the derivatives can be readily correlated with that of ferrocene. Splitting of the $^1E_{1g}$ and $^1E_{2g}$ excited states arising from the low-energy $e_{2g} \rightarrow e_{1g}$ transitions

Table 2

Electronic distributions in the series $Fe(Cp)_2X$ obtained from the INDO calculations

Atom charges and bond indices

X	Fe	*s*	*p*	*d*	C_1	C_2	C_4	X
H	−1.042	0.287	0.656	9.100	+0.100	+0.100	+0.100	+0.004
F	−1.073	0.286	0.649	8.138	+0.383	+0.069	+0.108	−0.314
Cl	−1.085	0.285	0.648	8.152	+0.289	+0.070	+0.109	−0.169
NH_2	−1.122	0.284	0.641	8.197	+0.250	+0.066	+0.117	−0.223
C_2H_4	−1.069	0.285	0.646	8.139	+0.129	+0.089	+0.106	−0.077
CH_3	−1.081	0.285	0.644	8.152	+0.169	+0.077	+0.109	−0.078

	$Fe-C_1$	$Fe-C_2$	$Fe-C_4$	C_1-C_2	C_2-C_4	C_4-C_5	C_1-X
H	0.346	0.346	0.346	1.271	1.271	1.271	0.940
F	0.325	0.334	0.334	1.232	1.290	1.254	0.854
Cl	0.335	0.329	0.339	1.233	1.299	1.245	0.944
NH_2	0.326	0.333	0.343	1.202	1.319	1.224	1.060
C_2H_4	0.336	0.343	0.340	1.215	1.299	1.248	0.958
CH_3	0.341	0.340	0.348	1.230	1.294	1.245	1.009

Iron d-orbital occupancies

	$d_{x^2-y^2}$	d_{xy}	d_{z^2}	d_{yz}	d_{xy}
H	1.983	1.069	1.994	1.069	1.983
F	1.983	1.125	1.994	1.053	1.983
Cl	1.983	1.132	1.994	1.059	1.983
NH_2	1.983	1.187	1.994	1.050	1.983
C_2H_4	1.983	1.116	1.994	1.062	1.983
CH_3	1.984	1.133	1.994	1.059	1.983

in ferrocene results in four energetically distinct electronic states originating from the electron promotions $d_{xy} \rightarrow d_{yz}$, $d_{x^2-y^2} \rightarrow d_{yz}$ and $d_{xy} \rightarrow d_{xz}$, $d_{x^2-y^2} \rightarrow d_{xz}$. Similarly the higher energy ${}^1E_{1g}$ ($a_{1g} \rightarrow e_{1g}$) is split into two components stemming from the transitions $d_{z^2} \rightarrow d_{yz}$ and $d_{z^2} \rightarrow d_{xz}$. This is in essential agreement with the CNDO results, although the orbital sequence of the virtual e_{1g} set is inverted, since the trends in the calculated lowest-energy excited states are found to correlate with the observed shifts,

$$ie,\ CH_3 > H > C_2H_4 > Cl > F > NH_2.$$

The close similarities exhibited by the absorption spectra of the $Fe(Cp)_2X$ series indicate that related trends might be expected in the bonding patterns of these species. Throughout the series, the energy positioning and extent of delocalisation of the molecular orbitals are remarkably similar, therefore the discrimination of explicit factors affecting the excited-state energies proves to be a formidable task. The metal-ring bonding, in particular the roles of the metal d_{xz} and d_{yz} orbitals, has considerable influence in the determination of excited-state properties. Even this partial interactive framework represents an extremely complex set of interactions. Nevertheless, it can be stated that the $d_{xz}-C_1$ interaction is of paramount importance, although the interdependent $d_{xz}-C_2$ and $d_{xz}-C_4$ interactions are also critical, whilst the $d_{yz}-C_1$ interaction is,

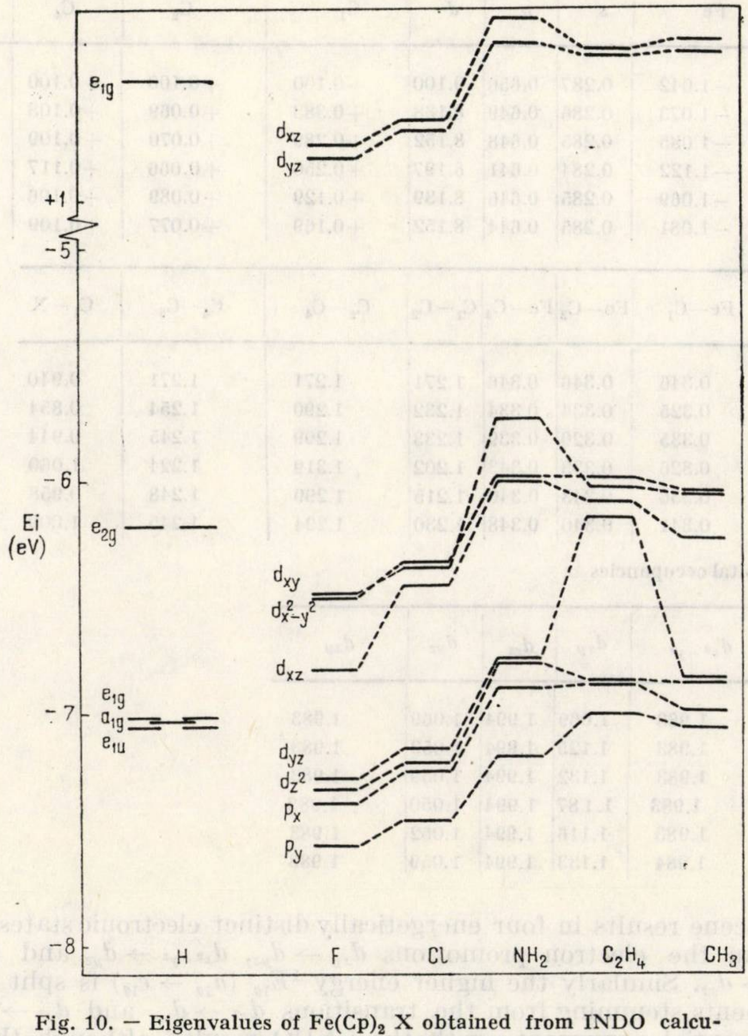

Fig. 10. — Eigenvalues of $Fe(Cp)_2X$ obtained from INDO calculations ($X = H, F, Cl, NH_2, C_2H_4$ and CH_3).

of course, unimportant. However, simple trends common to the entire series cannot be identified and the factors controlling the absorption spectra must be considered as a complex set of interrelated interactions involving primarily pseudo-e_{1g}—Cp(A) type bonding.

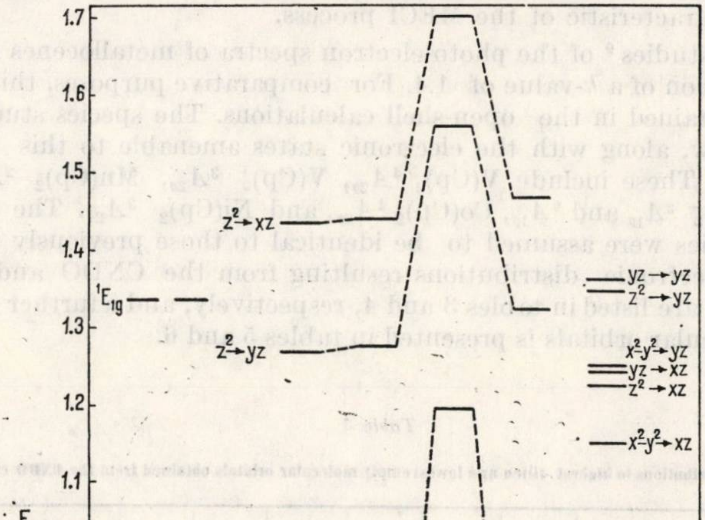

Fig. 11. — Excited-state energies of $Fe(Cp)_2X$ obtained from INDO calculations (X = H, F, Cl, NH_2, C_2H_4 and CH_3).

b) OPEN-SHELL CONFIGURATIONS

Single-determinantal unrestricted wavefunctions were evaluated within the open-shell Pople-Nesbet formalism.[25] This precludes the characterisation of spatially degenerate states which have previously been studied using the MECI calculational procedure. [9,26] We here make a further comparison of the CNDO and INDO levels of approximation in addition to an evaluation of the validity of Dewar's half-electron method [27] which is characteristic of the MECI process.

---

[25] J. A. Pople and R. K. Nesbet *J. Chem. Phys.* **22**, 5711 (1954).

Prior studies [9] of the photo-electron spectra of metallocenes resulted in the selection of a k-value of 1.4. For comparative purposes, this value has been retained in the open-shell calculations. The species studied are listed below, along with the electronic states amenable to this type of calculation. These include $V(Cp)_2$ $^4A_{2g}$, $V(Cp)_2^+$ $^3A_{2g}$, $Mn(Cp)_2$ $^2A_{1g}$ and $^6A_{1g}$, $Fe(Cp)_2^+$ $^2A_{1g}$ and $^6A_{1g}$, $Co(Cp)_2$ $^4A_{2g}$, and $Ni(Cp)_2$ $^3A_{2g}$. The molecular geometries were assumed to be identical to those previously employed. [9] The electronic distributions resulting from the CNDO and INDO calculations are listed in tables 3 and 4, respectively, and a further analysis of the molecular orbitals is presented in tables 5 and 6.

Table 3

Metal orbital contributions to highest filled and lowest empty molecular orbitals obtained from the CNDO calculations

Complex	State		a_{2u}*	a_{1g}*	e_{1u}*	e_{1g}*	a_{1g}	e_{2g}	e_{1u}	e_{1g}^2
$V(Cp)_2$	$^4\mathrm{A}_{2g}$	α	0.801	0.805	0.848	0.699	0.976	0.978	0.028	0.193
		β	0.801	0.803	0.848	0.697	0.978	0.979	0.028	0.194
$V(Cp)_2^+$	$^3A_{2g}$	α	0.830	0.810	0.837	0.627	0.978	0.978	0.031	0.221
		β	0.830	0.810	0.837	0.626	0.978	0.978	0.027	0.223
$Mn(Cp)_2$	$^6A_{1g}$	α	0.684	0.819	0.831	0.420	0.990	0.982	0.056	0.420
		β	0.684	0.814	0.813	0.577	0.990	0.990	0.076	0.370
$Mn(Cp)_2$	$^2A_{1g}$	α	0.649	0.817	0.824	0.738	0.990	0.992	0.063	0.225
		β	0.649	0.817	0.824	0.738	0.990	0.992	0.063	0.225
$Fe(Cp)_2^+$	$^6A_{1g}$	α	0.666	0.767	0.772	0.240	0.988	0.819	0.010	0.258
		β	0.666	0.755	0.749	0.232	0.990	0.974	0.053	0.368
$Fe(Cp)_2^+$	$^2A_{1g}$	α	0.537	0.724	0.711	0.465	0.988	0.951	0.043	0.364
		β	0.537	0.724	0.712	0.464	0.990	0.953	0.041	0.362
$Co(Cp)_2$	$^4A_{2g}$	α	0.387	0.774	0.729	0.296	0.992	0.968	0.057	0.444
		β	0.384	0.764	0.704	0.420	0.994	0.970	0.073	0.479
$Ni(Cp)_2$	$^3A_{1g}$	α	0.307	0.819	0.694	0.204	0.996	0.974	0.036	0.558
		β	0.304	0.808	0.664	0.433	0.996	0.978	0.089	0.518

---

[26] D. R. Armstrong, R. Fortune, P. G. Perkins and J.J.P. Stewart, *J. Chem. Soc., Faraday Trans. II*, **68**, 1839 (1972).

[27] M. J. S. Dewar, J. A. Hashmall and C. G. Venier, *J. Amer. Chem. Soc.*, **90**, 1953 (1968).

Table 4

Metal orbital contributions to highest filled and lowest empty molecular orbital obtained from the INDO calculations

Complex	State		$a_{2u}{}^*$	$a_{1g}{}^*$	$e_{1u}{}^*$	$e_{1g}{}^*$	a_{1g}	e_{2g}	e_{1u}	e_{1g}^2
$V(Cp)_2$	${}^4A_{2g}$	α	0.812	0.815	0.806	0.513	0.978	0.972	0.037	0.308
		β	0.805	0.814	0.556	0.697	0.978	0.978	0.018	0.199
$V(Cp)_2^+$	${}^3A_{2g}$	α	0.843	0.819	0.837	0.459	0.978	0.972	0.039	0.305
		β	0.843	0.821	0.845	0.626	0.978	0.978	0.032	0.237
$Mn(Cp)_2$	${}^6A_{1g}$	α	0.731	0.819	0.831	0.132	0.990	0.978	0.059	0.237
		β	0.696	0.815	0.819	0.620	0.990	0.994	0.081	0.326
$Mn(Cp)_2$	${}^2A_{1g}$	α	0.579	0.823	0.824	0.403	0.990	0.994	0.069	0.514
		β	0.536	0.828	0.837	0.767	0.992	0.994	0.052	0.201
$Fe(Cp)_2^+$	${}^6A_{1g}$	α	0.714	0.794	0.801	0.129	0.986	0.955	0.035	0.132
		β	0.684	0.771	0.771	0.266	0.990	0.968	0.067	0.439
$Fe(Cp)_2^+$	${}^2A_{1g}$	α	0.444	0.724	0.672	0.277	0.988	0.958	0.047	0.417
		β	0.406	0.715	0.673	0.408	0.990	0.972	0.042	0.394
$Co(Cp)_2$	${}^4A_{2g}$	α	0.324	0.792	0.719	0.165	0.994	0.992	0.042	0.362
		β	0.301	0.766	0.672	0.283	0.994	0.980	0.076	0.578
$Ni(Cp)_2$	${}^3A_{2g}$	α	0.175	0.828	0.527	0.161	0.996	0.996	0.059	0.557
		β	0.183	0.812	0.491	0.267	0.996	0.984	0.088	0.666

The ground state of the d^3 vanadocene [28, 29] is the high-spin spatially non-degenerate ${}^4A_{2g}$ state arising from the outer electronic configuration $(e_{2g})^2\,(a_{1g})^1$. This is correctly predicted from both the MECI calculations and the Pople-Nesbet calculations. Although the implementation of Dewar's method results in the outer electronic configuration $(e_{2g}\,\alpha)^{3/2}\,(e_{2g}\,\beta)^{3/2}$, the MECI process returns the configuration $(e_{2g}\,\alpha)^2\,(a_{1g}\alpha)^1$ as the most stable. The artificial degeneracy of the α and β levels imposed by Dewar's method is removed by explicit derivation of the spin-defined eigenfunctions. This results in different configurations for α and β spin, as delineated in Figure 12. Apart from those levels directly involved in the distribution of the three outer electrons, the α and β eigenvalue variations are found to be minimal. The INDO calculation results in reversal of the two highest filled levels, and this is consistent with the aforementioned relative placements of the e_{2g} and a_{1g} levels in ferrocene. The greater α and β eigenvalue differential arising from the INDO calculation is caused by larger variation in the molecular orbital localisations, as reflected by the metal atomic orbital contributions (Tables 3 and 4). This effect, which is particularly pronounced in the e_{1g} molecular orbitals, gives rise to significant spin densities associated with the metal d_{xz} and d_{yz} atomic orbitals (Tables 5 and 6). The spin densities associated with the d_{z^2}, $d_{x^2-y^2}$ and d_{xy} orbitals are close to unity, as expected from their high degree of localisation.

---

[28] R. Prins, P. Biloen and J. D. W. van Voorst, *J. Chem. Phys.*, **46**, 1216 (1967).

[29] R. Prins and J. D. W. van Voorst, *J. Chem. Phys.*, **49**, 4665 (196 8).

Table 5

Metal electron density distributions obtained from the CNDO calculations

Complex	State	Net charge on metal	Metal electronic configuration				Metal orbital occupancies					
			s	p	d		s	p_x	p_z	$d_{x^2-y^2}$	d_{xz}	d_{z^2}
$V(Cp)_2$	${}^4A_{2g}$	-0.29	0.320	0.778	4.191	α	0.166	0.135	0.119	0.990	0.299	0.988
						β	0.154	0.135	0.119	0.007	0.300	0.010
						$\alpha-\beta$	0.012	0.000	0.000	0.983	-0.001	0.978
$V(Cp)_2^+$	${}^3A_{2g}$	$+0.34$	0.318	0.832	3.508	α	0.159	0.146	0.124	0.991	0.371	0.011
						β	0.159	0.146	0.124	0.008	0.373	0.011
						$\alpha-\beta$	0.000	0.000	0.000	0.983	-0.002	0.000
$Mn(Cp)_2$	${}^6A_{1g}$	-0.04	0.329	0.869	5.842	α	0.165	0.148	0.121	0.998	0.999	0.994
						β	0.164	0.166	0.121	0.002	0.423	0.004
						$\alpha-\beta$	0.001	-0.022	0.000	0.986	0.576	0.990
$Mn(Cp)_2$	${}^2A_{1g}$	-0.20	0.323	0.843	6.027	α	0.165	0.151	0.119	0.998	0.260	0.994
						β	0.158	0.151	0.119	0.998	0.260	0.004
						$\alpha-\beta$	0.007	0.000	0.000	0.000	0.000	0.990
$Fe(Cp)_2^+$	${}^6A_{1g}$	$+0.19$	0.336	0.924	6.554	α	0.166	0.156	0.128	0.993	0.999	0.996
						β	0.170	0.178	0.128	0.018	0.766	0.006
						$\alpha-\beta$	-0.004	-0.022	0.000	0.975	0.233	0.990
$Fe(Cp)_2^+$	${}^2A_{1g}$	-0.29	0.324	0.866	7.105	α	0.164	0.155	0.123	0.992	0.534	0.996
						β	0.160	0.155	0.123	0.992	0.534	0.005
						$\alpha-\beta$	0.004	0.000	0.000	0.000	0.000	0.991
$Co(Cp)_2$	${}^4A_{2g}$	-0.34	0.323	0.874	8.140	α	0.160	0.150	0.120	0.996	0.999	0.997
						β	0.163	0.167	0.120	0.996	0.579	0.003
						$\alpha-\beta$	-0.003	-0.017	0.000	0.000	0.420	0.994
$Ni(Cp)_2$	${}^3A_{2g}$	-0.30	0.316	0.870	9.114	α	0.154	0.149	0.117	0.998	0.999	0.998
						β	0.162	0.168	0.119	0.998	0.566	0.998
						$\alpha-\beta$	-0.008	-0.019	-0.002	0.000	0.433	0.000

Table 6

Metal electron density distributions obtained from the INDO calculations

Complex	State	Net charge on metal	Metal electronic configuration			Metal orbital occupancies						
			s	p	d		s	p_x	p_z	$d_{x^2-y^2}$	d_{xz}	d^2
$V(Cp)_2$	$^4A_{2g}$	-0.64	0.314	0.773	4.556	α	0.165	0.141	0.116	0.993	0.487	0.991
						β	0.149	0.130	0.115	0.007	0.291	0.009
						$\alpha-\beta$	0.016	0.011	0.011	0.986	0.196	0.981
$V(Cp)_2^+$	$^3A_{2g}$	$+0.02$	0.314	0.823	3.846	α	0.159	0.152	0.120	0.993	0.539	0.013
						β	0.155	0.140	0.119	0.007	0.372	0.011
						$\alpha-\beta$	0.004	0.012	0.001	0.986	0.167	0.002
$Mn(Cp)_2$	$^6A_{1g}$	$+0.03$	0.338	0.900	5.730	α	0.172	0.162	0.118	0.999	0.999	0.996
						β	0.166	0.170	0.118	0.003	0.364	0.004
						$\alpha-\beta$	0.006	-0.008	0.000	0.996	0.635	0.992
$Mn(Cp)_2$	$^2A_{1g}$	-0.73	0.311	0.782	6.634	α	0.162	0.147	0.114	0.997	0.592	0.996
						β	0.149	0.131	0.112	0.996	0.282	0.004
						$\alpha-\beta$	0.013	0.016	0.002	0.001	0.360	0.992
$Fe(Cp)_2^+$	$^6A_{1g}$	$+0.22$	0.340	0.934	6.503	α	0.169	0.162	0.124	0.996	0.999	0.997
						β	0.171	0.181	0.124	0.023	0.732	0.006
						$\alpha-\beta$	-0.002	-0.019	0.000	0.972	0.267	0.991
$Fe(Cp)_2^+$	$^2A_{1g}$	-0.73	0.317	0.827	7.589	α	0.161	0.151	0.117	0.992	0.722	0.997
						β	0.156	0.146	0.116	0.989	0.590	0.006
						$\alpha-\beta$	0.005	0.005	0.001	0.003	0.132	0.991
$Co(Cp)_2$	$^4A_{2g}$	-0.58	0.321	0.847	8.415	α	0.158	0.144	0.114	0.996	0.999	0.998
						β	0.163	0.165	0.115	0.996	0.716	0.003
						$\alpha-\beta$	-0.005	-0.021	-0.001	0.000	0.283	0.995
$Ni(Cp)_2$	$^3A_{2g}$	-0.58	0.310	0.820	9.450	α	0.150	0.137	0.110	0.998	0.999	0.998
						β	0.160	0.162	0.112	0.998	0.732	0.998
						$\alpha-\beta$	-0.010	-0.025	-0.002	0.000	0.267	0.000

The prediction of a $^3A_{2g}$ ground state for the molecular ion $V(Cp)_2^+$ substantiates experimental inference [28, 29] of this ground state. The calculated ionisation potentials for the a_{1g} level of vanadocene, 5.05 and 6.32 eV for the CNDO and INDO calculations, respectively, compare favou-

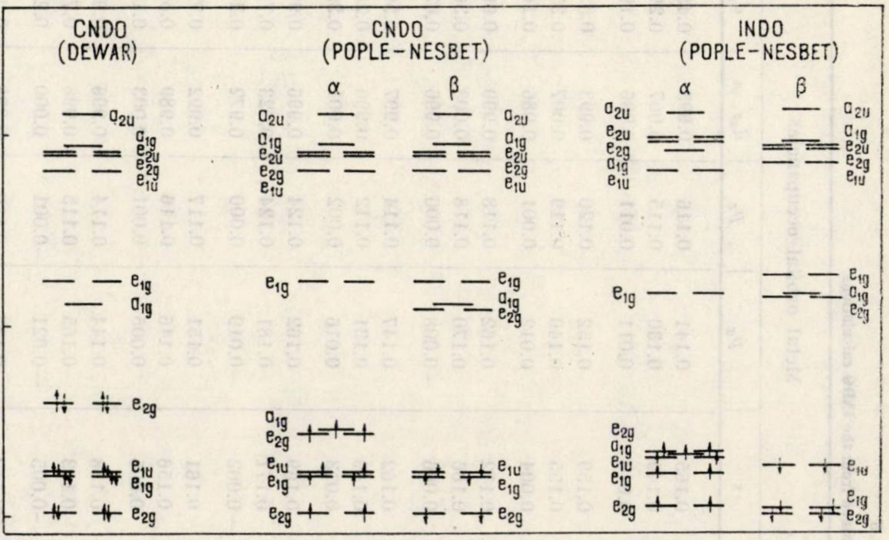
CNDO (DEWAR)
CNDO (POPLE-NESBET)
INDO (POPLE-NESBET)
α
β
10
0
-10
a2u
a1g
e2u
e2g
e1u
e1g
a1g
e2g
e1u
e1g
e2g

Fig. 12. — Molecular orbital diagram of the $^4A_{2g}$ state of $V(Cp)_2$.

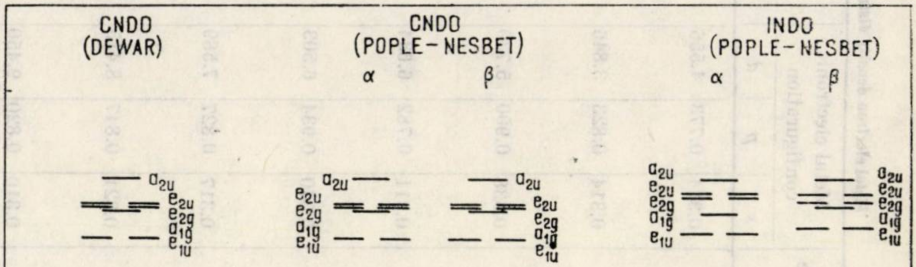
CNDO (DEWAR)
CNDO (POPLE-NESBET)
INDO (POPLE-NESBET)
α
β
10
0
-10
a2u
e2u
e2g
a1g
e1u
e1g
a1g
e2g
e1u
e1g
e2g

Fig. 13. — Molecular orbital diagram of the $^3A_{2g}$ state of $V(Cp)_2^+$.

rably with the observed value of 6.78 eV.[30] The energy level reorganisations brought about by ionisation (Figures 12 and 13) indicate the inapplicability of Koopmans'theorem.[14] The greatest differences between the α and β wavefunctions are again associated with the d_{xz} and d_{yz} orbitals and considerable spin density is accumulated in these orbitals by the INDO calculations.

Although the most likely ground state of chromocene is the ${}^3A_{2g}$ state,[9] the calculation resulted in an attempt to converge on a spatially degenerate ground state. This was due to the derivation of an incorrect energy level ordering.

The ${}^6A_{1g}(a_{1g})^1(e_{2g})^2(e_{1g})^2$ and ${}^2A_{1g}(a_{1g})^1(e_{2g})^4$ states of the d^5 manganocene have been studied and the molecular-orbital diagrams are given in Figure 14. Calculation shows these two states to be energetically similar, while experiment favours the high-spin ${}^6A_{1g}$ ground state.[31]

The CNDO and INDO calculations are at variance with respect to the absolute energy-level sequences. For the two electronic states considered, the CNDO calculations uniformly predict the common outer energy level order $e_{1g} > a_{1g} > e_{2g}$. The INDO calculations provide the alternative sequence $e_{1g} > e_{2g} > a_{1g}$, although the predominantly ligand-type e_{1g} and e_{1u} levels are now inserted between the e_{2g} and a_{1g}.

Comparison of the α and β wavefunctions shows that the greatest discrepancies arise in the constitutions of the e_{1g} type molecular orbitals. This effect is particularly pronounced in the INDO results leading to localisation of significant spin densities in the metal d_{xz} and d_{yz} atomic orbitals. Extensive charge transfer to the metal accompanies reduction in spin multiplicity due to electronic demotion to the more metal-localised e_{2g} molecular orbitals.

Similar effects are evident in the ${}^6A_{1g}$ and ${}^2A_{1g}$ states of the isoelectronic ferrocinium cation. The differences in electronic structures of $Mn(Cp)_2$ and $Fe(Cp)_2^+$ (Figures 14 and 15) are principally due to the relative degrees of divergence between the α and β spatial distributions as measured by the molecular-orbital coefficients.

The ground state of the formally d^7 cobaltocene is known[31] to be the low-spin ${}^2E_{1g}$ state arising from the component outer electronic configurations $(e_{2g})^4(a_{1g})^2(e_{1g})^1$. Unfortunately, this state cannot be studied within the Pople-Nesbet formalism adopted here and, consequently, the higher energy spatially non-degenerate ${}^4A_{2g}$ state was examined. This state results from the outer electronic configuration $(e_{2g})^4(a_{1g})(e_{1g})^2$ as shown in Figure 16. Depression of the a_{1g} eigenvalue relative to the ligand type e_{1g} and e_{1u} levels is found to result from the INDO calculation which inverts the energy level sequence a_{1g}, e_{2g} derived from the CNDO calculations. A comparable effect is manifest in the ${}^3A_{2g}(e_{2g})^1\,{}^4(a_{1g})\,{}^2(e_{1g})^2$ ground state of nickelocene, as shown in Figure 17. The close similarity in metal charges in these two species is due to the accommodation of the additional electron in the metal-localised a_{1g} molecular orbital.

Generally, both calculational procedures result in an excess of electron density being localised on the central metal atom. This is due, in part,

---

[30] S. Evans, M. L. H. Green, B. Jewitt, G. H. King and A. F. Orchard, *J. Chem. Soc., Faraday Trans. II*, **70**, 356 (1974).

[31] M. Nussbaum and J. Voitländer, *Z. Naturforsch.*, **20A**, 1417 (1965).

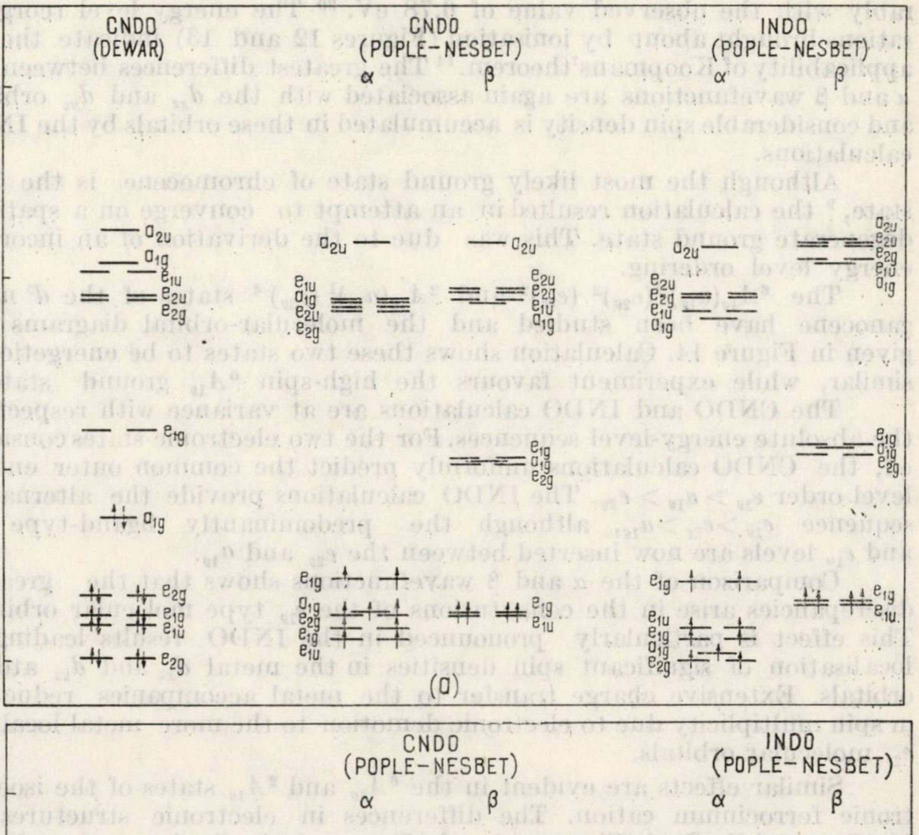
CNDO (DEWAR)
CNDO (POPLE-NESBET) α β
INDO (POPLE-NESBET) α β
20
10
0
-10
a_{2u}
a_{1g}
e_{1u}
e_{2u}
e_{2g}
e_{1g}
(a)
CNDO (POPLE-NESBET) α β
INDO (POPLE-NESBET) α β
20
10
0
-10
(b)

Fig.14. — Molecular orbital diagram of a) the ${}^6A_{1g}$ state and b) the ${}^2A_{1g}$ state of $Mn(Cp)_2$.

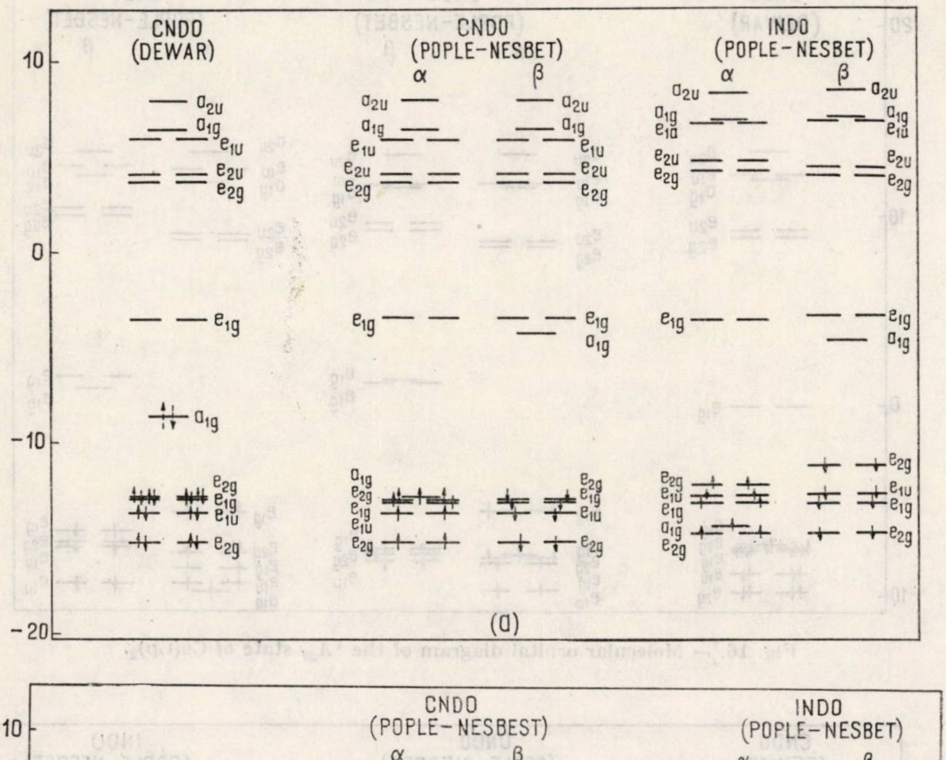
10
0
-10
-20
CNDO (DEWAR)
CNDO (POPLE-NESBET)
INDO (POPLE-NESBET)
α
β
a2u
a1g
e1u
e2u
e2g
e1g
a1g
e2g
e1g
e1u
e2g
(a)
10
0
-10
20
CNDO (POPLE-NESBEST)
INDO (POPLE-NESBET)
α
β
a2u
a1g
e1u
e2u
e2g
e1g
a1g
e2g
e1g
e2g
a1g
e1u
e2g
e1u
e1g
e2g
e2u
a1g
(b)

Fig. 15. — Molecular orbital diagram of a) the $^6A_{1g}$ state and b) the $^2A_{1g}$ state of Fe $(Cp)_2^+$.

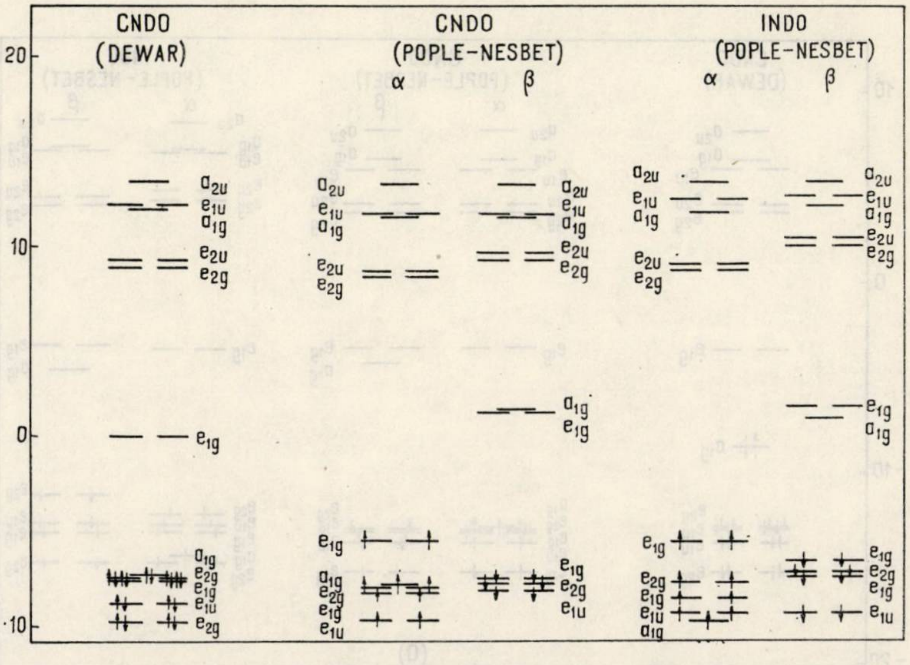
CNDO
(DEWAR)
CNDO
(POPLE-NESBET)
α
β
INDO
(POPLE-NESBET)
α
β
20
10
0
-10
a_{2u}
e_{1u}
a_{1g}
e_{2u}
e_{2g}
e_{1g}
a_{1g}
e_{2g}
e_{1g}
e_{1u}
e_{2g}
e_{1u}
a_{1g}

Fig. 16. – Molecular orbital diagram of the ${}^4A_{2g}$ state of $Co(Cp)_2$.

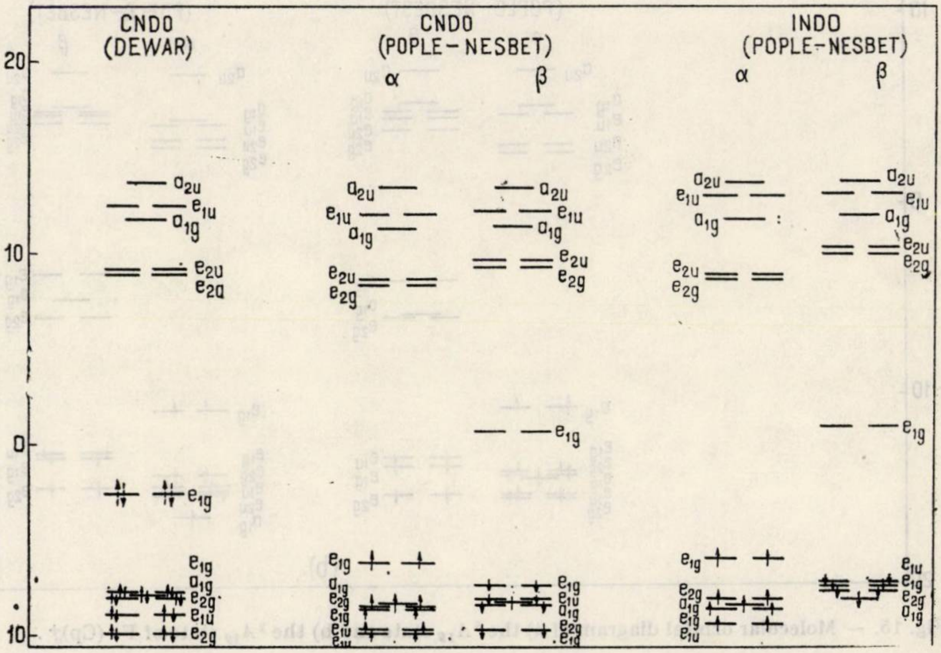
CNDO
(DEWAR)
CNDO
(POPLE-NESBET)
α
β
INDO
(POPLE-NESBET)
α
β
20
10
0
10
a_{2u}
e_{1u}
a_{1g}
e_{2u}
e_{2g}
e_{1g}
e_{1g}
a_{1g}
e_{2g}
e_{1u}
e_{2g}
e_{1u}
e_{1g}

Fig. 17. – Molecular orbital diagram of the ${}^3A_{2g}$ state of $Ni(Cp)_2$.

to the occurrence of occupied molecular orbitals of e_{1g} symmetry which contain significant contributions from the metal d_{xz} and d_{yz} orbitals and the electron density associated with these orbitals is further accentuated by the INDO calculations. In this and prior [9] studies of metallocenes, the $e_{2g}(d_{x^2-y^2}, d_{xy})$ and $a_{1g}(d_{z^2})$ molecular orbitals remain essentially metal-localised, in agreement both with experiment and with more rigorous calculation. [7] Although the concept of an energy-level sequence common to all metallocenes is open to doubt, the e_{1g} molecular orbitals which contain major contributions from the d_{xz} and d_{yz} metal atomic orbitals are more antibonding and more varied in their atomic orbital compositions than the corresponding e_{2g} and a_{1g} molecular orbitals. They have substantially more ligand character, which accounts for the increase in electron density associated with the metal when electrons are demoted from the e_{1g} to the e_{2g} or a_{1g} levels. Consequently, significant charge transfer accompanies change in multiplicity. Also, explicit derivations of the spin wavefunctions results in the introduction of skewed spatial electronic distributions. This effect is most pronounced in the e_{1g} molecular orbitals and the transfer of spin density to the d_{xz} and d_{yz} metal atomic orbitals is the major factor in determining the spin properties.

In conclusion, it may be stated that, while the approximate computational methods employed here do not afford a rigorously accurate portrayal of the electronic structure of metallocenes, the qualitative features of the bonding are adequately described and observed trends in the series considered are readily reproduced. Moreover, the INDO calculations afford a more realistic description of ground and open-shell states of molecules.

One of us (R. F.) gratefully acknowledges the award of a Crawford Bursary from the University of Strathclyde.

APPENDIX I

Metal electronic configuration used in the derivation of the core-matrix elements U_{ii}.

$$E(M, s^2 d^n) + 2U_{ss} + nU_{dd} + \frac{1}{2}(n+1)(n+2)F^\circ - 2n\left(\frac{1}{10}G_{sd}^2\right) - \frac{1}{2}n(n-1)\left[\frac{2}{63}F_{dd}^2 + \frac{2}{63}F_{dd}^4\right]$$

$$E(M, s^2 p^1 d^{n-1}) = 2U_{ss} + U_{pp} + (n-1)U_{dd} + \frac{1}{2}(n+1)(n+2)F^\circ - 2(n-1)\left(\frac{1}{10}G_{sd}^2\right) - 2\left(\frac{1}{6}G_{sp}^1\right) - \frac{1}{2}(n-1)(n-2)\left[\frac{2}{63}F_{dd}^2 + \frac{2}{63}F_{dd}^4\right] - (n-1)\left[\frac{1}{15}G_{pd}^1 + \frac{3}{70}G_{pd}^3\right]$$

$$E(M^+, s^2\,d^{n-1}) = 2U_{ss} + (n-1)\,U_{dd} + \frac{1}{2}n\,(n+1)\,F^\circ - 2(n-1)\left(\frac{1}{10}G^2_{sd}\right)$$

$$-\frac{1}{2}\,(n-1)\,(n-2)\left[\frac{2}{63}F^2_{dd} + \frac{2}{63}F^4_{dd}\right]$$

$$E(M^+, s^1\,d^n) = U_{ss} + n U_{dd} + \frac{1}{2}\,n(n+1)\,F^\circ - n\left(\frac{1}{10}G^2_{sd}\right)$$

$$-\frac{1}{2}\,n(n-1)\left[\frac{2}{63}F^2_{dd} + \frac{2}{63}F^4_{dd}\right]$$

$$U_{ss} = -I_s - (n+1)\,F^\circ + n\left(\frac{1}{10}G^2_{sd}\right)$$

$$U_{pp} = -I_p - (n+1)\,F^\circ + 2\left(\frac{1}{6}G^1_{sp}\right) + (n-1)\left[\frac{1}{15}G^1_{pd} + \frac{3}{70}G^3_{pd}\right]$$

$$U_{dd} = -I_d - (n+1)\,F^\circ + 2\left(\frac{1}{10}G^2_{sd}\right) + (n-1)\left[\frac{2}{63}F^2_{dd} + \frac{2}{63}F^4_{dd}\right]$$

APPENDIX II

Metal electronic configuration used in the derivation of the core-matrix elements U_{ii} for chromium.

$E(Cr, s^1\,d^5) = U_{ss} + 5\,U_{dd} + 15\,F^\circ - 5(1/10\,G^2_{sd}) - 10\ [2/63\,F^2_{dd} + 2/63\,F^4_{dd}]$

$E(Cr, s^1\,P^1\,d^4) = U_{ss} + U_{pp} + 4\,U_{dd} + 15\,F^\circ - (1/6\,G^1_{sp}) - 4$

$(1/10\,G^2_{sd}) - 4[1/15\,G^1_{pd} + 3/70\,G^3_{pd}] - 6\ [2/63\,F^2_{dd} + 2/63\,F^4_{dd}]$

$E(Cr^+, s^1\,d^4) = U_{ss} + 4\,U_{dd} + 10\,F^\circ - 4(1/10\,G^2_{sd}) - 6[2/63\ F^2_{dd} + 2/63\,F^4_{dd}]$

$E(Cr^+, d^5) = 5U_{dd} + 10\,F^\circ - 10\ [2/63\,F^2_{dd} + 2/63\,F^4_{dd}]$

$U_{ss} = -\,I_s - 5F^\circ + 5\,(1/10\,G^2_{sd})$

$U_{pp} = -\,I_p - 5\,F^\circ + (1/6\,G^1_{sp}) + 4[1/15\ G^1_{pd} + 3/70\,G^3_{pd}\,[$

$U_{dd} = -\,I_d - 5\,F^\circ + (1/10\,G^2_{sd}) + 4\ [2/63\,F^2_{dd} + 2/63\,F^4_{dd}]$

Revue Roumaine de Chimie, **23**, *8*, 1203–1212 (1978)

MEDIUMEINFLUSS BEI DER SOLVOLYSE VON ALKYLHALOGENIDEN. III[1]

BEMERKUNGEN ZUR LÖSUNGSMITTELABHÄNGIGKEIT DES KORRELATIONSFAKTORS LOG k GEGEN LOG $[H_2O]$

R. H. SCHUSTER * und I. A. SCHNEIDER**

*Zentrum für physikalische Chemie, Bukarest Str. Galaţi 31
**Institut für Chemie der Technischen Hochschule Iassy

Eingegangen am 17. September 1976

Im Falle von Solvolysen in wässerigem Medium wird in der Literatur die lineare Korrelation $\log k = a + \alpha \log [H_2O]$ angeführt, wo α als Reaktionsordnung in bezug auf Wasser gedeutet wird. Eine eingehendere Betrachtung dieser Korrelation ergibt, daß α lösungsmittelabhängig ist und ein umgekehrt proportionales Verhalten zur Aktivierungsenthalpie in Abbängigkeit von der Lösungsmittelzusammensetzung aufweist, woraus sich ein neuer physikalischer Sinn für α ergibt, der in Folge diskutiert wird.

Die Reaktionsgeschwindgkeit (RG) der Solvolyse eines Reaktanten X kann für ein Lösungsmittelgemisch A–B grundsätzlich durch den Ausdruck:

$$-\frac{dC_X}{dt} = kC_A^{\alpha} C_X^{\beta} + k' C_B^{\alpha'} C_X^{\beta'} = k C_A^{\alpha} C_X^{\beta} \left(1 + \frac{k' C_B^{\alpha'} C_X^{\beta'}}{k C_A^{\alpha} C_X^{\beta}}\right) \tag{1}$$

angegeben werden wobei C_A, C_B und C_X die jeweiligen Molkonzentrationen bedeuten. Ist nun der Unterschied zwischen k und k' sehr groß, wie im Falle von Wasser (A) und Alkoholen (B) oder ist B ein inertes Lösungsmittel, dann wird der Bruch in der Klammer des Ausdrucks (1) vernachlässigbar und, da sich die Konzentration C_A während der Reaktion nicht meßbar ändert, wird die beobachtete Reaktionsgeschwindigkeitskonstante (RGK):

$$k_{\text{beob.}} = kC_A^{\alpha} \tag{2}$$

oder

$$\log k_{\text{beob.}} = \log k + \alpha \log C_A \tag{2'}$$

---

[1] I. A. SCHNEIDER und R. H. SCHUSTER, *Rev. Roumaine Chim.*, (im Druck).

Es ist nun eine Sache der Einstellung des Beobachters in dieser Faktorenzerlegung der gefundenen RGK auch einen Sinn zu sehen. Etliche Male wurde das versucht, um eine Erklärung für den Lösungsmitteleffekt zu finden.[2–4] Dabei wurde der Exponent α als die Anzahl der Lösungsmittelmoleküle A die den Reaktanten im Übergangszustand umgeben (solvatisieren) definiert.

Graphisch erhaltene Werte für *t*-Butylchlorid und -bromid (*t*-BuCl, *t*-BuBr) liegen in hochwässerigen Acetongemischen bei 7 bzw. 6, wogegen im Falle der Solvolyse von Benzolsulfonsäureestern in Aceton-Wasser und Dioxan-Wasser Gemischen diese Werte eine gewisse Lösungsmittelabhängigkeit aufweisen. So wurden in einem großen Lösungsmittelbereich geringer Wasserkonzentration (10—50 Gew.% Wasser) graphisch konstante α-Werte (2,5—2,6) erhalten, die beim Übertritt in den Bereich hoher Wasserkonzentration (50—100 Gew. % Wasser) in wiederum konstante Werte von cca 6,0 umschlagen. Diese Beobachtungen erlaubten Tommila den Schluß zu ziehen, daß die α-Werte und der Substitutionsmechanismus in einer Beziehung zueinander stehen dürften. Dabei würden hohe α-Werte (6—7), da *t*-BuCl und *t*-BuBr diese Werte aufweisen einen SN_1 Mechanismus andeuten, wogegen niedere α-Werte ($\simeq 2$) einen Hinweis für einen SN_2 Vorgang etwa im Sinne eines push-pull Mechanismus,[5] darstellen sollten.

In einer vorangegangenen Arbeit [1] wurde aber bei der Solvolyse von *t*-BuCl in Aceton-Wasser Gemischen mittlerer Konzentration festgestellt, da ß α von kleineren Werten ausgehend, stetig und nichtlinear mit der Wasserkonzentration gegen Werte um 5—8 ansteigt. Da aber im Anfangsbereich keine Beschleunigung der Reaktion durch OH^- Ionen feststellbar ist, konnten wir uns nicht der Vorstellung Tommilas über eine Beziehung zwischen α und dem Reaktionsmechanismus anschließen. Gleichzeitig erschien es lohnenswert die Lösungsmittelabhängigkeit dieses Wertes für eine Reihe von Reaktanten und Lösungsmittelgemischen zu untersuchen. Es wurden ausschließlich Literaturdaten verwendet.

ERGEBNISSE UND DISKUSSION

Wegen der Ungenauigkeit der graphischen Darstellung berechneten wir die Neigung der Funktion log $k = f$ (log $[H_2O]$)für den Mittelpunkt des von zwei Konzentrationen i und j begrenzten Intervalls nach dem Ausdruck:

$$\alpha^{\frac{i+j}{2}} = \frac{\Delta \log k_{ij}}{\Delta \log [H_2O]_{ij}} = \frac{\log k_i/k_j}{\log [H_2O]_i/[H_2O]_j} \tag{3}$$

wobei die Fehlergrenze für den wirklichen α-Wert an sich viel zu klein ist um ein qualitatives Ergebnis in Frage zu stellen.

---

[2] E. Tommila, M. Tilikainen und A. Voipio, *Ann. Acad. Sci. Fennicae* AII, Nr. 65 (1955).

[3] E. Tommila, *Acta Chem. Scand.*, **9**, 975 (1955).

[4] E. A. Moelwyn-Hughes, *J. Chem. Soc.*, **1962**, 4301.

[5] C. G. Swain und W. P. Langsdorf, *J. Amer. Chem. Soc.*, **73**, 2813 (1951).

Die Berechnungen wurden vergleichsweise für wässerige und nichtwässerige Systeme angestellt. Aus Raummangel sind die verwendeten RGK nicht auch in die Tabellen einbezogen.

a) WÄSSERIGE SYSTEME

Aus Tabelle 1 und 2 geht eindeutig hervor, daß ein allgemeines lösunsgmittelabhängiges Verhalten der α-Werte, sowohl bei den Alkylhalogeniden, als auch bei den Benzolsulfonsäureestern vorliegt. Für sämtliche Reaktanten und Lösungsmittelgemische durchlaufen die experimentellen α-Werte, von, für Gemische kleinerer Wasserkonzentration ausgehend gültigen, niederen Werte (Mittelwerte bei cca 2,5) ansteigend ein eindeutiges Maximum um dann erneut abzufallen.

Tabelle 1

Berechnete α-Werte für die Solvolyse einiger Alkylhalogenide in Gemischen A – H_2O

RX	A	Wasser, Mol/l									T °C
		8,33	13,8	19,4	24,8	30,5	36,1	41,6	47,2	52,7	
t-BuCl[6]	MeOH	2,26	3,33	4,21	4,95	5,26	5,14	4,66	4,56	5,22	25
	EtOH	2,47	3,88	4,22	5,32	6,84	8,06	5,68	4,65	4,40	25
	Me_2CO	3,97	4,81	5,06	6,78	7,23	7,62	7,28	6,07	6,71	25
	Dioxan	3,50	4,61	5,32	5,96	7,67	7,50	5,03	5,36	5,78	25
t-BuBr[7]	MeOH	2,57	3,12	3,93	5,08	7,78	—	—	4,81	—	0
	EtOH	2,66	—	4,23	4,82	5,09	—	—	4,91	—	0
	EtOH	2,43	3,21	3,66	5,45	6,48	—	—	5,70	—	25
	Dioxan	—	4,83	5,48	6,43	6,81	6,51	—	5,33	—	0
α-PhEtCl[8]	EtOH	2,21	3,01	3,91	5,36	7,60	8,27	6,88	6,24	5,90	25
α-PhEtBr[7]	Dioxan	3,76	4,77	5,58	6,97	7,82	8,85	—	6,36	—	25
$(CH_3)_2PhC-CH_2Cl$[9]	EtOH	—	0,99	—	4,22	5,80	7,37	6,67	—	—	50
	MeOH	—	2,02	3,41	4,18	4,60	4,26	—	—	—	50
$(CH_3)_2PhC-CH_2Br$[9]	EtOH	2,09	2,72	—	4,15	5,55	7,41	6,53	—	—	50

---

[6] A. H. Fainberg und S. Winstein, *J. Amer. Chem. Soc.*, **78**, 2770 (1957).

[7] A. H. Fainberg und S. Winstein, *J. Amer. Chem. Soc.*, **79**, 1602 (1957).

[8] A. H. Fainberg und S. Winstein, *J. Amer. Chem. Soc.*, **79**, 1597 (1957).

[9] A. H. Fainberg und S. Winstein, *J. Amer. Chem. Soc.*, **79**, 1608 (1957).

Diese Maximumwerte liegen für Alkylhalogenide ziemlich unterschiedlicher Struktur zwischen 5—6, im Einklang mit dem von Moelwyn-Hughes erhaltenen Grenzwert für *t*-BuCl im Methanol-Wasser System. Daraus ist ersichtlich, daß eine komplizierte Lösungsmittelabhängigkeit der α-Werte vorliegt und daß kein Zusammenhang mit dem Reaktionsmechanismus (SN_1 oder SN_2) bestehen kann. Würde ein solcher im Sinne des Vorschlags von Tomilla existieren wäre ein Maximum der α-Werte für einen typischen SN_1-artigen Vorgang wie z.B. die Solvolyse der tertiären Alkylhalogenide gefolgt von einem Abfall dieser Werte gegen reines Wasser im Sinne unserer bisherigen Kenntnisse über Reaktionsmechanismen undenkbar. Wir sehen daher in unserem Befund eine Weiterentwickelung der Beobachtugen von Tommila im Sinne einer Lösungsmittelabhängigkeit der α-Werte entsprechend Gleichung (2′).

Tabelle 2

Berechetnete α-Werte für die Solvolyse einiger Alkyl-Benzolsulfonsäuereester in Aceton-Wasser

iPr—OSO_2Ph		nPr—OSO_2Ph		Et—OSO_2Ph	
H_2O Mol^2/l	α	H_2O Mol/l	α	H_2O Mol/l	α
53,9	6,06	—	—	54,7	2,62
50,7	5,41	51,4	2,83	52,7	5,26
48,2	11,59	—	—	48,5	3,26
45,2	6,89	—	—	—	—
43,7	5,48	43,8	5,48	—	—
38,1	6,22	36,1	3,91	38,8	3,69
27,7	1,89	24,9	1,03	27,7	2,67
15,8	2,50	15,8	1,95	13,8	1,84
5,75	2,01	7,00	1,62	—	—
3,65	2,25	—	—	3,85	1,56
2,80	1,05	—	—	2,30	1,72

Die Höhe der oben erwähnten, in wässerigen Gemischen allgemein auftretenden Maxima, bezogen auf den Wert bei 8,33 Mol/1 Wasser steigt in der Serie : Aceton < Dioxan < Methanol < Äthanol an.

Außerdem sind die Anfangswerte insbesondere für die weniger polaren Gemische, wie Dioxan-Wasser oder Aceton-Wasser größer als für Methanol-Wasser und Äthanol-Wasser, was wiederum gegen eine Auslegung der α-Werte als Mechanismuskriterium spricht, da ja polare Medien typische SN_1-artige Prozesse begünstigen sollten. Sogar bei typischen SN_1-Reaktanten, wie *t*-BuCl und *t*-BuBr liegen die Anfangswerte für α niedriger (etwa um 2,5), so daß der Vorschlag diesen Wert als Mechanismuskriterium zu werwenden, eher auf einer unvollständigen Untersuchung seiner Lösungsmittelabhängigkeit zurückzuführen ist, und kaum den Tatsachen entsprechen dürfte.

Wird nun wieder auf die herkömmliche Art den α-Wert zu deuten zurückgegriffen, als die Anzahl der Wassermoleküle die den Übergangszustand umgeben, so würde ein maximaler Wert desselben eine extreme Solvatation des Übergangszustandes bedeuten, was wiederum bei gleichbleibender Solvatation des Grundzustandes ein Minimum der Aktivierungsenergie zur Folge haben würde.

Ein Vergleich der Konzentrationsabhängigkeit der Aktivierungsenthalpie für *t*-BuCl, *t*-BuBr und Benzolsulfonsäureester in verschiedenen Lösungsmitteln mit dem Verlauf der α-Werte deutet auf eine auffallende Symmetrie hin (Abbildung 1, 2 und 3). Dem maximalen α-Wert entspricht

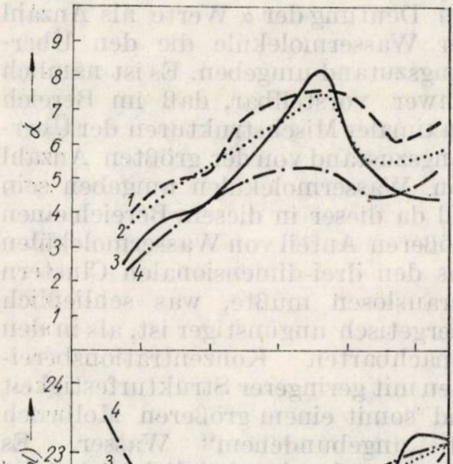

Abb. 1. Verlauf der α und $\Delta H^{\neq}$ Kurven für *t*-BuCl in Abhängigkeit des Logarithmus der Molkonzentration Wasser. 1 — Dioxan-H_2O; 2 — Me_2CO-H_2O; 3 — EtOH-H_2O; 4 — MeOH-H_2O.

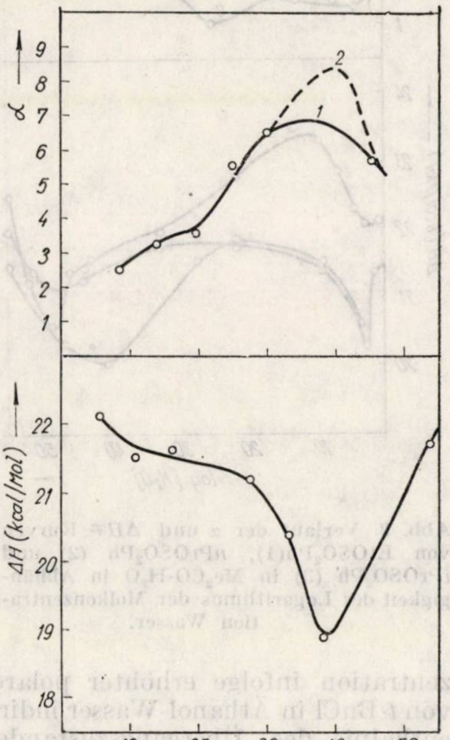

Abb.2. Verlauf der α und $\Delta H^{\neq}$ Kurven für *t*-BuBr in EtOH-H_2O in Abhängigkeit des Logarithmus der Molkonzentration Wasser.

ein minimaler $\Delta H^{\neq}$-Wert und die Form der $\Delta H^{\neq}$ Kurven ist in etwa das Spiegelbild der α-Kurven, ausgenommen der Bereich sehr hoher Wasserkonzentrationen (45—55, 55 Mol/l Wasser).

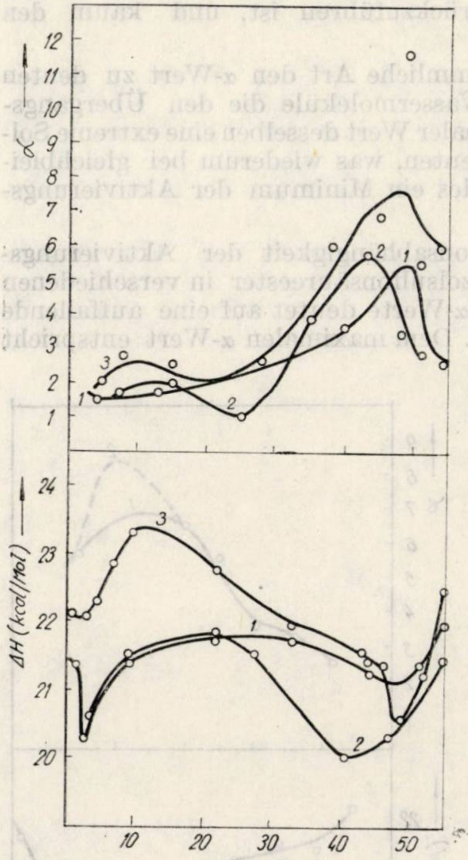

Abb. 3. Verlauf der α und $\Delta H^{\neq}$ Kurven von $EtOSO_2Ph$(1), $n$$PrOSO_2Ph$ (2) und $i$$PrOSO_2Ph$ (3) in Me_2CO-H_2O in Abhängigkeit des Logarithmus der Molkonzentration Wasser.

Dieser Befund würde auf den ersten Blick im Sinne der Definition der α-Werte sein, doch weisen laut Literaturangaben binäre wässerige Lösungsmittelsysteme aufgrund der speziellen Struktur des Wassers [10,11] Mischstrukturen auf, deren Stabilität bei einer bestimmten Konzentration des Gemisches ein Maximum erreicht.[12] Diesem Strukturmaximum entspricht eine minimale Solvatation des Grundzustandes, wodurch das $\Delta H^{\neq}$ Minimum der Solvolysereaktionen zu erklären ist. Dieses widerspricht nun wieder der oben angeführten Deutung der α-Werte als Anzahl der Wassermoleküle die den Übergangszutand umgeben. Es ist nämlich schwer vorstellbar, daß im Bereich maximaler Mischstrukturen der Übergangszustand von der größten Anzahl von Wassermolekülen umgeben sein soll da dieser in diesem Bereich einen größeren Anteil von Wassermolekülen aus den drei-dimensionalen Clustern herauslösen müßte, was schließlich energetisch ungünstiger ist, als in den benachbarten Konzentrationsbereichen mit geringerer Strukturfestigkeit und somit einem größeren Molbruch an „ungebundenem" Wasser. Es scheint viel wahrscheinlicher, daß die Solvatationsenthalpie eines stark polaren oder sogar ionisierten Übergangszustandes weniger sensibel als der Grundzustand gegen Strukturschwankungen des Lösungsmittels ist und eher leicht mit der Wasserkonzentration infolge erhöhter polarer Effekte ansteigt. So wurde im Falle von t-BuCl in Äthanol-Wasser indirekt festgestellt [13], daß die Solvatationsenthalpie des Übergangszustandes gegen hohe Wasserkonzentrationen

---

[10] G. Nemethy und H. Scheraga, *J. Chem. Phys.*, **36**, 3382 1962).

[11] H.S. Frank und W-Y. Wenn, *Discuss. Faraday Soc.*, **24**, 133 (1957).

[12] F. Franks und D. Ives, *Quart. Rev.*, **20**, 1 (1966).

[13] E. M. Arnett, W. G. Bentrude, J. J. Burke, und P. Mc C. Duggleby *J. Amer. Chem. Soc.*, **87**, 1541 (1965).

leicht ansteigt und im kritischen Strukturgebiet nur ein geringes Minimum durchläuft welches in diesem Sinne unwesentlich scheint.

Daher erscheint es angebracht, daß α-Werten eine andere Deutung als die Anzahl der den Übergangszustand umgebenden Wassermoleküle, zukommt. Für eine anschauliche Deutung der α-Werte gehen wir von dem Befund aus, daß die α- und $\Delta H^{\neq}$-Werte als Funktionen der Lösungsmittelkonzentration einen symmetrisch entgegengesetzten Verlauf aufweisen und daß die Solvatation des Grundzustandes zum Übergangszustand bedeutender von der Lösungsmittelkonzentration beeinflußt wird. Laut Eyring'scher Geschwindigkeitsgleichung[14]:

$$\ln k = \ln\left(\varkappa \frac{k_{\mathrm{B}}\, T}{h} K_0^{\mathrm{x}}\right) + \ln \frac{f_{\mathrm{A}}}{f_{\mathrm{A}\neq}} \qquad (4)$$

wird die Geschwindigkeitskonstante einer Solvolysereaktion vor allem von dem Verhältnis der Aktivitätskoeffizienten des Grundzustandes (f_{A}) und des Übergangszustandes ($f_{\mathrm{A}\neq}$) bestimmt. Dieses Verhältnis ist aber im Bereich der kompakteren Mischstrukturen am größten da hier der Grundzustand am schwächsten solvatisiert wird. Daraus ergibt sich aber für dieses Gebiet ein maximaler Anstieg der log k-Werte als Funktion der Lösungsmittelzusammensetzung, wie auch aus dem Schema in Abb. 4

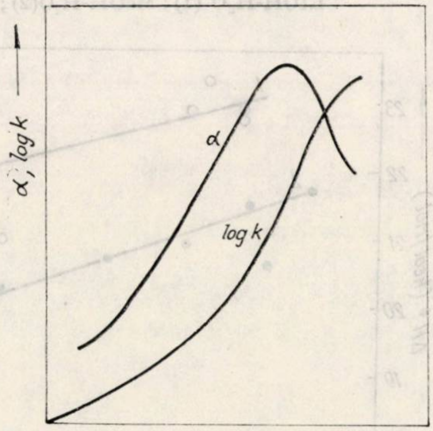

Abb. 4. Schematischer Verlauf der α und log k Werte in Abhängigkeit der Wasserkonzentration.

hervorgeht, wobei wir bemerken möchten, daß dieses Verhalten, mehr oder weniger betont in allen von uns untersuchten Beispielen aufzufinden war. Zu bemerken wäre fernerhin, daß der maximale Anstieg der log k-Werte genau in dem Bereich der höchsten α-Werte liegt, da beide Extremwerte auf dieselbe Ursache zurückzuführen sind. Auf diese Weise könnten aber letztlich auch die Aktivitätskoeffizienten bestimmt werden. Der

---

[14] K. J. Laidler und H. Eyring, *Ann. N. Y. Acad. Sci.*, **39**, 303 (1940).

α-Wert kann also eher als eine Funktion angesehen werden die dem Verhältnis der Solvatationsenergien des Grundzustandes und des Übergangszustandes Rechnung trägt.

Im Bereich geringerer Wasserkonzentrationen, bis zu Erreichen der Extremwerte von α oder $\Delta H^{\neq}$ besteht eine gute direkte Proportionalität zwischen diesen Größen. Diese Proportionalität ist wie aus Abbildung 5 hervorgeht leicht von dem Lösungsmittelsystem abhängig und weist für Äthanol-Wasser und Methanol-Wasser eine größere Neigung als für Aceton-Wasser und Dioxan-Wasser auf.

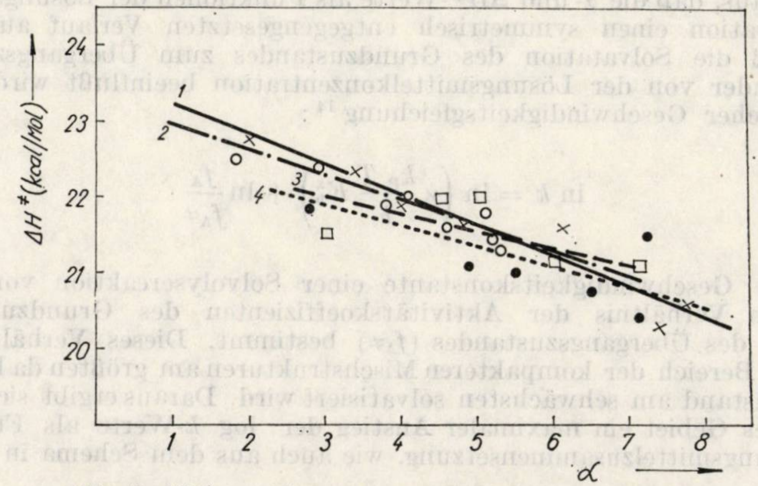

Abb. 5. $\Delta H^{\neq} - \alpha$ Korrelation für die Solvolyse von t-BuCl in EtOH-H_2O (1) ; MeOH-H_2O(2) ; Dioxan-H_2O (3 ; Me_2CO-H_2O (4).

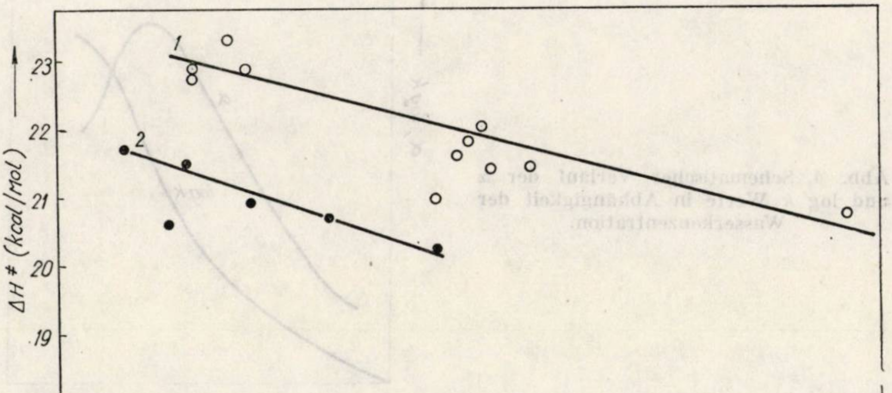

Abb. 6. $\Delta H^{\neq} - \alpha$ Korrellation für die Solvolyse von iPrOSO$_2$Ph (1) und nPrOSO$_2$Ph in Me_2CO-H_2O.

Auch für die aus den Ergebnissen von Tommila ermittelten α-Werten für Benzolsulfonsäuereester ist diese lineare Abhängigkeit vorhanden.

Interessanterweise ist die Neigung der $\Delta H^{\neq} - \alpha$ Geraden für Alkylchloride größer, als für die entsprechenden Alkylbromide, wobei der Einfluß des Alkylrests zweitrangig erscheint. Dieser Befund läßt wiederum darauf schließen, daß bestimmend für α das Solvatationsverhältnis des Grund- und Übergangszustandes ist.

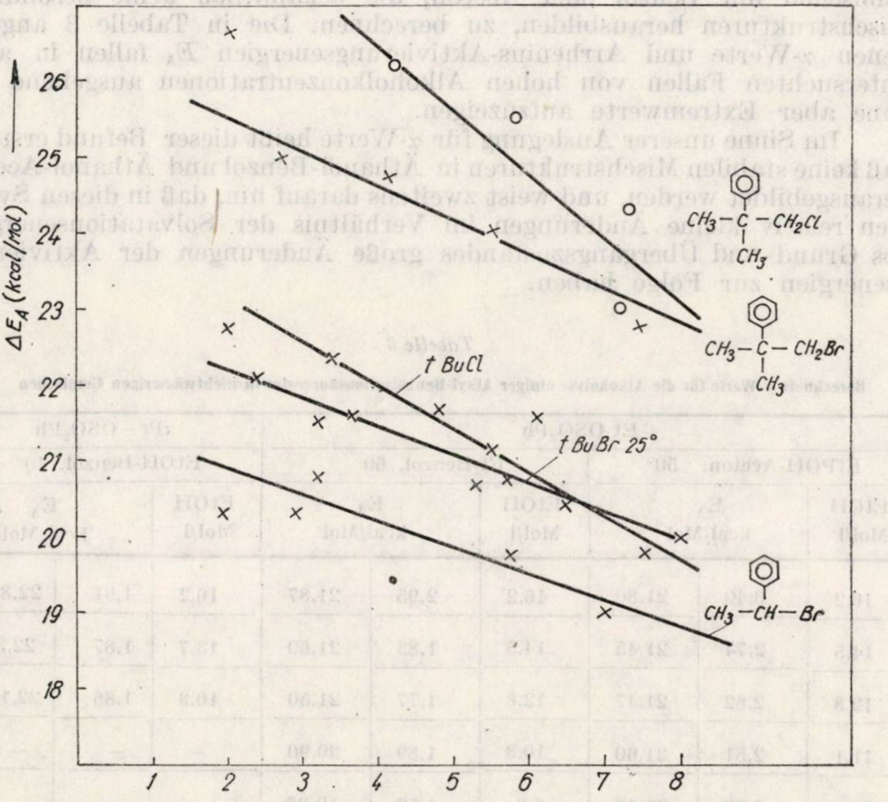

Abb. 7. $\Delta E_A - \alpha$ Korrelation für die Solvolyse einiger Alkylhalogenide EtOH-H_2O.

Im Bereich hoher Wasserkonzentrationen besteht die lineare Beziehung $\Delta H^{\neq} - \alpha$ nicht mehr wie aus Abb. 1 ersichtlich ist. Sowohl der Grund- als auch der Übergangszustand wird durch freie Wassermoleküle im selben Sinne solvatisiert.

b) NICHTWÄSSERIGE SYSTEME

Wie bekannt bilden auch Alkohole im flüssigen Zustand gewisse Strukturen, auch durch Wasserstoffbrückenbindung bedingt, die aber weit weniger stabil als die im Falle von Wasser sind. Es schien deshalb interessant im Vergleich zu wässerigen Gemischen α-Werte in Äthanol gemischen mit Benzol oder Aceton, die bekanntlich keine besonderen Mischstrukturen herausbilden, zu berechnen. Die in Tabelle 3 angegebenen α-Werte und Arrhenius-Aktivierungsenergien E_A fallen in allen untersuchten Fällen von hohen Alkoholkonzentrationen ausgehend ab, ohne aber Extremwerte aufzuzeigen.

Im Sinne unserer Auslegung für α-Werte heißt dieser Befund erstens, daß keine stabilen Mischstrukturen in Äthanol-Benzol und Äthanol-Aceton herausgebildet werden, und weist zweitens darauf hin, daß in diesen Systemen relativ kleine Änderungen im Verhältnis der Solvatationsenergien des Grund- und Übergangszustandes große Änderungen der Aktivierungsenergien zur Folge haben.

Tabelle 3

Berechnete α-Werte für die Alkoholyse einiger Alkyl-Benzolsulfonsäureester in nichtwässerigen Gemischen

Et-OSO_2Ph						iPr$-OSO_2$Ph		
EtPOH-Aceton, 50°			Et-Benzol, 60°			EtOH-Benzol, 40°		
EtOH Mol/l	E_A kcal/Mol		EtOH Mol/l	E_A kcal/Mol		EtOH Mol/l	E_A kcal/Mol	
16,2	3,40	21,80	16,2	2,95	21,87	16,2	1,91	22,80
14,5	2,74	21,45	14,5	1,83	21,60	13,7	1,87	22,35
12,8	2,62	21,47	12,8	1,77	21,50	10,3	1,86	22,10
11,1	2,51	21,60	10,3	1,89	20,90	—	—	—
9,4	2,39	21,40	6,8	1,52	19,96			
7,7	1,98	21,06	3,4	1,66	17,15			
6,0	1,58	21,53	1,3	2,05	15,10			
4,2	1,81	21,38	—	—	—	—	—	—

Wie immer benötigen wir weitere Belege für unsere Auslegungen, so daß es vorläufig wenig sinnvoll scheint eine weitere physikalische Bedeutung für die $\Delta H^{\neq} - \alpha$ Korrelation und das Solvatationsverhalten der Reaktanten zu suchen.

Revue Roumaine de Chimie, 23, 8, 1213 – 1232 (1978)

g-VALUES OF TRIGONALLY DISTORTED OCTAHEDRAL d^1 SYSTEMS : THE $Ti(H_2O)_6^{3+}$ COMPLEX ION IN FROZEN AQUEOUS SOLUTIONS

PAVLE I. PREMOVIČ
Department of Chemistry, University of Niš, Niš, Yugoslavia

Received June 9, 1976

MO expressions for the g-values of octahedral d^1 system with a relatively strong trigonal distortion, $D_{3d'}$, D_3 and C_{3v} symmetries, are derived in terms of a d_{z^2} ground state neglecting the contributions of charge-transfer terms. For the $Ti(H_2O)_6^{3+}$ complex ions in frozen aqueous solutions, where we assume that the metal-ligand bonding is rather ionic, this MO treatment is shown to be equivalent to that of the crystal field and offers a plausible interpretation for the recently published ESR g-values. This is demonstrated within the point-charge formalism by correlating theoretical $g_\perp$ — values with the angular distortion parameter θ.

INTRODUCTION

ESR studies of paramagnetic transition-metal complexes yield information about the distribution of the unpaired electrons and hence about the nature of the bonding between the metal ion and its ligands. There have been many reports concerning the application of ESR to trigonally distorted octahedral compounds of Ti(III), and of the interpretations of the ESR parameters in terms of crystal field parameters and the covalency of the metal-ligand bonding. Shifts of g-values from the free electron value as a measure of spin-orbit mixing of antibonding states into the ground state varies remarkably from compound to compound, for example, the g-values of titanium (III) acetylacetonate approach the free electron value while those of cesium titanium (III) alum show appreciable deviation from that value. The spin-lattice relaxation time also varies considerably from one system to another. In some cases the ESR could be observed only at liquid helium temperature, e.g. cesium titanium (III) alum while that of titanium (III) acetyl acetonate is readily observed at room temperature.

The ground state of a $3d^1$ ion such as Ti (III) is ^2D, separated in the free ion by a rather large energy, 80378 cm^{-1} from the first excited state (the $3d^1 - 4s^1$) transition.[1] An ideal octahedral crystal field, O_h symmetry, splits the ^2D state into a low lying $^2T_{2g}$ state and an upper ^2E_g state.

---

[1] C. E. Moore, "Atomc Energy Levels", US Bur. Stand. Circ. No. 467, 1964.

If the octahedron is distorted along the trigonal axes, the symmetry of the complex molecule is lowered from O_h to D_{3d}, D_3 or C_{3v} ; in all three cases the threefold degenerate level T_{2g} in O_h splits into one single and one twofold degenerate level. The twofold level E_g, in O_h, however, remains degenerate. The correlation diagram for d^1 ion in the trigonal crystal field is given in Figure 1.

The crystal field expressions for the g-values of octahedral Ti (III) complexes with some trigonal distortion have been discussed by Bleaney,[2] Jarrett,[3] Gladney and Swalen[4] and McGarvey[5] in terms of a $d_z^2 (= d_0)$ ground state. Ray[6] also considered this problem and derived expressions for the g-values in the presence of a crystal field of trigonal symmetry and covalent bonding. He expressed the g-values as a function of two parameters (P and Q in his terminology) in such a fashion that the quantitative estimates of the relative importance of the crystal-field parameters and the influence of covalent bonding are difficult to make. Interpretation of g-values in terms of these parameters does little to further chemical insight. McGarvey[7] presents equations for the g-values which are only an extension of the work of Ray and which include the effects of covalent bonding on the second order terms.

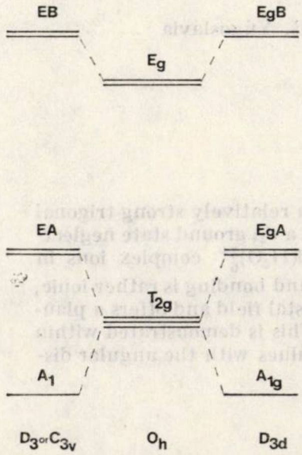

Fig. 1. — Splittings under trigonal distortion.

In the first part of this paper, we derive expressions for the g-tensor in terms of MO expansion coefficients for octahedral d^1 systems with a relatively strong trigonal distortion which have charge transfer bands at much higher energy than $d-d$ bands. This is done in order to illustrate the importance of certain terms which have usually been neglected in the past. In the second part, we attempt to show the sensitivity of the $g_\perp$-values to small angular departures from octahedral symmetry in trigonal systems. As an example we use the $Ti(H_2O)_6^{3+}$ complex ion in frozen aqueous solutions in which we assume that the covalency plays a minor role. In this case the MO formula for the $g_\perp$-value developed in the first part reduces to a relatively simple expression. Employing this expression and the point-charge calculation of Gerloch and coworkers,[8] theoretical $g_\perp$-values are obtained for this system. The following abbreviations will be used : CF = crystal field, PC = point-charge, and CT = charge transfer.

---

[2] B. Bleaney, *Proc. Phys. Soc. (London)*, **A63**, 407 (1950).

[3] B. H. S. Jarrett, *J. Chem. Phys.*, **42**, 1999 (1965).

[4] B. H. S. Gladney and J. D. Swalen, *J. Chem. Phys.*, **42**, 199 (1965).

[5] B. R. McGarvey, *Transition Metal Chem.*, **3**, 89 (1966).

[6] D. K. Ray, "Soviet Phys.-Solid State", **3**, 1838 (1962). See also *Nuovo Cimento*, **21**, 1 (1961).

[7] B. R. McGarvey, *J. Chem. Phys.*, **38**, 388 (1963).

[8] M. Gerloch, J. Lewis, G. G. Philips and P. N. Quested, *J. Chem. Soc.* (A), **(1970)**, 1941.

THE PRINCIPAL COMPONENTS OF THE g-TENSOR IN A TRIGONAL d^1 SYSTEM *

We shall consider a one electron-system, with the electron in the d_z^2 orbital, so that the ground state is A_{1g}^*. Only states of E_g symmetry can mix with ground state under perturbation of the angular momentum operator so that we need consider only MO's belonging to the representation a_{1g} and e_g. The coordinate axis system is shown in Figure 2. The z axis is chosen as the threefold axis. If the angle θ is defined as the angle between any bond and the principal rotation axis z, then a trigonal squash occurs when $\theta > 54.75°$ ($= \theta_{\text{oct}}$, the angle in O_h symmetry) and a trigonal elongation when $\theta < 54.75°$. The relevant antibonding MO's can be written down as :

$$a_{1g} = \alpha_1^* d_z^2 - \alpha_2^* \Phi\,(a_{1g}) \tag{1}$$

$$e_g\,1A = a_1 d_{x^2-y^2} - b_1 d_{xz} - \beta_2^* \Phi(e_g\,1A) \tag{2}$$

$$e_g\,2A = a_2 d_{xy} + b_2 d_{yz} - \gamma_2^* \Phi(e_g\,2A) \tag{3}$$

$$e_g\,1B = b_3 d_{x^2-y^2} + a_3 d_{xz} - \delta_2^* \Phi\,(e_g\,1B) \tag{4}$$

$$e_g\,2B = b_4 d_{xy} - a_4 d_{yz} - \varepsilon_2^* \Phi\,(e_g\,2B) \tag{5}$$

where the metal orbitals are the usual d functions, and the ligand functions, Φ, are group orbitals (or set of group orbitals) of appropriate symmetry.**

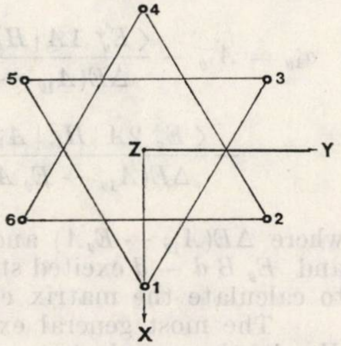

Fig. 2. — Definition of axes.

Notice that Ray[6] preferred to use as the metal orbitals the linear combinations

Symmetry	*Metal Orbital*
$a^1{}_g$	d_0
$e_g\,A$	$ad_2 - bd_{-1}$
	$ad_{-2} + bd_1$
$e_g\,B$	$bd_2 + ad_{-1}$
	$bd_{-2} - ad_1$

with the orthonormality condition $a^2 + b^2 = 1$. However, metal orbitals given by expressions (1) — (5) are found to be particularly convenient and simple here since matrix elements such as $<d|H_{1s}|\,d>$ and $<d|\hat{l}_x|\,d>$ can be more readily evaluated using table A.1. in Appendix A. Clearly, the two ways of writing the metal orbitals are equivalent and supplementary to each other.

---

* Although we are dealing in our treatment with the D_{3d} system, the results are applicable for the D_3 and C_{3v} systems. Note that in these cases the proper notation ought to be used (Figure 1).

** The wavefunctions (1)—(5), which describe MO's, will represent the states (denoted by capital letters) arising from the occupancy by the d^1 electron.

We now proceed to derive expressions for the principal $g_{\|}$ and $g_{\perp}$ components of the g-tensor in our trigonal d^1 system. To first order, the two ground-state spin functions in the presence of spin-orbit interaction will be

$$a_{1g}^{+} = A_{1g}^{+} - \frac{\langle E_g^{-}\, 1A \,|\, H_{ls} \,|\, A_{1g}^{+}\rangle}{\Delta E(A_{1g} \to E_g\, A)}\, E_g^{-}\, 1A - \frac{\langle E_g^{-} 1B \,|\, H_{ls} \,|\, A_{1g}^{+}\rangle}{\Delta E(A_{1g} \to E_g B)}\, E_g^{-}\, 1B - \frac{\langle E_g^{-}\, 2A \,|\, H_{ls} \,|\, A_{1g}^{+}\rangle}{\Delta E(A_{1g} \to E_g\, A)}\, E_g^{-}\, 2A - \frac{\langle E_g^{-}\, 2B \,|\, H_{ls} \,|\, A_{1g}^{+}\rangle}{\Delta E(A_{1g} \to E_g\, B)}\, E_g^{-}\, 2B \tag{6}$$

$$a_{1g}^{-} = A_{1g}^{-} - \frac{\langle E_g^{+}\, 1A \,|\, H_{ls} \,|\, A_{1g}^{-}\rangle}{\Delta E(A_{1g} \to E_g A)}\, E_g^{+} 1A - \frac{\langle E_g^{+}\, 1B \,|\, H_{ls}\, A_{1g}^{-}\rangle}{\Delta E(A_{1g} \to E_g B}\, E_g^{+}\, 1B - \frac{\langle E_g^{+}\, 2A \,|\, H_{ls} \,|\, A_{1g}^{-}\rangle}{\Delta E(A_{1g} \to E_g\, A)}\, E_g^{+} 2A - \frac{\langle E_g^{+}\, 2B \,|\, H_{ls} \,|\, A_{1g}^{-}\rangle}{\Delta E(A_{1g} \to E_g B)}\, E_g^{+}\, 2B \tag{7}$$

where $\Delta E(A_{1g} \to E_g A)$ and $\Delta E(A_{1g} \to E_g\, B)$ are the energies of the $E_g A$ and $E_g\, B\; d - d$ excited states. Before proceeding any further, it is useful to calculate the matrix elements in expressions (6) and (7).

The most general expression for the spin-orbit coupling operator, H_{ls}, in the one-electron case is

$$H_{ls} = \lambda_M(r_M)\, \hat{l}_M \hat{s} + \sum_{L=1}^{6} \lambda_L\, (r_L)\, \hat{l}_L\, \hat{s} \tag{8}$$

where r_k is the distance of the unpaired electron from the nucleus $k = M$, $L(=1 - 6)$, where the subscripts M and L denote the metal and the appropriate ligand atom, respectively; $\hat{l}_k$ is the orbital angular momentum operator for the unpaired electron centred on nucleus k; and $\lambda_k(r_k)$ is the atomic spin-orbit coupling constant for the appropriate orbital of atom k.

The operator $\hat{l} \cdot \hat{l}$ is written as

$$\hat{l} \cdot \hat{s} = \hat{l}_x\, \hat{s}_x + \hat{l}_y\, \hat{s}_y + \hat{l}_z\, \hat{s}_z \tag{9}$$

The functions obtained by the operation of the $\hat{l} \cdot \hat{s}$ operator are given in table A.1 (Appendix A).

Now we are in position to evaluate the various matrix elements in expression (6). Consider first the integral $\langle E_g^{-}\, 1A \,|H_{ls}\,|\, A_{1g}^{+}\rangle$, where the $E_g^{-} 1A$ is a $d{-}d$ excited state with the electron in the $e_g\, 1A$ antibonding MO as given by (2). Writing this integral out *in extenso*, we have

$$\langle a_1\, d_{x^2-y^2}^{-} - b_1 d_{xz}^{-} - \beta_2^{*}\, \Phi^{-}(e_g\, 1A) \,|\, H_{ls} \,|\, \alpha_1^{*}\, d_{z^2}^{2} - \alpha_2^{*} \Phi^{+}\, (a_{1g}) \rangle \tag{10}$$

Since λ_k is proportional to r_k^{-3} for hydrogen-like wavefunctions it seems reasonable to suppose that only one-center integrals of the type

$\langle\psi|\lambda_k(r_k)\,\hat{l}_k\hat{s}\,|\,\psi\rangle$ are significantly different from zero. There are only two terms to consider, given by (11) and (12).

$$-b_1\alpha_1^*\langle d_{xz}^-\,|\,\lambda_M(r_M)\,\hat{l}_M\,\hat{s}\,|\,d_{z^2}^+\rangle \tag{11}$$

$$\alpha_2^*\,\beta_2^*\langle\,\Phi^-(e_g\,1A)\,|\,\lambda_L(r_L)\,\hat{l}_L\cdot\hat{s}\,|\,\Phi^+(a_{1g})\,\rangle \tag{12}$$

The first of these (11) is simply equal to

$\frac{\sqrt{3}}{2}\,b_1\alpha_1^*\lambda_M$. Equation (12), after expansion of the ligand group orbitals,* is found to be zero.

We thus end up

$$-\langle\,E_g^-\,1A\,|\,H_{ls}\,|\,A_{1g}^+\,\rangle = -\frac{\sqrt{3}}{2}b_1\,\alpha_1^*\,\lambda_M \tag{13}$$

Similarly, we evaluate the rest of the integrals in equations (6) and (7) and the solutions are

$$-\langle\,E_g^-\,1B\,|\,H_{ls}\,|\,A_{1g}^+\,\rangle = \frac{\sqrt{3}}{2}\,a_3\,\alpha_1^*\,\lambda_M \tag{14}$$

$$-\langle\,E_g^-\,2A\,|\,H_{ls}\,|\,A_{1g}^+\,\rangle = \frac{\sqrt{3}}{2}\,\mathrm{i}b_2\,\alpha_1^*\,\lambda_M \tag{15}$$

$$-\langle\,E_g^-\,2B\,|\,H_{ls}\,|\,A_{1g}^+\,\rangle = -\frac{\sqrt{3}}{2}\,\mathrm{i}a_4\,\alpha_1^*\,\lambda_M \tag{16}$$

$$-\langle\,E_g^+\,1A\,|\,H_{ls}\,|\,A_{1g}^-\,\rangle = \frac{\sqrt{3}}{2}\,b_1\,\alpha_1^*\,\lambda_M \tag{17}$$

$$-\langle\,E_g^+\,1B\,|\,H_{ls}\,|\,A_{1g}^-\,\rangle = -\frac{\sqrt{3}}{2}\,a_3\,\alpha_1^*\,\lambda_M \tag{18}$$

$$-\langle\,E_{1g}^+\,2A\,|\,H_{ls}\,|\,A_{1g}^-\,\rangle = \frac{\sqrt{3}}{2}\,\mathrm{i}b_2\,\alpha_1^*\,\lambda_M \tag{19}$$

$$-\langle\,E_g^+\,2B\,|\,H_{ls}|\,A_{1g}^-\rangle = -\frac{\sqrt{3}}{2}\,\mathrm{i}a_4\alpha_1^*\,\lambda_M \tag{20}$$

*** These are obtained from the standard projection operator method.**

Introducing (13) — (16) and (17) — (20) into expressions (6) and (7), respectively, we get

$$a_{1g}^{+} = A_{1g}^{+} - \frac{\sqrt{3}\alpha_1^{*}\lambda_M}{2\Delta E(A_{1g} \rightarrow E_g A)} (b_1 E_g^{-}\, 1A - \mathrm{i} b_2\, E_g^{-}\, 2A) +$$

$$+ \frac{\sqrt{3}\alpha_1^{*}\lambda_M}{2\Delta E(A_{1g} \rightarrow E_g B)} (a_3 E_g^{-}\, 1B - \mathrm{i} a_4 E_g^{-}\, 2B) \tag{21}$$

$$a_{1g}^{-} = A_{1g}^{-} + \frac{\sqrt{3}\alpha_1^{*}\lambda_M}{2\Delta E(A_{1g} \rightarrow E_g A)} (b_1 E_g^{+}\, 1A + \mathrm{i} b_2\, E_g^{-}\, 2A) -$$

$$- \frac{\sqrt{3}\alpha_1^{*}\,\lambda_M}{\Delta E(A_{1g} \rightarrow E_g B)} (a_3 E_g^{+}\, 1B + \mathrm{i} a_4\, E_g^{-}\, 2B) \tag{22}$$

Throughout this paper we shall look at the case where the effective spin-orbit coupling constant λ_M of the d^1 complex ion in an octahedral ligand field of trigonal symmetry is much smaller than $\Delta E(A_{1g} \rightarrow E_g A)$. We shall consider this approximation valid for every system in which $\Delta E(A_{1g} \rightarrow E_g B) > 10\lambda_M$.

The basic theory of the Zeeman splitting in a trigonal d^1 system is given in Appendix B, expressions (23) and (24) being obtained for $g_{\parallel}$ and $g_{\perp}$.

$$g_{\parallel} = 2.0023 \tag{23}$$

$$g_{\perp} = 2 \cdot 0023 - 2\sqrt{3}\,\mathrm{i}\alpha_1^{*}\,\lambda_M \left(\frac{b_2 \langle e_g\, 2A \,|\, \hat{l}_x \,|\, a_{1g} \rangle}{\Delta E(A_{1g} \rightarrow E_g A)} - \frac{a_4 \langle e_g\, 2B \,|\, \hat{l}_x \,|\, a_{1g} \rangle}{\Delta E(A_{1g} \rightarrow E_g B)} \right) \tag{24}$$

We are now in position to derive the expressions for the g-values in terms of the CF model. In contrast to MO model, the CF approach supposes that partly-filled shells are pure d-orbitals. In this regard the expansion of the integrals $\langle e_g \,|\, \hat{l}_x \,|\, a_{1g} \rangle$* is rather simple and yields

$$\langle e_g\, 2A \,|\, \hat{l}_x \,|\, a_{1g} \rangle = -\mathrm{i}\sqrt{3}b_2 \tag{25}$$

$$\langle e_g\, 2B \,|\, \hat{l}_x \,|\, a_{1g} \rangle = \mathrm{i}\sqrt{3}a_4 \tag{26}$$

Since $\alpha_1^{*} = 1$ in CF model we can write

$$g_{\parallel} = 2.0023 \tag{27}$$

$$g_{\perp} = 2.0023 - \frac{6b_2^2\,\lambda_M}{\Delta E(A_{1g} \rightarrow E_g A)} - \frac{6a_4^2\,\lambda_M}{\Delta E(A_{1g} \rightarrow E_g B)} \tag{28}$$

---

* The functions obtained by the operation of $\hat{l}_x$ are given in table A.2 (Appendix A).

If the six ligand donor atoms to the d^1 ion are arranged in a nearly octahedral arrangement, then the symmetry is approximately octahedral in which case common approximation is to assume that $a_4 = a \sim \sqrt{\frac{2}{3}}$ and $b_2 = b \sim \sqrt{\frac{1^*}{3}}$ and we arrive at

$$g_{\|} = 2.0023 \tag{29}$$

$$g_{\perp} = 2.0023 - \frac{2\lambda_M}{\Delta E(A_{1g} \rightarrow E_g A)} - \frac{4\lambda_M}{\Delta E(A_{1g} \rightarrow E_g B)} \tag{30}$$

These are the so-called CF expressions for the principal components of the g-tensor of the d^1 metal ion in the CF of the octahedral symmetry with a strong trigonal distortion.

We proceed now to calculate the g-values in terms of the MO model. We shall calculate some of the matrix elements in detail in order to illustrate some interesting points. Consider first the integral $\langle e_g\, 2A \,|\, \hat{l}_x \,|\, a_{1g} \rangle$ which occurs in expression (24). We want to evaluate (31).

$$\langle\, a_2\, d_{xy} + b_2\, d_{yz} - \gamma_2^*\, \Phi(e_g\, 2A) \,|\, \hat{l}_x \,|\, \alpha_1^*\, d_{z^2} - \alpha_2^*\, \Phi(a_{1g}) \,\rangle \tag{31}$$

This is expanded as the sum of 6 terms. Integrals of the type $\langle d \,|\, \hat{l}_x \,|\, d \rangle$ are straightforward

$$a_2 \alpha_1^* \,\langle\, d_{xy} \,|\, \hat{l}_x \,|\, d_{z^2} \,\rangle = 0 \tag{32}$$

$$b_2 \alpha_1^* \,\langle d_{yz} \,|\, \hat{l}_x \,|\, d_{z^2} \,\rangle = -\mathrm{i}\sqrt{3}\, b_2 \alpha_1^* \tag{33}$$

That of the type $\langle \Phi \,|\, \hat{l}_x \,|\, \mathrm{d} \rangle$ is also straightforward and leads to metal-ligand group overlap integral

$$-\alpha_1^* \gamma_2^* \,\langle \Phi(e_g\, 2A) \,|\, \hat{l}_x \,|\, d_{z^2} \,\rangle = \mathrm{i}\sqrt{3}\, \alpha_1^* \gamma_2^*\, S(d_{yz'},\, e_g\, 2A) \tag{34}$$

Integrals of the type $\langle d \,|\, \hat{l}_x \,|\, \Phi \rangle$ can be easily calculated using the Hermitian property of $\hat{l}_x$, which may be defined by

$$\int \Phi^* \hat{l}_x\, \psi \mathrm{d}\tau = \int \psi \hat{l}_x^*\, \Phi^*\, \mathrm{d}\tau \tag{35}$$

Since in our case all Φ and ψ orbitals are real and $\hat{l}_x^* = -\hat{l}_x$, we have identity

$$\int \Phi^* \hat{l}_x\, \psi \mathrm{d}\tau = -\int \psi\, \hat{l}_x\, \Phi \mathrm{d}\tau \tag{36}$$

---

* The correctness of these assumed values will be discussed in detail under "Modification of the Lower E_g Wavefunctions and the g-Values" (See also Ref.[6]).

Terms of these types arising from the expansion of the integral $\langle e_g\, 2A | \hat{l}_x | a_{1g} \rangle$ are given

$$-a_2 \alpha_2^* \langle d_{xy} | \hat{l}_x | \Phi(a_{1g}) \rangle = \mathrm{i} a_2 \alpha_2^* S(d_{xz},\ a_{1g}) \tag{37}$$

$$-b_2 \alpha_2^* \langle d_{yz} | \hat{l}_x | \Phi(a_{1g}) \rangle = \mathrm{i} b_2 \alpha_2^* [S(d_{x^2-y^2},\ a_{1g}) + \sqrt{3} S(d_{z^2},\ a_{1g})] \tag{38}$$

The remaining term arising from the expansion of (32) is the sum of the matrix elements between ligand group orbitals and can be presented in a more convenient form

$$a_2^* \gamma_2^* \langle \Phi(e_g\, 2A) | \hat{l}_x | \Phi(a_{1g}) \rangle = \alpha_2^* \gamma_2^* R(e_g\, 2A,\ a_{1g}) \tag{39}$$

where $R(e_g\, 2A,\ a_{1g}) = \langle \Phi(e_g\, 2A) | \hat{l}_x | \Phi(a_{1g}) \rangle$.

The final result for the matrix element $\langle e_g\, 2A | \hat{l}_x | a_{1g} \rangle$ is given by

$$\begin{aligned} \langle E_g\, 2A | \hat{l}_x | A_{1g} \rangle = -\mathrm{i}\sqrt{3} b_2 \alpha_1^* \Big\{ 1 - \frac{\gamma_2^*}{b_2} S(d_{yz}\ e_g\, 2A) - \\ - \frac{a_2 \alpha_2^*}{\sqrt{3} b_2 \alpha_1^*} S(d_{xz},\ a_{1g}) - \frac{\alpha_2^*}{\sqrt{3} \alpha_1^*} [S(d_{x^2-y^2},\ a_{1g}) + \\ + \sqrt{3} S(d_{z^2},\ a_{1g})] + \alpha_2^* \gamma_2^* R(e_g\, 2A,\ a_{1g}) \Big\} \end{aligned} \tag{40}$$

The expansion of $\langle e_g\, 2B | \hat{l}_x | a_{1g} \rangle$ presents no additional complication and turns out to be

$$\begin{aligned} \langle e_g\, 2B | \hat{l}_x | a_{1g} \rangle = \mathrm{i}\sqrt{3} a_4 \alpha_1^* \Big\{ 1 + \frac{\varepsilon_2^*}{\sqrt{3} a_4} S(d_{yz},\ e_g\ 2B) + \\ + \frac{b_4 \alpha_2^*}{\sqrt{3} a_4 \alpha_1^*} S(d_{xz}\ e_g\ 2B) - \frac{\alpha_2^*}{\sqrt{3} \alpha_1^*} [S(d_{x^2-y^2},\ a_{1g}) + \\ + \sqrt{3} S(d_{z^2}, a_{1g})] + \alpha_2^* \varepsilon_2^* R(e_g\, 2B,\ a_{1g}) \Big\} \end{aligned} \tag{41}$$

where $R(e_g\, 2B,\ a_{1g}) = \langle \Phi(e_g\, 2B) | \hat{l}_x | \Phi(a_{1g}) \rangle$.

We are now in position to write down final expressions for the $g_{||}$ and $g_{\perp}$ principal components of the g-tensor. These are

$$g_{||} = 2.0023 \tag{42}$$

$$
\begin{aligned}
g_{\perp} = 2.0023 &- \frac{6b_2^2\,\alpha_1^{*\,2}\lambda_M}{\Delta E(A_{1g}\rightarrow E_gA)}\left\{1-\frac{\gamma_2^*}{b_2}S(d_{yz},\ e_g\,2A)-\right.\\
&-\frac{a_2\alpha_2^*}{\sqrt{3}b_2\,\alpha_1^*}S(d_{xz},\ a_{1g})-\frac{\alpha_2^*}{\sqrt{3}\alpha_1^*}\,[S(d_{x^2-y^2},\ a_{1g})+\\
&\left.+\sqrt{3}S(d_{z^2},\ a_{1g})]\right\}-\frac{6a_4^2\,\alpha_1^*\,\lambda_M}{\Delta E(A_{1g}\rightarrow E_gB)}\left\{1+\frac{\varepsilon_2^*}{\sqrt{3}a_4}S(d_{yz},\ e_g\,2B)+\right.\\
&\left.+\frac{b_4\alpha_2^*}{\sqrt{3}\alpha_1^*}S(d_{xz},\ e_g\,2B)-\frac{\alpha_2^*}{\sqrt{3}\alpha_1^*}\,[S(d_{x^2-y^2},\ a_{1g})+\sqrt{3}S(d_{z^2},\ a_{1g})]\right\}-\\
&-2\sqrt{3}\,\mathrm{i}\alpha_1^*\,\lambda_M[\alpha_2^*\,\gamma_2^*\,R(e_g\,2A,\ a_{1g})+\alpha_2^*\,\varepsilon_2^*\,R(e_g\,2B,\ a_{1g})]
\end{aligned}
\tag{43}
$$

Note that the expressions (42) and (43) are deficient in that they do not contain CT terms. Kon and Sharpless [9] showed that such terms could be important in the d^1 systems. However, many titanium (III) compounds to which our discussion is applicable exhibit CT bands at relatively high energies (〉 50000 cm^{-1}), so these CT terms are of minor importance. We shall later discuss such a system : the $Ti(H_2O)_6^{3+}$ complex ions in frozen aqueous solution.

DISCUSSION

Our expression (43) for the $g_{\perp}$ component is rather complicated. It seems therefore more instructive for our subsequent discussion to simplify this expression as follows :

$$
g_{\perp} = 2.0023 - \frac{6b_2^2\,\alpha_1^{*2}\,\lambda_M}{\Delta E(A_{1g}\rightarrow E_gA)}\,f_1 - \frac{6a_4^2\,\alpha_2^{*2}\,\lambda_M}{\Delta E(A_{1g}\rightarrow E_gB)}f_2 - C \tag{44}
$$

where f_1 and f_2 are

$$
\begin{aligned}
f_1 = 1 &- \frac{\gamma_2^*}{b_2}S(d_{yz},\ e_g\,2A)-\frac{a_2\alpha_2^*}{\sqrt{3}b_2\alpha_1^*}S(d_{xz},\ a_{1g})-\\
&-\frac{\alpha_2^*}{\sqrt{3}\alpha_1^*}\,[S(d_{x^2-y^2},\ a_{1g})-\sqrt{3}S(d_{z^2},\ a_{1g})]
\end{aligned}
\tag{45}
$$

$$
\begin{aligned}
f_2 = 1 &+ \frac{\varepsilon_2^*}{\sqrt{3}a_4}S(d_{yz},\ e_g\,2B)-\frac{b_4\alpha_2^*}{\sqrt{3}a_4\alpha_1}S(d_{xz},\ e_g\,2B)-\\
&-\frac{\alpha_2^*}{\sqrt{3}\alpha_1^*}\,[S(d_{x^2-y^2},\ a_{1g})+\sqrt{3}S(d_{z^2},\ a_{1g})]
\end{aligned}
\tag{46}
$$

---

[9] a. H. Kon and N. E. Sharpless, *J. Chem. Phys.*, **42**, 906 (1965).
b. H. Kon and N. E. Sharpless, *J. Chem. Phys.*, **43**, 1081 (1965).

and C is

$$C = 2\sqrt{3}i\alpha_1^* \lambda_M[\alpha_2^* \gamma_2^* R(e_g\, 2A,\ a_{1g}) + \alpha_2^* \varepsilon_2^* R(e_g\, 2B,\ a_{1g})] \tag{47}$$

In order to discuss the relative importance of the parameters f_1, f_2 and C in expression (44) we should have available the appropriate MO expansion coefficients and various overlap integrals. Unfortunately, it is not possible from the present experimental and theoretical data to give good numerical values either for the MO parameters describing the chemical bonding or for the overlap integrals. While detailed theoretical calculation of the parameters f_1, f_2 and C, i.e. the $g_\perp$ values, for an individual complex species will not be attempted here we shall try to use the simpler formula and content ourselves with the $Ti(H_2O)_6^{3+}$ complex ion in a frozen aqueous solution for which such formula is applicable.

TITANIUM (III) HEXA-AQUO COMPLEX IONS IN FROZEN AQUEOUS SOLUTIONS

The titanium (III) halides and titanium (III) sulphate have been studied both chemically and spectroscopically and are believed to contain only octahedrally solvated ions, Ti $(H_2O)_6^{3+}$.[10]

The broad weak band in the optical spectrum of the $Ti(H_2O)_9^{3+}$ complex ion is assigned to the $^2T_{2g} \rightarrow {}^2E_g$ transition.[10a] One interesting feature of the spectrum is the asymmetric character of the visible absorption band. This band consists of a broad maximum at $\sim 20300\ cm^{-1}$ with a pronounced shoulder at $\sim 17000\ cm^{-1}$. The splitting is considered to arise from a nuclear configurational instability in the excited state, i.e. from the Jahn-Teller effect. The perfect octahedral ion $Ti(H_2O)_6^{3+}$ cannot be stable because of the threefold degeneracy of the $^2T_{2g}$ ground state and a tetragonal distortion is required so that a nondegenerate ground state exists, i.e. ($^2B_{2g}$). However, the theoretical background of the Jahn-Teller effect gives no direct information concerning the magnitude of the deviation from octahedral symmetry, or a choice between a static and a dynamic equilibrium between limiting structures. It is, however, expected that the splitting of the $^2T_{2g}$ ground state will be smaller than that of the excited ^2E_g state.

Recently, Glebov[11] and Premovič and West[12] have reported that rapidly frozen (77 K) strongly acidic aqueous solutions of titanium (III) chloride, bromide, iodide or sulfate provide an identical spectrum from each sample with $g_{||} = 1.99$ and $g_\perp = 1.89$. Premovič and West's [12] analysis indicates that the local symmetry of the Ti (III) ions providing the signal is trigonal. It was proposed that these ions are $Ti(H_2O)_6^{3+}$ species* located in sites in the ice structure subject to strong crystal package forces.

---

[10] a. F. E. Ilse and H. Hartmann, *Z. phys. Chem.*, (*Leipzig*), **197**, 239 (1951).
b. H. Hartmann, H. L. Schläfer and K. H. Hansen, *Z. Anorg. Chem.*, **284**, 153 (1964).

[11] a. V. A. Glebov, *Zhur. strukt. Khim.*, **11**, 809 (1970).
b. V. A. Glebov, *Doklady Akad. Nauk S.S.S.R.*, **190**, 1378 (1970).

[12] P. I. Premovic and P. R. West, *Canad. J. Chem.*, **53**, 1630 (1975).

ESR and spectroscopic studies[13] and hexaquo complex ions of the transition metals of the iron group have convincingly demonstrated that chemical bonding between the central metal ion and water ligands is rather ionic. It is reasonable to suppose an analogous situation for the $Ti(H_2O)_6^{3+}$ complex ion. Moreover, another argument against the existence of covalent bonding in the $Ti(H_2O)_6^{3+}$ complex ion is the position of water in the neuphelauxetic series.[14] Those ligands which are known to form strong covalent bonds, such as Br^- and I^- have high positions in this series. Ligands which give rise to rather weak covalency in chemical bonding, such as F^-, have unusually low position in the series. Water, however, has a position very close to that of the fluoride ion, and this fact indicates that covalency of the chemical bonding between central metal ion and water ligands is likely to be rather weak. Since ionic bonding in the $Ti(H_2O)_6^{3+}$ complex ion implies that α_1^*, f_1 and f_2 are close to unity, C is close to zero, $a_4 = a$ and $b_2 = b$. The expressions (42) and (43) can be written

$$g_{\parallel} = 2.00 \tag{48}$$

$$g_{\perp} = 2.00 - \frac{6b^2\,\lambda_M}{\Delta E(A_{1g} \rightarrow E_gA)} - \frac{6a^2\,\lambda_M}{\Delta E(A_{1g} \rightarrow E_gB)} \tag{49}$$

These expressions are, of course, equivalent to the CF expressions (27) and (28).

Throughout this discussion, it has been assumed the ground-term splitting $\Delta E(A_{1g} \rightarrow E_gA) > 10\lambda_M$. Gladney and Swalen[4] have examined in detail ESR *g*-values calculated from a ^2D term perturbed by a $CF-D_3$ potential and spin-orbit coupling. They found that for *g*-values close to 2, the ratio $\lambda_M/\Delta E(A_{1g} \rightarrow E_gA) < 0.1 (\lambda_M/\delta < 0.1)$ in their terminology. Although their calculation suffers from all the deficiencies inherent in their CF approach, which neglects the relative importance of excited state admixture CF, we may reasonably suppose that this value for the ratio $\lambda_M/\Delta E(A_{1g} \rightarrow E_gA)$ is realistic and can meaningfully be used in our discussion.

As we stated above, very common device in order to reduce the number of unknowns either in the MO or CF expressions for the $g_{\parallel}$

---

* Although Ti(III) usually enters compounds into a site of local point symmetry C_3^4, the problem can frequently be discussed as one with D_{3d} point symmetry if the CF in the vicinity of Ti(III) is determined primarily by the charges in the six oxygen atoms of water ligands.

[13] a. C. J. BALLHAUSEN and H. B. GRAY, *Inorg. Chem.*, **1**, 111 (1962).
b. R. N. ROGERS and G. E. PAKE, *J. Chem. Phys.*, **33**, 1107 (1960).
c. K. DEARMOND, B. B. GARRETT and H. S. GUTOWSKY, *J. Chem. Phys.*, **42**, 1019 (1964).
d. M. GERLOCH and J. R. MILLER, *Progr. Inorg. Chem.*, **10**, 1 (1968).

[14] J. E. HUHEEY, "Inorganic Chemistry", Harper and Row, New York, 1972, p. 349.

and $g_\perp$ in a trigonal d^1 system is to regard the symmetry of this system approximately octahedral in which case $a \sim \sqrt{\frac{2}{3}}$ and $b \sim \sqrt{\frac{1}{3}}^{\,*}$. However such an assumption is questionable.

Recently, Gerloch and coworkers,[8] in their paper dealing with the magnetic properties of trigonally distorted iron (II) complexes, have pointed out the sensitivity of the magnetic properties to small angular departures from regular octahedral symmetry in trigonal systems. They emphasized that the analysis of magnetic data based on a constant geometry of the complex ion in different lattice environments is dangerous, in the trigonal case in particular, because of peculiarities of the angular functions with which the magnetic properties are associated. It therefore seems timely to reconsider the relationship between the *a* and *b* coefficients and features of structure of trigonal d^1 systems in the light of recent developments mentioned above.

MODIFICATION OF THE LOWER E_g WAVEFUNCTIONS AND THE g-VALUES

In trigonal symmetry the total CF potential may be represented by

$$V_{D_{3d}} = AY_2^0 + BY_4^0 + C(Y_4^3 - Y_4^{-3}) \tag{50}$$

for *d* orbitals, where *A*, *B*, and *C* are independent parameters. We may relate these parameters to features of structure and metal ion wavefunctions *via* the PC model. Instead of a potential parameterized by coefficients *A*, *B*, and *C* as in expression (50), this only involves the final matrix elements parameterized by *Dq*, *Cp* and θ. *Dq* and *Cp* are fourth-and second order radial parameters which do not involve the angular distortion parameter θ. Thus, the PC model separates distortion and radial parameters and allows a correlation with geometry of the complex ion.

Although it is inappropriate here to review the PC formalism developed by Gerloch and coworkers[8] it is instructive, however, to emphasize one aspect of their definitions, particularly *Dq*. Their definition of 10 *Dq*, which we use consistently throughout this paper, is identical, practically, with the $E_g - T_{2g}$ energy splitting, in octahedral symmetry. For our calculation we used for the cubic splitting 10 *Dq* a value of 20 300 cm^{-1} according to Hartmann and Schläfer.[10]

Initially, we do not know which value *Cp* parameter might take but Gerloch and coworkers [8] suggested that $5\ Dq \geqslant Cp \geqslant 2Dq$. However, their detailed analysis did not yield unambiguous results. In our case it is likely that *Cp* is at least greater than 4060 cm^{-1} ($2Dq$) so we ought to include in our calculation a range of values for this parameter, from 4060 cm^{-1} to 10150 cm^{-1} ($5Dq$).

---

* I.e., using a basis set of orbitals restricted to the cubic $^2T_{2g}$ and ^2E_g states. [15]

[15] C. J. BALLHAUSEN, "Introduction to Ligand Field Theory", McGraw-Hill, New York, 1962, p. 68.

Using a PC—CF model, as developed by Gerloch and coworkers[8], energy levels were calculated as functions of $Cp \geqslant 4060$ cm^{-1} and θ (and $Dq = 2030$ cm^{-1}).* Some typical results are shown in Figure 3. Analogous to the iron (II) case the behaviour of CF splittings for trigonal Ti (III) systems varies markedly with the magnitude of Cp. We observed that regardless of the magnitude of Cp coefficient a lowest-lying A_{1g} term is associated with a compressed octahedron ($\theta > 54.75°$), similarly a lowest-lying E_g term with an elongated octahedral system ($\theta < 54.75°$). Since our experimental g-values are only consistent with an A_{1g} ground state we conclude that the octahedron of the $Ti(H_2O)_6^{3+}$ complex ion in frozen aqueous solutions is trigonally compressed!

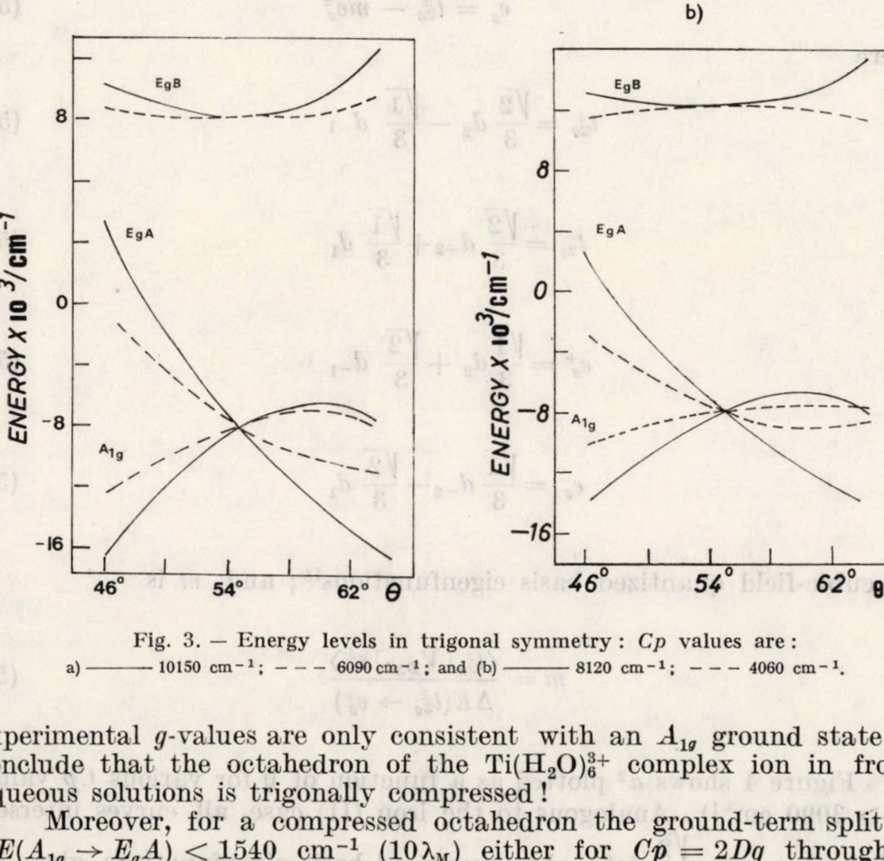

Fig. 3. — Energy levels in trigonal symmetry: Cp values are: a) ——— 10150 cm^{-1}; – – – 6090 cm^{-1}; and (b) ——— 8120 cm^{-1}; – – – 4060 cm^{-1}.

Moreover, for a compressed octahedron the ground-term splitting $\Delta E(A_{1g} \rightarrow E_gA) < 1540$ cm^{-1} ($10\lambda_M$) either for $Cp = 2Dq$ throughout angular range (Figure 3b) or for $\theta \leqslant$ ca. 56° regardless that Cp may be as high as $5Dq$ (Figure 3a). We note here that our calculation of the splitting $^2T_{2g}$ cubic-field ground term showed that when $Cp \sim Dq$ an E_g ground term persists throughout the angular range irrespective of the sense of distortion. These facts confirm our initial assumption that $Cp \geqslant 2Dq$. On the other hand, since we supposed that the ground-term splitting $\Delta E(A_{1g} \rightarrow E_gA) > 1540$ cm^{1-} ($10\lambda_M$) in the $Ti(H_2O)_6^{3+}$ complex ion in frozen aqueous solutions, we shall consider in our $g_\perp$ — calculation only the cases where this requirement is fulfilled.

---

*In this calculation we have assumed that there are equal and constant bond lengths.

Perhaps the most important point in our treatment of the $g_\perp$-values of the octahedral d^1 systems with a relatively strong trigonal distortion is the inclusion of the higher E_g into the lower E_g wavefunctions *via* trigonal field mixing. The coefficient a may be used as an indicator for the character of the lower E_g functions.

Simple perturbation theory suggests that the mixing coefficient m is given by

$$e_g = t_{2g}^{\pm} - m e_g^{\pm} \tag{51}$$

where

$$t_{2g}^{+} = \frac{\sqrt{2}}{3}\, d_2 - \frac{\sqrt{1}}{3}\, d_{-1} \tag{52}$$

$$t_{2g}^{-} = \frac{\sqrt{2}}{3}\, d_{-2} + \frac{\sqrt{1}}{3}\, d_1 \tag{53}$$

$$e_g^{+} = \frac{\sqrt{1}}{3} d_2 + \frac{\sqrt{2}}{3}\, d_{-1} \tag{54}$$

$$e_g^{-} = \frac{\sqrt{1}}{3}\, d_{-2} - \frac{\sqrt{2}}{3}\, d_1 \tag{55}$$

are cubic-field quantized basis eigenfunctions[15]; and, m is

$$m = \frac{\langle t_{2g}^{\pm} \mid V_{D3d} \mid e_g^{\pm} \rangle}{\Delta E(t_{2g}^{\pm} \rightarrow e_g^{\pm})} \tag{56}$$

Figure 4 shows a^2 plotted as a function of θ for various Cp values ($Cp \geqslant 3090$ cm^{-1}). Analogous to the iron (II) case, all curves intersect at θ_{oct} when $a^2 = \frac{\sqrt{2}}{3}$ (cf. cubic quantized basis eigenfunctions given by expressions (52) – (55)) as a result of the orthogonality of E_g and T_{2g} in ideal octahedral symmetry. Note that when Cp is $5Dq$, a compression of the octahedron by 5° causes a^2 to decrease by ca. 55% and b^2 (calculated using the orthonormality condition $a^2 + b^2 = 1$) to increase by ca. 52% ! Such a change in geometry, of course, would cause the same changes in the contributions to the $g_\perp$-value of the first (quadratic in b) and the second (quadratic in a) terms in expression (49). However, it should be noted that the first term is several times greater than the second term, since $\Delta E(A_{1g} \rightarrow E_g B) > \Delta E(A_{1g} \rightarrow E_g A)$ (Figure 3) and its contribution dominates the g-anisotropy. Consequently, a calculation of the energy levels (usually the $\Delta E(A_{1g} \rightarrow E_g A)$ transition) from experimental $g_{\perp}$-values based on the CF expression (30) would be, of course, irreconcilable with the optical or other data (magnetic relaxation, etc.). It has been customary to rationalize such discrepancies by introducing covalent bonding. This generally is done with Stevens'[16] orbital reduction factors * in the sense that it is possible to fit any ESR results without difficulty but not uniquely as the following idealized treatment shows.

The theoretical behaviour of $g_{\perp}$ values ** for the $Ti(H_2O)^{3+}$ complex ion as functions of θ ($\geqslant 56°$) for three representative values of Cp ($\geqslant 3Dq$), is shown in Figure 5. The $g_{\perp}$ values are clearly dependent on Cp. Notice particularly, for ca. $56° \leqslant \theta \leqslant 60°$ $g_{\perp}$ values vary rapidly. For example, with $Cp = 5Dq$, $g_{\perp}$, value increases from ca. 1.79 to ca. 1.91 as θ increases by only 4° from $\theta = 56°$. It is just this behaviour which is considered responsible for the g-anisotropy. Thus $g_{\perp}$ in this system can be significantly affected by small angular distortions, provided Cp is a large quan-

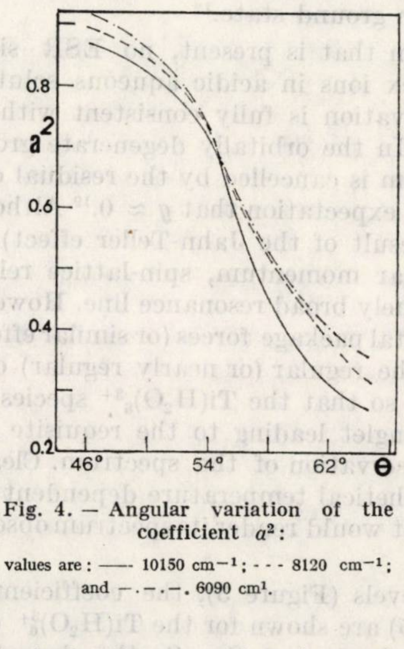

Fig. 4. — Angular variation of the coefficient a^2:

Cp values are : —— 10150 cm^{-1}; - - - 8120 cm^{-1}; and —·—·—. 6090 cm^{1}.

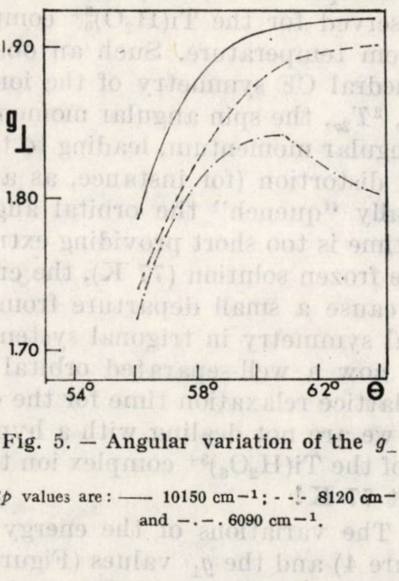

Fig. 5. — Angular variation of the $g_{\_}$:

Cp values are : —— 10150 cm^{-1}; - -·- 8120 cm^{-1}; and —.—. 6090 cm^{-1}.

---

[16] For a discussion of the significance of orbital reduction parameters in metal complexes see Ref. 13d.

* In our case, the orbital reduction factors are : $k_1 = \sqrt{f_1} \cdot \alpha_1^*$ and $k_2 = \sqrt{f_2}\, \alpha_1^*$.

** These are calculated using the expression (49).

tity. Assuming that the octahedron may only be *slightly* compressed, say $\theta - \theta_{oct} \leqslant 5°$, then it can be seen (Figure 5) that only $Cp = 5Dq$ may be compatible with experimental $g_\perp$ value of 1.89.[12] If the value is as large as 10150 cm^{-1} (i.e. $5Dq$) then the effective distortion angle θ can be as low as ca. 58.5° and the ground term splitting can be as high as ca. 5000 cm^{-1} (Figure 3b).

Gerloch and coworkers,[8] using the appropriate PC definitions, predicted, on the basis of the theoretical calculations of Ballhausen[17] and of Ballhausen and Acomon,[18] that $Cp \approx 5Dq$. In the light of this prediction and the findings in the present work a high value of Cp seems reasonable. Moreover, observation of the relatively sharp ESR spectra of the randomly oriented samples of the $Ti(H_2O)^{3+}$ complex ion in frozen aqueous solutions at 77 K would, also, indicate an excited state of a few thousand cm above the ground state.[12]

In spite of the unpaired electron that is present, no ESR signal is observed for the $Ti(H_2O)_6^{3+}$ complex ions in acidic aqueous solutions at room temperature. Such an observation is fully consistent with the octahedral CF symmetry of the ion. In the orbitally degenerate ground state, $^2T_{2g}$, the spin angular momentum is cancelled by the residual orbital angular momentum, leading to the expectation that $g \approx 0$.[19] Although small distortion (for instance, as a result of the Jahn-Teller effect) can partially "quench" the orbital angular momentum, spin-lattice relaxation time is too short providing extremely broad resonance line. However, in the frozen solution (77 K), the crystal package forces (or similar effects) may cause a small departure from the regular (or nearly regular) octahedral symmetry in trigonal system* so that the $Ti(H_2O)_6{}^{3+}$ species will have now a well-separated orbital singlet leading to the requisite long spin-lattice relaxation time for the observation of the spectrum. Clearly, then we are not dealing with a hypothetical temperature dependent process of the $Ti(H_2O_6)^{3+}$ complex ion that would render its spectrum observable at 77 K!

The variations of the energy levels (Figure 3), the coefficients a^2 (Figure 4) and the $g_\perp$ values (Figure 5) are shown for the $Ti(H_2O)_6^{3+}$ complex ion assuming that $\alpha_1^* \sim 1$, $f_1 = f_2 \sim 1$, and $C \sim O$; the departures from these conditions likely to be found in this complex ion would not change the overall patterns of the graphs and the qualitative and quantitative analyses must be similar.

---

[17] C. J. Ballhausen, *Mat. Fys. Medd. Dan. Vid. Selsk.*, **29**, 4 (1954).

[18] C. J. Ballhausen and E. M. Acomon, *Mat. Fys. Medd. Dan. Vid. Selsk.*, **31**, 2 (1958).

[19] A. Carington and A. D. McLachland, "Introduction to Magnetic Resonance with Applications to Chemistry and Chemical Physics", Harper and Row, New York, 1967, Chapt.10.

* This point emphasizes the danger of a ready comparison of data involving the complex ions in the same solutions in liquid and frozen states.

APPENDIX A

Table A.1

Functions obtained by the operation of the $\hat{l}\cdot\hat{s}$ operator on relevant atomic orbitals

	$\lvert x^2-y^2,+\rangle$	$\lvert xy,+\rangle$	$\lvert yz,+\rangle$	$\lvert xz,+\rangle$	$\lvert z^2,+\rangle$	$\lvert x^2-y^2,-\rangle$	$\lvert xy,-\rangle$	$\lvert yz,-\rangle$	$\lvert xz,-\rangle$	$\lvert z^2,-\rangle$
$x^2-y^2,+\lvert$	0	$-i$	0	0	0	0	0	$+i/2$	$+1/2$	0
$xy,+\lvert$	$+i$	0	0	0	0	0	0	$+1/2$	$-i/2$	0
$yz,+\lvert$	0	0	0	$i/2$	0	$-i/2$	$-1/2$	0	0	$-i\sqrt{3}/2$
$xz,+\lvert$	0	0	$-i/2$	0	0	$-1/2$	$+i/2$	0	0	$+\sqrt{3}/2$
$z^2,+\lvert$	0	0	0	0	0	0	0	$+i\sqrt{3}/2$	$-\sqrt{3}/2$	0
$x^2-y^2,-\lvert$	0	0	$+i/2$	$-1/2$	0	0	$+i$	0	0	0
$xy,-\lvert$	0	0	$-1/2$	$-i/2$	0	$-i$	0	0	0	0
$xz,-\lvert$	$-i/2$	$+i/2$	0	0	$-i\sqrt{3}/2$	0	0	0	$-i/2$	0
$xz,-\lvert$	$+1/2$	$+i/2$	0	0	$-\sqrt{3}/2$	0	0	$+i/2$	0	0
$z^2,-\lvert$	0	0	$+i\sqrt{3/2}$	$+\sqrt{3}/2$	0	0	0	0	0	0

Table A.2

Functions obtained by the operation of $\hat{l}_x$ on relevant atomic orbitals

	$\lvert d_{x^2-y^2}\rangle$	$\lvert d_{xy}\rangle$	$\lvert d_{yz}\rangle$	$\lvert d_{xz}\rangle$	$\lvert d_{z^2}\rangle$
$\hat{l}_x$	$-i\lvert d_{yz}\rangle$	$i\lvert d_{xz}\rangle$	$i[\lvert d_{x^2-y^2}\rangle + \lvert d_{z^2}\rangle]$	$i\lvert d_{xy}\rangle$	$-i\sqrt{3}\lvert d_{yz}\rangle$

APPENDIX B

We wish to find the effect of applying a magnetic field upon the doubly degenerate ground state of d^1 in a trigonal field of D_{3d}, D_3 and C_{3v} symmetries. The perturbation operator for this is given by

$$\mathrm{H}_{\mathrm{Zeeman}} = \beta_e(\hat{l} + 2.0023)\cdot\vec{H} = \beta_e\,(\hat{l}_z + 2.0023\,\hat{s}_z)H_z +$$

$$+\frac{1}{2}\,\beta_e\,[(\hat{l}_+ + 2.0023\,\hat{s}_+)\,H_- + (\hat{l}_- + 2.0023\,\hat{s}_-)\,H_+] \tag{B1}$$

where β_e is so called the Bohr magneton; $\hat{l}_\pm = \hat{l}_x \pm i\hat{l}_y$ and $\hat{s}_\pm = \hat{s}_x \pm i\hat{s}_y$ are the appropriate 'ladder' operators; and $H_\pm = H_x \pm iH_y$.

Since $\mathrm{H}_{\mathrm{Zeeman}}$ is much smaller than either $\Delta E(A_{1g} \rightarrow E_gA)$ or λ_M we can regard it as a perturbation operator acting on the two degenerate wavefunctions a_{1g}^+ and a_{1g}^- whose matrix in the basis of wavefunctions (21) and (22) is as it is given by (B2)

$$
\begin{array}{cc}
a_{1g}^{+} & a_{1g}^{-} \\
\left|\begin{array}{l}
<A_{1g}^{+} - \dfrac{\sqrt{3}\ \alpha_1^{*}\ \lambda_M}{2\Delta E\,(A_{1g}\to E_gA)}\,(b_1E_g^{-}\ 1A + \mathrm{i}b_2E_g^{-}\ 2A) + \\
+ \dfrac{\sqrt{3}\,\alpha_1^{*}\,\lambda_M}{2\,\Delta E(A_{1g}\to E_gB)}\,(a_3E_g^{-}\ 1B + \mathrm{i}a_4E_g^{-}\ 2B)\,| \\
\mathrm{H_{Zeeman}}\left|\ A_{1g}^{+} - \dfrac{\sqrt{3}\ \alpha_1^{*}\ \lambda_M}{2\,\Delta E(A_{1g}\to E_gA)}\,(b_1E_g^{-}\ 1A - \mathrm{i}b_2\ E_g^{-}\ 2A) +\right. \\
+ \dfrac{\sqrt{3}\ \alpha_1^{*}\ \lambda_M}{2\,\Delta E(A_{1g}\to E_gB)}\,(a_3\ E_g^{-}\ 1B - \mathrm{i}a_4\ E_g^{-}\ 2\ B) > -\ E
\end{array}\right. &
\left.\begin{array}{l}
<A_{1g}^{+} - \dfrac{\sqrt{3}\ \alpha_1^{*}\ \lambda_M}{2\,\Delta\ E(A_{1g}\to E_gA)}\,(b_1\ E_g^{-}\ 1A + \mathrm{i}b_2E_g^{-}\ 2A) + \\
+ \dfrac{\sqrt{3}\ \ \alpha_1^{*}\lambda_M}{2\,\Delta\ E(A_{1g}\to E_gB)}\,(a_3\ E_g^{-}\ 1B + \mathrm{i}a_4\ E_g^{-}\ 2B)\,| \\
\mathrm{H_{Zeemam}}\,|\ A_{1g}^{-} + \dfrac{\sqrt{3}\ \alpha_1^{*}\ \lambda_M}{2\,\Delta E(A_{1g}\to E_gA)}\,(b_1E_g^{+}\ 1A + \mathrm{i}b_2\ E_g^{+}\ 2A) - \\
- \dfrac{\sqrt{3}\ \alpha_1^{*}\ \lambda_M}{2\Delta E(A_{1g}\to E_gB)}\,(a_3\ E_g^{+}\ 1\ B + \mathrm{i}a_4\ E_g^{+}\ 2\ B) >
\end{array}\right| \\
\left|\begin{array}{l}
<A_{1g}^{-} + \dfrac{\sqrt{3}\ \alpha_1^{*}\ \lambda_M}{2\,\Delta E(A_{1g}\to E_gA)}\,(b_1\,E_g^{+}\,1A - \mathrm{i}b_2E_g^{+}\ 2A) - \\
- \dfrac{\sqrt{3}\ \ \alpha_1^{*}\ \lambda_M}{2\,\Delta E(A_{1g}\to E_gB)}\,(a_3E_g^{+}\,1B - \mathrm{i}a_4E_g^{+}2B)\,| \\
\mathrm{H_{Zeeman}}\,|\ A_{1g}^{+} - \dfrac{\sqrt{3}\ \alpha_1^{*}\ \lambda_M}{2\,\Delta E(A_{1g}\to E_gA)}\,(b_1\,E_g^{-}\ 1A - \mathrm{i}b_2\ E_g^{-}\ 2A) + \\
+ \dfrac{\sqrt{3}\ \ \alpha_1^{*}\ \lambda_M}{2\,\Delta E(A_{1g}\to E_gB)}\,(a_3\ E_g^{-}\ 1B - \mathrm{i}a_4\ E_g^{-}2\ B)>
\end{array}\right. &
\left.\begin{array}{l}
<A_{1g}^{-} + \dfrac{\sqrt{3}\ \ \alpha_1^{*}\ \lambda_M}{2\Delta E(A_{1g}\to E_gA)}\,(b_1\ E_g^{+}\ 1A - \mathrm{i}b_2\ E_g^{+}\ \ 2\ A) + \\
+ \dfrac{\sqrt{3}\ \ \alpha_1^{*}\ \ \lambda_M}{2\Delta E(A_{1g}\to E_gB)}\,(a_3\ E_g^{+}\ \ 1B\ -\ \mathrm{i}a_4\ E^{+}\ 2B)\,| \\
\mathrm{H_{Zeeman}}\left|\ A_{1g}^{-} + \dfrac{\sqrt{3}\alpha_1^{*}\lambda_M}{2\ \Delta\ E(A_{1g}\to E_gA)}\,(b_1E_g^{+}1\ A + \mathrm{i}b_2E_g^{+}2\ A) -\right. \\
- \dfrac{\sqrt{3}\alpha_1^{*}\lambda_M}{2\ \Delta\ E(A_{1g}\to E_gB)}\,(a_3E_g^{+}1B - \mathrm{i}a_4E_g^{+}2B) > -\ E
\end{array}\right|
\end{array}
\qquad \text{(B2)}
$$

This matrix is diagonal when the applied external magnetic field is along the z axis ($H_x = H_y = 0$). The matrix elements are given by

$$\langle a_{1g}^{+} | H_{\text{Zeeman}} | a_{1g}^{+} \rangle - E = \frac{1}{2} \cdot 2.0023 \ \beta_e H_z - E \tag{B3}$$

$$\langle a_{1g}^{-} | H_{\text{Zeeman}} | a_{1g}^{+} = 0 \tag{B4}$$

$$\langle a_{1g}^{+} | H_{\text{Zeeman}} | a_{1g}^{-} \rangle = 0 \tag{B5}$$

$$\langle a_{1g}^{-} | H_{\text{Zeeman}} | a_{1g}^{-} \rangle = - \frac{1}{2} \cdot 2.0023 \, \beta_e H_z - E \tag{B6}$$

The difference in energy of the eigenstates is then

$$\Delta E_z (= \Delta E_{\|}) = 2.0023 \ \beta_e H_z \tag{B7}$$

However, when the external magnetic field is along the x (or y) axis the matrix (B2) is non-diagonal, and the matrix elements are given by

$$\langle a_{1g}^{+} | H_{\text{Zeeman}} | a_{1g}^{+} \rangle - E = -E \tag{B8}$$

$$\begin{aligned} \langle a_{1g}^{-} | H_{\text{Zeeman}} | a_{1g}^{+} \rangle = \Bigg[& \frac{\sqrt{3} \ \alpha_1^{*} \lambda_M}{\Delta E(A_{1g} \rightarrow E_g A)} \ (b_1 \langle e_g \, 1A | \hat{l}_x | a_{1g} \rangle - \\ & - i b_2 \langle e_g \, 2A | \hat{l}_x | a_{1g} \rangle) - \frac{\sqrt{3} \ \alpha_1^{*} \lambda_M}{\Delta E(A_{1g} \rightarrow E_g B)} \ (a_3 \langle e_g \, 1B | \hat{l}_x | a_{1g} \rangle - \\ & - i a_4 \langle e_g \, 2B | \hat{l}_x | a_{1g} \rangle) \Bigg] \beta_e H_x + \frac{1}{2} \cdot 2.0023 \ \beta_e H_x \end{aligned} \tag{B9}$$

$$\begin{aligned} \langle a_{1g}^{+} | H_{\text{Zeeman}} | a_{1g}^{-} \rangle = \Bigg[& \frac{-\sqrt{3} \, \alpha_1^{*} \lambda_M}{\Delta E(A_{1g} \rightarrow E_g A)} \ (b_1 \langle e_g \, 1A | \hat{l}_x | a_{1g} \rangle + \\ & + i b_2 \langle e_g \, 2A | \hat{l}_x | A_{1g} \rangle) + \frac{\sqrt{3} \ \alpha_1^{*} \lambda_M}{\Delta E(A_{1g} \rightarrow E_g B)} \ (\langle a_3 \langle e_g \, 1B | l_x | a_{1g} \rangle + \\ & + i a_4 \langle e_g \, 2B | \hat{l}_x | a_{1g} \rangle) \Bigg] \beta_e H_x + \frac{1}{2} \cdot 2.0023 \, \beta_e H_x \end{aligned} \tag{B10}$$

$$\langle a_{1g}^{-} | H_{\text{Zeeman}} | a_{1g}^{-} \rangle - E = -E \tag{B11}$$

Solution of the matrix (B2) for this direction gives the energy splitting

$$\begin{aligned} \Delta E_x (= \Delta E_{\perp}) = -2\sqrt{3i} \, \alpha_1^{*} \ \lambda_M & \left[\frac{b_2 \langle e_g \, 2A | \hat{l}_x | a_{1g} \rangle}{\Delta E(A_{1g} \rightarrow E_g)} - \frac{a_4 \langle e_g 2 \, B | \hat{l}_x | a \ _{1g} \rangle}{\Delta E(A_{1g} \rightarrow E_g} \right] \\ & \beta_e H_x + 2.0023 \ \beta_e H_x \end{aligned} \tag{B12}$$

Note that terms quadratic in λ_M had been neglected since $\Delta E(A_{1g} \leftrightarrow E_g A)$, $\Delta E\ (A_{1g} \rightarrow E_g B) > \lambda_M$.

If we define $g_{||} = (g_z)$ and $g_\perp\ (= g_x = g_y)$ as

$$g_{||} = \frac{\Delta E_z}{\beta_e H_z} \tag{B13}$$

$$g_\perp = \frac{\Delta E_x}{\beta_e H_x} \tag{B14}$$

we end up with

$$g_{||} = 2.0023 \tag{B15}$$

$$g_\perp = 2.0023 - 2\sqrt{3}\mathrm{i}\alpha_1^* \lambda_M \left[\frac{b_2 \langle e_g 2A \,|\hat{l}_x|\, a_{1g}\rangle}{\Delta E(A_{1g} \rightarrow E_g\, A)} - \frac{a_4 \langle e_g 2B \,|\hat{l}_x|\, a_{1g}\rangle}{\Delta E A(_{1g} \rightarrow E_g B)} \right] \tag{B16}$$

We observe that the symmetry of the ligand field determines the axial symmetry of the g-tensor and, of course, the directions of its principal components. Moreover, since λ_M, $\Delta E(A_{1g} \rightarrow E_g A)$ and $\Delta E(A_{1g} \rightarrow E_g B)$ are positive, the $g_\perp$ principal component, of course, is less than the free electron value, 2.0023.

ACKNOWLEDGEMENTS. I thank Dr. S. Visaisouk for help and Dr. T. Dingle for criticism.

Revue Roumaine de Chimie, **23** *8*, 1233–1242 (1978)

CONCENTRATION FLUCTUATIONS IN CHEMICAL SYSTEMS WITH NONDEGENERATE REACTIONS

A THERMODYNAMIC APPROACH

M. VLAD and M. DRAGOŞ
Polytechnical Institute of Bucharest, Institute of Chemistry, Department of Physical Chemistry and Electrochemical Technology, Bd. Republicii 13, Bucharest, Romania

Received May 19, 1976

A general algorithm for calculating the equilibrium concentration fluctuations which occur in a closed system with nondegenerate reactions is developed and compared with the thermodynamical theory of fluctuations in open chemical systems and with the stochastic theory of reaction rates.

A. INTRODUCTION

The elaboration of a general method for calculating the magnitude of concentration fluctuations in chemical systems is of interest in connection with the theory of irreversible processes. In the equilibrium case, this can be done with the help of thermodynamical theory of fluctuations.[1–4] For an ideal open system (with or without chemical reactions), containing n molecular species, this theory leads to the following formula :[3]

$$\overline{\Delta N_i\, \Delta N_j} = \bar{N}_i\, \delta_{ij}, \qquad i, j = 1, \ldots, n \tag{1}$$

where N_i denotes the number of the molecular species i.

In the case of closed systems, some linear combinations of the random variables N_i $i = 1, \ldots, n$ are constrained not to fluctuate and then the formula (1) breaks down.

The purpose of this paper is to apply the thermodynamical theory of fluctuations to the case of a closed chemical system, with nondegenerate (independent) reactions. Before doing this we shall present the main results of the thermodynamic theory of fluctuations.[1–4]

1. For an adiabatic system, at equilibrium, characterized by n independent extensive variables x_i $i = 1, \ldots, n$ the covariance matrix

---

[1] R. F. Greene and H. B. Callen, *Phys. Rev.*, **83**, 1231 (1951).

[2] L. Landau and E. Lifchitz, "Physique Statistique", Ed. Mir. Moscou 1967, p. 414.

[3] P. Glansdorff and I. Prigogine, "Thermodynamic Theory of Structure, Stability and Fluctuations", Wiley-Interscience, London-New York-Sydney-Toronto, 1971.

[4] M. Lax, *Rev. Mod. Phys.*, **32**, 25 (1960).

$||\overline{(x_i - \bar{x}_i)(x_j - \bar{x}_j)}||$ is given by

$$\overline{\Delta\mathbf{X}\,\Delta\mathbf{X}^+} = \mathbf{g}^{-1} \tag{2}$$

where

$$\mathbf{g} = -\frac{1}{k}\left\|\left(\frac{\partial^2 S}{\partial x_i\,\partial x_j}\right)_{\text{eq}}\right\|,$$

S is the entropy of the system and k is Boltzmann's constant.

2. If the fluctuations are small, the probability distribution $P(x_1, \ldots$ $\ldots, x_n)\,\mathrm{d}x_1 \ldots \mathrm{d}x_n$ is approximately equal to :

$$P(\mathbf{X})\,\mathrm{d}^n\,\mathbf{X} \cong \sqrt{\frac{\det \mathbf{g}}{(2\pi)^n}}\,\exp\left(-\frac{1}{2}\sum_{i,j} g_{ij}\,\Delta x_i\,\Delta x_j\right)\mathrm{d}^n\mathbf{X}. \tag{3}$$

3. Supposing that the regression of the fluctuations obeys the linear law

$$\frac{\mathrm{d}\,\langle\Delta\mathbf{X}\rangle_{\mathbf{x}_0}}{\mathrm{d}t} = \mathbf{\Lambda}\langle\Delta\mathbf{X}\rangle_{\mathbf{x}_0} \tag{4}$$

and introducing the noise sources

$$\Phi_i = (\mathrm{d}\mathbf{X}/\mathrm{d}t - \mathbf{\Lambda}\mathbf{X})_i, \qquad i = 1, \ldots, n$$

one obtains

$$\overline{\Delta\mathbf{X}(t_1)\,\Delta\mathbf{X}^+(t_2)} = h(-\tau)\,\mathbf{E}(|\tau|)\,\overline{\Delta\mathbf{X}\Delta\mathbf{X}^+} + h(\tau)\,\overline{\Delta\mathbf{X}\Delta\mathbf{X}^+}\,\mathbf{E}^+(|\tau|), \tag{5}$$

$$\overline{\mathbf{\Phi}(t_1)\;\mathbf{\Phi}^+(t_2)} = -\delta(\tau)(\mathbf{\Lambda}\,\overline{\Delta\mathbf{X}\,\Delta\mathbf{X}^+} + \overline{\Delta\mathbf{X}\Delta\mathbf{X}^+}\mathbf{\Lambda}^+), \tag{6}$$

$$\overline{\Delta\mathbf{X}(\omega)\,\Delta\mathbf{X}(\omega')} = \frac{1}{(2\pi)^2}\iint_{-\infty}^{+\infty}\overline{\Delta\mathbf{X}(t_1)\Delta\mathbf{X}(t_2)}\;\mathrm{e}^{-i\omega t_1 - i\omega' t_2}\,dt_1\,dt_2 =$$

$$= \frac{1}{2\pi}\,\delta(\omega + \omega')\,[-(\mathbf{\Lambda} + \mathbf{I}i\omega')^{-1}\,\overline{\Delta\mathbf{X}\,\Delta\mathbf{X}^+} + \overline{\Delta\mathbf{X}\Delta\mathbf{X}^+}\,(\mathbf{I}\,i\omega - \mathbf{\Lambda}^+)^{-1}] \tag{7}$$

and

$$\overline{\mathbf{\Phi}(\omega)\,\mathbf{\Phi}(\omega')} = -\frac{1}{2\pi}\,\delta(\omega + \omega')\,(\mathbf{\Lambda}\overline{\Delta\mathbf{X}\Delta\mathbf{X}^+} + \overline{\Delta\mathbf{X}\,\Delta\mathbf{X}^+}\,\mathbf{\Lambda}^+) \tag{8}$$

where

$$\tau = t_2 - t_1,\ \mathbf{E}(t) = \exp\,(\mathbf{\Lambda}t)$$

and $h(\tau)$ is Heaviside's function.
All these results will be further useful to us.

B. THEORY

Let us consider a closed system at equilibrium with R nondegenerate elementary reactions

$$\sum_{i=1}^{n} \nu_{ij} A_i \underset{k'_j}{\overset{k_j}{\rightleftarrows}} \sum_{i=1}^{n} \nu'_{ij} A_i \quad j = 1, \ldots, R;\; 2 \geqslant \sum_i \nu_{ij}, \sum_i \nu'_{ij} \geqslant 1. \tag{9}$$

Since the chemical reactions (9) are nondegenerate, the rank of the stoechiometric matrix[5] $\mathbf{F} = ||\nu'_{ij} - \nu_{ij}||$ is R and then the composition of the system is completely determined by the advancements of the reactions $\xi_1, \ldots, \xi_R$. It follows that

$$\overline{\Delta\xi\, \Delta\xi^+} = \mathbf{g}^{-1} \tag{10}$$

with

$$\mathbf{g} = -\frac{1}{k}\left\| \left(\frac{\partial^2 S}{\partial \xi_i\, \partial \xi_j}\right)_{\mathrm{eq}} \right\|.$$

But

$$\Delta\mathbf{N} = \mathbf{F}\Delta\xi \tag{11}$$

whence we obtain

$$\frac{\partial}{\partial \xi_i} = \sum_k \frac{\partial N_k}{\partial \xi_i} \frac{\partial}{\partial N_k} = \sum_k f_{ki} \frac{\partial}{\partial N_k}. \tag{12}$$

Insertion of Eq. (12) into (10) yields

$$\mathbf{g} = -\frac{1}{k}\left\| \sum_{k,l} f_{ki} f_{lj} \left(\frac{\partial^2 S}{\partial N_k\, \partial N_l}\right)_{\mathrm{eq}} \right\|.$$

For an ideal mixture we have

$$\left(\frac{\partial^2 S}{\partial N_k\, \partial N_l}\right)_{\mathrm{eq}} = -k\, \frac{\delta_{kl}}{\bar{N}_k}$$

and hence

$$\mathbf{g} = \left\| \sum_l \frac{f_{li} f_{lj}}{\bar{N}_l} \right\| = \mathbf{F}^+\mathbf{D}^{-1}\mathbf{F} \tag{13}$$

where

$$\mathbf{D} = ||\delta_{ij} \bar{N}_i||.$$

---

[5] A. A. BEZDENEZHNYKH, "Inzhenernye metodî sostavlenia uravnenii skorostei reactsii rascheta kineticeskikh konstant", Izd. Khimia, Leningrad, 1973, p. 7.

Thus

$$\overline{\Delta\xi\Delta\xi^{+}} = (\mathbf{F}^{+}\,\mathbf{D}^{-1}\,\mathbf{F})^{-1}. \tag{13$'$}$$

As

$$\overline{\Delta\mathbf{N}\,\Delta\mathbf{N}^{+}} = \mathbf{F}\,\overline{\Delta\xi\,\Delta\xi^{+}}\,\mathbf{F}^{+}$$

we obtain

$$\overline{\Delta\mathbf{N}\Delta\mathbf{N}^{+}} = \mathbf{F}\mathbf{g}^{-1}\mathbf{F}^{+} = \mathbf{F}(\mathbf{F}^{+}\,\mathbf{D}^{-1}\,\mathbf{F})^{-1}\,\mathbf{F}^{+}. \tag{14}$$

Similarly

$$P(\xi)\,\mathrm{d}^{R}\xi \cong \sqrt{\frac{\det(\mathbf{F}^{+}\,\mathbf{D}^{-1}\,\mathbf{F})}{(2\pi)^{R}}}\,\exp\left(-\frac{1}{2}\,\Delta\xi^{+}\,\mathbf{F}^{+}\,\mathbf{D}^{-1}\,\mathbf{F}\,\Delta\xi\right)\mathrm{d}^{R}\ . \tag{15}$$

Considering that the regression of concentration fluctuations is described by the laws of chemical kinetics, we get

$$\frac{\mathrm{d}\,\langle\Delta\xi\rangle_{\xi_0}}{\mathrm{d}t} = \langle\mathbf{r}(\overline{\mathbf{N}} + \mathbf{F}\Delta\xi)\rangle_{\xi_0} \tag{16}$$

with

$$r_i = r_i' - r_j'',\ r_i' = k_i \prod_j N_j^{\nu_{ij}} \text{ and } r_i'' = k_i \prod_j N_j^{\nu'_{ji}}.$$

In the case of small fluctuations, Eq. (16) becomes :

$$\frac{\mathrm{d}\,\langle\Delta\xi\rangle_{\xi_0}}{\mathrm{d}t} \cong \langle\mathbf{r}(\overline{\mathbf{N}}) + \chi\mathbf{F}\Delta\xi\rangle_{\xi_0}. \tag{16$'$}$$

$$\left(\chi = ||\chi_{ij}|| = \left\|\frac{\partial r_i}{\partial \overline{N}_j}(\overline{\mathbf{N}})\right\| = \left\|\frac{\nu_{ij}\,r_i'(\overline{\mathbf{N}}) - \nu'_{ji}\,r_i''(\overline{\mathbf{N}})}{\overline{N}_j}\right\|\right)$$

The condition of macroscopic equilibrium

$$\mathrm{d}\overline{\mathbf{N}}/\mathrm{d}t = 0 \tag{17}$$

leads to

$$\mathbf{r}(\overline{\mathbf{N}}) = 0. \tag{18}$$

Indeed, from (17) it follows that

$$\mathrm{d}\overline{\mathbf{N}}/\mathrm{d}t = \mathbf{F}\mathrm{d}\overline{\xi}/\mathrm{d}t = \mathbf{F}\mathbf{r}(\overline{\mathbf{N}}) = 0. \tag{17$'$}$$

Since rank $\mathbf{F} = R$, Eqs. (17′) and (18) are equivalent. Eq. (18) express the principle of detailed balance [6] which in our case is a consequence of the macroscopic equilibrium. Comparing Eq. (4) with Eq. (16′) and taking into account that $\mathbf{r}(\bar{\mathbf{N}}) = 0$ we have :

---

[6] G. N. Lewis, *Proc. Nat. Acad. Sci. U.S.A.*, **11** 179 (1925).

$$\boldsymbol{\Lambda} = \boldsymbol{\chi}\mathbf{F}. \tag{16''}$$

Consequently

$$\overline{\Delta\boldsymbol{\xi}(t_1)\Delta\boldsymbol{\xi}^+(t_2)} = h\,(-\tau)\,\mathbf{E}(|\tau|)(\mathbf{F}^+\mathbf{D}^{-1}\mathbf{F})^{-1} + h(\tau)(\mathbf{F}^+\mathbf{D}^{-1}\mathbf{F})^{-1}\mathbf{E}^+(|\tau|), \tag{19}$$

$$\overline{\boldsymbol{\Phi}(t_1)\boldsymbol{\Phi}^+(t_2)} = -\delta(\tau)\,[\boldsymbol{\chi}\mathbf{F}(\mathbf{F}^+\mathbf{D}^{-1}\mathbf{F})^{-1} + (\mathbf{F}^+\mathbf{D}^{-1}\mathbf{F})^{-1}\boldsymbol{\chi}^+\mathbf{F}^+], \tag{20}$$

$$\overline{\Delta\boldsymbol{\xi}(\omega)\,\Delta\boldsymbol{\xi}^+(\omega')} = \frac{1}{2\pi}\,\delta(\omega+\omega')[-\boldsymbol{\chi}\mathbf{F} + \mathbf{I}\,\mathrm{i}\omega)^{-1}\,(\mathbf{F}^+\mathbf{D}^{-1}\mathbf{F})^{-1} + \\ + (\mathbf{F}^+\mathbf{D}^{-1}\mathbf{F})^{-1}\,(\mathbf{I}\mathrm{i}\omega - \mathbf{F}^+\boldsymbol{\chi}^+)^{-1}], \tag{21}$$

$$\overline{\boldsymbol{\Phi}\,(\omega)\,\boldsymbol{\Phi}^+\,(\omega')} = -\frac{1}{2\pi}\,\delta(\omega-\omega')\,[\boldsymbol{\chi}\mathbf{F}(\mathbf{F}^+\mathbf{D}^{-1}\mathbf{F})^{-1} + (\mathbf{F}^+\mathbf{D}^{-1}\mathbf{F})^{-1}\mathbf{F}^+\boldsymbol{\chi}^+], \tag{22}$$

$$\overline{\Delta\mathbf{N}(t_1)\,\Delta\mathbf{N}^+(t_2)} = h(-\tau)\,\mathbf{F}\mathbf{E}(|\tau|)\,(\mathbf{F}^+\mathbf{D}^{-1}\mathbf{F})^{-1}\,\mathbf{F}^+ + \\ + h(\tau)\,\mathbf{F}(\mathbf{F}^+\mathbf{D}^{-1}\mathbf{F})^{-1}\,\mathbf{E}^+(|\tau|)\,\mathbf{F}^+, \tag{23}$$

$$\overline{\boldsymbol{\Psi}(t_1)\,\boldsymbol{\Psi}^+(t_2)} = -\delta(\tau)\,[\mathbf{F}\boldsymbol{\chi}\mathbf{F}(\mathbf{F}^+\mathbf{D}^{-1}\mathbf{F})^{-1}\mathbf{F}^+ + \mathbf{F}(\mathbf{F}^+\mathbf{D}^{-1}\mathbf{F})^{-1}\,\mathbf{F}^+\boldsymbol{\chi}^+\mathbf{F}^+)], \tag{24}$$

$$\overline{\Delta\mathbf{N}\,(\omega)\,\Delta\mathbf{N}^+\,(\omega')} = \frac{1}{2\pi}\,\delta(\omega+\omega')\,[-\mathbf{F}(\boldsymbol{\chi}\mathbf{F} + \mathbf{I}\mathrm{i}\omega)^{-1}(\mathbf{F}^+\mathbf{D}^{-1}\mathbf{F})^{-1}\mathbf{F}^+ + \\ + \mathbf{F}(\mathbf{F}^+\mathbf{D}^{-1}\mathbf{F})^{-1}\,(\mathbf{I}\mathrm{i}\omega - \mathbf{F}^+\boldsymbol{\chi}^+)^{-1}\,\mathbf{F}^+] \tag{25}$$

and

$$\overline{\boldsymbol{\Psi}\,(\omega)\,\boldsymbol{\Psi}^+\,(\omega')} = -\frac{1}{2\pi}\,\delta(\omega+\omega')\,[\mathbf{F}\,\boldsymbol{\chi}\,\mathbf{F}(\mathbf{F}^+\mathbf{D}^{-1}\mathbf{F})^{-1}\mathbf{F}^+ + \\ + \mathbf{F}(\mathbf{F}^+\mathbf{D}^{-1}\mathbf{F})^{-1}\,\mathbf{F}^+\boldsymbol{\chi}^+\mathbf{F}^+] \tag{26}$$

where

$$\mathbf{E}(t) = \exp(\boldsymbol{\chi}\mathbf{F}t),$$

$$\boldsymbol{\Phi} = \mathrm{d}\boldsymbol{\xi}/\mathrm{d}t - \mathbf{r}(\bar{\mathbf{N}} + \mathbf{F}\Delta\boldsymbol{\xi})$$

and

$$\boldsymbol{\Psi} = \mathrm{d}\mathbf{N}/\mathrm{d}t - \mathbf{F}\mathbf{r}(\bar{\mathbf{N}} + \mathbf{F}\Delta\boldsymbol{\xi}).$$

The principle of microscopic reversibility[7] requires

$$\overline{\Delta\xi(t_1)\,\Delta\xi^+(t_2)} = \overline{\Delta\xi(t_2)\,\Delta\xi^+(t_1)} \tag{27}$$

and then

$$\mathbf{E}(\tau)\mathbf{g}^{-1} = \mathbf{g}^{-1}\mathbf{E}^+(\tau). \tag{28}$$

For the sake of simplicity we shall write Eq. (28) in an equilvalent form :

$$\mathbf{\Lambda}\mathbf{g}^{-1} = \mathbf{g}^{-1}\mathbf{\Lambda}^+. \tag{29}$$

The proof of the equivalence is the following :

a. Sufficiency

$$(28) \Rightarrow \left(\frac{\partial \mathbf{E}(\tau)}{\partial \tau}\right)_{\tau=0} \mathbf{g}^{-1} = \mathbf{g}^{-1}\left(\frac{\partial \mathbf{E}^+(\tau)}{\partial \tau}\right)_{\tau=0} \Rightarrow \mathbf{\Lambda}\mathbf{g}^{-1} = \mathbf{g}^{-1}\mathbf{\Lambda}^+.$$

b. Necessity

$$(29) \Rightarrow \mathbf{\Lambda}^l\,\mathbf{g}^{-1} = \mathbf{\Lambda}^{l-1}\mathbf{g}^{-1}\mathbf{\Lambda}^+ = \ldots = \mathbf{g}^{-1}\mathbf{\Lambda}^{+l} \Rightarrow$$

$$\Rightarrow \sum_{l=0}^{\infty} \frac{\tau^l\,\mathbf{\Lambda}^l}{l\,!}\,\mathbf{g}^{-1} = \mathbf{g}^{-1}\sum_{l=0}^{\infty}\frac{\tau^l\mathbf{\Lambda}^{+l}}{l!} \Rightarrow \mathbf{E}(\tau)\,\mathbf{g}^{-1} = \mathbf{g}^{-1}\mathbf{E}^+(\tau).$$

Eq. (29) can also be obtained using the thermodynamics of irreversible processes.[8] Within the framework of nonequilibrium thermodynamics, the regression equations takes the form :

$$\frac{\mathrm{d}\langle\Delta\xi_i\rangle_{\xi_0}}{\mathrm{d}t} = \sum_j \frac{L_{ij}}{T}\,\langle A_j\rangle_{\xi_0} \tag{30}$$

where

$$A_j = -\,RT\sum_\alpha f_{\alpha j}\ln\left(N_\alpha/\bar{N}_\alpha\right)$$

is the affinity of the *j*th reaction.

Whether the concentration fluctuations are small we can consider that :

$$A_j = -\,RT\sum_\alpha f_{\alpha j}\ln(1 + \sum_k f_{\alpha k}\,\Delta\,\xi_k/\bar{N}_\alpha) \cong$$

$$\cong -\,RT\sum_\alpha\sum_k f_{\alpha j}\,f_{\alpha k}\,\Delta\,\xi_k/\bar{N}_\alpha = -\,RT\sum_k g_{jk}\,\Delta\,\xi_k \tag{31}$$

whence we get

$$\frac{\mathrm{d}\,\langle\Delta\xi\rangle_{\xi_0}}{\mathrm{d}t} = -\,R\,\mathbf{L}\,\mathbf{g}\,\Delta\,\boldsymbol{\xi}. \tag{32}$$

---

[7] R. C. Tolman, *Phys. Rev.*, **23**, 699 (1926).

[8] S. R. de Groot and P. Mazur, "Non-Equilibrium Thermodynamics", North Holland Publ. Comp., Amsterdam, 1962.

From Eq. (4) and (32) it turns out that

$$\mathbf{\Lambda} = \chi \mathbf{F} = - R\,\mathbf{L}\,\mathbf{g}$$

or

$$\mathbf{L} = - \frac{1}{R}\, \chi\, \mathbf{F}\, \mathbf{g}^{-1} \tag{33}$$

and then the Onsager's reciprocal conditions [2,8]

$$\mathbf{L} = \mathbf{L}^{+}$$

may be written in the form

$$\mathbf{\Lambda g}^{-1} = (\mathbf{\Lambda g}^{-1}) = (\mathbf{g}^{-1})^{+}\, \mathbf{\Lambda}^{+} = \mathbf{g}^{-1}\, \mathbf{\Lambda}^{+}.$$

We find again, thus Eq. (29).

Further on, we shall prove that Eq. (29) follows from the condition of macroscopic equilibrium (17). Eq. (17) implies :

$$\mathbf{r}(\overline{\mathbf{N}}) = \mathbf{r}'(\overline{\mathbf{N}}) - \mathbf{r}''(\overline{\mathbf{N}}) = 0 \tag{18'}$$

or

$$\mathbf{r}'(\overline{\mathbf{N}}) = \mathbf{r}''(\overline{\mathbf{N}}) = \overline{\mathbf{r}} \tag{18''}$$

and hence

$$\chi = \left\| \frac{\nu_{ji}\, r'_i\,(\overline{\mathbf{N}}) - \nu'_{ji}\, r''_i\,(\overline{\mathbf{N}})}{\overline{\mathbf{N}}_j} \right\| = - \left\| \frac{f_{ji}\bar{r}_i}{\bar{N}_j} \right\| = -$$

$$= - \| \sum_{\alpha} \sum_{\beta} \bar{r}_i\; \delta_{i\alpha}\, f_{\beta\alpha}\;\; \delta_{\beta j}\; \bar{N}_j{}^{-1} \| = - \mathbf{Z F^{+} D^{-1}} \tag{34}$$

with

$$\mathbf{Z} = ||\bar{r}_i\; \delta_{ij}||.$$

Combining Eq. (13) with Eq. (34) we get

$$\mathbf{\Lambda g}^{-1} = \chi \mathbf{F g}^{-1} = -\mathbf{Z F^{+} D^{-1} F g^{-1}} = - \mathbf{Z g g^{-1}} = - \mathbf{Z}$$

and

$$\mathbf{g}^{-1} \mathbf{\Lambda}^{+} = - \mathbf{g}^{-1}\, (\mathbf{Z F^{+}\, D^{-1}\, F})^{+} = - \mathbf{g}^{-1}\, \mathbf{F^{+}\, D^{-1}\, F Z} = - \mathbf{Z}$$

whence

$$\mathbf{\Lambda g}^{-1} = \mathbf{g}^{-1}\, \mathbf{\Lambda}^{+}$$

i.e., in the case of a network with nondegenerate (independent) reactions, the principle of microscopic reversibility is fulfiled for any values of the rate constants and then for such systems do not exist ciclicity conditions of Wegscheider's type.[9,10]

C. EXAMPLES

As illustrations of the theory, we shall consider the following particular cases:

$$\textbf{1.}\ \sum_i \nu_i A_i \leftrightarrows \sum_i \nu'_i A_i \quad 2 \geqslant \sum_i \nu_i, \sum_i \nu'_i \geqslant 1, \tag{35}$$

$$\overline{\Delta\xi(t_1)\,\Delta\xi(t_2)} = \left(\sum_i \frac{f_i^2}{\bar{N}_i}\right)^{-1} \exp\left[-\,\bar{r}\left(\sum_i \frac{f_i^2}{\bar{N}_i}\right)|\tau|\right], \tag{36}$$

$$\overline{\Delta N_i(t_1)\,\Delta N_j(t_2)} = f_i f_j \left(\sum_i \frac{f_i^2}{\bar{N}_i}\right)^{-1} \exp\left[-\,\bar{r}\left(\sum_i \frac{f_i^2}{\bar{N}_i}\right)|\tau|\right], \tag{37}$$

$$\overline{\Delta\xi(\omega)\,\Delta\xi(\omega')} = \pi^{-1}\bar{r}\,\delta(\omega+\omega')\left[\omega'^2 + \bar{r}^2\left(\sum_i \frac{f_i^2}{\bar{N}_i}\right)^2\right]^{-1}, \tag{38}$$

$$\overline{\Delta N_i(\omega_1)\,\Delta N_j(\omega_2)} = \pi^{-1} f_i f_j\,\bar{r}\,\delta(\omega+\omega')\left[\omega'^2 + \bar{r}^2\left(\sum_i \frac{f_i^2}{\bar{N}_i}\right)^2\right]^{-1}. \tag{39}$$

$$\textbf{2.}\ A_1 \leftrightarrows A_2 \leftrightarrows A_3 \leftrightarrows \ldots \leftrightarrows A_{n+1},\ n = 1, 2, 3, \ldots \tag{40}$$

$$\overline{\Delta N_i\,\Delta N_j} = \delta_{ij}\,\bar{N}_i - \bar{N}_i\,\bar{N}_j / \sum_i \bar{N}_i. \tag{41}$$

$$\textbf{3.}\ \nu_1 A_1 \leftrightarrows \nu'_1 A_2;\ \nu_2 A_2 \leftrightarrows \nu'_2 A_3;\ 2 \geqslant \nu_1,\ \nu'_1,\ \nu_2,\ \nu'_2 \geqslant 1 \tag{42}$$

$$\overline{\Delta N_i\,\Delta N_j} = \delta_{ij}\,\bar{N}_i - \varphi_i\,\varphi_j\,\bar{N}_i\,\bar{N}_j / \sum_i \varphi_i^2\,\bar{N}_i. \tag{43}$$

with

$$\varphi_1 = \nu'_1\,\nu'_2,\ \varphi_2 = \nu_1\,\nu'_2 \text{ and } \varphi_3 = \nu_1\,\nu_2$$

$$\textbf{4.}\ A_1 + A_2 \leftrightarrows A_3,\ A_3 \leftrightarrows A_4 \tag{44}$$

---

[9] R. Wegscheider, *Z. phys. Chem.*, **39**, 257 (1902.)

[10] J. Z. Hearon, *Bull. Math. Biophys.*, **15**, 121 (1953).

$$\overline{\Delta \mathbf{N}\,\Delta \mathbf{N}^{+}} = \begin{bmatrix} \bar{N}_1 - \bar{N}_1^2 \dfrac{\bar{N}_1 + \bar{N}_3 + \bar{N}_4}{B} & \bar{N}_1 \bar{N}_2 \dfrac{\bar{N}_3 + \bar{N}_4}{B} & -\bar{N}_1 \bar{N}_3 \dfrac{\bar{N}_2}{B} & -\bar{N}_1 \bar{N}_4 \dfrac{\bar{N}_2}{B} \\ \bar{N}_2 \bar{N}_1 \dfrac{\bar{N}_3 + \bar{N}_4}{B} & \bar{N}_2 - \bar{N}_2^2 \dfrac{\bar{N}_1 + \bar{N}_3 + \bar{N}_4}{B} & -\bar{N}_2 \bar{N}_3 \dfrac{\bar{N}_1}{B} & -\bar{N}_2 \bar{N}_4 \dfrac{\bar{N}_1}{B} \\ -\bar{N}_3 \bar{N}_1 \dfrac{\bar{N}_2}{B} & -\bar{N}_3 \bar{N}_2 \dfrac{\bar{N}_1}{B} & \bar{N}_3 - \bar{N}_3^2 \dfrac{\bar{N}_1 + \bar{N}_2}{B} & -N_3 N_4 \dfrac{\bar{N}_1 + \bar{N}_2}{B} \\ -\bar{N}_4 \bar{N}_1 \dfrac{\bar{N}_2}{B} & -\bar{N}_4 \bar{N}_2 \dfrac{\bar{N}_1}{B} & -\bar{N}_4 \bar{N}_3 \dfrac{\bar{N}_1 + \bar{N}_2}{B} & \bar{N}_4 - \bar{N}_4^2 \dfrac{\bar{N}_1 + \bar{N}_2}{B} \end{bmatrix} \tag{45}$$

where

$$B = \bar{N}_1 \bar{N}_2 + \bar{N}_2 \bar{N}_3 + \bar{N}_1 \bar{N}_4 + \bar{N}_2 \bar{N}_3 + \bar{N}_2 \bar{N}_4$$

$$\mathbf{5.}\ A_1 \leftrightarrows A_2 + A_3,\ A_2 + A_3 \leftrightarrows A_4 \tag{46}$$

$$\overline{\Delta \mathbf{N}\,\Delta \mathbf{N}^{+}} = \begin{bmatrix} \bar{N}_1 - \bar{N}_1^2 \dfrac{\bar{N}_2 + \bar{N}_3'}{B'} & -\bar{N}_1 \bar{N}_2 \dfrac{\bar{N}_3}{B'} & -\bar{N}_1 \bar{N}_3 \dfrac{\bar{N}_2}{B'} & -N_1 N_4 \dfrac{\bar{N}_2 + \bar{N}_3}{B'} \\ -\bar{N}_2 \bar{N}_1 \dfrac{\bar{N}_3}{B'} & \bar{N}_2 - \bar{N}_2^2 \dfrac{\bar{N}_1 + \bar{N}_2 + \bar{N}_4}{B'} & \bar{N}_2 \bar{N}_3 \dfrac{\bar{N}_1 + \bar{N}_4}{B'} & \\ -\bar{N}_3 \bar{N}_1 \dfrac{\bar{N}_2}{B'} & \bar{N}_3 \bar{N}_2 \dfrac{\bar{N}_1 + \bar{N}_4}{B'} & \bar{N}_3 - \bar{N}_3^2 \dfrac{\bar{N}_1 + \bar{N}_3 + \bar{N}_4}{B'} & \bar{N}_3 \bar{N}_4 \dfrac{\bar{N}_2}{B'} \\ -\bar{N}_4 \bar{N}_1 \dfrac{\bar{N}_2 + \bar{N}_3}{B'} & -\bar{N}_4 \bar{N}_2 \dfrac{\bar{N}_3}{B'} & -\bar{N}_4 \bar{N}_3 \dfrac{\bar{N}_2}{B'} & \bar{N}_4 - \bar{N}_4^2 \dfrac{\bar{N}_2 + \bar{N}_3}{B'} \end{bmatrix} \tag{47}$$

with

$$B' = \bar{N}_1 \bar{N}_2 + \bar{N}_1 \bar{N}_3 + \bar{N}_2 \bar{N}_3 + \bar{N}_2 \bar{N}_4 + \bar{N}_3 \bar{N}_4$$

Examining Eqs. (41), (43), (45) and (47), we can notice that :

1. In the case of monomolecular reactions, the thermodynamic theory of fluctuations leads to the same results as the stochastic theory of reaction rates.[11,12]

2. If $N_i \ll \sum_i N_i$ (i.e., $R \gg 1$) the formula (1) is a good approximation of Eq. (14).

---

[11] D. A. Mc. Quarrie, *Adv. Chem. Phys.*, **15**, 149 (1969).

[12] M. Vlad and E. Segal, *Rev. Roumaine Chim.*, **21**, 667, 1311, 1319 (1976).

D. CONCLUSION

Throughout this paper we have calculated the magnitude of concentration fluctuations in a closed chemical system with R independent reactions, at equilibrium. The obtained results are in agreement with the stochastic theory of reaction rates.[11,12] We have shown that, for $R \gg 1$, the magnitude of fluctuations is the same, whether the system is open or closed.

ACKNOWLEDGEMENT. **We are indebted to E. Segal and V. Popa for their helpful suggestions.**

Revue Roumaine de Chimie, **23**, *8*, 1243–1249 (1978)

PHYSIKO-CHEMISCHE STUDIEN EINIGER THIOCARBOHYDRAZONE AROMATISCHER UND HETEROAROMATISCHER ALDEHYDE

SILVIA BARBU * und CONST. GH. MACAROVICI**
*Medizinisch-Pharmazeutisches Institut Cluj-Napoca, Pharmazeutische Fakultät,
Str. I. Creangă Nr. 12
**Babeş-Bolyai-Universität Cluj-Napoca, Chemie Fakultät
Str. Arany János Nr.11
Rumänien

Eingegangen am 24. Mai 1976

Es wurden einige Thiocarbohydrazone hergestellt, die von aromatischen und heterocyklischen Aldehyden abstammen (S-TCH, V-TCH I-TCH, N-TCH und T-TCH). um neue Liganden in die Koordinativchemie einzuführen. Die Thiocarbohydrazone wurden physikalisch-chemisch, derivatographisch und spektrophotometrisch im UV- und IR-Bereich untersucht.

Die Thiocarbohydrazone gehören einer Ligandenklasse an welche sowohl theoretisches — die Koordinationschemie betreffend — als auch praktisches Intresse für die Analytik aufweist und, dank ihrer biologischen Wirkung, auch für die Pharmakologie.

Die Thiocarbohydrazone, Kondensationsverbindungen des Thiocarbohydrazids mit Karbonylverbindungen, wurden zum ersten Mal von Stollé und Bowles erwähnt, die einige Bisthiocarbohydrazone synthetisierten.[1]

In einigen Arbeiten, welche sich mit Problemen der Chemie der Heterocyklen befassen, wird auch die Darstellung von Thiocarbohydrazonen erwähnt. [2–6]

Duval und Mitarbeiter, [7,8] synthetisierten einige Thiocarbohydrazone im Laufe ihrer Untersuchungen betreffend die analytischen Eigenschaften des Thiocarbohydrazids und studierten die erhaltenen Verbindungen thermogravimetrisch.

---

[1] R. Stollé und P. E. Bowles, *Ber. dtsch. chem. Ges.*, **41**, 1099 (1908).
[2] P. C. Guha und S. C. Dey, *J. Chem. Soc.*, **125**, 1215 (1924).
[3] W. Autenreith und H. Hetner, *Ber. dtsch. chem. Ges.*, **58**, 2151 (1925).
[4] R. Stollé und E. Gaertuer, *J. prakt. Chem.*, **132**, 209 (1931).
[5] J. Sandstrom, *Acta Chem. Scand.*, **14**, 1037 (1960).
[6] J. Sandstrom, *Acta Chem. Scand.*, **17**, 1595 (1963).
[7] C. Duval und T. B. Loc, *Compt. rend.*, **1955**, 1097.
[8] C. Duval und N. D. Young, *Mikrochim. Acta*, **1956**, 747.

Das Molekül der Thiocarbo-monohydrazone entspricht der allgemeinen Formel **1** und enthält die Azomethin-, Thiocarbonyl- und Hydrazingruppen mit elektronenabgebenden Eigenschaften.

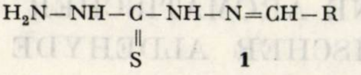

$$H_2N{-}NH{-}\underset{\underset{S}{\|}}{C}{-}NH{-}N{=}CH{-}R$$

1

1 A, $R = H$
1 S, $R = 2{-}C_6H_4OH$
1 V, $R = 3{-}MeO{-}4{-}HO{-}C_6H_3$
1 I, R = 4–Pyridyl
1 N, R = 3–Pyridyl
1 T, R = 2–Thienyl

Das Vorhandensein der Thiocarbonylgruppe im Molekül der Thiocarbohydrazone verleiht diesen fungizide Eigenschaften. In dieser Hinsicht werden Thiocarbo-monohydrazone und Bisthiocarbohydrazone, ausgehend von aliphatischen und aromatischen Aldehyden, synthetisiert.[9]

Zwecks Verwendung anderer Thiocarbohydrazone als Liganden, untersuchen wir in vorliegender Arbeit erst einmal das physikalisch-chemische Verhalten einiger von uns synthetisierten Thiocarbohydrazone und zwar: das Thiocarbohydrazon des Salicylaldehyds (S–TCH), des Vanillins (V–TCH), des Isonikotinaldehyds (I–TCH), des Nikotinaldehyds (N–TCH) und des Thiophen-2-carbaldehyds (T–TCH).

EXPERIMENTELLER TEIL

Das Thiocarbohydrazid wurde nach der von Burns[10] gegebenen Methode synthetisiert während die neuen, oben erwähnten Thiocarbohydrazone, durch Kondensationsreaktionen des Thiocarbohydrazids mit den entsprechenden Karbonylverbindungen hergestellt wurden (Tabelle 1).

Tabelle 1

Chemische Analyse und Schmp. der synthetisierten Thiocarbohydrazone 1

VERBINDUNG	N%		S%		Schmp. °C
	ber.	gef.	ber.	gef.	
1 S	26,63	26,28	15,25	15,45	185
1 V	23,31	22,95	13,34	13,55	148
1 I	35,87	35,60	16,42	16,20	205
1 N	35,87	36,00	16,42	16,15	210
1 T	27,97	28,08	32,01	32,30	185

Einer wäßrigen Thiocarbohydrazidlösung wird eine alkoholische Aldehydlösung im Molverhältnis 1 : 1 zugefügt. Das Gemisch wird 30 Minuten unter Rückfluß gekocht und dann abgekühlt. Der erhaltene, filtrierte Niederschlag wird mit einem Wasser-Alkohol-Gemisch (2 :1) gewaschen und durch Umkristallisierung aus Alkohol gereinigt.

Physikalische Messungen. Die Schmelzpunkte wurden mit Hilfe eines Apparates vom Typ Boëtius bestimmt. Die Derivatogramme wurden mit Hilfe eines Erdely-Paulik-Paulik Derivatographen aufgezeichnet. Die Elektronenspektren wurden mit Hilfe eines VSU-2P Carl Zeiss-Jena

---

[9] D. M. Wiles und T. Suprunchuk, *J. Med. Chem.*, **13**, 323 (1970).
[10] G. R. Burns, *Inorg. Chem.*, **7**, 2, 277 (1968).

Spektrophotometers, und die IR-Spektren mit Hilfe eines UR-10 Carl Zeiss-Jena Spektrophotometers, im Bereich 3600—400 cm^{-1} aufgenommen.

ERGEBNISSE UND DISKUSSIONEN

Thermisches Verhalten: Die Derivatogramme der Thiocarbohydrazone wurden im Vergleich zu dem des Thiocarbohydrazids ausgewertet und die erhaltenen Daten mit den Ergebnissen der stöchiometrischen Berechnung in Beziehung gebracht (Tabelle 2).

Tabelle 2

Thermische Effekte, aufgezeichnet bei der Pyrolyse der Thiocarbohydrazone 1.

Verbindung	Temperatur °C	Thermische Effekte, °C endo	exo	Gewichtsverlust % ber.	gef.	Phänomen
1 A	200	168	—	—	—	Schmelzen
	300		220	58,42	55,00	$2H_2N$-NH-Verlust
	400		305 370			
	500	495		41,68	45,00	S und C Verlust
	600		550			
1 S	200	180	—	—	—	Schmelzen
	300	280	220	40,45	43,45	Verlust der desulfurierten Seitenkette
	400	—	—			S-Verlust
	500	495		59,65	56,55	R-Pyrolyse
	700		610			
1 V	200	130	—	12,90	9,9	Schmelzen und NH_2-Verlust
	400			22,48	26,92	Verlust der restlichen Kette
	600	495		64,54	64,00	S-Verlust
	800		680			R-Pyrolyse
1 N	200	208				Verlust der desulfurierten Seitenkette
	300		235	43,56	44,92	
	400	305				S-Verlust
	500	445	500	56,42	55,08	
	600		550			R-Pyrolyse

Das Derivatogramm des Thiocarbohydrazids weist auf der DTA-Kurve einen den Schmelzvorgang begleitenden endothermen Effekt mit der thermischen Spitze bei 169° auf.

Die DTA-Kurven der Thiocarbohydrazone weisen zu Beginn einen analogen endothermen Effekt auf, der bei S-TCH den Schmelzvorgang, bei V-TCH und N-TCH den Schmelz-und Zersetzungsvorgang begleiten könnte. Die ATG-Kurven der beiden letztgenannten Substanzen zeigen einen Gewichtsverlust an.

Diese Ergebnisse stimmen mit den Schlußfolgerungen Duvals und Youngs[8] überein, die ein ähnliches Verhalten im Falle einiger Bisthiocarbohydrazone feststellten.

Im Einklang mit den Ergebnissen des derivatographischen Studiums kann man zwei Zersetzungsstufen für das Molekül der untersuchten Thiocarbohydrazone annehmen: unter 300° findet der Seitenkettenverlust statt, während bei höheren Temperaturen Schwefel abgespalten wird und die Pyrolyse des aromatischen oder heterocyklischen Restes, je nach der Aldehydart, stattfindet.

Die beiden Zersetzungsstufen sind von sehr starken exothermen Effekten begleitet, die der Verbrennung zugeschrieben werden.

Die aufgezeichneten endothermen Effekte über 300° können dem Schmelzen der entstandenen Zwischenprodukte nach der Zersetzung zugeschrieben werden. Die Differenzen zwischen den Ergebnissen der stöchiometrischen Berechnung und den Derivatogramm-Daten, für die verschiedenen Zersetzungsstufen, könnten der Interferenz und den Sublimierungsvorgängen zugeschrieben werden.

Die Elektronenspektren wurden für 10^{-4} M methanolische Thiocarbohydrazonlösung aufgenommen.

Die Absorptionsbanden sowie die Werte der molaren Extinktionskoeffizienten sind in Tabelle 3 wiedergegeben.

Tabelle 3

Elektronenspektrenbanden der Thiocarbohydrazone 1.

VERBINDUNG	$\pi - \pi^*$		Andere Banden			
	$\frac{\lambda \text{nm}}{\nu \text{cm}^{-1}}$	$\varepsilon \frac{\text{mol}}{\text{cm}^{-1}}$	$\frac{\lambda \text{nm}}{\nu \text{cm}^{-1}}$	$\varepsilon \frac{\text{mol}}{\text{cm}^{-1}}$	$\frac{\lambda \text{nm}}{\nu \text{cm}^{-1}}$	$\varepsilon \frac{\text{mol}}{\text{cm}^{-1}}$
1 S	330 30303	22440	300 30334	16545	—	—
1 V	300 30303	24150	230 43478	15210	—	—
1 I	300 30303	29950	255 29215	5775	230 43478	8165
1 N	320 31250	26000	245 40826	8500	—	—
1 T	330 30303	28239	265 37736	8680	230 43478	6810

Das Molekül der Thiocarbohydrazone enthält 2 Chromatophorgruppen: die Thion- und Azomethingruppe, die das Erscheinen von zwei Arten von Übergängen, $\pi - \pi^*$ und $n - \pi^*$, bedingen. Da der Übergang $n - \pi^*$ „verboten" ist, weist die entsprechende Bande eine geringe Intensität auf.

Im Spektrum der Thiocarbohydrazone fällt eine sehr starke Bande auf, die einem $\pi - \pi^*$-Übergang zugeschrieben wird und im Bereich über 300 nm liegt. Die Lage dieser Bande kann durch die geringe Elektronegativität der S- und N-Atome, deren π-Elektronen durch niedrigere Energiequanten aktiviert werden,[11] durch die Konjugation der Thioamid- und Azomethingruppe,[12] sowie durch die der Azomethingruppe und des vorhandenen Aldehydrestes, welche eine bathochrome Verschiebung herbeiführen, bedingt werden.

Im Spektrum der untersuchten Thiocarbohydrazone **1** erscheint die dem Übergang $n - \pi^*$ charakteristische Bande nicht, da sie vom Übergang $\pi - \pi^*$ verdeckt wird.

Nach Literaturangaben[13–15] kann in konjugierten Systemen die $\pi - \pi^*$ Bande die $n - \pi^*$ Bande um so mehr verdecken je ausgedehnter das konjugierte System ist, da die konjugierten Systeme nicht nur die Lage, sondern auch die Intensität der Bande (die im allgemeinen wächst) beeinflussen.

Im Spektrum der untersuchten Thiocarbohydrazone erscheinen Banden die kurzwelliger als 330 nm sind und eine geringere Intensität besitzen. Diese können dem Vorhandensein aromatischer oder heterocyklischer Ringe, sowie den an diesen Ringen vorhandenen Gruppen zugeschrieben werden; die nichtbeteiligten Elektronen der Atome dieser Gruppen sind im Falle des S-TCH und V-TCH mit dem aromatischen System konjugiert. Dadurch ist im Spektrum dieser Verbindungen die Intensität der Banden etwas größer.[16–18] Die von heterocyklischen Aldehyden abstammenden Thiocarbohydrazone weisen dieselben Banden auf, doch ist ihre Intensität etwas größer als im Pyridin- bzw. Thiophen-Spektrum, infolge der Konjugierung des heterocyklischen Systems mit der Azomethingruppe.[19,20]

Das Studium der IR-Spektren der Thiocarbohydrazone wurde auf Grund der Literaturdaten[9,10,21,22] bezüglich des Moleküls des Thiocarbohydrazids vorgenommen.

[11] C. N. R. Rao, „Ultraviolet and Visible Spectroscopy, Chemical Application" Bd. 2, Buterworths, London, 1967.

[12] J. Sandström, *Acta Chim. Scand.*, **17**, 937, 731, 1380 (1963).

[13] F. Bohlmann, *Chem. Ber.*, **84**, 490 (1951).

[14] J. R. Platt, *J. Chem. Phys.*, **18**, 1168 (1950).

[15] G. Young und W. Eyre, *J. Chem. Soc.*, **79**, 54 (1901).

[16] J. F. Music und F. A. Matsen, *J. Amer. Chem. Soc.*, **72**, 5256 (1950).

[17] W. W. Robertson und F. A. Matsen, *J. Amer. Chem. Soc.*, **72**, 5250 (1950).

[18] L. Doub und J. M. Vandenbelt, *J. Amer. Chem. Soc.*, **69**, 2714 (1947); **71**, 2414 (1949); **77**, 4535 (1955).

[19] S. Imanishi, *J. Chem. Phys.*, **19**, 389 (1951).

[20] R. P. Mariella und R. R. Raube, *J. Amer. Chem. Soc.*, **74**, 521 (1952).

[21] A. Braibanti, A. Tiripicchio und M. Tiripicchio Camellini, *J. Chem. Soc.*, **1972**, 2116.

[22] N. K. Dutt und C. N. Chakder, *J. Inorg. Nuclear. Chem.*, **32**, 2303 (1970); **33**, 393 (1971).

Tabelle 4

IR-Spektren der synthetisierten Thiocarbohydrazone 1 (cm^{-1}).

Verbindung \ Banden	ν_a NH$_2$ ν NH ν_s NH$_2$	δNH$_2$ νC = N	wNH νC−N δNH	νC−N νC=S	ρNH$_2$ νN−N νC=S δN−C−N		ν C−S δC−NN νCN	νC=S νC−N
					ρNH$_2$	νN−N		
1 S	3305 S 3270 3190 2990 3155 3285	1628	1560 m 1510 i	1280 i 1260 S 1210	1160 m	1020	965 m 820 schw	785 m 770 S 752 m
1 V	3420 i 3310 S 3190 3010	1610	1558 1522 1435	1280 i 1252 1213	1170 1130 i	1080 m 1038 i	980 m 970 950 867 i 825	770 m 745 schw
1 I	3285 i 3180 2990	1610	1575 1525	1280 i 1250 m 1210 m	1150 schw 1110 schw	1030 i	998 950 m 905 m 825	790 770 725
1 N	3280 3180 2995	1610 S 1600 i	1560 S 1520 1425 schw	1325 S 1280	1195 1150 schw 1140 schw	1090 m 1030 i	970 schw 940 890 schw 815 m	790 m 710 i
1 T	3275 3160 2970	1600 schw	1560 i 1510 i	1275 1283 i 1235 i	1410 schw	1090 schw 1050 schw 1025 m	930	780 s. schw 730 i

i = intensiv; m = mittel; schw = schwach; s.schw = sehr schwach; S = Schulter.

Die in Tabelle 4 gegebenen IR-Spektraldaten erlaubten uns folgende charakteristischen Bereiche festzulegen:

— der Bereich zwischen 3400—2900 cm^{-1} kann den Valenzschwingungen der NH- und NH_2-Gruppen zugeschrieben werden;

— der Bereich zwischen 1630—1400 cm^{-1} entspricht den D-eformationsschwingungen (δ) der NH_2 - Gruppe des Hydrazinrestes und der außerhalb der Ebene stattfindenden Schwingung (W) der NH-Gruppe. Ebenfalls in diesen Bereich fällt auch die Valenzschwingung der Azomethingruppe (ν C=N), die zwischen den Wellenzahlen 1630—1600 cm^{-1} auftritt;

— die Schwingungsarten ν C—N und ν C = S treten im Bereich zwischen 1325—1200 cm^{-1} auf. Die Anteiligkeit der potentiellen Energie dieser beiden Schwingungsarten im obengenannten Bereich wird in der Literatur widersprüchlich behandelt. Einige Autoren[10] nehmen das Vorherrschen der ν C—N-Schwingung, andere[22] wieder das der ν C=S Schwingung an.

Im Spektrum der von uns untersuchten Thiocarbohydrazone **1**, erscheint die den Schwingungsarten ν C—N und ν C=S zugeschriebene Bande bei 1280 cm^{-1} gespalten, wahrscheinlich infolge einer Veränderung der Geometrie des Moleküls die durch Kondensation des Thiocarbohydrazids mit Karbonylverbindungen hervorgerufen wird.[21]

Der Bereich zwischen 1200—1000 cm^{-1} wird den Schwingungen innerhalb der Ebene (ρ) der NH_2-Gruppe sowie den νN—H- und νN—C—N-Schwingungen zugeschrieben.

— Der Frequenzbereich zwischen 1000—700 cm^{-1} kann sowohl den ν—N—N—, νC=S, δ C—N—N—, ν C—N Schwingungsarten als auch den Pulsationsschwingungen der im Molekül anwesenden aromatischen oder heterocyklischen Ringe zugeschrieben werden.

Im Einklang mit vielen Literaturdaten[22-25] hat die ν N—N-Schwingungsart in diesem Bereich einen wichtigen Beitrag zu den Frequenzen zwischen 830—700 cm^{-1}.

---

[23] L. Sacconi und A. Sabatini, *J. Inorg. Nuclear Chem.*, **23**, 1389 (1963).

[24] K. Brodersen, *Z. anorg. Chem.*, **290**, 24 (1957).

[25] R. G. Snyder und J. C. Decius, *Spectrochim. Acta*, **13**, 280 (1959).

Revue Roumaine de Chimie, **23**, *8*, 1251–1259 (1978)

ELECTRONIC AND IR SPECTRA OF SOME NEW SQUARE-PLANAR COMPLEXES WITH Ni(d^8)—N(sp^2) BONDS

A. C. BANCIU

Centre of Physical Chemistry, Bucharest, Str. Dumbrava Roșie no. 23, Romania

Received August 3, 1976

Two new diamagnetic, therefore square-planar Ni(II) complexes with *sp*^{2} hybridized nitrogen atoms as donors were synthesized and their electronic and IR spectra were studied. The electronic spectra of these complexes have been interpreted in the terms of the ligand field theory.

Our previous papers [1–4] have reported on the synthesis and the physico-chemical properties of the new Ni(II) chelate complexes of type Ia, formed with organic ligands from the class of 1-methyl-2-carbethoxy-glyoxalanil-(1)-phenylhydrazones-(2), differently substituted at the benzene ring of the hydrazone group.

Recently, we have interpreted [4] the electronic spectra of type Ia complexes, in terms of ligand field theory.

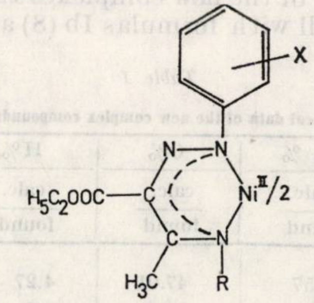

Ia: R = C_6H_5; 1: X = H
2,3: X = p; m$^-$ CH_3
4,5: X = p$^-$; m$^-$ OCH_3
6,7: X = p$^-$; m$^-$ NO_2

Ib: R = H; 1: X = H
2,3,4: X = p$^-$; m$^-$; o$^-$ CH_3
5,6,7: X = p$^-$; m$^-$; o$^-$ OCH_3
8,9: X = p$^-$; m$^-$ NO_2

---

[1] P. Spacu, A. C. Banciu and C. I. Lepădatu, *Rev. Roumaine Chim.*, **18**, 1143 (1973).
[2] A. C. Banciu and P. Spacu, *Rev. Roumaine Chim.*, **19**, 817 (1974).
[3] A. C. Banciu and P. Spacu, *Rev. Roumaine Chim.*, **19**, 1307 (1974).
[4] A. C. Banciu and C. I. Lepădatu, *Z. phys. Chem. (Frankfurt)*, **97**, 197 (1975).

From the same organic ligands, but conducting the complexation reaction with Ni(II) ions under conditions involving the splitting of the anil group from the molecule of the parent ligands, we obtained the chelate complexes nos. 1—7, of type Ib. These are formed by the Ni(II) ion with organic ligands belonging to the class of 1-methyl-2-carbethoxy-glyoxalimino-(1)-phenylhydrazones-(2), substituted at the benzene ring. The present paper describes two new chelate complexes of type Ib — *i. e.* the complexes Ib (8) and Ib (9) — with a thorough interpretation of their electronic spectra.

EXPERIMENTAL

The synthesis of the new chelate complexes was carried out as previously described, [1-3] in alcoholic aqueous solutions, in the presence of NH_3 solution.

The elemental analysis of the complexes was carried out by usual micromethods.

The IR spectra were recorded on a UR—10 Carl Zeiss (Jena) spectrophotometer, using KBr pellets.

The electronic absorption spectra were recorded in acetone solutions of $0.25 \times 10^{-4} - 2.5 \times 10^{-4}$ mole/l concentration, on a VSU—2 Carl Zeiss (Jena) spectrophotometer.

The electronic reflectance spectra were recorded on a VSU—1 Carl Zeiss (Jena) spectrophotometer, using MgO as standard.

The magnetic susceptibility measurements were performed at room temperature, according to the Faraday method, using $Hg[Co(NCS)_4]$ as standard.

RESULTS AND DISCUSSION

The analytical data of the new complexes Ib (8) and Ib (9) are listed in table 1. They agree well with formulas Ib (8) and Ib (9).

Table 1

Analytical data of the new complex compounds

Complex compound	Ni % calc. / found	C% calc. / found	H% calc. / found	N% calc. / found
I b(8)	9.57 9.4	47.01 46.8	4.27 4.9	18.27 18.8
I b(9)	9.57 9.3	47.01 47.0	4.27 4.9	18.27 18.3

The complexes are diamagnetic, therefore square-planar.

Like all the other complexes of type Ia and Ib, the new complexes Ib (8) and Ib (9) also contain a set of four sp^2 hybridized nitrogen atoms as donor atoms. These complexes too adopt a *trans* structure, in which the steric hindrances are minimized, compared to the corresponding *cis* structure.

The IR spectra. The IR spectrum of the complex Ib (9), together with the spectrum of the parent ligand used in its synthesis (which contains the anil group in its molecule), are systematized in table 2.

Table 2

The IR spectra (cm^{-1}) of the complex compound I b(9) and of the parent ligand(1-methyl-2-carbethoxy-glyoxalanil-(1)-*m*-nitrophenylhydrazone-(2))

Parent organic ligand	Complex compound I b (9)	Assignments
700 w–m	700 w–m	Deformation of benzene ring
	725 w–m	
735 w		Out-of-plane deformation of the C–H bond (γ–C–H) for the monosubstituted benzene
	740 s	
	760 m–s	
770 w–m	775 m–s	γ-C-H vibrations for the 1,3-disubstituted benzene
795 w–m	805 m	
815 w–m	825 sh	
845 w	845 sh	
885 w		
905 w	905 w–m	Symmetrical stretching vibration of the C–O–C bond
925 w		
	940 sh	
980 sh	980 w	Ring vibration of the benzene ring
1035 w–m	1035 m	
1075 s	1080 s	Asymmetrical stretching vibration of the C–O–C bond from the $COOC_2H_5$ group
	1100 vs	
1165 sh	1160 vs	
1180 s	1175 sh, s	
	1195 sh, s	Different vibrations of the C–O and $O-C_2H_5$ bonds from the $COOC_2H_5$ group
1230 m	1210 vs	
1280 m		C–N stretching vibration for the $m\text{-}NO_2\text{-}C_6H_4\text{-}NH\text{-}$ group
	1285 vs	
	1305 s	C–N stretching vibration for the $m\text{-}NO_2\text{-}C_6H_4 - N\langle$ group
	1330 vs	
1355 m–s	1350 vs	Symmetrical NO_2 stretching vibration
1380 w	1390 vs, broad	H_3C-C stretching vibration

Table 2 (continued)

Parent organic ligand	Complex compound I b (9)	Assignments
1430 w−m		
1455 w−m	1445 m	
1490 m	1480 w	C−C skeletal vibrations of the benzene ring
1520 sh		
1535 vs	1530 s	Vibrations of the conjugated C=N bonds and N=N bonds vibrations
	1555 m−s	
1585 w−m		
1625 w	1615 w	
1715 s	1695 vs	Stretching vibration of the C=O bond (ν CO) from the $COOC_2H_5$ group
2940 w	2945 w	Asymmetrical C−H stretching vibration from the CH_2 group
2980 w	2990 w	
3060 w	3100 w	C−H stretching vibrations of the substituted benzene ring
	3280 . . .	N−H stretching vibration from the imino, $>N-H$, group.
	3300 vs	

w = weak, m = medium; s = strong;
vs = very strong; sh = shoulder.

The organic ligand, involved in the formation of complex Ib (9), contains the *imino*, (= NH), group in its molecule, instead of the anil group. The ligand was formed as an intermediate during the synthesis reaction of the complex, without being isolated. Table 2 also exhibits the most probable assignments of the IR bands.

Certain domains are significant in these spectra, due to the indication provided both on similarities and on structural differences between the parent organic ligand and the metal complex compound Ib (9). Thus, the band of medium intensity, at 1280 cm^{-1}, assigned to the C−N stretching vibration in the m-NO_2-substituted C_6H_5-NH-group, appears only in the spectrum of the free ligand, which contains the free hydrazone group. Conversely, as a result of the structural changes produced by coordination, a very intense band, with maxima at 1285, 1305 and 1330 cm^{-1}, assigned to the C−N stretching vibration in the m-NO_2-substituted C_6H_5-$N\langle$ group, appears in the complex. The very intense band at 1350−1355 cm^{-1}, assigned to the symmetric NO_2 stretching vibration appears both in the parent free ligand and in the complex. This shows that from the molecule of the parent ligand the unsubstituted benzene ring has been split from the anil group, and not the m-NO_2-substituted benzene ring from the hydrazone group. The band assigned to the C=O stretching vibration from the carboxyethyl group, $-COOC_2H_5$, occurring at 1695 cm^{-1} in the free parent ligand, appears shifted by only 20 cm^{-1} in the complex. This shows that the carboxyethyl group has failed to participate in the coordination, a possibility which could not be *a priori* ignored. Otherwise, this band should have appeared markedly shifted,[5] at approx. 1635–1665 cm^{-1}, and this is obviously not the case. Finally, the very intense band, with the maximum located at 3280–3300 cm^{-1}, due to the N–H stretching vibration from the *imino* group, (=N–H), appears only in the spectrum of the complex. Apart from these, the other IR spectral data (Table 2) are also in good agreement with the formula Ib (9) of the complex.

The electronic spectra. Figure 1 exhibits the absorption spectra of the complexes Ib (8) and Ib (9), measured in acetone solutions within the 350–800 nm range. The low solubility of the complexes of type (Ib) has not permitted the preparation of more concentrated solutions, which would have helped to measure the absorption spectra at higher wavelengths than 800 nm under reasonable conditions (extinction values higher than 0.100).

In general, the electronic absorption spectra of the complexes Ib are quite similar to each other. They are also very similar to the already interpreted spectra[4] of the complexes Ia. Measured in acetone solutions, the latter present within the 350–1200 nm range four bands, which differ from each other in their intensity. They are: 1) a band due to the $\pi \rightarrow \pi^*$ transition of the organic ligand, at approx. 360 nm; 2) a band (shoulder) due to a charge-transfer (CT) transition, at approx. 500 nm; 3) a band (shoulder) due to a d–d spin-allowed transition, at approx. 600 nm and 4) a band due to a d–d spin-forbidden transition, at 1150 nm.

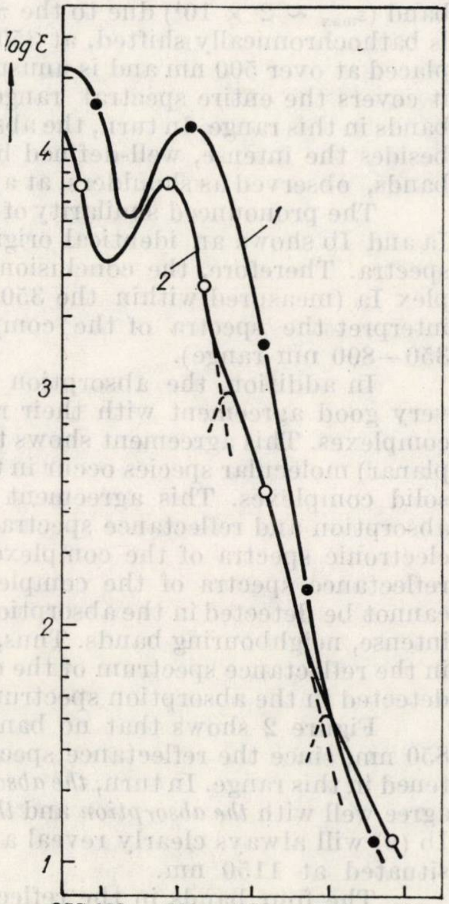

Fig. 1. — The absorption spectra of the complexes. *1* — complex compound Ib(8); *2* — complex compound Ib (9).

---

[5] L. J. BELLAMY, "The Infrared Spectra of Complex Molecules", Methuen, London, 1962.

All the differences existing between the spectra of the complexes Ia and Ib are easy to explain. Thus, in the complexes Ib, the band due to the $\pi \rightarrow \pi^*$ transition of the organic ligand is almost always hypsochromically shifted, to below 350 nm, outside of the investigated spectral range. The other bands, in the spectra of the complexes Ib appear roughly at similar wavelengths as in the complexes Ia. An explicable exception is presented by the spectrum of the complex Ib (8) (Figure 1). Compared to the spectra of the other complexes of type Ib, in this case the very intense band ($\varepsilon_{\max} \sim 2 \times 10^4$) due to the $\pi \rightarrow \pi^*$ transition of the organic ligand is bathochromically shifted, at 350 nm. The next band has its maximum placed at over 500 nm and is unusually intense ($\varepsilon_{\max} \sim 1 \times 10^4$). Therefore it covers the entire spectral range within 450—800 nm, obscuring other bands in this range. In turn, the absorption spectrum of the complex Ib (9), besides the intense, well-defined band at 490 nm, also reveals two more bands, observed as shoulders, at approx. 575 and approx. 700 nm.

The pronounced similarity of the absorption spectra of the complexes Ia and Ib shows an identical origin of the corresponding bands in these spectra. Therefore, the conclusions [4] drawn from the spectra of the complex Ia (measured within the 350—1200 nm range) can also be used to interpret the spectra of the complexes Ib (measured only within the 350—800 nm range).

In addition, the absorption spectra of the complexes Ib present a very good agreement with their reflectance spectra, measured on solid complexes. This agreement shows that similar (diamagnetic, hence square-planar) molecular species occur in the solutions of the complexes, as in the solid complexes. This agreement permits the simultaneous use of the absorption and reflectance spectra in the theoretical interpretation of the electronic spectra of the complexes Ib. This fact is important since the reflectance spectra of the complexes Ib also reveal some bands, which cannot be detected in the absorption spectra, being obscured by the more intense, neighbouring bands. Thus, the band appearing at approx. 740 nm in the reflectance spectrum of the complex Ib(9) (Figure 2) cannot be also detected in the absorption spectrum of the complex (Figure 1).

Figure 2 shows that no band occurs at wavelengths higher than 850 nm, since the reflectance spectrum of the complex Ib(9) is very flattened in this range. In turn, *the absorption spectra* of all complexes Ia (which agree well with *the absorption* and *the reflectance* spectrum of the complex Ib (9) will always clearly reveal a band in this domain, with a maximum situated at 1150 nm.

The four bands in the reflectance spectrum of the complex Ib (9), located at 490 nm (20400 cm^{-1}), ~ 570 nm (~ 17500 cm^{-1}), ~ 690 nm (~ 14500 cm^{-1}) and ~ 740 nm (~ 13500 cm^{-1}) will be assigned below. The first three of them are also present in the absorption spectrum of the complex Ib (9), at 490 nm, ~ 575 nm and ~ 700 nm.

The very high intensity ($\varepsilon_{\max} \sim 1 \times 10^4$) of the band at 490 nm indicates its positive charge-transfer (CT) origin.

The next two bands in the reflectance spectrum, at ~ 570 nm and ~ 690 nm, appear in the absorption spectrum (Figure 1) far less intense than the band at 490 nm. They may be reasonably assigned only to the following $d-d$ transitions: ${}^1A^a_{1g} \rightarrow {}^1A_{2g}$ (the band at ~ 570 nm ≈

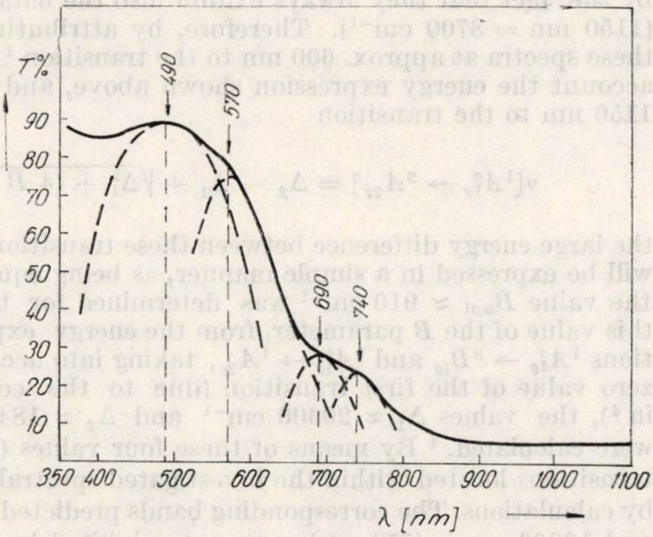

Fig. 2. — The reflectance spectrum of the complex compound Ib (9).

17500 cm^{-1}) and $^1A^a_{1g} \rightarrow {}^1B_{1g}$ (the band at ~ 690 nm ≈ 14500 cm^{-1}). The energy expressions of these transitions are [4]

$$\nu[{}^1A^a_{1g} \rightarrow {}^1A_{2g}] = \Delta_2 - \Delta_1 + \sqrt{\Delta_1^2 + (4B + C)^2} - C \quad (1)$$

$$\nu[{}^1A^a_{1g} \rightarrow {}^1B_{1g}] = \sqrt{\Delta_1^2 + (4B + C)^2} - 4B - C \quad (2)$$

B and C are the Racah parameters for the interelectronic repulsion radial integrals, and Δ_1 and Δ_2 are the energy distances between the "d" molecular antibonding levels illustrated in Figure 3.

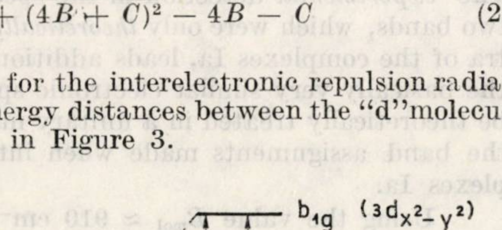

Fig. 3. — Antibonding "d" molecular levels for a square-planar complex, ML$_4$, with D_{4h} symmetry.

It has been observed that the small energy distance between these transitions, of only 3000 cm^{-1}, must be expressed by means of four parameters : B, C, Δ_1 and Δ_2. The above assignments are not arbitrary, as they would appear at a first glance. The assignments are identical with those made when explaining the absorption spectra of the complexes Ia (which agree very well with the reflectance and the absorption spectra of the complex Ib (9)). The interpretation of the spectra of the complexes Ia was facilitated by the fact that they always exhibit also the band at higher wavelengths (1150 nm = 8700 cm^{-1}). Therefore, by attributing the band located in these spectra at approx. 600 nm to the transition ${}^1A^a_{1g} \rightarrow {}^1B_{1g}$, taking into account the energy expression shown above, and assigning the band at 1150 nm to the transition

$$\nu[{}^1A^a_{1g} \rightarrow {}^3A_{2g}] = \Delta_2 - \Delta_1 + \sqrt{\Delta_1^2 + (4\,B + C)^2} - 3\,C \qquad (3)$$

the large energy difference between these transitions, of about 7500 cm^{-1}, will be expressed in a simple manner, as being equal to $2C(=8B)$. Thus, the value $B_{\mathrm{mol}} \approx 910$ cm^{-1} was determined for the complexes Ia. With this value of the B parameter, from the energy expressions of the transitions ${}^1A^a_{1g} \rightarrow {}^3B_{1g}$ and ${}^1A^a_{1g} \rightarrow {}^1A_{2g}$, taking into account the approximately zero value of the first transition (due to the considerations presented in [4]), the values $\Delta_1 \approx 20600$ cm^{-1} and $\Delta_2 \approx 18400$ cm^{-1} (i. e. $\Delta_1 \approx \Delta_2$) were calculated. [4] By means of these four values (B, C, Δ_1, Δ_2) two $d-d$ transitions located within the investigated spectral range were anticipated by calculations. The corresponding bands predicted at 14600 cm^{-1} (685 nm) and 13260 cm^{-1} (754 nm) were not exhibited by the absorption spectra of the complexes Ia, since they are obscured by more intense bands. Now, under the large shoulder between 650 — 800 nm the reflectance spectrum of the complex Ib (9) (Figure 2) reveals two bands, at approx. 690 nm and approx. 740 nm. The shoulder corresponding to the band at approx. 690 nm is also observed in the absorption spectrum of the complex Ib (9) (Figure 1). The *experimental* detection in the spectra of the complex Ib (9) of these two bands, which were only *theoretically* anticipated by means of the spectra of the complexes Ia, leads additional support to the assumption that the basically very similar electronic spectra of complexes Ia and Ib may be theoretically treated in a unitary manner. In addition, it supports also the band assignments made when interpreting the spectra of the complexes Ia.

Using the value $B_{\mathrm{mol}} \approx 910$ cm^{-1}, calculated from the absorption spectra of the complexes Ia, from the above energy expressions of the ${}^1A^a_{1g} \rightarrow {}^1A_{2g}$ and ${}^1A^a_{1g} \rightarrow {}^1B_{1g}$ transitions, it can be readily shown that $\Delta_1 \approx \Delta_2$. Therefore, the energy expression of the transition ${}^1A^a_{1g} \rightarrow {}^1A_{2g}$ helps to determine $\Delta_1 \approx 19800$ cm^{-1}

Assigning the last band in the reflectance spectrum of the complexes Ib (9), found at ~ 740 nm ($\approx$ 13500 cm^{-1}), to the spin-forbidden transition ${}^1A^a_{1g} \rightarrow {}^3E_g$ (like in complexes Ia), the following energy expression of this transition :

$$\nu[{}^1A^a_{1g} \rightarrow {}^3E_g] = \Delta_2 - \Delta_1 + \sqrt{\Delta_1^2 + (4B + C)^2} - 3B - C \qquad (4)$$

with the above indicated values of B_{mol} and Δ_1, helps to calculate the value $\Delta_2 \approx 18600$ cm^{-1}. Hence, the fact found in the interpretation of the absorption spectra of the complexes Ia, that $\Delta_1 \approx \Delta_2$, is again confirmed on the basis of the spectrum of complex Ib (9). In other words, the molecular antibonding $a_{1g}(3d_{z^2})$ level (resulted from the σ interaction of the $3d_{z^2}$ orbital of the Ni(II) ion with the sp^2 hybrid orbitals of the donor nitrogen atoms) is situated close to the molecular antibonding $e_g(3d_{xz}, 3d_{yz})$ level (resulted from the π interaction of the $3\,d_{xz}$ and $3\,d_{yz}$ orbitals of the Ni(II) ion with the $2\,p_z$ orbital of the donor nitrogen (Figure 3). The b_{2g} $(3\,d_{xy})$ level remains nonbonding in the studied complexes. This is so because there is no possibility for the formation of π coordinative bonds situated in the plane of the σ bonds (all the donor nitrogen atoms are found in sp^2 hybridization).

The small energy distance between the antibonding $e_g(3d_{xz}, 3d_{yz})$ and $a_{1g}(3\,d_{z^2})$ levels, as well as the nonbonding character of the $b_{2g}(3d_{xy})$ level seem to be characteristic of all the studied Ni(II) square-planar complexes having donor nitrogen atoms in sp^2 hybridization state.

Revue Roumaine de Chimie, 23, 8, 1261–1266 (1978)

DIVALENT MANGANESE COMPLEXES WITH LIGANDS CONTAINING O—N—N—O SEQUENCE

N. S. BIRADAR *, V. B. MAHALE and B. R. HAVINALE
Department of Chemistry, Karnatak University, Dharwar—580003, India

Received May 12, 1976

A few complexes of Mn(II) have been prepared by reacting manganese acetate with aroyl hydrazones in ethanol medium. The lemental analyses indicate 1 : 2 stoichiometry. On the basis of infrared spectral studies, it has been shown that the ligands coordinate through the oxygen of the carbonyl group and nitrogen of the azomethine group. Hence the ligands are shown to react in the keto form and the complexes have coordination number six.

INTRODUCTION

Of the several oxidation states of manganese, the oxidation state two has been extensively investigated.[1,2] It has been shown that bivalent manganese forms the complexes of coordination number four and six with a number of ligands. [3] Recently, hydrazones have been used as chelating agents for manganese. [4,5]

These hydrazones in the *keto form* may be identified as the monovalent tridentates if C=N, C=O groups along with OH take part in the bond formation and as bivalent tridentates in the *enol form*.

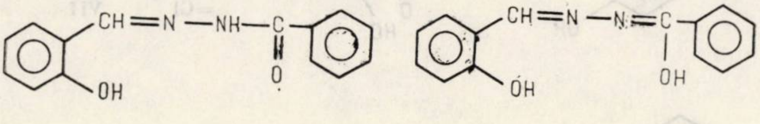

* For correspondence

---

[1] W. Klemm and H. Senff, *J. prakt. Chem.*, **154**, 73 (1939).

[2] [a] J. W. Wiley, G. N. Tyson, Jr. and J. S. Steller, *J. Amer. Chem. Soc.*, **64**, 963 (1942).
[b] A. K. Mukherjee and P. Ray, *J. Indian Chem. Soc.*, **32**, 633 (1955).
[c] S. J. Ebbs and L. T. Taylor, *Inorg. Nuclear Chem. Letters*, **10**, 1137 (1974).
[d] D. D. Ozha and R. K. Mehta, *J. Indian Chem. Soc.*, **52**, 370 (1975).

[3] F. A. Cotton and G. Wilkinson, "Advanced Inorganic Chemistry", Wiley Eastern, New Delhi, 1972.

[4] I. M. Issa. R. M. Issa, Y. M. Temerk and M. M. Ghoneim, *Monatsh.*, **104**, 963 (1973).

[5] K. K. Narang and A. Aggarwal, *Inorg. Chim. Acta*, **9**, 137 (1974).

A number of examples in which the ligands show varied behaviour depending on the reaction conditions is known in the literature. [5-8]

There is yet another type of bases containing two active and two coordinating centres and at the very outset these may be grouped under the class divalent tetradentates.

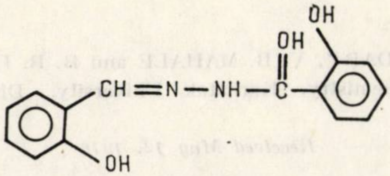

The data recently gathered emphasize that the information on the hydrazone complexes of Mn^{+2} is scanty.

The present work describes the synthesis, magnetic, and spectral properties of Mn^{+2} complexes with the following hydrazones.

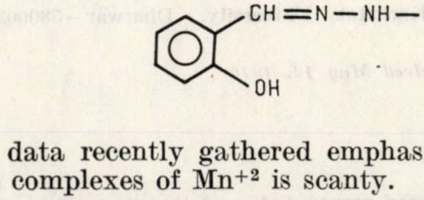

R=H I
=CH_3 II
=Cl III

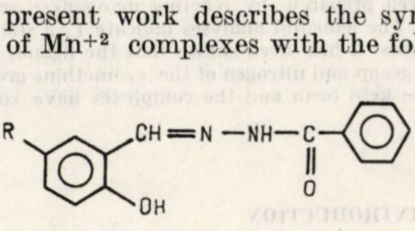

IV

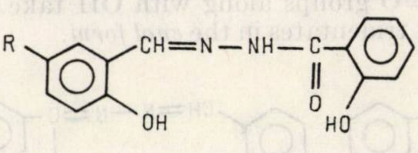

R=H V
=CH_3 VI
=Cl VII

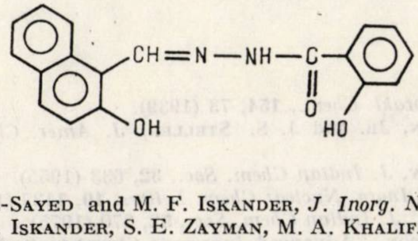

VIII

[6] L. El-Sayed and M. F. Iskander, *J. Inorg. Nuclear Chem.*, **33**, 435 (1971).

[7] M. F. Iskander, S. E. Zayman, M. A. Khalifa and L. El-Sayed, *J. Inorg. Nuclear Chem.*, **36**, 551 (1974).

[8] L. El-Sayed, M. F. Iskander and A. El-Toukhy, *J. Inorg. Nuclear Chem.*, **36**, 1739 (1974).

EXPERIMENTAL

MATERIALS AND METHOD

Ethyl benzoate, methylsalicylate and hydrazine hydrate used for preparing hydrazides were of reagent grade.

Manganese acetate was an analytical reagent. Benzoyl hydrazide and *o*-hydroxy-benzoylhydrazide were prepared according to the standard method [9] and substituted aldehydes were prepared according to Duff's [10] method.

The hydrazones were prepared by the reaction of benzoyl hydrazine or *o*-hydroxy-benzoylhydrazide (0.1M) with corresponding aldehyde (0.1M) in ethanol. The hydrazones were recrystallized from ethanol.

PREPARATION OF COMPLEXES

To an ethanolic solution containing (0.2M) of hydrazide and aldehyde, an aqueous manganese acetate solution (0.1M) was added. The reaction mixture was heated for a while on water bath and the complex precipitated was filtered and washed free from the ligand with ethanol and finally with ether and dried in vacuum over P_2O_5.

ELEMENTAL ANALYSIS

Manganese in the complexes was estimated volumetrically using EDTA by standard method [11] and nitrogen by Dumas method. The results of the elemental analyses are shown in table 1.

Table 1

Elemental analysis and magnetic moments of Mn(II) complexes with aroyl hydrazones

Ligand	Empirical formula	% Mn		% N		μ_{eff}, (298°K) B.M.
		Found	Calcd	Found	Calcd	
I	$Mn(C_{14}H_{11}N_2O_2)_2$	10.88	10.31	11.15	10.51	6.07
II	$Mn(C_{15}H_{13}N_2O_2)_2$	10.11	9.79	10.14	9.98	6.10
III	$Mn(C_{14}H_{10}ClN_2O_2)_2$	9.23	9.13	9.52	9.30	6.04
IV	$Mn(C_{18}H_{13}N_2O_2)_2$	8.61	8.68	8.80	8.85	6.00
V	$Mn(C_{14}H_{11}N_2O_3)_2$	10.08	9.72	9.82	9.91	6.00
VI	$Mn(C_{15}H_{13}N_2O_3)_2$	9.57	9.27	9.48	9.44	5.90
VII	$Mn(C_{14}H_{10}ClN_2O_3)_2$	9.08	8.67	8.45	8.83	6.00
VIII	$Mn(C_{18}H_{13}N_2O_3)_2$	8.27	8.26	8.13	8.42	5.80

PHYSICAL MEASUREMENTS

The magnetic measurements were made on a Gouy balance at room temperature using $Hg[Co(SCN)_4]$ as a calibrant. The electronic spectra of the complexes were recorded on a Beckmann DB spectrophotometer in the 350–2000 nm region. The infrared spectra of the ligands and the complexes in nujol mull were recorded on a Perkin-Elmer Model 700 spectrophotometer in the 4000 – 650 cm^{-1} region.

---

[9] A. I. Vogel, "A Text Book of Practical Organic Chemistry", Longmans, Green, London, 1968.

[10] J. C. Duff, *J. Chem. Soc.*, **1941**, 547.

[11] A. I. Vogel, "A Text Book of Quantitative Inorganic Analysis", Longmans Green, London, 1969.

Conductance measurements in DMSO were made on an ELICO CM-82 conductivity bridge with a cell having cell constant 0.829 cm^{-1}.

RESULTS AND DISCUSSION

The complexes are yellow in colour, insoluble in common organic solvents. However, they are soluble to a limited extent in DMF and DMSO. The results of the elemental analyses show that the complexes have 1 :2 stoichiometry.

CONDUCTANCE

The molar conductance values in DMSO at the concentration $\sim 10^{-3}$M are too small to measure for any dissociation of the complexes. Hence the complexes are nonelectrolytes.

MAGNETIC PROPERTIES

The magnetic moments obtained at room temperature for these complexes fall in the range of 5.80 – 6.10 B. M. suggesting the formation of spin free complexes. This closely agrees with the expected value about 5.9 B. M. for the magnetic moment of Mn(II) complexes.[12] The magnetic moments of both octahedral and tetrahedral Mn(II) complexes are close to 5.90 B.M. since a ^6S ground state persists in all the symmetries of Mn(II) complexes. These observations agree well with those of Poddar and coworkers.[13]

ELECTRONIC SPECTRA

Electronic transitions within the 3 d configuration for spin free Mn(II) species involve multiplicity changes and hence they are very weak in intensity.[3] Further the solubility of these complexes in DMSO is very low. In view of these facts, the electronic spectra are not obtained satisfactorily.

INFRARED SPECTRA

The important infrared frequencies of the ligands and the complexes are listed in table 2.

---

[12] B. N. Figgis and J. Lewis, "Progress in Inorganic Chemistry", Vol. 6, Interscience Publishers Inc., New York, 1964, p. 155.

[13] S. N. Poddar, K. Dey, J. Haldar and S. C. Nathsarkar, *J. Indian Chem. Soc.*, **47**, 743 (1970).

Infrared spectra of the ligands show a medium intensity band in the region 3220—3150 cm^{-1} due to ν (NH) vibration.[14] This band is retained in the complexes indicating that the ligands form complexes with Mn (II) in the *keto form*. The band due to intramolecular hydrogen bonded OH[15] in the region 2700—2600 cm^{-1} present in the ligands I—IV, is not observed in the complexes. This suggests that the hydrogen of the *o*-hydroxy group is replaced by the metal ion. In the complexes of the ligands V—VIII, however, the band is not vanished. This may be ascribed to the retainment of —OH group of the salicylhydrazide moiety. The ligands exhibit a strong band in the region 1670—1650 cm^{-1} due to ν (C=0)[16] and another in the region 1625—1610 cm^{-1} due to ν (C=N).[17] In almost all the complexes, peculiarly enough there is only one intense

Table 2

Important infrared frequencies (in cm^{-1}) of Mn(II) hydrazone complexes and their assignments

Ligand	ν(NH)	ν(C=0) + ν(C=N)	ν(C=C) + Amide II	ν(C—0)
I	3175	1610	1565 1545 1530	1295
II	3150	1615 1600	1562 1536	1300
III	3150	1600	1565 1555 1523	1300
IV	3175	1610	1592 1564 1520	1303
V	3220	1610	1600 1560 1545	1320
VI	3170	1600	1600 1550	1310
VII	3160	1605	1595 1555	1315
VIII	3220	1600	1600 1560 1540	1310

In the ligands, the following assignments may be made
ν(NH)∼3200cm^{-1}, ν (Intramolecular H—bonded OH) 2800—2700 cm^{-1}, ν(C=O) 1670—1650cm^{-1}, ν (C=N) 1625—1610 cm^{-1} and ν (C=O)∼1280 cm^{-1}

---

[14] C.N.R. Rao, "Chemical Applications of Infrared Spectroscopy", Academic Press, New York, London, 1963.

[15] H. H. Freedman, *J. Amer. Chem. Soc.*, **83**, 2900 (1961).

[16] A. E. Martin, *Nature*, **166**, 474 (1950).

[17] N. S. Biradar and V. H. Kulkarni, *J. Inorg. Nuclear Chem.*, **33**, 2451 (1971).

and broad band in the region 1615—1600 cm^{-1}. It may reasonably be assumed that both the C=O and C=N bands have merged and shifted to lower frequency. Thus hydrazones form coordinate bonds through the oxygen of C=0 and nitrogen of C = N with the metal ion. Two to three bands appearing in the region 1600—1520 cm^{-1} may be assigned to various stretching modes such as (C=C) skeletal and amide II on the basis of the previous observations.[5] There appears to be marked changes in ν(C—O); the band observed around 1280 cm^{-1} in ligands is shifted to higher frequency and appears in the region 1320—1295 cm^{-1} in the complexes.

All these above observations make us propose the following structure for the complexes in which Mn(II) is hexacoordinated.

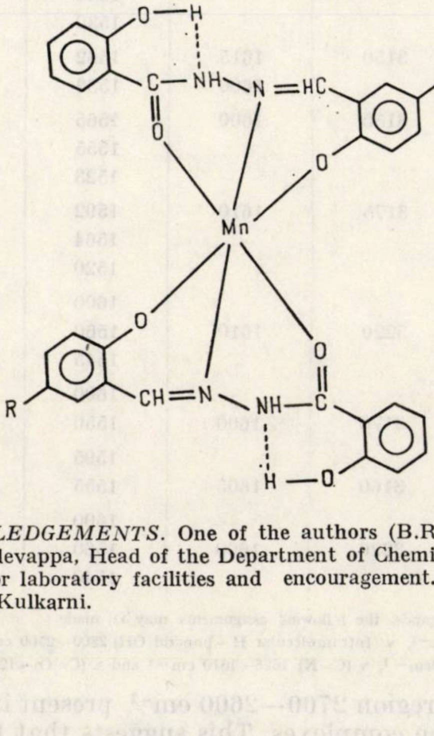

ACKNOWLEDGEMENTS. One of the authors (B.R.H.) is thankful to Prof. E. S. Jayadevappa, Head of the Department of Chemistry, Karnatak University, Dharwar, for laboratory facilities and encouragement. Thanks are also due to Dr. V. H. Kulkarni.

Revue Roumaine de Chimie, 23, 8, 1267–1273 (1978)

SUR LES COMPOSÉS DU TITANE(IV) AVEC DES BASES SCHIFF BI- ET TRI-DENTÉES

ANGELA KRIZA et MARTHA NASTA
Institut Politechnique de Bucarest,
Institut de Chimie, Faculté de Chimie,
89, Splaiul Independenţei, Bucarest, Roumanie

Reçu le 9 juillet 1976

Dans cet ouvrage on présente neuf nouveaux composés du titane (IV), obtenus du trichlorure d'éthoxytitane et des bases Schiff bi-et tridentées. L'analyse élémentaire, ainsi que l'étude spectrale dans le domaine IR ont indiqué pour les composés des bases Schiff tridentées une structure de complexes chélates, $TiCl_3$ (SB), le Ti(IV) ayant le chiffre de coordination 5. Avec des bases Schiff bidentées on a obtenu des composés du type $TiCl_2(SB)_2$, dont la molécule ne contient pas de liaisons donneur-accepteur N-Ti. Les spectres électroniques confirment les structures proposées pour les deux types de composés.

La littérature ne comprend pas une étude de synthèse concernant les complexes formés par le titane (IV) avec des bases Schiff. On a obtenu [1–5] des composés, des complexes moléculaires et des chélates, ayant le chiffre de coordination quatre ou six. Le chiffre de coordination cinq est plutôt rare pour le titane (IV).

Dans cet ouvrage nous présentons neuf nouveaux composés, obtenus par réaction du trichlorure d'éthoxytitane et des bases Schiff bi- et tridentées.

Les composés obtenus par réaction du trichlorure d'étoxytitane avec les bases Schiff bi- et tridentées sont des poudres intensément colorées, solubles en eau et alcools et insolubles en tétrachlorure de carbone, éther, benzène et chloroforme.

Les résultats de l'analyse élémentaire (tableau 1) prouvent que les composés obtenus peuvent être divisés dans deux types dont les stabilités sont différentes. Pour les composés avec des bases Schiff bidentées, obtenus par réaction 1 : 1 du trichlorure d'éthoxytitane et de la base Schiff (tableau 1,1–4), on peut proposer la formule $TiCl_3$(SB), tandis que les

---

[1] D. Negoiu et A. Kriza, *Anal. Univ. Buc.*, **20** (1971).
[2] D. Negoiu et A. Kriza, *Anal. Univ. Buc.*, **19**, 113 (1969).
[3] D. Negoiu et A. Kriza, *Anal. Univ. Buc.*, **19**, 31 (1970).
D. Negoiu, A. Kriza et M. Nasta, *Rev. Roumaine Chim.*, **19**, 1921 (1974).
[4] D. C. Bradley, M. B. Hurthstone et J. F. Rendall, *J. Chem. Soc. Chem. Comm. D.*, **12**, 672 (1969).
[5] A. D. Garnovski, V. I. Minkin, O. A. Osipov, V. T. Panioushkin, L. K. Isaeva et M. I. Knyazhanski, *Zhur. neorg. Khim.*, **12**, 2443 (1967).

Tableau 1

Données analytiques sur les composés $TiCl_x(SB)_{4-x}$ ($x = 2,3$)

Composé	Couleur	Ti%		N%		Cl%		C%		H%	
		calc.	dét.	calc.	dét.	calc.	dét.	calc.	dét.	calc.	dét.
$TiCl_3(SMEA)$	jaune foncé	14,79	14,26	4,32	4,59	32,95	34,02	33,83	34,67	3,13	3,29
$TiCl_3(SMPA)$	orange	14,40	13,20	4,21	4,19	31,99	31,55	36,13	36,79	3,61	3,86
$TiCl_3(SAPh)$	brun	13,03	13,29	3,81	3,91	28,98	29,24	42,46	42,71	2,72	2,61
$TiCl_3(SAPy)$	orange	13,63	13,29	7,97	7,57	30,96	28,85	40,96	41,03	2,56	2,67
$TiCl_2(BAPh)_2$	rouge	9,38	9,54	5,47	5,44	13,89	13,58	61,06	62,20	4,30	4,37
$TiCl_2(SMeA)_2$	rouge	12,4	11,6	—	—	18,4	19,6	—	—	—	—
$TiCl_2(SPrA)_2$	rouge	10,81	10,18	—	—	16,05	16,20	—	—	—	—
$TiCl_2(SPr^iA)_2$	rouge foncé	10,81	10,69	6,32	6,14	16,05	15,47	54,18	55,02	5,42	5,34
$TiCl_2(SBuA)_2$	rouge foncé	10,17	10,00	5,94	5,57	15,07	16,01	—	—	—	—

composés des ligands bidentés (tableau 1,5—9) sont du type $TiCl_2(SB)_2$ et ont été obtenus par réaction au rapport molaire 1 : 2.

Les composés $TiCl_3(SB)$ sont jaunes, orange ou bruns ; ils sont peu stables dans l'air et hydrolisent rapidement à cause de l'humidité atmosphérique ; ils fondent avec décomposition à environ 100°. Les composés du type $TiCl_2(SB)_2$ présentent une stabilité accrue dans l'air et se décomposent au-dessus de 200°, sans fondre.

Par réaction du trichlorure d'éthoxytitane avec des bases Schiff tridentées, au rapport molaire 1 :1, on remplace seulement le groupement éthoxy de la molécule du trichlorure d'éthoxytitane par une molécule d'azométhyne. La structure la plus probable pour les composés de ce type est une structure de complexe chélate (L) ; le ligand azométhynique est lié à l'atome métallique central par une liaison Ti—O et aussi par une liaison donneur-accepteur Ti—N, par l'intermédiaire du doublet électronique libre de l'azote azométhynique.

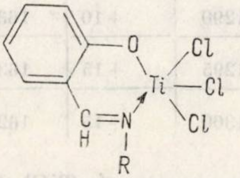

I

Pour confirmer la structure proposée on a déterminé les spectres IR des composés et des ligands et on a étudié les déplacements des bandes de vibration caractéristiques des groupements phénoxy, ν_{Ph-O}, et azométhyne, $\nu_{C=N}$, dans les spectres des composés par rapport aux spectres des ligands.

Les spectres des bases Schiff obtenues en partant des aminophénols ou des amino-alcools présentent (tableau 2) la bande caractéristique du groupement phénoxy, ν_{Ph-O}, à environ 1280 cm^{-1} et la bande caractéristique du groupement azométhyne, $\nu_{C=N}$, à environ 1600 cm^{-1} ; entre 3200—3600 cm^{-1} on remarque la bande large caractéristique du groupement hydroxyle libre. Dans le cas de la salicylalmonoéthanolamine et de la salicylalmonopropanolamine cette bande est due à l'hydroxyle aliphatique, car dans les spectres des azométhynes dérivées des amines aliphatiques correspondant aux amino-alcools elle n'apparaît pas.

Il est connu que dans la molécule des bases Schiff l'hydroxyle phénolique est chélaté par des liaisons hydrogène intramoléculaires avec l'azote azométhynique ; par conséquent dans les spectres IR de ces ligands apparaît une bande due à l'hydroxyle chélaté. D'après certains auteurs, cette bande est placée dans le domaine spectral 2800—3000 cm^{-1}. Dans les spectres IR de la salicylalmonoéthanolamine, de la salicylalmonopropanolamine et du salicylal-α-aminophénol il y a vraiment des bandes moins prononcées entre 2700 et 3100 cm^{-1} mais leur attribution est plutôt difficile.

Dans les spectres des composés 1—3 (tableau 2) la bande caractéristique du groupement phénoxy est déplacée vers des valeurs plus grandes des numéros d'onde, ce qui indique la réalisation des liaisons Ti—O—Ph

Le déplacement de ν_{Ph-O} vers des valeurs plus grandes est accompagnée par le déplacement de la bande caractéristique du groupement azométhyne, $\nu_{C=N}$, vers des fréquences plus basses (tabl. 2). Ce déplacement indique l'apparition des liaisons donneur-accepteur entre l'atome de titane et l'azote azométhynique.

Tableau 2

Spectres IR des azométhynes tridentées et de leurs composés $TiCl_3$ (SB)

Composé	ν_{Ph-O} (cm^{-1})			$\nu_{C=N}$ (cm^{-1})		
	ligand	composé	$\Delta\nu$	ligand	composé	$\Delta\nu$
$TiCl_3$(SMEA)	1280	1290	+10	1640	1608	−32
$TiCl_3$(SMPA)	1280	1290	+10	1630	1610	−20
$TiCl_3$(SAPh)	1280	1295	+15	1637	1610	−27
$TiCl_3$(SAPy)	1285	1300	+15	1620	1668	+48

Dans les spectres IR des composés $TiCl_3(SB)$ apparaît aussi la bande caractéristique de l'hydroxyle libre, une bande large, placée entre 3200 et 3400 cm^{-1}.

L'augmentation de la fréquence caractéristique du groupement phénoxy, en même temps que le déplacement de la fréquence caractéristique du groupement azométhyne vers des valeurs plus petites sont des épreuves spectrales qui indiquent nettement la formation des complexes chélates du type (I), contenant des cycles de six membres parmi lesquels l'atome de titane.

Donc les composés 1—3 contiennent des atomes de titane pentacoordinés ; ces composés sont très rarement mentionnés dans la littérature, le titane (IV) ayant comme caractéristique le chiffre de coordination six.

Quant au composé obtenu en partant du trichlorure d'éthoxytitane et de la salicylal-2-aminopyridine dans le spectre IR de ce composé on remarque un déplacement de 15 cm^{-1} de la bande ν_{Ph-O} vers des valeurs plus hautes par rapport au spectre de la salicylal-2-aminopyridine. Se sont donc formées des liaisons Ti-O-Ph.

La fréquence du cycle pyridinique qui apparaît à 1590 cm^{-1} est déplacée vers des valeurs plus grandes, ce qui indique, d'après Garnovski et ses collaborateurs,[5] l'apparition d'une liaison donneur-accepteur entre le titane et l'azote pyridinique.

Le fait que la fréquence $\nu_{C=N}$ apparaît déplacée vers des valeurs plus grandes nous empêche de faire d'autres considérations sur la structure de ce composé.

Par réaction du trichlorure d'éthoxytitane et des bases Schiff bidentées on remplace le groupement alcoxy, ainsi qu'un atome de chlore du chlorure d'éthoxytitane par deux molécules de base Schiff. En essayant d'obtenir des composés de type $TiCl_3(SB)$ avec des ligands bidentés, par rapport molaire 1 : 1, on a obtenu des mélanges probables de composés $TiCl_3(SB)$ et $TiCl_2(SB)_2$, séparables avec des solvants sélectifs.

Le tableau 3 contient des données spectrales IR sur les ligands bidentés et leurs composés avec le titane (IV).

Si des chélates s'étaient formés on aurait dû remarquer un déplacement du ν_{Ph-O} vers des valeurs plus grandes et un déplacement du $\nu_{C=N}$ vers des valeurs plus petites des numéros d'onde. Dans les spectres IR des composés on remarque des déplacements de la bande caractéristique du groupement phénoxy vers des valeurs plus grandes des fréquences, ce qui indique l'existence des liaisons Ti—O—Ph.

Tableau 3

Spectres IR des bases Schiff bidentées et de leurs composés $TiCl_2(SB)_2$

Composé	ν_{Ph-O} (cm^{-1}) ligand	composé	$\Delta\nu$	$\nu_{C=N}$ (cm^{-1}) ligand	composé	$\Delta\nu$
$TiCl_2(BAPh)_2$	1264	1275	+11	1635	1653	+18
$TiCl_2(SMeA)_2$	1290	1295	+5	1648	1680	+32
$TiCl_2(SPrA)_2$	1290	1300	+10	1640	1669	+29
$TiCl_2(S^iPrA)_2$	1290	1297	+7	1640	1655	+15
$TiCl_2(SBuA)_2$	1290	1298	+8	1642	1659	+17

On remarque aussi des déplacements positifs, assez grands de $\nu_{C=N}$, ce qui ne concorde pas avec la formation du cycle chélate. L'augmentation de la fréquence $\nu_{C=N}$ dans les spectres des composés par rapport à ceux des ligands peut être expliquée par la disparition des liaisons hydrogène qui existent dans la molécule du ligand azométhynique entre le groupement —OH phénolique et l'azote et la libération de l'azote du cycle quasi aromatique qui s'était ainsi formé.

Donc, les composés 5—9 du trichlorure d'éthoxytitane et des azométhynes aliphatiques bidentées, ainsi que du benzal-α-aminophénole ne sont pas de chélates, mais des composés du type (II), obtenus aussi par réaction au rapport molaire 1 : 2 du trichlorure d'éthoxytitane et des bases Schiff aromatiques bidentées.[3]

On peut aisément remarquer que le comportement différent des deux types de composés au chauffage et par contact avec l'air indique aussi une différence de structure.

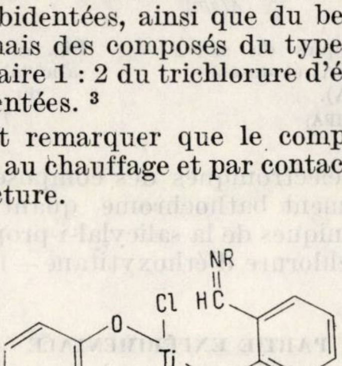

II

Une autre méthode qui pourrait confirmer les structures proposées pour les deux types de composés est offerte par les spectres électroniques. Dans les spectres électroniques des bases Schiff on remarque une bande intense dans l'ultraviolet à environ 260—280 nm et deux bandes dans le domaine visible du spectre : une bande intense à 360—370 nm et une autre, moins prononcée à environ 460 nm. Les deux bandes de 260 nm et 360 nm peuvent être attribuées au cycle aromatique de la salicylaldéhyde et, respectivement, au groupement azométhyne conjugué avec ce cycle benzénique.

Si des chélates sont formés, l'implication des électrons libres de l'azote azométhynique dans une liaison donneur-accepteur avec l'atome de titane produit un déplacement bathochrome de la bande de 370 nm. C'est ce que l'on observe dans le spectre électronique du composé $TiCl_3$ (SMEA) (fig. 1).

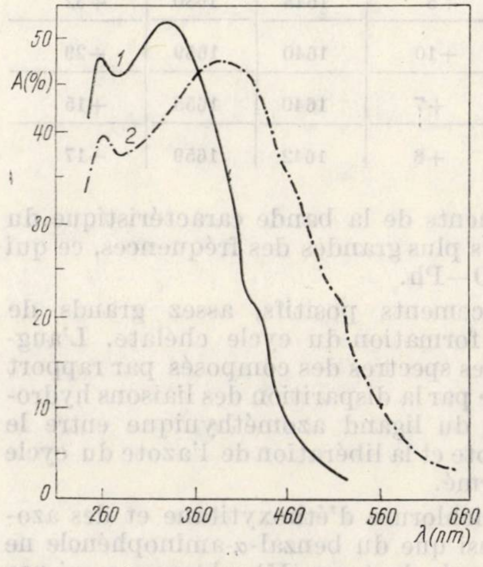

Fig. 1. — Spectres électroniques du salicylalmonoéthanolamine (SMEA) et du composé $TiCl_3$ (SMEA).
1, (SMEA) ; 2, $TiCl_3$(SMEA)

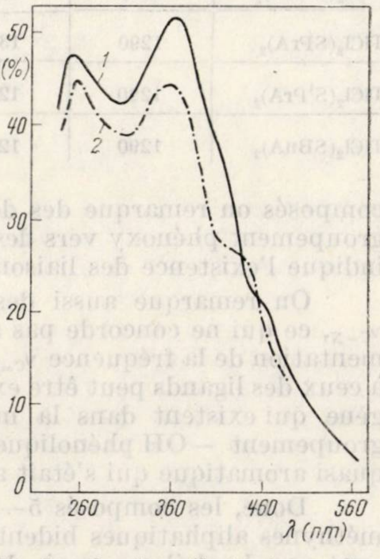

Fig. 2. — Spectres électroniques du salicylal-*i*-propylamine (S^iPrA) et du composé $TiCl_2(S^iPrA)_2$.
1, S^iPrA; 2, $TiCl_2(S^iPrA)_2$.

Dans les spectres électroniques des composés $TiCl_2$ $(SB)_2$ on ne remarque pas de déplacement bathochrome quant à la bande de 360 nm (voir les spectres électroniques de la salicylal-i-propylamine et du composé de ce ligand avec le trichlorure d'éthoxytitane — fig. 2).

PARTIE EXPÉRIMENTALE

1. *Bases Schiff.* Les bases Schiff employées en tant que ligands, leur couleur, leur point de fusion ou d'ébullition, ainsi que les analyses d'azote sont compris dans le tableau 4.

Les bases Schiff 1—8 (exception fait le n° 5) ont été préparées par réaction de la salicylaldéhyde et des amines, au rapport 1 : 1, dans du benzène. La réaction est exoterme et

Tableau 4

Bases Schiff

Base Schiff		Couleur	P.f. ou p. é.(°C/mm)	N%	
				calc.	dét.
Salicylalmonoéthanolamine	SMEA	jaune	142/1	8,48	8,50
Salicylalmonopropanolamine	SMPA	jaune	148/1	7,81	7,81
Salicylal-α-aminophénole	SAPh	rouge	184	6,57	6,62
Salicylal-2-aminopyridine	SAPy	jaune	62	14,12	14,05
Benzal-α-aminophénole	BAPh	marron	89,5	7,11	7,09
Salicylalméthylamine	SMeA	jaune	115/15	10,40	10,22
Salicylalpropylamine	SPrA	jaune	95/10	8,58	8,49
Salicylal-i-propylamine	$SPr^{i}A$	jaune	92/12	8,58	8,52
Salicylalbutylamine	SBuA	jaune	140/9	7,92	7,93

la solution change de couleur. On mène à l'ébullition pendant 2 heures, sous réflux; l'eau qui résulte par suite de la condensation a été écartée, ainsi que l'excès de benzène. Les bases Schiff ainsi obtenues ont été purifiées par distillation sous vide, ou par cristallisation de l'alcool.

Pour obtenir le benzal-α-aminophénole on passe un courant d'acyde chlorhydrique par une solution d'α-aminophénol. On ajoute une solution chaude de benzaldéhyde dans de l'alcool, puis on neutralise avec de l'acétate de sodium, quand on sépare une poudre marron, qui a été purifiée par cristallisation d'un mélange d'alcool : eau, 1 : 1.

2. *Trichlorure d'éthoxytitane.* La synthèse de trichlorure d'éthoxytitane par réaction du tétrachlorure de titane et de l'alcool éthylique a lieu dans du benzène, ou du chloroforme rigoureusement anhydrisés :

$$TiCl_4 + C_2H_5OH \rightarrow TiCl_3(OC_2H_5) + HCl$$

Le trichlorure d'éthoxytitane peut être purifié par distillation sous vide.

3. *Composés* $TiCl_x\,(SB)_{4-x}$. Etant donnée la sensibilité à l'humidité atmosphérique du trichlorure d'éthoxytitane et des composés mêmes, toutes les opérations nécessaires à la synthèse, la purification et, parfois, même à l'étude des composés doivent être faites sous azote anhydrisé et purifié et dans des solvants rigoureusement anhydrisés.

Pour obtenir les composés $TiCl_x(SB)_{4-x}$ on a mélangé 0,01 moles $TiCl_3(OC_2H_5)$, dans du tétrachlorure de carbone avec 0,01 ou 0,02 moles de base Schiff dissoutes dans le même solvant. Lorsqu'on a mélangé les deux solutions on a remarqué la séparation d'un solide. On mène à l'ébullition pendant deux heures. Le solide formé a été séparé sur une masse filtrante, sous azote, puis lavé au tétrachlorure de carbone, dans l'extracteur Soxhlet. Les composés ont été séchés « in vacuo ».

Revue Roumaine de Chimie, **23**, *8*, 1275–1278 (1978)

POTENTIOMETRIC STUDIES ON TERNARY COMPLEXES OF Zn(II)

V. KUMARI, R. C. SHARMA and G. K. CHATURVEDI,

Chemical Laboratories, Agra College, Agra, India

Received May 25, 1976

Potentiometric evidences have been cited for the formation of Zn(II)-TSA-en/pn/gly/tiron (where TSA = thiosalicylic acid, en = ethylenediamine, pn = 1,2-propylenediamine, gly = glycine, tiron = 1,2-dihydroxybenzene 3,5-disulphonic acid disodium salt). The formation constants (log K_{MAB}) and free energies of formation (ΔF°) have been calculated. The order of stability in terms of secondary ligands has been found to be as tiron> en> gly> pn.

INTRODUCTION

Potentiometric studies on Zn(II)-salicylic acid systems by Tandon et al.[1] indicate that salicylic acid has very little or no tendency to form complexes with Zn(II). Polarographic studies on the systems Zn(II)-TSA,[2] however, reveal the formation of 1 : 2 Zn(II)-TSA complexes. TSA complexes of Zn(II) and other transition metals have also been studied by Dubey and Kaul [3] and Ramamni and Shanmuganthan. In earlier communication [5] the authors have reported the results of potentiometric studies in Ni(II)-TSA-en/pn/gly/tiron ternary systems.[4] The results of pH-metric studies on similar systems with Zn(II), their formation constants (log K_{MAB}) and free energies of formation (ΔF°) are given and compared with those of Ni(II) systems, in this paper.

EXPERIMENTAL

All the chemicals used were of AnalaR BDH or E. Merck grade and en and pn were used as their dihydrochlorides. The concentrations of ligand solutions were checked by potentiometric titrations and Zn estimated gravimetrically as zinc ammonium phosphate pH changes during the titrations were recorded with a Philips Precision pH meter (PR 9405M) at 25 ± 1°C keeping the total volume (50 ml in 20% ethanol) ionic strength (0.1 M KNO_3), concentration (5×10^{-3} M in metal and ligand) constant at the beginning of titrations.

---

[1] G. Sharma and J. P. Tandon, *J. Inorg. Nuclear Chem.*, **32**, 1273 (1970).

[2] S. Prakash, P. C. Srivastava, A. M. Kumar and H. L. Nigam, *J. Electrochem. Soc. India*, **20**, 101 (1971).

[3] K. P. Dubey and M. K. Kaul, *Rev. Chim. Miner*, **8**, 819 (1971).

[4] R. Ramamni and S. P. Shanmuganthan, *Curr. Sci.*, **37**, 39 (1968).

[5] V. Kumari, R. C. Sharma and G. K. Chaturvedi, *J. Indian Chem. Soc.*, **52**, 84 (1975).

CALCULATIONS

pK values (Table 1) of the ligands were calculated by the method of Cheberek and Martell[6], formation constant (log K_{MAB}) by the method of Thompson and Loraas[7] and free energies of formation (ΔF°) from the expression $\Delta F^\circ = -RT \ln K_{MAB}$ (Table 2).

RESULTS AND DISCUSSION

Curve depicting the titration of thiosalicylic or *o*-mercaptobenzoic acid exhibits two inflections. The first inflection at $m = 1$, may be attributed to the titration of carboxylic proton and the second inflection at $m = 2$ in high pH range to the titration of proton of mercapto group.

In the curve *a* representing the titration of 1 : 1 Zn(II)—TSA, a sharp inflection at $m = 2$ may be correlated to the formation of 1 : 1 Zn(II)—TSA chelate, which probably disproportionates into 1 : 2 Zn(II)-TSA complex with the precipitation of metal hydroxide giving a second inflection at $m = 3$. This mechanism is supported by the observation that the initially formed insoluble white 1 : 1 Zn(II)—TSA species gradually dissolves probably, forming a soluble 1 : 2 Zn(II)-TSA complex and hydrated metal oxide.

Table 1

Dissociation constants of the ligands

Ligand	pK_1	pK_2
en	7.05	9.75
pn	6.91	9.78
gly	—	9.79
tiron	7.67	12.48[9]

Curve representing Zn(II)-en system exhibits a single inflection at $m = 3$. The precipitation commences at $m \sim 1.8$, probably indicating the disproportionation of 1 : 1 Zn(II)-en species into 1 : 2 Zn(II)-en complex and metal hydroxide just prior to its complete formation.[8]

Table 2

Formation constants and free energies of formation of the ternary complexes

System	log K_{MAB}	ΔF°(kcal/mole)
Zn(II)—TSA-en	4.89 ± 0.15	-6.65
Ni(II)—TSA-en[5]	6.09 ± 0.05	-8.28
Zn(II)—TSA-pn	3.26 ± 0.17	-4.43
Ni(II)—TSA-pn[5]	3.40 ± 0.18	-4.62
Zn(II)—TSA-gly	$3.78 + 0.19$	-5.14
Ni(II)—TSA-gly[5]	5.125 ± 0.015	-6.97
Zn(II)—TSA-tiron	7.04 ± 0.11	-9.58
Ni(II)—TSA-tiron[5]	7.88 ± 0.15	-10.71

---

[6] S. Cheberek and A. E. Martell, *J. Amer. Chem. Soc.*, **74**, 5052 (1952).

[7] L. C. Thompson and J. A. Loraas, *Inorg. Chem.*, **2**, 89 (1963).

[8] G. Sharma and J. P. Tandon, *Bulletin Pol. Des. Sci., Ser. Sci. Chim.*, **20**, 369 (1972).

[9] G. A. L. Heureux and A. E. Martell, *J. Inorg. Nuclear. Chem.*, **28**, 481 (1966).

In the case of Zn(II)-pn system, an ill-defined inflection and the slanting nature of the curve afterwards, probably indicate the formation of a weak 1 : 1 Zn(II)-pn complex which subsequently undergoes disproportionation forming 1 : 2 Zn(II)—pn and metal hydroxide.

In the curve representing the Zn(II)-gly system, the lowering in pH compared to glycine can be correlated to the complexation of the metal ion probably forming 1 : 1 chelate which however, disproportionates before its complete formation giving a single inflection at $m \sim 2$.

The curve representing Zn(II)-tiron system exhibits an inflection at $m \sim 2$, which may be correlated to the formation of Zn(II)-tiron complex which at higher pH probably forms a hydroxo complex, evidenced by a second inflection at $m \sim 3$.

Curves *b*, *c*, (Figure 1) represent 1 : 1 : 1 Zn(II)-TSA-en/pn and *d* and *e* (Figure 2) represent 1 : 1 : 1 Zn(II)-TSA-gly/tiron ternary systems. In all these cases the initial formation of 1 : 1 Zn(II)—TSA chelate is evidenced by (i) a white precipitate similar to that observed in the case

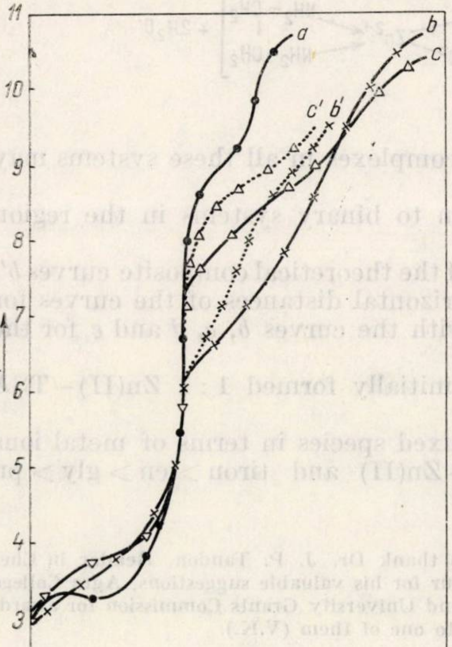

Fig. 1. — Curve $a = 1:1$ Zn(II)-TSA, $b = 1:1:1$ Zn(II)-TSA-en $c = 1:1:1$ Zn(II)-TSA-pn, *b′* and *c′* are corresponding theoretical composite curves. The curves representing the titrations of TSA and for the systems Zn(II)-en/pn have been omitted in this figure.

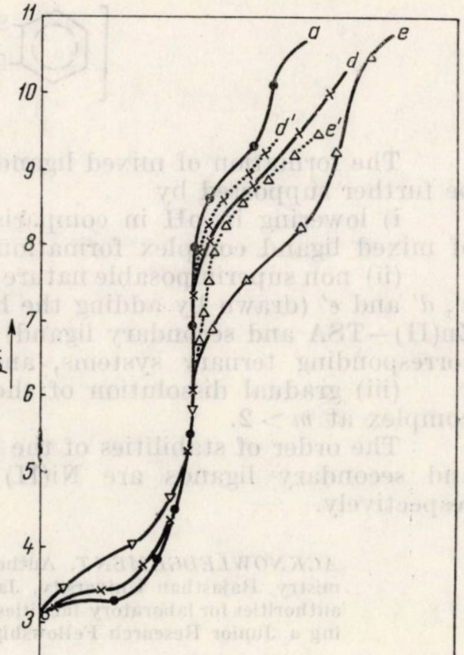

Fig. 2. — Curve $a = 1:1$ Zn(II) — TSA, $d = 1:1:1$ Zn(II)-TSA-gly, $e = 1:1:1$ Zn(II)-TSA-tiron, *d′* and *e′* are corresponding theoretical composite curves. The curves representing the titrations of TSA and for the systems Zn(II)-gly/tiron have been omitted in this figure.

of Zn(II)—TSA binary system, in the initial stages of titration; and (ii) an inflection at $m \sim 2$. Addition of the other ligand, however occurs afterwards an inflection at $m \sim 4$ (at $m \sim 3$ in the case of system involving glycine). The ill-defined nature of the inflections may be attributed to the weak nature of the ternary complexes. The stepwise addition of the two ligands may be shown as

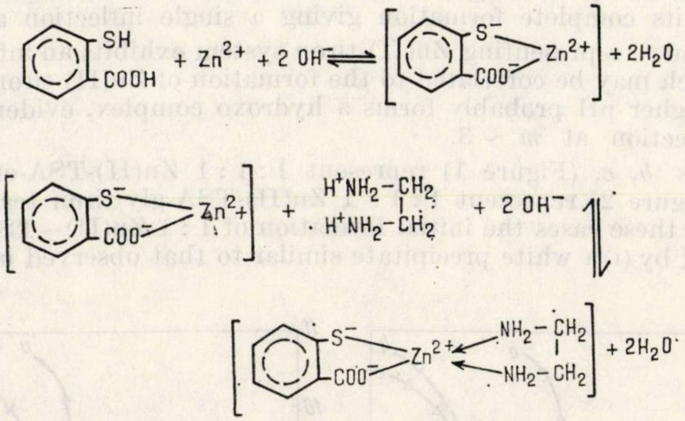

The formation of mixed ligand complexes in all these systems may be further supported by

i) lowering in pH in comparison to binary systems in the region of mixed ligand complex formation,

(ii) non superimposable nature of the theoretical composite curves b', c', d' and e' (drawn by adding the horizontal distances of the curves for Zn(II)—TSA and secondary ligand) with the curves b, c, d and e for the corresponding ternary systems, and

(iii) gradual dissolution of the initially formed 1 : 1 Zn(II)—TSA complex at $m > 2$.

The order of stabilities of the mixed species in terms of metal ions and secondary ligands are Ni(II) > Zn(II) and tiron > en > gly > pn respectively.

ACKNOWLEDGEMENT. Authors thank Dr. J. P. Tandon, Reader in Chemistry, Rajasthan University, Jaipur for his valuable suggestions, Agra College authorities for laboratory facilities and University Grants Commission for awarding a Junior Research Fellowship to one of them (V.K.).

Revue Roumaine de Chimie, **23**, *8*, 1279–1282 (1978)

POLAROGRAPHIC BEHAVIOUR OF COMPLEXES OF CADMIUM (II) AND LEAD (II) WITH 3-HYDROXYPYRIDINE-2-THIOL

R. S. SINDHU, K. B. PANDEYA and R. P. SINGH
Department of Chemistry, University of Delhi, Delhi-110007, India

Received May 5, 1976

Complexes of cadmium (II) and lead (II) complexes with 3-hydroxypyridine-2-thiol have been studied polarographically in 40% (v/v) methanol aqueous medium. The cadmium (II) complex has been studied by DeFord and Hume method ($\beta_1 = 27.9 \times 10^8$ and $\beta_2 = 26.3 \times 10^{11}$). In case of lead (II) complex the Lingane method has been applied. The value of the overall stability constant comes out to be 11.49×10^{13}.

INTRODUCTION

In as much as one considers shift in half-wave potential, $E_{\frac{1}{2}}$, complementary to chemical shifts due to complexation, polarography offers a very convenient tool for characterizing the nature of metal-ligand interaction. The present communication describes the results of polarographic studies on complex formation of cadmium (II) and lead (II) with 3-hydroxypyridine-2-thiol (abbreviated hereafter as HPT). Lead and cadmium are both toxic in nature and may be extracted from body with the help of chelating agents. Metal-ligand stability constant data have an important role in choice of suitable chelating agents. HPT has functional groups ideally situated for forming sterically favoured five membered chelate rings.

Polarographic studies on complex formation of cadmium (II) and lead (II) with other sulphur-oxygen donor ligands have been reported by earlier workers.[1–6]

EXPERIMENTAL

Reagent grade chemicals were used. The solutions of Cd(II) and Pb(II) were prepared in double distilled water. Solution of HPT was prepared in distilled methanol. The test solutions containing 1×10^{-4} M Cd(II) or Pb(II) and various concentrations of HPT were prepared keeping methanol to water ratio as 40% (v/v).

[1] H. L. Nigam and K. B. Pandeya, *Curr. Sci.*, **41**, 485 (1972).
[2] R. S. Saxena and Pratap Singh, *J. Indian Chem., Soc.*, **49**, 223 (1972).
[3] A. Saito and S. Himeno, *Bunseki Kagaku*, **21**, 1321 (1972).
[4] J. N. Gaur, R. C. Mehrotra, M. M. Palrecha, D. S. Jain, A. Kumar and C. M. Gupta, *J. Polarog. Soc.*, **14**, 122 (1968).
[5] P. C. Rawat and C. M. Gupta, *Experimenta Suppl.*, **18**, 535 (1971).
[6] R. S. Saxena and K. C. Gupta, *J. Indian Chem. Soc.*, **46**, 1045 (1969).

Ammonia buffer was used to maintain the pH as 9.0. KCl was used as supporting electrolyte ($\mu = 0.1$). Polarograms were recorded with a D.C. Manual Polarograph. Potentials were measured by a Leeds and Northrup Students potentiometer against a saturated calomel electrode. The dropping mercury electrode had the characteristics $m^{2/3}t^{1/6} = 2.132$ $mg^{2}t^{3-\frac{1}{2}}$, $h = 40$ cm. All the measurements were carried out at room temperature (35.0 ± 0.1°C). Purified nitrogen was passed through each solution to remove dissolved oxygen.

RESULTS AND DISCUSSION

The conventional $\log \frac{i}{id-i}$ vs. E_{de} plots of both the metal ions for various concentrations of HPT are straight lines with average reciprocal slope of (32 ± 1 mV). Plots of i_d against $(h_{eff})^{\frac{1}{2}}$ are straight lines. The results reflect that the electrode reactions are entirely two-electron reversible and diffusion controlled reductions. $E_{\frac{1}{2}}$ values for various ligand concentrations are given below in table 1.

Table 1

$E_{\frac{1}{2}}$ values at various ligand concentrations

Cd(II)HPT System $(E_{\frac{1}{2}})_s = 0.60$ V vs. S.C.E.		Pb(II)HPT System $(E_{\frac{1}{2}})_s = 0.386$ V vs. S.C.E	
Ligand concentration (mM)	$E_{1/2}$ (Volts vs./S.C.E.)	Ligand concentration/mM)	$E_{1/2}$ (Volts vs. S.C.E.)
2.0	0.817	2.0	0.655
3.0	0.828	4.0	0.669
4.0	0.836	5.0	0.675
6.0	0.846	6.0	0.680
7.0	0.849	8.0	0.687
8.0	0.853	9.0	0.691
9.0	0.856	10.0	0.692
10.0	0.858		

With increase in HPT concentration, the $E_{\frac{1}{2}}$ shifts towards more negative potential in both cases, showing the complex formation between the metal ions and the ligand. In Cd(II) HPT system, the plot of $E_{\frac{1}{2}}$ vs. $-\log C_x$ is found to be a smooth curve. The values of overall formation constants are determined by applying Deford and Hume treatment [7] as modified by Irving. [8] The values are obtained by plotting $F_{0-j}(X)$ functions against the ligand concentration (X) and then extrapolating them to zero ligand concentration (Figure 1). Since plots of $F_2(X)$ showed a horizontal line it reflects that only two complex species (1 : 1 and 1 : 2) are involved. Values of the formation constant obtained, are as $\beta_1 = 27.9 \times 10^8$ and $\beta_2 = 26.3 \times 10^{11}$.

In Pb(II) HPT system, the plot of $E_{\frac{1}{2}}$ vs. $-\log C_X$ is a straight line (Figure 2). From the slope of this plot, the number of ligand molecules

---

[7] D. D. DeFord and D. N. Hume, *J. Amer. Chem. Soc.*, **73**, 5321 (1951).

[8] H. Irving, *Adv. in Polarography*, **1**, 42 (1960).

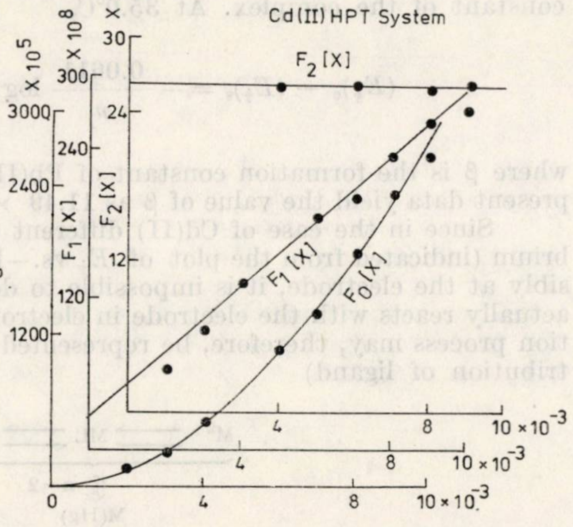

Fig. 1. — Plots of $F_j\,[X]$ Vs $[X]$.

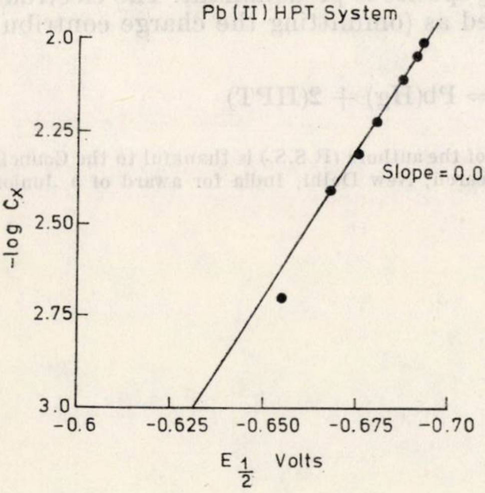

Fig. 2. — Plot of $E_{\frac{1}{2}}$ Vs $-\log C_X$.

attached to metal ion is calculated by using the equation

$$\frac{\Delta E_{\frac{1}{2}}}{\Delta \log C_X} = -p\,\frac{0.0611}{n} \qquad \text{(at 35°C)}$$

where p is the number of ligand molecules attached to the metal ion. The value of this slope being 0.620 in the present case, the value of p is obtained as 2, i.e., 1 : 2, metal; ligand complex is formed.

Lingane's method[9] has been used for calculating the formation constant of the complex. At 35.0°C,

$$(E_{\frac{1}{2}})_c - (E_{\frac{1}{2}})_s = -\frac{0.0611}{n}\log\beta - p\,\frac{0.0611}{n}\log C_X$$

where β is the formation constant of Pb(II) HPT chelate complex. The present data yield the value of β as 11.49×10^{13}.

Since in the case of Cd(II) different complex species are in equilibrium (indicated from the plot of $E_{\frac{1}{2}}$ vs. $-\log C_X$) and are reduced reversibly at the electrode, it is impossible to determine which of the species actually reacts with the electrode in electron transfer process. The reduction process may, therefore, be represented as (omitting the charge contribution of ligand)

$$\underbrace{M^{2+} \rightleftharpoons ML \rightleftharpoons ML_2}_{\substack{\Updownarrow\ n=2 \\ M(Hg)}}$$

In the case of lead(II), the ML_2 species is predominant. The electrode reaction may, therefore, be expressed as (ommitting the charge contribution of ligand).

$$Pb(HPT)_2^{2+} + 2_{\bar{e}} \Leftrightarrow Pb(Hg) + 2(HPT)$$

ACKNOWLEDGEMENT. One of the authors (R.S.S.) is thankful to the Council of Scientific and Industrial Research, New Delhi, India for award of a Junior Research Fellowship.

---

[9] J. J. Lingane, *Chem. Rev.*, **29**, 1 (1941).

Revue Roumaine de Chimie, **23**, *8*, 1283–1289, (1978)

ALUMINIUM CHLORIDE CATALYZED REACTIONS OF UNSATURATED ACIDS WITH BENZENE. XII[1]

METHYL ESTERS OF CYCLOHEXYLIDENEACETIC AND 1-CYCLOHEXENYLACETIC ACIDS

V. DRĂGUŢAN, ZS. ARVAY and ALICE MARIE GLATZ

Center of Organic Chemistry, Spl. Independenţei 202 B, Bucharest 15, Romania

Received May 20, 1977

The reaction of the methyl esters of cyclohexylideneacetic and 1-cyclohexenylacetic acids with benzene in the presence of aluminium chloride at 40—45° is described. Mixtures of esters phenylated in the 2, 3 or 4 position of the cyclohexane ring were obtained. In the 2 position the isomers *cis* and *trans* were formed, while in 3 and 4 positions the isomers were *cis* and *trans*, respectively. At 0—5° both kinetic and thermodynamic control of the reaction were evidenced.

The aluminium chloride catalyzed reactions of unsaturated alicyclic acids with benzene have been intensively studied.[2] In these studies it was shown that these reactions imply carbocations in which hydride ion shift rearrangements occur, that they are stereospecific involving the appearance of intermediate lactoid species and that the reaction products reach by isomerization an equilibrium ratio.

However, few data are known about the related reaction of the unsaturated alicyclic esters.[3]

In the reaction of ethyl 2-cyclopentenylacetate, Buu-Hoï and Cagniant [4] isolated ethyl 2-phenylcyclopentylacetate. Analogous results were obtained in the reactions with toluene, xylenes or acenaphtene.

Later on, Mousseron, Winternitz and Rouzier [5,6] demonstrated that the reaction product (obtained in the reaction with benzene) consists of ethyl *cis*-3-and *trans*-3-phenylcyclopentylacetate along with small amounts of the 2-phenyl isomer.

---

[1] Part XI, A. C. RĂZUŞ, ZS. ARVAY and A. M. GLATZ, *Rev. Roumaine Chim.*, **23**, 753(1978).

[2] See A. M. GLATZ, *Rev. Roumaine Chim.*, **19**, 455 (1974) and references cited in.

[3] R. KONCOS and B. S. FRIEDMAN in "Friedel-Crafts and Related Reactions", G. A. OLAH (editor), vol. II, Interscience, New York, 1964, p. 328.

[4] W. P. BUU-HOÏ and P. CAGNIANT, *Compt. rend.*, **220**, 744 (1945).

[5] M. MOUSSERON, F. WINTERNITZ and C. ROUZIER, *Bull. Soc. chim. France*, **1953**, 190.

[6] M. MOUSSERON, F. WITNTERNITZ and C. ROUZIER, *Bull. Soc. chim. France*, **1954**, 316.

The reaction of the methyl cyclopentylideneacetate, 1- and 2-cyclopentenylacetate was recently studied by Glatz, Răzuş *et al.* [7] In this reaction methyl 2- and 3-phenylcyclopentylacetate were formed as major products, their ratio depending on the starting material. The composition of this reaction mixture with respect to that of the corresponding acids was a proof for the mechanism through intermediate lactoid species proposed earlier for the acids [8].

Chuang and co-workers[9] carried out the reaction of ethyl 2-methyl-1-cyclohexenylacetate and 2-methylcyclohexylideneacetate and obtained ethyl 2-methyl-4-phenylcyclohexylacetate as the main product.

The recent results obtained in the reaction of cyclohexylideneacetic and 1-cyclohexenylacetic acids, [10] determined us to study in the present work the similar reaction of the corresponding methyl cyclohexylideneacetate (**1**) and 1-cyclohexenylacetate (**2**). We observed the formation of a mixture of the following compounds : methyl *trans*-2-(**3**), *cis*-2- (**4**), *cis*-3-(**5**) and *trans*-4-phenylcyclohexylacetate (**6**), the 1,3 and 1,4 isomers being the major products.

Table 1

The reaction of methyl cyclohexylideneacetate (1) and 1-cyclohexenylacetate (2) with benzene at 40–45°

Reactant	Reaction time, min.	Reaction mixture composition, %*					5 :6
		Starting m material	Methyl phenylcyclohexylacetates				
			3	4	5	6	
Ester **1**	0.5	9.2	1.2	1.4	35.7	44.4	0.8
	2	2.0	1.2	1.3	37.0	46.6	0.8
	5	1.0	1.3	1.2	38.7	49.5	0.8
	20	0.2	1.4	1.1	39.2	49.0	0.8
	60	—	1.4	1.1	44.5	46.8	0.95
	240	—	1.5	1.1	45.6	43.4	1.02
	480	—	1.5	1.1	46.2	43.0	1.05
Ester **2**	1	3.5	1.3	1.4	36.0	47.0	0.77
	5	1.0	1.3	1.3	37.5	48.5	0.77
	60	—	1.4	1.2	39.5	49.0	0.8
	240	—	1.5	1.1	44.0	47.0	0.95

* The remainder are many unidentified components.

Reaction at 40—45°. The reaction of esters **1** and **2** was carried out at 40—45° using a molar ratio ester : $AlCl_3$: benzene of 1 : 1.5 : 20. The reaction mixture composition was determined by v.p.c. at various reaction times (Table 1).

---

[7] A. C. Răzuş, Zs. Arvay, A. Haneş and A. M. Glatz, *Rev. Roumaine Chim.*, **21**, 727 (1976).

[8] A. M. Glatz, A. C. Răzuş, F. Badea and C. D. Neniţescu, *Rev. Roumaine Chim.*, **16**, 1567 (1971).

[9] Ch.-K. Chuang, J.-H. Chu and Y. -Sh. Koo, *Ber. dtsch. chem. Ges.*, **73**, 1347 (1940).

[10] V. Drăguţan, L. Stănescu and A. M. Glatz, *Rev. Roumaine Chim.*, **22**, 1045 (1977).

As it can be seen from the above results, the esters **1** and **2** gave 1,2-, 1,3- and 1,4-phenylated products. In contrast to the corresponding acids [10] both 1,2-disubstituted isomers, namely *trans*-2-(**3**) and *cis*-2-phenylcyclohexylacetate (**4**), were obtained. The *trans* and *cis* 1,2-disubstituted isomers were formed in small proportion reaching a maximum value of 2.6 and 2.7 %, respectively (Table 1).

The 1,3-and 1,4-disubstituted products were formed in nearly equal amounts, their ratio varying from 0.8 to 1.0. The final composition of the reaction mixture obtained from the ester **1** was **3** : **4** : **5** : **6** = 1.5 : 1.1 : : 46.2 : 43.0 after 8 hrs ; these values remained nearly constant on increasing the reaction time.

The data obtained in the reaction of the esters **1** and **2** could be explained by a reaction mechanism (involving intermediate carbocations) similar to that previously proposed for the corresponding acids[10] (scheme 1).

The carbocation **7** formed in a first step rearranges by 1,2-and 1,3-hydride ion shifts into the carbocations **8** and **9**. The latter could give either the final product, **5**, by an alkylation reaction or the carbocation **10** by hydride ion shift.

The formation of 1,2 isomers shows that in this reaction, in agreement with the results obtained with the methyl cyclopentylideneacetate, 1-and 2-cyclopentenylacetate [7] and unlike the reaction of cyclopentylidene-, cyclohexylidene-and 1-cyclohexenylacetic acids [8,10] intermediate lactoid species are not involved.

The small quantities of the isomers **3** and **4** and the predominance of the isomers **5** and **6** in the reaction mixture indicate that the competitive hydride ion shifts in the carbocations **7**, **8**, **9** and **10** occur faster than alkylation ; between the competitive hydride shifts an equilibrium favouring carbocations **9** and **10** is established.

From the above results it can be seen that at short reaction times the process is under kinetic control and then the products equilibrate thermodynamically. The compound *trans*-4 (**6**) isomerises into *cis*-3 (**5**) and a product mixture, in which the more stable compounds **5** and **6**[11] are the major products, is obtained. The isomerization of phenylcyclohexylacetates formed in the reaction of esters **1** and **2** with benzene is slower than the isomerization involved in the similar reaction of the corresponding acids [12] (Table 2). The smaller rate in the reaction of the esters can be accounted for by the deactivating effect of the carbomethoxy group.

Reaction at 0—5°. The reaction of ester **1** was carried out at 0—5° using the same ratios for the reactants. The reaction product consisted of the esters **3**, **4**, **5** and **6** in proportions differing from those obtained in the reaction at 40—45° (Table 3).

From the data obtained in the reaction at 0—5° the following can be inferred : a) as expected the conversion at low temperature was smaller

[11] E. L. Eliel, "Stereochemistry of Carbon Compounds", Mc. Graw-Hill, New York, 1962, p. 214.

[12] A. M. Glatz, V. Wertheimer and F. Badea, *Rev. Roumaine Chim.*, **19**, 87 (1974).

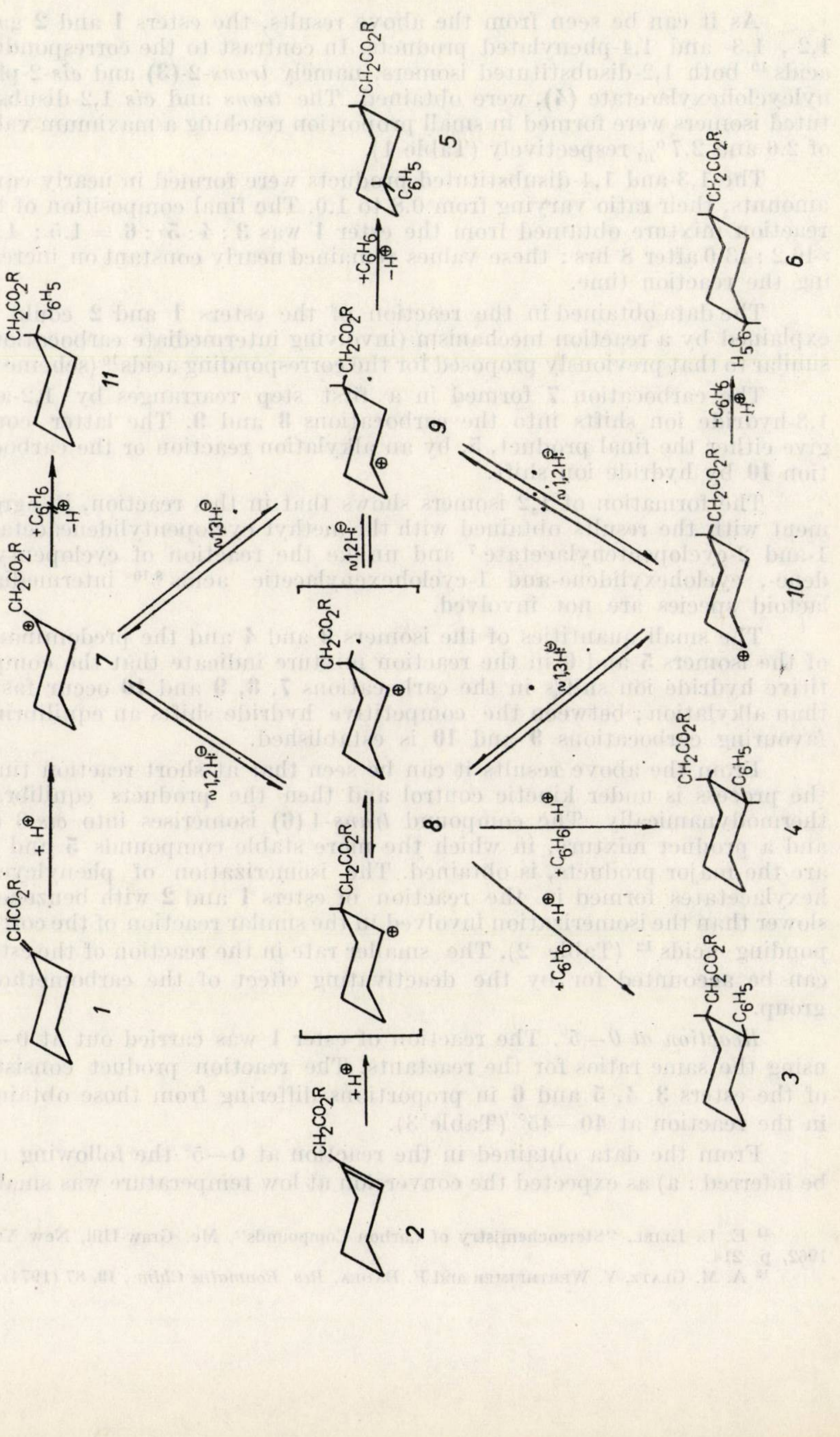
2
CH2CO2R
+H⊕
1
CHCO2R
+H⊕
7
CH2CO2R
+C6H6
−H⊕
11
CH2CO2R
C6H5
~1,2H⊕
~1,3H⊕
CH2CO2R
8
~1,2H⊕
+C6H6 −H⊕
CH2CO2R
~1,2H⊕
~1,3H⊕
9
CH2CO2R
+C6H6
−H⊕
5
CH2CO2R
C6H5
~1,3H⊕
10
CH2CO2R
+C6H6 −H⊕
4
CH2CO2R
C6H5
3
CH2CO2R
C6H5
+C6H6 −H⊕
6
CH2CO2R
C6H5

Table 2

The isomerisation of methyl phenylcyclohexylacetates

Reactant	Reaction time h	Reaction products %	
		5	**6**
Ester **5**	1	88.0	12.0
	4	83.5	16.5
Ester **6**	1	14.0	86.0
	4	32.0	68.0

Table 3

The reaction of methyl cyclohexylideneacetate (1) with benzene at 0–5°

Reaction time, min.	Starting material %	Methyl phenylcyclohexylacetates %			
		3	**4**	**5**	**6**
0.5	44.8	0.9	1.1	24.0	29.2
2	20.1	1.3	1.4	32.8	44.4
5	13.9	1.5	1.3	35.3	48.0
20	1.5	1.5	1.3	41.5	54.2
60	traces	1.5	1.2	42.3	55.0
240	traces	1.5	1.2	43.7	53.6
480	—	1.5	1.1	45.8	51.6

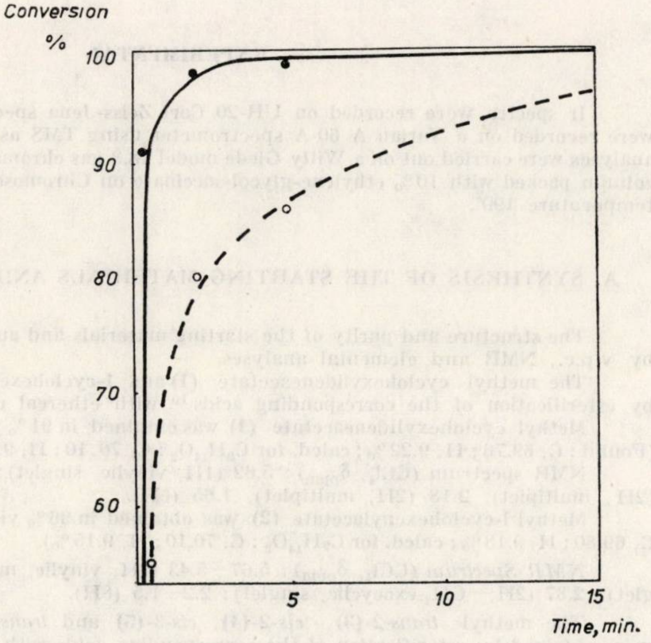

Fig. 1. — The dependence of conversion on reaction time at 40–45°(——) and 0–5°(- - -)

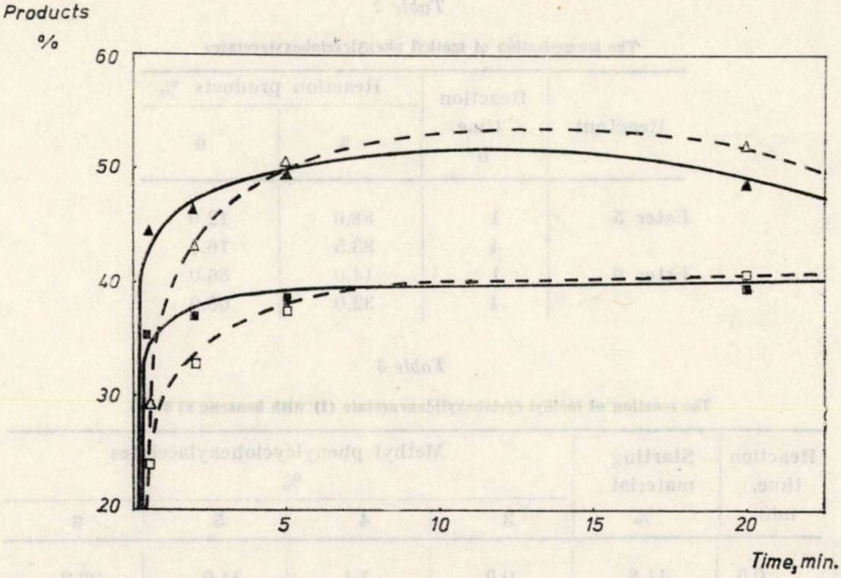

Fig. 2. — The variation of product concentrations with reaction time at 40−45° (—) and 0−5° (----)

than that at 40−45° (Figure 1) and b) the isomerization of phenylcyclohexylacetates takes place slower at 0−5° than in the reaction at 40−45° (Figure 2).

EXPERIMENTAL

Ir spectra were recorded on UR-20 Carl Zeiss-Jena spectrophotometer. NMR spectra were recorded on a Varian A 60-A spectrometer using TMS as internal standard. The v.p.c. analyses were carried out on a Willy Giede model 18.3 gas chromatograph using a 3 m × 4mm column packed with 10% ethylene-glycol-succinate on Chromosorb W (60−80 mesh); column temperature 190°.

A. SYNTHESIS OF THE STARTING MATERIALS AND AUTHENTIC SAMPLES

The structure and purity of the starting materials and authentic samples were checked by v.p.c., NMR and elemental analyses.

The methyl cyclohexylideneacetate **(1)** and 1-cyclohexenylacetate **(2)** were prepared by esterification of the corresponding acids [10] with ethereal diazomethane solution.

Methyl cyclohexylideneacetate **(1)** was obtained in 91% yield, b.p. 2 mm Hg= 84−85°. (Found : C, 69.76 ; H, 9.22% ; calcd. for $C_9H_{14}O_2$: C, 70.10 ; H, 9.15%).

NMR spectrum (CCl_4, δ_{ppm}) : 5.62 (1H, vinylic, singlet) ; 3.64 (3H, CH_3, singlet) ; 2.84 (2H, multiplet), 2.18 (2H, multiplet), 1.65 (6H).

Methyl 1-cyclohexenylacetate **(2)** was obtained in 96% yield, b.p.$_{2mm}$ 79−81°. (Found : C, 69.80 ; H, 9.18% ; calcd. for $C_9H_{14}O_2$: C, 70.10 ; H, 9.15%).

NMR Spectrum (CCl_4, δ_{ppm}) : 5.67−5.43 (1H, vinylic, multiplet) ; 3.67 (3H, CH_3, singlet) ; 2.87 (2H, $-CH_2$-exocyclic, singlet) ; 2.2−1.5 (8H).

The methyl *trans*-2-**(3)**, *cis*-2-**(4)**, *cis*-3-**(5)** and *trans*-4-phenylcyclohexylacetates**(6)** were obtained by esterification of the corresponding acids with diazomethane. [10]

B. REACTION OF METHYL CYCLOHEXYLIDENEACETATE (**1**) AND 1-CYCLOHEXENYLACETATE (**2**) WITH BENZENE AT 40–45°

To a stirred suspension of 5.24 g (39.3 mmol) of aluminium chloride in 40 ml anhydrous benzene, a solution of 4.0 g (26.0 mmol) methyl cyclohexylideneacetate (**1**) in 6.6. ml anhydrous benzene was added at 40–45°. The mixture was stirred at this temperature for 4 hrs. After cooling, the mixture was quenched in ice-water, extracted with ether, washed with a solution of 5% sodium bicarbonate and then with water to neutral reaction. The ethereal solution was dried over magnesium sulfate and the solvent removed by vacuum distillation; 4.9 g (82%) of a yellow liquid were obtained. (Found: C, 77.63; H, 8.90%; calcd. for $C_{15}H_{20}O_2$: C, 77.7 H, 8.62%).

The v.p.c. of the product indicated by comparison with authentic samples the following composition: 1.6% ester **3**, 1.1% ester **4**, 45.6% ester **5** and 43.4% ester **6**.

Similar experiments were carried out with the esters **1** and **2** at 10 hrs reaction time. At various intervals, samples were withdrawn and worked up as above. The product composition determined by v.p.c. is given in table 1.

C. THE ISOMERIZATION REACTION OF ESTERS **5** AND **6**.

0.2 g (1.4 mmol) of ester **5** in 2 ml anhydrous benzene were added to a stirred suspension of 0.3 g (2.2. mmol) aluminium chloride in 3 ml anhydrous benzene at 40–45°. After 1 h a sample was withdrawn, worked up as above and the product composition was determined by v.p.c. After 4 hrs the reaction mixture was quenched, worked up and the product analyzed in the usual manner. The product composition is given in table 2.

A similar experiment was run with the ester **6** and the results are given in table 2.

D. REACTION OF METHYL CYCLOHEXYLIDENEACETATE (**1**) WITH BENZENE AT 0–5°

The reaction of the ester **1** was carried out as described in section B with the difference that the reaction temperature was 0–5° and the ester solution was added quickly to avoid benzene crystallization. The product composition at various intervals determined by v.p.c. is given in table 3.

Revue Roumaine de Chimie, 23, 8, 1291–1301 (1978)

STUDIES IN SPECTRAL AND MAGNETIC PROPERTIES AND NON-ISOTHERMAL DECOMPOSITION OF PYRIDINE ADDUCTS OF SOME SALTS OF FATTY ACIDS

LEELA PARDESHI, A. RASHEED and R. A. BHOBE *
Department of Chemistry, Marathwada University, Aurangabad-431002, India

Received May 24, 1976

Pyridine adducts of some salts of fatty acids have been prepared and their magnetic and spectral properties studied. Non-isothermal decomposition studies of these salts by Freeman and Carroll method yield the order of decomposition and energies in one single step and these are reported with a possible connection between charge density of the metal ion and E_a values.

INTRODUCTION

The pyridine adducts of the salts of fatty acids do not seem to have attracted much attention and no proper investigation has been made of these adducts as seen from the perusal of the literature. Alfred Koening,[1] happens to be one worker who has attempted to study the pyridine adducts of chromium, cobalt, nickel and zinc stearates and copper and cobalt palmitates. His work was of preparatory type and in this he has studied the solubilities of the salts of fatty acids in a number of solvents.

The present study deals in spectral, magnetic and non-isothermal decomposition properties of the pyridine adducts of some salts of fatty acids and is mainly concerned with stages and kinetics of decomposition of these adducts by Freeman and Carroll method [2].

EXPERIMENTAL

Copper, nickel, chromium and cobalt stearates, palmitates and oleates were obtained by double decomposition method from the sodium salt of the organic acid and the chlorides of the respective metals. However, the purest variety of these salts was obtained by careful thermal decomposition of the pyridine adducts obtained by the procedure given below. These were the salts which were used for further investigation. All the salts used were of Anala R quality and pyridine was from E. Merck with B. pt. 115.3°. The pyridine adducts were prepared from the salts of fatty acids by refluxing calculated quantities of the salts with freshly distilled amine when blue, dark green, dirty green or pinkish adducts were obtained according to the salt of fatty acid used. Carbon, hydrogen and nitrogen in the adducts were determined by standard micro-analytical procedures. Copper, nickel, cobalt and chromium were estimated by well established method.

---

[1] Koening, *J. Amer. Chem. Soc.*, **63**, 951 (1941).

[2] E. S. Freeman and B. Carroll, *J. Phys. Chem.*, **62**, 394 (1958).

* Senior author to whom all correspondence should be addressed.

PHYSICAL MEASUREMENTS

The magnetic moments of the adducts were obtained by Gouy method. The temperatures were varied by circulating −5° and hot water of definite temperature through a jacket surrounding the sample.

Spectral measurements were made on SP-500 Unicam spectrophotometer. The reflectance spectra were recorded with the reflectance attachment of the spectrophotometer. The spectra of the solid adducts in the form of nujol mulls were taken by the method suggested by Cotton et al [3].

The non-isothermal decomposition studies of the adducts were made according to the procedure laid down by Freeman and Carroll . [2] The rise of temperature with time (dT/dt) was kept absolutely constant (0.609° per minute) and the thermocouple used for recording temperatures was calibrated very accurately with materials of known boilling points and melting temperatures.

RESULTS AND DISSCUSSION

The results of elemental analysis of the adducts are given in table 1.

The magnetic moments of the pyridine adducts of the copper salts alone are recorded here (Table 2) since they exhibited unusual behaviour in consistency with other Cu(II) alkonates [9]. The changes in the magnetic moments vary roughly from 1.50 B.M. at−5° to 1.76 B.M. at about 70°. These changes do not seem to be violent and hence polymerization process in the adducts, as against dimerisation, can be excluded from the

Table 1

Elemental analysis of the pyridine adducts

COMPOUND	FOUND				CALCULATED			
	%C	%H	%N	% Metal	%C	%H	%N	% Metal
$Cu_2C_{82}H_{150}O_8N_2$	69.16	9.98	1.86	8.94	69.44	10.58	1.97	8.96
$Cu_2C_{82}H_{141}O_8N_2$	69.28	9.94	1.84	8.89	69.83	10.07	1.98	9.01
$Cu_2C_{74}H_{134}O_8N_2$	68.16	10.33	1.94	9.84	68.04	10.26	2.15	9.73
$NiC_{41}H_{75}O_4N$	69.16	10.18	1.90	8.22	69.91	10.65	1.98	8.34
$NiC_{37}H_{67}O_4N$	68.19	10.14	2.12	9.11	68.54	10.34	2.16	9.07
$NiC_{41}H_{71}O_4N$	69.94	10.04	1.98	8.24	70.31	10.14	2.00	8.39
$CoC_{42}H_{72}O_4N$	70.33	10.12	1.94	8.39	70.69	10.09	1.96	8.27
$CrC_{37}H_{67}O_4N$	69.16	9.98	2.13	8.16	69.22	10.42	2.17	8.09

---

[3] F. A. Cotton, D. M. I. Goodgame and A. Sacco, *J. Amer. Chem. Soc.*, **83**, 415 (1961).

[4] B. N. Figgis and R. L. Martin, *J. Chem. Soc.*, **1956**, 3837.

Table 2

Magnetic data of the pyridine adducts of copper salts of fatty acids

$Cu_2(ST)_4$ (pyridine)$_2$; ST = stearate

Temp. K	269.3	284.6	310.0	336.0
$\chi_g \times 10^6$	0.541	0.569	0.671	0.745
$\chi_M \times 10^6$	767.2	806.4	949.1	1055.1
μ_{eff} (B.M.)	1.29	1.35	1.54	1.69

$Cu_2(OT)_4$ (pyridine)$_2$; OT = oleate

Temp. K	271.4	286.8	319.0	348.0
$\chi_g \times 10^6$	0.803	0.796	0.789	0.757
$\chi_M \times 10^6$	113.4	1121.4	1111.8	1067.4
μ_{eff} (B.M.)	1.56	1.61	1.69	1.73

$Cu_2(PT)_4$ (pyridine)$_2$; PT = palmitate

Temp. K	269.5	291.4	336.4	350.4
$\chi_g \times 10^6$	0.826	0.847	0.807	0.822
$\chi_M \times 10^6$	1078.1	1105.2	1053.8	1072.1
μ_{eff} (B.M.)	1.53	1.61	1.69	1.74

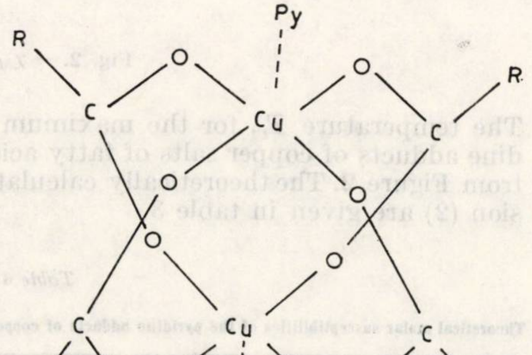

Fig. 1. — Binuclear structure. R = oleate, palmitate, stearate; Py = pyridine molecule.

present discussion. Binuclear structure, with oxygen bridges between copper and carbon as shown below, seems to be one possibility.

An exercise in calculated χ_M values for the pyridine adducts, on basically the same lines as those of Figgis and Martin,[5] yields the plots showing variation χ_M with T(as shown in Figure 2), the expression used for these calculation being

---

[5] R. L. Martin and H. Waterman, *J. Chem. Soc.*, **1957**, 2545 ; **1959**, 2960.

$$\chi_M \times 10^6 = \frac{g^2N^2\beta^2}{3kT}\left[1 + 1/3 \exp. \frac{J}{kT}\right]^{-1} + N\alpha \qquad (1)$$

When the terms $g^2N\beta^2/3k$ are reduced to 0.600 and J/k and $N\alpha$ are taken as 480 and 60 respectively expression (1) comes out to be

$$\chi_M \times 10^6 = (0.600/T)(1 + 1/3 \exp. 480/T)^{-1} + 60 \qquad (2)$$

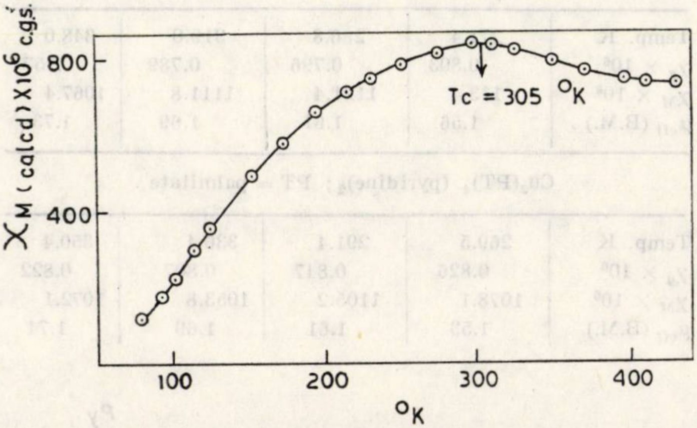

Fig. 2. — χ_M vs T.

The temperature T_c, for the maximum molar susceptibility of the pyridine adducts of copper salts of fatty acids, comes out to be 305 K as seen from Figure 2. The theoretically calculated values of χ_M by using expression (2) are given in table 3.

Table 3

Theoretical molar susceptibilities of the pyridine adducts of copper salts of fatty acids calculated from expression (2)

Temp. K	80	90	100	110	120	150
$\chi_M \times 10^6$	115.35	155.18	204.57	260.68	320.42	495.73
Temp. K	170	190	210	230	250	270
$\chi_M \times 10^6$	593.95	670.81	727.56	768.89	793.27	807.72
Temp. K	290	310	330	350	370	390
$\chi_M \times 10^6$	813.72	813.72	808.84	800.83	790.53	778.47
Temp. K	410	430				
$\chi_M \times 10^6$	765.33	751.52				

The spectral data presented in table 4 shows that the prominent bands of pure copper salts of fatty acids (copper palmite being taken at a representative salt) and their adducts with pyridine are around 15000 $(e \sim 100)$, 27,500 $(\theta \sim 60)$ and 14,000 cm^{-1} $(\theta \sim 80)$ 27,000 cm^{-1} $(\theta \sim 50)$ respectively. In the light of available data for the spectral transitions for Cu(II) ions in various possible environments, the tetrahedral geometry in the present case is clearly ruled out since no blank is drawn in the region $\sim$ 14,000 cm^{-1} to 25,000 cm^{-1} Graddon and Mockler[7] have pointed out that for copper complexes to be planar, a quartet grouped in two pairs, 10,000 cm^{-1} and 18,000 cm^{-1} is needed. From theoretical calculations Liehr[8] has predicted that a single band at 700 nm and a less defined shoulder at 510 nm should establish a square planar geometry for copper complexes. Spectral lines near about 700 nm are observed in the present case but the shoulder at 510 nm seems to have disappeared. According to Sacconi et al,[9] for copper complexes to be penta-coordinated with flattened pyramidal shape, the prominent bands should come out to be nearly 365 nm and 600 nm with high intensity. It is surprising to find that the wavelengths mentioned by Sacconi et al. fit in well with the spectral transitions observed in the present study with the difference that the intensities are few orders less than those observed for the pentacoordinated compounds of Coopper (II). It is difficult at this stage, to say very confidently, that the copper complexes studied in the present investigation are penta-coordinated since i) the extinction coefficients are low and ii) the absorption lines for the adducts are not far removed from those

Table 4

Electronic spectral data for copper (II) salt of palmitic acid and its pyridine adduct

Compound		$\lambda_{\max}$ $(\varepsilon)^a$	$\lambda_{\max}$ $(\varepsilon)^a$	λ max $(\varepsilon)^a$
COPPER(II)– PALMITATE :	Solution	668(106)	364.0(56)	284(450)
	Diff. reflectance	669.0(–)	359.0(–)	–
	Nujol Mull	671.0(–)	357.0(–)	–
COPPER(II)– PALMITATE-PYRIDINE ADDUCT	Solution	710.0(76)	374.5(46)	286(615)
	Diffuse reflectance.	712.0(–)	378.0(–)	–
	Nujol Mull	714.0(–)	379.0(–)	–

Values of $\lambda_{\max}$ in nm are given, followed by ε in brackets

---

[6] A. B. P. LEVER, "Inorganic Electronic Spectroscopy", Elsevier, Amsterdam, 1968, p. 359.

[7] D. P. GRADDON and G. M. MOCKLER, *Austral. J. Chem.*, **21**, 617 (1968).

[8] A. D. LIEHR, *J. Phys. Chem.*, **64**, 43 (1960).

[9] L. SACCONI, M. CIAMPOLINI, F. MAGGIO and F. P. CARASINO, *J. Inorg. Nuclear Chem.*, **19**, 73 (1961).

obtained for copper palmitate salt in benzene solution. However, structure (Figure 1) for dimer of copper salt accommodates the pyridine ligand extremely well.

NON-ISOTHERMAL DECOMPOSITION OF THE ADDUCTS

In this, kinetics of the decomposition of some typical pyridine adducts of the salts of fatty acids have been presented. There are two clear cut stages in the decomposition of the adducts. At the end of the first stage, all the pyridine molecules are let off which was confirmed by comparing the actual losses observed with those calculated theoretically. These calculations are presented in table 5. Table 6 lays out the order of reaction(b), the heat of activation in kilocalories/mole from the values of slopes(m) obtained from the plots of

$$\frac{\Delta \log \mathrm{d}w/\mathrm{d}t}{\Delta \log W_r} \text{ vs } \frac{\Delta\,(1/T)}{\Delta \log W_r}$$

These values were calculated from the loss time-curves, obtained according to the well established procedure given by Freeman and Carroll.[2] The loss time curves for the adducts, studied in the present investigation, are given in Figures 3 and 4 as curves *A*, *B*, *C* and *D*, *E*, *F*, respectively. It will be seen that there are two distinct stages in the decomposition of an adduct of the salts, namely of Cu(II), Ni(II), Co(II) and Cr(III). From the results given in table 5, it is clear that the percentage of decomposition in the first stage almost accurately corresponds with theoretically calculated losses, if all the pyridine molecules in a particular salt studied are supposed to be given off in that stage. It is reasonable to assume that, in the pyridine adducts of the type studied, the pyridine molecules are loosely bound and hence are easily lost at relatively low tempe-

Table 5

Weight (INmg) of the pyridine adducts subjected to thermal analysis and theoretically calculated and practically found losses of pyridine in adducts

Name of the aduct	Weight of the sample (mg)	Loss percent of pyridine molecules (calcd.)	Loss percent of pyridine molecules (found)
$Cr(PT)_2 \cdot$ Pyridine	221.91	12.32	12.36
$Co(PT)_2 \cdot$2-Pyridine	168.76	22.16	22.09
$Ni(PT)_2 \cdot$ Pyridine	306.44	12.19	12.17
$Cu_2(ST)_4$-2-Pyridine	256.84	11.15	11.14
$Cu_2(OT)_4$-2-Pyridine	274.76	11.08	11.06
$Cu_2(PT)_4$-2-Pyridine	274.96	12.11	12.12

ratures near about 70° to 90°. Again, it was ascertained by careful analysis of the residue, remaining after first stage, that it contained the purest sample of the salt of fatty acid. It is the contention of the present workers that diverse results regarding the dipole moments of salts of fatty acids, reported in literature, are mainly due to the age old method of preparation of salts of fatty acids by double descomposition where the possibility of basic salts of the fatty acid, being precipitated, exists. The fact that pyridine, even in the complexed state, is let off at fairly low temperatures, that is near about 65°, was observed by Duval[10] in his study of $Ni(Py)_4(NCS)_2$. Erdey and Liptay[11], Wendlant and Ali[12] and Muzumdar et al[13] have however reported dipyridinisation in the pyridine complexes, studied by them, took place in two stages beginning at 80°, the last traces of pyridine being let off at 290°. In the case of substituted pyridine adducts, it was noticed, that the ligands α-picoline, β-picoline, and γ-picoline were given off at near about 100°. Specific studies in the case of several Pt(II) complexes of α and β-picolines, undertaken by Ivanova[14], show typical endothermic peaks where α or β picoline is first given out. The idea in giving all these data was to establish, beyond doubt, that the decomposition of pyridine adducts, in which pyridine does not act as a firmly complexing ligand, but is in loose combination with the salts of fatty acid, the first step is bound to be depyridinisation and that too at comparatively lower temperatures. It is observed from the Figure 3 and 4 that the descomposition in the first stage is nearly complete, in almost all the cases, at near about 75° except in the case of copperoleate-pyridine adduct where it is ~ 65°, whereas in nickel palmitate-pyridine adduct it is slightly, higher, that is about 85°. Surprisingly, the range of plateau in which all the pyridine is given out and at the end of which salts of fatty acid start decomposing is the same for all and comparatively short, namely 6°. There cannot be any comparison between thermal dissociation of pyridine complexes of transition metal ions and pyridine adducts of the type studied in the present paper. It is generally observed that pyridine, in the metal complexes of transition metal ions, is let off in stages in some cases changing the stereochemistry of the complexes at every stage of its descomposition, the finest example of this being the Mn(II) pyridine complexes.[15]

The order of reaction (b) of the non-isothermal decomposition of pyridine from the adducts at the first stage and the Cu(II) salts or the salts of nickel, cobalt, and chromium at the second stage is given in table 6. The slope, m, incidently, gives the energy of activation E_a. Both these values b and m were obtained by the method of least squares. In a study of such type, it is futile to fit in the data of descomposition

---

[10] C. Duval, "Inorganic Thermogravimetric Analysis", Elsevier, Amsterdam, 1963, p. 361.

[11] L. Erdey and G. Liptay, *Periodica Polytechnica*, **7**, 223 (1963).

[12] W. W. Wendlandt and S. I. Ali, *Z. anorg. Chem.*, **337**, 6 (1965).

[13] A. K. Muzumdar, A. K. Mukherjee and A. K. Mukherjee, *J. Inorg. Nuclear.Chem.*, **26**, 2177 (1964).

[14] M. I. Ivanova., *Zhur. neorg. Khim.*, **2**, 1317 (1957); *Ibid.* **2**, 1324 (1957), *Ibid.* **2**, 1775 (1957).

[15] R. J. Allen, D. H. Brown, R. H. Nutall and D. W. A. Sharp, *J. Inorg. Nuclear Chem.*, **26**, 1885 (1964).

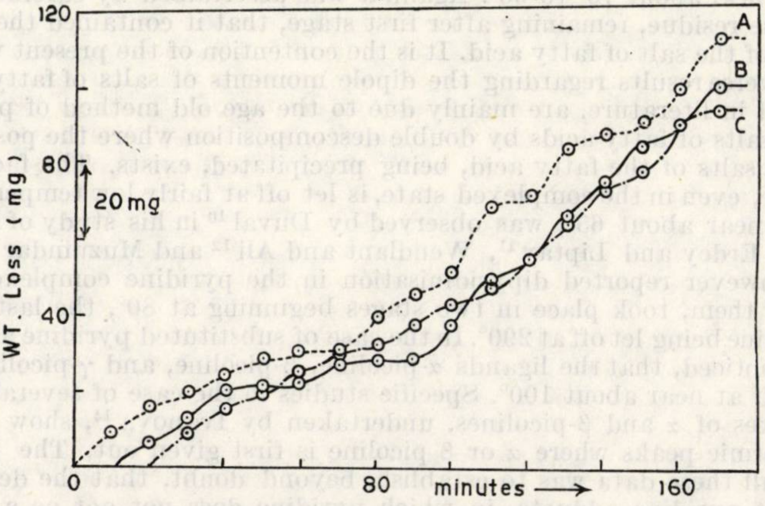

Fig. 3. — Weight loss versus minutes, curves *A*, *B*, *C*.

A — $Cu_2(OT)_4(pyridine)_2$; *B* — $Cu_2(ST)_4(pyridine)_2$; *C* — $Co_2(PT)_2(pyridine)_2$. The origin for the curves *B* and *D* is shifted by 10 and 20 minutes from the zero point for curve *A*.

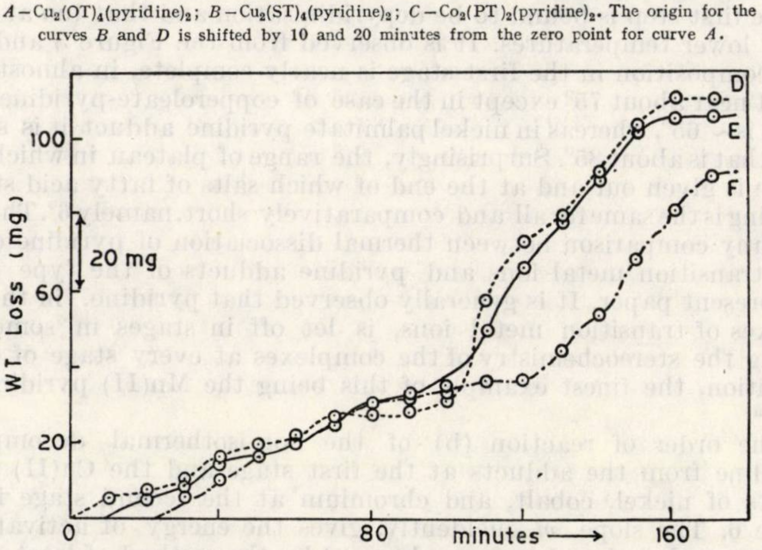

Fig. 4. — Weight Loss versus minutes, curved *D*, *E*, *F*,

D — $Cr(PT)_2$pyridine ; *E* — $Cu_2(PT)_4(pyridine)_2$; *F* — $Ni(PT)_2$pyridine. The origin for the curves *E* and *F* is shifted by 10 and 20 minutes from the zero point for curve *D*.

in expressions of the first, second or third order of kinetics of decomposition, since it is well known now that the decompositions of these types are seldom simple in nature and one should not expect an integer value as a solution for such kinetics. However, in almost all cases, barring that of Co(II) palmitate-pyridine adduct, the order, for depyridinisation, happens to be nearly zero, though the energies for these reactions vary from salt to salt.

Table 6

Non-isothermal decomposition studies of the pyridine adducts of the salts of fatty acids

System : *COPPER PALMITATE-PYRIDINE ADDUCT*

	a	b	c
First stage	0.27	1.06	m = 3.458×10^3
	0.51	1.61	b = 0.001
	0.58	2.04	E_a = 15.769 kcals/mole
	0.71	2.50	
Second stage	0.32	0.51	m = 7.174×10^3
	0.45	1.42	b = 1.79
	0.52	2.02	E_a = 32.712 kcals/mole
	0.63	2.71	

System : *COPPER STEARATE-PYRIDINE ADDUCT*

First stage	0.36	0.30	m = 1.588×10^3
	0.54	0.59	b = 0.23
	0.70	0.81	E_a = 7.241 kcals/mole
	0.92	1.15	
Second stage	0.22	0.22	m = 1.702×10^3
	0.28	0.34	b = 0.14
	0.42	0.60	E_a = 7.760 kcals/mole
	0.61	0.88	

System : *COPPER OLEATE-PYRIDINE ADDUCT*

First stage	0.08	0.04	m = 2.456×10^3
	0.15	0.10	b = 0.39
	0.22	0.15	E_a = 11.201 kcals/mole
	0.44	0.30	
Second stage	0.61	0.18	m = 0.253×10^3
	1.05	0.31	b = 0.03
	1.51	0.40	E_a = 1.151 kcals/mole
	2.25	0.61	

System : *NICKEL PALMITATE-PYRIDINE ADDUCT*

	a	b	c
First stage	0.19	0.11	m = 2.371×10^3
	0.27	0.30	b = 0.27
	0.33	0.45	E_a = 10.812 Kcals/mole
	0.52	0.81	
Second stage	0.18	0.15	m = 2.072×10^3
	0.26	0.31	b = 0.23
	0.33	0.45	E_a = 9.449 Kcals/mole
	0.52	0.85	

Table 6 (continued)

System : *COBALT PALMITATE-PYRIDINE ADDUCT*

First stage	0.38	1.04	$m = 0.879 \times 10^3$
	0.52	1.60	$b = 1.63$
	0.68	2.41	$E_a = 4.006$ Kcals/mole
	1.02	3.80	
Second stage	0.12	0.05	$m = 1.019 \times 10^3$
	0.35	0.31	$b = 0.07$
	0.56	0.51	$E_a = 4.647$ Kcals/mole
	0.76	0.72	

System : *CHROMIUM PALMITATE-PYRIDINE ADDUCT*

First stage	0.11	0.61	$m = 6.862 \times 10^3$
	0.18	1.12	$b = 0.04$
	0.25	1.50	$E_a = 31.290$ Kcals/mole
	0.34	2.22	
Second stage	0.17	0.02	$m = 3.60 \times 10^3$
	0.30	0.06	$b = 0.86$
	0.41	0.09	$E_a = 16.421$ Kcals/mole
	0.72	2.10	

a = The first column of data gives $\Delta (1/T) \Delta \log W_r$ values

b = In the second column are given the values of

$$-\frac{\Delta \log (dw/dt)}{\Delta \log W_r}$$

c = The values of slope m, the intercept b for each stage of decomposition are obtained by the method of least squares, m gives the value for E_a, the energy of activation and b values, the order of reaction i.e. decomposition.

In the discussion which follows, an attempt has been made to correlate the charge per unit area of the surface of the central ion such as a copper, cobalt, nickel and chromium with the energies of decomposition of the pyridine and substituted pyridine adducts.

A casual glance at the table 6 shows that the energies of activation involved in the decomposition of the pyridine molecule, are in the range of ~ 10 to 15 kcals/mole, except in the case of chromium adduct, where the energy is as high as 31.29 kcals/mole for letting off a single molecule of pyridine. If the charge densities per square cm of the ions Cu^{+2}. Cr^{+2} Co^{+2} and Ni^{+2} are estimated, they come out to be 24.88, 38.16, 21.38 and 24.08 e.s.u. cm^{-2}. Taking charge on cobalt ion as unity, the increase in the surface charge of the chromium ion comes out to be enormously large i.e. 78.5% higher ; the decreasing order of the charge density being Cu 16.39% and Ni 12 64%. The heavy charge on the surface of chromium ion presummably accounts for the exceptionally large activation energy involved in the decomposition stage. The datum for the E_a values for the decomposition of the copper oleate adduct is minimum and it is tempting to assume that the double bonded structure of the oleate anion puts a hindrance of some sort in the attachment of the pyridine molecule to the central Cu (II) ion. In the case of other adducts the order of reaction and the energies of activation involved, roughly parallel the charge density order of central metal ions, greater the charge density, greater seems the decomposition energy of the pyridine molecule and the decomposition of the salts of the metal ions with fatty acids. The energies of the decomposition of the pyridine molecule and the salt itself, in the case of Co(II) palmitate adduct, involves as low an energy as 4.0 and 4.65 kcals/mole respectively. This fits in well with the data presented in the table since cobalt ion had the minimum charge density per cm^2.

ACKNWOLEDGEMENTS. One of us, Miss Leela Pardeshi is indebted to the Marathwada University, Aurangabad, for the research fellowship which helped this project. A. Rasheed is grateful to Dr. D. D. Khanolkar and Principal R. S. Lawande, Yogeshwari Mahavidyalaya, Ambajogai, District Bhir, for allowing him to undertake this project in the Departamental laboratories and for constant encouragement.

Revue Roumaine de Chimie, **23**, *8*, 1303 – 1311 (1978)

ON THE POLYMERIZATION OF ACETYLENIC DERIVATIVES. XXXI

ELECTRON SPIN RESONANCE OF POLYARYLACETYLENE ISOMERS

SVETLANA DUMITRESCU, V. PERCEC and CR. I. SIMIONESCU
Institute of Macromolecular Chemistry "P. Poni",
Aleea Gr. Ghica Vodă, No. 41 A, Iaşi-6600,
Romania

Received November 23, 1976

The electronic spin resonance (ESR), spectra of isomeric structures of polyphenylacetylene (PPA), poly (α-ethynylnaphthalene) (Pα-EN), poly (β-ethynylnaphthalene) (Pβ-EN) and poly (N-ethynylcarbazole) (PEK), have been investigated as a function of temperature. Both in solution and in solid state, the unpaired spins concentration (N_s) of the *cis* polymers goes through a maximum at the *cis-trans* isomerization temperature. For *trans* polymers the Curie law is obeyed up to above their softening temperatures and for *cis* only for temperatures lower than that at which the polymer configuration is changed. The unpaired spins could be diradicals originated from π electrons released in the unpaired π orbitals from the main chain. The paramagnetic centers are dependent on polymer configuration, and are independent on polymer molecular weight.

Some previous papers reported the syntheses and properties of *cis* and *trans* isomers of PPA,[1,2,3] Pα-EN,[2-5] Pβ-EN[6,7] and PEK[8,9]. In the case of

---

[1] C. I. Simionescu, V. Percec and Sv. Dumitrescu, *J. Polymer Sci. Polym. Chem. Ed.*, **15**, 2497 (1977).

[2] C. I. Simionescu, Sv. Dumitrescu, I. Negulescu, V. Percec, M. Grigoraş, I. Diaconu, M. Leancă and L. Goraş, *Vysokomol. Soedineniya*, **A16**, 790 (**1974**).

[3] C. I. Simionescu, V. Percec and Sv. Dumitrescu, "XXIVth International Symposium on Macromolecules", Jerusalem, July 13–18, 1975, Abstract I. 1, p. 71.

[4] C. I. Simionescu, Sv. Dumitrescu, V. Percec, I. Negulescu and I. Diaconu, *J. Polymer Sci. Polym. Symposium. Ed.*, **42**, 201 (1973).

[5] C. I, Simionescu, Sv. Dumitrescu and V. Percec, *Polymer J.*, **8**, 313 (1976).

[6] C. I. Simionescu, Sv. Dumitrescu and V. Percec, "IVth Polymer Symposium", Varna, October 4–6, 1973, Preprints, Vol. I, p. 466.

[7] C. I. Simionescu, Sv. Dumitrescu and V. Percec, *Polymer J.*, **8**, 139 (1976).

[8] C. I. Simionescu, Sv. Dumitrescu and V. Percec, "XXIII IUPAC International Symposium on Macromolecules", Madrid, 1974, Preprint I.5–13.

[9] Sv. Dumitrescu. V. Percec and C. I. Simionescu, *J. Polymer Sci. Polym. Chem. Ed.* 2893, **15**, (1977).

the crystalline PPA, Ehrlich et al.[10-14] pointed out an order-disorder transition at about 120°. We showed that this transition represents in fact a *cis-trans* isomerization.[1,3] The *cis-trans* isomerization of *cis-transoidal* structure of PPA takes place in solution at about 120°.[1] The *cis-transoidal* and *cis-cisoidal* structures of PPA isomerize in solide state at temperatures higher than 120°. In this case the isomerization temperature depends on the heating time of the polymer sample.[1]

The *cis-cisoidal* structures of Pα-EN and Pβ-EN isomerize thermally at 240°[15] and 220°[3,7,15] respectively. The *cis-transoidal/cis—cisoidal* stereoblock structures of PEK isomerize thermally at temperatures which are dependent on the *cis-transoidal* vs. *cis-cisoidal* ratio of the given polymer (200—305°). All *cis-trans* thermal isomerization reactions of polyarylacetylenes are irreversible phenomena.

In this report the paramagnetism of polyarylacetylene isomers is investigated and its dependence on temperature and configuration is discussed.

EXPERIMENTAL

The amorphous *trans-cisoidal* polyarylacetylenes were synthesized by thermal bulk polymerization of the corresponding monomers at 140°. Polymer structures were discussed in previous papers, i. e., PPA [1,2], P α-EN, [4,5] P β-EN [6,7] PEK. [8,9] Insoluble and crystalline (60% crystallinity degree) *cis-cisoidal* PPA, soluble and low crystalline (5% crystallinity degree) *cis-transoidal* PPA, insoluble and high crystalline (80% crystallinity degree) *cis-cisoidal* Pα-EN, insoluble and crystalline (60% crystallinity degree) *cis-cisoidal* Pβ-EN, and soluble or insoluble and crystalline (60% crystallinity degree) PEK of *cis-transoidal/cis-cisoidal* stereoblock structure, were synthesized by polymerization of the corresponding acetylenic monomers in the presence of $AlEt_3$/$Fe(dmg)_2$. 2Py as catalytic system, according to the above mentioned papers. The following polymerization conditions were used: $Fe(dmg)_2$. 2Py = 5mole%; Al/Fe = 10 (molar ratio); (solvent+$AlEt_3$)/monomer=10 (volumic ratio); polymerization time=2 hrs; temperature=20°; solvent = toluene. Phenylacetylene polymers of different *cis* content were synthesized as was previously reported.[1]

The isomerization temperature of PEK is 300°[8,9]; the other polymers isomerize at temperatures given above. The thermal degradation of PEK starts at 260°, and at 300° the weight loss amounts 5.62%. The other polymers are stable in the temperature region in which they have been studied.

The ESR spectra were recorded on a JEOL model EPR spectrometer. The number of unpaired spins/g was comparatively calculated versus a spectrometer standard sample (DPPH).

RESULTS AND DISCUSSION

All isomers of polyarylacetylenes are paramagnetic, showing an ESR spectrum of Lorentz shape, characteristic of conjugated polymers ($g \simeq 2.003$).

---

[10] P. Ehrlich, R. J. Kern, E. D. Pierron and T. Provder, *J. Polymer Sci. Part B*, **5**, 911 (1967).

[11] P. Ehrlich, *J. Macromol. Sci., Phys.*, **2**, 153 (1968).

[12] H. Holob, P. Ehrlich and R. D. Allendoerfer, *Macromolecules*, **5**, 569 (1972).

[13] P. Ehrlich, E. C. Mertzlufft and R. D. Allendoerfer, *J. Polymer Sci. Polym. Letter Ed.*, **12**, 125 (1974).

[14] S. H. C. Chang, E. C. Mertzlufft, P. Ehrlich and R. D. Allendoerfer, *Macromolecules*, **8**, 642 (1975).

[15] C. I. Simionescu, Sv. Dumitrescu, V. Percec and M. Grigoraș, *Rev. Roumaine Chim.*, **22**, 1105 (1977).

Previously we reported that for the same polymer structure, the concentration of unpaired spins, N_S, does not depend on the molecular weight of the polymer.[5] This fact was recently confirmed by Ehrlich et al.[14] The difference between the N_S of crystalline and amorphous structures (Table 1) for PPA and Pβ-EN is of two and respectively of one order magnitude. Both polymers having crystalline structures exhibit a lower unpaired spins concentration than polymers with amorphous structures. Different values of N_S for crystalline and amorphous PPA were first time reported by Ehrlich et al.[10,11]

It is interesting to note that the structural units of PPA and Pβ-EN, i.e., corresponding to styrene and β-vinylnaphthalene, have a coplanar structure, while α-vinylnaphtalene and N-vinylcarbazole are not coplanar.[16]

All polymers with *trans-cisoidal* structures obey the Curie law (Figure 1) in the temperatures range of 20—200° i.e., up to above their softening temperatures (Table 1).

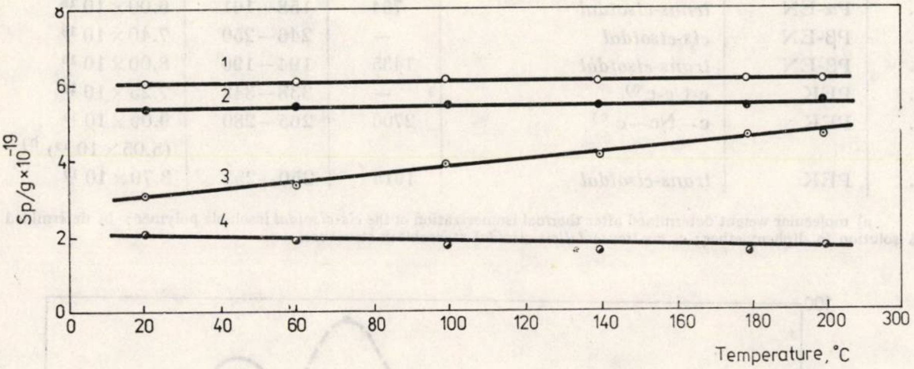

Fig. 1. — Temperature dependence of unpaired spins concentration for *trans-cisoidal* structure of:
1) Pα – EN; 2) Pβ – EN; 3) PPA; 4) PEK; heating time, 5 minutes.

For all polymers with *cis* configurations, the unpaired spins concentration goes through a maximum on heating but the polymers show a Curie dependence upon cooling. It means that the paramagnetism is dependent on the polymer conformation (Figures, 2, 3, 5—8).

The dependence of N_S upon temperature for solid state PPA having a *cis-transoidal* structure is presented in Figure 2. At short heating periods (i.e., the spectrum was recorded after 5 minutes of heating at the running temperature, curve 1), the N_s goes through a maximum at about 150°. When the same polymer was heated for two hours at the running temperature (curve 2, Figure 2) this maximum was shifted at about 120°. As a matter of fact these two maxima represent isomerization temperatures of *cis-transoidal* PPA for different thermal history.[1]

---

[16] L. H. Klemm, H. Ziffer, J. W. Sprague and W. Hodes, *J. Org. Chem.*, **20**, 190 (1955).

Table 1

E S R characteristic of polyarylacetylene isomers

No.	Polymer	Polymer structure	Mn	Softening temperature (°C)	Unpaired spins concentration vs. gram
1.	PPA	*cis-cisoidal* (90% *cis* content)	5000 a)	230–257	6.00×10^{17}
2.	PPA	*cis-cisoidal* (89% *cis* content)	5500 a)	238–243	2.00×10^{17}
3.	PPA	*cis-transoidal* (94% *cis* content)	4150	205–213	2.50×10^{19} (6.00×10^{18}) b)
4.	PPA	*cis-transoidal* (80% *cis* content)	3750	185–195	9.30×10^{19} (5.00×10^{18}) b)
5.	PPA	*trans-cisoidal*	850	120–124	3.02×10^{19}
6.	Pα-EN	*cis-cisoidal*	—	244–250	3.00×10^{19}
7.	Pα-EN	*trnas-cisoidal*	764	158–161	6.00×10^{19}
8.	Pβ-EN	*cis-cisoidal*	—	246–250	7.40×10^{18}
9.	Pβ-EN	*trans-cisoidal*	1435	194–196	8.00×10^{19}
10.	PEK	c-t/c-c c)	—	338–342	7.25×10^{19}
11.	PEK	c–t/c–c c)	2700	265–280	9.09×10^{19} (5.05×10^{19}) b)
12.	PEK	*trans-cisoidal*	1915	250–255	3.70×10^{19}

a) molecular weight determined after thermal isomerization of the *cis-cisoidal* insoluble polymer; b) determined as 10% solution in diphenylether; c) *cis-transoidal/cis-cisoidal* stereoblock structure.

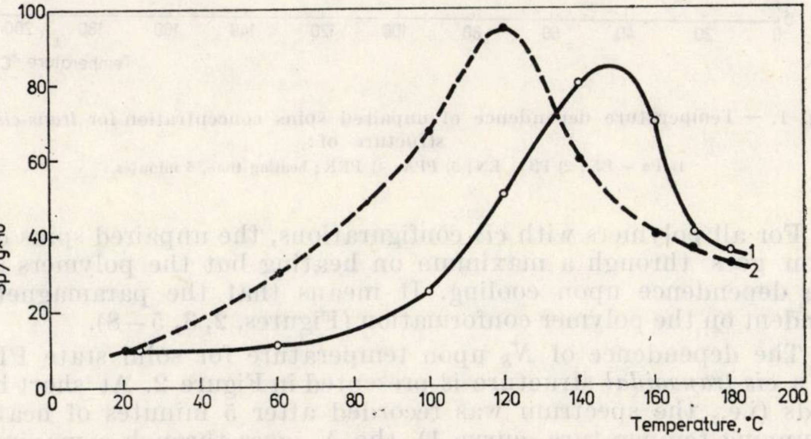

Fig. 2. — Temperature dependence of unpaired spins concentration for *cis-transoidal* structure of PPA (80% *cis* content):
1) Heating time, 5 minutes. 2) heating time, 2 hrs.

---

[17] M. I. Kushnerev, G. I. Bantirev, M. I. Cerkashin and A. A. Berlin, *Izvest. Akad. Nauk S.S.S.R., Otdel. khim. Nauk*, **10**, 2291 (1971).

[18] C. I. Simionescu, Sv. Dumitrescu, V. Percec and A. Stoleru, unpublished data.

[19] J. A. Pople and S. H. Walmsley, *Mol. Phys.*, **5**, 15 (1962).

This kind of dependence of N_s vs. temperature was for the first time reported by Ehrlich et al [11,12] in the case of high crystalline PPA, without any indications about its origin.

The same behaviour was observed in the case of *cis-transoidal* PPA in solution (Figure 3). In solution the maximum of N_S appears at about 120° irrespective of thermal history of the sample. At this temperature the ESR spectrum of PPA was well resolved (Figure 4).

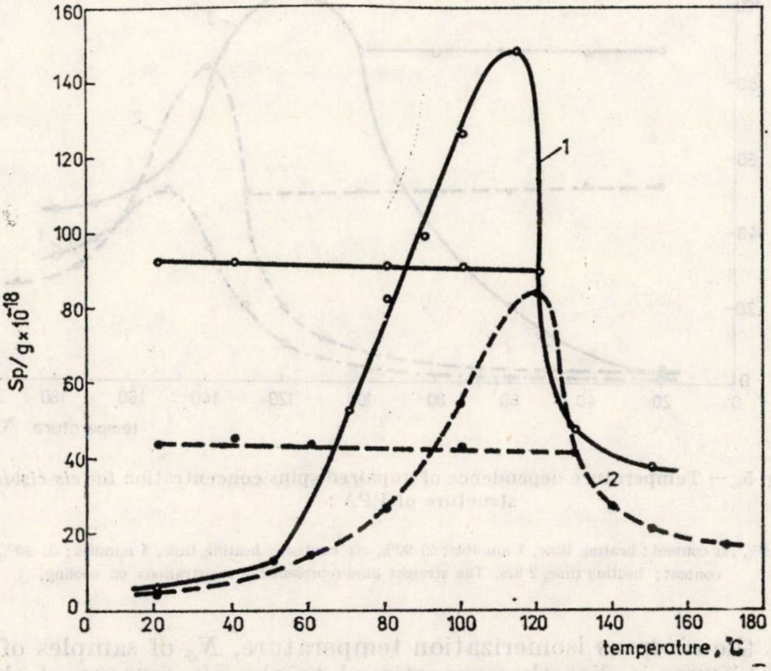

Fig. 3. — Temperature dependence of unpaired spins concentration for *cis-transoidal* structure of PPA (10 % solution in diphenylether):

1) 94% *cis* content; 2) 80% *cis* content; heating time, 5 minutes; the straight lines represent the registrations on cooling.

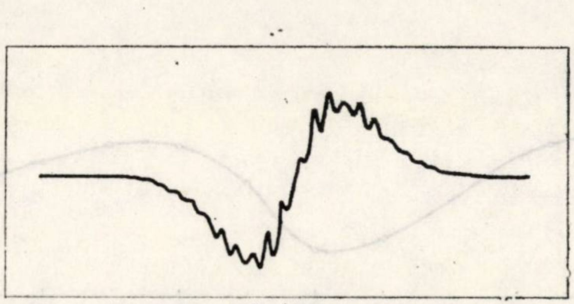

Fig. 4. — The hyperfine structure of 10 % *cis-transoidal* structure of PPA solution in diphenylether; temperature, 120°.

Based on NMR data we reported [1] that in solution the *cis-trans* isomerization of *cis-transoidal* structure of PPA occurs at about 120° for low heating periods. For the same duration of heating the *cis-transoidal* and *cis-cisoidal* PPA isomerize in solide state at higher temperatures.

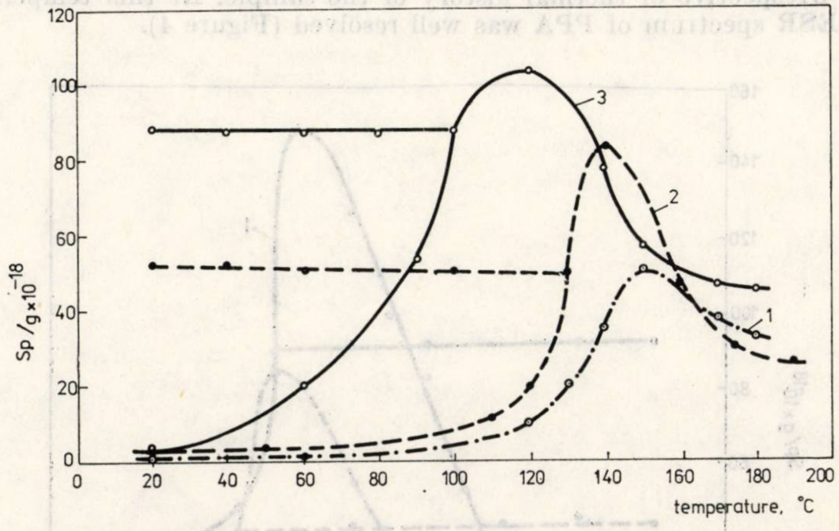

Fig. 5. — Temperature dependence of unpaired spins concentration for *cis-cisoidal* structure of PPA :

1) 89% *cis* content; heating time, 5 minutes; 2) 90% *cis* content; heating time, 5 minutes; 3) 90% *cis* content; heating time, 2 hrs. The straight lines represent the registrations on cooling.

At the *cis-trans* isomerization temperature, N_S of samples of similar thermal history is directly proportional to the *cis* content of the polymer (Figure 3).

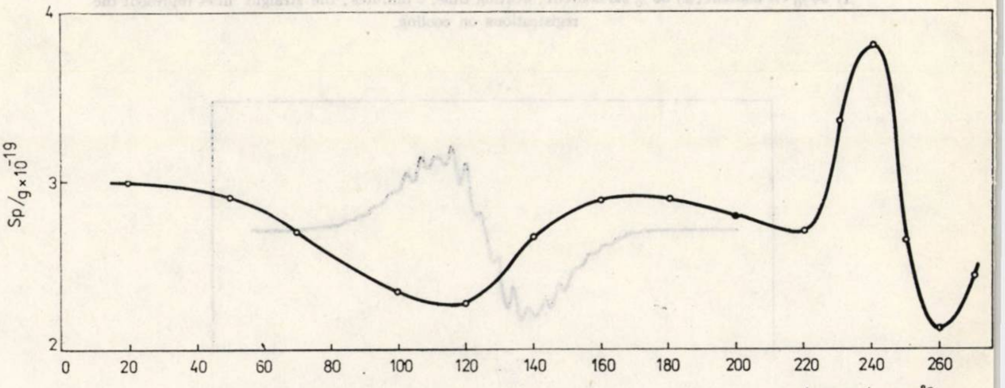

Fig. 6. — Temperature dependence of unpaired spins concentration for *cis-cisoidal* structure of Pα-EN. Heating time, 5 minutes.

Cis-cisoidal PPA behave like *cis-transoidal* structures (Figure 5). In the solid state the temperature at which N_s is maximum is dependent on thermal history of the polymer sample.

The *cis-cisoidal* structures of *P*α-EN (Figure 6), Pβ-EN (Figure 7) and the *cis-transoidal*/*cis-cisoidal* stereoblock structure of PEK (Figure 8) have shown a behaviour similar to *cis* structures of PPA, i.e., the N_S goes through a maximum at the temperature of *cis-trans* isomerization. The dependence of N_S vs. temperature for *cis-cisoidal* Pα-EN structure presents a minimum at 120° (Figure 6). This transition was not

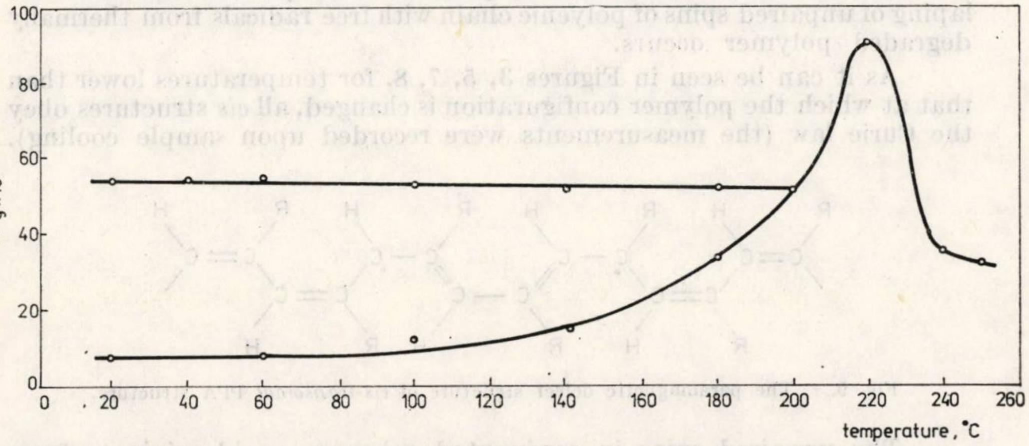

Fig. 7. — Temperature dependence of unpaired spins concentration for *cis-cisoidal* structure of Pβ-EN. The straight line represents the registration on cooling. Heating time, 5 minutes.

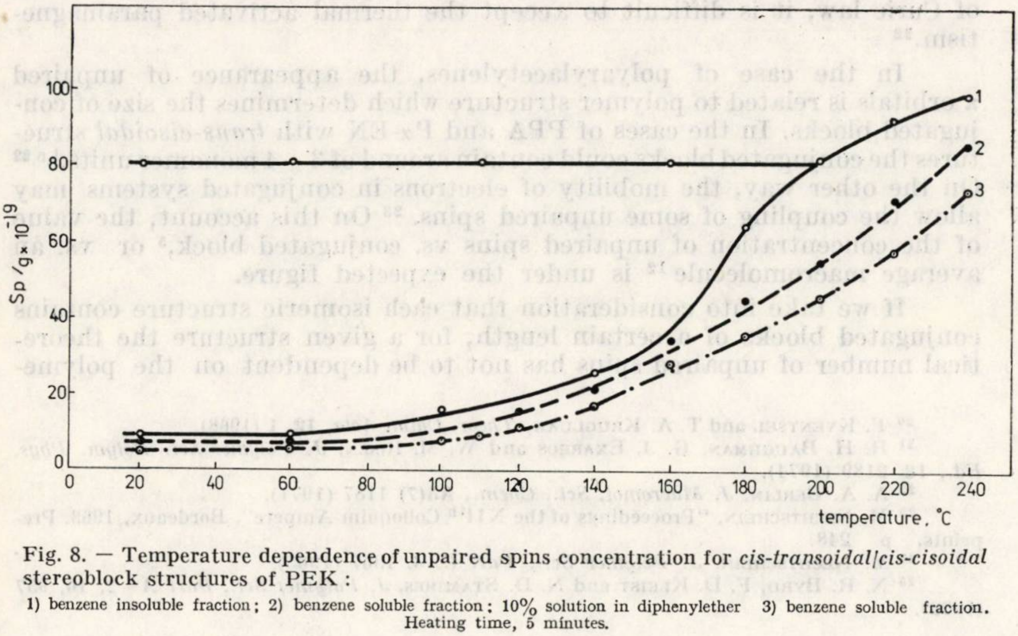

Fig. 8. — Temperature dependence of unpaired spins concentration for *cis-transoidal*/*cis-cisoidal* stereoblock structures of PEK :

1) benzene insoluble fraction; 2) benzene soluble fraction; 10% solution in diphenylether 3) benzene soluble fraction. Heating time, 5 minutes.

yet elucidated. The maximum of N_S (Figure 6) appears at the temperature of *cis-trans* isomerization (i.e., 240° for Pα-EN),[15] and *cis-cisoidal* structure of Pβ-EN (Figure 7) appears also at the isomerization temperature, namely at 220°.[7,15]

The *cis* structure of PEK which probably has a similar behaviour, was studied only up to 240° (Figure 8) because for higher temperatures the isomerization is acompanied by polymer decomposition, and an overlaping of unpaired spins of polyenic chain with free radicals from thermally degraded polymer occurs.

As it can be seen in Figures 3, 5, 7, 8, for temperatures lower than that at which the polymer configuration is changed, all *cis* structures obey the Curie law (the measurements were recorded upon sample cooling).

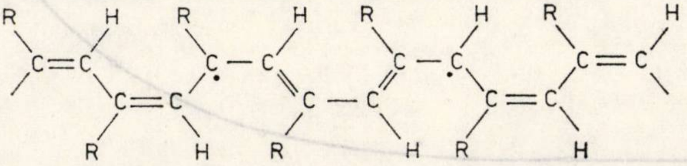

Fig. 9. — The paramagnetic defect structure of *cis-transoidal* PPA structure.

The unpaired spins in conjugated polymers could originate from unpaired π orbitals which appear from bond single-double alternation defects.[5,12,19–23] It is also suggested that the unpaired spins are diradicals which originate from π electron released in the rupture of skeletal π bonds (Figure 9).[12,20–23] According to our present results and to results reported by Ehrlich et al.[11,12,14] and Nechtschein[24,25] regarding the obeying of Curie law, it is difficult to accept the thermal activated paramagnetism.[22]

In the case of polyarylacetylenes, the appearance of unpaired π orbitals is related to polymer structure which determines the size of conjugated blocks. In the cases of PPA and Pα-EN with *trans-cisoidal* structures the conjugated blocks could contain around of 3—4 monomer units.[1,5,22] On the other way, the mobility of electrons in conjugated systems may allow the coupling of some unpaired spins.[23] On this account, the value of the concentration of unpaired spins vs. conjugated block,[5] or vs. an average macromolecule[12] is under the expected figure.

If we take into consideration that each isomeric structure contains conjugated blocks of a certain length, for a given structure the theoretical number of unpaired spins has not to be dependent on the polyme-

[20] F. Kventsel and T. A. Krugluak, *Theor. Chim. Acta*, **12**, 1 (1968).

[21] R. H. Baughman, G. J. Exarhos and W. M. Risen, *J. Polymer Sci. Polym. Phys. Ed.*, **12**, 2189 (1974).

[22] A. A. Berlin, *J. Macromol. Sci., Chem.*, **A5(7)** 1187 (1971).

[23] M. Nechtschein, "Proceedings of the XIIth Colloquim Ampere", Bordeaux, 1963, Preprints, p. 248.

[24] M. Nechtschein, *J. Polymer Sci., Part C.* **4**, 1367 (1965).

[25] N. R. Byrd, F. D. Kleist and N. D. Stamires, *J. Polymer Sci., Part A—2*, **10**, 957 (1972).

rization degree of the polymer. Consequently, the concentration of paramagnetic centers, for a certain isomeric structure of a given polyarylacetylene, depends on the following factors :

a) the length of the conjugated blocks, or in other words the steric structure of the macromolecule;

b) the mobility of electrons in macromolecule, which allows for the coupling of a part of unpaired spins;

c) the coplanarity of the monomer unit.

Thus,it is quite clear why the concentration of unpaired spins depends on steric structure of macromolecules (Table 1), which in turn imparts the length of conjugated blocks and consequently the number of unpaired π orbitals of the macromolecule.

In the crystalline polymers of *cis-cisoidal* structures (helix 3/1) in which the monomer units could adopt a coplanar form, the conjugation between the polyenic chain and aromatic substituent[17,18] is rendered possible, while in the *cis-transoidal* and *trans-cisoidal* amorphous polymer structures there is probably no conjugation between the polyenic chain and the aromatic substituent. In these conditions the last two structures release a greater number of unpaired π orbitals, and thus a higher concentration of unpaired spins appears. This is the case of different isomeric structures of PPA and Pβ-EN (Table 1).

The monomer units of Pα-EN and PEK could not be coplanar and no difference between the N_S of these crystalline and amorphous polymers has been observed (Table 1).

Evidently, the *cis-trans* thermal isomerization is a radicalic reaction. Consequently, we believe that at the isomerization temperature, the number of biradicals or of unpaired π orbitals is maximum and at the same time depends on the amount of *cis* units in the polymer.

The maximum values of N_S of PPA and Pβ-EN are higher than that of Pα-EN and PEK (Figures 2, 3, 5–8). This observation supports the releases of unpaired spins (i.e., the unpaired π orbitals) also by perturbation of the coplanarity between the polyenic chain and aromatic substituents, when this conjugation may exist.

The appearing of hyperfine structure at the isomerization temperature supports the existence of a structured radical in equilibrium with its unstructured precursor, and is not an evidence of a radical formed by irreversible degradation.[13,26]

ACKNOWLEDGEMENT. The authors would like to thank dr. R. Baican for ESR measurements.

---

[26] T. Masuda, N. Sasaki and T. Higashimura, *Macromolecules*, **8**, 717 (1975).

Revue Roumaine de Chimie, **23**, *8*, 1313–1323 (1978)

AMORPHOUS-CRYSTALLINE COUPLING IN POLYETHYLENE. VIII[1]

RELATIVISTIC EFFECTS IN DISCLINATION STATE FORMING PROCESSES

GH. DRĂGAN
Institute of Chemical Research, ICECHIM, Spl. Independenței 202,
Bucharest, Romania

Received August 2,1976

The study of the inductive effects during formation of the disclination state is continued by simultaneous annealing of two chlorinated samples originating from the same polyethylene. Effects of the individual and mixed annealing for dry and medium (with silicon oil) samples are respectively compared. Inductive coupling on six parameters deduced from DTA thermograms concerning T_m^1 and T_m^0 processes, has been studied. Samples in DTA scans do not keep the spatial symmetry from the annealing, like in the previous study, so that the observed modifications in the coupling nature are ascribed to the change of the reference temporal system by passing from the individual to the mixed annealing. In this way the observed results are in good agreement with the theoretical definition of the inductive element in topological thermodynamics by its relativistic effects on temporal systems of reference.

Previously proposed model[2] for the amorphous-crystalline coupling performed as a result of annealing of the lamellar defects decorated by photochlorination, establishes the formation of the disclination state at the interface between lamellar fragments and local amorphous domains. This process comes to be thermally activated on 110–130° temperature domain, both for the dry annealed samples and for the medium (with silicon oil) annealing ones. The coupling performed in the two cases, is indirectly studied on the already annealed samples (conditions denoted as *in vitro* system) by applying the Baughman–Turnbull's reasoning for the values measured from DTA thermograms concerning to T_m^1 and T_m^0 processes.[2] Purely dissipative coupling model[1] was trust to apply for the direct annealing process, but although the magnitude ($\alpha\Delta H_m \sim 10$ cal/g) exceeds the sensitivity of the used calorimeter,[1] no thermal effect was observed in this system defined as *in vivo*. However, by using the DTA system in isothermal conditions, an endothermal effect was observed associated to annealing process.[2] In this way a paradoxic situation was reached,[2] namely both the direct process (*in vivo* system) and the relaxation process of the disclination state in T_m^1 process (*in vitro* system) are endothermal effects concerning the same material. This result leads to the conclusion that the classical principle of the energy balance-sheet which considers the material as unitary system, is no more valid. New thermodynamic principles are required also by another important experimental result regarding the inductive coupling observed at simultaneous annealing of two samples of chlorinated polyethylene (CPE).[3] Model of the disclination state forming process[2] implies the existence of a viscous model characterized by an inductive element [4] expressed in topological representation.

---

[1] Part VII: Gh. Drăgan, *Rev. Roumaine Chim.*, **23**, 629 (1978).

[2] Gh. Drăgan, *Rev. Roumaine Chim.*, **21**, 1381 (1976).

Profound study of these morphological modifications in polyethylene (PE) and generally in composite systems, leads to the conclusion that the topological thermodynamics is the more appropriate representation for transformation processes in non-equilibrium systems. So far, in developing this formalism the following basic principles were established: the composite nature of the nonequilibrium systems and the temporal dependence of the topological variables.[5] The inductive element was subsequently defined by relativistic effects between temporal reference systems of time associated to the capacitive elements[4]. In fact these relativistic effects may be extended over the case of the purely dissipative coupling taking into account that for the crosslinking proces in epoxide resin-curing agent systems,[6] the kinetic equation suffers a modification of the temporal-relativistic type relative to the initial form. [1]

In the present work new results were reported concerning the inductive coupling during the processes of the formation of two disclination states by dry and medium annealing for two CPE sorts originating from the same PE sort previously denoted as LPE 3.[2,7] The inductive coupling was studied in conditions of individual annealing of two samples of the same sort, and by mixed annealing of two different samples. The results are interpreted using the amplitude parameters associated to T_m^1 and T_m^0 processes measured from DTA thermograms of the annealed samples (*in vitro* system). Since the DTA samples do not keep the annealing symmetry, the spatial dependence on annealing processes is removed remaining only the temporal dependene. In this way the relativistic effect of the inductive elements associated to dry and medium annealing, respectively, was clearly revealed by passing from the individual annealing system to the mixed annealing system.

EXPERIMENTAL

Materials. Two CPE samples obtained in different manners by chlorination in suspension from LPE 3 were used; CPE 31 directly obtained to 43.5% chlorine content by weight, and respectively CPE 32 obtained from LPE 3 previously annealed one hour at 125° and subsequently chlorinated to 40% chlorine content.

---

[3] Gh. Drăgan, *Rev. Roumaine Chim.*, **21**, 1537 (1976).

[4] Gh. Drăgan, *Revista de Chimie*, **29**, 214 (1978).

[5] Gh. Drăgan, *J. Thermal Anal.*, **9**, 405 (1976).

[6] Gh. Drăgan, *Rev. Roumaine Chim.*, in press.

[7] Gh. Drăgan, *Rev. Roumaine Chim.*, **20**, 687 (1975).

Table 1

The values of the six parameters : α, ΔH_m, h_2, $\alpha\Delta H_m$, h_1 and ΔH^1_m, measured from DTA scans of the CPE 31 and CPE 32 samples, dry or medium annealed in individual and mixed conditions. respectively (see the text)

α	DA CPE 31	CPE 32	ΔH_m DA (cal/g) CPE 31	CPE 32
V	0.558 ± 0.001	0.057 ± 0.007	22 ± 2.7	39 ± 3.8
VV	0.62 ± 0.02	0.068 ± 0.009	19 ± 3.6	37 ± 3.6
V	0.603 ± 0.009	0.10 ± 0.03	18 ± 1.2	36 ± 4.0
H	0.59 ± 0.01	0.07 ± 0.02	19 ± 2.1	38 ± 2.3
VV	0.54 ± 0.02	0.07 ± 0.01	17 ± 2.8	43 ± 3.7
VH	0.60 ± 0.01	0.07 ± 0.02	24 ± 1.7	41 ± 2.8
	MA		MA	
V	0.69 ± 0.07	0.08 ± 0.01	20 ± 1.7	45 ± 6.4
VV	0.71 ± 0.05	0.076 ± 0.008	21 ± 4.0	42 ± 3.7
V	0.65 ± 0.02	0.08 ± 0.02	20 ± 2.3	39 ± 3.0
H	0.66 ± 0.02	0.097 ± 0.008	16.2 ± 0.9	41 ± 5
VV	0.68 ± 0.05	0.12 ± 0.05	23 ± 3.6	53 ± 3.7
VH	0.71 ± 0.07	0.11 ± 0.01	21 ± 1.3	50 ± 4.9

h_2 (mm/g)	DA CPE 31	CPE 32	$\alpha\Delta H_m$ (cal/g) DA CPE 31	CPE 32
V	710 ± 30	150 ± 25	12.1 ± 0.50	2.2 ± 0.43
VV	610 ± 70	160 ± 27	11.8 ± 0.58	2.5 ± 0.48
V	610 ± 30	140 ± 57	10.5 ± 0.83	3.8 ± 0.65
H	600 ± 90	160 ± 53	11 ± 1.3	1.8 ± 0.20
VV	600 ± 120	170 ± 40	9 ± 1.7	2.8 ± 0.68
VH	700 ± 110	170 ± 20	14 ± 1.4	2 ± 1.1
	MA		MA	
V	410 ± 30	120 ± 26	8 ± 1.6	3.6 ± 0.81
VV	420 ± 26	110 ± 13	8 ± 1.6	3.2 ± 0.52
V	370 ± 28	100 ± 34	13.1 ± 1.4	3.2 ± 0.8
H	360 ± 40	120 ± 17	10.7 ± 0.4	3.9 ± 0.5
VV	430 ± 28	200 ± 28	8 ± 1.4	6.3 ± 0.78
VH	400 ± 44	200 ± 25	8.1 ± 0.48	5.4 ± 0.9

Table 1 *(continued)*

h_1 (mm/g)	DA CPE 31	DA CPE 32	ΔH_m^1 (cal/g) DA CPE 31	DA CPE 32
V	560 ± 27	2500 ± 300	10 ± 1.6	37 ± 2.2
VV	380 ± 72	2200 ± 110	7 ± 2.2	34 ± 2.2
V	400 ± 19	2200 ± 420	7 ± 1	32 ± 2.2
H	400 ± 48	2300 ± 75	8 ± 1.5	36 ± 1.4
VV	480 ± 30	2500 ± 130	8 ± 1.5	40 ± 2.2
VH	450 ± 85	2800 ± 100	10 ± 1.5	39 ± 1.8
	MA		MA	
V	190 ± 25	1400 ± 170	12 ± 1.6	31 ± 3.6
VV	170 ± 20	1300 ± 114	13 ± 3.0	39 ± 2.2
V	200 ± 24	1100 ± 195	7 ± 1	36 ± 2
H	190 ± 34	1100 ± 170	6 ± 1	37 ± 2
VV	200 ± 21	1400 ± 170	13 ± 2.5	47 ± 2.2
VH	170 ± 22	1300 ± 30	13 ± 1.0	45 ± 3.0

Annealing of these samples *in vivo* system was performed using the metallic block previously described. [3] All the samples were annealed in Pyrex tube during one hour at 124.8 ± 0.2° (the temperature of the ultrathermostate bath). The samples were dry annealed (DA) and in mixture with silicon oil Schuchardt 702, as medium annealing (MA), in proportion of 25% (CPE 31) and 30% (CPE 32), respectively. Inductive coupling effects during annealing for these two different conditions, were pursued by individual annealing of the same CPE samples, and for mixed annealing of both CPE samples, respectively. Both indivudal and mixed annealing were performed in vertical simultaneous annealing (VV) and vertical and horizontal annealing (VH). [3] (In mixed VH annealing, CPE 32 was always vertical). All annealed samples are referred to individually and vertically single annealed samples (V). For a brief expression of these cases the following notations were used : DCA and MCA for cross dry and medium annealing, respectively, for two samples of the same or different kind. For example CPE 32-DCA-CPE 31 denotes the CPE 32 sample simultaneously dry annealed with CPE 31 also dry sample.

DTA apparatus previously described, [2] uses cells with 3 mm inner diameter and 6 mm in heigh. In this way the DTA samples do not keep the annealing symmetry. The cylindrical samples from annealing were transversally cut at half with a rasor blade. From the two halves were prepared 3 DTA samples taking material from the two cutting regions in alluminium capsules. [2] All DTA scans were performed at 6.5°/min, so that for each set of 6 values it may evaluate the mean value and the associated root mean square deviation corresponding to each measured parameter. For the individually VV annealed samples, was taken material from the two samples. For reproducibility verification of the DTA scans, five scans on nearly quantities of indium were performed. The height and the melting heat (measured by planimetry) reproducibility is closer than ± 3%.

The magnitude values for T_m^1 and T_m^0 endotherms were related to the net weight of the samples excluding chlorine and the medium.

RESULTS AND DISCUSSIONS

The magnitude values corresponding to the T_m^1 and T_m^0 are gathered in table 1 for the samples annealed in the above mentioned *in vivo* conditions. For a good accuracy in interpretation, these values are expressed by mean values and their associated root mean square deviations calculated from the six individual values. The measured values are the following: the splitting coefficient $\alpha = h_2/(h_1 + h_2)$, the total enthalpy of melting ΔH_m(cal/g), the heights h_1 and h_2 corresponding to the endothermal effects T_m^0 and T_m^1, respectively (in mm/g), and the partial melting enthalpy associated to the processes, $\Delta H_m^1 = (1 - \alpha)\,\Delta H_m$ and $\sigma \Delta H_m$, respectively.[2] Inductive effects in these values are selected taking as reference the individual annealing (V) both for individual and mixed annealing in VV and VH conditions. For further discussions we quote the resulted values with "$-$" and "$+$", corresponding to the inductive non-coupling and coupling case, respectively. In Table 2 are selected all inductive coupling cases observed in the six considered parameters, regarding the individually annealed samples from the mixed annealed ones, respectively.

Table 2

Classification of the inductive coupling for the two disclination states about sign convention of the values from Table 1 (see the text)

	coupled samples	α	ΔH_m	h_2	$\alpha\Delta H_m$	h_1	ΔH_m^1
individual	CPE 32- DCA	$-$	$-$	$-$	$+$	$-$	$-$
	CPE 31 – MCA	$-$	$-$	$-$	$-$	$-$	$-$
mixt	CPE 31-DCA-CPE 32	$-$	$(+)$	$-$	$+$	$-$	$-$
	CPE 32-MCA-CPE31	$-$	$(+)$	$+$	$+$	$-$	$+$

CPE 31 sample has both in DA and MA system the splitting effect more pronounced than in CPE 32 sample. The lamellae break up [2,7] easier in CPE 31 sample by defect precipitation during annealing process. By LPE 3 annealing at 125° for an hour, the mobility of the conformation defect is greatly reduced, so that the diffusion of chlorine towards the lamellar defects strongly decreases. In Figure 1 is represented the kinetics of the lamellar thickening process for two sorts of PE similar to LPE 3, expressed as a dependence of the lamellar thickness ($\bar{D}_{001}$) and long period (L) versus annealing temperature. [8]

An exponential increase with annealing temperature is observed. This fact explains the weak T_m^1 process of the CPE 32 sample, and T_m^0 is almost unaffected by chlorination and annealing, relative to LPE 3 (with $\Delta H_m = 44.8$ cal/g). The disclination state proper to the annealed CPE 32 samples is more labile to the medium attack. As previously [2]

[8] a. N. Kusumoto, T. Yamamoto and M. Takayanagi, *J. Polymer Sci.*, **A−2**, 1173 (1971).

b. T. Kajiyama, T. Okada and M. Takayanagi, *J. Macromol. Sci.-Phys.*, **B9**, 35 (1974 .

observed silicon oil modifies the shape of T^1_m endotherm. In Table 3 the rations of the mean values for the six parameters obtained in MA system to these obtained in DA system are given.

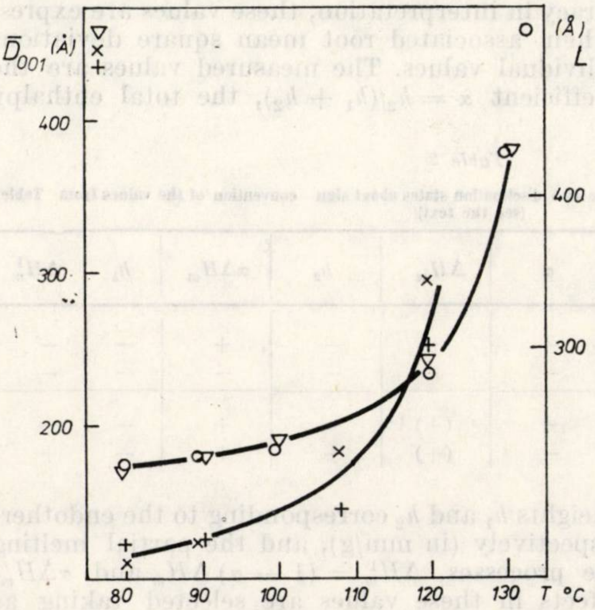

Fig. 1. — The kinetics of the thickening process for two linear PE species given as a dependence of the lamellar thickness ($\overline{D}_{001}$: ∇, ×, +) and long period (L : ○) on the annealing temperature: ∇, ○ PE Sholex 6150 C, reference [8a] ; ×, + PE Hizex 1200 J reference [8b].

The observations on the variation of these ratios in the presence of silicon oil relative to the two processes may be briefly reported as following.

— T^1_m : h_2 and $\alpha\Delta H_m$ proportionally decrease for CPE 31 sample, while for CPE 32, h_2 decreases and $\alpha\Delta H_m$ doubles ;

Table 3

The rations of the values of the six parameters in MA system to these obtained in DA system

	α	ΔH_m	h_2	$\alpha\,\Delta H_m$	h_1	ΔH^1_m
CPE 31	1.162	1.222	0.616	0.817	0.420	1.280
CPE 32	1.294	1.154	0.895	1.753	0.524	1.124

— T^0_m : h_1 and ΔH^1_m are similarly affected for both samples, namely h_1 decreases to the half, while ΔH^1_m slightly increases ;

— α and ΔH_m slightly increases in the presence of the silicon oil

The influence of silicon oil on the viscous relaxation process of the disclination state in CPE 32, explains the pronounced modifications of endothermal T^1_m effect in this sample.[2] To establish the influence manner of the silicon oil on this process, we take again the proposed model for the formation process (*in vivo* system) and for the relaxation process (*in vitro* system) of the twist disclination state. Figure 2a reproduces the disclination state performed by migration of the decorated defects along T direction in a local amorphous domain, and the establishment of shear stresses at the interface between lamellar fragments and local amorphous domain (dashed region).[2]

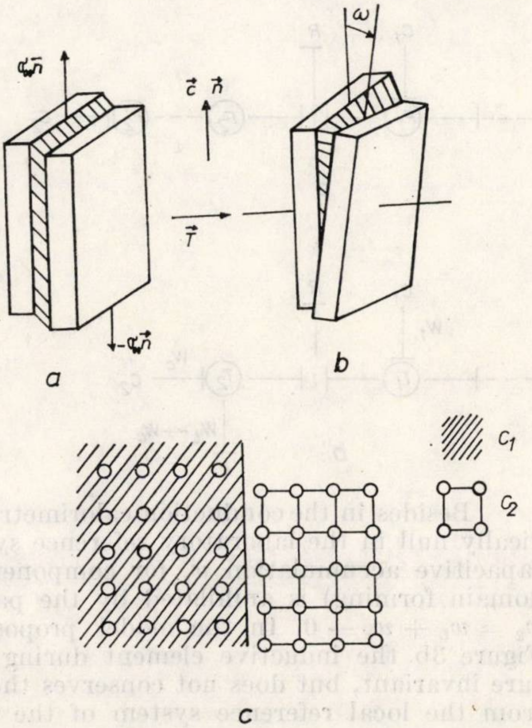

Fig. 2. — The model of the disclination state resulted by defects annealing (a); relaxation of the disclination state in endothermal T_m^1 effect (b); topological definition of the two components (c).

Behind heating over the melting temperature of the interlamellar order (T_m^1), the disclination state relaxes by reciprocal rotating and approaching of lamellar fragments (Figure 2b).[9,10] Both processes are characterized in the two calorimetric systems (in laboratory reference system) by endothermal fluxes.[2] We will try to explain this energetic paradox, by applying the principles of the topological thermodynamics. The migration of defects during annealing process may be expressed by a viscous mode of transfer and accumulation of the kinetic momentum between the two topological components in the internal circuit (Figure 2c).[4] At the defect *exit* by precipitation from the lamellar domain, a change in direction of the kinetic momentum is observed, which explains also the appearance of the shear stresses. This change in directions of the kinetic momentum is interpreted in topological language by an inductive element

[9] T. W. Chou, *J. Appl. Phys.*, **42**, 4931(1971).
[10] Gh. Drăgan, *Rev. Roumaine Chim.*, **23**, 261 (1978).

L in bond diagram of the internal circuit (Figure 3a), so that a supplimentary mechanical stress appears between the components, $\sigma_{00} = L\,(\mathrm{dv}/\mathrm{dt})$.[4]

For the used calorimetric system (the isothermal DTA system as *in vivo* system) we may rewrite the bond diagram by considering this process (Figure 3b), in reference to the same physical components C_1 and C_2 (Figure 2c).

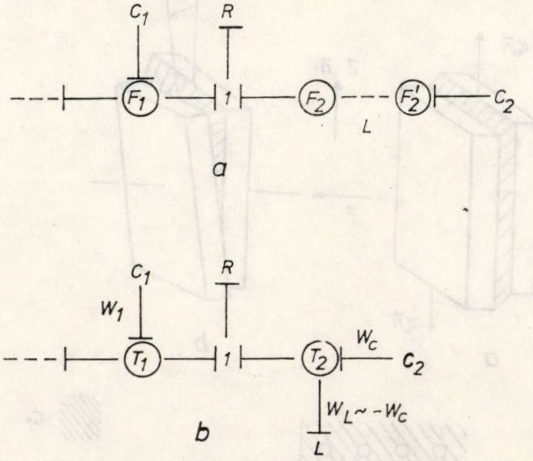

Fig. 3. — Bond diagrams of the internal circuit during defect annealing process in viscous mode representation (a) and as a thermal driven process (b), respectively.

Besides in the conduction calorimetric system[1] the flux w_2 is practically null in the laboratory reference system, we may assume that the capacitive accumulation w_c for component C_2 (by the local amorphous domain forming) is anihilated by the parasite flux $w_L \sim -w_c$, so that $w_2 = w_L + w_c \to 0$. In the model proposed by the bond diagram in Figure 3b the inductive element during annealing process is temperature invariant, but does not conserves the energetic heat flux by passing from the local reference system of the component C_2 to the reference system of the component C_1.[4] Energetic flux w_{L}, corresponds in the viscous mode to the disclination elastic energy[2] accumulated by the shear stresses σ_{00}.

In the DTA calorimetric system, the heat transfer between cells and thermostate, and the virtual transfer between cells,[5] are performed through a pure dissipative medium (by irradiation), in difference to the conduction calorimeter used in reference 1 where a capacitive element must be associated. The previous results[3] revealed on the other hand that the effect of the inductive element from the internal circuit is more pronounced by annealing in Pyrex than by annealing in brass. We may suppose that this dissipative element from the external circuit (in laboratory system) modifies the temporar-relativistic position of the laboratory reference system relative to the inductive element. This fact explains that in the isothermal DTA system as *in vivo* system the flux $w_2 \neq 0$, so that the endothermal effect is associated with the capacitive accumulation w_c.

Amorphous-crystalline coupling performed between the lamellar fragments and local amorphous domains behind the annealing, may be described by another diagram concerning the T_m process. To establish this coupling in the topological representation, we will take into account the following phenomenological facts:

(i) The previous study,[11] also the shape of the T_m^1 endotherms in the DTA system,[7] reveal that this process represents a first order transition (of order-disorder type) specific to the interlamellar order;

(ii) The magnitude values associated to this process (h_2, $\alpha\Delta H_m$) obey a thermally activated law verified by applying the Baughman-Turnbull reasoning;[2]

(iii) Both dry and medium annealed samples have the same activation energies;[2]

(iv) The DTA scans performed by cooling after heating scans with approximatively 30° over T_m^0, identically reproduce the exotherms corresponding to T_m^0 and T_m^1 processes, respectively. This fact is consistent with the previous observations[10] according to which it has been assumed that in the absence of an external field of stresses, the paracrystalline order from the solid state conserves in the melt. After the above observations it may be assume that the coupling becomes in T_m^1 process purely dissipative for the used calorimetric system, similar with the amorphous-crystalline coupling observed in LPE samples during T_m^0 process.[1] It rests to establish the origin of the flux $\alpha\Delta H_m$ during T_m^1 process. About the phenomenological proposed model,[2] the endotherm T_m^1 represents the relaxation of the disclination state by "delivering" of the elastic energy "accumulated" in the inductive element. In the newly performed coupling, the component C_2 (the local amorphous domain) dissipates this energy in the laboratory system of the calorimetric system,[6] so that the flux w_L, which is exothermal in the internal circuit of the *in vivo* system, becomes endothermal in T_m^1 process.

Silicon oil modifies the inductive coupling especially for CPE 32 sample where the local amorphous domains are more easily attacked. Change of the inductive element for the two disclination states associated to CPE 31 and CPE 32, respectively, leads to specific changes in the associated heat effects $\alpha\Delta H_m$ (Table 3). It may be observed that for the actual case in which the spatial symmetry of the thermal transfer from the annealing does not conserve, the splitting coefficient does not reveal semnificative coupling in any case of simultaneous annealing of two samples as it has been systematically observed by keping this thermal symmetry in the two calorimetric systems.[3] On the other hand it is important to note that the actual used annealing time (1 hr ~ 10^2 min) favours the increase of the errors as in the previous experiments.[3]

We may take again the cases of inductive coupling from Table 2 by the separating the individual and mixed coupling, respectively, and on the other hand relative to the inductive element by dry and medium annealing, respectively (Table 4). The values set (α, h_1, ΔH_m) separates by its unchanged behaviour at the passage from the individual to mixed and from dry to medium annealing, respectivelly. ΔH_m^1 remains invariant by passing from the individual to the mixed annealing, but modifies its behaviour at the passage from dry to medium annealing. Set $(\alpha\Delta H_m,\ h_2)$ which characterizes the T_m^1 process and in general the amorphous-crystaline coupling, has the same bahaviour for the two inductive elements in individual system, but specifically modifies at the passage to the mixed annealing, namely for dry annealing the inductive coupling conserves both in individual and mixed annealing to CPE 32 sample, while for medium annealing in the individual system the coupling is observed to CPE 31 sample, but in the mixed annealing this coupling is "transferred" to CPE 32 sample. This coupling set specifically behaves at the passage from the individual to mixed annealing for the two inductive elements DA and MA, respectively. We may express the inductive coupling by considering the matrix composed of the amplitude values associated to the process T_m^1 and T_m^0, respectively:

---

[11] GH. DRĂGAN, *Materiale Plastice*, **10**, 87 (1973).

Table 4

Inductive coupling behaviour of the two disclination states in the two annealing systems (individual and mixed), for dry and medium annealing, respectively

		CPE 32-DCA	CPE 31-DCA-CPE 32
DA	α	–	–
	h_1	–	–
	ΔH_m	–	–
	$\alpha\Delta H_m$	+	+
	h_2	–	–
	ΔH_m^1	–	–
		CPE 31-MCA	**CPE 32-MCA-CPE 31**
MA	α	–	–
	h_1	–	–
	ΔH_m	(+)	(+)
	$\alpha\Delta H_m$	+	+
	h_2	–	+
	ΔH_m^1	+	+

$$H = (T_m^1 \cdot T_m^0) = \begin{pmatrix} h_2 & h_1 \\ \alpha\Delta H_m & \Delta H_m^1 \end{pmatrix}.$$

In this way the inductive couplings from Table 4 may be expressed in short by the following diagram:

$$\begin{tikzcd}
\text{(individual)} & \text{(mixed)} & \\
\text{CPE 32 } (+,\ -) \arrow[r, dash, "C"] \arrow[d, dash, "L"'] & \text{CPE 31 } (+,\ -) \arrow[d, dash, "L"] & \text{(dry annealing)} \\
\text{CPE 31 } (+,\ +) \arrow[r, dash, "C"] & \text{CPE 32 } (+,\ +) & \text{(medium annealing)}
\end{tikzcd}$$

where in paranthesisis are given signs corresponding to the coupling observed in the matrix H. This diagram results to be commutative concerning the operations L and C which denote the change of the inductive element (in internal circuit) and the inductive coupling (in external circuit), respectively. In fact this diagram represents the change of the local reference system for which the inductive coupling is observed as a function of the two operations.

The inductive interaction observed during annealing process, may be compared to the scatering process in the two particles system. The relativistic effect observed by changing of the inertial reference system corresponds in the inductive coupling to the passage from the individual to mixed system of annealing, and the scattering matrix would correspond to the above defined matrix H.

Revue Roumaine de Chimie, **23**, *8*, 1325 – 1335 (1978)

ÉTUDE PHYSICO-CHIMIQUE DU POLYDIMÉTHYL-2,4-STYRÈNE OBTENU PAR POLYMÉRISATION CATIONIQUE

JACQUES CLAUS et ERNEST MARÉCHAL
Laboratoire de Chimie Macromoléculaire de l'Institut National Supérieur de Chimie Industrielle
de Rouen — B. P. 08 — 76130 — Mont-Saint-Aignan

Reçu le 17 juin 1976

Le diméthyl-2,4-styrène a été polymérisé en utilisant des amorceurs de natures diverses et à des concentrations différentes. Les polymères obtenus ont été fractionnés par chromatographie sur gel perméable (G. P. C.) préparative. Les fractions ont été étudiées par différentes méthodes physiques : osmométrie, diffusion de la lumière, viscosimétrie, G.P.C. analytique. Cette étude a été effectuée dans le benzène qui est un très bon solvant de ce polymère. Elle nous a permis d'établir les relations de Mark Houwink pour les polymères étudiés et de mettre en évidence l'apparition de branchements en fonction de la nature ou de la concentration de l'amorceur.

A. INTRODUCTION

Dans les travaux précédents, [1à4] l'influence électronique et stérique de divers substituants sur la polymérisation cationique de différents monomères a été étudiée.

Les méthylstyrènes ont en particulier fait l'objet de plusieurs études tant théoriques qu'expérimentales, et parmi ceux-ci, nous nous sommes intéressés plus spécialement aux polymères obtenus par amorçage cationique du diméthyl-2,4-styrène.

En étudiant les variations des viscosités intrinsèques des polymères obtenus, en fonction des conditions de polymérisations, nous avons, constaté que la nature et la concentration des amorceurs utilisés avaient un effet important sur les caractéristiques des matériaux obtenus. Afin de préciser cet effet, nous avons procédé à une étude approfondie de la structure des polymères obtenus dans diverses conditions d'amorçage. Pour cela, nous avons systématiquement étudié les grandeurs permettant de caractériser ces polymères en faisant appel aux techniques suivantes : fractionnement préparatif et analytique par chromatographie sur gel perméable, viscosimétrie en solution, osmométrie, diffusion de la lumière.

---

[1] A. Anton et E. Maréchal, *Bull. Soc. Chim. France*, **1971**, p. 3753.

[2] C. Bunel, S. Cohen, J. P. Laguerre et E. Maréchal, *Polymer Journal Japan*, **7**, 320 (1975).

[3] H. Garreau et E. Maréchal, *European Polym. J.*, **9**, 261 (1973).

[4] A. Anton et. E. Maréchal, *Bull. Soc. Chim. France*, **1971**, p. 2250.

L'étude suivante porte sur la détermination des grandeurs physicochimiques du polydiméthyl-2,4-styrène préparé en utilisant soit le dichloroéthylaluminium, soit le tétrachlorure de titane comme amorceur.

B. RÉSULTATS EXPÉRIMENTAUX

I. SYNTHÈSE DU MONOMÈRE

La méthode de synthèse décrite dans une étude précédente (1) a été reprise et optimisée de façon à obtenir de plus grandes quantités de monomère en une seule opération.

II. POLYMÉRISATION CATIONIQUE

a) *Méthode de polymérisation*. La méthode de polymérisation a été précédemment décrite. Nous l'avons reprise sans modification.[2]

b) *Conditions de polymérisation*. Tous les polymères obtenus ont été préparés dans les conditions suivantes :
Solvant : chlorure de méthylène, $[M] = 0{,}224$ mole. 1^{-1} $\theta = -70°$, $t = 5$ mn.
Nous avons étudié les variations de viscosité intrinsèque en fonction de la nature et de la concentration de l'amorceur. Elles sont représentées sur la figure 1. Dans tous les cas le rendement en polymère précipité par le méthanol est de 100%.

Afin d'étudier l'influence de la concentration et de la nature de l'amorceur sur les propriétés physico-chimiques du polymère, nous avons préparé quatre échantillons en quantité suffisante pour effectuer un fractionnement par G.P.C. préparative et étudier les fractions obtenues.

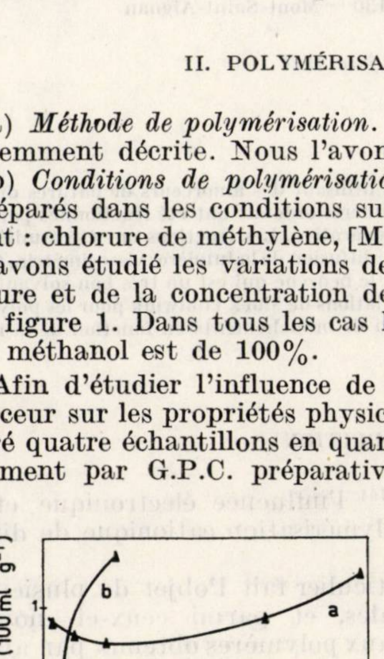

Fig. 1. — Polymérisation du diméthyl-2,4-styrène. Variations de $[\eta]$ (100 ml. g^{-1}) en fonction de [A] mole. 1^{-1}
Courbe a : Amorceur $EtCl_2Al$; Courbe b : Amorceur $TiCl_4$.

Les polymères ont été préparés dans les conditions d'amorçage suivantes :

$$S_I[AlC_2H_5Cl_2] = 0{,}048 \text{ mole. } 1^{-1}$$

$$S_{II}[AlC_2H_5Cl_2] = 0{,}1 \text{ mole. } 1^{-1}$$

$$S_{III} = [AlC_2H_5Cl_2] = 0{,}5 \text{ mole. } 1^{-1}$$

$$S_{IV}[TiCl_4] = 0{,}1 \text{ mole. } 1^{-1}$$

III. FRACTIONNEMENT

Chacun des polymères obtenus a été fractionné par G.P.C. préparative dans le benzène. Les solutions obtenues étant trop diluées pour faire l'objet de mesures par diffusion de la lumière, ont été précipitées par le méthanol puis rassemblées afin de former des lots de polymère d'environ 100 mg.

IV. ÉTUDE PHYSICO-CHIMIQUE

Toutes les déterminations ont été faites dans le benzène à l'exception des mesures osmométriques faites dans le toluène.

1) Viscosimétrie (benzène à 25°)

Nous avons déterminé la viscosité intrinsèque de chacune des fractions des différents polymères fractionnés. Les résultats sont donnés dans les tableaux 1 à 4.

Tableau 1

SI $[\eta] = 0{,}83 \quad 100\ \mathrm{cm^3g^{-1}}$

Fraction n°	1	2	3	4	5	6	7	8	9	10	11	12	13	14
$[\eta]$	2	1,2	1,1	1	0,9	0,8	0,75	0,7	0,6	0,55	0,5	0,4	0,3	0,2

Tableau 2

S II $[\eta] = 0{,}79$

Fraction n°	1	2	3	4	5	6	7	8	9	10	11	12
$[\eta]$	1,44	1,15	0,95	0,70	0,65	0,60	0,55	0,50	0,35	0,31	0,25	0,20

Tableau 3

S III $[\eta] = 1{,}19$

Fraction n°	1	2	3	4	5	6	7	8	9	10	11	12
$[\eta]$	2,28	1,80	1,19	1,08	1,05	1,02	0,98	0,95	0,90	0,90	0,88	0,88

Fraction n°	13	14	15	16	17	18	19
$[\eta]$	0,82	0,80	0,80	0,75	0,65	0,55	0,26

Tableau 4

S IV $[\eta] = 1{,}28$

F. n°	1	2	3	4	5	6	7	8	9	10	11	12	13	14
$[\eta]$	2,5	2,15	1,85	1,64	1,35	1,23	1,13	1,08	1,05	0,98	0,95	0,9	0,88	0,85

F. n°	15	16	17	18	19	20	21	22	23	24	25	26	27
$[\eta]$	0,80	0,80	0,7	0,65	0,65	0,65	0,60	0,56	0,58	0,56	0,43	0,30	0,14

2) Osmométrie (toluène à 37°)

Nous n'avons effectué les mesures que sur le polymère S II à seule fin de vérifier que les coefficients K et α de la loi de Mark Houwink obtenus par osmométrie nous redonnaient le même étalonnage en G.P.C. aux incertitudes de mesure près. Les résultats des mesures sont rassemblés dans le tableau 5.

Tableau 5

S II

Fraction n°	1	2	3	4	5	6	7	8	9	10	11	12
$\overline{M}_n \times 10^{-3}$	350	250	250	160	165	137	126,5	114	104	78	52,7	22

En représentant graphiquement (fig. 2) la variation de log $\overline{M}_n$ en fonction de log $[\eta]$, nous avons obtenu la relation suivante :

$$[\eta] = 6.10^{-6}\ \overline{M}_n^{0,97}\ 100\ \mathrm{cm}^3.\ g^{-1}$$

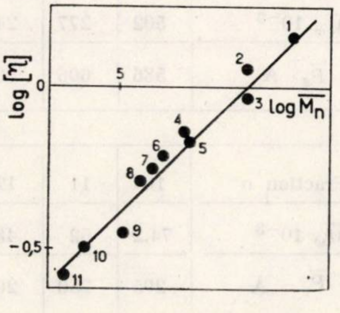

Fig. 2. — Polymérisation du diméthyl-2,4-styrène. Détermination de K et α pour l'échantillon SII.

3) Photogoniodiffusimétrie (benzène 20°)

a) *Détermination de l'incrément d'indice.* Nous avons obtenu sa valeur pour le diméthyl-2,4-styrène, dans le benzène, par réfractométrie différentielle :

$$\frac{\mathrm{d}n}{\mathrm{d}c} = 0{,}110\ \mathrm{ml.\ g^{-1}}$$

b) *Analyse des diagrammes de Zimm.* Nous avons tracé les diagrammes de Zimm pour toutes les fractions et nous avons déduit pour chacune d'elles les valeurs de la masse molaire moyenne en poids $\overline{M}_w$, et pour S I et S II les valeurs des rayons de giration $\overline{P}_z$. Les résultats sont donnés par les tableaux 6—9.

Tableau 6

SI

Fraction n°	1	2	3	4	5	6	7	8	9	10	11	12	13	14
$\overline{M}_w 10^{-3}$	1.630	463	424	360	360	300	290	270	259	190	190	150	110	73,5
$\overline{P}_z$ Å	650	606	580	540	500	500	480	450	440	410	400	350	310	300

Tableau 7

SII

Fraction n°	1	2	3	4	5	6	7	8	9
$\overline{M}_w$ 10^{-3}	502	277	249	210	208	171	112	105	102
$\overline{P}_z$ Å	586	606	590	415	420	360	310	310	320

Fraction n°	10	11	12
$\overline{M}_w$ 10^{-3}	74,2	52	48
$\overline{P}_z$ Å	295	250	200

Tableau 8

SIII

Fraction n°	1	2	3	4	5	6	7	8	9
$\overline{M}_w$ 10^{-3}	3.141	990	600	410	408	380	380	310	310

Fraction n°	10	11	12	13	14	15	16	17	18	19
$\overline{M}_w$ 10^{-3}	300	300	297	290	280	250	250	220	160	60

Tableau 9

SIV

Fraction n°	1	2	3	4	5	6	7	8	9	10
$\overline{M}_w$ 10^{-3}	6300	4100	3630	2950	1630	1400	1240	1090	1080	810

Fraction n°	11	12	13	14	15	16	17	18	19	20
$\overline{M}_w$ 10^{-3}	740	735	720	720	718	502	450	408	370	364

Fraction n°	21	22	23	24	25	26	27
$\overline{M}_w$ 10^{-3}	344	291	280	250	239	210	150

4) Relations de Mark Houwink

Elles sont obtenues ainsi qu'il l'a été indiqué dans la partie BIV 2 et sont données ci-dessous (unité 100 $cm^3 . g^{-1}$)

$$S_{I}\ [\eta] = 4{,}35\ 10^{-6}\ \overline{M_w}^{0{,}96}$$

$$S_{II}\ [\eta] = 3{,}8\ \ 10^{-6}\ \overline{M_w}^{0{,}96}$$

$$S_{III}\ [\eta] = 4{,}5\ \ 10^{-4}\ \overline{M_w}^{0{,}60}$$

$$S_{IV}\ [\eta] = 8\ \ \ 10^{-4}\ \overline{M_w}^{0{,}55}$$

5) Etude par chromatographie sur gel perméable

a) *Choix des colonnes et étalonnage.* Les colonnes utilisées pour cette étude nous ont permis de réaliser une séparation efficace des macromolécules ayant des masses comprises entre 2.10^3 et 2.10^6 environ. Nous avons réalisé un étalonnage « universel » de ces colonnes à l'aide d'échantillons étalons de masses molaires et de viscosités connues, en traçant la courbe $\log([\eta]M) = f(V_e)$ où V_e est le volume d'élution correspondant à l'étalon de masse M et de viscosité intrinsèque $[\eta]$. Cet étalonnage permet de calculer les masses molaires moyennes de toutes les substances macromoléculaires polydispersées, connaissant les coefficients K et α de la loi de Mark Houwink.

b) *Etude des différentes fractions par chromatographie sur gel perméable.* Pour chaque fraction les masses molaires $\overline{M_n}$ et $\overline{M_w}$ sont données par les relations suivantes. [5]

$$\overline{M_w} = K^{-\frac{1}{\alpha+1}} \sum \frac{h_i}{\sum h_i} ([\eta_i]M_i)^{\frac{1}{\alpha+1}}$$

$$\overline{M_n} = K^{-\frac{1}{\alpha+1}} \sum \frac{h_i}{\sum h_i \cdot \dfrac{1}{([\eta_i]M_i)^{\frac{1}{\alpha+1}}}}$$

dans lesquelles

— K et α sont les coefficients de Mark Houwink

— h_i est la hauteur du pic correspondant à un volume d'élution V_i

— $[\eta_i]M_i$ est la valeur donnée par la courbe d'étalonnage universel pour le volume V_i.

Nous avons ainsi recalculé les masses molaires moyennes de toutes les fractions de polydiméthyl-2,4-styrène.

Les différentes masses molaires mesurées par G.P.C. sont en bon accord avec celles mesurées par osmométrie et diffusion de la lumière.

---

[5] H. Benoît, Z. Grubisic, P. Rempp, D. Decker et J. G. Zilliox, *J. Chem. Phys.*, **63**, 1507 (1966).

C. ÉTUDE DU BRANCHEMENT

Si nous considérons les polymères S I et S II nous constatons que leurs coefficients α sont identiques. D'autre part, si nous portons sur le même graphique log $\overline{\rho}$ en fonction de log $\overline{M_w}$ pour ces deux polymères (fig. 3) nous constatons que les points représentatifs des différentes fractions des deux polymères s'alignent sur la même droite. On peut donc conclure en toute certitude que le degré de linéarité des deux polymères est identique.

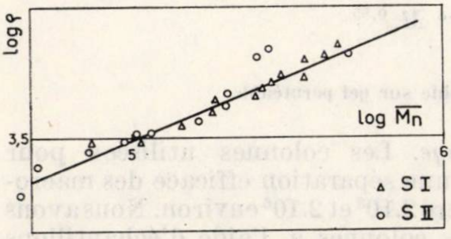

Fig. 3. — Polymérisation du diméthyl-2,4-styrène. Variations de log $\overline{\rho}$ (rayon de giration) avec log $\overline{M_w}$

Si nous considérons ensuite les deux polymères S II S III, nous constatons que pour S II = 0,96 et pour S III $\alpha = 0{,}6$. Ce qui correspond à des molécules plus branchées pour S III que pour S II. Cette constatation est confirmée par la figure 4 sur laquelle on a porté log $[\eta]$ en fonction de log $\overline{M_w}$ pour les deux polymères.

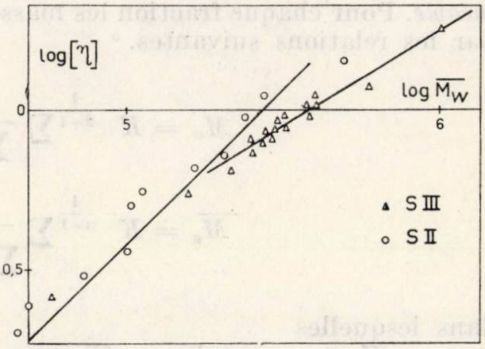

Fig. 4. — Polymérisation du diméthyl-2,4-styrène. Variations de log $[\eta]$ ($[\eta]$ en 100 ml. g^{-1}) avec log $\overline{M_w}$.
△ Echantillon SIII ; ○ Echantillon SI I

Les points représentatifs des fractions du polymère S IV sont alignés sur une droite située en dessous de la droite représentative des fractions du polymère S II. La viscosité intrinsèque d'une substance macromoléculaire de masse molaire donnée étant fonction de sa forme est maximum pour une molécule linéaire et est d'autant plus faible que les macromolécules sont plus branchées. Le graphique met donc en évidence l'apparition de macromolécules branchées pour le polymère SIII, et nous aboutissons à la même conclusion pour le polymère S IV.

D. INFLUENCE DES CONDITIONS D'AMORÇAGE

I. INFLUENCE DE LA CONCENTRATION DE L'AMORCEUR

Les polymères SI, SII, SIII ont été préparées dans ces conditions très voisines. Seule différait la concentration en dichloroéthylaluminium. En suivant l'évolution des propriétés des polymères obtenus nous pouvons en déduire deux types de comportement :

1) S_{II} a été préparé avec une concentration en amorceur double de celle employée pour S_I (0,1 au lieu de 0,05 mole. 1^{-1}). On constate que la linéarité des polymères obtenus est la même, seule varie leur masse molaire : Pour SI $\overline{M_w} = 340\,000$, $\overline{M_n} = 96\,000$, pour SII $\overline{M_w} = 190\,000$ $\overline{M_n} = 73\,000$

L'augmentation de la concentration en amorceur, en augmentant les sites actifs pour le même nombre de molécules monomères a provoqué une diminution de longueur des chaînes de polymère :

— de SII à SIII, la concentration en amorceur est multipliée par 5. Nous constatons deux phénomènes, d'une part une augmentation de la masse molaire : SIII $\overline{M_w} = 550000$

$$\overline{M_n} = 128000$$

d'autre part, une diminution de la linéarité des chaînes polymériques :

$$\alpha_{SII} = 0{,}96$$

$$\alpha_{SIII} = 0{,}6$$

Il semblerait donc que nous ayons en concurence deux types de réactions :

— d'une part, une réaction de propagation proprement dite où le carbocation polymère attaque une molécule monomère sur le site vinylique ce qui conduit à un allongement de la chaîne.

— d'autre part, des réactions de type Friédel et Crafts au cours desquelles le carbocation terminal réagit avec un des sites électrophiles du noyau benzénique d'une molécule de monomère ou de polymère, conduisant à la formation d'une chaîne latérale.

II. INFLUENCE DE LA NATURE DE L'AMORC EUR

Les polymères SII et SIV ont été préparées dans les mêmes con ditions de température et de concentration, seule la nature de l'amorceur diffère :

SII amorceur $C_2H_5AlCl_2$

SIV amorceur $TiCl_4$

Or on constate d'une part une augmentation très importante de la masse molaire dans le cas de SIV ($\overline{M_w} = 750\,000$, $\overline{M_n} = 178\,000$ au lieu de $\overline{M_w} = 190\,000$ et $\overline{M_n} = 73\,000$ pour SII), d'autre part une diminution considérable de la linéarité ($\alpha = 0{,}55$ au lieu de 0,96).

La longueur des chaînes obtenues est conditionnée par les valeurs relatives des constantes de propagation d'une part, de transfert et de terminaison d'autre part. Dans le cas du diméthyl-2,4-styrène la réaction de terminaison intramoléculaire est probablement essentiellement du type :

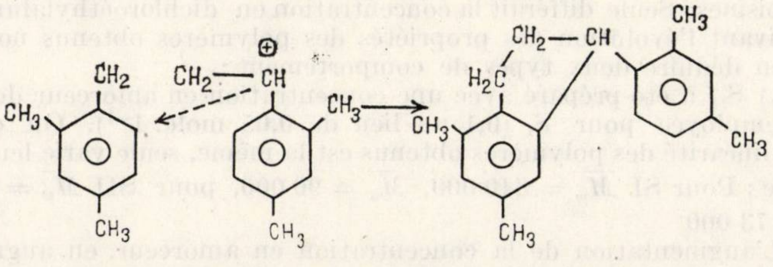

Cependant la superdélocalisabilité étant plus élevée sur le sommet 5 que sur le sommet 6, la réaction de terminaison aurait une contribution moins importante que la réaction intermoléculaire de transfert dont nous avons parlé précédemment et qui consiste essentiellement en une attaque électrophile du sommet 6.

Or, si la réaction de cyclisation intramoléculaire arrête la chaîne sans en augmenter la masse molaire, il n'en est pas de même pour la réaction intermoléculaire qui a, à la fois pour effet d'augmenter la masse molaire et le branchement. Le changement d'amorceur (c'est-à-dire de contre-ion) a donc eu pour effet essentiel de favoriser les réactions intermoléculaires de type Friedel et Crafts.

E. CONCLUSION

Toutes les mesures effectuées tendent à montrer que, selon les conditions de polymérisation, les chaînes de polymères peuvent être plus ou moins branchées, l'importance de branchement dépendant à la fois de la nature et de la concentration en amorceur.

Nous avons émis l'hypothèse que les branchements s'effectuaient par des réactions de Friedel et Crafts du type

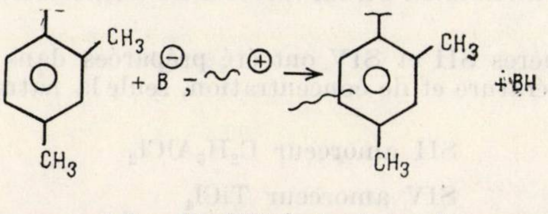

or les calculs de superdélocalisabilité, tant sur le monomère que sur le polymère montrent que ces réactions sont favorisées sur le sommet 5.

A fin de confirmer cette hypothèse nous avons entrepris de polymériser le triméthyl-2, 4, 5-styrène et de vérifier si l'importance des branchements est diminuée par la méthylation supplémentaire. D'autre part, afin de préciser quantitativement l'importance de la réaction de branchement nous avons entrepris de déterminer les constantes de transfert relatives à la polymérisation du diméthyl-2,4-styrène.

PARTIE EXPÉRIMENTALE

I. SYNTHÈSE ET POLYMÉRISATION

La synthèse est celle décrite par Anton. [1] La purification des réactifs et les polymérisations ont été menées comme dans nos derniers travaux. [2]

II. G.P.C. PRÉPARATIVES

Les fractionnements ont été effectués à l'aide d'un G. P. C. préparatif Waters chromatoprep 100, travaillant à température ambiante sur 3 colonnes de 120 cm, θ 5 cm garnies de Styragel B 3500 Å, 7, 5 · 10^4 Å et 5 · 10^5 Å avec un débit de benzène de 40 ml/mn. Nous avons opéré sur 4 à 5g de polymère dissous dans 500 cm^3 de benzène.

III. VISCOSITÉS INTRINSÈQUES

Elles sont mesurées en solution dans le benzène à l'aide de tubes de Ostwald.

IV. OSMOMÉTRIE

Nous avons utilisé un osmomètre à membrane Hewlett-Packard, travaillant à 37°. Les mesures sont effectuées dans le toluène sur quatre solutions C, $\frac{3c}{4}$, C/2, C/4, C variant de 1 à 2 pour cent.

V. DIFFUSION DE LA LUMIÈRE

a) *Mesure des incréments d'indice.* Nous avons utilisé le G. P. C. analytique démuni de ces colonnes que nous avons étalonné en injectant des mélanges benzène, tétrachlorure de carbone, d'indice donné, puis l'incrément d'indice a été déterminé en injectant des solutions de polymère en concentrations croissantes.

b) *Mesure des intensités diffusées.* Elles ont été effectuées sur un photogoniodiffusimètre SOFICA. Nous avons préparé 5 solutions du polymère dans le benzène de concentrations C, $\frac{4C}{5}$, $\frac{3C}{5}$, $\frac{2C}{5}$, C/5, C étant comprise entre 0,1 et 0,2 pour cent. Les solutions sont dépoussiérées par centrifugation à 15 000 t/mn pendant 2 heures.

c) *G.P.C. analytique.* Cette étude a été effectuée à l'aide d'un G. P. C. analytique Waters 501 travaillant à température ambiante. Nous avons opéré avec un jeu de 6 colonnes ayant une limite de perméabilité comprise entre 80 et 7 · 10^5 Å.

Les polymères à étudier sont dissous dans le benzène à des concentrations d'environ 0,4 pour cent. Le débit de benzène est de 60 ml/h. L'étalonnage a été effectué à l'aide de polystyrènes étalons commercialisés par Waters Associates.

Revue Roumaine de Chimie, **23**, *8*, 1337–1340 (1978)

COMPUTATION PROGRAM CONCERNING THE RESULTING COLOUR OF PIGMENT MIXTURES

CECILIA SAVII, T. P. TĂVALĂ, N. GR. BRÎNZAN and G. G. SAVII
Chemical Research Center, Timişoara, Bv. Mihai Viteazul 24, Romania

Received September 3, 1976

The computation of heteromorphic pigments colour, using a digital computer FELIX C 256, is performed. In order to obtain green tints, yellow pigments made from metallic sulphides — $(\mathrm{Zn}_{1-x}\,\mathrm{Cd}_x)\mathrm{S}$ — blue pigments with spinel structure — $\mathrm{CoO}\ [\mathrm{Cr}_{1-x}\mathrm{Al}_x]_2\mathrm{O}_3$ — and a white-grey pigment with rutile distorted crystal structure $\mathrm{Ti}_{1-3x}^{4+}\mathrm{Ca}_x^{2+}\mathrm{Sb}_{2x}^{5+}\mathrm{O}_2^{2-}$ taken in certain proportion were used. Based on the optical phenomena in the mass of the component pigments, the authors calculated the absorbance coefficients using the remission coefficients. A programme was written in FORTRAN IV language based on the least squares method for interpolating functions. The method is suited for generalization.

1. INTRODUCTION

The heteromorphic inorganic pigments are obtained by mixing up two or more pigments with a different colour and an analogous or different crystal structure.[1]

In order to obtain a desired colour, the relative amounts of the components can be computed from the spectrophotometric data or from the trichromatic colorimetric data, considering all optical phenomena occurring at the incidence of light on the layer of each pigment.[2] The data expressing the colour of each pigment are treated by means of a digital computer.

Franz Braun[3] indicated an analogical computing method of the mixture formula based on the formal linearization of the relation between the remission coefficient *R* and the absorption coefficient *K* of some powders. Some computation elements from the mentioned paper[3] were used in this paper in order to prepare a heteromorphic blueish- green pigment starting from three pigments : yellow, dark blue and white-grey, with different crystal structures.

Experimental spectrophotometric data of each pigment were treated by means of a numerical method for automatic computation.

---

[1] Iu. F. Petrov and V. P. Pîrkov, *Steklo i keramika*, **29**, 28 (1972).

[2] H. Weber, *Mitt. des Vereins Deutsche Email Fachleute*, **20**, 31 (1972).

[3] F. Braun, *Farbe und Lack*, **79**, 28 (1973).

2. EXPERIMENTAL

The colour of the heteromorphic pigment to be obtained was defined by the dominant wavelength — equal to 614 nm —and by the luminance—equal to 47.33—. These parameters involve a certain absorption coefficient K_d. The primary pigments were : a yellow pigment C_1, solid solution of zinc cadmium sulphide, $(Zn_{1-x}Cd_x)S$; a dark blue pigment C_2 with spinel structure, $CoO\,[Cr_{1-x}Al_x]_2O_3$; and a white-grey pigment C_3 with rutile distorted crystal structure, $Ti^{4+}_{1-3x}Ca^{2+}_{x}Sb^{5+}_{2x}O^{2-}_{2}$.

A reflection spectrum was determined for each primary pigment and also for the binary and the ternary mixtures, with reference to the white standard W. The white standard was a titanium dioxide powder of purity 99.00 %.

The reflection spectra were obtained by means of a UNICAM SP 800 spectrophotometer, adapted for micrometric powders.

The trichromatic coordinates were established using the MOMCOLOR Tristimulus colorimeter, Hungary, table 1.

Table 1

Principal spectral characteristics of the pigments

Symbol of the pigment	Chromaticity coordinates			Dominant wavelength	Luminance,
	x	y	z	λ_d, nm	Y
C_1	0.400	0.430	0.170	472.0	76.02
C_2	0.197	0.306	0.497	631.0	8.64
C_3	0.311	0.321	0.368	—	75.16
C	0.309	0.349	0.342	614.0	47.33

The powders were pressed in a special die at the $2.4 . 10^7\ N/m^2$ pressure, the obtained tablets had a plane and most diffusing surface.

The angular conditions of illumination and observation established by CIE in 1931 [4] were respected. The C illumination was used as radiation source.

The reflection spectra were used to determine the absorption coefficients K for the primary pigments, for three binary mixtures and a ternary mixture (Table 2).

Table 2

Experimental data

	nm	420	450	500	550	600	650	700	750
Absorbance	C_1	0.40	0.36	0.22	0.05	0.04	0.05	0.05	0.05
	C_2	0.46	0.46	0.45	0.60	0.62	0.61	0.38	0.16
	C_3	0.08	0.08	0.08	0.09	0.09	0.10	0.10	0.10
	C	0.26	0.25	0.23	0.25	0.25	0.25	0.14	0.09
	$C_1 + C_2$	0.44	0.40	0.32	0.39	0.39	0.38	0.23	0.13
	$C_1 + C_3$	0.32	0.28	0.19	0.09	0.10	0.11	0.11	0.11
	$C_2 + C_3$	0.26	0.26	0.26	0.33	0.33	0.32	0.19	0.16
	$C_1+C_2+C_3$	0.32	0.30	0.24	0.26	0.27	0.26	0.16	0.13

---

[4] W. D. WRIGHT, "The Measurement of Colour", Third Edition, HILGER& WATTS, LTD, London, 1964, p. 26.

The experimental data related to the absorption coefficients and the correction factors depending upon the particles size distribution in the powders mass were used to compute the absorption coefficients of the mixtures for eight wavelengths. The problem was solved by imposing the balanced quadrantal error between the absorption coefficients K_{am} of the experimentally obtained mixtures and the imposed absorption coefficients K_d of the desired pigment C, for eight wavelengths, to be minimal.

Therefore, a programme was developed and run on a FELIX C 256 digital computer.

3. RESULTS AND DISCUSSION

The theory which rules the tristimulus colorimetric system takes into account the influence exerted by the colour saturation on the linearity of the function $K = f(R)$ as well as that of the particle size distribution on optical phenomena.

The expression (1) given by Braun is used to find absorption coefficient of a ternary mixture.

$$K_{am} = X_1K_1 + X_2K_2 + X_3K_3 + \theta_1X_1X_2(K_1 + K_2) +$$
$$+ \theta_2X_1X_3(K_1+K_3) + \theta_3X_2X_3(K_2+K_3) + \theta_4X_1X_2X_3(K_1+K_2+K_3) \quad (1)$$

where :

— K_{am} is the absorption coefficient of the ternary mixture C ;

— K_1, K_2 and K_3 are the absorption coefficients of the three primary pigments, C_1, C_2 and C_3 ;

— X_1, X_2 and X_3 are the proportions of the three primary pigments, C_1, C_2, C_3, in the mixture C ;

— θ_1, θ_2, θ_3 and θ_4 are the correction factors depending on the particle size distribution.

When the proportion of the three primary pigments is expressed by a decimal fraction, their sum is unity :

$$X_1 + X_2 + X_3 = 1 \quad (2)$$

The absorption coefficients computed using the absorption spectra of the C_1, C_2, C_3 and C pigments, for certain wavelengths allowed to establish the interpolating functional relations :

$$K_i = f_i(\lambda) \quad (3)$$

where $i = 1, 2, 3$ for each primary pigment of the mixture, and :

$$\theta_j = \varphi_j(\lambda) \quad (4)$$

where $j = 1, 2, 3$ and 4.

The θ_j coefficients are calculated from the reflection spectra of all the binary mixtures and the ternary one, composed of equal proportions from each primary pigment.

Introducing equations (2) and (3) in the equation (1) one obtains :

$$K_{am} = F(X_1, X_2, \lambda) \quad (5)$$

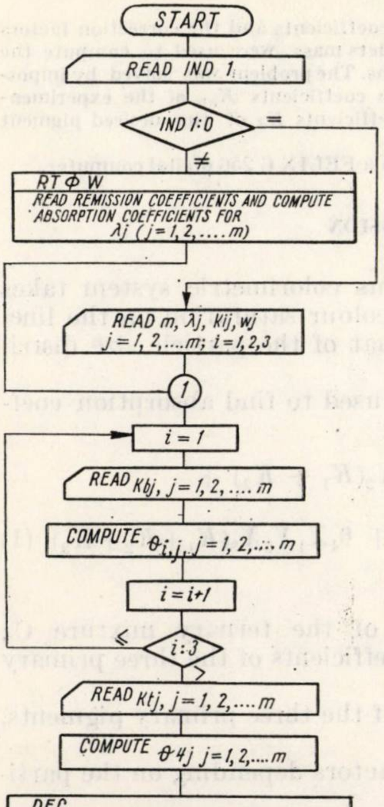
START
READ IND 1
IND 1:0
=
≠
RT Φ W
READ REMISSION COEFFICIENTS AND COMPUTE ABSORPTION COEFFICIENTS FOR λj (j = 1, 2, ... m)
READ m, λj, kij, wj
j = 1, 2,....m; i = 1, 2, 3
1
i = 1
READ Kbj, j = 1, 2, ... m
COMPUTE θi,j, j = 1, 2,.... m
i = i+1
i:3
<
>
READ Ktj, j = 1, 2,.... m
COMPUTE θ4j j = 1, 2,.... m
DEC
COMPUTE THE COEFFICIENTS Pli OF THE INTERPOLATING POLYNOMIAL:
Ki(λ) = Σ_{p=1}^{m-1} pl,i·λ^{l-1}, i = 1, 2, 3
DEC
COMPUTE THE COEFFICIENTS θli OF THE INTERPOLATING POLYNOMIAL:
θj(λ) = Σ_{l=1}^{m-1} θlj λ^{l-1}
READ n, λ d k, pK (Kd,k (k = 1, 2,...n)
GRADCON
MINIMIZE
φ(x1, x2) = Σ_{k=1}^{n} PK [Kam(x1, x2, λk) − Kd,k]^2
WRITE x1, x2, Kam, φ(x1, x2) FOR THE MINIMIZED FUNCTION
STOP

← Fig. 1. — Flow chart.

The condition for the balanced quadrantal error between the absorption coefficients K_{am} and the imposed absorption coefficients K_d, for eight wavelengths, to be minimal is expressed mathematically by the minimization of the function:

$$\Phi(X_1, X_2, \lambda) =$$

$$= \sum_{k=1}^{n} p_K [K_{am}(X_1, X_2, \lambda_K) - K_{d,K}]^2 \qquad (6)$$

Based on the above presented method the flow chart shown in Figure 1 was established.

The computation of the interpolating functions $K_i = f_i(\lambda)$ and $\theta_j = \varphi_j(\lambda)$ was carried out using Čebyšev polynomials. [5,6]

The conjugated gradients method [6] was used to minimize the function (6).

The results obtained, using a digital computer and the experimental data from table 2, as input data, are: $X_1 = 0.226$, $X_2 = 0.349$ and $X_3 = 0.425$.

4. CONCLUSIONS

The proposed method for computing a ternary mixture of pigments, in order to obtain a heteromorphic pigment with a desired colour, allows the study of more than one version in a short period and with great precision.

The use of the weighing factors p_K provides a greater malleability to the programme allowing the consideration of the importance and reliability of the pigments spectral characteristics for each wavelength.

The programme was run on a FELIX C 256 computer.

The method expressed by the above given example has a general character.

[5] B. Carnahan, H. A. Luther and J. O. Wilkes, "Applied Numerical Methods", J. Wiley & Sons Inc., New York, 1969.

[6] Ordinateur IRIS 50. SOUS-PROGRAMMES MATHEMATIQUES. Manual d'Utilisation, Paris, 1972.

Revue Roumaine de Chimie, **23**, *8*, 1341–1344 (1978)

FLASH PHOTOLYSIS STUDY OF TeO_3^{2-} ANION IN AQUEOUS SOLUTION

M. S. SUBHANI* and T. KAUSAR
Chemistry Department, University of Islamabad, Islamabad, Pakistan

Received April 28, 1976

Flash photolysis studies of TeO_3^{2-} anion in aqueous solution were carried out. Two transient species O_2^- and TeO_3^- with $\lambda_{max}=240$ nm and λ_{max} 355 nm were observed in oxygenated system. The rate constants for the second order decay of TeO_3^- and O_2^- radical anions were determined.

INTRODUCTION

Flash photolysis studies of simple inorganic anions have been the subject of various recent investigators [1-11].

In this paper the experimental results obtained on flash photolysis of TeO_3^{2-} anion in aqueous solution, are discussed. TeO_3^{2-} anion absorbs in the UV region and its spectrum has a long wavelength limit of 285 nm and the spectrum is classified as charge transfer to the solvent (C. tt. s) like to that of other similar anions. [12-14]

2. EXPERIMENTAL

All the chemicals used were of A. R. grade.
Sodium tellurite was prepared by the method described by Bagnall. [15]

---

* Present address : Department of Chemistry, University of Nigeria, Nsukka, Nigeria.

[1] M. S. Subhani and G. V. Buxton, *J. Chem. Soc. Trans.*, **68**, 958 (1972).

[2] M. S. Subhani and G. V. Buxton, *J. Chem Soc. Trans.*, **68**, 970 (1972).

[3] R. Sperling and A. Treinin, *J. Phys. Chem.*, **68**, 897 (1964).

[4] O. Amichai and A. Treinin, *J. Phys. Chem.*, **74**, 830 (1970).

[5] O. Amichai, G. Czapski and A. Treinin, *Israel J. Chem.*, **7**, 351 (1969).

[6] M. Danicls, E. V. Meyers and E. V. Belardo, *J. Phys. Chem.*, **72**, 389 (1968).

[7] G. Zimmerman, *J. Chem. Phys.*, **23**, 825 (1935).

[8] J. Barret, N. F. Fox and A. L. Mansell, *J. Phys. Chem.*, **69**, 2996 (1965).

[9] L. Farhas and F. S. Klein, *J. Chem. Phys.*, **16**, 866 (1948).

[10] A. Treinin and M. Yaacobi, *J. Phys. Chem.*, **68**, 2487 (1964).

[11] N. K. Bridge and M. S. Mathson, *J. Phys. Chem.* **64**, 1280 (1960).

[12] A. W. Albu and P. Goldfinger, *Z. Phys. Chem.*, **16B**, 388 (1932).

[13] K. Jablczynshi and H. Jablczynska, *Roczniki Chem.*, **10**, 579 (1930).

[14] A. D. Autrey and R. E. Connick, *J. Amer. Chem. Soc.*, **73**, 1842 (1951).

[15] K. W. Bagnall, "The Chemistry of Selenium, Tellurium and Polonium," Elsevier Publishing Co. Amsterdam, 1966, p. 74.

All solutions were prepared in triply distilled water just before photolysis. Solutions were deareated with the saturation of Ar gas and they were also saturated with N_2O and O_2 gas with the normal bubbling procedure.

The flash photolysis set up and the flash lamps used in the system were similar to those described elsewhere. [1]

RESULTS AND DISCUSSION

The flash photolysis of Ar saturated 10^{-2} M aqueous solution of sodium tellurite at natural pH gave rise to the formation of a transient species absorbing strongly in the wavelength region of 300 nm to 500 nm with $\lambda_{max} = 355$ nm as shown in Figure 1.

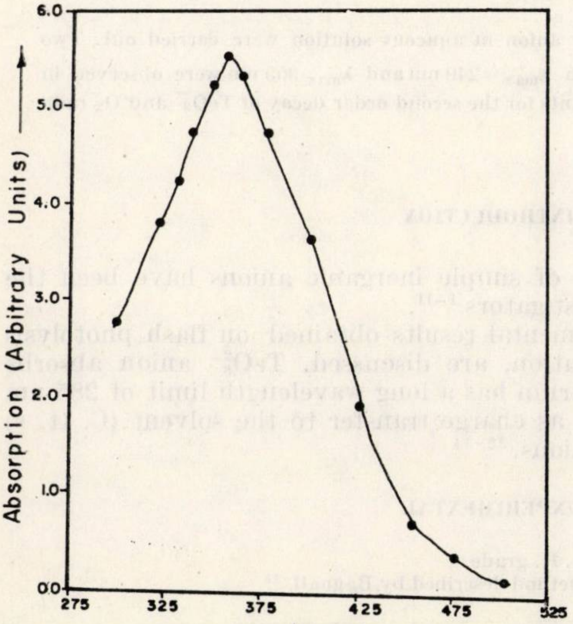

Fig. 1. — On flash photolysis of Ar saturated aqueous solution of TeO_3^{2-} at natural pH.

The species was found to decay by a second order process.

On flash photolysis of 10^{-2} M aqueous solution of TeO_3^{2-} anion saturated with N_2O at natural pH the same transient species was observed but the absorption was found to be increased twice to that of the observed one in the case of Ar saturated system.

On flash photolysis of oxygenated aqueous solution of TeO_3^{2-} anion at pH 5.5 two transient species were observed (Figure 2). One species has a maximum at about 240 nm and the other at 355 nm. The optical absorption spectra of both the species were recorded over the wave-length region 225–450 nm. The two species were found to decay by second order kinetics. The transient species absorbing in the far ultra violet region was identified as O_2^- radical anion. Its absorption spectrum, lifetime and decay are in agreement with the results of Czapski and Dorfman[16] and Adams et at.[17] The other transient with $\lambda_{max} = 335$ nm was observed in N_2O saturated or Ar saturated solution of TeO_3^{2-} was identified as TeO_3^- radical anion from its reported spectrum in the literature.[18] The flash photolysis results as mentioned above suggest that the transient species TeO_3^- radical anion is formed in the primary photo chemical process (2)

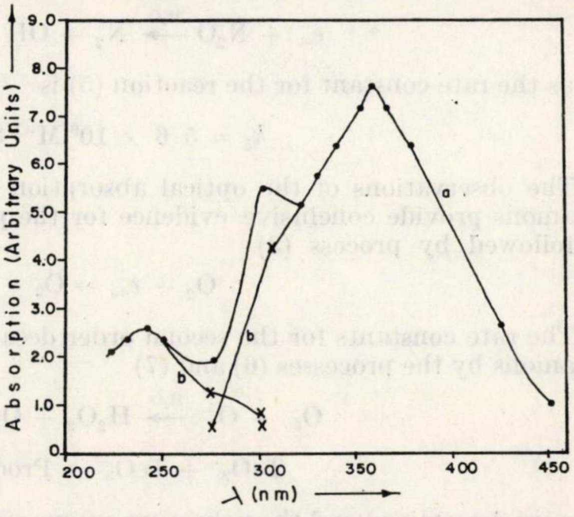

Fig. 2. — On flash photolysis of O_2 saturated TeO_3^{2-} aqueous solution at pH 5.5

● — (a) Complex spectra; × — (b) Resolved parts of the spectra.

$$TeO_3^{2-} + H_2O \xrightarrow{h\nu} TeO_3^{2-} + H_2^*O \tag{1}$$

$$TeO_3^{2-}\ H_2^* \longrightarrow TeO_3^- + e_{aq}^- \tag{2}$$

and the hydrated electron formed in reaction (2) reacts with O_2 present forming O_2^- radical anion by the process

$$O_2 + e_{aq}^- \rightarrow O_2^- \tag{3}$$

in oxygen saturated solution, thus giving rise to an absorbing spectrum with $\lambda_{max} = 240$ nm. As this species was not observed in the flash photolysis of Ar or N_2O saturated aqueous solution of TeO_3^{2-} anion it further confirms that the transient species is O_2^-. Its spectrum, kinetics and lifetime was in agreement with that reported in literature.[16,17]

The transient species TeO_3^- radical anion was also found in the flash photolysis of N_2O saturated solution of TeO_3^{2-} anion but its absorption was found to increase by a factor of two as compared to that of observed in Ar or O_2 saturated systems.

These results indicate that in N_2O saturated system TeO_3^- radical anion was also formed by reaction

$$OH + TeO_3^{2-} \rightarrow OH^- + TeO_3^- \tag{4}$$

---

[16] G. Czapski and L. M. Dorfman, *J. Phys. Chem.* **68**, 1169 (1964).

[17] G. E. Adams, J. W. Boag and B. D. Michael, *Proc. Roy. Soc.*, **A287**, 196, 321 (1965).

[18] G. E. Adams, J. W. Boag and B. D. Michael, *Trans. Faraday Soc.*, **61**, 1674 (1965).

suggested in the pulse radiolysis studies [18] in adition to the primary photolytic process (2).
The OH radicals participating in reaction (4) are produced by the reaction

$$e^-_{aq} + N_2O \xrightarrow{H_2O} N_2 + OH + OH^- \tag{5}$$

as the rate constant for the reaction (5) is

$$k_5 = 5 \cdot 6 \times 10^9 \, M^{-1} S^{-1}.^{19}$$

The observations of the optical absorption due to O_2^- and TeO_3^- radical anions provide conclusive evidence for the primary photolytic process (2) followed by process (3)

$$O_2 + e^-_{aq} \rightarrow O_2^- \tag{3}$$

The rate constants for the second order decay of the O_2^- and TeO_3^- radical anions by the processes (6) and (7)

$$O_2^- + O_2^- \xrightarrow{H_2O} H_2O_2 + O_2 + 2OH^- \tag{6}$$

$$TeO_3^- + TeO_3^- \rightarrow \text{Product} \tag{7}$$

were determined and the values are summerized in table 1.

The value for the extinction coefficient $\left(\varepsilon^{355\,\mathrm{nm}}_{\mathrm{Te\,O_3^-}}\right)$ was found to be in agreement with the reported value in literature. [18]

Table 1

(a) Rate constant for the 2nd order decay of O_2^- radical anion

	$(TeO_3^{2-}) = 2 \times 10^{-2}$ M		pH = 5.5
λ max (nm)	$2k/\varepsilon$ (Cm S^{-1})	ε (M^{-1} Cm^{-1})	k (M^{-1} S^{1-})
250	9.80×10^4	1030	4.95×10^7

b) Rate Constant for the 2nd order decay of TeO_3^- radical anion

	$(TeO_3^{2-}) = 2 \times 10^{-2}$M		pH = 5.5
λ max (nm)	$2k/\varepsilon$ (Cm S^{-1})	ε (M^{-1} Cm^{-1})	k (M^{-1} S^{-1})
355	4.2×10^5	3.5×10^3	7.3×10^8

---

[19] M. Anbar and P. Neta, *Internat. J. Appl. Radiation Isotopes*, **18**, 493 (1967).

Revue Roumanie de Chimie. **23**. *8*. 1345–1347 (1978)

LIQUID-LIQUID INTERFACES AS POTENTIOMETRIC ION-SENSORS. III[1]

THE n-OCTANOL-AQUEOUS SOLUTION INTERFACE IN THE ACID-BASE POTENTIOMETRIC TITRATION

MARIA MIOȘCU and MARIA GREBLĂ
Department of Analytical Chemistry, University of Cluj-Napoca,
Str. Arany János 11, Cluj-Napoca, Romania

Received August 2, 1976

The property of the n-octanol-aqueous solution interface to modify its electrical charge as a function of the composition of the aqueous solution, has been used to detect the equivalence point in a series of acid-base titrations. In order to check the accuracy, parallel titrations were also carried out with a glass electrode. Compared to previously investigated interfaces, better results have been obtained for some acids (H_2SO_4, H_2SeO_4, CH_3COOH), consisting in larger potential variations and shorter times required to attain the equilibrium.

In a series of previous papers the performances of liquid-liquid interfaces : n-butanol, [2] amyl alcohol, cyclohexanone, [1] cyclohexanol, [3] — aqueous solutions in the potentiometric acid-base titration have been studied.

In this context a study of the n-octanol-aqueous solution interface behaviour, in the acid-base potentiometric titration have been undertaken.

EXPERIMENTAL

The titrations were performed in a cell having the base area ~ 20 cm^2. An approximate 0.5 cm high octanol layer was applied over the solution to be titrated. The interface potential was overtaken with two calomel electrodes, the e.m.f. of the following cell being measured:

$$+ \text{ SCE} - \text{n-octanol/aqueous solution} - \text{SCE } (-)$$

Figure 1 shows the electrode function obtained during the titration of ~ 0.1 N HCl with 1 N KOH and of ~ 0.1 N KOH with 1 N HCl, the corresponding pH values being measured

---

[1] Part II : M. Mioșcu, M. Mureșan and E. Stejerean *Stud. Univ. Babeș-Bolyai Chem.* **2**, 5 (1973).

[2] C. Liteanu and M. Mioșcu, *Talanta*, **19**, 889 (1972).

[3] M. Mioșcu, I. Albu and M. Mureșan, *Chem. Analit.* **21**, 255 (1976).

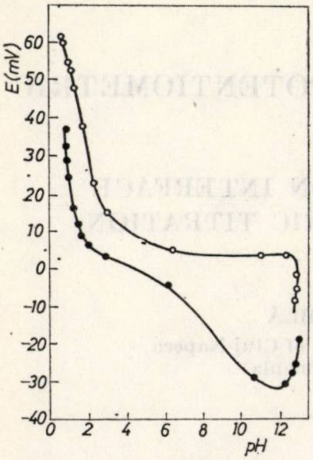

Fig .1. — Electrode functions : — ● — HCl ; —○— KOH

with a glass electrode. Between pH 4 — 12 very small potential changes are observed. The two rates of the curves differ following the equivalence point, influencing the shape of the titration curves too. The indication manner for such titration is based on the different loading of the interface before and after the equivalence point.

Figure 2 shows the titration curves for the following ~ 0.1 N strong acids : HCl, H_2SO_4 and HNO_3 with 1 N KOH. In all cases a clear potential change was noticed at the equivalence point. The titrations progressed well, the equilibria were rapidly established (less than 1 minute). We notice that in contrast with the response of other interfaces $^{1-3}$ in the presence of H_2SO_4, in this case the titration progresses very well, a higher potential change (≃ 100 mV) at the equivalence point being observed.

The weak acids titrations : H_2SeO_4, H_3PO_4, HCOOH and CH_3COOH in ~ 0.1 N concentration with 1 N KOH are shown in Figure 3. Similar to the H_2SO_4 titration, the H_2SeO_4 titration gives in the presence of this interface an unusually high potential jump. A different rate of the H_3PO_4 titration curve is observed resembling the classic potentiometric curves. The CH_3COOH titration curve progresses well, the equivalence point being well observed by a sudden potential variation. In contrast with the other studied interfaces, for which the CH_3COOH titration curve had a curious shape, for this interface the surface active action of CH_3COO^- ion is no more perceivable.

The titration curves of the ~ 0.1 N bases : KOH, $Ba(OH)_2$ and NH_4OH with 1 N HCl are shown in Figure 4. The titrations take place in good conditions, a clear potential jump being obtained at the equivalence point.

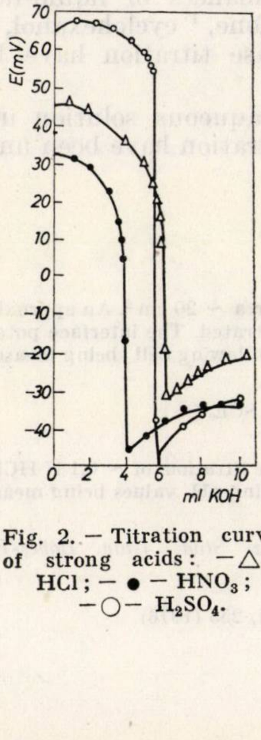

Fig. 2. — Titration curves of strong acids : —△— HCl ; — ● — HNO_3 ; —○— H_2SO_4.

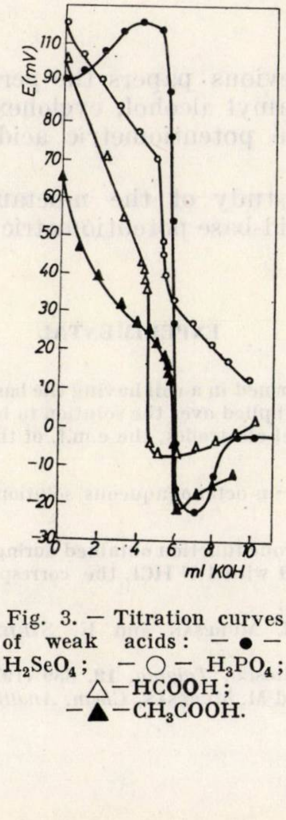

Fig. 3. — Titration curves of weak acids : — ● — H_2SeO_4 ; — ○ — H_3PO_4 ; △—HCOOH ; —▲—CH_3COOH.

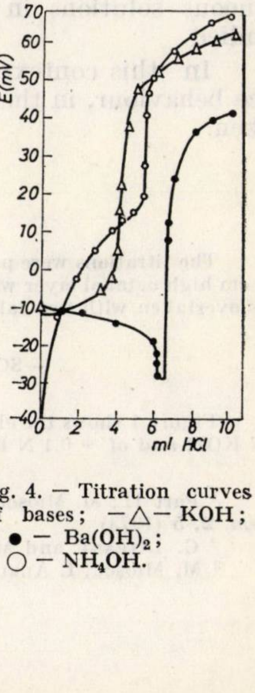

Fig. 4. — Titration curves of bases ; —△— KOH ; — ● — $Ba(OH)_2$; — ○ — NH_4OH.

RESULTS

In order to check the titrations accuracy, parallel titrations with glass electrodes have been performed, the equivalence volumes thus obtained being compared with the previous ones.

In the case of the acids titrations in the presence of the interface, the equivalence volumes have been graphically established at the cross-section of the two branches of the curve in the close proximity of the equivalence.

In the case of bases titrations the value of the equivalence has been given by the projection on the abscissa of the point which shows a clear potential rise. In the titrations with the glass-electrode the equivalence volumes have been established by calculation or by the Hahn-Weiler interpolation method. [4]

The results of all titrations are given in table 1.

Table 1

Results obtained for the titrations of acids and bases in the presence of n-octanol-aqueous solution interface

Titration	V_e(ml) interface	V_e (ml) glass elect.	Error %
HCl + KOH	6.10	6.12	−0.32
H_2SO_4 + KOH	5.50	5.55	−0.90
HNO_3 + KOH	3.95	3.91	+1.02
H_2SeO_4 + KOH	5.75	5.71	+0.70
H_3PO_4 + KOH	5.25	5.35	−1.80
HCOOH + KOH	4.55	4.54	+0.18
CH_3COOH+KOH	5.85	5.82	+0.51
KOH + HCl	4.05	4.01	+0.99
$Ba(OH)_2$ + HCl	6.55	6.52	+0.46
NH_4OH + HCl	5.64	5.64	—

The experimental results shown in this paper enable us to draw the conclusion that in potentiometric acid-base titrations the interface n-octanol-aqueous solution behaves similarly with other studied interfaces. An improvement concerning the magnitude of potential changes during the titration and the necessary time to attain equilibrium are observed. In some cases as in the titration of H_2SO_4, H_2SeO_4, CH_3COOH and KOH much better results have been obtained than in the similar titrations performed with other interfaces. The influence of the anion of the titrated acid upon the electric properties of the interface is lesser experienced in this case.

---

[4] L. F. Hahn and G. Weiler *Z,. analyt. Chem.*, **69**, 417 (1926).

Revue Roumaine de Chimie, 23, 8, 1349 (1978)

COMPTES RENDUS

STRUCTURE AND BONDING 28, Springer Verlag, Berlin, Heidelberg, New York, 1976, 131 p., 25 Figures and 15 Tables.

Under the title "Electrons in Oxygen- and Sulphur-containing Ligands", the 28th volume of Structure and Bonding includes three large chapters : the first one "Reversible Oxygenation" by R. W. Erkine and B. O. Field is concerned with the bonding modes of the dioxygen ligand in dioxygen complexes of type I, II(P), II(G), and the factors affecting their reversibility and stability. An historical survey illustrates the evolution of the corresponding ideas up to the present day, the older studies being restricted in a section, while more recent works, based on definitive structural data, are discussed in the other sections. By estimating the metal-dioxygen orbital overlap and the relative energies of the metal and dioxygen valence orbitals, an orientation criterion is required able to predict whether a II(P) or (II) G orientation is preferred. (II)G type complexes can lead to a reversible dioxygen adduct by an appropriate choice of ligand, while a reversible II(P) adduct can be isolated as long as bimolecular termination does not take place. Reversible type I dioxygen adducts are formed in solution, via bimolecular termination ; in aqueous media, they contain μ-hydroxo bridging in addition to the dioxygen bridging.

A special interest is accorded to the synthetic model of metal porphyrins, recently realized. For reversible oxygenation, in solution, at room temperature, it has been found necessary, the presence of sufficiently bulky substituents on the porphyrin ligand and an excess of the axial ligand, in order that the bimolecular termination could be prevented.

It is hoped that, based on the theoretical and experimental data presented in this work, the quantitative testable predictions, will progress significantly, in the near future.

In the second paper "Structural and Bonding Aspects in Phosphorous Chemistry-Inorganic Derivatives of Oxohalogeno Phosphoric Acids" by K. Dehnicke and A. F. Shihada, halophosphoric acids and phosphates of the type $[PO_3F]^{2-}$, $[PO_2F_2]^{2-}$, $[POSF_2]^-$, $[PO_2Cl_2]^-$, $[POSCl_2]^-$, $[PO_2Br_2]^-$ and $[PO_2FY]$ ($Y=Cl$, Br) are treated. One considers first free acids, especially in connection with the preparation methods and the properties of halophosphoric acids obtained in the last 10 years : HPO_3F, $HPO_2X_2(X=F, Cl)$ and $HPO_2FX(X=Cl, Br)$. Further, inorganic derivatives, mono- and difluorophosphates, difluoro- and dichloro-tiophosphates are discussed, paying much attention to dichloro and dibromo-phospahets, the most investigated of all hallophosphates.

A large part is accorded to structural investigations ; X-ray studies, vibrational and NMR spectroscopy and in some cases, Mössbauer spectra are mentioned as the main investigation methods for obtaining informations about structure and bonding in halophosphates. Crystal structures and stretching frequencies (cm^{-1}) of halophosphates as well as Mössbauer spectra of ^{119}tin and ^{57}iron halophosphates are listed in three comprehensive tables.

"Dithiocarbamates of transition group elements in Unsual Oxidation States" by J. Willemse, J. A. Cras, J. J. Steggerda and C. P. Keijzers is the 3rd and the last paper. After some short indications upon the oxidation state concept and the unsual oxidation state, the authors refer to the dithiocarbamato ligand, which can stabilise high oxidation states of the transition metals in its complexes. A review of dithiocarbamato complexes with transition metals from groups IV, V, VI, VII, VIII is presented, the oxidation states of each metal being indicated, as well as some characteristics of the respective complex. From the group I transition metal dithiocarbamato complexes, a large part is devoted to copper, which can have the oxidation state $+1, +2$, $+3$ in the different type complexes listed in table 2. An interesting phenomenon mentioned, is the occurrence of dithiocarbamates with copper in mixed oxidation states. Silver, gold and group II b metals, zinc, cadmium and mercury dithiocarbamatocomplexes are also considered. Interesting results are obtained from EPR studies about the Cu(II), Ag(II) and Au(II) dithiocarbamatocomplexes as well as from Mössbauer spectroscopy on Fe(III) complexes.

A comprehensive bibliography is given at the end of each chapter, the first one lists 282 references, the second 118 and the third 195 references. In addition an Authour-Index volume 1–28 is included.

This volume offers an occasion to know new areas in modern research of oxygen and sulphur containing ligands.

*C, **Mărculescu***

COMPTES RENDUS

STRUCTURE AND BONDING 28, Springer Verlag, Berlin, Heidelberg, New York 1976, 181 p., 25 Figures and 45 Tables.

Under the title "Electrons in Oxygen- and Sulphur-containing Ligands" the 28th volume of Structure and Bonding includes three large chapters; the first one "Reversible Oxygenation" by R. W. Erskine and B. O. Field is concerned with the bonding modes of the dioxygen ligand in dioxygen complexes of type I, II(P), II(G), and the factors affecting their reversibility and stability. An historical survey illustrates the evolution of the corresponding ideas up to the present day, the older studies being restricted in a section, while more recent works, based on definitive structural data, are discussed in the other sections. By estimating the metal-dioxygen orbital overlap and the relative energies of the metal and dioxygen valence orbitals, an orientation criterion is required able to predict whether a II(P) or II(G) orientation is preferred. II(G) type complexes can lead to a reversible dioxygen adduct by an appropriate choice of ligand, while a reversible II(P) adduct can be isolated as long as bimolecular termination does not take place. Reversible type I dioxygen adducts are formed in solution, via bimolecular termination; in aqueous media, they contain μ-hydroxo bridging in addition to the dioxygen bridging.

A special interest is accorded to the synthetic model of metal porphyrins, recently realized. For reversible oxygenation, in solution, at room temperature, it has been found necessary: the presence of sufficiently bulky substituents on the porphyrin ligand and an excess of the axial ligand, in order that the bimolecular termination could be prevented.

It is hoped that, based on the theoretical and experimental data presented in this work, the quantitative testable predictions will progress significantly in the near future.

In the second paper "Structural and Bonding Aspects in Phosphorus Chemistry-Inorganic Derivatives of Oxohalogeno Phosphoric Acids" by K. Dehnicke and A. F. Shihada, halophosphoric acids and phosphates of the type $[PO_2F_2]^-$, $[PO_2Cl_2]^-$, $[POSF_2]^-$, $[PO_2Cl_2]^-$, $[POSCl_2]^-$, $[PO_2Br_2]^-$ and $[PO_2XY]^-$ (Y=Cl, Br) are treated. One considers first free acids especially in connection with the preparation methods and the properties of halophosphoric acids obtained in the last 10 years: HPO_2F_2, HPO_2X_2 (X=F, Cl) and HPO_2FX (X=Cl, Br). Further inorganic derivatives, mono- and difluorophosphates, dichloro- and dichloro-thiophosphates are discussed, paying much attention to dichloro and dibromo phosphates, the most investigated of all halophosphates.

A large part is accorded to structural investigations: X-ray studies, vibrational and NMR spectroscopy, and in some cases, Mössbauer spectra are mentioned as the main investigation methods for obtaining informations about structure and bonding in halophosphates. Crystal structures and stretching frequencies of halophosphates as well as Mössbauer spectra of ^{119}Sn and ^{57}Fe from halophosphates are listed in three comprehensive tables.

"Dithiocarbamates of transition group elements in Unusual Oxidation States" by J. Willemse, J. A. Cras, J. J. Steggerda and C. P. Keijzers is the third and the last paper. After some short indications upon the oxidation state concept and the unusual oxidation state, the authors refer to the dithiocarbamate ligand, which can stabilise high oxidation states of the transition metals in its complexes. A review of dithiocarbamato complexes with transition metals from groups IV, V, VI, VII, VIII is presented, the oxidation states of each metal being indicated, as well as some characteristics of the respective complex. From the group I transition metal dithiocarbamato complexes, a large part is devoted to copper, which can have the oxidation state +1, +2, +3 in the different type complexes listed in table 2. An interesting phenomenon mentioned, is the occurrence of dithiocarbamates with copper in mixed oxidation states. Silver, gold and group II b metals, zinc, cadmium and mercury dithiocarbamatocomplexes are also considered. Interesting results are obtained from EPR studies about the Cu(II), Ag(II) and Au(II) dithiocarbamatocomplexes as well as from Mössbauer spectroscopy on Fe(III) complexes.

A comprehensive bibliography is given at the end of each chapter; the first one lists 282 references, the second 118 and the third 192 references. In addition an Author-Index volume 1—28 is included.

This volume offers an occasion to know new aspects of modern research of oxygen and sulphur containing ligands.

C. Mercorisu

NOTE POUR LES AUTEURS

La Revue Roumaine de Chimie publie des articles en anglais, français, russe, allemand ou espagnol. Les auteurs sont priés d'envoyer des articles et des comptes rendus inédits.

Les manuscrits seront dactylographiés à deux intervalles. La bibliographie, les tableaux et la légende des figures seront placés après le texte.

Si l'article fait partie d'une série numérotée, le titre de la partie précédente sera indiqué dans une note au bas de la première page.

Chaque article sera précédé d'un résumé comprenant quinze lignes au maximum.

Les références bibliographiques dans le texte seront faites par des exposants sans parenthèse et paraîtront comme des notes au bas de chaque page.

Les publications périodiques mentionnées dans la bibliographie seront présentées suivant les prescriptions internationales : le nom de l'auteur précédé de l'initiale du prénom, le titre de périodique abrégé conformément à Chemical Abstracts et souligné par une ligne, le numéro du tome, indiqué par des chiffres arabes et souligné par deux lignes, suivi de la première page de l'article ; à la fin, l'année de la parution sera placée entre parenthèses. Le numéro de la revue ne sera pas indiqué si les pages du volume sont numérotées consécutivement. Pour les revues dont les tomes ne sont pas numérotés (par ex. Bull. Soc. Chim. France, etc.), l'année de la parution soulignée par deux lignes précèdera l'indication de la page.

Les textes des livres inclueront : les noms des auteurs, les initiales du prénom, le titre du livre entre guillements et sans être souligné, le numéro du tome précédé par l'abréviation « vol. » (ou « Bd. »), le numéro de l'édition, les éditions (the publisher), la localité de la parution et la page de la référence précédée par l'abréviation « p. » (ou « S. »).

Les brevets seront indiqués comme suit : l'auteur ou la firme, le pays et le numéro du brevet, la data et la revue (Chem. Abstr.). Par ex. M. Jones (to Union Carbide co.), Brit. Pat. 601 238, 2 sept. 1959, Chem. Abstr., 54, 12808 (1960).

Si la référence n'a pas été lue en original, on indiquera aussi la revue de références consultée.

Les diagrammes seront tracés à l'encre de Chine sur papier calque. Les tableaux et les figures (en nombre strictement nécessaire) seront numérotés par des chiffres arabes et leur explication sera donnée dans la légende des figures. Prière de ne pas inscrire les mêmes données dans les tableaux et dans les figures. Chaque tableau aura un titre. On indiquera dans le texte la place approximative des tableaux et des figures. Les formules chimiques seront incluses dans le texte ; en outre, elles seront transcrites sur papier calque, à l'encre de Chine.

Les auteurs sont priés d'indiquer les caractères italiques (en soulignant les lettres au crayon), ainsi que tout autre caractère spécial ; les préfixes *ortho*, *meta*, *para*, *cis*, *trans*, etc. seront soulignés pour indiquer leurs caractères italiques et ne seront jamais écrits avec des majuscules.

Aucune correction à la main ne sera admise sur le manuscrit. Les corrections seront frappées à la machine. Les lettres grecques ou d'autres symboles spéciaux seront insérés à la main à l'encre clairement.

Le manuscrit sera signé par l'auteur.

Le colonne-titre aura 50 lettres au maximum.

L'entière responsabilité du contenu des articles appartient aux auteurs.

TRAVAUX PARUS AUX ÉDITIONS DE L'ACADÉMIE DE LA RÉPUBLIQUE SOCIALISTE DE ROUMANIE

I. ZUGRĂVESCU, MAGDA PETROVANU, **N-ylid Chemistry**, 1977, 396 p., 19 lei.

C. DRĂGULESCU, E. PETROVICI, **Chimie structurală modernă. Chimia coordinanţei 8** (La chimie structurale moderne. La chimie de la coordinence 8), 1977, 947 p., 70 lei.

I. G. MURGULESCU, **Introducere în Chimia fizică. Vol. I. 1. Atomi, molecule, legătură chimică** (Introduction à la Chimie physique, Ier vol. 1. Atomes, molécules, liaison chimique), 1976, 560 p., 36 lei.

E. P. BALTĂ, E. BALTĂ, **Introduction to the physical chemistry of the vitreous state**, coédition avec Abacus Press, 1976, 287 p., 31 lei.

H. I. GĂLĂŢEANU, **Radiochimia aplicată. Metode şi probleme** (La radiochimie appliquée. Méthodes et problèmes), 1976, 307 p., 19 lei.

CONST. V. UGLEA, **Cromatografia pe gel permeabil. Noi domenii de aplicare** (La chromatographie sur gel perméable. Nouveaux domaines d'application), 1976, 123 p., 6,75 lei.

FRANCISC A. GOTHARD, **Echilibre lichid-vapori. I. Baze teoretice şi metode de calcul** (Equilibres liquide-vapeurs. I. Bases théoriques et méthodes de calcul), 1975, 263 p., 2 pl., 28 lei.

CONST. GH. MARCOVICI, D. MARCOVICI, **Chimia oxizilor dubli şi utilizările lor** (La chimie des oxydes doubles et leur utilisation), 1975, 195 p., 13 lei.

M. AVRAM, **Antidăunători** (Pesticides), 1974, 496 p., 41 lei.

ELENA CEAUŞESCU, **Research work on synthesis and characterization of macromolecular compounds. Contributions**, 1974, 251 p., 20 lei.

DUMITRU COSTACHE, **Analiza chimică prin metoda cinetică** (L'Analyse chimique par la méthode cinétique), 1974, 251 p., 20 lei.

G. A. RĂDULESCU, **Proprietăţile ţiţeiurilor româneşti** (Les propriétés des pétroles roumains), 1974, 267 p., 2 pl., 18 lei.

CR. SIMIONESCU, VIORICA RUSAN, V. POPA, **Chimia algelor marine** (La chimie des algues marines), 1974, 212 p., 1 pl., 18 lei.

MARIA FITI, **Dozimetria chimică a radiaţiilor ionizante** (La dosimétrie chimique des radiations ionisantes), 1973, 240 p., 13,50 lei.

TIBERIU NĂSCUŢIU, **Metode radiochimice de analiză** (Méthodes radiochimiques d'analyse), 1973, 384 p., 23 lei.

CRISTOFOR SIMIONESCU, MARGARETA GRIGORAŞ, AGATA CERNĂTESCU-ASANDEI, GHEORGHE ROZMARIN, **Chimia lemnului în România. Plopul şi salcia** (La chimie du bois en Roumanie. Le peuplier et le saule), 1973, 299 p., 13 pl., 26 lei.

I. P. INFORMAŢIA c. 365

43426

Lei 25.—

F1103

ACADÉMIE DE LA RÉPUBLIQUE SOCIALISTE DE ROUMANIE

REFERÁLVA

REVUE ROUMAINE DE CHIMIE

TOME 23

N°s 9—10

Septembre—Octobre 1978

EDITURA ACADEMIEI REPUBLICII SOCIALISTE ROMÂNIA

Rev. Roumaine Chim.   RRCHAX, 23, *9—10*, p. 1351—1510 (1978). Bucarest

ACADÉMIE DE LA RÉPUBLIQUE SOCIALISTE DE ROUMANIE

COMITÉ DE RÉDACTION

Rédacteur en chef:

I. G. MURGULESCU, membre de l'Académie de la République Socialiste de Roumanie

Rédacteurs en chef adjoints:

A. T. BALABAN et V. EM. SAHINI, membres correspondants de l'Académie de la République Socialiste de Roumanie

Collège de rédaction:

EM. BRATU, ELENA CEAUŞESCU, ECATERINA CIORĂNESCU-NENITZESCU, CR. SIMIONESCU, membres de l'Académie de la République Socialiste de Roumanie; P. SPACU, membre correspondant de l'Académie de la République Socialiste de Roumanie; MARGARETA AVRAM, I. HAIDUC, D. I. MARCHIDAN, I. MOLDOVAN, G. NIAC et D. SĂNDULESCU

La Revue Roumaine de Chimie paraît 10 fois par an. Toute commande de l'étranger pour les travaux parus aux Editions de l'Académie de la République Socialiste de Roumanie sera adressée à ILEXIM-Departamentul Export-Import Carte (Livres)/Departamentul Export-Import Presă (Revues), P.O.B. 136—137 télex 11226, 3, str. 13 Decembrie, 70116 Bucarest, Roumanie

Les manuscrits, les livres et les revues proposés en échange, ainsi que toute correspondance seront envoyés à la rédaction:

REVUE ROUMAINE DE CHIMIE

125, Calea Victoriei, 71021 Bucarest, Roumanie, téléphone 50 76 80

EDITURA ACADEMIEI REPUBLICII SOCIALISTE ROMÂNIA

125, Calea Victoriei, 71021, Bucarest, Roumanie, téléphone 50 76 80

1978 DEC 1

ORSZÁGOS MŰSZAKI KÖNYVTÁR ÉS DOKUMENTÁCIÓS KÖZPONT

REVUE ROUMAINE DE CHIMIE

Tome 23, N°s 9–10 Septembre—Octobre 1978

LETIŢIA TOPOR and IVONA MOLDOVEANU, Thermodynamic properties of RbCl$-$CaCl$_2$ and CsCl$-$CaCl$_2$ molten systems 1353–1359

R D. CISMARU and MAGDALENA MOMIRLAN, On the aspect of oxides films formed on titanium in air at high temperatures 1361–1365

M. S. MASOUD, T. M. SALEM and F. M. ASHMAWY, Kinetics of oxidation of diethanolamine with hexacyanoferrate. III 1367–1372

R A. BANDI, Porous Z-two-phase electrodes. I. Raney-Ni-Ti-electrodes for anodic oxidation of methanol (in German) 1373–1376

S. P. JAIN and S. N. SRIVASTAVA, The stability of the solid stabilised emulsion with special reference to electrolytes 1377–1388

MARIA BREZEANU and MAGDALENA DINCULESCU, Polynuclear complex compounds of iron, cobalt and nickel. II. Bismuth – containing complex compounds 1389–1395

J. MARTIN GIL and F. J. MARTIN GIL, Synthesis and crystallographic data of complex uranyl sulphates : $UO_2(SO_4)_2K_2 . 2H_2O$ and $UO_2(SO_4)_3(NH_4)_4 . 4H_2O$ (in Spanish) 1397–1401

GH. MARCU, MARIANA RUSU and EUGENIA PERŢE, Thermal behavior of potassium bis-2-phospho-17-tungstouranate 1403–1408

J. R. MASAGUER, A. SOUSA-ALONSO, J. A. GARCÍA-VÁZQUEZ and A. BLANCO, Molecular charge-transfer complexes of iodine bromide with methylpyridines (in Spanish) 1409–1415

SILVIA PLOŞTINARU and P. SPACU, Fluorescence spectra of some Eu(III) and Tb(III) mixed ligand compounds 1417–1423

N. S. BIRADAR and B. R. PATIL, Titanium(IV) complexes with 2,2′-dihydroxychalkones 1425–1429

R B. R. ALEKSIĆ, A. TERLECKI-BARIČEVIĆ and M. AČIMOVIĆ, Electric conductivity of catalysts for the conversion of natural gas with water vapour 1431–1440

AURELIA GHENCIULESCU, L. ENESCU, HIRA LAL PRASAD, F. CHIRALEU, I. G. DINULESCU and MARGARET AVRAM, Chemistry of transition-metal organic compounds. I. On the reaction of ethyl diazoacetate with strained alkenes, catalyzed by π-allylpalladium chloride complexes 1441–1447

G. SURPĂŢEANU, M. CONSTANTINESCU and I. ZUGRĂVESCU, Experimental and theoretical study on the reaction of the loss of amido group from the pyridinium-cyano-amydo-methylide 1449–1453

Revue Roumaine Chim. 23, *9–10*, p. 1351–1510 (1978). Bucarest

P. SCHULZ and RADU VÎLCEANU, Kinetics and mechanism of the alkaline hydrolysis of hexamethoxy-cyclotriphosphazene and octamethoxy-cyclotetraphosphazene (in German) 1455–1459

C. LEONTE and EUGENIA CARP, The reaction of pyridinium-N-imine with picryl chloride, a route to 6-aza-benzo]a]indolizine system 1461–1463

A. M. EL-ABBADY, M. A. OMARA and M. TAHA MAHMOUD, Studies on the product obtained from Stobbe condensation between *o*-chlorobenzaldehyde and dimethyl homophthalate 1465–1469

F. URSEANU and C. DRĂGHICI, New cationic dye with dibenz [f, ij] isoquinoline [2,3-b] quinazoline-5,10-dione structure 1471–1474

R N. MOŞESCU, G. KALMUŢCHI, R. POPESCU and DEEA STEJARU, Separation and characterization of aromatic hydrocarbons from mineral oils by means of elution chromatography and of electronic absorption spectra (in French) 1475–1482

T. HODIŞAN, H. NAŞCU and VIORICA IANCU, Separation of acetic acid, salicylic acid, acetyl-salicylic acid and phenol by thin-layer chromatography on silica gel RG 1483–1487

R V. V. COŞOFREŢ, Some analytical applications of a new Ag^+-selective membrane electrode 1489–1498

MARIA ROMAN, CONSTANŢA PENCEA, DOINA CRISTU, I. MÎNZATU, A. CALBOREANU, O. SĂLĂGEAN, CRISTINA BRATU and GH. PETEU, Production of Iodine-123 for medical purposes 1499–1504

BOOK REVIEWS 1505–1509

Revue Roumaine de Chimie, **23**, *9–10*, 1353–1359 (1978)

THERMODYNAMIC PROPERTIES OF $RbCl-CaCl_2$ AND $CsCl-CaCl_2$ MOLTEN SYSTEMS

LETIŢIA TOPOR and IVONA MOLDOVEANU
Centre of Physical Chemistry, 31 str. Galaţi, Bucharest, Romania

Received June 9, 1976

The thermodynamic activities in molten $RbCl$-$CaCl_2$ and $CsCl$-$CaCl_2$ systems, as a composition function at 1373 K and 1423 K, have been determined from vapour pressure measurements. The partial molar free enthalpies and the excess partial molar free enthalpies have been deduced. Using the values obtained for the partial molar free enthalpies and the partial molar enthalpies from calorimetric measurements the partial molar entropies have been calculated. From the variation of these thermodynamic data as a composition function, the deviation from the ideal behaviour and the possibility of a local order has been deduced.

INTRODUCTION

Many thermodynamic studies concerning the charge-unsymmetrical fused salt systems have been accomplished in the last 15 years by different methods.

The studies concerning the charge unsymmetrical fused systems of alkaline earth halides and alkali halides are recent [1–11]. These systems have mainly been investigated by calorimetric and e.m.f. methods. Few experimental data exist for the charge unsymmetrical mixtures of alkaline earth halides with cesium or rubidium halides.

The enthalpy of mixing and the free enthalpy of mixing for the system $CaCl_2 + RbCl$, have been obtained by calorimetric [1], e.m.f. [2] and vapour pressure [6] measurements. For $CaCl_2 + CsCl$ system the enthalpy of mixing has been obtained by calorimetric[1] method and the free enthalpy from vapour pressure measurements[11].

---

[1] T. Østvold, *J. Phys. Chem.*, **76**, 1616 (1972).

[2] T. Østvold, *High Temp. Sci.*, **4**, 51(1972).

[3] J. J. Egan and J. Bracker, *J. Chem. Thermodynamics*, **6**, 9(1974).

[4] G. D. Robbins, T. Førland, T. Østvold, *Acta Chem. Scand.*, **22**, 3002 (1968).

[5] V. Ia. Deniscenko, A. G. Moracevski, *Zhur. priklad. Khim.*, **9**, 2110(1971).

[6] H. H. Emons, G. Bräutigam and D. Kögler, *Z. Chem. Heft.* **6**, 223 (1972).

[7] L. Topor and I. Moldoveanu, *Rev. Roumaine Chim.*, **21**, 495 (1976).

[8] T. Østvold "A Thermodynamic Study of Some Fused Salt Mixtures Containing Alkali and Alkaline Earth Chlorides, Bromides and Iodides" The Univ. of Trondheim, Norway, 1971.

[9] B. F. Markov and T. A. Tisura, *Ukrain. khim. Zhur.*, **39**, 757(1973).

[10] B. F. Markov, T. A. Tisura and A. N. Budarina, *Ukrain. khim. Zhur.*, **40**, 242 (1974); **38**, 823(1972).

[11] H. H. Emons and G. Bräutigam, *Rev. Roumaine Chim.*, **21**, 223 (1976).

We have determined the thermodynamic properties of $CaCl_2 + RbCl$ and $CaCl_2 + CsCl$ systems from vapour pressure measurements. The vapour pressure values obtained by Rodebush-Dixon method are given by the vapour pressure of molten alkali halides, those of the alkaline earth halide being negligible in these conditions.

EXPERIMENTAL

The quasi-static Rodebush-Dixon apparatus and the required procedure have been described previously.[12] The quartz cell was modified to permit the quantitative introduction of the weighted mixture. The new cell has been used first to study NaCl-$CaCl_2$ and KCl-$CaCl_2$ systems and has been described previously.[7]

The RbCl and CsCl Chemapol-Czechoslovakia and $CaCl_2$ analytical reagent grade Merck were used. RbCl and CsCl were dried 1–2 days at 373 K and them fused under a constant flow of HCl. $CaCl_2$ was dehydrated by fusing the salt in Ar stream and solidified by dropping the molten $CaCl_2$ in liquid CCl_4. All weighings of the samples and the filling of the cell were carried out in a drybox. The different compositions were obtained by the addition of a small quantity of RbCl or CsCl at the initial mixture. The small samples were taken out after measurements and the exact composition determined by potentiometrical titration of the total chlorine ions and complexometrical titration of calcium ions with complexon III.

The pressure values were measured with a mercury manometer using a Griffen & George Limited catethometer with a precision of 0.01 mm. The temperature was measured with Pt–PtRh thermocouple and maintained constant within ± 1° by a thermoregulator system.

RESULTS AND DISCUSSION

We have determined the vapour pressure of RbCl and CsCl in the molten mixture RbCl–$CaCl_2$ and CsCl–$CaCl_2$ at 1373 K and 1423 K. The activities of RbCl and CsCl in the mixture were calculated from the ratio of the vapour pressure of alkali halide in the molten mixtures and that of pure molten halides obtained previously.[13] The activity coefficients at different mole fractions have been calculated. The activity coefficients of molten $CaCl_2$ in mixture were obtained by graphical integration of Gibbs-Duhem equation. The partial molar free enthalpies of mixing ($\Delta\bar{G}_i$) and the excess partial molar free enthalpies ($\Delta\bar{G}_i^E$) were deduced from the equations :

$$\Delta\bar{G}_i = RT\ln a_i \tag{1}$$

$$\Delta\bar{G}_i^E = RT\ln\gamma_i \tag{2}$$

From these values the integral free enthalpies of mixing (ΔG) and the excess integral free enthalpies (ΔG^E) were calculated.

---

[12] I. G. Murgulescu and L. Topor, *Rev. Roumaine Chim.*, **11**, 1353 (1966).

[13] L. Topor, *J. Chem. Thermodynamics*, **4**, 739(1972).

The partial molar entropies of mixing were calculated from the partial molar enthalpies and the partial molar free enthalpies using the equation:

$$\Delta\bar{G}_i = \Delta\bar{H}_i - T\,\Delta\bar{S}_i$$

The partial molar enthalpies of mixing were calculated by derivation of the integral enthalpies of mixing equations determined by Østvold[1]. $\Delta\bar{H}_{\text{MeCl}}$ at 1100° and 1150° have been deduced by extrapolating the linear variation of $\Delta\bar{H}_{\text{MeCl}}$ vs. temperature from the range 810—894°.

The vapour pressure values of RbCl and CsCl in the mixture at 1373K, 1423 K and different molar fractions are presented in tables 1 and 2.

Table 1

Vapour pressures of RbCl (P_{RbCl}) in molten RbCl – CaCl$_2$ system at different mole fractions of RbCl (X_{RbCl})

X_{RbCl}	P_{RbCl} (mmHg)	
	$T = 1373$ K	$T = 1423$ K
0.13	1.89	3.06
0.19	2.98	5.28
0.27	5.54	8.90
0.32	7.47	13.48
0.40	10.83	20.23
0.48	14.99	27.57
0.57	21.77	37.76
0.67	33.03	56.16
0.76	46.76	76.27
0.85	59.72	96.68
1.00 *	78.37	122.80

* P^0_{RbCl}, vapour pressure of pure RbCl previously obtained.[13]

Table 2

Vapour pressures of CsCl (P_{CsCl}) in molten CsCl – CaCl$_2$ system at different mole fractions of CsCl (X_{CsCl})

X_{CsCl}	P_{CsCl} (mmHg)	
	$T = 1373$ K	$T = 1423$ K
0.12	2.20	4.79
0.21	5.80	11.17
0.30	10.10	19.53
0.40	18.18	32.31
0.50	29.97	51.41
0.57	41.77	69.80
0.70	72.26	116.80
0.81	98.57	159.32
1.00 *	123.90	194.90

* P^0_{CsCl}, vapour pressure of pure CsCl previously obtained.[13]

Figures 1–4 present the variation of the activities and the coefficients of activity vs. composition.

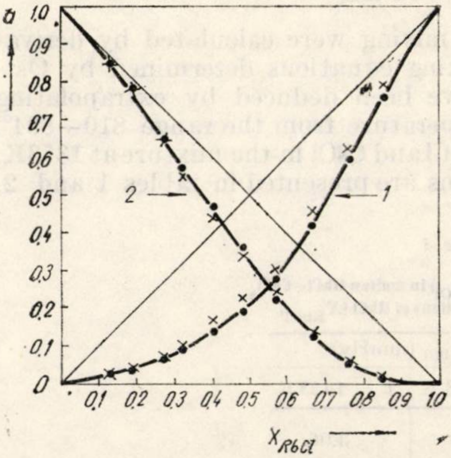

Fig. 1. — The activities of RbCl and $CaCl_2$ in molten RbCl-$CaCl_2$ system: 1 — a_{RbCl}; 2 — a_{CaCl_2}; ● —at 1373 K; X-at 1423 K.

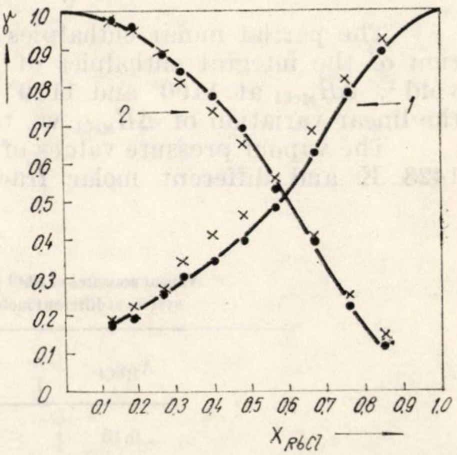

Fig. 2. — The activity coefficients of RbCl and $CaCl_2$ in molten RbCl—$CaCl_2$ system: 1 — γ_{RbCl}; 2—γ_{CaCl_2}; ●—at 1373 K; X—at 1423 K.

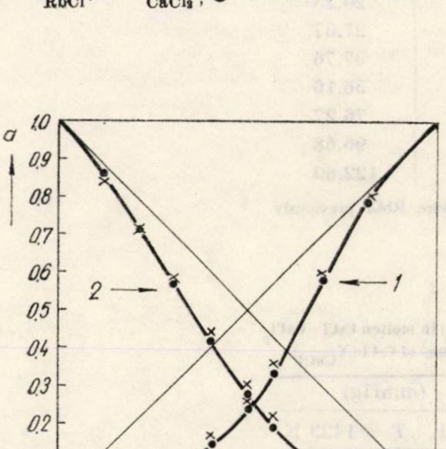

Fig. 3. — The activities of CsCl and $CaCl_2$ in molten CsCl-$CaCl_2$ system; 1—a_{CsCl}; 2—a_{CaCl_2}; ●—at 1373 K; X—at 1423 K.

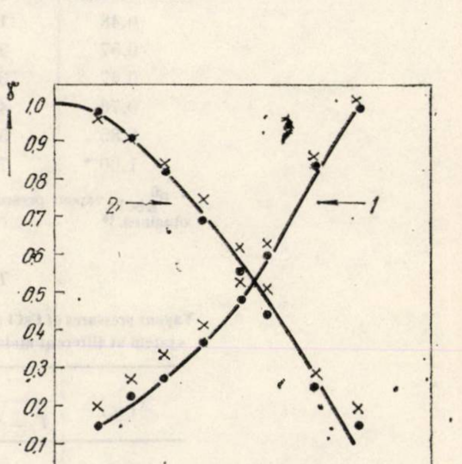

Fig. 4. — The activity coefficients of CsCl and $CaCl_2$ in molten CsCl—$CaCl_2$ system: 1—γ_{CsCl}; 2—γ_{CaCl_2}; ● — at 1373 K; X—at 1423 K.

The activities and the coefficients of activity show negative deviations from ideality for both systems.

The partial molar free enthalpies and the excess partial molar free enthalpies are negative and are presented in tables 3 and 4.

Table 3

The partial molar and excess partial molar free enthalpics of RbCl and $CaCl_2$ at different compositions

X_{RbCl}	$-\Delta \overline{G}$ (cal/mol)				$-\Delta \overline{G}^E$ (cal/mol)			
	$T = 1373$ K		$T = 1423$ K		$T = 1373$ K		$T = 1423$ K	
	RbCl	$CaCl_2$	RbCl	$CaCl_2$	RbCl	$CaCl_2$	RbCl	$CaCl_2$
0.13	10152.5	449.3	10431.2	465.6	4586.8	69.0	4667.4	65.68
0.19	8910.1	687.1	8889.9	760.9	4379.7	111.7	4203.0	154.78
0.27	7222.3	1182.1	7407.2	1222.6	3655.0	323.3	3713.3	331.0
0.32	6406.5	1526.6	6243.1	1658.3	3301.1	474.0	3023.3	568.4
0.40	5392.0	2098.3	5094.0	2302.1	2898.3	701.5	2509.3	866.2
0.48	4508.4	2791.6	4220.6	3063.0	2508.6	1010.9	2146.0	1211.5
0.57	3491.3	3993.2	3331.6	4051.5	1959.6	1610.7	1744.2	1665.5
0.67	2354.9	5565.7	2209.8	5683.8	1263.7	2543.8	1078.9	2547.9
0.76	1407.42	7989.0	1344.9	7914.4	659.5	4100.5	570.3	3884.1
0.85	740.4	11201.0	675.0	10753.8	298.0	6026.1	216.5	5400.9

Table 4

The partial molar and excess partial molar free enthalpies of CsCl and $CaCl_2$ at different compositions

^{x}CsCl	$-\Delta\overline{G}$ (cal/mol)				$-\Delta\overline{G}$ (cal/mol)			
	$T = 1373$ K		$T = 1423$ K		$T = 1373$ K		$T = 1423$ K	
	$CsCl_2$	$CaCl_2$	CsCl	$CaCl_2$	CsCl	$CaCl_2$	$CsCl_2$	$CaCl_2$
0.12	10947.5	874.1	10533.9	922.1	5169.7	74.7	4545.1	102.7
0.21	8332.2	1209.7	8090.7	1249.3	4090.5	270.4	3683.4	276.4
0.30	6848.5	1670.9	6503.2	1684.9	3567.9	536.5	3103.3	498.1
0.40	5224.9	2402.6	5071.9	2324.2	2727.6	991.4	2483.6	832.4
0.50	3866.5	3319.3	3764.7	3203.5	1977.2	1612.6	1803.8	1372.2
0.57	2964.2	4039.0	2901.2	3933.1	1432.3	2202.4	1313.5	1911.9
0.70	1470.2	5268.9	1442.7	5337.8	498.6	3739.7	435.5	3537.7
0.81	625.1	5881.9	569.5	5963.5	50.9	5208.0	−25.3	4570.5

The excess free enthalpies are negative and are presented in Figure 5 (for 1423 K) together with those of $NaCl + CaCl_2$,$KCl + CaCl_2$ systems obtained previously [7].

In Figure 6 are presented the excess free enthalpies obtained previously from e.m.f. measurements for $CaCl_2 + NaCl$ at 1098 K, $CaCl_2 + KCl$ at 1058 K systems [3] and vapour pressure measurements for $CaCl_2 + RbCl$ at 1173 K[6], $CaCl_2 + CsCl$ at 1243 K [11] systems.

The partial molar entropies and the integral entropies of RbCl and CsCl vs. composition are presented in Figures 7—10.

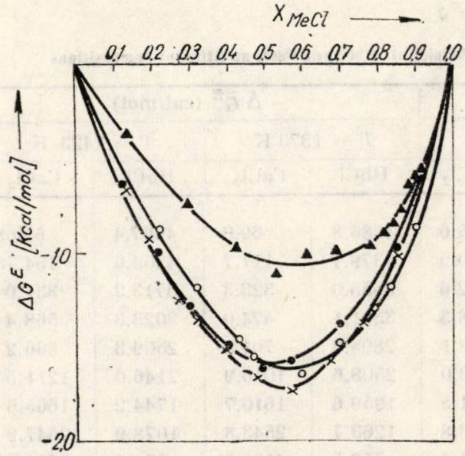

Fig. 5. — The excess free enthalpies for molten $CaCl_2-MeCl$ (Me — Na, K, Rb, Cs) systems at 1423 K:

▲ — $NaCl-CaCl_2$ system[7]; 0 — $KCl-CaCl_2$ system[7] X — $RbCl-CaCl_2$ system; ● $CsCl-CaCl_2$ system.

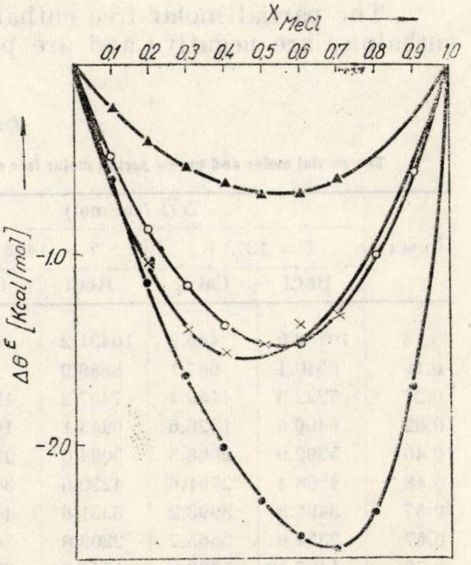

Fig. 6. — The excess free enthalpies for molten $CaCl_2-MeCl$ (Me = Na, CsK, Rb) systems obtained by other authors;

▲ $NaCl-CaCl_2$ system[3]; O—$KCl-CaCl_2$ system[3]; X—$RbCl-CaCl_2$ system[6] at 1173 K; ● $CsCl-CaCl_2$ system[11] at 1243 K.

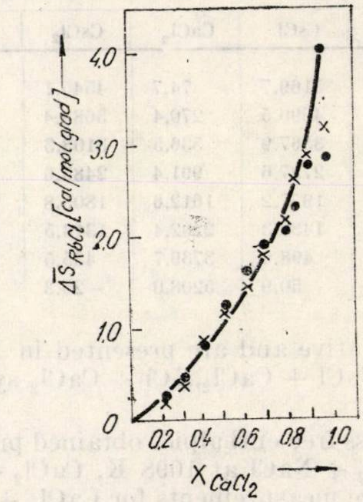

Fig. 7. — The partial molar entropy of RbCl in molten $RbCl-CaCl_2$ system; 0 at 1373 K; X — at 1423 K.

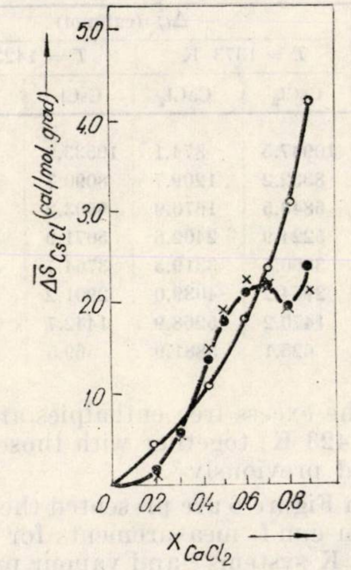

Fig. 8. — The partial molar entropy of CsCl in molten $CsCl-CaCl_2$ system; 0 — at 1373 K; X — 1423 K.

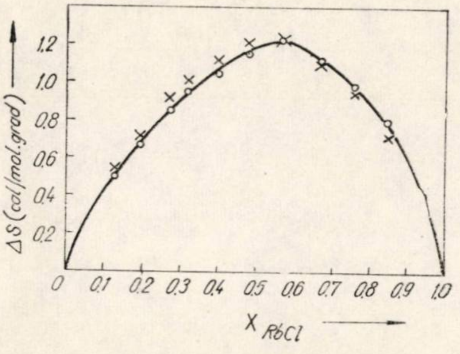

Fig. 9. — The integral entropies for molten RbCl—CaCl$_2$ system ;
0 — at 1373 K ; X — at 1423 K.

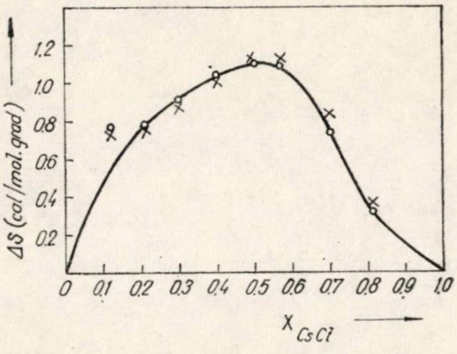

Fig. 10. — The integral entropies for molten CsCl—CaCl$_2$ system ;
0 — at 1373 K ; X — at 1423 K.

The excess free enthalpy values for $CaCl_2$ — MeCl (Me = Na, K, Rb, Cs) systems at lower temperatures (Figure 6) decrease from Na to Cs. At higher temperatures the excess free enthalpy values (Figure 5) for $CaCl_2$ — MeCl (Me = K, Rb, Cs) are not very different among them. With the increase of temperature, these systems show a tendency towards randomization. This tendency can be observed in the variation of the interaction parameter too [8].

In the $CaCl_2$ — MeCl (Me = Na, K, Rb, Cs) systems the tendency for association between the anions and the divalent cation is much weaker than in the other charge unsymmetrical mixtures ($MgCl_2$ — MeCl ; $NiCl_2$ — — MeCl ; $CoCl_2$ — MeCl, $FeCl_2$—MeCl, $CdCl_2$—MeCl ; $MnCl_2$—MeCl, Me — —alkaline ion) where the calorimetric determinations indicate a predominance of the $MeCl_4^{2-}$ species. [14,15] Although the polarizing strength of calcium ion is smaller, the negative deviations of thermodynamic properties in unsymmetrical mixtures involving Ca^{2+} can be explaind by a higher configurational order which decreases with the increase of the temperature. This local order may be due to the preferential association of Cl^- with the Ca^{2+} having higher charge densities than the alkali ions.

Other properties of $CaCl_2$ — MeCl (Me = Na, K, Rb, Cs) systems indicate the deviations from ideality : excess volums [16] ; excess electric conductibilities ; [17] the minimum of the interaction parameters vs. composition at $X_{CaCl_2} = 0.3$ for $CaCl_2$ — MeCl (Me = Rb, Cs) systems [1]. The enthalpies of formation of $MeCaX_3$ complex in $CaCl_2$ — MeCl (Me = K, Rb, Cs) mixtures have been obtained recently from calorimetric studies. [10] The values decrease from Cs to K (ΔH_{form} $CsCaCl_3 > \Delta H_{form}$ $RbCaCl_3 >$ $> \Delta H_{form}$ $KaCaCl_3$) the most stable complex being $CsCaCl_3$.

---

[14] G. N. PAPATHEODOROU, O. J. KLEPPA, *J. Inorg. Nuclear Chem.*, **33**, 1249 (1971); **32**, 889 (1970).

[15] O. J. KLEPPA, F. G. MCCARTY, *J. Phys. Chem.*, **70**, 1249 (1966).

[16] H. H. EMONS, *Chem. Zvesti*, **28**, 447 (1974).

[17] H. H. EMONS, G. BRÄUTIGAM and H. VOGT, *Z. anorg. Chem.*, **394**, 263 (1972).

Revue Roumaine de Chimie, **23**, *9–10*, 1361–1365 (1978)

ON THE ASPECT OF OXIDES FILMS FORMED ON TITANIUM IN AIR AT HIGH TEMPERATURES

D. CISMARU and MAGDALENA MOMIRLAN

Research Institute for Chemistry — Center of Physical Chemistry, Spl. Independenţei 202, Bucharest, Romania

Received November 8, 1977

Titanium oxide films obtained by the oxidation of titanium of a certain chemical composition in air at different temperatures ranging from 300° to 1 250°, at various time intervals — between one and seventeen hours — were studied. The colours of the oxide layers changed as temperature rose and oxidation time was longer. Tests were carried on to establish the temperature at which the oxide layer became independent of the metal holder. Titanium samples were kept in the reaction chamber for six hours under the conditions of gradual temperature growth from 700° to 900°. Some features of the titanium oxide layers formed at 1000° were studied. The titanium oxide films obtained at various temperatures were analysed with the scanning microscope.

INTRODUCTION

Titanium oxidation in air was studied by numerous researchers[1-10]. The studies carried at high temperatures have proved the change of the features of the oxide layer with variations in temperature and reaction time. In order to obtain accurate results constant temperature must be maintained in the reaction chamber and identical specimens should be used, both from the point of view of chemical composition and the preparation of the surface.

The observations on the changes in colour, on the thickness of the oxide layer and other properties, as well as the studies with the electronic microscope carried out on oxide films independent of the metal stand were a real help in interpreting the kinetic mechanism of titanium oxidation.

---

[1] C. Wagner, *Z. phys. Chem. (Frankfurt)*, **40B**, 455 (1938).

[2] M. D. Earle, *Phys. Rev.*, **61**, 56 (1942).

[3] P. Ehrlich, *Angew. Chem.*, **59A**, 163 (1947).

[4] M. H. Davies and C. E. Birchenall, *J. Metals*, **1951**, 877.

[5] J. T. Waber, *J. Chem. Phys.*, **20**, 734 (1952).

[6] V. L. Stout and M. D. Gibbsons, *J. Appl. Phys.*, **26**, 1488 (1955).

[7] J. P. Pemsler, *J. Electrochem.*, **105**, 315 (1958).

[8] G. Béranger, C. Marion and P. Lacombe, *J. Mat. Nucl.*, **20**, 337 (1966).

[9] B. Pieraggi and F. Dabosi, *J. Mat. Nucl.*, **54**, 224 (1974).

[10] P. Cremery and J. Bardolle, *Compt. rend.*, **282**, 627(1976).

EXPERIMENTAL

Titanium oxides obtained at different temperatures and oxidation time have been examined as regards colour and layer thickness.

The surfaces and oxide layers were examined by eyesight and with the optical and electronic microscope.

The specimens examined came from metallic titanium with the following chemical composition : 0.20 p.c. Fe ; 0.10 p.c. Si ; 0.10 p.c. Al ; 0.01 p.c. Ni ; 0.01 p.c. Cu ; 0.005 p.c. V ; 0.02 p.c. C ; 0.05 p.c. N_2 ; 0.19 p.c. O_2 ; oxidation has taken place in air, at constant temperatures of 300°, 550°, 850°, 1 000°, and 1 250°.

The surfaces of the metal specimens of titanium oxide formed at various temperatures were analysed by means of Jeol JSM 50 A – type scanning electronic microscope. Its resolution power was 100 Å, the acceleration voltage was 25 kV and the inclination anglef 45°.

The microstructures of the oxides have been photographed and the dimensions and shape of the particles have been examined.

RESULTS AND DISCUSSIONS

One may notice that if the reaction temperature is higher and the oxidation time is longer the outer aspect of the oxide film is altered, as well as its features.

At different reaction time the colour of the oxide layer changes from yellow at 300° to blue at 500°, violet at 550°, white at 850°, greyish-white at 900°, bright pink at 1000° and at 1 250° (Table 1).

The change in colour of the oxide layers, when the oxidation takes place at different temperatures is noticed. At very high temperatures (1000°) holes occur in the oxide layer, accelerating oxidation [11].

Our studies by means of the electronic microscope make us believe that the oxide formed is generally rutile, though the colour differs with temperature, but rutile can alter its colour with the growth in oxygen contents and with small quantities of other oxides [12-14].

The oxygen deficient structure may with Schottky symbols be expressed as :

$$\mathrm{Null} \rightleftharpoons 0_{\square}^{\cdot\cdot} + 2\theta + \frac{1}{2}\,\mathrm{O}_2$$

where "Null" designates a structure without defects, the squares are ion vacancies, the dots are positive excess charges, and θ are free electrons.

TiO_2 is an *n*-type conductor with decreasing oxygen content and the electrons can be captured according to one or both of the following equations:

---

[11] J. Bénard, "Oxydation des Métaux", Gauthier-Villard Editeur, Paris, 1964, p. 231.

[12] H. J. Engell and K. Hauffe, *Metall*, **6**, 285 (1952).

[13] R. C. DeVries and R. Roy, *Bull. Ceram.*, **33**, 370(1954).

[14] W. A. Weyl and T. Förland, *Ind. Eng. Chem.*, **42**, 257(1950).

$$O_{\square}^{\cdot\cdot} + \theta \rightleftharpoons O_{\square}. \text{ (blue F centre)}$$

$$Ti^{4+} + \theta \rightleftharpoons Ti^{3+}$$

When the oxygen content decreases the blue colour is more intensive, this usually meaning that the process of conduction electrons capture is taking place.

As regards adherence to the metal holder, it was seen that a transition point occurs at 800°. Up to 800° the oxide adheres to the metal holder and the layer formed is very thin. The granules of the oxide layer are homogenous in thickness in all crossections. Over 800° the layer has the aspect of a powdery film, compact white, which comes loose of the metal holder if only hit or even by itself when taken out of the furnace. Between 800° and 900° these properties are maintained, the film becoming darker — from white to yellowish and slightly grey.

The fact that the film comes loose at temperatures above 800° is explained by the appearance of a TiO layer which is partly independent and has the aspect of a fine powder. The TiO layer is formed between the metal and the TiO_2 layer, as a result of the decomposition of TiO_2 into TiO when the oxide layer cools. The preferential deposit of TiO leads to the destruction of the initial protective compact layer. As the TiO and Ti phases are mutually soluble, the thin TiO layer is less adherent to the metal, the formation of TiO being the cause of the oxide layer coming loose at over 800°.

At 1000° the inside layer is powdery and yellow, the outer one being compact and bright pink. Little violet stars implanted in the pink film can be noticed by means of binocular microscope. The oxide layer formed at 1000—1100° has a structure different from the other layers formed at other temperatures. The layer is ash-like on the outer side and easy to break. At 1000° the thickness of the oxide layer is not uniformous. At 1000° the thickness of the oxide layer is nevertheless greater than that of the layer formed at 800° and it keeps getting greater with oxidation time. (Table 1).

The oxide film deposited on metallic titanium consists of a number of parallel layers which cover one another like yellow tiles on the inside and pink-orange ones on the outside. The oxide layers are easy to break. The layers of oxide formed give the impression that the metal holder expanded into a number of parallel, breakable layers. This feature can be noticed at temperatures above 1000° too.

The observation continued at 1250°, when on a cross-section the layered oxide was perfectly noticeable, like a belt consisting of rows of tiles. Oxides formed at temperatures above 1100° have sections of variable thickness. The impurities in titanium have a bearing upon the mechanical properties of the oxide layer. Mg, Fe and Al have the tendency to

Table 1

Some properties (colour, thickness, aspect) of titanium oxide films, obtained at different temperatures

Oxidation temperature (°C)	Oxidation time (h)	Colour of exterior oxide film	Thickness of oxide film (mm)	Oxide aspect
300	17	golden-yellow	—	Not uniformously distributed on the metal holder
300—500	17	bright blue	—	Uniformously distributed, bright
550	12	violet	—	Mat, adherent to the metal holder
850	4	white	0.039	Powdery, partially adherent, coming off the metal holder here and there. Aspect of fine compact powder
700—900	6	white-slightly grey	0.063	Compact powder. It comes off the metal holder completely
1000	1	light yellow	0.069	Compact powder. It comes off the metal holder completely
	4	yellow-bright pink	0.310	Multi-layered. Parallel breakable layers
1250	17	bright pink	0.460	Parallel breakable layers

make the defect structure of TiO_2 grow, this leading to synterization, which can lessen the porosity of the oxide layers. The photographs taken by means of the scanning electronic microscope show the possibility of the appearance of a synterization effect at this temperature (1000°).

At 1250° the oxide is bright pink-orange on the exterior while on the interior, in cross-section, one can notice the adherence to the metal holder, like a row of parallel tiles, more intimately sticking one another than at 1000°.

Figures 1—6 show images of the surface of the oxided titanium at various temperatures.

When samples are kept at 1000° oxidation temperature for 1 h some crystals begin to take an elongated shape with multiple crystalline faces, showing a pronounced individualization. The size of the particles was determined when the samples were like that. The diagram of the particles distribution is shown in Figure 7.

The result of the analyses carried out by means of the scanning electronic microscope offered the possibility to draw some conclusions on the mechanism of titanium oxidation at various temperatures.

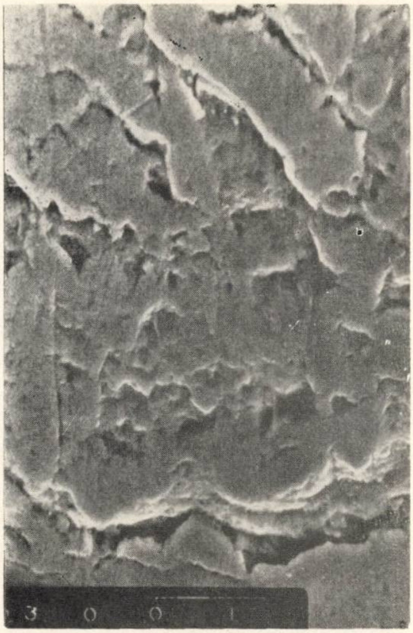

Fig. 1. — Surface of oxided titanium in air, for 17 hrs, at 300°. (× 1 000)

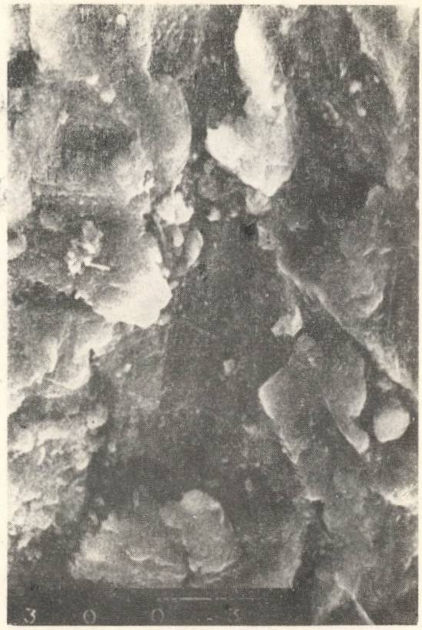

Fig. 2. — Surface of oxided titanium in air, for 12 hrs, at 550°. (× 3 000)

Fig. 3. — Surface of oxided titanium in air, for 4 hrs, at 850°. (× 3 000)

Fig. 4. — Surface of oxided titanium in air, for 1 h, at 1 000°. (× 3 000)

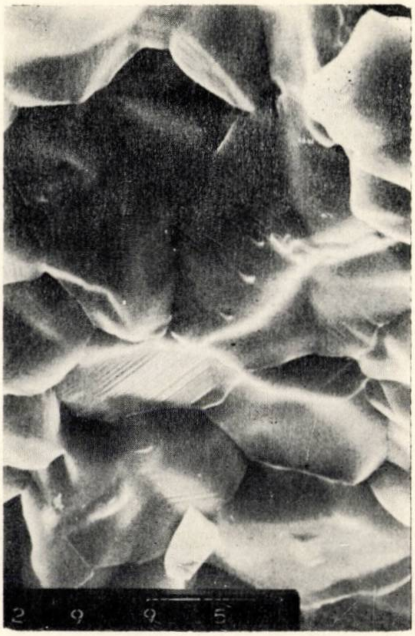

Fig. 5. — Surface of oxided titanium in air, for 4 hrs, at 1 000°. (× 3 000)

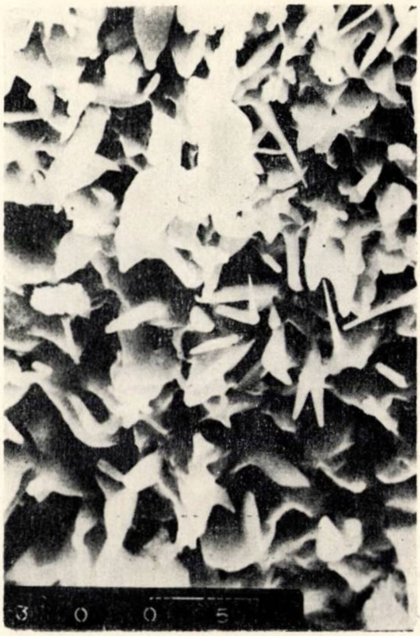

Fig. 6. — Surface of oxided titanium in air, for 17 hrs, at 1 250°. (× 3 000)

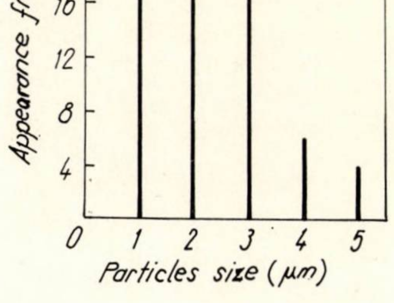

Fig. 7. — The particles distribution of surface of oxided titanium, for 1 h, at 1 000°.

CONCLUSIONS

As a result of the oxidation in air, at high temperatures, of titanium of a certain chemical composition, oxides are formed on its surface, which differ in form, structure and colour, depending on the oxidation time and temperature. A detailed analysis of the oxide layers was achieved by studying the colours and the surfaces by eyesight, by binocular microscope or by scanning electronic microscope.

The oxide layers formed at 300—500° essentially differ from those formed at 800° and from those formed at 1000—1250°. The conditions to obtain a fine oxide layer which comes off the metal holder were studied. It was noticed that starting at 800° at an oxidation time of 4 hours, the oxide layer was not uniformously adherent to the metal and came off partially. After 6 hours in the reaction chamber at a temperature from 700 to 900°, the oxide layer came off completely.

At 1000° the exterior layers were completely turned to ash. The oxide is formed of layers and becomes breakable, porperties which are maintained over 1000° also. The surfaces of oxide films formed at various temperatures were also studied by electronic microscopy.

Revue Roumaine de Chimie, **23**, *9–10*, 1367–1372 (1978)

KINETICS OF OXIDATION OF DIETHANOLAMINE WITH HEXACYANOFERRATE. III

M.S. MASOUD*[a], T. M. SALEM * and F. M. ASHMAWY**

* Faculty of Science, Chemistry Department, Alexandria University, Egypt

** Institute of Petroleum and Mining Engineering, Shebin
El-Khom, Egypt

Received August 28, 1976

The kinetic of oxidation of diethanolamine (DEA) with hexacyanoferrate III was studied. A spectrophotometric method was used to compute pK_a of DEA to be 9.15. Three moles of hexacyanoferrate III were required for the oxidation of DEA to CO_2, H_2O and H-CHO as final products. The effect of concentrations of the amine and the oxidising agent were discussed with an overall second order rate constant. The mechanism of the reaction was discussed. The kinetic and thermodynamic parameters were determined.

Ethanolamines have received much attention in studying the enzyme catalysed biochemical reaction [1]. These compounds and their complexes have many applications in industry [2] in the manufacture of plastics [3] and in the synthesis of ion exchange resins [4]. The interactions between transition metal ions and ethanolamines were studied in our laboratory [5-7].

Hexacyanoferrate III is well known for its powerful oxidising effect in alkaline media. It is described as one of the efficient electron abstracting reagents especially to complex ions and is one of the class of oxidising agents which passes through a reaction according to the following equation

$$[Fe(CN)_6]^{3-} + e \rightleftharpoons [Fe(CN)_6]^{4-}$$

This compound was used in the oxidation of glucose [8], 3-mercaptopropionic acid, [9] thiourea and thioacetamide[10]. The oxidation of triethanolamine with different oxidants gives various products mainly ammonia and formaldehyde.[11–16]

---

[a] To whom correspondance should be addressed.
Present address: P.O. Box 5516, Jeddah, Saudi Arabia.

[1] H. M. Week, *J. Amer. Ird. Assoc.*, **5**, 374 (1960).

[2] V. S. Klament, *Neft. Khoz*, **45**, 19 (1967).

[3] B. Elcmgren and A. Jchner, *Chem. Abstr.*, **55**, 15229 (1961).

[4] A. O. Sakubovic, *Polymer Sci.*, **1960**, 117.

[5] M. S. Masoud, *Ph. D. Thesis*, Faculty of Science, Alexandria, 1970.

[6] T. M. Salem, R. M. Issa and M. S. Masoud, *Egypt J. Chem.*, **16**, 283 (1973).

[7] M. S. Masoud, T. M. Salem and R. M. Issa, *Egypt J. Chem.*, **17**, 415 (1974).

[8] U. S. Mehrottra, M. C. Agrrwal and S. P. Muabram, *J. Phys. Chem.*, **72**, 1497 (1968).

[9] J. J. Bohning and K. Weiss, *J. Amer. Chem. Soc.*, **82**, 4724(1960).

[10] T. S. Thagarayan, *Chem. Rev.*, **58**, 439 (1958).

The present investigation was undertaken to in order to obtain kinetic evidence for the occurrence of the electron transfer in the oxidation of diethanolamine. Hexacyanoferrate III was chosen as an oxidant because it forms a stable reduction product through the gain of a single electron.[17]

EXPERIMENTAL

Aqueous potassium hexacyanoferrate III was prepared from Analar B.D.H., its concentration was checked by iodometry. [18] The reaction vessels were coated with black varnish to stop photochemical effects. The exact amount of the oxidising compound and sodium-hydroxide were mixed together at the appropiate concentrations. This mixture was added to required volume of the amine solution. The time for the ending of the reaction was three days. The progress of the relation was followed by estimating the unconsumed hexacyanoferrate III iodometrically. [19] The absorbance readings were recorded by using SP 800.

RESULTS AND DISCUSSION

A. Spectrophotometric determination of pK_a

The diethanolamine and its anion have different ultraviolet spectra. The absorbance at 224 nm was measured over wide range of $[OH^-]$ and the value of $[HN(C_2H_4O^{2-})_2]/[HN(C_2H_4OH)_2]$ was calculated in each case. The value of pK_a was calculated by a graphical method[20] involving extrapolation at infinite dilution according to the equation :

$$pK_w - pK_a = \log_{10} \frac{[HN(C_2H_4O^{2-})^2]}{[HN(C_2H_4OH)_2]} - \log [OH^-] + \log_{10} a_w f_{HN}(C_2H_4O^{2-})_2$$

where a_w and k_w are the activity and the ionic product of water respectively. Since $f = 1$ at infinite dilution, therefore by plotting $\log_{10} \frac{[HN(C_2H_4O^{2-})_2]}{[HN(C_2H_4OH)_2]} - \log [OH^-]$ versus $[OH^-]$ and by extrapolating to zero alkali concentration, a straight line is obtained, Figure 1, with an intercept equaling $pK_w - pK_a$ and amounting to 4.85.

---

[11] M. Smith and B. R. Willerfard, *J. Amer. Chem. Soc.*, **76**, 2502(1954).

[12] W. H. Dennis, L. A. Hill and B. D. Rosenbaltt, *J. Org. Chem.*, **1967**, 3783.

[13] E. T. Speakman and W. A. Waters, *J. Chem. Soc.*, **1955**, 40.

[14] E. J. Meehan, I. M. Kolthoff and H. Kakiuchi, *J. Phys. Chem.*, **66**, 1238 (1962).

[15] B. P. Sinha, O. P. Kachweha and R. C. Kapor, *J. Phys. Chem.*, **73**, 1627(1969).

[16] K. S. Shuks, P. C. Mathur and P. O. Bansal, *J. Inorg. Nuclear Chem.*, **35**, 1301(1973).

[17] F. Solymost, *Magyar Kém. Folyóirat*, **63**, 294(1957).

[18] A. I. Vogel, "Text Book of Quantitative Inorganic Analysis", Lowe & Brydone (Printers) Ltd, London, 1951, p. 356.

[19] A. I. Vogel, "Text Book of Quantitative Inorganic Analysis', Lowe & Brydone (Printers) Ltd, London, 1964, p. 345.

[20] C. H. Rochester, *Quart. Rev.*, **20**, 511 (1966).

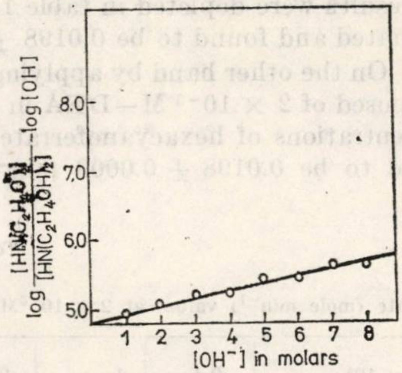

Fig. 1. — Det pK_a determination of DEA.

The pK_a obtained in the present case is 9.15, which is similar to that obtained by pH measurement.[5]

It is reasonable to compare the acidity of this compound with other compounds of similar stereochemistry. The pK_a values for methyl alcohol,[21] ethyl alcohol[21] and hydroxylamine[22] are 16.18 and 13.74 respectively. The decrease in the pK_a value of the diethanolamine compound with the previous three compounds could be related to steric effects.

B. Kinetic reactions

To determine the number of moles of the oxidising compound consumed per mole of the amine, a known amount of DEA was mixed with fifteen times its molar concentration of hexacyanoferrate III in 0.1 M NaOH solution. The mixture was then left for three days at room temperature, until the reaction was complete. The mode of the reaction could be suggested as follows :

$$HN(C_2H_4OH)_2 + 3OH^- + 3\,Fe(CN)_6^{3-} \rightarrow 4H - CHO + NH_3 +$$
$$+ H_3O^+ + 3\,Fe(CN)_6^{4-}$$

The formaldehyde was detected and determined using chromotropic colour reaction.[23] The concentration of the unreacted oxidant was determined iodometrically. These facilitate the calculation of the stoichiometry of the reaction. Similar products were observed in the oxidation of triethanolamine.[16]

The order of this reaction was determined in the following way First, by varying the concentration of the amine between $0.4 - 5 \times 10^{-3}$ while keeping that of the oxidising agent at 2×10^{-3} M in 25×10^{-3} M NaOH at 40° and by applying the first order rate equation, the following results were depicted in table 1. The velocity constant value (k) was evaluated and found to be $0.0198 \pm 0.0002\ \mathrm{min}^{-1}$.

---

[21] C. L. Friess, E. S. Lewis and A. Weissberger, "Investigations of Rate Mechanisms of Reactions", Vol. VIII, Part I, Interescience, New York, 1962, p. 201.

[22] M. N. Hughes, H. G. Nicklin and K. Shrimanker, *J. Chem. Soc. A* 1971, 3485.

[23] F. Feigl, "Spot Tests in Organic Analysis", 1960, p. 349.

On the other hand by applying the first order equation on a reaction composed of 2×10^{-3} M$-$DEA in 25×10^{-3}M NaOH at 40° an l variable concentrations of hexacyanoferrate III ($2-8 \times 10\ ^{3}$M), the k value was found to be $0.0198 \pm 0.0003\ \mathrm{min}^{-1}$.

Table 1

Rate (mole min^{-1}) values at 2×10^{-3}M-$\mathrm{Fe(CN)}_6^{3-}$ and 25×10^{-3} M $-$ NaOH at 40°

DEA $\times 10^3$	0.4	1	2	3	4	4
Rate(mole min^{-1})	0.004	0.0097	0.0198	0.0286	0.0396	0.0497

From the above results, an overall second order reaction is suggested. The energy of activation for this reaction was determined by measuring the rate of the reaction at different temperatures between 30$-$50° (5 degrees interval) by taking equimolar concentration of the amine and oxidising compound at 2×10^{-3}M in 25×10^{-3} M NaOH. Figure 2 shows the Arhenius plot between log k vs. $\dfrac{1}{T}$, from which $\Delta E = 7.92$ kcal.

The entropy of activation, ΔS, was calculated from the reaction :

$$\frac{\Delta S}{4.576} = \log K - 10.757 - \log T + \frac{\Delta H}{4.576\ T}$$

and found to be $-$ 49.82 e.u.

When consulting the effect of NaOH concentration on a solution containing equal concentrations of the amine and the oxidising compound (2×10^{-3}M) at 40°, the recorded rate was found to be affected by the alkali concentrations. This value increased lineraly with low [OH^-] up to 15×10^{-3}M while at higher [OH^-] it varied by the power 1.20, Figure 3. This may be probably due to the salt effect. This behaviour could be readily understood if a deprotonated species is involved in the rate determining step. The results are depicted in table 2.

Table 2

Rate (mole min^{-1}) values at 2×10^{-3} M-DEA and 2×10^{-3} M$-$Fe $\mathrm{(CN)}_6^{3-}$ at 40°

$\mathrm{NaOH}^- \times 10^3$M	5	10	15	20	25	30
Rate (mole min^{-1})	0.0036	0.0071	0.0104	0.0149	0.0198	0.0242

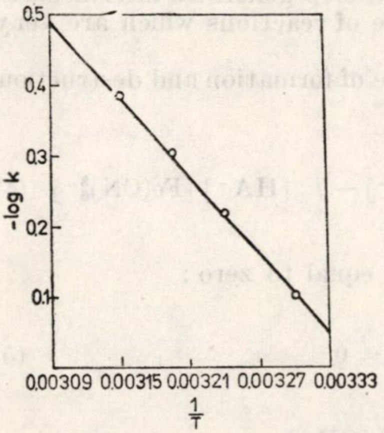

Fig. 2. — Arrhenious plot for the calculation of energy of activation.

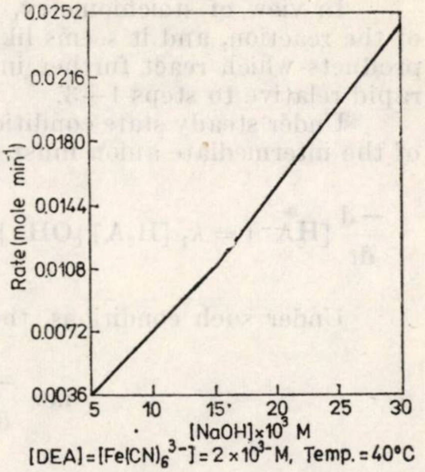

Fig. 3. — Effect of alkali concentrations on the rate of a reaction composed of $2 \times 10^{-}$M — of the amine and the oxidising compound at 40°.

C. Mechanism of the reaction

The diethanolamine compound is assumed to be subjected to an auto-oxidation in alkaline solution i.e. the fraction of the compound is present in an anionic deprotonated form involved in the rate determining step. The obtained entropy value suggests greater internal strain and some sort of steric hinderance in the compound.

Two distinct paths could be proposed for such mechanisms, either bimolecular collisions between the reacting molecules or reaction based on the formation and subsequent decomposition of an intermediate complex in composite reactions. The mechanism could be assumed to take place in three steps. The first depends on that the amine reacts with the alkali giving the intermediate anion as follows :

$$H_2A + OH^- \underset{K_{-1}}{\overset{K_1}{\rightleftharpoons}} HA^- + H_2O \qquad (1)$$

This reaction proceeds in a reversible manner.

In step 2 the intermediate anion reacts with the oxidant forming a complex Y which is followed by a fast step 3 that gives the product of the reaction. Step 2 with a rate k_2 may be fast or slow depending on the stability of the intermediate anion obtained in step 1. Step 3 is a relatively fast step with a rate k_3 giving the products of the reactions. Steps 2 and 3 can be represented as follows :

$$HA^- + Fe(CN)_6^{3-} \rightarrow Y \qquad (2)$$

$$Y \xrightarrow{k_3} (Fe(CN)_6^{4-} + \text{products} \qquad (3)$$

In view of stoichiometry, step 3 does not form the final products of the reaction, and it seems likely that this step generates intermediate products which react further in a sequence of reactions which are very rapid relative to steps 1—3.

Under steady state conditions, the rate of formation and destruction of the intermediate anion must be equal :

$$\frac{-\mathrm{d}}{\mathrm{d}t}[\mathrm{HA^-}] = k_1[\mathrm{H_2A}][\mathrm{OH^-}] - k_1[\mathrm{HA^-}] - k_2[\mathrm{HA^-}][\mathrm{Fe(CN)_6^{3-}}] \quad (4)$$

Under such conditions, this must be equal to zero :

$$\text{i.e. } \frac{-\mathrm{d}}{\mathrm{d}t}[\mathrm{HA^-}] = 0 \quad (5)$$

$$\therefore [\mathrm{HA^-}] = \frac{k_1[\mathrm{H_2A}][\mathrm{OH^-}]}{k_{-1} + k_2[\mathrm{Fe(CN)_6^{3-}}]} \quad (6)$$

$$..\frac{-\mathrm{d}}{\mathrm{d}t}[\mathrm{Fe(CN)_6^{3-}}] = k_2[\mathrm{HA^-}][\mathrm{Fe(CN)_6^{3-}}] + k_3[\mathrm{Y}][\mathrm{Fe(CN)_6^{3-}}] \quad (7)$$

Substituting for Ha⁻ :

$$\therefore \frac{-\mathrm{d}}{\mathrm{d}t}[\mathrm{Fe(CN)_6^{3-}}] = \frac{k_1k_2[\mathrm{H_2A}][\mathrm{OH^-}][\mathrm{Fe(CN)_6^{3-}}]}{k_{-1} + k_2[\mathrm{Fe(CN)_6^{3-}}]} + k_3[\mathrm{Y}][\mathrm{Fe(CN)_6^{3-}}] \quad (8)$$

If the reaction is controlled by step 2 as it is the slower and assuming $k_{-1} \gg k_2$ equation 8 could be formulated as follows :

$$\frac{-\mathrm{d}}{\mathrm{d}t}[\mathrm{Fe(CN)_6^{3-}}] = \frac{k_1k_2}{k_{-1}}[\mathrm{H_2A}][\mathrm{OH^-}][\mathrm{Fe(CN)_6^{3-}}] + k_3[\mathrm{Y}][\mathrm{Fe(CN)_6^{3-}}] \quad (9)$$

So, equation 9 involves that the interaction occurs between the amine and the negatively charged particles of both the alkali and the oxidising compounds.

Revue Roumaine de Chimie, 23, 9–10, 1373–1376 (1978)

PORÖSE ZWEIPHASENELEKTRODEN I.

RANEY-Ni-Ti-ELEKTRODEN FÜR ANODISCHE METHANOLOXIDATION

A. BANDI

Institut für Physikalische Chemie
Bukarest, Rumänien

Eingegangen am 6. November 1976

Es wurden verschiedene poröse Zweiphasenelektroden aus Raney-Ni-Ti Legierung, für anodische Methanoloxidation hergestellt. Der Einfluß des Preßdruckes auf die Porosität und elektrochemische Eigenschaften wurden untersucht.

Die von verschiedenen Autoren[1–4] durchgeführten Forschungen haben zu der Schlußfolgerung geführt, daß Raney-Ni als Katalysator zur Methanoloxidation in alkalischen Brennstoffzellen nur mit bescheidenen Ergebnissen verwendet werden kann. Veröffentlichungen jüngeren Datums[5–6] berichten über die Wirksamkeit der Raney-Ni-Mischkatalysatoren mit Ti, Mo, Fe, in der anodischen Oxidation des Wasserstoffs in alkalischen Lösungen.

In der vorliegenden Arbeit haben wir uns mit der Herstellung von Raney-Ni-Ti-Elektroden, zur Elektrooxidation des Methanols in alkalischen Lösungen, befaßt.

EXPERIMENTELLER TEIL

Die Elektroden wurden nach der von Justi und Winsel [1] vorgeschlagenen Methode (DSK-Elektroden) hergestellt. Es wurden folgende Materialien benützt:

— Nickelpulver aus Nickelkarbonyl (Ni–C), Korngröße 15 μ (Fluka-Schweiz).
Ni–AL–Ti Legierung (30–67–3%). Korngröße < 63 μ.

---

[1] E. Justi und A. Winsel, „Kalte Verbrennung“, Steiner Verlag, Wiesbaden, 1962, S. 241.

[2] L. Oniciu und A. Bandi, *Stud. Univ. Babeş Bolyai Chem.* 2, 47 (1969).

[3] H. H. Doehren und K. J. Euler, „Brennstoffelemente“, VDI Verlag, Düsseldorf, 1971, S. 55.

[4] F. V. Sturm und G. Richter, *Electrochim. Acta.* 10, 1169 (1965).

[5] G. Richter, „Deuxièmes Journées Internationales d'Etude des Piles a Combustible“, Bruxelles, 1967, S. 236.

[6] H. Cnobloch, M. Marchetto, H. Nischik, G. Richter und F. V. Sturm, „Deuxièmes Journées Internationales d'Etude des Piles a Combustible“, Bruxelles, 1967, S. 204.

Die röntgenographische Analyse der Ni—Al—Ti Legierung mit Korngröße unter 63 μ, unterstrich die Existenz von Al_3Ni (Phase β) und einer goßen Menge freien Aluminiums. Die intermetallischen Verbindungen mit Ti konnte man, des kleinen Ti Gehalts wegen, nicht hervorheben. Bei der Analyse eines Legierungspulvers mit der Korngröße unter 40 μ, fand man die gleichen Komponenten, aber kleinere Mengen von Al_3Ni und sehr viel freies Al. Dieses bestätigt die Feststellungen von Smrcek und Ministr, [7] daß die kleineren Fraktionen reicher in den weniger harten Phasen, in unserem Fall Al, vorhanden sind. Diese Fraktion wurde nicht in unseren Versuchen aufgenommen.

Das Ni—Al—Ti Pulver wurde mit Ni—C, im Verhälthis 1 : 2, gemischt und 24 Stunden lang homogenisiert.

Die Elektroden wurden in kreisförmige Plättchen, von 1 cm² großer Oberfläche und 0,7 mm Dicke, gepreßt. Der Preßdruck variierte zwischen 1110 und 3900 kgf/cm². Nachher wurden die Elektroden bei 650°C in Wasserstoffatmosphäre, 30 Minuten lang gesintert. Falls die Temperatur über 650° steigt, verläuft eine stark exotherme Reaktion und die Elektroden können nicht mehr aktiviert werden, das Aluminium löst sich nicht mehr in KOH, nicht einmal durch Kochen. Dieses wurde auch von anderen Autoren, [1] und zwar im Falle von Legierungen mit großem Aluminiumgehalt, bestätigt.

Die Elektroden wurden in 6M KOH bei 80°, 24 Stunden lang aktiviert.

Die elektrochemischen Bestimmungen wurden in einer konventionellen Zelle durchgeführt, wobei die Gegenelektrode (Platin), von der restlichen Zelle, durch eine Fritte getrennt wurde. Die Elektrodenpotentiale wurden gegen gesättigte Kalomelelektrode gemessen.

Zur Bestimmung der elektrochemischen Aktivität der Elektroden, wurden die Größen R_p (differentieller Polarisationswiderstand, Ω cm²) und i_{max} (maximaler Strom, mA/cm²), verwendet, die aus den potentiostatischen Stromspannungskurven entnommen wurden.

In Abb. 1 ist die potentiostatische Meßanordung abgebildet.

Mit Hilfe eines Quecksilberporosimeters wurde die Porosität der Proben bestimmt. In Rechnung wurden die Porenvolumina zwischen 75 und 75 000 Å gezogen.

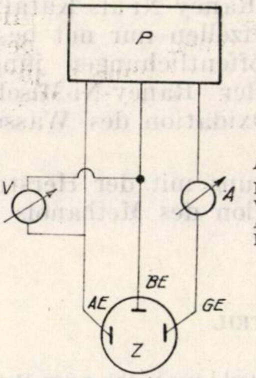

Abb. 1—Potentiostatische Meßanordnung:
P – Potentiostat:
V – Voltmeter;
A – Ampermeter; AE – Arbeitselektroden; BE – Bezugselektrode; GE – Gegenelektrode; Z – Zelle.

ERGEBNISSE UND DISKUSSIONEN

Die Elektrodenpotentiale der verschiedenen Elektroden sind der reversiblen Wasserstoffpotentialen, in derselben Lösung, nah. (siehe Tab. 1). Die Schnelligkeit der Wiedereinstellung der Ruhepotentiale, nach der die Elektroden polarisiert wurden, ist von der Dauer und Größe der Belastung abhängig. Wenn die Überspannung 120—150 mV nicht übertritt, stellt sich das Ruhepotential sehr schnell ein.

---

[7] K. SMRCEK und Z. MINISTR, *Metalloberfläche*, **25**, 195 (1971).

Die Strom-Spannungskurven der, mit verschiedenem Preßdruck hergestellten Elektroden, sind in Abb. 2 gezeichnet.

Die Ruhepotentiale (E_{st}), R_p und $i_{\max}$ der Elektroden, sind in der Tab. 1 wiedergegeben.

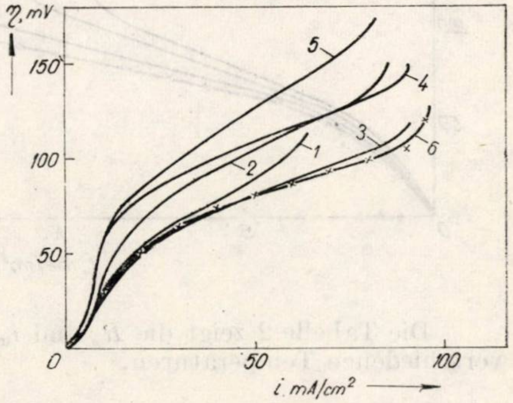

Abb. 2 — Strom-Spannungskurven der Raney-Ni-Ti-Elektroden bei 25° in 6M KOH und 2,5 M CH_3OH: *1* — 1110; *2* — 1670; *3* — 2230; *4* — 2750; *5* — 3350; *6* — 3900 kgf/cm².

Tabelle 1

Kenngrößen der Elektroden

Elektrode Nr.	1	2	3	4	5	6
P, Kgf/cm²	1110	1670	2230	2790	3350	3900
E_{st}, mV	−1070	−1080	−1070	−1090	−1085	−1070
R_p, Ω cm²	1,3	1,2	0,75	1,03	1,2	0,705
$i_{\max}$, mA/cm²	64,5	83	92,5	89,5	78	99,5
Porosität, %	39,6	38,4	37,6	37	36	27,6

Wie es aus der Tab. 1 ersichtlch ist, weisen den kleinsten Wert für R_p und damit die größte Aktivität, die Elektroden Nr. 3 und 6, auf. Die analytische Bestimmung des Aluminiumgehaltes in Elektroden ergab 4,8% im Verhältnis zu dem Anfangsaluminiumgehalt, Ausnahme bildet nur die Elektrode Nr. 6 (3900 kgf/cm²), wobei der Restaluminiumgehalt 20,4% betrug. Die etwa 5% Aluminium, die sehr fest gebunden sind, stören die elektrochemischen Bestimmungen nicht, während der 20%-ige Restaluminiumgehalt die anormalen Werte für $i_{\max}$ und R_p verursacht. Derselbe beeinflußt auch die Porosität der Elektrode, welche cca 30% niedriger als bei den anderen Elektroden ist.

Die Porosität, und damit auch die Aktivität, nimmt mit dem abnehmenden Preßdruck zu und erreicht ein Maximum (R_p minimal) bei den Elektroden Nr. 3 und 4. Wahrscheinlich ist hier eine optimale Porenstruktur und hohe spezifische Oberfläche erreicht.

Die Abb. 3 zeigt die Strom-Spannungskennlinien der Elektrode Nr. 3, aufgenommen bei verschiedenen Temperaturen in 6M KOH und 2,5M CH_3-OH.

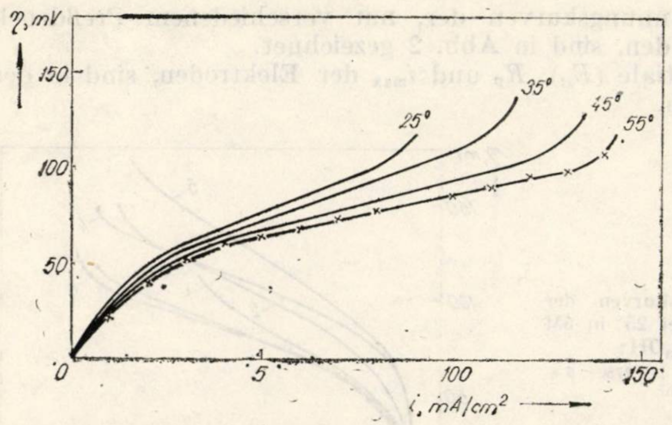

Abb. 3.— Strom-Spannung Kennlinien der Elektrode Nr. 3. Elektrolyt 6M KOH und 2,5 M CH_3OH bei 25°, 35°, 45°, 55°.

Die Tabelle 2 zeigt die R_p und i_{max} Werte der Elektrode Nr. 3 bei verschiedenen Temperaturen.

Tabelle 2

Kenngrößen der Elektrode Nr. 3

T, °C	25	35	45	55
R_p, Ω cm²	0,75	0,66	0,6	0,43
i_{max}, mA/cm²	91	115	135	143

Aus den vorliegenden Ergebnissen können wir schließen, daß der Raney-Ni-Ti Mischkatalysator für Methanoloxydation besser geeignet ist, als der Raney-Ni.[1-4] Die besten Ergebnisse erhält man mit der Elektrode Nr. 3 (Preßdruck 2230 kgf/cm²). Für diese Elektrode fanden wir $R_p = 0,75\ \Omega\ cm^2$ und $i_{max} = 91\ mA/cm^2$ bei 25°.

Revue Roumaine de Chimie 23, 9–10, 1377–1388 (1978)

THE STABILITY OF THE SOLID STABILISED EMULSION WITH SPECIAL REFERENCE TO ELECTROLYTES

S. P. JAIN and S. N. SRIVASTAVA
Chemical Laboratories, Agra College, Agra, India

Received September 11, 1976

The stability of the chromium hydroxide stabilised emulsion has been studied, which has been assessed by zeta potentials micro-electrophoretically. The interaction energies have also been calculated and the energy profiles have been plotted, the values obtained are consistent with the DLVO theory and are high enough. This is explained assuming the occurrence of secondary minima. The degree of aggregation *D* has been observed haemocytometrically and the obtained value of Van der Waals constant fitting the practical value of *D* is found to be 2.7×10^{-13}erg. The nature of adsorption has also been discussed in the light of calculated values of adsorption constants.

INTRODUCTION

The effect of addition of electrolytes on the stability of emulsions has been carried out by many workers.[1–12] The effect of added electrolyte on the electrophoretic mobility of O/W emulsions has been investigated by Stackelberg and Heindze,[13] who noticed that the double layer theory is adequate to explain the observed phenomena. In the present work it is proposed to study the stability of the emulsions stabilised by solid particles from partially flocculated sols specially in the light of DLVO theory[14–15] snd to examine the nature of flocculation which is expected to be reveraible.

[1] A. R. Martin and R. N. Hermann, *Trans. Faraday Soc.*, **37**, 30 (1941).

[2] L. Ya. Kremnev and N. I. Kuibina, *Kolloidn. Zhur.* **17**, 31 (1955) ; **9**, 392(1947).

[3] S. N. Srivastava, *Kolloid-Z.*, **173**, 137 (1960).

[4] A. King and G. W. Wrzeszinski, *Trans. Faraday Soc.*, **35**, 741 (1939).

[5] K. R. Lindfors, D. K. West, G. L. Blackmer and L. M. Carson, *J. Phys. Chem.*, **71**, 3057 (1967).

[6] H. A. Clowes, *J. Phys. Chem.*, **20**, 407 (1916).

[7] S. S. Bhatnagar, *J. Chem. Soc.*, **117**, 542 (1920).

[8] Hardy, *J. Physiol.*, **24**, 288 (1899) ; *Z. phys. Chem.*, **33**, 385 (1900) ; *Nature*, **109**, 226 (1921).

[9] H. Limburg, *Rec. Trav. chim.*, **45**, 772, 854, 875 (1926) ; Diss. Delft., (1924).

[10] F. Powis, *Z. phys. Chem.*, **20**, 747 (1941).

[11] J. J. Hermann, *Rec. Trav. chim*, **60**, 747 (1941).

[12] M. Van del Temple, *Rec. Trav. chim.*, **72**, 442 (1953) ; *J. Colloid Sci.*, **13**, 125 (1959).

[13] M. Von Stackelberg and H. Heindze, Forschungbber Writschafts — U. Verkehrsministeriums Nordrehein — Westfalen. N. 166, pp. 1—21 (1955).

[14] B. Derjaguin, *Trans. Faraday Soc.*, **36**, 203, 730 (1940) ; *J. Expt. Zhur. Phys. USSR*, **11**, 802 (1941) ;
B. Derjaguin and L. D. Landau, *Acta Phys. Chim. USSR*, **14**, 633 (1941).

[15] E. G. W. Verwey and J. Th. G. Overbeek, "Theory of Stability of Lyophobic Colloids", Elsevier Publ. Co., Amsterdam, 1948.

EXPERIMENTAL AND THEORETICAL

The electrophoretic mobility U measurements were carried by micro-electrophoresis apparatus using Northrop-Kunitz[16] type rectangular cell. The mobility was calculated by the following relation

$$U = \frac{d\,S\,A}{i\,t} \tag{1}$$

where d is the distance travelled by the particle in a time t under the influence of current i, S and A are the specific conductances of the emulsion and area of the cell respectively. The electrokinetic potential ξ was calculated with the Smoluchowsky equation applicable to the present system having $\varkappa a \gg 100$.

$$\xi = \frac{4\,\pi\,\eta}{\varepsilon}\,U \tag{2}$$

where η and ε are the coefficients of viscosity and dielectric constant of the dispersing medium respectively, a is the radius of the globules and $\varkappa$ is the thickness of the double layer.

The overall interaction energy V between the two double layers of the spherical particles is given by the following relation

$$V = V_A + V_R \tag{3}$$

where V_A and V_R are the attraction and repulsion energies. These were evaluated by the following equations[17]

$$V_A = -\frac{A\,a}{12\,H}\left(\frac{\lambda}{\lambda + 3.54\,H\,\Pi}\right) \tag{4}$$

valid for $H < 150$ Å

$$V_A = -\frac{A\,a}{\Pi}\left\{\frac{2.45\,\lambda}{120\;H^2} - \frac{\lambda^2}{1045\;H^3} + \frac{\lambda^3}{5.62\times 10^4\;H^4}\right\} \tag{5}$$

valid for $H > 150$ Å

$$V_R = \frac{\varepsilon a \psi_0^2}{2}\,\ln\,(1 + \exp.^{-H\varkappa}) \tag{6}$$

where H is the distance between the particles, λ is the London frequency taken equal to 1 000 Å, A is the Van der Waals constant taken equal to 2.8×10^{-13} erg. and ψ_0 is the surface potential here assumed to be equal to zeta potential.

The degree of aggregation D in case of reversible flocculation has been determined by the knowledge of depth of the secondary minima V using the following equation

$$D = 4\,\Pi\,a^3\,n_0 \int S^2\;\exp.\;(-\;V/kT)\;\mathrm{d}S \tag{7}$$

where S is calculated by the relation $S = 2 + \dfrac{H}{a}$, n_0 is the initial number of globules per c.c. in the emulsion, k is the Boltzmann constant, T is the temperature in absolute scale and a is the radius of the globules.

---

[16] J. H. Northrop and M. Kunitz, *J. Gen. Physiol*, **7**, 929 (1925).

[17] S. P. Jain and S. N. Srivastava, *Bull. Chem. Soc., Japan*, **43**, 3644(1970).

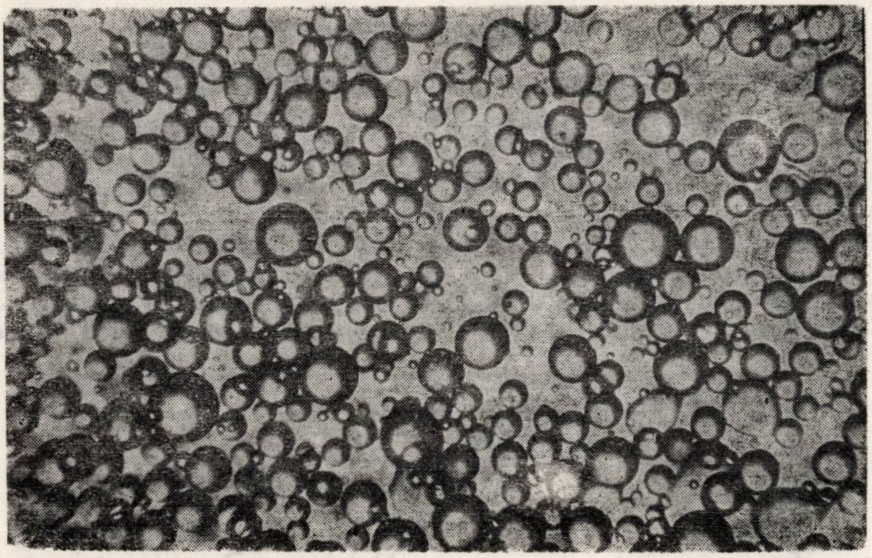

Fig. 1. — Microphotograph of the emulsion globules, 600 times magnified.

The change in charge density σ_c on adding small quantity of foreign ions is given by the Stern equation[17]

$$\sigma_c = \frac{N_1\, v\, e}{1 + \dfrac{55.6}{C}\,\exp.(\Delta G/kT)} \qquad (8)$$

where C is the molar concentration of the added electrolyte of valency v, N_1 the number of binding sites available per cm^2, e is the elementary charge and ΔG is the free energy of adsorption.

The size of the emulsion particles has been determined with the help of microphotograph, taken with Olympus Camera attached to the microscope (Figure 1) and the size distribution curve drawn in Figure 2, the average radius of the particles (a) is 1.8 μ. The pH of the emulsion was measured by Cambridge pH meter with an accuracy of ± 0.02 unit. All the reagents and chemicals used were of B. D. H. Analar grade. The emulsion was prepared by dispersing 10% of toluene (weighted with bromoform) in the partially flocculated (by the addition of potassium oxalate) sol. It was first hand shaken and then subjected to homogenisation in a stainless steel homogeniser.

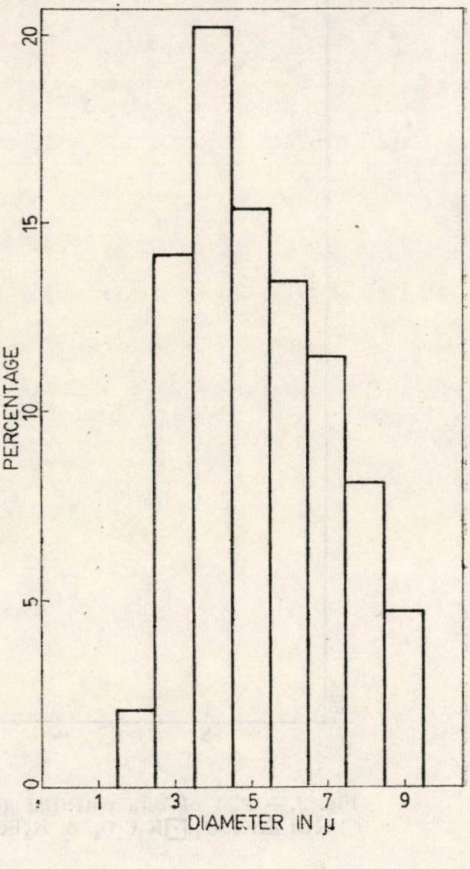

Fig. 2. — Size distribution curve of emulsion, mean radius 1.87 μ.

RESULTS AND DISCUSSION

The effect of electrolytes on zeta potential of the emulsion:

The electrokinetic potential in the presence of different electrolytes having different valent anions has been measured and plotted against log concentration in Figure 3. From the figure it is seen that the zeta potential decreases with the increasing concentration, the decrease is gradual with bromide while in the case of sulphate and oxalate it is sharp in comparison to monovalent anions. But in the case of tri and tetravalent anions at very low concentrations there is almost no change and on increasing the concentration a sharp decrease was observed. This sharp decrease is

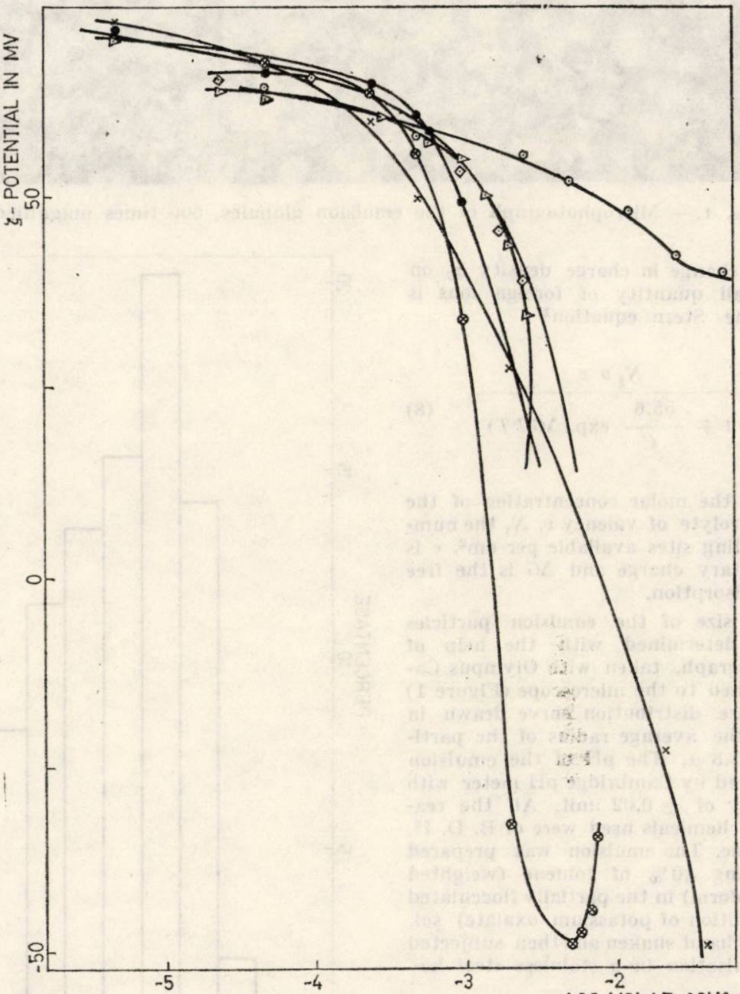

Fig. 3. — Plot of zeta potential against log molar concentration for ⊙ KBr, △K_2SO_4, ⊡$K_2C_2O_4$, × $K_3Fe(CN)_6$, ● $K_3(C_6H_7O_5)$, ⊗$K_4Fe(CN)_6$.

more in the case of tetravalent anion than in the trivalent one. On further increasing the concentration of anions the reversal of charge was observed.

On addition of monovalent and bivalent anions the compression in thickness of the double layer takes place, thus reducing the zeta slightly, even at very low range of concentration, but at higher concentration the effect of compressing the double layer prevails.[18] While polyvalent anions at low concentrations will interact with potential determining ions, a rearrangement of the dissolved ions across the interface takes place and thus they do not affect zeta potential much. But at higher concentrations, their adsorption at the surface of the particles takes place and compression of Gouy layer occurs resulting in the reduction of ψ_0 which ensures decrease in the zeta potential which may fall to zero. Particularly in emulsions which possess high value of the potential drop in the diffuse layer, the surface potential at 0/W interface appears to be highly sensitive to the concentration and kind of counter ions.

The excess of anions in the double layer may exceed the defficiency of the ions, having a charge of the same ions at the interface, and the presence of these excess ions at zero point of charge reverses the sign of the charge of the system and the sign of zeta potential. The increase in the zeta potential after charge reversal was obtained owing to the enhanced adsorption of these anions to the particle surface.

The absorbabilities of the anions mainly may be affected by the following factors, the nature of the anions, the polarizability, the nature of the inorganic ion in the surface of the chromium hydroxide and the hydrolysis of the electrolytes.[19-20] However, in the present case the hydrolysis of the electrolytes does not seem to be possible, when the anions are the counter ions because these anions can be more easily dehydrated than a normal cation and will go closer to the interface.[21] The other factors presumably will affect the bond strength of the adsorbed ions with potential determining ions.

The adsorption constants and free energies:

The adsorption constants have been calculated and tabulated in table 1. An increase in K_2 has been observed for the electrolytes having higher valencies of the anions while the value of N_1 decreases with electrolytes having higher valencies. In the initial stages of adsorption, the anions are adsorbed on the positively charged sites of the chromium hydroxide surface and that too, probably at points on the surface occupied by the potential determined by chromium ions. However, it is clear that the N_1 for electrolyte is greater than the surface excess of chromium ions since zeta potential shows a reversal of charge due to more adsorption of anions. Therefore, it appears to be a reasonable assumption that at certain concentrations, the electrolyte may be adsorbed directly to the surface at the sites other than occupied by potential determined by ions. Although, it is doubtful whether the absolute accuracy of N_1 is good enough to give certainty, nevertheless, the value of K_2, which determines the adsorbabilities, increases with the valency of the electrolytes and shows the existence of adsorption. The shift of the zero point of charge with increasing concentration towards the lower valency side expected theoretically with decreasing values of K_2 is in accordance with the observations of Ottewill, Rastogi and Watanabe.[22-23] The values of K_1/K_2 are the same for all the electrolytes for a particular system. Thus the agreement between the theory and experiment is good and denotes that coagulation with electrolytes (specially by anions) can be satisfactorily explained by the influence of adsorption on ψ_δ. This coagulation process seems to resemble the adsorption coagulation of Freundlich.

---

[18] H. Freundlich, *Z. phys. Chem.*, **73**, 385 (1910).

[19] G. Gouy, *Ann. Phys.*, **9**, 179 (1917).

[20] H. R. Kruyt and S. A. Troestra, *Kolloid. Beihefte*, **54**, 262, 277, 287 (1943).

[21] A. J. Rutgers and M. De. Snet, *Trans. Faraday Soc.*, **4**, 1764 (1945) ;
A. Frumkin, *Z. phys. Chem.*, **116**. 485 (1925).

Table 1

Adsorption constants and free energy for different electrolytes

Electrolyte (anionic)	K_1 coulomb litre/cm^2 mol.	K_2 litre/mol.	$\frac{K_1}{K_2} \times 10^6$ coulomb/cm^2	ΔG K.cals/mol.	N_1 groups/cm^2	Area/ molecule Å^2
$Fe(CN)_6^{---}$	6.90×10^{-4}	3.3×10^2	2.92	2.48	1.6×10^{13}	625
$Fe(CN)_6^{---}$	10.70×10^{-4}	8.6×10^2	2.83	2.73	0.4×10^{13}	2381

When all the sites are covered by anions, the value of the area occupied for trivalent and tetravalent anions is much higher. Thus a very little percentage of the area available is covered by the anions adsorbed. These anions are tightly bound in the Stern layer since they possess high free energy of adsorption. The value of ΔG obtained supports this view which is reasonably high as expected on the basis of electrostatic adsorption of potential determining sites. The value of free energy of adsorption (ΔG) increases with the valency of the anions. This indicates the influence of valency on their flocculating power because, smaller the free energy the greater is the amount of counter ions to reach the critical value of charge reversal concentration.

Potential energy curves:

The potential energy of the double layer around the particles has been calculated in the presence of different amount of different valent electrolytes and the energy curves have been plotted in the representative Figure 4. The height of maxima of energy profiles has also been tabulated in Table 2 from where it is obvious that for all the electrolytes the energy barriers are very high in the range of nearly 3000—4000 kT. Particles have to cross this energy barrier which is high enough for flocculation to occur and hence exhibit a high degree of stability. The presence of these high energy barriers is caused by the large size of these globules because both repulsive and attractive energies are proportional to the radius of

[22] R. H. OTTEWILL and A. WATANABE, *Kolloid-Z.*, **170**, 38, 132 (1960); **171**, 33 (1960)

[23] R. H. OTTEWILL, M. C. RASTOGI and A. WATANABE, *Trans. Fraday Soc.*, **56**, 854 (1960)

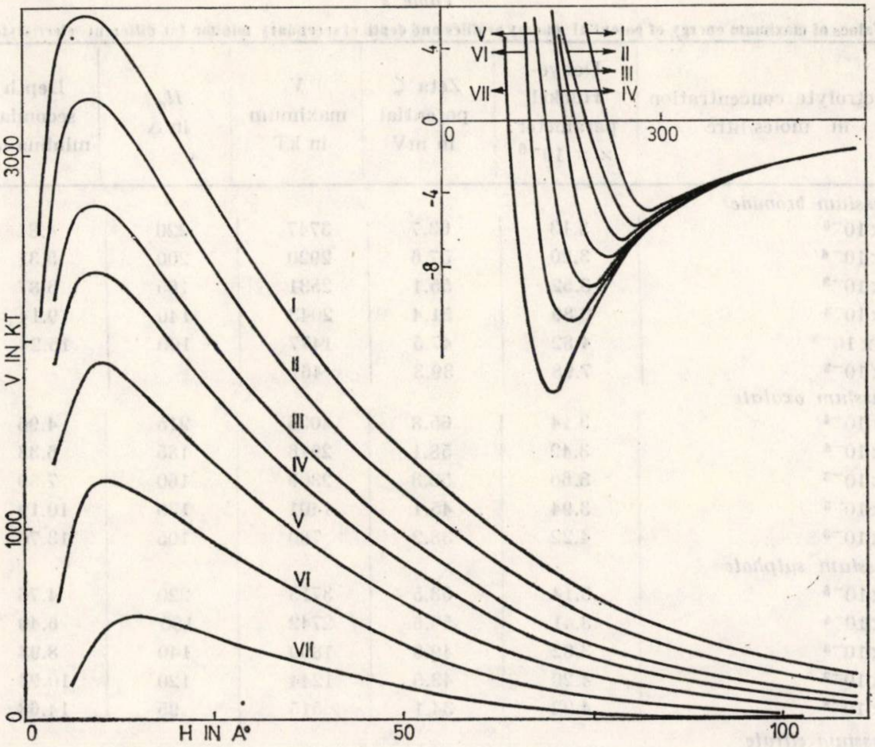

Fig. 4. — Plot of potential energies against distance of separation and elaborated secondary minima in the presence of K_2SO_4, *I* 5×10^{-5}, *II* 3×10^{-4}, *III* 6×10^{-4}, *IV* 1×10^{-3}, *V* 1.5×10^{-3} *VI* 2×10^{-3} and *VII* 2.5×10^{-3} moles/litre.

the particles. The extent of energy barriers depends upon the zeta potential and Debye-Huckel parameter ($\varkappa$) which invariably varies with the electrolyte content. The emulsions having zeta potentials nearly 35 mV and having the thickness of the double layer nearly 25 Å show that the flocculation occurs in the primary minima of a deep potential well of 40—60 kT, from where the particles cannot escape with thermal energy alone and are flocculated irreversibly.

The secondary minimum flocculation:

The existence of high energy barrier is sufficient to obviate the possibility of occurrence of flocculation in the primary minima, but the flocculation has been observed to occur. To account for this it was assumed that at larger distance attraction predominates and secondary minima occurs. The elaborated curves for showing the secondary minima are drawn in Figure 4, where the minima obtained in the energy contours are up to 5—10 kT deep where the droplets are still separated by about 150—250 Å, but are flocculated in loose aggregates. This reversible nature of flocculation is justified by the large size ($a = 1.87\ \mu$) of the particles with adsorbed solid chromium hydroxide. It was further verified by diluting the emulsion, when it was found that the particles disaggregated again.

Table 2

Values of maximum energy of potential energy profiles and depth of secondary minima for different electrolytes

Electrolyte concentration in moles/litre	Debye-Huckel parameter $\varkappa \times 10^{-6}$	Zeta ζ potential in mV	V maximum in kT	H_0 in Å	Depth of secondary minima in kT
Potassium bromide					
5.0×10^{-5}	3.13	63.7	3747	220	4.81
5.0×10^{-4}	3.20	57.6	2920	200	5.31
2.5×10^{-3}	3.52	55.1	2531	165	6.87
5.0×10^{-3}	3.89	51.4	2043	140	9.14
1.25×10^{-2}	4.82	47.5	1477	100	15.24
5.0×10^{-2}	7.98	39.3	461	—	—
Potassium oxalate					
1.0×10^{-4}	3.14	65.8	4035	215	4.96
6.0×10^{-4}	3.42	58.1	2916	185	6.33
1.0×10^{-3}	3.60	53.3	2309	160	7.50
1.8×10^{-3}	3.94	45.1	1401	130	10.19
2.5×10^{-3}	4.22	38.2	780	105	13.70
Potassium sulphate					
5.0×10^{-5}	3.14	63.5	3715	220	4.76
6.0×10^{-4}	3.41	56.6	2742	180	6.40
1.5×10^{-3}	3.82	49.9	1890	140	8.93
2.0×10^{-3}	4.20	43.5	1244	120	10.93
2.5×10^{-3}	4.22	34.1	515	95	14.68
Potassium citrate					
5.0×10^{-6}	3.12	71.9	4964	230	4.59
5.0×10^{-5}	3.17	66.2	4103	215	4.95
2.5×10^{-4}	3.37	64.5	3773	200	5.52
5.0×10^{-4}	3.63	57.1	2740	170	7.15
1.0×10^{-3}	4.02	49.0	1758	135	10.11
Potassium ferricyanide					
5.0×10^{-6}	3.12	73.0	5131	230	4.56
5.0×10^{-5}	3.17	63.9	3766	210	4.99
2.5×10^{-4}	3.37	59.6	3120	190	5.86
5.0×10^{-4}	3.60	49.4	1885	160	7.86
2.0×10^{-3}	4.76	26.6	149	—	—
Reversal					
2.0×10^{-2}	11.80	−24.5	—	—	—
6.5×10^{-2}	20.76	−106.8	5892	—	—
Potassium ferrocyanide					
5.0×10^{-6}	3.13	71.3	4871	230	4.61
5.0×10^{-5}	3.20	67.4	4242	215	4.92
2.5×10^{-4}	3.52	63.6	3602	180	6.46
5.0×10^{-4}	3.89	55.3	2470	148	8.74
1.0×10^{-3}	4.53	33.1	428	85	18.51
Reversal					
2.0×10^{-3}	5.60	−33.7	338	—	—
5.0×10^{-3}	7.98	−50.0	—	—	—
7.58×10^{-3}	9.57	−36.0	—	—	—

This type of secondary minima was also observed by few workers[17,24] in different systems but with the solid stabilised emulsions this has been reported for the first time.

The valency of the counter ions v and Debye-Huckel parameter $\varkappa$ have a profound influence on the position of the secondary minima as can be seen from the following equation :

$$H_m^2 \exp. (-\varkappa H_m) = 1.80 \times 10^{-9} \frac{v^2}{\varkappa\, \nu^2} \qquad (9)$$

and dependence has been shown in Figure 5. The distance at which secondary minima occurs decreases with the increase in the concentration of the electrolytes and the minima at the same particle distance can be obtained by higher concentration uni-univalent electrolyte than bivalent or polyvalent electrolytes.

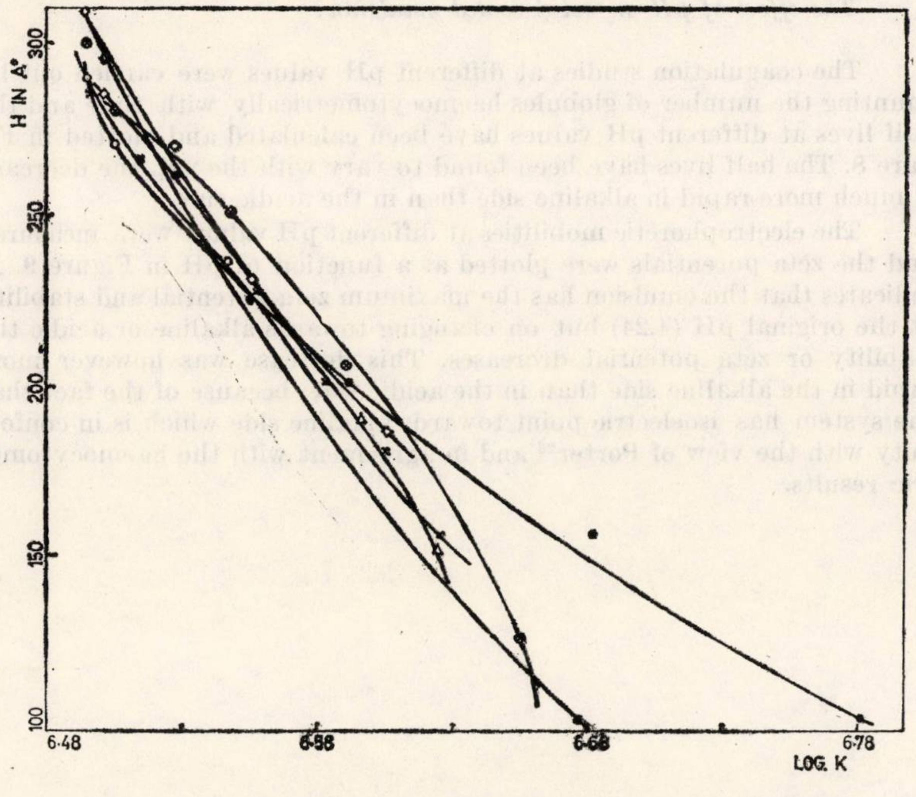

Fig. 5.—Plot of log Debye-Huckel constant $\varkappa$ against distance H_m in the presence of ⊙ KBr, △ $K_2C_2O_4$, × K_2SO_4, ⊡ $K_3(C_6H_7O_5)$, ● $K_3Fe(CN)_6$, ⊗ $K_4Fe(CN)_6$.

---

[24] M. Van Del Temple, Diss. Rubber Stichting, Delft, 1953.

Degree of aggregation and Van der Waals constant:

The degree of aggregation can be calculated by counting the number of singlets and doublets with time. In Figure 6, the number of individual drops remaining after association are plotted against time, these curves seem to level off after some time, indicating the reversible flocculation. The theoretical values of aggregation degree have also been calculated using different values of Van der Waals constant A with the help of depth of secondary minima and are plotted as a function of A in Figure 7. With the knowledge of the observed D, the value of A has been deduced and mean value of A for the oil (toluene) droplets coated with chromium hydroxide sol particles is found to be 2.7×10^{-13} erg, which seems to be reasonable and also agrees with the calculated values by physico-optical data.[25]

The effect of pH on solid coated emulsion:

The coagulation studies at different pH values were carried out by counting the number of globules haemocytometrically with time and the half lives at different pH values have been calculated and plotted in Figure 8. The half lives have been found to vary with the pH, the decrease is much more rapid in alkaline side than in the acidic side.

The electrophoretic mobilities at different pH values were measured and the zeta potentials were plotted as a function of pH in Figure 9. It indicates that the emulsion has the maximum zeta potential and stability at the original pH (4.24) but on changing towards alkaline or acidic the stability or zeta potential decreases. This decrease was however more rapid in the alkaline side than in the acidic side, because of the fact that the system has isoelectric point towards alkaline side which is in conformity with the view of Porter[26] and in agreement with the haemocytometric results.

---

[25] S. P. Jain and S. N. Srivastava, *Indian J. Chem.*, **9**, 973 (1971).

[26] E. E. Porter, "The Hydrous Oxide" by H. B. Weiser, New York, 1920, p. 91.

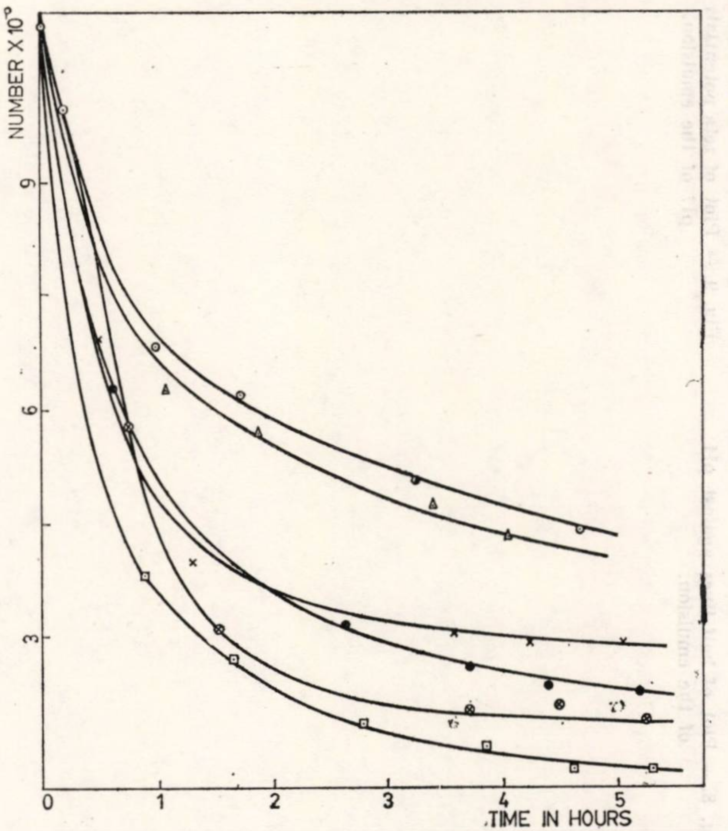

Fig. 6. — Plot of number of monomers per ml against time in hours in the presence of K_2SO_4 ⊙ 2.5×10^{-5}, △ 5.0×10^{-5}, × 3.0×10^{-4}, ● 1.0×10^{-3},. ⊗ 15×10^{-3}, ⊡ 2.5×10^{-3}.

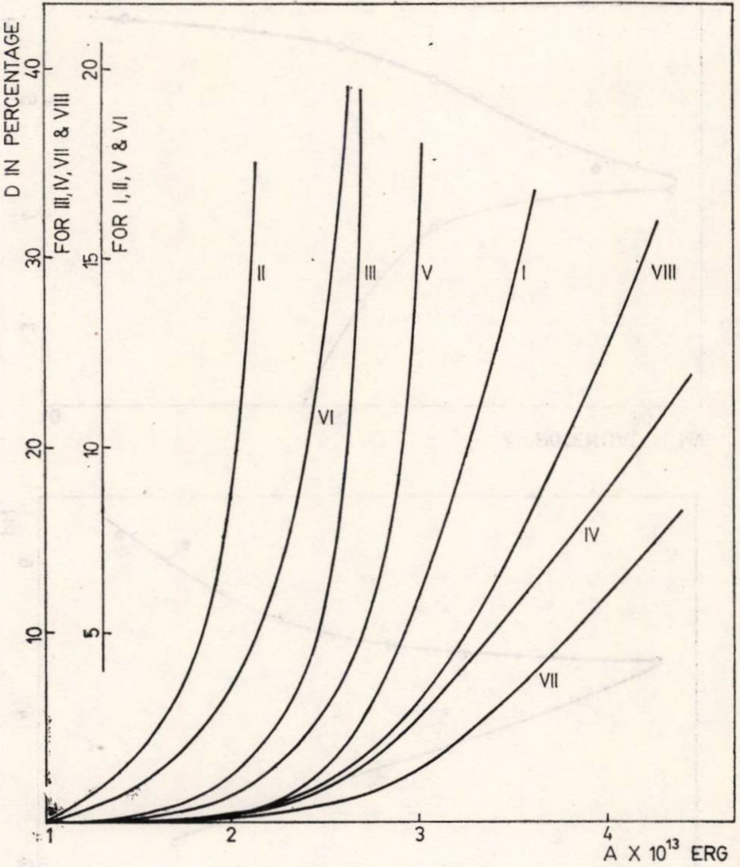

Fig. 7. — Plot of degree of aggregation against Van der Waals constant in the presence of *I* 5.0×10^{-5} KBr, *II* 1.5×10^{-3} K_2SO_4, *III* 1.0×10^{-3} and *IV* 1.0×10^{-4} $K_2C_2O_4$, *V* 2.5×10^{-4} K_3 $(C_6H_7O_5)$, *VI* 5.0×10^{-4} $K_3Fe(CN)_6$, *VII* 5.0×10^{-6} and *VIII* 5×10^{-5} $K_4Fe(CN)_6$.

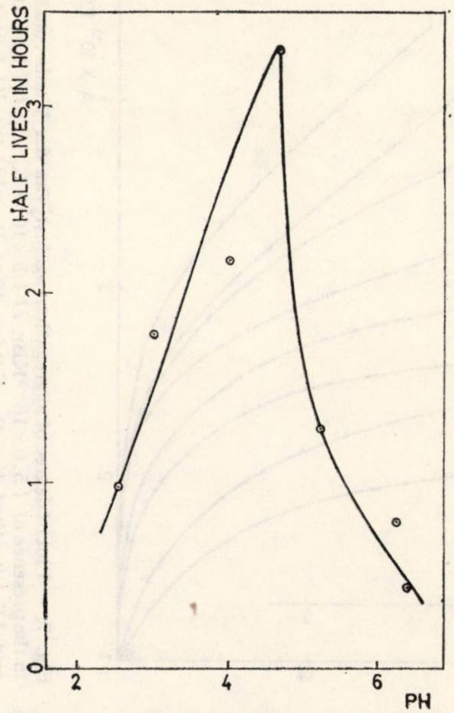

Fig. 8. — Plot of half lives against pH of the emulsion.

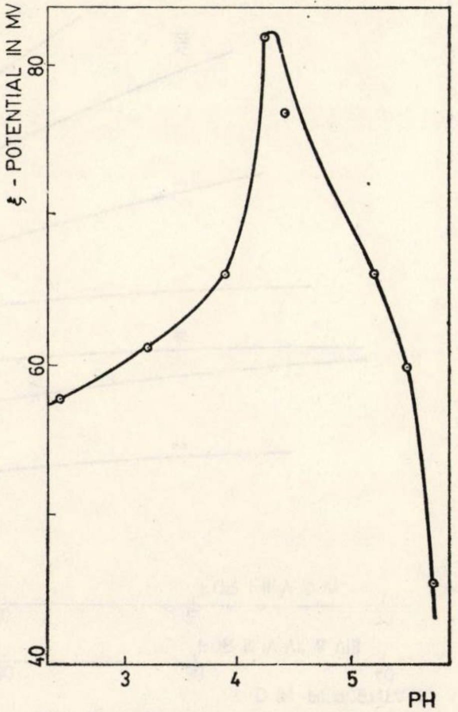

Fig. 9. — Plot of zeta potentials against pH of the emulsion.

Revue Roumaine de Chimie, **23**, *9–10*, 1389–1395 (1978)

POLYNUCLEAR COMPLEX COMPOUNDS OF IRON, COBALT AND NICKEL. II[1].

BISMUTH – CONTAINING COMPLEX COMPOUNDS

MARIA BREZEANU and MAGDALENA DINCULESCU

Polytechnic Institute of Bucharest, Laboratory of Inorganic Chemistry, Splaiul Independenţei, 202, Bucharest, Romania

Received January, 31, 1977

A series of polynuclear complex compounds containing iron, cobalt, nickel and bismuth were synthesized. They correspond to the following general formulas : $[Fe(BiOCl)X_3]$. $.2H_2O$, $Na[Fe(BiOCl)_2 X_4] . 2H_2O$, $X = Cl$, OH^-; $Na [M(BiOCl) Cl_3] \cdot 5H_2O$, $Na [M(BiOCl) Cl_2 (OH)] \cdot 5H_2O$, $Na_2 [M(BiOCl)_2Cl_4] \cdot 4H_2O$; $Na_2[M(BiOCl)_2Cl_2 (OH)_2]$. $.4H_2O$, in which $M = Co$ and Ni. These complex compounds were characterized by elemental chemical analysis, electronic and vibrational spectra.

A previous paper[1] has reported the results obtained in the synthesis and characterization of compounds formed in the system : $Fe X_3 - BiX_3 - NH_4OH$ where $X = NO_3^-$.

In order to establish the extent of the property of iron, cobalt and nickel ions to form polynuclear complex compounds with an element from the Vth main group, we have undertaken a study of the systems : $MX_n - BiX_3 -$ Base where $M = Fe(III)$, $Co(II)$, $Ni(II)$ $X = Cl^-$; Base $= NaOH$, NH_4OH.

The first stage of this study was concerned with the chemical and physico-chemical characterization of complex compounds formed in the mentioned systems, when the base was sodium hydroxide.

A series of polynuclear complex compounds which may be represented by the following general formulas : $[Fe(BiOCl)X_3] . 2H_2O$, $Na[Fe(BiOCl)_2X_4] . 2H_2O$, $X = Cl^-$, OH^-; $Na[M(BiOCl)Cl_3]. 5H_2O$, $Na[M(BiOCl)Cl_2(OH)] . 5H_2O$, $Na_2[M(BiOCl)_2Cl_4] . 4H_2O$, $Na_2[M(BiOCl)_2Cl_2(OH)_2] . 4H_2O$, in which $M = Co$ and Ni, have been obtained.

The compounds obtained were characterized by elemental analysis, vibrational and electronic spectra.

---

[1] Part I : M. Brezeanu and M. Dinculescu, *Rev. Chim. (Bucureşti)*, **23**, 641 (1977).

RESULTS AND DISCUSSION

The nature of species formed in the systems investigated was established by carrying out the synthesis under various conditions with regard to the following parameters :

- $MCl_n : BiCl_3$ ratio
- pH of the reaction medium
- nature of the base

To establish the contribution of the first parameter, i.e. the ratio of components, we maintained constant the amount of iron, cobalt, and nickel chloride, respectively, progressively varying the amount of bismuth chloride from a ratio of 1 : 1, 1 : 2, to excess.

The results obtained led to the conclusion that the maximum achievable M – Bi ratio in these compounds is 1 : 2, even when working in the presence of an excess of bismuth chloride. That means that the substances obtained are unitarian products not mixtures.

The presence of the BiOCl species as a ligand in the coordination sphere of such compounds is justified by the very marked tendency of bismuth (III) to hydrolyse even in acidic medium. The fact indicated by literature[2,3] that the BiOCl leads to a product with polymer structure only at high temperatures (700°) and on another hand that in combinations obtained, BiOCl is formed really in the reaction medium, gives us the permission to assert that in the combinations studied, it appears as a monomer unity.

The second parameter, i.e. the pH of the reaction medium, seems to influence the composition of coordination sphere.

Thus, the complex compounds obtained at a weakly acidic or neutral pH contain in their coordination sphere ligands such as bismuth oxichloride and chlorine. As the basicity of the reaction medium increases, chlorine ligands are gradually substituted by hydroxyl groups.

In the complex compounds of iron and bismuth, the substitution was complete, beginning even at pH = 10, whereas in the complex compounds of cobalt and nickel this was not possible even when an excess of sodium hydroxide was used.

For such compounds, only a partial chlorine substitution by hydroxyl groups occurs and with an excess of sodium hydroxide only $Na[M(BiOCl)Cl(OH)_2] \cdot 5H_2O$ (M = Co, Ni) is obtained, regardless of the $1MCl_2 : nBiCl_3$ ratio used.

Under the experimental conditions mentioned, the following complex compounds have been obtained :

– for a ratio $1MCl_n : 1BiCl_3$, M = Fe(III), Co(II), Ni(II) and pH = = 6–7, and 10 respectively, the compounds :

$$[Fe(BiOCl)X_3] \cdot 2H_2O,\ X = Cl^-,\ OH^-,\ Na[M(BiOCl)Cl_3] \cdot 5H_2O,$$
$$Na[M(BiOCl)Cl_2(OH)] \cdot 5H_2O,\ M = Co,\ Ni.$$

---

[2] "Gmelins Handbuch der Anorganischen Chemie" – Wismut – 1964, p. 692, p. 693.

[3] P. Pascal, "Nouveau Traite de Chimie Minerale", vol. 11, 1958, p. 753.

— for a ratio $1MCl_n : 2BiCl_3$ and the same pH values, compounds : $Na[Fe(BiOCl)_2X_4] . 2H_2O$, X = Cl^-, OH^-,

$Na_2[M(BiOCl)_2Cl_4] . 4H_2O$, $Na_2[M(BiOCl)_2Cl_2(OH)_2] . 4H_2O$, M = Co, Ni.

— by using an excess of sodium hydroxide (pH = 13—14), compounds $Na[M(BiOCl)Cl(OH)_2] . 5H_2O$, M = Co, Ni, regardless of the value of the $MCl_n : BiCl_3$ ratio.

Under these conditions, in the case of iron, the same compounds are obtained, i.e. : $[Fe(BiOCl)(OH)_3] . 2H_2O$ respectively $Na[Fe(BiOCl)_2(OH)_4] . 2H_2O$, at pH = 13 and pH = 10.

Based on electronic and vibrational spectra correlated with the elemental analysis, the complex compounds synthesized with a 1 : 1 ratio, were assigned a tetrahedral structure in which BiOCl acts as ligand alongside with the other chlorine ligands, respectively the hydroxyl group.

Based on the same data, the most probable structure of the compounds obtained at a 1 : 2 ratio was considered to be that in which M is hexacoordinated.

All these compounds exist in the form of one single modification. The iron complex compounds are brown, those of cobalt are blue-grey and those of nickel, green. Their colour turns lighter with the increase in the bismuth content of the compound. Similarly, within the limits of the same ratio, the colour turns darker with the increase in the basicity of the reaction medium.

By heating to 110°, the complex compounds synthesized undergo a weight loss, corresponding to the *n* water molecules which they contain.

I. R. SPECTRA

The investigation of vibrational spectra of most complex compounds synthesized has provided additional information on their structure.

The important spectral domains are those in which absorption is attributed to the vibration modes of the BiOCl molecule, of the lattice water and of the δ_{M-OH} stretching vibration in hydrocomplexes.

The characteristic frequencies and their probable assignments are presented in table 1.

The data shown in this table lead to the following findings :

— the presence in complex compounds containing the BiOCl ligand, of the characteristic frequency of the ν_{Bi-O} vibration mode, generally slightly modified ;[4]

— the presence in the spectra of all compounds, of bands corresponding to the three vibration modes characteristic for lattice water ;[5]

— the presence in the spectra of compounds containing the hydroxyl group of some bands in domain 970-1100 cm^{-1} attributed to the δ_{M-OH} stretching vibration.[5]

---

[4] A. Rulmont, *Compt. rend.*, **272**, 1364, (1971).

[5] K. Nakamoto, "The Infrared Spectra of Inorganic Compounds", Wiley, New-York, 1963, p. 156.

Table 1

Characteristic I. R. frequencies of synthesized complex compounds (cm^{-1})

Compound	$\nu Bi-O$	$\nu Bi-Cl$	$\delta M-OH$	νOH(str).	$\delta H-OH$	low frequencies
BiOCl	535–540	260	–	–	–	–
$[Fe(BiOCl)Cl_3]\cdot 2H_2O$	542	–	–	3440	1582	415
$[Fe(BiOCl)\ (OH)_3]\cdot 2H_2O$	540	–	1062	3440	1577	417
$[Co(BiOCl)Cl_3]Na\cdot 5H_2O$	547	–	–	3485	1630	414
$[Co(BiOCl)Cl(OH)_2]\ Na\cdot 5H_2O$	543	–	1042	3487	1590	414
$[Ni(BiOCl)Cl(OH)_2]Na\cdot 5H_2O$	545	–	1042	3486	1598	416
$[Fe(BiOCl)_2Cl_4]Na\cdot 2H_2O$	537	–	–	3430	1590	488
$[Fe(BiOCl)_2(OH)_4]Na\cdot 2H_2O$	537	–	1050	3448	1593	477
$[Co(BiOCl)_2Cl_4]Na_2\cdot 4H_2O$	542	–	–	3476	1632	423
$[Co(BiOCl)_2Cl_2(OH)_2]Na_2\cdot 4H_2O$	545	–	1049	3477	1586	425

An assignment of bands characteristic of the ν_{OH} valency vibration of the coordinated hydroxyl below 3500 cm^{-1} is not possible since the bands present in this domain overlap those belonging to the lattice water.

ELECTRONIC SPECTRA

The structure of the complex compounds obtained in the systems under consideration was elucidated by recording their electronic reflexion spectra.

An examination of such spectra enables to assign a tetrahedral configuration for complex compounds of the type: $[Fe(BiOCl)X_3]\,.\,2H_2O$, $X = Cl^-, OH^-$, $Na[M(BiOCl)Cl_3]\,.\,5H_2O$ and $Na[M(BiOCl)Cl(OH)_2]\,.\,5H_2O$ in which M = Co, Ni, the present bands being attributed as follows:

— the band of a very reduced intensity at about 800 nm, very likely to the $^4E \leftarrow {}^6A_1$ spin-forbidden transition, for a d^5 (Fe(III)) ion in a tetrahedral surrounding;

— the band at about 650 nm to the $^4T_1(P) \leftarrow {}^4A_2$ transition for a d^7 ion in a tetrahedral surrounding. Its fine structure is due to the spin-orbit coupling which determines the splitting of the $^4T_1(P)$ term[6].

— the bands at about 780 nm and 1200 nm, to the $^3T_1(P) \leftarrow {}^3T_1(F)$ transitions, respectively $^3A_2 \leftarrow {}^3T_1(F)$ in a tetrahedral surrounding of the Ni(II) ion.

[6] Y. Tanabe and S. Sugano, *J. Phys. Soc. Japan*, **6**, 457, (1954).

Figures 1, 2, and 3 exhibit the electronic reflexion spectra of compounds containing iron, cobalt, nickel and bismuth.

The examination of the electronic spectra of compounds $Na[Fe(BiOCl)_2X_4] . 2H_2O$, $X = Cl^-$, OH^-, $Na_2[M(BiOCl)_2Cl_4] . 4H_2O$,

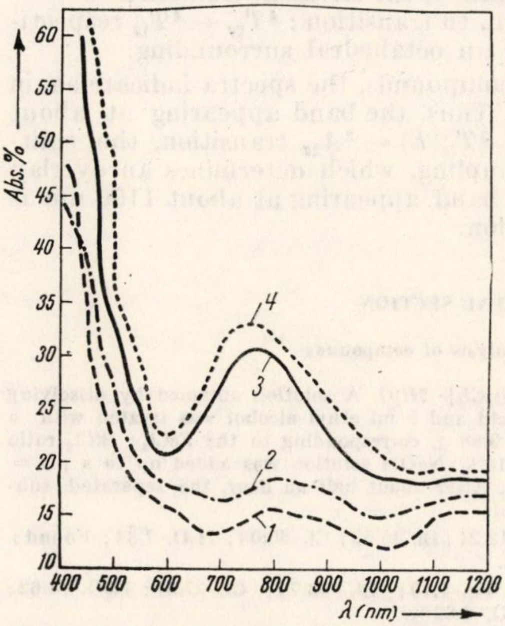

Fig. 1. — Electronic spectra of iron-containing compounds :

1. $[Fe(BiOCl)Cl_3].2H_2O$; 2. $[Fe(BiOCl)(OH)_3].2H_2O$; 3. $Na[Fe(BiOCl)_2Cl_4].2H_2O$; 4. $Na[Fe(BiOCl)_2(OH)_4].2H_2O$.

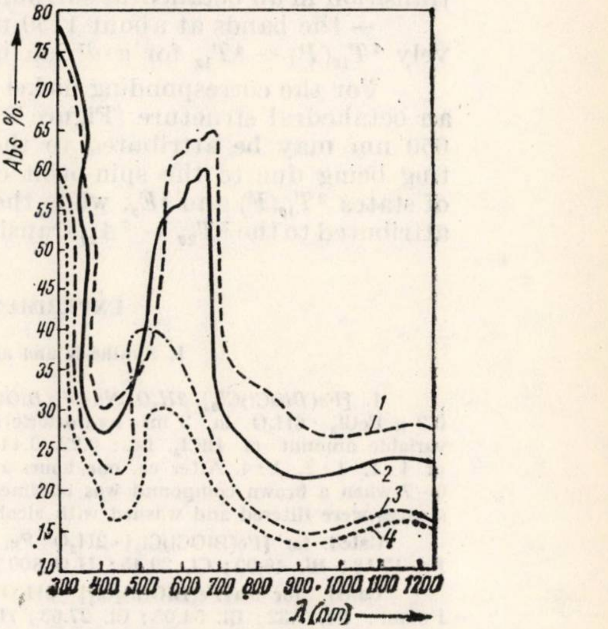

Fig. 2. — Electronic spectra of cobalt-containing compounds :

1. $Na[Co(BiOCl)Cl_3].5H_2O$; 2. $Na[Co(BiOCl)Cl(OH)_2].5H_2O$; 3. $Na_2[Co(BiOCl)_2Cl_4]. 4H_2O$; 4. $Na_2[Co(BiOCl)_2Cl_2(OH)_2]. 4H_2O$.

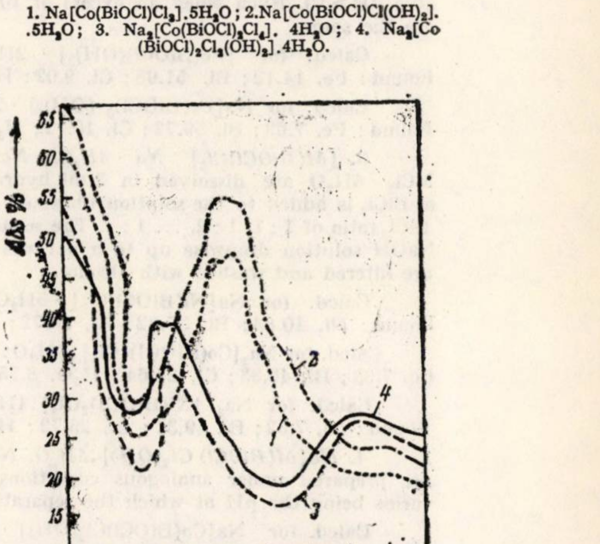

Fig. 3. — Electronic spectra of nickel-containing compounds :

1. $Na[Ni(BiOCl)Cl_3].5H_2O$; 2. $Na[Ni(BiOCl)Cl(OH)_2].5H_2O$; 3. $Na_2[Ni(BiOCl)_2Cl_4]. 4H_2O$; 4. $Na_2[Ni(BiOCl)_2Cl_2(OH)_2]. 4H_2O$.

$Na_2[M(BiOCl)_2Cl_2(OH)_2] . 4H_2O$ where M=Co, Ni, enables to conclude that their most probable structure is the octahedral one. The bands present in the spectra of compounds may be attributed thus:

— the band at about 780 nm, to the ${}^4T_{1g} \leftarrow {}^6A_{1g}$ spin-forbidden transition in an octahedral surrounding of the trivalent iron ion;

— the bands at about 1150 nm, to transition: ${}^4T_{2g} \leftarrow {}^4T_{1g}$ respectively ${}^4T_{1g}(P) \leftarrow {}^4T_{1g}$ for a d^7 ion in an octahedral surrounding.

For the corresponding nickel compounds, the spectra indicate again an octahedral structure (Figure 3). Thus, the band appearing at about 650 nm may be attributed to the ${}^3T_{1g}(F) \leftarrow {}^3A_{2g}$ transition, the splitting being due to the spin-orbit coupling, which determines an overlap of states ${}^3T_{1g}(F)$ and ${}^1E_g$, while the band appearing at about 1100 nm is attributed to the ${}^3T_{2g} \leftarrow {}^3A_{2g}$ transition.

EXPERIMENTAL SECTION

I. Synthesis and analysis of compounds

1. *$[Fe(BiOCl)Cl_3]. 2H_2O$, $Na\,[Fe(BiOCl)_2Cl_4] \cdot 2H_2O$.* A solution obtained by dissolving 0.2 g $FeCl_3 \cdot 6H_2O$ in 3 ml hydrocloric acid and 5 ml ethyl alcohol was treated with a variable amount of $BiCl_3$, i.e.: 0.22, 0.44, 0.88 g, corresponding to the $FeCl_3 : BiCl_3$ ratio of 1 : 1, 1 : 2, 1 : 4. After ca. one hour, a 10% NaOH solution was added up to a pH = 6−7 when a brown compound was obtained. After about half an hour, the separated substances were filtered and washed with alcohol.

Calcd. for $[Fe(BiOCl)Cl_3] \cdot 2H_2O$: Fe, 12.21; Bi, 45.53; Cl, 30.03; H_2O, 7.84; Found: Fe, 12.58; Bi, 46.00; Cl, 29.45; H_2O 800%.

Calcd. for $Na[Fe(BiOCl)_2Cl_4] \cdot 2H_2O$: Fe, 7.19; Bi, 53.72; Cl, 27.37; H_2O, 4.62; Found: Fe, 7.32; Bi, 54.05; Cl, 27.63; H_2O, 4.62%.

2. *$[Fe(BiOCl)\,(OH)_3]\ 2H_2O$, $Na[Fe(BiOCl)_2(OH)_4] . 2H_2O$.* The conditions for the preparation are identical with the above, except that the separation of compounds takes place at a pH$\geqslant$10. Even when an excess of 10% NaOH solution is added the reaction products are the same.

Calcd. for $[Fe(BiOCl)(OH)_3] \cdot 2H_2O$: Fe, 13.89; Bi, 51.86; Cl, 8.81; H_2O, 8.99; Found: Fe, 14.12; Bi, 51.98; Cl, 9.02; H_2O, 9.26%.

Calcd. for $Na[Fe(BiOCl)_2\,(OH)_4] \cdot 2H_2O$: Fe, 7.97; Bi, 59.37; Cl, 10.08; H_2O, 5.11; Found: Fe, 7.63; Bi, 59.72; Cl, 10.32; H_2O, 5.72%.

3. *$[M(BiOCl)Cl_3]\ Na \cdot 5H_2O$, $Na_2[M(BiOCl)_2Cl_4] \cdot 4H_2O$* where M = Co, Ni. 0.2g $MCl_2 \cdot 6H_2O$ are dissolved in 3 ml hydrochloric acid and 5 ml alcohol. A variable amount of $BiCl_3$ is added to the solution obtained, i.e. 0.26 g, 0.52 g, 1.05 g corresponding to a $MCl_2 : BiCl_3$ ratio of 1 : 1, 1 : 2, ... 1 : 4. The separation of compounds takes place by adding a 10% NaOH solution dropwise up to a pH = 6−7. After half an hour, the separated substances are filtered and washed with alcohol.

Calcd. for $Na[Ni(BiOCl)Cl_3] \cdot 5H_2O$: Ni, 10.94; Bi, 36.89; Cl, 26.43; H_2O, 16.66; Found: Ni, 10.83; Bi, 37,32: Cl, 26,72; H_2O, 16.68%.

Calcd. for $Na_2[Co(BiOCl)_2Cl_4] .4H_2O$: Co, 7.02; Bi, 49.76; Cl, 25.35; H_2O, 8.57; Found: Co, 7.33; Bi, 49.33; Cl, 25.64; H_2O, 8.75%,

Calcd. for $Na_2\,[Ni(BiOCl)_2Cl_4] .4H_2O$: Ni, 7.04; Bi, 49,75; Cl, 25.30; H_2O, 8. 63; Found: Ni, 7.52; Bi, 49.31; Cl, 25.72; H_2O, 8.90%.

4. *$Na[M(BiOCl)\,Cl_2(OH)] .5H_2O$. $Na_2[M(BiOCl)_2Cl_2(OH)_2]$. 4 H_2O.* These compounds are prepared under analogous conditions as the previous ones, the only parameter which varies being the pH at which the separation of compounds occurs (pH = 10).

Calcd. for $Na[Co(BiOCl)Cl_2(OH)] \cdot 5H_2O$: Co, 11.34; Bi, 40.19; Cl, 20.48; H_2O, 17.30; Found: Co, 11.62; Bi, 40.36; Cl, 20.58; H_2O, 17.90%.

Calcd. for $Na[Ni(BiOCl)Cl_2(OH)] \cdot 5H_2O$: Ni, 11.29; Bi, 40.21; Cl, 20.49; H_2O, 17.36; Found: Ni, 11.42; Bi, 40.46; Cl, 20.64; H_2O, 17.68%.

Calcd. for $Na_2[Co(BiOCl)_2Cl_2(OH)_2] \cdot 4H_2O$: Co, 7.34 ; Bi, 52.05 ; Cl, 17.68 ; H_2O, 8.96 ; Found : Co, 7.62 ; Bi, 52.38 ; Cl, 17.96, H_2O, 9.01 %.

Calcd. for $Na_2[Ni(BiOCl)_2Cl_2(OH)_2] \cdot 4H_2O$: Ni, 7.36 ; Bi, 52.08 ; Cl, 17.69 ; H_2O, 8.98 ; Found : Ni, 7.54 ; Bi, 52.46 ; Cl, 17.82, H_2O, 9.12 %.

It can be observed that for the complex compounds synthesized at points 1, 2, 3 and 4, the maximum M-Bi ratio that can be achieved is 1 : 2, even when working with an excess of $BiCl_3$.

5. $Na[M(BiOCl)Cl(OH)_2] \cdot 5H_2O$ (M = Co, Ni). The solution obtained by dissolving 0.2 g $MCl_2 \cdot 6H_2O$ in 3 ml hydrochloric acid and 5 ml alcohol, was treated with a variable amounts of $BiCl_3$, i.e. 0.22 g, 0.44 g 0.88 g corresponding to the $MCl_n : BiCl_3$ ratio of 1 : 1, 1 : 2 ... 1 : 4. By using an excess of sodium hydroxide (pH = 13—14) only compounds with the M — Bi ratio 1 : 1 have been obtained, regardless of the amount of bismuth chloride introduced.

The substances separated were filtered after half an hour and were thoroughly washed with alcohol.

Calcd. for $Na[Co(BiOCl)Cl(OH)_2] \cdot 5H_2O$: Co, 11.75 ; Bi, 41.63 ; Cl, 14.14 ; H_2O, 17.92 ; Found : Co, 11.93 ; Bi, 41.82 ; Cl, 14.63 ; H_2O, 18.36 %.

Calcd. for $Na[Ni(BiOCl)Cl(OH)_2] \cdot 5H_2O$: Ni, 11.77 ; Bi, 41.65 ; Cl, 14.16 ; H_2O, 17.95 ; Found : Ni, 11.58 ; Bi, 41.78 ; Cl, 14.71 ; H_2O, 18.63 %.

The sodium in the compounds was qualitatively determined on an ISP-28 spectrograph.

II. The electronic spectra were recorded using a VSU_1 spectrophotometer, with magnesium oxide as a reference.

III. The I.R. spectra were obtained by means of a UR- 20 spectrophotometer using potassium bromide pellets.

Revue Roumaine de Chimie, **23**, *9–10*, 1397–1401 (1978)

SINTESIS Y DATOS CRISTALOGRAFICOS DE SULFATOS COMPLEJOS DE URANILO: $K_2[UO_2(SO_4)_2]2H_2O$ Y $(NH_4)_4[UO_2(SO_4)_3]$. $4H_2O$

J. MARTIN GIL y F. J. MARTIN GIL

Departamento de Química Inorgánica. Facultad de Ciencias. Universidad de Valladolid. España

Recibido el 28 de julio, 1976

The synthesis and crystal data for the uranyl sulphate complexes of potassium, $K_2[UO_2(SO_4)_2]$. $2H_2O$, I, and ammonium, $(NH_4)_4$ $[UO_2(SO_4)_3] \cdot 4H_2O$, II, have been reported. Both compounds crystallize in the orthorhombic system with $a = 11{,}251$ Å, $b = 13{,}736$ Å, and $c = 7{,}372$ Å for I and $a = 12{,}403$ Å, $b = 13{,}608$ Å, and $c = 9{,}853$ Å for II. Both compounds contain 4 formula units/unit cell. The crystal data of the first compound are given along with those reported by Traill.

INTRODUCCION

Estudios sobre sulfatos dobles de uranilo concluyen afirmando la existencia de varios aniones complejos para un mismo ion metálico. Para compuestos con potasio se han propuesto las estequiometrías $K_2[(UO_2)_2(SO_4)_3] \cdot 5H_2O$[1], $K_2[UO_2(SO_4)_2] \cdot 2H_2O$[2] y $K_4[UO_2(SO_4)_3]$[3]. Del segundo complejo se han dado los parámetros cristalográficos por Traill[2] y han sido revisados por nosotros, encontrando una buena correspondencia entre ambos trabajos. Dos sulfatos complejos de uranilo y amonio han sido descritos en la bibliografía. El compuesto $(NH_4)_2\,[UO_2(SO_4)_2]$[2], es amarillo y monoclínico ; pertenece al grupo espacial : P2 1/n (C^5_{2h}), sus parámetros tienen por valores :

$$a = 20{,}53 \text{ Å},\ b = 7{,}30 \text{ Å},\ c = 7{,}74 \text{ Å, con } \beta = 99°25'$$

la red contiene 4 moléculas ; la densidad calculada tiene por valor 3,10 g cm^{-3} mientras que la densidad medida es de 3,07 g cm^{-3}. Según Staritzky[4] el sulfato doble $(NH_4)_2[(UO_2)_2(SO_4)_3] \cdot 5H_2O$ es ortorrómbico y la relación de sus ejes es la siguiente : $a : b : c = 1{,}00 : 1 : 0{,}91$.

En el presente trabajo damos la preparación de un nuevo sulfato complejo de uranilo y amonio, $(NH_4)_4[UO_2(SO_4)_3] \cdot 4H_2O$, y sus datos cristalográficos, en un avance para la determinación de su estructura.

---

[1] K. W. Bagnall, *MTP Internat. Rev. Sci.*, **7**, 151 (1972).

[2] R. J. Traill, *Am. Mineralogist*, **37**, 394 (1952).

[3] E. Rimbach, *Ber.*, **37**, 461 (1904).

[4] E. Staritzki y A. L. Truitt, *Décl. AECD*-3017 (1950).

Tabla 1

Diagrama *par* el sulfato de uranilo y posasio, $K_2[UO_2(SO_4)_2]\,2.H_2O$

Línea	2θ	d_{hkl} (Å)	I_{obs}	$1/d^2$		$h\ k\ l$
				Obs.	Calc.	
1	12,90	6,86	FF	0,0213	0,0212	0 2 0
2	14,40	6,15	DL	0,0264	0,0263	1 0 1
3	15,78	5,62	F	0,0316	0,0316	2 0 0
4	19,35	4,59	D	0,0475	0,0475 0,0477	1 2 1 0 3 0
5	20,80	4,27	D	0,0549	0,0556	1 3 0
6	24,15	3,69	D	0,0734	0,0736	0 0 2
7	25,30	3,52	DD	0,0807	0,0815	1 0 2
8	25,88	3,44	MF	0,0845	0,0848	0 4 0
9	26,20	3,40	D	0,0865	0,0868	1 1 2
10	27,00	3,30	D	0,0918	0,0923 0,0927	3 2 0 1 4 0
11	26,70	3,11	DD	0,1034	0,1032 0,1027	0 4 1 1 2 2
12	29,00	3,08	D	0,1054	0,1052	2 0 2
13	29,25	3,05	DD	0,1075	—	—
14	29,70	3,01	M	0,1104	0,1105 0,1107 0,1111	2 1 2 3 2 1 1 4 1
15	30,20	2,96	D	0,1141	—	—
16	30,95	2,89	DD	0,1197	0,1188	3 3 0
17	31,80	2,81	DD	0,1266	0,1264	2 2 0 4 0 0
18	32,70	2,74	D	0,1332	0,1325	0 5 0
19	33,60	2,67	DDD	0,1403	0,1404	1 5 0
20	35,00	2,56	DDD	0,1526	0,1529	2 3 2
21	35,70	2,51	DD	0,1587	0,1584	0 4 2
22	37,85 37,95	2,38 2,37	D D	0,1765 0,1780	— 0,1788	— 1 1 3
23	39,20 39,30	2,30 2,29	MF MF	0,1890 0,1907	0,1900 0,1908	2 4 2 0 6 0
24	40,20 40,40	2,24 2,23	DDD DDD	0,1993 0,2011	0,1987 0,2000	1 6 0 *4 0 2*
25	42,30 42,40	2,14	DD DD	0,2183	0,2187 0,2184	5 2 0 2 2 3
26	44,10	2,05	DD	0,2380	0,2371 0,2377	5 2 1 2 5 2
27	44,60	2,03	DDD	0,2427	0,2420	3 1 3
28	46,10	1,97	DD	0,2577	0,2579	3 2 3
29	48,50	1,88	DD	0,2829	0,2823 0,2820	5 4 0 2 4 3
30	53,10	1,72	DD	0,3380	0,3392	*0 8 0*
31	55,30	1,66	DD	0,3629	0,3631 0,3633	5 0 3 6 1 2

Tabla 1 continuación

Línea	2θ	d_{hkl} (Å)	I_{obs}	$1/d^2$ Obs.	$1/d^2$ Calc.	*h k l*
32	55,60	1,65	D	0,3673	0,3684	5 1 3
33	60,40	1,53	DDD	0,4271	0,4267 0,4275	0 5 4 7 2 1 3 6 3
34	67,50	1,39	DDD	0,5176	0,5168	2 5 6

SECCION EXPERIMENTAL

Preparación y propiedades

Por disolución de óxido U_3O_8 en ácido sulfúrico concentrado y posterior adición de una pequeña cantidad de perhidrol, tenemos una solución de sulfato de uranilo que origina cristales amarillo-verdosos y fluorescentes de fórmula $H_2[UO_2(SO_4)_2] \cdot x\,H_2O$. Para la preparación de los sulfatos complejos I y II interesa, mas que mezclar soluciones acuosas de ambos sulfatos, adicionar la del sulfato de metal alcalino a la solución fuertemente ácida del sulfato de uranilo. Si se desea, puede utilizarse el carbonato del metal, pero ha de mantenerse una alta acidez en el medio. De esta solución se obtienen los compuestos por cristalización en desecador de vacío sobre sosa caústica. Los cristales se separan por filtración a vacio de sus aguas madres y se secan con una corriente de aire descarbonatado y seco. Análisis: Calculados para $K_2[UO_2(SO_4)_2] . 2H_2O$: U, 41,30; SO_4, 33,33; K, 13,57; H_2O, 6,25. Encontrados para I: U, 40,95; SO_4, 33,65; K, 13,66; H_2O, 6.28. Calculados para $(NH_4)_4\,[UO_2(SO_4)_3] \cdot 4H_2O$: U, 33,88; SO_4, 41,02; NH_4, 10,27; H_2O, 10,25. Encontrados para II: U, 34,18; SO_4, 40,09; NH_4, 10,32; H_2O, 10,14.

Los cristales de los complejos son fluorescentes, su caracter como tales oscila de moderado a fuerte y son del tipo de la autunita, verde-amarillento, según la clasificación de Meixner.

Celda unidad y determinación del grupo espacial

Los diagramas de rayos X por el método del polvo para los compuestos I y II han sido obtenidos con un generador y difractómetro de rayos X Philips PW 1060/00, utilizando radiacción CuKα filtrada por Ni ($\lambda = 1{,}5418$ Å). Los diagramas muestran que ambos compuestos son ortorrómbicos y las ausencias sistemáticas de *h*00 y 00*l* para I y de *h*00 para II, si h ó

Tabla 2

Datos cristalográficos *para* $K_2[UO_2(SO_4)_2.2H_2O$

	Este estudio	Traill [2]
Sistema cristalino	Ortorrómbico	Ortorrómbico
Grupo espacial	P 2_122_1 (D_2^3)	Pmnb (D_{2h}^{16})
a, Å	11,251	11,55
b, Å	13,736	13,78
c, Å	7,372	7,28
V, Å	1139,3	1158,7
P.m. fórmula	576,43	576,43
Z, moléculas/celda	4	4
d(med.), g cm^{-3}	3,36	3,33
d(calc.), g cm^{-3}	3,36	3,30
Temp., °C	25	(25)

$l \neq 2n$, indican como grupos espaciales probables $P2_122_1$ (D_2^3) y p $P2_122$ (D_2^2) respectivamente. Los datos pertinentes a los cristales se dan en las tablas 1, 2, 3 y 4. Las densidades han sido determinadas mediante la técnica picnométrica habitual, usando tolueno como líquido de inmersión.

Tabla 3

Diagrama *para* el sulfato de uranilo y amonio $(NH_4)_4[UO_2(SO_4)_3] \cdot 4H_2O$

Línea	2θ	d_{hkl} (Å)	I_{obs}	$1/d^2$		*h k l*
				Obs.	Calc.	
1	12,96	6,83	FF	0,0214	0,0216	0 2 0
2	14,80	5,985	DD	0,0279	0,0281	1 2 0
3	15,95	5,55	D	0,0325	0,0319	0 2 1
4	16,79	5,28	M	0,0359	0,0363	2 0 1
5	17,40	5,10	D	0,0384	0,0384	1 2 1
6	17,79	4,98	MD	0,0403	0,0412	0 0 2
7	19,72	4,50	MD	0,0494	0,0486	0 3 0
8	22,40	3,97	D	0,0634	0,0639 0,0628	3 1 0 0 2 2
9	23,47	3,79	D	0,0696	0,0693	1 2 2
10	26,20	3,40	F	0,0865	0,0864	0 4 0
11	26,84	3,32	D	0,0907	0,0904	3 2 1
12	27,25	3,27	DD	0,0935	0,0927	0 0 3
13	27,60	3,23	DD	0,0959	0,0963 0,0967	1 3 2 0 4 1
14	28,90	3,09	DM	0,1047	0,1040 0,1051	4 0 0 3 1 2
15	31,15	2,87	D	0,1214	0,1208 0,1213	1 2 3 3 2 2
16	32,20	2,78	DD	0,1294	—	—
17	32,75	2,735	D	0,1337	0,1341	1 4 2
18	34,84	2,575	D	0,1508	0,1512	3 0 3
19	35,20	2,55	D	0,1538	0,1536	2 4 2
20	37,40	2,40	DD	0,1736	0,1728	3 2 3
21	37,70	2,39	DD	0,1751	*0,1762*	*0 5 2*
22	38,28	2,35	D	0,1811	—	—
23	39,75 40,25	2,27	D D	0,1941	0,1935 0,1944	3 5 0 0 6 0
24	43,95	2,06	DD	0,2357	0,2356	0 6 2
25	45,50	1,99	DD	0,2525	0,2529	3 6 0
26	47,70	1,91	DD	0,2741	0,2742 0,2749	4 1 4 0 7 1
27	48,95 49,25	1,90 1,86	DD DD	0,2770 0,2891	0,2768 0,2901	5 2 3 5 4 2
28	50,00	1,82	DD	0,3019	*0,2998*	*0 5 4*
29	51,30	1,78	D	0,3156	0,3160	3 0 5
30	53,85	1,70	DD	0,3460	0,3456	3 6 3
31	55,55	1,66	DD	0,3629	0,3638	1 7 3

Tabla 4

Datos cristalográficos *para* $(NH_4)_4\,[UO_2\,(SO_4)_3]\,.\,4H_2O$

Sistema cristalino	Ortorrómbico
Grupo espacial	p 2_122 (D_2^2)
a, Å	12,403
b, Å	13,608
c, Å	9,853
V, Å	1663,0
P.m. fórmula	702,49
Z, moléculas/celda	4
d(med.), g cm^{-3}	2,781
d(calc.), g cm^{-3}	2,806
Temp., °C	25

DISCUSION

Los datos cristalográficos del sulfato de uranilo y potasio son, excepto para varios detalles, concordantes con los dados por Traill[2]. La formulación de este sulfato doble como $UO_2K_2(SO_4)_2\,.\,2H_2O$, una vez demostrada[5] la naturaleza compleja de sales de este tipo, sugerimos debe modificarse a $K_2[UO_2(SO_4)_2]\,.\,2H_2O$. Otros sulfatos con este mismo anión complejo, $[UO_2(SO_4)_2]^{2-}$, de los que se dispone de datos cristalográficos son los de niquel[6] y magnesio (S. Rocha[7]). Son ortorrómbicos y el retículo es primitivo. Hace excepción el de amonio, $(NH_4)_2[UO_2(SO_4)_2]$, al que Traill da como monoclínico. Compuestos con este mismo catión pero con distinto anión complejo : $(NH_4)_2[(UO_2)_2(SO_4)_3]$ (Staritzky) y $(NH_4)_4[UO_2(SO_4)_3]$ (objeto del presente trabajo) son también ortorrómbicos.

---

[5] J. Ribas, J. Martin Gil y F. J. Martin Gil, *Quím. Anal.* **30**, 95 (1976).

[6] J. Martin Gil y F. J. Martin Gil, *Kristall u. Technik* **12**, K 55 (1977)

[7] S. Rocha, *Anais Acad. Brasil Cienc.*, **32**, 341 (1960).

Revue Roumaine de Chimie, **23**, *9–10*, 1403–1408 (1978)

THERMAL BEHAVIOR OF POTASSIUM bis-2-PHOSPHO-17-TUNGSTOURANATE

GH. MARCU, MARIANA RUSU and EUGENIA PERȚE
"Babeș-Bolyai" University, Chair of Inorganic
Chemistry, str. Arany Janoș, nr. 11, R-3400, Cluj-Napoca, Romania

Received November 19, 1976

The thermal behavior of the heteropoly compound K_{16} $[U(P_2W_{17}O_{61})_2]$.32 H_2O with the aid of TG analysis, DT analysis, IR spectroscopy and powder X-ray diffractometry was studied.

1. INTRODUCTION

Kehrmann[1] and Souchay[2] showed that the compounds of the phospho-9-tungstate series are formed at pH < 3.75, in concentrated solutions of Na_2WO_4 and Na_2HPO_4, after a long heating time. Pauling[3] suggested that the phosho-9-tungstate anion is a dimer and formulated the anion as follows :

$$[(PO_4)_2W_{18}O_{30}(OH)_{18}]^{6-}$$

After a weak alkaline treatment of the diphospho-18-tungstates, the unsaturated heteropoly tungstates of diphospho-17-tungstates series are obtained.[2]

In an attempt to replace the tungsten atom by another metal atom M^{m+} in the diphospho (diarseno)-18-tungstate compounds, Malik and Weakley[4,5] obtained 12 new species of diphospho(diarseno)-17-tungstate heteropoly compounds.

This class of compounds was also investigated by Tourné and coworkers.[6-8]

---

[1] F. Kehrmann, *Z. anorg. Chem.*, **4**, 138 (1893).

[2] P. Souchay and A. Tézé, *Compt. rend.*, **268**, 1804 (1969).

[3] L. Pauling, *J. Amer. Chem. Soc.*, **51**, 2868 (1929).

[4] S. A. Malik and T. J. R. Weakley, *Chem. Comm.*, **1967**, 1094.

[5] S. A. Malik and T. J. R. Weakley, *J. Chem. Soc.* (A), **1968**, 2647.

[6] C. M. Tourné, *Compt. rend.*, **266**, 702 (1968).

[7] C. M. Tourné and G. F. Tourné, *Compt. rend.*, **266**, 1363 (1968).

[8] C. M. Tourné and G. F. Tourné, *Bull. Soc. chim. France*, **4**, 1124(1969).

Baker[9] suggested for the heteropoly compounds of the series 1 : 2 : 17, the following formulation :

$$[(Y^{y-})M^{m+}O_5\,(P^{5+}\text{or } As^{5+})O_4)_2(W \text{ or } Mo)_{17}O_{48}]^{(10-m+y)-}$$

where Y^{y-} is a monodentate ligand.

The structure of the heteropoly compounds of the series 1 : 2 : 17 is a modification of the well-known "Dawson structure".[10]

The "modified Dawson structure" generally preserves all the characteristics of the "Dawson structure" the only modification being the fact that the metal ion M^{m+} replaces a W^{6+} atom and the occurrence of an unshared oxygen in the center of one of the 18 ligand octahedra.

Peakock[11] suggested that the bonds between the heteropoly ligands $P_2(As_2)W_{17}O_{61}{}^{10-}$ and lanthanides (as central atoms) are achieved only through the four external oxygens of each of the two ligands, without the participation of internal oxygen from the P—O or As—O bond, in the bonding to the lanthanide metal.

The present paper reports the results obtained in the investigation of the $K_{16}[U(P_2W_{17}O_{61})_2]\cdot 32\,H_2O$ heteropoly compound[12] and its transformations occurring in the temperature range 20—800° with the aid of TG and DT analysis, powder X-ray analysis and IR spectroscopy.

2. EXPERIMENTAL PART

2.1. Thermal analysis

The TGA and DTA measurements were performed with a Paulik Erdelyi derivatograph OD-102 type (without maintaining isothermal conditions, 4°/minute heating rate, 100 mg balance sensitivity, 710 mg sample weight. X-Ray diffraction measurements were performed with a diffractometer TUR-M-60 Dresden having a Debye-Scherrer chamber with Ni filter and Co anticathode ($\lambda_{Co}\ k_\alpha = 1.788896$ Å) at 50 kW, mA and 8 hour exposure time.

The diffractograms were recorded with a Vertical Goniometer PW-1050 with Cu anticathode, βNi filter and a scanning of 1°2θ/minute.

The IR absorption spectra were recorded in KBr pellets.

The density was controlled picnometrically, using ortodichlorbenzene as picnometric liquid, p. a., at 20°.

3. RESULTS AND DISCUSSIONS

3.1. Thermal Analysis

In Figure 1, the weight loss (TGA — Fig. 1.1.) its derivate (DTG — Fig. 1.2.), differential temperature (DTA — Fig. 1.3.) and the variation of temperature (T — Fig. 1.4.) are presented.

[9] L.C.W. Baker and J. S. Figgis, *J. Amer. Chem. Soc.*, **92**, 3794 (1970).

[10] H. Dawson, *Acta. Cryst.*, **6**, 113 (1953).

[11] R. D. Peacock, *J. Chem. Soc. (A)*, **1971**, 2028.

[12] Gh. Marcu, M. Rusu and A. V. Botar, *Rev. Roumaine Chim.*, **19**, 827 (1974).

The thermal dehydration process being at 40° occurs in 3 stages:

1) Between 40—140°, 20 hydration water molecules are eliminated, as shown by the endothermal effect at 110° and the weight loss of 3.7%;

2) Between 140—190°, 7 hydration water molecules are eliminated, as shown by the endothermal effect at 155° and the weight loss of 1.24%.

3) Between 190—400°, 5 hydration water molecules are eliminated, as shown by the endothermal effect at 205° and the weight loss of 0.97%.

The overall weight loss up to this temperature, calculated by addition of the weight losses in the three stages, is 5.91% and corresponds to 32 crystallization water molecules of zeolite nature. The elimination of these does not affect the parent structural lattice.

The destruction of complex and the formation of a new phase is evidenced by the exothermal peak at 513°.

The UO_2 formed in the decomposition process reacts with oxygen, as indicated by the approximately 0.05% weight increase on the TGA curve and the exothermal effect at 570°. By increasing the temperature, the elimination of some oxygen takes place, as indicated by a weight loss on TGA curve.

The stability range of the anhydrous compound is comprised between 400—500°.

For the characterization of the new formed phases and to explain the thermal effects, new samples were prepared by freezing the equilibria at different temperatures near the thermal transformation points indicated on DTA curve (Fig. 1.3.). These samples were analysed by powder X-ray analysis and IR spectrometry.

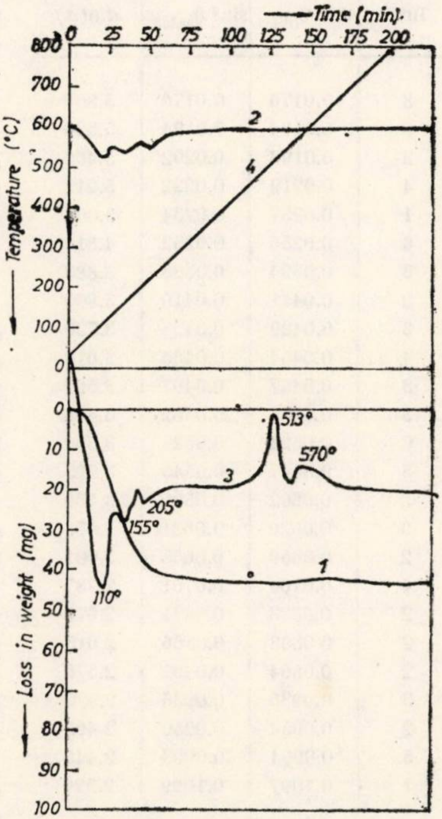

Fig. 1. — Thermogram of the $K_{16}[U(P_2W_{17}O_{61})_2] \cdot 32\ H_2O$ compound.

3.2. Powder X-Ray Diffraction Analysis

In table 1 the X-ray diffraction data, obtained for the $K_{16}[U(P_2W_{17}O_{61})_2] \cdot 32\ H_2O$ compound at room temperature, are listed.

The values obtained for the interplanar distance (*d*) represent the arithmetic mean of values calculated from Debyegramm and a diffractogram.

Table 1

$\sin^2\theta_{obs}$, $\sin^2\theta_{calcd}$ and d values for $K_{16}[U(P_2W_{17}O_{61})_2]\cdot 32H_2O$

Int*.	$\sin^2\theta_{obs.}$	$\sin^2\theta_{calcd.}$	d/n(Å)
3	0.0176	0.0176	5.807
2	0.0194	0.0194	5.536
2	0.0199	0.0202	5.462
4	0.0219	0.0222	5.212
1	0.0237	0.0234	5.008
6	0.0256	0.0252	4.819
5	0.0394	0.0398	3.883
2	0.0411	0.0410	3.800
3	0.0429	0.0428	3.720
4	0.0454	0.0455	3.616
3	0.0467	0.0467	3.567
3	0.0485	0.0482	3.498
6	0.0524	0.0527	3.366
5	0.0547	0.0545	3.295
2	0.0602	0.0599	3.139
9	0.0629	0.0631	3.073
2	0.0659	0.0655	3.001
4	0.0764	0.0761	2.787
2	0.0833	0.0831	2.670
2	0.0868	0.0866	2.615
2	0.0894	0.0892	2.576
3	0.0935	0.0936	2.520
2	0.0954	0.0950	2.495
5	0.0994	0.0993	2.445
1	0.1097	0.1099	2.326

Indexing, by the analytical method,[13] of the 23 lines gives the values $a_H = 11.63$ Å, and $c_H = 18.06$ Å respectively, which are characteristic for the hexagonal system. That our system is hexagonal is proved also by the fact that in the series of $\sin^2\theta$ values some values are divisible by 3.

Since in our case the relation $-h+k+1=3n$ is valid, we can deduce that our compound corresponds to the trigonal group with rhombohedral symmetry. In this case the relation between axes becomes $a = b = c$; $\alpha = \beta = \gamma < 120° \neq 90°$.

Based on X-ray diffraction data obtained for the compund $K_{16}[U(P_2W_{17}O_{61})_2]\cdot 32\,H_2O$ at room temperature and listed in table 1, the values $a = 9.018$ Å; $\alpha = 80°$ and $Z = 1$ were calculated, on the basis of the hexagonal system, trigonal group with rhombohedral symmetry. The compound has elemental cell dimensions very close to those given by other authors for the compounds of 1 : 2 : 17 tungstate series[14]; therefore we assume that this compound also presents a "modified Dawson" type structure, with the central U(IV) ion bonded through four external oxygen atoms of each of the two ligands.

In Figure 2 the relative intensity of diffraction lines depending on interplanar distances, is plotted for the compound $K_{16}[U(P_2W_{17}O_{61})_2]\cdot 32\,H_2O$ at 20°, for the compounds obtained by its heating at 500 and 800°, for the standard material obtained from a mixture of uranium, tungsten, phosphorus and potassium oxides, and for tetragonal WO_3.

The diffraction patterns are different, illustrating the different thermal transformation phase. At 20° the reflexes of rhombohedral structure are recorded which are preserved up to 500°, and prove that the dehydration process does not destroy the crystalline lattice, and that the anhydrous compound has a crystalline structure.

---

[13] R. W. D'Eye and E. Wait "X Ray Powder Photographe in Inorganic Chemistry", Butterworths, London, 1960, pp. 177.

[14] L. C. W. Baker, K. Eriks, M. T. Pope, M. Shibata, O. W. Rollins, J. H. Fang, V. S. Baker and L. L. Kohn, *J. Amer. Chem. Soc.*, **88**, 2329 (1966).

[15] O. Glemser, W. Holznagel, W. Hopte and E. Schwarzmann, *Z. Naturforsch.*, **20b**, 725 (1965).

At 800° the recorded reflexes differ from the precedent pattern, being nearly identical to diffraction pattern of the standard sample and even to the tetragonal WO_3, with very few differences. Consequently, the new crystalline phases formed by the decomposition of the complex is made-up of a chemically heterogeneous mixture in which predominates WO_3.

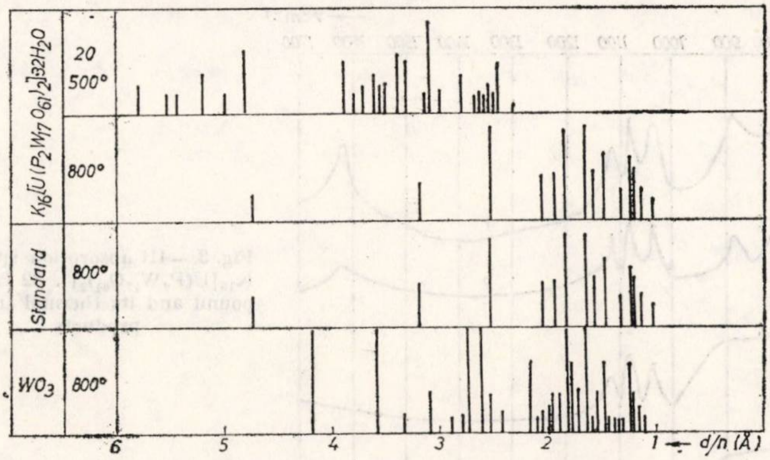

Fig. 2. – X-Ray diffraction pattern of $K_{16}[U(P_2W_{17}O_{61})_2] \cdot 32\ H_2O$ compound and its thermal treatment products.

From the values of a and α parameters determined by X-ray diffraction analysis and the density value ρ measured picnometrically, and using the formula :[13]

$$M = \frac{\rho\, a^3 (1 - 3\cos^2\alpha + 2\cos^3\alpha)^{1/2}}{1.6604 \,.\, Z}$$

where ρ = density in g/cm^3 ($\rho = 21.70\ g/cm^3$) ;
a = dimension of the elemental cell ($a = 9.018$ Å) ;
$\alpha = 80°40'$; $Z = 1$; the molecular mass of the heteropoly compound was calculated ; the value obtained $M = 9768$ is very close to the theoretical molecular mass, equal to 9766.

3.3. IR Absorption Spectra

The IR absorption spectra of the heteropoly compound and its 500° and 800° decomposition products are shown in Figure 3.

The absorption spectra of the compound held at room temperature and heated to 500°, show three absorption bands in the range 700–1000 cm^{-1}, due to valence vibrations of W–O and W–O–W bonds, which are generally characteristic to heteropoly tungstates.[15] The absorption maxima of 730–800 and 955 cm^{-1} are specific to heteropoly compounds having "Dawson structure".

At 1040 and 1080 cm^{-1} two absorption maxima are observed, which are attributed to the valence vibration of the P—O bond.[11]

The band at 1020 cm^{-1} is due to the vibration specific to U(IV)—O, the maximum at 1620 cm^{-1} being generated by the HOH deformation, present only on the spectrum of the parent compound. This latter maximum disappeares at 500°, at this temperature the dehydration process being terminated.

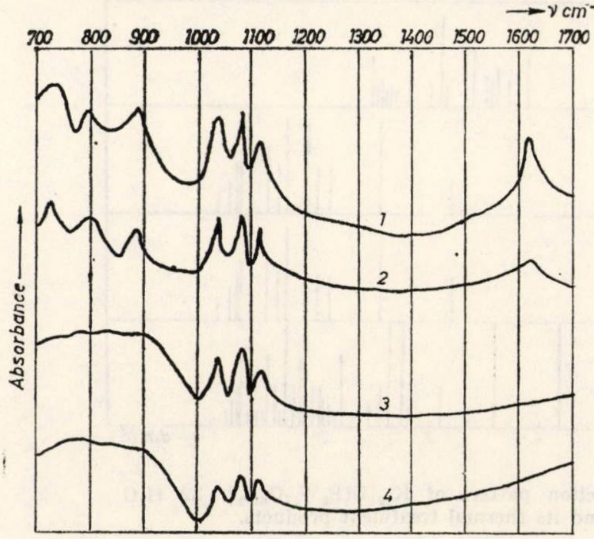

Fig. 3. — IR absorption spectra of $K_{16}[U(P_2W_{17}O_{61})_2]$. 32 H_2O compound and its thermal treatment products.

The product of heating to 800° exhibits a spectrum which contains a broad absorption band between 700 cm^{-1} and 1000 cm^{-1}, characteristic to the heterogen chemical system. The P—O band is preserved as indicated by the maximum at 1098 cm^{-1} and U(IV)—O by the maximum at 1020 cm^{-1}.

The standard sample made up of a mixture of oxides presents a spectrum identical to that of the product heated to 800°.

CONCLUSIONS

1. It was established that all the water in the heteropoly compound $K_{16}[U(P_2W_{17}O_{61}]_2]$. 32 H_2O is of zeolytical nature. Its elimination does not produce a modification in the structure of the compound. By thermal degradation of the compound, a heterogen mixture of oxides is obtained.

2. The heteropoly compound investigated crystallizes in hexagonal system, trigonal group with rhombohedral symmetry.

3. The molecular weight determined from X-ray diffraction data indicates that the heteropoly compound belongs to 1 : 2 : 17 tungstate series. This formulation is supported by the IR absorption data.

Revue Roumaine de Chimie, **23**, *9–10*, 1409–1415 (1978)

COMPLEJOS MOLECULARES DE TRANSFERENCIA DE CARGA. INTERACCION DE BROMURO DE YODO CON METIL PIRIDINAS

J. R. MASAGUER *, A. SOUSA-ALONSO, J. A. GARCÍA-VÁZQUEZ, A. BLANCO

Departamento de Química Inorgánica, Facultad de Ciencias, Universidad de Santiago

*** Actualmente en el Departamento de Química Inorgánica de la Universidad Autónoma de Madrid**

Recibido el 20 de septiembre 1976

Usando métodos calorimétricos se determinaron las entalpías de reacción, ΔH, para las interacciones de monobromuro de yodo con piridina (I), 2-metilpiridina (II), 3-metilpiridina (III) y 4-metilpiridina (IV) a 25° en ciclohexano como disolvente. Los valores de ΔH en kcal.mol^{-1} obtenidos son : $-(12,17 \pm 0,10)$ para (I) ; $-(12,57 \pm 0,11)$ para (II) ; $-(12,83 \pm 0,12)$ para (III) y $-(13,54 \pm 0,11)$ para (IV). Estos valores son discutidos e interpretados en función de los factores electrónicos y estéricos presentes en los complejos. Por otra parte se han caracterizado espectroscópicamente las bandas desplazadas del aceptor y las bandas de transferencia de carga de los complejos. Los resultados son discutidos e interpretados usando la teoría de Mulliken de los complejos de transferencia de carga.

By using calorimetric methods, enthalpies of reaction, ΔH, for the interaction of iodine monobromide with pyridine (I), 2-methylpyridine (II), 3-methylpyridine (III) and 4-methylpyridine (IV) have been measured at 25° in ciclohexane. The following values of ΔH (kcal.mol^{-1}) have been obtained : $-(12.17 \pm 0.10)$ for (I) ; $-(12.57 \pm 0.11)$ for (II) ; (-12.83 ± 0.12) for (III) and $-(13.54 \pm 0.11)$ for (IV). These values are discussed and interpreted in terms of electronic and steric effects. On the other hand, various spectral constants of the shift acceptor bands and the charge-transfer bands have been determined. The results are discussed and interpreted by using Mulliken's theory for charge-transfer complexes.

INTRODUCCION

Este trabajo fué realizado como parte de un programa para determinar las magnitudes termodinámicas asociadas con la formación de complejos moleculares de transferencia de carga de los halógenos e interhalógenos, así como los parámetros espectróscópicos asociados con dichos complejos.

En el anterior trabajo de esta serie [1] se estudiaron las interacciones de I_2 con piridina y metilpiridinas. Dado que los complejos moleculares de BrI están mucho menos estudiados, se decidió estudiar los complejos moleculares de dichas bases piridínicas con BrI.

---

[1] A. Sousa-Alonso, J. A. García-Vázquez, A. Blanco y J. R. Masaguer, *Acta Científica Compostelana*, **13**, 39 (1976).

PARTE EXPERIMENTAL

Ciclohexano, Merck, se lavó repetidas veces con ácido sulfúrico, hasta que la capa ácida quedó incolora, después de lo cual se lavó secuencialmente con agua destilada y una disolución diluída de sosa, hasta que la capa acuosa no dió reacción ácida. A continuación, el ciclohexano fué almacenado varios días sobre Cl_2Ca y refluído durante varias horas sobre hidruro cálcico, destilándose inmediatamente antes de su uso.

Piridina, Merck, fué refluída durante varias horas sobre hidruro cálcico, destilándose inmediatamente antes de su uso.

2-Metilpiridina, 3-metilpiridina y 4-metilpiridina, Merck, fueron refluídas sobre óxido de bario y destiladas inmediatamente antes de su uso.

Monobromuro de yodo, Schuchart, fué purificado por sucesivas cristalizaciones fraccionadas a partir de su fundido.

Con el fín de hacer los errores experimentales lo más pequeños posibles, las disoluciones fueron preparandas por pesada, y los datos de densidad necesarios para calcular las concentraciones fueron tomados de.[2]

Las medidas de absorbancia se han realizado en un espectrofotómetro Beckman DU cuyo compartimiento de cubetas había sido termostatado a 25°, haciendo circular a su través agua que provenía de un termostato.

Con el fín de evitar la posibilidad de existencia de reacciones secundarias que pudieran invalidar los resultados obtenidos, las medidas de la absorbancia se hicieron inmediatamente después de haber preparado las disoluciones, sin que en ningún caso hubieran transcurrido más de diez minutos entre la preparación de una disolución y la medida de su absorbancia.

El calorímetro utilizado fué construido en este departamento siguiendo un modelo descrito por Sunner y Wadsö.[3]

El calorímetro fué calibrado eléctricamente antes de cada experimento y comprobado midiendo la entalpía de disolucion de TRIS (trihidroximetilaminometano) en condiciones prefijadas. El valor obtenido, $-(7{,}130 \pm 0{,}006)$ $kcal.mol^{-1}$, está en satisfactoria concordancia con los valores encontrados por otros investigadores.[4]

Las funciones termodinámicas están expresadas en función de la caloría definida (cal $=$ $=$ 4,184 J) y se refiere al proceso isotérmico a 25°. La entalpía de reacción se calcula a partir de ε y $\log(R_i/R_f)$, en que ε es proporcional a la capacidad térmica total del sistema en cal por unidad de $\log(R_i/R_f)$, seindo R_i y R_f las resistencias del termistor al comienzo y al final de la reacción ó del período de calibrado, y $\log(R_i/R_f)$ es proporcional al cambio de temperatura.

El espectro de absorción del complejo molecular en disolución fué determinado mediendo la absorbancia de una disolución que contenía cantidades conocidas de monobromuro de yodo y base heterocíclica. Los experimentos se llevaron a cabo de forma que la concentración de base heterocíclica estuviese en suficiente exceso sobre la concentración de monobromuro de yodo, como para hacer que la cantidad de éste no complejado fuese prácticamente nula. La absorbancia debida a la base heterocíclica libre fué calculada a partir del coeficiente de extinción de la base a cada longitud de onda de medida y de la concentración de base libre calculada.

RESULTADOS Y DISCUSION

La interaccíon entre BrI y las bases piridínicas estudiadas puede ser descrita por medio de la reacción general:

$$\mathrm{BrI} + L \rightleftarrows \mathrm{BrIL} \tag{1}$$

en que L representa la base heterocíclica. Tal resultado fue conseguido por medio de una aplicación del método matricial descrito en,[5] y en la figura 1 se muestra la representacíon para el caso en que solo existen dos especies absorbentes.

---

[2] "Handbook of Chemistry and Physics", Chemical Rubber Publication Cº, (1961).

[3] S. Sunner y I. Wadsö, *Acta Chem. Scand*, **13**, 97 (1959).

[4] J. O. Hill, G. Ojelund y I. Wadsö, *J. Chem. Thermodynamics*, **1**, 111 (1968).

[5] J. S. Coleman, L. Varga y S. H. Martín, *Inorg. Chem.*, **9**, 1015 (1970).

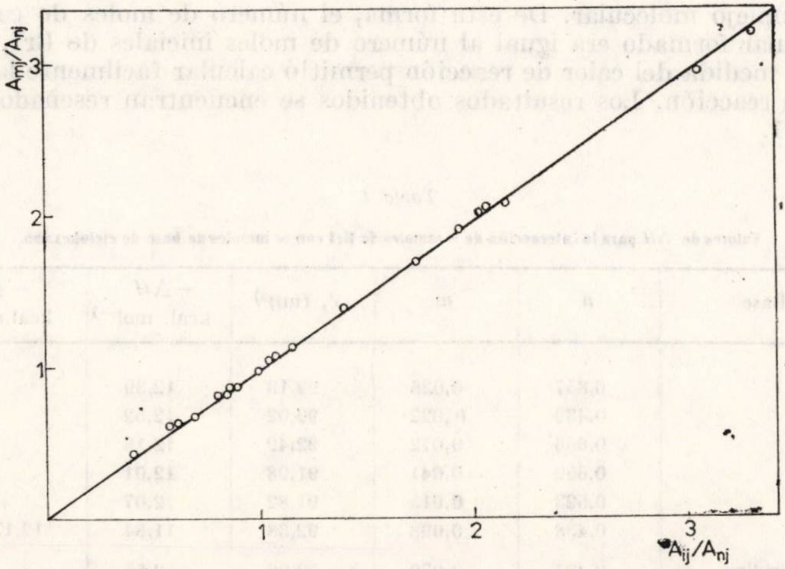

Fig. 1. — Gráfica resultante de la aplicación del método de Coleman,[5] suponiendo dos especies absorbentes en la disolución. A_{nj} representa la absorbancia de la disolución *n* a la longitud de onda *j*.

Datos termodinámicos

Para la medida de la constante de equilibrio fué elegida como magnitud extensiva de medida la absorbancia de disoluciones que contenía cantidades iniciales conocidas de monobromuro de yodo y base heterocíclica. En trabajos anteriores [6] se discuten las ecuaciones que ligan la absorbancia medida con la constante de equilibrio de la reacción (1) y los coeficientes de extinción de los complejos moleculares formados, así como el método *iterativo* seguido para procesar los datos experimentales. En el caso de los sistemas estudiados en este trabajo, no fué posible obtener una solución de las ecuaciones debido a problemas de convergencia, y lo único que pudo deducirse es que en todos los casos el valor de *K* era mayor que 15 000 $l.mol^{-1}$. Esto está en concordancia con los valores encontrados en Cl_4C para dichas interacciones. [7] Esto no es una consecuencia de errores cometidos en la obtención de los datos experimentales, sino una limitación inherente a los métodos de análisis lineal, dado que la estimación más optimista sostiene que no puede determinarse por medio de estos métodos valores de *K* superiores a 10^4 $l.mol^{-1}$. [8]

Sin embargo, aunque el valor de *K* no pudo ser determinado, el hecho de que su valor sea tan grande permitió el diseñar los experimentos calorimétricos de forma que todo el BrI fuese convertido prácticamente en complejo molecular. De esta forma, el número de moles de complejo molecular formado era igual al número de moles iniciales de BrI, por lo que la medida del calor de reacción permitió calcular fácilmente la entalpía de reacción. Los resultados obtenidos se encuentran reseñados en la tabla 1.

---

[6] J. R. Masaguer, A. Sousa-Alonso y J. Romero, *Anales real Soc. españ. Fís y Quím.*, **73**, 203 (1977).

[7] A. I. Popov y R. H. Rygg, *J. Amer. Chem., Soc.*, **79**, 4622 (1957); G. G. Aloisi, G. Beggiato y U. Mazzucato, *Trans. Faraday Soc.*, **66**, 3075 (1970).

[8] R. Olier y P. Clechet, *Thermochimica Acta*, **8**, 249 (1974).

Tabla 1

Valores de ΔH para la interacción de n mmoles de BrI con m mmoles de base de ciclohexano.

Base	n	m	V_t (ml)[a)]	$-\Delta H$ kcal. mol^{-1}	$-\overline{\Delta H}$ kcal.mol^{-1}
Piridina	0,857	0,026	92,13	12,39	
	0,439	0 ,022	92,02	12,52	
	0,666	0,072	92,42	12,16	
	0,652	0,041	91,98	12,01	
	0,523	0,015	91,82	12,07	
	0,438	0,098	92,38	11,84	12,17±0,10
2-metilpiridina	0,426	0,079	92,06	12,66	
	0,605	0,106	92,28	12,95	
	0,379	0,099	92,22	12,49	
	0,265	0,128	92,31	12,36	
	0,393	0,134	92,35	12,38	12,57±0,11
3-metilpiridina	0,530	0,095	92,10	12,93	
	0,589	0,086	92,03	13,10	
	0,317	0,079	91,98	12,64	
	0,716	0,137	92,19	13,09	
	0,284	0,094	91,94	12,35	
	0,589	0,145	92,23	12,87	12,83±0,12
4-metilpiridina	0,598	0,123	92,22	13,41	
	0,428	0,103	92,09	13,17	
	0,711	0,098	92,06	13,45	
	0,322	0,106	92,08	13,96	
	0,572	0,097	92,05	13,63	
	0,751	0,124	92,23	13,62	13,54±0,11

[a] V_t son los volúmenes totales de las disoluciones en el vaso calorimétrico.

Sacconi et al[9] han medido las entalpías de protonización de estas piridinas, y han encontrado que varía seqún la secuencia piridina$<$3-metilpiridina$<$2-metilpiridina$<$4-metilpiridina, estando sus valores en razonable concordancia con los valores encontrados posteriormente por Christensen et al.[10] Tal ordenación ha sido explicada en términos de efectos inductivos e hiperconjugativos.[11] Sin embargo, en el caso del BrI como aceptor, el orden de fuerza dadora es piridina $<$ 2-metilpiridina $<$ 3-metilpiridina $<$ 4-metilpiridina. Esto significa que en estos sistemas además de los efectos electrónicos existen otros no presentes en el caso del H^+ como aceptor y que son responsables de la disminución de la estabilidad del complejo de 2-metilpiridina. Tal efecto puede abscribirse a la existencia de impedimento estérico en el complejo, producido por el grupo CH_3 en posición *orto* con respecto al nitrógeno.

---

[9] L. Sacconi, P. Paoletti y M. Ciampolini, *J. Amer. Chem. Soc.*, **82**, 3831 (1960).

[10] J. J. Christensen, D. E. Smith, M. D. Slede y R. M. Izatt, *Thermochimica Acta*, **5**, 35 (1972).

La misma secuencia se observa en el caso de que el aceptor sea I_2[11], aunque en este caso los valores de ΔH son más pequeños. Esto puede atribuirse a un mayor valor de la afinidad electrónica del BrI que del I_2.

Parámetros espectroscópicos

Banda desplazada del aceptor. — La tabla 2 recoge las características más importantes de esta banda en los complejos estudiados en este trabajo.

Tabla 2

Parámetros espectroscópicos característicos de la banda desplazada del BrI en los complejos formados con las bases indicadas

Base	$\lambda^{a}_{max.}$ nm	$\varepsilon^{b}_{max.}$ $l \cdot cm^{-1} \cdot mol^{-1}$	$\nu_M - \nu^{c}_{0}$ cm^{-1}	$\Delta \nu^{d}_{1/2}$ cm^{-1}	f^{e}
Piridina	364	460	7310	4285	0,0091
2-metilpiridina	363	440	7387	5550	0,0112
3-metilpiridina	361	527	7464	5562	0,0135
4-metilpiridina	360	620	7618	6119	0,0174

[a] Longitud de onda del máximo; [b] coeficiente de extinción molar del máximo; [c] desplazamiento de la banda del BrI; [d] anchura de semibanda; [e] fuerza del oscilador.

Como puede verse, la banda de más baja energía del BrI experimenta un desplazamiento hipsocrómico, a la vez que su intensidad aumenta. Este fenómeno que se produce también en los complejos moleculares de I_2, está presente también en las interacciones del BrI con óxidos de piridina, y siendo los factores responsables los mismos [12]. Además, y como ya se indicó en (12), es de esperar que exista una correlación positiva entre ΔH y la magnitud del desplazamiento hipsocrómico por una parte, y por otra entre ΔH y la intensidad de la banda. Las figuras 2 y 3 demuestran que tal correlación existe.

Banda de transferencia de carga. — La tabla 3 recoge los datos espectroscópicos más característicos de la banda de transferencia de carga de los complejos moleculares estudiados.

De acuerdo con la teoría de Mulliken [13] de los complejos de transferencia de carga, debe existir una correlación positiva entre la frecuencia

---

[11] E. Klingsberg (Ed). "Heterocyclic Compounds", vol. 14; Pyridine and Derivatives, Part. I., Interscience, New York, 1960, p. 30.

[12] J. R. Masaguer, A. Sousa-Alonso, J. Sueiras y J. A. García-Vázquez, *Anales real Soc. españ. Fís. Quim.* **73**, 384 (1977).

[13] R. S. Mulliken y W. B. Person, "Molecular Complexes", Willey-Interscience, New York, (1969).

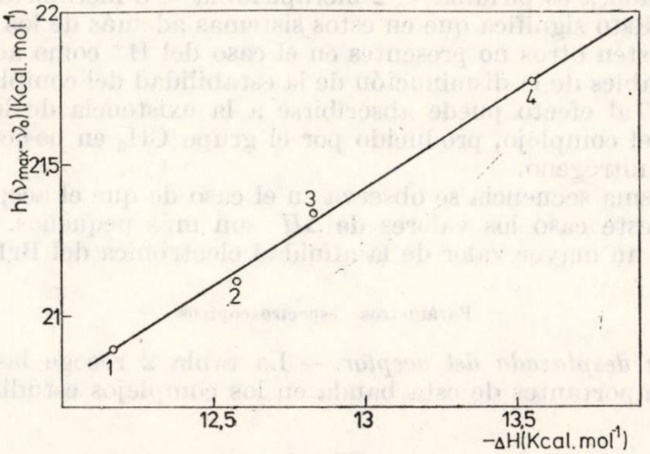

Fig. 2. — ΔH de la interacción de BrI con metilpiridina frente a la energía de desplazamiento de la banda de BrI:

1, piridina; *2*, 2-metilpiridina; *3*, 3-metilpiridina; *4*, 4-metilpiridina.

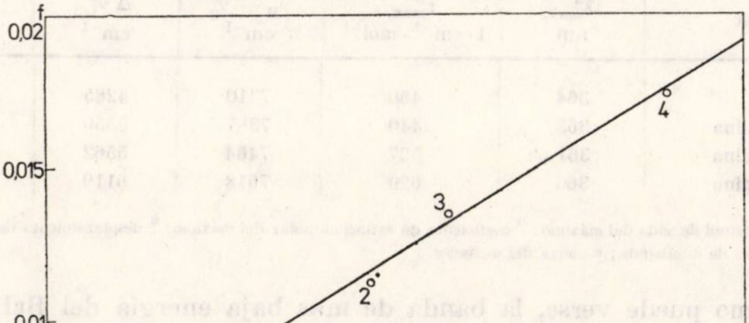

Fig. 3. — Fuerza del oscilador de la banda desplazada del BrI frente a ΔH de la interacción con metil piridinas:

1, piridina; *2*, 2-metilpiridina, *3*, 3-metilpiridina; *4*, 4-metilpiridina.

del máxima de absorción de la banda de transferencia de carga y el potencial de ionización del dador. En el caso de las bases aquí estudiadas dichos potenciales son: piridina 9,23 eV, 2-metilpiridina 9,02 eV, 3-metilpiridina 9,04 eV y 4-metilpiridina 9,04 eV[14]. Como puede verse, los valores de λ_{max} siguen muy aproximadamente la secuencia sugerida, aungue debe indicarse que muy probablemente las diferencias entre los valores de λ_{max} no sean significativas así como tampoco las diferencias en los potenciales de ionización.

---

[14] J. L. Franklin, J. G. Dillard, H. M. Rosenstock, J. T. Herron y K. Drakl, NSRDS-NBS26, U. S. Government Printing Office Washington, D. C. 1969.

Tabla 3

Parámetros espectroscópicos característicos de la banda de transferencia de carga en los complejos moleculares formado por BrI y las bases indicadas.

Base	λ_{max} nm	ε_{max} $l \cdot cm^{-1} \cdot mol^{-1}$	$\Delta\nu_{1/2}$ cm^{-1}	f
Piridina	220	35500	5809	0,948
2-metilpiridina	222	41000	5489	1,035
3-metilpiridina	221	48400	4976	1,107
4-metilpiridina	222	49400	5602	1,272

Además, la teoría de Mulliken predice que debe existir una correlación lineal entre ΔH de la interacción y la intensidad de las bandas de transferencia de carga. Como puede verse en la figura 4 tal predicción se cumple perfectamente en las interacciones de BrI con las bases piridínicas aquí estudiadas.

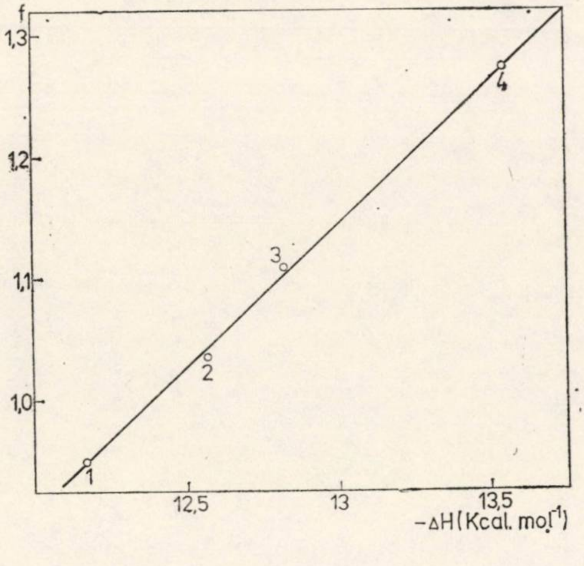

Fig. 4. — Fuerza del oscilador de la banda de transferencia de carga frente a ΔH de la interacción de BrI con metilpiridinas:

1, piridina; *2*, 2-metilpiridina; *3*, 3-metilpiridina; *4*, 4-metilpiridina.

que muy probablemente las diferencias entre los valores de λ_{max} no sean significativas así como tampoco las diferencias en los potenciales de ionización.

Tabla 7

Parámetros espectroscópicos característicos de las bandas de transferencia de carga en los complejos moleculares formados por BrI y las bases indicadas.

Base	λ_{max} nm	ε_{max} l·cm^{-1}·mol^{-1}	$\Delta\nu_{1/2}$ cm^{-1}	f
Piridina	230	33300	3509	0,848
2-metilpiridina	222	41000	5438	1,035
3-metilpiridina	224	45400	4975	1,107
4-metilpiridina	222	48400	5602	1,272

Además, la teoría de Mulliken predice que debe existir una correlación lineal entre ΔH de la interacción y la intensidad de las bandas de transferencia de carga. Como puede verse en la figura 4 tal predicción se cumple perfectamente en las interacciones de BrI con las bases piridínicas aquí estudiadas.

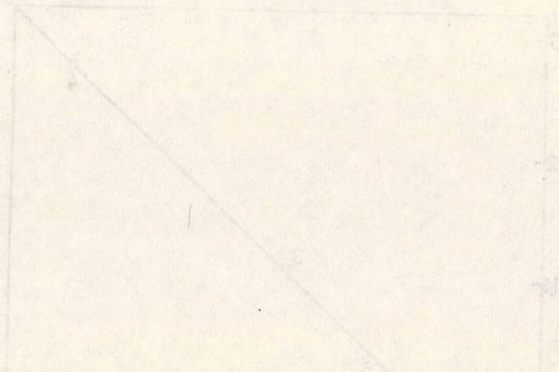

Fig. 4. — Fuerza del oscilador de la banda de transferencia de carga frente a ΔH de la interacción de BrI con metilpiridinas:
1, piridina; 2, 2-metilpiridina; 3, 3-metilpiridina; 4, 4-metilpiridina.

Revue Roumaine de Chimie, **23**, *9–10*, 1417–1423 (1978)

FLUORESCENCE SPECTRA OF SOME Eu(III) AND Tb(III) MIXED LIGAND COMPOUNDS

SILVIA PLOŞTINARU and P. SPACU
Center of Physical Chemistry, Spaiul Independenţei 202,
Bucharest, Romania

Received May 12, 1977

The work studies the fluorescence spectra of some Eu(III) and Tb(III) mixed ligand compounds, recorded at room temperature. The spectra of all studied Eu(III) complex compounds exhibit intense bands within the 550 – 650 nm range due to the $^5D_0 \rightarrow {}^7F_0$, $^5D_0 \rightarrow {}^7F_1$, $^5D_0 \rightarrow {}^7F_2$ transitions in the Eu(III) ion. The emission spectra of the Tb(III) complex compounds exhibit bands corresponding to the transitions from the $^5D_4$ excited level to the multiplets of ground level of Tb(III) ion.

The characteristic fluorescence of Eu(III) and Tb(III) complexes has been the subject of very interesting studies regarding the energy transfer process and the possibility to apply such complexes to laser technology.[1-4] The lanthanides ions embedded into organic chelates, whose donor atoms are oxygen or nitrogen, exhibit intense fluorescence properties when irradiated by UV light. These compounds absorb the UV radiation in the organic component of the molecule and re-emit the fluorescence radiation in the visible domain of the spectrum : the Eu(III) compounds in the orange region and the Tb(III) compounds in the green region.

In our previous papers[5-9] we have synthesized and studied under various aspects (UV and visible electronic spectra, IR spectra, thermogravimetry, etc.) a series of mixed complexes of lanthanides. These complexes are formed by lanthanides hydroxycarboxylates with bidentate neutral ligands having identical nitrogen or oxygen donor atoms. The complexes obtained by us are of interest from several points of view.

---

[1] A. Lempicki, H. Samelson and C. Brecher, *J. Chem. Phys.*, **41**, 1241 (1964).

[2] N. Filipescu, S. Bjorklund, N. Mc. Avoy and C. R. Hurt, *Canad. J. Chem.*, **45**, 1714 (1967).

[3] M. L. Bhaumik, and M. A. El. Sayed, *J. Chem. Phys.*, **42**, 787 (1965).

[4] W. M. Watson, R. P. Zerger, J. T. Yardley and G. D. Stucky, *Inorg. Chem.* **14**, 2675 (1975).

[5] P. Spacu and S. Ploştinaru, *Rev. Roumaine Chim.*, **17**, 697 (1972).

[6] P. Spacu and S. Ploştinaru, *Rev. Roumaine Chim.*, **18**, 971 (1973).

[7] S. Ploştinaru and P. Spacu, *Rev. Roumaine Chim.*, **18**, 2052 (1973).

[8] S. Ploştinaru and P. Spacu, *Rev. Roumaine Chim.*, **19**, 567 (1974).

[9] S. Ploştinaru, *Ph. D. Thesis*, Universitatea Bucureşti, 1973.

Thus, studies carried on in this direction have proved the possibility to enlarge the coordination sphere of lanthanides and hence the possibility to obtain complexes with large coordination numbers. Likewise, the complexes are of interest due to the intense fluorescence properties exhibited by some of them, i. e. those formed with Eu (III) and Tb(III) ions.

The present paper studies the fluorescence spectra of mixed complexes of the form:

LnL_2X_3 where: Ln = Eu(III) and Tb(III); L = 1,10-phenanthroline (phen) or 5,6-Dimethyl-1,10-phenanthroline (DMphen);
X = 5-chloro-2-hydroxybenzoic acid (ClSal) or (4-chloro-2hydroxy)phenylacetic acid (ClMand) or (4-bromo-2hydroxy)phenylacetic acid (BrMand);

$LnLX_3$ where: Ln = Eu(III) and Tb(III);
L = 2,2′dipyridyl-1,1’dioxide (dipyO$_2$);
X = 5-chloro-2-hydroxybenzoic acid (ClSal);

and also of the Eu(III) and Tb(III) simple salts formed with the acids of the corresponding hydroxycarboxylic acids.

EXPERIMENTAL

The synthesis and chemical analysis of the complexes herein studied have already been described elsewhere. [5,6,9]

The fluorescence spectra were measured on a Schimadzu-Q.V.-50 spectrofluorimeter, using an accessor for G.F.16 E fluorescence. The method of reflection on quartz plate in powders or films was applied to record the fluorescence spectra of compounds in solid state. The pelleting technique was also applied using KBr as dilutant. The Eu(III) complexes were excited by 3150 A° monochromatic radiation and for the Tb(III) complexes the excitation wavelength was 3400 A°.

RESULTS AND DISCUSSION

The fluorescence emission of Eu(III) and Tb(III) complexes is the result of an intramolecular energy transfer from the excited levels of the organic compound to the resonance levels of metal ions [10–12]. In his studies, Weissman [10] gave a scheme regarding the mechanism of intramolecular energy transfer. Figure 1 shows this mechanism in a simplified form.

According to this mechanism, the absorbed UV radiation excites the chelate to singlet state (S_1). The energy dissipation may take place in two ways: 1. A radiative transition to the ground state (S_0), i. e. $S_1 \rightarrow S_0$, which leads to a molecular fluorescence; 2. From the singlet excited state (S_1) one passes to the triplet state (T) by a nonradiative mechanism. A $T \rightarrow S_0$ radiative transition may occur henceforth (phosphorescence phenomenon) or an intramolecular energy transfer to the resonance levels (R)

---

[10] S. J. Weissman, *J. Chem. Phys.*, **10**, 214 (1942).

[11] M. L. Bhaumik, *J. Chem. Phys.*, **41**, 574 (1964).

[12] G. A. Crosby, R. E. Whan and R. M. Alire, *J. Chem. Phys.*, **34**, 743 (1961).

of the lanthanide ion. The fluorescence emission characteristic of the metal ion appears by a radiative transition from the resonance levels (*R*) to the ground state ^7F.

Other mechanisms regarding the intramolecular energy transfer have also been suggested.[11] The studies recently made in this field emphasize however the hypothesis advanced by Weissman and resumed by Crosby et al[12] in what the role of the triplet state is concerned. According to this mechanism, the lanthanides complexes will emit fluorescence radiations only if at least one of the metal ion resonance level from which the fluorescence emission occurs, is energetically situated below the ligand donor triplet level. Similarly, the life time of the donor triplet state must be longer than life time of the nonradiative transition on the metal ion excited level. If this is not the case, the spontaneous emission on the triplet state will hinder the achievement of the intramolecular energy transfer.

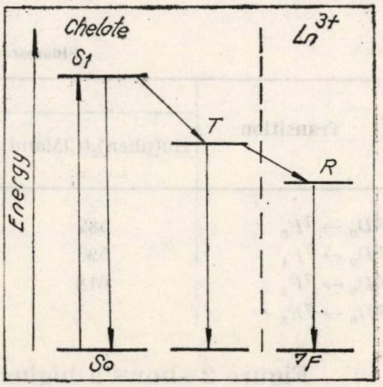

Fig. 1. — Intramolecular energy transfer scheme in the lanthanide complexes.

The fluorescence spectra studied in this paper were recorded in air, at room temperature. The data obtained in such conditions have enabled a comparison between the fluorescence intensity of Eu(III) and Tb(III) simple salts and that of corresponding mixed complexes. It was possible to estimate the influence of the neutral ligand (phen, DMphen, dipyO$_2$) on the fluorescence intensity of complexes. Likewise, it was possible to estimate the influence exerted on the fluorescence intensity when introducing substituents in the molecule of the neutral ligand. These data were obtained by maintaining the experimental conditions (slope, sensitivity of the device, λ excitation, concentration of active substance, etc.), for each set of determinations.

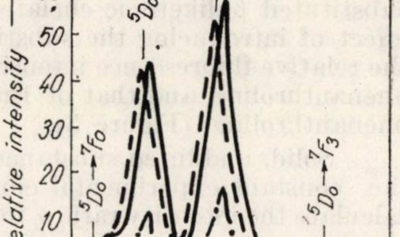

Fig. 2. — Fluorescence spectra of; —— Eu(phen)$_2$(ClSal)$_3$; ------ Eu dipyO$_2$ (ClSal)$_3$; — · — · —. Eu(ClSal)$_3$.

Figure 2 exhibits the fluorescence spectra obtained with some of the Eu(III) complexes under study (Eu(III) chlorosalicylate and the corresponding mixed complexes with 1,10-phenanthroline and 2,2′-dipyridyl-1,1′-dioxide).

The fluorescence spectra of the other studied compounds are very similar to those shown in Figure 2. The difference can only be seen in the band intensity. For the same hydroxycarboxylic acid, the relative fluorescence intensity of the complex varies in terms of the present neutral ligand as follows: DMphen>phen>dipyO$_2$. In general, the emission spectrum of all Eu(III) complexes has revealed intense bands in the 550—650 nm region (Table 1). The fluorescence in this domain is due to the ${}^5D_0 \rightarrow {}^7F_0$, ${}^5D_0 \rightarrow {}^7F_1, D_0 \rightarrow {}^7F_2$, ${}^5D_0 \rightarrow {}^7F_3$ transitions in Eu(III) ion. The assignments for observed transitions were made by analogy with the data reported in literature.[13]

Table 1

Fluorescence spectra of Eu(III) complexes

Transition	λ_{nm}			
	$Eu(phen)_2(ClMand)_3$	$Eu(phen)_2(BrMand)_3$	$Eu(DMphen)_2$ $(ClMand)_3$	$Eu(DMphen)_2$ $(BrMand)_3$
${}^5D_0 \rightarrow {}^7F_0$	582	580	582	581
${}^5D_0 \rightarrow {}^7F_1$	593	595	595	596
${}^5D_0 \rightarrow {}^7F_2$	618	618	618	618
${}^5D_0 \rightarrow {}^7F_3$	—	648	—	650

Figure 2 shows a higher fluorescence intensity for mixed complexes compared to the fluorescence intensity of the simple Eu(III) chlorosalicylate. The complexes formed with chloromandelic and bromomandelic acids have a similar behaviour. This intensity growth in mixed complexes is primarily explained by the fact that the intramolecular energy transfer in compounds containing chemical bonds with a certain covalency degree (the case of mixed complexes) is more efficient than in the compounds with ionic bonds.[14] Secondly, as shown by Butter and Kreher,[15] the fluorescence intensification is also due to the fact that the central metal ion found in a substrate of organic molecules is more isolated from external influences. This isolation reduces the nonradiative desactivation of the excited molecule. This accounts for the sensibly higher fluorescence of mixed complexes compared to that of simple complexes formed with hydroxycarboxylic acids.

The literature[16,17] describes the effect of introducing the substituents into the organic part of the complexes on the fluorescence intensity, on the quantum yield and on the band splitting, in a series of Eu(III) and Tb(III) substituted β-diketonic chelates. The present paper has investigated the effect of introducing the substituents, based on the comparison between the relative fluorescence intensity of Eu(III) chloromandelates with 1,10-phenanthroline and that of Eu(III) chloromandelates with 5,6-dimethylphenanthroline (Figure 3).

Solid, undiluted substances were used to this purpose, maintaining the constant experimental conditions. The data obtained, helped us to calculate the intensity ratio η for the two more intense transitions, ${}^5D_0 \rightarrow {}^7F_1$

[13] E. V. Sayre and S. Freed, *J. Chem. Phys.*, **24**, 1213 (1956).

[14] S. P. Sinha, *Z. Naturforsch.*, **20a**, 1665 (1965).

[15] E. Butter and Kreher, *Z. Naturforsch.*, **19a**, 434 (1964).

[16] F. Halverson, J. S. Brinen and J. R. Leto, *J. Chem. Phys.*, **41**, 2752 (1964).

[17] N. Filipescu, W. F. Sager and F. A. Serafin, *J. Phys. Chem.* **68**, 3324 (1964).

and ${}^5D_0 \rightarrow {}^7F_2$. η is defined as a ratio of the fluorescence intensity in the chelate with the substituted ligand, relative to that in the chelate with the nonsubstituted ligand. This represents a measure of the fluorescence intensity growth due to the substitution.[18] Table 2 presents the data necessary to calculate the η values for the above-mentioned complexes.

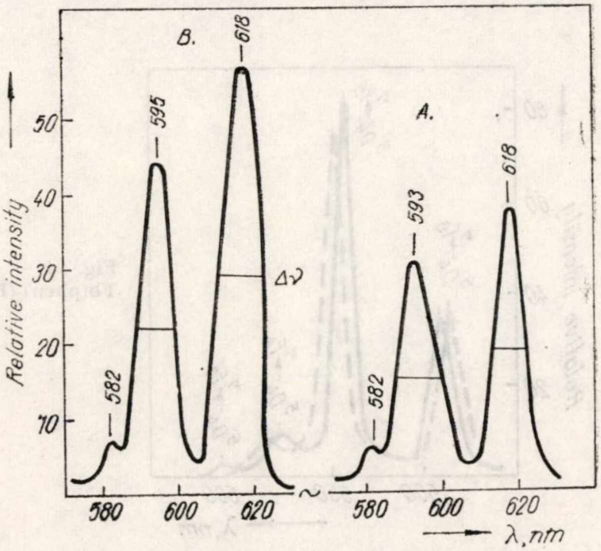

Fig. 3. — Fluorescence spectra of :
A. $Eu(phen)_2(ClMand)_3$;
B. Eu $(DMphen)_2$ $(ClMand)_3$.

Table 2

Data of fluorescence spectra

Transition nm	cm^{-1}	$\overline{\Delta \nu}$ cm^{-1}	$I_{max} \times \overline{\Delta \nu}$	Assignment
A. $Eu(phen)_2(ClMand)_3$				
582	17,182			${}^5D_0 \rightarrow {}^7F_0$
595	16,806	283	30.6×283	${}^5D_0 \rightarrow {}^7F_1$
618	16,181	189	38.0×189	${}^5D_0 \rightarrow {}^7F_2$
B. $Eu(DMphen)_2(ClMand)_3$				
582	17,182			${}^5D_0 \rightarrow {}^7F_0$
593	16,863	255	44.5×255	${}^5D_0 \rightarrow {}^7F_1$
618	16,181	230	57.5×230	${}^5D_0 \rightarrow {}^7F_2$

$\eta {}^5D_0 \rightarrow {}^7F_2 \cong 1.84$; $\eta {}^5D_0 \rightarrow {}^7F_1 \cong 1.30$

The values obtained $\eta\ {}^5D_0 \rightarrow {}^7F_2 \cong 1.84$ and $\eta\ {}^5D_0 \rightarrow {}^7F_1 \cong 1.30$ lead to the following conclusions :

— the methyl groups situated in 5,6 positions in 1,10-phenanthroline cause an increase in the electronic density around the donor nitrogen atoms and consequently the possibility of a larger overlapping between the ligand orbitals and the metal orbitals. This also results in a more efficient energy transfer, hence a growth of the fluorescence intensity.

---

[18] S. P. SINHA, *J, Inorg. Nuclear Chem.*, **28**, 189 (1966).

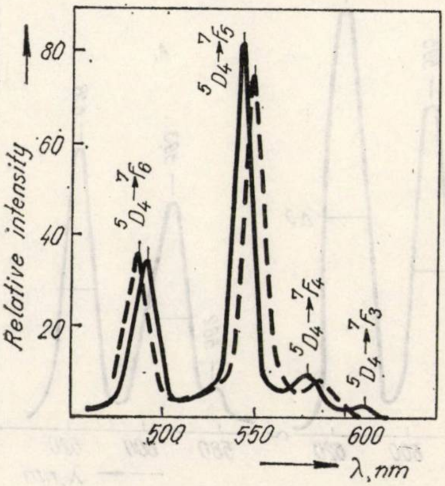

Fig. 4 — Fluorescence spectra of :——— Tb(phen)$_2$(BrMand)$_3$; ---- Tb(phen)$_2$ (ClSal)$_3$.

— the difference between the η values obtained for the two transitions suggests that the transition probability to the level ^7F is not of a similar order of magnitude, and that it varies in terms of the surrounding of the central metal ion.

The fluorescence spectra obtained with the Tb(III) complexes under study indicate bands corresponding to transitions from the excited level $^5D_4$ of Tb(f^8) to the multiplets of the ground level ^7F. The fluorescent emission occurs in the 400—600 nm region. Figure 4 illustrates the fluorescence spectra of Tb(III) mixed ligand compounds with 1,10-phenanthroline. Similar spectra were also obtained with mixed ligand complexes containing 2,2′dipyridyl-1. 1′dioxide as neutral ligand.The relative fluorescence intensity of mixed ligand complexes is higher than that of corresponding hydroxycarboxylates, also in the case of Tb(III). The difference observed is however much smaller, compared to that in the case of Eu(III) complexes. Moreover, the Tb(III) mixed ligand complexes with 5,6-dimethylphenanthroline, under similar experimental conditions, do not present fluorescence in contrast with the high band intensity observed in the case of Eu(III) complexe of the same type. Due to the particular similarity of the complexes of the two ions, formed with this neutral ligand, the absence of the fluorescent emission in the case of Tb(III) complexes can only be explained by associating it to the relative position of the triplet level of the organic ligand, relative to the resonance levels of the lanthanide ion.

The fluorescence of such complexes was also studied in solution. Due to their very reduced solubility, the solutions obtained (10^{-4}—10^{-5} moles/l in ethyl alcohol) fail to present a detectable fluorescence characteristic of metal ions. In this case, only a molecular fluorescence appears, characteristic of the organic ligand. This may be explained by the fact that an energy dissipation is produced in diluted solutions, the intramolecular energy transfer being far less efficient. Probably due to the collision with the solvent molecules, modifications appear in position of the ligand donor triplet levels and this hinders the fluorescent emission characteristic of the metal ions.

In the case of Eu(III) mixed ligand complexes containing 5-chlorosalicylic acid as hydroxycarboxylic acid, for which it was possible to obtain more concentrated solutions in acetone (10^{-2}moles/l), a fluorescent emission characteristic of the Eu(III) ion was observed.

In conclusion, the mixed ligand complexes studied in this paper, present a high fluorescence intensity which is very stable in time both in solid state and in very concentrated solutions.

ACKNOWLEDGEMENT. **We express our thanks to Dr. O. Horer of fluorescence laboratory of the Institute of Virology — Bucharest for assistance and helpful discussions.**

Revue Roumaine de Chimie, 23, *9–10*, 1425–1429 (1978)

TITANIUM(IV) COMPLEXES WITH 2,2′-DIHYDROXYCHALKONES

N. S. BIRADAR * and B. R. PATIL

(P. G. Centre Gulbarga) Department of Chemistry, Karnatak University, Dharwar-580003, India

Received August 2, 1976

A few complexes of titanium (IV) have been prepared by reacting 2,2′-dihydroxychalkones with titanium (IV) chloride in chloroform medium. The complexes are characterized by elemental analysis and molar conductance in DMF. The infrared spectra have been studied in the 4 000–400 cm^{-1} region. The titanium (IV) complexes formed with 2,2′-dihydroxy chalkones are shown to have hexacoordinated halogen bridged structures.

INTRODUCTION

In our previous paper [1] we have reported tin(IV) complexes with 2,2′-dihydroxychalkones and showed that they have chloro bridged hexacoordinated structures, on the basis of infrared spectral data. In this paper we wish to report titanium(IV) complexes with 2,2′-dihydroxychalkones. The probable structures have been expounded on the infrared spectral data obtained in the region 4000–400 cm^{-1}.

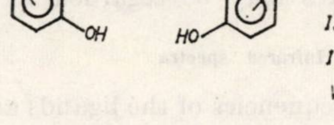

	R	R′
I	H	CH_3
II	CH_3	CH_3
III	Cl	CH_3
IV	CH_3	CH_3
V	Cl	Cl

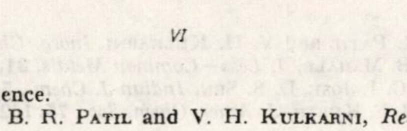

VI

---

* For correspondence.

[1] N. S. Biradar, B. R. Patil and V. H. Kulkarni, *Rev. Roumaine Chim.*, In Press.

EXPERIMENTAL

The chalkones (I — VI) were prepared according to the method reported in the literature.[2]

Preparation of the complexes

Titanium(IV) chloride of Reidel make was used as such without further purification for preparing the complexes.

Titanium(IV) chloride (0.01 mole) in little quantity of dry benzene was added to 0.012 mole of chalkone in dry chloroform with vigorous shaking. The reaction mixture was kept under reflux till the evalution of HCl gas ceased. Subsequently, the solvent was evaporated slowly and the residue was extracted with dry ether and filtered. The complex was washed thoroughly with ether and extracted in a soxhlet thimble with dry ether till it was free from the excess of reagent. The complex thus prepared was dried in vacuum over fused calcium chloride.

Analysis

Titanium in the complexes was estimated gravimetrically as TiO_2 and chloride determined gravimetrically as AgCl.

Physical measurements

The conductance measurements of the complexes in DMF were made with an ELICO conductivity bridge having a cell of cell constant 0.829 cm^{-1}. The infrared spectra of the ligands in Nujol mull were recorded on a Perkin Elmer Infracord 137-B in the region 4 000—650 cm^{-1}. The infrared spectra of the complexes in KBr pellet were recorded on a Perkin Elmer 337 recording spectrophotometer in the region 4 000—400 cm^{-1}.

RESULTS AND DISCUSSION

The complexes are dark red in colour and analyse for 1 : 1 stoichiometry (Table 1). These are not soluble in common organic solvents. However, to some extent, they are soluble in DMF. The insolubility of the complexes in common organic solvents hampered the molecular weight determination.

Molar conductivity

The molar conductance values in DMF at the concentration $\sim 10^{-3}$M are too small to account for the dissociation of the complexes in that solvent. Hence, these complexes may be regarded as non-electrolytes.

Infrared spectra

The important infrared frequencies of the ligands and their complexes are listed in table 2.

The medium intensity broad band observed in the region 3300—3200 cm^{-1} due to the intermolecular hydrogen bonded OH and the broad weak band with fine structure observed in the region 2675—2650 cm^{-1} due to the intramolecular H bonded OH[3] of the ligands are not observed

---

[2] N. S. Biradar, B. R. Patil and V. H. Kulkarni, *Inorg. Chim. Acta.*, **15**, 33 (1975).

[3a] N. S. Biradar, V. B. Mahale, *J. Less—Common Metals*, **31**, 159 (1973).

[b] K. K. Ramaswamy, C. I. Jose, D. S. Sen, *Indian J. Chem.*, **5**, 156 (1967).

[c] H. I. Hergert and B. F. Kurth, *J. Amer. Chem. Soc.*, **75**, 1622 (1953).

Table 1

Elemental analysis of titanium (IV) chalkonates

Lig. No.	Comp. No.	Empirical formula	% Ti	% Cl
I	VII	$(C_6H_{12}O_3)\ TiCl_2$	12.84 (12.91)	19.01 (19.14)
II	VIII	$(C_{17}H_{14}O_3)\ TiCl_2$	12.37 (12.45)	18.52 (18.45)
III	IX	$(C_{16}H_{11}ClO_3)\ TiCl_2$	11.73 (11.81)	11.44 (17.52)
IV	X	$(C_{16}H_{11}ClO_3)\ TiCl_2$	11.69 (11.81)	17.41 (17.52)
V	XI	$(C_{16}H_{10}Cl_2O_3)\ TiCl_2$	11.25 (11.35)	16.54 (16.63)
VI	XII	$(C_{19}H_{11}ClO_3)\ TiCl_2$	10.78 (10.85)	16.16 (16.09)

Note: The values in the parenthesis are the calculated values.

in the complexes. The phenolic C—O in the region 1280—1265 cm^{-1} of the ligands is shifted to higher frequency and is found in the region 1355—1290 cm^{-1}. These evidences are in favour of Ti—O bonds being present in the complexes due to the removal of the protons of the OH groups of 1 and 3 of the ligands.

The high intensity band observed in the region 1650—1640 cm^{-1} in the ligands assignable to the C=O stretching vibration [4] is shifted to the lower frequency in the complexes and merges with HC =CH vibration[5] in the region 1625—1600 cm^{-1} which appears in the region 1600—1580 cm^{-1} for the ligands. Medium to high intensity bands appearing in the region 1600—1470 cm^{-1} both for ligands and complexes are attributed to the aromatic C=C vibrations in view of the previous assignments. [1]

In the 600—400 cm^{-1} region along with the metal oxygen bands the skeletal vibrations of ligands also appear. Hence, it is difficult to warrant to conclusive assignments of the bands in this region. The assignments made in this region are therefore tentative and based on the previous reported data. [6]

---

[4] [a] C. N. R. Rao, "Chemical Applications of Infrared Spectroscopy" Academic Press, London, 1958.

[b] H. W. Thomson and P. J. Torkington, *J. Chem. Soc.*, **1945,** 640.

[c] N. L. Silver and D. W. Boykin (Jr.), *J. Org. Chem.*, **35,** 759 (1970).

[5] [a] N. K. Freeman, *J. Amer. Chem. Soc.*, **75,** 1859 (1953).

[b] D. N. Dhar and V. P. Gupta, *Indian J. Chem.*, **9,** 818 (1971).

[6] [a] K. Nakamoto and A. E. Martell, *J. Chem. Phys.*, **32,** 583 (1960).

[b] K. Nakamoto, P. J. McCarthy, A. Ruby and A. E. Martell, *J. Amer. Chem. Soc.*, **83,** 1272 (1961).

[c] K. Nakamoto, P. J. McCarthy and A. E. Martell, *J. Amer. Chem. Soc.*, **83,** 1272 (1961).

Table 2

Infrared frequencies (in cm^{-1}) of 2,2′-dihydroxy chalkones and their titanium (IV) complexes

S. No.	Assignments	I	VII	II	VIII	III	IX	IV	X	V	XI	VI	XII
1	Aromatic CH and −CH stretching vibration	2950	3050w 3000w 2900w 2850w	2900	3050w 3000w 2900w 2850w	2900	3050w 3000w 2900w 2850w	2950	3010w 2900w 2850w	2900	3050w 3000w 2900w 2850w	2900	3050w 3000w 2900w
2	Intermolecular H bonded OH stretching vibration	3200m	—	3300m	—	3200 br.m	—	3250m	—	3280m	—	3250 br.m	—
3	Intermolecular H bonded OH stretching vibration	2650 br. w	—	2675 br.w	—	2650 br.w	—	2675 br. w	—	2650 br. w	—	2650 br. w	—
4	C = 0 stretching vibration	1640s	1625s	1646s	1610s	1648s	1610s	1648s	1610s	1646s	1610m	1650s	1610m
5	HC = CH stretching vibration	1595m	—	1600m	—	1600s	—	1590s	—	1580m	—	1600m	1600m
6	Aromatic C = C stretching vibration	1570s 1495m 1480s	1550s 1500s —	1575s 1500m 1470m	1545s 1500m —	1558s — 1470s	1550sh 1540s 1490s	1575s 1525w 1470s	1550w 1545s 1490s	1580m — 1470s	1545s — 1490s	1525m — 1470s	1550sh 1510s —
7	Phenolic C = 0 stretching vibration	1265s	1290m	1275s	1295s	1280s	1315s	1280s	1320s	1286s	1300s	1290m	1300s
8	Ti−O stretching vibration	—	500s 440s	—	485m 435m	—	510s 480br. m 430br. m	—	510m 445 br.m	—	480m 430m	— —	510 br. w 480 br. m 440 br. w

w = weak; m = medium; s = strong; br = broad; sh = shoulder.
In most of these complexes C = 0 occurs at lower frequency amalgamated with HC = CH stretching frequency.

The medium to high intensity bands observed in the region 510–430 cm^{-1} are assigned to the ν(Ti—O) vibrations in view of the previous reports.[7]

The analytical (Table 1) and the spectral (Table 2) results suggest that the two hydroxy groups (1 and 3) of the chalkones have formed the bonds by loosing their protons and the coordinating bond is formed with the oxygen of the carbonyl group (2). Hence one can predict the following structure for these complexes :

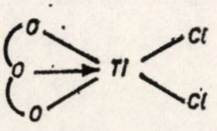

The construction of the models for these complexes does not favour the monomeric structure of the type shown above as the ligand involves much strain for such formulation. However a dimeric structure of the type shown below may be formed without much strain.

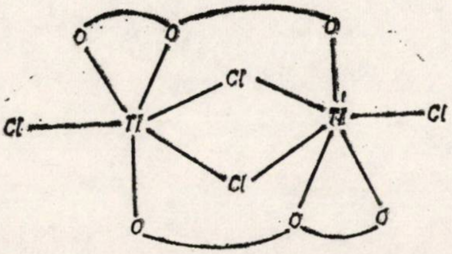

The molecular weights cannot be determined because of their insolubility in the common organic solvents. In analogy of our earlier paper,[1] the authors point out that the complexes might exist in a dimeric form.

Titanium exhibits coordination number six in these complexes as these complexes show nonelectrolytic behaviour in DMF.

[7a] C. D. Jordjevic, *Spectrochim. Acta*, **17**, 448 (1961).

[b] C. P. Prabhakaran and C. C. Patel, *J. Inorg. Nuclear Chem.*, **31**, 3316 (1969).

[c] B. C. Sharma and C. C. Patel, *Indian J. Chem.*, **8**, 747 (1970).

[d] J. A. Faniran and K. S. Patel, *J. Inorg. Nuclear Chem.*, **36**, 2261 (1974).

[e] K. Nakamoto, "Spectroscopy and Structure of Metal Chelate *Compounds*" (Edited by K. Nakamoto and P. J. McCarthy), p. 216, John Wiley, New York 1968).

[f] R. C. Fay and T. J. Pinnavia, *Inorg. Chem.*, **7**, 508 (1968).

[g] N. S. Biradar, V. H. Kulkarni and N. N. Sirmokadam, *J. Inorg. Nuclear Chem.*, **34**, 3651 (1972).

[h] Y. Kawasaki, T. Tanaka and R. Okawara, *Spectrochim., Acta*, **22A**, 157 (1966).

[i] S. C. Jain and R. Rivest, *J. Inorg. Nuclear Chem.*, **31**, 399 (1969).

Revue Roumaine de Chimie, **23**, *9–10*, 1431–1440 (1978)

ELECTRIC CONDUCTIVITY OF CATALYSTS FOR THE CONVERSION OF NATURAL GAS WITH WATER VAPOUR

B. R. ALEKSIĆ, A. TERLECKI-BARIČEVIĆ and M. AĆIMOVIĆ
Institute for Chemistry, Technology and Metallurgy,
Department for Catalysis, Beograd, Yugoslavia

Received July 20, 1976

Changes of electric conductivity of twelve different industrial catalysts for the steam reforming of methane and light hydrocarbons have been investigated in various atmospheres : reductive, oxidative and in vacuum, with the aim to follow the electric properties changes in the catalysts during their reduction by hydrogen. Catalysts have shown three different types of behaviour during reduction–oxidation cycles :

a) as semiconductors of the *p*-type being not reduced in investigated conditions ;

b) as a *p*-type semiconductors which undergo a partial reduction followed by the creation of nickel nuclei as a new type of carriers, and

c) catalysts changing from semiconductors to typical conductors and retaining the high conductivity after the re-oxidation treatment.

On the basis of the results obtained, correlation between electrical conductivity changes and reductibility of steam reforming catalysts seems to be possible.

The active component of the catalysts for the conversion of methane and light hydrocarbons with water vapour consists of metallic nickel obtained by the reduction of nickel oxide on the carrier, formed most frequently from aluminium oxide or the mixture of oxides or aluminates of calcium, magnesium and titane. The interaction of the carrier components and nickel oxide, under the conditions of catalyst synthesis or during exposure to higher temperatures and pressures under reaction conditions, can lead to the formation of more complex oxidative forms of nickel (aluminates, mixed oxides, solid solutions), which are not easily converted into the active form. Due to the fact that catalyst activity depends directly on the completeness of nickel conversion into the active metallic form, research workers are devoting large efforts to investigate the reduction process of supported nickel oxide.

In this work, the changes of electric conductivity during reduction by hydrogen of different types of industrial catalysts for the conversion of methane and light hydrocarbons with water vapour, have been investigated. Twelve different catalysts, classified into three groups, have been observed. The first and the second group (samples 1 — 5 and 6 — 9) comprise variants of the nickel on a carrier type catalyst made by two different producers, respectively, in order to modify its thermal, mechanical or catalytic properties. The remaining three catalysts in the third group (samples 10 — 12) are of a different origin, and they have been observed as well, because of their very widespread application. Investigations have been undertaken in order to remark the differences in the behaviour during the reduction of catalysts of different chemical composition, by following the changes of their electric conductivity in reductive atmosphere, as well as to contribute to the understanding of electric conductivity of these complex systems.

The so far investigations, concerned mainly the pure nickel oxides,[1-9] nickel oxides promoted with small quantities of other oxides — most frequently lithium or magnesium [10,11] as well as nickel oxides on aluminium oxide as a carrier. [12-15] In the work under [16] the possibility to follow the process of catalyst reduction by measuring the changes of magnetic susceptibility and electric conductivity, in situ, has been noticed.

EXPERIMENTAL

The chemical composition of the samples has been observed by semiquantitative spectrographic analysis on the spectrograph of high dispersity with a plate differential grate, and calculated by Hasler-Harvey method. Nickel content has been determined more precisely by complexometric analysis.

Electric conductivity has been determined by compensation method of resistance measurement in direct current of 4 V. Circular areas of the sample, shaped as a Rashig's ring, have been polished, in order to obtain a better contact with platinum plates used as electrodes.

The electric conductivity changes have been observed according to the following program of succesive steps:

I. The catalyst has been heated in vacuum of 10^{-5}mm Hg, up to 450° and has been kept at this temperature up to the point of resistance stabilization; it has been cooled after, and simultaneous measurements of conductivity have been done; the procedure of resistance stabilization at the highest temperature of the cycle has been applied during all the steps of this program; heating has been performed at the rate of 4°/min.

II. The purified hydrogen has been introduced on the cooled sample, and has been left to stay during the night; the catalysts have been heated in a hydrogen flow up to 450°,

---

[1] A. Bielański, J. Dereń, J. Haber, J. J. Stoczyński and T. Wilkowa, *Bull. Acad. polon. Sci., Ser. Sci. chim.*, **7**, 333 (1959).

[2] J. Dereń, Z. Jarzebski, S. Mrowec and T. Walec *Bull. Acad. polon. Sci. Ser. Sci. Chim.*, **19**, 147 (1971).

[3] J. Dereń, J. Haber and J. Stoczyński, *Bull. Acad. polon. Sci., Ser. Sci. chim.*, **9**, 245 (1961).

[4] R. P. Marcellini, R. E. Ranc and S. J. Teichner, "Actes 2e Congr. Intern. Catalyse", Technip, Paris, 1961, p. 289

[5] C. M. Osburn and R. W. West, *J. Phys. and Chem. Solids*, **32**, 1343 (1971).

[6] J. T. Richardson, *J. Catalysis*, **6**, 328 (1966).

[7] V. I. Savčenko and G. K. Boreskovi, *Kinetica i Kataliz*, **9**, 142 (1968).

[8] F. Wang, *J. Appl., Phys.*, **37**, 929 (1966).

[9] S. Mrowec and A. Podgorecka, *Zesz. Nauk, Aon. Krakow, Met. odlew.*, **48**, 31 (1973).

[10] J. Dereń, L. Stoch and J. Ziółkowski, *Zesz. Nauk, Aon, Krakow, Mat. Fiz. Ch.*, **6**, 59 (1971).

[11] G. Parravano, *J. Amer. Chem. Soc.*, **74**, 1194 (1952).

[12] I. V. Nicolescu, A. Popescu, A. Ionescu and L. Borbat, *Rev. Roumaine Chim.*, **11**, 357 (1966).

[13] Gh. Nedelcu and A. Mihai, *Rev. Chim.* (București), **22**, 369 (1971).

[14] L. A. Rudnickij, N. P. Maksimova and A. M. Alekseev, *Kinetica i Kataliz*, **14**, 1343 (1973).

[15] Ju. A. Tkač and V. T. Samojlenko, *Ukrain. khim. zhur.*, **36**, 965 (1970).

[16] O. Hello, *Gas. World*, **1967**. 726.

Table 1

Chemical composition of investigated samples

Group	Sample N°	Al	Ni		Ca	Mg	Si	K	Fe	Ti	U	Co	Cr	Sr
			s	c*										
	1	10	10	14.7	10	0.1	1	—	0.01	0.001	—	0.01	—	—
	2	5	5	21.8	5	1	1	—	1	0.1	—	0.1	0.001	0.001
I	3	10	5	9.8	10	0.5	1	1	0.2	3	—	0.01	0.02	—
	4	10	5	12.8	10	5	5	—	5	0.01	—	1	1	1
	5	10	5	10.3	1	1	1	—	1	0.2	—	0.05	0.1	0.05
	6	10	10	13.7	10	1	1	—	0.01	0.001	—	0.01	0.001	—
	7	10	5	9.0	10	1	1	1	0.1	0.006	—	3	0.02	—
II	8	10	5	12.3	10	0.8	1	1	0.1	0.006	—	0.05	0.06	—
	9	10	5	13.7	1	0.1	1	1	0.1	0.006	0.05	0.01	0.01	—
	10	10	10	20.0	10	1	0.5	—	0.01	—	—	0.006	0.004	0.06
	11	10	5	8.5	10	10	1	1	0.1	—	—	0.005	0.02	—
III	12	10	10	16.0	5	5	1	0.004	1	0.1	—	—	0.02	0.01

s — spectrochemical
c* — complexometric

kept at this temperature to the moment of stabilization and cooled with measurements of resistance changes; in the case in which stabilization has not been achieved during one working day, the procedure has been repeated until the constant resistance value at 450° has been reached.

III. The sample has been treated in vacuum, as under the item I.

IV. A flow of air has been introduced into the measuring cell, at room temperature; heating up to 450°, stabilization and sample cooling with measurements of conductivity, have been done afterwards.

V. The air has been desorbed from the sample by the procedure as under the item I.

RESULTS AND DISCUSSION

The chemical composition of the catalysts, according to the results of the semiquantitative spectrographic analysis, is shown in table 1. Nickel content was determined by complexometric analysis, also.

The chemical composition of the catalysts influences, certainly, the way of the electric conductivity in the samples; so, it has not been expected from the undertaken investigations to determine these very complex correlations, but only to remark the resulting effects.

The electric conductivity changes in function of temperature, obtained during cooling in different gaseous media, after particular cycle steps, are presented in Figure 1 for the first group, for the second group in Figure 2, and in Figure 3 for the third group of the investigated samples. On all figures, curves are signed by numbers 1 — 5, corresponding to particular steps of the cycle, as follows: 1 vacuum; 2. hydrogen; 3. vacuum after hydrogen; 4. air; 5. vacuum after air.

Three following different kinds of behaviour with no regard to the group to which catalysts belong, have been noticed:

a. Catalysts 2 (Figure 1b), 3 (Figure 1c), 5 (Figure 1e), 6 (Figure 2a), 7 (Figure 2b), 8 (Figure 2c) and 10 (Figure 3a) show the changes corresponding to the typical semiconductors of the *p*-type: in hydrogen, as donor gas, due to the chemisorption it comes to the decrease of electric conductivity, while in oxidation atmosphere, due to the acceptor character of oxygen, electric conductivity increases. During oxygen desorption in vacuum, conductivity decreases as the consequence of elimination of the nonstoichiometric oxygen from nickel oxide, due to which the number of the defects on catalyst surface has been reduced.

At the same time, the samples differ in size of conductivity and activation energy, which is the consequence of differences in chemical composition and processes of sample formation during their synthesis.

After the treatment of the samples 3, 5, 6, 7 and 10 in vacuum, after reduction, reoxidation and evacuation of reoxidized samples, considerable differences of the conductivity, versus the starting values, obtained in vacuum, have not been observed. Activation energies of conduction (Table 2) are not changed to a more important extent during the whole measurement cycle. The results obtained show that it has not come to a measurable reduction of the samples at the temperatures up to 450° in applied condi-

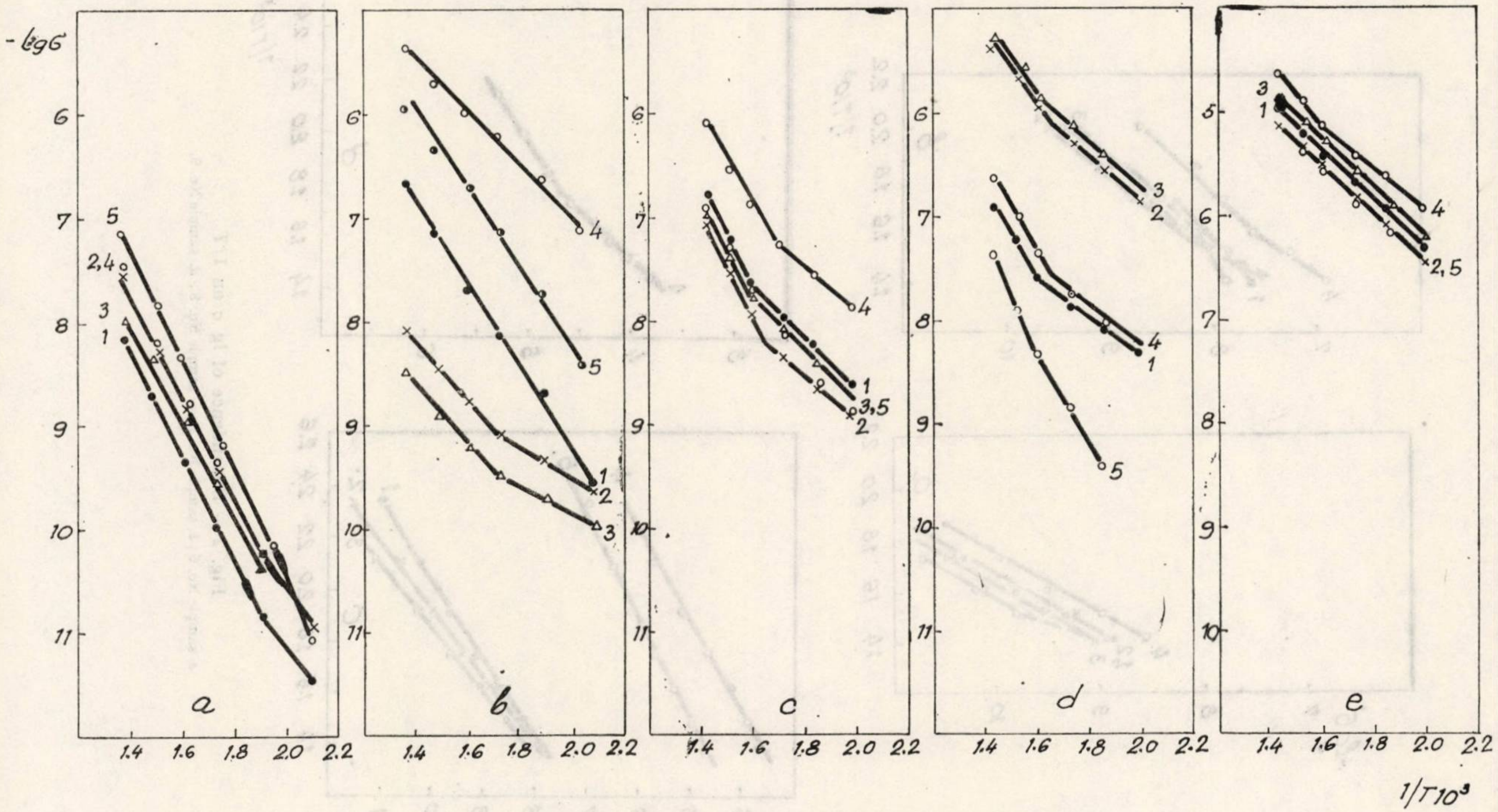

Fig. 1 — Dependence of lg σ on 1/*T*

a. sample No. 1 ; *b*. sample No. 2 ; *c*. sample No. 3 ; *d*. sample No. 4 ; *e*. sample No. 5.

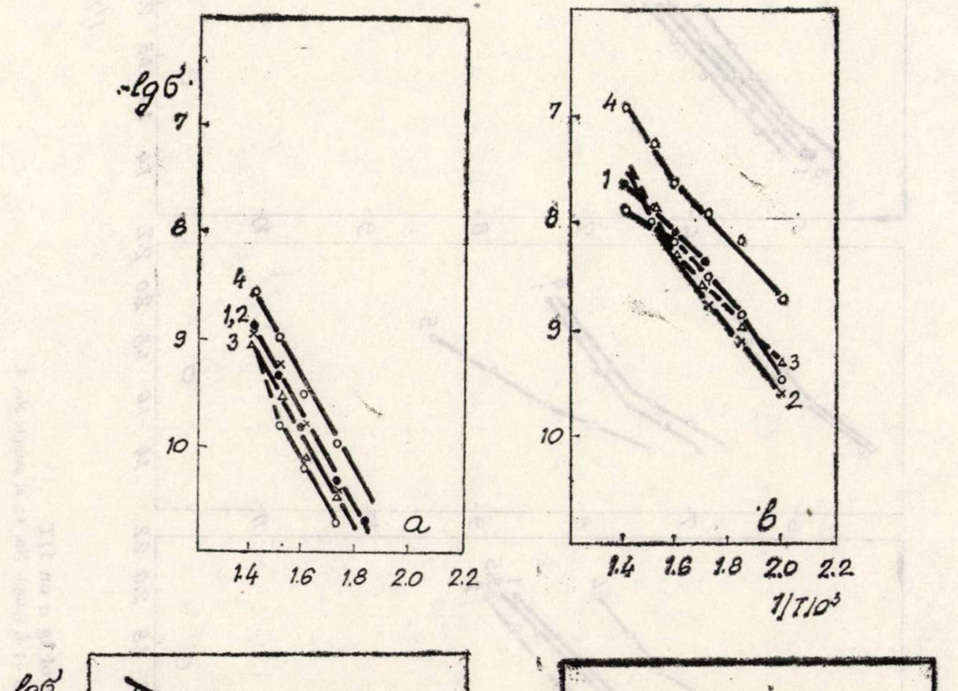

Fig. 2 — Dependence of lg σ on 1/*T*

a. sample No. 6 ; *b.* sample No. 7 ; *c.* sample No. 8 ; *d.* sample No. 9.

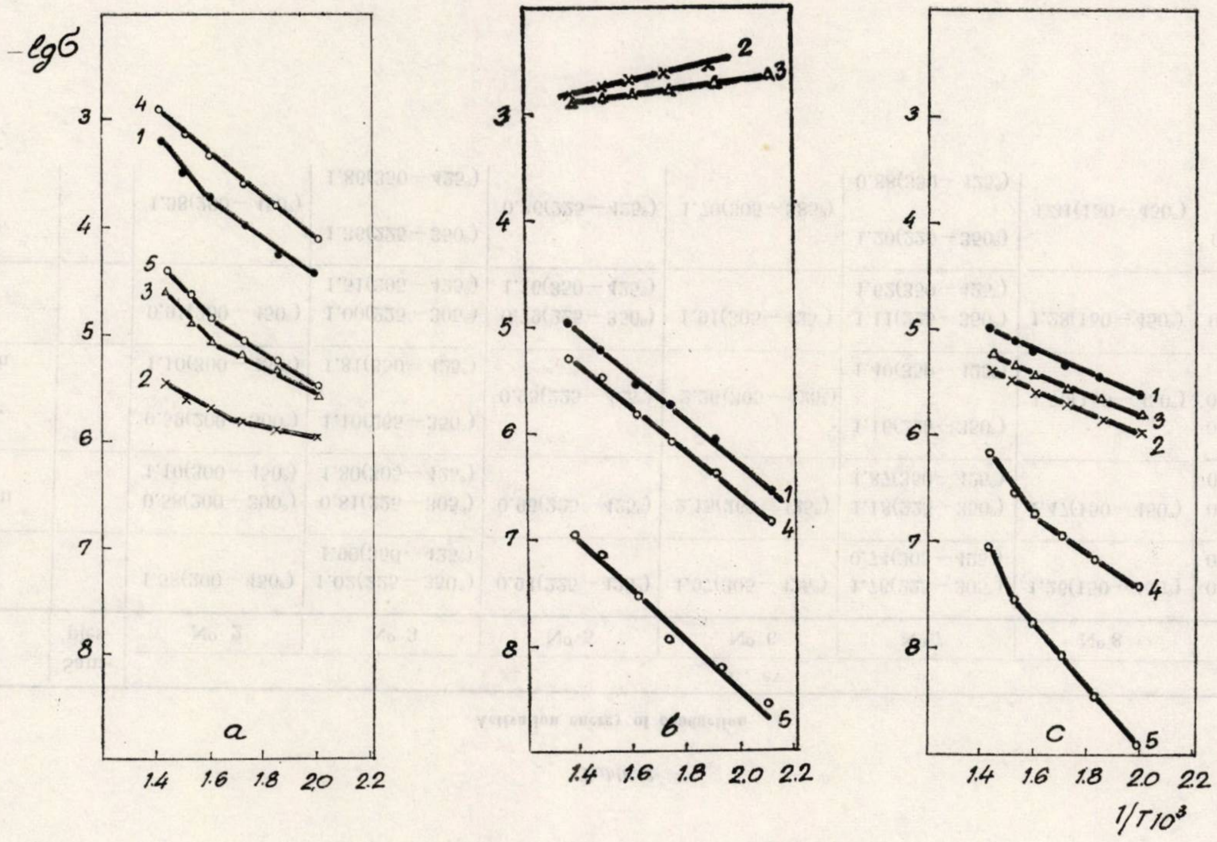

Fig. 3 — Dependence of lg σ on 1/T
a. sample No. 10 ; b. sample No. 11 ; c. sample No. 12.

Table 2

Activation energy of conduction

		Sam-ples	*E*, ev						
			Nº 2	Nº 3	Nº 5	Nº 6	Nº 7	Nº 8	Nº 10
1	Vacuum		1.58(200—450°)	1.02(225—350°) 1.90(350—425°)	0.94(225—425°)	1.97(305—425°)	1.76(225—305°) 0.74(305—425°)	1.26(150—450°)	0.37(225—305°) 0.99(305—425°)
2	Hydrogen		0.58(200—300°) 1.10(300—450°)	0.81(225—305°) 1.80(305—425°)	0.96(225—425°)	2.15(265—425°)	1.18(225—350°) 1.87(350—425°)	1.47(150—450°)	0.26(225—305°) 0.34(305—425°)
3	Vacuum, after hydrogen		0.59(200—300°) 1.10(300—450°)	1.10(265—350°) 1.81(350—425°)	0.95(225—425°)	2.26(305—425°)	1.16(225—350°) 1.40(350—425°)	1.70(150—450°)	0.55(225—350°) 0.98(350—425°)
4	Air		0.91(200—450°)	1.00(225—305°) 1.51(305—425°)	0.79(225—350°) 1.16(350—425°)	1.91(305—425°)	1.11(225—350°) 1.62(350—425°)	1.28(150—450°)	0.84(265—425°)
5	Vacuum, after air		1.38(200—450°)	1.36(225—350°) 1.86(350—425°)	0.86(225—425°)	1.70(305—385°)	1.20(225—350°) 0.88(350—425°)	1.31(150—450°)	0.65(225—350°) 1.14(350—425

tions, and that the effect of the same type of charge carriers in all the investigated gaseous media, is predominant.

In the case of samples 2 and 8, chemisorption of hydrogen and oxygen has led to the evident conductivity changes : during reoxidation of the samples a large number of defects in the structure of nickel oxide surface has been created and as the result a higher conductivity after hydrogen evacuation has been obtained ; however, the type of the defects has remained the same, as indicated by the activation energies of conductivity in vacuum before and after the measuring cycle, being of the same order of magnitude.

b. In samples 1 (Figure 1a), 4 (Figure 1d) and 12 (Figure 3c) it comes in donor gas atmosphere to a partial reduction of nickel oxide, as well as to the formation of new types of the defects ; this can be seen in the increase of conductivity, though the catalysts retain completely their semiconductive behaviour.

The increase of conductivity in donor gas can be explained by the formation of nuclei of elementary nickel by which it is possible to compensate the diminution of the number of vacancies of *p*-conductivity carriers, caused by hydrogen elimination from nickel oxide during reduction. The formation of elementary nickel nuclei and their further recrystallization can make free a part of carrier surface, so that the carrier can take part — to a rather large extent — into the catalyst surface conductivity. The effect of conductivity increase in hydrogen could not be ascribed to hydrogen hemisorption on the catalyst, because the sample conductivity has not been changed after hydrogen desorption.

Table 3

Activation energy of conduction

	Samples :	*E*, ev				
		N° 1	N° 4	N° 9	N° 11	N° 12
1	Vacuum	2.00(250—450°)	1.02(225—350°) 1.90(350—425°)	0.63(225—265°) 0.92(265—425°)	0.86(200—450°)	0.38(225—425°)
2	Hydrogen	1.98(250—450°)	0.81(225—305°) 1.80(305—425°)	—	—	0.38(225—450°)
3	Vacuum, after hydrogen	1.76(250—450°)	1.10(265—350°) 1.81(350—425°)	—	—	0.37(225—425°)
4	Air	2.18(250—450°)	1.00(225—305°) 1.51(305—425°)	—	0.84(200—450°)	0.69(225—350°) 1.22(350—425°)
5	Vacuum, after air	1.88(250—450°)	1.36(225—350°) 1.86(350—425°)	—	0.84(200—450°)	1.18(225—385°)

The changes of surface conductivity, due to the reoxidation of nickel are more evident in the samples 4 and 12, than in the sample 1.

Activation energies of conduction (Table 3) obtained for the samples 1 and 4 in the interval of higher temperatures have close values and they change slightly in different atmospheres, which obviously prove that in these samples, a similar type of defects is predominant.

c. Catalysts 9 (Figure 2d) and 11 (Figure 3b) are liable to the reduction in hydrogen to such an extent that become conductors themselves. Sample 9 retains its conductor behaviour even after the exposure to the oxidation atmosphere or to the desorption in vacuum. Sample 11 behaves similarly : it becomes a conductor during the reduction by H_2 (which can be seen in a negative temperature coefficient of the conductivity), but being exposed to reoxidation, it becomes again a semiconductor with the energy activation of conduction (Table 3) similar to the values before the reduction.

The fact that in the frame of each observed group of catalysts, including different modifications of the same basic type, different forms of electric conductivity in the investigated atmospheres occur, particularly in hydrogen, points out to the possibility to find out the correlations of the physical and chemical properties by which catalyst samples differ and their electric conductivity, as well as their reductibility.

Revue Roumaine de Chimie, **23**, *9–10*, **1441–1447** (1978)

CHEMISTRY OF TRANSITION-METAL ORGANIC COMPOUNDS. I

ON THE REACTION OF ETHYL DIAZOACETATE WITH STRAINED ALKENES, CATALYZED BY π-ALLYLPALLADIUM CHLORIDE COMPLEXES

AURELIA GHENCIULESCU, L. ENESCU, HIRA LAL PRASAD, F. CHIRALEU,
I. G. DINULESCU and MARGARET AVRAM

Laboratory of Organic Chemistry, National Institute of Chemistry,
Spl. Independenței 202 B, 76300 Bucharest 15, Romania

Received December 6, 1977

The reaction of ethyl diazoacetate with the polycyclic alkenes with strained double bond 1 – 4, in the presence of π-allylpalladium chloride complexes and copper bronze, is described. The structures of the stereoisomeric products 7 – 14 are discussed.

The intervention of transition-metal organic compounds as intermediates in a great number of catalytic routes for the synthesis of organic compounds is well known. The cyclopropanation of alkenes with ethyl diazoacetate is efficiently catalyzed by several transition metals[1] and their complexes.[2] The stereochemistry of the copper catalyzed reaction was the object of several studies.[1–4] The obtention of three-membered ring compounds by the decomposition of ethyl diazoacetate by π-allylpalladium chloride in the presence of alkenes was briefly reported,[5] but no data are available on the sterical course of the reaction nor on its limitations.

Our interest in the synthesis of small ring compounds and in the organic chemistry of palladium complexes[6] prompted us to investigate the catalytic ability of the recently obtained[7] di-μ-chloro-di-(1-chloro-1.2-diaryl-3-alkyl-π-allyl)-di-palladium complexes, in the cyclopropanation of some polycyclic alkenes.[8]

---

[1] D. Wendisch, "Carbocyclische Dreiring Verbindungen", in E. Müller, Houben – Weyl, "Methoden der Organischen Chemie", vol IV/3, G. Thieme Verlag, Stuttgart, 1971, p. 269.

[2] T. Aratani, Y. Yoneyoshi and T. Nagase, *Tetrahedron Letters*, **1975**, 1707; **1977**, 2599.

[3] P. Bessinet, R. Fraisse, R. Jaquier and P. Vaillefont, *Bull. Soc. Chim. France* **1960**, 1377.

[4] *a.* R. S. Sauers and P. E. Sonnet, *Tetrahedron*, **20**, 1029 (1964);
b. idem, *Chem. and Ind.*, **1963** 786.

[5] R. K. Armstrong, *J. Org. Chem.*, **31**, 618 (1968).

[6] I. G. Dinulescu, S. Staicu, F. Chiraleu and M. Avram, *J. Organometal. Chem.*, **140**, 91 (1977).

[7] S. Staicu, I. G. Dinulescu, F. Chiraleu and M. Avram, *J. Organometal. Chem.*, **113**, C 69 (1976).

[8] I. G. Dinulescu, L. Enescu, A. Ghenciulescu and M. Avram, *J. Chem. Research*, in press.

In this paper we report on the reaction of ethyl diazoacetate catalyzed by π-allylpalladium complexes or copper bronze, with the following polycyclic strained alkenes with norbornene skeleton : bezonorbornadiene (**1**), *exo*- and *endo*-benzocyclobutenonorbornene (**2** and **3**, respectively), and the dimethoxy alkene **4**.

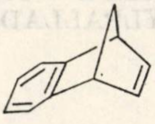
1

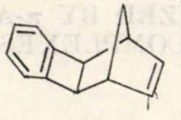
2

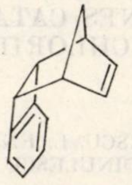
3

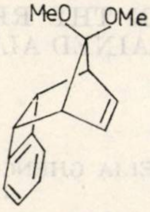

4

The cyclopropanations were carried out by treating the alkene with an excess of ethyl diazoacetate (EDA) in the presence of π-allylpalladium chloride complexes **5** or **6**, at room temperature (under cooling with ice-water). Each experiment was also performed according to the classical procedure, in the presence of copper bronze, at 120—130°.

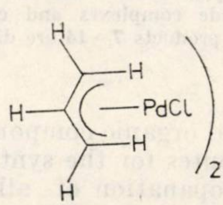

5

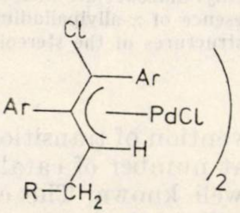

6

The crude reaction mixture were analysed by means of gas chromatography and NMR spectroscopy.

In the reaction catalyzed by π-allylpalladium chloride complexes **5** or **6**, benzonorbornadiene (**1**)[9] yielded quantitatively a mixture of almost equal amounts of two *exo*-cyclopropanation products with benzo [*f*] tricyclo [3.2.1.0 ^{2,4}]oct-6-ene skeleton : the *exo-anti*-ester **7** (m. p. 79°), and the *exo-syn*-ester **8** (m. p. 80°). In the reaction catalyzed by copper bronze, in addition to the two *exo*-cyclopropanation compounds, **7** and **8**, a third isomer, the *endo-anti*-ester **9**, was formed. (The molar ratios of the isomers **7**:**8** :**9** are 5 :1 :3).

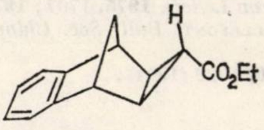

7

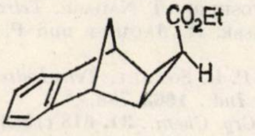

8

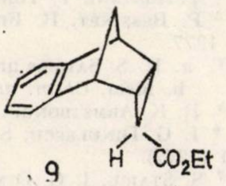

9

---

[9] T.F. Mich, E. J. Nienhouse, T. E. Farina and J. Tufariello, *J.Chem. Educ.*, **45,** 272 (1968).

The cyclopropanation of the alkenes **2—4**, under both experimental conditions, gave only the *exo*-cyclopropanated compounds with benzo [*c*]tetracyclo[4.3.1.0^{2,5} 0^{7,9}] dec-3-ene skeleton **(10—14)**. Thus with π-allylpalladium chloride complex as catalyts, the reaction of *exo*-benzocyclobutenonorbornene **(2)** [10] afforded, in almost quantitative yield, the *exo-anti*-ester **10** (m. p. 148°) and the *exo-syn*-ester **11** (oily), in the ratio 1 :1. In the copper catalyzed reaction the same mixture of esters **10** and 11, in the ratio 4 : 1, was obtained. The *endo*-benzocyclobutenonorbornene **(3)** [22] gave the *exo-anti*-ester **12** (m.p. 88°) and the *exo-syn*-ester **13** (m. p. 118°) in the ratio **1** :1 when organic palladium complexes were used as catalysts, and in the ratio 4 :1 in presence of copper bronze. In the reaction of the dimethoxy-alkene **4** [12], under both experimental conditions, only the *exo-anti*-ester **14** could be isolated together with some unreacted starting material.

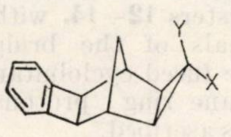

10 X = CO$_2$Et, Y = H
11 X = H, Y = CO$_2$Et

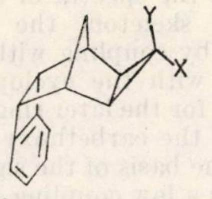

12 X = CO$_2$Et, Y = H
13 X = H, Y = CO$_2$Et

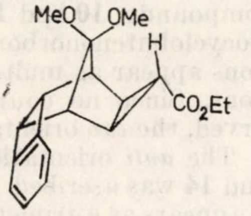

14

The structure and configuration of the products **7—14** were ascribed on the basis of NMR spectral data as well as on the basis of chemical behaviour. In order to establish the configuration of the cyclopropane ring as well as that of the carbethoxy groups, the chemical shift and the coupling constants of the cyclopropane ring protons were used, together with those of the bridgehead protons of the norbornene moiety. The systems investigated are fairly symmetric, so that the norbornene protons fused with the three- and the four-membered rings are magnetically equivalent. As already found for other norbornene derivatives, [13,14] the vicinal coupling constant between the bridgehead proton and an *endo* proton is small ; the signals appear nearly as singlets. The coupling constant of the bridgehead proton and an *exo* oriented proton has greater values and the signals are doublets or multiplets.

---

[10] L. Enescu and M. Avram, *Rev. Roumaine Chim.*, **22**, 1061 (1977).

[11] C. D. Nenitzescu, M. Avram and D. Dinu, *Chem. Ber.*, **90**, 2541 (1957).

[12] H. L. Prasad, Ph. D. Thesis, National Institute of Chemistry (Prof. M. Avram), Bucharest, 1978 ; J. A. Boulton and J. F.W. Mc Omie, *J. Chem. Soc.*, **1965**, 2549.

[13] M. Avram, F. Chiraleu, I. Pogany and I. G. Dinulescu, *Rev. Roumaine Chim.*, **15**, 1767 (1970).

[14] M. D. Gheorghiu, C. Drăghici and L. Pîrvulescu *Tetrahedron*, **33**, 3295 (1977) and literature therein cited.

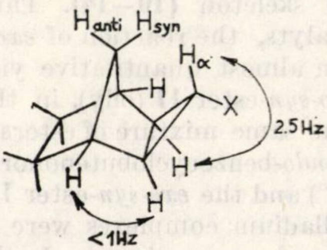

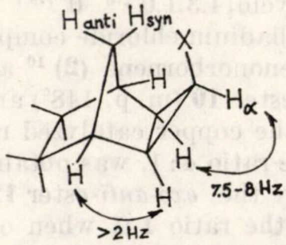

In the NMR spectra of the esters **7, 8, 10** and **11** the signal due to the bridgehead proton appears as singlet, indicating an *endo* orientation for the vicinal protons of the fused three- or four-membered rings, respectively. This feature suports the ascribed *exo* configuration for the cyclopropane ring in compounds **7** and **8** and for the three- and four-membered rings in compounds **10** and **11.** In the spectra of the esters **12—14,** with *endo*-benzocyclobutenonorbornene skeleton, the signals of the bridgehead protons appear as multiplet by coupling with the fused cyclobutane ring protons. Since no coupling with the cyclopropane ring protons were observed, the *exo* orientation for the later ring was ascribed.

The *anti* orientation of the carbethoxy groups in the esters **7, 10, 12** and **14** was ascribed on the basis of the signals due to the H-α proton. This appears as a triplet with a low coupling constant ($J = 2 . 5$ Hz) coupled with the other cyclopropane ring protons (doublet). The small value of this coupling constant was earlier found to be characteristic for *trans* oriented protons in a cyclopropane ring fused with norbornene skeleton. [4b] It is worth noting that in the compound **9** the small coupled triplet of this proton appears at a very high magnetic field (δ 0.22 ppm). This is possible only in the ascribed *endo* configuration of the cyclopropane ring and *anti* orientation of the carbethoxy group, in which this proton undergoes the strong shielding effect of the aromatic ring.

The *syn* orientation of the carbethoxy group in the esters **8, 11** and **13** results from the high values of the coupling constant of the H-α proton characteristic for *all-cis* cyclopropanic protons. [15] The signals of these protons appear in the form of an AB_2 system with $J_{AB} = 7{\cdot}5-8$ Hz. Further suport for the *syn* orientation of the carbethoxy group was obtained by the use of shift reagent technique. Thus on treatment with $Eu(FOD)_3$ [16] a strong shift was observed for the *anti*-H-α proton to lower magnetic field (part A of the AB_2 system) and for one of the methylene bridge proton (the *syn* oriented, in the neighbourhood of the carbethoxy group). A nonequivalency between the two CH_2 protons occurs, and a coupling ($J = 12.5$Hz) is observed.

The chemical behaviour in the epimerisation experiments (by heating with sodium alkoxyde in alcoholic solution) reveals the isomerisation

---

[15] L. M. JACKMAN and S. STERNHELL, "Applications of Nuclear Magnetic Resonance Spectroscopy in Organic Chemistry", 2nd Edn., Pergamon Press, Oxford, 1969, p. 286.

[16] FOD = 1.1.1.2.2.3.3-Heptafluoro-7. 7-dimethyl-octane-4.6-dionate ion.

(as well the transesterification, when methanol was used as solvent) of the *syn* esters into the more stable *anti* one.

In order to establish whether the preferred formation of the *anti* isomers in the copper catalyzed reaction is not due to the higher reaction temperatures compared with those of the palladium catalyzed reaction, benzonorbornadiene was treated with ethyl diazoacetate in presence of π-allylpalladium chloride complex at 120°. In the reaction product of this very violent reaction, the same mixture of equal amounts of the two *anti* and *syn* esters, **7** and **8** respectively, was evidenced.

Studies concerning the reaction of ethyl diazoacetate with other alkenes, aiming at establishing the role or the transition-metal organic intermediate on the stereochemistry of the cyclopropanation, are currently under way.

EXPERIMENTAL

IR spectra were recorded with a double beam UR 20 spectrophotometer. NMR spectra were determined with a Varian A-60 spectrometer. Gas chromatographic analyses was carried out a Chromatron gas chromatograph. The columns were 20% Methyl Sylicone SE 30 on Chronosorb W, 30–60 mesh, 2m × 0.5 mm; the column temperature was 180° (vaporizator temperature 220°); carrier gas: hydrogen, 50 ml/min.

Reaction of benzo [*c*] bicyclo [2.2.1] hepta-2.5-diene (I) with EDA

a. *In the presence of π-allylpalladium chloride complexes.* Into a cooled solution of 1.0 (6.65 mmoles) **1** and 20 mg π-allylpalladium chloride **5**[17], 1.20 g (10 mmoles) EDA were added dropwise, over a period ot two hours. The crude product, containing 50% **7** and 50% **8**, as found by glc, was chromatographied on alumina column. With petroleum ether as eluent *anti*-3-carbethoxy-*exo*-benzo [*f*] tricyclo [3.2.1.$0^{2\cdot4}$] oct-6-ene **(7)**, m.p. 80° (from methanol), was isolated.

IR (CCl_4) : ν_{CO} 1730 cm^{-}.^{1}

NMR (CCl_4, δ, ppm) 1.20–1.45 (m, 2H, H-8 *syn* and *anti*), 1.61 (d, 2H, H-2, H-4, $J = 2,5$ Hz), 2.45 (*t*, 1H, H-3, $J = 2.5$ Hz), 3.30 (s, 2H, H-1, H-5), 6.85–7.25 (m, 4H arom.); ethyl from ester: 1.18 (t, 3H, CH_3, $J = 6.0$ Hz), 4.02 (qu, 2H, CH_2, $J = 6.0$ Hz). With ether as eluent, *syn*-3-carbethoxy-*exo*-benzo [*f*] tricyclo [3.2.1.$0^{2\cdot4}$] oct-6-ene **(8)**, m.p. 79–80° (from methanol), was obtained.

IR (CCl_4) : ν_{CO} 1730 cm^{-1}.

NMR (CCl_4, δ, ppm): 1.10–1.35 (m, 4H, H-2, H-4, H-8 *syn* and *anti*), 2.05 (t, 1H, H-3, $J = 7.0$ Hz), 3.45 (s, 2H, H-1, H-5), 6.75–7.20 (m, 4 arom. H); ethyl from ester: 1.26 (t, 3H, CH_3, $J = 7.0$ Hz), 4.11 (qu, 2H, CH_2, $J = 7.0$ Hz).

The same results were obtained by using as catalyst di-μ-chloro-di-(1-chloro-1.2-diphenyl–2.5-dimethyl-hexenyl)-di-palladium **(6)**, Ar = phenyl, R = t-butyl) previously obtained from diphenylacetylene and t-butylethylene in, the presence of BNP.

b. *In the presence of copper bronze.* Into a suspension of 50 mg copper bronze in 2.0 g (14.06 mmoles) **1**, heated at 125°, 3.2 g (28 mmoles) EDA were added dropwise over a period of four hours. After removal of the catalyst, 2.50 g (78%) oily products were obtained, in which, by glc, the following compounds were evidenced: 57–62% *exo-anti*-ester **7**, 7–12% *exo-syn*-ester **8** and 30% *endo-anti*-ester **9**. By chromatography on alumina column with petroleum ether, several fractions were obtained. Some of these fractions were found to contain as chief products the esters *exo-anti* **7** and *exo-syn* **8**, respectively. A fraction contains the ester *endo-anti* **9** (*anti*-3-carbethoxy-*endo*-benzo [*f*] tricyclo [3.2.1.$0^{2\cdot4}$] oct-6-ene) in a very high concentration. However, it was not possible to isolate it in pure form, but the spectral parameters were established.

---

[17] R. HÜTTEL, *Synthesis*, **1970**, 225

NMR (CCl_4, δ, ppm) : 0.20 (t, 1H, H-3, $J = 2.5$ Hz), 1.20—1.40 (m, 2H, H-8 *syn* and *anti*), 2.23 (m, 2H, H-2, H-4), 3.41 (m, 2H, H-1, H-5), 6.85—7.25 (m, 4 arom. H) ; ethyl from ester : 1.08 (t, 3H, CH_3, $J = 7.0$ Hz), 3.90 (qu, 2H, CH_2, $J = 7.0$ Hz).

c. *In the presence of π-allylpalladium chloride* **(5)** *at high temperature.* Into a solution of 0.50 g (3.32 mmoles) **1** and 20 mg π-allylpalladium complex **5**, heated at 125°, 1.60 g (14 mmoles) EDA were droped carefully over a period of two hours. A very vigorous reaction takes place — and some time flame was observed. After cooling, a black oily (coloidal palladium) was obtained, which was purified by chromatography on alumina with ether, and analyzed by means of NMR and glc ; a content of 50 % **7** and 50 % **8** eas found.

Reaction of *exo*-benzo [*c*] tricyclo [4.2.1.0 $^{2 \cdot 5}$] nona-3.7-diene (2) with EDA

a. *In the presence of π-allylpalladium: chloride* **(5)**. A cooled solution of 1.50 g **2** of 60 % purity (0.90 g, 5.35 mmoles **2**) and 20 mg π-allylpalladium chloride **(5)** was treated dropwise, over a period of 3 hours, with 1.20 g (10.7 mmoles) EDA. Oily crystals were obtained (1.1 g, 80 %), for which a content of 50 % **10** and 50 % **11** was determined by glc.

Analysis : $C_{17}H_{18}O_2$ requires C, 80.28 ; 7.13 Found : C, 80.05 ; H, 7.09 %.

The oily crystals were triturated with 20 ml petroleum ether and filtered. The crystals thus obtained were chromatographied on alumina with petroleum ether, leading to 0.47 g (34.4 %) *anti*-8-carbethoxy-*exo,exo*-benzo [*c*] tetracyclo[4.3.1.$0^{2 \cdot 5}$. $0^{7 \cdot 9}$] dec-3-ene **(10)**, m.p. 148° (methanol).

IR (CCl_4) : $\nu_{C=O}$ 1730 cm^{-1} ; ν_{C-O} 1180 cm^{-1}.

NMR (CCl_4, δ, ppm) : 0.48 and 0.60 (m, 2H, H-10 *syn* and *anti*, AB system, $J = 11.0$ Hz), 1.46 (d, 2H, H-7, H-9, $J_{8 \cdot 9(7)} = 2.5$ Hz), 1.78 (t, 1H, H-8, $J_{8.9}$-= 2.5 Hz, 2.43 (s, 2H, H-1, H-6), 3.40 (s, 2H, H-2, H-5), 6.80—7.25 (m, 4 aromatic H) ; ethyl group : 1.23 (t, 3H, CH_3, $J = 7.0$ Hz), 4.09 (qu, 2H, CH_2, $J = 7.0$ Hz).

The petroleum ether solution was concentrated, and the oily residue was chromatographied on alumina column. Using as eluent petroleum ether, the following fractions were obtained : small quantities of unreacted **2** and then 0.45 g (75 %) benzotricyclene (present in the starting material together with **2**). With ether as eluent, *syn*-8-carbethoxy-*exo,exo*-benzo [c]tetracyclo [4.3.1.$0^{2 \cdot 5}0^{7 \cdot 9}$]dec-3-ene **(11)** (oily product) was obtained.

IR (CCl_4) : ν_{CO} 1730 cm^{-1}

NMR (CCl_1, δ, ppm) : 0.53 (s, 2H, H-10 *syn* and *anti*), 1.05—1.40 (m, 5H, H-7, H-9 and CH_3 from ethyl, which appears as a sharp triplet at 1.21 with $J = 7.0$ Hz), 2.55 (s, 2H, H-1 H-6), 3.33 (s, 2H, H-2, H-5), 4.03 (qu, 2H, CH_2 from ethyl, $J = 7.0$ Hz), 6.75—7.25 (m, 4 aromatic H). — NMR in presence of $Eu(FOD)_3$ at molar ratio 2.54 % : 0.68 and 0.96 (an AB system corresponding to H-10 *syn* and *anti*, $J = 12.5$ Hz), 1.15—1.55 (m, 5H, H-7, H-9, and CH_3 from ethyl, which appears as a sharp triplet at 1.36 with $J = 7.0$ Hz), 1.78 (1H, H-8, part A of an AB_2 system with $J = 8.0$ Hz), 2.70 (s, 2H, H-1, H-6), 3.41 (s, 2H, H-2, H-5), 4.44 (qu, 2H, CH_2 from ethyl, $J = 7.0$ Hz), 6.80—7.25 (m, 4 aromatic H).

b. *In the presence of copper bronze.* Into a well stirred suspension of 50 mg coopper bronze in 2.2 g **2** of 70 % purity (1.54 g, 9.15 mmoles **2**), 2.0 g (17.53 mmoles) EDA were added, at 125°, over a period of three hours. Methylene chloride was added, the copper was filtered off and the solvent was removed. The oily residue was chromatographied on alumina with ether, yielding 2.75 g (83 %) oily crystals, in which by glc a content of 80 % **10** and 20 % **11** was found.

From the reaction mixture, crystals of **10** were separated. The supernatant liquid, very soluble in petroleum ether, was chromatographied on SiO_2 column, with petroleum ether as eluent. The following compounds were obtained : benzotricyclene (from the starting material), *exo-anti*-ester **10** and *exo-syn*-ester **11**.

Reaction of *endo*-benzo [*c*] tricyclo [4.2.1.0. $^{2 \cdot 5}$] bona-3.7-diene (3) with EDA

a. *In the presence of π-allylpalladium chloride* **(5)**. To a vigorously stirred solution of 0.60 g (3.57 mmoles) **3** and 10 mg π-allylpalladium chloride **(5)**, 0.62 g (5.36 mmoles) EDA were added dropwise, over three hours, under cooling with cold water. The crude crystalline residue (0.82 g, 90 %), m.p. 70—95°, was found (by means of NMR spectra) to be a mixture of 50 % **12** with 50 % **13**. IR (CCl_4) : ν_{CO} 1730 cm^{-1}.

Analysis : $C_{17}H_{18}O_2$ requires C, 80.28 ; H, 7.13. Found : C, 80.49 ; H, 7.35 %.

By several recrystallizations from methanol, pure **12** and **13** were obtained.

anti-8-Carbethoxy-*endo,exo*-benzo[c]tetracyclo$[4.3.1.0^{2.5}0^{7.9}]$ dec-3-ene **(12)**, white crystals, m.p. 80°.

IR(CCl_4) : ν_{CO} 1730 cm^{-1}.

NMR (CCl_4, δ, ppm) : 0.90 (d, 2H, H-7, H-9, $J = 2.5$ Hz), 1.18 (m, 2H, H-10 *anti* and *syn*), 1.51 (t, 1H, H-8, $J_{8.9}$= 2,5 Hz), 2.55 (m, 2H, H-1, H-6), 3.60 (m, 2H, H-2, H—5), 7.85—7.20 (m, 4 aromatic H) ; the ethyl group appears at 1.11 (t, 3H, CH_3, $J = 7.0$ Hz) and 3.91 (qu, 2H, CH_2, $J = 7.0$ Hz).

syn-8-Carbethoxy-*endo, exo*-benzo[c]tetracyclo$[4.3.1.0^{2.5}0^{7.9}]$dec-3-ene **(13)**, white crystals, m.p. 118°.

IR (CCl_4) : ν_{CO} 1730 cm^{-1}.

NMR (CCl_4, δ, ppm) : 0.70 (2H, H-7, H-9) and 1.06 (1H, H-8), an AB_2 system with 7.5 Hz, 1.17 (m, 2H, H-10 *anti* and *syn*), 2.69 (m, 2H, H-1, H-6), 3.60 (m, 2H, H-2, H-5), 7.15—7.85 (m, 4 aromatic H) ; ethyl group : 1.24 (t, 3H, CH_3, $J = 7.0$ Hz) and 4.05 (qu, 2H, CH_2, $J = 7.0$ Hz).

b. *In the presence of copper bronze.* Into a vigorously stirred suspension of 50 mg copper bronze in 1.40 g (8.33 mmoles) **3**, heated at 125°, 2.0 g (17.53 mmoles) EDA were added dropwise over three hours. After cooling, the mixture was dissolved in methylene chloride, filtered, and the solvent was evaporated *in vacuo*.

The oily residue was chromatographied on aluminium oxide column. Using as eluent petroleum ether with 10% diethyl ether, 1.80 g (85%) crystalline mixture (m.p. 100—108°) of 75% **12** with 25% **13** (as resulted from NMR determinations), were obtained.

Reaction of 9,9-dimethoxy-benzo[c]tricyclo$[4.2.1.0^{2.5}]$ nona-3.7-diene (4) with EDA

a. *In the presence the of π-allylpalladium chloride* **(5)**. From 1.0 g (4.38 mmoles) **4**, 1.50 g (1.25 mmoles) EDA and 10 mg **5**, by the above described general procedure involving catalysis by organic palladium compounds, 1.70 g crude reaction product were obtained. By chromatography on alumina column with petroleum ether, two fractions were separated. The first one was found to contain 0.40 g (40%) starting material **4**.

From the second one, 0.50 g (37%) *anti*-8-carbethoxy-10.10-dimethoxy-*endo, exo*-benzo[c] tetracyclo$[4.3.1.0^{2.5}0^{7.9}]$oct-3-ene **(14)**, mp.p. 120° (from methanol), were obained.

IR(CCl_4) : ν_{CO}1735 cm^{-1}.

NMR (CCl_4, δ, ppm) : 0.86 (d, 2H, H-7, H-9, $J = 3.0$ Hz), 2.55 (broad s, 2H, H-1, H-6), 2.58 (tr, 1H, H-8, $J = 3.0$ Hz), 3.16 (s, 6H, 2 methoxy groups), 3.69 (m. 2H, H-2, H-5), 6.82—7.25 (m, 4 aromatic H) ; ethyl group : 1.11 (tr, 3H, CH_3, $J = 6.0$ Hz), 3.90 (qu, 2H, CH_2 $J = 6.0$ Hz).

b. *In the presence of copper bronze.* Using the above described procedure, from 2.0 (8.76 mmoles) **4,** 50 mg copper bronze and 2.4 g (mmoles) EDA, 3.5 g crude product were obtained. By chromatography on alumina column with petroleum ether, some starting material **4** and 0.70 g (25%) **14,** were obtained.

Epimerization of *exo-syn*-ester 8 into *exo-anti*-ester 7

1.0 g (4.38 mmoles) mixture of 50% **7** and 50%**8** and a solution of sodium ethoxide (prepared from 0.10 g sodium and 25 ml anhydrous ethanol) were boiled for 24 hours. Water (1 ml) and 1.0 g sodium hydroxide were added and the mixture was boiled for 4 hours. The solvent was removed, water (15 ml) was added, extracted with ether and the aqueous layer acidified. By extraction with ether, drying and solvent removal, 0.80 g (90%) *exo-anti*-acid were obtained ; m.p. 158°.

NMR ($CDCl_3$, δ, ppm) : 1.38 (s, 2H, H-8 *syn* and *anti*), 1.73 (d, 2H, H-2, H-4, $J = 2$ Hz), 2.51 (tr, 1H, H-3, $J = 2.0$ Hz), 3.38 (s, 2H, H-1, H-5), 6.92—7.32 (m, 4 aromatic H), 10.90 (s, 1H, COOH).

By boiling with ethanol in the presence of catalytic quantities of sulphuric acid, the *exo-anti*-ester **7** was formed. With methanol, *exo-anti*-methyl-ester (m.p. 88°) was obtained.

IR (CCl_4) : ν 1730 cm^{-1}.

NMR (CCl_4, δ, ppm) : 1.25 and 1.35 (2H, H-8, *syn* and *anti*, AB system, $J = 10.0$ Hz) 1.60 (d, 2H, H-2, H-4, $J = 2.5$ Hz), 2.45 (t, 1H, H-3, $J = 2.5$ Hz), 3.27 (s, 2H, H-1, H-5), 3.53 (s, 3H, $COOCH_3$), 6.80—7.20 (m, 4 arom. H).

anti-8-Carbethoxy-anti-exo-benzo[f]tetracyclo[4.3.1.0[illegible]]dec-3-ene (12), white crystals, m.p. 90°.

IR (CCl$_4$): ν_{CO} 1730 cm^{-1}.

NMR (CCl$_4$, δ, ppm): 0.90 (d, 2H, H-7, H-9, J = 2.5 Hz), 1.18 (m, 2H, H-10 anti and syn), 1.[illegible] (t, 1H, H-8, J = 2.5 Hz), 2.[illegible] (m, 2H, H-1, H-6), 3.[illegible] (m, 2H, H-2, H-5), 7.[illegible] – 7.30 (m, 4 aromatic H); the ethyl group appears at 1.11 (t, 3H, CH$_3$, J = 7.0 Hz) and 3.[illegible] (q, 2H, CH$_2$, J = 7.0 Hz).

syn-8-Carbethoxy-exo,exo-benzo[f]tetracyclo[[illegible]]non-3-ene (13), white crystals, m.p. 118°.

IR (CCl$_4$): ν_{CO} 1730 cm^{-1}.

NMR (CCl$_4$, δ, ppm): 0.70 (2H, H-7, H-9) and 1.05 (1H, H-8), in an AB$_2$ system with 7.5 Hz, 1.1[illegible] (m, 2H, H-10 anti and syn), 2.69 (m, 2H, H-1, H-6), 3.60 (m, 2H, H-2, H-5), 7.15 – 7.55 (m, 4 aromatic H); ethyl group: 1.24 (t, 3H, CH$_3$, J = 7.0 Hz) and 4.06 (q, 2H, CH$_2$, J = 7.0 Hz).

b. *In the presence of copper bronze.* Into a vigorously stirred suspension of 50 mg copper bronze in 1.40 g (8.43 mmoles) 5, heated at 125°, 2.0 g (17.53 mmoles) EDA were added dropwise over three hours. After cooling, the mixture was dissolved in methylene chloride, filtered, and the solvent was evaporated *in vacuo*.

The oily residue was chromatographed on aluminium oxide column. Using as eluent petroleum ether with 10% diethyl ether, 1.50 g (85%) crystalline mixture (m.p. 100 – 108°) of 75% 12 with 25% 13 (as resulted from NMR determinations), were obtained.

Reaction of 8,9-dimethoxy-benzo[f]tricyclo[4.2.1.0[illegible]]nona-3,7-diene (4) with EDA

a. *In the presence of π-allylpalladium chloride* (3). From 1.0 g (4.38 mmoles) 4, 1.50 g (13.15 mmoles) EDA and 10 mg 3, by the above described general procedure involving catalysis by organic palladium compounds, 1.70 g crude reaction product were obtained. By chromatography on alumina column with petroleum ether, two fractions were separated. The first one was found to contain 0.40 g (40%) starting material 4.

From the second one 0.80 g (57%) anti-3-carbethoxy-[illegible]-dimethoxy-endo, exo-benzo[f]tetracyclo[[illegible]]non-[illegible]-ene (14), m.p. 120° (from methanol), were obtained.

IR (CCl$_4$): ν_{CO} 1725 cm^{-1}.

NMR (CCl$_4$, δ, ppm): 0.85 (d, 2H, H-2, H-4, J = 3.0 Hz), 2.55 (broad s, 2H, H-1, H-5), 2.[illegible] (t, 1H, H-3, J = 3.0 Hz), 3.[illegible] (s, 6H, 2 methoxy groups), 3.80 (m, 2H, H-[illegible], H-[illegible]), 6.82 – 7.25 (m, 4 aromatic H); ethyl group: 1.11 (t, 3H, CH$_3$, J = 6.0 Hz), 3.90 (q, 2H, CH$_2$, J = 6.0 Hz).

b. *In the presence of copper bronze.* Using the above described procedure, from 2.0 g (8.[illegible] mmoles) 4, 50 mg copper bronze and 2.[illegible] g ([illegible] mmoles) EDA, 3.5 g crude product were obtained. By chromatography on alumina column with petroleum ether, some starting material 4 and 0.[illegible] g (25%) 14 were obtained.

Epimerization of exo-syn-ester 8 into exo-anti-ester 7

1.4 g 1:3 mixture of esters 7 and 8 and a solution of sodium ethoxide (prepared from 0.[illegible] g sodium and 25 ml anhydrous ethanol) were boiled for 24 hours. Water (1 ml) and 1.0 g sodium hydroxide were added and the mixture was boiled for 4 hours. The solvent was removed, water (15 ml) was added, extracted with ether and the aqueous layer acidified. By extraction with ether, drying and solvent removal, 0.80 g (80%) exo-anti-acid were obtained, m.p. 156°.

NMR (CDCl$_3$, δ, ppm): 1.[illegible] (s, 1H, H-8 syn and anti), 1.[illegible] (d, 2H, H-2, H-4, J = 3 Hz), 2.51 (t, 1H, H-3, J = 3.0 Hz), 3.38 (s, 2H, H-1, H-5), 6.92–7.32 (m, 4 aromatic H), 10.90 (s, 1H, COOH).

By boiling with ethanol in the presence of catalytic quantities of sulfuric acid, the exo-anti-ester 7 was formed. With methanol, exo-anti-methyl-ester (m.p. 65°) was obtained.

IR (CCl$_4$): ν_{CO} 1725 cm^{-1}.

NMR (CCl$_4$, δ, ppm): 1.[illegible] and 1.[illegible] (2H, H-8 syn and anti, AB system, J = 10.0 Hz), 1.[illegible] (d, 2H, H-2, H-4, J = 3.0 Hz), 2.[illegible] (t, 1H, H-3, J = 3.0 Hz), 3.22 (s, 2H, H-1, H-5), 3.53 (s, 3H, COOCH$_3$), 6.90 – 7.20 (m, 4 arom. H).

Revue Roumaine de Chimie, 23, *9–10*, 1449–1453 (1978)

EXPERIMENTAL AND THEORETICAL STUDY ON THE REACTION OF THE LOSS OF AMIDO GROUP FROM THE PYRIDINIUM-CYANO-AMYDO-METHYLIDE

G. SURPĂȚEANU [*], M. CONSTANTINESCU [**] and I. ZUGRĂVESCU [*]

[*] Organic Chemistry Department, Polytechnical Institute of Iassy 71 Splaiul Bahlui, Romania

[**] Computer Center of University "A. I. Cuza" Iassy, Romania

Received June 20, 1977

An experimental and theoretical study on the reaction of the loss of amido group from the ylide I R = NH_2 in acid medium was realized. The loss of amido group begins with the oxygen ylide atom protonation (scheme 3). ΔE_{total} (the total change in energy due to the partial formation of a bond) indicates the larger absolute value for the O–H (oxygen ylid hydrogen from the hydronium ion) interaction. The coefficients and the orbitals energies using a CNDO/2 method were obtained. A good agreement between experimental and theoretical results on the oxygen ylid protonation of ylid I (R = NH_2) was verified.

The carbanion disubstituted ylids of the type I (R = OC_2H_5, C_6H_5) in the acid medium lost the – COR group giving the cyanomethyl pyridinium salt XI respectively.[1]

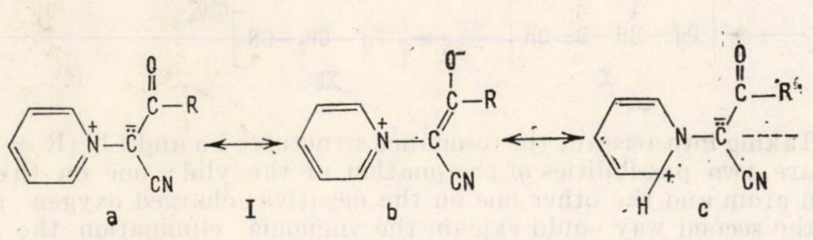

Taking into account that the negative charge, formally written on the carbon ylid atom, is delocalized on the all ylid carbanion, for these zwiterion systems one can write resonances structures of the type I a, b, c.

---

[1] F. Kröhnke, *Ber. dtsch. Chem. Ges.*, **72**, 83 (1939).

In a previous paper [2] we proposed the following mechanism fot the elimination reaction of the carbethoxy group from the ylid III :

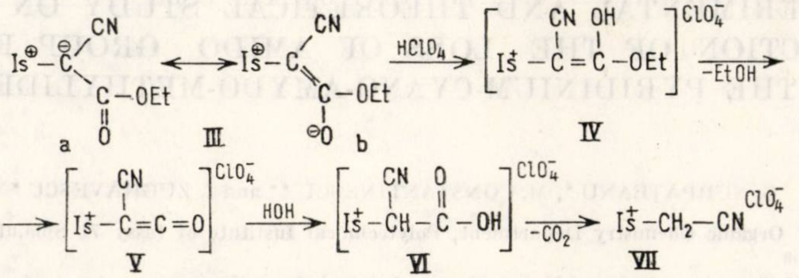

RESULTS AND DISCUSSIONS

In this paper we proposed an experimental and theoretical study (by the CNDO/2 method) on the loss of the amido group from the ylid I $R = NH_2$. The choice of this ylid is made because its geometry is known. [3]

In the reaction betweem ylid I $R = NH_2$, and perchloric acid in aqueous solution by slow heating, the salt XI is separated.

We supposed that this elimination reaction occurs by the same mechanism described in ref. [2] (scheme 3). The difference between these two mechanisms is the elimination of ethylic alchol in the first and of amonia in the second mechanism.

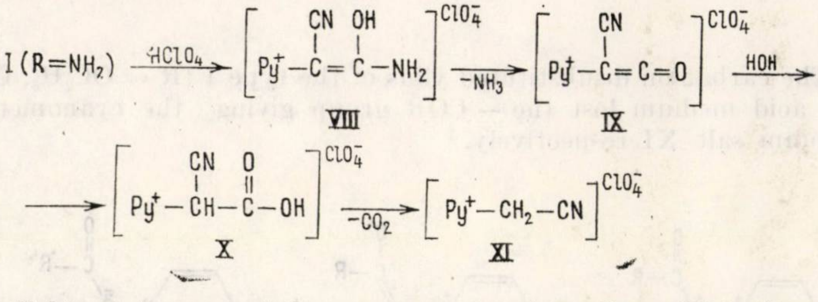

Taking into account the resonance structures I a and I b ($R = NH_2$) there are two possibilities of protonation of the ylid; one on the ylid carbon atom and the other one on the negative charged oxygen atom. Only the second way could explain the ammonia elimination, the water addition, the decarboxylation and finally the salt XI separation.

The CNDO/2 calculations of ylid I $R = NH_2$ were performed with its geometry described in paper. [3] The calculated atomic charges are presented in Figure 1.

---

[2] J. P. Catteau, P. Karafiloglou, A. Lablache — Combier., N. Lethan and G. Surpăţeanu, *Tetrahedron*, **32**, 461 (1976).

[3] G. Surpăţeanu and L. Devas, *Acta Cryst*. in print.

The larger negative charge (−0.6012) is on the oxygen atom, the ylid carbon atom has the negative charge of only −0.1389. The positive charge on the nitrogen ylid atom is not so high (+ 0.2958). The founded theoretical charges using the CNDO/2 method are in good agreement with those announced previously in the literature.[4,5] The negative charge on the all ylid carbanion and the positive charge on the pyridinium ring are delocalized.

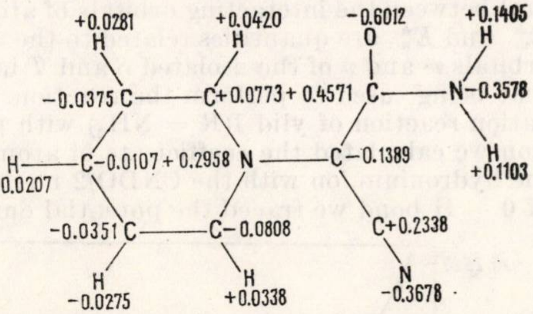

Fig. 1. — The calculated charges by CNDO/2 method for ylid I ($R = NH_2$)

The higher negative charge of the oxygen atom indicates that this atom could participate to a charge controlled reaction. In an orbital controlled reaction the electrophilic attack on the carbon atom is favourized because the sum $\Sigma\, C^2_{HOMO}$ of the coefficients of atomic orbitals from the high occupied molecular orbital of the carbon atom (0.4158) is larger than for the oxygen atom (0.3303) (Table 2). The above values were calculated by us using the coefficients of atomic orbital obtained with the CNDO/2 method.

For the next reactivity determinations we used the fundamental equation 1 of the generalized perturbation theory (G.P.) applied to the donor—acceptor interaction.[6,7,8]

$$\Delta E_{\text{total}} = \underset{\text{electrostatic term}}{-\frac{q_s q_t}{R_{st}}} + 2 \underset{\substack{\text{occupied orbi-}\\ \text{tals, } m\\ \text{of molecule } S}}{\sum} \underset{\substack{\text{unoccupied}\\ \text{orbitals } n \text{ of}\\ \text{molecule } T}}{\sum} \underset{\text{covalent term}}{\frac{(C_s^m C_t^n \, \Delta \beta_{st})^2}{E_m^* - E_n^*}} \qquad (1)$$

Where ΔE_{total} is the total charge in energy due to the partial formation of a bond between an atom s of the electron donor molecule S and an atom t the electron acceptor molecule T, in a solvent of effective dielectric constant ε ; q_s and q_t are the totale charges of atoms s and t in the isolated molecules ; R_{st} is the distance between the two atoms s and t for which

---

[4] J. P. Catteau, P. Karafiloglou, A. Lablache — Combier, N. Lethan and G. Surpăţeanu, *J. Electron. Spectroscop.*, in press.

[5] G. Surpăţeanu, J. P. Catteau, P. Karafiloglou and A. Lablache-Combier, *Tetrahedron Report*, **32**, 2647 (1976).

[6] R. F. Hudson and G. Klopman, *Tetrahedron Letters*, **12**, 1103 (1967).

[7] G. Klopman, *J. Amer. Chem. Soc.*, **90**, 223 (1968).

[8] G. Klopman "Chemical Reactivity and Reactions Paths", Wiley, New York, 1974, p. 61.

the interaction energy is calculated ; C_s^m are the coefficients of the atomic orbitals of atom s in the various molecular orbitals m of molecule S ; C_t^n are the coefficients of the atomic orbitals of atom t in the various molecular orbitals n of molecule T. $\Delta\beta_{st}$ is the change in the resonance integral between the interacting orbitals of atoms s and t at the distance R_{st} ; E_m^* and E_n^* are quantities related to the energy of the various molecular orbitals m and n of the isolated S and T molecules in the same medium as that being used to perform the reaction. Because we realized the protonation reaction of ylid I(R = NH_2) with perchloric acid in aqueous solution we calculated the coefficients of atomic orbitals and the energies of the hydronium ion with the CNDO/2 method. With the distance of 0.98 Å of 0 — H bond we traced the potential curve from Figure 2.

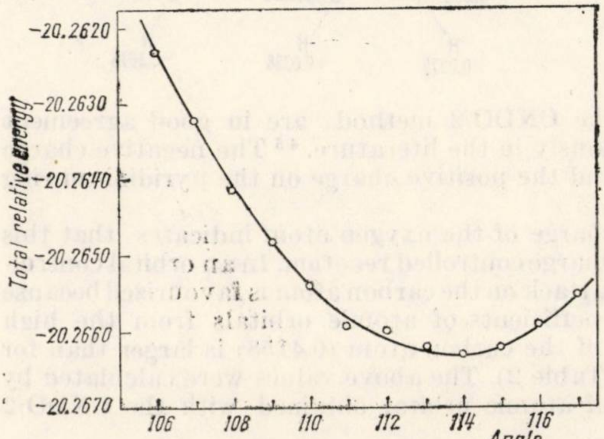

Fig. 2. — The total relative energy versus angle for the hydronium ion.

The minimum relative total energy of — 20.2663269043 u. a. of the hydronium ion for angle of 114° is found in table 1.

Table 1

The total relative energy versus angle for hydronium ion

Angle	ΔE_t (the total relative energy) u.a.
106	−20.2623138428
107	−20.2632446289
108	−20.2641143799
109	−20.2648468016
110	−20.2654418945
111	−20.2658691406
112	−20.2660432110
113	−20.2662963867
114	−20.2663269043
115	−20.2662200928
116	−20.2659301758
117	−20.2655639048

In the next calculations of ΔE_{total} we used the coefficients of unoccupied atomic orbitals of hydrogen atom from the unoccupied molecular orbitals of hydronium ion corresponding to this minimum value.

The used G. P. equation is the following

$$\Delta E_{\text{total}} = -\frac{q_s q_t}{R_{st} \, . \, \varepsilon} + 2 \sum \sum \frac{\sum_{1}^{4} (C_s^m \, . \, C_t^n \, \Delta\beta_{st})^2}{E_m - E_n} \qquad (2)$$

The sum $\sum_{1}^{4}$ indicates that the product $C_s^m \, . \, C_t^n$ is calculacted with the four atomic orbital coefficients ($2\,s$, $2p_x$, $2\,p_y$, $2p_z$) of the interacting carbon or oxygen and the 1s coefficients of the hydrogen atom. The energies E_m^* and E_n^* were replaced by their orbital energies E_m and E_n. The changes in the resonance integrals $\Delta\,\beta_{\text{OH}} = \Delta\,\beta_{\text{CH}} = \Delta\,\beta$ were considered equal between them. The ε value printed in calculations is 1 and the distances R_{st} in the transitional state were of 1.72 and 1.82 Å for the O—H and C — H interactions respectively.

The theoretical calculated ΔE_{total} are presented in table 2.

Table 2

The charges and ΔE_{total}

Atom	Total charge	$\Sigma^{C^2}_{\text{HOMO}}$	ΔE_{total}
$C^{(1)}$	-0.1389	0.4158	a) for O—H interaction
$O^{(2)}$	-0.6012	0.3303	$0.13-14.7452\ \Delta\beta^2$
$N^{(3)}$	$+0.2958$	—	b) for C—H interaction
$H^{(4)}$	$+0.3722$	—	$0.0284-7.3458\ \Delta\beta^2$

(1) ylid carbon atom; (2) ylid oxygen atom; (3) nitrogen from the pyridinium ring; (4) hydrogen from hydronium ion.

ΔE_{total} in the absolute value is bigger for the interaction ylid — hydronium ion, by the oxygen ylid atom with the hydrogen from the hydronium ion.

The both terms, electrostatically and covalently are larger for O — H interaction than for C—H interaction. Theoretically, the O — H interaction is energetically favorized. This theoretical result is experimentally verified because only the oxygen ylid atom protonation could explain the salt XI separation.

ACKNOWLEDGEMENTS. We express our sincere gratitude to Dr. C. Leonte for helpful discussion on the synthesis of these products.

Revue Roumaine de Chimie, **23**, *9–10*, 1455–1459 (1978)

KINETIK UND MECHANISMUS DER BASISCHEN HIDROLYSE VON HEXAMETHOXY-CYCLOTRIPHOSPHAZEN UND OCTAMETHOXY-CYCLOTETRAPHOSPHAZEN

PAUL SCHULZ und RADU VÎLCEANU
Chemiezentrum Timişoara des Zentralinstituts für Chemische
Forschung in Rumänien, Bd. Mihai Viteazul 24, 1900 Timişoara, Rumänien

Eingegangen am 27. Juli 1977

Die Hydrolyse von Hexamethoxy-cyclotriphosphazen und Octamethoxy-cyclotetraphosphazen in wäßriger Alkalihydroxydlösung führt nach Abspaltung der ersten Estergruppe in bimolekularer Kinetik glatt zum relativ stabilen entsprechenden P-oxo-cyclophosphazenat-anion, wobei der Sechsring etwa fünfmal schneller reagiert als der Achtring. Untersuchungen in mit ^{18}O markiertem Reaktionsmedium, die Aktivierungsparameter und die Umkehrung des üblichen Reaktivitätsverhältnisses zwischen Sechs- und Achtring machen einen nucleophilen Angriff des Hydroxylions am Methylkohlenstoffatom wahrscheinlich.

Kinetische Untersuchungen der Ringsubstitutionsreaktionen an Cyclophosphazenderivaten sind für die Aufklärung des vieldiskutierten Bindungscharakters im Phosphazenring von potentieller Bedeutung. Bisher betreffen vorliegende eingehendere kinetische Studien die Chloraustauschreaktion an Chlorphosphazenen verschiedener Ringgröße mit radioaktiv markierten Chloridionen von Sowerby, [1] Aminolysereaktionen (Goldschmidt und Licht [2–4]) und alkalische Hydrolysen der Fluoroalkyl-, Aryl- und Spiroarylenester cyclischer Phosphazene (Allcock und Walsh [5–7]). Außerdem liegen noch ältere kinetische Meßergebnisse vor, [8–10] deren Interpretation z. T. problematisch ist. [2] In den genannten Fällen wurde ein nucleophiler Substitutionsmechanismus am Phosphoratom (als direkter Ersatz *SN*2,[1,6,7] bzw. als Additions-Eliminierungsmechanismus, [2–4,11]) angenommen. Sofern sich die Untersuchungen auch auf das tetramere Analogon erstreckten, war eine 2-15-fache Zunahme der Reaktionsgeschwindigkeit festzustellen, die sich als qualitative Feststel-

[1] D. B. Sowerby, *J. Chem. Soc. (A)*, **1965**, 1369.

[2] J. M. E. Goldschmidt und E. Licht, *J. Chem. Soc. (A)*, **1971**, 2429.

[3] J. M. E. Goldschmidt und E. Licht, *J. Chem. Soc. Dalton*, **1972**, 728.

[4] J. M. E. Goldschmidt und E. Licht, *J. Chem. Soc. Dalton.*, **1972**, 732.

[5] H. R. Allcock und E. J. Walsh, *J. Amer. Chem. Soc.*, **91**, 3102 (1969).

[6] H. R. Allcock und E. J. Walsh, *J. Amer. Chem. Soc.*, **94**, 119 (1972).

[7] H. R. Allcock und E. J. Walsh, *J. Amer. Chem. Soc.*, **94**, 4538 (1972).

[8] J. V. Bailey und R. E. Parker, *Chem. and Ind.*, **1962**, 1823.

[9] T. Moeller und S. G. Kokalis, *J. Inorg. Nuclear Chem.*, **25**, 1397 (1963).

[10] M. Yokoyama und H. Cho, *Kogakuin Diagaku Kenkyu Hokoku*, **15**, 22, (1964); ***Chem. Abstr.***, **68**, 7026 (1968).

[11] S. K. Ray und R. A. Shaw, *Chem. and Ind.*, **1959**, 53.

lung auch aus präparativen Studien Rrgab, [12–14] und von verschiedenen Autoren auf die höhere Flexibilität des Achtrings zurückgeführt wird, die die im Substitutionsakt durchlaufenen Konformationsänderungen erleichtert. [1,6,7,9] Tab. 1. enthält repräsentative Werte des Reaktivitätsverhältnisses von Achtring und Sechsring. Sterische Faktoren, Solvatation und Verschiedenheit des Nucleophilen und der austretenden Gruppe bedingen eine erhebliche Streuung der Werte.

Tabelle 1

Reaktivitätsverhältnis ($R = k_{\text{Achtring}}/k_{\text{Sechsring}}$) bei nucleophilen Substitutionsreaktionen an Cyclophosphazenen

Cyclophosphazen (n = 3,4)	Nucleophiles Agens	Temperatur (°C)	R	Literatur
$(NPCl_2)_n$	Cl^{θ}	35	16,5	1
$[NP(OC_6H_5)_2]_n$	OH^{θ}	80	2	7
$[NP(OCH_2CF_3)_2]_n$	OH^{θ}	80	9	6
$[NP(OCH_2C_3F_7)_2]_n$	OH^{θ}	80	3	6

Die glatten Hydrolysereaktionen von Hexamethoxy-cyclotriphosphazen (I) und Octamethoxy-cyclotetraphosphazen (II): sind für ein kinetisches Studium gut geeignet. Dabei haben wir gefunden, daß (I) in wäßriger und wäßrig-alkoholischer Alkalihydroxydlösung etwa fünfmal schneller reagiert, als (II). [15] (Reaktivitätsverhältnis 0,2; vgl. Tab. 1) Zugleich konnten wir feststellen, daß die Reaktivitätsabnahme von (I) zum analogen Hexa-äthoxyderivat im Vergleich zu anderen Esterreihen

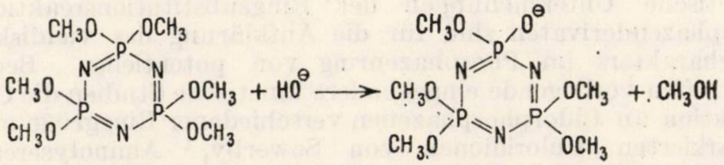

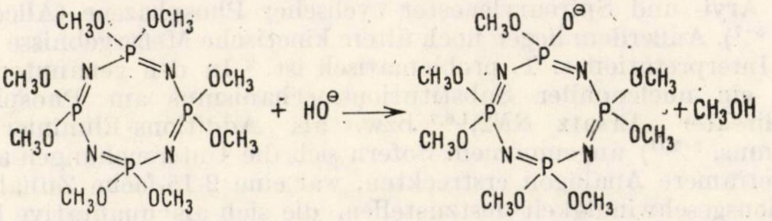

---

[12] B. Capon, K. Hills und R. A. Shaw, *Proc. Chem. Soc.*, **1962**, 390.

[13] B. Capon, K. Hills und R. A. Shaw, *J. Chem. Soc.* (*A*), **1965**, 4059.

[14] F. Seel und J. Langer, *Z. anorg. Chem.*, **295**, 316, (1958).

[15] R. Vîlceanu und P. Schulz, *Phosphorus*, **6**, 231 (1976).

des Phosphors ungewöhnlich groß ist. Hexaäthoxy-cyclotriphosphazen wird in wäßrig-alkoholischer, 1-normaler KOH-Lösung und 80° rund 200-mal langsamer verseift als (I).

Untersucht man die allgemeinen Faktoren, die das Reaktivitätsverhältnis von Sechs- und Achtring beeinflussen, bietet sich die Diskussion der Aktivierungsparameter als besonders aufschlußreich an. Die fast durchwegs höhere Basizität der Achtringe gegenüber analog substituierten Sechsringen [16,17] findet einen möglichen Ausdruck in den höhern Aktivierungsenthalpien bei der nucleophilen Achtringsubstitution am Phosphoratom.[6,7] Nun würde aber dieser Umstand allein eine Reaktivitätsabnahme beim Achtring im Vergleich zum Sechsring bewirken. Dieser Enthalpieeffekt wird aber durch meist bedeutend höhere Aktivierungsentropien[6,7] überkompensiert, woraus sich im Endergebnis die bekannte höhere Reaktivität der tetrameren Analogen ergibt. Dieser Entropieeffekt ist anscheinend Ausdruck der höheren konformationellen Freiheit des Achtrings.

Die von uns für die Raktionen (1) und (2) ermittelten Aktivierungsparameter sind in Tab. 2. zusammengefaßt. Die höhere Aktivierungsenthalpie bei (II) widerspiegelt die höhere Basizität des Achtrings (um 0,9 pK_a-Einheiten [16], gemessen durch Ringprotonierung) und ist wohl der Faktor, der das Reaktivitätsverhältnis in diesem Falle entscheidend beeinflußt. Offensichtlich entfällt hier der überkompensierende Beitrag der Aktivierungsentropie. Nimmt man nun an, daß das Hydroxylion am Methylkohlenstoff und nicht am Phosphor angreift, lassen sich die beschriebenen Befunde widerspruchsfrei zusammenfassen: Die höhere Flexibilität des Achtrings kann kinetisch nicht mehr wirksam werden, infolgedessen ändert sich das normale Reaktivitätsverhältnis, das für Substitutionen am Ringphosphor typisch ist. Zugleich findet auch die gewaltige Abnahme der Reaktionsgeschwindigkeit vom trimeren Methoxy- zum Äthoxyderivat eine Erklärung. Außerdem sind die gefundenen hohen Werte für die Aktivierungsenthalpien (Tab. 2.) bei nucleophilen Substitutionsreaktionen am α-Kohlenstoffatom üblich.

Tabelle 2

Aktivierungsparameter der Hydrolysereaktionen von (I) und (II) in 1-normaler wäßriger KOH-Lösung im Bereich 70–80°

	$\Delta H^{\ddagger}$(kcal/Mol)	$\Delta S^{\ddagger}$(cal/Mol . K)
$[NP(OCH_3)_2]_3$	$22{,}0 \pm 0{,}6$	$-14{,}1 \pm 2$
$[NP(OCH_3)_2]_4$	$23{,}7 \pm 0{,}6$	$-12{,}5 \pm 2$

Die untersuchten Hydrolysen weisen eine globale Kinetik zweiter Ordnung auf. Da in Gegenwart hoher Basenüberschüsse gearbeitet wurde, ergab sich zunächst eine Kinetik pseudo-erster Ordnung bezüglich (I) bzw. (II). Die bei jeweils drei Temperaturen gemessenen Geschwindigkeitskonstanten sind in Tab. 3. zusammengefaßt. Messungen in Gegenwart verschiedener Kaliumhydroxydkonzentrationen (wobei die Ionenstärke mit KNO_3 konstantgehalten wurde) die eine Abhängigkeit erster Ordnung von der Alkalikonzentration ergeben, bestätigen, daß eine globale Kinetik zweiter Ordnung vorliegt. (s. Tab. 4.).

---

[16] D. Feakins, W. A. Last, N. Neemuchwala und R. A. Shaw, *J. Chem. Soc.* **(A)** **1965**, 2804.

[17] D. Feakins, W. A. Last, N. Neemuchwala und R. A. Shaw, *Chem. and Ind.*, **1963, 164.**

Unsere Annahme, daß der nucleophile Angriff des Hydroxylions am Methylkohlenstoff stattfindet, wird ferner von Hydrolyseversuchen in ^{18}O-haltigem Wasser bestätigt, die ergaben, daß eine Sauerstoff Methyl-, und nicht eine Phosphor-Sauerstoffbindung gespalten wird. Bei diesen Versuchen bildet sich ^{18}O-haltiges Methanol, während die massenspektrometrisch erfaßten Molekülionen der in Trimethylsiloxyderivate umgewandelten Hydrolyseprodukte praktisch ^{18}O-frei sind.

Tabelle 3

Gefundene Geschwindigkeitskonstanten pseudo-erster Ordnung bei der Hydrolyse von (I) und (II) in 1-normaler wäßriger KOH-Lösung, (Sek^{-1})

	70,0°	75,0°	80,0°
$[NP(OCH_3)_2]_3$	$0{,}466 \cdot 10^{-4}$	$0{,}732 \cdot 10^{-4}$	$1{,}198 \cdot 10^{-4}$
$[NP(OCH_3)_2]_4$	$0{,}905 \cdot 10^{-5}$	$1{,}499 \cdot 10^{-5}$	$2{,}495 \cdot 10^{-5}$

Tabelle 4

Geschwindigkeit konstanten pseudo-erster Ordnung bei der Hydrolyse von (I) und (II) bei 80°, in Kaliumhydroxylösung verschiedener Konzentration, (Sek^{-1})

KOH-Konzentration (Mol/Liter)	Geschwindigkeitskonstanten	
	$[NP(OCH_3)_2]_3$	$[NP(OCH_3)_2]_4$
0,25	$0.275 \cdot 10^{-4}$	$0{,}600 \cdot 10^{-5}$
0,50	$0{,}570 \cdot 10^{-4}$	$1{,}212 \cdot 10^{-5}$
0,75	$0{,}869 \cdot 10^{-4}$	$1{,}850 \cdot 10^{-5}$
1,00	$1{,}198 \cdot 10^{-4}$	$2{,}495 \cdot 10^{-5}$

$$N_nP_n(OCH_3)_{2n} + {}^{18}OH^{\theta} \rightarrow CH_3^{18}OH + N_nP_n(OCH_3)_{2n-1}-{}_1O^{\theta} \quad (3)$$

$$N_nP_n(OCH_3)_{2n-1}O^{\theta} + ClSi(CH_3)_3 \rightarrow Cl^{\theta} + N_nP_n(OCH_3)_{2n-1}OSi(CH_3)_3 \quad (4)$$

Die Hydrolyse von (I) und (II) in D_2O ergab in beiden Fällen einen sekundären Lösungsmittelisotopeneffekt von $k_{H_2O}/k_{D_2O} = 0{,}86$ s. Tab. 5. Dieser Wert stimmt mit theoretischen Vorausberechnungen für bi-

Tabelle 5

Sekundärer Lösungsmittelisotopeneffekt bei der Hydrolyse von (I) und (II) in D_2O bei 80° und 1-normaler KOH-Konzentration

	k_{D_2O} (Sek^{-1})	k_{H_2O}/k_{D_2O}
$[NP(OCH_3)_2]_3$	$1{,}393 \cdot 10^{-4}$	0,860
$[NP(OCH_3)_2]_4$	$2{,}900 \cdot 10^{-5}$	0,860

molekulare Substitution durch Hydroxylionen am Kohlenstoffatom überein.[18,19] So z. B. weisen alkalische Hydrolysen von Sulfonsäurealkylestern einen wie oben definierten Isotopeneffekt von ebenfalls 0,86 auf.[18] Nun sind die k_{H_2O}/k_{D_2O} Werte im allgemeinen wenig mechanismusabhängig, stellen aber im vorliegenden Falle ein zusätzliches Argument im Sinne des vorgeschlagenen Mechanismus dar.

EXPERIMENTELLES

(I) und (II) wurden aus den entsprechenden Chloriden dargestellt,[20] und zweimal Petroläther umgelöst, bis die Schmelzpunkte den Literaturwerten entsprachen.

In einer Lösung von KOH in frisch destilliertem, kohlensäurefreiem Wasser entsprechender Konzentration wurden 0,2% (I) bzw. (II) gelöst und unter Stickstoffdruck filtriert. Die Hydrolysen wurden in einem thermostatisierten 30-ml-Mantelgefäß mit Magnetrührung, Rückflußkühler mit nachgeschalteter KOH-Säule und Thermometer durchgeführt. (Temperaturkonstanz ± 0,05°.) In entsprechenden Zeitabständen entnommene 1-ml-Proben werden rasch auf Zimmertemperatur abgekühlt.

In ein 2-ml-Schliffröhrchen werden 0,500 ml Probe und 0,500 ml Toluol p.a. mit einer Präzisions-Mikroliterspritze eindosiert. Der Inhalt wird kräftig durchgeschüttelt. (I) und (II) werden in der oberen klaren Tolulschicht gaschromatographisch erfaßt. (Säule: 5% Silikon OV−225 auf Gas-Chrom Q, 60−80 mesh; Länge 1 m, Innendurchmesser 5 mm, rostfreier Stahl; Trägergas Wasserstoff; Wärmeleitfähigkeitsdetektor; Temperatur 190° für (I) und 210° für (II)).

Der Hydrolysverlauf wurde anhand der Abnahme der Phosphazenesterkonzentration in mindestens zehn Meßpunkten verfolgt, bis zu Umsetzungen von über 80%.

Für die Untersuchungen in^{18}O-haltigem Wasser wurden jeweils 1 ml H_2O (^{18}O-Isotopengehalt 10%) mit 5% KOH und 5% (I) bzw. (II) in Phiolen eingeschmolzen und 3, bzw. 15 Stunden bei 80° gelagert. Vom Reaktionsgemisch wurden dann jeweils 0,05 ml abdestilliert und massenspektrometrisch untersucht. Die Auflösung des Geräts muß die Trennung des CH_3OH-Molekülions vom O_2-Molekülion gewährleisten. Der Destillationsrückstand wird mit Äthyläther (3-mal je 1 ml) extrahiert, mit 10% Schwefelsäure neutralisiert (pH = 4), mit Chloroform extrahiert (1 ml), und das Extrakt im Vakuum eingedampft. Der kristalline Rückstand wird mit 0,05 ml Trimethylchlorsilan und 0,05 ml Hexamethyldisilazan behandelt und nach 24-stündiger Lagerung unter strengstem Feuchtigkeitsausschluß, bei Zimmertemperatur, massenspektrometrisch untersucht. Das Molekülion-Multiplett wird mit dem analogen Signal einer Probe verglichen, die unter gleichen Bedingungen hydrolysiert und trimethylsilyliert wurde, mit dem Unterschied, daß das in diesem Ansatz verwendete Wasser ^{18}O-frei war. Der Vergleich zeigt, daß bei der Hydrolyse von (I) und (II) kein ^{18}O in das Produkt eingebaut wird.

---

[18] C. A. BUNTON und V. J. SHINER, *J. Amer. Chem. Soc.*, **83,** 3207 (1961).

[19] C. A. BUNTON und V. J. SHINER, *J. Amer. Chem. Soc.*, **83,** 42 (1961).

[20] B. W. FITZSIMMONS und R. A. SHAW, *J. Chem. Soc.* (*A*), **1964,** 1735.

Revue Roumaine de Chimie, 23, 9–10, 1461–1463 (1978

THE REACTION OF PYRIDINIUM-N-IMINE WITH PICRYL CHLORIDE, A ROUTE TO 6-AZA-BENZO [a]INDOLIZINE SYSTEM

C. LEONTE and EUGENIA CARP

Department of Organic and Macromolecular Chemistry, Polytechnic Institute, Calea 23 August 11, Iassy, Romania

Received December 15, 1976

Pyridinium-N-picrylimine, obtained by the arylation of pyridinium-N-imine with picryl chloride, yields, in the presence of piperidine, by loss of a NO_2 group, a cyclization product, the 7,9-dinitro derivative of 6-aza-benzo[a]indolizine.

The 'onium imines are isoelectronic with 'onium ylids and their chemistry is very similar. In this respect, we have found as well that, in the reaction with picryl chloride (PicCl, III), the pyridinium-N-imine (II) (formed *in situ* from N-aminopyridinium iodide, I) exhibits a remarkable similarity with the corresponding pyridinium ylids. [1]

When, to a chloroform solution of one mole of I and two moles triethylamine (NEt_3), a chloroform solution of one mole of III was added at ambient temperature, coral-red crystals of pyridinium-N-picrylimine (IV) were quantitatively isolated, m. p. 239° (decomp.). This arylation product of II is a weak base; an easily hydrolysable salt, N-picrylamino-pyridinium perchlorate (V) was obtained from IV and $HClO_4$, as colourless crystals, m. p. 255° (decomp.). The structure of IV results from the fact that the same product (mixed m. p., IR spectra) was obtained in a different way, starting from N-(2,4-dinitrophenyl)pyridinium chloride ("Zincke salt", VI). According to the known procedure for the preparation of pyridinium-N-imine derivatives,[2] from the ring-opening reaction of Zincke salt with picrylhydrazine ($PicNHNH_2$), 5-(2,4-dinitroanilino)-2,4-pentadienal picrylhydrazone (VII) was obtained in good yield, as dark red crystals, m. p. 171° (decomp.). The recyclization of VII (refluxing in acetic acid solution) yields the imine IV and 2,4-dinitroaniline.

[1a] W. AUGSTEIN, F. KRÖHNKE, *Liebigs Ann. Chem.*, **697**, 158 (1966); [b] D.–B. REUSCHLING, F. KRÖHNKE, *Chem. Ber.*, **104**, 2103 (1971).

[2a] H. BEYER, K. LEVERENZ, H. SCHILLING, *Angew. Chem.* **73**, 272 (1961); [b] H. BEYER, E. THIEME, *J. prakt. Chem.*, [4], **31**, 293 (1966); [c] Y. TAMURA, N. TSUJIMOTO, *Chem. and Ind.*, **1970**, 926; [d] Y. TAMURA, N. TSUJIMOTO, M. MANO, *Chem. and Pharm. Bull. (Japan)*, **19**, 130 (1971).

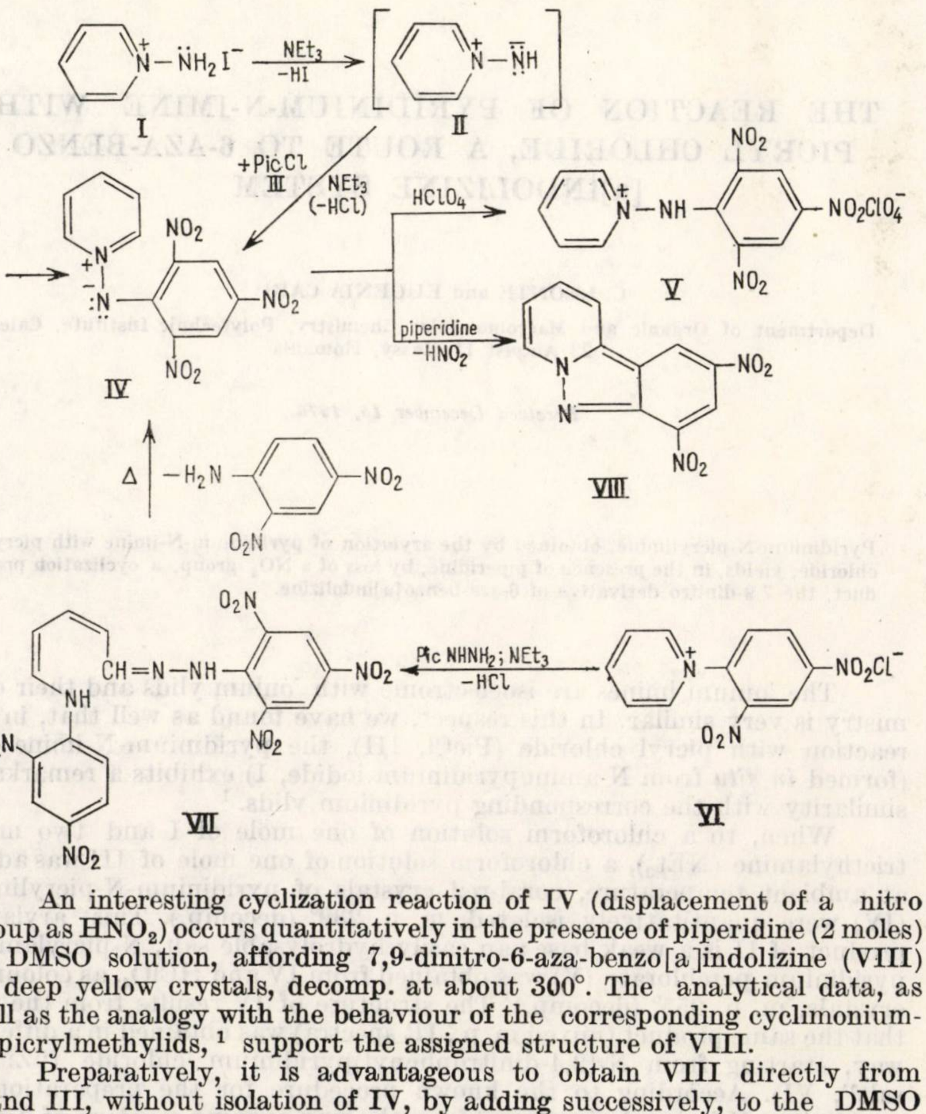

An interesting cyclization reaction of IV (displacement of a nitro group as HNO_2) occurs quantitatively in the presence of piperidine (2 moles) in DMSO solution, affording 7,9-dinitro-6-aza-benzo[a]indolizine (VIII) as deep yellow crystals, decomp. at about 300°. The analytical data, as well as the analogy with the behaviour of the corresponding cyclimonium-N-picrylmethylids,[1] support the assigned structure of VIII.

Preparatively, it is advantageous to obtain VIII directly from I and III, without isolation of IV, by adding successively, to the DMSO solution of the two reactants, NEt_3 (2 moles), and, after 30–45 minutes, piperidine (2 moles). If only NEt_3 (4 moles) is used as base in this procedure, the main product of the reaction is IV and the cyclization (IV → VIII) occurs only in a small extent.

EXPERIMENTAL

Pyridinium-N-picrylimine (*IV*). A. From I and III : A solution of 1.1 g (5 mmole) of I[3] in 25 ml of chloroform was treated with 1.4 ml (10 mmole) of triethylamine. After some time of shaking, to the violet-blue coloured solution, a solution of 1.24 g (5 mmole) of III in 25

---

[3] R. Gösl, A. Meuwsen, *Org. Synth.*, **43,** 1 (1963).

ml of chloroform was added. By filtration, successive washing with methanol, water, methanol and ethyl ether and recrystallization from 60 ml of glacial acetic acid, the product was quantitatively obtained as coral-red crystals, m.p. 239° (decomp.).
Analysis : $C_{11}H_7N_5O_6$ Calcd. : C, 43.28 ; H, 2.30 ; N, 22.95 ; Found : C, 43.42 ; H, 2.36 ; N, 23.00 %.

The compound is soluble with loss of colour in 1 : 1 diluted hydrochloric acid (salt formation), from which it may be again precipitated by dilution with water (hydrolysis). By treatment of an acetic acid solution of IV with 70 % perchloric acid and precipitation with ethyl ether, the salt V, as colourless crystals, m.p. 255° (decomp.) was obtained. The hydrolysis of V occurs even by exposure to atmospheric moisture.

B. From VII : A suspension of 0.5 g of VII in 10 ml of glacial acetic acid was refluxed for two hours. The reaction mixture was then allowed to stand overnight at room temperature. The product was isolated by filtration and recrystallization from glacial acetic acid. M.p. 239° (decomp.) ; there is no depression in the mixed m.p. with an authentic sample of IV (from the preceding procedure). The IR spectra are also identical.

In the filtrate obtained from the initial reaction mixture, 2,4-dinitroaniline was identified.

5-(2,4-Dinitroanilino)-2,4-pentadienal picrylhydrazone(VII). 1.2. g (5 mmole) of picrylhydrazine [4] was gradually added, under water cooling, to a solution of 1.4 g (5 mmole) of "Zincke salt" (VI)[5] in 3 ml of water and 12 ml of dioxan. To this mixture, with ice-water cooling, 0.7 ml (5 mmole) of NEt_3 was added. After several hours, by filtration of the cold solution, washing successively with dioxan, methanol, water, methanol and ethyl ether and recrystallization from dioxan — ethyl ether, dark red crystals of VII, m.p. 171° (decomp.), were obtained. The yield is 1.5 g (3 mmole).

7,9-Dinitro-6-aza-benzo[a]indolizine (VIII). A. From IV : To a solution of 0.61 g (2 mmole) of IV in 6 ml of DMSO, 0.4 ml (4 mmole) of piperidine was added, with stirring and water cooling. The reddish colour of the solution changes to dark violet and deep yellow crystals of VIII appear immediately in the reaction flask. The reaction mixture was left at room temperature for 3—4 hours and then, under ice-water cooling, 14 ml of 2N acetic acid was added ; after another hour, the product was filtered off, washed with water, methanol and ethyl ether. It was recrystallized from 20 ml of DMSO as deep yellow powder, decomp. at about 300° with previous redding. The yield is quantitative.
Analysis : $C_{11}H_6N_4O_4$ Calcd. : C, 51.16 ; H, 2.33 ; N, 21.71 ; Found : C, 51.40 ; H, 2.42 ; N, 22.02 %.

B. Directly from I : A solution of 2.22 g (10 mmole) of I and 2.48 g (10 mmole) of III in 30 ml of DMSO was treated, with stirring and under water cooling, with 2.8 ml (20 mmole) of NEt_3. After 30—45 minutes, 2 ml (20 mmole) of piperidine was dropped in. The reaction mixture was allowed to stand for two hours at room temperature. Under ice-water cooling, 70ml of 2N acetic acid was then slowly added and, after one hour, the product was filtered off, washed with water, methanol and ethyl ether and recrystallized from DMSO or DMFA. The yield is nearly quantitative.

In the above procedure the piperidine cannot be replaced by NEt_3, otherwise IV is obtained as a main product and only small quantities of VIII are formed.

---

[4] T. Curtius, G. M. Dedichen, *J. prakt. Chem.*, [2], **50**, 271 (1894).

[5] Th. Zincke, G. Heuser, W. Möller, *Liebigs Ann. Chem.*, **333**, 296 (1904).

Revue Roumaine de Chimie, **23**, *9–10*, 1465–1469 (1978)

STUDIES ON THE PRODUCT OBTAINED FROM STOBBE CONDENSATION BETWEEN *o*-CHLOROBENZALDEHYDE AND DIMETHYL HOMOPHTHALATE

A. M. EL-ABBADY *, M. A. OMARA and M. TAHA MAHMOUD
Chemistry Department, Faculty of Science, Tanta University, A.R.E.

Received July 12, 1976

o-Chlorobenzaldehyde is condensed with dimethyl homophthalate in the presence of potassium *t*-butoxide to give the γ-half-ester, *cis*-(o-$C_6H_4Cl/COOCH_3$) methyl α-(*o*-carboxyphenyl)-*o*-chlorocinnamate (I). This affords the dicarboxylic acid II on alkaline hydrolysis and the anhydride III on treatment with a dehydrating agent. Methanolysis of the anhydride gives the isomeric α-half-ester IV. The γ-half-ester yields on esterification the diester V, and on reduction in alkaline medium the dicarboxylic acid VI. Treatment of VI with acetyl chloride gives the anhydride VII, which on methanolysis affords the corresponding reduced α-half-ester VIII. The anhydride III, cyclises, on treatment with aluminium chloride, to give 4-chloro-2-(*o*-carboxyphenyl)inden-1-one IX, which on decarboxylation yields the 4-chloro-2-phenyl indenone X.

Recently different aldehydes and ketones [1-5] were condensed with homophthalic ester. In the case of benzaldehyde [1] the isolable product was claimed to be *trans*-($C_6H_5/COOCH_3$)methyl α-(*o*-carboxyphenyl) cinnamate.

However, in the present investigation we extended this study on *o*-chlorobenzaldehyde intending to see the effect of the *o*-chlorosubstituent on the reaction and the nature of the product. So *o*-chlorobenzaldehyde was condensed with dimethyl homophthalate in the presence of potassium *t*-butoxide. The isolated γ-halfester (85% yield) was proved to be *cis*-(o-$ClC_6H_4/COOCH_3$) methyl α-(*o*-carboxyphenyl)-*o*-chlorocinnamate I, on the following evidence and reactions (Chart 1).

---

* Present address : Sana'a University, Faculty of Science, Yemen Arab Republic, P.O.B. 1247.

[1] M. J. E. Loewenthal and R. J. Pappo, *J. Chem. Soc.*, **1952,** 4799.

[2] A. R. Pinder and J. B. Jones, *J. Chem. Soc.*, **1958,** 2612.

[3] J. N. Chatterjea and H. J. Mukherjea, *J. Indian Chem., Soc.*, **32,** 379, 446 (1960).

[4] J. N. Chatterjea, K. D. Banerji and H. M. Mukherjea, *J. Indian Chem. Soc.*, **40,** 45 (1963).

[5] J. N. Chatterjea, N. Parassed and K. D. Banerji, *J. Indian Chem. Soc.*, **41,** 93 (1964).

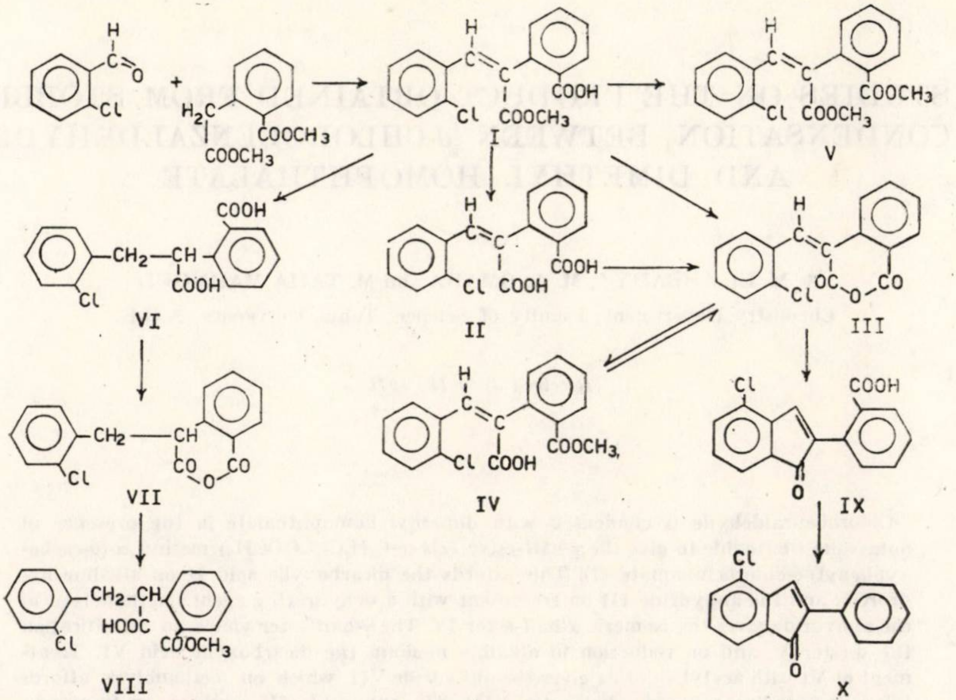

1) Its analytical data.

2) Its ir. spectrum which showed bands at 3100—3000, 2670, 1730, 1680, 1630 and 760 cm^{-1}, characteristic of ν OH for free and dimeric carboxylic acids, ν C=O of α, β-unsaturated esters and of aromatic acids, νC=C of olefinic linkages, and γ-CH of four adjacent hydrogen atoms, respectively.

3) Its u. v. spectrum (Table 1) characteristic for *trans*-stilbene moiety.

4) Its stability towards u. v. light (15 hrs. irradiations in benzene).

5) Its alkaline hydrolysis to give the corresponding dicarboxylic acid II which in its i. r. spectrum showed bands at 3000—2660, 1675, 1625 and 750 cm^{-1}, characteristic of ν OH of free and dimeric carboxylic acids, ν C=O of α, β-unsaturated and aromatic carboxylic acids, ν C=C of olefinic linkages, and γ-CH of four adjacent hydrogen atoms, respectively.

Treatment of the dicarboxylic acid II with acetyl chloride gave the corresponding anhydride III which showed a doublet at 1770 and 1730 cm^{-1}, characteristic of unsaturated six-membered ring anhydrides. Methanolysis of III gave the isomeric α-half-ester IV. The structure of IV was assigned from its analytical data, its i. r. spectrum which showed bands at 3090, 2660, 1725, 1680 and 769 cm^{-1}, characteristic of ν OH of monomeric and dimeric carboxylic acids, ν C=O of aromatic esters, ν C=O of α, β-unsaturated acids, and γ-CH of four adjacent hydrogen atoms, respectively, and from comparison of its electronic spectrum with that of the γ-half-ester I (Table 1). The isomeric α-half-ester IV failed to cyclise using concentrated sulphuric acid or phosphorus oxychloride and gave back the anhydride III.

6) Its further esterification with methanol and sulphuric acid to afford the corresponding diester V, which showed only one carbonyl band at 1730 cm^{-1} and an electronic spectrum similar to that of compounds I, II and IV (Table 1).

7) Its reduction with sodium amalgam in alkaline medium to give the corresponding reduced dicarboxylic acid VI in 85% yield which showed in its i. r. spectrum a carbonyl band at 1700 cm^{-1} (the ν C=C band of the olefinic linkage has disappeared) and possess a different electronic spectrum from that of the diacid II (Table 1).

Treatment of the reduced diacid with acetyl chloride gave the corresponding anhydride VII which showed a doublet at 1795 and 1760 cm^{-1}-characteristic of six-membered ring anhydrides. Methanolysis of VII gave the corresponding α-half-ester VIII, which showed in i. r. spectrum bands at 3080, 2660, 1745 and 1700 cm^{-1}, characteristic for ν OH of free and dimeric carboxylic acids, ν C=O of aliphatic acids and ν C=O for aromatic esters, respectively.

8) The failure of its cyclisation using conc. sulphuric acid, fused zinc chloride or phosphorus oxychloride; in these conditions the anhydride III was obtained.

However, on treating the anhydride III with anhydrous aluminium chloride in acetylene tetrachloride it gave the cyclised product, 4-chloro-2-(o-carboxyphenyl) inden-1-one (IX) in 47% yield. The structure of IX was established from: its analytical data, its i. r. spectrum which showed bands at 3360, 1720, 1700 and 760 cm^{-1}, characteristic of νOH of free carboxylic acids, ν C=O of α, β-unsaturated five-membered ring ketones, ν C=O of aromatic acids, and γ C—H of four adjacent hydrogen atoms, respectively, and finally its electronic spectrum (Table 1).

To be sure that no isomerisation had occurred during the cyclisation reaction, the half-ester I was treated with anhydrous aluminium chloride in acetylene tetrachloride (under the same conditions used for cyclisation reaction) and the product obtained was found to be the diacid II as shown by melting point and mixed melting point.

Decarboxylation of indenone acid IX with copper-bronze and pyridine gave 4-chloro-2-phenylindenone X, which showed one carbonyl band at 1700 cm^{-1} and two bands at 760 and 710 cm^{-1} characteristic of out-of-plane bending of five adjacent hydrogen atoms. The isolation of the indenone X confirmed the *trans*-stilbene moiety in the structure of the half-ester I and the anhydride III.

From the above data it is clear that the introduction of the chlorine atom in the o-position in the benzaldehyde molecule affected the nature of the Stobbe condensation reaction and its product in the following manner:

1) It facilitated the reaction and increased its yield.

2) It deactivated the phenyl ring towards the ring closure and accordingly facilitated the andydride formation.

Table 1

Electronic spectra of compounds

Compd.	λ_{max} (nm)	ε_{max}	λ_{max} (nm)	ε_{max}	λ_{max} (nm)	ε_{max}
I	216	23137	273	11760	293	10588
II	216	23100	265	13090	286	9060
IV	217	21390	272	12660	290	11790
V	219	31648	275	19000	290	17076
VI	214	25580	275	8870	—	—
VIII	217	21090	275	6150	—	—
IX	217	52727	269	30909	—	—
X	217	21000	235	18380	285	18271
					315	17500

EXPERIMENTAL

1 — Infrared spectra recorded as KBr disc using Unicam SP 200 spectrophotometer.
2 — Ultraviolet spectra were carried out using Unicam SP 8000 spectrophotometer.
3 — Melting points were not corrected.
4 — Elemental analysis were carried out by Cairo University Microanalytical unit.

cis-*Methyl α-(o-carboxyphenyl)-o-chlorocinnamate (I):*

The mixture of *o*-chlorobenzaldehyde (21 g, 0.15 mole) and dimethyl homophthalate (33 g, 0.16 mole) in *t*-butanol (50 ml) was added dropwise to a boiling solution of potassium *t*-butoxide (from 6.1 g potassium and 135 ml *t*-butanol) during 15 minutes. The mixture was worked-up as usual.[6] The solid product obtained was crystallized from benzene to give colourless crystals, m.p. 148°. Yield 40 g (85%).
Anal. Found : C, 64.7 ; H, 4.5 ; Cl, 11.0%

Calcd. for $C_{17}H_{13}O_4Cl$: C, 64.5 ; H, 4.1 ; Cl, 11.2%.

cis-α-(o-*carboxyphenyl*)-o-*chlorocinnamic acid (II):*

The γ-half-ester I (5 g, 0.016 mole) was refluxed with aqueous sodium hydroxide solution (50 ml, 10%) for 3 hours. The solid product obtained after acidifying with dilute hydrochloric acid, was crystallized from benzene/ethanol, m.p. 222–4°. Yield 4 g (88%).
Anal. Found : C, 63.3 ; H, 3.9 ; Cl, 11.5%.

Calcd. for $C_{16}H_{11}O_4Cl$: C, 63.5 ; H, 3.6 ; Cl, 11.7%.

cis-α-(o-*carboxyphenyl*)-o-*chlorocinnamic anhydride (III):*

The dicarboxylic acid II (2 g, 0.0066 mole) was refluxed with acetyl chloride (3 ml) for 5 hours. The excess acetyl chloride was removed by distillation. The solid residue obtained was dissolved in ether and extracted with sodium carbonate solution then with water. The ether was dried (Na_2SO_4) and then removed by distillation. The obtained solid was crystallized from benzene to give pale yellow needles, m.p. 174–5°. Yield 1.5 g (79%).
Anal. Found : C, 67.0 ; H, 3.8 ; Cl, 12.3%.

Calcd. for $C_{16}H_9O_3Cl$: C, 67.4 ; H, 3.3 ; Cl, 12.5%.

---

[6] Wm. S. Johnson, J. W. Patersen and W. P. Schnider, *J. Amer. Chem. Soc.*, **69**, 74 (1947).

cis-α-(*o-carbomethoxyphenyl*)-*o-chlorocinnamic acid* (*IV*) :

The anhydride III (0.7 g, 0.002 mole) was refluxed for 3 hours in methanol (30 ml). The solvent was then removed by distillation and the solid so obtained was crystallized from benzene to give crystals, m.p. 142°. Yield 0.7 g (89%).
Anal. Found : C, 64.7 ; H, 4.1 ; Cl, 10.9%.
Calcd. for $C_{17}H_{13}O_4Cl$: C, 64.5 ; H, 4.1 ; Cl, 11.2%.

cis-*methyl* α-(*o-carbomethoxyphenyl*)-*o-chlorocinnamate* (*V*) :

The solution of the γ-half-ester I (1 g, 0.003 mole) in dry methanol (30 ml) was treated with concentrated sulphuric acid (0.5 ml) then heated on a water-bath for 8 hours. The reaction mixture was cooled then worked-up as usual. The obtained solid was crystallized from petrol (b.p. 60—80°) to give colourless crystals, m.p. 95—6°. Yield 0.85 g (77%).
Anal. Found : C, 65.9 ; H, 4.8 ; Cl, 10.7%.
Calcd. for $C_{18}H_{15}O_4Cl$: C, 65.4 ; H, 4.5 ; Cl, 10.7%.

2-(*o-carboxyphenyl*)-3-(*o-chlorophenyl*)*propionic acid* (*VI*) :

The half-ester I (4 g, 0.012 mole) was dissolved in aqueous sodium hydroxide solution (40 ml, 5%) and treated with sodium amalgam (100 g, 10%) while heating on a water-bath. After the dissolution of sodium, the solution was decanted and acidified. The obtained solid was crystallized from benzene/ethanol to give colourless crystals, m.p. 172°. Yield 3.4 g (85%).
Anal. Found : C, 63.4 ; H, 4.4 ; Cl, 11.5%.
Calcd. for $C_{16}H_{13}O_4Cl$: C, 63.1 ; H, 4.3 ; Cl, 11.66%.

2-(*o-carboxyphenyl*)-3-(*o-chlorophenyl*) *propionic anhydride* (*VII*) :

The reduced dicarboxylic acid VI (1 g, 0.0032 mole) was refluxed with acetyl chloride (20 ml) for 3 hours on a water-bath. The excess acetyl chloride was removed by distillation, then worked-up as usual. The neutral solid so obtained was crystallized from benzene/petrol (b.p. 60—80°) to give colourless crystals, m.p. 83°. Yield 0.75 g (78%).
Anal. Found : C, 67.7 ; H, 4.5 ; Cl, 12.2%.
Calcd. for $C_{16}H_{11}O_3Cl$: C, 67.1 ; H, 3.9 ; Cl, 12.39%.

2-(*o-carbomethoxyphenyl*)-3-(*o-chlorophenyl*) *propionic acid* (*VIII*) :

The anhydride VII (0.8 g, 0.0027 mole) was refluxed in dry methanol (30 ml) for 3 hours. The excess methanol was then removed by distillation and the obtained solid was crystallized from benzene/petrol (b.p. 60—80°) to give colourless crystals, m.p. 110—11°. Yield 0.8 g (90%).
Anal. Found : C, 64.1 ; H, 4.9 ; Cl, 10.6%.
Calcd. for $C_{17}H_{15}O_4Cl$: C, 64.1 ; H, 4.7 ; Cl, 11.1%.

2-(*o-carboxyphenyl*)-*4-chloroinden-1-one* (*IX*) :

The solution of the anhydride III (0.85 g, 0.003 mole) in acetylene tetrachloride (20 ml) was treated with anhydrous aluminium chloride (0.9 g, 0.007 mole), then heated on a water-bath for 4 hours. The reaction mixture was worked-up as usual. The obtained product was crystallized from benzene to give pale yellow crystals, m.p. 200°. Yield 0.4 g (47%).
Anal. Found : C, 67.0 ; H, 3.7 ; Cl, 12.3%.
Calcd. for $C_{16}H_9O_3Cl$: C, 67.4 ; H, 3.3 ; Cl, 12.5%.
It gave dnp. of melting point 255° from benzene.

4-*chloro*-2-*phenylindenone* (*X*) :

Copper bronze (0.5 g) was added to a solution of the indenone acid IX (0.3 g, 0.001 mole) in pyridine (10 ml). The reaction mixture was refluxed for 10 hours, cooled then poured on cold dilute hydrochloric acid. The solid formed was washed with sodium carbonate solution, then crystallized from petroleum ether (b.p. 60—80°) to give pale yellow crystals, m.p. 171°. Yield 0.2 g (77%).
Anal. Found : C, 74.3 ; H, 3.4 ; Cl, 14.4%.
Calcd. for $C_{15}H_9OCl$: C, 74.8 ; H, 3.7 ; Cl, 14.8%.

Revue Roumaine de Chimie, 23, 9–10, 1471–1474 (1978)

NEW CATIONIC DYE WITH DIBENZ[f, ij]ISOQUINOLINE [2,3-b]QUINAZOLINE-5,10-DIONE STRUCTURE

F. URSEANU[a] and C. DRĂGHICI[b]

[a] Laboratory of Chemistry and Technology of Aromatic Intermediates and Dyes, Polytechnic Institute, Bucharest, Calea Victoriei 149

[b] Centre of Organic Chemistry, Bucharest, Romania

Received February 10, 1978

Syntheses for the preparation of new cationic dye with dibenz[f, ij]isoquinoline[2,3-b]quinazoline-5,10-dione structure are described.

1. INTRODUCTION

In a previous paper [1] we have presented the experimental results concerning the obtaining of new dispersion dyes with dibenz [f, ij] isoquinoline [2,3–b] quinazoline-5,10-dione structure. In the present work we report the syntheses carried out in order to prepare a new cationic dye I [2], having a similar structure with one of the already mentioned dispersion dyes II.

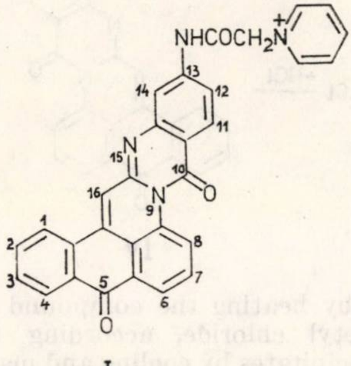

I

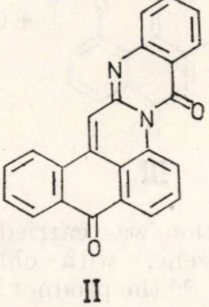

II

---

[1] F. Urseanu, L. Floru, I. Popescu, C. Drăghici and V. Zdrențu, *Rev. Roumaine Chim.*, **20**, 107 (1975).

[2] F. Urseanu, I. Popescu, V. Zdrențu and C. Drăghici, R. S. R. Pat. 65 603, Nov. 30, 1973.

2. SYNTHESIS OF NEW CATIONIC DYES

From the starting material 13-nitrodibenz[f,ij]isoquinoline [2,3—b] quinazoline-5,10-dione II, the cationic dye I was obtained based on the reactions given below:

2.1. Synthesis of 13-aminodibenz[f,ij]isoquinoline 2,3-b quinazoline—5,10-dione III

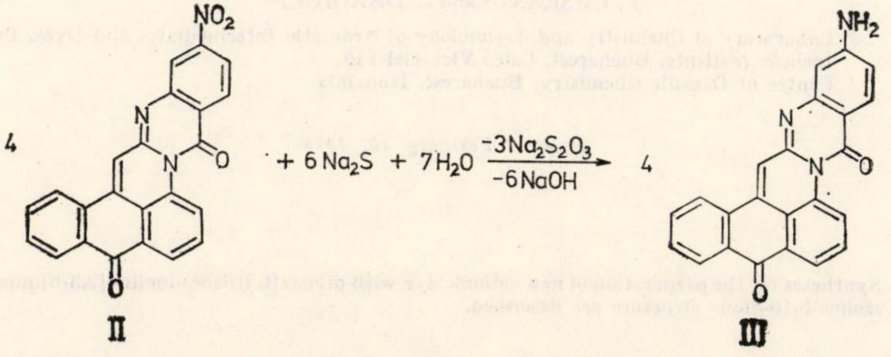

The product III was obtained from the compound II by the reduction of the nitro group with aqueous solution of sodium sulphide in N.N—dimethylformamide as solvent, according to literature procedures [3,4].

2.2. Synthesisis of 13-chloroacetylaminodibenz[f,ij]isoquinoline [2,3-b] quinazoline-5,10-dione IV

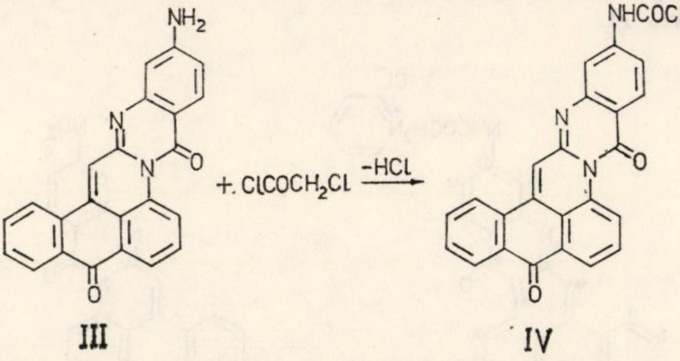

Acylation was carried out by heating the compound III in *ortho*-dichlorobenzene, with chloroacetyl chloride, according to literature procedures ; [3,5] the product IV precipitates by cooling and may be isolated by filtration.

---

[3] F. URSEANU, R. VINTILĂ and G. NAZARIE, *Rev. Chim. (București)*, **24**, 517 (1973).

[4] F. URSEANU and I. ZUGRĂVESCU, *Rev. Roumaine Chim.*, **18**(7), 1 211 (1973).

[5] F. URSEANU, C. DRĂGHICI and V. OLTEANU, *Rev. Roumaine Chim.*, **19** (11), 1 751 (1974).

2.3. Synthesis of the cationic dye I

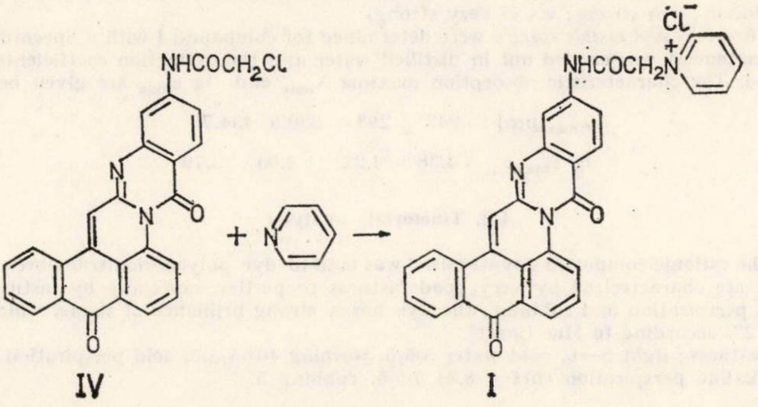

The compound IV was dissolved in nitrobenzene and treated with calculated amounts of pyridine, according to literature procedures; [3,5] the cationic dye I, thus formed by quanternization, is insoluble in nitrobenzene and it is isolated by filtration.

3. EXPERIMENTAL

3.1. 7.62 g (20 mmoles) compound II are dissolved in 120 ml N.N-dimethylformamide at 80−90°; in the solution resulted, a warm solution of 2 g Na_2S in 20 ml water is added dropwise for 30 minutes. The reaction is completed by heating at 95−98° for 3 hours (the mass colour turns gradually from yellow to brown). The formation of the amino group by reducing the nitro group is determined by a characteristic colour reaction, by the help of the Erlich reagent. Then, 240 ml water are added, the mass is cooled at 20°, neutralized with concentrated HCl at pH = 7, the precipitate formed is filtered, washed with 150 ml water and dried at 70−80°, yielding 6.38 g product III (91 % yield), which is a new compound (it may be used as yellow disperse dye for polyester fibres).

3.2. 6.32 g (18 mmoles) compound III are dissolved in 100 ml *ortho*-dichlorobenzene at 150−160°, then 1.52 ml (2.26 g; 20 mmoles) chloroacetyl chloride are added. The reaction is completed by heating at 175° for 2 hours. The mass is cooled at 10−15°, the precipitate formed is filtered, washed with 50 ml benzene and dried at 30−40° and p = 10 mm Hg, affording 7.38 g product IV (96 % yield).

3.3. 6.84 g (16 mmoles) compound IV are dissolved in 80 ml nitrobenzene at 120°, then 1.26 ml (1.3 g; 16.4 mmoles) pyridine are added. The reaction is completed by heating at 120−130° for 30 minutes. The precipitate formed is filtered at 20°, washed with 50 ml benzene and dried at 30−40° and p = 10 mm Hg; 7.82 g cationic dye I are thus obtained (96.6 % yield).

4. ANALYSES

The analysed compounds (IV and I) were previously purified. The compound IV was recrystallized from *ortho*-dichlorobenzene, while the cationic dye I was purified by dissolution in methanol, filtration and precipitation with ether. The purified compounds were subjected to spectral and tinctorial analyses.

4.1. Spectral analysis

Infrared, ultraviolet and visible spectra of the compounds were recorded.

IR spectra were recorded using a UR−10 spectrophotometer, in KBr pellet. Characteristic vibration frequencies ν [cm^{-1}]:

Compound IV : 685s ; 745s ; 970s ; 1601v.s ; 1646v.s ; 1452v.s ; 1721v.s.
Compound I : 736m ; 780s ; 980m ; 1378s ; 1495s ; 1540v.s ; 1590v.s ; 1636s ; 1665s ; 1694s.
(m = medium ; s = strong ; v.s = very strong)

Ultraviolet and visible spectra were determined for compound I with a Specord apparatus. The measurement was carried out in distilled water and the extinction coefficients ε_{max} were calculated. The characteristic absorption maxima λ_{max} and $\lg \varepsilon_{max}$ are given below :

λ_{max}[nm] :	243	293	330.5	434.7
$\lg \varepsilon_{max}$:	4.38	4.22	4.05	3.79

4.2. Tinctorial analysis

The cationic compound I synthesized was used to dye polyacrylonitrile fibres. The dyings obtained are characterized by very good fastness properties, especially by fastness to light, washing, perspiration and rubbing ; the dye has a strong brilliance of shade, which is named "yellow 2", according to Hue Chart[6].

Fastness : light 5—6, cold water 5/5/5, washing 40° 5/5/5, acid perspiration (pH = 5.5) 5/5/5, alkaline perspiration (pH = 8.4) 5/5/5, rubbing 5.

---

[9] C. I. Hue, "Indication Chart, American Association of Textile Chemists and Colourists" Lowell Institute, Lowell Massachusetts, USA.

Revue Roumaine de Chimie, **23,** *9–10,* 1475–1482 (1978)

LA SÉPARATION ET LA CARACTÉRISATION DES HYDROCARBURES AROMATIQUES DES HUILES MINÉRALES À L'AIDE DE LA CHROMATOGRAPHIE D'ÉLUTION ET DES SPECTRES ÉLECTRONIQUES D'ABSORPTION

N. MOŞESCU, G. KALMUŢCHI, R. POPESCU et DEEA STEJARU
Institut de recherche, génie chimique et projection des raffineries de pétrole
2000 Ploieşti, 291 A Bd. Republicii

Reçu le 25 février 1976

On a étudié des possibilités pour caractériser les structures des hydrocarbures aromatiques séparés des huiles moyennes et lourdes utilisant la combinaison chromatographie d'élution — spectrométrie en UV (200–350 nm) à base des bandes d'absorption caractéristiques, des effets dus aux groupes chromophores, des coefficients d'absorption et de la force de l'oscillateur.

Les procédés modernes de raffinage obligent à la connaissance des structures des hydrocarbures aromatiques contenus dans les huiles minérales. Pour l'étude de la structure des hydrocarbures aromatiques on applique des méthodes instrumentales de recherche telles que la spectrométrie de masse, la fluorescence, la chromatographie, la spectrométrie RMN.[1-6]

Dans cet ouvrage on présente des résultats de l'application de la combinaison chromatographie d'élution — spectrométrie en UV pour l'attribution des structures moléculaires de base aux hydrocarbures aromatiques mono-, bi-, tri- et tétra-nucléaires des huiles. On a établi entre les particularités des spectres électoniques en UV (200–350 nm), comme coefficients d'absorption, effets bathochromes, la force de l'oscillateur, une corrélation avec la structure moléculaire des hydrocarbures aromatiques mono-, bi- et tri-nucléaires séparés par chromatographie des huilles moyennes et des hydrocarbures aromatiques mono-, bi-, tri- et tétranucléaires séparés des huiles lourdes.

---

[1] K. I. Zimina, A. A. Poliakova. N. I. Lulova, A. G. Siriuk et S. A. Leontieva, "Panel Discussion. Preprint of the Proceedings of the 8th World Petroleum Congress", vol. 20, 1, 1971, p. 1–25.

[2] H. West "Panel Discussion. Preprint of the Proceedings of the 8th World Petroleum Congres", vol. 20, 3, 1971, p. 1–23.

[3] E. Hirsch et K. Altgelt, *Analyt. Chem.*, **42,** 1330 (1970).

[4] A. A. Poliakova, R. A. Hmelnitschi et I. M. Lukasenko, *Khimia i teknologia topliv i masel.*, **13,** 12 (1968).

[5] C. I. Robinsion et G. L. Cook *Analyt. Chem.*, **41,** 1548 (1969).

[6] R. Ţiţeica, N. Moşescu et G. Kalmuţchi *Rev. Roumaine Phys.*, **20,** 435 (1975).

PARTIE EXPÉRIMENTALE

On a étudié les spectres des hydrocarbures aromatiques mono-, bi- tri- et tétra-nucléaires purs et ceux des hydrocarbures aromatiques séparés par chromatographie des huiles moyennes et lourdes.

Les spectres ont été obtenus avec un spectrophotomètre SP—800 D Unicam, utilisant des cuves de quartz, ayant une épaisseur de couche de 1 cm et comme solvant de compensation on a utilisé le n-heptane de pureté spectrale. Les concentrations d'enregistrement ont été : $10^{-2}-10^{-4}$ g/100 ml de n-heptane spectral.

Les spectres obtenus sont présentés dans les figures 1—4.

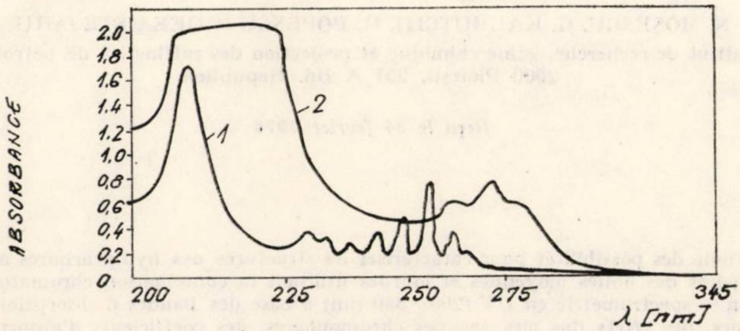

Fig. 1. — Spectres électroniques des hydrocarbures aromatiques mononucléaires.

1, Benzène, concentration 2.10^{-2} g/100 ml n-heptane ; *2*, Fraction séparée par chromatographie de l'huile, concentration 2.10^{-1} g/100 ml n-heptane.

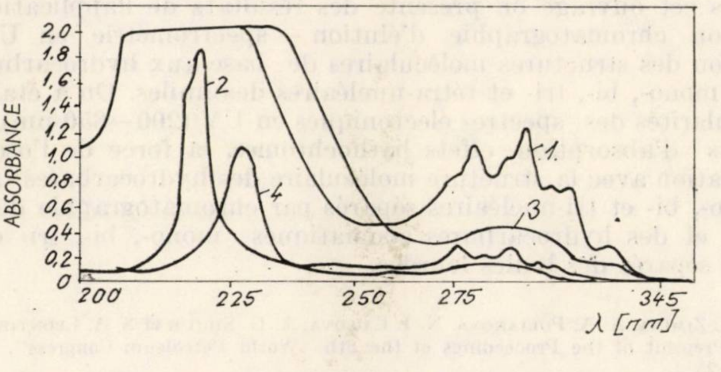

Fig. 2. — Spectres électroniques des hydrocarbures aromatiques binucléaires.

1, Naphtaline, concentration 2.10^{-3}g/100 ml n-heptane ; *2*, Naphtaline, concentration 2.10^{-4} g/100 ml n-heptane ; *3*, Fraction séparée par chromatographie de l'huile, concentration 2.10^{-3} g/100 ml n-heptane ; *4*, Fraction séparée par chromatographie de l'huile concentration 2.10^{-4} g/100 ml n-heptane.

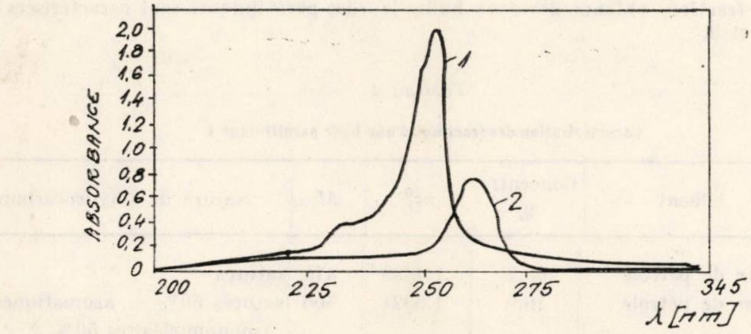

Fig. 3. — Spectres électroniques des hydrocarbures aromatiques trinucléaires.

1, Anthracène + phénanthrène, concentration 2.10 – ^{4}g/100 ml n-heptane; *2*, Fraction séparée par chromatographie de l'huile, concentration 2.10 – ^{4}g/100 ml n-heptane.

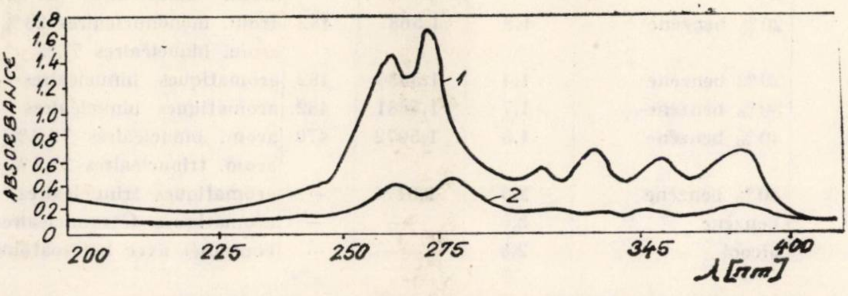

Fig. 4. — Spectres électroniques des hydrocarbures aromatiques tétranucléaires.

1, Chrysène, concentration 2.10 – ^{4}g/100 ml n-heptane; *2*, Fraction séparée par chromatographie de l'huile, concentration 2.10 – ^{4}g/100 ml n-heptane.

La séparation des huiles en fractions d'hydrocarbures aromatiques a été réalisée par la chromatographie d'élution d'après le schéma présenté dans la figure 5.

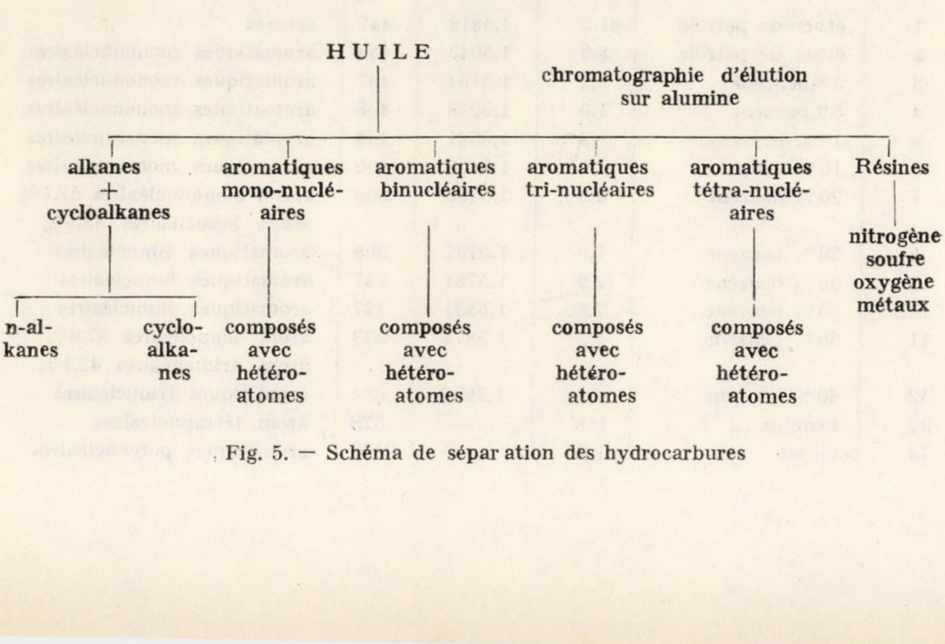
HUILE
chromatographie d'élution sur alumine
alkanes + cycloalkanes
aromatiques mono-nucléaires
aromatiques binucléaires
aromatiques tri-nucléaires
aromatiques tétra-nucléaires
Résines
nitrogène
soufre
oxygène
métaux
n-alkanes
cyclo-alkanes
composés avec hétéro-atomes
composés avec hétéro-atomes
composés avec hétéro-atomes
composés avec hétéro-atomes

Fig. 5. — Schéma de séparation des hydrocarbures

Ainsi les fractions obtenus des deux huiles lourdes paraffiniques sont caractérisées dans les tableaux 1 et 2.

Tableau 1

Caractérisation des fractions d'une huile paraffinique 1

Fraction N°	Eluent	Concentr. %	n_D^{20}	M	Nature de l'hydrocarbure
1	éther de pétrole	65,2	1,4883	475	saturés
2	éther de pétrole	10,9	1,5021	500	saturés 50 % + aromatiques mononucléaires 50 %
3	5 % benzène	2,3	1,5231	525	aromatiques mononucléaires
4	5 % benzène	1,6	1,5361	495	aromatiques mononucléaires
5	10 % benzène	3,2	1,5408	463	aromatiques mononucléaires
6	10 % benzène	2,0	1,5576	463	arom. mononucléaires 73 % arom. binucléaires 27 %
7	20 % benzène	1,8	1,5681	482	arom. mononucléaires 23 % arom. binucléaires 77 %
8	20 % benzène	1,4	1,5830	482	aromatiques binucléaires
9	30 % benzène	1,7	1,5881	482	aromatiques binucléaires
10	40 % benzène	1,5	1,5972	479	arom. binucléaires 72,3 % arom. trinucléaires 27,7 %
11	40 % benzène	2,6	1,6174	—	aromatiques trinucléaires
12	benzène	3,0	—	—	aromatiques tétranucléaires
13	alcool	2,8	—	—	composés avec hétéroatomes

Tableau 2

Caractérisation des fractions d'une huile paraffinique 2

Fraction N°	Eluent	Concentr. %	n_D^{20}	M	Nature de l'hydrocarbure
1	éther de pétrole	61,2	1,4818	447	saturés
2	éther de pétrole	8,2	1,5043	432	aromatiques mononucléaires
3	5 % benzène	3,2	1,5164	407	aromatiques mononucléaires
4	5 % benzène	1,0	1,5238	406	aromatiques mononucléaires
5	10 % benzène	5,2	1,5341	406	aromatiques mononucléaires
6	10 % benzène	2,0	1,5408	400	aromatiques mononucléaires
7	20 % benzène	2,6	1,5498	398	arom. mononucléaires 61,1 % arom. binucléaires 38,9 %
8	20 % benzène	7,0	1,5737	398	aromatiques binucléaires
9	30 % benzène	2,9	1,5781	397	aromatiques binucléaires
10	30 % benzène	2,8	1,5831	397	aromatiques binucléaires
11	40 % benzène	1,5	1,5874	393	arom. binucléaires 57,9 % arom. trinucléaires 42,1 %
12	40 % benzène	0,8	1,5923	384	aromatiques trinucléaires
13	benzène	0,8	—	378	arom. tétranucléaires
14	alcool	0,8	—	463	aromatiques polynucléaires

Les éluents utilisés pour obtenir les fractions ont été l'éther de pétrole pour les hydrocarbures saturés, et l'éther de pétrole avec 5%, 10%, 20%, 30% et 40% benzène pour les hydrocarbures aromatiques mononucléaires, binucléaires et trinucléaires, le benzène pour les aromatiques tétranucléaires et l'alcool pour les aromatiques polynucléaires et pour les composés avec hétéroatomes.

Ce choix des éluents a permis d'obtenir tant des fractions pures que des mélanges des hydrocarbures comme saturés avec aromatiques mononucléaires, aromatiques mononucléaires avec aromatiques binucléaires, binucléaires avec trinucléaires.

Pour avoir des données supplémentaires on a déterminé les indices de réfraction, qui ont confirmé l'attribution de la classe des hydrocarbures. De même on a déterminé par la méthode ébullioscopique le poids moléculaire des fractions séparées par la chromatographie.

RÉSULTATS ET DISCUSSIONS

On a établi les structures des hydrocarbures aromatiques en utilisant tant les particularités des spectres électroniques des hydrocarbures aromatiques purs que les spectres des hydrocarbures aromatiques séparés par chromatographie.

La répartition des hydrocarbures dans les deux huiles se présente comme suit :

Tableau 3

Répartition des hydrocarbures dans les deux huiles

	Saturés	Hydrocarbures aromatiques %				
		Mononucléaires	Binucléaires	Trinucléaires	Tétranucléaires	Composés avec hétéroatomes
huile 1	70,6	14,5	6,1	3,0	3,0	2,8
huile 2	61,2	21,2	14,6	1,4	1,6	—

Dans le tableau 4 sont présentés les coefficients d'absorption pour les hydrocarbures aromatiques mono-, bi-, tri- et tétra-nucléaires séparés par chromatographie des huiles moyennes et lourdes.

Les valeurs des coefficients indiquent que les fractions des hydrocarbures aromatiques qui existent dans les huiles ont des structures complexes, des noyaux naphténo-aromatiques fortement substitués. Il est évident que les coefficients d'absorption sont fonction de la nature du brut dont on a obtenu l'huile. Dans tous les cas, aux bandes des hydrocarbures séparés par chromatographie on observe, par rapport aux hydrocarbures purs, des effects bathochromes et une modification de la forme dans le sens de la disparition de la structure fine et l'élargissement des bandes d'absorption. Les coefficients d'extinction maximale ne tiennent pas compte de ce fait. Ainsi ces dernières années on a utilisé de plus en plus la force de l'oscillateur "f" pour caractériser l'intensité des transitions électroniques pour l'intervalle de fréquence d'une bande. Tenant compte que par l'introduction des substituants dans la molécule des hydrocarbures aromatiques se modifie la symétrie du cycle, l'influence de ces substituants peut être poursuivie

Tableau 4

Coefficients d'absorption pour les hydrocarbures aromatiques séparés d'une huile moyenne ou d'une huile lourde

Hydrocarbures aromatiques	Huile	K / g^{-1} cm^{+2}			
		λ = 220 . . . 230 nm	λ = 250 . . . 260 nm	λ = 260 . . . 290 nm	$\lambda \geqslant 300$ nm
mononucléaires	moyenne			11	
	lourde			8,8	
binucléaires	moyenne	2000		110	
	lourde	1535		320	
trinucléaires	moyenne		900		
	lourde		608,5		4,75
tétranucléaires	moyenne				
	lourde		517,5		35,3

en calculant la force de l'oscillateur.[7] Pour les hydrocarbures aromatiques mononucléaires et binucléaires on a pu obtenir ainsi des informations supplémentaires.

Par suite on présente des détails de structure pour les hydrocarbures aromatiques mono-, bi-, tri et tétra-nucléaires.

Ainsi les hydrocarbures aromatiques mononucléaires présentent trois bandes d'absorption caractéristiques, aux longueurs d'ondes $\lambda_1 = 266$, $\lambda_2 = 274$ et $\lambda_3 = 279$ nm avec des effets bathochromes $\Delta \lambda_1 = 12$, $\Delta \lambda_2 = 18$ et $\Delta \lambda_3 = 19$ nm par rapport à la bande "B" du benzène. Ces déplacements sont dus tant aux substituants du noyau, qu'à l'excitation locale des chromophores qui existent dans les molécules des hydrocarbures aromatiques des huiles. Il est évident que ces structures ne peuvent être attribuées aux composés "purs" mais à des structures (molécules) moyennes mixtes naphténo-aromatiques.

Les hydrocarbures aromatiques binucléaires présentent trois bandes d'absoption à $\lambda_1 = 225 - 230$ nm, $\lambda_2 = 285$ nm et $\lambda_3 = 325$ nm. Les effets bathochromes pour ces hydrocarbures sont plus faibles que pour les mononucléaires, étant : $\Delta \lambda_1 = 5 - 10$ nm, $\Delta \lambda_2 = 10$ nm et $\Delta \lambda_3 = 5$ nm. Ces bandes sont dues tant aux substituants du noyau qu'à l'excitation locale de quelques chromophores présents dans les structures des molécules moyennes des hydrocarbures aromatiques des huiles.

Utilisant les valeurs de la force de l'oscillateur "f" calculées pour un grand nombre des hydrocarbures aromatiques mononucléaires et binucléaires, [8,9] on a calculé les valeurs "f" pour les fractions des hydrocarbures aromatiques mononucléaires, mono- + bi-nucléaires et binucléaires séparés des deux huiles, présentées dans les tableaux 1 et 2. Ces valeurs sont présentées dans le tableau 5.

---

[7] R. Ţiţeica, V. Vîntu, A. Truţia et M. Popescu, *Rev. Phys.*, **6**, 225 (1961).

Les hydrocarbures aromatiques trinucléaires présentent deux groupes de bandes distinctes, une dans le domaine des petites longueurs d'onde, $\lambda_1 = 250 - 260$ nm, caractérisée par des absorptions fortes et une autre $\lambda_2 > 300$ nm, dans le domaine des grandes longueurs d'onde, ayant des intensités à peu près cent fois plus faibles par rapport aux bandes du domaine des petites longueurs d'onde.

Pour ces hydrocarbures on a utilisé seulement la bande à 255 nm, et on a attribué les structures suivantes :

— dérivés du phénântrène et de l'anthracène, mono-, bi- et trisubstitués ayant la formule C_nH_{2n-18}.

— hydrocarbures condensés du type naphténo-aromatique ayant la formule C_nH_{2n-20}.

Les hydrocarbures aromatiques tétranucléaires présentent des bandes d'absorption en deux régions, un doublet à $\lambda_1 = 257 - 267$ nm et à $\lambda_2 = 306 - 320$ nm. Les hydrocarbures aromatiques tétranucléaires étudiés présentent des bandes caractéristiques à $\lambda_1 = 265 - 275$ nm avec $\Delta \lambda_1 = 8$ nm et $\lambda_2 = 310 - 330$ nm avec $\Delta \lambda_2 = 4 - 10$ nm. Les effets bathochromes relativement grandes indiquent la présence des substituants donneurs d'électrons dans la structure aromatique de base.

A l'aide de la relation de Kaar [10] on a conclu que les hydrocarbures aromatiques tétranucléaires sont des hydrocarbures aromatiques condensés angulairement de la classe des phènes, appartenant aux :

— hydrocarbures aromatiques condensés angulairement du type chrysène, ayant la formule C_nH_{2n-24} et

— hydrocarbures condensés du type naphténo — aromatique ayant la formule C_nH_{2n-26}.

CONCLUSIONS

On a étudié des possibilités pour caractériser les structures des hydrocarbures aromatiques séparés des huiles moyennes et lourdes, utilisant la combinaison chromatographie d'élution — spectrométrie en UV (200 — 350 nm), à base des bandes d'absorption caractéristiques, des effets dus aux groupes chromophores, des coefficients d'absorption et de la force de l'oscillateur.

On a proposé des structures pour les hydrocarbures aromatiques mono-, bi-, tri- et tétra-nucléaires, ayant la formule C_nH_{2n-6} — $C_n H_{2n-26}$, séparés par chromatographie des huiles moyennes et lourdes, provenant des bruts de nature différente.

---

[8] N. Moşescu, Symposium "Metode moderne de analiză folosite în prelucrarea ţiţeiului şi petrochimie", Ploieşti, 1974, p. 24.

[9] R. Ţiţeica, N. Moşescu et G. Kalmuţchi, "XVIII^{1} Colloquium Spectroscopicum Internationale", Grenoble, 15—19. IX, 1975.

[10] C. Kaar, *Appl. Spectr.*, **13**, 15 (1959).

Tableau 5

Valeurs de la force de l'oscillateur et structures proposées pour les fractions séparées par chromatographie

Fractions	Domaine d'intégration	Solvant	Force de l'oscillateur "f"	Structures proposées
Huile paraffinique 1				
aromatiques mononucléaires	40800–34000	n-heptane	0,009439	— alkylbenzènes bi-, tri- et tétrasubstitués C_nH_{2n-6}
,, ,,	40400–33800	,,	0,007952	— tétralines bisubstitués C_nH_{2n-8}
,, ,,	40000–33600	,,	0,010294	— alkylcycloalkylbenzènes tétra- et pentasubstitués
aromatiques mono- + binucléaires	31500–30100	,,	0,000211	
,, ,, ,,	31200–29600	,,	0,000942	
aromatiques binucléaires	31200–29400	,,	0,002396	— alkylnaphtalines tri- et tétrasubstitués C_nH_{2n-12}
,, ,, ,,	31200–29600	,,	0,002935	— hydrocarbures naphténo-aromatiques C_nH_{2n-16}
Huile paraffinique 2				
aromatiques mononucléaires	40200–33600	,,	0,007432	— Les structures sont similaires aux structures de l'huile 1, mais les chaînes latérales sont plus longues. Les alkylbenzènes sont prédominants.
,, ,,	40400–33400	,,	0,005793	
,, ,,	40000–33200	,,	0,008432	
aromatiques mononucléaires + binucléaires	31200–29600	,,	0,000764	
aromatiques binucléaires	31200–29400	,,	0,003465	— alkylnaphtalines tri-, tétra- et pentasubstitués. Les chaînes latérales sont plus longues
,, ,,	31200–29400	,,	0,004321	

Revue Roumaine de Chimie, **23**, *9–10*, 1483–1487 (1978)

SEPARATION OF ACETIC ACID, SALICYLIC ACID, ACETYL-SALICYLIC ACID AND PHENOL BY THIN-LAYER CHROMATOGRAPHY ON SILICA GEL RG

T. HODIŞAN, H. NAŞCU and VIORICA IANCU
Chair of Analytical Chemistry, Department of Chemistry, "Babeş-Bolyai" University of Cluj-Napoca, Cluj-Napoca, str. Arany Ianos nr. 11, Romania

Received September 20, 1976

The optimum experimental conditions in order to resolve a four component mixture (acetic acid, salicylic acid, acetylsalicylic acid and phenol) on silica gel RG were studied. As criteria for selecting the solvent system, the information amount obtained by separation has been chosen. The test of 22 solvent systems on silica gel RG with pH=5.78 (10% aqueous suspension) proved that ethyl acetate — acetone (30 : 17, v/v) and chloroform — acetone (1 : 1, v/v) systems were efficiently.

In the survey of process for manufacturing acetylsalicylic acid the most difficult problem arisen is the separation of all components which take part in the technologic process, as starting materials (salicylic acid and phenol) as well as the synthesized products (acetylsalicylic acid and acetic acid). In this respect the thin-layer chromatography (TLC) on silica gel RG support and ethyl acetate — acetone (30 :17, v/v) and chloroform — acetone (1 :1, v/v) as solvent were used.

The literature shows no references concerning a mobile phase-stationary phase system for resolving this four component mixture. There are some mobile phase-stationary phase systems concerning the separation of phenols and phenolic acids on silica gel thin layers. [1-3]

The separation of phenol — salicylic acid mixture from industrial wastes, from a salicylic acid manufacturing plant, was studied by some of us elsewhere, [4] and a method for preventing water pollution with this two components was proposed.

Taking into account the fact that silica gel gives very good results in the separation of phenol and salicylic acid, Silica gel RG has been used as adsorbent in the present paper. On the other hand, the mobile phase

---

[1] N. A. Burges, H. M. Hurst and B. Walkden, *Geochim. et Cosmochim. Acta.* **28,** 1547 (1964); from "Chromatography" 2nd edition, E. Heftmann (ed), Reinhold, New York, 1967, p. 688.

[2] R. L. Layman, A. L. Livingstone, R. M. Bickoff and A. N. Booth, *J. Org. Chem.*, **23**, 756 (1958).

[3] D. Mc Hale, "Thin-Layer Chromatography", United Trade Press, London, 1964, p. 47.

[4] S. Gocan, T. Hodişan, H. Naşcu and C. Georgescu, *Rev. Roumaine Chim.*, (in press).

used for the separation of phenol from salicylic acid gives poor results in the case of this four components mixture and consequently other 22 solvent systems have been tested. In order to estimate the efficiency for an individual system, the information amount has been calculated, using the Shannon equation, by a procedure similar to that used by Simon and Lederer. [5] The Silica gel RG (which contains 20% gypsum) had the pH = = 5.78 (10% aqueous suspension). This silica gel has been proved in a preliminary investigation proper for this kind of separation.

In the present paper the hR_f values of four components were divided into groups which do not differ one by other more than 15 hR_f units; thus individual hR_f values appear taking part in a distinct group. The information amount has been calculated using the formula :

$$I = -\sum_i p_i \lg_2 p_i, \qquad (1)$$

where p_i is the probability of finding an hR_f value of a component within the group i. Suppose we have, for instance, four hR_f values : 61, 100, 80.5 and 0. The difference between individual values is higher than 15 so we have four groups. The probability of finding one of these values within the group is $1/4 = 0.25$. If we have other four hR_f values : 18.5, 60, 26 and 0, between 18.5 and 26 a difference lower than 15 exists so we have only three groups. The probability of finding an hR_f value within the group is 2/3 for the pair 18.5 and 26, and 1/3 for the other hR_f values.

The results obtained by such a procedure are given in table 1.

From, this table, it can be seen that, from the point of view of information theory, the most efficient systems are ethyl acetate — acetone and chloroform — acetone mixtures. This is the reason why these two solvents were used for the separation of our mixture.

Once established the solvent system which allowed the separation, the problem of determination of optimum composition of the two components of the mobile phase arises. These have been calculated by using the equation proposed by Turina and all. [6] The optimum composition is 30 : 17, v/v for ethyl acetate — acetone system and 1 : 1, v/v for chloroform — acetone system. In these conditions the separation of all four components is quantitative.

Another problem, which arises in this separation, is the pH of the chromatographic support. It can be seen that, all the four components have an acid character and, as showed by Stahl and Dumont, [7] in the case of ionisable components mixtures, the pH of support modifies to great extent the R_f values of these components. In this respect a study has been achieved concerning the variation of components R_f vs. the pH of support, by preparing Silica gel RG TLC plates with different pH values. The plates with acid silica gel were obtained by adding H_2SO_4 to the aqueous silica and gypsum slurry, and for basic ones, by adding KOH. The pH measure-

---

[5] J. Simon and M. Lederer, *J. Chromatog.*, **63**, 448 (1971).

[6] S. Turina, M. Trbozevic and M. Kastelan, *Analyt. Chem.*, **46**, 988 (1974).

[7] E. Stahl and E. Dumont, *J. Chromatog. Sci.*, **7**, 517 (1969).

Table 1

Amount of information obtained with 22 solvent systems

No.	Solvent system (v/v)	hR_f				I
		Salicylic acid	Phenol	Acetylsalicylic acid	Acetic acid	(bits)
1	Ethyl acetate-Ethanol (2 : 1)	53.5	68	61.5	0	0.8
2	,, (39 : 1)	40.5	53	45	0	0.8
3	Ethyl acetate-Benzene (1 : 1)	15.5	60	18	0	1.5
4	,, (9 : 4)	26	58.5	34	0	1.5
5	,, (30 : 1)	45.5	60	52	0	0.8
6	Ethyl acetate-Ethyl methyl ketone (1 :1)	84	100	93	0	1.5
7	Ethyl acetate-Ethyl ether (1 : 1)	54.5	64	62	0	0.8
8	Acetone-Pethroleum Ether (1 : 1)	16.5	61.5	21.5	0	1.5
9	Ethyl methyl ketone-Chloroform (1 : 1)	47.5	67	59.5	0	1.5
10	Ethyl methyl ketone-Pethroleum Ether (1 :1)	35.5	68	39.5	0	1.5
11	Ethanol-Acetone (1 : 1)	67	67.5	61	0	0.8
12	Acetone-Benzene (1 : 1)	58.5	64.5	56	0	0.8
13	Ethyl acetate-Chloroform (3 :1)	28.5	56	30	0	1.5
14	,, (1 :1)	18.5	60	26	0	1.5
15	,, (1 :3)	77.5	57	14	0	1.5
16	Ethyl acetate-Acetone (30 :17)	61	100	80.5	0	2.0
17	,, (6 :1)	34.5	63.5	36.5	0	1.5
18	,, (2 :1)	42.5	58.6	61.5	0	1.5
19	Ethyl acetate-Acetone (1 :1)	55.5	68	58.5	0	0.8
20	Chloroform-Acetone (1 :1)	26.5	72.5	57	0	2.0
21	,, (1.5 :1)	20.5	68	42.5	0	2.0
22	,, (5 :1)	15.5	65.5	19.5	0	1.5

ments were done after these layers were spreadead, dried and the layers were scraped down, weighed and introduced with the calculated amount of water in 50 ml Erlenmeyer stoppered flasks.

The visualization reagents used were the following :

a) aqueous solution $FeCl_3$ 1 % and $K_4\ Fe(CN)_6$ 1 %, freshly prepared, mixed 1 :1, for the detection of phenol and salicylic acid, and b) alcoholic solution 0.05 % brom cresol green, for the detection of acetic and acetylsalicylic acid.

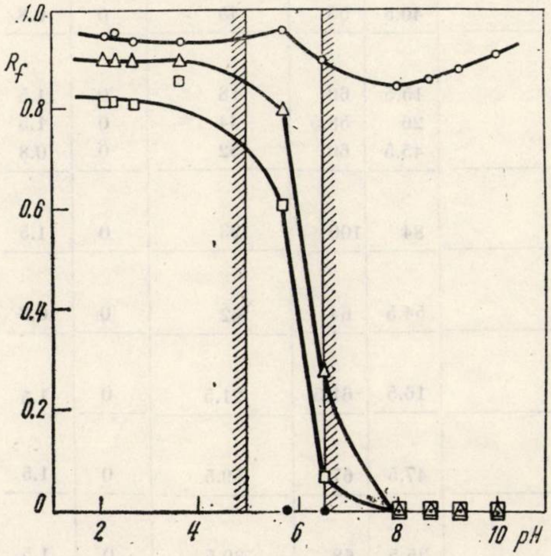

Fig. 1. — Variation of R_f values of mixture components vs. pH of support, using as mobile phase the system : ethyl acetate-acetone (30 : 17, v/v).

○ = phenol, Δ = acetylsalicylic acid, □ = salicylic acid, ● = acetic acid.

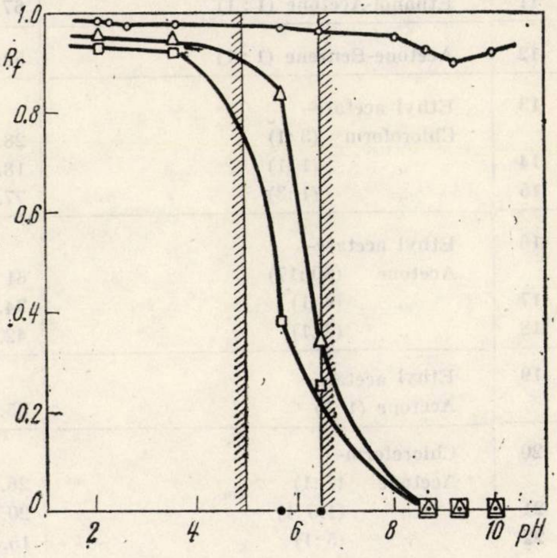

Fig. 2. — Variation of R_f values of mixture components vs. pH support using as mobile phase the system : chloroform-acetone (1 : 1, v/v).

○ = phenol, Δ = acetylsalicylic acid, □ = salicylic acid, ● = acetic acid.

At higher than 8 pH values the visualization of acetylsalicylic acid has been very poor and thus in this case the following visualization reagent has been used: c) aqueous solution of, freshly prepared, diazotized sulphanylic acid (sulphanylic acid 1.91 g/1, H_2SO_4 1 : 3 and $NaNO_2$ 3.40 g/1, 5 : 1 : 5) drying and spraying again with 10% aqueous KOH. With this reagent the phenol and salicylic acid could also be detected as yellow spots on the blue background given by the brom cresol green.

The results obtained for the two solvent systems are given in Figures 1 and 2. It can be seen that, in both cases a pH range exists in which the separation of the mixture occurs. The reproduction of this pH, with deviation of maximum 0.1 pH units in order to obtain a good quality separation, must be done.

In conclusion, the optimum experimental conditions in connection with the chromatographic support and mobile phase composition, for the separation of the four components mixture have been found.

Revue Roumaine de Chimie, **23**, 9–*10*, **1489–1498** (1978)

SOME ANALYTICAL APPLICATIONS OF A NEW Ag^+-SELECTIVE MEMBRANE ELECTRODE

V. V. COŞOFREŢ

Institute of Chemical-Pharmaceutical Research, Sos. Vitan 112, Bucharest — 4, Romania

Received September 29, 1976

The electrode, having as the liquid membrane the Ag(I) chelate of diketohydrindylidene-diketohydrindamine (DYDA) in benzene, presents a stable and reproducible electrode function in the range $10^{-1}-10^{-6}$ M Ag^+ and has a slope of 59.0 mV per decade. The selectivity coefficients, $K_{Ag^+,M^{Z+}}$, calculated by the separate-solution method, show that the electrode response is not affected by the presence of ordinary metallic cations. The electrode, having a response time of only several seconds, has been successfully used for the determination of various organic substances containing halogens or sulphur, as well as for the determination of some equilibrium constants in an aqueous medium for Ag^+-L (L = organic ligand) systems.

Following on the recent descriptions [1–7] at liquid membrane ion-selective electrodes based on metal chelates dissolved in organic solvents, we now describe the construction and analytical evaluation of a new liquid-state Ag^+-selective membrane electrode. Our liquid membrane consisted of the Ag(I) chelate of diketohydrindilidene-diketohydrindamine (DYDA) dissolved in benzene.

DYDA is formed in the reaction between ninhydrin (triketohydrindene hydrate) with aminoacids [8] and is more commonly known under the name of "Ruhemann's Purple".

This reaction has been studied from the mechanistic point of view by many authors starting with Ruhemann. On the basis of this reaction some methods were developed for the determination of amino acids. [9–12]

---

[1] V. V. Coşofreţ, *Rev. Chim. (Bucureşti)*, **25,** 836 (1975).

[2] G. E. Baiulescu, V. V. Coşofreţ and C. Cristescu, *Rev. Chim.* (*Bucureşti*), **26,** 429 (1975).

[3] J. Růžička and J. Chr. Tjell, *Analyt. Chim. Acta*, **51,** 1 (1970).

[4] G. E. Baiulescu and V. V. Coşofreţ, *Rev. Chim. (Bucureşti)*, **27,** 158 (1976).

[5] G. E. Baiulescu and V. V. Coşofreţ, *Rev. Chim* (*Bucureşti*), **26,** 1051 (1975).

[6] V. V. Coşofreţ, *Rev. Chim. (Bucureşti)*, **27,** 240 (1976).

[7] G. E. Baiulescu and V. V. Coşofreţ, *Talanta*, **23,** 677 (1976).

[8] S. Ruhemann, *J. Chem. Soc.*, **97,** 2025 (1960).

[9] E. W. Yemm and E. C. Cocking, *Analyst*, **80,** 209 (1955).

[10] A. M. Smith and A. H. Agiza, *Analyst*, **76,** 623 (1951).

[11] A. M. Smith and A. H. Agiza, *Analyst*, **76,** 619 (1951).

[12] Y. Shimizu-Shiga, *Kenritsu Tauky Daigaku Gakujutsu Zasshi*, **14,** 21 (1973).

Recently, the Hg(II) chelate of DYDA, dissolved in $CHCl_3$ has been used in order to obtain a liquid-state Hg^{2+}-selective membrane electrode.[7]

THEORETICAL

Between the Ag^+ ions from the aqueous phase and DYDA (noted HR) from the benzene, the following equilibrium is established :

$$(Ag^+)_{aq} + (HR)_0 \rightleftharpoons (AgR)_0 + (H^+)_{aq} \qquad (1)$$

where DYDA may be considered a weak acid ; the equilibrium constant, K, of the above reaction is given by

$$K = \frac{[AgR]_0\,[H^+]_{aq}}{[Ag^+]_{aq}\,[HR]_0} \qquad (2)$$

where indices aq and 0, refer to the aqueous and organic phases, respectively.

If the membrane (organic phase) contained only HR in benzene, the electrode potential would have been given by :

$$E = E_0 + \frac{RT}{F}\ln\frac{[H^+]_{aq}}{[HR]_0} \qquad (3)$$

where E_0 is the standard potential, valid for $[H^+]_{aq}/[HR]_0 = 1$. Combining equations (2) and (3) we get :

$$E = E_0 + \frac{RT}{F}\ln K\,\frac{[Ag^+]_{aq}}{[AgR]_0} \qquad (4)$$

or

$$E = E_0 + \frac{RT}{F}\ln K - \frac{RT}{F}\ln\,[AgR]_0 + \frac{RT}{F}\ln\,[Ag^+]_{aq} \qquad (5)$$

The first three terms of Eq.(5) can be incorporated in a constant E_0'; thus the Eq.(5) becomes:

$$E = E_0' + \frac{RT}{F}\ln\,[Ag^+]_{aq} \qquad (6)$$

This equation gives the variation of the membrane potential with the concentration of Ag^+ in the aqueous phase, assuming a membrane formed by the silver chelate of DYDA.

EXPERIMENTAL

Apparatus and reagents. E.m.f. measurements were performed at room temperature in mechanically stirred solutions, using an electronic potentiometric (Servogor®, Goerz Electro, Vienna). The potentiometric titration curves were recorded using a TTT 2 pH/mV meter with an ABU 12 Autoburette and Titrigraph SBR 2c recorder (Radiometer).

A saturated calomel electrode (type K 401, Radiometer) was used as reference electrode, and this was connected to the sample solution by a saturated KNO_3 bridge.

All reagents used were of analytical grade.

Preparation of the electroactive substance (the liquid membrane). In order to obtain the DYDA (the free acid) we proceeded as shown previously[7] but in this case we have used benzene as solvent. The organic phase is transferred to a separating funnel containing 20 ml of 10^{-2} M silver nitrate (pH 4.5) and the two phases are shaken for 2 minutes. (The volume of the organic phase (HR in benzene) was 50 ml and its concentration was 5×10^{-3}M). The aqueous phase is transferred to another separating funnel and shaken with 25 ml benzene. The organic phases are combined, dried by passage through anhydrous sodium sulphate and transferred to a 100 ml flask. This is the liquid membrane with an Ag(I) concentration of 5×10^{-4} M. The peak absorption of the solution is at 545 nm.

Construction of the electrode. This is done as described previously[2,13] by impregnating the support material (a hydrophobised graphyte rod) attached to the end of the Teflon tube, with the liquid membrane. The internal reference electrode is eliminated by use of a stainless-steel wire introduced into the graphyte rod.

The electrode is stored in liquid membrane.

RESULTS AND DISCUSSIONS

The electrode function. The e.m.f. measurements were made with the electrochemical cell :

$$\begin{array}{l|l|l|l} \text{Ag}^+\text{-selective} & & KNO_3 & \\ \text{membrane electrode} & Ag^+(C_{Ag^+}),\ \mu = 0.5\ (KNO_3) & \text{std.} & \text{SCE} \end{array} \qquad \text{(I)}$$

where C_{Ag^+} represents the Ag^+ concentration varying from 10^{-1} to 10^{-6} M. The e.m.f. of cell (I) is given by :

$$E_I = E'_0 + 0.059 \log [Ag^+] \qquad (7)$$

in the range $10^{-1} - 10^{-5}$ M Ag^+ concentration ; the slope of the electrode for the $10^{-5} - 10^{-6}$ M decade is only 53 mV. E'_0 represents the conditional standard potential of the electrode. The measurements were carried out at constant ionic strength ($\mu = 0.5$, KNO_3) and the junction potential was kept constant. In Figure 1 we present the plot $E_I - \log [Ag^+]$.

Extrapolating the curve from Figure 1 to $[Ag^+] = 1$ we obtain the conditional standard potential of the membrane electrode vs. SCE whose value is $E'_0 = 541$ mV. This is a value approaching that of the Ag^+-selective membrane electrodes constructed previously. This value depends on the concentration of the internal organic phase.

Influence of pH. As it is known, the membrane of the liquid state electrode changes in chemical nature depending on the pH of the solution in which it is introduced. Thus, the electrode will become H^+-sensitive in strongly acidic solutions. However, when using the electrode in alcaline solutions, the measured electrode potential will decrease as the alcalinity

---

[13] V. V. Coşofreţ, Doctoral thesis, Polytechnic Institute of Bucharest, Bucharest, 1975.

of the solution increases. The decrease is due to the precipitation of Ag^+ as Ag_2O under increasing alcalinity conditions. The influence of pH on the membrane potential at three Ag^+ concentrations is given in Figure 2. The pH was adjusted to the desired value with HNO_3 or NaOH. The linear range of the curves E(mV) vs . pH depends on $[Ag^+]_{aq}$.

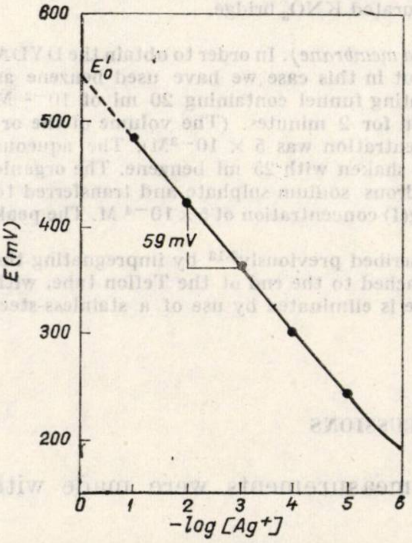

Fig. 1. — The electrode function.

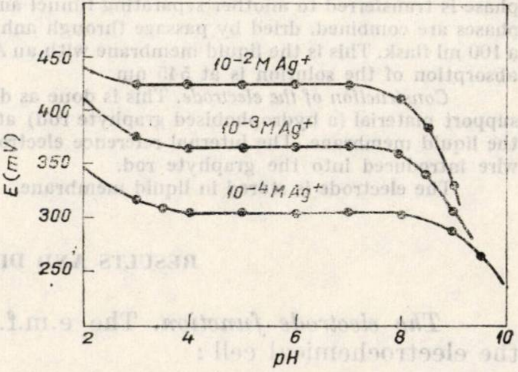

Fig. 2. — Influence of pH on the response of electrode for different $AgNO_3$ concentrations ($\mu = 0.5$, KNO_3).

Response time of the electrode. The response characteristics of the electrode were evaluated by introducing the electrode into silver nitrate solutions of different concentrations and noting the e.m.f. values as a function of time. The response time of the electrode is longest in the 10^{-6} and 10^{-5} M (ca. 3 min) solutions. In the concentrated solutions the response time of the electrode is of the order of a few seconds.

Selectivity of the electrode. Selectivity coefficients, $K_{Ag^+, M^{Z+}}$, were calculated by the method of Srinivasan and Rechnitz.[14] In this method, the potential of the ion-selective electrode in a solution containing Ag^+ at a given concentration (e.g.0.1 M) is compared with the potential of the same electrode in a solution containing the interfering cation, M^{Z+}. The concentration of M^{Z+} should be the same as that of the Ag^+ in the original solution.

The value of e.m.f. measured with the Ag^+-selective membrane electrode when in the electrochemical cell we have Ag^+ and the interferent ion M^{Z+}, is given by :

$$E = E'_0 + 0.059 \, (\log \, [Ag^+] + K_{Ag^+, M^{Z+}} [M^{Z+}]^{1/z}) \qquad (8)$$

---

[14] K. Srinivasan and G. A. Rechnitz, *Analyt. Chem.*, **41**, 1203 (1969).

However, when we have only the M^{Z+} species in the solution (thus $[Ag^+] = 0$) we have:

$$E_{II} = E'_0 + 0.059 \log K_{Ag^+, M^{Z+}} [M^{Z+}]^{1/Z} \quad (9)$$

In this case we used the following electrochemical cell:

Ag+-selective membrane electrode | $M^{Z+}(C_{M^{Z+}} = 0.1M), \mu = 0.5(KNO_3)$ | KNO_3 std. | SCE (II)

Substracting Eq.(7) from Eq. (9) and rearranging we get:

$$\log K_{Ag^+, M^{Z+}} = \frac{E_{II} - E_I}{0.059} + \log [Ag^+] - \log [M^{Z+}]^{1/Z} \quad (10)$$

The values of the selectivity coefficients were calculated for $[Ag^+] = [M^{Z+}] = 0.1$ M, where M^{Z+} represents the main metallic cations that form more or less stable chelates with DYDA. In all cases the nitrates were used at pH 1. The values of the selectivity coefficients may be seen in table 1.

Table 1

Selectivity coefficients, $K_{Ag^+, M^{Z+}}$ (The nitrates of the respective metals at a concentration of 0.1 M, pH = 1 and $\mu = 0.5, KNO_3$)

Interferent cation (M^{Z+})	$K_{Ag^+, M^{Z+}}$
Mn^{2+}	2.23×10^{-5}
Ni^{2+}	3.63×10^{-5}
Co^{2+}	3.54×10^{-5}
Mg^{2+}	3.71×10^{-5}
Zn^{2+}	4.07×10^{-5}
Al^{3+}	4.78×10^{-5}
Bi^{3+}	5.01×10^{-5}
Cd^{2+}	5.88×10^{-5}
Pb^{2+}	6.16×10^{-5}
Cu^{2+}	9.55×10^{-5}
Hg^{2+}	2.82×10^{-1}

It is seen from table 1, that only towards Hg^{2+} the electrode is not highly selective, because Hg^{2+} ions also form a stable chelate with DYDA.[7]

Reproducibility of potential measurements. The reproducibility was tested in the $10^{-1} - 10^{-6}$ M $AgNO_3$ range during a four-week period. The values in table 2 are the average of 12 measurements, and prove the excellent stability of the electrode.

ANALYTICAL USE

The good results obtained with this electrode at the potentiometric titration of halides, separately or in mixtures — see Figures 3 and 4 (the error of the determinations being less than ± 0.3%) lead us to the conclusion that the electrode might be used for the determination of some halogenated organic compounds used in drug industry. The results given in table 3 prove the rightness of our assumption. For the results in table 3 we used a 0.01 M $AgNO_3$ solution as titrant.

Table 2

Reproducibility of potential measurements (tested during four weeks). The values represent the average of 12 measurements

Ag^+, M	10^{-6}	10^{-5}	10^{-4}	10^{-3}	10^{-2}	10^{-1}
E(mV)	192±5	245±5	304±4	363±4	423±3	482±3

In the case of compounds 2,3 and 4 we used reflux hydrolysis for 1/2 hr with a 20% NaOH solution. The first five compounds from the table are important intermediates in organic synthesis, while the last ones are pharmacologically active compounds.

The electrode was also used successfully for the determination of some sulphur containing organic compounds.

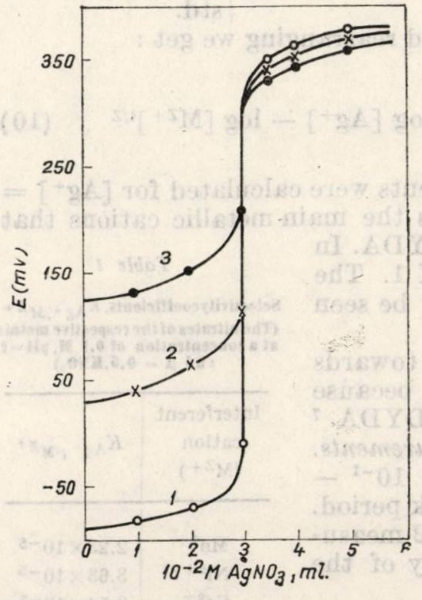

Fig. 3. — Potentiometric titration of I^- (1), Br^- (2) and Cl^- (3) (30 ml of 10^{-3} M from the respective potassium salt); pH = 2 – 3.

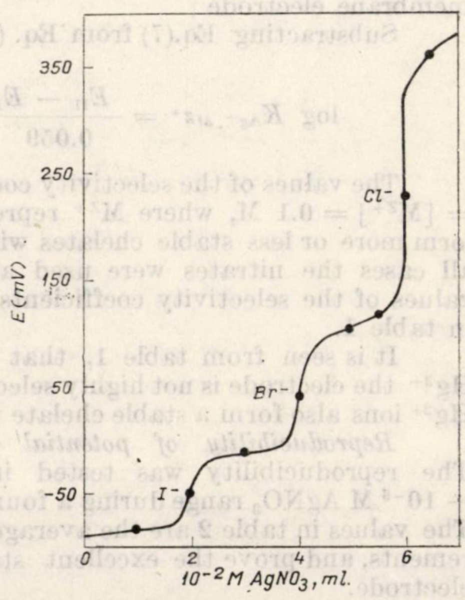

Fig. 4. — Potentiometric titration of $I^- + Br^- + Cl^-$ mixture (20 ml 10^{-3} M KI + 20ml 10^{-3}M KBr + 20 ml 10^{-3} M KCl); pH = 2.0.

In Figure 5 are presented some of the titration curves of thiourea at different concentrations. Thiourea was determined in the $10^{-1} - 10^{-4}$ M range. On the curves two potential jumps are to be seen, either of which could be used for the determination of thiourea from the sample. The volume of $AgNO_3$ corresponding to the first potential jump gives the exact quantity of thiourea, from the sample, while the volume corresponding to the second one gives twice the thiourea quantity from the sample.

Using a sulphide-selective membrane electrode, Pungor et al.[15] proved that following reactions take place:

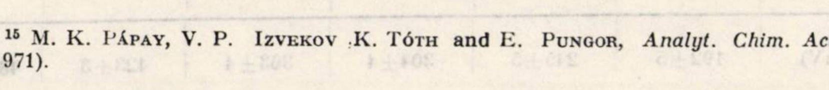

$$(H_2N)_2C=S + 2\,AgNO_3 \rightarrow Ag_2S + H_2N-C\equiv N + 2HNO_3 \qquad (11)$$

$$H_2N-C\equiv N + 2AgNO_3 \rightarrow Ag_2N-C\equiv N + 2HNO_3 \qquad (12)$$

---

[15] M. K. PÁPAY, V. P. IZVEKOV, K. TÓTH and E. PUNGOR, *Analyt. Chim. Acta*, **56**, 291 (1971).

Table 3

Potentiometric determination of some halogenated organic compounds using Ag+ — selective membrane electrode

No.	Organic compound	Taken (mg)	Found (mg)	Found (% X)
1.	Ethanolamine hydrochloride	2.436	2.449	36.56
	% $Cl_{theor.}$ = 36.37	4.872	4.858	36.27
		7.308	7.321	36.43
2.	Chlorethylamine hydrochloride	14.675	14.534	60.99
	% $Cl_{theor.}$ = 61.17	21.863	21.828	61.07
		29.150	29.122	61.11
3.	p-Acethylamino-benzene-sulphochloride	9.734	9.711	15.14
	% $Cl_{theor.}$ = 15.18	14.601	14.504	15.08
		19.468	19.253	15.01
4.	p-Toluene-sulphochloride	11.254	11.184	18.49
	% $Cl_{theor.}$ = 18.61	22.508	22.397	18.52
		33.762	33.430	18.43
5.	2-Amino-thiazoline hydrochloride	3.725	3.730	25.63
	% $Cl_{theor.}$ = 25.60	7.450	7.384	25.37
		11.175	11.115	25.46
6.	2, 3, 5, 6-Tetrahydro-6-phenyl	5.803	5.832	14.81
	imidazo (2,1-b) thiazole	8.705	8.615	14.58
	hydrochloride	11.606	11.590	14.72
	% $Cl_{theor.}$ = 14.74			
7.	4′-(β-Piperidine-ethoxy)-2-	16.254	16.202	8.75
	carbomethoxy-benzophenone	24.381	24.125	8.68
	hydrochloride	32.508	32.635	8.81
	% $Cl_{theor.}$ = 8.78			
8.	2,2′-Diphenyl-4-piperidino-	15.435	15.408	19.14
	butiramide methyl bromide	23.153	23.082	19.12
	% $Br_{theor.}$ = 19.18	30.870	30.962	19.24
9.	Novocaine hydrochloride	10.940	10.927	12.98
	% $Cl_{theor.}$ = 13.00	21.880	21.880	13.00
		32.820	32.714	12.96

Equation (11) corresponds to the first potential jump from the titration curves given in Figure 5 when Ag_2S precipitates. Equation (12) corresponds to the second potential jump, when silver cyanamide precipitates.

The electrode has also been used for the determination of the potassium alkyl-xanthates, that are important compounds in organic synthesis and in ore flotation. The above compounds are known to form highly insoluble compounds with Ag^+ :

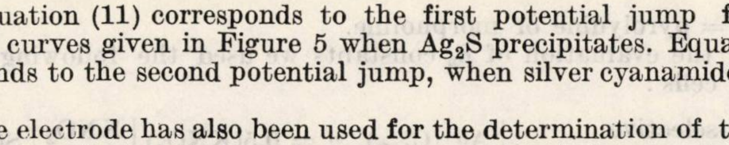

$$R - O - C\begin{matrix} /\!\!/ S \\ \backslash S^- K^+ \end{matrix} + Ag^+ \rightarrow R - O - C\begin{matrix} /\!\!/ S \\ \backslash S\,Ag \end{matrix} + K^+ \qquad (13)$$

In Figure 6 is shown a potentiometric titration curve of potassium ethylxanthate (conc. 10^{-3} M), using a 10^{-2} M $AgNO_3$ solution as titrant.

This electrode has been successfully used for the determination of some equilibrium constants in an aqueous medium for $Ag^+ - L$ (L = organic ligand) systems.

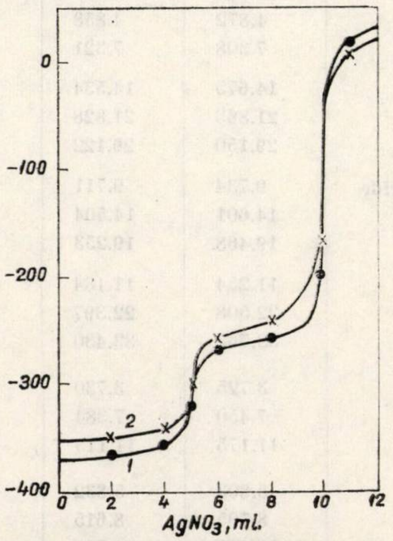

Fig. 5. — Potentiometric titration of thiourea at different concentrations with $AgNO_3$ solutions; 1 — 25 ml 10^{-2} M thiourea in 1M NaOH with 10^{-1} M $AgNO_3$; 2 — 25 ml 10^{-3} M thiourea in 1 M NaOH with 10^{-2} M $AgNO_3$.

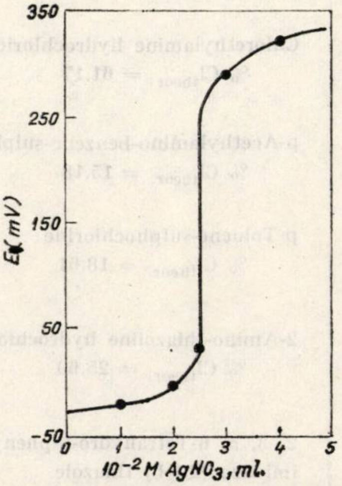

Fig. 6. — Potentiometric titration of 25 ml 10^{-3} potassium ethylxanthate with 10^{-2} M $AgNO_3$ solution.

The equilibrium:

$$Ag^+ + nL \rightleftharpoons [Ag\ L_n]^+ \tag{14}$$

is characterized by the equilibrium constant β_n:

$$\beta_n = \frac{[Ag\ L_n]^+}{[Ag^+][L]^n} \tag{15}$$

where L = pyrolydine or morpholine.

For the evaluation of β_n constants we used the following electrochemical cells:

$$\begin{array}{l|l|l|l}\text{Ag}^+\text{-selective membrane-electrode} & Ag^+(C^0_{Ag^+}),\ \mu = 0.5(KNO_3) & \begin{array}{c}KNO_3\\ \text{std.}\end{array} & \text{SCE}\end{array} \tag{III}$$

$$\begin{array}{l|l}\text{Ag}^+\text{-selective membrane-electrode} & Ag^+(C^0_{Ag^+}),\ \mu = 0.5\,(KNO_3),\ L(C_i),\ \mu = 0.5\,(KNO_3)\end{array}$$

$$\begin{array}{|l|l|}\begin{array}{c}KNO_3\\ \text{std.}\end{array} & \text{SCE}\end{array} \tag{IV}$$

E.m.f. of cells III and respectively IV are given by :

$$E_{\mathrm{III}} = E_0' + 0.059 \ \log C^0_{\mathrm{Ag}^+} = E_0' + 0.059 \log \frac{1}{V_0} \tag{16}$$

$$E_{\mathrm{IV}} = E_0' + 0.059 \log [\mathrm{Ag}^+] \tag{17}$$

assuming that $C^0_{\mathrm{L}} \gg C^0_{\mathrm{Ag}^+}$ and $C^0_{\mathrm{L}} \approx [\mathrm{L}]$, where : $C^0_{\mathrm{Ag}^+}$ is the initial concentration of Ag^+ in the cell ; $[\mathrm{Ag}^+]$ is the concentration at equilibrium of silver ; C^0_{L} is the initial concentration of pyrolyidine or morpholine (in great excess to the initial Ag^+ concentration) ; V_0 is the initial volume of $\mathrm{AgNO_3}$ solution.

From equations (16) and (17) by substracting and rearrangement we obtain :

$$\log \frac{C^0_{\mathrm{Ag}^+}}{\mathrm{Ag}^+} = \frac{E_{\mathrm{III}} - E_{\mathrm{IV}}}{0.059} = \log \psi \tag{18}$$

where ψ represents the Leden function.[16] Actually, for the calculation of the function we must take into account the dilution in the electrochemical cell due to the addition of a V volume of ligand. In these conditions, e.m.f. of the cell (III) will be given by the equation :

$$E'_{\mathrm{III}} = E_0' + 0.059 \ \log \frac{1}{V_0 + V} \tag{19}$$

From equations (16) and (19) we get :

$$E'_{\mathrm{III}} = E_{\mathrm{III}} - 0.059 \ \log \frac{V_0 + V}{V_0} \tag{20}$$

This equation together with equation (17) is used for the calculation of the ψ function.

Taking into account the β_n values (equation 15) the function becomes :

$$\psi = \frac{[\mathrm{Ag}^+] + \beta_1 [\mathrm{Ag}^+][\mathrm{L}] + \beta_2 [\mathrm{Ag}^+][\mathrm{L}]^2 + \ldots + \beta_n [\mathrm{Ag}^+][\mathrm{L}]^n}{[\mathrm{Ag}^+]} \tag{21}$$

or :

$$\psi = 1 + \beta_1[\mathrm{L}] + \beta_2 \ [\mathrm{L}]^2 + \ldots\ldots + \beta_n[\mathrm{L}]^n \tag{22}$$

where β_1, β_2, ..., β_n are the successive stability constants and [L] represents the concentration of the free ligand in complex, which is approximatively equal with the total concentration of the ligand. By the extrapolating functions of the $\psi_1 = \frac{\psi - 1}{[L]}$ and $\psi_2 = \frac{\psi_1 - \beta_1}{[L]}$ to $[L] \rightarrow 0$ we determined the successive stability constants.

---

[16] I. LEDEN, *Z. phys. Chem.*, **160**, 188 (1941).

In tables 4 and 5 are shown the determination results for Ag(I) – pyrolidine and Ag(I) – morpholine systems at 25° and $\mu = 0.5$ (KNO_3).

The present results are in good agreement with those obtained previously, using another Ag^+-selective membrane electrode.[13]

Table 4

Ag(I) – Pyrolidine system

$\mu = 0.5(KNO_3)$; $t = 25°$

No.	ΔE (V)	$C_L \times 10^2$	$\log \psi = \frac{\Delta E}{0.059}$	$\psi \times 10^{-1}$	$\psi_1 = \frac{\psi - 1}{[L]}$ $\times 10^{-3}$	$\psi_2 = \frac{\psi_1 - \beta_1}{L}$ $\times 10^{-6}$
1.	0.1127	1.0547	1.91016	8.13	7.614	0.660
2.	0.1259	1.3516	2.13389	13.61	9.995	0.691
3.	0.1313	1.4993	2.22542	16.80	11.138	0.699
4.	0.1403	1.7933	2.37796	23.88	13.260	0.703
5.	0.1460	2.0854	2.47457	29.82	14.251	0.652
6.	0.1540	2.3755	2.61017	40.75	17.122	0.693
7.	0.1598	2.6638	2.70847	51.11	19.149	0.694
8.	0.1649	2.9503	2.79491	62.36	21.103	0.693

$\beta_1 = 0.65 \times 10^3$ $\quad \beta_2 = 6.86 \times 10^5$

$\log\beta_1 = 2.81$ $\quad \log\beta_2 = 5.84$

Table 5

Ag(I) – Morpholine system

$\mu = 0.5(KNO_3)$; $t = 25°$

No.	ΔE (V)	$C_L \times 10^2$	$\log \psi = \frac{\Delta E}{0.059}$	ψ	$\psi_1 = \frac{\psi - 1}{[L]}$ $\times 10^{-2}$	$\psi_2 = \frac{\psi_1 - \beta_1}{[L]}$ $\times 10^{-5}$
1.	0.0476	0.9442	0.80678	6.41	5.728	0.421
2.	0.0545	1.1308	0.92373	8.39	6.535	0.423
3.	0.0605	1.3167	1.02542	10.60	7.290	0.421
4.	0.0665	1.5019	1.12712	13.40	8.256	0.433
5.	0.0714	1.6863	1.21017	16.22	9.025	0.431
6.	0.0759	1.8700	1.28644	19.34	9.807	0.431
7.	0.0843	2.2352	1.42881	26.84	11.560	0.438
8.	0.0911	2.5976	1.54406	35.00	13.098	0.436
9.	0.0970	2.9572	1.64406	44.06	14.651	0.433
10.	0.1024	3.3140	1.73359	34.15	16.038	0.431
11.	0.1071	3.6680	1.81525	65.35	17.543	0.431

$\beta_1 = 1.75 \times 10^2$ $\quad \beta_2 = 4.30 \times 10^4$

$\log\beta_1 = 2.24$ $\quad \log\beta_2 = 4.63$

Revue Roumaine de Chimie, **23**, *9–10*, 1499–1504 (1978)

PRODUCTION OF IODINE-123 FOR MEDICAL PURPOSES

MARIA ROMAN, CONSTANȚA PENCEA, DOINA CRISTU, I.MÎNZATU, A.CALBOREANU,
O. SĂLĂGEAN, CRISTINA BRATU and GH. PETEU
Institute of Atomic Physics, P.O. Box 5206, Bucharest, Romania

Received October 27, 1976

Iodine-123 at a radiochemical purity suitable for medical diagnostic application is produced with Cyclotron from natural antimony targets bombarded by particle beams of 26 MeV. The methods of target preparation, yields, radionuclidic impurities, chemical separation procedures and quality control are described.

INTRODUCTION

Iodine has been one of the most widely applied elements in the radiopharmaceuticals area and a considerable literature on radioiodinated compounds has been reported by A. P. Wolf *et al.* [1] The isotopes of iodine have been discussed by Myers [2] and Iya *et al*, [3] Tubis [4] reported on the general methods of preparation for the radioiodinated compounds.

From the various iodine isotopes, iodine-131 was one of the most extensively used in nuclear medicine until now, for the preparation of a large number of iodinated radiopharmaceuticals and only iodine-125 and iodine-132, were also generally used. The physical properties of iodine-123 make it recognized as the ideal radionuclide of iodine for imaging and diagnostic procedures in medicine. [5] This nuclide has a 13.3 hr. half-life and decays by electron capture followed by emission of 0.159 MeV photons with 84% abundance. [6] The absence of the undesirable electron emissioas well as its irradiation effects are significant advantages over other radion active isotopes of iodine. [7,8]

---

[1] A. P. Wolf, D. R. Christmas, J. S. Fowler and R. M. Lambrecht, "Symposium on New Development in Radiopharmaceuticals and Labelled Compounds", Copenhagen, March 26–30, 1973, IAEA–SM – 171 – 22, Vienna.

[2] W. G. Myers, "Radioisotopes of Iodine in Radioactive Pharmaceuticals", Proc. Symp. Oak Ridge 1965, USAEC, Conf. – 651111, 1966, p. 217 – 243.

[3] V. K. Iya, R. S. Mani and C. M. Desai in "Radioisotope Production and Quality Control", Tech. Rep. Ser. 128, IAEA, Vienna, 1971, p. 823.

[4] M. Tubis, in "Radioactive Pharmaceuticals", Proc. Symp. Oak Ridge 1965, USAEC, Conf. – 65111, 1966, p. 281.

[5] W. G. Myers and H. O. Anger, *J. Nucl. Med.*, **3**, 183 (1969).

[6] R. C. Ragaini, W. B. Walters, G. E. Gardon and P. A. Baedecker, *Nucl. Phys.*, **115**, 611 (1968).

[7] W. G. Myers "Transactions VIIth Int. Cong. of Internal Medicine", Vol. 2, Georg Thieme Verlag, Stuttgart, Germany (1963), p. 862.

[8] H. N. Wellman, J. F. Mark, B. I. Friedman and E. L. Saenger, *J. Nucl. Med.*, **9**, 359 (1968).

The substitution of iodine-131 with iodine-123 in thyroid studies could make an appreciable reduction in radiation dose to the thyroid while simultaneously yielding greatly improved images of the gland. The results of some clinical studies using ^{123}I have been reported by Myers[9] and Golden *et al.*[10] The advantages of ^{123}I over the very widely used ^{131}I have been also discussed elsewhere.[9–13]

LITERATURE DATA CONCERNING IODINE-123 PRODUCTION

Widespread application is still hampered by difficulties encountered in the production of this isotope. All methods proposed involve the use of particle accelerators and ^{123}I is produced either directly or indirectly, from the decay of ^{123}Xe($T_{1/2} = 2.1$ hr.). A rewiew of these methods has been made by Sodd *et al.*[13]

The most important problem is to ensure production of iodine-123 as free as possible from contamination by other isotopes of iodine, especially ^{124}I(4.2d), ^{125}I(56 d) and ^{126}I (13 d), which add somewhat to the radiation dose.

For the direct production of ^{123}I, tellurium and antimony targets have been used. The investigation of methods for the production of ^{123}I was started in 1962.[5] Hupf, Eldridge and Beaver[14] reported the production of ^{123}I by the ^{123}Te (p, n) ^{123}I reaction suggested by Myers and Anger.[5] They used 80% enriched tellurium-123 powder and the proton energy of the internal beam at the target (19.5 ± 0.5 MeV) was reduced to about 15.5 MeV after passing through the two layers of aluminium and the cooling water. From 2 hrs bombardments at currents of about 180 μA an average yield of 80.5 mCi/h. was obtained. When highly enriched ^{123}Te target material is used, the production of other, longer-lived iodine is very small. The ^{124}I, ^{125}I and ^{126}I activity in the product at the end of bombardment was less than 1.5% of the total ^{123}I activity.

Silvester, Sugden and Watson[15] reported on the preparation of iodine-123 by bombardment of natural antimony targets with α-particles of 21–30 MeV. They measured the relative yields of ^{123}I, ^{124}I, ^{125}I and ^{126}I, and found that the lowest ^{124}I ^{123}I ratio (0.7%) was obtained by employing a 25 MeV α-beam incident on a 17 mg/cm^2 antimony target. Under these conditions the yield of ^{123}I from 1 hr. bombardment at 30 μA was 150 μCi/μAh.

---

[9] W. G. Myers, *J. Nucl. Med.*, **7**, 390 (1966).

[10] W. G. Goolden, H. I. Glass and D. J. Silvester, *Brit. J. Radiol.*, **41**, 20 (1968).

[11] B. A. Rhodes, E. U. Buddemeyer, H. S. Stern and H. N. Wagner, *J. Nucl. Med.*, **7**, 385 (1966).

[12] K. E. Haloran, *Brit. J. Radiol.*, **37**, 101 (1964).

[13] V. J. Sodd, H. N. Wellman and B. M. Branson, *J. Nucl. Med.*, **10**, 136 (1969).

[14] H. B. Hupf, J. S. Eldrige and J. E. Beaver, *Int. J. Appl. Radiat. Isotopes*, **19**, 343 (1968).

[15] D. J. Silvester, J. Sugden and I. E. Watson, *Radiochem. Radioanal Letters*, **2**, 17 (1969).

Sodd, Blue, and Scholz[16] reported on the use of enriched ^{121}Sb (98, 40%) bombarded by α-particles of 25–36 MeV, and enriched ^{122}Te (95%) bombarded by deuterons of 6–9 MeV. The first system yielded up to 900 μCi ^{123}I/μAh, with about 1% iodine-124 contamination,whilst the latter yielded up to 100 μCi/μAh with about 0.1% ^{124}I contamination.

Dahl and Tilbury[17] used the irradiation of natural antimony plated on silver coated copper discs with 23 MeV ^{3}He particles to utilize the reaction $^{123}Sb(^{3}He^{2+}, 3n)\,^{123}I$ and obtained yields of about 24 μCi/μAh from 40 min. bombardments at about 150 μA. The ^{123}I made by this method contains 5% ^{124}I at the end of bombardment.

The principles involved in the indirect production of ^{123}I via its ^{123}Xe parent, free from highly undesirable beta emitters like ^{124}I and ^{126}I, were fully described by Blue and Sodd[18] who further outline the two experimental approaches that can be used.

The first is based on the reaction $^{122}Te(^{4}He, 3n)\,^{123}Xe$ in a generator type target with about 90% enriched ^{122}Te from which the ^{123}Xe formed during bombardment of target material is continuously swept out of the target vessel in a stream of helium.

Lambrecht and Wolf[19] report a "generator" system, making use of enriched ^{122}Te target material bombarded by α-particles of up to 46 MeV.

$^{122}Te(^{4}He, 3n)\ ^{123}Xe \xrightarrow[2.1h]{\beta^{+}Ec} {}^{123}I$ generator obtaining a yield of about 50 mCi

of ^{123}I, no ^{124}I could be detected in their product the only radiohalogen impurity is ^{125}I less than 0.2%.

In the second experimental approach, called the "cyclic" method, a period of bombardment is followed by a period during which the ^{123}Xe is removed from the target.

Lebowitz *et al.*[20] pointed out that proton beams of sufficiently high energy and intensity might be useful for the production of ^{123}Xe. They used target of ^{122}Te with particles of 37 MeV, or ^{123}Te with ^{3}He-particles of 30 MeV. The highest yield (about 750 μCi/μAh) was obtained using ^{123}Te and ^{3}He. Fusco *et al.*[21] used elementary iodine. In their method, they used a 58 MeV proton beam, making ^{123}Xe by the ^{127}I (p, 5 n) reaction, and led via ^{123}Xe to isolation of 24 mCi of ^{123}I in which the only impurity was ^{125}I less than 0.13%, from a 2 hrs bombardment.

Blue, Sodd and Scholz[22] using a much higher energy (about 576 MeV) protons and a natural xenon target showed that it is possible to produce up to 15 Ci of ^{123}Xe with a 470 MeV beam at 1 mA current for 1 hour.

---

[16] V. J. Sodd, J. W. Blue and K. L. Scholz, "Uses of Cyclotron in Chemistry, Metalurgy and Biology", Butterworths, London, 1970, p. 138.

[17] J. R. Dahl and R. S. Tilbury, *Int. J. Appl. Radiat Isotopes,* **23,** 431 (1972).

[18] J. W. Blue and V. J. Sodd "Use of Cyclotron in Chemistry, Metalurgy and Biology", Butterworths, London, 1970, p. 138.

[19] R. M. Lambrecht and A. P. Wolf, *Radiat. Research,* **52,** 32 (1972).

[20] E. Lebowitz, M. W. Greene and P. Richards, *Int. J. Appl. Radiat. Isotopes,* **21,** 489 (1971).

[21] M. A. Fusco, M. F. Peck, J. A. Jungerman, F. W. Zielinski, S. J. De Nardo and G. L. De Nardo, *J. Nucl., Med.,* **13,** 729 (1972).

[22] J. W. Blue, B. J. Sodd and K. L. Scholz, *J. Nucl. Med.,* **12,** 417 (1971).

Lindner, Brinkman *et al.* [23] describe a method for the production of ^{123}I which is different from that of Fusco *et al* [21] and is hybrid between the dynamic "loop" target principle with a circulating fluid and the "generator" target of Sodd *et al.* [18] They used two types of target fluids; CH_2I_2 and concentrated aqueous solutions of Li I without and with additional I_2. In conclusion, they report that the nuclear reaction ^{127}I(p, 5n) ^{123}Xe in combination with the dynamic "loop/generator" target principle offers a rather attractive indirect production method for ^{123}I wiht good yields and high radiochemical purity.

PRODUCTION AND SEPARATION OF IODINE-123

We report here on direct method to produce ^{123}I in natural antimony targets bombarded by α-particle beams of 26—27 MeV from Y-120 Cyclotron, using the ^{121}Sb(α, 2n) ^{123}I reaction. [5] From the various procedures for the isolation of radioiodine, [1-26] only the distillation procedures[14,15] and liquid-liquid extraction [6,24] are suitable for the separation of iodine from antimony. We performed the separation of the radioiodine from the irradiated target material, adopting the method of liquid-liquid extraction.

Our procedure is based on reduction of iodate formed during the dissolution of antimony in hydrochloric acid and nitric acid, with ferrous sulphate. The iodine is extracted with carbon tetrachloride.

EXPERIMENTAL

Target preparation and irradiation processing

Targets used in the production of ^{123}I are prepared by the electrodeposition of the natural antimony at the tequired thickness on a copper disc. The copper discs are first polished on one side to a mirror finish, and then cleaned with chloroform, acetone, nitric acid and water. The antimony layer is plated out to a thickness of 50—80 mg/cm^2 on the copper disc in electrolyte solution with SbO, 48 % HF and resorcinol. The current density 50 mA/cm^2 and the platinum chip anode.

Targets are bombarded with α-particles of 26 MeV at about 10 μA with the extracted beam of the Y—120 cyclotron. The yield of ^{123}I on target varies between 50 μCi and 100 μCi/μAh, on 1 hr. ^{124}I contamination from these irradiations is less than 1.5 % of the ^{123}I activity at the end of bombardment.

The ^{124}I relative contaminancy depends directly on the training on the full processing (i.e. irradiation time internal and the cooling time) as well as of the target thickness, and the nuclidic purity of the target.

Separation of the radioiodine

After bombardment, the antimony layer was scraped from its copper backing and was placed in a 500 ml distillation flask fitted with a water cooled column, with 50—100 ml of concentrated hydrochloric acid to which 50—60 μg iodide carrier were added. Then very carefully, in small partions, concentrated nitric acid (about 4—5 ml) was added to the reaction. The mixture was stirred constantly and gentle heated until all of antimony was dissolved and the iodine oxidized to iodate and periodate. The mixture was cooled and concentrated aqueous solution of $FeSO_4$ was added dropwise until the solution turned brown indicating formation of I_2. Then the elemental iodine was extracted with 10 ml of carbon tetrachloride. This extraction was repeated 4—5 times, each time after a waiting period of 15 min afforded about 85% of the iodine-123.

---

[23] L. Lindner, G. A. Brinkman, T. H. G. A. Suer, A. Schimmel, J. Th. Veenboer, F. H. S. Karten, J. Visser and C. J. Leurs, *"Symposium on New Development in Radiopharmaceuticals and Labelled Compounds"*, Compenhagen, March 26 — 30, 1973, IAEA — SM — 171 — — 63, Vienna.

[24] R. D. Neirincks, *Radiochem. Radional. Letters*, **5**, 205 (1970).

The organic fractions were collected in a beaker and 0.1 N NaOH solution was added, followed by addition of 0.2% $Na_2S_2O_3$ to reduce the I_2 to I^-. By evaporation of CCl_4, the ^{123}I was left in iodide form quantitatively in the aqueous phase. The aqueous solution was neutralized with 0.1 N hydrochloric acid, and evaporated to 10 ml giving a saline solution. The solution is ready for use after sterilization by filtration through a 0.22 filter membrane.

Quality Control

Radionuclide identification and measurements of the radioactivity were performed by the Heath[25] and Hupf[14] methods after chemical separation. The radionuclide purity was checked by gamma-ray spectrometry using a Ge(Li) multichannel analyser. The gammy ray spectrum was examined for radionuclidic impurities, especially ^{124}I, ^{125}I and ^{126}I. A gamma ray spectrum of iodine radioisotopes 24 hr. after EOB is shown in Figure 1, from which it can be seen the only contamination by ^{124}I. Iodine-123 ($T_{1/2} = 13$ h) decays to the KeV-gamma-ray state of ^{123}Te(stable). The iodine-124 ($T_{1/2} = 4.2$ d) content was determined by gamma-ray spectrometry using the 1695 KeV photopeak. After the iodine-123 and part of the iodine-124 had decayed, iodine-126 ($T_{1/2} = 13$ d) was determined in a similar manner using the 670 KeV photopeak. The iodine-125 ($T_{1/2} = 60$ d) was assayed[26] two months after the bombardment when all the other activities had decayed.

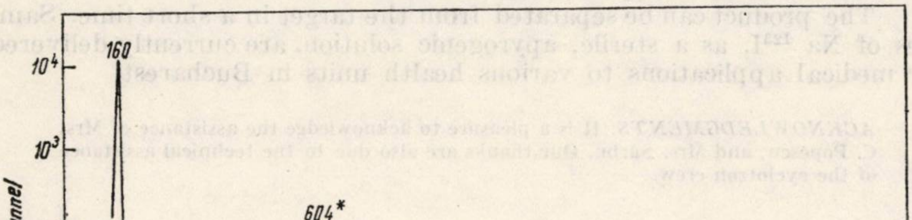

Fig. 1. — Gamma ray spectrum of ^{123}I. — Energies in KeV. * ^{124}I note that part of the 512 KeV peak is associated with ^{123}I.

The radiochemical purity and the purity control ^{123}I solution for medical use was carried out in accordance with literature data[27-28]. This involves chemical control, to verify that the ^{123}I is indeed present in the form of $Na^{123}I$ and not in an oxidized form and is determined by ascending paper chromatography in the presence of iodide and iodate carriers. Chromatography was carried out on 2 × 25 cm sheets of Watman No. 1 chromatographic paper dipped in a chromatographic mixture of three volumes of methanol to one volume of water for about 2 hrs. The respective position of the two compounds was shown by autoradiography. The average of R_f values in this system for iodide is 0.73 and iodate 0.5. We can confirm that the ^{123}I is present as iodide to an extent of 97%.

---

[25] R. L. Heath, "Scintillation Spectrometra", 2nd Ed., Vol. 1. USAEC. Rpt. IDO-16880—1, Idaho Operations Office, August 1964.

[26] J. E. Eldrige and P. Crowther, *Nucleonics*, **22,** 56 (1964).

[27] "Radioisotope Production and Quality Control" Tech. Rep. Ser. 128, IAEA, Vienna, 1971, p. 795.

[28] Y. Cohen, "Produits Pharmaceutiques", Rapport, CEA — No., 2150 (1962).

The chemical purity was checked by polarography for the detection of antimony. The antimony content was less than 0.001 mg/ml.

CONCLUSION

The ^{123}I prepared by this method contains between 0.8–1.5% ^{124}I at the end of bombardment. We can consider that despite this impurity of ^{124}I, ^{123}I is still preferable to the presently used ^{131}I in certain applications. For some cases, notably radioiodide investigations on young children and pregnant women, it is necessary to have the ^{124}I contamination lower than 1% at EOB.

The product can be separated from the target in a short time. Samples of Na ^{123}I, as a sterile, apyrogenic solution, are currently delivered for medical applications to various health units in Bucharest.

ACKNOWLEDGMENTS. It is a pleasure to acknowledge the assistance of Mrs. C. Popescu, and Mrs. Sârbu. Our thanks are also due to the technical assistance of the cyclotron crew.

Revue Roumaine de Chimie, 23, 9–10, 1505–1509 (1978)

COMPTES RENDUS

M. FLORESCU, "Tendinţe în dezvoltarea industriei chimice" (Trends in Chemical Industry Development), Bucharest, Ed. Tehnică, 1977, 366 p.

The book is the result of a careful documentation and deals with general problems regarding the present and the future of chemical industry. The modern chemical industry is a branch of technical and scientific activity whose rate of development is higher than those of other industries. The book which consists of 15 chapters offers a review of basic problems related to the trends in the development of chemical industry.

The first three chapters deal exhaustively with the role of chemical industry in the contemporary economic and social development, with the structure of chemical industry and its evolution. The topics of these chapters cover such matters as the complex utilization of natural gas, the chemistry of crude oil (the chemical processing of ethylene is considered a criterion for the evaluation of the level of development of modern chemistry) and the evolution of row material reserves.

Since the polymer chemistry enjoys a special place in chemical industry, chapter four deals exclusively with the trends of development of polymer production, the importance and the prospects of synthetic fibers as well as of synthetic rubber.

Chapter five is devoted to the problems raised by the tremendous investments required by renewing the technologies which in very short time become obsolete. A short review of investment development over the world is followed by considerations on the distribution of investments among the branches of Romanian chemical industry.

Special attention is given in chapter six to scientific and technological research. The topic of this chapter covers the role of basic, applied and development research, the role and implications of studies of polymer stereochemistry and the prospective tasks of Romanian chemical research. The next chapter, related to chapter six, is entitled "The technologic revolution in chemical industry" and deals with contemporary technologic trends, the role of chemical engineering, optimizing and automation of chemical processes, with catalytic processes in chemical industry and the economic efficiency of new technologic processes in large scale industrial production.

The next two chapters are devoted to natural and synthetic resources that may be processed by chemical industry, the structure and distribution of energy resources, the need for a rational utilization of natural energy resources and energy in chemical industry. The objectives of scientific development research related to achieving new energy technologies are also presented.

The role of chemistry in modern economy which seeks qualitatively higher utilization of natural resources, replacement of metals with plastic materials, the role of biochemistry and bioengineering and the implications of chemistry in the maintaining of ecologic equilibrium (pollution, recycling of wastes, Romania as part of the international effort to protect the environment and to interdict utilization of chemical weapons) make up the topic of chapter ten and eleven.

Chapter twelve treats the optimizing and modelling of technologic processes by cybernetization of chemical industry (computers, on line computers, special computer programs for chemistry).

The last three chapters of the book deal with the development of international co-operation in chemistry, the contribution of our country has brought to this, the development of world chemical industry, the influence of recessions, of economic and energy crises upon this development, the new rhythms of growth of demand and new structures of production and consumption.

The author awards a special attention to the program of socialist industrialization of our country according to the Programme of the Romanian Communist Party. Problems regarding the management of waters and the protection of the environment, the policy of promoting science and technical progress, the elaboration of prognoses for chemical industry are also considered.

The book supplies a rich bibliography (over 250 entries) and a very interesting set of tables (over 90) and graphs (60).

D. I. Marchidan

S. GÖRÖG and GY. SZÁSZ, *"Analysis of Steroid Hormone Drugs"* Akadémiai Kiadó, Budapest, 1978 (with Elsevier Scientific Publishing Company, Amsterdam) 426 pages.

This book is the first one devoted to the analysis of steroid hormone drugs. The task assumed by the authors seems to be a very difficult one, taking into account the large number (about 200) of steroid hormones and usual derivatives as well as the ever increasing number of papers dealing with the analysis of such compounds.

The book is primarily useful to chemists working in industrial and research laboratories (the biological and clinical methods of steroid analysis are not discussed).

The first three chapters, dealing with general problems of the field are : "Fundamental steroid hormone chemistry" (about 30 pages including an outline of steroid reactions of analytical importance) ; "Brief outline of the therapeutic use of steroid hormones" (15 pages) ; "Development of, and current trends in, methods of steroid hormone analysis" (10 pages, underlining the recent important growth of pharmaceutical and industrial steroid analysis and on the other side the marked increase of application of physical methods of analysis).

Chapter 4, "Chromatography of steroid hormones" (60 pages, 355 references), describes chromatographic techniques (with the exception of gas chromatography) applied to analysis of steroid drugs. After a theoretical introduction (comprising demonstrative exercises) the chromatographic methods (e.g. paper chromatograpy, thin-layer chromatography, adsorption chromatography) are described in a very practical manner, including numerous tables and detailed descriptions of the different techniques.

The following chapter is devoted to "Gas chromatography of steroid hormones" (30 pages, 164 references). Various important problems are discussed : possibilities and limitations of the method, advantages and disadvantages of derivatization, choice of derivatives, problems of qualitative and quantitative analysis, etc.

Chapter 6, "Methods of qualitative and quantitative analysis of steroid hormones" (100 pages, 311 references), is the most developed one in the book. All the physical methods utilized in steroid hormones analysis are described, namely : UV—VIS spectrophotometry, fluorimetry, IR spectroscopy, NMR spectroscopy, optical rotations, mass spectrometry and thermal methods. In addition some chemical reactions are mentioned : chromogenic, gravimetric and volumetric reactions. The practical character of this chapter is also worth mentioning. Numerous examples, tables, figures, reproductions of spectra (most of them recorded by the authors themselves) make the chapter a rich collection of useful data. However, the theoretical treatment of some physical methods does not appear to be well balanced. Thus, for the NMR spectroscopy there are four pages of theoretical principles, whereas for IR spectroscopy (which "nowadays... has become the most important method of identifying steroid hormones") such a theoretical approach lacks completely.

Chapter 7 deals with "Functional group analysis of steroid hormones" (about 90 pages, 307 references). The authors combine chemical reactions with physical methods for the analysis of the same functional group (e.g. $>C=O$; C_6H_5- ; $-COOR$; $HC\equiv C-$; side-chain etc.), which is certainly an original and very useful approach.

A minor mistake appears on pages 280/281, where in the structure of Girard *P* reagent a dimethylammonium moiety is included instead of a pyridinium one (from which even the initial *P* of the reagent name comes).

The last chapters of the book are devoted to "Assay of dosage forms" and to "Analysis of the raw materials for the semi-syntheses of steroid hormones".

In conclusion, the book is a very interesting one, filling a gap in the scientific literature. Due to the rich information, numerous data, tables, figures as well as the many practical aspects included, the book is not to be missed by chemists working in this field.

Mircea Banciu

ORGANIC CONDUCTORS AND SEMICONDUCTORS, Proceedings of the International Conference Siófok, Hungary, 1976 ; Edited by L. Pál, G. Grüner, A. Jánossy and J. Sólyom, Akadémiai Kiadó, Budapest — Springer Verlag, Berlin, 1977, 654 pp.

Organic conductors and semiconductors, in particular those of high conductivity, have lately acquired a growing interest. The International Conference on Organic Conductors and Semiconductors, held at Siófok (Hungary) in 1976, demonstrated that this field has stimulated research of both physicists and chemists, in a common effort in providing a theory of organic conductors and semiconductors, on the one hand and in producing materials of high efficiency, on the other hand.

The volume edited by Akadémiai Kiadó (with Springer Verlag, Berlin) includes beside the majority of the papers presented at this Conference, the abstract or the title of all the other lectures having no full text submitted. The papers, grouped in eight parts, follow the ordering of the Conference itself.

The works included in the first parts (I—IV) are essentially theoretical, with interest to the physicists concerned with the theory of conductors and semiconductors (I. One-dimensional Models ; II. Quasione-dimensional Models ; III. Impurity effects and disorder in one dimension ; IV. Phase transitions in TTF—TCNQ and related compounds). An excelent review of the theoretical investigation is written by Professor Morrel Cohen (The University of Chicago) in the paper "Disordered Quasi-one-dimensional Materials" (p. 225). The review covers the recent progress in only a few areas of the physics of semiconductors (Slante's theory of hopping conductivity in highly anisotropic materials, Theodorou's theory of the disordered, one-dimensional Hubbard model with application to the magnetic properties of NMP—TCNQ, the electron-phonon interaction as dynamic disorder, spin and charge ordering in donor-$(TCNQ)_2$ salts and surfaces of organic charge transfer salts ; 50 quotations).

The following parts (V—VIII), referring to the physical and chemical properties of organic semiconductors are both experimental and theoretical. Even if some of the papers included in these parts deal with the chemistry of organic semiconductors (for example : P. Delhaes *et. al.*, Physical Properties of Charge Transfer Complex with TCNQ and Iodine : Evidence of a Lattice Distortion, p. 493 ; J. Alizon *et. al.*, Investigations of High Conductivity Dipyranylidene and Dithiadipyranylidene — TCNQ Complexes, p. 563 ; Ch. Ivanova and V. Peneva, On the Conductivity of some Organic Dyes, p. 647), the emphasis is even there on the physics of such materials. The chemists desiring to be informed in the chemistry of this fascinating new area of research, will be disappointed to find out that most of the lectures with a chemical character are available only in abstract (for example : F. Wudl, G. A. Thomas, W. M. Walsh, Jr., and M. L. Kaplan, "New, Highly Conductive, Organic Solids" ; K. Bechgaard, C. Berg, J. R. Andersen and C. S. Jacobsen, "Organic Conductors Derived from Substituted Tetraselenafulvalenes", etc.). However, there are sufficient data and quoted literature, permitting to arise the interest of any chemist.

As apparent the Conference has mainly discussed the one-dimensional and quasi-one-dimensional organic semiconductors of the type of TTF—TCNQ (tetrathiafulvalene-tetracyanoquinodimethane) and TMTSF — TCNQ (tetramethyltetraselenafulvalene — TCNQ) and related compounds. The possible structures of these organic charge-transfer complexes, as well as the properties derived there from, are thoroughly discussed in a paper (A. N. Bloch, "Trends in Organic Conductors : Stabilization in the Nearly One-dimensional Metallic State", p. 317) including the bulk of the investigations on that subject (94 references).

Based on theoretical results, S. Suhai and G. Biczó (Hungary, p. 637) make suggestions for the synthesis of new organic compounds, likely to manifest similar behaviour as the known pair TTF—TCNQ. Their proposal, if experimentally proved, may completely reverse the chemical investigation of new compounds of high conductivity. Indeed, so far the organic charge transfer complexes used as semiconductors are built up from symmetrical compounds (TTF, TMTSF, TCNQ etc.). The authors consider that similar π-systems, with non-symmetrical molecules, may probably manifest a higher conductivity as the known complexes.

The results of the Conference, as well as the trends of the future investigations in this field are clearly expressed by Professor John Bardeen (Department of Physics, University of Illinois, Urbana) in his "Summary Remarks" (p. 13). Presenting the theoretical questions that attracted considerable attention at the Conference, he concludes that the field is much richer than he imagined a few years ago. His summary may stimulate interest and research of both physicists and chemists. In that way, even if addressed to theorists, the Proceedings of the Conference on Organic Conductors and Semiconductors may be useful to the chemical researcher.

Florin Badea

Lieng-Huang Lee (editor), "Characterization of Metal and Polymer Surfaces", vol. 1, Metal Surfaces, Academic Press, New York, 1977, 520 pp.

In the past decades, the field of metal surfaces has experienced rapid growth both in terms of industrial applications and academic interest. Reflecting this high level of activity, some leading authorities in physics and chemistry give a number of useful papers on both theoretical and experimental aspects of the characterization methods for metal surfaces. This volume contains proceedings of a Symposium on Advances in Characterization of Metal and Polymer Surfaces at the Centennial Meeting of the American Chemical Society, held in New York, April 1976.

This volume, devoted to metal surfaces, describes several techniques such as photoelectron and electron tunneling spectroscopy, secondary ion mass spectroscopy, scanning electron microscopy, reflectance spectroscopy, radiation analysis, Mössbauer spectroscopy, low energy electron diffraction (LEED), microprobe microscopy, infrared and laser Raman spectroscopy, ion microscopy, field-ion microscopy, electron spectroscopy for chemical analysis (ESCA), electron probe microanalysis, Auger electron spectroscopy, and atom-probe.

The book has the following contents :

Lieng-Huang Lee, Centennal Tribute : Surface Science and Polymer Technology.

Part I : Atom-Probe and Mössbauer Spectroscopy

E. W. Müller and S. V. Krishnaswamy, plenary lecture : Surface analysis at atomic level using the atom-probe.

G. W. Simmons and H. Leidheiser, Jr. : Applications of Mössbauer spectroscopy to the study of corrosion.

C. A. Clausen, and M. L. Good : Characterization of bulk and surface properties of heterogenous ruthenium catalysts by Mössbauer and ESCA techniques.

Discussion.

Part II : Auger Electron Spectroscopy and Electron Microprobe

M. L. Good : Introductory remarks.

R. L. Park, M. D. Boer and Y. Fukuda : Low energy electrons as a probe of solid surfaces.

I. M. Stewart : Surface characterization by electron microprobe.

J. T. Grant : Auger electron spectroscopy of solid surfaces.

C. E. Locke, J. H. Peavy, O. Rincon and M. Afzal : A study of passive film using Auger electron spectroscopy.

Discussion.

Part III : Low Energy Electron Diffraction

D. L. Allara : Introductory remarks.

P. J. Estrup : LEED studies of surface layers.

D. L. Adams and U. Landman : The use of direct methods in the analysis of LEED.

P. M. Marcus : Surface structure by analysis of "LEED" intensity measurements.

N. Stoner, A. V. van Hove and S. Y. Tong : Computation methods of LEED intensity spectra

Discussion.

Part IV : Secondary Ion Mass Spectroscopy

G. H. Morrison : Ion microscopy and surface analysis.

I. M. Stewart : Surface characterization by ion microprobe analyzer.

W. L. Baun : Study of adhesive bonding and bond failure surface using IIS—SIMS.

Discussion.

Part V : Photoelectron and Electron Tunneling Spectroscopy

R. R. Benerito : Introductory remarks.

D. M. Hercules : Surface characterization using electron spectroscopy (ESCA).

T. Rhodin and Ch. Brucker : Photoemission study of chemisorption on metals.

R. S. Haines : The study of organic reactions on the surface of magnetic pigments by X-ray photoelectron spectroscopy (ESCA).

K. P. Roenker and W. L. Baun : Molecular spectroscopy by inelastic electron tunneling.

Discussion.

Subject index and Author index.

The topics covered are of current interest for chemists and physicists who are seriously interested in the characterization of metal surfaces. The editor has done a commendable job of appealing to experts in the field.

Written for the researchers in university and in the electronics, computer, chemical, biomedical, auto, aerospace and other industries, this volume should also be very useful for advanced graduate students.

T. Chirulescu

B. RÅNBY and J. F. RABEK, "ESR Spectroscopy in Polymer Research", Springer-Verlag, Berlin Heidelberg New York, 1977, xiv + 410 p.

The book under review continues the series "Chemie, Physik und Technologie der Kunststoffe in Einzeldarstellungen", now entitled "Polymers/Properties and Applications".

The purpose of the book was to collect and present the available information on the applications of electron spin resonance (ESR) spectroscopy in polymer research. Starting from the first successful experimental observations, the authors (Dr. B. Rånby, professor, and Dr. J. F. Rabek, assistant professor, The Royal Institute of Technology, Stockholm, Sweden) review the results obtained up to now in this specific method in the study of polymer reactions.

The book is of interest both for those who want an introduction to this field, and for those already familiar with ESR spectroscopy. Treating in a coherent and extensive manner the literature published till now (original papers, reviews, discussions in monographs and books), it provides an important source of information for polymer and organic chemists, physicists, biologists, biochemists, and for students who are trained in the field.

The first three chapters (Generation of Free Radicals, Principles of ESR Spectroscopy, Experimental Instrumentation of Electron Spin Resonance) are addressed to those less familiar with this method and intend to encourage them to use it in polymer research. These chapters outline the fundamental principles of ESR and describe the instrumentation and the measurements techniques.

The long fourth chapter (111 pages), entitled "ESR Study of Polymerization Processes", is concerned with the study of polymerization processes by electron spin resonance. All the types of reactions are reviewed starting from homogeneous chain-growth polymerization, passing through polymerization initiated by mechano-radicals or by various free radical initiation systems, ionizing polymerization, photopolymerization, thermal polymerization, anionic and cationic polymerization, finally ending with heterogenous chain-growth polymerization. This extremely valuable chapter represents a remarkable reference source for researchers working in fields where polymerization processes are involved; it collects, practically, all the available information on the subject.

The fifth chapter — "ESR Study of Degradation Processes in Polymers" — organizes the material in four main parts (Radiation and Photo-Degradation of Polymers, Free Radicals Formed in Glow Discharge of Polymers, Anionic Degradation of Vinylaromatic Polymers, Reaction of Polymers with Hydroxy Radicals). The first part is the most extensive one, taking into consideration both organic and inorganic (sulphur-containing and siloxanes) polymers. The application of ESR spectroscopy in studying free radicals in biological systems is also reviewed, the attention of the authors being focused on cellulose and its derivatives, starch, lignin, wool and polynucleotides.

Chapters 6 (four pages) and 7 (thirteen pages) are devoted to "ESR Study of Polymers in Reactive Gases" and "ESR Studies of the Oxidation of Polymers", respectively. The last one ends with several pages dealing with "ESR Studies of Antioxidants", thus collecting the most important results in the domain.

Chapter 8 (ESR Studies of Molecular Fracture in Polymers) presents the up to date ESR investigations in the very complicated phenomenon that is molecular fracture in polymers. It appears clearly that ESR spectroscopy was successfully used in studying free radicals generated during fracture processes, processes of mechanical deformation, of grinding and machining of polymers.

Chapters 9—13 (ESR Studies of Graft Copolymerization, ESR Studies of Crosslinking, Application of Stable Free Radicals in Polymer Research, ESR Spectroscopy of Stable Polymer Radicals and their Low Molecular Analogues, and ESR Study of Ion-Exchange Resins, respectively) describe a number of the most modern developments of the method in the mentioned domains. One has to remark that some of these subjects have never been treated before in literature.

A total of 2519 references, part of them referring to the authors, own papers, end this very interesting book. The material is presented in a clear and concise manner, with tables, figures and diagrams wherever necessary. The work has a scientific unitary conception; the way in which the book is organized contributes to the understanding of the domain and to the development of fundamental and applicative research.

A special note for excellent printing could also be made.

Bogdan C. Simionescu

B. RÅNBY and J. F. RABEK, "ESR Spectroscopy in Polymer Research", Springer-Verlag, Berlin Heidelberg New York, 1977, xiv + 410 p.

The book under review continues the series "Chemie, Physik und Technologie der Kunststoffe in Einzeldarstellungen", now entitled "Polymers/Properties and Applications".

The purpose of the book was to collect and present the available information on the applications of electron spin resonance (ESR) spectroscopy in polymer research. Starting from the first successful experimental observations, the authors (Dr. B. Rånby, professor, and Dr. J. F. Rabek, assistant professor, The Royal Institute of Technology, Stockholm, Sweden) review the results obtained up to now in this specific method in the study of polymer reactions.

The book is of interest both for those who want an introduction to this field, and for those already familiar with ESR spectroscopy. Treating in a coherent and extensive manner the literature published till now (original papers, reviews, discussions in monographs and books), it provides an important source of information for polymer and organic chemists, physicists, biologists, biochemists, and for students who are trained in the field.

The first three chapters (Generation of Free Radicals, Principles of ESR Spectroscopy, Experimental Instrumentation of Electron Spin Resonance) are addressed to those less familiar with this method and intend to encourage them to use it in polymer research. These chapters outline the fundamental principles of ESR and describe the instrumentation and the measurements techniques.

The long fourth chapter (111 pages), entitled "ESR Study of Polymerization Processes", is concerned with the study of polymerization processes by electron spin resonance. All the types of reactions are reviewed starting from homogeneous chain growth polymerization, passing through polymerization initiated by mechano radicals or by various free radical initiation systems, ionizing polymerization, photopolymerization, thermal polymerization, anionic and cationic polymerization, finally ending with heterogeneous chain growth polymerization. This extremely valuable chapter represents a remarkable reference source for researchers working in fields where polymerization processes are involved; it collects, practically, all the available information on the subject.

The fifth chapter – "ESR Study of Degradation Processes in Polymers" – organizes the material in four main parts (Radiation and Photo-Degradation of Polymers, Free Radicals Formed in Glow Discharge of Polymers, Anionic Degradation of Vinylaromatic Polymers, Reaction of Polymers with Hydroxy Radicals). The first part is the most extensive one, taking into consideration both organic and inorganic (sulphur-containing and siloxanes) polymers. The application of ESR spectroscopy to studying free radicals in biological systems is also reviewed, the attention of the authors being focused on cellulose and its derivatives, starch, lignin, wool and polynucleotides.

Chapters 6 (four pages) and 7 (thirteen pages) are devoted to "ESR Study of Polymers in Reactive Gases" and "ESR Studies of the Oxidation of Polymers", respectively. The last one ends with several pages dealing with "ESR Studies of Antioxidants", thus collecting the most important results in the domain.

Chapter 8 (ESR Studies of Molecular Fracture in Polymers) presents the up to date ESR investigations in the very complicated phenomenon that is molecular fracture in polymers. It appears clearly that ESR spectroscopy was successfully used in studying free radicals generated during fracture processes, processes of mechanical deformation, of grinding and machining of polymers.

Chapters 9–13 (ESR Studies of Graft Copolymerization, ESR Studies of Crosslinking, Application of Stable Free Radicals in Polymer Research, ESR Spectroscopy of Stable Polymer Radicals and their Low Molecular Analogues, and ESR Study of Ion Exchange Resins, respectively) describe a number of the most modern developments of the method in the mentioned domains. One has to remark that some of these subjects have never been treated before in literature.

A total of 2519 references, part of them referring to the authors' own papers, end this very interesting book. The material is presented in a clear and concise manner, with tables, figures and diagrams wherever necessary. The work has a scientific unitary conception; the way in which the book is organized contributes to the understanding of the domain and to the development of fundamental and applicative research.

A special note for excellent printing could also be made.

Bogdan C. Simionescu

NOTE POUR LES AUTEURS

La Revue Roumaine de Chimie publie des articles en anglais, russe, allemand ou espagnol. Les auteurs sont priés d'envoyer des articles et des comptes rendus inédits.

Les manuscrits seront dactylographiés à deux intervalles. La bibliographie, les tableaux et la légende des figures seront placés après le texte.

Si l'article fait partie d'une série numérotée, le titre de la partie précédente sera indiqué dans une note au bas de la première page.

Chaque article sera précédé d'un résumé comprenant quinze lignes au maximum.

Les références bibliographiques dans le texte seront faites par des exposants sans parenthèse et paraîtront comme des notes au bas de chaque page.

Les publications périodiques mentionnées dans la bibliographie seront présentées suivant les prescriptions internationales : le nom de l'auteur précédé de l'initiale du prénom, le titre du périodique abrégé conformément à « Chemical Abstracts » et souligné par une ligne, le numéro du tome, indiqué par des chiffres arabes et souligné par deux lignes, suivi de la première page de l'article ; à la fin, l'année de la parution sera placée entre parenthèses. Le numéro de la revue ne sera pas indiqué si les pages du volume sont numérotées consécutivement. Pour les revues dont les tomes ne sont pas numérotés (par ex. Bull. Soc. Chim. France, etc.), l'année de la parution soulignée par deux lignes précédera l'indication de la page.

Les textes des livres ou traités inclueront : les noms des auteurs, les initiales du prénom, le titre du livre entre guillemets et sans être souligné, le numéro du tome précédé par l'abréviation « vol. » (ou « Bd. »), le numéro de l'édition, les éditions (the publisher), la localité de la parution et la page de la référence précédée par l'abréviation « p. » (ou « S. »).

Les brevets seront indiqués comme suit : l'auteur ou la firme, le pays et le numéro du brevet, la date et la revue (Chem. Abstr.). Par ex. M. Jones (to Union Carbide Co.), Brit. Pat. 601 238, 2 Sept. 1959, *Chem. Abstr.*, **54**, 12808 (1960).

Si la référence n'a pas été en original, on indiquera aussi la revue de références consultée.

Les diagrammes seront tracés à l'encre de Chine sur papier calque. Les tableaux et les figures (en nombre strictement nécessaire) seront numérotés par des chiffres arabes et leur explication sera donnée dans la légende des figures. Prière de ne pas inscrire les mêmes données dans les tableaux et les figures. Chaque tableau aura un titre. On indiquera dans le texte la place approximative des tableaux et des figures. Les formules chimiques seront incluses dans le texte ; en outre, elles seront transcrites sur papier calque, à l'encre de Chine.

Les auteurs sont priés d'indiquer les caractères italiques (en soulignant les lettres au crayon), ainsi que tout autre caractère spécial ; les préfixes *ortho*, *meta*, *para*, *cis*, *trans*, etc. seront soulignés pour indiquer leurs caractères italiques et ne seront jamais écrits avec des majuscules.

Aucune correction à la main ne sera admise sur le manuscrit. Les corrections seront frappées à la machine. Les lettres grecques ou d'autres symboles spéciaux seront insérés à la main à l'encre clairement.

Le manuscrit sera signé par l'auteur.

Le colonne-titre aura 50 lettres au maximum.

L'entière responsabilité du contenu des articles appartient aux auteurs.

TRAVAUX PARUS AUX ÉDITIONS DE L'ACADÉMIE DE LA RÉPUBLIQUE SOCIALISTE DE ROUMANIE

D. PURDELA (Sous la direction), **Nomenclatura Chimiei anorganice** (La nomenclature de la Chimie inorganique), 1977, 153 p., 11,50 lei.

DUMITRU NEGOIU, ANGELA KRIZA, **Poluanţi anorganici** (Polluants inorganiques dans l'air), 1977, 220 p., 16 lei.

I. ZUGRĂVESCU, MAGDA PETROVANU, **N-Ylid Chemistry**, 1977, 396 p., 19 lei.

C. DRĂGULESCU, E. PETROVICI, **Chimie structurală modernă. Chimia coordinanţei 8** (La chimie structurale moderne. La chimie de la coordinence 8), 1977, 947 p., 70 lei.

I. G. MURGULESCU, **Introducere în Chimia fizică. Vol. I. 1. Atomi, molecule, legătura chimică** (Introduction à la Chimie Physique, Ier vol. 1. Atomes, molécules, liaison chimique), 1976, 560 p., 36 lei.

E. P. BALTĂ, E. BALTĂ, **Introduction to the physical chemistry of the vitreous state**, coédition avec Abacus Press, 1976, 287 p., 31 lei.

H. I. GĂLĂŢEANU, **Radiochimia aplicată. Metode şi probleme** (La radiochimie appliquée. Méthodes et problèmes), 1976, 307 p., 19 lei.

CONST. V. UGLEA, **Cromatografia pe gel permeabil. Noi domenii de aplicare** (La chromatographie sur gel perméable. Nouveaux domaines d'application), 1976, 123 p., 6,75 lei.

FRANCISC A. GOTHARD, **Echilibre lichid-vapori. I. Baze teoretice şi metode de calcul** (Equilibres liquide-vapeurs. I. Bases théoriques et méthodes de calcul), 1976, 263 p., 2 pl., 28 lei.

CONST. GH. MACAROVICI, D. MACAROVICI, **Chimia oxizilor dubli şi utilizările lor** (La chimie des oxydes doubles et leur utilisation), 1975, 195 p., 13 lei.

M. AVRAM, **Antidăunători** (Pesticides), 1974, 496 p., 41 lei.

ELENA CEAUŞESCU, **Research work on synthesis and characterization of macromolecular compounds. Contributions**, 1974, 251 p., 20 lei.

DUMITRU COSTACHE, **Analiza chimică prin metoda cinetică** (L'Analyse chimique par la méthode cinétique), 1974, 251 p., 20 lei.

G. A. RĂDULESCU, **Proprietăţile ţiţeiurilor româneşti** (Les propriétés des pétroles roumains), 1974, 267 p., 2 pl., 18 lei.

CR. SIMIONESCU, VIORICA RUSAN, V. POPA, **Chimia algelor marine** (La chimie des algues marines), 1974, 212 p., 1 pl., 18 lei.

MARIA FITI, **Dozimetria chimică a radiaţiilor ionizante** (La dosimétrie chimique des radiations ionisantes), 1973, 240 p., 13,50 lei.

TIBERIU NĂŞCUŢIU, **Metode radiochimice de analiză** (Méthodes radiochimiques d'analyse), 1973, 384 p., 23 lei.

CRISTOFOR SIMIONESCU, MARGARETA GRIGORAŞ, AGATA CERNĂTESCU ASANDEI, GHEORGHE ROZMARIN, **Chimia lemnului în România. Plopul şi Salcia** (La Chimie du bois en Roumanie. Le peuplier et le saule), 1973, 299 p., 13 pl., 26 lei.

MIHAI FLORESCU, **Eficienţa economică a cercetării ştiinţifice** (L'efficience économique de la recherche scientifique), 1972, 115 p., 15 lei.

GEORGETA LĂZĂRESCU, **Sistematizarea informaţiilor în chimia organică** (Systématisation des informations en Chimie organique), 1972, 243 p., 1 pl., 10,50 lei.

1979 APR 19

I. P. Informaţia c. 444

43426

Lei 25.—

$45 (price per year)

F 1103

ACADÉMIE DE LA RÉPUBLIQUE SOCIALISTE DE ROUMANIE

REFERÁLVA

REVUE ROUMAINE DE CHIMIE

66

TOME 23
N°s 11–12
Novembre—Décembre 1978

EDITURA ACADEMIEI REPUBLICII SOCIALISTE ROMÂNIA

Rev. Roumaine Chim. RRCHAX, 23, *11–12*, p. 1511–1678 (1978), Bucarest

I

ACADÉMIE DE LA RÉPUBLIQUE SOCIALISTE DE ROUMANIE

COMITÉ DE RÉDACTION

Rédacteur en chef:

I. G. MURGULESCU, membre de l'Académie de la République Socialiste de Roumanie

Rédacteurs en chef adjoints:

A. T. BALABAN et V. EM. SAHINI, membres correspondants de l'Académie de la République Socialiste de Roumanie

Collège de rédaction:

EM. BRATU, ELENA CEAUŞESCU, ECATERINA CIORĂNESCU-NENITZESCU, C. DRĂGULESCU, CR. SIMIONESCU, membres de l'Académie de la République Socialiste de Roumanie; P. SPACU, membre correspondant de l'Académie de la République Socialiste de Roumanie; MARGARETA AVRAM, I. HAIDUC, D. I. MARGHIDAN, I. MOLDOVAN, G. NIAC et D. SĂNDULESCU

La Revue Roumaine de Chimie paraît 10 fois par an. Toute commande de l'étranger (fascicules ou abonnements) sera adressée à ILEXIM Departamentul Export-Import Carte (Livres)/Departamentul Export-Import Presă (Revues), P.O.Box 136—137 télex 11226, 3, str. 13 Decembrie, R-70116 Bucarest 12, Roumanie

Les manuscrits, les livres et les revues proposés en échange ainsi que toute correspondance seront envoyés à la rédaction :

REVUE ROUMAINE DE CHIMIE

23, str. Dumbrava Roşie, Bucarest, 9, Roumanie, téléphone 12 41 60

EDITURA ACADEMIEI REPUBLICII SOCIALISTE ROMÂNIA
125, Calea Victoriei, 71021 Bucarest, Roumanie, téléphone : 50 76 80

1979 JAN 1 9

REVUE ROUMAINE DE CHIMIE

Tome 23, N°s 11—12 Novembre—Décembre 1978

R O. RADOVICI, A. BANDI and C. CĂPĂŢ, Two phase porous electrodes. II. Influence of area on the activity of Raney-nickel-titanium-electrodes in the anodic oxidation of methanol (in German) . . . . 1513—1517

R RODICA MICU-SEMENIUC, TEREZIA DOBOŞ-ADAM and C. GH. MACAROVICI, Investigation of sulphonamides, benzamides and benzhydrazides. XXIV. Complex compounds of Cu(II) and Cd(II) with isomeric *ortho*-, *meta* and *para*-aminobenzamides . . . . 1519—1526

J. MARTIN GIL and F. J. MARTIN GIL, New complex uranyl sulphates. General study of IR spectra of these and other complexes (in Spanish) . . . 1527—1532

MARIA BREZEANU and MAGDALENA DINCULESCU, Polynuclear complex compounds of iron, cobalt and nickel. III. Bismuth — containing complex compounds . . . . 1533—1539

A. ABDEL MAKSOUD, G. HOSNI, O. HASSAN and S. SHAFIK, Reactions of 3′, 4′-dimethylchalcone and its derivatives . . . . 1541—1552

R LUMINIŢA VLĂDESCU and MIHAELA COSTACHE, Separation of elements Cu(II)—Zn(II)—Pb(II)—Fe(II), Fe(III) by means of ion exchangers (in French) . . . . 1553—1557

GH. MARCU, LETIŢIA GHIZDAVU and EUGENIA PERŢE, The study of cesium and thallium decatungstatediniobiosilicates in the solid state . . 1559—1565

A.F.M. FAHMY, M. A. EL-HASHASH, M. M. HABASHY and S. A. EL-WANNISE, Some reactions of 2-isopropyl-[4H]-3,1-benzoxazin-4-one . . . . . 1567—1573

I. SĂNDULESCU, OLGA ŞERBAN, S. DAVIDENCU, R. E. RUSSU and LIGIA FRUNZĂ, Formation and nature of active centres in solid oxid catalysts. III. Transalkylation of toluene on synthetic zeolite (in French) . . . . 1575—1579

M. A. EL-HASHASH and M. EL-KADY, Some reactions of β-aroyl-acrylic acid epoxides . . . . 1581—1588

TERESA KOWALSKA, Investigation of the autoxidation process of 1-dodecene 1589—1595

E. A. SOLIMAN, Some reactions with β-*p*-chlorobenzoylacrylic acids and β-*p*-toluyl-N-(*o*-carboxyphenyl)-acrylamide . . . . 1597—1605

P. K. MATHUR, Determination of isothiocyanatochromates using bromine monochloride . . . . 1607—1609

R GH. IONESCU, F. MATEI and AL. DUCA, Kinetic aspects of the oxidation reaction of gallic acid using an oxygen-selective electrode . . . . 1611—1617

Rev. Roumaine Chim. **23**, *11—12*, p. 1511—1678 (1978), Bucarest

4 M. S. SUBHANI and T. KAUSAR, Flash photolysis studies of aqueous solution of thiosulphate ion 1619–1626

4 M. S. SUBHANI and T. KAUSAR, Flash photolysis study of SeO_3^{2-} anion in aqueous solution 1627–1630

R ANIȘOARA BOLD and LUMINIȚA BĂLUȘESCU, The behaviour of α-bromostearic acid as extraction agent, I. Mechanism of copper(II) extraction . . 1631–1634

R CORNELIA LUCA, GABRIELA CHIȚANU, I. PETRARIU, A. AIRINEI and A. CARPOV, Retention of organic anions on strongly basic macroporous ion-exchangers 1635–1649

BOOK REVIEWS 1651–1653

AUTHOR INDEX 1655–1668

SUBJECT INDEX 1669–1677

Revue Roumaine de Chimie, **23**, *11–12*, 1513–1517 (1978)

PORÖSE ZWEIPHASENELEKTRODEN. II[1]

EINFLUSS DER OBERFLÄCHENGRÖSSE AUF DIE AKTIVITÄT DER RANEY-Ni-Ti-ELEKTRODEN IN DER ANODISCHEN METHANOLOXYDATION

O. RADOVICI, A. BANDI und C. CĂPĂŢ
Institut für Physikalische Chemie
Bukarest, Rumänien

Eingegangen am 6. November 1976

Aus Doppelschichtkapazitätsmessungen mit Hilfe der potentiostatischen Dreieckspannungsmethode, wurde die aktive Oberfläche von einigen porösen Raney-Ni-Ti-Elketroden ermittelt. Die Korrelation zwischen Oberflächengröße und elektrochemischen Eigenschaften wurde untersucht.

Die Größe der elektrochemisch aktiven Oberflächen der porösen Elektroden ist ein sehr wichtiger Faktor für die Bestimmung ihres elektrochemischen Verhaltens, ihrer Aktivität.[1] Die Ermittlung der Doppelschichtkapazität in hochkonzentrierten Elektrolyten ist die direkteste Art der Bestimmung der aktiven Oberfläche der Elektroden. Durch den Vergleich der Doppelschichtkapazität einer porösen Elektrode mit der Doppelschichtkapazität einer glatten Elektrode aus demselben Material, erhält man die aktive Oberfläche.

Zur Bestimmung der Doppelschichtkapazität der Raney-Ni-Elektroden, hat Richter[2] die Methode des potentiostatischen Potentialsprunges angewandt, welche Berndt[3] für poröse Ni-Sinterkörper benützt hatte. Da im Falle des potentiostatischen Potentialsprunges und vor allem bei der galvanostatischen Einschaltmethode,[2,4–7] der Ausschluß des faradayschen Stromes unmöglich ist, liefern diese Methoden fehlerhafte Ergebnisse.

Die Dreieckspannungsmethode, von Austin und Gagnon[8] vorgeschlagen, erlaubt eine Korrektur des faradayschen Stromes, wenn dieser, im Vergleich zum Aufladungsstrom, nicht zu hoch ist. Die Autoren[8] haben auf diese Weise die Doppelschichtkapazität verschiedener poröser Elektroden aus Ag, Ni, Kohle, bestimmt. In der Abb. 1 wird eine typische Strom-Zeit-Kurve, zusammen mit der Dreieckspannung, wiedergegeben.

---

[1] A. Bandi, *Rev. Roumaine Chim.*, **23**, 1373 (1978).

[2] G. Richter, „Deuxièmes Journées Internationales d'Etude des Piles a Combustible", Bruxelles, 1967, S. 236.

[3] D. Berndt, *Electrochim. Acta*, **10**, 1067 (1965).

[4] B. D. Cahan und P. Rüetschi, *J. Electrochem. Soc.*, **106**, 543 (1959).

[5] J. J. Mc Mullen und N. Hackerman, *J. Electrochem. Soc.*, **106**, 341 (1959).

[6] N. Laitinen und C. Genke, *J. Electrochem. Soc.*, **107**, 773 (1960).

[7] S. Gilman, *Electrochim. Acta*, **9**, 1025 (1964).

[8] L. G. Austin und E. G. Gagnon, *J. Electrochem. Soc.*, **120**, 251 (1973).

In der Abwesenheit des faradayschen Stromes verläuft die Strom-Zeit-Kurve mit der Zeitachse, bis zum Inversionspunkt der Spannung, parallel. Wenn auch faradayscher Strom anwesend ist, wächst (oder fällt) die Kurve mit der zunehmenden Spannung bis zum Inversionspunkt. In der unmittelbaren Nähe dieses Punktes sind die faradayschen Ströme ungefähr gleicher Größe, aber mit entgegengesetzten Zeichen, so, daß wir laut Tab. 1, schreiben können:

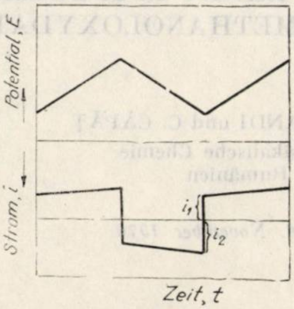

Abb. 1 Dreieckspannungsimpuls und die dazu gehörende Strom-Zeit-Kurve.

$$i_1 = i_f + kC_d \quad \text{und} \quad i_2 = -\,i_f + kC_d$$

wobei : k — die Potentialsänderung (mV/Sek.)
i_f — der faradaysche Strom (mA)
C_d — Doppelschichtkapazität (F)

Der Gesamtstrom i,

$$i = i_1 + i_2 = 2kC_d$$

wobei : $C_d = i/2k$

Die experimentellen Bedingungen werden so ausgesucht, daß die faradayschen Ströme aufs Minimum reduziert werden und, daß der distributive Effekt der Kapazität, durch die ungleiche Aufladung der Oberfläche und das Innere der Elektrode nicht auftritt.

In der vorliegenden Arbeit werden die Oberflächen einiger poröser Raney-Ni-Ti-Elektroden, zwecks ihrer Anwendung als Anoden in der Elektrooxydation des Methanols in alkalischen Lösungen, bestimmt.

EXPERIMENTELLER TEIL

Elektroden — Die Elektroden wurden nach der Methode Justi[9] aus Nickel Carbonil (Ni—C), Pulver Korngröße $< 15\,\mu$ und Ni—Al—Ti Legierung (30—67—3 %), Korngröße $< 63\,\mu$, hergestellt. Aus Pulvergemisch wurden runde Platten mit 1 cm² großer Fläche und 0,7 mm Dicke gepreßt. Der Preßdruck variierte zwischen 1110 und 3900 kgf/cm^2. Die Elektroden wurden bei 650° in Wasserstoffatmosphäre 30 Minuten lang gesintert und nachher in KOH bei 80°, 24 Stunden lang aktiviert.

---

[9] E. Justi und A. Winsel, „Kalte Verrennung", Steiner Verlag, Wiesbaden, 1962, S. 241.

Zur Bestimmung der Doppelschichtkapazität wurden die Elektroden, zwecks Auflösung des Restaluminiums, einer anodischen Polarisation unterzogen. Zur Bestimmung der elektrochemischen Aktivität der Elektroden wurden die Größen R_p, differentieller Polarisationswiderstand (Ω cm^2) und $i_{\max}$, maximaler Strom (mA/cm^2) gebraucht. Die Elektrodenpotentiale wurden gegen gesättigte Kalomelelektrode gemessen.

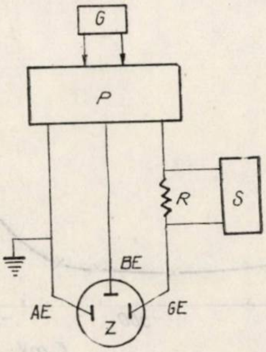

Abb. 2 Meßanordnung zur Bestimmung der Doppelschichtkapazität : P—Potentiostat ; G — Impulsgenerator ; S—Schreiber ; AE — Arbeitelektrode ; GE — Gegenelektrode ; BE — Bezugselektrode ; Z — Zelle. R — Widerstand.

Elektrolyten — Die elektrochemischen Versuche wurden in KOH 6M + CH_3OH 2,5 M bei 25° durchgeführt. Zur Bestimmung der Doppelschichtkapazität wurde KOH 6M verwendet, die Arbeitstemperatur war 40°. Die Temperatur wurde mit Hilfe eines Thermostates mit der Genauigkeit von ± 0,1° konstant gehalten.

Durchführung der Messungen — Die Meßanordnung, welche zur Bestimmung der Kapazität diente, wird in der Abb. 2 wiedergegeben.

Es wurden Impulsgenerator und Potentiostat Typ Tacussel benützt, die Strom-Zeit-Kurven werden mit Hilfe eines 8-Kanal Lichtschreibers Typ 8LS—201 RFT (DDR), aufgenommen. Die Gegenelektrode war Platinblech. Zur Berechnung der aktiven Oberfläche der porösen Elektroden wurde die Doppelschichtkapazität einer Ni-Blechelektrode in demselben Elektrolyten ermittelt.

Parallel zu den elektrochemischen Bestimmungen wurde die Oberfläche auch mit der BET-schen Methode, mit Hilfe einer in Rumänien hergestellten BET-Anlage, untersucht.

ERGEBNISSE UND DISKUSSIONEN

Die Kapazitätsänderung, abhängig von dem Potential der Ni-Blechelektrode, ist in der Abb. 3 wiedergegeben.

Aus Abb. 3 geht hervor, daß in einem großen Potentialbereich zwischen —300 und —800 V, die Doppelschichtkapazität konstant ist und einen Wert von 10μ F/cm^2 beträgt. Rechts und links dieses Potentialbereiches nehmen die Kapazitätswerte, wahrscheinlich wegen der ireversiblen Änderung der Oberfläche und des hohen faradayschen Stromes, zu. Ähnliche Ergebnisse wurden auch von Berndt [3] in KOH 1M erhalten. Zur Oberflächenberechnung der porösen Elektroden wurde der Kapazitätswert von 10μ F/cm^2 benützt.

In der Abb. 4 sind die BET-schen und die elektrochemisch ermittelten Oberflächenwerte wiedergegeben.

Man erkennt aus der Abb. 4 eine gute Übereinstimmung der BET-schen und der elektrochemisch ermittelten Werte. Starke Abweichung ist bei der Elektrode Nr. 6 zu bemerken, wobei die aus der differentiellen Kapazität berechnete Oberfläche viel größer ist, als die BET-Oberfläche.

Die Bestimmungen des Restaluminiums in angefertigten Elektroden zeigen einen großen Al-Gehalt für Elektrode Nr. 6, und zwar 20,4%, im Vergleich zu den anderen, wo der Aluminiumgehalt (im Verhältnis zu dem Anfangsaluminiumgehalt) nicht über 4,8% steigt. Wahrscheinlich erschwert der große Preßdruck (3900 kgf/cm²), welcher für die Elektrode Nr. 6 benützt wurde, die Auflösung des Aluminiums; daher der große Aluminiumgehalt und das verfälscht die Kapazitätsbestimmung. Bei den anderen Elektroden ist das 4,8%-ige Restaluminium sehr fest gebunden und beeinflußt die Kapazitätsbestimmung nicht.

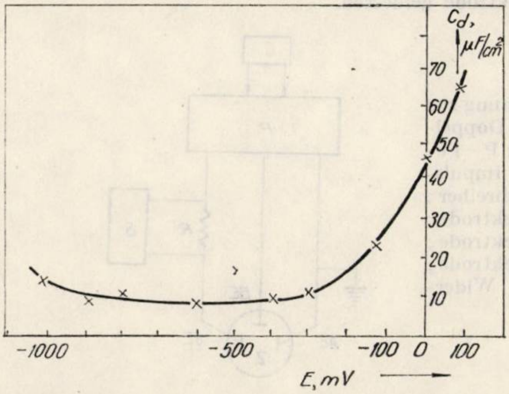

Abb. 3 Potentialabhängigkeit der Doppelschichtkapazität einer Ni-Elektrode in KOH 6M.

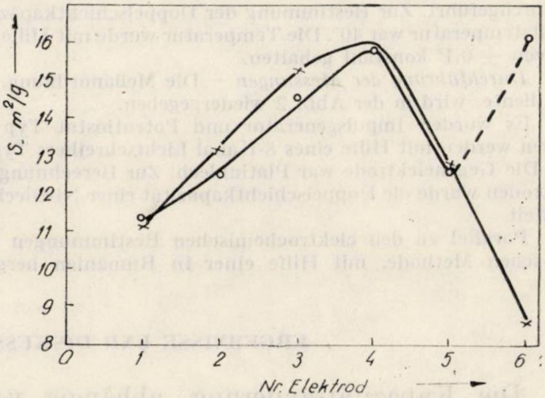

Abb. 4 BET — und aus der Kapazität berechnete Oberfläche der mit verschiedenem Preßdruck hergestellten Elektroden : × — BET-Oberfläche ; ○ — Aus der Kapazität berechnete Oberfläche (S_{Cd}).

In Tab. 1 sind die Kennwerte der Elektroden, R_p, i_{max}, und die aktive Oberfläche, wiedergegeben.

Tabelle 1

Kenngröße der Elektroden

Elektrode	1	2	3	4	5	6
P, kgf/cm²	1110	1670	2230	2790	3350	3900
R_p, Ω cm²	1,3	1,2	0,75	1,03	1,2	0,705
i_{max}, mA/cm²	64,5	83	92,5	89,5	78	99,5
S_{Cd}, m²/g	11,3	12,57	14,5	15,85	12,62	16,15

Die Wirksamkeit, oder die Aktivität einer Elektrode, kann man nach der Größe der aktiven Oberfläche beurteilen. Einige Autoren[10] behaupten, daß die Aktivität der Elektroden, linear oder exponential, mit der Oberfläche anwächst. In der Tab. 1 sieht man, daß R_p und $i_{\max}$ mit der zunehmenden Oberfläche bis zur Elektrode Nr. 3 (Preßdruck 2230 kgf/cm^2) abnehmen, bzw. wachsen, obwohl die Elektrode Nr. 4 (Preßdruck 2790 kgf/cm^2) eine größere spezifische Oberfläche besitzt. Das erklären wir mit der Änderung der Porenstruktur, verursacht von dem größeren Preßdruck. Demnach beeinflußt die Oberfläche der Elektroden ihre Aktivität, aber es ist wichtig, auch die richtige Porenstruktur erreicht zu haben, welche die Transportvorgänge begünstigt. Die Elektrode Nr. 6 (Preßdruck 3900 kgf/cm^2) hat R_p klein und $i_{\max}$ groß, obwohl Porosität[1] und BET-Oberfläche klein sind. Dieses anomale Verhalten erklären wir auch mit dem großen Restaluminiumgehalt.

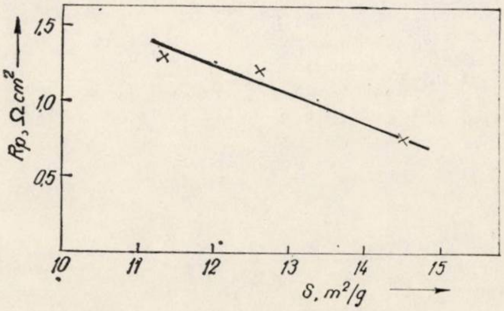

Abb. 5 Abhängigkeit der R_p-Werte von der Elektrodenoberfläche.

In Abb. 5 sind die R_p-Werte als Funktion der Oberfläche, für die Elektroden 1, 2, 3 aufgetragen und zeigen ein ungefähr lineares Verhalten.

Wir vermuten, daß die Aktivität mit der Oberfläche bis zu einem bestimmten Wert, in unserem Fall 14—15 m^2/g zunimmt, wenn die Porenstruktur unverändert ist und bleibt praktisch konstant, wenn die Oberfläche weiter wächst. Ähnliche Ergebnisse hat auch Smrček und Minstr[11] bei der anodischen Wasserstoffoxydation auf Raney-Ni-Elektroden gefunden.

---

[10] E. Y. Weissmann, *J. Electrochem. Soc.*, **114**, 658 (1967).

[11] K. Smrček und Z. Minstr, *Metalloberfläche*, **25**, 195 (1971).

Revue Roumaine de Chimie, **23**, *11–12*, 1519–1526 (1978)

INVESTIGATION OF SULPHONAMIDES, BENZAMIDES AND BENZHYDRAZIDES. XXIV*

COMPLEX COMPOUNDS OF Cu(II) AND Cd(II) WITH ISOMERIC *ortho-*, *meta* AND *para*-AMINOBENZAMIDES

RODICA MICU-SEMENIUC, TEREZIA DOBOŞ-ADAM and C. GH. MACAROVICI
"Babeş-Bolyai" University, Chemistry Department,
3400 Cluj-Napoca, Arany Janoş, 11, Romania

Received December 19, 1976

Within an investigation of aminobenzamides and related complexes, several new compounds derived from *ortho-*, *meta-* and *para*-aminobenzamide (abbreviated *o*-AB, *m*-AB and *p*-AB respectively) have been prepared, the structure of complexes was established and the coordination behaviour of isomeric benzamides was ascertained. This paper reports the results of investigation of Cu(II) and Cd(II) complex compounds with title aminobenzamides. The combination ratio was established by chemical analysis and photocolorimetric methods ; diffuse reflectance spectra, infrared and ESR spectra have been recorded. It was found that the complexes are either monomeric or polymeric, depending upon the coordinated ligand and the anionic partner. The complexes exhibit distorted octahedral or square planar geometries.

INTRODUCTION

Several complexes prepared from some metal salts with benzamide [1–5] are known. In these, the benzamide was found to coordinate through the oxygen of the amidic group.

In previous works we have investigated [6,7] the properties of aminobenzamides (abbreviated AB) and we prepared complexes of the type $MX_n(AB)_m$ [8–10] where M = Cu(II), Ag(I), Au(III), Zn(II), Cd(II),

---

[*] Preceding part is ref. 10

[1] S. Prasad and K. P. Srivastava, *J. Indian Chem. Soc.*, **35**, 793 (1958).

[2] R. Ch. Paul, R. B. Sreenathan and S. L. Chanda, *J. Inorg. Nuclear Chem.*, **28**, 1225 (1966).

[3] R. C. Aggarwal and P. P. Singh, *Z. anorg. Chem.*, **332**, 103 (1964).

[4] M. Gerrard, M.F. Lapertand and H.Pyszora, *J. Chem. Soc.*, **1960**, 2144 ; M. Gerrard, M. F. Lapertand and W. Wallis, *J. Chem. Soc.*, **1960**, 2141.

[5] M. B. Welch, R. S. Stephens and R. O. Ragsdale, *Inorg. Chim. Acta*, **2,** 367 (1968).

[6] C. Gh. Macarovici and C. Toma, *Studia Univ. Babeş-Bolyai Chem., fasc. IV*, **1958,** 42.

[7] C. Gh. Macarovici, V. Bota and C. Toma, *Studii şi Cercetări Chim. Acad. R. S. România, Fil. Cluj*, **1**, 75 (1960).

[8] C. Gh. Macarovici and C. Toma, *Studia Univ. Babeş-Bolyai Chem., fasc. II*, **1960,** 109.

[9] C. Gh. Macarovici and R. Micu-Semeniuc, *Studia Univ. Babeş-Bolyai Chem., fasc. I*, **1967**, 33 ; 97.

[10] C. Gh. Macarovici and R. Micu-Semeniuc, *Rev. Roumaine Chim.*, **12,** **1469** (1967).

Hg(II) ; X=Cl^-, 1/2 SO_4^{2-} ; m=1 or 2 and n = 1−3. On the basis of the known coordinative behaviour of aminobenzamides, an attempt to assign probable structures was made. In this paper we report the synthesis and spectral properties of some new aminobenzamide complexes.

EXPERIMENTAL PART

The aminobenzamides used as ligands were prepared according to literature data,[11-13] starting from *ortho-*, *meta-* and *para*-nitrobenzoic acids. The complexes were prepared in concentrated methanol solutions, from the metal salt and the appropiate aminobenzamide, taken in stoichiometric ratio. Variously coloured microcrystalline compounds have been obtained. Some are soluble in methanol and/or water, others are not. Usually, the soluble complexes exhibit sharp melting points, whereas those insoluble decompose at rather high temperatures. In table 1 elemental analysis data and some properties of the compounds prepared are given.

Table 1

Analysis and some properties of aminobenzamide compounds

Compounds	Colour	M.P.°C (D)	%M calc/found	%N calc/found	%Hal calc/found
1. $CuBr_2 \cdot 2$ *o*-AB	brown-redish	163	12.82/13.01	11.30/10.98	32.26/32.42
2. $CuBr_2 \cdot 2$ *m*-AB	brown	190	12.82/12.44	11.30/11.01	32.26/32.53
3. $CuBr_2 \cdot$ *p*-AB	yellow-green	(305)	17.96/17.51	8.34/ 8.68	44.47/44.98
4. $CuAc_2 \cdot$ *p*-AB *	green	(198)	20.01/20.24	8.81/ 8.63	—
5. $CuAc_2 \cdot 2$ *p*-AB *	green-blue	(272)	14.01/14.48	12.34/12.12	—
6. $Cu(ClO_4)_2 \cdot 2$ *o*-AB	green	247	11.88/11.98	10.47/10.20	—
7. $Cu(ClO_4)_2 \cdot$ *p*-AB	yellow-green	(208)	15.94/15.48	7.03/ 7.40	—
8. $CdCl_2 \cdot 2$ *o*-AB	white-yellow	163	24.67/24.12	12.29/12.48	15.59/15.16
9. $CdI_2 \cdot 2$ *o*-AB	grey	182	17.76/18.10	8.77/ 8.60	38.20/37.84
10. $CdI_2 \cdot 2$ *p*-AB	white-pink	(193)	17.76/17.94	8.77/ 8.96	38.20/37.78

* Ac = CH_3COO^-

The combination ratios in methanolic solutions were determined by P. Job's method [14] by using a FEK photocolorimeter (Soviet made) at λ = 413 nm on isomolar solutions (2.10^{-2} and 4.10^{-2} comparatively). The data obtained are given in table 2, together with previously obtained results.[8,9]

Diffuse reflectance spectra were recorded with a VSU−2G C. Zeiss, Jena spectrophotometer. The results are given in table 3.

ESR spectra of Cu(II) complexes were recorded with a JEOL JES−3B spectrometer, on crystalline samples, at room temperature. The ESR spectra are shown in Figure 1 and the spectral parameters are listed in table 4.

The infrared spectra of the complexes were recorded in KBr pellets with a UR−20 C. Zeiss, Jena apparatus. The assignment of bands in the spectra of complexes was made by comparison with those of the free aminobenzamide ligands and are listed in table 5.

RESULTS AND DISCUSSION

The elemental analyses of isolated complexes (Table 1) confirm the M : *n*L combination ratio (L = *o*−AB, *m*-AB, *p*-AB ; n = 1 or 2) found by continuous variations method in solutions [11] (Table 2). The combination ratio is not influenced by relative positions of amine and amide functions, or by the nature of the cations or anions involved. The combination ratio seems to be controlled only by the reaction conditions, especially by the starting stoichiometric reagents ratio.

---

[11] E. Reichenbach and F. Beilstein, *Liebigs Ann. Chem.*, **132,** 144 (1864).

[12] W. A. Jakobs and M. Heidelberger, *J. Amer. Chem. Soc.*, **39,** 1435 (1917).

[13] L. Mc. Master and F. F. Alimann, *J. Amer. Chem. Soc.*, **50,** 145 (1928).

[14] P. Job, *Ann. Chim. (France)*, **10,** 113 (1928).

Table 2

The combination ratio of aminobenzamides with some metallic salts

Combination ratio M : L	Aminobenzamide (-AB)	Metallic salts
1 : 1	*o*-AB	($CuCl_2$; $HgCl_2$) *
	m-AB	($HgCl_2$) *
	p-AB	($CuCl_2$; $AgNO_3AuCl_3$; $CdCl_2HgCl_2$) * $CuBr_2$; $Cu(ClO_4)_2$; $CuAc_2$ [a)] **
1 : 2	*o*-AB	($CuCl_2$; $CuSO_4$; $HgCl_2$) * ($CuBr_2$; $CuClO_4)_2$; $CdCl_2$; CdI_2 **
	m-AB	($CuCl_2$; $HgCl_2$) * $CuBr_2$ **
	p-AB	($CuSO_4$; $ZnSO_4$; $CdSO_4$; $HgCl_2$) * $CuAc_2$ [a)] ; CdI_2 **

* see reference [8; 9]

** this work

[a)] Ac = CH_3COO^-

The diffuse reflectance spectra of some Cu(II) complexes (Table 3) exhibit three well resolved bands, in the ranges 9,500 – 9,900 cm^{-1} ($^2B_{2g} \leftarrow {}^2B_{1g}$), 12,000 – 13,000 cm^{-1} ($^2E_g \leftarrow {}^2B_{1g}$) and 21,700 – 22,700 cm^{-1} ($^2A_{1g} \leftarrow {}^2B_{1g}$) characteristic of Cu(II) complexes.[15,16] This order of the Cu (II) ion terms was adopted since the second band in the recorded spectra is split for the first two compounds. This splittings can be understood only if the second transition involves a ^2E_g term, whose degeneration can be partly removed as a result of distorsions present in the complex molecule. The third band is more intense, probably due to contributions from charge transfer bands occurring above 25,000 cm^{-1}. The shapes and the positions of the bands suggest a D_{4h} local symmetry for the Cu(II) ion.

Table 3

Electronic transitions (diffuse reflectance spectra) of some aminobenzamide-copper(II) complexes (cm^{-1})

Compounds	$^2B_{2g} \leftarrow {}^2B_{1g}$	$^2E_g \leftarrow {}^2B_{1g}$	$^2A_{1g} \leftarrow {}^2B_{1g}$.
1. $CuBr_2 \cdot$ *p*-AB	9,500	12,900 12,000	21,700
2. $Cu(ClO_4)_2 \cdot$ *p*-AB	9,800	12,800 12,000	21,700
3. $CuSO_4 \cdot 2$ *p*-AB	9,900	13,500	22,700

---

[15] B. J. Hathaway and A. G. Tomlinson, *Coord. Chem. Rev.*, **5**, 1 (1970).

[16] B. J. Hathaway and D. E. Billing, *Coord. Chem. Rev.*, **5**, 143 (1970).

Two types of ESR spectra have been obtained : isotropic spectra (Figure 1*a*), with a single g value and $I_{\parallel}$ approximately equal to $I_{\perp}$ and axial type spectra (Figura 1*b*) with two values of the g factor and $I_{\parallel}$ differing from $I_{\perp}$. The data are listed in table 4.

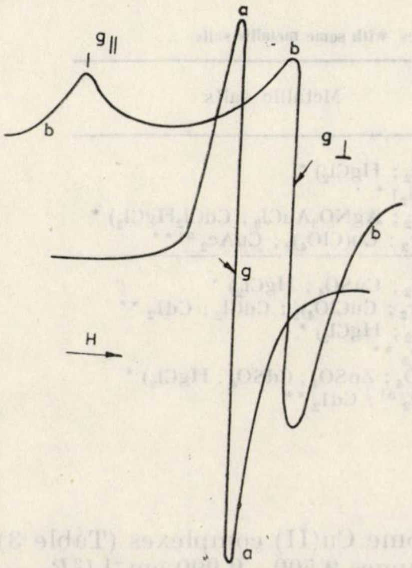

Fig. 1. — Types of ESR Spectra :
Isotropic Spectra : a) $CuBr_2 \cdot 2m$-AB
Axial Spectra : b) $CuBr_2 \cdot 2o$-AB

The isotropic spectra suggest that the copper(II) ion is in an octahedral configuration ($CuCl_2 \cdot 2$ *o*-AB and $CuBr_2 \cdot 2$ *m*-AB) with time-averaged distorsions.[16] A square planar geometry cannot, however, be rejected (e.g. for $CuBr_2 \cdot p$-AB and $Cu(ClO_2)_2 \cdot p$-AB).

The axial symmetry spectra suggest a compressed tetragonal distortions (for compounds with $g_{\min} < 2.04$).[16] Thus, the complex chloride exhibit a different behaviour from the other compounds. It seems that in the complex chlorides the distortions are of elongation type, whereas the remaining complexes exhibit compression distortions (Table 4). For the perchlorates and bromides planar geometries can also be postulated.

In the compound $CuCl_2 \cdot 2$ *o*-AB the Cu(II) ion seems to be six-coordinate rather than four-coordinate, as suggested previously,[10] having the local tetragonal axes of the molecular backbone, parallel to the magnetic field ($G > 4$).[15,16]

Among the compounds investigated by us, $CuCl_2 \cdot 2$ *m*-AB and $CuSO_4 \cdot 2$ *o*-AB exhibit some tendency to resolve the hyperfine structure of the ESR spectrum, with a hfs constant (A) relatively small (in the first approximation degree, ~30 gauss).

The parameters of the ESR spectra (Table 4) suggest that the local symmetry of the Cu(II) ion depends both on the nature of the isomeric aminobenzamide used and the nature of the anion. Isotropic and axial lines occur for *o*-, *m*- and *p*-aminobenzamides and Cl^-, Br^-, ClO_4^- and SO_4^{2-} anions. The six-coordination, suggested by ESR spectra, can be achieved only if a polymeric structure is formed through bridging ligands (either aminobenzamides or anionic group, see Figure 2). The spectra of complex perchlorates can be interpreted only if coordination of ClO_4^- is assumed, which was scarcely mentioned in the literature.[17-20]

---

[17] B. J. Hathaway and A. E. Underhill, *J. Chem. Soc.*, **1961**, 3091.
[18] F. A. Cotton and D. L. Weaver, *J. Amer. Chem. Soc.*, **87**, 4189 (1965).
[19] W. R. McWhinnie, G. C. Kulasingam and J. C. Draper, *J. Chem. Soc., A*, **1966**, 1199.
[20] L. Johansson, *Coord. Chem. Rev.*, **12**, 241 (1974).

In the infrared spectra the bands occurring in the ranges 3500—3100 cm^{-1} (stretching vibrations of amine and amide $-NH_2$ groups), 1715—1650 cm^{-1} (assigned to ν_{CO} valence vibrations, amide band I), 1650—1520 cm^{-1} (deformation vibration δ_{NH_2}, amide band II) and 1400 cm^{-1} (ν_{C-N} coupled with NH vibration, amide band III).[10,21,22]

Table 4

ESR parameters of some aminobenzamide-copper(II) complexes

Compounds	$\Delta H_{1/2}$ gss	$I_{\parallel}/I_{\perp}$	H gss	g
1. $CuCl_2 \cdot$ *o*-AB *	41.12	46/152	2971 3250	2.258 2.065
2. $CuCl_2 \cdot 2$ *o*-AB *	58.75	13/141	2970 3250	2.247 2.056
3. $CuCl_2 \cdot 2$ *m*-AB *	52.87	71/137	3086 3288	2.174 2.045
4. $CuCl_2 \cdot$ *p*-AB *	17.62	49/132	3241 3330	2.071 2.016
5. $CuBr_2 \cdot 2$ *o*-AB	88.13	47/103	3241 3319	2.070 2.022
6. $CuBr_2 \cdot 2$ *m*-AB	52.87	98/108	3231	2.078
7. $CuBr_2 \cdot$ *p*-AB	79.31	105/ 97	3280	2.047
8. $CuAc_2 \cdot$ *p*-AB **	105.20	69/ 86	3281	2.043
9. $Cu(ClO_4)_2 \cdot 2$ *o*-AB	21.64	55/139	3099 3307	2.166 2.030
10. $Cu(ClO_4)_2 \cdot$ *p*-AB	34.92	110/115	3292	2.035
11. $CuSO_4 \cdot 2$ *o*-AB *	93.96	64/162	2950 3283	2.327 2.043
12. $CuSO_4 \cdot 2$ *p*-AB *	20.37	89/142	3259 3294	2.060 2.038

* Synthesized by other authors — see ref.[9]

** Ac = CH_3COO-

It can be seen that the most dramatic changes caused by coordination of aminobenzamides occur in the stretching vibrations ν_{NH_2} range. Shifts of these bands towards lower energies are observed. The bands amide I, amide II and amide III, occur in the ranges reported in the literature for these bands, with only minor shifts from one complex to another (Table 5).

For all compounds containing *o*-AB the range of ν_{NH_2} vibrations are similar, namely: the bands due to $-NH_2$ (amine) groups occur at the same wave number or sometimes even higher than in the free ligands. Therefore, the $-NH_2$ group attached to the aromatic nucleus is not involved in coordination. Only the amide $-NH_2$ groups are shifted towards lower wave numbers, *i.e.* only these participate in coordination to the metal (Figure 2*a*). There are no other changes, except for the ν_{CO} band in Cd(II) complexes, where shifts of 20—22 cm^{-1} are observed. It is thus

---

[21] L. J. Bellamy, "The Infrared Spectra of Complex Molecules", Ed. II, Methuen Co LTD, London, J. Wiley, New-York, **1960**, p. 203—230.

[22] M. St. C. Flett, *Spectrochim. Acta*, **18**, 1537 (1962).

Table 5

Infrared spectra of aminobenzamide complexes (cm^{-1})

Compounds	ν_{aNH_2} amine	ν_{sNH_2} amine	ν_{aNH_2} amide	ν_{sNH_2} amide	ν_{CO}	ν_{CN}	
o-AB	3420	3330	3330	3200	1672	1460	1410
1. $CuBr_2 \cdot 2$ *o*-AB	3412	3342	3250	3142	1670	1443	1415
2. $Cu(ClO_4)_2 \cdot 2$ *o*-AB	3455	3350	3290	3245 3130sh	1668	1450	1410
3. $CuSO_4 \cdot 2$ *o*-AB **	3430	3340	3270	3130	1665	1435	1410
4. $CdCl_2 \cdot 2$ *o*-AB	3420	3320	3230	3175sh	1650	1460	1415
5. $CdI_2 \cdot 2$ *o*-AB	3425	3310	3220	3130sh	1652	1450	1425
m-AB	3470	3397	3360	3210	1700	1470	1412
6. $CuBr_2 \cdot 2$ *m*-AB	3365	3305	3290	3230	1670	1470	1412
p-AB	3471	3360sh	3335	3205	1650sh	1441	1400
7. $CuBr_2 \cdot$ *p*-AB	3415	3320	3270	3215	1670	1440	1410
8. $CuAc_2 \cdot$ *p*-AB *	3480	3380	3280	3220	1660sh	1445	1400
9. $CuAc_2 \cdot 2$ *p*-AB *	3480	3360	3230	3135sh	1660sh	1440	1408
10. $Cu(ClO_4)_2 \cdot$ *p*-AB	3415	3320	3270	3210 3150sh	1670	1430	1410
11. $CuSO_4 \cdot 2$ *p*-AB **	3470	3360	3250	3180	1680	1440	1415
12. $CdCl_2 \cdot$ *p*-AB	3390	3340	3280	3200	1675	1440	1410
13. $CdI_2 \cdot 2$ *p*-AB	3470	3380sh	3330	3200	1670	1440	1410
14. $CdSO_4 \cdot 2$ *p*-AB **	3390	3350	3280	3210	1670	1440	1410

* Ac = CH_3COO^-

** Synthesized by other authors – see ref.[9]

suggested that in these compounds the whole $-CO-NH_2$ (amide) group is involved in coordination (Table 5, Figure 2*b*).

The compound $CuBr_2 \cdot 2$*m*-AB exhibits marked band shifts for both amine $-NH_2$ (93 and 106 cm^{-1}) and amide $-NH_2$ (80 and 145 cm^{-1}) groups ; the other ranges are unaffected. This suggests that only nitrogen atoms participate in coordination, which is possible if the compound is a dimer (Figure 2*c*).

Two types of complexes with *p*-AB have been obtained : with one or two ligand molecules (Table 1). Their infrared spectra are different within the same type of compounds. Thus, for the 1M : 1*p*-AB type, those containing bromide, chloride and perchlorate exhibit shifts for both $-NH_2$ (amine and amide) groups, suggesting their coordination ; those containing acetate show only shifts of the bands assigned to amide $-NH_2$ groups, the amine $-NH_2$ groups being not involved in coordination. The first three compounds can be assigned structures of type 2*d*, and the last, a structure of type 2*b*.

The compounds with 1M : 2*p*-AB ratio are specific for each central metal atom. The copper (II) complexes exhibit shifts in the range 3500–3100 cm^{-1} only for the amide $-NH_2$ group, whereas in the cadmium complexes shifts are observed for both amine and amide $-NH_2$ groups. In the compounds $CuX_2 \cdot 2p-AB$ the central atom is probably four-coordinated, with two coordination sites occupied by the two *p*-AB molecules, the other two being occupied by the anion (X = SO_4^{2-} and Ac^-) (Figure 2*a*). The corresponding cadmium complexes might be dimers of the type 2*c*.

Unfortunately, the ν_{CO} range in the complex acetates are much complicated by the $-\mathrm{C}\genfrac{}{}{0pt}{}{\diagup \mathrm{O}}{\diagdown \mathrm{O}}$ group of the acetate anion, thus making the interpretation of the spectra rather difficult. The information obtained from infrared spectra is therefore not enough to afford an interpretation of their structure.

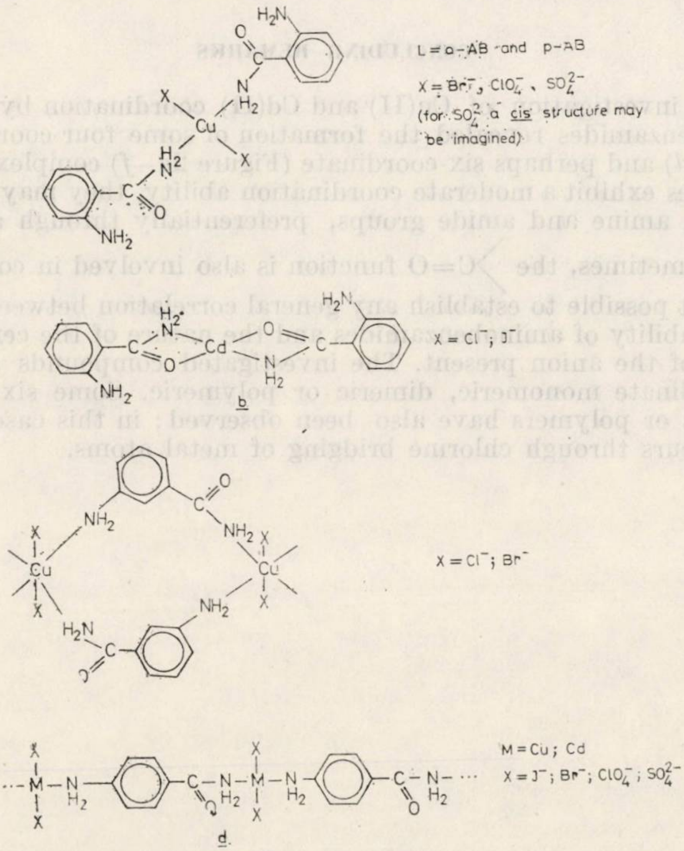
L = o-AB and p-AB
X = Br⁻, ClO₄⁻, SO₄²⁻
(for SO₄²⁻ a cis structure may be imagined)
Cu
Cd
X = Cl⁻; J⁻
b
X = Cl⁻; Br⁻
M = Cu; Cd
X = J⁻; Br⁻; ClO₄⁻; SO₄²⁻
d
L = p-AB
e
L = o-AB
f

Fig. 2. — Possible structures of aminobenzamide compounds.

The infrared spectra of complex sulfates and perchlorates suggest that these anions are involved in coordination. Thus, instead of two IR active bands, characteristic for a tetrahedral geometry, the spectra of these compounds exhibit two groups of bands, suggesting a coordinated anion of C_{3v} geometry.[23,24] These bands occur in the range ~ 1100 cm^{-1} (ν_3, F_4) and ~ 600 cm^{-1} (ν_4, F_2) : the complex sulfates show bands at 1125 and 1035 cm^{-1} for ν_3 and 645 and 600 cm^{-1} for ν_4 ; the perchlorates at 1125 and 1040 cm^{-1}, and respectively, at 650 and 600 cm^{-1}.

CONCLUDING REMARKS

The investigation of Cu(II) and Cd(II) coordination by *o*-, *m*- and *p*-aminobenzamides revealed the formation of some four-coordinate (Figure 2*a*--*d*) and perhaps six-coordinate (Figure 2*e*—*f*) complexes. Aminobenzamides exhibit a moderate coordination ability, they may coordinate with both amine and amide groups, preferentially through amide NH_2 group. Sometimes, the $>C=O$ function is also involved in coordination. It was not possible to establish any general correlation between the coordination ability of aminobenzamides and the nature of the central metal atom or of the anion present. The investigated compounds are mostly four-coordinate monomeric, dimeric or polymeric. Some six-coordinate monomers or polymers have also been observed; in this case polymerization occurs through chlorine bridging of metal atoms.

---

[23] K. Nakamoto, J. Fujita, S. Tanaka and M. Kobayashi, *J. Amer. Chem. Soc.*, **79**, 4909 (1957).

[24] P. S. K. Chia, L. F. Lindoy and S. E. Livingstone, *Inorg. Chim. Acta*, **2**, 459 (1968).

Revue Roumaine de Chimie, 23, 11–12, 1527–1532 (1978)

NUEVOS SULFATOS COMPLEJOS DE URANILO. ESTUDIO GLOBAL DE LOS ESPECTROS I. R. DE ESTAS Y OTRAS ESPECIES COMPLEJAS

J. MARTIN GIL y F. J. MARTIN GIL
Departamento de Química Inorgánica. Facultad de Ciencias.
Universidad de Valladolid (Spain)

Recibido el 1 de Octubre 1976

New uranyl sulfate complexes are reported in order to complete the table of possibilities of the complex species present in the $UO_2^{2+}-H_2SO_4-H_2O$ system. The species identified in the crystalline solids were $[(UO_2)_2(SO_4)_5]^{6-}$, $[(UO_2)_3(SO_4)_4]^{2-}$, $[(UO_2)_3(SO_4)_6]^{6-}$ and $[(UO_2)_4(SO_4)_7]^{6-}$. The i.r. spectra for these and another complexes which have been investigated in varying detail are discussed. Also in the work it is demonstrated that there is apparently no conexion between the asignments of the i.r. spectra reported and those of the species sorbed on ion exchangers.

Se dan nuevos sulfatos complejos de uranilo con el fin de completar el cuadro de posibilidades de las especies complejas presentes en el sistema $UO_2^{2+}-H_2SO_4-H_2O$. Las especies identificadas en los solidos cristalinos son $[(UO_2)_2(SO_4)_5]^{6-}$, $[(UO_2)_3(SO_4)_4]^{2-}$, $[(UO_2)_3(SO_4)_6]^{6-}$ y $[(UO_2)_4(SO_4)_7]^{6-}$. Los espectros i.r. para éstos y otros complejos, que han sido investigados con detalle, son objeto de discusion. También en el trabajo se demuestra que no hay aparentemente conexion entre las asignaciones de los espectros i.r. dados y los de las especies absorbidas en cambiadores de iones.

INTRODUCCION

En algunos trabajos previos [1–9] se han dado la preparación de sulfatos de uranilo con alcalinos, amonio, talio, magnesio, niquel, cobre y cinc, en los que se identificó la especie compleja $[UO_2(SO_4)_2]^{2-}$.

La existencia de los iones complejos $[UO_2(SO_4)_3]^{4-}$ y $[(UO_2)_2(SO_4)_3]^{2-}$ a pH inferior a 3,5 ha sido establecida.[10,11]

[1] J. A. Arfvedson, *Ann. Physik. Chem. Pogg.*, **1**, 245 (1824).

[2] J. J. Ebelmen, *Liebig's Ann. Chem.*, **3**, 286 (1842).

[3] E. Rimbach, *Ber.*, **37**, 461 (1904).

[4] M. Kohn, *Z. anorg. Chem.*, **59**, 111 (1908).

[5] F. De Coninck, *Ann. Chim. Phys.*, **28**, 5 (1903).

[6] A. Colani, *Bull. Soc. chim. France*, **43**, 736 (1928).

[7] R. J. Traill, *Am. Mineralogist*, **37**, 394 (1952).

[8] J. G. Ribas, J. Martin Gil y F. J. Martin Gil, *Quim. Anal. (IFQAAZ)*, **30**, 95 (1976).

[9] J. G. Ribas, J. Martin y F. J. Martin, *Energia Nuclear (Espana)*, **20**, 37 (1976).

[10] P. Pascal, »Nouveau Traité de Chimie Minérale (Uranium) », vol. 15 Masson et Cie, Ed., Paris, 1967.

[11] K. W. Bagnall, *MIP Internat. Review of Science — Inorg. Chem. — Series 1*, **7**, 151 (1972).

Considerando el hecho de que un aumento de acidez fuera el responsable del aumento de la complejidad de estas especies, empezamos a trabajar en medios más ácidos aún, a pH no superior a 1, obteniendo compuestos en los que, tal como esperábamos, interviene un número mayor de grupos uranilo y/o sulfato y de los que medidas de conductividad a temperaturas próximas a 0°C indican la existencia de aniones complejos. En recientes comunicaciones [8,9] hemos dado la preparación, propiedades y estudio termogravimétrico y espectral de compuestos con las especies complejas $[UO_2(SO_4)_4]^{6-}$, $[(UO_2)_2(SO_4)_4]^{4-}$ y $[(UO_2)_3(SO_4)_5]^{4-}$. En el presente trabajo, al aportar nuevos compuestos con las estequiometrías $(UO_2)_2(SO_4)_5M_3^{II}$, $(UO_2)_3(SO_4)_4M_2^{I}$, $(UO_2)_3(SO_4)_6M_2^{III}$ y $(UO_2)_4(SO_4)_7M_2^{II}$, completamos el cuadro de posibilidades de especies complejas con los iones uranilo y sulfato.

Un sumario de los compuestos preparados hasta la fecha se da en la Tabla 1.

Table 1

Sulfatos complejos de uranilo

$[UO_2(SO_4)_2]^{2-}$	$(Li^+, Na^+, K^+, Rb^+, Cs^+, NH_4^+, Tl^+, Mg^{2+}, Ni^{2+}, Cu^{2+}, Zn^{2+}, VO^{2+})$
$[UO_2(SO_4)_3]^{4-}$	$(Na^+, K^+, Rb^+, NH_4^+ \ Mg^{2+})$
$[UO_2(SO_4)_4]^{6-}$	(Co^{2+})
$[(UO_2)_2(SO_4)_3]^{2-}$	$(Na^+, K^+, Rb^+, Cs^+, NH_4^+)$
$[(UO_2)_2(SO_4)_4]^{4-}$	(Ce^{4+})
$[(UO_2)_2(SO_4)_5]^{6-}$	(Mg^{2+})
$[(UO_2)_3(SO_4)_4]^{2-}$	(Cs^+)
$[(UO_2)_3(SO_4)_5]^{4-}$	$(Na^+, Cd^{2+}, Hg^{2+}, Mn^{2+})$
$[(UO_2)_3(SO_4)_6]^{6-}$	(La^{3+})
$[(UO_2)_4(SO_4)_7]^{6-}$	(Cr^{3+})

PARTE EXPERIMENTAL

Método de preparación. Por cristalización, en desecador de vacio, de la solución fuertemente ácida en H_2SO_4 en la que se encuentran presentes ambos cationes (UO_2^{2+} y M^{n+}). Para mas detalles, consultar. [8] Los cristales de los complejos son amarillo-verdosos y fluorescentes.

Análisis. — Los sulfatos se han determinado gravimétricamente como sulfato de bario. El uranio ha sido pesado como U_3O_8. De los otros cationes, el lantano ha sido determinado por complexometria; el cromo (III), después de oxidado a cromo (VI), se precipitó como cromato de mercurio, se calcinó y se pesó como Cr_2O_3; el cesio y el magnesio se han determinado por AAS.
Resultados:
Sulfato de uranilo y magnesio, $(UO_2)_2(SO_4)_5Mg_3 \cdot 10\ H_2O$ — *Calc.*: U, 37,39; SO_4, 37,71; Mg, 5,72; H_2O, 14,14; *Encontr.*: U, 37,40 SO_4, 37,34; Mg, 4,77; H_2O, 13,71.

Sulfato de uranilo y cesio, $(UO_2)_3(SO_4)_4Cs_2 \cdot 2H_2O$ — *Calc.*: U, 47,73; SO_4, 25,68; Cs, 17,76; H_2O, 2,41. *Encontr.*: U, 46,84; SO_4, 25,60; Cs, 17,00; H_2O, 2,50.

Sulfato de uranilo y lantano, $(UO_2)_3(SO_4)_6La_2 \cdot 2H_2O$ — *Calc.*: U, 42,00; SO_4, 33,90; La, 16,34; H_2O, 2,12. *Encontr.*: U, 43,67; SO_4, 33,55; La, 15,56; H_2O, 2,10.

Sulfato de uranilo y cromo, $(UO_2)_4(SO_4)_7Cr_2 \cdot 10\ H_2O$ — *Calc.*: U, 46,75; SO_4, 33,01; Cr, 5,11; H_2O, 8,84. *Encontr.*: U, 46,13; SO_4, 32,10; Cr, 5,22; H_2O, 9,02.

Espectros infrarrojo. Los espectros de absorción i.r. de las muestras, en pastillaje de CsBr, han sido obtenidos entre 4.000 y 400 cm^{-1} con un espectrofotometro Pye-Unicam SP 1000.

RESULTADOS Y DISCUSION

Modos de vibración del ión uranilo en los complejos.

Los espectros i.r. de sales complejas del ión uranilo han recibido mucha atención a lo largo de estos años. De los modos de vibración podemos obtener información de la influencia de los ligandos situados en un plano perpendicular a la dirección axial O—U—O. Aparte de los cambios en la distancia U—O y, consecuentemente, en el orden de enlace, la linealidad del ión uranilo puede quedar afectada por los agentes complejantes. Son significativos los amplios márgenes para las frecuencias características que se dan en la bibliografia : la frecuencia de tensión simétrica, ν_1, se observa entre 960 y 890 cm^{-1}, la frecuencia de tensión asimétrica, ν_3, entre 1000 y 800 cm^{-1} y la vibración de deformación, ν_2, alrededor de 200 cm^{-1}.

Si el ión es lineal, solamente son activas en i.r. las frecuencias ν_3 y ν_2. Está muy bien establecido que la aparición de la banda correspondiente a ν_1 es coherente con una estructura angular del ión uranilo, en la que la vibración asimétrica sea más intensa que la simétrica correspondiente, hechos que se dan en los espectros de todos los complejos estudiados.

Heitner-Wirguin y Gantz[12], en su trabajo sobre les especies $[UO_2(SO_4)_2]^{2-}$ y $[UO_2(SO_4)_3]^{4-}$, absorbidas en cambiadores iónicos, identifican sólo una banda (a 910 y 905 cm^{-1}, respectivamente) que atribuyen a ν_3 y concluyen, en consecuencia, que el uranio retiene su linealidad al ser coordinado por los grupos sulfato.

Los espectros de los cristales de nuestros complejos, con éstas y otras estequiometrías, están en manifiesta desconexión con el trabajo anterior, no sólo en cuanto a la presencia bien definida en nuestros espectros de la banda atribuible al modo de vibración ν_1 (a 860 cm^{-1}), sino de la localización de ν_3 (a 940 cm^{-1}). Nuestras asignaciones (Tabla 2) están avaladas por la correspondencia entre ν_1 y ν_3 al obedecer las relaciones experimentales establecidas en la bibliografía :[13,14]

$$\nu_1 = 0{,}89\nu_3 + 21 \quad \text{y} \quad \nu_1 = 0{,}912\nu_3 - 1{,}04$$

Más aún, la resolución del espectrofotómetro ha permitido evidenciar el desdoblamiento de la banda ν_3 en la mayor parte de los complejos y de ν_1 en el caso particular $[UO_2(SO_4)_2]^{2-}$, consiguiéndose de este modo verificar el cumplimiento de las relaciones citadas entre los pares de picos correspondientes : 940 cm^{-1} (ν_3) y 858 cm^{-1} (ν_1) ; 954 cm^{-1} (ν_3) y 865 cm^{-1} (ν_1).

Dichas relaciones nos han servido también para advertir, en los espectros en los cuales ν_1 es única, que la banda atribuible a ese modo de vibración no es degenerada (como quizás pudiera pensarse) pues sólo se corresponde con uno de los componentes de ν_3 y no con los dos. La falta de la banda ν_1 atribuible al otro componente ν_3 indica que estamos ante un UO_2^{2+} lineal. Concluimos afirmando la coexistencia de dos agrupaciones diferentes UO_2^{2+}, curvada y lineal, en tales complejos (Tabla 2).

---

[12] C. Heitner-Wirguin y M. Gantz, *J. Inorg. Nuclear Chem.*, **35**, 3341 (1973).

[13] S. P. McGlynn, J. K. Smith y W. C. Neely, *J. Chem. Phys.*, **35**, 105 (1961).

[14] K. W. Bagnall y M. W. Wakerley, *J. Inorg. Nuclear Chem.*, **37**, 329 (1974).

Tabla 2

Frecuencias vibracionales, constantes de fuerza y distancias de enlace U–O de los sulfatos complejos de uranilo

	$[UO_2(SO_4)_2]^{2-}$	$[UO_2(SO_4)_3]^{4-}$	$[UO_2(SO_4)_4]^{6-}$
ν_3 (cm^{-1})	954 940	952 940	950 940
ν_1 (cm^{-1})	865 858	— 860	— 860
F_{U-O}(mdinas/Å)	7,461 7,266	7,438 7,290	7,411 7,290
$R_{U-O}(1)$ (Å)	1,722 1,727	1,723 1,729	1,724 1,729
$R_{U-O}(2)$ (Å)	1,686 1,699	1,687 1,694	1,688 1,694
	$[(UO_2)_2(SO_4)_3]^{2-}$	$[(UO_2)_2(SO_4)_4]^{4-}$	$[(UO_2)_2(SO_4)_5]^{6-}$
ν_3 (cm^{-1})	960 940	958 940	950–945
ν_1 (cm^{-1})	— 860	— 860	860
F_{U-O}(mdinas/Å)	7,539 7,290	7,520 7,290	7,343
$R_{U-O}(1)$ (Å)	1,720 1,729	1,721 1,729	1,724–1,726
$R_{U-O}(2)$ (Å)	1,682 1,694	1,682 1,694	1,688–1,691
	$[(UO_2)_3(SO_4)_4]^{2-}$	$[(UO_2)_3(SO_4)_5]^{4-}$	$[(UO_2)_3(SO_4)_6]^{6-}$
ν_3 (cm^{-1})	940 930	— 930	938 930
ν_1 (cm^{-1})	— 850 (835)	— 850	— 850
F_{U-O}(mdinas/Å)	7,275 7,154	7,154	7,247 7,154
$R_{U-O}(1)$ (Å)	1,727 1,730	1,730	1,728 1,730
$R_{U-O}(2)$ (Å)	1,694 1,700	1,700	1,696 1,700
	$[(UO_2)_4(SO_4)_7]^{6-}$		
ν_3 (cm^{-1})	947 931		
ν_1 (cm^{-1})	841		
F_{U-O}(mdinas/Å)	7,370 7,152		
$R_{U-O}(1)$ (Å)	1,725 1,730		
$R_{U-O}(2)$ (Å)	1,690 1,700		

En algunos espectros se observa una muy pequena banda alrededor de 900 cm^{-1}, que permitiría considerar en ciertos complejos un tercer vibrador UO_2^{2+}.

El desdoblamiento de bandas puede ser debido al "efecto de correlación de campo" en la celdilla unidad, en la que se espera que un número igual de moléculas puedan existir.

Si la celda elemental tiene cuatro moléculas, como en la sal $UO_2(SO_4)_2K_2 \cdot 2H_2O$,[15] y un centro de simetría, se puede considerar la interacción entre las vibraciones de $4/2=2$ agrupamientos UO_2^{2+}, conduciendo a la aparición de frecuencias inexistentes para un ión UO_2^{2+} aislado.

Estas últimas ideas, tomadas de los trabajos de varios autores [16-18] han de considerarse con prudente excepticismo, pues si bien ofrecen una explicación al fenómeno del desdoblamiento no son de aplicación general.

Se ha calculado la constante de fuerza para el enlace U—O y los valores obtenidos (Tabla 2) se han utilizado para determinar la distancia de enlace con dos ecuaciones de relación, la de Badger, debida a Jones [19] :

$$R_{U-O}(1) = \beta F_{U-O}^{-1/3} + d' \qquad (\beta = 1{,}08,\ d' = 1{,}17)$$

y la que es dada por McGlynn y col. en su trabajo [13] :

$$R_{U-O}(2) = 1{,}993\, F_{U-O}^{-1/3} + 0{,}666$$

Es lógico esperar que al incrementar el número de grupos sulfato coordinados ecuatorialmente al grupo $O \equiv U \equiv O$, se aprecie decrecimiento en el orden de enlace U—O, s.c., la distancia de enlace se haga mayor. A la vista de la Tabla 2 se observa que tales previsiones sólo se cumplen si forzamos los resultados, pues los valores de R_{U-O} (1 y 2) aumentan a medida que lo hace el número de grupos sulfato en las estequiometrías, pero de un modo muy leve y difícilmente apreciable (únicamente en la tercera cifra decimal). Las ligeras variaciones observadas se derivan de los débiles desplazamientos de la banda de uno de los componentes ν_3, ya que la localización del otro componente de ν_3 a 940 cm^{-1} y su correspondiente ν_1 a 860 cm^{-1} es prácticamente común.

Vibraciones fundamentales del ion sulfato.

El ion sulfato libre, de simetría T_d, tiene cuatro vibraciones fundamentales, dos de las cuales, ν_3 y ν_4, son activas en i.r. La simetría T_d se destruye por coordinación y cae a D_{2d}, C_{3v} ó C_{2v}. Si la bajada de simetría debe su origen a la coordinación del anión SO_4^{2-} por el metal, puede serlo de tres maneras : unidentada (C_{3v}), bidentada ó puenteada (ambas C_{2v}) en las que los modos normales de vibración se hacen activos en i.r. y las vibraciones degeneradas se separan.

En la Tabla 3 damos las correlaciones entre el grupo T_d y los grupos C_{2v} y C_{3v}.

Los sulfatos inorgánicos sencillos muestran una fuerte banda en la región 1215—1075 cm^{-1} atribuible a la ν_3 (F_2), seguida de la que debe asignarse a la vibración ν_1 (A_1) a 1020—970 cm^{-1}. Nuestros espectros dan una banda múltiple en el intervalo 1250—970 cm^{-1} con tres máximos a 1250 – 1220, 1120 y 1065 cm^{-1} y otra a 1010 cm^{-1} en correspondencia, pues, con el número de modos que debieran preveerse para las vibraciones de valencia ν_3 y ν_1 admitiendo simetría C_{2v}.

---

[15] J. Martin Gil y F. J. Martin Gil, esta Revista (en imprenta).

[16] J. Arenas, R. M. Rojas y J. Bermudez, *An. Quim.* (*ANQUBU*), **66**, 339 (1970).

[17] A. Ferrari, L. Cavalca y M. E. Tani, *Ann. Chim.*, **48**, 1230 (1958) ; **48**, 1244 (1958).

[18] H. Gerding, G. Prins y W. Gabes, *Rev. de Chim. Minerale*, **12**, 303 (1975).

[19] L. H. Jones, *Spectrochim. Acta*, **10**, 395 (1958) ; **11**, 409 (1959).

Tabla 3

Correlaciones entre el grupo de simetría T_d y los grupos C_{2v} y C_{3v}

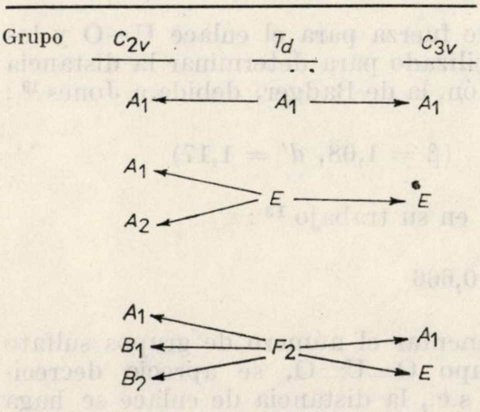

Una banda, fuerte y múltiple, con máximos a 645, 625 y 600 cm^{-1} ha sido también caracterizada, asignando los máximos a los tres modos A_1, B_1 y B_2 derivados de ν_4 (F_2).

La banda con picos a 480 (máximo) y 465 cm^{-1} puede ser atribuida a la vibración ν_2 (E).

Concluimos, en base a estos datos de desdoblamiento y posición, y siendo conscientes de que son difíciles de establecer con rigor, que los sulfatos tienen en los compuestos estudiados simetría C_{2v} (bidentada o puenteada). Reconocemos que con sólo datos de i.r. es arriesgado discernir entre sulfato unidentado (simetría C_{3v}) y los otros dos tipos citados. No obstante, al no disponer de estudios de polarización Raman, los datos i.r. deben ser aprovechados al máximo.

Curtis y al.[20] muestran que los sobretonos y bandas de combinación del grupo nitrato en los espectros de compuestos de uranilo pueden algunas veces ser utilizados para distinguir entre nitratos complejos monodentados y bidentados. Por ejemplo, la diferencia entre $\nu_2 + \nu_1$ y $\nu_2 + \nu_4$ es más grande en los bidentados (200 cm^{-1}) que en los monodentados (90 – 200 cm^{-1}). Los criterios aplicados por estos autores pueden ser de validez para los sulfatos complejos cuando aparezcan referencias de unidentados. En los trabajos sobre el ión $[UO_2(SO_4)_3]^{4-}$ el sulfato aparece como bidentado, pero no en base a razones deducidas de datos i.r. fundamentalmente, sino de otro tipo: Existe una presunción muy fuerte de que el número más usual de coordinación del grupo uranilo es seis. Serían precisos seis ligandos monodentados o tres bidentados y para estos autores[11,12,21] la elección fue obvia pues sólo contaban con tres grupos sulfato en su estequiometría. Razón a todas luces insuficiente para su aplicación a las restantes especies complejas.

Habría sido deseable que Heitner-Wirguin y Gantz[12] en la sección de su trabajo dedicada a espectros i.r. hubieran incluido el registro de los espectros o una tabla de frecuencias atribuibles a los iones sulfato pero sólo hacen constar la referencia a un pico a 645 cm^{-1} y de un modo más ambiguo aún que la asignación a ν_3 (UO_2^{2+}) ya referida.

---

[20] N. F. Curtis y Y. M. Curtis, *Inorg. Chem.*, **4**, 804 (1965).
[21] C. Deptula y S. Minc, *J. Inorg. Nuclear Chem.*, **29**, 221 (1967).

Revue Roumaine de Chimie, **23**, *11–12*, 1533–1539 (1978)

POLYNUCLEAR COMPLEX COMPOUNDS OF IRON, COBALT AND NICKEL. III[1]

BISMUTH – CONTAINING COMPLEX COMPOUNDS

MARIA BREZEANU and MAGDALENA DINCULESCU
Polytechnic Institute of Bucharest, Laboratory of Inorganic
Chemistry, Splaiul Independenţei, 202, Bucharest, Romania

Received March 2, 1977

A series of polynuclear complex compounds containing iron, cobalt, nickel and bismuth were synthesized. They correspond to the following general formulas : $[Fe(BiOCl)X_3]$, $[Fe(BiOCl)_2X_4]NH_4$; $[Co(BiOCl)_2X_2(H_2O)_2]$; $[Co(BiOCl)_2X_2]$, $X = Cl^-$, OH^- ; $[Co(BiOCl)Cl_3(H_2O)_2]NH_4$; $[Co(BiOCl)Cl_3]NH_4$; $[Co(BiOCl)Cl_2OH(H_2O)_2]NH_4$; $[Co(BiOCl)Cl_2OH]NH_4$. These complex compounds were characterized by elemental chemical analysis, electronic and vibrational spectra.

A previous paper [1] has reported the results obtained in the synthesis and characterization of compounds formed in the systems : $MX_n - BiX_3 -$ Base, were $M = Fe(III)$, $Co(II)$, $Ni(II)$, $X = Cl^-$, Base = NaOH.

In view of establishing the influence of the base used on the type of compounds which may be formed in such systems, the study of the same systems was extended using ammonia as a base.

A series of polynuclear complex compounds containing the mentioned elements were obtained and they may be represented by the following general formulas : $[Fe(BiOCl)X_3]$, $[Fe(BiOCl)_2X_4]NH_4$; $[Co(BiOCl)_2X_2(H_2O)_2]$; $[Co(BiOCl)_2X_2]$, $X = Cl^-$, OH^- ; $[Co(BiOCl)Cl_3(H_2O)_2]NH_4$; $[Co(BiOCl)Cl_3]NH_4$, $[Co(BiOCl)Cl_2OH(H_2O)_2]NH_4$, $[Co(BiOCl)Cl_2OH]NH_4$.

The compounds obtained were characterized by elemental analysis, vibrational and electronic spectra.

RESULTS AND DISCUSSION

The nature of species formed in the systems investigated was established by conducting the synthesis of these compounds under various conditions with regard to the following parameters : the $MX_n : BiX_3$ ratio and the pH of the reaction medium.

To establish the contribution of the first parameter, i.e. the ratio of components, we maintained constant the amount of iron, cobalt and nickel chloride, respectively, progressively varying the amount of bismuth chloride from a ratio of 1 : 1, 1 : 2, to excess.

---

[1] Part II : M. Brezeanu and M. Dinculescu, *Rev. Roumaine Chim.*, **9–10**, 1389 (1978).

It must be noted that for each system, the maximum amount of fixed bismuth chloride corresponds to a 1 : 2, $MCl_n : BiCl_3$ ratio even if a high excess of bismuth chloride is used in the synthesis.

The presence of the BiOCl species as a ligand in the coordination sphere of such compounds is justified by the very marked tendency of bismuth (III) to hydrolyse even in acidic medium. More than that the conditions established in order to obtain these combinations are practically the same as those indicated by literature for the obtaining of BiOCl.[2,3]

The second parameter, i.e. the pH of the reaction medium seems to influence the composition of the coordination sphere.

Syntheses were conducted at a $pH = 7, 10$ and ammonium hydroxide in excess ($pH = 12-13$). It was found that the total substitution (iron compounds) or the partial substitution (some cobalt compounds) of the chlorine ligands present in the coordination sphere with hydroxyl groups, takes place with the increasing basicity of the reaction medium, analogous to the MCl_n-BiCl_3-NaOH system. Unlike the latter, the total substitution of chlorine by hydroxyl was however possible for cobalt compounds in which the $CoCl_2-BiCl_3$ ratio is 1 : 2.

A series of polynuclear complex compounds containing the above mentioned elements have been obtained as a result of this study. They may be represented by the following general formulas :

— for a ratio $1\ MCl_n - 1\ BiCl_3$, M = Fe, Co, Ni and $pH = 6-7$ and 10 respectively, the compounds : $[Fe(BiOCl)X_3]$, $X = Cl^-, OH^-$; $[Co(BiOCl)Cl_3]NH_4$, $[Co(BiOCl)Cl_3(H_2O)_2]NH_4$, $[Co(BiOCl)Cl_2OH]NH_4$, $[Co(BiOCl)Cl_2OH(H_2O)_2]NH_4$.

— for a ratio $1\ MCl_n : 2\ BiCl_3$, $1\ MCl_n$: excess $BiCl_3$ respectively, and the same pH values, compounds : $[Fe(BiOCl)_2X_4]NH_4$, $[Co(BiOCl)_2X_2]$, $[Co(BiOCl)_2X_2(H_2O)_2]$, $X=Cl^-, OH^-$.

— by using an excess of ammonia ($pH = 12,13$), compounds : $[Co(BiOCl)Cl(OH)_2]NH_4$ and $[Co(BiOCl)Cl(OH)_2(H_2O)_2]NH_4$, regardless of the value of the $MCl_n : BiCl_3$ ratio. Under these conditions, in the case of iron, one obtains the same compounds as with a $pH = 10$, i.e. : $[Fe(BiOCl)(OH)_3]$ respectively $[Fe(BiOCl)_2(OH)_4]NH_4$.

It must be specified that for nickel the separation of such compounds was not possible under the mentioned conditions, a fact explained by the high stability of nickel hexamine which is formed in ammonia medium.

Like the analogous compounds in the system $FeCl_3-BiCl_3-NaOH$, the iron brown compounds exist under the form of one single modification.

A characteristic property of complex compounds containing bivalent cobalt as a central metal ion is their existence in two differently coloured modifications, i.e. light blue and light pink. The pink modification represents the stable species in solid state.

By heating to 110°, the pink compounds : $[Co(BiOCl)Cl_3(H_2O)_2]NH_4$, $[Co(BiOCl)Cl_2OH(H_2O)_2]NH_4$, $[Co(BiOCl)_2X_2(H_2O)_2]$, $X = Cl^-, OH^-$, change to the corresponding blue modifications.

---

[2] "Gmelins Handbuch der anorganischen Chemie" — Wismut — 1964, p. 692, p. 693.

[3] P. PASCAL, "Nouveau Traite de Chimie Minerale" vol. 11, 1958, p. 753.

This transition is accompained by a variation in weight corresponding to the loss of the two water molecules.

Based on electronic spectra, an octahedral structure was attributed to pink modifications and a tetrahedral one to the blue modifications. This fact leads to the conclusion that the two water molecules act as ligands contributing to the hexacoordination of the cobalt ion.

At room temperature, in time, the blue modifications turn pink again, hence the transformation is reversible.

Based on electronic and vibrational spectra correlated with the elemental chemical analysis, a tetrahedral structure was assigned to iron complex compounds : $[Fe(BiOCl)X_3]$, while an octahedral structure was assigned to compounds $[Fe(BiOCl)_2X_4]NH_4$, $X = Cl^-, OH^-$.

It seems that in such compounds and in cobalt compounds too, the BiOCl group acts as ligand alongside with the other chlorine ligands respectively the hydroxyl group.

In order to confirm the formula given to these combinations one has registered the spectrum of X beams : $[Fe(BiOCl)_2Cl_4]NH_4$. The fund noise being linear till the accentuation of Lorenz's factor shows that the substance analysed is not polymer. In the same way, from values of the reticular parameters so obtained, one reaches the conclusion that the main cell appears double — as dimensions — taking into account the parameter C (001).

I.R. SPECTRA

The vibration spectra of some of the complex compounds obtained were recorded, to obtain additional data on their structure.

The most important from this point of view are those spectral domains in which absorption is attributed to the vibration modes of the BiOCl molecule, of the OH^- and NH_4^+ ions.

In view of making the most exact possible assignment of absorption bands of the mentioned ligands, table 1 presents comparatively the vibration frequencies characteristic of the free and the coordinated ligands.

An examination of the data listed in this table shows the following :

— the presence in the spectra of all the investigated compounds of the characteristic ν_{Bi-O} vibration frequency at values close to those reported in the literature.[4] The existence of such frequencies represents a guarantee for the presence of ligand BiOCl in the compounds obtained.

— the presence in the spectra of compounds containing the hydroxyl group of the characteristic frequencies of its vibration modes in hydrocomplexes.

— the existence in the spectra of compounds containing the NH_4^+ ion of the three characteristic absorption bands, slightly modified.

The study of the vibration spectra of cobalt pink compounds also indicates the presence of some absorption bands in the domain 650—880 cm^{-1} which, according to Gamo [5] belong to the rocking and wagging

---

[4] A. Rulmont, *Compt. rend.*, **272**, 1364 (1971).

[5] J. Gamo, *Bull. Chem. Soc. Japan*, **760**, 1430 (1961).

Table 1

Characteristic I.R. freqeuncies of synthesized complex compounds (cm^{-1})

Compound	νBi−O	νBi−Cl	νOH	δM−OH	νNH_3	$\delta a(NH_3)$	$\delta s(NH_3)$
BiOCl	535−540	260	—	—	—	—	—
NH_4Cl	—	—	—	—	3138	1710	1403
OH(hidroxocomplexes)	—	—	3200− 3500	970 1100	—	—	—
$[Fe(BiOCl)(OH)_3]$	539	—	3436	1073	—	—	—
$[Fe(BiOCl)_2(OH)_4] \cdot NH_4$	538	—	3440	1060	3150	1706	1408
$[Fe(BiOCl)_2Cl_4] \cdot NH_4$	537	—	—	—	3146	1705	1410
$[Co(BiOCl)Cl_3(H_2O)_2]NH_4$ (pink)	538	—	—	—	3140	1705	1412
$[Co(BiOCl)Cl_3]NH_4$ (blue)	537	—	—	—	3139	1702	1410
$[Co(BiOCl)_2Cl_2(H_2O)_2]$ (pink)	537	—	—	—	—	—	—
$[Co(BiOCl)_2Cl_2]$ (blue)	538	—	—	—	—	—	—
$[Co(BiOCl)_2(OH)_2(H_2O)_2]$	536	—	3418	1068	—	—	—

vibration modes of the coordination water. Such absorption bands are not found in the spectra of blue corresponding compounds, a fact which is in agreement with the absence of the coordinated water in such compounds.

ELECTRONIC SPECTRA

Electronic reflexion spectra were recorded to obtain some information on the structure of complex compounds isolated in the systems under consideration.

A study of electronic spectra of compounds : $[Fe(BiOCl)X_3]$, $X = Cl^-$, OH^-, shows that their most likely structure is tetrahedral (Figure 1−1,2), the band at approximately 800 nm being attributed to the $E_4 \leftarrow {}^6A_1$ spin — forbidden transition.

The electronic spectra recorded for the compounds : $[Fe(BiOCl)_2X_4]NH_4$, $X = Cl^-, OH^-$, (Figure 1−3,4), may be satisfactorily interpreted in terms of an octahedral structure.

Thus the band appearing at about 780 nm is attributed to the spin forbidden transition ${}^4T_{1g} \rightarrow {}^6A_{1g}$, for a d^5 (Fe III) ion in an octahedral surrounding.

For the corresponding cobalt pink compounds $[Co(BiOCl)Cl_3(H_2O)_2]NH_4$, $[Co(BiOCl)Cl_2OH(H_2O)_2]NH_4$, $[Co(BiOCl)_2X_2(H_2O)_2]$, $X = Cl^-$, OH^- (Figure 2) the recorded electronic

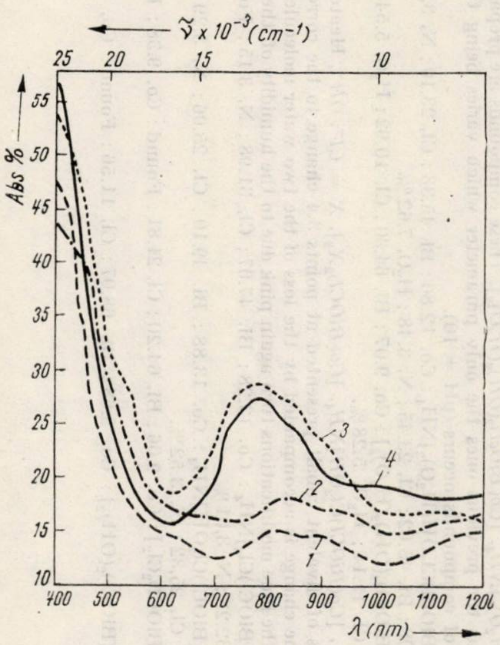

Fig. 1. — Electronic spectra of iron — containing compounds :

1. $[Fe(BiOCl)Cl_3]$; 2. $[Fe(BiOCl)(OH)_3]$;
3. $[Fe(BiOCl)_2Cl_4]NH_4$;
4. $[Fe(BiOCl)_2(OH)_4]NH_4$.

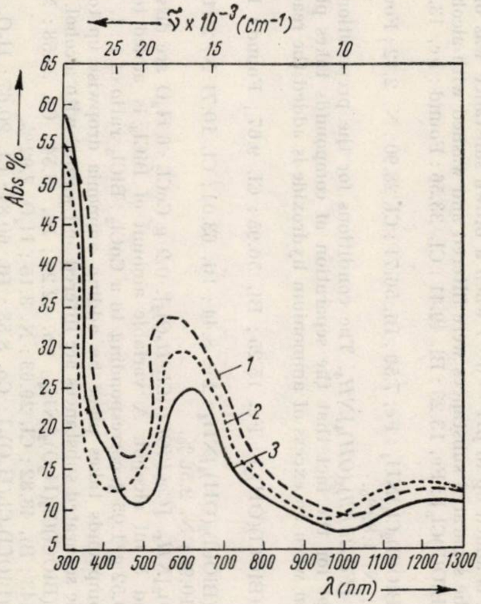

Fig. 2. — Electronic spectra of the pink cobalt compounds :

1. $[Co(BiOCl)Cl_3(H_2O)_2]NH_4$;
2. $[Co(BiOCl)Cl_2OH(H_2O)_2]NH_4$
3. $[Co(BiOCl)_2X_2(H_2O)_2]$.

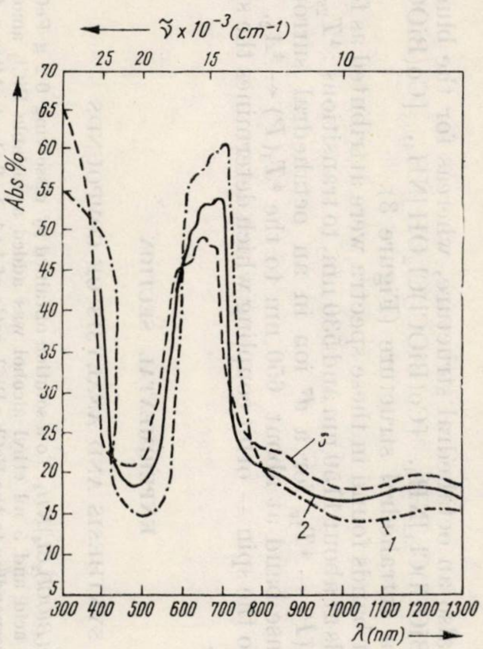

Fig. 3. — Electronic spectra of the blue cobalt compounds :

1. $[Co(BiOCl)Cl_3]NH_4$;
2. $[Co(BiOCl)Cl_2OH]NH_4$;
3. $[Co(BiOCl)_2X_2]$.

spectra indicate also an octahedral structure, whereas for the blue modifications : $[Co(BiOCl)Cl_3]NH_4$, $[Co(BiOCl)Cl_2OH]NH_4$, $[Co(BiOCl)_2X_2]$, $X = Cl^-$, OH^-, a tetrahedral structure (Figure 3).

The present bands found in these spectra were attributed as follows :

— the bands at about 1150 nm and 530 nm, to transitions : ${}^4T_{2g} \leftarrow {}^4T_{1g}$ respectively ${}^4T_{1g}(P) \leftarrow {}^4T_{1g}$ for a d^7 ion in an octahedral surrounding.

— the intense band at about 650 nm to the ${}^4T_1(P) \leftarrow {}^4A_2$. Its fine structure is due to the spin — orbit coupling which determines the splitting of the ${}^4T_1(P)_{\text{term}}$.

EXPERIMENTAL SECTION

I. SYNTHESIS AND ANALYSIS OF COMPOUNDS

1. $[Fe(BiOCl)Cl_3]$, $[Fe(BiOCl)_2Cl_4]NH_4$. To a solution obtained by dissolving 0.2 g $FeCl_3 \cdot 6H_2O$ in 3 ml hydrochloric acid and 5 ml ethyl alcohol was added a variable $BiCl_3$ amount, i.e. : 0.22, 0.44, 0.88 g, corresponding to the $FeCl_3 : BiCl_3$ ratio of 1 : 1, 1 : 2, 1 : 4. After a few hours of standing, ammonia is added up to pH = 6—7 when a brown substance was obtained. After about half an hour, the separated substances were filtered and washed with alcohol.

Calcd. for $[Fe(BiOCl)Cl_3]$: Fe, 13.23 ; Bi, 49.41 ; Cl, 33.56 ; Found : Fe, 13.32 ; Bi, 49.61 ; Cl, 33.86 %.

Calcd. for $[Fe(BiOCl)_2Cl_4]NH_4$: Fe, 7.59 ; Bi, 56.71 ; Cl, 28,90 ; N, 2.12 ; Found : Fe, 7.82 ; Bi, 57.08 ; Cl, 29.36 ; N, 1.89 %.

2. $[Fe(BiOCl)(OH)_3]$, $[Fe(BiOCl)_2(OH)_4]NH_4$. The conditions for the preparation are identical with the above except for the fact that the separation of compounds takes place beginning with a pH = 10. Even when an excess of ammonium hydroxide is added the reaction products will be the same.

Calcd. for $[Fe(BiOCl)(OH)_3]$: Fe, 15.25 ; Bi, 56.95 ; Cl, 9.67 ; Found : Fe, 15.62 ; Bi 57.12 ; Cl, 10.01 %.

Calcd. for $[Fe(BiOCl)_2(OH)_4]NH_4$: Fe, 8.44 ; Bi, 63.04 ; Cl, 10.71 N, 2.11 ; Found : Fe, 8.26 ; Bi, 63.46 ; Cl, 10.98 ; N, 2.56 %.

3. $[Co(BiOCl)Cl_3(H_2O)_2]NH_4$, $[Co(BiOCl)_2Cl_2(H_2O)_2]$. 0.2 g $CoCl_2 \cdot 6\,H_2O$ are dissolved in 3 ml hydrochloric acid and 5 ml alcohol. A variable amount of $BiCl_3$ is added to the solution obtained, i.e. 0.26 g, 0.52 g, 1.05 g, corresponding to a $CoCl_2 : BiCl_3$ ratio of 1 : 1, 1 : 2, . . . 1 : 4. The separation of compounds takes place by adding ammonia dropwise up to a pH = 6,7. After half an hour, the separated substances are filtered and washed with alcohol.

Calcd. for $[Co(BiOCl)Cl_3(H_2O)_2]NH_4$: Co, 12.29 ; Bi, 43.54 ; Cl, 29.58 ; N, 2.92 ; H_2O, 7.50 ; Found : Co, 12.43 ; Bi, 43.82 ; Cl, 29.63 ; N, 3.15 ; H_2O, 7.92 %.

Calcd. for $[Co(BiOCl)_2Cl_2(H_2O)_2]$: Co, 8.58 ; Bi, 60.84 ; Cl, 20.67 ; H_2O, 5.24 ; Found : Co, 8.91 ; Bi, 61.13 ; Cl, 20.83 ; H_2O, 5.78 %.

4. $[Co(BiOCl)Cl_2OH(H_2O)_2]NH_4$, $[Co(BiOcl)_2(OH)_2(H_2O)_2]$. These compounds are prepared under analogous conditions as the previous ones the only parameter which varies being the pH at which the separation of compounds occurs (pH = 10).

Calcd. for $[Co(BiOCl)Cl_2OH(H_2O)_2]NH_4$: Co, 12.80 ; Bi, 45.33 ; Cl, 23.10 ; N, 3.03 ; H_2O, 7.81 ; Found : Co, 13.08 ; Bi, 45.62 ; Cl, 23.45 ; N, 3.48 ; H_2O, 7.62 %.

Calcd. for $[Co(BiOCl)_2(OH)_2(H_2O)_2]$: Co, 9.07 ; Bi, 64.30 ; Cl, 10.92 ; H_2O, 5.54 ; Found : Co, 9.28 ; Bi, 64.62 ; Cl, 11.14 ; H_2O, 5.28 %.

5. $[Co(BiOCl)Cl_3]NH_4$, $[Co(BiOCl)Cl_2OH]NH_4$, $[Co(BiOCl)_2X_2]$, $X = Cl^-, OH^-$. Heated to 110° the pink modifications of divalent cobalt presented at points 3,4 change to the corresponding blue modifications. The change is accompanied by the loss of the two water molecules. Left in the air, in solid state, the blue modifications turn again pink due to the humidity of the medium.

Calcd. for $[Co(BiOCl)Cl_3]NH_4$: Co, 13.28 ; Bi, 47.07 ; Cl, 31.98 ; N, 3.15 ; Found : Co, 13.05 ; Bi, 46,65 ; Cl, 32.23 ; N, 3.01 %.

Calcd. for $[Co(BiOCl)Cl_2OH]NH_4$: Co, 13.88 ; Bi, 49.10 ; Cl, 25.06 ; N, 3.29 ; Found : Co, 14.07 ; Bi, 49.43 ; Cl, 25.32 ; N, 3.52 %.

Calcd. for $[Co(BiOCl)_2Cl_2]$: Co, 9.06 ; Bi, 64.20 ; Cl, 21.81 ; Found : Co, 9.38 ; Bi, 64.86 ; Cl, 22.15 %.

Calcd. for $[Co(BiOCl)_2(OH)_2]$: Co, 9.68 ; Bi, 68.07 ; Cl, 11.56 ; Found : Co, 9.92 ; Bi, 68.53 ; Cl, 11.93 %.

It can be observed that for the complex compounds synthesized until this point, the maximum M—Bi ratio (M = Fe, Co) that can be achieved in such compounds is 1 : 2, even when working an excess of bismuth chloride.

6. $[Co(BiOCl)Cl(OH)_2(H_2O)_2]NH_4$ *(pink)*, $[Co(BiOCl)Cl(OH)_2]NH_4$ *(blue)*. To the solution, obtained by dissolving 0.2 g $CoCl_2 \cdot 6\,H_2O$ in 3 ml hydrochloric acid and 5 ml alcohol, is added a variable $BiCl_3$ amount, i.e. : 0.22 g, 0.44 g, 0.88 g corresponding to the $CoCl_2 : BiCl_3$ ratio of 1 : 1, 1 : 2 . . . 1 : 4. By using in syntheses an excess of amonium hydroxide (pH = 12—13) it was possible to obtain only compounds in which the metal-bismuth ratio was 1 : 1, regardless of the amount of bismuth chloride involved.

The separated substances are filtered after half an hour and are thoroughly washed with alcohol.

Calcd. for $[Co(BiOCl)Cl(OH)_2(H_2O)_2]NH_4$ (pink) : Co, 8.98 ; Bi, 31.81 ; Cl, 32.42 ; N, 10.65 ; H_2O, 5.48% ; Found : Co, 9.02 ; Bi, 32.15 ; Cl, 32.98 ; N, 11.15 ; H_2O, 5.63%.

Calcd. for $[Co(BiOCl)Cl(OH)_2]NH_4$ (blue) : Co, 14.49 ; Bi, 51.10 ; Cl, 17.44 ; N, 3.44 ; Found : Co, 14.75 ; Bi, 51.62 ; Cl, 17.12 ; N, 3.89%.

II. The electronic spectra were recorded at room temperature using a VSU_1 spectrophotometer, with magnesium oxide as a reference.

III. The I.R. spectra were obtained by means of a UR—20 spectrophotometer using potassium pellets.

Revue Roumaine de Chimie, **23**, *11-12*, 1541-1552 (1978)

REACTIONS OF 3′,4′-DIMETHYLCHALCONE AND ITS DERIVATIVES

A. ABDEL MAKSOUD *, G. HOSNI *, O. HASSAN ** and S. SHAFIK **

* Chemistry Department, Faculty of Science, Ain Shams University
** Central National Research, Dokki, Cairo, E.A.R.

Received October 1, 1976

The alkylation of aromatic hydrocarbons with 3′,4′-dimethyl chalcone using Grignard and Friedel-Crafts reactions has been investigated. A number of pyrazolines and isoxazolines has been synthesized by the action of hydrazines and hydroxylamine-hydrochloride on chalcones. The reduction of pyrazolines with lithium-aluminium-hydride has been also investigated. The pyrazolines are converted to Mannich bases, and β-ketosulphide are prepared from the chalcone. The structures of these compounds have been studied both chemically and spectroscopically.

The reaction of chalcones with Grignard reagents has been reported.[1-3] The present investigation explored the alkylation of aromatic hydrocarbons with 3′, 4′-dimethylchalcone (1a) and 3,4-methylenedioxy-3′, 4′-dimethylchalcone (1b) with the Grignard reagents. Thus, treatment of chalcones 1a, b with methyl-iodide, phenyl-bromide, benzyl-chloride and/or α-naphthylmagnesium-bromide provided the 3,3-diarylpropiophenone derivatives (2a–h).

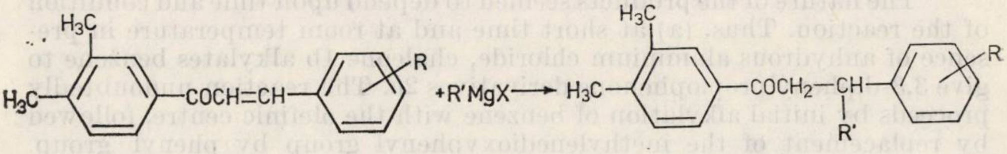

(1) **(2)**

a, R = H
b, R = $3,4-O_2CH_2$

	R	R′
a,	H	CH_3
b,	$3,4-O_2CH_2$	CH_3
c,	H	C_6H_5
d,	H	$C_6H_5CH_2$
e,	H	$C_{10}H_{7-(\alpha)}$
f,	$3,4-O_2CH_2$	C_6H_5
g,	$3,4-O_2CH_2$	$C_6H_5CH_2$
h,	$3,4-O_2CH_2$	$C_{10}H_{7-(\alpha)}$
i,	$C_6H_3(CH_3)_2(2,5)$	$C_6H_3(CH_3)_2(2,5)$
j,	$C_6H_4CH_3(p)$	$C_6H_4CH_3(p)$

---

[1] E. P. Kohler, *Am. Chem. J.*, **29**, 352 (1903).
[2] E. P. Kohler, *Am. Chem., J.*, **31**, 642 (1904).
[3] A. Sammour and M. Elkassaby, *U.A.R.J. Chem.* **13**, 409 (1970).

The followings come in support of the structures assigned to products 2 :

(1) Analytical values;

(2) i.r. Spectra of 20-g showed well defined absorption bands attributable for the carbonyl group at 1685—1680 cm^{-1};

(3) The products 2b—g gave hydrazone derivatives on treatment with hydrazine hydrate. The ir spectra of hydrazone derivatives lack the stretching frequency of $C=O$ but show the band of $C=N$ at 1620—1600 cm^{-1}.

(4) The products 2a, b, c, e, g, h gave oxime derivatives on treatment with hydroxylamine-hydrochloride. The infrared spectra of the oximes lack the stretching frequencies of $C=O$ and show bands of ν $C=N$ at 1610 cm^{-1};

(5) The product 2g reacts with benzaldehyde in the presence of potassium hydroxide to give the benzal derivative 3 showing that 2 has an active methylene group.

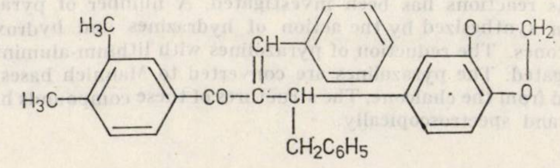

(3)

(6) Authentically, 3′, 4′-dimethylchalcone (1a) gave with benzene, under the Friedel-Crafts conditions, 2c, identified by melting point and mixed melting point experiment.

The alkylation of aromatic rings with chalcones in presence of anhydrous aluminium chloride has been reported.[3–10] This method has been applied in the present investigation to chalcones 1a, b with the same results.

The nature of the products seemed to depend upon time and condition of the reaction. Thus, (a) at short time and at room temperature in presence of anhydrous aluminium chloride, chalcone 1b alkylates benzene to give 3,3-diphenylpropiophenone derivatives 2c. The reaction undoubtedly proceeds by initial alkylation of benzene with the olefinic centre, followed by replacement of the methylenedioxyphenyl group by phenyl group.

This is confirmed from the reaction of 2f with benzene under the same conditions when 2c was obtained through replacement of the methylenedioxyphenyl group by phenyl group. Compounds 1a and 1b alkylate *p*-xylene in a similar manner to give only the compound 2i.

Also, 1a and 1b alkylate toluene in the same manner to give 2j. The structure of 2j was proved;

(a) Authentically via the reaction of 4,3′, 4′-trimethyl chalcone (1c) with *p*-tolylmagnesium bromide in dry ether to give 2j, identified by melting point and mixed melting point.

[4] D. VORLANDER, and A. FRIEDBERG, *Ber., dtsch. Chem. Ges.*, **56,** 1144 (1923).

[5] J. T. EASTON, D. B. BLACK, and R. C. FUSON, *J. Amer. Chem. Soc.*, **56,** 787 (1934).

[6] J. F. J. DIPPY and A. L. L. PALLUEL, *J. Chem. Soc.*, 1415 (1951).

[7] E. P. KOHLER, G. L. HERTAGE, and M. O. BURNLY, *Am. Chem. J.*, **44,** 60, (1910).

[8] K. O. JOSHI and A. K. JAUHER, *J. Indian Chem. Soc.*, **43,** 368 (1966).

[9] S. M. MUKHERJII, O. P. VIG, and N. MAHESHWAY, *J. Indian Chem. Soc.*, **43,** 9 (1957).

[10] J. COLONGE and L. PICHAT, *Bull. Soc. chim. France,* **15,** 177 (1949), **16,** 421 (1949).

(b) On the other hand, when the reaction time was prolonged at room temperature in the presence of anhydrous aluminium chloride and hydrogen chloride, the reaction of the chalcones 1a and 1b with toluene yielded directly indene derivative 4.

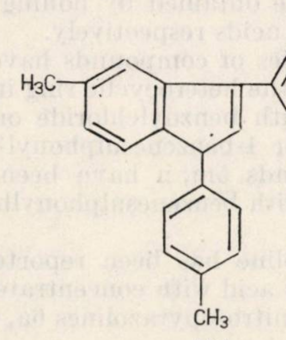

(4)

The reaction may proceed by initial alkylation of toluene with the olefinic centre accompanied by replacement of the phenyl and methylenedioxyphenyl group by tolyl group and followed by ring closure of the intermediate aryl-substituted propiophenones. This ring closure is accomplished by electrophilic intramolecular alkylation with β-arylcarbonyl compound yielding the indene derivative 4.

Pyrazolines are often formed by the direct action of hydrazines on the unsaturated carbonyl compounds.[11] In the present investigation the chalcones 1a, b were allowed to react with hydrazine hydrate in alcohol, acetic, formic, propionic and isobutyric acids to give the corresponding pyrazolines (5a—v).

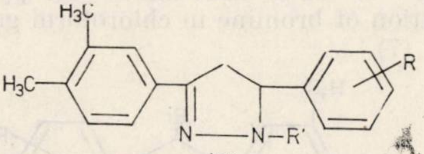

(5)

	R	R′		R	R′
a,	H	H	l,	$3,4-O_2CH_2$	COC_6H_5
b,	$3,4-O_2CH_2$	H	m,	H	$O_2SC_6H_5$
c,	H	$COCH_3$	n,	$3,4-O_2CH_2$	$O_2SC_6H_5$
d,	$3,4-O_2CH_2$	$COCH_3$	o,	$3,4-O_2CH_2$	CH_2CH_2CN
e,	H	CHO	p,	$3,4-O_2CH_2$	$CH_2CH_2CH_3$
f,	$3,4-O_2CH_2$	CHO	q,	H	$CH_2CH(CH_3)_2$
g,	H	$COCH_2CH_3$	r,	$3,4-O_2CH_2$	$CH_2CH(CH_3)_2$
h,	$3,4-O_2CH_2$	$COCH_2CH_3$	s,	H	C_6H_5
i,	H	$COCH(CH_3)_2$	t,	$3,4-O_2CH_2$	C_6H_5
j,	$3,4-O_2CH_2$	$COCH(CH_3)_2$	u,	H	$2,4C_6H_3(NO_2)_2$
k,	H	COC_6H_5	v,	$3,4-O_2CH_2$	$2,4C_6H_3(NO_2)_2$

---

[11] A. Sammour, M. I. B. Selim and G. H. Elsayed, *U.A.R.J. Chem.*, **14**, 235 (1971).

The i.r. spectra of 5a, c, f, g, i showed the $C{=}N$ stretching frequency at 1620—1600 cm^{-1}; compound 5a showed the NH stretching frequency at 3145 cm^{-1}; and 5c, f, g, i showed the CO stretching frequency in the region of 1670—1660 cm^{-1}.

3) Pyrazolines 5c—j can also be obtained by boiling 5a, b with acetic, formic, propionic and isobutyric acids respectively.

In this investigation a series of compounds have been prepared in order to study the behaviour of the heterocyclic ring in pyrazolines.

Pyrazolines 5a, b react with benzoylchloride or benzenesulphonyl chloride to give the 1-benzoyl-or 1-benzenesulphonyl-pyrazolines 5k—n.

Authentically the compounds 5m, n have been also prepared by the reaction of chalcones 1a, b with benzenesulphonylhydrazine in boiling alcohol.

The nitrosation of pyrazoline has been reported.[12] Treatment of pyrazolines 5a, b in hydrochloric acid with concentrated aqueous solution of sodium nitrite afforded the 1-nitrosopyrazolines 6a, b.

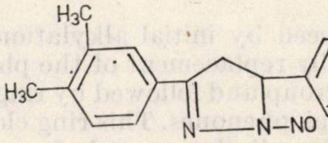

(6)

R
a, H
b, $3,4-O_2CH_2$

The i.r. spectrum of 6b showed the $C{=}N$ stretching frequency at 1620 cm^{-1} and of $N{-}N{=}O$ at 1380 cm^{-1}. The pyrazolines 5a, b when treated with a solution of bromine in chloroform gave the corresponding 4-bromopyrazolines (7).

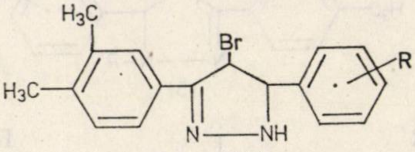

(7)

a, $R = H$
b, $R = 3,4-O_2CH_2$

Treatment of 5b with acrylonitrile afforded the 1-(β-cyanoethyl) pyrazoline (5*o*).

Cyanoethylation of pyrazoline is not unusual.[13]. Thus, treatment of methanolic solutions of pyrazolines 5a, b with secondary amines, namely piperidine and/or morpholine and aqueous formaldehyde yielded N-Mannich bases (8a, b).

---

[12] J. Elguero and R. Jacquier, *Bull. Soc. chim. France*, **3**, 769 (1965); *Chem. Abstr.*, **63**, 595 (1965).

[13] A. N. Kost and G. A. Golubeva, *Zhur. Obschei Khim.*, **30**, 494 (1960); *Chem. Abstr.*, **54**, 24671 (1960).

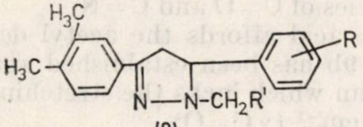

(8)

	R	R′
a,	H	NC_5H_{10}
b,	$3,4-O_2CH_2$	NC_4H_8O
c,	$3,4-O_2CH_2$	NC_5H_{10}

The i.r. spectra of 8a, b indicated the presence of C=N (1620 cm^{-1}) group.

It was stated previously [14] that the reduction of 4-ethyl-N-formyl-5-propyl-2-pyrazoline with lithium-aluminium-hydride in ether gives 4-ethyl-N-methyl-5-propylpyrazolidine. On the other hand, refluxing N-propyl-3,5,5-trimethyl-2-pyrazoline in toluene containing lithium-aluminium-hydride affords opening of the pyrazoline ring.

In the present investigation, it was found that two reactions can take place, namely, (a) only the reduction of the C=O with the formation of the corresponding N-alkylpyrazolines and, (b) reduction of both C=O and C=N groups with the formation of the corresponding N-alkylpyrazolidine. The nature of the products seemed to depend on time and conditions of the reaction.

Therefore, at short reaction time and in the presence of lithium-aluminium-hydride (1 : 1 mole) the pyrazolines 5h—j are reduced to the corresponding N-alkylpyrazolines (5p—r).

The structure of 5p—r has been established apart from the analytical data, by their i.r. spectra which show a band at 1620—1610 cm^{-1} characteristic of ν C=N and lack the stretching frequencies of NH and C=O groups.

On the other hand, when the reaction time was prolonged in the presence of excess of lithium-aluminium-hydride, the pyrazoline 5 l is reduced to the corresponding N-benzylpyrazolidine derivative (9a).

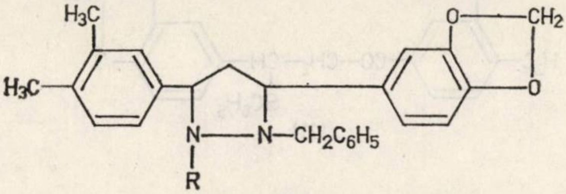

(9)

a, R = H
b, R = $COCH_3$

---

[14] A. N. Kost, M. A. Lapitskaya, G. A. Golubeva and S. M. Sernikova, *Zhur. Org. Khim.*, **4**, 752 (1969); *Chem. Abstr.*, **71**, 22063 (1969).

The structure of 9 has been established from :

1) Analytical data.

2) i.r. spectrum which showed a band corresponding to NH and lacks the stretching frequencies of C=O and C=N.

3) Boiling 9a in acetic acid affords the acetyl derivative 9b.

The structure of 9b has been established apart from the analytical data, by its i.r. spectrum which lacks the stretching frequency of NH and shows a band at 1660 cm^{-1} (ν C=O).

The action of phenylhydrazine and 2,4-dinitrophenylhydrazine has also been investigated. Thus the chalcones 1a, b were allowed to react with phenylhydrazine and 2 :4-dinitrophenylhydrazine in boiling alcohol to give the corresponding 1-aryl-pyrazolines (5s—v).

The behaviour of chalcones 1a, b towards the hydroxylamine-hydrochloride has now been investigated. Thus, the chalcones 1a, b were allowed to react with hydroxylamine-hydrochloride in boiling alcohol and gave the corresponding isoxazolines 10a, b.

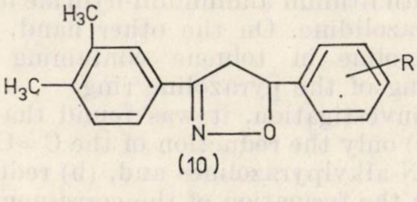

(10)

a, R = H

b, R = 3,4—O_2CH_2

The i.r. spectrum of 10b showed a band assigned to C=N (1610 cm^{-1}).

The behaviour of chalcones towards mercaptans has been reported.[15] In the present investigation the chalcone 1b reacts with thiophenol in the presence of piperidine to afford the β-ketosulphide 11. The i.r. spectrum of 11 showed a strong band at 1690 cm^{-1} (C=O). The structure of 11 was further confirmed by heating it with a slight excess of phenylhydrazine in acetic acid whereby 5t was obtained and identified by melting point and mixed melting point.

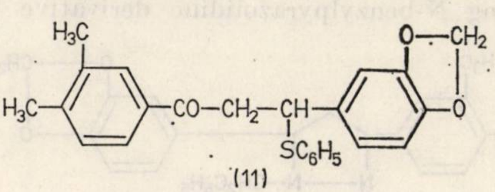

(11)

EXPERIMENTAL

i.r. Spectra were measured with a Unicam SP 1200 Spectrophotometer using KBr wafer technique. All melting points are uncorrected.

---

[15] A. Sammour and M. Elkassaby, *U.A.R.J. Chem.*, **13**, 243 (1970).

ACTION OF GRIGNARD REAGENTS ON CHALCONES 1. FORMATION OF 2

A solution of the chalcones (1a or b) (0.01 mole) in ether (200 ml) was added to an ethereal solution of methyl-, phenyl-, benzyl- or α-naphthyl-magnesium bromide (0.03 mole) during 30 min. The mixture was heated under reflux for 4 hrs, stood overnight at room temperature and then decomposed with ice-cold saturated aqueous ammonium chloride. The separated organic layer was washed with water and dried. On removal of the solvent the viscous oil obtained was triturated with light petrol (b.p. 40−60°) and the products were crystallized from the suitable solvent to give 2 as colourless crystals (Table 1).

Table 1

3,3-Diarylpropiophenones (2)

Compd	m.p. (°C)	Solvent	Formula	Analyses % Found C	H	Required C	H
2 a	48	pet. ether 40−60°	$C_{18}H_{20}O$	85. 8	8.00	85.67	7.99
2 b	65	pet. ether 40−60°	$C_{19}H_{20}O_3$	77. 3	6.9	77.00	6.80
2 c	109	ethanol	$C_{23}H_{22}O$	87. 6	7.1	87.86	7.05
2 d	90	pet. ether 60−80°	$C_{24}H_{24}O$	87. 8	7.3	87.76	7.36
2 e	89	pet. ether 60−80°	$C_{27}H_{24}O$	89.00	6.8	88.97	6.64
2 f	112	ethanol	$C_{24}H_{22}O_3$	80. 3	6.4	80.42	6.19
2 g	90	ethanol	$C_{25}H_{24}O_3$	80. 7	6.8	80.62	6.50
2 h	94	ethanol	$C_{28}H_{24}O_3$	82. 4	5.8	82.33	5.92

REACTION OF 2b−g WITH HYDRAZINE HYDRATE

A solution of 2 (0.01 mole) and hydrazine hydrate (0.01 mole) in ethanol (20 ml) was heated under reflux for 6 hrs. The solid separated after concentration and cooling the reaction mixture was crystallized from the suitable solvent to give the corresponding hydrazone (Table 2).

Table 2

Hydrazones of 2b−g

Hydrazone of	m.p. (°C)	solvent	Formula	Analyses % Found C	H	Required C	H
2 b	105	ethanol	$C_{19}H_{22}N_2O_2$	73.5	7.3	73.52	7.14
2 c	175	pet. ether 100−120°	$C_{23}H_{24}N_2$	84.3	7.5	84.10	7.37
2 d	123	ethanol	$C_{24}H_{26}N_2$	84.3	7.6	84.17	7.65
2 e	165	pet. ether 60−80°	$C_{27}H_{26}N_2$	85.8	7.1	85.67	6.92
2 f	117	*n*-butanol	$C_{24}H_{24}N_2O_2$	77.4	6.7	77.39	6.50
2 g	113	ethanol	$C_{25}H_{26}N_2O_2$	77.7	6.9	77.69	6.78

FORMATION OF OXIMES OF 2a, b, c, e, g, h

A mixture of 2 (0.01 mole) hydroxylamine hydrochloride (0.01 mole) and ethanol (20 ml) was heated under reflux for one hour. The reaction mixture was diluted with water and the obtained solid was crystallized from the suitable solvent to give the corresponding oxime (Table 3).

Table 3

Oximes of 2

oxime of	m.p. (°C)	solvent	Formula	Analyses % Found C	Found H	Required C	Required H
2 a	87	ethanol	$C_{18}H_{21}NO$	80. 8	8.00	80.86	7.92
2 b	135	ethanol	$C_{19}H_{21}NO_3$	73. 5	6.7	73.29	6.80
2 c	107	pet. ether 60−80°	$C_{23}H_{23}NO$	84.00	7.2	83.85	7.04
2 e	141	pet. ether 60−80°	$C_{27}H_{25}NO$	85. 4	6.7	85.45	6.64
2 g	124	pet. ether 100−120°	$C_{25}H_{25}NO_3$	77. 6	6.6	77.49	6.50
2 h	165	ethanol	$C_{28}H_{25}NO_3$	79. 5	6.1	79.41	5.95

REACTION OF 2g WITH BENZALDEHYDE. FORMATION OF 3

A solution of 2g (0.01 mole) and benzaldehyde (0.01 mole) in ethanol (10 ml) was treated with alcoholic potassium hydroxide solution (0.5 ml; 50%). The mixture was heated (steam-bath) for 4 hrs. The solid that separated on concentration and cooling was crystallized from pet. ether (60−80°) to give 3; m.p. 110°. Found: C, 83.5; H, 6.3 $C_{32}H_{28}O_3$ requires: C, 83.45; H, 6.13%.

REACTION OF 1a, b AND 2f WITH BENZENE IN THE PRESENCE OF ANHYDROUS ALUMINIUM CHLORIDE. FORMATION OF 2c

A solution of 1a, b or f (0.01 mole) in dry benzene (100 ml) was gradually added to a cooled suspension of anhydrous aluminium chloride (0.01 mole) in benzene (100 ml). The mixture was stirred at room temperature for one hour, and was then added to hydrochloric acid-ice. The separated benzene layer was dried, distilled and the solid obtained was crystallized from ethanol to yield colourless crystals of 2c, identified by m.p. and mixed m.p.

REACTION OF 1a, b WITH *p*-XYLENE AND TOLUENE. FORMATION OF 2i, j

A solution of the chalcone (1a or b) (0.01 mole) in dry *p*-xylene or toluene (100 ml) was added gradually to a cooled suspension solution of anhydrous aluminium chloride (0.01 mole) in *p*-xylene or toluene (100 ml). The mixture was stirred at room temperature for one hour and was then poured into HCl-ice. The organic layer was separated, dried and distilled. The viscous oils obtained were triturated by light petrol (b.p. 40−60°) and the products were crystallized from the suitable solvent to give 2i, j (Table 4).

Table 4

3,3-Diarylpropiophenones (2)

Compd	m.p. (°C)	solvent	formula	Analyses % Found C	Found H	Required C	Required H
2 i	84	pet. ether 60−80°	$C_{27}H_{30}O$	87.5	8.3	87.52	8.16
2 j	75	pet. ether 40−60°	$C_{25}H_{26}O$	87.8	7.6	87.67	7.65

PREPARATION OF AUTHENTIC SAMPLE OF (2j)

A solution of the chalcone (1c) (0.01 mole) in ether (200 ml) was added to an ethereal solution of *p*-tolylmagnesium bromide (0.03 mole) in the course of 30 min. The reaction mixture was heated under reflux for 4 hrs, left overnight at room temperature and then decomposed with ice-cold saturated ammonium chloride solution. The organic layer was separated, washed with water, dried and the solvent distilled. The viscous oil obtained was triturated with light petrol (b.p. 40—60°) the product was crystallized from pet. ether (40—60°) to give 2j identified by m.p. and mixed m.p.

REACTION OF 1a, b WITH TOLUENE. FORMATION OF 4

A solution of 1a, b (0.01 mole) in dry toluene was saturated with dry hydrogen chloride and anhydrous aluminium chloride (0.04 mole) was added. The suspension was stirred at room temperature for 15 hrs then added to HCl-ice. The toluene layer was separated, dried and distilled. The viscous oil obtained in each case was triturated with light petrol and the product was crystallized from pet. ether (100—120°) to give 4, identified by m.p. and mixed m.p. (216°); Found: C, 92.7; H, 7.5 $C_{25}H_{24}$ requires: C, 92.54; H, 7.46%.

ACTION OF HYDRAZINE HYDRATE ON CHALCONES 1a, b. FORMATION OF PYRAZOLINES (5a—j)

A solution of the chalcone 1 (0.01 mole) in ethyl alcohol, acetic acid, formic acid, propionic acid or isobutyric acid (50 ml) was treated with hydrazine hydrate (0.01 mole). The solution was refluxed for 6 hrs. The solids obtained after evaporation of the most part of the solvent under vacuo were crystallized from the suitable solvent to give 5a—j (Table 5).

Table 5

Pyrazolines (5)

Compd	m.p. (°C)	solvent	Formula	Analyses %			
				Found		Required	
				C	H	C	H
5 a	104	methanol	$C_{17}H_{18}N_2$	81.4	7.2	81.56	7.25
5 b	138	methanol	$C_{18}H_{18}N_2O_2$	73.5	6.2	73.45	6.16
5 c	112	pet. ether 80—100°	$C_{19}H_{20}N_2O$	78.1	6.9	78.05	6.90
5 d	166	ethanol	$C_{20}H_{20}N_2O_3$	71.1	6.1	71.41	5.99
5 e	117	pet. ether 40—60°	$C_{18}H_{18}N_2O$	77.7	6.5	77.67	6.52
5 f	153	ethanol	$C_{19}H_{18}N_2O_3$	70.9	5.6	70.79	5.63
5 g	121	pet. ether 40—60°	$C_{20}H_{22}N_2O$	78.7	7.3	78.40	7.24
5 h	131	ethanol	$C_{21}H_{22}N_2O_3$	71.7	6.4	71.98	6.33
5 i	151	ethanol	$C_{21}H_{24}N_2O$	78.9	7.7	78.71	7.55
5 j	155	ethanol	$C_{22}H_{24}N_2O_3$	72.5	6.7	72.5	6.64

REACTION OF PYRAZOLINES 5a, b WITH BENZOYL CHLORIDE AND BENZENESULPHONYL CHLORIDE. FORMATION OF PYRAZOLINES 5k—n

A mixture of 5 (0.01 mole) in pyridine (10 ml) was treated with benzoyl chloride or benzenesulphonyl chloride (1 ml) and the solution was heated on a water bath for one hour. The solution was poured into ice and the solid separated was crystallized from the suitable solvent to give the pyrazolines 5k—n (Table 6).

Table 6

Pyrazolines (5)

Compd	m.p. (°C)	solvent	Formula	Analyses % Found C	H	Required C	H
5 k	176	ethanol	$C_{24}H_{22}N_2O$	81.4	6.3	81.32	6.26
5 l	161	ethanol	$C_{25}H_{22}N_2O_3$	75.3	5.7	75.36	5.57
5 m	160	pet. ether 100−110°	$C_{23}H_{22}N_2O_2S$	70.6	5.6	70.77	5.64
5 n	215	benzene	$C_{24}H_{22}N_2O_4S$	66.5	5.2	66.35	5.06

PREPARATION OF AUTHENTIC SAMPLES OF 5m AND n

A solution of chalcone 1 (0.01 mol) in ethyl alcohol (20 ml) was treated with benzenesulphonyl-hydrazine (0.01 mole) and the solution was refluxed for 6 hrs. The solid separated after concentration and cooling was crystallized to give 5m and n, identified by m.p. and mixed m.p.

ACTION OF NITROUS ACID ON PYRAZOLINES 5a AND b. FORMATION OF 6a, b

A solution of pyrazolines 5 (0.01 mole) in hydrochloric acid (10 ml) was heated with a solution of sodium nitrite (0.03 mole) in water (3 ml). The reaction mixture was heated on a water bath for one hour, the solution was then poured into ice and the solid separated was crystalizzed from ethanol to give 6 (Table 7).

Table 7

1-nitrosopyrazolines (6)

Compd	m.p. (°C)	solvent	Formula	Analyses % Found C	H	Required C	H
6 a	150	ethanol	$C_{17}H_{17}N_3O$	73.1	6.3	73.09	6.13
6 b	146	ethanol	$C_{18}H_{17}N_3O_3$	66.8	5.4	66.86	5.30

ACTION OF BROMINE ON PYRAZOLINES 5a AND b. FORMATION OF 4-BROMOPYRAZOLINES 7

A solution of 5 (0.01 mole) in chloroform (20 ml) was treated with a solution of bromine (0.03 mole) in chloroform (20 ml). The solid product obtained after evaporation of chloroform was crystallized from benzene to give 7a and b (Table 8).

Table 8

4-bromopyrazolines (7)

Compd	m.p. (°C)	Formula	Analyses % Found C	H	Required C	H
7 a	103	$C_{17}H_{17}N_2Br$	62.3	5.2	62.00	5.16
7 b	156	$C_{18}H_{17}N_2O_2Br$	58.1	4.5	57.91	4.56

CYANOETHYLATION OF PYRAZOLINE 5b. FORMATION of 5*o*

A solution of pyrazoline 5 (0.01 mole), acrylonitrile (0.01 mole) ammonium chloride (0.02 mole) in water (10 ml) was heated for 8 hrs. The solid obtained, after extraction of the reaction mixture with ether and evaporation of the solvent, was crystallized from acetone to give 5*o* m.p.> 300°. Found : C, 72.81 ; H, 6.1 $C_{21}H_{21}N_3O_2$ requires : C, 72.60 ; H, 6.09 %.

MANNICH REACTION WITH THE PYRAZOLINES 5a AND b. FORMATION OF THE N-MANNICH BASES 8a—c

To a suspension of the pyrazolines 5a and b (0.01 mole) and the appropriate amine (morpholine or piperidine) (0.02 mole) in methanol, aqueous formaldehyde (35 %, 2.5 ml) was added. The reaction mixture was heated on a water bath for 5 hrs, kept overnight at room temperature, diluted with water and the resulting solid product crystallized from the suitable solvent to afford the N-Mannich bases 8a—c (Table 9).

Table 9

Mannich bases from pyrazolines (8)

Compd	m.p. (°C)	solvent	Formula	Analyses % Found C	Found H	Required C	Required H
8 a	163	pet. ether 60—80°	$C_{23}H_{29}N_3$	79.5	8.6	79.49	8.41
8 b	144	methanol	$C_{23}H_{27}N_3O_3$	70.3	6.7	70.20	6.92
8 c	146	methanol	$C_{24}H_{29}N_3O_2$	73.6	7.5	73.62	7.47

REDUCTION OF PYRAZOLINES 5h—j WITH LITHIUM-ALUMINIUM-HYDRIDE. FORMATION OF N-ALKYLPYRAZOLINES (5p—r)

A solution of 5 (0.01 mole), lithium-aluminium-hydride (0.01 mole) in dry ether (200 ml) was refluxed for one hour. The solid products obtained after filtration while hot and evaporation of the solvent were crystallized from the suitable solvent to give 5p—r (Table 10).

Table 10

N-alkylpyrazolines (5)

Compd	m.p. (°C)	solvent	Formula	Analyses % Found C	Found H	Required C	Required H
5 p	65	pet. ether 40—60°	$C_{21}H_{24}N_2O_2$	74.8	7.3	74.97	7.19
5 q	56	pet. ether 60—80°	$C_{21}H_{26}N_2$	82.5	8.4	82.31	8.55
5 r	79	pet. ether 40—60°	$C_{22}H_{26}N_2O_2$	75.4	7.5	75.40	7.48

REDUCTION OF PYRAZOLINE 5l WITH LITHIUM-ALUMINIUM-HYDRIDE. FORMATION OF N-BENZYLPYRAZOLIDINE (9a)

A solution of 5*l* (0.01 mole), lithium-aluminium-hydride (0.04 mole) in dry ether (20 ml) was refluxed for 15 hrs. The solid product obtained after filtration while hot and evaporation of the solvent was crystallized from ethanol to give 9a, m.p. 122° ; Found : C, 77.8 ; H, 6.8 $C_{25}H_{26}N_2O_2$ requires ; C, 77.69 ; H, 6.78 %.

ACETYLATION OF 9a. FORMATION of 9b

A solution of 9a (0.01 mole) in acetic acid (20 ml) was refluxed for 6 hrs. The solid separated after concentration and cooling was crystallized from ethanol to give 9b m.p. 140°; Found: C, 75.6; H, 6.7 $C_{27}H_{28}N_2O_3$ requires: C, 75.67; H, 6.59%.

CONDENSATION OF CHALCONES 1 WITH PHENYLHYDRAZINE, 2,4-DINITROPHENYL HYDRAZINE AND HYDROXYLAMINE. FORMATION OF PYRAZOLINES 5s–v AND ISOXAZOLINES 10a, b

A mixture of each of 1a and b (0.01 mole), and phenylhydrazine or 2,4-dinitrophenylhydrazine or hydroxylamine in ethanol (20 ml) was refluxed for 5 hrs. The products separated on cooling were crystallized from the suitable solvent to give the pyrazolines 5s–v and the isoxazolines 10a–b (Table 11).

Table 11

Pyrazolines (5) and isoxazolines (10)

Compd	m.p. (°C)	solvent	Formula	Analyses % Found C	Found H	Required C	Required H
5 s	136	ethanol	$C_{23}H_{22}N_2$	84.9	6.6	84.62	6.79
5 t	139	ethanol	$C_{24}H_{22}N_2O_2$	77.9	6.1	77.81	5.99
5 u	220	acetic acid	$C_{23}H_{20}N_4O_4$	66.5	4.9	66.33	4.84
5 v	243	benzene	$C_{24}H_{20}N_4O_6$	62.3	4.1	62.60	4.38
10 a	117	pet. ether. 100–120°	$C_{17}H_{17}NO$	81.1	6.5	81.24	6.82
10 b	120	pet. ether 100–120°	$C_{18}H_{17}NO_3$	73.5	5.9	73.20	5.80

ADDITION OF THIOPHENOL TO CHALCONE 1b. FORMATION OF 11

To a mixture of chalcone (0.01 mole), thiophenol (0.01 mole) and benzene (40 ml) 0.5 ml of piperidine was added and the mixture was vigorously shaked. After standing for 12 hrs, glacial acetic acid was dropwise added till the solution was acidic to phenolphthalein and the solvent was removed under vacuo leaving a crystalline residue which was crystallized from pet. ether (60–80°) to give 11 m.p. 90°; Found: C, 74.9; H, 5.8 $C_{24}H_{22}O_3S$ requires: C, 73.84; H 5.64%.

REACTION OF 11 WITH PHENYLHYDRAZINE. FORMATION OF 5t

Compound 11 (0.01 mole) in acetic acid (20 ml) was refluxed with phenylhydrazine (0.02 mole) for one hour. The solid product obtained after concentration and cooling was crystallized from ethanol to give 5t identified by m.p. and mixed m.p.

Revue Roumaine de Chimie, **23**, *11–12*, 1553–1557 (1978)

LA SÉPARATION DES ÉLÉMENTS Cu(II)–Zn(II)–Pb(II)–Fe(II), Fe(III) AU MOYEN DES RÉSINES ÉCHANGEUSES D'IONS

LUMINIȚA VLĂDESCU et MIHAELA COSTACHE
Laboratoire de Chimie Analytique, Faculté de Chimie, Institut de Chimie,
I.P.B., 202, Splaiul Independenței, Bucarest, Roumanie

Reçu le 13 novembre 1976

Dans le présent travail on a employé la β-alanine pour la complexation des ions Cu^{2+}, Zn^{2+}, Pb^{2+}, Fe^{2+} et Fe^{3+}. Prenant comme base la stabilité différente des combinaisons complexes formées, on a étudié les conditions optimales pour la séparation de ces éléments avec des résines échangeuses de cations. Après la fixation des combinaisons complexes formées, dans le cationit, l'élution a été effectuée en étapes successives avec de l'acide chlorhydrique : 0,5M pour le zinc, 1M pour le fer, 3M pour le plomb et 5M pour le cuivre. La méthode a été appliquée sur des mélanges synthétiques et sur des échantillons de laiton.

En utilisant des agents de complexation pour séparer le cuivre (II) et le zinc (II) avec des résines échangeuses d'ions, on a obtenu rapidement de très bons résultats. Dans ce but, dans la classe des amino-acides, on a employé la glycine.[1,2] Une série d'éléments, parmi lesquels le cuivre et le zinc, ont été séparés et déterminés semi-quantitativement par la méthode chromatographique de déplacement par des colonnes capillaires avec des résines échangeuses de cations.[3,4] De même, l'uranium a été séparé du cuivre, du zinc et d'autres éléments à l'aide des résines échangeuses d'anions en présence du même agent complexant.[5] Le zinc et le cadmium ont été séparés avec une résine cationique (Na^+) et la glycine[6] à pH = 8,5 et les éléments : V(V), Zr(IV), Ti(IV), Fe(II), Al(III), Cr(III), Ca(II), Mg(II) avec la β-alanine.[7]

Dans le présent travail on a employé la β-alanine pour la complexation des ions Cu^{2+}, Zn^{2+}, Pb^{2+}, Fe^{2+} et Fe^{3+}. Prenant comme base la stabilité différente des combinaisons complexes formées, on a étudié les conditions optimales pour la séparation de ces éléments, avec des résines échangeuses de cations. Après la fixation des combinaisons complexes

---

[1] S. S. Gupta et D. Mukerjee, *Z. analit. Chem.*, **213**, 38 (1965).
[2] N. T. Beck et J. Császár, *Acta Chim. Acad. Sci. Hung.*, **7**, 465 (1955).
[3] J. P. Quinche, *J. Chromatog.*, **13**, 203 (1964).
[4] J. P. Quinche et S. Quinche-Sax, *J. Chromatog.*, **32**, 162 (1968).
[5] E. Jercan et L. Dinoiu-Vlădescu, *Analyt. Chim. Acta*, **50**, 166 (1970).
[6] M. N. Zavereva, N. K. Cornovskaya et L. T. Kochurina, *Vestnik. Leningrad Univ., Fiz. Khim.*, **1974**, 153.
[7] L. Vlădescu et M. Costache, *Rev. Chim. (București)*, **27**, 1093 (1976).

formées dans le cationite, l'élution a été effectuée en étapes successives avec de l'acide chlorhydrique 0,5 M pour le Zn(II), 1M pour le Fe(II, III), 3M pour le Pb(II) et avec HCl 5M pour le Cu(II). La méthode a été appliquée sur des mélanges synthétiques et sur des échantillons de laiton.

PARTIE EXPÉRIMENTALE

MATÉRIAUX

- Les résines échangeuses de cations fortement acides, Merck I et Vionit CS$-$3.
- Solutions aqueuses 10^{-2}M de chlorures de Cu(II), Zn(II) et d'azotate de Pb(II) et Fe(II et III) à titre connu.
- Solution 10^{-2}M de complexon III (Serva).
- Solutions $5 \cdot 10^{-3}$, 10^{-2} et 10^{-1}M de β-alanine (Merck).
- Solutions aqueuses de HCl (Merck).

La détermination quantitative des ions a été effectuée par titrage complexonométrique.[8]

RÉSULTATS ET DISCUSSIONS

L'étude du comportement à l'échange cationique du cuivre (II) en présence de la β-alanine comme agent de complexation a montré la formation de combinaisons complexes très stables, de charge électropositive, les conditions optimales étant réalisées au pH = 5 et pour des teneurs 10^{-2} M en amino-acide.

En l'absence d'un agent de complexation, les ions Cu^{2+} et Zn^{2+} ne peuvent pas être séparés par élution à l'acide chlorhydrique, d'une résine échangeuse de cations fortement acide, parce qu'ils quittent la colonne ensemble, pour la même concentration en acide.

Les combinaisons complexes du cuivre, du zinc, du fer et du plomb avec la β-alanine peuvent être éluées, d'une colonne échangeuse de cations, avec des solutions de HCl de différentes concentrations. On a remarqué dans ce cas, l'apparition des éléments dans l'effluent, seulement pour certaines concentrations de l'acide, correspondant à la destruction des complexes (tableau 1).

Tableau 1

L'élution des éléments Cu(II), Zn(II), Pb(II) et Fe(II) d'un cationit avec HCl, après la complexation avec la β-alanine

HCl	Cu(II)		Zn(II)		Pb(II)		Fe(II)	
conc. M	introd. mg	élué mg	introd. mg	élué mg	introd. mg	élué mg	introd. mg	élué mg
0,1	1,01	—	0,65	—	0,51	—	0,78	—
0,3	1,01	—	0,65	—	0,51	—	0,78	—
0,5	1,01	—	0,65	0,63	0,51	—	0,78	0,70
1,0	1,01	—	0,65	0,68	0,51	—	0,78	0,75
3,0	1,01	—			0,51	0,47		
4,0	1,01	—			0,51	0,50		
5,0	1,01	0,98						
7,0	1,01	0,94						

---

[8] J. Pribil, "Complexonii în Chimia Analitică", Ed. tehnică, Bucarest, 1961.

Les données du tableau 1 montrent que le zinc peut être élué avec HCl 0,5 M, le fer avec HCl 1M, le plomb avec HCl 3M, et le cuivre avec HCl 5M.

Ensuite on a étudié l'action de la concentration de β-alanine sur l'élution des éléments avec les concentrations d'acide chlorhydrique établies. Les courbes d'élutions obtenues (fig. 1—4) montrent la nécessité d'un volume d'éluant d'autant plus grand, que la concentration de β-alanine augmente. C'est donc 10^{-2}M la concentration de β-alanine qu'il faut employer, pour réaliser plus rapidement la séparation.

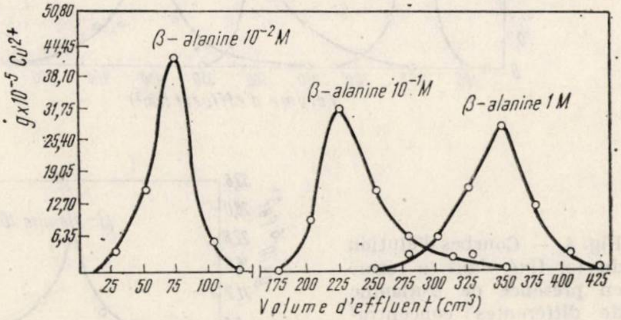

Fig. 1. — Courbes d'élution du cuivre fixé dans la résine en présence de β-alanine de différentes concentrations.

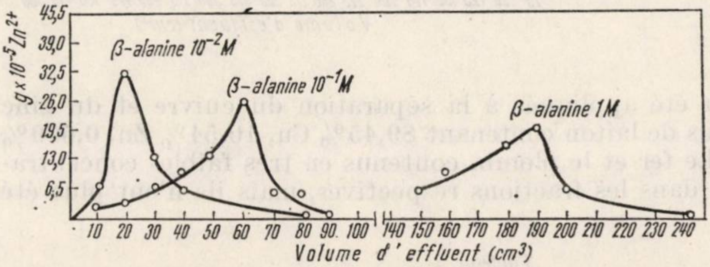

Fig. 2. — Courbes d'élution du zinc fixé dans la résine en présence de β-alanine de différentes concentrations.

Prenant comme base les résultats obtenus, on a effectué des séparations de mélanges binaires Cu(II)—Zn(II) contenant des quantités connues de ces deux cations. Les volumes nécessaires d'éluant ont été déterminés en traçant des courbes d'élution. Les cations Cu^{2+} et Zn^{2+} ont été transformés en combinaisons complexes, soit après leur fixation dans la résine échangeuse de cations, en passant une solutin 10^{-2}M de β-alanine par la colonne, soit avant, en mélangeant les réactants dans un entonnoir de séparation, de sorte que le cationite retienne directement les complexes formés.

Le premier procédé présente l'avantage d'utiliser des volumes plus petits de solution contenant l'échantillon et nécessite donc des colonnes moins longues que dans le second cas. Les résultats obtenus sont présentés dans le tableau 2.

On a tracé ensuite les courbes d'élution pour un mélange de solutions contenant du cuivre, du zinc, du fer et du plomb (fig. 5). Les éléments Fe(III) et Pb(II) ont été étudiés à cause de leur présence comme impuretés dans le laiton.

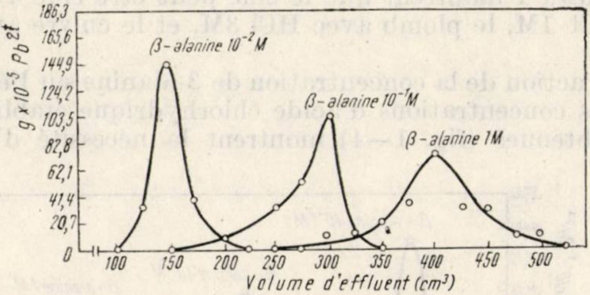

Fig. 3. — Courbes d'élution du plomb fixé dans la résine en présence de β-alanine de différentes concentrations.

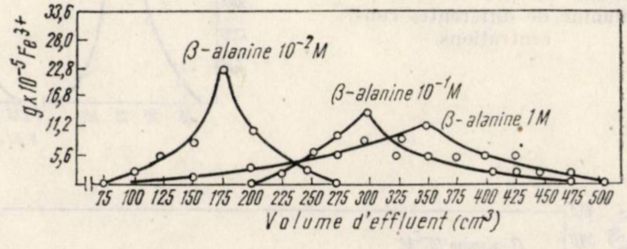

Fig. 4. — Courbes d'élution du fer fixé dans la résine en présence de β-alanine de différentes concentrations.

La méthode a été appliquée à la séparation du cuivre et du zinc dans des échantillons de laiton contenant 89,45% Cu, 10,54% Zn, 0,600% Fe et 0,005% Pb. Le fer et le plomb, contenus en très faibles concentrations, ont été élués dans les fractions respectives, mais ils n'ont plus été déterminés, de sorte que le tableau 3 comprend seulement les résultats concernant le cuivre et le zinc. La spectrographie d'émission des résidus obtenus par l'évaporation des fractions du cuivre et, respectivement du zinc, après la séparation, a montré l'absence totale d'autres ions. En utilisant des fixations et des élutions répétées les effluents du fer et respectivement du plomb étant collectés dans le même matras, on peut déterminer le contenu en ces éléments.

Tableau 2

Les résultats de la séparation de certains mélanges synthétiques de Cu(II) et Zn(II)

β-alanine conc M	HCl conc M	Cu(II)		Zn(II)	
		introduit mg	élué mg	introduit mg	élué mg
10^{-2}	0,5	1,01	—	0,65	0,63
	5,0		0,98		—
10^{-2}	0,5	0,50	—	0,65	0,68
	5,0		0,45		—
10^{-2}	0,5	3,03	—	0,32	0,30
	5,0		3,07		—

Il résulte que par la méthode proposée, on peut séparer les éléments Cu(II), Zn(II), Pb(II), et Fe(II, III) avec des résines échangeuses de cations, en utilisant la β-alanine comme agent de complexation et comme éluant l'acide chlorhydrique. En établissant les conditions optimales de travail, on a réalisé la séparation de ces éléments dans des mélanges synthétiques, ainsi que dans des échantillons de laiton.

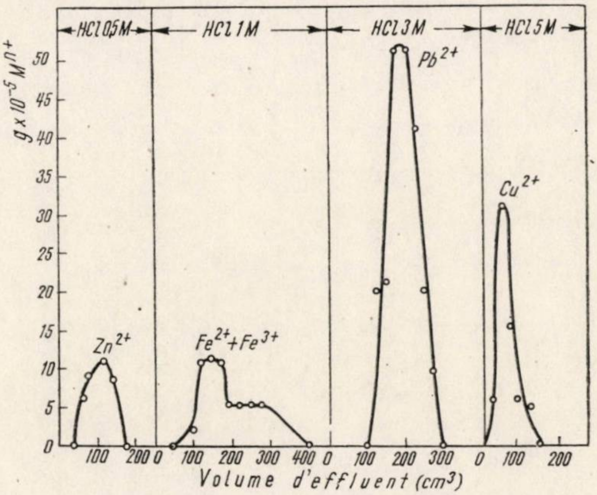

Fig. 5. — Courbes d'élution pour la séparation d'un mélange Cu(II) — Zn(II) — Pb(II) — Fe(II), Fe(III).

Tableau 3

Les résultats de la séparation des éléments (CuII) et Zb(II) dans le laiton

Quantité de laiton dans l'échantillon g	Cu(II)		Zn(II)	
	g	%	g	%
0,4438	0,3907	88,02	0,0490	11,04
0,4438	0,3866	87,40	0,0455	10,20
0,5992	0,5366	89,55	0,0585	9,7

Revue Roumaine de Chimie, **23**, *11–12*, 1559–1565 (1978)

THE STUDY OF CESIUM AND THALLIUM DECATUNGSTATEDINIOBIOSILICATES IN THE SOLID STATE

GH. MARCU, LETIŢIA GHIZDAVU and EUGENIA PERŢE

Department of Chemistry, University "Babeş-Bolyai"
Str. A. Janoş, Nr. 11, R–3400 Cluj-Napoca, Romania

Received November 23, 1976

The present paper deals with the heteropoly compounds $Cs_6[SiW_{10}Nb_2O_{40}] \cdot 4H_2O$ and $Tl_6[SiW_{10}Nb_2O_{40}] \cdot 7H_2O$ in solide state; their crystalline structures and thermal behaviour are studied.

As an extension of our studies on the decatungstatediniobiosilicate heteropoly compounds [1,2], we report the results obtained in the investigation of the $Cs_6[SiW_{10}Nb_2O_{40}] \cdot 4H_2O$ and $Tl_6[SiW_{10}Nb_2O_{40}] \cdot 7H_2O$ compounds in solid state, by the thermogravimetric and thermodifferential methods, completed with X-ray diffraction and IR absorption methods. The first two methods enable the continuous monitoring of the changes which occur during the temperature increase, while the last two methods indicate the characteristics of the phase in a given temperature range, its crystalline and moleculare structure.

EXPERIMENTAL

Cesium and thallium decatungstatediniobiosilicates were prepared by the direct reaction between freshly prepared decatungstatediniobiosilicic acid with the calculated amount of an aqueous solution of Cs_2SO_4 or $TlCH_3COO$.[1,2]

The products were crystallized twice and bright yellow rectangular prisms of $Cs_6[SiW_{10}Nb_2O_{40}] \cdot 4H_2O$ have been obtained. The thallium salt appears as a pale yellow precipitate with the formula $Tl_6[SiW_{10}Nb_2O_{40}] \cdot 7H_2O$. The elemental analysis confirmed these formulas.

The X-ray structure determination was made with the Debye-Scherrer method using crystalline powder. The crystallization system was determined using the analytical calculation procedure. A TUR-M 60 Dresden apparatus with a Debye-Scherrer chamber having 57.5 mm, a Co anticathode, a W filter at 50 kW and 7 mA was used for the Cs salt. For the Tl salt the anticathode was of Cu and a Ni filter was used. The exposure time was 8 hours.

The density was determined with a picnometer, using as density liquid analytical grade o-dichlorbenzene, at 20°.

---

[1] Gh. Marcu and L. Ghizdavu, *Rev. Roumaine Chim.*, **21**, 345 (1976).

[2] L. Ghizdavu, Ph. D. Thesis, Babeş-Bolyai University, Cluj-Napoca, 1975.

The thermal behaviour was studied with a Paulik-Erdely OD−102 type derivatograph up to 800°, without isothermal conditions, with a heating rate of 6°/min, the sample weight being 350 mg and the sensitivity of the balance 50 mg.

The IR absorption spectra were recorded on a UR−10 Karl Zeiss Jena apparatus. The sample was used in pellets with KBr.

RESULTS AND DISCUSSIONS

1. X-ray study. The X ray data for the $Cs_6[SiW_{10}Nb_2O_{40}]\cdot 4H_2O$ and $Tl_6[SiW_{10}Nb_2O_{40}]\cdot 7H_2O$ heteropoly compounds at room temperature are summarised in tables 1 and 2. From these data the elemental unit size $a = 11.78 \pm 0.03$Å was calculated. The odd and even values of the reflexion plane (Tables 1 and 2) show that these compounds crystalize in the cubic system, in a cubic primal lattice with a unit cell consisting of eight $Cs_6[SiW_{10}Nb_2O_{40}]\cdot 4H_2O$ or $Tl_6[SiW_{10}Nb_2O_{40}]\cdot 7H_2O$ molecules, with 1/8 appurtenance.

Table 1

The values of reflection plane indexes, line intensities and $\sin^2\theta$ values observed and calculated for $Cs_6[SiW_{10}Nb_2O_{40}]\cdot 4H_2O$

$\sum_i^n h_i^2$	Intensity*	$(\sin^2\theta)_{obs.}$	$(\sin^2\theta)_{calc.}$
6	1	0.03476	0.03462
10	1	0.05775	0.05770
12	10	0.06928	0.06924
14	2	0.08080	0.08078
16	9	0.09214	0.09232
18	2	0.10359	0.10386
22	9	0.12709	0.12694
26	9	0.15011	0.15002
30	7	0.17335	0.17310
32	9	0.18480	0.18644
38	10	0.21932	0.21921
40	1	0.23029	0.23080
44	3	0.25362	0.25392
48	1	0.27686	0.28696
50	10	0.28869	0.28850
58	1	0.33434	0.33466
62	10	0.35769	0.35774
65	8	0.37540	0.37505
73	1	0.42105	0.42121
77	1	0.44446	0.44429
85	1	0.49021	0.39035
86	1	0.49638	0.49612
89	1	0.51310	0.51343
91	1	0.52446	0.52497
93	1	0.53675	0.53651
96	1	0.55333	0.55382
101	1	0.58295	0.58267
105	1	0.60543	0.60575
115	1	0.66374	0.66345
121	1	0.69819	0.69807

* 9 − 10 − very strong; 7 − 8 − strong; 5 − 6 − medium; 3 − 4 − weak; 1 − 2 − very weak

The isomorphism and the unit cell similarity with the $Cs_3H_2[PMo_{10}V_2O_{40}]\cdot 1-2H_2O$, $Cs_3H[SiW_{12}O_{40}]\cdot 0-2H_2O$ and $Cs_5[PMo_{10}V_2O_{40}]\cdot 5H_2O$ [3,4] enabled us to assign them a "modified Keggin" structure.[5-7] According to this structural model the silicon atom forms a central tetrahedron and Nb^{5+} occupies randomly two of 12 octahedral sites in the tungsten-oxygen lattice, which belongs to the Keggin conventional structure shown below :

Table 2

The values of reflection plane indexes. line intensities and $\sin^2\theta$ values observed and calculated for $Tl_6[SiW_{10}Nb_2O_{40}]\cdot 7H_2O$

$\sum_i^n h_i^2$	Intensity*	$(\sin^2\theta)_{obs.}$	$(\sin^2\theta)_{calc.}$
8	1	0.03444	0.03424
10	1	0.04252	0.04280
13	2	0.05575	0.05564
14	8	0.05984	0.05984
19	2	0.08138	0.08132
22	2	0.09428	0.09415
25	1	0.10643	0.10700
38	6	0.16255	0.16264
41	5	0.17575	0.17548
46	1	0.19700	0.19688
51	1	0.21840	0.21828
61	1	0.26212	0.26108
64	1	0.27378	0.27392
106	1	0.45385	0.45368

* 9–10—very strong ; 7–8—strong ; 5–6—medium ; 3–4—weak ; 1–2—very weak

$$\left[\begin{array}{l} \quad (W_3O_{10})_2 \\ Si \\ \quad (NbW_2O_{10})_2 \end{array}\right]^{6-}$$

The correlation between the data from the X-ray analysis and the picnometric determination of the density, enabled us to determine the molecular weight of the studied compounds[8]. The densities thus obtained with a ±0.05 accuracy is $d = 3.64$ g/cm^3 and 4.14 g/cm^3 respectively, the molecular weights are close to those calculated, confirming the chemical formulas of these heteropoly compounds and a simple molecular structure (Table 3).

---

[3] A. V. Ablov, T. I. Malinovski and V. I. Dediu, *Zhur. neorg. Khim.*, **4,** 397 (1959).

[4] A. Suteu and L. Mîrza, *Lucrări ştiinţifice, Ser. mat. fiz. chim. (Oradea)*, **1972,** p. 55.

[5] J. F. Keggin, *Nature*, **131,** 968(1933).

[6] K. Y. Matsumoto, A. Kobayashi and Y. Sasaki, *Bull. Chem. Soc. Japan*, **48,** 3146 (1975).

[7] R. Allmann, *Acta Chem. Scand.*, **A 30,** 152(1976).

[8] R. W. D'Eye and E. Wait, "X-Ray Powder Photography in Inorganic Chemistry", Butterworths London, 1960, p. 177.

Table 3

The values of a, d, $M_{exp.}$ and $M_{theor.}$ for : $Cs_6[SiW_{10}Nb_2O_{40}]\cdot 4H_2O$ and $Tl_6[SiW_{10}Nb_2O_{40}]\cdot 7H_2O$ compounds

Formula	a(Å)	d(g/cm³)	$M_{exp.}$	$M_{theor.}$
$Cs_6[SiW_{10}Nb_2O_{40}]\cdot 4H_2O$	11.78	3.64	3584	3562
$Tl_6[SiW_{10}Nb_2O_{40}]\cdot 7H_2O$	11.78	4.14	4079	4045

2. Thermal study. From the thermal analysis curves for $Cs_6[SiW_{10}Nb_2O_{40}]\cdot 4H_2O$ and $Tl_6[SiW_{10}Nb_2O_{40}]\cdot 7H_2O$ given in Figures 1 and 2, two chemical processes are observed : the dehydration and the decomposition of the heteropoly compounds.

The dehydration of $Cs_6[SiW_{10}Nb_2O_{40}]\cdot 4H_2O$ (Figure 1, *1*) begins at 70° and proceeds through three stages : 70°–180° ; 180°–430° and 430°–450°. These stages correspond to two endothermal effects with the loss of three water molecules, with a slight shoulder at 160° and a maximum at 360° and an exothermal effect with a maximum at 435°. This suggests decomposition and rearrangement of the $[SiW_{10}Nb_2O_{40}]^{6-}$ anion (Figure 1, *2*).

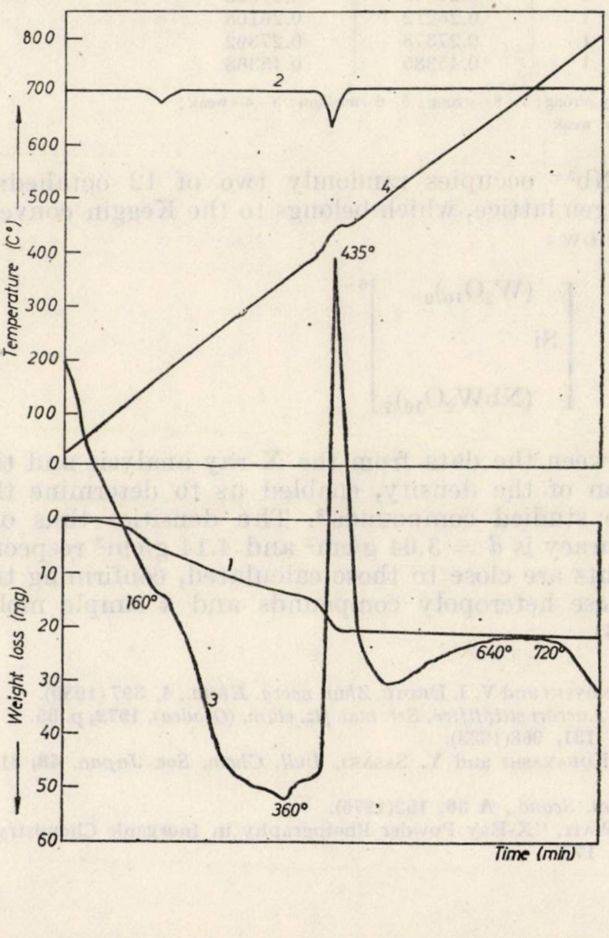

Fig. 1. — Thermoanalytical curves for $Cs_6[SiW_{10}Nb_2O_{40}]\cdot 4H_2O$; *1.* TG ; *2.* DTG ; *3.* DTA ; *4.* T°.

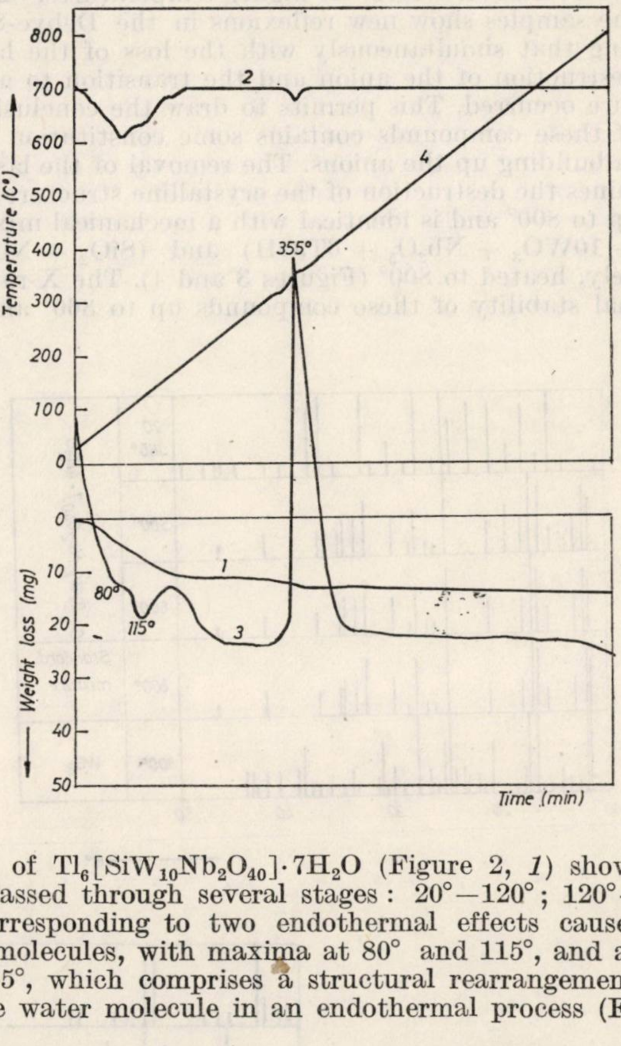

Fig. 2. — Thermoanalytical curves for $Tl_6[SiW_{10}Nb_2O_{40}]\cdot 7H_2O$; *1.* TG; *2.* DTG; *3.* DTA; *4.* T°.

The derivatogram of $Tl_6[SiW_{10}Nb_2O_{40}]\cdot 7H_2O$ (Figure 2, *1*) shows that dehydration had passed through several stages: 20°—120°; 120°—200° and 200°—400°, corresponding to two endothermal effects caused by the loss of 6 water molecules, with maxima at 80° and 115°, and an exothermal effect at 355°, which comprises a structural rearrangement, and the removal of one water molecule in an endothermal process (Figure 2, *2*).

In order to follow the transformations of the two heteropoly compounds with the rise of the temperature and to characterize the new formed phases, samples were prepared by heating the compounds for 30 minutes at various temperatures situated near the critical thermal points shown on the DTA curve (Figures 1, *3* and 2, *3*). The X-ray diffraction and IR curves of these samples are illustrated in Figures 3 and 4. These figures show that the parent cubic structure remained unchanged up to 360° for the Cs salt and up to 300° for the Tl salt. This conclusion is supported by the Debye-Scherrer diagram which remained unchanged in this range, in which they are only partially dehydrated. This fact showed that the water eliminated is of zeolite nature and occupies the empty sites between the large complex anions. These water molecules should be bonded through hydrogen bonds and their elimination does not modify the overall structure. At higher temperatures, 520° and 400° respectively, the samples show new reflexions in the Debye-Sherrer diagram, indicating that simultaneously with the loss of the last water molecules, the destruction of the anion and the transition to another crystalline structure occurred. This permits to draw the conclusion that the composition of these compounds contains some constitution water which participate in building up the anions. The removal of the last water molecules determines the destruction of the crystalline structure. The new phase is stable up to 800° and is identical with a mechanical mixture containing ($SiO_2 + 10WO_3 + Nb_2O_5 + 6TlOH$) and ($SiO_2 + Nb_2O_5 + 6CsOH$) respectively, heated to 800° (Figures 3 and 4). The X-ray data confirm the thermal stability of these compounds up to 360° and 300° respectively.

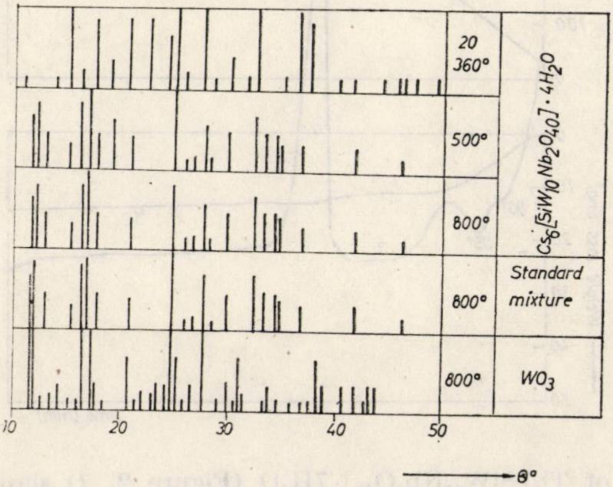

Fig. 3. — Debye-Scherrer diagrams of the $Cs_6[SiW_{10}Nb_2O_{40}] \cdot 4H_2O$ and of the standard mixture at various temperatures.

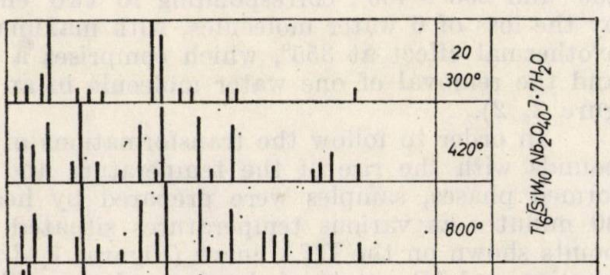

Fig. 4. — Debye-Scherrer diagrams of the $Tl_6[SiW_{10}Nb_2O_{40}] \cdot 7H_2O$ and of the standard mixture at various temperatures.

Above these temperatures there occurs a transition to a new crystalline phase, consisting of oxide mixtures, where the tetragonal lattice of tungsten trioxide prevails. [9]

3. The infrared absorption study. The IR spectra of $Cs_6[SiW_{10}Nb_2O_{40}]\cdot 4H_2O$ and $Tl_6[SiW_{10}Nb_2O_{40}]\cdot 7H_2O$ obtained at room temperature show absorption bands in the 790—1020 cm^{-1} region. Three absorption maxima were assigned to the valence vibration of W—O and W—O—W of the polytungstate structure, at 790, 920 and 980 cm^{-1} and a slight maximum at 1020 cm^{-1} was assigned to the Si—O—W bond. The fact that the absorption maxima are situated at wave numbers close to the related 1 : 12 compound the decatungstatesilicic acid with a Keggin structure, is interpreted as a proof of the Keggin structure of the studied compounds [10-13].

In the spectra of the products heated at 800°, a broad band between 850—900 cm^{-1} was obtained, identical to the IR spectra of the standard, a proof that the new crystalline phase is formed from mixed oxides, the chief constituent being WO_3.

CONCLUSIONS

1. The heteropoly compounds $Cs_6[SiW_{10}Nb_2O_{40}]\cdot 4H_2O$ and $Tl_6[SiW_{10}Nb_2O_{40}]\cdot 7H_2O$ crystallize in the primal cubic system with a modified Keggin structure. The unit cell site is $a = 11.78 \pm 0.03$ Å.

2. The IR spectra exhibit absorption bands in the 790—1020 cm^{-1} characteristic of Keggin structure.

3. The compounds have a thermal stability up to 360°, respectively 300°. Above this temperature a decomposition and consequently a change of the crystalline lattice occurs. X-ray diffraction data and IR spectra indicate a new crystalline phase, consisting of a mixture of oxides, the main component of which is WO_3.

---

[9] G. Kohlstrung, *Physica Status solidi (Berlin)*, **2,** 85 (1962).

[10] O. Glemser, W. Hölsnagel and E. Schwarzmann, *Z. Naturforsch.*, **20 b,** 725 (1965).

[11] G. Lange, H. Helm and K. Debrike, *Z. Naturforsch.*, **24 b,** 1498 (1969).

[12] C. M. Flynn Jr. and M. T. Pope, *Inorg. Chem.*, **10,** 2745 (1971).

[13] A. Duca and A. Pop, *Studii și Cercetări Chim. (Fil. Cluj)*, **12,** 35 (1961).

Revue Roumaine de Chimie, 23, 11–12, 1567–1573 (1978)

SOME REACTIONS OF 2-ISOPROPYL-[4H]-3,1-BENZOXAZIN-4-ONE

A. F. M. FAHMY, M. A. EL-HASHASH, M. M. HABASHY and S. A. El-WANNISE
Faculty of Science, Ain Shams University A.E.R., Egypt

Received November 4, 1976

Benzoxazone **1** reacted with primary aromatic amines to give **2a**, **2b** and **3**, with hydrazines to give **4a** and **4b**, with hydroxylamine hydrochloride to give **6**, with alcoholic ammonia to give **7**, with formamide to give **8**. Also **1** reacted with sodium azide to give **9**. Benzoxazone **1** reacted with toluene in the presence of anhydrous $AlCl_3$ to give **10**, and with phenylmagnesium bromide and benzylmagnesium chloride to give **11** and **12** respectively. Reaction of **1** with phosphorous pentachloride yields **13** which undergoes ring opening with *o*-toluidine followed by cyclization to give **14**.

It was stated previously that 3,1-benzoxazin-4-ones undergo ring opening reactions with different nucleophiles.[1–3] The present investigation deals with aminolysis of 2-isopropyl-[4H]-3,1-benzoxazin-4-one **(1)** with primary aromatic amines in boiling ethanol to give the corresponding 2-(arylcarbamoyl)-isobutroylanilides **(2a** and **2b)** and 2-(tolylcarbamoyl) aniline **(3)**. The formation of **3** is due to the attack of the more basic *p*-toluidine on the carbonyl group of the carbamoyl moiety.

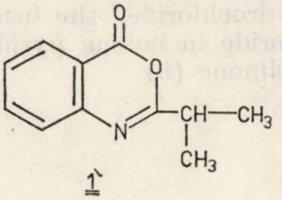

1

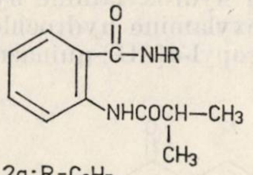

2a; R = C_6H_5
2b; R = *p*-Cl–C_6H_4

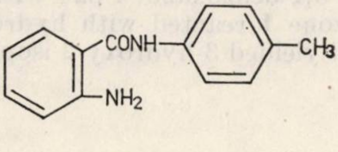

3

Structure of **2** was proved from the i.r. spectrum which showed $\nu_{CO's}$ (at 1670 and 1650 cm^{-1}) and $\nu_{NH's}$ (at 3300 and 3200 cm^{-1}) and other two bands (at 2970 and 2870 cm^{-1}) attributable to stretching frequencies of methyl groups and a weak band (at 2895 cm^{-1}) due to tertiary CH. The i.r.

---

[1] D. I. Zentmyer and E. C. Wagner, *J. Org. Chem.*, **14**, 967 (1949).

[2] M. T. Bogert and H. Ambrose, Soil, *J. Amer. Chem. Soc.*, **27**, 1305 (1905).

[3] A. Sammour, M. I. B. Selim and M. Abdo, *J. Chem. U.A.R.*, **14** (2) 197 (1971).

spectrum of **3** shows ν_{CO} (at 1660 cm^{-1}) and two ν_{NH} (at 3300 and 3180 cm^{-1}) for primary amines and amides.

Reaction of **1** with hydrazine hydrate or phenylhydrazine in boiling ethanol gave quinazolinones **4a** and **4b**.[3,4]

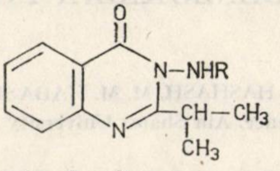

4a ; R = H
4b ; R = C_6H_5

The i.r. spectrum of **4a** shows ν_{CO} (at 1680 cm^{-1}), and ν_{NH} (at 3500 and 3340 cm^{-1}). The i.r. spectrum of **4b** shows ν_{CO} (at 1670 cm^{-1}), and ν_{NH} (at 3310 cm^{-1}).

Condensation of **4a** with benzaldehyde gave 3-(benzylideneamino)-4(3H)-quinazolinone (**5**).

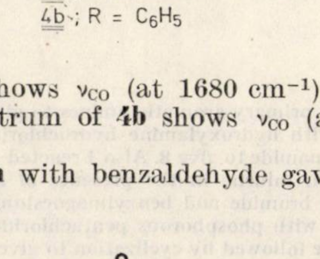

5

The i.r. spectrum of **5** was consistent with the proposed structure; it reveals no NH and the presence of bands (at 1690 and 1665 cm^{-1}) for $\nu_{C=O}$ and $\nu_{C=N}$ respectively.

By analogy with the recently reported reaction of 2-cyclohexyl-4H-3,1-benzoxazin-4-one with hydroxylamine hydrochloride,[4] the benzoxazone **1** reacted with hydroxylamine hydrochloride in boiling pyridine and yielded 3-hydroxy-2-isopropyl-4[3H]-quinazolinone (**6**).

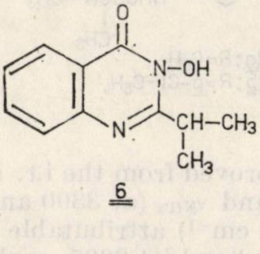

6

I.r. spectrum of **6** shows ν_{CO} (at 1670 cm^{-1}), and ν_{OH} (at 3100 cm^{-1} chelated).

[4] A. Sammour, A. F. M. Fahmy and M. Mahmoud, *Indian J. Chem.*, **11** (3) 222 (1973).

The benzoxazone **1** undergoes ammonolysis with alcoholic ammonia to give N-isobutroylanthranilamide **(7)**.

However reaction of **1** with formamide gives 2-isopropyl-4[3H]-quinazolinone **(8)** via ammonolysis followed by cyclization and hydrolysis.

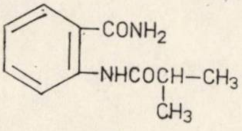

7

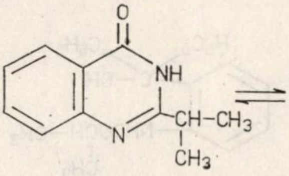

8a

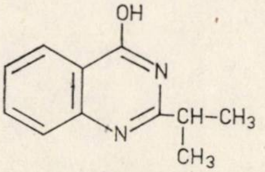

8b

The structure of **7** was confirmed from its i.r. spectrum which reveals NH bands (at 3360 and 3220 cm^{-1}) and two bands (at 1670 and 1640 cm^{-1}) for two carbonyls of primary and secondary amide.

I.r. spectrum of **8** shows ν_{OH} (at 3450 cm^{-1}), ν_{NH} (at 3160 cm^{-1}), ν_{CO} (at 1690 cm^{-1}) and two bands for two $\nu_{C=N}$ (at 1630 and 1620 cm^{-1}) which illustrate that 2-isopropyl-4[3H]-quinazolinone **(8)** exists in a lactam-lactim tautomeric equilibrium **(8a** and **8b)**.

In this investigation the hitherto unkown reaction of sodium azide with benzoxazone **1** was discovered. Benzoxazone **1** reacts with sodium azide in boiling acetic acid and yielded 1-(2-carboxyphenyl)-2-isopropyltetrazole **(9)**.

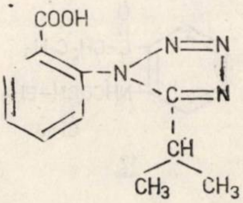

9

The structure of **9** was confirmed from its i.r. spectrum which shows $\nu_{C=O}$ of acid (at 1725 cm^{-1}), and a broad band (at 3430 cm^{-1}) attributable for ν_{OH} and other band in the region of 1100—900 cm^{-1} due to tetrazole ring.[5]

Reaction of **1** with $AlCl_3$ in toluene under the conditions of Fridel-Crafts reaction [4] gives 2-isobutroylamido-4-methylbenzophenone **(10)**.

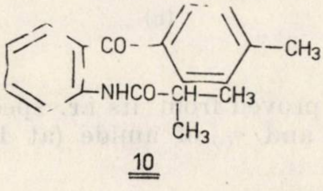

10

---

[5] W. I. Awad, A. F. M. Fahmy and A. Sammour, *J. Org. Chem.*, **30**, 2222 (1965).

The structure of **10** was confirmed from its i.r. spectrum which shows $\nu_{C=O}$ absorption of ketone (at 1682 cm^{-1}), $\nu_{C=O}$ of amide (at 1660 cm^{-1}) and ν_{NH} (at 3300 cm^{-1}).

Reaction of **1** with phenylmagnesium bromide gives *o*-isobutroylaminocarbinol **11**.[6]

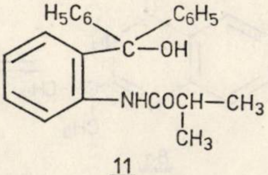

11

The i.r. spectrum of **11** agreed well with the proposed structure which shows $\nu_{C=O}$ (at 1680 cm^{-1}), ν_{NH} (at 3060 cm^{-1}) and ν_{OH} (at 3380 cm^{-1}).

However, benzylmagnesium chloride reacts with **1** to give *o*-isobutyroylamidodesoxybenzoin **(12)**, and not the corresponding carbinol as in the case of phenylmagnesium bromide. This is due to the greater steric crowding in the case of **12** which hinders further attack of benzylmagnesium chloride to give the expected carbinol, this assignment being based upon Cram's rule. This can be easily understood if we consider the possible conformers for **12** :

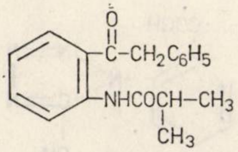

12

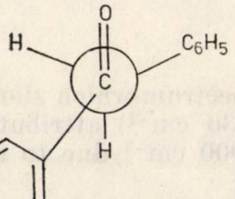

(a)

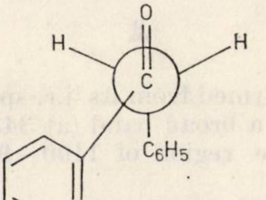

(b)

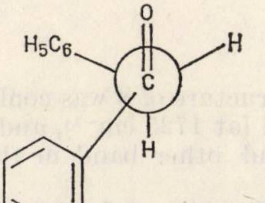

(c)

The structure of **12** was proved from its i.r. spectrum which shows ν_{CO} of ketone (at 1680 cm^{-1}) and ν_{CO} of amide (at 1660 cm^{-1}) and ν_{NH} (at 3240 cm^{-1}).

---

[6] A. Sammour, T. Zimaity and M. Abdo, *J. Chem. U.A.R.*, **16** (3) 215 (1973).

Reaction of **1** with phosphorus pentasulphide in dry xylene [7] gives 2-isopropylbenzothiazin-3,1[4H]-thione (**13**).

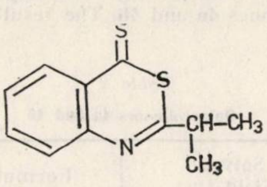

13

The assigned structure for the thione **13** is supported from its i.r. spectrum which shows $\nu_{C=S}$ (at 1340 cm^{-1}) and $\nu_{C=N}$ (at 1610 cm^{-1}). Reaction of **13** with *o*-toluidine by fusion gives 2-isopropyl-3-(*o*-tolyl) quinazolin-4-thione (**14**), via ring opening followed by cyclization.[8]

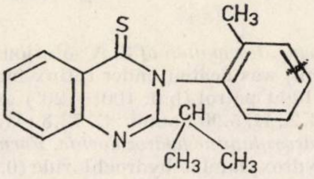

14

Infrared spectrum of **14** shows $\nu_{C=S}$ (at 1345 cm^{-1}), and $\nu_{C=N}$ (at 1630 cm^{-1}).

EXPERIMENTAL

The infrared absorption spectra were determined with an Unicam SP-1200 Spectrophotometer using KBr wafer technique ; all m.p. are uncorrected.

Action of primary amines on 2-isopropyl-4H-3,1-benzoxazin-4-one (**1**). *Formation of* **2a**, **2b** *and* **3**. A solution of **1** (0.01 mole) and primary aromatic amines, namely aniline, *p*-chloroaniline or *p*-toluidine (0.01 mole) in ethanol (40 ml) was heated under reflux for 5 hrs. The products **2a**, **2b** and **3** respectively that separated on cooling were recrystallized from the suitable solvent. The results are listed in table 1.

Table 1

2-(Arylcarbamoyl)isobutroylanilides (2) and 2-(*p*-tolylcarbamoyl)-aniline (3)

Compd.	m.p. (°C) colour	Solvent yield (%)	Formula	Analyses % Required		Analyses % Found
2a	160 colourless	benzene 75	$C_{17}H_{18}N_2O_2$	C H	72.24 6.38	71.90 5.98
2b	194 colourless	ethanol 67	$C_{17}H_{17}ClN_2O_2$	C H	64.54 5.37	64.00 5.30
3	130 colourless	ethanol 77	$C_{14}H_{14}N_2O$	C H	74.33 6.19	74.00 6.10

---

[7] L. J. Legrand, *Bull. Soc. chim., France*, **1960,** 337.

[8] A. Sammour, M. I. B. Selim, A. F. M. Fahmy and K. Elewah, *Indian J. Chem.* **11,** 437 (1973).

Action of hydrazines on **1**. *Formation of* **4a** *and* **4b**. A solution of benzoxazone 1 (0.01 mole) and hydrazine hydrate or phenylhydrazine (0.01 mole) in ethanol (40 ml) was heated under reflux for 6 hrs. The solid separated on cooling was recrystallized from suitable solvent to give the corresponding quinazolinones **4a** and **4b**. The results are given in table 2.

Table 2

Quinazolinones 4a and 4b

Compd.	m.p. (°C) Colour	Solvent Yield (%)	Formula	Analyses % Required	 Found
4a	80 colourless	light petrol (b.p. 100−120°) 82	$C_{11}H_{13}N_3O$	C 65.02 H 6.40	64.64 6.83
4b	127 colourless	ethanol 65	$C_{17}H_{17}N_3O$	C 73.12 H 6.09	72.92 6.24

Condensation of **4a** *with benzaldehyde. Formation of* **5**. A solution of **4a** (0.01 mole) and benzaldehyde (0.01 mole) in ethanol (50 ml) was heated under reflux for 6 hrs. The solid separated on cooling were recrystallized from light petrol (b.p. 100−120°) as colourless crystals ; m.p. 145° ; yield 75 % ; $C_{18}H_{17}N_3O$ Calc. C, 74.2 ; H, 5.90 Found : C, 73.8 ; H, 6.00 %

Reaction of benzoxazone **1** *with hydroxylamine hydrochloride. Formation of hydroxyquinazolinone* **6**. A mixture of **1** (0.01 mole) and hydroxylamine hydrochloride (0.03 mole) in dry pyridine (40 ml) was heated under reflux for 15 hrs. The reaction mixture was poured into cold dilute hydrochloric acid to give a solid which was recrystallized from benzene to give hydroxyquinazolinone **6** as colourless crystals which had m.p. 138° ; yield 75 % ; $C_{11}H_{12}N_2O_2$ Calc. C, 64.70 ; H, 5.90 Found : C, 64.50 ; H, 6.10 %

Action of alcoholic ammonia on benzoxazone **1**. *Formation of* **7**. An alcoholic solution of benzoxazone **1** (0.01 mole) was treated with excess alcoholic ammonia under reflux for 6 hrs. The solid produced after cooling was crystallized from ethanol to give N-isobutroylanthranilamide **(7)** as colourless crystals ; m.p. 166° ; yield 77 % ; $C_{11}H_{14}N_2O_2$ Calc. C, 64.70 ; H, 6.80 Found : C, 65.00 ; H, 7.25 %.

Action of formamide on the benzoxazone **1**. *Formation of quinazolinone* **8**. A mixture of benzoxazone **1** (0.01 mole) and formamide (0.015 mole) was heated at 175° in oil-bath for 3 hrs. The product obtained was recrystallized from benzene to give 2-isopropyl-4(3H)-quinazolinone **(8)** as colourless crystals ; m.p. 229° ; yield 68 % ; $C_{11}H_{12}N_2O$ Calc. C, 70.20 ; H, 6.40 Found : C, 70.20 ; H, 6.70 %.

Action of sodium azide on the benzoxazone **1**. *Formation of tetrazole* **9**. A mixture of benzoxazone **1** (0.01 mole) and sodium azide (0.015 mole) in boiling acetic acid (40 ml) was refluxed for 3 hrs. The product obtained after concentration was crystallized from benzene to give the tetrazole **9** as colourless crystals ; m.p. 120° ; yield 61 % ; $C_{11}H_{12}N_4O_2$ Calc. C, 56.80 ; H, 5.10 Found : C, 56.90 ; H, 5.55 %.

Friedel-Crafts reaction with **1**. *Formation of* **10**. To a solution of **1** (0.01 mole) in toluene (50 ml), aluminium chloride (0.04 mole) was added, a vigorous evolution of hydrogen chloride took place and a brown past precipitated. Stirring was continued for an additional 10 hrs at room temperature. The reaction mixture was then added to ice-cold hydrochloric acid, the organic layer was washed with water and excess solvent removed by steam distillation. The solid obtained was crystallized from light petrol (b.p. 80−100°) to give **10** as colourless crystals, m.p. 130° ; yield 51 % ; $C_{18}H_{19}NO_2$ Calc. C, 76.86 ; H, 6.76 Found : C, 77.34 ; H, 7.20 %.

Action of Grignard reagents on the benzoxazone **1**. *Formation of* 11 *and* **12**. A solution of **1** (0.01 mole) in dry benzene (100 ml) was treated with an ethereal solution of phenylmagnesium bromide or benzylmagnesium chloride (0.03 mole) in the course of 30 min. The reaction mixture was heated under reflux for 5 hrs, left overnight at room temperature, and then decomposed in the usual way. The viscous oil obtained was triturated with light petrol and the products were crystallized from the proper solvent to give the corresponding carbinol **11** and ketone **12**. The results are listed in table 3.

Action of phosphorus pentasulphide on the benzoxazone **1**. *Formation of* **13**. A solution of 1 (0.01 mole), P_2S_5 (0.02 mole) and dry xylene (100 ml) was heated under reflux for 6 hrs. The reaction mixture was filtered hot and concentrated. The product that separated on cooling was crystal-

Table 3

Carbinol 11 and ketone 12

Compd.	m.p.(°C) colour	Solvent yield (%)	Formula	Analyses % Required	
				Required	**Found**
11	155 colourless	benzene 63	$C_{23}H_{23}NO_2$	C 80.0 H 6.66	79.60 6.20
12	158 colourless	benzene 57	$C_{18}H_{19}NO_2$	C 76.86 H 6.76	77.45 6.90

lized from light petrol (b.p. 100—120°) to give 2-isopropyl-[4H]3,1-benzothiazin-4-thione **(13)** as red crystals; m.p. 105; yield 52%; Calc. $C_{11}H_{11}NS_2$ C, 59.70; H,4.90 Found: C, 59.90; H, 5.10%.

Action of o-toluidine on the thione **13**. *Formation of* **14**. A solution of 2-isopropyl-[4H]-3,1-benzothiazin-4-thione **(13)** (0.01 mole) and *o*-toluidine (0.01mole) in ethanol (50 ml) was heated under reflux for 5 hrs. The product that separated on cooling was crystallized from light petrol (b.p. 80—100°) to give **14** as pale yellow crystals; m.p. 125°; yield 57%; $C_{18}H_{18}N_2S$ Calc. C, 73.46; H, 6.12 Found: C, 73.51; H, 6.35%.

Revue Roumaine de Chimie, 23, *11–12*, 1575–1579 (1978)

LA GENÈSE ET LA NATURE DES CENTRES ACTIFS DANS LES CATALYSEURS ACIDES SOLIDES. III[1]

TRANSALKYLATION DU TOLUÈNE SUR LA ZÉOLITE SYNTHÉTIQUE HMgY

I. SĂNDULESCU, OLGA ŞERBAN, S. DAVIDENCU, R. E. RUSSU, LIGIA FRUNZĂ

Institut de Chimie, Département de Chimie Technologique et Catalyse, Splaiul Independenţei, 202, Bucarest 7

Reçu le 13 décembre 1976

On étudie l'influence du traitement thermique sur la nature et la concentration des centres acides, dans la zéolite synthétique HMgY. On étudie la corrélation entre l'activité catalytique dans la réaction de transalkylation du toluène et la concentration des centres acides déterminés par spectroscopie en IR en présence de pyridine adsorbée.

Dans le présent travail on étudie l'activité catalytique de la zéolite HMgY, dans la réaction de transalkylation du toluène[1–2] en corrélation avec la nature et la concentration des centres acides. Ces propriétés ont été modifiées par un traitement thermique différent de celui du catalyseur.

On sait que la réaction principale de transalkylation est accompagnée de réactions d'isomérisation et de désalkylation, qui peuvent être évaluées, en fonction de la force et de la concentration des centres actifs.[3–7]

RÉSULTATS EXPÉRIMENTAUX ET DISCUSSIONS

La réaction de transalkylation a été effectuée en système dynamique, isotherme, avec une couche fixe du catalyseur.

---

[1] I. V. Nicolescu, O. Şerban, I. Săndulescu et L. Stoicescu, *Rev. Roumaine Chim.*, **22,** 97 (1977).

[2] H. Matsumoto et Y. Morita, *Bull. Jap. Petrol. Inst.*, **10**, 26 (1968) ; **11**, 40 (1969).

[3] M. Saito, *J. Chem. Soc. Jap. Ind. Chem. Soc.*, **67,** 2506 (1965).

[4] V. J. Frillette et C. M. Munus, J. *Catalysis*, **4,** 504 (1965).

[5] I. I. Isakov et M. H. Minachev, *Neftekhimia*, **7,** 561 (1967).

[6] I. I. Isakov, M. H. Minachev et I. I. Usachev, *Izvest. Akad. Nauk. S.S.S.R., ser. Chim.*, **7,** 1588 (1973).

[7] I. V. Nicolescu, O. Şerban, A. Ionescu et O. Popescu-Vlădoianu, *Anal. Univ. Buc. XX,* **2,** 51 (1971).

Le catalyseur HMgY a subi un traitement thermique dans l'intervalle de température de 400 à 800°. On a utilisé une granulation du catalyseur de 1,25 à 1,6 mm qui supprime les phénomènes de diffusion.

L'analyse des produits de réaction a été effectuée à l'aide d'une colonne chromatographique de 6 m de longueur au diamètre de 4 mm. On a utilisé comme phase stationnaire bentone + diisodecilephtalate.

Les résultats expérimentaux ont été exprimés par la vitesse apparente de réaction, suivant la relation :

$$r_c = \frac{F_A}{W} X_c (\mathrm{mol \cdot g^{-1} \cdot h^{-1}}),$$

où : F_A — matière première (moles)
W — catalyseur (g)
X_c — conversion du toluène calculée des données chromatographyques.

Les données ont été exprimées aussi sous forme de rapport benzène/xylène (b/X).

La réaction de transalkylation a été étudiée en fonction des paramètres suivants : le traitement thermique du catalyseur, la température de réaction et la vitesse spatiale. L'étude de la réaction de transalkylation en fonction du traitement thermique de catalyseur (fig. 1), nous amène à constater que l'activité globale maximale du catalyseur est située à 600°, température à laquelle on considère que la concentration des centres actifs est maximale.

En représentant le rapport b/X en fonction de la température du traitement thermique, on constate d'après la figure 2, que la valeur maximale du rapport observée correspond toujours au catalyseur traité thermiquement à 600°C.

La réaction de transalkylation est optimale pour le rapport b/X = 1. Il résulte qu'aux températures de calcination comprises entre 400—500° et respectivement entre 700—800° la réaction de transalkylation est favorisée, mais entre 550—650° prédomine la réaction secondaire de désalkylation.

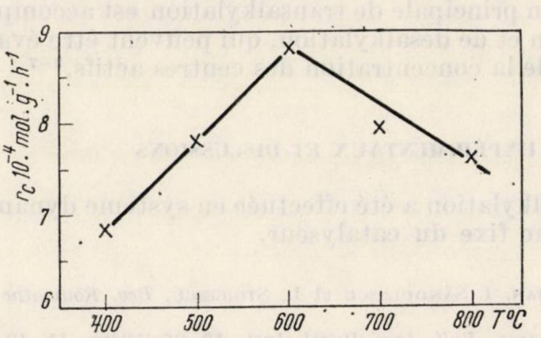

Fig. 1. — Variation de la vitesse apparente de réaction, r_c, en fonction de la température du traitement thermique du catalyseur.

Ce fait montre que le traitement thermique du catalyseur détermine la nature et la concentration des centres catalytiquement actifs. La variation du rapport L/B détermine le sens de la réaction catalytique, où *L* représente la concentration des centres Lewis, et B la concentration des centres Brönsted.

Comme suite de ces résultats, on a effectué la réaction de transalkylation sur le catalyseur traité thermiquement à 500°. On a étudié l'influence du temps de contact sur le sens de développement de la réaction.

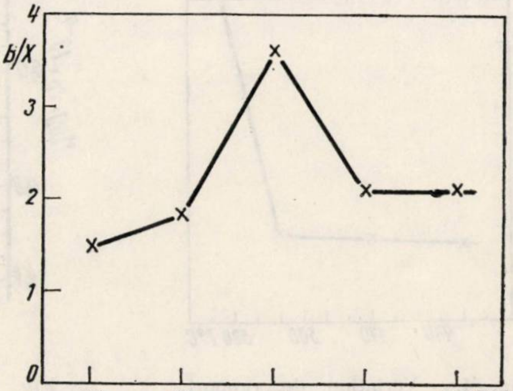

Fig. 2. — Variation du rapport b/X en fonction de la température du traitement thermique du catalyseur.

Il résulte de la représentation du rapport b/X en fonction de la vitesse spatiale que la valeur de la vitese spatiale pour laquelle on obtient un raport b/X optimal (figure 3) est de 0,5 h^{-1}.

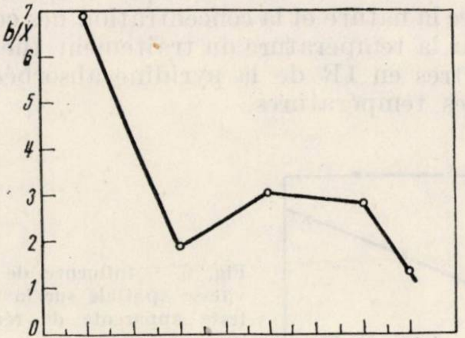

Fig. 3. — Variation du rapport b/X avec la vitesse spatiale.

Dans ce qui suit nous avons considéré cette valeur de la vitesse spatiale (0,5 h^{-1}).

En étudiant l'influence de la température sur le sens de la réaction, à la vitesse spatiale 0,5 h^{-1}, on constate (figure 4) que les températures de réaction au-dessous de 500° sont favorables à la réaction de transalkylation, mais des températures au-dessus de 500° déterminent une augmentation appréciable de la vitesse de désalkylation.

La représentation de la variation log r_c en fonction de 1/T (figure 5) nous a permis de calculer l'énergie d'activation dont la valeur est de 9,0 kcal/mole.

La représentation de la variation de la vitesse globale r_c en fonction de la vitesse spatiale (figure 6) à la température de réaction de 500° conduit à une droite qui passe par l'origine des axes des coordonnées, montrant que l'ordre de réaction est approximativement égal à l'unité.

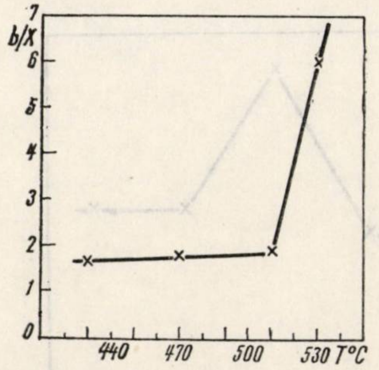

Fig. 4. — Variation du rapport b/X avec la température de réaction.

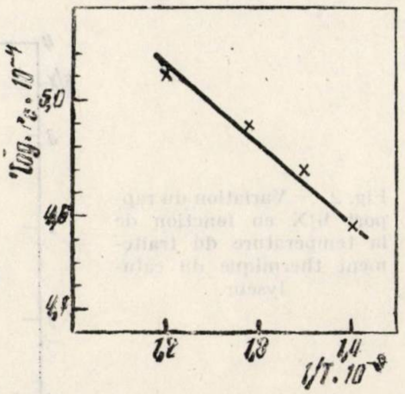

Fig. 5. — Variation du log r_c en fonction de 1/T.

En considérant l'activité du catalyseur zéolite synthétique HMgY en fonction de la température du traitement thermique on peut mettre en corrélation cette activité avec la nature et la concentration des centres L et B conditionnées toujours par la température du traitement thermique.

On a déterminé les spectres en IR de la pyridine absorbée sur le catalyseur calciné à différentes températures.

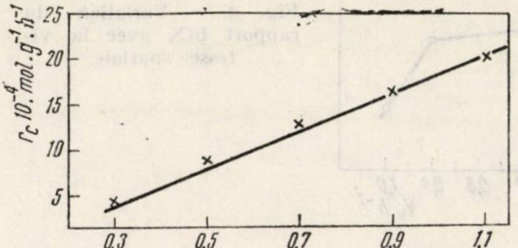

Fig. 6. — Influence de la vitesse spatiale sur la vitesse apparente de réaction.

Il en résulte de la figure 7 qu'à mesure que la température du traitement thermique augmente, il se produit un accroissement de l'intensité de la bande caractéristique aux centres *L* (1450 cm^{-1}), jusqu'à la température du traitement thermique de 700°, après laquelle pratiquement, ne se modifie plus.

L'intensité de la bande 1540 cm^{-1} attribuée aux centres B (fig. 8) présente un maximum évident pour des températures comprises entre 450–550°.

La variation du rapport LPy/BPy en fonction de la température du traitement thermique du catalyseur (fig. 9) a une variation faible jusqu'à la température de calcination de 600°, après quoi il se produit une augmentation significative de ce rapport.

Fig. 7. — Influence du traitement thermique du catalyseur sur l'intensité de la bande caractéristique aux centres L.

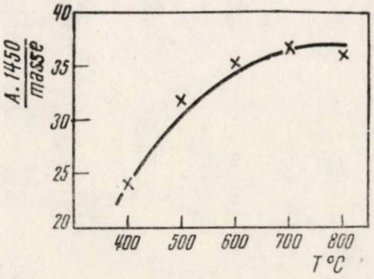

Le fait qu'on detérmine un maximum de la vitesse apparente de la réaction, ainsi que du rapport b/X à 600°, température de calcination, nous permet de conclure que le rapport LPy/BPy est le facteur déterminant du sens de la réaction, à savoir la réaction de transalkylation a lieu pour des valeurs faibles, tandis que la réaction de désalkylation pour de grands valeurs de ce rapport.

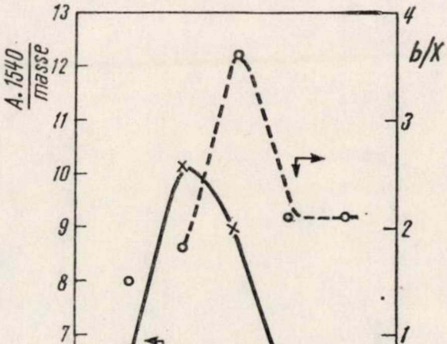

Fig. 8.— Influence du traitement thermique du catalyseur sur l'intensité de la bande caractéristique aux centres B.

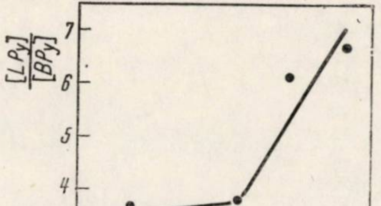

Fig. 9. — Modification du rapport LPy/BPy en fonction de traitement thermique du catalyseur.

Revue Roumaine de Chimie, **23**, *11–12*, 1581–1588 (1978)

SOME REACTIONS OF β-AROYL-ACRYLIC ACID EPOXIDES

M.A. EL-HASHASH and M. EL-KADY
Faculty of Science, Ain Shams University, Abbassia Cairo, Egypt

Received October 15, 1976

β-Aroylacrylic acids **1** react with hydrogen peroxide to give epoxides **2**, which react with sodium hydroxide and give diketones **3** together with glycolic acids **4**. Compounds **2a** and **2e** react with hydrazine to give pyrazolines **7**. Also the reaction of **2d** with hydroxylamine and amines has been described. Compound **2d** reacts with ethylbenzene under Friedel-Crafts conditions and yielded α, β-diphenyl-xenoyl propionic acid **13**.

In general, hydrogen peroxide reacts with α,β-unsaturated carbonyl compounds producing the corresponding α,β-epoxyketones.[1,2] This reaction has been applied on β-aroylacrylic acids in view of synthesis of the hitherto unknown α,β-epoxy-β-aroylacrylic acids. Thus, treatment of the alcoholic solutions of the β-aroylacrylic acid **1a, b** and **e** with hydrogen peroxide in alkaline medium yielded oily products which are believed to have structures like **2a**, **2b**, and **2e** respectively. On the other hand, **1c** and **1d** yielded **2c** and **2d** in a pure crystalline state.

$\mathrm{RCOCH{=}CHCOOH}$

1

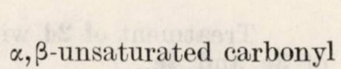

$$\mathrm{R{-}CO\,\underbrace{CH{-}CH}_{O}{-}COOH}$$

2

a : R = C_6H_5
b : R = $p\text{-}CH_3-C_6H_4$
c : R = $p\text{-}Cl-C_6H_4$
d : R = $p\text{-}C_6H_5-C_6H_4$

e : R =

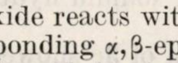

The proposed structures for **2c** and **2d** were supported by their infrared spectra which showed strong bands characteristic of two carbonyls, (1715 cm^{-1}, 1695 cm^{-1}) and epoxide linkage (1260 cm^{-1}). Structures **2a**

---

[1] A. Sammour and M. El-Kasaby, *U.A.R. J. Chem.*, **13,** 151 (1970).
[2] H. H. Wasserman and Norman E. Aubry, *J. Amer. Chem. Soc.*, 77, 590 (1955).

2b and **2e** were established by treatment of the oily products with sodium hydroxide solution[1] when a mixture of two products was obtained. One of these is the arylmethyl-1,2-diketone **3** and the other its rearranged arylmethylglycollic acids **4**.

R—CO—COCH$_3$

3

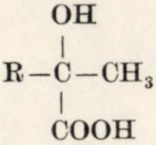

$$R-\overset{\overset{\displaystyle OH}{|}}{\underset{\underset{\displaystyle COOH}{|}}{C}}-CH_3$$

4

a : R = C_6H_5
b : R = p-$CH_3-C_6H_4$
c : R = p-$C_6H_5-C_6H_4$
d : R =

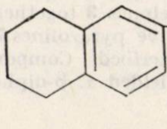

Treatment of **2d** with sodium hydroxide solution yielded a mixture of **3c** and **4c**.

The infrared spectrum of **3c** showed strong absorption bands in the carbonyl region at 1720 cm^{-1} and 1690 cm^{-1} such spectral characteristics being exhibited by 1,2-diketones. The diketone **3b** was identified as its 2,4-dinitrophenylhydrazone **5**, while the diketone **3d** was identified by converting it to 2(2-tetrahydronaphthyl)-3-methyl-quinoxaline **(6)** by reaction with *o*-phenylenediamine.

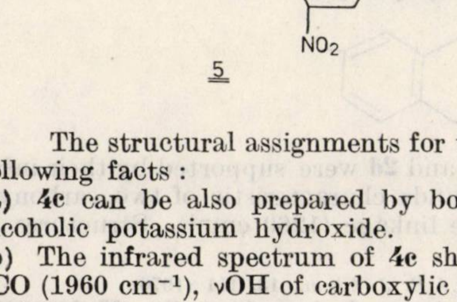

5

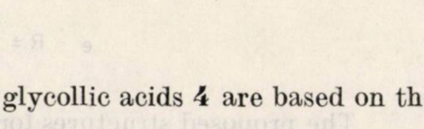

6

The structural assignments for the glycollic acids **4** are based on the following facts :

(a) **4c** can be also prepared by boiling the diketone **3c** with aqueous alcoholic potassium hydroxide.

(b) The infrared spectrum of **4c** showed strong bands characteristic of νCO (1960 cm^{-1}), νOH of carboxylic group (3000 cm^{-1}) and νOH band at (3450 cm^{-1}).

Recently [3-5] it has been shown that the oxirane ring 1,2-epoxyketones is opened with hydrazine. This reaction has been applied on the epoxides **2a** and **2e** with the same result. It is found that the oxirane ring is readily opened when the oils containing **2a** and **2e** are allowed to react with hydrazinehydrate in boiling alcohol, and yielded 3-aryl-4-hydroxy-5-carboxypyrazolines **7a** and **7b**.

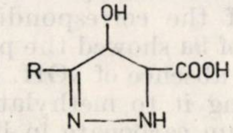

7

a : R = C_6H_5

b : R =

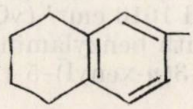

The assigned structure for the hydroxypyrazolines **7a** and **7b** were supported by the following :

(a) They give colour test for pyrazolines.[6]

(b) The infrared spectra showed the OH and NH stretching frequencies in the region of 3400 cm^{-1}, νCO at 1690 cm^{-1} and νC=N at 1610 cm^{-1}.

The NMR spectrum of **7a** (in $CDCl_3$) shows the following signals : a multiplet at δ 7.65 for 5H (aromatic protons), a singlet at δ 7 (OH), a singlet at δ 4.5 (NH) and a doublet at δ 2.2 corresponding to two aliphatic protons.

Compound **2d** reacts with 2,4-dinitrophenylhydrazine in boiling pyridine and yielded 1-(2′,4′-dinitrophenyl)-3-(*p*-xenyl)-4-hydroxy-5-carboxypyrazoline **(8)**. On the other hand, **2d** reacts with 2,4-dinitrophenylhydrazine in boiling alcohol in presence of concentrated sulphuric acid affording the pyrazole derivative **9a**.

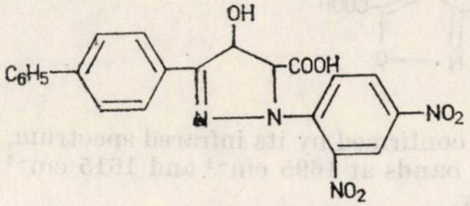

8

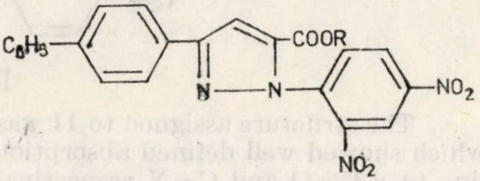

9

a : R = H
b : R = CH_3

---

[3] F. Piozzi and C. Fugant, *Ann. Chim (Ital.)*, **56**, 1248 (1966) ; *Chem. Abstr.* **67**, 73473 (1967).

[4] N. H. Cromwell and J. T. Martin, *J. Org. Chem.*, **33**, 1890 (1968).

[5] G. Kobayaschi, S. Furukawa and Y. Matsuda, *Yalagokuasshi*, **86**, 115 (19766) ; *Chem. Abstr*, **67**, 108594 (1967).

[6] V. Knorr, *Liebigs Ann. Chem.*, **238**, 200 (1887).

The assigned structure for **8** is supported by the followings :

(a) It gives colour test[7] for pyrazolines.

(b) It gives colour test with ferric chloride.

(c) I.R. Spectrum of **8** shows a well defined band in the region of 3440 cm^{-1} attributable for νOH, and other strong absorption bands at 1720 cm^{-1} (due to νCO of carboxylic group) and ($\nu C{=}N$) at 1610 cm^{-1}.

(d) Treatment of **8** with methanolic hydrochloric acid affected dehydration with formation of the corresponding pyrazole derivative **9a**. The infrared spectrum of **9a** showed the presence of νCO (1705 cm^{-1}), $\nu C{=}N$ (1620 cm^{-1}) and absence of νOH. Structure **9a** was confirmed chemically by subjecting it to methylation using dimethylsulphate and anhydrous potassium carbonate in boiling acetone[8] to give the methyl ester **9b** of pyrazole derivative.

Structure of **9b** is supported from the followings :

(a) I.R. Spectrum of **9b** showed strong absorption bands at 1730 cm^{-1} due to νCO of ester and 1610 cm^{-1} ($\nu C{=}N$).

(b) Compound **9b** reacts with benzylamine in boiling ethanol and yielded 1-(2′,4′-dinitrophenyl)-3(*p*-xenyl)-5-(N-benzylcarboxyaminde)-pyrazole **(10)**.

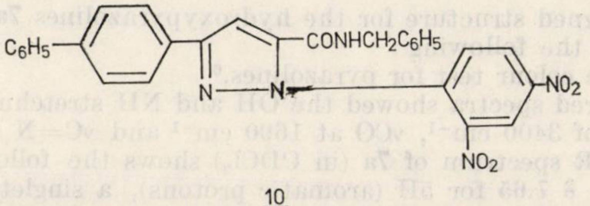

10

In the infrared spectrum of **10** the strong absorptions present at 1665 cm^{-1} and 1605 cm^{-1}, attributable to ν C=O and ν C=N are in accordance with the proposed structure.

The reaction of **2d** with hydroxylamine-hydrochloride in boiling pyridine yielded the isoxazole derivative **11**.

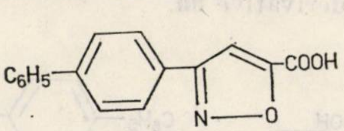

11

The structure assigned to **11** was confirmed by its infrared spectrum, which showed well defined absorption bands at 1695 cm^{-1} and 1615 cm^{-1} due to ν C=O and C=N respectively.

In chemical literature,[9,10] fission of epoxides with amines has been studied. In this study, this reaction was applied to the β-aroylacrylic acid epoxides. Thus, the epoxides **2d** and **2e** were allowed to react with amines, namely butylamine and benzylamine, in boiling alcohol, yielding the α-alkylamino-β-hydroxy-β-aroylpropionic acids **12**.

---

[7] B. H. Nicolet, *J. Amer. Chem. Soc.*, **57,** 1098 (1935).

[8] M. F. El-Newaihy and M. A. El-Hashash, *J. Chem. Soc.* (*c*) **1971,** 2373.

[9] I. G. Tischenko and P. M. Malashko, *Izvest. Akad. Nauk S.S.S.R. Otdel. khim. Nauk,* **6,** 103 (1969) ; *Chem. Abstr.,* **72,** 110 717 (1970).

[10] N. H. Cromwell, F. H. Schun Acher and J. L. Adeffang, *J. Amer. Chem. Soc.,* **83,** 974 (1961).

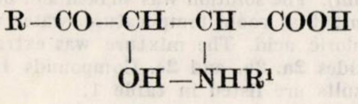

$$\underset{\textstyle OH}{R-CO-\overset{}{C}H}-\underset{\textstyle NHR^1}{CH}-COOH$$

12

a : R = p-$C_6H_5-C_6H_4$; $R^1 = C_4H_9$

b : R = p-$C_6H_5-C_6H_4$; $R^1 = CH_2C_6H_5$

c : R =

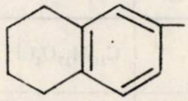

$R^1 = CH_2C_6H_5$

Investigation of the infrared spectra of **12** revealed strong absorption bands at about 3400 cm⁻¹, 3100 cm⁻¹ (ν OH, or ν NH) and at 1710 cm⁻¹, 1690 cm⁻¹ attributable for two ν C=O.

The alkylation of benzene with ethylene-oxide in presence of anhydrous-aluminium-chloride, giving rise to β-phenylethanol, has been reported frequently.[11,12] In the present work it has been observed that the reaction of ethylbenzene with epoxide **2d** in presence of anhydrous-aluminium-chloride yielded α,β-di(p-ethylphenyl)-β-(p-xenoyl) propionic acid **13**.

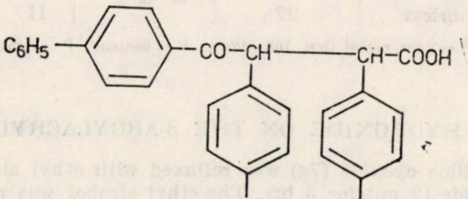

13

The infrared spectrum of **13** showed strong absorption at 1705 cm⁻¹ and 1682 cm⁻¹ due to two ν C=O, data which agree well with the proposed structure.

EXPERIMENTAL

The infrared absorption spectra were determined with a Unicam SP.-1200 Spectrophotometer using KBr Wafer technique, the NMR spectrum was determined with a Varian VN 1009 (S-60T) instrument, positions of peaks are expressed in δ values from TMS as internal standard.

---

[11] A. Schaarashmidt, L. Hermann and B. Szemzo, *Ber dtsch. chem. Ges.*, **58B**, 1914 (1925).

[12] E. T. Theimer, U.S.-Pat., 2, 043, 396 (1936); *Chem. Abstr.*, **30**, 6005 (1936).

EXPOSITION OF β-AROYLACRYLIC ACIDS

A solution of each of the β-aroylacrylic acid **1** (0.01 mole) in acetone (40 ml) and methyl alcohol (15 ml) was treated with 8% aqueous sodium hydroxide (12 ml) followed by hydrogen peroxide (30%; 5 ml). The solution was shaken and brought to boiling point during one hour and then left overnight at room temperature, water was then added and solution acidified with dilute hydrochloric acid. The mixture was extracted with ether compounds **1a**, **1b**, and **1e** gave oily epoxides **2a**, **2b**, and **2e**. Compounds **1c** and **1d** gave the crystalline products **2c** and **2d**. The results are listed in table 1.

Table 1

β-aroylacrylic acid epoxides (2), diketones (3) and glycolic acids (4)

Compd	m.p. (°C) colour	Solvent* yield (%)	Formula	Analyses %	
				Found	Required
2c	172 colourless	X 63	$C_{10}H_{17}O_4Cl$	C 53.21 H 3.26	52.98 3.09
2d	115 colourless	P* 65	$C_{16}H_{12}O_4$	C 71.33 H 4.19	71.63 4.51
3c	109 colourless	P 30	$C_{15}H_{12}O_2$	C 80.10 H 5.09	80.33 5.39
4b	126 colourless	P* 27	$C_{10}H_{12}O_3$	C 66.40 H 6.60	66.65 6.71
4c	205 colourless	B 22	$C_{15}H_{14}O_3$	C 74.67 H 5.57	74.36 5.83
4d	227 colourless	T 27	$C_{13}H_{16}O_3$	C 71.13 H 6.92	70.89 7.32

* X = xylene; P* = light petrol (b.p. 100 – 120°); B = benzene; P = light petrol (b.p. 80 – 100°); T = toluene

ACTION OF SODIUM HYDROXIDE ON THE β-AROYLACRYLIC ACID EPOXIDES

The oil or crystalline epoxide (7g) was refluxed with ethyl alcohol (10 ml) and 10% aqueous sodium hydroxide (2 ml) for 3 hrs. The ethyl alcohol was removed and water was added to the residue. The alkaline solution was extracted with ether (ethereal extract A). The alkaline layer on acidification gave the glycollic acids **4**. The ethereal extract (A) on evaporating yielded the diketones **3**. Compound **3a** was identified as its monoxime m.p. 165° while **4a** was identified as atrolactonic acid m.p. 118°. The results are listed in Table 1.

CONDENSATION OF 3b WITH 2,4-DINITROPHENYLHYDRAZINE. FORMATION OF DIHYDRAZONE 5

A solution of **3b** (2g) in ethanol (50 ml) was treated with 2,4-dinitrophenylhydrazine (0.03 mole) and the solution was refluxed for 5 hrs. The solid that separated after cooling was crystallized from xylene to give **5** as red crystals; m.p. 257°; yield 52% $C_{22}H_{18}N_8O_8$ Found: C, 50.92; H, 3.53; Required: C, 50.57; H, 3.44%.

CONDENSATION OF 3d WITH *o*-PHENYLENEDIAMINE. FORMATION OF THE QUINOXALINE 6

A solution of **3d** (0.01 mole) in ethyl alcohol (50 ml) was treated with *o*-phenylenediamine (0.01 mole). The reaction mixture was refluxed for two hours cooled, the quinoxaline **6** was separated and crystallized from benzene as pale yellow crystals m.p. 173°; yield 75%; $C_{19}H_{18}N_2$ Found: C, 83.40; H, 6.27; Required: C, 83.17; H, 6.61%.

CONVERSION OF THE DIKETONE 3c TO THE ACID 4c

Compound 3c (0.5 g ; 0.002 mole) was refluxed with ethyl alcohol (10 ml) and 10 % potassium hydroxide (5 ml) for two hours. Ethyl alcohol was distilled and water was added to the residue. On acidification with dilute sulphuric acid the acid **4c** separated and was crystallized from benzene-ethanol mixture to give crystals identified as **4c** by m.p. and mixed m.p. determination.

REACTION OF EXPOXIDES WITH HYDRAZINE. FORMATION OF 4-HYDROXY-PYRAZOLINES 7a AND 7b

The oil of **2a** or **2e** (2g) in 50 ml ethanol was heated with 3 ml 85 % hydrazine hydrate, refluxed for 10 hrs., and the reaction mixture poured into ice. The products were crystallized from the suitable solvent to give the hydroxypyrazolines **7a** and **7b**. The results are listed in table 2.

Table 2

Hydroxypyrazolines 7, and α-alkylamino-β-hydroxy-β-aroylpropionic acids 12

Compd	m.p. (°C) colour	solvent* yield(%)	Formula	Analyses %		
					Found	Required
7a	210 white	T 73	$C_{10}H_{10}N_2O_3$	C H	58.62 4.57	58.25 4.89
7b	208 white	X 69	$C_{14}H_{16}N_2O_3$	C H	64.20 5.80	64.60 6.20
12a	230 colourless	B 77	$C_{20}H_{23}NO_4$	C H	70.01 7.12	70.36 6.79
12b	105 colourless	P 63	$C_{23}H_{21}NO_4$	C H	73.27 5.93	73.58 5.64
12c	205 colourless	B 75	$C_{21}H_{23}NO_4$	C H	71.82 6.37	71.37 6.56

* T = toluene ; X = xylene ; B = benzene ; P = light petrol (b.p. 100–120°)

REACTION OF EPOXIDE 2d WITH 2,4-DINITROPHENYLHYDRAZINE. FORMATION OF 8

A solution of **2d** (0.01 mole) and 2,4-dinitrophenylhydrazine (0.01 mole) in pyridine (25 ml) was refluxed for 5 hrs. The product separated after pouring the solution on ice cold hydrochloric acid was crystallized from toluene to give **8** as yellow crystals m.p. 310°, yield 51 % $C_{22}H_{16}N_4O_7$. Found : C, 59.32 ; H, 3.83 ; Required : C, 58.93 ; H, 3.60 %

REACTION OF EPOXIDE 2d WITH 2,4-DINITROPHENYLHYDRAZINE. FORMATION OF 9a

To a solution of the epoxide **2d** (0.01 mole) in ethyl alcohol (50 ml) 2,4-dinitrophenylhydrazine (0.01 mole) and few drops of concetrated sulphuric acid were added, and the mixture was refluxed for 8 hrs. The reaction mixture on cooling gave the product which was crystallized from benzene as red needles to give the pyrazole **9a**, m.p. 217° yield 63 % $C_{22}H_{14}N_4O_6$ Found : C, 61.83 ; H, 3.48 Required ; C, 61.40 ; H, 3.28 %.

CONVERSION OF THE HYDROXYPYRAZOLINE **8** TO THE PYRAZOLE **9a**

A solution of the hydroxypyrazoline **8** (1g) in methanol (25 ml) was refluxed with dry hydrogen chloride then refluxed for 10 hrs. The product separated after cooling was crystallized from benzene (yield 60%) and identified as **9a** by m.p. and mixed m.p. determination.

METHYLATION OF THE PYRAXOLE **9a**. FORMATION OF METHYL ESTER **9b**

A mixture of pyrazole **9a**, dimethylsulphate, and anhydrous potassium carbonate (1 : 4 : 4 mole) in dry acetone was heated under reflux for 20—25 hrs. Excess of solvent was removed by distillation, and neutral product was isolated and crystallized from light petrol (b.p. 100—120°) to give methyl ester **9b** as pale yellow crystals, m.p. 175°, yield 75% $C_{23}H_{16}N_4O_6$ Found : C, 62.49 ; H. 3.81 ; Required : C, 62.16 ; H. 3.63%.

CONDENSATION OF **9b** WITH BENZYLAMINE. FORMATION OF **10**

A solution of **9b** (0.01 mole) and benzylamine (0.01 mole) in 40 ml ethanol was heated under reflux for 5 hrs. The solid separated on cooling was crystallized from ethanol to give **10** as colourless crystals m.p. 203°, yield 72%, $C_{29}H_{21}N_5O_5$ Found : C, 67.52 ; H, 4.37 ; Required : C, 67.04 ; H, 4.07%.

REACTION OF EPOXIDE **2d** WITH HYDROXYLAMINE HYDROCHLORIDE. FORMATION OF ISOXAZOLE **11**

A mixture of epoxide **2d** (0.01 mole) ; hydroxylamine-hydrochloride (0.02 mole) and pyridine (30 ml) was refluxed for 8 hrs. The product separated after pouring the solution into ice-cold dilute hydrochloric acid was crystallized from light petrol(b.p. 100—120°) to give the isoxazole **11** as colourless crystals m.p. 135°, yield 52%, $C_{16}H_{11}NO_3$ Found : C, 72.77 ; H, 4.53 ; Required : C, 72.44 ; H, 4.18%.

REACTION OF EPOXIDES **2d** AND **2e** WITH AMINES. FORMATION OF **12a**, **12b** and **12c**

A solution of epoxides **2d** and **2e** (0.01 mole) in 50 ml ethanol was treated with appropriate amine, namely butylamine and benzylamine (0.01 mole). The solution was heated under reflux for 3 hrs. The solid products after concentration and cooling were crystallized from the proper solvent to give α-alkylamino-β-hydroxy-β-aroylpropionic acids **12a**, **12b** and **12c**. The results are listed in table 2.

REACTION OF EPOXIDE **2d** WITH ETHYLBENZENE. FORMATION OF **13**

A solution of the epoxide **2d** (0.01 mole) in ethylbenzene was added gradually to a suspension of anhydrous-aluminium-chloride (Ca 0.03 mole) in a large excess of ethylbenzene (100 ml). The temperature of the reaction mixture was not allowed to rise above 30°. The suspension was stirred at room temperature for 8 hrs. The whole was then added to hydrochloric acid-ice. The excess of ethylbenzene was removed by steam distillation. The oily residue was dissolved in methanol. The solid obtained was crystallized form light petrol (b.p. 100—120°) to give **13** as colourless crystals, m.p. 192°, yield 53% $C_{32}H_{30}O_3$ Found : C, 82.87 ; H, 6.12 ; Required : C, 83.09 ; H, 6.54%.

Revue Roumaine de Chimie, **23**, *11–12*, 1589–1595 (1978)

INVESTIGATION OF THE AUTOXIDATION PROCESS OF 1-DODECENE

TERESA KOWALSKA
Institute of Chemistry, Silesian University, Katowice,
Poland

Received October 24, 1976

An attempt was made to trace the autoxidation of 1-dodecene by means of gas chromatography and tandem gas chromatography — mass spectrometry. The separation of the obtained autoxidation products by means of gas chromatography was performed using three different stationary phases, and the mass spectra of those products showing the highest yields were run. The importance of the mass spectra is mainly as "fingerprints" of the obtained products, due to the difficulty with the obtaining of molecular ions with the aliphatic compounds and thus with the elucidation of their molecular structures.

INTRODUCTION

Autoxidation of hydrocarbons with molecular oxygen creates an important problem both in the theoretical and practical aspect. Autoxidation of numerous hydrocarbons in liquid phase results with various important substances, which have a wide range of practical applications in manufacturing of artificial fibres, synthetics, surface active compounds, solvents etc.[1,2] Nevertheless the broad investigations, which might in the theoretical way fully explain the complex problems of kinetics and mechanism of hydrocarbon autoxidation, as well as the structures of the obtained oxidation products are an extremely difficult task. The majority of papers on these topics deal with some fragmentary aspects of the a/m problems.[2–5] This explains the necessity of further investigations on autoxidation of paraffins and olefins.

The main interest of this paper was concentrated on investigating the autoxidation process of 1-dodecene by means of gas chromatography and tandem gas chromatography — mass spectrometry techniques.

EXPERIMENTAL

Reagents. 1-Dodecene, "Fluka", Switzerland; this compound was of analytical grade and additionally purified by vacuum distillation (purity ≥ 99.5 %); Benzoyl peroxide, BDH, England, analytical grade.

[1] F. Broich, *Chem. Ing. Techn.*, **34**. 45 (1962).

[2] N. D. Chelok'yan, and E. V. Lebedev, *Neftepererabotka i Neftekhimiya*, **9**, 129 (1969).

[3] A. Greiner, *J. prakt. Chem.*, **38**, 199, 207 (1968).

[4] R. N. Abadsheva, and R. V. Kutsher, *Neftekhimiya*, **4**, 528 (1965).

[5] M. I. Farberov, G. D. Mantyukov, and S. I. Kryukov, *Neftekhimiya*, **4**, 584 (1965).

Equipment: The Pye-104 gas chromatograph (FID). Two columns used.
The metal column 2.5 mm inner diam. × 5 m length, 3% SE-30 on Chromosorb W (60—80 mesh); temp. 130°; carrier gas N_2, the flow rate 30 ml/min.
The glass column 2.5 mm inner diam. × 5 m length, 10% Apiezon L on Phasesep P (85—100 mesh); temp. 140°, carrier gas N_2, the flow rate 30 ml/min.
The Pye-104 gas chromatograph coupled through the silicone membrane separator with the A.E.I. MS-902S mass spectrometer; the ionisation current 70 eV, the separator temperature 200°, the source temperature ca. 200°, the chromatographic conditions as follows: the glass column 2.5 mm inner diam. × 5 m length, 5% Carbowax 20M on Chromosorb WPH (60—80 mesh), temp. of the oven 140°, carrier gas He, the flow rate 12 ml/min.
Conditions of running the autoxidation and performing the analyses.

The reaction of autoxidation of 1-dodecene was run with the help of oxygen from air, bubbled through the whole volume of hydrocarbon. For this purpose 2 ml of 1-dodecene with the addition of 0.5% benzoyl peroxide as an initiator was placed in a 10 ml pearshaped, three-necked reaction flask. The flask was equipped with a water-cooled condensor. The air was introduced through a cappillary with the flow rate of 20, 30 and 40 ml/min. On the basis of the preliminary experiments the optimum flow rate of air was established as 40 ml/min. The autoxidation reaction was run at 90±1° for 6 hrs. In the 0.5 hr intervals the course of reaction was controlled, using the chromatographic column with 3% SE-30 on Chromosorb W. At the end of the autoxidation process the detailed chromatographic separation of the obtained products was performed, using the chromatographic column with 10% Apiezon L on Phasesep P. The similar separation was repeated with 5% Carbowax 20M on Chromosorb WPH using the tandem GC-MS system and recording the mass spectra of the separated substances.

RESULTS AND DISCUSSION

The conditions of running the autoxidation of 1-dodecene aimed at the slow growth of the concentration of the reaction products in the mass of the oxidized substrate. As shown in Figure 1, one can point out 5 chemical compounds, which dominate in respect of their quantities, although their total yield is ca. 3%.

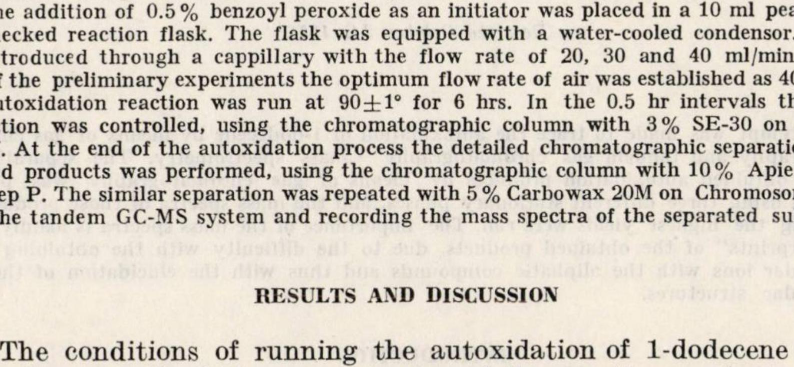

Fig. 1. — The gas chromatogram of the oxidized sample of 1-dodecene; The metal column 2.5 mm inner diam. × 5 m length, 3% SE-30 on Chromosorb W/60—80 mesh/, temp. 130°, carrier gas N_2, the flow rate 30 ml/min, FID; 1—5: the main products of autoxidation of 1-dodecene.

The chromatogram shown in Figure 1 demonstrates the unsatisfactory separation of the autoxidation products, with sufficient results only in the case of these substances, which produce the highest yields during the course of autoxidation. Therefore another column was used, with 10% Apiezon L on Phasesep P. With this column the better separation of the autoxidation products was obtained, with the good results also in the case of these products, which showed much lower yields during the course of the process. This separation is shown in Figure 2.

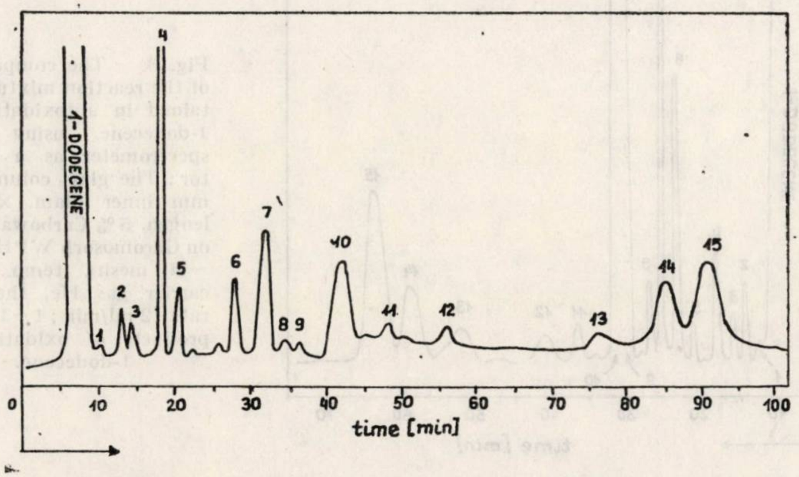

Fig. 2. — The gas chromatogram of the oxidized sample of 1-dodecene; The glass column 2.5 mm inner diam. × 5 m length, 10% Apiezon L on Phasesep P/85—100 mesh/, temp. 140°, carrier gas N_2, the flow rate 30 ml/min, FID; 1—15: the products of oxidation of 1-dodecene.

Now it ought to be mentioned that the application of chromatographic technique itself was insufficient to decide in a question, which product of autoxidation can be treated as a primary one, i.e. obtained directly from 1-dodecene through autoxidation. Taking into assumption the complex composition of the reaction mixture, including 15 separated products, both with higher and trace yields, the GC—MS characteristics of these substances were introduced. Applying the analytical conditions as described before, and the recorder coupled with the mass spectrometer, the separation of the autoxidation products on 5% Carbowax 20M on Chromosorb WPH was obtained and recorded as shown in Figure 3.

Comparing the chromatogram shown in Figure 1 with those presented in Figures 2 and 3 it was established that the five peaks 1—5 from Figure 1 correspond with the peaks 4, 6, 7, 10 and 15 from Figures 2 and 3. The additional confirmation was obtained through comparison of the corresponding mass spectra.

Although mass spectrometry is not the technique especially recommended in analysis of the aliphatic compounds, specially these medium- and long-chained ones,[6-8] which is due to their great susceptibility for

---

[6] P. Capella, M. Piretti, and A. Strocchi, *Riv. Ital. Sost. Grasse,* **46,** 659 (1969).

[7] R.T.M. Fraser, N. C. Paul, and L. Phillips, *J. Chem. Soc.* (*B*), **1970,** 1278.

[8] A. R. Burgess, D. K. Sen Sharma, and M.J.D. White, "Advances in Mass Spectrometry", Ed. E. Ken Drick, Elsevier, Amsterdam, 1968, pp. 345—356.

fragmentation along the whole carbon chain and thus the complex pattern of the obtained spectra, its application has also some definite value. The spectra presented in this paper serve mainly as "fingerprints", specially because none of them produces the molecular ion, which makes elucidation

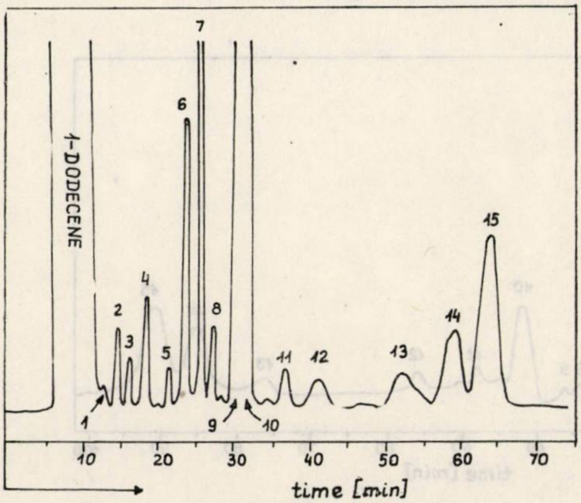

Fig. 3. — The composition of the reaction mixture obtained in autoxidation of 1-dodecene, using mass spectrometer as a detector; The glass column 2.5 mm inner diam. × 5 m length, 5% Carbowax 20M on Chromosorb WPH /60—80 mesh/, temp. 140°, carrier gas He, the flow rate 12 ml/min; 1—15: the products of oxidation of 1-dodecene.

of the corresponding structure possible. In Figures 4—8 the linear diagrams are shown of the mass spectra of these among the autoxidation products, which show the highest abundance, i.e. of the compounds, which are described as peaks 4, 6, 7, 10 and 15 in Figures 2 and 3.

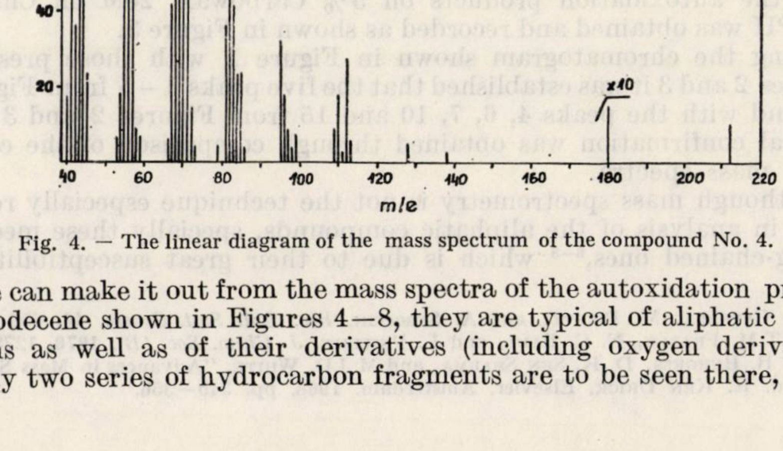

Fig. 4. — The linear diagram of the mass spectrum of the compound No. 4.

As one can make it out from the mass spectra of the autoxidation products of 1-dodecene shown in Figures 4—8, they are typical of aliphatic hydrocarbons as well as of their derivatives (including oxygen derivatives). Namely two series of hydrocarbon fragments are to be seen there, having

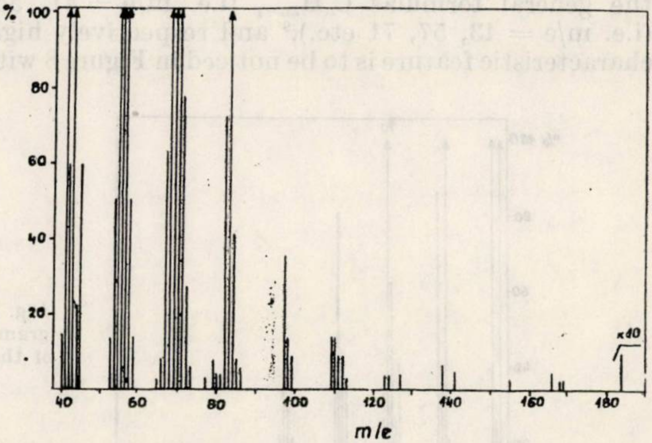

Fig. 5. — The linear diagram of the mass spectrum of the compound No. 6.

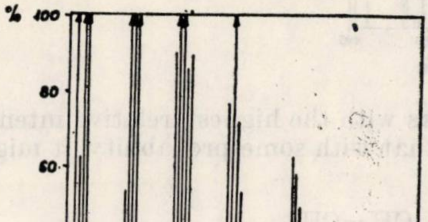

Fig. 6. — The linear diagram of the mass spectrum of the compound No. 7.

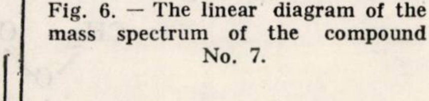

Fig. 7. — The linear diagram of the mass spectrum of the compound No. 10.

the general formulas C_nH_{2n-1} (i.e. m/e = 41, 55, 69 etc.) and C_nH_{2n+1} (i.e. m/e = 43, 57, 71 etc.),[9] and respectively high relative intensities. A characteristic feature is to be noticed in Figure 8 with the peak at m/e = 70.

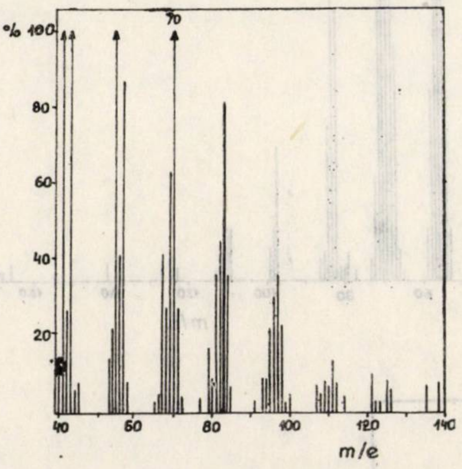

Fig. 8. — The linear diagram of the mass spectrum of the compound No. 15.

It belongs to the group of four peaks with the highest relative intensities, present in this spectrum. It seems that with some probability it might be ascribed to the below given ion :

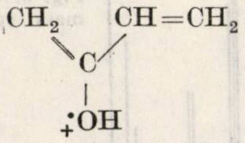

m/e = 70,

obtained in the following way :

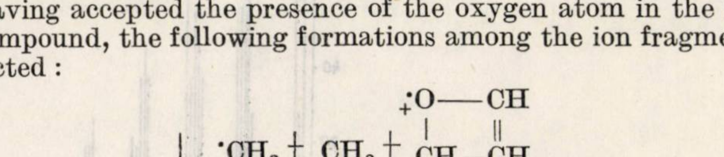

As an additional evidence for this sort of supposition the simultaneous specially high intensities of the peaks with m/e = 55, 69 and 83 may be given. Having accepted the presence of the oxygen atom in the molecule of this compound, the following formations among the ion fragments may be suspected :

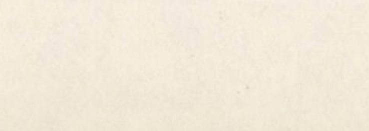

---

[9] A. R. Burgess, R.D.G. Lane, and D. K. Sen Sharma, *J. Chem. Soc.* (*B*) **1969**, 341.

obtained according to the following pattern :

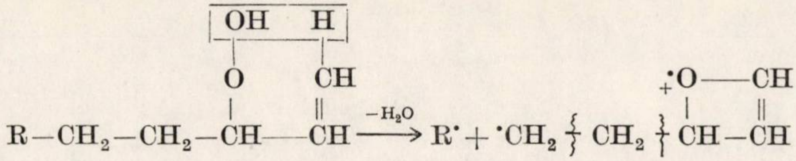

$$\begin{array}{lcccl}
 & \boxed{OH} & \boxed{H} & & \\
 & | & | & & \\
 & O & CH & & {}^{+}\dot{O}—CH \\
 & | & \| & & \;|\qquad\| \\
R-CH_2-CH_2- & CH & CH & \xrightarrow{-H_2O} R^{\cdot} + {}^{\cdot}CH_2 \wr CH_2 \wr & CH-CH
\end{array}$$

Such a mechanism would be analogical with one suggested by some authors on similar occasions [9,10] and the compound No. 15 from the presented chromatograms (Figures 2 and 3) could be the 1-dodecene hydroperoxide, which means the primary product of its autoxidation. On this basis the remaining products of autoxidation may possibly be accepted as the secondary products of this process, obtained in the further steps of the reaction. According to the contemporary theoretical interpretation of the autoxidation of olefins,[11] the secondary products are formed through the quick decay of hydroperoxides, resulting in the wide range of the final, more stable compounds.

Acknowledgement. I would like to thank Professor Dr. Józef Śliwiok for introducing me to the problems of autoxidation of aliphatic compounds and constant encouragement while working on this subject.

---

[10] H. Budzikiewicz, C. Djerassi, and D. H. Williams, "Interpretation of Mass Spectra of Organic Compounds", Holden-Day, San Francisco, 1964, p. 33.

[11] "Autoxidation and Antioxidants", Ed. W. O. Lundberg, Interscience Publishers, New York, 1961.

Revue Roumaine de Chimie, 23, 11–12, 1597–1605 (1978)

SOME REACTIONS WITH β-*p*-CHLOROBENZOYLACRYLIC ACIDS AND β-*p*-TOLUYL-N-(*o*-CARBOXYPHENYL)-ACRYLAMIDE

E. A. SOLIMAN
Faculty of Science, Ain Shams University Cairo, Egypt

Received November 8, 1976

The reaction of β-*p*-chlorobenzoylacrylic acid and β-*p*-toluyl-N-(*o*-carboxyphenyl)acrylamide with thiourea, amines and hydrazines has been investigated. Friedel-Crafts reaction with β-*p*-chlorobenzoylacrylic acid has been also described.

It is known that β-aroylacrylic acids reacts with thioureas [1,2] to give the corresponding 2-amino-4-hydroxy-5-aroylmethylthiazoles. This reaction has been now extended and explored. Thus reaction of β-*p*-chlorobenzoylacrylic acid (I) with thiourea or benzylthiourea gave 2-amino-4-hydroxy-5-*o*-chlorobenzoylmethylthiazoles IIIa and IIIb, respectively. But when this reaction was applied on the β-*p*-toluyl-N-(*o*-carboxyphenyl) acrylamide (II) it did not give the corresponding thiazole derivatives but gave 2-thio-1-(3-*p*-toluylacryloyl)urea derivatives IVa and IVb, respectively with elimination of anthranilic acid.

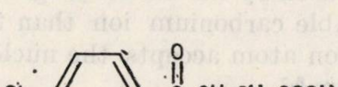

I

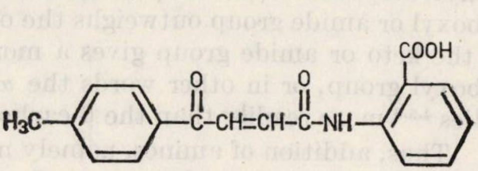

II

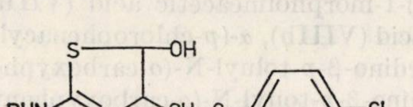

III

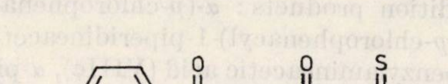

IV

a, $R = H$ b, $R = CH_2C_6H_5$

---

[1] R. Delaby, S. Danton and P. Chabrier, *Bull. Soc. chim. France*, 1961, 2061; *Chem. Abstr.*, 56, 14157 (1961).

[2] A. Sammour, M.IB. Selim and E. A. Soliman, *U.A.R. J. Chem.*, **15**; 311(1972).

The infrared spectra of compounds III showed bands in the region of 3320 cm^{-1} attributable to OH and NH groups, [3a] at 1710 cm^{-1} attributable to carbonyl group, [3b] and 1640 cm^{-1} attributable to C=N group of thiazole [3c].

The infrared spectra of compounds IV showed well-defined bands in the region of 3440 cm^{-1} (NH group), at 1720 cm^{-1} (C=O of ketone), 1680 cm^{-1} (C=O of amide),[3d] 1605 cm^{-1} (aliphatic C=C) [3c] and at 1270 cm^{-1} (C=S group).[3f]

As a point of interest, condensation of thiazoles III with hydrazine hydrate or hydroxylamine hydrochloride in boiling alcohol or in acetic acid gave 6-amino-3-(*p*-chlorophenyl)-1,4-dihydrothiazolo [5,4-*c*] pyridine (Va), 6-benzylamino-3-(*p*-chlorophenyl)-1,4-dihydrothiazolo [5,4-*c*] pyridine (Vb),6-amino-3-(*p*-chlorophenyl)-4*H*-thiazolo [4,5-*c*]-1,2-oxazine (VIa) and 6-benzylamino-3-(*p*-chlorophenyl)-4*H*-thiazolo [4,5-*c*]-1,2-oxazine (VIb), respectively.

The structures of compounds V and VI are supported by the infrared spectra which showed a well-defined band in the region of 3440 cm^{-1} (attributable to NH group), a stretching band at 1655 cm^{-1} (C=N group of thiazole) and a band at 1620 cm^{-1} (C=N group).

On the other hand, condensation of III with phenylhydrazine in boiling alcohol or in acetic acid gave 4′-[2-amino-5-hydroxy-4-thiazolyl]-4′-chloroacetophenone-phenylhydrazone (VIIa) and 4′-[benzylamino-5-hydroxy-4-thiazolyl]-4′-chloroacetophenonephenylhydrazone (VIIb).

The infrared spectra of compounds VII showed bands in the region of 3380 cm^{-1} (OH and NH group), 2920 cm^{-1} (CH_2group) [3g], 1640 cm^{-1} (C=N of thiazole), and 1620 cm^{-1} (C=N group).

In β-*p*-chlorobenzoylacrylic acid (I) or β-*p*-toluyl-N-(*p*-carboxyphenyl) acrylamide (II) the polarization of the double bond caused by the carboxyl or amide group outweighs the one caused by the carboxyl group, i.e. the keto or amide group gives a more stable carbonium ion than the carboxyl group, or in other words the α-carbon atom accepts the nucleophilies [4,5,6] more readily than the β-carbon atom [6,7].

Thus, addition of amines, namely morpholine, piperidine and benzylamine to a benzene solution of I or II yielded the corresponding addition products : α-(*p*-chlorophenacyl)-1-morpholineacetic acid (VIIIa) α-(*p*-chlorophenacyl)-1-piperidineacetic acid (VIIIb), α-(*p*-chlorophenacyl)-1-benzylamineacetic acid (VIIIc), α-piperdino-β-*p*-toluyl-N-(*o*-carboxyphenyl) propylamide (IXa) and α—benzylamino-β-*p*-touyl-N-(*o*-carboxyphenyl propylamide (IXb), respectively.

---

[3] L. J. BELLAMY "The Infrared Spectra of Complex Moleclues" Methuen, London, pp. [a] 249; [b] 132; [c] 277; [d] 204; [e] 34; [f] 355; [g] 13; [h] 162.

[4] N. H. CROMWELL, P. L. CRAGER, and K. E. COOK, *J. Amer. Chem. Soc.*, **78**, 4412 (1956).

[5] N. H. CROMWELL, and K. E. COOK, *J. Org. Chem.*, **23**, 1327 (1958).

[6] H. KATO and M. SCHIONA, *Nippon Kagaker Zasshi*, **88**, 2274 (1967).

[7] R. PUMMERER and E. BUCHTA, *Ber. dtsch. Chem. Gess.*, **69**, 1005(1936).

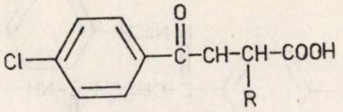

VIII

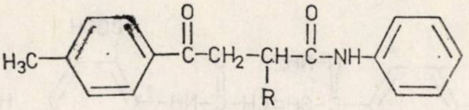

IX

a, R = NC_4H_8O
b, R = NC_5H_{10}
c, R = $NHCH_2C_6H_5$

a, R = NC_5H_{10}
b, R = $NHCH_2C_6H_5$

The infrared spectrum of VIIIb showed well-defined bands at 3560 cm^{-1} (OH group) 3h, 1720 cm^{-1} (C=O of carboxyl group), 1700 cm^{-1} (ketone group) and 2920 cm^{-1}, 2880 cm^{-1} (CH_2 group).

The infrared spectrum of IXa showed well-defined bands at 1680 cm^{-1} and 1700 cm^{-1} (C=O groups), 3420 cm^{-1} (NH group) and 2940 cm^{-1} (CH_2 group).

In general, phenylhydrazine reacts with α, β-unsaturated carbonyl compounds producing pyrazolines. This reaction has now been applied on β-*p*-chlorobenzoylacrylic acid (I) with hydrazine hydrate or phenylhydrazine. The corresponding 3-(*p*-chlorobenzoyl) acrylic acid hydrazone (Xa) and 3-(*p*-chlorobenzoyl) acrylic acid phenylhydrazone (Xb) were obtained without cyclization due to the decreased reactivity of the olefinic double bond in I (in comparison with unsaturated ketones).

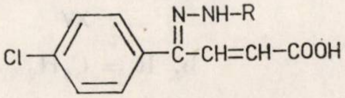

X

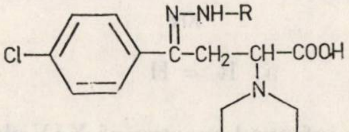

XI

a, R = H b, R = C_6H_5

The infrared spectrum of Xb showed well-defined bands at 1585 cm^{-1} (C=N), 3540 and 3440 cm^{-1} (OH and NH groups) and at 1600 cm^{-1} (olefinic C=C group).

Treatment of VIIIb with hydrazine hydrate or phenylhydrazine in alcohol was found to give α-(*p*-chlorophenacyl)-1-piperidineacetic acid hydrazone (XIa) and α-(*p*-chlorophenacyl)-1-piperidine acetic acid phenylhydrazone (XIb), respectively.

Condensation of VIIIb with hydrazine hydrate or phenylhydrazine in warm acetic acid gave the same hydrazone and phenylhydrazone derivatives Xa and Xb with elimination of the amine.

On the other hand, condensation of β-*p*-toluyl-N-(*p*-carboxyphenyl) acrylamide (II) with hydrazine hydrate or phenylhydrazine gave the corresponding hydrazone or cyclic products depending on the reaction conditions. In boiling alcohol it gave β-*p*-toluyl-N-(*o*-carboxyphenyl)acrylamide hydrazone (XII).

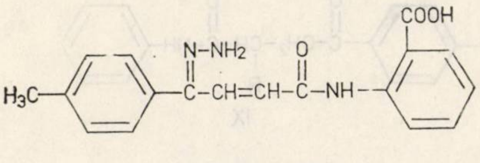
XII

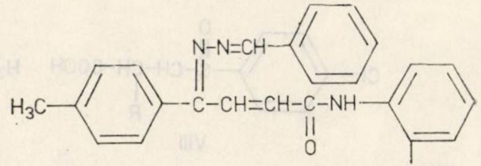
XIII

The infrared spectrum of XII showed well defined bands at 3420 cm^{-1} (OH and NH groups), 1690 cm^{-1} (C=O of the anilide), 1580 cm^{-1} (C=N) and 1605 cm^{-1} (aliphatic C=C group).

Compound XII can be easily condensed with benzaldehyde to give XIII.

Condensation of II with hydrazine hydrate or phenylhydrazine in boiling acetic acid gave two products 2-(2-*p*-toluylvinyl)-4H-3,1-benzoxazine-4-one hydrazone (XIVa), 2-(2-*p*-toluylvinyl)-4H-3,1-benzoxazine-4-one phenylhydrazone (XIVb) and the corresponding pyridazine derivatives XVa and XVb, respectively.

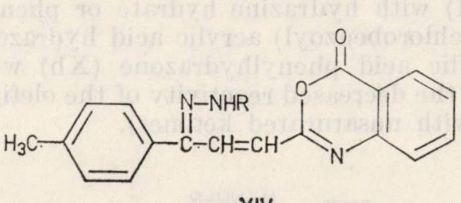
XIV

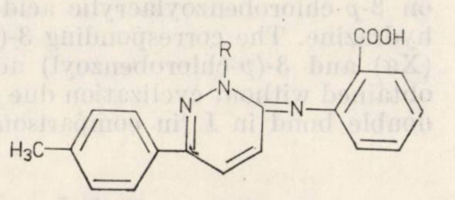
XV

a, R = H b, R = C_6H_5

The infrared spectra of XIV showed well-defined bands at 3410 cm^{-1} (NH group), 1595 cm^{-1} (C=N), 1720 cm^{-1} (C=O group) and 1605 cm^{-1} (aliphatic C=C group), whereas the infrared spectra of XV showed bands at 1580 cm^{-1} (C=N), 3480 cm^{-1} (OH group) and 1600 cm^{-1} (C=C group).

The structure of XIV has been established also via synthesis, by heating the hydrazone derivative XII with acetic anhydride.

On the other hand, reaction of XIVa with hydrazine hydrate in boiling alcohol (molar ratio 1 :1) gave 2-(2-*p*-toluylvinyl)-4H-3-aminoquinazoline-4-one hydrazone (XVI).

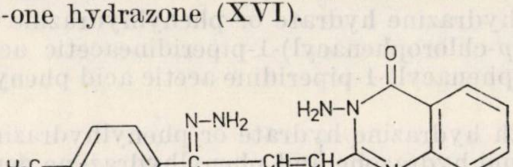
XVI

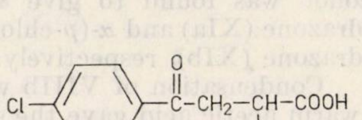
XVII

a, Ar = $C_6H_4CH_3(p)$
b, Ar = $C_6H_4C_2H_5(p)$
c, Ar = $C_6H_4OCH_3(p)$

Friedel-Crafts alkylation of β-benzoylacrylic acid takes place on α-carbon to the carbonyl group.[7] But addition of toluene, ethylbenzene and anisole to β-*p*-chlorobenzoylacrylic acid (I) under Friedel Crafts conditions, gave the corresponding α-(*p*-methylphenyl)-β-*p*-chlorobenzoylpropionic acid (XVIIa, α-(*p*-ethylphenyl)-β-*p*-chlorobenzoylpropionic acid (XVIIb) and α-(*p*-methoxyphenyl)-β-*p*-chlorobenzoylpropionic acid (XVIIc), respectively.[8]

The n.m.r. spectrum of XVIIb in $CDCl_3$ showed bands at δ values 7.95 (s), 7.80 (s), 7.35 (s), 7.30 (s) and 7.20 (s) (8H of substituted phenyl groups), 4.70 (m) (1H of $CH-COOH$), 2.75 (m) (2H of $-\underset{\underset{O}{\|}}{C}-CH_2$ group) 2.70 (m) (2H of CH_2 group adjacent to phenyl group) and 1.20 (t) (3H of CH_3 in CH_3-CH_2 group).

The infrared spectrum of XVIIa showed well defined bands at 3530 cm⁻¹ (OH group), 2880 cm⁻¹ (CH_2 group), 1720 cm⁻¹ ($C=O$ of carboxyl group) and 1690 cm⁻¹ ($C=O$ of ketone group).

Compounds XVIIa and XVIIb were easily dehydrated on boiling with acetic anhydride to give 3-(*p*-methylphenyl)-5-*p*-chlorophenyl-Δβ, γ-butenolide (XVIIIa) and 3-(*p*-ethylphenyl)-5-*p*-chlorophenyl-Δβ, γ-butenolide (XVIIIb), respectively.

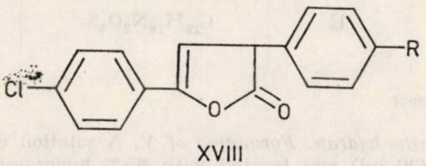

XVIII

a, $R = CH_3$ b, $R = CH_2CH_3$

The n.m.r. spectrum of XVIIIb show bands at δ values 7.90 (s), 7.80 (m), 7.65 (s), 7.40 (m) and 7.10 (m) (8H of substituted phenyl groups), 8.15 (s) (1H of $CH-\underset{\underset{O}{\|}}{C}-$ of 5-membered ring), 6.25 (s) (1H of $-CH=C$ group), 2.50 (m) (2H of CH_2- group adjacent to phenyl group) and 1.10 (t) (3H of CH_3 group in $-CH_2-CH_3$).

The infrared spectra of compounds XVIII showed defined bands at 1770 cm⁻¹ (lactone ring) and at 1600 cm⁻¹ (aliphatic $C=C$ group).

Condensation of XVIIa with hydrazine hydrate or phenylhydrazine in boiling alcohol gave 4-(*p*-tolyl)-6-*p*-chlorophenyl-2,3,4,5-tetrahydropyridazine-3-one (XIXa) and 2-phenyl-4-(*p*-tolyl)-6-*p*-chlorophenyl-2,3,4,5-tetrahydropyridazine-3-one (XIXb), respectively.

The infrared spectrum of XIXa showed well-defined bands at 1580 cm⁻¹ for ($C=N$) and 1710 cm⁻¹ ($C=O$ group).

---

[8] E. A. Khalaf, *Rev. Roumaine Chim.*, **18**, 2, 297 (1973).

EXPERIMENTAL

The infrared absorption spectra were determined with a Unicam SP 1200 Spectrophotometer using KBr Wafer technique. All melting points are not corrected.

Reaction of I and II with thioureas. Formation of III and IV.

A mixture of I or II (0.01 mole), thiourea (or benzylthiourea) (0.02 mole), ethanol (15 ml) was treated with 10 drops of glacial acetic acid. The mixture was then refluxed for 4 hrs. The solid which separated after evaporation of most of the solvent and cooling was crystallized from a proper solvent to give the thiazole derivatives IIIa (or IIIb) or thiourea derivatives IVa and IVb, respectively as colourless crystalls (yield 85 %). The results are listed in table 1.

Table 1

Thiazole III and thiourea IV derivatives

Compound	m.p. (°C)	Solvent*	Fomrula	Analysis (%)		
					Found	Required
IIIa	252	B/E	$C_{11}H_9ClN_2O_2S$	C H S	48.8 3.5 11.5	49.1 3.3 11.9
IIIb	214	B/E	$C_{18}H_{15}ClN_2O_2S$	C H N	59.9 4.1 8.7	60.2 4.1 8.9
IVa	244	E	$C_{12}H_{12}N_2O_2S$	C H S	57.6 4.4 12.8	58.0 4.8 12.9
IVb	222	E	$C_{19}H_{18}N_2O_2S$	C H N	67.2 5.5 8.2	67.4 5.6 8.2

* B = benzene ; E = ethanol

Reaction of III with hydrazine hydrate. Formation of V. A solution of thiazoles III (0.01 mole) in ethanol or acetic acid (20 ml) was treated with 85 % hydrazine hydrate (2 ml) and the solution was refluxed for 3 hrs. The solids which separated after cooling, were crystallized from suitable solvents to give the thiazolopyridazine Va and Vb as colourless crystals (yield 70 %). The results are listed in table 2.

Table 2

Thiazolo-pyridazine derivatives V

Compound	m.p. (°C)	Solvent *	Formula	Analysis (%)		
					Found	Required
Va	175	A	$C_{11}H_9N_4SCl$	C H N	49.3 3.4 20.9	49.9 3.4 21.2
Vb	149	E	$C_{18}H_{15}N_4SCl$	C H N	61.1 4.1 15.7	61.6 4.3 15.9

* A = acetic acid ; E = ethanol

Reaction of III with hydroxylamine hydrochloride. Formation of VI.

To a solution of III (0.01 mole) in ethanol (20 ml) hydroxalamine hydrochloride (0.01 mole) and a solution of sodium acetate (0.02 mole) in a few drops of water were added, then the mixture was refluxed for 5 hrs. The solid products formed after cooling were crystallized from ethanol to give thiazoloxazine derivatives VIa and VIb as colourless crystals (yield 50 %). The results are listed in table 3.

Table 3

Thiazolo-oxazine derivatives VI

Compound	m.p. (°C)	Formula		Analysis (%) Found	Analysis (%) Required
VIa	164.5	$C_{11}H_8N_3OSCl$	C H	49.6 3.1	49.7 3.0
VIb	210	$C_{18}H_{14}N_3OSCl$	C H	60.5 3.7	60.7 3.9

Reaction of III with phenylhydrazine. Formation of VII. A solution of III (0.01 mole) in ethanol or acetic acid (20 ml) was heated with phenylhydrazine (0.01 mole) under reflux for 3 hrs. The solid products formed after evaporation of most of the solvent and cooling were crystallized from proper solvent to give the phenylhydrazone derivatives VIIa and VIIb as pale yellow crystals (yield 75 %). The results are listed in table 4.

Table 4

Phenylhydrazone derivatives VII

Compound	m.p. (°C)	Solvent*	Formula		Analysis (%) Found	Analysis (%) Required
VIIa	164−5	B/E	$C_{17}H_{15}N_4OSCl$	C H	56.9 4.0	56.9 4.1
VIIb	182−3	E	$C_{24}H_{21}N_3OSCl$	C H	66.1 4.6	66.2 4.8

* B = benzene; E = ethanol

Reaction of I and II with amines. Formation of VIII and IX. To a solution of I or II (0.01 mole) in benzene (100 ml) the appropriate amine, namely, morpholine, piperidine or benzylamine (0.02 mole) was added. After standing at room temperature (10−15 min.) the separated products were crystallized from suitable solvent to give the corresponding addition products VIIIa−c and IXa and IXb as colourless crystals (yield 95 %). The results are listed in table 5.

Table 5

Addition products VIII and IX

Compound	m.p. (°C)	Solvent *	Formula		Analysis (%) Found	Analysis (%) Required
VIIIa	179−1	B/E	$C_{14}H_{16}NO_4Cl$	C H N	56.2 5.3 5.4	56.4 5.3 4.7
VIIIb	184−5	B/E	$C_{15}H_{18}NO_3Cl$	C H N	60.9 6.1 4.6	60.9 6.1 4.7
VIIIc	177−8	B/E	$C_{17}H_{16}NI_3Cl$	C H	63.9 5.1	64.2 5.0
IXa	112−3	P/B	$C_{22}H_{26}N_2O_2$	C H	75.0 7.0	75.4 7.4
IXb	195−6	B	$C_{24}H_{24}N_2O_2$	C H	77.2 6.3	77.4 6.4

* B = benzene; E = ethanol; P = petroleum ether (b.p. 100−120 °C)

Table 6

Hydrazone and phenylhydrazone derivatives X

Compound	m.p. (°C)	Formula	Analysis (%)		
				Found	Required
Xa	206–7	$C_{10}H_9N_2O_2Cl$	C	53.4	53.4
			H	4.1	4.0
			N	12.3	12.4
Xb	191–2	$C_{16}H_{13}N_2O_2Cl$	C	63.6	63.8
			H	4.3	4.3

Table 7

Condensation products XI, XII, XIV, XV, XVI and XIX

Componud	m.p. (°C)	Solvent*	Colour yield %	Formula	Analysis (%)		
						Found	Required
XIa	152–3	B/E	Yellow 85	$C_{15}H_{20}N_2O_2Cl$	C	60.6	60.9
					H	6.6	6.7
					N	9.2	9.4
XIb	134–5	E	Yellow 85	$C_{21}H_{24}N_2O_2Cl$	C	67.6	67.8
					H	6.2	6.4
					N	7.3	7.5
XII	300	B/E	colourless 65	$C_{18}H_{17}N_3O_3$	C	64.2	64.8
					H	5.0	5.1
					N	15.5	15.6
XIVa	89–90	B	colourless 75	$C_{18}H_{15}N_3O_2$	C	68.3	68.5
					H	4.4	4.7
					N	16.2	16.5
XIVb	187–8	E	Yellow 90	$C_{24}H_{19}N_3O_2$	C	73.5	73.6
					H	4.4	4.8
XVa	121–2	B/E	Yellow 70	$C_{18}H_{15}N_3O_2$	C	68.5	68.5
					H	4.6	4.7
					N	16.4	16.5
XVb	201–2	E	Yellow 75	$C_{24}H_{19}N_3O_2$	C	73.5	73.6
					H	4.6	4.8
XVI	208	E	colourless 80	$C_{18}H_{17}N_5O$	C	67.7	67.7
					H	5.3	5.3
					N	21.7	21.9
XIXa	177–8	B	Yellow 65	$C_{17}H_{14}N_2OCl$	C	68.5	68.5
					H	4.7	4.7
					N	9.2	9.4
XIXb	146–7	P	Yellow 80	$C_{23}H_{18}N_2OCl$	C	73.6	73.8
					H	4.8	4.8

* B = benzene; E = ethanol; P = petroleum ether (b.p. 80–100 °C)

Reaction of I with hydrazines. Formation of X. To a solution of I (0.01 mole) in glacial acetic acid (20 ml), hyrdazine hydrate or phenylhydrazine (0.02 mole) was added. A voluminous light yellow precipitate, immediately separated, dissolved after standing at room temperature for 24 hrs.

The reaction mixture was poured into ice and the separated solid was crystallized from a mixture of benzene and ethanol to give the hydrazone or phenylhydrazone derivatives Xy and Xb (yield 95%). The results are listed in table 6.

Reaction of VIIIb, II, XVIIa, XIVa. Formation of XI, XII, XIV, XV, XVI and XIX — A mixture of VIIIb, II, XIVa, or XVIIa (0.01 mole) hydrazine hydrate or phenylhydrazine (0.01 mole) and ethanol or acetic acid (20 ml) was refluxed for 6 hrs. The solid products formed after cooling were crystallized form proper solvent to give the corresponding condensation products XI, XII, XIV, XV, XVI and XIX, respectively. The results are listed in table 7.

Condensation of XII with benzaldehyde. Formation of XIII. A mixture of XII (0.01 mole), benzaldehyde (0.01 mole), ethanol (20 ml) and a few drops of piperidine was refluxed for 6 hrs. The solid product obtained after cooling and evaporation of most of the solvent was crystallized from ethanol to give XIII as colourless crystals, m.p. 182° (yield 80%) Found: C, 72.7; H, 4.9; N, 10.3%; $C_{25}H_{21}N_3O_3$ Required: C, 72.9; H, 5.1; N, 10.2%.

Friedel-Crafts alkylation of β-p-chlorobenzoylacrylic acid (I). Formation of α-aryl-β-p-chlorobenzoylpropionic acids (XVIIa-c). A solution of β-*p*-chlorobenzoylacrylic acid (0.01 mole) in aromatic hydrocarbon (toluene, ethylbenzene or anisole, 50 ml) was saturated with dry hydrogen chloride and aluminium chloride (0.04 mole) was added. The temperature of the reaction was maintained at 20—25°, stirring was continued for an additional 15 hrs. at room temperature. The reaction mixture was then added to a mixture of ice and HCl, the organic layer was washed with water and the excess solvent was removed by steam distillation. The organic material were extracted with ether and the ethereal solution was washed with 10% aqueous sodium carbonate solution. The alkaline solution was acidified with cold dilute hydrochloric acid. The products were crystallized from the suitable solvent to give α-aryl-β-*p*-chlorobenzoylpropionic acids (XVIIa—c) as colourless crystals (yield 65%). The results are listed in table 8.

Table 8

α-Aryl-β-*p*-chlorobenzoylpropionic acids XVII

Componud	m.p. (°C)	Solvent *	Fomrula	Analysis (%)		
					Found	Required
XVIIa	154—5	B/E	$C_{17}H_{15}O_3Cl$	C H	67.4 4.8	67.4 4.9
XVIIb	128—9	B	$C_{18}H_{17}O_3Cl$	C H	68.1 5.1	68.2 5.3
XVIIc	210—1	B/E	$C_{17}H_{15}O_3Cl$	C H	66.9 4.5	67.4 4.9

* B = benzene; E = ethanol

Dehydroation of XVII. Formation of XVIII. A solution of α-aryl-β-*p*-chlorobenzoylpropionic acid XVII (0.01 mole) in acetic anhydride (20 ml) was refluxed for 4 hrs. The solid obtained after concentration and cooling was crystallized from the suitable solvent to give the butenolides XVIIIa and XVIIIb (yield 70%). The results are listed in table 9.

Table 9

Furanone derivatives XVIII

Compound	m.p. (°C)	Solvent*	Formula	Analaysis (%)		
					Found	Required
XVIIIa	199—200	B	$C_{17}H_{18}O_2Cl$	C H	71.7 4.3	71.9 4.2
XVIIIb	215	B/E	$C_{18}H_{14}O_2Cl$	C H	72.6 4.4	72.6 4.7

* B = Benzene; E = ethanol

Revue Roumaine de Chimie **23**, *11–12*, 1607–1609 (1978)

DETERMINATION OF ISOTHIOCYANATOCHROMATES USING BROMINE MONOCHLORIDE

P. K. MATHUR
Department of Chemistry, Luchnow University, Lucknow — 226007, India

Received September 20, 1976

The present paper deals with the determination of potassium hexaisothiocyanatochromate (III) and Reinecke salt (ammonium tetraisothiocyanatodiamminechromate (III)) using bromine monochloride. A measured volume of the BrCl solution is treated with known volume of the isothiocyanatochromate solution. The contents are shaken and allowed to stand for about 10 minutes. Thereafter, the unreacted Br Cl is determined by adding 10% aqueous potassium iodide solution and titrating the liberated iodine with standard 0.1 N sodium thiosulphate solution.

1. INTRODUCTION

The well known Reinecke salt, $NH_4[Cr(NCS)_4-(NH_3)_2] \cdot H_2O$, and potassium hexaisothiocyanatochromate (III), $K_3[Cr(NCS)_6] \cdot 4H_2O$ have been widely used in the determination of various alkaloids, medicinally important organic bases and several metal ions. The quantitative determination of these salts is therefore of interest.

The pioneer work on the use of BrCl as an analytical reagent has been done by Schulek.[1] BrCl is a better oxidant than ICl because it gives larger equivalent for the consumption of the oxidant which leads to an improved accuracy.

BrCl solution is used for the oxidation of Reinecke salt and $K_3[Cr(NCS)_6]$ and unreacted BrCl solution is determined iodometrically. The reactions involved are given below :

$$BrCl + 2e^- = Br^- + Cl^- NH_4[Cr(NCS)_4(NH_3)_2] + 20\,H_2O = Cr^{3+} + NH_4^+ +$$

$$+ 4\,CNO^- + 2NH_4^+ + 38H^+ + 4SO_4^{2-} + 32e^- K_3[Cr(NCS)_6] + 30H_2O =$$

$$= Cr^{3+} + 3K^+ + 6CNO^- + 6SO_4^{2-} + 60H^+ + 48e^-$$

2. EXPERIMENTAL

The stock solution of BrCl was prepared by the method described in literature.[2–3] It may be noted that stock solutions of BrCl are reasonably stable and undergo no change for periods up to two weeks.

$K_3[Cr(NCS)_6] \cdot 4H_2O$ was prepared and standardised by slightly modifying the method adopted by Roesler.[4]

---

[1] E. Schulek and K. Burger, *Talanta,* **1,** 147 (1958).

[2] E. Schulek and K. Burger, *Ann. Univ. Sci., Budapest,* **2,** 133 (1960).

[3] C.G.R. Nair and R. Lalitha Kumari, *Indian J. Chem.,* **14A,** 115 (1976).

[4] J. Roesler, *Liebigs Ann. Chem.,* **141,** 185 (1867).

2.1 PROCEDURE

To measured volumes (20−60 ml) of the BrCl solution taken in 500 ml stoppered conical flasks, measured aliquots (20−60 ml) of the reductant, $K_3[Cr(NCS)_2]\cdot 4H_2O$ or Reinecke salt solution are added. The contents are shaken well and allowed to stand for 10 minutes. Thereafter, the unconsumed BrCl is determined by adding 20 ml of 10% aqueous KI solution and titrating the liberated I_2 with standard 0.1 N sodium thiosulphate solution. Blank titrations are performed concurrently for each experiment.

It may be noted from tables 1 and 2 that the number of equivalents of BrCl consumed per mole of $K_3[Cr(NCS)_6]$ and Reinecke salt are 48 and 32 respectively.

Table 1

Determination of $K_3[Cr(NCS)_6]\cdot 4H_2O$ with BrCl

Expt. No.	$K_3[Cr(NCS)_6]\cdot 4H_2O$ taken (m.mole)	BrCl consumed (m.mole)	Mole BrCl consumed per mole of $K_3[Cr(NCS)_6]\cdot 4H_2O$	$K_3[Cr(NCS)_6]\cdot 4H_2O$* found (m.mole)	% Error
1	0.02222	1.069	48.89	0.02227	+0.23
2	0.02794	1.344	48.10	0.02800	+0.21
3	0.03083	1.473	47.77	0.03069	−0.45
4	0.04444	2.143	48.21	0.04465	+0.48
5	0.05598	2.693	48.11	0.05611	+0.23
6	0.06166	2.955	47.92	0.06156	−0.16

* Assuming that 48 moles of oxidant are consumed per mole of $K_3[Cr(NCS)_6]\cdot 4H_2O$

Table 2

Determination of Reinecke salt with BrCl

Expt. No.	Reinecke salt (taken (m.mole)	BrCl consumed (m.mole)	Mole BrCl consumed per mole of Reinecke salt	Reinecke salt* found (m.mole)	% Error
1	0.04132	1.327	32.11	0.04148	+0.39
2	0.05165	1.656	32.07	0.05176	+0.21
3	0.06198	1.984	32.00	0.06200	+0.03
4	0.07231	2.310	31.95	0.07219	−0.17
5	0.08264	2.656	32.14	0.08291	+0.33

* Assuming that 32 moles of oxidant are consumed per mole of Reinecke salt

3. RESULTS AND DISCUSSION

For the determination of Reinecke salt using ICl, Nambisan Krishnan[5] has decomposed Reinecke salt by warming it with 5N NaOH for 10-15 minutes before oxidation with ICl and then acidifying with HCl to keep the overall acidity at about 5N. The addition of NaOH and subsequent neutralization by HCl has been eliminated in the determination of Reinecke salt using BrCl as oxidant. Moreover, BrCl is a better oxidant than ICl giving larger equivalent for the consumption of the oxidant and therefore leading to an improved accuracy. The numbers of equivalent of ICl and BrCl consumed for Reinecke salt are 24 and 32 respectively. The increased consumption of BrCl is due to its greater oxidising power, which enables the oxidation of CN^- to CNO^- in the Reinecke salt.

---

[5] P. N. Krishnan Nambisan, *Curr. Sci.*, **44**, 617 (1975).

ACKNOWLEDGEMENT. The author expresses his sincere thanks to Prof. S. S. Tewari, Head of the Chemistry Department, Lucknow University, for providing laboratory facilities and encouragement.

Revue Roumaine de Chimie, **23**, *11–12*, 1611–1617 (1978)

KINETIC ASPECTS OF THE OXIDATION REACTION OF GALLIC ACID USING AN OXYGEN-SELECTIVE ELECTRODE

GH. IONESCU, F. MATEI and AL. DUCA
Physical Chemistry and Analytical Chemistry Departments, Polytechnic Institute of Jassy, Splai Bahlui 71, Jassy, Romania

Received December 13, 1976

Using an oxygen-selective electrode, the principal kinetic aspects of the gallic acid oxidation in alkaline solution were investigated. The kinetic aspects under study were : the optimum response time of the electrode, the influence of pH on the catalytic activity of Co^{2+} ions, the influence of gallic acid concentration and the formal kinetic equation. These kinetic features are useful for analytical uses of this reaction for the analysis of Co^{2+}, Zn^{2+} and CN^- ions.

1. INTRODUCTION

The oxidation reaction of the gallic acid with ammonium persulphate has been studied by Jarabin and Szarvas[1] in conection with its use as qualitative test for vanadium traces determination. This reaction has also been studied by Fishman and Skougstad [2] with the aim of finding a new qualitative method for the spectrophotometrical analysis of vanadium traces in water.

By using the property of the gallic acid alkaline solutions of absorbing oxygen the authors of the present paper have evidenced the catalytic effect of Co^{2+} ions in oxidation reaction and settled the optimum conditions for the spectrophotometrical analysis of Co^{2+} ions traces. [3]

The fact that the oxidation of gallic acid in alkaline solution takes place on the count of the absorbed oxygen, suggested us to use an electrode sensitive to oxygen in order to study some kinetic aspects of gallic acid oxidation which will be taken into account for analytical uses of this reaction.

The following kinetic aspects were approached : the electrode optimum response, the influence of the pH and of gallic acid concentration on the catalytic activity of Co^{2+} ions and the formal kinetic equation.

---

[1] Z. Jarabin and P. Szarvas, *Acta Univ. Debrecen* (*Hung.*), **7**, 131 (1961).

[2] M. T. Fishman and W. M. Skougstad, *Analyt. Chem.*, **36**, 1643 (1964).

[3] Gh. Ionescu, N. Aelenei, and A. Duca, *Bul. Inst. Pol. Iaşi*, **22**, fasc. 1–2, 23 (1976).

2. EXPERIMENTAL

The experiments were run at 25° in a reaction mixture volume of 25 cm^3.

2.1. REAGENTS AND EQUIPMENT

The stock solutions were prepared with high purity reagents. The initial concentrations were the following: $c(AG) = 10^{-2}$ mol/l (AG = gallic acid), $c(Co^{2+}) = 10^{-2}$ mol/l, $c(NaOH) = 0.1$ mol/l, $c(BNa) = 0.2$ mol/l (BNa = natrium borate), $c(NH_4Cl) = 0.2$ mol/l, $c(NH_4OH) = 0.2$ mol/l. Bidistilled water and Jena glassware were used.

The oxygen-selective electrode used was of the Analytical Chemistry Laboratory-University of Cluj Napoca type, with silver cathode, lead anode and 0.1 N NaOH as electrolyte provided with polyethylene membrane. A microampermeter of 40 μA with a uniform scale of 140 divisions was used as measuring instrument for the electrode signal. The pH measurements were made by means of a Radiometer Copenhagen pH-meter 22 with glass-calomel electrodes.

2.2. THE OPTIMUM RESPONSE TIME OF ELECTRODE

The difference ΔX between the divisions indicated by the electrode in air and immersed in the reaction mixture was taken as measurable physical amount. This amount should be independent on the initial indication of the electrode in air but dependent on the reaction rate for a certain time interval.

In view of using this reaction for analysing the traces of catalyst (Co^{2+}) and some of its complexing reagent (CN^-), the optimum electrode response time was defined as the time for which the amount $\Delta X_c - \Delta X_n$ has the maximum value, where ΔX_c is the amount defined above for the catalyzed or inhibited reaction and ΔX_n for the uncatalyzed one. The experimental data are given in table 1.

*Table 1**

Dependence of the ΔX_n and ΔX_c amounts on the reaction time

t[min]	Borate buffer solution			Ammoniacal buffer solution		
	ΔX_n[div]	ΔX_c[div]	$\Delta X_c - \Delta X_n$[div]	ΔX_n[div]	ΔX_c[div]	$\Delta X_c - \Delta X_n$[div]
0.00	0	0	0	0	0	0
0.25	—	—	—	12	21	9
0.50	21	22	1	22	36	14
1.00	32	39	7	37	58	21
1.50	39	52	13	47	72	25
2.00	44	64	20	56	82	26
2.50	48	74	26	63	88	25
3.00	51	83	32	69	91	22
3.50	53	88	35	74	94	20
4.00	56	92	36	78	97	19
5.00	60	97	37	82	99	17

* ΔX_n and ΔX_c are the mean of five individual determinations.

Conditions were: pH = 10.1; $c(AG) = 1.6.10^{-3}$ mol.l^{-1}; $c(Co^{2+}) = 2.10^{-6}$ mol.l^{-1} for the borate buffer solution and pH = 9.55; $c(AG) = 5.10^{-4}$ mol.l^{-1}; $c(CO^{2+}) = 2.10^{-6}$ mol.l^{-1} for the ammoniacal buffer solution.

The existence of an optimum time with a maximum value of this difference results from the fact that the signal of the chosen analytical sensor is a function of the rate of several simultaneous processes, such as reaction within electrode, diffusion through membrane, the investigated chemical reaction, et al.

As results from diagrams in Figure 2, depicted based on the kinetic curves in Figure 1, the optimum electrode response time for the two

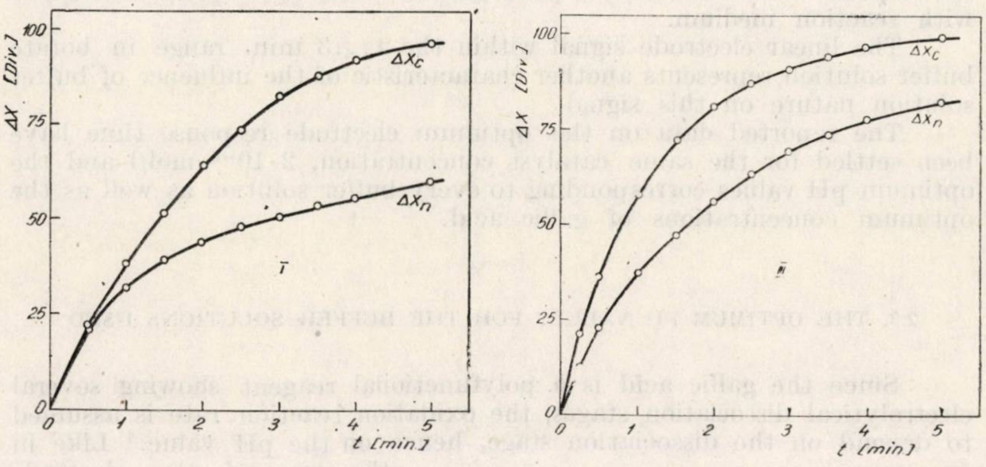

Fig. 1. — Dependence of the ΔX_n and ΔX_c amounts on the reaction times : *I*-in borate buffer solution ; *II*-in ammoniacal buffer solution ; $c(Co^{2+}) = 2 \cdot 10^{-6}$ mol.l^{-1}.

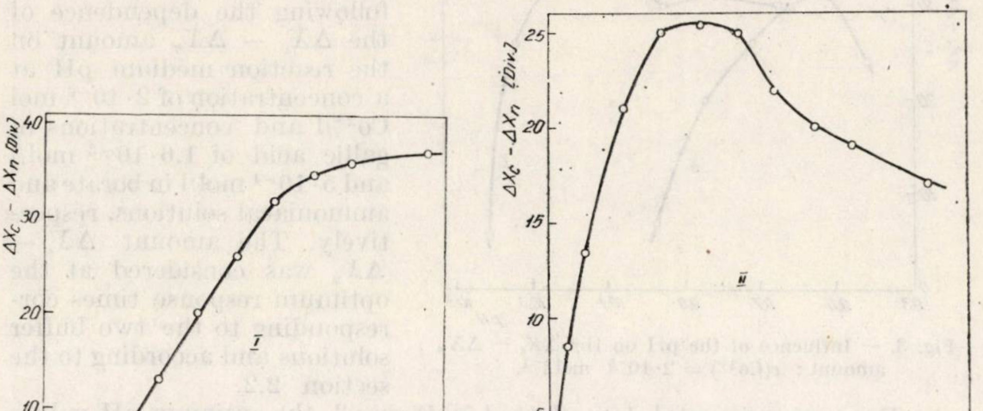

Fig. 2. — Dependence of the $\Delta X_c - \Delta X_n$ amount on the reaction times : *I*-in borate buffer solution ; *II*-in ammoniacal buffer solution ; $c(Co^{2+}) = 2 \cdot 10^{-6}$mol.l^{-1}.

buffer solutions is located within different ranges, namely $t \geqslant 3.5$ for the borate buffer solution and $1.5 \leqslant t \leqslant 2.5$ min. for the ammoniacal one. From t_0 the amount $\Delta X_c - \Delta X_n$ tends to a constant value for borate buffer solution and shows a maximum within the optimum time range for the ammoniacal buffer solution.

The difference in optimum times for the two buffer solutions might be explained by the existence of an induction period of about 0.5 . . .1 min. in the buffer borate solution, in contrast with the ammoniacal one where the response of the electrode is plain from the very moment of its contact with reaction medium.

The linear electrode signal within the 1. . .3 min. range in borate buffer solution represents another characteristic of the influence of buffer solution nature on this signal.

The reported data on the optimum electrode response time have been settled for the same catalyst concentration, $2 \cdot 10^{-6}$ mol/l and the optimum pH values corresponding to every buffer solution as well as the optimum concentrations of gallic acid.

2.3. THE OPTIMUM PH VALUES FOR THE BUFFER SOLUTIONS USED

Since the gallic acid is a polyfunctional reagent showing several electrolytical dissociation stages, the oxidation reaction rate is assumed to depend on the dissociation stage, hence on the pH value.[4] Like in the case of the electrode optimum response time, the influence of the reaction medium pH was studied by following the dependence of the $\Delta X_c - \Delta X_n$ amount on the reaction medium pH at a concentration of $2 \cdot 10^{-6}$ mol Co^{2+}/l and concentrations of gallic acid of $1.6 \cdot 10^{-3}$ mol/l and $5 \cdot 10^{-4}$ mol/l in borate and ammoniacal solutions, respectively. The amount $\Delta X_c - \Delta X_n$ was considered at the optimum response times corresponding to the two buffer solutions and according to the section 2.2.

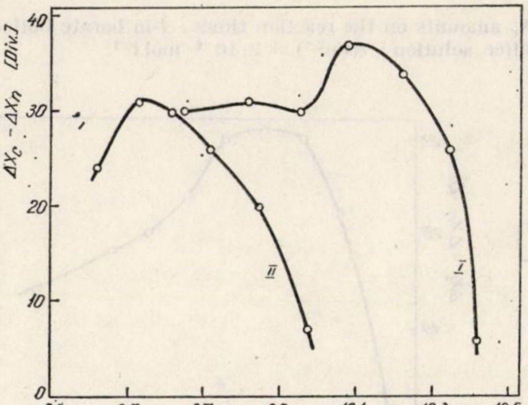

Fig. 3. — Influence of the pH on the $\Delta X_c - \Delta X_n$ amount : $c(Co^{2+}) = 2 \cdot 10^{-6}$ mol.l^{-1}.

From experimental data plotted in Figure 3, the optimum pH values are evidenced : 10.1 and 9.55 for borate and ammoniacal buffers, respectively. The difference in the two optimum pH values is probably due to the difference in the ionic strengths of the two buffer solutions which affects particularly the reaction rate within electrode.

---

[4] J. Bognar, *Mikrochim. Acta,* **6,** 901 (1961).

2.4. OPTIMUM CONCENTRATION OF GALLIC ACID

Since the oxygen initial concentration under the reaction conditions remains constant, being determined by oxygen solubility, the influence of the gallic acid concentration on the reaction rate was considered important.

For both buffer solutions a narrow concentration range of gallic acid was found experimentally in which the measured physical amount $\Delta X_c - \Delta X_n$ had the maximum value. The optimum concentration ranges of gallic acid in borate and ammoniacal buffers are of $1.6\cdot10^{-3}\ldots$ $\ldots2\cdot10^{-3}$ mol/l and $4\cdot10^{-4}\ldots6\cdot10^{-4}$ mol/l, respectively, Figure 4.

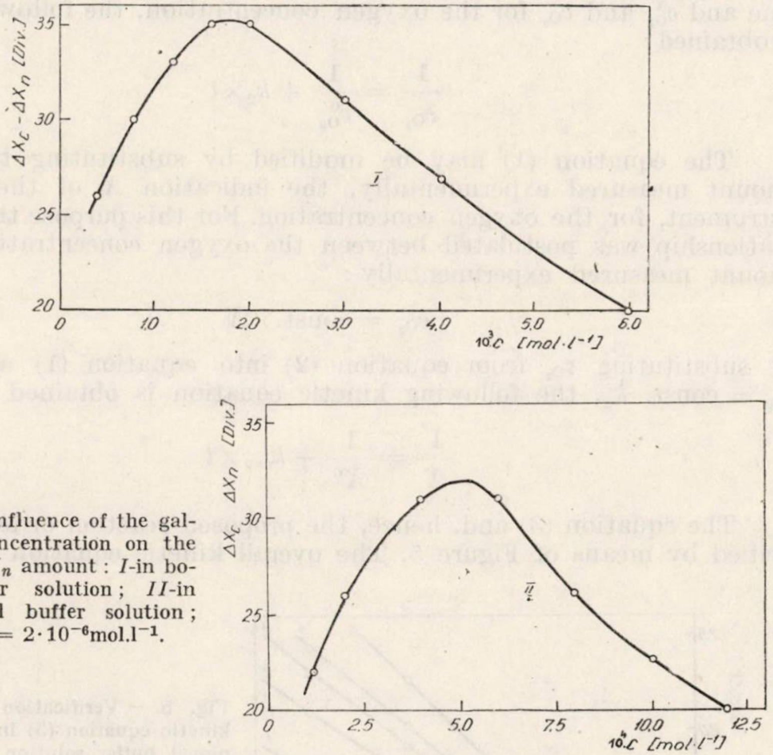

Fig. 4. — Influence of the gallic acid concentration on the $\Delta X_c - \Delta X_n$ amount : *I*-in borate buffer solution ; *II*-in ammoniacal buffer solution ; $c(Co^{2+}) = 2\cdot10^{-6}$mol.l^{-1}.

This influence might be explained by the change in the optimum pH value due to the acid pH of about 3.0 of the 10^{-2} mol/l gallic acid initial solution. Such an influence of the gallic acid concentration has also been evidenced by us in other papers.[3]

2.5. KINETIC EQUATION OF THE OXIDATION REACTION

The influence of gallic acid as both reagent and modifier of the optimum pH, restricts the possibility of deriving differentially a kinetic equation. Furthermore, for the second reagent, oxygen, the initial concentration cannot be modified, being determined by the oxygen solubility at the working temperature. For these reasons the more laborious and uncertain integral method was applied to derive the kinetic equation.[5]

The optimum concentration of gallic acid in ammoniacal buffer and that of the solved oxygen at 25°C were found practically equal. By assuming partial reaction orders with respect to every reactant as being 1, the following differential kinetic equation may be written:

$$-\frac{\mathrm{d}c_{O_2}}{\mathrm{d}t} = k_2 \times c_{AG} \times c_{O_2} = k_2 \times c_{O_2}^2$$

By integrating this equation between the limits 0 and t for the reaction time and $c_{O_2}^0$ and c_{O_2} for the oxygen concentration, the following solution is obtained:

$$\frac{1}{c_{O_2}} = \frac{1}{c_{O_2}^0} + k_2 \times t \qquad (1)$$

The equation (1) may be modified by substituting the physical amount measured experimentally, the indication X of the measuring instrument, for the oxygen concentration. For this purpose the following relationship was postulated between the oxygen concentration and the amount measured experimentally:

$$c_{O_2} = \text{const.} \times X \qquad (2)$$

By substituting c_{O_2} from equation (2) into equation (1) and putting $k_{\exp} = \text{const.}\ k_2$, the following kinetic equation is obtained:

$$\frac{1}{X} = \frac{1}{X^0} + k_{\exp} \times t \qquad (3)$$

The equation (3) and, hence, the proposed reaction order 2, may be verified by means of Figure 5. The overall kinetic equation is found to

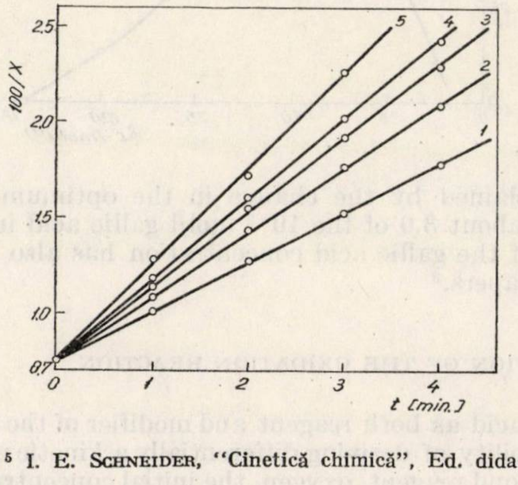

Fig. 5. — Verification of the kinetic equation (3) in ammoniacal buffer solution; conditions were: pH = 9.55; t = = 25°C; $c(AG) = 6.10^{-4}$ mol. l^{-1}; *1.* — $c(Co^{2+}) = 0$ mol.l^{-1}; *2* — $c(Co^{2+}) = 4.10^{-7}$ mol.l^{-1}; *3* — $c(Co^{2+}) = 8.10^{-7}$ mol.l^{-1}; *4* — $c(Co^{2+}) = 12.10^{-7}$ mol.l^{-1} *5* — $c(Co^{2+}) = 20.10^{-7}$ mol.l^{-1}

[5] I. E. Schneider, "Cinetică chimică", Ed. didactică şi pedagogică, Bucureşti, 1974, p. 27.

be satisfactory for both the uncatalyzed and catalyzed by Co^{2+} ions reactions.

Besides suggesting the overall kinetic picture, the equation (3) may be used for the rapid calculation of the k_{exp} which depends on the Co^{2+} concentration and could be used for plotting a standard diagram necessary for analysis of the Co^{2+} traces on the basis of this indicative reaction.

3. CONCLUSIONS

On the basis of the reported data, the following conclusions may be drawn :

1. The optimum response times of the electrode for the two buffer solutions are : $t \geqslant 3.5$ min. for the borate buffer solution and $1.5 \leqslant t \leqslant 2.5$ min. for the ammoniacal one. For the borate buffer solution an induction period of above 1 min. is required; also a linear response time of the electrode within 1...3 min. range being observed.

2. The optimum pH-values found were of 10.10 for the borate and 9.55 for the ammoniacal buffer solutions, respectively.

3. The optimum concentrations of gallic acid have two different values : $1.6 \cdot 10^{-3} \ldots 2 \cdot 10^{-3}$ mol/l for the borate buffer solution and $4 \cdot 10^{-4} \ldots 6 \cdot 10^{-4}$ mol/l for the ammoniacal one.

4. An overall kinetic order of 2 was found for the reaction in ammoniacal buffer solution.

Revue Roumaine de Chimie, **23**, *11–12*, 1619–1626 (1978)

FLASH PHOTOLYSIS STUDIES OF AQUEOUS SOLUTION OF THIOSULPHATE ION

M. S. SUBHANI * and T. KAUSAR
Department of Chemistry, University of Islamabad, Islamabad, Pakistan

Received March 27, 1976

Flash photolysis studies of aqueous solution of $S_2O_3^{2-}$ were carried out. Two transient species $S_2O_3^-$ and $S_2O_3^-$ with $\lambda_{max} = 380$ nm and $\lambda_{max} = 280$ nm absorbing in the wavelength region of 220–450 nm were observed, and their absorption spectra are reported. These species are found to decay by second order kinetics and the value for $\frac{2k}{\varepsilon}$ and $2k$ are reported.

The rate constant for the reaction

$$OH + S_2O_3^{2-} \rightarrow S_2O_3^- + OH^-$$

$$O^- + S_2O_3^{2-} \xrightarrow{H_2O} S_2O_3^- + 2OH^-$$

were also determined and are reported in this paper.

INTRODUCTION

The observation and reaction kinetics of transient species produced in photochemical reactions using the flash photolysis technique has been studied by many workers. However, relatively few investigations have been carried out in photolysis studies in vacuum U. V. region due to non availability of very pure silica reaction cells and other experimental difficulties.

The photochemical decomposition of inorganic anions in aqueous solution has been the subject of many investigators. [1–12] (Some qualitative investigations were carried out on the photochemical decomposition of $S_2O_3^{2-}$ ion in aqueous solution[7]). The results of the flash photolysis investigations of the thiosulphate ion in aqueous solution under different sets of conditions, to look for the various probable primary photochemical processes taking place on absorption of light by this ion, are discussed and presented in this paper.

---

* Present address: Department of Chemistry, University of Nigeria, Nsukka, Nigeria.

[1] (a) A.J. Allmand, P. W. Cunliffe and R. E. Maddison, *J. Chem. Soc.*, **1952**, 822. (b) A. J. Allmand, P. W. Cunliffe and R. E. Maddison, *J. Chem. Soc.*, **1927**, 655.

[2] A. J. Allmand and W. W. Weble, *Z. phys. Chem.*, **A 131**, 189 (1928).

[3] K. W. Young and A. J. Allmand, *Canad. J. Chem.*, **27B**, 318 (1949).

[4] G. V. Bunton, R. J. Williams, *Proc. Chem. Soc.*, **1962**, 141.

[5] G. V. Bunton and M. S. Subhani, *J. Chem. Soc. Faraday Trans.*, **68**, 958 (1972).

[6] G. V. Bunton and M. S. Subhani, *J. Chem. Soc. Faraday Trans.*, **68**, 970 (1972).

[7] R. Sperling and A. Treinin, *J. Phys. Chem.*, **768**, 897 (1964).

[8] O. Amichi, G. Czapski and A. Treinin, *Israel J. Chem.*, **7**, 351 (1969).

[9] L. Doglotti and E. Hayon, *J. Phys. Chem*, **71**, 2511 (1967).

[10] L. Farkas and F.S. Klein, *J. Chem, Phys.*, **16**, 886 (1948).

[11] A. Treinin, *Israel J. Chem.*, **9**, 103 (1970).

[12] N. K. Bridge and M. S. Matheson, *J. Phys. Chem.*, **64**, 1280 (1960).

EXPERIMENTAL

All the reagents used were of Analar grade and were used without further purification.

All solutions were prepared using water purified by triply distillation, radiolysis and photolysis.

Solutions to be photolysed were prepared just before irradition saturated with the required gas by the usual bubbling procedure[13] and its set up is shown in Figure 1.

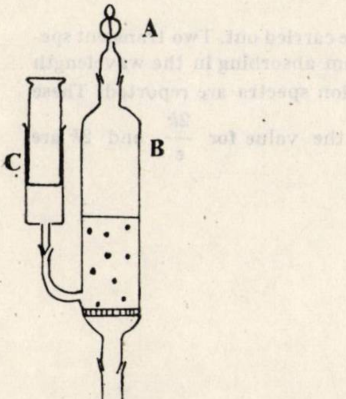

Fig. 1. — Bubbling system

A — outlet for gas; *B* — bubbler; *C* — Syringe; D_1 and D_2 — pre bubblers; *E* — freezing mixture container; *F* — gas inlet.

The pHs of the solutions were measured with a previously calibrated Pye pH meter. Fresh sample of solution was used for each measurements.

The detail of the flash photolysis set up and flash photolysis cell used in this work was very much similar to that have been described elsewhere.[5,14] The duration of flash was 20 micro seconds as shown in Figure 2.

The energy of the flash used was 680J. The optical detection system was the same as described elsewhere.[14] The signal fed to the Oscilloscope type Tektronix 545 B was displayed on the screen in the form of a trace. The traces on the oscilloscope were recorded on Poloroid type 410, (10,000 ASA) film using a Shackman-Land Camera. A typical trace is shown in Figure 3. These traces were magnified with the help of epidiascope and were traced on graphpaper for the plot of spectra and for kinetics studies of the transients produced. The concentration of thiosulphate anion was kept to the minimum in solution in order to avoid any interference with the transmission of monitoring light beam through the optical path in the photolytic cell due to sulpher produced on photolysis.

RESULTS AND DISCUSSIONS

The optical spectra of two transient species A and B were observed in the flash photolysis of 5×10^{-3}M sodium thiosulphate ions in aqueous solution at pH 4.5, natural and 12.2 respectively. A short lived trannsient (A) absorbing in the wave length region 340 nm to 450 nm with $\lambda_{max} = 380$ nm and a longer lived transient species (B) absorbing in the wavelength region of 220 nm to 400 nm with $\lambda_{max} = 280$ nm were recorded as shown in Figure 4.

---

[13] E. Collinson, K. W. Chambers, F. S. Dainton, W. A. Seddon and F. Wilkinson *Trans. Faraday Soc.*, **63**, 1699 (1967).

[14] M. S. Subhani, *J. Science and Mathematics*, **2**, (1976).

The transient A is most probably produced by the primary photochemical reaction

$$S_2O_3^{2-}\,H_2O \xrightarrow{h\nu} S_2O_3^{2-}\,H_2^*O \tag{1}$$

$$S_2O_3^{2-}\,H_2^*O \longrightarrow S_2O_3^{2-}\,H_2O \tag{2}$$

$$S_2O_3^{2-}H_2^*O \longrightarrow S_2O_3^{-} + e_{aq}^{-} \tag{3}$$

The recombination process of $S_2O_3^-$ radical anion and hydrated electron may also be occurring

$$S_2O_3^{-} + e_{aq}^{-} \longrightarrow S_2O_3^{2-}\,H_2^*O \tag{4}$$

The spectra with $\lambda_{max} = 380$ nm was assigned to be due to $S_2O_3^-$ radical anion as an identical short lived transient produced a pulse radiolysis of aqueous solution of thiosulphate ion was observed by Adams et al.[15] They suggested that the transient was produced by the oxidation $S_2O_3^{2-}$ ion by OH radical:

$$OH + S_2O_3^{2-} \longrightarrow S_2O_3^{-} + OH^{-} \tag{5}$$

and

$$\varepsilon_{380}^{S_2O_3^-} = 1.72\times10^{-3}\ M^{-1}\,Cm^{-1}$$

The yield of $S_2O_3^-$ transient was found to be increased by about 50% when N_2O saturated solution of 2×10^{-2} M $S_2O_3^{2-}$ ion at pH 4.5 was flash photolysed, as compared to that of 2×10^{-2} M $S_2O_3^{2-}$ ion Ar saturated solution at the same pH. The increase in yield is considered due to the reaction of OH radical with $S_2O_3^{2-}$ by reaction (5). The OH radicals involved in reaction (5) are produced by the reaction

$$N_2O + e_{aq}^{-} \rightarrow N_2 + (O^{-} \xrightarrow{H_2O} OH + OH^{-}) \tag{6}$$

and also by another primary photolytic process (7) (See latter)

$$S_2O_3^{2-}\,H_2^*O \rightarrow S_2O^{-} + OH + OH^{-}$$

The rate constant for the reaction (6) is $5.6\times10^{9}M^{-1}\,S^{-1}$.[16]
Thus the identification of the transient $S_2O_3^-$ radical anions support the primary photochemical process (3).

The transient B with $\lambda_{max} = 280$ nm is considered to be produced by another primary photochemical process represented by equation 7

$$S_2O_3^{2-}\,H_2^*O \rightarrow S_2O_2^{-} + OH + OH^{-} \tag{7}$$

and was suggested to be $S_2O_2^-$. On flash photolysis of Ar or N_2O saturated solution of same concentration of sodium thiosulphate at pH 4.5 and at

---

[15] G. E. Adams, J. W. Boag and B. D. Michael, *Trans. Faraday Soc.*, **61**, 1674 (1965).
[16] M. Anbar and P. Neta, *Inter J. Appl. Radiat. Isotope*, **18**, 493 (1967).

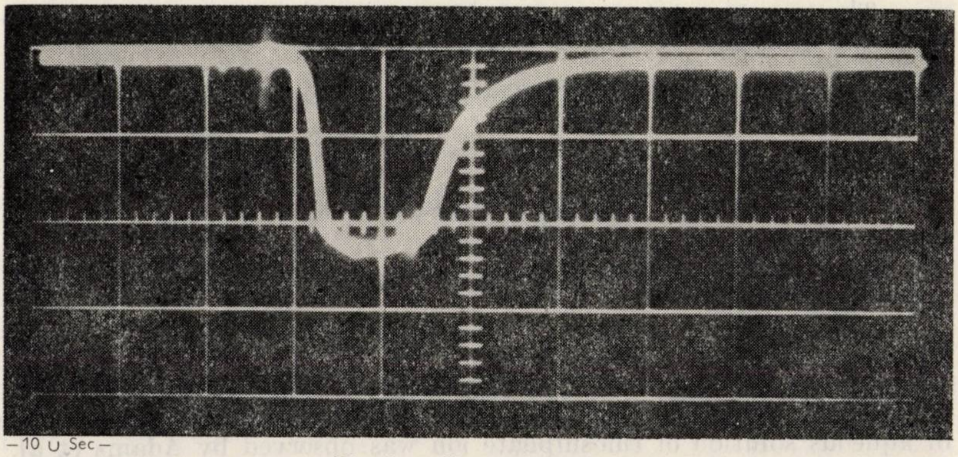

Fig. 2. — Shape of the flash

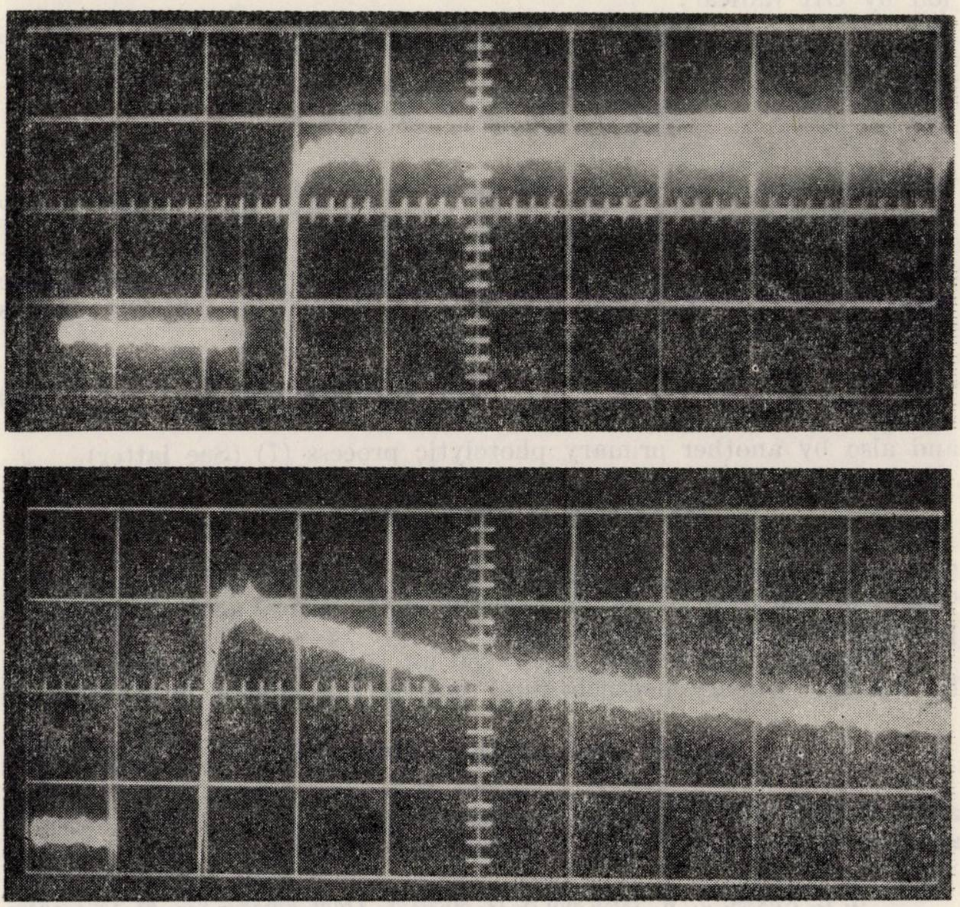

Fig. 3. — Typical traces

natural pH no change in the absorption spectrum and optical density due to $S_2O_2^-$ was observed which indicates that the species $S_2O_2^-$ was produced in primary photochemical process.

$$S_2O_3^{2-}\ H_2^*O \rightarrow S_2O_2^- + OH + OH^- \tag{7}$$

Sperling and Treinin[17] have assigned the band giving rise to the transient $S_2O_3^-$ as the allowed transion. $\Pi^* \leftarrow {}^n$ involving the non bonding electrons on the oxygen atom. It is suggested on this basis that $S_2O_2^-$ radical anion was produced as a result of a break of the S—O bond in $S_2O_3^{2-}$ ion.

On addition of OH radical scavenger such as methanol and formate ion in Ar saturated solution of 10^{-2}M sodium thiosulphate solution a decrease in yield of $S_2O_3^-$ radical anion by half of its magnitude in absence of methanol and formate ion was observed.

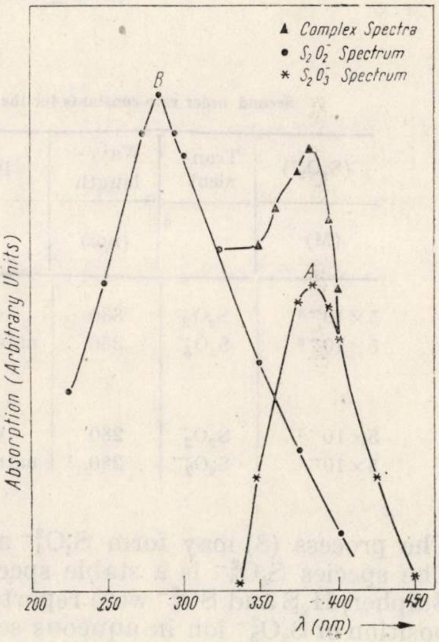

Fig. 4. — On flash photolysis of Ar saturated aqueous solution of $S_2O_3^{2-}$ at pH 4.5

A — absorption maximum of $S_2O_3^-$ radical anion ; B — absorption maximum of $S_2O_2^-$ radical anion.

These observations are the conclusive evidence that both the primary processes (3) and (7) are taking place and are occurring in equal magnitude.

The absorption due to $S_2O_2^-$ radical anion remained unaltered on flash photolysis of 10^{-2}M sodium thiosulphate at natural pH both in Ar and N_2O saturated solution, and in presence and absence of methanol or formate ions. This suggests that $S_2O_2^-$ is produced only as a result of the 2nd primary photochemical process (7) but not as a result of the decay of $S_2O_3^-$ radical anion.

Second order decay kinetics were observed both at $\lambda_{max}=380$ mm and $\lambda_{max}=275$ on flash photolysis of Ar saturated aqueous solution of $S_2O_3^{2-}$ at pH 4.5 and at natural pH so that :

$$S_2O_3^- + S_2O_3^- \rightarrow \text{product} \qquad (8)$$

$$S_2O_2^- + S_2O_2^- \rightarrow \text{product} \qquad (9)$$

The values of $\frac{2K}{\varepsilon}$ are shown in table 1.

Taking $\varepsilon_{380} = 1.72X10^3\ M^{-1}\ CM^{-1}$ reported by Adams et al.,[15] the value of 2K for $S_2O_3^-$ reaction was found to be :

$$(5.7 \pm 1.4)X10^9\ M^{-1}\ S^{-1}.$$

Table 1

Second order rate constants for the decay of $S_2O_3^-$ and $S_2O_2^-$ transient species

$(S_2O_3^-)$	Transient	Wavelength	pH	$2K$	$\frac{2K}{\varepsilon}$
(M)		(nm)		$M^{-1}\ S^{-1}$	$Cm\ S^{-1}$
5×10^{-3}	$S_2O_3^-$	380	4.5	$(5.7\pm1.4)10^6$	$(3.3\pm.4)10^9$
5×10^{-3}	$S_2O_3^-$	380	natural	$(5.6\pm1.2)\times10^6$	$(3.3+1.2)\times10^9$
				$\frac{2k}{\varepsilon}$	2k
5×10^{-3}	$S_2O_2^-$	280	4.5	$(4.2\pm0.5)\times10^4$	—
5×10^{-3}	$S_2O_2^-$	280	natural	$(4.5\pm0.5)\times10^4$	—

The process (8) may form $S_4O_6^{2-}$ as suggested by Sperling and Treinin.[17] The species $S_4O_6^{2-}$ is a stable species.

Sulpher, H_2S and SO_3^{2-} were reported as products of photochemical decomposition of $S_2O_3^{2-}$ ion in aqueous solution at natural pH.[17] These products may be formed as a result of the decay of $S_2O_3^{2-}$ and $S_2O_3^-$ and $S_2O_2^-$ radical anions and also by another photolytic process

$$S_2O_3^{2-} \xrightarrow{h\nu} SO_3^{2-} + S \qquad (10)$$

H_2S and SO_3^{2-} may be produced by the reaction of

$$e_{aq}^- + S_2O_3^{2-} \rightarrow SO_3^{2-} + S^- \qquad (11)$$

---

[17] R. Sperling and A. Treinin, *J. Phys. Chem.*, **68**, 897 (1964).

as $k\ (e_{aq}^- + S_2O_3^-) = 5.9 \times 10^8 \cdot M^{-1}\ sec^{-1}$ [18] and the HS formed in process (II) eventually converts to H_2S.

Flash photolysis studies of oxygen saturated solution of thiosulphate ion at pH 11.2 were carried out and the absorption spectrum in the wavelenth region 350 to 500 nm was recorded when absorption was found to be increased. On resolution of the complex spectrum (See Figure 5) another transient

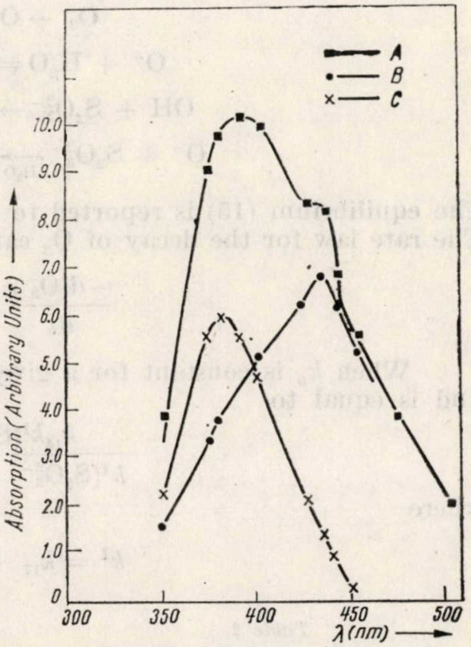

Fig. 5. — Oh flash photolysis of O_2 saturated aqueous solution of $S_2O_3^{2-}$ at pH 11.2.

A—complex spectra; B—spectrum of O_3^- radical anion; C—spectrum of $S_2O_3^-$ radical anion.

was identified as O_3^- radical anion on comparison with the spectrum of O_3^- reported in literature[8,19] and also to that of the radical anions $S_2O_3^-$. It is found that they do not absorb beyond 450 nm. Thus the peak appearing in the observed complex spectrum at 435 nm in addition to that at $\lambda_{max} = 380$ supported the production of O_3^- species and also the primary photochemical process

$$S_2O_3^{2-}\ H_2^*O \rightarrow S_2O_2^- + OH + OH^- \qquad (7)$$

followed by

$$OH + OH^- \rightleftharpoons O^- + H_2O \qquad (12)$$

and

$$O^- + O_2 \rightarrow O_3^- \qquad (13)$$

---

[18] M. S. Subhani, *Pak. J. ind. Science and Research*, (1976).

[19] D. Behar and G. Czapski, *Israel J. Chem.*, **6**, 43 (1968).

at pH 11.2. The transient species O_3^- was found to decay by first order kinetics. The ozonide ion is known to undergo unimolecular dissociation to O_2 and O^- [8,19]

$$O_3^- \rightarrow O_2 + O^- \tag{14}$$

In presence of $S_2O_3^{2-}$ the following mechanism for the first order decay kinetics of O_3^- radical anion can be suggested:

$$O^- + O_2 \rightarrow O_3^- \tag{13}$$

$$O_3^- \rightarrow O_2 + O^- \tag{14}$$

$$O^- + H_2O \rightleftharpoons OH + OH^- \tag{15}$$

$$OH + S_2O_3^{2-} \rightarrow S_2O_3^- + OH^- \tag{16}$$

$$O^- + S_2O_3^{2-} \xrightarrow[H_2O]{} S_2O_3^- + 2OH^- \tag{17}$$

The equilibrium (15) is reported to be rapidly established.[20]
The rate law for the decay of O_3 can be written as

$$\frac{-d(O_3^-)}{dt} = k_0(O_3^-) \tag{18}$$

When k_0 is constant for a given concentration of O_2 and $S_2O_3^{2-}$ ion and is equal to

$$\frac{k_{14}k^1(S_2O_3^{2-})}{k^1(S_2O_3^{2-}) + k_{13}(O_2)}$$

where

$$k^1 = k_{17} + k_{16}\,\frac{(H^+)}{K_{OH}}$$

Table 2

Rate constant for the decay of O_3^-
$(O_2) = 1.3 \times 10^{-3}M$

$10^3 \times (S_2O_3^{2-})$	pH	$10^{-3}k$ (s)
1.9	12	4.84
1.9	13	2.08
4.8	13	3.5

Table 3

k_{13} as 3.6×10^9 M^{-1} S^{-1} [21] and $pK_{OH} = 11.9$ [22]

Reaction	Rate constant
$O_3^- \rightarrow O_2 + O^-$	6.3×10^3 M^{-1} S^{-1}
$OH + S_2O_3^{2-} \rightarrow OH + S_2O_3^-$	9.8×10^9 M^{-1} S^{-1}
$O^- + S_2O_3^{2-} \rightarrow O^2 + S_2O_3^-$	4.3×10^8 M^{-1} S^{-1}

Thus the rate law (18) predict a first order decay provided $(S_2O_3^{2-})$ and (O_2) are kept' constant which is essentially true in the experiment report in this paper (See Table 2). The rate of decay O_3^- radical anion increases with increasing $(S_2O_3^{2-})$ and decreasing pH. The experimental results are consistent with the predictions. The values for the rate constants for the reactions (14), (16) and (17) are shown in table 3.

---

[20] G. V. Buxton, *Trans. Faraday Soc.*, **66**, 1656 (1970).
[21] G. V. Buxton, *Trans. Faraday Soc.*, **65**, 2150 (1969).
[22] J. Rabani and M. S. Matheson, *J. Phys. Chem.*, **70**, 761(1966).

Revue Roumaine de Chimie, **23**, *11–12*, 1627–1630 (1978)

FLASH PHOTOLYSIS STUDY OF SeO_3^{2-} ANION IN AQUEOUS SOLUTION

M. S. SUBHANI * and T. KAUSAR
Department of Chemistry, University of Islamabad, Islamabad, Pakistan

Received March 27, 1976

Flash photolysis studies of SeO_3^{2-} anion in aqueous system was carried out. The primary photolytic processes occurring are described and the optical absorption spectra of the short lived transients SeO_3^- ($\lambda_{max} = 430$ nm) and $\varepsilon_{430}^{SeO_3^-} = 1.4 \times 10^3\ M^{-1}\ cm^{-1}$ and the transient O_2^- radical anion ($\lambda_{max} = 240$ nm) were observed in oxygenated system. The rate constants for the 2nd order decay of SeO_3^- and O_2^- radical anions were evaluated. The primary photolytic process

$$SeO_3^{2-}H_2O^* \longrightarrow SeO_3^- + e_{aq}^-$$

was suggested for the photolysis of SeO_3^- anion.

INTRODUCTION

The absorption spectrum of selenite anion is observed in the ultraviolet region but the photochemistry has not been studied. It was thought that it would be interesting to look for the primary photolytic processes for the photolysis SeO_3^{2-} anion in aqueous solution.

In the present work the results on the flash photolysis study on SeO_3^{2-} anion are presented.

EXPERIMENTAL

All chemicals used were of A.R. grade. Sodium Selenite was prepared and purified by the method described by Bagnall.[1]

Solutions were prepared just before irradiation using water purified by triple distillation, radiolysis and photolysis.

These solutions were saturated with O_2, N_2O or Ar using normal bubbling technique.

The flash photolysis set up, flash lamps and detection system used were similar to those described elsewhere.[2,3]

The concentration of the solute used was kept to a minimum to reduce inner filter effects but sufficient to obtain enough transient.

---

* Present address: Department of Chemistry, University of Nigeria, Nsukka, Nigeria.

[1] K. W. Bagnall, "The Chemistry of Selenium, Tellurium, and Polonium", Elsevier Pub. Co. Amsterdam, 1966, p. 72.

[2] G. V. Bunton and M. S. Subhani, *J. Chem. Soc., Trans.*, **68**, 958 (1972).

[3] M. S. Subhani, *J. Science and Mathematics*, **2**, (1976).

RESULTS AND DISCUSSIONS

Flash photolysis of 10^{-2} M SeO_3^{2-} anion in aqueous solution at natural pH was carried out. A transient species absorbing in the wavelength region 350 to 600 nm was observed (see Figure 1) with $\lambda_{max} = 430$ nm. The same transient species was observed both in Ar saturated and N_2O saturated systems at natural pH (see Figure 1).

The species with $\lambda_{max} = 430$ nm was found to decay by second order kinetics. The decay rate was found to be the same both in presence of Ar and O_2 in the systems.

A second transient was observed in presence of oxygen absorbing in the wavelength region 220 to 300 nm with $\lambda_{max} = 240$ nm (see Figure 2). The species absorbs much less than the species with $\lambda_{max} = 430$ nm. and decay by a second order process (see Table 1).

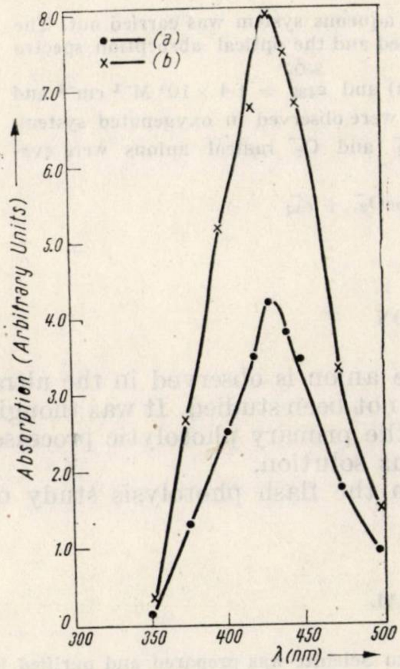

Fig. 1. — On flash photolysis of aqueous solution of SeO_3^{2-} anion at natural pH: (a) Ar Saturated; (b) N_2O Saturated.

Fig. 2. — On flash photolysis of O_2 saturated aqueous solution of SeO_3^{2-} anion at natural pH.

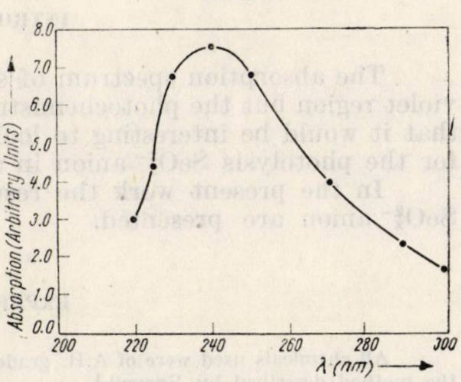

The above mentioned experimental observations can be explained on the basis that the main primary photolytic process resulting from the absorption of light by SeO_3^{2-} anion is due to change transfer to the solvent (C.t.t.S.) transition, similar to those suggested for SO_3^{2-} anion[3], resulting in the formation of SeO_3^- radical anion and solvated electron according to the process

$$SeO_3^{2-}\,H_2O \xrightleftharpoons{h\nu} SeO_3^{2-}\,H_2O^* \qquad (1)$$

$$SeO_3^{2-}\,H_2^*O \longrightarrow SeO_3^- + e_{aq}^- \qquad (2)$$

The electron produced in (2) forms an adduct with O_2 resulting in O_2^- radical anion

$$O_2 + e_{aq}^- \longrightarrow O_2^- \tag{3}$$

The species with $\lambda_{max} = 430$ nm was identified as to be SeO_3^- as reported in the pulse radiolysis work[4] and the species with $\lambda_{max} = 240$ nm was identified as O_2^- radical anion reported in the literature. [5,6]

In N_2O saturated solution of 10^{-2}M SeO_3^{2-} anion at natural pH no transient was observed at $\lambda_{max} = 240$ nm but the absorption due to SeO_3^- radical anion increased by a factor of almost two. This can be thus explained: e_{aq}^- reacts with N_2O in a reaction

$$N_2O + e_{aq}^- \longrightarrow N_2 + (O^- \xrightleftharpoons{H_2O} OH + OH^-) \tag{4}$$

and all the e_{aq}^- are practically scavenged by N_2O under the applied experimental conditions. Thus the reaction (3) is suppressed and the OH radicals produced in reaction (4) react with SeO_3^{2-} forming SeO_3^- radical anion by the reaction

$$SeO_3^{2-} + OH \rightarrow SeO_3^- + OH^- \tag{5}$$

and resulting in increase of SeO_3^- radical anion yield by a factor of 2.

The decay kinetics at 250 nm corresponds to the reaction

$$O_2^- + O_2^- \xrightarrow{H_2O} H_2O_2 + O_2 + 2OH^- \tag{6}$$

and that at $\lambda = 430$ nm is due to the decay of SeO_3^- by the process

$$SeO_3^- + SeO_3^- \rightarrow \text{Products} \tag{7}$$

the rate constants determined are summarized in table 1.

The value for the extinction coefficient for SeO_3^- radical anion at $\lambda_{max} = 430$ nm was established on the assumption that SeO_3^- and O_2^- radical anions are formed in equal amount just after the flash is over and from the knowledge of the extinction coefficient for O_2^- radical anion at $\lambda = 240$ nm, the ε for SeO_3^- radical anion at 430 nm or for that matter at any wavelength where SeO_3^- radical anion absorbs was determined. The value was in good agreement with the value reported in the literature.[4] Since under the experimental conditions used essentially none of the flash radiations was absorbed by water, the observations of the optical absorption spectra of SeO_3^- and O_2^- radical anions provide conclusive evidence for the primary photolytic process (2).

---

[4] G. E. Adams, J. W. Boag and B. D. Michael, *Trans. Faraday Soc.*, **61**, 1974 (1965).

[5] G. Czapski, L. M. Dorfman, *J. Phys. Chem.*, **68**, 1169 (1964).

[6] G. E. Adams, J. W. Boag and B. D. Michael, *Proc. Roy. Soc.*, **A 287**, 321 (1965).

Table 1

(a) Rate constant for the 2nd order decay of O_2^- at natural pH

λ (nm)	$(SeO_3^{2-})=10^{-2}$M. $\varepsilon(M^{-1}Cm^{-1})$	$2k/\varepsilon(Cm\ Sec^{-1})$	$k\ (M^{-1}Sec^{-1})$
250	1 030	9×10^4	4.6×10^7

(b) Rate constant for the 2nd order decay of (SeO_3^-) at natural pH

$(SeO_3^{2-})=10^{-2}$M.

(i) O_2 Saturated system :

λ(nm)	$2k/\varepsilon(Cm\ Sec^{-1})$	$\varepsilon(M^{-1}\ cm^{-1})$	$k\ (M^{-1}\ Sec^{-1})$
430	40×10^5	1.4×10^3	5.6×10^8

(ii) Ar Saturated system :

λ (nm)	$2k/\ \varepsilon(Cm\ Sec^{-1})$	$\varepsilon(M^{-1}\ Cm^{-1})$	$k\ (M^{-1}\ Sec^{-1})$
430	3.5×10^5	1.4×10^3	4.9×10^8

(i) Rate constant for the 2nd order decay of SeO_3^- at pH 12.5 in presence of Ar

λ(nm)	$2k/\ \varepsilon(Cm\ Sec^{-1})$	$\varepsilon(M^{-1}cm^{-1})$	$k\ (M^{-1}\ Sec^{-1})$
430	3.8×10^5	1.4×10^3	5.3×10^8

Revue Roumaine de Chimie, **23**, *11–12*, 1631–1634 (1978)

THE BEHAVIOUR OF α-BROMOSTEARIC ACID AS EXTRACTION AGENT. I

MECHANISM OF COPPER(II) EXTRACTION

ANIȘOARA BOLD and LUMINIȚA BĂLUȘESCU

Laboratory of Analytical Chemistry, Department of Chemistry and Chemical Engineering, Polytechnic Institute of Iassy, Splai Bahlui 71, Romania

Received November 12, 1976

The present paper studies the behaviour of α-bromostearic acid as extraction agent for copper(II). The dissociation constant and distribution ratio of the acid were determined. It was also established that the species extracted in the organic phase are of the type $CuR_2 \cdot 2HR$. A mechanism of Cu(II) extraction was suggested.

The results of the investigation on extraction of some transition elements with long chain fatty acids such as stearic, oleic and elaidic acids were reported in previous papers.[1-4].

Taking into account that the presence of a halogen in α-position of a carboxylic acid modifies its properties, we considered of interest to investigate the α-bromostearic acid as extraction agent.

In the present paper the results of investigating the extraction mechanism of copper(II) in the water–benzene–α-bromostearic acid system are reported.

EXPERIMENTAL

The α-bromostearic acid was obtained according to the procedure reported, [5] except that we used $POCl_3$ instead of amorphous phosphorus.

The purity of the acid obtained was confirmed by means of melting point, elemental analysis and I. R. spectrum. The I.R. spectra were recorded on a UNICAM SP-200 spectrophotometer.

The dissociation constant of the α-bromostearic acid was determined by potentiometric titration. Its value is equal to $(8.512 \pm 0.01) \times 10^{-7}$, and it is greater than that of stearic acid $(4.00 \pm 1) \times 10^{-8}$ with one order of magnitude.[1]

The organic phase required in extraction was obtained by dissolving the acid in benzene. The aqueous phase, containing Cu(II) was obtained as previously reported.[1]

The ionic strength was maintained constant to 0.1 with a 1 F $NaNO_3$ solution.

---

[1] S. Fișel and A. Bold, *Anal. Sti. Univ. "Al. I. Cuza" Iași, Sect.* I, **15**, 137 (1969).

[2] E. Bold and S. Fișel, *Rev. Roumaine Chim.*, **16**, 1775 (1971).

[3] E. Bold and S. Fișel, *Anal. Sti. Univ. "Al. I. Cuza"* Iași, *Sect*, I, **17**, 19 (1971).

[4] S. Fișel and A. Bold, *Anal. Sti. Univ. "Al. I. Cuza"*, *Iași, Sect. I*, **17**, 173 (1971).

[5] C. Hell and J. Sadomsky, *Ber. dtsch. chem. Ges.*, **24**, 2388 (1891).

Standardization of the extraction process was carried out by means of an automatic stirrer,[3] it was found that 150—250 periods are sufficient to attain the equilibrium.

The determination of copper in the two phases, and the pH measurements of the solutions, were done as in prior work.[1]

On the basis of the experimental data obtained, the distribution ratio (D) and the extraction degree (E%) have been computed.

DISCUSSION

It was found that the partition ratio of α-bromostearic acid (K_{HR}) between benzene and water depends on acid concentration in organic phase. The results are summarized in table 1.

Table 1

Partition of α-bromostearic acid between benzene and water (μ = 0.1, volume of phase 10 ml)

Initial concentration M × 10²	Concentration in the organic phase, M × 10²	Concentration in the aqueous phase, M × 10²	K_{HR}
36.12	33.67	2.340	14.46
18.00	17.56	0.450	39.02
11.90	11.89	0.103	115.42
7.80	7.70	0.031	251.24

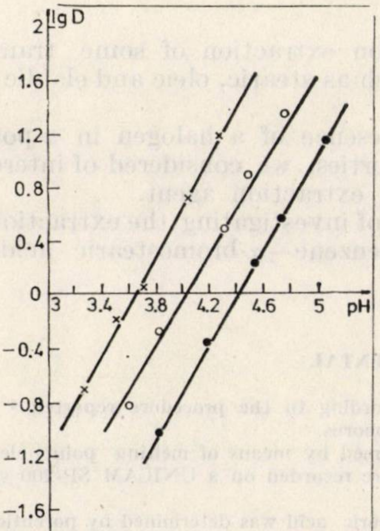

Fig. 1. — Extraction of Cu(II) with α-bromostearic acid. Variation of lg D vs. pH for solutions containing 2×10^{-3} M metal and various concentrations of fatty acid. × = 1×10^{-1} M; o = 5×10^{-2} M; ● = 2.5×10^{-2} M.

According to the data obtained, α-bromostearic acid is dimerized in benzene. On the basis of I. R. spectra, in the range of 1735—1800 cm^{-1}, a 1×10^{-1} M solution of α-bromostearic acid in benzene contains 75—80% dimer and 25—20% monomer.

The results of the lg D of Cu(II) vs. pH for different concentrations of acid are plotted in Figure 1.

Using the quantitative mathematical treatment of the extraction process as previously described,[1] the slope of the lg D lines was calculated. Its value is equal to 1.76 ($\simeq 2$). Taking into account this value, it can be concluded as a first approximation, that in aqueous phase the species involved in ion exchange is Cu^{2+}.

In order to establish the nature of species in the organic phase, as well as to determine the extraction curves in the optimum pH range, the plot $pH_{50\%}$ vs. logarithm of total concentration (C_{HR}) of carboxylic acid, in the organic phase (Figure 2) was used. The slope of the respective line is equal to 1.26 ; and x = the total number of α-bromostearic acid molecules participating in the extracted species was found to be equal to 4.43. It follows that in the presence of α-bromostearic acid Cu(II) is extracted in an acid form, of the type $CuR_2 \cdot 2HR$.

In order to establish the polymerization degree of the extracted species, the variation of logarithm of their distribution ratio (D) vs. pH for different concentrations of metal in aqueous phase was investigated. The experimental results are plotted in Figure 3.

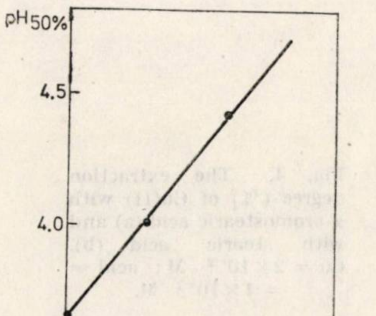

Fig. 2. — Extraction of Cu (II) with α-bromostearic acid. Relationship between pH of 50% extraction ($pH_{50\%}$) and lg C_{HR} slope = 1.25 ; x = 4.37

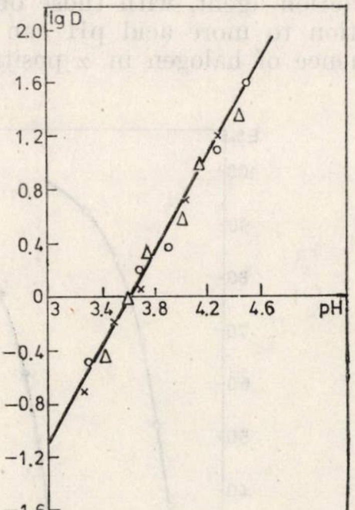

Fig. 3. — Extraction of Cu(II) with α-bromostearic acid. Variation of lg D vs. pH for different concentrations of the metal. o = 4×10^{-3} M ; × = 2×10^{-3} M ; △ = 1.33×10^{-3} M.

As follows from Figure 3, there is no significant dependence of lg D on the metal concentrations in aqueous phase, in the range between 1.33×10^{-3} M and 4×10^{-3} M. Therefore, it can be concluded that the extracted copper-containing species are monomeric.

According to the data presented above, we assume that the extraction mechanism of Cu(II) with α-bromostearic acid can be written as follows:

$$Cu^{2+} + 4HR \rightleftarrows CuR_2 \cdot 2HR + 2H^+$$

Table 2

The species formed in the extraction of Cu(II) with stearic and α-bromostearic acid

	Stearic acid	α-Bromostearic acid
n	2.1($\simeq$ 2)	1.76 ($\simeq$ 2)
x	3	4.37
m	1.9 ($\simeq$ 2)	1
species	$[CuR_2 \cdot HR]_2$	$CuR_2 \cdot 2HR$

Comparing the results obtained by using α-bromostearic acid as extraction agent, with those obtained with stearic acid,[1] a shift of extraction to more acid pH can be noticed. This fact can be due to the influence of halogen in α position.

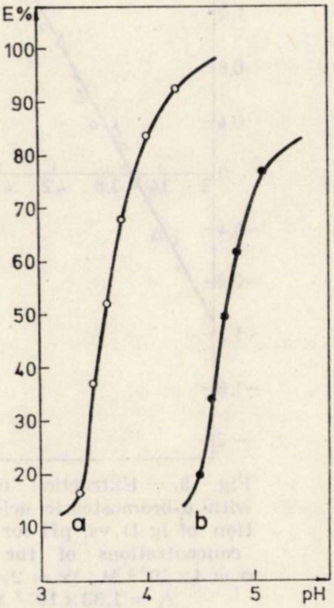

Fig. 4. — The extraction degree (%) of Cu(II) with α-bromostearic acid (a) and with stearic acid (b). $Cu = 2 \times 10^{-2}$ M; acid $= 1 \times 10^{-1}$ M.

The comparative results are presented in table 2.

The extraction degree (%). (Figure 4) with stearic acid is approximately 77% at pH = 5.1, while with α-bromostearic acid an extraction degree of 93% is achieved at pH = 4.28.

Revue Roumaine de Chimie, **23**, *11–12*, 1635–1649

RETENTION OF ORGANIC ANIONS ON STRONGLY BASIC MACROPOROUS ION-EXCHANGERS

CORNELIA LUCA, GABRIELA CHIŢANU, I. PETRARIU, A. AIRINEI
and A. CARPOV
Institute of Macromolecular Chemistry "Petru Poni" Aleea Gr. Ghica Vodă nr. 41 A,
Iassy, Romania

Received March 29, 1976

Eleven macroporous ion-exchangers having structural units of vinylbenzyltrimethylammonium have been synthetized by chloromethylation and amination of some ternary copolymers of styrene, divinylbenzene (DVB) and acrylic monomers. Different ternary copolymers have been obtained changing the nature of the inert and acrylic component and the concentration of divinylbenzene and acrylic monomer. The influence of ion-exchanger structure on the retention of some organic anions from aqueous solutions has been investigated and the specific adsorptions until the achieving of the equilibrium have been determined using alkali salts of some aromatic carboxylic and sulphonic acids. It has been observed that the chemical nature of the copolymer (i.e., copolymer composition) strongly influences retention of organic anions on the investigated ion-exchangers.

INTRODUCTION

The strongly basic ion-exchanging resins are especially used for water deionization. Because the pollution of the surface water with organic chemicals from industrial water increases continuously, there is an increasing interest for the investigation of the behaviour and efficiency of anion exchangers vs. the organic impurities within water. At the same time it is aiming at the synthesis of new types of anion exchangers that have to be "unpoisonable" vs. different chemicals are able to retain and then to eliminate as much as possible organic polluting materials. Usually these materials are aromatic carboxylic and sulphonic acids and their salts.

Retention of organic derivatives in the matrix of anion exchangers could take place either by ionic exchange or by physical interactions. Therefore it is dependent not only on the number and type of functional groups (i.e., the volume or weight capacity of ionic exchange) but also on the chemical and physical structure of the macromolecular matrix used for synthesis of the anion exchanger.

Investigations were devoted to retention of organic derivatives by anionic exchangers obtained both from styrene-divinylbenzene copolymers (gel type)[1-5] and from macroporous copolymers in presence of aliphatic hydrocarbons.[6-7] It was thus observed that both the retention rate of organic ions and its reversibility are favoured by macroporous structures. These structures could be obtained by copolymerization of styrene and DVB in presence of inert swelling components such as toluene[8] or of inert precipitating components either of small molecule such as aliphatic hydrocarbons[9] or of macromolecular character such as polystyrene.[10]

The macroporous structure is characterized by swelling porosity (i.e., the porosity which appears as a consequence of the polymer swelling in a suitable solvent). This kind of porosity is additional to permanent porosity (i.e., the dry state porosity of the polymer). The formation of the macroporous structure is highly determined by concentration of the crosslinking agent, especially when toluene is used as inert reaction component. In this case for concentrations of DVB of 18–20% an expanded structure is obtained i.e., for a new contact with the solvent the tridimensional matrix regains the shape it had during polymerization process. For a content of 27% SVB in copolymers the structure is intermediate between the expanded and macroporous structures and for contents of DVB higher than 35% permanent porous structures are formed.

When, at the copolymerization of DVB a polar monomer is added, e.g. acrylonitrile, alkyl methacrylates, etc., both the internal specific surface,[11] and the permanent porosity[12] of the obtained macroporous copolymers could be modified.

Therefore the aim of the present paper is the elucidation of the influence of copolymerization conditions and of the characteristics of copolymers styrene-DVB-acrylic derivative upon the retention from aqueous solutions of some aromatic carboxylic and sulphonic anions by macroporous anion-exchangers obtained from those copolymers. Consequently the following parameters of obtaining of macroporous support were varied :

— the nature of the inert component used at the copolymerization;
— DVB concentration;
— the nature and the concentration of the acrylic monomer used for synthesis of terpolymers.

---

[1] R. L. Gustafson and J. A. Lirio, *Ind. Eng. Chem. (Product Research and Development)*, **7**, 116 (1968).

[2] V. Talasek and J. Eliasek, *Coll. Czech. Chem. Comm.*, **34**, 2538 (1969).

[3] S. G. Alenitskaya and G. L. Starobinets, *Zhur. fiz. Khim.*, **43**, 2138 (1969).

[4] S. G. Alenitskaya and G. L. Starobinets, *Zhur. fiz. Khim.*, **43**, 2306, (1969).

[5] S. G. Alenitskaya and G. L. Starobinets, *Zhur. fiz. Khim.*, **43**, 2315 (1969).

[6] P. Martinola and G. Naumann, *Angew. Makromol. Chem.*, **4**, 185 (1968).

[7] P. Wolf and R. Schaaf, *Plaste Kaut.*, **18**, 21 (1971).

[8] J. R. Millar, E. G. Smith, W. S. Marr and T.R.E Kressman, *J. Chem. Soc.*, **33**, 218 (1963).

[9] J. Seidl, J. Malinsky, K. Dusek and W. Heitz, *Fortschr. Hochpolym. Forsch.*, **5**, 113 (1967).

[10] J. Seidl, J. Malinsky and E. Krejcar, *Chem. průmysl.*, **7**, 414 (1965).

[11] R. Wolf, R. Bachmann, H. Reuter, G. Schwachula D. Warnecke, W. Wohle and U. Krauss (R.D.G.), *Brit. Pat.* 1.020.907, Feb. **23**, 1966.

[12] Ig. Poinescu, S. Drăgan and S. Maxim (R.S.R.) *Rom. Pat.*, 67.211, June **13**, 1971.

EXPERIMENTAL

MATERIALS AND METHODS

Synthesis of anion-exchangers resins

The copolymers styrene-DVB-acrylic monomer were obtained[12] in presence of toluene, benzine and polystyrene as inert components. In each synthesis the feed composition was modified by changing the DVB concentration and the nature and the concentration of the acrylic derivative. The obtained copolymers were characterized by methanol coefficient (i.e., methanol vs. dried copolymer), w/w, toluene coefficient (i.e., toluene vs. dried copolymer w/w), specific density, (ρ_{sp}), apparent density, (ρ_{ap}) and permanent porosity (P%), the last one being calculated using the following equation :

$$P\% = \left(1 - \frac{\rho_{ap}}{\rho_{sp}}\right)\cdot 100$$

Copolymer compositions and characteristics are listed in table 1.

In order to obtain anionic exchangers having structural units of vinylbenzyltrimethyl ammonium the copolymers were chloromethylated with monochlorodimethylether using $ZnCl_2$ as catalyst and the obtained material was then aminated with trimethylamine (aqueous solution 24%).[13, 14]

PREPARATION OF ION-EXCHANGER SAMPLES

Samples of anion-exchangers were conditioned by alternate conversions to hydroxide and chloride forms with 4% aq. solutions of NaOH and HCl. After ultimate conversion to the chloride form, the resins were thoroughly rinced with de-ionized water until the complete removal of chlorine ions. All samples were dried at room temperature for 4–5 days. In order to determine the moisture content, amounts (1–2 g) of each sample were vacuum dried at 40° until the achieving of the constant weight. The exchange capacity of resins was determined by elution of chloride anion with 4% aq. solution of Na_2SO_4. The chloride level in solution was determined by titration with standard silver nitrate solution using a Copenhagen Radiometer TTT 1C.

REAGENTS

Sodium benzoate (NaB), sodium benzenesulphonate (NaBS), potassium α-naphtylacetat(KNA), sodium β-naphtalenesulphonate (NaNS) and sodium anthraquinone-2-sulphonate (NaAQS) were used in an aqueous solution of concentrations varying 10^{-1} and 10^{-2} M/1. The concentration of solutions before and after the contact with the anion exchanger were determined spectrophotometrically using a Unicam SP 200 ultraviolet spectrometer. The following wavelenghts were used (standard 1 cm quartz coll) : 224.5 mμ (NaB), 282.5 mμ (KNA) 263.0 mμ (NaBS), 320.5 mμ (NaNS) and 330.5 mμ (NaAQS).

RETENTION OF ORGANIC ANIONS

Owing to the fact that retention of organic derivatives on anion exchangers could take place also by ion-exchange according to eq.(1)

$$(R^+Cl^-) + (Na^+A^-) \rightleftarrows (R^+A^-) + (Na^+Cl^-)$$

---

[13] S. Maxim, Ig. Poinescu, S. Drăgan and M. Dima *Rev. Roumaine Chim.*, **17**, 1437 (1972).

[14] S. Maxim, Ig. Poinescu, D. Drăgan and M. Dima, *Rev. Roumaine Chim.*, **17**, 1447 (1972).

Table 1

Characteristics of copolymers used in synthesis of anion exchangers used for retention of organic derivatives

Run number	DVB %	Acrylic co-monomer %	Inert medium	Methanol coefficient w/w	Toluene coefficient w/w	ρ_{sp}	ρ_{ap}	P%
515	27	—	toluene	0.2600	1.7200	1.0600	1.0130	4.42
502	27	[a]AN ; 3	toluene	0.4600	1.8000	1.0918	0.9610	11.98
508	27	AN ; 5.22	toluene	0.4946	1.8778	1.0860	0.9227	15.05
510	27	AN ; 12.70	toluene	0.8697	1.8152	1.0860	1.0042	7.53
511	27	AN ; 16.90	toluene	1.2370	1.7962	1.0817	0.9160	15.30
507	20	AN ; 3.30	toluene	0.1055	1.7600	0.9900	—	—
503	35	AN ; 3	toluene	1.1680	1.8000	1.1620	0.9950	14.37
513	27	AN ; 3	poly-styrene	0.4740	0.5309	1.0687	0.7625	28.63
514	27	AN ; 3.41	benzine	1.4990	2.0150	1.0210	0.3926	61.60
522	27	[b]MMA ; 3	toluene	0.4020	1.8000	1.0180	1.0230	7.67
523	27	[c]BMA ; 3	toluene	0.4150	1.7790	1.1510	1.1120	3.39

[a] AN = acrylonitrile ; [b] MMA = methyl methacrylate ; [c] BMA = butyl methacrylate

instead of arylcarboxylic and arylsulphonic acids their salts were used in kinetic measurements in order to avoid the perturbation of ionic exchange equilibrium by:

— pH variation due to HCl resulted by ionic exchange with free arylcarboxylic and arylsulphonic acids:

$$(R^+Cl^-) + (H^+A^-) \rightleftarrows (R^+A^-) + (H^+Cl^-)$$

— low water solubility of some organic acids, such as 2-anthraquinone-sulphonic acid, in comparison with their alkali salts.

Retention of organic anions was carried out statically at room temperature (20°) as follows. Dried resin samples (1g) in chloride form were introduced in glass vessels containing known volumes of aqueous solutions of determined concentration organic derivatives. The volume of solution was taken in each case so that the amount of organic ion exceeded by $\sim$10% the exchange capacity of the resin. At known intervals of time liquid samples were taken out from vessels and the concentration of organic ions and chloride level was determined.

The amount of organic anion retained by anion exchanger was taken as the difference between the initial amount of organic material and that determined in liquid layer after the contact with resin. The specific adsorption, x/m, was then calculated as the number of mequiv. of organic anion retained by 1 g of dried resin and plotted vs. time in order to follow the retention of different organic anions.

RESULTS AND DISCUSSION

The influence of the nature of inert component used in synthesis of resins 502 (toluene), 513 (polystyrene) and 514 (benzine) on the retention of organic anions is given in Figures 1—5.

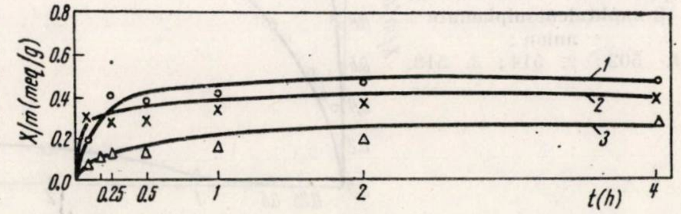

Fig. 1. — Influence of the nature of inert component used in copolymerization upon the retention of benzoate anion; *1.* 502; *2.* 514; *3.* 513.

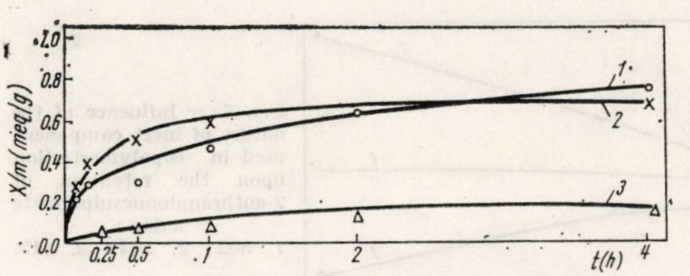

Fig. 2. — Influence of the nature of inert component used in copolymerization upon the retention of α-naphtylacetate anion: *1.* 502; *2.* 514; *3.* 513.

It can be seen from Figures 1 and 3 that the organic derivatives of molecular mass (M) less than 200, i.e. NaB (M = 144) and NaBS (M = = 180), are better retained by anion exchanger 502 (curves 1). For organic derivatives of higher molecular mass, i.e. KNA (M = 224), NaNS (M = = 230) and NaAQS (M = 310), the equilibrium is achieved faster for resin 514 than for resin 502. The specific adsorption is also higher for resin 514

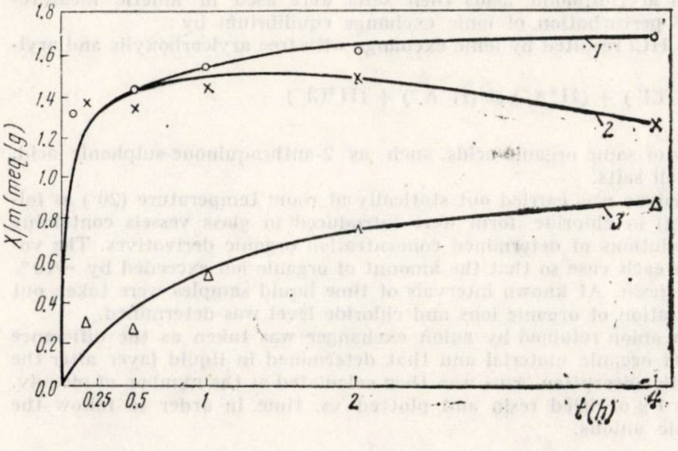

Fig. 3. — **Influence of the nature of inert component used in copolymerization upon the retention of benzenesulphonate anion : *1.* 502 ; *2.* 514 ; *3.* 513.**

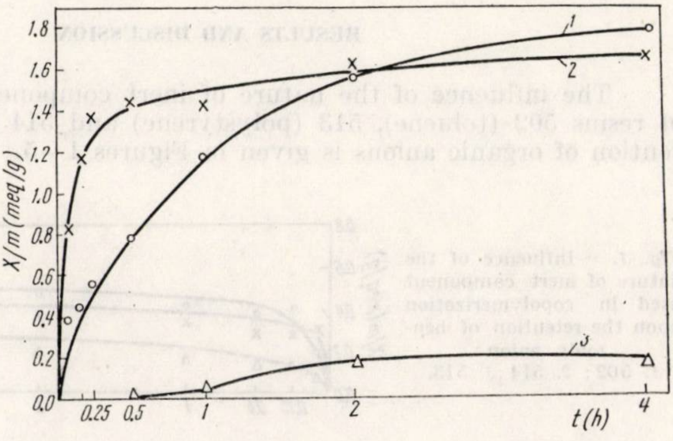

Fig. 4. — **Influence of the nature of inert component used in copolymerization upon the retention of β-naphtalenesulphonate anion : *1.* 502 ; *2.* 514 ; *3.* 513.**

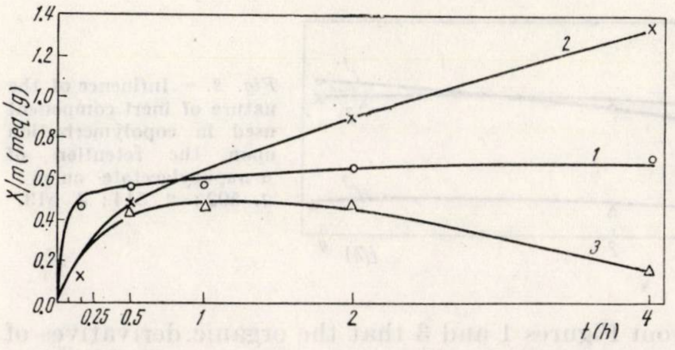

Fig. 5. — **Influence of the nature of inert component used in copolymerization upon the retention of 2-anthraquinonesulphonate anion : *1.* 502 ; *2.* 514 ; *3.* 513.**

than that corresponding to resin 502. The porest results were obtained when resin 513 was used (Figures 4 and 5).

This behaviour could be explained if the copolymerization conditions for resins 502,513 and 514 are taken into consideration. Different copolymerization conditions mean different tridimensional matrices for resulted polymers. Thus the resin 502 has an intermediate structure between an expanded structure and a macroporous structure, being characterized by a low permanent porosity (12%), while the resins 513 and 514 have macroporous structures of much higher permanent porosity: 27% and 62%, respectively (Table 1). Although a higher porosity determines an increased permeability for organic anions, sometimes these anions are better retained by expanded or intermediate structures. An explanation for this behaviour could be given based on findings of Millar et al.,[15] which reported that the anion exchangers of expanded structure swell better in water and make loose the compact domains of the tridimensional matrix allowing the access of some organic ions in sites where there are most of the functional groups able for ion exchange (e.g., the case of resin 502). The resins of high permanent porosity swell in water less than that of expanded structure due to the rigidity of the tridimensional matrix and organic ions can not penetrate the compact sites of the matrix and are uptaken only by its pores (e.g., resins 513 and 514). The number of functional groups in pores is much lower than that of compact sites so that a smaller amount of organic ions could be retained by ion exchange. This is the reason why benzoate and benzenesulphonate anions are retained better by resin 502 than by resins 514 and 513. Perhaps bulky organic anions such as KNA, NaNS and NaAQS cannot penetrate the compact sites of a resin having an expanded structure and swollen in water and are retained better by resins having a permanent porosity because they can get into the pores of macromolecular matrix. It explains thus the better retention of these bulky organic anions by resin 514 than by resin 502.

Perhaps the different behaviour in retention organic anions of resins 514 and 513 is due to the difference between specific surface of these two copolymers. It is known that the specific surface of copolymers obtained in presence of polystyrene is smaller than that of copolymers synthetized in presence of benzine. Regarding the retention of organic ions taking place onto the surface it is the anion exchanger 514 obtained in presence of benzine which will be favoured.

In order to put in evidence the influence of crosslinking on retention capacity of the resins obtained in presence of toluene, the following ion exchangers were used: 507 (20% DVB), 502 (27% DVB) and 503 (35% DVB). The obtained results are given in Figures 6–10).

It can be seen, as previously, that the anion exchanger 502 retains better the small organic anions than resins 503 and 507 and that the selectivity for certain large organic ions, such as β-naphtalene sulphonate and 2-anthraquinonesulphonate anions is higher for anion exchanger 503. The reason could be the higher permanent porosity of the copolymer 503 than that of the copolymer 502 (Table 1).

Comparative selectivities for organic anions of ternary copolymers containing as acrylic co-monomer acrylonitrile, AN, methylmethacrylate, MMA, or buthylmethacrylate, BMA, are presented in Figures 11–15.

---

[15] J. L. Millar, D. G. Smith, W. B. Marr and T.R.E. Kressman, *J. Chem. Soc.*, **34**, 2779 (1963).

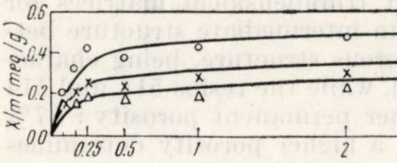

Fig. 6. — **Influence of DVB content in copolymer upon the retention of benzoate anion :** *1.* 502 ; *2.* 503 ; *3.* 507.

Fig. 7. — **Influence of DVB content in copolymer upon the retention of α-naphtylacetate anion :** *1.* 502 ; *2.* 503 ; *3.* 507.

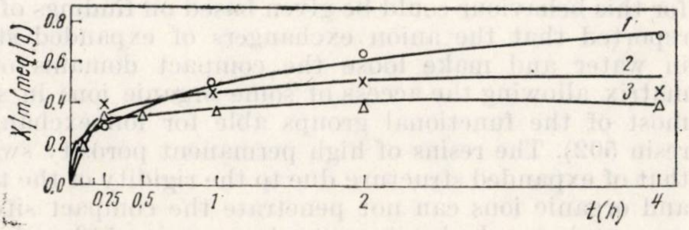

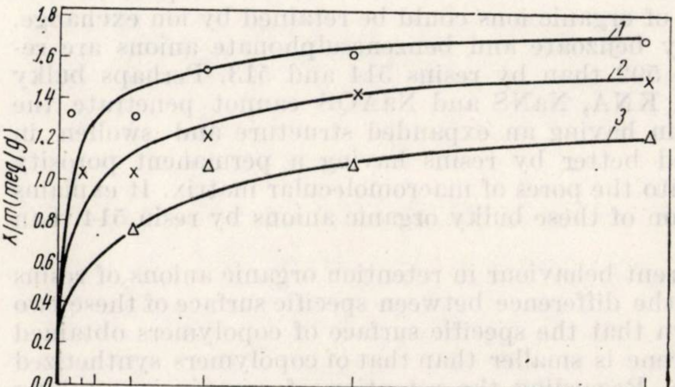

Fig. 8. — **Influence of DVB content in copolymer upon the retention of benzenesulphonate anion :** *1.* 502 ; *2.* 503 ; *3.* 507.

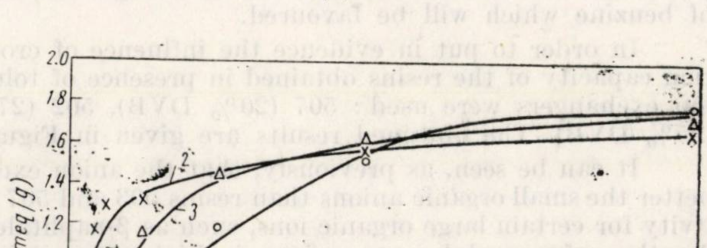

Fig. 9. — **Influence of DVB content in copolymer upon the retention of β-naphtalenesulphonate anion :** *1.* 502 ; *2.* 503 ; *3.* 507.

Fig. 10. — Influence of DVB content in copolymer upon the retention of 2-anthraquinonesulphate anion : *1.* 502 ; *2.* 503 ; *3.* 507.

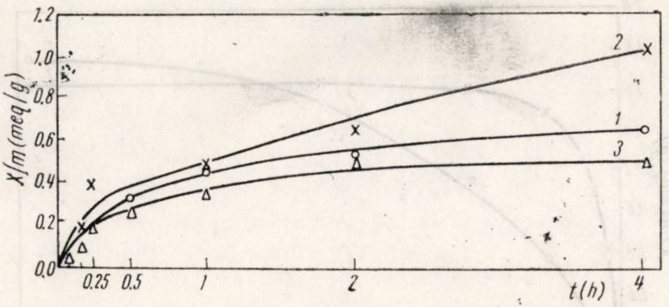

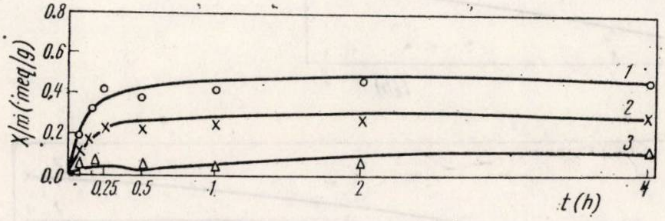

Fig. 11. — Influence of acrylic component from copolymer upon the retention of benzoate anion : *1.* 502 ; *2.* 523 ; *3.* 522.

Fig. 12. — Influence of acrylic component from copolymer upon the retention of α-naphtylacetate anion : *1.* 502 ; *2.* 523 ; *3.* 522.

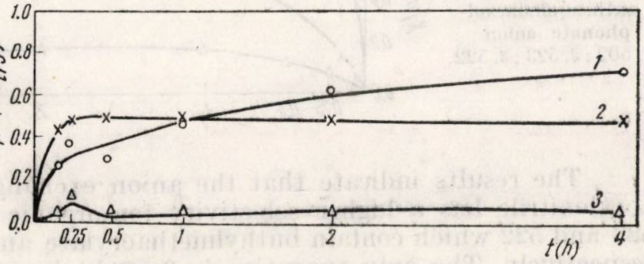

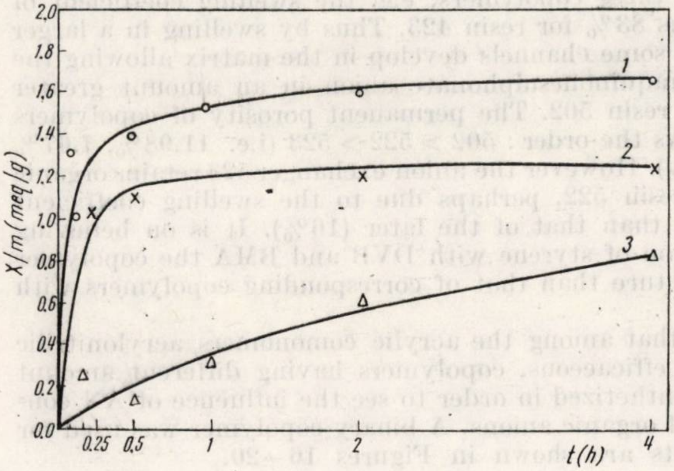

Fig. 13. — Influence of acrylic component from copolymer upon the retention of benzenesulphonate anion : *1.* 502 ; *2.* 523 ; *3.* 522.

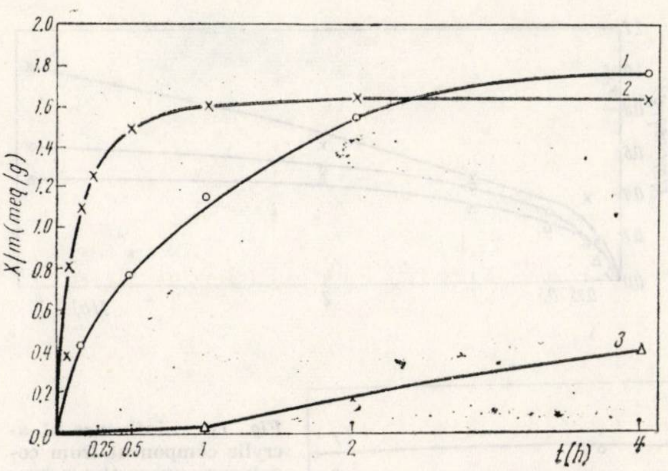

Fig. 14. — **Influence of acrylic component from copolymer upon the retention of β-naphtalenesulponate anion :**
1. 502 ; *2.* 523 ; *3.* 522.

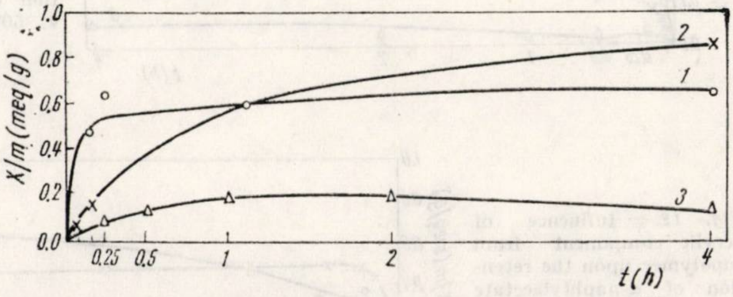

Fig. 15. — **Influence of acrylic component from copolymer upon the retention of 2-anthraquinonesulphonate anion :**
1. 502 ; *2.* 523 ; *3.* 522.

The results indicate that the anion exchanger 502 which contains acrylonitrile has a higher selectivity for organic anions than exchanger 523 and 522 which contain buthylmethacrylate and methylmethacrylate, respectively. The only exception is β-naphtalenesulphonate anion which is retained better by anion exchanger 523. The reason lies in swelling behaviour in water of these copolymers, e.g. the swelling coefficient of resin 502 is 50% versus 83% for resin 423. Thus by swelling in a larger extent of the resin 523 some channels develop in the matrix allowing the penetration of 2-anthraquinonesulphonate anion in an amount greater than that retained by resin 502. The permanent porosity of copolymers 502, 522 and 523 follows the order : 502 > 522 > 523 (i.e. 11.98%, 7.67% and 3.39%, respectively). However the anion exchanger 523 retains organic ions better than the resin 522, perhaps due to the swelling coefficient (83%) which is higher than that of the later (16%). It is on believing that by copolymerization of styrene with DVB and BMA the copolymer has a less packed structure than that of corresponding copolymers with AN and MMA.

Due to the fact that among the acrylic comonomers acrylonitrilic seems to be the most efficaceous, copolymers having different amount of acrylonitrile were synthetized in order to see the influence of AN content on the retention of organic anions. A binary copolymer was used for comparison. The results are shown in Figures 16—20.

Fig. 16. — **Influence of AN content in copolymer upon the retention of benzoate anion :**
1. **515 ;** *2.* **502 ;** *3.* **508 ;** *4.* **510 ;** *5.* **511.**

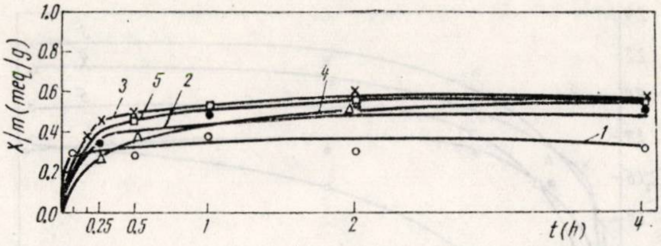

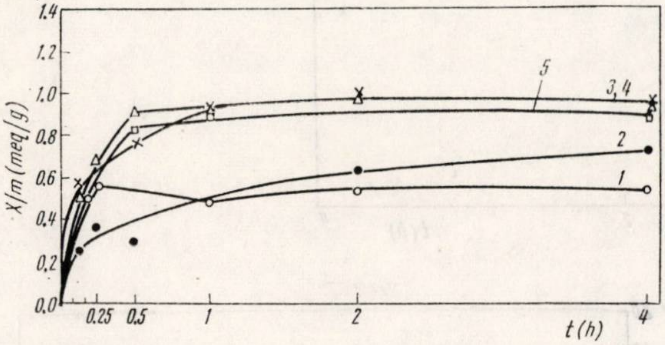

Fig. 17. — **Influence of AN content in copolymer upon the retention of α-naphtyl-acetate anion :**
1. **515 ;** *2.* **502 ;** *3.* **508 ;** *4.* **510 ;** *5.* **511.**

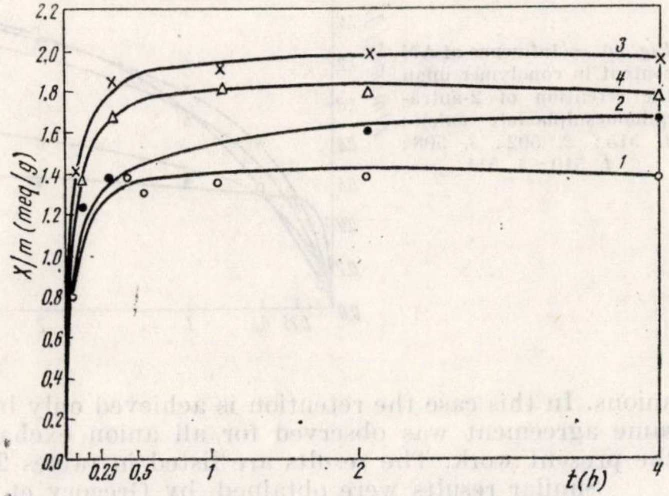

Fig. 18. — **Influence of AN content in copolymer upon the retention of benzene-sulphonate anion :**
1. **515 ;** *2.* **502 ;** *3.* **508 ;** *4.* **510.**

It appears that indifferently to the nature of organic anion, the maximum retention is obtained for an AN content in copolymers of 5%. The reason could be the high swelling coefficient of the anion exchanger 508 (5% AN), 100%.

The agreement between the specific retention of resins and the amount of chlorine exhanged from resin phase is good for carboxylic

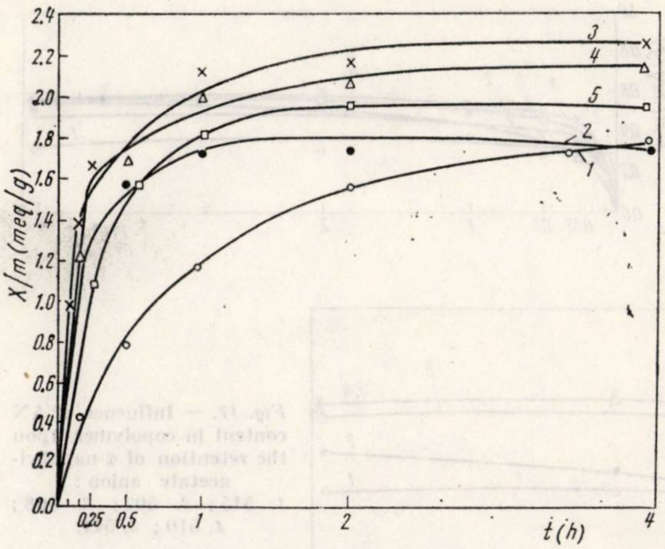

Fig. 19. — Influence of AN content in copolymer upon the retention of β-naphtalenesulphonate :
1. 515 ; *2.* 502 ; *3.* 508 ; *4.* 510 ; *5.* 511.

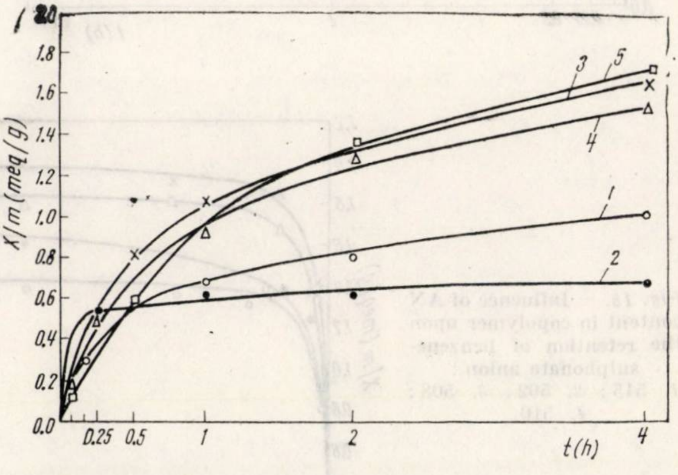

Fig. 20. — Influence of AN content in copolymer upon the retention of 2-antraquinonesulphonate anion :
1. 515 ; *2.* 502 ; *3.* 508 ; *4.* 510 ; *5.* 511.

anions. In this case the retention is achieved only by ionic exchange. The same agreement was observed for all anion exchangers investigated in the present work. The results are listed in tables 2 and 3.

Similar results were obtained by Gregory et al. who investigated the retention of some carboxylic anions derived from aliphatic acids by strongly basic anion exhangers.[16,17] At the retention of arylsulphonic anions, especially in the case of benzenesulphonic anion, some difference between specific retention and the amount of chloride exchanged from

---

[16] J. Gregory and M. J. Semmens, *J. Chem. Soc. Faraday Transactions*, **68**, 1045 (1972).

[17] M. Semmens and J. Gregory, *Environmental Science and Technology*, **8**, 834 (1974).

Table 2

Retention of benzoate anion in comparison with the amount of chlorine ions exchange from resin phase

Run number	Time min.	The amount of retained organic anion. mequiv./g dried resin	The amount of chlorine ions exchange from resin phase mequiv./g dried resin
502	15	0.41	0.46
	60	0.43	0.48
	120	0.48	0.53
508	30	0.47	0.49
	60	0.48	0.52
	120	0.49	0.54
510	30	0.26	0.31
	60	0.39	0.45
	120	0.52	0.56
513	30	0.21	0.21
	60	0.22	0.21
	120	0.31	0.31
514	15	0.34	0.36
	30	0.35	0.35
	60	0.40	0.41
503	30	0.35	0.38
	120	0.44	0.42
	240	0.49	0.48

Table 3

Retention of α-naphthy acetate anion in comparison with the amount of chlorine ions exchanges from resin phase

Run number	Time min.	The amount of retained organic anion mequiv./g dried resin	The amount of chlorine ions exchanged from resin phase mequiv./g dried resin
502	15	0.36	0.19
	60	0.46	0.45
	120	0.63	0.62
508	15	0.94	0.99
	30	0.97	1.02
	60	0.96	1.01
510	15	0.91	0.96
	30	0.94	1.00
	120	0.97	1.00
511	30	0.83	0.93
	240	0.93	1.00
513	60	0.09	0.12
	120	0.19	0.16
	240	0.23	0.26
514	15	0.66	0.70
	60	0.70	0.71
	120	0.76	0,75

Table 4

Retention of benzene sulphonic anion in comparison with the amount of chlorine ions exchanged from resin hase

Run nuber	Time min.	The amount of retained organic anion mequiv./g dried resin	The amount of chlorine ione exchanged from resin phase mequiv/g dried resin
502	15	1.96	1.12
	30	1.31	0.84
	120	1.63	0.98
	240	1.70	1.09
523	120	2.06	1.38
	240	2.13	1.38
503	120	2.37	1.15
	240	1.89	0.85
507	120	2.03	1.33
	240	2.16	1.39
514	60	1.70	1.18
	120	1.76	1.08

resin phase has been observed. It means that besides ionic exchange some phenomena of physical adsorption take place. The data are given in table 4.

The results also indicate that: a) the arylsulphonic anions are retained better than arylcarboxylic anions and b) in the series of arylcarboxylic anions specific retention follows the order KNA > NaB while in the series of arylsulphonic anions the order is inversed, i.e., NaBS > NaNS > NaAQS (Figure 21).

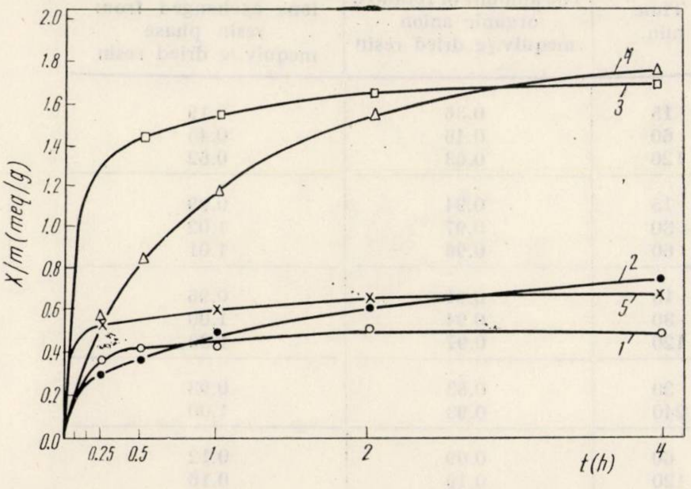

Fig. 21. — Retention of different organic anions on the anion exchanger 502: *1.* NaB; *2.* KNA; *3.* NaBS; *4.* NaNS *5.* NaAQS.

The most recent theories show that the selectivity of ion exchangers in processes of ionic exchange is given by difference between water-ion interaction (ion hydration) and water-water interaction (water structure) within resin phase and in the phase of external solution. The ion hydration influences the selectivity of resin not only by its size.[18]

The weaker the present acid of the anion the stronger the link formed with water (higher degree of hydration) is so that the diluted external solution will be prefered. It explains higher selectivities attained for retention of arylsulphonic anions in comparison with arylcarboxylic anions.

For the same series of organic anions the selectivies are perhaps dictated by alterations of water-water interactions due to the size of the organic ion.

The structure of water within resin phase is different from that within external solution; in solution phase the water has a structure much more ordered than within resin phase. Consequently in the ionic exchange process the larger ion is excluded from solution to resin phase where the water is less ordered (as far as the resin pores allow it). This kind of behaviour permits the water-ion and water-water interactions in the whole system.

CONCLUSIONS

1. The nature of inert component influences the retention from water of organic anions owing to the characteristics of macroporous structure formed. In some cases the expanded structure seems to be more efficient if the organic ion is not too large. For large anions more suitable are the structures having a permanent porosity and especially those obtained in presence of aliphatic hydrocarbons.

2. The acrylic component has a favourable influence upon the retention of organic anions. The best results were obtained with AN amounting 5% in copolymer composition.

3. In order to retain different organic impurities from water the characteristics of the ion exchanger must be adequate to the type of impurity.

---

[18] B. Chu, D. C. Whitney and R. M. Diamond, *J. Inorg. Nuclear Chem.*, **24**, 1405 (1962).

Revue Roumaine de Chimie, **23**, *11–12*, 1651–1653 (1978)

COMPTES RENDUS

A .D. JENKINS (Editor), "Progress in Polymer Science", vol. 5, No. 1 & No. 2 Pergamon Press, Oxford, New York, 1977.

For those working in polymer science, "Progress in Polymer Science" is meant to provide practical, rapid and comprehensive information on the newest aspects in the field of chemistry, physics materials science and molecular biology. The ideea of Pergamon Press to publish some review articles summarizing the developments and concepts in areas of particular importance is an excelent one and needs no further comments.

The first issue of the fifth volume ("Gas chromatographic measurmentes of polymer structure and interactions", 60 pages, author Derek G. Gray) contains an extensive article on the mentioned subject, summarizing recent applications where gas-chromatography has been used to investigate the structure and interactions of polymeric materials. The article deals with those cases in which the polymeric material under study is employed as a stationary phase in a gaschromatographic column.

The paper is divided into seven parts. In the first one (Introduction), some notions concerning the connection between gas-chromatographic measurements and equilibrium partition coefficients are given, these notions being specific for the development of gas-chromatographic technique in polymeric materials investigation.

The results obtained by different authors in employing GC to the study of the polymer-solvent interactions with several macromolecular compounds [poly)dimethylsiloxane), poly(isobutylene), poly(ethylene), etc] are analyzed and discussed in the second part (Thermodynamics of polymer solutions). This part is probably the most important one in connection with the application of GC on polymeric stationary phases.

Data concerning the interactions between two non-volatile components in a mixed stationary phase are also presented, followed by the techniques used to measure retention volumes and thermodynamical quantities at very low concentrations or at finite concentrations of the volatile component.

In the third section (Adsorption on solid polymer surfaces), application of the GC in characterization of solid surfaces, physical adsorption processes or molecular interactions between gases and solids are described.

Subsequent sections (part 4, Polymer crystallization studies, and part 5, The glass transition) provide information on the successes obtained in GC application to polymer crystallization and to glass transition, processes characterized by a discontinuity on the retention diagramm of the vapours on the polymeric stationary phase.

The review concludes (part 6, Misscellaneous applications, and part 7, Concluding remarks) with some observations on the applications (investigations on the compatibility of polymers, the rate of vaporus diffusion through polymers, the molecular weight measurements of oligomers, etc) and in the posibilities of the technique (the thermodynamic study of the polymer solutions at finite concentrations, of chemical modification of polymers etc).

The second issue of the volume ("Photochemical probes in polymers", 32 pages, authors J. L. R. Williams and R. C. Daly) is dealing with problems concerning polymer photochemistry and photochemistry in polymer matrices. The paper summarizes historically recent work on photochemistry which deals with the intimate molecular interactions occurring in polymer systems, rather than the gross macroscopic properties displayed by the sample. It considers the three generalized systems encountered where light absorbing chromophores or mers are considered in polymer systems, namely) (1) homopolymers $(mer_1)_n$, (2) copolymers $(mer_1)_n$-$(mer_2)_n$, and (3) small molecules added to (or dispersed in) photochemically inactive polymers or members of the first two groups.

The paper is divided into five parts — Introduction, The effects of free volume, thermal transition temperatures, mobility and polarity on photochemistry in polymer systems, Photoinduced mechanical effects in polymers, Photophysical processes in polymer matrices, and Commentary.

After a short — but complete — presentation of processes following the absorption of light by a photoreactive system, the attention of the authors is foccussed on the parameters influencing on photochemistry in polymer systems (the effects of free volume, thermal transition temperatures, mobility and polarity). All the important papers published in the field are reviewed, and different polymeric matrices containing small molecules are analysed too.

The photoinduced mechanical effects in polymer matrices and the photophysical processes in these matrices are also mentioned. Thus, the authors report the observations obtained in the photocontractile behaviour in the crosslinked photochromic polymeric systems and the occurrence of such photocontractile behaviour in biological photoprocesses.

The transfer, trapping or dissipation of the excitation energy in photophysical processes in polymer matrices, described in the last part of the paper, are analysed for different polymers (vinyl aromatic polymers, copolymers of styrene). The effects of side chain chromophore modification upon energy transport and photoemission spectra are underlined, and the modes of intramolecular energy migration are presented. The role of impurities in polymer luminescence is shown to be important, and the effect of pressure and temperature on fluorescent emission is pointed out.

Finally, the paper presents the results obtained in making effective use of energy migration, transfer and dissipiation or localization, to controll the light stability of commercial plastics. 108 references end this well documented review adressed to polymer scientists working in the field of photochemical processes.

Both papers represent a very rich informational material with outstanding documentation value, a dense thematic, and abundance of ideas and autoritive interpretation of the experimental data. All these are qualities with recommend not only the above discussed articles, but the whole series of volumes which have already appeared or will appear in the "Progress in Polymer Science".

Victor Bulacovschi and Bogdan Simionescu

RENATA REISFELD and CHRISTIAN K. JØRGENSEN, "Lasers and Excited States of Rare Earths", Springer-Verlag, Berlin-Heidelberg-New York, 1977, 226 pages (No. 1 in the "Inorganic Chemistry Concepts,' Series).

Beside conventional applications based on their familiar coherent light with negligible angular extension, lasers may provide in the not so distant future a much more valuable source of benefits for science, technology, and man. Time-resolved spectroscopy, effects of non-linear optics or nuclear fusion of light elements are but a few of such potential applications. This by itself would be reason to spare no effort in studying laser media and phaenomena.

The present state-of-the-art in the field of lasers based on rare earths is the subject matter of this book. Although the fluorescence of ruby had already been mentioned ten centuries earlier in "Thousand and One Nights", the laser was not achieved practically (by Maiman) until 1960. Since then, many lasing systems using di- and trivalent rare earths in a great variety of crystals, glasses and liquids were investigated. Beside the well known, Nd-glass laser, many other rare earth lasers were introduced, offering a wide choice of wavelengths and power outputs. Description of their principles in the book is attented by adequate considerations about excited state relaxation processes in solids and a thorough discussion of the optical transitions inolved. Several examples are given of existing (solid, vitreous, liquid and even gaseous) rare earth lasing systems. A separate chapter deals with the interrelation between the lanthanide spectra and the chemical bonding in rare earth comopounds, Another chapter discusses the energy transfer in rare earth systems, considering problems such as transfer probabilities, excitation migration, and phonon-assisted energy transfer. The energy transfer between lanthanides, on the one hand, and the uranyl ion or organic ligands, on the other, is thoroughly reviewed.

The last chapter of the book, "Applications and suggestions", makes a really fascinating reading indeed. Its main sections, each devoted to a particular laser application, are filled with many and varied considerations concerning the adequacy and feasibility of laser involvement in such modern and pregnant problems as laser-induced thermonuclear reactions, cathodoluminescence, interplanetary communications, geodesy and trigonometry in the Solar system, and holography. The laser-assisted isotope separation seems to be the only side overlooked by the authors.

The book bears the trademark of Professor Jorgensen's well known style, full of substance but also of (seemingly) peripheral considerations about the implications of the phenomena described, research suggestions, and historical remarks. Certain aspects of the ligand field theory are critically surveyed in passing and points of future development emphasized. The book may be helpful to all researchers concerned with the rare earth's involvement in laser effects, being at the same time an agreeable lecture for any quantum physicist or chemist.

Alex. Bulucelea

T. TÖRÖK, J. MIKA and E. GEGUS, "Emission Spectrochemical Analysis", Akadémiai Kiadó, Budapest, 1978, 692 p.

The book presents all practical aspects of emission spectrochemical analysis. It could be considered as a continuation of the book : J. Mika and. T. Török "Analytical Emission Spectroscopy Fundamentals" (joint edition of Akadémiai Kiadó, Budaptes and Butterworth, London, 1973) in which the same authors have extensively developed the theoretical aspects of emission spectroscopy.

After a brief introduction, chapter 2 presents in great detail (58 pages) all the aspects of sample preparation including the sampling of metals and alloys, non-conducting solid substances, solutions and gases.

Chapter 3 is devoted to an essential part of every sepctral equipment, the radiation source. The text (94 pages) is divided into four main sections treating the radiation sources used for investigation of : (1 metal samples, 2) solid non-conductors, 3) non-conducting liquids and solutions and (4) gases. Numerous figures (55) and details permit an easy understanding of the construction and operation of the various ansambles used in order to obtain the best results in each analysed case.

In the following chapter (80 pages) the conditions affecting line intensities are developed. The importance of different phenomena such as : diffusion, self-absorption, distribution of radiation in time and space etc., is presented and underlined for each factor by means of different examples including numerous tables and figures.

The following three chapters (5, 6 and 7) are devoted to spectral analysis, classified in : 1) spectrographic analysis (172 pages), 2) spectrometric analysis (62 pages) and 3) visual spectroscopic analysis (38 pages). Each of these chapters contains a lot of useful data concerning the equipment, technique and methods of evaluation. Other very interesting problems developed are those concerning the installation, work organization and economy of a spectral laboratory (spectrographic, spectrometric and spectroscopic one).

Chapter 8 gives useful information on evaluation of the results of measurements (error distribution, mean values, statistical determination of outlying results etc.

The book comprises also 138 pages of very useful data (not readily available elsewhere) presented as tbales (chapter 9). These tables include : 1) physico-chemical constants (boiling and melting points, enthalpies of evaporation and melting, molar standard entropies, ionization potentials, wavelength of the first and second resonance lines for all elements as well as molar enthalpies of formation form elements for important compounds and melting, boiling, sublimation or decomposition points for these compounds), 2) wavelength tables for spectrographic qualitative analysis, 3) tables of homologous line pairs for semiquantitative spectrographic analysis, 4) tables for quantitative spectrographic analysis (including numerical examples), 5) tables for visual spectroscopic analysis and 6) tables for error calculation of the results.

A very rich (but not exhaustive) reference list, divided to correspond to each section, completes the descriptive text of each chapter.

A detailed subject index ends this very interesting and practical book, which should be of a great value to all chemists working in this domain.

M. Banciu

field theory are critically surveyed in passing and points of future development emphasized. The book may be helpful to all researchers concerned with the rare earth's involvement in their effects being at the same time an agreeable lecture for any quantum physicist or chemist.

Alex. Vinogradov

T. TÖRÖK, J. MIKA and E. GEGUS, "Emission Spectrochemical Analysis". Akadémiai Kiadó, Budapest, 1978, 682 p.

The book presents all practical aspects of emission spectrochemical analysis. It could be considered as a continuation of the book J. Mika and T. Török "Analytical Emission Spectroscopy. Fundamentals" (joint edition of Akadémiai Kiadó, Budapest and Butterworth, London, 1974) in which the same authors have extensively developed the theoretical aspects of emission spectroscopy.

After a brief introduction, chapter 2 presents in great detail (38 pages) all the aspects of sample preparation including the sampling of metals and alloys, non-conducting solid samples, solutions and gases.

Chapter 3 is devoted to an essential part of every spectral equipment, the radiation source. The text (84 pages) is divided into four main sections treating the radiation sources used for investigation of: 1) metal samples, 2) solid non-conductors, 3) non-conducting liquids and solutions and (4) gases. Numerous figures (55) and details permit an easy understanding of the construction and operation of the various apparatus used in order to obtain the best results in each analysed case.

In the following chapter (40 pages) the conditions affecting the intensities are developed. The importance of different phenomena such as diffusion, self-absorption, distribution of radiation in time and space etc. is presented and underlined for each factor by means of different examples including numerous tables and figures.

The following three chapters (5, 6 and 7) are devoted to spectral analysis, classified as: 1) spectrographic analysis (172 pages), 2) spectrometric analysis (62 pages) and 3) visual spectroscopic analysis (36 pages). Each of these chapters contains a lot of useful data concerning the equipment, technique and methods of evaluation. Other very interesting problems developed are those concerning the installation, work organization and economy of a spectral laboratory (spectrographic, spectrometric and spectroscopic one).

Chapter 8 gives useful information on evaluation of the results of measurements (error distribution, mean values, statistical determination of notifying results, etc.

The book comprises also 132 pages of very useful data (not readily available elsewhere) presented as tables (Chapter 9). These tables include: 1) physico-chemical constants (boiling and melting points, enthalpies of evaporation and melting, molar standard entropies, ionization potentials, wavelength of the first and second resonance lines for all elements, as well as molar enthalpies of formation from elements for important compounds and melting, boiling, sublimation or decomposition points for these compounds); 2) wavelength tables for spectrographic qualitative analysis; 3) tables of homologous line pairs for semiquantitative spectrographic analysis; 4) tables for quantitative spectrographic analysis (including numerical examples); 5) tables for visual spectroscopic analysis and 6) tables for error calculation of the results.

A very rich (but not exhaustive) reference list, divided to correspond to each section, completes the descriptive text of each chapter.

A detailed subject index ends this very interesting and practical book, which should be of a great value to all chemists working in this domain.

M. Bercea

Revue Roumaine de Chimie, **23**, *11–12*, 1655–1668 (1978)

INDEX DES AUTEURS

A.

ABDEL HAMID H. A., voir EL-NEWAIHY M. F. . . . 73
ABDEL-HAY F. I., voir ANWAR M. . . . 1085
ABDEL NOUR A. R. O., voir HASSAN M. . . . 747
ABDU-SSALAM M. CACA, voir KHAN I. A. . . . 569
ABRAHAM M., M. POIRIER, Stability constant of FeCl$_4^-$ in molten NaFeCl$_4$ (in French) . . . 339
AČIMOVIĆ M., voir ALEKSIĆ B. R. . . . 1431
AGHERGHINEI I., Considerations upon rationalization of numerical integration of Mayo-Lewis equation . . . 445
AIKENS D., voir IDIŢOIU C. . . . 959
AIRINEI A., voir LUCA C. . . . 1 635
ALEKSIĆ B. R., A. TERLECKI-BARIČEVIĆ, M. AČIMOVIĆ, Electric conductivity of catalysts for the conversion of natural gas with water vapour . . . 1431
ANGHEL D.-F., G. POPESCU, Anionic surfactant analysis from micellar solutions . . . 251
ANGYALOSI I., voir CORDOŞ E. . . . 449
ANWAR M., F. I. ADBEL-HAY, M. FAHMY, Reactions on 2-phenyl-3-amino-4(2H) quinazolone . . . 1085
ANWER F. A., voir ETAIW S. H. . . . 79
ARMSTRONG D. R., R. FORTUNE, P. G. PERKINS, A molecular-orbital study of the ground and excited-state properties of metallocenes of the first-row transition-metal ions. II. . . . 1179
ARRANZ A., voir SENENT S. . . . 179
ARVAY ZS., voir DRĂGUŢAN V. . . . 1283
— , voir GLATZ A. M. . . . 595
— , voir RĂZUŞ A. C. . . . 753
ASHMAWY F. M., voir MASOUD M. S. . . . 1367
AVRAM M., voir GHENCIULESCU A. . . . 1441
AVRAMESCU F., D. A. ISĂCESCU, Heat of combustion of mono- and difurfurylidene acetone . . . 655
— , voir ISĂCESCU D. A. . . . 661
— , voir ISĂCESCU D. A. . . . 865
— , voir ISĂCESCU D. A. . . . 873

B.

BĂDILESCU S., V. TĂLPUŞ, R. RACOTĂ, Infrared spectral study of hydrogen bonding in ethyl alcohol absorbed in polyethylene sheets . . . 535
BAJPAI D. N., voir SINGH K. . . . 549
BALABAN A. T., Chemical graphs. XXXIII. Graphs for intramolecular rearrangements of tetragonal-pyramidal complexes . . . 733
— , I. I. STĂNOIU, F. CHIRALEU, Isotope effects in lanthanide-induced shifts of ^{1}H-NMR spectra of selectively side-chain deuteriated pyridines . . . 187
— , I. I. STĂNOIU, F. CHIRALEU, I. MOŢOC, Isotopic exchange of active methyl groups. XI. Kinetics of deuteriation of 2,6-diaryl-4-methylpyrylium salts . . . 143
— , M. D. GHEORGHIU, Solvent- and lanthanide-induced shifts in the ^{1}H-NMR spectra of 4-acetonylidene-2,6-dimethyl-[4H]pyran and its tautomeric protonated pyrylium cations . . . 1065

BALINT A. M., F. KEREK, Unidentate copper-amine complexes a statistical method to evaluate the dissociation constant of labile complexes 725
BALOG A., voir GÖNCZY F. 1093
BĂLUŞESCU L., voir BOLD A. 1 631
BANCIU A. C., Electronic and IR spectra of some new square-planar complexes with $Ni(d^8)$-$N(sp^2)$ bonds 1251
— , Electronic spectra and magnetic susceptibilities of some new tetrahedral chelate complexes with $Co(d^7)$-$N(sp^2)$ bonds 707
— , O. CONSTANTINESCU, P. SPACU, EPR study of chelate complexes with $Cu(II)$-$N(sp^2)$ bonds 215
BANDI A., Porous two-phase electrodes. I. Raney-Ni-Ti-electrodes for anodic oxidation of methanol (in German) 1373
— , voir RADOVICI O. 1 513
BANERJI K., SRIVASTAVA V. K. 1 049
BANYAI P., voir IONESCU N. I. 1 023
BARAN E. J., Vibrational spectrum of β-vanadyl sulfate (in German) 37
BĂRBÎNŢĂ E., voir PETRARIU I. 119
BARBU S., CONST. GH. MACAROVICI, Physico-chemical study of some thiocarbohydrazone of aromatic and heteroaromatic aldehydes (in German) 1 243
— , voir MACAROVICI CONST. GH. 1 035
BĂRCEANU G., voir CORDOŞ E. 287
BARRANS J., voir DESHERCES S. 203
BECHERESCU D., voir MARX F. 417
BELCEA I. M., voir MIHAIL R.. 681
BEŁTOWSKA-LEHMAN E., A. RIESENKAMPF, Conditions of electrodeposition as a factor influencing the properties of Ni-Fe thin films 883
BENDIC C., M. HILLEBRAND, V. E. SAHINI, Computer program for S. C. F.-C. I. calculations. I. Closed shell systems 3
BENŢIA TR., voir SCHELL H. D. 1 143
BHOBE R. A., voir PARDESHI L. 1 291
BIRADAR N. S., B. R. PATIL, Titanium (IV) complexes with 2,2′-dihydroxy-chalkones 1 425
— , V. B. MAHALE, B. R. HAVINALE, Four and six coordinate complex of $Zn(II)$ with aroyl hydrazones 55
— , V. E. MAHALE, B. R. HAVINALE, Divalent manganese complexes with ligands containing O—N—N—O sequence 1 261
BLAGA A. I., R. F. PAPE, T. CHIRILĂ, Acid-catalysed acetalisation. I. The influence of kind and concentration of acid catalysts on synthesis of bis-1,1(2′, 2′-ethylhexyloxy)-2-methyl-propane 581
BLANCO A., voir MASAGUER J. R. 1 409
BLEJOIU S. I., voir ROTARU P. 489
BODEA C., voir OŞIANU D. 573
BOGHINĂ C., voir CINCU C. 255
BOLD A., L. BĂLUŞESCU, The behaviour of α-bromostearic acid as extraction agent. I. Mechanism of copper(II) extraction 1 631
BOOK REVIEWS, 157, 158, 159, 160, 309, 310, 311, 467, 468, 637, 637, 638, 825, 825, 985, 986, 987, 987, 1 157, 1 157, 1 158, 1 349, 1 505, 1 506, 1 506, 1 507, 1 508, 1 509, 1 651, 1 652, 1 653 . . . .
BOZEŞANU M., voir MURGULESCU I. G. 991
BRATU C., voir ROMAN M.. . . . . 1 499
BREAZU D., voir GÖNCZY F. 1 093
BREZEANU M., I. JITARU, Nickel(II) coordination compounds with 3-amino-1-propanol 909
— , voir JITARU I. 559
— , M. DINCULESCU, Polynuclear complex compounds of iron, cobalt and nickel. II. Bismuth-containing complex compounds 1 389
— , M. DINCULESCU, Polynuclear complex compounds of iron, cobalt and nickel. III. Bismuth-containing complex compounds 1 533
— , M. DINCULESCU, Polynuclear complex compounds of iron, cobalt and nickel. III. Mercury-containing complex compounds 699
BRÎNZAN N. GR., voir SAVII C. 1 337

BRÎNZOI V., voir CONSTANTINESCU E. . . . 527
— , voir CONSTANTINESCU E. . . . 673
BUCHWALD M., voir MANTSCH O. (in German) . . . 921
BULCOVSCHI V., voir SIMIONESCU CR. I. . . . 89
BUTUCELEA A., R. GRIGOROVICI, Vibrational symmetry coordinates for some arsenic chalcogenides . . . 651
— , voir SAHINI V. E. . . . 643

C.

CACHAZA J. M., J. CASADO, A. VARELA, Study of Arbuzov reactions. II. Reactions between trialkylphosphites and ethyl bromides (in Spanish) . . . 233
CALBOREANU A., voir ROMAN M. . . . 1 499
CAMPANELLA L., T. FERRI, D. GOZZI, Pyridinemonocarboxylate ion selective electrodes . . . 281
CĂPĂŢ C., voir RADOVICI O. . . . 1 513
CARP E., voir LEONTE C. . . . 1 461
CARPOV A., voir LUCA C. . . . 1 653
CASADO J., voir CACHAZA J. M. . . . 233
CHATURVEDI G. K., voir KUMARI V. . . . 1 275
CHIFU E., M. TOMOAIA, E. NICOARĂ, A. OLTEANU, Isozeaxanthin films at the oil/water and air/water interfaces . . . 1 163
CHIRALEU F., voir BALABAN A. T. . . . 143
— , voir BALABAN A. T. . . . 187
— , voir GHENCIULESCU A. . . . 1 441
CHIRILĂ T., voir BLAGA A. I. . . . 581
CHIŢANU G., voir LUCA C. . . . 1 653
CINCU C., C. BOGHINĂ, Unperturbed dimensions of copolymers. Poly(N-vinylcaprolactam-diethylfurmarate) alternating copolymers . . . 255
CIOBANU A., N. LUCHIAN, V. HAMCIUC, Cyclic organosilicon compounds. Reaction of 1,4-dilithium-1,1,4,4-tetraphenylbutane with organodichlorosilanes . . . 943
CIOHODARU L., C. RENŢIA, I. ZAMFIRESCU, Electronic structure of some stilbene derivatives. VII. MO-LCI-PPP calculations for some polynitro-*trans*-stilbene derivatives . . . 853
CIOPEC M., voir MARCHIDAN D. I. . . . 19
CISMARU D., M. MOMÎRLAN, On the aspect of oxides films formed on titanium in air at high temperatures . . . 1 361
CLACK D. W., M. MONSHI, Molecular orbital calculations on transition metal complexes. XII. Unpaired electron distributions . . . 495
CLAUS J., E. MARÉCHAL, Physico-chemical study of poly (2,4-dimethyl-styrene) obtained by cationic polymerisation (in French) . . . 1 325
CONSTANTIN V., voir SAHINI V. E. . . . 163
— , voir SAHINI V. E. . . . 315
— , voir SAHINI V. E. . . . 479
CONSTANTINESCU E., V. BRÎNZOI, Anodic oxidation of cyclohexanol . . . 673
— , V. BRÎNZOI, Anodic oxidation of primary alcohols . . . 527
CONSTANTINESCU M., voir SURPĂŢEANU G. . . . 1 449
— , voir ZUCA ŞT. . . . 995
CONSTANTINESCU O., voir BANCIU A. C. . . . 215
CONSTANTINESCU T., ŞT. ENACHE, R. VASILIEV, Microreactions combined with thin-layer chromatography for the identification of phenothiazine drugs 967
CORDOŞ E., G. BĂRCEANU, Evaluation of a methane-oxygen-air flame for atomic emission . . . 287
— , I. ANGYLOSI, C. DIMITRESCU, An automatic system for cyclic chronopotentiometry . . . 449
CORMOŞ L., A. POP, L. ORBU, Contributions to the study of the catalytic activity of some $nSiO_2.mAl_2O_3.xH_2O$ systems in the decomposition reaction of cumene hydroperoxide. V. Influence of the reaction medium . . . 225
COŞOFREŢ V. V., Some analytical applications of a new Ag^+— selective membrane electrode . . . 1 489
COSTACHE M., voir VLĂDESCU L. . . . 1 553

CRĂCIUNEANU R., E. FLOREAN, Behaviour of 1-actyl-4-aryl-thiosemicarbazides towards heavy metal ions. IV. Behaviour of Ni(II) towards 1-benzoyl-4-arylthiosemicarbazides (in German) 397

CRISTESCU C., voir DRIMUŞ I. 407

CRISTU D., voir ROMAN M. 1 499

CUJBĂ M., voir PETRARIU I. 797

D.

DESHERCES S., J. BARRANS, J. L. ROUBATY, Synthesis of 4-hydroxy-Δ^2-oxadiazolines-1,2,4 (in French) 203

DAVIDENCO S., voir SĂNDULESCU I. 1 575

DIMITRESCU C., voir CORDOŞ E. 449

DINCULESCU M., voir BREZEANU M. 699

— , voir BREZEANU M. 1 389

— , voir BREZEANU M. 1 553

DINULESCU I. G., voir GHENCIULESCU A. 1 441

DOBOŞ-ADAM T., voir MICU-SEMENIUC R. 1 519

DORDEA E., voir ROMAN L. (in French) 929

DOSS S. H., Sultam synthesis (in German) 577

DRĂGAN GH., Amorphous-crystalline coupling in polyethylene. V. Lamellar recrystallization in shear history 261

— , Amorphous-crystalline coupling in polyethylene. VI. The study of the morphological changes in high molecular weight polyethylene by compounding with polypropylene 435

— , Amorphous-crystalline coupling in polyethylene. VII. Study of the crystallization kinetics in the approximation of the purely thermal disipative coupling 629

— , Amorphous-crystalline coupling in polyethylene. VIII. Relativistic effects in disclination state forming processes 1 313

DRĂGHICI C., voir GLATZ A. M. 595

— , voir URSEANU F. 1 471

DRAGOŞ M., voir VLAD M. 1 233

DRĂGUŢAN V., ZS. ARVAY, A. M. GLATZ, Aluminium chloride catalyzed reaction of unsaturated acids with benzene. XII. Methyl esters of cyclohexylidene-acetic and 1-cyclohexenylacetic acids 1 283

— , voir GLATZ A. M. 595

DRIMUŞ I., PAPAHAGI, On the influence of the chain length of n-alkanes on the composition of monocarboxylic acids formed by catalytic autooxidation of n-alkanes in liquid phase with molecular oxygen (in German) 209

— , L. PAPAHAGI, C. CRISTESCU, Degradation of peroxides obtanied by thermal oxidation of n-dodecane with molecular oxygen. I. Thermal degradation of samples obtained at various conversions. II. Separation of a peroxidic concentrate from n-dodecane oxidized at a low conversion ; thermocatalytic degradation of this concentrate (in German) 407

DRUŢĂ I., voir PETROVANU M. 781

DUCA AL., voir IONESCU GH. 1 611

DUMITRESCU S., V. PERCEC, CR. I. SIMIONESCU, On the polymerization of acetylenic derivatives. XXXI. Electron spin resonance of polyarylacetylene isomers 1 303

DUMITRIU S., voir SIMIONESCU CR. I. 89

DWIVEDI B. K., voir SINGH K. 549

E.

ECHIM-GROSU M., voir ROMAN L. (in French) 929

EL-ABBADY A. M., M. A. OMARA, M. T. MAHMOUD, Studies on the product obtained from Stobbe condensation between *o*-chlorobenzaldehyde and dimethyl homophthalate 1 465

EL-HASHASH M. A., M. EL-KADY, Some reactions of β-aroyl-acrylic acid epoxides 1 581

— , voir FAHMY A. F. M. 1 567

EL-KADY M., voir EL-HASHASH M. A. 1 581
EL-KASHEF H. S., voir HAMMAM A. S. 587
— , voir ISSA I. M. 617
EL-NEWAIHY M. F., E. I. ENAYAT, M. R. SALEM, H. A. ABDEL HAMID, Condensation of 3,4-disubstituted benzophenones with dimethyl homophthalate 73
EL-SAMAHY A. A., voir ISSA I. M. 617
EL-WANNISE S. A., voir FAHMY A. F. M. 1 567
ENACHE ŞT., voir CONSTANTINESCU T. 967
ENAYAT E. I., voir EL-NEWAIHY M. F. 73
ENESCU L., voir GHENCIULESCU A. 1 441
ETAIW S. H., F. A. ANWER, F. M. ISSA, Electronic spectra and structure of 4-arylhydrazono-3-methyl-5-pyrazolones 79

F.

FADDA A. A., voir KHALIL A. M. 935
FAHMY A. F. M., M. A. EL-HASHASH, M. M. HABASHY, S. A. EL-WANNISE, Some reactions of 2-isopropyl-[4H]-3,1-benzoxazin-4-one 1 567
FAHMY M., voir ANWAR M. 1 085
FAROQI Z. H., voir KHAN I. A. 569
FATEEN A. E. K., A. M. KADDAH, Spiro-3-arylidene-1,2,3,4-tetrahydronaphthalen-4-ones. II. Synthesis of spiropyrazolines 791
— , and A. M. KADDAH, Y. M. NAGUIB, Spiro-3-arylidene-1,2,3,4-tetrahydronaphthalen-4-ones. I. Reactions with amines and Friedel-Crafts reactions 759
FĂTU D., Decomposition of solids by volumetric measurements: kinetic study (in French) 1 029
FELDMAN D., voir SIMIONESCU CR. I. 237
FERRARI L., voir SENENT S. 179
FERRI T., voir CAMPANELLA L. 281
FLOREAN E., voir CRĂCIUNEANU R. 397
— , voir ROMAN L. (in French) 929
FLORU L., voir TĂRĂBĂŞEANU-MIHĂILĂ C. 977
— , voir TĂRĂBĂŞEANU-MIHĂILĂ C. 1 079
FORTUNE R., voir ARMSTRONG D. R. 1 179
FRUNZĂ L., voir SĂNDULESCU I. 1 575

G.

GARCÍA-VÁZQUEZ J. A., voir MASAGUER J. R. 1 409
GAUR H. C., voir JAIN R. K. 555
GEORGESCU C., voir GOCAN S. 265
GHENCIULESCU A., L. ENESCU, H. L. PRASAD, F. CHIRALEU, I. G. DINULESCU, M. AVRAM, Chemistry of transition-metal organic compounds. I. On the reaction of ethyl diazoacetate with strained alkenes, catalyzed by π-allylpalladium chloride complexes 1 441
GHEORGHIU M. D., voir BALABAN A. T. 1 065
GHERASIM G. M., L. STOICESCU-CRIVETZ, Thermal and photoinduced polymerization of N,N′-bismaleimide 111
GHIZDAVU L., voir MARCU GH. 1 559
GIRDHAR K. K., Spectrophotochemical studies of the kinetics of the conversion of ferrocyanide to ferricyanide in the presence of hydrogen peroxide 819
GLATZ A. M., V. DRĂGUŢAN, Zs. ARVAY, C. DRĂGHICI, A. C. RĂZUŞ, Different behaviour of isomeric arylbenzylketones towards phosphorus pentachloride 595
— , voir DRĂGUŢAN V. 1 283
— , voir RĂZUŞ A. C. 753
GOCAN S., C. KONNERT, H. VOIK, Separation of polyphenols by thin layer chromatography with orthogonal temperature gradient (in German) 133
— , T. HODIŞAN, H. NAŞCU, C. GEORGESCU, Separation and determination of phenol and salicylic acid in industrial wastes 265

GÖNCZY F., A. BALOG, E. VARGHA, D. BREAZU, I. HALLER, Peptides. XVI. The use of β-dicarbonyl-N-protected methionine and tryptophan in peptide synthesis 1 093

GOZZI D., voir CAMPANELLA L. 281

GREBLĂ M., voir MIOŞCU M. 1 345

GRIGOROVICI R., voir BUTUCELEA A. 651

— , voir SAHINI V. E. 643

GUTMAN I., M. RANDIĆ, N. TRINAJSTIĆ, Kekulé structures and topology. III. On inseparability of Kekulé structures 383

H.

HABASHY M. M., voir FAHMY A. F. M. 1 567

HALLER I., voir GÖNCZY F. 1 093

HAMCIUC V., voir CIOBANU A. 943

HAMMAM A. S., H. S. EL-KASHEF, Heterocyclic quinones. X. Synthesis and antibacterial screening of new thiazolocarbazoloquinones 587

HASSAN M., A. R. O. ABDEL NOUR, A. M. SATTI, The kinetics and reactions of some aryl-substituted epoxides with t-butoxide in t-butanol 747

HASSAN O., voir MAKSOUD A. A. 1 541

HAVINALE B. R., voir BIRADAR N. S. 55

— , voir BIRADAR N. S. 1 261

HILLEBRAND M., voir BENDIC C. 3

HODIŞAN T., H. NAŞCU, V. IANCU, Separation of acetic acid, salicylic acid and phenol by thin-layer chromatography on silica gel RG 1 483

— , voir GOCAN S. 265

— , voir LITEANU C. 125

HOPÎRTEAN E., E. ŞTEFĂNIGĂ, Liquid membrane-electrodes. XII. Liquid membrane-electrodes for perchlorate, thiocyanate, tetrafluoroborate and nitrate based on triphenylmethane dyes 137

— , E. VERESS, Ion selective membrane-electrodes for organic analysis. I. Liquid membrane-electrode for some organic anions based on cetylpyridinium salt 273

HOPÎRTEAN I., voir MAGER S. 1 061

HOROWITZ O., On triazines. LVI. HMO calculations for derivatives of 1,3,5-triazine (in German) 603

HOSNI G., voir MAKSOUD A. A. 1 541

I.

IANCU V., voir HODIŞAN T. 1 483

IDIŢOIU C., D. AIKENS, Cyclic voltammetry determination of α, α′-dimethylphenyl hydroperoxide 959

IONESCU GH., F. MATEI, AL. DUCA, Kinetic aspects of the oxidation reaction of gallic acid using an oxygen-selective electrode 1 611

IONESCU L. G., Entropy of some simple gas-water clathrates 45

IONESCU N. I., P. BANYAI, Influence of oxygen on the dark conductivity of metal-free phthalocyanine 1 023

IORDACHE D., On the vibrational anharmonicities of the furan molecule 301

ISĂCESCU D. A., F. AVRAMESCU, Reaction mechanism for the condensation of furfural with acetone catalysed by sodium hydroxide 661

— , F. AVRAMESCU, Reaction mechanism for the condensation of furfural with acetone in the catalysis of sodium hydroxide. II. The activated complex and its catalytic action 865

— , F. AVRAMESCU, Reaction mechanism for the condensation of furfural with acetone in the catalysis of sodium hydroxide. III. Solvent influence on the nature of the activated complex and on its catalytic action 873

— , voir AVRAMESCU F. 655

ISSA F. M., voir ETAIW S. H. 79

ISSA I. M., A. A. EL SAMAHY, R. M. ISSA, H. S. EL KASHEF, Preparation and spectrophotometric studies of some quinoneanils 617

ISSA R. M., voir ISSA I. M. 617

J.

JAIN R. K., H. C. GAUR, Generalized potential-time equation for A. C. chronopotentiometry : application to quasi-reversible processes . . . 555
JAIN S. P., S. N. SRIVASTAVA, The stability of the solid stabilised emulsion with special reference to electrolytes . . . 1 377
JITARU I., M. BREZEANU, Cobalt complex compounds with 3-amino-1-propanol 559
— , voir BREZEANU M. . . . 909
JOSHI B. C., voir SRIMALI S. S. . . . 613

K.

KADDAH A. M., voir A. E. K. FATEEN . . . 759
— , voir A. E.-K. FATEEN . . . 791
KAKKAR K. K., D. C. RUPAINWAR, Extraction of thallium (III) from its chloride and bromide solutions with isoamyl alcohol (IAA) and amyl acetate (AA) . . 1 139
KALMUŢCHI G., voir MOŞESCU N. . . . 1 475
KATYAL M., voir SINGH A. K. . . . 1 153
KAUSAR T., voir SUBHANI M. S. . . . 1 619
— , voir SUBHANI M. S. . . . 1 341
— , voir SUBHANI M. S. . . . 1 627
KAUSAR Z., voir SUBHANI M. S. . . . 1 129
KEREK F., voir BALINT A. M. . . . 725
KHALID M., voir SUBHANI M. S. . . . 1 117
KHALIL A. M., A. A. FADDA, M. M. YOUSIF, The action of aryl-amines on 3-aryl-5-arylmethylenerhodamines . . . 935
KHAN I. A., ABDU-SSALAM M. CACA, Z. H. FAROOQI, Studies on coordination compounds, 2-thiosalicylic acid complexes of copper (II) . . . 569
KHAS H., voir RAO G. N. . . . 1 149
KLAFKOWSKI W., voir SWINARSKI A. . . . 171
KNOP J. V., N. TRINAJSTIĆ, M. MILUN, S. PEJAKOVIĆ, Conformational analysis and electronic structure of thienylpyridines . . . 103
KONNERT C., voir GOCAN S. . . . 133
KOWALSKA T., Investigation of the autoxidation process of 1-dodecene . . . 1 589
KRIZA A., M. NASTA, On titanium (IV) compounds with Schiff bi- and three-dentate bases (in French) . . . 1 267
KUMAR S., voir SRIMALI S. S. . . . 613
KUMAR V., voir RAO G. N. . . . 1 149
KUMARI V., R. C. SHARMA, G. K. CHATURVEDI, Potentiometric studies on ternary complexes of Zn(II) . . . 1 275

L.

LAMBRINO V. D., R. S. NISTOR, Determination of the repartition of elements in a bentonite by means of X-ray analyzer with electronic microprobe (in French) 625
LĂZĂRESCU M. F., voir LĂZĂRESCU V. . . . 861
LĂZĂRESCU V., M. F. LĂZĂRESCU, Highly pure gallium obtained by a simple technique . . . 861
LECA M., voir VÎLCU R. . . . 1 171
LEONTE C., E. CARP, The reaction of pyridinium-N-imine with picryl chloride, a route to 6-aza-benzo [a] indolizine system . . . 1 461
LITEANU C., T. HODIŞAN, Optimization of the separation process in temperature gradient chromatography. II. Determination of the minimum chromatographing time necessary for the separation of some component mixtures by applying a constant temperature gradient . . . 125
LUCA C., G. CHIŢANU, I. PETRARIU, A. AIRINEI, A. CARPOV, Retention of organic anions on strongly basic macroporous ion-exchangers . . . 1 635
— , voir PETRARIU I. . . . 797
— , voir PETRARIU I. . . . 951
— , voir PETRARIU I. . . . 1 109
LUCHIAN N., voir CIOBANU A. . . . 943

M.

MACAROVICI C. GH., S. BARBU, Metallocomplexes of salicylaldehyde-thiocarbohydrazone (in German) 1 035
— , voir BARBU S. 1 243
— , voir MICU-SEMENIUC R. 1 519
MAGER S., I. HOPÎRTEAN, F. PAIU, R. ŢĂRANU, Determination of benzaldehyde in the catalytical oxidation products of toluene, by gas chromatography 1 061
— , voir VĂGĂONESCU M. 63
MAHALE V. E., voir BIRADAR N. S. 55
— , voir BIRADAR N. S. 1 261
MAHMOUD M. T., voir EL-ABBADY A. M. 1 465
MAI VAN TRI, voir PETROVANU M. 781
MAKSOUD A. A., G. HOSNI, O. HASSAN, S. SHAFIK, Reactions of 3′,4′-dimethylchalcone and its derivatives 1 541
MALIK S. A., voir QURESHI A. M.. 269
MÁNOK F., CS. VARHELYI, On the α-dioximine complexes of transition metals. LVI. Some aspects of the polarographic behaviour of the azido-bis-dimethylglyoximine complexes of cobalt (III) 917
MANTSCH O., M. BUCHWALD, 16-Methyl Reichstein S 21-acetate from 16-dehydropregnenolone acetate (in German) 921
MARANDIUC D., voir SCHMIDT W. 295
MARCHIDAN D. I., M. CIOPEC, Thermodynamic properties of maleic, trimellitic and pyromellitic anhydrides. 19
MARCU GH., L. GHIZDAVU, E. PERŢE, The study of cesium and thallium decatungstatediniobiosilicates in the solid state 1 559
— , M. RUSU, E. PERŢE, Thermal behaviour of potassium bis-2-phospho-17-tungstouranate 1 403
MĂRCULESCU B., voir TĂRĂBĂŞANU-MIHĂILĂ C.. 977
— , voir TĂRĂBĂŞANU-MIHĂILĂ C. 1 079
MARECHAL E., voir CLAUS J. 1 325
MARTIN GIL F. J., voir MARTIN GIL J. 1 397
— , voir MARTIN GIL J. 1 527
MARTIN GIL J., F. J. MARTIN GIL, New complex uranyl sulphates. General study of IR spectra of these and other complexes (in Spanish) 1 527
— , F. J. MARTIN GIL, Synthesis and crystallographic data of comlex uranyl sulphates: $UO_2(SO_4)_2K_2 \cdot 2H_2O$ and $UO_2(SO_4)_3(NH_4)_4 \cdot 4H_2O$ (in Spanish) . 1 397
MARX F., I. MENESSY, D. BECHERESCU, On the formation of high-melting carbides in plasma 417
MASAGUER J. R., A. SOUSA-ALONSO, J. A. GARCÍA-VÁZQUEZ, A. BLANCO, Molecular charge-transfer complexes of iodine bromide with methylpyridines (in Spanish) 1 409
MASOUD M. S., T. M. SALEM, F. M. ASHMAWY, Kinetics of oxidation of diethanolamine with hexacynoferrate. III. 1 367
MATA F., voir SENENT S. (in Spanish) 841
MATEESCU M. A., voir SCHELL H. D. 1 143
MATEI F., voir IONESCU GH. 1 611
MATHUR P. K., Determination of isothiocyanatochromates using bromine monochloride 1 607
MEGHEA A., The kinetics of the oxidation of aniline with sodium chlorite 1 005
MENESSY I., voir MARX F. 417
MICU-SEMENIUC R., T. DOBOŞ-ADAM, C. GH. MACAROVICI, Investigation of sulphonamides, benzamides and benzhydrazides. XXIV. Complex compounds of Cu(II) and Cd(II) with isomeric *ortho-*, *meta* and *para*-aminobenzamides . . 1 519
MIHAIL R., C. V. RADU, I. M. BELCEA, Methods for complex reaction systems equilibrium computation 681
MILUN M., voir KNOP J. V. 103
MINCU G., voir MURGULESCU I. G. 471
MÎNZATU I., voir ROMAN M.. . . . . 1 499
MIOŞCU M., M. GREBLĂ, Liquid-liquid interfaces as potentiometric ion-sensors. III. The n-octanol-aqueous solution interface in the acid-base potentiometric titration 1 345

MIRZA M. Y., Practical indications for the preparation of ^{99m}-Tc generator for medical use 429
MISRA B. B., voir SRIVASTAVA V. K. 377
MOLDOVEANU I., voir TOPOR L. 1 353
MOLDOVEANU S., A new type of parametrization among the approximate SCF-LCAO-MO methods 453
MOMIRLAN M., voir CISMARU D. 1 361
MONSHI M., voir CLACK D. W. 495
MOROȘANU C. E., E. SEGAL, *In situ* evaluation of the chemical vapor deposition rates of some thin films on silicon by infrared interference 515
MOȘESCU N., G. KALMUȚCHI, R. POPESCU, D. STEJARU, Separation and characterization of aromatic hydrocarbons from mineral oils by means of elution chromatography and of electronic absorption spectra (in French) 1 475
MOȚOC I., voir BALABAN A. T. 143
MRACEC M., Z. SIMON, Hybridization of dicoordinated trivalent phosphorus in conjugated six-membered rings 769
MUNTEANU L., voir VĂGĂONESCU M. 63
MUREȘAN N., voir NEGOIU D. 371
MURGULESCU I. G., G. MINCU, Kinetics and mechanism of oxidoreduction. Reaction of the bisoxalatodiaquo Co(III) complex with iodide ion in acid medium 471
— , M. BOZEȘANU, Some peculiarities of the slow oxiation reaction of methane 991

N.

NAGUIB Y. M., voir A. E.-K. FATEEN 759
NAȘCU H., voir GOCAN S. 265
— , voir HODIȘAN T. 1 483
NASTA M., voir KRIZA A. 1 267
NEAGU L. M., voir PETRARIU I. 951
— , voir PETRARIU I. 1 109
NEGOIU D., M. NEGOIU, Complex compounds with tri-*p*-xylylphosphine 1 043
— , V. MUREȘAN, N. MUREȘAN, Contributions to the chemistry of thiocomplexes. VI. Complex compounds of Pt(II) with thioamides of the dibenzofuran series 371
NEGOIU M., voir NEGOIU D. 1 043
NEMEȘ A., voir SCHMIDT W. 295
NIAC G., voir ROTARU P. 489
NICOARĂ E., voir CHIFU E. 1 163
— , voir OȘIANU D. 573
NICOLESCU A., M. UDREA, G. POPA, Comparative study of the adsorption of some cyclic hydrocarbons on active alumina-support for catalysts. I. Determination of adsorption isotherms and of various characteristic thermodynamic values 361
NISTOR R. S., voir LAMBRINO V. D. 625
NUȚĂ V., voir SIMIONESCU CR. I. 237

O.

ODOCHIAN L., I. A. SCHNEIDER, Some remarks on the heterogeneous character of the low temperature cracking of methane in silica vessels 835
OLTEANU A., voir CHIFU E. 1 163
OLTEANU M., voir VÎLCU R. 1 171
OMARA M. A., voir EL-ABBADY A. M. 1 465
ONCESCU T., voir VASILESCU A. 1 055
ORBU L., voir CORMOȘ L. 225
OȘIANU D., E. NICOARĂ, C. BODEA, Inchain-epoxides of carotenoids. VI. Isomerizations and rearrangements of canthaxanthin-inchain-epoxides 573
OSTROGOVICH G., voir SCHMIDT W. 295

P.

PAIU F., voir MAGER S. 1 061
PANDEYA K. B., voir SINDHU R. S. 1 279
PAPAHAGI L., voir DRIMUȘ I. 209
— , voir DRIMUȘ I. 407

PAPE R. F., voir BLAGA A. I. 581

PARDESHI L., A. RASHEED, R. A. BHOBE, Studies in spectral and magnetic properties and non-isothermal decomposition of pyridine adducts of some salts of fatty acids 1 291

PATIL B. R., voir BIRADAR N. S. 1 425

PEJAKOVIĆ S., voir KNOP J. V. 103

PEÑA M. A. DE LA, voir SENENT S. (in Spanish) 841

PENCEA C., voir ROMAN M. 1 499

PERCEC V., voir DUMITRESCU S. 1 303

PERKINS P. G., voir ARMSTRONG D. R. 1 179

PERŢE E., voir MARCU GH. 1 403

— , voir MARCU GH. 1 559

PESHEV O., A remark on oxygen adsorption at semiconducting CdS 1 003

PETEU GH., voir ROMAN M. 1 499

PETRARIU I., E. BĂRBÎNŢĂ, Interaction between chloromethylated styrene-divinylbenzene and dimethylformamide 119

— , L. M. NEAGU, C. LUCA, IG. POINESCU, P. PETRARIU, Degradation of anion exchangers in agressive medium. V. Effect of hydroxyl ions in the presence of ferric chloride on chemical stability of type I macroporous anion exchangers 951

— , L. M. NEAGU, IG. POINESCU, C. LUCA, P. PETRARIU, Degradation of anion exchangers in aggressive medium. VI. Effect of hydroxyl ions in the presence of $CuCl_2$ on the chemical stability of macroporous strongly basic quaternary ammonium anion exchangers 1 109

— , M. CUJBĂ, IG. POINESCU, C. LUCA, Degradation of anion exchangers in aggressive medium. IV. Chemical stability of type I macroporous anion exchangers with binary and ternary structure in basic medium 797

— , voir LUCA C. 1 653

PETRARIU P. voir PETRARIU I.. 951

— , voir PETRARIU I. 1 109

PETROVANU M., I. DRUŢĂ, MAI VAN TRI, Pyridazinium-ylids. IX. Addition of aryl-pyridazinium-ylids on activated olefins 781

PLOŞTINARU S., P. SPACU, Fluorescence spectra of some Eu(III) and Tb(III) mixed ligand compounds 1 417

POINESCU IG., voir PETRARIU I. 797

— , voir PETRARIU I. 951

— , voir PETRARIU I. 1 109

POIRIER M., voir ABRAHAM M. 339

POP A., voir CORMOŞ L. 225

POPA G., voir NICOLESCU A. 361

POPA V. I., voir SIMIONESCU CR. I. 89

POPESCU G., voir ANGHEL D. F. 251

POPESCU R., voir MOŞESCU N. 1 475

PRAKASH O., voir SINGH R. 667

PRAKASH S., voir SINGH R. 667

PRASAD H. L., voir GHENCIULESCU A. 1 441

PREMOVIĆ P. I., *g*-Values of trigonally distorted octahedral d^1 systems : the $Ti(H_2O)_6^{3+}$ complex ion in frozen aqueous solutions 1 213

Q.

QURESHI A. M., S. A. MALIK, A modified non cyanide scheme for the qualitative chemical analysis of the group II A sulphides 269

R.

RACOTĂ R., voir BĂDILESCU S. 535

RADOVICI O., A. BANDI, C. CĂPĂŢ, Two phase porous electrodes. II. Influence of area on the activity of Raney-nickle-titanium-electrodes in the anodic oxidation of methanol (in German) 1 513

RADU C. V., voir MIHAIL R. 681

RĂDULESCU M., Study of the influence of fluoride contamination on the corrosion of zircaloy-2 in water and steam at high temperature (in French) 351

RĂDULESCU N., C. SÂRBU, Solvent and medium basicity effects on the reaction of 5-chloro-2-pentanone with sodium methoxide 197

RANDIĆ M., voir GUTMAN I.. 383

RAO G. N., V. KUMAR, H. KHAS, Polarography of methioninate complexes of cadmium (II), lead (II) and zinc (II) 1 149

RASHEED A., voir PARDESHI L. 1 291

RĂZUŞ A. C., ZS. ARVAY, A. M. GLATZ, Aluminium chloride catalyzed reactions of unsaturated acids with benzene. XI. Isomerizations during the reaction of benzene with 4-methyl-2-pentenoic acid 753

— , voir GLATZ A. M. 595

RENŢEA C., voir CIOHODARU L. 853

RIESENKAMPF A., voir BEŁTOWSKA-LEHMAN E. 883

ROMAN L., E. FLOREAN, M. ECHIM-GROSU, E. DORDEA, Study of the reaction between Pb(II) and 5-mercapto-2-amino-1,3,4-thiadiazole. Analytical applications (in French) 929

ROMAN M., C. PENCEA, D. CRISTU, I. MÎNZATU, A. CALBOREANU, O. SĂLĂGEAN, C. BRATU, GH. PETEU, Production of iodine-123 for medical purposes 1 499

ROTARU P., G. NIAC, S. I. BLEJOIU, Method for calculating heats of decomposition from thermogravimetric data (in French) 489

ROUBATY J. L., voir DESCHERCES 203

RUPAINWAR D. C., voir KAKKAR K. K. 1 139

RUSU M., voir MARCU GH. 1 403

RUSSU R. E., voir SĂNDULESCU I. 1 575

S.

SAHINI V. E., L. TELEA, Molecular interaction in anisidine. III. IR spectra and heats of dilution 483

— , R. GRIGOROVICI, A. BUTUCELEA, A modified Urey-Bradley force field for hexahalodisilanes 643

— , V. CONSTANTIN, I. ŞERBAN, Determination of ionization potentials using a Mi-1305 mass spectrometer 479

— , V. CONSTANTIN, I. ŞERBAN, C. VLĂDESCU, Electron impact-induced fragmentation of dibenzo /b,e/oxepin-11-one and dibenzo /b, e/thiepin-11-one 163

— , V. CONSTANTIN, I. ŞERBAN, C. VLĂDESCU, Electron-impact-induced fragmentation of some dibenzo [b, e]thiepines 315

— , voir BENDIC C. 3

SĂLĂGEAN O., voir ROMAN M. 1 499

SALEM M. R., voir EL-NEWAIHY M. F. 73

SALEM T. M., voir MASOUD M. S. 1 367

SĂNDULESCU I., O. ŞERBAN ,S. DAVIDENCO, R. E. RUSSU, L. FRUNZĂ, Formation and nature of active centres in solid oxid catalysts. III. Transalkylation of toluene on synthetic zeolite (in French) 1 575

SÂRBU C., voir RĂDULESCU N. 197

SATTI A. M., voir HASSAN M. 747

SAVII C., T. P. TĂVALĂ, N. GR. BRÎNZAN, G. G. SAVII, Computation program concerning the resulting colour of pigment mixtures 1 337

SAVII G. G., voir SAVII C. 1 337

SCHELL H. D., M. ŞERBAN, M. A. MATEESCU, TR. BENŢIA, Acid and alkali amylose ionic exchanger (in German) 1 143

SCHMIDT W., D. MARANDIUC, A. NEMEŞ, G. OSTROGOVICH, Enhancement of exactitude and reduction of time in planimetry of this layer chromatograms (in German). 295

SCHNEIDER I. A., voir ODOCHIAN L. 835

— , voir SCHUSTER R. H. 1 203

SCHULZ P., R. VÎLCEANU, Kinetics and mechanism of the alkaline hydrolysis of hexamethoxy-cyclotriphosphazene and octamethoxy-cyclotetraphosphazene (in German) 1 455

SCHUSTER R. H., I. A. SCHNEIDER, The environment influence on solvolysis of alkyl halides. III. Observations concerning the solvent dependence of correlation factor log *k versus* log [H_2O] (in German) 1 203

SECARĂ A., A. TURCU, E. SEGAL, Kinetic investigation of some molecular complexes between 1,3,7,9-tetranitrophenothiazine-5-oxide and amines 147

SEGAL E., voir MOROȘANU C. E. 515

— , voir SECARĂ A. 147

— , voir VLAD M. 999

SENENT S., F. MATA, M. A. DE LA PEÑA, Kinetic study of the oxidation of tertiary amines by permanganate (in Spanish) 841

— , L. FERRARI, ARRANZ A., Kinetic study of the reduction of Cr(VI) by hydrazine (in Spanish) 179

ȘERBAN I., voir SAHINI V. E. 163

— , voir SAHINI V. E. 315

— , voir SAHINI V. E. 479

ȘERBAN M., Lindemann law of melting 1 013

— , voir SCHELL H. D. 1 143

ȘERBAN O., voir SĂNDULESCU I. 1 575

SHAFIK S., voir MAKSOUD A. A. 1 541

SHARMA D., voir SRIMALI S. S. 613

SHARMA R. C., voir KUMARI V. 1 275

SIMIONESCU B., voir SIMIONESCU CR. I. 89

SIMIONESCU CR. I. 1 303

— , D. FELDMAN, V. NUȚĂ, Coopolymerization of acrylonitrile with methacrylic esters in the presence of organo-metallic catallysts 237

— , S. DUMITRIU, V. I. POPA, V. BULACOVSCHI, B. SIMIONESCU, Chemical model for the synthesis of living matter (in French) 89

SIMON Z., voir MRACEC M. 769

SINDHU R. S., K. B. PANDEYA, R. P. SINGH, Polarographic behaviour of complexes of cadmium (II) and lead (II) with 3-hydroxypyridine-2-thiol 1 279

SINGH A. K., M. KATYAL, R. P. SINGH, Spectrophotometric determination of iridium (III) with substituted pyrimidinethiols 1 153

SINGH C., voir SRIVASTAVA V. K. 377

SINGH K., The limiting apparent molal volumes of ions in N-methylacetamide . . 31

— , D. N. BAJPAI, B. K. DWIVEDI, Apparent molal volumes of some common salts in methanol-water mixtures 549

SINGH R., S. PRAKASH, O. PRAKASH, Thermodynamic properties of binary liquid mixtures 667

SINGH R. P., voir SINDHU R. S. 1 279

— , voir SINGH A. K. 1 153

SOLIMAN E. A., Some reactions with β-*p*-chlorobenzoylacrylic acids and β-*p*-toluyl-N-(*o*-carboxyphenyl)-acrylamide 1 597

SOUSA-ALONSO A., voir MASAGUER J. R. 1 409

SPACU P., voir BANCIU A. C. 215

— , voir PLOȘTINARU S. 1 417

SRIMALI S. S., N. D. SHARMA, S. KUMAR, B. C. JOSHI, Proton-catalysed rearrangement of sulphonamide to sulphone. I. Conversion of substituted arylquinolylamine sulphonamide to the isomeric substituted diarylsuphone 613

SRIVASTAVA G. P., voir SRIVASTAVA V. K. 1 049

SRIVASTAVA S. N., voir JAIN S. P. 1 377

SRIVASTAVA V. K., C. SINGH, B. B. MISRA, Protection of DNA by metal coordinates — A simple stoichiometric study 377

— , K. BANERJI, G. P. SRIVASTAVA, Dielectric behaviour of DNA-metal complexes 1 049

STĂNOIU I. I., voir BALABAN A. T. 143

— , voir BALABAN A. T. 187

ȘTEFĂNIGĂ E., voir HOPÎRTEAN E. 137

STEJARU D., voir MOȘESCU N. 1 475

STERNBERG S., M. TERZI, Surface tension of simple fused halides 325

—, T. VIȘAN, Cyclic voltammetry of strontium deposition and dissolution in molten potassium nitrate 505

STOICESCU-CRIVETZ L., voir GHERASIM G. M. 111

SUBHANI M. S., Study of the influence of the dielectric constant on the reaction between simple inorganic anions in solution 719

— , M. KHALID, Pulse radiolysis and flash photolysis studies of SeO$_4^{2-}$ anion in aqueous solution 1 117

— , T. KAUSAR, Flash photolysis studies of aqueous solution of thiosulphate ion 1 619

— , T. KAUSAR, Flash photolysis study of SeO$_3^{2-}$ anion in aqueous solution 1 627

— , T. KAUSAR, Flash photolysis study of TeO$_3^{2-}$ anion in aqueous solution . . 1 341

— , Z. KAUSER, Flash photolysis decomposition of sulphate and sulphite anions in aqueous solution 1 129

SURPĂŢEANU G., M. CONSTANTINESCU, I. ZUGRĂVESCU, Experimental and theoretical study on the reaction of the loss and amido group from the pyridinium-cyano-amydo-methylide 1 449

SWINARSKI A., W. KLAFKOWSKI, Influence of the origin of iron oxide on the catalytic activity of the catalyst (in French) 171

T.

TĂLPUŞ V., voir BĂDILESCU S. 535

TĂRĂBĂŞANU-MIHĂILĂ C., C. ZAHARIA, L. FLORU, F. URSEANU, B. MĂRCULESCU, Heterocyclic compact condensed systems. IV. Linear bis pyrazolo [2,3-d] [8,9-d] *trans*-quinacridone 1 079

— , and F. URSEANU, L. FLORU, B. MĂRCULESCU, Heterocyclic compact condensed systems. III. Isomer 9-amino-thiazolo[4,5-f] indazole 977

ŢĂRANU R., voir MAGER S. 1 061

TĂVALĂ T. P., voir SAVII C. 1 337

TELEA L., voir SAHINI V. E. 483

TERLECKI-BARIČEVIĆ A., voir B. R. ALEKSIĆ 1 431

TERZI M., voir STERNBERG S. 325

THÉOBALD F., Oxides and oxide hydrates of vanadium IV, V and intermediate oxidation state (in French) 887

TÖKES B., Polarographic investigations of the chemical constitution and reaction mechanisms of organic peroxides. I. Conditions of the polarographic analysis of organic peroxides (in Russian) 805

TOMOAIA M., voir CHIFU E. 1 163

TOPOR L. I. MOLDOVEANU, Thermodynamic properties of $RbCl-CaCl_2$ and $CsCl-CaCl_2$ molten systems 1 353

TRINAJSTIĆ N., voir GUTMAN I. 383

— , voir KNOP J. V. 103

TURCU A., voir SECARĂ A. 147

U.

UDREA M., voir NICOLESCU A. 361

URSEANU F., C. DRĂGHICI, New cationic dye with dibenz [f, ij] isoquinoline [2,3-b] quinazoline-5,10-dione structure 1 471

— , voir TĂRĂBĂŞANU-MIHĂILĂ C. 977

— , voir TĂRĂBĂŞANU-MIHĂILĂ C. 1 079

V.

VĂGĂONESCU M., S. MAGER, L. MUNTEANU, Molecular complexes of nitrophenols with hexamethylenetetramine and their isomers 63

VARELA A., voir CACHAZA J. M. 233

VARGHA E., voir GÖNCZY F. 1 093

VÁRHELYI CS., voir MÁNOK F. 917

VASILESCU A., T. ONCESCU, Dynamics of the ligand exchange in uranyl bis-(chelated) complexes. II. Configurational rearrangement of bis-(benzoylacetonate) uranyl chelate 1 055

VASILIEV R. 967
VERESS E., voir HOPÎRTEAN E. 273
VÎLCEANU R., voir SCHULTZ P. 1 455
VÎLCU R., M. LECA, M. OLTEANU, Contraction of polyacrylamides in electrolyte solutions 1 171
VIŞAN T., voir STERNBERG S. 505
VLAD M., Fluctuation phenomena in diffusion 541
— , Perturbation approaches for kinetics of isotope exchange reactions 523
— , E. SEGAL, Langmuir's rate equation for catalytic heterogeneous reactions and the principle of detailed balance 999
— , M. DRAGOŞ, Concentration fluctuations in chemical systems with nondegenerate reactions. A thermodynamic approach 1 233
VLĂDESCU C., voir SAHINI V. E. 163
— , voir SAHINI V. E. 315
VLĂDESCU L., and M. COSTACHE, Separation of elements Cu(II)-Zn(II)-Pb(II)-Fe(II), Fe(III) by means of ion exchangers (in French) 1 553
VOIK H., voir GOCAN S. 133

Y.

YOUSIF M. M., voir KHALIL A. M. 935

Z.

ZAHARIA L., voir TĂRĂBĂŞANU-MIHĂILĂ C. 1 079
ZAMFIRESCU I., voir CIOHODARU L. 853
ZUCA ŞT., Electrical conductivity and the structure of binary molten alkali halide mixtures 829
— , M. CONSTANTINESCU, Cationic tracer-diffusion, coefficients in molten (Tl-Alk)NO_3 systems 995
ZUGRĂVESCU I., voir SURPĂŢEANU G. 1 449

Revue Roumaine de Chimie, **23**, *11–12*, 1669–1677 (1978)

INDEX DES SUJETS

1978

A.

Acetic acid, salicylic acid, acetyl-salicylic acid and phenol by thin-layer chromatography on silica gel RG, Separation of—, T. HODIŞAN, H. NAŞCU and V. IANCU 483
Acid-catalysed acetalisation. I. The influence of kind and concentration of acid catalysts on synthesis of bis-1, 1-(2′,2′-ethylhexyloxy)-2-methylpropane, A. I. BLAGA, R. F. PAPE and T. CHIRILĂ 581
1-Acyl-4-aryl-thiosemicarbazides towards heavy metal ions. IV. Behaviour of Ni(II) towards 1-benzoyl-4-aryl-thiosemicarbazides, Behaviour of —, R. CRĂCIUNEANU and E. FLOREAN 397
Adsorption of some cyclic hydrocarbons on active alumina-support for catalysts. I. Determination of adsorption isotherms and of various characteristic thermodynamic values, Comparative study of the-, A. NICOLESCU, M. UDREA and G. POPA 361
Alkyl halides. III. Observations concerning the solvent dependence of correlation factor log *k versus* log $[H_2O]$, The environment influence on solvolysis of —, R. H. SCHUSTER and I. A. SCHNEIDER 1 203
Aluminium chloride catalysed reactions of unsaturated acids with benzene. XI. Isomerizations during the reaction of benzene with 4-methyl-2-pentenoic acid, A.C. RĂZUŞ, ZS. ARVAY and A. M. GLATZ 753
Aluminium chloride catalysed reactions of unsaturated acids with benzene. XII. Methyl esters of cyclohexylidene-acetic and 1-cyclohexenylacetic acids. V. DRĂGUŢAN, ZS. ARVAY and A. M. GLATZ 1 283
Amylose ionic exchanger, Acid and alkali —, H. D. SCHELL, M. ŞERBAN, M. A. MATEESCU and TR. BENŢIA 1 143
Aniline with sodium chlorite, The kinetics of the oxidation of —, A. MEGHEA . . . 1 005
Anion exchangers in aggressive medium. IV. Chemical stability of type I macroporous anion exchangers with binary and ternary structure in basic medium, Degradation of —, I. PETRARIU, M. CUJBA, IG. POINESCU and C. LUCA . . . 797
Anion exchangers in aggressive medium. VI. Effect of hydroxyl ions in the presence of $CuCl_2$ on the chemical stability of macroporous strongly basic quaternary ammonium anion exchangers, Degradation of —, I. PETRARIU, M. L. NEAGU, IG. POINESCU, C. LUCA and P. PETRARIU 1 109
Anionic surfactant analysis from micellar solutions, D. F. ANGHEL and G. POPESCU 251
Anodic oxidation of cyclohexanol, E. CONSTANTINESCU and V. BRÎNZOI. . . . 673
Anodic oxidation of primary alcohols, E. CONSTANTINESCU and V. BRÎNZOI 527
Apparent molal volumes of some common salts in methanol-water mixtures, K. SINGH, D. N. BAJPAI and B. K. DWIVEDI 549
Arbuzov reactions. II. Reactions between trialkylphosphites and ethyl bromides, Study of —, J. M. CACHAZA, J. CASADO and A. VARELA 233
Aromatic hydrocarbons from mineral oils by means of elution chromatography and of electronic absorption spectra, Separation and characterization of—, N. MOŞESCU, G. KALMUŢCHI, R. POPESCU and D. STEJARU 1 475
β-Aroyl-acrylic acid epoxides, Some reactions of —, M.A. EL-HASHASH and M. EL-KADY 1 581
Aryl-amines on 3-aryl-5-arylmethylenerhodanines, The action of —, A. M. KHALIL, A. A. FADDA and M. M. YOUSIF. 935
Arylbenzylketones towards phosphours pentachloride, Different behaviour of isomeric —, A. M. GLATZ, V. DRĂGUŢAN, ZS. ARVAY, C. DRĂGHICI and A. C. RĂZUŞ 595
Atomic emission, Evaluation of a methane-oxygen-air flame for —, E. CORDOŞ and G. BĂRCEANU 287

B.

Basicity effects on the reaction of 5-chloro-2-pentanone with sodium methoxide. Solvent and medium —, N. RĂDULESCU and C. SÂRBU 197

Bentonite by means of X-ray analyzer with electronic microprobe, Determination of the repartition of elements in a —, V. D. LAMBRINO and R. S. NISTOR 625

Benzaldehyde in the catalytical oxidation products of toluene by gas chromatography, Determination of —, S. MAGER, I. HOPÂRTEAN, F. PAIU and R. ŢĂRANU 1 061

Benzophenones with dimethyl homophtalate, Condensation of 3,4-disubstituted — —, M. F. EL-NEWAIHY, E. I. ENAYAT, M. R. SALEM and H. A. ABDEL HAMID 73

BOOK REVIEWS 157, 158, 159, 160, 308, 310, 311, 467, 468, 637, 637, 638, 825, 825, 985, 986, 987, 987, 1 157, 1 157, 1 158, 1 349, 1 505, 1 506, 1 506, 1 507, 1 509 . . . .

α-Bromostearic acid as extraction agent. I. Mechanism of copper(II) extraction, The behaviour of —, A. BOLD and L. BĂLUŞESCU 1 631

C.

Carbides in plasma, On the formation of high-melting —, F. MARX, I. MENESSY and D. BECHERESCU 417

Carotenoids. VI. Isomerizations and rearrangements of canthaxanthin-inchain-epoxides, Inchain-epoxides of —, D. OŞIANU, E. NICOARĂ and C. BODEA 573

Catalytic activity of some $nSiO_2.mAl_2O_3\cdot xH_2O$ systems in the decomposition reaction of cumene hydroperoxide. V. Influence of the reaction medium, Contributions to the study of the —, L. CORMOŞ, A. POP and L. ORBU 225

Catalytic heterogeneous reactions and the principle of detailed balance, Langmuir's rate equation for —, M. VLAD and E. SEGAL 999

Cationic tracer-diffusion coefficients in molten $(Tl\text{-}Alk)NO_3$ systems, ŞT. ZUCA and M. CONSTANTINESCU 995

Cesium and thallium decatungstatediniobiosilicates in the solid state, The study of —, GH. MARCU, L. GHIZDAVU and E. PERŢE 1 559

Chelate complexes with $Co(d^7)$-$N(sp^2)$ bonds, Electronic spectra and magnetic susceptibilites of some new tetrahedral —, A. C. BANCIU 707

Chelate complexes with $Cu(II)$-$N(sp^2)$ bonds, EPR study of —, A. C. BANCIU, O. CONSTANTINESCU and P. SPACU 215

Chemical graphs. XXXIII. Graphs for intramolecular rearrangements of tetragonal-pyramidal complexes, A. T. BALABAN 733

β-*p*-Chlorobenzoylacrylic acids and β-*p*-toluoyl-N-(*o*-carboxyphenyl)-acrylamide, Some reactions with —, E. A. SOLIMAN 1 597

Chloromethylated styrene-divinylbenzene and dimethylformamide, Interaction between —, I. PETRARIU and E. BĂRBÎNŢĂ 119

Chronopotentiometry : application to quasi-reversible processes, Generalized potential-time equations for A. C. —, R. K. JAIN and H. C. GAUR 555

Clathrates, Entropy of some simple gas-water —, L. G. IONESCU 45

Cobalt complex compounds with 3-amino-1-propanol, I. JITARU and M. BREZEANU 559

Complex compounds with tri-*p*-xylylphosphine, D. NEGOIU and M. NEGOIU . . . 1 043

Complex uranyl sulphates. General study of IR spectra of these and other complexes, New —, J. MARTIN GIL and F. J. MARTIN GIL 1 527

Complex uranyl sulphates $UO_2(SO_4)_2K_2.2H_2O$ and $UO_2(SO_4)_3(NH_4)_4\cdot 4H_2O$, Synthesis and crystallographic data of —, J. MARTIN GIL and F. J. MARTIN GIL . . . 1 397

Complexes of cadmium (II) and lead (II) with 3-hydroxypyridine-2-thiol, Polarograhpic behaviour of —, R. S. SINDHU, K. B. PANDEYA and R. P. SINGH . . . 1 279

Complexes of cadmium (II), lead (II) and zinc (II), Polarography of methioninate —, G. N. RAO, V. KUMAR and H. KHAS 1 149

Complexes of transition metals. LVI. Some aspects of the polarographic behaviour of the azido-dimethylglyoximine complexes of cobalt(III), On the α-dioximine —, F. MÁNOK, and CS. VÁRHELYI 917

Complexes of Zn(II), Potentiometric studies on ternary —, V. KUMARI, R. C. SHARMA and G. K. CHATURVEDI 1 275

Complexes with $Ni(d^8)$-$N(sp^2)$ bonds, Electronic and IR spectra of some new square-planar —, A. C. BANCIU 1 251

Computer program for S.C.F.—C.I. calculations I. Closed shell systems, C. BENDIC, M. HILLEBRAND and V. E. SAHINI 3

Concentration fluctuations in chemical systems with nondegenerate reactions. A thermodynamic approach, M. VLAD and M. DRAGOȘ 1 233

Condensation between *o*-chlorobenzaldehyde and dimethyl homophthalate, Studies on the product obtained from Stobbe —, A. M. EL-ABBADY, M. A. OMARA and M. TAHA MAHMOUD 1 465

Condensation of furfural with acetone catalysed by sodium hydroxide, Reaction mechanism for the —, D. A. ISĂCESCU and F. AVRAMESCU 661

Condensation of furfural with acetone in the catalysis of sodium hydroxide. II. The activated complex and its catalytic action, Reaction mechanism for the —, D. A. ISĂCESCU and F. AVRAMESCU 865

Condensation of furfural with acetone in the catalysis of sodium hydroxide. III. Solvent influence on the nature of the activated complex and on its catalytic action, Reaction mechanism for the —, D. A. ISĂCESCU and F. AVRAMESCU . . 873

Coordinate complexes of Zn(II) with aroyl hydrazones, Four and six —, N. S. BIRADAR, V. B. MAHALE and B. R. HAVINALE 55

Copolymerization of acrylonitrile with methacrylic esters in the presence of organometallic catalysts, CR. I. SIMIONESCU, D. FELDMAN and V. NUȚĂ . . 237

Copper-amine complexes, a statistical method to evaluate the dissociation constant of labile complexes, Unidentate —, A. M. BALINT and F. KEREK 725

Copper (II), Studies on coordination compounds, 2-thiosalicylic acid complexes of —, I. A. KHAN, ABDU-SSALAM M. CACA and Z. H. FAROOQI 569

Corrosion of zircaloy-2 in water and steam at high temperature, Study of the influence of fluoride contamination the —, M. RĂDULESCU 351

Cracking of methane in silica vesels, Some remarks on the heterogeneous character of the low temperature —, L. ODOCHIAN and I. A. SCHNEIDER. 835

Cyclic chronopotentiometry, An automatic system for —, E. CORDOȘ, I. ANGYALOSI and C. DIMITRESCU 449

Cyclic organosilicon compounds. Reaction of 1,4-dilithium-1,1,4,4-tetraphenylbutane with organodichlorosilanes, A. CIOBANU, N. LUCHIAN and V. HAMCIUC 943

Cyclic voltammetry determination of α, α'-dimethylphenyl hydroperoxide, C. IDIȚOIU and D. AIKENS 959

Cyclic voltammetry of strontium deposition and dissolution in molten potassium nitrate, S. STERNBERG and T. VIȘAN 505

D.

Dark conductivity of metal-free phthalocyanine, Influence of oxygen on the —, N. I. IONESCU and P. BANYAI 1 023

Decomposition of solids by volumetric measurements : kinetic study, D. FĂTU . . 1 029

Degradation of anion exchangers in agressive medium V. Effect of hydroxyl ions in the presence of ferric chloride on chemical stability of type I macroporous anion exchangers, I. PETRARIU, L. M. NEAGU, C. LUCA, IG. POINESCU and P. PETRARIU 951

Dielectric behaviour of DNA — metal complexes, V. K. SRIVASTAVA, P. K. BANERJI and G. P. SRIVASTAVA 1 049

Dielectric constant on the reaction between simple inorganic anions in solution, Study of the influence of the —, M. S. SUBHANI. 719

Diethanolamine with hexacyanoferrate. III. Kinetics of oxidation of —, M. S. MASOUD, T. M. SALEM and F. M. ASHMAWY 1 367

Diffusion, Fluctuation phenomena in —, M. VLAD 541

3′,4′-Dimethylchalcone and the derivatives, Reactions of —, A. ABDEL MAKSOUD, G. HOSNI, O. HASSAN and S. SHAFIK 1 541

1-Dodecene, Investigation of the autoxidation process of —, T. KOWALSKA 1 589

Dye with dibenz [f, ij] isoquinoline [2,3-b]quinazoline-5,10-dione structure, New cationic —, F. URSEANU and C. DRĂGHICI 1 471

E.

Electrodeposition as a factor influencing the properties of Ni—Fe thin films, Conditions of —, E. BEŁTOWSKA-LEHMAN and A. RIESENKAMPF 883

Electrolytes, The stability of the solid stabilised emulsion with special reference to —, S. P. JAIN and S. N. SRIVASTAVA 1 377

Electron impact-induced fragmentation of dibenzo [b, e] oxepin-11-one and dibenzo [b, e]thiepin-11-one, V. E. SAHINI, V. CONSTANTIN, I. ȘERBAN and C. VLĂDESCU 163

Electron-impact-induced fragmentation of some dibenzo[b, e] thiepines, V. E. SAHINI, V. CONSTANTIN, I. ȘERBAN and C. VLĂDESCU 315

Electronic spectra and structure of 4-arylhydrazono-3-methyl-5-pyrazolones, S. H. ETAIW, F. A. ANWER and F. M. ISSA 79

Elements Cu(II)-Zn(II)-Pb(II)-Fe(II), Fe(III) by means of ions exchangers, Separation of —, L. VLĂDESCU and M. COSTACHE 1 553

Epoxides with *t*-butoxidein *t*-butanol, The kinetics and reactions of some aryl-substituted —, M. HASSAN, A. R. O. ABDEL NOUR and A. M. SATTI 747

Equilibrium computation, Methods for complex reaction systems —, R. MIHAIL, C. V. RADU and I. M. BELCEA 681

F.

Fatty acids, Studies in spectral and magnetic properties and non-isothermal decomposition of pyridine adducts of some salts of fatty acids, L. PARDESHI, A. RASHEED and R. A. BHOBE 1 291

Ferricyanide in the presence of hydrogen peroxide, Spectrophotometrical studies of the kinetics of the conversion of ferrocyanide to —, K. K. GIRDHAR 819

Flash photolysis decomposition of sulphate and sulphite anions in aqueous solution, M. S. SUBHANI and Z. KAUSER 1 129

Flash photolysis studies of aqueous solution of thiosulphate ion, M. S. SUBHANI and T. KAUSAR 1 619

Flash photolysis study of SeO_3^{2-} anion in aqueous solution, M.S. SUBHANI and T. KAUSAR 1 627

Flash photolysis study of TeO_3^{2+} anion in aqueous solution, M. S. SUBHANI and T. KAUSAR 1 341

Furan molecule, On the vibrational anharmonicities of the —, D. IORDACHE . . . 301

G.

Gallic acid using an oxygen-selective electrode, Kinetic aspects of the oxidation reaction of —, GH. IONESCU, F. MATEI ann AL. DUCA 1 611

Gallium obtained by a simple technique, Highly pure —, V. LĂZĂRESCU and M. F. LĂZĂRESCU 861

H.

Heat of combustion of mono- and difurfurylidene acetone, F. AVRAMESCU and D. A. ISĂCESCU 655

Heats of decomposition from thermogravimteric data, Method for calculating —, P. ROTARU, G. NIAC and S. I. BLEJOIU 489

Heterocyclic compact condensed systems. III. Isomer 9-aminothiazolo[4,5-f]indazole, C. TĂRĂBĂȘANU-MIHĂILĂ, F. URSEANU, L. FLORU and B. MĂRCULESCU 977

Heterocyclic compact condensed systems. IV. Linear bis pyrazolo[2,3-d], 8,9-d *trans*-quinacridone, C. TĂRĂBĂȘANU-MIHĂILĂ, C. ZAHARIA, L. FLORU, F. URSEANU and B. MĂRCULESCU 1 079

Heterocyclic quinones, X. Synthesis and antibacterial screening of new thiazolocarbazoloquinones, A. S. HAMMAM and H. S. EL-KASHEF 587

Hexahalodisilanes, A modified Urey-Bradley force field for —, V. E. SAHINI, R. GRIGOROVICI and A. BUTUCELEA 643

Hexamethoxy-cyclotriphosphazene and octamethoxy-cyclotetraphosphazenes. Kinetics and mechanism of the alkaline hydrolysis of —, P. SCHULZ and R. VÎLCEANU 1 455

I.

Iodine-123 for medical purposes, Production of —, M. ROMAN, C. PENCEA, D. CRISTU, I. MÎNZATU, A. CALBOREANU, O. SĂLĂGEAN, C. BRATU and GH. PETEU 1 499

Ion selective membrane-electrodes for organic analysis. I. Liquid membrane-electrode for some organic anions based on cetylpyridinium salt, E. HOPÎRTEAN and E. VERESS 273

Ionization potentials using a MI-1305 mass spectometer, Determination of —, V. E. SAHINI, V. CONSTANTIN and I. ŞERBAN 479

Iridium (III) with substituted pyrimidinethiols, Spectrophotometric determination of —, A. K. SINGH, M. KATYAL and R. P. SINGH. 1 153

Iron oxide on the catalytic activity of the catalyst, Influence of the origin of —, A. SWINARSKI and W. KLAFKOWSKI 171

2-Isopropyl-[4H]-3,1-benzonazin-4-one, Some reactions of —, A. F. M. FAHMY, M. A. EL-HASHASH, M. M. HABASHY and S. A. EL-WANNISE 1 567

Isothiocyanatochromates using bromine monochloride, Determination of —, P. K. MATHUR 1 607

Isotope effects in lanthanide — induced shifts of ^{1}H-NMR spectra of selectively side--chain deuteriated pyridines, A. T. BALABAN, I.I. STĂNOIU and F. CHIRALEU 187

Isotopic exchange of active methyl groups. XI. Kinetics of deuteriation of 2,6-diaryl-4-methylpyrylium salts, A. T. BALABAN, I. I. STĂNOIU, F. CHIRALEU and I. MOŢOC 143

Isozeaxanthin films at the oil/water and air/water interfaces, E. CHIFU, M. TOMOAIA, E. NICOARĂ and A. OLTEANU. 1 163

K.

Kekulé structures and topology. III. On inseparability of Kekulé structures, I. GUTMAN, M. RANDIĆ and N. TRINAJSTIĆ 383

L.

Layer chromatograms, Enhancement of exactitude and reduction of time in planimetry of thin —, W. SCHMIDT, D. MARANDIUC, A. NEMEŞ and G. OSTROGOVICH 295

Liquid-liquid interfaces as potentiometric ion-sensors. III. The n-octanol-aqueous solution interface in the acid-base potentiometric titration, M. MIOŞCU and M. GREBLĂ 1 345

Liquid membrane-electrodes. XII. Liquid membrane-electrodes for perchlorate, thiocyanate, tetrafluoroborate and nitrate based on triphenylmethane dyes, E. HOPÎRTEAN, and E. ŞTEFĂNIGĂ 137

Living matter, Chemical model for the synthesis of —, CR. I. SIMIONESCU, S. DUMITRIU, V. I. POPA, V. BULACOVSCHI and B. SIMIONESCU 89

M.

Manganese complexes with ligands containing O—N—N—O sequence, Divalent —, N. S. BIRADAR, V. B. MAHALE and B. R. HAVINALE 1 261

Melting, Lindemann law of —, M. ŞERBAN. 1 013

Membrane electrode, Some analytical applications of a new Ag$^+$-selective—, V. V. COŞOFREŢ 1 489

Metallocenes of the first-row transition-metal ions. II. A molecular-orbital study of the ground and excited -state properties of —, D. R. ARMSTRONG, R. FORTUNE and P. G. PERKINS 1 179

Metallocomplexes of salicylaldehyde-thiocarbohidrazone, C. GH. MACARAOVICI and S. BARBU 1 035

Methane, Some pecularities of the slow oxidation reaction of —, I. G. MURGULESCU and M. BOZEŞANU 991

16 α-Methyl Reichstein S 21-acetate from 16-dehydropregnenolone acetate, O. MANTSCH and M. BUCHWALD 921

Mixed ligand compounds, Fluorescence spectra of some Eu(III) and Tb(III) —, S. PLOŞTINARU and P. SPACU 1 417

Molal volumes of ions in N-methylacetamide, The limiting apparent —, K. SINGH 31

Molecular charge-transfer complexes of iodine bromide with methylpyridines, J. R. MASAGUER, A. SOUSA-ALONSO, J. A. GARCÍA-VÁZQUEZ and A. BLANCO 1 409

Molecular complexes between 1,3,7,9-tetranitrophenothiazine-5-oxide and amines, Kinetic investigation of some —, A. SECARĂ, A. TURCU and E. SEGAL 147

Molecular complexes of nitrophenols with hexamethylenetetramine and their isomers, M. VĂGĂONESCU, S. MAGER and L. MUNTEANU 63

Molecular interactions in anisidine. III. IR spectra and heats of dilution, V. E. SAHINI and L. TELEA 483

Molecular orbital calculations on transition metal complexes. XII. Unpaired electron distributions, D. W. CLACK and M. MONSHI 495

Molten alkali halide mixtures, Electrical conductivity and the structure of binary —, ŞT. ZUCA 829

Monocarboxylic acids formed by catalytic autoxidation of n-alkanes in liquid phase with molecular oxygen, On the influence of the chain length of n-alkanes on the composition of —, I. DRIMUŞ and L. PAPAHAGI 209

N.

Natural gas with water vapour, Electric conductivity of catalysts for the conversion of —, B. R. ALEKSIĆ, A. TERLECKI-BARIČEVIĆ and M. AČIMOVIĆ 1431

Nickel(II) coordination compounds with 3-amino-1-propanol, M. BREZEANU and I. JITARU 909

O.

Organic anions on strongly basic macroporous ion-exchangers, Relation of —, C. LUCA, G. GHIŢANU, I. PETRARIU, A. AIRINEI and A. CARPOV 1 653

Oxidation of tertiary amines by permanganate, Kinetic study of the —, S. SENENT, F. MATA and M. A. de la PEÑA 841

Oxides films formed on titanium in air at high temperature, On the aspect of —, D. CISMARU and M. MOMIRLAN 1 361

Oxidoreduction. Reaction of the bisoxalatodiaquo Co(II) complex with iodide ion in acid medium, Kinetics and mechanism of —, I. G. MURGULESCU and G. MINCU 471

Oxygen adsorption at semiconducting CdS, A remark on —, O. PESHEV 1 003

P.

Parametrization among the approximate SCF-LCAO-MO methods, A new type of —, S. MOLDOVEANU 453

Pb(II) and 5-mercapto-2-amino-1,3,4-thiadiazole. Analytical applications, Study of the reaction between —, L. ROMAN, E. FLOREAN, M. ECHIM-GROSU and C. DORDEA 929

Peptides. XVI. The use of β-dicarbonyl N-protected methionine and tryptophan in peptide synthesis, F. GÖNCZY, A. BALOG, E. VARGHA, D. BREAZU and I. HALLER 1 093

Peroxides. I. Conditions of the polarographic analysis of organic peroxides, Polarographic investigations of the chemical constitution and reaction mechanisms of organic —, B. TŐKES 805

Peroxides obtained by thermal oxidation of n-dodecane with molecular oxygen. I. Thermal degradation of samples obtained at various conversions. II. Separation of a peroxidic concentrate from n-dodecane oxidized at a law conversion ; thermocatalytic degradation of this concentrate, Degradation of —, I. DRIMUȘ, L. PAPAHAGI and C. CRISTESCU 407

Perturbation approaches for kinetics of isotope exchange reactions, M. VLAD . . . 523

Phenol and salicylic acid in industrial wastes, Separation and determination of —, S. GOCAN, T. HODIȘAN, H. NAȘCU and C. GEORGESCU 265

Phenothiazine drugs, Microreactions combined with thin-layer chromatography for the identification of —, T. CONSTANTINESCU, ȘT. ENACHE and R. VASILIEV 967

Phosphorus in conjugated six-membred rings, Hybridization of dicoordinated trivalent and tetracoordinated pentavalent —, M. MRACEC and Z. SIMON 769

Pigment mixtures, Computation program concerning the resulting colour of —, C. SAVII, T. P. TĂVALĂ, N. GR. BRÎNZAN and G. G. SAVII 1337

Polyacrylamides in electrolyte solutions, Contraction of —, R. VÎLCU, M. LECA and M. OLTEANU 1 171

Poly(2,4-dimethyl-styrene) obtained by cationic polymerization, Physico-chemical study of —, J. CLAUS and E. MARÉCHAL 1 325

Polyethylene. V. Lamellar recrystallization in shear history, Amorphous-crystalline coupling in —, GH. DRĂGAN 261

Polyethylene. VI. The study of the morphological changes in high molecular weight polyethylene by compounding with polypropylene, Amorphous — crystalline coupling in —, GH. DRĂGAN 435

Polyethylene. VII. Study of the crystallization kinetics in the approximation of the purely termal disipative coupling, Amorphous-crystalline coupling in —, GH. DRĂGAN 629

Polyethylene. VIII. Relativistic effects in disclination state forming processes, Amorphous-crystalline coupling in —, GH. DRĂGAN 1 313

Polyethylene sheets, Infrared spectral study of hydrogen bonding in ethyl alcohol absorbed in —, S. BĂDILESCU, V. TĂLPUȘ and R. RACOTĂ 535

Polymerization of acetylenic derivatives. XXXI. Electron spin resonance of polyaryl-acetylene isomers, On the —, S. DUMITRESCU, V. PERCEC and CR. I. SIMIONESCU 1 303

Polymerization of N.N'-bismaleimide, Thermal and photoinduced —, G. M. GHERASIM and L. STOICESCU-CRIVETZ 111

Polynuclear complex compounds of iron, cobalt and nickel. II. Bismuth-containing complex compounds, M. BREZEANU, and M. DINCULESCU 1 389

Polynuclear complex compounds of iron, cobalt and nickel. III. Bismuth-containing complex compounds, M. BREZEANU and M. DINCULESCU 1 533

Polynuclear complex compounds of iron, cobalt and nickel. III. Mercury-containing complex compounds, M. BREZEANU and M. DINCULESCU 699

Polyphenols by thin layer chromatography with orthogonal temperature gradient, Separation of —, S. GOCAN, C. KONNERT and H. VOIK 133

Porous electrodes. II. Influence of area on the activity of Raney-nickel-titanium-electrodes in the anodic oxidation of methanol, Two phase —, O. RADOVICI, A. BANDI and C. CĂPĂȚ 1 513

Porous two- phase electrodes. I. Raney-Ni-Ti-electrodes for anodic oxidation of methanol, A. BANDI 1 373

Potassium bis-2-phospho-17-tungstouranate, Thermal behaviour of —, GH. MARCU, M. RUSU and E. PERȚE 1 403

Preparation of ^{99m}-Tc generator for medical use, Practical indications for the —, M. Y. MIRZA 429

Protection of DNA by metal coordinates — A simple stoichiometric study, V. K. SRIVASTAVA, C. SINGH and B. B. MISRA. 377

Pulse radiolysis and flash photolysis studies of SeO_4^{2-} anion in aqueous solution, M. S. SUBHANI and M. KHALID 1 117

Pyridazinium-ylids. IX. Addition of aryl-pyridazinium-ylids on activated olefins, M. PETROVANU, I. DRUȚĂ and MAI VAN TRI 781

Pyridinemonocarboxylate ion selective electrodes, L. CAMPANELLA, T. FERRI and D. GOZZI 281

Pyridinium-cyano-amydo-methylide, Experimental and theoretical study on the reaction of the loss and amido group from the —, G. SURPĂȚEANU, M. CONSSTANTINESCU and I. ZUGRĂVESCU 1 449

Pyridinium-N-imine with picryl chloride, a route to 6-aza-benzo [a] indolizine system, The reaction of —, C. LEONTE and E. CARP 1 461

Pyrylium cations, Solvent- and lanthanide-induced shifts in the ^{1}H-NMR spectra of 4-acetonylidene-2,6-dimethyl[4H]pyran and its tautomeric protonated —, A. T. BALABAN and M. D. GHEORGHIU 1 065

Q.

Quinazolone, Reactions on 2-phenyl-3-amino-4(3H)-, M. ANWAR, F. I. ABDEL-HAY and M. FAHMY 1 085

Quinoneanils, Preparation and spectrophotometric studies of some —, I. M. ISSA, A. A. EL SAMAHY, R. M. ISSA and H. S. EL KASHEF 617

R.

Rationalization of numerical integration of Mayo-Lewis equation, Considerations upon —, I. AGHERGHINEI 445

Reduction of Cr(VI) by hydrazine, Kinetic study of the —, S. SENENT, L. FERRARI and A. ARRANZ 179

S.

Solid oxid catalysts. III. Transalkylation of toluene on synthetic zeolite, Formation and nature of active centres in —, I. SĂNDULESCU, O. ŞERBAN, S. DAVIDENCO, R. E. RUSSU and L. FRUNZĂ 1 575

Spiro-3-arylidene-1,2,3,4-tetrahydronaphthalene-4-ones. I. Reactions with amines and Friedel-Crafts reactions, ABD EL-KADER FATEEN, A. M. KADDAH and Y. M. NAGUIB 759

Spiro-3-arylidene-1,2,3,4-tetrahydronaphthalene-4-ones. II. Synthesis of spiropyrazolines ABD EL-KADER FATEEN and M. KADDAH 791

Stability constant of $FeCl_4^-$ in molten $NaFeCl_4$, M. ABRAHAM and M. POIRIER 339

Stilbene derivatives. VII. MO-LCI-PPP calculations for some polynitro-*trans*-stilbene derivatives, Electronic structure of some —, L. CIOHODARU, C. C. RENŢIA and I. ZAMFIRESCU 853

Sulphides, A modified non cyanide scheme for the qualitative chemical analysis of the group II A —, A. M. QURESHI and S. A. MALIK 269

Sulphonamide to sulphone. I. Conversion of substituted aryl-quinolylamine sulphonamide to the isomeric substituted diarylsulphone, Proton-catalysed rearrangement of —, S. S. SRIMALI, N. D. SHARMA, S. KUMAR and B. C. JOSHI 613

Sulphonamides, benzamides and benzohydrazides. XXIV. Complex compounds of Cu(II) and Cd(II) with isomeric *ortho-*, *meta* and *para*-amino-bezamides, Investigation of —, R. MICU-SEMENIUC, T. DOBOS-ADAM and C. GH. MACAROVICI 1 519

Sultam synthesis, S. H. DOSS 577

Surface tension of simple fused halides, S. STERNBERG and M. TERZI 325

Synthesis of 4-Hydroxy-Δ^2-oxadiazolines-1,2,4, S. DESHERCES, J. BARRANS and J. L. ROUBATY 203

T.

Temperature gradient chromatography. II. Determination of the minimum chromatographing time necessary for the separation of some component mixtures, by applying a constant temperature gradient, Optimization of the separation process in —, C. LITEANU and T. HODIŞAN 125

Thallium (III) from its chloride and bromide solutions with isoamyl alcohol (IAA) and amyl acetate (AA), Extraction of —, K. K. KAKKAR and D. C. RUPAINWAR 1 139

Thermodynamic properties of binary liquid mixtures, R. SINGH, S. PRAKASH and O. PRAKASH 667

Thermodynamic properties of maleic, trimellitic and pyromellitic anhydrides, D. I. MARCHIDAN and M. CIOPEC 19

Thermodynamic properties of $RbCl\text{-}CaCl_2$ and $CsCl\text{-}CaCl_2$ molten systems, L. TOPOR and I. MOLDOVEANU 1 353

Thienylpyridines, Conformational analysis and electronic structure of —, J. V. KNOP, N. TRINAJSTIĆ, M. MILUN and S. PEJAKOVIĆ 103

Thin films on silicon by infrared interference, *In situ* evaluation of the chemical vapor deposition rate of some —, C.-E. MOROŞANU and E. SEGAL 515

Thiocarbohydrazone of aromatic and heteroaromatic aldehydes, Physico-chemical study of some —, S. BARBU and C. GH. MACAROVICI 1 243

Thiocomplexes. VI. Complex compounds of Pt(II) with thioamides of the dibenzofuran series, Contributions to the chemistry of —, D. NEGOIU, V. MUREŞAN and N. MUREŞAN 371

Titanium (IV) complexes with 2,2′-dihydroxychalkones, N. S. BIRADAR and B. R. PATIL 1 425

Titanium (IV) compounds with Schiff bi- and three-dentate bases, On —, A. KRIZA and M. NASTA 1 267

Transition-metal organic compounds. I. On the reaction of ethyl diazoacetate with strained alkenes, catalyzed by π-allylpalladium chloride complexes, Chemistry of —, A. GHENCIULESCU, L. ENESCU, H. L. PRAŞAD, F. CHIRALEU, I. G. DINULESCU and M. AVRAM 1 441

Triazines. LVI. HMO calculations for derivatives of 1,3,5-triazine, On —, O. HOROWITZ 603

Trigonally distorted octahedral d^1 systems : the $Ti(H_2O)_6^{3+}$ complex ion in frozen aqueous solutions, *g*-Values of —, P. I. PREMOVIČ 1 213

U.

Unperturbated dimensions of copolymers. Poly(N-vinylcaprolactam-diethylfumarate) alternating copolymer, C. CINCU and C. BOGHINĂ 255

Uranyl bis-(chelated) complexes. II. Configurational rearrangement of bis-(benzoylacetonate) uranyl chelate, Dynamics of the ligand exchange in —, A. VASILESCU and T. ONCESCU 1 055

V.

Vanadium in IV, V and intermediate oxidation state, Oxides and oxide hydrates of —, F. THÉOBALD 887

Vibrational spectrum of β-vanadylsulphate, E. J. BARAN 37

Vibrational symmetry coordinates for some arsenic chalcogenides, A. BUTUCELEA and R. GRIGOROVICI 651

NOTE POUR LES AUTEURS

La Revue Roumaine de Chimie publie des articles en anglais, français, russe, allemand ou espagnol. Les auteurs sont priés d'envoyer des articles et des comptes rendus inédits.

Les manuscrits seront dactylographiés à deux intervalles. La bibliographie, les tableaux et la légende des figures seront placés après le texte.

Si l'article fait partie d'une série numérotée, le titre de la partie précédente sera indiqué dans une note au bas de la première page.

Chaque article sera précédé d'un résumé comprenant quinze lignes au maximum.

Les références bibliographiques dans le texte seront faites par des exposants sans parenthèse et paraîtront comme des notes au bas de chaque page.

Les publications périodiques mentionnées dans la bibliographie seront présentées suivant les prescriptions internationales : le nom de l'auteur précédé de l'initiale du prénom, le titre du périodique abrégé conformément à « Chemical Abstracts » et souligné par une ligne, le numéro du tome, indiqué par des chiffres arabes et souligné par deux lignes, suivi de la première page de l'article ; à la fin, l'année de la parution sera placée entre parenthèses. Le numéro de la revue ne sera pas indiqué si les pages du volume sont numérotées consécutivement. Pour les revues dont les tomes ne sont pas numérotés (par ex. Bull. Soc. Chim. France, etc.), l'année de la parution soulignée par deux lignes précédera l'indication de la page.

Les textes des livres ou traités inclueront : les noms des auteurs, les initiales du prénom, le titre du livre entre guillemets et sans être souligné, le numéro du tome précédé par l'abréviation « vol. » (ou « Bd. »), le numéro de l'édition, les éditions (the publisher), la localité de la parution et la page de la référence précédée par l'abréviation « p. » (ou « S. »).

Les brevets seront indiqués comme suit : l'auteur ou la firme, le pays et le numéro du brevet, la date et la revue (Chem. Abstr.). Par ex : M. Jones (to Union Carbide Co.), Brit, Pat. 601 238, 2 Sept. 1959, *Chem. Abstr.*, **54**, 12808 (1960).

Si la référence n'a pas été lue en original, on indiquera aussi la revue de références consultée.

Les diagrammes seront tracés à l'encre de Chine sur papier calque. Les tableaux et les figures (en nombre strictement nécessaire) seront numérotés par des chiffres arabes et leur explication sera donnée dans la légende des figures. Prière de ne pas inscrire les mêmes données dans les tableaux et les figures. Chaque tableau aura un titre. On indiquera dans le texte la place approximative des tableaux et des figures. Les formules chimiques seront incluses dans le texte ; en outre, elles seront transcrites sur papier calque, à l'encre de Chine.

Les auteurs sont priés d'indiquer les caractères italiques (en soulignant les lettres au crayon) ainsi que tout autre caractère spécial ; les préfixes *ortho*, *meta*, *para*, *cis*, *trans*, etc. seront soulignés pour indiquer leurs caractères italiques et ne seront jamais écrits avec des majuscules.

Aucune correction à la main ne sera admise sur le manuscrit. Les corrections seront frappées à la machine. Les lettres grecques ou d'autres symboles spéciaux seront insérés à la main à l'encre clairement.

Le manuscrit sera signé par l'auteur.

Le colonne-titre aura 50 lettres au maximum.

L'entière responsabilité du contenu des articles appartient aux auteurs.

TRAVAUX PARUS AUX ÉDITIONS DE L'ACADÉMIE DE LA RÉPUBLIQUE SOCIALISTE DE ROUMANIE

DUMITRU NEGOIU, ANGELA KRISA, **Poluanţi anorganici în aer** (Polluants inorganiques en l'air), 1977, 220 p.

D. PURDELA (sous la direction), **Nomenclatura chimiei anorganice** (La nomenclature de la chimie inorganique), 1977, 153 p.

I. ZUGRĂVESCU, MAGDA PETROVANU, **N-Ylid Chemistry**, 1977, 396 p.

C. DRĂGULESCU, E. PETROVICI, **Chimie structurală modernă. Chimia coordinanţei 8** (La chimie strcturale moderne. La chimie de la coordinence 8), 1977, 947 p.

I. G. MURGULESCU, **Introducere în Chimia fizică. Vol. I. 1. Atomi, molecule, legătură chimică** (Introduction à la Chimie Physique, Ier vol. 1. Atomes, molécules, liaison chimique), 1976, 560 p.

E. P. BALTĂ, E. BALTĂ, **Introduction to the physical chemistry of the vitreous state**, coédition avec Abacus Press, 1976, 287 p.

M. I. GĂLĂŢEANU, **Radiochimia aplicată. Metode şi probleme** (La radiochimie appliquée. Méthodes et problèmes), 1976, 307 p.

CONST. V. UGLEA, **Cromatografia pe gel permeabil. Noi domenii de aplicare** (La chromatographie sur gel perméable. Nouveaux domaines d'application), 1976, 123 p.

FRANCISC A. GOTHARD, **Echilibre lichid-vapori. I. Baze teoretice şi metode de calcul** (Equilibres liquide-vapeurs. I. Bases théoriques et méthodes de calcul), 1975, 263 p., 2 pl.

CONST. GH. MACAROVICI, D. MACAROVICI, **Chimia oxizilor dubli şi utilizările lor** (La chimie des oxydes doubles et leur utilisation), 1975, 195 p.

M. AVRAM, **Antidăunători** (Pesticides), 1974, 496 p.

ELENA CEAUŞESCU, **Research work on synthesis and characterization of macromolecular compounds. Contributions**, 1974, 251 p.

DUMITRU COSTACHE, **Analiza chimică prin metoda cinetică** (L'Analyse chimique par la méthode cinétique), 1974, 251 p.

G. E. RĂDULESCU, **Proprietăţile ţiţeiurilor româneşti** (Les propriétés des pétroles roumains), 1974, 267 p., 2 pl.

CR. SIMIONESCU, VIORICA RUSAN, V. POPA, **Chimia algelor marine** (La chimie des algues marines), 1974, 212 p., 1 pl.

MARIA FITI, **Dozimetria chimică a radiaţiilor ionizante** (La dosimétrie chimique des radiations ionisantes), 1973, 240 p.

TIBERIU NĂŞCUŢIU, **Metode radiochimice de analiză** (Méthodes radiochimiques d'analyse), 1973, 384 p.

CRISTOFOR SIMIONESCU, MARGARETA GRIGORAŞ, AGATA CERNĂTESCU ASANDEI, GHEORGHE ROZMARIN, **Chimia lemnului în România. Plopul şi salcia** (La Chimie du bois en Roumanie. Le peuplier et le saule), 1973, 299 p., 13 pl.

MIHAI FLORESCU, **Eficienţa economică a cercetării ştiinţifice** (L'efficience économique de la recherche scientifique), 1972, 115 p.

GEORGETA LĂZĂRESCU, **Sistematizarea informaţiilor în chimia organică** (Systématisation des informations en Chimie organique), 1972, 243 p., 1 pl.

I. P. INFORMAŢIA c. 510

43426

Lei 25—

$45 (price per year)